frontiers | Research Topics

Clinicopathological factors and staging in gastrointestinal cancers

Edited by
Qi Liu, Chang-In Choi, Shouki Bazarbashi, Ravindra Deshpande and Sanjit Mukherjee

Published in
Frontiers in Oncology
Frontiers in Surgery
Frontiers in Medicine

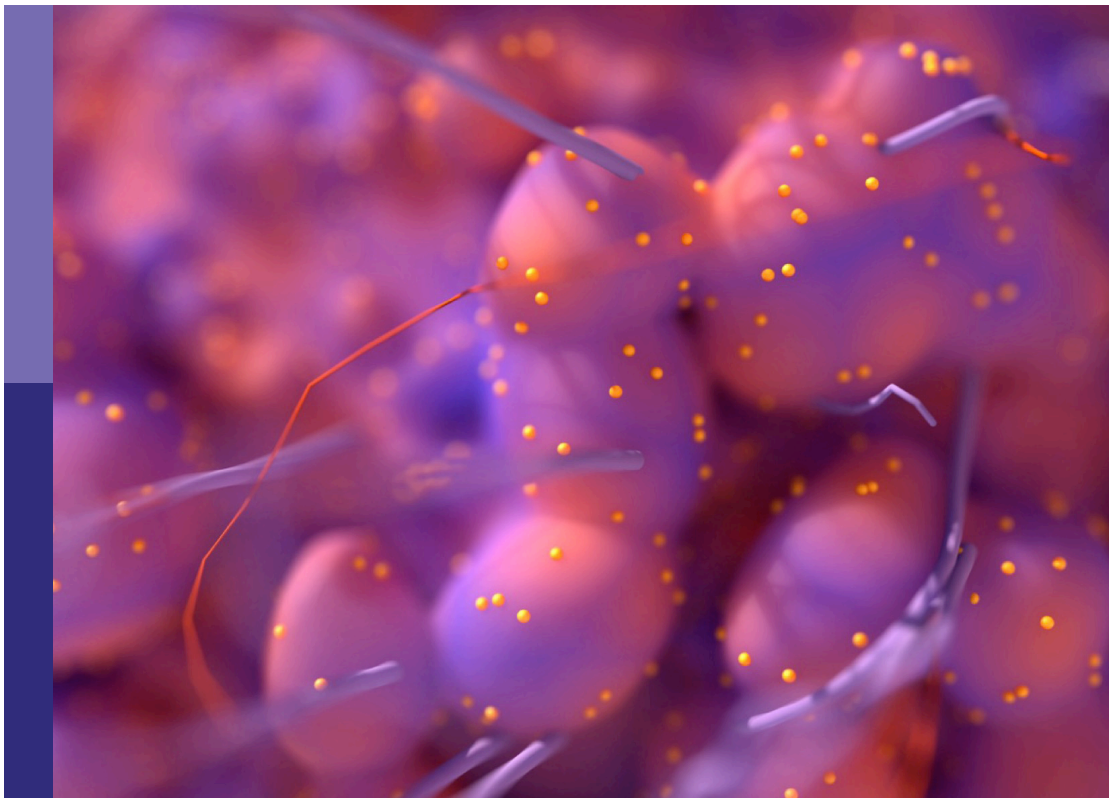

FRONTIERS EBOOK COPYRIGHT STATEMENT

The copyright in the text of individual articles in this ebook is the property of their respective authors or their respective institutions or funders. The copyright in graphics and images within each article may be subject to copyright of other parties. In both cases this is subject to a license granted to Frontiers.

The compilation of articles constituting this ebook is the property of Frontiers.

Each article within this ebook, and the ebook itself, are published under the most recent version of the Creative Commons CC-BY licence. The version current at the date of publication of this ebook is CC-BY 4.0. If the CC-BY licence is updated, the licence granted by Frontiers is automatically updated to the new version.

When exercising any right under the CC-BY licence, Frontiers must be attributed as the original publisher of the article or ebook, as applicable.

Authors have the responsibility of ensuring that any graphics or other materials which are the property of others may be included in the CC-BY licence, but this should be checked before relying on the CC-BY licence to reproduce those materials. Any copyright notices relating to those materials must be complied with.

Copyright and source acknowledgement notices may not be removed and must be displayed in any copy, derivative work or partial copy which includes the elements in question.

All copyright, and all rights therein, are protected by national and international copyright laws. The above represents a summary only. For further information please read Frontiers' Conditions for Website Use and Copyright Statement, and the applicable CC-BY licence.

ISSN 1664-8714
ISBN 978-2-8325-2221-9
DOI 10.3389/978-2-8325-2221-9

About Frontiers

Frontiers is more than just an open access publisher of scholarly articles: it is a pioneering approach to the world of academia, radically improving the way scholarly research is managed. The grand vision of Frontiers is a world where all people have an equal opportunity to seek, share and generate knowledge. Frontiers provides immediate and permanent online open access to all its publications, but this alone is not enough to realize our grand goals.

Frontiers journal series

The Frontiers journal series is a multi-tier and interdisciplinary set of open-access, online journals, promising a paradigm shift from the current review, selection and dissemination processes in academic publishing. All Frontiers journals are driven by researchers for researchers; therefore, they constitute a service to the scholarly community. At the same time, the *Frontiers journal series* operates on a revolutionary invention, the tiered publishing system, initially addressing specific communities of scholars, and gradually climbing up to broader public understanding, thus serving the interests of the lay society, too.

Dedication to quality

Each Frontiers article is a landmark of the highest quality, thanks to genuinely collaborative interactions between authors and review editors, who include some of the world's best academicians. Research must be certified by peers before entering a stream of knowledge that may eventually reach the public - and shape society; therefore, Frontiers only applies the most rigorous and unbiased reviews. Frontiers revolutionizes research publishing by freely delivering the most outstanding research, evaluated with no bias from both the academic and social point of view. By applying the most advanced information technologies, Frontiers is catapulting scholarly publishing into a new generation.

What are Frontiers Research Topics?

Frontiers Research Topics are very popular trademarks of the *Frontiers journals series*: they are collections of at least ten articles, all centered on a particular subject. With their unique mix of varied contributions from Original Research to Review Articles, Frontiers Research Topics unify the most influential researchers, the latest key findings and historical advances in a hot research area.

Find out more on how to host your own Frontiers Research Topic or contribute to one as an author by contacting the Frontiers editorial office: frontiersin.org/about/contact

Clinicopathological factors and staging in gastrointestinal cancers

Topic editors

Qi Liu — Fudan University, China

Chang-In Choi — Pusan National University Hospital, Republic of Korea

Shouki Bazarbashi — King Faisal Specialist Hospital & Research Centre, Saudi Arabia

Ravindra Deshpande — Wake Forest University, United States

Sanjit Mukherjee — National Institutes of Health (NIH), United States

Citation

Liu, Q., Choi, C.-I., Bazarbashi, S., Deshpande, R., Mukherjee, S., eds. (2023). *Clinicopathological factors and staging in gastrointestinal cancers*. Lausanne: Frontiers Media SA. doi: 10.3389/978-2-8325-2221-9

Table of contents

11 Editorial: Clinicopathological factors and staging in gastrointestinal cancers
Ravindra Deshpande

13 A Novel Nomogram Based on Hepatic and Coagulation Function for Evaluating Outcomes of Intrahepatic Cholangiocarcinoma After Curative Hepatectomy: A Multi-Center Study of 653 Patients
Yunshi Cai, Bohan Zhang, Jiaxin Li, Hui Li, Hailing Liu, Kunlin Xie, Chengyou Du and Hong Wu

23 Impact of Inadequate Number of Lymph Nodes Examined on Survival in Stage II Colon Cancer
Qi Wu, Zhiyuan Zhang, Yijiao Chen, Jiang Chang, Yudong Jiang, Dexiang Zhu and Ye Wei

29 Diabetes Mellitus Increases the Risk of Hepatocellular Carcinoma After Direct-Acting Antiviral Therapy: Systematic Review and Meta-Analysis
Szilárd Váncsa, Dávid Németh, Péter Hegyi, Zsolt Szakács, Ádám Farkas, Szabolcs Kiss, Péter Jenő Hegyi, Anna Kanjo, Patrícia Sarlós, Bálint Erőss and Gabriella Pár

39 Albumin-To-Alkaline Phosphatase Ratio as a Novel and Promising Prognostic Biomarker in Patients Undergoing Esophagectomy for Carcinoma: A Propensity Score Matching Study
Xianying Zhu, Dongni Chen, Shuangjiang Li, Wenbiao Zhang, Yongjiang Li, Xiaoyu Wang, Jian Zhou and Zhesheng Wen

59 Predicting Survival of Patients With Rectal Neuroendocrine Tumors Using Machine Learning: A SEER-Based Population Study
Xiaoyun Cheng, Jinzhang Li, Tianming Xu, Kemin Li and Jingnan Li

70 Systemic Therapy for Microsatellite Instability Small Bowel Adenocarcinoma With Mesenteric Vascular Embolism as Initial Symptom: A Case Report
Zhongyi Dong, Xiang Xia and Zizhen Zhang

77 Comparison of Vascular Invasion With Lymph Node Metastasis as a Prognostic Factor in Stage I-III Colon Cancer: An Observational Cohort Study
Jung Hoon Bae, Ji Hoon Kim, Bong-Hyeon Kye, Abdullah Al-Sawat, Chul Seung Lee, Seung-Rim Han, In Kyu Lee, Sung Hak Lee and Yoon Suk Lee

86 Decrease in Blood Neutrophil-to-Lymphocyte Ratio Indicates Better Survival After Neoadjuvant Chemotherapy in Patients With Advanced Gastric Cancer
Ziyi Liu, Yahang Liang, Xiaolong Tang and Hui Qu

96 Comparing the Expressions of Vitamin D Receptor, Cell Proliferation, and Apoptosis in Gastric Mucosa With Gastritis, Intestinal Metaplasia, or Adenocarcinoma Change
Li-Wei Chen, Liang-Che Chang, Chung-Ching Hua, Tzu-Chien Cheng and Chin-Chan Lee

106 Prognostic Enigma of Pancreatic Solid Pseudopapillary Neoplasm: A Single-Center Experience of 63 Patients
Xinbo Wang, Daojun Zhu, Wei Bao, Min Li, Sizhen Wang and Rongxi Shen

114 Comparison of Four Lymph Node Stage Methods for Predicting the Prognosis of Distal Cholangiocarcinoma Patients After Surgery
Xiuyi Huang, Xiaoya Niu, Zhen You, Youlin Long, Fan Luo and Hui Ye

123 Clinicopathological Features Combined With Immune Infiltration Could Well Distinguish Outcomes in Stage II and Stage III Colorectal Cancer: A Retrospective Study
Jiazi Ren, Linfeng Xu, Siyu Zhou, Jian Ouyang, Weiqiang You, Nengquan Sheng, Li Yan, Du Peng, Lu Xie and Zhigang Wang

136 Metastasis Pattern and Survival Analysis in Primary Small Bowel Adenocarcinoma: A SEER-Based Study
Yanmei Gu, Haixiao Deng, Daijun Wang and Yumin Li

151 Higher Lymph Node Metastasis Rate and Poorer Prognosis of Intestinal-Type Gastric Cancer Compared to Diffuse-Type Gastric Cancer in Early-Onset Early-Stage Gastric Cancer: A Retrospective Study
Chao-Tao Tang and Si-Hai Chen

166 Incidence, Risk Factors and Prognosis of T4a Gastric Cancer: A Population-Based Study
Zhiya Hu, Ziyi Zuo, Han Miao, Zhijie Ning and Youyuan Deng

182 Significance of Lymph Node Metastasis in the Treatment of Gastric Cancer and Current Challenges in Determining the Extent of Metastasis
Shinichi Kinami, Hitoshi Saito and Hiroyuki Takamura

196 Development and Validation of a New Lymph Node Ratio-Based Staging System for Ampullary Carcinoma After Curative Pancreaticoduodenectomy
Xiaojie Zhang, Chongyuan Sun, Zefeng Li, Tongbo Wang, Lulu Zhao, Penghui Niu, Chunguang Guo, Yingtai Chen, Xu Che and Dongbing Zhao

207 Adding Consolidation Capecitabine to Neoadjuvant Chemoradiotherapy for Locally Advanced Rectal Cancer: A Propensity-Matched Comparative Study
Yifang Fang, Chengmin Sheng, Feng Ding, Weijie Zhao, Guoxian Guan and Xing Liu

216 Survival Analysis in Gastrointestinal Neuroendocrine Carcinoma With Bone Metastasis at Diagnosis
Genlian Chen, Qiang Xu, Shengjun Qian, Zhan Wang and Shicheng Wang

223 Establishment and Analysis of an Individualized Immune-Related Gene Signature for the Prognosis of Gastric Cancer
Mengying Li, Wei Cao, Bingqian Huang, Zhipeng Zhu, Yaxin Chen, Jiawei Zhang, Guodong Cao and Bo Chen

240 The Importance of Being "That" Colorectal pT1: A Combined Clinico-Pathological Predictive Score to Improve Nodal Risk Stratification
Alessandro Gambella, Enrico Costantino Falco, Giacomo Benazzo, Simona Osella-Abate, Rebecca Senetta, Isabella Castellano, Luca Bertero and Paola Cassoni

250 The Sex Features of Patients With Solid Pseudopapillary Neoplasms of the Pancreas: A Retrospective Study
Guangmin Wei, Qiong Luo, Jiankai Fang, Xiaolou Li, Yanhong Shi, Yuqiong Li and Liqi Sun

259 Perioperative Serum Scoring Systems Predict Early Recurrence and Poor Prognosis of Resectable Pancreatic Cancer
Shengnan Li, Gengpu Zhang, Yang Lu, Tiansuo Zhao, Chuntao Gao, Weishuai Liu, Yongjun Piao, Yanan Chen, Chongbiao Huang, Antao Chang and Jihui Hao

272 Machine Learning-Based Radiological Features and Diagnostic Predictive Model of Xanthogranulomatous Cholecystitis
Qiao-Mei Zhou, Chuan-Xian Liu, Jia-Ping Zhou, Jie-Ni Yu, You Wang, Xiao-Jie Wang, Jian-Xia Xu and Ri-Sheng Yu

281 Prognostic Significance of SOCS3 in Patients With Solid Tumors: A Meta-Analysis
Xia Zheng, Jie Shao, Sihui Wei, Yu Gu and Jun Qian

290 Characteristic of Perineural Invasion in Hilar Cholangiocarcinoma Based on Whole-Mount Histologic Large Sections of Liver
Si-Yuan Wang, Nan Jiang, Jian-Ping Zeng, Shao-Qing Yu, Ying Xiao and Shuo Jin

299 UHMK1 Is a Novel Marker for Personalized Prediction of Pancreatic Cancer Prognosis
Yiqiao Luo, Shanshan Han, Bin Yan, Huihui Ji, Lian Zhao, Jury Gladkich and Ingrid Herr

314 The Application Value of Syndecan-2 Gene Methylation for Colorectal Cancer Diagnosis: A Clinical Study and Meta-Analyses
Congbo Yue, Yaping Zhang, Yanlei Wang, Zhenhong Zhang, Mengjiao Zhang, Huayang Wang, Wendan Chen, Ziqi Shang, Yiwei Xin, Xin Zhang and Yi Zhang

325 The Prognostic Significance and Gene Expression Characteristics of Gastric Signet-Ring Cell Carcinoma: A Study Based on the SEER and TCGA Databases
Junren Ma, Yan Meng, Xin Zhou, Limei Guo and Wei Fu

343 Establishment of a Dynamic Nomogram for Predicting the Risk of Lymph Node Metastasis in T1 Stage Colorectal Cancer
Zitao Liu, Chao Huang, Huakai Tian, Yu Liu, Yongshan Huang and Zhengming Zhu

355 Prognostic Value of Lymph Node Evaluation in Stage II Small Bowel Adenocarcinoma: An Updated Analysis of Surveillance, Epidemiology, and End Results Database
Zhen Liu, Kun Liu, Jiale Gao, Chao Jing, Yanhong Ma, Shu Zheng and Jianzhen Shan

363 Progression Patterns and Post-Progression Survival in Recurred Intrahepatic Cholangiocarcinoma Patients: A Novel Prognostic Nomogram Based on Multicenter Cohorts
Chongyu Zhao, Chaobin He, Jiawei Lu, Xin Huang, Cheng Chen and Xiaojun Lin

375 An Efficient Nomogram for Discriminating Intrahepatic Cholangiocarcinoma From Hepatocellular Carcinoma: A Retrospective Study
Yuan-Quan Si, Xiu-Qin Wang, Cui-Cui Pan, Yong Wang and Zhi-Ming Lu

384 The Effect of Anlotinib Combined with anti-PD-1 in the Treatment of Gastric Cancer
Wubin Zheng, Guoqiang Sun, Zhitao Li, Fan Wu, Guangshun Sun, Hongyong Cao, Jin Zhou and Yong Ma

394 Prognostic Nomogram Based on the Metastatic Lymph Node Ratio for $T_{1-4}N_{0-1}M_0$ Pancreatic Neuroendocrine Tumors After Surgery
Jingxiang Shi, Sifan Liu, Jisen Cao, Shigang Shan, Chaoyi Ren, Jinjuan Zhang and Yijun Wang

406 Berberine as a Potential Agent for the Treatment of Colorectal Cancer
Xi Jiang, Zhongxiu Jiang, Min Jiang and Yan Sun

420 Impact of Examined Lymph Node Count on Precise Staging and Long-term Survival After Neoadjuvant Therapy for Carcinoma of the Esophagus: A SEER Database Analysis
Tao Bao, Lei Bao and Wei Guo

429 Splenic Volume, an Easy-To-Use Predictor of HCC Late Recurrence for HCC Patients After Hepatectomy
Tongdi Fang, Guo Long, Xingyu Mi, Wenxin Su, Lei Mo and Ledu Zhou

440 The Percentage of Signet Ring Cells Is Inversely Related to Aggressive Behavior and Poor Prognosis in Mixed-Type Gastric Cancer
Luigi Marano, Maria Raffaella Ambrosio, Luca Resca, Ludovico Carbone, Osvaldo Carpineto Samorani, Roberto Petrioli, Vinno Savelli, Maurizio Costantini, Lara Malaspina, Karol Polom, Ivano Biviano, Daniele Marrelli and Franco Roviello

450 Comparison of Four Lymph Node Staging Systems in Gastric Adenocarcinoma after Neoadjuvant Therapy – A Population-Based Study
Lai Hongkun, Zheng Jiabin and Li Yong

467 Commentary: The Tumor Markers and Blood Inflammation Markers Are More Likely to Be the Indicators for Differentiating Benign and Malignant Pancreatic Mucinous Cystic Neoplasms
Jiang Liu, Ying Xing and Liqi Sun

469 Adjuvant Chemotherapy Benefit in Elderly Stage II/III Colon Cancer Patients
Xin Chen, Junhao Tu, Xiaolan Xu, Wen Gu, Lei Qin, Haixin Qian, Zhenyu Jia, Chuntao Ma and Yinkai Xu

477 Integration of Inflammation-Immune Factors to Build Prognostic Model Predictive of Prognosis and Minimal Residual Disease for Hepatocellular Carcinoma
Xin Xu, Ao Huang, De-Zhen Guo, Yu-Peng Wang, Shi-Yu Zhang, Jia-Yan Yan, Xin-Yu Wang, Ya Cao, Jia Fan, Jian Zhou, Xiu-Tao Fu and Ying-Hong Shi

487 Clinicopathological and Prognostic Value of USP22 Expression in Gastric Cancer: A Systematic Review and Meta-Analysis and Database Validation
Yuhang Wang, Zirui Jia, Jiacheng Gao, Tingting Zhou, Xiangwen Zhang and Guo Zu

496 Hepatic Arterial Infusion Chemotherapy With Folfirinox or Oxaliplatin Alone in Metastatic Colorectal Cancer
Violaine Randrian, Simon Pernot, Baptiste Sionneau, Denis Smith, Annie Lim, Yann Touchefeu, Claire Gallois, Anthony Turpin, Sahir Javed, Rosine Guimbaud, Pascale Rivera, Mehdi Karoui, Edouard Auclin and Julien Taieb

504 Type-1 Grade 2 Multi-Focal Gastric Neuroendocrine Tumors Secondary to Chronic Autoimmune Gastritis
Ziqi Yu, Aiyao Wang, Chong Hu, Tao Yu and Jianyong Chen

510 Efficacy of Postoperative Adjuvant Transcatheter Arterial Chemoembolization in Hepatocellular Carcinoma Patients With Microscopic Portal Vein Invasion
Yiwen Qiu, Yi Yang, Tao Wang, Shu Shen and Wentao Wang

523 Development and Validation of Nomogram for Predicting Survival of Primary Liver Cancers Using Machine Learning
Rui Chen, Beining Hou, Shaotian Qiu, Shuai Shao, Zhenjun Yu, Feng Zhou, Beichen Guo, Yuhan Li, Yingwei Zhang and Tao Han

533 Surgical Treatment of Intraductal Papillary Neoplasm of the Bile Duct: A Report of Two Cases and Review of the Literature
Binjie Li, Zhiqiang Liu, Zhuo Meng, Mingyang Li, Weijun Tian and Quanyan Liu

540 Regulation of Gamma-Aminobutyric Acid Transaminase Expression and Its Clinical Significance in Hepatocellular Carcinoma
Xiaoqiang Gao, Xiaodong Jia, Moyan Xu, Jiao Xiang, Jin Lei, Yinyin Li, Yinying Lu and Shi Zuo

556 Efficacy and Safety of Camrelizumab in Combination with Docetaxel+S-1 Sequenced by Camrelizumab+S-1 for Stage III (PD-1+/MSI-H/EBV+/dMMR) Gastric Cancer: Study Protocol for a Single-Center, Prospective, Open-Label, Single-Arm Trial
Zhongyi Dong, Bo Ni, Linxi Yang, Yujing Guan, Chunchao Zhu, Enhao Zhao, Gang Zhao, Xiang Xia and Zizhen Zhang

564 SOX30 Overexpression Reflects Tumor Invasive Degree, Lymph Node Metastasis and Predicts Better Survival in Colorectal Cancer Patients: A Long-Term Follow-Up Cohort Study
Chao Li, Pengfei Li, Lulu Yu, Qingsen Sun, Bin Gu, Yanhua Sun and Liansheng Sun

572 Anti-colon Cancer Effects of *Dendrobium officinale* Kimura & Migo Revealed by Network Pharmacology Integrated With Molecular Docking and Metabolomics Studies
Shengchang Tao, Jinyan Li, Huan Wang, Shaobo Ding, Weichao Han, Ruirong He, Zhiyao Ren and Gang Wei

594 Diagnostic Performance of LI-RADS Version 2018 for Primary Liver Cancer in Patients With Liver Cirrhosis on Enhanced MRI
Xinai Liu, Xiaoyan Ni, Yubo Li, Chun Yang, Yi Wang, Chunzheng Ma, Changwu Zhou and Xin Lu

603 Undifferentiated Pleomorphic Sarcoma of the Duodenal Papilla: A Rare Case and Worth Discussing History
Jianlong Wang, Bin Liu, Jiachao Hou and Tao Li

611 Overexpression of OAS1 Is Correlated With Poor Prognosis in Pancreatic Cancer
Lingling Lu, Huaxiang Wang, Jian Fang, Jiaolong Zheng, Bang Liu, Lei Xia and Dongliang Li

623 The Prognostic Value of Adjuvant Chemotherapy in Colon Cancer With Solitary Tumor Deposit
Qiangkang Lin, Huizhen Zhou, Si Shi, Jixu Lin and Wangxin Yan

631 Exploring the scope of 4sb and 12a lymph node dissection for cT2-4 lower third gastric cancer: Study protocol for a prospective cohort trial
Haiqiao Zhang, Zhi Zheng, Xiaoye Liu, Jun Cai, Jie Yin and Jun Zhang

641 Comparison of Long-Term Oncologic Outcomes Between Surgical T4 and T3 in Patients Diagnosed With Pathologic Stage IIA Right Colon Cancer
Youngbae Jeon, Kug Hyun Nam, Seok Won Choi, Tae Sik Hwang and Jeong-Heum Baek

649 Intestinal Microbiota in Colorectal Adenoma-Carcinoma Sequence
Hanju Hua, Yanhong Sun, Xinjue He, Yi Chen, Lisong Teng and Chao Lu

658 Serum levels of IL-6 and CRP can predict the efficacy of mFOLFIRINOX in patients with advanced pancreatic cancer
Feifei Shen, Chuan Liu, Weiguo Zhang, Sijia He, Fan Wang, Jingjue Wang, Qi Li and Fei Zhou

671 Association of preoperative albumin–bilirubin with surgical textbook outcomes following laparoscopic hepatectomy for hepatocellular carcinoma
Fei-Qi Xu, Tai-Wei Ye, Dong-Dong Wang, Ya-Ming Xie, Kang-Jun Zhang, Jian Cheng, Zun-Qiang Xiao, Si-Yu Liu, Kai Jiang, Wei-Feng Yao, Guo-Liang Shen, Jun-Wei Liu, Cheng-Wu Zhang, Dong-Sheng Huang and Lei Liang

679 Comparison of clinicopathologic characteristics and survival outcomes between invasive IPMN and invasive MCN: A population-based analysis
Zhen Yang and Guangjun Shi

690 The prognostic significance of inflammation-immunity-nutrition score on postoperative survival and recurrence in hepatocellular carcinoma patients
Yuxin Liang, Zilong Zhang, Deyuan Zhong, Chunyou Lai, Zonglin Dai, Haibo Zou, Tianhang Feng, Jin Shang, Ying Shi and Xiaolun Huang

702 Exploring pathological signatures for predicting the recurrence of early-stage hepatocellular carcinoma based on deep learning
Wei-Feng Qu, Meng-Xin Tian, Jing-Tao Qiu, Yu-Cheng Guo, Chen-Yang Tao, Wei-Ren Liu, Zheng Tang, Kun Qian, Zhi-Xun Wang, Xiao-Yu Li, Wei-An Hu, Jian Zhou, Jia Fan, Hao Zou, Ying-Yong Hou and Ying-Hong Shi

716 A nomogram for predicting 10-year cancer specific survival in patients with pathological T3N0M0 rectal cancer
Shuang Liu, Shanfei Yang, Haina Yu, Huilong Luo, Gong Chen, Yuanhong Gao, Rui Sun and Weiwei Xiao

727 Clinical outcome comparison of laparoscopic radical antegrade modular pancreatosplenectomy vs. laparoscopic distal pancreatosplenectomy for left-sided pancreatic ductal adenocarcinoma surgical resection
Nan Niu, Yuhui He, Yiping Mou, Sijia Meng, Peng Xu, Yucheng Zhou, Weiwei Jin, Chao Lu, Yunyun Xu, Qicong Zhu and Tao Xia

734 Lymph node ratio is a superior predictor in surgically treated early-onset pancreatic cancer
Yangyang Zheng, Zhenhua Lu, Xiaolei Shi, Tianhua Tan, Cheng Xing, Jingyong Xu, Hongyuan Cui and Jinghai Song

747 Case report: A rare occurrence of triple malignancy of the stomach, rectum and liver in a single patient
Cancan Jin, Jiangnan Hu, Kirthikaa Balapattabi, Brian Wang, Sizhe Hu, Kangyi Wang, Liangbin Fu, Xiaokang Zhao, Feng Qian and Zhen Wang

754 Modification of the eighth AJCC/UICC staging system for perihilar cholangiocarcinoma: An alternative pathological staging system from cholangiocarcinoma-prevalent Northeast Thailand
Chaiwat Aphivatanasiri, Prakasit Sa-Ngiamwibool, Sakkarn Sangkhamanon, Piyapharom Intarawichian, Waritta Kunprom, Malinee Thanee, Piya Prajumwongs, Narong Khuntikeo, Attapol Titapun, Apiwat Jareanrat, Vasin Thanasukarn, Tharatip Srisuk, Vor Luvira, Kulyada Eurboonyanun, Julaluck Promsorn, Watcharin Loilome, Aileen Wee and Supinda Koonmee

774 Combined clinical features and MRI parameters for the prediction of VEGFR2 in hepatocellular carcinoma patients
Laizhu Zhang, Chunxiao Cheng, Binghua Li, Jun Chen, Jin Peng, Yajuan Cao, Yang Yue, Xiaoli Mai and Decai Yu

784 PN3b as an independent risk factor for poor prognosis and peritoneal recurrence in Borrmann type IV gastric cancer: A retrospective cohort study
Yiran Chen, Yanyan Chen, Liping Wen, Laizhen Tou, Haiyong Wang and Lisong Teng

795 Tumor burden score dictates prognosis of patients with combined hepatocellular cholangiocarcinoma undergoing hepatectomy
Gang Deng, Jun-kai Ren, Hai-tao Wang, Liang Deng, Zu-bing Chen, You-wen Fan, Ya-jun Tang, Tong Zhang and Di Tang

frontiers | Frontiers in Oncology

TYPE Editorial
PUBLISHED 05 April 2023
DOI 10.3389/fonc.2023.1193216

Check for updates

OPEN ACCESS

EDITED AND REVIEWED BY
Aali Jan Sheen,
Manchester Royal Infirmary,
United Kingdom

*CORRESPONDENCE
Ravindra Deshpande
rdeshpan@wakehealth.edu

SPECIALTY SECTION
This article was submitted to Surgical Oncology, a section of the journal Frontiers in Oncology

RECEIVED 24 March 2023
ACCEPTED 31 March 2023
PUBLISHED 05 April 2023

CITATION
Deshpande R (2023) Editorial: Clinicopathological factors and staging in gastrointestinal cancers.
Front. Oncol. 13:1193216.
doi: 10.3389/fonc.2023.1193216

COPYRIGHT
© 2023 Deshpande. This is an open-access article distributed under the terms of the Creative Commons Attribution License (CC BY). The use, distribution or reproduction in other forums is permitted, provided the original author(s) and the copyright owner(s) are credited and that the original publication in this journal is cited, in accordance with accepted academic practice. No use, distribution or reproduction is permitted which does not comply with these terms.

Editorial: Clinicopathological factors and staging in gastrointestinal cancers

Ravindra Deshpande*

Department of Cancer Biology, Wake Forest University School of Medicine, Winston-Salem, NC, United States

KEYWORDS

gastric cancer, TNM system, prognosis, therapy, treatment

Editorial on the Research Topic
Clinicopathological factors and staging in gastrointestinal cancers

Gastric cancer (GC) represents the most prevalent malignancy in the globe with second highest mortality (1). GC to occur more frequently in men than women with average age over 60 with advanced stage at diagnosis making the prognosis poor (2). The incidence of GC observed to decline in last few decades and this is mainly attributed to decreased prevalence of *Helicobacter Pylori* infection and change in lifestyle habits such as smoking, food storage and preservation (3). GC patients are treated with surgery. The choice of surgical resection affected by few cofounding factors such as histological grade of tumor, location and TNM category. Irrespective of this, relapse is observed in most of the patients (4). On treatment front, neoadjuvant chemotherapy in combination with radiation is chosen to prevent the tumor dissemination (5). In GC with locally advanced and metastatic form, patients treated with modified approaches such as targeted therapy, and immunotherapy. At the same time, more advanced approaches such as tumor vaccines, adoptive cell therapy are pondered (6). The proposed ways curated to achieve greater clinical benefit with personal and comprehensive diagnosis.

Gastric cancer diagnosis is based on invasion extent of primary tumor (T-stage), lymph node status (N-stage), and distant spread (M-stage), also known as TNM system (7). However, this system is not perfect and additional parameters such as distant spread, tumor micro environmental markers, treatment effects and circulating biomarkers viewed as attractive targets. In view of this, the Research Topic 'Clinicopathological Factors and Staging in Gastrointestinal Cancers' sheds light on four important aspects including, the refinement of GC staging system; prognostic prediction based on GCstaging; survival analyses of clinicopathological factors in GC and treatment choices in GC.

A total of 09 articles published on refinement of staging system (Wu et al, Ren et al., Zhang et al., Liu et al., Bao et al., Hongkun et al., Jeon et al., Yue et al.),. Among these reports, Ren et al describes the retrospective study to use of immunoscores to distinguish the outcomes in stage II and III colorectal cancer. Zhang et al. proposes to use the Lymph node metastasis (LNM) based staging system to predict prognosis in ampullary carcinoma (AC) cases where as Wu et al., note that the overall survival was comparable in N0 stage with N1 stage when less than 8 lymph nodes were present and therefore proposes to give emphasis in stage II colon cancer with less than 8 lymph nodes. Jeon et al., compares the

surgical outcomes in surgical and pathological stages of colon cancer patients and infers that there is significant difference exists between surgical T4 and T3 in pathologic stage IIA.

Prognosis in gastric cancer patients with identical TNM stage and receiving the similar treatment is observed to be different (8), presenting the need of personalized biomarkers and tailored therapies to yield clinically significant results. Pathomics signature derived from hematoxylin and eosin stained slides of gastric cancer patients to assign prognostic benefit associated with adjuvant chemotherapy (9). In present topic, 17 articles have shed light on the refinement of existing system to accurately predict prognosis (Cheng et al., Bae at al., Gu et al., Huang at al., Hu at al., Tang and Chen, Chen at al., Li et al., Li et al., Marano et al., Li et al., Lu et al., Liu et al., Zheng et al., Chen et al., Zheng et al., Wang et al.),. The published studies propose to use expression pattern of uniquely expressed genes to understand the clinicopathological features and accurately predict the survival. For instance, Wang et al., observed that USP22 expression in gastric cancer tissues is associated with lymph node and distant metastasis and TNM grade. Zheng et al., Lu et al. perform data analysis from the TCGA database to identify OAS1 to be overexpressed in pancreatic cancer tissue and associated with poor survival. Authors also conform the OAS1 expression in pathological tissues and note that apoptosis, Notch signaling and p53 pathways were associated with OAS1 expression. On similar note, Li et al. examines the expression of SOX30 in 195 CRC and adjacent tissues and observe that its expression was decreased in CRC tissue and negatively associated with tumor size and lymph node metastasis. This collection also features 04 review and systematic review of meta analysis articles (Kinami et al., Jiang et al., Váncsa et al., Yue et al.),. Kinami et al. summarizes the importance of determining lymph node metastasis in diagnosis of gastric cancer. Xi Jiang et al. reviews the anti-tumor effects of berberine (BBR) in CRC. Authors note that BBR exerts antitumor effect in CRC by regulating microbiota and mucosal barrier function and attest to use this drug for chemotherapy. In addition, Zhang et al., attempts to develop prediction model using vascular endothelial growth factor receptor 2 (VEGFR2) immunohistochemistry in 206 HCC patients. Authors also uses contrast-enhanced MRI parameters in predicting VEGFR2 expression. In another interesting study, Gao et al., uses bioinformatics approaches to examine the DNA methylation, copy number variation and regulated miRNAs of Gamma-aminobutyric acid transaminase (ABAT) in HCC. Author's infer that ABAT expression was lower in HCC and miR-135a-5p may be the upstream regulatory miRNA for ABAT. Immunotherapy is well recognized treatment for HCC and know to improve therapeutic response. Presently, one of the attractive strategy is to use tyrosine kinase inhibitors synergizing with immune checkpoint inhibitors including anti-PD-1/PD-L1 (10). Zheng et al., screens 880 drugs to identify Anlotinib downregulates PD-L1 expression and may benefit with anti PD-1 inhibitor in clinical setting for GC.

Together, the brief overview of the articles presented here provide the glimpse of updates on use of prognostic and clinicopathological factors in affecting the gastric cancer staging and eventually the treatment course.

Author contributions

The author confirms being the sole contributor of this work and has approved it for publication.

Conflict of interest

The author declares that the research was conducted in the absence of any commercial or financial relationships that could be construed as a potential conflict of interest.

Publisher's note

All claims expressed in this article are solely those of the authors and do not necessarily represent those of their affiliated organizations, or those of the publisher, the editors and the reviewers. Any product that may be evaluated in this article, or claim that may be made by its manufacturer, is not guaranteed or endorsed by the publisher.

References

1. Norwood DA, Montalvan EE, Dominguez RL, Morgan DR. Gastric cancer: Emerging trends in prevention, diagnosis, and treatment. *Gastroenterol Clin North Am* (2022) 51:501–18. doi: 10.1016/j.gtc.2022.05.001

2. Wang S, Zheng R, Arnold M, Abnet C, Zeng H, Zhang S, et al. Global and national trends in the age-specific sex ratio of esophageal cancer and gastric cancer by subtype. *Int J Cancer* (2022) 151:1447–61. doi: 10.1002/ijc.34158

3. Petryszyn P, Chapelle N, Matysiak-Budnik T. Gastric cancer: Where are we heading? *Dig Dis* (2020) 38:280–5. doi: 10.1159/000506509

4. Lordick F, Carneiro F, Cascinu S, Fleitas T, Haustermans K, Piessen G, et al. Gastric cancer: ESMO clinical practice guideline for diagnosis, treatment and follow-up. *Ann Oncol* (2022) 33:1005–20. doi: 10.1016/j.annonc.2022.07.004

5. Li GZ, Doherty GM, Wang J. Surgical management of gastric cancer: A review. *JAMA Surg* (2022) 157:446–54. doi: 10.1001/jamasurg.2022.0182

6. Smyth EC, Nilsson M, Grabsch HI, van Grieken NC, Lordick F. Gastric cancer. *Lancet* (2020) 396:635–48. doi: 10.1016/S0140-6736(20)31288-5

7. Sano T, Coit DG, Kim HH, Roviello F, Kassab P, Wittekind C, et al. Proposal of a new stage grouping of gastric cancer for TNM classification: International gastric cancer association staging project. *Gastric Cancer* (2017) 20:217–25. doi: 10.1007/s10120-016-0601-9

8. Cheong JH, Yang HK, Kim H, Kim WH, Kim YW, Kook MC, et al. Predictive test for chemotherapy response in resectable gastric cancer: A multi-cohort, retrospective analysis. *Lancet Oncol* (2018) 19:629–38. doi: 10.1016/S1470-2045(18)30108-6

9. Chen D, Fu M, Chi L, Lin L, Cheng J, Xue W, et al. Prognostic and predictive value of a pathomics signature in gastric cancer. *Nat Commun* (2022) 13:6903. doi: 10.1038/s41467-022-34703-w

10. Deshpande RP, Sharma S, Watabe K. The confounders of cancer immunotherapy: Roles of lifestyle, metabolic disorders and sociological factors. *Cancers (Basel)* (2020) 12. doi: 10.3390/cancers12102983

frontiers in Oncology

ORIGINAL RESEARCH
published: 12 July 2021
doi: 10.3389/fonc.2021.711061

A Novel Nomogram Based on Hepatic and Coagulation Function for Evaluating Outcomes of Intrahepatic Cholangiocarcinoma After Curative Hepatectomy: A Multi-Center Study of 653 Patients

Yunshi Cai[1†], Bohan Zhang[1†], Jiaxin Li[1], Hui Li[1], Hailing Liu[1], Kunlin Xie[1], Chengyou Du[2] and Hong Wu[1*]*

[1] Department of Liver Surgery & Liver Transplantation, State Key Laboratory of Biotherapy and Cancer Center, West China Hospital, Sichuan University and Collaborative Innovation Center of Biotherapy, Chengdu, China, [2] Department of Hepatobiliary Surgery & Liver Transplantation, The First Affiliated Hospital of Chongqing Medical University, Chongqing, China

Background and Aims: Hepatic and coagulation function are routine laboratory tests prior to curative hepatectomy. The prognostic value of gamma-glutamyl transpeptidase (GGT) to platelet ratio (GPR) and international normalized ratio (INR) in surgically treated patients with intrahepatic cholangiocarcinoma (ICC) remains unclear.

Methods: ICC patients received curative hepatectomy in two west China centers were included. Time-dependent ROC curves were conducted to compare established indexes with prognostic value for ICC. GPR-INR score was introduced and evaluated using the Time-dependent AUC curve and Kaplan-Meier survival analysis. A novel nomogram based on the GPR-INR score was proposed; Harrell's C-index, calibration curve and decision curve analysis were used to assess this nomogram.

Results: A total of 653 patients were included. The areas under ROC curves of GPR and INR in OS and RFS were superior to other indexes. Patients with a high GPR-INR score (1,2) presented significantly decreased overall survival (OS) and recurrence-free survival (RFS); GPR-INR sore, along with several clinicopathological indexes were selected into the nomogram, the calibration curve for OS probability showed good coincidence between the nomogram and the actual surveillance. The C-index of the nomogram was 0.708 (derivation set) and 0.746 (validation set), which was more representative than the C-indexes of the GPR-INR score (0.597, 0.678). In decision curve analysis, the net benefits of the nomogram in derivation and validation set were higher than Barcelona Clinic Liver Cancer staging (BCLC) classification and American Joint Committee on Cancer (AJCC) TNM 8th staging system.

OPEN ACCESS

Edited by:
Qi Liu,
Fudan University, China

Reviewed by:
Patryk Lipiński,
Children's Memorial Health Institute (IPCZD), Poland
Osama Elbahr,
Menofia University, Egypt
Francesco Fleres,
ASST Valtellina e Alto Lario, Italy

***Correspondence:**
Hong Wu
wuhong@scu.edu.cn
Chengyou Du
duchengyou@126.com

†These authors have contributed equally to this work and share senior authorship

Specialty section:
This article was submitted to Surgical Oncology, a section of the journal Frontiers in Oncology

Received: *17 May 2021*
Accepted: *28 June 2021*
Published: *12 July 2021*

Citation:
Cai Y, Zhang B, Li J, Li H, Liu H, Xie K, Du C and Wu H (2021) A Novel Nomogram Based on Hepatic and Coagulation Function for Evaluating Outcomes of Intrahepatic Cholangiocarcinoma After Curative Hepatectomy: A Multi-Center Study of 653 Patients. Front. Oncol. 11:711061. doi: 10.3389/fonc.2021.711061

Conclusions: The proposed nomogram generated superior discriminative ability to established staging systems; it is profitable to applicate this nomogram in clinical practice.

Keywords: gamma-glutamyl transpeptidase, GGT to platelet ratio, intrahepatic cholangiocarcinoma, international normalized ratio, nomogram

INTRODUCTION

Liver cancer remains the second leading cause of tumor-related death in Asia, America and Africa, which leads to nearly 548,400 male deaths and 233,300 female deaths annually (1). Intrahepatic cholangiocarcinoma (ICC) is one of the subtypes of cholangiocarcinoma which originates in the secondary bile ducts of the liver, which accounts for 10% to 30% of all primary liver malignancies, ranks only after hepatocellular carcinoma (2, 3). The reported global incidence of ICC increased from 0.32-0.44 to 0.85-1.18 per 100,000 population for the past half-century, the mortality rate rose synchronously from 0.1 to 1.5 per 100,000 population, highest in Asian population (1.4 per 100,000) compared with the white (0.8 per 100,000) and the black people (0.7 per 100,000) (4–7). Consistent with HCC, liver cirrhosis and HBV, HCV infections are the most relevant risk factors for ICC; other established factors including parasite infection, hepatolithiasis, primary sclerosing cholangitis, and bile-duct cyst (8, 9). ICC is associated with rapid progression, early recurrence and unsatisfying outcomes, 75% of the patients die within one year since diagnosis and the 5-year overall survival remains under 5% (4, 10). Surgical resection remains the buttress for treatment of ICC; however, survival following resection of ICC remains restrained; the median disease-specific survival time in patients received resection is 36 months (11), the 5-year overall survival rate of patients underwent R0 or R1 resection is 28% (12). Gemcitabine, fluoropyrimidine and Cisplatin-based systematic chemotherapy is beneficial to patients with recurrent, advanced or metastatic ICCs, but the median survival time was generally less than 12 months (7). Therefore, precise prognostic indexes or models are needed for evaluating the survival of surgical candidates thus improve outcomes.

Clinical and histopathological parameters including tumor size, vascular invasion, lymph node status and extrahepatic metastasis have been proved relevant with the survival of ICC patients (11, 13). These parameters are commonly used in tumor staging of the American Joint Committee on Cancer (AJCC) TNM system (14). In addition to the tumor staging system, serum markers such as carcinoembryonic antigen (CEA) and cancer antigen 19-9 (CA19-9) have been proved as independent risk factors in predicting the prognosis of ICC patients (15). Inflammatory models including neutrophil-to-lymphocyte ratio (NLR), platelet-to-lymphocyte ratio (PLR) and systemic immune-inflammation index (SII) (16) were introduced recently to predict prognosis of ICC patients; moreover, preoperative hepatic function indexes such as fibrosis-4 score (FIB-4) and albumin-bilirubin score (ALBI) also play crucial roles in predicting survival of HCC patients (17). Gamma-glutamyl transpeptidase(GGT)-to-platelet ratio (GPR), firstly defined by Lemoin et al. (18), is a more accurate marker than FIB-4 in staging HBV-related liver fibrosis; its value in predicting HCC development was further validated by Korean researchers (19). Model for end-stage liver disease (MELD) is a general standard for evaluating survival of end-stage liver disease patients and liver transplantation recipients, international normalized ratio (INR) is applied to assess coagulation function in this model (20). Furthermore, elevated INR level is associated with poor long-term outcome of HCC after hepatic resection (21). However, the prognostic value of these hepatic function parameters and coagulation indexes in ICC patients remain largely unknown.

In the present study, we compared several inflammatory, hepatic function and coagulation indexes, aimed to identify and validate the most valuable prognostic indicators for ICC patients after curative liver resection. Moreover, we hoped to establish a simple and feasible preoperative scoring system to evaluate outcomes of surgically treated ICC patients.

MATERIALS AND METHODS

Study Population

A total of 665 surgically treated ICC patients at two west China medical centers, West China hospital of Sichuan University and the First Affiliated Hospital of Chongqing Medical University, were sequentially included. 535 patients received the operation at the West China Hospital during December 2008 and December 2017 were enrolled as derivation set to assess the parameters and establish the nomogram, 130 patients received the operation at the First Affiliated Hospital of Chongqing Medical University between May 2010 and December 2015 were included as the validation set to verify the effectiveness of the model. The inclusion criteria were as follow: (1) histologically diagnosed ICC; (2) underwent hepatectomy with curative intent firstly;

Abbreviations: GGT, gamma-glutamyl transpeptidase; GPR, GGT to platelet ratio; ICC, intrahepatic cholangiocarcinoma; INR, international normalized ratio; AUROC, the area under receiver operating characteristic curves; C-index, concordance-index; OS, overall survival; RFS, recurrence-free survival; BCLC staging classification, Barcelona Clinic Liver Cancer staging classification; AJCC TNM system, American Joint Committee on Cancer TNM system; HCC, hepatocellular carcinoma; HBV, hepatitis B virus; HCV, hepatitis C virus; CEA, carcinoembryonic antigen; CA19-9, cancer antigen 19-9; NLR, neutrophil-to-lymphocyte ratio; PLR, platelet-to-lymphocyte ratio; SII, systemic immune-inflammation index; FIB-4, fibrosis-4 score; ALBI, albumin-bilirubin score; MELD, Model for end-stage liver disease; TACE, transarterial chemoembolization; RFA, radiofrequency ablation; ALT, alanine aminotransferase; AST, aspartate aminotransferase; AFP, alpha-fetoprotein; MVI, microvascular invasion; DCA, decision curve analysis; PTCD, percutaneous transhepaticcholangial drainage.

exclusion criteria: (1) patients received preoperative transarterial chemoembolization (TACE), radiofrequency ablation (RFA), radiotherapy, targeting therapy, or other anti-tumor treatment; (2) insufficient hepatic functional reserve for liver resection; (3) extrahepatic metastasis; (4) positive surgical margin; (5) tumor rupture; (6) patients without complete clinical data and follow-up information. Written informed consents were obtained from all participants or their relatives. This study was approved by the ethics committee of West China Hospital of Sichuan University and the First Affiliated Hospital of Chongqing Medical University, in line with the guidelines of the 1975 Declaration of Helsinki.

Data Collection and Follow-Up

All the clinical and histopathological information were obtained from the hospital electronic medical records. Preoperative data were collected as follows: neutrophil, lymphocyte and platelet counts; bilirubin, albumin and GGT levels; alanine aminotransferase (ALT), aspartate aminotransferase (AST) and INR levels; HBV and HCV loads. Moreover, the serum tumor markers including alpha-fetoprotein (AFP), carcino-embryonic antigen (CEA) and carbohydrate antigen 19-9 (CA19-9) levels were collected. the GPR was defined as GGT level (U/L) divided by platelet counts (10^9/L); platelet-to-lymphocyte ratio (PLR) was calculated from platelet counts divided by lymphocyte counts; systemic immune-inflammation index (SII) was calculated from ($neutrophil(10^9/L) \times Platelet(10^9/L)$)/ $Lymphocyte(10^9/L00$; fibrosis-4 index (FIB-4) was calculated from $(ALT(U/L) \times age(year))/(platelet(10^9/L) \times \sqrt{AST(U/L)})$; ALBI was calculated by the following formula: (log_{10} $bilirubin$ $(mol/L) \times 0.66) - (albumin(g/L) \times 0.085)$. X-tile software (22) was used to determine the cut-off values of these indexes and patients were stratified according to the cut-offs. Clinical and histopathological features including ascites, liver cirrhosis, numbers of nodules, diameter of tumor, differentiation, hepatolithiasis, lymph node status, microvascular invasion (MVI), macrovascular invasion, perineural invasion and extrahepatic metastasis were also obtained. MVI was defined as the presence of tumor cells in vessels or in vascular space lined by the epithelial cells under the microscope; macrovascular invasion was defined as radiologically or macroscopically identified large vessel invasion. Para-aortic lymph node invasion was considered as extrahepatic metastasis. All included patients were stratified according to the 8th edition of AJCC staging manual and the Barcelona Clinic Liver Cancer (BCLC) staging classification (14, 23). Postoperative follow-up was conducted per month within 1 year, and then every 3 months within two years, then every 6 months thenceforth, serum tumor markers and contrast-enhanced ultrasonography or CT scan were used to monitor the recurrence of tumor. For patients who had difficulties going back to the hospital for routine examination due to distance or traffic issues, we recommend them to exam in local medical institutions and re-check the findings through telephone and Internet follow-up surveys. At the end of follow-up in December 2017, 8 patients (5 patients in West China Hospital and 3 in the First Affiliated Hospital of Chongqing Medical University) lost to follow-up. 4 patients in the First Affiliated Hospital of Chongqing medical university were withdrawn due to incomplete medical records (pathology report or preoperative laboratory indexes).

Statistical Analysis

The software of EmpowerStats (http://www.empowerstats.com) and R (https://www.r-project.org, v3.6.3) were used for statistical analysis, data was presented as mean ± standard deviation (SD) or proportion. Comparison of categorical and continuous variables between groups were performed with Student's *t*-test and Pearson's x^2 test, respectively. Non-parametric Mann-Whitney U test was used to analysis the data with abnormal distribution. The ideal cut-off values of GPR, INR, PLR, SII, FIB-4 and ALBI were determined by using X-tile software (http://medicine.yale.edu/lab/rimm/research/software). The discriminative ability of the indexes was assessed by the area under receiver operating characteristic curves (AUROC) or time-dependent AUROC *via* the "survivalROC" package in R. Kaplan-Meier curves were depicted according to the cut-off values of GPR, INR and GPR-INR score, and their differences between groups were determined by comparing the cumulative survival of included ICC patients using the log-rank test. Cox proportional hazards regression model was used to identify potential prognostic factors for overall survival (OS), clinicopathological indexes with $P<0.2$ in the univariate model were incorporated into the multivariate Cox regression model, and the nomogram was generated accordingly. Harrell's concordance index (c-index) and calibration curves were applied to evaluate the availability of the nomogram; comparisons between the nomogram and other staging systems were achieved by using decision curve analysis (DCA) *via* the "rmda" package in R. $P<0.05$ was considered statistically significant.

RESULTS

Patients Characteristics at Baseline

530 patients [256 (48.3%) male, mean (SD) age, 57.2 (10.7) years] in West China Hospital and 123 patients [71 (57.7%) male, mean (SD) age, 58.2 (11.1) years] in the First Affiliated Hospital of Chongqing Medical University were finally recruited into the derivation set and validation set, respectively. Liver cirrhosis was detected in 148 (27.9%) patients in the derivation set and 16 (13%) patients in the validation set; all patients were stratified into Child-Pugh grade A, in derivation set, 451 (85.1%) patients were 5 points and 79 (14.9%) were 6 points; in the validation set, 93 (75.6%) were 5 points and 30 (24.4%) were 6 points. Nearly 30% of the patients were with multiple tumors in both cohorts, and tumor diameter on average was greater than 5 cm (5.9 ± 2.7 cm in derivation set and 6.2 ± 1.4 cm in validation set). More than half of the patients in both sets were with poor tumor differentiation (63.4% in derivation set and 73.2% in validation set). 53 (10%) patients in derivation set and 15 (12.1%) patients in the validation set were with microvascular invasion, 138 (26%) patients in derivation set and 30 (24.4%) patients in the

validation set were with elevated serum CA19-9 level (≥22U/ml); additionally, 88 (16.6%) patients in derivation set and 23 (18.7%) patients in validation set suffered from hepatolithiasis. Patients' characteristics at baseline were summarized in **Table 1**.

GPR and INR Were Related to Increased Risk of Prognosis

The preoperative inflammatory, hepatic function and coagulation function indexes including GPR, INR, PLR, SII, FIB-4 and ALBI were calculated based on the patients' data of derivation set, X-tile software was adopted to confirm the optimal cut-off values of these indexes (**Supplemental Figure 1**) with minimal *P*-value from log-rank x^2 test (GPR: 0.7, INR: 1.1, PLR: 104.4, SII: 683, ALBI: -0.8). The discriminative capability of these indexes to 1-,3- and 5-year OS and RFS were compared by using ROC; the AUC of GPR, SII and INR were superior to that of PLR, FIB-4 and ALBI (**Supplemental Figure 2**). Considering that both the values of GPR and SII were impacted by the platelet counts, the GPR and INR were selected. Patients were stratified into four groups according to the cut-off values of GPR and INR (group A: GPR<0.7, group B: GPR≥0.7; group C: INR<1.1, group D: INR≥1.1) with the strongest discriminative ability, the correlation between baseline characteristics with GPR and INR of the patients in derivation seta was demonstrated in **Table 2**. There were 354 patients in group A and 176 patients in group B; compared to group A, group B presented with the following distinctions: more male patients and fewer female patients (*P*=0.01), higher prevalence of macrovascular invasion (*P*<0.001), biliary invasion (*P*<0.001), higher Child-Pugh score (*P*=0.002), lower prevalence of liver capsule invasion (*P*<0.001), lower CA19-9 level (*P*=0.027), lower rate of the presence of positive HBsAg (*P*=0.029). Based on the cut-off of INR, 457 patients were classified into Group C and 73 in Group D; in comparison to Group C, Group D presented with: higher rate of male patients (*P*=0.003), higher rate of the presence of liver cirrhosis (*P*<0.01), higher rate of positive HBsAg (*P*<0.001) and Hepatitis C antibody (*P*=0.008), lower prevalence of liver capsule invasion (*P*=0.044), lower Child-Pugh score (*P*=0.001). There was no significant difference in other characteristics among these groups. The basic features of patients in the validation set were shown in **Supplemental Table 1**. Kaplan-Meier analysis suggested that the patients with GPR<0.7 had better OS and RFS than those with GPR≥0.7 (median OS: 25.8 months *vs.* 23.1 months), in consistence with GPR, the OS and RFS of the patients with INR<1.1 also superior to the patients with higher INR (median OS: 25.4 months *vs.* 21.3 months) (**Supplemental Figure 3**).

TABLE 1 | Baseline characteristics of patients.

Variables	Deveriation set (n=530)	Validation set (n=123)
Age, mean ± SD	57.2±10.7	58.2±11.1
Gender, n (%)		
Male	256(48.3%)	71(57.7%)
Female	274(51.7%)	52(42.3%)
Cirrhosis, n (%)	148(27.9%)	16(13.0%)
Ascite, n (%)	50(9.4%)	60(48.8%)
Child score, n (%)		
5	451(85.1%)	93(75.6%)
6	79(14.9%)	30(24.4%)
Multiple tumors, n (%)	157(29.6%)	36(29.3%)
Tumor size (cm), mean ± SD	5.9±2.7	6.2±1.4
Poor tumor differentiation, n (%)	336(63.4%)	90(73.2%)
Hepatolithiasis, n (%)	88(16.6%)	23(18.7%)
Microvascular invasion, n (%)	53(10.0%)	15(12.1%)
Macrovascular invasion, n (%)	123(23.2%)	25(20.3%)
Lymph node metastasis, n (%)	129(24.3%)	35(28.5%)
Biliary invasion, n (%)	53(10.0%)	63(51.2%)
Perineural invasion, n (%)	77(14.5%)	29(23.6%)
Liver capsule invasion	325(61.3%)	65(52.8%)
CA19-9, n (%)		
≥22U/ml	138(26.0%)	30(24.4%)
<22U/ml	346(65.3%)	93(75.6%)
Not available	46(8.7%)	0(0%)
HBsAg (positive),n(%)	153(28.9%)	22(17.9%)
HCV, n (%)	3(0.6%)	0(0%)
TNM stage, n (%)		
I-II	173(32.6%)	45(36.6%)
III-IV	357(67.4%)	78(63.4%)
BCLC stage		
0-A	268(50.6%)	47(38.2%)
B-C	262(49.4%)	76(61.8%)
INR grade		
<1.1	457(86.2%)	80(65.0%)
≥1.1	73(13.8%)	43(35.0%)
GPR grade		
<0.7	354(66.8%)	55(44.7%)
≥0.7	176(33.2%)	68(55.3%)
Overall survival, month, mean ± SD	24.9±21.4	26.2±20.8

CA19-9, cancer antigen 19-9; HBsAg, hepatitis B surface antigen; HCV, hepatitis C virus; BCLC stage, Barcelona Clinic Liver Cancer stage; INR, international normalized ratio; GPR, gamma-glutamyl transpeptidase to platelet ratio.

The Proposal of GPR-INR Score

1 point was allocated to GPR≥0.7 or INR≥1.1; therefore, the GPR-INR score composed of 0, 1 or 2 points was generated in the derivation set. Patients were stratified into three groups according to the GPR-INR score, the patients with GPR-INR score 1 had better 1-,3-,5-year OS and RFS rates than those with GPR-INR score 2 (OS: 64.9%, 20.8%, 5.4% vs. 43.7%, 10.4%, 4.2%; RFS: 41.4%, 14.1%, 4.4% *vs.* 29.2%, 6.3%, 2.1%), but worse than those with GPR-INR score 0 (OS: 64.9%, 20.8%, 5.4% *vs.* 82.7%, 30.2%, 12.9%; RFS: 41.4%, 14.1%, 4.4% vs. 62.7%, 22.1%, 10.3%) (**Figures 1C, D**). Moreover, we found that GPR-INR score surpasses GPR or INR in predicting OS and RFS through the result of time-dependent AUROC analysis (**Figures 1A, B**). To further estimate the clinical efficacy of the GPR-INR score in the prediction of OS and RFS, subgroup analysis using univariate Cox regression was applied based on gender (male or female), age (<60 or ≥60 years), tumor numbers (solitary or multiple), tumor diameters (<5 or ≥5 cm), with or without liver cirrhosis, hepatolithiasis, microvascular invasion, macrovascular invasion, lymph node metastasis, perineural and liver capsule invasion, tumor differentiation (well-moderate or poor), CA19-9 level (<22 or ≥22 U/ml), Child-Pugh score (5 or 6), TNM stage (I-II or III-IV) and BCLC classification (0-A or B-C). Although it failed to attain statistical significance in several subgroups (patients with cirrhosis, hepatolithiasis, MVI, perineural invasion etc.), the tendency of poor OS and RFS in patients with high GPR-INR score was accordant (**Figure 2**).

TABLE 2 | Univariate and multivariate analyses to determine independent predictors of overall survival.

Variables	Univariate analysis			Multivariate analysis		
	HR	95%CI	P value	HR	95%CI	P value
Gender, Female/Male	0.821	0.658-1.023	0.078			
Age	0.995	0.987-1.008	0.708	0.833	0.643-1.078	0.165
Cirrhosis	1.274	1.002-1.619	0.047	1.511	1.145-1.993	0.003
Hepatolithiasis	1.323	1.005-1.751	0.046	1.344	0.976-1.851	0.07
Tumor number,Multiple/single	1.712	1.359-2.156	<0.0001	1.587	1.074-2.346	0.02
Tumor size,≥5/<5(cm)	1.212	0.969-1.517	0.092	1.237	0.941-1.626	0.126
Tumor differentiation, Undifferentiation-Poor/Moderate-Well	2.053	1.555-2.712	<0.0001	1.881	1.396-2.535	<0.0001
Microvascular invasion	1.719	1.236-2.391	0.001	1.009	0.696-1.465	0.958
Macrovascular invasion	1.181	0.914-1.526	0.203			
Lymph node metastasis	2.353	1.856-2.981	<0.0001	1.775	1.326-2.377	0.0001
Liver capsule invasion	1.078	0.858-1.352	0.517			
Perineural invasion	1.564	1.161-2.109	0.003	1.5466	1.088-2.197	0.015
GPR-INR score						
0	Reference			Reference		
1	1.806	1.395-2.341	<0.0001	1.436	1.059-1.946	0.019
2	3.233	2.226-4.696	<0.0001	2.794	1.833-4.258	<0.0001
CA199 grade ≥22/<22(U/ml)	2.166	1.621-2.895	<0.0001	2.018	1.471-2.769	<0.0001
HBV	1.131	0.889-1.437	0.317			
HCV	1.865	0.597-5.828	0.283			
TNM stage,III-IV/I-II	1.397	1.075-1.815	0.012	1.045	0.711-1.535	0.821
BCLC stage,B-C/0-A	1.608	1.276-2.028	<0.0001	1.201	0.874-1.649	0.256

CA19-9, cancer antigen 19-9; HBV, hepatitis B virus; HCV, hepatitis C virus; BCLC stage, Barcelona Clinic Liver Cancer stage; INR, international normalized ratio; GPR, gamma-glutamyl transpeptidase to platelet ratio.

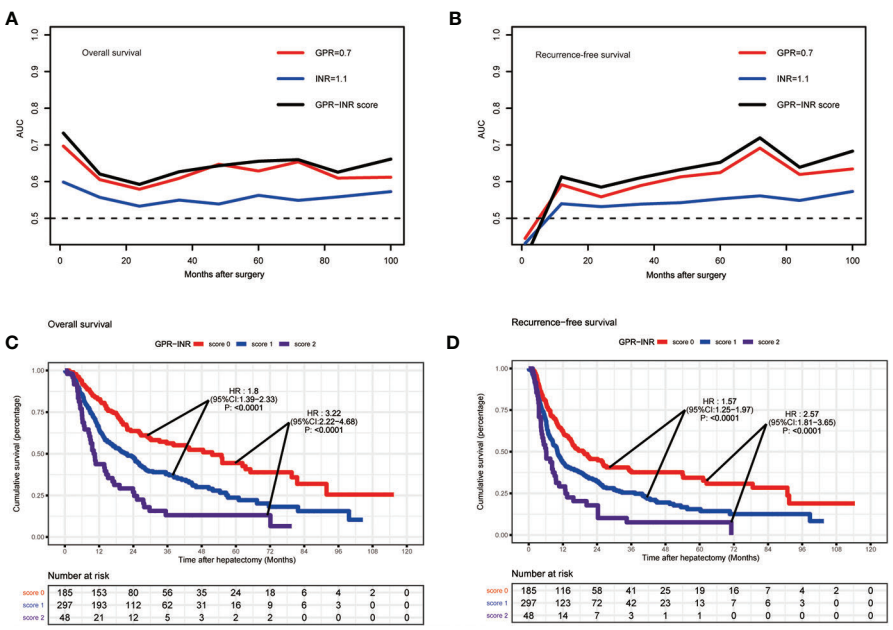

FIGURE 1 | The predictive ability of GPR-INR score for OS and RFS in the derivation set. **(A, B)** The time-dependent AUC curves of GPR, INR and GPR-INR score, the AUROC of the GPR-INR score was higher than that of the GPR and the INR for RFS and OS prediction. **(C, D)** Kaplan–Meier curves of the patients in the derivation set for OS and RFS, GPR-INR score 1 had better RFS and OS than GPR-INR score 2, worse RFS and OS than GPR-INR score 0.

Development and Validation of GPR-INR Nomogram for OS

Univariate and multivariate Cox proportional hazards regression models were used to identify independent prognostic factors for overall survival; multivariate analysis exhibited that liver cirrhosis, hepatolithiasis, multiple tumors, tumor with poor differentiation, lymph node metastasis, perineural invasion, CA19-9 and GPR-INR score were independent risk factors for overall survival. The prognostic nomogram that combined all independent risk factors for OS was developed on the basis of the patients of derivation set (**Figure 3**). C-index was compared between GPR-INR and the prognostic nomogram in the prediction of overall survival; the results suggested that the prognostic nomogram was more accurate in the evaluation of OS than the GPR-INR score (**Table 3**). The calibration curves for the probability of 3- and 5-year overall survival in derivation and validation sets were plotted, the results demonstrated an optimal accordance between the nomogram prediction and actual observation in both sets (**Figures 4A–D**). In addition, the GPR-INR nomogram was compared with two conventional systems in staging liver cancer, the BCLC and the AJCC 8th edition staging systems, by using decision curve analysis. As shown in **Figures 4E, F**, the GPR-INR nomogram displayed superior net benefits within a wider range of threshold probability to the other two systems in predicting overall survival for the patients of both derivation and validation sets. The results suggested that the GPR-INR nomogram was a beneficial predictive model in predicting postoperative long-term outcomes for surgically treated ICC patients.

DISCUSSION

The present study evaluated the potential effectiveness of preoperative inflammatory, hepatic and coagulation indexes in the prediction of outcomes for ICC patients following surgical resection; GPR and INR showed the greatest prognostic value among several indexes and were integrated into GPR-INR score for the first time. Moreover, a nomogram based on the GPR-INR score and other clinicopathological features identified by multivariable analysis was built and validated in derivation and validation sets. The result of this study suggested that the GPR-

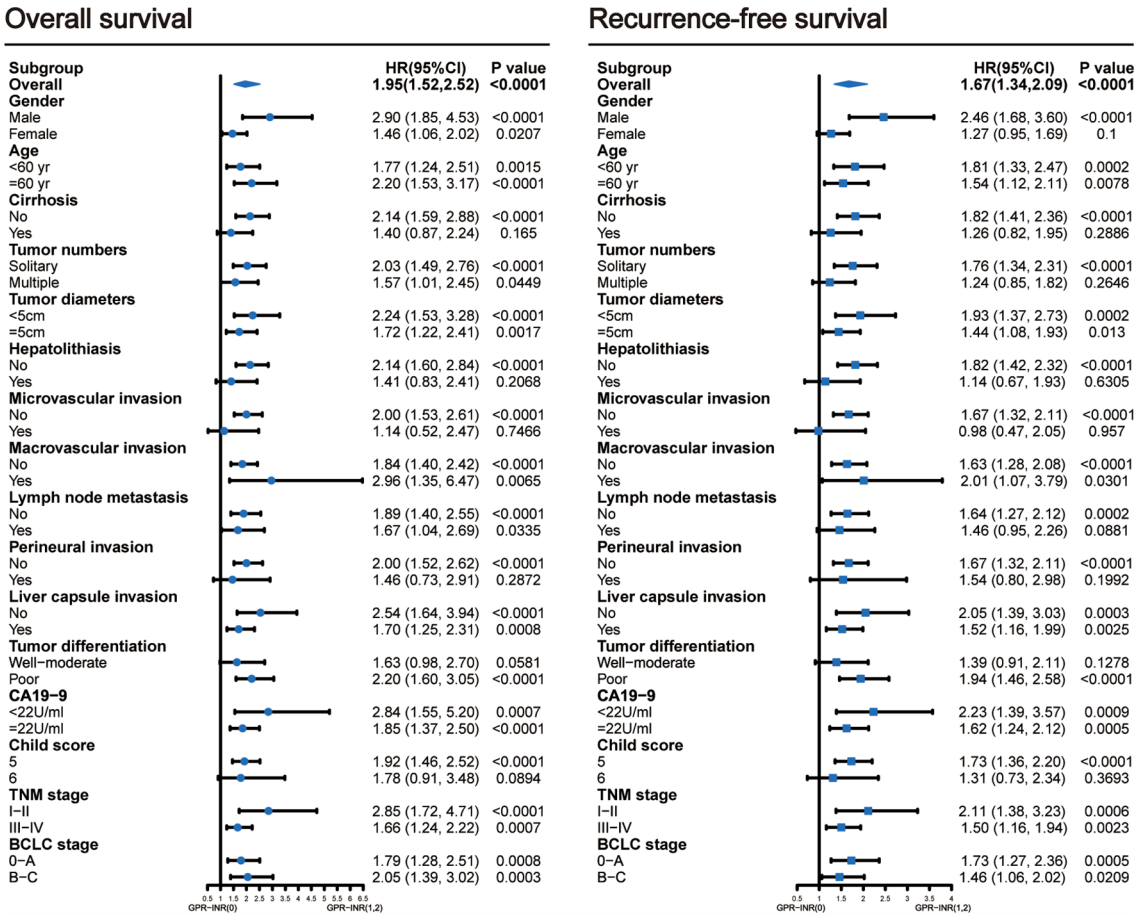

FIGURE 2 | Subgroup analyses using univariable Cox regression to assess the discrimination ability of the GPR-INR score for overall survival and recurrence-free survival in patients with different clinical characteristics. CI, confidence interval.

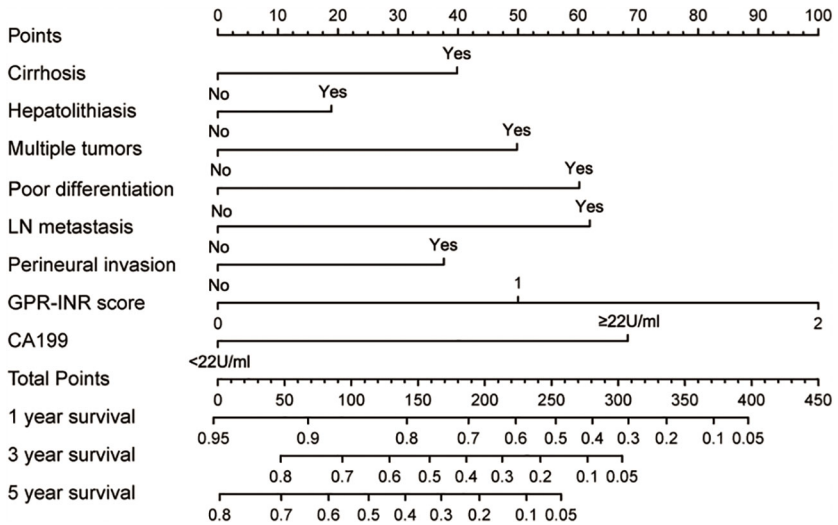

FIGURE 3 | The GPR-INR nomogram. (To use the nomogram, the patient's value was located on each variable axis, and a line was drawn to determine the individual points. The sum of these points was located on the total points axis, and a line was drawn downward to determine the likelihood of 1-, 3- or 5-year OS). CA-199, preoperative serum CA 19-9 level; LN metastasis, regional lymph node metastasis.

TABLE 3 | Comparisons of the values of two models in predicting prognosis of overall survivals among the patients in derivation and validation cohort.

Models	C-index
Derivation cohort	
GPR-INR score	0.597
GPR-INR nomogram	0.708
Validation corhort	
GPR-INR score	0.678
GPR-INR nomogram	0.746

INR, international normalized ratio; GPR, gamma-glutamyl transpeptidase to platelet ratio; C-index, Harrell's concordance-index.

INR score was an independent predictor for OS and RFS in patients with different clinical characteristics. Furthermore, with greater predictive power than BCLC and AJCC 8th staging systems, the GPR-INR nomogram was an optimal scoring system in the prediction of long-term outcomes for ICC patients undergoing curative hepatectomy.

There is accumulating evidence indicating that preoperative serum biomarkers play a crucial role in predicting the prognosis of liver cancer patients. The lymphocyte-based indexes including PLR, NLR, LMR and SII have been introduced as potential prognostic markers for patients with HCC (16, 24) and ICC (25) following curative liver resection. Liver function indexes including bilirubin, albumin, alkaline phosphatase (ALP), gamma-glutamyl transpeptidase (GGT), aspartate aminotransferase (AST) and alanine aminotransferase (ALT), are essential serum markers to determine the hepatic reserve function and feasibility of liver resection, on the basis of these indexes, several scoring systems including ALBI, FIB-4, AGR, AAPR and APRI, have been validated as efficient prognostic indicators for liver cancer patients (17, 26, 27). Several studies have reported that GPR demonstrated prognostic value in HCC (19, 28); however, the predictive capability of GPR for the survival of surgically treated ICC patients is unknown. As a critical indicator of coagulation function, although INR has been proposed as a promising prognostic marker in patients with HCC and biliary tract cancer (21, 29), its predictive effect in patients with ICC has not been studied separately.

Since the first prognostic nomogram for ICC was developed by Shen et al. (3), various nomograms based on different parameters have proliferated. Baseline characteristics and histopathological features were integrated by Omar et al. to build a model in predicting long-term outcomes for ICC patients following hepatectomy; the C-index for this model was 0.692 (30). Liang et al. proposed a nomogram based on radiological findings and TNM stage to predict the early recurrence of ICC (31). Tumor-related features including tumor stroma, tumor number, lymph node metastasis and MVI were combined by Jing et al. (32), with a C-index of 0.745. Xing et al. put forward a nomogram on the basis of ALBI grade to predict OS for patients with recurrent ICC (33). However, the nomogram containing preoperative hepatic and coagulation function for ICC has not yet been established.

In the current study, ROC analysis of 1-, 3-, 5-year postoperative outcome revealed that the GPR, INR and SII were superior predictive markers to predict OS and RFS in patients with ICC following surgical resection. Their predictive ability was greater than PLR, FIB-4 and ALBI, inconsistent with the tendency of the previous study in HCC patients (19). X-tile analysis determined the optimal cut-off value for the GPR and the INR. Survival analysis demonstrated that patients with a high GPR (≥0.7) and INR (≥1.1) had worse OS and RFS than those with a low GPR and INR (**Supplemental Figure 3**). High GPR and INR were more likely to present in ICC patients with liver

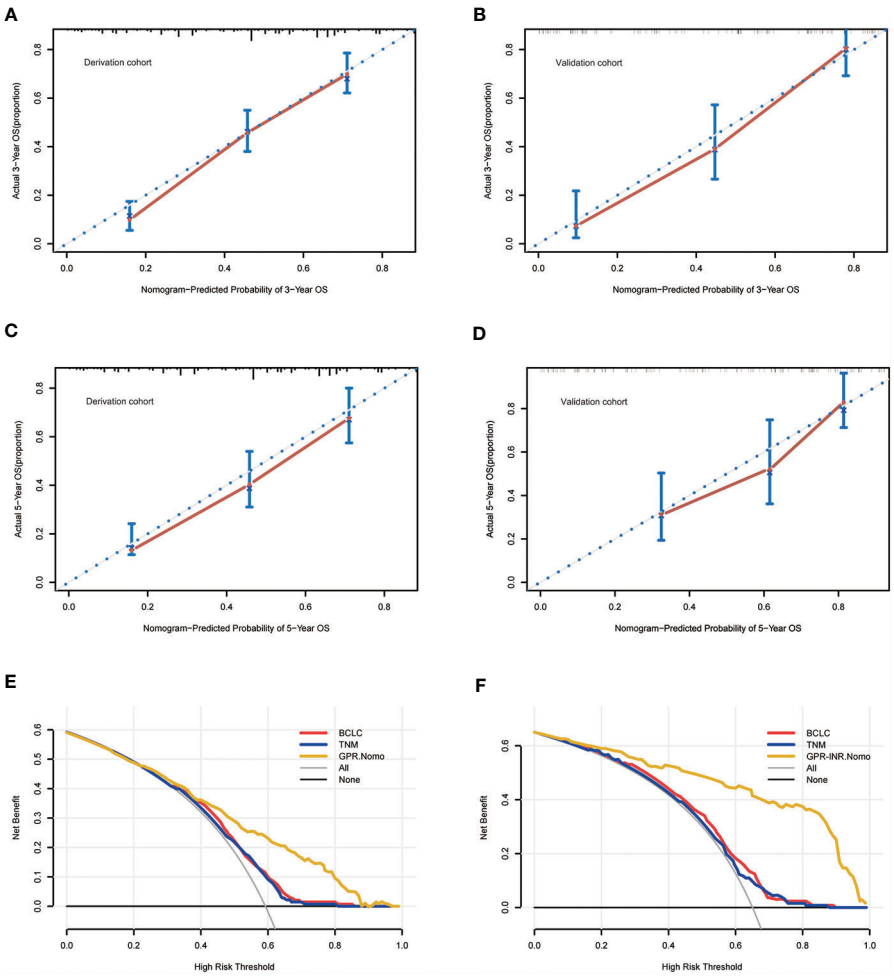

FIGURE 4 | The calibration curves for predicting the OS of the patients at 3 years in the derivation set **(A)** and validation set **(B)** and at 5 years in the derivation set **(C)** and validation set **(D)**. The decision curve analysis for the BCLC staging system, the AJCC 8th TNM system and the GPR-INR nomogram in the derivation set **(E)** and the validation set **(F)**.

cirrhosis, vascular and liver capsule invasion, indicating that the preoperative GPR and INR were related to the basic liver condition and tumor progression. These findings demonstrated that GPR and INR were both valuable preoperative prognostic markers for ICC patients following hepatectomy.

In order to further improve the prognostic power, the GPR and INR were integrated into the GPR-INR score; time-dependent analysis suggested that the discriminative power of the GPR-INR score was consistently greater than that of the GPR or INR in predicting long-term outcomes for surgically treated ICC patients. Patients were stratified into 3 groups according to the GPR-INR score; the ICC patients with higher GPR-INR score had worse OS and RFS in Kaplan-Meier survival analysis. In addition, the GPR-INR score remained a risk factor for OS and RFS in various subgroups.

In comparison with the GPR-INR score, the prognostic markers evaluated in this study, including SII, FIB-4, ALBI and PLR, failed to derive independent prognostic value in multivariate analysis. A prior study showed that a high preoperative PLR was an independent risk factor for OS and RFS (34); in this study, PLR was also associated with OS in univariate analysis but lost its predictive power in multivariate study, the results were inconsistent with the research from Japan (25). Similarly, the ALBI and SII showed no independent predictive utility in OS and the FIB-4 demonstrated no correlation with OS in both univariate and multivariate analysis in this study, maybe because of their common relationship with the platelet counts and weaker prognostic value than GPR-INR score. On that account, we conclude that compared with these established predictors, the GPR-INR score could more accurately predict the prognosis of ICC patients following liver resection.

For the purpose of building a more accurate prediction model, clinicopathological characteristics of ICC patients were included in the evaluation. Liver cirrhosis, hepatolithiasis, multiple tumors, poor tumor differentiation, lymph node

metastasis, perineural invasion, CA19-9 and GPR-INR score were identified as risk factors for OS in univariate analysis. Multivariate analysis also identified the GPR-INR score as an independent risk factor for OS, along with CA19-9, liver cirrhosis and four histopathological factors (multiple tumors, poor tumor differentiation, lymph node metastasis, perineural invasion). These factors were further integrated into the GPR-INR nomogram, the predicted 3- and 5-year OS were in good agreements with the actual OS. In comparison with the single use of the GPR-INR score, the C-index of the GPR-INR nomogram demonstrated greater stratifying ability. Importantly, the BCLC and the AJCC TNM systems are the most commonly used staging systems worldwide (35, 36); the decision curve analysis indicated that the GPR-INR nomogram had superior clinical usefulness when compared with the two conventional systems.

There are several shortcomings that warrant consideration in this study. Firstly, although this was a multi-center study, both centers were located in the western region of China; due to the high prevalence of hepatolithiasis in this region, the accuracy of the GPR-INR nomogram might be limited by the etiology and retrospective design, further prospective international multi-institutional studies were needed to certify our initial findings. Secondly, few patients admitted for obstructive jaundice received preoperative percutaneous transhepaticcholangial drainage (PTCD) due to safety concerns; thus the GGT and bilirubin levels might be fluctuant. Third, a small number of patients received retreatment in other medical institutions after tumor recurrence; consequently, this study failed to assess the influence of postoperative treatment for recurrent ICC, which might alter the OS. In addition, the underlying mechanisms for the impact of the coagulation and hepatic functions on the survival of ICC patients were not analyzed in the present study; basic researches are required using *in vivo* and *in vitro* experiments to explore the concrete mechanisms.

CONCLUSIONS

A preoperative GPR-INR score was a validated independent prognostic marker for surgically treated ICC patients, superior to the well-established inflammatory and liver functional indexes. Moreover, the GPR-INR nomogram represented a more reliable model than the AJCC 8th and BCLC systems. With its low cost, objectivity and accessibility, it was profitable to consider the GPR-INR nomogram as a substitute model in risk stratification for ICC patients after curative hepatic resections.

DATA AVAILABILITY STATEMENT

The original contributions presented in the study are included in the article/**Supplementary Material**. Further inquiries can be directed to the corresponding authors.

ETHICS STATEMENT

This study complied with Helsinki declaration of 1975. The ethics committee of West China Hospital of Sichuan University and the First Affiliated Hospital of Chongqing Medical University approved the protocols.

AUTHOR CONTRIBUTIONS

YC, HW, and CD: conceptualization. YC and BZ: data curation. YC, HL, and HlL: formal analysis. CD and HW: supervision. YC, BZ, and KX: writing—original draft. All authors contributed to the article and approved the submitted version.

FUNDING

This work was supported by grants from the National Key Technologies R&D Program (2018YFC1106800), the Natural Science Foundation of China (81972747, 81872004, 81800564, 81770615, 81700555 and 81672882), the Science and Technology Support Program of Sichuan Province (2019YFQ0001, 2018SZ0115, 2017SZ0003), the Science and Technology Program of Tibet Autonomous Region (XZ201801-GB-02) and the 1.3.5 project for disciplines of excellence, West China Hospital, Sichuan University (ZYJC18008), 2021 Sichuan Science and Technology Plan Project "International cooperation in science and technology innovation/technological innovation cooperation in Hong Kong, Macao and Taiwan", Artificial intelligence assisted precise diagnosis and minimally invasive treatment of liver tumor diseases (2021YFH0095).

SUPPLEMENTARY MATERIAL

The Supplementary Material for this article can be found online at: https://www.frontiersin.org/articles/10.3389/fonc.2021.711061/full#supplementary-material

REFERENCES

1. Ferlay J, Colombet M, Soerjomataram I, Mathers C, Parkin DM, Piñeros S, et al. Estimating the Global Cancer Incidence and Mortality in 2018: GLOBOCAN Sources and Methods. *Int J Cancer* (2019) 144(8):1941–53. doi: 10.1002/ijc.31937
2. Rizvi S, Khan SA, Hallemeier CL, Kelley RK, Gores GJ. Cholangiocarcinoma - Evolving Concepts and Therapeutic Strategies. *Nat Rev Clin Oncol Feb* (2018) 15(2):95–111. doi: 10.1038/nrclinonc.2017.157
3. Wang Y, Li J, Xia Y, Gong R, Wang K, Yan Z, et al. Prognostic Nomogram for Intrahepatic Cholangiocarcinoma After Partial Hepatectomy. *J Clin Oncol* (2013) 31(9):1188–95. doi: 10.1200/JCO.2012.41.5984
4. Shaib YH, Davila JA, McGlynn K, El-Serag HB. Rising Incidence of Intrahepatic Cholangiocarcinoma in the United States: A True Increase? *J Hepatol* (2004) 40(3):472–7. doi: 10.1016/j.jhep.2003.11.030
5. Saha SK, Zhu AX, Fuchs CS, Brooks GA. Forty-Year Trends in Cholangiocarcinoma Incidence in the U.S.: Intrahepatic Disease on the Rise. *Oncologist* (2016) 21(5):594–9. doi: 10.1634/theoncologist.2015-0446

6. Razumilava N, Gores GJ. Cholangiocarcinoma. *Lancet* (2014) 383 (9935):2168–79. doi: 10.1016/S0140-6736(13)61903-0
7. Bridgewater J, Galle PR, Khan SA, Llovet JM, Park W, Patel T, et al. Guidelines for the Diagnosis and Management of Intrahepatic Cholangiocarcinoma. *J Hepatol Jun* (2014) 60(6):1268–89. doi: 10.1016/j.jhep.2014.01.021
8. Razumilava N, Gores GJ. Classification, Diagnosis, and Management of Cholangiocarcinoma. *Clin Gastroenterol Hepatol Jan* (2013) 11(1):13–21.e1; quiz e3-4. doi: 10.1016/j.cgh.2012.09.009
9. Tyson GL, El-Serag HB. Risk Factors for Cholangiocarcinoma. *Hepatol Jul* (2011) 54(1):173–84. doi: 10.1002/hep.24351
10. Yasser S, Hashem BE. The Epidemiology of Cholangiocarcinoma. *Semin Liver Dis* (2004) 24:115–25. doi: 10.1055/s-2004-828889
11. Endo I, Gonen M, Yopp AC, Dalal KM, Zhou Q, Klimstra D, et al. Intrahepatic Cholangiocarcinoma: Rising Frequency, Improved Survival, and Determinants of Outcome After Resection. *Ann Surg Jul* (2008) 248 (1):84–96. doi: 10.1097/SLA.0b013e318176c4d3
12. Farges O, Fuks D, Boleslawski E, Le Treut YP, Castaing D, Laurent A, et al. Influence of Surgical Margins on Outcome in Patients With Intrahepatic Cholangiocarcinoma: A Multicenter Study by the AFC-IHCC-2009 Study Group. *Ann Surg* (2011) 254(5):824–29; discussion 830. doi: 10.1097/SLA.0b013e318236c21d
13. Choi SB, Kim KS, Choi JY, Park SW, Choi JS, Lee W, et al. The Prognosis and Survival Outcome of Intrahepatic Cholangiocarcinoma Following Surgical Resection: Association of Lymph Node Metastasis and Lymph Node Dissection With Survival. *Ann Surg Oncol Nov* (2009) 16(11):3048–56. doi: 10.1245/s10434-009-0631-1
14. Chun YS, Pawlik TM, Vauthey JN. 8th Edition of the AJCC Cancer Staging Manual: Pancreas and Hepatobiliary Cancers. *Ann Surg Oncol Apr* (2018) 25 (4):845–7. doi: 10.1245/s10434-017-6025-x
15. Luo X, Yuan L, Wang Y, Ge R, Sun Y, Wei G. Survival Outcomes and Prognostic Factors of Surgical Therapy for All Potentially Resectable Intrahepatic Cholangiocarcinoma: A Large Single-Center Cohort Study. *J Gastrointest Surg* (2014) 18(3):562–72. doi: 10.1007/s11605-013-2447-3
16. Sellers CM, Uhlig J, Ludwig JM, Stein SM, Kim HS. Inflammatory Markers in Intrahepatic Cholangiocarcinoma: Effects of Advanced Liver Disease. *Cancer Med* (2019) 8(13):5916–29. doi: 10.1002/cam4.2373
17. Toyoda H, Kumada T, Tada T, Yama T, Mizuno K, Sone Y, et al. Differences in the Impact of Prognostic Factors for Hepatocellular Carcinoma Over Time. *Cancer Sci* (2017) 108(12):2438–44. doi: 10.1111/cas.13406
18. Lemoine M, Shimakawa Y, Nayagam S, Khalil M, Suso P, Lloyd J, et al. The Gamma-Glutamyl Transpeptidase to Platelet Ratio (GPR) Predicts Significant Liver Fibrosis and Cirrhosis in Patients With Chronic HBV Infection in West Africa. *Gut* (2016) 65(8):1369–76. doi: 10.1136/gutjnl-2015-309260
19. Park YE, Kim BK, Park JY, Kim DY, Ahn SH, Han KH, et al. Gamma-Glutamyl Transpeptidase-to-Platelet Ratio Is an Independent Predictor of Hepatitis B Virus-Related Liver Cancer. *J Gastroenterol Hepatol* (2017) 32 (6):1221–9. doi: 10.1111/jgh.13653
20. Kamath PS, Kim WR. Advanced Liver Disease Study G. *Model end-stage liver Dis (MELD) Hepatol* (2007) 45(3):797–805. doi: 10.1002/hep.21563
21. Haruki K, Shiba H, Saito N, Horiuchi T, Fujiwara Y, Furukawa K, et al. Risk Stratification Using a Novel Liver Functional Reserve Score of Combination Prothrombin Time-International Normalized Ratio to Albumin Ratio and Albumin in Patients With Hepatocellular Carcinoma. *Surgery* (2018) 164 (3):404–10. doi: 10.1016/j.surg.2018.02.022
22. Robert LC, Marisa DF, David LR. X-Tile: A New Bio-Informatics Tool for Biomarker Assessment and Outcome-Based Cut-Point Optimization. *Clin Cancer Res* (2004) 10:7252–9. doi: 10.1158/1078-0432.CCR-04-0713
23. Josep ML, Concepcio B, Jordi B. Prognosis of Hepatocellular Carcinoma: The BCLC Staging Classification. *Semin Liver Dis* (1999) 19(3):329–38. doi: 10.1055/s-2007-1007122
24. Ha Y, Mohamed Ali MA, Petersen MM, Harmsen WS, Therneau TM, Lee LC, et al. Lymphocyte to Monocyte Ratio-Based Nomogram for Predicting Outcomes of Hepatocellular Carcinoma Treated With Sorafenib. *Hepatol Int Sep* (2020) 14(5):776–87. doi: 10.1007/s12072-020-10076-4
25. Ohira M, Yoshizumi T, Yugawa K, Kosai-Fujimoto Y, Inokuchi S, Motomura T, et al. Association of Inflammatory Biomarkers With Long-Term Outcomes After Curative Surgery for Mass-Forming Intrahepatic Cholangiocarcinoma. *Surg Today Apr* (2020) 50(4):379–88. doi: 10.1007/s00595-019-01905-7
26. Li H, Li J, Wang J, Liu H, Cai B, Wang G, et al. Assessment of Liver Function for Evaluation of Long-Term Outcomes of Intrahepatic Cholangiocarcinoma: A Multi-Institutional Analysis of 620 Patients. *Front Oncol* (2020) 10:525. doi: 10.3389/fonc.2020.00525
27. Shen J, Tang L, Zhang X, Peng W, Wen T, Li C, et al. A Novel Index in Hepatocellular Carcinoma Patients After Curative Hepatectomy: Albumin to Gamma-Glutamyltransferase Ratio (AGR). *Front Oncol* (2019) 9:817. doi: 10.3389/fonc.2019.00817
28. Luo D, Li H, Hu J, Zhang M, Zhang S, Wu L, et al. Development and Validation of Nomograms Based on Gamma-Glutamyl Transpeptidase to Platelet Ratio for Hepatocellular Carcinoma Patients Reveal Novel Prognostic Value and the Ratio Is Negatively Correlated With P38MAPK Expression. *Front Oncol* (2020) 10:548744. doi: 10.3389/fonc.2020.548744
29. Schweitzer N, Fischer M, Kirstein MM, Berhane S, Kottas M, Sinn M, et al. Risk Estimation for Biliary Tract Cancer: Development and Validation of a Prognostic Score. *Liver Int* (2017) 37(12):1852–60. doi: 10.1111/liv.13517
30. Hyder O, Marques H, Pulitano C, Marsh JW, Alexandrescu S, Bauer TW, et al. A Nomogram to Predict Long-Term Survival After Resection for Intrahepatic Cholangiocarcinoma: An Eastern and Western Experience. *JAMA Surg* (2014) 149(5):432–8. doi: 10.1001/jamasurg.2013.5168
31. Liang W, Xu L, Yang P, Zhang L, Wan D, Huang Q, et al. Novel Nomogram for Preoperative Prediction of Early Recurrence in Intrahepatic Cholangiocarcinoma. *Front Oncol* (2018) 8:360. doi: 10.3389/fonc.2018.00360
32. Jing CY, Fu YP, Huang JL, Zhang MX, Yi Y, Gan W, et al. Prognostic Nomogram Based on Histological Characteristics of Fibrotic Tumor Stroma in Patients Who Underwent Curative Resection for Intrahepatic Cholangiocarcinoma. *Oncologist* (2018) 23(12):1482–93. doi: 10.1634/theoncologist.2017-0439
33. Xing KL, Lu LH, Huang X, He CB, Song YD, Guo RP, et al. A Novel Prognostic Nomogram for Patients With Recurrence of Intrahepatic Cholangiocarcinoma After Initial Surgery. *Front Oncol* (2020) 10:434. doi: 10.3389/fonc.2020.00434
34. Chen Q, Dai Z, Yin D, Yang LX, Wang Z, Xiao YS, et al. Negative Impact of Preoperative Platelet-Lymphocyte Ratio on Outcome After Hepatic Resection for Intrahepatic Cholangiocarcinoma. *Med (Baltimore)* (2015) 94(13):e574. doi: 10.1097/MD.0000000000000574
35. Tsilimigras DI, Bagante F, Sahara K, Moris D, Hyer JM, Wu L, et al. Prognosis After Resection of Barcelona Clinic Liver Cancer (BCLC) Stage 0, A, and B Hepatocellular Carcinoma: A Comprehensive Assessment of the Current BCLC Classification. *Ann Surg Oncol* (2019) 26(11):3693–700. doi: 10.1245/s10434-019-07580-9
36. Ronnekleiv-Kelly SM, Pawlik TM. Staging of Intrahepatic Cholangiocarcinoma. *Hepatobiliary Surg Nutr* (2017) 6(1):35–43. doi: 10.21037/hbsn.2016.10.02

Conflict of Interest: The authors declare that the research was conducted in the absence of any commercial or financial relationships that could be construed as a potential conflict of interest.

Copyright © 2021 Cai, Zhang, Li, Li, Liu, Xie, Du and Wu. This is an open-access article distributed under the terms of the Creative Commons Attribution License (CC BY). The use, distribution or reproduction in other forums is permitted, provided the original author(s) and the copyright owner(s) are credited and that the original publication in this journal is cited, in accordance with accepted academic practice. No use, distribution or reproduction is permitted which does not comply with these terms.

frontiers in Oncology

ORIGINAL RESEARCH
published: 20 September 2021
doi: 10.3389/fonc.2021.736678

Impact of Inadequate Number of Lymph Nodes Examined on Survival in Stage II Colon Cancer

Qi Wu[†], *Zhiyuan Zhang*[†], *Yijiao Chen*[†], *Jiang Chang*[†], *Yudong Jiang*, *Dexiang Zhu*[*] *and Ye Wei*[*]

Department of General Surgery, Zhongshan Hospital, Fudan University, Shanghai, China

OPEN ACCESS

Edited by:
Ravindra Deshpande, Wake Forest School of Medicine, United States

Reviewed by:
Nazri Mustaffa, Universiti Sains Malaysia (USM), Malaysia
Paul Willemsen, Hospital Network Antwerp (ZNA), Belgium
Wenlong Gu, Jianhu People's Hospital, China

***Correspondence:**
Ye Wei
wei.ye@zs-hospital.sh.cn
Dexiang Zhu
zhu.dexiang@zs-hospital.sh.cn

[†]*These authors have contributed equally to this work*

Specialty section:
This article was submitted to Surgical Oncology, a section of the journal Frontiers in Oncology

Received: *05 July 2021*
Accepted: *27 August 2021*
Published: *20 September 2021*

Citation:
Wu Q, Zhang Z, Chen Y, Chang J, Jiang Y, Zhu D and Wei Y (2021) Impact of Inadequate Number of Lymph Nodes Examined on Survival in Stage II Colon Cancer. Front. Oncol. 11:736678. doi: 10.3389/fonc.2021.736678

Background: Inadequate number of lymph nodes examined was not uncommon. We aimed to assess the clinical role of inadequate number of lymph nodes examined in stage II colon cancer.

Methods: The cancer data used in our study were obtained from the SEER (Surveillance, Epidemiology and End Results) program. Using the chi-square test, all the variables obtained in our study were compared based on whether patients had enough (≥12) lymph nodes examined. Kaplan–Meier analysis was used for overall survival (OS) analysis, and log-rank test was applied to compare different N stages with the total number of lymph nodes examined. Multivariate analysis was carried out by creating a Cox proportional hazard model to assess the prognostic roles of different variables.

Results: In total, 80,296 stage II/III colon cancer patients were recruited for our study. N0 stage with <8 lymph nodes examined would present with a worse prognosis compared to N1 stage (5-year OS rates, 51.6% vs. 57.1%, $p < 0.001$). Multivariate analyses indicated that OS of N0 stage with <8 lymph nodes examined was similar to that of N1 stage after adjusting for other recognized prognostic factors [hazard ratios (HRs) = 1.051, 95% confidence intervals (CIs) = 1.014–1.090, $p = 0.018$].

Conclusions: N0 stage with less than eight lymph nodes examined in stage II colon cancer presented with no better OS compared to that of N1 stage. Stage II colon cancer with less than eight lymph nodes examined needed to be given greater emphasis in clinical practice.

Keywords: number, lymph nodes, survival, stage II colon cancer, retrospective

INTRODUCTION

Colon adenocarcinoma was ranked as one of the most frequent malignant tumors worldwide (1). The tumor node metastasis (TNM) cancer staging system proposed by the American Joint Committee on Cancer (AJCC) has been widely used to guide treatment plans and evaluate prognosis of colon cancer patients. Based on this staging system, the most obvious difference between stage II and stage III colon cancer was the presence of pathological lymph node metastasis.

Recommended by the American College of Pathologists (ACP) and the American Joint Committee on Cancer (AJCC), the pathological examination of lymph nodes should be at least 12 in the surgical specimen, which has become the general consensus to ensure accurate nodal staging in colon cancer patients (2, 3). It was reported by researchers that the least number of lymph nodes examined was 13 to identify more than 90% local lymph node metastasis (4). In spite of that, inadequate number of lymph nodes examined was not uncommon. Inadequate number of lymph nodes examined might lead to inaccurate assessment for lymph node involvement, which would misguide clinical treatment decisions and adversely affect patient outcomes (5, 6).

It was previously reported in a big retrospective study that the number of lymph nodes examined ranged between 5.5 and 21.3 lymph nodes, and the average lymph node harvest was 11.7, which was less than the recommended minimum lymph nodes examined (7). In the present study, using the data from a big cancer database with long-term follow-up, we aimed to evaluate the prognostic value of inadequate number of lymph nodes examined in stage II colon cancer.

MATERIALS AND METHODS

Patients

The cancer data used in our study were obtained from the SEER (Surveillance, Epidemiology and End Results) program. Established by the National Cancer Institute, it collected and updated de-identified patient information regarding cancer incidence, clinicopathological characteristics, treatment modalities, survival, etc.

The patient flow diagram is shown in **Supplementary Figure S1**. From 2004 to 2010, patients diagnosed with colon cancer were identified using the NCI SEER*Stat software (version 8.3.5). All patients meeting the following criteria were eligible for inclusion in the present study: (1) with surgical resection; (2) with active follow-up; (3) without distant metastasis; (4) with positive histological confirmation; (5) T3 or T4; (6) with exact number of nodes examined; and (7) adenocarcinoma histology. Besides stage II colon cancer, we have also recruited stage III (stage T3–4 with lymph node metastasis) patients to compare the prognosis of inadequate lymph nodes examined and pathological lymph node positivity.

The following demographic and clinicopathologic characteristics including tumor grade, gender, the time of diagnosis, TNM stage, race, tumor histology, and the receipt of chemotherapy were subsequently required from this cancer database. For N stage, it has been divided into different subgroups according to the examined number of lymph nodes to assess the clinical role of inadequate number of lymph nodes examined in stage II colon cancer.

Statistical Analyses

In the present study, overall survival (OS) was considered to be the outcome of interest. OS was defined as the time from the date of diagnosis with colon cancer to time of death. In the first, using the chi-square test, all the variables obtained in our study were compared based on whether patients had enough (≥12) lymph nodes examined.

Kaplan–Meier analysis was used for OS analysis, and the log-rank test was applied to compare different node stages with the number of lymph nodes examined in total. According to the above variables, multivariate analysis was carried out by creating a Cox proportional hazard model to assess the clinical role of different variables with 95% confidence intervals (CIs) and hazard ratios (HRs). Analyses were performed by using IBM SPSS Statistics for Windows, Version 25.0. (IBM Corp., Armonk, NY). In our analyses, only tests producing a two-sided $p < 0.05$ would reach statistical significance.

RESULTS

Patients' Demographics and Clinical Characteristics

In total, 80,296 stage II/III colon cancer patients were recruited for our study; demographic and clinicopathologic characteristics including tumor grade, gender, the time of diagnosis, TNM stage, race, tumor histology, and the receipt of chemotherapy were then acquired from this cancer database. Besides stage II colon cancer, we have also recruited stage III (stage T3–4 with lymph node metastasis) patients to compare the prognosis of inadequate lymph nodes examined and pathological lymph node positivity.

In total, male patients accounted for 48.0% (38,537). As shown in **Figure 1**, the median number of lymph nodes examined was 16, and there was a total of 45,146 (56.2%) deaths at end of the follow-up. The demographic and clinicopathological characteristics of colon cancer patients were listed (**Table 1**). In all, 58,799 patients (73.2%) had more than 12 lymph nodes examined. The results of chi-square test also indicated that white patients ($p = 0.013$), ≤75 years old ($p < 0.001$), T3 stage ($p = 0.034$), stage N2 ($p < 0.001$), poor/anaplastic grade ($p < 0.001$), female ($p < 0.001$), mucinous/signet ring cell histology ($p < 0.001$), and later year of diagnosis ($p < 0.001$) were more likely to have enough (≥12) lymph nodes examined.

Inadequate Number of Lymph Nodes Examined Had Poor Prognosis

In **Figure 2**, patients would present with worse OS as the number of lymph nodes examined decreased in node-negative cases—<4 lymph nodes (5-year OS rate = 46.2%) was more likely to have decreased OS compared with <8 lymph nodes (5-year OS rate = 54.1%; $p < 0.001$), <8 lymph nodes was more likely to have decreased OS compared with <12 lymph nodes (5-year OS rate= 60.2%; $p < 0.001$), and < 12 lymph nodes was more likely to have worse OS compared with more than 12 lymph nodes examined (5-year OS rate = 69.0%; $p < 0.001$). Moreover, results of Kaplan–Meier analyses indicated that <8 lymph nodes with node negativity was even more likely to have decreased OS compared with N1 stage (5-year OS rates, 54.1% *vs.* 57.1%, $p < 0.001$).

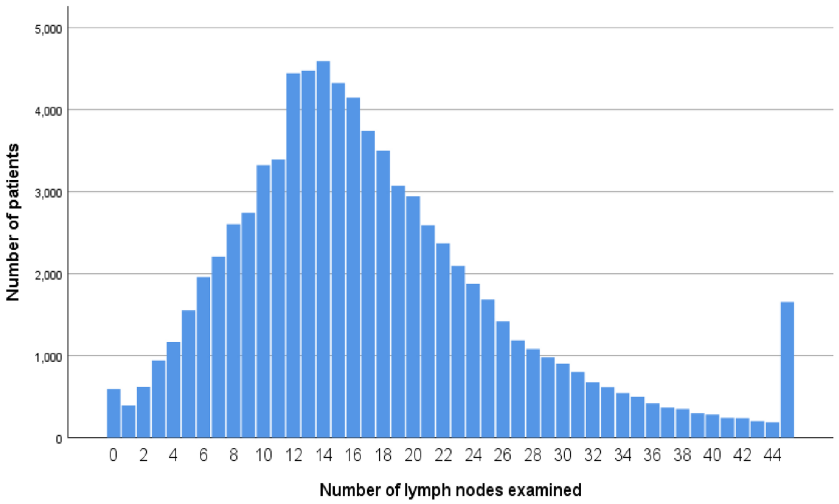

FIGURE 1 | Distribution of numbers of lymph node retrieved.

TABLE 1 | Demographics and clinical characteristics.

Characteristics	No. of lymph nodes examined (%)		*p*-value
	<12 (*n* = 21,497)	≥12 (*n* = 58,799)	
Race			0.013
White	17,340 (80.7)	47,882 (81.4)	
Black	2,547 (11.8)	6,536 (11.1)	
Other	1,610 (7.5)	4381 (7.5)	
Age at diagnosis			<0.001
≤75 years	11,660 (54.2)	36,608 (62.3)	
>75 years	9,837 (45.8)	22,191 (37.7)	
T stage			0.034
T3	17,951 (83.5)	49,464 (84.1)	
T4	3,546 (16.5)	9,335 (15.9)	
N stage			<0.001
N0	12,789 (59.5)	31,748 (54.0)	
N1	6,374 (29.7)	16,079 (27.3)	
N2	2,334 (10.9)	10,972 (18.7)	
Tumor grade			<0.001
High/Moderate	16,700 (77.7)	43,430 (73.9)	
Poor/Anaplastic	4,328 (20.1)	14,318 (24.4)	
Unknown	469 (2.2)	1,051 (1.8)	
Sex			<0.001
Male	10,575 (49.2)	27,962 (47.6)	
Female	10,922 (50.8)	30,837 (52.4)	
Histology			<0.001
Adenocarcinoma	19,287 (89.7)	51,692 (87.9)	
Mucinous/signet ring cell	2,210 (10.3)	7,107 (12.1)	
Year of diagnosis			<0.001
2004–2007	15,878 (73.9)	30,885 (52.5)	
2008–2010	5,619 (26.1)	27,914 (47.5)	
Chemotherapy			<0.001
No	15,267 (71.0)	38,086 (64.8)	
Yes	6,230 (29.0)	20,713 (35.2)	

In addition, multivariate analyses were conducted based on the Cox proportional hazards model with the recognized prognostic factors included, which showed that patients would present with worse OS as the number of lymph nodes examined decreased in node-negative cases. Moreover, patients with N1 stage were prone to having better OS compared to N0 stage with <4 lymph nodes examined (HR = 0.909, 95%CI = 0.860–0.962, p = 0.001; **Table 2**).

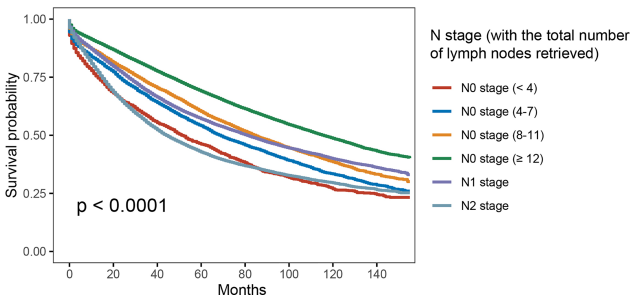

FIGURE 2 | Kaplan–Meier survival curves for colon cancer patients according to number of lymph node retrieved.

The Comparison of OS Between Node Positivity and Inadequate Lymph Nodes Examined

To better evaluate the clinical role of inadequate number of lymph nodes examined in stage II colon cancer, we then compared the OS difference between node-positive patients and node-negative patients (with inadequate lymph nodes examined).

As shown in **Figure 3**, with the combination of less than four lymph nodes and less than eight lymph nodes examined together in node-negative patients, it was found that N0 stage with <8 lymph nodes examined would present with worse OS compared

TABLE 2 | Multivariate analyses on overall survival in colon cancer.

Characteristics	Overall survival		
	HR (95% CI)	SE	*p*-value
Race			<0.001
White	Reference		
Black	1.196 (1.161–1.232)	0.015	<0.001
Other	0.780 (0.750–0.812)	0.020	<0.001
Age at diagnosis			<0.001
≤75 years	Reference		
>75 years	2.524 (2.474–2.576)	0.010	
Histology			0.005
Adenocarcinoma	Reference		
Mucinous/signet ring cell	1.042 (1.013–1.072)	0.015	
T stage			<0.001
T3	Reference		
T4	1.650 (1.611–1.689)	0.012	
N stage			<0.001
N0 stage (<4 lymph nodes)	Reference		
N0 stage (<8 lymph nodes)	0.810 (0.759–0.864)	0.033	<0.001
N0 stage (<12 lymph nodes)	0.690 (0.649–0.733)	0.031	<0.001
N0 stage (≥12 lymph nodes)	0.541 (0.512–0.572)	0.028	<0.001
N1 stage	0.909 (0.860–0.962)	0.029	0.001
N2 stage	1.389 (1.311–1.471)	0.029	<0.001
Tumor grade			<0.001
High/Moderate	Reference		
Poor/Anaplastic	1.147 (1.122–1.172)	0.011	<0.001
Unknown	1.131 (1.059–1.208)	0.033	<0.001
Sex			<0.001
Male	Reference		
Female	0.839 (0.824–0.855)	0.010	
Year of diagnosis			0.547
2004–2007	Reference		
2008–2010	1.006 (0.986–1.026)	0.010	
Chemotherapy			<0.001
No	Reference		
Yes	0.586 (0.572–0.600)	0.012	

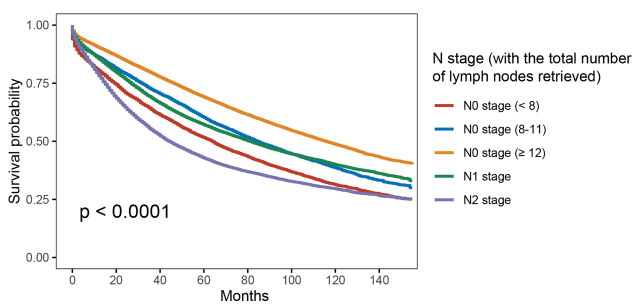

FIGURE 3 | Kaplan–Meier survival curves for colon cancer patients according to the number of lymph node retrieved (with the combination of less than four lymph nodes and less than eight lymph nodes examined together).

to stage N1 (5-year OS rates, 51.6% vs. 57.1%, $p < 0.001$). The results also showed that the survival difference between N0 stage with <12 lymph nodes examined and N1 stage was not statistically significant ($p = 0.918$). Then, multivariate analyses were conducted based on the Cox proportional hazard model with the recognized prognostic factors included; the results

TABLE 3 | Multivariate analyses on overall survival in colon cancer (with the combination of less than four lymph nodes and less than eight lymph nodes retrieved together).

Characteristics	Overall survival		
	HR (95% CI)	SE	*p*-value
Race			<0.001
White	Reference		
Black	1.195 (1.161–1.231)	0.015	<0.001
Other	0.780 (0.750–0.812)	0.020	<0.001
Age at diagnosis			<0.001
≤75 years	Reference		
>75 years	2.524 (2.474–2.575)	0.010	
Histology			0.005
Adenocarcinoma	Reference		
Mucinous/signet ring cell	1.041 (1.012–1.072)	0.015	
T stage			<0.001
T3	Reference		
T4	1.651 (1.612–1.690)	0.012	
N stage			<0.001
N0 stage (<8 lymph nodes)	Reference		
N0 stage (<12 lymph nodes)	0.798 (0.764–0.833)	0.022	<0.001
N0 stage (≥12 lymph nodes)	0.626 (0.605–0.648)	0.018	<0.001
N1 stage	1.051 (1.014–1.090)	0.018	0.006
N2 stage	1.606 (1.545–1.669)	0.020	<0.001
Tumor grade			<0.001
High/Moderate	Reference		
Poor/Anaplastic	1.146 (1.122–1.172)	0.011	<0.001
Unknown	1.136 (1.064–1.213)	0.033	<0.001
Sex			<0.001
Male	Reference		
Female	0.839 (0.824–0.855)	0.010	
Year of diagnosis			0.508
2004–2007	Reference		
2008–2010	1.007 (0.987–1.027)	0.010	
Chemotherapy			<0.001
No	Reference		
Yes	0.586 (0.572–0.600)	0.012	

indicated that the OS of N0 stage with <8 lymph nodes was similar to that of N1 stage after adjusting for other recognized prognostic factors (HR = 1.051, 95%CI = 1.014–1.090, $p = 0.018$; **Table 3**).

DISCUSSION

The high and increasing incidence of colon cancer around the world made the related studies a hot topic in recent years (8–11). In this study, we aimed to evaluate the clinical role of inadequate number of lymph nodes examined in stage II colon cancer, with comparison of node positivity in stage III colon cancer.

With a median follow-up time of 75 months, 80,296 colon cancer patients were enrolled in the whole cohort. Therefore, this was a large retrospective study with long-term follow-up, and it has added more credibility to our main findings. The median number of lymph nodes examined in total was 16, which exceeded the recommended number of lymph nodes examined according to the clinical recommendations of AJCC and ACP. Our results have revealed that up to 26.8% of all the colon cancer patients did not have adequate retrieval of the recommended

number of lymph nodes. However, adequate lymphadenectomy has been suggested for colon cancer, and recent studies showed that increased number of lymph nodes examined for pathological identification would contribute to improved OS in colon cancer, indicating the necessity of finding ways to increase the number of lymph nodes examined (12–15).

To the best of our knowledge, the present population-based study was the largest one that has addressed the clinical role of inadequate lymph node examined in stage II colon cancer. It was found that white race, younger age, later tumor stage, advanced tumor grade, female, mucinous/signet ring cell histology, and later year of diagnosis were prone to being associated with enough (≥12) lymph nodes removed. Previous studies also reported that the length of the bowel resection and the location of ligation of the blood vessels (such as a higher ligation in a complete excision) could affect the number of lymph nodes retrieved (16). Apart from that, several other factors such as the extent and the technique of surgical dissection, physiological factors, and the pathologist's work experience and technical level were also found to exert an effect on the lymph nodes examined (17–19).

Using Kaplan–Meier method, our initial analysis indicated that N0 stage with <4 lymph nodes examined would present with worse OS compared with N1 stage (46.2% *vs.* 57.1%, $p < 0.001$). Moreover, N0 stage with less than eight but more than four lymph nodes examined (5-year OS rate = 54.1%) also presented with worse OS compared with N1 stage ($p < 0.001$). In addition, multivariate analyses were conducted based on the Cox proportional hazards model with the recognized prognostic factors included; the results showed that the OS of N1 stage had 9.1% decreased risk of overall mortality compared with less than four lymph nodes in node-negative patients after adjusting for other recognized factors.

Therefore, we have combined less than four lymph nodes with more than four but less than eight lymph nodes examined together in node-negative patients. The Kaplan–Meier survival analyses indicated that N0 stage with <8 lymph nodes examined would present with worse OS compared to stage N1 (5-year OS rates, 51.6% *vs.* 57.1%, $p < 0.001$). Other recognized prognostic characteristics were then taken account into multivariate analyses, which indicated that the OS of N0 stage with <8 lymph nodes examined was similar to that of N1 stage.

In our analyses, the result that survival of N0 stage with less than eight lymph nodes examined was comparable to that of N1 stage was parallel to previous findings (3, 14, 20). As early as 2002, it was reported by Cianchi and his colleagues (20) that the 5-year survival rate of the Dukes B patients with <8 retrieved lymph nodes was similar to that of the Dukes C patients. Then, in 2005, Sarli et al. (14) recruited 745 stage II and 493 stage III colorectal cancer patients in Italy and found that patients with stage III tumor with only one to three positive lymph nodes had a similar 5-year survival rate (52.6%) compared with that of patients with stage II colon cancer with less than nine lymph nodes examined in total (51.3%).

Similarly in 2009, one British study showed that the survival of Duke's B (stage II) colorectal cancer patients with less than nine lymph nodes examined in total was not better than that of Duke's C (stage III) disease patients (3). In spite of that, it was noteworthy that the abovementioned three studies did not enroll enough cases to evaluate the prognostic value of inadequate number of lymph nodes examined in stage II colon cancer. Moreover, in the present study, with 80,296 patients recruited from a big cancer database, we concluded that N0 stage with less than eight lymph nodes examined in stage II colon cancer presented with similar OS compared to that of N1 stage. Stage II colon cancer with less than eight lymph nodes examined needed to be given greater emphasis in clinical practice.

As suggested by the clinical recommendations of European Society for Medical Oncology, some clinical factors such as pT4 stage, bowel obstruction or tumor perforation, lymph nodes sampling <12, lymphatic or vascular or peripheral invasion, and poorly differentiated tumor were listed as risk characteristics in stage II disease (21). Recently, some researchers have questioned the efficacy of chemotherapy in high-risk stage II colon cancer patients (22–24). In 2018, it was also reported by some American researchers that adjuvant chemotherapy was not associated with improved survival if less than 12 lymph nodes was deemed as the sole high-risk factor (25). The number of enrolled patients in the current study was sufficiently large to give us confidence that the results were high in reliability to evaluate the clinical role of inadequate number of lymph nodes examined in stage II colon cancer. The results of our analyses, together with what have been discussed above, made us believe that stage II colon cancer with less than eight lymph nodes examined needed to be given greater emphasis in clinical practice. However, it should be recognized that preoperative chemotherapy and postoperative chemotherapy were mixed up as chemotherapy and thus analyzing whether neoadjuvant treatment would have effect on the number of lymph nodes examined because of the limitation of this cancer database. Improvements in technology and research in oncology have greatly improved the prognosis of colon cancer patients in the past decade, which may have an influence on the findings of our study. Moreover, the selection bias would also exist in a study with retrospective design. Therefore, it would be interesting to carry out a prospective study to further explore the clinical role of less than eight lymph nodes examined in offering adjuvant therapy in stage II colon cancer.

CONCLUSIONS

Our study showed that OS of N0 stage with less than eight lymph nodes examined was comparable to that of N1 stage in stage II colon cancer. Therefore, stage II colon cancer with less than 8 lymph nodes examined needed to be given greater emphasis in clinical practice. It would be interesting to carry out a prospective study to further explore the clinical role of less than eight lymph nodes examined in offering adjuvant therapy in stage II colon cancer.

DATA AVAILABILITY STATEMENT

The raw data are available from the corresponding author upon reasonable request.

AUTHOR CONTRIBUTIONS

DZ and YW conceived and designed the study. QW and ZZ contributed to the acquisition of data. QW, YC, JC, and YJ interpreted the data. QW wrote the first draft of the manuscript. DZ and YW reviewed and edited the manuscript. All authors contributed to the article and approved the submitted version.

SUPPLEMENTARY MATERIAL

The Supplementary Material for this article can be found online at: https://www.frontiersin.org/articles/10.3389/fonc.2021.736678/full#supplementary-material

Supplementary Figure 1 | Patient selection flow diagram.

REFERENCES

1. Bray F, Ferlay J, Soerjomataram I, Siegel RL, Torre LA, Jemal A. Global Cancer Statistics 2018: GLOBOCAN Estimates of Incidence and Mortality Worldwide for 36 Cancers in 185 Countries. *CA Cancer J Clin* (2018) 68 (6):394–424. doi: 10.3322/caac.21492
2. Edge SB, Compton CC. The American Joint Committee on Cancer: The 7th Edition of the AJCC Cancer Staging Manual and the Future of TNM. *Ann Surg Oncol* (2010) 17(6):1471–4. doi: 10.1245/s10434-010-0985-4
3. Fretwell VL, Ang CW, Tweedle EM, Rooney PS. The Impact of Lymph Node Yield on Duke's B and C Colorectal Cancer Survival. *Colorectal Dis* (2010) 12 (10):995–1000. doi: 10.1111/j.1463-1318.2009.01966.x
4. Scott KW, Grace RH. Detection of Lymph Node Metastases in Colorectal Carcinoma Before and After Fat Clearance. *Br J Surg* (1989) 76(11):1165–7. doi: 10.1002/bjs.1800761118
5. Xie D, Song X, Tong L. Stage Migration Resulting From Inadequate Number of Examined Lymph Nodes Impacts Prognosis in Stage II Colon Cancer After Radical Surgery. *Int J Colorectal Dis* (2021) 36(5):959–69. doi: 10.1007/s00384-020-03794-6
6. Cai Y, Cheng G, Lu X, Ju H, Zhu X. The Re-Evaluation of Optimal Lymph Node Yield in Stage II Right-Sided Colon Cancer: Is a Minimum of 12 Lymph Nodes Adequate? *Int J Colorectal Dis* (2020) 35(4):623–31. doi: 10.1007/s00384-019-03483-z
7. Tekkis PP, Smith JJ, Heriot AG, Darzi AW, Thompson MR, Stamatakis JD. A National Study on Lymph Node Retrieval in Resectional Surgery for Colorectal Cancer. *Dis Colon Rectum* (2006) 49(11):1673–83. doi: 10.1007/s10350-006-0691-2
8. Li Y, Zeng C, Hu J, Pan Y, Shan Y, Liu B, et al. Long non-Coding RNA-SNHG7 Acts as a Target of miR-34a to Increase GALNT7 Level and Regulate PI3K/Akt/mTOR Pathway in Colorectal Cancer Progression. *J Hematol Oncol* (2018) 11(1):89. doi: 10.1186/s13045-018-0632-2
9. La Vecchia S, Sebastián C. Metabolic Pathways Regulating Colorectal Cancer Initiation and Progression. *Semin Cell Dev Biol* (2020) 98:63–70. doi: 10.1016/j.semcdb.2019.05.018
10. Liu Q, Luo D, Cai S, Li Q, Li X. Circulating Basophil Count as a Prognostic Marker of Tumor Aggressiveness and Survival Outcomes in Colorectal Cancer. *Clin Transl Med* (2020) 9(1):6. doi: 10.1186/s40169-019-0255-4
11. Kaminski MF, Robertson DJ, Senore C, Rex DK. Optimizing the Quality of Colorectal Cancer Screening Worldwide. *Gastroenterology* (2020) 158(2):404–17. doi: 10.1053/j.gastro.2019.11.026
12. Nelson H, Petrelli N, Carlin A, Couture J, Fleshman J, Guillem J, et al. Guidelines 2000 for Colon and Rectal Cancer Surgery. *J Natl Cancer Inst* (2001) 93(8):583–96. doi: 10.1093/jnci/93.8.583
13. Vather R, Sammour T, Kahokehr A, Connolly AB, Hill AG. Lymph Node Evaluation and Long-Term Survival in Stage II and Stage III Colon Cancer: A National Study. *Ann Surg Oncol* (2009) 16(3):585–93. doi: 10.1245/s10434-008-0265-8
14. Sarli L, Bader G, Iusco D, Salvemini C, Mauro DD, Mazzeo A, et al. Number of Lymph Nodes Examined and Prognosis of TNM Stage II Colorectal Cancer. *Eur J Cancer* (2005) 41(2):272–9. doi: 10.1016/j.ejca.2004.10.010
15. Chang GJ, Rodriguez-Bigas MA, Skibber JM, Moyer VA. Lymph Node Evaluation and Survival After Curative Resection of Colon Cancer: Systematic Review. *J Natl Cancer Inst* (2007) 99(6):433–41. doi: 10.1093/jnci/djk092
16. Sun J, Dong M, Xiao X. Efficacy, Functional Outcome and Post-Operative Complications of Total Abdominal Colectomy With Ileorectal Anastomosis vs. Segmental Colectomy in Hereditary non-Polyposis Colorectal Cancer. *Exp Ther Med* (2018) 16(3):1603–12. doi: 10.3892/etm.2018.6380
17. Mekenkamp LJ, van Krieken JH, Marijnen CA, van de Velde CJ, Nagtegaal ID. Lymph Node Retrieval in Rectal Cancer is Dependent on Many Factors–the Role of the Tumor, the Patient, the Surgeon, the Radiotherapist, and the Pathologist. *Am J Surg Pathol* (2009) 33(10):1547–53. doi: 10.1097/PAS.0b013e3181b2e01f
18. Thorn CC, Woodcock NP, Scott N, Verbeke C, Scott SB, Ambrose NS. What Factors Affect Lymph Node Yield in Surgery for Rectal Cancer? *Colorectal Dis* (2004) 6(5):356–61. doi: 10.1111/j.1463-1318.2004.00670.x
19. Miller ED, Robb BW, Cummings OW, Johnstone PA. The Effects of Preoperative Chemoradiotherapy on Lymph Node Sampling in Rectal Cancer. *Dis Colon Rectum* (2012) 55(9):1002–7. doi: 10.1097/DCR.0b013e3182536d70
20. Cianchi F, Palomba A, Boddi V, Messerini L, Pucciani F, Perigli G, et al. Lymph Node Recovery From Colorectal Tumor Specimens: Recommendation for a Minimum Number of Lymph Nodes to be Examined. *World J Surg* (2002) 26(3):384–9. doi: 10.1007/s00268-001-0236-8
21. Labianca R, Nordlinger B, Beretta GD, Mosconi S, Mandalà M, Cervantes A, et al. Early Colon Cancer: ESMO Clinical Practice Guidelines for Diagnosis, Treatment and Follow-Up. *Ann Oncol* (2013) 24 Suppl 6:vi64–72. doi: 10.1093/annonc/mdt354
22. Babaei M, Balavarca Y, Jansen L, Lemmens V, van Erning FN, van Eycken L, et al. Administration of Adjuvant Chemotherapy for Stage II-III Colon Cancer Patients: An European Population-Based Study. *Int J Cancer* (2018) 142 (7):1480–9. doi: 10.1002/ijc.31168
23. O'Connor ES, Greenblatt DY, LoConte NK, Gangnon RE, Liou JI, Heise CP, et al. Adjuvant Chemotherapy for Stage II Colon Cancer With Poor Prognostic Features. *J Clin Oncol* (2011) 29(25):3381–8. doi: 10.1200/JCO.2010.34.3426
24. Kim MK, Won DD, Park SM, Kim T, Kim SR, Oh ST, et al. Effect of Adjuvant Chemotherapy on Stage II Colon Cancer: Analysis of Korean National Data. *Cancer Res Treat* (2018) 50(4):1149–63. doi: 10.4143/crt.2017.194
25. Babcock BD, Aljehani MA, Jabo B, Choi AH, Morgan JW, Selleck MJ, et al. High-Risk Stage II Colon Cancer: Not All Risks Are Created Equal. *Ann Surg Oncol* (2018) 25(7):1980–5. doi: 10.1245/s10434-018-6484-8

Conflict of Interest: The authors declare that the research was conducted in the absence of any commercial or financial relationships that could be construed as a potential conflict of interest.

Publisher's Note: All claims expressed in this article are solely those of the authors and do not necessarily represent those of their affiliated organizations, or those of the publisher, the editors and the reviewers. Any product that may be evaluated in this article, or claim that may be made by its manufacturer, is not guaranteed or endorsed by the publisher.

Copyright © 2021 Wu, Zhang, Chen, Chang, Jiang, Zhu and Wei. This is an open-access article distributed under the terms of the Creative Commons Attribution License (CC BY). The use, distribution or reproduction in other forums is permitted, provided the original author(s) and the copyright owner(s) are credited and that the original publication in this journal is cited, in accordance with accepted academic practice. No use, distribution or reproduction is permitted which does not comply with these terms.

frontiers in Medicine

SYSTEMATIC REVIEW
published: 18 October 2021
doi: 10.3389/fmed.2021.744512

Diabetes Mellitus Increases the Risk of Hepatocellular Carcinoma After Direct-Acting Antiviral Therapy: Systematic Review and Meta-Analysis

*Szilárd Váncsa[1,2], Dávid Németh[1], Péter Hegyi[1,2,3], Zsolt Szakács[1], Ádám Farkas[1], Szabolcs Kiss[1,4], Péter Jenő Hegyi[1], Anna Kanjo[1,4,5], Patrícia Sarlós[6], Bálint Erőss[1,3] and Gabriella Pár[6]**

[1] Institute for Translational Medicine, Medical School, University of Pécs, Pécs, Hungary, [2] János Szentágothai Research Centre, University of Pécs, Pécs, Hungary, [3] Centre for Translational Medicine, Semmelweis University, Budapest, Hungary, [4] Doctoral School of Clinical Medicine, University of Szeged, Szeged, Hungary, [5] Heim Pál National Pediatric Institute, Budapest, Hungary, [6] Department of Gastroenterology, First Department of Medicine, Medical School, University of Pécs, Pécs, Hungary

OPEN ACCESS

Edited by:
Ravindra Deshpande, Wake Forest School of Medicine, United States

Reviewed by:
Eric Yoshida, University of British Columbia, Canada
Shyam Kottilil, University of Maryland, Baltimore, United States

***Correspondence:**
Gabriella Pár
pargabriella@gmail.com

Specialty section:
This article was submitted to Gastroenterology, a section of the journal Frontiers in Medicine

Received: *20 July 2021*
Accepted: *23 September 2021*
Published: *18 October 2021*

Citation:
Váncsa S, Németh D, Hegyi P, Szakács Z, Farkas Á, Kiss S, Hegyi PJ, Kanjo A, Sarlós P, Erőss B and Pár G (2021) Diabetes Mellitus Increases the Risk of Hepatocellular Carcinoma After Direct-Acting Antiviral Therapy: Systematic Review and Meta-Analysis. Front. Med. 8:744512. doi: 10.3389/fmed.2021.744512

Background: Hepatitis C virus (HCV)-infected patients treated with direct-acting antivirals (DAAs) are still at risk of developing hepatocellular carcinoma (HCC) after sustained virologic response (SVR). This study aimed to investigate the role of diabetes mellitus (DM) as a potential predictive risk factor in developing *de novo* HCC in HCV-infected patients after DAA treatment.

Methods: This study was registered on PROSPERO under registration number CRD42021230457. We performed a systematic search in four medical databases from inception through November 3rd, 2020. Studies were eligible if they reported on HCV-infected patients treated with DAAs and compared the frequency of *de novo* HCC in patients with and without DM. We calculated pooled odds ratios, unadjusted (UHR), and adjusted hazard ratios (AHR) with 95% confidence intervals (CIs) in meta-analysis.

Results: We included 30 articles in our systematic review and meta-analysis. DM proved to be a significant risk factor of HCC in DAA-treated HCV patients in unadjusted (*UHR* = 1.44, CI: 1.15–1.79) and adjusted analyses (*AHR* = 1.31, *CI*: 1.06–1.62). In the group of patients achieving SVR after DAA therapy, DM increased the risk of HCC in unadjusted (*UHR* = 1.3, CI: 1.09–1.51) analysis; however, in adjusted results, the risk was non-significant (*AHR* = 1.07, CI: 0.89–1.28). In patients with advanced liver fibrosis, DM was a risk factor for HCC in adjusted (*AHR* = 1.36, CI: 1.03–1.8), but not in unadjusted analysis (*UHR* = 1.11, CI: 0.8–1.42).

Conclusions: DM is an independent risk factor of *de novo* HCC after DAA treatment in HCV-infected patients.

Systematic Review Registration: https://www.crd.york.ac.uk/prospero/display_record.php?RecordID=230457, identifier: CRD42021230457.

Keywords: chronic hepatitis, glucose metabolism, prognosis, carcinogenesis, liver cancer

INTRODUCTION

Hepatocellular carcinoma (HCC) is a major cause of cancer-related death worldwide (1). One of the most important causes of HCC is hepatitis C virus (HCV) infection, accounting for 20% of all HCC cases (2). Among patients with chronic HCV, the lifetime prevalence of HCC ranges between 1 and 3%. However, in patients with HCV-related cirrhosis, the proportion of HCC can reach as high as 7% during the follow-up (3).

Since introducing new direct-acting antivirals (DAA), the cure rate among HCV patients approaches 90–100% (4). This high sustained virological response rate (SVR) has been associated with a reduced risk of liver-related and overall mortality. However, according to recent publications, the risk of HCC in DAA-treated patients decreases, but it is not eliminated (4, 5). Therefore, it is clinically important to identify patients carrying a high risk of HCC development after DAA treatment.

The most highlighted risk factor for HCC development is advanced fibrosis or cirrhosis (5). The eradication of HCV may stop the progression of liver disease or even cause fibrosis regression; however, the risk of HCC persists after eradication. This risk is multifactorial, and it can be influenced by other conditions such as chronic alcohol consumption, non-alcoholic fatty liver disease, or type 2 diabetes mellitus (T2DM) (6).

Previously T2DM was associated with a higher risk of HCC, regardless of other toxic factors, such as alcohol consumption or steatosis (7). In HCV patients, this increased risk was present both in pre- and post-interferon treatment (8). However, in DAA-treated HCV patients, the role of T2DM as a risk factor of HCC development is still contradictory. The study of Benhammou et al. (9) found that diabetes was independently associated with increased risk of mortality [hazard ratio (HR) = 1.25, 95% confidence interval (CI): 1.16–1.48] and HCC (HR = 1.32, 95% CI: 1.01–1.72) in DAA-treated HCV patients, however, in a population not excluding previous HCC cases. Another large retrospective study, multivariate analysis found an increased risk of HCC in patients with DM (HR = 2.52, 95% CI: 1.06–5.87) (10). Other studies did not find an association between pre-DAA treatment DM and risk of HCC in sustained virological responders (11, 12). To our knowledge, no meta-analysis assessed the connection between DM and HCC development after DAA therapy for HCV.

Our study aimed to assess the risk of HCC in patients with DM after DAA therapy for HCV to resolve the contradictory results in this topic. We hypothesized that DM increases the risk of HCC development after DAA treatment.

METHODS AND MATERIALS

We conducted our systematic review and meta-analysis according to the recommendations proposed by the Cochrane Collaboration (13), and we report our study following the Preferred Reporting Items for Systematic Reviews and Meta-Analyses (PRISMA) 2020 Statement (**Supplementary Table 1**) (14). The study protocol was registered onto the International Prospective Register of Systematic Reviews (PROSPERO, registration number CRD42021230457, see https://www.crd.york.ac.uk/prospero). We did not deviate from the initial protocol.

Systematic Search

MEDLINE (via PubMed), Embase, Cochrane Central Register of Controlled Trials (CENTRAL), and Web of Science databases were searched for relevant publications. We searched the mentioned databases from inception to November 3rd, 2020. The search strategy included the following keywords: {["direct acting antiviral" OR boceprevir OR glecaprevir OR grazoprevir OR paritaprevir OR simeprevir OR telaprevir OR voxilaprevir OR daclatasvir OR elbasvir OR ledipasvir OR ombitasvir OR pibrentasvir OR velpatasvir OR dasabuvir OR sofosbuvir] AND "hepatitis C" AND (carcinoma OR cancer OR tumor OR malign OR neoplasm)}. No language or any other restrictions were used during the search.

Selection and Eligibility of Studies

The yield of the search was imported into a reference management program, EndNote v9.0 (Clarivate Analytics, Philadelphia, PA, USA). After removing duplicate studies, two independent authors searched the library by title, abstract, and full-text for relevant articles. Disagreements were resolved by discussion at the level of abstract and full-text selection, while at the level of title selection, the selected studies were merged.

Eligible full-text articles reported on HCV patients (P) treated with any DAA treatment and compared the outcome of patients with and without DM (E and C). Regarding the definition of DM, we used the one reported in each included article. Since most of the articles did not define the type of DM, we did not differentiate between the types. The outcome of interest (O) was the incidence of *de novo* HCC. Studies with a mean follow-up period of at least six months were included in our analysis because of the time necessary for HCC development. All included articles excluded previous cases of HCC. Previous unsuccessful treatment with IFN-based therapy was not an exclusion criterion; however, studies were excluded if patients received combined DAA and IFN treatment. Eligible articles reported on the proportion of HCC in patients with and without DM or reported their results using unadjusted or adjusted Cox hazard models. Regarding study design, descriptive studies were excluded. In the case of overlapping populations, we selected the studies with the greatest number of participants.

Data Extraction

Two review authors extracted the data independently. Disagreements were resolved by consensus. A standardized form was used for data extraction, which included: first author, the year of publications, study population, study period, study site (country), study design, demographic characteristics of the included patients, follow-up period, characteristics of hepatitis C virus infection, relative measure for the risk of HCC in patients with and without DM, event rate in patients with and without DM, and information for assessing the risk of bias in the studies. Unadjusted and adjusted results were extracted separately.

Data Synthesis

All statistical analysis of the data was conducted using the Stata 15.1 SE program package (Stata Corp LLC, College Station, TX, USA) and Comprehensive Meta-Analysis (version 3, Biostat Inc., Englewood, NJ, USA). We calculated pooled hazard ratios (HRs) with 95% confidence intervals (CIs) from unadjusted and adjusted results (UHR and AHR, respectively), and pooled odds ratios (ORs) with 95% CIs from 2 x 2 tables (HCC vs. no-HCC, and DM vs. no-DM groups). UHR and AHR were pooled separately. Random effects model was used to calculate the pooled estimates using the DerSimonian-Laird method (15). If the HR was reported with an asymmetrical CI, the article was excluded from the meta-analysis.

Heterogeneity was tested with I^2 and χ^2 tests; p-value < 0.1 indicated statistically significant heterogeneity. Heterogeneity are presented in the results section and on the forest plots. Publication bias was assessed by the Egger's test and by visual analysis of Funnel plots. To investigate heterogeneity, we performed a random-effect meta-regression analysis between the mean follow-up period after DAA treatment and the rate of HCC in each included article. Publication bias assessment and meta-regression were performed if there were at least 10 studies included in the analysis. Except for heterogeneity, a p-value < 0.05 was considered statistically significant.

A subgroup analysis was carried out with articles reporting only on patients achieving a SVR after DAA treatment (Occurrence of hepatocellular carcinoma in patients with sustained virological response). Furthermore, articles reporting on patients with advanced liver fibrosis with and without SVR were analyzed in a subgroup (Occurrence of hepatocellular carcinoma in patients with advanced liver fibrosis (METAVIR F3-F4) and Occurrence of hepatocellular carcinoma in patients with advanced liver fibrosis (METAVIR F3-F4) achieving sustained virological response, respectively). In sub-group analysis advanced liver fibrosis was defined as METAVIR stage

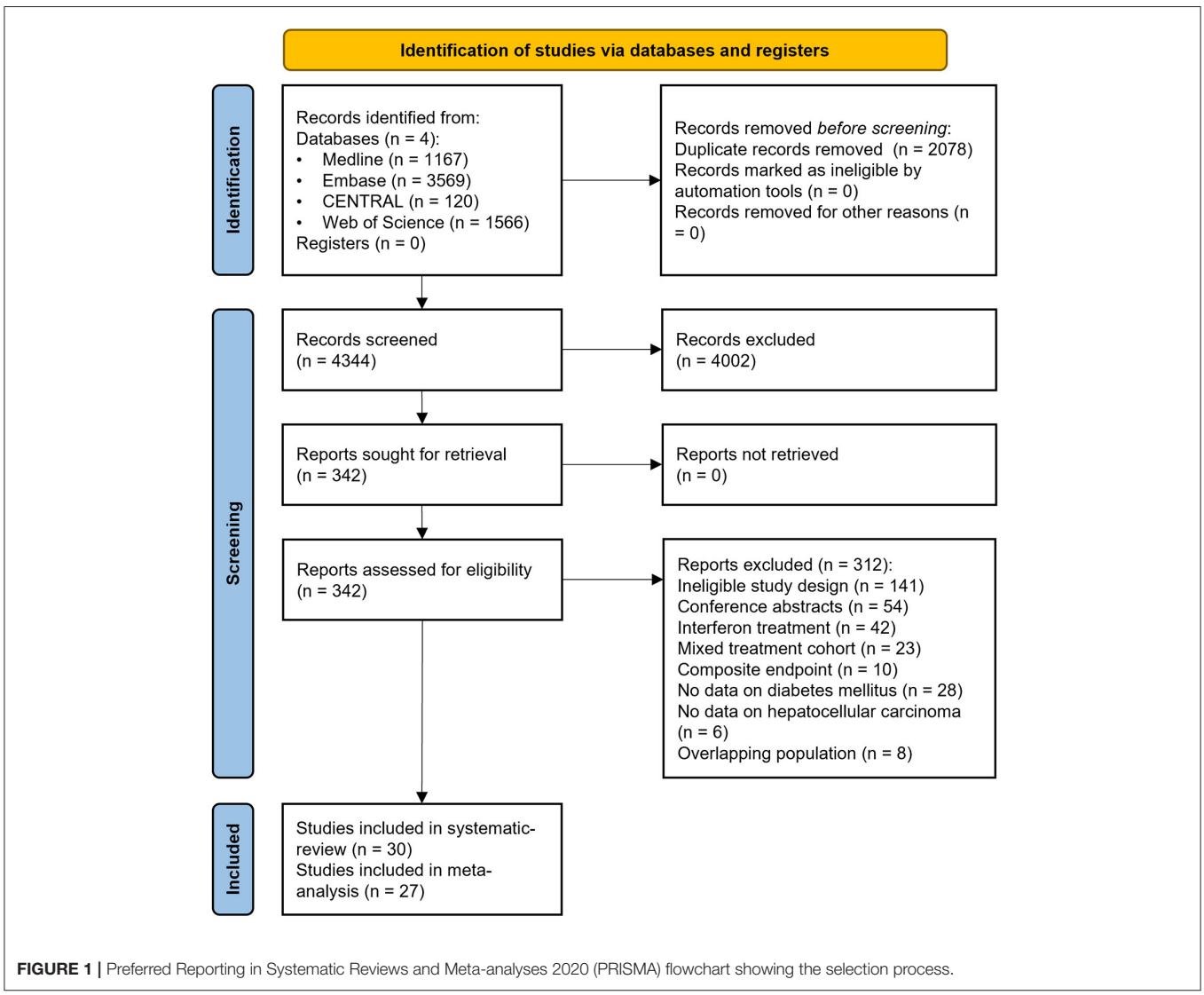

FIGURE 1 | Preferred Reporting in Systematic Reviews and Meta-analyses 2020 (PRISMA) flowchart showing the selection process.

F3 and/or F4 (16), since articles reported on the stage of fibrosis differently.

Risk of Bias Assessment in Individual Studies

Two review authors independently assessed the risk of bias for each included study using the Quality in Prognostic Studies (QUIPS) tool (17). Disagreements were resolved by consensus. Methodological details of the assessment are summarized in **Supplementary Appendix 1**. We used the Risk-of-bias VISualization (robvis) web-based tool to visualize summary plots of the assessed domains (18).

RESULTS

Search and Selection

We detailed the selection process in **Figure 1**. Our search strategy yielded a total of 6,422 records. After duplicate removal and selection by title and abstract, 342 articles were eligible for full-text assessment. We included 30 observational studies in our qualitative synthesis (10, 12, 19–43); however, we excluded three articles from the quantitative synthesis due to asymmetric CIs (11, 44, 45).

Basic Characteristics of the Included Studies

The main characteristics of the included articles are summarized in **Table 1**. The eligibility criteria of each included article are summarized in **Supplementary Table 2**. Out of the 30 included articles, 17 were published from Europe, nine from Asia, two from North America, one from South America, and one from Africa. The mean follow-up period ranged between 6 and 45 months, and the rate of HCC ranged between 1 and 34.3%. Generally, *de novo* HCC was assessed every 3 to 6 months after DAA treatment using abdominal imaging (ultrasound, computed tomography, or magnetic resonance). The follow-up policies of the included articles are summarized in **Supplementary Table 3**.

Occurrence of Hepatocellular Carcinoma in all the Included Articles

Overall, 13 articles reported unadjusted and eight adjusted HRs on the risk of HCC in patients with and without DM. The odds of HCC at the end of the follow-up period were reported in 19 articles.

Based on 13 articles with 35,373 patients, our results show that DM is associated with an increased risk of HCC after DAA treatment in unadjusted results ($UHR = 1.44$, CI: 1.15–1.79; heterogeneity $I^2 = 38\%$, $p = 0.08$; **Figure 2**). A similar result was found in the pool of eight studies ($n = 30{,}416$) reporting adjusted analysis ($AHR = 1.31$, CI: 1.06–1.62; $I^2 = 18.7\%$, $p = 0.282$; **Supplementary Figure 1**). The odds to develop HCC were also higher at the end of the follow-up period in patients with DM than those without DM (5.2 vs. 3%; respectively, $OR = 1.68$, CI: 1.35–2.08; $I^2 = 30\%$, $p = 0.106$; **Supplementary Figure 2**).

Meta-regression analysis showed no significant correlation between mean follow-up months and the risk of HCC in patients with DM (**Supplementary Figures 3**, **4**).

Occurrence of Hepatocellular Carcinoma in Patients With Sustained Virological Response

In the subgroup analysis of five studies reporting on patients who achieved SVR after DAA treatment ($n = 22{,}791$ patients), the risk of HCC was higher in patients with DM ($UHR = 1.3$, CI: 1.09–1.51; $I^2 = 2.9\%$, $p = 0.404$; **Figure 3**). The difference was not significant in adjusted models, although only three articles ($n = 21{,}229$) were included in this analysis ($AHR = 1.07$, CI: 0.89–1.28; $I^2 = 0\%$, $p = 0.890$; **Supplementary Figure 5**). We found a significant difference in the proportion of HCC in patients with DM compared to those without DM after successful DAA treatment (4.9 vs. 3%; $OR = 1.71$, CI: 1.22–2.4; $I^2 = 28.8\%$, $p = 0.198$; **Supplementary Figure 6**).

Occurrence of Hepatocellular Carcinoma in Patients With Advanced Liver Fibrosis (METAVIR F3-F4)

In the subgroup of patients with advanced liver fibrosis, eight articles with 12,373 reported on unadjusted and six articles on adjusted results ($n = 30{,}705$). DM was associated with an increased risk of HCC in adjusted ($AHR = 1.36$, CI: 1.03–1.8; $I^2 = 34.4\%$, $p = 0.178$; **Supplementary Figure 7**), but not in unadjusted analyses ($UHR = 1.11$, CI: 0.8–1.42; $I^2 = 0\%$, $p = 0.505$; **Supplementary Figure 8**). The odds of HCC were higher in DM patients with advanced liver fibrosis compared to patients without DM (5.5 vs. 4.3%; $OR = 1.51$, CI: 1.15–1.99; $I^2 = 39.1\%$, $p = 0.073$; **Supplementary Figure 9**).

Occurrence of Hepatocellular Carcinoma in Patients With Advanced Liver Fibrosis (METAVIR F3-F4) Achieving Sustained Virological Response

We were unable to assess the risk in unadjusted and adjusted hazard models. The rate of HCC was not significantly higher in patients with DM compared to those without DM (5.7 vs. 3.9%; $OR = 1.67$, CI: 0.91–3.07; $I^2 = 51\%$, $p = 0.106$; **Supplementary Figure 10**).

Risk of Bias Assessment

The results of the risk of bias assessment of individual studies are summarized in **Supplementary Table 4**. Out of the six assessed domains, the prognostic factor measurement was attributed moderate or high risk of bias in 24 of the included articles due to missing definition of DM (**Supplementary Figures 11**, **12**). In **Supplementary Table 5** we summarized the parameters included in multivariate adjustment in each included article.

The assessment of publication bias could only be performed in the case of three comparisons. We did not detect the presence of publication in these comparisons (see **Supplementary Figures 13–15** for funnel plots and Egger's test alfa value).

TABLE 1 | Basic characteristics of included studies.

References	Study site	Study type	No of patients (female %)	Age (years)†	Follow up period (months)†	F3/F4 rate (subgroup)‡	Genotype (GT)	DM (% of total)	SVR rate	Overall HCC rate
Calvaruso et al. (19)	Italy	prospective	2249 (43)	65.4	14.0	100%	GT1a/1b/2/3/4/other	30	95.2%	3.5%
Ciancio et al. (20)	Italy	prospective	893 (42)	59.6	44.5	67%	GT1a/1b/2a/2c/3/4/5/6	16	100%	2.5%
Conti et al. (21)	Italy	prospective	344 (40)	63.0	6.0	100%	GT1/2/3/4	17	91.6%	3.2%
Degasperi et al. (10)	Italy	retrospective	505 (40)	63.0	25.0	100%	GT1b/other	19	96.4%	5.5%
Faillaci et al. (22)	Italy	prospective	155 (33)	62.2	N/A	100%	GT1a/1b/2/3/4	18	90.3%	13.6%
Gardini et al. (23)	Italy	retrospective	416 (42)	63.3	18.2	100%	GT1a/1b/2/3/4	24	<100%	7%
Ide et al. (24)	Japan	prospective	2552 (61)	64.6	22.6	30%	GT1/2	20	100%	2.8%
Janjua et al. (25)	Canada	retrospective	3905 (33)	N/A	12.0	14% (0%, 100%)	GT1/2/3/other	20	92.5%	1%
Kanwal et al. (26)	USA	retrospective	18076 (4)	61.6	35.0	38% (0%, 100%)	GT1/2/3/other	43	100%	3%
Lleo et al. (27)	Italy	prospective	1766 (38)	61.7	12.0	100%	GT1a/1b/2/3/4	20	95.1%	2.8%
Alonso Lopez et al. (28)	Spain	prospective	993 (45)	61.7	45.0	100%	N/A	17	100%	3.6%
Mariño et al. (29)	Spain	retrospective	1123 (40)	59.3	19.6	100%	GT1/other	19	95.2%	6.4%
Mecci et al. (30)	UK	prospective	245 (25)	57.0	32.4	100%	GT1/3/other	29	80.4%	34.3%
Mettke et al. (31)	Germany	prospective	158 (45)	59.0	14.7	100%	GT1a/1b/2/3/4/other	23	100%	3.8%
Nagata et al. (44)	Japan	prospective	752 (55)	69.0	21.6	33%	GT1a/1b/2a/2b/3a/other	15	96.0%	1.1%
Nakagawa et al. (32)	Japan	prospective	947 (54)	65.9	24.2	28%	N/A	12	100%	2.7%
Ogasawara et al. (33)	Japan	retrospective	398 (61)	70.0	39.6	51%	GT1b	10	100%	4.8%
Ogawa et al. (11)	Japan	prospective	1675 (56)	66.0	17.0	18%	GT1/2	18	100%	2.7%
Ozeki et al. (34)	Japan	retrospective	769 (59)	64.0	35.0	19%	GT1/2	12	100%	2.3%
Piñero et al. (12)	Latin America	prospective	1400 (52)	58.0	16.0	56% (100%)	GT1a/1b/2/3/4/other	15	97.0%	2.1%
Pons et al. (35)	Spain	prospective	572 (51)	63.7	34.8	100%	GT1/2/3/4	22	100%	4.4%
Quaranta et al. (36)	Italy	prospective	3114 (44)	59.0	38.9	N/A	GT1/2/3/4/5	14	94.9	1.4%
Rinaldi et al. (37)	Italy	prospective	985 (45)	67.0	12.0	100%	GT1/2/3/4	13	98.1%	3.6%
Romano et al. (38)	Italy	prospective	3917 (38)	58.1	17.9	100%	GT1a/1b/2/3/4/other	11	93.9%	1.4%
Sangiovanni et al. (39)	Italy	prospective	1161 (41)	65.0	17.0	100%	GT1a/1b/2/3/4	21	96%	4.1%
Shiha et al. (40)	Egypt	prospective	2372 (48)	N/A	23.6	100%	GT4	20	100%	4.6%
Tani et al. (45)	Japan	retrospective	1088 (50)	68.0	13.8	18%	GT1a/1b/2/3/4/6	16	100%	2.6%
Tayyab et al. (41)	Pakistan	prospective	662 (51)	50.0	12.0	49%	GT3/other	28	91.9%	6.3%
Watanabe et al. (42)	Japan	prospective	1174 (54)	66.0	24.0	N/A	GT1/2	15	100%	2.8%
Yoshimasu et al. (43)	Japan	retrospective	211 (48)	63.0	21.0	N/A	GT1a/1b/2a/2b	13	91.5%	1%

† *mean or median.*

‡ *advanced liver fibrosis and cirrhosis based on METAVIR scores (F3 and F4).*

HCC, hepatocellular carcinoma; GT, genotype; SVR, sustained viral response.

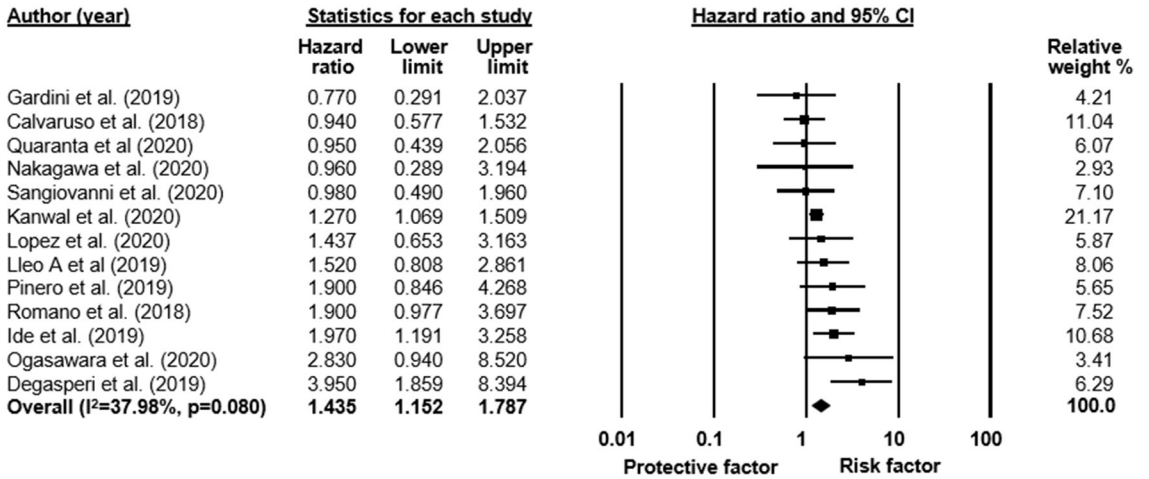

FIGURE 2 | Forest plot with pooled unadjusted hazard ratio, representing the risk of HCC in all patients with and without DM after HCV treatment with DAA therapy.

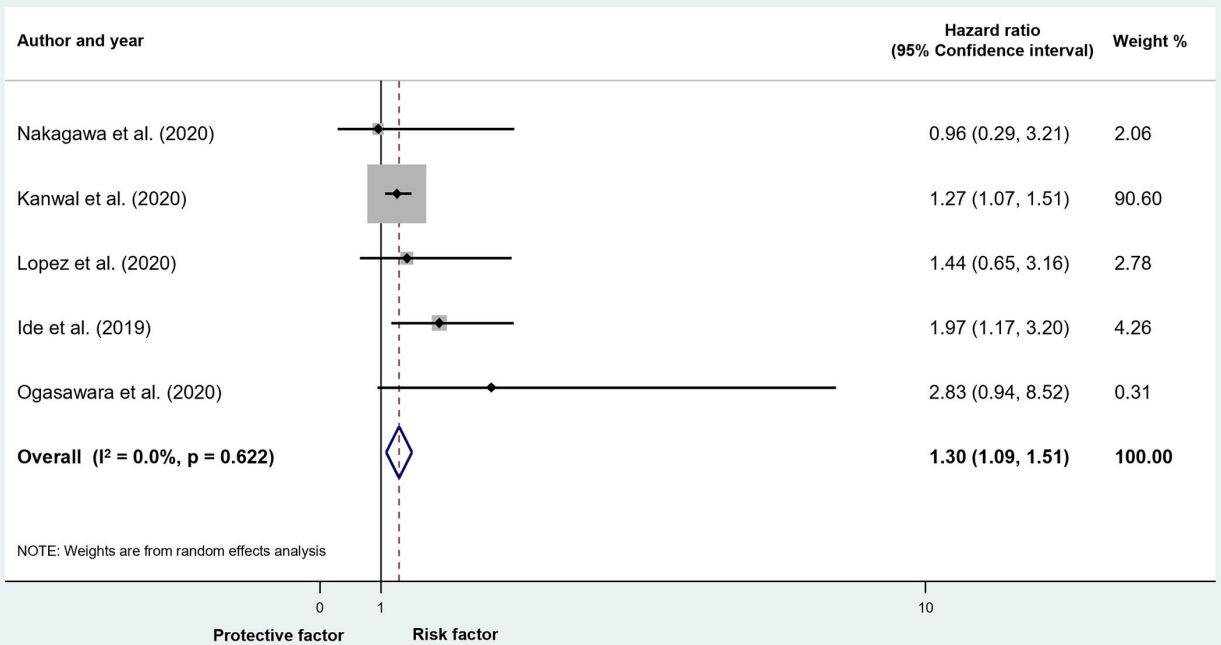

FIGURE 3 | Forest plot with pooled unadjusted hazard ratio, representing the risk of HCC in patients with and without DM who achieved sustained virological response after HCV treatment with DAA therapy.

DISCUSSION

In our meta-analysis, we aimed to analyze the association between DM and the risk of HCC after all DAA treatments for HCV infection, as successful antiviral therapy is known to reduce but does not eliminate the risk of developing HCC. We found an increased risk of HCC among patients with DM in unadjusted and adjusted analyses. In the subgroups with SVR or advanced liver fibrosis, the risk was also increased.

Based on current guidelines, a thorough clinical assessment is recommended every six months after successful DAA treatment in patients with advanced fibrosis or cirrhosis (METAVIR F3 and F4). The European Association for the Study of the Liver (EASL), in their 2020 recommendations on treatment of hepatitis C, highlights DM as a co-factor for liver disease and recommends a closer follow-up of these patients after treatment for HCV (4). However, the guideline does not refer to an increased risk of HCC in patients with DM. The American Association for the

Study of Liver Diseases (AASLD) recommends surveillance for HCC only in patients with cirrhosis. For non-cirrhotic patients, the recommended follow-up is as in non-HCV infected patients, without specification on DM (46).

Our results are consistent with previous results. In the general population, T2DM was associated with a moderately increased risk of HCC incidence (risk ratio = 2.23, 95% CI: 1.68–2.96) (47). We found a similar, 1.7-fold increased odds of HCC after DAA treatment in patients with DM, which was comparable in subgroups as well. On the other hand, diabetes with HCV infection increases the risk of HCC by 2 to 3-folds, which is higher than the risk in patients with DM after DAA treatment (48). In a review of prospective studies, the risk of HCC after DAA treatment was between 2.1 and 5.4% after median follow-up periods of few months and 33.4 months (49). In our results, HCC occurrence was similar in patients with DM between 4.9 and 5.7%, while in patients without DM being lower, between 3 and 4.3%.

The risk of HCC after DAA treatment is most probably multifactorial. In an experimental study, authors found a decreased expression of inhibitory checkpoint receptors upon innate immune cells after DAA therapy in HCV patients (50). This may favor decreased immune surveillance against tumor cells. HCV infection-induced epigenetic modifications associated with HCC risk, such as H3K27ac, persist after DAA treatment (51). On the other hand, liver comorbidities such as metabolic associated fatty liver disease or alcohol consumption were highlighted as risk factors of HCC (5). Metabolic risk factors, such as metabolic syndrome, obesity, or insulin resistance, may further increase the risk of HCC through the presence of low-grade chronic inflammation (48). Furthermore, T2DM contributes to fibrosis progression after DAA therapy, which is a risk of HCC (52).

There is a two-way association between HCV infection and DM (53). Hepatitis C infection was showed to significantly increase the odds of DM, compared to different control groups (54). It is estimated that up to 33% of chronic hepatitis C patients have DM, which is influenced by increased age, male gender, duration of infection, and other risk factors (55). The underlying mechanisms include hepatic steatosis, an increase in reactive oxygen agents, and inflammatory cytokines, which lead to insulin resistance (53). On the other hand, DM leads to the progression of hepatic fibrosis in HCV infection (56), which starts early in infection and involves oxidative stress, inflammation, and oncogenesis (57).

The risk of HCC was different in the included articles. In the study of Benhammou et al. (9), an increased risk of *de novo* and recurrent HCC was found in T2DM patients without cirrhosis (*AHR* = 1.32, 95%CI: 1.01–1.72) but not in those with cirrhosis (*AHR* = 1.06, 95%CI: 0.92–1.23). However, patients with previous HCC were not excluded. Overall, in this study, the authors did not find an increased risk of HCC in patients with T2DM, but they concluded that pre-DAA diabetes increases mortality and liver-related events in patients with and without SVR. Two other studies analyzed the subgroup of patients without cirrhosis (25, 26), neither of them found a significant difference between patients with and without T2DM (*AHR* = 3.08, 95%CI: 0.93–10.17; *AHR* = 0.98, 95%CI: 0.67–1.44, respectively). We did not have enough data to analyze the risk in patients without cirrhosis.

The highest risk of HCC among patients with DM was found in the study of Degasperi et al. (10); they reported a 3-year cumulative incidence of 16% in patients with diabetes and 4% in patients without diabetes ($p < 0.001$). The proportion of HCC increased with other risk factors; in diabetic male patients with a liver stiffness >30 kPa, 50% developed *de novo* HCC. The longest follow-up in the included studies was a median of 45 months (28). The risk of HCC did not differ in this study in patients with DM. However, based on our analysis, the mean follow-up period did not correlate with the risk of HCC.

One study analyzed the combined risk of *de novo* and recurrent HCC in diabetic patients by multivariate Cox regression analysis (20). In this study, the duration of DM > 10 years, family history of DM, and no improvement of DM were not associated with an increased incident HCC ($p > 0.05$), while insulin therapy was an unfavorable predictor (*HR* = 4.11, 95% CI: 1.20–14.13). Iuliano et al. (58) reported on the risk of HCC based on the duration of DM. In patients with and without metabolic syndrome, the risk increased with longer duration; however, the risk was higher in those with metabolic syndrome ($p = 0.002$). On the other hand, Mecci et al. (30) demonstrated that both in the early (<6 months) and late (>6 months) HCC groups, DM was present in a higher proportion compared to the non-HCC group (36 and 33% vs. 19%, respectively); although the difference was significant only in the late group ($p < 0.05$). These results suggest that the increased risk in patients with DM is constantly present.

Lastly, Romano et al. (38) analyzed the risk of HCC in the presence of one or more risk factors. In patients with DM, the cumulative proportion of HCC was 3%, while DM with hepatitis B surface antigen (HBsAg) positivity and APRI score ≥2.5 increased the risk up to 18%. In addition to these, Child-Turcotte Pugh B further increased the proportion of HCC to 29%. Based on these results, the presence of DM with additional risk factors will result in a much higher increase in the proportion of HCC.

The proper control of DM should be carried out in both pre- and post-DAA treatment to decrease the risk of liver fibrosis progression and HCC development. Successful treatment of HCV with DAA contributes to a reduced glycated hemoglobin level (mean difference = 0.45, 95% CI: 0.3–0.6), which may further decrease the risk of HCC (59). Furthermore, in a systematic review of metformin's protective effect in diabetic patients, authors found a reduced risk of HCC (*OR* = 0.47; 95% CI: 0.28–0.8) (60).

Strengths and Limitation

Our study has several strengths. First, we registered the pre-study protocol and followed it wholly. Second, we managed to include a substantial number of articles with a high number of patients. Third, we could pool adjusted HR results. On the other hand, our study has limitations.

Most importantly, the definition of DM was missing in most of the articles, carrying a high risk of bias. Studies mainly included patients with advanced liver disease or a high proportion of

them; therefore, it is hard to generalize our results. The follow-up period was relatively short in most of the studies and was different among studies; it is possible that the higher risk of HCC would drop after longer follow-ups. Authors used other methods to screen for HCC; however, all of them used abdominal imaging. Besides prospective studies, we included retrospective cohort analyses as well. Lastly, some of the results carry a moderate risk of statistical heterogeneity.

Implication for Practice

Overall, successful antiviral treatment reduces but does not eliminate the risk of HCC. Additionally, the risk of HCC is higher in patients with advanced liver fibrosis and DM, so they should be followed up more closely after HCV eradication with DAAs. Other conditions potentially increasing liver fibrosis progression must be assessed and handled correctly.

Implication for Research

Further studies are needed to clarify the risk of HCC in DAA-treated DM populations, based on the duration, treatment, and complications of DM. It is a question of whether the adequate treatment of DM decreases the risk of HCC in patients with SVR. Lastly, cost-effectiveness studies should be initiated to determine the proper follow-up period (3 vs. 6 months) in a high-risk group of patients.

CONCLUSION

There is an increased risk of HCC development in patients with DM compared to patients without DM after DAA treatment for HCV infection.

DATA AVAILABILITY STATEMENT

The original contributions presented in the study are included in the article/**Supplementary Material**, further inquiries can be directed to the corresponding author.

AUTHOR CONTRIBUTIONS

SV: conceptualization, project administration, formal analysis, writing—original draft. DN: conceptualization, formal analysis, visualization, writing—original draft. PH: conceptualization, funding acquisition, writing—review and editing. ZS and ÁF: conceptualization, data curation, writing—review and editing. SK: conceptualization, methodology, writing—review and editing. PH, AK, and PS: conceptualization, writing—review and editing. BE: conceptualization, methodology, visualization, writing—original draft. GP: conceptualization, supervision, writing—original draft. All authors certify that they have participated sufficiently to take public responsibility for the content, including participation in the concept, design, analysis, writing, or revision of the manuscript.

FUNDING

Funding was provided by an Economic Development and Innovation Operative Programme Grant (GINOP-2.3.4-15-2020-00010) and by a Human Resources Development Operational Programme Grant (EFOP-3.6.2-16-2017-00006, EFOP-3.6.1.-16-2016-00004), both co-financed by the European Union (European Regional Development Fund) within the framework of the Széchenyi 2020 Program. Furthermore, funding was provided by the ÚNKP-20-3-I-PTE-604, a New National Excellence Program of the Ministry for Innovation and Technology from the source of the National Research, Development, and Innovation Fund (for SV). Sponsors had no role in the design, data collection, analysis, interpretation, and manuscript preparation.

SUPPLEMENTARY MATERIAL

The Supplementary Material for this article can be found online at: https://www.frontiersin.org/articles/10.3389/fmed.2021.744512/full#supplementary-material

REFERENCES

1. Ferlay J, Ervik M, Lam F, Colombet M, Mery L, Piñeros M, et al. *Global Cancer Observatory: Cancer Today*. Lyon: International Agency for Research on Cancer (2020). Available online at: https://gco.iarc.fr/today (accessed April 15, 2021).
2. de Martel C, Maucort-Boulch D, Plummer M, Franceschi S. World-wide relative contribution of hepatitis B and C viruses in hepatocellular carcinoma. *Hepatology.* (2015) 62:1190–200. doi: 10.1002/hep.27969
3. Hajarizadeh B, Grebely J, Dore GJ. Epidemiology and natural history of HCV infection. *Nat Rev Gastroenterol Hepatol.* (2013) 10:553–62. doi: 10.1038/nrgastro.2013.107
4. Pawlotsky JM, Negro F, Aghemo A, Berenguer M, Dalgard O, Dusheiko G, et al. EASL recommendations on treatment of hepatitis C: final update of the series? *J Hepatol.* (2020) 73:1170–218. doi: 10.1016/j.jhep.2020.08.018
5. Negro F. Residual risk of liver disease after hepatitis C virus eradication. *J Hepatol.* (2021) 74:952–63. doi: 10.1016/j.jhep.2020.11.040
6. Ioannou GN. HCC surveillance after SVR in patients with F3/F4 fibrosis. *J Hepatol.* (2021) 74:458–65. doi: 10.1016/j.jhep.2020.10.016
7. Davila JA, Morgan RO, Shaib Y, McGlynn KA, El-Serag HB. Diabetes increases the risk of hepatocellular carcinoma in the United States: a population based case control study. *Gut.* (2005) 54:533. doi: 10.1136/gut.2004.052167
8. Desbois AC, Cacoub P. Diabetes mellitus, insulin resistance and hepatitis C virus infection: a contemporary review. *World J Gastroenterol.* (2017) 23:1697–711. doi: 10.3748/wjg.v23.i9.1697
9. Benhammou JN, Moon AM, Pisegna JR, Su F, Vutien P, Moylan CA, et al. Nonalcoholic fatty liver disease risk factors affect liver-related outcomes after direct-acting antiviral treatment for Hepatitis C. *Dig Dis Sci.* (2020) 66:2394–406. doi: 10.1007/s10620-020-06457-2
10. Degasperi E, D'Ambrosio R, Iavarone M, Sangiovanni A, Aghemo A, Soffredini R, et al. Factors associated with increased risk of *de novo* or recurrent hepatocellular carcinoma in patients with cirrhosis treated with direct-acting antivirals for HCV infection. *Clin Gastroenterol Hepatol.* (2019) 17:1183–91. doi: 10.1016/j.cgh.2018.10.038
11. Ogawa E, Furusyo N, Nomura H, Dohmen K, Higashi N, Takahashi K, et al. Short-term risk of hepatocellular carcinoma after hepatitis C virus eradication following direct-acting anti-viral treatment. *Aliment Pharmacol Ther.* (2018) 47:104–13. doi: 10.1111/apt.14380

12. Piñero F, Mendizabal M, Ridruejo E, Herz Wolff F, Ameigeiras B, Anders M, et al. Treatment with direct-acting antivirals for HCV decreases but does not eliminate the risk of hepatocellular carcinoma. *Liver Int.* (2019) 39:1033–43. doi: 10.1111/liv.14041
13. Higgins JP, Thomas J, Chandler J, Cumpston M, Li T, Page MJ, et al. *Cochrane Handbook for Systematic Reviews of Interventions, 2nd Edn*. Chichester: John Wiley & Sons (2019). doi: 10.1002/9781119536604
14. Page MJ, McKenzie JE, Bossuyt PM, Boutron I, Hoffmann TC, Mulrow CD, et al. The PRISMA 2020 statement: an updated guideline for reporting systematic reviews. *BMJ.* (2021) 372:n71. doi: 10.1136/bmj.n71
15. DerSimonian R, Laird N. Meta-analysis in clinical trials. *Control Clin Trials.* (1986) 7:177–88. doi: 10.1016/0197-2456(86)90046-2
16. The French METAVIR. Cooperative Study Group. Intraobserver and interobserver variations in liver biopsy interpretation in patients with chronic hepatitis C. *Hepatology.* (1994) 20:15–20. doi: 10.1002/hep.1840200104
17. Hayden JA, van der Windt DA, Cartwright JL, Côté P, Bombardier C. Assessing bias in studies of prognostic factors. *Ann Intern Med.* (2013) 158:280–6. doi: 10.7326/0003-4819-158-4-201302190-00009
18. McGuinness LA, Higgins JPT. Risk-of-bias VISualization (robvis): An R package and Shiny web app for visualizing risk-of-bias assessments. *Res Synth Methods.* (2020) 12:55–61. doi: 10.1002/jrsm.1411
19. Calvaruso V, Cabibbo G, Cacciola I, Petta S, Madonia S, Bellia A, et al. Incidence of hepatocellular carcinoma in patients with HCV-associated cirrhosis treated with direct-acting antiviral agents. *Gastroenterology.* (2018) 155:411–21. doi: 10.1053/j.gastro.2018.04.008
20. Ciancio A, Giuseppe Ribaldone D, Dotta A, Giordanino C, Sacco M, Fagoonee S, et al. Long-term follow-up of diabetic and non-diabetic patients with chronic hepatitis c successfully treated with direct acting antiviral agents. *Liver Int.* (2020) 41:276–87. doi: 10.1111/liv.14676
21. Conti F, Buonfiglioli F, Scuteri A, Crespi C, Bolondi L, Caraceni P, et al. Early occurrence and recurrence of hepatocellular carcinoma in HCV-related cirrhosis treated with direct-acting antivirals. *J Hepatol.* (2016) 65:727–33. doi: 10.1016/j.jhep.2016.06.015
22. Faillaci F, Marzi L, Critelli R, Milosa F, Schepis F, Turola E, et al. Liver angiopoietin-2 is a key predictor of *de novo* or recurrent hepatocellular cancer after hepatitis C virus direct-acting antivirals. *Hepatology.* (2018) 68:1010–24. doi: 10.1002/hep.29911
23. Gardini AC, Foschi FG, Conti F, Petracci E, Marisi G, Buonfiglioli F, et al. Immune inflammation indicators and ALBI score to predict occurrence and recurrence of hepatocellular carcinoma in HCV-related cirrhosis treated with direct-acting antivirals. *Dig Liver Dis.* (2018) 51:681–8. doi: 10.1016/j.dld.2018.01.055
24. Ide T, Koga H, Nakano M, Hashimoto S, Yatsuhashi H, Higuchi N, et al. Direct-acting antiviral agents do not increase the incidence of hepatocellular carcinoma development: a prospective, multicenter study. *Hepatol Int.* (2019) 13:293–301. doi: 10.1007/s12072-019-09939-2
25. Janjua NZ, Wong SL, Darvishian M, Butt ZA Yu AM, Binka M, et al. The impact of SVR from direct-acting antiviral- and interferon-based treatments for HCV on hepatocellular carcinoma risk. *J Viral Hepat.* (2020) 27:781–93. doi: 10.1111/jvh.13295
26. Kanwal F, Kramer JR, Asch SM, Cao Y, Li L, El-Serag HB. Long-term risk of hepatocellular carcinoma in HCV patients treated with direct acting antiviral agents. *Hepatology.* (2020) 71:44–55. doi: 10.1002/hep.30823
27. Lleo A, Aglitti A, Aghemo A, Maisonneuve P, Bruno S, Persico M, et al. Predictors of hepatocellular carcinoma in HCV cirrhotic patients treated with direct acting antivirals. *Dig Liver Dis.* (2019) 51:310–7. doi: 10.1016/j.dld.2018.10.014
28. Alonso López S, Manzano ML, Gea F, Gutiérrez ML, Ahumada AM, Devesa MJ, et al. A Model based on noninvasive markers predicts very low hepatocellular carcinoma risk after viral response in hepatitis C virus–advanced fibrosis. *Hepatology.* (2020) 72:1924–34. doi: 10.1002/hep.31588
29. Mariño Z, Darnell A, Lens S, Sapena V, Díaz A, Belmonte E, et al. Time association between hepatitis C therapy and hepatocellular carcinoma emergence in cirrhosis: relevance of non-characterized nodules. *J Hepatol.* (2019) 70:874–84. doi: 10.1016/j.jhep.2019.01.005
30. Mecci AJ, Kemos P, Leen C, Lawson A, Richardson P, Khakoo SI, et al. The association between hepatocellular carcinoma and direct-acting anti-viral treatment in patients with decompensated cirrhosis. *Aliment Pharmacol Ther.* (2019) 50:204–14. doi: 10.1111/apt.15296
31. Mettke F, Schlevogt B, Deterding K, Wranke A, Smith A, Port K, et al. Interferon-free therapy of chronic hepatitis C with direct-acting antivirals does not change the short-term risk for *de novo* hepatocellular carcinoma in patients with liver cirrhosis. *Aliment Pharmacol Ther.* (2018) 47:516–25. doi: 10.1111/apt.14427
32. Nakagawa M, Nawa N, Takeichi E, Shimizu T, Tsuchiya J, Sato A, et al. Mac-2 binding protein glycosylation isomer as a novel predictive biomarker for patient survival after hepatitis C virus eradication by DAAs. *J Gastroenterol.* (2020) 55:990–9. doi: 10.1007/s00535-020-01715-6
33. Ogasawara N, Saitoh S, Akuta N, Sezaki H, Suzuki F, Fujiyama S, et al. Advantage of liver stiffness measurement before and after direct-acting antiviral therapy to predict hepatocellular carcinoma and exacerbation of esophageal varices in chronic hepatitis C. *Hepatol Res.* (2020) 50:426–38. doi: 10.1111/hepr.13467
34. Ozeki I, Nakajima T, Suii H, Tatsumi R, Yamaguchi M, Arakawa T, et al. Predictors of hepatocellular carcinoma after hepatitis C virus eradication following direct-acting antiviral treatment: relationship with serum zinc. *J Clin Biochem Nutr.* (2020) 66:245–52. doi: 10.3164/jcbn.19-98
35. Pons M, Rodriguez-Tajes S, Esteban JI, Marino Z, Vargas V, Lens S, et al. Non-invasive prediction of liver-related events in patients with HCV-associated compensated advanced chronic liver disease after oral antivirals. *J Hepatol.* (2020) 72:472–80. doi: 10.1016/j.jhep.2019.10.005
36. Quaranta MG, Ferrigno L, Monti M, Filomia R, Biliotti E, Iannone A, et al. Advanced liver disease outcomes after hepatitis C eradication by human immunodeficiency virus infection in PITER cohort. *Hepatol Int.* (2020) 14:362–72. doi: 10.1007/s12072-020-10034-0
37. Rinaldi L, Perrella A, Guarino M, De Luca M, Piai G, Coppola N, et al. Incidence and risk factors of early HCC occurrence in HCV patients treated with direct acting antivirals: a prospective multicentre study. *J Transl Med.* (2019) 17:292. doi: 10.1186/s12967-019-2033-x
38. Romano A, Angeli P, Piovesan S, Noventa F, Anastassopoulos G, Chemello L, et al. Newly diagnosed hepatocellular carcinoma in patients with advanced hepatitis C treated with DAAs: a prospective population study. *J Hepatol.* (2018) 69:345–52. doi: 10.1016/j.jhep.2018.03.009
39. Sangiovanni A, Alimenti E, Gattai R, Filomia R, Parente E, Valenti L, et al. Undefined/non-malignant hepatic nodules are associated with early occurrence of HCC in DAA-treated patients with HCV-related cirrhosis. *J Hepatol.* (2020) 73:593–602. doi: 10.1016/j.jhep.2020.03.030
40. Shiha G, Mousa N, Soliman R, Nnh Mikhail N, Adel Elbasiony M, Khattab M. Incidence of HCC in chronic hepatitis C patients with advanced hepatic fibrosis who achieved SVR following DAAs: a prospective study. *J Viral Hepat.* (2020) 27:671–9. doi: 10.1111/jvh.13276
41. Tayyab GUN, Rasool S, Nasir B, Rubi G, Abou-Samra AB, Butt AA. Hepatocellular carcinoma occurs frequently and early after treatment in HCV genotype 3 infected persons treated with DAA regimens. *BMC Gastroenterol.* (2020) 20:93. doi: 10.1186/s12876-020-01249-4
42. Watanabe T, Tokumoto Y, Joko K, Michitaka K, Horiike N, Tanaka Y, et al. Predictors of hepatocellular carcinoma occurrence after direct-acting antiviral therapy in patients with hepatitis C virus infection. *Hepatol Res.* (2019) 49:136–46. doi: 10.1111/hepr.13278
43. Yoshimasu Y, Furuichi Y, Kasai Y, Takeuchi H, Sugimoto K, Nakamura I, et al. Predictive factors for hepatocellular carcinoma occurrence or recurrence after direct-acting antiviral agents in patients with chronic hepatitis C. *J Gastrointestin Liver Dis.* (2019) 28:63–71. doi: 10.15403/jgld.2014.1121.281.hpc
44. Nagata H, Nakagawa M, Asahina Y, Sato A, Asano Y, Tsunoda T, et al. Effect of interferon-based and -free therapy on early occurrence and recurrence of hepatocellular carcinoma in chronic hepatitis C. *J Hepatol.* (2017) 67:933–9. doi: 10.1016/j.jhep.2017.05.028
45. Tani J, Morishita A, Sakamoto T, Takuma K, Nakahara M, Fujita K, et al. Simple scoring system for prediction of hepatocellular carcinoma occurrence after hepatitis C virus eradication by direct-acting antiviral treatment: all Kagawa liver disease group study. *Oncol Lett.* (2020) 19:2205–12. doi: 10.3892/ol.2020.11341

46. AASLD-IDSA. *Recommendations for Testing, Managing, and Treating Hepatitis C*. (2021). Available online at: http://www.hcvguidelines.org (accessed April 15, 2021).
47. Wang P, Kang D, Cao W, Wang Y, Liu Z. Diabetes mellitus and risk of hepatocellular carcinoma: a systematic review and meta-analysis. *Diabetes Metab Res Rev*. (2012) 28:109–22. doi: 10.1002/dmrr.1291
48. Dash S, Aydin Y, Widmer KE, Nayak L. Hepatocellular carcinoma mechanisms associated with chronic HCV infection and the impact of direct-acting antiviral treatment. *J Hepatocell Carcinoma*. (2020) 7:45–76. doi: 10.2147/JHC.S221187
49. Rinaldi L, Nevola R, Franci G, Perrella A, Corvino G, Marrone A, et al. Risk of hepatocellular carcinoma after HCV clearance by direct-acting antivirals treatment predictive factors and role of epigenetics. *Cancers*. (2020) 12:1351. doi: 10.3390/cancers12061351
50. Szereday L, Meggyes M, Berki T, Miseta A, Farkas N, Gervain J, et al. Direct-acting antiviral treatment downregulates immune checkpoint inhibitor expression in patients with chronic hepatitis C. *Clin Exp Med*. (2020) 20:219–30. doi: 10.1007/s10238-020-00618-3
51. Hamdane N, Jühling F, Crouchet E, El Saghire H, Thumann C, Oudot MA, et al. HCV-induced epigenetic changes associated with liver cancer risk persist after sustained virologic response. *Gastroenterology*. (2019) 156:2313-29.e7. doi: 10.1053/j.gastro.2019.02.038
52. Shiha G, Soliman R, Mikhail N, Ibrahim A, Serwah A-H, Khattab M. Changes in hepatic fibrosis stages after achieving SVR following direct-acting anti-viral treatment: a prospective study. *GastroHep*. (2020) 2:39–48. doi: 10.1002/ygh2.384
53. Hammerstad SS, Grock SF, Lee HJ, Hasham A, Sundaram N, Tomer Y. Diabetes and hepatitis C: a two-way association. *Front Endocrinol*. (2015) 6:134. doi: 10.3389/fendo.2015.00134
54. White DL, Ratziu V, El-Serag HB. Hepatitis C infection and risk of diabetes: a systematic review and meta-analysis. *J Hepatol*. (2008) 49:831–44. doi: 10.1016/j.jhep.2008.08.006
55. Elhawary EI, Mahmoud GF, El-Daly MA, Mekky FA, Esmat GG. Abdel-Hamid M. Association of HCV with diabetes mellitus: an Egyptian case-control study. *Virol J*. (2011) 8:367. doi: 10.1186/1743-422X-8-367
56. Mohamed AA, Loutfy SA, Craik JD. M Hashem AG, Siam I. Chronic hepatitis c genotype-4 infection: role of insulin resistance in hepatocellular carcinoma. *Virol J*. (2011) 8:496. doi: 10.1186/1743-422X-8-496
57. Siddique A, Kowdley KV. Insulin resistance and other metabolic risk factors in the pathogenesis of hepatocellular carcinoma. *Clin Liver Dis*. (2011) 15:281–96. doi: 10.1016/j.cld.2011.03.007
58. Iuliano N, Pafundi PC, Acierno C, Monaco L, Fascione MC, Mastrocinque D, et al. Impact of type II diabetes on HCC appearance in patients treated with direct acting antivirals. *World J Cancer Res*. (2018) 5:e1048. doi: 10.32113/wcrj_20183_1048
59. Carnovale C, Pozzi M, Dassano A, D'Addio F, Gentili M, Magni C, et al. The impact of a successful treatment of hepatitis C virus on glyco-metabolic control in diabetic patients: a systematic review and meta-analysis. *Acta Diabetol*. (2019) 56:341–54. doi: 10.1007/s00592-018-1257-1
60. Cunha V, Cotrim HP, Rocha R, Carvalho K, Lins-Kusterer L. Metformin in the prevention of hepatocellular carcinoma in diabetic patients: a systematic review. *Ann Hepatol*. (2020) 19:232–7. doi: 10.1016/j.aohep.2019.10.005

Conflict of Interest: The authors declare that the research was conducted in the absence of any commercial or financial relationships that could be construed as a potential conflict of interest.

Publisher's Note: All claims expressed in this article are solely those of the authors and do not necessarily represent those of their affiliated organizations, or those of the publisher, the editors and the reviewers. Any product that may be evaluated in this article, or claim that may be made by its manufacturer, is not guaranteed or endorsed by the publisher.

Copyright © 2021 Váncsa, Németh, Hegyi, Szakács, Farkas, Kiss, Hegyi, Kanjo, Sarlós, Erőss and Pár. This is an open-access article distributed under the terms of the Creative Commons Attribution License (CC BY). The use, distribution or reproduction in other forums is permitted, provided the original author(s) and the copyright owner(s) are credited and that the original publication in this journal is cited, in accordance with accepted academic practice. No use, distribution or reproduction is permitted which does not comply with these terms.

frontiers in Oncology

ORIGINAL RESEARCH
published: 20 October 2021
doi: 10.3389/fonc.2021.764076

Albumin-To-Alkaline Phosphatase Ratio as a Novel and Promising Prognostic Biomarker in Patients Undergoing Esophagectomy for Carcinoma: A Propensity Score Matching Study

Xianying Zhu[1,2†], *Dongni Chen*[3†], *Shuangjiang Li*[1,4†], *Wenbiao Zhang*[1,5], *Yongjiang Li*[1,6], *Xiaoyu Wang*[1], *Jian Zhou*[1,5*] and *Zhesheng Wen*[1,7*]

[1] State Key Laboratory of Oncology in South China, Collaborative Innovation Center for Cancer Medicine, Sun Yat-Sen University Cancer Center, Guangzhou, China, [2] Intensive Care Unit, Sun Yat-Sen University Cancer Center, Sun Yat-Sen University, Guangzhou, China, [3] Department of Thoracic Surgery, Nanfang Hospital, Southern Medical University, Guangzhou, China, [4] Department of Endoscopy and Laser, Sun Yat-Sen University Cancer Center, Sun Yat-Sen University, Guangzhou, China, [5] Department of Medical Imaging, Sun Yat-Sen University Cancer Center, Sun Yat-Sen University, Guangzhou, China, [6] Department of Nuclear Medicine, Sun Yat-Sen University Cancer Center, Sun Yat-Sen University, Guangzhou, China, [7] Department of Thoracic Oncology, Sun Yat-Sen University Cancer Center, Sun Yat-Sen University, Guangzhou, China

OPEN ACCESS

Edited by:
Qi Liu,
Fudan University, China

Reviewed by:
Erkan Topkan,
Başkent University, Turkey
Beatrice Aramini,
University Hospital of Modena, Italy

***Correspondence:**
Zhesheng Wen
wenzhsh@sysucc.org.cn
Jian Zhou
zhoujian@sysucc.org.cn

[†]These authors have contributed equally to this work

Specialty section:
This article was submitted to Surgical Oncology, a section of the journal Frontiers in Oncology

Received: *25 August 2021*
Accepted: *04 October 2021*
Published: *20 October 2021*

Citation:
Zhu X, Chen D, Li S, Zhang W, Li Y, Wang X, Zhou J and Wen Z (2021) Albumin-To-Alkaline Phosphatase Ratio as a Novel and Promising Prognostic Biomarker in Patients Undergoing Esophagectomy for Carcinoma: A Propensity Score Matching Study. Front. Oncol. 11:764076. doi: 10.3389/fonc.2021.764076

Background: Albumin-to-alkaline phosphatase ratio (AAPR) has been reported as a novel prognostic predictor for numerous solid tumors. We aimed to assess the prognostic role of preoperative AAPR in surgically resectable esophageal squamous cell carcinoma (ESCC) by a propensity score matching (PSM) analysis with predictive nomograms.

Methods: Our study was conducted in a single-center prospective database between June 2009 and December 2012. Kaplan-Meier analysis was used to distinguish the difference in survival outcomes between patients stratified by an AAPR threshold. Multivariable Cox proportional hazards regression model was finally generated to specify independent prognostic markers for the entire and PSM cohorts.

Results: A total of 497 patients with ESCC were included in this study. An AAPR of 0.50 was determined as the optimal cutoff point for prognostic outcome stratification. Patients with AAPR<0.50 had significantly worse overall survival (OS), and progression-free survival (PFS) compared to those with AAPR≥0.50 (Log-rank P<0.001). This significant difference remained stable in the PSM analysis. Multivariable analyses based on the entire and PSM cohorts consistently showed that AAPR<0.50 might be one of the most predominant prognostic factors resulting in unfavorable OS and PFS of ESCC patients undergoing esophagectomy (P<0.001). The nomograms consisting of AAPR and other independent prognostic factors further demonstrated a plausible predictive accuracy of postoperative OS and PFS.

Conclusion: AAPR can be considered as a simple, convenient and noninvasive biomarker with a significant prognostic effect in surgically resected ESCC.

Keywords: albumin-to-alkaline phosphatase ratio, esophageal squamous cell carcinoma, prognosis, prediction, esophagectomy

1 INTRODUCTION

1.1 Background

Esophageal cancer (EC) ranks seventh in global cancer incidence and sixth in cancer-specific mortality (1). EC can be subdivided into esophageal adenocarcinoma and esophageal squamous cell carcinoma (ESCC). The latter is extremely prevalent across the EC hotspots worldwide, accounting for approximately 90% of all histological subtypes (2). Despite recent advances in the development of minimally invasive techniques, optimization of chemoradiotherapy regimens, and innovations in molecularly targeted therapies, the post-treatment prognosis of EC has remained discouraging in decades, with 5-year survival rates ranging from 10% to 20% (3, 4). Esophagectomy, as the mainstay of curative treatment for EC, is still considered a life-threatening gastrointestinal procedure with high mortality rates ranging from 8% to 23% (5–7). Therefore, it becomes crucial to delve into a series of putative prognostic markers that can accurately predict the outcome of the procedure and help to draw up an individualized treatment plan in advance for EC patients intending to undergo esophagectomy.

There is growing evidence that systemic immuno-nutritional status, which can be conveniently and effectively characterized by peripheral blood biomarkers, plays a pivotal role in the pathogenesis and progression of cancers, and further contributes to being a determinant of cancer-related prognosis (4, 8–11). Serum albumin (sALB), a traditional serum biochemical marker synthesized by the liver, has been widely used to reflect the nutritional reserve of the host and considered as a prognostic indicator for malignant tumors (12–14). Alkaline phosphatase (ALP), another hydrolase widely accepted as a disease marker of the hepatobiliary system, bone, and kidney, has also been correlated with postoperative survival of cancer patients (15). In summary, a novel and simple scoring system by integrating sALB with serum ALP, named albumin-to-alkaline phosphatase ratio (AAPR), has been constantly validated as a reliable prognostic indicator across a wide range of malignant tumors, regardless of their treatment options (12, 16–24). However, to our knowledge, the potential prognostic value of AAPR has not yet been explored in patients undergoing esophagectomy for EC.

1.2 Objectives

Considering these issues, the purpose of this propensity score matching (PSM) study was to provide a comprehensive assessment of preoperative AAPR as a validated prognostic biomarker for surgically resectable ESCC.

2 MATERIALS AND METHODS

2.1 Study Design and Protocol

Our study was a PSM analysis performed in the ESCC database prospectively maintained in our cancer center. We received formal approval from the Institutional Review Board (No: GZR 2018-120) and performed all relevant procedures compliant with the Declaration of Helsinki. Finally, we completed this report following the Strengthening the Reporting of Cohort Studies in Surgery (STROCSS) 2019 Guideline (25).

2.2 Participant Selection

2.2.1 Settings

We evaluated clinical and survival data of consecutive patients who underwent esophagectomy for ESCC in our inpatient unit between June 2009 and December 2012.

2.2.2 Inclusion and Exclusion Criteria

The following criteria were performed to determine the suitability of patients for inclusion or exclusion:

(i) Patients with surgically resectable ESCC diagnosed by routine histology were included. Esophageal adenocarcinoma or benign diseases would be excluded;

(ii) Esophagectomy *via* Ivor-Lewis, Sweet and McKeown procedures and esophageal reconstruction with a gastric tube were included. Transhiatal esophagectomy would be excluded;

(iii) Peripheral hematological and biochemical indices must be obtained within seven days prior to the procedure. To ensure the objectivity and accuracy of the analyzed data, the scarcity of complete medical records and follow-up characteristics would not be considered;

(iv) Patients receiving neoadjuvant chemotherapy or chemoradiotherapy would not be considered to minimize potential confounding effects caused by changes in peripheral blood composition after preoperative anticancer therapy, which might complicate the prognostic impact of AAPR;

(v) Patients with concurrent or prior malignancies would not be considered, with the aim to avoid the additional assumption of carcinomatous tissues outside of the esophagus on the host immuno-nutritional reserve, and thus attenuate potential bias risks in the prognostic factor analysis.

2.3 Follow-Up Survey

Regular follow-up assessments began on the day of surgery and then during in-hospital observation, every three months for the first two years, every six months for the next three years, and then annually until death or the final follow-up date of December 2018. Follow-up assessments included routine laboratory tests, computed tomography scans of head and neck, chest and abdomen, and endoscopy when necessary.

2.4 Measures and Definitions of Outcome Data

2.4.1 Patient Characteristics

(i) Basic patient information included: age (years), sex (male/female), and body mass index (BMI, kg/m^2);

(ii) Patients' preoperative comorbidities included: gastrointestinal comorbidities (including chronic gastritis, gastroduodenal ulcers, gastroduodenal bleeding, gastroesophageal reflux disease, caustic stricture of the esophagus, and alimentary tract polyps), cardiovascular comorbidities (including hypertension, coronary artery disease, valvular heart disease, cerebrovascular disease, cardiac arrhythmias, chronic heart failure and peripheral artery disease), diabetes mellitus, respiratory comorbidities (including chronic obstructive pulmonary

disease, emphysema, tuberculosis, pneumonia, asthma, bronchiectasis and interstitial lung diseases), hepatobiliary comorbidities (including cirrhosis, hepatitis B, hepatitis C, severe fatty liver and cholelithiasis);

(iii) Pathological parameters of the patients included: grade of differentiation (well/moderate/poor), vascular invasion (present/absent), lymphatic invasion (present/absent), perineural and neural invasion (present/absent), tumor size (cm), tumor invasion (T stage), lymph node metastasis (LNM, N stage) and TNM stage. Tumor staging was estimated by our experienced pathologists according to the 8th edition of the AJCC/UICC TNM staging system of ESCC (26).

2.4.2 Acquisition of Peripheral Blood Markers

Blood sampling for each included patient was performed by our experienced nurses within seven days prior to esophagectomy. The following peripheral blood biomarkers would be collected from complete blood counts and biochemical tests: sALB (g/L), ALP (U/L), C-reactive protein (CRP, mg/L), neutrophil count (10^9/L), and lymphocyte count (10^9/L). AAPR was calculated by dividing the level of sALB by the level of serum ALP (sALB/ALP). Also, neutrophil to lymphocyte ratio (NLR) was derived from the total numbers of neutrophils and lymphocytes and used for further survival analysis.

2.4.3 Grouping Criteria of AAPR

We used a free online statistical tool constructed on the R framework (https://molpathoheidelberg.shinyapps.io/CutoffFinder_v1/), the *Cutoff Finder*, to determine the optimal cutoff point for AAPR in predicting postoperative survival. We could then compare clinicopathological characteristics and surgical outcomes of the two groups of patients stratified by this threshold of AAPR. In addition, prognostic significance of AAPR was further analyzed in all subgroups that were stratified according to patients' clinicopathological characteristics.

2.4.4 Outcomes of Interest

The primary endpoint and the secondary endpoint for survival outcome evaluation were overall survival (OS) and progression-free survival (PFS), respectively. OS was defined as the time interval between esophagectomy and the date of death from any cause or censor at final follow-up. PFS was defined as the time interval between esophagectomy and the date of radiological or histological detection of cancerous recurrence or metastasis (4, 27).

Another one secondary objective was to estimate the differences in postoperative complications, 30-day mortality and 90-day mortality between the two AAPR groups. Postoperative complications were defined as any Clavien-Dindo classification grade ≥ III complication occurred during hospitalization (28). Thirty-day mortality and 90-day mortality were defined as any death within 30 and 90 days after surgery.

2.5 Surgical Procedure and Combined Treatment Modality

McKeown, Sweet, and Ivor-Lewis esophagectomies were all standard surgical approaches for treating ESCC at our institution. In addition, reconstruction of the gastric tube with an anastomosis in the cervical incision was generally performed through the posterior mediastinal route. A two-field lymphadenectomy was indicated for middle to lower thoracic ESCC, while a three-field lymphadenectomy was indicated for upper thoracic ESCC. Finally, a feeding tube was routinely placed into the stomach or duodenum at the end of the procedure.

Regarding adjuvant therapy after esophagectomy, a detailed chemotherapy regimen based on cisplatin plus fluoropyrimidine and/or radiotherapy would be finalized according to patients' baseline conditions and pathological findings.

2.6 Statistical Analysis

The following statistical methods in our study were completed using IBM SPSS 26.0 software (IBM SPSS Statistics, Version 22.0. Armonk, NY: IBM Corp) and R Studio version 4.0.3 (R Foundation for Statistical Computing, Vienna, Austria). Statistical significance was indicated by a two-sided test P value less than 0.050.

We used Pearson's chi-square test, Yates' correction test and Fisher exact test to compare categorical data and Mann-Whitney U test to compare continuous data [mean ± standard deviation (SD); median and interquartile range (IQR)], respectively.

Kaplan-Meier curve with Log-rank test was applied to analyze the differences in OS and PFS among different patient groups.

We further performed time-dependent receiver operating characteristic (t-ROC) analysis, a special ROC analysis for time-to-event variables, to estimate the ability of AAPR, sALB, ALP, NLR, and CRP to discriminate between the predictive accuracy of postoperative survival throughout the follow-up period. In addition, their areas under curve (AUCs) would be inferred and compared.

In our PSM analysis, a nearest neighbor matching algorithm by caliper matching with a specified distance at 0.20 SD of the logarithm of the propensity score was utilized to help adequately balance the baseline characteristics between the two AAPR groups. Finally, a 1:1 pair of well-matched patients was generated based on their propensity scores. Furthermore, neither sALB nor ALP, critical factors in the direct establishment of AAPR, would be considered in the PSM procedure (12).

The relationships between all estimated characteristics and survival outcomes were initially explored through univariable Cox proportional hazards regression analysis. Thereafter, any clinicopathological parameter with P<0.15 was included in multivariable Cox proportional hazards regression models, and hazard ratios (HRs) with 95% confidence intervals (CIs) were then generated to indicate which factors could play a significant prognostic role in predicting OS and PFS.

We further displayed nomograms graphically mapping multivariable Cox proportional hazards regression models built on independent prognostic contributors. In the prognostic nomogram, each predictive covariable was assigned a score from 0 to 100 based on its point scale bar, and the probability of survival was then represented by the cumulative points mapped by all these covariables. In addition, we computed Harrell's concordance statistic (C-statistic) to measure the goodness-of-fit of each multivariable Cox proportional hazards

regression model. Finally, we plotted calibration curves to reveal the consistency between survival outcomes predicted by nomograms and the real-world survival outcomes.

3 RESULTS

3.1 Patient Demographics and Outcomes

3.1.1 Participant Population and Primary Demographics

From June 2009 to December 2012, a total of 661 patients underwent esophagectomy at an inpatient unit in our institution. **Figure 1** shows a flowchart of the entire process of participant selection. During the study period, 497 patients have met all eligibility criteria, completed the entire follow-up assessment, and were ultimately enrolled in the current study (**Figure 1**). Their primary demographic data are summarized in **Table 1**.

3.1.2 Patient Characteristics

The entire cohort included 404 (81.3%) male and 93 (18.7%) female patients with a mean age of 59.15 ± 9.29 years and a mean BMI of 21.51 ± 3.24 kg/m^2. A total of 125 (25.2%) patients were diagnosed preoperatively with one or more types of comorbidities (**Table 1**). Postoperative pathological evaluation showed that 95 (19.1%) patients, 248 (49.9%) patients and 154 (31.0%) patients were classified as TNM stage I, II and III ESCC, respectively. There were 52.3% of the cohort (260 patients) confirmed with the presence of LNM (N_{1-3} stage). Other pathological records are also detailed in **Table 1**. Finally, 189 (38.0%) patients received adjuvant chemotherapy (175) and/or adjuvant radiotherapy (56) after esophagectomy.

3.1.3 Laboratory Markers

The mean values regarding sALB, ALP, CRP, neutrophil count, and lymphocyte count in all included patients were 43.04 ± 3.22 g/L, 70.57 ± 19.19 U/L, 6.16 ± 11.44, 4.67 ± 1.87 10^9/L, and 1.96 ± 0.61 10^9/L. In addition, both AAPR and NLR could thus be obtained with mean values of 2.65 ± 1.61 and 0.65 ± 0.17, respectively, as shown in **Table 1**.

3.1.4 AAPR Evaluation

On the basis of biostatistical results generated by the *Cutoff Finder*, various cutoff points for AAPR were statistically significant for prognostic prediction, and an AAPR of 0.50 was finally recognized as the optimal cutoff point, as shown in **Figure 2A**. Therefore, 86 (17.3%) patients were classified into the AAPR<0.50 group, and the remaining 411 (82.7%) patients were classified into the AAPR≥0.50 group (**Table 1** and **Figure 2B**).

3.1.5 Postoperative Outcomes

The median follow-up time for our surgical cohort was 53 (1-114) months. Until the final follow-up date, the rates of OS and PFS were 42.7% and 38.2%, respectively. In-hospital outcomes are also detailed in **Table 1**. There were 88 (17.7%) patients developed with Clavien-Dindo grade ≥ III complications in the perioperative period. The 30-day and 90-day mortality rates for the entire cohort were 0.6% (3 cases) and 2.6% (13 cases), respectively.

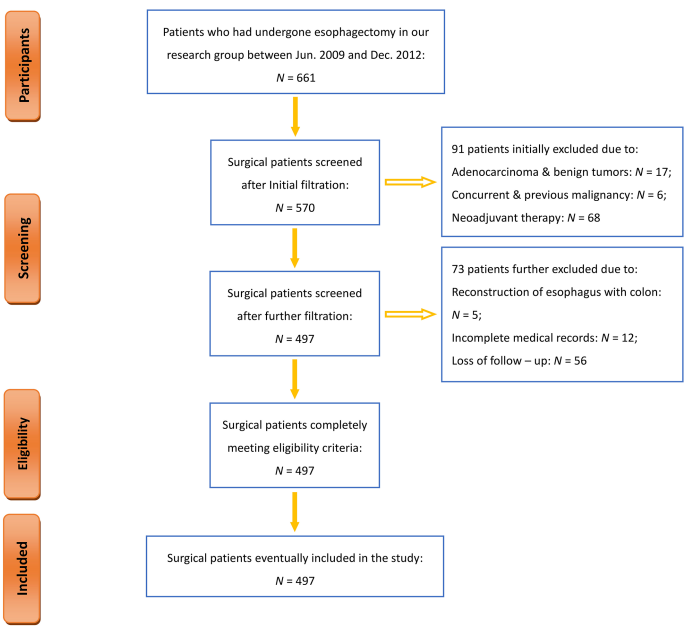

FIGURE 1 | Flowchart of the inclusion and exclusion of participants.

TABLE 1 | Patient characteristics and in-hospital outcomes of the entire cohort.

Characteristics	Entire Cohort			*P* Value
	Total (*N* = 497)	AAPR ≥ 0.50 (*N* = 411)	AAPR < 0.50 (*N* = 86)	
Age (Years)				
Mean ± SD	59.15 ± 9.29	59.11 ± 9.38	59.34 ± 8.92	0.91
Median (IQR)	59 (53 - 66)	59 (53 - 65)	58 (54 - 66)	
Gender (n, %)				
Female	93 (18.7%)	78 (19.0%)	15 (17.4%)	0.74
Male	404 (81.3%)	333 (81.0%)	71 (82.6%)	
Body Mass Index (kg/m^2)				
Mean ± SD	21.51 ± 3.24	21.69 ± 3.28	20.67 ± 2.89	0.003
Median (IQR)	21.26 (19.47 - 23.56)	21.47 (19.59 - 23.72)	20.20 (18.41 - 22.28)	
Gastrointestinal Comorbidity (n, %)				
Absent	468 (94.2%)	385 (93.7%)	83 (96.5%)	0.31
Present	29 (5.8%)	26 (6.3%)	3 (3.5%)	
Cardio-Cerebrovascular Comorbidity (n, %)				
Absent	427 (85.9%)	353 (85.9%)	74 (86.0%)	0.97
Present	70 (14.1%)	58 (14.1%)	12 (14.0%)	
Diabetes Mellitus (n, %)				
Absent	483 (97.2%)	400 (97.3%)	83 (96.5%)	0.96
Present	14 (2.8%)	11 (2.7%)	3 (3.5%)	
Respiratory Comorbidity (n, %)				
Absent	475 (95.6%)	392 (95.4%)	83 (96.5%)	0.86
Present	22 (4.4%)	19 (4.6%)	3 (3.5%)	
Hepatobiliary Comorbidity (n, %)				
Absent	478 (96.2%)	394 (95.9%)	84 (97.7%)	0.63
Present	19 (3.8%)	17 (4.1%)	2 (2.3%)	
Neutrophil to Lymphocyte Ratio				
Mean ± SD	2.65 ± 1.61	2.58 ± 1.65	2.96 ± 1.40	0.004
Median (IQR)	2.26 (1.70 - 3.17)	2.21 (1.68 - 3.00)	2.65 (1.87 - 3.91)	
C - Reactive Protein (mg/L)				
Mean ± SD	6.16 ± 11.44	5.40 ± 10.18	9.80 ± 15.73	< 0.001
Median (IQR)	2.33 (1.01 - 5.60)	2.05 (0.91 - 4.66)	4.95 (2.32 - 9.56)	
AAPR Value				
Mean ± SD	0.65 ± 0.17	0.69 ± 0.15	0.44 ± 0.06	< 0.001
Median (IQR)	0.62 (0.54 - 0.74)	0.66 (0.59 - 0.76)	0.46 (0.40 - 0.48)	
Differentiation Grade (n, %)				
Well	116 (23.3%)	95 (23.1%)	21 (24.4%)	0.77
Moderate	226 (45.5%)	185 (45.0%)	41 (47.7%)	
Poor	155 (31.2%)	131 (31.9%)	24 (27.9%)	
Vascular Invasion (n, %)				
Absent	457 (92.0%)	380 (92.5%)	77 (89.5%)	0.37
Present	40 (8.0%)	31 (7.5%)	9 (10.5%)	
Lymphatic Invasion (n, %)				
Absent	464 (93.4%)	386 (93.9%)	78 (90.7%)	0.28
Present	33 (6.6%)	25 (6.1%)	8 (9.3%)	
Perineurium & Neural Invasion (n, %)				
Absent	468 (94.2%)	392 (95.4%)	76 (88.4%)	0.012
Present	29 (5.8%)	19 (4.6%)	10 (11.6%)	
Tumor Size (cm)				
Mean ± SD	3.79 ± 1.57	3.67 ± 1.57	4.33 ± 1.45	< 0.001
Median (IQR)	4.0 (3.0 - 5.0)	3.5 (2.5 - 4.5)	4.0 (3.5 - 5.0)	
T Stage (n, %)				
T_1	54 (10.9%)	49 (11.9%)	5 (5.8%)	0.25
T_2	92 (18.5%)	75 (18.2%)	17 (19.8%)	
T_3	351 (70.6%)	287 (69.8%)	64 (74.4%)	
N Stage (n, %)				
N_0	237 (47.7%)	201 (48.9%)	36 (41.9%)	0.58
N_1	219 (44.1%)	178 (43.3%)	41 (47.7%)	
N_2	24 (4.8%)	18 (4.4%)	6 (7.0%)	
N_3	17 (3.4%)	14 (3.4%)	3 (3.5%)	
TNM Stage (n, %)				
I	95 (19.1%)	76 (18.5%)	19 (22.1%)	0.67
II	248 (49.9%)	205 (49.9%)	43 (50.0%)	

(Continued)

TABLE 1 | Continued

Characteristics	Entire Cohort			*P* Value
	Total (*N* = 497)	AAPR ≥ 0.50 (*N* = 411)	AAPR < 0.50 (*N* = 86)	
III	154 (31.0%)	130 (31.6%)	24 (27.9%)	
Adjuvant Chemotherapy (n, %)				
Not Received	322 (64.8%)	266 (64.7%)	56 (65.1%)	0.94
Received	175 (35.2%)	145 (35.3%)	30 (34.9%)	
Adjuvant Radiotherapy (n, %)				
Not Received	441 (88.7%)	366 (89.1%)	75 (87.2%)	0.62
Received	56 (11.3%)	45 (10.9%)	11 (12.8%)	
Postoperative Complications (n, %)				
Absent	409 (82.3%)	345 (83.9%)	64 (74.4%)	0.035
Present	88 (17.7%)	66 (16.1%)	22 (25.6%)	
30 - Day Mortality (n, %)				
Absent	494 (99.4%)	408 (99.3%)	86 (100%)	1.0
Present	3 (0.6%)	3 (0.7%)	0 (0%)	
90 - Day Mortality (n, %)				
Absent	484 (97.4%)	403 (98.1%)	81 (94.2%)	0.095
Present	13 (2.6%)	8 (1.9%)	5 (5.8%)	

AAPR, Albumin to Alkaline Phosphatase Ratio; IQR, Interquartile Range; SD, Standard Deviation.

3.2 Discriminatory Power of Peripheral Blood Biomarkers

Figure 3 shows the dynamic AUCs derived from the t-ROC analysis for all estimated peripheral blood markers. The AUCs for AAPR predicting postoperative survival ranged from 0.57 to 0.63 throughout the follow-up assessment, especially after ≥ 2 years at follow-up, showing a better discriminatory capacity than CRP and NLR. AAPR had significant predictive roles regarding 1-year OS, 3-year OS, 5-year OS, and 10-year OS with AUCs of 0.60, 0.60, 0.58, and 0.62, respectively (P<0.050).

3.3 Comparison Between AAPR Groups in the Entire Cohort

3.3.1 Preoperative AAPR and Patient Characteristics

Table 1 exhibits demographic differences in perioperative characteristics between the two AAPR groups. We found that patients with AAPR<0.50 had a significantly lower BMI (P=0.003), significantly larger tumor size (P<0.001), and a significantly higher percentage of perineural/neural invasion compared with patients with AAPR≥0.50. There were no significant differences in other clinicopathological features between the two AAPR groups.

3.3.2 Preoperative AAPR and In-Hospital Outcomes

Postoperative complication rate was found to be significantly higher in patients with AAPR<0.50 than in those with AAPR≥0.50 (25.6% vs. 16.1%; P=0.035; **Table 1**). There was no significant difference in 30-day mortality (0% vs. 0.7%; P=1.0) or 90-day mortality (5.8% vs. 1.9%; P=0.095) between the two AAPR groups (**Table 1**).

3.3.3 Preoperative AAPR and Survival Outcomes

Kaplan-Meier survival analysis revealed that the mean OS time estimates for the AAPR<0.50 and AAPR≥0.50 groups were 1267 ± 134 (95% CI: 1004-1530) days and 2082 ± 68 (95% CI: 1948-2216) days, respectively. Patients with AAPR<0.50 and with AAPR≥0.50 had an OS rate of 22.1% and 47.0% after follow-up, respectively. In addition, the mean PFS time estimates for the AAPR<0.50 and AAPR≥0.50 groups were 1138 ± 133 (95% CI: 877-1399) days and 1877 ± 71 (95% CI: 1737-2016) days, respectively. The PFS rates after follow-up for patients with AAPR<0.50 and with AAPR≥0.50 were 19.8% and 42.1%. Thus, both OS and PFS were significantly shorter in patients with AAPR<0.50 than those with AAPR≥0.50 (Log-rank P<0.001; **Figures 4A, B**).

3.3.4 Univariable and Multivariable Analysis on Prognostic Factors of OS

Univariable Cox proportional hazards regression analysis based on the entire patient cohort showed that for each additional unit of age (P<0.001), BMI (P=0.010), NLR (P=0.008) and tumor size (P<0.001), male population (P=0.025), cardiovascular comorbidity (P=0.024), AAPR<0.50 (P<0.001), vascular invasion (P=0.001), lymphatic invasion (P=0.001), T_3 stage tumor (P<0.001), LNM (P<0.001), adjuvant chemotherapy (P<0.001), and adjuvant radiotherapy (P=0.024) were significantly associated with postoperative OS, as shown in **Table 2**.

After adjustment by all covariable estimates holding P<0.15, multivariable Cox proportional hazards regression analysis showed that for every 1 year increase in age (HR: 1.037; 95% CI: 1.022-1.052; P<0.001), every 1 kg/m^2 increase in BMI (HR: 0.950; 95% CI: 0.910-0.992; P=0.020), AAPR<0.50 (HR: 1.92; 95% CI: 1.44-2.54; P<0.001), T_3 stage tumor (HR: 1.39; 95% CI: 1.04-1.85; P=0.027), LNM (HR: 2.44; 95% CI: 1.85-3.22; P<0.001), adjuvant chemotherapy (HR: 1.39; 95% CI: 1.04-1.85; P=0.024), and the occurrence of postoperative complications (HR: 1.42; 95% CI: 1.04-1.92; P=0.025) could be independent prognostic factors for OS in ESCC patients undergoing esophagectomy (**Table 2**).

Finally, we constructed a prognostic nomogram incorporating all the above independent indicators to represent a visual and comprehensive risk evaluation scale for predicting postoperative OS, as shown in **Figure 5A**. We found that both LNM and AAPR were the most predominant predictors of postoperative OS in ESCC patients (P<0.001). This nomogram based on AAPR and other independent predictors presented a significant contribution to the

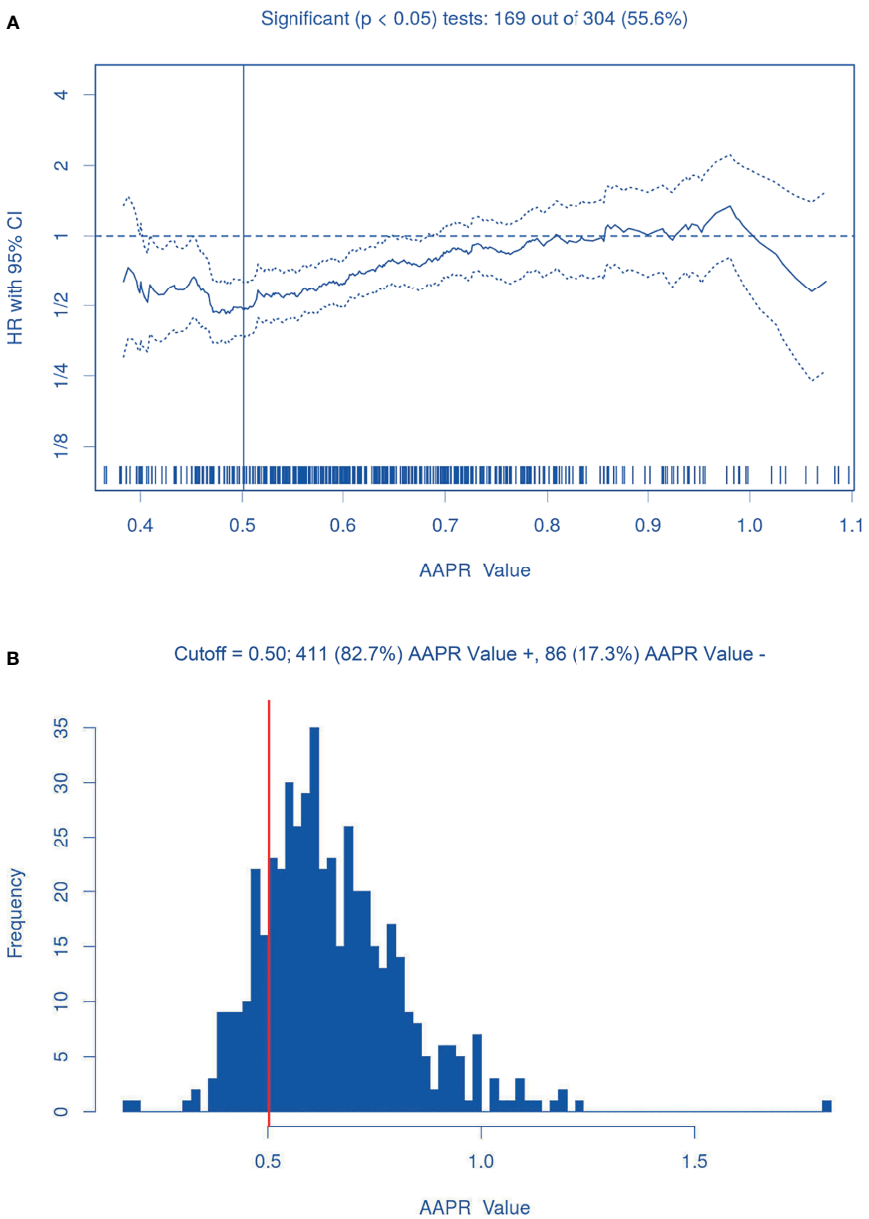

FIGURE 2 | The AAPR optimal cutoff point (0.50). **(A)** Hazard ratios for overall survival according to the cutoff points for preoperative AAPR; **(B)** Patient distribution according to preoperative AAPR. The vertical line indicates the threshold value of AAPR with the most significant split in Log-rank test.

discrimination of OS probability with a C-statistic of 0.71 (95% CI: 0.62-0.80; *P*<0.001). **Figures 5B-E** are calibration curves assessing the predictive strength of our nomogram for OS probability. These curves showed a significant agreement between the OS predicted by our nomogram and the real-world OS at different follow-up periods.

3.3.5 Univariable and Multivariable Analysis on Prognostic Factors of PFS

Univariable Cox proportional hazards regression analysis based on the entire patient cohort showed that for each additional unit of age (*P*=0.023), BMI (*P*=0.013) and tumor size (*P*<0.001), male population (*P*=0.033), AAPR<0.50 (*P*<0.001), vascular invasion (*P*=0.001), lymphatic invasion (*P*=0.002), T_3 stage tumor (*P*<0.001), LNM (*P*<0.001), adjuvant chemotherapy (*P*<0.001), and adjuvant radiotherapy (*P*<0.001) were significantly associated with postoperative PFS (**Table 2**).

Multivariable Cox proportional hazards regression models built on clinicopathological parameters showing *P*<0.15 further demonstrated that for every 1 year increase in age (HR: 1.027; 95% CI: 1.013-1.041; *P*<0.001), every 1 kg/m^2 increase in BMI (HR: 0.943; 95% CI: 0.904-0.983; *P*=0.006), every 0.5 cm increase

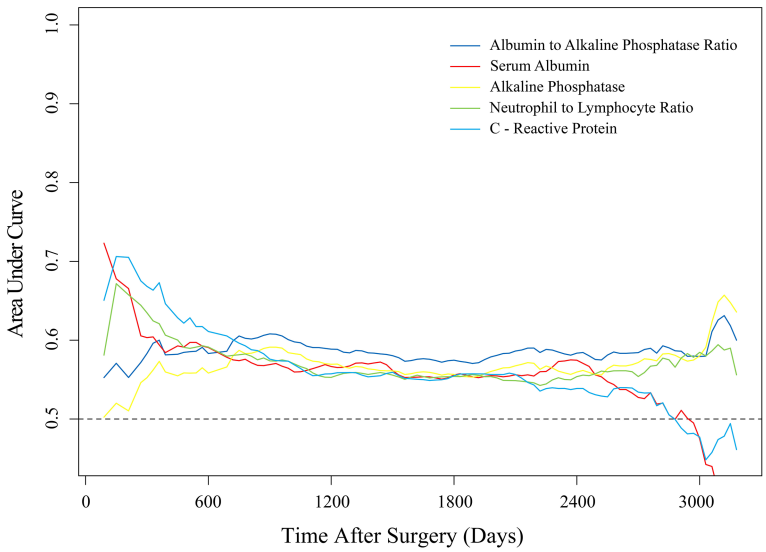

FIGURE 3 | Time-dependent ROC analysis of the discriminatory ability of laboratory-assayed biomarkers for postoperative survival during follow-up.

in tumor size (HR: 1.101; 95% CI: 1.016-1.194; *P*=0.019), AAPR<0.50 (HR: 1.66; 95% CI: 1.25-2.18; *P*<0.001), LNM (HR: 2.06; 95% CI: 1.59-2.68; *P*<0.001), adjuvant chemotherapy (HR: 1.64; 95% CI: 1.25-2.16; *P*<0.001), and adjuvant radiotherapy (HR: 1.47; 95% CI: 1.06-2.06; *P*=0.022) were determined to be independent predictors of PFS in surgically resected ESCC (**Table 2**).

Finally, **Figure 6A** indicates a prognostic nomogram integrated by all the independent predictors of PFS mentioned above. LNM, AAPR, and adjuvant chemotherapy were the prognostic indicators contributing the most to postoperative PFS (*P*<0.001). The C-statistic of this nomogram was 0.70 (95% CI: 0.61-0.78), which had statistical significance when applied to differentiate the probability of PFS (*P*<0.001). In addition, as shown in **Figures 6B-E**, all calibration curves also showed a significant agreement between the nomogram-predicted PFS and the real-world PFS at different follow-up periods.

3.4 Subgroup Analysis on the Prognostic Value of AAPR

As the subgroup survival results indicated, an unfavorable prognostic value of AAPR<0.50 for OS and PFS remained significantly reliable across all subgroups stratified by age, grade of differentiation, presence of perineural and neural invasion, tumor size, T stage, N stage, TNM stage, and occurrence of postoperative complications (**Figures 7A, B**).

In addition, AAPR<0.50 was significantly associated with more inferior OS in all subgroups of BMI, preoperative comorbidity, adjuvant therapy, and male patients without vascular or lymphatic invasion. Moreover, AAPR<0.50 was also significantly associated with more inferior PFS in the subgroups of male gender, BMI <24 kg/m^2, absence of preoperative comorbidity, absence of vascular or lymphatic invasion, and patients not receiving adjuvant therapy.

3.5 Comparison Between AAPR Groups in the PSM Cohort

3.5.1 PSM Cohort Generation

We determined BMI, NLR, CRP, perineural and neural invasion, and tumor size, all of which differed significantly between the two AAPR groups and were further engaged in the PSM procedure (**Figure 8**). As a result, this PSM analysis yielded 75 fully matched pairs of patients grouped by preoperative AAPR, as shown in **Table 3**.

3.5.2 Preoperative AAPR and In-Hospital Outcomes

In the PSM cohort, there was no significant difference between patients with AAPR<0.50 and those with AAPR≥0.50 in terms of postoperative complication rate (26.7% vs. 22.7%; *P*=0.57), 30-day mortality rate (1.3% vs. 1.3%; *P*=1.0), or 90-day mortality rate (6.7% vs. 2.7%; *P*=0.44) (**Table 3**).

3.5.3 Preoperative AAPR and Survival Outcomes

Kaplan-Meier survival analysis based on the PSM cohort showed that the mean OS time estimates for the AAPR<0.50 and AAPR≥0.50 groups were 1308 ± 148 (95% CI: 1017-1598) days and 2219 ± 157 (95% CI: 1911-2527) days, respectively. Patients with AAPR<0.50 and with AAPR≥0.50 had an OS rate of 24.0% and 53.3% after follow-up. In addition, the mean PFS time estimates for the AAPR<0.50 and AAPR≥0.50 groups were 1203 ± 146 (95% CI: 917-1489) days and 2112 ± 164 (95% CI: 1791-2434) days, respectively. The PFS rates after follow-up for patients with AAPR<0.50 and with AAPR≥0.50 were 21.3% and 50.7%, respectively. Thus, in the PSM cohort, patients with AAPR<0.50 had significantly worse outcomes of both OS and PFS than those with AAPR≥0.50 (Log-rank *P*<0.001; **Figures 9A, B**).

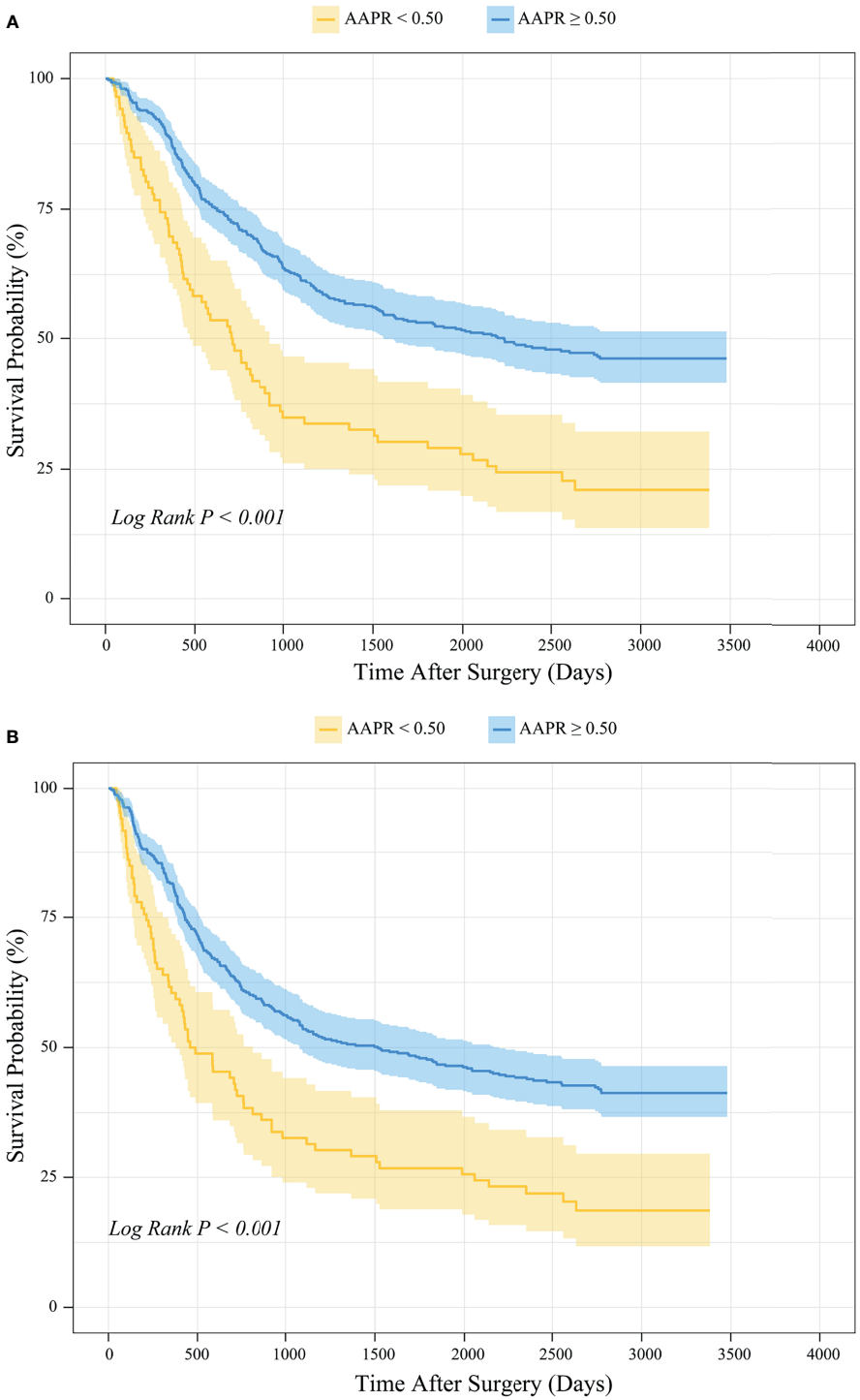

FIGURE 4 | Kaplan-Meier survival analysis of **(A)** OS and **(B)** PFS between patients stratified by preoperative AAPR.

3.5.4 Univariable and Multivariable Analysis on Prognostic Factors of OS

Univariable Cox proportional hazards regression analysis revealed that for every 1 year increase in age (P=0.013), AAPR<0.50 (P<0.001), LNM (P<0.001), and the occurrence of postoperative complications (P=0.017) were significantly associated with shortened OS of ESCC patients in the PSM cohort (**Table 4**). Subsequently, in multivariable Cox proportional hazards regression

TABLE 2 | Univariable and multivariable analyses of the prognostic factors in the entire cohort.

Characteristics	Overall Survival				Progression Free Survival			
	Univariable Analysis		Multivariable Analysis		Univariable Analysis		Multivariable Analysis	
	HR with 95%CI	*P* Value	HR with 95%CI	*P* Value	HR with 95%CI	*P* Value	HR with 95%CI	*P* Value
Age (Per 1 Year Increase)	1.025 (1.012 - 1.038)	<0.001	1.037 (1.022 - 1.052)	<0.001	1.014 (1.002 - 1.026)	0.023	1.027 (1.013 - 1.041)	<0.001
Gender								
Female	Reference				Reference			
Male	1.46 (1.05 - 2.02)	0.025	1.25 (0.89 - 1.76)	0.19	1.40 (1.03 - 1.91)	0.033	1.22 (0.88 - 1.68)	0.23
Body Mass Index (Per 1 kg/m^2 Increase)	0.949 (0.912 - 0.987)	0.010	0.950 (0.910 - 0.992)	0.020	0.953 (0.917 - 0.990)	0.013	0.943 (0.904 - 0.983)	0.006
Gastrointestinal Comorbidity								
Absent	Reference				Reference			
Present	1.11 (0.69 - 1.79)	0.66			1.08 (0.68 - 1.71)	0.75		
Cardio-Cerebrovascular Comorbidity								
Absent	Reference				Reference			
Present	1.43 (1.05 - 1.96)	0.024	1.21 (0.87 - 1.70)	0.26	1.30 (0.96 - 1.77)	0.095	1.28 (0.92 - 1.77)	0.14
Diabetes Mellitus								
Absent	Reference				Reference			
Present	0.91 (0.43 - 1.92)	0.80			0.97 (0.48 - 1.95)	0.92		
Respiratory Comorbidity								
Absent	Reference				Reference			
Present	1.10 (0.63 - 1.91)	0.74			0.93 (0.53 - 1.62)	0.79		
Hepatobiliary Comorbidity								
Absent	Reference				Reference			
Present	1.19 (0.68 - 2.07)	0.54			1.15 (0.66 - 2.01)	0.62		
Neutrophil to Lymphocyte Ratio (Per Unit Increase)	1.090 (1.023 - 1.16)	0.008	1.053 (0.969 - 1.144)	0.22	1.062 (0.997 - 1.131)	0.061	0.991 (0.917 - 1.071)	0.82
C - Reactive Protein (Per 1 mg/L Increase)	1.007 (0.999 - 1.016)	0.11	0.990 (0.978 - 1.001)	0.082	1.005 (0.997 - 1.014)	0.22		
Albumin to Alkaline Phosphatase Ratio								
≥ 0.50	Reference				Reference			
< 0.50	2.11 (1.60 - 2.78)	<0.001	1.92 (1.44 - 2.54)	<0.001	1.93 (1.48 - 2.53)	<0.001	1.66 (1.26 - 2.18)	< 0.001
Differentiation Grade								
Well - Moderate	Reference				Reference			
Poor	1.13 (0.89 - 1.45)	0.32			1.16 (0.92 - 1.47)	0.21		
Vascular Invasion								
Absent	Reference				Reference			
Present	1.92 (1.32 - 2.79)	0.001	1.66 (0.61 - 4.55)	0.32	1.90 (1.31 - 2.74)	0.001	2.15 (0.87 - 5.30)	0.096
Lymphatic Invasion								
Absent	Reference				Reference			
Present	2.02 (1.36 - 3.01)	0.001	1.10 (0.37 - 3.25)	0.86	1.85 (1.24 - 2.74)	0.002	0.72 (0.27 - 1.92)	0.51
Perineurium & Neural Invasion								
Absent	Reference				Reference			
Present	1.48 (0.94 - 2.34)	0.091	1.00 (0.60 - 1.66)	1.0	1.39 (0.89 - 2.17)	0.14	1.10 (0.68 - 1.79)	0.69
Tumor Size (Per 0.5 cm Increase)	1.160 (1.082 - 1.244)	<0.001	1.090 (0.999 - 1.189)	0.054	1.160 (1.085 - 1.241)	<0.001	1.101 (1.016 - 1.194)	0.019
T Stage								
T_1 - T_2	Reference				Reference			
T_3	1.70 (1.29 - 2.24)	<0.001	1.39 (1.04 - 1.85)	0.027	1.59 (1.23 - 2.07)	<0.001	1.23 (0.93 - 1.62)	0.15
N Stage								
N_0	Reference				Reference			
N_1 - N_3	2.83 (2.21 - 3.64)	<0.001	2.44 (1.85 - 3.22)	< 0.001	2.72 (2.14 - 3.46)	<0.001	2.06 (1.59 - 2.68)	< 0.001
TNM Stage								
I - II	Reference				Reference			
III	1.44 (0.89 - 1.47)	0.29			1.17 (0.93 - 1.49)	0.19		
Adjuvant Chemotherapy								
Not Received	Reference				Reference			
Received	1.59 (1.26 - 2.01)	<0.001	1.39 (1.04 - 1.85)	0.024	1.94 (1.55 - 2.44)	<0.001	1.64 (1.25 - 2.16)	< 0.001

(Continued)

TABLE 2 | Continued

Characteristics	Overall Survival				Progression Free Survival			
	Univariable Analysis		Multivariable Analysis		Univariable Analysis		Multivariable Analysis	
	HR with 95%CI	*P* Value	HR with 95%CI	*P* Value	HR with 95%CI	*P* Value	HR with 95%CI	*P* Value
Adjuvant Radiotherapy								
Not Received	Reference				Reference			
Received	1.46 (1.05 - 2.03)	0.024	1.05 (0.73 - 1.50)	0.79	2.13 (1.57 - 2.89)	<0.001	1.47 (1.06 - 2.06)	0.022
Postoperative Complications								
Absent	Reference				Reference			
Present	1.33 (0.99 - 1.78)	0.056	1.42 (1.04 - 1.92)	0.025	1.15 (0.86 - 1.54)	0.33		

CI, Confidence Interval; HR, Hazard Ratio.

analysis, all of them were further identified as independent prognostic biomarkers of postoperative OS after adjustment for other clinicopathological characteristics with $P<0.15$. In addition, LNM (HR: 2.56; 95% CI: 1.66-3.94; $P<0.001$) and AAPR<0.50 (HR: 2.40; 95% CI: 1.56-3.69; $P<0.001$) showed the most substantial prognostic significance associated with unfavorable OS in surgically resected ESCC (**Table 4**). A multivariable Cox proportional hazards regression model consisting of AAPR and other independent prognostic predictors had a significant discriminatory power for OS probability as indicated by a C-statistic of 0.71 (95% CI: 0.57-0.86; $P<0.001$).

3.5.5 Univariable and Multivariable Analysis on Prognostic Factors of PFS

In univariable Cox proportional hazards regression analysis, we found that for every 1 year increase in age ($P=0.017$), AAPR<0.50 ($P<0.001$), LNM ($P<0.001$), and the occurrence of postoperative complications ($P=0.042$) were significantly associated with worsening PFS of ESCC patients in the PSM cohort (**Table 4**). Multivariable Cox proportional hazards regression model on clinicopathological covariables with $P<0.15$ further suggested that for every 1 year increase in age (HR: 1.029; 95% CI: 1.004-1.054; $P=0.020$), every 1 kg/m^2 increase in BMI (HR: 0.923; 95% CI: 0.852-0.999; $P=0.048$), AAPR<0.50 (HR: 2.30; 95% CI: 1.50-3.53; $P<0.001$), and LNM (HR: 2.47; 95% CI: 1.57-3.89; $P<0.001$) could be regarded as independent predictors of postoperative PFS (**Table 4**). Finally, the multivariable Cox proportional hazards regression model involving AAPR and other independent prognostic predictors had a significant discriminatory power for the probability of PFS with a C-statistic of 0.71 (95% CI: 0.56-0.86; $P<0.001$).

4 DISCUSSION

4.1 Key Results and Interpretations

Since Chan et al. (16) first introduced this simply synthetic biomarker based on sALB and serum ALP for estimating the outcome of the procedure in hepatocellular carcinoma, AAPR has been widely demonstrated to be promisingly indicative of post-treatment prognosis in a series of malignant tumors, including nasopharyngeal carcinoma (17), urothelial carcinoma (18), cholangiocarcinoma (19), lung cancer (12, 20), bladder cancer (21), and pancreatic cancer (22, 23). Several recent evidence-based literature reviews have also provided comprehensive results suggesting a potent prognostic impact of AAPR in human solid tumors, regardless of their histological origins (15, 24). However, until recently, there was no investigation aimed at the clinical significance of AAPR in surgically resected ESCC.

To our knowledge, our study was the first to employ a PSM analysis to elucidate potential prognostic effects of preoperative AAPR on OS and PFS in surgically resected ESCC. An AAPR of 0.50 was considered to be the threshold for prognostic outcome stratification of ESCC patients in our cohort. Patients with AAPR<0.50 had a significantly lower BMI, significantly larger tumor size, significantly higher NLR and CRP, and a significantly higher proportion of perineural and neural invasion than patients with AAPR≥0.50. Similar to previous reports in surgical oncology, we found that a decreased level of preoperative AAPR was significantly associated with poorer survival outcomes following esophagectomy for cancer. In our study, by applying an optimal cutoff point of 0.50, AAPR could play a considerable role in the effective risk stratification of OS and PFS in surgical patients with ESCC. In addition, we further established two nomograms based on preoperative AAPR with the aim to predict the probability of OS and PFS comprehensively. After calibration, AAPR<0.50 and LNM were finally identified as the two most apparent susceptibility factors for death from any cause or cancer progression in the present cohort of ESCC patients.

One of our study focuses was to determine the prognostic utility of AAPR in patients undergoing esophagectomy for ESCC *via* both Cox proportional hazards regression analysis and PSM analysis. PSM has been widely validated as an excellent statistical alternative that collapsed all potential confounders into a single value that matches each subject between study groups with well-balanced baseline characteristics, thus providing an effective way to circumvent the ontological limitations of classical multivariable regression modeling (8, 10, 12). Given such concerns, a total of 75 well-matched pairs of patients were extracted by reviewing the propensity scores of the two AAPR groups. Finally, AAPR was found to exhibit substantial

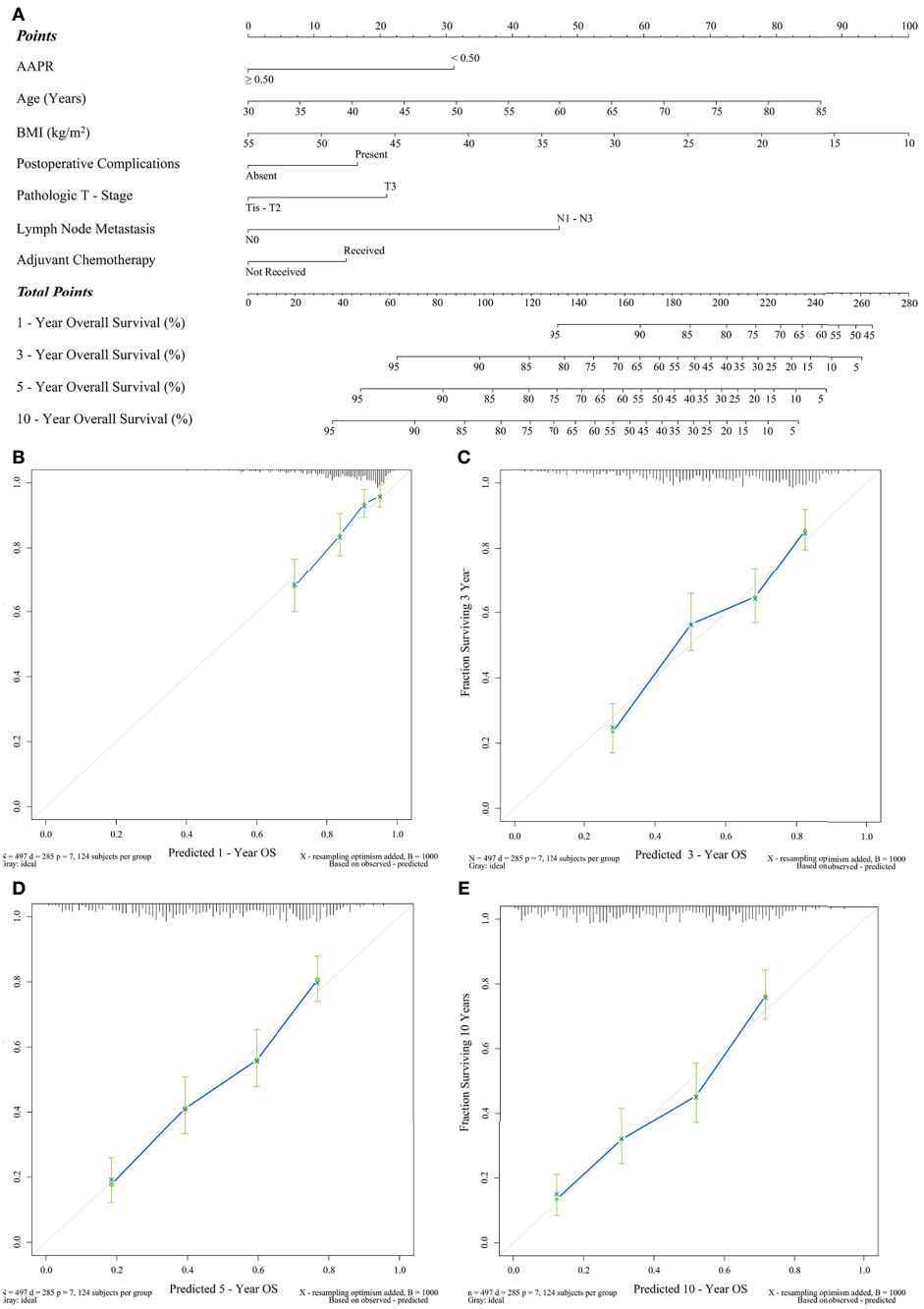

FIGURE 5 | Prediction of OS by preoperative AAPR. **(A)** AAPR composite nomogram and its calibration curves **(B)** 1-year OS, **(C)** 3-year OS, **(D)** 5-year OS, and **(E)** 10-year OS.

prognostic impact in the entire cohort, and was also validated as a independent prognostic biomarker for OS and PFS in the PSM cohort.

Another highlight of our study was a comprehensive survival analysis of the prognostic roles of AAPR in a specific set of ESCC patient subgroups. Our findings confirmed that AAPR remained statistically reliable for predicting OS and PFS of ESCC patients in most subgroups stratified by clinicopathological characteristics. Furthermore, we observed no significant difference in either OS or PFS between patients with AAPR<0.50 and with AAPR≥0.50 in both women and patients with vascular or lymphatic invasive tumors. We speculated that the limited sample size of these two subgroups might have weakened the demonstrative power of Cox proportional hazards regression models derived.

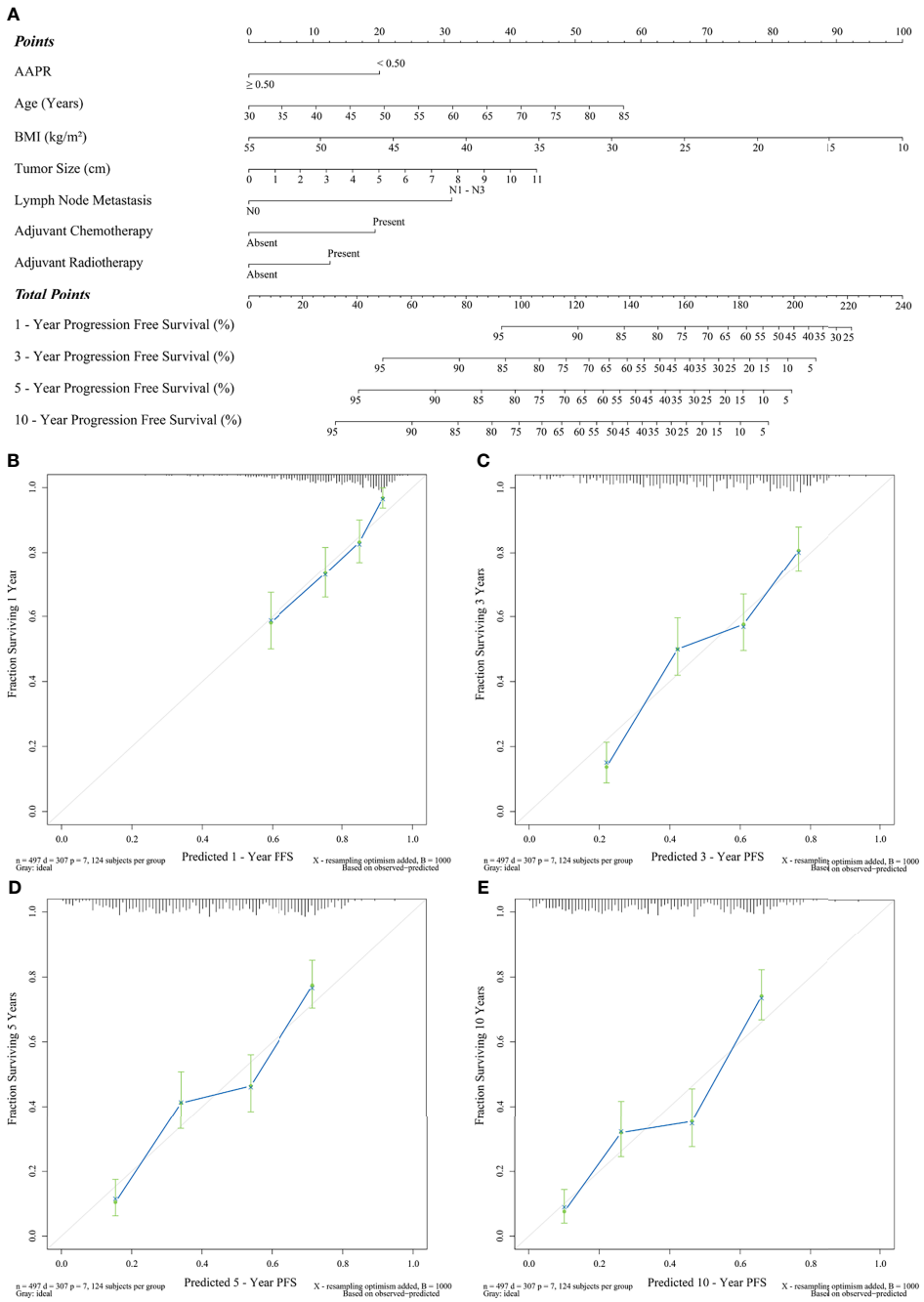

FIGURE 6 | Prediction of PFS by preoperative AAPR. **(A)** AAPR composite nomogram and its calibration curves **(B)** 1-year PFS, **(C)** 3-year PFS, **(D)** 5-year PFS, and **(E)** 10-year PFS.

The following possible biological mechanisms may help to elucidate the links between AAPR and prognosis of surgically resected ESCC. Firstly, hypoalbuminemia characterized by a decline in sALB has not only been considered as a promising indicator of suppression of host immune-nutritional reserve, but also as a potential diagnostic biomarker for human malignancies (14). Hypoalbuminemia also performs as one of the cardinal markers of cachexia during the carcinomatous progression, which is defined as a multifactorial syndrome characterized by an ongoing skeletal muscle loss that cannot be fully reversed by conventional nutritional support and eventually aggravates a functional impairment according to the Washington and Delphi consensus (29), especially throughout the disease trajectory of ESCC (30). In addition, as a negative acute-phase protein, sALB

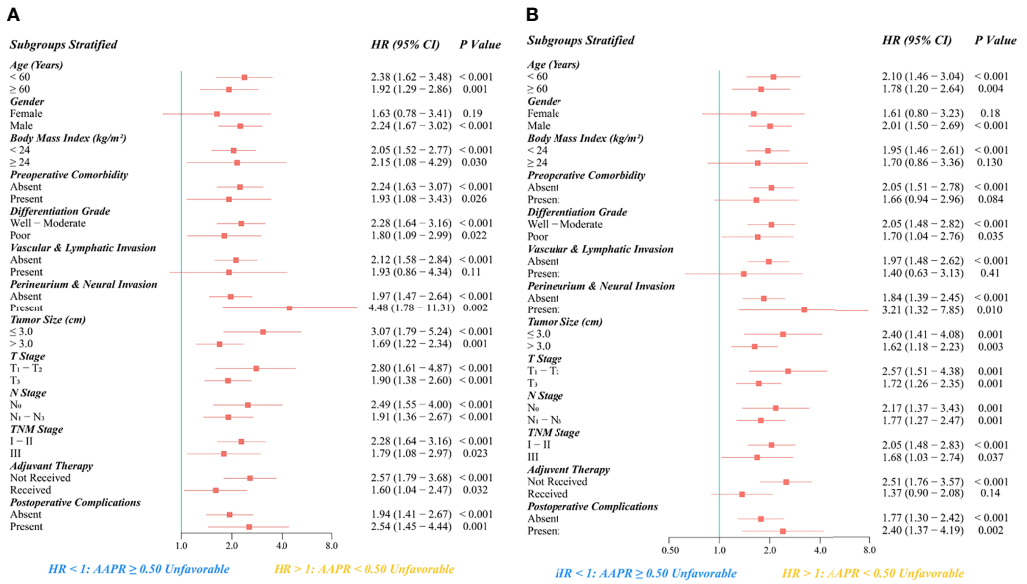

FIGURE 7 | Subgroup analysis regarding the prognostic significance of preoperative AAPR on **(A)** OS and **(B)** PFS after esophagectomy for ESCC.

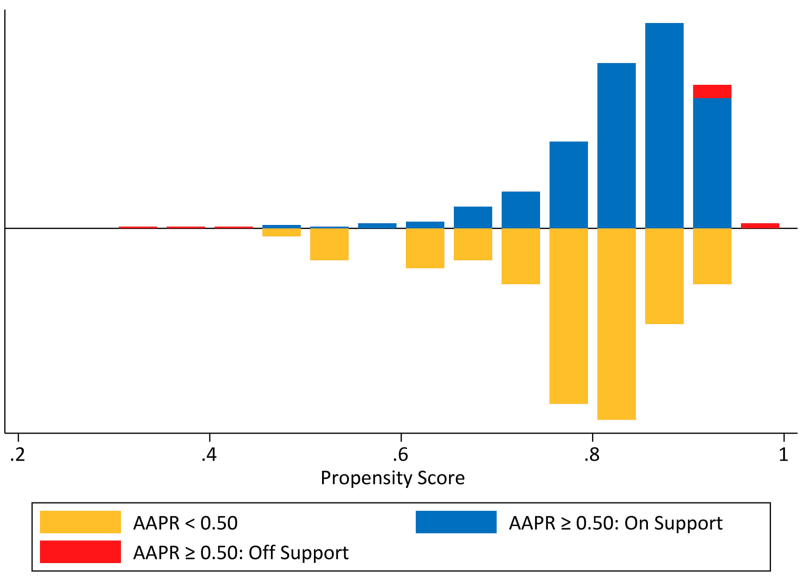

FIGURE 8 | Mirrored histogram presenting the propensity score distribution and the overlap between unmatched and matched samples in the two AAPR groups.

has also been used to reveal changes in the systemic inflammatory response, as hepatocyte synthesis of sALB can be influenced by the biological activity of pro-inflammatory cytokines. Both malnutrition and inflammation contribute to the development of hypoalbuminemia, which leads to impaired surgical tolerance due to an impaired ability to withstand acute injury (8, 10, 12). At the same time, sALB maintains its physiological properties as an antioxidant transporter. Therefore, hypoalbuminemia may impair antitumor immunity and response to adjuvant therapy, leading to unfavorable post-surgical prognosis (15).

Secondly, serum ALP is a hydrolytic enzyme mainly concentrated in the liver, bone, and kidney that catalyze the hydrolytic processes and phosphate transfer in an alkaline environment. An extensive body of evidence suggest that elevated ALP levels can indicate oxidative stress, which is induced by inflammation together with fast-growing tumors, contributing to the production of reactive oxygen species that damage the DNA,

TABLE 3 | Patient characteristics and in-hospital outcomes of the propensity score matched cohort.

Characteristics	Propensity Score Matched Cohort			*P* Value
	Total (*N* = 150)	AAPR ≥ 0.50 (*N* = 75)	AAPR < 0.50 (*N* = 75)	
Age (Years)				
Mean ± SD	59.61 ± 9.39	59.81 ± 10.05	59.40 ± 8.74	0.63
Median (IQR)	60 (54 - 66)	60 (53 - 68)	58 (54 - 66)	
Gender (n, %)				
Female	25 (16.7%)	11 (14.7%)	14 (18.7%)	0.51
Male	125 (83.3%)	64 (85.3%)	61 (81.3%)	
Body Mass Index (kg/m^2)				
Mean ± SD	20.70 ± 2.84	20.52 ± 2.75	20.88 ± 2.94	0.58
Median (IQR)	20.24 (18.50 - 22.66)	20.08 (18.49 - 22.66)	20.38 (18.51 - 22.84)	
Gastrointestinal Comorbidity (n, %)				
Absent	144 (96.0%)	72 (96.0%)	72 (96.0%)	1.0
Present	6 (4.0%)	3 (4.0%)	3 (4.0%)	
Cardio-Cerebrovascular Comorbidity (n, %)				
Absent	127 (84.7%)	61 (81.3%)	66 (88.0%)	0.26
Present	23 (15.3%)	14 (18.7%)	9 (12.0%)	
Diabetes Mellitus (n, %)				
Absent	146 (97.3%)	73 (97.3%)	73 (97.3%)	1.0
Present	4 (2.7%)	2 (2.7%)	2 (2.7%)	
Respiratory Comorbidity (n, %)				
Absent	145 (96.7%)	72 (96.0%)	73 (97.3%)	1.0
Present	5 (3.3%)	3 (4.0%)	2 (2.7%)	
Hepatobiliary Comorbidity (n, %)				
Absent	146 (97.3%)	73 (97.3%)	73 (97.3%)	1.0
Present	4 (2.7%)	2 (2.7%)	2 (2.7%)	
Neutrophil to Lymphocyte Ratio				
Mean ± SD	2.95 ± 1.45	2.99 ± 1.47	2.91 ± 1.43	0.76
Median (IQR)	2.62 (1.86 - 3.81)	2.73 (1.89 - 3.79)	2.56 (1.70 - 3.91)	
C - Reactive Protein (mg/L)				
Mean ± SD	7.98 ± 11.13	7.81 ± 11.96	8.16 ± 10.32	0.080
Median (IQR)	3.54 (1.47 - 8.89)	2.78 (1.02 - 10.58)	4.39 (2.22 - 8.79)	
AAPR Value				
Mean ± SD	0.55 ± 0.15	0.67 ± 0.13	0.44 ± 0.05	< 0.001
Median (IQR)	0.50 (0.46 - 0.63)	0.62 (0.57 - 0.76)	0.46 (0.41 - 0.48)	
Differentiation Grade (n, %)				
Well	39 (26.0%)	20 (26.7%)	19 (25.3%)	0.88
Moderate	71 (47.3%)	34 (45.3%)	37 (49.3%)	
Poor	40 (26.7%)	21 (28.0%)	19 (25.3%)	
Vascular Invasion (n, %)				
Absent	136 (90.7%)	68 (90.7%)	68 (90.7%)	1.0
Present	14 (9.3%)	7 (9.3%)	7 (9.3%)	
Lymphatic Invasion (n, %)				
Absent	138 (92.0%)	69 (92.0%)	69 (92.0%)	1.0
Present	12 (8.0%)	6 (8.0%)	6 (8.0%)	
Perineurium & Neural Invasion (n, %)				
Absent	136 (90.7%)	68 (90.7%)	68 (90.7%)	1.0
Present	14 (9.3%)	7 (9.3%)	7 (9.3%)	
Tumor Size (cm)				
Mean ± SD	4.27 ± 1.68	4.26 ± 1.85	4.28 ± 1.51	0.94
Median (IQR)	4.0 (3.0 - 5.0)	4.0 (3.0 - 5.0)	4.0 (3.0 - 5.0)	
T Stage (n, %)				
T_1	12 (8.0%)	7 (9.3%)	5 (6.7%)	0.71
T_2	27 (18.0%)	12 (16.0%)	15 (20.0%)	
T_3	111 (74.0%)	56 (74.7%)	55 (73.3%)	
N Stage (n, %)				
N_0	73 (48.7%)	41 (54.7%)	32 (42.7%)	0.39
N_1	65 (43.3%)	30 (40.0%)	35 (46.7%)	
N_2	7 (4.7%)	2 (2.7%)	5 (6.7%)	
N_3	5 (3.3%)	2 (2.7%)	3 (4.0%)	
TNM Stage (n, %)				
I	34 (22.7%)	17 (22.7%)	17 (22.7%)	0.84
II	75 (50.0%)	36 (48.0%)	39 (52.0%)	

(Continued)

TABLE 3 | Continued

Characteristics	Propensity Score Matched Cohort			*P* Value
	Total (*N* = 150)	AAPR ≥ 0.50 (*N* = 75)	AAPR < 0.50 (*N* = 75)	
III	41 (27.3%)	22 (29.3%)	19 (25.3%)	
Adjuvant Chemotherapy (n, %)				
Not Received	103 (68.7%)	54 (72.0%)	49 (65.3%)	0.38
Received	47 (31.3%)	21 (28.0%)	26 (34.7%)	
Adjuvant Radiotherapy (n, %)				
Not Received	133 (88.7%)	68 (90.7%)	65 (86.7%)	0.44
Received	17 (11.3%)	7 (9.3%)	10 (13.3%)	
Postoperative Complications (n, %)				
Absent	113 (75.3%)	58 (77.3%)	55 (73.3%)	0.57
Present	37 (24.7%)	17 (22.7%)	20 (26.7%)	
30 - Day Mortality (n, %)				
Absent	148 (98.7%)	74 (98.7%)	74 (98.7%)	1.0
Present	2 (1.3%)	1 (1.3%)	1 (1.3%)	
90 - Day Mortality (n, %)				
Absent	143 (95.3%)	73 (97.3%)	70 (93.3%)	0.44
Present	7 (4.7%)	2 (2.7%)	5 (6.7%)	

AAPR, Albumin to Alkaline Phosphatase Ratio; IQR, Interquartile Range; SD, Standard Deviation.

protein, and lipid, and promote active mutagenic metabolism (12, 31). In addition, increased cellular permeability in cancer-related inflammation can also increase intracellular ALP concentration and activity (32). Therefore, serum ALP can be considered a valuable marker of carcinogenesis, cancer cell proliferation and metastasis (29).

4.2 Clinical Significance

All our findings provide evidence to support the inclusion of a value of AAPR in routine risk assessment prior to esophagectomy to better distinguish patients who have a higher probability of suffering an unfavorable prognosis. AAPR is directly extrapolated from sALB and serum ALP, both of which can be easily and inexpensively obtained through peripheral chemistry test in the routine clinical practice. In addition, the predictive accuracy of postoperative survival in ESCC patients can be improved by identifying their AAPR levels early before surgery. Thus, more accurate prognostic prediction would thus facilitate the development of more individualized treatment plans to improve anti-inflammatory and nutritional care, enhance the tolerance of surgery, and limit potential adverse events.

4.3 Limitations

There were several notable limitations of this study.

First, this study was a retrospective analysis on a single-center prospectively collected database that was not externally validated. Therefore, due to the inherent limitations of retrospective nature, potential selection bias might have still attenuated the demonstrative strength of AAPR as a reliable prognostic marker for surgically resectable ESCC, despite our attempts to conduct a well-designed PSM analysis of the included patients based on our reasonably stringent eligibility criteria. In addition, the limited sample size of a single institution might also have negatively affected the strength of evidence in our study. Therefore, we strongly recommend additional multicenter prospective studies in the future to better control for potential confounding covariables to validate the clinical implication of AAPR in surgically resectable ESCC.

Second, the value of AAPR in this study was a single time-point measure preoperatively. However, AAPR was usually a dynamic serum biomarker which significantly fluctuated over time. It would also be essentially meaningful to explore the changes of AAPR during the follow-up period. Hence, a prospective validating analysis aimed on the dynamic prognostic roles of AAPR in surgically resectable ESCC can be regarded as a crucial area of investigation in the future.

Third, serum ALP comprises a heterogeneous group of isozymes presented only in intestinal, placental, and reproductive tissues, which are substantially different from the tissue-nonspecific types mainly produced by the liver, bone, and kidney (32). Unfortunately, ALP isozyme analysis was not a routine laboratory test at our institution during the study period. We suggest that different assays for the source of ALP may further help to understand possible biological mechanisms underlying the prognostic role of AAPR in ESCC.

Fourth, potential differences in the salvage procedures outside our institution might exist during the disease course between the two AAPR groups, which had probably altered the ESCC prognosis in favor of one group in an unintentional manner.

Finally, there was no consensus on the threshold for AAPR in surgical oncology. In the latest studies, the selective cutoff points for AAPR varied.

5 CONCLUSIONS

In conclusion, our study suggests that preoperative AAPR can be a promising prognostic predictor of OS and PFS in patients undergoing esophagectomy for ESCC. As a simple, convenient, and noninvasive biomarker from routine biochemical tests, AAPR shows excellent potential to help improve the predictive effectiveness of current risk stratification tools for the prognosis

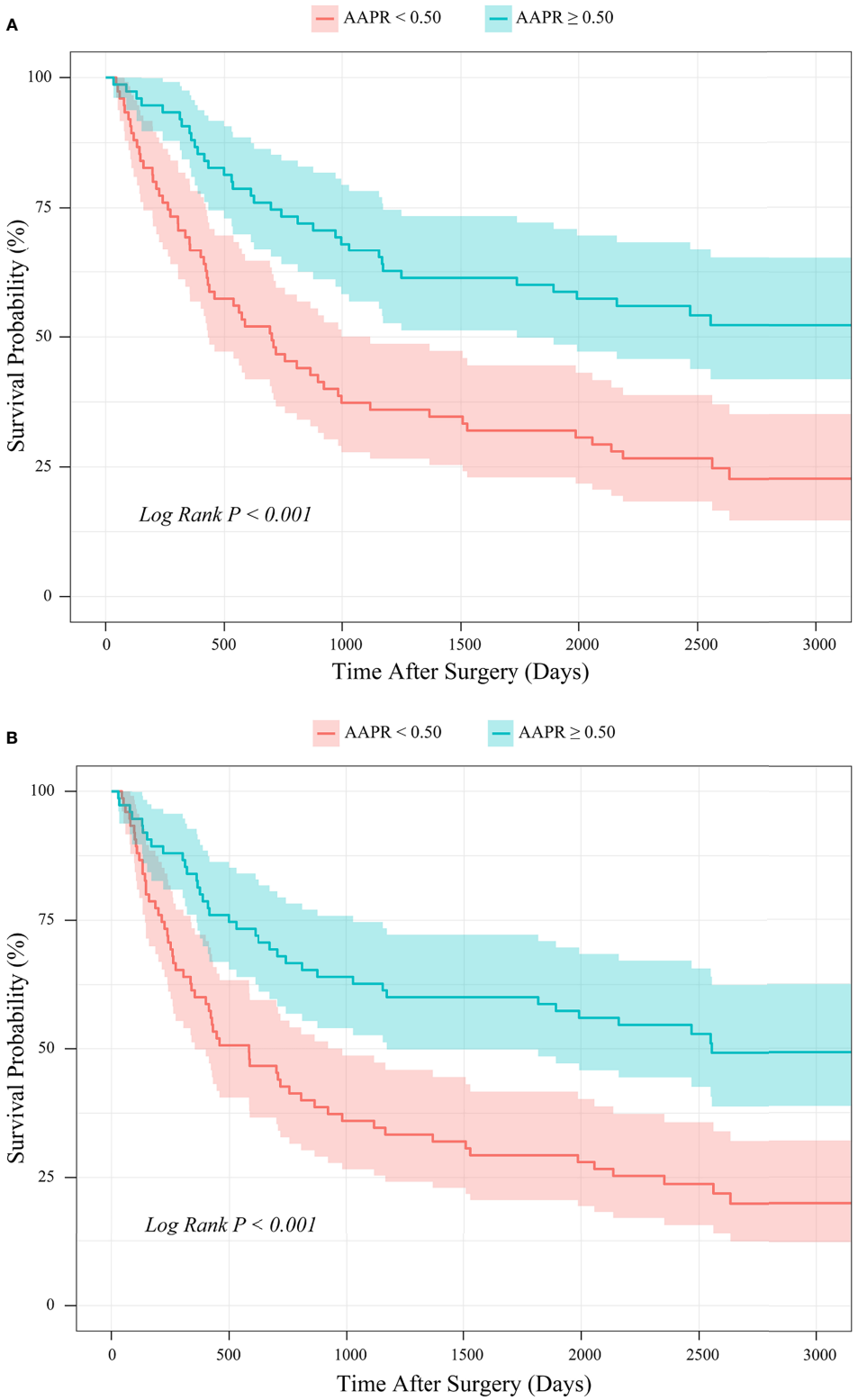

FIGURE 9 | PSM-based Kaplan-Meier survival analysis of **(A)** OS and **(B)** PFS between patient groups stratified by preoperative AAPR.

TABLE 4 | Univariable and multivariable analyses of the prognostic factors in the propensity score matched cohort.

Characteristics	Overall Survival				Progression Free Survival			
	Univariable Analysis		Multivariable Analysis		Univariable Analysis		Multivariable Analysis	
	HR with 95%CI	*P* Value	HR with 95%CI	*P* Value	HR with 95%CI	*P* Value	HR with 95%CI	*P* Value
Age (Per 1 Year Increase)	1.028 (1.006 - 1.051)	0.013	1.028 (1.005 - 1.051)	0.018	1.026 (1.005 - 1.048)	0.017	1.029 (1.004 - 1.054)	0.020
Gender								
Female	Reference				Reference			
Male	1.06 (0.61 - 1.85)	0.83			1.01 (0.59 - 1.73)	0.97		
Body Mass Index (Per 1 kg/m^2 Increase)	0.945 (0.877 - 1.019)	0.14	0.926 (0.855 - 1.003)	0.060	0.947 (0.880 - 1.019)	0.140	0.923 (0.852 - 0.999)	0.048
Gastrointestinal Comorbidity								
Absent	Reference				Reference			
Present	1.24 (0.45 - 3.37)	0.68			1.18 (0.43 - 3.21)	0.75		
Cardio-Cerebrovascular Comorbidity								
Absent	Reference				Reference			
Present	1.29 (0.74 - 2.25)	0.37			1.25 (0.72 - 2.17)	0.43		
Diabetes Mellitus								
Absent	Reference				Reference			
Present	0.37 (0.05 - 2.62)	0.32			0.35 (0.05 - 2.49)	0.29		
Respiratory Comorbidity								
Absent	Reference				Reference			
Present	1.09 (0.34 - 3.43)	0.89			0.96 (0.30 - 3.03)	0.94		
Hepatobiliary Comorbidity								
Absent	Reference				Reference			
Present	1.26 (0.40 - 3.98)	0.70			1.12 (0.35 - 3.53)	0.85		
Neutrophil to Lymphocyte Ratio (Per Unit Increase)	1.094 (0.943 - 1.248)	0.26			1.058 (0.920 - 1.216)	0.43		
C - Reactive Protein (Per 1 mg/L Increase)	1.000 (0.982 - 1.019)	0.99			1.004 (0.986 - 1.021)	0.68		
Albumin to Alkaline Phosphatase Ratio								
≥ 0.50	Reference				Reference			
< 0.50	2.34 (1.53 - 3.57)	<0.001	2.40 (1.56 - 3.69)	<0.001	2.26 (1.49 - 3.42)	<0.001	2.30 (1.50 - 3.53)	<0.001
Differentiation Grade								
Well - Moderate	Reference				Reference			
Poor	1.16 (0.74 - 1.82)	0.51			1.32 (0.86 - 2.03)	0.21		
Vascular Invasion								
Absent	Reference				Reference			
Present	1.35 (0.70 - 2.61)	0.37			1.31 (0.68 - 2.52)	0.42		
Lymphatic Invasion								
Absent	Reference				Reference			
Present	1.08 (0.52 - 2.24)	0.83			1.03 (0.50 - 2.12)	0.94		
Perineurium & Neural Invasion								
Absent	Reference				Reference			
Present	1.26 (0.63 - 2.51)	0.52			1.17 (0.59 - 2.33)	0.66		
Tumor Size (Per 0.5 cm Increase)	1.050 (0.934 - 1.180)	0.41			1.084 (0.967 - 1.216)	0.17		
T Stage								
T_1 - T_2	Reference				Reference			
T_3	1.34 (0.83 - 2.16)	0.23			1.19 (0.76 - 1.88)	0.45		
N Stage								
N_0	Reference				Reference			
N_1 - N_3	2.60 (1.69 - 3.99)	<0.001	2.56 (1.66 - 3.94)	<0.001	2.66 (1.75 - 4.04)	<0.001	2.47 (1.57 - 3.89)	<0.001
TNM Stage								
I - II	Reference				Reference			
III	1.17 (0.75 - 1.82)	0.49			1.32 (0.86 - 2.02)	0.21		
Adjuvant Chemotherapy								
Not Received	Reference				Reference			
Received	1.27 (0.82 - 1.95)	0.28			1.44 (0.95 - 2.19)	0.087	1.25 (0.76 - 2.06)	0.38
Adjuvant Radiotherapy								
Not Received	Reference				Reference			
Received	1.20 (0.66 - 2.15)	0.55			1.73 (1.00 - 3.02)	0.052	1.02 (0.55 - 1.88)	0.96

(Continued)

TABLE 4 | Continued

Characteristics	Overall Survival				Progression Free Survival			
	Univariable Analysis		Multivariable Analysis		Univariable Analysis		Multivariable Analysis	
	HR with 95%CI	*P* Value	HR with 95%CI	*P* Value	HR with 95%CI	*P* Value	HR with 95%CI	*P* Value
Postoperative Complications								
Absent	Reference				Reference			
Present	1.72 (1.10 - 2.69)	0.017	1.62 (1.03 - 2.55)	0.036	1.58 (1.02 - 2.45)	0.042	1.43 (0.90 - 2.25)	0.13

CI, Confidence Interval; HR, Hazard Ratio.

of surgically resected ESCC. As the present study still has some limitations, future multicenter prospective studies are urgently needed to confirm and validate our findings.

DATA AVAILABILITY STATEMENT

The raw data supporting the conclusions of this article will be made available by the authors, without undue reservation.

ETHICS STATEMENT

The studies involving human participants were reviewed and approved by the Institutional Review Board of Sun Yat-Sen University Cancer Center (No: GZR 2018-120) and performed all relevant procedures compliant with the Declaration of Helsinki. The patients/participants provided their written informed consent to participate in this study.

AUTHOR CONTRIBUTIONS

We formally declare that all the authors' individual contributions are as follows. Conceptualization and Supervision, SL and ZW. Data curation, DC, XZ, JZ, and ZW. Formal analysis and Methodology, SL, WZ, and YL. Funding acquisition, ZW. Investigation, XZ, SL, and DC. Project administration, SL, JZ, and ZW. Resources, DC, WZ, JZ, and ZW. Software, SL and YL. Validation, XZ, DC, SL, WZ, and YL. Visualization, SL and XW. Writing - original draft, XZ, DC, and SL. Writing - review and editing, XZ, JZ, and ZW. All authors contributed to the article and approved the submitted version.

FUNDING

This study was supported by the National Natural Science Foundation (No. 81871986).

ACKNOWLEDGMENTS

We give special thanks to Mrs. Hong Xie and Mrs. Peng Wang, from the Department of Medical English, West China School of Medicine, Sichuan University, Chengdu, China, for their English language editing to this manuscript.

REFERENCES

1. Sung H, Ferlay J, Siegel RL, Laversanne M, Soerjomataram I, Jemal A, et al. Global Cancer Statistics 2020: GLOBOCAN Estimates of Incidence and Mortality Worldwide for 36 Cancers in 185 Countries. *CA Cancer J Clin* (2021) 71(3):209–49. doi: 10.3322/caac.21660
2. GBD 2017 Oesophageal Cancer Collaborators. The Global, Regional, and National Burden of Oesophageal Cancer and its Attributable Risk Factors in 195 Countries and Territories, 1990-2017: A Systematic Analysis for the Global Burden of Disease Study 2017. *Lancet Gastroenterol Hepatol* (2020) 5 (6):582–97. doi: 10.1016/S2468-1253(20)30007-8
3. Siegel RL, Miller KD, Fuchs HE, Jemal A. Cancer Statistics, 2021. *CA Cancer J Clin* (2021) 71(1):7–33. doi: 10.3322/caac.21654
4. Wang Q, Peng L, Han Y, Li T, Dai W, Wang Y, et al. Preoperative Serum Sodium Level as a Prognostic and Predictive Biomarker for Adjuvant Therapy in Esophageal Cancer. *Front Oncol* (2021) 10:555714. doi: 10.3389/fonc.2020.555714
5. Ilson DH, van Hillegersberg R. Management of Patients With Adenocarcinoma or Squamous Cancer of the Esophagus. *Gastroenterology* (2018) 154(2):437–51. doi: 10.1053/j.gastro.2017.09.048
6. Li SJ, Wang ZQ, Li YJ, Fan J, Zhang WB, Che GW, et al. Diabetes Mellitus and Risk of Anastomotic Leakage After Esophagectomy: A Systematic Review and Meta-Analysis. *Dis Esophagus* (2017) 30(6):1–12. doi: 10.1093/dote/dox006
7. Yang J, Liu X, Cao S, Dong X, Rao S, Cai K. Understanding Esophageal Cancer: The Challenges and Opportunities for the Next Decade. *Front Oncol* (2020) 10:1727. doi: 10.3389/fonc.2020.01727
8. Li S, Wang H, Yang Z, Zhao L, Lv W, Du H, et al. Naples Prognostic Score as a Novel Prognostic Prediction Tool in Video-Assisted Thoracoscopic Surgery for Early-Stage Lung Cancer: A Propensity Score Matching Study. *Surg Endosc* (2021) 35(7):3679–97. doi: 10.1007/s00464-020-07851-7
9. Feng JF, Zhao JM, Chen S, Chen QX. Naples Prognostic Score: A Novel Prognostic Score in Predicting Cancer-Specific Survival in Patients With Resected Esophageal Squamous Cell Carcinoma. *Front Oncol* (2021) 11:652537. doi: 10.3389/fonc.2021.652537
10. Li SJ, Zhao L, Wang HY, Zhou HN, Ju J, Du H, et al. Gustave Roussy Immune Score Based on a Three-Category Risk Assessment Scale Serves as a Novel and Effective Prognostic Indicator for Surgically Resectable Early-Stage Non-Small-Cell Lung Cancer: A Propensity Score Matching Retrospective Cohort Study. *Int J Surg* (2020) 84:25–40. doi: 10.1016/j.ijsu.2020.10.015
11. Hao J, Chen C, Wan F, Zhu Y, Jin H, Zhou J, et al. Prognostic Value of Pre-Treatment Prognostic Nutritional Index in Esophageal Cancer: A Systematic Review and Meta-Analysis. *Front Oncol* (2020) 10:797. doi: 10.3389/fonc.2020.00797
12. Li SJ, Lv WY, Du H, Li YJ, Zhang WB, Che GW, et al. Albumin-To-Alkaline Phosphatase Ratio as a Novel Prognostic Indicator for Patients Undergoing Minimally Invasive Lung Cancer Surgery: Propensity Score Matching

Analysis Using a Prospective Database. *Int J Surg* (2019) 69:32–42. doi: 10.1016/j.ijsu.2019.07.008
13. Guner A, Cho M, Kim YM, Cheong JH, Hyung WJ, Kim HI. Prognostic Value of Postoperative Neutrophil and Albumin: Reassessment One Month After Gastric Cancer Surgery. *Front Oncol* (2021) 11:633924. doi: 10.3389/fonc.2021.633924
14. Loftus TJ, Brown MP, Slish JH, Rosenthal MD. Serum Levels of Prealbumin and Albumin for Preoperative Risk Stratification. *Nutr Clin Pract* (2019) 34 (3):340–8. doi: 10.1002/ncp.10271
15. An L, Yin WT, Sun DW. Albumin-To-Alkaline Phosphatase Ratio as a Promising Indicator of Prognosis in Human Cancers: Is it Possible? *BMC Cancer* (2021) 21(1):247. doi: 10.1186/s12885-021-07921-6
16. Chan AW, Chan SL, Mo FK, Wong GL, Wong VW, Cheung YS, et al. Albumin-To-Alkaline Phosphatase Ratio: A Novel Prognostic Index for Hepatocellular Carcinoma. *Dis Markers* (2015) 2015:564057. doi: 10.1155/2015/564057
17. Kim JS, Keam B, Heo DS, Han DH, Rhee CS, Kim JH, et al. The Prognostic Value of Albumin-To-Alkaline Phosphatase Ratio Before Radical Radiotherapy in Patients With Non-Metastatic Nasopharyngeal Carcinoma: A Propensity Score Matching Analysis. *Cancer Res Treat* (2019) 51(4):1313–23. doi: 10.4143/crt.2018.503
18. Tan P, Xie N, Ai J, Xu H, Xu H, Liu L, et al. The Prognostic Significance of Albumin-To-Alkaline Phosphatase Ratio in Upper Tract Urothelial Carcinoma. *Sci Rep* (2018) 8(1):12311. doi: 10.1038/s41598-018-29833-5
19. Xiong JP, Long JY, Xu WY, Bian J, Huang HC, Bai Y, et al. Albumin-To-Alkaline Phosphatase Ratio: A Novel Prognostic Index of Overall Survival in Cholangiocarcinoma Patients After Surgery. *World J Gastrointest Oncol* (2019) 11(1):39–47. doi: 10.4251/wjgo.v11.i1.39
20. Zhou S, Jiang W, Wang H, Wei N, Yu Q. Predictive Value of Pretreatment Albumin-to-Alkaline Phosphatase Ratio for Overall Survival for Patients With Advanced Non-Small Cell Lung Cancer. *Cancer Med* (2020) 9(17):6268–80. doi: 10.1002/cam4.3244
21. Li S, Lu S, Liu X, Chen X. Association Between the Pretreatment Albumin-To-Alkaline Phosphatase Ratio and Clinical Outcomes in Patients With Bladder Cancer Treated With Radical Cystectomy: A Retrospective Cohort Study. *Front Oncol* (2021) 11:664392. doi: 10.3389/fonc.2021.664392
22. Haksoyler V, Topkan E. Prognostic Utility of Prechemoradiotherapy Albumin-To-Alkaline Phosphatase Ratio in Unresectable Locally Advanced Pancreatic Carcinoma Patients. *Gastroenterol Res Pract* (2021) 2021:6647145. doi: 10.1155/2021/6647145
23. Acikgoz Y, Bal O, Dogan M. Albumin-To-Alkaline Phosphatase Ratio: Does It Predict Survival in Grade 1 and Grade 2 Neuroendocrine Tumors? *Pancreas* (2021) 50(1):111–7. doi: 10.1097/MPA.0000000000001720
24. Tian G, Li G, Guan L, Yang Y, Li N. Pretreatment Albumin-to-Alkaline Phosphatase Ratio as a Prognostic Indicator in Solid Cancers: A Meta-Analysis With Trial Sequential Analysis. *Int J Surg* (2020) 81:66–73. doi: 10.1016/j.ijsu.2020.07.024
25. Agha R, Abdall-Razak A, Crossley E, Dowlut N, Iosifidis C, Mathew G, et al. STROCSS 2019 Guideline: Strengthening the Reporting of Cohort Studies in Surgery. *Int J Surg* (2019) 72:156–65. doi: 10.1016/j.ijsu.2019.11.002
26. Rice TW, Ishwaran H, Hofstetter WL, Kelsen DP, Apperson-Hansen C, Blackstone EH, et al. Recommendations for Pathologic Staging (pTNM) of Cancer of the Esophagus and Esophagogastric Junction for the 8th Edition AJCC/UICC Staging Manuals. *Dis Esophagus* (2016) 29(8):897–905. doi: 10.1111/dote.12533
27. Kataoka K, Nakamura K, Mizusawa J, Kato K, Eba J, Katayama H, et al. Surrogacy of Progression-Free Survival (PFS) for Overall Survival (OS) in Esophageal Cancer Trials With Preoperative Therapy: Literature-Based Meta-Analysis. *Eur J Surg Oncol* (2017) 43(10):1956–61. doi: 10.1016/j.ejso.2017.06.017
28. Dindo D, Demartines N, Clavien PA. Classification of Surgical Complications: A New Proposal With Evaluation in a Cohort of 6336 Patients and Results of a Survey. *Ann Surg* (2004) 240(2):205–13. doi: 10.1097/01.sla.0000133083.54934.ae
29. Fearon K, Strasser F, Anker SD, Bosaeus I, Bruera E, Fainsinger RL, et al. Definition and Classification of Cancer Cachexia: An International Consensus. *Lancet Oncol* (2011) 12(5):489–95. doi: 10.1016/S1470-2045(10)70218-7
30. Anandavadivelan P, Lagergren P. Cachexia in Patients With Oesophageal Cancer. *Nat Rev Clin Oncol* (2016) 13(3):185–98. doi: 10.1038/nrclinonc.2015.200
31. Mantovani A, Allavena P, Sica A, Balkwill F. Cancer-Related Inflammation. *Nature* (2008) 454(7203):436–44. doi: 10.1038/nature07205
32. Namikawa T, Ishida N, Tsuda S, Fujisawa K, Munekage E, Iwabu J, et al. Prognostic Significance of Serum Alkaline Phosphatase and Lactate Dehydrogenase Levels in Patients With Unresectable Advanced Gastric Cancer. *Gastric Cancer* (2019) 22(4):684–91. doi: 10.1007/s10120-018-0897-8

Conflict of Interest: The authors declare that the research was conducted in the absence of any commercial or financial relationships that could be construed as a potential conflict of interest.

Publisher's Note: All claims expressed in this article are solely those of the authors and do not necessarily represent those of their affiliated organizations, or those of the publisher, the editors and the reviewers. Any product that may be evaluated in this article, or claim that may be made by its manufacturer, is not guaranteed or endorsed by the publisher.

Copyright © 2021 Zhu, Chen, Li, Zhang, Li, Wang, Zhou and Wen. This is an open-access article distributed under the terms of the Creative Commons Attribution License (CC BY). The use, distribution or reproduction in other forums is permitted, provided the original author(s) and the copyright owner(s) are credited and that the original publication in this journal is cited, in accordance with accepted academic practice. No use, distribution or reproduction is permitted which does not comply with these terms.

frontiers in Surgery

ORIGINAL RESEARCH
published: 03 November 2021
doi: 10.3389/fsurg.2021.745220

Predicting Survival of Patients With Rectal Neuroendocrine Tumors Using Machine Learning: A SEER-Based Population Study

Xiaoyun Cheng[1,2], *Jinzhang Li*[3], *Tianming Xu*[1,2], *Kemin Li*[1,2] *and Jingnan Li*[1,2]*

[1] *Department of Gastroenterology, Peking Union Medical College Hospital, Chinese Academy of Medical Sciences and Peking Union Medical College, Beijing, China,* [2] *Key Laboratory of Gut Microbiota Translational Medicine Research, Peking Union Medical College Hospital, Chinese Academy of Medical Sciences and Peking Union Medical College, Beijing, China,* [3] *Department of Physiology and Pathophysiology, School of Basic Medical Sciences, Capital Medical University, Beijing, China*

Background: The number of patients diagnosed with rectal neuroendocrine tumors (R-NETs) is increasing year by year. An integrated survival predictive model is required to predict the prognosis of R-NETs. The present study is aimed at exploring epidemiological characteristics of R-NETs based on a retrospective study from the Surveillance, Epidemiology, and End Results (SEER) database and predicting survival of R-NETs with machine learning.

Methods: Data of patients with R-NETs were extracted from the SEER database (2000–2017), and data were also retrospectively collected from a single medical center in China. The main outcome measure was the 5-year survival status. Risk factors affecting survival were analyzed by Cox regression analysis, and six common machine learning algorithms were chosen to build the predictive models. Data from the SEER database were divided into a training set and an internal validation set according to the year 2010 as a time point. Data from China were chosen as an external validation set. The best machine learning predictive model was compared with the American Joint Committee on Cancer (AJCC) seventh staging system to evaluate its predictive performance in the internal validation dataset and external validation dataset.

Results: A total of 10,580 patients from the SEER database and 68 patients from a single medical center were included in the analysis. Age, gender, race, histologic type, tumor size, tumor number, summary stage, and surgical treatment were risk factors affecting survival status. After the adjustment of parameters and algorithms comparison, the predictive model using the eXtreme Gradient Boosting (XGBoost) algorithm had the best predictive performance in the training set [area under the curve (AUC) = 0.87, 95%CI: 0.86–0.88]. In the internal validation, the predictive ability of XGBoost was better than that of the AJCC seventh staging system (AUC: 0.90 vs. 0.78). In the external validation, the XGBoost predictive

OPEN ACCESS

Edited by:
Qi Liu,
Fudan University, China

Reviewed by:
Ilze Strumfa,
Riga Stradinš University, Latvia
Andrea Botticelli,
Sapienza University of Rome, Italy

***Correspondence:**
Jingnan Li
pumcjnl@126.com

Specialty section:
This article was submitted to Surgical Oncology, a section of the journal Frontiers in Surgery

Received: *26 July 2021*
Accepted: *04 October 2021*
Published: *03 November 2021*

Citation:
Cheng X, Li J, Xu T, Li K and Li J (2021) Predicting Survival of Patients With Rectal Neuroendocrine Tumors Using Machine Learning: A SEER-Based Population Study. Front. Surg. 8:745220. doi: 10.3389/fsurg.2021.745220

model (AUC = 0.89) performed better than the AJCC seventh staging system (AUC = 0.83).

Conclusions: The XGBoost algorithm had better predictive power than the AJCC seventh staging system, which had a potential value of the clinical application.

Keywords: rectal neuroendocrine tumors, machine learning, predictive model, SEER database, rectal cancer

INTRODUCTION

Gastroenteropancreatic neuroendocrine tumors (GEP-NETs) are heterogeneous malignancies that originate from gastrointestinal peptidergic neurons and neuroendocrine cells. The rectum is one of the most common primary sites of GEP-NETs. As mass screening for gastrointestinal cancer has become more widespread and endoscopy has advanced, the number of patients diagnosed with rectal neuroendocrine tumors (R-NETs) is increasing year by year. In the United States, the Surveillance, Epidemiology, and End Results (SEER) registry database show that the incidence of R-NETs increased from 0.2 per 100,000 in 1973 to 0.86 per 100,000 in 2004 (1). Although the 5-year survival is high overall (range, 83%−94%), patients with nodal disease and distant metastases have a poor prognosis and high rates of mortality (2). Early study based on the SEER estimated the 5-year survival of localized, regional, and distant metastatic R-NETs were 90, 62, and 24%, respectively (3). Therefore, effective models to predict the prognosis of R-NETs are required.

Tumor–node–metastasis (TNM) staging system proposed by the American Joint Committee on Cancer (AJCC) and the European Neuroendocrine Tumor Society (ENETS) and pathology classification proposed by the World Health Organization have been considered as prognostic systems of R-NETs. However, these systems mainly include tumor size, organ invasion, mitotic count, and Ki-67 as predictors (1, 4, 5). Many other factors, such as age, sex, tumor numbers, or treatment, are not involved. Previous studies are heterogeneous when the respective roles of staging and grading are compared (6), so an integrated survival predictive model composed of various clinicopathological characteristics is immediately needed.

Recently, the use of artificial intelligence for medicine has drawn much attention, especially in model data. In artificial intelligence, machine learning can help analyze implicit useful information from a large number of data and reveal the relationship between data. Multiple machine learning algorithms could be used in building predictive models.

The present study is aimed at exploring epidemiological characteristics of R-NETs based on a retrospective study from the SEER database and predicting the survival of R-NETs with machine learning algorithms.

MATERIALS AND METHODS

Participants

For this research, data of patients with R-NETs were extracted from the SEER database (2000–2017), using the SEER* Stat software version 8.3.6.1. The primary site code (C20.9, rectum, NOS) and the following International Classification of Diseases for Oncology, Third Edition (ICD-O-3), histology codes were used to identify cases with R-NETs: 8240 (Carcinoid tumor), 8246 (Neuroendocrine carcinoma), and 8249 (Atypical carcinoid tumor). We included cases with cancer diagnosed microscopically and excluded cases with cancer diagnosed solely by autopsy or death certificate.

Data including age at diagnosis, sex, race, grade, tumor size, survival months, distant metastasis, surgery type, AJCC seventh stage, death status were retrieved from the SEER database. The main outcome measure was overall survival. In addition, we collected data of patients with R-NETs in Peking Union Medical College Hospital from January 2012 to January 2016. The same encoding was adopted as the SEER database to validate the predictive model. Patients with missing data were excluded. Since the predictive model needed to classify the data, we chose the 5-year survival status as the target of the predictive model. The patients included in the study were who died during the 5-year follow-up and survived for >5-year follow-up period. Because the follow-up period was not long enough to obtain an accurate 5-year survival status, we excluded patients who survived for <5-year follow-up period.

Data Preprocessing

In this study, data were preprocessed according to the characteristics of the SEER database. For the text record, we used label encode to convert it into numerical values to facilitate data processing by machine learning algorithms. For unordered categorical variables with three or more categories, we used one hot encode to convert them into multiple binary categorical variables, so the data could be used more effectively.

For the sake of interpretability, we simplified partial data. The primary site surgery was simplified to tumor destruction, tumor resection, no surgery, and an unknown type of surgery. In addition, the data of tumor size were simplified to tumor size larger than 1 cm or not. For the missing data in the database, we calculated the Euclidean distance between each case and used the mean values of the five closest cases to estimate and fill in the missing values. This method is called the k-Nearest Neighbors approach (7).

For most machine learning algorithms, when variables range from 0 to 1, the optimum conditions are obtained. Data were scaled to the range from 0 to 1 at the preprocessing stage to boost the efficiency of machine learning algorithms.

Establishment of Predictive Model

We used Python's scikit-learn 0.24.1 package to construct a machine learning predictive model (8). The scikit-learn

0.24.1 package is widely used because it includes common machine learning algorithms. In this study, we selected six common machine learning algorithms to build predictive models. Among the support vector machine algorithms, we chose the C-Support Vector Classification (SVC) and Nu-SVC with the radial basis function kernel. Among the ensemble-based algorithms, we chose the random forest (RF) algorithm, AdaBoost algorithm, and eXtreme Gradient Boosting (XGBoost) algorithm. The Naive Bayes (NB) algorithm is also considered to have a good predictive ability, so we also chose it to build a predictive model. For comparison, we chose the AJCC seventh staging system as a representative of clinically used predictive models.

Feature Selection

First, we used all the demographic characteristics, tumor grade, tumor size, tumor metastasis, and other descriptive information obtained from the SEER database as the features to optimize the predictive power of the machine learning models. We used the machine learning algorithms described above to establish preliminary predictive models under default conditions and used Shapley additive explanations (SHAP) to assess the importance of each feature. SHAP is a method of interpreting machine learning predictive models. It can analyze the impact of each feature of each patient on the predictive results (9). Integrating the SHAP results of all preliminary predictive models, features that are considered important in all preliminary predictive models are used as the final features of the machine learning model.

Ten-Fold Cross-Validation

Ten-fold cross-validation is a commonly used method to evaluate predictive capacity in the process of constructing machine learning predictive models. Due to the characteristics of machine learning algorithms, the data used in the training process cannot be used to test the trained predictive model again. Therefore, when we evaluated machine learning predictive models, the data from the SEER database were divided into training data and test data. In the 10-fold cross-validation process, we equally divided the data into 10 sets, from where one set was selected as training data and the remaining 9 were testing data. The training data were used to train machine learning predictive models, and then the testing data were used to calculate the receiver operating characteristic (ROC) curve and area under the curve (AUC) of the predictive model. The results obtained with 10 repetitions and the average ROC curve over the generated 10 different ROC curves were employed to assess the performance of the predictive model.

Parameter Adjustment

The parameter settings of the machine learning algorithms will affect the predictive ability of the predictive model and each machine learning classifier has different parameter settings. In the present study, we used the grid-search algorithm to determine the optimal parameters for each machine learning algorithm.

We used the potential range of optimal parameters to establish the predictive model one by one and used 10-fold cross-validation to compare the predictive ability of the predictive model relying on parameter combinations. Then we selected

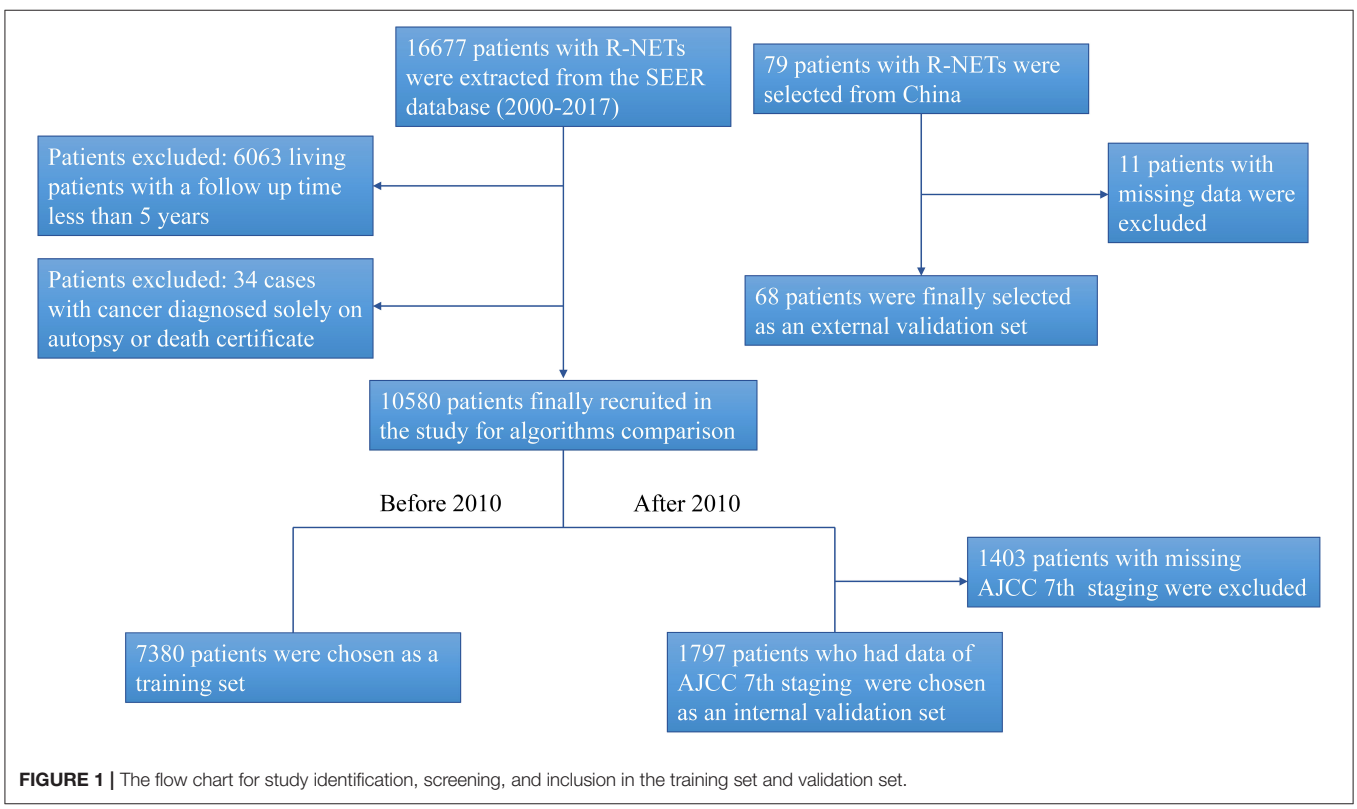

FIGURE 1 | The flow chart for study identification, screening, and inclusion in the training set and validation set.

TABLE 1 | Main characteristics of the patients.

Variable	Overall	Survived for more than 5-year follow-up	Died during the 5-year follow-up	*P*-value
Age (years)	56.3 ± 11.9	55.1 ± 11.2	64.5 ± 13.0	<0.001
Gender (%)				<0.001
Male	5,267 (49.8%)	4,418 (48.1%)	849 (60.8%)	
Female	5,313 (50.2%)	4,765 (51.9%)	548 (39.2%)	
Race (%)				<0.001
White	6,099 (57.6%)	5,280 (57.5%)	819 (58.6%)	
Black	2,516 (23.8%)	2,111 (23.0%)	405 (29.0%)	
Others	1,537 (14.5%)	1,369 (14.9%)	168 (12.0%)	
NA	428 (4.0%)	423 (4.6%)	5 (0.4%)	
Histology type (%)				<0.001
Carcinoid tumor	9,560 (90.4%)	8,677 (94.5%)	883 (63.2%)	
Neuroendocrine carcinoma	1,004 (9.5%)	503 (5.5%)	501 (35.9%)	
Atypical carcinoid tumor	16 (0.2%)	3 (0.0%)	13 (0.9%)	
Surgical treatment (%)				<0.001
No surgery	2,106 (19.9%)	1,573 (17.1%)	533 (38.2%)	
Tumor destruction	34 (0.3%)	30 (0.3%)	4 (0.3%)	
Tumor resection	8,306 (78.5%)	7,467 (81.3%)	839 (60.1%)	
Surgery, unknown type	25 (0.2%)	19 (0.2%)	6 (0.4%)	
NA	109 (1.0%)	94 (1.0%)	15 (1.1%)	
Tumor size (cm)				<0.001
<1	3,119 (29.5%)	2,889 (31.5%)	230 (16.5%)	
1–2	645 (6.1%)	539 (5.9%)	106 (7.6%)	
>2	477 (4.5%)	198 (2.2%)	279 (20.0%)	
NA	6,339 (59.9%)	5,557 (60.5%)	782 (56.0%)	
Tumor numbers	1.00 (1.00–1.00)	1.00 (1.00–1.00)	1.00 (1.00–2.00)	<0.001
Regional lymph nodes invasion (%)				<0.001
Negative	10,079 (95.3%)	8,835 (96.2%)	1,244 (89.0%)	
Positive	193 (1.8%)	88 (1.0%)	105 (7.5%)	
NA	308 (2.9%)	260 (2.8%)	48 (3.4%)	
Grade (%)				<0.001
Well differentiated	1,783 (16.9%)	1,559 (17.0%)	224 (16.0%)	
Moderately differentiated	354 (3.3%)	287 (3.1%)	67 (4.8%)	
Poorly differentiated	266 (2.5%)	36 (0.4%)	230 (16.5%)	
Undifferentiated	111 (1.0%)	12 (0.1%)	99 (7.1%)	
NA	8,066 (76.2%)	7,289 (79.4%)	777 (55.6%)	
TNM staging (%)				<0.001
I	1,417 (13.4%)	1,271 (13.8%)	146 (10.5%)	
II	128 (1.2%)	99 (1.1%)	29 (2.1%)	
III	67 (0.6%)	27 (0.3%)	40 (2.9%)	
IV	185 (1.7%)	16 (0.2%)	169 (12.1%)	
NA	8,783 (83.0%)	7,770 (84.6%)	1,013 (72.5%)	
Summary staging (%)				<0.001
In situ	39 (0.4%)	37 (0.4%)	2 (0.1%)	
Localized	8,648 (81.7%)	7,897 (86.0%)	751 (53.8%)	
Regional	205 (1.9%)	97 (1.1%)	108 (7.7%)	
Distant	447 (4.2%)	59 (0.6%)	388 (27.8%)	
NA	1,241 (11.7%)	1,093 (11.9%)	148 (10.6%)	
Total	10,580	9,183	1,397	

NA refers to the count of missing values.

parameter combinations with the best predictive capacity. This process is called the grid-search algorithm. By changing the ranges of parameters, the best parameter combination of the machine learning algorithm was finally obtained.

Evaluation of Predictive Models

The predictive power built by six machine learning algorithms was assessed by a 10-fold cross-validation procedure. For comparisons based on the ROC curves and the AUC, we selected the predictive model with the best predictive power as the representative of the machine learning predictive model. To compare with traditional predictive models, we used the AJCC seventh staging system as the representative of traditional predictive models. The data from the SEER database for the period 2000–2009 were used as the training set, and the data from the SEER database for the period 2010–2017 were used as the internal validation set. In the internal validation set, we also deleted patients with missing AJCC staging. External validation with a cohort from Peking Union Medical College Hospital was performed. The training set was used to train the machine learning predictive model. We calculated the ROC curve and the AUC of predictive models using the internal validation set and the external validation set for internal and external validation. We compared the best machine learning predictive model with the AJCC seventh staging system to evaluate their predictive performance. In addition, we used the parametric approach based on Platt's logistic model to calibrate model-predicted probabilities and calculated the Brier score to evaluate the calibration performance of the predictive model.

Statistical Analysis

R 4.0.4 was used for data description and statistical analysis. According to whether continuous variables satisfied the normal distribution, data expressed as mean ± standard deviation or median, first, and third quartiles. We used Student's *t*-test or the Mann–Whitney *U* test for statistical analysis. Categorical variables were expressed by frequency (*n*) and percentage (%).

TABLE 2 | Multivariable Cox regression results.

Characteristics	B	*P* value	HR value	HR 95%CI
Female	0.359	<0.001	0.699	0.643–0.760
Race—White		<0.001		
Black	0.371	<0.001	1.449	1.320–1.592
Other	0.180	0.006	0.835	0.733–0.950
NA	1.787	<0.001	0.167	0.087–0.323
Histologic type—carcinoid tumor		<0.001		
Neuroendocrine carcinoma	0.482	<0.001	1.619	1.378–1.901
Atypical carcinoid tumor	1.334	<0.001	3.796	2.168–6.645
Grade—well differentiated		<0.001		
Moderately differentiated	0.106	0.378	1.112	0.879–1.406
Poorly differentiated	0.798	<0.001	2.221	1.802–2.738
Undifferentiated	0.800	<0.001	2.225	1.714–2.888
NA	0.059	0.383	0.942	0.825–1.077
Summary stage—*In situ*		<0.001		
Localized	0.089	0.828	1.093	0.490–2.438
Regional	1.153	0.006	3.169	1.386–7.246
Distant	2.109	<0.001	8.241	3.641–18.655
NA	0.073	0.861	1.075	0.477–2.423
Surgical approach—no surgery		<0.001		
Tumor destruction	0.333	0.326	0.717	0.369–1.393
Unknown type	0.309	<0.001	0.734	0.661–0.815
Tumor resection	0.142	0.674	1.153	0.594–2.237
NA	0.048	0.820	0.954	0.633–1.436
Tumor size <1 cm		0.022		
1–2 cm	0.250	0.009	1.284	1.066–1.546
>2 cm	0.249	0.011	1.283	1.059–1.554
NA	0.104	0.084	1.110	0.986–1.248
Tumor numbers	0.358	<0.001	1.431	1.359–1.507
Age	0.058	<0.001	1.060	1.056–1.064

NA refers to the count of missing values.
HR, hazard rate.

We conducted Chi-square test or Fisher's exact test for statistical analysis. Net reclassification index (NRI) was deployed to compare the performance improvement of the predictive model. *P*-value of <0.05 was considered statistically significant, and all *P* values were two sided.

RESULTS

Patient Characteristics

A total of 16,677 patients with R-NETs were extracted from the SEER database and a total of 79 patients with R-NETs were collected from Peking Union Medical College Hospital according to the inclusion criteria. Based on the exclusion criteria, a total of 10,580 patients from the SEER database and 68 patients from Peking Union Medical College Hospital were finally included in the analysis (**Figure 1**). Basic characteristics of patients from the SEER database were summarized in **Table 1**, the median age of the study group was 56.3 years old and 49.8% were male. Many baseline characteristics were significantly different between the patients who survived for more than 5-years of the follow-up period and patients who died during the 5-year follow-up period.

TABLE 3 | Features used in machine learning predictive models.

General information	
	Age (years)
	Gender
	Race
	Rural or urban
Tumor information	
	Histologic type
	Grade
	Summary stage
	Surgical approach
	Tumor size (mm)
	Metastasis (Bone, Liver, Brain)
	Farthest extension of tumors (mm)
	Tumor numbers

Survival Factors Associated With the Prognosis With R-NETs

In the cohort of SEER database patients, multivariable Cox regression analysis showed that age, gender, race, histologic type, tumor size, tumor number, summary stage, and surgical treatment were independent prognostic factors for the 5-year survival status (**Table 2**). It was found that older age, increased tumor grade, larger tumor size, more tumor numbers, and advanced staging could significantly decrease the 5-year survival. Also, histologic type of atypical carcinoid tumor was associated with a worse survival outcome than the histologic type of carcinoid tumor and neuroendocrine carcinoma. The female gender was a protective factor for the 5-year survival status.

Feature Analysis

In the cohort of SEER database patients, we evaluated all machine learning predictive models using the SHAP method, and finally, we selected 12 features that were considered important features in all machine learning predictive models (**Table 3**). The SHAP summary plot of the predictive model ordered 12 features based on their impact on the 5-year survival status in **Figure 2**. The higher SHAP value of a feature indicates the greater possibility of a 5-year survival. The color of the dot represents a large or small feature value. Red indicates that the feature value is large, purple indicates that the feature value is close to the overall average, and blue indicates that the feature value is small. Take age as an

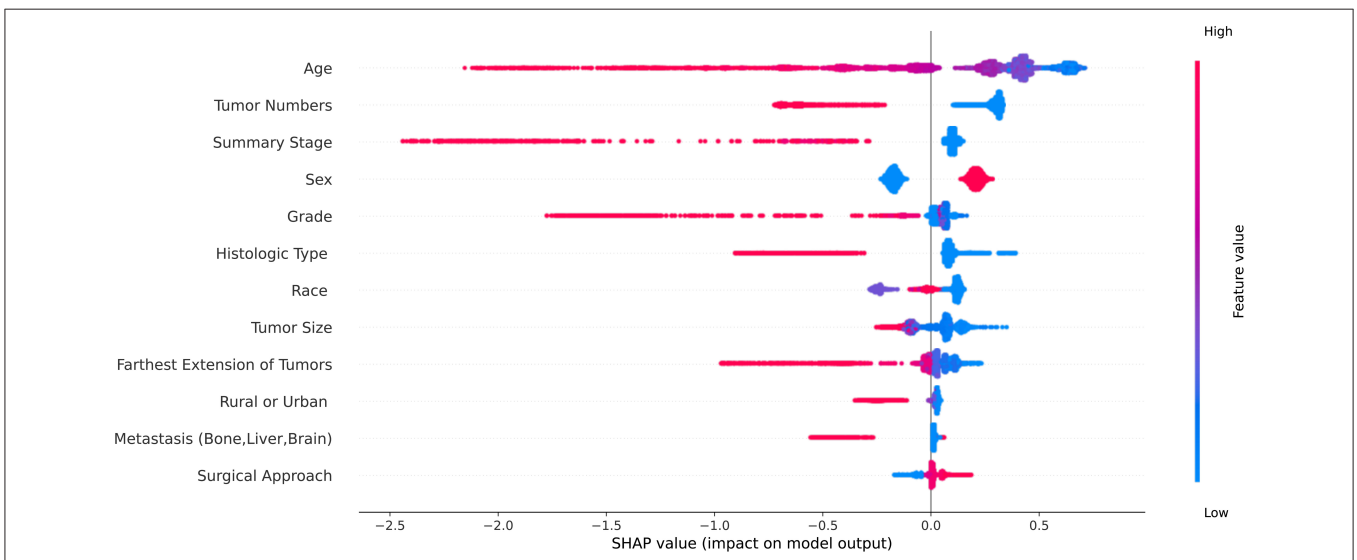

FIGURE 2 | The Shapley additive explanations summary plot of the predictive model ordered 12 features based on their impact on the 5-year survival status. The red dot represents the high value of the feature and the blue dot represents the low value of the feature.

example, we found that older age was associated with the lower likelihood of 5-year survival.

Model Evaluation

The SEER database started recording the seventh edition of the AJCC staging system for R-NETs in 2010. To further evaluate the predictive performance of the AJCC seventh staging system and the machine learning predictive model, we chose patients from the SEER database during the 2000–2009 period as the training set, involving a total of 7,380 patients. Based on the data from 2010 to 2017, we excluded patients without the AJCC seventh staging. Finally, a total of 1,797 patients were selected in the internal validation set (**Figure 1**).

Clinical characteristics of the training set and internal validation set were summarized in **Table 4**. First, we used the training set to establish and train machine learning models. After parameters adjustment and algorithms comparison, the AUC values of six machine learning models were higher than 0.78, thereby demonstrating a good predictive ability of predictive models (**Figure 3**). As described in **Table 4**, the AUC of SVC was 0.80 (95%CI: 0.78–0.82), the AUC of Nu-SVC was 0.79 (95%CI: 0.78–0.81), the AUC of RF was 0.85 (95%CI: 0.83–0.86), the AUC of Ada Boost was 0.84 (95%CI: 0.83–0.85), the AUC of NB was 0.78 (95%CI: 0.76–0.80), and the AUC of XGBoost was 0.87 (95%CI: 0.86–0.88). Among them, the predictive model using the XGBoost algorithm had the best predictive performance. Subsequently, we compared the XGBoost model and the AJCC seventh staging system for predicting the 5-year survival status in R-NETs.

Internal Validation

We analyzed the predictive performance of the machine learning predictive model and the AJCC seventh staging system in the internal validation set. We calibrated the machine learning model using the parametric approach based on Platt's logistic model, the Brier score obtained from the machine learning predictive model was 0.084, indicating good calibration and discriminative ability. The ROC curve of machine learning predictive models (AUC = 0.90, 95% CI: 0.89–0.92) was better than the ROC curve of AJCC seventh staging system (AUC = 0.78, 95% CI: 0.76–0.80). The sensitivity of machine learning models was not inferior to the traditional AJCC staging system, and a high specificity was also observed (**Figure 4**; **Table 5**). Compared with the AJCC seventh staging system, more patients were correctly classified by machine learning predictive models (NRI = 0.151, 95%CI: 0.103–0.199, $P<0.001$).

External Validation

To evaluate the performance of machine learning predictive models, we collected data of 68 patients with R-NETs from Peking Union Medical College Hospital as the external validation set. The basic characteristics of 68 patients are summarized in **Table 6**. In external validation, the machine learning predictive model had a better degree of calibration and its Brier score is 0.080. Although the number of data was relatively small, the ROC curve of the machine learning predictive model (AUC = 0.89, 95%CI: 0.77–1.00) was still superior to the ROC curve of

TABLE 4 | Main characteristics of training set and internal validation set.

Variable	Training set	Internal validation set	*P* value
Age (years)	56.1 ± 12.0	56.6 ± 11.8	0.107
Gender (%)			0.969
Male	3,663 (49.6%)	891 (49.6%)	
Female	3,717 (50.4%)	906 (50.4%)	
Race (%)			0.001
White	4,381 (59.4%)	1,001 (55.7%)	
Black	1,688 (22.9%)	442 (24.6%)	
Others	1,043 (14.1%)	305 (17.0%)	
NA	268 (3.6%)	49 (2.7%)	
Histology type (%)			<0.001
Carcinoid tumor	6,964 (94.4%)	1,391 (77.4%)	
Neuroendocrine carcinoma	409 (5.5%)	402 (22.4%)	
Atypical carcinoid tumor	7 (0.1%)	4 (0.2%)	
Surgical treatment (%)			<0.001
No surgery	1,385 (18.8%)	262 (14.6%)	
Tumor destruction	29 (0.4%)	2 (0.1%)	
Tumor resection	5,885 (79.7%)	1,522 (84.7%)	
Surgery, unknown type	17 (0.2%)	5 (0.3%)	
NA	64 (0.9%)	6 (0.3%)	
Tumor size (cm)			<0.001
<1	1,754 (23.8%)	1,251 (69.6%)	
1∼2	388 (5.3%)	227 (12.6%)	
>2	215 (2.9%)	218 (12.1%)	
NA	5,023 (68.1%)	101 (5.6%)	
Tumor numbers	1.00 (1.00–1.00)	1.00 (1.00–1.00)	0.135
Regional lymph nodes invasion (%)			<0.001
Negative	7,051 (95.5%)	1,726 (96.0%)	
Positive	130 (1.8%)	60 (3.3%)	
NA	199 (2.7%)	11 (0.6%)	
Grade (%)			<0.001
Well differentiated	720 (9.8%)	667 (37.1%)	
Moderately differentiated	164 (2.2%)	120 (6.7%)	
Poorly differentiated	125 (1.7%)	108 (6.0%)	
Undifferentiated	48 (0.7%)	47 (2.6%)	
NA	6,323 (85.7%)	855 (47.6%)	
TNM staging (%)			–
I	0 (0.0%)	1,417 (78.9%)	
II	0 (0.0%)	128 (7.1%)	
III	0 (0.0%)	67 (3.7%)	
IV	0 (0.0%)	185 (10.3%)	
NA	7,380 (100.0%)	0 (0.0%)	
Summary staging (%)			<0.001
In situ	30 (0.4%)	0 (0.0%)	
Localized	6,130 (83.1%)	1,543 (85.9%)	
Regional	125 (1.7%)	66 (3.7%)	
Distant	223 (3.0%)	188 (10.5%)	
NA	872 (11.8%)	0 (0.0%)	
5–Year survival	6,618 (89.7%)	1,413 (78.6%)	<0.001
Total	7,380	1,797	

NA refers to the count of missing values.

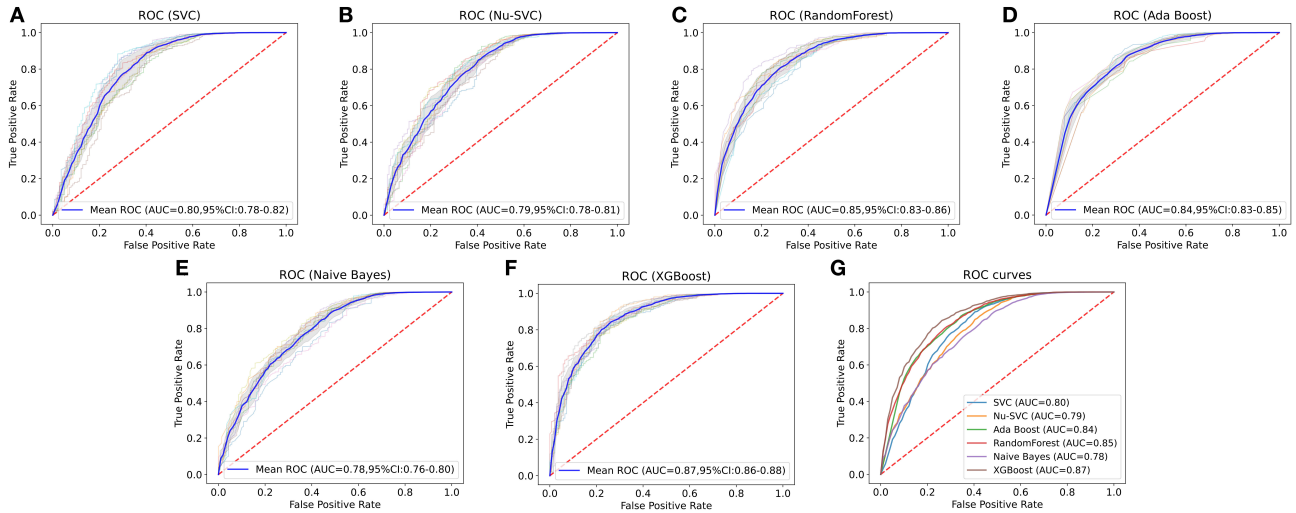

FIGURE 3 | Comparison of the AUCs of six machine learning algorithms. The predictive model using the eXtreme Gradient Boosting (XGBoost) algorithm had the best predictive performance. SVC, C-Support Vector Classification; RF, random forest; NB, Naive Bayes.

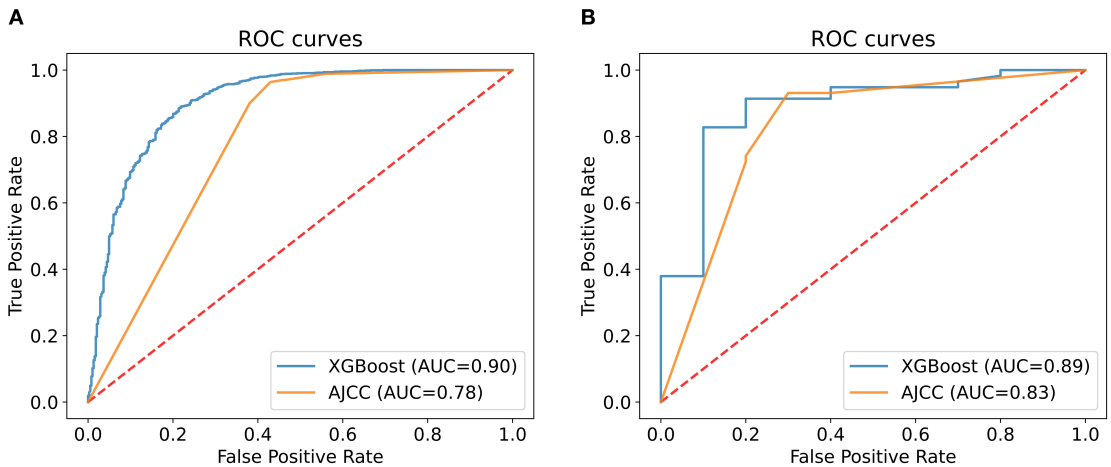

FIGURE 4 | Comparison of the XGBoost model and the AJCC seventh staging system. The area under the curve (AUC) of the XGBoost model to predict 5-year survival status was larger than that of the AJCC seventh staging system in both internal **(A)** and external validation **(B)**.

AJCC seventh staging system (AUC = 0.83, 95% CI: 0.66–0.99) (**Figure 4**; **Table 5**). In addition, more patients were correctly classified by the machine learning predictive model (NRI = 0.190, 95%CI: 0.089–0.291, $P < 0.001$).

DISCUSSION

In this study, we constructed prognostic models through six common machine learning algorithms based on clinical features. To our knowledge, this is the first study to use machine learning algorithms predicting the survival status of patients with R-NETs. As the result showed, these models had a good predictive ability based on a large number of patient data from the SEER database. Our study proved that machine learning predictive models performed better than the AJCC staging system. In both internal validation and external validation, the XGBoost model performed best among all the models overall.

Machine learning can discern patterns from large datasets. Identified patterns are then used to encode a mathematical model, which applies to new data for further validation (10). Applications of machine learning in medicine are being used in disease diagnosis, prognosis, therapy development, and treatment assessment. As the number of data grows, machine learning algorithms will develop more accurate predictive power. Because NETs are relatively rare tumors, only a few machine learning applications studies have focused on NETs. Most research studies have focused on disease diagnosis, such as imaging parameters (11), pathological manifestations (12), or biomarker analysis (13). The SEER registry database effectively compensates for the deficiencies in the clinical data in traditional

TABLE 5 | Performance of machine learning predictive models and the AJCC seventh staging system.

Predictive models	AUC	95% CI of AUC
Machine learning predictive models		
SVC	0.80	0.78–0.82
Nu–SVC	0.79	0.78–0.81
Random Forest	0.85	0.83–0.86
Ada Boost	0.84	0.83–0.85
Naïve Bayes	0.78	0.76–0.80
XGBoost	0.87	0.86–0.88
Internal validation		
Machine Learning (XGBoost)	0.90	0.89–0.92
AJCC seventh staging system	0.78	0.76–0.80
External validation		
Machine Learning (XGBoost)	0.89	0.77–1.00
AJCC seventh staging system	0.83	0.66–0.99

AJCC, American Joint Committee on Cancer; AUC, area under the curve; SVC, support vector classification; XGBoost, eXtreme gradient boosting.

research centers. Using the SEER database from 1973 to 2014, research has found that the models developed with classic machine learning algorithms performed well in survival prediction of pancreas neuroendocrine tumors (14). At present, there is no relevant literature report about machine learning prognostic models of patients with R-NETs.

A gradual increase of patients with R-NETs has highlighted the need for a more comprehensive and refined system for disease prognosis. To date, a variety of prognostic predictive systems have been established. In 2008, a study developed a new TNM staging system through data from the SEER database. Primary tumor size, depth of invasion, lymph node involvement, and distant metastasis were related to the prognosis of R-NETs (15). Fields et al. indicated that the number of positive locoregional lymph nodes was an independent factor to estimate survival of R-NETs (16). In another recent study by Capurso and colleagues, the prognostic role of the ENETs staging and grading systems was evaluated in rectal neuroendocrine neoplasms. They reported that the presence of metastatic disease at diagnosis and the proliferative index was associated with overall and progression-free survival (6). Feng and collaborators developed a nomogram predicting the overall survival of R-NETs. They found that age, sex, tumor size, and TNM stage were independently correlated with prognosis (17). Apart from these, we found out that tumor numbers, race, and surgical approach also influenced prognosis.

Prognostic risk models based on a single anatomical stage or pathological grade have some limitations. They mainly relate to the depth of tumor invasion, tumor size, involvement of lymph nodes, the presence of metastatic disease, and the Ki-67 index. The machine learning model based on multiple factors is expected to be a more effective tool in predicting the prognosis. Machine learning can process a large number of data in a short time, and it has certain advantages in comparison with the traditional methods. Currently, logistic regression is the

TABLE 6 | Main characteristics of SEER database and China database.

Variable	SEER database	China database	*P*-value
Age (years)	56.3 ± 11.9	49.3 ± 11.9	<0.001
Gender (%)			0.447
Male	5,267 (49.8%)	37 (54.4%)	
Female	5,313 (50.2%)	31 (45.6%)	
Race (%)			<0.001
White	6,099 (57.6%)	0 (0.0%)	
Black	2,516 (23.8%)	0 (0.0%)	
Others	1,537 (14.5%)	68 (100.0%)	
NA	428 (4.0%)	0 (0.0%)	
Histology type (%)			0.329
Carcinoid tumor	9,560 (90.4%)	58 (85.3%)	
Neuroendocrine carcinoma	1,004 (9.5%)	10 (14.7%)	
Atypical carcinoid tumor	16 (0.2%)	0 (0.0%)	
Surgical treatment (%)			0.086
No surgery	2,106 (19.9%)	5 (7.4%)	
Tumor destruction	34 (0.3%)	0 (0.0%)	
Surgery, unknown type	8,306 (78.5%)	63 (92.6%)	
Tumor resection	25 (0.2%)	0 (0.0%)	
NA	109 (1.0%)	0 (0.0%)	
Tumor size (cm)			<0.001
<1	3,119 (29.5%)	37 (54.4%)	
1–2	645 (6.1%)	23 (33.8%)	
>2	477 (4.5%)	8 (11.8%)	
NA	6,339 (59.9%)	0 (0.0%)	
Tumor numbers	1.00 (1.00–1.00)	1.00 (1.00–1.00)	–
Regional lymph nodes invasion (%)			<0.001
Negative	10,079 (95.3%)	54 (79.4%)	
Positive	193 (1.8%)	14 (20.6%)	
NA	308 (2.9%)	0 (0.0%)	
Grade (%)			<0.001
Well differentiated	1,783 (16.9%)	50 (73.5%)	
Moderately differentiated	354 (3.3%)	16 (23.5%)	
Poorly differentiated	266 (2.5%)	2 (2.9%)	
Undifferentiated	111 (1.0%)	0 (0.0%)	
NA	8,066 (76.2%)	0 (0.0%)	
TNM staging (%)			<0.001
I	1,417 (13.4%)	44 (64.7%)	
II	128 (1.2%)	1 (1.5%)	
III	67 (0.6%)	13 (19.1%)	
IV	185 (1.7%)	10 (14.7%)	
NA	8,783 (83.0%)	0 (0.0%)	
Summary staging (%)			<0.001
In situ	39 (0.4%)	6 (8.88%)	
Localized	8,648 (81.7%)	47 (69.1%)	
Regional	205 (1.9%)	4 (5.9%)	
Distant	447 (4.2%)	11 (16.2%)	
NA	1,241 (11.7%)	0 (0.0%)	
5-Year survival	9,183 (86.8%)	58 (85.3%)	0.715
Total	10,580	68	

NA refers to the count of missing values.

most frequently used traditional analytical statistical algorithm, which can determine risk predictive factors in the short term (18). However, clinical characteristics often have a non-linear relationship, which makes logistic regression sometimes fail to obtain the desired results. Machine learning can use algorithms and statistical models to identify data and learn from the data, which can handle non-linear data (19). Therefore, many researchers support the use of more advanced machine learning algorithms to build predictive models for big data analysis. In most studies, the performance of machine learning models is better than that of logistic regression.

The challenges of building machine learning models include multicollinearity, incorrect imputation, data leakage, neglecting feature scaling, and normalization, which will cause overfitting, loss of feature importance interpretability, and model instability. Using a clear validation set, feature importance analysis, and standard techniques provides efficient approaches for establishing prognostic models (20). As shown in **Table 1**, some information was missing in the database. We used the k-Nearest Neighbors approach to avoid incorrect imputation. During the validation process, we used the algorithm to automatically split the data into a training set and a validation set, thus ensuring a clean validation set.

The ultimate purpose of constructing predictive models is to facilitate clinical decision making. We built an accessible online application (https://gastrointestinal.github.io/NET/) based on the XGBoost algorithm for the convenience of clinical practice.

Despite its merits, this study has certain limitations. First, this was a retrospective study, so the potential for selective bias was inevitable. Second, because R-NETs were a rare disease in China, the sample size of external validation is relatively small. Although machine learning models showed good predictive performance with the currently small dataset, they require a larger scale study for external validation in the future. Third, we cannot analyze the appropriateness of medication due to the lack of detailed drug regimens in the SEER database. Finally, machine learning predictive models do not provide a predictive scoring system. This limits their applications in routine clinical practice. However, the online application we have established could be more conveniently combined with the electronic medical record system to help clinical decision making.

In summary, we explored and analyzed the demographic characteristics of patients with R-NETs and used machine learning algorithms to establish survival predictive models. The XGBoost algorithm had better predictive power than the AJCC staging system, which had a potential clinical application value.

DATA AVAILABILITY STATEMENT

The datasets presented in this study can be found in online repositories. The names of the repository/repositories and accession number(s) can be found below: Data of patients with R-NETs were extracted from the SEER database (2000–2017), using the SEER* Stat software version 8.3.6.1. (https://staging.seer.cancer.gov).

AUTHOR CONTRIBUTIONS

JingL: designed the study. KL,TX, and JinL: material preparation, data collection, and analysis. XC: wrote the manuscript. All authors commented on previous versions of the manuscript, read, and approved the final manuscript.

FUNDING

This study was supported by the National Natural Science Foundation of China (81770559) and the Chinese Academy of Medical Sciences (CAMS) Initiative for Innovative Medicine (CAMS-2016-I2M-1-007).

ACKNOWLEDGMENTS

The authors thank the SEER database for the detailed data.

REFERENCES

1. Caplin M, Sundin A, Nillson O, Baum RP, Klose KJ, Kelestimur F, et al. ENETS Consensus Guidelines for the management of patients with digestive neuroendocrine neoplasms: colorectal neuroendocrine neoplasms. *Neuroendocrinology.* (2012) 95:88–97. doi: 10.1159/000335594
2. McDermott FD, Heeney A, Courtney D, Mohan H, Winter D. Rectal carcinoids: a systematic review. *Surg Endosc.* (2014) 28:2020–6. doi: 10.1007/s00464-014-3430-0
3. Yao JC, Hassan M, Phan A, Dagohoy C, Leary C, Mares JE, et al. One hundred years after "carcinoid": epidemiology of and prognostic factors for neuroendocrine tumors in 35,825 cases in the United States. *J Clin Oncol.* (2008) 26:3063–72. doi: 10.1200/JCO.2007.15.4377
4. Amin MB, Edge SB. *AJCC Cancer Staging Manual*. New York, NY: Springer (2017).
5. Bosman FT, Carneiro F, Hruban RH, Theise ND. *WHO classification of tumours of the digestive system*. Geneva: World Health Organization (2010).
6. Capurso G, Gaujoux S, Pescatori LC, Panzuto F, Panis Y, Pilozzi E, et al. The ENETS TNM staging and grading system accurately predict prognosis in patients with rectal NENs. *Dig Liver Dis.* (2019) 51:1725–30. doi: 10.1016/j.dld.2019.07.011
7. Troyanskaya O, Cantor M, Sherlock G, Brown P, Hastie T, Tibshirani R, et al. Missing value estimation methods for DNA microarrays. *Bioinformatics.* (2001) 17:520–5. doi: 10.1093/bioinformatics/17.6.520
8. Pedregosa F, Varoquaux G, Gramfort A, Michel V, Thirion B, Grisel O, et al. Scikit-learn: machine learning in python. *J Mach Learn Res.* (2011) 12:2825–30.
9. Lundberg SM, Lee SI. A unified approach to interpreting model predictions. *Adv Neur In.* (2017) 17–30.
10. Scott IA. Demystifying machine learning—a primer for physicians. *Intern Med J.* (2021) 1–18. doi: 10.1111/imj.15200
11. Zhang T, Zhang Y, Liu X, Xu H, Chen C, Zhou X, et al. Application of radiomics analysis based on CT combined with machine learning in diagnostic of pancreatic neuroendocrine tumors patient's pathological grades. *Front Oncol.* (2020) 10:521831. doi: 10.3389/fonc.2020.521831
12. Govind D, Jen KY, Matsukuma K, Gao G, Olson KA, Gui D, et al. Improving the accuracy of gastrointestinal neuroendocrine tumor grading with deep learning. *Sci Rep.* (2020) 10:11064. doi: 10.1038/s41598-020-67880-z

13. Kjellman M, Knigge U, Welin S, Thiis-Evensen E, Gronbaek H, Schalin-Jantti C, et al. A plasma protein biomarker strategy for detection of small intestinal neuroendocrine tumors. *Neuroendocrinology.* (2020) 30:20. doi: 10.1159/000510483
14. Song Y, Gao S, Tan W, Qiu Z, Zhou H, Zhao Y. Multiple machine learnings revealed similar predictive accuracy for prognosis of PNETs from the surveillance, epidemiology, and end result database. *J Cancer.* (2018) 9:3971–8. doi: 10.7150/jca.26649
15. Landry CS, Brock G, Scoggins CR, McMasters KM, Martin RC. A proposed staging system for rectal carcinoid tumors based on an analysis of 4701 patients. *Surgery.* (2008) 144:460–6. doi: 10.1016/j.surg.2008.05.005
16. Fields AC, McCarty JC, Ma-Pak L, Lu P, Irani J, Goldberg JE, et al. New lymph node staging for rectal neuroendocrine tumors. *J Surg Oncol.* (2019) 119:156–62. doi: 10.1002/jso.25307
17. Feng X, Wei G, Wang W, Zhang Y, Zeng Y, Chen M, et al. Nomogram for individually predicting overall survival in rectal neuroendocrine tumours. *BMC Cancer.* (2020) 20:865. doi: 10.1186/s12885-020-07328-9
18. Collins GS, Reitsma JB, Altman DG, Moons KG. Transparent reporting of a multivariable prediction model for individual prognosis or diagnosis (TRIPOD): the TRIPOD statement. *Ann Intern Med.* (2015) 162:55–63. doi: 10.7326/M14-0697
19. Hamet P, Tremblay J. Artificial intelligence in medicine. *Metabolism.* (2017) 69S:S36–S40. doi: 10.1016/j.metabol.2017.01.011
20. Gilvary C, Madhukar N, Elkhader J, Elemento O. The missing pieces of artificial intelligence in medicine. *Trends Pharmacol Sci.* (2019) 40:555–64. doi: 10.1016/j.tips.2019.06.001

Conflict of Interest: The authors declare that the research was conducted in the absence of any commercial or financial relationships that could be construed as a potential conflict of interest.

Publisher's Note: All claims expressed in this article are solely those of the authors and do not necessarily represent those of their affiliated organizations, or those of the publisher, the editors and the reviewers. Any product that may be evaluated in this article, or claim that may be made by its manufacturer, is not guaranteed or endorsed by the publisher.

Copyright © 2021 Cheng, Li, Xu, Li and Li. This is an open-access article distributed under the terms of the Creative Commons Attribution License (CC BY). The use, distribution or reproduction in other forums is permitted, provided the original author(s) and the copyright owner(s) are credited and that the original publication in this journal is cited, in accordance with accepted academic practice. No use, distribution or reproduction is permitted which does not comply with these terms.

frontiers in Medicine

CASE REPORT
published: 08 November 2021
doi: 10.3389/fmed.2021.764233

Systemic Therapy for Microsatellite Instability Small Bowel Adenocarcinoma With Mesenteric Vascular Embolism as Initial Symptom: A Case Report

*Zhongyi Dong†, Xiang Xia and Zizhen Zhang**

Department of Gastrointestinal Surgery, Renji Hospital, School of Medicine, Shanghai Jiao Tong University, Shanghai, China

Background: Small bowel adenocarcinoma are relatively rare tumors of the digestive system. Due to the lack of specific screening methods, patients are often diagnosed at an advanced stage. At present, there is no specific surgical guidance and chemotherapy regimen for small bowel adenocarcinoma. Here, we report a rare small bowel adenocarcinoma case with mesenteric vascular embolization and microsatellite instability, in which palliative surgery combined with chemotherapy and anti-Programmed cell death protein 1(PD-1) therapy resulted in complete remission.

Case Presentation: The patient was a 55-year-old man who was admitted for suspected small bowel adenocarcinoma combined with incomplete ileus, mesenteric vascular occlusion and distant metastasis. We performed palliative surgery to remove adenocarcinoma as well as relieve obstruction. Then according to the pathological and immunohistochemical results (Stage IV and microsatellite instability), we used XELOX regimen combined with anti-PD-1 therapy. In last 2 years follow up, this patient achieved complete remission.

Conclusions: The possibility of small intestinal tumor should be considered in patients with mesenteric vascular obstruction. PD-1 blockade is an effective therapy for small bowel adenocarcinoma with microsatellite instability.

Keywords: case reports, intestinal cancers, immune checkpoint inhibitor, mesenteric vascular occlusion, palliative care

OPEN ACCESS

Edited by:
Qi Liu,
Fudan University, China

Reviewed by:
Firdaus Hayati,
Universiti Malaysia Sabah, Malaysia
Amitabh Kumar Upadhyay,
Tata Steel, India

***Correspondence:**
Zizhen Zhang
zhangzizhen@renji.com

†ORCID:
Zhongyi Dong
orcid.org/0000-0002-5586-2260

Specialty section:
This article was submitted to Gastroenterology, a section of the journal Frontiers in Medicine

Received: *25 August 2021*
Accepted: *19 October 2021*
Published: *08 November 2021*

Citation:
Dong Z, Xia X and Zhang Z (2021) Systemic Therapy for Microsatellite Instability Small Bowel Adenocarcinoma With Mesenteric Vascular Embolism as Initial Symptom: A Case Report. Front. Med. 8:764233. doi: 10.3389/fmed.2021.764233

INTRODUCTION

Although the small intestine occupies most of the length and surface area of the digestive tract, primary small intestine cancer is still a relatively rare tumor of the digestive system, which accounts for only about 3% of cancers occuring in this system (1). The most affected segment was duodenum, including 46–82% of the cases, followed by jejunum (11–31%) and ileum (7–21%) (2). But unlike other cancers of the digestive system, such as stomach and esophagus, the incidence of small intestinal malignancies has continued to rise over the past decade (3). Small bowel adenocarcinoma is estimated to be accounting for about 30–45% of the total cases, with a 5-year overall survival rate in

patients at stage IV of 42% (4). The advanced patients usually have a delayed clinical presentation and non-specific symptoms such as abdominal pain, nausea and gastrointestinal bleeding (2). Herein, we report a case of microsatellite-unstable (MSI-H) advanced small bowel adenocarcinoma with mesenteric vascular occlusion as the initial symptom which is quite unusual.

CASE PRESENTATION

Without apparent inducement, a 55-year-old male patient was admitted for upper-middle abdominal pain with acid reflux, fullness and weakness for 1 week. Contrast-enhanced Computed tomography (CT) of the abdomen showed a small bowel mass with multiple enlarged lymph nodes in the right middle abdomen. The superior and inferior mesenteric vein trunks and their major tributaries were nearly occluded at the level adjacent to the tumor [**Figures 1(A1–D1)**].

The patient had no previous noteworthy medical history. And the patient did not smoke or consume alcohol. There was no noteworthy family medical history, such as cancer or small intestinal diseases. The patient had been in good physical condition, and had a good spirit.

Physical examination revealed normal abdominal findings. The abdomen was soft and flat, with no gurgling, bloating or tenderness. All other vital signs were stable. Laboratory tests showed a decrease in neutrophil percentage (43.5%, Normal range: 50–70%), a decrease in hemoglobin (95 g/L, Normal range: 120–160 g/L), and an increase in platelet count (386 * 10^9L, Normal range: 100–300*10^9/L). Prothrombin time increased (14.30 s, Normal range: 11–13 s) and fibrinogen content increased (4.64 g/L, Normal range: 2–4 g/L). The special tumor markers of digestive system (Alpha-fetoprotein, Carbohydrate antigen199, Carcinoembryonic antigen, Carbohydrate antigen724) were in the normal range. In addition, on chest scan, scattered fibrous tissues and emphysema were found in both lungs.

The patient underwent a laparoscopic exploration and small bowel adenocarcinoma resection. The tumor was located in the small intestine 20 cm away from the ligament of Treitz. The size of the tumor was 6 * 5 * 5 cm. The tumor had invaded the serosa and caused incomplete obstruction. Meanwhile, multiple swollen lymph nodes could be found in the mesentery root and around the abdominal aorta, some of which has fused into a mass (**Figure 2**). Pathological specimens showed that this patient was grade II adenocarcinoma of the small intestine (7 * 4 * 1.3 cm), with the invasion of the serosa. Lymph nodes in the intestinal wall (1/1) showed metastasis and there were even three cancerous nodules. The upper and lower margins of the specimen were negative. Immunohistochemical results showed that cytokeratin CK7(−), cytokeratin CK20(+), Ki-67(70%), p53(+), MLH1(+), PMS2(+), MSH2(—/+), MSH6(−) (**Figure 3**).

By histopathology and imaging, the patient was considered to have metastatic adenocarcinoma of the small intestine. Immunohistochemical results showed that the MMR gene-associated protein was missing, indicating that it was microsatellite-unstable (MSI-H) small bowel adenocarcinoma and the anti-PD-1 therapy was presumed to be suitable. Based on the follow-up a month later, we treated with XELOX (Oxaliplatin 200 mg, St, IV; Capecitabine 1000 mg, BID, d1-14), taking a course of 3 weeks. The platinum drug was discontinued due to the toxicity after an eight-course of treatment, and Capecitabine continued to be administered orally alone for 10 courses. In addition, we combined the PD-1 inhibitor (200 mg, ST, IV) in 18 sessions. The patient was followed up regularly for 11 months after surgical resection, and there was no evidence of recurrence. After intensive care by medical staff and family, the patient's condition was greatly relieved. Now he was considered to be in complete remission according to the Fluorodeoxyglucose-positron emission tomography (FDG-PET) image and other assessment [**Figures 1(A2–D2)**, **4**].

DISCUSSION AND CONCLUSION

Small intestinal malignancies are still rare, but due to the improvement of medical technology, the detection rate of these malignancies has been increasing in recent years (5). There is a high degree of diversity in the anatomic distribution and histological morphology of small intestinal malignant tumors. Small bowel adenocarcinoma is one of the most common types and it is usually found at the advanced stage due to the absence of obvious symptoms and the lack of specific testing methods (6). Lymph node metastasis and hematogenous metastasis are the most common forms of small bowel adenocarcinoma. But the small intestinal mucosa is rich in lymph node tissue, so it is prone to metastasize through lymph nodes in the early stage. The five-year survival rate was higher when the tumor was localized (85%), but the rate was only 3–5% for patients with distant metastasis (stage IV) (7).

Due to the low incidence of small bowel adenocarcinoma and the limited data available, its pathogenesis is still unknown but the risk factors are considered to be similar to those of colorectal cancer. Poor lifestyle, eating habits and some special diseases such as smoking, alcohol abuse, higher BMI, inflammatory bowel disease, inherited cancer syndrome, all increase the risk (2). The researchers compared changes in DNA copy number between small bowel cancer, stomach cancer and colorectal cancer, and found that small bowel adenocarcinoma was more similar to colorectal cancer (8). The above reasons lead to the fact that most of the existing treatment for the small bowel malignancies refer to colorectal cancer.

This case, a 55-year-old man, had suspected multiple metastases in the lymph nodes surrounding the superior mesenteric vessels and the abdominal aorta on the first imaging examination. After a thorough examination and laparoscopic exploration, he was diagnosed with stage IV small bowel adenocarcinoma. His clinical course demonstrates that small bowel adenocarcinoma is usually asymptomatic in the

Abbreviations: CT, Computed tomography; FDG-PET, Fluorodeoxyglucose-positron emission tomography; PD-1, Programmed cell death protein 1; MSI-H, Microsatellite-unstable; dMMR, deficient mismatch repair.

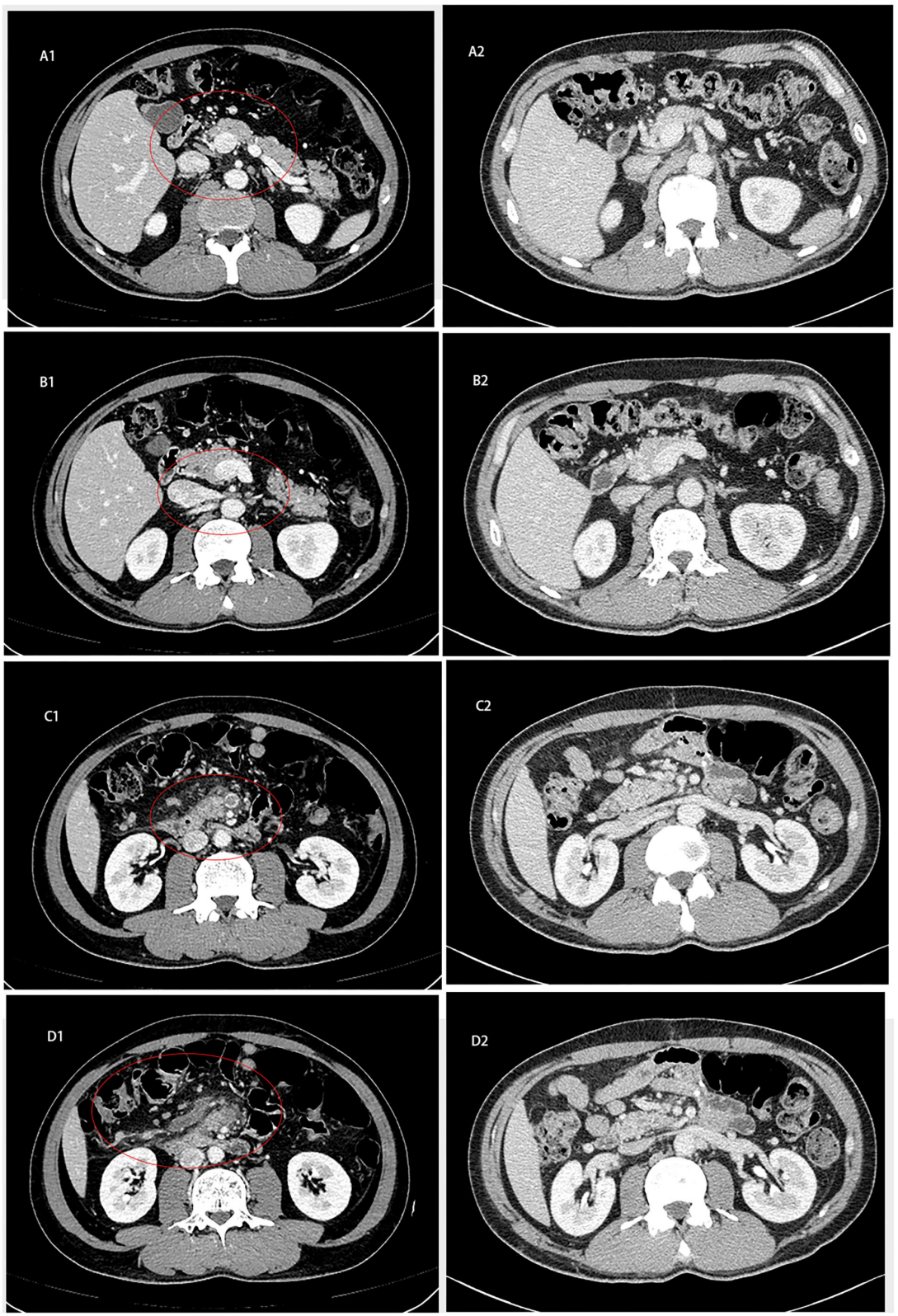

FIGURE 1 | Abdominal computed tomography of patient. **(A1–D1)** Contrast-enhanced CT on February 2, 2020 showed that the small intestine in the right middle abdomen was occupied by tumor with multiple enlarged lymph nodes. **(A2–D2)** Abdominal CT on October 6, 2020 showed that the obstruction of intestinal lumen was relieved after operation 2020.

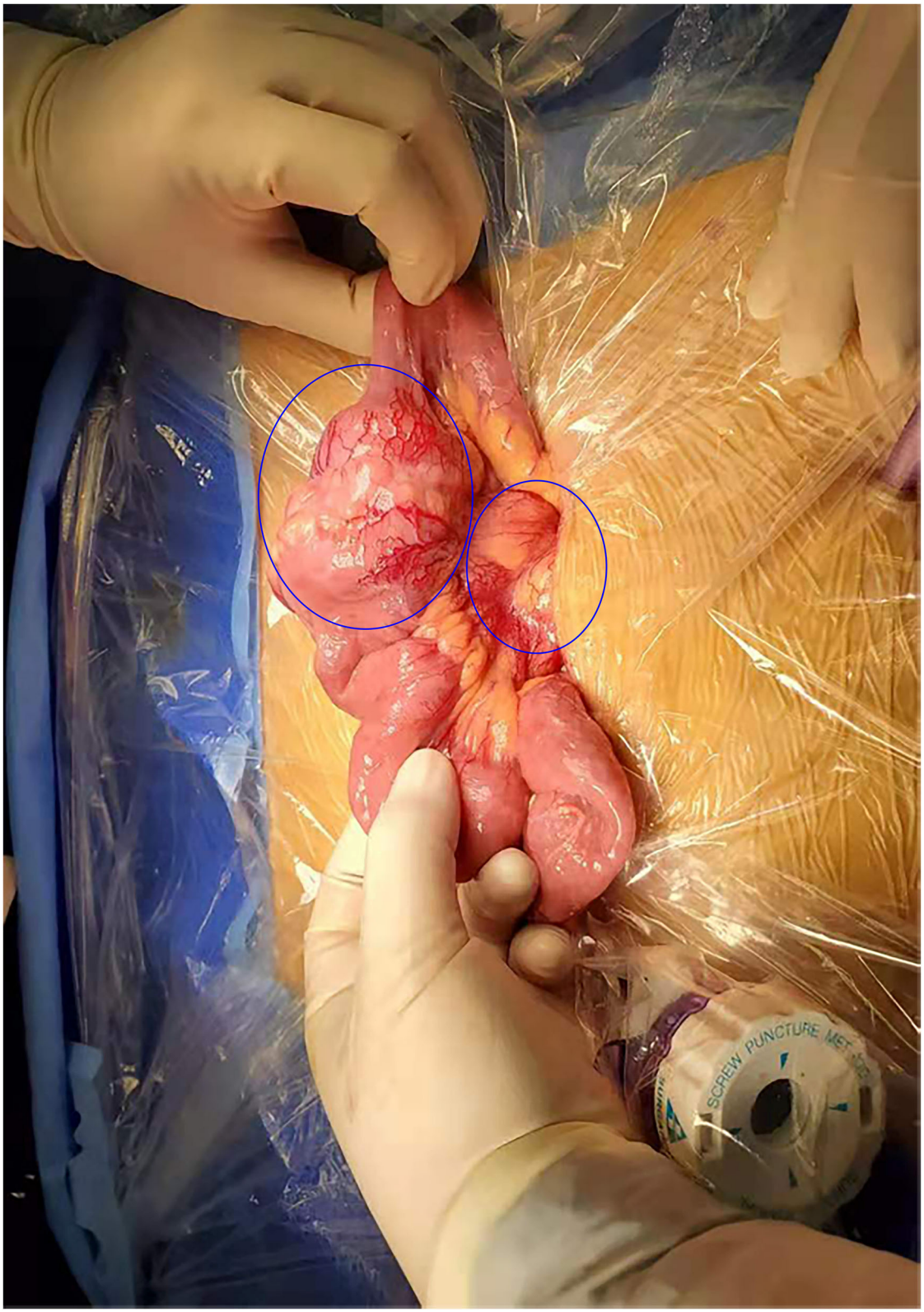

FIGURE 2 | Surgical findings. Enlarged lymph nodes were identified in the root of the mesentery in addition to the mass tumor in the small intestine.

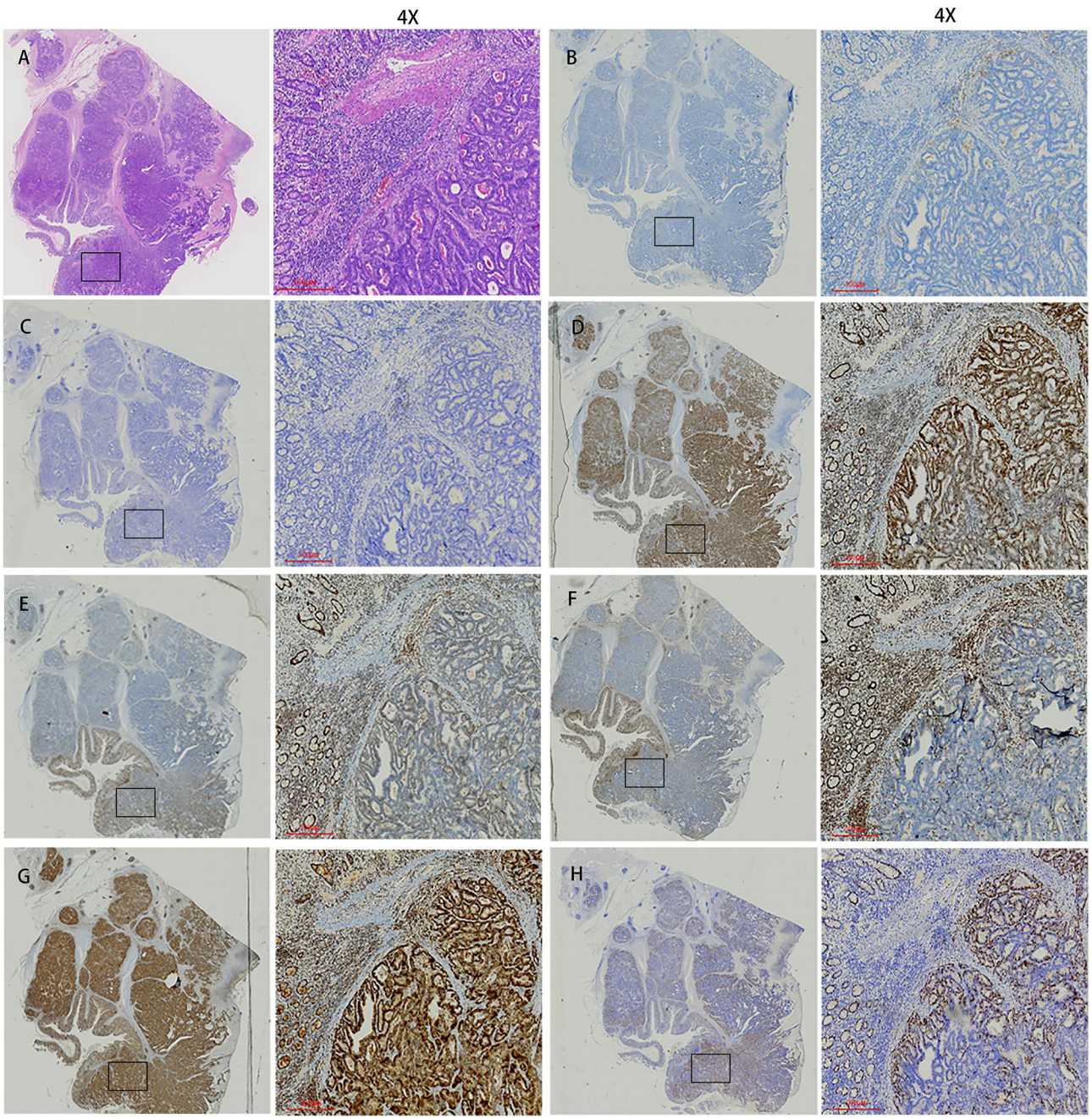

FIGURE 3 | Histopathological findings and immunohistochemistry. **(A)** Histological findings showed tumor cells with cytoplasm rich in eosinophilic granules and clear nucleoli that showed dense proliferation. **(B)** PD-1. **(C)** PD-L1. **(D)** MLH1. **(E)** MSH2. **(F)** MSH6. **(G)** PMS2. **(H)** Ki67. The first image in each group was viewed from a macro perspective. The scale bars of second picture in each group was 300 μm.

early stages and may present with systemic anemia or local obstruction in the late stages. But unlike other small bowel adenocarcinoma patients, our patient presented with a typical mesenteric vascular embolism as the first symptom such as abdominal pain, distension and acid reflux. Therefore, we performed surgery (laparoscopic exploration and small bowel adenocarcinoma resection). During the operation, the tumor was found to have invaded the serosa, and a large mass caused an incomplete obstruction. For localized adenocarcinoma of the small intestine, surgical complete resection (R0) and total regional lymph node resection are the only methods to achieve a curative outcome (7). However, there is still no relevant research data to guide surgical techniques (9). Most small bowel adenocarcinomas with distant metastases can't be

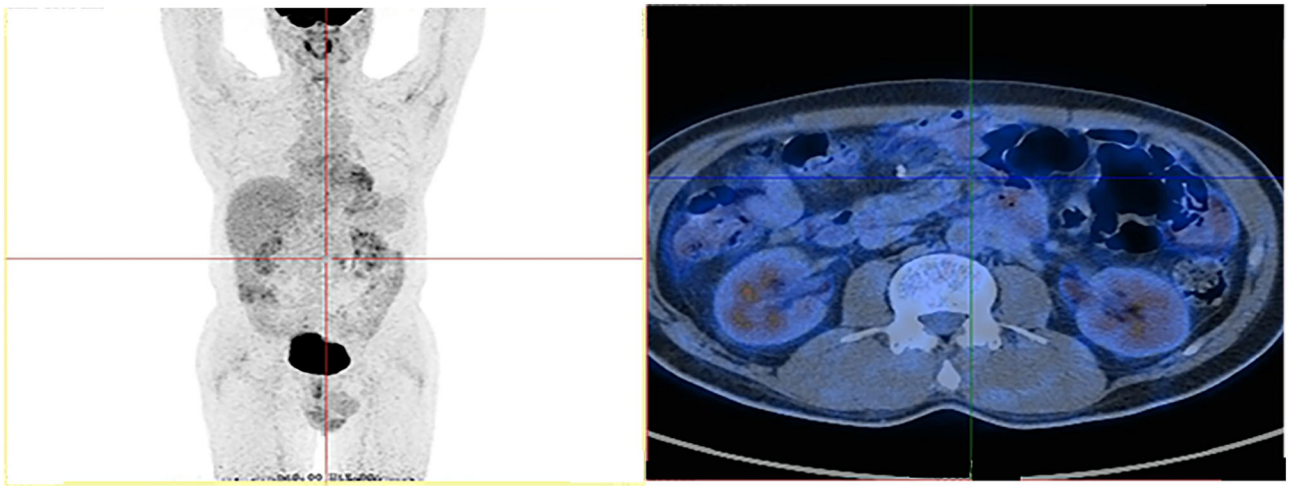

FIGURE 4 | FDG-PET scan shows no metastatic lesions and lymph node.

removed, and even in some patients with only limited visceral metastases, there is little evidence to support resection of metastases (4).

Combined with postoperative histopathologic and immunohistochemical findings, we gave the patient XELOX regimen in combination with PD-1 blockade. Small bowel adenocarcinoma has traditionally been considered to respond poorly to chemotherapy. Although no randomized trial has demonstrated the benefit of systemic chemotherapy in patients who have distant metastases, several retrospective studies have shown a significant increase in overall and disease-free survival (10–14). A number of studies have evaluated the efficacy of CAPEOX in patients with advanced small bowel adenocarcinoma, and the response rate to this regimen is significantly higher than the rate to conventional therapy 5-fluorouracil/adriamycin/mitomycin C. In terms of safety, the most common side effects of XELOX are neutropenia, complete blood count reduction, nausea and vomiting. In contrast, the incidence of severe side effects of 5-fluorouracil/adriamycin/mitomycin C was extremely high (68%) (15). What's more, the level of Ki67 can predict cancer progression as a biological maker of cell proliferation (16). The patients with high expression of Ki67 have better response to chemotherapy compared to patients with low Ki67 expression. Immunotherapy, such as Bevacizumab and Regorafenib, also plays a potential role due to the microsatellite instability and high tumor burden (17). At present, the chemotherapy regimen of small bowel adenocarcinoma mainly refers to colorectal cancer, mainly fluorouracil. Based on these data, Folfox, CAPEOX with or without Bevacizumab as a first-line treatment for advanced small bowel adenocarcinoma (4).

Recent studies have found that most patients with small bowel adenocarcinoma express high levels of PD-1, suggesting that checkpoint inhibitor therapy may play a role. The Mismatch repair gene (MMR gene), which includes MLH-1, PMS-2, MSH-2, and MSH-6, plays an important part in the repair of DNA homologous recombination repair. MMR gene missing causes deficiency (dMMR), which results in microsatellite instability. Small bowel adenocarcinoma has a higher incidence of dMMR than colorectal cancer, making checkpoint inhibitors an important treatment option for some patients (18). Our patient was diagnosed as MSI-H and dMMR small bowel adenocarcinoma and showed significant benefit after continued treatment with PD-1 blockade. The remaining fused lymph nodes were completely relieved by this therapy. A multicenter, Phase II Pembrolizumab has been shown to be effective in the treatment of patients with advanced small bowel adenocarcinoma and has been shown to be effective in the treatment of refractory dMMR colorectal and non-colorectal tumors such as breast cancer, melanoma and lung cancer (19). At present, there is no report of XELOX in combination with immunotherapy for small bowel adenocarcinoma. Our patient could tolerate this combination without specific side effects during the whole treatment.

In general, the prognosis of advanced small bowel adenocarcinoma is poor. In this case, the patient presents with mesenteric vascular embolism as the initial symptom, which provided an extra basis and thinking for clinical diagnosis of small bowel adenocarcinoma. Palliative surgery can help relieve obstruction in cases where radical surgery is not possible. At the same time, systematic chemotherapy combined with anti-PD-1 therapy can control the MSI-H small bowel adenocarcinoma patient' s disease progression and improve disease-free survival or overall survival.

DATA AVAILABILITY STATEMENT

The original contributions presented in the study are included in the article/supplementary material, further inquiries can be directed to the corresponding author/s.

ETHICS STATEMENT

Written informed consent was obtained from the individual(s) for the publication of any potentially identifiable images or data included in this article.

AUTHOR CONTRIBUTIONS

ZD: drafting the manuscript. XX: acquisition of data. ZZ: conception and design. All authors: revision, adaptation, and final approval of the manuscript.

FUNDING

The study was sponsored by the National Natural Science Foundation of China (Grant Numbers: 81972206), which supported data collection, analysis, and manuscript writing.

ACKNOWLEDGMENTS

We kindly thank the editor and reviewers for careful review and valuable comments, which have led to a significant improvement of the manuscript. Radiologists and anatomic pathologist contributed CT, PET scan and histology figures of this paper.

REFERENCES

1. Siegel RL, Miller KD, Jemal A. Cancer statistics, 2019. *CA Cancer J Clin.* (2019) 69:7–34. doi: 10.3322/caac.21551
2. Aparicio T, Zaanan A, Svrcek M, Laurent-Puig P, Carrere N, Manfredi S, et al. Small bowel adenocarcinoma: epidemiology, risk factors, diagnosis and treatment. *Dig Liver Dis.* (2014) 46:97–104. doi: 10.1016/j.dld.2013.04.013
3. Legue LM, Bernards N, Gerritse SL, van Oudheusden TR, de Hingh IH, Creemers GM, et al. Trends in incidence, treatment and survival of small bowel adenocarcinomas between 1999 and 2013: a population-based study in The Netherlands. *Acta Oncol.* (2016) 55:1183–9. doi: 10.1080/0284186X.2016.1182211
4. Benson AB, Venook AP, Al-Hawary MM, Arain MA, Chen YJ, Ciombor KK, et al. Small bowel adenocarcinoma, version 1.2020, NCCN clinical practice guidelines in oncology. *J Natl Compr Canc Netw.* (2019) 17:1109–33. doi: 10.6004/jnccn.2019.0043
5. Barsouk A, Rawla P, Barsouk A, Thandra KC. Epidemiology of cancers of the small intestine: trends, risk factors, and prevention. *Med Sci (Basel).* (2019) 7:46. doi: 10.3390/medsci7030046
6. Bojesen RD, Andersson M, Riis LB, Nielsen OH, Jess T. Incidence of, phenotypes of and survival from small bowel cancer in Denmark, 1994-2010: a population-based study. *J Gastroenterol.* (2016) 51:891–9. doi: 10.1007/s00535-016-1171-7
7. Dabaja BS, Suki D, Pro B, Bonnen M, Ajani J. Adenocarcinoma of the small bowel: presentation, prognostic factors, and outcome of 217 patients. *Cancer.* (2004) 101:518–26. doi: 10.1002/cncr.20404
8. Haan JC, Buffart TE, Eijk PP, van de Wiel MA, van Wieringen WN, Howdle PD, et al. Small bowel adenocarcinoma copy number profiles are more closely related to colorectal than to gastric cancers. *Ann Oncol.* (2012) 23:367–74. doi: 10.1093/annonc/mdr122
9. Zhang S, Yuan W, Zhang J, Chen Y, Zheng C, Ma J, et al. Clinicopathological features, surgical treatments, and survival outcomes of patients with small bowel adenocarcinoma. *Medicine (Baltimore).* (2017) 96:e7713. doi: 10.1097/MD.0000000000007713
10. Fishman PN, Pond GR, Moore MJ, Oza A, Burkes RL, Siu LL, et al. Natural history and chemotherapy effectiveness for advanced adenocarcinoma of the small bowel: a retrospective review of 113 cases. *Am J Clin Oncol.* (2006) 29:225–31. doi: 10.1097/01coc.0000214931.01062.01
11. Halfdanarson TR, McWilliams RR, Donohue JH, Quevedo JF, A. single-institution experience with 491 cases of small bowel adenocarcinoma. *Am J Surg.* (2010) 199:797–803. doi: 10.1016/j.amjsurg.2009.05.037
12. Czaykowski P, Hui D. Chemotherapy in small bowel adenocarcinoma: 10-year experience of the British Columbia Cancer Agency. *Clin Oncol (R Coll Radiol).* (2007) 19:143–9. doi: 10.1016/j.clon.2006.12.001
13. Koo DH, Yun SC, Hong YS Ryu MH, Lee JL, Chang HM, et al. Systemic chemotherapy for treatment of advanced small bowel adenocarcinoma with prognostic factor analysis: retrospective study. *BMC Cancer.* (2011) 11:205. doi: 10.1186/1471-2407-11-205
14. Aydin D, Sendur MA, Kefeli U, Umut Unal O, Tastekin D, Akyol M, et al. Evaluation of prognostic factors and treatment in advanced small bowel adenocarcinoma: report of a multi-institutional experience of Anatolian Society of Medical Oncology (ASMO). *J BUON.* (2016) 21:1242–9.
15. Xiang XJ, Liu YW, Zhang L, Qiu F, Yu F, Zhan ZY, et al. A phase II study of modified FOLFOX as first-line chemotherapy in advanced small bowel adenocarcinoma. *Anticancer Drugs.* (2012) 23:561–6. doi: 10.1097/CAD.0b013e328350dd0d
16. Yang C, Zhang J, Ding M, Xu K, Li L, Mao L, et al. Ki67 targeted strategies for cancer therapy. *Clin Transl Oncol.* (2018) 20:570–5. doi: 10.1007/s12094-017-1774-3
17. Takayoshi K, Kusaba H, Uenomachi M, Mitsugi K, Makiyama C, Makiyama A, et al. Suggestion of added value by bevacizumab to chemotherapy in patients with unresectable or recurrent small bowel cancer. *Cancer Chemother Pharmacol.* (2017) 80:333–42. doi: 10.1007/s00280-017-3371-0
18. Klose J, Lasitschka F, Horsch C, Strowitzki MJ, Bruckner T, Volz C, et al. Prognostic relevance of programmed death-ligand 1 expression and microsatellite status in small bowel adenocarcinoma. *Scand J Gastroenterol.* (2020) 55:321–9. doi: 10.1080/00365521.2020.1734073
19. Le DT, Uram JN, Wang H, Bartlett BR, Kemberling H, Eyring AD, et al. PD-1 blockade in tumors with mismatch-repair deficiency. *N Engl J Med.* (2015) 372:2509–20. doi: 10.1056/NEJMoa1500596

Conflict of Interest: The authors declare that the research was conducted in the absence of any commercial or financial relationships that could be construed as a potential conflict of interest.

Publisher's Note: All claims expressed in this article are solely those of the author and do not necessarily represent those of their affiliated organizations, or those of the publisher, the editors and the reviewers. Any product that may be evaluated in this article, or claim that may be made by its manufacturer, is not guaranteed or endorsed by the publisher.

Copyright © 2021 Dong, Xia and Zhang. This is an open-access article distributed under the terms of the Creative Commons Attribution License (CC BY). The use, distribution or reproduction in other forums is permitted, provided the original author(s) and the copyright owner(s) are credited and that the original publication in this journal is cited, in accordance with accepted academic practice. No use, distribution or reproduction is permitted which does not comply with these terms.

frontiers in Surgery

ORIGINAL RESEARCH
published: 10 November 2021
doi: 10.3389/fsurg.2021.773019

Comparison of Vascular Invasion With Lymph Node Metastasis as a Prognostic Factor in Stage I-III Colon Cancer: An Observational Cohort Study

*Jung Hoon Bae[1], Ji Hoon Kim[2], Bong-Hyeon Kye[3], Abdullah Al-Sawat[4], Chul Seung Lee[1], Seung-Rim Han[1], In Kyu Lee[1], Sung Hak Lee[5] and Yoon Suk Lee[1]**

[1] Division of Colorectal Surgery, Department of Surgery, Seoul St. Mary's Hospital, College of Medicine, The Catholic University of Korea, Seoul, South Korea, [2] Division of Colorectal Surgery, Department of Surgery, Incheon St. Mary's Hospital, College of Medicine, The Catholic University of Korea, Incheon, South Korea, [3] Division of Colorectal Surgery, Department of Surgery, St. Vincent's Hospital, College of Medicine, The Catholic University of Korea, Suwon-Si, South Korea, [4] Department of Surgery, College of Medicine, Taif University, Taif, Saudi Arabia, [5] Department of Hospital Pathology, Seoul St. Mary's Hospital, College of Medicine, The Catholic University of Korea, Seoul, South Korea

OPEN ACCESS

Edited by:
Qi Liu,
Fudan University, China

Reviewed by:
Matteo Riccò,
Azienda Unità Sanitaria Locale-IRCCS di Reggio Emilia, Italy
Avik Mandal,
All India Institute of Medical Sciences (Patna), India

***Correspondence:**
Yoon Suk Lee
yslee@catholic.ac.kr

Specialty section:
This article was submitted to Surgical Oncology, a section of the journal Frontiers in Surgery

Received: 09 September 2021
Accepted: 18 October 2021
Published: 10 November 2021

Citation:
Bae JH, Kim JH, Kye B-H, Al-Sawat A, Lee CS, Han S-R, Lee IK, Lee SH and Lee YS (2021) Comparison of Vascular Invasion With Lymph Node Metastasis as a Prognostic Factor in Stage I-III Colon Cancer: An Observational Cohort Study. Front. Surg. 8:773019. doi: 10.3389/fsurg.2021.773019

Purpose: This study aimed to evaluate the prognostic impact of vascular invasion (VI) in comparison with that of lymph node metastasis (LNM) in non-metastatic colon cancer.

Methods: Patients who underwent curative surgery for stage I-III colon cancer were divided into four groups depending on the status of VI and LNM (Group I: VI-/LNM-; Group II: VI+/LNM-; Group III: VI-/LNM+; Group IV: VI+/LNM+). Group III was subdivided according to the nodal (N) stage (Group IIIA: VI-/N1; Group IIIB: VI-/N2). Oncological outcomes were compared between Groups II and III.

Results: In total, 793 non-metastatic colon cancer patients were included. Group II [hazard ratio (HR) 2.34, 1.01–5.41] and Group III (HR 1.91, 1.26–2.89) were independently associated with poor disease-free survival (DFS). The 5-year DFS rates were comparable in Groups II (71.6%) and III (72.5%) ($P = 0.637$). When Group III was subdivided into Groups IIIA and IIIB, DFS deteriorated in the following order: Groups IIIA, II, and IIIB. The 5-year DFS rates were 79.7, 71.6, and 61.4% in Groups IIIA, II, and IIIB, respectively. Group II had a tendency toward early recurrence. The 1- and 2-year DFS rates were 76.3 and 71.6% in Group II and 88.3 and 79.8% in Group III, respectively ($P = 0.067$ and 0.247). All recurrences in Group II were distant metastases.

Conclusion: VI is a prognostic factor as significant as LNM and may be a stronger prognostic factor than N1 stage in non-metastatic colon cancer. Furthermore, a potential association was observed between VI and recurrence patterns, such as early recurrence and distant metastasis.

Keywords: colonic neoplasms, vascular invasion, lymph node metastasis, prognosis, recurrence

INTRODUCTION

Colon cancer is one of the most common cancers worldwide (1). Standard treatment for non-metastatic colon cancer is curative resection, followed by adjuvant chemotherapy, in selected patients (2, 3). The survival benefit of adjuvant chemotherapy in patients with conventional tumor-node-metastasis (TNM) stage III has been well established (2, 3). Most guidelines recommend adjuvant chemotherapy after curative resection for stage III colon cancer with lymph node metastasis (LNM). In contrast, for stage II colon cancer without LNM, even with high-risk factors, adjuvant chemotherapy is considered an optional treatment modality after curative surgery (2, 3). Generally, high-risk features in colon cancer are as follows: T4 tumors, poorly differentiated tumors, positive margin involvement, <12 lymph nodes (LNs) examined, obstruction, perforation, perineural invasion, lymphatic invasion, and vascular invasion (VI) (2, 3).

Distant metastasis occurs through vascular and lymphatic channels in colon cancer (4–9). However, the conventional TNM staging system categorizes non-metastatic colon cancer into stages I-II and stage III depending only on the status of LNM within the lymphatic pathway (10, 11). The staging system is considered a strong predictor of long-term oncological outcomes.

However, the staging system does not include factors associated with the vascular system, which is a main metastatic pathway. Hence, the impact of vascular metastasis on oncological outcomes has been underestimated compared to that of lymphatic metastasis in the staging system. However, as the vascular system does not have a gateway like LN, we hypothesized that the tumor cells would spread through the vascular channel more aggressively and faster than that through the lymphatic system. In this respect, VI is an important risk factor for distant metastasis through the vascular system, and VI has already been reported in several studies as a significant prognostic factor for colon cancer (12–15). However, there is a lack of literature that directly compares the prognostic effects of VI and LNM. Thus, this study aimed to evaluate the prognostic impact of VI compared to that of LNM in stage I-III colon cancer.

MATERIALS AND METHODS

Patients and Data Collection

Patients who underwent curative surgery for primary colon carcinoma between March 2004 and December 2015 at Incheon St. Mary's Hospital were consecutively included in this study ($n = 905$). Patients without data on VI ($n = 14$), those with intramucosal carcinoma ($n = 27$), and those who had a synchronous malignancy at the time of diagnosis or recurrence within 90 days postoperatively ($n = 71$) were excluded. Finally, 793 patients with stage I-III colon cancer were enrolled (**Figure 1**). This study was conducted by retrospectively reviewing the data, and the follow-up was completed in August 2019.

Patients demographics, clinicopathological characteristics, recurrence, and survival data were collected from the hospital's colon cancer patient registry. Patients with comorbidities were classified according to the American Society of Anesthesiologists (ASA) score. Right-sided colon was defined as cecum, ascending colon, hepatic flexure colon, and transverse colon. Left-sided colon was defined as splenic flexure colon, descending colon, sigmoid colon, and recto-sigmoid colon above the peritoneal reflection.

Pathological stage was classified according to the Eighth American Joint Cancer Committee TNM classification system (10, 11). In addition to VI, we recorded lymphatic invasion, perineural invasion, number of examined LNs, and histological grade as high-risk features. A favorable histological grade was defined as well or moderately differentiated adenocarcinoma. A poor histological grade was defined as poorly differentiated adenocarcinoma, mucinous carcinoma, or signet ring cell carcinoma. The presence of lymphovascular invasion was assessed for through hematoxylin and eosin (H&E)-staining. According to the current pathology practice guidelines (16), when the tumor cells involve small vessels with an unequivocal endothelial lining, such as lymphatics, capillaries, and postcapillary venules, it was considered lymphatic (small vessel) invasion. In contrast, when carcinoma was present in vessels with an identifiable thick smooth muscle layer or elastic lamina, this was considered vascular (large vessel) invasion (**Figure 2**).

This study was approved by the Institutional Review Board of the Ethics Committee of the College of Medicine, The Catholic University of Korea (OC19RESI0035). An informed consent statement was obtained from all patients, and the procedures were carried out in accordance with the ethical standards of the committee responsible for human experimentation and with the guidelines of the Helsinki Declaration, 1975, as revised in 1983. All patient records were anonymized and deidentified before the analysis.

Study Design

The patients were divided into four groups depending on the status of VI and LNM, regardless of the TNM stage. Group I included patients without VI and LNM (VI-/LNM-); Group II, those with VI and without LNM (VI+/LNM-); Group III, those without VI and with LNM (VI-/LNM+); and Group IV, those with both VI and LNM (VI+/LNM+). Subsequently, we subdivided Group III into Groups IIIA and IIIB according to the N stage. Group IIIA included patients without VI and with N1 stage (metastasis in 1–3 regional LNs), and Group IIIB, those without VI and with N2 stage (metastasis in four or more regional LNs) (**Figure 1**).

Follow-Up Schedule and Clinical Outcomes

Surveillance was performed every 3–6 months until 2 years postoperatively and then every 6–12 months until 5 years postoperatively. Tumor markers including carcinoembryonic antigen and carbohydrate antigen 19-9, abdominopelvic computed tomography (CT), and chest CT were performed according to the surveillance schedule. Adjuvant chemotherapy was recommended for patients with stage III and for those with stage II who had at least one high-risk feature. The decision to

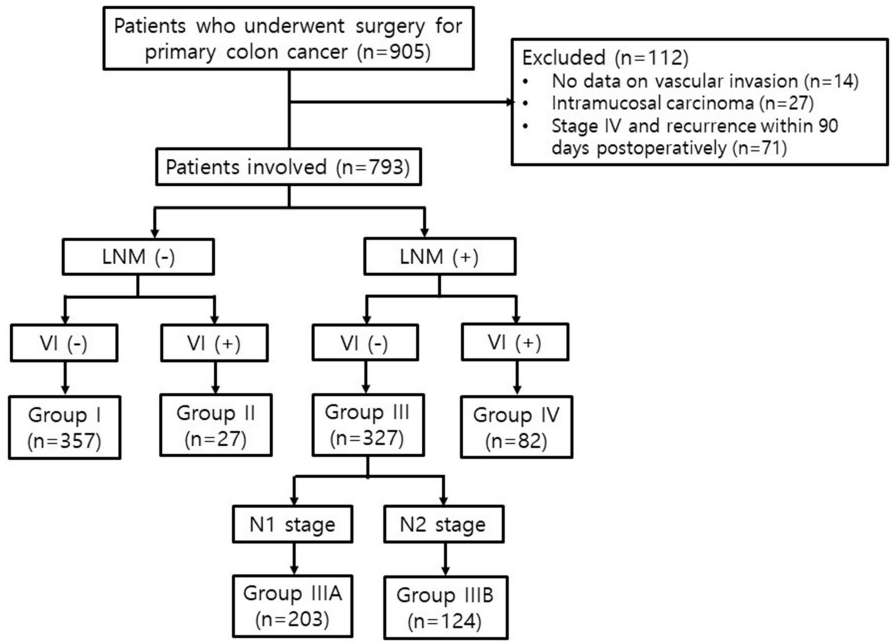

FIGURE 1 | Study flow chart. VI, vascular invasion; LNM, lymph node metastasis.

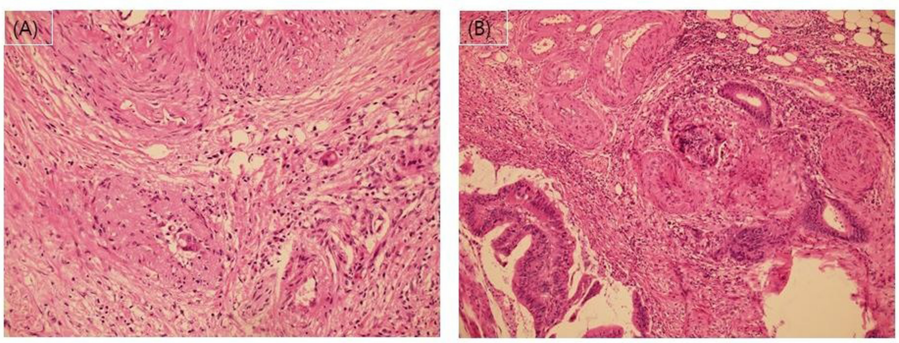

FIGURE 2 | (A) and **(B)** Microphotographs of vascular invasion using hematoxylin and eosin staining.

perform chemotherapy was made taking into consideration the patient's performance status and consent.

The primary outcome was disease-free survival (DFS), which was defined as the interval from the date of surgery until the date of disease recurrence detection by radiological or pathological examination or, in case of no recurrence, until the date of last follow-up. Overall survival (OS) was defined as the interval from the date of surgery until the date of death or last follow-up.

Statistical Analyses

The categorical variables of the groups were compared using the chi-square or Fisher's exact test. DFS and OS rates were calculated using the Kaplan-Meier method, and survival curves were compared among the groups using the log-rank test. The univariate prognostic significance of variables was determined using the Cox proportional hazard model. Variables significantly related to survival rate in the univariate analysis were subsequently included in the multivariate analysis employing the Cox multiple regression model. All statistical analyses were performed using SPSS software for Windows (version 25.0; IBM Corp., Armonk, NY, USA). Two-tailed P-values of <0.05 were considered statistically significant.

RESULTS

Baseline Characteristics Related to VI

In total, 793 patients with stage I-III colon cancer were included in the study. Median follow-up duration was 48 months (interquartile range 29–65). The mean age of the patients was 63.6 $\pm$ 12.5 years, the male-to-female ratio was 1.18:1, and 131 patients (16.5%) had an ASA score $\geq$3. Tumors were localized to the right-sided colon in 304 (38.3%) and the left-sided colon

TABLE 1 | Patient's clinico-pathological characteristics according to the presence of vascular invasion (VI).

Variables	Total patients (*N* = 793)	No VI (%) (*N* = 684, 86.3%)	VI (%) (*N* = 109, 13.7%)	*P*
Age > 65 years	397 (50.1)	341 (49.9)	56 (51.4)	0.768
Sex, female	363 (45.8)	320 (46.8)	43 (39.4)	0.153
ASA score, ≥3	131 (16.5)	111 (16.2)	20 (18.3)	0.580
Tumor location				0.220
Right-sided	304 (38.3)	268 (39.2)	36 (33.0)	
Left-sided	489 (61.7)	416 (60.8)	73 (67.0)	
Surgical approach				0.858
Laparoscopic	738 (93.1)	637 (93.1)	101 (92.7)	
Conventional	55 (6.9)	47 (6.9)	8 (7.3)	
Combined resection, yes	109 (13.7)	96 (14.0)	13 (11.9)	0.553
T4 tumor	147 (18.5)	106 (15.5)	41 (37.6)	<0.001
LN metastasis, yes	409 (51.6)	327 (47.8)	82 (75.2)	<0.001
Stage				<0.001
I	54 (6.8)	52 (7.6)	2 (1.8)	
II	330 (41.6)	305 (44.6)	25 (22.9)	
III	409 (51.6)	327 (47.8)	82 (75.2)	
LN harvest, <12	71 (9.0)	61 (8.9)	10 (9.2)	0.931
Histological grade, poor	76 (9.6)	54 (7.9)	22 (20.2)	<0.001
Lymphatic invasion, yes	362 (45.6)	265 (38.7)	97 (89.0)	<0.001
Perineural invasion, yes	291 (36.7)	225 (32.9)	66 (60.6)	<0.001
Adjuvant chemotherapy, yes	575 (72.5)	485 (70.9)	90 (82.6)	0.011
Recurrence, yes	153 (19.3)	121 (17.7)	32 (29.4)	0.004
Local recurrence, yes	17 (2.1)	14 (2.0)	3 (2.8)	0.718

VI, vascular invasion; ASA, American Society of Anesthesiologist; T, tumor; LN, lymph node.
Proportion are presented for categorical data (%).

in 489 patients (61.7%). The operation was performed by the laparoscopic approach in 738 (93.1%) and the conventional approach in 55 (6.9%) patients. Adjuvant chemotherapy was administered to 575 (72.5%), and recurrence was observed in 153 patients (19.3%).

VI was observed in 109 patients (13.7%). The patients' clinicopathological characteristics were compared according to the status of VI (**Table 1**). Patients with VI demonstrated significantly higher rates of lymphatic invasion (89.0 vs. 38.7%; $P < 0.001$), perineural invasion (60.6 vs. 32.9%; $P < 0.001$), poor histological grade (20.2 vs. 7.9%; $P < 0.001$), T4 tumor (37.6 vs. 15.5%; $P < 0.001$), and LNM (75.2 vs. 47.8%; $P < 0.001$) than those without VI. Adjuvant chemotherapy was performed more in patients with VI than in those without VI (82.6 vs. 70.9%; $P = 0.011$). The recurrence rate was higher in patients with VI than in those without VI (29.4 vs. 17.7%; $P = 0.004$). However, local recurrence rates were not different (2.8 vs. 2.0%; $P = 0.718$).

Baseline Characteristics According to the Groups

Of the 793 patients, 357 (45.0%) were included in Group I, 27 (3.4%) in Group II, 327 (41.2%) in Group III, and 82 (10.3%) in Group IV. The patients' clinicopathological characteristics are listed according to their respective groups in **Table 2**. Group IV (VI+/LNM+) had the highest rates of T4 tumor ($P < 0.001$), poor histological grade ($P < 0.001$), lymphatic invasion ($P < 0.001$), and perineural invasion ($P < 0.001$) among the groups. The recurrence rate was the highest in Group IV (30.5%) and the lowest in Group I (11.5%) ($P < 0.001$). There was no difference in local recurrence rates among the Groups ($P = 0.388$).

No significant differences were observed between Groups II (VI+/LNM-) and III (VI-/LNM+) in baseline characteristics, except for the sex ratio; patients in Group II were predominantly male ($P = 0.030$). Adjuvant chemotherapy was administered in 77.8 and 81.7% of patients in Groups II and III, respectively ($P = 0.619$). Recurrence rates were 25.9 and 24.5% in Groups II and III, respectively ($P = 0.865$).

Survival Outcomes

The outcomes of the univariate and multivariate analyses to identify significant prognostic factors for DFS and OS are shown in **Tables 3**, **4**, respectively. The univariate analysis showed that both VI [hazard ratio (HR) 1.98; 95% confidence interval (CI) 1.34–2.92] and LNM (HR 2.26; 95% CI 1.60–3.17) were significant prognostic factors for poor DFS. Multivariate analysis revealed that Group II (HR 2.34; 95% CI 1.01–5.41), Group III (HR 1.91; 95% CI 1.26–2.89), Group IV (HR 2.34; 95% CI 1.33–4.14), poor histological grade (HR 1.66; 95% CI 1.07–2.59), and T4 tumors (HR 2.08; 95% CI 1.44–3.01) were independently associated with poor DFS. Lymphatic invasion and perineural invasion were not detected as significant prognostic factors for DFS.

Both VI (HR 2.21; 95% CI 1.37–3.58) and LNM (HR 1.87; 95% CI 1.22–2.88) were significant prognostic factors for poor OS in the univariate analysis. In the multivariate analysis, high ASA score (HR 1.64; 95% CI 1.01–2.66), T4 tumor (HR 1.98; 95% CI 1.21–3.23), poor histological grade (HR 2.11; 95% CI 1.24–3.61), and Group IV (HR 2.92; 95% CI 1.40–6.08) were independently associated with poor OS. Adjuvant chemotherapy was an independent favorable prognostic factor for OS (HR 0.33; 95% CI 0.20–0.53).

The Kaplan-Meier curves for DFS and OS are shown according to the groups (**Figure 3**). Patients in Groups II (VI+/LNM-) and III (VI-/LNM+) had poorer prognosis than those in Group I (VI-/LNM-). Group IV (VI+/LNM+) showed the worst prognosis among the groups regarding DFS and OS ($P < 0.001$ and $P < 0.001$). The 5-year DFS rates were 86.6, 71.6, 72.5, and 64.4% in Groups I, II, III, and IV, respectively. The 5-year OS rates were 91.9, 80.6, 83.8, and 76.2% in Groups I, II, III, and IV, respectively.

Comparison of Oncological Outcomes Between Groups II (VI+/LNM-) and III (VI-/LNM+)

A survival analysis including only Groups II and III was performed to directly compare the prognostic impact of VI

TABLE 2 | Patient's clinico-pathological characteristics according to the groups.

Variables	Group I VI-, LNM- (*N* = 357)	Group II VI+, LNM- (*N* = 27)	Group III VI-, LNM+ (*N* = 327)	Group IV VI+, LNM+ (*N* = 82)	*P*[a]	*P*[b]
Age > 65 years	180 (50.4)	18 (66.7)	161 (49.2)	38 (46.3)	0.316	0.082
Sex, female	152 (42.6)	8 (29.6)	168 (51.4)	35 (42.7)	0.033	0.030
ASA score, ≥ 3	56 (15.7)	6 (22.2)	55 (16.8)	14 (17.1)	0.836	0.435
Tumor location					0.518	0.174
Right-sided	140 (39.2)	7 (25.9)	128 (39.1)	29 (35.4)		
Left-sided	217 (60.8)	20 (74.1)	199 (60.9)	53 (64.6)		
Surgical approach					0.422	1.000
Laparoscopic	338 (94.7)	25 (92.6)	299 (91.4)	76 (92.7)		
Conventional	19 (5.3)	2 (7.4)	28 (8.6)	6 (7.3)		
Combined resection, yes	45 (12.6)	2 (7.4)	51 (15.6)	11 (13.4)	0.520	0.399
T4 tumor	30 (8.4)	6 (22.2)	76 (23.2)	35 (42.7)	<0.001	0.904
Stage					<0.001	<0.001
I	52 (14.6)	2 (7.4)	0	0		
II	305 (85.4)	25 (92.6)	0	0		
III	0	0	327 (100)	82 (100)		
LN harvest, <12	39 (10.9)	4 (14.8)	22 (6.7)	6 (7.3)	0.165	0.125
Histological grade, poor	18 (5.0)	2 (7.4)	36 (11.0)	20 (24.4)	<0.001	0.753
Lymphatic invasion, yes	67 (18.8)	21 (77.8)	198 (60.6)	76 (92.7)	<0.001	0.077
Perineural invasion, yes	93 (26.1)	12 (44.4)	132 (40.4)	54 (65.9)	<0.001	0.678
Adjuvant systemic chemotherapy, yes	218 (61.1)	21 (77.8)	267 (81.7)	69 (84.1)	<0.001	0.619
Recurrence, yes	41 (11.5)	7 (25.9)	80 (24.5)	25 (30.5)	<0.001	0.865
Local recurrence, yes	5 (1.4)	0 (0.0)	9 (2.8)	3 (3.7)	0.388	1.000

VI, vascular invasion; LNM, lymph node metastasis; ASA, American Society of Anesthesiologist; T, tumor; LN, lymph node.
[a]*P-value comparing all groups.*
[b]*P-value comparing only group II (VI+/LNM-) and group III (VI-/LNM+).*
Proportion are presented for categorical data (%).

TABLE 3 | Disease-free survival in stage I-III colon cancer patients.

	Univariate analysis		Multivariate analysis	
Variables	**HR (95% CI)**	***P***	**HR (95% CI)**	***P***
Age ≥ 65	1.29 (0.94–1.77)	0.119		
Sex, female	0.90 (0.65–1.24)	0.512		
ASA score, ≥ 3	1.24 (0.82–1.89)	0.304		
Tumor location, left-sided	0.98 (0.71–1.36)	0.912		
T4 tumor	2.75 (1.96–3.85)	<0.001	2.08 (1.44–3.01)	<0.001
LN metastasis, yes	2.26 (1.60–3.17)	<0.001		
LN harvest, <12	1.01 (0.57–1.79)	0.970		
Histological grade, poor	2.05 (1.32–3.16)	0.001	1.66 (1.07–2.59)	0.024
VI, yes	1.98 (1.34–2.92)	0.001		
Lymphatic invasion, yes	1.89 (1.37–2.61)	<0.001	1.04 (0.70–1.55)	0.847
Perineural invasion, yes	1.52 (1.11–2.09)	0.010	1.09 (0.77–1.56)	0.617
Adjuvant systemic chemotherapy, yes	0.84(0.58–1.21)	0.340		
Group				
I (VI-, LNM-)	Reference		Reference	
II (VI+, LNM-)	2.78 (1.25–6.20)	0.012	2.34 (1.01–5.41)	0.048
III (VI-, LNM+)	2.31 (1.59–3.37)	<0.001	1.91 (1.26–2.89)	0.002
IV (VI+, LNM+)	3.29 (2.00–5.42)	<0.001	2.34 (1.33–4.14)	0.003

HR, hazard ratio; CI, confidence interval; ASA, American Society of Anesthesiologist; T, tumor; LN, lymph node; VI, vascular invasion; LNM, lymph node metastasis.

TABLE 4 | Overall survival in stage I-III colon cancer patients.

	Univariate analysis		Multivariate analysis	
Variables	**HR (95% CI)**	***P***	**HR (95% CI)**	***P***
Age ≥ 65	1.96 (1.29–3.00)	0.002	1.53 (0.97–2.39)	0.066
Sex, female	0.67 (0.43–1.02)	0.062		
ASA score, ≥ 3	2.07 (1.30–3.30)	0.002	1.64 (1.01–2.66)	0.044
Tumor location, left-sided	0.94 (0.61–1.43)	0.754		
T4 tumor	2.59 (1.67–4.01)	<0.001	1.98 (1.21–3.23)	0.007
LN metastasis, yes	1.87 (1.22–2.88)	0.004		
LN harvest, <12	1.62 (0.88–2.97)	0.122		
Histological grade, poor	2.54 (1.52–4.26)	<0.001	2.11 (1.24–3.61)	0.006
VI, yes	2.21 (1.37–3.58)	0.001		
Lymphatic invasion, yes	1.79 (1.18–2.72)	0.006	1.21 (0.71–2.06)	0.481
Perineural invasion, yes	1.38 (0.92–2.10)	0.124		
Adjuvant systemic chemotherapy, yes	0.43(0.28–0.65)	<0.001	0.33 (0.20–0.53)	<0.001
Group				
I (VI-, LNM-)	Reference		Reference	
II (VI+, LNM-)	2.03 (0.71–5.79)	0.185	1.72 (0.57–5.22)	0.340
III (VI-, LNM+)	1.71 (1.06–2.76)	0.029	1.66 (0.85–3.27)	0.141
IV (VI+, LNM+)	3.26 (1.81–5.90)	<0.001	2.92 (1.40–6.08)	0.004

HR, hazard ratio; CI, confidence interval; ASA, American Society of Anesthesiologist; T, tumor; LN, lymph node; VI, vascular invasion; LNM, lymph node metastasis.

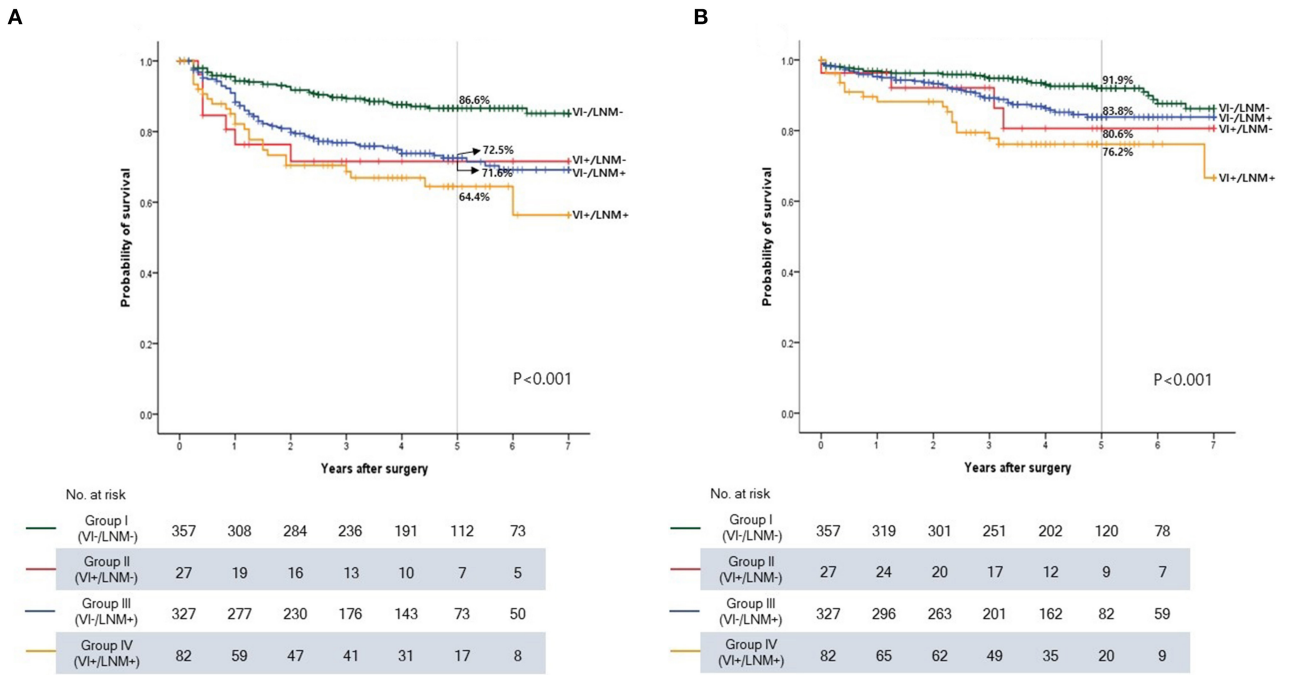

FIGURE 3 | Kaplan-Meier survival curve according to the groups in stage I-III colon cancer. **(A)** Disease-free survival. **(B)** Overall survival. VI, vascular invasion; LNM, lymph node metastasis.

and LNM. No significant differences in DFS and OS were observed between Groups II and III ($P = 0.637$ and $P = 0.697$) (**Figures 4A,B**).

However, the 1- and 2-year DFS rates tended to be lower in Group II than in Group III. The 1-year DFS rates were 76.3% in Group II and 88.3% in Group III ($P = 0.067$), and the 2-year DFS rates were 71.6% in Group II and 79.8% in Group III ($P = 0.247$). In contrast, the 5-year DFS rates were almost the same between the two groups (71.6% and 72.5% in Groups II and III, respectively).

Subsequently, Group III was subdivided into Groups IIIA (VI-/N1) and IIIB (VI-/N2) on the basis of the N stage, and the oncological outcomes were compared to those in Group II (VI+/N0). The Kaplan-Meier curve showed that DFS and OS deteriorated in the following order: Groups IIIA, II, and IIIB (**Figures 4C,D**). The 5-year DFS rates were 79.7, 71.6, and 61.4% in Groups IIIA, II, and IIIB, respectively. The 5-year OS rates were 87.1, 80.6, and 78.1% in Groups IIIA, II, and IIIB, respectively.

Recurrence Patterns

No differences in recurrence patterns such as distant metastasis, local recurrence, or recurrence in the liver, lung, or peritoneum were observed between patients in Groups II and III (**Table 5**) with recurrences. However, all recurrences were distant metastasis in Group II. In contrast, local recurrence was observed in nine patients (11.3%) in Group III.

DISCUSSION

In colon cancer, the TNM staging system is very simple because LNM is the only criterion for stage III (10). However, overemphasis on LNM in the staging system is controversial. Many studies have reported the poor prognostic impact of high-risk features other than LNM (17–21). One study showed the relationship between the number of high-risk features and prognosis, demonstrating that the 5-year OS rate was <20% in patients with stage II colon cancer with four or more high-risk features (20).

In this study, we compared the prognostic impact of VI, one of the high-risk features, with that of LNM, the criteria for stage III in the TNM staging system. We divided the patients into groups depending on their VI and LNM statuses, and no significant difference between the prognostic impacts of VI and LNM was found. Furthermore, despite no statistical significance, the 5-year DFS rate in VI+/N0 patients (71.6%) was lower than that in VI-/N1 patients (79.7%) and higher than that in VI-/N2 patients (61.4%). These findings suggest that the prognostic impact of VI may be somewhere between those of N1 and N2 in the TNM staging system.

Another interesting point of this study was the recurrence pattern. Seven recurrences occurred in VI+/LNM- patients, and all seven (100%) occurred within 2 years. Of the seven recurrences, six cases (85.7%) occurred within 1 year after surgery, and one case (14.3%) occurred 24 months after surgery. In VI-/LNM+ patients, there were 36 (45.0%) recurrences within 1 year and 61 (76.3%) recurrences within

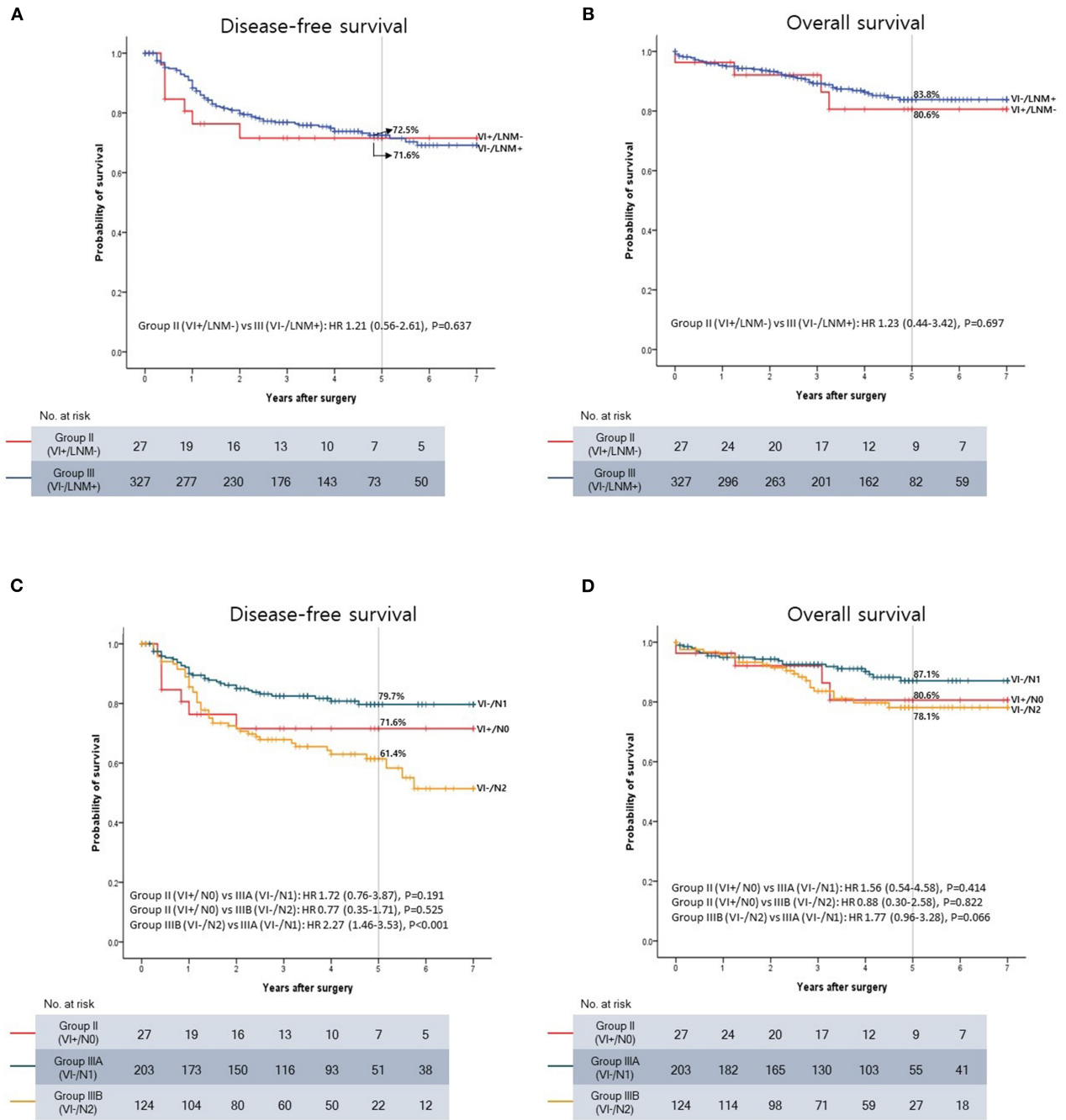

FIGURE 4 | Kaplan-Meier survival curve. **(A)** Disease-free survival (DFS) between VI+/LNM- and VI-/LNM+ patients. **(B)** Overall survival (OS) between VI+/LNM- and VI-/LNM+ patients. **(C)** DFS between VI+/LNM-, VI-/N1, and VI-/N2 patients. **(D)** OS between VI+/LNM-, VI-/N1, and VI-/N2 patients.

2 years among the 80 recurrences in total. The 1-year DFS rates were 76.3% in VI+/LNM- patients and 88.3% in VI-/LNM+ patients, and the 2-year DFS rates were 71.6% in VI+/LNM- patients and 79.8% in VI-/LNM+ patients. Additionally, all recurrences in VI+/LNM- patients were distant metastasis. In contrast, 11.3% of the recurrences in VI-/LNM+ patients were local recurrences. Although there was no statistical significance, VI+/LNM- was found to be associated with early recurrence and distant metastasis compared with VI-/LNM+. In this study, the proportion of VI+/LNM- patients who underwent chemotherapy was 77.8%, comparable to the number of VI-/LNM+ patients who underwent chemotherapy (81.7%). Therefore, the postoperative factors affecting oncological outcomes were minimized.

TABLE 5 | Recurrence types of recurrent patients in groups II and III.

Variables	Group II VI+, LNM- (*N* = 7)	Group III VI-, LNM+ (*N* = 80)	*P*
Liver metastasis, yes	3 (42.9)	33 (41.3)	1.000
Lung metastasis, yes	2 (28.6)	26 (32.5)	1.000
Peritoneal metastasis, yes	2 (28.6)	17 (21.3)	0.644
Distant metastasis, yes	7 (100.0)	75 (93.8)	1.000
Local recurrence, yes	0 (0.0)	9 (11.3)	1.000

VI, vascular invasion; LNM, lymph node metastasis.
Proportion are presented for categorical data (%).

Distant metastasis is the most common cause of death in patients with cancer (22, 23), and it is known to occur through vascular and lymphatic channels (4–9). Lymphatic drainage occurs in the following order: epicolic/paracolic LN, intermediate LN, and apical LN in colon cancer (24), and an association between the location of a regional LNM and disease recurrence has been reported (25, 26). Therefore, complete mesocolic excision (CME) and central vessel ligation (CVL), including the removal of apical LNs, are considered standard procedures in colon cancer surgery. Indeed, many studies have reported that CME and CVL contributed to better survival outcomes (27–29). When surgeons perform adequate CME and CVL procedures, the risk for metastasis through lymphatic channels can be reduced. For example, in stage III colon cancer without apical LNM, theoretically, the possibility of distant metastasis through lymphatic channels is negated by surgery with CME and CVL if there is no skip LNM. In contrast, the vascular system differs from the lymphatic system because it does not have a gateway like LNs. On the basis of these facts, tumor cell dissemination would be more aggressive and faster when tumor cells were transported through the vascular system than through the lymphatic system. In this study, we performed CME and CVL in all patients and demonstrated that VI is not only a poor prognostic factor similar to LNM, but also an indicator of early recurrence.

This study had several limitations. First, as this study was retrospective, inherent and unintentional selection bias cannot be dismissed. However, the selection bias was minimized because the clinicopathological factors, which can affect the prognosis, were not different between VI+/LNM- and VI-/LNM+ patients. Even the proportions of patients who received adjuvant chemotherapy among VI+/LNM- and VI-/LNM+ patients were comparable. Second, the sample size was small. The 1- and 2-year DFS rates of VI+/LNM- patients were lower than those of VI-/LNM+ patients. Furthermore, VI tended to be a stronger prognostic factor than metastasis in 1–3 regional LNs (N1 stage). However, these differences were not statistically significant. Third, we did not include MSI status as a prognostic factor in this study. According to the ESMO guideline, vascular invasion is classified as a minor prognostic parameter for stage II risk assessment (3). The guideline recommends that adjuvant therapy be determined based on the MSI status in intermediate-risk stage II colon cancer. The study center has evaluated the MSI status as a prognostic factor since 2013. Therefore, most of them have no data on MSI status. Since adjuvant chemotherapy was performed for stage II colon cancer with at least one risk factor regardless of MSI status, compared with current ESMO guideline, some of the patients included in this study underwent overtreatment. Finally, the detection rate of VI was low in this study (13.7%). Recent studies have reported detection rates of VI ranging from 19 to 34% (12–14, 17, 18, 20). This difference may be due to the staining method. One study investigated the detection rate of VI in 93 patients with T3 or T4 colorectal cancer and reported that it increased from 15.1% in the original pathological report when using H&E staining to 48.4% when using elastic stain (30). During the study period, we used H&E staining for the detection of VI, which could result in a low VI detection rate. This may be the reason why only a small population belonged to Group II (VI+/LNM-). Therefore, a large-scale multicenter study using elastin staining as a method to detect VI is needed to clarify the results of this study.

In conclusion, we demonstrated that VI is a prognostic factor as significant as LNM and may be a stronger prognostic factor than the N1 stage in non-metastatic colon cancer. Furthermore, the result provided the first insights into a potential association between VI and recurrence patterns, such as early recurrence and distant metastasis. Therefore, this study suggests that adjuvant chemotherapy should be considered in stage II colon cancer with VI. A large-scale multicenter study using an advanced staining method would help to clarify the prognostic impact of VI.

DATA AVAILABILITY STATEMENT

The original contributions presented in the study are included in the article/supplementary material, further inquiries can be directed to the corresponding author/s.

ETHICS STATEMENT

The studies involving human participants were reviewed and approved by Institutional Review Board of the Ethics Committee of the College of Medicine, the Catholic University of Korea (OC19RESI0035). Written informed consent for participation was not required for this study in accordance with the national legislation and the institutional requirements.

AUTHOR CONTRIBUTIONS

YL: conceptualization and writing-review and editing. JK and YL: data curation. JB: formal analysis, software, and writing–original draft. JB, CL, S-RH, JK, and YL: investigation. JB, B-HK, AA-S, SL, and YL: methodology. JB and YL: project administration. JB, JK, and YL: resources. B-HK, IL, and YL: supervision and validation. JB, SL, and YL: visualization.

REFERENCES

1. Siegel RL, Miller KD, Jemal A. Cancer statistics, 2019. *CA Cancer J Clin.* (2019) 69:7–34. doi: 10.3322/caac.21551
2. Benson AB, III rd, Venook AP, Cederquist L, Chan E, Chen YJ, Cooper HS, et al. Colon cancer, version 1.2017, NCCN clinical practice guidelines in oncology. *J Natl Compr Canc Netw.* (2017) 15:370–98. doi: 10.6004/jnccn.2017.0036
3. Argilés G, Tabernero J, Labianca R, Hochhauser D, Salazar R, Iveson T, et al. Localised colon cancer: ESMO clinical practice guidelines for diagnosis, treatment and follow-up. *Ann Oncol.* (2020) 31:1291–305. doi: 10.1016/j.annonc.2020.06.022
4. Springfield DS. Mechanisms of metastasis. *Clin Orthop Relat Res.* (1982) 169:15–9. doi: 10.1097/00003086-198209000-00003
5. Royston D, Jackson DG. Mechanisms of lymphatic metastasis in human colorectal adenocarcinoma. *J Pathol.* (2009) 217:608–19. doi: 10.1002/path.2517
6. Ferris RL, Lotze MT, Leong SP, Hoon DS, Morton DL. Lymphatics, lymph nodes and the immune system: barriers and gateways for cancer spread. *Clin Exp Metastasis.* (2012) 29:729–36. doi: 10.1007/s10585-012-9520-2
7. Witte MH, Dellinger MT, McDonald DM, Nathanson SD, Boccardo FM, Campisi CC, et al. Lymphangiogenesis and hemangiogenesis: potential targets for therapy. *J Surg Oncol.* (2011) 103:489–500. doi: 10.1002/jso.21714
8. Holopainen T, Bry M, Alitalo K, Saaristo A. Perspectives on lymphangiogenesis and angiogenesis in cancer. *J Surg Oncol.* (2011) 103:484–8. doi: 10.1002/jso.21808
9. Pantel K, Brakenhoff RH. Dissecting the metastatic cascade. *Nat Rev Cancer.* (2004) 4:448–56. doi: 10.1038/nrc1370
10. Hari DM, Leung AM, Lee JH, Sim MS, Vuong B, Chiu CG, et al. AJCC cancer staging manual 7th edition criteria for colon cancer: do the complex modifications improve prognostic assessment? *J Am Coll Surg.* (2013) 217:181–90. doi: 10.1016/j.jamcollsurg.2013.04.018
11. Jin M, Frankel WL. Lymph node metastasis in colorectal cancer. *Surg Oncol Clin N Am.* (2018) 27:401–12. doi: 10.1016/j.soc.2017.11.011
12. Betge J, Pollheimer MJ, Lindtner RA, Kornprat P, Schlemmer A, Rehak P, et al. Intramural and extramural vascular invasion in colorectal cancer: prognostic significance and quality of pathology reporting. *Cancer.* (2012) 118:628–38. doi: 10.1002/cncr.26310
13. Gibson KM, Chan C, Chapuis PH, Dent OF, Bokey L. Mural and extramural venous invasion and prognosis in colorectal cancer. *Dis Colon Rectum.* (2014) 57:916–26. doi: 10.1097/DCR.0000000000000162
14. Parnaby CN, Scott NW, Ramsay G, MacKay C, Samuel L, Murray GI, et al. Prognostic value of lymph node ratio and extramural vascular invasion on survival for patients undergoing curative colon cancer resection. *Br J Cancer.* (2015) 113:212–9. doi: 10.1038/bjc.2015.211
15. Skancke M, Arnott SM, Amdur RL, Siegel RS, Obias VJ, Umapathi BA. Lymphovascular invasion and perineural invasion negatively impact overall survival for stage II adenocarcinoma of the colon. *Dis Colon Rectum.* (2019) 62:181–8. doi: 10.1097/DCR.0000000000001258
16. Kim BH, Kim JM, Kang GH, Chang HJ, Kang DW, Kim JH, et al. Standardized pathology report for colorectal cancer, 2nd Edition. *J Pathol Transl Med.* (2020) 54:1–19. doi: 10.4132/jptm.2019.09.28
17. Petersen VC, Baxter KJ, Love SB, Shepherd NA. Identification of objective pathological prognostic determinants and models of prognosis in Dukes' B colon cancer. *Gut.* (2002) 51:65–9. doi: 10.1136/gut.51.1.65
18. Leijssen LGJ, Dinaux AM, Amri R, Taylor MS, Deshpande V, Bordeianou LG, et al. Impact of intramural and extramural vascular invasion on stage II-III colon cancer outcomes. *J Surg Oncol.* (2019) 119:749–57. doi: 10.1002/jso.25367
19. Babcock BD, Aljehani MA, Jabo B, Choi AH, Morgan JW, Selleck MJ, et al. High-risk stage II colon cancer: not all risks are created equal. *Ann Surg Oncol.* (2018) 25:1980–5. doi: 10.1245/s10434-018-6484-8
20. Amri R, England J, Bordeianou LG, Berger DL. Risk stratification in patients with stage II colon cancer. *Ann Surg Oncol.* (2016) 23:3907–14. doi: 10.1245/s10434-016-5387-9
21. Amri R, Bordeianou LG, Sylla P, Berger DL. Association of radial margin positivity with colon cancer. *JAMA Surg.* (2015) 150:890–8. doi: 10.1001/jamasurg.2015.1525
22. Edwards BK, Noone AM, Mariotto AB, Simard EP, Boscoe FP, Henley SJ, et al. Annual report to the nation on the status of cancer, 1975-2010, featuring prevalence of comorbidity and impact on survival among persons with lung, colorectal, breast, or prostate cancer. *Cancer.* (2014) 120:1290–314. doi: 10.1002/cncr.28509
23. Pachmayr E, Treese C, Stein U. Underlying mechanisms for distant metastasis - molecular biology. *Visc Med.* (2017) 33:11–20. doi: 10.1159/000454696
24. Merrie AE, Phillips LV, Yun K, McCall JL. Skip metastases in colon cancer: assessment by lymph node mapping using molecular detection. *Surgery.* (2001) 129:684–91. doi: 10.1067/msy.2001.113887
25. Kobayashi H, Enomoto M, Higuchi T, Uetake H, Iida S, Ishikawa T, et al. Clinical significance of lymph node ratio and location of nodal involvement in patients with right colon cancer. *Dig Surg.* (2011) 28:190–7. doi: 10.1159/000323966
26. Liang JT, Lai HS, Huang J, Sun CT. Long-term oncologic results of laparoscopic D3 lymphadenectomy with complete mesocolic excision for right-sided colon cancer with clinically positive lymph nodes. *Surg Endosc.* (2015) 29:2394–401. doi: 10.1007/s00464-014-3940-9
27. Bertelsen CA, Neuenschwander AU, Jansen JE, Wilhelmsen M, Kirkegaard-Klitbo A, Tenma JR, et al. Disease-free survival after complete mesocolic excision compared with conventional colon cancer surgery: a retrospective, population-based study. *Lancet Oncol.* (2015) 16:161–8. doi: 10.1016/S1470-2045(14)71168-4
28. Merkel S, Weber K, Matzel KE, Agaimy A, Gohl J, Hohenberger W. Prognosis of patients with colonic carcinoma before, during and after implementation of complete mesocolic excision. *Br J Surg.* (2016) 103:1220–9. doi: 10.1002/bjs.10183
29. Storli KE, Sondenaa K, Furnes B, Nesvik I, Gudlaugsson E, Bukholm I, et al. Short term results of complete (D3) vs. standard (D2) mesenteric excision in colon cancer shows improved outcome of complete mesenteric excision in patients with TNM stages I-II. *Tech Coloproctol.* (2014) 18:557–64. doi: 10.1007/s10151-013-1100-1
30. Hwang C, Lee S, Kim A, Kim YG, Ahn SJ, Park DY. Venous invasion in colorectal cancer: impact of morphologic findings on detection rate. *Cancer Res Treat.* (2016) 48:1222–8. doi: 10.4143/crt.2015.429

Conflict of Interest: The authors declare that the research was conducted in the absence of any commercial or financial relationships that could be construed as a potential conflict of interest.

Publisher's Note: All claims expressed in this article are solely those of the authors and do not necessarily represent those of their affiliated organizations, or those of the publisher, the editors and the reviewers. Any product that may be evaluated in this article, or claim that may be made by its manufacturer, is not guaranteed or endorsed by the publisher.

Copyright © 2021 Bae, Kim, Kye, Al-Sawat, Lee, Han, Lee, Lee and Lee. This is an open-access article distributed under the terms of the Creative Commons Attribution License (CC BY). The use, distribution or reproduction in other forums is permitted, provided the original author(s) and the copyright owner(s) are credited and that the original publication in this journal is cited, in accordance with accepted academic practice. No use, distribution or reproduction is permitted which does not comply with these terms.

frontiers in Surgery

ORIGINAL RESEARCH
published: 16 November 2021
doi: 10.3389/fsurg.2021.745748

Decrease in Blood Neutrophil-to-Lymphocyte Ratio Indicates Better Survival After Neoadjuvant Chemotherapy in Patients With Advanced Gastric Cancer

Ziyi Liu[1], *Yahang Liang*[1], *Xiaolong Tang*[2*] *and Hui Qu*[2*]

[1] *Department of Clinical Medicine, Qilu Medical College of Shandong University, Jinan, China,* [2] *Department of General Surgery, Qilu Hospital of Shandong University, Jinan, China*

OPEN ACCESS

Edited by:
Qi Liu,
Fudan University, China

Reviewed by:
Alex Giakoustidis,
Aristotle University of Thessaloniki, Greece
Alessandro Rizzo,
Sant'Orsola-Malpighi Polyclinic, Italy

***Correspondence:**
Xiaolong Tang
tangxl666@foxmail.com
Hui Qu
quhuidoctor@163.com

Specialty section:
This article was submitted to Surgical Oncology, a section of the journal Frontiers in Surgery

Received: *22 July 2021*
Accepted: *12 October 2021*
Published: *16 November 2021*

Citation:
Liu Z, Liang Y, Tang X and Qu H (2021) Decrease in Blood Neutrophil-to-Lymphocyte Ratio Indicates Better Survival After Neoadjuvant Chemotherapy in Patients With Advanced Gastric Cancer. Front. Surg. 8:745748. doi: 10.3389/fsurg.2021.745748

Introduction: Gastric cancer is the fifth most commonly diagnosed tumor and is the fourth leading cause of cancer-related mortality, worldwide. Due to the low rate of early diagnosis, approximately two-thirds of patients are first diagnosed at an advanced stage. Neoadjuvant chemotherapy (NAC) is recommended for patients with advanced gastric cancer (AGC). The neutrophil-to-lymphocyte ratio (NLR), a combined inflammatory and immunogenic factor, has been universally used for predicting outcomes in AGC patients. Given that NLR is a dynamic process, in this study, we investigated the value of NLR change for the prediction of chemotherapeutic responses and prognosis in patients with AGC.

Methods: We retrospectively enrolled 111 patients with AGC who underwent NAC following curative surgery. Patients were divided into two groups according to the NLR change after chemotherapy into the increased and decreased groups. Outcome measures were overall survival (OS) and disease-free survival (DFS). Univariate was calculated by Kaplan-Meier method. Multivariate analysis was performed using the Cox proportional hazards regression model.

Results: Post-chemotherapy, NLR increased in 36 patients and decreased in 75 patients. After a median follow-up time of 19 months, six patients developed local recurrence, 23 developed distant recurrence, and 34 died. Patients with reduced post-chemotherapy NLR showed significantly longer OS ($p < 0.001$) and DFS ($p < 0.001$). A decrease in the NLR after NAC was an independent indicator associated with better OS ($p < 0.001$) and DFS ($p < 0.001$).

Conclusions: In patients with AGC, a decrease in NLR after NAC indicated better survival. NLR change could serve as a robust indicator for the efficiency of NAC and prognostic prediction in patients with AGC.

Keywords: advanced gastric cancer, neutrophil-to-lymphocyte ratio, neoadjuvant chemotherapy, dynamic change, overall survival, disease-free survival

INTRODUCTION

Globally, over a million new cases and 769,000 deaths due to gastric cancer (GC) were diagnosed in 2020, making it the fifth most commonly diagnosed cancer and the fourth leading cause of cancer-related deaths. In particular, the incidence rate of GC is the highest in East Asia (1). Due to the absence of specific early symptoms in gastric cancer (2), ∼70% of patients are first diagnosed in an advanced stage (3). Complete surgical resection remains the only curative method for patients with advanced gastric cancer (AGC) (4). However, even after adequate gastric resection, the 5-year survival rate remains at ∼25% (5). To improve the prognosis of patients with AGC, multidisciplinary therapies including neoadjuvant chemotherapy (NAC), targeted therapy (6), surgery, immunotherapy, and chemoradiotherapy are recommended by the latest National Comprehensive Cancer Network (NCCN) guidelines (7).

To evaluate the effect of NAC, clinical response and post-operative histopathological examination have been widely used. But these evaluations are not comprehensive which can further influence the selection of post-operative therapeutic strategies. Therefore, other factors, such as inflammatory responses should be considered while evaluating the efficacy of NAC and identifying the patients who could benefit from NAC with potentially better prognosis.

The relationship between systemic inflammation and cancer progression has been generally studied (8–10). Several inflammatory markers, for instance, C-reactive protein (CRP), leukocytes, neutrophils, lymphocytes, monocytes, macrophages, and platelet counts are associated with various cancer types (11–15). Beyond these, the neutrophil-to-lymphocyte ratio (NLR) has gained increased attention in recent years. A meta-analysis comprising of 100 studies consisting of 40,559 patients shows that high NLR is associated with an adverse overall survival (OS) (HR = 1.81, 95% CI = 1.67 to 1.97; $p < 0.001$) in many solid tumors (16). NLR has also been universally identified as a promising prognostic factor for patients with AGC. Low pre-treatment NLR indicates a favorable prognosis for both OS and disease-free survival (DFS) (17, 18).

Most researchers emphasize the predictive value of NLR in patients with AGC who undergo curative gastrectomy, while only a few commit to the importance of NLR in patients receiving NAC. Additionally, current clinical studies have not reached a consensus on the specific value of NLR. The selection of parameters, such as median, mean, or the cutoff value varies in each article, which further weakens the application of NLR. However, to date, NLR remains dynamic (19). The change in NLR after chemotherapy can better reflect the process of tumor-related immune responses in the body. The purpose of this study was to investigate the applicability of NLR change in the prediction of chemotherapeutic response and prognosis in patients with AGC.

Abbreviations: AGC, advanced gastric cancer; NAC, neoadjuvant chemotherapy; NLR, neutrophil-to-lymphocyte ratio; DFS, disease-free survival; OS, overall survival; AJCC, American Joint Committee on Cancer; NCCN, National Comprehensive Cancer Network; MODS, multiple organ dysfunction syndrome.

PATIENTS AND METHODS

Patients

A total of 111 patients with AGC who underwent NAC and curative gastrectomy at the Department of Gastrointestinal Surgery, Affiliated Qilu Hospital, Shandong University, between August 2016 and December 2019 were enrolled retrospectively in this study. Pathological staging was performed according to the 8th edition of the American Joint Committee on Cancer (AJCC) Cancer Staging Manual. Patients with the following conditions were excluded: distant metastases or peritoneal implantation, previous chemotherapy or radiotherapy treatment, simultaneous malignancies other than GC, and recurrent or metastasis GC confirmed by histopathology or cytology. Post-operative telephonic follow-up was performed for 6 months to 3 years or till death.

Treatment Regime

Before curative gastrectomy, patients were mainly administered with one of three chemotherapeutic regimens as follows: S-1 + oxaliplatin (SOX), oxaliplatin + capecitabine (XELOX), 5-Fu + leucovorin + oxaliplatin + docetaxel (mFLOT); SOX regimen: Oral tegafur–gimeracil oteracil potassium capsule (S-1) 100 mg/m^2 on days 1–14, oxaliplatin 130 mg/m^2 on day 1, followed by seven days of rest, and SOX regimen was repeated every 3 weeks for up to 3–8 cycles; XELOX regimen: oxaliplatin, 150 mg/m^2, by intravenous infusion, on day 1, capecitabine, 1,000 mg/m^2, orally, twice/day on days 1–14. XELOX was repeated every 3 weeks for up to 3–6 cycles. Lastly, mFLOT regimen: 24-h 5-FU 2200 mg/m^2, leucovorin 200 mg/m^2, oxaliplatin 75 mg/m^2, docetaxel 45 mg/m^2, by intravenous infusion, on day 1 of each 14-day cycle for up to 4 cycles.

NLR Assessment

For all patients, a routine blood examination was performed at two stages: (1) Pre-chemotherapy: within 1 week before the initial day of chemotherapy; (2) post-chemotherapy: after finishing the last dose of chemotherapy and within 1 week before surgery. Patients were divided into two, namely, increased and decreased groups, based on their variations in NLR after NAC.

Statistical Analysis

Clinical response was defined based on OS and DFS. OS was calculated from the first day of NAC till death due to any cause or last contact. DFS was calculated from the initial date of NAC until disease recurrence, death, or last contact. Clinicopathological characteristics were analyzed using the Chi-square test. OS and DFS were calculated by the Kaplan-Meier method and analyzed for significance by the log-rank test. Variables that were clinically relevant or showed a univariable association ($p < 0.1$) with the outcomes (DFS and OS) were included in the subsequent multivariate Cox proportional-hazard regression model. Given the number of available events, we carefully chose the variables for inclusion to ensure simplicity in the final model. All data were analyzed using the SPSS 25.0 statistical software. $P < 0.05$ was considered statistically significant.

RESULTS

Clinicopathological Characteristics

Patient Characteristics

Table 1 shows the clinicopathological characteristics of the 111 enrolled patients (83 male; 28 female) with a median age of 58 years (range: 32–81 years).

Blood Examination Data

The median pre-chemotherapy and post-chemotherapy NLR were 2.28 and 1.75, respectively. According to NLR change after chemotherapy, 36 patients were classified in the increased NLR group, while 75 patients were in the decreased NLR group.

Prognostic Values

A total of six patients showed local recurrence and 23 patients showed distant metastasis. Thirty four patients died during the follow-up. Among them, 28 patients had tumor-related deaths and six patients died due to multiple organ dysfunction syndrome (MODS) or other reasons.

Comparison of Survival Outcome Between NLR Increased and Decreased Groups

Kaplan-Meier survival curve was plotted, and the log-rank test was used to analyze OS and DFS. NLR increased in 36 patients after chemotherapy, including 29 patients having an NLR greater than the median post-chemotherapy value of 1.75, while eight patients had NLR <1.75. NLR decreased in 75 patients after chemotherapy, with seven patients having an NLR >1.75, while 48 patients had an NLR <1.75.

According to the median post-chemotherapy NLR of 1.75 and the change in NLR after chemotherapy, all 111 patients were further divided into the following 4 subgroups: NLR $\geq$ 1.75 + decrease; NLR $\geq$ 1.75 + increase; NLR < 1.75 + decrease; and NLR < 1.75 + increase. By the end of the follow-up, the OS and DFS rates of NLR $\geq$ 1.75 + decrease group were 72.5 and 67.4%, respectively. In the NLR < 1.75 + decrease group, the OS and DFS rates were 76.4 and 74.3%, respectively. The median OS and DFS were 14.0 months and 13.0 months, respectively, in the NLR $\geq$ 1.75 + increase group. In the NLR < 1.75 + increase group, the median OS and DFS were 15.3 months and 14.3 months, respectively.

Patients with decreased NLR after NAC showed significantly favorable outcomes as compared to those with an increased NLR in both OS ($p < 0.001$) and DFS ($p < 0.001$) rates (**Figure 1**). Low post-chemotherapy NLR (<1.75) patients showed significantly longer OS ($p = 0.002$) and DFS ($p = 0.002$) than those with high post-chemotherapy NLR (≥1.75) (**Figure 2**). Interestingly, patients with high (≥1.75) but reduced post-chemotherapy NLR showed better OS ($p = 0.036$) and DFS ($p = 0.039$) than those with low (<1.75) but increased post-chemotherapy NLR (**Figure 3**). Among the high NLR (≥1.75) patients, those with decreased NLR showed longer OS ($p = 0.001$) and DFS ($p = 0.001$) than those with an increased NLR. Similarly, among the low NLR (<1.75) patients, those with decreased NLR showed

TABLE 1 | Clinicopathological features.

Variables	Change of NLR			*p* value
	Total (*n*)	Increase (*n* = 36)	Decrease (*n* = 75)	
Sex				0.150
Male	83	30	53	
Female	28	6	22	
Age (yr)				0.939
<60	58	19	39	
≥60	53	17	36	
Chemotherapy regimen				0.281
SOX	63	18	45	
XELOX	10	6	4	
FLOT	13	4	9	
Others	25	8	17	
Differentiation				0.130
High & medium	42	10	32	
Low, signet-ring cell carcinoma, mucinous adenocarcinoma	69	26	43	
Tumor size (cm)				0.939
<5	53	17	36	
≥5	58	19	39	
Tumor location				0.197
Upper 1/3	40	9	31	
Meddle 1/3	38	13	25	
Lower 1/3	33	14	19	
pT stage				0.739
1	7	2	5	
2	14	3	11	
3	48	18	30	
4	42	13	29	
Lymphatic metastasis				0.353
Yes	80	28	52	
No	31	8	23	
Venous invasion				0.920
Yes	47	15	32	
No	64	21	43	
Post-chemotherapy NLR				<0.001
<1.75	55	7	48	
≥1.75	56	29	27	
Recurrence				0.662
Yes	6	1	5	
No	105	35	70	
Metastasis				0.077
Yes	23	11	12	
No	88	25	63	
Outcome				<0.001
Alive	77	13	64	
Death	34	23	11	

NLR, neutrophil-to-lymphocyte ratio; pT, pathological T stage; DFS, disease-free survival; CI, confidence interval; HR, hazard ratio.

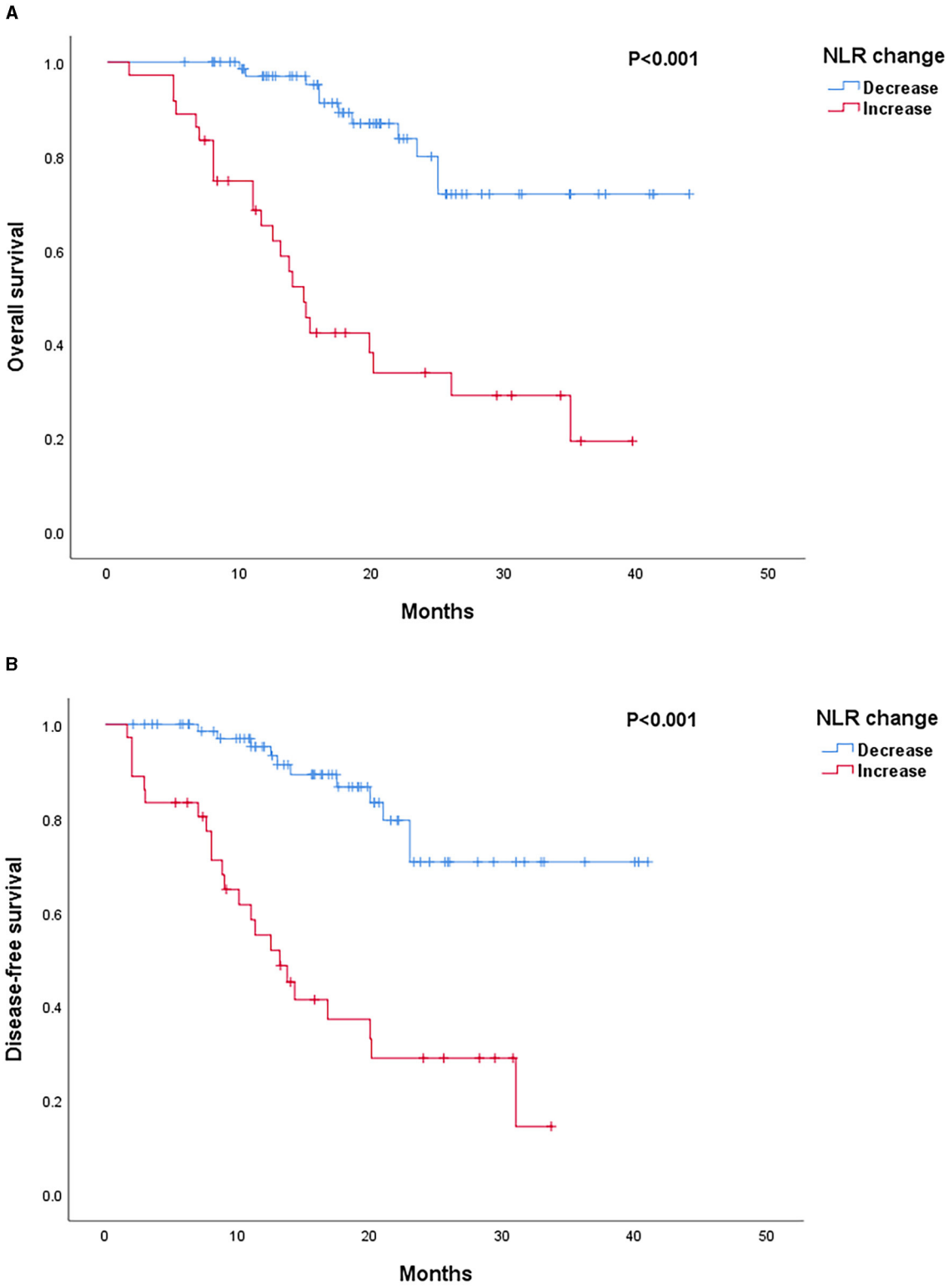

FIGURE 1 | (A) Survival outcomes according to neutrophil-to-lymphocyte ratio (NLR) change. Kaplan–Meier curves of OS. **(B)** Survival outcomes according to NLR change. Kaplan–Meier curves of DFS.

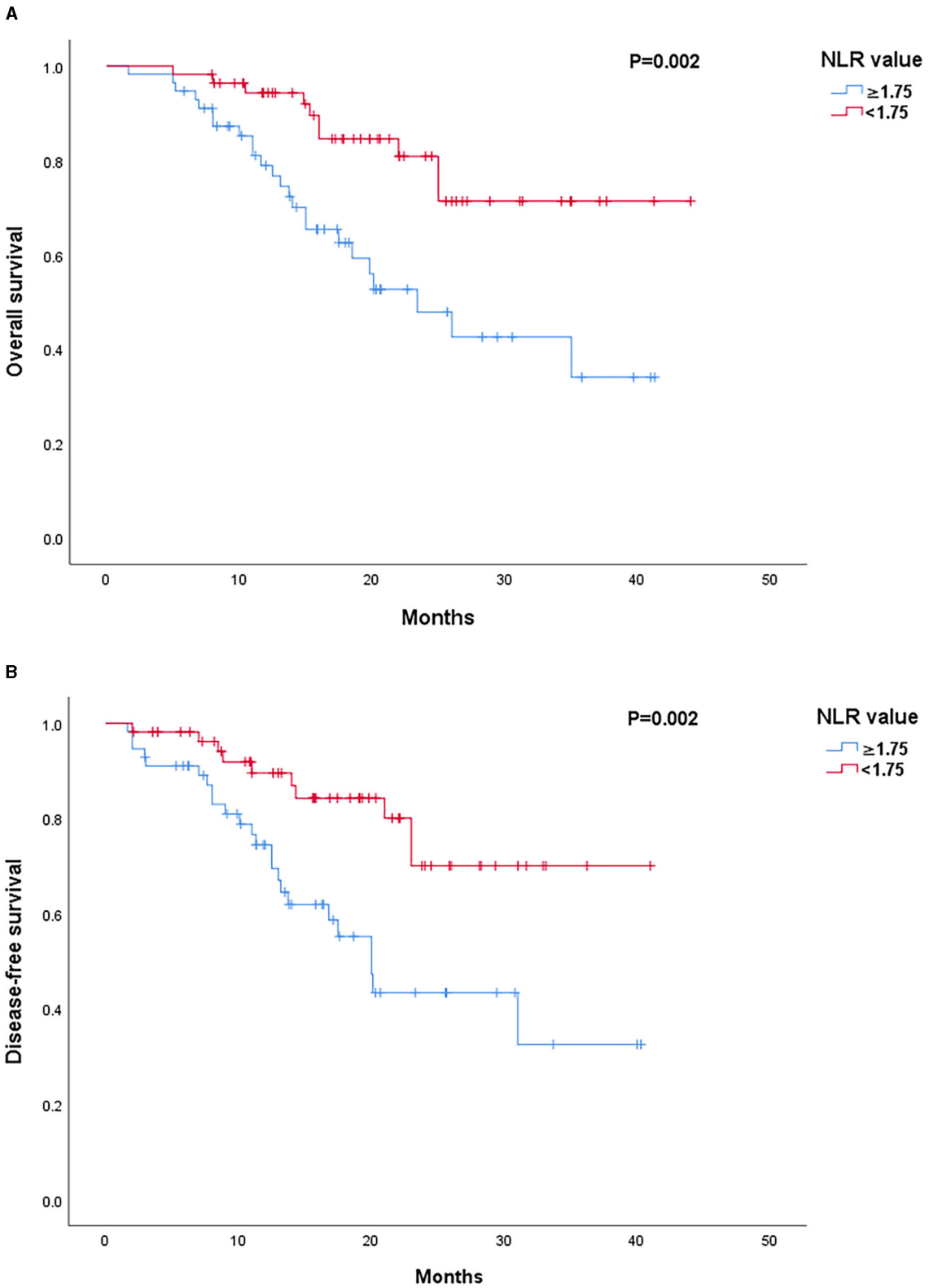

FIGURE 2 | (A) Survival outcomes according to post-chemotherapy NLR value. Kaplan–Meier curves of OS. **(B)** Survival outcomes according to post-chemotherapy NLR value. Kaplan–Meier curves of DFS.

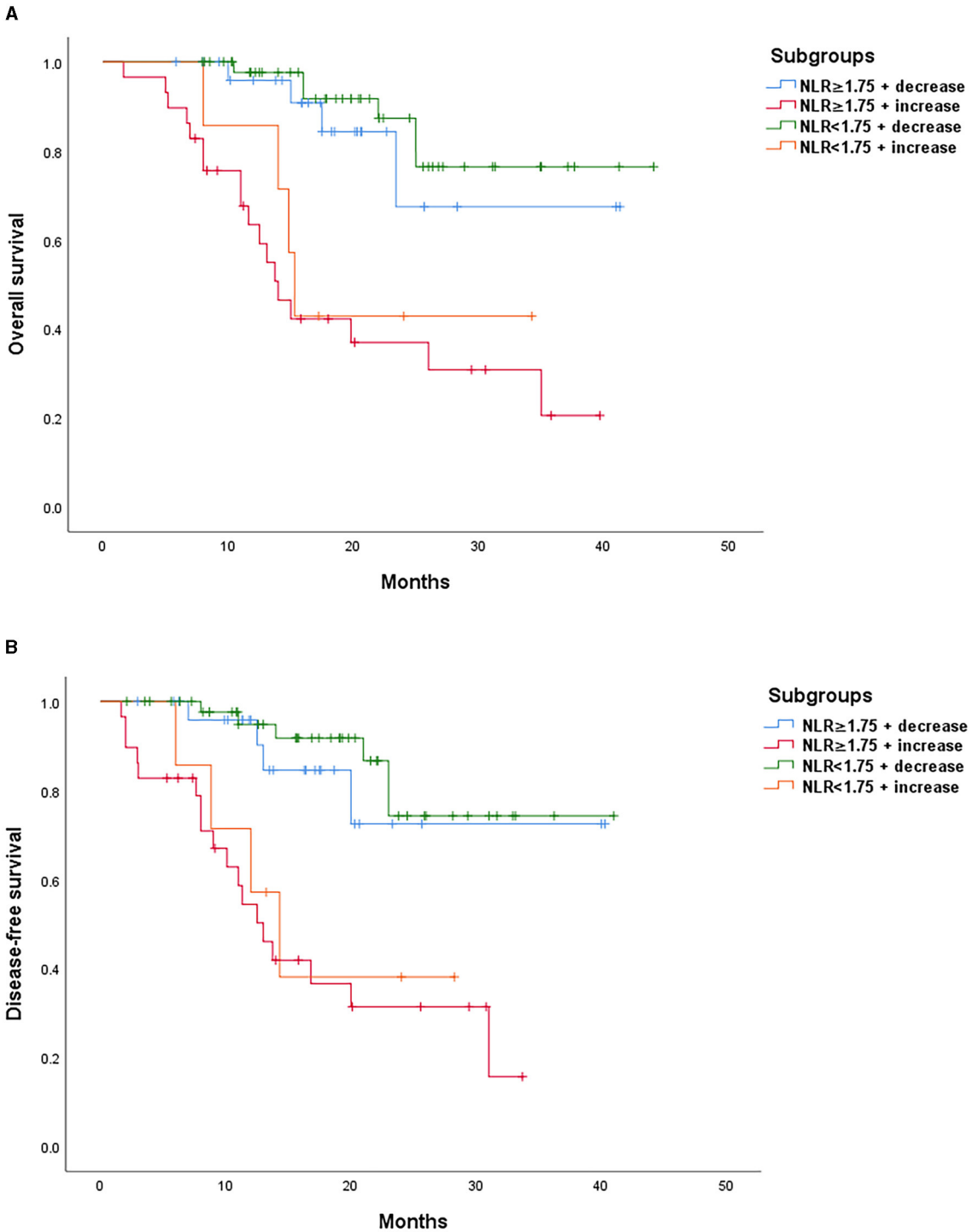

FIGURE 3 | (A) Survival outcomes according to subgroups. Kaplan–Meier curves of OS. **(B)** Survival outcomes according to subgroups. Kaplan–Meier curves of DFS.

longer OS ($p = 0.001$) and DFS ($p = 0.005$) than those with an increased NLR. As for the increased NLR group, there were no statistically significant differences between patients with high NLR (≥1.75) or low NLR (<1.75) in both OS ($p = 0.519$) and DFS ($p = 0.672$). Similar trends were observed in the decreased NLR group, and OS ($p = 0.425$) and DFS ($p = 0.460$) showed no significant differences among patients with high NLR (≥1.75) or low NLR (<1.75).

TABLE 2 | Univariate and multivariate analysis for overall survival (OS) in patients with advanced gastric cancer (AGC), who received neoadjuvant chemotherapy (NAC).

	Univariate	Multivariate		
Variables	***P*-value**	**HR**	**95%CI**	***P*-value**
Sex	0.408			
Male/female				
Age (yr)	0.413			
<60/≥60				
Chemotherapy regimen	0.486			
SOX/XELOX/FLOT/others				
Differentiation	0.029	0.485	0.246–1.537	0.299
High & medium/Low, signet-ring cell carcinoma, mucinous adenocarcinoma				
Tumor size (cm)	0.714			
<5/≥5				
Tumor location	0.004	1.127	0.981–9.713	0.054
Upper/meddle/lower				
pT stage	0.454			
1/2/3/4				
Lymphatic metastasis	0.698			
Yes/no				
Venous invasion	0.039	0.473	0.289–1.342	0.227
Yes/no				
Recurrence	0.168			
Yes/no				
Metastasis	<0.001	1.920	0.062–0.345	<0.001
Yes/no				
Pre-chemotherapy NLR	0.403			
<2.28/≥2.28				
Post-chemotherapy NLR	0.002	0.516	0.202–1.763	0.350
<1.75/≥1.75				
Change of NLR	<0.001	1.945	2.180–22.438	0.001
Increase/decrease				

NLR, neutrophil-to-lymphocyte ratio; pT, pathological T stage; DFS, disease-free survival; CI, confidence interval; HR, hazard ratio.

TABLE 3 | Univariate and multivariate analysis for disease-free survival (DFS) in patients with AGC, who received NAC.

	Univariate	Multivariate		
Variables	***P*-value**	**HR**	**95%CI**	***P*-value**
Sex	0.496			
Male/female				
Age (yr)	0.482			
<60/≥60				
Chemotherapy regimen	0.469			
SOX/XELOX/FLOT/others				
Differentiation	0.024	0.661	0.208–1.280	0.153
High & medium/low, signet-ring cell carcinoma, mucinous adenocarcinoma				
Tumor size (cm)	0.797			
<5/≥5				
Tumor location	0.003	0.720	0.679–6.218	0.203
Upper/meddle/lower				
pT stage	0.454			
1/2/3/4				
Lymphatic metastasis	0.660			
Yes/no				
Venous invasion	0.034	0.440	0.294–1.410	0.271
Yes/no				
Recurrence	0.131			
Yes/no				
Metastasis	<0.001	1.742	0.075–0.407	<0.001
Yes/no				
Pre-chemotherapy NLR	0.357			
<2.28/≥2.28				
Post-chemotherapy NLR	0.002	0.511	0.199–1.813	0.365
<1.75/≥1.75				
Change of NLR	<0.001	1.753	1.861–17.900	0.002
Increase/decrease				

NLR, neutrophil-to-lymphocyte ratio; pT, pathological T stage; DFS, disease-free survival; CI, confidence interval; HR, hazard ratio.

Prognostic Factors

Prognostic factors for DFS and OS were analyzed using univariate and multivariate analyses based on the Kaplan-Meier method and Cox regression model, respectively. Univariate analysis for OS showed that differentiation ($p = 0.029$), tumor location ($p = 0.004$), venous invasion ($p = 0.039$), metastasis ($p < 0.001$), post-chemotherapy NLR value ($p = 0.002$), and NLR change ($p < 0.001$) were significant risk factors (**Table 2**). Additionally, the significant risk factors for DFS were differentiation ($p = 0.024$), tumor location ($p = 0.003$), venous invasion ($p = 0.034$), metastasis ($p < 0.001$), post-chemotherapy NLR value ($p = 0.002$), and NLR change ($p < 0.001$, **Table 3**).

Factors that showed a univariable association ($p < 0.1$) with DFS or OS were included further in the multivariate Cox proportional-hazard regression model. According to multivariate analysis, metastasis (HR 0.147, 95% CI 0.062–0.345; $p < 0.001$) and NLR change (HR 1.920, 95% CI 2.180–22.438; $p < 0.001$) were independently associated with poor OS (**Table 2**), metastasis (HR 1.742, 95% CI 0.075–0.407; $p < 0.001$), and NLR change (HR 1.753, 95% CI 1.861–17.900; $p < 0.001$) were also independently associated with poor DFS (**Table 3**).

DISCUSSION

In this study, we investigated the prognostic value of NLR change in 111 patients with AGC who had received NAC. Patients were grouped according to the change in NLR after chemotherapy, and further sub-grouped according to their post-chemotherapy values of NLR. The results showed that regardless of whether their NLR was high (≥1.75) or low (<1.75) after chemotherapy, the survival in patients with decreased NLR after NAC was significantly better as compared to those with increased NLR (*p*

< 0.001). Interestingly, patients with decreased and high post-chemotherapy NLR had significantly longer OS ($p = 0.036$) and DFS ($p = 0.039$) than those with increased and low post-chemotherapy NLR, even if their NLR value were greater than the median value of 1.75. Decreased NLR after NAC could function as an independent prognostic indicator of better OS ($p < 0.001$) and DFS ($p < 0.001$). We confirmed that a decrease in NLR after NAC indicated better survival in patients with AGC. More importantly, NLR change could serve as a robust biomarker for the evaluation of chemotherapeutic response and outcomes in patients with AGC, which could further help in the selection of subsequent treatment strategies. To our best knowledge, this is the first study that proved the prognostic significance of NLR change after NAC in patients with AGC.

Since the relationship between inflammation and cancer was put forward by Rudolf Virchow over 150 years ago (20), the role of inflammation in the pathogenesis and development of malignant neoplasms has been widely studied for several tumors (21–23). There is a complex interaction between tumor-host immunity and inflammatory response. The damage to tissue due to tumors can trigger a series of immune responses both locally and in the whole body. Although the accumulation of various immune cell types in tumors represent part of the anti-tumor response, they, in turn, are repolarized for pro-tumorigenic functions, including the inhibition of cytotoxic immune-cell recruitment (24).

NLR, a combination biomarker, reflects the inflammatory response. In cancer, neutrophils are a vital component of the tumor microenvironment (25) that facilitate tumor progression by provoking mutation in tumor suppressor genes, driving angiogenesis, secreting enzymes and cytokines to promote proliferation and metastasis, remodeling extracellular matrix, and immunosuppression (26, 27). While, lymphocytes, triggered by the systemic inflammatory response, expose depression in innate cellular immunity as indicated by the increase in T8 suppressor lymphocytes and a decrease in T4 helper lymphocytes (28). Consequently, high NLR promotes tumor growth and inhibits anti-tumor response, ultimately leading to unfavorable prognosis in patients.

Although the role of NLR in predicting survival in patients with AGC has been confirmed in previous studies (29–31), the clinical values of NLR remain unclear in patients with AGC who have undergone NAC. Another non-negligible limitation in the existing studies is that the selection of NLR value parameters, such as median, mean, or the cutoff value derived from the ROC curve, varies between articles, which further weakens the applicability of NLR due to the lack of a uniform standard. NLR is a dynamic process. When inflammatory reactions and immune responses of the body are imbalanced, the anti-tumor action weakens and tumor growth-promoting effects are seen. The change in NLR is reflective of the transformation of this balance. Therefore, we bridged the NLR change with tumor outcomes and NAC efficiency in this study. Two key findings have emerged as follows: first, the decrease in NLR after NAC indicated resolution of inflammation or better chemotherapeutic response; second, decreased NLR after NAC implied better survival in patients with AGC. Our research addressed some previous limitations of existing studies and provided convenient and meaningful information for clinical practice. Theoretically, NLR change as an inflammation marker can better reflect the dynamic processes in the body. Clinically, NLR change can help in evaluating the efficiency of NAC. Prognostic stratification based on NLR change may guide physicians to incorporate a specific treatment regimen based on the performance of the patient. For example, drugs may be re-prescribed for targeted action in the poor prognosis group. Further studies are needed to validate this speculation. Additionally, early diagnosis and multidisciplinary therapies would be research hotspots in the future. NLR combined with traditional tumor markers and examinations may benefit to early screening outcomes in patients with GC. Besides, NLR change reflects the balance between inflammatory and immune responses in AGC patients. Thus, our study could provide strong evidence for the development of immunotherapy.

However, some limitations remain unaddressed in our study. First, this was a retrospective study at a single institution that enrolled a smaller number of patients. It is hard to draw a generalized conclusion as the populations in the present study do not represent all patients with AGC. Second, uniform NAC regimens and cycles were not administered to all patients enrolled in this study. Although more than 40% of the patients underwent a SOX treatment regimen, other regimens were also recommended. Failing to identify this information accurately could lead to a selection bias. Finally, we did not consider drug administration history which could influence the immune status (e.g., aspirin, NSAIDs, and corticosteroids). Hence, prospective clinical trials, multi-institutional enrolment, adequate sample sizes, and a single chemotherapeutic regimen should be considered in future investigations.

CONCLUSION

In conclusion, NLR change reflects the dynamicity between tumor inflammatory and immune responses. Decrease in NLR value after NAC corresponded to a good chemotherapeutic response and improved survival rates. Patients with AGC with decreased NLR after NAC showed more favorable OS and DFS. We confirmed that NLR change was a reliable and easily available prognostic factor for patients with AGC who had undergone NAC.

DATA AVAILABILITY STATEMENT

The raw data supporting the conclusions of this article will be made available by the authors, without undue reservation.

ETHICS STATEMENT

Written informed consent was obtained from the individual(s) for the publication of any potentially identifiable images or data included in this article.

AUTHOR CONTRIBUTIONS

ZL: investigation, resources, visualization, roles and writing—original draft, and writing—review and editing. YL: formal analysis and software. XT: data curation and project administration. HQ: conceptualization, funding acquisition, methodology, supervision, and validation. All authors contributed to the article and approved the submitted version.

REFERENCES

1. Sung H, Ferlay J, Siegel RL, Laversanne M, Soerjomataram I, Jemal A, et al. Global cancer statistics 2020: GLOBOCAN estimates of incidence and mortality worldwide for 36 cancers in 185 countries. *CA Cancer J Clin*. (2021) 71:209–49. doi: 10.3322/caac.21660
2. Karimi P, Islami F, Anandasabapathy S, Anandasabapathy S, Kamangar F. Gastric cancer: descriptive epidemiology, risk factors, screening, and prevention. *Cancer Epidemiol Biomarkers Prev*. (2015) 23:700–13. doi: 10.1158/1055-9965.EPI-13-1057
3. Tan Z. Recent advances in the surgical treatment of advanced gastric cancer: a review. *Med Sci Monit*. (2019) 25:3537–41. doi: 10.12659/MSM.916475
4. Johnston FM, Beckman M. Updates on management of gastric cancer. *Curr Oncol Rep*. (2019) 21:1–9. doi: 10.1007/s11912-019-0820-4
5. Claassen YHM, Hartgrink HH, Dikken JL, de Steur WO, van Sandick JW, van Grieken NCT, et al. Surgical morbidity and mortality after neoadjuvant chemotherapy in the CRITICS gastric cancer trial. *Eur J Surg Oncol*. (2018) 44:613–9. doi: 10.1016/j.ejso.2018.02.004
6. Ricci AD, Rizzo A, Lorena F, Llimpe R, Di Fabio F, De Biase D, et al. Novel HER2-directed treatments in advanced gastric carcinoma : another paradigm shift? *Cancers*. (2021) 13:1664. doi: 10.3390/cancers13071664
7. Nicole McMillian N, Lenora Pluchino MA, Ajani JA, D'Amico TA, Chair V, Bentrem DJ, et al. *NCCN Guidelines Version 2.2021 Gastric Cancer Continue NCCN Guidelines Panel Disclosures*. (2021).
8. Chen DS, Mellman I. Elements of cancer immunity and the cancer-immune set point. *Nature*. (2017) 541:321–30. doi: 10.1038/nature21349
9. Mantovani A, Allavena P, Sica A, Balkwill F. Cancer-related inflammation. *Nature*. (2008) 454:436–44. doi: 10.1038/nature07205
10. Coussens LM, Werb Z. Inflammation and cancer. *Nature*. (2002) 420:860–7. doi: 10.1038/nature01322
11. East JM, Hogan J, Samaha G, Medani M, Mackerricher W, Polinkevych S, et al. Ratios derived from an array of standard haematological indices predict the oncological outcome in colon cancer. *Color Dis*. (2014) 16:442–9. doi: 10.1111/codi.12561
12. Ishizuka M, Nagata H, Takagi K, Iwasaki Y, Kubota K. Combination of platelet count and neutrophil to lymphocyte ratio is a useful predictor of postoperative survival in patients with colorectal cancer. *Br J Cancer*. (2013) 109:401–7. doi: 10.1038/bjc.2013.350
13. Kemal Y, Demirag G, Ekiz K, Yücel I. Mean platelet volume could be a useful biomarker for monitoring epithelial ovarian cancer. *J Obstet Gynaecol*. (2014) 34:515–8. doi: 10.3109/01443615.2014.912620
14. Kemal Y, Yucel I, Ekiz K, Demirag G, Yilmaz B, Teker F, et al. Elevated serum neutrophil to lymphocyte and platelet to lymphocyte ratios could be useful in lung cancer diagnosis. *Asian Pacific J Cancer Prev*. (2014) 15:2651–4. doi: 10.7314/APJCP.2014.15.6.2651
15. Rihawi K, Ricci AD, Rizzo A, Brocchi S, Marasco G, Pastore LV, et al. Tumor-associated macrophages and inflammatory microenvironment in gastric cancer : novel translational implications. *Int J Mol Sci*. (2021) 7:3805. doi: 10.3390/ijms22083805
16. Templeton AJ, McNamara MG, Šeruga B, Vera-Badillo FE, Aneja P, Ocaña A, et al. Prognostic role of neutrophil-to-lymphocyte ratio in solid tumors: a systematic review and meta-analysis. *J Natl Cancer Inst*. (2014) 106:dju124. doi: 10.1093/jnci/dju124
17. Hirahara T, Arigami T, Yanagita S, Matsushita D, Uchikado Y, Kita Y, et al. Combined neutrophil-lymphocyte ratio and platelet-lymphocyte ratio predicts chemotherapy response and prognosis in patients with advanced gastric cancer. *BMC Cancer*. (2019) 19:672. doi: 10.1186/s12885-019-5903-y
18. Zhang L-X, Wei Z-J, Xu A-M, Zang JH. Can the neutrophil-lymphocyte ratio and platelet-lymphocyte ratio be beneficial in predicting lymph node metastasis and promising prognostic markers of gastric cancer patients? Tumor maker retrospective study. *Int J Surg*. (2018) 56:320–7. doi: 10.1016/j.ijsu.2018.06.037
19. Szor DJ, Dias AR, Pereira MA, Fernando M, Pertille K, Zilberstein B, et al. Neutrophil-lymphocyte ratio change after curative gastrectomy for gastric cancer : a subgroup analysis. *Einstein*. (2020) 18:eAO4860. doi: 10.31744/einstein_journal/2020AO4860
20. Balkwill F, Mantovani A. Inflammation and cancer: back to Virchow? *Lancet*. (2001) 357:539–45. doi: 10.1016/S0140-6736(00)04046-0
21. Diakos CI, Charles KA, McMillan DC, Clarke SJ. Cancer-related inflammation and treatment effectiveness. *Lancet Oncol*. (2014) 15:e493–503. doi: 10.1016/S1470-2045(14)70263-3
22. Greten FR, Grivennikov SI. Inflammation and cancer: triggers, mechanisms, and consequences. *Immunity*. (2019) 51:27–41. doi: 10.1016/j.immuni.2019.06.025
23. Elinav E, Nowarski R, Thaiss CA, Hu B, Jin C, Flavell RA. Inflammation-induced cancer: crosstalk between tumours, immune cells and microorganisms. *Nat Rev Cancer*. (2013) 13:759–71. doi: 10.1038/nrc3611
24. De Visser KE, Eichten A, Coussens LM. Paradoxical roles of the immune system during cancer development. *Nat Rev Cancer*. (2006) 6:24–37. doi: 10.1038/nrc1782
25. Fridman WH, Zitvogel L, Sautès-Fridman C, Kroemer G. The immune contexture in cancer prognosis and treatment. *Nat Rev Clin Oncol*. (2017) 14:717–34. doi: 10.1038/nrclinonc.2017.101
26. Jaillon S, Ponzetta A, Di Mitri D, Santoni A, Bonecchi R, Mantovani A. Neutrophil diversity and plasticity in tumour progression and therapy. *Nat Rev Cancer*. (2020) 20:485–503. doi: 10.1038/s41568-020-0281-y
27. Xu A-M, Huang L, Zhu L, Wei Z-J. Significance of peripheral neutrophil-lymphocyte ratio among gastric cancer patients and construction of a treatment-predictive model: a study based on 1131 cases. *Am J Cancer Res*. (2014) 4:189–95.
28. Lee S, Oh SY, Kim SH, Lee JH, Kim MC, Kim KH, et al. Prognostic significance of neutrophil lymphocyte ratio and platelet lymphocyte ratio in advanced gastric cancer patients treated with FOLFOX chemotherapy. *BMC Cancer*. (2013) 13:350. doi: 10.1186/1471-2407-13-350
29. Wang H, Ding Y, Li N, Wu L, Gao Y, Xiao C, et al. Prognostic value of neutrophil–lymphocyte ratio, platelet–lymphocyte ratio, and combined neutrophil–lymphocyte ratio and platelet–lymphocyte ratio in stage IV advanced gastric cancer. *Front Oncol*. (2020) 10:841. doi: 10.3389/fonc.2020.00841
30. Aldemir MN, Turkeli M, Simsek M, Yildirim N, Bilen Y, Yetimoglu H, et al. Prognostic value of baseline neutrophil-lymphocyte and platelet-lymphocyte ratios in local and advanced gastric cancer patients. *Asian Pacific J Cancer Prev*. (2015) 16:5933–7. doi: 10.7314/APJCP.2015.16.14.5933
31. Rae I, Jun C, Park C, Hyuk C, Jung P, Jo H. Pre-treatment neutrophil to lymphocyte ratio as a prognostic marker to predict chemotherapeutic

response and survival outcomes in metastatic advanced gastric cancer. *Gastric Cancer*. (2014) 17:703–10. doi: 10.1007/s10120-013-0330-2

Conflict of Interest: The authors declare that the research was conducted in the absence of any commercial or financial relationships that could be construed as a potential conflict of interest.

Publisher's Note: All claims expressed in this article are solely those of the authors and do not necessarily represent those of their affiliated organizations, or those of the publisher, the editors and the reviewers. Any product that may be evaluated in this article, or claim that may be made by its manufacturer, is not guaranteed or endorsed by the publisher.

Copyright © 2021 Liu, Liang, Tang and Qu. This is an open-access article distributed under the terms of the Creative Commons Attribution License (CC BY). The use, distribution or reproduction in other forums is permitted, provided the original author(s) and the copyright owner(s) are credited and that the original publication in this journal is cited, in accordance with accepted academic practice. No use, distribution or reproduction is permitted which does not comply with these terms.

frontiers in Medicine

ORIGINAL RESEARCH
published: 22 November 2021
doi: 10.3389/fmed.2021.766061

Comparing the Expressions of Vitamin D Receptor, Cell Proliferation, and Apoptosis in Gastric Mucosa With Gastritis, Intestinal Metaplasia, or Adenocarcinoma Change

Li-Wei Chen[1,2]*, *Liang-Che Chang*[3], *Chung-Ching Hua*[4], *Tzu-Chien Cheng*[3] and *Chin-Chan Lee*[2,4]

[1] Department of Gastroenterology and Hepatology, Chang-Gung Memorial Hospital and University at Keelung, Keelung, Taiwan, [2] Community Medicine Research Center, Chang-Gung Memorial Hospital and University at Keelung, Keelung, Taiwan, [3] Department of Pathology, Pathology Chang-Gung Memorial Hospital and University at Keelung, Keelung, Taiwan, [4] Department of Internal Medicine, Internal Medicine Chang-Gung Memorial Hospital and University at Keelung, Keelung, Taiwan

OPEN ACCESS

Edited by:
Ravindra Deshpande, Wake Forest School of Medicine, United States

Reviewed by:
Gargi Mahapatra, Wake Forest Baptist Medical Center, United States
Angela Verma, University of Maryland, Baltimore, United States
Praveen Kumar Allu, University of Pennsylvania, United States

***Correspondence:**
Li-Wei Chen
leiwei@cgmh.org.tw

Specialty section:
This article was submitted to Gastroenterology, a section of the journal Frontiers in Medicine

Received: *28 August 2021*
Accepted: *27 October 2021*
Published: *22 November 2021*

Citation:
Chen L-W, Chang L-C, Hua C-C, Cheng T-C and Lee C-C (2021) Comparing the Expressions of Vitamin D Receptor, Cell Proliferation, and Apoptosis in Gastric Mucosa With Gastritis, Intestinal Metaplasia, or Adenocarcinoma Change. Front. Med. 8:766061. doi: 10.3389/fmed.2021.766061

Background: This study aimed to compare the expression of vitamin D receptor (VDR), cell proliferation, and apoptosis in the gastric mucosa of patients with gastritis, intestinal metaplasia (IM), and adenocarcinoma using artificial intelligence.

Material and Methods: This study retrospectively enrolled patients at the Keelung Chang Gung Memorial Hospital from November of 2016 to June, 2017, who were diagnosed with gastric adenocarcinoma. The inclusion criteria were patients' pathologic reports that revealed all compartments of *Helicobacter pylori* infection, gastritis, IM, and adenocarcinoma simultaneously in the same gastric sample. Tissue slides after immunohistochemical (IHC) staining were transformed into digital images using a scanner and counted using computer software (QuPath and ImageJ). IHC staining included PA1-711 antibody for VDR, Ki67 antigen for proliferation, and M30 antibody CK18 for apoptosis.

Results: Twenty-nine patients were included in the IHC staining quantitative analysis. The mean age was 69.1 ± 11.3 y/o. Most (25/29, 86.2%) patients had poorly differentiated adenocarcinoma. The mean expression of Ki67 and CK18 increased progressively from gastritis and IM to adenocarcinoma, with statistical significance ($P < 0.05$). VDR expression did not correlate with Ki67 or CK18 expression. Survival time was only correlated with tumor stage (correlation coefficient = −0.423, P value < 0.05), but was not correlated with the expression of VDR, Ki67, and CK18.

Conclusion: Ki67 expression and CK18 expression progressively increased in the areas of gastritis, IM, and adenocarcinoma. No correlation between VDR expression and Ki67 or CK18 expression was found in this study.

Keywords: adenocarcinoma, stomach neoplasm, cell proliferation, apoptosis, artificial intelligence, Ki67 antigen, keratin 18, receptor calcitriol

INTRODUCTION

Gastritis and intestinal metaplasia (IM) are common findings in patients with *Helicobacter pylori* (*H. pylori*) infection (1, 2). The prevalence of IM in patients with *H. pylori* infection is 30–40% at the age of 50 years old (1, 2). Gastric epithelial hyperproliferation has been observed in patients with gastritis and IM caused by *H. pylori* infection (3–5). Previous studies have also revealed that IM is associated with an increased risk of gastric cancer (6–9). Detection of IM in gastric adenocarcinoma samples is a common histological finding (9).

Apoptotic cells are rare in the glandular neck region (the generative cell zone) of normal gastric mucosa. With progression of atrophic gastritis, the generative cell zone shifts downward and a relatively large number of apoptotic cells occur (10). *H. pylori* infection induces apoptosis in gastric epithelial cells (10). The effect of *H. pylori* apoptosis could result from molecules produced by *H. pylori* or the host immune/inflammatory response (10). Molecules such as cytotoxin (VacA), lipopolysaccharide, or nitric oxide may directly induce apoptosis (10, 11). Many cytokines produced by type 1 T helper cells, such as TNF-α and IFN-γ, markedly potentiate apoptosis. The balance between cell proliferation and apoptosis is important for carcinogenesis in precancerous lesions, such as IM and *H. pylori* infection (10, 11).

Gut epithelial vitamin D receptor (VDR) signaling appears to play an essential role in controlling mucosal inflammation and thus could be a useful therapeutic target in the management of some gastrointestinal diseases (12). Although 1, 25-Dihydroxyvitamin D [1, 25 $(OH)_2D3$] is not produced by the stomach, it affects the immune regulatory responses via the VDR of the stomach (13–15). Vitamin D deficiency has been associated with risk of several cancers including gastric cancer (16). VDR is a superfamily of steroid hormone receptors that act as a transcription factor for a target gene. Moreover, 1, 25 $(OH)_2D3$ was reported to be associated with the inhibition of cell cycle progression, induction of cell apoptosis, and differentiation of various types of cancer cells. Hence, 1, 25 $(OH)_2D3$ has been reported to inhibit proliferation and anti-tumor effects via VDR (15, 16). VDR was also reported to play an important role in gastric mucosa homeostasis and host protection against *H. pylori* infection (13). VDR could regulate cathelicidin antimicrobial protein (CAMP) and has an antimicrobial activity against *H. pylori* (13, 17). Past studies found an important role of the VDR/CAMP pathway in innate immunity and an anti-inflammatory mechanism of vitamin D. VDR mRNA expression levels were significantly up-regulated in *H. pylori*-infected patients and positively correlated with chronic inflammation scores. There was a significant positive correlation between VDR and CAMP mRNA expression in *H. pylori*-positive gastric mucosa (13). In animal model study using wild-type and VDR knockdown mice to demonstrate that VitD3 inhibits H. pylori infection by enhancing the expression of VDR and CAMP. VDR knockdown mice were more susceptible to H. pylori infection. In cultured mouse primary gastric epithelial cells, VitD3/VDR complex binds to the CAMP promoter region to increase its expression (17).

1, 25 (OH)2D3 binding to VDR could transcriptionally activate the expression of a number of target genes, finally executing the antitumor functions. A lot of genes have been identified as its direct targets, such as p21 (18, 19) and c-Myc (20) which are involved in different signaling pathways during tumor genesis. A previous study has shown that vitamin D suppresses proliferation and stimulates cell cycle arrest in gastric cancer cells but not in immortalized normal gastric cells (12). Vitamin D has increased p21 expression and decreased cyclin-dependent kinase 2 (CDK2) expression via VDR route (12).

The hypothesis of this study was that patients infected with *H. pylori* might have gastritis, gastric IM, and gastric adenocarcinoma. VDR expression in the stomach may differ in the areas of gastritis, IM, and gastric adenocarcinoma. When compared with the area of gastritis, the pathologic presentation of cell proliferation and apoptosis may be different in the areas of IM and adenocarcinoma. A progressive increase or decrease in cell proliferation or apoptosis may be detected in the areas of gastritis, IM, and gastric cancer, respectively.

The current study aimed to evaluate VDR expression, cell proliferation, and apoptosis in gastric adenocarcinoma samples using digital quantitative immunohistochemistry (IHC) statin analyses. In this study we aimed to:

1. Compare the Expression of VDR, Cell Proliferation (by Ki67 Statin), and Apoptosis (by CK18 Staining) in three Different Parts, Including Gastritis (non-Dysplasia or Tumor), IM (Premalignant Area), and Gastric Adenocarcinoma (Malignant Site) by Artificial Intelligence (AI) Using Computer Software to Prevent Manual or Inter-Observer Bias for IHC Score Counting;
2. Analyze the Association Between VDR Expression, Cell Proliferation, and Apoptosis;
3. Elucidate Whether High VDR Expression Is Associated With Higher or Lower Cell Proliferation and Apoptosis;
4. Analyze the Correlation of Survival Time With Tumor Stage and three IHC Stain Expressions.

MATERIALS AND METHODS

Subjects and Tissue Samples

This study retrospectively enrolled patients who were diagnosed with gastric adenocarcinoma at the Keelung Chang Gung Memorial Hospital (KCGMH) from November of 2016 to June 2017. Gastric samples that were confirmed as malignant after pathologic examination were stored in the tissue bank of KCGMH. For a patient with both endoscopic biopsy and surgical resection specimens, samples from surgical resection were used for IHC staining expression analyses in this study. For patients without an operation for gastric malignancy, endoscopic biopsy samples were used for IHC analyses. The inclusion criteria were patients' pathologic reports that revealed all compartments of *H. pylori* infection, gastritis, IM, and adenocarcinoma simultaneously in the same gastric sample. The exclusion criteria were incomplete records of demographic data, tumor stage, and clinical course.

Patient demographics, tumor location in the stomach, tumor stage, and survival time were recorded. No chemotherapy, radiotherapy, or other therapies were performed in these patients before endoscopic biopsy or surgical resection. Two pathologists (Dr. Chang LC and Dr. Cheng TC) provided all the equipment and histological examinations. Every specimen was reviewed by an experienced pathologist (Dr. Chang LC) under microscopic examination to localize the areas of gastritis, IM, and adenocarcinoma. Commercial kits for IHC staining and publicly available software applications for digital image creation and quantitative analysis were used. This study was approved by the Ethics Committee of the Chang Gung Memorial Hospital (IRB No 103-7463A3, 105-4426C).

Histology and IHC Stain for *H. pylori* Detection and IM

Histology (hematoxylin and eosin) and IHC *H. pylori* antibody staining (polyclone, Zytomed Systems GmbH, Berlin, Germany) were performed to confirm *H. pylori* infection. Histological sections of all specimens were routinely examined to determine gastritis, IM, and malignancy. Because the gastric mucosa adjacent to malignancy is always infiltrated by inflammatory cell, a diagnosis of gastritis is made for this non-tumor, non-IM mucosa by pathologists. IM was detected based on the morphological features in the stomach observed by H&E and Alcian blue staining (6, 21).

Digital Quantitative Analyses for IHC Images

Tissue sections were cut from the tissue blocks at 4 μm and stained with H&E and IHC. The slides were scanned at 400 × magnification using a Hamamatsu Nanozoomer S360 scanner and NDP image (Hamamatsu, Japan). Digital data analysis was performed using computer software to prevent manual or inter-observer bias for IHC score counting. The computer softwares ImmunoRatio (ImageJ plugin) (22) and QuPath (23) were applied for digital slide bioimage analyses (24–26). The application of ImmunoRatio calculates the percentage of positively stained nuclear area (labeling index) by using a color deconvolution algorithm for separating the staining components (diaminobenzidine and hematoxylin) and adaptive thresholding for nuclear area segmentation (25). Every digital image was quantitatively analyzed in three adjacent areas: gastritis, IM, and adenocarcinoma.

Ki-67 Antigen for Epithelial Cell Proliferation

Antigen Ki-67 IHC staining was performed using a DAKO autostain agent (Cytomation, Carpinteria, CA, USA). The REAL EnVision Detection System, Peroxidase/diaminobenzidine (DAB) (K5007, DAKO), was used to visualize the staining.

PA1-711 Antibody for VDR

After appropriate blocking and management of gastric tissue, VDR staining was performed using an anti-VDR polyclonal antibody (PA1-711, Thermo Scientific, Fremont, CA, USA).

M30 CytoDEATH Antibody for Detecting Apoptosis

Mouse monoclonal antibody (Clone M30, mouse IgG2b) was used to detect apoptosis in epithelial cells (caspase cleavage product of cytokeratin 18, CK18). Apoptosis was detected by applying the M30-antibody to fixed samples, and then secondary detection systems were used for IHC staining. The M30 CytoDEATH antibody (Roche Diagnostics GmbH, Mannheim, Germany) binds to a caspase-cleaved, formalin-resistant epitope of the CK 18 cytoskeletal protein (27).

Gastric Cancer Stage

Gastric cancer staging was performed according to the American Joint Committee on Cancer (AJCC, 7th edition) (28).

Statistical Analysis

Continuous data are expressed as mean ± standard deviation (SD). A two-sample *t*-test was used to compare the mean values. Categorical data were analyzed using chi-square and Fisher exact tests. One-way analysis of variance (ANOVA) was used to compare the mean values of multiple samples. The Scheffe method was applied for *post-hoc* analysis. All statistical tests were two-tailed. Differences were considered statistically significant at $p < 0.05$. Statistical analyses were performed using the Statistical Package for the Social Sciences (version 18.0) for Windows (PASW, Chicago, IL, USA).

RESULTS

Initially, 69 gastric tissue samples were collected from the tissue bank of KCGMH. Among these 69 samples, 32 originated from the same patients (from endoscopic biopsy and surgical resection). Five samples were inadequate for IHC staining examination. We were unable to trace the origins of three samples. Finally, 29 patients (24 surgical resections and 5 endoscopic biopsies) were included in the IHC staining analysis (**Figure 1**, Study flow). IHC stains of PAI 711 antibody (VDR), Ki67 antigen (cell proliferation), and M30 antibody CK18 (cell apoptosis) were performed for all samples from these 29 patients.

The demographic and clinical characteristics of the patients are listed in **Table 1**. The mean age was 69.1 ± 11.3 y/o. Most (25/29, 86.2%) patients had poorly differentiated adenocarcinoma. The tumors were located in the gastric antrum (22/29, 75.9%), body (6/29, 20.7%), and cardiac (1/29, 3.4%). Tumor stages at diagnosis were stage I (13/29, 44.8%), stage II (2/29, 6.9%), stage III (6/29, 20.7%), and stage IV (8/29, 27.6%).

Digital images of *H. pylori* infection (H&E and antibody stain, **Figure 2**). **Figures 3**, **4** reveals digital images of H&E and CK18 stain in different sites (total, gastritis, IM, and adenocarcinoma). Digital analyses of IHC expression using ImageJ and ImmunoRatio software are presented in **Figure 5**. **Figure 6** reveals different cell types (moderate differentiation and well-differentiation) gastric adenocarcinoma and IHC (VDR, Ki67 and CK18) stain.

The expression levels of PAI 711 antibody (VDR), Ki67 antigen (cell proliferation), and M30 antibody CK18 (cell apoptosis) among gastritis, IM, and adenocarcinoma are listed

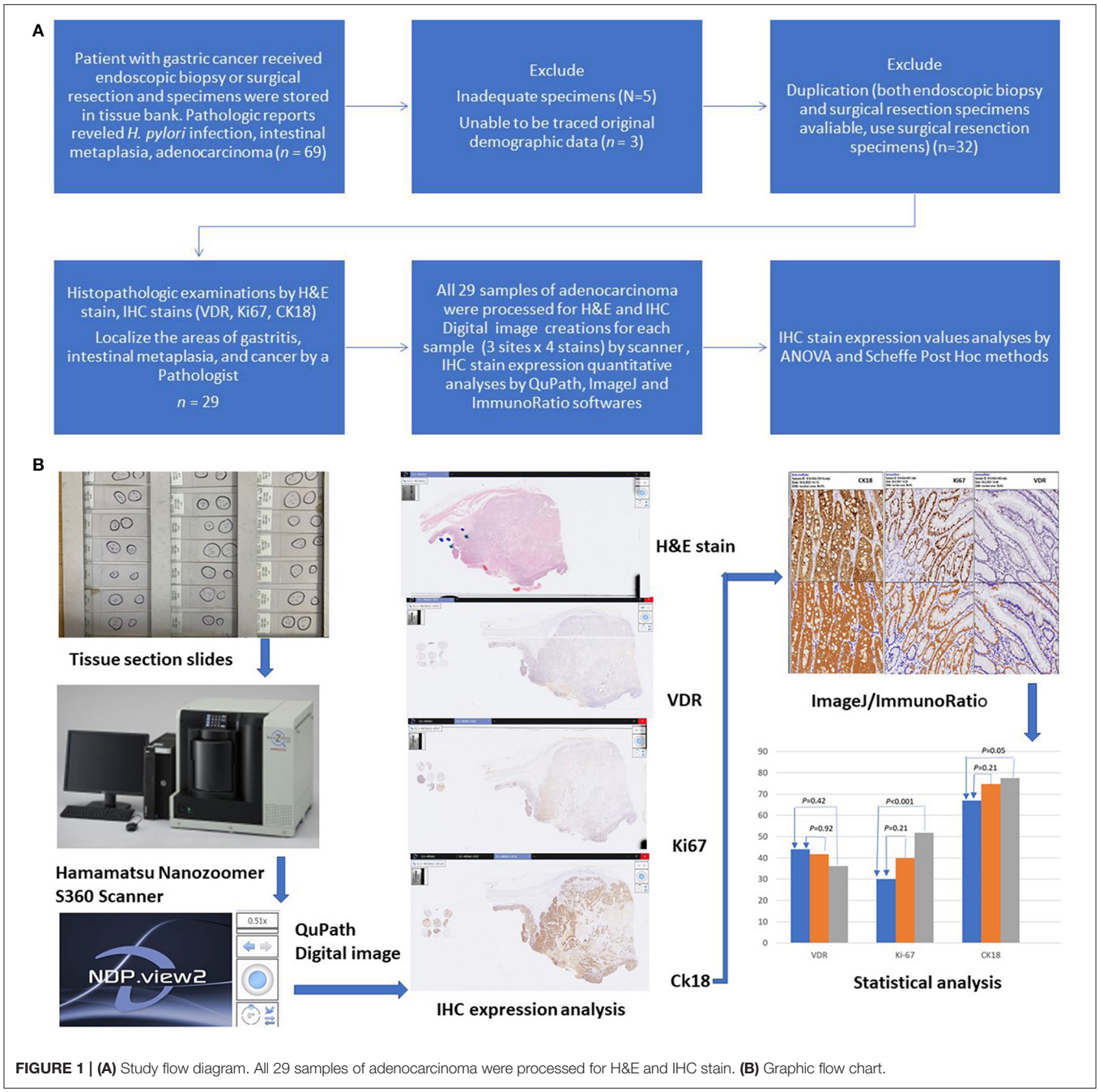

FIGURE 1 | (A) Study flow diagram. All 29 samples of adenocarcinoma were processed for H&E and IHC stain. **(B)** Graphic flow chart.

in **Table 2**. The mean expression of Ki67 and CK18 increased significantly ($P < 0.05$) from gastritis, IM to adenocarcinoma. However, mean values of VDR expression were no statistical difference among gastritis, IM, and adenocarcinoma by ANOVA ($P = 0.404$).

Table 3 shows the Scheffe *post-hoc* analysis. The main location for a different expression of Ki67 and CK18 were between gastritis and cancer. The expression of Ki67 and CK18 was similar between the IM (premalignancy) and adenocarcinoma (malignancy) sites (**Figure 7**).

When a correlation analysis between VDR and Ki67 or CK18 was performed, VDR expression was not correlated with Ki67 or CK18 expression in gastritis, IM and adenocarcinoma site (**Table 4**).

Compare the VDR expression in gastritis, IM, and adenocarcinoma between male and female patients. There was no statistical difference of mean VDR expression between male and female patients in the gastritis (42.2 ± 25.0 vs. 48.9 ± 27.7, $P = 0.58$), IM (41.8 ± 17.3 vs. 41.7 ± 14.7, $P = 0.73$), and adenocarcinoma (36.6 ± 18.8 vs. 36.6 ± 18.5, $P = 0.98$).

Survival time was only correlated with tumor stage (correlation coefficient = −0.423, *P*-value < 0.05), but was not correlated with the expression of VDR, Ki67, and CK18.

DISCUSSION

VDR could regulate cathelicidin antimicrobial protein (CAMP) and has an antimicrobial activity against *H. pylori* (13, 17). Past studies found an important role of the VDR/CAMP pathway in innate immunity and an anti-inflammatory mechanism of vitamin D (13, 17). VDR mRNA expression levels were significantly up-regulated in *H. pylori*-infected patients and positively correlated with chronic inflammation scores. There was a significant positive correlation between VDR and CAMP mRNA expression in *H. pylori*-positive gastric mucosa (13). Previous studies have shown that VDR expression may control the expression of cell proliferation and apoptosis (14–16, 29–31). Wen et al. (32) demonstrated that VDR was lowest in cancer tissues (positive rate = 57.61%), compared to premalignant (73.64%) and normal tissues (82.61%), with a statistically significant difference ($P = 0.001$). A decline in VDR expression was observed in normal, premalignant, and malignant gastric tissues, especially in poorly differentiated tissues. In our study,

TABLE 1 | Demography and clinical characters.

Age (y/o)	69.1 ± 11.3
Gender (F/M)	12/17
Adenocarcinoma type (tubular/other)	(27/2)
Tumor location (antrum/body/cardiac)	22/6/1
Differentiation (poor/moderate/well)	25/4/0
Operation (with/without) after diagnosis	24/5
Operation type (BI/BII/Total gastrectomy)	14/8/2
Tumor stage (I/II/III/IV)	13/2/6/8
Chemotherapy (with/without) after diagnosis	15/14
Mean survival days (stage I/II/III/IV)	2631/1472/920/274

IM, intestinal metaplasia; BI, Billroth's I subtotal gastrectomy; BII, Billroth's II subtotal gastrectomy; Total, total gastrectomy.

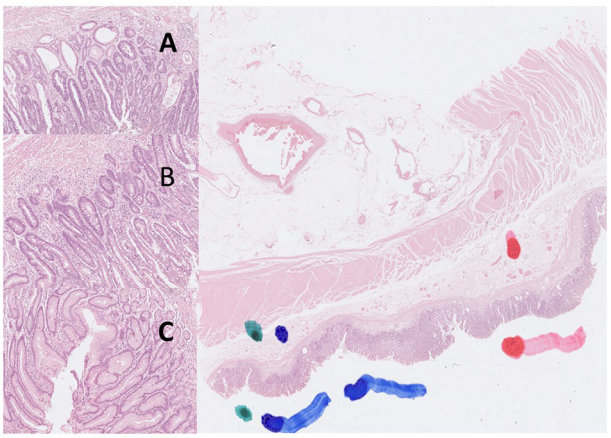

FIGURE 3 | Digital pictures of H&E stain created by Hamamatsu Nanozoomer S360 scanner and QuPath software (40X). The color markers were made by a pathologist to localize the targeted areas (green color: gastritis; blue color: intestinal metaplasia; red color: gastric adenocarcinoma). **(A)** adenocarcinoma, **(B)** intestinal metaplasia, **(C)** gastritis.

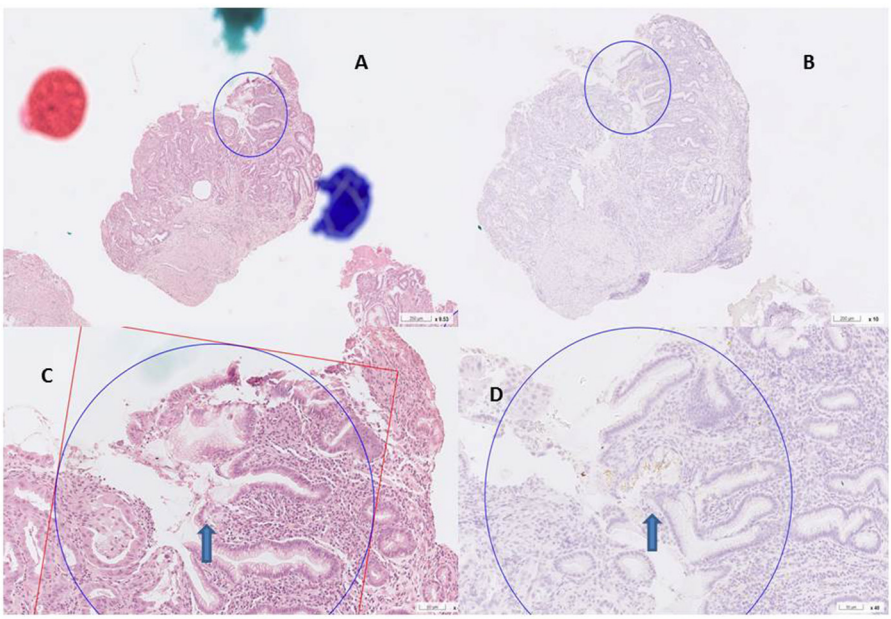

FIGURE 2 | *H. pylori* infection H&E and antibody stain. **(A,B)** H& E stain, curved bacilli within the mucus of epithelim (arrow). **(C,D)** anti *H. pylori* antibody stain (arrow).

there was no statistically difference of VDR expression (44.1%, 41.8%, 36.1% in gastritis, IM, and malignant tissue, respectively; $P = 0.404$) was detected. The main reason for the difference in results between Wen et al. (32) and our study may be due to the different methods for VDR expression evaluation. In Wen et al. study, VDR expression was presented as a positive rate (PR), which was similar to qualitative analysis (positive or negative). Moreover, some gastritis or IM tissues were collected from patients without gastric cancer. In our study, quantitative digital analyses were performed to prevent intra-or inter-observer bios. All three parts (gastritis, IM, and cancer) were adjacent and came from the same patient. Because the major type of gastric adenocarcinoma was poorly differentiated in this study, similar VDR expression in the mucosa adjacent to the tumor may be found in patients with poorly differentiated gastric adenocarcinoma.

The relationship between serum vitamin D deficiency and gastric cancer development remains under debate (13–15, 33, 34). Because 1, 25 $(OH)_2D3$ is not produced by the stomach, 1, 25 $(OH)_2D3$ affects the immune regulatory responses via the VDR of the stomach (12–14). However, no serum vitamin D level was recorded in this study because checking the vitamin D level was not a regular guideline for gastric adenocarcinoma treatment. To understand the relationship between serum vitamin D level and gastric VDR expression, it is necessary to include more patients with serum vitamin D and VDR expression in the gastric mucosa by endoscopic biopsy.

It is common to disclose increased proliferation and decreased apoptosis in malignant cells (10). Our hypothesis was an increased Ki67 (cell proliferation) and a deceased CK18 (apoptosis) in cancer, but the results of our study revealed that both Ki67 and CK18 expression increased in IM and malignant tissues. Apoptosis is defined by characteristic changes in nuclear morphology, including chromatin condensation and fragmentation, overall cell shrinkage, and blebbing of the plasma membrane. CK18 expression was high (mean 77.6%) in gastric

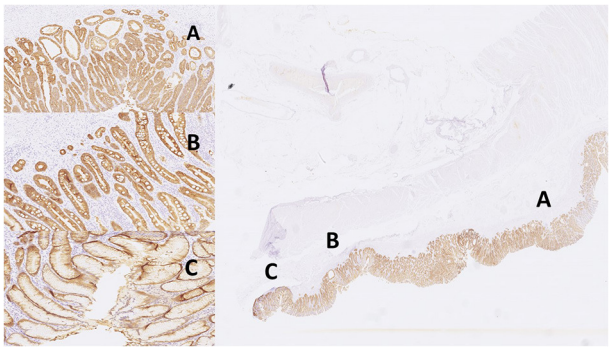

FIGURE 4 | Images of IHC expression by CK18 stain in different sites. Right: total; left top: gastritis; left middle: IM; left bottom: adenocarcinoma. **(A)** adenocarcinoma, **(B)** intestinal metaplasia, **(C)** gastritis.

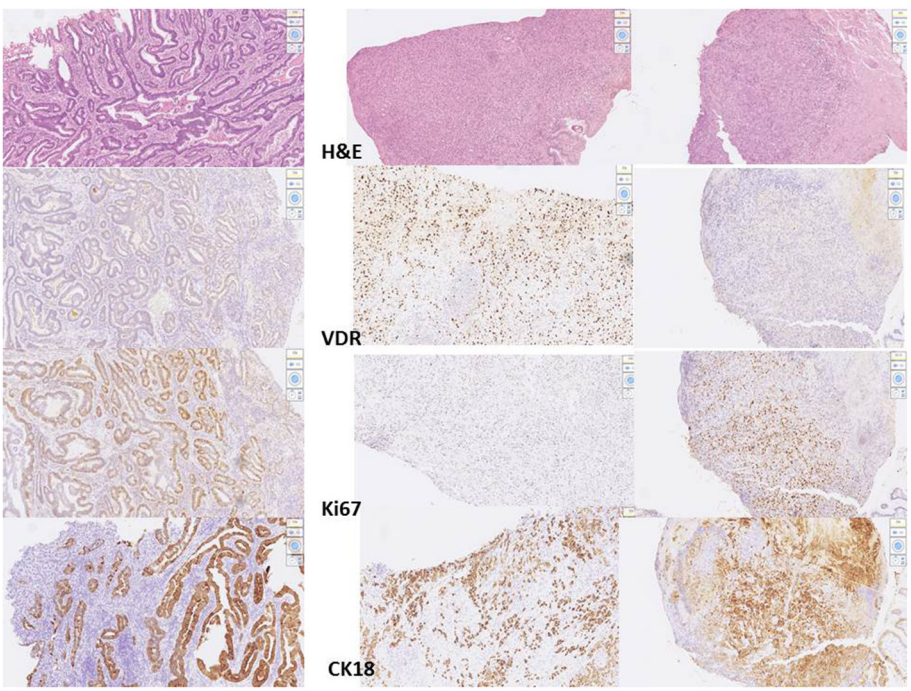

FIGURE 5 | Digital images for different cell type of adenocarcinoma from 3 patients. Left: moderate differentiated adenocarcinoma, stage III. Middle: poor differentiated adenocarcinoma, stage I. Right: poor differentiated adenocarcinoma, stage III. From the top to the bottom: H&E stain, VDR, Ki67, CK18 stain processed by scanner and QuPath software.

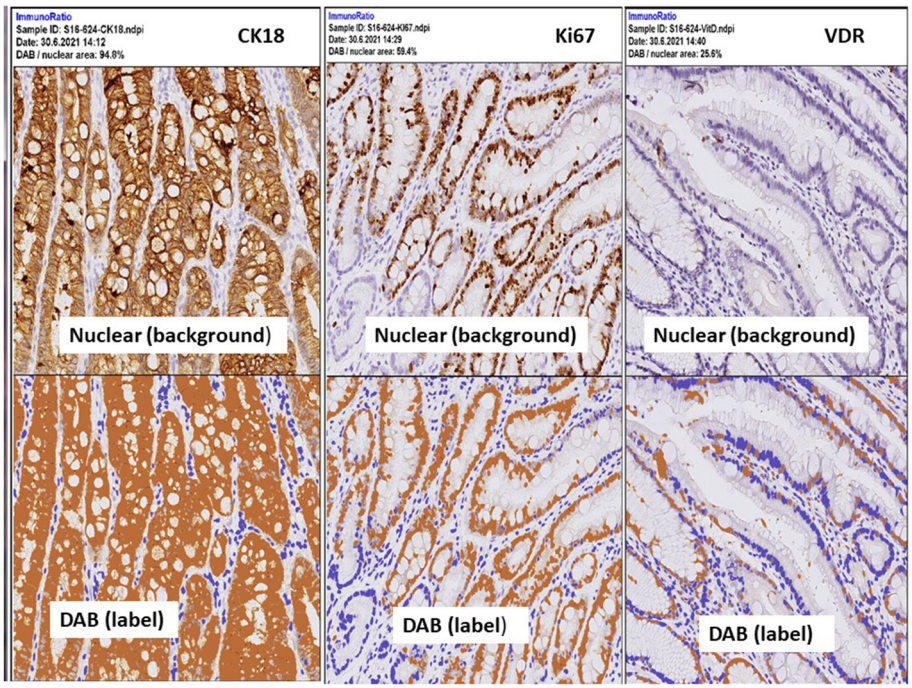

FIGURE 6 | IHC expressions by ImmunoRatio (ImageJ plugin software) processed from one patient with stage I, poor differentiated type gastric adenocarcinoma. Upper panel: the original hematoxylin image (total cell). Lower panel: "DAB" indicates labeled cells, a pseudo-colored image showing the segmented staining components. Labeling index is calculated by the percentage of DAB (positively stained cells) divided the total cell. Left: 94.8% by CK18, middle: 59.4% by Ki67, right: 25.8% by VDR.

TABLE 2 | The mean expressions of VDR, Ki67, and CK18 among gastritis, IM and cancer.

	Mean expression (%) in targeted areas			
IHC stain	**Gastritis**	**IM**	**Cancer**	***P*-value**
VDR	44.1 ± 26.4	41.8 ± 16.9	36.1 ± 19.7	0.404
Ki67	30.1 ± 18.4	39.9 ± 18.5	51.8 ± 21.8	<0.001
CK18	66.9 ± 19.8	74.7 ± 15.0	77.6 ± 14.7	0.047

IHC stain, immunohistochemical stain; Gastritis, inflammation but relatively normal gastric mucosa adjacent to malignancy; IM, intestinal metaplasia adjacent to malignancy; Cancer, gastric adenocarcinoma; VDR, PA1-711 for vitamin D receptor; Ki67, antigen Ki-67 stain for epithelial cell proliferation; CK18, cytokeratin 18, M30 CytoDEATH antibody for detecting apoptosis; P-value, ANOVA analysis.

TABLE 3 | Scheffe *post hoc* analysis among different stains and locations.

Stain	**VDR**		**Ki67**		**CK18**	
Location	**Gastritis**	**IM**	**Gastritis**	**IM**	**Gastritis**	**IM**
Adenocarcinoma+						
Coefficient	−7.362	−5.103	21.128	11.931	10.638	2.851
P-value	0.421	0.659	0.000	0.069	0.057	0.809

+ Post hoc compare the expression of IHC between adenocarcinoma and gastritis or intestinal metaplasia.

adenocarcinoma in the current study. The expression of CK18 was also high in the non-tumor gastritis mucosa in the current study (mean 66.9%).

Chronic inflammation and IM are associated with increased apoptosis but primarily occur at the mucosal surface and not in the deeper layers (27). In the current study, the mucosa of gastritis was adjacent to the IM and the malignant areas. Chronic inflammation may induce high CK18 expression (35). Previous studies on apoptosis in gastric adenocarcinoma mostly used cell lines and the counting score for apoptosis was variable (10, 35). CK18 expression in the mucosa of gastritis adjacent to IM and gastric adenocarcinoma (especially poor differentiation type) may be high in nature. An imbalance between cell proliferation and apoptosis may be the reason and mechanism of carcinogenesis (10, 17). Wagner et al. (29) found decreased apoptotic activity following increased proliferation in chronic *H. pylori* infection; they assumed that increased proliferation might play a role in carcinogenesis.

In normal gastric mucosa, apoptotic cells are rare and in the generative cell zone near glandular neck region. When the sequential change of atrophic gastritis, IM, and dysplasia, the number of apoptotic cells increase (10). Numerous molecules produced by *H. pylori* including cytotoxin (VacA), lipopolysaccharide, monochloramine, and nitric oxide may directly induce apoptosis. Moreover, *H. pylori*-stimulated host inflammatory/immune responses lead to release of a large

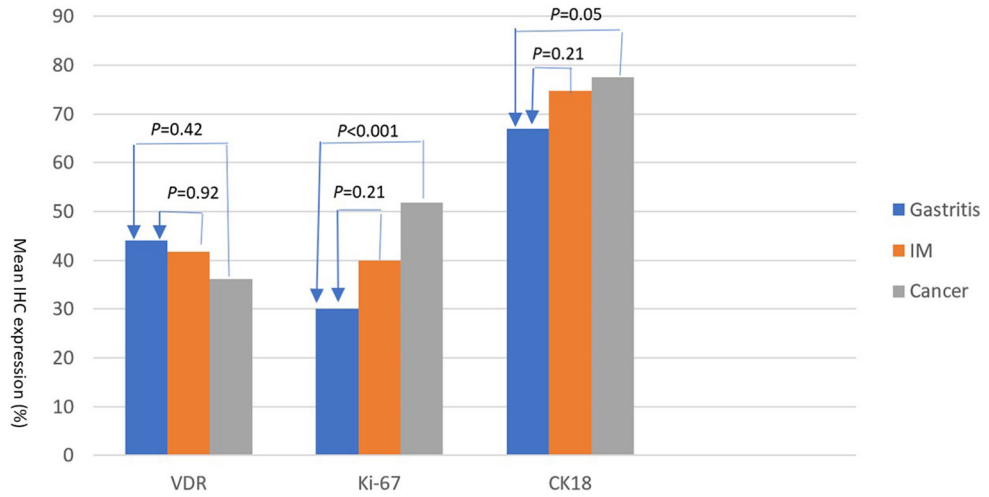

FIGURE 7 | IHC expressions (%) (Y axis) of VDR, Ki67, and CK18 (X axis) in areas of gastritis, IM, and cancer. The expression of each IHC stain in IM (orange bar) and cancer (gray bar) is compared with the expression in gastritis (blue bar). *P*-values are presented at the top of each comparison (Scheffe *post-hoc* analysis).

TABLE 4 | Correlation the expressions between VDR and Ki67 or CK18 in different sites.

Area referred factor	Compared factor	Correlation coefficient	*P*-value
Gastritis			
VDR	Ki67	0.142	0.462
	CK18	−0.121	0.531
IM			
VDR	Ki67	0.171	0.375
	CK18	−0.302	0.111
Cancer			
VDR	Ki67	0.066	0.736
	CK18	0.103	0.597

amount of cytokines. Cytokines produced by type 1 T helper cells, such as TNF-alpha and IFN-gamma, markedly potentiate apoptosis (10, 36).

This study applied artificial intelligence (AI) methods, including a high-resolution scanner (Hamamatsu Nanozoomer S360 scanner) for digital image creation, QuPath, and ImageJ/ImmunoRatio software for IHC scoring. This software could be downloaded freely from specific webs. The strength of AI use is rapid and avoids intra- or inter-observer bios. AI for IHC score counting is easier than traditional manual counting. The preparing of samples in this study were paraffin-embedded tissue sections from tissue bank. Paraffin-embedded tissues are frequently used for pathological examinations, included IHC analyses. Patients who get *H. pylori* infection may develop the conditions of gastritis, IM and gastric adenocarcinoma, which conditions could be detected in one slicing slide from the surgical or biopsy specimens. IHC examination could evaluate the expressions of VDR, Ki67 and CK18 with precise locations in one slide simultaneously. However, there are some limitations to use AI for quantitative IHC tests like our study. First, the precisely targeted areas for scanning and scoring still depend on the pathologists in our study. Second, reports issued the correlation between IHC quantitative analyses and gene expressions in this field of *H. pylori* related gastric adenocarcinoma are rarely now. Third, the application of ImageJ/ImmunoRatio software for other different IHC examinations may require further studies. Hence, further studies are needed for validation and clarification the correlation between digital IHC quantitative tests and gene expression examination.

Conclusively, cell proliferation by Ki67 expression and apoptosis by CK18 expression progressively increased in the areas of gastritis, IM, and adenocarcinoma. Ki67 expression positively correlated with CK18 expression in gastritis. No association between VDR expression and Ki67 or CK18 expression was found in this study. Survival time was only correlated with tumor stage, but was not correlated with the expression of VDR, Ki67, and CK18.

DATA AVAILABILITY STATEMENT

The original contributions presented in the study are included in the article, further inquiries can be directed to the corresponding author.

ETHICS STATEMENT

The Institutional Review Board of the Chang-Gung Memorial Hospital approved this research (IRB No. 103-7463A3, 105-4426C). All participants agreed to the study conditions

and provided informed consent before the enrollment in this study.

AUTHOR CONTRIBUTIONS

L-WC, L-CC, and C-CH contributed to conception and design of the study. L-WC organized the database, wrote the first draft of the manuscript, and got the grant. L-WC, C-CH, and C-CL performed the statistical analysis. L-WC and L-CC wrote sections of the manuscript. L-CC and T-CC provided all the equipment and histological examinations. All authors contributed to manuscript revision, read, and approved the submitted version.

FUNDING

This study was supported by the Chang Gung Medical Foundation and Keelung Chang Gung Memorial Hospital Tissue Bank (CRRPG 2H0052).

ACKNOWLEDGMENTS

The authors thank two assistants from the Community Medicine Research Center, Chia-Wen Hsieh and Mi-Sio Huang for assisting with sample preparation from the tissue bank and clinical data collection.

REFERENCES

1. Wong BC, Lam SK, Wong WM, Chen JS, Zheng TT, Feng RE, et al. *Helicobacter pylori* eradication to prevent gastric cancer in a high-risk region of China: a randomized controlled trial. *JAMA*. (2004) 291:187–94. doi: 10.1001/jama.291.2.187
2. Asaka M, Sugiyama T, Nobuta A, Kato M, Takeda H, Graham DY. Atrophic gastritis and intestinal metaplasia in Japan: results of a large multicenter study. *Helicobacter*. (2001) 6:294–9. doi: 10.1046/j.1523-5378.2001.00042.x
3. Bechi P, Balzi M, Becciolini A, Maugeri A, Raggi CC, Amorosi A, et al. *Helicobacter pylori* and cell proliferation of the gastric mucosa: possible implications for gastric carcinogenesis. *Am J Gastroenterol*. (1996) 91:271–6.
4. Ierardi E, Francavilla R, Panella C. Effect of *Helicobacter pylori* eradication on intestinal metaplasia and gastric epithelium proliferation. *Ital J Gastroenterol Hepatol*. (1997) 29:470–5.
5. Peek RM Jr, Moss SF, Tham KT, Holt PR, Tham KT, Blaser MJ, et al. *Helicobacter pylori* cagA+ strains and dissociation of gastric epithelial cell proliferation from apoptosis. *J Nat Cancer Inst*. (1997) 89:863–8. doi: 10.1093/jnci/89.12.863
6. Correa P, Piazuelo B, Wilson KT. Pathology of gastric intestinal metaplasia: clinical implications. *Am J Gastroenterol*. (2010) 105:493–8. doi: 10.1038/ajg.2009.728
7. Sung JJY, Lin SR, Ching JYL, Zhou LY, To KF, Wang RT, et al. Atrophy and intestinal metaplasia one year after cure of H pylori infection: a prospective, randomized study. *Gastroenterology*. (2000) 119:7–14. doi: 10.1053/gast.2000.8550
8. Leung WK, Lin SR, Ching JYL, To KF, Ng EK, Chan FK, et al. Factors predicting progression of gastric intestinal metaplasia: results of a randomised trial on Helicobacter pylori eradication. *Gut*. (2004) 53:1244–9. doi: 10.1136/gut.2003.034629
9. Zhang C, Yamada N, Wu YL, Wen M, Matsuhisa T, Matsukura N. Helicobacter pylori infection, glandular atrophy and intestinal metaplasia in superficial gastritis, gastric erosion, erosive gastritis, gastric ulcer and early gastric cancer. *World J Gastroenterol*. (2005) 11:791–6. doi: 10.3748/wjg.v11.i6.791
10. Xia HH, Talley NJ. Apoptosis in gastric epithelium induced by Helicobacter pylori infection: implications in gastric carcinogenesis. *Am J Gastroenterol*. (2001) 96:16–26. doi: 10.1016/S0002-9270(00)02240-1
11. Yousefi B, Mohammadlou M, Abdollahi M, Salek Farrokhi A, Karbalaei M, Keikha M, et al. Epigenetic changes in gastric cancer induction by Helicobacter pylori. *J Cell Physiol*. (2019) 234:21770–84. doi: 10.1002/jcp.28925
12. Li M, Li L, Zhang L, Hu W, Shen J, Xiao Z, et al. 1,25-Dihydroxyvitamin D3 suppresses gastric cancer cell growth through VDR- and mutant p53-mediated induction of p21. *Life Sci*. (2017) 179:88–97. doi: 10.1016/j.lfs.2017.04.021
13. Guo L, Chen W, Zhu H, Chen Y, Wan X, Yang N, et al. Helicobacter pylori induces increased expression of the vitamin d receptor in immune responses. *Helicobacter*. (2013) 19:37–47. doi: 10.1111/hel.12102
14. Ben C, Qiu WZ, Wang DS, Luo HY, Zhang DS, Wang ZQ, et al. Prognostic effects of 25-hydroxyvitamin D levels in gastric cancer. *J Trans Med*. (2012) 10:16–20. doi: 10.1186/1479-5876-10-16
15. Bao A, Li Y, Tong Y, Zheng H, Wu W, Wei C. Tumor-suppressive effects of 1,25-dihydroxyvitamin D3 in gastric cancer cells. *Hepato Gastroenterol*. (2013) 60:943–8. doi: 10.5754/hge121003
16. Du C, Yang S, Zhao X, Dong H. Pathogenic roles of alterations in vitamin D and vitamin D receptor in gastric tumorigenesis. *Oncotarget*. (2017) 8:29474–86. doi: 10.18632/oncotarget.15298
17. Zhou A, Li L, Zhao G, Min L, Liu S, Zhu S, et al. Vitamin D3 inhibits helicobacter pylori infection by activating the VitD3/VDR-CAMP pathway in mice. *Front Cell Infect Microbiol*. (2020) 10:566730. doi: 10.3389/fcimb.2020.566730
18. Saramaki A, Banwell CM, Campbell MJ, Carlberg C. Regulation of the human p21(waf1/cip1) gene promoter via multiple binding sites for p53 and the vitamin D3 receptor. *Nucleic Acids Res*. (2006) 34:543–54. doi: 10.1093/nar/gkj460
19. Rao A, Coan A, Welsh JE, Barclay WW, Koumenis C, Cramer SD. Vitamin D receptor and p21/WAF1 are targets of genistein and 1,25-dihydroxyvitamin D3 in human prostate cancer cells. *Cancer Res*. (2004) 64:2143–7. doi: 10.1158/0008-5472.CAN-03-3480
20. Salehi-Tabar R, Nguyen-Yamamoto L, Tavera-Mendoza LE, Quail T, Dimitrov V, An BS, et al. Vitamin D receptor as a master regulator of the c-MYC/MXD1 network. *Proc Natl Acad Sci USA*. (2012) 109:18827–32. doi: 10.1073/pnas.1210037109
21. Capelle LG, de Vries AC, Haringsma J, Ter Borg F, de Vries RA, Bruno MJ, et al. The staging of gastritis with the OLGA system by using intestinal metaplasia as an accurate alternative for atrophic gastritis. *Gastrointest Endosc*. (2010) 71:1150–8. doi: 10.1016/j.gie.2009.12.029
22. *ImmunoRatio 1.0c.Jar Downloaded*. Available online at: https://wsiserver.jilab.fi/old-jvsmicroscope-software/ (accessed March 7, 2019).
23. *QuPath version 0.23 Downloaded*. Available online at: https://qupath.github.io/ (accessed September 27, 2020).
24. Schneider CA, Rasband WS, Eliceiri KW. NIH Image to ImageJ: 25 years of image analysis. *Nat Meth*. (2012) 9:671–5. doi: 10.1038/nmeth.2089
25. Tuominen VJ, Ruotoistenmäki S, Viitanen A, Jumppanen M, Isola J. ImmunoRatio: a publicly available web application for quantitative image analysis of estrogen receptor (ER), progresterone receptor (PR), and Ki-67. *Breast Cancer Res*. (2012) 12:R56. doi: 10.1186/bcr2615
26. Bankhead P, Loughrey MB, Fernández JA, Dombrowski Y, McArt DG, Dunne PD, et al. QuPath: open source software for digital pathology image analysis. *Sci Rep*. (2017) 7:16878. doi: 10.1038/s41598-017-17204-5
27. Leers MPG, Lgen WK, Rklund VB, Bergman T, Tribbick G, Persson B, et al. Immunocytochemical detection and mapping of a cytokeratin 18 neo-epitope exposed during early apoptosis. *J Pathol*. (1999) 187:567–72. doi: 10.1002/(SICI)1096-9896(199904)187:5<567::AID-PATH288>3.0.CO;2-J
28. Washington K. 7th edition of the AJCC cancer staging manual: stomach. *Ann Surg Oncol*. (2010) 17:3077–9. doi: 10.1245/s10434-010-1362-z

29. Wagner S, Beil W, Westermann J, Logan RPH, Bock CT, Trautwein C, et al. Regulation of gastric epithelial cell growth by *Helicobacter pylori*: Evidence for a major role of apoptosis. *Gastroenterology*. (1997) 113:1836–47. doi: 10.1016/S0016-5085(97)70003-9
30. Deeb KK, Trump DL Johnson CS. Vitamin D signaling pathways in cancer: potential for anticancer therapeutics. *Cancer*. (2007) 7:684–700. doi: 10.1038/nrc2196
31. Feldman D, Krishnan AV, Swami S, Giovannucci E, Feldman BJ. The role of vitamin D in reducing cancer risk and progression. *Nat Rev Cancer*. (2014) 14:342–57. doi: 10.1038/nrc3691
32. Wen Y, Da M, Zhang Y, Peng L, Yao J, Duan Y. Alterations in vitamin D signaling pathway in gastric cancer progression: a study of vitamin D receptor expression in human normal, premalignant, and malignant gastric tissue. *Int J Clin Exp Pathol*. (2015) 8:13176–84.
33. Khayatzadeh S, Feizi A, Saneei P, Esmaillzadeh A. Vitamin D intake, serum Vitamin D levels, and risk of gastric cancer: a systematic review and meta-analysis. *J Res Med Sci*. (2015) 20:790–6. doi: 10.4103/1735-1995.168404
34. Kwak JH, Paik JK. Vitamin D status and gastric cancer: a cross-sectional study in Koreans. *Nutrients*. (2020) 12:2004. doi: 10.3390/nu12072004
35. van Grieken NCT, Meijer GA, Hausen A, Meuwissen SGM, Baak JPA, et al. Increased apoptosis in gastric mucosa adjacent to intestinal metaplasia. *J Clin Pathol*. (2003) 56:358–62. doi: 10.1136/jcp.56.5.358
36. Charitos IA, D'Agostino D, Topi S, Bottalico L. 40 years of helicobacter pylori: a revolution in biomedical thought. *Gastroenterol Insights*. (2021) 12:111–35. doi: 10.3390/gastroent12020011

Conflict of Interest: The authors declare that the research was conducted in the absence of any commercial or financial relationships that could be construed as a potential conflict of interest.

Publisher's Note: All claims expressed in this article are solely those of the authors and do not necessarily represent those of their affiliated organizations, or those of the publisher, the editors and the reviewers. Any product that may be evaluated in this article, or claim that may be made by its manufacturer, is not guaranteed or endorsed by the publisher.

Copyright © 2021 Chen, Chang, Hua, Cheng and Lee. This is an open-access article distributed under the terms of the Creative Commons Attribution License (CC BY). The use, distribution or reproduction in other forums is permitted, provided the original author(s) and the copyright owner(s) are credited and that the original publication in this journal is cited, in accordance with accepted academic practice. No use, distribution or reproduction is permitted which does not comply with these terms.

frontiers in Surgery

ORIGINAL RESEARCH
published: 22 November 2021
doi: 10.3389/fsurg.2021.771587

Prognostic Enigma of Pancreatic Solid Pseudopapillary Neoplasm: A Single-Center Experience of 63 Patients

Xinbo Wang[1]*, *Daojun Zhu*[1], *Wei Bao*[2], *Min Li*[1], *Sizhen Wang*[1] and *Rongxi Shen*[1]

[1] Research Institute of General Surgery, Jinling Hospital, Nanjing University Medical School, Nanjing, China, [2] Department of Pathology, Jinling Hospital, Nanjing University Medical School, Nanjing, China

OPEN ACCESS

Edited by:
Ravindra Deshpande,
Wake Forest School of Medicine,
United States

Reviewed by:
Angela Verma,
University of Maryland, Baltimore,
United States
Praveen Kumar Allu,
University of Pennsylvania,
United States
Deepak Babu,
Case Western Reserve University,
United States

***Correspondence:**
Xinbo Wang
wxinbo2008@163.com

Specialty section:
This article was submitted to Surgical Oncology, a section of the journal Frontiers in Surgery

Received: 06 September 2021
Accepted: 20 October 2021
Published: 22 November 2021

Citation:
Wang X, Zhu D, Bao W, Li M, Wang S and Shen R (2021) Prognostic Enigma of Pancreatic Solid Pseudopapillary Neoplasm: A Single-Center Experience of 63 Patients. Front. Surg. 8:771587. doi: 10.3389/fsurg.2021.771587

Background: Studies investigating prognostic factors of solid pseudopapillary neoplasm (SPN) have been published with conflicting findings.

Methods: Retrospective analysis of 63 consecutive cases of SPN in our institution from January 2010 to December 2019 was carried out. The clinicopathological features, treatment practices along with survival associations were collected and analyzed.

Results: Fifteen patients (23.8%) were male, and 48 (76.2%) were female, with a median age of 34.0 ± 14.5 years. The larger tumor size was correlated with the more mixed components ($p = 0.000$) and the higher Ki-67 index ($p = 0.042$). No recurrence was found in the nine patients whose tumors fulfilled the WHO criteria for malignancy due to the presence of at least perineural invasion (6.4%), angiovascular invasion (2.3%), and/or adjacent organ invasion (6.4%). Microscopic infiltrative growth was detected in 9 (14.3%) tumors, which was correlated significantly with the WHO criteria ($p = 0.002$), capsule invasion ($p = 0.005$), and pancreatic parenchyma invasion ($p = 0.001$), but not with disease-free survival ($p = 0.13$). CD99 was found to be positively expressed in 88.9% (40/45) of tumors and more likely to have depressed Ki-67 index ($p = 0.016$). After a median follow-up of 58 months, only two patients (3.2%) had a recurrence after their first operation outside of our hospital. No patient died due to tumor progression.

Conclusions: Although survival is favorable with aggressive surgery, it is actually difficult to assess the prognostic factors of resected SPNs. Future investigations into the role of clinicopathological evaluation will unveil the prognostic enigma of pancreatic SPN after resection.

Keywords: malignant, pancreas, prognosis, solid pseudopapillary neoplasm, surgical management

INTRODUCTION

Solid pseudopapillary neoplasm (SPN) is a rare pancreatic tumor, which was first defined by Frantz in 1959 and classified as a potential malignant neoplasm by WHO in 2010 (1). The biologic behaviors of SPN are mostly less aggressive in spite of the tumor phenotype and classically present as large, solitary, well-circumscribed lesions with female predominance (2). However, up to 5–15% of patients demonstrate gross malignant features, such as invasion of adjacent organs or distant metastases, at the time of diagnosis or during the long-term follow-up after surgery (3). Because of its rarity and overall indolent but malignant course, SPN has not been well-studied, and standard staging tools have been questioned. Similarly, one of the biggest challenges in managing patients with SPN lies in predicting tumor behavior at the time of presentation (4). The WHO criteria of malignancy, which focused on microscopic features of malignancy, cannot be always equated with predicting the clinical malignant prognosis of SPN, nor were immunohistochemical stains, including the proliferative index Ki67 (5, 6).

Studies of investigating prognostic factors of SPN discuss plausible theories of the malignant potential of this enigmatic disease. Wu et al. (7) found that male patients had significantly poorer overall survival and disease-specific survival than female patients. Yin et al. (8) suggested that disrupted capsule, large tumor size, and pancreatic tail localization were viewed as the malignant SPN phenotype. Tang et al. (9) reported that peripancreatic lymphadenopathy on preoperative radiologic images was associated with malignancy in patients with SPN. Fu et al. (10) highlighted the proliferate index detected by Ki-67 in predicting the adverse outcome after an operation for SPN, but some study advocated the importance of pathologic evaluation in risk assessment in patients with SPNs (11, 12). Some authors disapproved the parenchyma-preserving resection on accounting of tumor recurrence (13), while others advocated function-preserving surgical approaches (14). Recent study based on the molecular alterations found that micro-RNA expression patterns in tumor might be able to predict metastatic spread of SPNs after surgery (15).

In this study, to validate the aforementioned prognostic factors usability in SPN and penetrate into the nature of this tumor, we described the clinicopathologic features, treatment practices, and outcome of 63 patients with SPNs in our institution.

MATERIALS AND METHODS

Data were extracted from the prospectively maintained databases of the patients operated for SPN at Research Institute of General Surgery, Jinling Hospital, Nanjing University Medical School, over a period of 10 years from January 2010 to December 2019. All 63 consecutive patients were identified and included in the study population. All patients underwent standard evaluation by routine blood investigations, including serum levels of carcinoembryonic antigen (CEA) and carbohydrate antigen 19-9 (CA19-9), and enhanced CT and/or MRI were examined before surgery. The type of resection was determined by the location and extent of the tumor with R0 resection as the primary aim. Minimally invasive and parenchyma sparing procedures would be performed in case that the definite diagnosis of SPN was reached through the preoperatively imaging and/or cytology. In particular, enucleations were carried out only when there was a safe distance between the tumor and the main pancreatic duct. According to the International Study Group on Pancreatic Surgery (ISGPS) classification (16), postoperative complications were defined as complications occurring within 30 days of surgery. Complications were graded as per the Clavien-Dindo classification (17). All of the tumors were pathologically confirmed to SPN by histological and immunohistochemical findings. Based on the WHO 2010 criteria, SPNs were classified as malignant if they showed invasion of either pancreatic tissue, peripancreatic nerves, or the vessels. Patients were followed up every 3 months for the first 1 year, every 6 months for the next year, and annually thereafter. Collected data included the clinicopathological and survival outcome from the hospital records and telephone interviews.

Statistical Analysis

All statistical analyses were performed by SPSS ver. 21 (SPSS, Inc., IBM, Chicago, IL). Descriptive variables such as mean, SD, frequency, and rates were calculated. Statistical differences were detected using the independent samples *t*-test, Mann–Whitney *U*-test, or chi-square test when appropriate. Overall survival and disease-free survival were compared by Kaplan–Meier method.

RESULTS

Patient Characteristics

It can be clearly found that the diagnosis of SPNs has progressively increased over 10 years in our institution, which is also in line with the reported significant increase in the incidence of SPN in the past decade. In total, 63 patients (15 males and 48 females) underwent surgical exploration for SPNs, ranging in age from 11 to 70 years (median 34 years). Demographic characteristics are described in **Table 1**. Nearly half of the patients (52.4%) had symptoms, of which abdominal pain was the most frequent (25.4%). Tumor markers, such as CA19-9, CA125, and CEA, were almost in the normal range. The localization of the tumor was in the head and neck in 25 patients (39.7%), including one with tumor recurrent *in situ*, and 38 in the body and tail (60.3%), including one with liver and retroperitoneal metastasis. The mean tumor size at diagnosis was 4.9 ± 2.4 cm in diameter. In the preoperative imaging (CT and/or MRI scan), most tumors (90.5%) were not accompanied by pancreatic duct dilatation. Tumors had radiologically heterogeneous (solid and cystic) features in 35 patients (55.5%). Solid features were found in 26 patients (41.3%), and cystic features were found in two patients (3.2%).

Sixty-one patients (96.8%) underwent curative surgery with negative margin (R0 resection). The type of operations included pancreaticoduodenectomy (15, 23.9%), distal pancreatectomy with splenectomy (22, 34.9%), and spleen-preserving distal pancreatectomy (15, 23.8%). Parenchyma-preserving

TABLE 1 | Demographic characteristics of 63 patients with SPN.

Clinical Features	Frequency (%) Mean ± SD
Gender	
Male	15 (23.8)
Female	48 (76.2)
Age (years)	34.0 ± 14.5
BMI (Kg/m^2)	22.5 ± 3.3
Symptoms	
No	30 (47.6)
Yes	33 (52.4)
Ca 19.9 >37 U/ml	2 (3.2)
Tumor location	
Head + neck	25 (39.7)
Body + tail	38 (60.3)
Size at radiology, cm	4.9 ± 2.4
Radiologic features	
Solid	26 (41.3)
Cystic	2 (3.2)
Mixed	35 (55.5)
Main pancreatic duct dilatation	6 (9.5)
Vascular encasement at radiology	1 (1.6)
Recurrence lesions at radiology	2 (3.2)
Type of surgery	
Enucleation	5 (7.9)
Distal pancreatectomy	22 (34.9)
Distal, spleen-preserving	14 (22.2)
Classical whipple	12 (19.1)
PPPD	3 (4.8)
Central pancreatectomy	5 (7.9)
Palliative surgery*	2 (3.2)
Surgical complications	
Hemorrhage	3 (4.8)
Pancreatic fistula	7 (11.1)
DGE	2 (3.2)
Pancreatitis	1 (1.6)
Postoperative hospital stay, days	14.6 ± 12.0

Palliative surgery includes metastasectomy and/or laparotomy.
PPPD, Pylorus-preserving pancreatoduodenectomy; DGE, Delayed gastric emptying.

procedures included central pancreatectomy (5, 7.9%) and tumor enucleation (5, 7.9%). No lymphadenectomy was performed. Notably, one patient was found to have lung squamous cell carcinoma before the surgery, so the simultaneous implementation of distal pancreatectomy and thoracoscopic lobectomy was performed. Only two patients (3.2%) who developed recurrence after their first operation outside of our hospital had debulking operations (R2). One patient who experienced retroperitoneal metastasis and peritoneal seeding after 5 years of distal pancreatectomy underwent metastasectomy. The other patient who experienced local recurrence in the pancreatic head after 7 years of tumor enucleation underwent laparotomy and tumor biopsy due to the encasement of the portal vein and its branches.

TABLE 2 | Pathological features of the 63 resected SPN (at primary tumor operation).

Clinical features	Frequency (%) Mean ± SD
Size at gross pathology (cm)	5.3 ± 2.7
Macroscopic features	
Solid	26 (41.3)
Cystic	2 (3.2)
Mixed	35 (55.5)
Synchronous multifocal growth	1 (1.6)
Microscopic growth pattern	
Expansive growth	54 (85.7)
Infiltrative growth	9 (14.3)
Calcifications	6 (9.5)
Perineural invasion	4(6.4)
Angiovascular invasion	2(3.2)
Adjacent organ invasion	4(6.4)
Spleen	2(3.2)
Splenic vein/portal vein	1(1.6)
Duodenum	1(1.6)
Pancreatic parenchyma invasion	17 (27.0)
Capsule invasion	21 (33.3)

The median postoperative hospital stay was 14.6 days (ranging from 4 to 64 days). A total of 13 (20.6%) patients experienced postoperative complications. The most common morbidity following pancreatectomy was the postoperative pancreatic fistula (7, 11.1%). There were no reoperations or mortalities.

Pathological and Immunohistochemistry Features

Pathological features are displayed in **Table 2**. Some selected clinicopathologic characteristics used to forecast recurrence were compared and are illustrated in **Table 3**. Of the 18 patients (28.6%) preoperatively misdiagnosed with other pancreatic neoplasms, the cystic neoplasms accounted for almost half of the preoperative misdiagnoses (8/18, 44.4%). SPN also had distinctive pathologic features, ranging from purely solid to purely cystic. It was noted that the larger tumor size was correlated significantly with the more mixed components (**Table 3**; $p = 0.000$) and the higher Ki-67 index ($p < 0.042$). Only one male patient was identified synchronous multifocal SPN by three tumors (3*3*2.8 cm, 1.3*1.2*0.8 cm, and 0.6*0.6*0.4 cm), which were all well-capsulated in the pancreatic head. Of note, 21 cases (33.3%) invaded the pancreatic capsule and 17 cases (27%) had pancreatic parenchyma invasion. According to the 2010 WHO classification for malignant SPNs, nine (14.3%) fulfilled inclusion criteria of the presence of at least one of the following: angiovascular infiltration (3.2%), perineural invasion (6.4%), and adjacent organ invasion (6.4%). None of these malignant characters was confirmed in the two recurrent patients at their pathological analysis of the primary tumor, but the metastasectomy specimens fulfilled WHO criteria for a malignant SPN: one with microscopic infiltrative growth

TABLE 3 | Comparison of selected clinicopathologic characteristics used to forecast recurrence (at primary tumor operation).

Characteristics	Tumor size			Microscopic growth pattern			CD99 stain			Total
	≤5 cm ($n = 36$)	>5 cm ($n = 27$)	*P-value*	Expansive ($n = 54$)	Infiltrative ($n = 9$)	*P-value*	Negative ($n = 5$)	Positive ($n = 40$)	*P-value*	($n = 63$)
Age (years)	36.7 ± 14.9	30.4 ± 13.5	0.473	34.4 ± 14.6	31.7 ± 14.8	0.616	37.8 ± 21.6	33.8 ± 14.2	0.459	34.0 ± 14.5
Tumor size (cm)	—	—	—	5.0 ± 2.6	4.3 ± 1.3	0.083	5.5 ± 2.4	5.0 ± 2.5	0.719	4.9 ± 2.4
Ki-67 (%)	2.7 ± 2.7	3.7 ± 3.8	**0.042**	3.3 ± 3.2	3.6 ± 4.6	0.276	5.0 ± 4.6	2.7 ± 2.7	**0.016**	3.3 ± 3.1
Gender			0.232			0.363			0.303	—
Male	11	4		12	3		0	12		15
Female	25	23		42	6		5	28		48
Tumor location			0.882			0.245			0.157	
Head + neck	14	11		20	5		2	16		25
Body + tail	22	16		34	4		3	24		38
WHO criteria			0.117			**0.002**			0.211	
Benign	33	21		50	4		3	34		54
Malignant	3	6		4	5		2	6		9
Macroscopic features			**0.000**			0.054			0.317	
Solid	22	4		20	6		1	17		26
Cystic	2	0		1	1		0	2		2
Mixed	12	23		33	2		4	21		35
Microscopic growth pattern			0.177						0.568	
Expansive growth	29	25		—	—	—	5	32		54
Infiltrative growth	7	2		—	—	—	0	8		9
Capsule invasion	10	11	0.28	14	7	**0.005**	2	13	0.737	21
Pancreatic parenchyma invasion	11	6	0.461	10	7	**0.001**	2	10	0.598	17
Perineural invasion	1	3	0.179	3	1	0.469	0	3	0.526	4
Angiovascular invasion	0	2	0.097	1	1	0.267	0	0	—	2

Bold values indicate statistical significance.

pattern and perineural invasion, and the other one with adjacent organ invasion. Notably, microscopic infiltrative growth was detected in 9 (14.3%) patients and more likely to be identified as malignant (**Table 3**; $p = 0.002$). We also found that the microscopic infiltrative growth was correlated significantly with the capsule invasion ($p = 0.005$) and pancreatic parenchyma invasion ($p = 0.001$), but not with the perineural invasion or angiovascular invasion ($p > 0.05$). No lymph nodes were pathologically confirmed to be metastatic.

Immunohistochemical analysis was performed in selected cases. The proliferation index (Ki-67) ranged from 0 to 15 (median, 3.3). Six cases showed Ki-67 index >5% and 3 cases >10%. β-Catenin and CD56 were positively expressed in 100% (47/47), CD10 in 89.5% (34/38), pancytokeratin in 52.3% (23/44), and neuron-specific enolase (NSE) in 66.7% (10/15). Chromogranin A was negative in 95.8% (44/46) of tumors, and synaptophysin negative in 37.3% (22/59) of tumors. In keeping with the known histological features of SPN, CD99 was found to be positively expressed in 88.9% (40/45) of tumors. Interestingly, the Ki-67 index of CD99-negative patients (**Figure 1**) was significantly higher than that of CD99-positive patients (**Table 3**; $p = 0.016$). In addition, the high female prevalence was reiterated with the positive expression of progesterone receptors in 93.1% (27/29) of tumors.

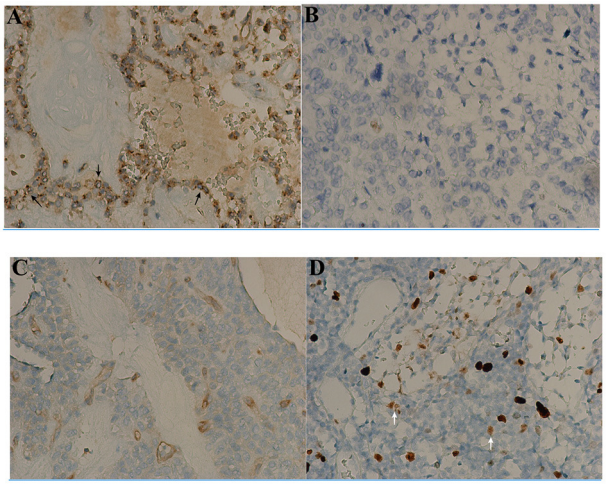

FIGURE 1 | Immunohistochemical findings of CD99 and Ki-67 index in solid-pseudopapillary neoplasms (SPN) after surgery (x200). The tumor appears to have a particular dot-like paranuclei expression of CD99 (black arrow, **A**) with low Ki-67 index 1% **(B)**. The other tumor appearing to be negative for CD99 expression **(C)** has much high Ki-67 index 10% (white arrow, **D**).

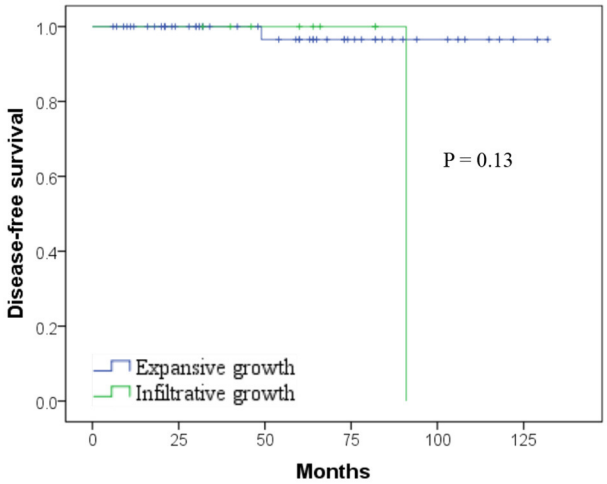

FIGURE 2 | Kaplan–Meier curves showing no difference in disease-free survival (DFS) after surgery for solid pseudopapillary neoplasm (SPN) according to the microscopic infiltrative/expansive growth pattern ($p = 0.13$).

Follow-up

The final follow-up date was June 30, 2020. The median follow-up period was 58 months, ranging from 6 to 132 months. Except the female patient who died of lung cancer 16 months after simultaneous implementation of distal pancreatectomy and thoracoscopic lobectomy, no patient died of disease directly. Of the two recurred female patients, one was alive with locally advanced recurrent lesion in the pancreatic head at 96 months and the other one was alive with a single liver metastasis lesion after multiple subsequent metastasectomy at 124 months. There was no difference in disease-free survival (DFS) after surgery for SPN according to the microscopic infiltrative growth pattern or expansive growth pattern (**Figure 2**; $p = 0.13$), nor were all the clinical pathological and immunohistochemistry features, including the negative correlations between CD99 and Ki67 index. The 1-, 3-, and 5-year DFS rates were 100, 98.4, and 96.8%, respectively. The 1-, 3-, and 5-year overall survival (OS) rates were 100, 98.4, and 98.4%, respectively.

DISCUSSION

Because of the rarity of SPNs and the non-extensive case series present in literature, the biological behavior and risk factors for malignancy still failed to be clarified (3). The clinical data of the present series reinforce that the lack of histologic and clinical parameters to predict malignant behavior can also be pertaining to the favorable prognosis and long survival rate of SPNs.

Clinically, most studies reported that SPNs tended to occur in young female patients (18). However, our data were truly different as the ratio of male to female was 1:3.2, which was far fewer than the Western reports and similar to the Chinese reports (19). This difference possibly stems from fact that the incidence rate of male patients is rising and the difference of incidence rates comes from a different epidemiology of SPNs in different centers and regions. There was no difference in the age, tumor size, and location at diagnosis stroke between males and females. SPNs occurred more frequently in the body and tail of the pancreas. Nearly half of SPNs (52.4%) were incidentally discovered even though tumor size tended to be usually large with a median diameter of 5.3 cm, which is similar to other's reports (20). It was noted that the larger tumor size was correlated significantly with the more mixed components ($p = 0.000$) and the higher Ki-67 index ($p < 0.042$), not with the malignant potential ($p = 0.117$). The characteristic feature of SPN is the combination of solid pseudopapillae with fibrovascular stalks and cystic component with varied degeneration and hemorrhage (6). Some studies had shown a relationship between the tumor size >5 cm, tumor necrosis, high index of Ki-67, and SPNs with malignant potential (3, 6, 16). Our findings further corroborated that the combination of Ki-67 and the tumor size might be more informative than Ki-67 alone to predict the malignant potential (21).

Of note, one male patient in our cohort was identified synchronous multifocal SPN with three tumors well-capsulated macroscopically, which has not been reported in the literature so far. These multifocal tumors had perineural invasion with positive expression of β-catenin and CD56 and the high index of Ki-67 ranging from 10 to 15%. The pathogenesis of this tumor remains unclear. Kosmahl et al. (22) speculated that SPNs might originate from genital ridge-related cells, substantiated by the closeness of the genital ridges to the pancreatic anlage during embryogenesis. This might explain why one patient presented here has 18 years of menopause since 2002, whereas she suffered repeated recurrence and liver metastasis. The histogenesis of SPN remains unclear despite the extensive research using immunohistochemistry, electron microscopy, and

molecular biology (23). Molecular and genetic studies on the synchronous multifocal SPN may reveal some new insights into the tumorigenesis of SPN.

The focus of this study was to evaluate the predictive value of the WHO criteria for malignant potential of SPNs from the perspective of surgical prognosis. The tumors of nine patients (14.3%) fulfilled the WHO criteria for malignancy, which was consistent with the data analyzed in large literature (24). Nevertheless, none of these nine patients experienced a recurrence. Despite a 100% negative predictive value, as the only two recurred patients did not accomplish those criteria in their primary tumors, the positive predictive value remains low. Some studies with large numbers of SPNs also failed to show a correlation between the microscopic malignant features and clinically evident malignance of SPNs (6, 24). In our study, microscopic infiltrative growth detected in nine (14.3%) patients was correlated significantly with the WHO criteria for malignance ($p = 0.002$), the capsule invasion ($p = 0.005$), and pancreatic parenchyma invasion ($p = 0.001$). Few literatures had previously studied the significance of infiltrative growth pattern in SPNs (12). Although infiltrative growth is not equal to malignant transformation from a low-grade to a high-grade malignancy or easy to relapse, it is related to the WHO malignant criteria and deserves attention. Some studies (25) have strived to delineate the pathologic features, including diffuse growth, extensive necrosis, dedifferentiation, and sarcomatoid features, necessary to its aggressive behavior or metastatic potential. It is essential to search for the high-grade morphologic features for identifying the aggressive SPNs. Our findings indicate that the accumulation of extensive clinical data is still required for this enigmatic disease.

The predictive value of Ki-67 index in evaluating the malignant potential of SPNs still remains controversial (21). The Ki-67 index higher than 5% may be a predictor of tumor recurrence in spite of its prognostic role not exploring or validating (26). Some studies regarded that Ki-67 was not associated with malignancy (3). The lack of signs of microscopic invasion in the surgical specimen should not discard a malignant potential of the tumor (27). In our cohort, the Ki-67 index was both <1% in the primary tumors in the only two recurred patients. One patient had the Ki-67 index 2% in the locally advanced recurrent lesions. And the other patient experiencing repeated recurrence and liver metastasis had Ki-67 index increased progressively with the increase in the number of metastases, from the initial tumor <1–15% of the last metastasectomy. Not only because Ki67% is a dynamic and evolutionary process as a proliferation marker protein, but also because it is highly expressed in proliferative cells, it is definitely not accurate to use Ki-67 alone as a predictor of tumor recurrence. Consistent with our finding, Walter et al. (28) also found that the Ki-67 index was 2% in the primary tumor, 10% in ovarian lesions, and 20% in liver metastases. It is recommended to review the assertive clinical features, such as local pancreatic or extrapancreatic invasion and metastases apart from the WHO microscopy criteria (1), since the clinicopathological features of SPN appear to be unreliable in assessing its biological behavior (5). Moreover, investigating the cause of the genetic variation of SPN may have enabled us to delineate the potential molecular pathways involved in recurrence (23).

The somewhat diverse immunohistochemical features of SPN lead to uncertainty in its origin (4). It is important to critically evaluate the diagnostic and prognostic utility of all the known markers. SPN appears to be highly unique expression of CD99 (29), and this dot-like paranuclei staining pattern was present in 88.9% (40/45), and the Ki-67 index of CD99-negative patients was significantly higher than that of CD99-positive patients ($p = 0.016$) in our series. There are few reports to investigate the role of CD99 expression in the prognostic value and efficacy assessment, so the evaluation value of immunohistochemistry in SPN may be deliberately emphasized. To our knowledge, the phenomenon of CD99 in downregulation of the proliferative activity by Ki-67 index has not been described in pancreatic SPNs to date. CD99 is involved in crucial biological processes, such as cell adhesion, migration, death, differentiation, immune responses, and tumorigenesis (30). Loss from the membrane and paranuclear localization of CD99 may result in the dysfunction of this adhesion molecule, and thus "discohesion" of SPN cells (31). However, CD99 plays an intriguing and dual role in different cell types. In particular, it corresponds to the cell malignancy or the oncosuppression in tumors (32). In gastric adenocarcinoma (33) and pulmonary carcinoid tumors (34), the decreased expression of CD99 was strongly associated with high proliferative activity, poor survival, and a heightened risk of metastasis formation, which may be related to increased migratory/invasion cell capabilities (35). Although the molecular basis underlying CD99 expression in SPN is still poorly understood, further investigations into the role of CD99 in the development of SPN are needed.

Another issue is the risk of parenchyma-preserving resection during the prognostic assessment for SPN recurrence. Few studies focus on analyzing an association of recurrence and initial type of operative procedure (2). One of the largest reports of 202 enucleations failed to provide information on the potential relationship between recurrence and the initial type of surgery (24). Although they did not analyze the recurrence events in relation to surgical procedures, the correlation between local approaches and non-radical resection seemed to be reasonable, according to the high risk for residual tumor or local recurrence (13). All the parenchyma-sparing surgery, including 5 (7.9%) in enucleation and 5 (7.9%) in central pancreatectomy, was performed radically (R0 resection) with no recurrence in our cohort. One of the two recurred patients experienced local recurrence 84 months after tumor enucleation in a county hospital and has survived for 96 months from the first surgery. This case further verified the conclusion that the local non-radical pancreatectomy for SPN was prone to recurrence (36).

The limitations to this study included the small number of cases and the retrospective nature, which might locate inconsistency in reporting pathologic data. In our cohort, none of the WHO criteria for malignance, infiltrative growth pattern, or the high Ki-67 index (≥4 or 5%) was confirmed in the primary tumor of the two recurred patients,

but the metastasectomy specimens fulfilled some of the malignant characters. Moreover, the immunohistochemistry was heterogeneous due to using different panel of antibodies among different specimens, as CD99 was performed in selected cases (45/63). SPN was dismissed from mind by many pathologists and clinicians in the past, who focused much on diagnosis rather than clinicopathological characteristics with survival associations (14). Future research based on standardized clinicopathological evaluation of pancreatic SPN will be able to further unveil the prognostic enigma of pancreatic SPN after resection.

CONCLUSION

Although aggressive surgery is the main method of management of pancreatic SPNs with favorable survival, it is generally difficult to assess the prognostic factors of resected SPNs. Our findings further corroborated that the current clinicopathological criteria for malignant potential SPNs should be deliberated. Future investigations into the role of clinicopathological evaluation will be able to further unveil the prognostic enigma of pancreatic SPN after resection.

DATA AVAILABILITY STATEMENT

The original contributions presented in the study are included in the article/supplementary material, further inquiries can be directed to the corresponding author/s.

ETHICS STATEMENT

The studies involving human participants were reviewed and approved by the Ethics Committee of Jinling Hospital, Nanjing University Medical School. The patients/participants provided their written informed consent to participate in this study.

AUTHOR CONTRIBUTIONS

XW was involved in the identification, selection, and management of patient cases, and wrote and revised the manuscript. DZ, ML, SW, and RS was involved in the management of patient cases and data acquisition, analysis, and interpretation. WB performed the histological images analysis and reviewed the manuscript. All authors read and approved the final manuscript.

REFERENCES

1. Bosman FT, Carneiro F, Hruban RH. *WHO Classification of Tumours of the Digestive System*. Lyon: 4th edn. Vol. 3. World Health Organization (2010).
2. Hanada K, Kurihara K, Itoi T, Katanuma A, Sasaki T, Hara K, et al. Clinical and pathological features of solid pseudopapillary neoplasms of the pancreas: a nationwide multicenter study in Japan. *Pancreas.* (2018) 47:1019–26. doi: 10.1097/MPA.0000000000001114
3. Kang CM, Choi SH, Kim SC, Lee WJ, Choi DW, Kim SW, et al. Predicting recurrence of pancreatic solid pseudopapillary tumors after surgical resection: a multicenter analysis in Korea. *Ann Surg.* (2014) 260:348–55. doi: 10.1097/SLA.0000000000000583
4. La Rosa S, Bongiovanni M. Pancreatic solid pseudopapillary neoplasm: key pathologic and genetic features. *Arch Pathol Lab Med.* (2020) 144:829–37. doi: 10.5858/arpa.2019-0473-RA
5. Naar L, Spanomichou D, Mastoraki A, Smyrniotis V, Arkadopoulos N. Solid pseudopapillary neoplasms of the pancreas: a surgical and genetic enigma. *World J Surg.* (2017) 41:1871–81. doi: 10.1007/s00268-017-3921-y
6. Jutric Z, Rozenfeld Y, Grendar J, Hammill CW, Cassera MA, Newell PH, et al. Analysis of 340 patients with solid pseudopapillary tumors of the pancreas: a closer look at patients with metastatic disease. *Ann Surg Oncol.* (2017) 24:2015–22. doi: 10.1245/s10434-017-5772-z
7. Wu J, Mao Y, Jiang Y, Song Y, Yu P, Sun S, et al. Sex differences in solid pseudopapillary neoplasm of the pancreas: a population-based study. *Cancer Med.* (2020) 9:6030–41. doi: 10.1002/cam4.3180
8. Yin Q, Wang M, Wang C, Wu Z, Yuan F, Chen K, et al. Differentiation between benign and malignant solid pseudopapillary tumor of the pancreas by MDCT. *Eur J Radiol.* (2012) 81:3010–8. doi: 10.1016/j.ejrad.2012.03.013
9. Tang X, Zhang J, Che X, Chen Y, Wang C. Peripancreatic lymphadenopathy on preoperative radiologic images predicts malignancy in pancreatic solid pseudopapillary neoplasm. *Int J Clin Exp Med.* (2015) 8:16315–21.
10. Yang F, Yu X, Bao Y, Du Z, Jin C, Fu, et al. Prognostic value of Ki-67 in solid pseudopapillary tumor of the pancreas: Huashan experience and systematic review of the literature. *Surgery.* (2016) 159:1023–31. doi: 10.1016/j.surg.2015.10.018
11. Estrella J, Li L, Rashid A, Wang H, Katz M, Fleming J, et al. Solid pseudopapillary neoplasm of the pancreas: clinicopathologic and survival analyses of 64 cases from a single institution. *Am J Clin Path.* (2014) 38:147–57. doi: 10.1097/PAS.0000000000000141
12. Marchegiani G, Andrianello S, Massignani M, Malleo G, Maggino L, Paiella S, et al. Solid pseudopapillary tumors of the pancreas: specific pathological features predict the likelihood of postoperative recurrence. *J Surg Oncol.* (2016) 114:597–601. doi: 10.1002/jso.24380
13. Tjaden C, Hassenpflug M, Hinz U, Klaiber U, Klauss M, Buchler MW, et al. Outcome and prognosis after pancreatectomy in patients with solid pseudopapillary neoplasms. *Pancreatology.* (2019) 19:699–709. doi: 10.1016/j.pan.2019.06.008
14. Liu M, Liu J, Hu Q, Xu W, Liu W, Zhang Z, et al. Management of solid pseudopapillary neoplasms of pancreas: a single center experience of 243 consecutive patients. *Pancreatology.* (2019) 19:681–5. doi: 10.1016/j.pan.2019.07.001
15. Cohen SJ, Papoulas M, Graubardt N, Ovdat E, Loewenstein S, Kania-Almog J, et al. Micro-RNA expression patterns predict metastatic spread in solid pseudopapillary neoplasms of the pancreas. *Front Oncol.* (2020) 10:328. doi: 10.3389/fonc.2020.00328
16. Bassi C, Marchegiani G, Dervenis C, Sarr M, Abu Hilal M, Adham M, et al. The 2016 update of the International Study Group (ISGPS) definition and grading of postoperative pancreatic fistula: 11 years after. *Surgery.* (2017) 161:584–91. doi: 10.1016/j.surg.2016.11.014
17. Dindo D, Demartines N, Clavien PA. Classification of surgical complications: a new proposal with evaluation in a cohort of 6336 patients and results of a survey. *Ann Surg.* (2004) 240:205–13. doi: 10.1097/01.sla.0000133083.54934.ae
18. Huffman BM, Westin G, Alsidawi S, Alberts SR, Nagorney DM, Halfdanarson TR, et al. Survival and prognostic factors in patients with solid pseudopapillary neoplasms of the pancreas. *Pancreas.* (2018) 47:1003–7. doi: 10.1097/MPA.0000000000001112
19. Wang P, Wei J, Wu J, Xu W, Chen Q, Gao W, et al. Diagnosis and treatment of solid-pseudopapillary tumors of the pancreas: a single institution experience with 97 cases. *Pancreatology.* (2018) 18:415–9. doi: 10.1016/j.pan.2017.12.012
20. Xu Y, Zhao G, Pu N, Nuerxiati A, Ji Y, Zhang L, et al. One hundred twenty-one resected solid pseudopapillary tumors of the pancreas: an 8-year single-institution experience at Zhongshan hospital, shanghai, China. *Pancreas.* (2017) 46:1023–8. doi: 10.1097/MPA.0000000000000885

21. Yang F, Wu W, Wang X, Zhang Q, Bao Y, Zhou Z, et al. Grading solid pseudopapillary tumors of the pancreas: the Fudan prognostic index. *Ann Surg Oncol.* (2021) 28:550–9. doi: 10.1245/s10434-020-08626-z
22. Kosmahl M, Seada L, Jänig U, Harms D, Klöppel G. Solid–pseudopapillary tumor of the pancreas: its origin revisited. *Virchows Arch.* (2000) 436:473–80. doi: 10.1007/s004280050475
23. Guo M, Luo G, Jin K, Long J, Cheng H, Lu Y, et al. Somatic genetic variation in solid pseudopapillary tumor of the pancreas by whole exome sequencing. *Int J Mol Sci.* (2017) 18:81. doi: 10.3390/ijms18010081
24. Law JK, Ahmed A, Singh VK, Akshintala VS, Olson MT, Raman SP, et al. A systematic review of solid-pseudopapillary neoplasms: are these rare lesions? *Pancreas.* (2014) 43:331–7. doi: 10.1097/MPA.0000000000000061
25. Watanabe Y, Okamoto K, Okada K, Aikawa M, Koyama I, Yamaguchi H. A case of aggressive solid pseudopapillary neoplasm: comparison of clinical and pathologic features with non-aggressive cases. *Pathol Int.* (2017) 67:202–7. doi: 10.1111/pin.12516
26. Yu P, Cheng X, Du Y, Yang L, Xu Z, Yin W, et al. Solid pseudopapillary neoplasms of the pancreas: a 19-year multicenter experience in China. *J Gastrointest Surg.* (2015) 19:1433–40. doi: 10.1007/s11605-015-2862-8
27. Geers C, Moulin P, Gigot JF, Weynand B, Deprez P, Rahier J, et al. Solid and pseudopapillary tumor of the pancreas-review and new insights into pathogenesis. *Am J Surg Pathol.* (2006) 30:1243–9. doi: 10.1097/01.pas.0000213311.28682.b2
28. Walter T, Hommell-Fontaine J, Hervieu V, Adham M, Poncet G, Dumortier J, et al. Primary malignant solid pseudopapillary tumors of the gastroduodenal area. *Clin Res Hepatol Gastroenterol.* (2011) 35:227–33. doi: 10.1016/j.clinre.2011.01.004
29. Guo Y, Yuan F, Deng H, Wang HF, Jin XL, Xiao JC. Paranuclear dot-like immunostaining for CD99: a unique staining pattern for diagnosing solid-pseudopapillary neoplasm of the pancreas. *Am J Surg Pathol.* (2011) 35:799–806. doi: 10.1097/PAS.0b013e318219c036
30. Pasello M, Manara MC, Scotlandi K. CD99 at the crossroads of physiology and pathology. *J Cell Commun Signal.* (2018) 12:55–68. doi: 10.1007/s12079-017-0445-z
31. Li L, Li J, Hao C, Zhang C, Mu K, Wang Y, et al. Immunohistochemical evaluation of solid pseudopapillary tumors of the pancreas: the expression pattern of CD99 is highly unique. *Cancer Lett.* (2011) 310:9–14. doi: 10.1016/j.canlet.2011.04.017
32. Manara MC, Pasello M, Scotlandi K. CD99: a cell surface protein with an oncojanus role in tumors. *Genes.* (2018) 9:159. doi: 10.3390/genes9030159
33. Lee JH, Kim SH, Wang LH, Choi YL, Kim YC, Kim JH, et al. Clinical significance of CD99 down-regulation in gastric adenocarcinoma. *Clin Cancer Res.* (2007) 13:2584–91. doi: 10.1158/1078-0432.CCR-06-1785
34. Pelosi G, Fraggetta F, Sonzogni A, Fazio N, Cavallon A, Viale G. CD99 immunoreactivity in gastrointestinal and pulmonary neuroendocrine tumours. *Virchows Arch.* (2000) 437:270–4. doi: 10.1007/s004280000240
35. Zucchini C, Manara MC, Pinca RS, De Sanctis P, Guerzoni C, Sciandra M, et al. CD99 suppresses osteosarcoma cell migration through inhibition of ROCK2 activity. *Oncogene.* (2014) 33:1912–21. doi: 10.1038/onc.2013.152
36. The European Study Group on Cystic Tumours of the Pancreas. European evidence-based guidelines on pancreatic cystic neoplasms. *Gut.* (2018) 67:789–804. doi: 10.1136/gutjnl-2018-316027

Conflict of Interest: The authors declare that the research was conducted in the absence of any commercial or financial relationships that could be construed as a potential conflict of interest.

Publisher's Note: All claims expressed in this article are solely those of the authors and do not necessarily represent those of their affiliated organizations, or those of the publisher, the editors and the reviewers. Any product that may be evaluated in this article, or claim that may be made by its manufacturer, is not guaranteed or endorsed by the publisher.

Copyright © 2021 Wang, Zhu, Bao, Li, Wang and Shen. This is an open-access article distributed under the terms of the Creative Commons Attribution License (CC BY). The use, distribution or reproduction in other forums is permitted, provided the original author(s) and the copyright owner(s) are credited and that the original publication in this journal is cited, in accordance with accepted academic practice. No use, distribution or reproduction is permitted which does not comply with these terms.

frontiers in Oncology

ORIGINAL RESEARCH
published: 03 December 2021
doi: 10.3389/fonc.2021.779761

Comparison of Four Lymph Node Stage Methods for Predicting the Prognosis of Distal Cholangiocarcinoma Patients After Surgery

Xiuyi Huang[1], *Xiaoya Niu*[1], *Zhen You*[1], *Youlin Long*[2], *Fan Luo*[1] *and Hui Ye*[1]*

[1] Department of Biliary Surgery, West China Hospital, Sichuan University, Chengdu, China, [2] Chinese Evidence-Based Medicine Center, West China Hospital, Sichuan University, Chengdu, China

OPEN ACCESS

Edited by:
Ravindra Deshpande, Wake Forest School of Medicine, United States

Reviewed by:
Naresh Damuka, Wake Forest School of Medicine, United States
Praveen Kumar Allu, University of Pennsylvania, United States

***Correspondence:**
Hui Ye
yehuimd@163.com

Specialty section:
This article was submitted to Gastrointestinal Cancers: Hepato Pancreatic Biliary Cancers, a section of the journal Frontiers in Oncology

Received: *19 September 2021*
Accepted: *16 November 2021*
Published: *03 December 2021*

Citation:
Huang X, Niu X, You Z, Long Y, Luo F and Ye H (2021) Comparison of Four Lymph Node Stage Methods for Predicting the Prognosis of Distal Cholangiocarcinoma Patients After Surgery. Front. Oncol. 11:779761. doi: 10.3389/fonc.2021.779761

Background: The metastatic status of regional lymph nodes is an effective risk factor for the prognosis of distal cholangiocarcinoma (dCCA). But existing lymph node staging is not accurate enough and is susceptible to interference. This study aims to explore the predictive ability of the log odds of positive lymph nodes (LODDS) staging system of dCCA compared with existing lymph node staging systems.

Methods: A total of 928 dCCA patients were selected from the Surveillance, Epidemiology, and End Results (SEER) database as the training cohort, and 207 dCCA patients from West China Hospital who underwent surgery were reviewed as the validation cohort. The least absolute shrinkage and selection operator (LASSO) and multivariate Cox regression were conducted to identify the most meaningful factors relevant to prognosis. The performance of four lymph node stage systems was compared by a model-based approach.

Result: Age at diagnosis, pathological grade, American Joint Committee on Cancer (AJCC) tumor 7th T stage, tumor size, radiotherapy, chemotherapy, and lymph node stage system were independent prognostic factors. The model with the LODDS system had a better model fit with the highest C-index (0.679) and 1-/3-/5- area under the receiver operating characteristic curve (AUC) (0.739/0.671/0.658) as well as the lowest Akaike information criterion (AIC) (5,020.52). External validation results from 207 dCCA patients showed a C-index of 0.647 and 1-/3-/5-AUC of 0.740/0.683/0.589. Compared with the lymph node ratio (LNR), AJCC 8th N system, and 7th N system, the 5-year net reclassification improvement (NRI) of the LODDS system was 0.030 (95% CI: –0.079 to 0.147), 0.042 (95% CI: –0.062 to 0.139), and 0.040 (95% CI: –0.057 to 0.146), respectively. The integrated discrimination improvement (IDI) of LODDS improved compared with the LNR model (0.016; 95% CI: –0.001 to 0.036), AJCC 8th N system (0.020; 95% CI: 0.003–0.037), and AJCC 7th N system (0.019; 95% CI: 0.002–0.036). Decision curve analysis (DCA) also shows a greater net benefit of LODDS. In lymph node-negative patients, LODDS reveals a positive linear relationship with the hazard ratio (HR).

The stage capacity of LODDS in a subgroup analysis stratified by examined lymph node number (ELNN) was consistent.

Conclusions: The LODDS lymph node stage system has superior predictive performance as compared with the LNR, AJCC 7th, and 8th lymph node stage systems. Meanwhile, LODDS has a more detailed staging ability and good stability.

Keywords: distal cholangiocarcinoma (dCCA), log odds of positive lymph node (LODDS), lymph node stage, prognosis ability, modeling

INTRODUCTION

Distal cholangiocarcinoma (dCCA) is a malignant tumor located at the common bile duct, accounting for 20%–30% of all cholangiocarcinoma. Hitherto, the primary treatment for dCCA is radical surgical resection, such as pancreaticoduodenectomy and lymphadenectomy (1, 2). Due to the lower resection rate and the higher recurrence rate after surgery, the prognosis of dCCA is poor, and the 5-year survival rate for patients only ranges from 20% to 50% (3, 4). Many studies reported that the metastatic status of regional lymph nodes is a strong risk factor of prognosis (5–8). An accurate lymph node stage system is required to evaluate the tumor stage precisely and direct the appropriate postoperative adjuvant therapy for resectable dCCA after surgery.

The most commonly employed lymph node staging system so far is the American Joint Committee on Cancer (AJCC) tumor TNM staging system. In the AJCC 7th edition, the lymph node stage system of dCCA was based on the location of lymph node metastasis. The 8th edition lymph node stage was reclassified into N0 (no regional lymph node metastasis), N1 (1 to 3 regional lymph node metastasis), and N2 (≥4 regional lymph node metastasis) according to the regional positive lymph node number (PLNN). The 8th version also suggests that at least 12 lymph nodes need to be examined to ensure the accuracy of staging. However, dissection of more than 12 lymph nodes is a challenge sometimes due to the complexity of the surgical area and the skills of surgeons. Thus, a better lymph node staging system is required for the prognosis prediction of dCCA.

Lymph node ratio (LNR), which is the ratio of PLNN to examined lymph node number (ELNN), has been proposed as an indicator of lymph node staging. Several studies have confirmed that the LNR is a promising indicator of the prognosis of dCCA (4, 9–12). Log odds of positive lymph nodes (LODDS) is the log of the ratio of PLNN to negative lymph node number (NLNN). LODDS is theoretically more accurate than the LNR staging, especially in patients with negative lymph nodes. Good predictive ability in tumors has been shown in gallbladder cancer, hilar cholangiocarcinoma, colon cancer, gastric cancer, breast cancer, and thyroid cancers (13–18). However, the effect of LODDS has not been investigated in dCCA. Considering the latest lymph node stage method of dCCA conveying the significance of the number of lymph nodes toward prognosis, the LODDS may play a more important role in dCCA patients. In this study, we compare the performance of the LODDS staging system with three other lymph node staging systems (LNR system, AJCC 8th N staging system, and AJCC 7th N staging system) and explore more value of LODDS as a prognosis factor for dCCA after surgery.

METHOD

Study Design and Data Source

The Surveillance, Epidemiology, and End Results (SEER) database is an open-source clinical database. It collects cancer incidence data from population-based cancer registries covering approximately 34.6% of the U.S. population. The inclusion criteria are patients diagnosed with dCCA between 2004 and 2018 in the SEER database. The exclusion criteria are 1) patients who did not undergo surgery or surgery information is unclear; 2) patients with more than one *in situ* malignancy; 3) patients without certain lymph node accounts; and 4) patients who died in the first month after surgery. The process flowchart of the training cohort is shown in **Figure 1**. The primary outcome was overall survival (OS), which was defined as the time from diagnosis to death from any cause. The last follow-up date was November 31, 2020. The study was conducted following the Declaration of Helsinki. The Ethical Committee of The West China Hospital of Sichuan University has approved the research, and informed consent was obtained from all patients. The SEER database is an open-access database, and all patient information has been de-identified, so informed consent of the training set was waived.

Handing of Variables

The variables we collected include the age at dCCA diagnosis, sex, race, histology, AJCC TNM stage, pathological grade, tumor size, ELNN, PLNN, NLNN, radiotherapy, and chemotherapy information, survival time, and vital status. The AJCC 8th lymph node stage was deduced by using the PLNN and metastasis region. Owing to lack of the information on the depth of bile duct infiltration in the database, the AJCC 7th T stage was still used in this study. LODDS is calculated by log [(0.05 + PLNN)/(0.05 + NLNN)], and the result of LODDS in this study ranges from −2.95 to 2.37. The LNR is the ratio of PLNN/ELNN, and the result ranges from 0 to 1.

Handling of Missing Data

The missing data in the present study were about 14.5% including 70 cases in grade, 24 cases in TNM system, and 74 cases in tumor size. Some of the cases with more than one value

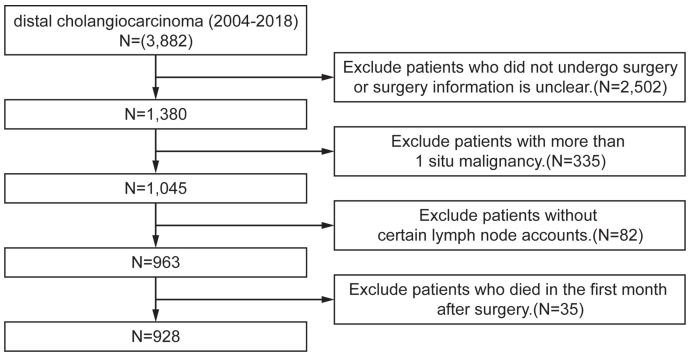

FIGURE 1 | Flowchart of the data process for training set.

are missing. By analyzing the relationship between the missing values and variables, we take that the data were missing at random. To fill the missing values, the multiple imputation method based on chained equations was performed 15 times. All the variables except survival time and status are included in the imputation procedure.

Predictor Transformation and Selection

To increase utility and carry out further research, X-tile 3.6.1 software (Yale University School of Medicine, New Haven, CT, USA) was used to identify the optimal cutoff value of variables. The program calculates the cutoff value with significant differences by selecting the highest χ^2 value and uses a standard log-rank test to calculate the p-value (19). The cutoff values of age are 78 years; the tumor size was categorized as <20, 20 to 34, and ≥ 34 mm. LODDS was divided into three categories: LODDS1–3, <−2.0, −2.0 to −0.4, and ≥−0.4. The LNR was stratified into LNR1–3: <0.1, 0.1 to 0.3, and ≥0.3. The rest of the category variables were classified according to the classification criteria of the SEER database.

The least absolute shrinkage and selection operator (LASSO) *via* 10-fold cross-validation was conducted firstly. Twelve variables were selected with the lambda value that produces the minimum mean cross-validated error: age at diagnosis, race, pathological grade, AJCC 7th T stage, LODDS, tumor size, NLNN, radiotherapy, and chemotherapy. Then the selected variables above, as well as the AJCC 7th N stage, AJCC 8th N stage, and LNR, were incorporated into multivariable Cox regression.

Model Construction, Comparison, and Validation

Cox proportional hazard models of four N staging systems (LODDS system, LNR system, AJCC 8th N staging system, and AJCC 7th N staging system) based on the variables screened above are constructed. The proportionality of hazards in Cox models was tested based on the Schoenfeld residuals, and chemotherapy was considered as a time-dependent covariable. Thus, a step function was used to estimate the hazard ratio (HR) according to the median OS, and the observation period was split into ≤26 and >26 months. Akaike information criterion (AIC), C-index, and the area under the receiver operating characteristic curve (AUC) of 1/3/5 years of four models were compared. The net reclassification improvement (NRI) and the integrated discrimination improvement (IDI) were calculated to cross-sectionally compare the predictive power of LODDS with other lymph node staging systems. The levels of year risk are derived from the event rate (20). Decision curve analysis (DCA) was used to compare the clinical availability and utility of four lymph node stage models. Finally, external validation of the model was carried out by using patients filtered at the West China Hospital of Sichuan University.

Statistical Analysis

The group differences of categorical and continuous variables were determined by the chi-square test and Kruskal–Wallis H test, respectively. The Cox proportional hazards regression model of four lymph node stages was constructed, the survival curve of each model was depicted by the Kaplan–Meier analysis, and the differences were tested by a log-rank method. Statistical analyses were carried out with R software version 4.0.4. A p-value <0.05 was regarded as significant.

RESULTS

Demographic and Clinical Characteristics

928 patients in total diagnosed with dCCA between 2004 and 2018 from the SEER database were selected as the training cohort. 207 patients diagnosed with dCCA at the West China Hospital of Sichuan University from 2009 to 2018 were collected as the validation cohort. The baseline characteristics of the training cohort and validation cohort are summarized in **Table S1**. For the training set, the median follow-up time was 45 months; the median OS was 26 months; and 3- and 5-year survival was 37.7% and 26%, respectively. The median age was 67 years (interquartile range (IQR): 59.3–73.0); more patients were male (66.6%); the median size of tumors was 22 mm (IQR: 15.0–30.0); more than half of patients received chemotherapy; and 31.2% of patients received radiation therapy. The median and

mean values of ELNN are 14.0 and 15.0, respectively; the median and mean values of PLNN are 1 and 1.7, respectively.

Prognostic Factors for Distal Cholangiocarcinoma Patients

Variables were then subjected to multivariate Cox regression such as age at diagnosis, sex, race, pathological grade, AJCC 7th T stage, LODDS, LNR, tumor size, ELNN, PLNN, radiotherapy, and chemotherapy filtered by LASSO regression. The HRs of the variables above with corresponding 95% CIs are presented in **Table 1**. Age at diagnosis, pathological grade, tumor size, chemotherapy, and lymph node stage system were closely associated with the OS of dCCA ($p < 0.05$). Though the p-value of radiotherapy is not significant in multivariate Cox regression (HR = 0.92, $p = 0.463$), it was still regarded as a predictor since relevant studies have shown the improved prognosis of dCCA with radiotherapy (21–24). Finally, seven variables were ascertained to construct the model: age at diagnosis, pathological grade, AJCC 7th T stage, tumor size, radiotherapy, chemotherapy, and lymph node stage system. The variance inflation factor value for all variables is between 1 and 5, which means moderate multicollinearity between variables in the model and does not need to be adjusted (25).

Comparison of Four Lymph Node Staging Systems and Validation

The strata method of four N staging systems in the Kaplan–Meier survival were all statistically significant for OS of dCCA ($p < 0.0001$, log-rank; **Figure 2**), indicating that the four lymph node stage systems are all well predictive of prognosis for dCCA. **Table 2** lists and compares the model parameters of four models. The C-index for the LODDS, LNR, AJCC 8th, and 7th N systems were 0.679, 0.672, 0.667, and 0.666, respectively. The AIC values of four lymph node stages were 5,020.52, 5,036.77, 5,041.48, and 5,044.56. The 1-year AUC values for four lymph node stages were 0.739, 0.728, 0.718, and 0.715. The 3-year AUC values for four lymph node stages were 0.671, 0.655, 0.664, and 0.665. The 5-year AUC values for four lymph node stages were 0.658, 0.653, 0.643, and 0.644. The LODDS system had the best model fit with the highest C-index and 1-/3-/5-AUC as well as the lowest AIC. For this reason, LODDS was considered the most accurate way of lymph node staging for the prognosis of dCCA patients. NRI and

TABLE 1 | Multivariate Cox regression analysis of factors associated with overall survival.

Variables		Multivariate analysis		
		HR	95% CI	p-Value
Age, year	≤78	Reference		
	>78	1.55	1.17–2.05	0.002**
Race	White	Reference		
	Black	0.85	0.61–1.2	0.356
	Other	0.89	0.71–1.11	0.305
Grade	Well, I	Reference		
	Moderately, II	1.14	0.84–1.54	0.398
	Poorly, III	1.43	1.05–1.95	0.025*
7th T stage	T1	Reference		
	T2	1.39	0.96–2.03	0.085
	T3	2.04	1.42–2.94	<0.001***
	T4	2.04	1.23–3.39	0.006**
7th N stage	N0	Reference		
	N1	2.20	0.66–7.29	0.198
8th N stage	N0	Reference		
	N1	0.43	0.13–1.51	0.190
	N2	0.57	0.15–2.17	0.414
LODDS	LODDS 1	Reference		
	LODDS 2	1.70	1.21–2.38	0.002**
	LODDS 3	4.32	2.16–8.63	<0.001***
LNR	LNR 1	Reference		
	LNR 2	1.04	0.77–1.41	0.793
	LNR 3	0.51	0.26–1.01	0.054
Tumor size (cm)	≤20	Reference		
	20–34	1.07	0.87–1.31	0.519
	>34	1.67	1.32–2.12	<0.001***
NLNN	—	0.99	0.97–1	0.026*
Chemotherapy	None/unknown	Reference		
	Yes	0.71	0.57–0.88	0.002**
Radiotherapy	None/unknown	Reference		
	Yes	0.92	0.74–1.15	0.463

HR, hazard ratio; T, tumor; N, node; LODDS, log odds of positive lymph nodes; LNR, positive lymph node ratio; PLNN, positive lymph nodes number; NLNN, negative lymph node number.
**p-Values <0.05.*
***p-Values <0.01.*
****p-Values <0.001.*

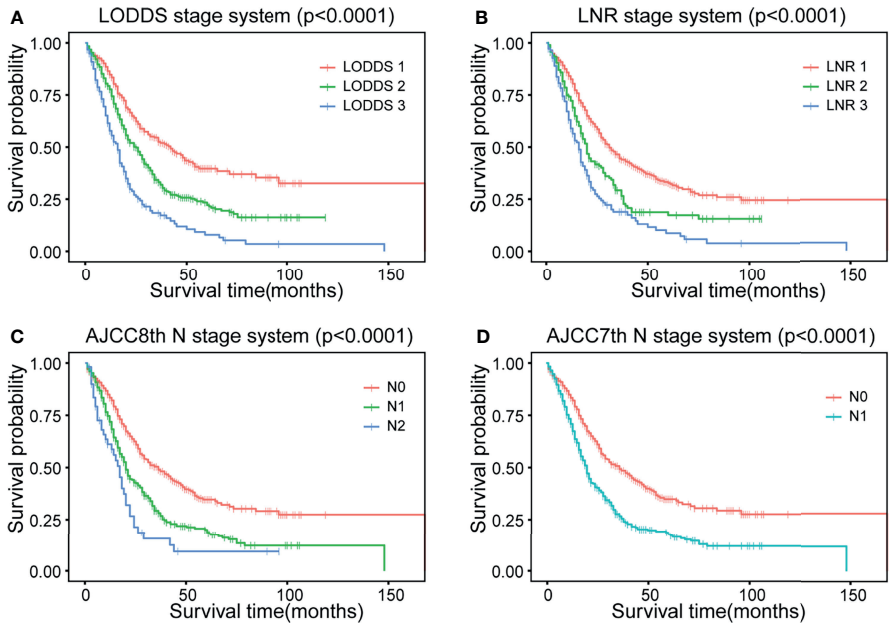

FIGURE 2 | Kaplan–Meier curves of four different lymph node staging systems. **(A)** LODDS system, **(B)** LNR system, **(C)** AJCC 8th N stage, and **(D)** AJCC 7th N stage. LODDS, log odds of positive lymph nodes; LODDS1, <–2.0; LODDS2, –2.0 to –0.4; LODDS3, ≥–0.4; LNR, lymph node ratio; LNR1, <0.1; LNR2, 0.1 to 0.3; LNR3, ≥0.3; AJCC, American Joint Committee on Cancer. AJCC 8th: N0, no regional lymph node metastasis; N1, 1 to 3 regional lymph node metastasis; N2, ≥4 regional lymph node metastasis. AJCC 7th: N0, no regional lymph node metastasis; N1, positive regional lymph nodes. OS, overall survival.

TABLE 2 | The comparison of four lymph node stage system.

System	LODDS	LNR	8th N stage†	7th N stage†
AIC	5,020.52	5,036.77	5,041.48	5,044.56
AUC (1-year)	0.739	0.728	0.718	0.715
AUC (3-year)	0.671	0.655	0.664	0.665
AUC (5-year)	0.658	0.653	0.643	0.644
C-index	0.679	0.672	0.667	0.666
LODDS model performance compared with other models				
NRI (5-year)	—	0.030 (–0.079 to 0.147)	0.042 (–0.062 to 0.139)	0.040 (–0.057 to 0.146)
NRI (events)	—	–0.027 (–0.077 to 0.024)	–0.024 (–0.065 to 0.026)	–0.024 (–0.061 to 0.024)
NRI (non-events)	—	0.057 (–0.053 to 0.176)	0.064 (–0.034 to 0.153)	0.064 (–0.034 to 0.164)
IDI (5-year)	—	0.016 (–0.001 to 0.036)	0.020 (0.003 to 0.037)	0.019 (0.002 to 0.036)

LODDS, log odds of positive lymph nodes; LNR, positive lymph node ratio; AIC, Akaike information criterion; AUC, the area under the receiver operating characteristic curve; NRI, net reclassification improvement; IDI, integrated discrimination improvement.

†*American Joint Committee on Cancer TNM staging system.*

IDI were calculated to measure the reclassification improvements of LODDS (**Table 2**). The 5-year NRI values of LODDS vs. LNR, AJCC 8th, and AJCC 7th N systems were 0.030 (95% CI: –0.079 to 0.147), 0.042 (95% CI: –0.062 to 0.139), and 0.040 (95% CI: –0.057 to 0.146). The 5-year IDI values of LODDS vs. LNR, AJCC 8th, and 7th N systems were 0.016 (95% CI: –0.001 to 0.036), 0.020 (95% CI: 0.003–0.037), and 0.019 (95% CI: 0.002–0.036), respectively. All values of NRI and IDI are greater than zero, which implies that LODDS can better differentiate between high- and low-risk dCCA patients after surgery, especially for low-risk patients who are classified as high risk by the original staging approach. The DCA curve shows that the LODDS system has the highest net benefits among the four lymph node stage systems, which indicates better performance in prognostic predictions for dCCA (**Figure 3**).

External validation results from 207 dCCA patients showed a C-index of 0.6476 and 1-/3-/5-AUC of 0.740/0.683/0.589, respectively. The results indicate a good predictive ability of LODDS in the Asian population. And the accurate predictive capability of LODDS also has been proved in DCA curve (**Figure 3**).

Relationship Between the Number of Lymph Nodes and Staging

When all tested lymph nodes are negative, the LNR value is equal to 0 and the N stage of both AJCC 7th and 8th is N0. But the

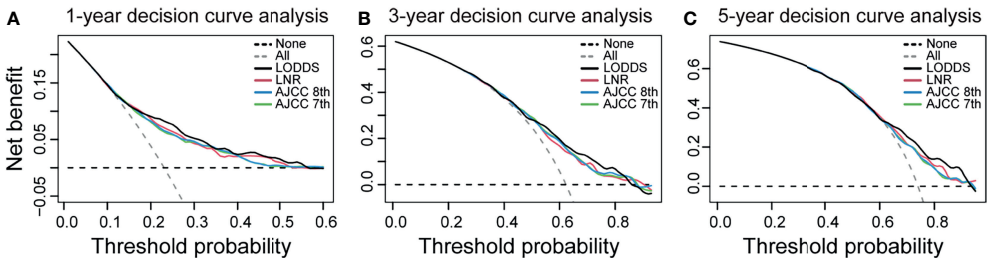

FIGURE 3 | Decision curve analysis for the LODDS system, LNR system, AJCC 8th N stage, and AJCC 7th N stage. **(A)** 1-year decision curve analysis. **(B)** 3-year decision curve analysis. **(C)** 5-year decision curve analysis. The x-axis indicates net benefit when all patients are considered as not having the outcome, and the y-axis indicates net benefit when all patients are considered as having the outcome. The LODDS has the highest net benefit over the other three lymph node models mostly. LODDS, log odds of positive lymph nodes; LNR, lymph node ratio; AJCC, American Joint Committee on Cancer.

LODDS value still varies based on the number of lymph nodes detected. We explored the correlations between HR and LODDS when PLNN = 0. **Figure 4** shows a positive linear relationship between LODDS and HR. This suggests that the ELNN in lymph node-negative patients is prognostically relevant and that LODDS has the ability to predict risk in this condition.

To investigate the impact of ELNN on prognosis and staging accuracy, the effect of ELNN controlling for the risk of death was evaluated in **Table S2**. Patients' outcomes significantly improved when the ELNN is more than 15. We additionally performed subgroup-stratified analyses, identifying the stage accuracy of four systems stratified by ELNN. The cutoff value of ELNN is 15. The Kaplan–Meier survival shows that there is a significant difference in the prognosis of AJCC 7th and AJCC 8th N stages stratified by ELNN = 15 (**Figure 5**). But the p-value was not significant in all strata of the LODDS and LNR staging systems. This suggests that AJCC 7th and 8th N stage methods tend to be influenced by the ELNN while the LODDS and LNR are less disturbed by ELNN. Thus, the LODDS and LNR perform better in improving staging accuracy in cases of an inadequate number of lymph nodes detected.

Chemotherapy and Prognosis

When the data were modeled as a step function by adjusting the covariates, we discover that there was a negative association between chemotherapy and mortality until approximately 12 months after surgery (HR = 0.41, 95% CI: 0.30–0.56, $p < 0.001$), after which there was a positive association between chemotherapy exposure and mortality (**Table S3**). This phenomenon gives us an unexpected discovery that chemotherapy may be associated with improved early prognosis.

DISCUSSION

The importance of lymph node metastasis status when assessing disease prognosis is necessary to be taken into account. Thus, an appropriate method for lymph node staging is helpful when guiding the therapy of dCCA after surgery. In the 7th edition of the AJCC TNM staging system, the N staging is mainly distinguished by the presence of regional lymph node metastasis. Several studies have confirmed that the number of regional PLNN can reflect the effect of lymph node metastasis on the prognosis of dCCA better when compared with the presence of lymph node metastases alone (26–30). The other two retrospective studies also found that patients with more than 11 lymph nodes removed had a better prognosis (31, 32). Besides, a large multicenter cohort studied by Kang et al. concluded that PLNN detection rates become stabilized when the total number of dissected lymph nodes was more than 12 (33). Thus, the 8th version adopted the regional PLNN as the N stage. To ensure the staging accuracy, the recommended minimum number of lymph nodes to be detected is 12 (34). In our study, the association with prognosis was not significant when the cutoff value of ELNN was 12 (HR = 0.92, 95% CI: 0.777–1.090, p = 0.335). However, with

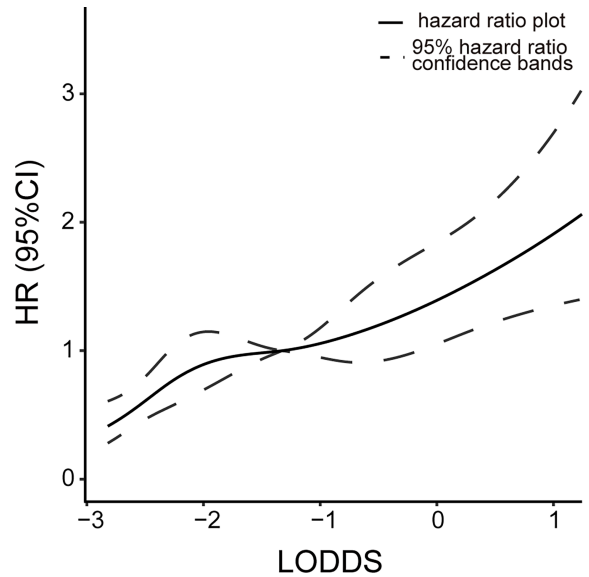

FIGURE 4 | Relationship between the risk of death and LODDS value at LNR = 0. Continuous line, hazard ratio plot; dotted lines, 95% hazard ratio confidence bands. LODDS, log odds of positive lymph nodes; LNR, lymph node ratio.

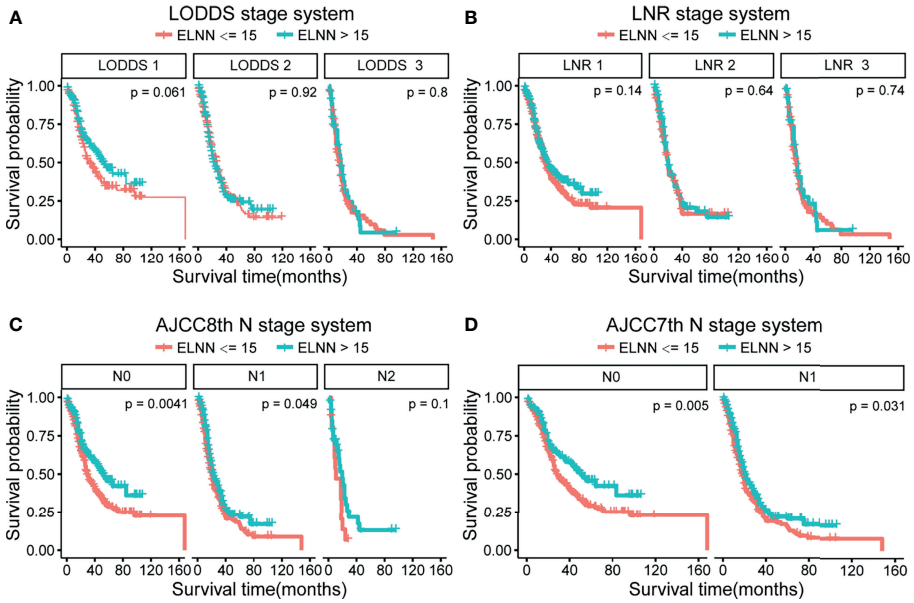

FIGURE 5 | Kaplan–Meier survival curve according to N stage for the four lymph node staging systems stratified by ELNN=15. **(A)** LODDS system, **(B)** LNR system, **(C)** AJCC 8th N stage, and **(D)** AJCC 7th N stage. LODDS, log odds of positive lymph nodes; ELNN, examined lymph node number; LNR, lymph node ratio; AJCC, American Joint Committee on Cancer; OS, overall survival.

more than 15 lymph nodes, the dissection prognosis was improved significantly. One reason for the discrepancy may be that the SEER database lacks information for excluding high-risk patients, such as marginal status.

Although examining an adequate number of lymph nodes can help stage precisely, we also need to consider the accuracy of staging when the ELNN is inadequate. The LNR staging system combined with ELNN and PLNN compensates for the impact of insufficient ELNN on staging. A meta-analysis found that LNR = 0.2 is the ideal cutoff value for risk stratification of dCCA patients with radical resection (4), while the optimal cutoff value based on prognosis was between 0.45 and 0.17 (11, 12, 29, 30). Similar cutoff values were obtained in our study by using X-tile software: LNR1-3: <0.1, 0.1 to 0.3, and ≥0.3. However, the LNR is also incomplete. The LNR value becomes 0 or 1 when PLNN is 0 or all examined lymph nodes are positive, which lacks the corresponding discriminatory ability (35). LODDS is the log of the ratio of PLNN to NLNN. It could stage the lymph node condition when the PLNN is 0 or fully positive as well. The linear relationship between LODDS and HR at PLNN = 0 depicted in our study suggests that LODDS has good discriminating power in lymph node-negative patients. The value of LODDS in the fully positive lymph node patients is not calculated due to few samples. To evaluate the predictive power of different N stages when considering ELNN, subgroup analysis was performed to compare survival curves of four lymph node stages. Since the detection of 12 lymph nodes suggested by previous articles does not significantly impact the prognosis in our study, we choose 15 as the cutoff value of ELNN. Both the LODDS and LNR models are unaffected by staging migration arising from the number of lymph nodes detected. This demonstrates the advantages of LODDS staging from another aspect. However, since the SEER database lacks other information on relevant risk factors, it may affect the results.

To identify the prognostic value of LODDS, this study calculated the values of C-index, AIC, and AUC of the four lymph node stage models, and the LODDS presented the best performance overall. The universality of the conclusion was verified by using data from our medical center. The result showed the superiority of LODDS as a lymph node stage system and also performs a good predictive ability in the Asian population. Eventually, the NRI, IDI values, and DCA curves exhibited improvement compared with the AJCC 8th staging system, AJCC 7th N staging system, and LNR staging system. This further confirmed the predictive accuracy of LODDS.

In addition, we observed a time-varying correlation between chemotherapy and time-related hazard. Chemotherapy significantly decreased the risk of mortality in the first year after surgery but has no significant improvement in prognosis beyond 1 year, which may indicate that chemotherapy improves the early prognosis of dCCA patients after surgery. Besides, we take radiotherapy as a predictor based on clinical experience. The conduction of radiotherapy for dCCA has not come to a global agreement. Several studies have revealed that postoperative chemoradiotherapy improves the prognosis of patients significantly, especially for patients with R1 resection and regional LN metastases. But the effect is not remarkable when chemotherapy or radiotherapy is given alone (21–24, 36–38). In our study, radiotherapy was not significant for OS improvement but benefit prognosis when excluding patients with negative

regional lymph node metastasis (HR = 0.725, p = 0.006). We can reasonably assume that radiotherapy improves the prognosis of high-risk patients from previous studies. However, large prospective randomized controlled trials are required for exploring the effect of adjuvant therapy on dCCA. Meanwhile, jaundice, high fibrinogen level, and alcohol consumption could be associated with a poor prognosis of dCCA after pancreatoduodenectomy (39). But we could not take these factors into account in the analysis due to a lack of information in the SEER database. This might limit our model's performance. To the extent of our knowledge, this study is the first one that investigates the predictive value of the LODDS lymph node staging system in dCCA. The results demonstrated that LODDS staging outperformed the AJCC staging and LNR staging. Nevertheless, some shortcomings still exist in this study. First, the data in the SEER database are retrospective and therefore was exposed to selection bias. Second, some other vital information related to the tumor, like marginal status, tumor markers, AJCC 8th T stage, and jaundice, is not recorded in the SEER database, which may affect the accuracy of the prediction model. Third, the cutoff values of LODDS and tumor size are calculated from the log-rank test, and their validity needs to be further confirmed in large samples of clinical practice.

CONCLUSION

For patients with dCCA, the LODDS lymph node stage system seems to have a superior ability to predict survival compared with the AJCC staging system and LNR systems. Particularly, it compensates for the migration of the AJCC lymph node stage system better when the number of lymph nodes examined is low, as well as the accurate stage of lymph node-negative patients. Hence, the LODDS lymph node stage may be a promising predictor.

DATA AVAILABILITY STATEMENT

The original contributions presented in the study are included in the article/**Supplementary Material**. Further inquiries can be directed to the corresponding author.

ETHICS STATEMENT

The studies involving human participants were reviewed and approved by the Ethics Committee on Biomedical Research, West China Hospital of Sichuan University. The patients/participants provided their written informed consent to participate in this study.

AUTHOR CONTRIBUTIONS

XH: conceptualization, methodology, survey, data analysis, and writing—original draft. ZY: methodology, survey, and data analysis. XN: survey and data collection. YL: methodology and data analysis. FL: data collection. HY: writing—review and editing, and supervision. All authors contributed to the article and approved the submitted version.

ACKNOWLEDGMENTS

The authors would like to thank Dr. Shuang Dai from the West China Hospital of Sichuan University for providing technical help.

SUPPLEMENTARY MATERIAL

The Supplementary Material for this article can be found online at: https://www.frontiersin.org/articles/10.3389/fonc.2021.779761/full#supplementary-material

REFERENCES

1. Khan SA, Tavolari S, Brandi G. Cholangiocarcinoma: Epidemiology and Risk Factors. *Liver Int* (2019) 39 Suppl 1:19–31. doi: 10.1111/liv.14095
2. Valle JW, Kelley RK, Nervi B, Oh DY, Zhu AX. Biliary Tract Cancer. *Lancet* (2021) 397(10272):428–44. doi: 10.1016/s0140-6736(21)00153-7
3. Wang M, Chen Z, Guo P, Wang Y, Chen G. Therapy for Advanced Cholangiocarcinoma: Current Knowledge and Future Potential. *J Cell Mol Med* (2021) 25(2):618–28. doi: 10.1111/jcmm.16151
4. Chin KM, Di Martino M, Syn N, Ielpo B, Hilal MA, Goh BKP, et al. Re-Appraising the Role of Lymph Node Status in Predicting Survival in Resected Distal Cholangiocarcinoma - A Meta-Analysis and Systematic Review. *Eur J Surg Oncol* (2021) 47(6):1267–77. doi: 10.1016/j.ejso.2021.01.004
5. Murakami Y, Uemura K, Hayashidani Y, Sudo T, Hashimoto Y, Ohge H, et al. Prognostic Significance of Lymph Node Metastasis and Surgical Margin Status for Distal Cholangiocarcinoma. *J Surg Oncol* (2007) 95(3):207–12. doi: 10.1002/jso.20668
6. Zhou Y, Liu S, Wu L, Wan T. Survival After Surgical Resection of Distal Cholangiocarcinoma: A Systematic Review and Meta-Analysis of Prognostic Factors. *Asian J Surg* (2017) 40(2):129–38. doi: 10.1016/j.asjsur.2015.07.002
7. Ito Y, Abe Y, Egawa T, Kitago M, Itano O, Kitagawa Y. Predictive Factors of Early Recurrence in Patients With Distal Cholangiocarcinoma After Pancreaticoduodenectomy. *Gastroenterol Res Pract* (2018) 2018:6431254. doi: 10.1155/2018/6431254
8. Suzuki S, Shimoda M, Shimazaki J, Maruyama T, Oshiro Y, Nishida K, et al. Number of Positive Lymph Nodes and Lymphatic Invasion are Significant Prognostic Factors After Pancreaticoduodenectomy for Distal Cholangiocarcinoma. *Clin Exp Gastroenterol* (2019) 12:255–62. doi: 10.2147/ceg.S207333
9. Oshiro Y, Sasaki R, Kobayashi A, Murata S, Fukunaga K, Kondo T, et al. Prognostic Relevance of the Lymph Node Ratio in Surgical Patients With Extrahepatic Cholangiocarcinoma. *Eur J Surg Oncol* (2011) 37(1):60–4. doi: 10.1016/j.ejso.2010.10.011
10. Zhang JW, Chu YM, Lan ZM, Tang XL, Chen YT, Wang CF, et al. Correlation Between Metastatic Lymph Node Ratio and Prognosis in Patients With Extrahepatic Cholangiocarcinoma. *World J Gastroenterol* (2015) 21(14):4255–60. doi: 10.3748/wjg.v21.i14.4255
11. Li X, Lin H, Sun Y, Gong J, Feng H, Tu J. Prognostic Significance of the Lymph Node Ratio in Surgical Patients With Distal Cholangiocarcinoma. *J Surg Res* (2019) 236:2–11. doi: 10.1016/j.jss.2018.10.044
12. You Y, Shin YC, Choi DW, Heo JS, Shin SH, Kim N, et al. Proposed Modification of Staging for Distal Cholangiocarcinoma Based on the Lymph Node Ratio Using Korean Multicenter Database. *Cancers (Basel)* (2020) 12(3):762. doi: 10.3390/cancers12030762

13. Li P, Song L. A Novel Prognostic Nomogram for Patients With Surgically Resected Perihilar Cholangiocarcinoma: A SEER-Based Study. *Ann Transl Med* (2021) 9(1):54. doi: 10.21037/atm-20-3130
14. Occhionorelli S, Andreotti D, Vallese P, Morganti L, Lacavalla D, Forini E, et al. Evaluation on Prognostic Efficacy of Lymph Nodes Ratio (LNR) and Log Odds of Positive Lymph Nodes (LODDS) in Complicated Colon Cancer: The First Study in Emergency Surgery. *World J Surg Oncol* (2018) 16(1):186. doi: 10.1186/s12957-018-1483-6
15. Wang J, Hassett JM, Dayton MT, Kulaylat MN. The Prognostic Superiority of Log Odds of Positive Lymph Nodes in Stage III Colon Cancer. *J Gastrointest Surg* (2008) 12(10):1790–6. doi: 10.1007/s11605-008-0651-3
16. Spolverato G, Ejaz A, Kim Y, Squires MH, Poultsides G, Fields RC, et al. Prognostic Performance of Different Lymph Node Staging Systems After Curative Intent Resection for Gastric Adenocarcinoma. *Ann Surg* (2015) 262 (6):991–8. doi: 10.1097/sla.0000000000001040
17. Chen LJ, Chung KP, Chang YJ, Chang YJ. Ratio and Log Odds of Positive Lymph Nodes in Breast Cancer Patients With Mastectomy. *Surg Oncol* (2015) 24(3):239–47. doi: 10.1016/j.suronc.2015.05.001
18. Tang J, Jiang S, Gao L, Xi X, Zhao R, Lai X, et al. Construction and Validation of a Nomogram Based on the Log Odds of Positive Lymph Nodes to Predict the Prognosis of Medullary Thyroid Carcinoma After Surgery. *Ann Surg Oncol* (2021) 28(8):4360–70. doi: 10.1245/s10434-020-09567-3
19. Camp RL, Dolled-Filhart M, Rimm DL. X-Tile: A New Bio-Informatics Tool for Biomarker Assessment and Outcome-Based Cut-Point Optimization. *Clin Cancer Res* (2004) 10(21):7252–9. doi: 10.1158/1078-0432.Ccr-04-0713
20. Cook NR, Paynter NP. Performance of Reclassification Statistics in Comparing Risk Prediction Models. *Biom J* (2011) 53(2):237–58. doi: 10.1002/bimj.201000078
21. Shi XQ, Zhang JY, Tian H, Tang LN, Li AL. Role of Adjuvant (Chemo) Radiotherapy for Resected Extrahepatic Cholangiocarcinoma: A Meta-Analysis. *J Zhejiang Univ Sci B* (2020) 21(7):549–59. doi: 10.1631/jzus.B1900691
22. Im JH, Park JS, Yoon DS, Lee DK, Kim JW, Lee IJ. Risk Factors Associated With Locoregional Failure and Estimation of Survival After Curative Resection for Patients With Distal Bile Duct Cancer. *Sci Rep* (2019) 9 (1):5061. doi: 10.1038/s41598-019-41622-2
23. Lee J, Kang SH, Noh OK, Chun M, Oh YT, Kim BW, et al. Adjuvant Concurrent Chemoradiation Therapy in Patients With Microscopic Residual Tumor After Curative Resection for Extrahepatic Cholangiocarcinoma. *Clin Transl Oncol* (2018) 20(8):1011–7. doi: 10.1007/s12094-017-1815-y
24. Matsuda T, Fujita H, Harada N, Kunimoto Y, Tanaka T, Kimura T, et al. Impact of Adjuvant Radiation Therapy for Microscopic Residual Tumor After Resection of Extrahepatic Bile Duct Cancer. *Am J Clin Oncol* (2013) 36 (5):461–5. doi: 10.1097/COC.0b013e31825494ab
25. Hsieh FY, Lavori PW, Cohen HJ, Feussner JR. An Overview of Variance Inflation Factors for Sample-Size Calculation. *Eval Health Prof* (2003) 26 (3):239–57. doi: 10.1177/0163278703255230
26. Yoshida T, Matsumoto T, Sasaki A, Morii Y, Aramaki M, Kitano S. Prognostic Factors After Pancreatoduodenectomy With Extended Lymphadenectomy for Distal Bile Duct Cancer. *Arch Surg* (2002) 137(1):69–73. doi: 10.1001/archsurg.137.1.69
27. Murakami Y, Uemura K, Hayashidani Y, Sudo T, Ohge H, Sueda T. Pancreatoduodenectomy for Distal Cholangiocarcinoma: Prognostic Impact of Lymph Node Metastasis. *World J Surg* (2007) 31(2):337–42. doi: 10.1007/s00268-006-0224-0
28. Hong SM, Cho H, Lee OJ, Ro JY. The Number of Metastatic Lymph Nodes in Extrahepatic Bile Duct Carcinoma as a Prognostic Factor. *Am J Surg Pathol* (2005) 29(9):1177–83. doi: 10.1097/01.pas.0000160978.77833.d7
29. Kiriyama M, Ebata T, Aoba T, Kaneoka Y, Arai T, Shimizu Y, et al. Prognostic Impact of Lymph Node Metastasis in Distal Cholangiocarcinoma. *Br J Surg* (2015) 102(4):399–406. doi: 10.1002/bjs.9752
30. Lyu S, Li L, Zhao X, Ren Z, Cao D, He Q. Prognostic Impact of Lymph Node Parameters in Distal Cholangiocarcinoma After Pancreaticoduodenectomy. *World J Surg Oncol* (2020) 18(1):262. doi: 10.1186/s12957-020-02040-1
31. Ito K, Ito H, Allen PJ, Gonen M, Klimstra D, D'Angelica MI, et al. Adequate Lymph Node Assessment for Extrahepatic Bile Duct Adenocarcinoma. *Ann Surg* (2010) 251(4):675–81. doi: 10.1097/SLA.0b013e3181d3d2b2
32. Moon A, Choi DW, Choi SH, Heo JS, Jang KT. Validation of T Stage According to Depth of Invasion and N Stage Subclassification Based on Number of Metastatic Lymph Nodes for Distal Extrahepatic Bile Duct (EBD) Carcinoma. *Med (Baltimore)* (2015) 94(50):e2064. doi: 10.1097/md.0000000000002064
33. Kang JS, Higuchi R, He J, Yamamoto M, Wolfgang CL, Cameron JL, et al. Proposal of the Minimal Number of Retrieved Regional Lymph Nodes for Accurate Staging of Distal Bile Duct Cancer and Clinical Validation of the Three-Tier Lymph Node Staging System (AJCC 8th Edition). *J Hepatobiliary Pancreat Sci* (2020) 27(2):75–83. doi: 10.1002/jhbp.690
34. Amin MB, Greene FL, Edge SB, Compton CC, Gershenwald JE, Brookland RK, et al. The Eighth Edition AJCC Cancer Staging Manual: Continuing to Build a Bridge From a Population-Based to a More "Personalized" Approach to Cancer Staging. *CA Cancer J Clin* (2017) 67(2):93–9. doi: 10.3322/caac.21388
35. Johnson PM, Porter GA, Ricciardi R, Baxter NN. Increasing Negative Lymph Node Count is Independently Associated With Improved Long-Term Survival in Stage IIIB and IIIC Colon Cancer. *J Clin Oncol* (2006) 24(22):3570–5. doi: 10.1200/jco.2006.06.8866
36. Kim YS, Hwang IG, Park SE, Go SI, Kang JH, Park I, et al. Role of Adjuvant Therapy After R0 Resection for Patients With Distal Cholangiocarcinoma. *Cancer Chemother Pharmacol* (2016) 77(5):979–85. doi: 10.1007/s00280-016-3014-x
37. Wang ML, Ke ZY, Yin S, Liu CH, Huang Q. The Effect of Adjuvant Chemotherapy in Resectable Cholangiocarcinoma: A Meta-Analysis and Systematic Review. *Hepatobiliary Pancreat Dis Int* (2019) 18(2):110–6. doi: 10.1016/j.hbpd.2018.11.001
38. Bergeat D, Turrini O, Courtin-Tanguy L, Truant S, Darnis B, Delpero JR, et al. Impact of Adjuvant Chemotherapy After Pancreaticoduodenectomy for Distal Cholangiocarcinoma: A Propensity Score Analysis From a French Multicentric Cohort. *Langenbecks Arch Surg* (2018) 403(6):701–9. doi: 10.1007/s00423-018-1702-1
39. Chen Q, Li J, Jin B, Wu X, Shi Y, Xu H, et al. Prognostic Nomogram That Predicts Overall Survival of Patients With Distal Cholangiocarcinoma After Pancreatoduodenectomy. *Cancer Manag Res* (2020) 12:10303–10. doi: 10.2147/cmar.S276393

Conflict of Interest: The authors declare that the research was conducted in the absence of any commercial or financial relationships that could be construed as a potential conflict of interest.

Publisher's Note: All claims expressed in this article are solely those of the authors and do not necessarily represent those of their affiliated organizations, or those of the publisher, the editors and the reviewers. Any product that may be evaluated in this article, or claim that may be made by its manufacturer, is not guaranteed or endorsed by the publisher.

Copyright © 2021 Huang, Niu, You, Long, Luo and Ye. This is an open-access article distributed under the terms of the Creative Commons Attribution License (CC BY). The use, distribution or reproduction in other forums is permitted, provided the original author(s) and the copyright owner(s) are credited and that the original publication in this journal is cited, in accordance with accepted academic practice. No use, distribution or reproduction is permitted which does not comply with these terms.

frontiers in Oncology

ORIGINAL RESEARCH
published: 03 December 2021
doi: 10.3389/fonc.2021.776997

Clinicopathological Features Combined With Immune Infiltration Could Well Distinguish Outcomes in Stage II and Stage III Colorectal Cancer: A Retrospective Study

Jiazi Ren[1†], Linfeng Xu[2,3†], Siyu Zhou[1†], Jian Ouyang[2], Weiqiang You[1], Nengquan Sheng[1], Li Yan[1], Du Peng[4], Lu Xie[2*] and Zhigang Wang[1*]*

[1] Department of General Surgery, Shanghai Jiao Tong University Affiliated Sixth People's Hospital, Shanghai, China, [2] Shanghai Center for Bioinformation Technology, Shanghai Institute for Biomedical and Pharmaceutical Technologies, Shanghai, China, [3] School of Health Science and Engineering, University of Shanghai for Science and Technology, Shanghai, China, [4] Department of Colorectal Surgery, Xinhua Hospital, Shanghai Jiao Tong University School of Medicine, Shanghai, China

OPEN ACCESS

Edited by:
Qi Liu,
Fudan University, China

Reviewed by:
Xinqun Li,
University of Texas MD Anderson Cancer Center, United States
Gianni Lazzarin,
Abano Terme Hospital, Italy

***Correspondence:**
Zhigang Wang
wangzhigang72@sjtu.edu.cn
Lu Xie
luxiex2017@outlook.com
Du Peng
dupeng@xinhuamed.com.cn

†These authors have contributed equally to this work and share first authorship

Specialty section:
This article was submitted to Surgical Oncology, a section of the journal Frontiers in Oncology

Received: 14 September 2021
Accepted: 15 November 2021
Published: 03 December 2021

Citation:
Ren J, Xu L, Zhou S, Ouyang J, You W, Sheng N, Yan L, Peng D, Xie L and Wang Z (2021) Clinicopathological Features Combined With Immune Infiltration Could Well Distinguish Outcomes in Stage II and Stage III Colorectal Cancer: A Retrospective Study. Front. Oncol. 11:776997. doi: 10.3389/fonc.2021.776997

Background: The Immunoscore predicts prognosis in patients with colorectal cancer (CRC). However, a few studies have incorporated the Immunoscore into the construction of comprehensive prognostic models in CRC, especially stage II CRC. We aimed to construct and validate multidimensional models integrating clinicopathological characteristics and the Immunoscore to predict the prognosis of patients with stage II–III CRC.

Methods: Patients (n = 254) diagnosed with stage II–III CRC from 2009 to 2016 were used to generate Cox models for predicting disease-free survival (DFS) and overall survival (OS). The variables included basic clinical indicators, blood inflammatory markers, preoperative tumor biomarkers, mismatch repair status, and the Immunoscore ($CD3^+$ and $CD8^+$ T-cell densities). Univariate and multivariate Cox proportional regressions were used to construct the prognostic models for DFS and OS. We validated the predictive accuracy and ability of the prognostic models in our cohort of 254 patients.

Results: We constructed two predictive prognostic models with C-index values of 0.6941 for DFS and 0.7138 for OS in patients with stage II–III CRC. The Immunoscore was the most informative predictor of DFS (11.92%), followed by pN stage, carcinoembryonic antigen (CEA), and vascular infiltration. For OS, the Immunoscore was the most informative predictor (8.59%), followed by pN stage, age, CA125, and CEA. Based on the prognostic models, nomograms were developed to predict the 3- and 5-year DFS and OS rates. Patients were divided into three risk groups (low, intermediate, and high) according to the risk scores obtained from the nomogram, and significant differences were observed in the recurrence and survival of the different risk groups ($p < 0.0001$). Calibration curve and time-dependent receiver operating characteristic (ROC) analysis showed good accuracy of our models. Furthermore, the decision curve analysis indicated

that our nomograms had better net benefit than pathological TNM (pTNM) stage within a wide threshold probability. Especially, we developed a website based on our prognostic models to predict the risks of recurrence and death of patients with stage II–III CRC.

Conclusions: Multidimensional models including the clinicopathological characteristics and the Immunoscore were constructed and validated, with good accuracy and convenience, to evaluate the risks of recurrence and death of stage II–III CRC patients.

Keywords: clinicopathological features, Immunoscore, colorectal cancer, prognostic, model

INTRODUCTION

Colorectal cancer (CRC) is a highly prevalent and dangerous global disease. In 2020, CRC ranked the third (10%) in morbidity and the second (9.4%) in mortality in the world (1). The morbidity and mortality of CRC in China ranked the second (12.2%) and the fifth (9.5%) (1), respectively. Despite improvements in diagnosis and treatment technology, 30% of stage II–III CRC patients still suffer recurrence after radical surgery (2), which seriously affects patient prognosis. Currently, the pathological TNM (pTNM) staging system based on the 8th edition of the American Joint Committee on Cancer (AJCC) is the main standard in prognostic evaluation, adjuvant treatment, and follow-up strategy in patients after curative CRC surgery (3). However, in clinical practice, discordances are usually observed between pTNM stage-based predictions and the actual outcomes. For example, some patients with stage II CRC have worse prognosis than some patients with stage III CRC (4, 5). Therefore, the prognostic information provided by the current evaluation system is limited. The major reasons for this include the lack of immune infiltration, tumor genetic status, and DNA mismatch repair (MMR) status, among others. Although some researchers have explored new indicators to improve prognosis prediction (6, 7), their clinical application is still very limited. Accordingly, it is of great importance and urgent clinical significance to explore approaches with good clinical feasibility and accuracy to predict the risks of recurrence and death of CRC patients.

In colon cancer, Galon et al. proposed the Immunoscore concept (8), which is a quantification of $CD3^+$ and $CD8^+$ T cells in the tumor core (CT) and invasive margin (IM). A multicenter international collaboration group verified the prognostic value of the Immunoscore in stage I–III colon cancer, and the relative contribution of Immunoscore was the largest among all risk factors, even more than that of the pTNM staging system. Notably, the combination of the Immunoscore and clinical indicators significantly improved the predictive accuracy for overall survival (9). These studies suggest that the Immunoscore could be a powerful complement to the existing prognostic evaluation systems.

In addition to the Immunoscore, the tumor location characteristics (10, 11), molecular characteristics (12–14), preoperative tumor markers (15, 16), and tumor inflammatory status (17) are all closely related to CRC prognosis. However, the specificity and the accuracy of the various risk factors are low when used in isolation, making it difficult to accurately assess the prognosis of CRC, whereas the integration of multiple factors into one model will greatly improve the prognostic value (6). Therefore, the construction of a comprehensive CRC prognostic model would be beneficial in improving the accuracy of prognosis prediction. Currently, some groups have used this idea to construct prognostic models for stage III colon cancer (18, 19). However, a comprehensive prognostic model for stage II CRC still remains to be explored.

To solve the above issues, we integrated 18 variables, including the basic clinical indicators, preoperative serum tumor markers, blood inflammatory markers, MMR status, and the Immunoscore, and used the Cox risk proportion model to build new multidimensional models for predicting the recurrence and survival in patients with stage II–III CRC. Our study generated accurate and feasible approaches to prognosis prediction for patients with stage II–III CRC, providing new insights into improving the current prognostic evaluation system and the quality of decision-making for postoperative follow-up and adjuvant treatment.

Abbreviations: AJCC, American Joint Committee on Cancer; CT, the core of the tumor; CSA, tumor cross-sectional area; C-index, concordance index; CIs, confidence intervals; CRC, colorectal cancer; CA19-9, carbohydrate antigen 19-9; CEA, carcinoembryonic antigen; CA125, carbohydrate antigen 125; DFS, disease-free survival; HR, hazard ratio; IM, invasive margin; iAUC, integrated area under the ROC curve; K-M, Kaplan–Meier; MSI, microsatellite instability; MSS, microsatellite stable; MMR, mismatch repair; dMMR, deficient mismatch repair; pMMR, proficient mismatch repair; NLR, neutrophil-to-lymphocyte ratio; OS, overall survival; PLR, platelet-to-lymphocyte ratio; pTNM, pathological TNM based on the 8th edition of AJCC; ROC, receiver operating characteristic; SITC, Society for Immunotherapy of Cancer; VILINI, vascular infiltration, lymphatic infiltration and nerve infiltration.

MATERIALS AND METHODS

Study Population and Data Collection

This study was a single-center retrospective study registered in the Chinese Clinical Trial Registry (approval no. ChiCTR2000041147). Our study was approved by the Ethics Committee of Shanghai Jiao Tong University Affiliated Sixth People's Hospital (approval no. 2020-253). The cohort from Shanghai Jiao Tong University Affiliated Sixth People's Hospital was used to develop and validate the model. All patients were pathologically diagnosed with stage II–III CRC between January 2009 and December 2016. Written informed

consent was obtained for this study. Patients fulfilling the criteria patients were excluded: 1) age <18 years; 2) had emergency surgery; 3) had multiple primary carcinoma; 4) with incomplete clinical data; 5) died within 30 days; 6) lost to follow-up; and 7) underwent preoperative adjuvant therapy.

In our study, clinical features such as gender, age, pTNM stage, tumor location, tumor cross-sectional area (CSA), tumor long axis, tumor differentiation, lymphatic infiltration, vascular infiltration, nerve infiltration, neutrophil-to-lymphocyte ratio (NLR), platelet-to-lymphocyte ratio (PLR), preoperative tumor markers [carcinoembryonic antigen (CEA), carbohydrate antigen 19-9 (CA19-9), and CA125], and the MMR status were collected. Patient clinical data were mainly provided by examination of their medical history and by the Electronic Medical Record Department. Pathological staging was based on the 8th AJCC criterion for CRC. NLR and PLR were calculated as (neutrophil count)/(lymphocyte count) and (platelet count)/(lymphocyte count), respectively. Preoperative tumor markers were examined within 1 week before surgery. All patients were followed up according to the current National Comprehensive Cancer Network (NCCN) guidelines, including analysis of serum tumor markers, colonoscopy, chest X-ray, and CT (or MRI). Patient follow-up data were updated by telephone, email, and medical history. Disease-free survival (DFS) was defined as the time from surgery to cancer metastasis or recurrence. Overall survival (OS) was defined as the time from surgery to death.

Immunohistochemical Analysis

Immunostaining of $CD3^+$ and $CD8^+$ T cells was performed on formalin-fixed paraffin-embedded sections. Antigen retrieval was conducted with an EDTA buffer (pH 9.0) for 90 s, followed by quenching of endogenous peroxidase activity by 3% H_2O_2 for 30 min at room temperature. Sections were incubated at 4°C with primary antibodies: rabbit anti-human monoclonal antibody against CD3 (EP41; ZSGB-BIO, Beijing, China) and rabbit anti-human monoclonal antibody against CD8 (SP16; ZSGB-BIO, Beijing, China). Revelation with the Ultra DAB IHC Detection Kit (Maxim, Fuzhou, China) and counterstaining with Harris hematoxylin were performed. Counterstained slides were scanned at ×40 magnification (NanoZoomer S360, Hamamatsu, Japan) to generate a whole slide imaging file in NDPI format. CT was the core of the tumor, and the invasive margin (IM) was defined as a region of 500-μm width surrounding the CT. The CT and IM regions were manually marked on the whole slide using QuPath software (20), in which hematoxylin/eosin-stained sections were used to help CT/IM labeling. Two independent pathologists, who were blinded to the patients' clinical information, participated in the analysis to avoid the interference of necrotic areas and to verify the location of the CT/IM. Positive CD3 and CD8 cells within the CT and IM areas were obtained *via* QuPath software (20), and the densities of CD3 and CD8 were quantified by the number of cells per square millimeter in both CT and IM. The concordance in the semi-quantitative evaluation between CD3 and CD8 was determined by two independent pathologists.

For every patient, the densities of $CD3^+$ and $CD8^+$ cells in the CT and IM regions ($CD3_{CT}$, $CD3_{IM}$, $CD8_{CT}$, and $CD8_{IM}$) were converted into percentiles (0%–100%) based on our cohort, as described by Galon et al. (9). The mean of the four percentiles ($CD3_{CT}$, $CD3_{IM}$, $CD8_{CT}$, and $CD8_{IM}$) was then calculated and converted into a percentile Immunoscore. In a three-category Immunoscore analysis, a 0%–25% density was scored as low, 25%–70% density was scored as intermediate, and 70%–100% density was scored as high (9). In our study, we found that a low (0%–25%) and an intermediate (25%–70%) Immunoscore in the three-category Immunoscore had similar clinical outcomes (DFS). Consequently, we combined the low-Immunoscore (0%–25%) and intermediate-Immunoscore (25%–70%) groups as the low-Immunoscore group (0%–70%) in a two-category Immunoscore, in which a 0%–70% density was scored as low and 70%–100% was scored as high. Samples were excluded from the analysis if counts were missing from a tumor region, if there was improper histology (e.g., broken tissue, atypical CT/IM, excessive necrotic cavity, excessive mucous area, etc.), or if the staining intensity was regarded as low.

The tumor DNA MMR status was determined by immunohistochemical analysis of MMR proteins (MLH1, MSH2, MSH6, and PMS2) on formalin-fixed paraffin-embedded sections. The conditions of having deficient MMR (dMMR; loss of at least one MMR protein) and proficient MMR (pMMR) were denoted as microsatellite instability (MSI) and microsatellite stability (MSS), respectively. Two independent pathologists, who were blinded to the patients' clinical information, participated in the analysis to verify the MMR status.

Statistical Analysis

The association between the clinicopathological characteristics and the Immunoscore was analyzed *via* a chi-squared test. All numeric variables were tested for normality using the Shapiro–Wilk test.

To develop the prognostic model, we performed univariate analysis of all variables using Cox proportional hazards regression. Subsequently, the significant variables ($p < 0.05$) were analyzed with the multivariate Cox proportional hazards regression. After removing the non-significant covariates in the multivariate analysis, a final multivariable Cox regression model was constructed. A nomogram was constructed to predict the 3- and 5-year DFS/OS probabilities with the total points of all variables. The risk score was the linear predictor of the Cox model built on our cohort with selected variables. To evaluate the predictive accuracy of the different variables or models, we used the integrated area under the receiver operating characteristic (ROC) curve (iAUC) with 1,000× bootstrap resampling. The performances of the models were compared using likelihood ratio tests, when the models were nested. The relative importance of each variable to the risks of recurrence and death was estimated using the χ^2 from Harrell's rms R package (version 6.0-1).

Model performance was evaluated with the concordance index (C-index) and corrected 1,000 times by bootstrapping. The calibration curves of the nomogram were drawn for 3- and 5-year DFS/OS to evaluate the accuracy of the model by comparing the DFS/OS probabilities between observations and predictions. A time-dependent ROC was used to compare the discrimination between our nomogram and pTNM. Patients

were classified into three risk groups (high, intermediate, and low) according to the risk scores obtained from the nomogram: the 30% with the highest scores were designated the "high" risk group, the 30% with the lowest scores the "low" group, and the remaining 40% as the "intermediate" group. The Kaplan–Meier (K-M) method was applied to estimate the survival probabilities. Hazard ratios (HRs) and 95% confidence intervals (CIs) were estimated, and a log-rank test was used to determine the statistical differences between different groups. Decision curve analysis was conducted using the ggDCA package in R (version 1.2) to determine the clinical usefulness of the nomogram *via* quantifying the net benefits at different threshold probabilities (21).

Data processing, data analysis, and figures were performed and produced in R language (version 4.0.3). All analyses were two sided, and $p < 0.05$ was considered statistically significant.

RESULTS

Study Design and Patient Characteristics

A total of 1,048 patients with stage II–III CRC were collected between January 2009 and December 2016 from Shanghai Jiao Tong University Affiliated Sixth People's Hospital (**Supplementary Figure S1**). After clinical quality control, there were 735 eligible patients with complete clinical data. Formalin-fixed paraffin-embedded sections of tumor samples from 350 out of the 735 patients were collected and the Immunoscore data were retrieved between 2020 and 2021. Within the 350 samples, 96 were excluded due to mismatch in the quality control, among which 67 patients were excluded after histology quality control, 20 patients were excluded after staining quality control, and 9 patients were excluded due to missing staining data. Subsequently, only eligible patients with qualified immunohistochemical data samples ($n = 254$) were finally included in the development and validation of the prognostic models.

The characteristics of our study population are shown in **Table 1**. In total, 60.0% of patients were males, and the median age of all patients was 66.0 years (IQR = 56–76 years). One hundred fifty-one (59.0%) patients had stage II and 103 (41.0%) had stage III CRC. Colon tumors located on the left and right sides were 73 (29.0%) and 84 (33.0%), respectively, and 97 (38.0%) patients had rectum tumors. The degree of differentiation in more than half of the tumors was identified as moderate or well (147, 58.0%), and 107 (42.0%) patients had a poor level. Of the patients, 235 (93.0%) showed MSS and only 19 (7.0%) showed MSI. Seventy-seven (30.0%) patients had a relapse, and 74 (29.0%) patients died. The median follow-up time for all patients was 53.0 months.

The median densities of $CD3^+$ T cells in CT and IM were 227/mm^2 (14–2,061/mm^2) and 629/mm^2 (38–2,359/mm^2), respectively, and those of $CD8^+$ T cells were 119/mm^2 (8–1,832/mm^2) and 340/mm^2 (13–1,365/mm^2), respectively. More than half of CRC patients had a low Immunoscore (189, 74.0%), while 26.0% (65) of patients had a high Immunoscore (**Table 1**).

To study the association between the Immunoscore and other characteristics in the tumor microenvironment, we performed chi-squared test analysis (**Supplementary Table S1**). We did not find any relationship between the Immunoscore and other characteristics, except for the microsatellite status. The results showed that a high Immunoscore was found more frequently than a low Immunoscore in tumors with dMMR (14.0% *vs*. 5.0%, $p = 0.0468$). Although tumor location was not significantly associated with the Immunoscore ($p = 0.0689$), it showed some trends, and a high Immunoscore was found to be less frequent in tumors in right-sided colon cancer (**Supplementary Table S1**).

Validation of the Two-Level Categorical Immunoscore for Predicting DFS and OS

Representative images of $CD3^+$ and $CD8^+$ T-lymphocyte immunostaining on formalin-fixed paraffin-embedded sections are provided in **Figure 1**. The CT and IM areas of the tumor were manually marked on the whole slide using QuPath software (20), in which hematoxylin/eosin-stained sections were used to help in CT/IM labeling. We validated the two-level categorical Immunoscore (**Supplementary Figure S2**) whose prognostic impact was previously shown in an international validation study in TNM stage I–III colon cancers (9). When tumors were categorized into predetermined low (0%–70%) and high (70%–100%) groups, a low Immunoscore was associated with a statistically significant and poorer DFS ($p = 0.0390$) and OS ($p = 0.0070$). The 3-year DFS for low *vs*. high Immunoscore was 68.7% *vs*. 82.5%, and the 3-year OS was 75.9% *vs*. 87.4%. The 5-year DFS for low *vs*. high Immunoscore was 62.6% *vs*. 77.3%, and the 5-year OS was 63.1% *vs*. 82.1% (**Supplementary Figure S2**). For consistency with prior work, the associations between DFS and OS were also shown for percentile Immunoscore and three-level categorical Immunoscore (9) (**Supplementary Table S2**).

Association of Clinicopathological Variables and Immunoscore With DFS and OS

To screen the prognostic factors, we performed univariate analysis. Our results suggested that the pT stage, pN stage, lymphatic infiltration, CEA, and the Immunoscore were significantly associated with DFS and OS in CRC patients ($p < 0.05$) (**Supplementary Table S2**). Vascular infiltration affected DFS, but not OS, whereas age, NLR, and CA125 affected OS, but not DFS ($p < 0.05$) (**Supplementary Table S2**).

Compared to patients with T1, T2, and T3 tumors, patients with T4 tumors had significantly worse DFS (HR = 2.05, 95% CI = 1.11–3.80, $p = 0.0226$) and OS (HR = 2.58, 95% CI = 1.32–5.04, $p = 0.0054$) (**Supplementary Table S2**). Patients with N2 had statistically significant and worse DFS (HR = 3.98, 95% CI = 2.34–6.78, $p < 0.0001$) and OS (HR = 4.27, 95% CI = 2.47–7.37, $p < 0.0001$) than patients with N0. Patients with N1 also had worse OS (HR = 2.05, 95% CI = 1.11–3.80, $p = 0.0226$), but not DFS, than patients with N0 (**Supplementary Table S2**). Patients with lymphatic infiltration displayed a statistically significant association with DFS ($p < 0.05$) and OS ($p < 0.05$) (**Supplementary Table S2**) and were therefore included in the

TABLE 1 | Clinicopathological and molecular characteristics of patients with stage II–III colorectal cancer (CRC).

Variable	Patients (*n* = 254)
Gender, *n* (%)	
Female	101 (40.0)
Male	153 (60.0)
Age	
Median	66.0
Interquartile range	56.0–76.0
pT stage, *n* (%)	
T1, T2, T3	61 (24.0)
T4	193 (76.0)
pN stage, *n* (%)	
N0	151 (59.0)
N1	67 (26.0)
N2	36 (14.0)
pTNM stage, *n* (%)	
II	151 (59.0)
III	103 (41.0)
Tumor location, *n* (%)	
Left colon	73 (29.0)
Right colon	84 (33.0)
Rectum	97 (38.0)
Tumor CSA, *n* (%)	
<16	123 (48.0)
≥16	131 (52.0)
Tumor long axis, *n* (%)	
<4.5	124 (49.0)
≥4.5	130 (51.0)
Degree of tumor differentiation, *n* (%)	
Moderate and well	147 (58.0)
Poor	107 (42.0)
Lymphatic infiltration, *n* (%)	
Absent	108 (43.0)
Present	146 (57.0)
Vascular infiltration, *n* (%)	
Absent	224 (88.0)
Present	30 (12.0)
Nerve infiltration, *n* (%)	
Absent	14 (6.0)
Present	240 (94.0)
NLR	
Median	2.2
Interquartile range	1.6–3.5
PLR	
Median	7.3
Interquartile range	103.0–216.1
CEA	
Median	3.9
Interquartile range	2.0–9.5
CA19-9	
Median	12.0
Interquartile range	6.8–24.1
CA125	
Median	10.8
Interquartile range	8.3–16.7
MMR, *n* (%)	
dMMR	19 (7.0)
pMMR	235 (93.0)
Immunoscore, *n* (%)	
Low	189 (74.0)
High	65 (26.0)
Metastasis or recurrence, *n* (%)	
No	177 (70.0)
Yes	77 (30.0)
Survival status, *n* (%)	
Alive	180 (71.0)
Dead	74 (29.0)

CSA, tumor cross-sectional area; NLR, neutrophil-to-lymphocyte ratio; PLR, platelet-to-lymphocyte ratio; dMMR, deficient mismatch repair; pMMR, proficient mismatch repair.

multivariable Cox models. An increased level of CEA was associated with shorter DFS ($p < 0.0001$) and OS ($p < 0.01$), which achieved statistical significance (**Supplementary Table S2**). In the univariate analysis, the Immunoscore was analyzed as a two-level categorical variable, and a high Immunoscore was associated with a statistically significant and better DFS (HR = 0.54, 95% CI = 0.30–0.98, $p = 0.0421$) and OS (HR = 0.41, 95% CI = 0.21–0.80, $p = 0.0092$) (**Supplementary Table S2**). For consistency with prior studies, the associations with DFS and OS were also shown for the percentile Immunoscore and three-level categorical Immunoscore (9), and both were protective prognostic factors for DFS ($p < 0.05$) and OS ($p < 0.05$) (**Supplementary Table S2**). The MMR status was not prognostic either in DFS ($p = 0.5753$) or OS ($p = 0.3085$) (**Supplementary Table S2**). Subsequently, all variables statistically significant in the univariate analysis were entered into the multivariate Cox proportional hazards regression analysis.

Construction of Prognostic Models Using Multivariate Cox Proportional Hazards Regression Analyses

Multivariate Cox proportional hazards regression analysis for DFS and OS revealed that the pN stage, vascular infiltration, CEA, and the Immunoscore were independently associated with DFS ($p < 0.05$) (**Table 2**), and age, pN stage, CEA, CA125, and the Immunoscore were independently associated with OS ($p < 0.05$) (**Table 2**) in our cohort. The predictive accuracy of the Immunoscore was evaluated by determining the time-dependent AUC (**Supplementary Figure S3**). For DFS, the predictive accuracy of the Immunoscore was found to be similar to that of the PLR ($p > 0.05$) and was superior to that of gender, age, tumor location, tumor CSA, tumor long axis, tumor differentiation, nerve infiltration, NLR, CA19-9, CA125, or MMR ($p < 0.05$), however was lower than that of pT stage, pN stage, lymphatic infiltration, vascular infiltration, and CEA ($p < 0.05$) (**Supplementary Figure S3A**). For OS, the predictive accuracy of the Immunoscore was found to be similar to that of pT stage ($p > 0.05$) and was superior to that of gender, age, tumor location, tumor CSA, tumor long axis, tumor differentiation, lymphatic infiltration, vascular infiltration, nerve infiltration, NLR, PLR, CA19-9, or MMR ($p < 0.05$), however was lower than that of pN stage, CEA, and CA125 ($p < 0.05$) (**Supplementary Figure S3B**). Furthermore, adding preoperative serum tumor markers (CEA, CA19-9, and CA125) or the Immunoscore to a model that combined all clinical variables (gender, age, pT stage, pN stage, tumor location, tumor CSA, tumor long axis, tumor differentiation, lymphatic infiltration, vascular infiltration, and nerve infiltration) significantly improved both DFS (likelihood ratio: $p = 0.0052$

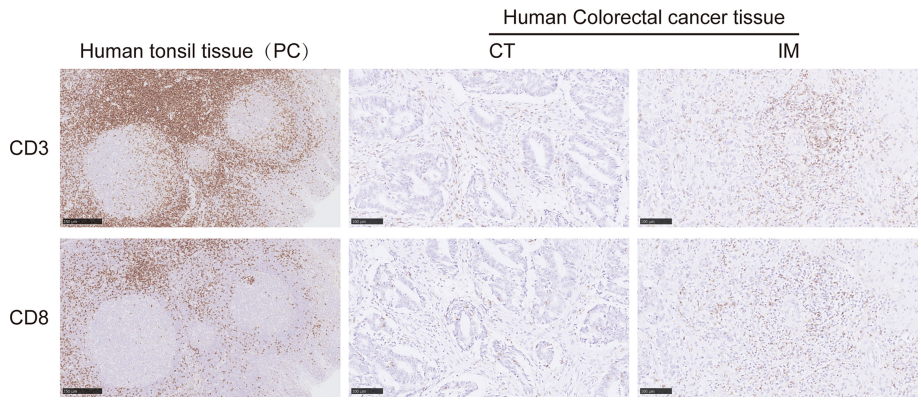

FIGURE 1 | Representative immunohistochemical images of $CD3^+$ and $CD8^+$ T cells on formalin-fixed paraffin-embedded sections from human colorectal cancer (CRC) tissue. Representative images of $CD3^+$ T cells in the CT (*middle upper panel*) and IM (*right upper panel*) and $CD8^+$ T cells in the CT (*middle lower panel*) and IM (*right lower panel*). Human tonsil tissues were stained as positive controls for CD3 and CD8 positive staining (*left upper* and *lower panels*). CT, the core of the tumor; IM, invasive margin.

and $p = 0.0276$, respectively) and OS (likelihood ratio: $p = 0.0004$ and $p = 0.0117$, respectively) prediction (**Supplementary Figures S3A, B**). Therefore, clinical variables, preoperative serum tumor markers, and the Immunoscore were all required to optimize the determination of patient prognosis.

Variables that were statistically significant in the multivariate Cox analysis were used to develop the final prognostic models, which included independent variables that were associated with DFS and OS. Finally, four indicators were selected for the prognostic model of DFS in CRC, including pN stage, vascular infiltration, CEA, and the Immunoscore (**Table 2**), and five indicators were selected for OS prediction in CRC, including age, pN stage, CEA, CA125, and the Immunoscore (**Table 2**).

The final model was then used to generate a nomogram to predict the DFS (**Figure 2A**) and OS (**Figure 2B**) rates for individual patients in clinical practice. The nomogram assigns points to each variable and allows predicting the DFS/OS probabilities at 3 and 5 years using the total points of all variables. The risk scores were generated as a linear predictor of the Cox model and were calculated as follows: 1) risk score for DFS in CRC patients: (0*N0 + 0.1488*N1 + 1.2511*N2) + 0.7320*(vascular infiltration) + 0.3625*ln(CEA value) + −0.7759*(Immunoscore); 2) risk score for OS in CRC patients: 0.0336*age + (0*N0 + 0.5231*N1 + 1.7046*N2) + 0.2192*ln(CEA value) + 0.4896*ln(CA125 value) + −0.8166*(Immunoscore).

We analyzed the relative importance of all variables in the final multivariable model, and the results revealed that the pN stage (41.64%) had the largest impact on DFS, followed by CEA (34.26%), vascular infiltration (12.18%), and then the Immunoscore (11.92%) (**Figure 3A**). For OS, the pN stage

TABLE 2 | Multivariate Cox proportional hazards regression analysis for disease-free survival (DFS) and overall survival (OS).

Variable	Disease-free survival		Overall survival	
	HR (95% CI)	*p*-value	HR (95% CI)	*p*-value
Age			1.96 (1.32–2.91)	0.0009
pT stage	0.65 (0.35–1.24)	0.1934	1.92 (0.96–3.83)	0.0640
pN stage				
N1 *vs*. N0	1.16 (0.66–2.05)	0.6087	1.69 (0.96–2.98)	0.0707
N2 *vs*. N0	3.49 (2.03–6.02)	<0.0001	5.50 (3.05–9.92)	<0.0001
Lymphatic infiltration				
Present *vs*. absent	0.74 (0.38–1.46)	0.3882	0.77 (0.40–1.49)	0.4385
Vascular infiltration				
Present *vs*. absent	2.08 (1.18–3.65)	0.0108		
CEA	1.75 (1.36–2.27)	<0.0001	1.40 (1.05–1.87)	0.0202
CA125			1.41 (1.14–1.73)	0.0012
NLR			1.06 (0.99–1.14)	0.1118
Immunoscore				
High *vs*. low	0.46 (0.25–0.84)	0.0117	0.44 (0.22–0.87)	0.0179
C-index	0.6941		0.7138	

CEA and CA125 are processed by logarithmic transformation (base e).

CI, confidence interval; HR, hazard ratio; CEA, carcinoembryonic antigen; CA125, carbohydrate antigen 125; NLR, neutrophil-to-lymphocyte ratio.

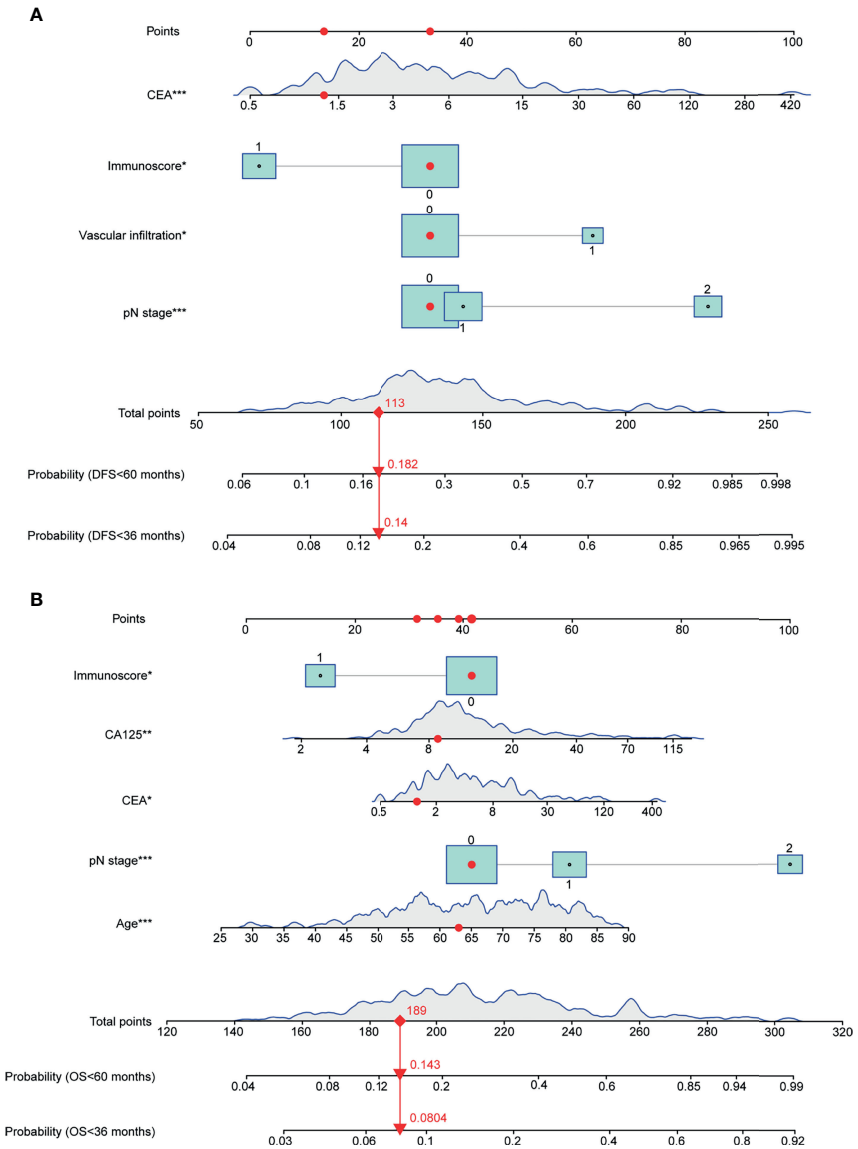

FIGURE 2 | Nomograms for predicting the 3- and 5-year DFS/OS probabilities based on multivariable Cox models. **(A)** Nomogram for DFS prediction. **(B)** Nomogram for OS prediction. Continuous or category variables were shown by *peaks* or *rectangles*, respectively. The distribution of the peak represents the distribution of sample size, and the *size of the rectangles* represents the sample size within each category. The nomograms assign points to each variable, and the 3- and 5-year DFS/OS probabilities were predicted by the total points of all variables. The *red points* and *arrows* give an example for DFS and OS prediction. OS, overall survival; DFS, disease-free survival (*P < 0.05, **P < 0.01, ***P < 0.001).

(50.08%) had the largest impact, followed by age (16.94%), CA125 (16.12%), CEA (8.28%), and then the Immunoscore (8.59%) (**Figure 3B**).

Evaluation and Determination of the Accuracy and Predictive Power of the Prognostic Models

The C-index of the nomogram was 0.6941, corrected with 1,000 permutations, for DFS in CRC in our cohort (**Table 2**). The C-index of our OS model was 0.7138, corrected with 1,000 permutations (**Table 2**). Notably, the C-index of pTNM based on the 8th edition of AJCC was 0.6456 for DFS and was 0.6647 for OS. The calibration curves for CRC based on the nomograms showed very good agreement between the predicted and observed probabilities of DFS and OS at 3 and 5 years (**Figures 4A–D**). Consistently, our nomogram also showed a slightly higher prognostic accuracy than the pTNM stage from 30 to 70 months for both DFS (3-year AUC: nomogram = 0.74, pTNM = 0.69; 5-year AUC: nomogram = 0.75, pTNM = 0.71) (**Figure 4E**) and OS (3-year AUC: nomogram = 0.75, pTNM =

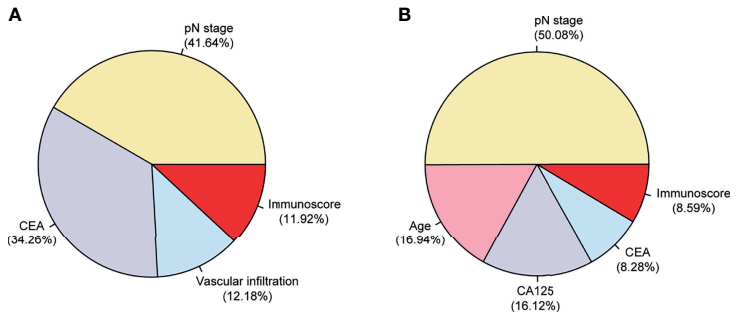

FIGURE 3 | Relative contributions (in percent) of each variable to DFS/OS in the final multivariable Cox models in 254 patients with stage II–III colorectal cancer (CRC). The relative importance of each variable to the risks of DFS **(A)** and OS **(B)**. OS, overall survival; DFS, disease-free survival.

0.68; 5-year AUC: nomogram = 0.78, pTNM = 0.74) (**Figure 4F**) in the time-dependent ROC analysis.

According to the risk scores obtained from the nomogram, the patients were categorized into three risk groups: 30% of patients with the highest scores classified as "high", 30% with the lowest scores as "low", and the rest (40%) as "intermediate". Consequently, the cutoff values were 0.269/0.887 for DFS and 3.435/4.344 for OS in CRC. K-M curves were applied to compare the survival differences. The K-M curve analysis showed statistically significant differences among the different risk groups ($p < 0.0001$) (**Figures 5A, B**). In the subgroup analysis, it was found that the correlation between nomogram-based risk stratification and DFS/OS was significant both in the subsets of stage II (DFS: $p = 0.0017$; OS: $p = 0.0014$) (**Figures 5C, D**) and stage III (DFS: $p = 0.0028$; OS: $p = 0.0031$) (**Figures 5E, F**) patients. Therefore, the risk scores generated based on our prognostic models efficiently distinguished the prognosis of patients with stage II or III CRC.

Based on our prognostic models, some patients previously believed to have a high risk of relapse or death rate were found to be at low risk. The classification of patients with stage III CRC into the low-risk ($T_{1-3}N_1$) and high-risk (T_4 or N_2) groups is routinely used to guide the treatment of adjuvant FOLFOX (folinic acid–fluorouracil–oxaliplatin) or CAPOX (capecitabine–oxaliplatin) in clinical practice (22). Based on this classification, our cohort included 17 low-risk ($T_{1-3}N_1$) and 86 high-risk (T_4 or N_2) patients with stage III CRC. As the number of patients in the low-risk group was too low, we only analyzed the high-risk group using our prognostic models. The analysis showed that our nomogram could significantly identify a group of patients with good OS, but not DFS, within clinically high-risk stage III CRC (**Supplementary Figures S4A, B**). Furthermore, we performed a similar analysis in patients with stage II CRC. High-risk stage II CRC had the characteristics of positive biomarkers for vascular infiltration, lymphatic infiltration, or nerve infiltration (VILINI$^+$) or T_4 stage II, whereas low-risk CRC was negative for VILINI markers (VILINI$^-$) and T_{1-3} stage II (22). Our cohort included two low-risk (VILINI$^-$ and T_{1-3}) and 149 high-risk (VILINI$^+$ or T_4) patients with stage II CRC. As the number of patients in the low-risk (VILINI$^-$ and T_{1-3}) group was too low, we only analyzed the high-risk (VILINI$^+$ or T_4) group using our prognostic models. The analysis showed that our nomogram could significantly identify a group of patients with very good DFS and OS within clinically high-risk stage II CRC (**Supplementary Figures S4C, D**). These results suggest that our new multidimensional models could improve patient prognosis prediction.

To determine the clinical usefulness of our nomograms, a decision curve analysis for the nomogram based on our model and pTNM stage was performed, as shown in **Figure 6**. By applying our prognostic models, a higher net benefit than that for the strategy of accepting or rejecting interventions for every patient could be achieved when the risk thresholds for DFS range from 12% to 100% at 3 years (**Figure 6A**) and from 16% to 100% at 5 years (**Figure 6B**) and for OS from 6% to 80% at 3 years (**Figure 6C**) and from 15% to 100% at 5 years (**Figure 6D**). Especially, at 3 years, if the threshold probability ranged from 0.12 to 0.30 and from 0.43 to 1.00, our prognostic models for DFS showed a better net benefit than that of pTNM stage (**Figure 6A**); at 5 years, if the threshold probability ranged from 0.16 to 0.36 and from 0.53 to 1.00, our prognostic models for DFS showed a better net benefit than that of pTNM stage (**Figure 6B**). As for the prognostic models for OS at 3 years, if the threshold probability ranged from 0.06 to 0.22 and from 0.27 to 0.80, our nomogram showed a better net benefit than that of pTNM stage (**Figure 6C**); at 5 years, our nomogram showed a better net benefit than that of pTNM stage if the threshold probability ranged from 0.15 to 0.37 and from 0.47 to 1.00 (**Figure 6D**).

Website-Based Tool for Predicting the Prognosis of Stage II–III CRC

Based on the two prognostic models of the 254 patients from our cohort, we developed a website for predicting the risks of recurrence (DFS) and death (OS) of stage II–III CRC patients (http://www.biostatistics.online/liuyuan2). The scoring system based on our model was built into the website, and the prediction results, including risk stratification (high/intermediate/low) and recurrence/survival probabilities at different times, could be obtained after inputting the model variable values. It is easy to

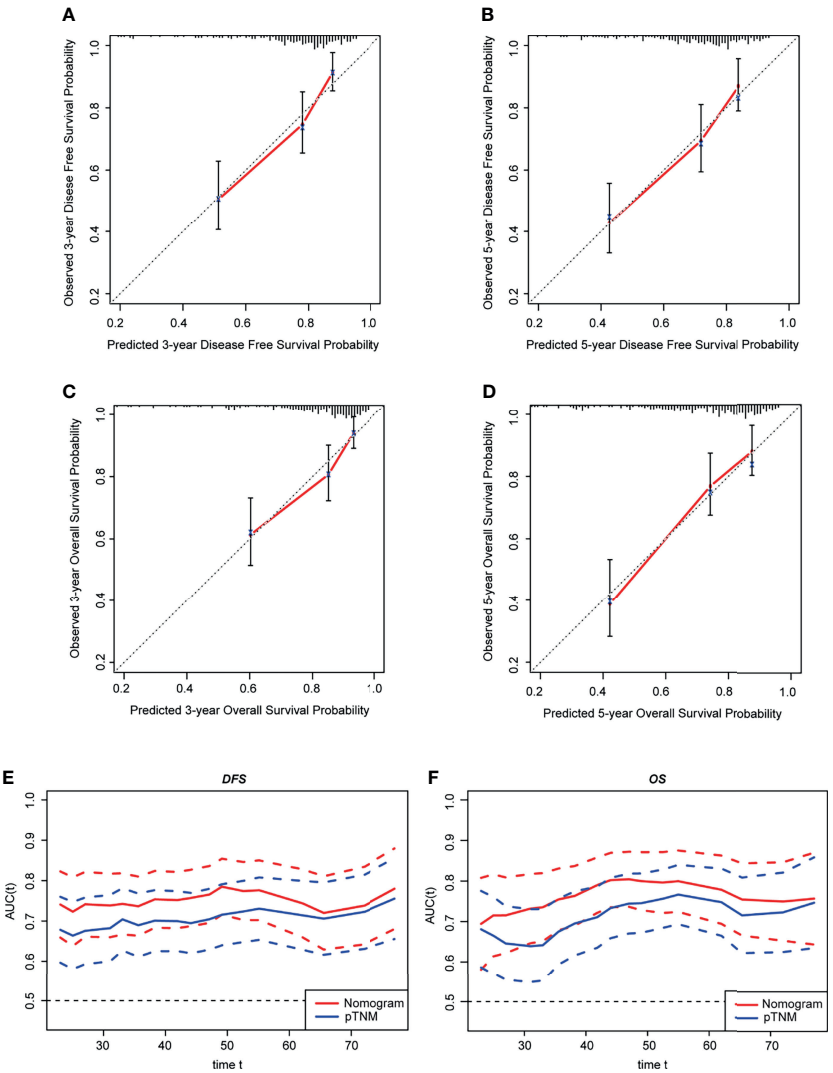

FIGURE 4 | Prognostic accuracy of the nomograms in 254 patients with stage II–III colorectal cancer (CRC). **(A, B)** Calibration curves for 3-year **(A)** and for 5-year **(B)** DFS. **(C, D)** Calibration curves for 3-year **(C)** and for 5-year **(D)** OS. **(E, F)** Time-dependent ROC curves comparing the prognostic accuracy of the nomograms with pTNM stage for DFS **(E)** and OS **(F)**. The *x*-axis in **(A–D)** shows the predicted 3- and 5-year DFS/OS probabilities by the nomogram, and the *y*-axis shows the observed 3- and 5-year DFS/OS probabilities. *Dashed lines* represent perfect prediction (accuracy is 100%), and *red solid lines* represent the actual prediction. ROC, receiver operating characteristic; pTNM, pathological TNM based on the 8th edition American Joint Committee on Cancer (AJCC); OS, overall survival; DFS, disease-free survival.

operate and friendly to clinicians, which is very helpful for the generalization and application of our models.

DISCUSSION

Postoperative recurrence and metastasis are the main factors affecting the survival of CRC patients after radical surgery. If the recurrence risk of CRC can be accurately predicted, more active interventions could be taken for high-risk patients and, therefore, they may have better survival benefits. Given the incomplete prognostic information of the present pTNM staging system, we integrated 18 variables including basic clinical indicators, preoperative serum tumor markers, blood inflammatory markers, MMR status, and the Immunoscore to generate prognostic models to evaluate the prognosis of stage II–III CRC. The model performance was validated and showed good accuracy and predictive ability. Furthermore, we developed a website based on our prognostic models, which is easy to use and of great convenience for the generalization and application of our models.

In this study, we validated the two-level categorical Immunoscore in patients with stage II–III CRC in our cohort whose prognostic impact was previously validated in stage I–III colon cancers (9). The MMR status was not a statistically significant factor for DFS/OS in our univariate analysis, and this could be attributed to the small sample size in our cohort (only 19 patients

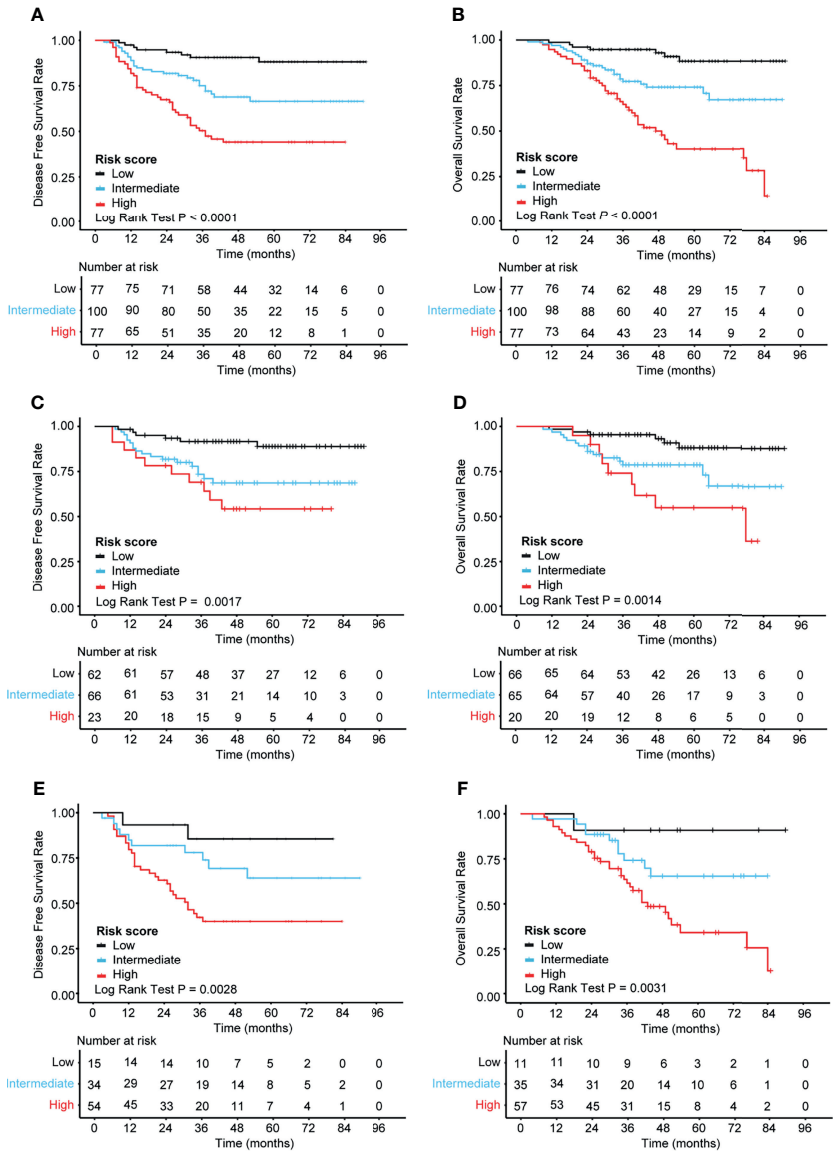

FIGURE 5 | Kaplan–Meier analysis of the different risk groups in 254 patients with stage II–III colorectal cancer (CRC). **(A, B)** K-M curves for DFS **(A)** and OS **(B)** in all patients (*n* = 254). **(C, D)** K-M curves for DFS **(C)** and OS **(D)** in patients with stage II CRC (*n* = 151). **(E, F)** K-M curves for DFS **(E)** and OS **(F)** in patients with stage III CRC (*n* = 103). The log-rank test was performed to determine statistical differences. K-M, Kaplan–Meier; OS, overall survival; DFS, disease-free survival.

with MSI from the total 254 patients). In the chi-squared test analysis, we found that a high Immunoscore was more frequent than a low Immunoscore in tumors with dMMR. It is possible that the beneficial effect of a dMMR status for prognosis prediction could be attributed to its ability to induce strong antitumor immunity (which corresponds to a high Immunoscore) (18).

Recurrence risk stratification of patients is especially important for guiding clinicians to avoid both under- and overtreatment. Consequently, there is an urgent need to develop models that can accurately evaluate their prognosis and improve risk stratification management. This would guide patients regarding adjuvant chemotherapy and improve their treatment. The classification of patients with stage III CRC into low-risk ($T_{1-3}N_1$) and high-risk (T_4 or N_2) groups is routinely used to guide the treatment of adjuvant FOLFOX or CAPOX in clinical practice (22). As for stage II CRC patients, the NCCN and the European Society for Medical Oncology (ESMO) guidelines suggest that adjuvant chemotherapy may be considered in patients with high-risk features such as T4 staging, poor tumor differentiation, and the presence of lymphatic infiltration, vascular infiltration, or nerve infiltration (3, 23, 24). However, serum tumor markers, molecular characteristics, and the tumor immune microenvironment were not included in the determinants of chemotherapy decisions. Recently, a study by the Multicenter International Society for Immunotherapy of Cancer (SITC) of the

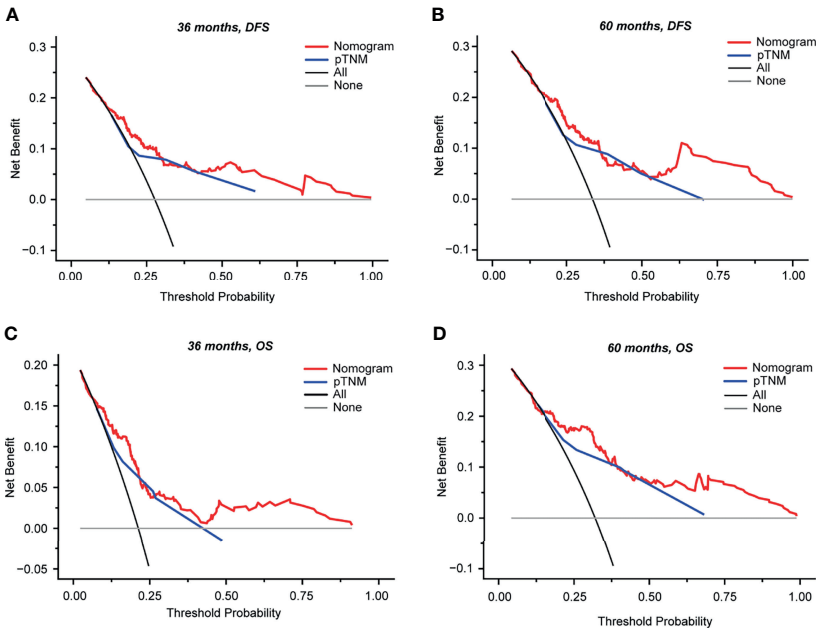

FIGURE 6 | Decision curve analysis (DCA) of the nomograms and model comparisons with pTNM stage in 254 patients with stage II–III colorectal cancer (CRC). DCA was performed to determine the clinical usefulness of the nomogram *via* quantifying the net benefits at different threshold probabilities. The *x*-axis and *y*-axis represent the threshold probability and net benefit, respectively. **(A, B)** DCA curves for DFS at 36 months **(A)** and at 60 months **(B)**. **(C, D)** DCA curves for OS at 36 months **(C)** and at 60 months **(D)**. *Gray horizontal lines* denote that none of the patients received intervention. *Black lines* represent all patients who received intervention. *Red lines* represent the net benefit of model prediction. *Blue lines* represent the net benefit of pTNM prediction. DCA, decision curve analysis; OS, overall survival; DFS, disease-free survival; pTNM, pathological TNM based on the 8th edition of the American Joint Committee on Cancer (AJCC).

consensus Immunoscore demonstrated the prediction of chemotherapy response in stage III colon cancer (25). This study showed that patients with a high Immunoscore significantly benefit from chemotherapy treatment, while patients with a low Immunoscore did not. Similarly, a randomized phase 3 clinical trial (IDEA) in 1,062 stage III colon cancer patients confirmed the predictive value of the Immunoscore on chemotherapy response (26). Therefore, the tumor immune microenvironment may play an important role in guiding the strategy for postoperative chemotherapy. Presently, the Sinicrope group and the Ghiringhelli group have developed comprehensive prognostic models including the Immunoscore for stage III colon cancer (18, 19). However, a comprehensive prognostic model containing the Immunoscore for stage II CRC still remains to be explored. Our cohort included 151 stage II CRC patients and 103 stage III CRC patients, so the prognostic models we developed can act as a good supplement to the models from the Sinicrope and Ghiringhelli groups for predicting stage II–III CRC outcomes.

Currently, there is no lack of research on early warning models for CRC recurrence (6, 7, 18, 19, 27, 28), but problems still exist. For example, patient data cannot include complete patient information and novel risk factors, or the indicators are not easy to obtain and of high cost, etc. Considering the clinical operation and cost, models with theoretically high predictive accuracy may not perform well in clinical practice, so it is not easy to achieve a balance between feasibility and accuracy. Our models have considerable advantages. Firstly, the abundant candidate variables provide relatively complete information for model construction, which helps to construct a model of high precision. Secondly, most of the variables included in this study, except for the Immunoscore (which can be obtained by immunohistochemistry with low cost and high consistency across different centers), are indicators of routine clinical tests, which are easy to obtain. Thirdly, we developed comprehensive prognostic models including the Immunoscore for stage II–III CRC, especially for stage II CRC. Fourthly, we built in a model scoring system to develop a model-based website, which greatly simplifies the scoring process and is therefore very user-friendly and beneficial to the generalization of our models. Finally, our prognostic models can make personalized patient predictions, which could contribute to the development of more precise medicine. Nevertheless, our models also have some shortcomings that need to be improved. Firstly, since this is a single-center retrospective study, it may produce selective bias and bring limitations regarding the generalizability of the model. Secondly, as our patients were collected from 2009 to 2016, at which time the *BRAF*/*KRAS*/*NRAS*/*HRAS* gene mutation state was not yet routinely screened for, our dataset lacked this information. Finally, due to the lack of an external dataset with matched sample type and variables, our models were only validated in the internal cohort. In our future work, we will validate our models in an independent external dataset.

Furthermore, we will increase the number of research centers and sample size to expand the generalizability and application of our models.

In conclusion, we validated the two-level categorical Immunoscore in patients with stage II–III CRC. Furthermore, comprehensive models including clinicopathological indicators and the Immunoscore were constructed and validated, with good accuracy and convenience, to evaluate the risks of recurrence and death of stage II–III CRC patients. Our prognostic models may provide new insights into improving the current prognosis evaluation system and the quality of subsequent decision-making for postoperative follow-up and adjuvant treatment.

DATA AVAILABILITY STATEMENT

The raw data supporting the conclusions of this article will be made available by the authors, without undue reservation.

ETHICS STATEMENT

The studies involving human participants were reviewed and approved by the Ethics Committee of Shanghai Jiao Tong University Affiliated Sixth People's Hospital. The patients/participants provided written informed consent to participate in this study.

AUTHOR CONTRIBUTIONS

JR and SZ designed the study and interpreted the data. JR wrote the manuscript and collected the immunochemistry data and the related quantification data. ZW and DP amended the manuscript. WY, LY, and NS collected the clinicopathological and follow-up data from Shanghai Jiao Tong University Affiliated Sixth People's Hospital. WY collected and stored the formalin-fixed paraffin-embedded sections for $CD3^+$ and $CD8^+$ T-cell staining. LFX, JO, and LX performed model construction and validation using the R language. LFX developed the website for predicting the prognosis of CRC. All authors contributed to the article and approved the submitted version.

FUNDING

This work was supported by the Shanghai Municipal Education Commission-Gaofeng Clinical Medicine Grant Support (no. 20172023), China Postdoctoral Science Foundation (no. 2021M692121), National Natural Science Foundation of China (no. 82101833 and no. 31870829), Shanghai Municipal Health Commission, and the Collaborative Innovation Cluster Project (no. 2019CXJQ02).

ACKNOWLEDGMENTS

We sincerely thank the Ethics Committee and the Electronic Patients' Record Department. Thanks to Dr. Yaobing Chen from Biossci Biotechnology Co., Ltd for his warm help on immunohistochemical-related issues.

SUPPLEMENTARY MATERIAL

The Supplementary Material for this article can be found online at: https://www.frontiersin.org/articles/10.3389/fonc.2021.776997/full#supplementary-material

Supplementary Figure 1 | Study design.

Supplementary Figure 2 | Validation of prognostic value of the two-level categorical Immunoscore in 254 patients. The Kaplan-Meier (K-M) method was applied to estimate DFS **(A)** and OS **(B)** probabilities at different times, and the log-rank test was performed to determine statistical differences. A 0–70% percentile Immunoscore was considered as low-Immunoscore, and a 70%-100% was considered as high-Immunoscore. K-M, Kaplan-Meier; OS, overall survival; DFS, disease-free survival.

Supplementary Figure 3 | Predictive accuracy on DFS/OS of Immunoscore and other clinicopathological variables, or combined variables in 254 patients with stage II-III CRC. The integrated area under the ROC curve (iAUC) with 1000 × bootstrap resampling was used to evaluate the predictive accuracy on DFS **(A)** and OS **(B)** of different variables. Likelihood ratio tests were used for model performance comparison when the models were nested. OS, overall survival; DFS, disease-free survival; VILINI, vascular infiltration, lymphatic infiltration and nerve infiltration; CSA, tumor cross-sectional area; NLR, neutrophil-to-lymphocyte ratio; PLR, platelet-to-lymphocyte ratio; MMR, mismatch repair. *P < 0.05, **P < 0.01, ***P < 0.001.

Supplementary Figure 4 | The nomograms improved patient prognosis prediction in clinical high-risk patients with stage II and stage III. **(A)** K-M DFS curve based on our nomogram in clinical high-risk stage III CRC patients (T4 or N2, n=86). **(B)** K-M OS curve based on our nomogram in high-risk stage III CRC patients (T4 or N2, n=86). **(C)** K-M DFS curve based on our nomogram in high-risk stage II CRC patients (VILINI+ or T4, n=149). **(D)** K-M OS curve based on our nomogram in high-risk stage II CRC patients (VILINI+ or T4, n=149). The log-rank test was performed to determine statistical differences. K-M, Kaplan-Meier; VILINI, vascular infiltration, lymphatic infiltration and nerve infiltration. OS, overall survival; DFS, disease-free survival.

REFERENCES

1. Sung H, Ferlay J, Siegel RL, Laversanne M, Soerjomataram I, Jemal A, et al. Global Cancer Statistics 2020: GLOBOCAN Estimates of Incidence and Mortality Worldwide for 36 Cancers in 185 Countries. *CA Cancer J Clin* (2021) 71(3):209–49. doi: 10.3322/caac.21660
2. You YN, Rustin RB, Sullivan JD. Oncotype DX(®) Colon Cancer Assay for Prediction of Recurrence Risk in Patients With Stage II and III Colon Cancer: A Review of the Evidence. *Surg Oncol* (2015) 24(2):61–6. doi: 10.1016/j.suronc.2015.02.001
3. Benson AB, Venook AP, Al-Hawary MM, Cederquist L, Chen YJ, Ciombor KK, et al. NCCN Guidelines Insights: Colon Cancer, Version 2.2018. *J Natl Compr Canc Netw* (2018) 16(4):359–69. doi: 10.6004/jnccn.2018.0021
4. Kim MJ, Jeong SY, Choi SJ, Ryoo SB, Park JW, Park KJ, et al. Survival Paradox Between Stage IIB/C (T4N0) and Stage IIIA (T1-2N1) Colon Cancer. *Ann Surg Oncol* (2015) 22(2):505–12. doi: 10.1245/s10434-014-3982-1

5. You W, Sheng N, Yan L, Chen H, Gong J, He Z, et al. The Difference in Prognosis of Stage II and III Colorectal Cancer Based on Preoperative Serum Tumor Markers. *J Cancer* (2019) 10(16):3757–66. doi: 10.7150/jca.31660
6. Zhang JX, Song W, Chen ZH, Wei JH, Liao YJ, Lei J, et al. Prognostic and Predictive Value of a microRNA Signature in Stage II Colon Cancer: A microRNA Expression Analysis. *Lancet Oncol* (2013) 14(13):1295–306. doi: 10.1016/s1470-2045(13)70491-1
7. Zhou Z, Mo S, Dai W, Ying Z, Zhang L, Xiang W, et al. Development and Validation of an Autophagy Score Signature for the Prediction of Post-Operative Survival in Colorectal Cancer. *Front Oncol* (2019) 9:878. doi: 10.3389/fonc.2019.00878
8. Mlecnik B, Tosolini M, Kirilovsky A, Berger A, Bindea G, Meatchi T, et al. Histopathologic-Based Prognostic Factors of Colorectal Cancers Are Associated With the State of the Local Immune Reaction. *J Clin Oncol* (2011) 29(6):610–8. doi: 10.1200/jco.2010.30.5425
9. Pagès F, Mlecnik B, Marliot F, Bindea G, Ou FS, Bifulco C, et al. International Validation of the Consensus Immunoscore for the Classification of Colon Cancer: A Prognostic and Accuracy Study. *Lancet* (2018) 391(10135):2128–39. doi: 10.1016/s0140-6736(18)30789-x
10. Brulé SY, Jonker DJ, Karapetis CS, O'Callaghan CJ, Moore MJ, Wong R, et al. Location of Colon Cancer (Right-Sided Versus Left-Sided) as a Prognostic Factor and a Predictor of Benefit From Cetuximab in NCIC CO.17. *Eur J Cancer* (2015) 51(11):1405–14. doi: 10.1016/j.ejca.2015.03.015
11. Petrelli F, Tomasello G, Borgonovo K, Ghidini M, Turati L, Dallera P, et al. Prognostic Survival Associated With Left-Sided vs Right-Sided Colon Cancer: A Systematic Review and Meta-Analysis. *JAMA Oncol* (2017) 3(2):211–9. doi: 10.1001/jamaoncol.2016.4227
12. Guinney J, Dienstmann R, Wang X, de Reyniès A, Schlicker A, Soneson C, et al. The Consensus Molecular Subtypes of Colorectal Cancer. *Nat Med* (2015) 21(11):1350–6. doi: 10.1038/nm.3967
13. Taieb J, Le Malicot K, Shi Q, Penault-Llorca F, Bouché O, Tabernero J, et al. Prognostic Value of BRAF and KRAS Mutations in MSI and MSS Stage III Colon Cancer. *J Natl Cancer Inst* (2017) 109(5):djw272. doi: 10.1093/jnci/djw272
14. Taieb J, Zaanan A, Le Malicot K, Julié C, Blons H, Mineur L, et al. Prognostic Effect of BRAF and KRAS Mutations in Patients With Stage III Colon Cancer Treated With Leucovorin, Fluorouracil, and Oxaliplatin With or Without Cetuximab: A *Post Hoc* Analysis of the PETACC-8 Trial. *JAMA Oncol* (2016) 2(5):643–53. doi: 10.1001/jamaoncol.2015.5225
15. Konishi T, Shimada Y, Hsu M, Tufts L, Jimenez-Rodriguez R, Cercek A, et al. Association of Preoperative and Postoperative Serum Carcinoembryonic Antigen and Colon Cancer Outcome. *JAMA Oncol* (2018) 4(3):309–15. doi: 10.1001/jamaoncol.2017.4420
16. Thomsen M, Skovlund E, Sorbye H, Bolstad N, Nustad KJ, Glimelius B, et al. Prognostic Role of Carcinoembryonic Antigen and Carbohydrate Antigen 19-9 in Metastatic Colorectal Cancer: A BRAF-Mutant Subset With High CA 19-9 Level and Poor Outcome. *Br J Cancer* (2018) 118(12):1609–16. doi: 10.1038/s41416-018-0115-9
17. Diakos CI, Charles KA, McMillan DC, Clarke SJ. Cancer-Related Inflammation and Treatment Effectiveness. *Lancet Oncol* (2014) 15(11): e493–503. doi: 10.1016/s1470-2045(14)70263-3
18. Sinicrope FA, Shi Q, Hermitte F, Zemla TJ, Mlecnik B, Benson AB, et al. Contribution of Immunoscore and Molecular Features to Survival Prediction in Stage III Colon Cancer. *JNCI Cancer Spectr* (2020) 4(3):pkaa023. doi: 10.1093/jncics/pkaa023
19. Reichling C, Taieb J, Derangere V, Klopfenstein Q, Le Malicot K, Gornet JM, et al. Artificial Intelligence-Guided Tissue Analysis Combined With Immune Infiltrate Assessment Predicts Stage III Colon Cancer Outcomes in PETACC08 Study. *Gut* (2020) 69(4):681–90. doi: 10.1136/gutjnl-2019-319292
20. Bankhead P, Loughrey MB, Fernández JA, Dombrowski Y, McArt DG, Dunne PD, et al. QuPath: Open Source Software for Digital Pathology Image Analysis. *Sci Rep* (2017) 7(1):16878. doi: 10.1038/s41598-017-17204-5
21. Vickers AJ, Elkin EB. Decision Curve Analysis: A Novel Method for Evaluating Prediction Models. *Med Decis Making* (2006) 26(6):565–74. doi: 10.1177/0272989x06295361
22. Grothey A, Sobrero AF, Shields AF, Yoshino T, Paul J, Taieb J, et al. Duration of Adjuvant Chemotherapy for Stage III Colon Cancer. *N Engl J Med* (2018) 378(13):1177–88. doi: 10.1056/NEJMoa1713709
23. Glynne-Jones R, Wyrwicz L, Tiret E, Brown G, Rödel C, Cervantes A, et al. Rectal Cancer: ESMO Clinical Practice Guidelines for Diagnosis, Treatment and Follow-Up. *Ann Oncol* (2017) 28(suppl_4):iv22–40. doi: 10.1093/annonc/mdx224
24. Benson AB, Venook AP, Al-Hawary MM, Arain MA, Chen YJ, Ciombor KK, et al. Colon Cancer, Version 2.2021, NCCN Clinical Practice Guidelines in Oncology. *J Natl Compr Canc Netw* (2021) 19(3):329–59. doi: 10.6004/jnccn.2021.0012
25. Mlecnik B, Bifulco C, Bindea G, Marliot F, Lugli A, Lee JJ, et al. Multicenter International Society for Immunotherapy of Cancer Study of the Consensus Immunoscore for the Prediction of Survival and Response to Chemotherapy in Stage III Colon Cancer. *J Clin Oncol* (2020) 38(31):3638–51. doi: 10.1200/jco.19.03205
26. Pagès F, André T, Taieb J, Vernerey D, Henriques J, Borg C, et al. Prognostic and Predictive Value of the Immunoscore in Stage III Colon Cancer Patients Treated With Oxaliplatin in the Prospective IDEA France PRODIGE-GERCOR Cohort Study. *Ann Oncol* (2020) 31(7):921–9. doi: 10.1016/j.annonc.2020.03.310
27. Weiser MR, Landmann RG, Kattan MW, Gonen M, Shia J, Chou J, et al. Individualized Prediction of Colon Cancer Recurrence Using a Nomogram. *J Clin Oncol* (2008) 26(3):380–5. doi: 10.1200/jco.2007.14.1291
28. Hsu L, Jeon J, Brenner H, Gruber SB, Schoen RE, Berndt SI, et al. A Model to Determine Colorectal Cancer Risk Using Common Genetic Susceptibility Loci. *Gastroenterology* (2015) 148(7):1330–9.e14. doi: 10.1053/j.gastro.2015.02.010

Conflict of Interest: The authors declare that the research was conducted in the absence of any commercial or financial relationships that could be construed as a potential conflict of interest.

Publisher's Note: All claims expressed in this article are solely those of the authors and do not necessarily represent those of their affiliated organizations, or those of the publisher, the editors and the reviewers. Any product that may be evaluated in this article, or claim that may be made by its manufacturer, is not guaranteed or endorsed by the publisher.

Copyright © 2021 Ren, Xu, Zhou, Ouyang, You, Sheng, Yan, Peng, Xie and Wang. This is an open-access article distributed under the terms of the Creative Commons Attribution License (CC BY). The use, distribution or reproduction in other forums is permitted, provided the original author(s) and the copyright owner(s) are credited and that the original publication in this journal is cited, in accordance with accepted academic practice. No use, distribution or reproduction is permitted which does not comply with these terms.

frontiers in Surgery

ORIGINAL RESEARCH
published: 07 December 2021
doi: 10.3389/fsurg.2021.759162

Metastasis Pattern and Survival Analysis in Primary Small Bowel Adenocarcinoma: A SEER-Based Study

Yanmei Gu[1†], *Haixiao Deng*[1†], *Daijun Wang*[1] *and Yumin Li*[1,2*]

[1] *Department of General Surgery, Lanzhou University Second Hospital, The Second Clinical Medical College of Lanzhou University, Lanzhou, China,* [2] *Key Laboratory of Digestive System Tumors of Gansu, Lanzhou, China*

OPEN ACCESS

Edited by:
Sanjit Mukherjee, National Institutes of Health (NIH), United States

Reviewed by:
Yi Liao, Affiliated Hospital of Southwest Medical University, China
Yuqian Feng, Zhejiang Chinese Medical University, China

***Correspondence:**
Yumin Li
liym@lzu.edu.cn

[†] *These authors have contributed equally to this work and share first authorship*

Specialty section:
This article was submitted to Surgical Oncology, a section of the journal Frontiers in Surgery

Received: *16 August 2021*
Accepted: *25 October 2021*
Published: *07 December 2021*

Citation:
Gu Y, Deng H, Wang D and Li Y (2021) Metastasis Pattern and Survival Analysis in Primary Small Bowel Adenocarcinoma: A SEER-Based Study. Front. Surg. 8:759162. doi: 10.3389/fsurg.2021.759162

Background: Small bowel adenocarcinoma (SBA) is a rare gastrointestinal tumor with high malignancy. The aim of this study was to comprehensively evaluate the distant metastasis pattern and establish nomograms predicting survival for SBA.

Methods: From 2010 to 2015, patients diagnosed with SBA were identified based on the Surveillance, Epidemiology, and End Results (SEER) database. Kaplan–Meier survival analysis was applied to compare survival differences between metastasis patterns. Then, univariate and multivariate cox analyses were applied to screened out independent prognostic factors of cancer-specific survival (CSS) and overall survival (OS), and identify the risk factors for metastasis of SBA. To assess the discrimination and calibration of nomograms, the concordance index (C-index), calibration curves, receiver-operating characteristic curve (ROC), and decision curve analysis (DCA) were calculated.

Results: Kaplan–Meier curves revealed that metastasis patterns were significantly correlated with CSS ($p < 0.001$) and OS ($p < 0.001$). Then, the metastasis pattern was showed to be an independent prognostic factor of OS and CSS in patients with SBA, as well as age, grade, T stage, N stage, surgery, retrieval of regional lymph nodes, and chemotherapy. Combining these factors, we constructed prognostic nomograms, which suggested that the metastasis pattern made the greatest contribution to the survival of patients with SBA. Nomograms for OS and CSS had a C-index of 0.787 and 0.793, respectively. Calibration curves showed an excellent agreement between probability and actual observation in the training and validation cohort. Decision curve analysis also exhibited its clinical value with an improved net benefit. In addition, the models we constructed had better prognostic accuracy and clinical utility than traditional TNM staging based on C-index and ROC. Further, Cox regression analysis showed that old age, poor differentiation, N2, and not receiving chemotherapy were the risk factors for prognosis in patients with metastatic SBA.

Conclusion: As an independent prognostic factor, the metastasis pattern exhibited the greatest predictive effect on OS and CSS for patients with SBA. Adjuvant chemotherapy had a positive effect on the survival of patients with SBA. Nomograms for predicting

3-and 5-year OS and CSS of patients with SBA were constructed, which could identify patients with higher risk and might be superior in predicting the survival of patients with SBA than TNM staging.

Keywords: small bowel adenocarcinoma, cancer-specific survival, overall survival, nomogram, metastasis

INTRODUCTION

Small bowel adenocarcinoma (SBA) often occurred in the glandular epithelium, accounting for about 36.9% in small intestinal cancer, and SBA, which mostly located in the duodenum, is the second most common histological type (1, 2). Due to the lack of specific symptoms and the narrow structure, it is difficult to diagnose SBA at the early stage (1). Moreover, the patients with SBA often need individual treatment, which depends on the original occurring position based on surgical resection, chemotherapy, radiation, and immunotherapy (3–5). Although complicated therapies were applied, the prognosis of patients with SBA with a median survival of 37% months remain poorly (6). Therefore, it is urgent to conduct an accurate prognostic analysis of patients with SBA to individualized treatment and monitoring.

Like other tumors, SBA can metastasize to the liver, lung, brain, and bone, with the liver being the dominant site of metastasis (7). Distant metastasis of SBA is one of the main causes of death. However, limited by the small sample size, few studies have analyzed and summarized the relationship between these metastasis sites and prognostic factors of multiple metastases. Therefore, it is important to identify SBA patients with early metastasis and take timely intervention measures. Patients undergoing radical surgery often die from distant metastases of the disease, suggesting the role of adjuvant chemotherapy (8).

Nomogram is a convenient and effective statistical prediction tool, widely used in cancer prognosis research (9, 10). However,

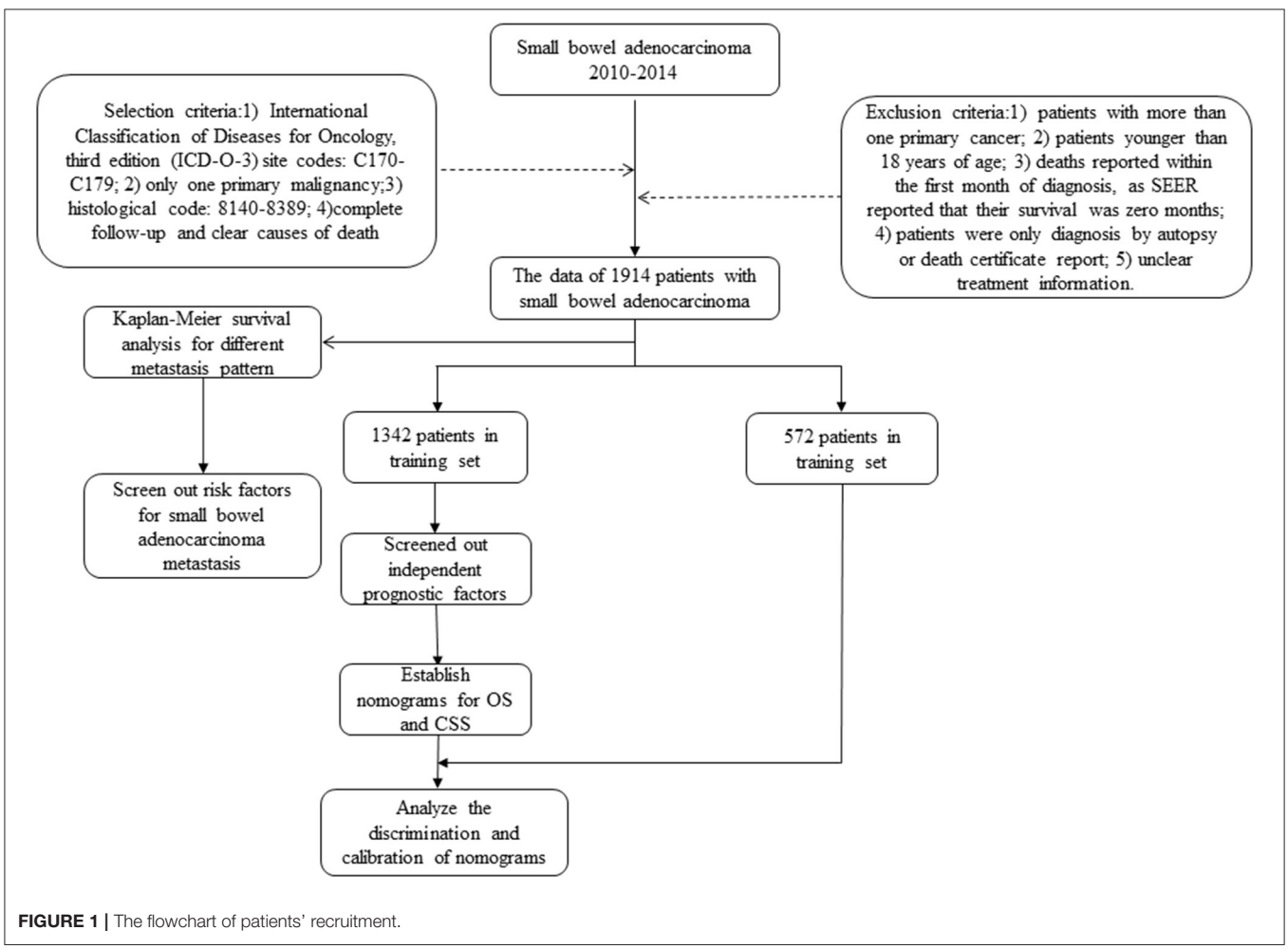

FIGURE 1 | The flowchart of patients' recruitment.

TABLE 1 | Patients' baseline clinicopathological characteristics.

Characteristics	Training cohort	Validation cohort	Total	*P*-value
	1,342 (70.1%)	**572 (29.9%)**	**1,914 (100%)**	
Age				0.242
<60	454 (33.8)	177 (30.9)	631 (33.0)	
60–69	377 (28.1)	170 (29.7)	547 (28.6)	
70–79	290 (21.6)	142 (24.8)	432 (22.6)	
≥80	221 (16.5)	83 (14.5)	304 (15.9)	
Sex				0.341
Female	604 (45.0)	271 (47.4)	875 (45.7)	
Male	738 (55.0)	301 (52.6)	1,039 (54.3)	
Primary site				0.089
Duodenum	762 (56.8)	315 (55.1)	1,077 (56.3)	
Jejunum	233 (17.4)	81 (14.2)	314 (16.4)	
Ileum	199 (14.8)	105 (18.4)	304 (15.9)	
Other	148 (11.0)	71 (12.4)	219 (11.4)	
Grade				0.865
I/II	815 (60.7)	345 (60.3)	1,160 (60.6)	
III/IV	527 (39.3)	227 (39.7)	754 (39.4)	
T stage				0.682
T1/T2	223 (16.6)	87 (15.2)	310 (16.2)	
T3	425 (31.7)	194 (33.9)	619 (32.3)	
T4	555 (41.4)	228 (39.9)	783 (40.9)	
TX	139 (10.4)	63 (11.0)	202 (10.6)	
N stage				0.417
N0	681 (50.7)	279 (48.8)	960 (50.2)	
N1	377 (28.1)	161 (28.1)	538 (28.1)	
N2	211 (15.7)	106 (18.5)	317 (16.6)	
NX	73 (5.4)	26 (4.5)	99 (5.2)	
Metastasis status				0.594
No	959 (71.5)	415 (72.6)	1,374 (71.8)	
Liver metastasis	166 (12.4)	58 (10.1)	224 (11.7)	
Bone/Brain/Lung metastasis	37 (2.8)	15 (2.6)	52 (2.7)	
≥2 sites	28 (2.1)	16 (2.8)	44 (2.3)	
Other	152 (11.3)	68 (11.9)	220 (11.5)	
Surgery				0.157
No	368 (27.4)	139 (24.3)	507 (26.5)	
Yes	974 (72.6)	433 (75.7)	1,407 (73.5)	
Retrieval of regional lymph nodes				0.089
0	492 (36.7)	180 (31.5)	672 (35.1)	
1–3	118 (8.8)	52 (9.1)	170 (8.9)	
≥4	732 (54.5)	340 (59.4)	1,072 (56.0)	
Radiation				0.702
No	1,231 (91.7)	517 (90.4)	1,748 (91.3)	
Yes	111 (8.3)	55 (9.6)	166 (8.7)	
Chemotherapy				0.112
No	675 (50.3)	265 (46.3)	940 (49.1)	
Yes	667 (49.7)	307 (53.7)	974 (50.9)	

the factors that affect tumor progression are complex and diverse. The nomogram can integrate and analyze various prognostic factors of individuals, simplify the classification of patients in clinical trials, and quantify the individualized outcome of patients (11, 12). Therefore, nomogram specially designed for predicting the survival of SBA is promising. This study aimed to establish the models for predicting cancer-specific survival (CSS) ($P < 0.001$) and overall survival (OS) of SBA and explore the effects of metastasis pattern on the prognosis of SBA. The Surveillance, Epidemiology, and End Results (SEER) database can provide us with corresponding data, which contains a wealth of large-scale information on tumor epidemiology, such as various clinical information and social information for specific populations (13–15).

MATERIALS AND METHODS

Patients

The cancer incidence information collected by SEER database includes data from 18 cancer registries, covering approximately 34.6% of the US population. Data on patients diagnosed with SBA were selected from 2010 to 2014, since the information on cancer metastasis sites was available from 2010 in SEER. The inclusion criteria for patients were based on International Classification of Diseases for Oncology, third edition (ICD-O-3) site codes: C170-C179 (C170: Duodenum, C171: Jejunum, C172: Ileum, C173: Meckels diverticulum, C178: Overlapping lesion of small intestine, C179: Small intestine), only one primary malignancy, histological code: 8140-8389, complete follow-up, and clear causes of death (**Supplementary Table 1**). Exclusion criteria were as follows: (1) patients with more than one primary cancer; (2) patients younger than 18 years of age; (3) deaths reported within the first month of diagnosis, as SEER reported that their survival was 0 months; (4) patients were only diagnosed by autopsy or death certificate report; and (5) unclear treatment information (**Figure 1**). Finally, a total of 1,914 patients were included.

Study Variables

The factors identified in the analysis included age, race, sex, marital status, primary site, histologic grade, TNM stage, surgery, chemotherapy, radiation, retrieval of reginal lymph nodes, the causes of death, and follow-up information. The endpoints of the study were OS and CSS. Overall survival is defined as the time from diagnosis to death, and CSS is the time from diagnosis to death from SBA.

Statistical Analyses

All cases meeting the inclusion criteria were included in our study, which were divided into training cohort and validation cohort in a ratio of 7:3 by a random split method. Chi-square test was performed for the basic clinicopathological characteristics of the two cohorts. Kaplan–Meier survival analysis was used to calculate the correlation between different metastasis pattern and OS and CSS, and the log-rank test was performed to compare the significance of survival curves. All variables were evaluated by univariate and multivariate Cox regression analyses to assess the correlation between each characteristic and OS and CSS, and to identify the risk factors for metastasis of SBA. Based on the results of Cox regression analysis, nomograms were constructed for predicting 3- and 5-year OS and CSS. Concordance index (C-index) was used to evaluate the predictive ability of nomograms (16, 17). Concordance index of 0.5 indicates that the model has no predictive power, while a C-index of 1.0 indicates perfect. Receiver-operating characteristic curve (ROC) can also verify nomogram. In addition, calibration curves were drawn to assess the prognosis and actual outcome of survival. To measure the clinical application of nomogram, decision curve analysis (DCA)

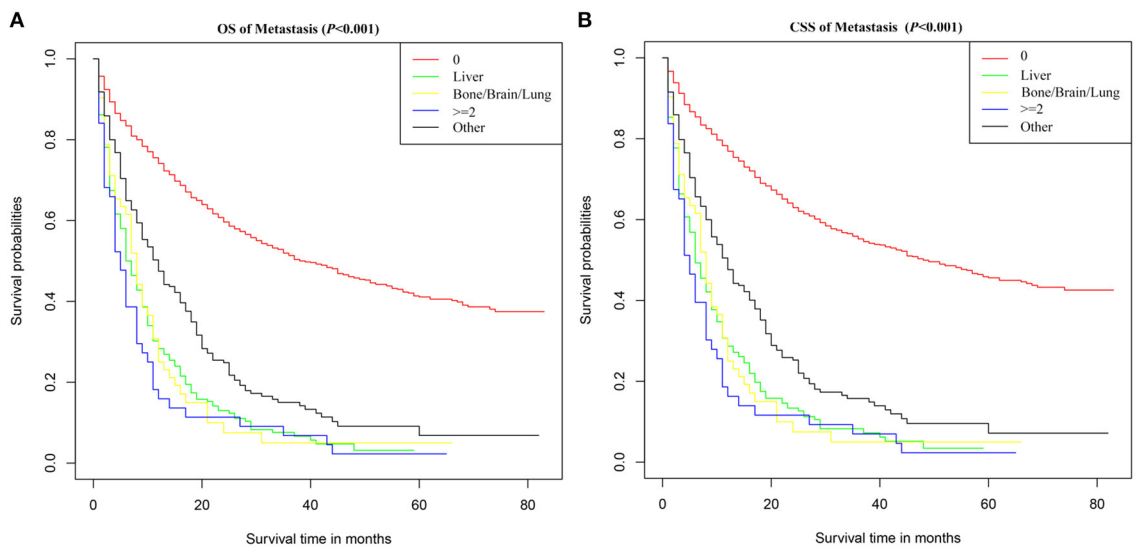

FIGURE 2 | Survival curves of **(A)** OS and **(B)** CSS for SBA according to metastasis pattern. 0, no metastasis; ≥2, metastasis to at least two sites; Other, metastasis occurred, but the SEER database did not provide the site of metastasis.

TABLE 2 | Univariate Cox regression analysis for overall survival and cancer-specific survival in small bowel adenocarcinoma (training cohort).

Characteristics	Overall survival		Cancer specific survival	
	HR (95%CI)	*P*-value	HR (95%CI)	*P*-value
Age				
<60	Reference		Reference	
60–69	1.231(1.021–1.484)	0.030	1.249(1.028–1.518)	0.025
70–79	1.739(1.437–2.104)	<0.001	1.904(1.559–2.324)	<0.001
≥80	2.434(1.994–2.971)	<0.001	2.417(1.943–3.006)	<0.001
Sex				
Female	Reference		Reference	
Male	1.070(0.932–1.230)	0.338	1.132(0.977–1.313)	0.099
Primary site				
Duodenum	Reference		Reference	
Jejunum	0.548(0.446–0.673)	<0.001	0.591(0.476–0.734)	<0.001
Ileum	0.573(0.464–0.708)	<0.001	0.652(0.528–0.806)	<0.001
Other	0.726(0.577–0.913)	0.006	0.741(0.580–0.945)	0.016
Grade				
I/II	Reference		Reference	
III/IV	1.757(1.529–2.019)	<0.001	1.874(1.618–2.170)	<0.001
T stage				
T1/T2	Reference		Reference	
T3	0.638(0.507–0.802)	<0.001	0.520(0.409–0.663)	<0.001
T4	1.328(1.083–1.629)	0.006	1.111(0.898–1.374)	0.333
TX	3.511(2.730–4.515)	<0.001	3.034(2.340–3.935)	<0.001
N stage				
N0	Reference		Reference	
N1	1.317(1.120–1.549)	<0.001	1.220(1.025–1.453)	0.025
N2	1.306(1.074–1.588)	0.007	1.382(1.132–1.688)	<0.002
NX	2.382(1.803–3.146)	<0.001	2.605(1.945–3.488)	<0.001
Metastasis status				
No	Reference		Reference	
Liver metastasis	4.354(3.600–5.266)	<0.001	4.164(3.405–5.091)	<0.001
Bone/Brain/Lung metastasis	4.490(3.172–6.354)	<0.001	4.796(3.426–6.715)	<0.001
≥2 sites	4.972(3.365–7.346)	<0.001	7.760(3.278–6.913)	<0.001
Other	2.939(2.408–3.588)	<0.001	2.815(2.283–3.471)	<0.001
Surgery				
No	Reference		Reference	
Yes	0.210(0.181–0.243)	<0.001	0.203(0.174–0.237)	<0.001
Retrieval of regional lymph nodes				
0	Reference		Reference	
1–3	0.499(0.389–0.639)	<0.001	0.473(0.365–0.615)	<0.001
≥4	0.299(0.258–0.346)	<0.001	0.274(0.234–0.320)	<0.001
Radiation				
No	Reference		Reference	
Yes	1.163(0.914–1.479)	0.219	1.083(0.847–1.386)	0.525
Chemotherapy				
No	Reference		Reference	
Yes	0.825(0.719–0.947)	0.006	0.787(0.680–0.911)	0.001

TABLE 3 | Multivariate Cox regression analysis for OS and CSS in SBA patients (training cohort).

Characteristics	Overall survival		Cancer specific survival	
	HR (95%CI)	*P*-value	HR (95%CI)	*P*-value
Age				
<60	Reference		Reference	
60–69	1.271(1.046–1.544)	0.016	1.215(0.996–1.483)	0.056
70–79	1.783(1.453–2.190)	<0.001	1.610(1.296–2.000)	<0.001
≥80	2.024(1.607–2.550)	<0.001	2.233(1.742–2.862)	<0.001
Sex				
Female	Reference		Reference	
Male	1.171(1.012–1.355)	0.034	1.195(1.022–1.397)	0.026
Primary site				
Duodenum	Reference		Reference	
Jejunum	0.831(0.654–1.055)	0.127	0.928(0.723–1.191)	0.555
Ileum	0.884(0.695–1.124)	0.314	1.082(0.844–1.389)	0.533
Other	1.039(0.809–1.334)	0.532	1.030(0.787–1.347)	0.831
Grade				
I/II	Reference		Reference	
III/IV	1.612(1.395–1.863)	<0.001	1.786(1.529–2.085)	<0.001
T stage				
T1/T2	Reference		Reference	
T3	1.108(0.863–1.422)	0.421	0.927(0.713–1.205)	0.572
T4	1.692(1.348–2.122)	<0.001	1.608(1.272–2.033)	<0.001
TX	1.786(1.361–2.344)	<0.001	1.325(1.004–1.750)	0.047
N stage				
N0	Reference		Reference	
N1	1.414(1.180–1.693)	<0.001	1.445(1.191–1.754)	<0.001
N2	2.112(1.675–2.664)	<0.001	2.330(1.830–2.967)	<0.001
NX	0.930(0.689–1.256)	0.636	0.991(0.720–1.363)	0.955
Metastasis status				
No	Reference		Reference	
Liver metastasis	2.762(2.205–3.461)	<0.001	2.316(1.830–2.932)	<0.001
Bone/Brain/Lung metastasis	2.857(1.971–4.142)	<0.001	2.432(1.699–3.480)	<0.001
≥2 sites	3.236(2.135–4.905)	<0.001	2.970(1.995–4.420)	<0.001
Other	2.108(1.694–2.623)	<0.001	1.921(1.526–2.418)	<0.001
Surgery				
No	Reference		Reference	
Yes	0.445(0.335–0.591)	<0.001	0.419(0.310–0.566)	<0.001
Retrieval of regional lymph nodes				
0	Reference		Reference	
1–3	1.085(0.801–1.470)	0.598	1.343(0.823–1.563)	0.441
≥4	0.610(0.469–0.793)	<0.001	0.500(0.377–0.664)	<0.001
Radiation				
No	Reference		Reference	
Yes	1.127(0.874–1.454)	0.357	0.987(0.760–1.283)	0.923
Chemotherapy				
No	Reference		Reference	
Yes	0.502(0.426–0.592)	<0.001	0.547(0.459–0.651)	<0.001

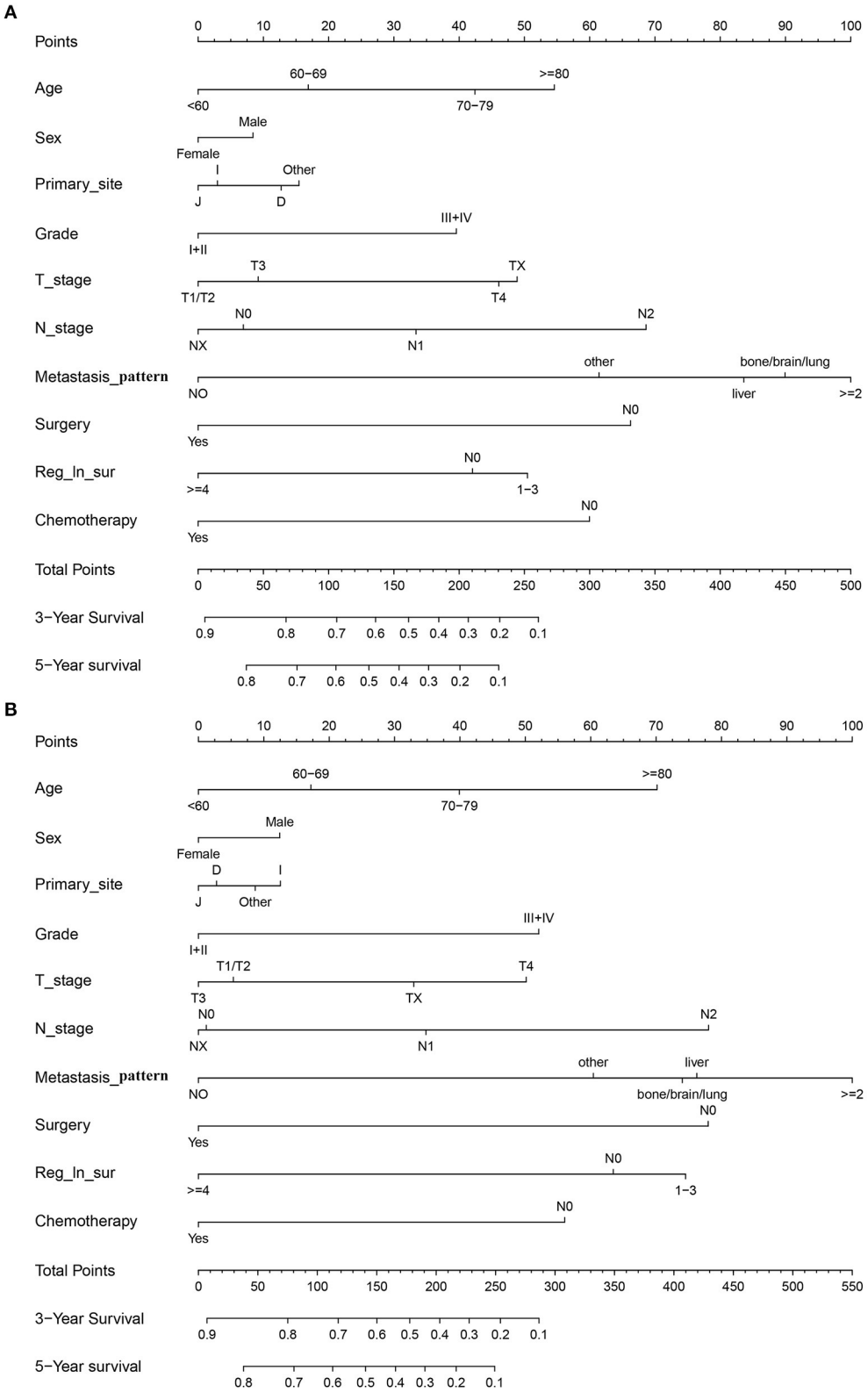

FIGURE 3 | Nomograms of SBA for predicting 3- and 5-year survival **(A)** OS and **(B)** CSS.

TABLE 4 | Detailed scores of prognostic factors in the OS and CSS nomogram.

Characteristic	OS nomogram	CSS nomogram
Age		
<60	0	0
60–69	17	17
70–79	42	40
≥80	55	70
Sex		
Female	0	0
Male	8	12
Primary site		
Duodenum	13	3
Jejunum	0	0
Ileum	3	13
Other	15	9
Grade		
I+II	0	0
III+IV	40	52
T stage		
T1+T2	0	5
T3	9	0
T4	46	50
TX	49	33
N stage		
N0	7	1
N1	33	35
N2	69	78
NX	0	0
Metastasis status		
No	0	0
Liver metastasis	84	76
Bone/Brain/Lung metastasis	90	74
≥2 sites	100	100
Other	61	60
Surgery		
No	66	78
Yes	0	0
Retrieval of regional lymph nodes		
No	42	63
1–3	50	75
≥4	0	0
Chemotherapy		
No	60	56
Yes	0	0

was applied (18, 19). SPSS software and R statistical software were used for the analysis. A P-value < 0.05 was considered statistically significant.

RESULTS

Patient Characteristics

This study included 1,914 patients with SBA in SEER database from 2010 to 2015. Random split-sample method was used to randomly divide patients into training cohort ($n = 1{,}342$) and validation cohort ($n = 572$). Training cohort information was used to create nomogram, and validation cohort was applied to build external verification of nomogram. As shown in **Table 1**, age ($p = 0.242$), sex ($p = 0.341$), primary site ($p = 0.089$), grade ($p = 0.865$), T stage ($p = 0.682$), N stage ($p = 0.417$), metastasis status ($p = 0.594$), surgery ($p = 0.157$), retrieval of reginal lymph nodes ($p = 0.089$), radiation ($p = 0.702$), and chemotherapy ($p = 0.112$) were all factors that were similar between two groups.

Survival Analysis for Different Metastasis Pattern

In order to evaluate the impact of different metastasis patterns on OS and CSS in patients with SBA, Kaplan–Meier survival analysis was performed on all patients. As shown in **Figure 2A**, the difference in OS among different metastasis pattern was statistically significant ($p < 0.001$).The survival was highest for SBA patients without metastasis, followed by patients with liver and bone/brain/lung metastasis, and the worst in patients with multiple metastases. Furthermore, the Kaplan–Meier survival analysis on CSS in patients with SBA was consistent with the results of OS (**Figure 2B**).

Independent Prognostic Factors for OS and CSS

In the training cohort, we determined that age, marital status, primary site, grade, T stage, N stage, metastasis pattern, surgery, retrieval of regional lymph nodes, and chemotherapy are related to OS and CSS by univariate Cox regression analysis (**Table 2**). In order to further judge whether these factors can be used as independent prognostic factors, we conducted a multivariate Cox regression analysis (**Table 3**). The results showed that age, grade, T stage, N stage, metastasis pattern, surgery, retrieval of regional lymph nodes, and chemotherapy were identified as independent prognostic factors for OS and CSS, which were further included in the construction of nomogram. From the clinical point of view, we also considered tumor primary site as the parameter of the nomogram (**Figure 3**). Nomogram showed that the metastatic pattern of SBA had the greatest impact on the prognosis, of which liver metastasis accounted for a large proportion, and surgery, N stage, and chemotherapy also made great contribution to prognosis. Age, grade, T stage, and retrieval of reginal lymph nodes showed a moderate effect on OS (**Figure 3A**). However, in the nomogram for CSS, the metastasis pattern was the greatest contributor, followed by surgery, N stage, and retrieval of reginal lymph nodes (**Figure 3B**). According to the individual characteristics of patients with SBA, the scores of each variable were added to correspond to the total score to predict the OS and CSS at 3- and 5-years. The detailed score of each variable is shown in **Table 4**.

In the training cohort, the C-index of nomogram for predicting CSS and OS was 0.793 (95% CI 0.785–0.801) and 0.787 (95% CI 0.780–0.794), respectively. However, the C-index of TNM staging for CSS and OS was 0.702 (95% CI 0.692–0.712) and 0.696 (95% CI 0.687–0.705). In the validation cohort, the C-index of nomogram for CSS was 0.796 (95%

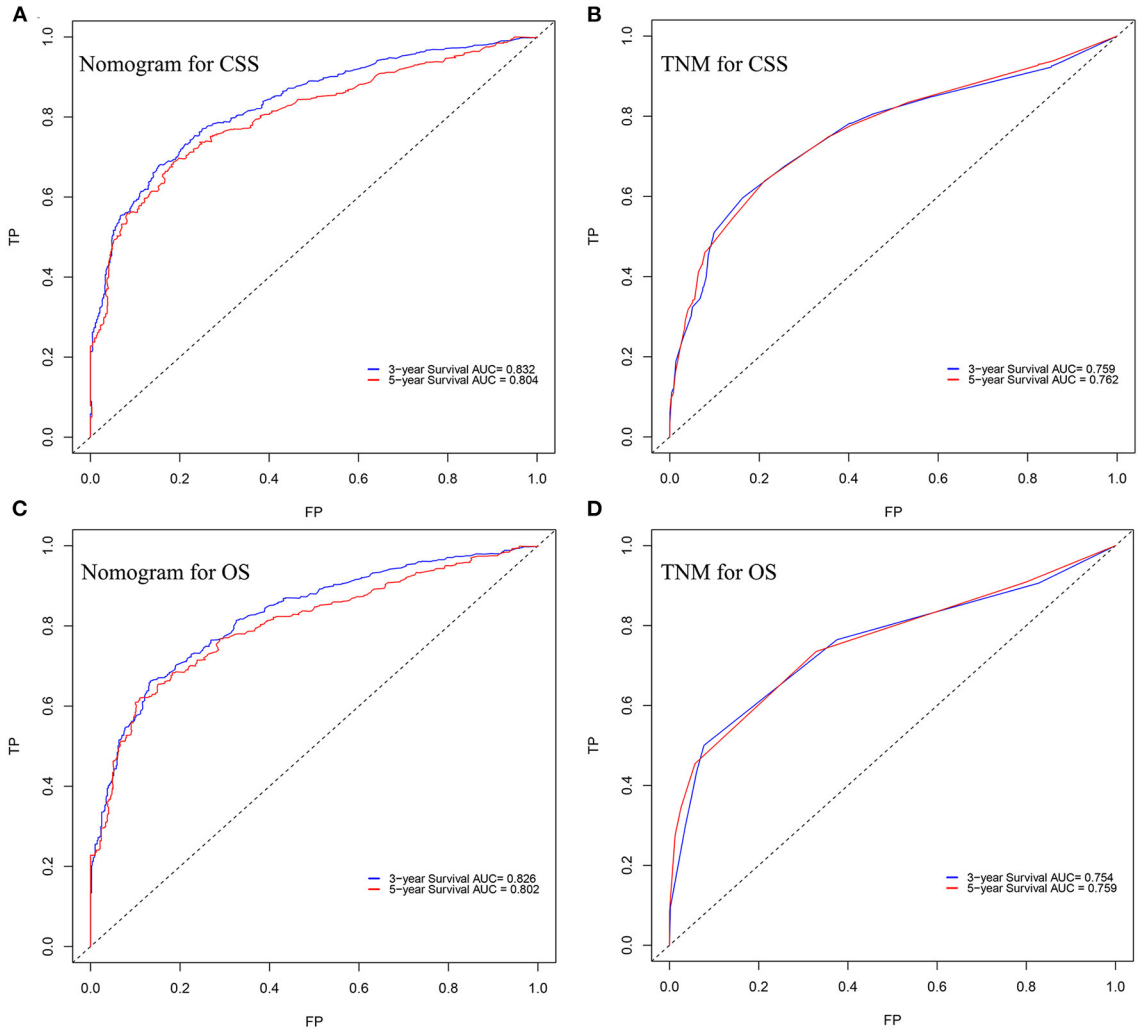

FIGURE 4 | ROC curves of the nomogram for predicting **(A)** CSS and **(B)** OS at 3- and 5-year point. ROC curves of the TNM staging for predicting **(C)** CSS and **(D)** OS.

CI 0.785–0.807) and that for OS was 0.762 (95% CI 0.749–0.775), which were higher than those of TNM staging [CSS: 0.718 (95% CI 0.704–0.732); OS: 0.678 (95% CI 0.663–0.693)]. The higher the C-index, the more suitable of the model for patients with SBA. By comparing the discrimination capability of nomogram with the 7th edition of AJCC TNM staging, ROC analysis showed that the nomograms we constructed also demonstrated a superior survival predictability than the 7th AJCC TNM staging system (**Figure 4**). Furthermore, the calibration and prediction curves of nomograms for the 3- and 5-year survival rates of patients exhibited a perfect correlation in the training cohort, indicating that nomograms for CSS and OS were well-validated (**Figures 5A,C,E,G**). In the validation cohort, the results showed the same reliability of the model (**Figures 5B,D,F,H**). Decision curve analysis indicated that the models had significantly positive net benefits within the risk of death in both cohorts, demonstrating that nomograms had good clinical value in predicting OS and CSS at 3- and 5-years (**Figure 6**).

Risk Factors for SBA Distant Metastasis

We then identified the risk factors that were significantly associated with distant metastatic SBA. Among the variables studied, advanced age, tumor origin in the duodenum, poor differentiation, lack of surgical treatment at the primary site and regional lymph node dissection, and lack of radiotherapy and chemotherapy were significantly associated with OS and CSS in patients with metastatic SBA (**Table 5**). Variables that were statistically significant in the univariate analysis were selected for inclusion in the multivariate analysis for OS. As shown in **Table 6**, advanced age ($p = 0.015$), poor differentiation ($p < 0.001$), N2 stage ($p = 0.009$), absence of regional lymph node dissection ($p = 0.007$), and not receiving chemotherapy ($p < 0.001$) were significantly associated with poor prognosis in patients with

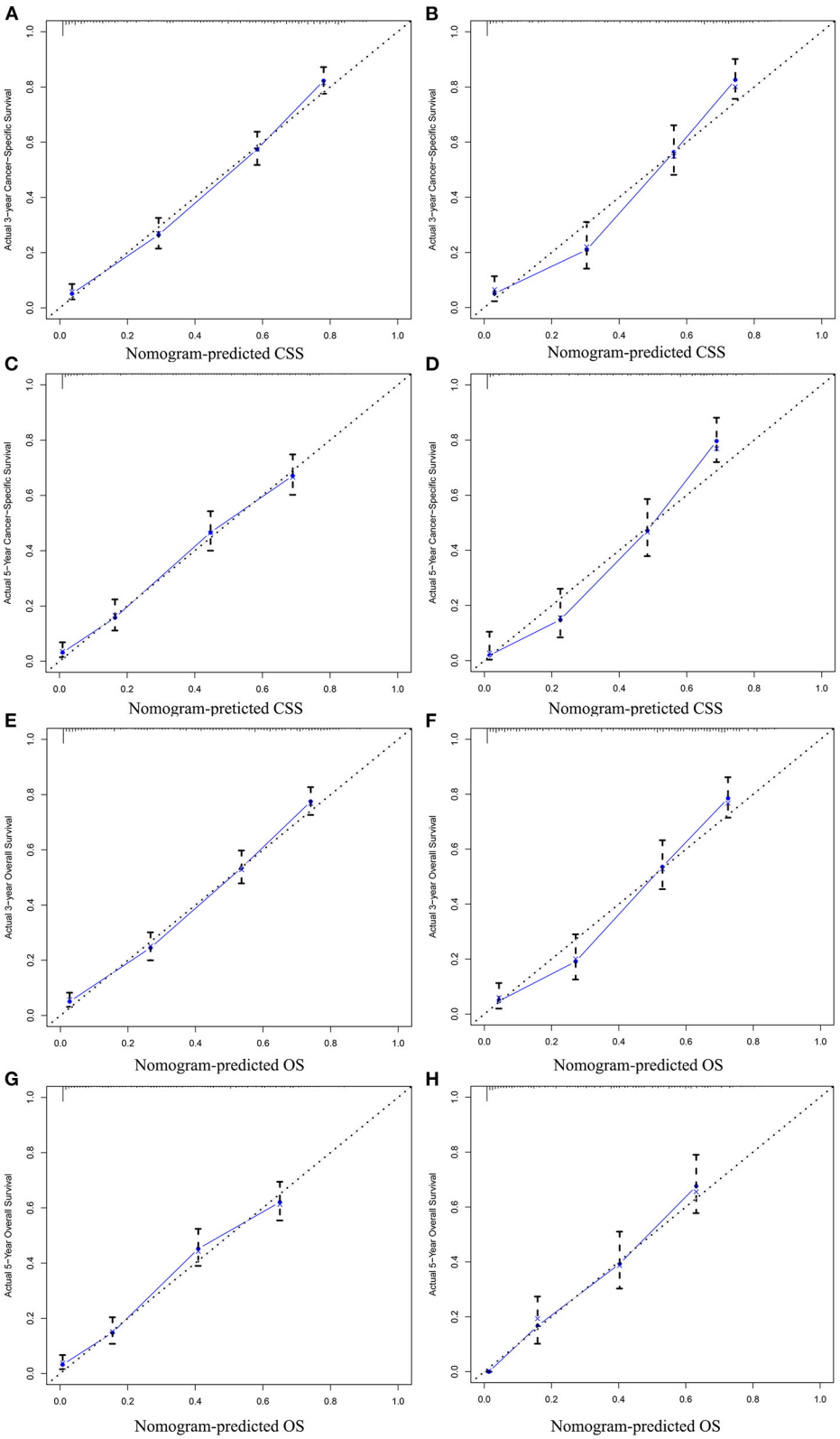

FIGURE 5 | Calibration plots for predicting CSS at 3-year **(A)** training cohort and **(B)** validation cohort; calibration plots for predicting CSS at 5-year **(C)** training cohort and **(D)** validation cohort; calibration plots for predicting OS at 3-year **(E)** training cohort and **(F)** validation cohort; calibration plots for predicting OS at 5-year **(G)** training cohort, and **(H)** validation cohort.

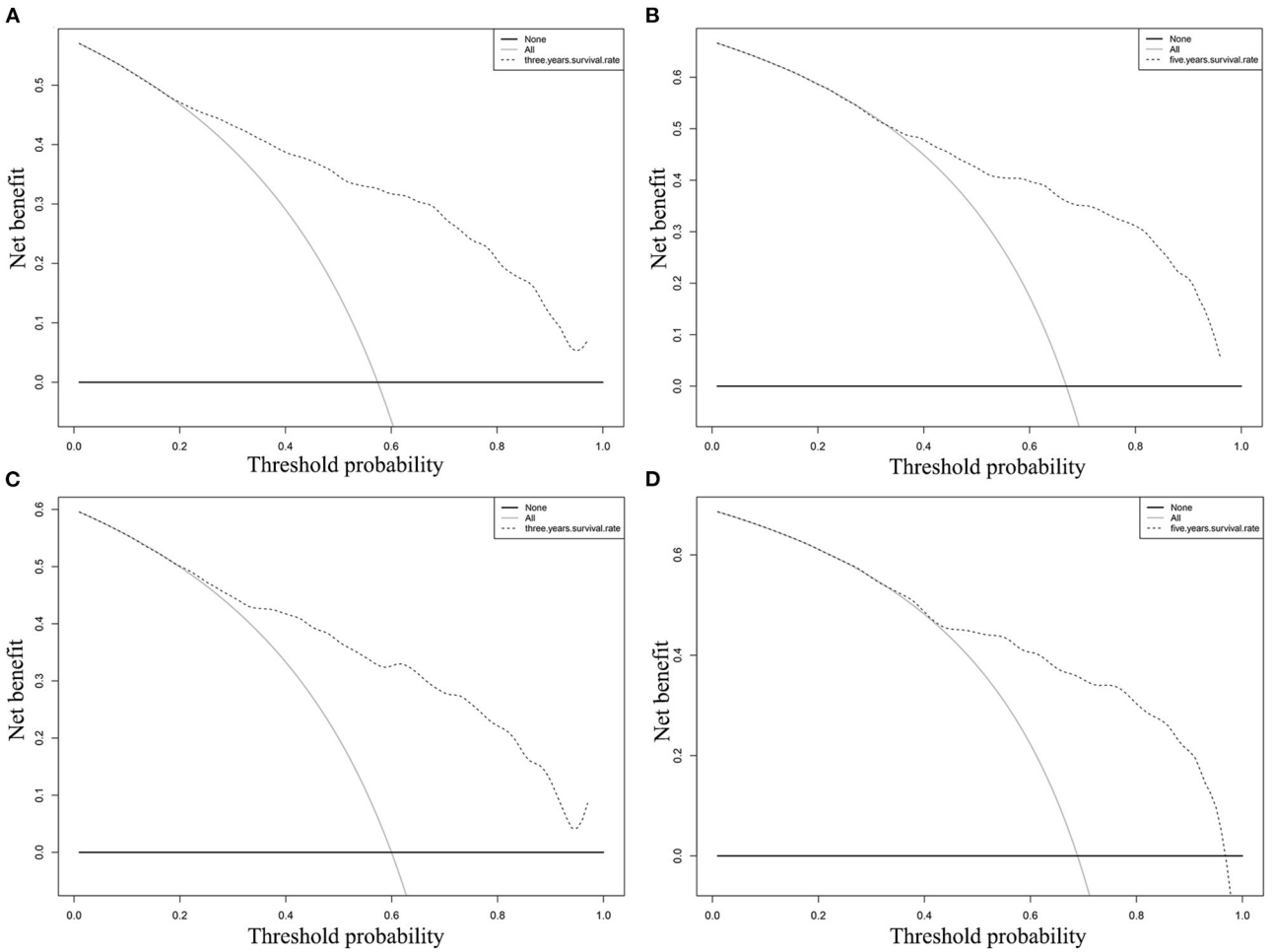

FIGURE 6 | DCA of the nomogram for predicting CSS at **(A)** 3-year and **(B)** 5-year point; DCA of the nomogram for predicting OS at **(C)** 3-year and **(D)** 5-year point.

metastatic SBA. Similar results were observed in the multivariate analysis for CSS.

DISCUSSION

The malignant small bowel tumor is a rare gastrointestinal tumor, accounting for about 5% of all gastrointestinal tumors (20). Small bowel adenocarcinoma is one of the most common histological subtypes, which has been found to have a very bad prognosis (21). The AJCC TNM staging system neglects taking some significant factors into consider, though it is applied to predict the survival of patients with SBA. Although recent study has constructed a prognostic model for SBA, this study ignores the impact of adjuvant chemotherapy, radiotherapy, lymph node dissection, and tumor metastasis patterns on the survival of patients with SBA (22). Compared with previous prognostic models, our study established the most comprehensive nomogram for patients with SBA. Concordance index, calibration curves, ROC, and DCA all proved good predictive ability and clinical application of nomograms. The new model showed more predictability than the 7th edition of AJCC TNM staging system both in the training test and in the validation set. We further identify the risk factors of patients with metastatic SBA.

Age, tumor grade, T stage, and N stage were shown to be independent prognostic factors for OS and CSS in patients with SBA, consistent with previous studies (6, 20, 23, 24). Old age was one of the factors for the poor prognosis of many malignant tumors, which may be attributed to the decline of the patient's body resistance. Poorly differentiated or undifferentiated of tumors often led to the malignant progression; thus, it was the factor affecting the survival. In addition, our model indicated that T4 and N2 were the important risk factors for patients with SBA. In a prospective study based on 347 patients with SBA, T4 ($p = 0.001$) was correlated with a higher risk of death, which was an independent prognostic factor for OS in patients with SBA (25). Another retrospective study also emphasized T4 as an independent prognostic factor (26). Previous retrospective studies have shown that lymph node involvement has adverse effects on patients with SBA (7). It should be noted that

TABLE 5 | Univariate Cox regression analysis for survival in SBA patients with metastasis.

Characteristics	Overall survival		Cancer specific survival	
	HR (95%CI)	*P*-value	HR (95%CI)	*P*-value
Age				
<60	Reference		Reference	
60–69	1.191(0.945–1.497)	0.139	1.179(0.933–1.490)	0.167
70–79	1.517(1.189–1.934)	<0.001	1.504(1.175–1.926)	0.001
≥80	2.115(1.590–2.814)	<0.001	2.206(1.639–2.970)	<0.001
Sex				
Female	Reference		Reference	
Male	1.062(0.884–1.275)	0.521	1.051(0.872–1.267)	0.602
Marital status				
Married	Reference		Reference	
Unmarried	1.078(0.894–1.299)	0.433	1.075(0.888–1.302)	0.459
Unknown	1.292(0.835–1.998)	0.250	1.328(0.850–2.075)	0.213
Primary site				
Duodenum	Reference		Reference	
Jejunum	0.497(0.383–0.645)	<0.001	0.499(0.381–0.652)	<0.001
Ileum	0.584(0.440–0.774)	<0.001	0.587(0.442–0.781)	<0.001
Other	0.758(0.575–1.000)	0.051	0.742(0.558–0.988)	0.041
Grade				
I/II	Reference		Reference	
III/IV	1.396(1.164–1.673)	<0.001	1.391(1.156–1.675)	<0.001
T stage				
T1/T2	Reference		Reference	
T3	0.678(0.494–0.931)	0.016	0.669(0.485–0.924)	0.015
T4	0.724(0.552–0.950)	0.020	0.721(0.548–0.949)	0.019
TX	1.300(0.966–1.750)	0.084	1.323(0.979–1.788)	0.068
N stage				
N0	Reference		Reference	
N1	0.790(0.636–0.980)	0.032	0.800(0.642–0.998)	0.048
N2	0.829(0.643–1.068)	0.146	0.854(0.660–1.107)	0.233
NX	1.038(0.752–1.434)	0.820	1.058(0.760–1.472)	0.738
Surgery				
No	Reference		Reference	
Yes	0.491(0.408–0.591)	<0.001	0.487(0.4026–0.588)	<0.001
Retrieval of regional lymph nodes				
0	Reference		Reference	
1–3	0.621(0.450–0.858)	0.004	0.608(0.435–0.850)	0.004
≥4	0.509(0.412–0.628)	<0.001	0.505(0.407–0.627)	<0.001
Radiation				
No	Reference		Reference	
Yes	1.664(1.195–2.317)	0.003	1.633(1.167–2.285)	0.004
Chemotherapy				
No	Reference		Reference	
Yes	0.477(0.395–0.577)	<0.001	0.462(0.381–0.561)	<0.001

surgery, number of lymph node dissection, and chemotherapy have strong prognostic values for patients with CSS and OS, demonstrating the positive effect of surgical treatment and systemic chemotherapy on patients with SBA. At present, surgery remains the main treatment option for patients with SBA, while radical surgical resection and adequate lymph node dissection are important means to improve the prognosis of patients. In many past studies, adjuvant chemotherapy could significantly improve OS and disease-free survival (DFS) (27, 28). Another retrospective study pointed out that adjuvant chemotherapy did not improve the OS and DFS of patients with SBA after surgery (29). In our study, patients receiving chemotherapy had a lower risk of survival (HR = 0.502, $P < 0.001$), suggesting that adjuvant chemotherapy has a positive effect on improving

TABLE 6 | Multivariate Cox regression analysis for survival in SBA patients with metastasis.

Characteristics	Overall survival		Cancer specific survival	
	HR (95%CI)	*P*-value	HR (95%CI)	*P*-value
Age				
<60	Reference		Reference	
60–69	1.221(0.964–1.545)	0.097	1.214(0.955–1.544)	0.113
70–79	1.261(0.979–1.626)	0.073	1.236(0.954–1.601)	0.109
≥80	1.462(1.076–1.987)	0.015	1.512(1.098–2.082)	0.011
Primary site				
Duodenum	Reference		Reference	
Jejunum	0.759(0.552–1.044)	0.09	0.802(0.575–1.118)	0.192
Ileum	0.865(0.600–1.247)	0.436	0.932(0.641–1.356)	0.714
Other	1.187(0.866–1.628)	0.286	1.202(0.868–1.664)	0.267
Grade				
I/II	Reference		Reference	
III/IV	1.600(1.325–1.932)	<0.001	1.564(1.290–1.897)	<0.001
T stage				
T1/T2	Reference		Reference	
T3	0.999(0.709–1.410)	0.999	0.992(0.699–1.408)	0.965
T4	0.925(0.688–1.244)	0.604	0.928(0.687–1.254)	0.626
TX	1.179(0.869–1.600)	0.291	1.211(0.889–1.649)	0.224
N stage				
N0	Reference		Reference	
N1	1.059(0.843–1.331)	0.623	1.100(0.869–1.392)	0.430
N2	1.517(1.108–2.078)	0.009	1.576(1.145–2.170)	0.005
NX	0.911(0.650–1.278)	0.590	0.962(0.680–1.361)	0.825
Surgery				
No	Reference		Reference	
Yes	0.708(0.495–1.014)	0.059	0.714(0.495–1.029)	0.071
Retrieval of regional lymph nodes				
0	Reference		Reference	
1–3	0.991(0.673–1.460)	0.963	0.976(0.655–1.455)	0.906
≥4	0.601(0.416–0.869)	0.007	0.567(0.389–0.826)	0.003
Radiation				
No	Reference		Reference	
Yes	1.156(0.814–1.640)	0.419	1.133(0.794–1.615)	0.492
Chemotherapy				
No	Reference		Reference	
Yes	0.456(0.371–0.561)	<0.001	0.442(0.357–0.546)	<0.001

the prognosis of patients with SBA. However, radiotherapy had no significant effect on the prognosis of SBA based on the Cox analysis. For solid tumors, there were still uncertainties in dose selection, time, and toxicity of radiotherapy (30). Due to the rare incidence of small intestinal adenocarcinoma, the analysis of the effect of therapies was limited by the small sample size, so the effect of radiation on patients with SBA was still controversial (21, 23, 26, 28). In addition, studies have shown that the primary tumor site was an independent prognostic factor in patients with SBA (31, 32). This may be attributed to the fact that the early diagnosis rate of SBA that originated in the duodenum was higher than that of jejunum and ileum tumors, and they were treated relatively early. In univariate Cox analysis, the primary tumor site was significant, but multivariate regression analysis suggested negative results.

Among the included variables, the metastatic pattern was a significant independent prognostic factor and was positively correlated with the risk of death of the patient. The results of survival analysis were consistent. Small bowel adenocarcinoma patients with more than two metastasis sites had a significantly negative prognosis in this model. The study showed poor OS in patients with metastatic SBA, consistent with our study (33). Based on the results of univariate Cox analysis, multivariate Cox regression again emphasized that poorly differentiated, N2, and absence of chemotherapy were negatively associated with OS and CSS in metastatic SBA patients. A systematic

review of seven prospective studies revealed that adjuvant chemotherapy was effective for unresectable or metastatic SBA (34). In a retrospective analysis of patients with metastatic SBA, patients who received palliative chemotherapy had a median OS of 9.3 months, significantly better than those who did not receive chemotherapy (35). These studies suggested that adjuvant chemotherapy had a certain benefit in improving the prognosis of metastatic SBA. However, the current SBA chemotherapy regimens mostly refer to other gastrointestinal malignancies, and the efficacy of different chemotherapy regimens varies greatly. In a multicenter retrospective analysis, oxaliplatin-based chemotherapy regimens were found to significantly improve the prognosis of patients with metastatic SBA compared with cisplatin (36). Limitations of our study were the lack of detailed protocols for chemotherapy and targeted therapy regimens and the absence of a history of Crohn's disease.

In summary, we have established and verified two clinically effective nomograms predicting OS and CSS for patients with primary SBA at 3- and 5-years, based on a large number of people. The prognosis of metastatic SBA is poor. Advanced age, poor differentiation, and N2 are the risk factors for metastatic SBA. Adjuvant chemotherapy can improve the prognosis of metastatic SBA to a certain extent.

DATA AVAILABILITY STATEMENT

The original contributions presented in the study are included in the article/**Supplementary Material**, further inquiries can be directed to the corresponding author/s.

AUTHOR CONTRIBUTIONS

YG, HD, and YL designed the research and wrote the manuscript. YG and HD processed and analyzed the data. DW assisted in the data processing. YL conceived of the study and coordinated the study. All authors gave final approval for publication.

SUPPLEMENTARY MATERIAL

The Supplementary Material for this article can be found online at: https://www.frontiersin.org/articles/10.3389/fsurg.2021.759162/full#supplementary-material

REFERENCES

1. Benson AB, Venook AP, Al-Hawary MM, Arain MA, Chen YJ, Ciombor KK, et al. Small bowel adenocarcinoma, version 1.2020, NCCN clinical practice guidelines in oncology. *J Natl Compr Canc Netw.* (2019) 17:1109–33. doi: 10.6004/jnccn.2019.0043
2. Giuffrida P, Vanoli A, Di Sabatino A. Survival in Crohn's disease-associated small bowel adenocarcinoma. *Gut.* (2021) 70:997–8. doi: 10.1136/gutjnl-2020-322364
3. Aparicio T, Svrcek M, Henriques J, Afchain P, Lièvre A, Tougeron D, et al. Panel gene profiling of small bowel adenocarcinoma: results from the NADEGE prospective cohort. *Int J Cancer.* (2021) 148:1731–42. doi: 10.1002/ijc.33392
4. Latham A, Shia J, Patel Z, Reidy-Lagunes DL, Segal NH, Yaeger R, et al. Characterization and clinical outcomes of DNA mismatch repair-deficient small bowel adenocarcinoma. *Clin Cancer Res.* (2021) 27:1429–37. doi: 10.1158/1078-0432.CCR-20-2892
5. Pedersen KS, Foster NR, Overman MJ, Boland PM, Kim SS, Arrambide KA, et al. ZEBRA: a multicenter phase II study of pembrolizumab in patients with advanced small-bowel adenocarcinoma. *Clin Cancer Res.* (2021) 27:3641–8. doi: 10.1158/1078-0432.CCR-21-0159
6. Sakae H, Kanzaki H, Nasu J, Akimoto Y, Matsueda K, Yoshioka M, et al. The characteristics and outcomes of small bowel adenocarcinoma: a multicentre retrospective observational study. *Br J Cancer.* (2017) 117:1607–13. doi: 10.1038/bjc.2017.338
7. Dabaja BS, Suki D, Pro B, Bonnen M, Ajani J. Adenocarcinoma of the small bowel: presentation, prognostic factors, and outcome of 217 patients. *Cancer.* (2004) 101:518–26. doi: 10.1002/cncr.20404
8. Halfdanarson TR, McWilliams RR, Donohue JH, Quevedo JF. A single-institution experience with 491 cases of small bowel adenocarcinoma. *Am J Surg.* (2010) 199:797–803. doi: 10.1016/j.amjsurg.2009.05.037
9. Wang S, Yang L, Ci B, Maclean M, Gerber DE, Xiao G, et al. Development and validation of a nomogram prognostic model for SCLC patients. *J Thorac Oncol.* (2018) 13:1338–48. doi: 10.1016/j.jtho.2018.05.037
10. Liao Y, Yin G, Fan X. The positive lymph node ratio predicts survival in T(1-4)N(1-3)M(0) non-small cell lung cancer: a nomogram using the SEER database. *Front Oncol.* (2020) 10:1356. doi: 10.3389/fonc.2020.01356
11. He Y, Zhu Z, Chen Y, Chen F, Wang Y, Ouyang C, et al. Development and validation of a novel diagnostic nomogram to differentiate between intestinal tuberculosis and Crohn's disease: a 6-year prospective multicenter study. *Am J Gastroenterol.* (2019) 114:490–9. doi: 10.14309/ajg.0000000000000064
12. Tanadini-Lang S, Rieber J, Filippi AR, Fode MM, Streblow J, Adebahr S, et al. Nomogram based overall survival prediction in stereotactic body radiotherapy for oligo-metastatic lung disease. *Radiother Oncol.* (2017) 123:182–8. doi: 10.1016/j.radonc.2017.01.003
13. Liang W, He J, Shen Y, Shen J, He Q, Zhang J, et al. Impact of examined lymph node count on precise staging and long-term survival of resected non-small-cell lung cancer: a population study of the US SEER database and a Chinese multi-institutional registry. *J Clin Oncol.* (2017) 35:1162–70. doi: 10.1200/JCO.2016.67.5140
14. Doll KM, Rademaker A, Sosa JA. Practical guide to surgical data sets: surveillance, epidemiology, and end results (SEER) database. *JAMA Surg.* (2018) 153:588–9. doi: 10.1001/jamasurg.2018.0501
15. Abdel-Rahman O. Challenging a dogma: five-year survival does not equal cure in all colorectal cancer patients. *Expert Rev Anticancer Ther.* (2018) 18:187–92. doi: 10.1080/14737140.2018.1409625
16. Moskowitz CS. Using free-response receiver operating characteristic curves to assess the accuracy of machine diagnosis of cancer. *Jama.* (2017) 318:2250–1. doi: 10.1001/jama.2017.18686
17. Harrell FE Jr, Lee KL, Mark DB. Multivariable prognostic models: issues in developing models, evaluating assumptions and adequacy, and measuring and reducing errors. *Stat Med.* (1996) 15:361–87. doi: 10.1002/(SICI)1097-0258(19960229)15:4<361::AID-SIM168>3.0.CO;2-4
18. Zhang Z, Rousson V, Lee WC, Ferdynus C, Chen M, Qian X, et al. Decision curve analysis: a technical note. *Ann Transl Med.* (2018) 6:308. doi: 10.21037/atm.2018.07.02
19. Van Calster B, Wynants L, Verbeek JFM, Verbakel JY, Christodoulou E, Vickers AJ, et al. Reporting and interpreting decision curve analysis: a guide for investigators. *Eur Urol.* (2018) 74:796–804. doi: 10.1016/j.eururo.2018.08.038
20. Aparicio T, Zaanan A, Svrcek M, Laurent-Puig P, Carrere N, Manfredi S, et al. Small bowel adenocarcinoma: epidemiology, risk factors, diagnosis and treatment. *Dig Liver Dis.* (2014) 46:97–104. doi: 10.1016/j.dld.2013.04.013
21. Delaunoit T, Neczyporenko F, Limburg PJ, Erlichman C. Small bowel adenocarcinoma: a rare but aggressive disease. *Clin Colorectal Cancer.* (2004) 4:241–8; discussion 249–51. doi: 10.3816/CCC.2004.n.023

22. Zheng Z, Zhou X, Zhang J, Zhao B, Chen C, Liu X, et al. Nomograms predict survival of patients with small bowel adenocarcinoma: a SEER-based study. *Int J Clin Oncol.* (2021) 26:387–98. doi: 10.1007/s10147-020-01813-8
23. Koo DH, Yun SC, Hong YS Ryu MH, Lee JL, Chang HM, et al. Systemic chemotherapy for treatment of advanced small bowel adenocarcinoma with prognostic factor analysis: retrospective study. *BMC Cancer.* (2011) 11:205. doi: 10.1186/1471-2407-11-205
24. Hong SH, Koh YH, Rho SY, Byun JH, Oh ST, Im KW, et al. Primary adenocarcinoma of the small intestine: presentation, prognostic factors and clinical outcome. *Jpn J Clin Oncol.* (2009) 39:54–61. doi: 10.1093/jjco/hyn122
25. Aparicio T, Henriques J, Manfredi S, Tougeron D, Bouché O, Pezet D, et al. Small bowel adenocarcinoma: results from a nationwide prospective ARCAD-NADEGE cohort study of 347 patients. *Int J Cancer.* (2020) 147:967–77. doi: 10.1002/ijc.32860
26. Huffman BM, Jin Z, Yadav S, Patel S, Nagorney DM, Truty MJ, et al. Novel prognostic factors in resected small bowel adenocarcinoma. *Clin Colorectal Cancer.* (2019) 18:218–25. doi: 10.1016/j.clcc.2019.05.002
27. Li N, Shen W, Deng W, Yang H, Ma Y, Bie L, et al. Clinical features and the efficacy of adjuvant chemotherapy in resectable small bowel adenocarcinoma: a single-center, long-term analysis. *Ann Transl Med.* (2020) 8:949. doi: 10.21037/atm-20-1503
28. Ecker BL, McMillan MT, Datta J, Mamtani R, Giantonio BJ, Dempsey DT, et al. Efficacy of adjuvant chemotherapy for small bowel adenocarcinoma: a propensity score-matched analysis. *Cancer.* (2016) 122:693–701. doi: 10.1002/cncr.29840
29. Aydin D, Sendur MA, Kefeli U, Unal OU, Tastekin D, Akyol M, et al. Evaluation of prognostic factors and adjuvant chemotherapy in patients with small bowel adenocarcinoma who underwent curative resection. *Clin Colorectal Cancer.* (2017) 16:220–7. doi: 10.1016/j.clcc.2016.08.002
30. Tzeng CW, Fiveash JB, Heslin MJ. Radiation therapy for retroperitoneal sarcoma. *Expert Rev Anticancer Ther.* (2006) 6:1251–60. doi: 10.1586/14737140.6.8.1251
31. Wilhelm A, Galata C, Beutner U, Schmied BM, Warschkow R, Steffen T, et al. Duodenal localization is a negative predictor of survival after small bowel adenocarcinoma resection: a population-based, propensity score-matched analysis. *J Surg Oncol.* (2018) 117:397–408. doi: 10.1002/jso.24877
32. Falcone R, Romiti A, Filetti M, Roberto M, Righini R, Botticelli A, et al. Impact of tumor site on the prognosis of small bowel adenocarcinoma. *Tumori.* (2019) 105:524–8. doi: 10.1177/0300891619839297
33. Rompteaux P, Gagnière J, Gornet JM, Coriat R, Baumgaertner I, Lecomte T, et al. Resection of small bowel adenocarcinoma metastases: results of the ARCAD-NADEGE cohort study. *Eur J Surg Oncol.* (2019) 45:331–5. doi: 10.1016/j.ejso.2018.11.012
34. Nishikawa Y, Hoshino N, Horimatsu T, Funakoshi T, Hida K, Sakai Y, et al. Chemotherapy for patients with unresectable or metastatic small bowel adenocarcinoma: a systematic review. *Int J Clin Oncol.* (2020) 25:1441–9. doi: 10.1007/s10147-020-01703-z
35. Legué LM, Bernards N, Lemmens VE, de Hingh IH, Creemers GJ, van Erning FN. Palliative chemotherapy for patients with synchronous metastases of small-bowel adenocarcinoma: a reflection of daily practice. *Unit Eur Gastroenterol J.* (2019) 7:1380–8. doi: 10.1177/2050640619858211
36. Zaanan A, Costes L, Gauthier M, Malka D, Locher C, Mitry E, et al. Chemotherapy of advanced small-bowel adenocarcinoma: a multicenter AGEO study. *Ann Oncol.* (2010) 21:1786–93. doi: 10.1093/annonc/mdq038

Conflict of Interest: The authors declare that the research was conducted in the absence of any commercial or financial relationships that could be construed as a potential conflict of interest.

Publisher's Note: All claims expressed in this article are solely those of the authors and do not necessarily represent those of their affiliated organizations, or those of the publisher, the editors and the reviewers. Any product that may be evaluated in this article, or claim that may be made by its manufacturer, is not guaranteed or endorsed by the publisher.

Copyright © 2021 Gu, Deng, Wang and Li. This is an open-access article distributed under the terms of the Creative Commons Attribution License (CC BY). The use, distribution or reproduction in other forums is permitted, provided the original author(s) and the copyright owner(s) are credited and that the original publication in this journal is cited, in accordance with accepted academic practice. No use, distribution or reproduction is permitted which does not comply with these terms.

frontiers in Medicine

ORIGINAL RESEARCH
published: 23 December 2021
doi: 10.3389/fmed.2021.758977

Higher Lymph Node Metastasis Rate and Poorer Prognosis of Intestinal-Type Gastric Cancer Compared to Diffuse-Type Gastric Cancer in Early-Onset Early-Stage Gastric Cancer: A Retrospective Study

*Chao-Tao Tang and Si-Hai Chen**

Department of Gastroenterology, The First Affiliated Hospital of Nanchang University, Nanchang, China

OPEN ACCESS

Edited by:
Chang-In Choi,
Pusan National University Hospital,
South Korea

Reviewed by:
Yf Gu,
Zhejiang University, China
Shanming Ruan,
Zhejiang Chinese Medical University, China

****Correspondence:***
Si-Hai Chen
chensihai19911011@163.com

Specialty section:
This article was submitted to Gastroenterology, a section of the journal Frontiers in Medicine

Received: *15 August 2021*
Accepted: *24 November 2021*
Published: *23 December 2021*

Citation:
Tang C-T and Chen S-H (2021) Higher Lymph Node Metastasis Rate and Poorer Prognosis of Intestinal-Type Gastric Cancer Compared to Diffuse-Type Gastric Cancer in Early-Onset Early-Stage Gastric Cancer: A Retrospective Study. Front. Med. 8:758977. doi: 10.3389/fmed.2021.758977

Background: The incidence of early-onset gastric cancer (GC) that was diagnosed at <50 years is increasing, but there is a knowledge gap on early-onset early-stage GC (EEGC) that was defined as early-onset GC limited to the mucosa or submucosa. Therefore, we comprehensively analysed the clinical features based on Lauren type.

Methods: Logistic and Cox analyses were used to investigate risk factors for lymph node metastasis (LNM) and prognosis, respectively. Propensity score matching (PSM) was used to adjust confounding factors. Protein mass spectrometry analysis was used to explore the molecular mechanism of LNM.

Result: Our study included 581 patients with EEGC from the Surveillance, Epidemiology, and End Results (SEER) database and 226 patients with EEGC from our own centre. We identified intestinal type, T1b stage, and tumour size (>3 cm) as risk factors for LNM using SEER and our own data. We also found that the prognosis of patients with intestinal-type EEGC was poorer than patients with diffuse-type EEGC, and T1b stage and positive LNM were hazard factors for survival. After analysing the expression of proteins between positive and negative LNM in the intestinal or diffuse type, we found no similar proteins between these groups. The differentially expressed genes (DEGs) in the intestinal type functioned as epithelial cell signalling in *Helicobacter pylori*. The DEGs in the diffuse type functioned in the tricarboxylic acid cycle (TCA cycle) and oxidative phosphorylation.

Conclusion: For EEGC, our study was the first report to demonstrate that the intestinal type was a risk factor for LNM and survival compared to the diffuse type, and the oncogenic expression promoting the occurrence of LNM was different. These findings suggest that clinicians should pay more attention to intestinal-type EEGC than diffuse-type EEGC.

Keywords: lymph node metastasis, Lauren type, survival, early-onset, early gastric cancer

INTRODUCTION

Global cancer statistics reported that gastric cancer (GC) was the fifth most common tumour in incidence in 2020, and is ranked fourth in cancer-related mortality (1). The incidence and mortality of GC steadily declined over the last decade, especially for non-cardia GC. However, a recent notable finding was that the incidence of GC increased in young patients aged ≤50 years (2, 3). Several studies named cases diagnosed at >50 years as early-onset GC (4–6). Lauren classification was proposed in 1965, and it has been widely used in clinical applications. There are two main types, an intestinal type and a diffuse type (7). Intestinal-type GC is characterised by tubular and glandular structures, and diffuse-type GC lacks cell-to-cell interactions (7). Diffuse GC is more likely an inherited GC caused by CDH1 germline mutations that encode E-cadherin protein and mutant p53, and intestinal-type GC is more frequently associated with claudin 6 overexpression (8). The diffuse type correlates with the genomic stable type, and the intestinal type is associated with the chromosomal instability type (5). The intestinal type has a closer relationship with *Helicobacter pylori* (*H.p.)* compared to the diffuse type, which is why the incidence of the intestinal type is diminished and the diffuse type GC is increased (9, 10). The diffuse type is prone to peritoneal metastasis, and the intestinal type has a higher risk of liver metastasis. Therefore, the recurrence patterns are also different between types (11). The prognosis is controversial based on the Lauren classification (8, 12). Early-stage gastric cancer (EGC), which comprises T1 tumours irrespective of lymph node metastasis (LNM), is a special type of cancer. EGC tumours are limited to the mucosa or submucosa, which have accounted for an increasing proportion with the rapid advocation of endoscopy, with a ratio of up to 60% (13). The proportion of early-onset GC is rare, and its features remain a knowledge gap for most clinical doctors and researchers. However, early-onset GC is more aggressive than traditional GC, which has prompted many researchers to focus on this research area (4, 14). Comparisons of the clinical features, prognosis and genomic features between intestinal-type and diffuse-type GC in early-onset early-stage GC (EEGC) were not performed. Therefore, we examined all the above work, and the results elucidate these differences.

Our manuscript included 581 EEGC cases based on the Lauren classification and 226 patients with EEGC from the First Affiliated Hospital of Nanchang University to analyse the differences in LNM, prognosis and genomic expression and found that intestinal-type EEGC had a higher rate of LNM and poorer prognosis. Intestinal-type EEGC and diffuse-type EEGC with LNM had different genomic expressions.

METHODS

Extraction of Patient Data

All patient data were extracted from the SEER database and the First Hospital of Nanchang University. For extracting patient data from the SEER database using National Cancer Institute's SEER*Stat software (version 8.3.6), we designated the following inclusion criteria: (1) patients who were <50 years old and were diagnosed with T1 stage GC on histological examination; (2) patients with detailed records of survival information; (3) patients with concrete information of race, histological grade, examined lymph nodes (LNs), and tumour diameter; and (4) all patients who underwent surgery without chemotherapy before surgery. The following exclusion criteria were used: patients with unknown information about our included clinical features, such as tumour site and N stage; and patients who were not diagnosed with intestinal (M8140, M8211, M8010, and M8144) or diffuse type (M8145, M8490, and M8142) (9) disease. To extract patient data from our centre, we selected patients who were diagnosed from January 2011 to January 2020 to collect the clinical characteristics. The following inclusion criteria were used: (1) patients who were diagnosed with T1 stage GC by pathology and aged <50 years; (2) patients who did not receive preoperative adjuvant therapy; and (3) patients who had Lauren classification information. The exclusion criteria included (1) patients without records of T stage, N stage, and lymphatic invasion and (2) patients with severe diseases, such as cirrhosis, renal failure, and cardiac failure. All our patients were followed up *via* telephone or we-chat, and patients who missed their follow-up were excluded when we analysed the difference in prognosis. The concrete information of patients from the SEER database is listed in **Table 1**, and information on patients extracted from our centre is shown in **Table 2**.

Definition of Variables

The clinical features extracted from the SEER database included sex, race, primary tumour site, pathological grade, N stage, and examined LNs. Some additional features in our patients included *H.p.*, smoking, drinking, invasive depth, family history, and lymphatic invasion. All patients were divided into intestinal-type and diffuse-type EEGC according to the definition. Sex was recorded as male and female. The race was separated into white, black, and other races. Primary sites included cardia, fundus, body, antrum, and overlapping tumours. The pathological grade was divided into four groups: well, moderately, poorly differentiated, and undifferentiated. N stage was recorded as negative (No) and positive (Yes). Tumour size was divided into ≤3 cm and >3 cm according to previous studies (15). Examined LNs were divided into <16 and ≥16 according to certain guidelines (16). Smoking, drinking, family history, and lymphatic invasion were listed as negative (No) and positive (Yes). The main observation features included LNM, overall survival (OS), and cancer-specific survival (CSS).

Protein Mass Spectrometry Analysis

The entire process was completed by Shanghai Luming Biological Technology Co., Ltd. We collected paraffin tissue from 12 patients, including three pairs of intestinal-type EEGC with positive LNM or negative LNM and three pairs of diffuse-type EEGC, which underwent propensity score matching (PSM). All analyses were performed using a fusion mass spectrometer (Thermo, USA) equipped with an Easyspray source (Thermo, USA). All labelled samples were mixed with equal amounts

Abbreviations: EEGC, early-onset early-stage GC; PSM, propensity score matching; DEGs, differentially expressed genes; LNM, lymph node metastasis; H.p, Helicobacter pylori; SEER, Surveillance, Epidemiology, and End Results Program; OS, overall survival; CSS, cancer-specific survival; OR, odd ratio.

TABLE 1 | Basic characteristics of patients diagnosed with gastric cancer (GC) based on Lauren type in T1 stage from January 2010 to January 2015 in the SEER database.

Variables	Total (%)	Intestinal type	Diffuse type	*P* Value
n	581	297	284	
Age				0.0019
20–29	35 (6.02%)	19 (6.40%)	16 (5.63%)	
30–39	135 (23.24%)	51 (17.17%)	84 (29.58%)	
40–45	411 (70.74%)	227 (76.43%)	184 (64.79%)	
Race				0.4387
White	393 (67.64%)	204 (68.69%)	189 (66.55%)	
Black	87 (14.97%)	47 (15.82%)	40 (14.08%)	
Other	101 (17.38%)	46 (15.49%)	55 (19.37%)	
Sex				<0.001
Male	313 (53.87%)	193 (64.98%)	120 (42.25%)	
Female	268 (46.13%)	104 (35.02%)	164 (57.75%)	
Lymph node metastasis				0.0001
No	418 (71.94%)	193 (64.98%)	225 (79.23%)	
Yes	163 (28.06%)	104 (35.02%)	59 (20.77%)	
Tumour site				<0.001
Cardia	140 (24.1%)	112 (37.71%)	28 (9.86%)	
Fundus	21 (3.61%)	9 (3.03%)	12 (4.22%)	
Body	69 (11.88%)	33 (11.11%)	36 (12.68%)	
Antrum	216 (37.18%)	88 (29.63%)	128 (45.07%)	
Overlappping/NOS	146 (25.13%)	66 (22.22%)	80 (28.17%)	
T stage				0.002
T1a	284 (48.88%)	123 (41.41%)	161 (56.69%)	
T1b	297 (51.12%)	174 (58.59%)	123 (43.31%)	
Tumour size				<0.001
≤3cm	17 (2.93%)	17 (5.72%)	0 (0.00%)	
>3cm	564 (92.07%)	280 (94.28%)	284 (100%)	
Examined LNs				0.0017
≤16	493 (84.85%)	266 (89.56%)	227 (79.93%)	
>16	88 (15.15%)	31 (10.44%)	57 (20.07%)	
Cell differentiation				<0.001
Well/moderately differentiated	125 (21.51%)	114 (38.38%)	11 (3.87%)	
Poorly differentiated/undifferentiated	456 (78.49%)	183 (61.62%)	273 (96.13%)	

of tandem mass tag (TMT) reagent. The samples were loaded by a capillary trap column (100 μm × 2 cm, RP-C18, Thermo Fisher) and separated using a capillary analytical column (15 cm × 75 μm, RP-C18, Thermo Fisher) on an EASY-nLCTM 1200 system (Thermo, USA). Full MS scans were acquired in the mass range of 350–1,500 m/z with a mass resolution of 1,20,000, and the AGC target value was set at 4e5. The 10 most intense peaks in MS were fragmented using higher-energy collisional dissociation with a collision energy of 38. MS/MS spectra were obtained with a resolution of 50,000 with an Automatic Gain Control (AGC) target of 5e4 and a maximum injection time of 86 ms. The fusion dynamic exclusion was set for 45 s and was run under positive mode. Spectronaut was used to perform a thorough search of all of the raw data against the sample protein database. A database search was performed with trypsin digestion specificity. Alkylation on cysteine was considered a fixed modification in the database search. The protein, peptide, and PSM false discovery rates (FDRs) were set to 0.01. For Data independent acquisition (DIA) data, the quantification FDR was also set to 0.05.

Statistical Analysis

For basic statistical analysis, all extracted patients were divided into intestinal-type and diffuse-type EEGC according to Lauren classification, and the differences in the included clinical characteristics were compared using Pearson's chi-squared test. Univariate and multivariate logistic regression analyses were used to investigate the potential risk factors associated with LNM, and Cox regression analysis was used for the analysis of prognostic factors. All results are shown as odds ratios (ORs) and hazard ratios (HRs) with 95% CIs. For the imbalance between the two groups, we performed PSM to obtain new data for analysis, and the calliper value was set as 0.02. The effect was balanced when the $P > 0.05$. As

TABLE 2 | Basic information of patients with GC based on Lauren type in T1 stage from our hospital diagnosed from January 2011 to January 2019.

Variables	Total	Intestinal type (IT)	Diffuse type (DT)	Mixed type (MT)	*P* value (IT/DT)
Total	226	101	88	37	
Age (median)	41	41	40	40	
Sex					0.017
Man	104 (46.02%)	57 (56.44%)	34 (38.64%)	13 (35.14%)	
Female	122 (53.98%)	44 (43.56%)	54 (61.36%)	24 (64.86%)	
Paris type					0.182
IIa/IIb	53 (23.45%)	20 (19.80%)	27 (30.68%)	6 (16.22%)	
IIc/III	173 (76.55%)	81 (80.20%)	61 (69.32%)	31 (83.78%)	
Histopatholo-gic type					-
Tubular adenocarcinoma	101 (44.69%)	101 (100%)	0 (0.00%)	0 (0.00%)	-
Signet ring cell carcinoma	26 (11.50%)	0 (0.00%)	26 (29.55%)	0 (0.00%)	-
Low adhesion carcinoma	62 (27.43%)	0 (0.00%)	62 (70.45%)	0 (0.00%)	-
Mixed carcinoma	37 (16.37%)	0 (0.00%)	0 (0.00%)	100 (100%)	
Tumour site					0.279
Fundus	3 (1.33%)	2 (1.98%)	1 (1.14%)	0 (0.00%)	
Body	40 (17.70%)	14 (13.86%)	20 (22.73%)	6 (16.22%)	
Antrum	183 (80.97%)	85 (84.16%)	67 (76.14%)	31 (83.78%)	
Hp Positive					0.745
No	81 (35.84%)	32 (31.68%)	31 (35.23%)	18 (48.65%)	
Yes	55 (24.34%)	25 (24.75%)	24 (27.27%)	6 (16.22%)	
Unknown	90 (39.82%)	44 (43.56%)	33 (37.50%)	13 (35.14%)	
Cell differentiation					<0.001
Poorly differentiated	121 (53.54%)	16 (15.84%)	76 (86.36%)	29 (78.38%)	
Moderately differentiated	92 (40.71%)	82 (81.19%)	5 (5.68%)	5 (13.51%)	
Well differentiated	10 (4.42%)	3 (2.97%)	7 (7.95%)	0 (0.00%)	
Unknown	3 (1.33%)	0 (0.00%)	0 (0.00%)	3 (8.11%)	
Tumour size					0.308
≤3 cm	133 (58.85%)	64 (63.37%)	49 (55.68%)	20 (54.05%)	
>3 cm	93 (41.15%)	37 (36.63%)	39 (44.32%)	17 (45.95%)	
Examined_LNs					0.62
<16	29 (12.83%)	15 (14.85%)	11 (12.5%)	3 (8.11%)	
≥16	197 (87.17%)	86 (85.15%)	77 (87.50%)	34 (91.89%)	
Smoking					0.109
No	166 (73.45%)	68 (67.33%)	69 (78.41%)	29 (78.38%)	
Yes	60 (26.55%)	33 (32.67%)	19 (21.59%)	8 (21.62%)	
Drinking					0.125
No	178 (78.76%)	75 (74.26%)	74 (84.09%)	29 (78.38%)	
Yes	48 (21.24%)	26 (25.74%)	14 (15.91%)	8 (21.62%)	
Depth					0.227
T1a	119 (52.65%)	49 (48.51%)	50 (56.82%)	20 (54.05%)	
T1b	107 (47.35%)	52 (51.49%)	38 (43.18%)	17 (45.95%)	
N stage					0.031
No	177 (78.32%)	73 (72.28%)	75 (85.23%)	29 (78.38%)	
Yes	49 (21.68%)	28 (27.72%)	13 (14.77%)	8 (21.62%)	
N1	31 (13.72%)	18 (17.82%)	9 (10.23%)	4 (10.81%)	
N2	12 (5.31%)	6 (5.94%)	3 (3.41%)	3 (8.11%)	
N3	6 (2.65%)	4 (3.96%)	1 (1.14%)	1 (2.70%)	
Lymphatic invasion				+	0.033
No	202 (89.38%)	88 (87.13%)	83 (94.32%)	30 (81.08%)	
Yes	24 (10.62%)	13 (12.87%)	3 (3.41%)	7 (18.92%)	
Family history					0.65
No	193 (85.40%)	85 (84.16%)	76 (86.36%)	32 (86.49%)	
Yes	33 (14.60%)	16 (15.84%)	12 (13.64%)	5 (13.51%)	

described in our previous study (17), we completed the process in R software and determined the *P*-value using Pearson's chi-squared test. We examined the correlations with LNM between intestinal-type and diffuse-type EEGC using univariate logistic analysis and used univariate Cox regression analysis to assess whether intestinal-type and diffuse-type EEGC had different survival. All statistical analyses were performed using R software, and all associated packages of R software were obtained from the software program's website (https://cran.r-project.org/web/packages/). The student's *t*-test was used for continuous variables with a Gaussian distribution, and the non-parametric Kruskal–Wallis rank-sum test was used for non-normally distributed continuous variables or ordinal categorical variables. The chi-squared test was performed using SPSS (version 24.0). The results were statistically significant when the $P < 0.05$.

RESULTS

Basic Information of Patients From the SEER Database and Our Hospital

According to the flowchart in **Supplementary Figure S1**, we included 581 patients with EEGC, 297 intestinal-type and 284 diffuse-type GC patients. The flowchart in **Supplementary Figure S2** shows that we enrolled 226 patients with EEGC, which included 101 intestinal-type patients, 88 diffuse-type patients, and 37 mixed-type patients who were diagnosed from January 2011 to January 2020. The basic information of patients from the SEER database is listed in **Table 1**, and information on patients from our hospital is shown in **Table 2**. Patients with diffuse-type were younger and more likely to be female than patients with intestinal-type ($P < 0.05$) (**Table 1**). Diffuse-type GC was superior to be poorly

TABLE 3 | Univariate and multivariate logistic regression model for exploring the potential risk factors for lymph node metastasis (LNM) in patients from the SEER database.

Variables	Univariate analysis	*P* Value	Multivariate analysis	*P* Value
Age				
20–29	Reference	-		
30–39	1.25 (0.553–2.827)	0.592		
40–45	0.891 (0.414–1.916)	0.768		
Race				
White	Reference	-		
Black	0.659 (0.379–1.145)	0.139		
Other	0.861 (0.527–1.406)	0.549		
Sex				
Male	Reference	-	Reference	-
Female	0.588 (0.406–0.853)	0.005	0.749 (0.502–1.118)	0.749
Lauren type				
Intestinal type	Reference	-	Reference	-
Diffuse type	0.487 (0.335–0.707)	<0.001	0.375 (0.240–0.586)	<0.001
Tumour site		0.001		0.157
Cardia	Reference	-	Reference	-
Fundus	1.125 (0.445–2.846)	0.084	1.332 (0.501–3.547)	0.566
Body	0.57 (0.304–1.067)	0.079	0.695 (0.359–1.345)	0.28
Anturm	0.398 (0.247–0.639)	<0.001	0.6081 (0.311–1.053)	0.013
Overlappping/NOS	0.495 (0.297–0.825)	0.007	0.354 (0.24–0.586)	0.076
T stage				
T1a	Reference	-	Reference	-
T1b	1.698 (1.212–2.946)	0.034	1.98 (1.352–3.146)	0.014
Tumour size				
≤3 cm	Reference	-	Reference	-
>3 cm	1.711 (1.072–2.733)	0.024	3.62 (1.957–5.633)	<0.001
Examined LNs				
≤16	Reference	-		
>16	0.688 (0.409–0.894)	0.012		
Cell differentiation				
Well/moderately differentiated	Reference	-		
Poorly differentiated/undifferentiated	-	-		

differentiated GC and had more examined LNs ($P < 0.05$). Diffuse-type GC was superior to poorly differentiated GC and had more examined LNs ($P < 0.05$). However, we found that intestinal-type EEGC was more likely positive for LNM (35.02 vs. 20.77%, $P = 0.0001$) and invasive (T1b, 58.59 vs. 43.31%, $P = 0.002$). Our patients with diffuse-type GC were more likely to be female and have poor differentiation ($P < 0.05$) (**Table 2**), and patients with intestinal-type GC tended to have positive LNM (27.72 vs. 14.77%, $P = 0.031$) and lymphatic invasion (12.87 vs. 3.41%, $P = 0.033$). We also found that patients with mixed-type GC had high rates of LNM (21.62%) and lymphatic invasion (18.92%). However, we did not compare mixed-type GC with the other two types due to the limited sample of the type.

Comparison of LNM and Identification of Risk Factors for LNM in Patients With Intestinal-Type and Diffuse-Type EEGC

To investigate the risk factors for LNM, we performed univariate logistic regression analysis. The SEER data (**Table 3**) revealed that advanced T stage (T1b vs. T1a, OR, 1.98, $P = 0.014$) and larger tumour size (>3 cm vs. <3 cm, OR,

TABLE 4 | Univariate and multivariate logistic regression model for exploring the potential risk factors for LNM in patients from our hospital.

Variables	Univariate analysis	*P* Value	Multivariate analysis	*P* Value
Age				
20–39 years	Reference	-		
40–45 years	1.473 (0.722–3.006)	0.287		
Sex				
Man	Reference	-	Reference	-
Female	3.209 (1.496–6.88)	0.003	4.308 (1.702–10.9)	0.002
Paris type				
IIa/IIb	Reference	-		
IIc/III	1.251 (0.528–2.966)	0.611		
Hp Positive				
No	Reference	-		
Yes	0.877 (0.399–1.924)	0.743		
Unknown	0.847 (0.373–1.921)	0.691		
Cell differentiation				
Poorly differentiated	Reference	-		
Moderately/well differentiated	1.001 (0.488–2.055)	0.997		
Unknown	-	-		
Tumour size				
≤3 cm	Reference	-	Reference	-
>3 cm	2.29 (1.135–4.623)	0.021	2.423 (1.038–5.653)	0.041
Examined LNs				
<16	Reference	-		
≥16	1.036 (0.359–2.929)	0.962		
Smoking				
No	Reference	-		
Yes	1.063 (0.808–1.561)	0.052		
Drinking				
No	Reference	-		
Yes	0.391 (0.13–1.177)	0.095		
Depth				
T1a	Reference	-	Reference	-
T1b	2.275 (1.114–4.645)	0.024	2.259 (0.965–5.289)	0.046
Lauren type				
Intestinal type	Reference	-	Reference	-
Diffuse type	0.452 (0.217–0.94)	0.034	0.358 (0.147–0.873)	0.024
Lymphatic invasion				
No	Reference	-	Reference	-
Yes	25.062 (6.743–93.15)	<0.001	24.285 (5.878–100.46)	<0.001
Family history				
No	Reference	-		
Yes	1.552 (0.628–3.834)	0.341		

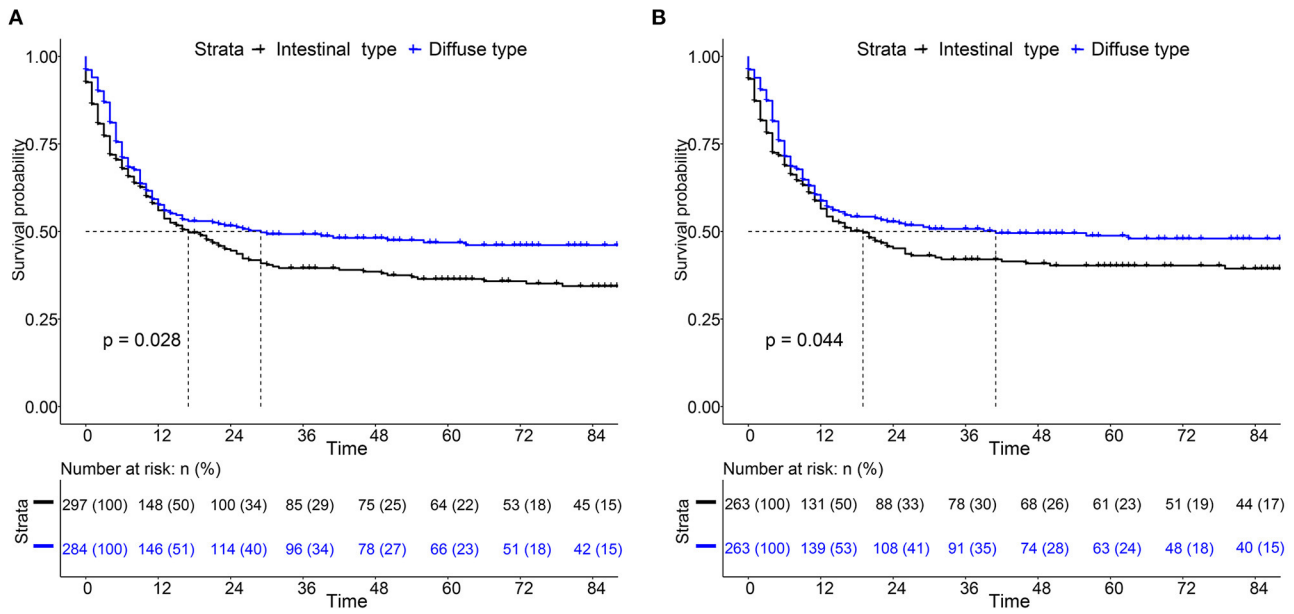

FIGURE 1 | Comparison of survival between intestinal type and diffuse type early-onset early-stage GC (EEGC). **(A,B)** K-M survival curve of overall survival (OS) and cancer-specific survival (CSS) between the two groups, respectively.

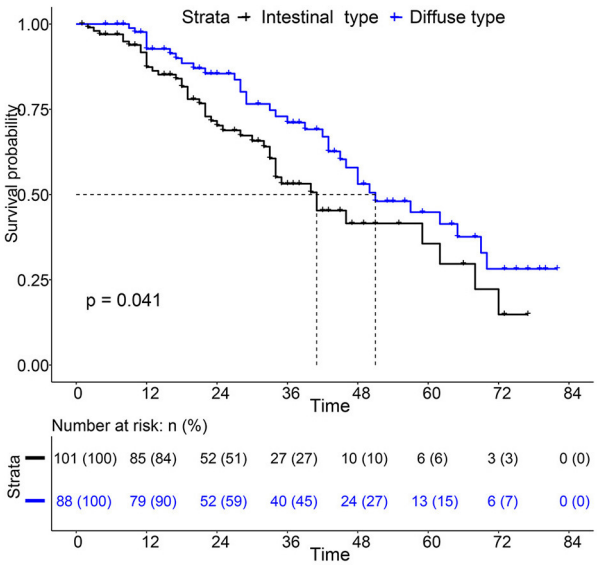

FIGURE 2 | K-M survival curve between Intestinal type and diffuse type EEGC was performed with data from our hospital.

3.62, $P < 0.001$) were risk factors. We found that diffuse-type GC was less likely to cause LNM (OR, 0.375; 95% CI, 0.24–0.586, $P < 0.001$). For our patients (**Table 4**), women tended to have positive LNM (OR, 4.308; 95% CI, 1.701–10.9, $P = 0.002$), larger tumour size, T1b stage, and positive lymphatic invasion (OR, 24.285; 95% CI, 5.878–100.46, $P < 0.001$). We found that diffuse type was a protective factor for LNM (OR, 0.358; 95% CI, 0.147–0.873). To adjust the confounding factors between the diffuse type and intestinal type, we performed PSM by matching 102 intestinal-type with 102 diffuse-type GC to determine whether Lauren type was associated with LNM. We found that the intestinal type was frequently associated with positive LNM (35.02 vs. 20.77%, $P = 0.001$) (**Supplementary Table S1**).

Comparison of Survival and Identification of Risk Factors for Survival Between Patients With Intestinal-Type EEGC and Patients With Diffuse-Type EEGC

For the survival between the two types, we first plotted the Kaplan-Meier curve (K-M curve) survival curve of the SEER data and our data. As shown in **Figure 1**, patients with diffuse-type had a better prognosis of OS and CSS ($P < 0.05$). Our own data also revealed that diffuse type was a protective factor for prognosis ($P < 0.05$) (**Figure 2**). Because some clinical features were not balanced in the SEER data, we performed PSM to eliminate confounding factors that correlated with survival (**Supplementary Table S2**) and found that patients with diffuse-type disease had a better prognosis (**Figure 3**). To explore related hazard factors, we performed univariate and multivariate Cox analyses, which suggested that positive LNM, T1b stage, and intestinal type were independent risk factors for patients with EEGC from the SEER data and our centre (**Table 5** and **Figure 4**).

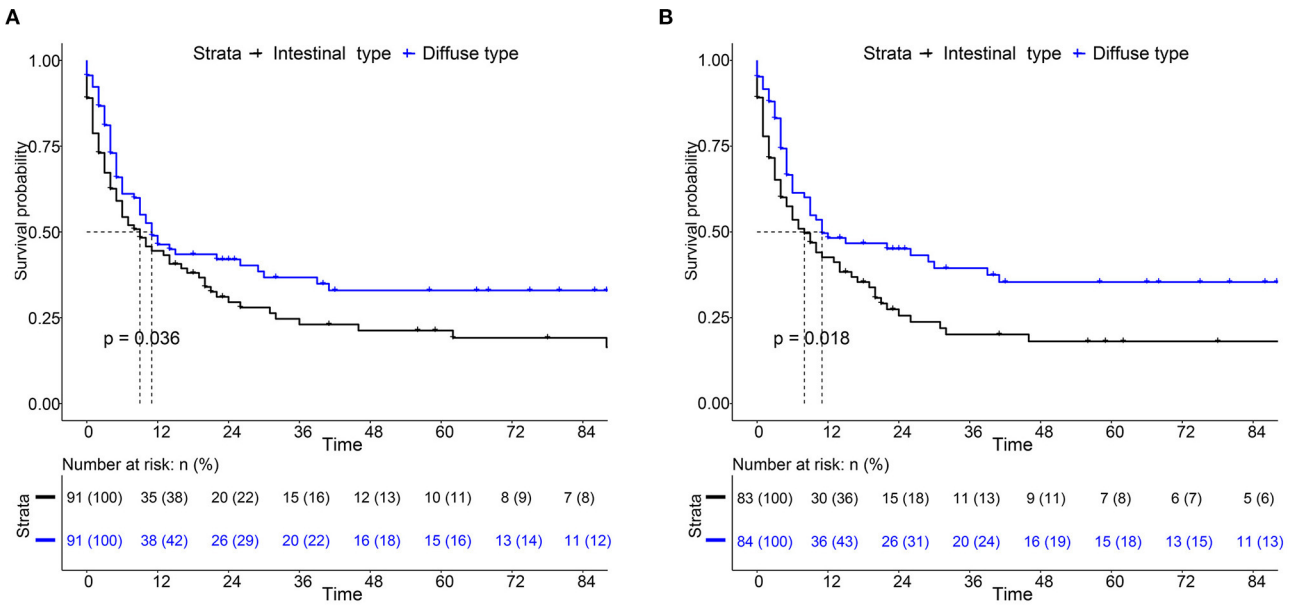

FIGURE 3 | K-M survival curve of OS **(A)** and CSS **(B)** between intestinal type and diffuse type EEGC after propensity score matching (PSM) by SEER data.

Mass Spectrometry Analysis Found Several Special Proteins Associated With LNM Between Intestinal-Type and Diffuse-Type EEGC

Based on the results of our analysis, we considered that intestinal-type EEGC was prone to LNM, but the mechanism was not clear. Therefore, to explore the potential causes, we performed mass spectrometry analysis by extracting proteins from EEGC tissue blocked in wax. Regardless of intestinal-type or diffuse-type EEGC, we matched three patients who had positive LNM with three patients without LNM to exclude the influence of confounding factors. As shown in **Figure 5**, we found upregulated and downregulated genes in the two types of EEGC (**Figures 5A,B**), including 26 upregulated and seven downregulated genes in intestinal-type EEGC with positive LNM, and 46 upregulated and 58 downregulated genes in diffuse-type EEGC with LNM (**Figure 5C**). However, there were no common genes between these groups (**Figure 5D**). Detailed information on differentially expressed genes (DEGs) is shown in heat plots in **Supplementary Figure S3** (intestinal type) and **Supplementary Figure S4** (diffuse type), and the corresponding annotations are shown in **Supplementary Tables S3**,**S4**. For the intestinal type, the seven downregulated genes were UBE2E2, RDH11, IGF2R, ADDGRE5, PLCG2, SIRT2, and CD99, and the upregulated genes included DCTN6, SAE1, RNF185, and PEX19 (**Supplementary Table S3**). The upregulated genes in the diffuse type included FN1, SERPINB6, MUC6, and LAMB3, and the downregulated genes included HIP1R, PANK4, NDUFA2, and ITGA9 (**Supplementary Table S4**). Further GO analysis showed that DEGs in intestinal-type GC were involved in several biological processes, such as autophagy, DNA damage, and receptor signalling pathways, which were primarily plasma membrane, extracellular exosome, and other cellular components (**Figure 6A**). Unlike the intestinal type, the diffuse-type DEGs were primarily involved in mitochondrial ATP synthesis and glyoxylate metabolic processes, which consisted of extracellular exosomes, mitochondria, and other cellular components (**Figure 6B**). Kyoto Encyclopedia of Genes and Genomes (KEGG) pathway analysis found that DEGs in intestinal-type GC functioned in epithelial cell signalling in *H.p.* infection, followed by peroxisome and endocytosis (**Figure 7A**). We found that DEGs in the diffuse type were involved in the citrate cycle (TCA cycle), glycolysis/gluconeogenesis, and oxidative phosphorylation (**Figure 7B**). We constructed a protein-protein interaction network using Cytoscape software (**Figures 7C,D**). As shown in **Figure 7C**, we found that the UBE2E2, HTT, LYN, SIRT2, IGF2R, and SAE1 proteins had many interacting proteins. Unlike the intestinal type, the network was more complicated among DEGs (**Figure 7D**). FN1, ATP5F, and PDHX almost interacted with other DEGs.

DISCUSSION

Nowadays, few studies focused on early-onset GC in the T1 stage. Our study included 581 patients with EEGC from the SEER database and 226 patients with EEGC from our own centre. Both data revealed that intestinal type, T1b stage, and tumour size (>3 cm) were risk factors for LNM and intestinal type, T1b stage and positive LNM were hazard factors for survival. The DEGs in the intestinal type functioned as epithelial cell signalling in *H.p.*, and DEGs in the diffuse type functioned in the TCA cycle and oxidative phosphorylation. To our knowledge, this report is

TABLE 5 | Univariate and multivariate cox regression model for exploring the potential risk factors for patients' overall survival (OS) from SEER database.

Variables	Univariate analysis	*P* Value	Multivariate analysis	*P* Value
Age				
20–29	Reference	-		
30–39	1.441 (0.816–2.546)	0.208		
40–45	1.184 (0.69–2.033)	0.54		
Race				
White	Reference	-		
Black	1.248 (0.929–1.675)	0.141		
Other	0.722 (0.517–1.09)	0.056		
Sex				
Male	Reference	-		
Female	0.893 (0.714–1.118)	0.324		
Lymph node metastasis				
No	Reference	-	Reference	-
Yes	1.949 (1.546–2.456)	<0.001	2.118 (1.522–2.946)	<0.001
Tumour site				
Cardia	Reference	-		
Fundus	1.4 (0.796–2.462)	0.242		
Body	0.924 (0.632–1.352)	0.685		
Anturm	0.611 (0.453–0.825)	0.001		
Overlappping/NOS	1.163 (0.864–1.564)	0.319		
T stage				
T1a	Reference	-	Reference	-
T1b	2.153 (1.56–3.262)	0.022	2.068 (1.468–3.469)	0.035
Tumour size				
≤3 cm	Reference	-	Reference	-
>3 cm	1.667 (1.24–2.241)	0.001	1.708 (1.341–3.41)	<0.001
Lauren type				
Intestinal type	Reference	-	Reference	-
Diffuse type	0.792 (0.633–0.991)	0.041	0.644 (0.498–0.831)	0.001
Examined LNs				
≤16	Reference	-	Reference	-
>16	0.807 (0.624–0.968)	0.021	0.901 (0.821–1.238)	0.051
Cell differentiation				
Well/moderately differentiated	-	-		
Poorly differentiated/undifferentiated	-	-		

the first study to elucidate the differences in clinical features and genomic expression between intestinal- and diffuse-type EEGC.

For the two histological subtypes based on the Lauren type, some studies described the different clinical characteristics. Intestinal-type GC was superior to older patients compared to diffuse-type GC, which is also reported by other studies (9, 18). Some studies found that the incidence of the intestinal type increased faster than the diffuse type, and it was more frequent in male patients (11, 19). Therefore, this result may explain why the ratio of male patients with intestinal-type GC was larger than diffuse-type GC. Consistent with our results that the number of examined LNs was different between intestinal type and diffuse type, Arco et al. also found that the number of examined LNs varied in the Lauren type (20). Other differences in T stage, tumour site, and tumour site between intestinal-type and diffuse-type EEGC were reported in other studies (21). Unlike our previous knowledge that diffuse-type advanced GC was a risk factor for LNM (22–25), we found that intestinal type in EEGC was a risk factor associated with LNM (26). Other studies suggested a comparable rate of LNM between diffuse-type and intestinal-type GC for early-stage GC (21). Several reasons may explain these contradictory results. First, early-onset GC was not like conventional GC. Regardless of genomic mutation or inductive factors, they are distinct diseases (11, 27). Early-onset GC exhibited an E-cadherin-high, cyclooxygenase-2 (COX-2)-low, trefoil factor 1 (TFF1)-expressing phenotype, and COX-2 overexpression and loss of TFF1 were found in conventional cancers (28, 29). Second, diffuse-type and intestinal-type early-onset GC were also different, which may result in different clinical manifestations. For example, diffuse-type GC had a more

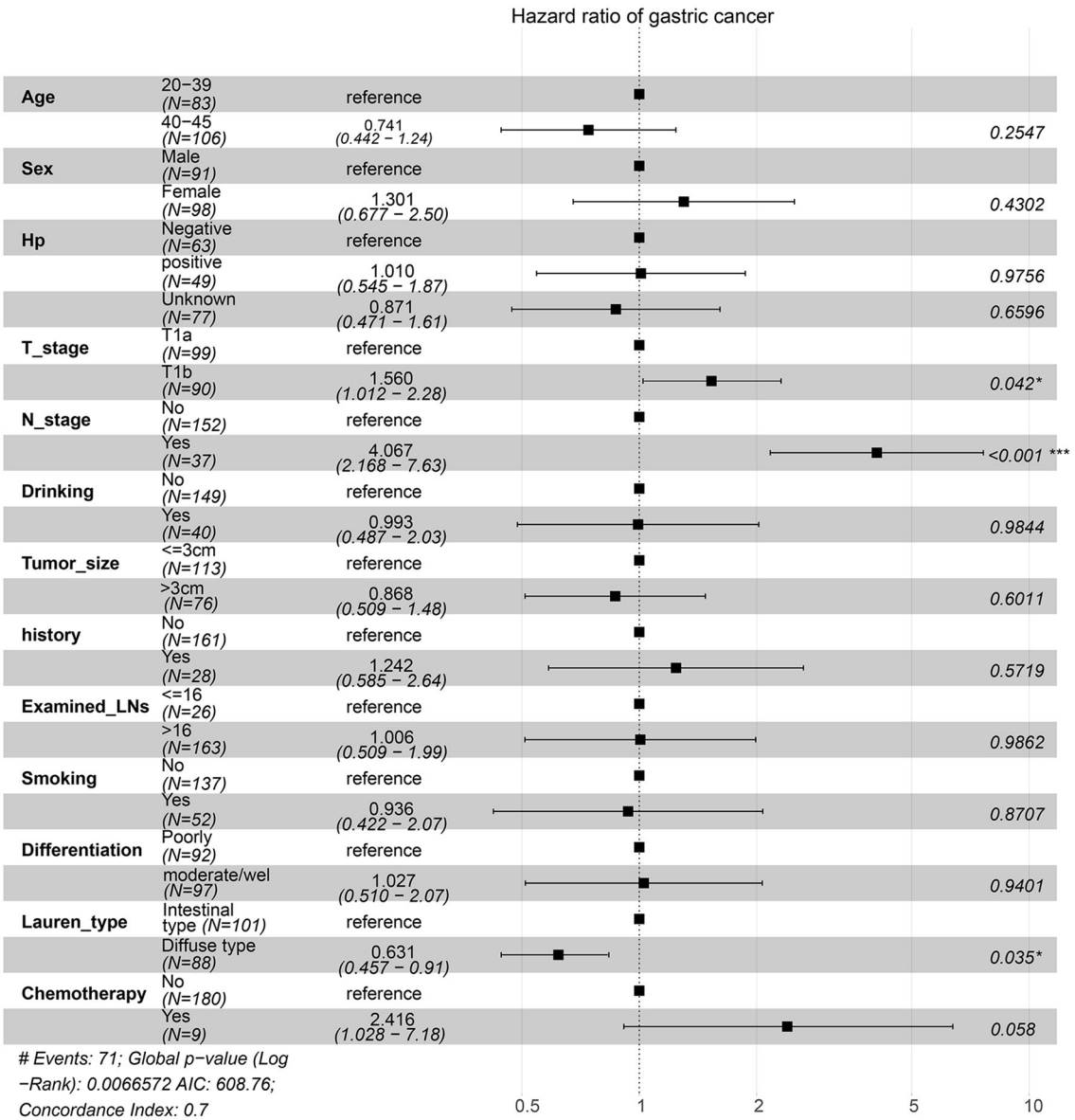

FIGURE 4 | Risk factors associated with survival were identified by multivariate Cox regression analysis using the information of patients from our centre.

germline mutation phenotype in CDH1, and intestinal-type GC was more likely due to *H.p.* infection (29, 30). Other than the Lauren type associated with LNM, in line with our results, some studies also reported submucosal tumour invasion, lympho-vascular invasion, and high-grade tumour differentiation as risk factors for LNM (31, 32).

To determine the association between Lauren classification and survival, we compared the disparity of survival in patients with diffuse-type and intestinal-type EEGC. To the best of our knowledge, this report is the first study to compare their survival. For conventional GC, several studies reported that patients with intestinal-type had better survival than patients with diffuse-type (18, 33), but some studies suggested that diffuse-type early GC was similar or better than intestinal-type GC (21, 34, 35). Our results of the K-M survival curve and Cox regression analysis before or after PSM showed that patients with intestinal-type EEGC had a worse prognosis, which sufficiently supported that intestinal-type EEGC was a risk factor for survival.

For the proteogenomic characterisation of early-onset GC, most studies focused on the diffuse type (36). Diffuse-type GC and intestinal-type GC are heterogeneous diseases with different molecular subtypes. For example, intestinal-type GC had a higher rate of microsatellite-unstable tumours, and diffuse-type GC had more mesenchymal-like types. Different genomic expression levels predicted different prognoses and recurrences

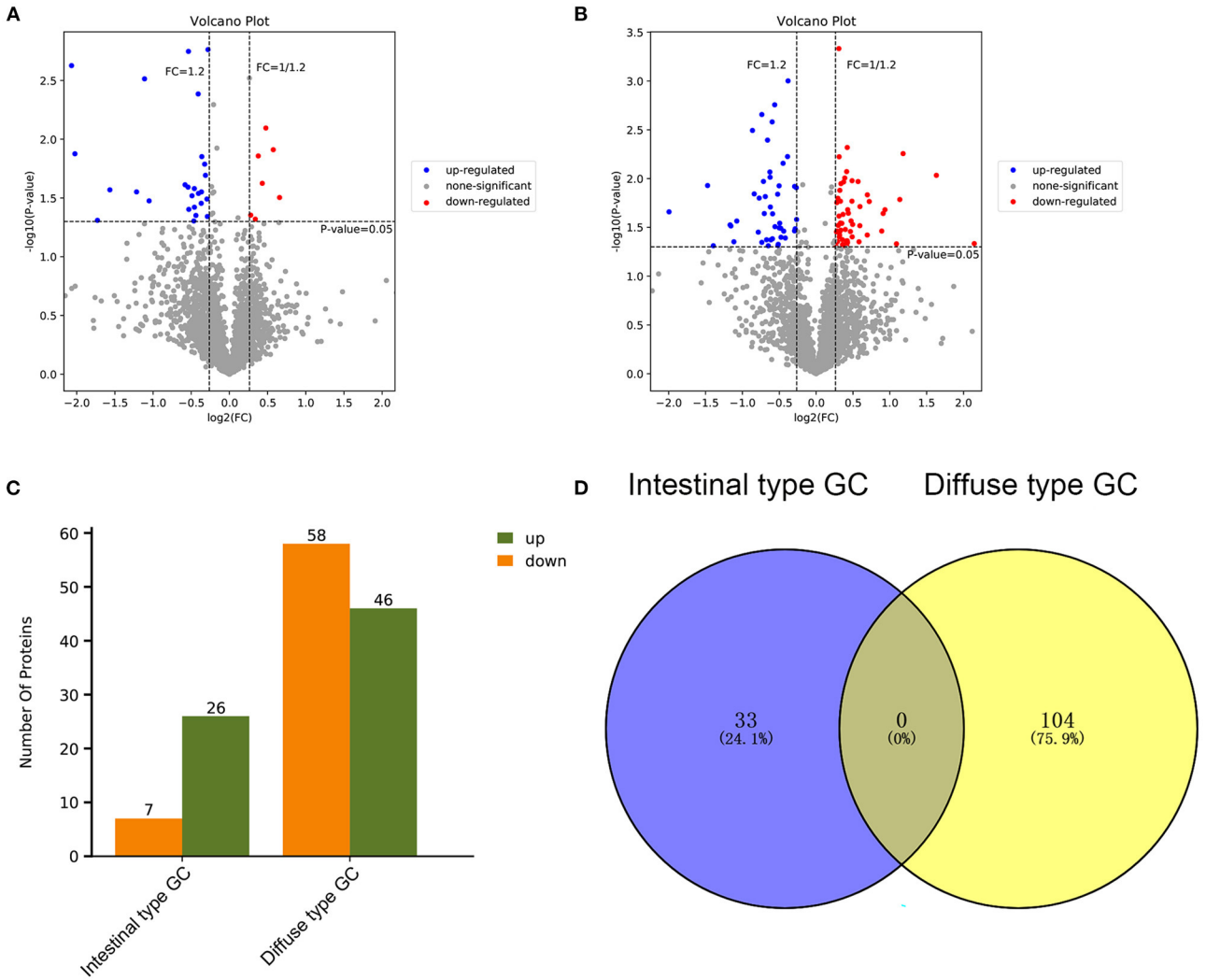

FIGURE 5 | Differentially expressed genes (DEGs) of patients with positive LNM were investigated by performing protein mass spectrometry analysis compared to patients with negative lymph node metastasis (LNM) between intestinal type EEGC and diffuse type EEGC. **(A,B)** The DEGs were shown by volcano plot between intestinal type EEGC **(A)** and diffuse type EEGC **(B)**. **(C)** The histogram was performed to show the total DEGs between the two types. **(D)** Venn plot was performed to assess whether there were common DEGs between the two types.

(36, 37). Mun et al. performed an integrated proteogenomic analysis in young diffuse-type GC and found that many DEGs, such as MUC5B, CDH1, and LAMC1, were associated with phosphorylation or glycosylation, which may activate somatic mutations (38). Consistent with these findings, our results found that DEGs, such as LAMB and MUC6, were involved in the TCA cycle and oxidative phosphorylation. These DEGs were associated with metabolism and tumour invasion. Our study found that DEGs in the intestinal type were highly associated with *H.p.* infection, such as SAE1, RDH11, and RNF185. As indicated in epidemiological studies, *H.p.* infection was an important factor for intestinal-type GC (39). Previous studies showed that DEGs in intestinal-type GC were involved in *H.p.*-induced inflammation, and nuclear factor (NF)-κB signalling and proteins related to nitric oxide synthase or DNA damage promote the development and invasion of intestinal-type GC (39–41). Therefore, our results were similar to a previous study, which suggests that our results are reliable. However, our results were only based on three pairs of GC waxed tissue with negative or positive LNM, which may cause a limited number of DEGs and may be less convincing. To some extent, performing PSM reduces confounding factors and enhances reliability. Therefore, our DEGs between EEGC with negative LNM and EEGC with positive LNM may explain why intestinal-type EEGC had a higher rate of LNM than diffuse-type EEGC.

CONCLUSION

In conclusion, our study was the first report to demonstrate the clinical characteristics between intestinal-type EEGC and diffuse-type EEGC and found that the intestinal type was a

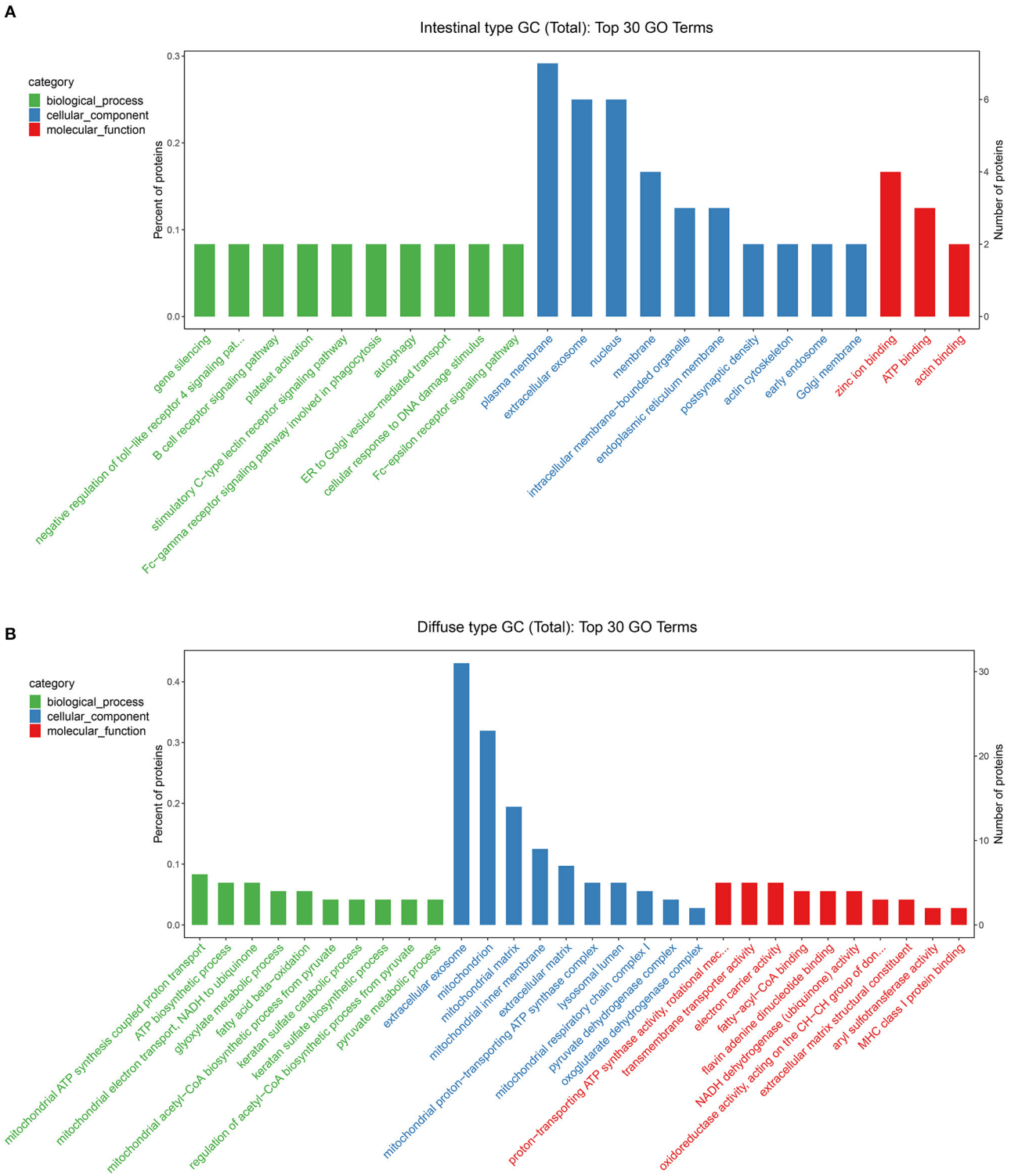

FIGURE 6 | Gene Ontology (GO) analysis was performed to evaluate the biological process, cellular component, and molecular function of DEGs between intestinal type EEGC **(A)** and diffuse type EEGC **(B)**.

risk factor for LNM and survival. The oncogenic expression promoting the occurrence of LNM for the intestinal type was different from the diffuse type, which suggests that the mechanisms of LNM between the intestinal type and the diffuse type are unique. These findings may implicate that clinicians could recommend shorter follow-up intervals or maybe adjuvant

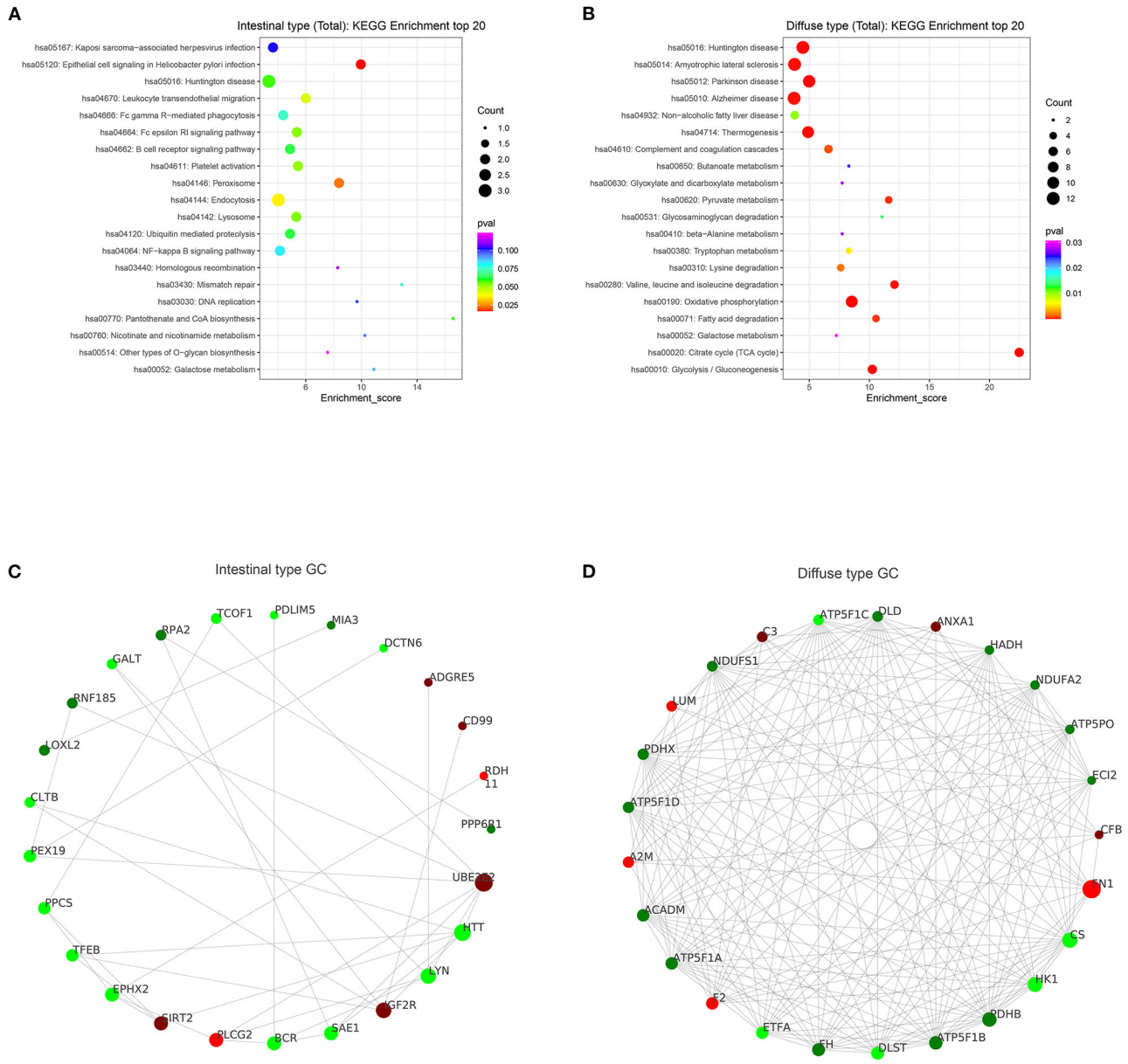

FIGURE 7 | KEGG enrichment and protein interaction were performed according to DEGs. **(A,B)** results of KEGG enrichment between intestinal type EEGC **(A)** and diffuse type EEGC **(B)**. **(C,D)** results of protein-protein interaction between intestinal type EEGC **(C)** and diffuse type EEGC **(D)**.

therapy to intestinal-type EEGC than diffuse-type EEGC because of the higher rate of LNM and poorer rate of survival, however, the interesting findings would deserve being demonstrated by a larger-population study.

DATA AVAILABILITY STATEMENT

The original contributions presented in the study are included in the article/**Supplementary Material**, further inquiries can be directed to the corresponding author/s.

ETHICS STATEMENT

The studies involving human participants were reviewed and approved by First Affiliated Hospital of Nanchang University. The patients/participants provided their written informed consent to participate in this study.

AUTHOR CONTRIBUTIONS

S-HC and C-TT: experiment performing, data analysis, and manuscript writing. S-HC: project development. All authors contributed to the article and approved the submitted version.

FUNDING

Youth cultivation project of the Institute of First Affiliated Hospital of Nanchang University (YFYPY202023).

SUPPLEMENTARY MATERIAL

The Supplementary Material for this article can be found online at: https://www.frontiersin.org/articles/10.3389/fmed.2021.758977/full#supplementary-material

REFERENCES

1. Sung H, Ferlay J, Siegel RL, Laversanne M, Soerjomataram I, Jemal A et al. Global cancer statistics 2020: GLOBOCAN estimates of incidence and mortality worldwide for 36 cancers in 185 countries. *CA Cancer J Clin.* (2021) 71:209–49. doi: 10.3322/caac.21660
2. Arnold M, Park JY, Camargo MC, Lunet N, Forman D, Soerjomataram I. Is gastric cancer becoming a rare disease? A global assessment of predicted incidence trends to 2035. *Gut.* (2020) 69:823–9. doi: 10.1136/gutjnl-2019-320234
3. Heer EV, Harper AS, Sung H, Jemal A, Fidler-Benaoudia MM. Emerging cancer incidence trends in Canada: The growing burden of young adult cancers. *Cancer.* (2020) 126:4553–62. doi: 10.1002/cncr.33050
4. Zhao LY, Hu JK. Early-onset gastric cancer is quite distinct from late-onset gastric cancer. *Surgery.* (2020) 167:883. doi: 10.1016/j.surg.2019.08.018
5. Setia N, Wang CX, Lager A, Maron S, Shroff S, Arndt N, et al. Morphologic and molecular analysis of early-onset gastric cancer. *Cancer.* (2020) 127:103–14. doi: 10.1002/cncr.33213
6. Herrera-Pariente C, Capó-García R, Díaz-Gay M, Carballal S, Muñoz J, Llach J, et al. Identification of new genes involved in germline predisposition to early-onset gastric cancer. *Int J Mol Sci.* (2021) 22: 1310. doi: 10.3390/ijms22031310
7. Lauren P. The two histological main types of gastric carcinoma. Diffuse and so-called intestinal-type carcinoma. An attempt at a histo-clinical classification. *Acta Pathol Microbiol Scand.* (1965) 64:31–49. doi: 10.1111/apm.1965.64.1.31
8. Huang X, Feng Z, Jiang Y, Li J, Xiang Q, Guo S, et al. VSIG4 mediates transcriptional inhibition of Nlrp3 and Il-1β in macrophages. *Sci Adv.* (2019) 5:eaau7426. doi: 10.1126/sciadv.aau7426
9. Tang CT, Zeng L, Yang J, Zeng C, Chen Y. Analysis of the incidence and survival of gastric cancer based on the lauren classification: a large population-based study using SEER. *Front Oncol.* (2020) 10:1212. doi: 10.3389/fonc.2020.01212
10. Correa P. Gastric cancer: overview. *Gastroenterol Clin North Am.* (2013) 42:211–7. doi: 10.1016/j.gtc.2013.01.002
11. Bergquist JR, Leiting JL, Habermann EB, Cleary SP, Kendrick ML, Smoot RL, et al. Early-onset gastric cancer is a distinct disease with worrisome trends and oncogenic features. *Surgery.* (2019) 166:547–55. doi: 10.1016/j.surg.2019.04.036
12. Berlth F, Bollschweiler E, Drebber U, Hoelscher AH, Moenig S. Pathohistological classification systems in gastric cancer: diagnostic relevance and prognostic value. *World J Gastroenterol.* (2014) 20:5679–84. doi: 10.3748/wjg.v20.i19.5679
13. Bertuccio P, Chatenoud L, Levi F, Praud D, Ferlay J, Negri E, et al. Recent patterns in gastric cancer: a global overview. *Int J Cancer.* (2009) 125:666–73. doi: 10.1002/ijc.24290
14. Kolb JM, Leong S, Westbrook LM, Patel SG. Aggressive case of early onset gastric cancer; identifying the knowledge gap. *Gut.* (2020) 70:828–52. doi: 10.1136/gutjnl-2019-320453
15. Yura M, Yoshikawa T, Otsuki S, Yamagata Y, Morita S, Katai H, Nishida T. Is surgery alone sufficient for treating T1 gastric cancer with extensive lymph node metastases? *Gastric Cancer.* (2020) 23:349–55. doi: 10.1007/s10120-019-01006-x
16. Coburn N, Cosby R, Klein L, Knight G, Malthaner R, Mamazza J, et al. Staging and surgical approaches in gastric cancer: a clinical practice guideline. *Curr Oncol.* (2017) 24:324–31. doi: 10.3747/co.24.3736
17. Tang CT, Chen Y, Zeng C. Prognostic analysis of gastric signet ring cell carcinoma and mucinous carcinoma: a propensity score-matched study and competing risk analysis. *Aging (Albany NY).* (2020) 12:22059–77. doi: 10.18632/aging.104048
18. Chen YC, Fang WL, Wang RF, Liu CA, Yang MH, Lo SS, et al. Clinicopathological variation of lauren classification in gastric cancer. *Pathol Oncol Res.* (2016) 22:197–202. doi: 10.1007/s12253-015-9996-6
19. Milne AN, Offerhaus GJ. Early-onset gastric cancer: Learning lessons from the young. *World J Gastrointest Oncol.* (2010) 2:59–64. doi: 10.4251/wjgo.v2.i2.59
20. Díaz Del Arco C, Estrada Muñoz L, Sánchez Pernaute A, Ortega Medina L, García Gómez de. Las Heras S, García Martínez R, et al. Development of a simplified tumor-lymph node ratio classification system for patients with resected gastric cancer: A western study. *Ann Diagn Pathol.* (2021) 50:151677. doi: 10.1016/j.anndiagpath.2020.151677
21. Li ZY, Zhang QW, Teng LM, Zhang CH, Huang Y. Comparable rates of lymph node metastasis and survival between diffuse type and intestinal type early gastric cancer patients: a large population-based study. *Gastrointest Endosc.* (2019) 90:84–95.e10. doi: 10.1016/j.gie.2019.03.002
22. Du J, Shen Y, Yan W, Wang J. Risk factors of lymph node metastasis in the splenic hilum of gastric cancer patients: a meta-analysis. *World J Surg Oncol.* (2020) 18:233. doi: 10.1186/s12957-020-02008-1
23. Chu YN Yu YN, Jing X, Mao T, Chen YQ, Zhou XB, et al. Feasibility of endoscopic treatment and predictors of lymph node metastasis in early gastric cancer. *World J Gastroenterol.* (2019) 25:5344–55. doi: 10.3748/wjg.v25.i35.5344
24. Fang WL, Huang KH, Lan YT, Chen MH, Chao Y, Lo SS, et al. The risk factors of lymph node metastasis in early gastric cancer. *Pathol Oncol Res.* (2015) 21:941–6. doi: 10.1007/s12253-015-9920-0
25. Ronellenfitsch U, Lippert C, Grobholz R, Lang S, Post S, Kähler G, et al. Histology-based prediction of lymph node metastases in early gastric cancer as decision guidance for endoscopic resection. *Oncotarget.* (2016) 7:10676–83. doi: 10.18632/oncotarget.7221
26. Yim K, Jang WM, Lee SH. Modified tumor budding as a better predictor of lymph node metastasis in early gastric cancer: possible real-world applications. *Cancers (Basel).* (2021) 13:3045. doi: 10.3390/cancers13143405
27. Giryes A, Oweira H, Mannhart M, Decker M, Abdel-Rahman O. Exploring the differences between early-onset gastric cancer and traditional-onset gastric cancer. *J Gastrointest Oncol.* (2018) 9:1157–63. doi: 10.21037/jgo.2018.06.11
28. Milne AN, Carvalho R, Morsink FM, Musler AR, de Leng WW, Ristimäki A, et al. Early-onset gastric cancers have a different molecular expression profile than conventional gastric cancers. *Mod Pathol.* (2006) 19:564–72. doi: 10.1038/modpathol.3800563
29. Cho SY, Park JW, Liu Y, Park YS, Kim JH, Yang H, et al. Sporadic early-onset diffuse gastric cancers have high frequency of somatic CDH1 alterations, but low frequency of somatic RHOA mutations compared with late-onset cancers. *Gastroenterology.* (2017) 153:536–49.e526. doi: 10.1053/j.gastro.2017.05.012
30. Tiwari SK, Manoj G, Kumar GV, Sivaram G, Hassan SI, Prabhakar B, et al. Prognostic significance of genotyping Helicobacter pylori infection in patients in younger age groups with gastric cancer. *Postgrad Med J.* (2008) 84:193–7. doi: 10.1136/pgmj.2007.065060
31. Bausys R, Bausys A, Vysniauskaite I, Maneikis K, Klimas D, Luksta M, et al. Risk factors for lymph node metastasis in early gastric cancer patients: Report from Eastern Europe country- Lithuania. *BMC Surg.* (2017) 17:108. doi: 10.1186/s12893-017-0304-0
32. Milhomem LM, Milhomem-Cardoso DM, da Mota OM, Mota ED, Kagan A, Filho JBS. Risk of lymph node metastasis in early gastric cancer and indications for endoscopic resection: is it worth applying the east rules to the west? *Surg Endosc.* (2021) 35:4380–8. doi: 10.1007/s00464-020-07932-7
33. Qiu MZ, Cai MY, Zhang DS, Wang ZQ, Wang DS Li YH, et al. Clinicopathological characteristics and prognostic analysis of Lauren

classification in gastric adenocarcinoma in China. *J Transl Med.* (2013) 11:58. doi: 10.1186/1479-5876-11-58
34. Lee JY, Gong EJ, Chung EJ, Park HW, Bae SE, Kim EH, et al. The characteristics and prognosis of diffuse-type early gastric cancer diagnosed during health check-ups. *Gut Liver.* (2017) 11:807–12. doi: 10.5009/gnl17033
35. Pyo JH, Ahn S, Lee H, Min BH, Lee JH, Shim SG, et al. Clinicopathological features and prognosis of mixed-type T1a gastric cancer based on Lauren's classification. *Ann Surg Oncol.* (2016) 23:784–91. doi: 10.1245/s10434-016-5549-9
36. Kim SK, Kim HJ, Park JL, Heo H, Kim SY, Lee SI, et al. Identification of a molecular signature of prognostic subtypes in diffuse-type gastric cancer. *Gastric Cancer.* (2020) 23:473–82. doi: 10.1007/s10120-019-01029-4
37. Cristescu R, Lee J, Nebozhyn M, Kim KM, Ting JC, Wong SS, et al. Molecular analysis of gastric cancer identifies subtypes associated with distinct clinical outcomes. *Nat Med.* (2015) 21:449–56. doi: 10.1038/nm.3850
38. Mun DG, Bhin J, Kim S, Kim H, Jung JH, Jung Y, et al. Proteogenomic characterization of human early-onset gastric cancer. *Cancer Cell.* (2019) 35:111–24.e110. doi: 10.1016/j.ccell.2018.12.003
39. Pucułek M, Machlowska J, Wierzbicki R, Baj J, Maciejewski R, Sitarz R. Helicobacter pylori associated factors in the development of gastric cancer with special reference to the early-onset subtype. *Oncotarget.* (2018) 9:31146–62. doi: 10.18632/oncotarget.25757
40. Milne AN, Sitarz R, Carvalho R, Carneiro F, Offerhaus GJ. Early onset gastric cancer: on the road to unraveling gastric carcinogenesis. *Curr Mol Med.* (2007) 7:15–28. doi: 10.2174/156652407779940503
41. Kim HS, Kim JW, Hwang IG, Lee HS, Kim WH. Expression of DNA damage response markers in early-onset or familial gastric cancers. *Asian Pac J Cancer Prev.* (2019) 20:1369–76. doi: 10.31557/APJCP.2019.20.5.1369

Conflict of Interest: The authors declare that the research was conducted in the absence of any commercial or financial relationships that could be construed as a potential conflict of interest.

Publisher's Note: All claims expressed in this article are solely those of the authors and do not necessarily represent those of their affiliated organizations, or those of the publisher, the editors and the reviewers. Any product that may be evaluated in this article, or claim that may be made by its manufacturer, is not guaranteed or endorsed by the publisher.

Copyright © 2021 Tang and Chen. This is an open-access article distributed under the terms of the Creative Commons Attribution License (CC BY). The use, distribution or reproduction in other forums is permitted, provided the original author(s) and the copyright owner(s) are credited and that the original publication in this journal is cited, in accordance with accepted academic practice. No use, distribution or reproduction is permitted which does not comply with these terms.

frontiers in Medicine

ORIGINAL RESEARCH
published: 05 January 2022
doi: 10.3389/fmed.2021.767904

Incidence, Risk Factors and Prognosis of T4a Gastric Cancer: A Population-Based Study

Zhiya Hu[1†], *Ziyi Zuo*[2†], *Han Miao*[3], *Zhijie Ning*[4*] and *Youyuan Deng*[5*]

[1] Department of Pharmacy, The Third Hospital of Changsha, Changsha, China, [2] The First Clinical College, Wenzhou Medical University, Wenzhou, China, [3] Department of Clinical Medicine, Dalian University, Dalian, China, [4] Department of Neurology, Fengcheng Hospital, Shanghai, China, [5] Department of General Surgery, Xiangtan Central Hospital, Xiangtan, China

OPEN ACCESS

Edited by:
Chang-In Choi,
Pusan National University Hospital,
South Korea

Reviewed by:
Kaibo Guo,
Zhejiang Chinese Medical University, China
Leonardo Frazzoni,
University of Bologna, Italy

***Correspondence:**
Zhijie Ning
ningzj17@163.com
Youyuan Deng
dengyouyuan@smail.hunnu.edu.cn

[†]These authors have contributed equally to this work and share first authorship

Specialty section:
This article was submitted to Gastroenterology, a section of the journal Frontiers in Medicine

Received: 31 August 2021
Accepted: 24 November 2021
Published: 05 January 2022

Citation:
Hu Z, Zuo Z, Miao H, Ning Z and Deng Y (2022) Incidence, Risk Factors and Prognosis of T4a Gastric Cancer: A Population-Based Study. Front. Med. 8:767904. doi: 10.3389/fmed.2021.767904

Background: T4a gastric cancer (GC) is a subtype of advanced GC (AGC), which urgently needs a comprehensive grade method for better treatment strategy choosing. The purpose of this study was to develop two nomograms for predicting the prognosis of patients with T4a GC.

Methods: A total of 1,129 patients diagnosed as T4a GC between 2010 and 2015 were extracted from the Surveillance, Epidemiology, and End Result (SEER) program database. Univariate and multivariate Cox analyses were performed to explore the independent predictors and to establish nomogram for overall survival (OS) of the patients, whereas competing risk analyses were performed to find the independent predictors and to establish nomogram for cancer-specific survival (CSS) of the patients. The area under the curve (AUC), calibration curve, decision curve analysis (DCA), and Kaplan–Meier analysis were performed to evaluate the nomograms.

Results: Older age, larger tumor size, black race, signet ring cell carcinoma (SRCC), more lymph node involvement, the absence of surgery, the absence of radiotherapy, and the absence of chemotherapy were identified as independent prognostic factors for both OS and CSS. In the training cohort, the AUCs of the OS nomogram were 0.760, 0.743, and 0.723 for 1-, 3-, and 5-year OS, whereas the AUCs of the CSS nomogram were 0.724, 0.703, and 0.713 for 1-, 3-, and 5-year CSS, respectively. The calibration curve and DCA indicated that both nomograms can effectively predict OS and CSS, respectively. The abovementioned results were also confirmed in the validation cohort. Stratification of the patients into high- and low-risk groups highlighted the differences in prognosis between the two groups both in training and in validation cohorts.

Conclusions: Age, tumor size, race, histologic type, N stage, surgery status, radiotherapy, and chemotherapy were confirmed as independent prognostic factors for both OS and CSS in patients with T4a GC. Two nomograms based on the abovementioned variables were constructed to provide more accurate individual survival predictions for them.

Keywords: nomogram, T4a gastric cancer, prognosis, overall survival, cancer-specific survival, SEER

INTRODUCTION

Gastric cancer (GC) is the fifth malignancy and ranks third in cancer-related mortality worldwide (1). Advanced gastric cancer (AGC) is a common type of GC with a poor prognosis, and the 5-year survival rate is <20% (2, 3). Even if radical resection, the 5-year survival rate is only 30–50% (4). Currently, neoadjuvant therapy and radical resection combined with chemotherapy have been systematically used for patients with AGC (5). However, due to the high risk of distant metastasis, the survival of these patients was still unsatisfactory.

As an important branch of patients with AGC, patients with T4a GC have their unique characteristics. According to the 8th version of the TNM staging system of the American Joint Committee on Cancer (AJCC), T4a GC was defined as the tumor perforating serosa (6). Owing to the presence of incurable factors including distant lymph node involvement, peritoneal metastasis, and hematogenous metastasis, the outcomes of traditional treatments varied distinctly in this group of patients (7, 8). Further, with the complexity of the prognosis and its influencing factors, there are still challenges in assessing the prognosis precisely and individually. Therefore, an effective grading and stratification system of T4a GC is of great importance for treatment choosing prior to operation to have a higher chance of curative resection and reduce postoperative morbidity and mortality (9). However, for T4a GC, the relevant study is still lacking.

The nomogram is a practical tool in medical practice, which could pictorially represent a multivariable model. Recently, nomograms mostly concentrate on the patients of early-stage or under single treatment, and they mostly adequate for prognosis predicting intraoperatively or postoperatively (10–16). However, there still few nomograms integrating all the relevant clinicopathologic characters for patients with T4a GC. In this study, based on the Surveillance, Epidemiology, and End Result (SEER) program database, we aimed to identify the prognostic factors of patients with T4a GC and develop nomograms to predict overall survival (OS) and cancer-specific survival (CSS).

MATERIALS AND METHODS

Patients

All patients with first primary GC between 2010 and 2015 with SEER Stat 3.6.1 were included. The SEER database is publicly available without any personal information. The inclusion criteria were as follows: (1) first primary T4a GC and (2) follow up greater than or equal to 1 month. Meanwhile, patients without clear baseline information, tumor characteristics, and treatment data were excluded. Patients who meet the abovementioned criteria were randomly divided into the training set (70%) and the validation set (30%). In this study, the nomograms were constructed based on the training set and were validated by the validation set.

Variables

The variables utilized in this study were age at diagnosis, sex, race, histologic type, tumor size, tumor grade, N stage, marriage status, insurance status, surgery, radiotherapy, and chemotherapy. Age and tumor size were transferred into categorical variables, and the cutoff values were calculated by X-tile software (17). In this study, age and tumor size were divided into low, medium, and high levels. N stage was described as N0, N1, N2, and N3. Tumor grade was classified as well differentiated (I), moderately differentiated (II), poorly differentiated (III), and undifferentiated anaplastic (IV). In this study, OS and CSS were considered as outcomes. The OS was defined as the time interval from the date of primary diagnosis to the date of death caused by any cause, and the CSS was defined as the time interval from the date of primary diagnosis to the date of GC-specific death.

Statistical Analysis

The univariate and multivariate Cox analyses were performed to explore the independent prognostic factors and establish the nomogram for predicting the OS of patients with T4a GC, whereas competing risk analyses were performed to find the independent predictors and to establish nomogram for CSS of the patients. Besides, the time-dependent receiver operating characteristic (ROC) curve for the nomograms was established, and the area under the curve (AUC) was calculated to show the discrimination of the nomograms. Calibration curves were established to compare the probability between nomogram-predicted and observed outcomes, and the decision curve analysis (DCA) was used to explore the clinical utilization of the nomograms. Further, we categorized the patients into high- and low-risk groups according to their median risk score, survival analysis was performed to probe the difference in prognosis between the two groups using the Kaplan–Meier method, and the log-rank test was performed. Moreover, two nomograms were verified with the validation cohort. In this study, all statistical analyses were performed with SPSS 25.0 and R software (version 3.6.1), and a $p < 0.05$ (two-tailed) was considered statistically significant.

RESULTS

Baseline Patient Demographics

In our study, to explore the difference in clinicopathological factors between patients with T4a and other GC, all the clinicopathological data of patients with GC were extracted and comparison showed a distinct difference between patients with T4a and other GC in all the variables included in this study (**Table 1**). Besides, a total of 1,129 patients with T4a GC were included and were randomly divided into the training cohort ($n = 793$) and the validation cohort ($n = 336$). The baseline demographics and clinicopathologic characteristics are listed in **Table 2**. The optimal cutoff value of tumor size and age at diagnosis were calculated separately for OS and CSS. Tumor size was divided into ≤31 mm, 32–90 mm, and ≥91 mm based on OS, and the same grouping was also concluded based on CSS. Moreover, the optimal cutoff value of age at diagnosis was identified as 65 and 80 years based on OS status and CSS.

TABLE 1 | Clinical characteristics between patients with T4a and non-T4a GC.

Variables		T4a GC *n* = 1,446 (%)	Non-T4a GC *n* = 8,292 (%)	*p*
Age [mean (SD)]		64.69 (14.18)	66.16 (13.15)	**<0.001**
Race				**<0.001**
	White	901 (62.31)	5,713 (68.9)	
	Black	192 (13.28)	1,014 (12.23)	
	Other	353 (24.41)	1,565 (18.87)	
Sex				**<0.001**
	Female	632 (43.71)	2,775 (33.47)	
	Male	814 (56.29)	5,517 (66.53)	
Histologic type				**<0.001**
	Adenocarcinoma	974 (67.36)	6,750 (81.4)	
	Mucinous adenocarcinoma	52 (3.6)	184 (2.22)	
	Signet ring cell carcinoma	420 (29.05)	1,358 (16.38)	
Tumor size				**<0.001**
	Low	247 (17.08)	3,391 (40.89)	
	Middle	973 (67.29)	4,348 (52.44)	
	High	226 (15.63)	553 (6.67)	
Grade				**<0.001**
	I	14 (0.97)	552 (6.66)	
	II	235 (16.25)	2,672 (32.22)	
	III	1,161 (80.29)	4,915 (59.27)	
	IV	36 (2.49)	153 (1.85)	
AJCC stage				**<0.001**
	I	0 (0)	2,455 (29.61)	
	II	174 (12.03)	2,000 (24.12)	
	III	955 (66.04)	2,430 (29.31)	
	IV	317 (21.92)	1,407 (16.97)	
N				**<0.001**
	N0	244 (16.87)	3,815 (46.01)	
	N1	284 (19.64)	2,385 (28.76)	
	N2	300 (20.75)	1,116 (13.46)	
	N3	618 (42.74)	976 (11.77)	
M				**<0.001**
	M0	1,129 (78.08)	6,885 (83.03)	
	M1	317 (21.92)	1,407 (16.97)	
Insurance				**0.017**
	No	60 (4.15)	246 (2.97)	
	Yes	1,386 (95.85)	8,046 (97.03)	
Marriage				**0.009**
	No	588 (40.66)	3,071 (37.04)	
	Yes	858 (59.34)	5,221 (62.96)	

Bold values indicate the corresponding variable have statistical significance (P < 0.05).

Identification of Prognosis Factors

The results of the univariate analysis for predicting OS of patients with T4a GC in the training cohort are shown in **Table 3**; the significant OS-related variables were age, race, tumor size, N stage, grade, histologic type, marriage status, surgery, radiotherapy, and chemotherapy. These factors were further included in the multivariate Cox analysis. Finally, age, tumor size, race, N stage, surgery status, radiotherapy, and chemotherapy were identified as independent prognostic factors for OS in patients with T4a GC. Moreover, to facilitate the clinical utilities of the model, we added the variable of histological type into the final model for its biological plausibility. In addition, the same analyses were reperformed in the whole cohort, and we concluded the same conclusions as mentioned above (**Supplementary Table 1**).

For identifying prognostic factors related to CSS of patients with T4a GC, multivariate competing risk model analyses were performed, and age, tumor size, race, N stage, surgery

TABLE 2 | Baseline information of 1,129 patients T4aN0-3M0 gastric cancer.

		Whole cohort (n = 1,129)	Training cohort (n = 793)	Validation cohort (n = 336)
Age		65.65 ± 14.01	65.34 ± 14.01	66.37 ± 14.02
Race				
	Black	154 (13.64%)	113 (14.25%)	41 (12.20%)
	White	694 (61.47%)	482 (60.78%)	212 (63.10%)
	Other	281 (24.89%)	198 (24.97%)	83 (24.70%)
Sex				
	Female	500 (44.29%)	345 (43.51%)	155 (46.13%)
	Male	629 (55.71%)	448 (56.49%)	181 (53.87%)
Histologic type				
	Adenocarcinoma	754 (66.78%)	537 (67.72%)	217 (64.58%)
	Mucinous adenocarcinoma	34 (3.01%)	24 (3.03%)	10 (2.98%)
	Signet ring cell carcinoma	341 (30.20%)	232 (29.26%)	109 (32.44%)
Tumor size		62.43 ± 43.50	63.09 ± 46.54	60.88 ± 35.34
Grade				
	I	12 (1.06%)	9 (1.13%)	3 (0.89%)
	II	173 (15.32%)	126 (15.89%)	47 (13.99%)
	III	920 (81.49%)	641 (80.83%)	279 (83.04%)
	IV	24 (2.13%)	17 (2.14%)	7 (2.08%)
N stage				
	N0	196 (17.36%)	137 (17.28%)	59 (17.56%)
	N1	219 (19.40%)	161 (20.30%)	58 (17.26%)
	N2	246 (21.79%)	170 (21.44%)	76 (22.62%)
	N3	468 (41.45%)	325 (40.98%)	143 (42.56%)
Surgery performed		1,076 (95.31%)	748 (94.33%)	328 (97.62%)
Radiotherapy performed		466 (41.28%)	321 (40.48%)	145 (43.15%)
Chemotherapy performed		751 (66.52%)	518 (65.32%)	233 (69.35%)
Insurance		1,089 (96.46%)	762 (96.09%)	327 (97.32%)
Married		664 (58.81%)	464 (58.51%)	200 (59.52%)

status, radiotherapy, and chemotherapy were identified as independent prognostic factors for CSS in patients with T4a GC (**Table 4**). Moreover, to facilitate the clinical utilities of the model, we added the variable of histological type into the model for its biological plausibility. In addition, the same analyses were reperformed in the whole cohort, and we concluded the same conclusions as mentioned above (**Supplementary Table 2**).

Construction of Nomograms

Based on the multivariate Cox analysis and multivariate competing risk model, two nomograms to predict 1-, 3-, and 5-year OS and CSS that integrated the abovementioned independent factors were conducted (**Figures 1**, **2**). As for these two nomograms, we can obtain the corresponding survival probability of each patient by adding up all points that correspond to each predictor. The ROC curve demonstrated the discrimination of the nomograms. The AUCs of the nomogram for predicting 1-, 3-, and 5-year OS were 0.760, 0.743, and 0.723, respectively (**Figures 3A–C**). The AUCs of the nomogram that predicting 1-, 3-, and 5-year CSS were 0.724, 0.703, and 0.713, respectively (**Figures 4A–C**). The calibration curves of OS (**Figures 5A–C**) and CSS (**Figures 6A–C**) showed optimal predictive accuracy. Moreover, DCA of 1-, 3-, and 5-year OS (**Figures 5D–F**) and CSS (**Figures 6D–F**) showed that the nomograms had a higher net benefit in the training cohort which indicated a favorable clinical utilization.

Validation of the Nomograms

To estimate the performance of the nomograms, external validation was performed, and the results demonstrated that the nomograms also have favorable outcomes in the validation cohort. The AUCs of the nomogram for predicting 1-, 3-, and 5-year OS were 0.729, 0.711, and 0.772, respectively (**Figures 3D–F**). The AUCs of the nomogram that predicting 1-, 3-, and 5-year CSS were 0.699, 0.712, and 0.753, respectively (**Figures 4D–F**). The calibration curves for the OS (**Figures 7A–C**) and CSS (**Figures 8A–C**) probabilities further validated the nomograms. Moreover, DCA of 1-, 3-, and 5-year OS (**Figures 7D–F**) and CSS (**Figures 8D–F**) also confirmed that the nomograms have favorable clinical utilization in the validation cohort.

TABLE 3 | Univariate and multivariate Cox analyses for the OS of patients with T4aN0-3M0 GC in the training cohort.

		Univariate Cox			Multivariate Cox		
		HR	**95% CI**	***p-value***	**HR**	**95%CI**	***p*-value**
Age							
	Low			Reference			
	Middle	**1.311**	**1.085–1.583**	**0.005**	**1.332**	**1.098–1.615**	**0.004**
	High	**1.896**	**1.508–2.382**	**0.000**	**1.561**	**1.216–2.005**	**0.000**
Race							
	White			Reference			
	Black	0.981	0.767–1.254	0.876	1.101	0.855–1.416	0.456
	Other	**0.760**	**0.617–0.936**	**0.010**	**0.702**	**0.568–0.867**	**0.001**
Sex (male)		1.026	0.866–1.216	0.765			
Histologic type							
	Adenocarcinoma			Reference			
	Mucinous adenocarcinoma	0.833	0.479–1.449	0.518	0.815	0.465–1.426	0.473
	Signet ring cell carcinoma	**1.251**	**1.044–1.498**	**0.015**	1.162	0.958–1.409	0.127
Size							
	Low			Reference			
	Middle	**1.323**	**1.043–1.678**	**0.021**	1.130	0.883–1.447	0.332
	High	**2.064**	**1.543–2.762**	**0.000**	**1.625**	**1.195–2.209**	**0.002**
Grade							
	I			Reference			
	II	1.200	0.483–2.981	0.694	0.818	0.326–2.051	0.669
	III	1.986	0.822–4.801	0.128	1.353	0.552–3.318	0.509
	IV	**3.126**	**1.134–8.619**	**0.028**	1.882	0.672–5.274	0.229
N stage							
	N0			Reference			
	N1	1.241	0.926–1.662	0.148	**1.360**	**1.008–1.836**	**0.044**
	N2	1.220	0.911–1.633	0.182	**1.461**	**1.082–1.972**	**0.013**
	N3	**1.880**	**1.460–2.421**	**0.000**	**2.035**	**1.550–2.670**	**0.000**
Surgery performed		**0.398**	**0.292–0.543**	**0.000**	**0.294**	**0.212–0.407**	**0.000**
Radiotherapy performed		**0.609**	**0.511–0.726**	**0.000**	**0.750**	**0.611–0.920**	**0.006**
Chemotherapy performed		**0.551**	**0.464–0.655**	**0.000**	**0.591**	**0.476–0.733**	**0.000**
Insurance (yes)		0.820	0.540–1.245	0.351			
Married (yes)		**0.815**	**0.688–0.966**	**0.019**	0.961	0.803–1.150	0.664

Bold values indicate the corresponding variable have statistical significance (P < 0.05).

Risk Stratification for Patients With T4a GC

As mentioned above, for patients with T4a GC, risk stratification is of great importance in downgrading the GC prior to resection, thus improving the treatment management and the chance of curative resection. Therefore, we further stratified the patient into high- and low-risk groups based on the median risk score. Kaplan–Meier survival analysis showed favorable OS and CSS in the low-risk group compared with the high-risk group (**Figures 9A,B**). In the validation cohort, a favorable prognosis was also observed in the low-risk group for both OS and CSS (**Figures 9C,D**).

Comparison Between the Novel Nomograms and AJCC Stage System

To further estimate the performance and clinical value of the nomograms in this study, we further compared the nomograms with AJCC stage system in the whole study cohort using ROC curve analysis, and results show that the nomograms also have favorable outcomes compared with AJCC stage system. The AUCs of the nomogram for predicting 1-, 3-, and 5-year OS were 0.757, 0.729, and 0.746, respectively (**Figure 10A**), whereas the AUCs of AJCC stage system were 0.584, 0.613, and 0.641, respectively (**Figure 10B**). The AUCs of the nomogram for predicting 1-, 3-, and 5-year CSS were 0.717, 0.706, and 0.723, respectively (**Figure 10C**), whereas the AUCs of AJCC stage system were 0.585, 0.620, and 0.647 (**Figure 10D**), separately.

DISCUSSION

In this study, older age, larger tumor size, black race, signet ring cell carcinoma (SRCC), more lymph node involvement, the absence of surgery, the absence of radiotherapy, and the

TABLE 4 | Multivariate competing risk model analysis of CSS for each variable in T4aN0-3M0 patients with T4aN0-3M0 GC in the training cohort.

		HR	95% CI	*p*
Age				
	Low		Reference	
	Middle	1.126	0.917–1.382	0.260
	High	**1.330**	**1.001–1.767**	**0.049**
Race				
	White		Reference	
	Black	0.995	0.758–1.305	0.970
	Other	**0.676**	**0.541–0.845**	**0.001**
Sex (male)		1.078	0.894–1.300	0.430
Histologic type				
	Adenocarcinoma		Reference	
	Mucinous adenocarcinoma	0.705	0.371–1.341	0.290
	Signet ring cell carcinoma	1.191	0.968–1.466	0.099
Size				
	Low		Reference	
	Middle	1.136	0.889–1.451	0.310
	High	**1.582**	**1.151–2.173**	**0.005**
Grade				
	I		Reference	
	II	0.932	0.343–2.527	0.890
	III	1.471	0.556–3.893	0.440
	IV	2.475	0.857–7.149	0.094
N stage				
	N0		Reference	
	N1	1.360	0.980–1.889	0.066
	N2	**1.561**	**1.134–2.148**	**0.006**
	N3	**1.972**	**1.472–2.642**	**0.000**
Surgery performed		**0.341**	**0.230–0.504**	**0.000**
Radiotherapy performed		**0.699**	**0.571–0.856**	**0.001**
Chemotherapy performed		**0.667**	**0.530–0.839**	**0.001**
Insurance (yes)		0.798	0.494–1.289	0.360
Married (yes)		0.933	0.764–1.139	0.490

Bold values indicate the corresponding variable have statistical significance (P < 0.05).

absence of chemotherapy were found to be negatively associated with both OS and CSS in patients with T4a GC. Based on that, two nomograms for predicting the 1-, 3-, and 5-year OS and CSS of patients with T4a GC were constructed and validated. Discrimination, calibration, and clinical utilization analysis further confirmed that the nomograms we constructed were of favorable effectiveness and accuracy. The proposed nomograms also showed favorable ability to categorize patients with T4a GC into high- and low-risk groups with significant differences in OS and CSS.

As described before, owing to the presence of incurable factors such as distant lymph node involvement, peritoneal metastasis, and hematogenous metastasis, patients with T4a GC always suffered from distinctly different outcomes of traditional treatments (7, 8). In this study, we compared the clinicopathological factors and also other factors between patients with T4a and other GC and found T4a GC always accompanied with larger tumor size, more severe tumor grade, more lymph node invasion, and distant metastasis, which may lead to a worse clinical outcome. Moreover, with the complexity of the prognosis and its influencing factors, there are still challenges in assessing the prognosis precisely and individually. Therefore, this study paved a new way in assessing the patients' potential risk under different clinicopathological backgrounds and different medical procedures. Based on the validations and the comparison between models that widely used, we hope that the novel nomograms could better assist the clinical practice.

To date, there are many nomograms for GC, and they have shown clinical utilization from different aspects. In the postoperative perspective, the nomogram from Memorial Sloan-Kettering Cancer Center (MSKCC) was conducted to predict the survival probability of patients with GC after an R0 resection (14). From the intraoperative perspective, the PMN stage system was introduced recently to make a better treatment decision for patients with AGC (13). In addition to these studies, there also have different nomograms that integrated biomarkers (10)

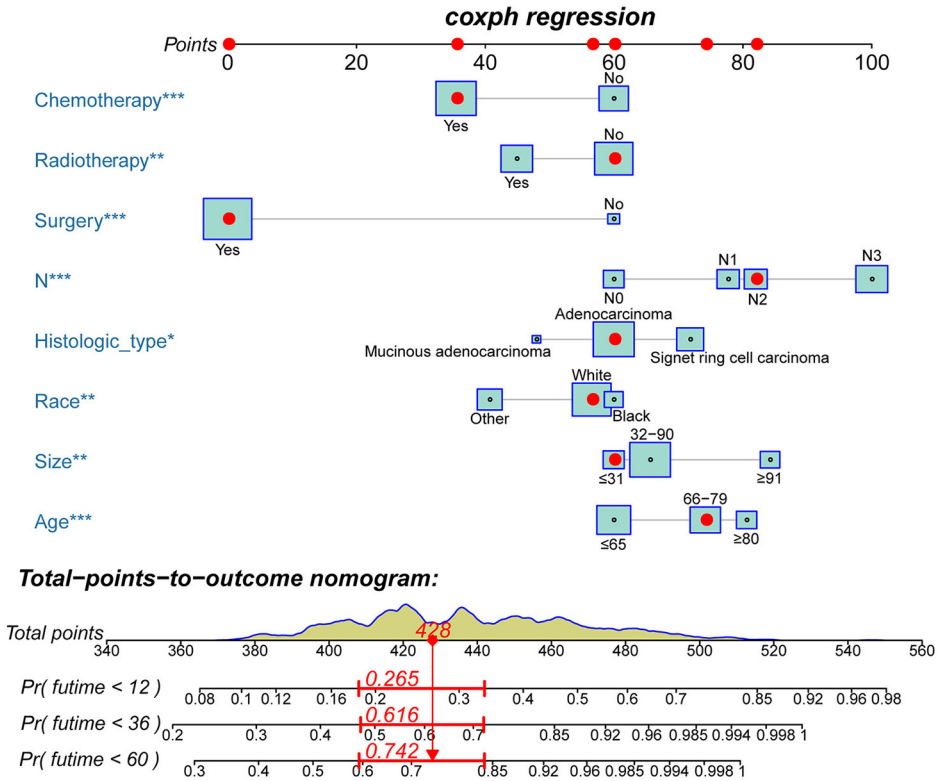

FIGURE 1 | The novel nomogram to predict 1-, 3-, and 5-year OS of patients with T4a GC.

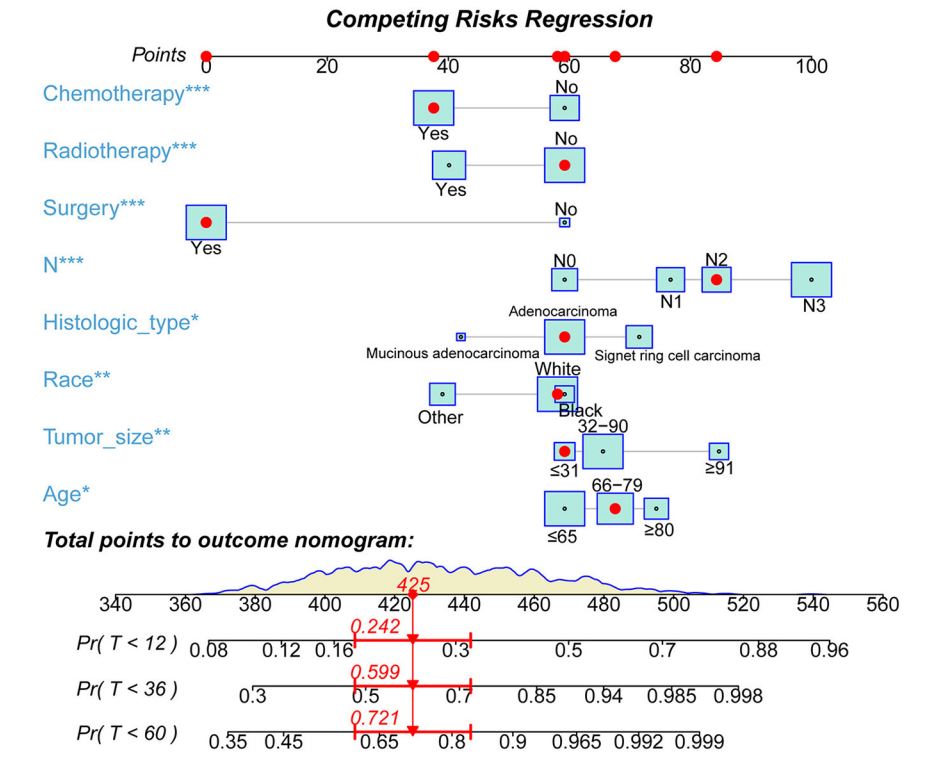

FIGURE 2 | The novel nomogram to predict 1-, 3-, and 5-year CSS of patients with T4a GC.

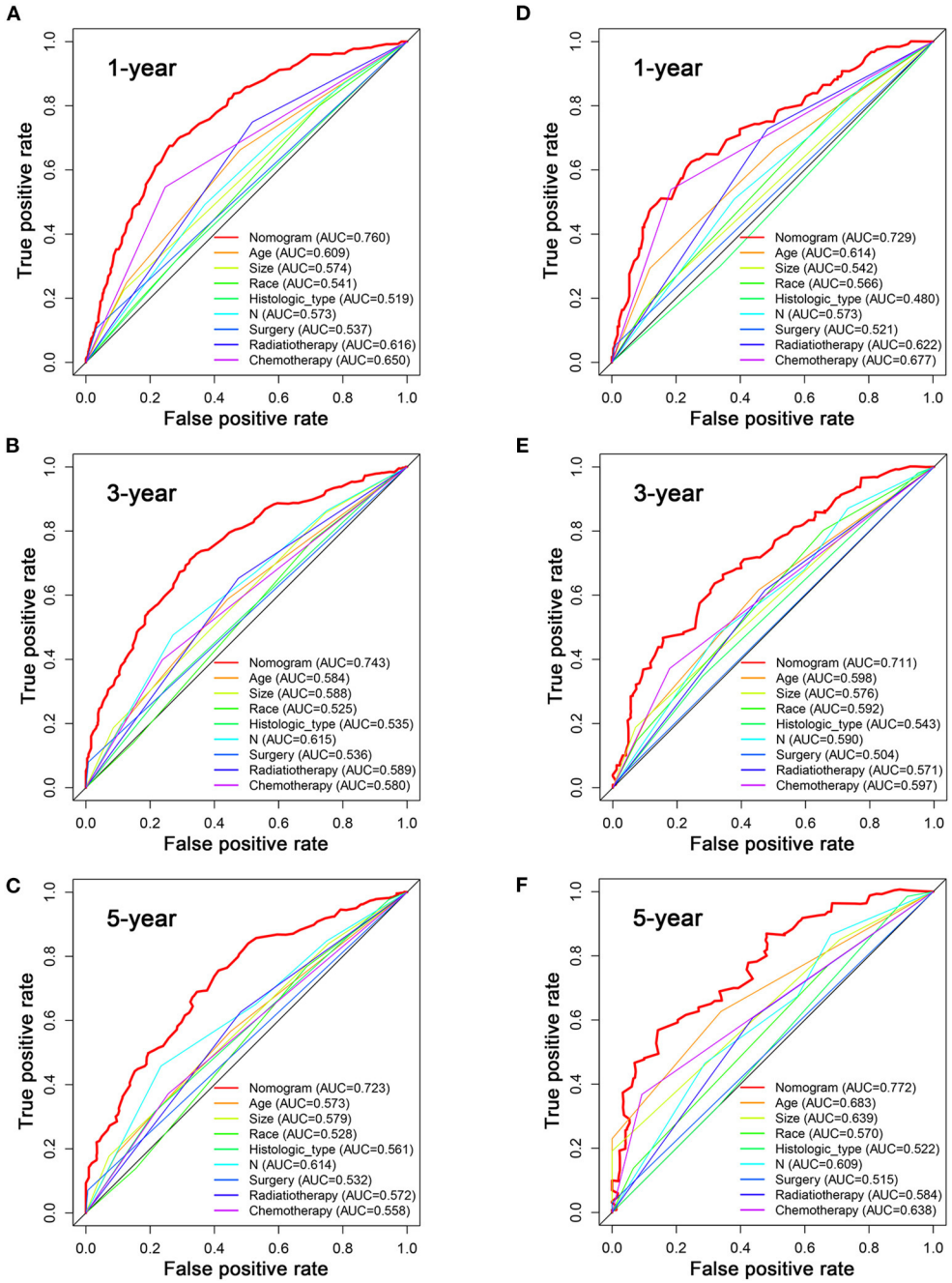

FIGURE 3 | The ROC curves for predicting patients' OS of nomogram and all independent predictors at 1 **(A)**, 3 **(B)**, and 5 years **(C)** in the training cohort and at 1 **(D)**, 3 **(E)**, and 5 years **(F)** in the validation cohort.

and other clinical characters (11). Recently, collagen nomograms have provided a new direction to evaluate the recurrence and metastasis of GC (18); moreover, with the continuous progress of radiomics, nomograms based on radiomics signatures also paved a new way for the diagnosis and evaluation of GC (12).

Compared with the abovementioned studies, our nomograms have several improvements. First, most of the studies were focused on the survival status of whole patients with GC or AGC (10–16, 18). Instead, we went a step further and focused on T4a GC in the subdivided perspective. Owing to the complexity of the prognosis and its influencing factors, a precision stratification is crucial to apply individual and also neoadjuvant therapies to downgrade the GC prior to surgery thus enhancing the opportunity for a curative resection (9) and maximize the benefits of patients. So, we integrated various prognostic factors that appeared in the previous studies to

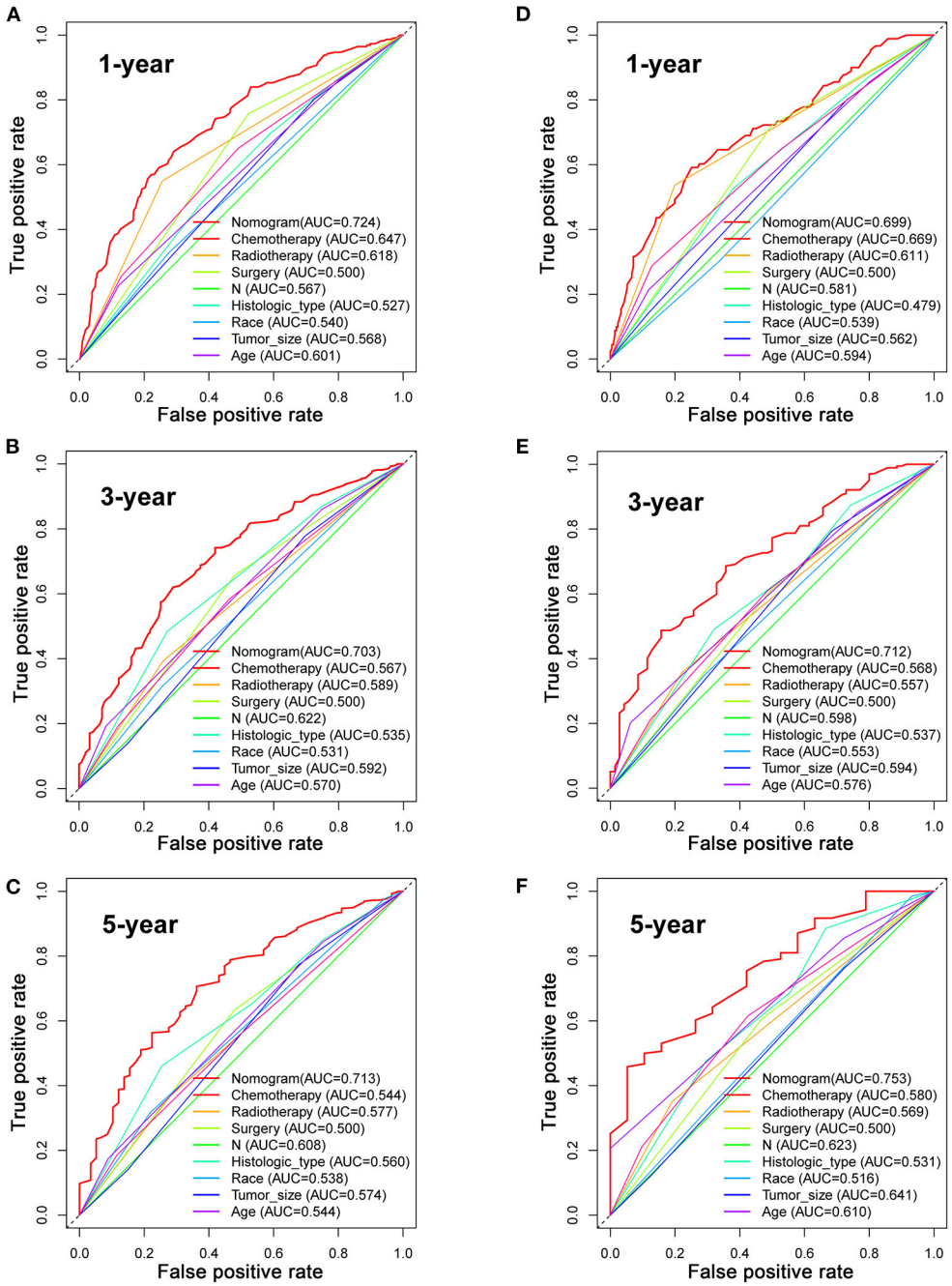

FIGURE 4 | The ROC curves for predicting patients' CSS of nomogram and all independent predictors at 1 **(A)**, 3 **(B)**, and 5 years **(C)** in the training cohort and at 1 **(D)**, 3 **(E)**, and 5 years **(F)** in the validation cohort.

construct a more comprehensive prognosis model for patients with T4a GC, which also meets the requirements of precision medicine. Second, most of the studies were based on a single-centered database with a limited number of patients. Compared with this, we extracted 1,129 patients from the SEER database and performed a large cohort population-based study. Third, we further stratified patients with T4a GC into high- and low-risk groups based on the median risk score, which step closer to the clinical practice and provided a detailed stratification method for a better treatment decision of surgeons. Finally, in the construction and validation of the nomograms, ROC curves, calibration curves, and DCA analysis were used to estimate the performance of the nomograms, such a comprehensive analysis is also an important improvement in our research.

In our study, surgery, radiotherapy, and chemotherapy were associated with a better prognosis. Radical resection is still an

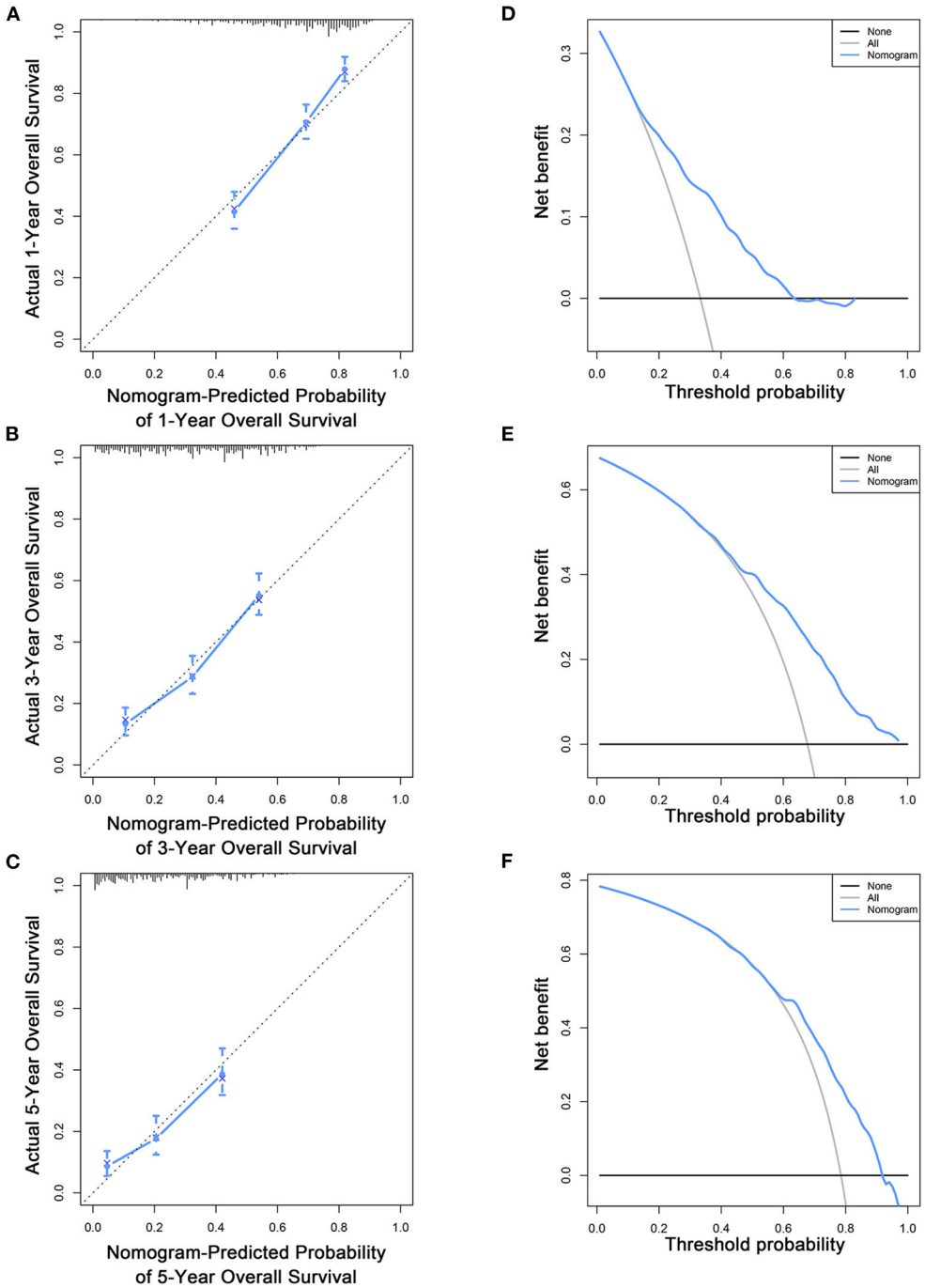

FIGURE 5 | Calibration curves **(A–C)** and DCA **(D–F)** of the nomogram for predicting patients' OS at 1, 3, and 5 years in the training cohort.

important method for the treatment of GC, but there were also studies with opposite views. According to the research of Martin et al. (19), for patients with T4 GC, resection of two or more adjacent organs for achieving R0 resection will increase the risk of postoperative morbidity and mortality, but that does not contradict our conclusion. In the research of Li et al. (9), patients who underwent R0 resection have a higher survival rate than that of R1/2 without radical resection, and most of the postoperative morbidities were mild complications that only need short-term medical intervention, so radical treatment including resection of multiple adjacent organs is still recommended. Since patients with GC with peritoneal invasion still inevitably face the risk of metastasis and recurrence after resection, Dikken et al. (20) found that

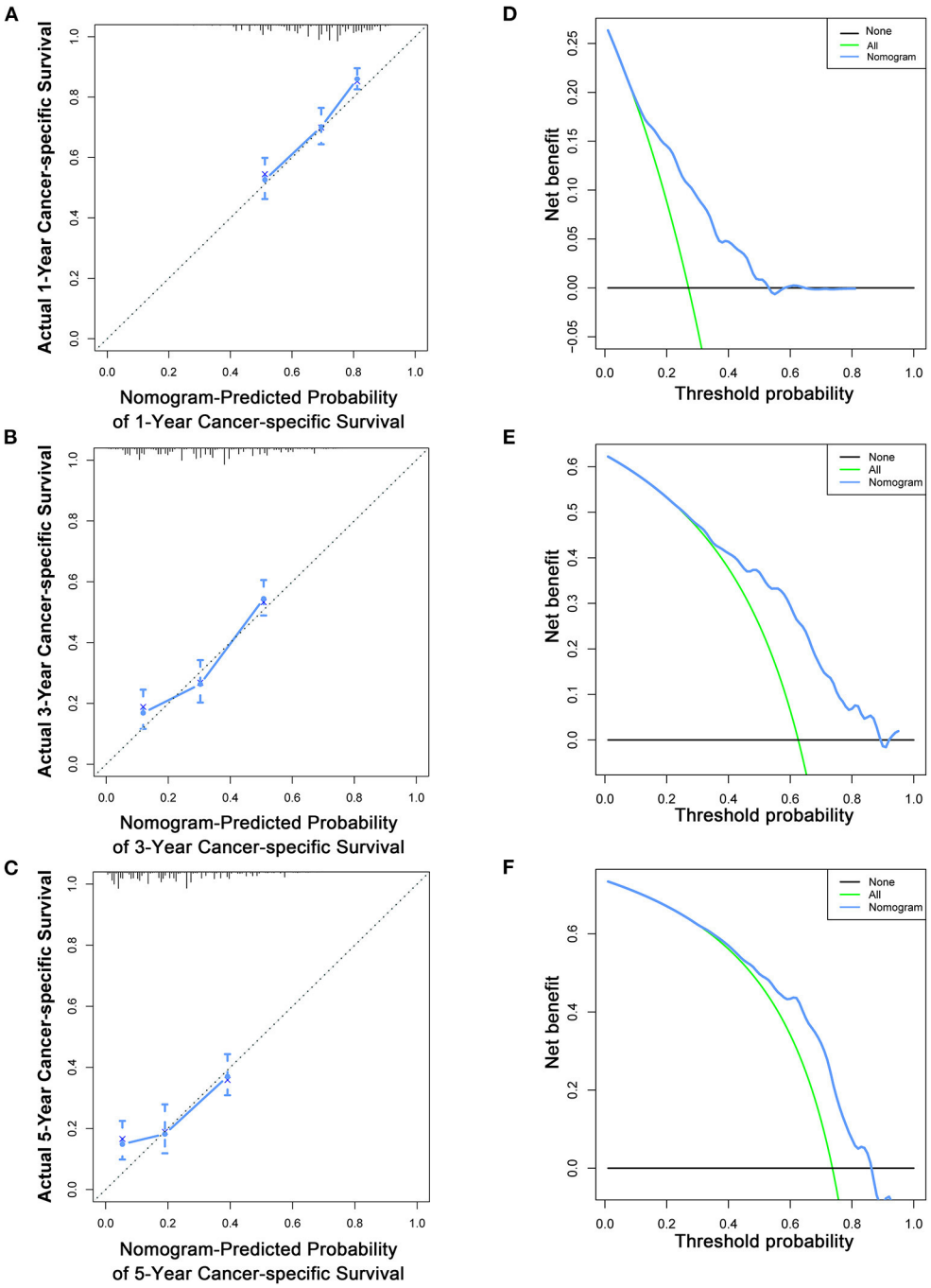

FIGURE 6 | Calibration curves **(A–C)** and DCA **(D–F)** of the nomogram for predicting patients' CSS at 1, 3, and 5 years in the training cohort.

after D1 surgery, the addition of chemoradiotherapy had a major impact on reducing recurrence. The same conclusion was also introduced by Ozden et al. (21). In the recent years, the concept of adjuvant therapy has gradually entered the scene. Theoretically, if chemotherapy can reduce the size of GC tissue thus achieving the purpose of downgrading, the possibility of complete resection will be promoted, and the micrometastasis will also be eliminated to a certain extent. Yoshikawa et al. (22) also demonstrated that preoperative adjuvant chemotherapy may have a potential role in promoting the survival of patients with T3/T4 GC. In conclusion, for T4a GC, radical resection combined with multimodality therapy may be an effective means to improve the survival rate, but effective treatment strategies are still controversial.

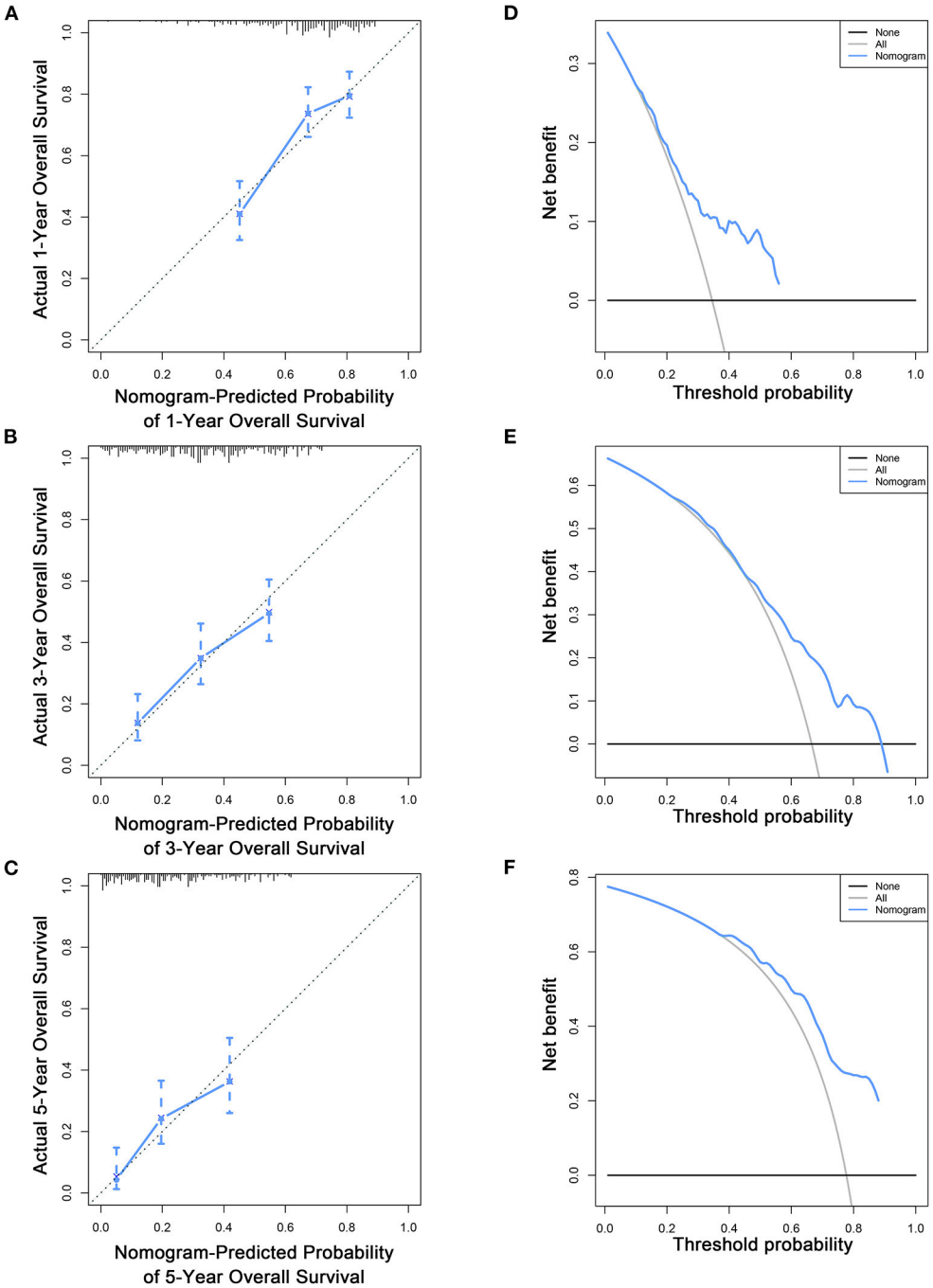

FIGURE 7 | Calibration curves **(A–C)** and DCA **(D–F)** of the nomogram for predicting patients' OS at 1, 3, and 5 years in the validation cohort.

It is still controversial that whether tumor size should be an important prognostic factor. Lee et al. (23) found that the size of the tumor had little correlation with survival or recurrence in patients with node-negative AGC, compared with those who emphasized the prognostic value of tumor size (24, 25). In addition, Lee et al. suggested that the confounding of GC types with significantly different prognosis may lead to their conclusion. Despite that, Deng et al. (26) have demonstrated that tumor size could enhance the survival discriminations in patients with T4a GC. Theoretically, a larger tumor size might relate to a higher biologic malignancy, for patients with T4a GC; peritoneal metastasis contributed greatly to the postoperative mortality (27), which might explain the reason why tumor size showed favorable utilization in the prognosis prediction of

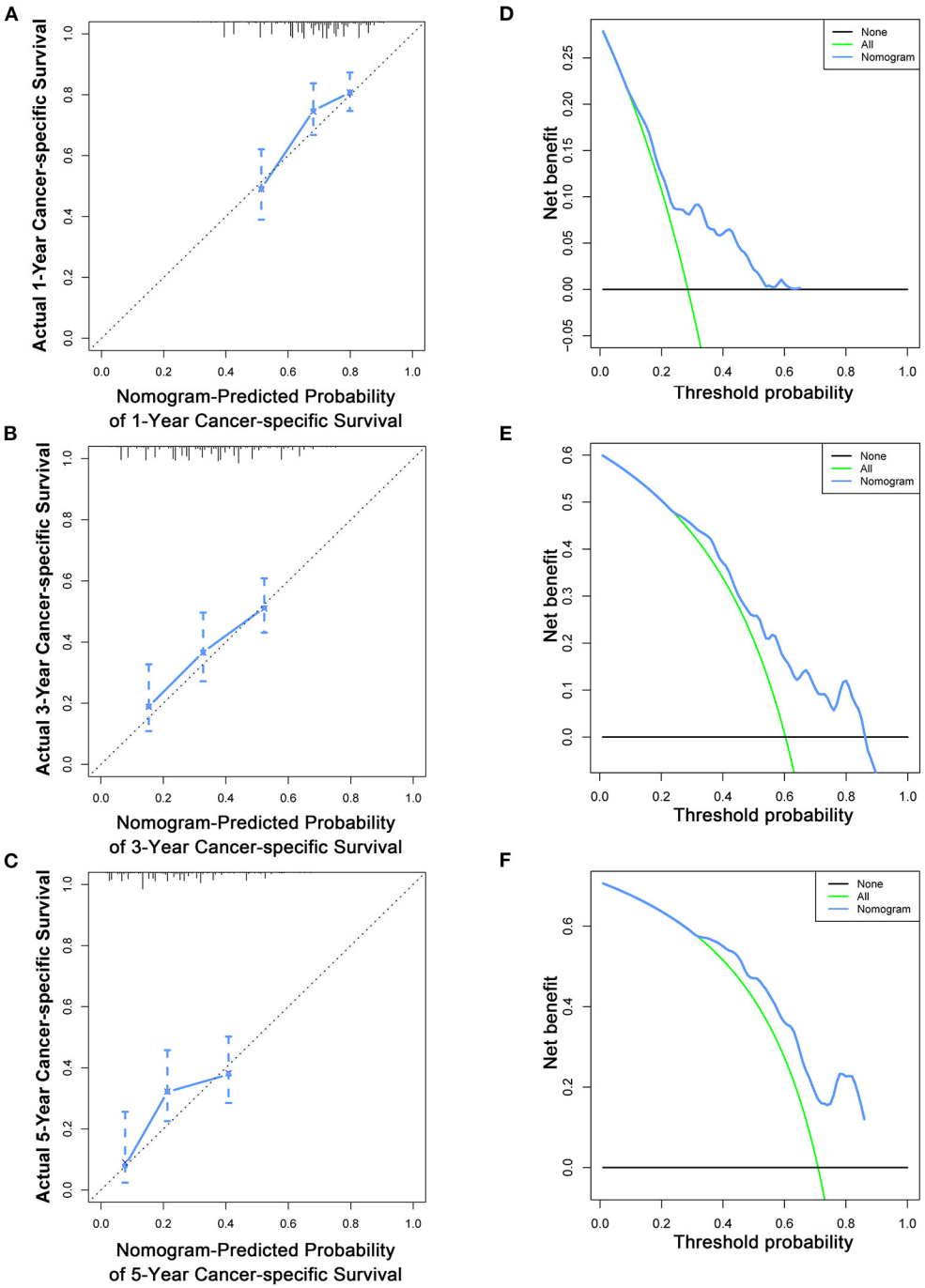

FIGURE 8 | Calibration curves **(A–C)** and DCA **(D–F)** of the nomogram for predicting patients' CSS at 1, 3, and 5 years in the validation cohort.

patients with T4a GC. In addition to the tumor size, another important prognostic factor is the histopathological type. In this study, the pathological types including SRCC, mucinous adenocarcinoma, and adenocarcinoma were considered, and the results of both univariate and multivariate analysis showed that the pathological type of T4a GC was significantly correlated with the prognosis. Among them, SRCC was associated with a worse prognosis, whereas the prognosis of patients with mucinous adenocarcinoma was relatively better. In the study of Yang et al. (28), SRCC accompanied by "migratory cancerous embolus of lymphatic" showed a high malignant phenotype, and the 5-year survival rate was only 15.9%, whereas that rate of mucinous gastric carcinoma (MGC) was only 19.4%. Although different pathological types play different roles in the formation

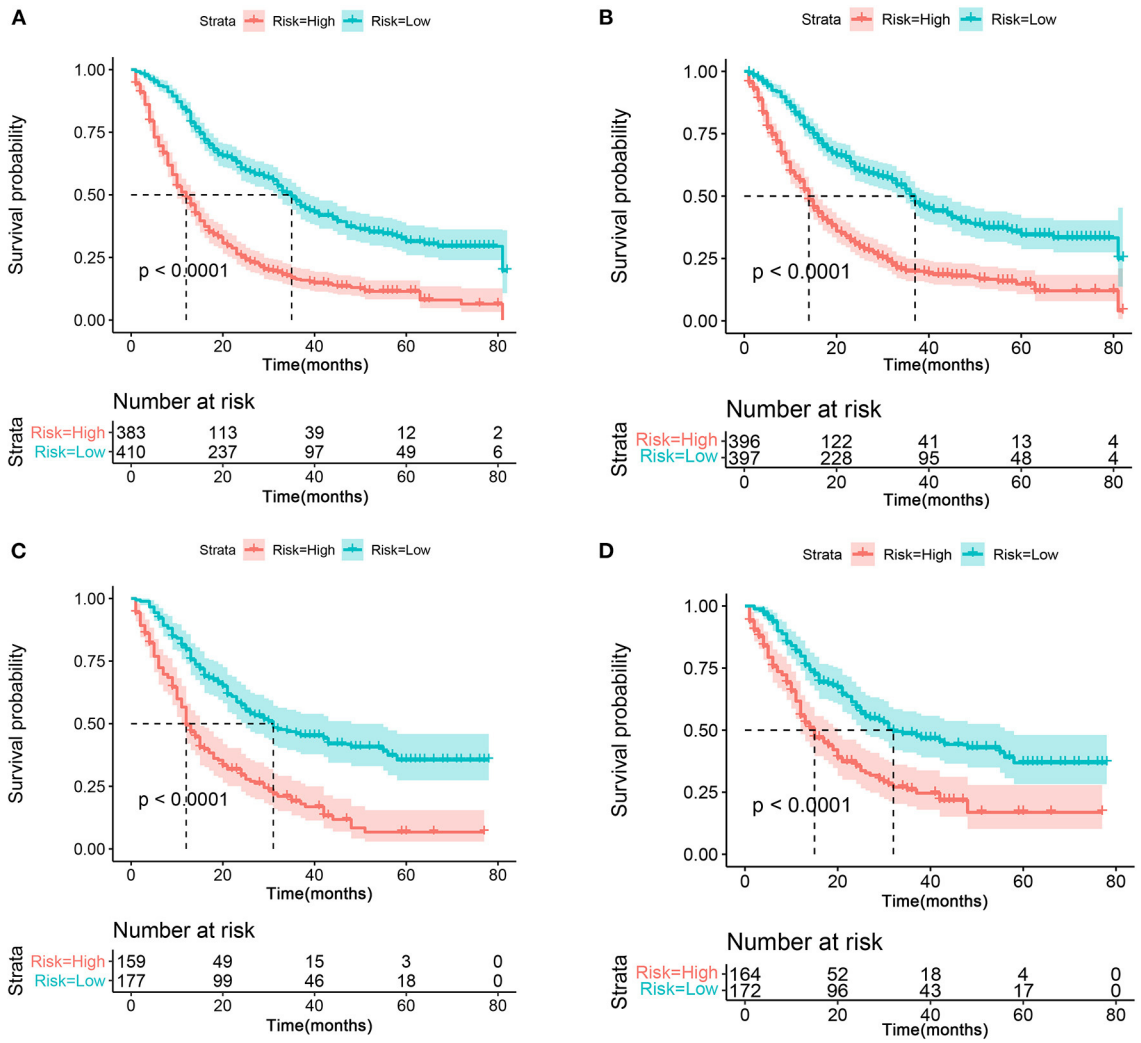

FIGURE 9 | The Kaplan–Meier survival curve of risk group stratification for OS **(A)** and CSS **(B)** in the training cohort. The Kaplan–Meier survival curve of risk group stratification for OS **(C)** and CSS **(D)** in the validation cohort.

of malignant phenotypes, the prognosis of these two types is not favorable. Thus, early detection and precise prognosis prediction are important in forming treatment strategies and prolong the survival of patients. Bozkaya et al. (29) also showed that patients with SRCC had worse prognosis and survival probability than MGC, and the degree of lymph node invasion was significantly correlated with OS, which was consistent with this study. Although, there were few studies discussed the difference between adenocarcinoma and the above two pathological types, it is undeniable that the malignant degree of tumor cells plays an important role in the prognosis of patients with T4a GC.

Several limitations of this study need to be acknowledged. First, since this study is a retrospective study based on the SEER database, information and selection bias might have been introduced. Second, the SEER database does not provide the access to detailed clinical information, tumor depth, metastatic sites, and operation methods were not documented, with detailed treatment strategy information, and the exploration of the prognosis of different treatment strategy might be possible. Additionally, the reason why some patients did not undergo surgery is unclear. Third, the nomogram constructed in this study could only predict OS and CSS to a maximum of 5 years due to the limited follow-up period. Despite these limitations, this is still a large population-based study that investigated the prognostic factors of patients with T4a GC, and the favorable clinical utilization of the nomogram was further confirmed.

CONCLUSIONS

This study identified age, tumor size, race, histologic type, N stage, surgery status, radiotherapy, and chemotherapy as prognostic factors for both OS and CSS in patients with T4a GC. These factors were incorporated to construct the nomograms,

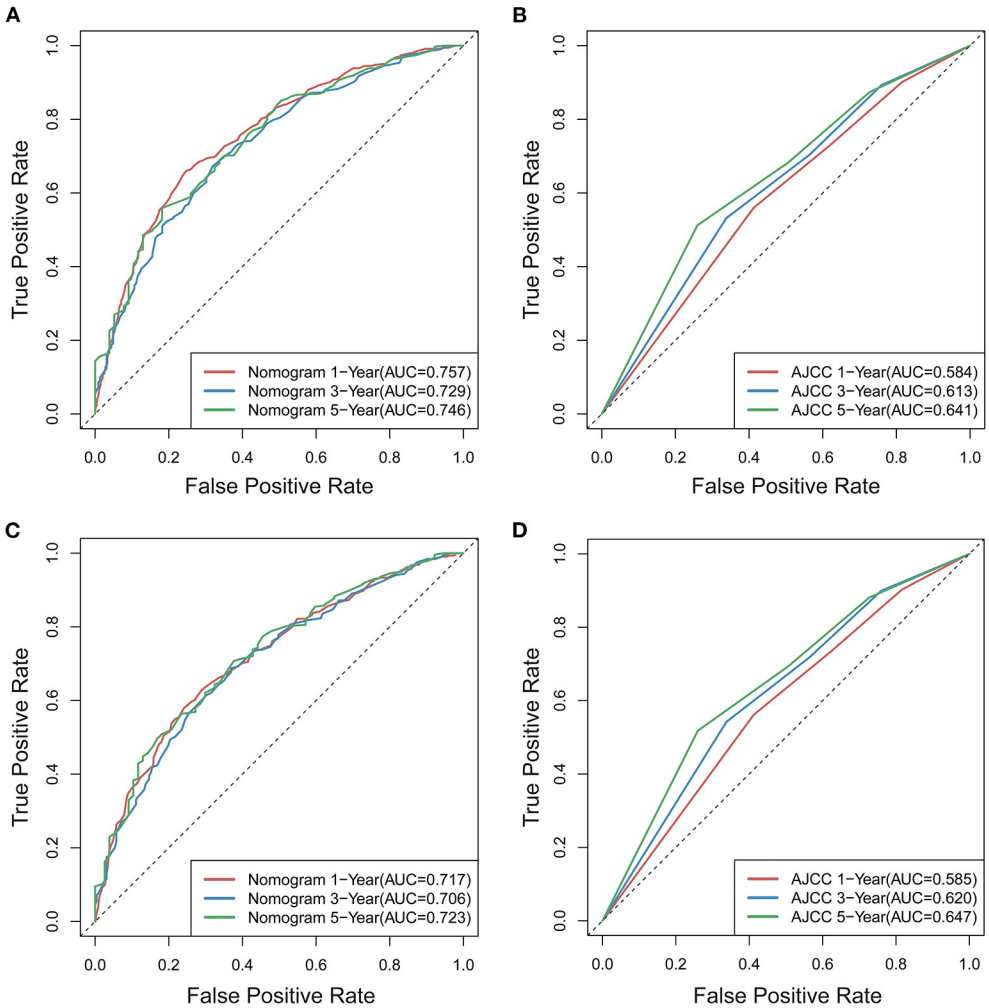

FIGURE 10 | Comparison of ROC curves for predicting patients' OS at 1, 3, and 5years between novel nomogram **(A)** and AJCC model **(B)**, for predicting patients' CSS at 1, 3, and 5years between novel nomogram **(C)** and AJCC model **(D)**.

and the nomograms may assist with patient assessments and help physicians to make an appropriate clinical decision.

DATA AVAILABILITY STATEMENT

The original contributions presented in the study are included in the article/**Supplementary Material**, further inquiries can be directed to the corresponding author.

AUTHOR CONTRIBUTIONS

ZH, YD, and ZZ conducted the experiments. ZH, YD, and HM analyzed the data. ZZ wrote the manuscript. ZN contributed to the conception of the present research and was responsible for approving the version before publication. All authors participated in the design, manuscript revision, read, and approved the submitted version.

FUNDING

The research was supported by the National College Students Innovation and Entrepreneurship Training Program (202010343034) and Zhejiang Province Science and Technology Plan Research and Xinmiao Talent Program (2019R413001 and 2020R413018).

SUPPLEMENTARY MATERIAL

The Supplementary Material for this article can be found online at: https://www.frontiersin.org/articles/10.3389/fmed.2021.767904/full#supplementary-material

REFERENCES

1. Bray F, Ferlay J, Soerjomataram I, Siegel RL, Torre LA, Jemal A. Global cancer statistics 2018: GLOBOCAN estimates of incidence and mortality worldwide for 36 cancers in 185 countries. *CA Cancer J Clin.* (2018) 68:394–424. doi: 10.3322/caac.21492
2. Glehen O, Mohamed F, Gilly FN. Peritoneal carcinomatosis from digestive tract cancer: new management by cytoreductive surgery and intraperitoneal chemohyperthermia. *Lancet Oncol.* (2004) 5:219–28. doi: 10.1016/s1470-2045(04)01425-1
3. Fujitani K, Yang HK, Mizusawa J, Kim YW, Terashima M, Han SU, et al. Gastrectomy plus chemotherapy versus chemotherapy alone for advanced GC with a single non-curable factor (REGATTA): a phase 3, randomised controlled trial. *Lancet Oncol.* (2016) 17:309–18. doi: 10.1016/s1470-2045(15)00553-7
4. Neugut AI, Hayek M, Howe G. Epidemiology of gastric cancer. *Semin Oncol.* (1996) 23:281–91.
5. Menges M, Hoehler T. Current strategies in systemic treatment of gastric cancer and cancer of the gastroesophageal junction. *J Cancer Res Clin Oncol.* (2009) 135:29–38. doi: 10.1007/s00432-008-0425-z
6. Gretschel S, Siegel R, Estévez-Schwarz L, Hünerbein M, Schneider U, Schlag PM. Surgical strategies for gastric cancer with synchronous peritoneal carcinomatosis. *Br J Surg.* (2006) 93:1530–5. doi: 10.1002/bjs.5513
7. Fukuda N, Sugiyama Y, Wada J. Prognostic factors of T4 gastric cancer patients undergoing potentially curative resection. *World J Gastroenterol.* (2011) 17:1180–4. doi: 10.3748/wjg.v17.i9.1180
8. Zhu BY, Yuan SQ, Nie RC Li SM, Yang LR, Duan JL, et al. Prognostic factors and recurrence patterns in T4 gastric cancer patients after curative resection. *J Cancer.* (2019) 10:1181–8. doi: 10.7150/jca.28993
9. Li MZ, Deng L, Wang JJ, Xiao LB, Wu WH, Yang SB, et al. Surgical outcomes and prognostic factors of T4 gastric cancer patients without distant metastasis. *PLoS ONE.* (2014) 9:e107061. doi: 10.1371/journal.pone.0107061
10. Huang C, Liu Z, Xiao L, Xia Y, Huang J, Luo H, et al. Clinical significance of serum CA125, CA19-9, CA72-4, and fibrinogen-to-lymphocyte ratio in gastric cancer with peritoneal dissemination. *Front Oncol.* (2019) 9:1159. doi: 10.3389/fonc.2019.01159
11. Chen S, Chen X, Nie R, Ou Yang L, Liu A, Li Y, et al. A nomogram to predict prognosis for gastric cancer with peritoneal dissemination. *Chin J Cancer Res.* (2018) 30:449–59. doi: 10.21147/j.issn.1000-9604.2018.04.08
12. Huang W, Zhou K, Jiang Y, Chen C, Yuan Q, Han Z, et al. Radiomics nomogram for prediction of peritoneal metastasis in patients with gastric cancer. *Front Oncol.* (2020) 10:1416. doi: 10.3389/fonc.2020.01416
13. Chen QY, Liu ZY, Zhong Q, Jiang W, Zhao YJ Li P, et al. An intraoperative model for predicting survival and deciding therapeutic schedules: a comprehensive analysis of peritoneal metastasis in patients with advanced gastric cancer. *Front Oncol.* (2020) 10:550526. doi: 10.3389/fonc.2020.550526
14. Dikken JL, Baser RE, Gonen M, Kattan MW, Shah MA, Verheij M, et al. Conditional probability of survival nomogram for 1-, 2-, and 3-year survivors after an R0 resection for gastric cancer. *Ann Surg Oncol.* (2013) 20:1623–30. doi: 10.1245/s10434-012-2723-6
15. Kattan MW, Karpeh MS, Mazumdar M, Brennan MF. Postoperative nomogram for disease-specific survival after an R0 resection for gastric carcinoma. *J Clin Oncol.* (2003) 21:3647–50. doi: 10.1200/jco.2003.01.240
16. Han DS, Suh YS, Kong SH, Lee HJ, Choi Y, Aikou S, et al. Nomogram predicting long-term survival after d2 gastrectomy for gastric cancer. *J Clin Oncol.* (2012) 30:3834–40. doi: 10.1200/jco.2012.41.8343
17. Camp RL, Dolled-Filhart M, Rimm DL. X-tile: a new bio-informatics tool for biomarker assessment and outcome-based cut-point optimization. *Clin Cancer Res.* (2004) 10:7252–9. doi: 10.1158/1078-0432.Ccr-04-0713
18. Chen D, Liu Z, Liu W, Fu M, Jiang W, Xu S, et al. Predicting postoperative peritoneal metastasis in gastric cancer with serosal invasion using a collagen nomogram. *Nat Commun.* (2021) 12:179. doi: 10.1038/s41467-020-20429-0
19. Martin RC. 2nd, Jaques DP, Brennan MF, Karpeh M. Achieving RO resection for locally advanced gastric cancer: is it worth the risk of multiorgan resection? *J Am Coll Surg.* (2002) 194:568–77. doi: 10.1016/s1072-7515(02)01116-x
20. Dikken JL, Jansen EP, Cats A, Bakker B, Hartgrink HH, Kranenbarg EM, et al. Impact of the extent of surgery and postoperative chemoradiotherapy on recurrence patterns in gastric cancer. *J Clin Oncol.* (2010) 28:2430–6. doi: 10.1200/jco.2009.26.9654
21. Ozden S, Ozgen Z, Ozyurt H, Gemici C, Yaprak G, Tepetam H, et al. Survival in gastric cancer in relation to postoperative adjuvant therapy and determinants. *World J Gastroenterol.* (2015) 21:1222–33. doi: 10.3748/wjg.v21.i4.1222
22. Yoshikawa T, Omura K, Kobayashi O, Nashimoto A, Takabayashi A, Yamada T, et al. A phase II study of preoperative chemotherapy with S-1 plus cisplatin followed by D2/D3 gastrectomy for clinically serosa-positive gastric cancer (JACCRO GC-01 study). *Eur J Surg Oncol.* (2010) 36:546–51. doi: 10.1016/j.ejso.2010.04.011
23. Lee IS, Yook JH, Kim TH, Kim HS, Kim KC, Oh ST, et al. Prognostic factors and recurrence pattern in node-negative advanced gastric cancer. *Eur J Surg Oncol.* (2013) 39:136–40. doi: 10.1016/j.ejso.2012.10.008
24. Kim DY, Seo KW, Joo JK, Park YK Ryu SY, Kim HR, et al. Prognostic factors in patients with node-negative gastric carcinoma: a comparison with node-positive gastric carcinoma. *World J Gastroenterol.* (2006) 12:1182–6. doi: 10.3748/wjg.v12.i8.1182
25. Maehara Y, Tomoda M, Tomisaki S, Ohmori M, Baba H, Akazawa K, et al. Surgical treatment and outcome for node-negative gastric cancer. *Surgery.* (1997) 121:633–9. doi: 10.1016/s0039-6060(97)90051-9
26. Deng J, Zhang R, Pan Y, Ding X, Cai M, Liu Y, et al. Tumor size as a recommendable variable for accuracy of the prognostic prediction of gastric cancer: a retrospective analysis of 1,521 patients. *Ann Surg Oncol.* (2015) 22:565–72. doi: 10.1245/s10434-014-4014-x
27. Kunisaki C, Akiyama H, Nomura M, Matsuda G, Otsuka Y, Ono HA, et al. Surgical outcomes in patients with T4 gastric carcinoma. *J Am Coll Surg.* (2006) 202:223–30. doi: 10.1016/j.jamcollsurg.2005.10.020
28. Yang XF, Yang L, Mao XY, Wu DY, Zhang SM, Xin Y. Pathobiological behavior and molecular mechanism of signet ring cell carcinoma and mucinous adenocarcinoma of the stomach: a comparative study. *World J Gastroenterol.* (2004) 10:750–4. doi: 10.3748/wjg.v10.i5.750
29. Bozkaya Y, Erdem GU, Ozdemir NY, Demirci NS, Hocazade C, Yazici O, et al. Comparison of clinicopathological and prognostic characteristics in patients with mucinous carcinoma and signet ring cell carcinoma of the stomach. *Curr Med Res Opin.* (2017) 33:109–16. doi: 10.1080/03007995.2016.1239192

Conflict of Interest: The authors declare that the research was conducted in the absence of any commercial or financial relationships that could be construed as a potential conflict of interest.

Publisher's Note: All claims expressed in this article are solely those of the authors and do not necessarily represent those of their affiliated organizations, or those of the publisher, the editors and the reviewers. Any product that may be evaluated in this article, or claim that may be made by its manufacturer, is not guaranteed or endorsed by the publisher.

Copyright © 2022 Hu, Zuo, Miao, Ning and Deng. This is an open-access article distributed under the terms of the Creative Commons Attribution License (CC BY). The use, distribution or reproduction in other forums is permitted, provided the original author(s) and the copyright owner(s) are credited and that the original publication in this journal is cited, in accordance with accepted academic practice. No use, distribution or reproduction is permitted which does not comply with these terms.

frontiers in Oncology

REVIEW
published: 07 January 2022
doi: 10.3389/fonc.2021.806162

Significance of Lymph Node Metastasis in the Treatment of Gastric Cancer and Current Challenges in Determining the Extent of Metastasis

Shinichi Kinami[1,2*], *Hitoshi Saito*[2] *and Hiroyuki Takamura*[1]

[1] Department of Surgical Oncology, Kanazawa Medical University, 1-1 Daigaku, Uchinada-machi, Kahoku-gun, Japan, [2] Department of General and Gastroenterologic Surgery, Kanazawa Medical University Himi Municipal Hospital, Himi City, Japan

OPEN ACCESS

Edited by:
Sanjit Mukherjee, National Institutes of Health (NIH), United States

Reviewed by:
Mei Wang, Jiangsu University, China
Toshiyuki Kosuga, Saiseikai Shigaken Hospital, Japan

***Correspondence:**
Shinichi Kinami
kinami@kanazawa-med.ac.jp

Specialty section:
This article was submitted to Surgical Oncology, a section of the journal Frontiers in Oncology

Received: *31 October 2021*
Accepted: *13 December 2021*
Published: *07 January 2022*

Citation:
Kinami S, Saito H and Takamura H (2022) Significance of Lymph Node Metastasis in the Treatment of Gastric Cancer and Current Challenges in Determining the Extent of Metastasis. Front. Oncol. 11:806162. doi: 10.3389/fonc.2021.806162

The stomach exhibits abundant lymphatic flow, and metastasis to lymph nodes is common. In the case of gastric cancer, there is a regularity to the spread of lymph node metastasis, and it does not easily metastasize outside the regional nodes. Furthermore, when its extent is limited, nodal metastasis of gastric cancer can be cured by appropriate lymph node dissection. Therefore, identifying and determining the extent of lymph node metastasis is important for ensuring accurate diagnosis and appropriate surgical treatment in patients with gastric cancer. However, precise detection of lymph node metastasis remains difficult. Most nodal metastases in gastric cancer are microscopic metastases, which often occur in small-sized lymph nodes, and are thus difficult to diagnose both preoperatively and intraoperatively. Preoperative nodal diagnoses are mainly made using computed tomography, although the specificity of this method is low because it is mainly based on the size of the lymph node. Furthermore, peripheral nodal metastases cannot be palpated intraoperatively, nodal harvesting of resected specimens remains difficult, and the number of lymph nodes detected vary greatly depending on the skill of the technician. Based on these findings, gastrectomy with prophylactic lymph node dissection is considered the standard surgical procedure for gastric cancer. In contrast, several groups have examined the value of sentinel node biopsy for accurately evaluating nodal metastasis in patients with early gastric cancer, reporting high sensitivity and accuracy. Sentinel node biopsy is also important for individualizing and optimizing the extent of uniform prophylactic lymph node dissection and determining whether patients are indicated for function-preserving curative gastrectomy, which is superior in preventing post-gastrectomy symptoms and maintaining dietary habits. Notably, advancements in surgical treatment for early gastric

cancer are expected to result in individualized surgical strategies with sentinel node biopsy. Chemotherapy for advanced gastric cancer has also progressed, and conversion gastrectomy can now be performed after downstaging, even in cases previously regarded as inoperable. In this review, we discuss the importance of determining lymph node metastasis in the treatment of gastric cancer, the associated difficulties, and the need to investigate strategies that can improve the diagnosis of lymph node metastasis.

Keywords: gastric cancer, lymph node metastasis, MDCT, sentinel node, staging

INTRODUCTION

Lymph node metastasis is an important determinant of disease progression in patients with gastric cancer. The stage of gastric cancer without distant metastasis is determined based on the depth of invasion and the degree of lymph node metastasis (1–3). In recent years, determining the degree of lymph node metastasis after gastric cancer surgery has become essential for selecting appropriate adjuvant therapy and improving prognosis, as the effect of adjuvant chemotherapy in suppressing recurrence has become clear (4–8). In addition, given that it can be cured to some extent by prophylactic lymph node dissection, preoperative diagnosis of lymph node metastasis is an important factor when planning surgical treatment for patients with gastric cancer (9–11). For these reasons, numerous studies have investigated the diagnosis, pathophysiology, and treatment of lymph node metastasis in the context of gastric cancer (12–14). However, diagnosis of nodal metastasis remains difficult in these patients, and several problems with detection remain unresolved. In this review, we discuss the importance of determining lymph node metastasis in the treatment of gastric cancer and the associated difficulties.

CHARACTERISTICS OF LYMPH NODE METASTASIS IN PATIENTS WITH GASTRIC CANCER

Lymph node metastasis is a common form of metastasis in patients with gastric cancer (9). Cancer that invades within the submucosa is defined as early gastric cancer, regardless of the presence or absence of metastasis (15). The rate of hematogenous metastasis in patients with early gastric cancer is approximately 0.2% (16), and peritoneal metastasis is unlikely to occur (17), whereas the incidence of lymph node metastasis is approximately 10% (18). The relatively high rate of lymph node metastasis in patients with gastric cancer can be attributed to the abundant lymphatic flow in the stomach (19, 20). Indeed, there is a rich lymphatic network in the submucosa, and immunohistological staining using D2-40 have revealed that there are abundant lymphatic vessels near the muscularis mucosae (21). This physiological environment explains the frequency of lymph node metastasis even in cases of early gastric cancer (19, 21).

The incidence of lymph node metastasis in gastric cancer is closely related to the depth of invasion (17). According to the database of the Cancer Institute Hospital of the Japan Foundation for Cancer Research, which is considered the most reliable large-scale database, the nodal metastasis rates according to pathological depth of invasion are 2.3% for mucosal, 21.9% for submucosal, 64.2% for proper muscle-subserosal, and 86.6% for serosal exposure cancers (17).

Previously, pioneers in gastric cancer surgery in Japan classified regional lymph nodes along the arteries, examined lymphatic flow using tracers, and tabulated the sites of lymph node metastasis (2, 3), revealing that there is a regularity in the spread of lymph node metastases in patients with gastric cancer. **Table 1** shows that the rate of lymph node metastasis of early gastric cancer varies considerably according to station number (17, 22), based on data from representative articles. It can be seen that the lymph node metastasis rate varies considerably with the station number. Lymph nodes and lymphatic system of gastric cancer exhibit a stratified structure, consisting of three layers: the perigastric nodes and nodes along the left gastric artery; the nodes around the celiac artery, along the proper hepatic artery, and the suprapancreatic nodes; and the deeper para-aortic lymph nodes (**Figure 1**). The station numbers and definitions of the lymph nodes, which are important for gastric cancer staging and surgical treatment are precisely stated in **Table 2**. These nodes approximately correspond to group 1, 2, and 3 lymph nodes in the old Japanese Classification of Gastric Carcinoma, respectively (23). Most nodal metastases in early gastric cancer are confined to group 1 nodes, the rate of metastasis to group 2 nodes is low, and metastasis to group 3 nodes is rare. Lymph node metastases are thought to spread along with the lymphatic flow from group 1 to group 2 and then to group 3. In other words, lymph node metastasis of gastric cancer spreads from the perigastric nodes, *via* the suprapancreatic nodes and nodes around the celiac artery, to the para-aortic nodes, following which it flows out to the systemic circulation (**Figure 2**). Currently, the regional lymph nodes for gastric cancer are defined as No. 1 to No. 12 and No. 14v, and other nodal metastases are considered distant metastases (2, 3).

In many cancers, lymph node metastasis is an important surrogate marker of survival prognosis and an important factor when considering postoperative adjuvant therapy. The prognosis of gastric cancer also worsens as the number of lymph node metastases increases (24–27). A previous study reported that survival curves clearly deviate according to the number of lymph node metastases, based on analysis of data in the registry of the Japanese Society of Gastric Cancer, a high-quality dataset that

TABLE 1 | The precise incidence of nodal metastasis of early gastric cancer in previous studies with large number of cases.

		Nakajima (17)	Tanaka (22)
Total no. of cases		3630	2368
Perigastric nodes	#1	0.90%	0.97%
	#2	0.11%	0.08%
	#3	5.9%	4.6%
	#4	3.9%	3.2%
	#5	0.47%	0.51%
	#6	3.4%	2.4%
Nodes along left gastric artery	#7	1.1%	1.4%
Suprapancreatic nodes	#8a	1.1%	0.63%
	#9	1.1%	0.72%
	#11p	0.36%	0.42%
	#11d	0.03%	0.00%
Nodes at the hilum of spleen	#10	0.08%	0.00%
Nodes along proper hepatic artery	#12a	0.06%	0.00%
Para-aortic nodes	#16	0.25%	0.00%

The percentage of each column represents the metastatic ratio per patients of the lymph nodes in each station.

includes information for half of all patients undergoing gastric cancer surgery in Japan (9).

The Z0011 study demonstrated that additional axillary nodal dissection after sentinel node biopsy does not improve prognosis in patients with breast cancer (28–30). Similarly, in many carcinomas, lymph node metastasis is thought to be important for accurate staging, but prophylactic nodal dissection does not improve prognosis (31–35). In contrast, the therapeutic effect of prophylactic lymph node dissection in patients with gastric cancer has been verified. The rate of nodal metastasis for early gastric cancer is approximately 10% (18), but the 5-year survival rate after gastrectomy with prophylactic nodal dissection is as high as 98% (9–11). In cases of advanced gastric cancer, D2 (nodal dissection up to group 2 nodes) is associated with better prognosis than D1 (dissection of perigastric nodes only) (36, 37). This phenomenon seems to be a unique feature of gastric cancer. It is presumed that the major difference between gastric cancer and breast cancer is related to the anatomical location of the lymph nodes. Breast cancer that has metastasized to the axillary lymph nodes can easily develop systemic metastases from these nodes. In contrast, the lymphatic system of gastric cancer exhibits a stratified structure (**Figures 1**, **2**), and there exists a state in which metastatic foci are localized around the stomach and not spread throughout the body, which is presumed to account for the prophylactic effect of lymph node dissection.

Previous studies have elucidated the molecular mechanisms involved in lymph node metastasis (38–41). Among them, the initial and most important process is lymphangiogenesis (42–44), which is regulated by members of the vascular endothelial growth factor (VEGF) family and their receptors (43–46). Cell migration is another important process in nodal metastasis, and Wnt-5a is thought to be among the cell migration-associated molecules involved in gastric cancer (47, 48). In addition, it is well accepted that cancer stem cells play a significant role in nodal metastasis of gastric cancer (48–50) (**Figure 3**).

STANDARD LYMPH NODE DISSECTION STRATEGY FOR GASTRIC CANCER

Lymph node dissection for gastric cancer was well studied in Japan during the 20th century. Following the studies related to the frequency of lymph node metastasis and the prognosis of nodal dissection, the results were consolidated by the Japanese Research Society for Gastric Cancer, which revised the classification of station numbers and proposed extent of nodal dissection. In the past, the extent of nodal dissection was determined based on the location of gastric cancer (23), and strategies were based on the results of retrospective studies. The importance of prospective studies is now recognized in the field of surgical treatment. Since lymph node dissection allows for an accurate pathological diagnosis of nodal metastasis, leading to so-called stage migration (51–53), retrospective studies may overestimate the effect of lymph node dissection. Thus, the actual outcome of nodal dissection can only be evaluated in prospective studies.

Two prospective clinical trials were conducted to determine the influence of the extent of nodal dissection in gastric cancer surgery. One is JCOG9501 trial (53–56). At that time, approximately 10% of patients with para-aortic nodal metastasis survived for 5 years if these nodes were dissected (51). To verify the efficacy of para-aortic nodal dissection, a prospective randomized clinical trial was conducted, in which patients with advanced gastric cancer were randomly assigned to two treatment groups: the study group with lymph node dissection up to D2 plus para-aortic lymph node (PAN) dissection and the control group with nodal dissection up to D2 only. The results indicated that PAN dissection did not significantly influence outcomes, as there was little difference in the incidence of complications (55) or survival prognosis (54) between the two groups. In this study, metastases were histologically detected in 8.5% of patients who underwent D2 plus PAN dissection, and the 5-year overall survival rate was 18.2%. Given that nature of prospective randomized trials, these

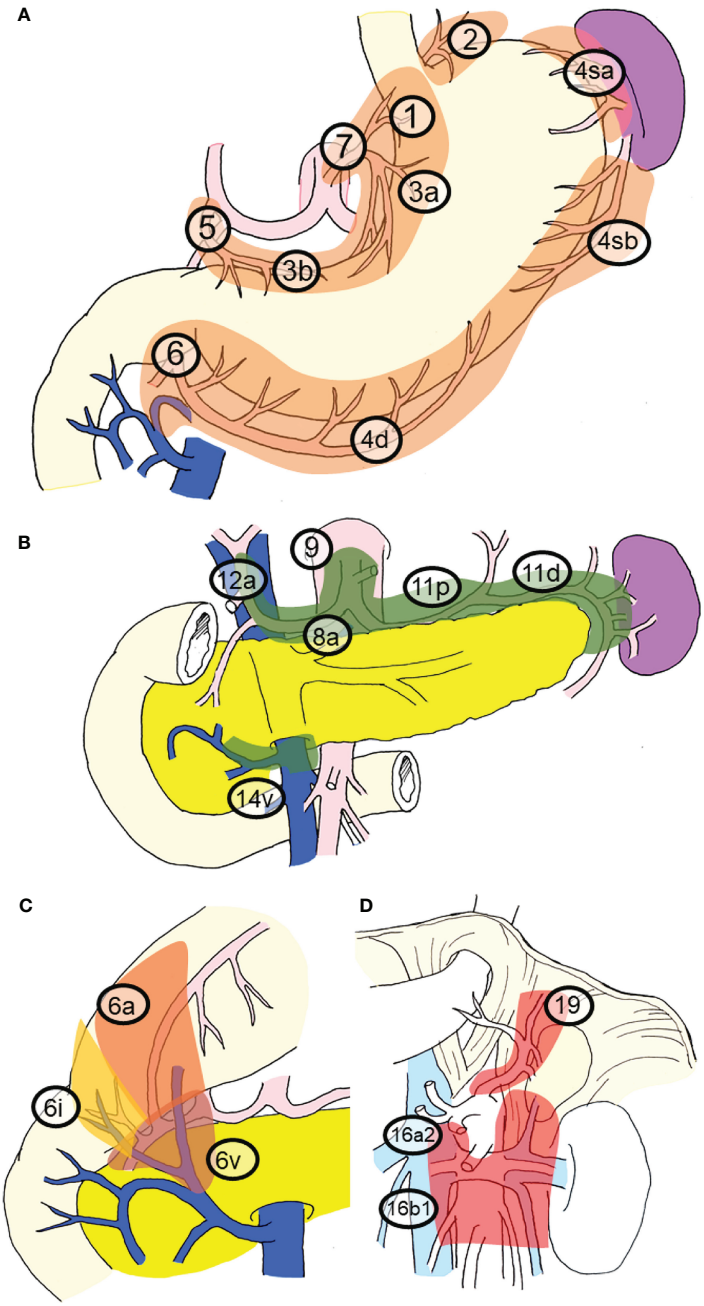

FIGURE 1 | Regional lymph nodes and station numbers in gastric cancer. This classification and the station numbers are based on the Japanese Classification of Gastric Carcinoma. The details of the nodal station numbers have been described in **Table 2**. **(A)** Perigastric nodes and nodes along the left gastric artery. These nodes nearly correspond to group 1 nodes. **(B)** Nodes around the celiac artery, along the proper hepatic artery and suprapancreatic nodes. These nodes nearly correspond to the group 2 nodes. **(C)** The subcategory of No. 6 nodes. **(D)** Nodes in deeper layers. Para-aortic lymph nodes and No. 19 nodes. These nodes nearly correspond to group 3 nodes.

findings support the notion that some patients with latent pathological PAN metastases can survive for 5 years without dissection. In other words, although extended lymph node dissection may be effective for accurate staging, it does not improve survival.

Another important prospective trial was the aforementioned Dutch trial (36, 57), which compared the therapeutic effects of D1 and D2. This trial is significant in that a famous Japanese gastric surgeon provided guidance on the surgical techniques in the Netherlands. Initially, there was no difference in the 5-year

TABLE 2 | The station numbers and the definitions of the lymph nodes which are important for gastric cancer staging and surgical treatment.

Perigastric nodes	
#1	Nodes at the left side of cardia, including those along the first branch of the ascending limb of the left gastric artery
#2	Nodes at the right side of cardia, including those along the esophagocardiac branch of the left subphrenic artery
#3a	Nodes at the lesser curvature of stomach along the branches of the left gastric artery
#3b	Nodes at the lesser curvature of stomach along the second branch and distal part of the right gastric artery
#4sa	Nodes along the short gastric arteries
#4sb	Nodes at the left side of greater curvature along the left gastroepiploic artery
#4d	Nodes at the right side of greater curvature along the second branch and distal part of the right gastroepiploic artery
#5	Suprapyloric nodes along the first branch and proximal part of the right gastric artery
#6a	Infrapyloric nodes along the first branch and proximal part of the right gastroepiploic artery
#6v	Nodes along the confluence of the right gastroepiploic vein
#6i	Nodes along the infrapyloric artery and vein
Nodes along the left gastric artery	
#7	Nodes along the trunk of the left gastric artery between its root and the ascending branch
Suprapancreatic nodes	
#8a	Nodes at the anterosuperior side of the common hepatic artery
#9	Nodes around the celiac artery
#11p	Nodes at the proximal half side along the splenic artery
#11d	Nodes at the distal half side along the splenic artery
Others of the regional lymph nodes	
#12a	Nodes along the proper hepatic artery (left side nodes of the hepatoduodenal ligament)
#14v	Nodes along the superior mesenteric vein
Para-aortic nodes (PAN)	
#16a2 lateral	Left side of para-aortic nodes between the upper margin of the origin of the celiac artery and the lower border of the left renal vein
#16a2 inter	Right side of para-aortic nodes between the upper margin of the origin of the celiac artery and the lower border of the left renal vein
#16b1 lateral	Left side of para-aortic nodes between the lower border of the left renal vein and the upper border of the origin of the inferior mesenteric artery
#16b1 inter	Right side of para-aortic nodes between the lower border of the left renal vein and the upper border of the origin of the inferior mesenteric artery
Other important nodes	
#8p	Nodes at the posterior side of the common hepatic artery
#13	Nodes on the posterior surface of the pancreas head cranial to the duodenal papilla
#19	Nodes along the left subphrenic artery
#20	Paraesophageal nodes at the diaphragmatic esophageal hiatus

survival rate between the D1 and D2 groups (57); however, after 15 years of follow-up, survival outcomes were better among patients who had undergone D2 than among those who had undergone D1 (36). The initial lack of difference in survival was attributed to the relatively greater invasiveness and apparently higher surgery-related mortality of D2 than D1. This study exposed the difficulties of prospective trials of surgical treatment in terms of quality control and evaluation methods. Nevertheless, it was important for demonstrating the superiority of D2 over D1 in patients with advanced gastric cancer. When the results of the JCOG9501 and Dutch trials are integrated, they demonstrate that D2 can improve the prognosis for advanced gastric cancer but that D2 plus PAN dissection has no effect. Furthermore, the integrated results indicate that Asian patients can tolerate the invasiveness of lymph node dissection while Western patients not.

After the clear survival advantages of adjuvant chemotherapy and adjuvant chemoradiotherapy for gastric cancer, prospective studies on lymph node dissection have become less common. Therefore, even though there is a consensus that appropriate prophylactic lymph node dissection improves prognosis, there is not enough evidence to determine the appropriate extent of dissection. The appropriate dissection range for gastric cancer in Western patients and patients with early gastric cancer, obesity, or comorbidities remains to be determined, and the superiority of D2 over D1+ remains unresolved. Currently, the range of D2 is specified for each gastrectomy method in the Japanese guidelines (58, 59), but the validity of each is unknown because no prospective studies have been conducted.

CHALLENGES IN THE PREOPERATIVE DIAGNOSIS OF LYMPH NODE METASTASIS IN GASTRIC CANCER

Preoperative diagnosis of lymph node metastasis is essential for planning proper surgical treatment. However, it is difficult (60), and two factors make the preoperative diagnosis of nodal metastasis difficult: (a) The regional lymph nodes are in the abdominal cavity, and (b) approximately half of lymph node metastases are microscopic (61, 62). According to a recent study on diagnostic imaging (61), which classified metastatic lymph nodes based on microscopic metastatic morphology, 42.5% of metastatic lymph nodes in gastric cancer were of the small nodular type and peripheral type. Lesion volumes for these types are smaller than those for the large nodular and diffuse types.

Researchers have also examined the significance of ultrasonography for diagnosing lymph node metastasis; however, several studies have demonstrated that gastric cancer ultrasonography does not play a major role in diagnosing lymph node metastasis (60, 63, 64). The most important regional lymph

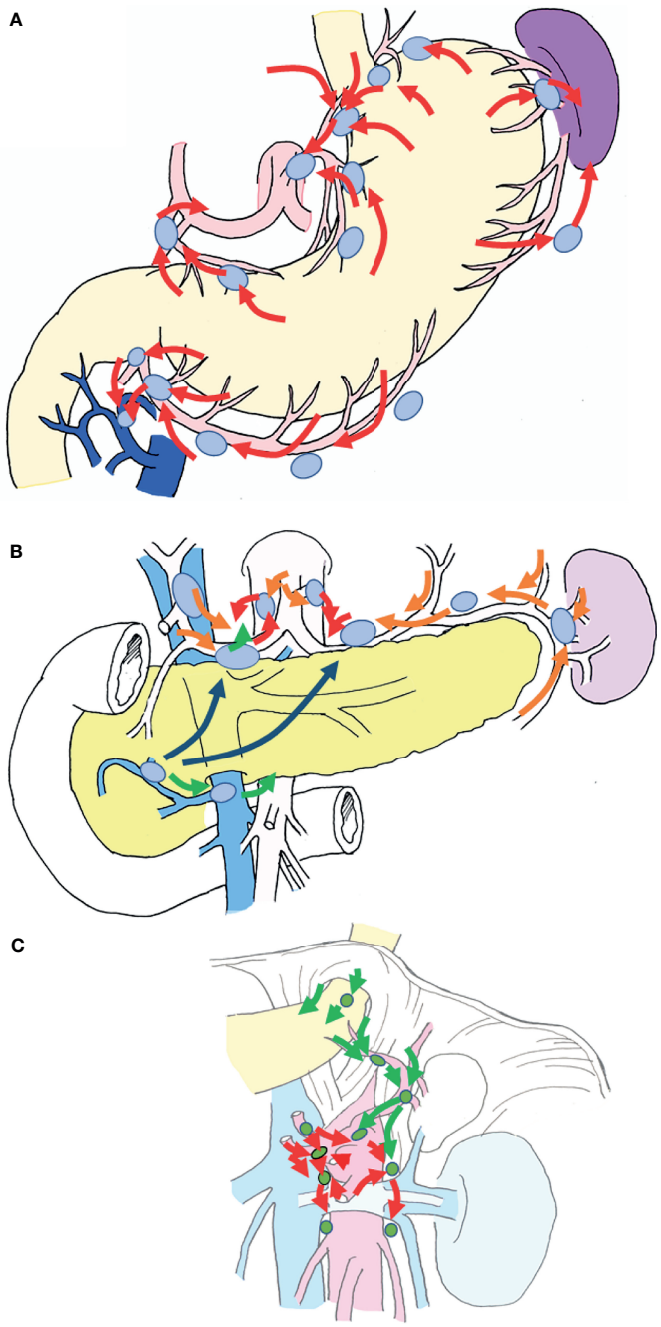

FIGURE 2 | Schematic diagram of the lymphatic system of the stomach. The lymphatic flow of the stomach spreads from the perigastric nodes, *via* the suprapancreatic nodes and nodes around the celiac artery, to the para-aortic nodes, following which it enters the systemic circulation. **(A)** Lymphatic flow from the gastric wall is directed to the root of each artery *via* nearby perigastric nodes (red arrows). **(B)** The lymphatic flow into the root of each artery flows *via* suprapancreatic nodes (orange arrows) and out to the paraaortic nodes from the left and right of the celiac artery (red arrows). There are also routes from #8a to #8p (the posterior side of the common hepatic artery), and routes from #6 to the root of the superior mesenteric artery *via* #14v (green arrows). Routes from #6 to the suprapancreatic nodes *via* the lymphatics under the pancreatic capsule are also available (indigo arrows). **(C)** Lymphatic flow around the celiac artery and the superior mesenteric artery lead to the paraaortic nodes, which are the terminal lymph nodes of gastric cancer (red arrows). A route from the left dorsal side of the cardia to #16a2 lateral nodes *via* #19, along the left subphrenic artery also exists (green arrows).

nodes in breast cancer are the axillary lymph nodes, which are located under the skin, making ultrasonographic diagnosis easy and ultrasound-guided needle biopsy possible (65–67). On the other hand, since the regional lymph nodes of gastric cancer are in the abdominal cavity, it is difficult to make an ultrasonographic diagnosis from the body surface unless the patient has advanced metastasis, and needle biopsy is not possible. Endoscopic ultrasonography allows for observation

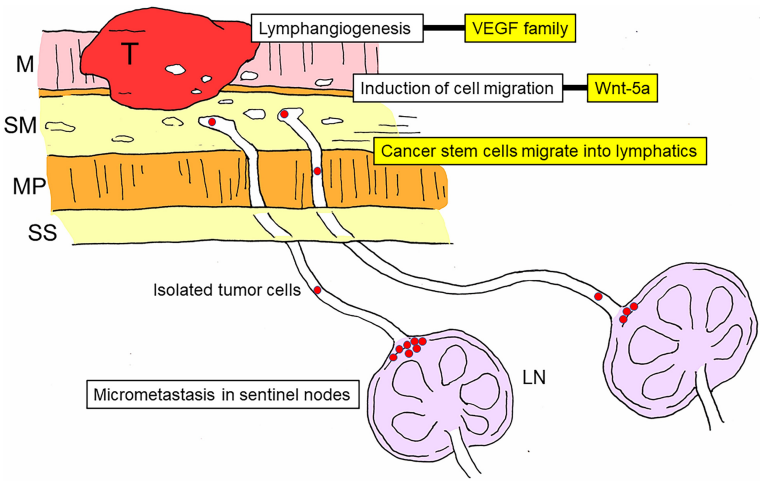

FIGURE 3 | Schematic diagram of the development and molecular mechanisms of nodal metastasis in gastric cancer. Lymph node metastasis can be divided into multiple stages: lymphangiogenesis, induction of cell migration, invasion of cancer stem cells into the lymphatic system, arrival of cancer stem cells in sentinel lymph nodes, and establishment of micrometastasis in the marginal sinus. The vascular endothelial growth factor (VEGF) family is involved in lymphangiogenesis, and Wnt-5a is involved in the induction of cell migration. T, tumor; M, mucosal layer; SM, submucosal layer; MP, proper muscle layer; SS, subserosal layer; LN, lymph node; VEGF, vascular endothelial growth factor.

within the lumen of the stomach and is more useful than ultrasonography on the body surface (68–70). In esophageal cancer, many of the regional lymph nodes are within the mediastinum around the esophagus; therefore, endoscopic ultrasonography, endoscopic ultrasound-guided elastography, and ultrasound-guided needle biopsy are extremely useful for preoperative diagnosis of lymph node metastasis (70–73). On the other hand, in gastric cancer, although most of the regional lymph nodes are located near the stomach, they lie within the perigastric mesentery (e.g., omentum), and the arteriovenous system runs in the immediate vicinity. Thus, even with endoscopic ultrasonography, it is difficult to visualize regional lymph nodes using ultrasound-guided needle biopsy (60, 74).

Computed tomography (CT) is the most important tool for preoperative nodal diagnosis of gastric cancer (60), and its diagnostic accuracy has increased with technological improvements in equipment (75). Currently, multi-detector spiral CT (MDCT) is widely used (75–82). The advantages of MDCT include objective anatomical imaging and superior spatial resolution. At present, with three-dimensional imaging and multi-planar reconstruction technology, it is possible to determine the precise position and shape of lymph nodes in all directions using different sections. However, even with MDCT, the preoperative nodal diagnosis of gastric cancer is not always satisfactory (81, 82). In a multicenter study concerning preoperative diagnosis of stage III gastric cancer, the sensitivity and specificity of the diagnostic method were 62.5% and 65.7%, respectively (81). A standard nodal diagnosis by MDCT is made based on the assumption that the size of the metastatic lymph node is large (60, 61, 75–82). However, metastatic nodes are not necessarily large (61, 62). In addition, the increased resolution does not mean that all regional lymph nodes can be visualized (61), and accurate calculation of diagnostic ability is difficult given the difficulty in achieving one-to-one correspondence between imaging and pathological diagnosis. In a recent article, the threshold from the receiver operating characteristic (ROC) curve was 7.6 mm in the long axis, and the sensitivity and specificity of the diagnostic method were 86.8% and 80.1%, respectively. However, after one-to-one correspondence based on accurate mapping and measurement of nodal size on resected specimens, the sensitivity and specificity were 91.4% and 47.3%, respectively, even when using the same threshold (61). The reason for such high sensitivity is that large nodes are often metastatic, while the low specificity can be explained by the fact that many metastatic nodes in gastric cancer are small. In this study, 56.3% of the metastatic nodes were below the threshold (61). Thus, patients diagnosed as positive for metastasis using MDCT are extremely likely to be positive for metastasis, but it is difficult to make a definitive diagnosis in node-negative patients. In other words, although MDCT diagnosis is beneficial for advanced gastric cancer, it is not suitable for confirming node-negative early gastric cancer (61, 82). One meta-analysis has indicated that the diagnostic ability of MDCT for lymph node metastasis of gastric cancer was greater for cases with exposed serosa than for cases without serosa exposure (75).

Positron emission tomography-CT (PET-CT) and magnetic resonance imaging (MRI) have also been used for preoperative imaging of lymph node metastasis (60, 80, 83–88), although neither has surpassed the diagnostic ability of MDCT (60). It is difficult to visualize microscopic metastases, even with PET-CT (83, 84). Although attempts have been made to diagnose nodal metastasis with MR lymphography using an ultrasmall superparamagnetic iron oxide (USPIO) contrast medium (88), no sufficient diagnostic results have been reported.

Some articles have reported attempts to improve the diagnostic imaging accuracy for nodal metastasis in gastric

cancer. Since diagnostic imaging can determine not only the presence and size of lymph nodes but also the morphology, attempts have been made to improve its accuracy in diagnosing metastasis by taking these factors into consideration. EUS not only identifies perigastric lymph nodes, it also visualizes some internal structure of the lymph nodes, which can sometimes lead to the detection of the intranodal metastatic lesions (89–91). In MDCT, attempts are being made to recognize metastasis from the aspect ratio of lymph nodes and contrast pattern (60, 61, 76). Since the sizes of the regional lymph nodes in gastric cancer vary depending on the lymph node stations, attempt have been reported to set different threshold values for each station, without making it uniform (79).

AN ATTEMPT TO PREDICT LYMPH NODE METASTASIS IN EARLY GASTRIC CANCER BY USING NOMOGRAM AND MOLECULAR MAKERS

There is a limit to diagnosing the presence of lymph node metastasis on diagnostic imaging for gastric cancer. However, if the presence of lymph node metastasis can be inferred from the state of the primary lesion, it may be possible to compensate for the uncertainty in diagnostic imaging. The rate of lymph node metastasis in advanced gastric cancer is high, and the degree of lymph node metastasis is of more importance than the presence or absence of lymph node metastasis. Therefore, it is more important to predict the presence or absence of lymph node metastasis in early gastric cancer than in advanced gastric cancer.

Attempts to calculate regression equations or nomograms for diagnosing the possibility of lymph node metastasis from the clinicopathological factors of early gastric cancer have been reported (92–95). However, unlike extracting the conditions for node-negative patients, attempts to diagnose node-positive patients are not always successful. This type of study generally analyzes patients (who have undergone surgical resection) based on tumor size, site of occupation, histology, depth of invasion, and lymphovascular invasion in resected specimens, but since many of these factors are known after resection, it is difficult to pin-point patients with metastases using only the factors available before surgery.

In order to solve this problem, an attempt to predict the presence of lymph node metastasis by adding molecular markers to clinicopathological factors has been reported. Microarray analysis has led to the observation of gene expressions involved in invasion and metastasis. In gastric cancer as well, upregulation and downregulation of many genes have been observed in relation to lymph node metastasis in basic studies (96–98). However, few molecular markers have proven useful in diagnosing lymph node metastasis in actual clinical specimens. These include VEGF-C (43, 44), EGFR (99), E-cadherin (100, 101), CD44v6 (102), and p53 (103, 104). Unfortunately, these are still in the research stage and have not yet been used in clinical practice. A reason for this is that the usefulness of these assays varies depending on the researcher (102); the heterogeneity of the expression site of the molecular marker may be another reason. In addition, a weak reason is that this is an indirect diagnosis, which does not directly diagnose lymph node metastasis.

INTRAOPERATIVE DIAGNOSIS OF LYMPH NODE METASTASIS IN GASTRIC CANCER

Researchers have investigated the accuracy of evaluating lymph node metastasis in early gastric cancer *via* sentinel lymph node biopsy (105–108). A sentinel node is defined as a node that directly receives lymphatic drainage from a primary tumor (109). The results of a multicenter prospective study indicated that the sentinel node concept is also valid for early gastric cancer (106). The subject of sentinel node biopsy is a clinical node-negative patient, and although the spread of metastasis is unknown, sentinel node biopsy exhibits excellent performance, making it complementary to MDCT diagnosis (18, 110).

Unfortunately, sentinel node biopsy cannot overcome all the disadvantages of MDCT. First, sentinel node biopsy is beneficial only for patients within the indication, as it is feasible only for cT1N0 gastric cancer of less than 5 cm in size. There are also problems specific to gastric cancer sentinel node biopsy, including the use of lymphatic basin dissection as the standard method, which results in the need for dissection of some regional nodes. Therefore, unlike in cases of breast cancer, sentinel node biopsy is difficult to perform prior to gastrectomy (110). Another disadvantage is that it is technically difficult and requires extensive medical resources (18).

As with other carcinomas, sentinel node biopsy for gastric cancer is advantageous in its capacity for ultra-staging and omitting unnecessary nodal dissection in node-negative patients. As with axillary dissection in patients with breast cancer, researchers have investigated the value of sentinel node biopsy as an indicator for the application of function-preserving curative gastrectomy, which omits nodal dissection and reduces the extent of gastrectomy in patients with gastric cancer. A prospective clinical trial is currently ongoing (108, 111).

CHALLENGES IN THE PATHOLOGICAL INVESTIGATION OF LYMPH NODE METASTASIS IN GASTRIC CANCER

Although it is not often mentioned, there are some pitfalls in the pathological determination of lymph node metastases in gastric cancer, including the accuracy of the number of lymph nodes to be examined and the physical limitations in determining pathological metastasis.

In the old Japanese Classification of Gastric Carcinoma (112), the N stage was determined based on the location of lymph node metastasis. At this time, staging was possible when the presence or absence of metastasis of the most distal lymph node was known and harvesting all dissected lymph nodes was not always

necessary. However, with this method, an accurate N stage cannot be determined until a certain extent of lymph node dissection is performed. Currently, the N stage is determined based on the number of metastatic lymph nodes (2, 3). This method is useful for generalization because it does not require complicated grouping or extended nodal dissection. However, all dissected lymph nodes must now be sent to pathology for staging, making it necessary to harvest all lymph nodes removed.

Gastric cancer has many regional lymph nodes, many of which are small, and metastases can occur even in these small lymph nodes (61, 62), which makes harvesting the nodes difficult. However, until now, the accuracy of node harvesting has been neglected (113, 114). Worldwide, harvested nodes are likely to be handled by pathologists. The "palpitation method" for discriminating lymph nodes is probably the most practiced method worldwide and can be performed by pathologists (113), but the number of lymph nodes is larger when examined by surgeons or at a specialized facility (115–117). In clinical practice, more than 15 lymph nodes are often targeted for harvesting (118). However, the actual number of affected lymph nodes is higher, and previous studies have reported that the number of lymph nodes harvested after D2 distal gastrectomy can exceed 40 (113, 119, 120). Many reports have suggested that a greater number of harvested lymph nodes is associated with better prognosis (121–123). In other words, although lymph node harvesting is an important prognostic factor, quality control remains inadequate. The packet submission method has been proposed as a strategy for improving accuracy (115, 124, 125). Although the detection accuracy of the fat-cleaning method has also been reported (126), the time and effort required for fixation, dyeing, and harvesting are extensive.

There are also physical limitations to pathological determination of nodal metastasis. In general, lymph node metastasis is determined *via* microscopic examination of the largest section containing the hilus after hematoxylin and eosin (H&E) staining (2, 3). However, this method can only detect metastatic lesions in the section and may not detect metastasis in the initial image. Lymph node metastasis is thought to progress from cancer cells that flow from the primary lesion into the lymphatic system and reach the marginal sinuses of nodes (110), and the initial images reflect isolated tumor cells (ITCs) and micrometastases. The IJCC staging manual defines an ITC as a metastatic lesion of 0.2 mm or less and a micrometastasis as a metastatic lesion of 2 mm or less (1). Although ITCs do not affect the prognosis of gastric cancer (127), micrometastasis is often reported to worsen the prognosis (128, 129). In other words, when metastasis is determined *via* microscopic examination of the H&E-stained section as usual, a certain degree of error must be considered when determining the number of metastases. For accurate detection of all micrometastases, all retrieved lymph nodes should be subjected to multiple sectioning at 2-mm intervals, which is not practical. An alternative to multiple sectioning is molecular diagnosis of homogenized whole lymph nodes (129). However, there are also challenges to overcome in molecular diagnosis, such as the selection of the gene amplification method, primer selection, contamination, pseudogenes, and cost, making it impractical for use in actual clinical practice. Furthermore, how the results of molecular diagnosis should be used to determine prognosis remains unknown.

CURRENT STATE AND FUTURE DEVELOPMENTS IN THE EVALUATION OF LYMPH NODE METASTASIS IN GASTRIC CANCER

To a certain extent, nodal metastasis of gastric cancer can be cured *via* lymph node dissection when limited to the perigastric nodes. Therefore, preoperative nodal diagnosis is important for planning surgical treatment in patients with gastric cancer. In the case of advanced gastric cancer, MDCT can be used for preoperative nodal diagnosis to some extent, although it is difficult to distinguish node-negative patients with early gastric cancer using this method. Sentinel node biopsy can overcome some of the disadvantages of MDCT.

Postoperative nodal metastatic status is also important when determining the strategy for adjuvant chemotherapy after gastrectomy. However, since the degree of nodal metastasis is determined based on the number of metastatic nodes, it should be noted that there are potential problems with the accuracy of harvesting and a possibility of underestimating micrometastasis. A practical solution to this problem would be to add a safety margin when performing lymph node dissection in patients undergoing gastrectomy.

In the remainder future developments surrounding lymph node metastasis in gastric cancer will be discussed.

Advancements in CT equipment and diagnosis are expected to continue. Improvements in artificial intelligence (AI) supported diagnosis will likely increase the accuracy of nodal diagnosis, rather than finer resolution and more detailed 3D construction (130–132). Although lymph node morphology and contrast patterns have been useful for nodal diagnosis (133), AI diagnosis is likely to surpass this. Advances in intraoperative nodal diagnosis are also expected. Indeed, recent studies have attempted to detect tumor antigens, enzymes produced by tumors, or stromal reactions surrounding metastases using fluorescence observation for rapid intraoperative diagnosis of metastasis (134–140).

Controlling the accuracy of harvesting remains critical, therefore, thorough analysis of the associated difficulties are required to develop simple standardized methods with better accuracy and objectivity than the palpitation method. The most promising method is the fat-dissociation method (113), which has been reported to be useful for shortening the time and improving the accuracy of node harvesting in patients with gastric cancer. Other methods such as indocyanine green fluorescence and methylene blue staining methods have also been proposed (141, 142).

In addition, therapeutic strategies targeting lymph node metastases, especially sentinel lymph node metastases in the

case of molecular targeting therapy, have been considered (143). If such techniques prove useful, the significance of lymph node metastasis will extend beyond a mere basis for staging, and it will become an essential factor when planning more effective adjuvant therapy and treatment strategies for recurrence.

Chemotherapy for advanced gastric cancer has also progressed, and conversion gastrectomy can be performed after downstaging with chemotherapy, even in patients who are not eligible for radical resection (144, 145). It is important to diagnose nodal metastasis and determine its influence on therapeutic efficacy in such patients. To further enhance the effect of conversion gastrectomy following chemotherapy, prompt judgments of diagnosis and the chemotherapeutic effect are essential. Currently, PET-CT is useful; however, there are expectations for improved CT diagnosis using AI.

AUTHOR CONTRIBUTIONS

SK was responsible for the scientific conception of the study and writing of the manuscript. All authors (SK, HS, and HT) contributed to the literature review, data analysis, drafting, editing, critical revision of the manuscript, and approval of the final version of the manuscript.

REFERENCES

1. Brierley J, Gospodarowicz M, Wittekind C. *UICC TNM Classification of Malignant Tumours. 8th*. Chichester: Wiley (2017).
2. Japanese Gastric Cancer Association. *Japanese Classification of Gastric Carcinoma. 15th*. Tokyo: Kanehara Shuppan (2017).
3. Japanese Gastric Cancer Association. Japanese Classification of Gastric Carcinoma: 3rd English Edition. *Gastric Cancer* (2011) 14(2):101–12. doi: 10.1007/s10120-011-0041-5
4. Cunningham D, Allum WH, Stenning SP, Thompson JN, Van de Velde CJHV, Nicolson M, et al. Perioperative Chemotherapy Versus Surgery Alone for Resectable Gastroesophageal Cancer. *N Engl J Med* (2006) 355 (1):11–20. doi: 10.1056/NEJMoa055531
5. Ronellenfitsch U, Schwarzbach M, Hofheinz R, Kienle P, Kieser M, Slanger TE, et al. Perioperative Chemo(Radio)Therapy Versus Primary Surgery for Resectable Adenocarcinoma of the Stomach, Gastroesophageal Junction, and Lower Esophagus. *Cochrane Database Syst Rev* (2013) 31(5):CD008107. doi: 10.1002/14651858.CD008107.pub2
6. Sasako M, Sakuramoto S, Katai H, Kinoshita T, Furukawa H, Yamaguchi T, et al. Five-Year Outcomes of a Randomized Phase III Trial Comparing Adjuvant Chemotherapy With S-1 Versus Surgery Alone in Stage II or III Gastric Cancer. *J Clin Oncol* (2011) 29(33):4387–93. doi: 10.1200/JCO.2011.36.5908
7. Noh SH, Park SR, Yang HK, Chung HC, Chung IJ, Kim SW, et al. Adjuvant Capecitabine Plus Oxaliplatin for Gastric Cancer After D2 Gastrectomy (Classic): 5-Year Follow-Up of an Open-Label, Randomised Phase 3 Trial. *Lancet Oncol* (2014) 15(12):1389–96. doi: 10.1016/S1470-2045(14)70473-5
8. Yoshida K, Kodera Y, Kochi M, Ichikawa W, Kakeji Y, Sano T, et al. Addition of Docetaxel to Oral Fluoropyrimidine Improves Efficacy in Patients With Stage III Gastric Cancer: Interim Analysis of JACCRO GC-07, a Randomized Controlled Trial. *J Clin Oncol* (2019) 37(15):1296–304. doi: 10.1200/JCO.18.01138
9. Katai H, Ishikawa T, Akazawa K, Isobe Y, Miyashiro I, Oda I, et al. Five-Year Survival Analysis of Surgically Resected Gastric Cancer Cases in Japan: A Retrospective Analysis of More Than 100,000 Patients From the Nationwide Registry of the Japanese Gastric Cancer Association(2001–2007). *Gastric Cancer* (2018) 21(1):144–54. doi: 10.1007/s10120-017-0716-7
10. Kikuchi S, Kuroda S, Nishizaki M, Kagawa T, Kanzaki H, Kawahara Y, et al. Management of Early Gastric Cancer That Meet the Indication for Radical Lymph Node Dissection Following Endoscopic Resection: A Retrospective Cohort Analysis. *BMC Surg* (2017) 17(1):72. doi: 10.1186/s12893-017-0268-0
11. Lee JH, Yom CK, Han HS. Comparison of Long-Term Outcomes of Laparoscopy-Assisted and Open Distal Gastrectomy for Early Gastric Cancer. *Surg Endosc* (2009) 23(8):1759–63. doi: 10.1007/s00464-008-0198-0
12. Deng JY, Liang H. Clinical Significance of Lymph Node Metastasis in Gastric Cancer. *World J Gastroenterol* (2014) 20(14):3967–75. doi: 10.3748/wjg.v20.i14.3967
13. Coburn N, Cosby R, Klein L, Knight G, Malthaner R, Mamazza J, et al. Staging and Surgical Approaches in Gastric Cancer: A Systematic Review. *Cancer Treat Rev* (2018) 63:104–15. doi: 10.1016/j.ctrv.2017.12.006
14. Kumagai K, Sano T, Natsugoe S eds. Part III Lymph Node Metastasis: Clinical Significance Gastric Cancer. In: *Lymph Node Metastasis in Gastrointestinal Cancer*. Singapore: Springer Nature Singapore Pte Ltd. p. 267–82. doi: 10.1007/978-981-10-4699-5_14
15. Tasaka S. National Survey of Early Gastric Cancer (Japanese). *Gastroenterol Endosc* (1962) 4:4–14.
16. Koufuji K, Takeda J, Hashimoto K, Tanaka T, Kakegawa T. Early Gastric Cancer Associated With Synchronous Liver Metastasis. *Kurume Med J* (1991) 38(4):271–4. doi: 10.2739/kurumemedj.38.271
17. Nakajima S, Yamaguchi T. Gastric Cancer Database of the Cancer Institute Hospital 1946–2004 (Japanese). *Tokyo: Kanehara Shuppan* (2006).
18. Kinami S, Nakamura N, Tomita Y, Miyata T, Fujita H, Ueda N, et al. Precision Surgical Approach With Lymph-Node Dissection in Early Gastric Cancer. *World J Gastroenterol* (2019) 25(14):1640–52. doi: 10.3748/wjg.v25.i14.1640
19. Lehnert T, Erlandson RA, Decosse JJ. Lymph and Blood Capillaries of the Human Gastric Mucosa. A Morphologic Basis for Metastasis in Early Gastric Carcinoma. *Gastroenterology* (1985) 89(5):939–50. doi: 10.1016/0016-5085(85)90192-1
20. Alexander JS, Ganta VC, Jordan PA, Witte MH. Gastrointestinal Lymphatics in Health and Disease. *Pathophysiology* (2010) 17(4):315–35. doi: 10.1016/j.pathophys.2009.09.003
21. Yonemura Y, Endou Y, Tabachi K, Kawamura T, Yun HY, Kameya T, et al. Evaluation of Lymphatic Invasion in Primary Gastric Cancer by a New Monoclonal Antibody, D2-40. *Hum Pathol* (2006) 37(9):1193–9. doi: 10.1016/j.humpath.2006.04.014
22. Tanaka N, Katai H, Taniguchi H, Saka M, Morita S, Fukagawa T, et al. Surgical Treatment for Early Gastric Cancer (in Japanese With English Abstract). *Stomach Intest* (2009) 44:700–6. doi: 10.11477/mf.1403101642
23. Japanese Gastric Cancer Association. *Japanese Classification of Gastric Carcinoma. 13th*. Tokyo: Kanehara Shuppan (1999).
24. Makino M, Moriwaki S, Yonekawa M, Oota M, Kimura O, Kaibara N. Prognostic Significance of the Number of Metastatic Lymph Nodes in Patients With Gastric Cancer. *J Surg Oncol* (1991) 47(1):12–6. doi: 10.1002/jso.2930470104
25. Ichikura T, Tomimatsu S, Okusa Y, Uefuji K, Tamakuma S. Comparison of the Prognostic Significance Between the Number of Metastatic Lymph Nodes and Nodal Stage Based on Their Location in Patients With Gastric Cancer. *J Clin Oncol* (1993) 11(10):1894–900. doi: 10.1200/JCO.1993.11.10.1894
26. Wu CW, Hsieh MC, Lo SS, Tsay SH, Lui WY, P'eng FK. Relation of Number of Positive Lymph Nodes to the Prognosis of Patients With Primary Gastric Adenocarcinoma. *Gut* (1996) 38(4):525–7. doi: 10.1136/gut.38.4.525
27. Karpeh MS, Leon L, Klimstra D, Brennan MF. Lymph Node Staging in Gastric Cancer: Is Location More Important Than Number? An Analysis of 1,038 Patients. *Ann Surg* (2000) 232(3):362–71. doi: 10.1097/00000658-200009000-00008
28. Giuliano AE, Hunt KK, Ballman KV, Beitsch PD, Whitworth PW, Blumencranz PW, et al. Axillary Dissection vs No Axillary Dissection in Women With Invasive Breast Cancer and Sentinel Node Metastasis: A

Randomized Clinical Trial. *JAMA* (2011) 305(6):569–75. doi: 10.1001/jama.2011.90
29. Giuliano AE, Ballman KV, McCall L, Beitsch PD, Brennan MB, Kelemen PR, et al. Effect of Axillary Dissection vs No Axillary Dissection on 10-Year Overall Survival Among Women With Invasive Breast Cancer and Sentinel Node Metastasis: The ACOSOG Z0011 (Alliance) Randomized Clinical Trial. *JAMA* (2017) 318(10):918–26. doi: 10.1001/jama.2017.11470
30. Jatoi I, Benson JR, Toi M. De-Escalation of Axillary Surgery in Early Breast Cancer. *Lancet Oncol* (2016) 17(10):e430–41. doi: 10.1016/S1470-2045(16)30311-4
31. Anania G, Davies RJ, Arezzo A, Bagolini F, D'Andrea V, Graziosi L, et al. Rise and Fall of Total Mesorectal Excision With Lateral Pelvic Lymphadenectomy for Rectal Cancer: An Updated Systematic Review and Meta-Analysis of 11,366 Patients. *Int J Colorectal Dis* (2021) 36(11):2321–33. doi: 10.1007/s00384-021-03946-2
32. de Lima Vazquez V, Sachetto T, Perpetuo NM, Carvalho AL. Prognostic Factors for Lymph Node Metastasis From Advanced Squamous Cell Carcinoma of the Skin of the Trunk and Extremities. *World J Surg Oncol* (2008) 6(6: 73):73. doi: 10.1186/1477-7819-6-73
33. Panici PB, Maggioni A, Hacker N, Landoni F, Ackermann S, Campagnutta E, et al. Systematic Aortic and Pelvic Lymphadenectomy Versus Resection of Bulky Nodes Only in Optimally Debulked Advanced Ovarian Cancer: A Randomized Clinical Trial. *J Natl Cancer Inst* (2005) 97(8):560–6. doi: 10.1093/jnci/dji102
34. Nimura Y, Nagino M, Takao S, Takada T, Miyazaki K, Kawarada Y, et al. Standard Versus Extended Lymphadenectomy in Radical Pancreatoduodenectomy for Ductal Adenocarcinoma of the Head of the Pancreas: Long-Term Results of a Japanese Multicenter Randomized Controlled Trial. *J Hepatobiliary Pancreat Sci* (2012) 19(3):230–41. doi: 10.1007/s00534-011-0466-6
35. Hu H, Xu G, Du S, Luo Z, Zhao H, Cai J. The Role of Lymph Node Dissection in Intrahepatic Cholangiocarcinoma: A Multicenter Retrospective Study. *BMC Surg* (2021) 21(1):359. doi: 10.1186/s12893-021-01363-4
36. Songun I, Putter H, Kranenbarg EM, Sasako M, van de Velde CJ. Surgical Treatment of Gastric Cancer: 15-Year Follow-Up Results of the Randomised Nationwide Dutch D1D2 Trial. *Lancet Oncol* (2010) 11(5):439–49. doi: 10.1016/S1470-2045(10)70070-X
37. Wu CW, Hsiung CA, Lo SS, Hsieh MC, Chen JH, Li AF, et al. Nodal Dissection for Patients With Gastric Cancer: A Randomised Controlled Trial. *Lancet Oncol* (2006) 7(4):309–15. doi: 10.1016/S1470-2045(06)70623-4
38. Zhu T, Hu X, Wei P, Shan G. Molecular Background of the Regional Lymph Node Metastasis of Gastric Cancer. *Oncol Lett* (2018) 15(3):3409–14. doi: 10.3892/ol.2018.7813
39. Eccles SA, Welch DR. Metastasis: Recent Discoveries and Novel Treatment Strategies. *Lancet* (2007) 369(9574):1742–57. doi: 10.1016/S0140-6736(07)60781-8
40. Langheinrich MC, Schellerer V, Perrakis A, Lohmüller C, Schildberg C, Naschberger E, et al. Molecular Mechanisms of Lymphatic Metastasis in Solid Tumors of the Gastrointestinal Tract. *Int J Clin Exp Pathol* (2012) 5(7):614–23.
41. Achen MG, Stacker SA. Molecular Control of Lymphatic Metastasis. *Ann NY Acad Sci* (2008) 1131:225–34. doi: 10.1196/annals.1413.020
42. Sundar SS, Ganesan TS. Role of Lymphangiogenesis in Cancer. *J Clin Oncol* (2007) 25(27):4298–307. doi: 10.1200/JCO.2006.07.1092
43. Yonemura Y, Endo Y, Tabata K, Kawamura T, Yun HY, Bandou E, et al. Role of VEGF-C and VEGF-D in Lymphangiogenesis in Gastric Cancer. *Int J Clin Oncol* (2005) 10(5):318–27. doi: 10.1007/s10147-005-0508-7
44. Amioka T, Kitadai Y, Tanaka S, Haruma K, Yoshihara M, Yasui W, et al. Vascular Endothelial Growth Factor-C Expression Predicts Lymph Node Metastasis of Human Gastric Carcinomas Invading the Submucosa. *Eur J Cancer* (2002) 38(10):1413–9. doi: 10.1016/s0959-8049(02)00106-5
45. Kitadai Y. Angiogenesis and Lymphangiogenesis of Gastric Cancer. *J Oncol* (2010) 2010:468725. doi: 10.1155/2010/468725
46. Stacker SA, Achen MG, Jussila L, Baldwin ME, Alitalo K. Lymphangiogenesis and Cancer Metastasis. *Nat Rev Cancer* (2002) 2(8):573–83. doi: 10.1038/nrc863
47. Kurayoshi M, Oue N, Yamamoto H, Kishida M, Inoue A, Asahara T, et al. Expression of Wnt-5a Is Correlated With Aggressiveness of Gastric Cancer by Stimulating Cell Migration and Invasion. *Cancer Res* (2006) 66(21):10439–48. doi: 10.1158/0008-5472.CAN-06-2359
48. Yamamoto H, Kitadai Y, Yamamoto H, Oue N, Ohdan H, Yasui W, et al. Laminin Gamma2 Mediates Wnt5a-Induced Invasion of Gastric Cancer Cells. *Gastroenterology* (2009) 137(1):242–52, 252.e1, 252.e1–252.e6. doi: 10.1053/j.gastro.2009.02.003
49. Takaishi S, Okumura T, Tu S, Wang SS, Shibata W, Vigneshwaran R, et al. Identification of Gastric Cancer Stem Cells Using the Cell Surface Marker CD44. *Stem Cells* (2009) 27(5):1006–20. doi: 10.1002/stem.30
50. Wakamatsu Y, Sakamoto N, Oo HZ, Naito Y, Uraoka N, Anami K, et al. Expression of Cancer Stem Cell Markers ALDH1, CD44 and CD133 in Primary Tumor and Lymph Node Metastasis of Gastric Cancer. *Pathol Int* (2012) 62(2):112–9. doi: 10.1111/j.1440-1827.2011.02760.x
51. Takashima S, Kosaka T. Results and Controversial Issues Regarding a Para-Aortic Lymph Node Dissection for Advanced Gastric Cancer. *Surg Today* (2005) 35(6):425–31. doi: 10.1007/s00595-004-2976-1
52. Sano T, Katai H, Sasako M, Maruyama K. Problems of International Standardization of Gastric Cancer Surgery (Japanese). *Nihon Geka Gakkai Zasshi* (2001) 102(10):758–63.
53. Yoshikawa T, Sasako M, Sano T, Nashimoto A, Kurita A, Tsujinaka T, et al. Stage Migration Caused by D2 Dissection With Para-Aortic Lymphadenectomy for Gastric Cancer From the Results of a Prospective Randomized Controlled Trial. *Br J Surg* (2006) 93(12):1526–9. doi: 10.1002/bjs.5487
54. Sasako M, Sano T, Yamamoto S, Kurokawa Y, Nashimoto A, Kurita A, et al. D2 Lymphadenectomy Alone or With Para-Aortic Nodal Dissection for Gastric Cancer. *N Engl J Med* (2008) 359(5):453–62. doi: 10.1056/NEJMoa0707035
55. Sano T, Sasako M, Yamamoto S, Nashimoto A, Kurita A, Hiratsuka M, et al. Gastric Cancer Surgery: Morbidity and Mortality Results From a Prospective Randomized Controlled Trial Comparing D2 and Extended Para-Aortic Lymphadenectomy - Japan Clinical Oncology Group Study 9501. *J Clin Oncol* (2004) 22(14):2767–73. doi: 10.1200/JCO.2004.10.184
56. Tsujinaka T, Sasako M, Yamamoto S, Sano T, Kurokawa Y, Nashimoto A, et al. Influence of Overweight on Surgical Complications for Gastric Cancer: Results From a Randomized Control Trial Comparing D2 and Extended Para-Aortic D3 Lymphadenectomy (JCOG9501). *Ann Surg Oncol* (2007) 14(2):355–61. doi: 10.1245/s10434-006-9209-3
57. Bonenkamp JJ, Hermans J, Sasako M, van de Velde CJ, Welvaart K, Songun I, et al. Extended Lymph-Node Dissection for Gastric Cancer. *N Engl J Med* (1999) 340(12):908–14. doi: 10.1056/NEJM199903253401202
58. Japanese Gastric Cancer Association. *Japanese Gastric Cancer Treatment Guidelines 2021. 6th*. Tokyo: Kanehara Shuppan (2021).
59. Japanese Gastric Cancer Association. Japanese Gastric Cancer Treatment Guidelines 2018 5th Ed. *Gastric Cancer* (2021) 24:1–21. doi: 10.1007/s10120-020-01042-y
60. Kwee RM, Kwee TC. Imaging in Assessing Lymph Node Status in Gastric Cancer. *Gastric Cancer* (2009) 12(1):6–22. doi: 10.1007/s10120-008-0492-5
61. Jiang ZY, Kinami S, Nakamura N, Miyata T, Fujita H, Takamura H, et al. Diagnostic Ability of Multi-Detector Spiral Computed Tomography for Pathological Lymph Node Metastasis of Advanced Gastric Cancer. *World J Gastrointest Oncol* (2020) 12(4):435–46. doi: 10.4251/wjgo.v12.i4.435
62. Noda N, Sasako M, Yamaguchi N, Nakanishi Y. Ignoring Small Lymph Nodes can be a Major Cause of Staging Error in Gastric Cancer. *Br J Surg* (1998) 85(6):831–4. doi: 10.1046/j.1365-2168.1998.00691.x
63. Smeets AJ, Zonderland HM, van der Voorde F, Laméris JS. Evaluation of Abdominal Lymph Nodes by Ultrasound. *J Ultrasound Med* (1990) 9(6):325–31. doi: 10.7863/jum.1990.9.6.325
64. Liao SR, Dai Y, Huo L, Yan K, Zhang L, Zhang H, et al. Transabdominal Ultrasonography in Preoperative Staging of Gastric Cancer. *World J Gastroenterol* (2004) 10(23):3399–404. doi: 10.3748/wjg.v10.i23.3399
65. Alvarez S, Añorbe E, Alcorta P, López F, Alonso I, Cortés J. Role of Sonography in the Diagnosis of Axillary Lymph Node Metastases in Breast Cancer: A Systematic Review. *AJR* (2006) 186(5):1342–8. doi: 10.2214/AJR.05.0936
66. Swinson C, Ravichandran D, Nayagam M, Allen S. Ultrasound and Fine Needle Aspiration Cytology of the Axilla in the Pre-Operative Identification

of Axillary Nodal Involvement in Breast Cancer. *Eur J Surg Oncol* (2009) 35 (11):1152–7. doi: 10.1016/j.ejso.2009.03.008
67. Gipponi M, Fregatti P, Garlaschi A, Murelli F, Margarino C, Depaoli F, et al. Axillary Ultrasound and Fine-Needle Aspiration Cytology in the Preoperative Staging of Axillary Node Metastasis in Breast Cancer Patients. *Breast* (2016) 30:146–50. doi: 10.1016/j.breast.2016.09.009
68. Mocellin S, Marchet A, Nitti D. EUS for the Staging of Gastric Cancer: A Meta-Analysis. *Gastrointest Endosc* (2011) 73(6):1122–34. doi: 10.1016/j.gie.2011.01.030
69. Mocellin S, Pasquali S. Diagnostic Accuracy of Endoscopic Ultrasonography (EUS) for the Preoperative Locoregional Staging of Primary Gastric Cancer. *Cochrane Database Syst Rev* (2015) 6(2):CD009944. doi: 10.1002/14651858.CD009944.pub2
70. Tamanini G, Cominardi A, Brighi N, Fusaroli P, Lisotti A. Endoscopic Ultrasound Assessment and Tissue Acquisition of Mediastinal and Abdominal Lymph Nodes. *World J Gastrointest Oncol* (2021) 13 (10):1475–91. doi: 10.4251/wjgo.v13.i10.1475
71. Paterson S, Duthie F, Stanley AJ. Endoscopic Ultrasound-Guided Elastography in the Nodal Staging of Oesophageal Cancer. *World J Gastroenterol* (2012) 18(9):889–95. doi: 10.3748/wjg.v18.i9.889
72. Harrington C, Smith L, Bisland J, López González EL, Jamieson N, Paterson S, et al. Mediastinal Node Staging by Positron Emission Tomography-Computed Tomography and Selective Endoscopic Ultrasound With Fine Needle Aspiration for Patients With Upper Gastrointestinal Cancer: Results From a Regional Centre. *World J Gastrointest Endosc* (2018) 10(1):37–44. doi: 10.4253/wjge.v10.i1.37
73. Sazuka T, Akai T, Uesato M, Horibe D, Kuboshima M, Kitabayashi H, et al. Assessment for Diagnosis of Lymph Node Metastasis in Esophageal Cancer Using Endoscopic Ultrasound Elastography. *Esophagus* (2016) 13:254–63. doi: 10.1007/s10388-016-0521-0
74. Bentrem D, Gerdes H, Tang L, Brennan M, Coit D. Clinical Correlation of Endoscopic Ultrasonography With Pathologic Stage and Outcome in Patients Undergoing Curative Resection for Gastric Cancer. *Ann Surg Oncol* (2007) 14(6):1853–9. doi: 10.1245/s10434-006-9037-5
75. Luo M, Lv Y, Guo X, Song H, Su G, Chen B. Value and Impact Factors of Multidetector Computed Tomography in Diagnosis of Preoperative Lymph Node Metastasis in Gastric Cancer: A PRISMA-Compliant Systematic Review and Meta-Analysis. *Medicine* (2017) 96(33):e7769. doi: 10.1097/MD.0000000000007769
76. Wang J, Zhong L, Zhou X, Chen D, Li R. Value of Multiphase Contrast-Enhanced CT With Three-Dimensional Reconstruction in Detecting Depth of Infiltration, Lymph Node Metastasis, and Extramural Vascular Invasion of Gastric Cancer. *J Gastrointest Oncol* (2021) 12(4):1351–62. doi: 10.21037/jgo-21-276
77. Jiang M, Wang X, Shan X, Pan D, Jia Y, Ni E, et al. Value of Multi-Slice Spiral Computed Tomography in the Diagnosis of Metastatic Lymph Nodes and N-Stage of Gastric Cancer. *J Int Med Res* (2019) 47(1):281–92. doi: 10.1177/0300060518800611
78. Kubota K, Suzuki A, Shiozaki H, Wada T, Kyosaka T, Kishida A. Accuracy of Multidetector-Row Computed Tomography in the Preoperative Diagnosis of Lymph Node Metastasis in Patients With Gastric Cancer. *Gastrointest Tumors* (2017) 3(3–4):163–70. doi: 10.1159/000454923
79. Saito T, Kurokawa Y, Takiguchi S, Miyazaki Y, Takahashi T, Yamasaki M, et al. Accuracy of Multidetector-Row CT in Diagnosing Lymph Node Metastasis in Patients With Gastric Cancer. *Eur Radiol* (2015) 25(2):368–74. doi: 10.1007/s00330-014-3373-9
80. Choi JI, Joo I, Lee JM. State-Of-the-Art Preoperative Staging of Gastric Cancer by MDCT and Magnetic Resonance Imaging. *World J Gastroenterol* (2014) 20(16):4546–57. doi: 10.3748/wjg.v20.i16.4546
81. Fukagawa T, Katai H, Mizusawa J, Nakamura K, Sano T, Terashima M, et al. A Prospective Multi-Institutional Validity Study to Evaluate the Accuracy of Clinical Diagnosis of Pathological Stage III Gastric Cancer (JCOG1302A). *Gastric Cancer* (2018) 21(1):68–73. doi: 10.1007/s10120-017-0701-1
82. Ohashi M, Morita S, Fukagawa T, Wada T, Kushima R, Onaya H, et al. Evaluation of 64-Channel Contrast-Enhanced Multi-Detector Row Computed Tomography for Preoperative N Staging in Ct2-4 Gastric Carcinoma. *World J Surg* (2016) 40(1):165–71. doi: 10.1007/s00268-015-3318-8
83. Yang QM, Kawamura T, Itoh H, Bando E, Nemoto M, Akamoto S, et al. Is PET-CT Suitable for Predicting Lymph Node Status for Gastric Cancer? *Hepatogastroenterology* (2008) 55(82–83):782–5.
84. Park K, Jang G, Baek S, Song H. Usefulness of Combined PET/CT to Assess Regional Lymph Node Involvement in Gastric Cancer. *Tumori* (2014) 100 (2):201–6. doi: 10.1700/1491.16415
85. Kawanaka Y, Kitajima K, Fukushima K, Mouri M, Doi H, Oshima T, et al. Added Value of Pretreatment (18)F-FDG PET/CT for Staging of Advanced Gastric Cancer: Comparison With Contrast-Enhanced MDCT. *Eur J Radiol* (2016) 85(5):989–95. doi: 10.1016/j.ejrad.2016.03.003
86. Choi JY, Shim KN, Kim SE, Jung HK, Jung SA, Yoo K. The Clinical Value of 18F-Fluorodeoxyglucose Uptake on Positron Emission Tomography/Computed Tomography for Predicting Regional Lymph Node Metastasis and Non-Curative Surgery in Primary Gastric Carcinoma. *Korean J Gastroenterol* (2014) 64(6):340–7. doi: 10.4166/kjg.2014.64.6.340
87. Borggreve AS, Goense L, Brenkman HJF, Mook S, Meijer GJ, Wessels FJ, et al. Imaging Strategies in the Management of Gastric Cancer: Current Role and Future Potential of MRI. *Br J Radiol* (2019) 92(1097):20181044. doi: 10.1259/bjr.20181044
88. Tokuhara T, Tanigawa N, Matsuki M, Nomura E, Mabuchi H, Lee SW, et al. Evaluation of Lymph Node Metastases in Gastric Cancer Using Magnetic Resonance Imaging With Ultrasmall Superparamagnetic Iron Oxide (USPIO): Diagnostic Performance in Post-Contrast Images Using New Diagnostic Criteria. *Gastric Cancer* (2008) 11(4):194–200. doi: 10.1007/s10120-008-0480-9
89. Catalano MF, Sivak MV, Rice T, Gragg LA, Van Dam JV. Endosonographic Features Predictive of Lymph Node Metastasis. *Gastrointest Endosc* (1994) 40(4):442–6. doi: 10.1016/s0016-5107(94)70206-3
90. Faige DO. EUS in Patients With Benign and Malignant Lymphadenopathy. *Gastrointest Endosc* (2001) 53(6):593–8. doi: 10.1067/mge.2001.114060
91. Shimoyama S, Yasuda H, Hashimoto M, Tatsutomi Y, Aoki F, Mafune K, et al. Accuracy of Linear-Array EUS for Preoperative Staging of Gastric Cardia Cancer. *Gastrointest Endosc* (2004) 60(1):50–5. doi: 10.1016/s0016-5107(04)01312-4
92. Shida A, Fujioka S, Kawamura M, Takahashi N, Ishibashi Y, Nakada K, et al. Prediction of Lymph Node Metastasis in Patients With Submucosa-Invading Early Gastric Cancer. *Anticancer Res* (2014) 34(8):4471–4.
93. Fujii M, Egashira Y, Akutagawa H, Nishida T, Nitta T, Edagawa G, et al. Pathological Factors Related to Lymph Node Metastasis of Submucosally Invasive Gastric Cancer: Criteria for Additional Gastrectomy After Endoscopic Resection. *Gastric Cancer* (2013) 16(4):521–30. doi: 10.1007/s10120-012-0215-9
94. Zheng Z, Zhang Y, Zhang L, Li Z, Wu X, Liu Y, et al. A Nomogram for Predicting the Likelihood of Lymph Node Metastasis in Early Gastric Patients. *BMC Cancer* (2016) 16:92. doi: 10.1186/s12885-016-2132-5
95. Zhao LY, Yin Y, Li X, Zhu CJ, Wang YG, Chen XL, et al. A Nomogram Composed of Clinicopathologic Features and Preoperative Serum Tumor Markers to Predict Lymph Node Metastasis in Early Gastric Cancer Patients. *Oncotarget* (2016) 7(37):59630–9. doi: 10.18632/oncotarget.10732
96. Hippo Y, Taniguchi H, Tsutsumi S, Machida N, Chong JM, Fukayama M, et al. Global Gene Expression Analysis of Gastric Cancer by Oligonucleotide Microarrays. *Cancer Res* (2002) 62(1):233–40.
97. Inoue H, Matsuyama A, Mimori K, Ueo H, Mori M. Prognostic Score of Gastric Cancer Determined by cDNA Microarray. *Clin Cancer Res* (2002) 8 (11):3475–9.
98. Oue N, Hamai Y, Mitani Y, Matsumura S, Oshimo Y, Aung PP, et al. Gene Expression Profile of Gastric Carcinoma: Identification of Genes and Tags Potentially Involved in Invasion, Metastasis, and Carcinogenesis by Serial Analysis of Gene Expression. *Cancer Res* (2004) 64(7):2397–405. doi: 10.1158/0008-5472.can-03-3514
99. Jin EH, Lee DH, Jung SA, Shim KN, Seo JY, Kim N, et al. Clinicopathologic Factors and Molecular Markers Related to Lymph Node Metastasis in Early Gastric Cancer. *World J Gastroenterol* (2015) 21(2):571–7. doi: 10.3748/wjg.v21.i2.571
100. Yoshii T, Miyagi Y, Nakamura Y, Kobayashi O, Kameda Y, Ohkawa S. Pilot Research for the Correlation Between the Expression Pattern of E-Cadherin-β-Catenin Complex and Lymph Node Metastasis in Early Gastric Cancer. *Tumori* (2013) 99(2):234–8. doi: 10.1700/1283.14198

101. Piccolo G, Zanghı` A, Di Vita M, Bisagni P, Lecchi F, Cavallaro A, et al. The Role of E-Cadherin Expression in the Treatment of Western Undifferentiated Early Gastric Cancer: Can a Biological Factor Predict Lymph Node Metastasis? *PloS One* (2020) 15(4):e0232429. doi: 10.1371/journal.pone.0232429
102. Eom BW, Joo J, Park B, Jo MJ, Choi SH, Cho SJ, et al. Nomogram Incorporating CD44v6 and Clinicopathological Factors to Predict Lymph Node Metastasis for Early Gastric Cancer. *PloS One* (2016) 11(8):e0159424. doi: 10.1371/journal.pone.0159424
103. Wang YW, Zhu ML, Wang RF, Xue WJ, Zhu XR, Wang LF, et al. Predictable Factors for Lymph Node Metastasis in Early Gastric Cancer Analysis of Clinicopathologic Factors and Biological Markers. *Tumour Biol* (2016) 37 (7):8567–78. doi: 10.1007/s13277-015-4721-3
104. Yin XY, Pang T, Liu Y, Cui HT, Luo TH, Lu ZM, et al. Development and Validation of a Nomogram for Preoperative Prediction of Lymph Node Metastasis in Early Gastric Cancer. *World J Surg Oncol* (2020) 18(1):2. doi: 10.1186/s12957-019-1778-2
105. Miwa K, Kinami S, Taniguchi K, Fushida S, Fujimura T, Nonomura A. Mapping Sentinel Nodes in Patients With Early-Stage Gastric Carcinoma. *Br J Surg* (2003) 90(2):178–82. doi: 10.1002/bjs.4031
106. Kitagawa Y, Takeuchi H, Takagi Y, Natsugoe S, Terashima M, Murakami N, et al. Sentinel Node Mapping for Gastric Cancer: A Prospective Multicenter Trial in Japan. *J Clin Oncol* (2013) 31(29):3704–10. doi: 10.1200/JCO.2013.50.3789
107. Takeuchi H, Goto O, Yahagi N, Kitagawa Y. Function-Preserving Gastrectomy Based on the Sentinel Node Concept in Early Gastric Cancer. *Gastric Cancer* (2017) 20(Suppl 1):53–9. doi: 10.1007/s10120-016-0649-6
108. Park JY, Kim YW, Ryu KW, Nam BH, Lee YJ, Jeong SH, et al. Assessment of Laparoscopic Stomach Preserving Surgery With Sentinel Basin Dissection Versus Standard Gastrectomy With Lymphadenectomy in Early Gastric Cancer-A Multicenter Randomized Phase III Clinical Trial (SENORITA Trial) Protocol. *BMC Cancer* (2016) 16(16):340. doi: 10.1186/s12885-016-2336-8
109. Morton DL, Wen DR, Wong JH, Economou JS, Cagle LA, Storm FK, et al. Technical Details of Intraoperative Lymphatic Mapping for Early Stage Melanoma. *Arch Surg* (1992) 127(4):392–9. doi: 10.1001/archsurg.1992.01420040034005
110. Kinami S, Kosaka T, Natsugoe S eds. Part IV Sentinel Node Navigation Surgery: Methodology: Dye and Isotope Method. In: *Lymph Node Metastasis in Gastrointestinal Cancer*. Singapore: Springer Nature Singapore Pte Ltd. p. 305–21. doi: 10.1007/978-981-10-4699-5_16
111. Kamiya S, Takeuchi H, Fukuda K, Kawakubo H, Takahashi N, Mitsumori N, et al. A Multicenter Non-Randomized Phase III Study of Sentinel Node Navigation Surgery for Early Gastric Cancer. *Jpn J Clin Oncol* (2021) 51 (2):305–9. doi: 10.1093/jjco/hyaa179
112. Japanese Gastric Cancer Association. Japanese Classification of Gastric Carcinoma - 2nd English Edition. *Gastric Cancer* (1998) 1(1):10–24. doi: 10.1007/s101209800016
113. Kinami S, Ohnishi T, Nakamura N, Jiang ZY, Miyata T, Fujita H, et al. Efficacy of the Fat-Dissociation Method for Nodal Harvesting in Gastric Cancer. *World J Gastrointest Surg* (2020) 12(6):277–86. doi: 10.4240/wjgs.v12.i6.277
114. Ambrosio MRA, Perotti B, Cavazzana A, Arganini M. How Surgeon and Pathologist Cooperation may Drive Toward a More Efficient Nodes Harvesting in Gastric Cancer Surgery. *Updates Surg* (2021) 73(5):2025–8. doi: 10.1007/s13304-021-01030-6
115. Ikoma N, Estrella JS, Hofstetter WL, Ajani JA, Fournier KF, Mansfield PF, et al. Surgeon Assessment of Gastric Cancer Lymph Node Specimens With a Video of Technique. *J Gastrointest Surg* (2018) 22(11):2013–9. doi: 10.1007/s11605-018-3880-0
116. Morgan JW, Ji L, Friedman G, Senthil M, Dyke C, Lum SS. The Role of the Cancer Center When Using Lymph Node Count as a Quality Measure for Gastric Cancer Surgery. *JAMA Surg* (2015) 150(1):37–43. doi: 10.1001/jamasurg.2014.678
117. Bunt AM, Hermans J, van de Velde CJ, Sasako M, Hoefsloot FA, Fleuren G, et al. Lymph Node Retrieval in a Randomized Trial on Western-Type Versus Japanese-Type Surgery in Gastric Cancer. *J Clin Oncol* (1996) 14(8):2289–94. doi: 10.1200/JCO.1996.14.8.2289
118. Amin MB, Edge S, Greene F, Byrd DR, Brookland RK, Washington MK, et al. *AJCC Cancer Staging Manual. 8th*. New York: Springer (2017).
119. Inaki N, Etoh T, Ohyama T, Uchiyama K, Katada N, Koeda K, et al. A Multi-Institutional, Prospective, Phase II Feasibility Study of Laparoscopy-Assisted Distal Gastrectomy With D2 Lymph Node Dissection for Locally Advanced Gastric Cancer (JLSSG0901). *World J Surg* (2015) 39(11):2734–41. doi: 10.1007/s00268-015-3160-z
120. Hu Y, Huang C, Sun Y, Su X, Cao H, Hu J, et al. Morbidity and Mortality of Laparoscopic Versus Open D2 Distal Gastrectomy for Advanced Gastric Cancer: A Randomized Controlled Trial. *J Clin Oncol* (2016) 34(12):1350–7. doi: 10.1200/JCO.2015.63.7215
121. Smith DD, Schwarz RR, Schwarz RE. Impact of Total Lymph Node Count on Staging and Survival After Gastrectomy for Gastric Cancer: Data From a Large US-Population Database. *J Clin Oncol* (2005) 23(28):7114–24. doi: 10.1200/JCO.2005.14.621
122. Macalindong SS, Kim KH, Nam BH, Ryu KW, Kubo N, Kim JY, et al. Effect of Total Number of Harvested Lymph Nodes on Survival Outcomes After Curative Resection for Gastric Adenocarcinoma: Findings From an Eastern High-Volume Gastric Cancer Center. *BMC Cancer* (2018) 18(1):73. doi: 10.1186/s12885-017-3872-6
123. Lu J, Wang W, Zheng CH, Fang C, Li P, Xie JW, et al. Influence of Total Lymph Node Count on Staging and Survival After Gastrectomy for Gastric Cancer: An Analysis From a Two-Institution Database in China. *Ann Surg Oncol* (2017) 24(2):486–93. doi: 10.1245/s10434-016-5494-7
124. Cao Y, Xiong L, Deng S, Shen L, Li J, Wu K, et al. The Effect of Perigastric Lipolymphatic Tissue Grouping by Surgeon on the Number of Pathologic Sampled Lymph Nodes After Radical Gastrectomy. *Med (Baltimore)* (2018) 97(27):e11411. doi: 10.1097/MD.0000000000011411
125. Wang P, Zhang K, Xi H, Liang W, Xie T, Gao Y, et al. Lymph Node Yield Following Packet Submission After Isolation by Surgeon During Gastrectomy. *Cancer Manag Res* (2019) 11:9871–81. doi: 10.2147/CMAR.S211218
126. Candela FC, Urmacher C, Brennan MF. Comparison of the Conventional Method of Lymph Node Staging With a Comprehensive Fat-Clearing Method for Gastric Adenocarcinoma. *Cancer* (1990) 66(8):1828–32. doi: 10.1002/1097-0142(19901015)66:8<1828::aid-cncr2820660830>3.0.co;2-z
127. Fukagawa T, Sasako M, Ito S, Nakanishi H, Iinuma H, Natsugoe S, et al. The Prognostic Significance of Isolated Tumor Cells in the Lymph Nodes of Gastric Cancer Patients. *Gastric Cancer* (2010) 13(3):191–6. doi: 10.1007/s10120-010-0556-1
128. Huang JY, Xu YY, Li M, Sun Z, Zhu Z, Song YX, et al. The Prognostic Impact of Occult Lymph Node Metastasis in Node-Negative Gastric Cancer: A Systematic Review and Meta-Analysis. *Ann Surg Oncol* (2013) 20(12):3927–34. doi: 10.1245/s10434-013-3021-7
129. Arigami T, Uenosono Y, Yanagita S, Ishigami S, Natsugoe S. Gastric Cancer in Lymph Node Metastasis in Gastrointestinal Cancer. In: Natsugoe S, editor. *Part II Lymph Node Micrometastasis: Clinical Aspect*. Springer: Springer Nature Singapore Pte Ltd (2019). p. 209–33. doi: 10.1007/978-981-10-4699-5_10
130. Gao Y, Zhang ZD, Li S, Guo YT, Wu QY, Liu SH, et al. Deep Neural Network-Assisted Computed Tomography Diagnosis of Metastatic Lymph Nodes From Gastric Cancer. *Chin Med J (Engl)* (2019) 132(23):2804–11. doi: 10.1097/CM9.0000000000000532
131. Li C, Zhang S, Zhang H, Pang L, Lam K, Hui C, et al. Using the K-Nearest Neighbor Algorithm for the Classification of Lymph Node Metastasis in Gastric Cancer. *Comput Math Methods Med* (2012) 2012:876545. doi: 10.1155/2012/876545
132. Niu PH, Zhao LL, Wu HL, Zhao DB, Chen YT. Artificial Intelligence in Gastric Cancer: Application and Future Perspectives. *World J Gastroenterol* (2020) 26(36):5408–19. doi: 10.3748/wjg.v26.i36.5408
133. Liu S, Shi H, Ji C, Zheng H, Pan X, Guan W, et al. Preoperative CT Texture Analysis of Gastric Cancer: Correlations With Postoperative TNM Staging. *Clin Radiol* (2018) 73(8):756.e1–9. doi: 10.1016/j.crad.2018.03.005
134. Matsumoto T, Murayama Y, Matsuo H, Okochi K, Koshiishi N, Harada Y, et al. 5-ALA-Assistant Automated Detection of Lymph Node Metastasis in Gastric Cancer Patients. *Gastric Cancer* (2020) 23(4):725–33. doi: 10.1007/s10120-020-01044-w
135. Tsujimoto H, Morimoto Y, Takahata R, Nomura S, Yoshida K, Hiraki S, et al. Theranostic Photosensitive Nanoparticles for Lymph Node Metastasis of

Gastric Cancer. *Ann Surg Oncol* (2015) 22(Suppl 3):S923–8. doi: 10.1245/s10434-015-4594-0

136. Eisenberg DP, Adusumilli PS, Hendershott KJ, Chung S, Yu Z, Chan MK, et al. Real-Time Intraoperative Detection of Breast Cancer Axillary Lymph Node Metastases Using a Green Fluorescent Protein-Expressing Herpes Virus. *Ann Surg* (2006) 243(6):824–830; discussion 830. doi: 10.1097/01.sla.0000219738.56896.c0
137. Tummers WS, Miller SE, Teraphongphom NT, van den Berg NS, Hasan A, Longacre TA, et al. Detection of Visually Occult Metastatic Lymph Nodes Using Molecularly Targeted Fluorescent Imaging During Surgical Resection of Pancreatic Cancer. *HPB (Oxf)* (2019) 21(7):883–90. doi: 10.1016/j.hpb.2018.11.008
138. Shinden Y, Ueo H, Tobo T, Gamachi A, Utou M, Komatsu H, et al. Rapid Diagnosis of Lymph Node Metastasis in Breast Cancer Using a New Fluorescent Method With γ-Glutamyl Hydroxymethyl Rhodamine Green. *Sci Rep* (2016) 9:6, 27525. doi: 10.1038/srep27525
139. Cho HJ, Lee S, Park SJ, Lee YD, Jeong K, Park JH, et al. Tumor Microenvironment-Responsive Fluorogenic Nanoprobe for Ratiometric Dual-Channel Imaging of Lymph Node Metastasis. *Colloids Surf B Biointerf* (2019) 179:9–16. doi: 10.1016/j.colsurfb.2019.03.047
140. Mieog JSD, Achterberg FB, Zlitni A, Hutteman M, Burggraaf J, Swijnenburg RJ, et al. Fundamentals and Developments in Fluorescence-Guided Cancer Surgery. *Nat Rev Clin Oncol* (2022) 19:9–22. doi: 10.1038/s41571-021-00548-3
141. Kusano M, Ono H, Danjo Y, Kawamata F, Tajima Y, Ohtsubo S, et al. Chapter14: Fluorescent Navigation Surgery for Gastrointestinal Tract Cancers: Detection of Sentinel Nodes, Tumor Tattooing, and Harvesting of Lymph Nodes. In: Kusano M, Kokudo N, Toi M, Kaibori M, editors. *ICG Fluorescence Imaging and Navigation Surgery*. Tokyo: Springer Nature Japan (2016). p. 165–74. doi: 10.1007/978-4-431-55528-5_14
142. Aoyama T, Fujikawa H, Cho H, Ogata T, Shirai J, Hayashi T, et al. A Methylene Blue–Assisted Technique for Harvesting Lymph Nodes After Radical Surgery for Gastric Cancer: A Prospective, Randomized, Controlled Study. *Am J Surg Pathol* (2015) 39(2):266–73. doi: 10.1097/PAS.0000000000000336
143. Mansouri N, Movafagh A, Sayad A, Heidary Pour A, Taheri M, Soleimani S, et al. Targeting of BUB1b Gene Expression in Sentinel Lymph Node Biopsies of Invasive Breast Cancer in Iranian Female Patients. *Asian Pac J Cancer Prev* (2016) 17(S3):317–21. doi: 10.7314/apjcp.2016.17.s3.317
144. Yoshida K, Yamaguchi K, Okumura N, Tanahashi T, Kodera Y. Is Conversion Therapy Possible in Stage IV Gastric Cancer: The Proposal of New Biological Categories of Classification. *Gastric Cancer* (2016) 19(2):329–38. doi: 10.1007/s10120-015-0575-z
145. Terashima M, Yoshida K, Rha SY, Bae JM, Li G, Katai H, et al. International Retrospective Cohort Study of Conversion Therapy for Stage IV Gastric Cancer 1 (CONVO-GC-1). *J Clin Oncol* (2018) 36(15_suppl):4042–2. doi: 10.1200/JCO.2018.36.15_suppl.4042

Conflict of Interest: The authors declare that the research was conducted in the absence of any commercial or financial relationships that could be construed as a potential conflict of interest.

Publisher's Note: All claims expressed in this article are solely those of the authors and do not necessarily represent those of their affiliated organizations, or those of the publisher, the editors and the reviewers. Any product that may be evaluated in this article, or claim that may be made by its manufacturer, is not guaranteed or endorsed by the publisher.

Copyright © 2022 Kinami, Saito and Takamura. This is an open-access article distributed under the terms of the Creative Commons Attribution License (CC BY). The use, distribution or reproduction in other forums is permitted, provided the original author(s) and the copyright owner(s) are credited and that the original publication in this journal is cited, in accordance with accepted academic practice. No use, distribution or reproduction is permitted which does not comply with these terms.

frontiers in Oncology

ORIGINAL RESEARCH
published: 20 January 2022
doi: 10.3389/fonc.2021.811595

Development and Validation of a New Lymph Node Ratio-Based Staging System for Ampullary Carcinoma After Curative Pancreaticoduodenectomy

Xiaojie Zhang[1], Chongyuan Sun[1], Zefeng Li[1], Tongbo Wang[1], Lulu Zhao[1], Penghui Niu[1], Chunguang Guo[1], Yingtai Chen[1], Xu Che[1,2] and Dongbing Zhao[1*]*

[1] Department of Pancreatic and Gastric Surgical Oncology, National Cancer Center/National Clinical Research for Cancer/Cancer Hospital, Chinese Academy of Medical Sciences and Peking Union Medical College, Beijing, China, [2] Department of Hepatobiliary and Pancreatic Surgery, National Cancer Center/National Clinical Research Center for Cancer/Cancer Hospital & Shenzhen Hospital, Chinese Academy of Medical Sciences and Peking Union Medical College, Shenzhen, China

Background: Lymph node metastasis (LNM) is closely associated with the prognosis of ampullary carcinoma (AC). The purpose of this study is to explore the relationship between lymph node ratio (LNR) and the prognosis of patients with AC after curative pancreaticoduodenectomy and to establish a new LNR-based staging system.

Methods: AC patients in the Cancer Hospital, Chinese Academy of Medical Sciences, between 1998 and 2020 were retrospectively reviewed as the training cohort; and AC patients in the Surveillance, Epidemiology, and End Results (SEER) database between 2010 and 2018 were obtained as the validation cohort. Within the training group, Kaplan–Meier survival analyses and Cox proportional hazards regression were conducted to assess the prognostic value of LNR and establish a new LNR-based staging system. Then, the new staging system was compared with the 8th American Joint Committee on Cancer (AJCC) TNM staging system in both the training and validation cohorts.

Results: A total of 264 patients in the training cohort and 199 patients in the validation cohort were enrolled. Significant overall survival (OS) difference was observed between LNR-low stage and LNR-high stage in both training ($p = 0.001$) and validation cohorts ($p < 0.001$). Then a new LNR-based staging system was developed. Under the new system, the number of patients in the training cohort and validation cohort of stage I, stage II, and stage III was 30 (11%) vs. 18 (9%), 190 (72%) vs. 96 (48%), and 44 (17%) vs. 85 (43%), respectively. The new staging system classified patients with respect to survival better than did the 8th AJCC TNM staging system.

OPEN ACCESS

Edited by:
Ravindra Deshpande, Wake Forest School of Medicine, United States

Reviewed by:
Satheesh Sengodan, National Cancer Institute at Frederick, United States
Gargi Mahapatra, Wake Forest Baptist Medical Center, United States

***Correspondence:**
Xu Che
yixuetg@foxmail.com
Dongbing Zhao
dbzhao@cicams.ac.cn

Specialty section:
This article was submitted to Surgical Oncology, a section of the journal Frontiers in Oncology

Received: *09 November 2021*
Accepted: *15 December 2021*
Published: *20 January 2022*

Citation:
Zhang X, Sun C, Li Z, Wang T, Zhao L, Niu P, Guo C, Chen Y, Che X and Zhao D (2022) Development and Validation of a New Lymph Node Ratio-Based Staging System for Ampullary Carcinoma After Curative Pancreaticoduodenectomy. Front. Oncol. 11:811595. doi: 10.3389/fonc.2021.811595

Conclusions: The new LNR-based staging system had better discriminability for predicting survival in AC patients after curative pancreaticoduodenectomy. More data are needed for further validation.

Keywords: ampullary adenocarcinoma, lymph node metastasis, lymph node ratio (LNR), SEER, prognosis, staging system

INTRODUCTION

Ampullary carcinoma (AC) is a relatively rare tumor arising from the ampulla of Vater, with an incidence of around 0.6 cases in 100,000 people (1–3). Generally, AC patients are diagnosed at an early stage due to early symptoms of biliary obstruction (4, 5). At present, curative pancreaticoduodenectomy (Whipple) remains the mainstay of treatment for AC. It has been reported the rate of lymph node metastasis (LNM) ranges from 20% to 50% (1). Despite many clinicopathologic characters are associated with prognosis for AC patients, LNM is still one of the most crucial risk factors (1, 6–25).

The number of involved lymph nodes occupies a significant part in the current TNM Classification of Malignant Tumors (TNM) staging system proposed by the American Joint Committee on Cancer (AJCC). Nevertheless, debates still exist about the node stage for AC patients. Previous studies showed some differences when conducting subgroup analysis according to the number of LNM (1, 9, 13, 15, 19, 21). Recently, a retrospective study enrolled 111 patients who underwent Whipple surgery found that patients with ≥3 local LNMs had similar survival time as compared with the patients with distant LNM (1). Moreover, the total number of harvested lymph nodes is also a vital prognostic factor in AC (8, 12, 15, 17). In view of this, some studies evaluated node staging for AC based on lymph node ratio (LNR) (7, 9, 11, 18, 23). Yet the cutoff value of LNR varied across studies. Moreover, whether the LNR could replace the current N staging has not been evaluated.

Therefore, in the present study, we assessed the prognostic value of the total harvested number of lymph nodes and LNR for AC patients after curative Whipple surgery. Additionally, we conducted a comparative analysis of the current lymph node categories of AC in the eighth edition of the AJCC staging guidelines. Furthermore, we used a separate cohort from the Surveillance, Epidemiology, and End Results (SEER) database for further external validation.

MATERIALS AND METHODS

Patients

Clinicopathologic data of ampullary adenocarcinoma patients who underwent curative pancreaticoduodenectomy in the Cancer Hospital, Chinese Academy of Medical Sciences, between 1998 and 2020 were retrospectively collected as the training cohort. We then excluded some patients according to the following criteria: i) patients diagnosed with neuroendocrine tumors, adenoma, and other rare tumor types; ii) patients with zero regional lymph node examined; iii) death within a month after the operation due to complications and other reasons; and iv) patients with missing or incomplete clinicopathologic information. In total, 264 patients were enrolled in the training cohort.

Persistent data of AC patients in the SEER database between 2010 and 2018 were obtained as validation cohort using the SEER * State v8.3.6 tool on July 8, 2021. Selection items were as follows: i) primary site—labeled = "C24.1-Ampulla of Vater"; ii) ICD-O-3 Hist/behav = "/3: adenocarcinoma, NOS"; and iii) diagnostic confirmation = "Microscopically confirmed." The main exclusion criteria were as follows: i) AC was not the first primary malignant tumor; ii) patients did not receive pancreaticoduodenectomy; iii) patients with zero regional lymph node examined; and iv) some important information was unknown, such as staging, tumor size, number of regional lymph nodes examined, and number of LNM. Eventually, a total of 199 patients were included in the validation cohort.

Covariates and Outcomes

The major covariates include gender, age, preoperative jaundice, intraoperative transfusion, operation time, tumor size, differentiation, number of regional lymph nodes examined, LNR, AJCC TNM stage (8th edition), blood vessel invasion, postoperative complications, and adjuvant treatment. LNR was defined as the ratio of the number of LNM to the total number of regional lymph nodes examined.

Follow-up data in the training cohort were collected through telephone and outpatient reexaminations. In total, 62 patients were lost to follow-up, and the follow-up rate was 76.5%. The primary outcome was overall survival (OS), which was defined as the time interval from diagnosis to the most recent follow-up date or date of death. The second outcomes were disease-free survival (DFS) and cancer-specific survival (CSS). DFS was defined as the time from surgery to the local recurrence or distant metastasis. CSS was calculated as the time from diagnosis to the most recent follow-up date or date of death caused by AC.

Statistical Analysis

To determine the optimal cutoff values, we used X-tile software (version 3.6.1) and converted the continuous variables into categorical variables before conducting statistical analyses. Univariable survival analysis was conducted using the training cohort according to the Cox proportional hazards regression model. Then covariates with $p < 0.2$ were included in Cox multivariate regression to find independent prognostic factors. Hazard ratios (HRs) and their 95% CI were presented.

Based on the survival analysis results, we developed a new LNR-based staging system for AC after curative Whipple surgery. The prognostic performances of the novel staging and the 8th AJCC TNM stage were compared in the training cohort and validation cohort with OS, DFS, and CSS as outcomes.

All statistical analyses were conducted with IBM SPSS statistics 21 (IBM Corp, Armonk, NY, United States). The GraphPad Prism software (version 8.0.2) was utilized to generate survival curves. A two-sided test with $p \leq 0.05$ was considered to be statistically significant.

RESULTS

Demographic and Clinicopathologic Data

A total of 264 patients in the training cohort and 199 patients in the validation cohort were enrolled. The detailed demographic and clinicopathologic data were depicted in **Table 1**. The median number of total regional examined lymph nodes in the training and validation cohorts was 11 (interquartile range (IQR): 7–18) and 15 (IQR: 11–20), respectively. LNM occurred in 29.5% AC patients in the training cohort, while in 66.3% AC patients in the validation cohort. Furthermore, the number of N1 stage and N2 stage in the training and validation cohorts was 25% vs. 44.7%, and 4.5% vs. 21.6%, respectively. The median of LNR in the training and validation cohorts was 0.00 (IQR: 0.00–0.05) and 0.08 (IQR: 0.00–0.21), respectively. According to the X-tile analysis results, LNR was divided into three groups: LNR = 0, 0 < LNR ≤ 0.1, and LNR > 0.1 (**Supplementary Figure 1**). In the LNR = 0 group, all the patients were at the N0 stage. In the 0 < LNR ≤ 0.1 group, all the patients were at the N1 stage. In the LNR > 0.1 group, 32/44 patients were at the N1 stage and 12/44 patients at the N2 stage in the training cohort, while 44/87 patients were at the N1 stage and 43/87 patients at the N2 stage in the validation cohort.

TABLE 1 | The clinicopathologic characteristics of the AC patients in the training and validation cohorts.

Characteristic	Training cohort		Validation cohort	
	N = 264	%	N = 199	%
Sex				
Male	147	55.7%	114	57.3%
Female	117	44.3%	85	42.7%
Age				
≤47	58	22.0%	14	7.0%
48–68	173	65.5%	103	51.8%
≥69	33	12.5%	82	41.2%
Preoperative biliary drainage				
No	207	78.4%		
Yes	57	21.6%		
Intraoperative transfusion				
No	122	46.2%		
Yes	142	53.8%		
Operation time				
≤6 h	190	72.0%		
>6 h	74	28.0%		
Tumor size				
≦2.7 cm	177	67.0%	139	69.8%
>2.7 cm	87	33.0%	60	30.2%
Differentiation				
Poor	96	36.4%	71	35.7%
Moderate	113	42.8%	107	53.8%
Well	55	20.8%	21	10.6%
Regional nodes examined [median, IQR]	11 [7–18]		15 [11–20]	
≤6	58	22.0%	15	7.5%
>6	206	78.0%	184	92.5%
LNR [median, IQR]	0.00 [0.00–0.05]		0.08 [0.00–0.21]	
0	186	70.5%	67	33.7%
≤0.1	34	12.9%	45	22.6%
>0.1	44	16.7%	87	43.7%
T stage				
T1	30	11.4%	18	9.0%
T2	103	39.0%	54	27.1%
T3	131	49.6%	127	63.8%
N stage				
N0	186	70.5%	67	33.7%
N1	66	25.0%	89	44.7%
N2	12	4.5%	43	21.6%
TNM stage				
I	113	42.8%	33	16.6%
II	74	28.0%	34	17.1%
III	77	29.2%	132	66.3%
Blood vessel invasion				
No	201	76.1%		
Yes	63	23.9%		
Postoperative complications				
No	161	61.0%		
Yes	103	39.0%		
Adjuvant treatment				
No	176	66.7%		
Yes	61	23.1%		
Unknown	27	10.2%		

AC, ampullary carcinoma; IQR, interquartile range; LNR, lymph node ratio.

Survival Outcomes

In the training cohort, the median OS was 36 (IQR: 22–62) months. The 1-year, 3-year, and 5-year DFS rates were 68.8%, 33.5%, and 25.6%, respectively. The 1-year, 3-year, and 5-year OS rates were 89.3%, 58.6%, and 44.1%, respectively. The Kaplan–Meier survival curve is shown in **Figures 1A, B**.

In the validation cohort, the median OS was 41 (IQR: 17–62) months. The 1-year, 3-year, and 5-year CSS rates were 86.7%, 64.7%, and 56.0%, respectively. The 1-year, 3-year, and 5-year OS rates were 85.3%, 58.6%, and 47.7%, respectively. The Kaplan–Meier survival curve is shown in **Figures 1C, D**.

Survival Analysis for the Training Cohort

Univariate analysis revealed that age (≥69 years), tumor size (≥2.7 cm), poor differentiation, T3 stage, LNR (>0.1), and blood vessel invasion were risk factors for OS in AC patients, while tumor size (≥2.7 cm), poor differentiation, T3 stage, the number of total regional examined lymph nodes (<6), LNR (>0.1), and blood vessel invasion were risk factors for DFS in AC patients. Multivariate analysis showed that only LNR (>0.1) (HR: 2.557, 95% CI: 1.377–4.747, $p = 0.003$) was the independent risk factor for OS in AC patients, while T3 stage (HR: 3.654, 95% CI: 1.290–10.350, $p = 0.015$) and LNR (>0.1) (HR: 2.418, 95% CI: 1.352–4.324, $p = 0.003$) were independent risk factors for DFS in AC patients. The detailed results of Cox regression were demonstrated in **Tables 2** and **3**.

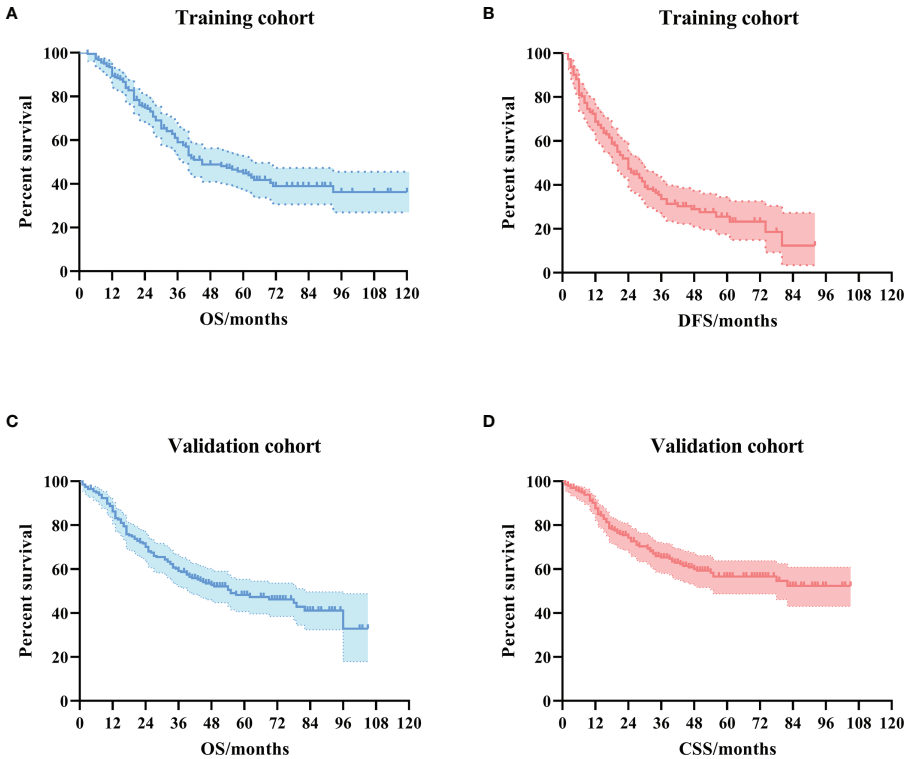

FIGURE 1 | The Kaplan–Meier survival curves for ampullary carcinoma patients after curative pancreaticoduodenectomy. **(A)** OS curve in the training cohort. **(B)** DFS curve in the training cohort. **(C)** OS curve in the validation cohort. **(D)** CSS curve in the validation cohort. OS, overall survival; DFS, disease-free survival; CSS, cancer-specific survival.

Then we conducted survival analysis including the variables age, tumor size, differentiation, T stage, N stage, blood vessel invasion, postoperative complications, and adjuvant treatment. The univariate survival curves based on the N stage are depicted in **Figure 2**. The multivariate analysis results demonstrated no significant difference in the survival (**Table 4**).

Proposed a New Lymph Node Ratio-Based Staging System

Based on the results of survival analysis, we developed a new LNR-based staging system for AC after curative pancreaticoduodenectomy. Patients were divided into LNR-low stage and LNR-high stage in the new LNR-based staging system, considering that there was no significant survival difference between the LNR = 0 group and 0 < LNR ≤ 0.1 group. The detailed new staging system is illustrated in **Figure 3**.

Validation of the New Lymph Node Ratio-Based Staging System

According to the new staging system, we then re-staged the patients in the training cohort and validation cohort. Under the new staging system, the number of patients in the training cohort and validation cohort of stage I, stage II, and stage III was 30 (11%) vs. 18 (9%), 190 (72%) vs. 96 (48%), and 44 (17%) vs. 85 (43%), respectively. The detailed proportions are demonstrated in **Supplementary Figure 3**.

Kaplan–Meier univariate survival curves stratified by LNR in the training cohort and validation cohort are depicted in **Figure 4** and demonstrated a significant difference in survival ($p \leq 0.001$). Subsequently, we compared the new stage and the current 8th AJCC TNM stage in the training cohort and validation cohort. The results revealed that the survival curves of different tumor stages could clearly be distinguished from each other (**Figure 5**).

DISCUSSION

The current study demonstrated that LNR was a more powerful prognostic factor than the current N stage according to the 8th AJCC staging system. We established a new staging system by substituting LNR stage for the N stage and divided LNR into LNR-low stage and LNR-high stage with the best cutoff value of 0.1. By comparing the survival curves of the training cohort and the validation cohort, we found that the LNR-based staging system had better clinical benefits than the 8th AJCC TNM staging system.

LNR has been confirmed as a prognostic factor of AC patients, but no uniform cutoff threshold for LNR has been

TABLE 2 | Univariate and multivariate Cox regression analyses of OS of the AC patients in the training cohort.

Characteristic	Univariable analysis		Multivariable analysis	
	HR [95% CI]	*p*-Value	HR [95% CI]	*p*-Value
Sex				
Male	Reference			
Female	0.908 [0.607–1.358]	0.638		
Age				
≤47	Reference		Reference	
48–68	1.359 [0.789–2.343]	0.269	1.349 [0.758–2.400]	0.308
≥69	2.091 [1.003–4.361]	0.049	1.356 [0.581–3.163]	0.481
Preoperative biliary drainage				
No	Reference			
Yes	0.964 [0.583–1.594]	0.887		
Intraoperative transfusion				
No	Reference			
Yes	0.844 [0.567–1.258]	0.405		
Operation time				
≤6 h	Reference			
>6 h	1.236 [0.803–1.905]	0.336		
Tumor size				
≦2.7 cm	Reference		Reference	
>2.7 cm	1.724 [1.145–2.595]	0.009	1.200 [0.750–1.921]	0.447
Differentiation				
Poor	Reference			
Moderate	0.937 [0.605–1.449]	0.769	0.855 [0.529–1.382]	0.522
Well	0.470 [0.260–0.849]	0.012	0.677 [0.330–1.391]	0.289
T stage				
T1	Reference		Reference	
T2	1.490 [0.686–3.235]	0.314	1.299 [0.562–3.001]	0.540
T3	3.319 [1.578–6.981]	0.002	2.230 [0.914–5.439]	0.078
Regional nodes examined				
≤6	Reference		Reference	
>6	1.453 [0.892–2.369]	0.134	1.109 [0.640–1.922]	0.712
LNR				
0	Reference		Reference	
≤0.1	1.740 [0.984–3.075]	0.057	1.471 [0.776–2.787]	0.236
>0.1	2.596 [1.588–4.245]	<0.001	2.557 [1.377–4.747]	0.003
Blood vessel invasion				
No	Reference		Reference	
Yes	1.587 [1.018–2.473]	0.042	1.015 [0.603–1.707]	0.956
Postoperative complications				
No	Reference		Reference	
Yes	1.487 [0.992–2.227]	0.054	1.519 [0.998–2.311]	0.051
Adjuvant treatment				
No	Reference		Reference	
Yes	1.353 [0.864–2.119]	0.186	0.613 [0.345–1.089]	0.095
Unknown	4.717 [1.704–13.054]	0.003	2.969 [0.861–10.236]	0.085

OS, overall survival; AC, ampullary carcinoma; LNR, lymph node ratio.

established. Kim et al. retrospectively analyzed 71 patients with AC who underwent adjuvant chemotherapy after radical resection and found that LNR > 0.15 was an independent risk factor for OS (10). In an analysis of 212 AC patients who received radical surgery in Taiwan, LNR > 0.056 indicated poor DFS and OS (11). Similarly, a study by Falconi et al. explored multiple cutoff values (LNR = 0, 0 < LNR ≤ 0.2, 0.2 < LNR ≤ 0.4, LNR > 0.4) in AC patients and found that high LNR was associated with OS (23). Moreover, a high LNR (≥0.15) was closely associated with decreased time to distant recurrence than low LNR (LNR = 0, and 0.01 ≤ LNR ≤ 0.14) in AC patients after surgery (18). However, some previous studies revealed that LNR was not an independent significant prognostic factor in AC patients (16, 19, 21). In the present study, we confirmed LNR as a significant prognostic factor in AC patients after curative pancreaticoduodenectomy and estimated the cutoff value of 0.1. Such a difference in the cutoff value of LNR might be related to several factors. Firstly, the difference in social characteristics and ethnicity across studies may responsible for this discrepancy. Secondly, dissection of the lymph nodes was the major factor influencing the total number of resected lymph nodes and LNR. In the present study, we only included AC patients after curative pancreaticoduodenectomy and excluded other radical surgery modes. Thirdly, the difference in the follow-up time and adjuvant treatment in each study may also affect the results.

In the current 8th AJCC staging system, the number of metastatic lymph nodes is the basis of N stage. The prognostic

TABLE 3 | Univariate and multivariate Cox regression analyses of DFS of the AC patients in the training cohort.

Characteristic	Univariable analysis		Multivariable analysis	
	HR [95% CI]	*p*-Value	HR [95% CI]	*p*-Value
Sex				
Male	Reference			
Female	0.967 [0.647–1.446]	0.872		
Age				
≤47	Reference			
48–68	1.283 [0.765–2.153]	0.345		
≥69	1.228 [0.551–2.737]	0.616		
Preoperative biliary drainage				
No	Reference			
Yes	0.889 [0.538–1.467]	0.644		
Intraoperative transfusion				
No	Reference			
Yes	0.822 [0.552–1.223]	0.333		
Operation time				
≤6 h	Reference			
>6 h	0.952 [0.605–1.497]	0.831		
Tumor size				
≦2.7 cm	Reference		Reference	
>2.7 cm	1.704 [1.134–2.561]	0.010	1.388 [0.879–2.190]	0.159
Differentiation				
Poor	Reference		Reference	
Moderate	1.016 [0.659–1.566]	0.944	0.957 [0.602–1.521]	0.854
Well	0.466 [0.255–0.851]	0.013	0.913 [0.415–2.012]	0.822
T stage				
T1	Reference		Reference	
T2	1.874 [0.783–4.485]	0.158	2.461 [0.937–6.461]	0.067
T3	4.372 [1.881–10.161]	0.001	3.654 [1.290–10.350]	0.015
Regional nodes examined				
≤6	Reference		Reference	
>6	0.601 [0.374–0.968]	0.036	0.610 [0.356–1.046]	0.072
LNR				
0	Reference		Reference	
≤0.1	1.368 [0.803–2.330]	0.249	1.274 [0.727–2.231]	0.398
>0.1	2.436 [1.483–4.002]	<0.001	2.418 [1.352–4.324]	0.003
Blood vessel invasion				
No	Reference		Reference	
Yes	1.802 [1.168–2.779]	0.008	0.928 [0.557–1.546]	0.774
Postoperative complications				
No	Reference			
Yes	1.306 [0.866–1.971]	0.203		
Adjuvant treatment				
No	Reference		Reference	
Yes	1.436 [0.939–2.198]	0.095	0.662 [0.367–1.054]	0.078
Unknown	Not available	0.966	Not available	0.960

DFS, disease-free survival; AC, ampullary carcinoma; LNR, lymph node ratio.

value of different numbers of LNM has been explored in many studies (1, 12, 13, 15). It was worth noting that in a recent study, the investigators demonstrated that nearly 16.8% AC patients with pathologic negative lymph nodes were estimated to have undetected LNM through nodal staging score (6). Meanwhile, patients with a high nodal staging score generally had longer OS (6). However, in our cohort, we found the current N stage was not an independent prognostic factor for AC patients. A possible explanation is that the extent of lymphadenectomy and the primary sites of metastatic lymph nodes were also crucial factors for survival (1).

Currently, no consensus has been reached regarding the lymphadenectomy for the AC patients due to limited cases. The AJCC recommends that at least 12 lymph nodes should be dissected for AC patients (1). Some previous studies have revealed that an increasing number of resected lymph nodes might improve the positive rate of lymph nodes and prolong the survival time (8, 12, 17). In the present study, we found no significant relationship between the total number of lymph nodes and prognosis. Several reasons might account for this apparent discrepancy. Firstly, the location of metastatic lymph nodes of AC patients may be different in different studies. A recent study demonstrated that the prognosis was worse in AC patients with regional lymph nodes metastasis in other sites than only in the pancreatic head region (1). Secondly, in our study, more AC patients have negative lymph nodes and early pathologic stage. Therefore, the survival may not reach statistical differences.

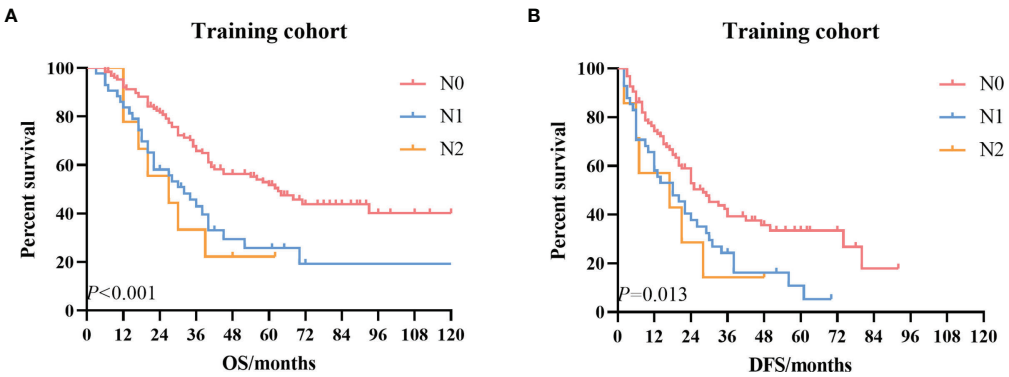

FIGURE 2 | The Kaplan–Meier survival curves according to the N stage. **(A)** OS curve in the training cohort. **(B)** DFS curve in the training cohort. OS, overall survival; DFS, disease-free survival.

On the basis of our analysis, we established a new staging system-based LNR and replaced the current 8th AJCC N staging for the first time. The new LNR-based staging system shows certain advantages over the 8th AJCC TNM staging system in both the training cohort and validation cohort. Under the new staging system, LNR is used to correlate LNM and surgical dissection quality. On the one hand, even if the numbers of metastatic lymph nodes are high in some AC patients, they are in

TABLE 4 | Multivariate Cox regression analyses contained N stage in the AC patients.

Characteristic	OS		RFS	
	HR [95% CI]	*p*-Value	HR [95% CI]	*p*-Value
Age				
≤47	Reference			
48–68	1.288 [0.726–2.287]	0.387		
≥69	1.355 [0.580–3.164]	0.483		
Tumor size				
≦2.7 cm	Reference		Reference	
>2.7 cm	1.223 [0.757–1.975]	0.411	1.305 [0.823–2.072]	0.258
Differentiation				
Poor	Reference		Reference	
Moderate	0.861 [0.531–1.396]	0.544	0.970 [0.607–1.550]	0.900
Well	0.694 [0.337–1.427]	0.32	1.013 [0.467–2.200]	0.973
T stage				
T1	Reference		Reference	
T2	1.319 [0.571–3.045]	0.517	2.660 [1.011–6.995]	0.047
T3	2.212 [0.903–5.418]	0.082	3.997 [1.412–11.314]	0.009
Regional nodes examined				
≤6	Reference		Reference	
>6	1.032 [0.596–1.785]	0.911	0.527 [0.314–0.882]	0.015
N stage				
0	0.450 [0.177–1.141]	0.093	0.451 [0.173–1.177]	0.104
1	0.843 [0.342–2.081]	0.712	0.735 [0.287–1.884]	0.522
2	Reference		Reference	
Blood vessel invasion				
No	Reference		Reference	
Yes	1.082 [0.647–1.811]	0.763	1.019 [0.623–1.667]	0.939
Postoperative complications				
No	Reference			
Yes	1.539 [1.013–2.339]	0.044		
Adjuvant treatment				
No	Reference		Reference	
Yes	0.648 [0.364–1.156]	0.142	0.649 [0.381–1.104]	0.111
Unknown	3.032 [0.828–11.109]	0.094		

AC, ampullary carcinoma; OS, overall survival; RFS, recurrence-free survival.

Stage-New	T	LNR	M
ⅠA	1	Low	0
ⅡA	2	Low	0
ⅡB	3	Low	0
ⅠB	1	High	0
ⅢA	2	High	0
ⅢB	3	High	0
Ⅳ	Any	Any	M1

FIGURE 3 | A new LNR-based staging system for ampullary carcinoma after curative pancreaticoduodenectomy. LNR, lymph node ratio.

the LNR-low staging due to thorough lymph node dissection. On the other hand, the new system avoids to a certain extent the incomplete lymph node dissection leading to a lower N stage of AC patients who have the LNR-high stage in fact. However, the new LNR-based staging system still needs to be validated in future larger prospective cohorts.

To our knowledge, this single-center cohort study has the largest size evaluating LNR in AC patients after curative

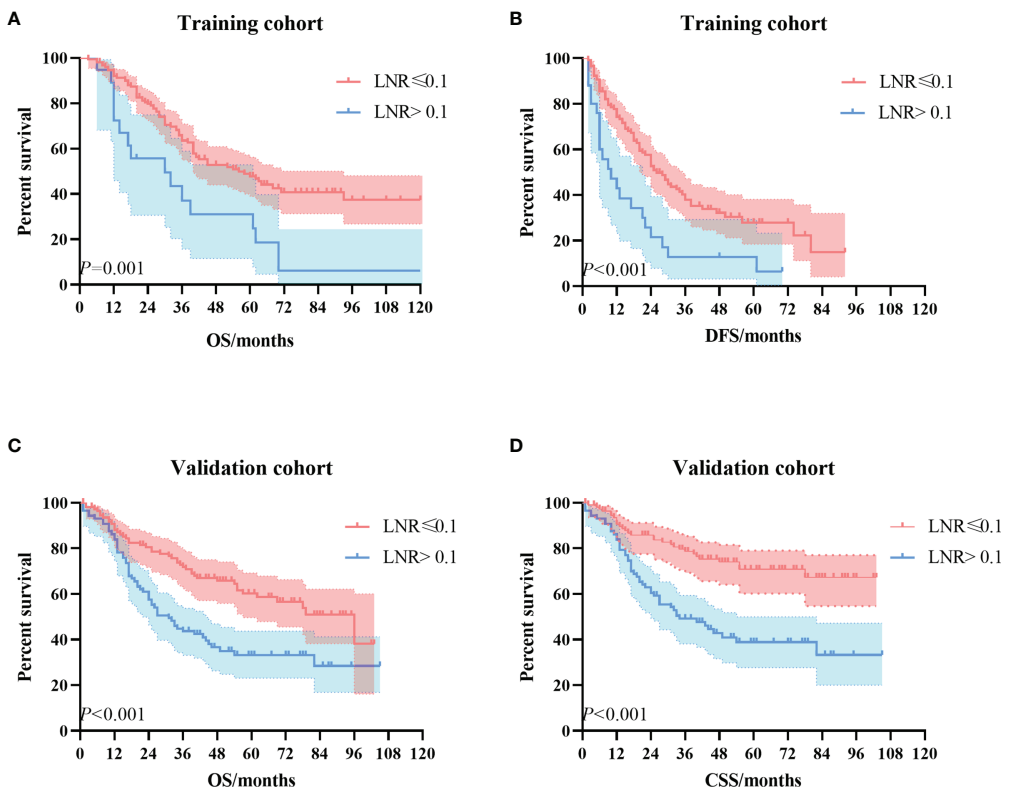

FIGURE 4 | The Kaplan–Meier survival curves according to the LNR stage. **(A)** OS curve in the training cohort. **(B)** DFS curve in the training cohort. **(C)** OS curve in the validation cohort. **(D)** CSS curve in the validation cohort. LNR, lymph node ratio; OS, overall survival; DFS, disease-free survival; CSS, cancer-specific survival.

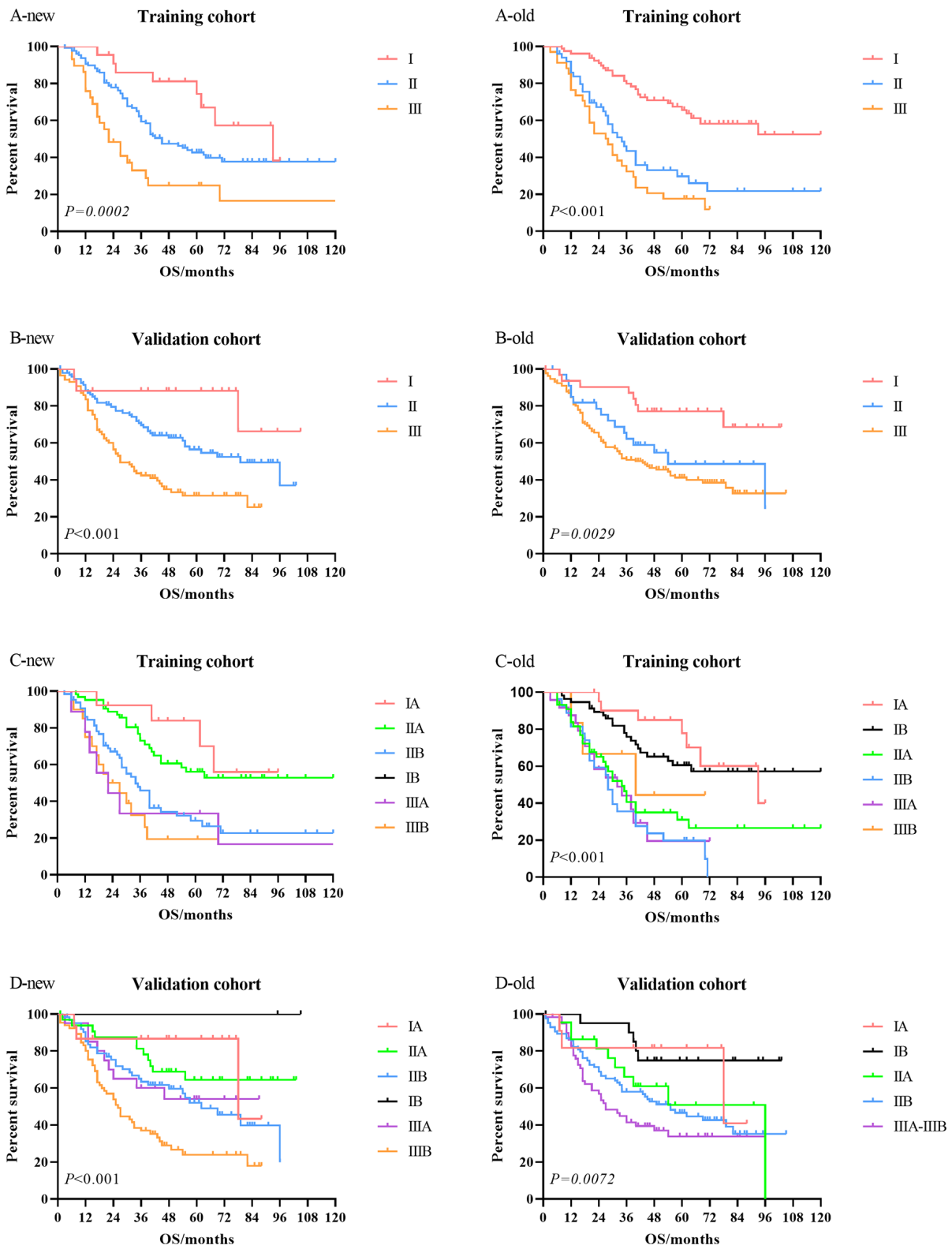

FIGURE 5 | Comparison of the Kaplan–Meier survival curves between LNR-based staging system (new) and current 8th AJCC TNM staging system (old) in the training cohort and validation cohort. LNR, lymph node ratio; AJCC, American Joint Committee on Cancer.

pancreaticoduodenectomy. Moreover, we incorporated LNR into the staging system for the first time and established a new staging system. In order to verify the clinical benefit of the new LNR-based staging system, we used data from the SEER database for validation. Despite these strengths, we acknowledged several potential limitations that should be considered objectively. Firstly, this was a single-center retrospective study with a limited number of patients and clinical variables. Secondly, some missing important clinical data, such as adjuvant treatment and the levels of tumor biomarkers, might have a certain impact on the results of this study. Thirdly, some patients had shorter follow-up time, and the rate of loss to follow-up was relatively high.

CONCLUSIONS

In conclusion, the present study demonstrated that LNR was an independent prognostic factor in AC patients after curative pancreaticoduodenectomy. Survival analysis revealed that the new LNR-based staging system had better clinical benefits than the 8th AJCC TNM staging system. However, further prospective studies with larger patients are necessary to validate the new LNR-based staging system.

DATA AVAILABILITY STATEMENT

The raw data supporting the conclusions of this article will be made available by the authors, without undue reservation.

ETHICS STATEMENT

Ethical review and approval were not required for the study on human participants in accordance with the local legislation and institutional requirements. Written informed consent for participation was not required for this study in accordance with the national legislation and the institutional requirements.

AUTHOR CONTRIBUTIONS

1) Guarantor of integrity of the entire study: XC and DZ. 2) Study concepts and design: XZ and DZ. 3) Provision of study materials or patients: XZ, CS, and ZL. 4) Collection and assembly of data: XZ, LZ, PN, TW, XC, YC, and CG. 5) Statistical analysis: XZ. 6) Manuscript preparation: all authors. 7) Manuscript editing: all authors.

SUPPLEMENTARY MATERIAL

The Supplementary Material for this article can be found online at: https://www.frontiersin.org/articles/10.3389/fonc.2021.811595/full#supplementary-material

Supplementary Figure 1 | The optimal cut-off value of LNR according to the X-tile software.

Supplementary Figure 2 | The optimal cut-off value of total number of lymph nodes examined according to the X-tile software.

Supplementary Figure 3 | The proportions of patients in the training cohort and validation cohort under the new staging system.

REFERENCES

1. Matsui S, Yamamoto Y, Sugiura T, Okamura Y, Ito T, Ashida R, et al. The Prognostic Relevance of the Number and Location of Positive Lymph Nodes for Ampulla of Vater Carcinoma. *World J Surg* (2021) 45(1):270–8. doi: 10.1007/s00268-020-05770-1
2. Albores-Saavedra J, Schwartz AM, Batich K, Henson DE. Cancers of the Ampulla of Vater: Demographics, Morphology, and Survival Based on 5,625 Cases From the SEER Program. *J Surg Oncol* (2009) 100(7):598–605. doi: 10.1002/jso.21374
3. Benhamiche AM, Jouve JL, Manfredi S, Prost P, Isambert N, Faivre J. Cancer of the Ampulla of Vater: Results of a 20-Year Population-Based Study. *Eur J Gastroenterol Hepatol* (2000) 12(1):75–9. doi: 10.1097/00042737-200012010-00014
4. Zimmermann C, Wolk S, Aust DE, Meier F, Saeger HD, Ehehalt F, et al. The Pathohistological Subtype Strongly Predicts Survival in Patients With Ampullary Carcinoma. *Sci Rep* (2019) 9(1):12676. doi: 10.1038/s41598-019-49179-w
5. Imamura T, Yamamoto Y, Sugiura T, Okamura Y, Ito T, Ashida R, et al. The Prognostic Relevance of the New 8th Edition of the Union for International Cancer Control Classification of TNM Staging for Ampulla of Vater Carcinoma. *Ann Surg Oncol* (2019) 26(6):1639–48. doi: 10.1245/s10434-019-07238-6
6. Huang XT, Huang CS, Li JH, Xu QC, Yin XY. Use of Nodal Staging Score in Evaluating the Accuracy of Pathologic Nodal Status in Node-Negative Ampullary Carcinoma. *J Gastrointest Surg Off J Soc Surg Aliment Tract* (2021) 25(4):1001–9. doi: 10.1007/s11605-020-04572-z
7. Agalar C, Aysal A, Unek T, Egeli T, Ozbilgin M, Akturk N, et al. The Role of Log Odds of Positive Lymph Nodes in Predicting the Survival After Resection for Ampullary Adenocarcinoma. *Pathol Oncol Res POR* (2020) 26(1):467–73. doi: 10.1007/s12253-019-00584-6
8. Nassour I, Christie A, Choti MA, Mansour JC, Minter RM, Polanco PM, et al. Determining the Adequate Examined Lymph Node Count in Resected Ampullary Adenocarcinoma-A National Cohort Study. *J Gastrointest Surg Off J Soc Surg Aliment Tract* (2018) 22(5):792–801. doi: 10.1007/s11605-018-3737-6
9. Kwon J, Kim K, Chie EK, Kim BH, Jang JY, Kim SW, et al. Prognostic Relevance of Lymph Node Status for Patients With Ampullary Adenocarcinoma After Radical Resection Followed by Adjuvant Treatment. *Eur J Surg Oncol J Eur Soc Surg Oncol Br Assoc Surg Oncol* (2017) 43(9):1690–6. doi: 10.1016/j.ejso.2017.05.024
10. Kim K, Chie EK, Jang JY, Kim SW, Han SW, Oh DY, et al. Prognostic Significance of Nodal Ratio in Patients Undergoing Adjuvant Chemoradiotherapy After Curative Resection for Ampullary Cancer. *Am J Clin Oncol* (2016) 39(4):346–9. doi: 10.1097/coc.0000000000000075
11. Hsu CH, Chen TD, Tsai CY, Hsu JT, Yeh CN, Jan YY, et al. Prognostic Value of the Metastatic Lymph Node Ratio in Patients With Resectable Carcinoma of Ampulla of Vater. *Medicine* (2015) 94(42):e1859. doi: 10.1097/md.0000000000001859
12. Chen SC, Shyr YM, Chou SC, Wang SE. The Role of Lymph Nodes in Predicting the Prognosis of Ampullary Carcinoma After Curative Resection. *World J Surg Oncol* (2015) 13:224. doi: 10.1186/s12957-015-0643-1
13. Balci S, Basturk O, Saka B, Bagci P, Postlewait LM, Tajiri T, et al. Substaging Nodal Status in Ampullary Carcinomas has Significant Prognostic Value: Proposed Revised Staging Based on an Analysis of 313 Well-Characterized Cases. *Ann Surg Oncol* (2015) 22(13):4392–401. doi: 10.1245/s10434-015-4499-y
14. Okano K, Asano E, Kushida Y, Kamada H, Mori H, Suzuki Y. Factors Influencing Lymph Node Metastasis in Patients With Ampullary Adenocarcinoma. *Digest Surg* (2014) 31(6):459–67. doi: 10.1159/000370251

15. Kang HJ, Eo SH, Kim SC, Park KM, Lee YJ, Lee SK, et al. Increased Number of Metastatic Lymph Nodes in Adenocarcinoma of the Ampulla of Vater as a Prognostic Factor: A Proposal of New Nodal Classification. *Surgery* (2014) 155(1):74–84. doi: 10.1016/j.surg.2013.08.004
16. Pomianowska E, Westgaard A, Mathisen Ø, Clausen OP, Gladhaug IP. Prognostic Relevance of Number and Ratio of Metastatic Lymph Nodes in Resected Pancreatic, Ampullary, and Distal Bile Duct Carcinomas. *Ann Surg Oncol* (2013) 20(1):233–41. doi: 10.1245/s10434-012-2592-z
17. Partelli S, Crippa S, Capelli P, Neri A, Bassi C, Zamboni G, et al. Adequacy of Lymph Node Retrieval for Ampullary Cancer and its Association With Improved Staging and Survival. *World J Surg* (2013) 37(6):1397–404. doi: 10.1007/s00268-013-1995-8
18. Roland CL, Katz MH, Gonzalez GM, Pisters PW, Vauthey JN, Wolff RA, et al. A High Positive Lymph Node Ratio Is Associated With Distant Recurrence After Surgical Resection of Ampullary Carcinoma. *J Gastrointest Surg Off J Soc Surg Aliment Tract* (2012) 16(11):2056–63. doi: 10.1007/s11605-012-2015-2
19. Sakata J, Shirai Y, Wakai T, Ajioka Y, Akazawa K, Hatakeyama K. Assessment of the Nodal Status in Ampullary Carcinoma: The Number of Positive Lymph Nodes Versus the Lymph Node Ratio. *World J Surg* (2011) 35(9):2118–24. doi: 10.1007/s00268-011-1175-7
20. de Paiva Haddad LB, Patzina RA, Penteado S, Montagnini AL, da Cunha JE, Machado MC, et al. Lymph Node Involvement and Not the Histophatologic Subtype is Correlated With Outcome After Resection of Adenocarcinoma of the Ampulla of Vater. *J Gastrointest Surg Off J Soc Surg Aliment Tract* (2010) 14(4):719–28. doi: 10.1007/s11605-010-1156-4
21. Sierzega M, Nowak K, Kulig J, Matyja A, Nowak W, Popiela T. Lymph Node Involvement in Ampullary Cancer: The Importance of the Number, Ratio, and Location of Metastatic Nodes. *J Surg Oncol* (2009) 100(1):19–24. doi: 10.1002/jso.21283
22. van der Gaag NA, ten Kate FJ, Lagarde SM, Busch OR, van Gulik TM, Gouma DJ. Prognostic Significance of Extracapsular Lymph Node Involvement in Patients With Adenocarcinoma of the Ampulla of Vater. *Br J Surg* (2008) 95 (6):735–43. doi: 10.1002/bjs.6076
23. Falconi M, Crippa S, Domínguez I, Barugola G, Capelli P, Marcucci S, et al. Prognostic Relevance of Lymph Node Ratio and Number of Resected Nodes After Curative Resection of Ampulla of Vater Carcinoma. *Ann Surg Oncol* (2008) 15(11):3178–86. doi: 10.1245/s10434-008-0099-4
24. Bogoevski D, Chayeb H, Cataldegirmen G, Schurr PG, Kaifi JT, Mann O, et al. Nodal Microinvolvement in Patients With Carcinoma of the Papilla of Vater Receiving No Adjuvant Chemotherapy. *J Gastrointest Surg Off J Soc Surg Aliment Tract* (2008) 12(11):1830–7. doi: 10.1007/s11605-008-0683-8
25. Sakata E, Shirai Y, Yokoyama N, Wakai T, Sakata J, Hatakeyama K. Clinical Significance of Lymph Node Micrometastasis in Ampullary Carcinoma. *World J Surg* (2006) 30(6):985–91. doi: 10.1007/s00268-005-7985-8

Conflict of Interest: The authors declare that the research was conducted in the absence of any commercial or financial relationships that could be construed as a potential conflict of interest.

Publisher's Note: All claims expressed in this article are solely those of the authors and do not necessarily represent those of their affiliated organizations, or those of the publisher, the editors and the reviewers. Any product that may be evaluated in this article, or claim that may be made by its manufacturer, is not guaranteed or endorsed by the publisher.

Copyright © 2022 Zhang, Sun, Li, Wang, Zhao, Niu, Guo, Chen, Che and Zhao. This is an open-access article distributed under the terms of the Creative Commons Attribution License (CC BY). The use, distribution or reproduction in other forums is permitted, provided the original author(s) and the copyright owner(s) are credited and that the original publication in this journal is cited, in accordance with accepted academic practice. No use, distribution or reproduction is permitted which does not comply with these terms.

frontiers in Surgery

ORIGINAL RESEARCH
published: 27 January 2022
doi: 10.3389/fsurg.2021.770767

Adding Consolidation Capecitabine to Neoadjuvant Chemoradiotherapy for Locally Advanced Rectal Cancer: A Propensity-Matched Comparative Study

Yifang Fang[1†], *Chengmin Sheng*[2†], *Feng Ding*[1†], *Weijie Zhao*[1†], *Guoxian Guan*[1*] and *Xing Liu*[1*]

[1] Department of Colorectal Surgery, The First Affiliated Hospital of Fujian Medical University, Fuzhou, China, [2] Fuzhou Medical College of Nanchang University, Fuzhou, China

OPEN ACCESS

Edited by:
Qi Liu,
Fudan University, China

Reviewed by:
Takahiro Hiratsuka,
Oita University, Japan
Cihangir Akyol,
Ankara University, Turkey
Mohammad Mohammadianpanah,
Shiraz University of Medical Sciences, Iran

***Correspondence:**
Xing Liu
fjmufylx@163.com
Guoxian Guan
fjxhggx@163.com

[†] These authors have contributed equally to this work

Specialty section:
This article was submitted to Surgical Oncology, a section of the journal Frontiers in Surgery

Received: 04 September 2021
Accepted: 27 December 2021
Published: 27 January 2022

Citation:
Fang Y, Sheng C, Ding F, Zhao W, Guan G and Liu X (2022) Adding Consolidation Capecitabine to Neoadjuvant Chemoradiotherapy for Locally Advanced Rectal Cancer: A Propensity-Matched Comparative Study. Front. Surg. 8:770767. doi: 10.3389/fsurg.2021.770767

Aim: To determine whether adding consolidation capecitabine chemotherapy without lengthening the waiting period influences pathological complete response (pCR) and short-term outcome of locally advanced rectal cancer (LARC) receiving neoadjuvant chemoradiotherapy (NCRT).

Method: Totally, 545 LARC who received NCRT and radical resection between 2010 and 2018 were enrolled. Short-term outcome and pCR rate were compared between patients with and without additional consolidation capecitabine. Logistic analysis was performed to identify predictors of pCR.

Results: After propensity score matching, 229 patients were matched in both NCRT and NCRT-Cape groups. Postoperative morbidity was comparable between groups except for operation time, which is lower in the NCRT group (213.2 ± 67.4 vs. 227.9 ± 70.5, $p = 0.025$). Two groups achieved similar pCR rates (21.8 vs. 22.7%, $p = 1.000$). Tumor size (OR = 0.439, $p < 0.001$), time interval between NCRT and surgery (OR = 1.241, $p = 0.003$), and post-NCRT carcinoembryonic antigen (OR = 0.880, $p = 0.008$) were significantly correlated with pCR in patients with LARC. A predictive nomogram was constructed with a C-index of 0.787 and 0.741 on internal and external validation.

Conclusion: Adding consolidation capecitabine chemotherapy without lengthening CRT-to-surgery interval in LARC patients after NCRT does not seem to impact pCR or short-term outcome. A predictive nomogram for pCR was successful, and it could support treatment decision-making.

Keywords: rectal neoplasm, neoadjuvant chemoradiotherapy, capecitabine, prognosis, propensity score matched analysis

INTRODUCTION

Neoadjuvant chemoradiotherapy (NCRT) and radical surgery have become the standard treatment for locally advanced rectal cancer (LARC) (1). The benefits of this multimodal treatment have been well-documented, namely, tumor downsizing and downstaging, increased radical resection rate, and better local tumor control (2–4). Approximately 10–30% of LARC patients following NCRT

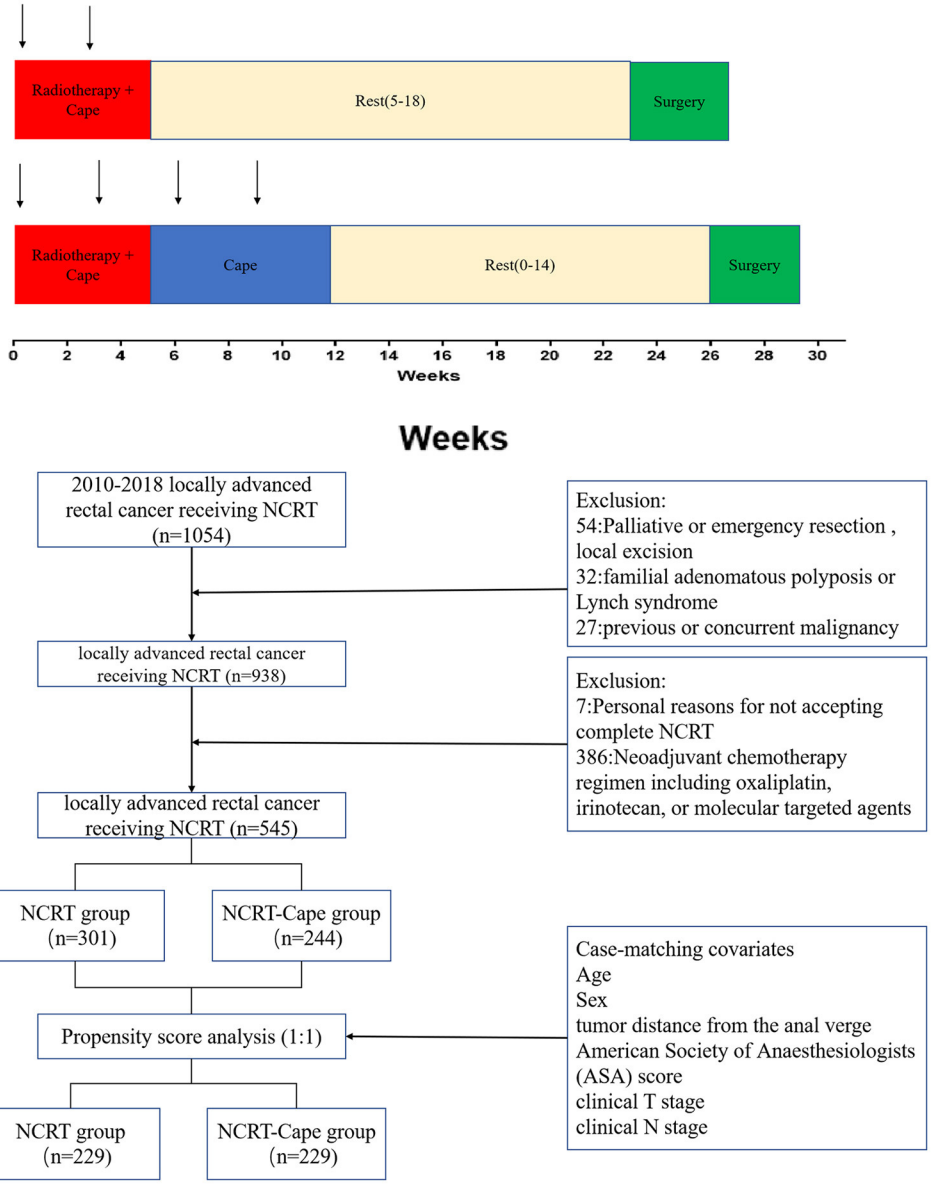

FIGURE 1 | The protocol of the neoadjuvant chemoradiotherapy in the two groups. NCRT, neoadjuvant chemoradiotherapy; NCRT-Cape, neoadjuvant chemoradiotherapy, and additional capecitabine chemotherapy.

will develop a pathological complete response (pCR), together with a low recurrence rate (5–7).

Given the superior oncological outcome, organ preservation with a "watch and wait" strategy or local excision, has been proposed to patients achieving pCR to improve the quality of life and anal sphincter preserving rate. Consequently, increasing pCR rate has become a primary endpoint of clinical trials, which might increase patients with LARC who could potentially benefit from organ-preservation strategies. Many strategies have been adopted to maximize the pCR rate, namely, dose-escalated radiation (8), intensified neoadjuvant treatment [induction (9) or consolidation chemotherapy (1, 8, 10–16)], and lengthening the CRT-to-surgery interval (17).

Standard NCRT protocol using a continuous infusional 5-fluorouracil (5-Fu) for radiation sensitization has been shown to achieve tumor downstaging, but no improved overall survival. Growing evidence has demonstrated that the addition of oxaliplatin to NRT acquires equivalent oncological outcomes when compared to fluoropyrimidine-based CRT, but increases toxicities and cost (18–22). The inconvenience of using an intravenous continuous infusion of 5-FU resulted in the development of an oral fluoropyrimidine, capecitabine. A meta-analysis (23) has demonstrated equivalent efficacy of capecitabine

TABLE 1 | Patient characteristics in patients with LARC after NCRT.

Characteristics	Unmatched patients			Propensity-matched patients		
	NCRT ($n = 301$)	NCRT-Cape ($n = 244$)	*p*-value	NCRT ($n = 229$)	NCRT-Cape ($n = 229$)	*p*-value
Sex (%)			0.857			1.000
Male	193 (64.1)	159 (65.2)		148 (64.6)	148 (58.4)	
Female	108 (35.9)	85 (34.8)		81 (35.4)	81 (35.4)	
Age (years)	57.4.0 ± 11.4	56.0 ± 10.7	0.131	57.3 ± 11.4	56.3 ± 10.4	0.348
ASA score (%)			0.842			0.922
1	214 (71.1)	179 (73.4)		167 (72.9)	169 (73.8)	
2	83 (27.6)	62 (25.4)		58 (25.3)	59 (24.9)	
3	4 (1.3)	3 (1.2)		4 (1.7)	3 (1.3)	
Distance from the anal verge (cm)	6.1 ± 2.3	6.7 ± 2.5	**0.002**	6.3 ± 2.5	6.4 ± 2.3	0.656
Time interval between CRT and surgery (weeks)	9.5 ± 1.5	9.3 ± 1.6	0.311	9.5 ± 1.5	9.5 ± 2.6	0.925
Histopathology (%)			0.656			0.248
pCR	64 (21.3)	53 (21.3)		154 (98.1)	157 (100.0)	
Adenocarcinoma	219 (72.8)	173 (70.9)		154 (98.1)	157 (100.0)	
Signet ring cell carcinoma	17 (5.6)	15 (6.1)		3 (1.9)	0 (0.0)	
Mucinous adenocarcinoma	1 (0.3)	3 (1.2)		17 (5.6)	17 (5.6)	
Tumor size	2.6 ± 1.3	2.5 ± 1.3	0.699	2.5 ± 1.2	2.5 ± 1.2	0.485
Clinical T stage (%)			0.063			0.070
T2 + 3	128 (42.5)	84 (34.3)		102 (44.5)	82 (35.8)	
T4	173 (57.5)	160 (65.6)		127 (55.5)	147 (64.2)	
Clinical N stage (%)			0.320			0.446
N0	34 (11.3)	21 (8.6)		27 (11.8)	21 (3.0)	
N+	267 (88.7)	223 (91.4)		202 (88.2)	208 (90.8)	

LARC, locally advanced rectal cancer; NCRT, neoadjuvant chemoradiotherapy; NCRT-Cape, neoadjuvant chemoradiotherapy and additional capecitabine chemotherapy; ASA, American society of anesthesiologists; CRT, chemoradiotherapy. Bold values indicate of statistical significance.

and infusional 5-Fu in the neoadjuvant setting, suggesting capecitabine to be an alternative to 5-Fu-based CRT for LARC.

In this article, we aimed to determine whether adding 2 cycles of consolidation capecitabine without lengthening CRT-to-surgery interval influences pCR rate and short-term outcome of LARC patients after NCRT. In addition, we sought to identify post-CRT determinants for pCR, and to construct a nomogram that might be helpful during organ preservation strategy decision-making.

PATIENTS AND METHOD

Patient Eligibility

We performed a retrospective study based on propensity score matching. Between October 2010 and January 2018, patients with LARC who underwent curative resection and received capecitabine-based NCRT from our database. Patient inclusion criteria were: (1) clinical stage II or III (cT3/4 or cN1/2) disease; (2) pathologically proven rectal adenocarcinomas; and (3) tumors distance <12 cm from the anal verge. Exclusion criteria included: (1) neoadjuvant chemotherapy regimen, namely, oxaliplatin, irinotecan, or molecular targeted agents; (2) previous or concurrent malignancy; (3) emergency or palliative resection; and (4) transanal local excision. This study was approved by the Institutional Review Board of Fujian Medical University Union Hospital (2013051).

Treatment Protocol and Follow-Up

Patient assessments were performed at baseline for tumor staging using a digital rectal examination, colonoscopy, chest radiography, abdominopelvic MRI, and/or transrectal ultrasound. Preoperative radiotherapy consisted of 45 Gy to the pelvis for 5 weeks (180 cGy/25 fractions) and a tumor boost of 5.4 Gy. Concomitant chemotherapy was administered with oral capecitabine (825 mg/m^2 two times daily from day 1 to day 14 per cycle, a total of two cycles during the pre-operative radiotherapy). The treatment decision whether or not to add two-cycle consolidation capecitabine chemotherapy to NCRT was based on the disease stage. Surgery was carried out 6–20 weeks after the completion of radiation. Surgical techniques, namely, total mesorectal excision and high ligation of the inferior mesenteric artery, were routinely performed. After 3–4 weeks from surgery, adjuvant chemotherapy (FOLFOX or CapeOX) was considered for patients for 6 months. The treatment schema of our study is presented in **Figure 1**.

Patients were followed four times in the first 3 years, then twice for the next 2 years, and annually thereafter. Patient follow-up lasted until death or the cut-off date of October 31, 2018.

TABLE 2 | Operative and post-operative outcomes in patients with LARC after NCRT.

Characteristics	NCRT (n = 229)	NCRT-Cape (n = 229)	p-value
Operative time (min)	213.2 ± 67.4	227.9 ± 70.5	**0.025**
Estimated blood loss (ml)	76.5 ± 88.8	79.2 ± 81.9	0.417
Surgery approach			0.516
Laparoscopic	158 (69.0)	155 (67.6)	
Open	53 (23.1)	49 (21.4)	
Robotic	18 (7.9)	25 (10.9)	
Post-operative hospital stay (days)	8.3 ± 5.5	9.0 ± 6.3	0.183
Post-operative complications	33 (14.4)	40 (17.5)	0.444
30 days readmission	1 (0.4)	1 (0.4)	1.000
Peri-CRT complications*	64 (27.9)	62 (27.1)	0.917
Major	7 (3.1)	1 (0.4)	0.068
Sphincter-saving procedure	203 (88.6)	204 (89.1)	1.000
Lymph nodes retrieved	12.4 ± 7.7	12.5 ± 6.4	0.832
Metastatic lymph nodes	0.5 ± 1.3	0.5 ± 1.5	0.840
CRM involvement	0 (0)	2 (0.9)	0.499
Pathological TNM stage			0.957
0	50 (21.8)	52 (22.7)	
I	59 (25.8)	63 (27.5)	
II	58 (25.3)	57 (24.9)	
III	60 (26.2)	58 (24.5)	
IV	2 (0.9)	1 (0.4)	
TRG grade			**0.026**
0	51 (21.8)	52 (22.7)	1.000
1	84 (36.7)	61 (26.6)	**0.027**
2	77 (33.6)	105 (45.9)	**0.010**
3	17 (7.4)	11 (4.8)	0.330
Perineural invasion	11 (4.8)	12 (5.2)	1.000
Vascular invasion	11 (4.8)	9 (3.9)	0.820

**Some patients experienced more than one complication, and categorized as. NCRT, neoadjuvant chemoradiotherapy; NCRT-Cape, neoadjuvant chemoradiotherapy and additional capecitabine chemotherapy; CRM, circumferential resection margin; TRG, tumor regression grade. Bold values indicate of statistical significance.*

Definitions

Tumor distance from the anal verge was estimated by digital rectal examination, pre-operative MRI evaluation, and intraoperative findings during the operation. Tumor response to NCRT was graded according to Rectal Cancer Tumor Regression Grade (TRG) method (24). pCR was defined as no viable tumor cells in the primary site or the lymph nodes. Postoperative morbidity was classified according to the Clavien–Dindo classification (25).

Statistical Analysis

To minimize group differences, we performed a 1:1 propensity score matching analysis by using R Version 3.5.1 (Vienna, Austria). Statistical analyses were performed using SPSS version 23.0 (SPSS INC., Chicago, IL, USA). Categorical variables were presented as numbers and compared using the chi-square test or Fisher's exact test as appropriate. Continuous variables were expressed as means ± SD and analyzed using Student's t-test. The logistic regression model was used to identify independent predictors for pCR, and a predictive nomogram was developed by the R project. To validate the results, patients were randomly divided into training ($n = 420$) and validation ($n = 125$) cohorts by using SPSS. The nomogram went through internal and external validation. $p < 0.05$ was considered statistically significant.

RESULTS

Patient Characteristics

The baseline features of patients with LARC are presented in **Table 1**. Totally 545 patients with LARC were included. After propensity score matching, 229 patients receiving standard NCRT (NCRT group) and 229 patients treated with NCRT and additional 2 cycles of consolidation capecitabine chemotherapy (NCRT-Cape group) were matched. After matching, between-group baseline characteristics were well-balanced, such as age, gender, American Society of Anesthesiologists grade, interval time between NCRT and surgery, distance from the anal verge, clinical T and N stage.

Perioperative Outcomes

Surgical results are listed in **Table 2**. Estimated blood loss, surgical approach, and preserve organ rate were comparable between the two groups (**Table 2**). The operation time in the NCRT group was significantly lower than that of the NCRT-Cape group (213.2 ± 67.4 vs. 227.9 ± 70.5, $p = 0.025$), compared to. Postoperative morbidity was similar between two groups (14.4 vs. 17.5%, $p = 0.444$). No group difference was observed in post-operative hospital stay and 30 days readmission ($p = 0.183$, $p = 1.000$, respectively). Complication severity was similar in the two groups. Similarly, no significant difference was observed in peri-NCRT complications between groups ($p = 0.917$). No re-operation was found in either group. Likewise, no perioperative mortality occurred in the two groups.

Pathological Outcomes

Adding consolidation capecitabine chemotherapy had no impact on lymph node retrieved and metastatic lymph nodes ($p = 0.832$, $p = 0.840$, respectively). With regard to tumor response to NCRT, a lower proportion of good response (TRG1: 36.7 vs. 26.6%, $p = 0.028$) and a higher proportion of partial response (TRG2: 33.6 vs. 45.9%, $p = 0.010$) were noted in patients in the NCRT-Cape group. However, additional administration of 2 cycles of consolidation capecitabine chemotherapy did not increase pCR rate compared to standard NCRT group (21.8 vs. 22.7%, $p = 1.000$, **Figure 2**). Positive circumferential resection margin rates were comparable between both groups, and tumor size ($p = 0.499$, $p = 0.485$). A pathological TNM stage was similar between two groups ($p = 0.957$). Similarly, perinerval and vascular invasion did not differ between two groups ($p = 1.000$, $p = 0.820$, respectively).

Predictive Factors of pCR

To identify risk factors for pCR in LARC, logistic regression analysis was performed in 545 patients (before propensity score matching). In univariate analysis, adding consolidation capecitabine chemotherapy (OR = 0.954, p = 0.476) was not correlated with pCR in patients with LARC. Tumor size (OR = 0.428, $p < 0.001$), interval time between NCRT and surgery (OR = 1.141, p = 0.036), pre-NCRT clinical T stage (OR = 0.641, p = 0.027), pre-NCRT clinical N stage (OR = 0.514, p = 0.031), lymph nodes harvested (OR = 0.955, p = 0.008), and post-NCRT carcinoembryonic antigen (CEA) (OR = 0.872, p = 0.003) were significantly correlated with pCR in patients with LARC. On multivariate analysis, tumor size (OR = 0.439, $p < 0.001$), and interval time between NCRT and surgery (OR = 1.241, p = 0.003), and post-NCRT CEA (OR = 0.880, p = 0.008) were significant risk factors for pCR in patients with LARC (**Table 3**).

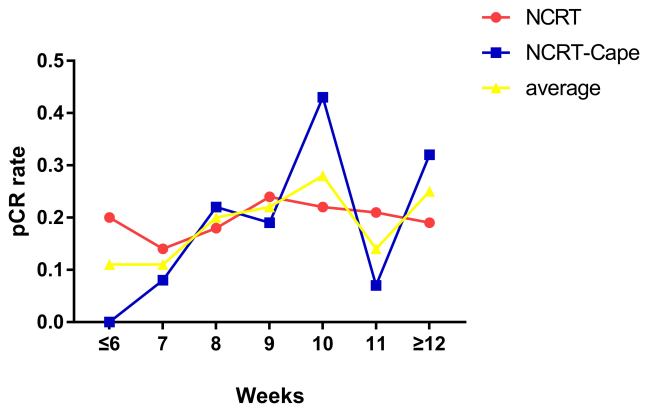

FIGURE 2 | The relationship between time intervals and pCR rates. NCRT, neoadjuvant chemoradiotherapy; NCRT-Cape, neoadjuvant chemoradiotherapy, and additional capecitabine chemotherapy.

Nomogram for pCR

Based on results from multivariate analysis, a predicting nomogram for pCR was developed, as demonstrated in **Figure 3A**. By summing up the score of each variable, a straight line could be drawn to obtain the predicted pCR rate. The C-index of the nomogram was 0.78 (95% CI 0.73–0.83). The calibration curve (**Figure 3B**) showed good performance upon internal validation between the predicted and actual probability of pCR. Upon external validation, the C-index of the nomogram was 0.73 (95% CI 0.63–0.83), and the calibration curve (**Figure 3C**) showed good accordance between predicted and observed probabilities of pCR.

TABLE 3 | Univariate and multivariate analysis of predictive factors for pCR in locally advanced rectal cancer patients (n = 545).

Variables	Univariate analysis			Multivariate analysis		
	HR	95% CI	*P*-Value	HR	95% CI	*P*-Value
Sex, male/female	1.383	0.908–2.105	0.926			
Age	0.999	0.980–1.017	0.886			
ASA	0.916	0.594–1.411	0.689			
Distance from the anal verge	0.927	0.850–1.011	0.088			
Tumor size	0.428	0.334–0.548	**<0.001**	0.439	0.338–0.570	**<0.001**
Surgery approach						
Laparoscopic	Reference	Reference	0.724			
Open	1.141	0.530–2.455	0.736			
Robotic	1.348	0.582–3.122	0.486			
Sphincter-Saving procedure	0.584	0.279–1.221	0.153			
Operative time (min)	0.998	0.995–1.002	0.337			
Estimated blood loss (ml)	0.998	0.995–1.001	0.284			
Time interval between NCRT and surgery	1.141	1.009–1.291	**0.036**	1.241	1.074–1.434	**0.003**
Pre-NCRT cT stage	0.641	0.432–0.950	**0.027**	0.710	0.460–1.096	0.123
Pre-NCRT cN stage	0.514	0.281–0.941	**0.031**	0.707	0.355–1.407	0.323
Post-Operative hospital stay	0.969	0.927–1.014	0.175			
Lymph nodes harvested	0.955	0.924–0.988	**0.008**	0.985	0.948–1.022	0.420
Post-NCRT CEA level	0.872	0.795–0.956	**0.003**	0.880	0.802–0.967	**0.008**
Post-NCRT CA19-9 level	0.993	0.979–1.007	0.309			
Post-Operative complications	0.821	0.456–1.475	0.666			
Plus capecitabine	0.954	0.632–1.440	0.822			
Reduce the dose	1.237	0.246–6.210	0.796			
NCRT complications	1.139	0.721–1.800	0.577			

NCRT, neoadjuvant chemoradiotherapy; NCRT-Cape, neoadjuvant chemoradiotherapy, and additional capecitabine chemotherapy; CRM, circumferential resection margin; TRG, tumor regression grade, HR, hazard ratio; CI, confidential interval. Bold values indicate of statistical significance.

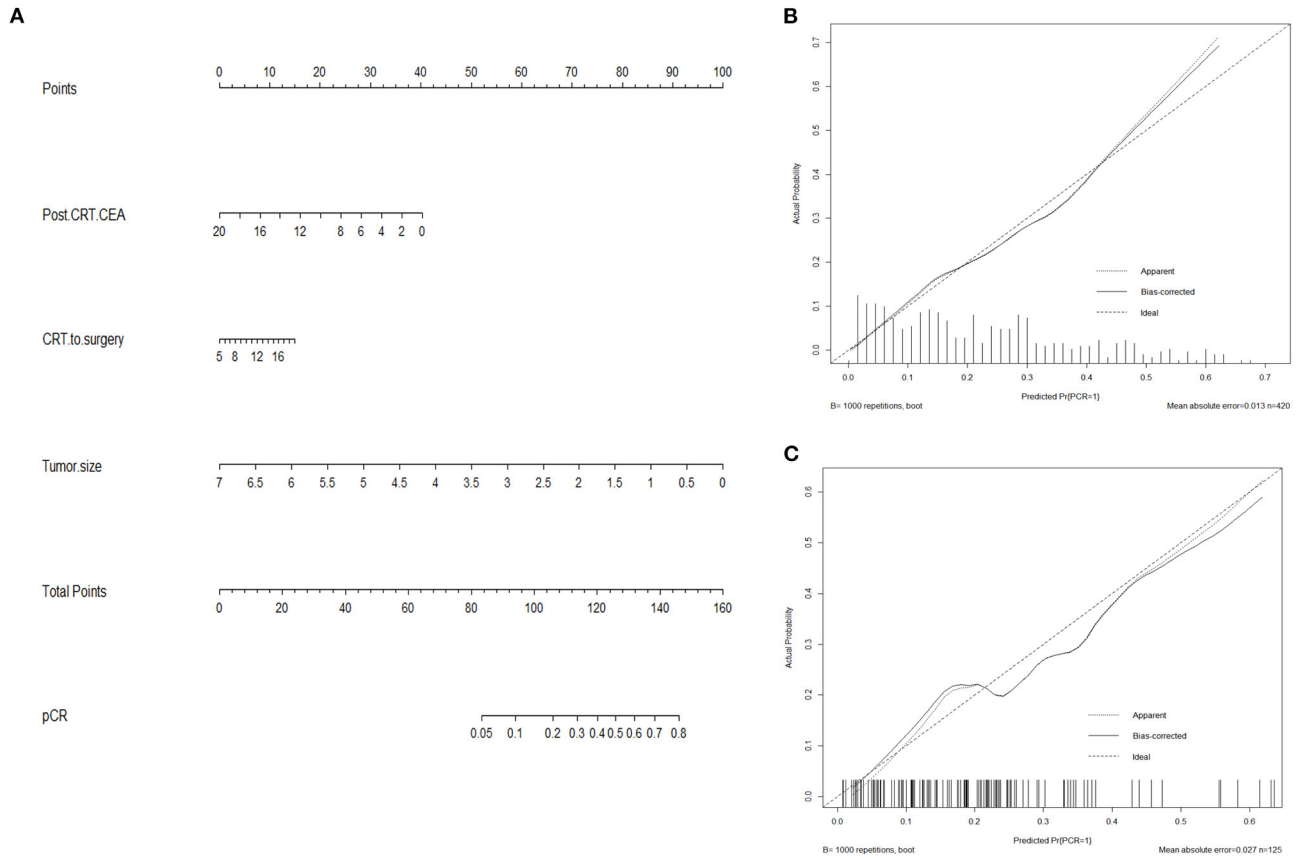

FIGURE 3 | Nomogram predicting pCR **(A)** and calibration curves with internal **(B)** and external **(C)** validation. **(A)** A score for each variable can be obtained at the top scale, and the sum of scores indicates a predictive probability of pCR. **(B,C)** The solid line indicates the actual performance of our nomogram, and the dashed line represents the prediction by an ideal model. CEA, carcinoembryonic antigen.

DISCUSSION

A great effort has been made to maximize tumor response to NCRT, in which pCR is selected as a surrogate endpoint. Herein, we investigated the efficacy of adding consolidation capecitabine chemotherapy without changing the CRT-to-surgery interval for patients with LARC. The result demonstrated that adding 2 cycles of consolidation capecitabine to NCRT had no impact on the short-term perioperative outcome, and did not result in an increase in pCR rates. Additionally, by incorporating post-NCRT significant predictive factors in Logistic analysis, we built a nomogram for pCR that might assist in decision-making about organ-preserving strategies.

Fluoropyrimidine-based (5-FU or capecitabine) pre-operative chemoradiotherapy is the standard care for LARC. Incorporation of oxaliplatin to fluoropyrimidine-based CRT has been shown to acquire equivalent oncological outcomes but increase toxicities (18–22). Accumulating evidence has proposed capecitabine to be an alternative to 5-FU, the efficacy of XELOX (capecitabine and oxaliplatin) was comparable with that of the FOLFOX4 regimen (5-FU/folinic acid plus oxaliplatin) (26). In addition, using oral capecitabine instead of infusional 5-FU during NCRT has been shown to be correlated with improved tumor response and lower toxicity, and a comparable pCR rate is compared to pre-operative 5-FU-based NCRT (27–29). It has been demonstrated that nCRT with capecitabine is safe and well-tolerated in the ACCORD/PRODIGD 2 phase III trial (30).

To improve tumor response without increasing perioperative complications, we added 2 cycles of consolidation capecitabine chemotherapy in the waiting period to the standard NCRT regimen. Our preliminary results demonstrated that additional two-cycle consolidation capecitabine did not increase the incidence of peri-CRT complications, such as hand-foot syndrome, fatigue, and diarrhea, suggesting this regimen might be well-tolerated.

Meanwhile, we used propensity score matching to reduce selection bias; between-group baseline characteristics were well-balanced after matching. No negative effect on surgical outcome was observed when patients were administered two-cycle consolidation capecitabine to NCRT. Regarding surgical morbidity, the severity of post-operative complications and post-operative hospital stay were found comparable between the two groups. No reoperation and perioperative mortality occurred in the two groups. Together, these results indicated the

safety of adding 2 cycles of consolidation capecitabine to the NCRT regimen.

To further explore the efficacy of adding consolidation capecitabine to NCRT on tumor response, we compared the pCR rates between the two groups. The addition of consolidation capecitabine to NCRT did not significantly improve pCR rate. The absolute ypCR rate difference between groups was very small and not statistically significant. Similar results were found in a recent phase II OIGIT-01 Trial (31). We suggested that radiosensitization by using capecitabine might have already maximized tumor responses to NCRT, leaving little room for improvement with the addition of two-cycle consolidation capecitabine chemotherapy.

The optimal timing of surgery after NCRT is still controversial (32). Surgery beyond 8 weeks after completion of radiotherapy might increase pelvic fibrosis and rectal edema, leading to intraoperative technical difficulties and increased surgical complications. On the other hand, the pCR rate might increase by prolongation of the NCRT-to-surgery interval (17, 33–36). Herein, we analyzed the relationship between pCR and NCRT-to-surgery interval. The result revealed that longer interval time correlated with increased pCR rate. Results from Logistic regression demonstrated that interval time was a significant risk factor for pCR than the consolidation capecitabine chemotherapy.

Additionally, after adjustment for confounding factors, tumor size, and post-NCRT CEA level were significant risk factors for pCR in patients with LARC. To facilitate the decision-making regarding organ-preserving strategies, we developed a nomogram predicting pCR. This nomogram has a reliable C-index on internal and external validation. The incorporation of specific molecular and genetic markers into the predicting nomogram would enhance the performance of the model. Nowadays, delivery of "total neoadjuvant therapy" (TNT) strategies is becoming increasingly popular to improve the pCR rates (37), allowing a group of patients to benefit from full-dose adjuvant chemotherapy and finally a less-invasive organ preservation strategy (38–41). However, the definite role of TNT strategies is still unveiled.

There are several limitations that warrant discussion. First, this study was subjected to selection bias owing to its retrospective nature. To minimize selection bias between groups, we performed propensity score analysis. Second, our predictive model was based on a single-center retrospective analysis. It requires further external validation in a large population from multiple institutions. Another limitation was that this study focused on the pCR rate, a surrogate marker of oncological outcomes. Further studies focused on the long-term oncological outcomes are needed to further confirm the results of our study. Nevertheless, our study adds to the understanding of the efficacy of adding capecitabine to standard NCRT.

Our study suggested that additional studies in a large-scale population are needed to confirm these results.

DATA AVAILABILITY STATEMENT

The original contributions presented in the study are included in the article/**Supplementary Material**, further inquiries can be directed to the corresponding author/s.

ETHICS STATEMENT

Studies relative to humans in this article were approved by the Ethics Committee of The Fujian Medical University Union Hospital (2013051). The patients/participants provided their written informed consent to participate in this study.

AUTHOR CONTRIBUTIONS

YFF, CMS, FD, WJZ, GXG, and XL designed the experiments, performed the experiments, analyzed the data, and wrote the article. All authors contributed to the article and approved the submitted version.

FUNDING

This study was supported by the National Foundation of China (No. 82172800), Science Foundation of the Fujian Province (No. 2019J0105), Special Financial Foundation of Fujian Provincial (No. 2015-1297 and 2020B1050), the Startup Fund for Scientific Research, Fujian Medical University (2017XQ1029 and 2018QH2027), and the Professor Development Foundation of Fujian Medical University (No. JS11006). Talent programs granted from The First Affiliated Hospital of Fujian Medical University (YJRC3600). Joint Funds for the Innovation of Science and Technology, Fujian Province (2020Y9125).

SUPPLEMENTARY MATERIAL

The Supplementary Material for this article can be found online at: https://www.frontiersin.org/articles/10.3389/fsurg.2021.770767/full#supplementary-material

REFERENCES

1. Heald RJ, Husband EM, Ryall RD. The mesorectum in rectal cancer surgery–the clue to pelvic recurrence. *Br J Surg.* (1982) 69:613–6. doi: 10.1002/bjs.1800691019
2. Sauer R, Becker H, Hohenberger W, Rödel C, Wittekind C, Fietkau R, et al. Preoperative versus postoperative chemoradiotherapy for rectal cancer. *N Engl J Med.* (2004) 351:1731–40. doi: 10.1056/NEJMoa040694
3. Mohiuddin M, Winter K, Mitchell E, Hanna N, Yuen A, Nichols C, et al. Randomized phase II study of neoadjuvant combined-modality chemoradiation for distal rectal cancer: radiation therapy oncology group trial 0012. *J Clin Oncol.* (2006) 24:650–5. doi: 10.1200/JCO.2005.03.6095
4. van Gijn W, Marijnen CA, Nagtegaal ID, Kranenbarg EM, Putter H, Wiggers T, et al. Preoperative radiotherapy combined with total mesorectal excision for resectable rectal cancer: 12-year follow-up of the multicentre, randomised controlled TME trial. *Lancet Oncol.* (2011) 12:575–82. doi: 10.1016/S1470-2045(11)70097-3

5. Park IJ, You YN, Agarwal A, Skibber JM, Rodriguez-Bigas MA, Eng C, et al. Neoadjuvant treatment response as an early response indicator for patients with rectal cancer. *J Clin Oncol.* (2012) 30:1770–6. doi: 10.1200/JCO.2011.39.7901
6. Maas M, Nelemans PJ, Valentini V, Das P, Rödel C, Kuo LJ, et al. Long-term outcome in patients with a pathological complete response after chemoradiation for rectal cancer: a pooled analysis of individual patient data. *Lancet Oncol.* (2010) 11:835–44. doi: 10.1016/S1470-2045(10)70172-8
7. Roh MS, Colangelo LH, O'Connell MJ, Yothers G, Deutsch M, Allegra CJ, et al. Preoperative multimodality therapy improves disease-free survival in patients with carcinoma of the rectum: NSABP R-03. *J Clin Oncol.* (2009) 27:5124–30. doi: 10.1200/JCO.2009.22.0467
8. São Julião GP, Habr-Gama A, Vailati BB, Aguilar PB, Sabbaga J, Araújo S, et al. Is neoadjuvant chemoradiation with dose-escalation and consolidation chemotherapy sufficient to increase surgery-free and distant metastases-free survival in baseline cT3 rectal cancer. *Eur J Surg Oncol.* (2018) 44:93–9. doi: 10.1016/j.ejso.2017.11.010
9. Wiltshire KL, Ward IG, Swallow C, Oza AM, Cummings B, Pond GR, et al. Preoperative radiation with concurrent chemotherapy for resectable rectal cancer: effect of dose escalation on pathologic complete response, local recurrence-free survival, disease-free survival, and overall survival. *Int J Radiat Oncol Biol Phys.* (2006) 64:709–16. doi: 10.1016/j.ijrobp.2005.08.012
10. Fernández-Martos C, Pericay C, Aparicio J, Salud A, Safont M, Massuti B, et al. Phase II, randomized study of concomitant chemoradiotherapy followed by surgery and adjuvant capecitabine plus oxaliplatin (CAPOX) compared with induction CAPOX followed by concomitant chemoradiotherapy and surgery in magnetic resonance imaging-defined, locally advanced rectal cancer: grupo cancer de recto 3 study. *J Clin Oncol.* (2010) 28:859–65. doi: 10.1200/JCO.2009.25.8541
11. Fernandez-Martos C, Garcia-Albeniz X, Pericay C, Maurel J, Aparicio J, Montagut C, et al. Chemoradiation, surgery and adjuvant chemotherapy versus induction chemotherapy followed by chemoradiation and surgery: long-term results of the Spanish GCR-3 phase II randomized trial†. *Ann Oncol.* (2015) 26:1722–8. doi: 10.1093/annonc/mdv223
12. Myerson RJ, Tan B, Hunt S, Olsen J, Birnbaum E, Fleshman J, et al. Five fractions of radiation therapy followed by 4 cycles of FOLFOX chemotherapy as preoperative treatment for rectal cancer. *Int J Radiat Oncol Biol Phys.* (2014) 88:829–36. doi: 10.1016/j.ijrobp.2013.12.028
13. Markovina S, Youssef F, Roy A, Aggarwal S, Khwaja S, DeWees T, et al. Improved metastasis- and disease-free survival with preoperative sequential short-course radiation therapy and FOLFOX chemotherapy for rectal cancer compared with neoadjuvant long-course chemoradiotherapy: results of a matched pair analysis. *Int J Radiat Oncol Biol Phys.* (2017) 99:417–26. doi: 10.1016/j.ijrobp.2017.05.048
14. Abboud H, Petrak A, Mealy M, Sasidharan S, Siddique L, Levy M. Treatment of acute relapses in neuromyelitis optica: steroids alone versus steroids plus plasma exchange. *Mult Scler.* (2016) 22:185–92. doi: 10.1177/1352458515581438
15. Cercek A, Goodman KA, Hajj C, Weisberger E, Segal NH, Reidy-Lagunes DL, et al. Neoadjuvant chemotherapy first, followed by chemoradiation and then surgery, in the management of locally advanced rectal cancer. *J Natl Compr Canc Netw.* (2014) 12:513–9. doi: 10.6004/jnccn.2014.0056
16. Bujko K, Wyrwicz L, Rutkowski A, Malinowska M, Pietrzak L, Kryński J, et al. Long-course oxaliplatin-based preoperative chemoradiation versus 5 × 5 Gy and consolidation chemotherapy for cT4 or fixed cT3 rectal cancer: results of a randomized phase III study. *Ann Oncol.* (2016) 27:834–42. doi: 10.1093/annonc/mdw198.20
17. Du D, Su Z, Wang D, Liu W, Wei Z. Optimal interval to surgery after neoadjuvant chemoradiotherapy in rectal cancer: a systematic review and meta-analysis. *Clin Colorectal Cancer.* (2018) 17:13–24. doi: 10.1016/j.clcc.2017.10.012
18. De Felice F, Benevento I, Magnante AL, Musio D, Bulzonetti N, Caiazzo R, et al. Clinical benefit of adding oxaliplatin to standard neoadjuvant chemoradiotherapy in locally advanced rectal cancer: a meta-analysis : oxaliplatin in neoadjuvant treatment for rectal cancer. *BMC Cancer.* (2017) 17:325. doi: 10.1186/s12885-017-3323-4
19. Gérard JP, Azria D, Gourgou-Bourgade S, Martel-Laffay I, Hennequin C, Etienne PL, et al. Comparison of two neoadjuvant chemoradiotherapy regimens for locally advanced rectal cancer: results of the phase III trial ACCORD 12/0405-Prodige 2. *J Clin Oncol.* (2010) 28:1638–44. doi: 10.1200/JCO.2009.25.8376
20. Rödel C, Graeven U, Fietkau R, Hohenberger W, Hothorn T, Arnold D, et al. Oxaliplatin added to fluorouracil-based preoperative chemoradiotherapy and postoperative chemotherapy of locally advanced rectal cancer (the German CAO/ARO/AIO-04 study): final results of the multicentre, open-label, randomised, phase 3 trial. *Lancet Oncol.* (2015) 16:979–89. doi: 10.1016/S1470-2045(15)00159-X
21. Aschele C, Cionini L, Lonardi S, Pinto C, Cordio S, Rosati G, et al. Primary tumor response to preoperative chemoradiation with or without oxaliplatin in locally advanced rectal cancer: pathologic results of the STAR-01 randomized phase III trial. *J Clin Oncol.* (2011) 29:2773–80. doi: 10.1200/JCO.2010.34.4911
22. Benson AB, Venook AP, Al-Hawary MM, Cederquist L, Chen YJ, Ciombor KK, et al. Rectal cancer, version 2.2018, NCCN clinical practice guidelines in oncology. *J Natl Compr Canc Netw.* (2018) 16:874–901. doi: 10.6004/jnccn.2018.0061
23. Zou XC, Wang QW, Zhang JM. Comparison of 5-FU-based and capecitabine-based neoadjuvant chemoradiotherapy in patients with rectal cancer: a meta-analysis. *Clin Colorectal Cancer.* (2017) 16:e123–123e139. doi: 10.1016/j.clcc.2017.01.009
24. Wheeler JM, Warren BF, Mortensen NJ, Ekanyaka N, Kulacoglu H, Jones AC, et al. Quantification of histologic regression of rectal cancer after irradiation: a proposal for a modified staging system. *Dis Colon Rectum.* (2002) 45:1051–6. doi: 10.1007/s10350-004-6359-x
25. Dindo D, Demartines N, Clavien PA. Classification of surgical complications: a new proposal with evaluation in a cohort of 6336 patients and results of a survey. *Ann Surg.* (2004) 240:205–13. doi: 10.1097/01.sla.0000133083.54934.ae
26. Cassidy J, Saltz L, Twelves C, Van Cutsem E, Hoff P, Kang Y, et al. Efficacy of capecitabine versus 5-fluorouracil in colorectal and gastric cancers: a meta-analysis of individual data from 6171 patients. *Ann Oncol.* (2011) 22:2604–9. doi: 10.1093/annonc/mdr031
27. Fernández-Martos C, Nogué M, Cejas P, Moreno-García V, Machancoses AH, Feliu J. The role of capecitabine in locally advanced rectal cancer treatment: an update. *Drugs.* (2012) 72:1057–73. doi: 10.2165/11633870-000000000-00000
28. Hofheinz RD, Wenz F, Post S, Matzdorff A, Laechelt S, Hartmann JT, et al. Chemoradiotherapy with capecitabine versus fluorouracil for locally advanced rectal cancer: a randomised, multicentre, non-inferiority, phase 3 trial. *Lancet Oncol.* (2012) 13:579–88. doi: 10.1016/S1470-2045(12)70116-X
29. Chan AK, Wong AO, Jenken DA. Preoperative capecitabine and pelvic radiation in locally advanced rectal cancer–is it equivalent to 5-FU infusion plus leucovorin and radiotherapy. *Int J Radiat Oncol Biol Phys.* (2010) 76:1413–9. doi: 10.1016/j.ijrobp.2009.03.048
30. François E, Azria D, Gourgou-Bourgade S, Jarlier M, Martel-Laffay I, Hennequin C, et al. Results in the elderly with locally advanced rectal cancer from the ACCOR12/PRODIGE 2 phase III trial: tolerance and efficacy. *Radiother Oncol.* (2014) 110:144–9. doi: 10.1016/j.radonc.2013.10.019
31. Golo D, But-Hadzic J, Anderluh F, Brecelj E, Edhemovic I, Jeromen A, et al. Induction chemotherapy, chemoradiotherapy and consolidation chemotherapy in preoperative treatment of rectal cancer - long-term results of phase II OIGIT-01 trial. *Radiol Oncol.* (2018) 52:267–74. doi: 10.2478/raon-2018-0028
32. Glimelius B. Optimal time intervals between pre-operative radiotherapy or chemoradiotherapy and surgery in rectal cancer. *Front Oncol.* (2014) 4:50. doi: 10.3389/fonc.2014.00050
33. Figueiredo N, Panteleimonitis S, Popeskou S, Cunha JF, Qureshi T, Beets GL, et al. Delaying surgery after neoadjuvant chemoradiotherapy in rectal cancer has no influence in surgical approach or short-term clinical outcomes. *Eur J Surg Oncol.* (2018) 44:484–9. doi: 10.1016/j.ejso.2018.01.088
34. Garcia-Aguilar J, Smith DD, Avila K, Bergsland EK, Chu P, Krieg RM. Optimal timing of surgery after chemoradiation for advanced rectal cancer: preliminary results of a multicenter, nonrandomized phase II prospective trial. *Ann Surg.* (2011) 254:97–102. doi: 10.1097/SLA.0b013e3182196e1f
35. Rombouts A, Hugen N, Elferink M, Nagtegaal ID, de Wilt J. Treatment interval between neoadjuvant chemoradiotherapy and surgery in rectal cancer patients: a population-based study. *Ann Surg Oncol.* (2016) 23:3593–601. doi: 10.1245/s10434-016-5294-0

36. Petrelli F, Sgroi G, Sarti E, Barni S. Increasing the interval between neoadjuvant chemoradiotherapy and surgery in rectal cancer: a meta-analysis of published Studies. *Ann Surg.* (2016) 263:458–64. doi: 10.1097/SLA.0000000000000368
37. Garcia-Aguilar J, Chow OS, Smith DD, Marcet JE, Cataldo PA, Varma MG, et al. Effect of adding mFOLFOX6 after neoadjuvant chemoradiation in locally advanced rectal cancer: a multicentre, phase 2 trial. *Lancet Oncol.* (2015) 16:957–66. doi: 10.1016/S1470-2045(15)00004-2
38. Probst CP, Becerra AZ, Aquina CT, Tejani MA, Wexner SD, Garcia-Aguilar J, et al. Extended intervals after neoadjuvant therapy in locally advanced rectal cancer: the key to improved tumor response and potential organ preservation. *J Am Coll Surg.* (2015) 221:430–40. doi: 10.1016/j.jamcollsurg.2015.04.010
39. Nilsson PJ, van Etten B, Hospers GA, Påhlman L, van de Velde CJ, Beets-Tan RG, et al. Short-course radiotherapy followed by neo-adjuvant chemotherapy in locally advanced rectal cancer–the RAPIDO trial. *BMC Cancer.* (2013) 13:279. doi: 10.1186/1471-2407-13-279
40. Martens MH, Maas M, Heijnen LA, Lambregts DM, Leijtens JW, Stassen LP, et al. Long-term outcome of an organ preservation program after neoadjuvant treatment for rectal cancer. *J Natl Cancer Inst.* (2016) 108:djw171. doi: 10.1093/jnci/djw171
41. Beets GL, Figueiredo NF, Beets-Tan RG. Management of rectal cancer without radical resection. *Annu Rev Med.* (2017) 68:169–82. doi: 10.1146/annurev-med-062915-021419

Conflict of Interest: The authors declare that the research was conducted in the absence of any commercial or financial relationships that could be construed as a potential conflict of interest.

Publisher's Note: All claims expressed in this article are solely those of the authors and do not necessarily represent those of their affiliated organizations, or those of the publisher, the editors and the reviewers. Any product that may be evaluated in this article, or claim that may be made by its manufacturer, is not guaranteed or endorsed by the publisher.

Copyright © 2022 Fang, Sheng, Ding, Zhao, Guan and Liu. This is an open-access article distributed under the terms of the Creative Commons Attribution License (CC BY). The use, distribution or reproduction in other forums is permitted, provided the original author(s) and the copyright owner(s) are credited and that the original publication in this journal is cited, in accordance with accepted academic practice. No use, distribution or reproduction is permitted which does not comply with these terms.

frontiers in Surgery

ORIGINAL RESEARCH
published: 28 January 2022
doi: 10.3389/fsurg.2022.820725

Survival Analysis in Gastrointestinal Neuroendocrine Carcinoma With Bone Metastasis at Diagnosis

Genlian Chen[1†], Qiang Xu[2†], Shengjun Qian[3†], Zhan Wang[3] and Shicheng Wang[4*]*

[1] Department of Orthopedics, People's Hospital of Pan'an County, Jinhua, China, [2] Department of Orthopedics, Xuzhou Central Hospital, Xuzhou, China, [3] Department of Orthopedic Surgery, The Second Affiliated Hospital, Zhejiang University School of Medicine, Hangzhou, China, [4] Department of Orthopedic Surgery, Ningbo No.6 Hospital, Ningbo, China

Purpose: Gastrointestinal neuroendocrine carcinoma (NEC) with bone metastasis is rarely reported. The purpose of this study is to explore the prognosis and risk factors of such patients.

Patients and Methods: We retrospectively reviewed patients diagnosed as gastrointestinal NECs with bone metastasis at diagnosis from 2010 to 2016 by using the Surveillance, Epidemiology and End Results (SEER) database. Predictors of overall survival (OS) and cancer-specific survival (CSS) were analyzed by univariable and multivariable Cox analyses. Kaplan–Meier plots were constructed to show the correlation between independent predictors and survival.

Results: A total of 330 gastrointestinal NEC patients with bone metastasis at diagnosis were included for analysis. Over half of patients were male and older than 60 years old. The most common primary site of gastrointestinal NEC with bone metastasis was the pancreas. The prognosis of gastrointestinal NEC with bone metastasis (3-year OS and CSS rates: 16.7 and 17.0%) was very poor. On Cox multivariable analysis, age over 60 years old, no surgery, and lung metastasis were independent predictors of decreased OS and CSS.

Conclusions: We identified three independent factors associated with prognosis among gastrointestinal NEC patients with bone metastasis, namely age, surgery, and lung metastasis. For younger gastrointestinal NEC patients with bone metastasis, surgical resection of primary tumors as well as actively treating lung metastasis might be useful for prolonging survival.

Keywords: gastrointestinal, neuroendocrine carcinoma, bone metastasis, survival, risk factors

OPEN ACCESS

Edited by:
Sanjit Mukherjee, National Institutes of Health (NIH), United States

Reviewed by:
Jun-Gang Zhang, Zhejiang Provincial People's Hospital, China
Abhisek Bhattacharya, National Institutes of Health (NIH), United States

***Correspondence:**
Zhan Wang
wangzhanhz@zju.edu.cn
Shicheng Wang
woson004@gmail.com

[†] These authors have contributed equally to this work

Specialty section:
This article was submitted to Surgical Oncology, a section of the journal Frontiers in Surgery

Received: *23 November 2021*
Accepted: *03 January 2022*
Published: *28 January 2022*

Citation:
Chen G, Xu Q, Qian S, Wang Z and Wang S (2022) Survival Analysis in Gastrointestinal Neuroendocrine Carcinoma With Bone Metastasis at Diagnosis. Front. Surg. 9:820725. doi: 10.3389/fsurg.2022.820725

INTRODUCTION

Neuroendocrine carcinoma (NEC) is a poorly differentiated subtype of neuroendocrine neoplasms (NENs) according to the 2019 World Health Organization (WHO) classification (1). Although NECs are commonly considered as rare, they have a rising incidence in recent years (2–4). NECs are characterized by poorly differentiated morphology as well as a high proliferation capacity (Ki−67 proliferation index > 20%) (5). Moreover, NECs are often presented with metastasis at diagnosis or advanced status and have a poor prognosis (6–8). Lung is the common site of NECs, while

gastrointestinal NECs are rarely seen and account for about 35–55% of all extra-pulmonary NECs (9). Gastrointestinal NECs mainly arise from the esophagus, stomach, pancreas, colon and rectum and common metastatic sites for NECs include liver, lung and bone (8, 10).

Various treatment options are available for curative and palliative treatment of gastrointestinal NECs, including surgical resection, chemotherapy, and radiotherapy (11). However, treatment outcomes of gastrointestinal NECs remain poor (12). Due to the rarity of gastrointestinal NECs, there are limited researches regarding the treatment and survival of metastatic gastrointestinal NECs. As far as we know, clinical studies on survival analysis of gastrointestinal NECs with bone metastasis are lacking. Therefore, we conducted a population-based study by applying the Surveillance, Epidemiology and End Results (SEER) database to investigate the clinical characteristics and prognostic factors for gastrointestinal NECs with bone metastasis. Our findings may bring insight into gastrointestinal NECs with bone metastasis and provide a survival benefit on survival.

MATERIALS AND METHODS

Study Population

This study retrospectively reviewed patients diagnosed as gastrointestinal NECs with bone metastasis at presentation by using the U.S National Cancer Institute's SEER database (Version 8.3.8) between 2010 and 2016. This population-based database collects information on cancer patients in 18 registries, covering approximately 30% of cancer cases in the U.S (www.seer.cancer.gov). Ethical review is not required for the present study because the public database does not contain information to identify patients.

Histological types were defined by the following International Classification of Diseases for Oncology, 3rd edition (ICD-O-3) code 8246/3 (neuroendocrine carcinoma, NOS). The primary sites were defined, including the esophagus, stomach, liver, pancreas, small intestine, cecum, appendix, colon, rectum, anus, gallbladder, biliary tract and other GI sites. Cases diagnosed not by histopathological examinations were excluded. In the present study, clinicopathological data, sociological data and treatment data were included for analysis. Surgery or radiotherapy in this study refers to the primary sites (13). Based on previous literature (14, 15), overall survival (OS) and cancer specific survival (CSS) are defined as the time from initial diagnosis to death due to any cause and NEC, respectively.

Statistical Methods

All statistical analyses were performed by using IBM SPSS Statistics (Version 22). First, univariable Cox regression analyses were performed to select significant survival predictors. Then, significant risk factors from univariable analyses were integrated into multivariate Cox regression analysis to identify independent risk factors. Meanwhile, hazard ratios (HRs) and 95% confidence intervals (CIs) were calculated. Survival curves of independent risk factors were constructed with the Kaplan-Meier method. Variables with two-tailed $p < 0.05$ were considered statistically significant.

TABLE 1 | Demographics of 330 gastrointestinal neuroendocrine carcinoma with bone metastasis at diagnosis.

Variable	Value
Race	
White	261 (79.1%)
Black	43 (13.0%)
Others	26 (7.9%)
Gender	
Female	123 (37.3%)
Male	207 (62.7%)
Age (years)	
≤60	125 (37.9%)
>60	205 (62.1%)
Tumor location	
Colon and rectum	83 (25.2%)
Pancreas, liver, stomach	164 (49.7%)
Others	83 (25.2%)
Tumor size (cm)	
<5	110 (33.3%)
≥5	85 (25.8%)
Unknown	135 (40.9%)
Surgery	
Yes	34 (10.3%)
No	296 (89.7%)
Radiotherapy	
Yes	108 (32.7%)
No	222 (67.3%)
Chemotherapy	
Yes	180 (54.5%)
No	150 (45.5%)
Brain metastasis	
No	294 (89.1%)
Yes	21 (6.4%)
Unknown	15 (4.5%)
Liver metastasis	
No	73 (22.1%)
Yes	251 (76.1%)
Unknown	6 (1.8%)
Lung metastasis	
No	234 (70.9%)
Yes	78 (23.6%)
Unknown	18 (5.5%)
Marital status	
Married	183 (55.5%)
Others	131 (39.7%)
Unknown	16 (4.8%)
Dead	
Yes	257 (77.9%)
No	73 (22.1%)
1-year OS rate	39.50%
1-year CSS rate	40.00%
3-year OS rate	16.70%
3-year CSS rate	17.00%

OS, overall survival; CSS, cancer-specific survival.

TABLE 2 | Univariate Cox analysis of survival in gastrointestinal neuroendocrine carcinoma with bone metastasis.

Variable	OS		CSS	
	HR (95% CI)	*P*	HR (95% CI)	*P*
Race				
White	1		1	
Black	1.139 (0.792–1.639)	0.482	1.102 (0.754–1.611)	0.615
Others	0.921 (0.575–1.475)	0.732	0.930 (0.580–1.490)	0.762
Gender				
Female	1		1	
Male	0.961 (0.745–1.239)	0.758	0.984 (0.758–1.277)	0.902
Age (years)				
≤60	1		1	
>60	1.355 (1.050–1.749)	0.2	1.317 (1.016–1.708)	0.037
Tumor location				
Colon and rectum	1		1	
Pancreas, liver, stomach	0.801 (0.596–1.076)	0.14	0.801 (0.594–1.080)	0.146
Others	0.830 (0.586–1.174)	0.292	0.817 (0.572–1.167)	0.265
Tumor size (cm)				
<5	1		1	
≥5	1.335 (0.969–1.840)	0.077	1.303 (0.936–1.814)	0.117
Surgery				
Yes	1		1	
No	1.811 (1.168–2.808)	0.008	1.781 (1.148–2.765)	0.01
Radiotherapy				
Yes	1		1	
No	1.000 (0.772–1.296)	0.998	0.992 (0.762–1.293)	0.955
Chemotherapy				
Yes	1		1	
No	0.982 (0.763–1.263)	0.887	0.942 (0.727–1.221)	0.651
Brain metastasis				
No	1		1	
Yes	1.412 (0.883–2.257)	0.15	1.585 (0.977–2.570)	0.062
Liver metastasis				
No	1		1	
Yes	1.136 (0.842–1.532)	0.406	1.145 (0.842–1.556)	0.389
Lung metastasis				
No	1		1	
Yes	1.519 (1.145–2.015)	0.004	1.560 (1.167–2.086)	0.003
Marital status				
Married	1		1	
Others	1.020 (0.792–1.314)	0.878	0.992 (0.766–1.286)	0.953

TABLE 3 | Multivariate Cox regression analysis of survival in gastrointestinal neuroendocrine carcinoma with bone metastasis.

Variable	OS		CSS	
	HR (95% CI)	*P*	HR (95% CI)	*P*
Age (years)				
≤60	1		1	
>60	1.376 (1.064–1.779)	0.015	1.328 (1.024–1.723)	0.033
Surgery				
Yes	1		1	
No	1.738 (1.120–2.698)	0.014	1.726 (1.111–2.681)	0.015
Lung metastasis				
No	1		1	
Yes	1.534 (1.155–2.038)	0.003	1.564 (1.169–2.092)	0.003

RESULTS

Patients Characteristics

In total, 330 patients with gastrointestinal NEC and bone metastasis at diagnosis extracted from the SEER database were eligible for the analysis. **Table 1** summarized the demographics of all patients. Of all patients, 79.1% were white and 62.7% were males. Over half of patients (62.1%) were aged over 60 years old. 25.2% ($n = 83$) of patients were located in the colon and rectum, 49.7% ($n = 164$) of patients were located in the pancreas, liver, stomach, and 18.31% of patients ($n = 63$) were located in other sites. Tumor size distribution was <5 cm 33.3%, ≥5 cm 25.8%, and unknown 40.9%. In terms of treatment methods, 34 (10.3%) patients received surgery, 108 (32.7%) received radiotherapy, and 180 (54.5%) received chemotherapy. Liver metastasis (76.1%) was more common than brain metastasis (6.4%) or lung metastasis (23.6%). Over half of the patients (55.5%) were married. One-year OS and CSS rate for all patients were 39.5 and 40%, respectively.

Survival Analysis

On univariable analysis, variables found to be significantly associated with both OS and CSS were age, surgery, and lung metastasis (**Table 2**). There was no significant difference in OS or CSS in terms of race, gender, tumor location, tumor size, radiotherapy, chemotherapy, brain metastasis, liver metastasis, and marital status (**Table 2**).

Three significant risk factors for OS and CSS identified in the univariable Cox analysis were integrated into the multivariable analysis. Multivariable analysis revealed age, surgery, and lung metastasis were significant predictors for both OS and CSS (**Table 3**). Additionally, the Kaplan–Meier survival curves showed that patients with age ≤60 years old (**Figure 1**), surgery (**Figure 2**), or no lung metastasis (**Figure 3**), had increased OS and CSS.

DISCUSSION

Previous studies indicated that NEC patients were prone to metastasis. Although some studies reported the prognosis of gastrointestinal NEC, few studies have been conducted on the prognosis of gastrointestinal NEC with bone metastasis. To our knowledge, this is the largest study investigating the clinical characteristics, and prognosis of gastrointestinal NEC patients with bone metastasis. The 3-year CSS rate of these patients was only 17%, which suggested a poor outcome. Moreover, significant independent predictors affecting gastrointestinal NEC with bone metastasis included age, lung

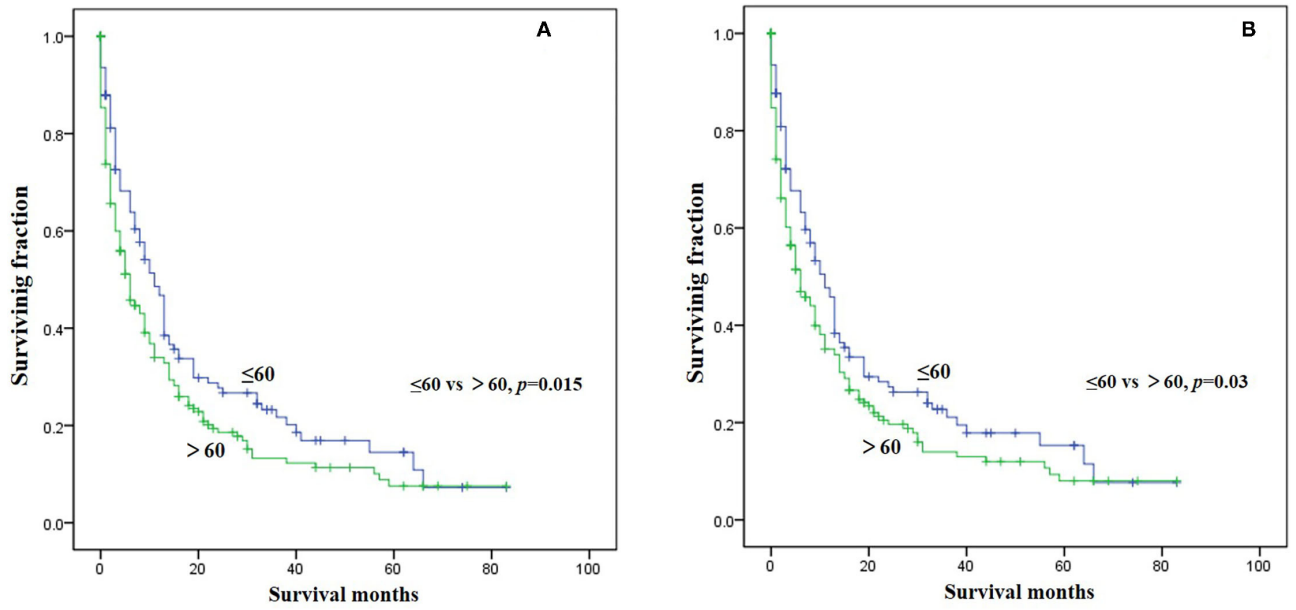

FIGURE 1 | Kaplan-Meier method estimated survival in gastrointestinal NEC with bone metastasis at diagnosis stratified by age. **(A)** OS, **(B)** CSS (OS, overall survival; CSS, cancer-specific survival).

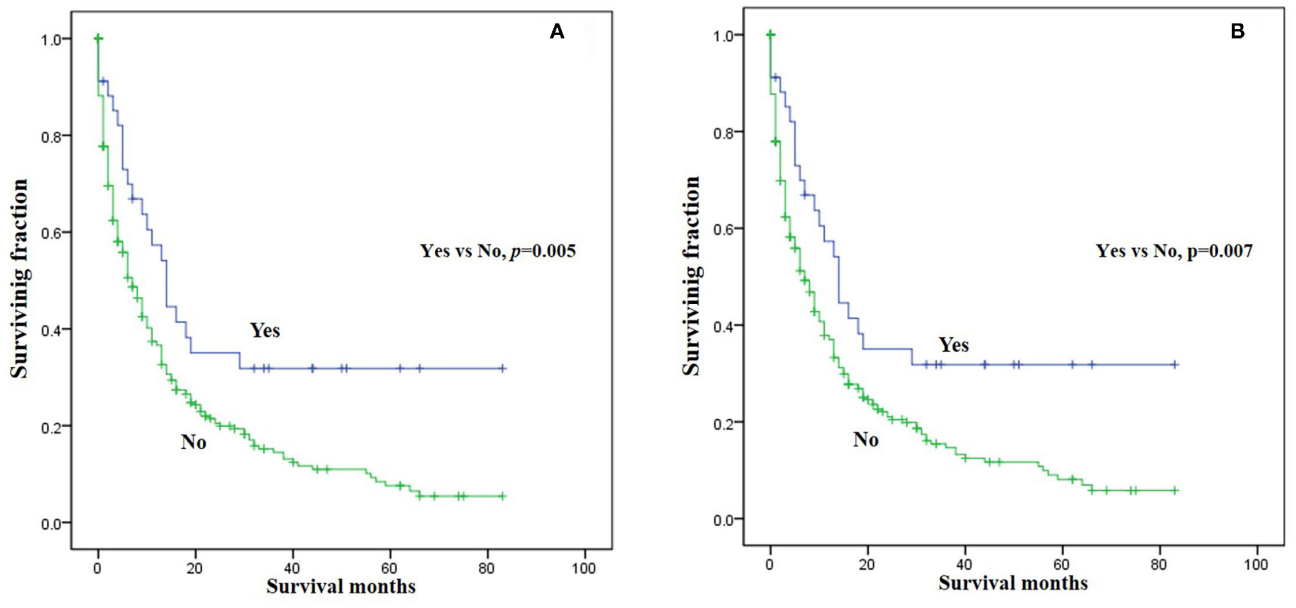

FIGURE 2 | Kaplan-Meier method estimated survival in gastrointestinal NEC with bone metastasis at diagnosis stratified by surgery. **(A)** OS, **(B)** CSS (OS, overall survival; CSS, cancer-specific survival).

metastasis, and surgery. The results of this study may help clinicians develop appropriate treatment strategies and provide reasonable treatment suggestions for patients.

No significant difference on survival was observed in univariate analysis among patients with different races. Interestingly, some studies on lung neuroendocrine neoplasms revealed race was an independent survival predictor (16, 17). Patients over 60 years old are generally considered the elderly. Based on previous literature (18, 19), we divided the patients' age into >60 years old and ≤60 years old for convenient analysis. Multivariate analysis revealed that age under 60 years were associated with improved OS and CSS, which was in line with previous studies (20–22). There is no significant difference in survival time between male and female patients.

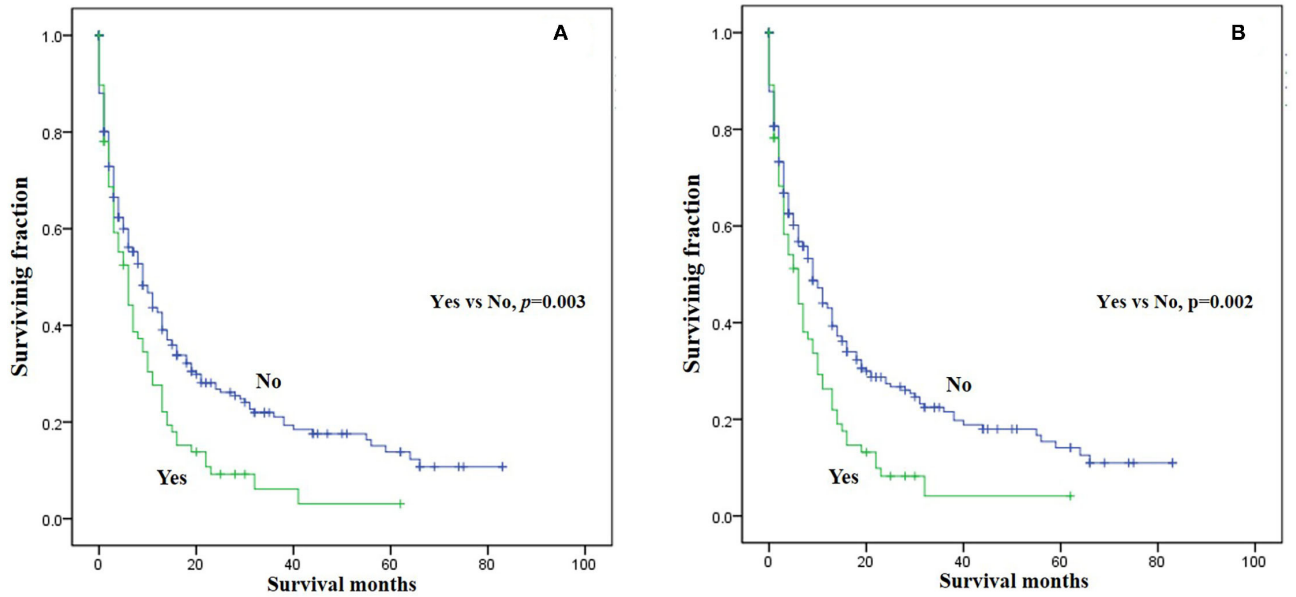

FIGURE 3 | Kaplan-Meier method estimated survival in gastrointestinal NEC with bone metastasis at diagnosis stratified by lung metastasis. **(A)** OS, **(B)** CSS (OS, overall survival; CSS, cancer-specific survival).

The most common primary site of gastrointestinal NEC with bone metastasis was the pancreas. Additionally, no significant difference was observed in OS and CSS among patients with different primary tumor locations. Based on previous literature (23, 24), we divided the tumor size into ≥5 cm and <5 cm for convenient analysis. For many primary malignant tumors, tumor size is often one of the important factors affecting the prognosis of patients (25, 26). In contrast to our traditional knowledge, we noted that tumor size in the current study was not correlated with survival. Further studies are needed to confirm this finding.

Treatment patterns and outcomes of gastrointestinal NEC patients especially metastatic ones have not been well-described. Our multivariable results highlighted the role of surgical resection in prolonging the survival, which was consistent with the situation of non-metastatic patients (12). Sorbye et al. (9) recommended that chemotherapy treatment should be performed for advanced gastrointestinal NEC patients. However, our studies found that chemotherapy or radiotherapy did not improve the prognosis of those patients. Although liver metastasis was most common in gastrointestinal NEC patients with bone metastasis, it was not an independent risk factor for prognosis. Additionally, the presence of brain metastasis was not associated with a decreased survival. Of note, these patients were secondly complicated with lung metastasis, which was recognized as an independent risk factor for the decreased prognosis. Therefore, actively treating lung metastasis may have positive effect on survival. Marital status had no association with survival in this study. In accordance with these findings, we suggested that for younger gastrointestinal NEC patients with bone metastasis, surgical resection of primary tumors as well as actively treating lung metastasis might be useful for prolonging survival.

Some limitations of the present study should be noted. First, this study has retrospective nature, which can lead to bias. Second, detailed therapy information is not available in the database. Third, local recurrence or distal metastasis data during follow-up were not recorded in the database. Additionally, due to the small sample size and few independent risk factors in this study, we did not build a prediction model. Future studies can attempt to build predictive models. Although this study has these limitations, it has important implications for managing these patients.

CONCLUSIONS

This is the largest study of survival analysis on gastrointestinal NEC patients with bone metastasis. Age, surgery and lung metastasis were identified as independent risk factors of survival. Resection of primary tumors as well as actively treating lung metastasis can prolong the survival of this special cohort. However, multicenter co-operative studies should be performed to confirm our findings in the future.

DATA AVAILABILITY STATEMENT

The raw data supporting the conclusions of this article will be made available by the authors, without undue reservation.

ETHICS STATEMENT

Ethical review and approval was not required for the study on human participants in accordance with the

local legislation and institutional requirements. Written informed consent for participation was not required for this study in accordance with the national legislation and the institutional requirements.

AUTHOR CONTRIBUTIONS

SW and ZW conceived and designed the study. GC, QX, and SQ collected the data. GC, QX, and SQ performed the statistical analysis. GC wrote the manuscript and SW and ZW revised it. All authors read and approved the final manuscript.

FUNDING

This work was supported by the China Postdoctoral Science Foundation (2021M692792), National Natural Science Foundation of China (82103499), and Zhejiang Provincial Natural Science Foundation (LQ22H160040).

REFERENCES

1. Shi H, Qi C, Meng L, Yao H, Jiang C, Fan M, et al. Do neuroendocrine carcinomas and mixed neuroendocrine-non-neuroendocrine neoplasm of the gastrointestinal tract have the same prognosis? A SEER database analysis of 12,878 cases. *Ther Adv Endocrinol Metabol.* (2020) 11:2042018820938304. doi: 10.1177/2042018820938304
2. Yao JC, Hassan M, Phan A, Dagohoy C, Leary C, Mares JE, et al. One hundred years after "carcinoid": epidemiology of and prognostic factors for neuroendocrine tumors in 35,825 cases in the United States. *J Clin Oncol.* (2008) 26:3063–72. doi: 10.1200/JCO.2007.15.4377
3. Korse CM, Taal BG, van Velthuysen ML, Visser O. Incidence and survival of neuroendocrine tumours in the Netherlands according to histological grade: experience of two decades of cancer registry. *Eur J Cancer.* (2013) 49:1975–83. doi: 10.1016/j.ejca.2012.12.022
4. Dasari A, Shen C, Halperin D, Zhao B, Zhou S, Xu Y, et al. Trends in the incidence, prevalence, and survival outcomes in patients with neuroendocrine tumors in the United States. *JAMA Oncol.* (2017) 3:1335–42. doi: 10.1001/jamaoncol.2017.0589
5. Pellat A, Cottereau AS, Terris B, Coriat R. Neuroendocrine carcinomas of the digestive tract: what is new? *Cancers.* (2021) 13:3766. doi: 10.3390/cancers13153766
6. Wang Z, Li W, Chen T, Yang J, Luo L, Zhang L, et al. Retrospective analysis of the clinicopathological characteristics of gastrointestinal neuroendocrine neoplasms. *Exp Ther Med.* (2015) 10:1084–8. doi: 10.3892/etm.2015.2634
7. Koumarianou A, Chatzellis E, Boutzios G, Tsavaris N, Kaltsas G. Current concepts in the diagnosis and management of poorly differentiated gastrointestinal neuroendocrine carcinomas. *Endokrynol Polska.* (2013) 64:60–72.
8. Cai W, Tan Y, Ge W, Ding K, Hu H. Pattern and risk factors for distant metastases in gastrointestinal neuroendocrine neoplasms: a population-based study. *Cancer Med.* (2018) 7:2699–709. doi: 10.1002/cam4.1507
9. Sorbye H, Welin S, Langer SW, Vestermark LW, Holt N, Osterlund P, et al. Predictive and prognostic factors for treatment and survival in 305 patients with advanced gastrointestinal neuroendocrine carcinoma (WHO G3): the NORDIC NEC study. *Ann Oncol.* (2013) 24:152–60. doi: 10.1093/annonc/mds276
10. Lokesh KN, Anand A, Lakshmaiah KC, Babu KG, Lokanatha D, Jacob LA, et al. Clinical profile and treatment outcomes of metastatic neuroendocrine carcinoma: a single institution experience. *South Asian J Cancer.* (2018) 7:207–9. doi: 10.4103/sajc.sajc_176_17
11. Morita M, Taguchi K, Kagawa M, Nakanoko T, Uehara H, Sugiyama M, et al. Treatment strategies for neuroendocrine carcinoma of the upper digestive tract. *Int J Clin Oncol.* (2020) 25:842–50. doi: 10.1007/s10147-020-01631-y
12. Fang C, Wang W, Zhang Y, Feng X, Sun J, Zeng Y, et al. Clinicopathologic characteristics and prognosis of gastroenteropancreatic neuroendocrine neoplasms: a multicenter study in South China. *Chin J Cancer.* (2017) 36:51. doi: 10.1186/s40880-017-0218-3
13. Wang Z, Cheng Y, Chen S, Shao H, Chen X, Wang Z, et al. Novel prognostic nomograms for female patients with breast cancer and bone metastasis at presentation. *Ann Transl Med.* (2020) 8:197. doi: 10.21037/atm.2020.01.37
14. Wang Z, Wu B, Zhou Y, Huang X, Pan W, Liu M, et al. Predictors of the survival of primary and secondary older osteosarcoma patients. *J Cancer.* (2019) 10:4614–22. doi: 10.7150/jca.32627
15. Wang Z, Li S, Li Y, Lin N, Huang X, Liu M, et al. Prognostic factors for survival among patients with primary bone sarcomas of small bones. *Cancer Manag Res.* (2018) 10:1191–9. doi: 10.2147/CMAR.S163229
16. Yang Q, Xu Z, Chen X, Zheng L, Yu Y, Zhao X, et al. Clinicopathological characteristics and prognostic factors of pulmonary large cell neuroendocrine carcinoma: a large population-based analysis. *Thoracic Cancer.* (2019) 10:751–60. doi: 10.1111/1759-7714.12993
17. Shah S, Gosain R, Groman A, Gosain R, Dasari A, Halfdanarson TR, et al. Incidence and survival outcomes in patients with lung neuroendocrine neoplasms in the United States. *Cancers.* (2021) 13:1753. doi: 10.3390/cancers13081753
18. Liu D, Wu J, Lin C, Andriani L, Ding S, Shen K, et al. Breast subtypes and prognosis of breast cancer patients with initial bone metastasis: a population-based study. *Front Oncol.* (2020) 10:580112. doi: 10.3389/fonc.2020.580112
19. Lin F, Duan J, Lin Y, Wu H, Xu G, Guo X, et al. Survival and risk factors in patients with liposarcoma with distant metastasis. *Am J Transl Res.* (2020) 12:2071–82.
20. Alese OB, Jiang R, Shaib W, Wu C, Akce M, Behera M, et al. High-grade gastrointestinal neuroendocrine carcinoma management and outcomes: a national cancer database study. *Oncologist.* (2019) 24:911–20. doi: 10.1634/theoncologist.2018-0382
21. Yuan G, Zhan C, Zhu D, Xie H, Wei T, Lu T, et al. Population-based analysis of esophageal large cell neuroendocrine carcinoma between 2004 and 2015. *J Thoracic Dis.* (2019) 11:5480–8. doi: 10.21037/jtd.2019.11.34
22. Russolillo N, Vigano L, Razzore P, Langella S, Motta M, Bertuzzo F, et al. Survival prognostic factors of gastro-enteric-pancreatic neuroendocrine tumors after primary tumor resection in a single tertiary center: comparison of gastro-enteric and pancreatic locations. *Eur J Surg Oncol.* (2015) 41:751–7. doi: 10.1016/j.ejso.2015.02.011
23. Cao L, Zhao L, Wang M, Zhang XH, Yang ZC, Liu YP. Clinicopathological characteristics and prognosis of pulmonary large cell neuroendocrine carcinoma aged ≥65 years. *PeerJ.* (2019) 7:e6824. doi: 10.7717/peerj.6824
24. Xu B, Chu Y, Hu Q, Song Q. The clinicopathological features and overall survival of patients with gastric neuroendocrine carcinoma. *Technol Cancer Res Treat.* (2021) 20:15330338211055340. doi: 10.1177/15330338211055340
25. Zhang Y, Wu Z, Wang X, Li C, Chang J, Jiang W, et al. Development and external validation of a nomogram for predicting the effect of tumor size on survival of patients with perihilar cholangiocarcinoma. *BMC Cancer.* (2020) 20:1044. doi: 10.1186/s12885-020-07501-0
26. Ren S, Wang Z, Huang X, Sun L, Shao J, Ye Z. Prognostic factors for postoperative survival among patients with rhabdomyosarcoma of

the limbs. *Cancer Manag Res.* (2018) 10:4181–9. doi: 10.2147/CMAR.S175734

Conflict of Interest: The authors declare that the research was conducted in the absence of any commercial or financial relationships that could be construed as a potential conflict of interest.

Publisher's Note: All claims expressed in this article are solely those of the authors and do not necessarily represent those of their affiliated organizations, or those of the publisher, the editors and the reviewers. Any product that may be evaluated in this article, or claim that may be made by its manufacturer, is not guaranteed or endorsed by the publisher.

Copyright © 2022 Chen, Xu, Qian, Wang and Wang. This is an open-access article distributed under the terms of the Creative Commons Attribution License (CC BY). The use, distribution or reproduction in other forums is permitted, provided the original author(s) and the copyright owner(s) are credited and that the original publication in this journal is cited, in accordance with accepted academic practice. No use, distribution or reproduction is permitted which does not comply with these terms.

frontiers in Surgery

ORIGINAL RESEARCH
published: 31 January 2022
doi: 10.3389/fsurg.2022.829237

Establishment and Analysis of an Individualized Immune-Related Gene Signature for the Prognosis of Gastric Cancer

Mengying Li[1,2†], *Wei Cao*[1†], *Bingqian Huang*[1,2], *Zhipeng Zhu*[1,2], *Yaxin Chen*[1,2], *Jiawei Zhang*[1*], *Guodong Cao*[1*] and *Bo Chen*[1*]

[1] Department of General Surgery, First Affiliated Hospital of Anhui Medical University, Hefei, China, [2] Department of Clinical Medicine, Anhui Medical University, Hefei, China

OPEN ACCESS

Edited by:
Sanjit Mukherjee,
National Institutes of Health (NIH),
United States

Reviewed by:
Ke Xu,
Clinical Medical College and the First Affiliated Hospital of Chengdu Medical College, China
Qian Chen,
Guangxi Medical University Cancer Hospital, China

***Correspondence:**
Jiawei Zhang
ayfyzjw@163.com
Guodong Cao
ayfycgd@163.com
Bo Chen
chenbo831116@163.com

[†] These authors have contributed equally to this work

Specialty section:
This article was submitted to Surgical Oncology, a section of the journal Frontiers in Surgery

Received: 05 December 2021
Accepted: 05 January 2022
Published: 31 January 2022

Citation:
Li M, Cao W, Huang B, Zhu Z, Chen Y, Zhang J, Cao G and Chen B (2022) Establishment and Analysis of an Individualized Immune-Related Gene Signature for the Prognosis of Gastric Cancer. Front. Surg. 9:829237. doi: 10.3389/fsurg.2022.829237

A growing number of studies have shown that immunity plays an important clinical role in the process of gastric cancer (GC). The purpose of this study was to explore the function of differentially expressed immune-related genes (DEIRGs) of GC, and construct a gene signature to predict the overall survival (OS) of patients. Gene expression profiles and clinical data of GC patients were downloaded from TCGA and GEO databases. Combined with immune-related genes (IRGs) downloaded from the ImmPort database, 357 DEIRGs in GC tissues and adjacent tissues were identified. Based on the analysis of Lasso and Cox in the training set, a prognostic risk scoring model consisting of 9 (RBP7, DES, CCR1, PNOC, SPP1, VIP, TNFRSF12A, TUBB3, PRKCG) DEIRGs was obtained. Functional analysis revealed that model genes may participate in the formation and development of tumor cells by affecting the function of cell gap junction intercellular communication (GJJC). According to the model score, the samples were divided into high-risk and low-risk groups. In multivariate Cox regression analysis, the risk score was an independent prognostic factor (HR = 1.674, 95% CI = 1.470–1.907, $P < 0.001$). Survival analysis showed that the OS of high-risk GC patients was significantly lower than that of low-risk GC patients ($P < 0.001$). The area under the receiver operating characteristic curve (ROC) of the model was greater than other clinical indicators when verified in various data sets, confirming that the prediction model has a reliable accuracy. In conclusion, this study has explored the biological functions of DEIRGs in GC and discovered novel gene targets for the treatment of GC. The constructed prognostic gene signature is helpful for clinicians to determine the prognosis of GC patients and formulate personalized treatment plans.

Keywords: gastric cancer, immune gene, prognosis, computational biology, biomarker

INTRODUCTION

Gastric cancer (GC) is the fifth most common cancer and the third most common cause of cancer death worldwide (1), and is one of the most common malignant tumors of the digestive system (2). However, GC at an early stage of discomfort symptoms are less or not obvious. Most GC patients have reached the stage of inoperable radical treatment at the time of diagnosis. Therefore, timely

adjustment of clinical treatment strategy according to prognostic monitoring plays a crucial role in the treatment of GC (3). Tumor pathology (T), lymph node biopsy (N) and distant organ metastasis (M) are the main criteria to determine the prognosis of patients at present, but the prognosis of patients under the same TNM stage is also very different (4). In recent years, it has been observed that the prognosis of GC is not only related to the pathological stage, but also the tumor immune state may have an important influence on the prognosis of patients (5).

The immune microenvironment including anti-epidemic effector cells and molecules, plays an important role in the occurrence, development and clinical outcome of cancer. In recent years, tumor immunotherapy, as a novel treatment method, based on the human immune system, has demonstrated remarkable clinical effects by using immunoregulation to play an anti-tumor role. Immunotherapies such as immune checkpoint inhibitors and monoclonal antibodies can modulate the immune function of the body by changing the tumor microenvironment and producing an anti-tumor immune response (6). In GC, antibodies against PD-1 or PD-L1 can reverse the formation of tumor immunosuppressive microenvironment and exert anti-tumor effects (7). Immune cell infiltration is a major factor affecting the prognosis of GC. Foxp3-expressing regulatory T (Treg) cells into tumor tissue has been shown to be associated with poor prognosis in cancer patients (8). A variety of tumor immunotherapies related to natural killer cells have also entered the clinical trial stage (9). However, the abnormal changes in the gene expression profile related to immunity and the molecular mechanism of tumor immunity remain unclear (10). Continued detailed analysis of the immunological signatures of the tumor microenvironment will help to rapidly develop multiple novel immunotherapeutic strategies and identify potential biomarkers for clinical benefit (11).

Although many prognostic biomarkers have been discovered, such as carcinoembryonic antigen (CEA), carbohydrate antigen 199 (CA199), carbohydrate antigen 724 (CA724), which have been widely used in clinical practice (12). However, their effectiveness can be affected by various factors, and the prediction ability of a single indicator is insufficient (13). Instead, genetic markers provide better predictive performance, such genetic signatures are widely used for molecular diagnosis, individualized therapy, and accurate survival prediction (14), and multi-gene prognostic models can guide clinicians in choosing more appropriate treatments (15). Considering the significance of immunity, it is reasonable to conclude that IRGs has broad promise of GC prognostic evaluation, and that the polygene signatures generated by various algorithms will be better than single molecules in predicting prognosis. Numerous researchers have conducted research in this area. For example, Xie et al. (16) recently reported a 12 immue-related signature based on patients with breast cancer.

With the development of high-throughput sequencing technology, the combination of microarray data and bioinformatics has been widely used to identify a variety of cancer prognostic targets (17). In this study, based on immune-related genes that can reflect the infiltration of immune cells, a novel and reliable multi-gene risk scoring model was established to improve the prognosis of GC patients. Identification of core immune genes and pathways provides new therapeutic targets and generates new insights about GC progression.

MATERIALS AND METHODS

Data Source

The RNA sequencing data and clinical data of all GC patients were downloaded from the Cancer Genome Atlas (TCGA) database (https://cancergenome.nih.gov) and Gene Expression Omnibus (GEO) database (http://www.ncbi.nlm.nih.gov/gds) including GSE84437, GSE57303. The immune gene data were obtained from the Immunology Database and Analysis Portal (ImmPort) (https://immport.niaid.nih.gov). The tumor-related transcription factor data were derived from the Cistrome (http://cistrome.org/) database. For TCGA and GEO data sets, the expression profiles were converted from probe level to the corresponding gene symbols based on each group of annotation files, and further standardized. By examining the data, only patients with complete clinical survival information were used for follow-up analysis.

Identification of DEIRGs and Differentially Expressed Tumor-Related Transcription Factors

Differentially expressed genes (DEGs) in GC and normal tissues were screened from the gene matrix downloaded from the TCGA database using Package "limma" of R4.0.5 software (The screening criteria were FDR < 0.05 and $|\log2FC| > 1$). The intersection of IRGs and DEGs was used to obtain the DEIRGs in GC and normal tissues. Similarly, DETFs in GC and normal tissues were identified.

Enrichment Analysis of DEIRGs and Protein Interaction Analysis

In order to annotate and analyze the biological functions of prognostic immune genes, we used the DAVID6.8 database (https://david.ncifcrf.gov) to perform Gene Ontology enrichment analysis (GO) and Kyoto Encyclopedia of Genes and Genomes (KEGG) Pathway analysis, the enrichment results with $P < 0.05$ were retained. Among them, KEGG utilizes its comprehensive database resources to analyze genetic information and make quantitative predictions on higher-level and more complex cell activities and biological behaviors. GO analysis selects three major categories: Biological Process (BP), Cell Component (CC) and Molecular Function (MF) to display the enrichment results. The protein interaction network was established by using STRING (http://string-db.org), and the interaction parameters were set as a composite score >0.9. Cytoscape software was used to reconstruct the network and cluster filtering was performed using the MCODE plug-in: Degree cut-off = 2, node score cut-off = 0.2, Max depth = 100, k-score = 2.

Identification and Analysis of Prognostic Differentially Expressed IRGs

In the data set GSE84437, except for patients with incomplete clinical information and survival time <30 d, a total of 431 patients with GC were obtained. The samples were randomly divided into a training set (216 cases) and a test set (215 cases). In the training set, the PDEIRGs were evaluated by univariate Cox regression analysis. Meanwhile, by calculating the correlation coefficient between DETFs and PDEIRGs in GC, the regulatory network in GC was constructed. In addition, KEGG was used to explore the underlying immune molecular mechanisms and immune pathways.

Establishment and Verification of a Prognostic Risk Scoring Model

In the training set, Lasso regression analysis was used to further analyze the PDEIRGs, so as to avoid over-fitting of the model. Based on the lambda.min method, the best possible PDEIRGs that may be used to establish the model were selected. According to the multivariate Cox regression analysis, the hazard ratio (HR) of each gene was calculated, and the final prognostic risk scoring model was established based on the linear combination of expression levels: Risk score (RS) = β1*expRNA1+ β2*expRNA2+…+βn*expRNAn, among them, β is the regression coefficient of the corresponding factor obtained by multivariate Cox regression analysis. ExpRNA is the expression of the corresponding RNA.

The sample RS was calculated according to the formula, and the patients with GC were divided into high-risk and low-risk groups based on the median value of the sample risk value. In order to further confirm and verify the prognostic value of the model, we used the R language "survival" package for Kaplan-Meier analysis and log-rank test in the training set to evaluate the survival time of the two groups of patients. Besides, we drew the ROC curve with the "survivalROC" package to verify the accuracy of the model. At the same time, the "pheatmap" package was adopted to draw the risk curve. In the same way, internal verification was carried out in the testing set and the overall set, while external verification was carried out in the GSE57303 and TCGA data sets. Then, based on the above model, we built a nomogram using "rms" package to better predict the prognosis of patients with GC.

Correlation Analysis Between 9-Gene Signature and Immune Cell Infiltration

In order to figure out whether this model can reflect the status of the tumor immune microenvironment of patients with GC, we explore the correlation between 9-gene signature and the amount of immune cell infiltration through TIMER (https://cistrome.shinyapps.io/timer/) immune cell database and CIBERSORT. The Pearson correlation coefficient test was used to estimate the relationship between the expression of model genes and the content of different types of immune cells.

Statistical Methods

All statistical analysis used R software 4.0.5 (Institute for Statistics and Mathematics, Vienna, Austria; https//www.r-project.org/). The following R software packages were used for further data analysis: limma, survival, survivalROC, pheatmap, rms etc. For all tests, $P<0.05$ was considered statistically significant.

RESULTS

Identification of DEIRGs and DETFs in GC

The Wilcoxon rank sum test was used to analyze 375 GC and 32 normal gastric samples in TCGA GC data set. A total of 6,739 DEGs were screened by differential expression analysis (FDR < 0.05, |log2FC| > 1). In addition, 2,483 IRGs were downloaded from the ImmPort database containing 17 categories, including tumor necrosis factor family members, transforming growth factor β family members, chemokines and cytokine receptors, interleukins, interferons, etc. In R language, 357 DEIRGs were obtained by intersection of IRGs and all DEGs, including 204 up-regulated DEIRGs and 153 down-regulated DEIRGs. The heat map and volcano map of DEIRGs were drawn (**Figures 1A,C**). In the same way, DETFs in GC tissues were analyzed. Compared with adjacent tissues, 71 DETFs were found in GC tissues, and the heat map and volcanic map of DETFs were plotted (**Figures 1B,D**).

Functional Enrichment Analysis and Establishment of PPI Network of DEIRGs

Functional analysis including KEGG and GO pathways was performed on these DEIRGs. KEGG pathway analysis revealed that these genes are mainly enriched in the cell cycle and vascular smooth muscle contraction process (**Figure 2A**). GO analysis showed that the biological processes of these genes are mainly involved in: muscle system processes, organelle fission, DNA-binding transcription activation activity, RNA polymerase II-specific binding to glycosaminoglycans, and the main cell components are: extracellular matrix and collagen extracellular matrix (**Figures 2B–D**).

PPI network was established based on 357 DEIRGs, and then a plug-in called MCODE of Cytoscape was used to identify the most significant collaborative regulation module. The score value of a node reflected the density of the node and the surrounding nodes. The top 2 significant modules were selected and are shown in **Figures 2E1,E2**, of which APLNR and STAT1 called seed genes that had the highest score in the modules. For the sake of convenience, we named these modules the APLNR and STAT1 modules, respectively. In the APLNR module, 496 edges involving 32 nodes were formed in the network, and CXCL8, CXCL12, CXCL1 CXCL10 were the remarkable nodes, as they had more connection with other genes of the module. The STAT1 module had 22 nodes with 127 degrees, and ICAM1, EDN1, STAT1, and GCG had higher degree values. Based on the online Kaplan-Meier Plotter database, it was found that high expression of APLNR was associated with poor prognosis of GC, while high expression of STAT1 was associated with good prognosis of GC (both $P < 0.005$) (**Supplementary Figure 1**).

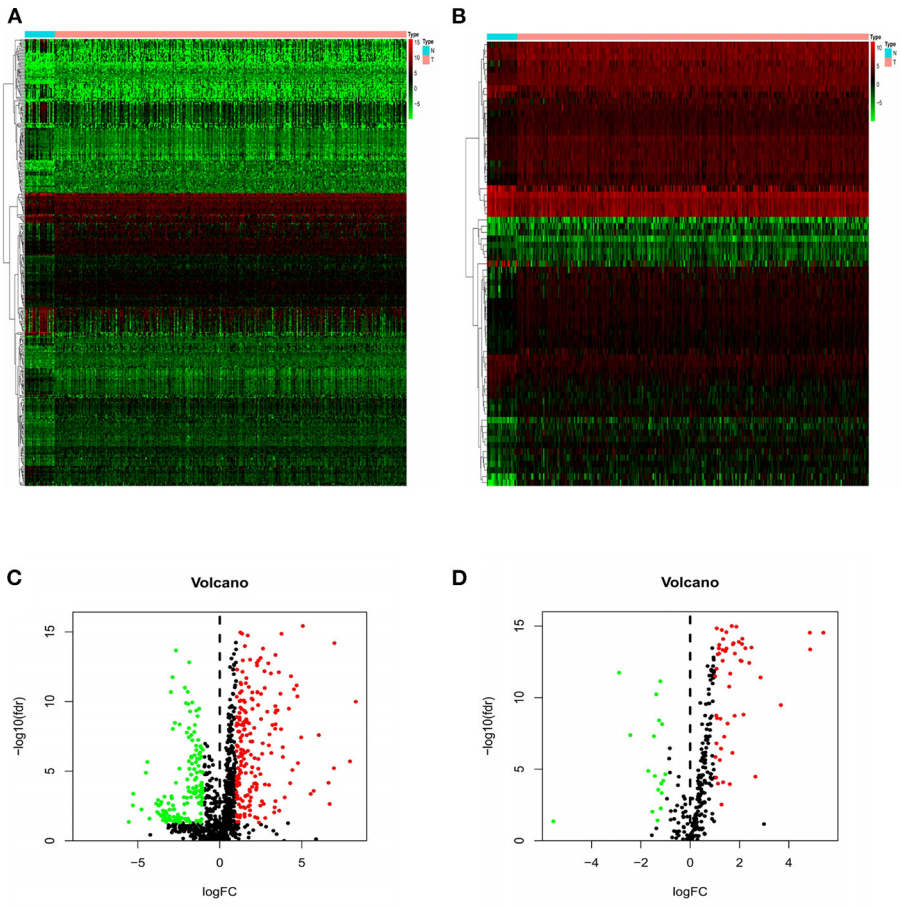

FIGURE 1 | Heat maps and volcanic maps of IRGs and TFs expression. The differential expression heat maps of IRGs **(A)** and TFs **(B)**. The differential expression volcanic maps of IRGs **(C)** and TFs **(D)**. The heat map abscissa represents the sample: the blue area represents normal tissue and the red area represents tumor tissue; the ordinate represents the gene. On the volcano map, the green area represents the down-regulated differential genes and the red area represents the up-regulated genes.

Identification of PDEIRGs and Establishment of a Regulatory Network

Due to the more sufficient number of patient samples in the GSE84437 data set, the expression of 357 DEIRGs identified in TCGA database was analyzed by univariate Cox analysis to identify PDEIRGs. The data showed that the expression of 35 DEIRGs was significantly related to OS in patients with GC (all $P < 0.05$) (**Figure 3A**). In order to further explore the role of PDEIRGs in the regulatory network, the relationship between PDEIRGs and DETFs was analyzed. The correlation between 71 DETFs and 35 PDEIRGs was detected (correlation coefficient > 0.4 and $P < 0.001$). The results showed that there was a significant correlation between 14 DETFs and 23 PDEIRGs (**Supplementary Table 1**). In addition, Cytoscape software was utilized to develop a TFs regulatory network to reveal direct correlations (**Figure 3B**). In order to explore the potential immune molecular mechanisms and immune pathways underlying the PDEIRGs, we conducted a functional analysis. It showed that they mainly focused on peptide ligand-binding receptors, positive regulation of response to external stimulus, allograft rejection, angiogenesis, etc. (**Figure 3C**).

Establishment of a Prognostic Risk Scoring Model Based on IRGs

In order to identify the best model for predicting prognosis, we used Lasso regression analysis and multivariate Cox regression analysis to perform screening of variables on high-dimensional mRNA expression profile data. After 100 times of 10-fold cross-validation and optimization by Cox analysis (**Figures 4A1,A2**), the 9 genes (RBP7, DES, SPP1, VIP, TNFRSF12A, TUBB3, CCR1, PNOC, and PRKCG) obtained were determined as risk genes in the prognosis model as shown in the forest graph (**Figure 4B**). The high-risk genes were negatively correlated with the prognosis of patients, and the low-risk genes were positively correlated with the prognosis of patients. In the model, RBP7, DES, SPP1, VIP, TNFRSF12A, and TUBB3 were high-risk genes, and CCR1, PNOC, and PRKCG were low-risk genes. Extracting the coefficients of multivariate Cox analysis

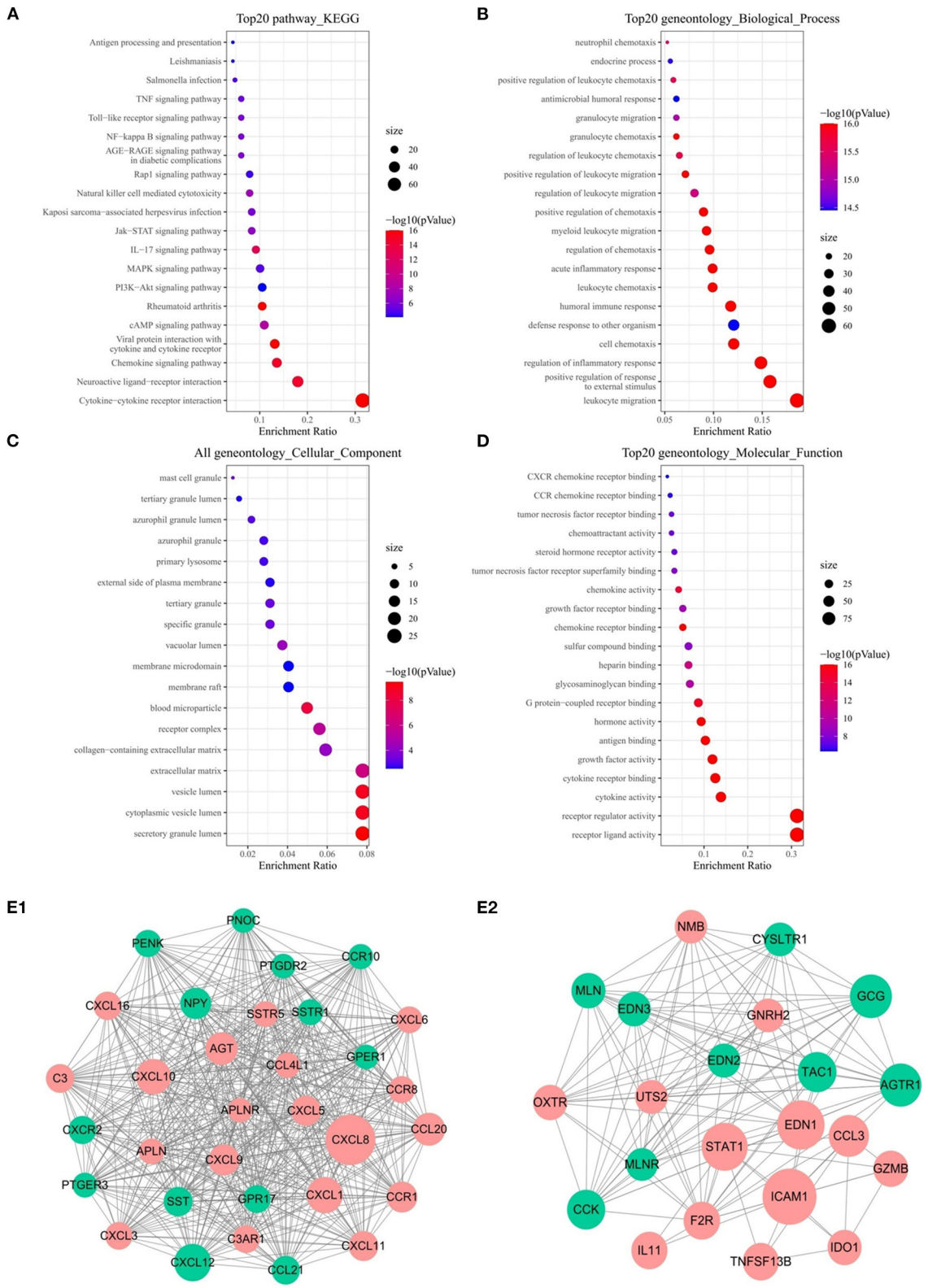

FIGURE 2 | Functional enrichment analysis of 357 DEIRGs and significant modular analysis based on PPI network. Top 20 KEGG terms **(A)**. Top 20 GO terms of GO: BP **(B)**. Top 20 GO terms of GO: CC **(C)**. Top 20 GO terms of GO: MF **(D)**. PPI network of the APLNR module **(E1)**. PPI network of the STAT1 module **(E2)**. In A, B, C and D, terms are sorted by the number of genes enriched. In **(E1,E2)**, red stands for up-regulated and green stands for down-regulated genes. The size of the node represents the number of proteins that interact with the specified protein.

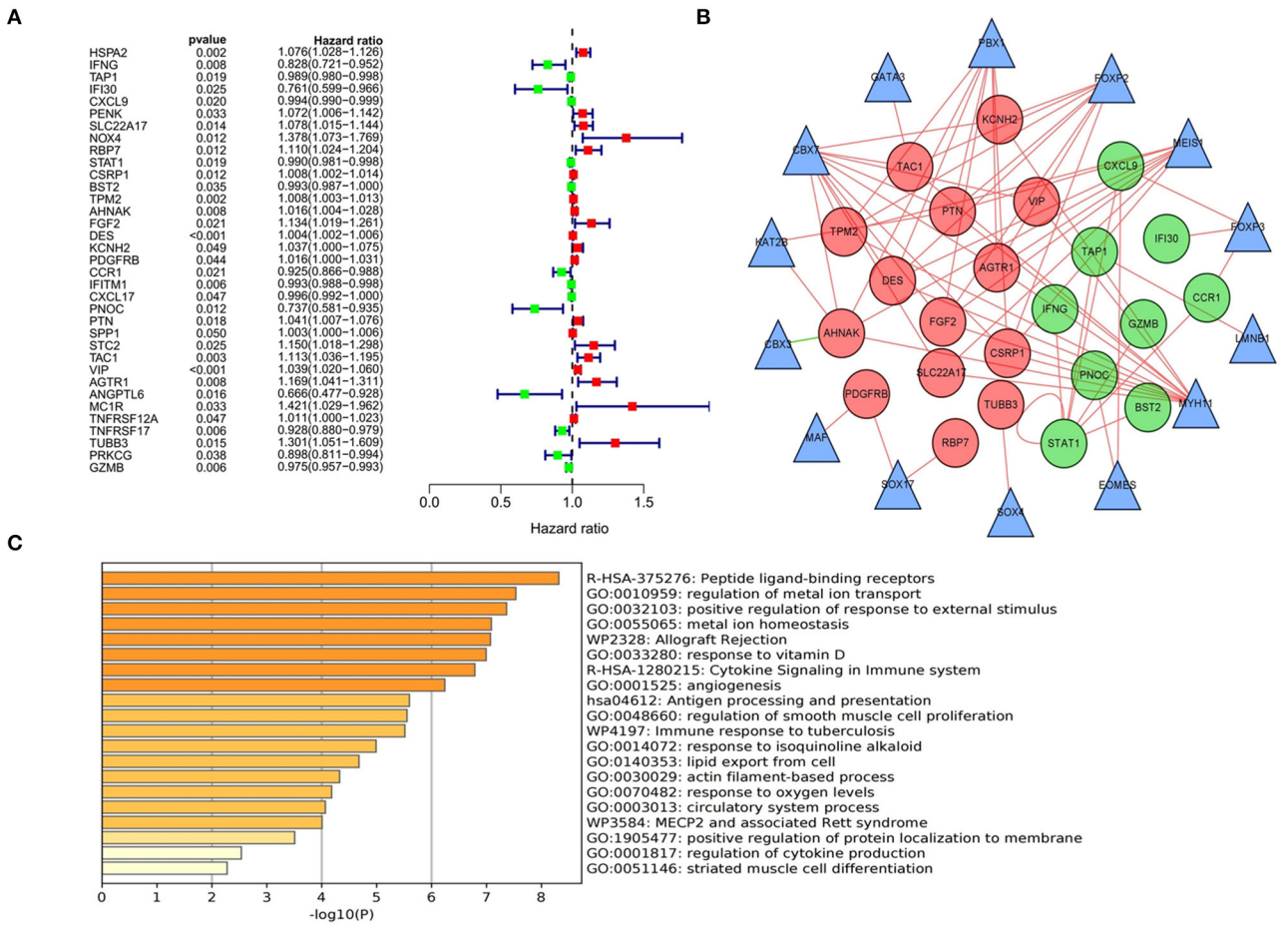

FIGURE 3 | Identification, functional enrichment of PDEIRGs and construction of TF-based regulatory network in GC. **(A)** A forest diagram of PDEIRGs through univariate Cox analysis. The red mark indicates that HR value of the immune gene is >1 (high risk), and the green mark indicates that HR value of the immune gene is <1 (low risk). **(B)** TF-based regulatory network. The red and green dots represent PDEIRGs, the triangles represent DETFs that correlated with PDEIRGs in terms of their mRNA expression. **(C)** Functional analysis.

of mRNAs from the Lasso and Cox regression model: Risk score = (0.111005431) * RBP7 expression + (0.002868645) * DES expression + (−0.089069349) * CCR1 expression + (−0.26816701) * PNOC expression + (0.003158221) * SPP1 expression + (0.021454067) * VIP expression + (0.017371273) *TNFRSF12A expression + (0.274538183) * TUBB3 expression + (−0.080069838)*PRKCG expression.

In the training set, patients were classified according to the risk score and divided into high-risk group and low-risk group. The risk score distribution and survival status of high-risk and low-risk patients were shown in the **Figures 5A1–A3**. The survival time of GC patients decreased with the increase in risk score. Survival analysis was performed in high-risk and low-risk groups with R "survival" package. The Kaplan–Meier curve showed that the prognosis of patients in high-risk group was poorer. The 5-year OS of high-risk patients is 44.3%, while the 5-year OS of low-risk patients is 73.0%, the difference is statistically significant (P = 1.261e−06) (**Figure 5B**). In order to further verify the accuracy of the prognosis evaluation model and other clinical indicators, we used the R "survivalROC" package to draw multiple ROC curves. The results showed that the AUC of the model was 0.811 (**Figure 5C**), which was significantly higher than other clinical indicators, indicating that the risk scoring model had a satisfying predictive performance.

Verification of Independent Risk Factors for GC

In addition, in the training set, we used the pathological characteristics in clinical data as the independent variable and patient survival time as a dependent variable for Cox univariate regression analysis. The results suggested that T stage, N stage and prognostic risk model were high-risk factors affecting the prognosis of GC. Taking the risk factors of GC as an independent variable and survival time as a dependent variable, the Cox multivariate regression analysis was conducted. The results indicated that the risk score of the risk scoring model was an independent risk factor affecting the prognosis of patients with GC (**Table 1**).

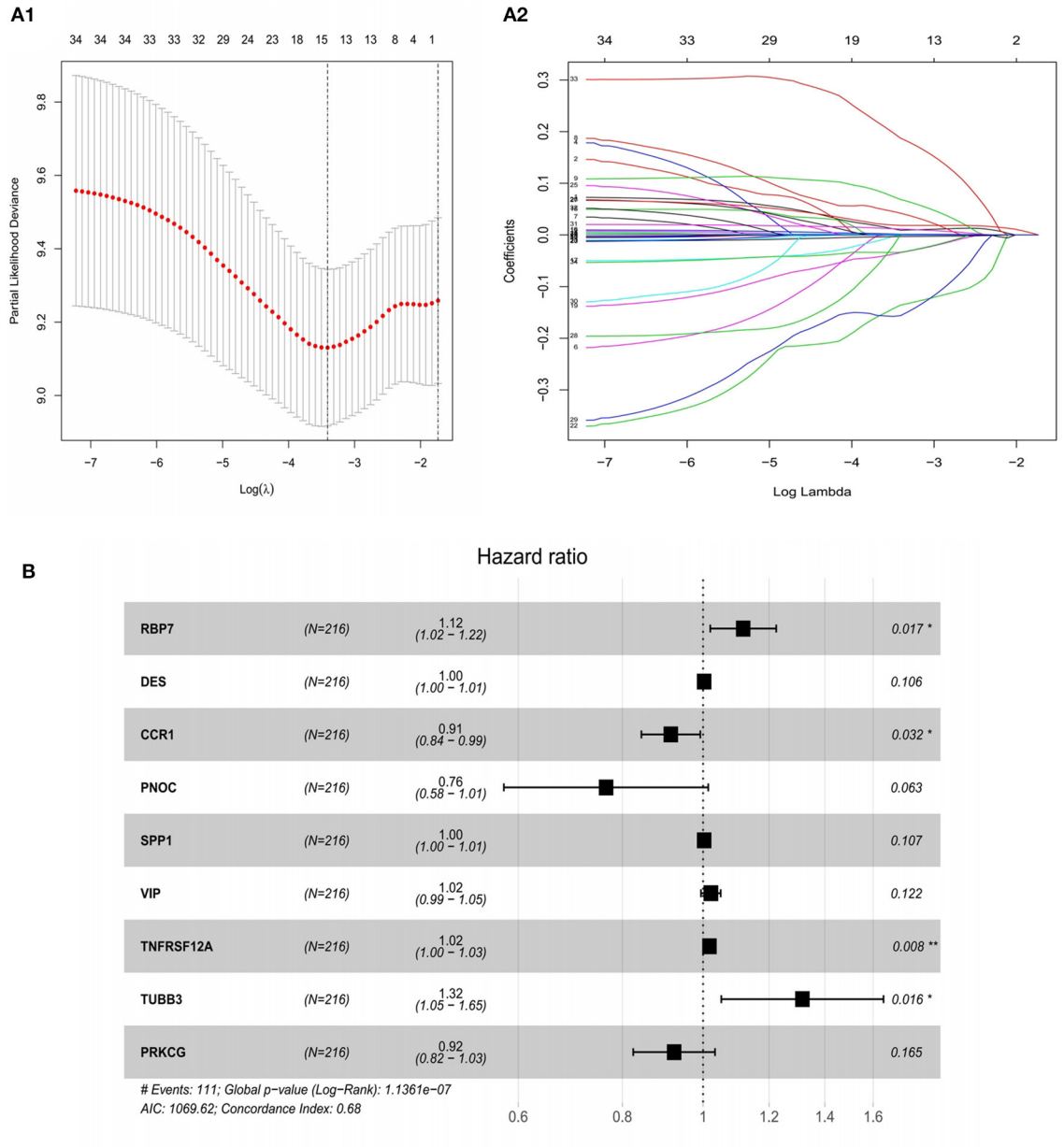

FIGURE 4 | Construction of a risk assessment model by Lasso and Cox regression analysis in the training group. **(A1)** Selection of the optimal parameter (lambda) in the Lasso model for GC. **(A2)** Lasso coefficient profiles of genes in GC. A coefficient profile plot was generated against the log (lambda) sequence. **(B)** After optimization by Cox analysis, 9 mRNAs were selected to construct the risk assessment model as shown in the forest graph. $^{**}P < 0.01$; $^{*}P < 0.05$.

Internal Validation of Prognostic Risk Scoring Model

The model was internally validated through the test set and the overall patients set. Firstly, 215 patient samples in the test set were classified according to the risk score of the model and divided into high-risk group and low-risk group. The risk score distribution and survival status of internal validation samples were shown in the **Figures 6A1,B1,C1**. The average survival time of cases was shorter and the number of deaths was larger in high-risk group, while the expression of 9 mRNAs in the high-risk group and the low-risk group was different. The Kaplan-Meier curve in the testing validation sample showed that the prognosis of patients in high-risk group was poorer ($P = 3.386e{-}03$) (**Figure 7A1**). The 5-year OS rate of high-risk patients was 49.0%, while that of low-risk patients was 70.0%. The area of the risk score of the internal validation sample under the AUC value

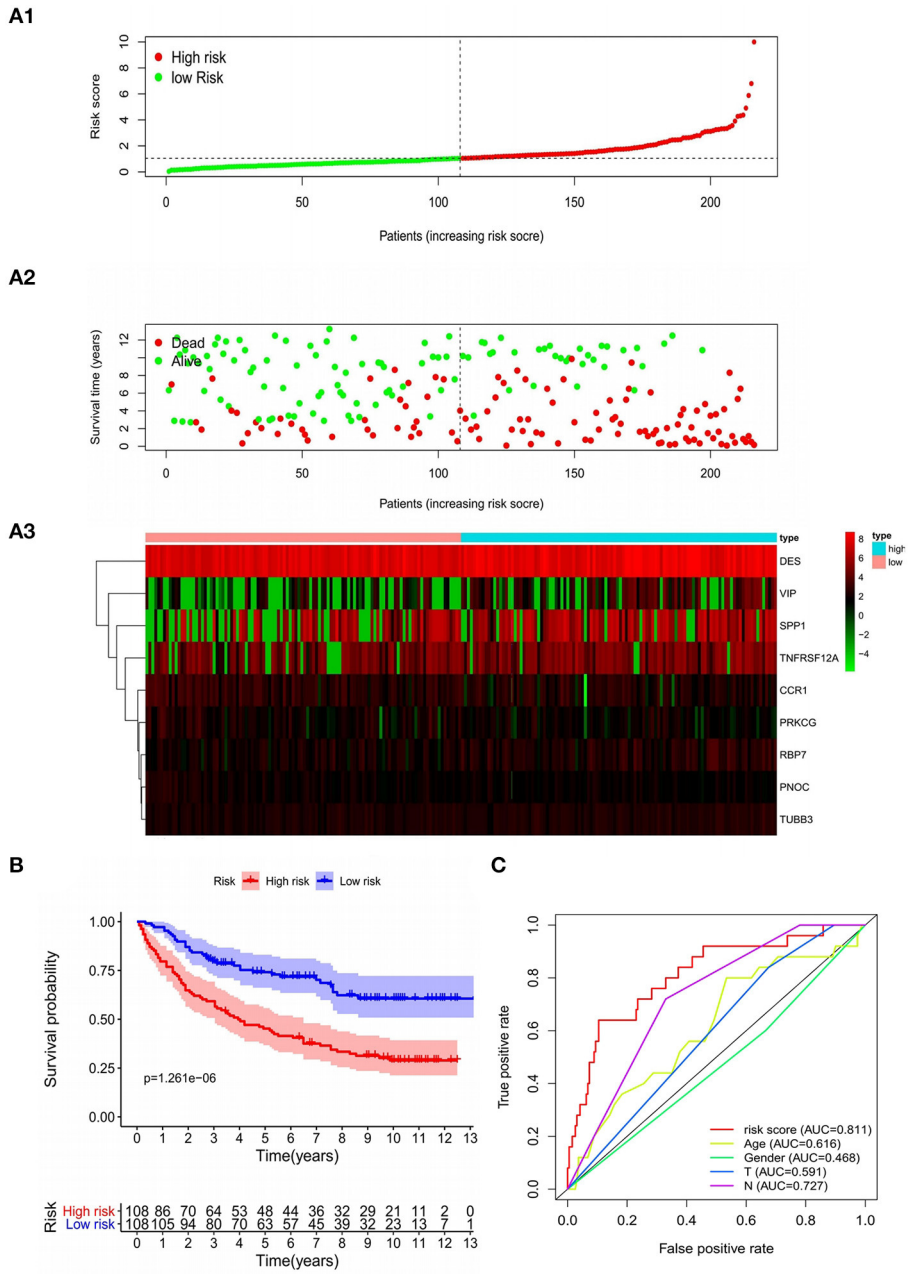

FIGURE 5 | Characteristics of the prognostic model in the training group. **(A1,A2)** The distribution of risk score, patients' survival and status for GC. The black dotted line divided patients into high-risk group and low-risk group. **(A3)** Heat map of gene expression profiles in prognostic model for GC. **(B)** Kaplan-Meier survival analysis of patients stratified by the median risk score. **(C)** The ROC curve was applied to assess the predictive performance of the model compared to other clinical features.

of ROC was 0.683, which was significantly greater than other clinical indicators (**Figure 7B1**).

The training set and the testing set were combined into an overall patients set. As depicted in **Figures 6A2,B2,C2**, the survival status of high-risk patients is also not as good as that of low-risk patients, while the expression of 9 mRNAs in the high-risk group and the low-risk group was still different. As shown in the Kaplan-Meier survival curve (**Figure 7A2**), OS of patients in high-risk group was shorter than that in low-risk group ($P < 0.001$). The AUC of risk score was 0.735, which was significantly higher than other indicators (**Figure 7B2**).

External Validation of Prognostic Risk Scoring Model

In addition, the model was externally validated in GSE57303 and TCGA GC. In GSE57303, 70 patient samples were classified

according to the risk score of the model and divided into high-risk group and low-risk group. The risk score distribution and survival status of the external validation sample are consistent with the previous results (**Figures 6A3,B3,C3**). The Kaplan-Meier curve shows that the survival time of patients with low-risk score is significantly longer than that of patients with high-risk score ($P = 9.439e{-}08$) (**Figure 7A3**). The AUC values of the 3-, 5-year survival rate for patients were 0.747, 0.701, proving that the Cox model has a satisfying prognostic predictive ability (**Figure 7B3**). In TCGA GC containing 319 patient samples, the model still showed a good prognosis (**Supplementary Figures 2A–C**). Based on the clinical information of gastric cancer patients in TCGA database, including age, gender, stage, T, M, N, we constructed a prediction model of clinical predictive indicators based on Lasso regression analysis, and plotted the ROC curve of the model. The results showed that the AUC value was less than that of our 9-gene model. That is to say, the prediction performance of immune prediction model is superior to clinical prediction model (**Supplementary Figure 4**). The above all prove that the model had a reliable accuracy and the Cox model was preferable to other single indicators in predicting prognosis.

TABLE 1 | Univariate and multivariate Cox regression analysis of the training set.

Covariates	Univariate analysis		Multivariate analysis	
	HR(95% CI)	*P*	HR(95% CI)	*P*
Age	1.016 (0.999–1.033)	0.062056	1.021 (1.003–1.038)	**0.02092**
Gender	1.129 (0.758–1.680)	0.550738	1.003 (0.657–1.531)	0.987295
T	1.597 (1.156–2.205)	**0.00447**	1.436 (1.025–2.011)	**0.03557**
N	1.669 (1.356–2.054)	**1.33E−06**	1.458 (1.168–1.818)	**0.00084**
riskScore	1.746 (1.537–1.983)	**1.01E−17**	1.674 (1.470–1.907)	**7.46E−15**

Bold indicates that the result is meaningful.

Construction of the Nomogram

In order to provide clinicians with quantitative methods to predict the prognosis of GC patients, we established a nomogram using rms package based on TCGA-GC, which combined with the various predictors of the prognosis of GC patients, patient age and risk score (**Figure 8A**). Further, The calibration curves and DCA curves of 1, 3, and 5 years showed that the 1-, 3-, and 5-year survival rate of GC patients predicted by the nomogram coincides well with the actual survival rate, which indicated that the nomogram we have established can better predict the survival rate of GC patients (**Figures 8B1–B3,C1–C3**). In addition, the nomogram constructed based on GSE84437 has also been well-verified by the calibration curve (**Supplementary Figures 3A,B**).

Correlation Analysis Between Model Genes and Pathological Characteristics

GO and KEGG pathway analysis were employed to identify the biological function of the model genes (**Table 2**). The R language "Beeswarm" package was used to further study the relationship between gene distribution and clinical parameter stratified. It was found that the expressions of RBP7, CCR1, and PNOC were positively correlated with clinical grade. DES, CCR1, VIP, TNFRSF12A, and TUBB3 were positively correlated with the clinical stage. CCR1, SPP1, TNFRSF12A, and TUBB3 were

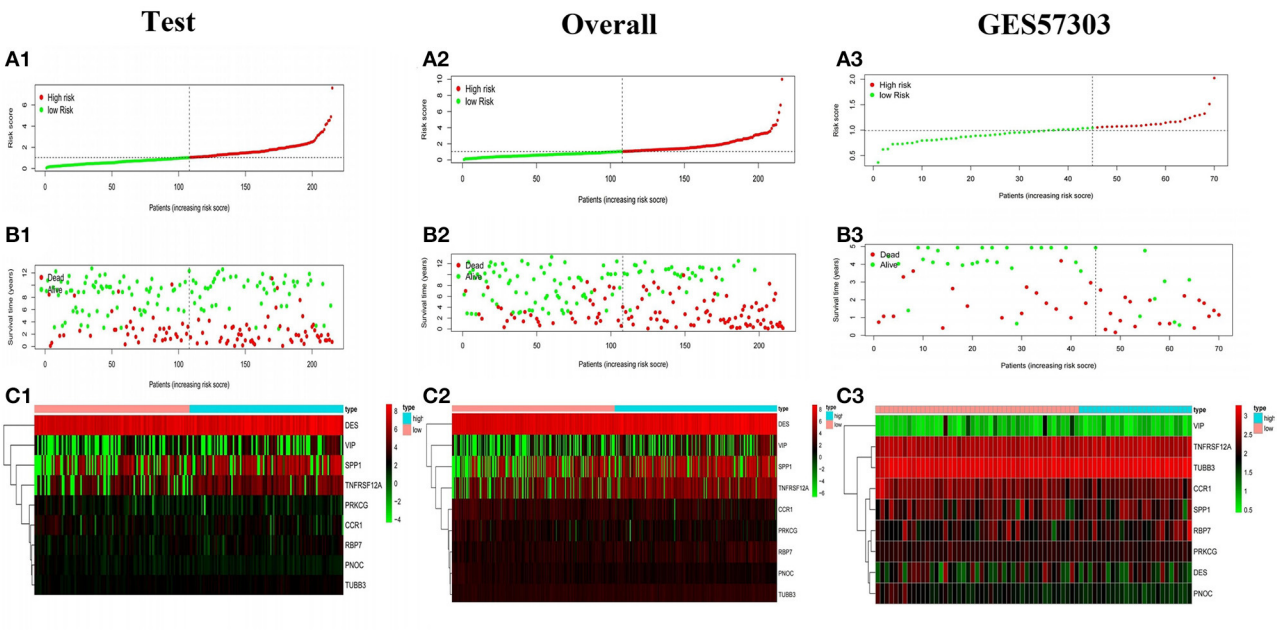

FIGURE 6 | Survival status of gastric cancer patients with different risk scores. The distribution of risk score **(A1)**, survival time **(B1)**, heat map **(C1)** of the test set. **(A2,B2,C2, A3,B3,C3)** The distribution of risk score, survival time, heat map of the overall internal validation set and GSE57303 external validation set.

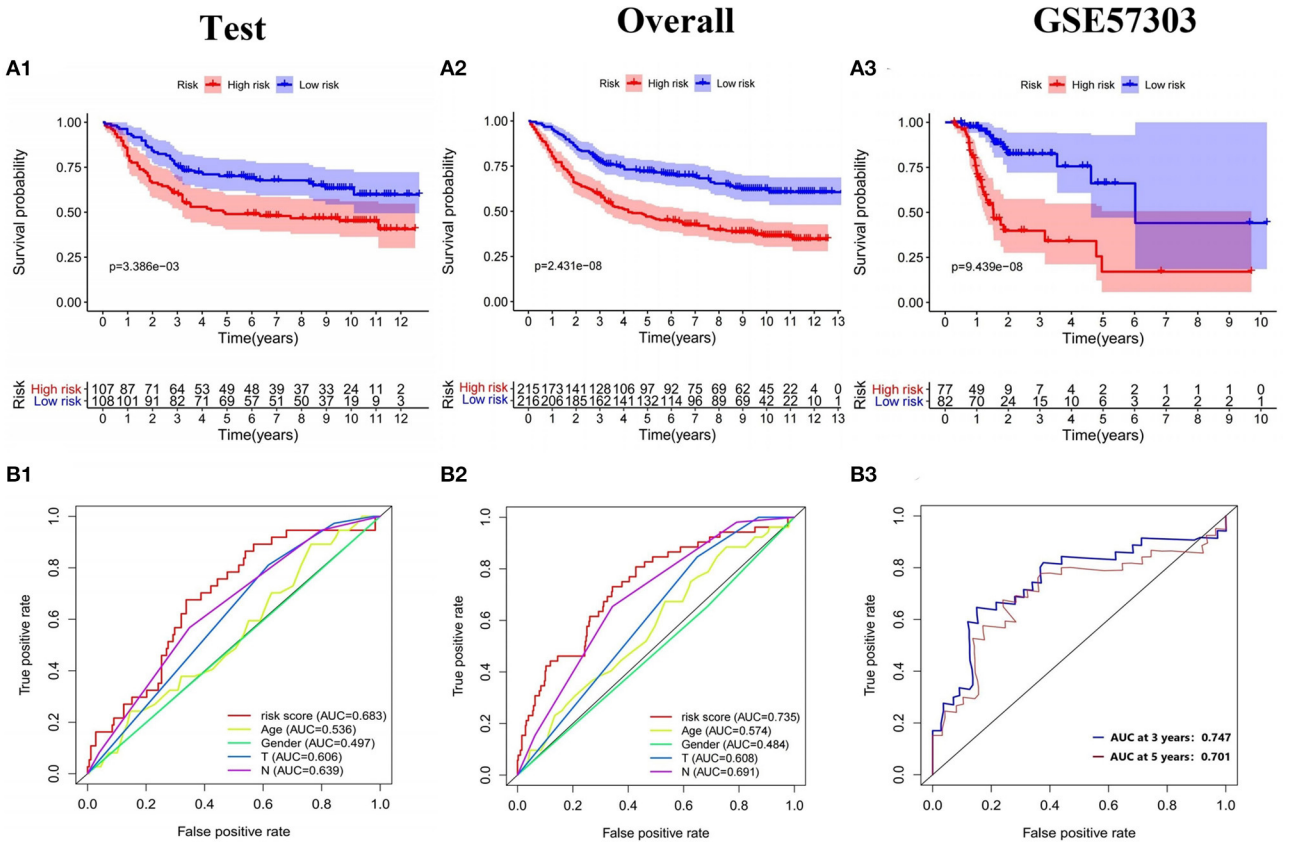

FIGURE 7 | Validation of the prognostic model. **(A1–A3)** K-M survival analysis and **(B1–B3)** ROC curve of the test set, the overall internal validation set and GSE57303 external validation set.

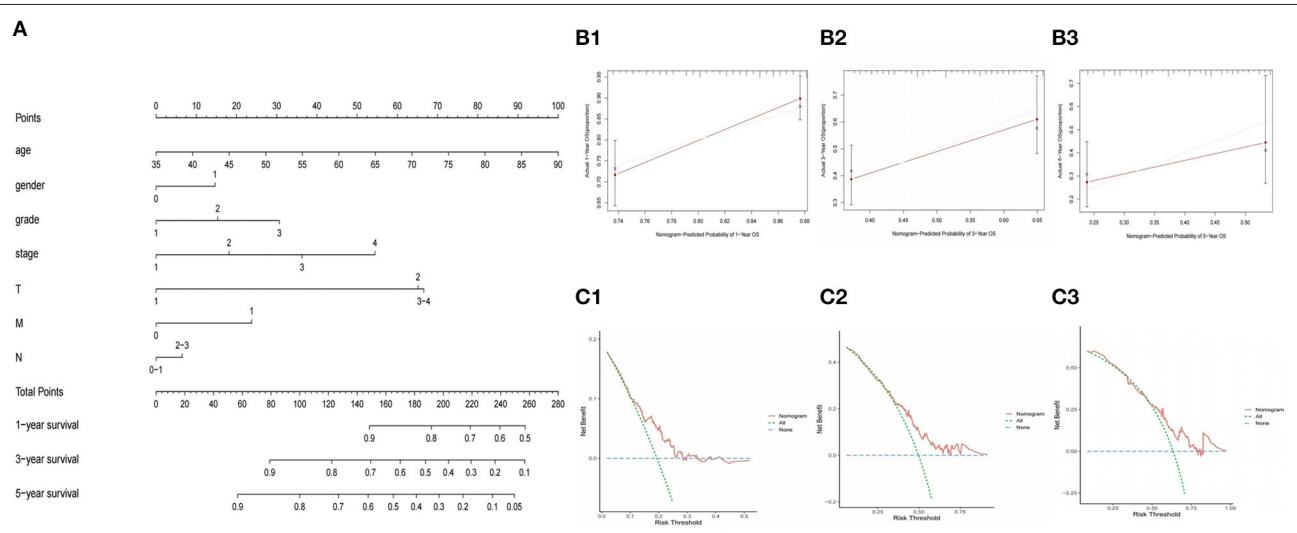

FIGURE 8 | Construction and validation of nomogram to predict the probability of 1-year, 3-year, and 5-year survival rate in GC. **(A)** Nomogram of prognostic model. **(B1–B3)** Verification of nomogram capability in the TCGA database. **(C1–C3)** Verification of DCA curves in the TCGA database.

TABLE 2 | Enrichment analysis of genes in the model.

Term ID	Term description	Strength	False discovery rate	Matching proteins in the network
GO:0005184	Neuropeptide hormone activity	2.18	0.0082	PNOC, VIP
GO:0005200	Structural constituent of cytoskeleton	1.61	0.0461	TUBB3, DES
GO:0048018	Receptor ligand activity	1.15	0.0461	PNOC, VIP, SPP1
hsa04540	Gap junction	1.7	0.0461	PRKCG, TUBB3
HSA-1280215	Cytokine Signaling in Immune system	1.12	0.0472	CCR1, TNFRSF12A

positively correlated with T stage. DES and VIP were positively correlated with N stage (all $P < 0.05$) (**Figure 9**). In order to study the protein expression of 9 genes in normal tissues and gastric cancer tissues, we searched the Human Protein Atlas (HPA) database and obtained the immunohistochemical results of 8 genes (**Figure 10**). The results of immunohistochemistry showed that the protein expression levels of RBP7, DES, SPP1, VIP, and PRKCG in gastric cancer tissues were higher than those in normal tissues, while PNOC, TNFRSF12A, and TUBB3 proteins are less expressed in gastric cancer tissues than normal tissues. However, the immunohistochemical results of CCR1 were not found in the database.

Correlation Analysis Between 9-Gene Model and Immune Cell Infiltration

In order to further study the relationship between the 9-gene signature and immune cells, the gene expression data of the samples in the TCGA cohort and the gene expression profiles of 22 kinds of immune cells were analyzed by CIBERSORT software, and the contents of various immune cells in the samples were estimated. According to the risk value calculated by the model, patients are divided into high and low risk groups, we found that the risk score calculated based on 9-gene signature was found to be significantly correlated with the infiltration of 9 types of immune cells, including Plasma cells, T cells regulatory (Tregs), Macrophages M0, etc. (**Figures 11A,B**).

The correlation between RBP7, DES, CCR1, PNOC, SPP1, VIP, TNFRSF12A, TUBB3, PRKCG genes and the amount of immune cell infiltration was explored by TIMER. Spearman correlation analysis was used for correlation analysis. As shown in the table, the expressions of CCR1, PNOC, and VIP genes were significantly correlated with tumor purity, B cell infiltration, CD8+T cell infiltration, CD4+T cell infiltration, macrophage infiltration, neutrophil infiltration and dendritic cell infiltration, and the differences were statistically significant. There was a significant correlation between DES gene expression and tumor purity, B cell infiltration, CD8+T cell infiltration, CD4+T cell infiltration, macrophage infiltration, and dendritic cell infiltration, and the differences were all statistical significance. The expression of other genes was significantly related to tumor purity and the infiltration of one or more immune cells, and the differences were all statistically significant (all $P < 0.05$) (**Supplementary Table 2**).

The Effect of Immunotherapy in High- and Low-Risk Groups

In addition, in order to explore the effect of immunotherapy in high- and low-risk groups, the tumor immune dysfunction and rejection (TIDE) calculation framework was used to simulate the two main mechanisms of tumor immune evasion and provide predictive results for immunotherapy. Elevated TIDE indicates that the patient has inhibitory cells that inhibit T cell infiltration and does not respond to immunotherapy. We found that the score of the high-risk group was significantly higher than that of the low-risk group, that is, there were more obvious immune dysfunction and immune rejection, indicating that the immunotherapy effect of patients in the high-risk group were often poor (**Figures 11C1–C3**).

DISCUSSION

GC is a type of highly heterogeneous malignant tumor, with a rising incidence worldwide, poor prognosis and high mortality (18). There is evidence that commonly used clinicopathological parameters (such as TNM stage, age, sex, viral infection, and serum CEA levels) are insufficient to accurately predict patient outcomes (19). Therefore, it is necessary to identify sensitive and stable GC prognostic biomarkers to improve treatment. At present, models based on genetic signatures have been reported in a variety of cancers, such as ovarian cancer, lung adenocarcinoma, and soft tissue sarcoma (20–22). Immunotherapy involves changes in genes, metabolism, inflammation and tumor microenvironment, and the mechanisms are complex. Considering that cell atypia and even canceration often occur in a microenvironment of dense inflammatory cells, the study of tumor genomics and changes in the tissue microenvironment is a new challenge (23).

Based on TCGA database, this study utilized R language to screen out the DEIRGs in GC tissues. Combined with detailed clinical data in GSE84437, Lasso and Cox analysis was applied to screen genes closely related to the prognosis of patients in 358 DEIRGs. In the end, 9 mRNAs were selected to form a prognostic model. Survival analysis, ROC curve and risk curve were used in the training set, validation set and external validation set to verify the accurate prediction performance of the model. In order to independently predict patient survival, the model was combined with other clinical variables to construct a nomogram for better clinical application. At the same time, we performed gene expression and clinical correlation analysis on the model genes discovered in the study, and found a number of genes closely related to the patient's clinical status, providing a basis for finding reliable genetic biological targets.

In tumor cells, an inactivated, pleiotropic transcription factor simultaneously coordinates the expression of a large family of

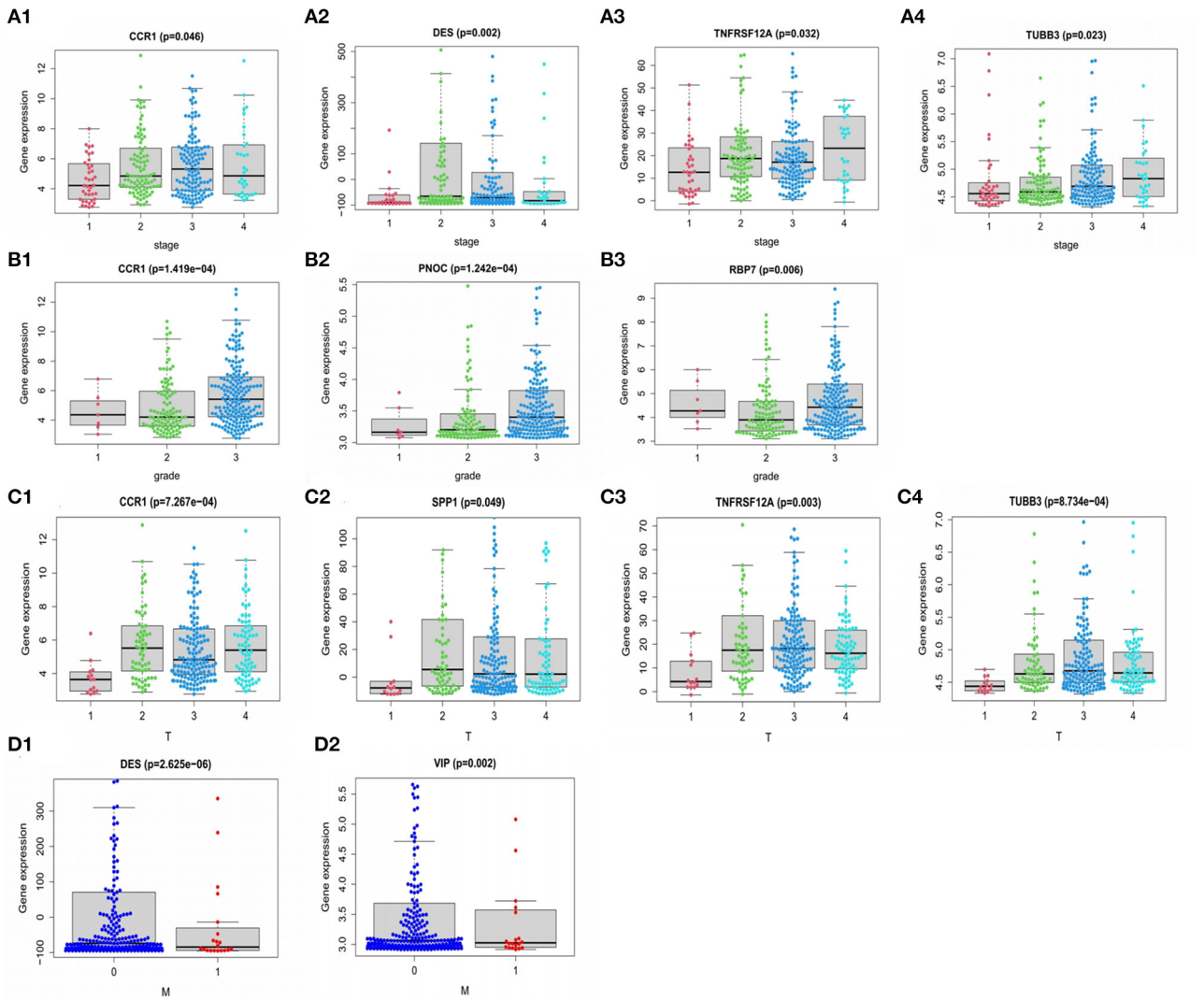

FIGURE 9 | Relationship of PDEIRGs with patients' clinical characteristics of GC. **(A1–A4)** Immune gene CCR1, DES, TNFRSF12A, TUBB3 had significant clinical correlation with stage. **(B1–B3)** CCR1, PNOC, RBP7 had significant clinical correlation with grade. **(C1–C4)** CCR1, SPP1, TNFRSF12A, TUBB3 had significant clinical correlation with T stage. **(D1,D2)** DES, VIP had a significant clinical correlation with the M stage.

responding genes, causing them to act together to produce the phenotype of the cancer cell (24). In our work, there is a statistically significant correlation between multiple DETFs and PDEIRGs. Transcription factors play a direct role in regulating immune-related genes. Among these TFs, FOX family and Chromobox family were found to be closely related to the occurrence and development of GC. Experiments have shown that Treg-like immunosuppressive effects can occur after inducing initial T cells to express FOXP3 *in vitro* or *in vivo*, indicating that FOXP3 is a key factor in controlling the expression of immunosuppressive molecules (25). High expression of CBX7 can enhance the clonal proliferation, migration and invasion of GC cells, promote the self-renewal of GC stem-like cells, and reduce the sensitivity of GC cells to chemotherapy drugs (26). It can be deduced that the targeted therapy of TFs will become an important direction of tumor research in the future.

Furthermore, the results of functional annotation showed that the genes in the model played key roles in receptor ligand activity, gap junction, and cytokine signal transduction. It is worth noting that mediated GJIC is one of the most common way of communication between cells (27), in regulating cell growth, differentiation and apoptosis plays an important role, inhibition of GJIC function or defects can make the former around tumor cells or cells lose normal cell growth regulation and autonomy, and then develop into tumor cells, It is an important mechanism of promoting carcinogenesis stage (28, 29). The research on the mechanism of the influence of model genes on gap junction can be regarded as our subsequent research direction. In addition, immune cell infiltration plays

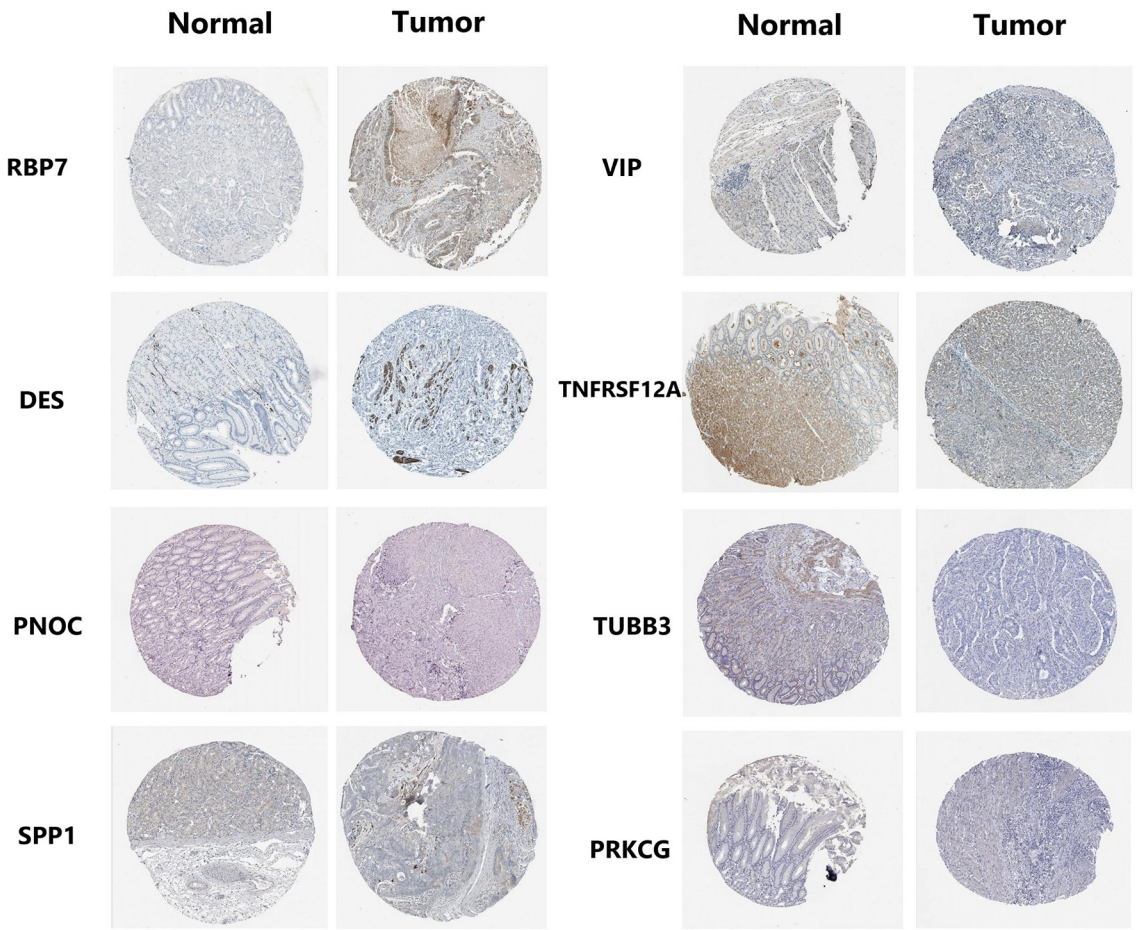

FIGURE 10 | Expression profiles of 8 genes in normal stomach tissues and gastric adenocarcinoma tissues. Immunohistochemical results were obtained from HPA database.

an important role in tumor development. Previous studies have found that the accumulation of tumor-associated macrophages is associated with poor clinical prognosis (30). Dendritic cells play a critical role in the initial activation of tumor immunity (31). The expression of multiple genes in the model was significantly correlated with the infiltration of various immune cells and tumor purity, which also indicated that our model could effectively predict the prognosis of GC patients.

According to previous studies, the genes identified in our work regarded as independent prognostic factors for GC were often found to be involved in tumor occurrence and development. CCR1 is a member of the β-chemokine receptor family. Chemokines are an important component of the tumor microenvironment. CC chemokines produced by tumor cells and tumor-related cells can affect the proliferation, migration and invasion of cancer cells (32, 33). Interestingly, this study found that the high expression of CCR1 was significantly related to the good prognosis of GC patients, whether CCR1 can participate in the GC process through chemokine antagonism is our next step. The protein of TUBB3 is mainly expressed in neurons and may be involved in neurogenesis and axon guidance and maintenance (34). Cao et al. (35) found that the expression of TUBB3 is significantly correlated with the clinicopathologic characteristics of gastric cancer patients, such as age, sex and family history. It may be a potential biomarker for prognosis and chemotherapy guidance. TNFRSF12A is the receptor of TNFSF12/TWEAK, which can promote angiogenesis and endothelial cell proliferation, and regulate cell adhesion to matrix proteins. Wu et al. (36) found that the decrease of TNFRSF12A expression in thyroid cancer indicates a poor prognosis. RBP7 encoded proteins are members of the cellular retinol binding protein (CRBP) family, and their members are necessary for vitamin A stability and metabolism (37). Previous studies have shown that RBP4, as a member of the same family, its receptor is a strong transformation medium and drives malignant transformation in human breast and colon cancer cells (38). Elmasry M's study (39) showed that RBP7 is also a clinical prognostic biomarker and is associated with tumor invasion and EMT of colon cancer. Moreover, in our work, we found that RBP7 is a high-risk factor for GC, so figuring out how RBP7 drives these malignant features and how it affects the transcriptome of gastrointestinal tumor cells is our next research direction.

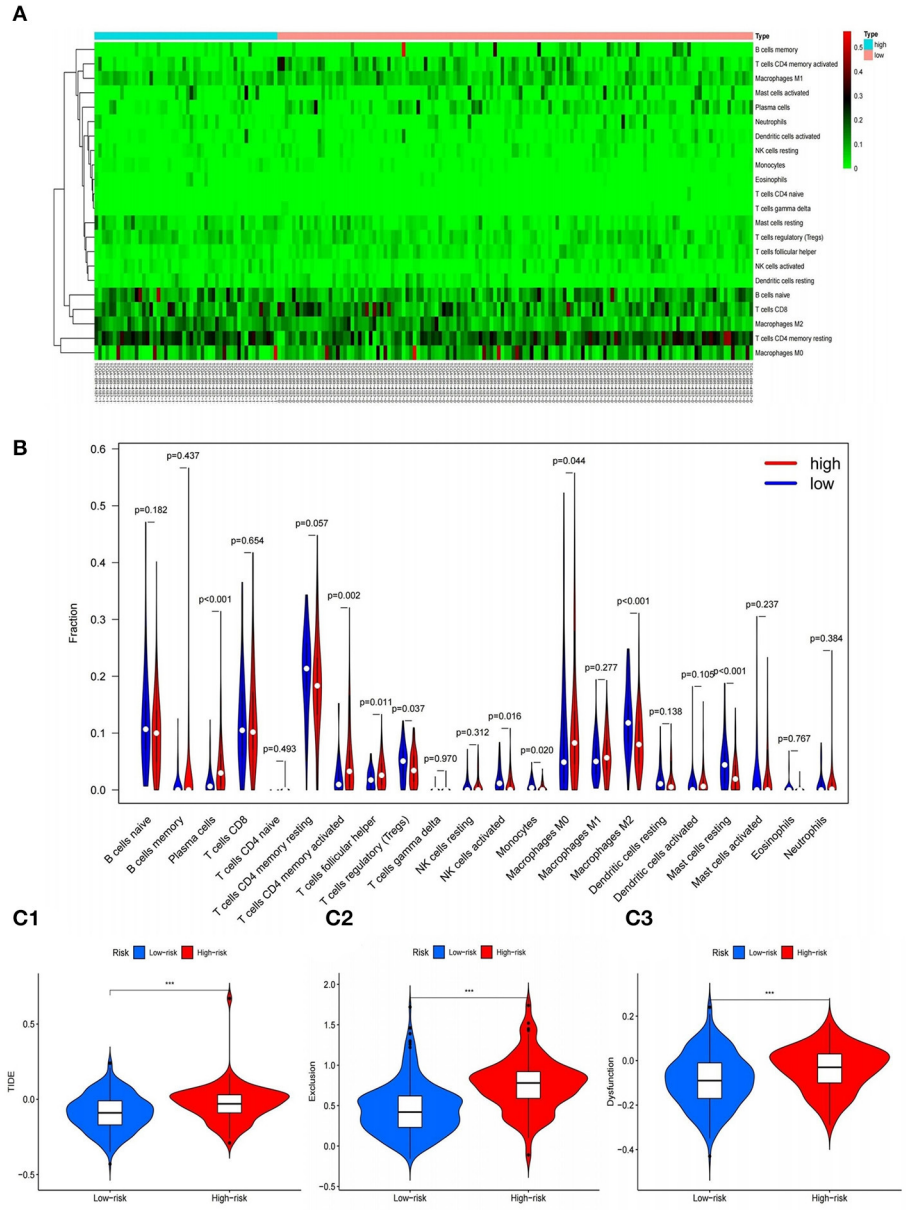

FIGURE 11 | Correlation of gene model with immune cell infiltration and immunotherapy. **(A,B)** Heat and violin plots of differences in immune cell infiltration in high and low risk groups. **(C1–C3)** Violin plots of differences in TIDE between high and low risk groups. ***$P < 0.001$.

In addition to these genes, several other genes in the study also have intriguing biological implications. VIP is a neuropeptide belonging to the family of G protein-coupled receptors, which can activate cAMP-response element binding protein by regulating the cAMP/PKA signaling pathway (40). It involves in gastric smooth muscle relaxation, vasodilation and gastric juice secretion. Zygulska et al. (41) found that overexpression of vasoactive intestinal peptide (VIP) receptors may occur in human surface gastrointestinal malignant tumors; Balkwill et al. (42) found that neurotransmitter secretion is increased in the inflammatory response caused by cancer. Based on these, it is inferred that the increased expression of VIP and its receptor may be related to cancer-related inflammation. SPP1 is primarily located in the extracellular matrix, mainly involved in the adhesion of cell matrix, osteogenization, anticellulation apoptosis, cell attachment, immunocyte chemokine, and other biological processes. According to reports, SPP1 can promote tumor cell survival, regulate tumor-related angiogenesis and inflammatory responses (43), closely related to lung cancer, ovarian cancer, colon cancer, head and neck squamous cancer and adverse prognosis closely related (44, 45). There has been no previous report on SPP1 and GC, but this study, based on bioinformatics, first found that SPP1 is a risk factor for GC prognosis, and its mechanism of tumor action needs further

study and demonstration. Moreover, it is worth noting that STAT1 and APLNR are the seed genes in the module, and their role in tumors has been confirmed, which is consistent with the results of this study. It has been suggested that STAT1 serves as a tumor suppressor by promoting the expression of p21waf, caspase 3 and caspase 7 to activate pro-apoptotic pathways (46). APLNR is the receptor for Apelin. In various cancers, Apelin expression increases, and the Apelin/APLNR axis play an essential role in tumor development by enhancing angiogenesis, metastasis, cell proliferation, and cancer stem cell development and drug resistance (47).

Based on a search of previous literature, a prognostic model based on gene signatures has been established in a variety of cancers and its feasibility has been verified. However, few studies have integrated multiple data sets in GC to explore immune gene regulatory networks and establish reliable prognostic models, as well as in-depth analysis of its molecular mechanism. This study innovatively screened the immune genes with prognostic significance in GC, and combined with reliable statistical methods to construct a prognostic risk model based on 9 immune-related genes. Multiple data sets in different platforms proved that the model relative to other clinical staging method had more excellent performance and reliable prediction. In addition, we found that the model gene was not only related to GC stage and grade, but also reflected the immune microenvironment of GC, providing insights for immunotherapy. The traditional TNM gastric cancer staging system cannot be used to accurately predict whether patients will benefit from adjuvant chemotherapy. The establishment of this model completes the existing staging system, and can guide accurate prognosis judgments and treatment options.

However, this study also has some limitations. First, the risk scoring model needs to be further validated in multi-center clinical trials and prospective studies. Secondly, the function of 9 immune genes still needs to be further analyzed. In various studies on GC, the prognostic risk model of GC described in this article has not been reported previously. This study used bioinformatics methods to establish a prognostic model consisting of RBP7, DES, CCR1, PNOC, SPP1, VIP, TNFRSF12A, TUBB3, and PRKCG, and proved its prognostic value in GC. The nomogram established in combination with the risk score can clinically predict the OS of patients with GC after resection. It is worth noting that this study provides a new immunological perspective and a new basis for immunotherapy of GC. This model may be a new and accurate prediction tool for evaluating whether GC patients can benefit from immunotherapy.

CONCLUSIONS

In summary, based on the TCGA and GEO data set, we have identified DEIRGs expressed in GC tissues. We established a reliable multi-gene joint prediction model, which is beneficial to improve the prognosis of patients. Moreover, this study found several prognostic markers worth exploring: APLNR is a risk factor for GC, so blocking the Apelin/APLNR axis to inhibit the development of gastric cancer is a promising new therapy. In addition, CCR1 and STAT1 are protective factors for gastric cancer. The enhancement of the pro-apoptotic pathway of STAT1 has the potential to inhibit GC. Whether CCR1 can participate in the GC process through chemokine antagonism is our next step.

DATA AVAILABILITY STATEMENT

The datasets presented in this study can be found in online repositories. The names of the repository/repositories and accession number(s) can be found in the article/**Supplementary Material**.

AUTHOR CONTRIBUTIONS

ML designed, analyzed the data, and wrote the manuscript. WC helped to prepare the dataset and participated in the discussion. YC and ZZ helped to search for some relevant papers for this research. BH analyzed the data and generated the figures and tables. BC and GC guided the research process. All authors read and approved the final manuscript.

FUNDING

This work was supported by the National Natural Science Foundation of China (81602425), the Anhui Quality Engineering Project (2020jyxm0898 and 2020jyxm0910), the Anhui Health Soft Science Research Project (2020WR01003), and the Key Research and Development Program of Anhui Province (201904a07020045).

SUPPLEMENTARY MATERIAL

The Supplementary Material for this article can be found online at: https://www.frontiersin.org/articles/10.3389/fsurg.2022.829237/full#supplementary-material

Supplementary Figure 1 | Kaplan-Meier analysis of the impact of the 2 seed genes on the prognosis of GC patients.

Supplementary Figure 2 | Validation of the prognostic model in TCGA GC set.

Supplementary Figure 3 | Construction and validation of nomogram in GEO database.

Supplementary Figure 4 | ROC curve of predictive model based on clinical predictive indicators.

Supplementary Figure 5 | Boxplot of differential expression of CCR1 in gastric cancer and normal tissues.

Supplementary Table 1 | Correlation between TFs and immuneGenes.

Supplementary Table 2 | Analysis of the relationship between PDEIRGs and immune cell infiltration.

Additional File 6 | Differentially expressed immune-related genes of GC.

Additional File 7 | Clinical information of patients in TCGA cohort.

Additional File 8 | Clinical information of patients in GSE57303 cohort.

Additional File 9 | Clinical information of patients in GSE84433 cohort.

Additional File 10 | Correlation and regulatory relationship between TF and genes in the prognostic model.

REFERENCES

1. Smyth EC, Nilsson M, Grabsch HI, van Grieken NC, Lordick F. Gastric cancer. *Lancet*. (2020) 396:635–48. doi: 10.1016/S0140-6736(20)31288-5
2. Song Z, Wu Y, Yang J, Yang D, Fang X. Progress in the treatment of advanced gastric cancer. *Tumour Biol*. (2017) 39:1010428317714626. doi: 10.1177/1010428317714626
3. Mastoraki A, Benetou C, Mastoraki S, Papanikolaou IS, Danias N, Smyrniotis V, et al. The role of surgery in the therapeutic approach of gastric cancer liver metastases. *Indian J Gastroenterol*. (2016) 35:331–6. doi: 10.1007/s12664-016-0683-7
4. Zhang LL, Xu F, Song D, Huang MY, Huang YS, Deng QL, et al. Development of a nomogram model for treatment of nonmetastatic nasopharyngeal carcinoma. *JAMA Netw Open*. (2020) 3:e2029882. doi: 10.1001/jamanetworkopen.2020.29882
5. Chan TA, Yarchoan M, Jaffee E, Swanton C, Quezada SA, Stenzinger A, et al. Development of tumor mutation burden as an immunotherapy biomarker: utility for the oncology clinic. *Ann Oncol*. (2019) 30:44–56. doi: 10.1093/annonc/mdy495
6. Xu P, Liang F. Nanomaterial-based tumor photothermal immunotherapy. *Int J Nanomed*. (2020) 15:9159–80. doi: 10.2147/IJN.S249252
7. Dammeijer F, van Gulijk M, Mulder EE, Lukkes M, Klaase L, van den Bosch T, et al. The PD-1/PD-L1-checkpoint restrains t cell immunity in tumor-draining lymph nodes. *Cancer Cell*. (2020) 38:685–700.e8. doi: 10.1016/j.ccell.2020.09.001
8. Ma K, Li X, Lv J, Liu Z, Zhang L, Cong H, et al. Correlations between CD4+ FoxP3+ Treg and expression of FoxM1 and Ki-67 in gastric cancer patients. *Asia Pac J Clin Oncol*. (2021) 17:e63–9. doi: 10.1111/ajco.13302
9. Lee DA. Cellular therapy: adoptive immunotherapy with expanded natural killer cells. *Immunol Rev*. (2019) 290:85–99. doi: 10.1111/imr.12793
10. Choi IK, Wang Z, Ke Q, Hong M, Paul DW Jr, Fernandes SM, et al. Mechanism of EBV inducing anti-tumour immunity and its therapeutic use. *Nature*. (2021) 590:157–62. doi: 10.1038/s41586-020-03075-w
11. Kawazoe A, Shitara K, Boku N, Yoshikawa T, Terashima M. Current status of immunotherapy for advanced gastric cancer. *Jpn J Clin Oncol*. (2021) 51:20–7. doi: 10.1093/jjco/hyaa202
12. Feng F, Tian Y, Xu G, Liu Z, Liu S, Zheng G, et al. Diagnostic and prognostic value of CEA, CA19-9, AFP and CA125 for early gastric cancer. *BMC Cancer*. (2017) 17:737. doi: 10.1186/s12885-017-3738-y
13. Lai JZ, Zhu YY, Liu Y, Zhou LL, Hu L, Chen L, et al. Abscopal effects of local radiotherapy are dependent on tumor immunogenicity. *Front Oncol*. (2021) 11:690188. doi: 10.3389/fonc.2021.690188
14. Yu Y, Feng X, Cang S. A two-microRNA signature as a diagnostic and prognostic marker of pancreatic adenocarcinoma. *Cancer Manag Res*. (2018) 10:1507–15. doi: 10.2147/CMAR.S158712
15. Yuan GQ, Wei NL, Mu LY, Wang XQ, Zhang YN, Zhou WN, et al. A 4-miRNAs signature predicts survival in glioblastoma multiforme patients. *Cancer Biomark*. (2017) 20:443–52. doi: 10.3233/CBM-170205
16. Xie P, Ma Y, Yu S, An R, He J, Zhang H. Development of an immune-related prognostic signature in breast cancer. *Front Genet*. (2020) 10:1390. doi: 10.3389/fgene.2019.01390
17. Gómez-Vela F, Divina F, García-Torres M. computational methods for the analysis of genomic data and biological processes. *Genes*. (2020) 11:1230. doi: 10.3390/genes11101230
18. Usui G, Matsusaka K, Mano Y, Urabe M, Funata S, Fukayama M, et al. DNA methylation and genetic aberrations in gastric cancer. *Digestion*. (2021) 102:25–32. doi: 10.1159/000511243
19. Matsuoka T, Yashiro M. Biomarkers of gastric cancer: current topics and future perspective. *World J Gastroenterol*. (2018) 24:2818–32. doi: 10.3748/wjg.v24.i26.2818
20. Bao M, Zhang L, Hu Y. Novel gene signatures for prognosis prediction in ovarian cancer. *J Cell Mol Med*. (2020) 24:9972–84. doi: 10.1111/jcmm.15601
21. Li P, Cao G, Zhang Y, Shi J, Cai K, Zhen L, et al. FHL3 promotes pancreatic cancer invasion and metastasis through preventing the ubiquitination degradation of EMT associated transcription factors. *Aging*. (2020) 12:53–69. doi: 10.18632/aging.102564
22. Shen R, Liu B, Li X, Yu T, Xu K, Ma J. Development and validation of an immune gene-set based prognostic signature for soft tissue sarcoma. *BMC Cancer*. (2021) 21:144. doi: 10.1186/s12885-021-07852-2
23. Ladányi A, Tímár J. Immunologic and immunogenomic aspects of tumor progression. *Semin Cancer Biol*. (2020) 60:249–61. doi: 10.1016/j.semcancer.2019.08.011
24. Salokas K, Weldatsadik RG, Varjosalo M. Human transcription factor and protein kinase gene fusions in human cancer. *Sci Rep*. (2020) 10:14169. doi: 10.1038/s41598-020-71040-8
25. Sato Y, Passerini L, Piening BD, Uyeda MJ, Goodwin M, Gregori S, et al. Human-engineered Treg-like cells suppress FOXP3-deficient T cells but preserve adaptive immune responses *in vivo*. *Clin Transl Immunol*. (2020) 9:e1214. doi: 10.1002/cti2.1214
26. Ma T, Ma N, Chen JL, Tang FX, Zong Z, Yu ZM, et al. Expression and prognostic value of Chromobox family members in gastric cancer. *J Gastrointest Oncol*. (2020) 11:983–98. doi: 10.21037/jgo-20-223
27. Vicario N, Turnaturi R, Spitale FM, Torrisi F, Zappalà A, Gulino R, et al. Intercellular communication and ion channels in neuropathic pain chronicization. *Inflamm Res*. (2020) 69:841–50. doi: 10.1007/s00011-020-01363-9
28. Navarrete M, Salazar-Onfray F, Tittarelli A. Flow cytometry evaluation of gap junction-mediated intercellular communication between cytotoxic T cells and target tumor cells. *Methods Mol Biol*. (2021) 2346:225–36. doi: 10.1007/978-1-0716-1581-2
29. Sinyuk M, Mulkearns-Hubert EE, Reizes O, Lathia J. Cancer connectors: connexins, gap junctions, and communication. *Front Oncol*. (2018) 8:646. doi: 10.3389/fonc.2018.00646
30. Xue Y, Tong L, LiuAnwei Liu F, Liu A, Zeng S, Xiong Q, et al. Tumor-infiltrating M2 macrophages driven by specific genomic alterations are associated with prognosis in bladder cancer. *Oncol Rep*. (2019) 42:581–94. doi: 10.3892/or.2019.7196
31. Wang W, Erbe AK, DeSantes KB, Sondel PM. Donor selection for ex vivo-expanded natural killer cells as adoptive cancer immunotherapy. *Future Oncol*. (2017) 13:1043–7. doi: 10.2217/fon-2017-0039
32. Korbecki J, Kojder K, Simińska D, Bohatyrewicz R, Gutowska I, Chlubek D, et al. CC chemokines in a tumor: a review of pro-cancer and anti-cancer properties of the ligands of receptors CCR1, CCR2, CCR3, and CCR4. *Int J Mol Sci*. (2020) 21:8412. doi: 10.3390/ijms21218412
33. Eum HH, Kwon M, Ryu D, Jo A, Chung W, Kim N, et al. Tumor-promoting macrophages prevail in malignant ascites of advanced gastric cancer. *Exp Mol Med*. (2020) 52:1976–88. doi: 10.1038/s12276-020-00538-y
34. Jin S, Park SE, Won D, Lee ST, Han SH, Han J. TUBB3 M323V syndrome presents with infantile nystagmus. *Genes*. (2021) 12:575. doi: 10.3390/genes12040575
35. Cao Y, Zhang G, Wang P, Zhou J, Gan W, Song Y, et al. Clinical significance of UGT1A1 polymorphism and expression of ERCC1, BRCA1, TYMS, RRM1, TUBB3, STMN1 and TOP2A in gastric cancer. *BMC Gastroenterol*. (2017) 17:2. doi: 10.1186/s12876-016-0561-x
36. Wu ZH, Niu X, Wu GH, Cheng Q. Decreased expression of TNFRSF12A in thyroid gland cancer predicts poor prognosis: a study based on TCGA data. *Medicine*. (2020) 99:e21882. doi: 10.1097/MD.0000000000021882
37. Luck K, Kim DK, Lambourne L, Spirohn K, Begg BE, Bian W, et al. A reference map of the human binary protein interactome. *Nature*. (2020) 580:402–8. doi: 10.1038/s41586-020-2188-x
38. Karunanithi S, Levi L, DeVecchio J, Karagkounis G, Reizes O, Lathia JD, et al. RBP4-STRA6 pathway drives cancer stem cell maintenance and mediates high-fat diet-induced colon carcinogenesis. *Stem Cell Rep*. (2017) 9:438–50. doi: 10.1016/j.stemcr.2017.06.002
39. Elmasry M, Brandl L, Engel J, Jung A, Kirchner T, Horst D. RBP7 is a clinically prognostic biomarker and linked to tumor invasion and EMT in colon cancer. *J Cancer*. (2019) 10:4883–91. doi: 10.7150/jca.35180
40. Siddappa PK, Vege SS. Vasoactive intestinal peptide-secreting tumors: a review. *Pancreas*. (2019) 48:1119–25. doi: 10.1097/MPA.0000000000001402
41. Zygulska AL, Furgala A, Kaszuba-Zwoińska J, Krzemieniecki K, Gil K. Changes in plasma levels of cholecystokinin, neurotensin, VIP and PYY in gastric and colorectal cancer - preliminary results. *Peptides*. (2019) 122:170148. doi: 10.1016/j.peptides.2019.170148

42. Balkwill F, Mantovani A. Inflammation and cancer: back to Virchow? *Lancet*. (2001) 357:539–45. doi: 10.1016/S0140-6736(00)04046-0
43. Wei T, Bi G, Bian Y, Ruan S, Yuan G, Xie H, et al. The significance of secreted phosphoprotein 1 in multiple human cancers. *Front Mol Biosci*. (2020) 7:565383. doi: 10.3389/fmolb.2020.565383
44. Maleš J, Mihalj H, Šestak A, Kralik K, Smolić M. osteopontin levels in patients with squamous metastatic head and neck cancer. *Medicina*. (2021) 57:185. doi: 10.3390/medicina57020185
45. Ji X, Liu Y, Mei F, Li X, Zhang M, Yao B, et al. SPP1 overexpression is associated with poor outcomes in ALK fusion lung cancer patients without receiving targeted therapy. *Sci Rep*. (2021) 11:14031. doi: 10.1038/s41598-021-93484-2
46. Deng H, Zhen H, Fu Z, Huang X, Zhou H, Liu L. The antagonistic effect between STAT1 and Survivin and its clinical significance in gastric cancer. *Oncol Lett*. (2012) 3:193–9. doi: 10.3892/ol.2011.423
47. Masoumi J, Jafarzadeh A, Khorramdelazad H, Abbasloui M, Abdolalizadeh J, Jamali N. Role of Apelin/APJ axis in cancer development and progression. *Adv Med Sci*. (2020) 65:202–13. doi: 10.1016/j.advms.2020.02.002

Conflict of Interest: The authors declare that the research was conducted in the absence of any commercial or financial relationships that could be construed as a potential conflict of interest.

Publisher's Note: All claims expressed in this article are solely those of the authors and do not necessarily represent those of their affiliated organizations, or those of the publisher, the editors and the reviewers. Any product that may be evaluated in this article, or claim that may be made by its manufacturer, is not guaranteed or endorsed by the publisher.

Copyright © 2022 Li, Cao, Huang, Zhu, Chen, Zhang, Cao and Chen. This is an open-access article distributed under the terms of the Creative Commons Attribution License (CC BY). The use, distribution or reproduction in other forums is permitted, provided the original author(s) and the copyright owner(s) are credited and that the original publication in this journal is cited, in accordance with accepted academic practice. No use, distribution or reproduction is permitted which does not comply with these terms.

frontiers in Medicine

ORIGINAL RESEARCH
published: 14 February 2022
doi: 10.3389/fmed.2022.837876

The Importance of Being "That" Colorectal pT1: A Combined Clinico-Pathological Predictive Score to Improve Nodal Risk Stratification

Alessandro Gambella[1†], *Enrico Costantino Falco*[1†], *Giacomo Benazzo*[1], *Simona Osella-Abate*[2], *Rebecca Senetta*[3], *Isabella Castellano*[1], *Luca Bertero*[1*] and *Paola Cassoni*[1]

[1] Pathology Unit, Department of Medical Sciences, University of Turin, Turin, Italy, [2] Molecular Pathology Unit, "Città della Salute e della Scienza di Torino" University Hospital, Turin, Italy, [3] Pathology Unit, Department of Oncology, University of Turin, Turin, Italy

OPEN ACCESS

Edited by:
Qi Liu,
Fudan University, China

Reviewed by:
Valeria Barresi,
University of Verona, Italy
Antonio Ieni,
University of Messina, Italy

***Correspondence:**
Luca Bertero
luca.bertero@unito.it

[†] These authors have contributed equally to this work and share first authorship

Specialty section:
This article was submitted to Gastroenterology, a section of the journal Frontiers in Medicine

Received: 17 December 2021
Accepted: 14 January 2022
Published: 14 February 2022

Citation:
Gambella A, Falco EC, Benazzo G, Osella-Abate S, Senetta R, Castellano I, Bertero L and Cassoni P (2022) The Importance of Being "That" Colorectal pT1: A Combined Clinico-Pathological Predictive Score to Improve Nodal Risk Stratification. Front. Med. 9:837876. doi: 10.3389/fmed.2022.837876

The management of endoscopically resected pT1 colorectal cancer (CRC) relies on nodal metastasis risk estimation based on the assessment of specific histopathological features. Avoiding the overtreatment of metastasis-free patients represents a crucial unmet clinical need. By analyzing a consecutive series of 207 pT1 CRCs treated with colectomy and lymphadenectomy, this study aimed to develop a novel clinicopathological score to improve pT1 CRC metastasis prediction. First, we established the clinicopathological profile of metastatic cases: lymphovascular invasion (OR: 23.8; CI: 5.12–110.9) and high-grade tumor budding (OR: 5.21; CI: 1.60–16.8) correlated with an increased risk of nodal metastasis, while age at diagnosis >65 years (OR: 0.26; CI: 0.09–0.71) and high tumor-infiltrating lymphocytes (OR: 0.19; CI: 0.06–0.59) showed a protective effect. Combining these features, we built a five-tier risk score that, applied to our series, identified cases with a higher risk (score $\geq$ 2) of nodal metastasis (OR: 7.7; CI: 2.4–24.4). Notably, a score of 0 was only assigned to cases with no metastases (13/13 cases) and all the score 4 samples (2/2 cases) showed nodal metastases. In conclusion, we developed an effectively combined score to assess pT1 CRC nodal metastasis risk. We believe that its adoption within a multidisciplinary pT1 unit could improve patients' clinical management and limit surgical overtreatment.

Keywords: colorectal carcinoma, pT1, lymph node metastasis, predictive score, age at diagnosis, tumor budding, lymphovascular invasion, tumor-infiltrating lymphocytes

INTRODUCTION

Screening programs improved the early detection of colorectal cancers (CRCs) (1–5) but raised a new clinical issue: the management of endoscopically resected pT1 colorectal tumors (pT1 CRC).

According to the Tumor Node Metastasis (TNM) classification of malignant tumors, pT1 CRC is defined by the presence of submucosal invasion and represents the earliest stage with metastatic potential (6). Specifically, nodal metastasis in this setting has been reported in up to 15% of pT1 CRC cases (7, 8).

Following pT1 CRC endoscopic resection, two different approaches can be undertaken: either conservative endoscopic follow-up (9, 10) or surgical resection enabling nodal status assessment (11–13). This choice is guided by the risk of node metastasis which is estimated according to specific histopathological parameters which stratify these tumors in low- and high-risk pT1 CRC (14, 15). The ultimate clinical aim is to balance staging/therapeutic benefits with surgical risks and consequences (16, 17).

Regarding the analyzed histopathological features, tumor budding, lymphovascular invasion, tumor grading, and micro staging repeatedly resulted to be significantly associated with nodal involvement: currently, in the presence of even one of these morphological features, surgical resection is proposed, thus favoring lymph node metastases identification but also increasing the percentages of cases submitted to surgery with no lymph node involvement (7, 18).

Based on this observation, a significant subgroup of patients is overtreated (19, 20). In these cases, colectomy with lymphadenectomy is stadiative rather than curative, and it exposes patients to surgery-related morbidity and mortality risks that could be avoided through improved patient selection. Improvement of the risk estimation of nodal metastasis in this setting is an unmet clinical need and would help avoid these risks. In particular, it has to be considered that most of the patients without evidence of node metastasis after surgery were surgically treated because of the presence of a single high-risk parameter, thus novel approaches should focus on developing combined multiparametric scores (7, 8, 18, 21).

Fostered by this state of the art, this study aims to improve pT1 CRC risk stratification by proposing a novel and effective clinicopathological predictor score of nodal metastases, established through the analysis of a comprehensive range of clinical and histopathological features in a large consecutive series of pT1 CRC, surgically treated at a tertiary referral institution.

MATERIALS AND METHODS

Dataset Construction

This is a retrospective study based on a consecutive series of surgically resected pT1 CRC samples (colectomy plus lymphadenectomy) collected from the pathology archives of the "Città della Salute e della Scienza" University Hospital in Turin and diagnosed from January 2010 to March 2019. Demographic, clinical, and histopathological data were extracted from the diagnostic reports, and then pseudo-anonymized by a Unit member not involved in the study. Cases receiving neoadjuvant treatment (*i.e.,* chemoradiotherapy) or lacking material for histological revision were excluded. A final series of 207 samples were collected.

Our study was based on the assessment of hematoxylin-eosin (H&E) slides only as per routine practice at our institution. Original H&E slides were retrieved and then independently reviewed by three pathologists (AG, LB, and PC). Disagreements were discussed and jointly resolved by consensus. Histopathological features were assessed and scored according to published studies and international guidelines (**Figure 1**).

In particular, a tumor "bud" was defined as a cluster of less than five cells located at the invasive front of the tumor (22–24). Based on the clusters quantity, tumor budding was further stratified into a low (less than five clusters per hotspot in a field measuring 0.785 mm^2) and high grade (equal or more than five clusters per hotspot in a field measuring 0.785 mm^2) according to a binary system as reported in the literature (8, 22, 25, 26).

Lymphovascular invasion was reported whether tumor cells were identified within endothelial-outlined peritumoral stromal vessels (24). Tumor differentiation grade was attributed according to the least differentiated tumoral component (24). The depth and width of submucosal invasion were assessed and analyzed using 1 and 4 mm cutoff values, respectively (27–29).

Regarding the tumor-infiltrating lymphocytes (TILs) assessment, standardized international definition criteria are currently lacking, particularly in the pT1 CRC setting. Therefore, we graded TILs with a semi-quantitative three-tier approach, evaluating the quantity and location of lymphocytes. In particular, we considered only TILs outlining tumor cells at the invasive tumor front, whereas TILs/lymphocytes interspersed within the tumor bulk and/or located in superficial tumor layers were neglected to avoid potential confounders related to luminal/mechanic injury and tumor superficial erosion/necrosis. Then, cases with no peritumoral lymphocytes were reported as "absent TILs," whereas "high TILs" were cases with lymphocytes continuously outlining tumor cells at the tumor invasive front and extending in the Surrounding stroma. "Mild TILs" referred to all the cases with intermediate features (interrupted outlining and/or infiltrate limited to tumor cells surrounding area) (**Figure 2**).

The clinical and histopathological features evaluated in this study are reported in **Table 1**, whereas the overall study design is represented in **Figure 3**.

Statistical Analysis

Statistical analyses were performed with the Stata 15.0 statistical software (StataCorp, College Station, TX, USA.), applying proper tests for categorical (Pearson's Chi-squared -χ2- test) and numerical variables (T Student's test, Wilcoxon signed-rank test). Bonferroni correction was performed for multiple groups correlations. Univariate binary logistic regression analyses were performed to assess the correlation between the lymph node metastatic status and other variables, calculating relative Odds Ratio (OR) and 95% CI. Statistical analyses were considered significant according to the standard p-value < 0.05.

RESULTS

Clinical and Histopathological Features

Our population presented a median age of 70 years (interval: 37–90) and was mainly composed of female patients (114 cases; 55.1%). Most of the collected lesions were non-pedunculated polyps (177 cases; 85.5%), sited in the sigmoid-rectal tract (113 cases; 54.6%), and 46 specifically located in the rectum (22.2%), without synchronous polyps elsewhere (165 cases; 79.7%). Most

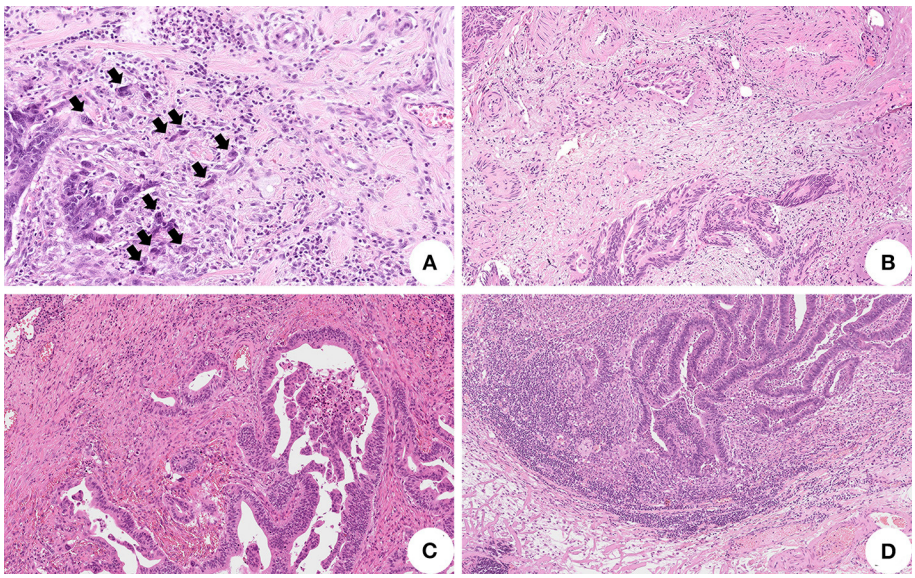

FIGURE 1 | Histopathological features associated with lymph node metastasis in pT1 colorectal cancer (CRC). **(A)** High-grade tumor budding represented by equal or more than five clusters of less than five tumor cells at the invasive front of the tumor (black arrows) (original magnification: 200X); **(B)** Tumor cells invasion of peritumoral stromal vessels representing lymphovascular invasion (original magnification: 100X); **(C)** Absent/mild tumor-infiltrating lymphocytes surrounding tumor cells (original magnification: 100X); **(D)** High tumor-infiltrating lymphocytes facing the invasive tumor front (original magnification: 100X).

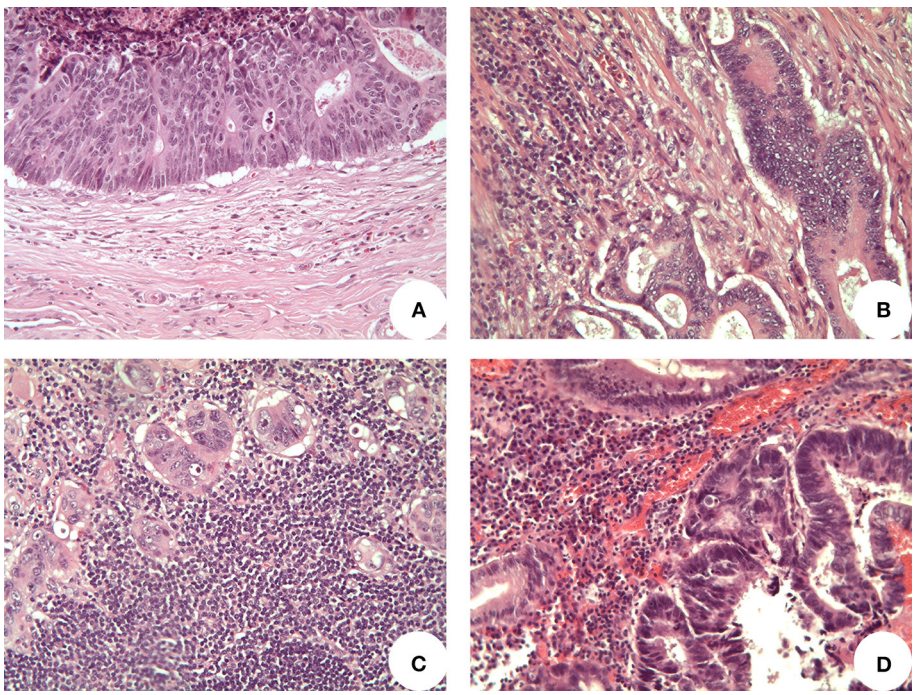

FIGURE 2 | Representative images of tumor infiltrating lymphocytes (TILs) (original magnification 200x). **(A)** "Absent TILs" cases presented no lymphocytes at the invasive front of tumor; **(B)** "mild TILs" cases showed scattering lymphocytes partially surrounding tumor cells; **(C)** "high TILs" cases presented several lymphocytes continuously outlining tumor cells at the invasive tumor front and extending in the surrounding stroma; **(D)** lymphocytes located in superficial tumor layers were not considered, as well as lymphocytes within the tumor bulk.

cases presented an infiltrative growth pattern (134 cases; 64.7%) and were graded as moderately differentiated (G2) (169 cases; 81.6%), while mucinous features were frequently absent (173 cases; 83.6%). TILs were mild in most cases (165 cases; 79.7%), while high-grade tumor budding and lymphovascular invasion were observed in a minority (8.7 and 3.9%, respectively) of cases.

TABLE 1 | Clinical and histopathological variables evaluated in our study.

Characteristic		Total ($n = 207$)	Percentage (%)
Gender	Male	93	44.9
	Female	114	55.1
Age	Median (interval)	70 (37–90)	–
Age	<65	66	31.9
	≥65	141	68.1
Morphology	Non pedunculated	177	85.5
	Pedunculated	30	14.5
Site	Cecum-Right	69	33.3
	Transverse	14	6.8
	Left	11	5.3
	Sigmoid-rectum	113	54.6
	Sigmoid	67	32.4
	Rectum	46	22.2
Simultaneous polyps	Absent	165	79.7
	Present	42	20.3
Grade	Well differentiated (G1)	31	15.0
	Moderately differentiated (G2)	169	81.6
	Poorly differentiated (G3)	7	3.4
Mucinous feature	Absent	173	83.6
	Present	34	16.4
Lymphovascular	Absent	199	96.1
invasion	Present	8	3.9
TILs	Absent	24	11.6
	Mild	165	79.7
	High	18	8.7
Tumor budding	Low-grade	189	91.3
	High-grade	18	8.7
Sampled lymph nodes	<12	88	42.5
	≥12	119	57.5
Lymph nodes	Absent	189	91.3
metastasis	Present	18	8.7
Growth pattern	Expansive	73	35.3
	Infiltrative	134	64.7
Depth of invasion	<1 mm	22	10.6
	≥1 mm	185	89.4
Width of invasion	<4 mm	44	21.3
	≥4 mm	163	78.7

With regards to the Ueno's method for pT1 micro-staging (28), most of the lesions presented a depth of invasion ≥ 1 mm (185 cases; 89.4%) and a width of invasion ≥ 4 mm (163 cases; 78.7%). All clinical and histopathological data are reported in **Table 1**.

Lymph Node Metastasis: Defining "That" pT1 Profile

We analyzed the association between all the assessed variables and lymph node involvement to build our predictive risk score.

We registered 18 cases with lymph node metastasis (8.7%). In this population, we observed that nodal involvement was correlated with younger age (cut-off: 65 years) ($p = 0.005$), presence of lymphovascular invasion ($p < 0.001$), absent/mild TILs ($p = 0.006$), and high-grade tumor budding ($p = 0.003$) (**Table 2**).

The univariate logistic regression confirmed these data, revealing that lymphovascular invasion (OR: 23.8; CI: 5.12–110.9) and high-grade tumor budding (OR: 5.21; CI: 1.60–16.8) were significantly associated with an increased risk of nodal metastasis, while age at diagnosis >65 years (OR: 0.26; CI: 0.09–0.71) and high TILs (OR: 0.19; CI: 0.06–0.59) showed a protective effect (**Table 3**).

Fostered by the increasing evidence supporting both tumor budding relevance in pT1 CRC risk assessment and its relationship with lymphovascular invasion, we decided to stratify our population according to this parameter to verify its significance in our series. We compared samples with low-grade (189 cases; 91.3%) and high-grade (18 cases; 8.7%) tumor budding observing that high-grade tumor budding strongly correlated with lymph node metastasis ($p = 0.003$) and with lymphovascular invasion ($p < 0.001$), as well. In addition, the univariate logistic regression confirmed that lymphovascular invasion (OR: 13.21; CI: 2.98–58.55) was significantly correlated with high-grade tumor budding.

Finally, we also analyzed the role of tumor grade, another variable routinely used to predict lymph nodes metastasis (7), but we did not identify any correlation with lymph node metastasis ($p = 0.456$).

Since our consecutive series included also 88 cases with <12 sampled lymph nodes and considering the higher risk of recurrence and understanding associated with this sampling, we decided to perform the same analysis excluding non-metastatic cases (N0) with <12 lymph nodes (n = 79) and performed our analysis in the resulting series [thus composed of metastatic cases (N+) and non-metastatic cases (N0) with > 12 lymph nodes (n = 128)]. In this subgroup, we observed the same significant correlations between nodal involvement and clinical-pathologic variables [younger age ($p = 0.006$), presence of lymphovascular invasion ($p < 0.001$), absent/mild TILs ($p = 0.006$), and high-grade tumor budding ($p = 0.008$)], confirmed by univariate logistic regression [lymphovascular invasion (OR: 20.7; CI: 3.65–118.1) and high-grade tumor budding (OR: 4.90; CI: 1.39–17.2) associated with an increased risk of nodal metastasis; age at diagnosis >65 years (OR: 0.24; CI: 0.09–0.70) and high TILs (OR: 0.16; CI: 0.05–0.49) associated with a protective effect].

Prediction of Lymph Node Metastasis: Assembling the Combined Score

Based on these results, we combined the features significantly related to lymph node metastasis (i.e., age at diagnosis, tumor budding, lymphovascular invasion, and TILs) to build our clinico-histopathological metastatic risk score.

We conferred at one point that any of the following features were present: age at diagnosis <65-year, high-grade tumor budding, presence of lymphovascular invasion, and absent/mild

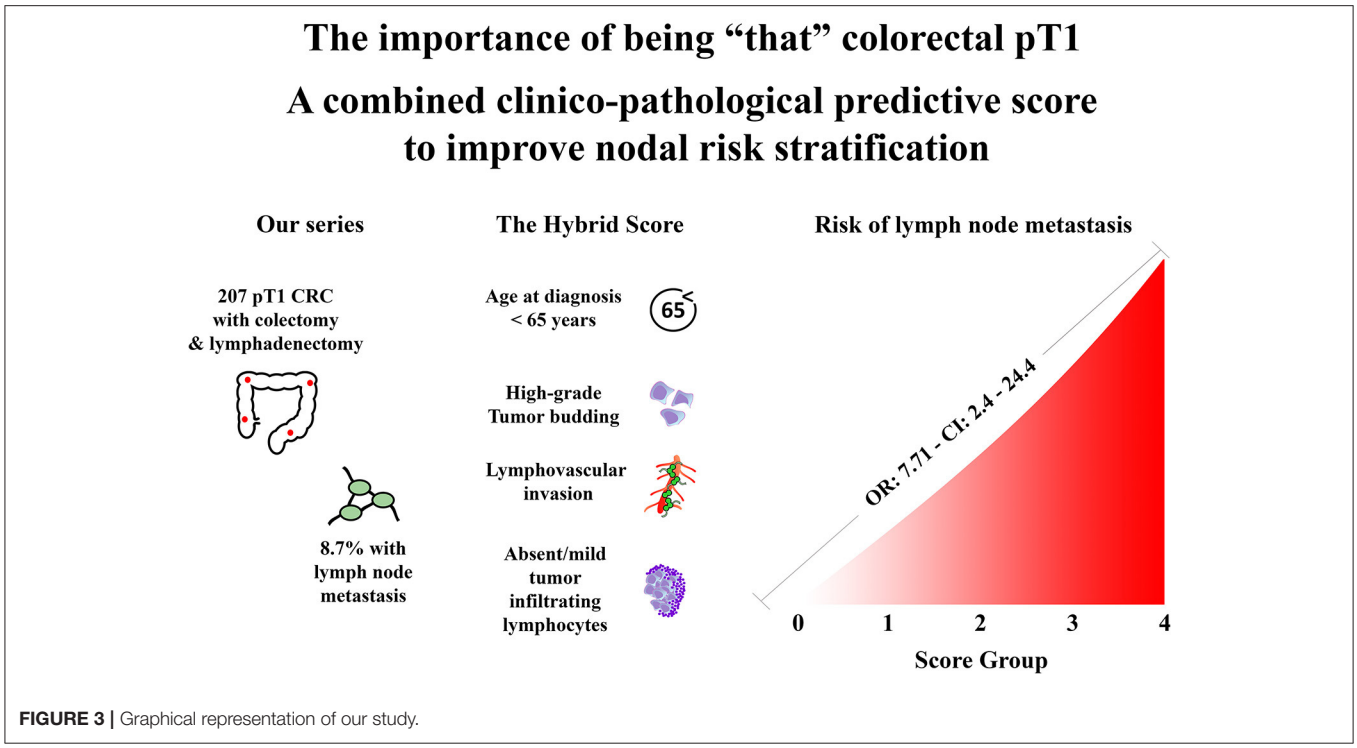

FIGURE 3 | Graphical representation of our study.

TILs. Therefore, the score would define five possible subgroups ranging from Score 0 (no variables) to Score 4 (all variables simultaneously present).

Applying the score to the whole population, scores 1 and 2 were the most represented groups (121 cases and 63 cases, respectively). Nodal metastasis significantly correlated with our score stratification ($p < 0.001$) and, of note, no metastatic cases were observed in the score 0 groups (n = 13), whereas all score 4 cases (n = 2) presented lymph node metastasis (**Table 4**).

In addition, the correlation ($p < 0.001$) was maintained even when comparing cases with a score ≥2 and cases with a score of 0 or 1 (**Table 5**).

Univariate logistic regression also confirmed the correlation between these two clusters: score ≥2 cases presented a significantly higher risk of nodal metastasis compared to score 0 and 1 cases (OR: 7.71; CI: 2.4–24.4) (**Table 6**).

These analyses were also performed in the previously described subgroup [N+ and N0 with >12 lymph nodes (n = 128)], showing similar outcomes either considering the scoring groups separately (**Table 7**) or clustered in score 0/1 vs. score ≥2 (**Table 7**), the latter confirmed by univariate logistic regression (**Table 8**).

DISCUSSION

This study aimed to enhance the clinical management of endoscopically resected pT1 CRC by identifying and combining metastasis-correlated clinicopathological features in a predictive score of nodal metastasis.

Our series of retrospective consecutive pT1 CRC presented a percentage of nodal metastasis (8,7%) in agreement with the literature range of 4.9–16.9% (7, 8, 19, 21). This data shows that, to date, a large number of cases are potentially overtreated and exposed to significant surgical-related risks without certain benefits except for achieving definitive pathological tumor staging.

Until now, the prediction of CRC pT1 nodal status has been based on histopathological features alone assessed on endoscopically-resected specimens. According to the current international guidelines, the presence of even one single histopathological parameter among poorly differentiated tumors (G3), high-grade tumor budding, lymphovascular invasion, and submucosal invasion ≥1 mm depth or ≥ 4 mm width is routinely used to assign a high risk of node metastasis, aiming for identifying any potential metastatic case but leading to the surgical overtreatment of patients with no metastatic disease (11, 13, 28–33). Of note, these features proved to correlate with node metastasis although a somewhat disappointing interobserver agreement (34, 35). In our study, we confirmed lymphovascular invasion and high-grade tumor budding, and additionally identified absent/mild TILs and younger age (cut-off: 65 years) as relevant features related to nodal involvement and, therefore, we combined them to build our risk score.

Among these, tumor budding and lymphovascular invasion have been thoroughly studied and their association with nodal metastasis is well recognized (8, 18, 33, 36). Recent evidence also suggested that these features are intertwined and could represent two sides of the same coin, ultimately leading to lymph node metastasis (21) since cells composing the tumor "buds" were

TABLE 2 | Distribution of clinical data and pathological features based on lymph nodes metastasis.

			Lymph node metastasis		
		Total ($n = 207$)	**No** ($n = 189$)	**Yes** ($n = 18$)	***p*-value**
Gender	Male	93	106	8	0.343
	Female	114	83	10	
Age	Median (interval)	70 (37–90)	70 (43–90)	62 (37–85)	0.025
Age	<65	66	55	11	0.005
	≥65	141	134	7	
Morphology	Non pedunculated	177	164	13	0.094
	Pedunculated	30	25	5	
Site	Cecum-Right	69	63	6	0.997
	Transverse	14	13	1	
	Left	11	10	1	
	Sigmoid-rectum	113	103	10	
Simultaneous polyps	Absent	165	150	15	0.689
	Present	42	39	3	
Mucinous feature	Absent	34	31	3	0.635
	Present	173	158	15	
Lymphovascularinvasion	Absent	199	186	13	< 0.001
	Present	8	3	5	
TILs	Absent	24	18	6	0.006
	Mild	165	153	12	
	High	18	18	0	
Tumor budding	Low-grade	189	176	13	0.003
	High-grade	18	13	5	
Sampled lymphnodes	<12	88	79	9	0.236
	≥12	119	110	9	
Growth pattern	Expansive	73	70	3	0.084
	Infiltrative	134	119	15	
Depth of invasion	<1 mm	22	20	2	0.945
	≥1 mm	185	169	16	
Width of invasion	<4 mm	44	42	2	0.271
	≥4 mm	163	147	16	

TABLE 3 | Univariate logistic regression analysis between clinico-pathological variables and lymph nodes metastasis.

	OR	**CI**	***p*-value**
Gender (Male vs. Female)	1.59	0.60–4.22	0.346
Age (linear)	0.93	0.88–0.97	0.003
Age (>65-year-old)	0.26	0.09–0.71	0.008
Lymphovascular invasion	23.8	5.12–110.9	< 0.001
High-grade tumor budding	5.21	1.60–16.8	0.006
High TILs	0.19	0.06–0.59	0.004
Pedunculated morphology	2.52	0.82–7.68	0.103
Grading	2.28	0.63–8.29	0.210
Sampled lymph nodes >12	0.72	0.27–1.89	0.503
Sigmoid-rectum site	1.04	0.39–2.76	0.931

TABLE 4 | Correlation analysis between the score group and presence of lymph node metastasis.

Score group	**Lymph node metastasis**		***p*-value**
	No	**Yes**	
0	13	0	<0.001
1	117	4	
2	54	9	
3	5	3	
4	0	2	

found to be also responsible for the invasion of nearby stromal lymphovascular vessels. These cells exhibited epithelial and mesenchymal markers suggesting the activation of the epithelial-mesenchymal transition process, an aggressive tumor phenotype associated with poor survival and resistance to therapy (37–41). Our data support their strong reciprocal intertwining and their influence on lymph nodes metastasis development.

TABLE 5 | Correlation analysis clustering cases with score <2 vs. score ≥2.

Score group	Lymph node metastasis		*p*-value
	No	Yes	
0–1	130	4	<0.001
2–4	59	14	

TABLE 6 | Univariate logistic regression evaluating our score outcomes predicting lymph node metastasis.

		OR	CI	*p*-value
Score group (clustered score)	Score 2–4 vs. score 0–1	7.71	2.4–24.4	0.001

TABLE 7 | Correlation analysis between the score groups and presence of lymph nodes metastasis in the N+ plus N0 with >12 lymph nodes subgroup.

Score group	Lymph node metastasis		*p*-value
	No	Yes	
0	7	0	<0.001
1	71	4	
2	29	9	
3	3	3	
4	0	2	
0–1	78	4	<0.001
2–4	32	14	

TABLE 8 | Univariate logistic regression evaluating the association between the score groups and lymph node metastasis in the N+ plus N0 with >12 lymph nodes cases.

		OR	CI	*p*-value
Score group (clustered score)	Score 2–4 vs. score 0–1	8,2	2.5–26.7	0.001

Our results also demonstrate that TILs are significantly correlated with the risk of harboring a nodal metastasis, a finding in agreement with the established role of the immune system in influencing CRC growth and survival (42–45). However, it should be noted that so far, studies evaluating the role of TILs in CRC mainly focused on advanced disease settings. The few reports addressing pT1 CRC provided conflicting results. (43, 44, 46–48). A univariate analysis of 102 endoscopically resected pT1 CRCs reported an increased number of CD3 positive TILs in the metastatic group, but this finding was not confirmed by multivariate analysis (21). No correlations were observed analyzing the CD8 positive TILs (21). Differently, a recent study by Kang et al. analyzed the distribution and mean numbers of CD3, CD8, and FOXP3 positive lymphocytes in pT1 CRC and identified a significant association between lymph node metastasis and a lower number of CD8 positive lymphocytes located within the tumor core (49). In the present study, we demonstrated a correlation between absent/mild TILs and a higher risk of nodal involvement. This association seems to be particularly relevant since none of our cases with high TILs presented nodal metastasis, while the four score 1 cases presenting nodal metastasis received this score exactly due to the presence of absent/mild TILs. We believe that TILs could become a significant histopathological feature of pT1 CRC, representing a morphological counterpart of tumor immunobiology and immune system activation against tumor growth. In this regard, our results support the relevance of this parameter in shaping tumor invasiveness even at early disease stages, but further studies should specifically investigate TILs in early CRC to confirm their predictive significance in terms of nodal metastasis and provide additional insights on their mechanistic role and develop specific guidelines regarding their assessment.

Lastly, the predictive significance of age at diagnosis is of particular interest since it shows the importance of clinical variables even in this early oncological setting. Moreover, whereas the assessment of histopathological features alone can be hampered by inter-observer variability (50), age at diagnosis is not. Younger age is also known to be related to more aggressive CRC lesions (51–54).

We did not confirm micro staging (≥1 mm depth and ≥4 mm width of invasion) nor tumor grading as potential risk factors of nodal involvement. Similar evidence has been recently reported in the literature: in particular, micro staging reliability in pT1 CRC has been questioned for the significant influence of technical processing and lesion morphology on its interpretation; similarly, the importance of tumor grading as a predictive marker has been found to be overall limited compared with other morphological features (55–59).

In the practical daily routine, some pT1 CRC cases, although close to the recommended cut-off, did not meet the required number of harvested lymph nodes. Indeed, this is a limitation that actually occurs, potentially impacting the pT1 CRC staging (60, 61). Aiming to develop a score that can be applied in a "real-world" pT1 CRC series, we preferred to also maintain these cases and test our score in both scenarios, thus considering either all cases (including the ones with <12 lymph nodes) or the subgroup of N+ and N0 >12 only cases. Indeed, our score maintains the same level of statistic and clinical significance, further confirming its practical relevance.

We acknowledge that our study presents some potential limitations, including its retrospective nature and the limited, although considerable, sample size. Moreover, future studies should investigate the efficacy of the here proposed approach on endoscopic resection samples.

Ultimately, our score improves the overall identification of patients who would benefit from a surgical approach following endoscopically resected pT1 CRC compared to the evidence reported so far in the literature (62–64). It should also be noted that balancing the risks due to over-and undertreatment is extremely challenging when dealing with an early tumor stage. Identifying subgroups of patients, no matter how small, with very low or very high metastatic risks is particularly important since it allows to confidently propose a therapeutic option to these patients. Our score enabled this result since no score 0 patient

showed nodal metastasis, while all score 4 had metastatic disease. Although the sample sizes of these groups were particularly limited, these promising results warrant further validation. Among patients with intermediate-risk scores (score 1–3), we observed a progressive increase of nodal metastasis (score 1: 3.4%, score 2: 16.7%, score 3: 60.0%), a piece of information that would not have been available by employing the conventional dichotomized approach. This stratified risk assessment could help tailor patients' management by multidisciplinary boards.

In conclusion, despite some limitations, including the retrospective and single-institutional nature, our study allowed us to develop a novel multiparametric score combining evidence-based histopathological features with age at diagnosis as a clinical variable. Our score represents an effective system to estimate the lymph node metastasis risk, superior to the current single parameter-based risk assessment. Further multi-centric and ideally prospective studies are recommended to confirm our findings and enable the adoption of the proposed score within multidisciplinary CRC tumor boards to guide patients' management.

DATA AVAILABILITY STATEMENT

The raw data supporting the conclusions of this article will be made available by the authors, without undue reservation.

ETHICS STATEMENT

The studies involving human participants were reviewed and approved by the Institutional Review Board (or Ethics Committee) of the University of Turin (approval number: DSM-ChBU n° 03/2020, approved in October 2020). Written informed consent for participation was not required for this study in accordance with the national legislation and the institutional requirements.

AUTHOR CONTRIBUTIONS

LB and PC: conceptualization and funding acquisition. AG, EF, GB, SO-A, RS, IC, LB, and PC: methodology and writing—review and editing. AG, EF, GB, SO-A, and LB: formal analysis. AG and EF: writing—original draft preparation. All authors contributed to the article and approved the submitted version.

FUNDING

This research was funded by the Rete Oncologica del Piemonte e della Valle d'Aosta (Oncology Network of Piedmont and Aosta Valley-Italy; Grant to LB and PC, no specific grant number available).

REFERENCES

1. Collaborators GBDCC. The global, regional, and national burden of colorectal cancer and its attributable risk factors in 195 countries and territories, 1990–2017: a systematic analysis for the Global Burden of Disease Study 2017. *Lancet Gastroenterol Hepatol.* (2019) 4:913–33. doi: 10.1016/S2468-1253(19)30345-0
2. Amri R, Bordeianou LG, Sylla P, Berger DL. Impact of screening colonoscopy on outcomes in colon cancer surgery. *JAMA Surg.* (2013) 148:747–54. doi: 10.1001/jamasurg.2013.8
3. Gupta N, Kupfer SS, Davis AM. Colorectal cancer screening. *JAMA.* (2019) 321:2022–3. doi: 10.1001/jama.2019.4842
4. Kahi CJ, Imperiale TF, Juliar BE, Rex DK. Effect of screening colonoscopy on colorectal cancer incidence and mortality. *Clin Gastroenterol Hepatol.* (2009) 7:770–5. doi: 10.1016/j.cgh.2008.12.030
5. Kahi CJ, Anderson JC, Rex DK. Screening and surveillance for colorectal cancer: state of the art. *Gastrointest Endosc.* (2013) 77:335–50. doi: 10.1016/j.gie.2013.01.002
6. Brierley JG, M.; Wittekind, C. *TNM classification of malignant tumors*. Eighth ed: John Wiley & Sons, Ltd. (2017).
7. Bosch SL, Teerenstra S, de Wilt JH, Cunningham C, Nagtegaal ID. Predicting lymph node metastasis in pT1 colorectal cancer: a systematic review of risk factors providing rationale for therapy decisions. *Endoscopy.* (2013) 45:827–34. doi: 10.1055/s-0033-1344238
8. Cappellesso R, Luchini C, Veronese N, Lo Mele M, Rosa-Rizzotto E, Guido E, et al. Tumor budding as a risk factor for nodal metastasis in pT1 colorectal cancers: a meta-analysis. *Hum Pathol.* (2017) 65:62–70. doi: 10.1016/j.humpath.2017.04.013
9. Bianco F, Arezzo A, Agresta F, Coco C, Faletti R, Krivocapic Z, et al. Practice parameters for early colon cancer management: Italian society of colorectal surgery (societa Italiana di chirurgia colo-rettale; SICCR) guidelines. *Tech Coloproctol.* (2015) 19:577–85. doi: 10.1007/s10151-015-1361-y
10. Kim JB, Lee HS, Lee HJ, Kim J, Yang DH, Yu CS, et al. Long-term outcomes of endoscopic vs. surgical resection of superficial submucosal colorectal cancer. *Dig Dis Sci.* (2015) 60:2785–92. doi: 10.1007/s10620-015-3530-2
11. Steele RJ, Pox C, Kuipers EJ, Minoli G, Lambert R, International Agency for Research on C. European guidelines for quality assurance in colorectal cancer screening and diagnosis. *Endoscopy.* (2012) 44:SE140–50. doi: 10.1055/s-0032-1309802
12. Quirke P, Risio M, Lambert R, von Karsa L, Vieth M, International Agency for Research on C. European guidelines for quality assurance in colorectal cancer screening and diagnosis. *Endoscopy.* (2012) 44:SE116–30. doi: 10.1055/s-0032-1309797
13. Labianca R, Nordlinger B, Beretta GD, Mosconi S, Mandala M, Cervantes A, et al. Early colon cancer: ESMO Clinical Practice Guidelines for diagnosis, treatment and follow-up. *Ann Oncol.* (2013) 24:vi64-72. doi: 10.1093/annonc/mdt354
14. Hassan C, Wysocki PT, Fuccio L, Seufferlein T, Dinis-Ribeiro M, Brandao C, et al. Endoscopic surveillance after surgical or endoscopic resection for colorectal cancer: European Society of Gastrointestinal Endoscopy (ESGE) and European Society of Digestive Oncology (ESDO) Guideline. *Endoscopy.* (2019) 51:266–77. doi: 10.1055/a-0831-2522
15. Hassan C, Antonelli G, Dumonceau JM, Regula J, Bretthauer M, Chaussade S, et al. Post-polypectomy colonoscopy surveillance: European Society of Gastrointestinal Endoscopy (ESGE) Guideline - Update 2020. *Endoscopy.* (2020) 52:687–700. doi: 10.1055/a-1185-3109
16. Ikematsu H, Yoda Y, Matsuda T, Yamaguchi Y, Hotta K, Kobayashi N, et al. Long-term outcomes after resection for submucosal invasive colorectal cancers. *Gastroenterology.* (2013) 144:551–9. doi: 10.1053/j.gastro.2012.12.003
17. Hohenberger W, Weber K, Matzel K, Papadopoulos T, Merkel S. Standardized surgery for colonic cancer: complete mesocolic excision and central ligation–technical notes and outcome. *Colorectal Dis.* (2009) 11:354–64; discussion 64–5. doi: 10.1111/j.1463-1318.2008.01735.x
18. Zhang Q, Wang L, Huang D, Xu M, Weng W, Ni S, et al. Pathological risk factors for lymph node metastasis in patients with submucosal invasive colorectal carcinoma. *Cancer Manag Res.* (2019) 11:1107–14. doi: 10.2147/CMAR.S181740
19. Senore C, Giovo I, Ribaldone DG, Ciancio A, Cassoni P, Arrigoni A, et al. Management of Pt1 tumors removed by endoscopy during colorectal cancer

screening: outcome and treatment quality indicators. *Eur J Surg Oncol.* (2018) 44:1873–9. doi: 10.1016/j.ejso.2018.09.009
20. Backes Y, Elias SG, Groen JN, Schwartz MP, Wolfhagen FHJ, Geesing JMJ, et al. Histologic factors associated with need for surgery in patients with pedunculated T1 colorectal carcinomas. *Gastroenterology.* (2018) 154:1647–59. doi: 10.1053/j.gastro.2018.01.023
21. Cappellesso R, Nicole L, Zanco F, Lo Mele M, Fassina A, Ventura L, et al. Synchronous nodal metastatic risk in screening detected and endoscopically removed pT1 colorectal cancers. *Pathol Res Pract.* (2020) 216:152966. doi: 10.1016/j.prp.2020.152966
22. Ueno H, Murphy J, Jass JR, Mochizuki H, Talbot IC. Tumor 'budding' as an index to estimate the potential of aggressiveness in rectal cancer. *Histopathology.* (2002) 40:127–32. doi: 10.1046/j.1365-2559.2002.01324.x
23. Lugli A, Kirsch R, Ajioka Y, Bosman F, Cathomas G, Dawson H, et al. Recommendations for reporting tumor budding in colorectal cancer based on the international tumor budding consensus conference (ITBCC) 2016. *Mod Pathol.* (2017) 30:1299–311. doi: 10.1038/modpathol.2017.46
24. Nagtegaal ID, Odze RD, Klimstra D, Paradis V, Rugge M, Schirmacher P, et al. The 2019 WHO classification of tumors of the digestive system. *Histopathology.* (2020) 76:182–8. doi: 10.1111/his.13975
25. Ferlitsch M, Moss A, Hassan C, Bhandari P, Dumonceau JM, Paspatis G, et al. Colorectal polypectomy and endoscopic mucosal resection (EMR): European Society of Gastrointestinal Endoscopy (ESGE) Clinical Guideline. *Endoscopy.* (2017) 49:270–97. doi: 10.1055/s-0043-102569
26. Trinh A, Ladrach C, Dawson HE, Ten Hoorn S, Kuppen PJK, Reimers MS, et al. Tumor budding is associated with the mesenchymal colon cancer subtype and RAS/RAF mutations: a study of 1320 colorectal cancers with Consensus Molecular Subgroup (CMS) data. *Br J Cancer.* (2018) 119:1244–51. doi: 10.1038/s41416-018-0230-7
27. Wang LM, Guy R, Fryer E, Kartsonaki C, Gill P, Hughes C, et al. The Ueno method for substaging pT1 colorectal adenocarcinoma by depth and width measurement: an interobserver study. *Colorectal Dis.* (2015) 17:674–81. doi: 10.1111/codi.12910
28. Ueno H, Mochizuki H, Hashiguchi Y, Shimazaki H, Aida S, Hase K, et al. Risk factors for an adverse outcome in early invasive colorectal carcinoma. *Gastroenterology.* (2004) 127:385–94. doi: 10.1053/j.gastro.2004.04.022
29. Watanabe T, Itabashi M, Shimada Y, Tanaka S, Ito Y, Ajioka Y, et al. Japanese Society for cancer of the colon and rectum (JSCCR) guidelines 2010 for the treatment of colorectal cancer. *Int J Clin Oncol.* (2012) 17:1–29. doi: 10.1007/s10147-011-0315-2
30. Nascimbeni R, Burgart LJ, Nivatvongs S, Larson DR. Risk of lymph node metastasis in T1 carcinoma of the colon and rectum. *Dis Colon Rectum.* (2002) 45:200–6. doi: 10.1007/s10350-004-6147-7
31. Kitajima K, Fujimori T, Fujii S, Takeda J, Ohkura Y, Kawamata H, et al. Correlations between lymph node metastasis and depth of submucosal invasion in submucosal invasive colorectal carcinoma: a Japanese collaborative study. *J Gastroenterol.* (2004) 39:534–43. doi: 10.1007/s00535-004-1339-4
32. Kawachi H, Eishi Y, Ueno H, Nemoto T, Fujimori T, Iwashita A, et al. A three-tier classification system based on the depth of submucosal invasion and budding/sprouting can improve the treatment strategy for T1 colorectal cancer: a retrospective multicenter study. *Mod Pathol.* (2015) 28:872–9. doi: 10.1038/modpathol.2015.36
33. Graham RP, Vierkant RA, Tillmans LS, Wang AH, Laird PW, Weisenberger DJ, et al. Tumor budding in colorectal carcinoma: confirmation of prognostic significance and histologic cutoff in a population-based cohort. *Am J Surg Pathol.* (2015) 39:1340–6. doi: 10.1097/PAS.0000000000000504
34. Harris EI, Lewin DN, Wang HL, Lauwers GY, Srivastava A, Shyr Y, et al. Lymphovascular invasion in colorectal cancer: an interobserver variability study. *Am J Surg Pathol.* (2008) 32:1816–21. doi: 10.1097/PAS.0b013e3181816083
35. Hacking S, Angert M, Jin C, Kline M, Gupta N, Cho M, et al. Tumor budding in colorectal carcinoma: an institutional interobserver reliability and prognostic study of colorectal adenocarcinoma cases. *Ann Diagn Pathol.* (2019) 43:151420. doi: 10.1016/j.anndiagpath.2019.151420
36. Lee SJ, Kim A, Kim YK, Park WY, Kim HS, Jo HJ, et al. The significance of tumor budding in T1 colorectal carcinoma: the most reliable predictor of lymph node metastasis especially in endoscopically resected T1 colorectal carcinoma. *Hum Pathol.* (2018) 78:8–17. doi: 10.1016/j.humpath.2018.02.001
37. Meyer SN, Galvan JA, Zahnd S, Sokol L, Dawson H, Lugli A, et al. Co-expression of cytokeratin and vimentin in colorectal cancer highlights a subset of tumor buds and an atypical cancer-associated stroma. *Hum Pathol.* (2019) 87:18–27. doi: 10.1016/j.humpath.2019.02.002
38. Zlobec I, Berger MD, Lugli A. Tumor budding and its clinical implications in gastrointestinal cancers. *Br J Cancer.* (2020) 123:700–8. doi: 10.1038/s41416-020-0954-z
39. Grigore AD, Jolly MK, Jia D, Farach-Carson MC, Levine H. Tumor budding: the name is EMT. *Partial EMT. J Clin Med.* (2016) 5(5). doi: 10.3390/jcm5050051
40. Jager T, Neureiter D, Fallaha M, Schredl P, Kiesslich T, Urbas R, et al. The potential predictive value of tumor budding for neoadjuvant chemoradiotherapy response in locally advanced rectal cancer. *Strahlenther Onkol.* (2018) 194:991–1006. doi: 10.1007/s00066-018-1340-0
41. Miyata H, Yoshioka A, Yamasaki M, Nushijima Y, Takiguchi S, Fujiwara Y, et al. Tumor budding in tumor invasive front predicts prognosis and survival of patients with esophageal squamous cell carcinomas receiving neoadjuvant chemotherapy. *Cancer.* (2009) 115:3324–34. doi: 10.1002/cncr.24390
42. Galon J, Costes A, Sanchez-Cabo F, Kirilovsky A, Mlecnik B, Lagorce-Pages C, et al. Type, density, and location of immune cells within human colorectal tumors predict clinical outcome. *Science.* (2006) 313:1960–4. doi: 10.1126/science.1129139
43. Narayanan S, Kawaguchi T, Peng X, Qi Q, Liu S, Yan L, et al. Tumor infiltrating lymphocytes and macrophages improve survival in microsatellite unstable colorectal cancer. *Sci Rep.* (2019) 9:13455. doi: 10.1038/s41598-019-49878-4
44. Xiao B, Peng J, Wang Y, Deng Y, Ou Q, Wu X, et al. Prognostic value of tumor infiltrating lymphocytes combined with PD-L1 expression for patients with solitary colorectal cancer liver metastasis. *Ann Transl Med.* (2020) 8:1221. doi: 10.21037/atm-20-2762a
45. Liu S, Kong P, Wang X, Yang L, Jiang C, He W, et al. Tumor microenvironment classification based on T-cell infiltration and PD-L1 in patients with mismatch repair-proficient and -deficient colorectal cancer. *Oncol Lett.* (2019) 17:2335–43. doi: 10.3892/ol.2018.9826
46. Zhao Y, Ge X, He J, Cheng Y, Wang Z, Wang J, et al. The prognostic value of tumor-infiltrating lymphocytes in colorectal cancer differs by anatomical subsite: a systematic review and meta-analysis. *World J Surg Oncol.* (2019) 17:85. doi: 10.1186/s12957-019-1621-9
47. Bupathi M, Wu C. Biomarkers for immune therapy in colorectal cancer: mismatch-repair deficiency and others. *J Gastrointest Oncol.* (2016) 7:713–20. doi: 10.21037/jgo.2016.07.03
48. Baldin P, Van den Eynde M, Mlecnik B, Galon J. Immunity to live: an immunopathoscore using the consensus Immunoscore to best define the risk of recurrence and death in stage IV metastatic patients. *Oncoimmunology.* (2020) 9:1826133. doi: 10.1080/2162402X.2020.1826133
49. Kang J, Choi YJ, Kim IK, Lee HS, Kim H, Baik SH, et al. LASSO-based machine learning algorithm for prediction of lymph node metastasis in T1 colorectal cancer. *Cancer Res Treat.* (2021) 53:773–83. doi: 10.4143/crt.2020.974
50. Gijsbers K, de Graaf W, Moons LMG, Ter Borg F. High practice variation in risk stratification, baseline oncological staging, and follow-up strategies for T1 colorectal cancers in the Netherlands. *Endosc Int Open.* (2020) 8:E1117–E22. doi: 10.1055/a-1192-3545
51. Guo K, Feng Y, Yuan L, Wasan HS, Sun L, Shen M, et al. Risk factors and predictors of lymph nodes metastasis and distant metastasis in newly diagnosed T1 colorectal cancer. *Cancer Med.* (2020) 9:5095–113. doi: 10.1002/cam4.3114
52. Xu X, Zhang C, Ni X, Wu J, Pan C, Wang S, et al. Population-based analysis on predictors for lymph node metastasis in T1 colon cancer. *Surg Endosc.* (2020) 34:4030–40. doi: 10.1007/s00464-019-07192-0
53. Meyer JE, Cohen SJ, Ruth KJ, Sigurdson ER, Hall MJ. Young age increases risk of lymph node positivity in early-stage rectal cancer. *J Natl Cancer Inst.* (2016) 108(1). doi: 10.1093/jnci/djv284
54. Xie X, Yin J, Zhou Z, Dang C, Zhang H, Zhang Y. Young age increases the risk for lymph node metastasis in patients with early colon cancer. *BMC Cancer.* (2019) 19: 803. doi: 10.1186/s12885-019-5995-4
55. Masaki T, Sugiyama M, Matsuoka H, Abe N, Izumisato Y, Goto A, et al. Clinical utility of grading criteria for submucosal invasion in the

prognosis of T1 colorectal carcinomas. *J Gastroenterol.* (2003) 38:37–44. doi: 10.1007/s005350300004
56. Rasheed S, Bowley DM, Aziz O, Tekkis PP, Sadat AE, Guenther T, et al. Can depth of tumor invasion predict lymph node positivity in patients undergoing resection for early rectal cancer? a comparative study between t1 and t2 cancers. *Colorectal Dis.* (2008) 10:231–8. doi: 10.1111/j.1463-1318.2007.01411.x
57. Yim K, Won DD, Lee IK, Oh ST, Jung ES, Lee SH. Novel predictors for lymph node metastasis in submucosal invasive colorectal carcinoma. *World J Gastroenterol.* (2017) 23:5936–44. doi: 10.3748/wjg.v23.i32.5936
58. Ueno H, Kajiwara Y, Shimazaki H, Shinto E, Hashiguchi Y, Nakanishi K, et al. New criteria for histologic grading of colorectal cancer. *Am J Surg Pathol.* (2012) 36:193–201. doi: 10.1097/PAS.0b013e318235edee
59. Shivji S, Conner JR, Barresi V, Kirsch R. Poorly differentiated clusters in colorectal cancer: a current review and implications for future practice. *Histopathology.* (2020) 77:351–68. doi: 10.1111/his.14128
60. Son SM, Woo CG, Lee OJ, Lee SJ, Lee TG, Lee HC. Factors affecting retrieval of 12 or more lymph nodes in pT1 colorectal cancers. *J Int Med Res.* (2019) 47:4827–40. doi: 10.1177/0300060519862055
61. Aldecoa I, Montironi C, Planell N, Pellise M, Fernandez-Esparrach G, Gines A, et al. Endoscopic tattooing of early colon carcinoma enhances detection of lymph nodes most prone to harbor tumor burden. *Surg Endosc.* (2017) 31:723–33. doi: 10.1007/s00464-016-5026-3
62. Yoda Y, Ikematsu H, Matsuda T, Yamaguchi Y, Hotta K, Kobayashi N, et al. A large-scale multicenter study of long-term outcomes after endoscopic resection for submucosal invasive colorectal cancer. *Endoscopy.* (2013) 45:718–24. doi: 10.1055/s-0033-1344234
63. Asayama N, Oka S, Tanaka S, Nagata S, Furudoi A, Kuwai T, et al. Long-term outcomes after treatment for pedunculated-type T1 colorectal carcinoma: a multicenter retrospective cohort study. *J Gastroenterol.* (2016) 51:702–10. doi: 10.1007/s00535-015-1144-2
64. Barel F, Auffret A, Cariou M, Kermarrec T, Samaison L, Bourhis A, et al. High reproducibility is attainable in assessing histoprognostic parameters of pT1 colorectal cancer using routine histopathology slides and immunohistochemistry analyses. *Pathology.* (2019) 51:46–54. doi: 10.1016/j.pathol.2018.10.007

Conflict of Interest: The authors declare that the research was conducted in the absence of any commercial or financial relationships that could be construed as a potential conflict of interest.

Publisher's Note: All claims expressed in this article are solely those of the authors and do not necessarily represent those of their affiliated organizations, or those of the publisher, the editors and the reviewers. Any product that may be evaluated in this article, or claim that may be made by its manufacturer, is not guaranteed or endorsed by the publisher.

Copyright © 2022 Gambella, Falco, Benazzo, Osella-Abate, Senetta, Castellano, Bertero and Cassoni. This is an open-access article distributed under the terms of the Creative Commons Attribution License (CC BY). The use, distribution or reproduction in other forums is permitted, provided the original author(s) and the copyright owner(s) are credited and that the original publication in this journal is cited, in accordance with accepted academic practice. No use, distribution or reproduction is permitted which does not comply with these terms.

frontiers in Oncology

ORIGINAL RESEARCH
published: 18 February 2022
doi: 10.3389/fonc.2022.844182

The Sex Features of Patients With Solid Pseudopapillary Neoplasms of the Pancreas: A Retrospective Study

Guangmin Wei[1], Qiong Luo[1], Jiankai Fang[1], Xiaolou Li[1], Yanhong Shi[1], Yuqiong Li[2] and Liqi Sun[2,3]**

[1] Department of Oncology, Mengchao Hepatobiliary Hospital of Fujian Medical University, Fuzhou, China,
[2] Department of Gastroenterology, Changhai Hospital, Second Military Medical University, Shanghai, China,
[3] Department of Gastroenterology, 72nd Group Army Hospital, Huzhou University, Huzhou, China

Background: Solid pseudopapillary neoplasms of the pancreas (SPNs) in male patients are more frequently reported. The aim of the study was to evaluate the sex features of SPN and the risk factors that predict tumor recurrence.

Methods: From 2013 to 2019, patients who were pathologically confirmed to have SPNs were retrospectively reviewed. The baseline study parameters were compared between males and females. A logistic regression model was established to identify the independent risk factors for tumor recurrence.

Results: In total, 221 patients were included in this study. Of them, 53 patients (24.0%) were males. Male patients were older than female patients (39.1 vs 31.6 years, P=0.001), and the tumor size in male patients was smaller than that in female patients (50.38 vs 39.65 mm, P=0.038). The preoperative imaging diagnostic accuracy was significantly higher in females than in males (70.5% vs 54%, P=0.02). SPNs in male patients tended to be misdiagnosed with other malignant tumors (37.7% vs 10.7%, P<0.0001), with a more solid component observed in images (66.8% vs 24.7%, P<0.0001). For immunohistochemical staining, the expression of beta catenin was significantly lower in male patients (P=0.002), and the expression of vimentin was the opposite (P=0.01). The overall survival rate and disease-free survival were not different. Based on multivariate analysis, older age [hazard ratio (HR)= 1.094, 95% confidence interval (CI): 1.005-1.190] and KI 67 index grade III (HR=12.029, 95% CI: 2.399-60.311) were independent risk factors for tumor recurrence.

Conclusion: The clinical and imaging features of SPN in males were not in full accord with those in females; however, the differences did not influence prognosis.

Keywords: pancreas, solid pseudopapillary tumor, survival, risk factors, retrospective study

OPEN ACCESS

Edited by:
Sanjit Mukherjee, National Institutes of Health (NIH), United States

Reviewed by:
Stefano Francesco Crinò, University of Verona, Italy
Attila Zalatnai, Semmelweis University, Hungary
Cheng-Peng Li, Peking University Cancer Hospital, China

****Correspondence:***
Yuqiong Li
liyuqiong1122@163.com
Liqi Sun
zjhzslqsmmu@qq.com

Specialty section:
This article was submitted to Gastrointestinal Cancers: Hepato Pancreatic Biliary Cancers, a section of the journal Frontiers in Oncology

Received: *27 December 2021*
Accepted: *25 January 2022*
Published: *18 February 2022*

Citation:
Wei G, Luo Q, Fang J, Li X, Shi Y, Li Y and Sun L (2022) The Sex Features of Patients With Solid Pseudopapillary Neoplasms of the Pancreas: A Retrospective Study. Front. Oncol. 12:844182. doi: 10.3389/fonc.2022.844182

INTRODUCTION

Solid pseudopapillary neoplasms (SPNs) are uncommon. These tumors account for approximately 0.9%-2.7% of all exocrine pancreatic neoplasms (1, 2) and approximately 3%-5% of pancreatic cystic neoplasms (3, 4). The tumor is an epithelial-originated low-grade malignant neoplasm with the possibility of locally advanced, recurrent, and metastatic disease. Complete surgical resection is recommended as the main treatment for SPN (5).

SPNs occur predominantly in young women, with an overall female-male ratio of 9.8:1 reported in previous studies (1, 2). However, more male patients were identified in recent studies, with a female-male ratio ranging from 5:1 to 3:1 (6–9). The phenomenon that more male SPN patients have been identified has attracted increasing attention from clinicians and researchers (10).

Previous studies identified that progesterone receptors were present in 79%-100% of cases with SPN (11, 12). Moreover, the imaging features were different between male and female patients (13–15). In general, we hypothesized that progesterone may play a role in the biological behavior and clinical characteristics of SPN, which needs to be further clarified. However, a limited number of studies have focused on the impact of sex on the prognosis of patients with SPN. The conclusion was inconsistent (2, 7, 16, 17). The sample size in most of these studies was small, and the study cohort in one study was extracted from a database with nonstandard data included (7). Therefore, this study aims to compare the clinicopathological features and prognosis between males and females with SPN based on a relatively large cohort study from 2 pancreatic disease centers in China.

METHODS

Study Population

We conducted a retrospective study at Changhai Hospital affiliated with Navy/Second Medical University. The Institutional Review Board approved the study. Patients who underwent surgical resection from January 2013 to June 2019 for pathologically identified SPN were included in our study. The following inclusion criteria were applied: (1) patients pathologically diagnosed with SPN; (2) patients whose full electronic medical records and imaging records could be obtained; and (3) patients whose follow-up data could be obtained. Exclusion criteria included (1) specimens obtained from reresections; (2) concomitant other neoplasms on final pathology (e.g., neuroendocrine tumor, cholangiocarcinoma); and (3) patients with unavailable pathological and follow-up data. The selection procedure of the study participants is presented in **Figure 1**.

The decision on surgical treatment was made by multidisciplinary hepatopancreatobiliary teams. If the lesion was diagnosed as a pancreatic cystic lesion by imaging modality, the surgical indications followed the International Consensus Guideline (18). If diagnosed with invasive cancer, the surgery indications would follow the European Society for Medical Oncology guidelines (19). The choices of surgical procedures depended on the location, degree, extent of diseases and experiences of the surgeon.

Perioperative Management

The operations for SPN were performed by experienced surgeons in Changhai hospital. Before surgery, routine preoperative examinations were performed to exclude surgical contraindications. These routine examinations included electrocardiogram, pulmonary function, coagulation function, liver function, renal function, electrolyte and hemoglobin.

After surgery, amylase analysis from drainage fluid was performed to determine whether postoperative pancreatic fistula (POPF) existed. Routine blood examinations were performed to determine whether infection existed and whether antibiotics were used. Plain CT was performed to determine whether pancreatic fluid collection existed and to detect the causes of infection. If any clinically significant complications occurred, further treatments were needed.

Study Parameters

The parameters included in our study were composed of five parts: baseline characteristics, imaging data, pathological outcomes, short-term complications and long-term follow-up data.

The baseline characteristics included age, sex, initial symptoms, hospital stay days and surgical methods. The surgical methods included pancreatoduodenectomy (PD), total pancreatectomy (TP), distal pancreatectomy (DP), central pancreatectomy (CP) and enucleation.

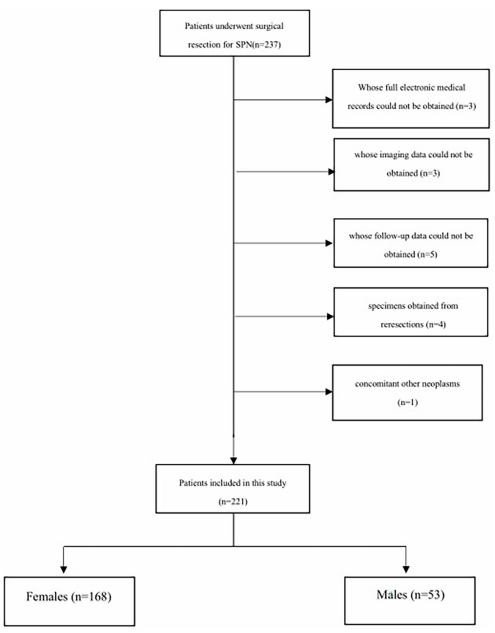

FIGURE 1 | Flowchart presenting the selection process of studies.

The imaging data included tumor size, location, imaging diagnoses by radiologists and proportion of solid components. The tumor might be located in head/body/tail/multiple sites of the pancreas. If multiple tumors occurred, only the size of the largest tumor was measured. The proportion of solid components was evaluated by T2 sequences obtained by contrast-enhanced MRI. If the proportion of the solid component was inconsistent on different layers, only the largest proportion was measured. The imaging diagnosis was divided into 2 parts: diagnostic accuracy (the diagnostic conclusions were SPNs) and surgical indication accuracy [diagnostic conclusions were malignancy, SPNs, neuroendocrine tumor (NET)].

The pathological outcomes included margin status, peripheral tissue invasion status and immunohistochemical outcomes. Positive margin status was defined as a tumor component ≤5 mm from the incisal margin. Peripheral tissue invasion status consisted of perineural invasion, vascular invasion, cancerization of ducts, lymphatic metastasis, common bile duct invasion, peripancreatic fat invasion, spleen invasion and duodenum invasion. The immunohistochemical outcomes included the Ki-67 index, beta-catenin, lymphoid enhancer-binding factor (LEF1), cyclin D1 and vimentin, which were measured in all included cases. The Ki-67 index of the tumor was divided into 3 grades: < 3%, 3%-20% and >20% (20).

Short-term complications were adverse events that occurred within 30 days after surgery, including POPF, delayed gastric emptying, hemorrhage, abdominal infection and bile leakage. The grade of complications was based on the Clavien-Dindo score. Complications that scored Clavien Dindo grade III or greater were considered severe complications.

The long-term follow-up data included long-term complications (exocrine insufficiency, endocrine insufficiency, alimentary stricture), disease-free survival (DFS) rate and overall survival (OS) rate. Follow-up data were obtained from telephone interviews and/or outpatient interviews in this study. Endocrine insufficiency was defined as a fasting plasma glucose level > 7.0 mmol/L and/or the need for diet modification, oral medication, or insulin use to control plasma glucose levels. Exocrine insufficiency was defined as symptoms (steatorrhea or weight loss) resolving after pancreatic enzyme supplementation (21). Recurrence was defined as a local or a metastatic tumor confirmed by radiology or histology during postoperative follow-up.

Statistical Analysis

The patients were divided into 2 groups according to their sex: male group and female group. The parameters were compared between the 2 groups. Quantitative parameters were expressed as the medians and range. Continuous data are reported as the mean ± standard deviation (SD) or as the median and range according to the distribution of the parameter. Categorical parameters were compared between the 2 groups using χ^2 or Fisher's exact test. Kaplan–Meier survival curves were established to estimate and compare the RFS rate and OS rate between the 2 groups. A logistic regression model was established to identify the independent risk factors for tumor recurrence. Statistical analysis was performed using SPSS version 22.0 (SPSS Inc., Chicago, IL, United States), and survival curves were drawn using GraphPad Prism (version 7.00). All tests were two-sided, and a P value < 0.05 was considered statistically significant.

RESULTS

Patient Characteristics

From January 2013 to December 2018, 221 patients who underwent pancreatic surgery were included in our study. All tumors were confirmed as SPNs according to the final histology examination. Among them, 53 patients (25.1%) were males, and 168 patients (74.9%) were females. The mean age of the overall study cohort was 33.3 years ± 12.7. Male patients were older than female patients (39.1 vs 31.6 years, t=3.283, P=0.001).

The majority of them were incidentally found (158/221, 71.5%). In the patients who were symptomatic, abdominal pain was the most common symptom (40/63, 63.5%), followed by abdominal distension (12/63, 19.0%), nausea and vomiting (8/63, 12.7%) and jaundice (3/63, 4.8%). The proportion of initial symptoms was not significantly different between males and females (χ^2 = 5.37, P=0.251).

In male patients, PD was performed in 13 patients (24.5%), DP was performed in 25 patients (47.2%), CP was performed in 10 patients (18.9%) and enucleation was performed in 5 patients (9.5%). No TP was performed in male patients. In female patients, PD was performed in 48 patients (28.6%), DP was performed in 82 patients (48.8%), CP was performed in 20 patients (11.9%), enucleation was performed in 8 patients (4.8%) and TP was performed in 10 patients (6.0%). The proportion of surgical methods was also not significantly different between males and females (χ^2 = 4.28, P=0.37).

The mean hospital stay was 12.53 days ± 6.87, with no difference between the 2 groups (14.24 vs 12.1 days, t=2.131, P=0.08).

The baseline characteristics of the study cohort are shown in **Table 1**.

Imaging Data

The tumor size for the overall study cohort was 47.98 ± 27.75 mm, with a significantly larger tumor size in female patients (50.38 vs 39.65 mm, P=0.038). In the male group, 23/5/4/21 tumors were located in multiple head/body/tail sites of the pancreas, while 67/19/19/63 tumors were located in multiple head/body/tail sites of the pancreas. The tumor location was not different between the 2 groups (χ^2 = 0.482, P=0.92).

All patients underwent preoperative imaging evaluations. The imaging diagnoses were correct, which means that the diagnosis was SPN, which was observed in 146 patients (66.9%). In the male group, 28 patients (54.0%) had correct imaging diagnoses. In the female group, 118 patients (70.5%) had correct imaging diagnoses. SPNs in male patients tended to be misdiagnosed with malignant tumors more often than SPNs in female patients (37.7% vs 10.7%, χ^2 = 20.662, P<0.0001). The diagnostic accuracy was significantly higher in the female group (χ^2 = 5.446, P=0.02). SPNs in male patients tended to be misdiagnosed with malignant tumors more often than SPNs in female patients (37.7% vs 10.7%, χ^2 = 20.662, P<0.0001).

TABLE 1 | Baseline characteristics and imaging data stratified by gender.

	Male (N=53)	Female (N=168)	*P* value
Age(years), mean ±SD	39.1±12.7	31.6±12.2	0.001
Symptoms, N%			0.251
incidentally found	42(79.2)	116(69.0)	
abdominal pain	10(18.9)	30(17.9)	
abdominal distension	0(0)	12(7.1)	
nausea and vomiting	0(0)	8(4.8)	
jaundice	1(1.9)	2(1.2)	
Surgical methods, N%			0.370
PD	13(24.5)	48(28.6)	
DP	25(47.2)	82(48.8)	
CP	10(18.9)	28(16.7)	
TP	0(0)	10(6.0)	
enucleation	5(9.4)	8(4.8)	
Hospital stays (days), mean ±SD	14.2±9.3	12.0±6.0	0.08
Tumor size (mm), mean ±SD	39.6±22.8	50.4±28.7	0.038
Tumor location (head/body/tail/ diffuse**), N%**	23/5/4/21	67/19/19/63	0.92
Imaging diagnoses, N%			
SPN	28(54.0)	118(70.5)	0.02
Malignant tumor	20(37.7)	18(10.7)	<0.0001
neuroendocrine tumor	1(1.9)	11(6.5)	0.192
other benign tumors	4(7.5)	21(12.8)	0.321
Imaging diagnoses for having surgical indications, N%	49(92.5)	147(87.5)	0.519
Solid component, N%			
Completely solid	25(47.2)	40(23.8)	0.001
Completely cystic	0(0)	32(19.0)	<0.001
>50% solid component	23(43.4)	55(32.7)	0.157
<50% solid component	5(9.4)	41(24.4)	0.043
Average solid component proportion, %	66.8	24.7	<0.001

SD, standard deviation; SPN, Solid pseudopapillary neoplasm; PD, pancreatoduodenectomy; TP, total pancreatectomy; DP, distal pancreatectomy; CP, central pancreatectomy.

Moreover, 49 male patients (92.5%) were diagnosed with having surgical indications (28 SPNs, 20 malignant tumors, 1 NET). Meanwhile, 147 male patients (87.5%) were diagnosed with having surgical indications (118 SPNs, 18 malignant tumors, 11 NETs). The diagnostic accuracy of having surgical indication was not significantly different between the 2 groups (χ^2 = 0.415, P=0.519). However, SPNs in male patients tended to be misdiagnosed with malignant tumors more often than SPNs in female patients (37.7% vs 10.7%, χ^2 = 20.662, P<0.0001).

Completely cystic tumors were observed in 0 and 32 (19.0%) male and female patients, respectively. Completely solid tumors were observed in 25 (47.2%) and 40 (23.8%) male and female patients, respectively. Tumors that had a solid component <50% were observed in 5 (9.4%) and 41 (24.4%) males and females, respectively. Tumors that had a solid component >50% were observed in 23 (43.4%) and 55 (32.7%) males and females, respectively. The mean solid component was 66.8% ± 24.5 for male patients and 24.7% ± 20.5 for female patients, which was significantly higher in male patients (t=23.67, P<0.0001). The imaging data of the study cohort are shown in **Table 1**.

Pathological Outcomes

According to the pathological specimens in male patients, a positive margin status was observed in 3 patients (5.7%), and peripheral tissue invasion was observed in 4 patients (7.5%)

For immunohistochemical staining, beta catenin was expressed in 47 cases (89.2%), cyclin D1 was expressed in 50 cases (94.6%), LEF1 was expressed in 33 cases (62.3%), and vimentin was expressed in 44 cases (83.0%). Grade I Ki67 was identified in 47 tumors (88.7%), Grade II Ki67 was identified in 4 tumors (7.5%) and Grade III Ki67 was identified in 2 tumors (3.8%).

In female patients, positive margin status was observed in 14 patients (8.3%), and peripheral tissue invasion was observed in 11 patients (6.5%). For immunohistochemical staining, beta catenin was expressed in 165 cases (98.2%), cyclin D1 was expressed in 164 cases (97.6%), LEF1 was expressed in 105 cases (62.5%), and vimentin was expressed in 108 cases (64.3%). Grade I Ki67 was identified in 141 tumors (83.9%), Grade II Ki67 was identified in 25 tumors (14.9%) and Grade III Ki67 was identified in 2 tumors (1.2%).

Comparing the pathological outcomes between the 2 groups. Positive margin status and peripheral tissue invasion were not different between the 2 groups (χ^2 = 0.405 and 0.564, P=0.524 and 0.489). The expression of Cyclin D1 and LEF1 was not significantly different between the 2 groups ($\chi2$ = 0.463, 0.059, P=0.541, 0.808). The Ki67 grade was not different between the 2 groups ($\chi2$ = 1.263, P=0.532). However, the expression of beta catenin was significantly lower in male patients ($\chi2$ = 9.377, P=0.002), and the expression of vimentin was significantly higher in male patients ($\chi2$ = 6.584, P=0.01). The pathological outcomes of the study cohort are shown in **Table 2**.

Short-Term Complications

In the male group, perioperative complications occurred in 10 patients (18.9%). POPF grade II or above developed in 2 patients (2/10, 20.0%), delayed gastric emptying developed in 2 patients

TABLE 2 | Pathological outcomes stratified by gender.

	Male (N=53)	Female (N=168)	*P* value
Positive margin status, N%	3(5.7)	14(8.3)	0.524
peripheral tissue invasion, N%	4(7.5)	11(6.5)	0.489
Immunohistochemical staining, N%			
Beta Catenin	47(88.7)	165(98.2)	0.002
Cyclin D1	50(94.3)	164(97.6)	0.541
LEF1	33(62.3)	105(62.5)	0.808
Vimentin	44(83.0)	118(64.3)	0.01
KI 67 grade, N%			0.532
Grade I	47(88.7)	141(83.9)	
Grade II	4(7.5)	25(14.9)	
Grade III	2(3.8)	2(1.2)	

LEF1, Lymphoid enhancer-binding factor.

(2/10, 20.0%), abdominal infection developed in 4 patients (4/10, 40.0%), bleeding developed in 1 patient (1/10, 10.0%), and 1 patient (1/10, 10.0%) developed both delayed gastric emptying and abdominal infection. Three complications (3/10, 30%) scored Clavien Dindo grade III or above and were considered severe complications.

In the female group, perioperative complications occurred in 30 patients (17.9%). Five patients (5/30, 16.7%) developed severe POPF, 6 patients (6/30, 20.0%) developed delayed gastric emptying, 5 patients developed abdominal infection (5/30, 16.7%), 9 patients developed bleeding (9/30, 3%), and 5 patients (5/30, 16.7%) developed severe POPF, abdominal infection and bleeding. Ten complications (10/30, 33.3%) scored Clavien Dindo grade III or above and were considered severe complications.

The overall perioperative complication rate and severe complication rate were comparable between the groups ($\chi 2$ = 0.028 and 0.00, P=0.868 and 1.0). The short-term complications of the study cohort are presented in **Table 3**.

Long-Term Follow-Up Data

In the male group, alimentary strictures were observed in 1 patient (1.9%). Three patients (5.7%) experienced pancreatic endocrine insufficiency, and 11 patients (20.8%) experienced exocrine insufficiency. Two patients (3.8%) experienced both pancreatic exocrine insufficiency and endocrine insufficiency. In the female group, alimentary strictures were observed in 1 patient (0.6%). Five patients (3.0%) experienced pancreatic endocrine insufficiency, and 31 patients (18.5%) experienced exocrine insufficiency. Ten patients (6.0%) experienced both pancreatic exocrine insufficiency and endocrine insufficiency. The incidence rates of long-term complications were not different between the 2 groups ($\chi 2$ = 0.002, P=0.963).

The final follow-up date was September 30, 2021. The median follow-up period was 54 months (27-105 months). Only 2 patients died due to perioperative complications (both in the female group), and the 3-, 5-, and 8-year overall survival (OS) rates were estimated to be 99.1%, 99.1%, and 99.1%, respectively. In total, 10 patients (4.5%) developed recurrence in the overall study cohort, with 7 patients (5 local recurrence and 2 liver metastasis) in the female group and 3 patients (2 local recurrence and 1 liver metastasis) in the male group. The median time to recurrence was 50 months (range 6–76 months). The 3-, 5-, and 8-year RFS rates were estimated at 98.6%, 96.2%, and 95.3% for the study cohort, respectively. The 3-, 5-, and 8-year RFS rates for the male group were 96.2%, 94.3%, and 94.3%, respectively. The 3-, 5-, and 8-year RFS rates for the female group were 99.4%, 97.0%, and 95.8%, respectively. Kaplan–Meier analysis and the log-rank test showed

TABLE 3 | Short-term complications and long-term follow-up data stratified by gender.

	Male (N = 53)	Female (N = 168)	*P* value
Short-term complications			
POPF grade II or above, N%	2(3.8)	5(3.0)	0.773
Delayed gastric emptying, N%	2(3.8)	6(3.6)	0.945
Abdominal infection, N%	4(7.7)	5(3.0)	0.142
Bleeding, N%	1(1.9)	9(5.4)	0.289
Two or more complications occurred, N%	1(1.9)	5(3.0)	0.67
Claviene Dindo grade III or above, N%	3(5.7)	10(6.0)	1.00
Long-term follow up data			
Alimentary stricture, N%	1(1.9)	1(0.6)	0.423
Pancreatic endocrine insufficiency, N%	3(5.7)	5(3.0)	0.362
pancreatic exocrine insufficiency, N%	11(20.8)	31(18.5)	0.710
Both endocrine and exocrine	2(3.8)	10(6.0)	0.542
insufficiency, N% Death, N%	0(0)	2(1.2)	1.00
Tumor recurrence, N%	3(5.7)	7(4.2)	0.648

POPF, postoperative pancreatic fistula.

that the recurrence rate was not significantly different between the groups ($\chi 2 = 1.286$, P=0.206) (**Figure 2**). The long-term follow-up data of the study cohort are presented in **Table 3**.

The Risk Factors for Tumor Recurrence

The parameters, including age, symptoms, surgical method, tumor size, tumor location, margin status, peripheral tissue invasion and immunohistochemical staining, were included in univariate analysis (**Table 4**). The results demonstrated that older age (42.4 vs 32.9 years, P=0.05), large tumor size (67.9 vs 47.1 mm, P=0.04) and a high KI 67 index were significantly associated with tumor recurrence, and the three parameters were included in multivariate logistic regression analysis. Moreover, sex was also included in multivariate analysis to adjust the baseline features.

Based on multivariate analysis, older age [hazard ratio (HR)= 1.094, 95% confidence interval (CI): 1.005-1.190, P=0.039] and KI 67 index grade III (HR=12.029, 95% CI: 2.399-60.311, P=0.002) were independent risk factors for tumor recurrence (**Table 5**).

DISCUSSION

In this study, we analyzed the data of 221 patients with SPN. The primary aim of the study was to identify sex features of SPNs. The second aim of the study was to identify the biological behaviors of SPNs and the risk factors associated with tumor recurrence. Our multiple retrospective study with a large sample size could significantly gain knowledge of SPN.

SPNs can occur at any age but are mainly observed in young women in their 30s (22). In our study, 168 patients were women with a mean age of 31.6 years. However, about one fourth of the patients were male. Data on the characteristics of male patients are scarce. In our study, we identified that male patients were associated with older age, smaller tumor size and more solid components on imaging. The results were consistent with previous studies (14, 23). Beyond these, we observed that male SPNs were previously misdiagnosed by radiologists. SPNs in male patients tended to be misdiagnosed with malignant tumors. However, imaging diagnoses greatly influence the treatment modality and operation type choices. Therefore, the differential diagnosis of SPN for male patients should receive more attention from radiologists. The application of endoscopic ultrasound (EUS) maybe a better solution. Preoperative EUS and EUS guided tissue acquisition allowed pancreatic SPN diagnosis in 80%-90 cases (24, 25). Moreover, the Ki67 index can be measured by the specimens obtained by EUS guided tissue biopsy (26). Hence, in patients whose imaging diagnoses are indeterminate, EUS should be performed.

The difference in male and female SPN may be due to sex hormones (27, 28). Progesterone may participate in the pathogenesis of SPN (29). Some cases reported that SPN grew rapidly during pregnancy (30, 31). Moreover, the estrogen receptor was strongly expressed in tumor tissues. The proliferative action of estrogen *in vitro* was also identified (32). Therefore, the sex features of SPN may be due to exposure to progesterone and/or estrogen during the reproductive period in females (7).

Surgical resection is the standard treatment choice for SPNs. The overall prognosis is excellent for SPNs, with a cure rate of > 95% following complete surgical resection (1, 33). In our study, we also found that the prognosis of SPN was favorable. After surgery, the 3-, 5-, and 8-year OS rates were estimated to be 99.1%, 99.1%, and 99.1%, and the 3-, 5-, and 8-year RFS rates were estimated to be 98.6%, 96.2%, and 95.3%, respectively. At the time of resection, only 7.5% of the patients had peripheral tissue invasion. After long-term follow-up, only 2 patients died due to perioperative complications, and 10 patients experienced tumor recurrence. DFS and OS differences between males and females were not observed in our study. This conclusion was consistent with the study by Cai et al. (16) with 16 cases included. However, Wu et al. (7) and Huffman et al. (17) concluded that female sex was associated with improved survival in which the data were obtained from the National Cancer

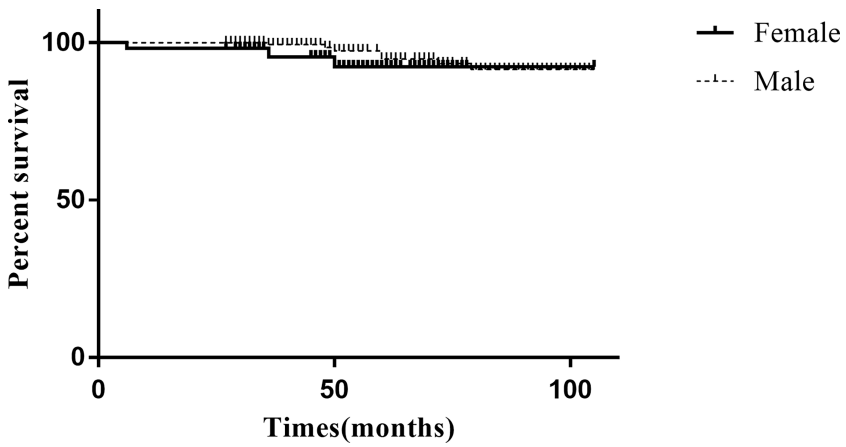

FIGURE 2 | Kaplan–Meier curves for recurrence rate according to the sex.

TABLE 4 | Univariate analysis for predication of tumor recurrence.

	Recurrence (N = 10)	No recurrence (N = 211)	*P* value
Age(years), mean ±SD	42.4±14.7	32.9±12.5	0.050
Symptoms, N%			
incidentally found	5(50)	153(72.5)	0.123
abdominal pain	4(40)	36(17.1)	0.155
abdominal distension	0(0)	12(5.7)	1.00
nausea and vomiting	0(0)	8(3.8)	1.00
jaundice	1(10)	2(0.9)	0.13
Surgical methods, N%			
PD	3(30)	58(27.5)	1.00
DP	4(40)	103(48.8)	0.586
CP	1(10)	37(17.5)	0.537
TP	0(0)	10(4.7)	1.00
enucleation	2(20)	11(5.2)	0.210
Tumor size (mm), mean ±SD	67.9±35.0	47.1±27.2	0.041
Tumor location (head/body/tail/ diffuse**), N%**	4/0/1/5	86/24/22/79	0.491
Positive margin status, N%	1(10)	2(0.9)	0.13
peripheral tissue invasion, N%	1(10)	3(1.4)	0.17
Immunohistochemical staining, N%			
Beta Catenin	9(90)	203(96.2)	0.332
Cyclin D1	10(100)	204(96.7)	0.808
LEF1	6(60)	132(62.6)	0.786
Vimentin	7(70)	155(73.5)	0.758
KI 67 grade, N%			<0.001
Grade I (n=188)	3	185	
Grade II (n=29)	4	25	
Grade III (n=4)	3	1	

Center database. The reason may be that the baseline characteristics of the included patients were different from those in our study. In their study, most of their data were obtained from white and black patients. Their sex hormone levels were different from those of Asian patients. Moreover, the average age of male patients was much older than that in our study, and older age was identified as an independent risk factor for tumor recurrence in our study. Therefore, the selection bias of the included patients may contribute to the difference.

The pathological outcomes were also analyzed in our study. More than 90% of the patients could reach margin-negative surgical resection. Peripheral tissue invasion was rare observed. Some previous studies concluded that lymph node metastasis and positive margin status may be risk factors for poor prognosis of SPN (34, 35). However, this relationship was not identified in our study. The inconsistent conclusion may be due to the small number of lymph node metastasis and positive margin status patients included in our study, and statistical bias may exist. Although numerous biomarkers over the years have been documented to have value in diagnosing SPNs (36–38), there are still no specific immunohistochemical biomarkers for SPNs at present. Only the biomarkers tested in our center were included in our study. The Cyclin D1 expressed in almost all SPNs. Beta Catenin was more specific in female patients, and Vimentin was more specific in male patients. The results may be especially helpful in building pathological diagnoses in tissues obtained by endoscopic ultrasound-guided fine needle biopsy (EUS-FNB). The dose obtained by EUS-FNB tissue is always not as high as that obtained by surgical specimens. However, the conclusion needs further verified.

Ki67 indicates the proliferation of cells. The Ki-67 index has prognostic significance for SPN patients (9, 39). In our study, 3 of the 4 patients who had a grade III Ki67 index experienced tumor recurrence. The recurrence HR for grade III Ki 67 index was 12.03. SPN patients with a grade III Ki67 index were at very high risk of tumor recurrence. A continuous surveillance approach should be adopted in these patients. The cutoff level of the Ki-67 index in our study was based on the criteria for pNETs. For SPT, the optimal cutoff level of Ki-67 needs recalculation. In the studies by Yang et al. (39) and Wu et al. (40), a Ki-67 index

TABLE 5 | Multivariate analysis for predication of tumor recurrence.

	HR (95%CI)	*P* value
Age	1.094(1.005-1.190)	0.039
Gender	1.593(0.258-5.678)	0.22
Tumor size	1.015(0.973-1.059)	0.484
KI 67 grade		
Grade I	1.0	
Grade II	2.589(0.202-33.196)	0.465
Grade III	12.029(2.399-60.311)	0.002

greater than 4% was set as the cutoff level. However, only 3 and 4 patients in their studies developed tumor recurrence. Significant statistical bias might exist in their studies. Therefore, we did not adopt the criteria in our study. Due to the small number of cases of SPN, the optimal cutoff level of the Ki-67 index may be difficult to determine due to the small recurrence and death rate.

Patients who had distant metastasis were not included in our study due to the lack of surgical indications. Unresectable SPN remains the most important predictor of poor prognosis in all experiences (41). Nonsurgical treatments have been scarcely investigated, and no standardized protocol exists for this subset of patients. Chemotherapy agents such as cisplatin, 5-fluorouracil and gemcitabine have been proposed in some cases with uncertain results (42). Recently, radiotherapy and targeted therapy have also been reported to treat unresectable or recurrent SPNs in case reports (43, 44). Based on the conclusions in our study, investigating the possible estrogen-dependent behavior of SPN could perhaps open the way to new nonsurgical treatment strategies.

Our study had several limitations worth discussing. First, its retrospective nature prevented us from making stronger conclusions. The second limitation was the relatively small sample size. Due to the rarity of SPNs, SPN cases, especially recurrent SPNs, were not common in our center. More multicenter prospective studies with large sample sizes are necessary to better understand SPNs.

CONCLUSION

The incidence of SPN in males was not as low as that previously reported. Male SPN patients were associated with older age, smaller tumor size and more solid components on imaging. For immunohistochemical staining, Cyclin D1 was expressed in almost all SPNs. Beta Catenin was more specific in female patients, and Vimentin was more specific in male patients. Positive margin status, peripheral tissue invasion, postoperative complications, DFS and OS were not significantly different between males and females, which indicated that the prognoses of SPNs in males and females were similar. Elderly age and Ki67 index grade III were independent risk factors for tumor recurrence. Further prospective studies with large sample sizes are needed to verify the findings of our study.

DATA AVAILABILITY STATEMENT

The raw data supporting the conclusions of this article will be made available by the authors, without undue reservation.

ETHICS STATEMENT

The studies involving human participants were reviewed and approved by The Institutional Review Board of Changhai Hospital. The patients provided their written informed consent to participate in this study.

AUTHOR CONTRIBUTIONS

GW, QL, YL, and LS conceived and designed the experiments. YL have made data acquisition. JF, XL, and YS analyzed the data.GW, QL, and LS wrote the manuscript. All authors contributed to the article and approved the submitted version.

REFERENCES

1. Papavramidis T, Papavramidis S. Solid Pseudopapillary Tumors of the Pancreas: Review of 718 Patients Reported in English Literature. *J Am Coll Surg* (2005) 200(6):965–72. doi: 10.1016/j.jamcollsurg.2005.02.011
2. Machado MC, Machado MA, Bacchella T, Jukemura J, Almeida JL, Cunha JE. Solid Pseudopapillary Neoplasm of the Pancreas: Distinct Patterns of Onset, Diagnosis, and Prognosis for Male Versus Female Patients. *Surgery* (2008) 143 (1):29–34. doi: 10.1016/j.surg.2007.07.030
3. Scholten L, van Huijgevoort NCM, van Hooft JE, Besselink MG, Del Chiaro M. Pancreatic Cystic Neoplasms: Different Types, Different Management, New Guidelines. *Visc Med* (2018) 34(3):173–7. doi: 10.1159/000489641
4. Stark A, Donahue TR, Reber HA, Hines OJ. Pancreatic Cyst Disease: A Review. *JAMA* (2016) 315(17):1882–93. doi: 10.1001/jama.2016.4690
5. Lubezky N, Papoulas M, Lessing Y, Gitstein G, Brazowski E, Nachmany I, et al. Solid Pseudopapillary Neoplasm of the Pancreas: Management and Long-Term Outcome. *Eur J Surg Oncol* (2017) 43(6):1056–60. doi: 10.1016/j.ejso.2017.02.001
6. Liu M, Liu J, Hu Q, Xu W, Liu W, Zhang Z, et al. Management of Solid Pseudopapillary Neoplasms of Pancreas: A Single Center Experience of 243 Consecutive Patients. *Pancreatology* (2019) 19(5):681–5. doi: 10.1016/j.pan.2019.07.001
7. Wu J, Mao Y, Jiang Y, Song Y, Yu P, Sun S, et al. Sex Differences in Solid Pseudopapillary Neoplasm of the Pancreas: A Population-Based Study. *Cancer Med* (2020) 9(16):6030–41. doi: 10.1002/cam4.3180
8. Yao J, Song H. A Review of Clinicopathological Characteristics and Treatment of Solid Pseudopapillary Tumor of the Pancreas With 2450 Cases in Chinese Population. *BioMed Res Int* (2020) 2020:2829647. doi: 10.1155/2020/2829647
9. Yang F, Wu W, Wang X, Zhang Q, Bao Y, Zhou Z, et al. Grading Solid Pseudopapillary Tumors of the Pancreas: The Fudan Prognostic Index. *Ann Surg Oncol* (2021) 28(1):550–9. doi: 10.1245/s10434-020-08626-z
10. Omiyale AO. Solid Pseudopapillary Neoplasm of the Pancreas. *World J Hepatol* (2021) 13(8):896–903. doi: 10.4254/wjh.v13.i8.896
11. Yeh TS, Jan YY, Chiu CT, Ho YB, Chen TC, Lee KF, et al. Characterisation of Oestrogen Receptor, Progesterone Receptor, Trefoil Factor 1, and Epidermal Growth Factor and its Receptor in Pancreatic Cystic Neoplasms and Pancreatic Ductal Adenocarcinoma. *Gut* (2002) 51(5):712–6. doi: 10.1136/gut.51.5.712
12. Nguyen NQ, Johns AL, Gill AJ, Ring N, Chang DK, Clarkson A, et al. Clinical and Immunohistochemical Features of 34 Solid Pseudopapillary Tumors of the Pancreas. *J Gastroenterol Hepatol* (2011) 26(2):267–74. doi: 10.1111/j.1440-1746.2010.06466.x
13. Park MJ, Lee JH, Kim JK, Kim YC, Park MS, Yu JS, et al. Multidetector CT Imaging Features of Solid Pseudopapillary Tumours of the Pancreas in Male Patients: Distinctive Imaging Features With Female Patients. *Br J Radiol* (2014) 87(1035):20130513. doi: 10.1259/bjr.20130513
14. Shi S, Zhou Y, Hu C. Clinical Manifestations and Multi-Slice Computed Tomography Characteristics of Solid Pseudopapillary Neoplasms of the Pancreas Between Males and Females. *BMC Med Imaging* (2019) 19(1):87. doi: 10.1186/s12880-019-0390-9

15. Sasaki Y, Ishikawa T, Kawashima H, Ohno E, Shimoyama Y, Ishikawa E, et al. Gender Difference in the Transabdominal Ultrasound Findings of Solid-Pseudopapillary Neoplasm. *Pancreatology* (2020) 20(5):997–1003. doi: 10.1016/j.pan.2020.06.016
16. Cai YQ, Xie SM, Ran X, Wang X, Mai G, Liu XB. Solid Pseudopapillary Tumor of the Pancreas in Male Patients: Report of 16 Cases. *World J Gastroenterol* (2014) 20(22):6939–45. doi: 10.3748/wjg.v20.i22.6939
17. Huffman BM, Westin G, Alsidawi S, Alberts SR, Nagorney DM, Halfdanarson TR, et al. Survival and Prognostic Factors in Patients With Solid Pseudopapillary Neoplasms of the Pancreas. *Pancreas* (2018) 47(8):1003–7. doi: 10.1097/MPA.0000000000001112
18. Tanaka M, Fernández-del Castillo C, Adsay V, Chari S, Falconi M, Jang JY, et al. International Consensus Guidelines 2012 for the Management of IPMN and MCN of the Pancreas. *Pancreatology* (2012) 12(3):183–97. doi: 10.1016/j.pan.2012.04.004 Erratum in: *Ann Oncol*. 2017 Jul 1;28(suppl_4):iv167-8
19. Ducreux M, Cuhna AS, Caramella C, Hollebecque A, Burtin P, Goéré D, et al. Cancer of the Pancreas: ESMO Clinical Practice Guidelines for Diagnosis, Treatment and Follow-Up. *Ann Oncol* (2015) 26(Suppl 5):v56–68. doi: 10.1093/annonc/mdv295
20. Inzani F, Petrone G, Rindi G. The New World Health Organization Classification for Pancreatic Neuroendocrine Neoplasia. *Endocrinol Metab Clin North Am* (2018) 47(3):463–70. doi: 10.1016/j.ecl.2018.04.008
21. Faitot F, Gaujoux S, Barbier L, Novaes M, Dokmak S, Aussilhou B, et al. Reappraisal of Pancreatic Enucleations: A Single-Center Experience of 126 Procedures. *Surgery* (2015) 158(1):201–10. doi: 10.1016/j.surg.2015.03.023
22. Ye J, Ma M, Cheng D, Yuan F, Deng X, Zhan Q, et al. Solid-Pseudopapillary Tumor of the Pancreas: Clinical Features, Pathological Characteristics, and Origin. *J Surg Oncol* (2012) 106(6):728–35. doi: 10.1002/jso.23195
23. Hu S, Huang W, Lin X, Wang Y, Chen KM, Chai W. Solid Pseudopapillary Tumour of the Pancreas: Distinct Patterns of Computed Tomography Manifestation for Male Versus Female Patients. *Radiol Med* (2014) 119 (2):83–9. doi: 10.1007/s11547-013-0327-2
24. Karsenti D, Caillol F, Chaput U, Perrot B, Koch S, Vuitton L, et al. Safety of Endoscopic Ultrasound-Guided Fine-Needle Aspiration for Pancreatic Solid Pseudopapillary Neoplasm Before Surgical Resection: A European Multicenter Registry-Based Study on 149 Patients. *Pancreas* (2020) 49 (1):34–8. doi: 10.1097/MPA.0000000000001460
25. Crinó SF, Brandolese A, Vieceli F, Paiella S, Conti Bellocchi MC, Manfrin E, et al. Endoscopic Ultrasound Features Associated With Malignancy and Aggressiveness of Nonhypovascular Solid Pancreatic Lesions: Results From a Prospective Observational Study. *Ultraschall Med* (2021) 42(2):167–77. doi: 10.1055/a-1014-2766
26. Paiella S, Landoni L, Rota R, Valenti M, Elio G, Crinò SF, et al. Endoscopic Ultrasound-Guided Fine-Needle Aspiration for the Diagnosis and Grading of Pancreatic Neuroendocrine Tumors: A Retrospective Analysis of 110 Cases. *Endoscopy* (2020) 52(11):988–94. doi: 10.1055/a-1180-8614
27. Naar L, Spanomichou DA, Mastoraki A, Smyrniotis V, Arkadopoulos N. Solid Pseudopapillary Neoplasms of the Pancreas: A Surgical and Genetic Enigma. *World J Surg* (2017) 41(7):1871–81. doi: 10.1007/s00268-017-3921-y
28. Pettinato G, Di Vizio D, Manivel JC, Pambuccian SE, Somma P, Insabato L. Solid-Pseudopapillary Tumor of the Pancreas: A Neoplasm With Distinct and Highly Characteristic Cytological Features. *Diagn Cytopathol* (2002) 27 (6):325–34. doi: 10.1002/dc.10189
29. Zou Y, Huang Y, Hong B, Xiang X, Zhou B, Wei S. Comparison of the Clinicopathological Features of Pancreatic Solid Pseudopapillary Neoplasms Between Males and Females: Gender Does Matter. *Histol Histopathol* (2020) 35(3):257–68. doi: 10.14670/HH-18-156
30. Ganepola GA, Gritsman AY, Asimakopulos N, Yiengpruksawan A. Are Pancreatic Tumors Hormone Dependent?: A Case Report of Unusual, Rapidly Growing Pancreatic Tumor During Pregnancy, Its Possible Relationship to Female Sex Hormones, and Review of the Literature. *Am Surg* (1999) 65(2):105–11.
31. Huang TT, Zhu J, Zhou H, Zhao AM. Solid Pseudopapillary Neoplasm of Pancreas in Pregnancy Treated With Tumor Enucleation: Case Report and Review of the Literature. *Niger J Clin Pract* (2018) 21(9):1234–7. doi: 10.4103/njcp.njcp_39_18
32. Tognarini I, Tonelli F, Nesi G, Martineti V, Galli G, Gozzini A, et al. *In Vitro* Effects of Oestrogens, Antioestrogens and SERMs on Pancreatic Solid Pseudopapillary Neoplasm-Derived Primary Cell Culture. *Cell Oncol* (2010) 32(5-6):331–43. doi: 10.1155/2010/459862
33. Law JK, Ahmed A, Singh VK, Akshintala VS, Olson MT, Raman SP, et al. A Systematic Review of Solid-Pseudopapillary Neoplasms: Are These Rare Lesions? *Pancreas* (2014) 43(3):331–7. doi: 10.1097/MPA.0000000000000061
34. Chen H, Huang Y, Yang N, Yan W, Yang R, Zhang S, et al. Solid-Pseudopapillary Neoplasm of the Pancreas: A 63-Case Analysis of Clinicopathologic and Immunohistochemical Features and Risk Factors of Malignancy. *Cancer Manag Res* (2021) 13:3335–43. doi: 10.2147/CMAR.S304981
35. Gao H, Gao Y, Yin L, Wang G, Wei J, Jiang K, et al. Risk Factors of the Recurrences of Pancreatic Solid Pseudopapillary Tumors: A Systematic Review and Meta-Analysis. *J Cancer* (2018) 9(11):1905–14. doi: 10.7150/jca.24491
36. Li L, Li J, Hao C, Zhang C, Mu K, Wang Y, et al. Immunohistochemical Evaluation of Solid Pseudopapillary Tumors of the Pancreas: The Expression Pattern of CD99 is Highly Unique. *Cancer Lett* (2011) 310(1):9–14. doi: 10.1016/j.canlet.2011.04.017
37. Singhi AD, Lilo M, Hruban RH, Cressman KL, Fuhrer K, Seethala RR. Overexpression of Lymphoid Enhancer-Binding Factor 1 (LEF1) in Solid-Pseudopapillary Neoplasms of the Pancreas. *Mod Pathol* (2014) 27(10):1355–63. doi: 10.1038/modpathol.2014.40
38. Din NU, Rahim S, Abdul-Ghafar J, Ahmed A, Ahmad Z. Clinicopathological and Immunohistochemical Study of 29 Cases of Solid-Pseudopapillary Neoplasms of the Pancreas in Patients Under 20 Years of Age Along With Detailed Review of Literature. *Diagn Pathol* (2020) 15(1):139. doi: 10.1186/s13000-020-01058-z
39. Yang F, Yu X, Bao Y, Du Z, Jin C, Fu D. Prognostic Value of Ki-67 in Solid Pseudopapillary Tumor of the Pancreas: Huashan Experience and Systematic Review of the Literature. *Surgery* (2016) 159(4):1023–31. doi: 10.1016/j.surg.2015.10.018
40. Wu JH, Tian XY, Liu BN, Li CP, Zhao M, Hao CY. Clinicopathological Features and Prognostic Factors of Solid Pseudopapillary Neoplasms of Pancreas. *Pak J Pharm Sci* (2019) 32(1(Special)):459–64.
41. Farhat W, Ammar H, Amine Said M, Mizouni A, Bouazzi A, Abdessaied N, et al. Solid Pseudopapillary Neoplasm of the Pancreas: A Report of 10 Cases and Literature Review. *ANZ J Surg* (2020) 90(9):1683–8. doi: 10.1111/ans.15701
42. Ansari D, Elebro J, Tingstedt B, Ygland E, Fabricius M, Andersson B, et al. Single-Institution Experience With Solid Pseudopapillary Neoplasm of the Pancreas. *Scand J Gastroenterol* (2011) 46(12):1492–7. doi: 10.3109/00365521.2011.627448
43. Dyas AR, Johnson DT, Rubin E, Schulick RD, Kumar Sharma Y. Yttrium-90 Selective Internal Radiotherapy as Bridge to Curative Hepatectomy for Recurrent Malignant Solid Pseudopapillary Neoplasm of Pancreas: Case Report and Review of Literature. *J Surg Case Rep* (2020) 2020(9):rjaa325. doi: 10.1093/jscr/rjaa325
44. Wang X, Zhu D, Bao W, Li M, Wang S, Shen R. Case Report: Targeted Therapy for Metastatic Solid Pseudopapillary Neoplasm of the Pancreas With CTNNB1 and PTEN Mutations. *Front Oncol* (2021) 11:729151. doi: 10.3389/fonc.2021.729151

Conflict of Interest: The authors declare that the research was conducted in the absence of any commercial or financial relationships that could be construed as a potential conflict of interest.

Publisher's Note: All claims expressed in this article are solely those of the authors and do not necessarily represent those of their affiliated organizations, or those of the publisher, the editors and the reviewers. Any product that may be evaluated in this article, or claim that may be made by its manufacturer, is not guaranteed or endorsed by the publisher.

Copyright © 2022 Wei, Luo, Fang, Li, Shi, Li and Sun. This is an open-access article distributed under the terms of the Creative Commons Attribution License (CC BY). The use, distribution or reproduction in other forums is permitted, provided the original author(s) and the copyright owner(s) are credited and that the original publication in this journal is cited, in accordance with accepted academic practice. No use, distribution or reproduction is permitted which does not comply with these terms.

frontiers in Oncology

ORIGINAL RESEARCH
published: 21 February 2022
doi: 10.3389/fonc.2022.841819

Perioperative Serum Scoring Systems Predict Early Recurrence and Poor Prognosis of Resectable Pancreatic Cancer

Shengnan Li[1†], Gengpu Zhang[1†], Yang Lu[1], Tiansuo Zhao[1], Chuntao Gao[1], Weishuai Liu[1], Yongjun Piao[2], Yanan Chen[2], Chongbiao Huang[1], Antao Chang[1*] and Jihui Hao[1*]*

[1] Department of Pancreatic Cancer, Tianjin Medical University Cancer Institute and Hospital, National Clinical Research Center for Cancer, Key Laboratory of Cancer Prevention and Therapy, Tianjin's Clinical Research Center for Cancer, Tianjin, China, [2] School of Medicine, Nankai University, Tianjin, China

OPEN ACCESS

Edited by:
Qi Liu,
Fudan University, China

Reviewed by:
Stephan Kersting,
Universitätsmedizin Greifswald, Germany
Ming Cui,
Peking Union Medical College Hospital (CAMS), China

***Correspondence:**
Jihui Hao
haojihui@tjmuch.com
Antao Chang
changantao@tjmuch.com
Chongbiao Huang
chhuang@tmu.edu.cn

[†]These authors have contributed equally to this work

Specialty section:
This article was submitted to Gastrointestinal Cancers: Hepato Pancreatic Biliary Cancers, a section of the journal Frontiers in Oncology

Received: 22 December 2021
Accepted: 21 January 2022
Published: 21 February 2022

Citation:
Li S, Zhang G, Lu Y, Zhao T, Gao C, Liu W, Piao Y, Chen Y, Huang C, Chang A and Hao J (2022) Perioperative Serum Scoring Systems Predict Early Recurrence and Poor Prognosis of Resectable Pancreatic Cancer. Front. Oncol. 12:841819. doi: 10.3389/fonc.2022.841819

Objective: Some patients with pancreatic ductal adenocarcinoma (PDAC) are prone to rapid recurrence or metastasis after radical resection. However, evaluation methods for effectively identifying these patients are lacking. In this study, we established perioperative serum scoring systems to screen patients with early recurrence and poor prognosis.

Methods: We systematically analysed 44 perioperative serum parameters, including systemic inflammatory parameters, coagulation system parameters, tumor markers, and 18 clinicopathological characteristics of 218 patients with radical resection in our centre. Univariate Cox regression and LASSO regression models were used to screen variables. Kaplan-Meier survival analysis was used to compare relapse-free survival and overall survival. Multivariate Cox regression was used to evaluate the independent risk variables. AUC and C-index were used to reveal the effectiveness of the models. In addition, the effectiveness was also verified in an independent cohort of 109 patients.

Results: Preoperative systemic immune coagulation cascade (SICC) (including increased neutrophil to lymphocyte ratio, decreased lymphocyte to monocyte ratio, increased platelet and fibrinogen) and increased postoperative tumor markers (TMs) (CA199, CEA and CA242) were independent risk factors for early recurrence of resectable pancreatic cancer. On this basis, we established the preoperative SICC score and postoperative TMs score models. The patients with higher preoperative SICC or postoperative TMs score were more likely to have early relapse and worse prognosis. The nomogram based on preoperative SICC, postoperative TMs, CACI, smoking index, vascular cancer embolus and adjuvant chemotherapy can effectively evaluate the recurrence rate ($AUC_{1\ year}$: 0.763, $AUC_{2\ year}$: 0.679, $AUC_{3\ year}$: 0.657) and overall survival rate ($AUC_{1\ year}$: 0.770, $AUC_{3\ year}$: 0.804, $AUC_{5\ year}$: 0.763).

Conclusion: Preoperative SICC and postoperative TMs can help identify resectable PDAC patients with early recurrence and poor prognosis.

Keywords: systemic immune inflammation, coagulation system, tumor marker, resectable pancreatic cancer, early recurrence, prognosis

INTRODUCTION

Pancreatic ductal adenocarcinoma (PDAC) is one of the most lethal malignancies with a 5-year survival rate of 10%, mainly caused by insidious rapid recurrence or metastasis (1). Surgical resection is currently the most effective treatment for PDAC. However, only approximately 20% of patients have the opportunity to undergo radical resection at the time of diagnosis (2). Meanwhile, approximately half of these patients who underwent surgery can receive follow-up adjuvant chemotherapy (3, 4). Unfortunately, about a quarter of these patients will rapidly relapse within 6 months after surgery, but may benefit from neoadjuvant chemotherapy (5–7). Therefore, screening out these patients with high risk of early recurrence for precision medicine and early intervention could be an effective strategy to improve their prognosis and survival. However, there is no accessible evaluation system in clinic at present, driving us to establish new models for effective prediction of the early recurrence and overall survival (OS) of patients with resectable PDAC.

An increasing number of studies have shown that systemic immune inflammation amongst patients with cancer is closely related to their poor prognosis (8, 9). Neutrophils, lymphocytes, platelets, monocytes and the combinations of these factors, such as neutrophil-to-lymphocyte ratio (NLR), platelet-to-lymphocyte ratio (PLR) and lymphocyte-to-monocyte ratio (LMR), are associated with the prognosis of cancer patients (10–12). For example, lots of studies have demonstrated a causal relationship between neutrophils and metastasis (13–15). Meanwhile, it has been reported that the activation of platelets and the coagulation system also play essential roles in the progression of cancer (16). However, some studies have also reported that the proper use of these inflammatory parameters as prognostic factors is depended on the level of serum bilirubin (17). In addition, the intrinsic mechanisms of cancer cell heterogeneity between tumor-bearing hosts also largely determine metastasis driven by systemic immune inflammation (18). Hence, the effect of systemic immune inflammation on the prognosis of cancer patients may depend on the results of the comprehensive effects of the internal tumor microenvironment.

Currently, the most common tumor marker for PDAC in clinical practice is carbohydrate antigen 19-9 (CA19-9), but its usefulness in prognostic monitoring is limited because of low sensitivity and low specificity (19). In recent years, several pathological indexes, such as tumor size, tumor location, lymph node metastasis, TNM stage and pathological grade have been reported to possibly affect OS or disease recurrence of PDAC (20, 21). Meanwhile, serum index like serum alkaline phosphatase (ALP) in patients with early PDAC has also been reported to be significantly correlated with OS (22). However, the relationship between the baseline levels of other serum indexes, i.e., serum bilirubin, containing total bilirubin (TBIL) and direct bilirubin (DBIL), or albumin (ALB) and the prognosis of patients with PDAC remains controversial, and need to be further investigated (23, 24). Previous studies mainly focused on the limited parameters 1 month or more before or after surgery, whilst disregarding the influence of these indicators during the perioperative period, which in fact, is more crucial for predicting the prognosis of resectable PDAC (25). In this study, we evaluated the comprehensive effects of pathological indexes, systemic inflammation indicators, coagulation system parameters, tumor markers and other serum parameters on the early recurrence and the prognosis of resectable PDAC during the perioperative period. Our data indicated that preoperative systemic immune coagulation cascade (SICC) [including NLR, LMR, platelet and fibrinogen (Fbg)] and postoperative tumor markers (TMs) [CA19-9, carcinoembryonic antigen (CEA) and carbohydrate antigen 242 (CA242)] were pivotal in prediction of early recurrence and low survival of PDAC patients with radical resection. On this basis, we constructed a series of evaluation systems for effectively identifying PDAC patients with rapid recurrence or metastasis after radical resection, which may help clinicians make medical decisions and provide individualised treatment to patients with resectable PDAC.

Abbreviations: AJCC, American joint committee on cancer; AUC, area under the curve; CA19-9, carbohydrate antigen 19-9; CA242, carbohydrate antigen 242; CACI, Charson age comorbidity index; CEA, carcinoembryonic antigen; CI, confidence interval; RFS, relapse-free survival; HR, hazard ratio; LASSO, least absolute shrinkage and selection operator; LMR, lymphocyte to monocyte ratio; NAR, neutrophil to albumin ratio; NLR, neutrophil to lymphocyte ratio; OS, overall survival; PAR, platelet to albumin ratio; PDAC, pancreatic ductal adenocarcinoma; PLR, platelet to lymphocyte ratio; PNI, prognostic nutrition index ROC, receiver operating characteristic; SICC, Systemic immune coagulation cascade; TMs, Tumor markers.

MATERIALS AND METHODS

Patients and Samples

This study recruited 327 PDAC patients with radical resection under the National Comprehensive Cancer Network (NCCN) guidelines from March 2012 to December 2018 at Tianjin Medical University Cancer Institute and Hospital (TJMUCIH) (26). All patients had intact abdominal CT or MRI imaging and other baseline information. No patients had local vascular invasion and portal vein invasion/resection or arterial resection. All enrolled patients did not receive neoadjuvant therapy before radical resection. The inclusion criteria included: 1) No arterial tumor contact (celiac axis, superior mesenteric artery, or common hepatic artery); 2) No tumor contact with the superior mesenteric vein or portal vein or ≤180° contact without vein contour irregularity; 3) Without any form of anti-tumor treatment before operation; 4) Patients with pancreatic ductal adenocarcinoma confirmed by histopathology. The exclusion criteria were as follows: 1) patients with non-R0 resection; 2) histopathologically confirmed patients with non-PDAC; 3) patients who died within 3 months after the operation; 4) patients whose informed consent was not signed or follow-up records were incomplete; 5) patients who had a history of other malignant tumors; 6) patients who received neoadjuvant chemotherapy; 7) Patients whose tumor invaded the celiac artery, superior mesenteric artery, and/or common hepatic artery. These patients were randomly assigned to the training group (218 patients) and the validation group (109 patients) at the ratio 2:1. This retrospective study had been approved by the Ethics Committee of the TJMUCIH.

Histopathology Characteristics

Tumor tissues were collected during the operation with their pathological information, which include, vascular cancer embolus, capsule invasion, perineural invasion, tumor size, regional lymph node metastasis and pathological grade. Smoking index, alcohol consumption, diabetes, abdominal pain and body weight were also recorded. The Charson age comorbidity index (CACI) was calculated on the basis of the prospectively maintained institutional database, and 4 points were used to determine the cutoff value as described in published references (5). R0 resection was evaluated by two independent pathologists according to the statement of the International Pancreatic Surgery Group (27). When the distance between the tumor and the closest resection margin was greater than 1 mm, the resection margin (R) was defined as R0, otherwise it was defined as R1. All the patients were classified in accordance with the 8th edition of the American Joint Committee on Cancer.

Tumor Biomarker and Laboratory Testing

Tumor markers (CA19-9, CEA and CA242), liver function indexes (ALB, ALP, TBIL, DBIL, gamma-glutamyltransferase and lactate dehydrogenase), systemic inflammatory parameters [neutrophils, platelets, lymphocytes, monocytes, NLR, PLR, LMR, prognostic nutrition index (PNI), neutrophil-to-ALB ratio (NAR) and platelet-to-ALB ratio (PAR)] and coagulation parameters [prothrombin time (PT), international normalised ratio (INR), activated partial thrombin time (APTT), Fbg, thrombin time (TT) and d-dimer DD] were collected 7 days before operation. Amongst them, liver function and systemic inflammatory parameters must be retested 1 week later the operation. Tumor markers should be re-examined 30 days later after operation. A total of 44 serum parameters, including preoperative and postoperative, were included in the current study. X-Tile software was used to automatically calculate the cutoff value of all the parameters and model scores (28).

Follow Up of Patients

We followed the criteria of RECIST1.1, combined with imaging evaluation to judge the objective progress of tumor. All enrolled patients were continuously followed up, which was performed jointly by surgeons, physicians and radiologists. Patients were re-examined every 3 months in the first 2 years after operation, including imaging and tumor markers detection. If the results were stable, the interval of re-examination could be changed to once a year. Early recurrence was defined as recurrence within 1 year after radical resection as described before (5). OS was defined as the time between the date of surgery and the date of death due to any reason or the last follow-up. The median follow-up times of the training and validation groups were 41 months and 40 months, respectively; and the median survival times were 19 months and 20 months, respectively.

Identification of Independent Risk Factors

To identify and verify the independent prognostic value of risk factors, we first performed univariate Cox regression analysis on 44 perioperative blood parameters using the R studio software (version 1.3.1056). Compared with the traditional stepwise regression method, LASSO regression punished the overfitting of data by constructing penalty coefficients, which reduced the interference of collinearity influencing factors between data. LASSO regression can actively select from a large number of variables with multicollinearity, reducing the possibility of data over fitting by constructing penalty coefficients (29). Then, 18 variables with p value less than 0.05 were further included in the LASSO (least absolute shrinkage and selection operator) regression analysis to screen out the variables related to early recurrence. During the LASSO regression, two analyses, the shrinkage coefficient diagram and the 10-fold cross-validation diagram were used to screen out the final perioperative serological factors that affect the early recurrence of PDAC patients with radical resection in the training cohort. The shrinkage coefficient diagram was used to determine the candidate variables that entered the model with the variation of λ value. As the value of λ increased, the greater the degree of model compressed, the less the number of candidate variables entered the model. The 10-fold cross-validation diagram was used to determine the lambda.min, which referred to the lambda value of the best model to control the decline of partial likelihood deviance. On this basis, 4 preoperative factors (platelets, Fbg, NLR and LMR) and 3 postoperative parameters (CA19-9, CEA and CA242) were screened out for the establishment of preoperative SICC and postoperative TMs scores.

Construction and Validation of Nomograms

The preoperative SICC and postoperative TMs scores established by univariate Cox and LASSO regression as two variable parameters, together with the clinicopathological characteristics of patients, a total of 20 parameters, were included in univariate and multivariate Cox regression analysis, and further determined all independent risk factors associated with early recurrence and OS in patients. On this basis, the factors associated with the recurrence of PDAC patients after radical resection were identified as: preoperative SICC, postoperative TMs, CACI, vascular cancer embolus and adjuvant chemotherapy. The factors associated with overall survival were preoperative SICC, postoperative TMs, CACI, smoking index, vascular cancer embolus, and adjuvant chemotherapy. By taking into account all the variables, nomograms were established. The total points of each patient were calculated by the score model, and then divided into the high-score and low-score groups.

Statistical Analysis

R Studio version 1.3.1056 was used for statistical analysis. Data comparison and correlation between groups were determined *via* nonparametric tests, chi-squared tests or Fisher accuracy as indicated. Univariate and multivariate Cox ("survival" package in R) and LASSO regression ("glmnet" package in R) were applied to analyse risk factors that affect prognosis. p-value and hazard ratio (HR) were calculated *via* Cox regression to determine the prognostic factors. The Kaplan-Meier method was used to compare survival between groups. The receiver operating characteristic (ROC) curve and the concordance index (C-index) were used to evaluate the performance of predictive model for recurrence or prognosis. Area under the curve (AUC)

values were compared by Z-test. $p<0.05$ was considered statistically significant.

RESULTS

Patient Characteristics

A total of 327 patients with radical resection were recruited for this study, and then randomly divided into the training group (218) and the validation group (109), with the same average age of 60 years. In the training group, 201 (92.2%) patients were younger than 70 years, and 124 (56.9%) patients were male, and 128 (58.7%) patients had a CACI greater than or equal to 4. In addition, 149 cases (68.3%) were located in the head and uncinate process of the pancreas, while 69 cases (31.7%) were in the body and tail. 108 patients (49.5%) were in stage I (21 patients in stage IA and 87 patients in stage IB), 93 patients (42.7%) were in stage II (30 patients in stage IIA and 63 patients in stage IIB), and 17 patients (7.8%) were in stage III due to the presence of more than 3 lymph node metastases. Based on the pathological features, there were 35 patients (16.0%) in T1-stage (tumor size ≤ 2), 134 patients (61.5%) in T2-stage (2 < tumor size ≤ 4cm), and 49 patients (22.5%) in T3-stage (tumor size > 4cm). 80 patients (36.7%) had lymph node metastasis that were confirmed by pathology, including 63 patients with N1-stage and 17 patients with N2-stage. Furthermore, 177 patients (81.2%) received gemcitabine-based systemic chemotherapy after resection (**Table 1**).

Similarly, we also analysed the constituent ratio of each clinicopathological feature in the validation group, and compared with that in the training group. As expected, most of the clinicopathological features did not differ statistically between the two groups, except the differentiation degree and the ratio of patients that received adjuvant chemotherapy (**Table 1**), suggesting an entirely acceptable homogeneity between these two cohorts.

Identification of Parameters Related to Early Recurrence

On the basis of published studies and clinical experience, 44 blood parameters that might have been perceived as contributing to the postoperative early recurrence of PDAC patients were initially selected in the training group, and then evaluated using the Cox regression models (**Figure 1A**). In the univariate survival analysis, 18 of the 44 variables were statistically corelated with early recurrence of PDAC patients after radical resection (**Table 2**). We next analysed the correlation of these 18 variables, and determined that they were interrelated rather than independent influencing variables (**Figure 1B** and **Supplementary Table 1**).

Compared with the traditional stepwise regression method, LASSO regression punished the over fitting of data by constructing penalty coefficient, which reduced the interference of collinearity influencing factors between data. Therefore, we used LASSO regression to further analyze these 18 variables. The shrinkage coefficient diagram may force and generate coefficients that are exactly 0 during operation. It is selected to retain non-zero variables in the model and generate a set of more relevant and interpretable prediction values to build the optimal model. As the value of λ increased, the greater the degree of model compressed, the less the number of candidate variables entered the model (**Figure 1C**). The 10-fold cross-validation diagram was used to determine the lambda.min, which referred to the lambda value of the best model to control the decline of partial likelihood deviance. The lambda.min was calculated as 0.07373468 (**Figure 1D**). At this time, the factors entering the model that significantly affected the early recurrence after radical resection only included 4 preoperative factors (platelets, Fbg,

TABLE 1 | Clinicopathological characteristics of patients in the training and validation groups.

Characteristics	Training (n)	Validation (n)	P-value
Total	218	109	–
Age, median (range)(years)	60 (39-80)	60 (36-84)	–
(<70 years vs. ≥70 years)	201 vs. 17	96 vs. 13	0.223
Gender (Male vs. Female)	124 vs. 94	73 vs. 36	0.079
CACI (≥4 vs. <4)	128 vs. 90	64 vs. 45	1.000
Smoking index (<400 vs. ≥400)	152 vs. 66	78 vs. 31	0.732
Alcohol consumption (No vs. Yes)	166 vs. 52	84 vs. 25	0.854
Family cancer history (No vs. Yes)	184 vs. 34	88 vs. 21	0.403
Diabetes (Absent vs. Present)	162 vs. 56	79 vs. 30	0.722
Pain (Present vs. Absent)	125 vs. 93	63 vs. 46	0.937
Weight loss (Present vs. Absent)	107 vs. 111	59 vs. 50	0.390
Tumor location (Head and Uncinate process vs. Body and Tail)	149 vs. 69	75 vs. 34	0.933
Differentiation (Poor vs. Well/Moderate)	147 vs. 71	60 vs. 49	0.028
Tumor size (≤4.0 cm vs. >4.0cm)	169 vs. 49	87 vs. 22	0.635
Regional lymph (N0 vs. N1 and N2)	138 vs. 80	77 vs. 32	0.187
Pathological stage (I and IIA vs. IIB and III)	138 vs. 80	77 vs. 32	0.187
Pancreatic capsule invasion (Present vs. Absent)	159 vs. 59	83 vs. 26	0.533
Perineural invasion (Present vs. Absent)	111 vs. 107	65 vs. 44	0.136
Vascular cancer embolus (Absent vs. Present)	185 vs. 33	93 vs. 16	0.913
Adjuvant chemotherapy (yes vs. no)	177 vs. 41	77 vs. 32	0.031

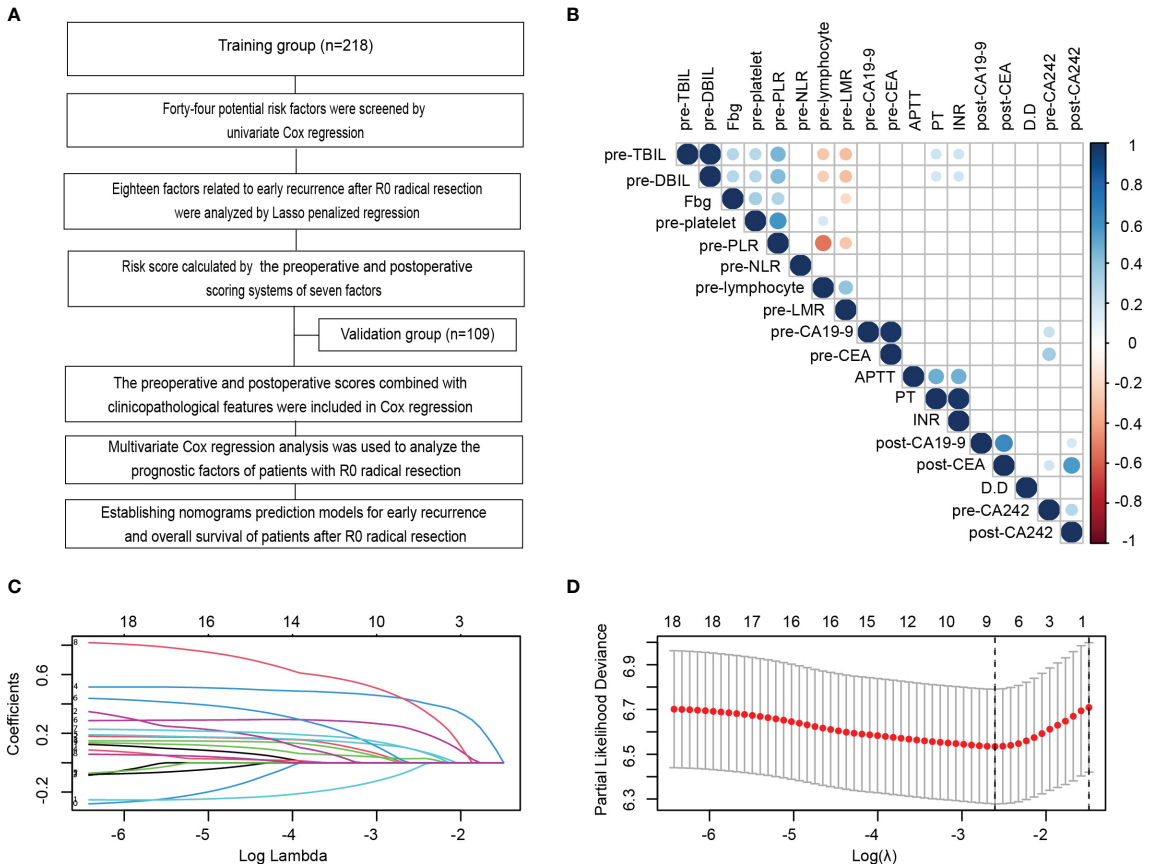

FIGURE 1 | Identification and establishment of scoring systems related to serum indexes for early recurrence during the perioperative period. **(A)** Flowchart of the establishment of scoring systems and nomograms for the early recurrence and long-term prognosis of PDAC patients after radical resection in this study. **(B)** Correlation analysis amongst 18 variables with p values less than 0.05 in the univariate Cox analysis of the training cohort. **(C, D)** LASSO analysis of the 18 variables with $p < 0.05$ in the univariate Cox regression analysis to screen out the perioperative serological factors that affect the early recurrence of PDAC patients with radical resection in the training cohort. Shrinkage coefficient diagram was shown in **(C)**. Each curve represented the change track of each candidate variable coefficient. As the value of λ increased, the greater the degree of model compressed, the less the number of candidate variables entered the model. Ten-fold cross-validation diagram showed the determination of the best λ Value **(D)**.

NLR and LMR) and 3 postoperative parameters (CA19-9, CEA and CA242). According to the screening variable coefficient, we established the preoperative and postoperative scoring formulas as follows:

$$\text{Preoperative SICC score} = 0.414{*}\text{platelet} + 0.096{*}\text{Fbg} + 0.028{*}\text{NLR} - 0.055{*}\text{LMR}$$

$$\text{PostoperativeTMs score} = 0.428{*}\text{CA19} - 9 + 0.097{*}\text{CEA} + 0.028{*}\text{NLR} + 0.232{*}\text{CA242}$$

$$\text{Total score} = \text{Preoperative SICC score} + \text{Postoperative TMs score}$$

Based on these formulas, we calculated the preoperative SICC and postoperative TMs of each patient, and then used X-Tile to determine their best cutoff values for prediction of early recurrence. Eventually, the cutoff values of preoperative SICC and postoperative TMs for effectively predicting early recurrence of PDAC patients after radical resection were set as 0.4 and 0.6, respectively.

ROC Curves of the Scoring Systems

To evaluate the accuracy of our newly developed scoring systems in predicting early recurrence, we determined the ROC curves of our preoperative and postoperative scoring systems, as well as the currently used tumor markers (CA19-9, CEA, CA242), and the five independent inflammatory markers (neutrophils, platelets, lymphocytes, monocytes and ALB) or even their combinations (NLR, PLR, LMR, PNI, NAR and PAR) during the preoperative and postoperative period in the training group, and then compared their performance in predicting early recurrence of PDAC patients (**Table 3**). Encouragingly, our data indicated that the AUC of our preoperative SICC was significantly higher than

TABLE 2 | Univariate Cox regression analysis of 44 perioperative blood parameters in patients with PDAC after radical resection.

Parameters	Beta	HR (95% CI for HR)	Wald.Test	p.value
[a] Pre-CA19-9 (<942.4 vs. ≥942.4)	0.652	1.920 (1.310-2.820)	11.10	<0.001
Pre-CEA (<8.03 vs. ≥8.03)	0.441	1.550 (1.050-2.300)	4.82	0.028
Pre-CA242 (<14.93 vs. ≥14.93)	0.407	1.500 (1.100-2.040)	6.72	0.010
[b] Post-CA19-9 (<31.11 vs. ≥31.11)	1.110	3.030 (2.240-4.100)	51.40	<0.001
Post-CEA (<2.56 vs. ≥2.56)	0.517	1.680 (1.240-2.260)	11.50	<0.001
Post-CA242 (<11.68 vs. ≥11.68)	0.822	2.280 (1.680-3.080)	28.30	<0.001
Pre-neutrophils (<3.73 vs. ≥3.73)	0.272	1.310 (0.976-1.760)	3.24	0.072
Pre-lymphocytes (<1.4 vs. ≥1.4)	-0.334	0.716 (0.532-0.964)	4.85	0.028
Pre-monocytes (<0.43 vs. ≥0.43)	0.088	1.090 (0.812-1.470)	0.34	0.561
Pre-platelets (<329 vs. ≥329)	0.728	2.070 (1.400-3.070)	13.10	<0.001
Pre-ALB (<46.5 vs. ≥46.5)	0.231	1.260 (0.850-1.870)	1.33	0.250
Pre-NLR (<1.95 vs. ≥1.95)	0.628	1.870 (1.340-2.610)	13.70	<0.001
Pre-PLR (<191.96 vs. ≥191.96)	0.450	1.570 (1.150-2.140)	7.91	0.005
Pre-LMR (<4.7 vs. ≥4.7)	-0.359	0.699 (0.503-0.970)	4.59	0.032
Pre-PNI (<54.15 vs. ≥54.15)	0.113	1.120 (0.796-1.570)	0.42	0.518
Pre-NAR (<0.09 vs. ≥0.09)	0.141	1.150 (0.857-1.550)	0.87	0.350
Pre-PAR (<7.71 vs. ≥7.71)	0.042	1.040 (0.696-1.560)	0.04	0.839
Pre-ALP (<68 vs. ≥68)	0.182	1.200 (0.745-1.930)	0.56	0.454
Pre-TBIL (<382.1 vs. ≥382.1)	0.631	1.880 (1.110-3.200)	5.43	0.020
Pre-DBIL (<189.9 vs. ≥189.9)	0.541	1.720 (1.080-2.740)	5.16	0.023
Pre-GGT (<19 vs. ≥19)	0.169	1.180 (0.811-1.730)	0.76	0.382
Pre-LDH (<142 vs. ≥142)	0.542	1.720 (0.878-3.370)	2.50	0.114
Post-neutrophils (<6.54 vs. ≥6.54)	0.248	1.280 (0.940-1.750)	2.46	0.117
Post-lymphocytes (<1.39 vs. ≥1.39)	0.139	1.150 (0.853-1.550)	0.84	0.360
Post-monocytes (<0.67 vs. ≥0.67)	0.209	1.230 (0.912-1.670)	1.85	0.174
Post-platelets (<409 vs. ≥409)	0.241	1.270 (0.931-1.740)	2.28	0.131
Post-ALB (<33.3 vs. ≥33.3)	0.228	1.260 (0.901-1.750)	1.81	0.178
Post-NLR (<4.38 vs. ≥4.38)	0.152	1.160 (0.855-1.590)	0.93	0.334
Post-PLR (<327.94 vs. ≥327.94)	0.110	1.120 (0.807-1.550)	0.44	0.505
Post-LMR (<0.74 vs. ≥0.74)	0.733	2.080 (0.772-5.610)	2.10	0.147
Post-PNI (<39.40 vs. ≥39.40)	0.298	1.350 (0.955-1.900)	2.88	0.090
Post-NAR (<0.15 vs. ≥0.15)	0.296	1.340 (0.932-1.940)	2.51	0.113
Post-PAR (<14.49 vs. ≥14.49)	0.050	1.050 (0.713-1.550)	0.06	0.800
Post-ALP (<69 vs. ≥69)	0.567	1.760 (0.781-3.980)	1.87	0.172
Post-TBIL (<218.9 vs. ≥218.9)	0.597	1.820 (0.674-4.900)	1.40	0.238
Post-DBIL (<24.9 vs. ≥24.9)	0.204	1.230 (0.862-1.750)	1.29	0.256
Post-GGT (<68 vs. ≥68)	0.241	1.270 (0.902-1.800)	1.89	0.169
Post-LDH (<223.19 vs. ≥223.19)	0.149	1.160 (0.844-1.600)	0.84	0.360
PT (<11.1 vs. ≥11.1)	0.401	1.490 (1.110-2.010)	6.94	0.008
INR (<1.04 vs. ≥1.04)	0.392	1.480 (1.090-2.010)	6.24	0.013
APTT (<21.5 vs. ≥21.5)	0.611	1.840 (1.000-3.390)	3.84	0.049
Fbg (<3.851 vs. ≥3.851)	0.517	1.680 (1.240-2.270)	11.20	0.001
TT (<17.1 vs. ≥17.1)	0.349	1.420 (0.848-2.370)	1.77	0.184
D-D (<295.82 vs. ≥295.82)	0.359	1.430 (1.000-2.040)	3.90	0.048

[a]*Pre-,means preoperative;* [b]*Post-,means postoperative.*

those of CA19-9 (0.659 vs 0.536; p=0.006), CEA (0.659 vs 0.543; p=0.01) and CA242 (0.659 vs 0.554; p=0.044), as well as neutrophils (0.659 vs 0.552; p=0.010), platelets (0.659 vs 0.569; p=0.004), lymphocytes (0.659 vs 0.560; p=0.041), monocytes (0.659 vs 0.504; p<0.001) and ALB (0.659 vs 0.508; p=0.001), or even NLR (0.659 vs 0.599; p=0.032), PLR (0.659 vs 0.568; p=0.009), LMR (0.659 vs 0.570; p=0.047), PNI (0.659 vs 0.503; p=0.003), NAR (0.659 vs 0.526; p=0.010) and PAR (0.659 vs 0.510; p<0.001) (**Figures 2A, B** and **Table 3**), suggesting that the preoperative application of SICC was more accurate than the currently used tumor and inflammatory markers in predicting early recurrence.

Interestingly, compared with the preoperative SICC, after operation more attention should be given to the changes in tumor markers, which were more effective than that of the postoperative immune indexes for prediction of early recurrence (**Figures 2C, D** and **Table 3**). Although the AUC between the postoperative TMs (0.683) and the independent postoperative tumor markers (CA19-9, 0.617; CEA, 0.588; CA242, 0.637) was no statistical difference, postoperative TMs still provided the maximum AUC value in predicting early recurrence (**Figure 2C** and **Table 3**). In addition, no statistical difference was observed among the preoperative SICC, postoperative TMs and total scores for predicting early recurrence (**Table 3**), suggesting that our new scoring systems may help doctors evaluate the early recurrence of PDAC patients both at preoperative and postoperative stage.

TABLE 3 | Comparison of the area under curve (AUC) of the blood scoring systems and inflammatory markers.

Parameters	pre[a]			post[b]		
	AUC (95%CI)	*p* value	*p* value[c]	AUC (95%CI)	*p* value	*p* value[d]
CA19-9	0.536 (0.491-0.582)	0.063	0.006	0.617 (0.558-0.677)	<0.001	0.424
CEA	0.543 (0.500-0.587)	0.030	0.010	0.588 (0.522-0.654)	0.005	0.120
CA242	0.554 (0.487-0.622)	0.059	0.044	0.637 (0.572-0.701)	<0.001	0.601
Neutrophils	0.552 (0.486-0.618)	0.063	0.010	0.546 (0.480-0.612)	0.345	0.006
Platelets	0.569 (0.526-0.613)	0.002	0.004	0.538 (0.477-0.599)	0.113	0.005
Lymphocytes	0.560 (0.497-0.624)	0.033	0.041	0.519 (0.452-0.586)	0.707	0.002
Monocyte	0.504 (0.437-0.571)	0.457	<0.001	0.527 (0.461-0.594)	0.211	0.001
Albumin	0.508 (0.460-0.556)	0.377	0.001	0.561 (0.498-0.623)	0.029	0.017
NLR	0.599 (0.536-0.663)	0.001	0.032	0.546 (0.480-0.612)	0.084	0.005
PLR	0.568 (0.509-0.627)	0.014	0.009	0.526 (0.469-0.583)	0.186	0.001
LMR	0.570 (0.498-0.625)	0.028	0.047	0.522 (0.496-0.549)	0.042	<0.001
PNI	0.503 (0.445-0.560)	0.466	0.003	0.564 (0.505-0.624)	0.017	0.018
NAR	0.526 (0.459-0.592)	0.227	0.010	0.550 (0.492-0.608)	0.043	0.005
PAR	0.510 (0.463-0.557)	0.340	<0.001	0.504 (0.454-0.554)	0.435	<0.001
Preoperative SICC	0.659 (0.586-0.733)	<0.001	–	–	–	0.633
Postoperative TMs	–	–	0.633	0.683 (0.608-0.758)	<0.001	–
Total score	0.719 (0.653-0.786)	<0.001	0.118	0.719 (0.653-0.786)	<0.001	0.083

[a]*Indicates preoperative serum index.*
[b]*Indicates postoperative serum index.*
[c]*The AUC values between preoperative SICC and other inflammatory factors were compared by Z-test.*
[d]*The AUC values between postoperative TMs and other inflammatory factors were compared by Z-test.*

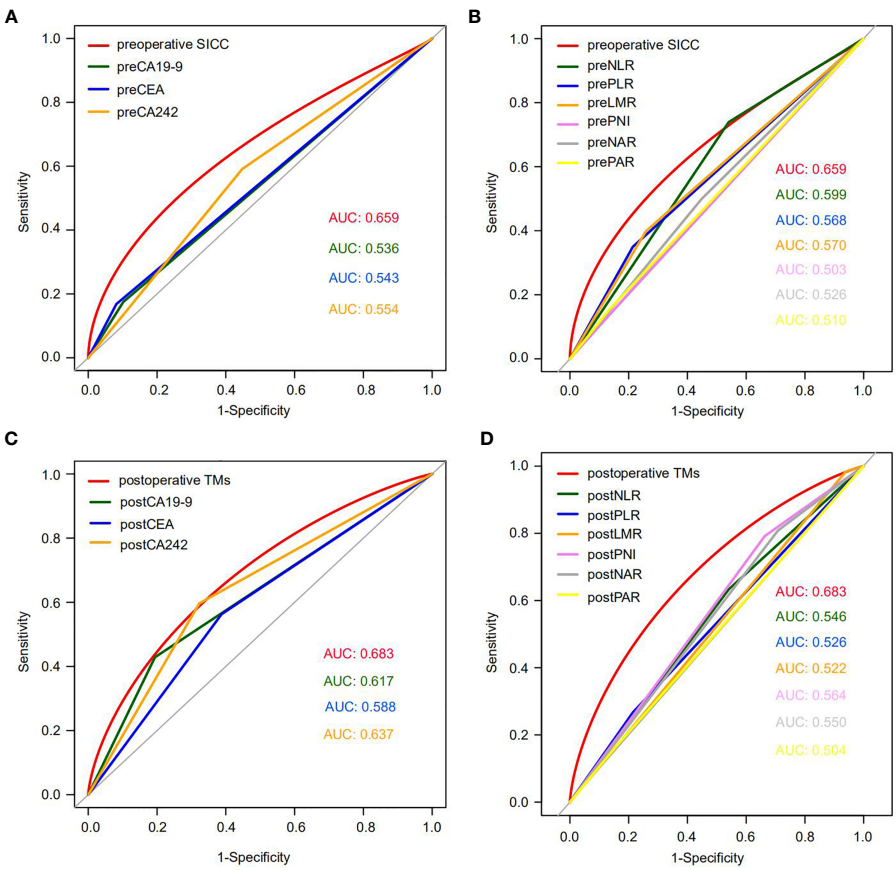

FIGURE 2 | The ROC curves of preoperative SICC, postoperative TMs, tumor markers and six combinations of inflammatory factors in the training cohort. **(A)** Comparison of the ROC curves for early recurrence between preoperative SICC and preoperative tumor markers for PDAC patients who underwent radical resection. **(B)** Comparison of the ROC curves for early recurrence between preoperative SICC and preoperative six combinations of inflammatory markers. **(C)** Comparison of the ROC curves for early recurrence between postoperative TMs and postoperative tumor markers. **(D)** Comparison of the ROC curves for early recurrence between postoperative TMs and postoperative six combinations of inflammatory markers.

Prognostic Stratification Value of Serum Scoring Systems for Patients With Resectable PDAC

To further investigate the accuracy of the serum scoring systems in predicting the recurrence and long-term prognosis of patients with resectable PDAC, we performed univariate and multivariate Cox analysis in the training group to assess the efficacy of preoperative SICC and postoperative TMs score, as well as the clinical pathological variables for predicting the relapse-free survival (RFS) and overall survival (OS) of patients. In the univariate Cox analysis, preoperative SICC ≥ 0.4, postoperative TMs ≥ 0.6, CACI ≥ 4, lymph node metastasis, vascular cancer embolus, high pathological stage and no postoperative adjuvant chemotherapy were the risk factors for both recurrence and poor OS. In addition, poor pathological differentiation was also a risk factor for recurrence, but not for poor OS, while smoking index ≥ 400 was just the opposite. Moreover, incorporating the aforementioned variables into multivariate Cox analysis indicated that preoperative SICC ≥ 0.4, postoperative TMs ≥ 0.6, CACI ≥ 4, vascular cancer embolus and not receiving adjuvant chemotherapy were independent risk factors for both early recurrence and poor OS (**Table 4**).

Notably, Kaplan-Meier survival analysis demonstrated that patients with preoperative SICC ≥ 0.4 displayed much lower survival times than that with preoperative SICC < 0.4 both in RFS (median survival: 5 vs 12 months) and OS (median survival: 12 vs 22 months) (**Figures 3A, B**). Similarly, patients with postoperative TMs ≥ 0.6 or total score ≥ 0.6 also represented the poor RFS (median survival: 5 vs 15 months in both scores) and OS (median survival: 12 vs 28 months in postoperative TMs, 11 vs 28 months in total score) when compared to the patients with lower score (**Figures 3C–F**). Furthermore, in accordance with patients' total score and recurrence prognosis distribution (**Figure 3G**), and by comparing with the actual recurrence rate and survival rate, the total score predicted the early recurrence and long-term survival of patients with C-index values of 0.680 and 0.678, respectively (**Figure 3H**), suggesting a high efficiency of this scoring system.

To confirmed these data, we next performed the same analysis in the validation group with a cohort of 109 patients. As expected, all of our newly developed preoperative SICC, postoperative TMs and total scores could effectively evaluate the RFS and OS of the patients in the validation group (**Supplementary Figures 1A–F**). Meanwhile, the total score was very consistent in predicting the early recurrence and long-term survival of patients over these two cohorts (**Supplementary Figures 1G, H**). Altogether, these results demonstrated that our scoring systems may be helpful for effectively identifying PDAC patients with rapid recurrence or metastasis after radical resection.

Construction and Verification of Nomograms for Early Recurrence and Long-Term Prognosis Prediction

On the basis of the aforementioned multivariate Cox regression model, we then established two independent nomograms for

TABLE 4 | Univariate and multivariate analysis of recurrence and long-term prognosis in the training group.

Characteristics	Relapse-free survival		Overall survival	
	HR (95%CI)	p-value	HR (95%CI)	p-value
Univariate analysis				
Preoperative SICC (≥0.4 vs. <0.4)	6.540 (2.800-15.300)	<0.001	5.770 (2.490-13.400)	<0.001
Postoperative TMs (≥0.6 vs. <0.6)	4.090 (2.460-6.830)	<0.001	5.620 (3.350-9.440)	<0.001
Gender (Male vs. Female)	0.855 (0.630-1.160)	0.314	0.733 (0.535-1.00)	0.052
Age (≥70 years vs. <70 years)	0.962 (0.546-1.700)	0.893	0.979 (0.543-1.760)	0.943
CACI (≥4 vs. <4)	1.700 (1.240-2.330)	<0.001	2.150 (1.540-3.000)	<0.001
Smoking Index (≥400 vs. <400)	1.270 (0.913-1.760)	0.157	1.490 (1.080-2.070)	0.016
Alcohol consumption (yes vs. no)	1.090 (0.764-1.560)	0.630	1.290 (0.909-1.840)	0.153
Diabetes (yes vs. no)	1.090 (0.777-1.540)	0.610	0.960 (0.672-1.370)	0.822
Abdominal pain (yes vs. no)	1.270 (0.929-1.720)	0.135	1.210 (0.880-1.660)	0.244
Weight loss (yes vs. no)	0.963 (0.712-1.300)	0.806	1.120 (0.824-1.530)	0.466
Operation procedure (PD vs. DP)	0.885 (0.644-1.220)	0.453	0.830 (0.600-1.150)	0.259
Differentiation (Poor vs. well/moderate)	1.420 (1.020-1.970)	0.037	1.250 (0.892-1.740)	0.196
Tumor size (>4.0cm versus ≤4.0 cm)	1.100 (0.765-1.580)	0.611	1.360 (0.949-1.940)	0.094
lymph node (N) (0 vs. 1 and 2)	1.280 (1.010-1.620)	0.043	1.370 (1.090-1.740)	0.007
Positive lymph node ratio (>0.2 vs. ≤0.2)	1.380 (0.934-2.050)	0.105	1.550 (1.050-2.290)	0.028
Pancreatic capsule invasion (Present vs. Absent)	0.963 (0.689-1.340)	0.824	1.070 (0.753-1.510)	0.721
Perineural invasion (Present vs. Absent)	1.050 (0.776-1.420)	0.758	1.080 (0.794-1.470)	0.626
Vascular cancer embolus (Present vs. Absent)	1.660 (1.100-2.500)	0.015	1.510 (1.010-2.270)	0.044
Pathological stage (I/IIA vs. IIB/III)	1.390 (1.010-1.900)	0.041	1.420 (1.030-1.940)	0.031
Adjuvant chemotherapy (yes vs. no)	1.710 (1.160-2.540)	0.007	2.410 (1.650-3.530)	<0.001
Multivariate analysis				
Preoperative SICC (≥0.4 vs. <0.4)	4.646 (1.887-11.438)	<0.001	2.834 (1.161-6.915)	0.022
Postoperative TMs (≥0.6 vs. <0.6)	3.205 (1.891-5.434)	<0.001	3.821 (2.187-6.676)	<0.001
CACI (≥4 vs. <4)	1.414 (1.017-1.966)	0.039	1.630 (1.140-2.329)	0.007
Smoking Index (≥400 vs. <400)	–	–	1.553 (1.110-2.172)	0.010
Vascular cancer embolus (Present vs. Absent)	1.702 (1.080-2.684)	0.022	1.709 (1.114-2.624)	0.014
Adjuvant chemotherapy (yes vs. no)	1.551 (1.026-2.347)	0.038	1.745 (1.162-2.621)	0.007

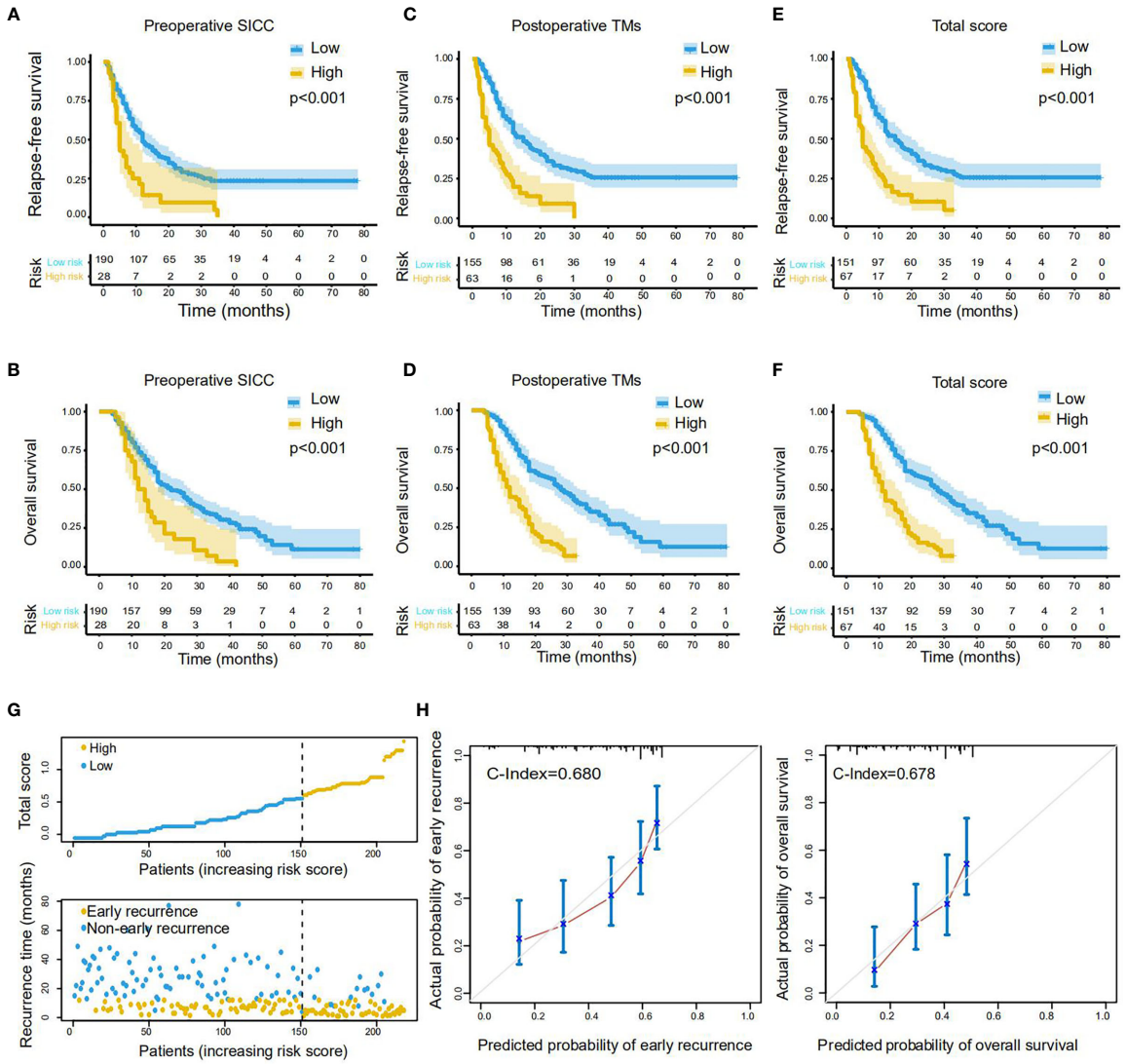

FIGURE 3 | Performance of the scoring systems on RFS and OS prediction in the training cohort. **(A, B)** The Kaplan-Meier survival curves of RFS **(A)** and OS **(B)** for PDAC patients with low or high preoperative SICC ($Value_{cutoff}$ = 0.4). **(C, D)** The Kaplan-Meier survival curves of RFS **(C)** and OS **(D)** for patients with low or high postoperative TMs ($Value_{cutoff}$ = 0.6). **(E, F)** The Kaplan-Meier survival curves of RFS **(E)** and OS **(F)** for patients with low or high total score ($Value_{cutoff}$ = 0.6). **(G)** Distribution of the total score and related recurrence data in the training cohort. **(H)** Calibration plot for the internal validation of the total score on RFS (left) and OS (right) evaluation. The Y-axis represents the actual rate. The X-axis represents the predicted rate. Each cutoff value was calculated *via* X-Tile.

predicting recurrence at 1, 2 or 3 years and survival at 1, 3 or 5 years, respectively. The factors for predicting recurrence and survival both included CACI, vascular cancer embolus, adjuvant chemotherapy, preoperative SICC and postoperative TMs (**Figures 4A, B**). Besides, the smoking index was also involved in the survival prediction (**Figure 4B**). To assess the efficacy of these two nomograms in recurrence and survival prediction, we determined their ROC curves for RFS and OS evaluation in the training cohort. The results indicated that AUC values of 1-, 2- and 3-years RFS were 0.763, 0.679 and 0.657 (**Figure 4C**), while the 1-, 3- and 5-year OS were 0.770, 0.804 and 0.763, respectively (**Figure 4D**), representing a great performance for these two nomograms in predicting recurrence and survival of PDAC after radical resection.

According to the nomograms, we next calculated the patient risk score in recurrence and prognosis prediction. By using the X-tile plot, we finally determined the cutoff values of recurrence and survival as 191 and 185, respectively, and then divided the training cohort into high-risk and low-risk groups. As expected, in contrast with the low-risk group, high-risk group were more likely to suffer from relapse (p<0.001), and displayed much worse OS rates (p<0.001) (**Figures 4E, F**).

Simultaneously, we also performed the same analysis in the validation cohort and obtained the consistent results that our newly

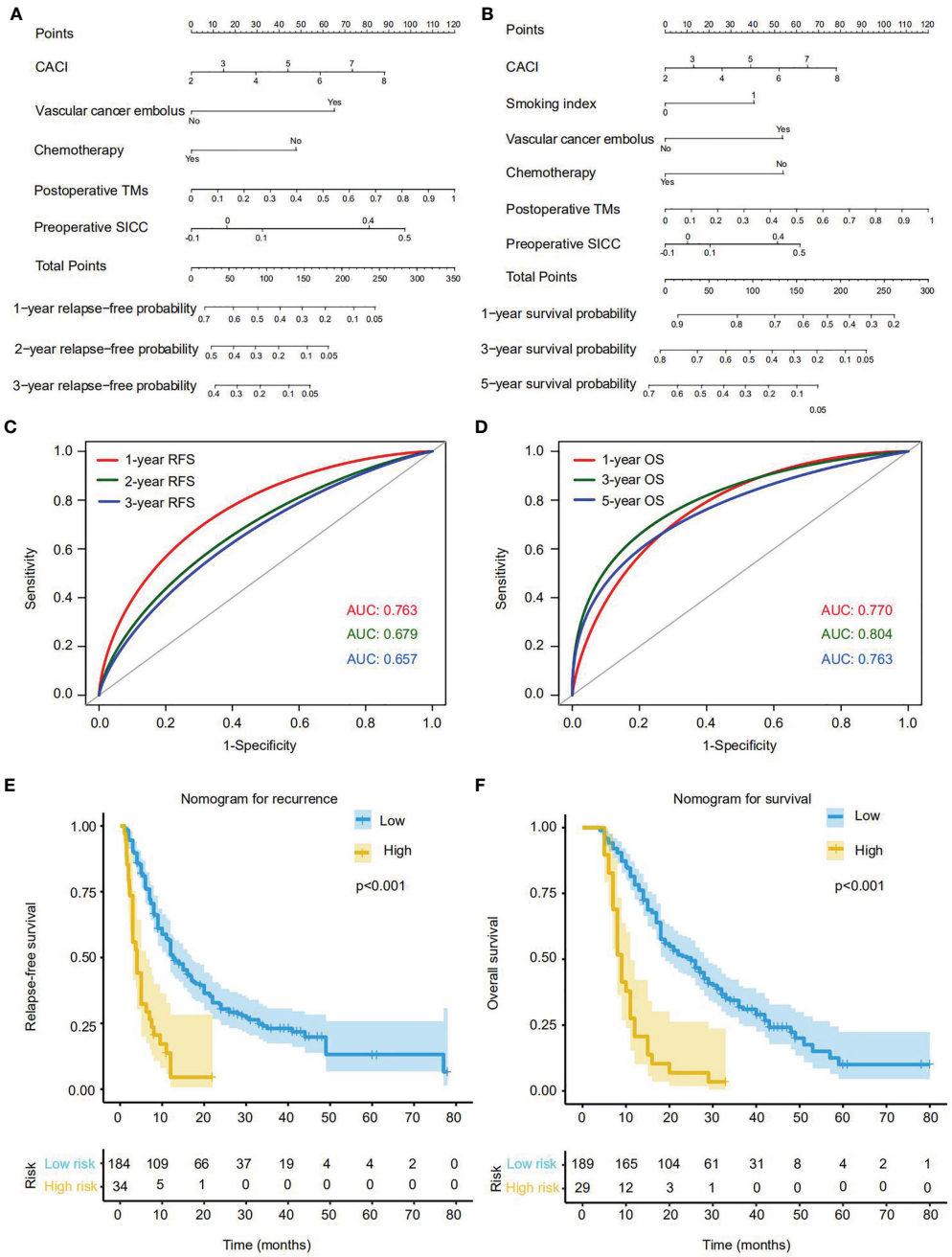

FIGURE 4 | Establishment and effectiveness evaluation of nomograms for predicting the recurrence or OS rate of PDAC patients with radical resection in the training cohort. **(A)** Nomogram for predicting 1-, 2- and 3-year recurrence. **(B)** Nomogram for predicting 1-, 3- and 5-year OS. **(C)** The ROC curves and AUC values of the nomogram for 1-, 2- and 3-year recurrence predictions. **(D)** The ROC curves and AUC values of the nomogram for 1-, 3- and 5-year OS predictions. **(E, F)** The Kaplan-Meier survival curves of RFS **(E)** and OS **(F)** for patients with low or high score according to the nomograms ($cutoff_{recurrence}$ = 191; $cutoff_{survival}$ = 185). Each cutoff value was calculated *via* X-Tile.

established nomograms could effectively predict the recurrence and survival of PDAC patients with radical resection. (**Supplementary Figure 2A-D**). Thus, we have developed a series of accessible scoring systems and nomograms that display high potential to help clinicians identify resectable PDAC patients with high risk of early recurrence and metastasis for precision medicine and early intervention.

DISCUSSION

Clinically, some PDAC patients who underwent radical resection experienced rapid recurrence and metastasis after operation, but may benefit from neoadjuvant chemotherapy (5). By setting the time threshold for early recurrence at 12

months, approximately 53.8% (176/327) patients in our cohorts experienced early recurrence after radical resection. Thus, an effective and accessible evaluation system for accurately identifying these patients is urgently needed in clinic, but is currently lacked. Current evaluation systems just consider limited parameters 1 month or more before or after surgery, whilst disregarding the indicators during the perioperative period, which in fact, is more crucial for the prognosis prediction of resectable PDAC (25). In this study, we recruited 327 PDAC patients with radical resection from our centre and randomly divided into two cohorts (the training and validation groups). In the training cohort, 44 perioperative serum parameters during the perioperative period, including systemic inflammatory system parameters, coagulation system parameters, tumor markers and other parameters, were systematically analysed to determine factors that may affect early recurrence. After univariate Cox screening, variables with p value less than 0.05 were included in the LASSO regression model to undergo a more rigorous screening process. Our data indicated that 4 preoperative parameters (platelets, Fbg, NLR and LMR) and 3 postoperative parameters (CA19-9, CEA and CA242) were important risk factors for early recurrence of PDAC patients after radical resection, which was very consistent in the validation cohort. These findings suggested that more attention should be given to coagulation cascades and systemic inflammatory response before operation and tumor markers changes after operation.

The coagulation and immune systems play important roles in the occurrence and development of tumors (30, 31). The interaction between platelets and tumor cells is a prerequisite for tumor blood metastasis, which could help tumor cells escape from immunosurveillance, and facilitates proliferation and colonisation (32, 33). It is well known that Fbg is closely related to the development of inflammation-driven malignant tumors through promoting proliferation, angiogenesis and the expression of key inflammatory mediators (30). A meta-analysis of 15371 patients showed that an increase in plasma Fbg before treatment was significantly associated with a decrease in the survival of patients with solid tumors (34). Lots of studies have confirmed that many systemic immune factors and their combinations, such as neutrophils (35), lymphocytes (36), monocytes (37), platelets (38), ALB (39), NLR (40), PLR (41), LMR (42), NAR (43) and PAR (44) could predict the prognosis of patients. Amongst them, neutrophils and monocytes are regarded as risk factors for the prognosis, while lymphocytes are considered as protective factors for tumor patients (37, 45), which is consistent with our findings.

CA19-9 is well-known as the preferred biomarker that is recommended in NCCN guidelines for the clinical management of PDAC (46). However, it should be noted that the sensitivity of CA19-9 in patients with early PDAC is much lower than that with late PDAC (47). Besides, CEA and CA242 are other two commonly used tumor markers in clinic. Notably, the patients with positive expression of more than two of these tumor markers have significantly shorter survival time than that with only one or no expression (19). Interestingly, a retrospective cohort study reported that patients with elevated preoperative CEA that returned to normal after colon cancer resection did not exhibit a higher risk of recurrence in contrast with normal preoperative CEA, suggesting that preoperative CEA was not a risk factor for postoperative recurrence. Instead, patients with elevated postoperative CEA were more prone to recurrence within 1 year after operation (48). This study further supports our results that postoperative but not preoperative tumor markers were risk factors for early recurrence of PDAC patients who underwent radical resection. That would mean more attention should be given to the postoperative tumor markers for monitoring the prognosis of resectable PDAC patients.

All of the parameters involved in this study are necessary inspection indicators for PDAC patients during the perioperative period. Therefore, our newly developed evaluation systems are very accessible, and will not increase the financial burden of patients. However, it should be noted that our study still has several limitations. Firstly, although huge number of parameters were considered in the beginning, just limited variables were finally involved in the evaluation models. Secondly, this study was a single-centre retrospective study, so the representativeness of these systems is limited, and need to be further investigate. In the future, we will continue to improve these scoring systems and nomograms by including more indicators and expanding the patient cohort to multi-centre.

In conclusion, we established preoperative SICC and postoperative TMs scoring models for effectively predicting early recurrence and prognosis of PDAC patients after radical resection, whose scores were identified as independent risk factors for recurrence and long-term survival in our cohorts. Moreover, on the basis of these scoring systems, we further constructed nomogram models for the accurate evaluation of the RFS and OS of PDAC patients who underwent radical resection. Thus, our study has provided a series of effective evaluation systems that may help clinicians identify PDAC patients with high risk of early recurrence and metastasis for individualised treatment.

DATA AVAILABILITY STATEMENT

The raw data supporting the conclusions of this article will be made available by the authors, without undue reservation.

ETHICS STATEMENT

The studies involving human participants were reviewed and approved by Tianjin Medical University Cancer Institute and Hospital. The patients/participants provided their written informed consent to participate in this study.

AUTHOR CONTRIBUTIONS

SL: conceptualization, methodology, data curation, formal analysis, investigation, validation, visualization, writing-original draft. GZ: conceptualization, methodology, data curation, formal analysis, investigation, writing-original draft. YL: methodology, data curation, formal analysis, validation, investigation. TZ: resources, data curation, formal analysis. CG: resources, data curation, formal analysis. WL: data curation, formal analysis. YP: methodology, formal analysis, validation. CH: conceptualization, formal analysis, supervision, funding acquisition. YC: writing-review and editing. AC: conceptualization, formal analysis, investigation, supervision, project administration, funding acquisition, writing-review and editing. JH: conceptualization, resources, supervision, funding acquisition, writing-review and editing.

FUNDING

This work was supported by the National Key Research and Development Program of China (2021YFA1201100), the National Natural Science Foundation of China (grants 82030092, 81720108028, 82072657, 81802432, 82072716, 81802433, 82072659, 82173295, 81871968, 81871978, 82072691 and 82103006), the programs of Tianjin Prominent Talents, Tianjin Eminent Scholars, Tianjin Natural Science Foundation (18JCJQJC47800,19JCJQJC63100, 19JCYBJC26200 and 20JCQNJC01330).

ACKNOWLEDGMENTS

We sincerely thank all participants who have contributed to this study.

SUPPLEMENTARY MATERIAL

The Supplementary Material for this article can be found online at: https://www.frontiersin.org/articles/10.3389/fonc.2022.841819/full#supplementary-material

Supplementary Figure 1 | Verification of the performance of preoperative SICC and postoperative TMs scoring systems on RFS and OS evaluation in the validation cohort. **(A-B)** The Kaplan-Meier survival curves of RFS **(A)** and OS **(B)** for PDAC patients with low or high preoperative SICC ($Value_{cutoff}$ = 0.4). **(C, D)** The Kaplan-Meier survival curves of RFS **(C)** and OS **(D)** for patients with low or high postoperative TMs ($Value_{cutoff}$ = 0.6). **(E, F)** The Kaplan-Meier survival curves of RFS **(E)** and OS **(F)** for patients with low or high total score ($Value_{cutoff}$ = 0.6). **(G)** Distribution of the total score and related recurrence data in the validation cohort. **(H)** Calibration plot for the external validation of the total score on RFS (left) and OS (right) evaluation. The Y-axis represents the actual rate. The X-axis represents the predicted rate. Each cutoff value was calculated *via* X-Tile.

Supplementary Figure 2 | Verification of the nomograms for predicting the recurrence or OS rate of PDAC patients with radical resection in the validation cohort. **(A)** The ROC curves and AUC values of the nomogram for 1-, 2- and 3-year recurrence predictions in the validation cohort. **(B)** The ROC curves and AUC values of the nomogram for 1-, 3- and 5-year OS predictions in the validation cohort. **(C, D)** The Kaplan-Meier survival curves of RFS **(C)** and OS **(D)** for patients of the validation cohort with low or high score according to the nomograms ($cutoff_{recurrence}$ = 191; $cutoff_{survival}$ = 185). Each cutoff value was calculated *via* X-Tile.

REFERENCES

1. Mizrahi JD, Surana R, Valle JW, Shroff RT. Pancreatic Cancer. *Lancet* (2020) 395(10242):2008–20. doi: 10.1016/S0140-6736(20)30974-0
2. Kamisawa T, Wood LD, Itoi T, Takaori K. Pancreatic Cancer. *Lancet* (2016) 388(10039):73–85. doi: 10.1016/S0140-6736(16)00141-0
3. Mayo SC, Gilson MM, Herman JM, Cameron JL, Nathan H, Edil BH, et al. Management of Patients With Pancreatic Adenocarcinoma: National Trends in Patient Selection, Operative Management, and Use of Adjuvant Therapy. *J Am Coll Surg* (2012) 214(1):33–45. doi: 10.1016/j.jamcollsurg.2011.09.022
4. Merkow RP, Bilimoria KY, Tomlinson JS, Paruch JL, Fleming JB, Talamonti MS, et al. Postoperative Complications Reduce Adjuvant Chemotherapy Use in Resectable Pancreatic Cancer. *Ann Surg* (2014) 260(2):372–7. doi: 10.1097/SLA.0000000000000378
5. Groot VP, Gemenetzis G, Blair AB, Rivero-Soto RJ, Yu J, Javed AA, et al. Defining and Predicting Early Recurrence in 957 Patients With Resected Pancreatic Ductal Adenocarcinoma. *Ann Surg* (2019) 269(6):1154–62. doi: 10.1097/SLA.0000000000002734
6. Mokdad AA, Minter RM, Zhu H, Augustine MM, Porembka MR, Wang SC, et al. Neoadjuvant Therapy Followed by Resection Versus Upfront Resection for Resectable Pancreatic Cancer: A Propensity Score Matched Analysis. *J Clin Oncol* (2017) 35(5):515–22. doi: 10.1200/JCO.2016.68.5081
7. O'Reilly EM, Ferrone C. Neoadjuvant or Adjuvant Therapy for Resectable or Borderline Resectable Pancreatic Cancer: Which Is Preferred? *J Clin Oncol* (2020) 38(16):1757–9. doi: 10.1200/JCO.19.03318
8. Diakos CI, Charles KA, McMillan DC, Clarke SJ. Cancer-Related Inflammation and Treatment Effectiveness. *Lancet Oncol* (2014) 15(11):e493–503. doi: 10.1016/S1470-2045(14)70263-3
9. McAllister SS, Weinberg RA. The Tumour-Induced Systemic Environment as a Critical Regulator of Cancer Progression and Metastasis. *Nat Cell Biol* (2014) 16(8):717–27. doi: 10.1038/ncb3015
10. Naumann P, Eberlein J, Farnia B, Liermann J, Hackert T, Debus J, et al. Cachectic Body Composition and Inflammatory Markers Portend a Poor Prognosis in Patients With Locally Advanced Pancreatic Cancer Treated With Chemoradiation. *Cancers (Basel)* (2019) 11(11):1655. doi: 10.3390/cancers11111655
11. Zhang K, Hua YQ, Wang D, Chen LY, Wu CJ, Chen Z, et al. Systemic Immune-Inflammation Index Predicts Prognosis of Patients With Advanced Pancreatic Cancer. *J Transl Med* (2019) 17(1):30. doi: 10.1186/s12967-019-1782-x
12. Dolan RD, Laird BJA, Horgan PG, McMillan DC. The Prognostic Value of the Systemic Inflammatory Response in Randomised Clinical Trials in Cancer: A Systematic Review. *Crit Rev Oncol Hematol* (2018) 132:130–7. doi: 10.1016/j.critrevonc.2018.09.016
13. Coffelt SB, Wellenstein MD, de Visser KE. Neutrophils in Cancer: Neutral No More. *Nat Rev Cancer* (2016) 16(7):431–46. doi: 10.1038/nrc.2016.52
14. Coffelt SB, Kersten K, Doornebal CW, Weiden J, Vrijland K, Hau CS, et al. IL-17-Producing Gammadelta T Cells and Neutrophils Conspire to Promote Breast Cancer Metastasis. *Nature* (2015) 522(7556):345–8. doi: 10.1038/nature14282
15. Szczerba BM, Castro-Giner F, Vetter M, Krol I, Gkountela S, Landin J, et al. Neutrophils Escort Circulating Tumour Cells to Enable Cell Cycle Progression. *Nature* (2019) 566(7745):553–7. doi: 10.1038/s41586-019-0915-y
16. Gay LJ, Felding-Habermann B. Contribution of Platelets to Tumour Metastasis. *Nat Rev Cancer* (2011) 11(2):123–34. doi: 10.1038/nrc3004
17. Aziz MH, Sideras K, Aziz NA, Mauff K, Haen R, Roos D, et al. The Systemic-Immune-Inflammation Index Independently Predicts Survival and Recurrence in Resectable Pancreatic Cancer and Its Prognostic Value

Depends on Bilirubin Levels: A Retrospective Multicenter Cohort Study. *Ann Surg* (2019) 270(1):139–46. doi: 10.1097/SLA.0000000000002660
18. Wellenstein MD, Coffelt SB, Duits DEM, van Miltenburg MH, Slagter M, de Rink I, et al. Loss of P53 Triggers WNT-Dependent Systemic Inflammation to Drive Breast Cancer Metastasis. *Nature* (2019) 572(7770):538–42. doi: 10.1038/s41586-019-1450-6
19. Ni XG, Bai XF, Mao YL, Shao YF, Wu JX, Shan Y, et al. The Clinical Value of Serum CEA, CA19-9, and CA242 in the Diagnosis and Prognosis of Pancreatic Cancer. *Eur J Surg Oncol* (2005) 31(2):164–9. doi: 10.1016/j.ejso.2004.09.007
20. Hori S, Shimada K, Ino Y, Oguro S, Esaki M, Nara S, et al. Macroscopic Features Predict Outcome in Patients With Pancreatic Ductal Adenocarcinoma. *Virchows Arch* (2016) 469(6):621–34. doi: 10.1007/s00428-016-2026-6
21. Shen CN, Goh KS, Huang CR, Chiang TC, Lee CY, Jeng YM, et al. Lymphatic Vessel Remodeling and Invasion in Pancreatic Cancer Progression. *EBioMedicine* (2019) 47:98–113. doi: 10.1016/j.ebiom.2019.08.044
22. Xiao Y, Lu J, Chang W, Chen Y, Li X, Li D, et al. Dynamic Serum Alkaline Phosphatase Is an Indicator of Overall Survival in Pancreatic Cancer. *BMC Cancer* (2019) 19(1):785. doi: 10.1186/s12885-019-6004-7
23. Feng L, Gu S, Wang P, Chen H, Chen Z, Meng Z, et al. Pretreatment Values of Bilirubin and Albumin Are Not Prognostic Predictors in Patients With Advanced Pancreatic Cancer. *Cancer Med* (2018) 7(12):5943–51. doi: 10.1002/cam4.1848
24. Yagyu T, Saito H, Sakamoto T, Uchinaka EI, Morimoto M, Amisaki M, et al. Preoperative Albumin-Bilirubin Grade as a Useful Prognostic Indicator in Patients With Pancreatic Cancer. *Anticancer Res* (2019) 39(3):1441–6. doi: 10.21873/anticanres.13260
25. Fernandez-del Castillo C, Morales-Oyarvide V, McGrath D, Wargo JA, Ferrone CR, Thayer SP, et al. Evolution of the Whipple Procedure at the Massachusetts General Hospital. *Surgery* (2012) 152(3 Suppl 1):S56–63. doi: 10.1016/j.surg.2012.05.022
26. Al-Hawary MM, Francis IR, Chari ST, Fishman EK, Hough DM, Lu DS, et al. Pancreatic Ductal Adenocarcinoma Radiology Reporting Template: Consensus Statement of the Society of Abdominal Radiology and the American Pancreatic Association. *Gastroenterology* (2014) 146(1):291–304.e1. doi: 10.1053/j.gastro.2013.11.004
27. Bockhorn M, Uzunoglu FG, Adham M, Imrie C, Milicevic M, Sandberg AA, et al. Borderline Resectable Pancreatic Cancer: A Consensus Statement by the International Study Group of Pancreatic Surgery (ISGPS). *Surgery* (2014) 155 (6):977–88. doi: 10.1016/j.surg.2014.02.001
28. Camp RL, Dolled-Filhart M. Rimm DL. X-Tile: A New Bio-Informatics Tool for Biomarker Assessment and Outcome-Based Cut-Point Optimization. *Clin Cancer Res* (2004) 10(21):7252–9. doi: 10.1158/1078-0432.CCR-04-0713
29. McEligot AJ, Poynor V, Sharma R, Panangadan A. Logistic LASSO Regression for Dietary Intakes and Breast Cancer. *Nutrients* (2020) 12(9):2652. doi: 10.3390/nu12092652
30. Steinbrecher KA, Horowitz NA, Blevins EA, Barney KA, Shaw MA, Harmel-Laws E, et al. Colitis-Associated Cancer Is Dependent on the Interplay Between the Hemostatic and Inflammatory Systems and Supported by Integrin Alpha(M)beta(2) Engagement of Fibrinogen. *Cancer Res* (2010) 70 (7):2634–43. doi: 10.1158/0008-5472.CAN-09-3465
31. Janssen LME, Ramsay EE, Logsdon CD, Overwijk WW. The Immune System in Cancer Metastasis: Friend or Foe? *J Immunother Cancer* (2017) 5(1):79. doi: 10.1186/s40425-017-0283-9
32. Schlesinger M. Role of Platelets and Platelet Receptors in Cancer Metastasis. *J Hematol Oncol* (2018) 11(1):125. doi: 10.1186/s13045-018-0669-2
33. Haemmerle M, Stone RL, Menter DG, Afshar-Kharghan V, Sood AK. The Platelet Lifeline to Cancer: Challenges and Opportunities. *Cancer Cell* (2018) 33(6):965–83. doi: 10.1016/j.ccell.2018.03.002
34. Perisanidis C, Psyrri A, Cohen EE, Engelmann J, Heinze G, Perisanidis B, et al. Prognostic Role of Pretreatment Plasma Fibrinogen in Patients With Solid Tumors: A Systematic Review and Meta-Analysis. *Cancer Treat Rev* (2015) 41 (10):960–70. doi: 10.1016/j.ctrv.2015.10.002
35. Ocana A, Nieto-Jimenez C, Pandiella A, Templeton AJ. Neutrophils in Cancer: Prognostic Role and Therapeutic Strategies. *Mol Cancer* (2017) 16 (1):137. doi: 10.1186/s12943-017-0707-7
36. Wu Y, Ye S, Goswami S, Pei X, Xiang L, Zhang X, et al. Clinical Significance of Peripheral Blood and Tumor Tissue Lymphocyte Subsets in Cervical Cancer Patients. *BMC Cancer* (2020) 20(1):173. doi: 10.1186/s12885-020-6633-x
37. Hong YM, Yoon KT, Hwang TH, Cho M. Pretreatment Peripheral Neutrophils, Lymphocytes and Monocytes Predict Long-Term Survival in Hepatocellular Carcinoma. *BMC Cancer* (2020) 20(1):937. doi: 10.1186/s12885-020-07105-8
38. Sulibhavi A, Asokan S, Miller MI, Moreira P, Daly BD, Fernando HC, et al. Peripheral Blood Lymphocytes and Platelets Are Prognostic in Surgical Pt1 Non-Small Cell Lung Cancer. *Ann Thorac Surg* (2020) 109(2):337–42. doi: 10.1016/j.athoracsur.2019.09.006
39. Matsuda S, Takeuchi H, Kawakubo H, Takemura R, Maeda Y, Hirata Y, et al. Validation Study of Fibrinogen and Albumin Score in Esophageal Cancer Patients Who Underwent Esophagectomy: Multicenter Prospective Cohort Study. *Ann Surg Oncol* (2021) 28(2):774–84. doi: 10.1245/s10434-020-08958-w
40. Templeton AJ, McNamara MG, Seruga B, Vera-Badillo FE, Aneja P, Ocana A, et al. Prognostic Role of Neutrophil-to-Lymphocyte Ratio in Solid Tumors: A Systematic Review and Meta-Analysis. *J Natl Cancer Inst* (2014) 106(6): dju124. doi: 10.1093/jnci/dju124
41. Li B, Zhou P, Liu Y, Wei H, Yang X, Chen T, et al. Platelet-To-Lymphocyte Ratio in Advanced Cancer: Review and Meta-Analysis. *Clin Chim Acta* (2018) 483:48–56. doi: 10.1016/j.cca.2018.04.023
42. Cho U, Park HS, Im SY, Yoo CY, Jung JH, Suh YJ, et al. Prognostic Value of Systemic Inflammatory Markers and Development of a Nomogram in Breast Cancer. *PloS One* (2018) 13(7):e0200936. doi: 10.1371/journal.pone.0200936
43. Li R, Sun Z, Song S, He X, Shi X, Li Z, et al. NARFIB: A Novel Prognostic Score Based on the Neutrophil-To-Albumin Ratio and Fibrinogen Can Predict the Prognosis of Gastrointestinal Stromal Tumors. *Cancer Manag Res* (2020) 12:11183–90. doi: 10.2147/CMAR.S281375
44. Shindoh J, Kawamura Y, Kobayashi Y, Kiya Y, Sugawara T, Akuta N, et al. Platelet-Albumin Score as a Sensitive Measure for Surgical Risk Prediction and Survival Outcomes of Patients With Hepatocellular Carcinoma. *J Gastrointest Surg* (2019) 23(1):76–83. doi: 10.1007/s11605-018-3871-1
45. Fan Z, Luo G, Gong Y, Xu H, Qian Y, Deng S, et al. Prognostic Value of the C-Reactive Protein/Lymphocyte Ratio in Pancreatic Cancer. *Ann Surg Oncol* (2020) 27(10):4017–25. doi: 10.1245/s10434-020-08301-3
46. Tempero MA, Malafa MP, Chiorean EG, Czito B, Scaife C, Narang AK, et al. Pancreatic Adenocarcinoma, Version 1.2019. *J Natl Compr Canc Netw* (2019) 17(3):202–10. doi: 10.6004/jnccn.2019.0014
47. Bilici A. Prognostic Factors Related With Survival in Patients With Pancreatic Adenocarcinoma. *World J Gastroenterol* (2014) 20(31):10802–12. doi: 10.3748/wjg.v20.i31.10802
48. Konishi T, Shimada Y, Hsu M, Tufts L, Jimenez-Rodriguez R, Cercek A, et al. Association of Preoperative and Postoperative Serum Carcinoembryonic Antigen and Colon Cancer Outcome. *JAMA Oncol* (2018) 4(3):309–15. doi: 10.1001/jamaoncol.2017.4420

Conflict of Interest: The authors declare that the research was conducted in the absence of any commercial or financial relationships that could be construed as a potential conflict of interest.

Publisher's Note: All claims expressed in this article are solely those of the authors and do not necessarily represent those of their affiliated organizations, or those of the publisher, the editors and the reviewers. Any product that may be evaluated in this article, or claim that may be made by its manufacturer, is not guaranteed or endorsed by the publisher.

Copyright © 2022 Li, Zhang, Lu, Zhao, Gao, Liu, Piao, Chen, Huang, Chang and Hao. This is an open-access article distributed under the terms of the Creative Commons Attribution License (CC BY). The use, distribution or reproduction in other forums is permitted, provided the original author(s) and the copyright owner(s) are credited and that the original publication in this journal is cited, in accordance with accepted academic practice. No use, distribution or reproduction is permitted which does not comply with these terms.

frontiers in Oncology

ORIGINAL RESEARCH
published: 24 February 2022
doi: 10.3389/fonc.2022.792077

Machine Learning-Based Radiological Features and Diagnostic Predictive Model of Xanthogranulomatous Cholecystitis

Qiao-Mei Zhou[1], Chuan-Xian Liu[2], Jia-Ping Zhou[1], Jie-Ni Yu[1], You Wang[3], Xiao-Jie Wang[1], Jian-Xia Xu[4] and Ri-Sheng Yu[1]**

[1] Department of Radiology, The Second Affiliated Hospital, Zhejiang University School of Medicine, Hangzhou, China, [2] Department of Radiology, Jiaxing Hospital of Traditional Chinese Medicine, Jiaxing, China, [3] Department of Radiology, Sir Run Run Shaw Hospital, Zhejiang University School of Medicine, Hangzhou, China, [4] Department of Radiology, The Second Affiliated Hospital, Zhejiang Chinese Medical University, Hangzhou, China

OPEN ACCESS

Edited by:
Qi Liu,
Fudan University, China

Reviewed by:
Faten Limaiem,
Hôpital Mongi Slim, Tunisia
Dimitrios Schizas,
National and Kapodistrian University of Athens, Greece

***Correspondence:**
Ri-Sheng Yu
risheng-yu@zju.edu.cn
Jian-Xia Xu
xjx129@163.com

Specialty section:
This article was submitted to Gastrointestinal Cancers: Hepato Pancreatic Biliary Cancers, a section of the journal Frontiers in Oncology

Received: 09 October 2021
Accepted: 31 January 2022
Published: 24 February 2022

Citation:
Zhou Q-M, Liu C-X, Zhou J-P, Yu J-N, Wang Y, Wang X-J, Xu J-X and Yu R-S (2022) Machine Learning-Based Radiological Features and Diagnostic Predictive Model of Xanthogranulomatous Cholecystitis. Front. Oncol. 12:792077. doi: 10.3389/fonc.2022.792077

Background: Xanthogranulomatous cholecystitis (XGC) is a rare benign chronic inflammatory disease of the gallbladder that is sometimes indistinguishable from gallbladder cancer (GBC), thereby affecting the decision of the choice of treatment. Thus, this study aimed to analyse the radiological characteristics of XGC and GBC to establish a diagnostic prediction model for differential diagnosis and clinical decision-making.

Methods: We investigated radiological characteristics confirmed by the RandomForest and Logistic regression to establish computed tomography (CT), magnetic resonance imaging (MRI), CT/MRI models and diagnostic prediction model, and performed receiver operating characteristic curve (ROC) analysis to prove the effectiveness of the diagnostic prediction model.

Results: Based on the optimal features confirmed by the RandomForest method, the mean area under the curve (AUC) of the ROC of the CT and MRI models was 0.817 (mean accuracy = 0.837) and 0.839 (mean accuracy = 0.842), respectively, whereas the CT/MRI model had a considerable predictive performance with the mean AUC of 0.897 (mean accuracy = 0.906). The diagnostic prediction model established for the convenience of clinical application was similar to the CT/MRI model with the mean AUC and accuracy of 0.888 and 0.898, respectively, indicating a preferable diagnostic efficiency in distinguishing XGC from GBC.

Conclusions: The diagnostic prediction model showed good diagnostic accuracy for the preoperative discrimination of XGC and GBC, which might aid in clinical decision-making.

Keywords: gallbladder cancer, radiological features, diagnostic prediction model, RandomForest, Xanthogranulomatous cholecystitis (XGC)

INTRODUCTION

Xanthogranulomatous cholecystitis (XGC) is a rare and chronic inflammatory lesion of the gallbladder characterised by special types of granulomas and foamy cells (1). Epidemiological data from previous studies showed that the incidence of XGC was 1.3%–1.9% and that in India was 8.8%, with little difference in sex among regions (2). Goodman and Ishak described XGC as a special pathological entity in 1981 (3). Although XGC is benign, it is locally aggressive and may affect nearby organs such as the liver, duodenum, colon, and common bile duct (4). It may be misdiagnosed as gallbladder cancer (GBC) or may coexist with GBC because the inflammatory process involved resembles that of GBC in a macroscopic view.

The clinical manifestations and biological examination of XGC are nonspecific and similar to acute or chronic cholecystitis (5). Several studies have reported some imaging features that highly suggest XGC, including diffuse thickening of the gallbladder wall, continuous mucosal lines, intramural hypoattenuating nodules, and the presence of gallstones in the background of chronic gallbladder disease (6, 7). Approaches based on image analysis to guide the most appropriate treatment decisions have been intensively studied (8), and the applications of artificial intelligence (9), machine learning (10), and deep learning (11) in radiology images have been increasingly explored. Imaging tools such as computed tomography (CT) and magnetic resonance imaging (MRI) are generally utilised for clinical evaluation of gallbladder diseases, so analysis of their unique radiological features through machine learning may be a better method to distinguish XGC from GBC (12).

Laparoscopic cholecystectomy is the current gold standard for the treatment of benign gallbladder diseases. However, the high conversion rate of laparoscopic cholecystectomy to open cholecystectomy in XGC is related to the difficulty in distinguishing GBC (13). Moreover, surgeons may perform improper surgery owing to the misdiagnosis of GBC (14). In this study, we retrospectively analysed 60 cases of XGC and 93 cases of GBC confirmed by histopathology to establish a diagnostic prediction model for XGC and GBC based on CT and MRI features to help clinical decision-making on the appropriate treatment method for patients with XGC.

METHODS

Patients

The flow chart of patient screening is presented in **Figure 1**. Patients with an inflammatory lesion originating in the gallbladder from the Second Affiliated Hospital of Zhejiang University School of Medicine from 2011 to 2021 and pathologically confirmed as XGC or GBC were included in the study population. These patients had satisfactory CT and MRI data and did not receive chemotherapy or radiotherapy. However, owing to limited data and poor imaging quality, some patients were excluded. The final study cohort comprised 60 patients with XGC and 93 patients with GBC. Our institutional review board approved this retrospective study and waived the requirement for patient consent.

Image Acquisition

Multidetector-row CT (SOMATOM Definition Flash; Siemens Healthcare) was used to perform abdominal CT examinations. All patients underwent a plain scan under the fasting state initially and then received an injection of 100-mL contrast agent at 3-4 mL/s into the antecubital vein for enhanced scan. The arterial, portal vein, and equilibrium phases were obtained at 25, 60, and 100 s after the injection of the contrast agent.

A 3.0-T magnet (Signa or Discovery 750; GE Healthcare) with an eight-channel torso-phased array coil was used to obtain axial T1-weighted images (T1WI), T2-weighted images (T2WI), contrast-enhanced images and diffusion-weighted imaging (DWI) of all patients. Dynamic breath-hold imaging acquisitions were performed at 25–32, 45–52, 75–82, and 135–142 s after contrast enhancement to obtain the arterial, portal venous, equilibrium, and delayed phases. The imaging parameters of MRI were as follows: repetition time/echo time (TR/TE) of 205/3.2msec (or 3.9/1.8msec) and 6000/102.5msec (or 12000/86.3msec); the matrix of 256x256, the standard field of view of 4mm; the slice thickness of 4mm with no interslice gap. The parameters of DWI were as follows: TR/TE=1300/60.6msec or 6000/52.5 mec; water selective excitation for fat suppression; 5 mm thickness; matrix size of 128x128; field of view of 36x36cm; the number of shots of 6; slice thickness/gap of 5 mm/1.0 mm; 20 axial slices; scan time of 144s; b value of 0 and 600 s/mm2.

Image Analysis

The original images were evaluated separately by two experienced abdominal radiologists who were blinded to patients' pathological results. The variables of CT imaging were as follows: gallstones (no, gallbladder stones, intrahepatic bile duct stones, and extrahepatic bile duct stones), bile duct dilation (no, intrahepatic bile duct, extrahepatic bile duct, and intra and extrahepatic bile ducts), gallbladder cavity (normal, atrophy, and dilation), gallbladder morphology (regular and irregular), gallbladder wall thickness (≤10 and ≥10 mm), gallbladder wall thickening pattern (focal and diffuse), CT strengthening method (persistent, delayed, and other), intramural nodules (no, focal ≤20%, and diffuse >20%), intramural fat, mucosal lines (continuous, partly continuous, and disrupted), abnormal enhancement of adjacent liver parenchyma, liver/gallbladder interface (clear and blurred), fat around the gallbladder (clear and blurred), liver involvement, involvement of adjacent tissues outside the liver, peripheral lymph nodes (no, ≤10 mm, and >10 mm).

The variables of MRI were as follows: T1WI signal of the thickened cyst wall (high, equal, low, and mix), T2WI signal of the thickened cyst wall (high, equal, low, and mixed), MRI

Abbreviations: XGC, xanthogranulomatous cholecystitis; GBC, gallbladder cancer; CT, computed tomography; MRI, magnetic resonance imaging; RF, Random Forest; AUC, the area under the curve; ROC, the receiver operating characteristic curve; T1WI, T1 weighted imaging; T2WI, T1 weighted imaging; DWI, diffusion-weighted magnetic resonance imaging; ADC, apparent diffusion coefficient.

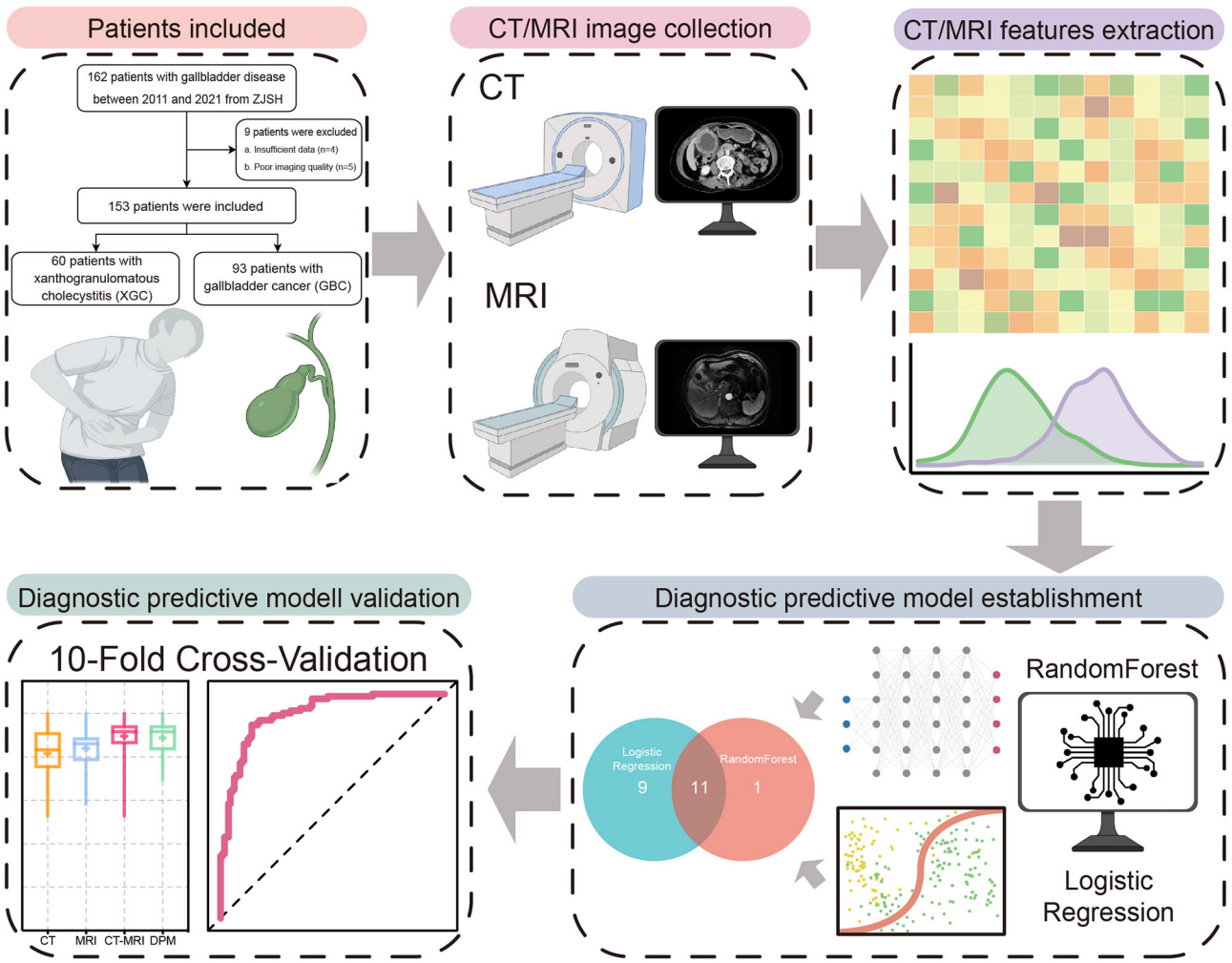

FIGURE 1 | Schematic of research workflow and patient selection flowchart.

strengthening method (persistent, delayed, and other), T1WI signal of intramural nodules (no, high, equal, and low), T1WI signal of intramural nodules (no, high, equal, and low), lipid signal, bile signal, DWI (high, slightly high, and equal), apparent diffusion coefficient (ADC) (equal and low), and mucosal enhancement (no, obvious, and mild).

Model Construction and Validation

The general technical workflow is presented in **Figure 1**. CT, MRI, and CT/MRI RandomForest (RF) classifiers were built based on the extracted CT and MRI image features. The "randomForest" package of R software (ver. 3.6.3; R Foundation for Statistical Computing, Vienna, Austria) was used to run the RF classifiers. Ten-fold cross-validation was performed to adjust the parameters of the classifiers and to determine the best diagnostic model during the training process. Univariate analysis was performed to evaluate the selected radiological features and their association with the above model. Finally, the most predictive parameters were used to construct the optimal diagnosis model using the RF method for distinguishing XGC from GBC.

Statistical Analysis

SPSS ver. 26.0 (IBM Corp., Armonk, NY, USA), and R software (ver. 3.6.3; R Foundation for Statistical Computing, Vienna, Austria) were used to process all data. Continuous variables are presented as median with standard deviation and categorical variables as the number with a percentage. The same variables between the two groups were compared using the Mann–Whitney U-test for continuous non-normally distributed variables and chi-square or Fisher's exact test for categorical variables. Variables that were statistically significant in the univariate analysis were obtained using ridge regression analysis to minimise multicollinearity, followed by the Logistic regression model. The models constructed using RF were validated using 10-fold cross-validation. Statistical significance was defined with a two-sided p-value of <0.05.

TABLE 1 | Imaging features in XGC and GBC patients.

Features	Xanthogranulomatous Cholecystitis (n = 60)		Gallbladder Cancer (n = 93)		*P**
	n	%	n	%	
CT Features					
Gallstones					<0.001
No	4	6.7%	46	49.4%	
Gallbladder stones	54	90.0%	46	49.4%	
Intra-hepatic bile duct stones	1	1.7%	0	0.0%	
Extra-hepatic bile duct stones	1	1.7%	1	1.2%	
Bile duct dilation					<0.001
No	33	55.0%	53	57.0%	
Intra-hepatic bile duct	1	1.7%	17	18.3%	
Extra-hepatic bile duct	22	36.7%	8	8.6%	
Intrahepatic and extrahepatic bile duct	4	6.7%	15	16.1%	
Gallbladder cavity					0.021
Normal	3	5.0%	13	14.0%	
Atrophy	48	80.0%	76	81.7%	
Dilation	9	15.0%	4	4.3%	
Gallbladder morphology					0.002†
Regular	15	25.0%	6	6.5%	
Irregular	45	75.0%	87	93.5%	
Gallbladder wall thickness					0.407
≤ 10mm	15	25.0%	18	18.4%	
> 10mm	45	75.0%	75	80.6%	
Gallbladder wall thickening pattern					<0.001
Focal	14	23.3%	49	52.7%	
Diffuse	46	76.7%	44	47.3%	
CT strengthening method					0.012
Persistent	27	45.0%	61	65.6%	
Delay	31	51.7%	26	28.0%	
Other	2	3.3%	6	6.5%	
Intramural nodules					<0.001
No	21	35.0%	52	55.9%	
Focal (≤ 20%)	23	38.3%	36	38.7%	
Diffuse (> 20%)	16	26.7%	5	5.4%	
Intramural fat					0.177
No	42	70.0%	74	79.6%	
Yes	18	30.0%	19	20.4%	
Mucosal lines					<0.001
Continuous	20	33.3%	1	1.1%	
Partly continuous	28	46.7%	60	64.5%	
Disrupted	12	20.0%	32	34.4%	
Abnormal enhancement of adjacent liver parenchyma					0.001
No	11	18.3%	41	44.1%	
Yes	49	81.7%	52	55.9%	
Liver/gallbladder interface					0.008
Clear	15	25.0%	43	46.2%	
Blurred	45	75.0%	50	53.8%	
Fat around the gallbladder					0.001
Clear	13	21.7%	46	49.5%	
Blurred	47	78.3%	47	50.5%	
Liver involvement					0.004
No	46	76.7%	50	53.8%	
Yes	14	23.3%	43	46.2%	
Involve adjacent tissues outside the liver					0.927
No	26	43.3%	41	44.1%	
Yes	34	56.7%	52	55.9%	
Peripheral lymph nodes					0.001
No	44	73.3.0%	42	45.2%	
≤ 10 mm	13	21.7%	27	29.0%	
> 10mm	3	5.0%	24	25.8%	
MRI Features					
T1WI signal of thickened cyst wall					0.085
High	3	5.0%	4	4.3%	

(Continued)

TABLE 1 | Continued

Features	Xanthogranulomatous Cholecystitis (n = 60)		Gallbladder Cancer (n = 93)		*P**
	n	%	n	%	
Equal	22	36.7%	41	44.1%	
Low	23	38.3%	42	45.2%	
Mix	12	20.0%	6	6.5%	
T2WI signal of thickened cyst wall					0.001
High	5	8.3%	14	15.1%	
Equal	37	61.7%	48	51.6%	
Low	7	11.7%	28	30.1%	
Mix	11	18.3%	3	3.2%	
MRI strengthening method					0.725
Persistent	17	28.3%	28	30.1%	
Delay	37	61.7%	59	63.4%	
Other	6	10.0%	6	6.5%	
T1WI signal of intramural nodules					<0.001
No	5	8.3%	68	73.1%	
High	10	16.7%	3	3.2%	
Equal	24	40.0%	14	15.1%	
Low	21	35.0%	8	8.6%	
T2WI signal of intramural nodules					<0.001
No	5	8.3%	68	73.1%	
High	38	63.3%	20	21.5%	
Equal	15	25.0%	5	5.4%	
Low	2	3.4%	0	0.0%	
Lipid signal					<0.001
No	22	36.7%	82	88.2%	
Yes	38	63.3%	11	11.8%	
Bile signal					0.218
No	42	70.0%	56	60.2%	
Yes	18	30.0%	37	39.8%	
DWI					0.004
High	21	35.0%	58	62.4%	
Slightly high	30	50.0%	27	29.0%	
Equal	9	15.0%	8	8.6%	
ADC					<0.001
Equal	44	73.3%	30	32.3%	
Low	16	26.7%	63	67.7%	
Mucosal enhancement					<0.001
No	6	10.0%	39	41.9%	
Obvious	39	65.0%	21	22.6%	
Mild	15	25.0%	33	35.5%	

Calculated by Chi-Square test; †calculated by Fisher exact test.

RESULTS

Imaging Features

A comparison of CT and MRI features is summarised in **Table 1**. There were significant differences in the features of gallstones, bile duct dilation, gallbladder cavity, gallbladder morphology, gallbladder wall thickening pattern, strengthening method, intramural nodules, mucosal lines, abnormal enhancement of adjacent liver parenchyma, liver/gallbladder interface, fat around the gallbladder, liver involvement, and peripheral lymph nodes and T2WI signal of the thickened cyst wall, T1WI signal of intramural nodules, T2WI signal of intramural nodules, lipid signal, DWI, ADC, and mucosal enhancement.

RF Model

Based on the characteristics of the collected CT and MRI scans, the RF method was performed to establish three differential diagnosis models of XGC and GBC. In the training process, 10-fold cross-validation was performed 10 times to adjust the parameters of the classifier. Performance evaluation was conducted using the mean AUC. The AUCs of the CT and MRI models were 0.817 and 0.839, respectively, with corresponding accuracies of 0.837 and 0.842. The CT/MRI model showed good discrimination between XGC and GBC with an AUC of 0.897. Additionally, the CT/MRI model showed a high diagnostic performance with an accuracy of 0.906 (**Figures 2A, B**), thereby confirming the diagnostic importance of radiological features for the recognition of XGC. Furthermore, the Gini index can be used to judge the importance of different variables in the RF model (**Figure 2C**).

Diagnostic Predictive Model

A total of 20 imaging features showed statistical differences in the univariate analysis through Logistic regression (**Figure 2D**).

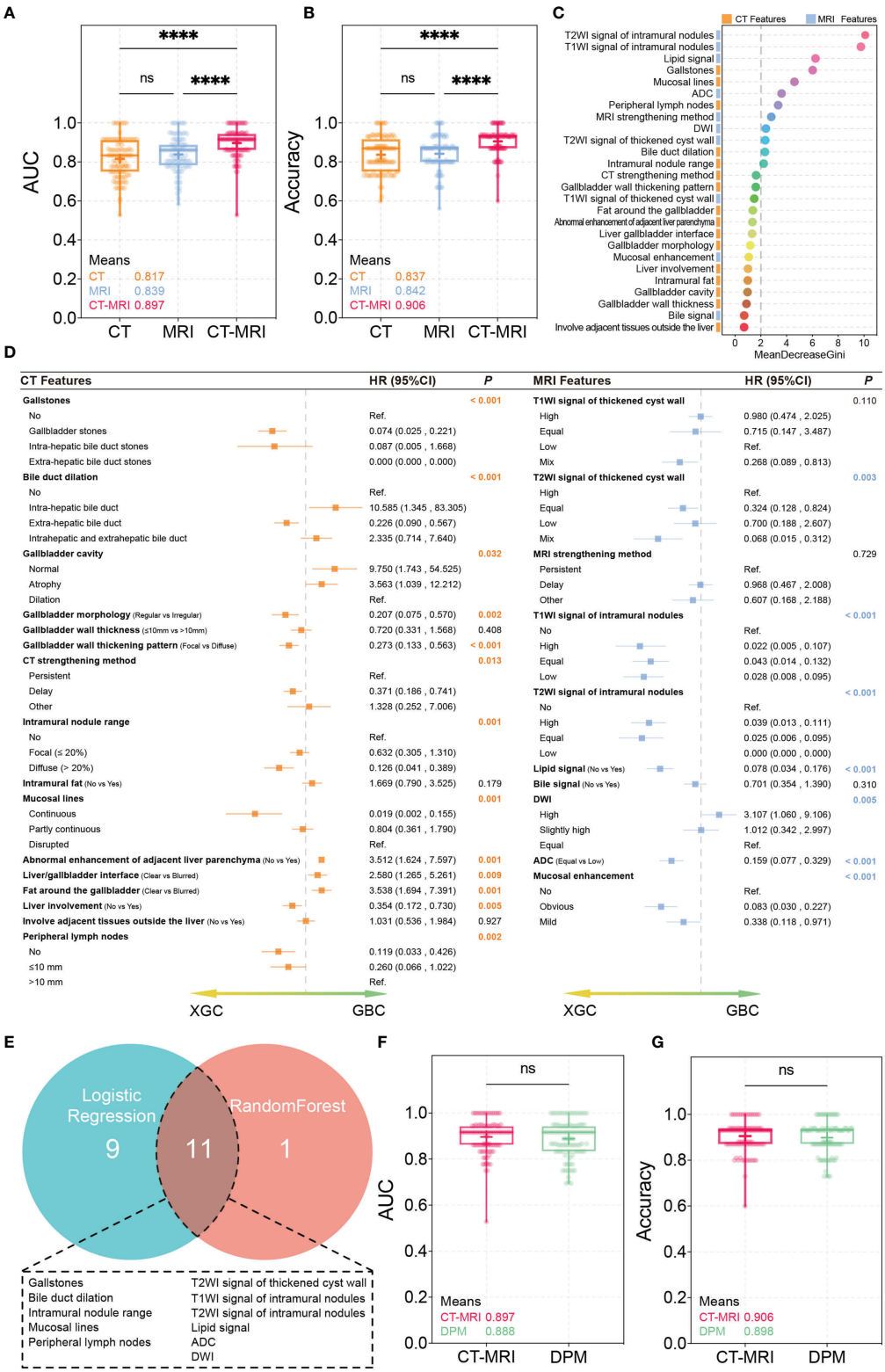

FIGURE 2 | RandomForest and Logistic regression test results. **(A, B)** AUC and accuracy of the CT, MRI, CT/MRI models. ****$P < 0.0001$; ns, not significant, Mann-Whitney U Test. **(C)** The importance of variables measured using the CT/MRI model with the Random Forest Gini Index. **(D)** Logistic regression for univariate analysis. **(E)** Correlation of variables obtained using random forest and logistic regression. **(F, G)** AUC and accuracy of the CT/MRI model and diagnosis prediction model. ns, not significant, Mann-Whitney U Test.

To lapply the above diagnostic system conveniently in practice, important imaging features extracted by the two machine learning methods were integrated to further build a new differential diagnosis model. A total of 11 imaging features were retained, including those of gallstones, bile duct dilation, intramural nodules, mucosal lines, and peripheral lymph nodes and T2WI signal of the thickened cyst wall, T1WI signal of intramural nodules, T2WI signal of intramural nodules, lipid signal, ADC, and DWI (**Figure 2E**).

Subsequently, we constructed a diagnostic predictive model using these 11 parameters using the RF method. Ten times of 10-fold cross-validation was performed to evaluate the reliability and reproducibility of the diagnostic predictive model. Finally, the average AUC and accuracy of the diagnostic prediction model were 0.888 and 0.898, respectively, which are similar to those of the primary CT/MRI model (**Figures 2F, G**). Interestingly, the comparison of ROCs verified using the Mann–Whitney U-test showed no statistical difference between the two models, indicating that the diagnostic predictive model made full use of the value of the CT/MRI model. These features were ranked according to their relevance to the differential diagnosis as follows: T2WI signal of intramural nodules, T1WI signal of intramural nodules, lipid signal, gallstones, mucosal lines, ADC, peripheral lymph nodes, DWI, T2WI signal of the thickened cyst wall, bile duct dilation, and intramural nodules.

DISCUSSION

XGC was originally considered a malignant disease process; however, many studies have now confirmed its benign course (15), which is characterised by a focal or diffuse destructive inflammatory process, followed by significant macrophage and foam cell infiltrations and hyperplastic fibrosis. Concerning the pathogenesis of XGC, the most widely accepted theory is that the extravasation of bile through the ruptured Rokitansky-Aschoff sinus or increased internal pressure of the biliary tract causes small mucosal ulcers (16). Extensive inflammatory fibrosis results in the thickening of the gallbladder wall and the formation of multiple yellowish-brown nodules (17). The inflammatory process often spreads to adjacent organs, thereby forming a tumour-like mass around the gallbladder (18). Since XGC is often misdiagnosed as GBC, which leads to unnecessary radical surgical excision, it is important to distinguish between XGC and GBC before surgery.

Although ultrasound is a clinically preferred and ubiquitous imaging method, its specificity for XGC is low (12). Clinically, CT and MRI are widely used to distinguish between XGC and GBC because of their convenience and non-invasiveness (19). We reviewed a large amount of literature in the early stages and incorporated the reported potential radiological features that may distinguish XGC from GBC into the initial model. Using the RF algorithm and Logistic regression method, it was shown that

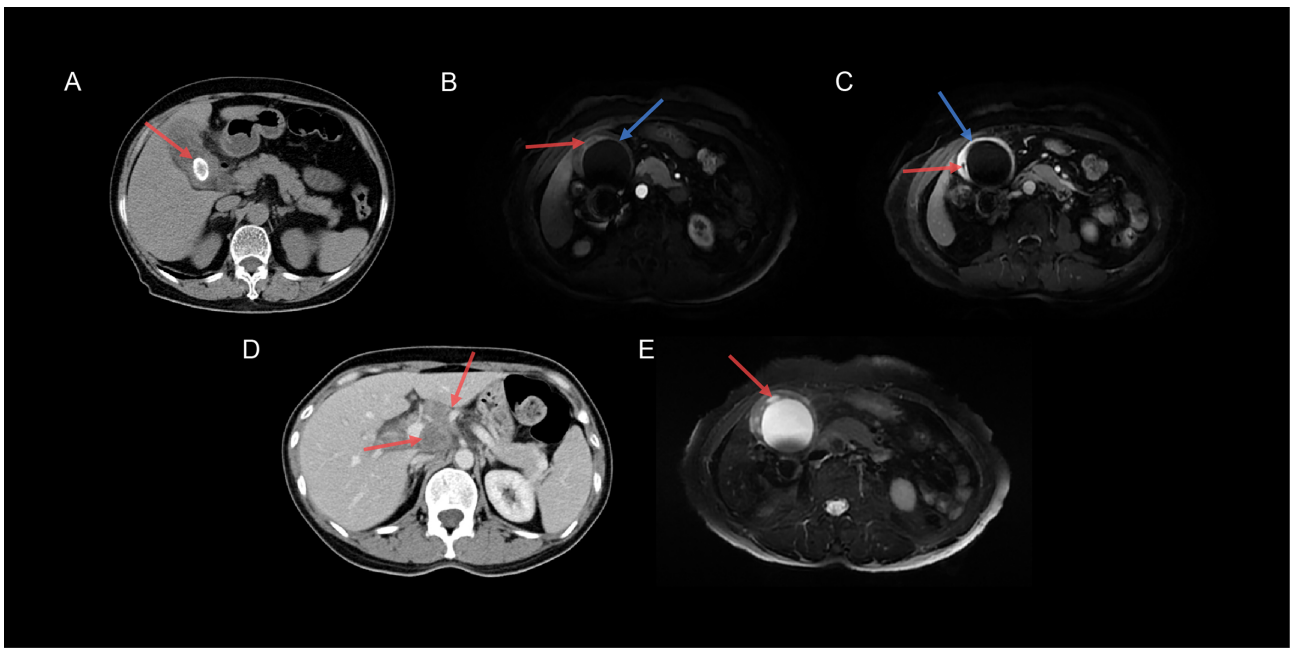

FIGURE 3 | Typical images of XGC and GBC specimens. **(A)** The CT transverse section revealed cholecystolithiasis (red arrow) in a 46-year-old women with XGC. **(B)** Axial T1-weighted MRI-enhanced image showed low-intensity nodules (red arrow) in the gallbladder wall, and the continuous mucosal line was significantly enhanced (blue arrow) in the arterial phase. **(C)** Axial T1-weighted MRI-enhanced image showed that the gallbladder wall was obviously enhanced; however, the intramural nodules were unenhanced (red arrow), and the mucosal line was intact (blue arrow) in the delayed phase. **(D)** Axial CT image demonstrated two lymph nodes (>10 mm) in the hilar (red arrow) in a 46-year-old women with GBC. **(E)** Axial T2-weighted MRI-enhanced image demonstrated that the gallbladder wall was apparently thickened with multiple high-intensity nodules (red arrow).

the diagnostic prediction model had a stronger ability to distinguish between XGC and GBC with an AUC of 0.888 and an accuracy of 0.898. This model, constructed with outstanding clinical applicability, summarised 11 radiological features and had high diagnostic performance, thereby confirming the importance of imaging features in the differential diagnosis of XGC and GBC.

CT findings included gallstones, mucosal lines, peripheral lymph nodes, bile duct dilation, and intramural nodules. Studies have shown that the development of XGC may be related to gallstones (17, 20), similar to our findings (**Figure 3A**). Additionally, intramural hypodense nodules, continuous mucosal lines, and absence of intrahepatic bile duct dilatation suggested XGC (**Figures 3B, C**). Goshima et al. reported that three of the five CT features that meet the XGC characteristics can provide high accuracy in distinguishing XGC from GBC (21), which is consistent with our results. Peripheral lymphadenopathy (>10 mm) was an independent factor in the diagnosis of GBC (**Figure 3D**), which may help in the correct preoperative diagnosis of XGC. As for the MRI features, the high-signal area of the T2WI corresponded to the area of significant xanthogranulomas (**Figure 3E**), which is consistent with a previous finding (22). The lipid signal of XGC nodules was owing to tissue cell phagocytosis and accumulation of extravasated bile and bile lipids. Ogawa et al. showed that the positive signal rate with DWI was significantly higher in GBC than in benign gallbladder diseases (23). DWI and ADC may play a significant role in distinguishing XGC from GBC because they are beneficial for distinguishing malignant and benign lesions.

XGC should be operated immediately once diagnosed to prevent complications owing to its invasiveness and destructiveness (24). Compared with open surgery, laparoscopic cholecystectomy has a shorter operating time and shorter postoperative hospital stay (25), which indicates that in some strictly selected cases, laparoscopic surgery is superior to open surgery for XGC treatment (4). Our predictive diagnosis model can distinguish XGC from GBC through adequate preoperative evaluation, helps clinical decision-making, and reduces the incidence of postoperative complications. Despite the high accuracy of the predictive diagnosis model, intraoperative diagnosis is still necessary because XGC may coexist with GBC. The frequency of coexistence of these two lesions was approximately 19.6% in India (26). However, there was no coexistence of XGC and GBC in our study, which is one of the limitations of this study. Owing to the retrospective study design, patients with only a single examination and obvious imaging findings were not included, so there may be an inherent selection bias. On the other hand, there were individual variables that have reported differences; however, they were not significant in our study cohort, indicating that more patients may need to be introduced in future studies.

CONCLUSION

We established a diagnostic prediction model for XGC using the RF method and logistic regression. The model contains 11 important critical variables, including T2WI signal of intramural nodules, T1WI signal of intramural nodules, lipid signal, gallstones, mucosal lines, ADC, peripheral lymph nodes, DWI, T2WI signal of the thickened cyst wall, bile duct dilation, and intramural nodules. This diagnostic prediction model has exhibited good discrimination between XGC and GBC, thus providing significant assistance in clinical practice.

DATA AVAILABILITY STATEMENT

The raw data supporting the conclusions of this article will be made available by the authors, without undue reservation.

ETHICS STATEMENT

The studies involving human participants were reviewed and approved by The Second Affiliated Hospital of Zhejiang University School of Medicine (Approval numbers 20210806). Written informed consent for participation was not required for this study in accordance with the national legislation and the institutional requirements.

AUTHOR CONTRIBUTIONS

QZ conceived the study and drafted the manuscript. Ri-Sheng Yu and JX helped critically revise the manuscript for important intellectual content. QZ, CL and JZ performed the research. JY, YW and XW helped analyse data. All authors contributed to the article and approved the submitted version.

FUNDING

This study was supported by grants from the Zhejiang Medical and Health Science and Technology Plan Project (Grant Numbers 2019KY476).

REFERENCES

1. Zhao F, Lu PX, Yan SX, Wang GF, Yuan J, Zhang SZ, et al. CT and MR Features of Xanthogranulomatous Cholecystitis: An Analysis of Consecutive 49 Cases. *Eur J Radiol* (2013) 82(9):1391–7. doi: 10.1016/j.ejrad.2013.04.026
2. Hale M, Roberts K, Hodson J, Scott N, Sheridan M, Toogood G. Xanthogranulomatous Cholecystitis: A European and Global Perspective. *HPB Off J Int Hepato Pancreato Biliary Assoc* (2014) 16(5):448–58. doi: 10.1111/hpb.12152
3. Goodman Z, Ishak K. Xanthogranulomatous Cholecystitis. *Am J Surg Pathol* (1981) 5(7):653–9. doi: 10.1097/00000478-198110000-00007

4. Cui Y, Zhang H, Zhao E, Cui N, Li Z. Differential Diagnosis and Treatment Options for Xanthogranulomatous Cholecystitis. *Med Principles Pract Int J Kuwait University Health Sci Centre* (2013) 22(1):18–23. doi: 10.1159/000339659
5. Suzuki H. Specific Radiological Findings, If Present, can Offer High Accuracy for the Differentiation of Xanthogranulomatous Cholecystitis and Gallbladder Cancer. *Ann Transl Med* (2020) 8(11):662. doi: 10.21037/atm.2020.03.193
6. Truant S, Chater C, Pruvot F-R. Greatly Enlarged Thickened Gallbladder. *JAMA Surg* (2015) 150(3):267–8. doi: 10.1001/jamasurg.2014.492
7. Feng L, You Z, Gou J, Liao E, Chen L. Xanthogranulomatous Cholecystitis: Experience in 100 Cases. *Ann Transl Med* (2020) 8(17):1089. doi: 10.21037/atm-20-5836
8. Loukas C, Frountzas M, Schizas D. Patch-Based Classification of Gallbladder Wall Vascularity From Laparoscopic Images Using Deep Learning. *Int J Comput Assisted Radiol Surg* (2021) 16(1):103–13. doi: 10.1007/s11548-020-02285-x
9. Shoshan Y, Bakalo R, Gilboa-Solomon F, Ratner V, Barkan E, Ozery-Flato M, et al. Artificial Intelligence for Reducing Workload in Breast Cancer Screening With Digital Breast Tomosynthesis. *Radiology* (2022) p:211105. doi: 10.1148/radiol.211105
10. Reiazi R, Arrowsmith C, Welch M, Abbas-Aghababazadeh F, Eeles C, Tadic T, et al. Prediction of Human Papillomavirus (HPV) Association of Oropharyngeal Cancer (OPC) Using Radiomics: The Impact of the Variation of CT Scanner. *Cancers* (2021) 13(9). doi: 10.3390/cancers13092269
11. Gao R, Zhao S, Aishanjiang K, Cai H, Wei T, Zhang Y, et al. Deep Learning for Differential Diagnosis of Malignant Hepatic Tumors Based on Multi-Phase Contrast-Enhanced CT and Clinical Data. *J Hematol Oncol* (2021) 14(1):154. doi: 10.1186/s13045-021-01167-2
12. Bo X, Chen E, Wang J, Nan L, Xin Y, Wang C, et al. Diagnostic Accuracy of Imaging Modalities in Differentiating Xanthogranulomatous Cholecystitis From Gallbladder Cancer. *Ann Transl Med* (2019) 7(22):627. doi: 10.21037/atm.2019.11.35
13. Makimoto S, Takami T, Hatano K, Kataoka N, Yamaguchi T, Tomita M, et al. Xanthogranulomatous Cholecystitis: A Review of 31 Patients. *Surg Endosc* (2021) 35(7):3874–80. doi: 10.1007/s00464-020-07828-6
14. Giudicelli X, Rode A, Bancel B, Nguyen A, Mabrut J. Xanthogranulomatous Cholecystitis: Diagnosis and Management. *J Visceral Surg* (2021) 158(4):326–36. doi: 10.1016/j.jviscsurg.2021.02.004
15. Nacif L, Hessheimer A, Rodríguez Gómez S, Montironi C, Fondevila C. Infiltrative Xanthogranulomatous Cholecystitis Mimicking Aggressive Gallbladder Carcinoma: A Diagnostic and Therapeutic Dilemma. *World J Gastroenterol* (2017) 23(48):8671–8. doi: 10.3748/wjg.v23.i48.8671
16. Rahman J, Tahir M, Sonawane S. Xanthogranulomatous Cholecystitis: A Diagnostic Challenge for Radiologists, Surgeons, and Pathologists. *Cureus* (2020) 12(8):e10007. doi: 10.7759/cureus.10007
17. Kwon A, Matsui Y, Uemura Y. Surgical Procedures and Histopathologic Findings for Patients With Xanthogranulomatous Cholecystitis. *J Am Coll Surgeons* (2004) 199(2):204–10. doi: 10.1016/j.jamcollsurg.2004.03.018
18. Garcea G, Rajesh A, Dennison A. Surgical Management of Cystic Lesions in the Liver. *ANZ J Surg* (2013) 83:516–22. doi: 10.1111/ans.12049
19. Singh VP, Rajesh S, Bihari C, Desai SN, Pargewar SS, Arora A. Xanthogranulomatous Cholecystitis: What Every Radiologist Should Know. *World J Radiol* (2016) 8(2):183–91. doi: 10.4329/wjr.v8.i2.183
20. Uchiyama K, Ozawa S, Ueno M, Hayami S, Hirono S, Ina S, et al. Xanthogranulomatous Cholecystitis: The Use of Preoperative CT Findings to Differentiate it From Gallbladder Carcinoma. *J Hepato-biliary-pancreatic Surg* (2009) 16(3):333–8. doi: 10.1007/s00534-009-0067-9
21. Goshima S, Chang S, Wang J, Kanematsu M, Bae K, Federle M. Xanthogranulomatous Cholecystitis: Diagnostic Performance of CT to Differentiate From Gallbladder Cancer. *Eur J Radiol* (2010) 74(3):e79–83. doi: 10.1016/j.ejrad.2009.04.017
22. Shuto R, Kiyosue H, Komatsu E, Matsumoto S, Kawano K, Kondo Y, et al. CT and MR Imaging Findings of Xanthogranulomatous Cholecystitis: Correlation With Pathologic Findings. *Eur Radiol* (2004) 14(3):440–6. doi: 10.1007/s00330-003-1931-7
23. Ogawa T, Horaguchi J, Fujita N, Noda Y, Kobayashi G, Ito K, et al. High B-Value Diffusion-Weighted Magnetic Resonance Imaging for Gallbladder Lesions: Differentiation Between Benignity and Malignancy. *J Gastroenterol* (2012) 47(12):1352–60. doi: 10.1007/s00535-012-0604-1
24. Srinivas G, Sinha S, Ryley N, Houghton P. Perfidious Gallbladders - a Diagnostic Dilemma With Xanthogranulomatous Cholecystitis. *Ann R Coll Surgeons Engl* (2007) 89(2):168–72. doi: 10.1308/003588407X155833
25. Frountzas M, Schizas D, Liatsou E, Economopoulos K, Nikolaou C, Apostolou K, et al. Presentation and Surgical Management of Xanthogranulomatous Cholecystitis. *Hepatobiliary Pancreatic Dis Int HBPD Int* (2021) 20(2):117–27. doi: 10.1016/j.hbpd.2021.01.002
26. Krishnani N, Shukla S, Jain M, Pandey R, Gupta R. Fine Needle Aspiration Cytology in Xanthogranulomatous Cholecystitis, Gallbladder Adenocarcinoma and Coexistent Lesions. *Acta Cytol* (2000) 44(4):508–14. doi: 10.1159/000328522

Conflict of Interest: The authors declare that the research was conducted in the absence of any commercial or financial relationships that could be construed as a potential conflict of interest.

Publisher's Note: All claims expressed in this article are solely those of the authors and do not necessarily represent those of their affiliated organizations, or those of the publisher, the editors and the reviewers. Any product that may be evaluated in this article, or claim that may be made by its manufacturer, is not guaranteed or endorsed by the publisher.

Copyright © 2022 Zhou, Liu, Zhou, Yu, Wang, Wang, Xu and Yu. This is an open-access article distributed under the terms of the Creative Commons Attribution License (CC BY). The use, distribution or reproduction in other forums is permitted, provided the original author(s) and the copyright owner(s) are credited and that the original publication in this journal is cited, in accordance with accepted academic practice. No use, distribution or reproduction is permitted which does not comply with these terms.

frontiers in Surgery

SYSTEMATIC REVIEW
published: 28 February 2022
doi: 10.3389/fsurg.2021.802143

Prognostic Significance of SOCS3 in Patients With Solid Tumors: A Meta-Analysis

Xia Zheng[1,2†], *Jie Shao*[1,2†], *Sihui Wei*[3], *Yu Gu*[1,2*] *and Jun Qian*[1,2*]

[1] Oncology Department, Affiliated Hospital of Nanjing University of Chinese Medicine, Nanjing, China, [2] Oncology Department, Jiangsu Province Hospital of Chinese Medicine, Nanjing, China, [3] Oncology Department, Third People's Hospital of Province, Wuhan, China

OPEN ACCESS

Edited by:
Qi Liu,
Fudan University, China

Reviewed by:
Marco Massani,
ULSS2 Marca Trevigiana, Italy
Alessandro Rizzo,
National Cancer Institute Foundation (IRCCS), Italy
Andrea Laurenzi,
University Hospital of Bologna Policlinico S. Orsola-Malpighi, Italy
Ziv Radisavljevic,
Brigham and Women's Hospital and Harvard Medical School, United States

***Correspondence:**
Jun Qian
jun_qian@njucm.edu.cn
Yu Gu
guyugg@njucm.edu.cn

[†]These authors have contributed equally to this work and share first authorship

Specialty section:
This article was submitted to Surgical Oncology, a section of the journal Frontiers in Surgery

Received: 26 October 2021
Accepted: 31 December 2021
Published: 28 February 2022

Citation:
Zheng X, Shao J, Wei S, Gu Y and Qian J (2022) Prognostic Significance of SOCS3 in Patients With Solid Tumors: A Meta-Analysis. Front. Surg. 8:802143. doi: 10.3389/fsurg.2021.802143

Background: The identification of reliable biomarkers for predicting disease recurrence and the survival of patients with cancer is of great importance. Numerous previous studies have revealed that the abnormal expression of the suppressor of cytokine signaling 3 (SOCS3) was associated with patient outcomes. However, these results were inconsistent. The aim of the present study was to assess the prognostic value of SOCS3 in patients with solid tumors.

Methods: Studies focusing on the prognostic value of SOCS3 in solid tumors were searched for in the PubMed, Embase, Web of Science, and Scopus databases. We included studies that compared disease-free survival (DFS) and overall survival based on different levels of SOCS3. Other outcomes (e.g., Edmondson grading, tumor size, tumor vascular invasion, lymph node invasion, and distant metastasis) were also considered. The hazard ratio (HR)/risk ratio (RR) and corresponding 95% CI were determined.

Results: Twelve studies with 1,551 patients were included in this meta-analysis. The pooled analysis demonstrated that the higher expression of SOCS3 was significantly associated with better disease-free survival (HR:0.36, 95% CI:0.17–0.77, $P < 0.001$) and overall survival (HR:0.45, 95% CI:0.32–0.62, $P < 0.001$) compared with low expression. Moreover, SOCS3 expression was closely correlated with the Edmondson grading [odds ratio (OR):0.77, 95% CI:0.61–0.98, $P = 0.033$], vascular invasion (OR:0.63, 95% CI:0.52–0.78, $P < 0.001$), and distant metastasis (OR:0.73, 95% CI:0.51–1.03, $P = 0.076$). However, the levels of SOCS3 were not significantly associated with tumor size (OR:0.85, 95% CI:0.71–1.03, $P = 0.090$) and lymph node invasion (OR:0.73, 95% CI:0.51–1.03, $P = 0.076$).

Conclusion: Increased SOCS3 expression in tumor mass was associated with better DFS and OS, suggesting it might be a novel and reliable biomarker for predicting the risk of cancer recurrence and mortality.

Keywords: suppressor of cytokine signaling 3 (SOCS3), solid tumor, prognosis, meta-analysis, radical resection

INTRODUCTION

According to the most recently published data, the global cancer-related morbidity and mortality rates in 2020 were estimatedto be 19.3 and 10.0 million, respectively. This evidence revealed that malignancy has become a major public health concern (1). Surgical resection is considered the main curative therapeutic strategy for most types of solid tumors. However, most patients with such tumors experience postoperative recurrence. Although chemotherapy, radiotherapy, and targeted therapy have made remarkable progress in cancer treatment, patients' survival remains limited. Immunotherapy, especially for immune checkpoint inhibitors, has been applied in a variety of tumors and prolonged patients' survival significantly. Immune-based combinations have been recommended as the first-line therapy in most malignancies such as hepatocellular carcinoma (HCC) (2, 3). Nonetheless, some patients did not respond to this novel treatment option with unsatisfactory survival. According to previous studies, it is necessary to identify biomarkers to predict the outcomes in patients who received immune-based therapy (4). Thus far, risk factors linked to patients' outcomes have been poorly understood. Therefore, the identification of hypersensitive and specific biomarkers for predicting patient outcomes is urgently warranted.

Currently, various clinicopathological factors (e.g., Edmondson grading, tumor size, lymph nodes invasion, and distant metastasis) have been recognized as common predictors of patient outcome. Accordingly, multiple tumor staging systems (e.g., TNM) have been developed and applied to the management of cancer in clinical practice. However, the accuracy of these systems remains unsatisfactory.

Owing to their inhibitory effect on multiple cytokine-related signaling pathways, members of the suppressor of cytokine signaling (SOCS) protein family are considered potential prognostic molecules in patients with cancer. Particularly, it has been found that the SOCS 3 (SOCS3) expression is lower in tumor tissues compared with adjacent tissues; this difference in expression may influence patient outcomes (5, 6). Interestingly, SOCS3 acts as a double-edged sword in the regulation of cancer biology. For example, a recent study suggested that SOCS3 inhibited the proliferation of breast cancer cells *in vitro* (7). However, another study demonstrated that SOCS3 mediated interferon-α resistance in renal cell carcinoma (8).

Although SOCS3 methylation has been demonstrated as a reliable prognostic factor in HBV infection-related HCC cases (9), previous clinical studies have yielded inconsistent data regarding the prognostic significance of SOCS3. Multiple retrospective cohort studies revealed that elevated SOCS3 expression was correlated with favorable disease-free survival (DFS) and overall survival (OS) in patients with HCC (10, 11), colorectal cancer (12), gastric cancer (13–15), breast cancer (16), cholangiocarcinoma (17), ovarian cancer (18), and prostatic cancer (19). However, Jiang et al. (20). have demonstrated that the expression of SOCS3 cannot predict the postoperative risk of tumor recurrence in patients with HCC. Conversely, a study reported by Bekki et al. (21) suggested that higher levels of SOCS3 were associated with an increased risk of recurrence in undifferentiated pleomorphic sarcoma.

Therefore, we performed a meta-analysis of data collected from published research studies to re-assess the prognostic value of SOCS3 in patients with solid tumors.

METHODS

Search Strategy

Published studies potentially related to solid tumors and SOCS3 expression were extracted from the PubMed, Embase, Scopus, and Web of Science databases in October 2020. The keywords "cancer," "carcinoma," "suppressor of cytokine signaling 3," and "prognosis," as well as related abbreviations, were used for the screening and identification of candidate studies to be included in the meta-analysis. Multiple synonyms were also utilized.

Inclusion and Exclusion Criteria

Eligible studies were identified using the following criteria: (1) research addressing the relationship between the outcomes of patients with solid tumors and SOCS3 expression, (2) detection of SOCS3 expression in tumor tissues using immunohistochemistry, and (3) confirmation of all solid tumors through pathological examination.

The exclusion criteria for this meta-analysis were: (1) other types of publications (i.e., reviews, conference abstracts, case reports, or comments); (2) *in vivo* or *in vitro* research studies; (3) lack of data on DFS or OS; (4) use of data from public databases; and (5) lack of hazard ratios (HRs) and 95% confidence intervals (CIs) as effective measurements.

Data Management and Outcome Assessment

Using the aforementioned criteria, available articles were independently selected and reviewed by two investigators through abstract and full-text reading. In case of disagreement between the investigators, a consensus was reached through discussion with a senior investigator. The HRs and 95% CIs of OS and DFS were collected and recognized as effective measurements. Univariate and multivariate analyses were performed, and the studies or data with more accurate HRs and 95% CIs were subsequently selected for the meta-analysis.

Quality Assessment

The UK Cochrane Center of Evidence (2009) was used to estimate the level of evidence in the studies. The quality of the retrospective cohort studies was assessed using the Newcastle–Ottawa scale (22). This scale consists of three factors, namely the selection of patients, comparability of the study groups, and assessment of outcome. The maximum total score is nine; scores $\geq$6 denoted high-quality studies and were also a pre-setting selection criterion in this report.

Statistical Analysis

Hazard ratios (HRs) and the corresponding 95% CIs were calculated to pool the functional outcomes. Statistical heterogeneity among the studies was assessed using chi-square

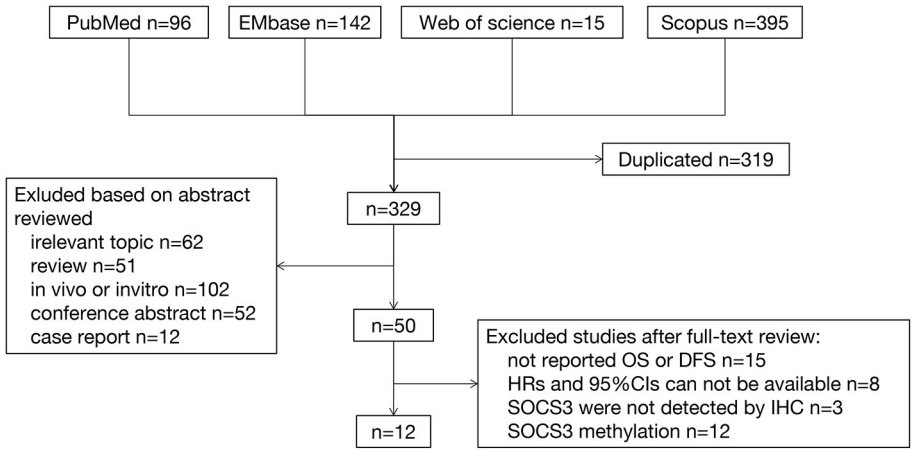

FIGURE 1 | Flow of studies selection.

TABLE 1 | Characteristics of included studies.

References	Country	Mean age (year)	n (male%)	Cancer type	Stage	Treatment options	Follow-up time (month)	Analysis variate	Outcomes	Level of evidence	NOS
Chen et al. (10)	China	na	74 (91.9%)	HCC	pT1-3N0M0 (8th)	Surgery	60.0	M	OS	2a	8
Bekki et al. (21)	Japan	na	75 (40%)	UPS	II-IV (7th)	na	na	M	OS	2a	7
Chu et al. (12)	China	68.72	88 (52.3%)	CRC	I-IV (7th)	Surgery	46.62	M	OS	2a	8
Deng et al. (15)	China	57.4	107 (66.45)	GC	na	Surgery	37.0	M	OS	2a	8
Jiang et al. (20)	China	51.4	176 (84.1%)	HCC	na	Surgery	56.5	M	DFS, OS	2a	9
Li et al. (14)	China	57.0	186 (68.8%)	GC	I-IV (6th)	Surgery	40.7	M	OS	2a	8
Pierconti et al. (19)	Italy	na	65 (100%)	PCa	pT2-3N0M0 (7th)	Radical prostatectomy	na	M	DFS	2a	6
Shang et al. (18)	China	54.0	136 (0%)	OC	I-IV (FIGO)	Surgery	na	M	OS	2a	6
Wang et al. (17)	China	61.1	86 (37.2%)	CCA	I-IVA (7th)	Surgery	23.0	M	OS	2a	8
Xu et al. (13)	China	48.0	105 (65.7%)	GC	I-IV (7th)	Surgery	30.0	M	OS	2a	8
Ying et al. (16)	China	52.8	367 (0%)	BC	I-III (7th)	Surgery	43.3	M	DFS	2a	7
Zhao et al. (11)	China	50.4	85 (78.8%)	HCC	na	Surgery	30.0	M	DFS, OS	2a	8

HCC, hepatocellular carcinoma; UPS, Undifferentiated Pleomorphic Sarcoma; Pca, prostate cancer; CRC, colorectal cancer; OC, ovarian cancer; GC, gastric cancer; BC, breast cancer; CCA, cholangiocarcinoma; DFS, disease-free survival; OS, overall survival; M, multivariate analysis.

tests, with $P < 0.05$ or $I^2 > 50\%$ denoting statistical significance. In the absence of evident heterogeneity, a fixed-effects model was utilized; otherwise, a random-effects model was selected to minimize the heterogeneity, followed by subgroup and sensitivity analyses. Funnel plots, Egger's test, and Begg's test were used to examine publication bias. All statistical analyses were performed using the STATA version 14.0 (StataCorp, College Station, TX, USA) software.

RESULTS

Characteristics of Selected Articles

After removing duplicated publications ($n = 319$), 329 articles were selected for screening. By scanning the titles and abstracts of these articles, 279 publications were excluded; of those, 62 were unrelated, 51 were reviews, 102 described *in vivo* or *in vitro* studies, 52 were conference abstracts, and 12 were case reports. According to the aforementioned criteria, 38 studies were excluded for the following reasons: (1) lack of data on DFS and OS ($n = 15$), (2) lack of HRs and 95% CIs ($n = 8$), (3) lack of immunohistochemistry analysis for the detection of SOCS3 expression, and (4) exclusive focus on SOCS3 methylation ($n = 12$) (**Figure 1**).

In total, 1,551 patients from 12 retrospective cohort studies were included in the present analysis (10–21). The level of evidence was 2a. Based on the Newcastle–Ottawa Scale, all studies received a quality score of 6–9 (**Table 1**).

Predictive Role of SOCS3 in DFS and OS

Four studies including 693 patients investigated the relationship between SOCS3 expression and the risk of tumor recurrence.

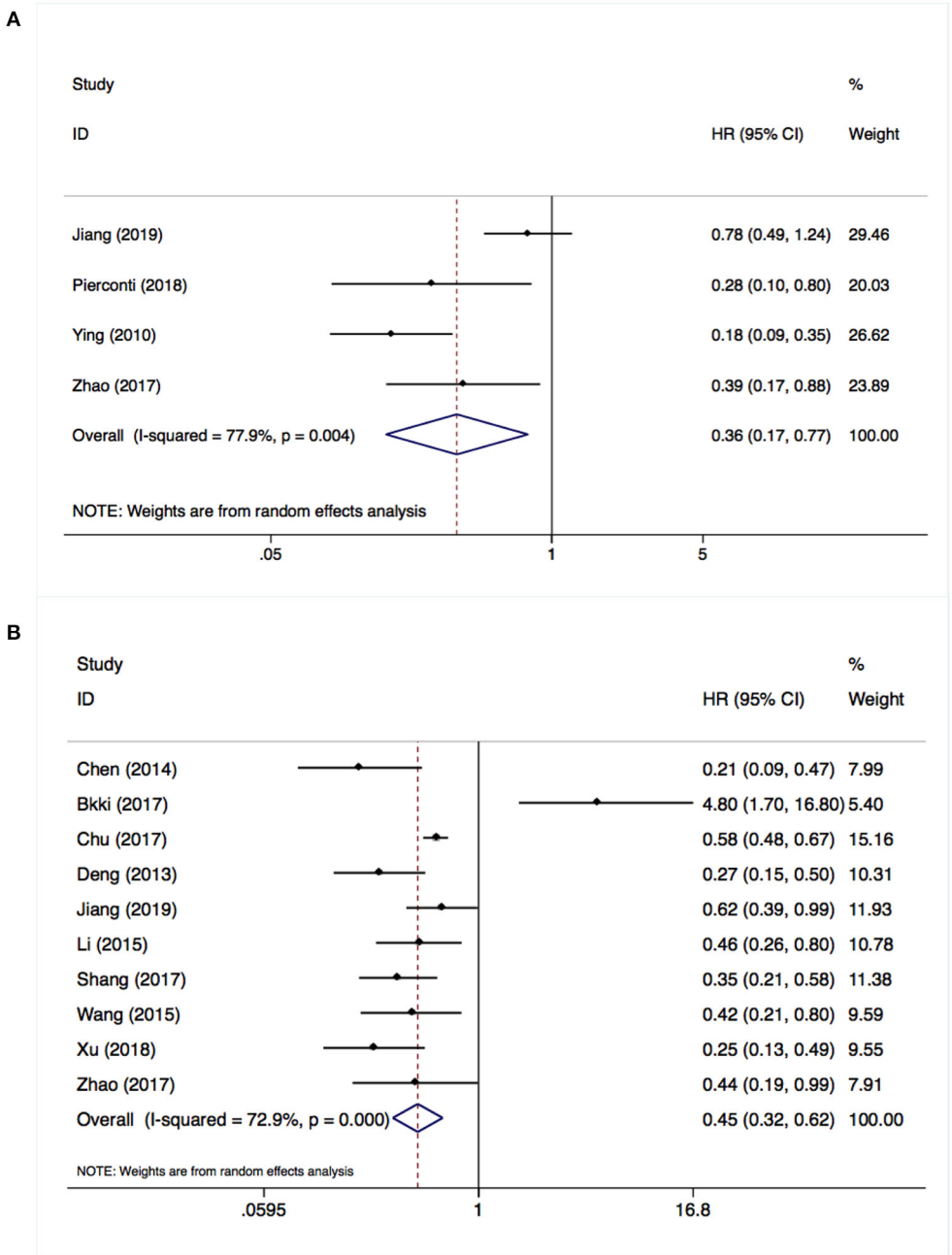

FIGURE 2 | Overexpressed suppressor of cytokine signaling 3 (SOCS3) was associated with better disease-free survival **(A)** and overall survival **(B)**.

Considering the degree of heterogeneity (I^2 = 77.9%), a random-effects model was utilized for the analysis of these data. We found that an elevated SOCS3 expression in tumor tissues was significantly correlated with better DFS (HR:0.36, 95% CI:0.17–0.77, $P < 0.001$) vs. low expression (**Figure 2A**). Similarly, a pooled analysis of 10 studies with 1,119 cases using the random-effects model (I^2 = 72.9%) revealed that higher levels of SOCS3 were significantly associated with better OS vs. low levels (HR:0.45, 95% CI:0.32–0.62, $P < 0.001$) (**Figure 2B**, **Table 2**).

Correlation Between SOCS3 Expression and Clinicopathological Features

Eight studies involving 1,118 patients focused on the relationship between SOCS3 expression and Edmondson grading. A pooled analysis with a random-effects model (I^2 = 72.9%) revealed that the lower expression of SOCS3 was correlated with poorly differentiated tumors [risk ratio (RR):0.77, 95% CI:0.61–0.98, $P = 0.033$] (**Figure 3A**). However, according to the results of a meta-analysis of seven studies using a random-effects model (I^2 = 67.2), SOCS3 expression was not associated

TABLE 2 | Results of meta-analysis of interested outcomes.

Outcomes/pathological factors	Cohort number	Case number	HR/RR(95%CI)-Model	*P*	Heterogeneity		Public bias	
					I^2 (%)	*P*	Egger test *P*	Begg test *P*
DFS	4	693	0.36 (0.17–0.77)-random	<0.001	77.9	0.004	0.381	0.734
OS	10	1,119	0.45 (0.32–0.62)-random	<0.001	72.9	<0.001	0.437	0.371
Differentiation (III–IV vs. I–II)	8	1,118	0.77 (0.61–0.98)-random	0.033	72.9	<0.001	0.612	0.902
Tumor size (large vs. small)	7	1,183	0.85 (0.71–1.03)-random	0.090	67.2	0.006	0.110	0.230
Vascular invasion (present vs. absence)	6	876	0.63 (0.52–0.78)-fixed	<0.001	9.40	0.356	0.856	1.000
Lymph nodes metastasis (with vs. without)	8	1,252	0.73 (0.51–1.03)-random	0.076	85.0	<0.001	0.915	1.000
Distance metastasis (with vs. without)	4	557	0.56 (0.40–0.78)-fixed	<0.001	34.2	0.208	0.107	0.308

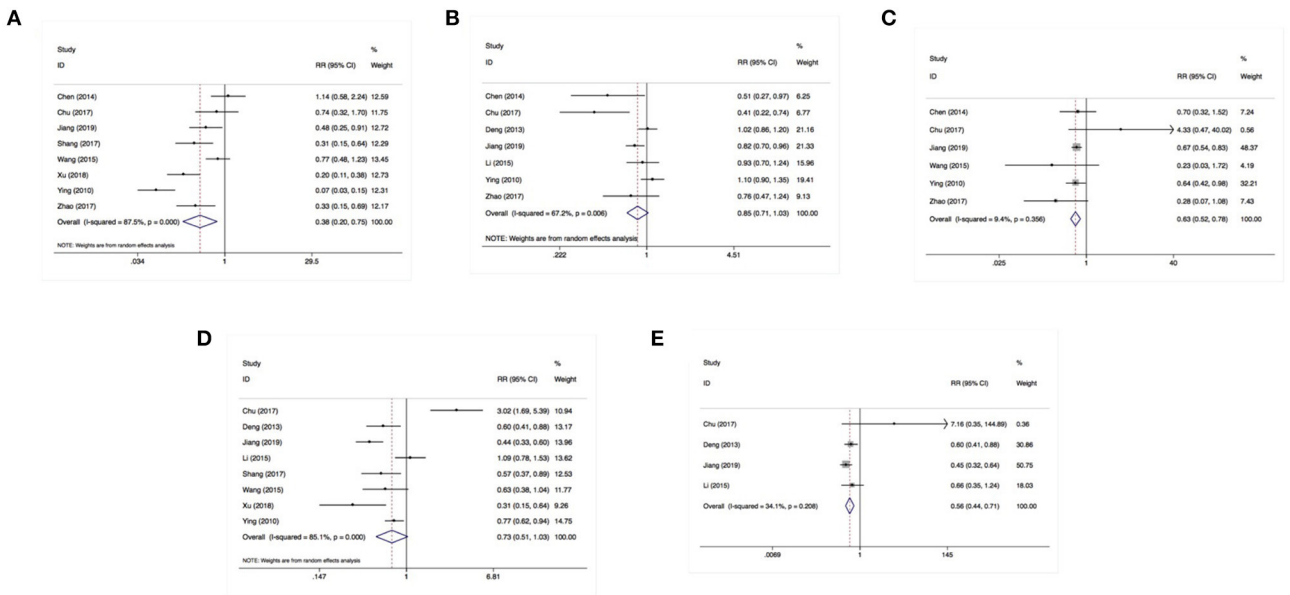

FIGURE 3 | SOCS3 expression was associated with Edmondson grading **(A)**, vascular invasion **(C)**, distant metastasis **(E)** instead of tumor size **(B)** or lymph nodes invasion **(D)**.

with tumor size (RR:0.85, 95% CI:0.71–1.03, $P = 0.090$) (**Figure 3B**).

Using a fixed-effects model ($I^2 = 9.40\%$), a pooled analysis of six studies (including 876 cases) demonstrated that the lower expression of SOCS3 increased the risk of tumor vascular invasion (RR:0.63, 95% CI:0.52–0.78, $P < 0.001$) (**Figure 3C**). In contrast, an analysis of eight studies with a random-effects model ($I^2 = 85.0\%$) revealed that SOCS3 expression did not have an obvious impact on lymph node invasion (RR:0.73, 95% CI:0.51–1.03, $P = 0.076$) (**Figure 3D**). An analysis of four studies with a fixed-effects model showed that higher SOCS3 expression significantly reduced the risk of metastasis vs. low expression (RR:0.56, 95% CI:0.40–0.78, $P < 0.001$) (**Figure 3E**).

Sensitivity, Stratification, and Bias Analysis

For the sensitivity analysis, we employed a leave-one-out approach to examine the stability of the pooled analysis results concerning DFS and OS. The exclusion of any single study did not alter the statistical significance of the results, indicating that the results of this meta-analysis were stable and robust (**Figures 4A,B**).

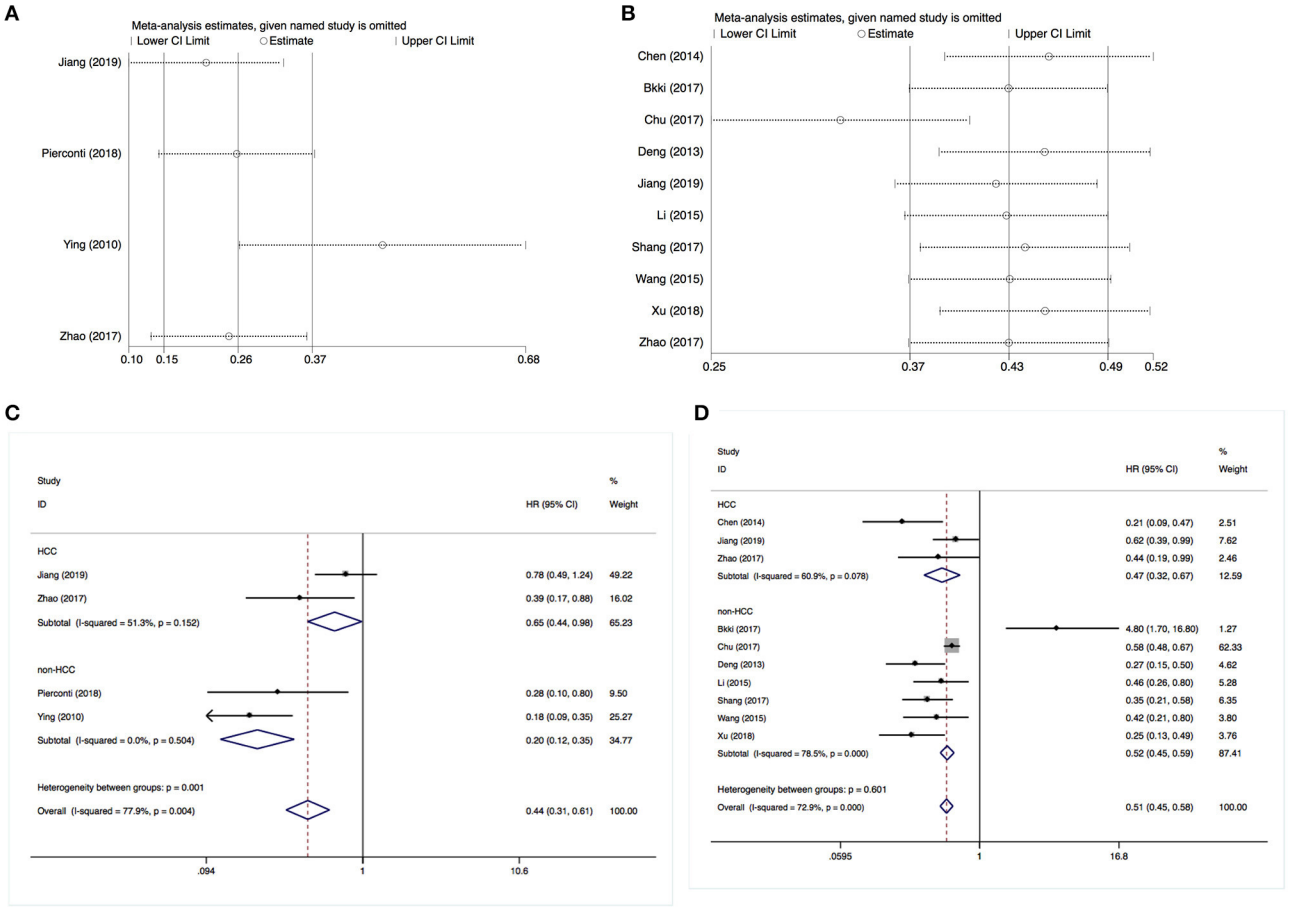

FIGURE 4 | Sensitivity and stratification analysis results. **(A)** Sensitivity analysis of disease-free survival. **(B)** Sensitivity analysis of overall survival. **(C)** Stratification analysis of disease-free survival. **(D)** Stratification analysis of overall survival.

Subsequently, we performed a stratification analysis by the studies that enrolled HCC ($n = 3$) or non-HCC cases. It revealed that an increased SOCS3 expression was associated with a better DFS and OS in both patients with HCC or other types of solid tumor cases (**Figures 4C,D**). These results were consistent with the above pooled analysis.

Publication bias was investigated using Begg's and Egger's tests, as well as funnel plots. All *P*-values obtained from Egger's and Begg's tests for each endpoint were >0.05 (**Table 2**). Additionally, the visual inspection of the funnel plots did not show obvious asymmetry for the DFS (**Figure 5A**) or OS (**Figure 5B**) analyses. These results confirmed the absence of publication bias risk among the included studies in the present meta-analysis.

DISCUSSION

Due to the heterogeneity of cancer, the exploration of reliable prognostic biomarkers is highly important in the era of precision medicine. According to preclinical research studies, SOCS3 is a differently expressive gene between tumors and adjacent tissues (7, 23). However, its prognostic value in patients with cancer remains poorly understood. In the present study, we screened the available literature and performed a meta-analysis to assess the correlation between SOCS3 expression and the risk of cancer relapse and mortality. The findings demonstrated that higher SOCS3 expression in tumor tissues was associated with a significantly better DFS and OS compared with low expression. The results were stable without obvious publication bias. Meanwhile, we uncovered that SOCS3 was obviously related to Edmondson grading, vascular invasion, and metastasis instead of with tumor size and lymph nodes invasion. Generally, a few genes perform different effects on tumor biology or reflect inconsistent clinicopathological features. We believe the different results were mainly due to the limited sizes of available studies and different cancer types. According to these results, SOCS3 may be a novel prognostic biomarker in patients with solid tumors.

The exact mechanism through which SOCS3 affects patient outcomes remains unclear. Nevertheless, its inhibitory effect on multiple cytokine-related signaling pathways has been widely

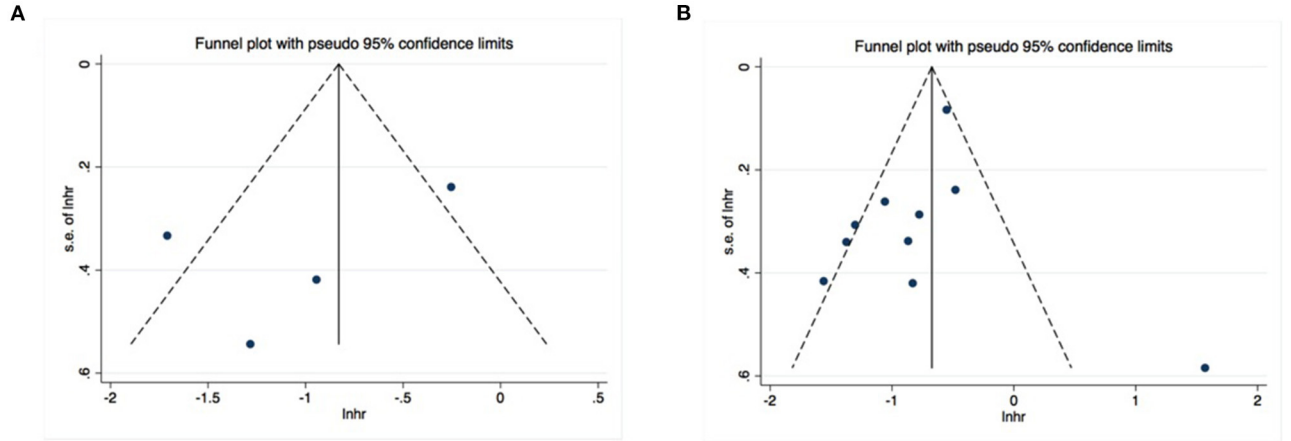

FIGURE 5 | No significant publication bias existed in the pooled analysis about disease-free survival **(A)** or overall survival **(B)**.

acknowledged. The incidence and progression of cancer may be ascribed to a variety of cytokines and growth factors, which are abundant in the tumor microenvironment (TME). In fact, a complex network of growth exists in TME and plays a critical role in cell-cell communication. The interaction of these cytokines with their receptors activates multiple signaling pathways, thus resulting in cell proliferation, angiogenesis, immune escape, and other biological processes which are hallmarks of cancer.

As mentioned above, members of the SOCS family of genes exert their anti-cancer function by inhibiting multiple signaling pathways related to cytokines and growth factors. In particular, SOCS3 mainly suppresses the activity of the interleukin 6/Janus kinase/signal transducer and the activator of the transcription 3 (IL6/JAK/STAT3) pathway in a feedback manner (24). It has been reported that SOCS3 is frequently silenced by hypermethylation and suppresses cell growth in human lung cancer (25). An *in vivo* study revealed that SOCS3 deficiency would induce gastric cancer by enhancing the STAT3 signaling pathway (26).

Cytokine IL6 is secreted by tumor cells or tumor stem cells and can promote cancer progression by mediating drug resistance, immune escape, angiogenesis, and metabolic disorder (27). Therefore, IL6 is considered an effective anti-cancer target. Accordingly, several monoclonal antibodies against IL6 or its receptor have been investigated in early-phase clinical trials for the treatment of hematological malignancy (28, 29), prostate cancer (30), renal cancer (31), and ovarian cancer (32). Targeting IL6 has shown a favorable safety profile and promising efficacy in the field of cancer management.

STAT3 is activated by JAK and IL6 and is a multi-function gene. Based on previous findings, STAT3 can facilitate cancer progression by increasing the expression of programmed cell death 1 ligand 1 (PD-L1), vascular epidermal growth factor A (VEGFA), matrix metalloproteinase (MMP), etc. (33). Importantly, STAT3 phosphorylation has been linked to worse and better prognosis in patients with solid tumors and hematological malignancy, respectively (34, 35). A previous meta-analysis confirmed that the overexpression of p-STAT3 was significantly correlated with poor outcomes in patients with cancer (36–38). Therefore, STAT3 is commonly considered a potential anti-cancer target (39). Recently, multiple promising STAT3 inhibitors have been used in clinical trials for the treatment of patients with cancer. Based on these data, we propose that the SOCS3-induced suppression of the IL6/JAK/STAT3 pathway may be one of the main mechanisms influencing patient outcomes (40).

To our knowledge, this is the first meta-analysis confirming the prognostic value of SOCS3 in patients with solid tumors. In clinical practice, SOCS3 could be recommended as a general molecular to be detected in tumor mass, which may assist physicians in recognizing high-risk patients and, consequently, achieve precision management. However, a well-designed prospective study is necessary to validate the prognostic value of SOCS3 in cancer patients.

However, some limitations in the present study should be acknowledged. Firstly, all included investigations were retrospective cohort studies with a modest level of evidence. Secondly, most participants in these studies were from Asian countries (e.g., China and Japan), which may restrict the applicability of these findings to populations residing in other regions. Thirdly, the heterogeneity detected in the present study may result from the quality of the studies included and multiple tumor types. Lastly, the cut-off value of SOCS3 expression in each study was inconsistent; this inconsistency may have affected our results.

CONCLUSION

The anti-oncogene SOCS3 may be a novel biomarker for predicting the outcomes of patients with solid tumors. This molecule can be applied to clinical practice and may be a therapeutic target.

DATA AVAILABILITY STATEMENT

The original contributions presented in the study are included in the article/supplementary material. Further inquiries can be directed to the corresponding author.

AUTHOR CONTRIBUTIONS

JQ and YG: conception and design. XZ: data analysis and interpretation. JS and SW: collection and assembly of data. All authors wrote the manuscript and approved the final version of the manuscript.

FUNDING

This study was funded by National Traditional Chinese Medicine Inheritance and Innovation Platform Construction Project by National Administration of Traditional Chinese Medicine, College Project of Jiangsu Province Hospital of Chinese Medicine (NO. Y2020CX570).

REFERENCES

1. Sung H, Ferlay J, Siegel RL, Laversanne M, Soerjomataram I, Jemal A, et al. Global cancer statistics 2020: GLOBOCAN estimates of incidence and mortality worldwide for 36 cancers in 185 countries. *CA Cancer J Clin.* (2021) 71:209–49. doi: 10.3322/caac.21660
2. Rizzo A, Ricci AD, Brandi G. Immune-based combinations for advanced hepatocellular carcinoma: shaping the direction of first-line therapy. *Future Oncol.* (2021) 17:755–7. doi: 10.2217/fon-2020-0986
3. Rizzo A, Dadduzio V, Ricci AD, Massari F, Di Federico A, Gadaleta-Caldarola G, et al. Lenvatinib plus pembrolizumab: the next frontier for the treatment of hepatocellular carcinoma? *Expert Opin Investig Drugs.* (2021) 1–8. doi: 10.1080/13543784.2021.1948532
4. Rizzo A, Brandi G. Biochemical predictors of response to immune checkpoint inhibitors in unresectable hepatocellular carcinoma. *Cancer Treat Res Commun.* (2021) 27:100328. doi: 10.1016/j.ctarc.2021.100328
5. Zhou QY, Peng PL, Xu YH. MiR-221 affects proliferation and apoptosis of gastric cancer cells through targeting SOCS3. *Eur Rev Med Pharmacol Sci.* (2019) 23:9427–35. doi: 10.26355/eurrev_201911_19436
6. Ghafouri-Fard S, Oskooei VK, Azari I, Taheri M. Suppressor of cytokine signaling (SOCS) genes are downregulated in breast cancer. *World J Surg Oncol.* (2018) 16:226. doi: 10.1186/s12957-018-1529-9
7. Barclay JL, Anderson ST, Waters MJ, Curlewis JD. SOCS3 as a tumor suppressor in breast cancer cells, and its regulation by PRL. *Int J Cancer.* (2009) 124:1756–66. doi: 10.1002/ijc.24172
8. Tomita S, Ishibashi K, Hashimoto K, Sugino T, Yanagida T, Kushida N, et al. Suppression of SOCS3 increases susceptibility of renal cell carcinoma to interferon-α. *Cancer Sci.* (2011) 102:57–63. doi: 10.1111/j.1349-7006.2010.01751.x
9. Zhang X, You Q, Zhang X, Chen X. SOCS3 methylation predicts a poor prognosis in HBV infection-related hepatocellular carcinoma. *Int J Mol Sci.* (2015) 16:22662–75. doi: 10.3390/ijms160922662
10. Chen L, Huang X, Zhang W, Liu Y, Chen B, Xiang Y, et al. Correlation of PD-L1 and SOCS3 co-expression with the prognosis of hepatocellular carcinoma patients. *J Cancer.* (2020) 11:5440–8. doi: 10.7150/jca.46158
11. Zhao R, Chen K, Zhou J, He J, Liu J, Guan P, et al. The prognostic role of BORIS and SOCS3 in human hepatocellular carcinoma. *Medicine.* (2017) 96:e6420. doi: 10.1097/MD.0000000000006420
12. Chu Q, Shen D, He L, Wang H, Liu C, Zhang W. Prognostic significance of SOCS3 and its biological function in colorectal cancer. *Gene.* (2017) 627:114–22. doi: 10.1016/j.gene.2017.06.013
13. Xu W, Fu J, Wu H, Sun W. Human epidermal growth factor receptor 2 expressions and Janus-activated kinase/signal transducer and activator of transcription 3-suppressor of cytokine signaling 3 pathway may be associated with clinicopathological features and prognosis of gastric cancer. *J Cancer Res Ther.* (2018) 14(Suppl):S311–8. doi: 10.4103/0973-1482.235348
14. Li G, Xu J, Wang Z, Yuan Y, Li Y, Cai S, et al. Low expression of SOCS-1 and SOCS-3 is a poor prognostic indicator for gastric cancer patients. *J Cancer Res Clin Oncol.* (2015) 141:443–52. doi: 10.1007/s00432-014-1838-5
15. Deng J, Jiao X, Liu H, Wu L, Zhang R, Wang B, et al. Lymph node metastasis is mediated by suppressor of cytokine signaling-3 in gastric cancer. *Tumour Biol.* (2013) 34:3627–36. doi: 10.1007/s13277-013-0944-3
16. Ying M, Li D, Yang L, Wang M, Wang N, Chen Y, et al. Loss of SOCS3 expression is associated with an increased risk of recurrent disease in breast carcinoma. *J Cancer Res Clin Oncol.* (2010) 136:1617–26. doi: 10.1007/s00432-010-0819-6
17. Wang Y, Wan M, Zhou Q, Wang H, Wang Z, Zhong X, et al. The prognostic role of SOCS3 and A20 in human cholangiocarcinoma. *PLoS ONE.* (2015) 10:e0141165. doi: 10.1371/journal.pone.0141165
18. Shang AQ, Wu J, Bi F, Zhang YJ, Xu LR, Li LL, et al. Relationship between HER2 and JAK/STAT-SOCS3 signaling pathway and clinicopathological features and prognosis of ovarian cancer. *Cancer Biol Ther.* (2017) 18:314–22. doi: 10.1080/15384047.2017.1310343
19. Pierconti F, Martini M, Cenci T, Larocca LM. The immunohistochemical analysis of SOCS3 protein identifies a subgroup of prostatic cancer biopsies with aggressive behavior. *Appl Immunohistochem Mol Morphol.* (2018) 26:324–9. doi: 10.1097/PAI.0000000000000438
20. Jiang LH, Hao YL, Zhu JW. Expression and prognostic value of HER-2/neu, STAT3 and SOCS3 in hepatocellular carcinoma. *Clin Res Hepatol Gastroenterol.* (2019) 43:282–91. doi: 10.1016/j.clinre.2018.09.011
21. Bekki H, Kohashi K, Yamada Y, Iura K, Ishii T, Maekawa A, et al. Phosphorylation of STAT3 in undifferentiated pleomorphic sarcoma is correlated with a favorable prognosis. *Pathobiology.* (2017) 84:161–9. doi: 10.1159/000448524
22. Lo CK, Mertz D, Loeb M. Newcastle-ottawa scale: comparing reviewers' to authors' assessments. *BMC Med Res Methodol.* (2014) 14:45. doi: 10.1186/1471-2288-14-45
23. Zhang S, Wang W, Wang E, Qiu X. SOCS3 expression is inversely correlated with Pyk2 in non-small cell lung cancer and exogenous SOCS3 inhibits proliferation and invasion of A549 cells. *Pathology.* (2012) 44:434–40. doi: 10.1097/PAT.0b013e328354ffdf
24. Yu T, Zuo Y, Cai R, Huang X, Wu S, Zhang C, et al. SENP1 regulates IFN-γ-STAT1 signaling through STAT3-SOCS3 negative feedback loop. *J Mol Cell Biol.* (2017) 9:144–53. doi: 10.1093/jmcb/mjw042
25. He B, You L, Uematsu K, Zang K, Xu Z, Lee AY, et al. SOCS-3 is frequently silenced by hypermethylation and suppresses cell growth in human lung cancer. *Proc Natl Acad Sci U S A.* (2003) 100:14133–8. doi: 10.1073/pnas.2232790100
26. Inagaki-Ohara K, Mayuzumi H, Kato S, Minokoshi Y, Otsubo T, Kawamura YI, et al. Enhancement of leptin receptor signaling by SOCS3 deficiency induces development of gastric tumors in mice. *Oncogene.* (2014) 33:74–84. doi: 10.1038/onc.2012.540
27. Kumari N, Dwarakanath BS, Das A, Bhatt AN. Role of interleukin-6 in cancer progression and therapeutic resistance. *Tumour Biol.* (2016) 37:11553–72. doi: 10.1007/s13277-016-5098-7
28. Kurzrock R, Voorhees PM, Casper C, Furman RR, Fayad L, Lonial S, et al. A phase I, open-label study of siltuximab, an anti-IL-6 monoclonal antibody, in patients with B-cell non-Hodgkin lymphoma, multiple myeloma, or castleman disease. *Clin Cancer Res.* (2013) 19:3659–70. doi: 10.1158/1078-0432.CCR-12-3349
29. Orlowski RZ, Gercheva L, Williams C, Sutherland H, Robak T, Masszi T, et al. A phase 2, randomized, double-blind, placebo-controlled study of siltuximab (anti-IL-6 mAb) and bortezomib versus bortezomib alone in patients with relapsed or refractory multiple myeloma. *Am J Hematol.* (2015) 90:42–9. doi: 10.1002/ajh.23868

30. Karkera J, Steiner H, Li W, Skradski V, Moser PL, Riethdorf S, et al. The anti-interleukin-6 antibody siltuximab down-regulates genes implicated in tumorigenesis in prostate cancer patients from a phase I study. *Prostate.* (2011) 71:1455–65. doi: 10.1002/pros.21362
31. Rossi JF, Négrier S, James ND, Kocak I, Hawkins R, Davis H, et al. A phase I/II study of siltuximab (CNTO 328), an anti-interleukin-6 monoclonal antibody, in metastatic renal cell cancer. *Br J Cancer.* (2010) 103:1154–62. doi: 10.1038/sj.bjc.6605872
32. Dijkgraaf EM, Santegoets SJ, Reyners AK, Goedemans R, Wouters MC, Kenter GG, et al. A phase I trial combining carboplatin/doxorubicin with tocilizumab, an anti-IL-6R monoclonal antibody, and interferon-α2b in patients with recurrent epithelial ovarian cancer. *Ann Oncol.* (2015) 26:2141–9. doi: 10.1093/annonc/mdv309
33. Yu H, Jove R. The STATs of cancer–new molecular targets come of age. *Nat Rev Cancer.* (2004) 4:97–105. doi: 10.1038/nrc1275
34. Pan YM, Wang CG, Zhu M, Xing R, Cui JT, Li WM, et al. STAT3 signaling drives EZH2 transcriptional activation and mediates poor prognosis in gastric cancer. *Mol Cancer.* (2016) 15:79. doi: 10.1186/s12943-016-0561-z
35. Pectasides E, Egloff AM, Sasaki C, Kountourakis P, Burtness B, Fountzilas G, et al. Nuclear localization of signal transducer and activator of transcription 3 in head and neck squamous cell carcinoma is associated with a better prognosis. *Clin Cancer Res.* (2010) 16:2427–34. doi: 10.1158/1078-0432.CCR-09-2658
36. Tong M, Wang J, Jiang N, Pan H, Li D. Correlation between p-STAT3 overexpression and prognosis in lung cancer: a systematic review and meta-analysis. *PLoS ONE.* (2017) 12:e0182282. doi: 10.1371/journal.pone.0182282
37. Wu P, Wu D, Zhao L, Huang L, Shen G, Huang J, et al. Prognostic role of STAT3 in solid tumors: a systematic review and meta-analysis. *Oncotarget.* (2016) 7:19863–83. doi: 10.18632/oncotarget.7887
38. Kong H, Zhang Q, Zeng Y, Wang H, Wu M, Zheng T, et al. Prognostic significance of STAT3/phosphorylated-STAT3 in tumor: a meta-analysis of literatures. *Int J Clin Exp Med.* (2015) 8:8525–39.
39. Furtek SL, Backos DS, Matheson CJ, Reigan P. Strategies and approaches of targeting STAT3 for cancer treatment. *ACS Chem Biol.* (2016) 11:308–18. doi: 10.1021/acschembio.5b00945
40. Okusaka T, Ueno H, Ikeda M, Mitsunaga S, Ozaka M, Ishii H, et al. Phase 1 and pharmacological trial of OPB-31121, a signal transducer and activator of transcription-3 inhibitor, in patients with advanced hepatocellular carcinoma. *Hepatol Res.* (2015) 45:1283–91. doi: 10.1111/hepr.12504

Conflict of Interest: The authors declare that the research was conducted in the absence of any commercial or financial relationships that could be construed as a potential conflict of interest.

Publisher's Note: All claims expressed in this article are solely those of the authors and do not necessarily represent those of their affiliated organizations, or those of the publisher, the editors and the reviewers. Any product that may be evaluated in this article, or claim that may be made by its manufacturer, is not guaranteed or endorsed by the publisher.

Copyright © 2022 Zheng, Shao, Wei, Gu and Qian. This is an open-access article distributed under the terms of the Creative Commons Attribution License (CC BY). The use, distribution or reproduction in other forums is permitted, provided the original author(s) and the copyright owner(s) are credited and that the original publication in this journal is cited, in accordance with accepted academic practice. No use, distribution or reproduction is permitted which does not comply with these terms.

frontiers in Oncology

ORIGINAL RESEARCH
published: 08 March 2022
doi: 10.3389/fonc.2022.855615

Characteristic of Perineural Invasion in Hilar Cholangiocarcinoma Based on Whole-Mount Histologic Large Sections of Liver

Si-Yuan Wang[1,2†], *Nan Jiang*[1,2†], *Jian-Ping Zeng*[1,2], *Shao-Qing Yu*[1,2], *Ying Xiao*[3] *and Shuo Jin*[1,2*]

[1] Beijing Tsinghua Changgung Hospital, School of Clinical Medicine, Institute for Precision Medicine, Tsinghua University, Beijing, China, [2] State Key Laboratory of Precision Measurement Technology and Instruments, Department of Precision Instrument, Tsinghua University, Beijing, China, [3] Department of Pathology, Beijing Tsinghua Changgung Hospital, Beijing, China

OPEN ACCESS

Edited by:
Qi Liu,
Fudan University, China

Reviewed by:
Amira Kamal El-hawary,
Mansoura University, Egypt
Francesca Marcon,
Ca 'Granda Foundation Maggiore Policlinico Hospital (IRCCS), Italy

***Correspondence:**
Shuo Jin
jsa01263@163.com

†These authors have contributed equally to this work and share first authorship

Specialty section:
This article was submitted to Gastrointestinal Cancers: Hepato Pancreatic Biliary Cancers, a section of the journal Frontiers in Oncology

Received: 15 January 2022
Accepted: 14 February 2022
Published: 08 March 2022

Citation:
Wang S-Y, Jiang N, Zeng J-P, Yu S-Q, Xiao Y and Jin S (2022) Characteristic of Perineural Invasion in Hilar Cholangiocarcinoma Based on Whole-Mount Histologic Large Sections of Liver. Front. Oncol. 12:855615. doi: 10.3389/fonc.2022.855615

Background & Objective: Perineural invasion is an important biological feature of hilar cholangiocarcinoma (HCCA). We developed a whole-mount histologic large sections (WHLS) of the liver to evaluate peripheral nerve invasion (PNI) of HCCA.

Methods: Using sampling, fixation, dehydration, embedding, sectioning, hematoxylin and eosin (H&E) and immunohistochemical (IHC) staining, and scanning, the characteristics of intrahepatic and extrahepatic PNI in 20 patients with Bismuth type III and type IV HCCA were analyzed with WHLS. Correlation between the characteristics of nerve invasion and tumor size, vascular invasion (artery, portal vein), degree of differentiation, microvascular invasion (MVI), carbohydrate antigen19-9 (CA19-9), and differentiation degree of HCCA was statistically evaluated.

Results: The WHLS of the liver was successfully established, which enabled us to observe intrahepatic and extrahepatic distribution of HCCA and whether surrounding tissues including nervous, blood, and lymph vessels were infiltrated. Extrahepatic and intrahepatic PNI were identified in 20 (100%) patients and 1 (5.0%) patient, respectively. Vessel density decreased in most invaded nerves presented by CD-34, which correlated with 100% of poorly differentiated and 83% of moderately differentiated tumors ($P<0.008$).

Conclusion: This study established a WHLS of the liver that can be used for clinical diagnosis and research, and confirmed that extrahepatic PNI is prevalent, but intrahepatic nerve invasion is rare and does not accompany the invasion scope of bile ducts in types III and IV HCCA. In addition, moderately and poorly differentiated malignant tumors are more prone to PNI, independent of blood supply.

Keywords: panoramic immunohistochemistry, whole-mount histologic large sections, tumor biological behavior, pathological digital imaging, pathological methodology

Abbreviations: HCCA, hilar cholangiocarcinoma; PNI, peripheral nerve invasion; H&E, hematoxylin-eosin staining; IHC, immunohistochemical staining; WHLS, whole-mount histologic large sections.

1 INTRODUCTION

Hilar cholangiocarcinoma (HCCA) is the most common type of cholangiocarcinoma, and is characterized by high morbidity, high mortality rates, and poor prognosis (1–5). According to previous studies, the proportion of peripheral nerve invasion (PNI) in HCCA is around 38.8%-84.5% (6–10), and the overall survival rate of patients with PNI is significantly shorter than of those without PNI (11–13). In types III and IV HCCA, the invasion scope in the perihilar region is significantly larger than that of types I and II, and the tumor invades further along the intrahepatic bile duct. However, whether there is a difference between intrahepatic and extrahepatic PNI has not been clearly determined. Owing to limitations of the study area and due to tissue discontinuity, traditional pathological methods have not been able to provide solutions to this problem (14–16). Therefore, a whole-mount histologic large sections (WHLS) technology for hepatectomy specimens larger than 10 cm × 10 cm is urgently needed to panoramically analyze the characteristics of nerve invasion in HCCA.

WHLS technology was first introduced in 1994 for the diagnosis and staging of breast, prostate, endometrial, and lung cancers as well as brain tumors (15, 17–19). However, no systematic studies on hepatic WHLS larger than 5cm have been reported.

We have developed a WHLS system that includes dehydration, tissue embedding, sectioning, hematoxylin and eosin (H&E), immunohistochemical (IHC) staining and digital scanning for hepatectomy specimens larger than 10 × 10cm. Through this system, we can observe the characteristics of intrahepatic and extrahepatic PNI in Bismuth III and IV types of HCCA. Besides, WHLS can display the entire tumor, its surrounding tissues, the intrahepatic lesions, the incision margin, and the surrounding microenvironment.6

2 MATERIALS AND METHODS

Twenty patients were diagnosed with Bismuth types III and IV HCCA and underwent hemihepatectomy or trisegmenthepatectomy from July 2018 to February 2021. The preparation and staining methods of WHLS were as follows. IHC staining of S100, CD-34, and D2-40 was performed to visualize the nerve, lymph vessels, and blood vessels. Clinical and pathological information including tumor size, vascular invasion, degree of differentiation, microvascular invasion (MVI), and carbohydrate antigen19-9 (CA19-9) were recorded and analyzed. We used the broad definition of PNI as tumor cell invasion in, around, and through the nerves (5).

2.1 Establishment of Hepatic WHLS

2.1.1 Equipment and Apparatus Used to Prepare WHLS

The customized glass slide dimensions were 127 mm × 102 mm × 1.1 mm and the customized cover glass dimensions were 120 mm × 100 mm × 0.13 mm. The study area of WHLS was approximately 60 times larger than that of traditional pathological sections. Other equipment included a Leica ASP300S tissue processor (Leica Microsystems, Wetzlar, Germany), a Sakura IVS-410 microtome (Sakura Finetek Japan Co. Ltd., Tokyo, Japan), and a Sakura Tissue-Tek TEC5 embedding machine (Sakura Finetek Japan Co. Ltd.).

2.1.2 First and Second Fixation Stages

In the first fixation stage, the resected liver specimens were dissected and photographed. Ten percent (v/v) neutral formalin fixation solution was injected into the liver specimens including the hepatic arteries, portal veins, and bile duct systems to ensure complete tissue fixation. In the second fixation stage, the specimens were immersed in 10-fold volumes of 10% (v/v) formalin for 24 h.

2.1.3 Tissue Sampling of WHLS

Specimens were taken along a plane parallel to the axial abdominal enhanced CT (**Supplement Figure 1A**). Continuous cross-sections, 8–10 mm in thickness, were sampled. The starting sites from the distal end of the tumor until the intrahepatic tumor disappeared.

2.1.4 Third Fixation Stage

HCCA cross-sections, 8–10 mm in thickness, were sampled for the second time. To ensure the smoothness of the specimens, the thickness of each section was controlled within 4–5 mm using the embedding frame as a guide (**Supplement Figure 1B**). The modified tissue was placed in a tenfold volume of 10% (v/v) neutral formalin, re-fixed for several days.

2.1.5 Dehydration

This procedure is a critical step in WHLS preparation. Here, a suitable dehydration procedure was established after several preliminary experiments. The sections were placed in a Leica ASP300S dehydrator (Leica Microsystems) under normal pressure. The dehydration procedure is shown in **Supplement Table 1**.

2.1.6 Tissue Embedding and Paraffin Impregnation

For WHLS, a glass culture dish approximately 30 cm in diameter, was used for paraffin impregnation and embedding (**Supplement Figure 1C**). Dental forceps were then used to adjust and press the tissue and ensure that it was neither curled nor deformed. **Supplement Figure 1D** shows the properly prepared paraffin-embedded tissues.

2.1.7 Tissue Sectioning

The Sakura IVS-410 microtome and Sakura disposable 18-cm custom blade were used for slicing. Serial sections were obtained at a distance of 2 mm from the beginning of the common hepatic duct tumor until the proximal liver tumor disappeared along a plane parallel to the axial abdominal enhanced CT. The temperature of the Leica spreading sink (Leica Microsystems) was set to 39°C while the temperature of the Leica baking table (Leica Microsystems) was set to 75°C. High-flow humidification was critical during sectioning.

2.1.8 H&E Staining

The steps of H&E staining are listed in **Supplement Table 2**.

2.1.9 IHC Staining

After deparaffinization and antigen retrieval, all sections were incubated with primary anti-S-100 antibody, anti-CD34 antibody, and anti-D2-40 antibody (Abcam, USA) overnight at room temperature. After washing with PBS-T, all sections were incubated with secondary antibody (Abcam, USA) for 60 min at room temperature. Finally, xylene was used for transparency, and neutral gum was used to seal the tablets.

2.1.10 Digital Scanning and Interpretation of WHLS Features

Tissue sections were digitally scanned with the Olympus VS200 panoramic digital scanner (Olympus Corp., Tokyo, Japan). Characteristics of the scanned WHLS were interpreted with Olyvia software (Olympus Corp.). This program freely expanded and contracted WHLS at a maximum magnification ≥ 400×. All features of the HCCA were interpreted by three senior members of the Department of Pathology. In case there was a lack of consensus among the three pathologists, a fourth was consulted to interpret the features.

2.2 Statistical Analysis

Results are expressed as means ± standard deviation. Statistical analyses were carried out using the chi square test t-test, and Mann–Whitney U test by SPSS v25.0. A p value of less than 0.05 was considered statistically significant.

3 RESULTS

The clinicopathological characteristics of the 20 cases are shown in **Table 1**. According to the Bismuth-Corlette classification, 12 patients were type III (60%) and 8 patients were type IV (40%). Pathological analysis shows that there were 11 infiltrating (55%), 3 nodular (15%), and 6 sclerotic (30%) types. A total of 15 (75%) patients underwent hemihepatectomy and 5 (25%) patients underwent trisegment hepatectomy.

3.1 Display of WHLS in HCCA

The WHLS of HCCA in **Figures 1A, B** included the caudate lobe and the hilum. Moreover, adipose, nerve tissue, vessels, and lymph nodes in the hepatic hilar region could also be observed.

3.2 Display of the Caudate Lobe and Hilum in HCCA

The caudate lobe region and hilar region shown in **Figure 1A** were enlarged to obtain **Figures 2A–F**. The arrangements of the hepatocytes, Glisson system, and other features of the tissues in the caudate lobe and hilum were clearly visible. Furthermore, the cancerous bile duct and changes in the surrounding environment could be comprehensively mapped.

3.3 Display of Hepatic Margin and Peripheral Portal Area

Figure 3A is an enlargement of the local incision margin shown in **Figure 1A** and clearly demonstrates hepatocyte morphology and hepatocyte cord structure. **Figure 3B** is an enlargement of the distal peripheral portal area and clearly demonstrates the morphological characteristics of the bile ducts and their relationship with neighboring tissues. **Figure 3C** shows the internal hepatic parenchyma and the central vein and the surrounding hepatocytes are clearly visible.

3.4 Display of Intrahepatic and Extrahepatic Nerves, Blood Vessels, and Lymph Vessels

Through S-100, CD-34, and D2-40 IHC staining, combined with HE staining results, the distribution of intrahepatic and extrahepatic nerves, vessels, and lymph-vessels was clearly displayed (**Figures 4A–D**).

3.5 Characteristics and Risk Factors of PNI

After H&E and IHC staining, the intrahepatic and extrahepatic nerves and vessels of excised liver specimens were clearly

TABLE 1 | Demographic and preoperative data.

	No. of patients (n = 20)
Age (years)	66.1 (44-79)
Sex ratio (M: F)	9: 11
Bismuth type	
III A	6 (30%)
III B	6 (30%)
IV	8 (40%)
Surgical operation	
Right hemitectectomy	8 (40%)
Left hemitectectomy	7 (35%)
Right trisegment hepatectectomy	2 (10%)
Left trisegment hepatectectomy	3 (15%)
Pathological type	
Infiltrating	11 (55%)
Sclerotic	6 (30%)
Nodular	3 (15%)

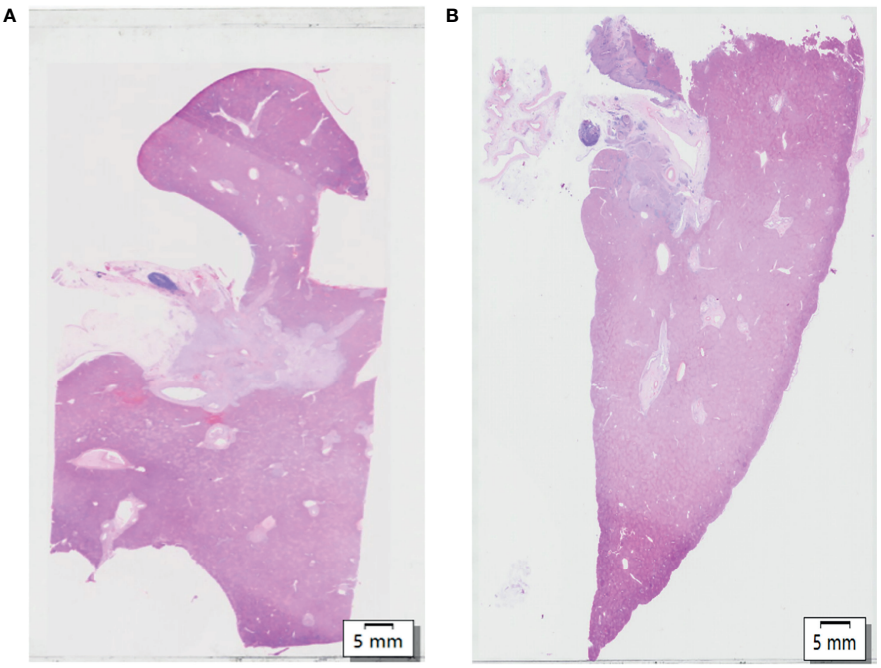

FIGURE 1 | **(A, B)** Hematoxylin and eosin (H&E) of whole-mount histologic large sections (WHLS) in Hilar cholangiocarcinoma (HCCA). Scale bar, 5 mm.

displayed. Among the 20 patients, the rate of PNI was 100%. For the 20 treated cases, extrahepatic and intrahepatic PNI were identified in 20 (100%) patients and 1 (5.0%) patient, respectively (**Figures 5A, B** and **Table 2**). The pathological type in the patients with intrahepatic PNI was infiltrating (Bismuth IIIB). When the nerve was invaded by tumors, vessel density decreased in 16 patients (80%) and showed no change in 4 patients (20%) as shown by CD34 IHC staining (**Figures 5C, D**). The decreased vessel density in PNI was highly statistically correlated with the degree of tumor differentiation, which occurred in 100% of poorly differentiated and 83% of moderately differentiated tumors (P<0.008, **Table 3**). Moreover, our study confirmed that vessel density decrease in PNI was not statistically associated with tumor size, Bismuth type, vascular invasion (including hepatic artery and portal vein), CA-199, MVI, or Ki-67.

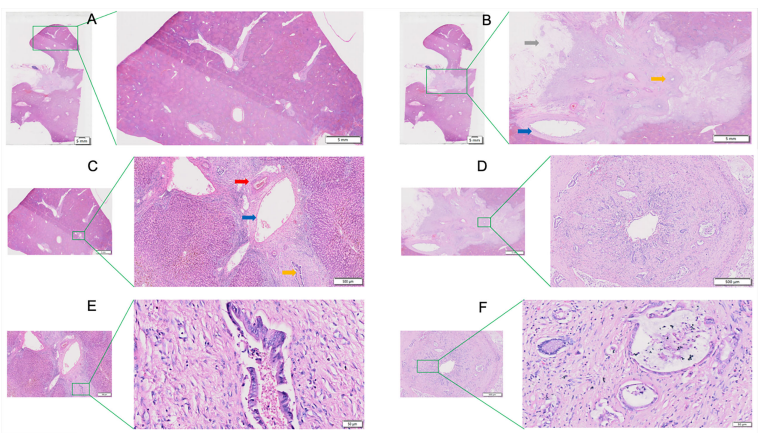

FIGURE 2 | View of the caudate lobe by WHLS in HCCA. **(A)** Large portal areas visible within caudate lobes. Scale bar, 5 mm. **(B)** Tissues in the hilar region including portal vein (blue arrow), bile duct (yellow arrow), adipose tissue(grey arrow). Scale bar, 5 mm. **(C)** Arterioles (red arrow), portal vein (blue arrow), and bile ducts (yellow arrow) in caudate lobular portal area. Scale bar, 500um. **(D)** Cancerous bile duct. Scale bar, 500 μm. **(E)** Bile ducts in caudate lobular portal area. Scale bar, 50 μm. **(F)** Adenocarcinoma in cancerous bile duct. Scale bar, 50 μm.

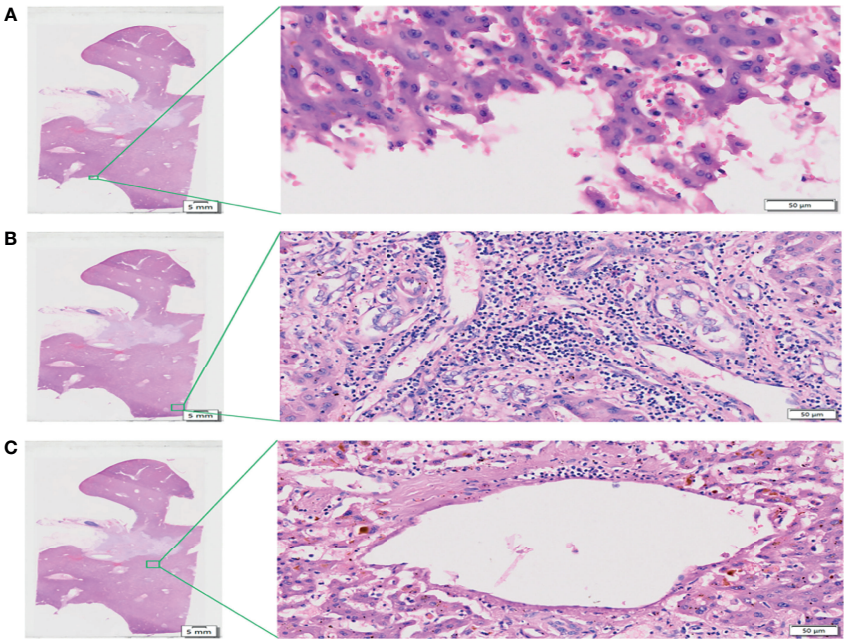

FIGURE 3 | View of the liver incision margin, distal peripheral portal area, and internal hepatic parenchyma of WHLS in HCCA. **(A)** Local liver incision margin. Scale bar, 50 μm. **(B)** Distal peripheral portal area. Scale bar, 50 μm. **(C)** Internal hepatic parenchyma. Scale bar, 50 μm.

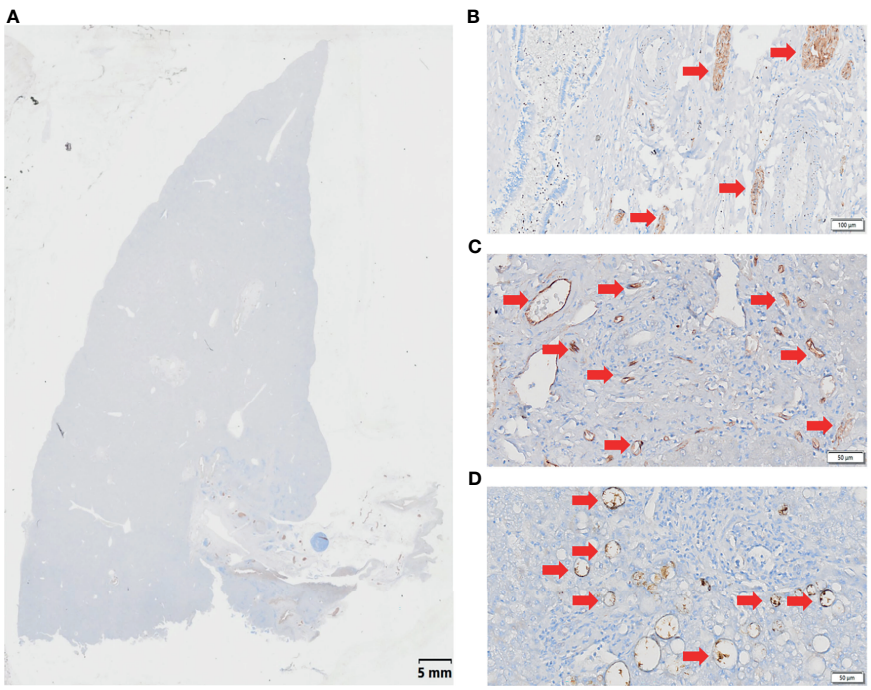

FIGURE 4 | Immunohistochemical (IHC) staining of WHLS in HCCA. **(A)** IHC staining. Scale bar, 5 mm. **(B)** S-100 staining demonstrates nerve distribution in the liver. The red arrows show nerve tissue. Scale bar, 50 μm. **(C)** CD34 staining demonstrates vascular distribution in the liver. The red arrows show blood vessels. Scale bar, 100 μm. **(D)** D2-40 staining demonstrates lymphatic distribution in the liver. The red arrows show lymphatic vessels. Scale bar, 50 μm.

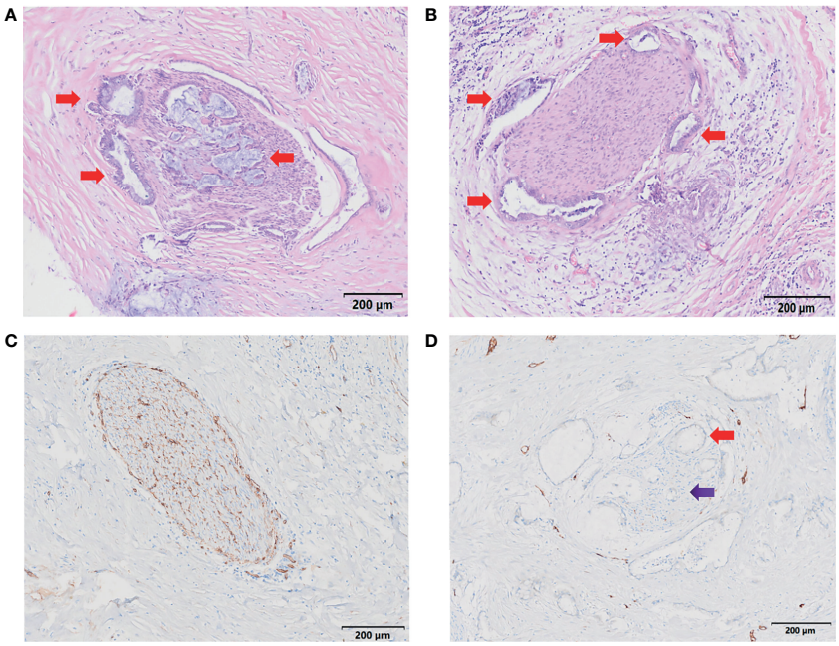

FIGURE 5 | Characteristics of PNI. **(A, B)** H&E staining demonstrates nerve invasion (red arrows), including both perineural invasion **(A, B)** and intraneural invasion **(A)**. Scale bar, 200 μm. **(C)** Distribution of blood supply to normal nerves (S-100 staining). Scale bar, 200 μm. **(D)** Blood supply distribution of PNI (S-100 staining); the red arrow shows tumor invasion of the nerve, and the purple arrow shows decreased blood supply to the nerve. Scale bar, 200 μm.

4 DISCUSSION

In this study, we developed a WHLS that clarified the incidence of PNI in types III and IV HCCA, and the characteristics of the blood supply of the PNI inside the liver were further clarified. Moreover, the panoramic digital pathology system provided a relatively more complete qualitative diagnosis after exploring the scope of invasion and the biological behavior of the tumor.

4.1 Establishment of WHLS

A three-stage tissue fixation scheme was adopted in this study. The first involved perfusion fixation. The perfusion liquid penetrated as far as possible into the liver parenchyma and prevented the sloughing of the intrahepatic duct epithelium. The second stage aimed to increased specimen hardness and enabled the application of the third fixation stage. In the third stage, specimens were further processed into thin lamellae,

TABLE 2 | Characteristics of PNI.

	Intrahepatic PNI	Extrahepatic PNI	CD34
1	Negative	Positive	Decrease
2	Negative	Positive	Decrease
3	Negative	Positive	Decrease
4	Negative	Positive	Decrease
5	Negative	Positive	Decrease
6	Negative	Positive	Normal
7	Negative	Positive	Normal
8	Negative	Positive	Decrease
9	Negative	Positive	Decrease
10	Negative	Positive	Decrease
11	Negative	Positive	Decrease
12	Negative	Positive	Decrease
13	Positive	Positive	Decrease
14	Negative	Positive	Decrease
15	Negative	Positive	Decrease
16	Negative	Positive	Normal
17	Negative	Positive	Decrease
18	Negative	Positive	Normal
19	Negative	Positive	Decrease
20	Negative	Positive	Decrease

TABLE 3 | Risk factors of PNI.

	Decrease of blood supply	Normal blood supply	P value
Pathological Type			0.487
Nodular	3 (18.8%)	0 (0.0%)	
Infiltrating	9 (56.3%)	2 (50%)	
Sclerotic	4 (25.0%)	2 (50%)	
Bismuth type			0.255*
III	11 (68.8%)	1 (25%)	
IV	5 (31.3%)	3 (75%)	
Vascular invasion (A)			0.619*
positive	7 (87.5%)	9 (25%)	
negative	1 (12.5%)	3 (75%)	
Vascular invasion (P)			0.582*
positive	9 (90.0%)	7 (70%)	
negative	1 (10.0%)	3 (30%)	
Differentiation			0.008
low	6 (37.5%)	0 (0.0%)	
moderate	10 (62.5%)	2 (50.0%)	
high	0 (0.0%)	2 (50.0%)	
MVI			1.000*
negative	13 (81.3%)	4 (100.0%)	
positive	3 (18.8%)	0 (0.0%)	
CA-199	565.80 (107.85, 1178.80)	1178.80 (536.61, 3194.27)	0.104
Ki-67	20.0% (15.0%, 35.0%)	20.0% (18.5%, 35.0%)	0.739

**Fisher exact test; A, hepatic artery; P, portal vein; MVI, microvascular invasion; CA19-9, carbohydrate antigen 19-9.*

approximately 4-5 mm thick, facilitating an even more profound fixation of the liver parenchyma to prevent autolysis.

To the best of our knowledge, no prior studies have reported on the systemic dehydration of liver tissue specimens > 10 cm in size (14, 17, 19). Dehydration for large liver tissue pathological investigations should endeavor to prevent wrinkling, maintain tissue hardness, and facilitate sectioning. In this study, we developed a series of dehydration procedures suitable for whole-mount liver that fully dehydrated the tissue samples and minimized shrinkage. Prolonged tissue dehydration at low alcohol concentrations (70%) effectively increases dehydration efficiency within the liver parenchyma. The amount of time in which tissues are soaked in high alcohol concentrations is minimized. In this way, tissue shrinkage is avoided, and the tissue surface remains smooth.

In this study, we performed H&E staining and IHC staining manually after optimizing it through repeated preliminary tests. **Supplement Table 2** shows that the H&E staining time for large sections was approximately 84-86 min. Adenocarcinoma, the surrounding liver tissue, and its nuclear morphology were clearly visible in the pathological liver sections stained by this technique. In addition, the morphology of all accessory arteries, blood vessels, and lymphatic and nerve tissues could be plainly seen.

4.2 PNI Characteristics

Previous studies have reported that there are great differences in the probability of nerve invasion in HCCA (6, 12, 20–22). Moreover, the characteristics of nerve invasion and whether it is accompanied by intrahepatic bile duct invasion in types III and IV of HCCA are not clear. Our study established a WHLS of the liver to show that the rate of PNI was prevalent (100%) in Bismuth types III and IV HCCA. This may indicate that, compared with types I and II HCCA, the biological behavior of extrahepatic PNI in types III and IV HCCA was increased owing to the large infiltration range in the perihilar region. We have further confirmed the pattern of the PNI using WHLS, suggesting that PNI was more common in the extrahepatic (100%) than in the intrahepatic (5.0%) area. This result confirmed that PNI in types III and IV HCCA was not accompanied by intrahepatic bile duct invasion. A previous study demonstrated that when tumor cells invade nerve fibers, the number of blood vessels in the peripheral tissues increase (5, 23, 24). By using WHLS, our study revealed that the blood supply was rich and well distributed in normal nerves. However, there was a decrease in the density of vessels in PNI in most cases of III and IV HCCA, indicating that these two types of HCCA may not rely on blood supply for invading nerves. We also found that this biological behavior was more common in tumors with low (100%) and moderate (83%) differentiation (P<0.008). These results suggest that the moderately and poorly differentiated malignant tumors are more prone to PNI independent of blood supply.

In conclusion, this study established a WHLS of the liver that can be used for clinical diagnosis and research, and confirmed that extrahepatic PNI is prevalent in types III and IV HCCA, but intrahepatic PNI is rare and does not accompany the invasion scope of the bile duct. The decrease in vessel density in PNI was closely related to tumor differentiation. The more undifferentiated the HCCA, the more likely will be the biological behavior of PNI independent of blood supply to appear.

DATA AVAILABILITY STATEMENT

The raw data supporting the conclusions of this article will be made available by the authors, without undue reservation.

ETHICS STATEMENT

The studies involving human participants were reviewed and approved by Beijing Tsinghua Changgung Hospital Ethics Committee. Written informed consent for participation was not required for this study in accordance with the national legislation and the institutional requirements.

AUTHOR CONTRIBUTIONS

Conceptualization, S-YW, NJ, and SJ. Methodology, S-YW. Software, S-YW and S-QY. Validation, NJ, J-PZ, and SJ. Formal analysis, S-YW. Investigation, S-YW. Resources, SJ. Data curation, YX. Writing—original draft preparation, NJ and S-YW. Writing—review and editing, SJ. Visualization, S-QY. Supervision, SJ. Project administration, J-PZ. All authors have read and agreed to the published version of the manuscript.

FUNDING

National Natural Science Foundation of China (No. 82000484, No. 81930119, No. 82090050, No. 82090053). Research and Cultivation Program of Beijing Municipal Hospital (No. PX2018038).

ACKNOWLEDGMENTS

The authors wish to thank Dr Jin-Lian Zhou for the technological help.

SUPPLEMENTARY MATERIAL

The Supplementary Material for this article can be found online at: https://www.frontiersin.org/articles/10.3389/fonc.2022.855615/full#supplementary-material

Supplementary Figure 1 | Histologic tissue sampling, second tissue sampling, and paraffin embedding of hilar cholangiocarcinoma (HCCA) pathological tissue. **(A)** Whole-mount histologic large sections (WHLS) taken along the axial CT direction. **(B)** Pathological tissue sampling after second fixation. **(C)** Paraffin embedding of HCCA pathological tissue. **(D)** HCCA pathological tissue embedding being prepared.

REFERENCES

1. Razumilava N, Gores GJ. Cholangiocarcinoma. *Lancet* (2014) 383 (9935):2168–79. doi: 10.1016/s0140-6736(13)61903-0
2. Valle JW, Kelley RK, Nervi B, Oh D-Y, Zhu AX. Biliary Tract Cancer. *Lancet* (2021) 397(10272):428–44. doi: 10.1016/s0140-6736(21)00153-7
3. Poruk KE, Pawlik TM, Weiss MJ. Perioperative Management of Hilar Cholangiocarcinoma. *J Gastrointest Surg* (2015) 19(10):1889–99. doi: 10.1007/s11605-015-2854-8
4. Lewis HL, Rahnemai-Azar AA, Dillhoff M, Schmidt CR, Pawlik TM. Current Management of Perihilar Cholangiocarcinoma and Future Perspectives. *Chirurgia (Bucur)* (2017) 112(3):193–207. doi: 10.21614/chirurgia.112.3.193
5. Liebig C, Ayala G, Wilks JA, Berger DH, Albo D. Perineural Invasion in Cancer: A Review of the Literature. *Cancer* (2009) 115(15):3379–91. doi: 10.1002/cncr.24396
6. Hu HJ, Jin YW, Shrestha A, Ma WJ, Wang JK, Liu F, et al. Predictive Factors of Early Recurrence After R0 Resection of Hilar Cholangiocarcinoma: A Single Institution Experience in China. *Cancer Med* (2019) 8(4):1567–75. doi: 10.1002/cam4.2052
7. Seyama Y, Kubota K, Sano K, Noie T, Takayama T, Kosuge T, et al. Long-Term Outcome of Extended Hemihepatectomy for Hilar Bile Duct Cancer With No Mortality and High Survival Rate. *Ann Surg* (2003) 238(1):73–83. doi: 10.1097/01.Sla.0000074960.55004.72
8. Robles R, Figueras J, Turrión VS, Margarit C, Moya A, Varo E, et al. Spanish Experience in Liver Transplantation for Hilar and Peripheral Cholangiocarcinoma. *Ann Surg* (2004) 239(2):265–71. doi: 10.1097/01.sla.0000108702.45715.81
9. Su CH, Tsay SH, Wu CC, Shyr YM, King KL, Lee CH, et al. Factors Influencing Postoperative Morbidity, Mortality, and Survival After Resection for Hilar Cholangiocarcinoma. *Ann Surg* (1996) 223: (4):384–94. doi: 10.1097/00000658-199604000-00007
10. Yamaguchi K, Chijiiwa K, Saiki S, Shimizu S, Tanaka M. Carcinoma of the Extrahepatic Bile Duct: Mode of Spread and its Prognostic Implications. *Hepatogastroenterology* (1997) 44(17):1256–61. doi: 10.1002/(SICI)1097-0347(199709)19:6<535::AID-HED11>3.0.CO;2-4
11. Nimura Y, Kamiya J, Kondo S, Nagino M, Uesaka K, Oda K, et al. Aggressive Preoperative Management and Extended Surgery for Hilar Cholangiocar Cinoma: Nagoya Experience. *J Hepato Biliary Pancreatic Surg* (2000) 7 (2):155–62. doi: 10.1007/s005340050170
12. Tan X, Sivakumar S, Bednarsch J, Wiltberger G, Heij LR. Nerve Fibers in the Tumor Microenvironment in Neurotropic Cancer—Pancreatic Cancer and Cholangiocarcinoma. *Oncogene* (2020) 40:899–908. doi: 10.1038/s41388-020-01578-4
13. Aloe L, Rocco ML, Balzamino BO, Micera A. Nerve Growth Factor: Role in Growth, Differentiation and Controlling Cancer Cell Development. *J Exp Clin Cancer Res* (2016) 35(1):116–23. doi: 10.1186/s13046-016-0395-y
14. Mukhopadhyay S, Feldman MD, Abels E, Ashfaq R, Beltaifa S, Cacciabeve NG, et al. Whole Slide Imaging Versus Microscopy for Primary Diagnosis in Surgical Pathology. *Am J Surg Pathol* (2017) 00(00):1–14. doi: 10.1097/PAS.0000000000000948
15. Lazutkin AA, Shuvaev SA, Barykina NV. Click Histochemistry for Whole-Mount Staining of Brain Structures. *MethodsX* (2019) 6:1986–91. doi: 10.1016/j.mex.2019.09.011
16. Volynskaya Z, Evans AJ, Asa SL. Clinical Applications of Whole-Slide Imaging in Anatomic Pathology. *Adv Anat Pathol* (2017) 24(4):215–21. doi: 10.1097/PAP.0000000000000153
17. Cimadamore A, Cheng L, Lopez-Beltran A, Mazzucchelli R, Luciano R, Scarpelli M, et al. Added Clinical Value of Whole-Mount Histopathology of Radical Prostatectomy Specimens: A Collaborative Review. *Eur Urol Oncol* (2021) 4(4):558–69. doi: 10.1016/j.euo.2020.08.003
18. Ebel JJ, Shabsigh A, Sharp DS, Zynger DL. Whole-Mount Evaluation of Penectomies for Penile Cancer: Feasibility, Cost and Comparison to Routine Sectioning. *Histopathology* (2013) 63(1):64–73. doi: 10.1111/his.12149
19. Clarke GM, Eidt S, Sun L, Mawdsley G, Zubovits JT, Yaffe MJ. Whole-Specimen Histopathology: A Method to Produce Whole-Mount Breast Serial Sections for 3-D Digital Histopathology Imaging. *Histopathology* (2007) 50 (2):232–42. doi: 10.1111/j.1365-2559.2006.02561.x
20. Kovalenko YA, Zharikov YO, Kukeev IA, Vishnevsky VA, Chzhao AV. Predictors of Outcomes in Surgery for Hilar Cholangiocarcinoma. *Khirurgiia (Mosk)* (2018) 10):5–11. doi: 10.17116/hirurgia20181015
21. Chen S-H, Zhang B-Y, Zhou B, Zhu C-Z, Sun L-Q. Perineural Invasion of Cancer: A Complex Crosstalk Between Cells and Molecules in the Perineural Niche. *Am J Cancer Res* (2019) 9(1):1–21.
22. Mansfield SD, Barakat O, Charnley RM, Jaques BC, O'Suilleabhain CB, Atherton PJ, et al. Management of Hilar Cholangiocarcinoma in the

North of England: Pathology, Treatment, and Outcome. *J World J Gastroenterol* (2005) 11(48):7625–30. doi: 10.3748/wjg.v11.i48.7625
23. Li CG, Zhou ZP, Tan XL, Zhao ZM. Perineural Invasion of Hilar Cholangiocarcinoma in Chinese Population: One Center's Experience. *World J Gastrointest Oncol* (2020) 12(4):457–66. doi: 10.4251/wjgo.v12.i4.457
24. Shen FZ, Zhang BY, Feng YJ, Jia ZX, An B, Liu CC, et al.. Current Research in Perineural Invasion of Cholangiocarcinoma. *J Exp Clin Cancer Res* (2010) 29 (1):1–7. doi: 10.1186/1756-9966-29-24

Conflict of Interest: The authors declare that the research was conducted in the absence of any commercial or financial relationships that could be construed as a potential conflict of interest.

Publisher's Note: All claims expressed in this article are solely those of the authors and do not necessarily represent those of their affiliated organizations, or those of the publisher, the editors and the reviewers. Any product that may be evaluated in this article, or claim that may be made by its manufacturer, is not guaranteed or endorsed by the publisher.

Copyright © 2022 Wang, Jiang, Zeng, Yu, Xiao and Jin. This is an open-access article distributed under the terms of the Creative Commons Attribution License (CC BY). The use, distribution or reproduction in other forums is permitted, provided the original author(s) and the copyright owner(s) are credited and that the original publication in this journal is cited, in accordance with accepted academic practice. No use, distribution or reproduction is permitted which does not comply with these terms.

frontiers in Oncology

ORIGINAL RESEARCH
published: 10 March 2022
doi: 10.3389/fonc.2022.834647

UHMK1 Is a Novel Marker for Personalized Prediction of Pancreatic Cancer Prognosis

*Yiqiao Luo, Shanshan Han, Bin Yan, Huihui Ji, Lian Zhao, Jury Gladkich and Ingrid Herr**

Molecular OncoSurgery, Section Surgical Research, Department of General, Visceral and Transplant Surgery, University of Heidelberg, Heidelberg, Germany

OPEN ACCESS

Edited by:
Qi Liu,
Fudan University, China

Reviewed by:
Sakthivel Muniyan,
University of Nebraska Medical Center, United States
Jesse Bakke,
Central Michigan University, United States

***Correspondence:**
Ingrid Herr
i.herr@uni-heidelberg.de

Specialty section:
This article was submitted to Gastrointestinal Cancers: Hepato Pancreatic Biliary Cancers, a section of the journal Frontiers in Oncology

Received: *13 December 2021*
Accepted: *16 February 2022*
Published: *10 March 2022*

Citation:
Luo Y, Han S, Yan B, Ji H, Zhao L, Gladkich J and Herr I (2022) UHMK1 Is a Novel Marker for Personalized Prediction of Pancreatic Cancer Prognosis. Front. Oncol. 12:834647. doi: 10.3389/fonc.2022.834647

Pancreatic ductal adenocarcinoma (PDAC) is among the leading causes of cancer mortality, and new therapeutic options are urgently needed. Long noncoding RNA H19 (H19) is known to promote PDAC progression, but the downstream genes of H19 are largely unknown. Five PDAC cell lines, nonmalignant pancreatic cells, TCGA, GEO-derived pancreatic tissues (malignant, n=413; nonmalignant, n=234), a pancreatic tissue array (n=96), and pancreatic tissues from our clinic (malignant, n=20; nonmalignant, n=20) were examined by a gene array, RT-qPCR, Western blotting, MTT, colony formation, wound-healing, siRNA-mediated gene silencing, bioinformatics, xenotransplantation, and immunohistochemistry assays. The cell cycle inhibitor, UHMK1, was identified to have the strongest correlation with H19. UHMK1 expression was enhanced in PDAC, and high UHMK1 expression correlated with tumor stage, and lower overall survival. siRNA-mediated UHMK1 downregulation inhibited progression signaling. siRNA-mediated downregulation of H19 or UHMK1 inhibited tumor proliferation and xenograft growth. Based on the correlation between UHMK1 expression and clinical parameters, we developed a nomogram that reliably predicts patient prognosis and overall survival. Together, we characterized UHMK1 as an H19-induced oncogene and verified it as a novel PDAC prognostic marker for overall survival.

Keywords: pancreatic cancer, long noncoding RNA, UHMK1, tumor marker, nomogram

Abbreviations: AUC, Area under the curve; CAM, Chorioallantois membrane; DCA, Decision curve analysis; ES, Enrichment score; FDR, False discovery rate; GEPIA, Gene expression profiling interactive analysis; GO, Gene Ontology; GSEA, Gene Set Enrichment Analysis; GSVA, Gene Set Variation Analysis; siH19-1, H19 siRNA No. 1; siH19-2, H19 siRNA No. 2; H&E, Hematoxylin and eosin; LncRNA, Long noncoding RNA; MSigDB, Molecular Signature Database; MTT, 3-(4,5-dimethylthiazol-2-yl)-2,5-diphenyltetrazolium bromide; OS, Overall survival; PDAC, Pancreatic ductal adenocarcinoma; ROC, Receiver operating characteristic; UHMK1, U2AF homology motif kinase 1; NES, Normalized enrichment score.

INTRODUCTION

Pancreatic ductal adenocarcinoma (PDAC) is one of the leading causes of cancer mortality worldwide and is characterized by late diagnosis, early metastasis, and high therapy resistance (1). Despite worldwide efforts, therapeutic options for PDAC are limited (2, 3), and improvement is urgently needed.

Long noncoding RNAs (lncRNAs) are noncoding RNAs that contain more than 200 nucleotides (4). LncRNAs epigenetically regulate gene expression by modulating transcriptional activities, posttranscriptional activities, genomic imprinting, and other biological processes (5). Recently, the lncRNA H19 (H19) has been identified as a cancer promotor in different cancer types (6–9). H19 is highly expressed in PDAC, and it promotes proliferation, migration, and metastasis (6, 10–12). We identified the innate anti-viral immunity gene APOBEC3G as a major H19 downstream gene (12, 13) and demonstrated that the downregulation of H19 or APOBEC3G by siRNA or the bioactive agent sulforaphane prevented H19-mediated PDAC progression features as demonstrated by assays for colony formation, migration, invasion, Smad2 phosphorylation and tumor xenograft growth (12). Nevertheless, the function of additional, yet unknown, H19 target genes needs to be clarified.

The U2AF homology motif kinase 1 (UHMK1) was initially identified as a regulator of cyclin-dependent kinase inhibitors and the cell cycle regulator, p27 (Kip1) (14). Moreover, a more ubiquitous role of UHMK1 in cellular signaling is known, e.g., as a regulator of splicing factors 1 (15, 16), and RNA-binding proteins (17). Recently, a function of UHMK1 in the progression of hepatocellular carcinoma (18), gastric cancer (19), and ovarian cancer (20) has been reported, but the function of UHMK1 in PDAC is unclear.

Here, we demonstrated a high correlation between H19 and UHMK1, because the siRNA-mediated downregulation of H19 resulted in strong inhibition of UHMK1 RNA and protein expression. We further explored the role of UHMK1 in PDAC and found that high UHMK1 expression correlated with a shorter overall survival of PDAC patients. siRNA-mediated knockdown of UHMK1 expression was associated with reduced viability, clonogenicity, and migration. The inhibition of both H19 and UHMK1 prevented PDAC xenograft growth. Using UHMK1 expression and clinical data, we constructed a prognostic nomogram with high accuracy, which provides a new clinical tool to predict the prognosis of PDAC patients and aid in the treatment decision-making process.

RESULTS

UHMK1 Is Highly Expressed in PDAC, Which Can be Inhibited by SiRNA-Mediated Downregulation of H19

Recently it was shown that H19 is highly expressed in PDAC and we demonstrated that the siRNA-mediated downregulation of H19 inhibited progression features of PDAC (10, 12). To further investigate these promising results, the aim of the present study was to identify H19 mediators and to explore their function in PDAC progression. H19 expression was inhibited in MIA-PaCa2 cells by lipotransfection of two H19 siRNA constructs, whose functionalities were recently confirmed (12), along with a nonsense siRNA control. RNA was isolated 24 h after transfection, and gene array analysis was performed. Bioinformatics evaluation revealed 49 differentially expressed genes for siH19-1 and 30 differentially expressed genes for siH19-2 (**Supplementary Figures S1A, B**). Using the UpSetR R package, we selected six candidate genes associated with siH19-1 and siH19-2 as shown by volcano plots (**Figure 1A**) and a Venn diagram (**Supplementary Figure S1C**). At the top of the H19-downregulated candidate genes was UHMK1, closely followed by MIGA1, SERPINB9, and SGPL1, whereas ZNF56 and ZNF616 were upregulated by H19. Based on the online database TIMER 2.0, Pearson correlation analysis detected a positive correlation between UHMK1 and SGPL1, SERPINB9, and MIGA1 with R=0.524, R=0.296, and R=0.798, respectively, as presented by dot plots (**Supplementary Figure S2A**). By utilizing GEPIA online database, we figured out that each of these genes was significantly upregulated in PDAC patient tissues compared to nonmalignant pancreatic tissues (**Supplementary Figure S2B**). These results suggested that H19 drives the progression of PDAC not only through UHMK1 but also through several downstream genes simultaneously.

To verify these results, we lipotransfected siH19-1 and siH19-2 along with a nonsense siRNA control into BxPc-3, AsPC-1, and MIA-PaCa2 cells. After 24 h, total RNA was extracted, and UHMK1 expression was examined by RT-qPCR. The RNA expression of UHMK1 was significantly downregulated after knockdown by both siH19 constructs in all cell lines examined (**Figure 1B**). Because siH19-1 was most potent in the downregulation of UHMK1 mRNA expression, we used siH19 for all subsequent experiments. Next, we studied UHMK1 mRNA expression by RT-qPCR in the nonmalignant pancreas cell line, CRL-4023, and five PDAC cell lines. Compared to CRL-4023 cells, there was significantly increased UHMK1 expression in four of the five PDAC cell lines (**Figure 1C**). We confirmed that knockdown of H19 decreased UHMK1 expression in protein level by Western blot analysis (**Figure 1D** and **Supplementary Figure S3**). To evaluate UHMK1 protein expression in PDAC tissue from patients, we performed immunohistochemistry on PDAC tissues (n=20) and nonmalignant pancreatic tissues (n=20), which were obtained from brain-dead donors (**Table S1**). The expression level of UHMK1 was quantified by counting the percentage of UHMK1-positive cells of 10 randomly chosen vision fields of each tissue by two independent researchers with experience in pancreas histology who were blinded to the conditions. High, medium, low, and no expression was scored as 3, 2, 1, and 0, respectively. We discovered higher UHMK1 expression in PDAC tissues compared to nonmalignant, inflamed pancreatic tissue (**Figure 1E**), which can be seem in the representative staining (**Figure 1F**).

Increased UHMK1 Expression Correlates With the Clinical Stage of PDAC

To examine UHMK1 expression in different cancer stages, we performed immunohistochemistry using a commercially available pancreatic cancer tissue array with 91 malignant tissues and 5 nonmalignant pancreatic tissues along with patient information on clinical stage and pathology grade (**Table S2**). UHMK1-positive cells were quantified by

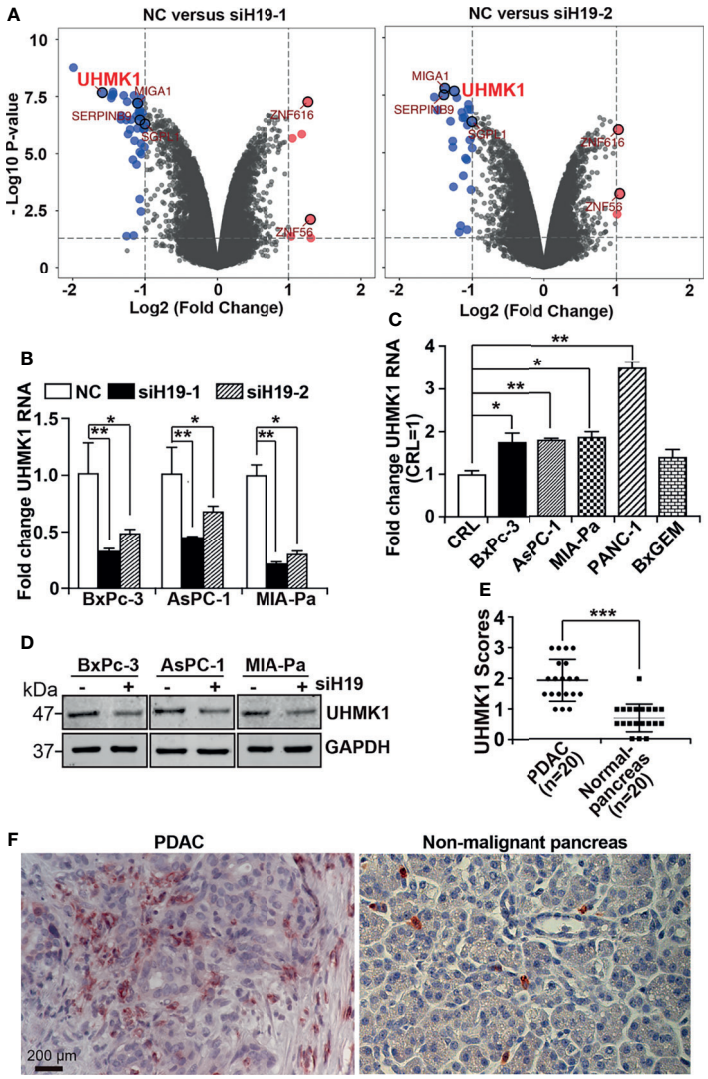

FIGURE 1 | LncRNA H19-induced UHMK1 is highly expressed in PDAC. **(A)** Volcano plot showing differentially expressed genes in MIA-PaCa2 cell line depleted for lncRNA H19 using the siRNAs siH19-1 (left panel) and siRNAs siH19-2 (right panel), in comparison with cells transfected with a nonsense siRNA control (NC). The threshold was set to a $\log_2$ (fold change) >1 and a P value <0.05. Vertical axis corresponds to the statistical significance level provided as the -Log10 P value. The horizontal dashed gray line shows the P-value cutoff (-log10 1.3 ≙ P = 0.05) with points above the line having P values <0.05. The vertical gray dashed line indicates 1-fold changes/doubling (log2-fold change of 1), The six most significantly differentially regulated genes were MIGA1, SERPINB9, SGPL1, ZNF616, ZNF56, and UHMK1. **(B)** UHMK1 mRNA expression in the PDAC cell lines BxPc-3, AsPC-1 and MIA-PaCa2 after depletion of lncRNA H19, compared with control cells (NC). **(C)** UHMK1 mRNA expression in CRL-4023 (CRL), and the PDAC cell lines BxPc-3, AsPC-1, MIA-PaCa2, PANC-1, and BxGEM, The data were normalized to the expression of CRL-4023 cells. **(D)** GAPDH served as a loading control. The protein sizes in kilodaltons (kDa) are shown on the right. The crude Western blot images are shown in Figure S2. **(E)** UHMK1 protein expression was detected in paraffin-embedded human tissue derived from PDAC (n = 20) or nonmalignant (normal) pancreata (n = 20) by performing immunohistochemistry. Cell nuclei were stained with hematoxylin. **(F)** Representative images of UHMK1 expression in PDAC and nonmalignant pancreatic tissues are shown. The scale bar indicates 200 μm. *$P < 0.05$, **$P < 0.01$, and ***$P < 0.001$.

microscopy and the use of a scoring system (**Figure 2A**). Whereas the expression of UHMK1 was low to absent in normal pancreatic tissue, its expression was increased corresponding to malignancy as shown by representative images and a diagram (**Figure 2B**). Together, UHMK1 expression positively correlated with the clinical stage because the expression was lower in stage I, higher in stage II, and low to absent in nonmalignant pancreatic tissues. Unfortunately, we were unable to calculate the significance of advanced stages III/IV because only 6 tissues for these stages were available.

UHMK1 Is an Independent Marker for Overall Survival

To examine the impact of UHMK1 in PDAC, we screened TCGA and GTX online databases based on GEPIA for the presence of UHMK1 expression data in PDAC tissues. We found a

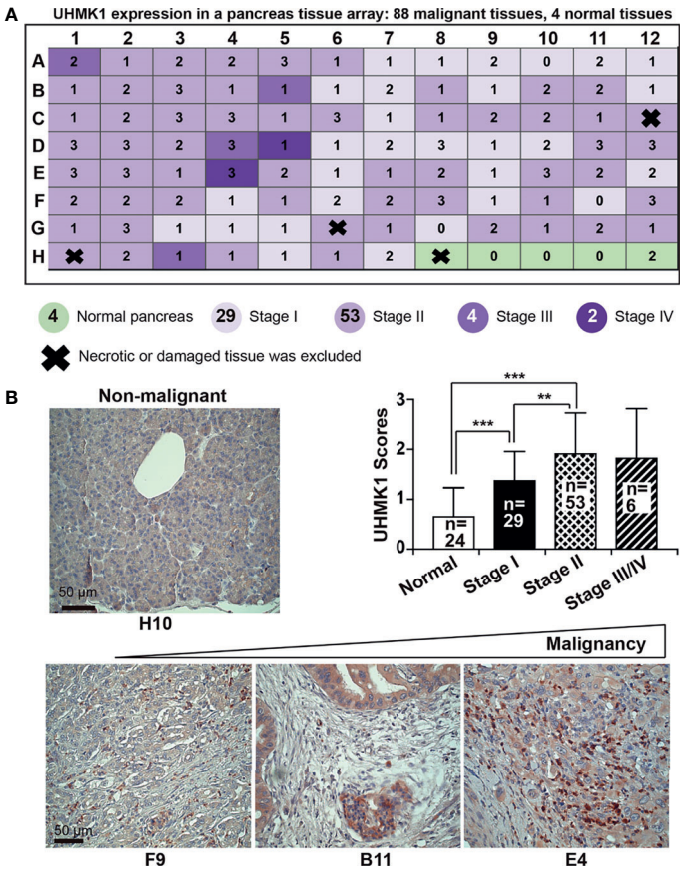

FIGURE 2 | UHMK1 expression is related to PDAC tumor stage. **(A)** UHMK1 expression was examined by immunohistochemical staining of a commercially available PDAC tissue microarray with paraffin-embedded pancreatic tissue, which contained 91 malignant tissues from stage I to IV and 5 normal pancreatic tissues. Four tissues of the microarray were necrotic or damaged and were therefore excluded from the evaluation, and these tissues are indicated by thick black crosses on the schematic. The expression of UHMK1 was evaluated by immunohistochemistry under 400× magnification. The expression level was quantified by counting the positive, dark-brown cells per tissue by two independent researchers with expertise in pancreas histology who were blinded by the conditions. UHMKI expression was scored based on the following scale: high UHMK1 expression, 3; medium UHMK1 expression, 2; low UHMK1 expression, 1; and no UHMK1 expression, 0. **(B)** Representative images of UHMK1 expression in normal pancreatic tissue and in tissues of different PDAC stages are shown. Because there were only four nonnecrotic tissues from the nonmalignant pancreas available in this tissue array, we included data from the 20 previously examined nonmalignant pancreatic tissues. The mean expression of UHMK1 according to the previously scored values is shown. The scale bar indicates 50 µm. $^{**}P < 0.01$, and $^{***}P < 0.001$.

significant upregulation of UHMK1 in PDAC tissues (n=179) compared to nonmalignant pancreatic tissues (n=171) (**Figure 3A**). These data were confirmed by extracting data from the GEO online database, demonstrating that UHMK1 was more highly expressed in PDAC tissues (n=63, n=24, and n=36) than in nonmalignant paracancerous tissues (n=36) (**Supplementary Figure S4A**). Similarly, *in silico* analysis using the GEPIA database revealed significant UHMK1 upregulation in malignant tissues of other tumor entities compared to adjacent nonmalignant tissues, including breast invasive carcinoma, cervical squamous cell carcinoma and endocervical adenocarcinoma, lymphoid neoplasm diffuse large B-cell lymphoma, esophageal carcinoma, skin cutaneous melanoma, stomach adenocarcinoma, and thymoma (**Supplementary Figure S4B**). The correlation between UHMK1 expression and overall survival was then evaluated by the Kaplan-Meier plotter online database. We divided the available mRNA expression data into high and low UHMK1 expression groups according to the best cutoff value and found a significant association between high UHMK1 expression and shorter overall survival of PDAC patients (**Figure 3B**). To investigate whether UHMK1 expression is an independent risk factor and appropriate for predicting the prognosis of PDAC, a statistical survival model was developed. By performing univariate Cox regression analysis, we examined survival with respect to a single variable and found that UHMK1 expression (P=0.027), age (P=0.019), grade (P=0.007), pTNM stage (P=0.037), and radiation therapy (P=0.014) significantly and independently predicted the overall survival of PDAC patients (**Figure 3C**). Because one variable influences the other, we investigated survival with respect to all identified variables simultaneously by multivariate Cox analysis, which identified UHMK1 (P=0.045), grade (P=0.004), and radiation therapy (P=0.01) as significant risk factors for the prediction of overall survival in PDAC. These data suggested

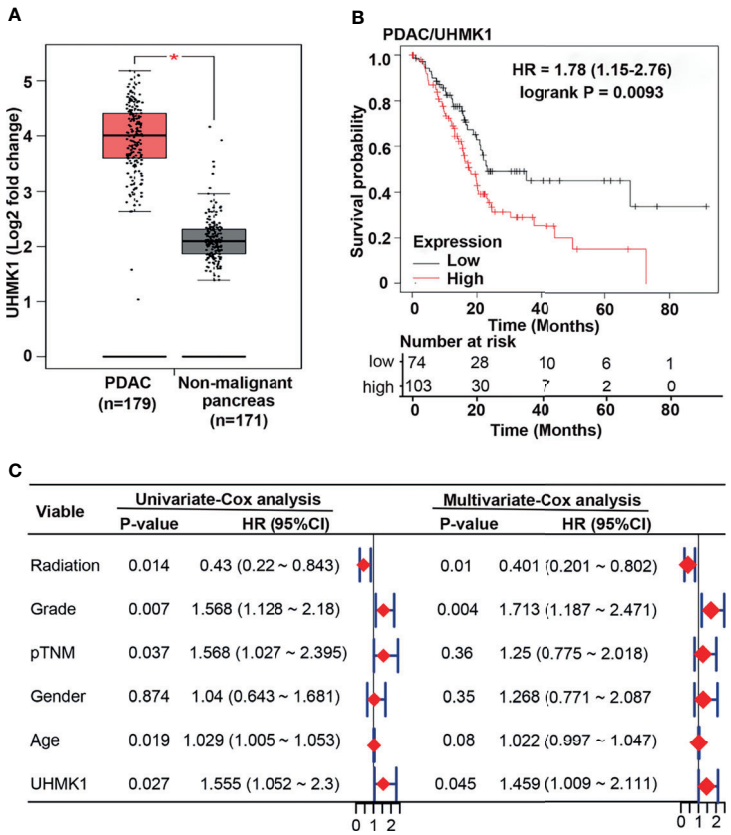

FIGURE 3 | UHMK1 expression correlates with the survival of PDAC patients. **(A)** Using the GEPIA online database, available expression data of UHMK1 in human PDAC (n = 179) and normal pancreatic (n = 171) tissues were identified, and the expression levels with the means ± SD are shown in the diagram. *$P < 0.05$. Red columns represent PDAC tissue, and gray columns represent tissue from nonmalignant pancreatic tissues. **(B)** Kaplan-Meier analysis of UHMK1 in PDAC. The best cutoff was defined as followed: All possible cutoff values between the lower and higher quartiles are computed, and the best performing threshold is used as a cutoff. The cutoff value was 2390, and the expression range of the probe was 331–5779. The patient data were split according to the cutoff values <2390 = low UHMK1 expression (black line), including 74 patients, and >2390 = high UHMK1 expression (red line), including 103 patients. The Y-axis shows the survival probability, which is the proportion of units that survive beyond a specified time, which is given by the X-axis (Time/Months). The hazard ratio (HR) of 1.78 indicates a 1.78× higher risk of death for patients in the high UHMK1 expression group. The number at risk indicates the number of survivors at the corresponding time point. **(C)** PDAC patients' clinical data were downloaded from TCGA database, and univariate and multivariate Cox regression analyses were performed in the R studio environment. The risk of death in PDAC patients is expressed as the hazard ratio (HR) according to application of radiation treatment, the tumor grade, the pathologically evaluated tumor/node/metastasis status (pTNM), sex, age, and the level of UHMK1 expression. HR=1 indicates lack of association. HR > 1 indicates an increased risk, and HR < 1 indicates a lower risk. The HR is represented by red diamonds on a scale from 0 to 2.

that UHMK1 expression is an appropriate parameter for the prediction of the prognosis of PDAC patients.

UHMK1 Is Associated With Cancer-Related Pathways

To highlight the biological function of UHMK1 expression, we analyzed PDAC samples with adjacent information from 19,590 genes, which were selected from TCGA-PAAD database using the TCGAbiolinks R package. Using the median UHMK1 expression in PDAC tissue as the threshold, data were divided into a group with high UHMK1 expression (n=88) and a group with low UHMK1 expression (n=89). These data were evaluated by gene ontology (GO) analysis based on GSEA and the databases "biological processes", "cellular components", and "molecular functions" were chosen respectively and the resulting top 5 items are shown according to NES. Regarding the dataset "biological processes", cytokinesis, membrane protein intracellular domain proteolysis, regulation of DNA templated transcription initiation, regulation of protein export from nucleus, and regulation of translational initiation were found to be enriched (**Figure 4A** and **Table S3**). As for the dataset "cellular components", cytoplasmic stress granule, early endosome, nuclear inner membrane, nuclear membrane and ribonucleoprotein granule were enriched (**Figure 4B** and **Table S3**). In terms of molecular functions, the double stranded RNA binding, phosphatidylinositol binding, protein serine threonine kinase activator activity, RNA polymerase binding and single stranded RNA binding were enriched (**Figure 4C** and **Table S3**).

To further highlight the functional impact of high UHMK1 expression in PDAC, we performed GSVA analysis. A heatmap

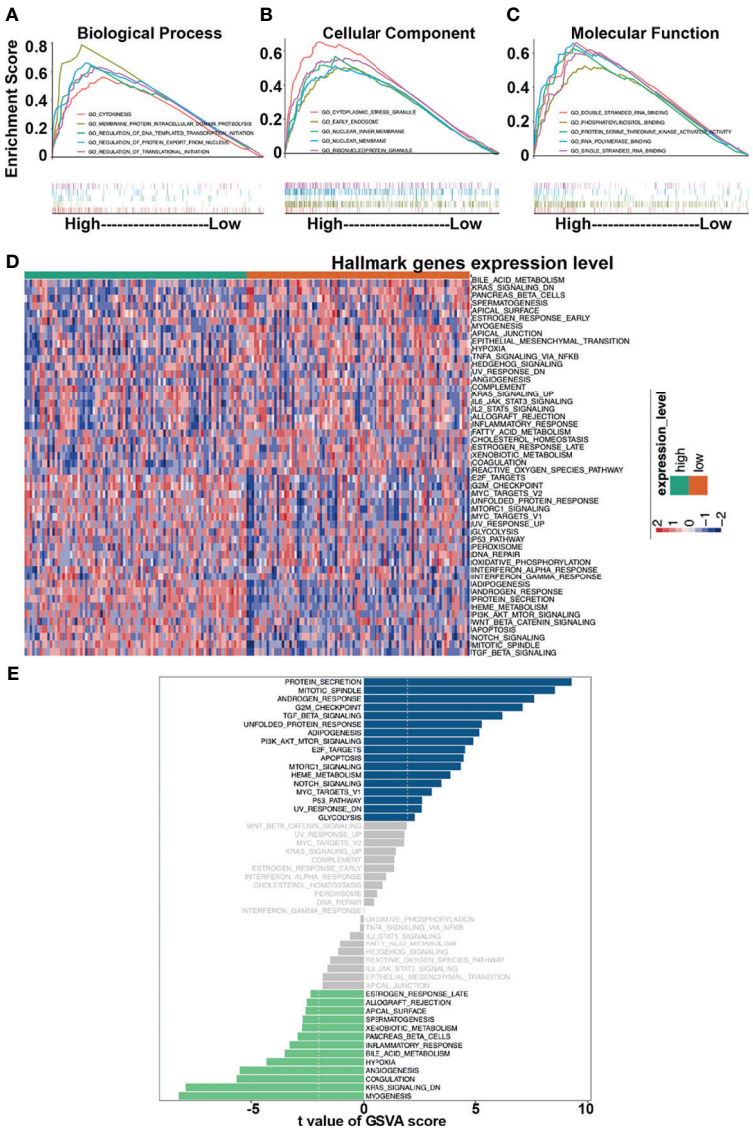

FIGURE 4 | Functional analysis of UHMK1. GO analysis was performed in GSEA software. Top five items are shown. The number of permutations was set to 1000. The top 5 items are shown for each analysis based on the normalized enrichment score (NES). **(A)** Biological process. **(B)** Cellular component. **(C)** Molecular function. **(D)** Hallmark gene sets, which represent specific well-defined biological states or process, were chosen as related gene sets. The R package "GSVA" was utilized to perform GSVA analysis. A heatmap which presents the expression levels of Hallmark pathways relative to high and low expression of UHMK1 is shown. Red: high UHMK1 expression. Blue: low UHMK1expression within a scale from 2 to -2 as indicated. **(E)** mRNA expression of 177 samples was extracted from the TCGA-PAAD database. According to the median of the UHMK1 expression, two groups of high and low UHMK1 expression were split and uploaded to the R-Studio environment and examined by GSVA analysis and the use of the R package "limma". The threshold was set to t value <2. Samples with high UHMK1 had some gene pathways upregulated (blue bars)/downregulated (green bars).

was created according to high and low expression of UHMK1. The heatmap was illustrated the enrichment level of each samples in hallmark pathways. Red represented high enrichment score, blue represented low enrichment score (**Figure 4D**). Finally, the differential gene expression between these two groups was evaluated by GSVA and the limma R package, and the results are presented as a bar plot (**Figure 4E**). Significant changes in cancer-related pathways occurred, and alterations were found in protein secretion, cell cycle progression, and signaling pathways, including the TGF-β, PI3K/AKT/mTOR, apoptosis, mTORC1, Notch, Myc, and p53 pathways.

Knockdown of UHMK1 Suppresses Viability, Migration, and Colony Formation

To evaluate the effect of UHMK1 on PDAC progression, we lipotransfected BxPc-3, AsPC-1, and MIA-PaCa2 cells with four different UHMK1 siRNA constructs and evaluated the expression

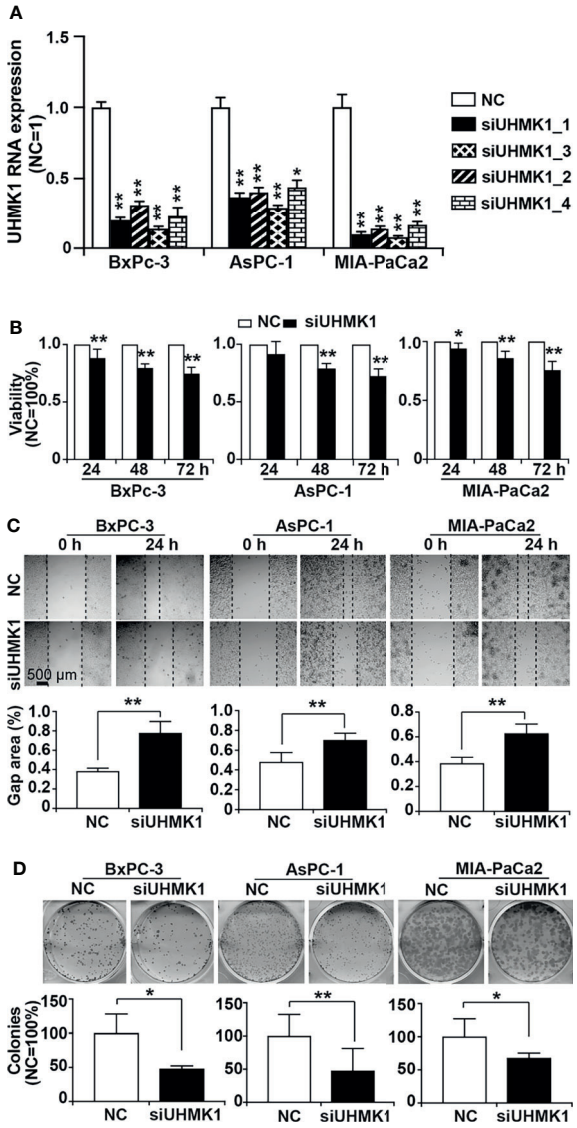

FIGURE 5 | Knockdown of UHMK1 suppresses tumor progression features. **(A)** Four different siRNA constructs of UHMK1 (siUHMK_1, siUHMK1_2, siUHMK1_3, and siUHMK1_4) along with a nonsense siRNA control (NC) were transfected into BxPc-3, AsPC-1, and MIA-PaCa2 cells. RNA was harvested 24 h later, and the expression of UHMK1 was detected by RT-qPCR. The UHMK1 expression levels were normalized to the β-actin housekeeping gene. The fold change of UHMK1 expression was normalized to that in the NC control group, which was set to 1. **(B)** BxPc-3, AsPC-1, and MIA-PaCa2 cells were transfected with siUHMK1 or a nonsense siRNA control (NC). Cell viability was detected by MTT assay at 24 h, 48 h, and 72 h after transfection. The NC control was set to 1. **(C)** Would healing assay. The closure of the wounded region was examined by microscopy 24 h after scratching. Representative images are shown, and the dotted line indicates the gap. The percentage of the gap area was evaluated by ImageJ, and the mean width ± SD is shown in the diagrams. **(D)** Similarly, 24 h after transfection, cells were seeded into 6-well plates at a low density of 400 cells/well and cultured in regular cell culture medium for 14 days. After washing with PBS and fixing with 4% PFA, cells were stained with 0.05% Coomassie blue, and representative images are shown. The number of colonies consisting of at least 50 cells per plate was counted, and the means ± SD are shown in the diagrams. The NC controls were set to 100%. $^{*}P < 0.05$ and $^{**}P < 0.01$.

of UHMK1 by RT-qPCR 24 h later. The expression of UHMK1 was strongly inhibited by all siRNAs in all PDAC cells compared to the siRNA control (**Figure 5A**). Among all siRNA constructs, siUHMK1-1 had the strongest and most significant inhibitory effect. Therefore, siUHMK1-1 was used for all subsequent experiments. To assess the impact of UHMK1 on cell viability, transfection of siUHMK1-1 and NC was followed by a MTT assay at 24, 48, and 72 h. The knockdown of UHMK1 significantly inhibited cell viability at all time points, but the effect was time-dependent and most pronounced at 72 h, the percentage ± standard deviation was calculated (BxPc-3: 74.8% ± 0.05; AsPC-1: 72.9% ± 0.06; MIA-PaCa2: 75.8% ± 0.07) (**Figure 5B**). Similarly, we evaluated the effect of UHMK1 on stem cell progression features by scratch and colony-forming assays. Upon UHMK1 knockdown and inhibition of

proliferation by serum starvation, we found a significantly slower closure of the wounded region (**Figure 5C**), and UHMK1-deficient cells formed significantly fewer colonies (**Figure 5D**). Above all, MTT assay suggested UHMK1 affected cell viability, wound healing assay gave us a hint that UHMK1 involved in cell migration and colony forming assay indicated that UHMK1 influenced the capacity of colony forming. These results suggested that UHMK1 drives PDAC progression.

Downregulation of H19 or UHMK1 Inhibits Tumor Growth

To evaluate the effect of UHMK1 on tumor growth, we lipotransfected MIA-PaCa2 cells with siH19, siUHMK1, or a control siRNA construct followed by xenotransplantation to the CAM of fertilized chicken eggs at day 9 of chick development. Tumors were resected at day 18, and the tumor volume was determined. Compared to the control, depletion of H19 or UHMK1 rendered smaller tumors in the resected xenografts (**Figure 6A**). Immunohistochemical staining of xenograft sections with Ki-67 demonstrated that proliferation was significantly inhibited by siH19 or siUHMK1 as evaluated by counting the percentage of positively stained cells, as shown in a diagram along with representative staining (**Figure 6B**). To verify the correlation of H19 and UHMK1 expression *in vivo*, we detected UHMK1 expression by immunohistochemistry in H19-deficient xenografts and found a significant downregulation of UHMK1 (**Figure 6C**). To exclude that siH19 or siUHMK1 might have reduced the tumor size by interference with chick development, we confirmed that the weight of each individual chick was not altered between the groups and that liver necrosis did not occur (**Supplementary Figures S5A, B**).

UHMK1 Expression Is an Appropriate Nomogram Prediction Factor

Because nomograms are widely used in oncology to predict personalized prognosis and treatment (21, 22), we added the obtained UHMK1 expression data to a nomogram, containing the confirmed prognostic factors of "age", "tumor grade", and "radiation therapy" (**Figure 7A**), which were obtained from TCGA online database. The nomogram was constructed using the "RMS package" in the R studio environment. Scoring points were assigned to each parameter on the individual point scale axes. A total score was calculated by adding the individual points, then projecting the total points to the lower total points scale, which enabled prediction of the 1-, 3-, and 5-year overall survival rates. The allocation of scoring points per individual parameter in the nomogram model is shown in **Supplemental Table S4**. To control how accurately the nomogram predicts survival, we measured the AUC-ROC performance using R language as previously described (23). The AUC values predicted by our nomogram for the 1-, 3-, and 5-year overall survival rates were 0.718, 0.712, and 0.775, respectively (**Figure 7B**), suggesting that our nomogram is an acceptable prediction model (21, 22). Finally, we performed a DCA control experiment to identify the range of threshold probabilities in which the nomogram is of value, the magnitude of benefit, and if the nomogram is worth using in general (24). By DCA, we found that the standardized net benefit of the nomogram model (purple line) was higher than each single item, which gave us a hint that the constructed nomogram had superior clinical utility for PDAC patients (**Figure 7C**). These data indicated that the use of the constructed nomogram to predict prognosis is of greater benefit than using each individual parameter alone.

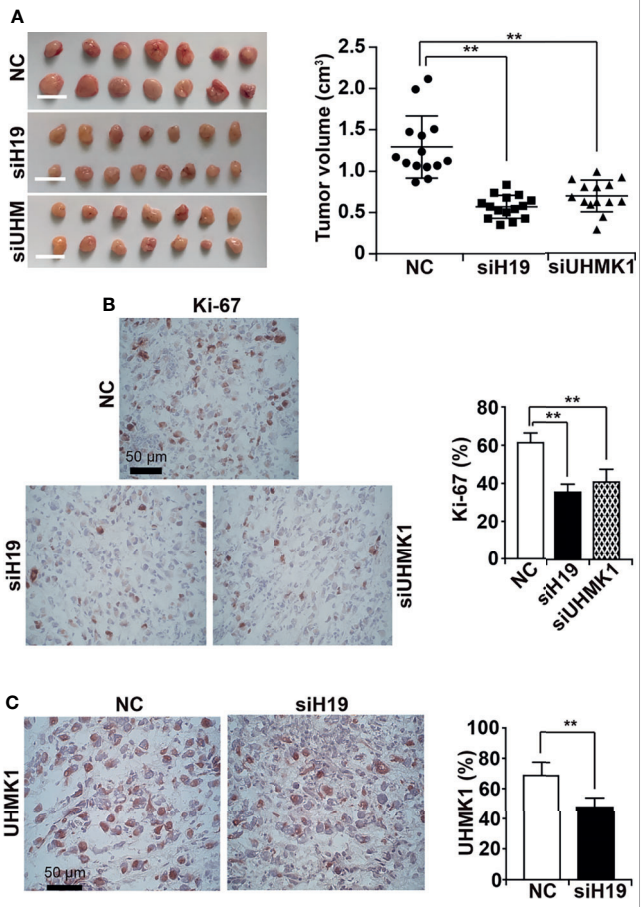

FIGURE 6 | Knockdown of H19 or UHMK1 inhibits tumor growth *in vivo*. **(A)** siH19, siUHMK1, and a nonsense siRNA control (NC) were transfected into MIA-PaCa2 cells. After 24 h, 10^6 cells of each group were transplanted onto the CAM of each egg (n = 15 eggs/group) on developmental day 9 of the chick embryo. Tumor xenografts were resected on day 18 of chick development, and representative images are shown on the left. The individual xenograft volumes and the mean volumes of each group are presented on the right. **(B)** The expression of the Ki-67 proliferation marker was detected by immunohistochemistry in frozen xenograft sections. Representative images using 400× magnification are shown, and the scale bar represents 50 μm. The percentage of Ki-67-positive cells was quantified by counting the dark red-stained cells in 10 randomly chosen vision fields of each tissue by two independent examiners who were blinded by the conditions. **(C)** The expression of UHMK1 was detected and the percentage of the positive UHMK1 signal was quantified. $^{**}P < 0.01$.

DISCUSSION

Here, we demonstrated that the UHMK1 nuclear kinase is induced by lncRNA H19 and showed that both UHMK1 and

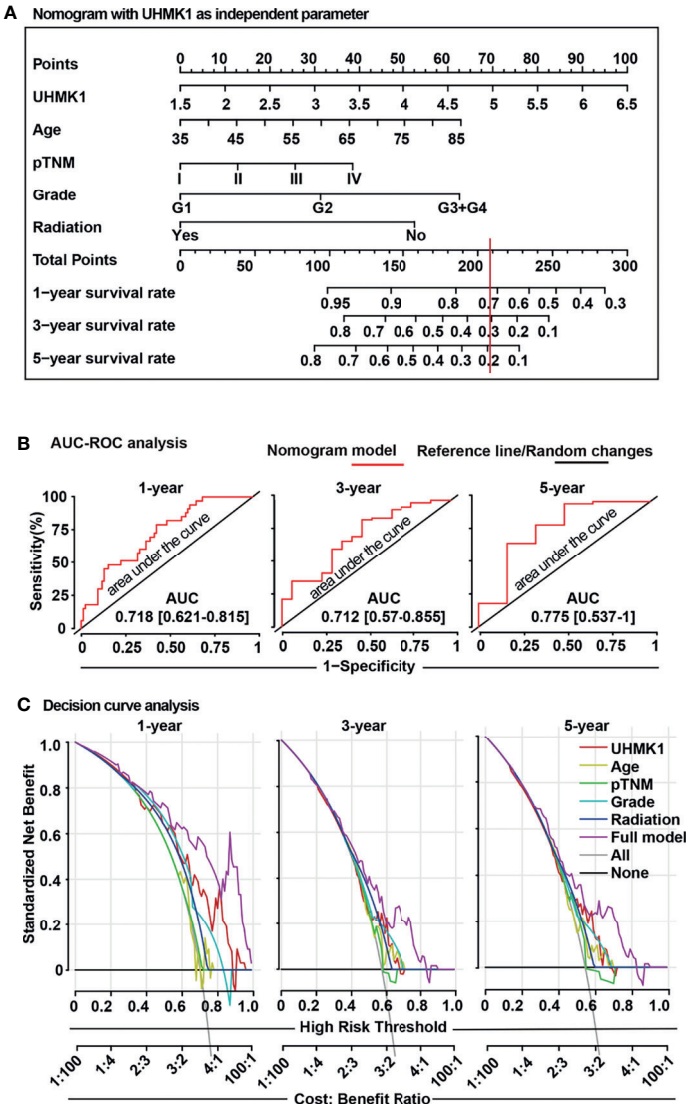

FIGURE 7 | The UHMK1 nomogram reliably predicts the survival probability of PDAC patients. **(A)** A nomogram was constructed using the "RMS package" in R studio software with specific codes. UHMK1 expression data from PDAC patients (n =129) with available clinicopathological parameters were downloaded from TCGA database. Based on univariate Cox regression analysis, a nomogram was established for the prediction of 1-, 3-, and 5-year overall survival. The single parameters of this nomogram were level of UHMK1 expression on a scale from 1.5 to 6.5, age on a scale from 35 to 85, pathologically evaluated tumor/node/metastasis status (pTNM) based on stages I to IV, grade based on G1 to G4 stages, and application of radiation. To estimate the survival probability, the points for each variable was read and summed. A straight line from the sum of all points on the total points axis was then drawn to the 1-, 3-, and 5-year survival axes to determine the respective survival rate. For example, a 60-year-old patient (31 points), who had UHMK1 expression level 5 (70 points), G2 tumor grade (31 points), and TNM stage III (25 points) but who did not undergo radiation therapy (51 points), received a total of 208 points. By drawing a vertical line (red) passing the total points scale at 208, the corresponding 1-, 3-, and 5-year overall survival rates for this patient are 72%, 30%, and 19%, respectively. **(B)** To confirm the predictive power of the nomogram, an "area under the curve" (ROC-AUC) analysis was performed using the "survivalROC", "survival", and "riskRegression" R packages in R studio software. The red line represents the nomogram model, and the black line is the reference line for random changes. **(C)** A "decision curve analysis" (DCA) was established to compare the clinical benefits of the nomogram. The "rmda" R package was used in R studio software with specific codes. The gray line represents the treat-all-patients scheme (All), and the black line represents the treat-none scheme (None). The single parameters of UHMK1 expression, age, pTNM, grading, radiation therapy, or all together (full model) were evaluated, and the results are presented in the diagram. The Y-axis represents the standardized net benefit, which is a positive constant quantifying the expected benefit of intervention for a case. The X-axis represents the high-risk threshold, which summarizes the costs and benefits of intervention. The cost:benefit ratio is a ratio of standardized net benefit with or without intervention.

H19 are strongly involved in PDAC progression. We inhibited H19 expression and performed gene array and bioinformatics analysis along with functional experiments to verify UHMK1 as the top candidate of downregulated genes, closely followed by SGPL1, MIGA1, and SERPINB9. We further investigated UHMK1 expression in PDAC tissues and nonmalignant pancreatic tissues, and we correlated the results to associated clinicopathological data. Elevated UHMK1 levels correlated with

advanced TNM stages and predicted the overall survival rate. We established a nomogram with the risk factor of UHMK1 expression and showed that UHMK1 is a reliable parameter and independent predictor of the overall survival of PDAC patients.

We focused on studying UHMK1 because it was at the top of the H19-downregulated candidate genes and because its function in PDAC was previously unknown. To define the role of UHMK1, we assessed the mRNA and protein levels of UHMK1 in PDAC and other tumor entities as well as in nonmalignant pancreatic tissues. We found low UHMK1 expression in nonmalignant pancreatic cells and tissues. In contrast, UHMK1 expression was remarkably increased in several PDAC cell lines and tissues. Furthermore, we detected a significant upregulation of UHMK1 expression in advanced breast cancer, cervical squamous cell carcinoma and endocervical adenocarcinoma, lymphoid neoplasm, diffuse large B-cell lymphoma, esophageal carcinoma, skin cutaneous melanoma, stomach adenocarcinoma, and thymoma. Our results are consistent with previous work, demonstrating enhanced UHMK1 expression in clinical PDAC specimens, PDAC cell lines (25), gastric cancer (19), liver cancer cells (18), and leukemia cells (26).

Our findings imply that depletion of UHMK1 expression inhibited cell viability by performing MTT assay. Meanwhile, we performed wound healing and colony forming assays to confirm our result. *In vivo*, by staining proliferation marker Ki-67 of xenograft tissue which were resected from CAM, we confirmed that the knockdown of UHMK1 expression suppressed the Ki-67 and thereby proliferation. By GSVA, we demonstrated that high expression of UHMK1 correlated with the enrichment of signaling pathways involved in the regulation of the cell cycle, including TGF-β PI3K-AKT-mTOR, Notch, p53 and others. Although the current knowledge about the cellular function of UHMK1 is limited, it is known that UHMK1 signaling is associated with DNA replication, spliceosome biology, and cell cycle regulation (18). A previous study has used FACS sorting to generate UHMK1-deficient cells, which have a reduced number of cells in the S phase and G2/M phases of mitosis (18). These data are in line with another report, confirming that UHMK1 expression leads to cell cycle progression (26). However, there are also contradictory data indicating that UHMK1 silencing does not affect cell cycle progression in U937 leukemia cells (27). The probable reason might be the different microenvironment between solid tumor and non-solid tumor. Finally, one report has indicated that COX5B regulates tumor growth by modulating the AMPK-UHMK1-ERK signaling cascade in hepatoma (28). Interestingly, UHMK1 promotes the progression of gastric cancer through reprogramming of nucleotide metabolism (19). Additionally, YAP-dependent induction of UHMK1 has been reported to support the nuclear enrichment of the MYBL2 oncogene, leading to the proliferation of hepatocellular carcinoma cells as demonstrated in YAP-deficient mice and human hepatocellular carcinoma tissues (18). UHMK1 has been detected as an autoantibody biomarker for serous ovarian cancer using an ELISA platform against a total of 153 serum samples (63 cases with 30 benign disease controls and 60 healthy controls) (20).

Therefore, the signaling pathways underlying the observed UHMK1-regulated progression of PDAC are quite complex and involve the regulation of UHMK1 by lncRNA H19 according to our findings. However, H19 is not the only lncRNA involved in UHMK1 regulation because Xu et al., 2021 stated that lncRNA EBLN3P regulates UHMK1 expression by sponging miR323a-3p, thereby promoting colorectal cancer progression (29). Although it is unknown whether the latter described mechanism is also involved in PDAC progression, our data were consistent with the notion that reduced expression of H19 inhibits PDAC metastasis, which involves the H19-mediated regulation of miR-194 and let-7 (6, 10, 30). Upon siRNA-mediated inhibition of H19 expression, we observed reduced cell viability, migration, invasion, and tumor growth as shown here and in our previous study (12). H19 may exert these effects by inducing several downstream genes. For example, the APOBEC3G tumor promoter is preferentially induced upon induction of H19 expression by the sulforaphane bioactive agent (12). In addition to UHMK1, we detected other strong H19-induced candidate genes, and the H19-mediated upregulation of SGPL1, MIGA1, and SERPINB9 may work together with UHMK1 as we detected a strong correlation of high expression of all of these genes in PDAC tissue but not in nonmalignant pancreatic tissue.

To confirm our results, we performed *in vivo* experiment using fertilized chicken eggs for tumor xenotransplantation. We understand that the mouse model is most common used in researches. However, our former studies illustrated that the pancreatic xenografts can grow fast in fertilized chicken eggs, and the morphology and the expression patterns, progression markers and PDAC markers were comparable with primary patient tissues and their xenograft copies (31). In addition, the tumor environment in chicken egg xenografts were similar compared to primary patient tumors and mouse xenografts (32). Furthermore, we would like to mention that both the subcutaneous xenografts in mouse model and chicken egg xenografts model have their limitations, and cannot entire reflect the pro-fibrotic nature, immunosuppressive tumor microenvironment of PDAC (33). Our constructed chick egg model was several used to successfully established tumor xenotransplantation to the CAM for measuring the tumor growth (12, 34–36). A major advantage of the chicken egg model is that it has natural immunodeficiency. At days 8-9 of chick embryonal development, the blood vessel network is dense enough to bear the growth of the tumor xenograft. On day 18, we resected the xenografts for the reason that the chick hatches on day 21. Therefore, the fertilized chicken eggs are well suited for the short-term studies. By the use of this model, we confirmed that knockdown of UHMK1 and H19 significantly inhibited PDAC xenograft growth but did not completely inhibit it. Likewise, immunohistochemistry confirmed that UHMK1 and Ki-67 expression in xenograft tissue were significantly but not completely reduced following siRNA-mediated knockdown of UHMK1 and H19. To ensure that the siRNA-mediated knockdown was lasting for several days, we transfected the siRNA constructs immediately prior to xenotransplanation.

One may speculate that a complete knockout of UHMK1 or H19, e.g. by the use of CRISPR/Cas would have resulted in an even more pronounced inhibition of tumor xenograft growth.

By constructing a statistical survival model, we correlated high UHMK1 expression with a worse prognosis and shorter survival of PDAC patients compared to the parameters of pTNM stage, grading, age, and application of radiation therapy. Unfortunately, we could not compare UHMK1 expression to the effects of the standard chemotherapy regimens, gemcitabine, nab-paclitaxel, or FOLFIRINOX, because a significant number of patient data were not available in online databases.

Finally, we combined UHMK1 expression and clinical parameters to establish a novel prognostic nomogram that individually predicts the 1-, 3-, and 5-year overall survival rates of PDAC patients. To illustrate the reliability of our nomogram, we compared our AUC value to a PDAC nomogram that was constructed by Liu et al., 2021 (37), who reported AUC values of 0.713, 0.753, and 0.823 for 1-, 3-, and 5-year survival, respectively. Liu's results suggested their constructed nomogram model had the superior predictive power with AUC value more than 0.7. Correspondingly, the AUC values in our nomogram model were 0.718, 0.712, and 0.775 for 1-, 3-, and 5-year survival, respectively. These data demonstrated the satisfactory prediction accuracy of our nomogram as well. According to the AUC and the clinical net benefit control experiments, our nomogram illustrated a better prediction of overall survival compared to the generally accepted prediction parameters of age, pTNM stage, grading, and application of radiation therapy. Nonetheless, before our nomogram can be used clinically, further validation by multicenter, large-scale clinical trials is necessary. Because we calculated online results from different online databases, it may have led to a batch effect, indicating that systematic technical differences can occur when samples are processed and measured in different batches (38).

In conclusion, we characterized UHMK1 as a new lncRNA H19-induced gene and highlighted the function of UHMK1 as a novel progression and prognostic marker and therapeutic target in PDAC. Moreover, the novel UHMK1-based nomogram model provides a more convenient and accurate prediction of the overall survival rate of PDAC patients.

MATERIALS AND METHODS

Tumor Cell Lines

The established human PDAC cell lines, MIA-PaCa2 (RRID : CVCL_0428), BxPc-3 (RRID : CVCL_0186), PANC-1 (RRID : CVCL_0480), and AsPC-1 (RRID : CVCL_0152), as well as the nonmalignant pancreatic ductal cell line, CRL-4023 (RRID : CVCL_C466), were obtained from the American Type Culture Collection (ATCC, Manassas, VA, USA). Gemcitabine-resistant BxGEM cells were selected from parental BxPc-3 cells (RRID : CVCL_0186), as described (39). PDAC cells were cultured at 37°C in high glucose DMEM (Sigma, Deisenhoffen, Germany), 10% FBS (Sigma), and 25 mmol/L HEPES (Thermo Fisher, Dreieich, Germany). CRL-4023 cells were cultured in 75% DMEM without glucose, 2 mM L-glutamine, 1.5 g/L sodium bicarbonate, and 25% M3 Base medium (Incell Corporation LLC, San Antonio, TX, USA). Mycoplasma-negative cultures were ensured monthly by PlasmoTest™ (*In vivo*Gen, San Diego, CA, USA). All cell lines have been authenticated by SNP profiling (Multiplexion, Heidelberg, Germany).

Patient Tissues

Malignant pancreatic tissues from anonymous patients (n=20) and nonmalignant pancreatic tissues from anonymous brain-dead donors (n=20) were provided by the tissue bank of the European Pancreatic Cancer Center Heidelberg. According to the World Health Organization (WHO), conventional clinical and histological criteria established the clinical diagnoses (**Supplementary Table S1**).

SiRNA Transfection

PDAC cells were seeded at a concentration of 2×10^5/well in 6-well plates and cultured in serum-reduced OptiMEM® for 12 hours. AllStars Negative Control siRNA, FlexiTube siRNA siH19-1, FlexiTube siRNA siH19-2, and FlexiTube siRNA directed against human UHMK1 (QIAGEN, Hilden, Germany) were transfected at a concentration of 50 nM using Lipofectamine 2000 (Thermo Fisher Scientific, Dreieich, Germany) according to the manufacturer's instructions. After 4 h of transfection, the supernatant was discarded, and regular cell culture medium was added. The cells were used for experiments after 24, 48 or 72 h of incubation.

mRNA Microarray Profiling

MIA-PaCa2 cells were lipotransfected with a nonsense siRNA control or specific siH19-1 and siH19-2 siRNAs (QIAGEN, Hilden, Germany) as described above. The RNeasy Kit (QIAGEN, Hilden, Germany) was used to isolate mRNA. Microarray analysis was performed at the Microarray-Analytic Center of the Medical Faculty Mannheim using the Clariom™ D Assay (Thermo Fisher Scientific, Dreieich, Germany). Heatmaps and volcano plots were created with R Studio (https://rstudio.com/products/rstudio/). The "limma" R package was applied to normalize the data and to identify differentially expressed genes between control cells and siH19-1 or siH19-2-transfected cells. Genes with a fold change >1 and a P value <0.05 were considered significantly differentially regulated genes. The results were prepared as heatmaps or volcano plots using the "ggplot2" R package.

mRNA Extraction and RT-qPCR

The RNeasy Mini Kit (QIAGEN, Hilden, Germany) was used to isolate mRNA. For reverse transcription, the High-Capacity RNA-to-DNA™ Kit (Thermo Fisher Scientific, Dreieich, Germany) was utilized according to the manufacturer's instructions. DNA was amplified using PowerUp™ SYBR™ Green Master Mix (Thermo Fisher Scientific, Germany) by RT-qPCR. The following primer sequences were used: UHMK1 forward, 5′-AGAGAAACCATGGGCAGAAG-3′; UHMK1 reverse, 5′-CAAGCCATGAAACAGCATCT-3′; β-actin forward, 5′-AATCGTGCGTGACATTAAGGAG-3′; and β-actin reverse, 5′-ACTGTGTTGGCGTACAGGTCTT-3. The concentration of each primer was 500 nM. The gene expression

levels were normalized to the β-actin housekeeping gene. The qPCR conditions were as follows: 40 cycles of denaturation at 95°C for 15 sec, annealing at 56°C for 15 sec, and extension at 72°C for 1 min. The results are presented as the relative expression value, which was calculated by the $2^{-\Delta\Delta Ct}$ method (40).

Western Blot Analysis

After treatment, cells were lysed with RIPA lysis buffer (Abcam, Cambridge, UK), and total protein was purified by a standard protocol. Protein concentration was determined by the BCA Protein Assay Kit (Abcam, Cambridge, UK). Before SDS-PAGE separation, the samples were denatured by boiling for 5 min and then kept on ice. The separated proteins were transferred from the gel to a PVDF membrane by a semidry system. The membrane was blocked by incubation in 3% BSA solution, incubated with primary antibodies, washed, and incubated with IRDye® infrared dye-conjugated secondary antibodies (LI-COR Biosciences, Bad Homburg, Germany). The infrared intensity was measured with an Odyssey CLx Infrared Imaging System (LI-COR). Rabbit polyclonal antibodies against UHMK1 (PA550622, Invitrogen, Germany), GAPDH (Cell Signaling Technology, Danvers, MA, USA), and IRDye® 800CW goat anti-rabbit IgG secondary antibody (LI-COR) were used.

Immunohistochemical Staining

Immunohistochemistry on 6-µm frozen or paraffin-embedded tissue sections was performed as previously described (41). Primary antibodies included rabbit polyclonal antibodies against UHMK1 (PA550622, Invitrogen, Germany) and Ki67 (Abcam, Cambridge, UK). Goat anti-rabbit biotinylated IgG (Vector, Burlingame, CA, USA) was the secondary antibody. ImageJ was used to calculate the intensity of the signal emitted from positively stained cells.

Gene Expression Profiling Interactive Analysis (GEPIA)

GEPIA is an online database (http://gepia.cancer-pku.cn) that contains tumor data from The Cancer Genome Atlas (TCGA, https://www.cancer.gov/about-nci/organization/ccg/research/structural-genomics/tcga) and the Genotype-Tissue Expression (GTEx, https://gtexportal.org/home/) databases. GEPIA was used to analyze the expression of UHMK1 in tumor and normal tissue derived from PDAC and other tumor entities.

Tumor IMmune Estimation Resource 2.0 (TIMER 2.0)

TIMER (http://timer.cistrome.org) is a comprehensive resource for systematical analysis in diverse cancer types to explore immune association, cancer exploration, and immune estimation. Within the TIMER database, a Pearson correlation analysis was performed to compare the expression of UHMK1 with SGPL1, SERPINB9, and MIGA1.

Kaplan-Meier Plotter Survival Analysis

UHMK1 was identified as a survival biomarker by Kaplan-Meier survival analysis and the Kaplan-Meier plotter online database (https://kmplot.com/analysis/), which contains expression data from 54,000 genes with corresponding survival data from 21 different tumor entities, including PDAC. The Kaplan-Meier plotter database includes TCGA, GEO, and EGA. The purpose of this online database is to discover and validate survival biomarkers. The Kaplan-Meier plotter online database was used to detect the overall survival rate of patients with low or high UHMK1 expression in PDAC tissue samples. Auto select best cutoff was chosen in the analysis.

Cox Regression Analysis

The clinical data of PDAC patients were downloaded from the TCGA database, and univariate and multivariate Cox regression analyses were performed in the R studio environment. The risk of death in PDAC patients is expressed as the hazard ratio (HR) according to application of radiation treatment, the tumor grade, the pathologically evaluated tumor/node/metastasis status (pTNM), sex, age, and the level of UHMK1 expression. HR=1 indicates lack of association. HR>1 indicates an increased risk, and HR<1 indicates a lower risk.

Gene Set Enrichment Analysis (GSEA) and Gene Set Variation Analysis (GSVA)

GSEA 4.0.3 software was used for gene set enrichment analysis. GSEA is a computational method that determines whether an *a priori* defined set of genes shows statistically significant, concordant differences between two biological states (42). Gene Ontology (GO) analysis was conducted using the GSEA software, which was download from Molecular Signature Database (MSigDB) (https://www.gsea-msigdb.org/gsea/msigdb). The GSVA R package was used for gene set variation analysis (GSVA) in the R Studio environment. The h.all.v7.1.symbols.gmt gene set database (https://www.gsea-msigdb.org/gsea/msigdb) was used for enrichment analyses. For the GSVA, the related gene sets, including c5.bp.v7.1.symbols.gmt, c5.cc.v7.1.symbols.gmt, and c5.mf.v7.1.symbols.gmt, were downloaded from MSigDB (https://www.gsea-msigdb.org/gsea/msigdb).

Cell Viability Assay

Twenty-four hours after transfecting with siUHMK1, BxPc-3, AsPC-1 and MIA-PACA2 (5×10^4 cells/well) were seeded into 96-well microplates. After transfection of siUHMK1 at 24, 48, and 72h, 10 µL of 3-(4,5-dimethylthiazol-2-yl)-2,5-diphenyltetrazolium bromide (MTT) was added and incubated for 4 h. Depending on active NADPH-dependent cellular oxidoreductase enzymes, which are present in the functional mitochondria of viable cells, MTT was reduced to insoluble, purple formazan. Subsequently, the medium was carefully discarded, and 200 µL of DMSO was added to dissolve the formazan crystals by shaking on a plate shaker. The color intensity was quantified at a wavelength of 560 nm by spectrophotometry. The viability was evaluated by subtracting the DMSO background, calculating the mean values of each group (n=8), and calculating the standard deviations. The controls of each cell line were set to 100%.

Wound-Healing Assay

Twenty-four hours after lipotransfection, 5×10^5 cells/well were seeded in 6-well plates. Upon reaching a confluency of approximately 90%, a scratch was made with the tip of a 10-µL

pipette in the middle of the cell layer, and this time point was set as 0 h. Cells were washed twice with PBS, and the width of the gap area was determined. Cells were then cultured in serum-free medium to stop proliferation. After incubation for 24 h and 48 h at 37°C, images were acquired using a Nikon Eclipse TS 100-F inverted microscope. The width of the gap area was measured with ImageJ (https://imagej.net/Downloads).

Colony-Forming Assay

Twenty-four hours after lipotransfection, 400 cells/well were seeded in 6-well plates and cultured without medium change for 14 days. Cells were then washed with 10 mL of PBS and fixed with 2 mL of 4% paraformaldehyde (PFA) for 10 min. The fixation solution was replaced with 2 mL of 70% EtOH, which was incubated for 10 min. Finally, cells were stained with 0.05% Coomassie Blue, washed with water, and dried overnight. The percentage of colonies was evaluated by normalizing the number of transfected cell colonies to the number of colonies obtained from cells transfected with the negative control siRNA.

Tumor Xenotransplantation

Fertilized chicken eggs were purchased from a local ecological hatchery (Geflügelzucht Hockenberger, Eppingen, Germany), and the eggs were prepared for transplantation as previously described (43). Before xenotransplantation, MIA-PaCa2 cells were transfected with siH19, siA3G, or negative control siRNA. At day 9 of chick development, 10^6 transfected MIA-PaCa2 cells/egg were transplanted onto the chorioallantois membrane (CAM) as previously described (43). At day 18 of chick development, the embryos were humanely euthanized by injection of 10 µL of a 25 mg/ml Ketanest® solution (Pfizer Pharma PFE GmbH, Berlin, Germany) into a CAM vessel followed by resection of the tumor xenografts. The tumor volume was measured 3-dimensionally by a USB microscope camera (eScope, Oitez, Hong Kong), and digital image editing was performed using a customized mount.

Construction of a UHMK1-Based Nomogram

Nomographical two-dimensional alignment charts (nomograms) are widely used for individual prediction of cancer prognosis (21). By using univariate Cox regression analysis, cancer-related variables can be filtered for nomogram construction (44). Based on the univariate Cox regression analysis of UHMK1 expression and clinical data in TCGA database, a nomogram was constructed to predict the 1-, 3-, and 5-year overall survival rates using the "RMS package" in R studio. To further confirm the superiority of the nomogram, the area under the curve (AUC) was implemented to evaluate the accuracy of prognostic prediction of the nomogram, while receiver operating characteristic (45) analysis was used to determine the sensitivity and specificity. Decision curve analysis (DCA) was used to compare the clinical benefits of the constructed nomogram. The "survivalROC", "survival", "riskRegression", and "rmda" R packages were also used.

Data Extraction From GEO

Three independent datasets, GSE57495, GSE77435, and GSE15471, were downloaded from GEO (http://www.ncbi.nlm.nih.gov/geo/). The GSE57495, GSE77435, and GSE15471 datasets included 63 PDAC tissues, 24 PDAC tissues, and 36 PDAC tissues, respectively, with 36 matched normal paracancerous tissues, and they were analyzed for UHMK1 expression.

Statistical Analysis

The quantitative data are presented as the mean values and standard deviations from at least three independent experiments. The significance of the data was analyzed with Student's t test, which was corrected for multiple comparisons with the Bonferroni-Holm method. A Pearson correlation analysis was performed to measure the linear correlation between two variables, including UHMK1 expression vs. SGPL1 expression, SERPIMB9 expression, or MIGA1 expression. JMP software (SAS, Heidelberg, Germany) was used to analyze the gene microarray data. R studio software version 4.0.3 was also used for statistical analyses. $P<0.05$ was considered statistically significant. In GSEA, a false discovery rate (FDR) of 5% was used to adjust for multiple testing. *$P<0.05$, **$P<0.01$, and ***$P<0.001$.

DATA AVAILABILITY STATEMENT

The datasets presented in this study can be found in online repositories. The names of the repository/repositories and accession number(s) can be found in the article/**Supplementary Material**.

ETHICS STATEMENT

Patient materials were obtained under the approval of the Ethical Committee of the University of Heidelberg after receiving written informed consent from patients. The diagnoses were established by conventional clinical and histological criteria according to the WHO and the anonymous patient data are provided. All surgical resections were indicated by the principles and practice of oncological therapy. Established tumor cell lines were xenotransplanted to fertilized chicken eggs. Since the chick embryo until day 18 of development is not considered as animal, an animal ethics statements is not required.

AUTHOR CONTRIBUTIONS

IH and YL, conception and design. YL and SH, development of methodology. YL, SH, BY, HJ, LZ, and JG, acquisition of data. YL, BY, and IH, analysis and interpretation of data. YL and IH, writing, review, and revision of the manuscript. All authors contributed to the article and approved the submitted version.

FUNDING

This study was supported by the China Scholarship Council in the form of scholarships to YL and SH. IH was supported by grants from the German Research Council (DFG HE 3186/15–1),

Karsten Burmeister - BIMAG Bau- und Industriemaschinen GmbH, Heidelberger Stiftung Chirurgie, Dietmar Hopp-Stiftung, and Klaus Tschira Stiftung.

ACKNOWLEDGMENTS

We are grateful to C. de la Torre and S. Bauer for excellent technical support. We thank the PancoBank of our clinic (Medical Director: M.W. Büchler) for providing anonymous patient data (U. Hinz), and the collection and processing of pancreatic specimens supported by the team of the European Pancreas Center (N. Giese, B. Bentzinger, K. Ruf) and funded by the Heidelberger Stiftung Chirurgie, the Federal Ministry of Education and Research (BMBF 01GS08114), and the Biomaterial Bank Heidelberg/BMBH (P. Schirmacher; BMBF 01EY1101).

SUPPLEMENTARY MATERIAL

The Supplementary Material for this article can be found online at: https://www.frontiersin.org/articles/10.3389/fonc.2022.834647/full#supplementary-material

REFERENCES

1. Ferlay J, Soerjomataram I, Dikshit R, Eser S, Mathers C, Rebelo M, et al. Cancer Incidence and Mortality Worldwide: Sources, Methods and Major Patterns in GLOBOCAN 2012. *Int J Cancer* (2015) 136:E359–86. doi: 10.1002/ijc.29210
2. Siegel RL, Miller KD, Jemal A. Cancer Statistics, 2020. *CA: Cancer J Clin* (2020) 70:7–30. doi: 10.3322/caac.21590
3. Neoptolemos JP, Kleeff J, Michl P, Costello E, Greenhalf W, Palmer DH. Therapeutic Developments in Pancreatic Cancer: Current and Future Perspectives. *Nat Rev Gastroenterol Hepatol* (2018) 15:333–48. doi: 10.1038/s41575-018-0005-x
4. Zhang S, Qin C, Cao G, Xin W, Feng C, Zhang W. Systematic Analysis of Long Noncoding RNAs in the Senescence-Accelerated Mouse Prone 8 Brain Using RNA Sequencing. *Mol Ther Nucleic Acids* (2016) 5:e343. doi: 10.1038/mtna.2016.57
5. Fatica A, Bozzoni I. Long non-Coding RNAs: New Players in Cell Differentiation and Development. *Nat Rev Genet* (2014) 15:7–21. doi: 10.1038/nrg3606
6. Yoshimura H, Matsuda Y, Yamamoto M, Michishita M, Takahashi K, Sasaki N, et al. Reduced Expression of the H19 Long non-Coding RNA Inhibits Pancreatic Cancer Metastasis. *Lab Investig J Tech Methods Pathol* (2018) 98:814–24. doi: 10.1038/s41374-018-0048-1
7. Han J, Han B, Wu X, Hao J, Dong X, Shen Q, et al. Knockdown of lncRNA H19 Restores Chemo-Sensitivity in Paclitaxel-Resistant Triple-Negative Breast Cancer Through Triggering Apoptosis and Regulating Akt Signaling Pathway. *Toxicol Appl Pharmacol* (2018) 359:55–61. doi: 10.1016/j.taap.2018.09.018
8. Li P, Tong L, Song Y, Sun J, Shi J, Wu Z, et al. Long Noncoding RNA H19 Participates in Metformin-Mediated Inhibition of Gastric Cancer Cell Invasion. *J Cell Physiol* (2018). doi: 10.1002/jcp.27269
9. Ren J, Ding L, Zhang D, Shi G, Xu Q, Shen S, et al. Carcinoma-Associated Fibroblasts Promote the Stemness and Chemoresistance of Colorectal Cancer by Transferring Exosomal lncRNA H19. *Theranostics* (2018) 8:3932–48. doi: 10.7150/thno.25541
10. Sun Y, Zhu Q, Yang W, Shan Y, Yu Z, Zhang Q, et al. LncRNA H19/miR-194/PFTK1 Axis Modulates the Cell Proliferation and Migration of Pancreatic Cancer. *J Cell Biochem* (2019) 120:3874–86. doi: 10.1002/jcb.27669
11. Ma L, Tian X, Guo H, Zhang Z, Du C, Wang F, et al. Long Noncoding RNA H19 Derived miR-675 Regulates Cell Proliferation by Down-Regulating E2F-1 in Human Pancreatic Ductal Adenocarcinoma. *J Cancer* (2018) 9:389–99. doi: 10.7150/jca.21347
12. Luo Y, Yan B, Liu L, Yin L, Ji H, An X, et al. Sulforaphane Inhibits the Expression of Long Noncoding RNA H19 and Its Target APOBEC3G and Thereby Pancreatic Cancer Progression. *Cancers* (2021) 13:827. doi: 10.3390/cancers13040827
13. Wu J, Pan TH, Xu S, Jia LT, Zhu LL, Mao JS, et al. The Virus-Induced Protein APOBEC3G Inhibits Anoikis by Activation of Akt Kinase in Pancreatic Cancer Cells. *Sci Rep* (2015) 5:12230. doi: 10.1038/srep12230
14. Boehm M, Yoshimoto T, Crook MF, Nallamshetty S, True A, Nabel GJ, et al. A Growth Factor-Dependent Nuclear Kinase Phosphorylates P27(Kip1) and Regulates Cell Cycle Progression. *EMBO J* (2002) 21:3390–401. doi: 10.1093/emboj/cdf343
15. Manceau V, Swenson M, Le Caer JP, Sobel A, Kielkopf CL, Maucuer A. Major Phosphorylation of SF1 on Adjacent Ser-Pro Motifs Enhances Interaction With U2AF65. *FEBS J* (2006) 273:577–87. doi: 10.1111/j.1742-4658.2005.05091.x
16. Manceau V, Kielkopf CL, Sobel A, Maucuer A. Different Requirements of the Kinase and UHM Domains of KIS for its Nuclear Localization and Binding to Splicing Factors. *J Mol Biol* (2008) 381:748–62. doi: 10.1016/j.jmb.2008.06.026
17. Pedraza N, Ortiz R, Cornadó A, Llobet A, Aldea M, Gallego C. KIS, a Kinase Associated With Microtubule Regulators, Enhances Translation of AMPA Receptors and Stimulates Dendritic Spine Remodeling. *J Neurosci: Off J Soc Neurosci* (2014) 34:13988–97. doi: 10.1523/JNEUROSCI.1573-14.2014
18. Wei T, Weiler SME, Tóth M, Sticht C, Lutz T, Thomann S, et al. YAP-Dependent Induction of UHMK1 Supports Nuclear Enrichment of the Oncogene MYBL2 and Proliferation in Liver Cancer Cells. *Oncogene* (2019) 38:5541–50. doi: 10.1038/s41388-019-0801-y
19. Feng X, Ma D, Zhao J, Song Y, Zhu Y, Zhou Q, et al. UHMK1 Promotes Gastric Cancer Progression Through Reprogramming Nucleotide Metabolism. *EMBO J* (2020) 39:e102541. doi: 10.15252/embj.2019102541
20. Katchman BA, Chowell D, Wallstrom G, Vitonis AF, LaBaer J, Cramer DW, et al. Autoantibody Biomarkers for the Detection of Serous Ovarian Cancer. *Gynecol Oncol* (2017) 146:129–36. doi: 10.1016/j.ygyno.2017.04.005
21. Balachandran VP, Gonen M, Smith JJ, DeMatteo RP. Nomograms in Oncology: More Than Meets the Eye. *Lancet Oncol* (2015) 16:e173–80. doi: 10.1016/S1470-2045(14)71116-7
22. Iasonos A, Schrag D, Raj GV, Panageas KS. How to Build and Interpret a Nomogram for Cancer Prognosis. *J Clin Oncol* (2008) 26:1364–70. doi: 10.1200/JCO.2007.12.9791
23. Mandrekar JN. Receiver Operating Characteristic Curve in Diagnostic Test Assessment. *J Thorac Oncol* (2010) 5:1315–6. doi: 10.1097/JTO.0b013e3181ec173d
24. Vickers AJ, Elkin EB. Decision Curve Analysis: A Novel Method for Evaluating Prediction Models. *Med Decis Making* (2006) 26:565–74. doi: 10.1177/0272989X06295361
25. Idichi T, Seki N, Kurahara H, Fukuhisa H, Toda H, Shimonosono M, et al. Molecular Pathogenesis of Pancreatic Ductal Adenocarcinoma: Impact of Passenger Strand of pre-miR-148a on Gene Regulation. *Cancer Sci* (2018) 109:2013–26. doi: 10.1111/cas.13610
26. Nakamura S, Okinaka K, Hirano I, Ono T, Sugimoto Y, Shigeno K, et al. KIS Induces Proliferation and the Cell Cycle Progression Through the Phosphorylation of p27Kip1 in Leukemia Cells. *Leuk Res* (2008) 32:1358–65. doi: 10.1016/j.leukres.2008.02.012
27. Barbutti I, Machado-Neto JA, Arfelli VC, de Melo Campos P, Traina F, Saad STO, et al. The U2AF Homology Motif Kinase 1 (UHMK1) is Upregulated Upon Hematopoietic Cell Differentiation. Biochimica Et Biophysica Acta. *Mol Basis Dis* (2018) 1864:959–66. doi: 10.1016/j.bbadis.2018.01.004
28. Chu YD, Lin WR, Lin YH, Kuo WH, Tseng CJ, Lim SN, et al. COX5B-Mediated Bioenergetic Alteration Regulates Tumor Growth and Migration by Modulating AMPK-UHMK1-ERK Cascade in Hepatoma. *Cancers* (2020) 12:1646–69. doi: 10.3390/cancers12061646

29. Xu XH, Song W, Li JH, Huang ZQ, Liu YF, Bao Q, et al. Long Non-Coding RNA EBLN3P Regulates UHMK1 Expression by Sponging miR-323a-3p and Promotes Colorectal Cancer Progression. *Front Med (Lausanne)* (2021) 8:651600. doi: 10.3389/fmed.2021.651600
30. Ma C, Nong K, Zhu H, Wang W, Huang X, Yuan Z, et al. H19 Promotes Pancreatic Cancer Metastasis by Derepressing Let-7's Suppression on its Target HMGA2-Mediated EMT. *Tumour Biol* (2014) 35:9163–9. doi: 10.1007/s13277-014-2185-5
31. Zhao Z, Bauer N, Aleksandrowicz E, Yin L, Gladkich J, Gross W, et al. Intraductal Papillary Mucinous Neoplasm of the Pancreas Rapidly Xenografts in Chicken Eggs and Predicts Aggressiveness. *Int J Cancer* (2018) 142:1440–52. doi: 10.1002/ijc.31160
32. Naumann P, Fortunato F, Zentgraf H, Buchler MW, Herr I, Werner J. Autophagy and Cell Death Signaling Following Dietary Sulforaphane Act Independently of Each Other and Require Oxidative Stress in Pancreatic Cancer. *Int J Oncol* (2011) 39:101–9. doi: 10.3892/ijo.2011.1025
33. Yu M, Tannock IF. Targeting Tumor Architecture to Favor Drug Penetration: A New Weapon to Combat Chemoresistance in Pancreatic Cancer? *Cancer Cell* (2012) 21:327–9. doi: 10.1016/j.ccr.2012.03.002
34. Liu L, Salnikov AV, Bauer N, Aleksandrowicz E, Labsch S, Nwaeburu C, et al. Triptolide Reverses Hypoxia-Induced Epithelial-Mesenchymal Transition and Stem-Like Features in Pancreatic Cancer by NF-kappaB Downregulation. *Int J Cancer* (2014) 134:2489–503. doi: 10.1002/ijc.28583
35. Aleksandrowicz E, Herr I. Ethical Euthanasia and Short-Term Anesthesia of the Chick Embryo. *ALTEX* (2015) 32:143–7. doi: 10.14573/altex.1410031
36. Yin L, Xiao X, Georgikou C, Yin Y, Liu L, Karakhanova S, et al. MicroRNA-365a-3p Inhibits C-Rel-Mediated NF-kappaB Signaling and the Progression of Pancreatic Cancer. *Cancer Lett* (2019) 452:203–12. doi: 10.1016/j.canlet.2019.03.025
37. Liu X, Chen B, Chen J, Sun S. A Novel Tp53-Associated Nomogram to Predict the Overall Survival in Patients With Pancreatic Cancer. *BMC Cancer* (2021) 21:335. doi: 10.1186/s12885-021-08066-2
38. Leek JT, Johnson WE, Parker HS, Jaffe AE, Storey JD. The Sva Package for Removing Batch Effects and Other Unwanted Variation in High-Throughput Experiments. *Bioinf (Oxford England)* (2012) 28:882–3. doi: 10.1093/bioinformatics/bts034
39. Fan P, Zhang Y, Liu L, Zhao Z, Yin Y, Xiao X, et al. Continuous Exposure of Pancreatic Cancer Cells to Dietary Bioactive Agents Does Not Induce Drug Resistance Unlike Chemotherapy. *Cell Death Dis* (2016) 7:e2246. doi: 10.1038/cddis.2016.157
40. Livak KJ, Schmittgen TD. Analysis of Relative Gene Expression Data Using Real-Time Quantitative PCR and the 2(-Delta Delta C(T)) Method. *Methods* (2001) 25:402–8. doi: 10.1006/meth.2001.1262
41. Kallifatidis G, Labsch S, Rausch V, Mattern J, Gladkich J, Moldenhauer G, et al. Sulforaphane Increases Drug-Mediated Cytotoxicity Toward Cancer Stem-Like Cells of Pancreas and Prostate. *Mol Ther* (2011) 19:188–95. doi: 10.1038/mt.2010.216
42. Subramanian A, Kuehn H, Gould J, Tamayo P, Mesirov JP. GSEA-P: A Desktop Application for Gene Set Enrichment Analysis. *Bioinf (Oxford England)* (2007) 23:3251–3. doi: 10.1093/bioinformatics/btm369
43. Nwaeburu CC, Aleksandrowicz E, Bauer N, Zhao Z, Herr I. MicroRNA In Vivo Delivery to Human Pancreas Tumor Xenografts on Chicken Eggs. *Protocol Exchange* (2017) doi: 10.1038/nprot.2017.126
44. Wu M, Li X, Zhang T, Liu Z, Zhao Y. Identification of a Nine-Gene Signature and Establishment of a Prognostic Nomogram Predicting Overall Survival of Pancreatic Cancer. *Front Oncol* (2019) 9:996. doi: 10.3389/fonc.2019.00996
45. Owen KL, Brockwell NK, Parker BS. JAK-STAT Signaling: A Double-Edged Sword of Immune Regulation and Cancer Progression. *Cancers* (2019) 11:2002–28. doi: 10.3390/cancers11122002

Conflict of Interest: The authors declare that the research was conducted in the absence of any commercial or financial relationships that could be construed as a potential conflict of interest.

Publisher's Note: All claims expressed in this article are solely those of the authors and do not necessarily represent those of their affiliated organizations, or those of the publisher, the editors and the reviewers. Any product that may be evaluated in this article, or claim that may be made by its manufacturer, is not guaranteed or endorsed by the publisher.

Copyright © 2022 Luo, Han, Yan, Ji, Zhao, Gladkich and Herr. This is an open-access article distributed under the terms of the Creative Commons Attribution License (CC BY). The use, distribution or reproduction in other forums is permitted, provided the original author(s) and the copyright owner(s) are credited and that the original publication in this journal is cited, in accordance with accepted academic practice. No use, distribution or reproduction is permitted which does not comply with these terms.

frontiers in Medicine

SYSTEMATIC REVIEW
published: 15 March 2022
doi: 10.3389/fmed.2022.753545

The Application Value of Syndecan-2 Gene Methylation for Colorectal Cancer Diagnosis: A Clinical Study and Meta-Analyses

Congbo Yue[1†], Yaping Zhang[1†], Yanlei Wang[2], Zhenhong Zhang[3], Mengjiao Zhang[1], Huayang Wang[1], Wendan Chen[1], Ziqi Shang[1], Yiwei Xin[1], Xin Zhang[1] and Yi Zhang[1*]*

[1] Department of Clinical Laboratory, Qilu Hospital of Shandong University, Jinan, China, [2] Department of General Surgery, Qilu Hospital of Shandong University, Jinan, China, [3] Jinan AXZE Medical Test Laboratory, Jinan, China

OPEN ACCESS

Edited by:
Qi Liu,
Fudan University, China

Reviewed by:
Hicham Mansour,
Mohamed Premier University, Morocco
Xie Li,
Shandong University, China
Weijing He,
UT Health San Antonio, United States

****Correspondence:***
Xin Zhang
xinzhang@sdu.edu.cn
Yi Zhang
yizhang@sdu.edu.cn

† These authors have contributed equally to this work

Specialty section:
This article was submitted to Gastroenterology, a section of the journal Frontiers in Medicine

Received: *05 August 2021*
Accepted: *07 February 2022*
Published: *15 March 2022*

Citation:
Yue C, Zhang Y, Wang Y, Zhang Z, Zhang M, Wang H, Chen W, Shang Z, Xin Y, Zhang X and Zhang Y (2022) The Application Value of Syndecan-2 Gene Methylation for Colorectal Cancer Diagnosis: A Clinical Study and Meta-Analyses. Front. Med. 9:753545. doi: 10.3389/fmed.2022.753545

Objective: Syndecan-2 (SDC2) methylation has been previously reported as a sensitive biomarker for the early detection of colorectal cancer (CRC). Droplet digital PCR (ddPCR) is the latest development of PCR technology. It can accurately detect and quantify the target sequence of nucleic acid. ddPCR is widely used in research and clinical diagnosis. In the present study, we aimed to develop a ddPCR method to detect SDC2 gene methylation and evaluate the diagnostic value of SDC2 gene methylation.

Methods: First, a ddPCR method was developed to measure SDC2 methylation in stool samples collected from 51 cases of normal, 23 cases of adenoma, and 86 cases of CRC. Subsequently, a meta-analysis of existing studies was conducted to judge the diagnostic value of SDC2 gene methylation in CRC. PUBMED, EMBASE, Web of Science, and Scopus databases were searched for relative studies. Meta-analysis was performed using Meta Disc 1.4 and STATA 15.0 software.

Results: The ddPCR showed that the linearity, sensitivity, and specificity for the detection of SDC2 gene methylation could be down to 0.1% methylation level and 5 ng of methylated DNA input. In 109 cases of CRC, 107 cases could be detected, and the sensitivity was 98.17%. The median value of the percentage of methylated reference (PMR) in colorectal adenoma and CRC patients was significantly higher compared with the normal individuals ($p < 0.001$). In addition, we found that the PMR value was associated with the clinical staging of CRC. The difference of PMR in stage II and stage IIIA was statistically significant ($p < 0.05$). Moreover, the meta-analysis showed that 11 out of 87 studies were identified to report the feasibility of SDC2 gene methylation as a method to diagnose early CRC. The pooled sensitivity and specificity of SDC2 gene methylation test for CRC were 0.80 [95% *CI* (0.68–0.88)] and 0.93 [95% *CI* (0.91–0.94)], respectively. The pooled diagnostic odds ratio (DOR) and area under curve (AUC) were 52.46 [95% *CI* (30.43–90.45)] and 0.94 [95% *CI* (0.92, 0.96)], respectively.

Conclusions: The ddPCR method was more sensitive and convenient to detect SDC2 gene methylation, and the pooled analysis showed that methylated SDC2 was a valuable biomarker for the non-invasive detection of CRC.

Keywords: droplet digital PCR, diagnostic value, colorectal cancer, SDC2 gene methylation, biomarker

INTRODUCTION

Colorectal cancer (CRC) is the third most common cancer diagnosed worldwide. Every year, more than 945,000 people develop CRC globally, leading to about 492,000 CRC-related deaths (1). If CRC metastasizes, the average 5-year survival rate is estimated to be below 10%, while such rate may be as high as 90% if CRC can be detected in the early stage (2). The importance of diagnosis tools for early detection of CRC has been recognized worldwide. At present, colonoscopy is considered the "gold standard" for CRC diagnosis. It can show lesions more accurately and remove lesions at the same time, but it is invasive and associated with unpleasant intestinal preparation and the risk of intestinal perforation (3). The immunochemical fecal occult blood test (iFOBT), a non-invasive CRC diagnosis approach that uses antibodies against human globulin, has reduced CRC mortality by 15–33% (4, 5). However, this test is characterized by frequent false-negative and false-positive results (6). Therefore, it is urgently necessary to develop a non-invasive and more accurate diagnosis method to promote an early diagnosis of CRC.

DNA methylation is a major manifestation of epigenetics, involving a wide range of disease, such as Alzheimer's disease, diabetic nephropathy, and cancer (7). Abnormal methylation is the core of carcinogenesis, which usually leads to gene expression defects (8). Methylation of tumor suppressor genes is an early event in many tumors and may be one of the first changes related to tumorigenesis (9, 10). Many studies have identified specific DNA methylation sites, such as SEPT9, as biomarkers for CRC detection (11). Methylation status is tissue-specific and constant between several tissue types in different patients. Therefore, gene methylation has certain advantages as a biomarker for cancer detection (12). Brock's study found that methylation in the promoter regions of p16, CDH13, APC, and RASSF1A was associated with the early recurrence of lung cancer (13). Sobhani's study demonstrated that hypermethylation of the Wif1 promoter, the gene regulating the Wnt pathway, serves as diagnostic marker for early CRC (14). However, the value of methylation biomarkers in circulating tumor DNA (ctDNA) in CRC diagnosis and early detection needs further study. Syndecan-2 (SDC2), also called fibroglycan, encodes a transmembrane (type I) heparan sulfate proteoglycan. Hypermethylation of SDC2 has been reported in malignant glioma (15). SDC2 has been identified as a new potential epigenetic biomarker, which can be used to detect CRC using the CpG microarray method. Moreover, SDC2 shows a very high frequency of methylation even in the early stage. Therefore, SDC2 methylation can be used as a potential biomarker for the early detection of CRC.

To further confirm the diagnostic value of SDC2 gene methylation in CRC, we first developed a new technology of droplet digital PCR (ddPCR) to detect SDC2 gene methylation to improve the sensitivity of methylation detection. The principle of this method is that a DNA sample is divided into more than 10,000 droplets, and PCR amplification of template molecules takes place in each droplet (16). The simple readout of droplet partitions as a binary code of one (positive) and zero (negative) represents the "digital" aspect of the technique, and when the final droplet number is more than 10,000, the associated data fits a Poisson distribution (17). This method can be used to directly and simply calculate the copy number of DNA in the sample without a standard curve. Since ddPCR is an end-point PCR approach, it is not affected by the change of reaction efficiency. The high precision of this technology does not require repeated holes, which saves samples and time, and it also effectively allows the accurate quantitation of precious samples (18). In recent years, ddPCR has been more and more used in clinical practice because it can detect and quantify rare alleles more reliably, and it has the advantages of simplicity and rapidity (19). However, there are no reports about the use of ddPCR in the detection of SDC2 gene methylation and its application in the diagnosis of CRC. Therefore, we used ddPCR to detect SDC2 gene methylation and analyzed its application value in patients with CRC. Then, we conducted a meta-analysis of relevant studies to further study the diagnostic value of SDC2 gene methylation in CRC.

METHODS AND MATERIALS

Patient and Sample Collection

All patients with CRC were from the Qilu Hospital of Shandong University. This study was approved by the Medical Ethics Committee of Qilu Hospital of Shandong University, and all subjects gave written informed consent to participate. Briefly, stool samples (∼5 g) were collected from 43 patients with CRC, 23 patients with adenoma, and 51 normal individuals before bowel preparation. Another 43 CRC cases were received 1 week after colonoscopy but before surgery. The specimens were kept in 15 ml preservative buffer, followed by immediate storage at −80°C.

DNA Extraction and Quantification

A QIAamp DNA Mini Kit (Qiagen) was used to extract DNA from stools according to the manufacturer's instructions. NanoDrop One (Thermo Scientific) was adopted to determine the concentration of DNA.

Sequence-Specific Capture

Each capture reaction was carried out by adding 300 μl of stool DNA to an equal volume of 6 mol/L guanidine isothiocyanate solution (Sigma). The SDC2 gene capture probe was CGGTACTCTGCTCCGGATTCGTGTGC (20). After incubation at room temperature for 4 h, 50 μl prepared Dynabeads M-280 streptavidin (Thermo Fisher Scientific) was added to the solution, and the mixture was incubated at room temperature for 1 h. The bead/hybrid capture complexes were then washed two times with 1× wash buffer (1.0 mol/L NaCl, 5 mmol/L Tris-HCl pH 7.5, and 0.5 mmol/L EDTA) and then eluted with 50 μl nuclease-free water containing 20 ng/ml transfer RNA (Sigma). Target gene SDC2 was captured in one reaction.

Bisulfite Conversion of DNA

DNA was bisulfite-treated using EZ DNA Methylation-Gold™ Kit (Zymo Research) according to the manufacturer's instructions. Briefly, DNA was added to the bisulfite treatment reaction. The sample tube was placed in a thermal cycler with

the following steps: 98°C for 10 min; 64°C for 2.5 h, and storage at 4°C for up to 20 h. After the final wash step, DNA was eluted with 10 μL M-Elution buffer. The DNA transformed by sodium bisulfite should be used as soon as possible or stored at −80°C for later use. Repeated freezing and thawing were strongly discouraged as >3 freeze-thaw cycles could lead to DNA fragmentation that impaired PCR amplification.

Droplet Digital PCR

Methylated copies of the SDC2 gene and the reference gene C-LESS (insensitive to CpG methylation status) were quantified using the QX200™ AutoDG Droplet Digital™ PCR System (Bio-Rad). **Supplementary Table 1** shows the primer and probe sequences of SDC2 (21) and C-LESS (22) for this assay. The SDC2 reaction mixture consisted of 1x ddPCR Supermix for Probes (Bio-Rad), 900 nM of each primer, 250 nM of the probe, and 20 ng bisulfite-converted DNA template. The C-LESS reaction mixture consisted of 1x ddPCR Supermix for Probes (Bio-Rad), 900 nM of each primer, 500 nM of the probe, and 20 ng bisulfite-converted DNA template. Samples were loaded into the DG32™ Automated Droplet Generator Cartridges (Bio-Rad). Then, the droplets were transferred to a 96-well PCR plate and placed into a C1000 TouchTM Thermal Cycle with 96-Deep well Reaction Module (Bio-Rad). **Supplementary Table 2** lists the PCR cycling conditions. Data were analyzed using the QuantaSoft software (Bio-Rad). For each experiment, the following control samples were included: positive control well [Universal Methylated DNA (EMD Millipore)], negative control well [Universal Unmethylated DNA (EMD Millipore)], and non-template-control (NTC) well. The number of positive droplets in the negative control wells should be zero, which indicated the optimal specificity of the assay. In addition, NTC wells should also produce zero positive droplets, which reflected optimal laboratory practices. To obtain a measure of SDC2 gene methylation for each sample, the percentage of methylated reference (PMR) was the ratio of SDC2 to C-LESS in DNA extracted from fecal sample compared with the ratio of SDC2 to C-LESS in positive control (fully methylated DNA).

For quality control purposes, samples that generated <100 positive droplets per well for the C-LESS reaction were excluded.

Real-Time Methylation-Specific PCR (QMSP)

Real-time methylation-specific PCR (qMSP) was used to detect SDC2 methylation in DNA samples from 43 stool specimens of CRC. PCR was conducted in a 25-μl reaction system consisting of 400 nmol/L of each primer, 200 nmol/L of each probe, 5 mmol/L Mg^{2+}, 400 mmol/L dNTPs, 0.1 U/ml GoTaq Hot Start Polymerase (Promega), and 1× buffer. For cell line and tissue samples, 1 μl bisulfite-converted DNA was added to the PCR reaction, while 5 μl bisulfite-converted captured stool DNA was used for stool samples. PCR was performed on a LightCycler 96 (Roche Diagnostics). Briefly, after an initial denaturation step at 95°C for 5 min, the amplifications were carried out with 10 cycles at a melting temperature of 95°C for 20 s, an annealing temperature of 62°C for 30 s, and an extension temperature of 70°C for 30 s, followed by 40 cycles at a melting temperature of 95°C for 20 s, an annealing temperature of 58°C for 60 s, and an extension temperature of 72°C for 30 s. Finally, a cooling step at 37°C for 30 s was conducted. Each plate consisted of bisulfite-treated DNA samples, positive and negative controls, and water blanks.

Statistical Analysis

In the present study, GraphPad Prism 8 software was used to analyze the data. Pearson's correlation coefficient was used to verify the linearity of ddPCR detection. Non-parametric Kruskal–Wallis test was adopted to compare ctDNA concentration among different groups. The value of $p < 0.05$ was considered statistically significant.

Meta-Analysis Methods

Study Selection Criteria

Inclusion criteria were set as follows: the techniques and target gene were clearly stated in articles; the target gene was verified by the detection of tumor samples; and sufficient data to construct a diagnostic table, such as true positive (TP), false positive (FP), false negative (FN), and true negative (TN).

Exclusion criteria were set as follows: experiments based on cell lines or animal models; studies were not written in English; and duplicate publications, reviews, letters, technical reports, case reports, or comments.

Search Strategy

The databases, such as EMBASE, PUBMED, Web of Science, and Scopus were searched using the keywords "SDC2," or "syndecan-2," and "colorectal cancer," or "colorectal carcinoma," or "colorectal tumor" to identify all relevant studies. Titles and abstracts of the articles identified through the keyword search were screened against the study selection criteria. Potentially relevant articles were retrieved for the evaluation of full texts.

Quality Assessment

The quality assessment of the articles was estimated using the revised Quality Assessment of Diagnostic Accuracy Studies 2 (QUADAS-2) guidelines. With signaling questions, the risk of bias and concerns regarding applicability were judged as "yes," "unclear," and "no."

Data Extraction

Studies included throughout the process were evaluated by two reviewers, and in the case of disagreement, consensus could be reached through discussion between authors or submission to a third reviewer. The following information was extracted: (1) general information and relevant clinical information of the literature: such as title, country, year of publication, and author; and (2) diagnostic parameters of the literature: the detection value of SDC2 gene methylation and its extracted diagnostic four grid parameters, such as TP, FP, TN, and FN.

Meta-Analysis

First, the four grid table data, the author, and the year extracted from the studies were input into Stata15.0 software to estimate the pooled sensitivity, specificity, positive likelihood ratio, negative likelihood ratio, diagnostic odds ratio (DOR), and

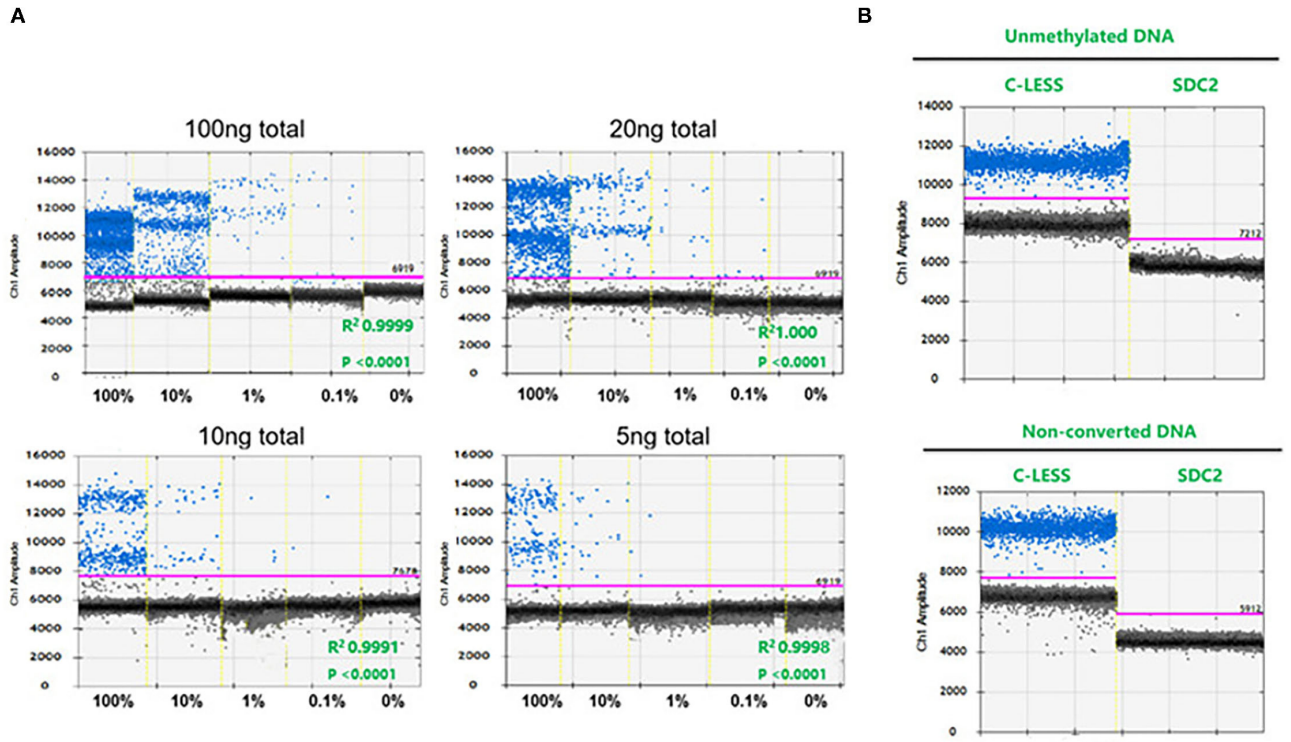

FIGURE 1 | The sensitivity, specificity, and analytical range of the SDC2 gene methylation by droplet digital PCR (ddPCR) assay. **(A)** Serial 1:10 dilution of bisulfite-converted fully methylated control DNA ($n = 3$ independent replicates). **(B)** Unmethylated control DNA and non-converted DNA.

95% *CI*. Statistical heterogeneity was assessed by I^2 statistics. Generally speaking, $I^2 < 25\%$ indicated small heterogeneity, I^2 between 25 and 70% reflected medium heterogeneity, and if $I^2 > 70\%$, it was considered to have high heterogeneity. Forest plots for the pooled sensitivity, specificity, positive likelihood ratio, negative likelihood ratio, and DOR of SDC2 gene methylation were generated for detecting CRC. Summary receiver operating characteristic (SROC) curves were plotted to assess the accuracy of SDC2 gene methylation for the detection of CRC. A *Z*-test was applied to examine the statistical difference of the areas under SROC curves (AUC).

In addition, the subgroup analyses were performed to estimate the effect of sample sources on the diagnostic performance of SDC2 gene methylation and explore heterogeneity using Meta Disc 1.4 (when the number of intergroup studies was <4, Stata 15.0 could not be used for the subgroup analysis). The presence of publication bias was tested by Deeks' funnel plot analysis.

All the analyses were conducted using Meta-Disc software 1.4 and Stata 15.0. Statistical tests presented were two-sided, and a $p < 0.05$ was considered statistically significant.

RESULTS

Development of DdPCR Assay for the Detection of SDC2 Gene Methylation

In the present study, we primarily aimed to evaluate the performance of ddPCR in detecting SDC2 methylation in the terms of sensitivity, specificity, and analytic range. The sensitivity and analytical range of SDC2 methylation analysis were determined by measuring the lower limit of detection. We used four different DNA quantities, such as 100, 20, 10, and 5 ng. Additionally, we prepared 10-fold serial dilutions of a fully-methylated control DNA in the back of fully unmethylated control DNA. The assay could be performed with an input DNA amount of as low as 5 ng, and the results showed good linearity over the titration series (100, 10, 1, 0.1, and 0%). Methylation of SDC2 could be detected down to 0.1% by ddPCR. The ddPCR could cope with a reduced amount of input DNA (**Figure 1A**). **Supplementary Figure 1** shows the copies/well of various methylation levels over a range of concentrations. We chose 20 ng as the amount of DNA input. No positive droplets were detected when unmethylated control DNA or non-bisulfate-treated fully-methylated DNA was used as the input (**Figure 1B**), confirming the specificity of the assay for methylated DNA.

High Sensitivity of DdPCR Assay for the Analysis of SDC2 Gene Methylation

We detected the methylation of the SDC2 gene in stool samples (51 cases of normal individuals, 23 cases of patients with adenoma, and 86 cases of patients with CRC) using ddPCR, and the methylation of SDC2 promoter was calculated as PMR using fully-methylated control DNA as a reference. The results showed that in 109 cases of CRC, 107 cases could be detected, and the sensitivity was 98.17%. The median value of PMR in colorectal adenoma and patients with CRC was significantly higher compared with the normal group ($p < 0.001$). There

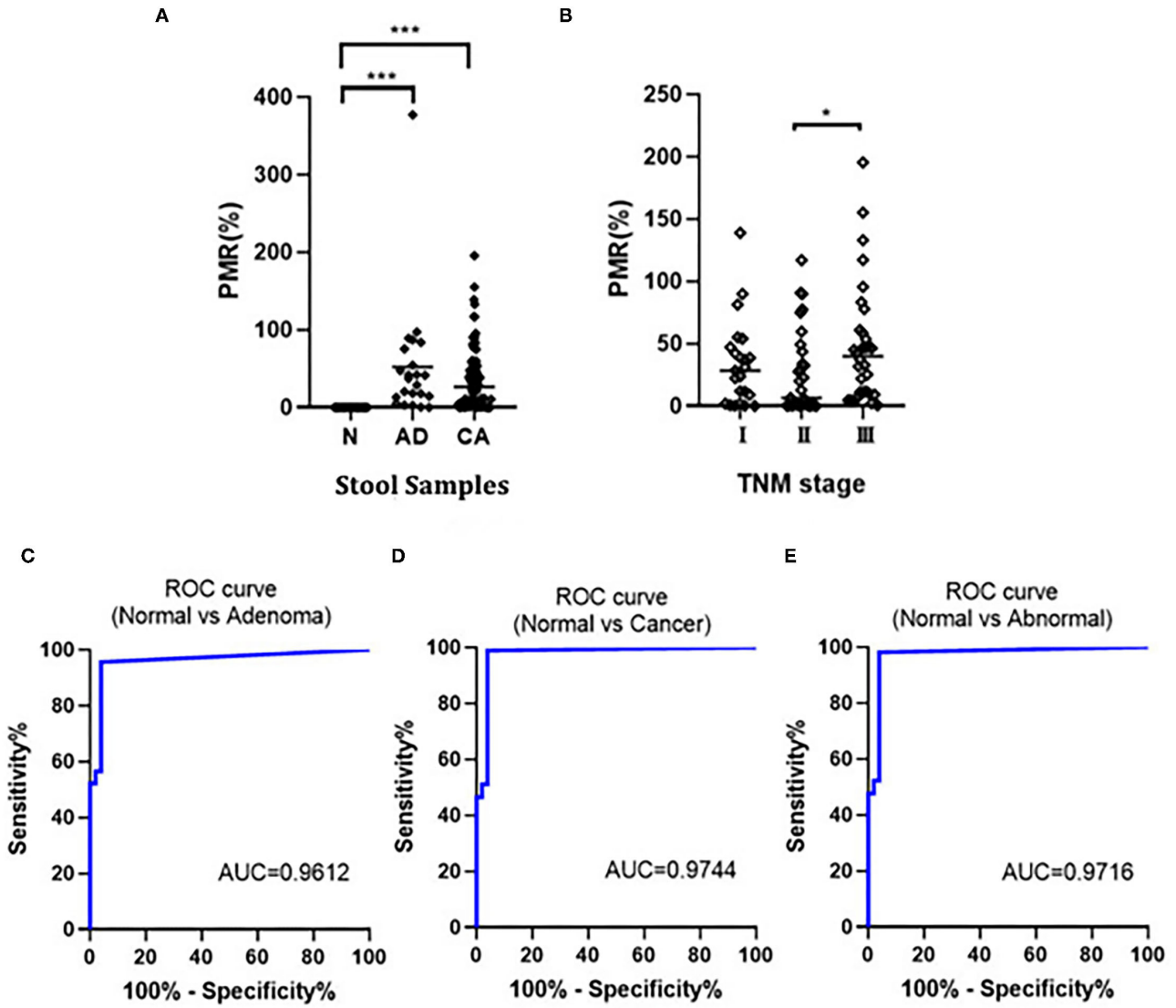

FIGURE 2 | (A) Comparison of SDC2 percentage of methylated reference (PMR) in normal (N), colorectal adenoma (AD), and colorectal cancer (CRC) (CA). ***$p <$ 0.001; **(B)** Correlation of SDC2 PMR in stool samples with CRC stages. *$p < 0.05$; **(C–E)** Receiver operating characteristic (ROC) curves to verify the diagnostic performance of SDC2 gene methylation.

was no statistically significant difference between colorectal adenoma and patients with CRC (**Figure 2A**). Moreover, we found that the PMR value was associated with the clinical staging of CRC. The difference of PMR in stage II and stage III was statistically significant (**Figure 2B**). No significant relationships were observed between SDC2 methylation and clinical features, such as age, sex, tumor size, and tumor location (unpaired *t*-test, $p > 0.05$; **Table 1**). Then, we conducted ROC curves and calculated the AUC to verify the diagnostic performance of SDC2 gene methylation by ddPCR on CRC. The results showed that the AUC was 0.9612, 0.9744, and 0.9716 for discriminating normal from adenoma, cancer, and abnormal, respectively (**Figures 2C–E**). This finding suggested that SDC2 gene methylation possessed important diagnostic value for CRC. The result of qMSP detection showed that 29 of 43 patients with CRC were positive, and the sensitivity was 67.44%. Therefore, the method of ddPCR was better than qMSP.

Literature Search Result and Quality Assessment for Meta-Analysis

Figure 3 shows that 91 studies were identified from the initial literature search. After the removal of 57 duplicates, the first round of title and abstract review was conducted, and 20 articles were excluded because they were overview, system review, and conference submission, or not related to SDC2 gene methylation detection for CRC. For the 14 remaining articles, a full-text review was conducted, and three of them were excluded due to

TABLE 1 | PMR results according to the clinical characteristics of colorectal cancer patients in this study.

Characteristics (number)	PMR (%) Median (25th and 75th percentile)	*P*
Sex		
Male (64)	20.27 (3.11, 48.95)	0.48
Female (45)	29.34 (9.84, 54.59)	
Age		
≤50 (29)	42.15 (7.430, 56.79)	0.35
>50 (80)	20.35 (2.850, 47.78)	
Tumor size		
≤4 (54)	26.80 (4.085, 48.74)	0.87
>4 (55)	28.72 (4.170, 59.78)	
Location		
Left (96)	29.03 (5.623, 54.90)	0.06
Right (13)	5.70 (0.460, 40.51)	
TNM stage		
I (23)	28.35 (1.920, 47.11)	0.03
II (27)	6.640 (0.820, 43.63)	
III (35)	39.97 (10.62, 60.28)	

the following reasons: no full text, no useful data in articles, and articles in Chinese. Finally, 11 eligible studies were included in the final review. The total number of cases included was 2,523, the minimum number of cases included was 64, and the maximum number was 490. Colonoscopy was used as the gold standard in all studies. **Table 2** lists the characteristics and diagnostic parameters of the included studies. Moreover, we assessed the quality of the 11 articles according to the QUADAS-2 assessment tool (**Supplementary Figure 2**).

Diagnostic Accuracy of Methylated SDC2

Supplementary Figure 3 summarizes the diagnostic performance of SDC2 for the detection of CRC. Meta-analysis was carried out on 11 included studies by using the random-effects model. The results showed that the combined sensitivity was 0.80 [95% *CI* (0.68, 0.88)], the specificity was 0.93 [95% *CI* (0.91, 0.94)], the positive likelihood ratio was 11.36 [95% *CI* (9.22, 14.01)], the negative likelihood ratio was 0.22 [95% *CI* (0.13, 0.35)], and the diagnostic ratio was 52.46 [95% *CI* (30.43, 90.45)]. The I^2 of the combined sensitivity, combined specificity, positive likelihood ratio, negative likelihood ratio, and diagnostic ratio was 97.35, 54.25, 31.23, 98.57, and 100.00%, respectively, indicating that there was heterogeneity caused by non-threshold effect among the studies. Sensitivity analyses were performed to explore the sources of heterogeneity, and **Figure 4** shows the results of sensitivity analysis. After the study of Rasmussen, S. L. was removed, the heterogeneity test was carried out again, and I^2 was not decreased compared with the previous value.

Subgroup Analysis

To evaluate the potential impact of factors, such as sample sources, and explore the sources of heterogeneity, we further

TABLE 2 | Characteristics and diagnostic parameters of the included studies.

Author	Country	Year	Sample sources	Number of cases	Gold standard	Method	TP	FP	FN	TN	Sensitivity	Specificity	AUC
An, S. and T. J. Oh	USA	2019	Serum	168	Colonoscopy	RT-qPCR	107	7	10	44	0.915	0.863	0.937
Chen, Y., et al.	China	2019	Serum	225	Colonoscopy	RT-qPCR	79	5	32	109	0.712	0.956	0.881
Rasmussen, S. L., et al.	Denmark	2017	Serum	295	Colonoscopy	RT-qPCR	47	6	146	96	0.244	0.941	0.887
Oh, T., et al.	South Korea	2013	Serum	256	Colonoscopy	RT-qPCR	114	6	17	119	0.87	0.952	0.927
Zhao, G., et al.	China	2019	Plasma	283	Colonoscopy	RT-qPCR	81	7	36	159	0.692	0.958	0.886
Bartak, B. K., et al.	Hungary	2017	Plasma	84	Colonoscopy	RT-qPCR	42	1	5	36	0.89	0.97	0.93
Han, Y. D., et al.	South Korea	2019	Stool	490	Colonoscopy	RT-qPCR	221	24	24	221	0.902	0.902	0.902
Niu, F., et al.	China	2017	stool	373	Colonoscopy	RT-qPCR	159	12	35	167	0.811	0.933	0.92
Oh, T. J., et al.	South Korea	2017	stool	72	Colonoscopy	RT-qPCR	45	2	5	20	0.9	0.909	0.933
Sun, M., et al.	China	2019	Stool	213	Colonoscopy	RT-qPCR	72	9	33	99	0.686	0.917	0.8
Park, Y. S., et al.	South Korea	2018	Bowel lavage fluid (BLF)	64	Colonoscopy	RT-qPCR	8	6	2	48	0.8	0.89	0.844

TP, Ture Positive; FP, False Positive; FN, False Negative; TN, True Negative.

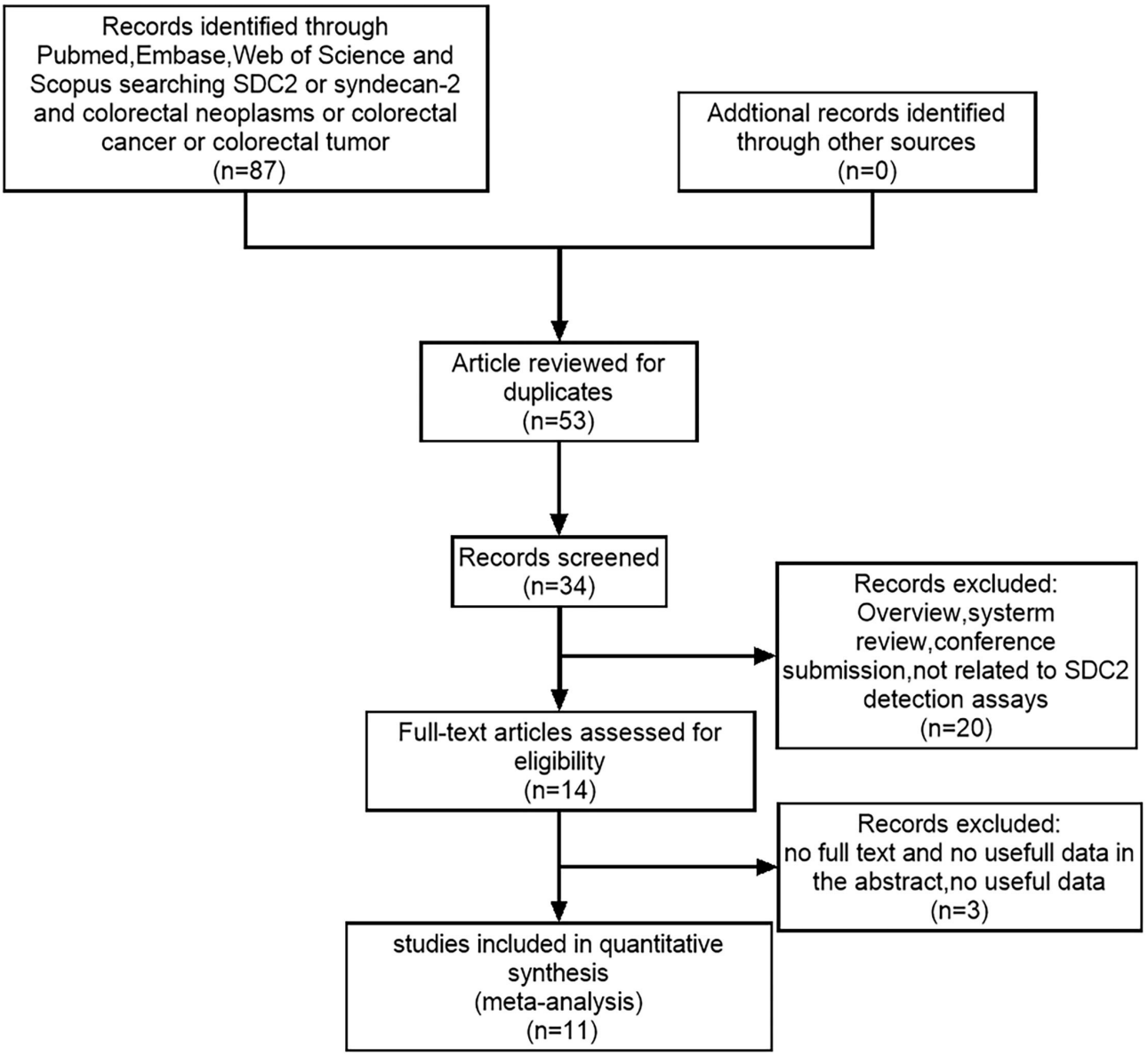

FIGURE 3 | The PRISMA flow diagram for literature selection from relevant studies for this meta-analysis. The design of the diagram and the screening of the literature were based on the PRISMA statement for reporting meta-analysis.

analyzed the factors of sample sources in different groups (**Supplementary Figure 4**). Since there was only one study about SDC2 gene methylation test in bowel lavage fluid as CRC test, there was no subgroup analysis. The sensitivity of methylation detection of SDC2 gene in stool samples was 0.84 [95% *CI* (0.80–0.87)], in serum samples was 0.75 [95% *CI* (0.68–0.81)], and that in plasma samples was 0.63 [95% *CI* (0.59–0.67)] ($p < 0.05$). The negative likelihood ratio of methylation detection of SDC2 gene in fecal samples is 0.18 [95% *CI* (0.10–0.31)], in serum samples is 0.24 [95% *CI* (0.06–1.05)], and in plasma samples is 0.20 [95% *CI* (0.07–0.58)] ($p < 0.05$). The specificity, positive predictive value, and DOR obtained by subgroup analysis were not statistically significant ($p > 0.05$). Therefore, the sample source was the source of heterogeneity.

Summary Operating Characteristics Analyses

We further constructed SROC curves to verify the diagnostic performance of SDC2 gene methylation on CRC. The pooled AUC was 0.94 [95% *CI* (0.92, 0.96)] (**Figure 5A**), indicating that the methylation of the SDC2 gene had a significant diagnostic value as a detection indicator of CRC. The overall bias of the included studies was tested using the Deeks' funnel plot. The

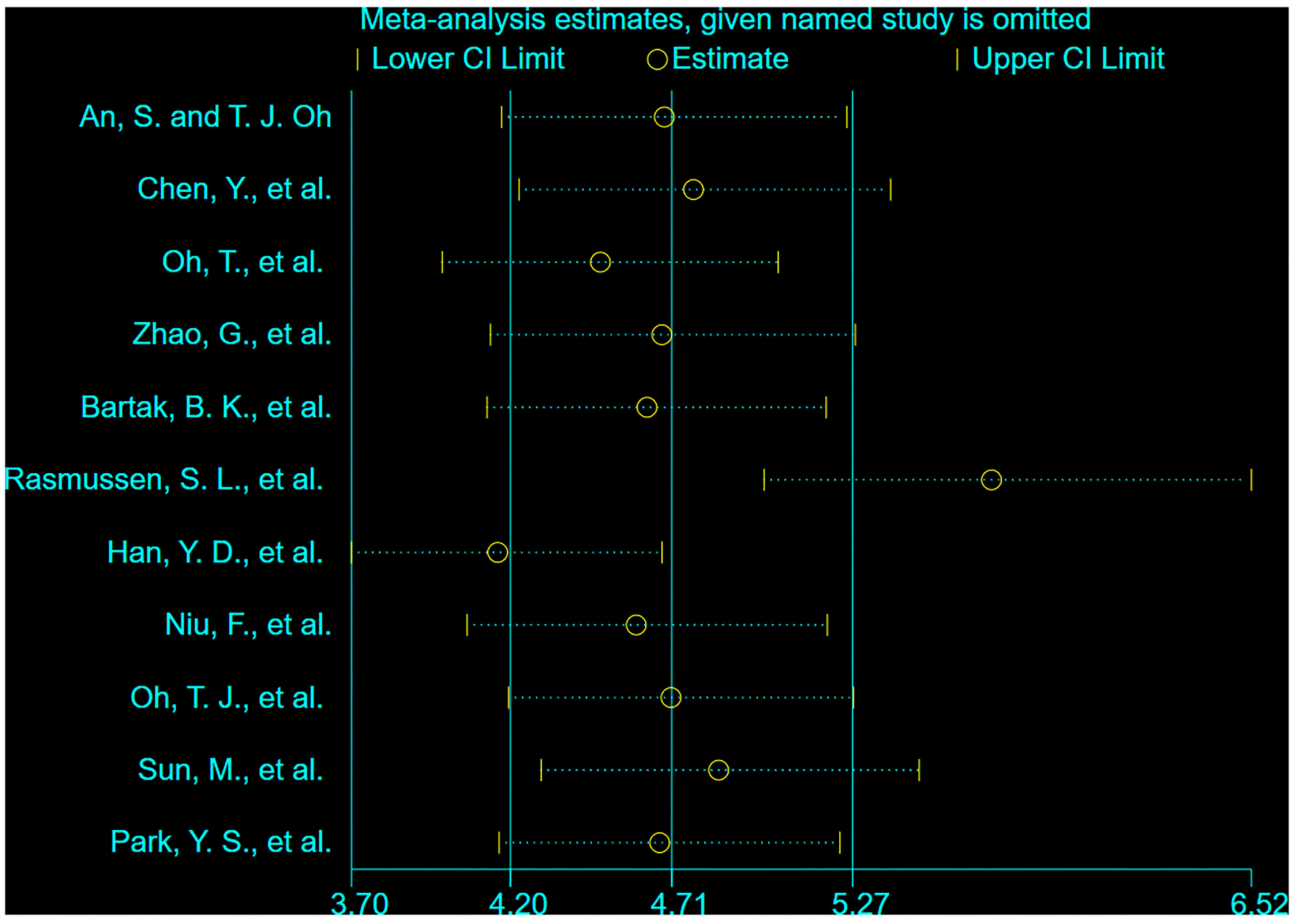

FIGURE 4 | The sensitivity analysis of the included studies.

value of p of 0.86 indicated that the distribution of studies was symmetric, and there was no systematic bias across all studies analyzed in this study (**Figure 5B**).

DISCUSSION

Although surgical techniques, neoadjuvant chemotherapy regimens, and new therapeutic strategies of various drugs have developed greatly in the field of CRC treatment in recent years, many patients with CRC still develop into advanced or metastatic CRC, leading to the poor prognosis of these patients (23). Therefore, it is urgently necessary to find more effective biomarkers in the early diagnosis and targeted treatment of CRC.

PCR has been widely used to detect DNA methylation. The first-generation PCR is based on the PCR amplification of DNA digested by methylation-sensitive restriction enzyme (24). Then, there is a more flexible method, called MSP, which uses bisulfite to treat DNA fragments, converts unmethylated cytosine into uracil through deamination, and designs primers for the transformed DNA. The quantitative detection ability of DNA methylation has been greatly enhanced by fluorescence quantitative PCR (MethyLight). In MethyLight, primers and probes are designed for bisulfite transformation, and DNA sequence and quantitative information can be obtained in a real-time manner (25). Despite its advantages over MSP, MethyLight is still susceptible to PCR inhibitors and has limited sensitivity to detect rare methylation reactions. Therefore, the traditional qMSP is often unable to achieve the required precision and sensitivity for methylation detection (26). The next generation sequencing (NGS) can also detect rare mutations but with a lower technical sensitivity than ddPCR, unless (potentially costly) high sequencing depth is reached (27). Here, we described a novel and highly sensitive assay for the detection of methylated DNA based on ddPCR. We detected 109 tissues of CRC using ddPCR and calculated PMR using the FM control DNA as a reference. The results showed that in 109 cases of CRC, 107 cases could be detected, and the sensitivity was 98.17%. Additionally, we calculated PMR using the number of copies/20 μl well. The median value of PMR in colorectal adenoma and patients with CRC was significantly higher compared with the normal individuals ($p < 0.001$). Moreover, we found that the PMR value was associated with the clinical staging of CRC. The difference of PMR in stage II and stage III was statistically significant ($p < 0.05$). The above-mentioned results indicated that SDC2 gene methylation had a

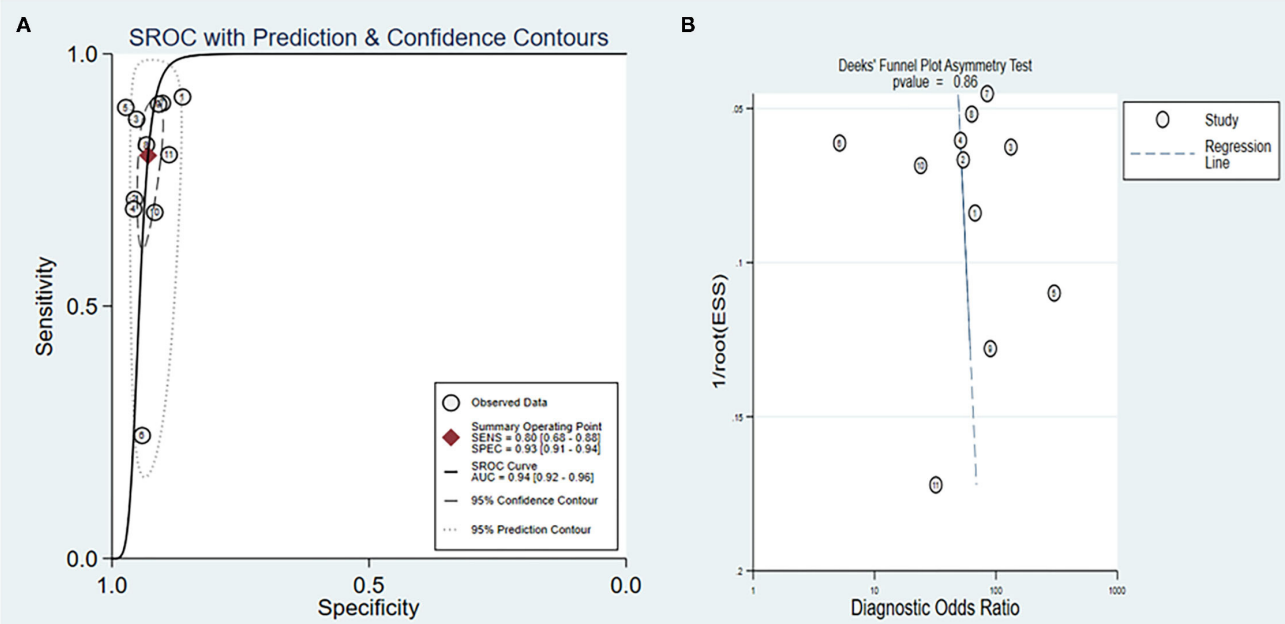

FIGURE 5 | (A) Summary ROC (SROC) curve for SDC2; **(B)** Deeks' funnel plot asymmetry test for all studies included in this meta-analysis.

certain value in the diagnosis of patients with CRC. To further prove this point, we conducted a meta-analysis.

In this meta-analysis, 11 articles meeting the inclusion criteria were included through database retrieval and manual retrieval, with a total of 2,523 samples. According to the QUADAS-2 quality evaluation standard, the quality of all the literature included in the evaluation was of medium and high quality, and the bias mainly focused on the selection of research objects and the two parts of the diagnostic test to be evaluated. The combined sensitivity, specificity, and DOR of 11 studies were 80, 93, and 52.46%, respectively, and the positive likelihood ratio and negative likelihood ratio were 11.36 and 0.22, respectively. We found that the sensitivity of ddPCR (98.17%) to detect SDC2 gene methylation was much higher compared with the quantitative PCR (qPCR). The positive likelihood ratio was more than 10, and the negative likelihood ratio was <0.1, indicating that the index had high accuracy. In addition, the AUC of the combined ROC curve of SDC2 gene methylation for cancer diagnosis was 0.94. It is generally considered that AUC of 0.5–0.7 indicates low diagnosis accuracy, 0.7–0.9 indicates medium diagnosis accuracy, and above 0.9 indicates high diagnosis accuracy (28). It indicated that SDC2 gene methylation had high efficiency for cancer diagnosis. To evaluate the potential impact of factors including sample sources, we further analyzed the factors of sample sources in different groups. We found that the sample source was the source of heterogeneity. It also suggested that the accuracy of methylation of the SDC2 gene in fecal samples was higher compared with plasma, serum, and intestinal lavage samples.

When the subgroup analysis was conducted to compare the differences between sample sources, we found an interesting question. It is well known that the difference between serum and plasma is the lack of clotting factors and fibrinogen due to the solidification process. However, according to the results of subgroup analysis, the sensitivity of serum and plasma was 63 and 75%, respectively. At present, the consensus is that plasma samples are more suitable for ctDNA analysis compared with serum in clinical application (29). Although serum usually produces higher levels of cell-free DNA (cfDNA) (30), it may contain the higher concentrations of DNA released during the dissolution of circulating leukocytes (such as, neutrophils), which may reduce the relative proportion of ctDNA (25). Serum collection requires coagulation at room temperature, which also increases the risk of cytolysis and ctDNA degradation. If the detection of SDC2 gene methylation can be applied in clinical practice, plasma collected from patients may be preferable to serum samples. However, we could not make a definitive conclusion due to the limited number of samples. Subsequent studies on relevant aspects should be carried out for verification.

There are some limitations in this study. First, we only used CRC stool samples to detect SDC2 gene methylation. This accurate and sensitive method should be focused on the methylation detection of cfDNA (serum, plasma, or urine) in future studies, providing a greater value for clinical application. Second, the number of studies used for the meta-analysis is small. Besides, we have strict requirements on the data included in the literatures, some authors of related articles did not provide the original data. The limited number of samples in this study might affect the results of meta-analysis. Third, the purpose of this study was to explore the methylation of the SDC2 gene as a biomarker of CRC detection. However, the cancer pathological stages and the limited number of samples in this study might affect meta-analysis results. Finally, this study we only used single marker (SDC2) for CRC detection. Studying a multiplex of markers could give more strength to this

study. For example, Mazouji, O's group and other researchers have demonstrated the diagnostic role of several non-invasive methylation biomarkers in CRC detection, such as WIF, NPY, PENK, SEPT9, VIM, Alx4, and others (31). The role of multi-target stool DNA testing in CRC diagnosis has attracted more and more attention. Imperiale, T. F's research showed that multi-target stool DNA testing can significantly detect more cancers in asymptomatic persons with an average risk of colorectal cancer (32).

CONCLUSIONS

Collectively, SDC2 gene methylation had high efficiency in the diagnosis of CRC, which might be used as an important reference index for CRC detection. The results of subgroup analysis showed that the diagnostic efficiency of SDC2 gene methylation in feces was higher compared with other sample sources. However, more investigations are still required in future research. We found that ddPCR was more sensitive and convenient to detect SDC2 gene methylation.

DATA AVAILABILITY STATEMENT

The raw data supporting the conclusions of this article will be made available by the authors, without undue reservation.

AUTHOR CONTRIBUTIONS

CY and YaZ created the figure and wrote the manuscript. YW, ZZ, MZ, HW, WC, ZS, YX, XZ, and YiZ provided comments and suggestions. All authors have read and approved the final manuscript.

FUNDING

This study was sponsored by the National Natural Science Foundation of China (81972005 and 81702815), the Natural Science Foundation of Shandong Province (ZR201910220159), Shandong Medical and Health Technology Development Project (2018WSB20002), and the Key Technology Research and Development Program of Shandong Province (2019GSF108247).

SUPPLEMENTARY MATERIAL

The Supplementary Material for this article can be found online at: https://www.frontiersin.org/articles/10.3389/fmed.2022.753545/full#supplementary-material

Supplementary Figure 1 | The copies/well of various methylation levels (100, 10, 1, 0.1, and 0%) over a range of concentrations (from 100 to 5 ng).

Supplementary Figure 2 | The study quality of included studies.

Supplementary Figure 3 | Forest plots for the SDC2 gene methylation tests on the detection of colorectal cancer (CRC). **(A)** Combined sensitivity and specificity forest plots. **(B)** Combined positive likelihood ratio and negative likelihood ratio forest plots. **(C)** Combined diagnostic ratio forest plots.

Supplementary Figure 4 | Subgroup analysis of the detection of CRC by methylation of SDC2 gene from different sample sources, such as stool, serum, and plasma. **(A–E)** The pooled sensitivity, specificity, positive likelihood, and negative likelihood of SDC2 gene methylation from different sample sources, respectively.

Supplementary Table 1 | The primer and probe sequences for assay.

Supplementary Table 2 | ddPCR cycling conditions.

REFERENCES

1. Weitz J, Koch M, Debus J, Höhler T, Galle PR, Büchler MW. Colorectal cancer. *Lancet.* (2005) 365:153–65. doi: 10.1016/S0140-6736(05)17706-X
2. Moody L, Dvoretskiy S, An R, Mantha S, Pan YX. The Efficacy of miR-20a as a Diagnostic and Prognostic Biomarker for Colorectal Cancer: A Systematic Review and Meta-Analysis. *Cancers (Basel).* (2019) 11:1111. doi: 10.3390/cancers11081111
3. Sun M, Liu J, Hu H, Guo P, Shan Z, Yang H, et al. A novel panel of stool-based DNA biomarkers for early screening of colorectal neoplasms in a Chinese population. *J Cancer Res Clin Oncol.* (2019) 145:2423–32. doi: 10.1007/s00432-019-02992-2
4. Brenner DE, Rennert G. Fecal DNA Biomarkers for the Detection of Colorectal Neoplasia: Attractive, but Is It Feasible? *JNCI: J Natl Cancer Inst.* (2005) 97:1107–9. doi: 10.1093/jnci/dji244
5. Lenhard K, Bommer GT, Asutay S, Schauer R, Brabletz T, Göke B, et al. Analysis of promoter methylation in stool: a novel method for the detection of colorectal cancer. *Clin Gastroenterol Hepatol.* (2005) 3:142–9. doi: 10.1016/S1542-3565(04)00624-X
6. Kanthan R, Senger JL, Kanthan SC. Fecal molecular markers for colorectal cancer screening. *Gastroenterol Res Pract.* (2012) 2012:184343. doi: 10.1155/2012/184343
7. Ao C, Gao L, Yu L. Research progress in predicting DNA methylation modifications and the relation with human diseases. *Curr Med Chem.* (2021) 29:822–36. doi: 10.2174/0929867328666210917115733
8. Luo H, Zhao Q, Wei W, Zheng L, Yi S, Li G, et al. Circulating tumor DNA methylation profiles enable early diagnosis, prognosis prediction, and screening for colorectal cancer. *Sci Transl Med.* (2020) 12:1–11. doi: 10.1126/scitranslmed.aax7533
9. Stephen B, Baylin PAJ. A decade of exploring the cancer epigenome - biological and translational implications. *Nat Rev Cancer.* (2011) 11:726–34. doi: 10.1038/nrc3130
10. Baylin SB, Jones PA. Epigenetic Determinants of Cancer. *Cold Spring Harb Perspect Biol.* (2016) 8:a019505. doi: 10.1101/cshperspect.a019505
11. Toyota M, Ho C, Ahuja N, Jair KW, Li Q, Ohe-Toyota M, et al. Identification of differentially methylated sequences in colorectal cancer by methylated CpG island amplification. *Cancer Res.* (1999) 59:2307–12.
12. Gai W, Sun K. Epigenetic Biomarkers in Cell-Free DNA and Applications in Liquid Biopsy. *Genes (Basel).* (2019) 10:32. doi: 10.3390/genes10010032
13. Brock MV, Hooker CM, Ota-Machida E, Han Y, Guo M, Ames S, et al. DNA methylation markers and early recurrence in stage I lung cancer. *N Engl J Med.* (2008) 358:1118–28. doi: 10.1056/NEJMoa0706550
14. Amiot A, Mansour H, Baumgaertner I, Delchier JC, Tournigand C, Furet JP, et al. The detection of the methylated Wif-1 gene is more accurate than a fecal occult blood test for colorectal cancer screening. *PLoS ONE.* (2014) 9:e99233. doi: 10.1371/journal.pone.0099233
15. Chen WD, Han ZJ, Skoletsky J, Olson J, Sah J, Myeroff L, et al. Detection in fecal DNA of colon cancer-specific methylation of the nonexpressed vimentin gene. *J Natl Cancer Inst.* (2005) 97:1124–32. doi: 10.1093/jnci/dji204
16. Park YS, Kim DS, Cho SW, Park JW, Jeon SJ, Moon TJ, et al. Analysis of Syndecan-2 Methylation in Bowel Lavage Fluid for the Detection of Colorectal Neoplasm. *Gut Liver.* (2018) 12:508–15. doi: 10.5009/gnl17357
17. Foltz G, Yoon JG, Lee H, Ryken TC, Sibenaller Z, Ehrich M, et al. DNA methyltransferase-mediated transcriptional silencing in malignant glioma: a

combined whole-genome microarray and promoter array analysis. *Oncogene.* (2009) 28:2667–77. doi: 10.1038/onc.2009.122
18. Hayashi M, Guerrero-Preston R, Sidransky D, Koch WM. Paired box 5 methylation detection by droplet digital PCR for ultra-sensitive deep surgical margins analysis of head and neck squamous cell carcinoma. *Cancer Prev Res (Phila).* (2015) 8:1017–26. doi: 10.1158/1940-6207.CAPR-15-0180
19. Sze MA, Abbasi M, Hogg JC, Sin DD. A comparison between droplet digital and quantitative PCR in the analysis of bacterial 16S load in lung tissue samples from control and COPD GOLD 2. *PLoS ONE.* (2014) 9:e110351. doi: 10.1371/journal.pone.0110351
20. Hindson BJ, Ness KD, Masquelier DA, Belgrader P, Heredia NJ, Makarewicz AJ, et al. High-throughput droplet digital PCR system for absolute quantitation of DNA copy number. *Anal Chem.* (2011) 83:8604–10. doi: 10.1021/ac202028g
21. Strain MC, Richman DD. New assays for monitoring residual HIV burden in effectively treated individuals. *Curr Opin HIV AIDS.* (2013) 8:106–10. doi: 10.1097/COH.0b013e32835d811b
22. Olmedillas-Lopez S, Garcia-Arranz M, Garcia-Olmo D. Current and Emerging Applications of Droplet Digital PCR in Oncology. *Mol Diagn Ther.* (2017) 21:493–510. doi: 10.1007/s40291-017-0278-8
23. Niu F, Wen J, Fu X, Li C, Zhao R, Wu S, et al. Stool DNA Test of Methylated Syndecan-2 for the Early Detection of Colorectal Neoplasia. *Cancer Epidemiol Biomarkers Prev.* (2017) 26:1411–9. doi: 10.1158/1055-9965.EPI-17-0153
24. Lissa D, Ishigame T, Noro R, Tucker MJ, Bliskovsky V, Shema S, et al. HOXA9 methylation and blood vessel invasion in FFPE tissues for prognostic stratification of stage I lung adenocarcinoma patients. *Lung Cancer.* (2018) 122:151–9. doi: 10.1016/j.lungcan.2018.05.021
25. Stengel D, Bauwens K, Sehouli J, Ekkernkamp A, Porzsolt F. A likelihood ratio approach to meta-analysis of diagnostic studies. *J Med Screen.* (2003) 10:47–51. doi: 10.1258/096914103321610806
26. Handsaker RE, Van Doren V, Berman JR, Genovese G, Kashin S, Boettger LM, et al. Large multiallelic copy number variations in humans. *Nat Genet.* (2015) 47:296–303. doi: 10.1038/ng.3200
27. Mansour H, Ouhajjou A, Bajic VB, Incitti R. Next-Generation Sequencing at High Sequencing Depth as a Tool to Study the Evolution of Metastasis Driven by Genetic Change Events of Lung Squamous Cell Carcinoma. *Front Oncol.* (2020) 10:1215. doi: 10.3389/fonc.2020.01215
28. Zuccotti M, Grant M, Monk M. Polymerase chain reaction for the detection of methylation of a specific CpG site in the G6pd gene of mouse embryos. *Methods Enzymol.* (1993) 225:557–67. doi: 10.1016/0076-6879(93)25036-2
29. Herman JG, Graff JR, Myöhänen S, Nelkin BD, Baylin SB. Methylation-specific PCR: a novel PCR assay for methylation status of CpG islands. *Proc Natl Acad Sci U S A.* (1996) 93:9821–6. doi: 10.1073/pnas.93.18.9821
30. Eads CA, Lord RV, Wickramasinghe K, Long TI, Kurumboor SK, Bernstein L, et al. Epigenetic patterns in the progression of esophageal adenocarcinoma. *Cancer Res.* (2001) 61:3410–8.
31. Mazouji O, Ouhajjou A, Incitti R, Mansour H. Updates on Clinical Use of Liquid Biopsy in Colorectal Cancer Screening, Diagnosis, Follow-Up, and Treatment Guidance. *Front Cell Dev Biol.* (2021) 9:660924. doi: 10.3389/fcell.2021.660924
32. Imperiale TF, Ransohoff DF, Itzkowitz SH, Levin TR, Lavin P, Lidgard GP, et al. Multitarget stool DNA testing for colorectal-cancer screening. *N Engl J Med.* (2014) 370:1287–97. doi: 10.1056/NEJMoa1311194

Conflict of Interest: The authors declare that the research was conducted in the absence of any commercial or financial relationships that could be construed as a potential conflict of interest.

Publisher's Note: All claims expressed in this article are solely those of the authors and do not necessarily represent those of their affiliated organizations, or those of the publisher, the editors and the reviewers. Any product that may be evaluated in this article, or claim that may be made by its manufacturer, is not guaranteed or endorsed by the publisher.

Copyright © 2022 Yue, Zhang, Wang, Zhang, Zhang, Wang, Chen, Shang, Xin, Zhang and Zhang. This is an open-access article distributed under the terms of the Creative Commons Attribution License (CC BY). The use, distribution or reproduction in other forums is permitted, provided the original author(s) and the copyright owner(s) are credited and that the original publication in this journal is cited, in accordance with accepted academic practice. No use, distribution or reproduction is permitted which does not comply with these terms.

frontiers in Surgery

ORIGINAL RESEARCH
published: 17 March 2022
doi: 10.3389/fsurg.2022.819018

The Prognostic Significance and Gene Expression Characteristics of Gastric Signet-Ring Cell Carcinoma: A Study Based on the SEER and TCGA Databases

Junren Ma[1†], *Yan Meng*[1†], *Xin Zhou*[1,2*], *Limei Guo*[3*] *and Wei Fu*[1,2*]

[1] *Department of General Surgery, Peking University Third Hospital, Beijing, China,* [2] *Peking University Third Hospital Cancer Center, Beijing, China,* [3] *Department of Pathology, Peking University Third Hospital, Beijing, China*

OPEN ACCESS

Edited by:
Qi Liu,
Fudan University, China

Reviewed by:
Eliana Saul Furquim Werneck Abdelhay,
National Cancer Institute (INCA), Brazil
Chih-Yang Wang,
Taipei Medical University, Taiwan

***Correspondence:**
Xin Zhou
zhouxinasd@sina.cn
Limei Guo
guolimei@bjmu.edu.cn
Wei Fu
fuwei@bjmu.edu.cn

[†] *These authors have contributed equally to this work*

Specialty section:
This article was submitted to Surgical Oncology, a section of the journal Frontiers in Surgery

Received: *20 November 2021*
Accepted: *07 February 2022*
Published: *17 March 2022*

Citation:
Ma J, Meng Y, Zhou X, Guo L and Fu W (2022) The Prognostic Significance and Gene Expression Characteristics of Gastric Signet-Ring Cell Carcinoma: A Study Based on the SEER and TCGA Databases. Front. Surg. 9:819018. doi: 10.3389/fsurg.2022.819018

Purpose: This study is based on the Surveillance, Epidemiology, and End Results (SEER) program to explore the prognostic differences between signet-ring cell carcinoma (SRC) and intestinal-type gastric carcinoma (ITGC). This study is also based on gene sequencing data from The Cancer Genome Atlas (TCGA) to identify unique genetic contributions to the prognostic differences between the two subtypes of gastric cancer.

Patients and Methods: The clinical data were based on the SEER database from 2004 to 2015. Kaplan–Meier (KM) curves were used to compare 5-year overall survival (OS), and Cox regression was used for univariate and multivariate analyses. Gene expression profiles were obtained from TCGA database, and differentially expressed genes (DEGs) were screened. Functional enrichment analysis, protein interaction and survival analysis will be further carried out. Genes of interest were verified by the Human Protein Atlas, immunohistochemistry, and encyclopedia of Cancer Cell Lines (CCLE). The relationship between genes of interest and immune cell infiltration was also analyzed by Tumor Immune Estimation Resource (TIMER).

Results: Compared with ITGC patients, SRC patients were more likely to be female, tended to be younger, and have a greater tumor distribution in the middle and lower stomach ($p < 0.01$). SRCs showed a significantly better prognosis than ITGCs ($p < 0.01$) in early gastric cancer (EGC), while the prognosis of SRCs was significantly worse than ITGCs ($p < 0.05$) in advanced gastric cancer (AGC). A total of 256 DEGs were screened in SRCs compared to ITGCs, and the enrichment analysis and protein interactions revealed that differential genes were mainly related to extracellular matrix organization. Thrombospondin1 (THBS1) and serpin peptidase inhibitor, clade E, member 1 (SERPINE1) are significantly differentially expressed between SRC and ITGC, which has been preliminarily verified by immunohistochemistry and open-source databases. THBS1 and SERPINE1 are also associated with multiple immune cell infiltrates in gastric cancer.

Conclusions: There were significant differences in the clinicopathological features and prognosis between SRC and ITGC. These results suggest that SRC and ITGC may be two distinct types of tumors with different pathogeneses. We found many

codifferentially expressed genes and important pathways between SRC and ITGC. THBS1 and SERPINE1 were significantly differentially expressed in the two types of gastric cancer, and may have potentially important functions.

Keywords: signet-ring cell carcinoma, intestinal-type gastric cancer, clinical stages, prognostic factor, genomic profile

INTRODUCTION

With the advancements to the standard treatment of *Helicobacter pylori* (HP), the overall incidence of gastric cancer is declining (1). However, the incidence of signet-ring cell carcinoma (SRC) is increasing each year (2). SRC is a subtype of gastric cancer with a large amount of mucus (3) and is generally considered to have a poor prognosis (4, 5). In recent years, some studies in Asia have shown that the prognosis of SRC is closely related to clinical stage (6–13). SRC has a good prognosis in the early stage and a relatively worse prognosis in the advanced stage. Only a few western studies have analyzed SRC vs. non-signet ring cell carcinoma (NSRC), but the preliminary conclusion is not consistent with that of Eastern countries (14, 15). Intra-tumor heterogeneity may lead to unexpected bias; hence, the need to compare SRC with intestinal-type gastric carcinoma (ITGC). Meanwhile, the expression characteristics of SRC at the gene level have not been specifically and clearly explained. The purpose of this study was to investigate the prognostic significance of SRC and ITGC based on the Surveillance, Epidemiology, and End Results (SEER) database and the gene expression characteristics of both types of cancer based on The Cancer Genome Atlas (TCGA) database.

METHODS

Clinical Data

Clinical data were obtained from 18 SEER registries, and records from 2004 to 2007 were analyzed for this study. Data used for analysis included age, sex, race, tumor location, surgical treatment, pathological stage, lymph node metastasis status, and survival status. SRC is defined as adenocarcinoma in which more than 50% of the tumor consists of isolated or small groups of malignant cells containing intracytoplasmic mucin (3). Early gastric cancer (EGC) is defined as a tumor limited to the mucosa or submucosa, regardless of lymph nodal status (16). Advanced gastric cancer (AGC) is defined as tumor invasion beyond the submucosa. The International Classification of Diseases (ICD) code 8490/3 was used to identify SRC patients, while the codes 8140/3, 8144/3, 8210/3, 8211/3, 8260/3, 8261/3, 8262/3, and 8283/3 were used for ITGC patients. For the 57,200 patients with SRC and ITGC, the exclusion criteria were as follows: unknown surgery status (n = 32,341), unknown staging (n = 908), unknown differential (n = 1,481), race, tumor size, unknown tumor location (n = 4,250), survival time < 1 month (n = 1,031), <18 years old (n = 4), M1 (n = 1,662) (**Figure 1**). The final analysis patients (N = 16,123) were divided into three groups according to the WHO histological type: well-to-moderately differentiated adenocarcinoma (WMD, n = 6,107), poorly differentiated adenocarcinoma (PD, n = 6,518), and SRC (n = 3,498).

RNA Sequencing Data

The RNA sequencing data of SRC and ITGC patients were obtained from the TCGA database. The inclusion criteria of gastric cancer samples were as follows: (i) gene expression profiling of SRC and ITGC were available in the dataset; (ii) the ICD code 8490/3 was used to identify SRC patients, while the codes 8144/3, 8211/3, and 8260/3 were used for ITGC patients. Finally, 12 SRC patients and 150 ITGC patients were enrolled in this study. Our workflow for the bioinformatics analysis of TCGA databases is illustrated in **Figure 2**.

Genome Sequencing Data Analysis

The RNA sequencing results of enrolled patients were obtained from TCGA data portal (https://tcga-data.nci.nih.gov/tcga/). They were normalized and processed with TCGAbiolinks of R software (17). The TCGAbiolinks principle of differential analysis was first used to convert the count matrix into an edgeR object (18), and then it assigned the same discrete estimate to each gene. Then, a pairwise test was used to identify the differential expression patterns between SRC and ITGC. Finally, the error detection rate (FDR) correction was used to obtain the output and identify differentially expressed genes (DEGs). The parameters set for the differential expression analysis were FDR < 0.05 with $|Log_2FC| > 1$.

Analysis and Validation of Interest Genes

Gene Ontology (GO) and Kyoto Encyclopedia of Genes and Genomes (KEGG) pathway enrichment analyses and protein–protein interaction (PPI) analysis were then performed using Metascape (http://metascape.org) (19). Kaplan–Meier (KM) plots of the genes of interest were constructed. The overall survival (OS) was analyzed, and the log-rank test was performed. Pearson's test was used for pairwise gene expression correlation analysis of the genes of interest. A $p < 0.05$ was considered to be significant.

Immunohistochemical methods were used to verify the genes of interest in postoperative pathological tissues of gastric cancer in our hospital. The pathological tissues were obtained from postoperative specimens from Peking University Third Hospital and included SRC and ITGC tissues. These samples were evaluated by an independent pathologist. Tissues (5 mm thick) were deparaffinized and treated with 3% H_2O_2-CH_3OH for 15 min to block endogenous peroxidase. Samples were submerged in a pH 6.0 or 9.0 buffer in a pressure cooker for antigen retrieval and then incubated at 37°C

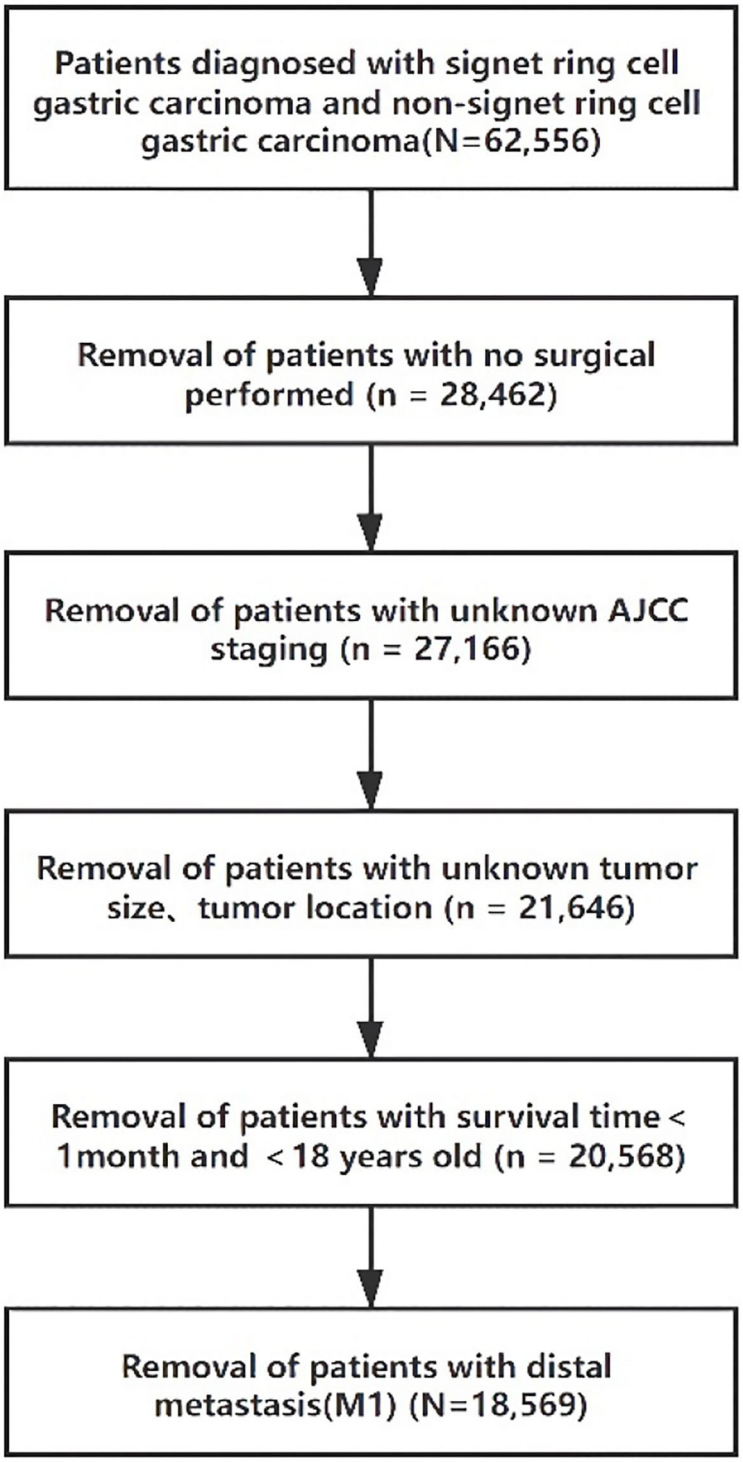

FIGURE 1 | Flow diagram of selected cases in the surveillance, epidemiology, and end results database.

for 2 h with antibodies against thrombospondin 1 (Abcam, ab1823, 1:50) and PAI1 (Abcam, ab125687, 1:50). After washing with phosphate-buffered saline (PBS), the sections were incubated with horseradish peroxidase (HRP)-conjugated IgG (ZSGB—Bio, PV-6000) at room temperature for 30 min and then stained with a 3,3N-diaminobenzidine tetrahydrochloride

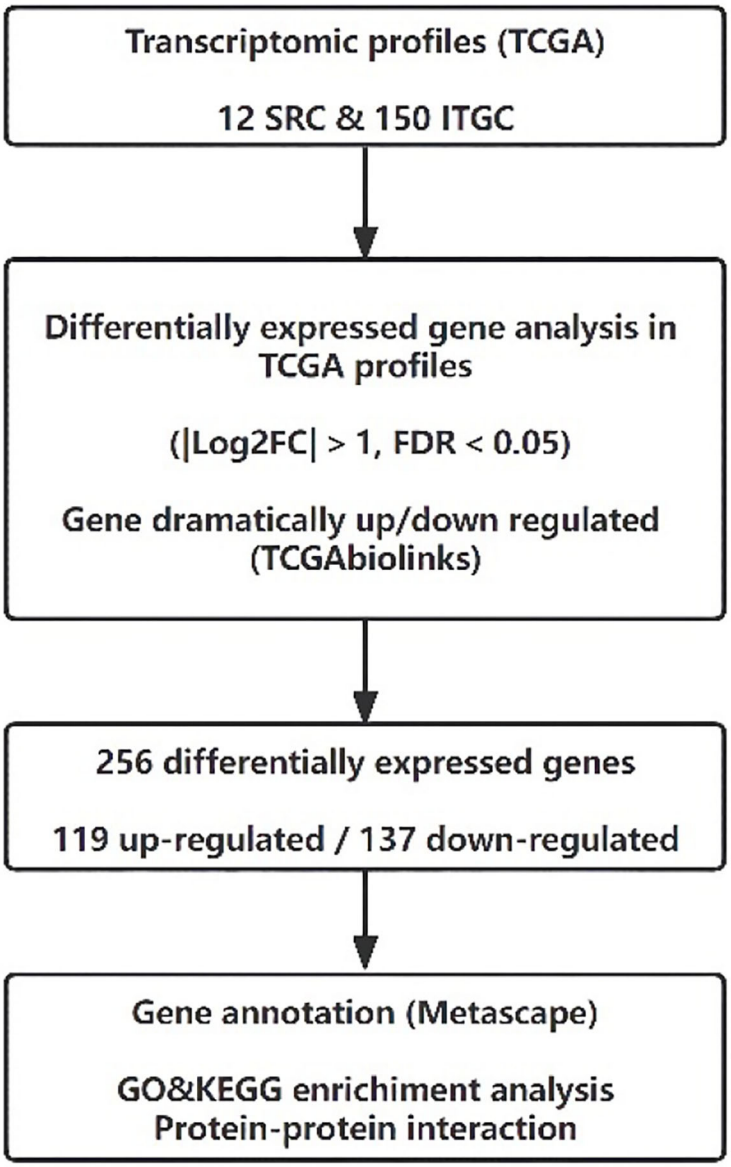

FIGURE 2 | Flow diagram of transcriptomic profiles in The Cancer Genome Atlas database.

(DAB) detection system kit (ZSGB-Bio, ZLI-9018). Protein expression and localization were detected under light microscopy and analyzed by Nikon Diagram Program (NDP) view (version 2.6.8).

We used the Human Protein Atlas and Encyclopedia of Cancer Cell Lines (CCLE) databases to verify the expression of genes of interest in pathological tumor tissues and tumor cell lines. We also use Tumor Immune Estimation Resource (TIMER) (http://cistrome.org/TIMER) (20) to further explore the clinical effects of differential genes and different immune invasions infiltrates.

Statistical Analysis

Continuous variables and categorical variables were compared by *t*-test and chi-square analysis, respectively. The KM method was used to calculate the survival rate, and then the survival curves were compared by the log-rank test. Univariate and multivariate analyses were performed by the Cox regression risk model. All data analyses were performed by SPSS version 24.0.

This study conforms to the Strengthening the reporting of cohort studies in surgery (STROCSS) criteria (21). Because all the original data come from open-source databases, ethical review is unnecessary.

TABLE 1 | Comparison of clinicopathological characteristics in early gastric cancer.

	SRC 75,417.7%	WMD 240,056.2%	*p1* (SRC&WMD)	PD 111,726.1%	*p2* (SRC&PD)
Age (Mean ± SD)	63.4 ± 13.5	70.6 ± 10.6	<0.01	68.9 ± 11.2	<0.01
≤60 years old	29,038.5%	42,817.8%		24,421.8%	
>60 years old	46,461.5%	197,282.2%		87,378.2%	
Gender			<0.01		<0.01
Male	35,947.6%	159,766.5%		70,763.3%	
Female	39,552.4%	80,333.5%		41,036.7%	
Size (Mean ± SD)	22.8 ± 19.4	22.3 ± 18.7	0.541	26.3 ± 19.8	<0.01
≤2 cm	43,858.1%	139,658.2%		54,849.1%	
>2 cm	31,641.9%	100,441.8%		56,950.9%	
Race			0.412		0.423
White	49,365.4%	162,567.7%	0.239	70,763.3%	0.349
Black	8,911.8%	25,210.5	0.324	14,212.7%	0.543
American Indian	60.8%	150.6%	0.612	70.6%	0.657
Asian/Pacific Islander	16,622%	50,821.2%	0.623	26,123.4%	0.489
Location			<0.01		<0.01
Upper	12,416.4%	95,539.8%	<0.01	38,334.3%	<0.01
Middle	29,238.7%	56,723.6%	<0.01	32,328.9%	<0.01
Lower	30,240.1%	79,633.2%	<0.01	36,232.4%	<0.01
Whole	364.8%	823.4%	0.093	494.4%	0.671
pN			<0.01		<0.01
N–	60,480.1%	209,687.3%	<0.01	83,474.7%	<0.01
N+	15,019.9%	30,412.7%	<0.01	28,325.3%	<0.01

SRC, signet ring cell carcinoma; WMD, well-to-moderately differentiated adenocarcinoma; PD, poorly differentiated adenocarcinoma; SD, standard deviation.

RESULTS

Clinicopathological Characteristics

The clinicopathologic characteristics of patients with EGC and AGC are shown in **Tables 1**, **2**, respectively. Of the 16,123 gastric cancer patients, 4,271 patients (26.5%) had EGC, and 11,852 patients (73.5%) had AGC. There was a statistically significant difference ($p < 0.01$) in histological type between the EGC patients and the AGC patients.

In patients with EGC, SRC was more common in younger patients and female patients than WMD (age: $p < 0.01$; sex: $p < 0.01$) and PD (age: $p < 0.01$; sex: $p < 0.01$). There was no significant difference in tumor size between the SRC and the WMD, but tumor size was smaller in SRC than PD ($p < 0.01$). Furthermore, there were more middle and lower third tumor locations and less upper third locations in SRC ($p < 0.01$). The SRC patients had less lymph node metastasis (LNM) than PD ($p < 0.01$) patients and more LNM than WMD ($p < 0.01$) patients.

In patients with AGC, SRC was more common in younger, female patients, and the tumor size was larger than that of WMD (age: $p < 0.01$; sex: $p < 0.01$; size: $p < 0.01$) and PD (age: $p < 0.01$; sex: $p < 0.01$; size: $p < 0.01$). There were more Asian/Pacific islanders in the SRC group than in the WMD group ($p = 0.016$). SRCs were more frequently located in the middle and lower third of the stomach than WMDs ($p < 0.01$) and PDs ($p < 0.01$), and SRCs presented a more diffuse infiltration growth pattern ($p < 0.01$). In the tumor stage (T) and lymph node (N) stage, the proportion of SRC patients with stage T4 and N3 disease was higher than that of WMD ($p < 0.01$) and PD ($p < 0.01$) patients.

Survival

The median follow-up was 35 months. The KM curves for different clinical stages are shown in **Figure 3**. In general, the OS of WMD was significantly better than that of SRC and PD ($p < 0.01$), and there was no significant difference between SRC and PD.

Notably, when the patients were divided into EGC and AGC by pathological stage, SRC showed a significantly better prognosis than both WMD and PD in EGC ($p < 0.01$). However, this result was reversed in AGC; that is, SRC demonstrated a significantly worse prognosis than WMD ($p < 0.01$) and PD ($p = 0.041$). Regardless of EGC or AGC, PD has a worse prognosis than WMD ($p < 0.01$).

Mortality Predictors

We performed an unadjusted analysis of OS for EGC and AGC and performed a multivariate analysis using Cox's proportional hazard model after adjustments for sex, age, race, location, tumor size, and pathological stage.

In EGC, the univariate analysis showed that SRC was associated with a reduction in mortality compared to WMD (*HR*: 0.702; 95% *CI*: 0.611–0.807; $p < 0.01$) and PD (*HR*: 0.628; 95%

TABLE 2 | Comparison of clinicopathological characteristics in advanced gastric cancer.

	SRC 2744,23.2%	WMD 3707,31.2%	*P1* (SRC&WMD)	PD 5401,45.6%	*P2* (SRC&PD)
Age (Mean ± SD)	62.2 ± 13.5	68.6 ± 11.5	<0.01	67.8 ± 12.4	<0.01
≤60 years old	120,343.8%	87,523.6%		147,227.3%	
>60 years old	154,156.2%	283,276.4%		392,972.7%	
Gender			<0.01		<0.01
Male	148,354%	262,370.8%		359,966.6%	
Female	126,146%	108,429.2%		180,233.4%	
Size (Mean ± SD)	56.2 ± 36.3	47.0 ± 24.6	<0.01	51.8 ± 27.1	<0.01
≤5 cm	144,852.8%	237,063.9%		312,057.8%	
>5 cm	129,647.1%	133,736.1%		228,142.2%	
Race			0.062		0.486
White	1857,67.7%	2541,68.5%	0.457	3696,68.4%	0.488
Black	350,12.8%	521,14.1%	0.127	686,12.7%	0.946
American Indian	23,0.8%	37,1%	0.462	29,0.5%	0.137
Asian/Pacific Islander	514,18.7%	608,16.4%	0.016	990,18.3%	0.654
Location			<0.01		<0.01
Upper	56,720.7%	153,241.3%	<0.01	196,336.3%	<0.01
Middle	87,631.9%	86,923.4%	<0.01	144,626.8%	<0.01
Lower	97,635.6%	111,430.1%	<0.01	162,130%	<0.01
Whole	32,511.8%	1,925.2%	<0.01	3,716.9%	<0.01
pT			<0.01		<0.01
T2	38,414%	95,725.8%	<0.01	89,416.6%	<0.01
T3	119,943.7%	195,452.7%	<0.01	283,152.4%	<0.01
T4	116,142.3%	79,621.5%	<0.01	167,631%	<0.01
pN			<0.01		<0.01
N0	68,825.1%	152,441.1%	<0.01	147,627.3%	0.036
N1	83,230.3%	140,137.8%	<0.01	207,638.4%	<0.01
N2	62,722.8%	52,914.3%	<0.01	113,921.1%	0.056
N3	59,721.8%	2,536.8%	<0.01	71,013.1%	<0.01

SRC, signet ring cell carcinoma; WMD, well-to-moderately differentiated adenocarcinoma; PD, poorly differentiated adenocarcinoma; SD, standard deviation.

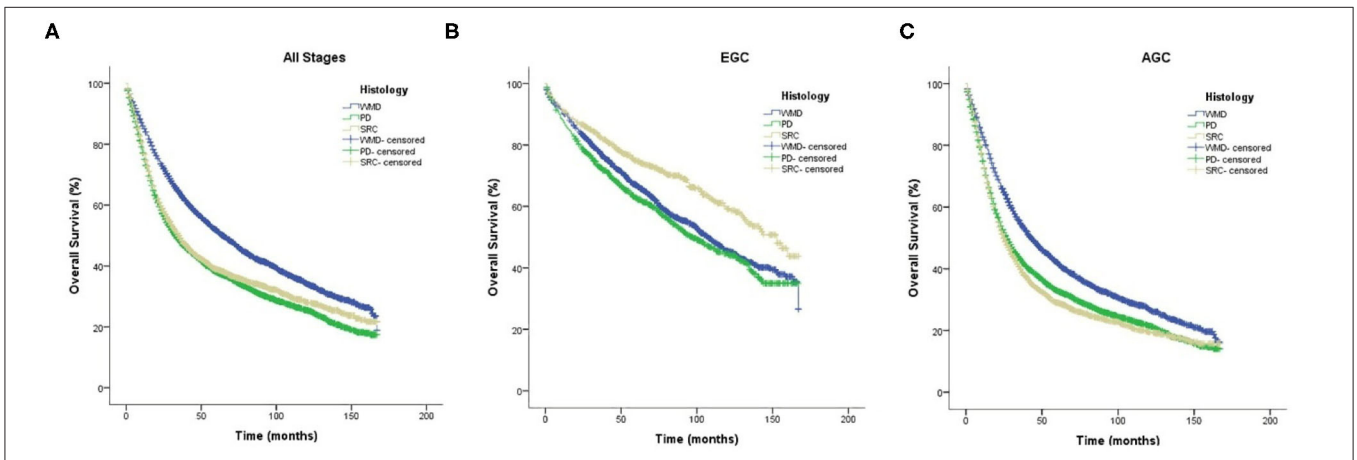

FIGURE 3 | Kaplan–Meier survival curves comparing overall survival in signet-ring cell carcinoma and non-signet-ring cell carcinoma are shown for **(A)** all stages, **(B)** early gastric cancer, and **(C)** advanced gastric cancer.

TABLE 3 | Univariate and multivariate analyses of prognostic factors for overall survival in early gastric cancer.

	Univariate			Multivariate		
	HR	**95%CI**	***p***	**HR**	**95%CI**	***p***
Gender (Male)	1.226	1.111∼1.353	<0.01	1.204	1.088∼1.332	<0.01
Age (≤60)	0.379	0.328∼0.437	<0.01	0.363	0.313∼0.42	<0.01
Race						
White (vs. API)	1.547	1.363∼1.756	<0.01	1.501	1.314∼1.715	<0.01
Location						
Middle (vs. Upper)	0.794	0.705∼0.895	<0.01	0.828	0.729∼0.94	<0.01
Lower (vs. Upper)	0.817	0.730∼0.913	<0.01	0.86	0.761∼0.972	<0.01
Histology						
SRC (vs. ITGC)	0.677	0.592∼0.775	<0.01	0.826	0.719∼0.949	<0.01
SRC (vs. WMD)	0.702	0.611∼0.807	<0.01	0.859	0.744∼0.992	0.039
SRC (vs. PD)	0.628	0.539∼0.730	<0.01	0.767	0.657∼0.896	<0.01
Tumor size (≤2 cm)	0.793	0.722∼0.87	<0.01	0.893	0.811∼0.984	0.022
pN (N–)	0.693	0.571∼0.715	<0.01	0.647	0.575∼0.727	<0.01

HR, hazard ratio; CI, Confidence interval; SRC, signet ring cell carcinoma; WMD, well-to-moderately differentiated adenocarcinoma; PD, poorly differentiated adenocarcinoma; ITGC, intestinal-type gastric carcinoma; API, Asian/Pacific Islander.

TABLE 4 | Univariate and multivariate analyses of prognostic factors for overall survival in advanced gastric cancer.

	Univariate			Multivariate		
	HR	**95% CI**	***p***	**HR**	**95% CI**	***p***
Gender (Male)	1.021	0.976∼1.068	0.366	1.013	0.967∼1.061	0.589
Age (≤60)	0.710	0.676∼0.745	<0.01	0.620	0.590∼0.652	<0.01
Race						
White (vs. API)	1.276	1.202∼1.355	<0.01	1.292	1.216∼1.374	<0.01
Location						
Middle (vs. Upper)	0.877	0.829∼0.928	<0.01	0.822	0.775∼0.871	<0.01
Lower (vs. Upper)	0.969	0.919∼1.022	0.245	0.904	0.855∼0.956	<0.01
Histology						
SRC (vs. ITGC)	1.178	1.12∼1.238	<0.01	1.126	1.068∼1.188	<0.01
SRC (vs. WMD)	1.374	1.294∼1.458	<0.01	1.259	1.182∼1.182	<0.01
SRC (vs. PD)	1.058	1.002∼1.116	0.041	1.058	1.001∼1.119	0.048
Tumor size (≤5 cm)	0.805	0.771∼0.841	<0.01	0.965	0.922∼1.01	0.122
pT						
T3 (vs. T2)	1.564	1.468∼1.667	<0.01	1.343	1.258∼1.433	<0.01
T4 (vs. T2)	2.274	2.127∼2.430	<0.01	1.843	1.719∼1.976	<0.01
pN						
N1 (vs. N0)	1.519	1.437∼1.605	<0.01	1.397	1.321∼1.478	<0.01
N2 (vs. N0)	1.915	1.796∼2.041	<0.01	1.731	1.620∼1.849	<0.01
N3 (vs. N0)	2.789	2.601∼2.992	<0.01	2.442	2.269∼2.628	<0.01

HR, hazard ratio; CI, Confidence interval; SRC, signet ring cell carcinoma; WMD, well-to-moderately differentiated adenocarcinoma; PD, poorly differentiated adenocarcinoma; ITGC, intestinal-type gastric carcinoma; API, Asian/Pacific Islander.

CI: 0.539–0.730; $p < 0.01$), as shown in **Table 3**. Multivariate analysis showed that SRC was an independent protective factor for OS in EGC compared with WMD (*HR*: 0.859, 95% *CI*: 0.744–0.992, $p = 0.039$) and PD (*HR*: 0.767, 95% *CI*: 0.657–0.896, $p < 0.01$).

Meanwhile, in AGC, the univariate analysis showed that SRC was associated with increased mortality compared to WMD (*HR*: 1.374; 95% *CI*: 1.294–1.458; $p < 0.01$) and PD (*HR*: 1.058; 95% *CI*: 1.002–1.116; $p = 0.041$), as shown in **Table 4**. Multivariate analysis showed that SRC was an independent risk predictor for OS in AGC compared with WMD (*HR*: 1.259, 95% *CI*: 1.182–1.182, $p < 0.01$) and PD (*HR*: 1.058, 95% *CI*: 1.001–1.119, $p = 0.048$).

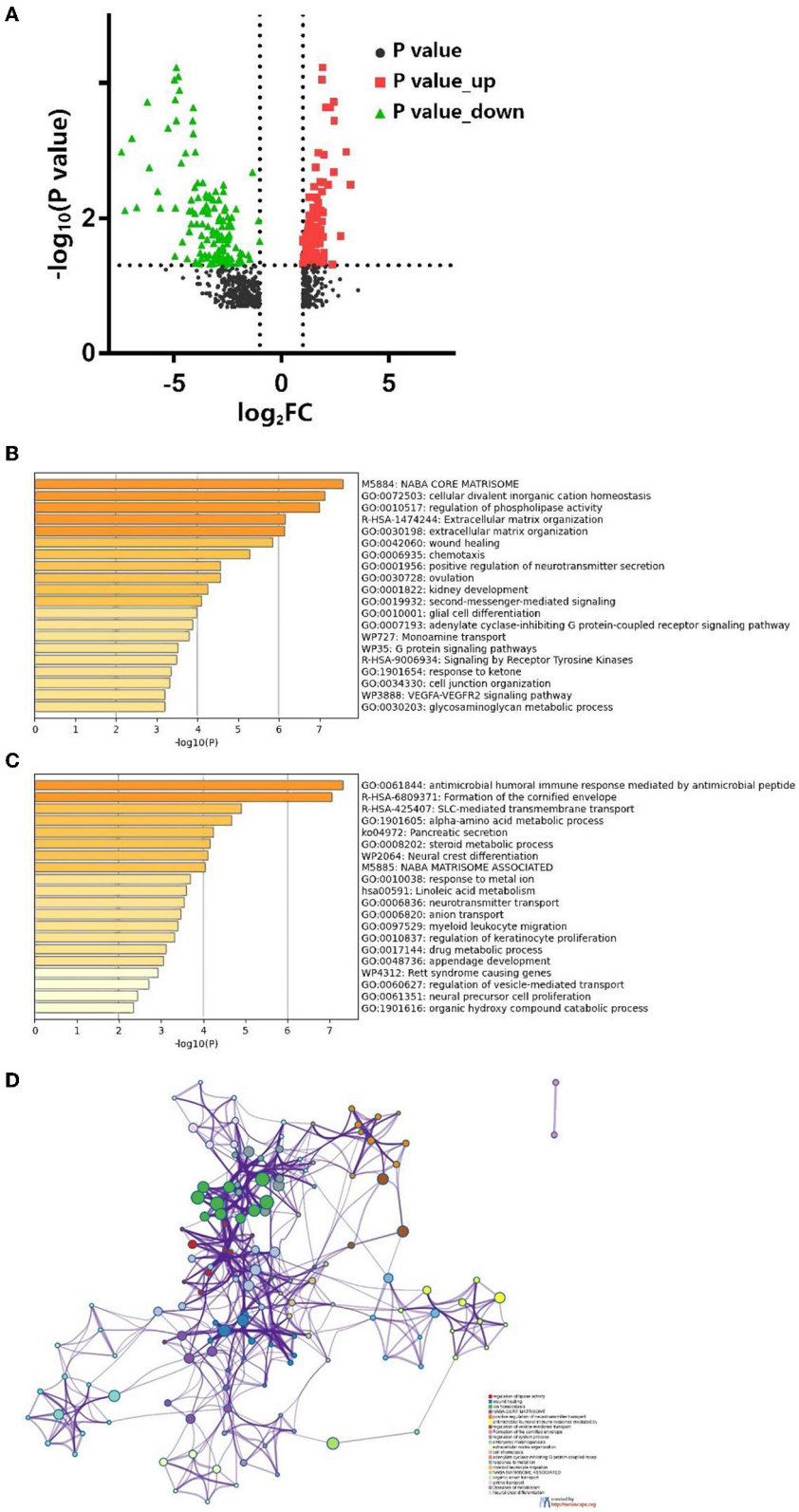

FIGURE 4 | (A) Volcano map of differentially expressed genes. Bar graph of enriched terms across differentially expressed genes are shown for **(B)** up-regulate, **(D)** down-regulate, and **(C)** network of enriched terms colored by cluster ID, each node represents an enriched term. Nodes that share the same cluster ID are typically close to each other and terms with a similarity >0.3 are connected by edges.

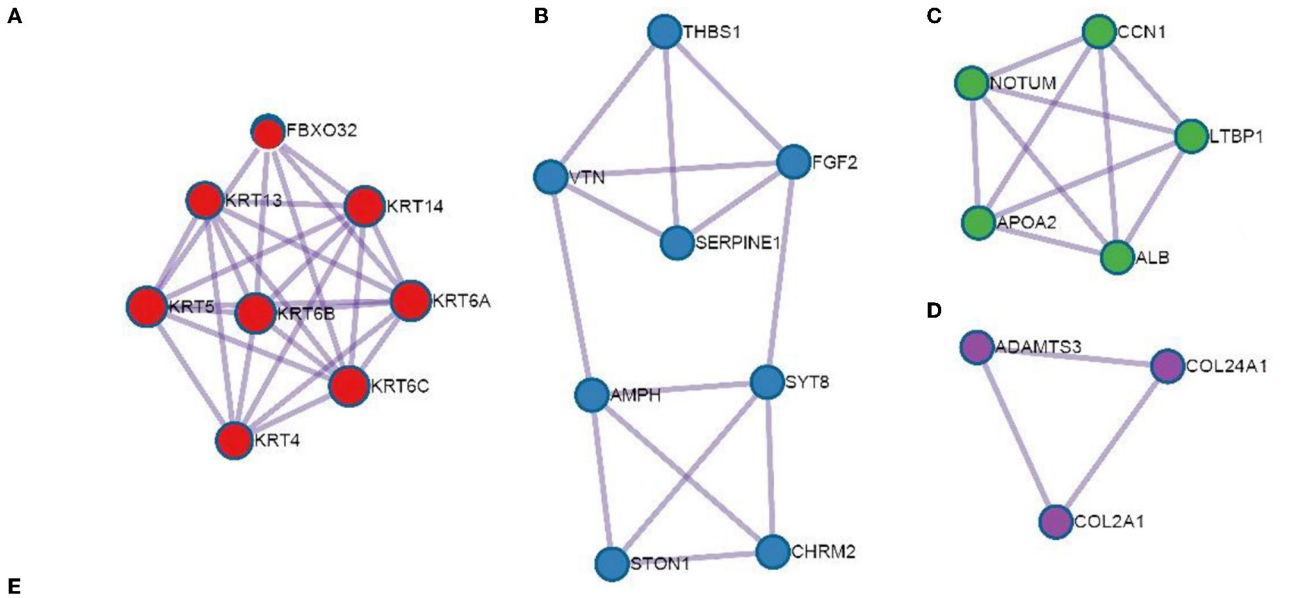

E

Network	Annotation
MCODE_ALL	R-HSA-6809371: Formation of the cornified envelope R-HSA-1474244: Extracellular matrix organization R-HSA-6805567: Keratinization
MCODE_1	R-HSA-6809371: Formation of the cornified envelope R-HSA-6805567: Keratinization
MCODE_2	GO:0006897: endocytosis GO:0061045: negative regulation of wound healing GO:1903035: negative regulation of response to wounding
MCODE_3	R-HSA-8957275: Post-translational protein phosphorylation R-HSA-381426: Regulation of Insulin-like Growth Factor (IGF) transport and uptake by Insulin-like Growth Factor Binding Proteins (IGFBPs)
MCODE_4	R-HSA-1650814: Collagen biosynthesis and modifying enzymes R-HSA-1474290: Collagen formation R-HSA-1474244: Extracellular matrix organization

FIGURE 5 | Protein–protein interaction network is shown for: **(A)** MCODE 1, **(B)** MCODE 2, **(C)** MCODE 3, and **(D)** MCODE 4. The resultant network contains the subset of proteins that form physical interactions with at least one other member in the list. If the network contains between 3 and 500 proteins, the Molecular Complex Detection (MCODE) algorithm has been applied to identify densely connected network components. Gene ontology enrichment analysis was applied to each MCODE network for **(E)**.

Gene Expression Signatures of SRC and ITGC

We used the edgeR package (18) ($|\text{Log}_2\text{FC}| > 1$, FDR < 0.05) to identify DEGs. In total, 256 codifferentially expressed genes (119 upregulated and 137 downregulated) were found and are shown in volcano plots (**Figure 4A**). Further functional annotation was performed on these 256 genes to determine the meaningful biological processes in SRC. A bar graph of the enriched terms across the differentially expressed genes is shown in **Figures 4B,D**, and the network was visualized using Cytoscape (22) (**Figure 4C**).

The results revealed that the biological processes primarily associated with the upregulated genes included the NABA core matrisome cellular divalent inorganic cation homeostasis, the regulation of phospholipase activity and extracellular matrix (ECM) organization. Furthermore, the downregulated genes were associated with the antimicrobial humoral immune response mediated by antimicrobial peptides and the formation

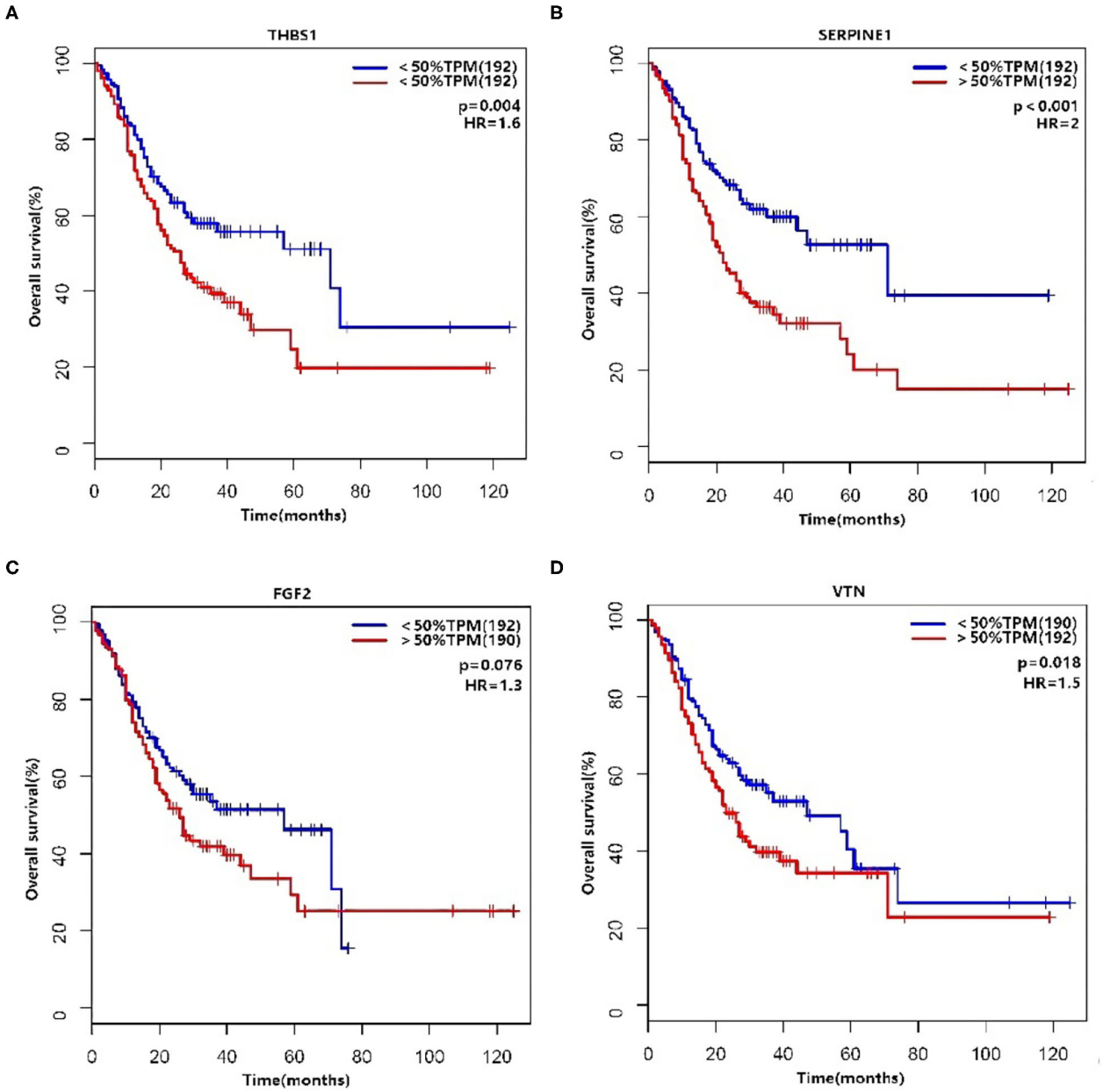

FIGURE 6 | Survival analysis are shown for **(A)** THBS1, **(B)** SERPINE1, **(C)** FGF2, and **(D)** VTN.

of the cornified envelope. PPI enrichment analysis was performed with the following databases: Search tool for the retrival of interacting genes/proteins (STRING) (23), The Biological General Repository for Interaction Datasets (BioGrid) (24), OmniPath (25), and InWeb_IM (25). The molecular complex detection (MCODE) algorithm (26) was used to cluster the PPI network (**Figures 5A–D**) and GO enrichment analysis was applied to each MCODE network (**Figure 5E**). We found that the protein interactions were mainly related to the formation of the cornified envelope, ECM organization, and keratinization.

There was an interaction between Thrombospondin1 (THBS1), serpin peptidase inhibitor, clade E, member 1 (SERPINE1), VTN, and FGF2. We used the median to classify high and low expression in terms of the expression level (TPM, transcripts per million). The KM method was used to calculate the survival rate between them (**Figure 6**), and then the survival curves were compared by the log-rank test. We found that THBS1, SERPINE1, and VTN were statistically related to OS ($p < 0.05$). The Pearson correlation coefficient was used

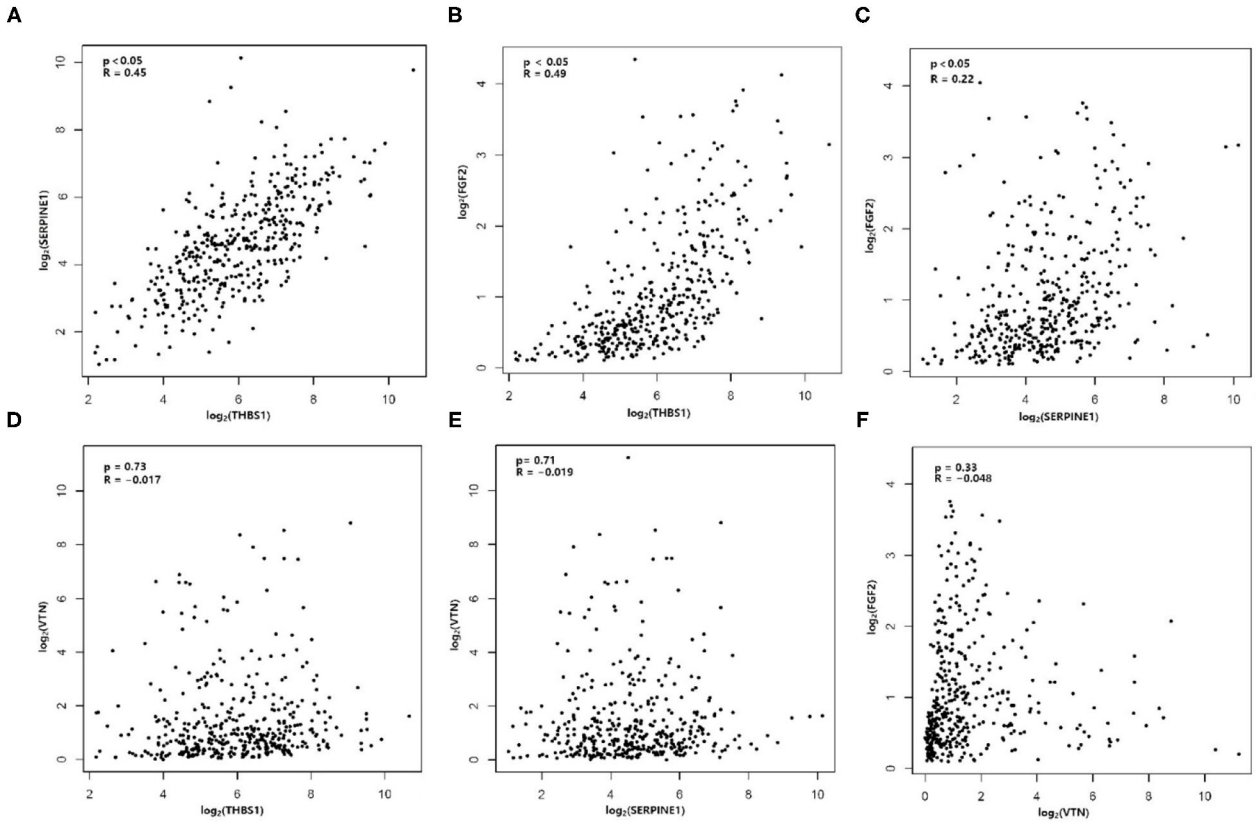

FIGURE 7 | Correlation analysis is shown for **(A)** THBS1 and SERPINE1, **(B)** THBS1 and FGF2, **(C)** SERPINE1 and FGF2, **(D)** THBS1 and VTN, **(E)** SERPINE1 and VTN, and **(F)** VTN and FGF2.

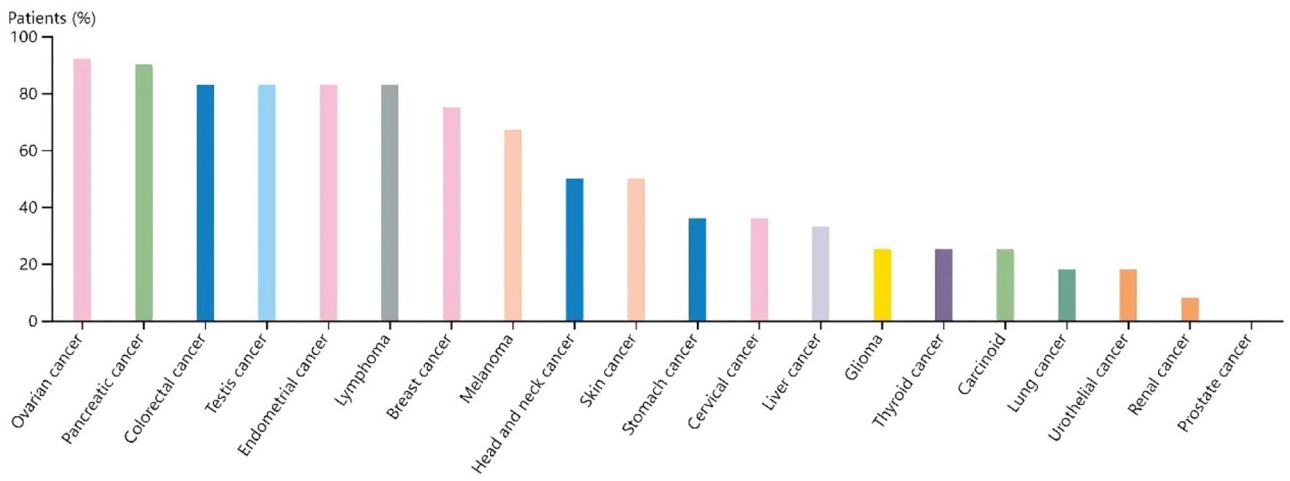

FIGURE 8 | THBS1 showed moderate to strong membranous staining in malignant tumor cells, with occasional cytoplasmic staining. SERPINE1 was negatively expressed in all tumor tissues *via* The Human Protein Atlas.

for correlation analysis (**Figure 7**) based on the TPM of the DEGs and showed that THBS1, SERPINE1, and FGF2 were correlated.

Validation of the Genes of Interest

Differential gene expression analysis suggested that THBS1 and SERPINE1 were significantly differentially expressed in the two

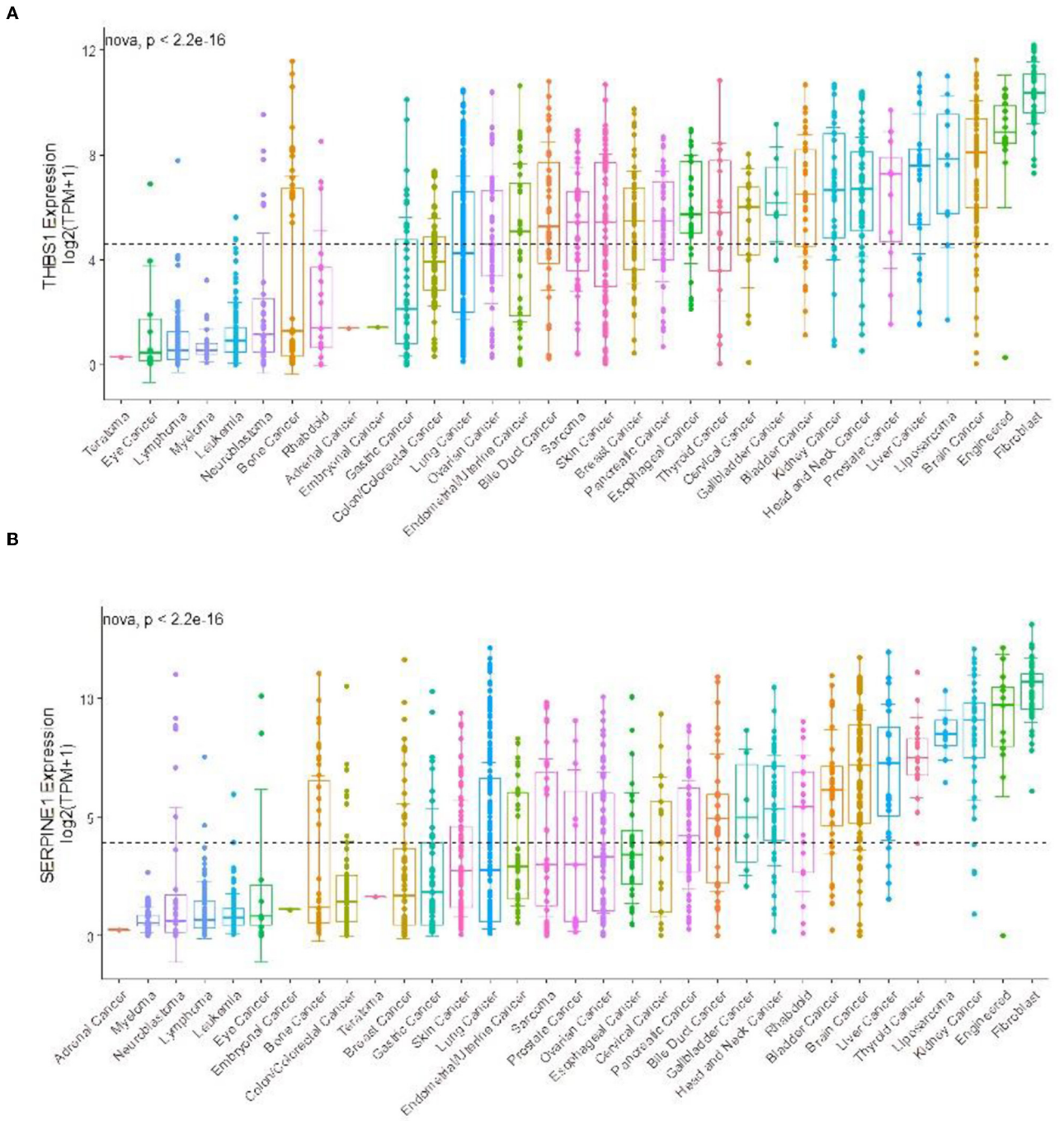

FIGURE 9 | Gene expression in different cancer cell lines for **(A)** THBS1 and **(B)** SERPINE1. The black dotted lines represent the average expression of all tumors, and the horizontal lines in the middle of each boxplot represent the median expression of individual tumors.

types of gastric cancer, correlation analysis found a correlation between the two genes, and prognostic analysis suggested that THBS1 and SERPINE1 might have potential functions in SRC. We performed gene validation in the Human Protein Atlas and found that gastric cancers were partly positive for THBS1 (**Figure 8**).

In the CCLE database, THBS1 was found to be highly expressed in many tumor cell lines but only moderately expressed in gastric cancer (**Figure 9**). Then, gastric cancer cell lines were analyzed, and SERPINE1 and THBS1 were found to be relatively higher in metastatic tumor cell lines (**Figure 10**).

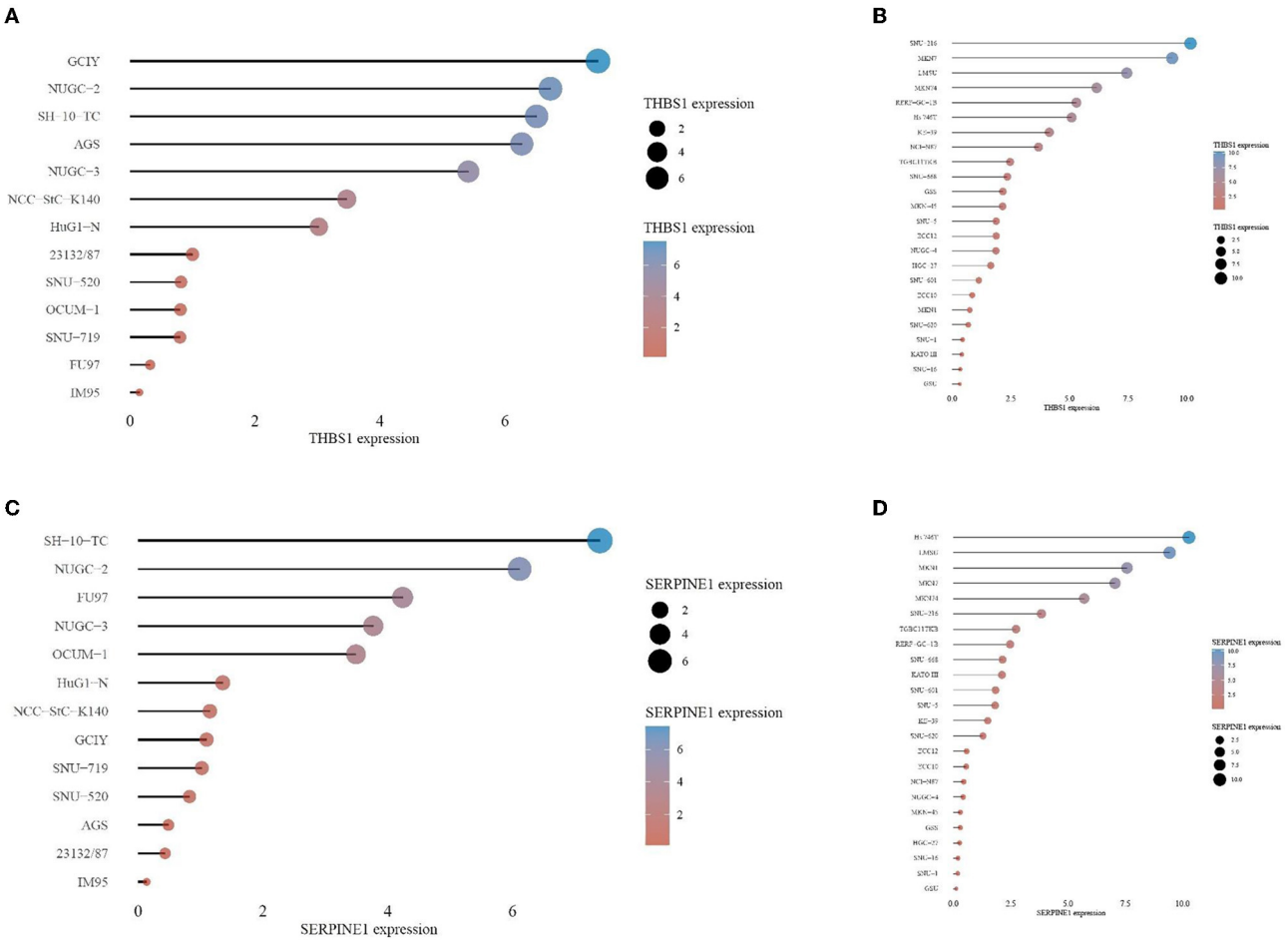

FIGURE 10 | Gene expression levels in different gastric cancer cell lines for **(A)** THBS1 in primary cancer cell, **(B)** SERPINE1 in primary cancer cell, **(C)** THBS1 in metastasis cancer cell, and **(D)** SERPINE1 in metastasis cancer cell.

For further confirmation of these genes at the protein level, we performed immunohistochemical staining in human samples (**Figure 11**). In EGC, there was no significant difference in the expression of THBS1 and ITGC in two types of gastric cancer, while in AGC, the expression of THBS1 and SERPINE1 in SRC was higher than that in ITGC (**Table 5**). In SRC, the expression of THBS1 and SERPINE1 was significantly higher in AGC than in EGC. In ITGC, the expression of THBS1 in AGC was significantly higher than that in EGC, while the expression of SERPINE1 in EGC was not significantly different from that in AGC (**Table 6**).

Tumor Immune Infiltration Analysis

The TIMER was used to explore the immunological microenvironment and identified correlations between levels of immune infiltration and expressions of the THBS1 and SERPINE1 in gastric cancer (**Figure 12**).

Survival analysis showed that macrophages ($p = 0.004$) and neutrophils ($p = 0.033$) were significantly associated with gastric cancer. THBS1 expression was significantly positively linked with immune infiltration of purity ($r = -0.183$, $p < 0.001$), CD8+ T cells ($r = 0.25$, $p = 1.09 \times 10^{-6}$), CD4+ T cells ($r = 0.334$, $p = 5.33 \times 10^{-11}$), macrophages ($r = 0.601$, $p = 1.07 \times 10^{-37}$), neutrophils ($r = 0.343$, $p = 1.11 \times 10^{-11}$), and DCs ($r = 0.448$, $p = 1.07 \times 10^{-19}$). The SERPINE1 expression was significantly positively linked with immune infiltration of purity ($r = -0.168$, $p = 0.001$), B cells ($r = -0.111$, $p = 0.033$), CD8+ T cells ($r = 0.149$, $p = 0.004$), macrophages ($r = 0.310$, $p = 1.05 \times 10^{-9}$), neutrophils ($r = 0.248$, $p = 1.29 \times 10^{-6}$), and DCs ($r = 0.209$, $p = 5.02 \times 10^{-5}$).

DISCUSSION

In recent years, a growing number of studies in Asian countries has shown that the prognosis of SRC depends on the pathological grading and staging, with better outcomes in SRC than in NSRC in EGC and a reversal in AGC (6–13). Previous studies using the SEER database did not show significant differences between SRC and NSRC (14, 15, 27). Gastric cancer is a mixture of

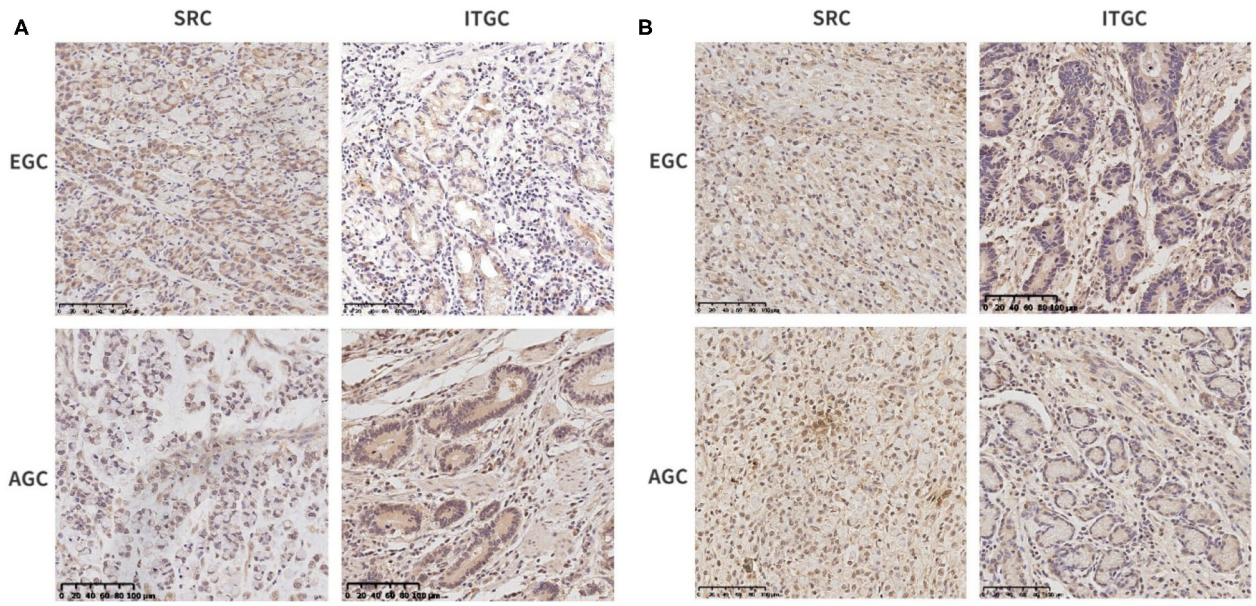

FIGURE 11 | Immunohistochemical staining of SRC and intestinal-type gastric carcinoma (ITGC) samples for **(A)** THBS1 and **(B)** SERPINE1. The blue color stood for nuclear staining and the yellow color for target protein staining (scale bars: 100 μm).

TABLE 5 | Expression of THBS1 and SERPINE1 in signet-ring cell carcinoma and non-signet ring cell carcinoma.

	SRC		ITGC		*p*
	+	−	+	−	
EGC					
THBS1	5	26	4	19	0.902
SERPINE1	6	24	6	15	0.478
AGC					
THBS1	19	3	13	9	0.042
SERPINE1	17	5	10	12	0.030

SRC, signet ring cell carcinoma; ITGC, intestinal-type gastric carcinoma; EGC, early gastric cancer; AGC, advanced gastric cancer.

TABLE 6 | Expression of THBS1 and SERPINE1 in early gastric cancer and advanced gastric cancer.

	EGC		AGC		*p*
	+	−	+	−	
SRC					
THBS1	5	26	19	3	<0.01
SERPINE1	6	24	17	5	<0.01
ITGC					
THBS1	4	19	13	9	<0.01
SERPINE1	6	15	10	12	0.252

SRC, signet ring cell carcinoma; ITGC, intestinal-type gastric carcinoma; EGC, early gastric cancer; AGC, advanced gastric cancer.

various subtypes of tumors, and previous studies have shown that the clinical characteristics of different tumor types vary greatly (28–30). The cause of such results may be the heterogeneity of the tumor, which is induced by the different selection criteria. The currently recognized cause of intestinal-type gastric cancer is long-term chronic atrophic inflammation (31), the pathogenesis of other types of gastric cancer is unknown, and the clinicopathological characteristics and prognosis vary from one type to another. This study selected only ITGC and SRC, excluding mucinous adenocarcinoma, mixed adenocarcinoma, and other rare types.

Our results suggest that the clinical characteristics of SRC differ significantly from those of intestinal-type gastric adenocarcinoma. One difference is that SRC develops at an earlier age, approximately 7 years earlier than ITGC. The second difference lies in the sex distribution. Approximately half of patients with SRC are female, even though gastric cancer is generally considered to be a predominantly male cancer (32). Studies have shown that younger women have higher levels of estrogen receptors, so sex hormones may play a role in age and sex differences (33, 34). Other studies have shown that more than 80.0% of SRCs express estrogen receptors and are more likely to metastasize to the ovary, suggesting that SRCs have a higher affinity for estrogen (35). SRCs exhibit more middle and lower third tumor locations than the upper locations in the total population and are more likely to present with diffuse infiltrating gastric cancer in AGC. Some studies show that Mist1+ stem cells in the gastric isthmus can be transformed into SRCs in the absence of E-cadherin (36), which may be why SRCs are more frequently located in the middle third

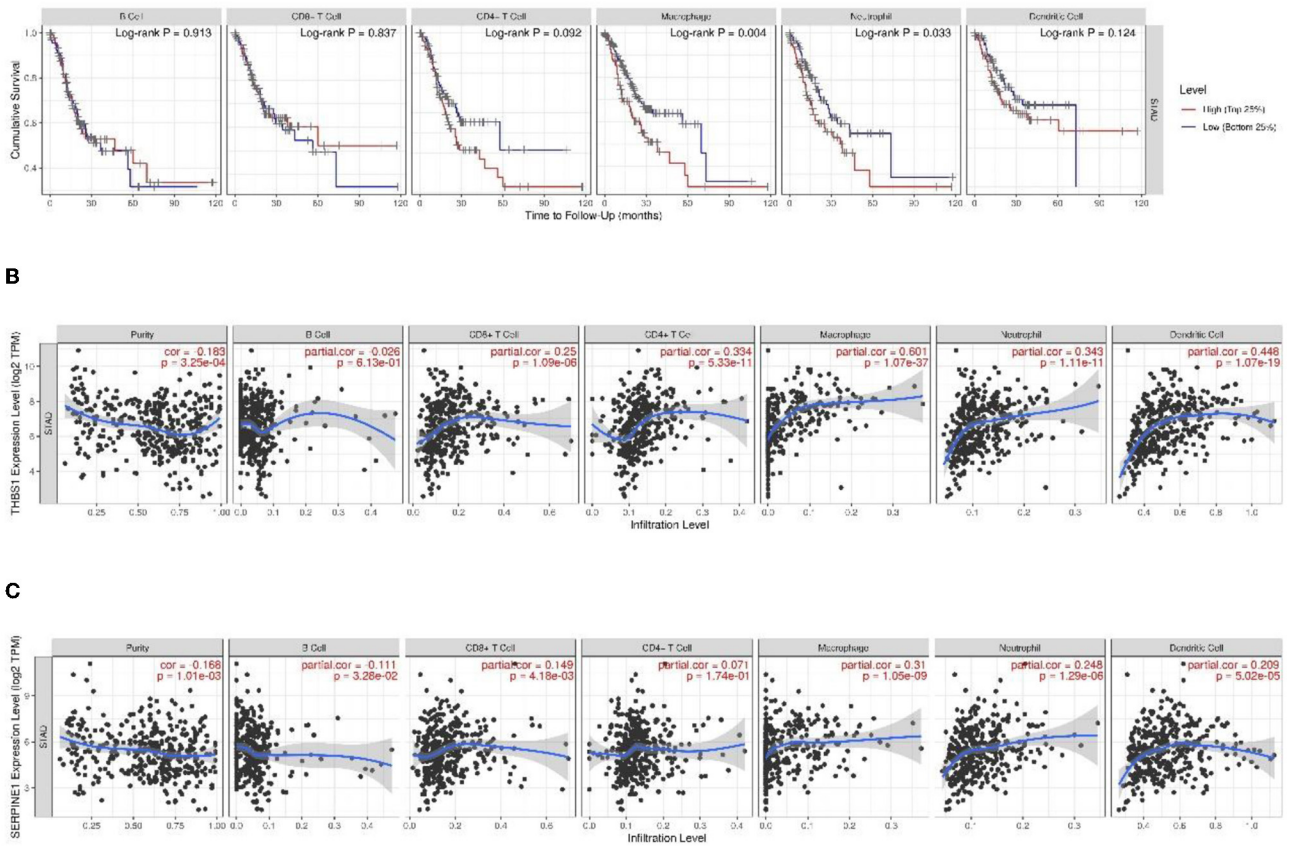

FIGURE 12 | (A) Kaplan–Meier curves of gastric cancer stratified by immune cell abundance. Correlation with levels of immune infiltration (purity, B cells, CD8+ T cells, CD4+ T cells, macrophages, neutrophils, and dendritic cells) for **(B)** THBS1 and **(C)** SERPINE1. The correlation measurement is indicated by the partial correlation value using Spearman's partial rho and the statistical significance of the *p*-value.

of the stomach. All of these findings reinforce the idea that SRC and ITGC may be two completely different diseases (37, 38).

Herein, we believe that stage adjustment is necessary to analyze the prognosis of SRC. SRC was associated with a better prognosis in early gastric cancer but a worse survival in advanced gastric cancer. These results may suggest that mutated genes controlling SRC progression may play a role in later stages of the disease. However, no studies have been conducted to elucidate how the gene level causes a difference in clinicopathological features between SRC and ITGC.

We identified 256 DEGs (119 upregulated and 137 downregulated) between SRC and ITGC in TCGA data, which may help us further explore the key reasons for the differential prognosis of the two types of gastric cancer. The genes THBS1, SERPINE1, VTN, and FGF2 were identified as genes of interest through functional enrichment analysis and PPI analysis. GO enrichment analysis showed that they were mainly related to biological processes such as wound healing, cell chemotaxis, and ECM tissue. These biological processes are at the core of our enrichment term network and may be closely related to the characteristics of SRC. Further survival analysis showed that THBS1, SERPINE1, and VTN were significantly associated with the prognosis of gastric cancer. Correlation analysis showed that THBS1, SERPINE, and FGF2 were correlated. In our study, it was found that the expression of THBS1 and SERPINE1 was significantly different in SRC and ITGC, as well as in EGC and AGC. It is reasonable to assume that THBS1 and SERPINE1 may have potentially important functions.

According to our study, SRC has more T4 and N3 distribution in pathological stages than ITGC; this may be the reason why SRC shows more malignancy in AGC than ITGC. Thrombospondin1 is an extracellular glycoprotein that has been shown to play a role in cell invasion and migration (39). Some studies have confirmed that THBS-1 protein is mainly located in myofibroblasts of the tumor stroma and is significantly associated with lymph node metastasis of gastric cancer (40). It has also been proven that FGF7/FGFR2 signaling promotes the invasion and migration of gastric cancer by upregulating THBS1 (41). Serpin peptidase inhibitor, clade E, member 1 can prevent excessive proteolysis and maintain

the integrity of the ECM, which is necessary for capillary morphogenesis, cell migration, and tumor invasion (42). Studies have shown that the lncRNA NKX2-1-AS1 can activate the VEGFR-2 signaling pathway through SERPINE1 to promote tumor progression and angiogenesis in gastric cancer (43). Tumor cell line validation also showed higher expression of THBS1 and SERPINE1 in metastatic cancer cell lines. Given the role of THBS1 and SERPINE1 in tumor invasion and metastasis, it may explain the higher degree of malignancy in advanced SRC to some extent.

We also performed a correlation analysis of tumor-infiltrating immune cells. In gastric cancer, macrophages and neutrophils are significantly associated with prognosis. THBS1 and SERPINE1 were associated with multiple immune cell infiltrates, with the correlation between THBS1 and macrophages up to 0.601 ($p = 1.07 \times 10^{-37}$). Tumor-associated macrophages (TAM) are important components of tumor microenvironment and regulate tumor progression. TAM can secrete matrix metalloproteinase (MMP), serine protease and cathepsin to mediate ECM degradation and cell–ECM interaction to promote tumor cell invasion and migration (44, 45).

There are some limitations in our study that must be considered. First, although the use of a large database can reduce the bias due to differences in patient distribution to some extent, these data also limited our study because perioperative chemotherapy, which is critical to prognosis, was missing. The surgery type and the extent of lymph node dissection (D1, D2) were not recorded in patients who underwent surgical resection. Therefore, more cohort studies should be conducted.

Second, two parts of this study were obtained from the SEER database and TCGA database, and both are maintained by the National Cancer Institute. Although the inclusion criteria for the two parts of this study were basically the same, due to the defects of the database itself, there was a huge difference in the proportion of SRC and ITGC cases. Thus, it is not appropriate for us to add other features to the grouping. These deficiencies may have partially influenced the results, as evidenced by the fact that CDH1 (46) and CDS1 expression did not differ between two groups. Moreover, since the number of SRCs in the TCGA database is too small, it is difficult to conduct grouping for subsequent analysis of genes of interest. Although our results were validated by immunohistochemistry, more studies on the single-cell sequencing of SRC are needed. Further mechanistic validation for the genes of interest will be further implemented.

CONCLUSIONS

There were significant differences in the clinicopathological features and prognosis between SRC and ITGC. These results suggest that SRC and ITGC may be two distinct types of tumors with different pathogeneses. We found many codifferentially expressed genes and important pathways between SRC and ITGC. THBS1 and SERPINE1 were significantly differentially expressed in the two types of gastric cancer, and may have potentially important functions.

DATA AVAILABILITY STATEMENT

The original contributions presented in the study are included in the article/supplementary material, further inquiries can be directed to the corresponding author.

ETHICS STATEMENT

Ethical review and approval was not required for the study on human participants in accordance with the local legislation and institutional requirements. Written informed consent for participation was not required for this study in accordance with the national legislation and the institutional requirements.

AUTHOR CONTRIBUTIONS

JM analyses the data and statistics and drafted the manuscripts. YM was responsible for literature search, manuscript preparation, and contributed to some of the pictures. WF, LG, and XZ responsible for the design of the study, reviewed the manuscript, provided feedback, and provided financial support. All authors contributed to the article and approved the submitted version.

FUNDING

This work was supported by grants from the National Natural Science Foundation of China (No. 82003153), Beijing Municipal Science and Technology Commission (No. Z131100004013036), and National Multidisciplinary Cooperative Diagnosis and Treatment Capacity Building Project for Major Diseases: Comprehensive Diagnosis and Treatment of gastrointestinal Tumors (No. A63445-24).

REFERENCES

1. Lee YC, Chiang TH, Chou CK, Tu YK, Liao WC, Wu MS, et al. Association between helicobacter pylori eradication and gastric cancer incidence: a systematic review and meta-analysis. *Gastroenterology*. (2016) 150:1113–24.e5. doi: 10.1053/j.gastro.2016.01.028
2. Henson DE, Dittus C, Younes M, Nguyen H, Albores-Saavedra J. Differential trends in the intestinal and diffuse types of gastric carcinoma in the United States, 1973-2000: increase in the signet ring cell type. *Arch Pathol Lab Med*. (2004) 128:765–70. doi: 10.5858/2004-128-765-DTITIA
3. Nagtegaal ID, Odze RD, Klimstra D, Paradis V, Rugge M, Schirmacher P, et al. The 2019 WHO classification of tumours of the digestive system. *Histopathology*. (2020) 76:182–8. doi: 10.1111/his.13975
4. Kim JP, Kim SC, Yang HK. Prognostic significance of signet ring cell carcinoma of the stomach. *Surg Oncol*. (1994) 3:221–7. doi: 10.1016/0960-7404(94)90037-X

5. Piessen G, Messager M, Leteurtre E, Jean-Pierre T, Mariette C. Signet ring cell histology is an independent predictor of poor prognosis in gastric adenocarcinoma regardless of tumoral clinical presentation. *Ann Surg.* (2009) 250:878–87. doi: 10.1097/SLA.0b013e3181b21c7b
6. Maehara Y, Sakaguchi Y, Moriguchi S, Orita H, Korenaga D, Kohnoe S, et al. Signet ring cell carcinoma of the stomach. *Cancer.* (1992) 69:1645–50. doi: 10.1002/1097-0142(19920401)69:7<1645::AID-CNCR2820690702>3.0.CO;2-X
7. Yokota T, Kunii Y, Teshima S, Yamada Y, Saito T, Kikuchi S, et al. Signet ring cell carcinoma of the stomach: a clinicopathological comparison with the other histological types. *Tohoku J Exp Med.* (1998) 186:121–30. doi: 10.1620/tjem.186.121
8. Kim DY, Park YK, Joo JK, Ryu SY, Kim YJ, Kim SK, et al. Clinicopathological characteristics of signet ring cell carcinoma of the stomach. *ANZ J Surg.* (2004) 74:1060–4. doi: 10.1111/j.1445-1433.2004.03268.x
9. Chiu CT, Kuo CJ, Yeh TS, Hsu JT, Liu KH, Yeh CN, et al. Early signet ring cell gastric cancer. *Dig Dis Sci.* (2011) 56:1749–56. doi: 10.1007/s10620-010-1487-8
10. Kwon KJ, Shim KN, Song EM, Choi JY, Kim SE, Jung HK, et al. Clinicopathological characteristics and prognosis of signet ring cell carcinoma of the stomach. *Gastric Cancer.* (2014) 17:43–53. doi: 10.1007/s10120-013-0234-1
11. Chon HJ, Hyung WJ, Kim C, Park S, Kim JH, Park CH, et al. Differential prognostic implications of gastric signet ring cell carcinoma: stage adjusted analysis from a single high-volume center in Asia. *Ann Surg.* (2017) 265:946–53. doi: 10.1097/SLA.0000000000001793
12. Kao YC, Fang WL, Wang RF, Li AF, Yang MH, Wu CW, et al. Clinicopathological differences in signet ring cell adenocarcinoma between early and advanced gastric cancer. *Gastric Cancer.* (2019) 22:255–63. doi: 10.1007/s10120-018-0860-8
13. Huang KH, Chen MH, Fang WL, Lin CH, Chao Y, Lo SS, et al. The clinicopathological characteristics and genetic alterations of signet-ring cell carcinoma in gastric cancer. *Cancers (Basel).* (2020) 12:2318. doi: 10.3390/cancers12082318
14. Taghavi S, Jayarajan SN, Davey A, Willis AI. Prognostic significance of signet ring gastric cancer. *J Clin Oncol.* (2012) 30:3493–8. doi: 10.1200/JCO.2012.42.6635
15. Cui J, Liang H, Deng J, Ding X, Wang X, Zhang L, et al. [Clinicopathological features and prognostic analysis of patients with signet ring cell gastric carcinoma]. *Zhonghua Zhong Liu Za Zhi.* (2015) 37:367–70. doi: 10.3760/cma.j.issn.0253-3766.2015.05.011
16. Japanese Gastric Cancer Association. Japanese classification of gastric carcinoma: 3rd English edition. *Gastric Cancer.* (2011) 14:101–12. doi: 10.1007/s10120-011-0041-5
17. Colaprico A, Silva TC, Olsen C, Garofano L, Cava C, Garolini D, et al. TCGAbiolinks: an R/Bioconductor package for integrative analysis of TCGA data. *Nucleic Acids Res.* (2016) 44:e71. doi: 10.1093/nar/gkv1507
18. McCarthy DJ, Chen Y, Smyth GK. Differential expression analysis of multifactor RNA-Seq experiments with respect to biological variation. *Nucleic Acids Res.* (2012) 40:4288–97. doi: 10.1093/nar/gks042
19. Zhou Y, Zhou B, Pache L, Chang M, Khodabakhshi AH, Tanaseichuk O, et al. Metascape provides a biologist-oriented resource for the analysis of systems-level datasets. *Nat Commun.* (2019) 10:1523. doi: 10.1038/s41467-019-09234-6
20. Li T, Fan J, Wang B, Traugh N, Chen Q, Liu JS, et al. TIMER: a web server for comprehensive analysis of tumor-infiltrating immune cells. *Cancer Res.* (2017) 77:e108–e10. doi: 10.1158/0008-5472.CAN-17-0307
21. Agha R, Abdall-Razak A, Crossley E, Dowlut N, Iosifidis C, Mathew G, et al. STROCSS 2019 guideline: strengthening the reporting of cohort studies in surgery. *Int J Surg.* (2019) 72:156–65. doi: 10.1016/j.ijsu.2019.11.002
22. Shannon P, Markiel A, Ozier O, Baliga NS, Wang JT, Ramage D, et al. Cytoscape: a software environment for integrated models of biomolecular interaction networks. *Genome Res.* (2003) 13:2498–504. doi: 10.1101/gr.1239303
23. Szklarczyk D, Gable AL, Lyon D, Junge A, Wyder S, Huerta-Cepas J, et al. STRING v11: protein-protein association networks with increased coverage, supporting functional discovery in genome-wide experimental datasets. *Nucleic Acids Res.* (2019) 47:D607–D13. doi: 10.1093/nar/gky1131
24. Stark C, Breitkreutz BJ, Reguly T, Boucher L, Breitkreutz A, Tyers M. BioGRID: a general repository for interaction datasets. *Nucleic Acids Res.* (2006) 34(Database issue):D535–D9. doi: 10.1093/nar/gkj109
25. Li T, Wernersson R, Hansen RB, Horn H, Mercer J, Slodkowicz G, et al. A scored human protein-protein interaction network to catalyze genomic interpretation. *Nat Methods.* (2017) 14:61–4. doi: 10.1038/nmeth.4083
26. Bader GD, Hogue CW. An automated method for finding molecular complexes in large protein interaction networks. *BMC Bioinformatics.* (2003) 4:2. doi: 10.1186/1471-2105-4-2
27. Lin CL, Zhu GW, Huang YJ, Zheng W, Yang SG, Ye JX. Operable gastric adenocarcinoma with different histological subtypes: cancer-specific survival in the United States. *Saudi J Gastroenterol.* (2020) 26:46–52. doi: 10.4103/sjg.SJG_406_19
28. Hoerr SO, Hazard JB, Bailey D. Prognosis in carcinoma of the stomach in relation to the microscopic type. *Surg Gynecol Obstet.* (1966) 122:485–94.
29. Kawamura H, Kondo Y, Osawa S, Nisida Y, Okada K, Isizu H, et al. A clinicopathologic study of mucinous adenocarcinoma of the stomach. *Gastric Cancer.* (2001) 4:83–6. doi: 10.1007/PL00011728
30. Park JM, Jang YJ, Kim JH, Park SS, Park SH, Kim SJ, et al. Gastric cancer histology: clinicopathologic characteristics and prognostic value. *J Surg Oncol.* (2008) 98:520–5. doi: 10.1002/jso.21150
31. Hoffmann W. Current status on stem cells and cancers of the gastric epithelium. *Int J Mol Sci.* (2015) 16:19153–69. doi: 10.3390/ijms160819153
32. Sipponen P, Correa P. Delayed rise in incidence of gastric cancer in females results in unique sex ratio (M/F) pattern: etiologic hypothesis. *Gastric Cancer.* (2002) 5:213–9. doi: 10.1007/s101200200037
33. Matsui M, Kojima O, Kawakami S, Uehara Y, Takahashi T. The prognosis of patients with gastric cancer possessing sex hormone receptors. *Surg Today.* (1992) 22:421–5. doi: 10.1007/BF00308791
34. Ryu WS, Kim JH, Jang YJ, Park SS, Um JW, Park SH, et al. Expression of estrogen receptors in gastric cancer and their clinical significance. *J Surg Oncol.* (2012) 106:456–61. doi: 10.1002/jso.23097
35. Yang XF, Yang L, Mao XY, Wu DY, Zhang SM, Xin Y. Pathobiological behavior and molecular mechanism of signet ring cell carcinoma and mucinous adenocarcinoma of the stomach: a comparative study. *World J Gastroenterol.* (2004) 10:750–4. doi: 10.3748/wjg.v10.i5.750
36. Hayakawa Y, Ariyama H, Stancikova J, Sakitani K, Asfaha S, Renz BW, et al. Mist1 expressing gastric stem cells maintain the normal and neoplastic gastric epithelium and are supported by a perivascular stem cell niche. *Cancer Cell.* (2015) 28:800–14. doi: 10.1016/j.ccell.2015.10.003
37. Hohenberger P, Gretschel S. Gastric cancer. *Lancet.* (2003) 362:305–15. doi: 10.1016/S0140-6736(03)13975-X
38. Tan IB, Ivanova T, Lim KH, Ong CW, Deng N, Lee J, et al. Intrinsic subtypes of gastric cancer, based on gene expression pattern, predict survival and respond differently to chemotherapy. *Gastroenterology.* (2011) 141:476–85, 485.e1–e11. doi: 10.1053/j.gastro.2011.04.042
39. Jayachandran A, Anaka M, Prithviraj P, Hudson C, McKeown SJ, Lo PH, et al. Thrombospondin 1 promotes an aggressive phenotype through epithelial-to-mesenchymal transition in human melanoma. *Oncotarget.* (2014) 5:5782–97. doi: 10.18632/oncotarget.2164
40. Lin XD, Chen SQ, Qi YL, Zhu JW, Tang Y, Lin JY. Overexpression of thrombospondin-1 in stromal myofibroblasts is associated with tumor growth and nodal metastasis in gastric carcinoma. *J Surg Oncol.* (2012) 106:94–100. doi: 10.1002/jso.23037
41. Huang T, Wang L, Liu D, Li P, Xiong H, Zhuang L, et al. FGF7/FGFR2 signal promotes invasion and migration in human gastric cancer through upregulation of thrombospondin-1. *Int J Oncol.* (2017) 50:1501–12. doi: 10.3892/ijo.2017.3927
42. Devy L, Blacher S, Grignet-Debrus C, Bajou K, Masson V, Gerard RD, et al. The pro- or antiangiogenic effect of plasminogen activator inhibitor 1 is dose dependent. *FASEB J.* (2002) 16:147–54. doi: 10.1096/fj.01-0552com
43. Teng F, Zhang JX, Chen Y, Shen XD, Su C, Guo YJ, et al. LncRNA NKX2-1-AS1 promotes tumor progression and angiogenesis *via* upregulation of SERPINE1 expression and activation of the VEGFR-2 signaling pathway in gastric cancer. *Mol Oncol.* (2021) 15:1234–55. doi: 10.1002/1878-0261.12911

44. Liang W, Huang X, Carlos CJJ, Lu X. Research progress of tumor microenvironment and tumor-associated macrophages. *Clin Transl Oncol.* (2020) 22:2141–52. doi: 10.1007/s12094-020-02367-x
45. Yan Y, Zhang J, Li JH, Liu X, Wang JZ, Qu HY, et al. High tumor-associated macrophages infiltration is associated with poor prognosis and may contribute to the phenomenon of epithelial-mesenchymal transition in gastric cancer. *Onco Targets Ther.* (2016) 9:3975–83. doi: 10.2147/OTT.S103112
46. Ma YR, Siegal GP, Wei S. Reacquisition of E-cadherin expression in metastatic deposits of signet-ring cell carcinoma of the upper gastrointestinal system: a potential anchor for metastatic deposition. *J Clin Pathol.* (2017) 70:528–32. doi: 10.1136/jclinpath-2016-203959

Conflict of Interest: The authors declare that the research was conducted in the absence of any commercial or financial relationships that could be construed as a potential conflict of interest.

Publisher's Note: All claims expressed in this article are solely those of the authors and do not necessarily represent those of their affiliated organizations, or those of the publisher, the editors and the reviewers. Any product that may be evaluated in this article, or claim that may be made by its manufacturer, is not guaranteed or endorsed by the publisher.

Copyright © 2022 Ma, Meng, Zhou, Guo and Fu. This is an open-access article distributed under the terms of the Creative Commons Attribution License (CC BY). The use, distribution or reproduction in other forums is permitted, provided the original author(s) and the copyright owner(s) are credited and that the original publication in this journal is cited, in accordance with accepted academic practice. No use, distribution or reproduction is permitted which does not comply with these terms.

frontiers in Surgery

ORIGINAL RESEARCH
published: 21 March 2022
doi: 10.3389/fsurg.2022.845666

Establishment of a Dynamic Nomogram for Predicting the Risk of Lymph Node Metastasis in T1 Stage Colorectal Cancer

*Zitao Liu, Chao Huang, Huakai Tian, Yu Liu, Yongshan Huang and Zhengming Zhu**

Department of Gastrointestinal Surgery, The Second Affiliated Hospital of Nanchang University, Nanchang, China

Background: Accurate prediction of the risk of lymph node metastasis in patients with stage T1 colorectal cancer is crucial for the formulation of treatment plans for additional surgery and lymph node dissection after endoscopic resection. The purpose of this study was to establish a predictive model for evaluating the risk of LNM in patients with stage T1 colorectal cancer.

Methods: The clinicopathological and imaging data of 179 patients with T1 stage colorectal cancer who underwent radical resection of colorectal cancer were collected. LASSO regression and a random forest algorithm were used to screen the important risk factors for LNM, and a multivariate logistic regression equation and dynamic nomogram were constructed. The C index, Calibration curve, and area under the ROC curve were used to evaluate the discriminant and prediction ability of the nomogram. The net reclassification index (NRI), comprehensive discriminant improvement index (IDI), and clinical decision curve (DCA) were compared with traditional ESMO criteria to evaluate the accuracy, net benefit, and clinical practicability of the model.

Results: The probability of lymph node metastasis in patients with T1 colorectal cancer was 11.17% (20/179). Multivariate analysis showed that the independent risk factors for LNM in T1 colorectal cancer were submucosal invasion depth, histological grade, CEA, lymphovascular invasion, and imaging results. The dynamic nomogram model constructed with independent risk factors has good discrimination and prediction capabilities. The C index was 0.914, the corrected C index was 0.890, the area under the ROC curve was 0.914, and the accuracy, sensitivity, and specificity were 93.3, 80.0, and 91.8%, respectively. The NRI, IDI, and DCA show that this model is superior to the ESMO standard.

Conclusion: This study establishes a dynamic nomogram that can effectively predict the risk of lymph node metastasis in patients with stage T1 colorectal cancer, which will provide certain help for the formulation of subsequent treatment plans for patients with stage T1 CRC after endoscopic resection.

Keywords: T1 stage colorectal cancer, lymph node metastasis (LNM), random forest, LASSO regression algorithm, dynamic nomogram

OPEN ACCESS

Edited by:
Qi Liu,
Fudan University, China

Reviewed by:
Gaetano Luglio,
University of Naples Federico II, Italy
Yuming Jiang,
Stanford University, United States

****Correspondence:***
Zhengming Zhu
zzm8654@163.com

Specialty section:
This article was submitted to Surgical Oncology, a section of the journal Frontiers in Surgery

Received: *30 December 2021*
Accepted: *16 February 2022*
Published: *21 March 2022*

Citation:
Liu Z, Huang C, Tian H, Liu Y, Huang Y and Zhu Z (2022) Establishment of a Dynamic Nomogram for Predicting the Risk of Lymph Node Metastasis in T1 Stage Colorectal Cancer. Front. Surg. 9:845666. doi: 10.3389/fsurg.2022.845666

INTRODUCTION

Colorectal cancer is a common malignant cancer of the digestive tract and has the third-highest mortality rate among all cancers worldwide (1). In recent years, with the improvement of people's health awareness, the popularization of colorectal cancer screening programs and the improvement of endoscopic systems, many early colorectal cancers have been diagnosed and treated early (2, 3). At the same time, many T1 colorectal cancer patients who previously required radical surgical treatment can be cured by endoscopic mucosal resection (4). Previous studies have shown that the probability of lymph node metastasis in T1 colorectal patients is 7 to 16% (5–7). Therefore, accurate assessment of the risk of lymph node metastasis in patients with T1 colorectal cancer is an important factor in prognosis and whether additional surgical treatment is needed after endoscopic resection (8). At present, the assessment of LNM at stage T1 is mainly based on pathological specimens after endoscopic resection and related guidelines, such as those of the National Cancer Network (NCCN), European Society of Medical Oncology (ESMO), and Japanese Society of Colorectal Cancer (JSCCR). The risk factors for LNM are the depth of submucosal invasion (>1,000 μm), histological grade, vascular and lymphatic invasion, and tumor budding. Currently, there are some controversies regarding tumor budding as a risk factor for T1 stage colorectal cancer LNM, and only the JSCCR has included it in the guidelines (9–11). If patients have one or more risk factors, they are considered to be at high risk for LNM and require additional surgery and lymph node dissection. However, the way that patients are classified into low-risk and high-risk groups have led to a decrease in the positive predictive value of LNM and the result of overtreatment (12). According to the current guidelines, the incidence rate of LNM is ∼10%, which means that many patients without lymph node metastasis have undergone unnecessary additional surgery, and there is a 1.5–3% probability of postoperative death. In addition, artificial anal surgery may be required for some patients with low stage T1 rectal cancer (13). Therefore, to reduce unnecessary surgery and provide suitable treatment for patients, it is necessary to establish a prediction model for accurately predicting LNM.

At present, although some studies have constructed scoring systems to stratify the risk of LNM for T1 colorectal cancer, Jung et al. constructed a nomogram prediction model that included five pathological factors (vascular invasion, submucosal invasion depth, tumor budding, differentiation grade, and adenoma background), with an AUC of 0.812 and a 95% CI of (0.770, 0.855) (6). Miyachi et al. constructed a prediction model that included five clinicopathological factors (mucosal muscular state, sex, vascular lymphatic invasion, differentiation grade, and tumor budding) (5). These models have the good discriminatory ability, but the risk factors included are mainly pathological factors, some of which are controversial. Recently, some studies have predicted the risk of LNM by observing the morphology and location of tumors and endoscopic features (ulcer depression, mucosal hypertonia, morphological changes, nodular eminence in the ulcer center, etc.) through endoscopic systems. However, because this study is a single-center study and endoscopic features such as LNM prediction factors are controversial, its clinical application is limited (7). There are also some studies that predict the risk of LNM through genomics and biomarkers. For example, Ozawa et al. found that high expression of five microRNAs (MIR32, MIR181B, MIR193B, MIR195, and MIR411) is closely related to lymph node metastasis of T1 colorectal cancer. The area under the ROC curve of this model is 0.83 (14). Kishida et al. found that the loss of ARID1A expression is related to LNM in T1 colorectal cancer (15). Kandimalla et al. showed the expression of 8 genes (AMT, MMP9, FOXA1, LYZ, MMP1, C2CD4A, PIGR, and RCC1) was related to LNM in T1 colorectal cancer. The area under the ROC curve of the prediction model was 0.88 (95% CI: 0.79–0.97) (16). Although these tumor markers can predict the risk of LNM relatively accurately, the complicated operation process limits their clinical application value.

Multi-slice spiral CT (MDCT) and MRI are routine imaging examinations for preoperative clinical evaluation of lymph node status in colorectal cancer patients. Lymph node metastasis is diagnosed through imaging features, including maximum short-axis diameter of lymph nodes, irregular morphology, necrosis of lymph node center, calcification of lymph nodes, the uneven density of lymph nodes, etc. (17–22). Although studies have shown that the accuracy of MDCT scanning in predicting LNM is 59–71% and that the accuracy, sensitivity, and specificity of MRI in predicting LNM are 92.5, 80–85, and 95%, respectively (17, 18, 23), there are few studies on T1 colorectal cancer. Therefore, this study constructs a prediction model based on the clinicopathological factors and imaging manifestations of patients to evaluate the risk of lymph node metastasis in stage T1 colorectal cancer and provides a reference for the formulation of subsequent treatment plans for stage T1 colorectal cancer patients after endoscopic resection.

METHODS

This research was approved by the Ethics Committee of the Second Affiliated Hospital of Nanchang University and implemented according to the Declaration of Helsinki Ethical Standards.

Study Patients

This study included 179 patients with stage T1 colorectal cancer who underwent radical resection of colorectal cancer at the Gastrointestinal Surgery Department of the Second Affiliated Hospital of Nanchang University from January 2010 to October 2020, including 103 males and 76 females, with a median age 59.5 ± 11.8 years old, 59 cases of colon cancer, and 120 cases of rectal cancer. The inclusion criteria were as follows: 1. Patients with stage T1 colorectal cancer were treated by radical resection of colorectal cancer, and postoperative pathology was confirmed as stage T1 colorectal cancer. 2. No neoadjuvant radiotherapy or chemotherapy before surgery; 3. Patients without other tumors; and 4. Complete preoperative clinical data; Patients with familial polyposis, Lynch syndrome history, and ulcerative colitis were excluded.

Colorectal cancer patients underwent surgery according to CME or TME principles with intestinal resection and

lymph node dissection. The surgical methods mainly included open surgery, laparoscopic-assisted radical colorectal cancer surgery, and complete laparoscopic radical colorectal cancer surgery.

Assessment of Clinicopathological Factors

The clinicopathological characteristics of the patients were extracted from the hospital's electronic health record system, and retrospective data were collected, including sex, age, smoking history, tumor markers (CEA, CA199) and hemoglobin, neutrophil ratio, lymphocyte ratio, fibrinogen, and prealbumin values at the time of the patient's first admission. The location of the tumor was divided into the following: right colon (ileocecal, ascending colon, and liver flexure of colon), left colon (splenic flexure of the colon, descending colon, and sigmoid colon), and rectum. The size of the tumor was measured according to the maximum diameter of the tumor under endoscopy. The tumor morphology under endoscopy was divided into two types according to the Paris standards: polyp type and non-polyp type, where the polyp type includes the pedicle polyp type and non-pedicle polyp type, and the non-polyp type includes the flat raised type and depressed type (24). The depth of submucosal invasion was divided into SM1, SM2, and SM3 according to Kudo's standard (25). According to the histological classification of colorectal cancer by the World Health Organization, cancers were divided into low and high grades. Low-grade cancers include highly differentiated and moderately differentiated adenocarcinoma, while high-grade cancers include poorly differentiated adenocarcinoma, signet ring cell carcinoma, mucinous adenocarcinoma, and neuroendocrine carcinoma. Lymphovascular invasion is defined as the appearance of tumor cells in the stroma of microvessels or the lymphatic space. The background of adenoma was defined by the continuity of adenoma tissue and resected cancer tissue under a microscope.

Interpretation of CT and MRI Images

All the patients with colon cancer underwent plain or enhanced CT scans of the whole abdomen before the operation, and all patients with rectal cancer underwent pelvic MRI and plain or enhanced CT scans of the whole abdomen before the operation. Patients ate a digestible juicy diet within 2 days before undergoing a plain CT scan or enhanced CT scan of the whole abdomen and took oral laxatives to clean the intestinal tract one day before the MRI examination. A CT scan was performed with a 64-slice multispiral CT scanner, with a slice thickness of 5 mm. MRI was performed with 3.0 T MRI, and T1WI, T2WI, and DWI were performed. All case images were independently evaluated by 2 experienced chief radiologists (specializing in abdominal CT or MRI), and the status of peri-intestinal lymph nodes was evaluated in combination with the endoscopy results. If the two results were inconsistent, they would be re-evaluated by another chief radiologist, and the results would be determined after comprehensive analysis. Whether lymph nodes appeared on the image was recorded, as was the maximum value of the short axis of the lymph nodes, though it was ignored when the size of the suspected lymph nodes was <3 mm because they are difficult to distinguish from vascular structures and non-specific soft tissue density. Patients with rectal cancer underwent MDCT and MRI examinations. If only one examination had positive imaging manifestations, the results of the positive imaging manifestations were recorded. If both examinations had positive imaging manifestations at the same time, the MRI results were the main images considered.

Statistical Analysis

The normality of the data was analyzed by the single sample K–S test. If the measurement data were normally distributed, they were expressed as the mean ± SD; otherwise, they were described by the median and quartile range. Categorical variables were described by the ratio and 95% CI. In the univariate analysis, a *t*-test or Mann-Whitney *U* test was used for measurement data, and the chi-square test was used for categorical variables, LASSO regression, and the random forest algorithm were used to screen the risk factors for LNM, and then the important risk factors were included in the construction of the logistic regression equation. The best cut-off value of important risk factors was determined by ROC curve analysis. To visualize the analysis of the data, a dynamic nomogram was constructed to calculate the risk of LNM. The C index, corrected C index, area under the ROC curve, and calibration curve were used to evaluate the prediction ability of the model. The calibration curve was internally verified by the bootstrap method, and the net reclassification index (NRI), comprehensive discriminant improvement index (IDI), and clinical decision curve (DCA) were compared with the traditional ESMO standard to evaluate the accuracy, net benefit, and clinical practicability of the model.

All data were analyzed using SPSS 24.0 (SPSS Inc., Chicago, IL, USA) and R (version x64 4.0.3), including the rms, corrplot, glmnet, randomforest, rsconnect, DynNom, rmda, PredictABEL, and other toolboxes. $P < 0.05$ indicated the statistical significance.

RESULTS

Clinical Characteristics

The study showed that 20 patients had LNM (11.17%), including 14 males and 6 females, aged 58.5 ± 14.9 years. A total of 159 patients (88.83%) had no LNM, including 89 males and 70 females, aged 59.6 ± 11.4 years. There were 125 cases with negative lymph nodes on imaging, and 54 cases were found to have enlarged lymph nodes. The minimum value was 3 mm, the maximum value was 11 mm, and the best cut-off value was 5 mm. Patients with enlarged lymph nodes were divided into two groups: 0–5 and > 5 mm. In the patients with the LNM group, 3 cases had negative lymph nodes on imaging, 8 cases had lymph nodes 0–5 mm in size, and 9 cases had lymph nodes > 5 mm in size. In the patients without LNM, 122 cases had negative lymph nodes on imaging, 24 cases had lymph nodes 0–5 mm in size, and 13 cases had lymph nodes > 5 mm in size. Age ($P = 0.889$), sex ($P = 0.233$), smoking history ($P = 0.543$), tumor location ($P = 0.141$), hemoglobin ($P = 0.486$), fibrinogen ($P = 0.699$), preoperative CA199 level ($P = 0.486$), the ratio

TABLE 1 | Clinicopathological and imaging features of patients with stage T1 colorectal cancer.

Factors	Total	LNM (–)	LNM (+)	*P*-value
Age (year)	59.5 ± 11.8	59.6 ± 11.4	58.5 ± 14.9	0.889
Sex				
Male	103 (57.5%)	89 (86.4%)	14 (13.6%)	0.233
Female	76 (42.5%)	70 (92.1%)	6 (7.9%)	
Smoking				
No	153 (85.5%)	135 (88.2%)	18 (11.8%)	0.543
Yes	26 (14.5%)	24 (92.3%)	2 (7.7%)	
Tumor size (cm)				
≤2	53 (29.6%)	51 (96.2%)	2 (3.8%)	0.042
>2	126 (70.4%)	108 (85.7%)	18 (14.3%)	
Tumor location				
Right colon	17 (9.5%)	17 (100%)	0 (0%)	0.141
Left colon	42 (23.5%)	38 (90.5%)	4 (9.5%)	
Rectum	120 (67.0%)	104 (86.7%)	16 (13.3%)	
Background adenoma				
No	44 (24.6%)	35 (79.5%)	9 (20.5%)	0.025
Yes	135 (75.4%)	124 (91.9%)	11 (8.1%)	
Depth of submucosal invasion				
Sm1	63 (35.2%)	62 (98.4%)	1 (1.6%)	0.002
Sm2	46 (25.7%)	42 (91.3%)	4 (8.7%)	
Sm3	70 (39.1%)	55 (78.6%)	15 (21.4%)	
Histologic grade				
Low	173 (96.6%)	158 (91.3%)	15 (8.7%)	<0.001
High	6 (3.4%)	1 (16.7%)	5 (83.3%)	
Lymphovascular invasion				
No	165 (92.2%)	150 (90.9%)	15 (9.1%)	0.002
Yes	14 (7.8%)	9 (64.3%)	5 (35.7%)	
Tumor type				
Polyp type	76 (42.5%)	72 (94.7%)	4 (5.3%)	0.032
Non-polyp type	103 (57.5%)	87 (84.5%)	16 (15.5%)	
Imaging results				
Node negative	125 (69.8%)	122 (97.6%)	3 (2.4%)	<0.001
Node size (0–5 mm)	32 (17,9%)	24 (75%)	8 (25%)	
Node size (>5 mm)	22 (12.3%)	13 (59.1%)	9 (40.9%)	
Hemoglobin (g/L)	125 ± 18.0	125.5 ± 17.6	120 ± 20.7	0.486
Fibrinogen (g/L)	2.83 ± 0.81	2.84 ± 0.82	2.72 ± 0.69	0.699
Preoperative CEA (ng/ml)				
≤5	165 (92.2%)	151 (91.5%)	14 (8.5%)	<0.001
>5	14 (7.8%)	8 (57.1%)	6 (42.9%)	
Preoperative CA199 (ng/ml)	13.54 ± 10.67	13.1 ± 10.26	16.8 ± 13.3	0.486
Neutrophil to lymphocyte ratio	2.69 ± 2.14	2.66 ± 2.20	2.98 ± 1.71	0.350
Fibrinogen to prealbumin ratio	0.01 ± 0.007	0.01 ± 0.007	0.01 ± 0.005	0.325

of neutrophils to lymphocytes ($P = 0.350$), and the ratio of fibrinogen to prealbumin ($P = 0.325$) were not associated with lymph node metastasis in stage T1 colorectal cancer **(Table 1)**.

Univariate and Multivariate Analysis

Univariate analysis showed that tumor size ($P = 0.042$), adenoma background ($P = 0.025$), submucosal invasion depth ($P = 0.002$), histological grade ($P < 0.001$), vascular and lymphatic invasion ($P = 0.002$), tumor type ($P = 0.032$), imaging results ($P < 0.001$) and preoperative CEA ($P < 0.001$) were related to lymph node metastasis in T1 colorectal cancer **(Table 1)**. Multivariate analysis showed that submucosal invasion depth (OR =14. 997, $P = 0.043$), histological grade (OR = 42. 071, $P = 0.006$), preoperative CEA (OR = 5. 60, $P = 0.028$), vascular and lymphatic invasion (OR = 23. 891, $P = 0.002$), lymph node size 0–5 mm (OR = 5. 284, $P = 0.049$) and lymph node size > 5 mm (OR = 19. 074, $P =$

TABLE 2 | Multivariate analysis of risk factors for lymph node metastasis in T1 colorectal cancer.

Risk factors	B	SE	Wals	*P*-value	OR (95%CI)
Depth of submucosal invasion					
Sm1	1 (reference)				
Sm2 or Sm3	2.708	1.336	4.11	0.043	14.997 (1.094, 205.592)
Histologic grade					
Low	1 (reference)				
High	3.739	1.354	7.624	0.006	42.071 (2.959, 598.106)
CEA (ng/ml)					
≤5	1 (reference)				
>5	1.723	0.786	4.805	0.028	5.60 (1.20, 26.134)
Imaging results					
Node negative	1 (reference)				
Node size (0–5 mm)	1.665	0.847	3.867	0.049	5.284 (1.005, 27.766)
Node size (>5 mm)	2.948	0.847	12.11	0.001	19.074 (3.625, 100.374)
Lymphovascular invasion					
No	1 (reference)				
Yes	3.174	1.031	9.483	0.002	23.891 (3.17, 180.073)

0.001) were independent risk factors for lymph node metastasis in T1 colorectal cancer **(Table 2)**.

LASSO Regression and Random Forest Algorithm

To avoid the influence of confounding factors, 8 significant factors from the univariate analysis were included in the LASSO regression, and variables were re-evaluated. Finally, 6 non-zero coefficient variables were included in the multivariate analysis. These factors were vascular lymphatic invasion, histological grade, imaging results, preoperative CEA, submucosal invasion depth, and tumor type **(Figures 1A,B)**. In addition, the random forest algorithm was used to analyze the 8 factors that were of great significance in the single factor analysis, and the importance of the variables was ranked. The greater the Gini coefficient, the greater the importance of the factor. The imaging results ranked first, followed by histological grade, vascular and lymphatic invasion, preoperative CEA, and submucosal invasion depth **(Figure 1C)**.

Receiver Operating Characteristic Curve

Figure 1D shows the area under the curve of independent risk factors for lymph node metastasis in T1 colorectal cancer. According to ROC curve analysis, the cut-off value of the maximum diameter of the short axis of the enlarged lymph node on imaging was 5 mm. The area under the curve of vascular and lymphatic invasion was 0.597, 95% CI (0.451, 0.742), the sensitivity was 25%, and the specificity was 94.3. The area under the curve of the histological grade was 0.622, 95% CI (0.473, 0.771), the sensitivity was 25%, and the specificity was 99%. The area under the curve of the depth of submucosal invasion was 0.673, 95% CI (0.570, 0.776), the sensitivity was 95%, and the specificity was 39.6%. The area under the curve of preoperative CEA was 0.631, 95% CI (0.478, 0.772), the sensitivity was 30%, and the specificity was 95%. The area under the curve of the imaging results was 0.826, 95% CI (0.726, 0.926), the sensitivity was 85%, and the specificity was 76.6%. The results showed that only the imaging results had good sensitivity and specificity in predicting LNM, while the sensitivity or specificity of other factors was relatively low **(Table 3)**.

Nomogram Construction

Based on the results of logistic analysis, *R* was used to construct a prediction model **(Figure 2)**, and each risk factor was assigned a value. The score of no vascular lymphatic invasion was 0, and the score of accompanying vascular lymphatic invasion was 85. The preoperative CEA $\leq$ 5 ng/ml score was 0, and the preoperative CEA $>$ 5 ng/ml score was 46; 0 points indicated low-grade cancer, and 100 points indicated high-grade cancer. The submucosal invasion depth sm1 was 0, and sm2 or sm3 was 72. On imaging, the negative lymph nodes were 0 points, and the enlarged lymph nodes were 45 points for 0–5 mm and 79 points for $>$ 5 mm. The total score of the prediction model was 382, suggesting that the risk of lymph node metastasis in T1 colorectal cancer was $>$ 99%, and the risk of LNM was predicted by the sum of the scores (**Table 4**). The C index of the model was 0.914, the corrected C index was 0.890, the accuracy, sensitivity, and specificity were 93.3, 80, 91.8%, respectively, and the area under the ROC curve **(Table 5)** was 0.914 **(Figure 3A)**. These results reflect that the prediction model has better discrimination ability and higher accuracy. The calibration curve also shows that the prediction model is highly consistent with the actual situation **(Figure 3B)**. In addition, for the convenience of clinicians, we constructed a dynamic nomogram (https://liuzitao.shinyapps.io/dynnomapp/). When using this program, we only need to input the information for five patient variables, and we can immediately obtain the risk probability of LNM and the 95% CI.

According to the ESMO guidelines, we constructed model 3 (composed of vascular lymphatic invasion, submucosal invasion depth, and histological grade) and added variable factors for

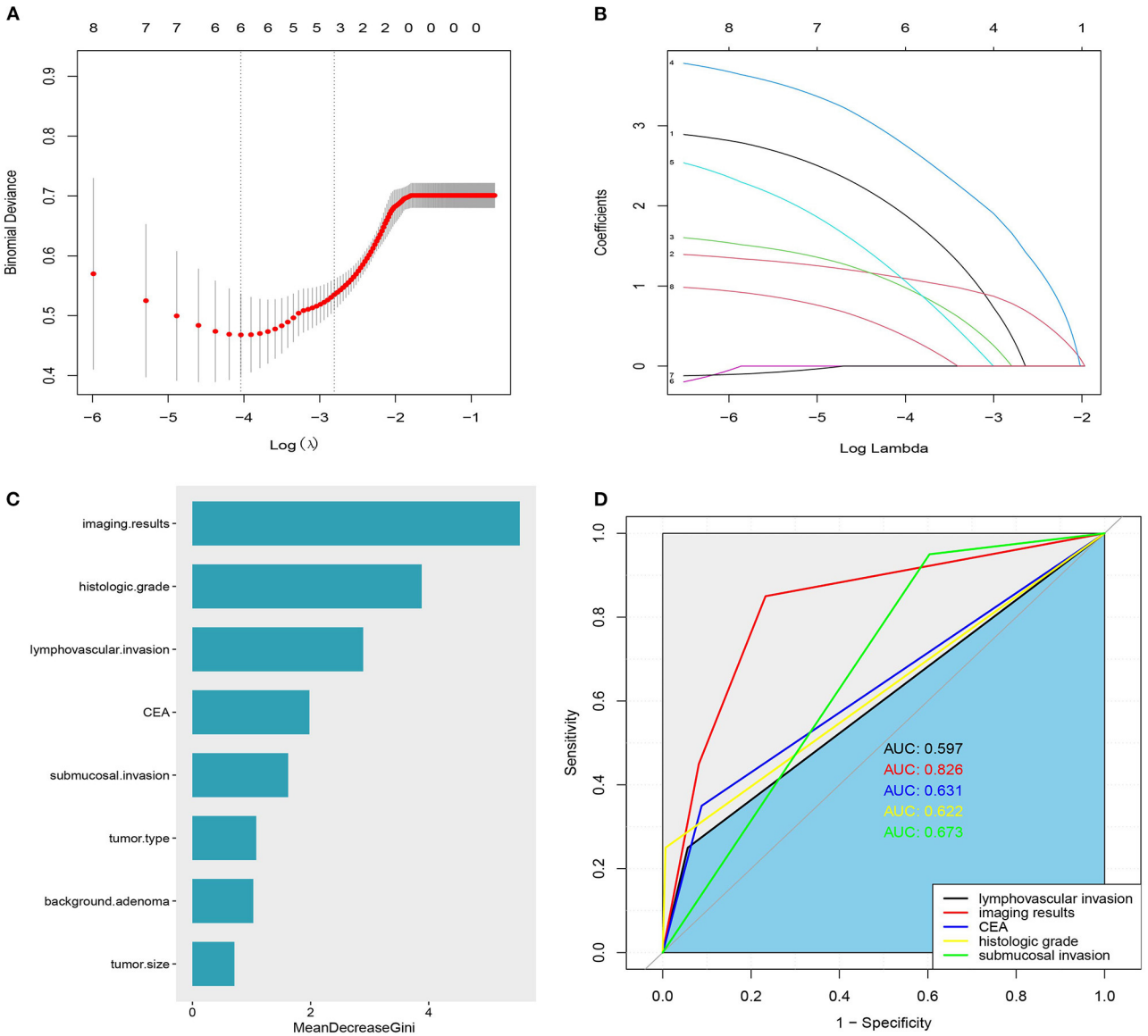

FIGURE 1 | (A) Variable selection using the least absolute shrinkage and selection operator (LASSO) regression model. **(B)** Lasso coefficients were shown for 8 variables: 1: Lymphovascular invasion, 2: imaging results, 3: CEA,4: Histologic grade, 5: depth of submucosal invasion, 6: tumor size, 7: adenoma background, and 8: tumor type. **(C)** The importance of LNM related factors in T1 colorectal cancer was ranked. **(D)** ROC curve of independent risk factors of LNM in T1 colorectal cancer.

TABLE 3 | Independent risk factors for LNM in T1 colorectal cancer of ROC curve.

Factors	AUC	95%CI	Sensitivity (%)	Specificity (%)	Cut-off value
Lymphovascular invasion	0.597	(0.451, 0.742)	25.0	94.3	
Histologic grade	0.622	(0.473, 0.771)	25.0	99.0	
submucosal invasion	0.673	(0.570, 0.776)	95.0	39.6	
CEA	0.631	(0.478, 0.772)	30.0	95.0	
Imaging results	0.826	(0.726, 0.926)	85.0	76.6	5 mm

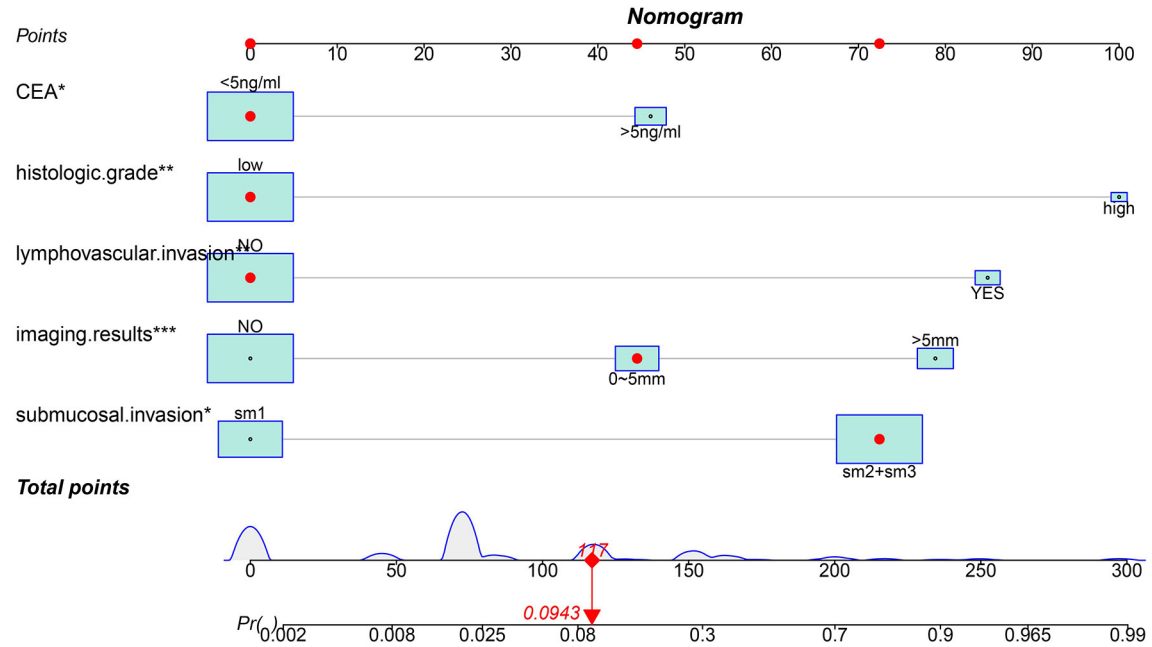

FIGURE 2 | The nomogram for predicting lymph node metastasis in T1 colorectal cancer.

TABLE 4 | The relationship between total points and risk of LNM in T1 colorectal cancer.

Total points	Risk of LNM
<100	<5%
101–119	6–10%
120–140	11–20%
141–155	21–30%
156–167	31–40%
168–177	41–50%
178–188	51–60%
189–200	61–70%
201–214	71–80%
215–236	81–90%
237–256	91–95%
257–300	95–99%
>300	>99%

preoperative CEA on the basis of model 3 to construct model 2. Compared with the ESMO guideline standard (model 3), the NRI of our prediction model (model 1) and model 2 were 21.8, 95% CI (−2.95,46.59), and 13.7, 95% CI (−4.22, 31.64), respectively, and the comprehensive discrimination improvement index (IDI) was 12.58, 95% CI (1.85, 23.31), $P = 0.021$, and 4.05, 95% CI (−0.83, 8.93), $P = 0.104$, respectively **(Table 5, Figure 4A)**. These results show that our predictive model (model 1) is significantly superior to the ESMO guideline standard (model 3) and model 2 in predicting LNM.

A clinical decision curve (DCA) was drawn to compare the clinical utility and net benefit of our prediction model with ESMO guidelines (Model 3) and Model 2 **(Figure 4B)**. The DCA curve shows that our prediction model has better clinical practicability than the other two models and obtains greater net benefits.

DISCUSSION

At present, there is some controversy about whether additional surgical treatment is needed for patients with stage T1 colorectal cancer after endoscopic resection and negative margins. Previous studies have shown that in stage T1 colorectal cancer, the 5-year overall survival rate (OS) of patients without lymph node metastasis is significantly higher than that of patients with lymph node metastasis (26). Therefore, accurate assessment of lymph node status in T1 colorectal cancer patients after endoscopic resection is an important factor in the formulation of treatment strategy and prognosis. Relevant guidelines such as the National Cancer Network (NCCN), the European Society of Medical Oncology (ESMO), and the Japanese Society of Colorectal Cancer (JSCCR) indicate that pathological factors such as vascular lymphatic invasion, histological grade, depth of submucosal invasion, and tumor budding are closely related to lymph node metastasis, and the aforementioned pathological factors are taken as indications for additional surgery after endoscopic resection (9–11). The multivariate analysis in this study also showed that vascular lymphatic invasion, histological grade, and depth of submucosal invasion were independent risk factors for lymph node metastasis in T1 colorectal cancer. In addition, preoperative CEA level and imaging results were also independent risk factors for LNM. Since tumor budding was not included in this study,

TABLE 5 | Comparison of three model capabilities.

	AUC	Sensitivity	Specificity	NRI	95%CI (%)	IDI	95%CI (%)	IDI *P*-value
Model1	0.914	80.0%	91.8%	21.8%	(−2.95, 46.59)	12.58%	(1.85, 23.31)	0.021
Model2	0.850	65.0%	96.2%	13.7%	(−4.22, 31.64)	4.05%	(−0.83, 8.93)	0.104
Model3	0.817	50.0%	98.7%	reference	reference	reference	reference	reference

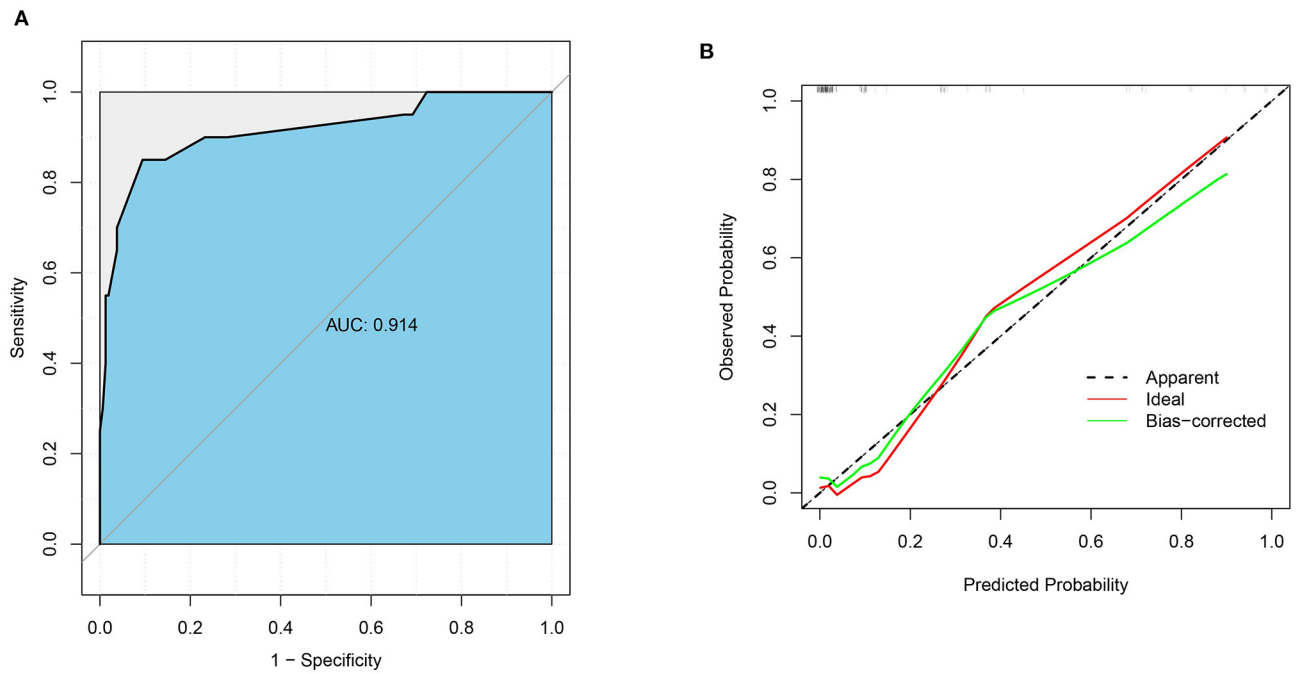

FIGURE 3 | (A) ROC Curve Area of Prediction Model. **(B)** Calibration Curve of Nomogram Model.

comparing our prediction model with ESMO guidelines, it was found that the prediction model of this study has significantly better discrimination ability, accuracy, and clinical practicability for LNM than ESMO guidelines.

There is no doubt that vascular lymphatic invasion and differentiation grade are important factors in predicting LNM. Ichimasa et al. predicted the risk of LNM in T1 colorectal cancer through artificial intelligence analysis. The results showed that the importance of vascular lymphatic invasion and histological grade in the model was significantly greater than that of other clinicopathological factors (27). Our research also confirms this result. The cause of lymph node metastasis in high-histological grade tumors is generally related to a poor degree of differentiation in tumor cells, such as poorly differentiated adenocarcinoma, signet ring cell carcinoma, mucinous adenocarcinoma, and neuroendocrine carcinoma. These tumor cells have stronger invasion ability and are more likely to invade surrounding tissues, especially lymphatic tissues (28). In addition, vascular lymphatic invasion and high histological grade are also closely related to prognosis (26).

In this study, the depth of submucosal invasion was measured according to the Kudo criteria (sm1, sm2, and sm3). Multivariate analysis showed that the depth of submucosal invasion was also an independent risk factor for LNM, but compared with other clinicopathological features, the depth of submucosal invasion was the least important. According to the guidelines of the Japan Colorectal Cancer Society in 2019, when the submucosal invasion depth is <1,000 μm or close to 1,000 μm, the probability of lymph node metastasis is extremely low, at 1.3% (95% CI is 0–2.4%), and there is even no possibility of lymph node metastasis (10). Kitajima et al. also showed that a submucosal invasion depth <1,000 μm, a probability of LNM of 0, and a submucosal invasion depth >1,000 μm were risk factors for lymph node metastasis (29). Recently, some studies have suggested that a submucosal invasion depth >1,000 μm is a risk factor for LNM. Some controversy exists. Miyachi et al. reported that LNM occurred in 5 out of 61 lesions with submucosal invasion depths <1,000 μm (8.2%) (5), and Suh et al. also found that LNM occurred in 12 out of 98 SM1 lesions (12.2%) (30). In this study, it was also found that one case (1.6%) of SM1 had LNM. In Ei Kudo et al. and other studies, the risk of LNM for stage T1 colorectal cancer was analyzed through big data artificial intelligence algorithms. The results showed that the discrimination ability of the model that did not include

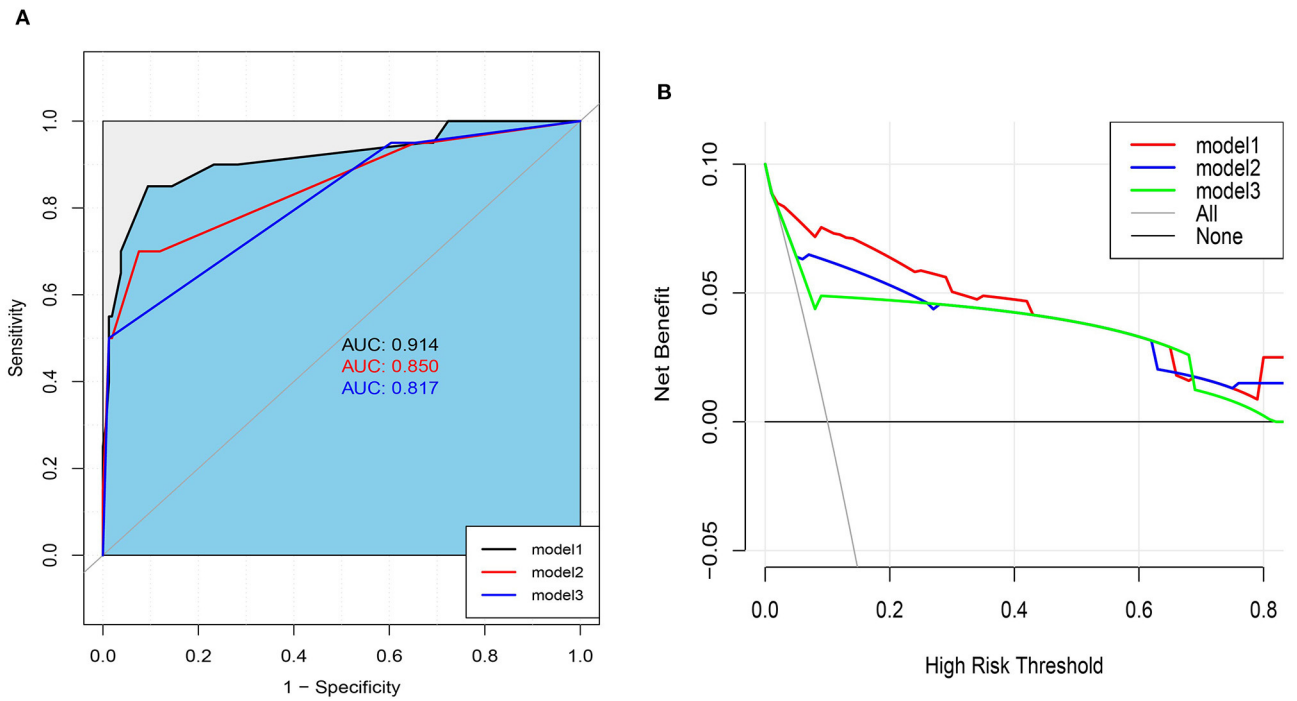

FIGURE 4 | (A) Area under ROC Curve of Three Models. **(B)** Decision Curve analysis for Nomogram and ESMO Guidelines (model 3) and model 2 in Predicting LNM Risk of T1 Colorectal Cancer.

tumor budding and submucosal invasion depth as predictive factors was better than that of the Japanese Colorectal Cancer Society (JSCCR) guidelines (31). In addition, the measurement of submucosal invasion depth has certain problems in the observation consensus of different pathologists, and different tumor types and diagnostic techniques will also affect the final results (32, 33). Therefore, the depth of submucosal invasion as a risk factor for LNM needs further study.

Most colorectal cancers evolve from adenomatous polyps, but ∼30% of cancers appear directly in the form of cancer nests without adenoma evolution (34–36). Previous studies have shown that a lack of adenoma background is closely related to LNM in T1 colorectal cancer (30). Studies by Ryul Oh et al. have shown that a lack of adenoma background is an independent risk factor for LNM (6), but studies by Miyachi et al. and Ichimasa et al. have shown that a lack of adenoma background is not significantly related to LNM (5, 27). In this study, univariate analysis showed that a lack of adenoma background was significantly associated with LNM, but multivariate analysis showed that a lack of adenoma background was not an independent risk factor for LNM. Recently, some studies have shown that clinicopathological features such as age, sex, tumor location, and tumor size are also related to LNM. For example, the risk of LNM for rectal cancer is higher than that for colon cancer (7, 37), the probability of LNM for women is significantly higher than that for men (5, 38, 39), and the risk of LNM for young patients is higher than that for patients of other ages (38, 40). However, as predictors of LNM, these clinicopathological factors are still debatable, and more research is needed to further confirm their predictive ability.

Many studies have confirmed that tumor markers have certain clinical value in evaluating lymph node metastasis, recurrence, distant metastasis, and prognosis of colorectal cancer (41, 42). However, there are some controversies about the clinical value of tumor markers in LNM evaluation of T1 colorectal cancer. Sun et al's research found that an increase in preoperative CA724 levels is a good predictor of LNM in T1 colorectal cancer (26). Mo et al.'s research showed that there is a certain correlation between preoperative CEA level and LNM (43). Guo et al.'s research was based on the SEER database and analyzed the risk factors for LNM in T1 colorectal cancer; it confirmed that the preoperative CEA level is related to LNM (38). In our study, we also found that an increase in the preoperative CEA level was an independent risk factor for LNM, but there was no obvious correlation between the preoperative CA199 level and LNM. Therefore, future research on tumor markers will help us to further understand the risk of LNM in T1 colorectal cancer.

The National Cancer Network (NCCN) recommends enhanced CT scans and MRI as effective imaging examinations for evaluating preoperative lymph node status of advanced colorectal cancer (9, 44). Radiologists evaluate lymph node status through imaging features, including the maximum diameter of the short axis of the lymph node, shape, lymph node density, and calcification (17–22). However, many criteria are not suitable for the preoperative assessment of lymph node status in T1 colorectal cancer. Previous studies indicated that if the

maximum diameter of the short axis of lymph nodes on CT images is >1 cm, it is indicative of the metastatic lymph nodes (17, 45). If the maximum diameter of the short axis of lymph nodes on MRI images is >8 mm, the shape is irregular, the boundary unclear and other characteristics, it is indicative of metastatic lymph nodes (46). With the continuous improvement of CT and MRI equipment, lymph nodes as small as 5 mm can be detected on CT and MRI. In addition, pathologists have found that many lymph nodes smaller than 5 mm have metastasis. Therefore, an optimal cut-off value of lymph node size is very important for preoperative evaluation of lymph node status in T1 colorectal cancer. Choi et al. showed that the best cut-off value of the maximum diameter of the lymph node short axis was 4.1 mm, and the sensitivity and specificity were 78.6 and 75%, respectively (47). The best cut-off value in Kitaguchi et al. was 4.0 mm, and the sensitivity, specificity, accuracy, and negative predictive value of CT were 84, 69, 71, and 97%, respectively. The sensitivity, specificity, accuracy, and negative predictive value of MRI were 94, 23, 33, and 95%, respectively (48). The best cut-off value in this study was 5.0 mm. According to the cut-off value, the patients were divided into the imaging-negative lymph node group, the 0–5 mm group, and the > 5 mm group. The sensitivity and specificity were 85.0 and 76.6%, respectively, and the AUC was 0.826. These results show that a cut-off value of 5 mm is the standard and has a better ability to distinguish the status of lymph nodes before surgery. Therefore, preoperative combined imaging examination is helpful for accurately evaluating the status of lymph nodes before surgery. However, because of the lack of MRI examinations in colon cancer patients in this study, it is impossible to distinguish the diagnostic efficacy of CT and MRI for LNM in T1 colorectal cancer.

There are some limitations to this study. First, this study is a single-center retrospective study, and the sample size is relatively small, so there may be some selection bias. Therefore, the results need further verification with multicenter, big data research. Second, our prediction model has not been externally verified, which limits its value for clinical use to a certain extent. Third, all the patients in the study underwent radical surgery. Therefore, there may be some errors in the application of these risk factors to evaluate the lymph node status of patients after endoscopic resection, and further research is required.

CONCLUSION

The prediction model of this study can accurately predict the risk of T1 stage colorectal lymph node metastasis, provide some help for whether patients with T1 stage colorectal cancer need additional surgical treatment after endoscopic resection, and help to reduce unnecessary operations.

DATA AVAILABILITY STATEMENT

The original contributions presented in the study are included in the article/**Supplementary Material**, further inquiries can be directed to the corresponding author.

ETHICS STATEMENT

The studies involving human participants were reviewed and approved by the Second Affiliated Hospital of Nanchang University. The patients/participants provided their written informed consent to participate in this study.

AUTHOR CONTRIBUTIONS

ZL designed the study, analyzed the data, and wrote the manuscript with contributions from all the authors. YL, HT, and YH collected the clinical data. YH, CH, and ZZ provided the critical comments for this article. All the authors read and approved the final version of the article.

SUPPLEMENTARY MATERIAL

The Supplementary Material for this article can be found online at: https://www.frontiersin.org/articles/10.3389/fsurg.2022.845666/full#supplementary-material

REFERENCES

1. Siegel RL, Miller KD, Jemal A. Cancer statistics, 2020.*CA: Can J Clinic.* (2020) 70:7–30.doi: 10.3322/caac.21590
2. Bretthauer M, Kaminski MF, Løberg M, Zauber AG, Regula J, Kuipers EJ, et al. Population-based colonoscopy screening for colorectal cancer: a randomized clinical trial. *JAMA Int Med.* (2016) 176:894–902. doi: 10.1001/jamainternmed.2016.0960
3. Amri R, Bordeianou LG, Sylla P, Berger DL. Impact of screening colonoscopy on outcomes in colon cancer surgery. *JAMA Surg.* (2013) 148:747–54. doi: 10.1001/jamasurg.2013.8
4. Saitoh Y, Inaba Y, Sasaki T, Sugiyama R, Sukegawa R, Fujiya M. Management of colorectal T1 carcinoma treated by endoscopic resection. *Digestiv Endoscop Offic J Japan Gastroenterologic Endoscop Soc.* (2016) 28:324–9. doi: 10.1111/den.12503
5. Miyachi H, Kudo SE, Ichimasa K, Hisayuki T, Oikawa H, Matsudaira S, et al. Management of T1 colorectal cancers after endoscopic treatment based on the risk stratification of lymph node metastasis. *J Gastroenterol Hepatol.* (2016) 31:1126–32. doi: 10.1111/jgh.13257
6. Oh JR, Park B, Lee S, Han KS, Youk EG, Lee DH, et al. Nomogram development and external validation for predicting the risk of lymph node metastasis in T1 colorectal cancer. *Cancer Res Treat.* (2019) 51:1275–84. doi: 10.4143/crt.2018.569
7. Yasue C, Chino A, Takamatsu M, Namikawa K, Ide D, Saito S, et al. Pathological risk factors and predictive endoscopic factors for lymph node metastasis of T1 colorectal cancer: a single-center study of 846 lesions. *J Gastroenterol.* (2019) 54:708–17. doi: 10.1007/s00535-019-01564-y
8. Chok KS, Law WL. Prognostic factors affecting survival and recurrence of patients with pT1 and pT2 colorectal cancer. *World J Surg.* (2007) 31:1485–90.doi: 10.1007/s00268-007-9089-0
9. Benson AB, Venook AP, Al-Hawary MM, Cederquist L, Chen YJ, Ciombor KK, et al. Rectal Cancer, Version 2.2018, NCCN clinical practice guidelines in oncology. *J Nat Comprehen Cancer Netw JNCCN.* (2018) 16:874–901. doi: 10.6004/jnccn.2018.0061
10. Hashiguchi Y, Muro K, Saito Y, Ito Y, Ajioka Y, Hamaguchi T, et al. Japanese Society for Cancer of the Colon and Rectum (JSCCR) guidelines 2019 for the treatment of colorectal cancer. *Int J Clinic Oncol.* (2020) 25:1–42. doi: 10.1007/s10147-019-01485-z

11. Glynne-Jones R, Wyrwicz L, Tiret E, Brown G, Rödel C, Cervantes A, et al. Rectal cancer: ESMO Clinical Practice Guidelines for diagnosis, treatment and follow-up. *Annals Oncol official J Euro Soc Med Oncol.* (2017) 28 (suppl_4):iv22-iv40.doi: 10.1093/annonc/mdx224
12. Ha RK, Han KS, Sohn DK, Kim BC, Hong CW, Chang HJ, et al. Histopathologic risk factors for lymph node metastasis in patients with T1 colorectal cancer. *Annal Surgic Treat Res.* (2017) 93:266–71. doi: 10.4174/astr.2017.93.5.266
13. Vermeer NCA, Backes Y, Snijders HS, Bastiaannet E, Liefers GJ, Moons LMG, et al. National cohort study on postoperative risks after surgery for submucosal invasive colorectal cancer. *BJS open.* (2019) 3:210–7. doi: 10.1002/bjs5.50125
14. Ozawa T, Kandimalla R, Gao F, Nozawa H, Hata K, Nagata H, et al. A MicroRNA Signature Associated With Metastasis of T1 Colorectal Cancers to Lymph Nodes. *Gastroenterology.* (2018) 154:844–8.e7. doi: 10.1053/j.gastro.2017.11.275
15. Kishida Y, Oishi T, Sugino T, Shiomi A, Urakami K, Kusuhara M, et al. Associations between loss of ARID1A expression and clinicopathologic and genetic variables in t1 early colorectal cancer. *Am J Clinic Pathol.* (2019) 152:463–70.doi: 10.1093/ajcp/aqz062
16. Kandimalla R, Ozawa T, Gao F, Wang X, Goel A. Gene expression signature in surgical tissues and endoscopic biopsies identifies High-Risk T1 colorectal cancers. *Gastroenterology.* (2019) 156:2338–41. doi: 10.1053/j.gastro.2019.02.027
17. Kijima S, Sasaki T, Nagata K, Utano K, Lefor AT, Sugimoto H. Preoperative evaluation of colorectal cancer using CT colonography, MRI, and PET/CT. *World J Gastroenterol.* (2014) 20:16964–75. doi: 10.3748/wjg.v20.i45.16964
18. Zhou L, Wang JZ, Wang JT, Wu YJ, Chen H, Wang WB, et al. Correlation analysis of MR/CT on colorectal cancer lymph node metastasis characteristics and prognosis. *Euro Rev Med Pharmacologic Sci.* (2017) 21:1219–25.
19. Xu H, Zhao W, Guo W, Cao S, Gao C, Song T, et al. Prediction model combining clinical and mr data for diagnosis of lymph node metastasis in patients with rectal cancer. *J Magnet Resonan Imaging : JMRI.* (2021) 53:874–83. doi: 10.1002/jmri.27369
20. Li M, Zhang J, Dan Y, Yao Y, Dai W, Cai G, et al. A clinical-radiomics nomogram for the preoperative prediction of lymph node metastasis in colorectal cancer. *J Translat Med.* (2020) 18:46. doi: 10.1186/s12967-020-02215-0
21. Li XT, Sun YS, Tang L, Cao K, Zhang XY. Evaluating local lymph node metastasis with magnetic resonance imaging, endoluminal ultrasound and computed tomography in rectal cancer: a meta-analysis. *Colorect Dis Offic J Assoc Coloproctol Great Br Ireland.* (2015) 17:O129–35. doi: 10.1111/codi.12909
22. Chen Y, Wen Z, Liu Y, Yang X, Ma Y, Lu B, et al. Value of high-resolution MRI in detecting lymph node calcifications in patients with rectal cancer. *Acad Radiol.* (2020) 27:1709–17. doi: 10.1016/j.acra.2020.01.003
23. Mizukami Y, Ueda S, Mizumoto A, Sasada T, Okumura R, Kohno S, et al. Diffusion-weighted magnetic resonance imaging for detecting lymph node metastasis of rectal cancer. *World J Surg.* (2011) 35:895–9. doi: 10.1007/s00268-011-0986-x
24. The Paris endoscopic classification of superficial neoplastic lesions: esophagus, stomach, and colon: November 30 to December 1, (2002). *Gastrointestinal Endoscopy.* (2003) 58:S3-43. doi: 10.1016/S0016-5107(03)02159-X
25. Kudo S, Tamegai Y, Yamano H, Imai Y, Kogure E, Kashida H. Endoscopic mucosal resection of the colon: the Japanese technique. *Gastrointestinal Endoscopy Clinic N Am.* (2001) 11:519–35. doi: 10.1016/S1052-5157(18)30059-X
26. Sun ZQ, Ma S, Zhou QB, Yang SX, Chang Y, Zeng XY, et al. Prognostic value of lymph node metastasis in patients with T1-stage colorectal cancer from multiple centers in China. *World J Gastroenterol.* (2017) 23:8582–90.doi: 10.3748/wjg.v23.i48.8582
27. Ichimasa K, Kudo SE, Mori Y, Misawa M, Matsudaira S, Kouyama Y, et al. Artificial intelligence may help in predicting the need for additional surgery after endoscopic resection of T1 colorectal cancer. *Endoscopy.* (2018) 50:230–40.doi: 10.1055/s-0043-122385
28. Derwinger K, Kodeda K, Bexe-Lindskog E, Taflin H. Tumour differentiation grade is associated with TNM staging and the risk of node metastasis in colorectal cancer. *Acta Oncologica.* (2010) 49:57–62. doi: 10.3109/02841860903334411
29. Kitajima K, Fujimori T, Fujii S, Takeda J, Ohkura Y, Kawamata H, et al. Correlations between lymph node metastasis and depth of submucosal invasion in submucosal invasive colorectal carcinoma: a Japanese collaborative study. *J Gastroenterol.* (2004) 39:534–43. doi: 10.1007/s00535-004-1339-4
30. Suh JH, Han KS, Kim BC, Hong CW, Sohn DK, Chang HJ, et al. Predictors for lymph node metastasis in T1 colorectal cancer. *Endoscopy.* (2012) 44:590–5. doi: 10.1055/s-0031-1291665
31. Kudo SE, Ichimasa K, Villard B, Mori Y, Misawa M, Saito S, et al. Artificial intelligence system to determine risk of T1 Colorectal cancer metastasis to lymph node. *Gastroenterology.* (2021) 160:1075–84.e2. doi: 10.1053/j.gastro.2020.09.027
32. Barel F, Auffret A, Cariou M, Kermarrec T, Samaison L, Bourhis A, et al. High reproducibility is attainable in assessing histoprognostic parameters of pT1 colorectal cancer using routine histopathology slides and immunohistochemistry analyses. *Pathology.* (2019) 51:46–54. doi: 10.1016/j.pathol.2018.10.007
33. Kouyama Y, Kudo SE, Miyachi H, Ichimasa K, Hisayuki T, Oikawa H, et al. Practical problems of measuring depth of submucosal invasion in T1 colorectal carcinomas. *Int J Colorect Dis.* (2016) 31:137–46. doi: 10.1007/s00384-015-2403-7
34. Vogelstein B, Fearon ER, Hamilton SR, Kern SE, Preisinger AC, Leppert M, et al. Genetic alterations during colorectal-tumor development. *New Engl J Med.* (1988) 319:525–32. doi: 10.1056/NEJM198809013190901
35. Kikuchi-Yanoshita R, Konishi M, Ito S, Seki M, Tanaka K, Maeda Y, et al. Genetic changes of both p53 alleles associated with the conversion from colorectal adenoma to early carcinoma in familial adenomatous polyposis and non-familial adenomatous polyposis patients. *Cancer Res.* (1992) 52:3965–71.
36. Shimoda T, Ikegami M, Fujisaki J, Matsui T, Aizawa S, Ishikawa E. Early colorectal carcinoma with special reference to its development de novo. *Cancer.* (1989) 64:1138–46.
37. Wang H, Wei XZ, Fu CG, Zhao RH, Cao FA. Patterns of lymph node metastasis are different in colon and rectal carcinomas. *World J Gastroenterol.* (2010) 16:5375–9. doi: 10.3748/wjg.v16.i42.5375
38. Guo K, Feng Y, Yuan L, Wasan HS, Sun L, Shen M, et al. Risk factors and predictors of lymph nodes metastasis and distant metastasis in newly diagnosed T1 colorectal cancer. *Cancer Med.* (2020) 9:5095–113. doi: 10.1002/cam4.3114
39. Lee YJ, Huh JW, Shin JK, Park YA, Cho YB, Kim HC, et al. Risk factors for lymph node metastasis in early colon cancer. *Int J Colorect Dis.* (2020) 35:1607–13. doi: 10.1007/s00384-020-03618-7
40. Rönnow CF, Arthursson V, Toth E, Krarup PM, Syk I, Thorlacius H. Lymphovascular infiltration, not depth of invasion, is the critical risk factor of metastases in early colorectal cancer: retrospective population-based cohort study on prospectively collected data, including validation. *Annals Surg.* (2022) 275:e148–e54. doi: 10.1097/SLA.0000000000003854
41. Gao Y, Wang J, Zhou Y, Sheng S, Qian SY, Huo X. Evaluation of Serum CEA, CA19-9, CA72-4, CA125 and ferritin as diagnostic markers and factors of clinical parameters for colorectal cancer. *Sci Rep.* (2018) 8:2732. doi: 10.1038/s41598-018-21048-y
42. Bramsen JB, Rasmussen MH, Ongen H, Mattesen TB, Ørntoft MW, Árnadóttir SS, et al. Molecular-Subtype-specific biomarkers improve prediction of prognosis in colorectal cancer. *Cell reports.* (2017) 19:1268–80.doi: 10.1016/j.celrep.2017.04.045
43. Mo S, Zhou Z, Dai W, Xiang W, Han L, Zhang L, et al. Development and external validation of a predictive scoring system associated with metastasis of T1-2 colorectal tumors to lymph nodes. *Clinic Translat Med.* (2020) 10:275–87. doi: 10.1002/ctm2.30
44. Benson AB, Venook AP, Al-Hawary MM, Cederquist L, Chen YJ, Ciombor KK, et al. NCCN Guidelines insights: colon cancer, version 2.2018. *J Nat Comprehens Cancer Netw : JNCCN.* (2018) 16:359–69. doi: 10.6004/jnccn.2018.0021

45. Nerad E, Lahaye MJ, Maas M, Nelemans P, Bakers FC, Beets GL, et al. Diagnostic accuracy of CT for local staging of colon cancer: a systematic review and meta-analysis. *AJR Am J Roentgenol.* (2016) 207:984–95. doi: 10.2214/AJR.15.15785
46. Al-Sukhni E, Milot L, Fruitman M, Beyene J, Victor JC, Schmocker S, et al. Diagnostic accuracy of MRI for assessment of T category, lymph node metastases, and circumferential resection margin involvement in patients with rectal cancer: a systematic review and meta-analysis. *Annal Surg Oncol.* (2012) 19:2212–23. doi: 10.1245/s10434-011-2210-5
47. Choi J, Oh SN, Yeo DM, Kang WK, Jung CK, Kim SW, et al. Computed tomography and magnetic resonance imaging evaluation of lymph node metastasis in early colorectal cancer. *World J Gastroenterol.* (2015) 21:556–62. doi: 10.3748/wjg.v21.i2.556
48. Kitaguchi D, Sasaki T, Nishizawa Y, Tsukada Y, Ito M. Long-term outcomes and lymph node metastasis in patients receiving radical surgery for pathological T1 lower rectal cancer. *World J Surg.* (2019) 43:649–56. doi: 10.1007/s00268-018-4824-2

Conflict of Interest: The authors declare that the research was conducted in the absence of any commercial or financial relationships that could be construed as a potential conflict of interest.

Publisher's Note: All claims expressed in this article are solely those of the authors and do not necessarily represent those of their affiliated organizations, or those of the publisher, the editors and the reviewers. Any product that may be evaluated in this article, or claim that may be made by its manufacturer, is not guaranteed or endorsed by the publisher.

Copyright © 2022 Liu, Huang, Tian, Liu, Huang and Zhu. This is an open-access article distributed under the terms of the Creative Commons Attribution License (CC BY). The use, distribution or reproduction in other forums is permitted, provided the original author(s) and the copyright owner(s) are credited and that the original publication in this journal is cited, in accordance with accepted academic practice. No use, distribution or reproduction is permitted which does not comply with these terms.

frontiers in Oncology

ORIGINAL RESEARCH
published: 25 March 2022
doi: 10.3389/fonc.2022.865745

Prognostic Value of Lymph Node Evaluation in Stage II Small Bowel Adenocarcinoma: An Updated Analysis of Surveillance, Epidemiology, and End Results Database

Zhen Liu[1,2†], *Kun Liu*[3,4,5,6†], *Jiale Gao*[3,4,5,6], *Chao Jing*[3,4,5,6], *Yanhong Ma*[1], *Shu Zheng*[2*] and *Jianzhen Shan*[1*]

[1] Department of Oncology, The First Affiliated Hospital, Zhejiang University School of Medicine, Hangzhou, China, [2] Cancer Institute (Key Laboratory for Cancer Intervention and Prevention, China National Ministry of Education, Zhejiang Provincial Key Laboratory of Molecular Biology in Medical Sciences), The Second Affiliated Hospital, Zhejiang University School of Medicine, Hangzhou, China, [3] Department of General Surgery, Beijing Friendship Hospital, Capital Medical University, Beijing, China, [4] Clinical Center for Colorectal Cancer, Capital Medical University, Beijing, China, [5] Beijing Key Laboratory of Cancer Invasion and Metastasis Research, Beijing, China, [6] National Clinical Research Center for Digestive Diseases, Beijing, China

OPEN ACCESS

Edited by:
Qi Liu,
Fudan University, China

Reviewed by:
Imerio Angriman,
University of Padua, Italy
Eva Lieto,
University of Campania
Luigi Vanvitelli, Italy
Felipe Luz,
Hospital do Câncer em Uberlândia - Grupo Luta Pela Vida, Brazil

***Correspondence:**
Shu Zheng
zhengshu@zju.edu.cn
Jianzhen Shan
shanjz@zju.edu.cn

[†]These authors have contributed equally to this work

Specialty section:
This article was submitted to Surgical Oncology, a section of the journal Frontiers in Oncology

Received: 30 January 2022
Accepted: 03 March 2022
Published: 25 March 2022

Citation:
Liu Z, Liu K, Gao J, Jing C, Ma Y, Zheng S and Shan J (2022) Prognostic Value of Lymph Node Evaluation in Stage II Small Bowel Adenocarcinoma: An Updated Analysis of Surveillance, Epidemiology, and End Results Database. Front. Oncol. 12:865745. doi: 10.3389/fonc.2022.865745

Background: Due to the lack of large-scale clinical trials, the treatment strategies of small bowel adenocarcinoma (SBA) are controversial, especially for stage II patients. According to the National Comprehensive Cancer Network (NCCN) guideline, few lymph nodes (LNs) examined (<5 for duodenum or <8 for jejunal/ileal primary location) are one of the high-risk features for stage II patients, for whom adjuvant chemotherapy is recommended. This consensus is originally drawn from data in the Surveillance, Epidemiology, and End Results Database (SEER) between 1988 and 2010. However, the surgical modalities and chemotherapy strategies changed a lot after 2004 for SBA patients. The previous data may not represent a true picture of current therapeutics. Thus, we reanalyzed the SEER database and updated the cutoff point of LN numbers resected with respect to cancer-specific survival (CSS) using the latest SEER information.

Methods: Patients diagnosed with stage II SBA and who underwent curative surgery between 2004 and 2018 were extracted from the SEER database. CSS was calculated using the Kaplan–Meier method and compared by log-rank test. Maximum survival differences based on total LNs examined for duodenal and jejunoileal tumors were determined separately with the cut-point analysis and maximum log-rank χ^2 statistic. A nomogram model was constructed based on the multivariate Cox analysis to predict 5- and 10-year CSS and was then validated with an internal cohort.

Results: A total of 935 stage II SBA patients met the inclusion criteria. The greatest difference in survival was found in patients who had removal of at least 5 LNs for duodenal and 12 LNs for jejunoileal tumors. Multivariate Cox analysis showed that age, T stage, histology grade, primary site, and LN numbers were independent prognostic factors for survival. The C index of nomogram model was 0.701 (95% CI, 0.661–0.741, $p < 0.001$).

Conclusions: The number of LNs harvested is an important prognostic factor for survival in stage II SBA patients. LN number examined <5 remains a high-risk factor for duodenum, but the cutoff point for jejunal/ileal tumors should rise from 8 to 12. Appropriate radical lymphadenectomy should be performed in stage II SBA surgery.

Keywords: small bowel adenocarcinoma, lymph node evaluation, cancer-specific survival, stage II patient, SEER database

INTRODUCTION

Small bowel adenocarcinoma (SBA) is an uncommon cancer of the gastrointestinal tract, which accounts for less than 5% of all gastrointestinal malignancies (1). SBA is generally defined as duodenal, jejunal, and ileal adenocarcinoma. Its mechanisms are poorly understood (2). Due to the lack of large-scale, multicenter, randomized controlled trials, the optimal therapeutics are controversial. The clinical practices on SBAs usually follow the guidelines of colorectal cancers (CRCs), in which surgery is the main strategy for early-stage disease and chemotherapy for advanced disease (3).

Radical resection is the standard treatment for stage II SBAs. However, the efficacy of adjuvant treatment for these patients is unclear. Previous studies reported that the number of lymph nodes (LNs) removed during surgery is an essential indicator for evaluating the severity and survival of patients (4). The National Comprehensive Cancer Network (NCCN) guideline of SBA (Version 2.2021) suggested that inadequate LNs examined (<5 for duodenal or <8 for jejunal/ileal primary tumor location) was one of the high-risk features for stage II SBA patients, for whom adjuvant chemotherapy was recommended. This consensus was drawn from two studies conducted by Thuy et al. and Overman et al., which analyzed SBA patients from the Surveillance, Epidemiology, and End Results Database (SEER) (5, 6). The former study included patients from 1988 to 2010 and the latter from 1988 to 2005.

Nevertheless, the treatment strategies for intestinal cancers have changed a lot based on findings of several large clinical trials in the past 20 years, which remarkably prolonged the survival time of patients. Before the 2000s, 5-fluorouracil (5-FU) monotherapy was the standard adjuvant chemotherapy choice for CRC and SBA patients (7). Combined regimens of oxaliplatin and 5-FU have emerged as a new standard of care since 2002 (8, 9). Targeted anticancer agents such as bevacizumab and cetuximab have been approved by the Food and Drug Administration (FDA) since 2004 (10, 11). The advances of these new drugs improved clinical survival outcomes significantly.

Another fact is that surgical modalities for SBA and CRC improved a lot in the past 20 years. By analyzing data from the SEER database, we found that the median number of total LNs removed during surgery increased from 6 in 2004 to 15 in 2018 in stage II SBA patients.

Thus, we speculate that, since LNs as an essential prognostic factor, the data before the 2000s may not exactly represent the current strategies for SBA treatment, especially for patients with stage II disease. In this study, we updated the LN number as a risk factor for stage II SBA patients with the latest data from the SEER database between 2004 and 2018 and indeed found that the cutoff value of LNs removed for jejunum and ileum should be changed.

MATERIALS AND METHODS

Patients

All patients diagnosed as SBA (ICD-O-3:8140, 8143, 8144, 8145, 8210, 8211, 8220, 8255, 8260, 8261, 8262, 8263, 8310, 8480, 8481, and 8490) were extracted from the SEER database (http://seer.cancer.gov/) with SEER*Stat Software (version 8.3.9.2). To ensure comparable treatment methods with current clinical practice, only patients diagnosed after 2004 were included. Parameters included age, sex, tumor size, primary tumor site, LNs examined, distant metastasis, histological grade, surgery, survival time, and survival status. Tumor size and extension (T), LN metastases (N), and distance metastases status (M) were combined to classify patients to stage I to IV according to the American Joint Committee on Cancer (AJCC) 8th edition cancer staging system. Stage II patients with complete clinical information who underwent surgery and SBA as the first diagnosed tumor were included for further analysis.

Cut-Point Analysis for Total Lymph Nodes

Cancer-specific survival (CSS) was calculated using the Kaplan–Meier method, and comparisons were analyzed by the log-rank test. Patients were censored if they died from causes other than SBA or if they were alive at follow-up. Maximum survival differences based on total LNs examined were determined separately with the cut-point analysis and maximum log-rank χ^2 statistic (12). The point with maximum likelihood ratio chi-square value was selected as the optimal cut-point. The number of LNs removed lower than the cut-point value was regarded as high risk, while the LNs equal or higher than the cut-point value were marked as low risk.

Nomogram Construction

Patients were randomly assigned to a training cohort (70%) and a validation cohort (30%).

Univariate correlations between prognostic variables and CSS were carried out using the Kaplan–Meier method and log-rank test. Factors with a significant difference from univariate analysis were further analyzed in a multivariate Cox proportional hazards model. A nomogram model was constructed based on the training cohort to predict the 5- and 10-year CSS with the rms

package in R software version 3.5.1. The nomogram was then validated on the validation cohort. The discriminative capacity of the nomogram was evaluated with the concordance index (C-index). Calibration plots were constructed to compare the calibrations between nomogram-predicted and actual survival.

Statistical Analysis

Means and SDs for continuous variables were determined using descriptive statistics. Categorical and discrete variables were compared with the χ^2 test. Continuous variables were expressed as median with interquartile range. Student's t-test was used to compare means. Multivariate analyses were performed by multivariate Cox proportional hazards regression model using IBM SPSS (vision 26.0). Nomogram was generated by R software with the "rms" package (www.r-project.org). Hazard ratios (HRs) and their 95% CI were calculated. A two-sided p-value <0.05 was considered statistically significant.

Ethics Statement

This study was exempted from Institutional Review Board review because the SEER database contained no personal identifiers.

RESULTS

Patient Characteristics

From 2004 to 2018, 8,960 adults were diagnosed with SBA. A total of 2,694 cases were excluded because it was not their first diagnosed tumor, and 631 cases were excluded due to missing survival time (survival month was 0 or unknown). Out of 5,635 primary SBA patients, 1,327 patients were under stage II. The numbers of LN resected were unknown among 13 patients. The primary site of 209 patients was unspecified, and 170 patients did not undergo surgery. Finally, a total of 935 SBA patients with stage II and underwent surgery were enrolled, including 413 (44.2%) in the duodenum and 522 (55.8%) in the jejunoileum (**Figure 1**).

As shown in **Table 1**, two patient cohorts were comparable with respect to gender, age, grade, ethnicity, and area. However, the median number of LNs resected was prone to be higher in the duodenum than jejunoileal cohort, which was 11 (95% CI, 10–12) and 9 (95% CI, 8–11), respectively. There were more patients with the T4 stage in the duodenum (43.6%) than the jejunoileum (36.6%).

Cut-Point Analysis for Total Lymph Nodes

To identify the optimum cut-point number of LNs that should be resected during surgery, maximum log-rank χ^2 analysis was performed. We found that the greatest difference in survival was found in patients who had removals of at least 5 LNs for duodenal and 12 LNs for jejunoileal tumors (**Table 2**).

Kaplan–Meier survival curves are shown in **Figure 2**. Patients above the cut-off point showed greater benefits in median survival for both duodenal (HR: 0.39, 95% CI, 0.26 to 0.58, Pearson's chi-square: 20.69, $p < 0.0001$) and jejunoileal tumors (HR: 0.71, 95% CI, 0.52 to 0.98, Pearson's chi-square: 4.253, $p = 0.0392$).

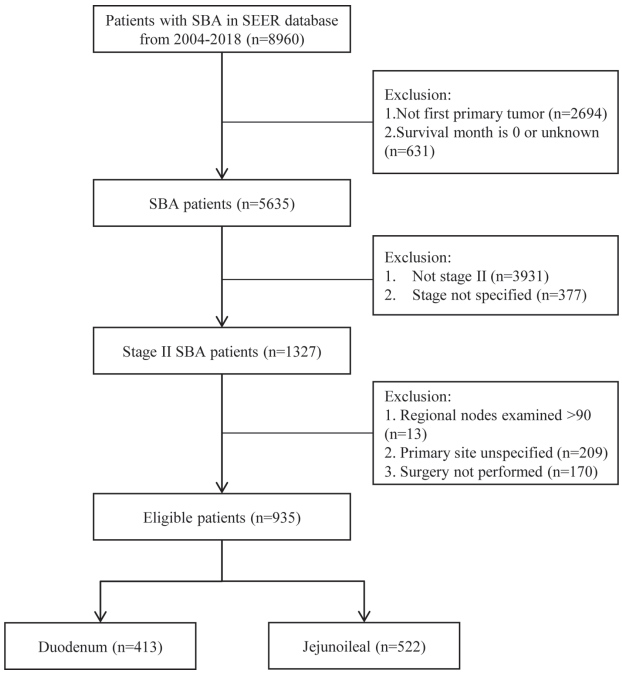

FIGURE 1 | Flowchart demonstrating the selection processes of cases from SEER database used in this analysis. SBA, small bowel adenocarcinoma; SEER, Surveillance, Epidemiology, and End Results Database.

Multivariable Survival Analysis

Many factors were found to influence the CSS. The multivariate Cox regression was performed to explore potential factors that might be associated with the survival time. As shown in **Table 3**, age, T stage, histology grade, primary site, and LNs examined were independent prognostic factors for survival.

We can see that older age (≥45 years), T4, and higher histology grade were negative prognostic factors. Tumors located in the jejunoileum had a better CSS than in the duodenum (HR: 0.745, 95% CI, 0.565–0.981, $p < 0.05$). LN risks based on the cut-point analysis (5 for duodenum and 12 for jejunoileum) were significantly related to CSS (low risk/high risk, HR: 0.522, 95% CI, 0.401–0.678, $p < 0.001$).

Nomogram Construction and Validation

The multivariate Cox regression model revealed that CSS was associated with age, T stage, pathological grade, tumor location, and LNs risks. Based on these variables, we established a CSS nomogram to predict the 5- and 10-year survival rates of SBA patients.

The nomogram in **Figure 3** shows that pathological grade at diagnosis was the greatest contributor to the prognosis, followed by T stage, LN risk, age, and primary site. The C index of this model was 0.701 (95% CI, 0.661–0.741, $p < 0.001$).

We performed an internal validation of this nomogram. The results showed that the C-index of the validation nomogram was 0.687 (95% CI 0.653–0.721, $p < 0.001$). The area under the curve (AUC) of 10-year survival was 0.72 (95% CI 0.66–0.79) for the training cohort and 0.70 (0.64–0.75) for the validation cohort (**Figures 4A, B**).

TABLE 1 | Clinicopathological characteristics of patients with small bowel adenocarcinoma.

	Entire cohort, n = 935	Duodenum, n = 413	Jejunoileum, n = 522
Gender (%)			
Male	482 (51.6)	211 (51.1)	271 (51.9)
Female	453 (48.4)	202 (48.9)	251 (48.1)
Age (%)			
<45	94 (10.1)	37 (9.0)	57 (10.9)
45–64	394 (42.1)	164 (39.7)	230 (44.1)
≥65	447 (47.8)	212 (51.3)	235 (45.0)
T stage (%)			
T3	564 (60.3)	233 (56.4)	331 (63.4)
T4	371 (39.7)	180 (43.6)	191 (36.6)
Median number of LNs examined (95% CI)	10 (9-11)	11 (10-12)	9 (8-11)
Histology grade (%)			
Well	94 (10.1)	34 (8.2)	60 (11.5)
Moderate	490 (52.4)	206 (50.0)	284 (54.4)
Poor	250 (26.7)	120 (29.1)	130 (24.9)
Undifferentiated	15 (1.6)	7 (1.7)	8 (1.5)
Unknown	86 (9.2)	46 (11.1)	40 (7.7)
Year diagnosed (%)			
2004–2008	281 (30.1)	132 (32.0)	149 (28.5)
2009–2013	310 (33.2)	137 (33.2)	173 (33.1)
2014–2018	344 (36.8)	144 (34.9)	200 (38.3)
Ethnicity (%)			
White	712 (76.1)	324 (78.5)	388 (74.3)
Black	167 (17.9)	63 (15.3)	104 (19.9)
Asian	43 (4.6)	22 (5.3)	21 (4.0)
Others	13 (1.4)	4 (0.9)	9 (1.7)
Area (%)			
Urban	838 (89.6)	375 (90.18)	463 (88.7)
Rural	97 (10.4)	38 (9.2)	59 (11.3)

LNs, lymph nodes.

TABLE 2 | Cut-point analyses for detecting optimal number of lymph nodes with respect to cancer-specific survival.

No. of LNs examined	Duodenum		Jejunoileum	
	χ^2	p-Value	χ^2	p-Value
1 vs. ≥2	12.95	0.0003	1.17	0.2795
≤2 vs. ≥3	11.73	0.0006	1.973	0.1602
≤3 vs. ≥4	9.54	0.002	2.281	0.131
≤4 vs. ≥5	**20.69**	**<0.0001**	1.823	0.1769
≤5 vs. ≥6	19.76	<0.0001	1.184	0.2766
≤6 vs. ≥7	17.84	<0.0001	1.268	0.2602
≤7 vs. ≥8	10.76	0.001	1.968	0.1606
≤8 vs. ≥9	14.03	0.0002	3.478	0.0622
≤9 vs. ≥10	11.72	0.0006	3.476	0.0623
≤10 vs. ≥11	10.06	0.0015	3.486	0.0619
≤11 vs. ≥12	15.65	<0.0001	**4.253**	**0.0392**
≤12 vs. ≥13	13.95	0.0002	3.168	0.0751
≤13 vs. ≥14	13.72	0.0002	3.672	0.0553
≤14 vs. ≥15	13.15	0.0003	3.418	0.0645
≤15 vs. ≥16	13.83	0.0002	3.713	0.054
≤16 vs. ≥17	14.2	0.0002	4.061	0.0439
≤17 vs. ≥18	12.72	0.0004	3.244	0.0717

Values in bold indicate the highest χ^2 and statistical significance.
LNs, lymph nodes.

Calibration plots revealed a strong correlation between predictions estimated by the nomogram and actual observations for both the training and validation cohorts, especially for the 10-year CSS (**Figures 4C, D**).

DISCUSSION

SBA treatment is challenging, given its relative rarity and advanced stage of diagnosis. Due to the lack of large-scale,

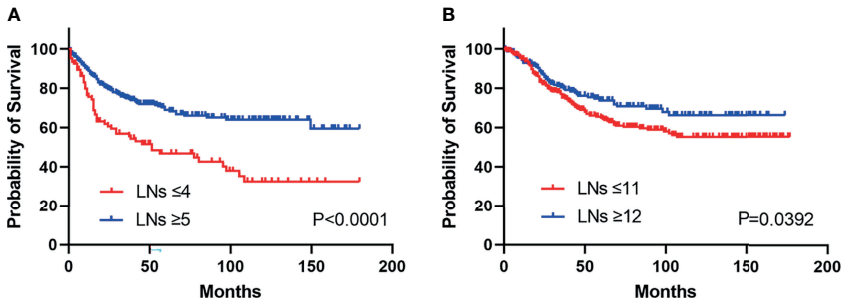

FIGURE 2 | Kaplan–Meier curves illustrate cancer-specific survival stratified by lymph node risk in patients with duodenal (HR: 0.39, 95% CI, 0.26 to 0.58, p < 0.0001) **(A)** and jejunoileal tumors (HR: 0.71, 95% CI, 0.52 to 0.98, p = 0.0392) **(B)**. LNs, lymph nodes.

TABLE 3 | Multivariate Cox regression analyses of patients with small bowel carcinoma.

	HR	95% CI	p-Value
Age at diagnosis			
<45	Reference		
45–64	1.069	0.679–1.683	0.772
≥65	1.787	1.152–2.773	0.009
T stage			<0.001
T3	Reference		
T4	2.076	1.635–2.636	<0.001
Histology grade			
Well	Reference		
Moderate	1.412	0.884–2.256	0.148
Poor	1.827	1.125–2.967	0.014
Undifferentiated	2.425	1.060–5.550	0.035
Unknown	1.297	0.631–2.670	0.479
Primary site			
Duodenum	Reference		
Jejunoileum	0.744	0.565–0.981	0.036
LNs examined			
High risk	Reference		
Low risk	0.521	0.401–0.678	<0.001

HR, hazard ratio; LNs, lymph nodes.

multicenter, randomized, controlled trials, the treatment strategies usually follow the consent of patients with CRCs. It is well accepted that patients with stage II CRC should be divided into a high-risk group and low-risk group according to several postoperative histology features, such as T4, grade 3 or 4, lymphovascular or perineural invasion, and <12 LNs examined (13). Patients with these high-risk features should receive adjuvant chemotherapy after the initial surgery (14). Similar evaluations had also been made for SBA. High-risk features for stage II SBA patients include T4 stage, close or positive surgical margins, few LNs examined (<5 for duodenal or <8 for jejunal/ileal primary tumor location), or tumor perforation according to NCCN guidelines. Our study focused on one of these features, LNs examined, and found that the optimal cut-off numbers for stage II SBA patients should be updated to 12 for jejunal/ileal primary tumor location, which was consistent with stage II CRC patients.

The recommendation of LN risks in the NCCN guideline (<5 for duodenal or <8 for jejunal/ileal primary tumor location) is drawn from patients in the SEER database from 1988 to 2010 and 1988 to 2005 (5, 6). However, the treatment strategies changed significantly in recent years. A recent study demonstrated that the LN numbers in NCCN guidelines (<5 for duodenal or <8 for jejunal/ileal primary tumor location) did not discriminate SBA patients from high and low risk (p = 0.166) (15). In **Figure 5**, we can see that the median number of surgical removed LNs in stage II SBA patients is increasing, from 6 (95% CI, 6–8) in 2004 to 15 (95% CI, 8–17) in 2018. On the other hand, the addition of oxaliplatin to fluorouracil-based chemotherapy has become the standard treatment since 2002, which is more efficient than 5-FU monotherapy (9). Targeted anticancer agents such as bevacizumab and cetuximab have been developed since 2004. These strategies improved survival time significantly. Thus, the outcomes of SBA patients before 2004 may not represent a true picture of current treatments.

Our study updated the survival data using the latest SEER database in patients with stage II SBA diagnosed between 2004 and 2018. We demonstrated that patients with stage II SBA and

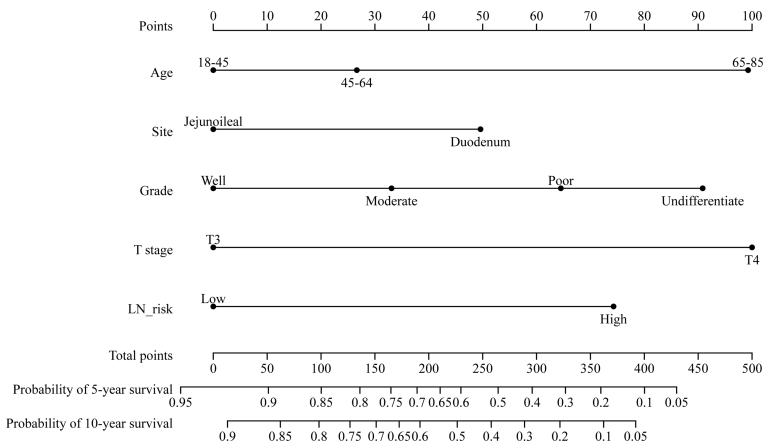

FIGURE 3 | Nomogram predicting the 5- and 10-year cancer-specific survival of patients with stage II small bowel adenocarcinoma. LN risk, lymph node risk.

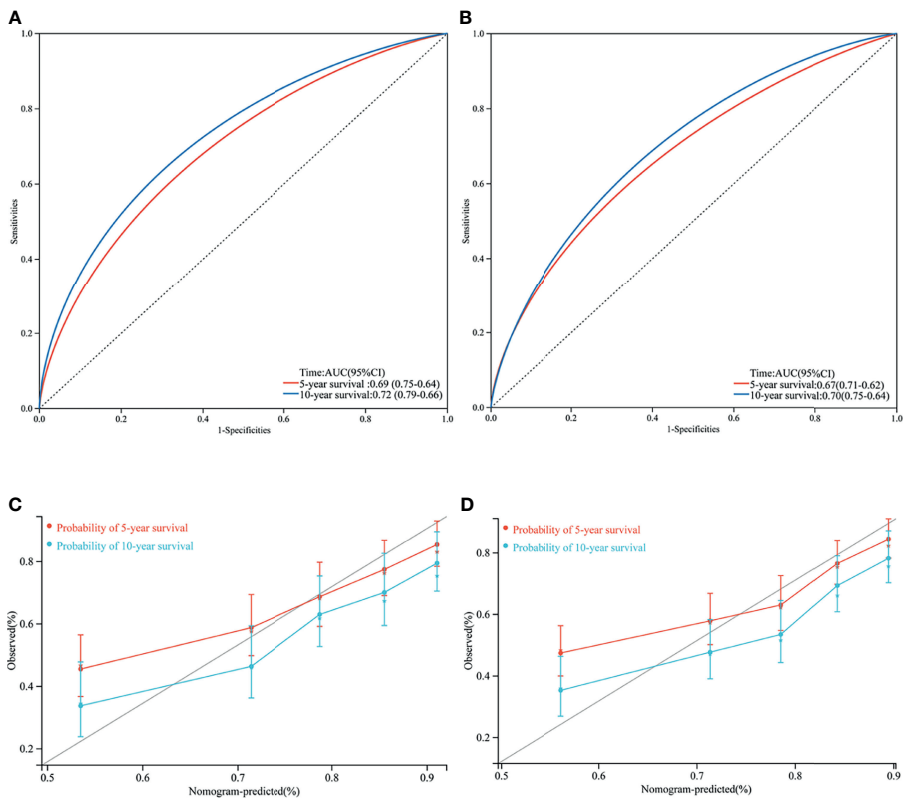

FIGURE 4 | Area under curve (AUC) of the training set **(A)** and validation set **(B)**; 5- and 10- year cancer-specific survival according to the training set **(C)** and the validation set **(D)**.

total examined LNs <5 for duodenal tumors or <12 for jejunal/ileal primary tumors were at high risk. These patients may benefit from adjuvant chemotherapy. We also established a nomogram to predict the 5- and 10-year survival rates of SBA patients, which was more accurate than the AJCC staging system.

Several limitations exist in our analysis. There is a lack of treatment information in the SEER database, such as surgical margins, tumor perforation, chemotherapy regimen, recurrence, and molecular features. We cannot compare the survival outcome directly between patients with and without adjuvant

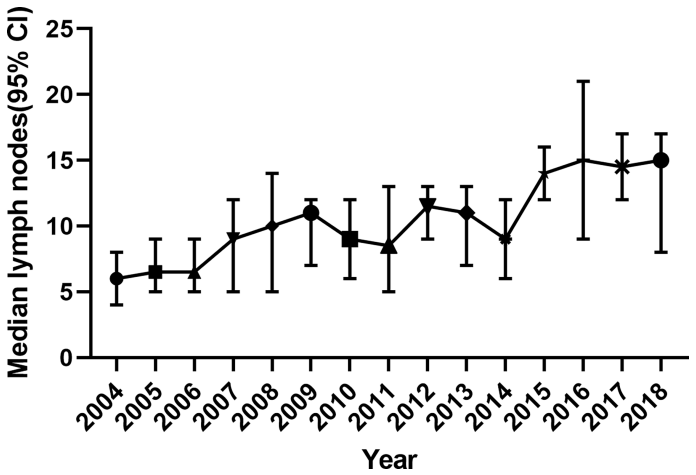

FIGURE 5 | The number of surgically removed lymph nodes in stage II SBA patients from 2004 to 2018, indicated by median and 95% CI. SBA, small bowel adenocarcinoma.

chemotherapy. SEER database is retrospective, and we excluded patients with incomplete information, which may lead to selection bias. Though 935 patients were finally included in our study, large multicenter, randomized clinical trials are strongly needed to further confirm the conclusion. The BALLAD trial (NCT02502370) is ongoing, which is the first prospective trial designed to recruit 100 participants and to assess the benefit of adjuvant chemotherapy versus observation alone in patients with stage I–III SBA. Primary outcomes are 3-year disease-free survival and overall survival (OS), with expected results in 2023.

CONCLUSION

The total number of LNs harvested is an important prognostic factor of survival in stage II SBA. Patients with total examined LNs <5 for duodenal or <12 for jejunal/ileal primary tumor are at high risk. Sufficient LN dissection is recommended for stage II SBA patients.

DATA AVAILABILITY STATEMENT

The original contributions presented in the study are included in the article/supplementary material. Further inquiries can be directed to the corresponding authors.

ETHICS STATEMENT

Ethical review and approval were not required for the study on human participants in accordance with the local legislation and institutional requirements. Written informed consent for participation was not required for this study in accordance with the national legislation and the institutional requirements.

AUTHOR CONTRIBUTIONS

ZL, SZ, and JS designed the study. ZL, KL, JG, CJ, and YM collected and analyzed the data. ZL and KL organized the manuscript. All authors have read and approved the final manuscript.

FUNDING

This work is supported by grants from the National Natural Science Foundation of China (81602635), Zhejiang Provincial Natural Science Foundation (LY21H160042), and Zhejiang Medical and Health Project (2017205840, 2018274816, 2019334185).

ACKNOWLEDGMENTS

The authors appreciate the contribution of the SEER database.

REFERENCES

1. Aparicio T, Zaanan A, Svrcek M, Laurent-Puig P, Carrere N, Manfredi S, et al. Small Bowel Adenocarcinoma: Epidemiology, Risk Factors, Diagnosis and Treatment. *Dig Liver Dis* (2014) 46(2):97–104. doi: 10.1016/j.dld.2013.04.013
2. Delaunoit T, Neczyporenko F, Limburg PJ, Erlichman C. Pathogenesis and Risk Factors of Small Bowel Adenocarcinoma: A Colorectal Cancer Sibling? *Am J Gastroenterol* (2005) 100(3):703–10. doi: 10.1111/j.1572-0241.2005.40605.x
3. Reynolds I, Healy P, McNamara DA. Malignant Tumours of the Small Intestine. *Surgeon* (2014) 12(5):263–70. doi: 10.1016/j.surge.2014.02.003
4. Pedersen KS, Raghav K, Overman MJ. Small Bowel Adenocarcinoma: Etiology, Presentation, and Molecular Alterations. *J Natl Compr Canc Netw* (2019) 17(9):1135–41. doi: 10.6004/jnccn.2019.7344

5. Overman MJ, Hu CY, Wolff RA, Chang GJ. Prognostic Value of Lymph Node Evaluation in Small Bowel Adenocarcinoma: Analysis of the Surveillance, Epidemiology, and End Results Database. *Cancer* (2010) 116(23):5374–82. doi: 10.1002/cncr.25324
6. Tran TB, Qadan M, Dua MM, Norton JA, Poultsides GA, Visser BC. Prognostic Relevance of Lymph Node Ratio and Total Lymph Node Count for Small Bowel Adenocarcinoma. *Surgery* (2015) 158(2):486–93. doi: 10.1016/j.surg.2015.03.048
7. Singhal N, Singhal D. Adjuvant Chemotherapy for Small Intestine Adenocarcinoma. *Cochrane Database Syst Rev* (2007) 3:CD005202. doi: 10.1002/14651858.CD005202.pub2
8. Ibrahim A, Hirschfeld S, Cohen MH, Griebel DJ, Williams GA, Pazdur R. FDA Drug Approval Summaries: Oxaliplatin. *Oncologist* (2004) 9(1):8–12. doi: 10.1634/theoncologist.9-1-8
9. Overman MJ, Kopetz S, Wen S, Hoff PM, Fogelman D, Morris J, et al. Chemotherapy With 5-Fluorouracil and a Platinum Compound Improves Outcomes in Metastatic Small Bowel Adenocarcinoma. *Cancer* (2008) 113 (8):2038–45. doi: 10.1002/cncr.23822
10. Strickler JH, Hurwitz HI. Bevacizumab-Based Therapies in the First-Line Treatment of Metastatic Colorectal Cancer. *Oncologist* (2012) 17(4):513–24. doi: 10.1634/theoncologist.2012-0003
11. Alekshun T, Garrett C. Targeted Therapies in the Treatment of Colorectal Cancers. *Cancer Control* (2005) 12(2):105–10. doi: 10.1177/107327480501200205
12. Altman DG, Lausen B, Sauerbrei W, Schumacher M. Dangers of Using "Optimal" Cutpoints in the Evaluation of Prognostic Factors. *J Natl Cancer Inst* (1994) 86(11):829–35. doi: 10.1093/jnci/86.11.829
13. Boland CR, Goel A. Prognostic Subgroups Among Patients With Stage II Colon Cancer. *N Engl J Med* (2016) 374(3):277–8. doi: 10.1056/NEJMe1514353
14. Simillis C, Singh H, Afxentiou T, Mills S, Warren OJ, Smith JJ, et al. Postoperative Chemotherapy Improves Survival in Patients With Resected High-Risk Stage II Colorectal Cancer: Results of a Systematic Review and Meta-Analysis. *Colorectal Dis* (2020) 22(10):1231–44. doi: 10.1111/codi.14994
15. Vanoli A, Grillo F, Guerini C, Neri G, Arpa G, Klersy C, et al. Prognostic Role of Mismatch Repair Status, Histotype and High-Risk Pathologic Features in Stage II Small Bowel Adenocarcinomas. *Ann Surg Oncol* (2021) 28(2):1167–77. doi: 10.1245/s10434-020-08926-4

Conflict of Interest: The authors declare that the research was conducted in the absence of any commercial or financial relationships that could be construed as a potential conflict of interest.

Publisher's Note: All claims expressed in this article are solely those of the authors and do not necessarily represent those of their affiliated organizations, or those of the publisher, the editors and the reviewers. Any product that may be evaluated in this article, or claim that may be made by its manufacturer, is not guaranteed or endorsed by the publisher.

Copyright © 2022 Liu, Liu, Gao, Jing, Ma, Zheng and Shan. This is an open-access article distributed under the terms of the Creative Commons Attribution License (CC BY). The use, distribution or reproduction in other forums is permitted, provided the original author(s) and the copyright owner(s) are credited and that the original publication in this journal is cited, in accordance with accepted academic practice. No use, distribution or reproduction is permitted which does not comply with these terms.

frontiers | Frontiers in Oncology

ORIGINAL RESEARCH
published: 08 April 2022
doi: 10.3389/fonc.2022.832038

Progression Patterns and Post-Progression Survival in Recurred Intrahepatic Cholangiocarcinoma Patients: A Novel Prognostic Nomogram Based on Multicenter Cohorts

Chongyu Zhao[1†], Chaobin He[1†], Jiawei Lu[2†], Xin Huang[1], Cheng Chen[3] and Xiaojun Lin[1*]*

[1] Department of Pancreatobiliary Surgery, State Key Laboratory of Oncology in South China, Collaborative Innovation Center for Cancer Medicine, Sun Yat-sen University Cancer Center, Guangzhou, China, [2] Department of Oncology, The Second Hospital of Dalian Medical University, Dalian, China, [3] Department of Cardiology, The First Affiliated Hospital of Dalian Medical University, Dalian, China

Background: The post-progression survival (PPS) of recurred intrahepatic cholangiocarcinoma (iCCA) patients relates to the characteristics of tumor progression. Moreover, the prediction model of PPS in those patients has not been well established. This study aimed at developing a novel nomogram for predicting PPS in recurred iCCA patients.

Method: Clinical characteristics were retrospectively collected in 396 patients diagnosed with iCCA from cohorts of Sun Yat-sen University Cancer Center (SYSUCC) and the First Hospital of Dalian Medical University (FHDMU). The PPS in patients with different progression patterns was investigated. The nomogram of PPS was established with the Cox regression model in the primary cohort. Then the nomogram was verified in the external validation cohort.

Results: Liver progression was the commonest pattern (42.08%) in recurred iCCA patients, while patients with local LN progression had significantly better PPS than those with other patterns. The independent prognostic factors comprised elevated CEA levels, tumor differentiation, N stage 8th, adjuvant therapy, Local LN metastasis, Liver Metastasis only, and Multiple Metastasis. The nomogram constructed on these factors achieved satisfied C-indexes of 0.794 (95% CI 0.769–0.828) and 0.827 (0.779–0.876) for the training and validation cohorts, respectively. These values were significantly higher than those of the 8th TNM stage system (all $p < 0.001$). The recurred iCCA patients could be precisely classified into high- and low-risk groups according to the cutoff point of this nomogram ($p < 0.01$).

OPEN ACCESS

Edited by:
Qi Liu,
Fudan University, China

Reviewed by:
Chongyi Jiang,
Fudan University, China
Duilio Pagano,
Mediterranean Institute for Transplantation and Highly Specialized Therapies (ISMETT), Italy
Nasrin Borumandnia,
Shahid Beheshti University of Medical Sciences, Iran

***Correspondence:**
Xiaojun Lin
linxj@sysucc.org.cn
Chaobin He
hechb@sysucc.org.cn

†These authors have contributed equally to this work

Specialty section:
This article was submitted to Gastrointestinal Cancers: Hepato Pancreatic Biliary Cancers, a section of the journal Frontiers in Oncology

Received: *09 December 2021*
Accepted: *09 March 2022*
Published: *08 April 2022*

Citation:
Zhao C, He C, Lu J, Huang X, Chen C and Lin X (2022) Progression Patterns and Post-Progression Survival in Recurred Intrahepatic Cholangiocarcinoma Patients: A Novel Prognostic Nomogram Based on Multicenter Cohorts. Front. Oncol. 12:832038. doi: 10.3389/fonc.2022.832038

Conclusion: The investigation of progression patterns and the development of this nomogram can offer new evidence to precisely postoperative and post-progression management of iCCA patients.

Keywords: intrahepatic cholangiocarcinoma, post-progression survival, recurrence, prognosis, nomogram

INTRODUCTION

Intrahepatic cholangiocarcinoma (iCCA) is composed of heterogeneous malignancies that originate from, hence displaying pathological characteristics of the biliary track, or trans-differentiate from hepatocytes (1, 2). Radical surgical resection offers the only treatment option that increases potential long-term survival for iCCA patients. It has been reported in numerous studies that overall survival of iCCA patients ranges from 17% to 42% after surgery (3–6), resulting in the rise of recurrence rates in these patients. In patients with 26-month median disease-free survival, recurrence rates were reported to be up to 50%–60% (7).

Additionally, the outcomes of recurred iCCA patients could be determined by various factors. In a previous study in patients with recurrence in pancreatic ductal adenocarcinoma, it was observed that the patients with multiple metastases showed significantly distinct outcomes as compared to those with "liver only" metastasis, suggesting that different survival outcomes in patients could be resulted from different progression patterns (8). Moreover, in the efforts of developing effective adjuvant therapy for iCCA patients, treatments after operation were proven to improve the outcomes in patients with recurrence (9). Consequently, the number of patients with post-progression survival (PPS) have been accounting for an increasing proportion in overall survival (OS), and the vital role of post-progression survival in recurred iCCA patients is now well-established. Even though there were several predictive stage systems estimating the OS or progression-free survival (PFS) of iCCA patients, to date there remains no established model to predict the outcome for patients in the category of PPS (10). To better stratify the patients for precise medical intervention, it would be instrumental to construct a predictive system of PPS in iCCA patients.

Herein, in the present study, we sought to compare the PPS in iCCA patients with different progression patterns in multicenter patient cohorts and establish a prognostic nomogram to predict the PPS of iCCA patients after radical surgical resection based on multicenter cohorts.

METHOD

Patients' Characteristics

396 consecutive patients pathologically diagnosed with iCCA who underwent radical surgical resection at Sun Yat-sen University Cancer Center (SYSUCC) and the First Affiliated Hospital of Dalian Medical University (FHDMU) were preliminarily enrolled in the present study (289 patients from SYSUCC between January 2000 and December 2018 as the primary cohort and 107 patients from FHDMU between May 2013 and December 2019 as the validation cohort). Variables of the total patients related to preoperative baseline characteristics, liver function, tumor marker, pathological diagnosis, tumor progression, and time to death or last visit were collected from the medical record, as shown in **Supplementary Table 1**. The two cohorts of this study owned the same indications and contraindications to resection. Then a total of 280 recurred patients were finally enrolled in the recurrence cohort (200 patients from the primary cohort and 78 patients from the validation cohort). Previously researched inflammation-based indexes were calculated and analyzed as well. This study obtained the written informed consent from all the patients and was approved by the ethics committees of two participating centers.

Follow-up and Survival Outcomes

The routine postoperative follow-up began at 30 days after resection, then each 3 months for the first year and 6 months until death or dropout. Patterns and timing of recurrence were obtained at regular follow-up, which consisted of regular abdominal CT, carcinoembryonic antigen (CEA) measurement, and carbohydrate antigen 19-9 (CA19-9) measurement. "Elevated CEA" was defined as CEA value >5ng/ml; other threshold values of those characteristics are exhibited in **Supplementary Table 1**. Additional imaging examinations were conducted to determine patterns of recurrence in necessary. Follow-up data of two cohorts were retrieved on November 30, 2020. The outcome variables of this study, PPS, were calculated from the date of tumor progression to the date of death or last follow-up.

Progression Patterns

Imaging findings were the primary methods to confirm the progression patterns. While the imaging findings were ambiguous about recurrence or progression, biopsy was conducted. The progression patterns were described by the first location of recurrence. The demarcation point distinguishing early and late progression was defined as 2 years after surgical resection as previous studies (11). The term "Local LN" referred to local lymph-node metastasis. The term "Liver" referred to isolated hepatic recurrence, while the term "Multiple" referred to multiple metastases.

Statistical Analysis

Categorical variables were analyzed in whole numbers and proportions. Proportions were compared using the chi-square test or the Fisher exact test. The Mann–Whitney U test was

conducted to compare the distributions of continuous variables. Survival curves were calculated using the Kaplan–Meier method and then compared with the log-rank test. The multivariable analysis of the predictive factors of PPS was performed using the Cox regression model. Then the nomogram was constituted based on the multivariable analysis in the training cohort. The predictive performance was measured by Harrell's concordance index (C-index) and assessed with calibration curves and survival curves. SPSS software version 22 (SPSS Inc., Chicago, IL, USA) and R software version 4.1.1 (R Development Core Team; http://www.r-project.org) were used. All statistical inferences were based on two-sided p values, with values <0.05 taken to indicate statistical significance. Particularly, those variables which had $p < 0.2$ in the univariable analysis were included in the multivariable regression analysis.

RESULTS

Characteristics of Patients

The preoperative clinical, surgical, and postoperative pathological demographics of the recurred iCCA patients in the primary and validation cohorts are exhibited in **Table 1**. The primary cohort consisted of 111 (38.4%) female and 178 (61.6%) male patients with a median age of 56 years. A total of 130 (45.0%) patients had received chemotherapy after resection. As for the validation cohort, 45 females (42.1%) and 62 males (57.9%) with a median age of 64 years were enrolled. Thirty-five (32.7%) patients had received chemotherapy after resection. There were no significant differences in baseline characteristics between the two cohorts.

The general survival outcomes were as follows: in the primary cohort, the 1-, 2-, and 3-year OS rates were 78.2%, 64.9%, and 52.2%, respectively; the 1-, 2-, and 3-year PFS were 48.5%, 35.4%, and 31.5% while the 1-, 2-, 3-year PPS were 49.6%, 30.5%, and 19.8%, respectively; in the validation cohort, the 1-, 2-, 3-year OS rates were 61.8%, 40.4%, and 32.7% and the 1-, 2-, and 3-year PFS were 44.7%, 29.3%, and 21.0% while the 1-, 2-, and 3-year PPS were 53.8%, 24.3%, and 2.6%, respectively.

Comparisons of PPS Classified by Progression Patterns

The progression patterns of iCCA patients after surgery were classified into 5 subgroups (**Figure 1A**): Local LN, Liver only, Local plus Liver, Multiple, and Others. Particularly, there were 17 patients in the "Others" group, including 10 patients with isolated lung metastasis, 4 patients with single distant metastasis, and 2 patients with other non-typical metastasis. Although the most optimistic survival curve was observed in this group, the "Others" progression pattern was not included in the subsequent analysis because of its heterogeneity and minor sample size.

Liver progression was the commonest pattern since there were 85 (42.08%) patients who had isolated hepatic progression, followed by Local progression (41 patients, 20.30%) and Multiple progression (40 patients, 19.80%), while Local plus Liver was the rarest pattern (19 patients, 9.41%). Patients with liver progression had the longest median PPS of 17.70 months (95% CI 12.476–22.924), followed by patients with Local LN metastasis (median PPS 16.13 months, 95% CI 9.021–23.246) and Local plus Liver progression (median PPS 10.57 months, 95% CI 3.266–17.867).

The comparisons of PPS between Local LN and Liver showed no significant differences (**Figure 1B**); apart from this result, Local LN had significantly higher survival rates ($p < 0.05$) than Local plus Liver (**Figure 1C**) and Multiple (**Figure 1D**). In addition, the comparisons of PPS between Liver and Local plus Liver (**Figure 1E**), between Liver and Multiple (**Figure 1F**), and between Local plus Liver and Multiple (**Figure 1G**) revealed that the former owned a higher PPS rate ($p < 0.05$) than the latter. Overall, patients with local LN progression had significantly higher survival rates than those with other progression patterns. On the contrary, multiple metastases corresponded with the poorest rates among these patterns.

Prognostic Factors of PPS

The primary cohort was employed to conduct univariable and multivariable analyses and further establish the predictive nomogram. The univariable analysis identified 16 factors significantly correlating to PPS (**Table 2**). The Cox-regression analysis was conducted on the basis of univariable analysis. As a result, the multivariable analysis defined CEA (HR, 2.102; 95% CI 1.318–3.071; $p < 0.001$), tumor differentiation (HR, 6.125; 95% CI 1.228–30.456; $p = 0.027$), N stage 8th (HR, 6.077; 95% CI 0.680–54.274; $p = 0.036$), after-operation therapy (HR, 0.474; 95% CI 0.315–0.713; $p < 0.001$), Local LN metastasis (HR, 0.938; 95% CI 0.852–1.291; $p = 0.041$), Liver Metastasis only (HR, 0.881; 95% CI 0.709–1.093; $p = 0.039$), and Multiple Metastases (HR, 0.434; 95% CI 0.335–0.561; $p < 0.001$) as independent prognostic factors of PPS (**Table 2**). The PPS survival curves stratified by these factors are shown in **Figure 2**.

Construction and Validation of Nomogram for PPS Prediction

According to the independent prognostic factors defined in the multivariable analysis, a nomogram was constructed to predict 1- and 2-year PPS for postoperative progressed iCCA patients (**Figure 3**). This nomogram could evaluate the probability of survival outcomes by adding up the scores for each variable. An objectively high agreement could be observed between actual and predicted survival in the calibration plots of both primary (**Figures 4A, B**) and validation cohorts (**Figures 4C, D**). The C-indexes of the present nomogram in the primary and validation cohorts were 0.794 (95% CI 0.769–0.828) and 0.827 (95% CI 0.532–0.678), respectively; these values were significantly higher than those of the 8th TNM stage system (**Table 3**). To further evaluate the performance of our nomogram, the decision curve analysis was carried out in both the primary and validation cohorts (**Figure 5**); the nomogram also showed more outstanding performance than the 8th TNM staging system did for PPS prediction in recurred iCCA patients. Furthermore, the total point of every patient in the primary

TABLE 1 | Clinical and pathological characteristics of recurred iCCA patients in the primary cohort (SYSUCC cohort) and validation cohort (FHDMU cohort).

Variables	Primary cohort (n = 202)	Validation cohort (n = 78)	Variables	Primary cohort (n = 202)	Validation cohort (n = 78)
Gender			mGPS		
Male	68 (33.7%)	33 (42.3%)	0	152 (75.2%)	26 (33.3%)
Female	134 (66.3%)	45 (57.7%)	1	47 (23.3%)	31 (39.7%)
Age (years)			2	3 (1.49%)	21 (26.9%)
≤60 years	74 (36.6%)	53 (67.9%)	Microvascular invasion		
>60 years	128 (63.4%)	25 (32.1%)	Absence	159 (78.7%)	69 (88.5%)
Progression period			Presence	43 (21.3%)	9 (11.5%)
Early	149 (73.8%)	56 (71.8%)	Lymph-vessel invasion		
Late	16 (7.92%)	8 (10.3%)	Absence	187 (92.6%)	–
Medium	37 (18.3%)	14 (17.9%)	Presence	15 (7.43%)	–
Progression patterns			Macrovascular invasion		
Liver	85 (42.1%)	29 (37.2%)	Absence	187 (92.6%)	69 (88.5%)
Liver+Local	19 (9.41%)	11 (14.1%)	Presence	15 (7.43%)	9 (11.5%)
Local	41 (20.3%)	8 (10.3%)	Satellite sites		
Multiple	40 (19.8%)	23 (29.5%)	Absence	125 (61.9%)	77 (98.7%)
Others	17 (8.42%)	7 (8.97%)	Presence	77 (38.1%)	1 (1.3%)
WBC count ($\times10^9$/L)			Adjacent organ invasion		
≤10	176 (87.1%)	66 (84.6%)	Absence	173 (85.6%)	75 (96.2%)
>10	26 (12.9%)	12 (15.4%)	Presence	29 (14.4%)	3 (3.85%)
HGB (g/L)			Tumor size		
≤175	17 (8.42%)	22 (28.2%)	≤5cm	64 (31.7%)	35 (44.9%)
>175	185 (91.6%)	56 (71.8%)	≤5cm	138 (68.3%)	43 (55.1%)
PLT (×109/L)			LN metastasis		
≤350	195 (96.5%)	73 (93.6%)	Absence	162 (80.2%)	70 (89.7%)
>350	7 (3.47%)	5 (6.41%)	Presence	40 (19.8%)	8 (10.3%)
ALT (U/L)			Positive LN number:		
≤50	159 (78.7%)	41 (52.6%)	0	162 (80.2%)	70 (89.7%)
>50	43 (21.3%)	37 (47.4%)	1	17 (8.42%)	2 (2.56%)
AST (U/L)			2	10 (4.95%)	1 (1.28%)
≤40	171 (84.7%)	43 (55.1%)	4	6 (2.97%)	2 (2.56%)
>40	31 (15.3%)	35 (44.9%)	5	3 (1.49%)	2 (2.56%)
ALP (U/L)			6	3 (1.49%)	–
≤125	110 (54.5%)	16 (20.5%)	>6	1 (0.50%)	1 (1.28%)
>125	92 (45.5%)	62 (79.5%)	Tumor differentiation		
GGT (U/L)			Low	24 (11.9%)	2 (2.56%)
≤60	63 (31.2%)	10 (12.8%)	Medium/high	178 (88.1%)	76 (97.4%)
>60	139 (68.8%)	68 (87.2%)	T stage 8th		
ALB (g/L)			1	18 (8.91%)	62 (79.5%)
>40	4 (1.98%)	27 (34.6%)	2	22 (10.9%)	3 (3.85%)
≤40	198 (98.0%)	51 (65.4%)	3	141 (69.8%)	10 (12.8%)
TBIL (μmol/L)			4	21 (10.4%)	3 (3.85%)
≤20.5	180 (89.1%)	42 (53.8%)	N stage 8th		
>20.5	22 (10.9%)	36 (46.2%)	Absence	162 (80.2%)	70 (89.7%)
IBIL (μmol/L)			Presence	40 (19.8%)	8 (10.3%)
≤15	187 (92.6%)	51 (65.4%)	TNM 8th		
>15	15 (7.43%)	27 (34.6%)	IA	18 (8.91%)	24 (30.8%)
HBsAg			IB	21 (10.4%)	35 (44.9%)
Absence	108 (53.5%)	–	II	24 (11.9%)	2 (2.56%)
Presence	94 (46.5%)	–	IIIA	84 (41.6%)	6 (7.69%)
CA19-9 (U/mL)			IIIB	55 (27.9%)	11 (14.1%)
≤35	81 (40.1%)	20 (25.6%)	After operation therapy		
>35	121 (59.9%)	58 (74.4%)	Absence	78 (38.6%)	51 (65.4%)
CEA (ng/mL)			Presence	124 (61.4%)	27 (34.6%)
≤5	139 (68.8%)	43 (55.1%)	LN7 metastasis		
>5	63 (31.2%)	35 (44.9%)	Absence	198 (98.0%)	78 (100%)
NLR			Presence	4 (1.98%)	0 (0%)
<2.62	124 (61.4%)	24 (30.8%)	LN8 metastasis		
≥2.62	78 (38.6%)	54 (69.2%)	Absence	194 (96.0%)	73 (93.6%)
PLR			Presence	8 (3.96%)	5 (6.41%)
<104.85	117 (57.9%)	17 (21.8%)	LN9 metastasis		
≥104.85	85 (42.1%)	61 (78.2%)	Absence	196 (97.0%)	–
SII			Presence	6 (2.97%)	–
0	47 (23.3%)	17 (21.8%)	LN12 metastasis		

(Continued)

TABLE 1 | Continued

Variables	Primary cohort (n = 202)	Validation cohort (n = 78)	Variables	Primary cohort (n = 202)	Validation cohort (n = 78)
1	155 (76.7%)	61 (78.2%)	Absence	177 (87.6%)	68 (87.2%)
LCR			Presence	25 (12.4%)	10 (12.8%)
0	12 (5.94%)	–	LN13 metastasis		
1	190 (94.1%)	–	Absence	194 (96.0%)	74 (94.9%)
PNI			Presence	8 (3.96%)	4 (5.13%)
0	189 (93.6%)	36 (46.2%)	LN14 metastasis		
1	13 (6.44%)	42 (53.8%)	Absence	201 (99.5%)	–
PI			Presence	1 (0.50%)	–
0	143 (70.8%)	24 (30.8%)	LN16 metastasis		
1	50 (24.8%)	44 (56.4%)	Absence	199 (98.5%)	–
2	9 (4.46%)	10 (12.8%)	Presence	3 (1.49%)	–

cohort was calculated according to the constructed nomogram, then the cutoff point was computed using the R package "cutoff." All the patients in this study were categorized into High- and Low-risk groups according to the cutoff point of 48. The PPS rates of patients in the low-risk group were significantly higher than those in the high-risk group in both primary (**Figure 6A**) and validation cohorts (**Figure 6B**).

DISCUSSION

Intrahepatic cholangiocarcinoma is a type of heterogeneous hepatobiliary malignancies with increasing incidence worldwide. Compared to HCC, patients with iCCA often suffer from worse overall survival, progression-free survival, and post-progression survival (12). Even after radical surgical resection, the 5-year survival rate rarely exceeded 30% (13, 14). The primary reason responsible for the poor outcomes is recurrence, which occurred in 50%–70% surgically resected iCCA patients (14–16). There have been several studies that concentrated on evaluation and prediction of postoperative recurrence (15, 17–20). However, there is a lack of research that focused on post-progression survival in iCCA patients. Therefore, it is necessary to establish an efficient tool to evaluate and predict PPS in these patients. In the present study, we analyzed the survival outcomes and the patterns of recurrence in multicenter cohorts of iCCA patients. Independent PPS prognostic predictive factors were then adjusted to the multiple characteristics of the tumor and features of progression. Finally, a novel nomogram that could accurately stratify patients into subgroups with distinct prognosis based on the potential PPS rates was established and validated.

In the last few decades, there have been encouraging progresses in optimizing surgical techniques, developing scheme and medicine of adjuvant therapy, and raising public awareness to the iCCA and its high recurrence rate. Several previous studies have revealed that PPS represented up to two-thirds of patients in breast cancer (21), non-small cell lung cancer (22), and ovarian cancer (23). Clearly, PPS represents an increasing important factor in outcomes of cancer patients. Given the relationship between PPS and progression and adjuvant therapy in this study, PPS could be an independent indicator of the outcomes in recurred iCCA patients.

Progression pattern, defined by the first recurred location, plays a vital role in PPS prediction, especially the metastasis progression patterns which had the highest assignment in our

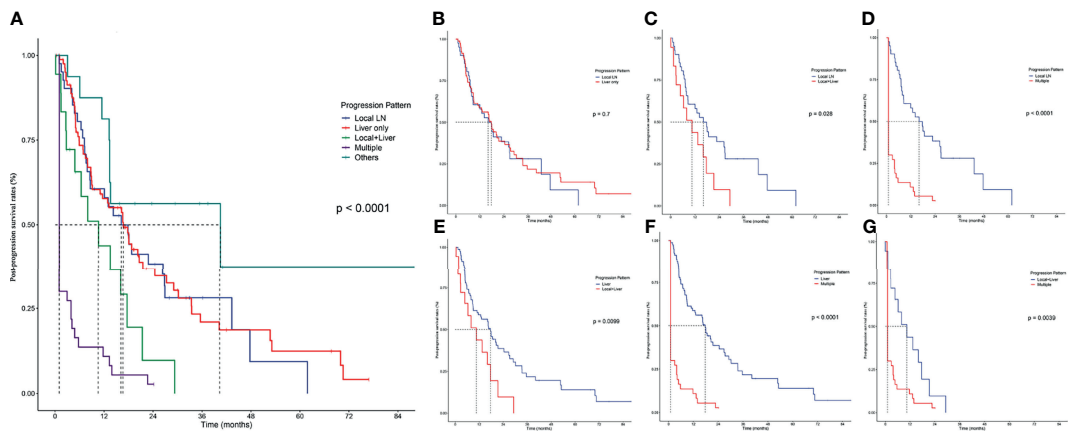

FIGURE 1 | Pairwise comparison of post-progression survival in patients with different progression patterns. **(A)** PPS stratified by all progression patterns. Stratification of patients by comparing the following progression patterns: **(B)** Local LN vs. Liver only; **(C)** local LN vs. Local+Liver; **(D)** local LN vs. Multiple; **(E)** Liver vs. Local+Liver; **(F)** Liver vs. Multiple; **(G)**, Local+Liver vs. Multiple.

TABLE 2 | Univariate and multivariate analysis of prognostic factors of PPS.

Characteristics	Levels	PPS					
		Univariate analysis			Multivariate analysis		
		HR	95%	p	HR	95%	p
Age (years)	≤60 years	Reference					
	>60 years	1.090	0.784–1.516	0.609			
Gender	Male	Reference					
	Female	1.041	0.744–1.456	0.814			
WBC count (×10^9/L)	≤10	Reference			Reference		
	>10	2.006	1.296–3.105	0.002	0.872	0.384–1.976	0.742
HGB (g/L)	≤175	Reference					
	>175	1.228	0.662–2.277	0.515			
PLT (×109/L)	≤350	Reference					
	>350	0.542	0.239–1.232	0.144	1.632	0.513–5.194	0.407
ALT (U/L)	≤50	Reference					
	>50	1.242	0.846–1.824	0.269			
AST (U/L)	≤40	Reference					
	>40	0.976	0.620–1.546	0.917			
GGT (U/L)	≤60	Reference			Reference		
	>60	1.599	1.111–2.303	0.012	1.120	0.177–5.688	0.989
ALP (U/L)	≤125	Reference			Reference		
	>125	2.035	1.463–2.833	<0.001	1.316	0.851–2.036	0.217
ALB (g/L)	>40	Reference			Reference		
	≤40	1.200	0.978–1.472	0.081	1.135	0.797–1.614	0.483
TBIL (mmol/L)	≤20.5	Reference					
	>20.5	1.292	0.778–2.147	0.323			
IBIL (mmol/L)	≤15	Reference					
	>15	0.901	0.473–1.714	0.750			
NLR	<2.62	Reference			Reference		
	≥2.62	1.432	1.030–1.990	0.033	0.776	0.473–1.273	0.315
LMR	<4.06	Reference			Reference		
	≥4.06	0.786	0.569–1.087	0.145	0.902	0.579–1.405	0.648
PLR	<104.85	Reference			Reference		
	≥104.85	1.371	0.988–1.903	0.059	1.167	0.753–1.809	0.489
SII	0	Reference			Reference		
	1	1.435	0.975–2.112	0.067	1.121	0.662–1.899	0.670
LCR	0	Reference					
	1	0.943	0.495–1.796	0.858			
PNI	0	Reference					
	1	0.880	0.448–1.730	0.712			
PI				<0.001			0.534
	0	Reference			Reference		
	1	0.500	0.241–1.036	0.062	0.587	0.112–3.085	0.529
	2	1.146	0.537–2.444	0.724	0.992	0.326–3.016	0.989
mGPS				<0.001			0.996
	0	Reference			Reference		
	1	0.811	0.199–3.299	0.770	1.053	0.148–7.512	0.959
	2	1.709	0.412–7.083	0.460	1.012	0.177–5.788	0.989
HBsAg	Absence	Reference			Reference		
	Presence	0.762	0.550–1.055	0.101	0.716	0.459–1.118	0.142
CA 19-9 (U/mL)	≤35	Reference					
	>35	1.190	0.856–1.656	0.301			
CEA (ng/mL)	≤5	Reference			Reference		
	>5	2.640	1.866–3.735	<0.001	1.807	1.147–2.847	0.011
Microvascular invasion	Absence	Reference					
	Presence	1.049	0.704–1.563	0.815			
Lymph-vessel invasion	Absence	Reference					
	Presence	1.201	0.691–2.088	0.516			
Macrovascular invasion	Absence	Reference					
	Presence	1.417	0.764–2.628	0.268			
Satellite sites	Absence	Reference					
	Presence	1.216	0.876–1.690	0.243			
Adjacent organ invasion	Absence	Reference					
	Presence	1.106	0.695–1.760	0.670			

(Continued)

TABLE 2 | Continued

Characteristics	Levels	PPS					
		Univariate analysis			Multivariate analysis		
		HR	95%	p	HR	95%	p
Tumor size	≤5 cm	Reference			Reference		
	≤5 cm	2.376	1.615–3.495	<0.001	1.424	0.856–2.366	0.173
Liver capsule invasion	Absence	Reference					
	Presence	0.880	0.631–1.228	0.452			
Tumor differentiation	Low	Reference			Reference		
	Medium/High	5.926	1.425–24.641	0.014	1.059	0.694–1.615	0.038
T stage 8th				0.104			0.822
	1	Reference			Reference		
	2	1.149	0.582–2.269	0.689	1.674	0.148–18.987	0.677
	3	1.316	0.701–2.470	0.393	1.381	0.354–5.387	0.642
	4	0.953	0.548–1.658	0.864	1.308	0.383–4.462	0.668
N stage 8th	Absence	Reference			Reference		
	Presence	1.537	1.049–2.250	0.027	5.793	0.364–8.118	0.041
TNM 8th				0.041			0.074
	I	Reference			Reference		
	II	0.948	0.547–1.645	0.850	1.452	0.109–19.306	0.778
	IIIa	0.999	0.589–1.693	0.996	2.335	0.462–11.799	0.305
	IIIb	0.687	0.464–1.017	0.060	1.381	0.316–6.031	0.667
After operation therapy	Absence	Reference			Reference		
	Presence	0.496	0.357–0.690	<0.001	0.521	0.343–0.791	0.002
Local LN metastasis	Absence	Reference			Reference		
	Presence	1.116	0.913–1.365	0.013	0.710	0.313–1.613	0.037
Liver metastasis only	Absence	Reference			Reference		
	Presence	1.246	1.056–1.471	0.009	1.236	0.627–2.439	0.041
Local+Liver Metastasis	Absence	Reference			Reference		
	Presence	0.811	0.614–1.070	0.139	1.559	0.583–4.167	0.376
Multiple metastasis	Absence	Reference			Reference		
	Presence	0.480	0.395–0.582	<0.001	5.911	2.742–12.744	<0.001
Progression period	Early	Reference					
	Late	1.240	0.850–1.810	0.264			
LN7 metastasis	Absence	Reference					
	Presence	1.114	0.274–4.533	0.880			
LN8 metastasis	Absence	Reference			Reference		
	Presence	1.447	0.834–2.509	0.188	1.026	0.387–2.716	0.960
LN9 metastasis	Absence	Reference			Reference		
	Presence	1.998	0.814–4.906	0.131	1.181	0.280–4.978	0.821
LN12 metastasis	Absence	Reference			Reference		
	Presence	1.462	1.065–2.008	0.019	1.281	0.721–2.276	0.399
LN13 metastasis	Absence	Reference					
	Presence	0.953	0.420–2.162	0.907			
LN14 metastasis	Absence	Reference					
	Presence	0.049	0.000–526.981	0.525			
LN16 metastasis	Absence	Reference					
	Presence	1.238	0.394–3.893	0.714			

nomogram. This observation indicated that the post-progression survival was primarily determined by recurrence-related factors rather than the primary characteristics of the tumor. In accordance with literatures, in the current study it was observed that liver metastasis accounted for the majority of progression patterns, followed by local LN metastasis and multiple metastases, while local plus liver metastasis contributed to a small proportion of tumor progression (15, 18, 20, 24). The reason why liver metastasis accounted for the majority of patterns may be in connection with the portal vein metastatic slant of iCCA. Liver and local progression patterns shared similar PPS rates and displayed significantly better outcomes when compared to other patterns, while multiple progression patterns resulted in the worst PPS outcome. Notably, there was no difference between liver metastasis and local metastasis in PPS. The median PPS of these two patterns is 12–14 months. It is the belongingness to local isolated progression which liver metastasis and local metastasis have in common. This further indicates that with positive and appropriate adjuvant therapy, local isolated progression, whether single liver metastasis or single local LN metastasis, could lead to a relatively better PPS. On the other hand, local multiple-progression pattern and liver plus local led to a relatively worse PPS survival compared to liver or single local multiple progression pattern, but still much better than multiple-metastasis patterns.

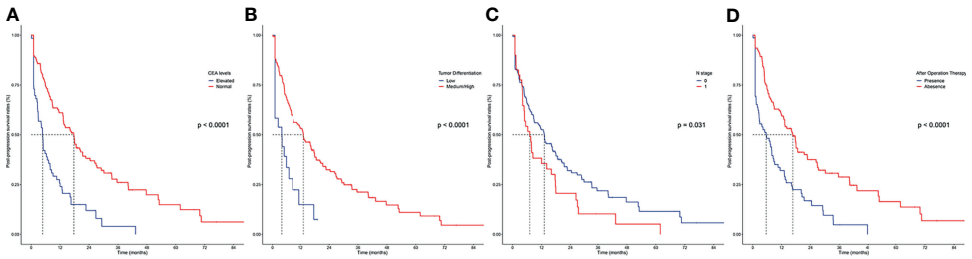

FIGURE 2 | Kaplan–Meier curves for post-progression survival in patients with iCCA in the SYSUCC cohort stratified by the significant prognostic factor defined by the Cox-regression analysis. **(A)** CEA levels; **(B)** tumor differentiation; **(C)** N stage; **(D)** after operation therapy.

Opposite to the previous studies and our anticipation, progression period, defined as time to recurrence or metastasis, had no significant prognostic prediction value to PPS (11, 18). This result might be interfered by the patients' compliance as they might not have conducted the check-back schedule regularly. On the other hand, it is worth noting that there are a series of the difficulties in identifying tumor progression by imaging examinations. In addition, receiving adjuvant treatments in the early-progression patients often resulted in better PPS.

Similar to previous studies, we observed in the current studies that CEA, as a vital tumor marker, was an independent prognostic factor for PPS in iCCA patients (25, 26). Elevated CEA levels often indicated higher tumor burden and worse malignant characteristics in iCCA, which has further implication as poor treatment responses. Besides, tumor markers such as CEA may also have powerful prognostic value in predicting the survival of iCCA patients. Further, pathological features of primary tumor are equally crucial as CEA levels in our model. A previous study showed that tumors of poorly histopathologic stage promote the development of metastasis and shorten survival times by secreting molecules such as E-cadherin and epidermal growth factor (27). Whether or not positive lymph nodes were uncovered in pathological diagnosis is also involved in the nomogram. Different from HCC, in which lymph node metastasis were rarely observed, iCCA often spreads through the lymphatic system (19). As a result, intraoperative lymphadenectomy is highly recommended by guidelines and most studies (9, 28).

The potential benefits of postoperative adjuvant therapy in iCCA remained controversial (29). In this present study, we demonstrated for the first time that postoperative adjuvant therapy provided clinical benefits in PPS of iCCA patients. Compared to breast cancer and lung cancer, the treatment responses of iCCA to chemotherapy, targeted therapy, and immunotherapy are shown to be underwhelming in plenty of studies through the past decades (9). However, with the continuous efforts in the development of novel therapeutics, a few recent clinical trials reported that chemotherapy led to improved survival for iCCA patients with lymph node metastasis or advanced tumor stages (30, 31). Similarly, in the current study, significant differences in PPS were observed between patients who did receive postoperative therapies and those who did not. Our results demonstrated that conventional adjuvant therapy benefited the PPS of iCCA patients. As for the patients at high risk for recurrence, the treatment scheme should be adjusted based on clinical observations in more intensive monitoring.

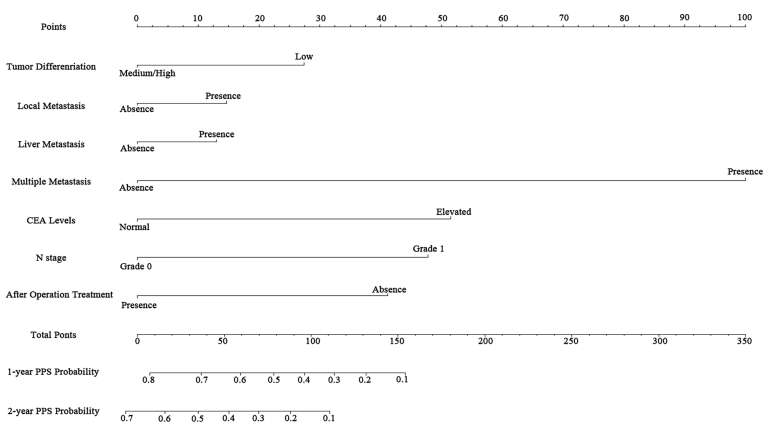

FIGURE 3 | Nomogram for predicting the 1- and 2-year post-progression survival rates in patients with iCCA.

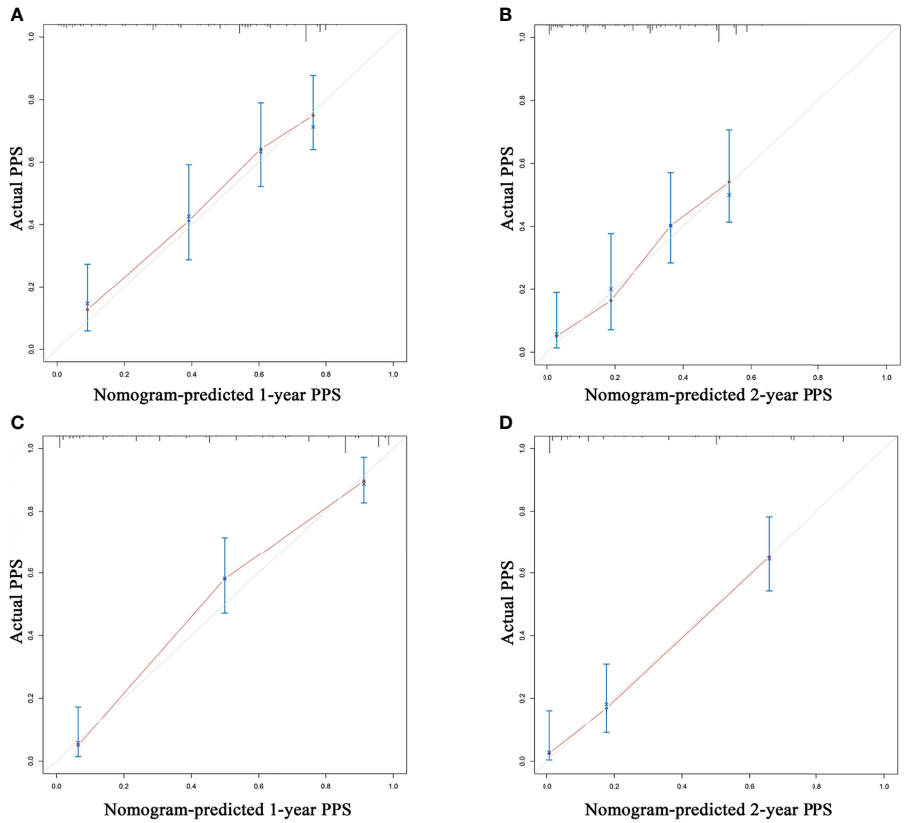

FIGURE 4 | The calibration curve for predicting post-progression survival at 1 year and 2 years in the training cohort **(A, B)** and validation cohort **(C, D)**.

Finally, we constructed a novel nomogram based on these independent prognostic factors and further calculated the cutoff of the total points. In accordance with the cutoff point, patients in primary cohorts and validation cohorts were classified into high-risk and low-risk subgroups, respectively. The patients at high risk demonstrated significantly poorer PPS than those who are at low risk in both cohorts. Therefore, this validated nomogram could accurately stratify patients into subgroups with significantly different PPS rates. Moreover, it may provide assistance with intensive monitoring and determining of adjuvant therapy for recurred iCCA patients.

There were several limitations in the present study. First, although we have studied patients from multicenter cohorts, only four progression patterns were analyzed in this study. An extended follow-up period is warranted to obtain additional information and provide more precise tumor progression patterns after surgical resection. Secondly, the retrospective data can sometimes be obscure since the specific regimens as well as the lengths of the therapy period were unavailable in this study. Thirdly, there are systematic bias of a retrospective study caused by the incomplete adherence to postoperative follow-up protocol. Fourth, the molecular analysis was not studied in the present study; the underlying mechanisms between poor PPS and the significantly prognostic factors were valuable to lucubrate. Last, the sample size of this present study was not numerous enough; further extensive large, trans-regional

TABLE 3 | Comparisons of the C-index with the nomogram and 8th TNM stage system in the primary cohort and validation cohorts.

System		PPS	
		C-index	p
Primary cohort	Nomogram	0.794 (0.769–0.828)	<0.001
	TNM stage	0.577 (0.476–0.674)	
Validation cohort	Nomogram	0.827 (0.779–0.876)	<0.001
	TNM stage	0.605 (0.532–0.678)	

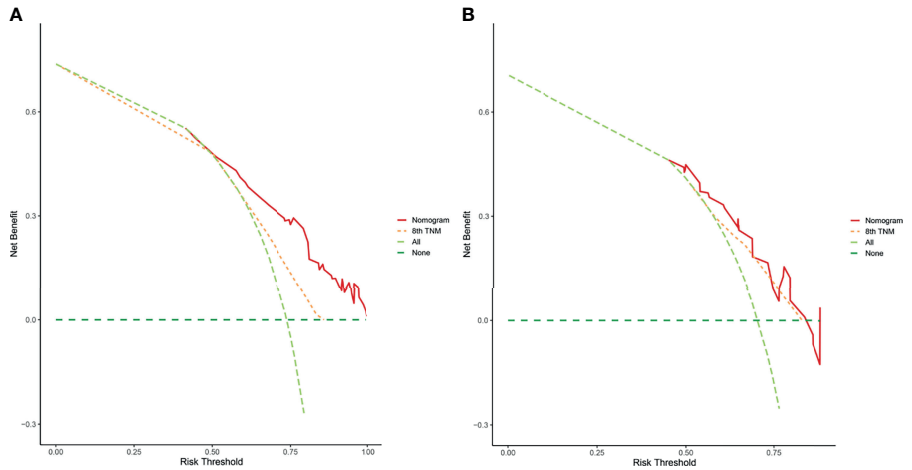

FIGURE 5 | The decision curve analysis of this nomogram for predicting PPS in the primary **(A)** and validation **(B)** cohorts.

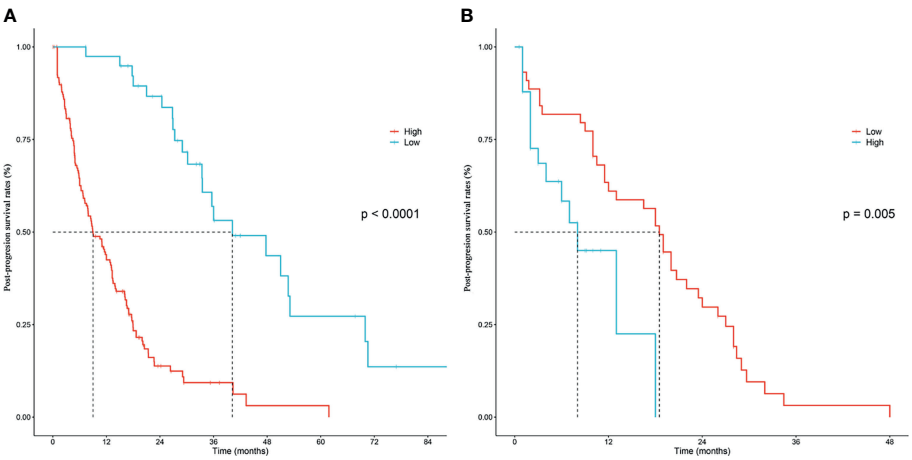

FIGURE 6 | Kaplan–Meier post-progression survival stratified by the nomogram score in the training cohort **(A)** and validation cohort **(B)**, respectively.

studies were needed to verify the prognostic power of this novel nomogram.

CONCLUSION

To our knowledge, the current study is the first to construct a nomogram for PPS of recurred iCCA patients in multicenter patient cohorts. We analyzed the PPS of different progression patterns of iCCA and further established a novel nomogram to predict PPS in postoperative recurred iCCA patients. In addition to the primary tumor features, the inclusion of progression patterns ensured the better prognostic prediction by this nomogram. Besides, the current study was conducted in diverse patient populations from the multicenter cohorts, which further strengthened the predictive power of the novel nomogram. Therefore, this novel nomogram could help clinicians to predict the PPS of recurred iCCA patients. The patients which were classified into the high-risk group by this nomogram should be monitored more frequently. Early and regular adjuvant therapy would also benefit those patients with high risk in this nomogram.

DATA AVAILABILITY STATEMENT

The raw data supporting the conclusions of this article will be made available by the authors, without undue reservation.

ETHICS STATEMENT

Ethical approval/written informed consent was not required for the study of animals/human participants in accordance with the local legislation and institutional requirements.

AUTHOR CONTRIBUTIONS

Study concept: XL. Study design: CZ, CH, JL. Drafting of the manuscript: CZ, CH, JL. Data collection: CZ, CH, JL, CC, XH. Data analysis: CH, CZ, JL, XH. Critical revision of the manuscript: XL. All authors contributed to the article and approved the submitted version.

FUNDING

This work was supported by grants from the National Natural Science Funds (No. 82102166), Guangdong Basic and Applied Basic Research Foundation (2020A1515110954), and Sun Yat-sen University Grant for Medical Humanities Practice and Teaching (No. 23000-18008023).

ACKNOWLEDGMENTS

We acknowledge the Medical Records Department of Sun Yat-sen University Cancer Center for collecting the survival data of the patients. We thank the patients who were included in this study.

SUPPLEMENTARY MATERIAL

The Supplementary Material for this article can be found online at: https://www.frontiersin.org/articles/10.3389/fonc.2022.832038/full#supplementary-material

REFERENCES

1. Fan B, Malato Y, Calvisi DF, Naqvi S, Razumilava N, Ribback S, et al. Cholangiocarcinomas can Originate From Hepatocytes in Mice. *J Clin Invest* (2012) 122:2911–5. doi: 10.1172/JCI63212
2. Sekiya S, Suzuki A. Intrahepatic Cholangiocarcinoma can Arise From Notch-Mediated Conversion of Hepatocytes. *J Clin Invest* (2012) 122:3914–8. doi: 10.1172/JCI63065
3. Tamandl D, Herberger B, Gruenberger B, Puhalla H, Klinger M, Gruenberger T. Influence of Hepatic Resection Margin on Recurrence and Survival in Intrahepatic Cholangiocarcinoma. *Ann Surg Oncol* (2008) 15:2787–94. doi: 10.1245/s10434-008-0081-1
4. Shimada K, Sano T, Nara S, Esaki M, Sakamoto Y, Kosuge T, et al. Therapeutic Value of Lymph Node Dissection During Hepatectomy in Patients With Intrahepatic Cholangiocellular Carcinoma With Negative Lymph Node Involvement. *Surgery* (2009) 145:411–6. doi: 10.1016/j.surg.2008.11.010
5. Paik KY, Jung JC, Heo JS, Choi SH, Choi DW, Kim YI. What Prognostic Factors are Important for Resected Intrahepatic Cholangiocarcinoma? *J Gastroenterol Hepatol* (2008) 23:766–70. doi: 10.1111/j.1440-1746.2007.05040.x
6. Uenishi T, Kubo S, Yamazaki O, Yamada T, Sasaki Y, Nagano H, et al. Indications for Surgical Treatment of Intrahepatic Cholangiocarcinoma With Lymph Node Metastases. *J Hepatobil Pancreat Surg* (2008) 15:417–22. doi: 10.1007/s00534-007-1315-5
7. Endo I, Gonen M, Yopp AC, Dalal KM, Zhou Q, Klimstra D, et al. Intrahepatic Cholangiocarcinoma: Rising Frequency, Improved Survival, and Determinants of Outcome After Resection. *Ann Surg* (2008) 248:84–96. doi: 10.1097/SLA.0b013e318176c4d3
8. He C, Sun S, Zhang Y, Lin X, Li S. A Novel Nomogram to Predict Survival in Patients With Recurrence of Pancreatic Ductal Adenocarcinoma After Radical Resection. *Front Oncol* (2020) 10:1564. doi: 10.3389/fonc.2020.01564
9. Bridgewater J, Galle PR, Khan SA, Llovet JM, Park JW, Patel T, et al. Guidelines for the Diagnosis and Management of Intrahepatic Cholangiocarcinoma. *J Hepatol* (2014) 60:1268–89. doi: 10.1016/j.jhep.2014.01.021
10. Ogasawara S, Chiba T, Ooka Y, Suzuki E, Kanogawa N, Saito T, et al. Post-Progression Survival in Patients With Advanced Hepatocellular Carcinoma Resistant to Sorafenib. *Invest New Drugs* (2016) 34:255–60. doi: 10.1007/s10637-016-0323-1
11. Zhang XF, Beal EW, Bagante F, Chakedis J, Weiss M, Popescu I, et al. Early Versus Late Recurrence of Intrahepatic Cholangiocarcinoma After Resection With Curative Intent. *Br J Surg* (2018) 105:848–56. doi: 10.1002/bjs.10676
12. Zhou XD, Tang ZY, Fan J, Zhou J, Wu ZQ, Qin LX, et al. Intrahepatic Cholangiocarcinoma: Report of 272 Patients Compared With 5,829 Patients With Hepatocellular Carcinoma. *J Cancer Res Clin Oncol* (2009) 135:1073–80. doi: 10.1007/s00432-009-0547-y
13. Mavros MN, Economopoulos KP, Alexiou VG, Pawlik TM. Treatment and Prognosis for Patients With Intrahepatic Cholangiocarcinoma: Systematic Review and Meta-Analysis. *JAMA Surg* (2014) 149:565–74. doi: 10.1001/jamasurg.2013.5137
14. Spolverato G, Kim Y, Alexandrescu S, Marques HP, Lamelas J, Aldrighetti L, et al. Management and Outcomes of Patients With Recurrent Intrahepatic Cholangiocarcinoma Following Previous Curative-Intent Surgical Resection. *Ann Surg Oncol* (2016) 23:235–43. doi: 10.1245/s10434-015-4642-9
15. Hyder O, Hatzaras I, Sotiropoulos GC, Paul A, Alexandrescu S, Marques H, et al. Recurrence After Operative Management of Intrahepatic Cholangiocarcinoma. *Surgery* (2013) 153:811–8. doi: 10.1016/j.surg.2012.12.005
16. Sulpice L, Rayar M, Boucher E, Pracht M, Meunier B, Boudjema K. Treatment of Recurrent Intrahepatic Cholangiocarcinoma. *Br J Surg* (2012) 99:1711–7. doi: 10.1002/bjs.8953
17. Miwa S, Miyagawa S, Kobayashi A, Akahane Y, Nakata T, Mihara M, et al. Predictive Factors for Intrahepatic Cholangiocarcinoma Recurrence in the Liver Following Surgery. *J Gastroenterol* (2006) 41:893–900. doi: 10.1007/s00535-006-1877-z
18. Doussot A, Gonen M, Wiggers JK, Groot-Koerkamp B, DeMatteo RP, Fuks D, et al. Recurrence Patterns and Disease-Free Survival After Resection of Intrahepatic Cholangiocarcinoma: Preoperative and Postoperative Prognostic Models. *J Am Coll Surgeons* (2016) 223:493–505.e492.doi: 10.1016/j.jamcollsurg.2016.05.019
19. Chan K-M, Tsai C-Y, Yeh C-N, Yeh T-S, Lee W-C, Jan Y-Y, et al. Characterization of Intrahepatic Cholangiocarcinoma After Curative Resection: Outcome, Prognostic Factor, and Recurrence. *BMC Gastroenterol* (2018) 18:180. doi: 10.1186/s12876-018-0912-x
20. Jeong S, Cheng Q, Huang L, Wang J, Sha M, Tong Y, et al. Risk Stratification System to Predict Recurrence of Intrahepatic Cholangiocarcinoma After Hepatic Resection. *BMC Cancer* (2017) 17:464. doi: 10.1186/s12885-017-3464-5
21. Saad ED, Katz A, Buyse M. Overall Survival and Post-Progression Survival in Advanced Breast Cancer: A Review of Recent Randomized Clinical Trials. *J Clin Oncol* (2010) 28:1958–62. doi: 10.1200/JCO.2009.25.5414

22. Rutkowski J, Saad ED, Burzykowski T, Buyse M, Jassem J. Chronological Trends in Progression-Free, Overall, and Post-Progression Survival in First-Line Therapy for Advanced NSCLC. *J Thorac Oncol* (2019) 14:1619–27. doi: 10.1016/j.jtho.2019.05.030
23. Sundar S, Wu J, Hillaby K, Yap J, Lilford R. A Systematic Review Evaluating the Relationship Between Progression Free Survival and Post Progression Survival in Advanced Ovarian Cancer. *Gynecol Oncol* (2012) 125:493–9. doi: 10.1016/j.ygyno.2011.12.420
24. Song S, Kim K, Chie EK, Kim S, Park HJ, Yi NJ, et al. Locoregional Recurrence After Curative Intent Resection for Intrahepatic Cholangiocarcinoma: Implications for Adjuvant Radiotherapy. *Clin Transl Oncol* (2015) 17:825–9. doi: 10.1007/s12094-015-1312-0
25. Jaklitsch M, Petrowsky H. The Power to Predict With Biomarkers: Carbohydrate Antigen 19-9 (CA 19-9) and Carcinoembryonic Antigen (CEA) Serum Markers in Intrahepatic Cholangiocarcinoma. *Transl Gastroenterol Hepatol* (2019) 4:23. doi: 10.21037/tgh.2019.03.06
26. Moro A, Mehta R, Sahara K, Tsilimigras DI, Paredes AZ, Farooq A, et al. The Impact of Preoperative CA19-9 and CEA on Outcomes of Patients With Intrahepatic Cholangiocarcinoma. *Ann Surg Oncol* (2020) 27:2888–901. doi: 10.1245/s10434-020-08350-8
27. Kohei Shibata TM, Yada K. Factors Predicting Recurrence After Resection of Pancreatic Ductal Carcinoma. *Pancreas* (2005) 31:69–73. doi: 10.1097/01.mpa.0000166998.04266.88
28. Amini N, Ejaz A, Spolverato G, Maithel SK, Kim Y, Pawlik TM. Management of Lymph Nodes During Resection of Hepatocellular Carcinoma and Intrahepatic Cholangiocarcinoma: A Systematic Review. *J Gastrointest Surg* (2014) 18:2136–48. doi: 10.1007/s11605-014-2667-1
29. Rizvi S, Gores GJ. Pathogenesis, Diagnosis, and Management of Cholangiocarcinoma. *Gastroenterology* (2013) 145:1215–29. doi: 10.1053/j.gastro.2013.10.013
30. Machairas N, Lang H, Jayant K, Raptis DA, Sotiropoulos GC. Intrahepatic Cholangiocarcinoma: Limitations for Resectability, Current Surgical Concepts and Future Perspectives. *Eur J Surg Oncol* (2020) 46:740–6. doi: 10.1016/j.ejso.2020.01.028
31. Kelley RK, Bridgewater J, Gores GJ, Zhu AX. Systemic Therapies for Intrahepatic Cholangiocarcinoma. *J Hepatol* (2020) 72:353–63. doi: 10.1016/j.jhep.2019.10.009

Conflict of Interest: The authors declare that the research was conducted in the absence of any commercial or financial relationships that could be construed as a potential conflict of interest.

Publisher's Note: All claims expressed in this article are solely those of the authors and do not necessarily represent those of their affiliated organizations, or those of the publisher, the editors and the reviewers. Any product that may be evaluated in this article, or claim that may be made by its manufacturer, is not guaranteed or endorsed by the publisher.

Copyright © 2022 Zhao, He, Lu, Huang, Chen and Lin. This is an open-access article distributed under the terms of the Creative Commons Attribution License (CC BY). The use, distribution or reproduction in other forums is permitted, provided the original author(s) and the copyright owner(s) are credited and that the original publication in this journal is cited, in accordance with accepted academic practice. No use, distribution or reproduction is permitted which does not comply with these terms.

frontiers | Frontiers in Oncology

ORIGINAL RESEARCH
published: 11 April 2022
doi: 10.3389/fonc.2022.833999

An Efficient Nomogram for Discriminating Intrahepatic Cholangiocarcinoma From Hepatocellular Carcinoma: A Retrospective Study

Yuan-Quan Si[1†], Xiu-Qin Wang[1,2†], Cui-Cui Pan[1], Yong Wang[1] and Zhi-Ming Lu[1*]*

[1] Department of Clinical Laboratory, Shandong Provincial Hospital Affiliated to Shandong First Medical University, Jinan, China, [2] School of Basic Medicine, Shandong First Medical University, Jinan, China

OPEN ACCESS

Edited by:
Qi Liu,
Fudan University, China

Reviewed by:
Federico Ravaioli,
University of Bologna, Italy
Jose M. Ramia,
Hospital General Universitario de Alicante, Spain
Hani Susianti,
University of Brawijaya, Indonesia

***Correspondence:**
Zhi-Ming Lu
luzhiming@sdu.edu.cn
Yong Wang
sdwangyong@126.com

[†]These authors have contributed equally to this work

Specialty section:
This article was submitted to Gastrointestinal Cancers: Hepato Pancreatic Biliary Cancers, a section of the journal Frontiers in Oncology

Received: *12 December 2021*
Accepted: *07 March 2022*
Published: *11 April 2022*

Citation:
Si Y-Q, Wang X-Q, Pan C-C, Wang Y and Lu Z-M (2022) An Efficient Nomogram for Discriminating Intrahepatic Cholangiocarcinoma From Hepatocellular Carcinoma: A Retrospective Study. Front. Oncol. 12:833999. doi: 10.3389/fonc.2022.833999

Objective: This study aims to establish a nomogram and provide an effective method to distinguish between intrahepatic cholangiocarcinoma (ICC) and hepatocellular carcinoma (HCC).

Methods: A total of 1,591 patients with HCC or ICC hospitalized at Shandong Provincial Hospital between January 2016 and August 2021 were included and randomly divided into development and validation groups in a ratio of 3:1. Univariate and multivariate analyses were performed to determine the independent differential factors between HCC and ICC patients in the development cohort. By combining these independent differential factors, the nomogram was established for discriminating ICC from HCC. The accuracy of the nomogram was estimated by using receiver operating characteristic (ROC) curve and decision curve analysis (DCA). Furthermore, the predictive nomogram was assessed in the internal testing set.

Results: Through multivariate analysis, independent differential factors between HCC and ICC involved hepatitis B virus (HBV), logarithm of alpha-fetoprotein (Log AFP), logarithm of protein induced by vitamin K absence or antagonist-II (Log PIVKA-II), logarithm of carbohydrate antigen 199 (Log CA199), and logarithm of carbohydrate antigen 125 (Log CA125). A nomogram was finally established by incorporating these five independent differential factors. Comparing a model of conventional tumor biomarkers including AFP and CA199, the nomogram showed a better distinction between ICC and HCC. The area under the ROC curve (AUC) of ICC diagnosis was 0.951 (95% CI, 0.938–0.964) for the nomogram. The results were consistent in the validation cohort with an AUC of 0.958 (95% CI, 0.938–0.978). After integrating patient preferences into the analysis, the DCA showed that using this nomogram to distinguish ICC and HCC increased more benefit compared with the conventional model.

Conclusion: An efficient nomogram has been established for the differential diagnosis between ICC and HCC, which may facilitate the detection and diagnosis of ICC. Further use of the nomogram in multicenter investigations will confirm the practicality of the tool for future clinical application.

Keywords: intrahepatic cholangiocarcinoma, hepatocellular carcinoma, nomogram, alpha-fetoprotein, PIVKA-II, CA199, CA125

INTRODUCTION

Primary liver cancer (PLC) is the sixth most common cancer and the third leading cause of cancer-related death worldwide in 2020, which includes HCC and ICC, and mixed hepatocellular–cholangiocarcinoma carcinoma according to different cell origin (1). Among them, ICC derived from the epithelial cell of intrahepatic bile duct is the second most common liver malignancy (2). Although ICC is not as common as HCC, its incidence rate has risen sharply in recent years without clear etiology (3, 4).

However, due to the different molecular mechanisms of carcinogenesis, the survival and prognosis of ICC are worse than HCC. Despite recent advances in basic research and clinical trials, it is reported that the 5-year survival rate of ICC is only about 30%. As a malignant neoplasm, ICC often shares some common hazard factors and clinical features with HCC, which is a challenge for the differential diagnosis of ICC and HCC. With this in mind, it is urgent to find an effective and specific method that can provide early prediction value for the differential diagnosis of ICC and HCC (5–7).

The gold standard of differential diagnosis between ICC and HCC relies on pathological examination yet in the current clinical practice (4). The two tumor markers (AFP and CA199) are the most commonly used cancer biomarkers to distinguish ICC and HCC. However, the diagnostic specificity and sensitivity of these biomarkers are still not satisfactory (8–11). Although lots of research have been carried out to study the characteristics of ICC and seek new differential diagnostic markers to distinguish ICC from HCC, their effects in clinical application still remain weak (12, 13). In view of the lack of highly specific and sensitive predictive biomarkers to diagnose ICC, the establishment of predictive models including independent factors may be a feasible way to resolve the issue. Nomograms are recently described as simple graphical systems, which may be more accurate than traditional methods in preoperative diagnosis and prognostic evaluation for a variety of malignant tumors, including liver cancer and pancreatic adenocarcinoma (14–16). In order to distinguish between ICC and HCC before surgery without pathological verification, our study is to establish and verify the nomogram model for the differential diagnosis of ICC and HCC based on demographic characteristics and the results of routine laboratory tests.

MATERIALS AND METHODS

Patients

A total of 1,591 patients with HCC or ICC who received curative surgery for PLC at Shandong Provincial Hospital between January 2016 and August 2021 were included in this retrospective study. The patients were selected according to the inclusion and elimination criteria, just as shown in **Figure 1**. The inclusion criteria entailed pathologically confirmed HCC or ICC patients over the age of 18. The reasons for exclusion were as follows: (1) incomplete clinical information; (2) mixed hepatocellular–cholangiocellular carcinoma or other types of liver tumor; (3) with medical history of other cancers; (4) with preoperative treatments. Patients who met the inclusion and exclusion criteria were divided into development and validation groups randomly in a ratio of 3:1. All procedures involving human participants have been approved by the Shandong Provincial Hospital Research Ethics Committee. The data were anonymous, and the requirement for informed consent was therefore waived (17).

Clinicopathological Variables

Demographic variables including age, gender, hepatitis B history, hepatitis C history and clinicopathological staging of ICC and HCC were obtained. Serum examination included AFP, AFP-L3%, PIVKA-II, carcinoembryonic antigen (CEA), CA199, CA125, alanine transaminase (ALT), aspartate transaminase (AST), γ-glutamyl transpeptidase (GGT), total bilirubin (TBIL), direct bilirubin (DBIL), total protein (TP), albumin (ALB), red blood cell (RBC), white blood cell (WBC), and platelet (PLT). In our study, the contents of these tests were detected respectively before undergoing scheduled surgery. AFP and AFP-L3 were detected by the method of immunofluorescence on automatic electrophoresis fluorescence immunoassay instrument (mTAS Wako i30, Japan). AFP-L3% was measured by the AFP-L3 divided by the AFP. PIVKA-II was measured using chemiluminescence enzyme immunoassay on automatic chemiluminescence immunoassay analyzer (LUMIPULSE®G1200, Japan). Detection of CEA, CA199, and CA125 was performed using an automatic electrochemiluminescence analyzer (Roche Diagnostics, Mannheim, Germany). Serum levels of ALT, AST, GGT, TP, ALB, TBIL, and DBIL were analyzed using automatic biochemical analyzer (AU5831, USA). The values of PLT, RBC and WBC were measured with fully automated hematology analyzer (Sysmex XN-9000, Sysmex, Kobe, Japan). The above reagents required were all original kits, and the tests were carried out in strict accordance with the standard operation procedures.

Statistical Analysis

Numerical variables were expressed as mean with standard deviation (SD) or median with interquartile range (IQR), which were compared by Student's *t*-test or Mann–Whitney

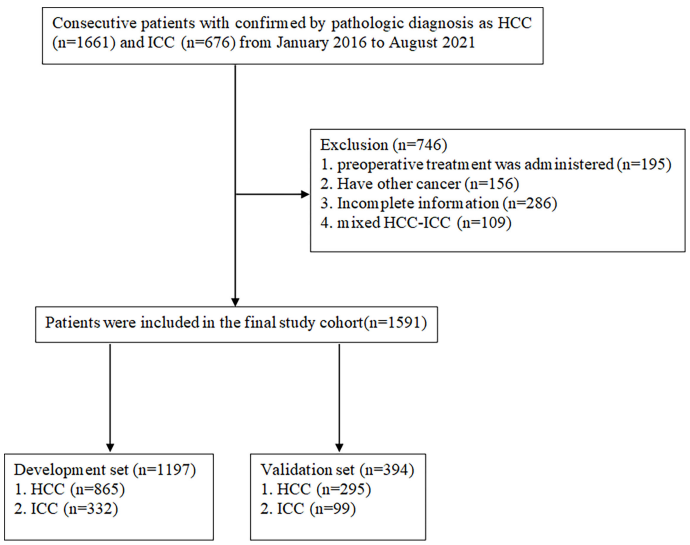

FIGURE 1 | Flowchart detailing the patient selection process and exclusion criteria.

test, respectively. Categorical variables were expressed as frequencies and compared using Pearson's χ^2 test or Fisher exact test. Log transformation was performed for these variables with skewed distributions such as AFP, AFP-L3%, PIVKA-II, CEA, CA199, CA125, ALT, AST, GGT, TBIL, and DBIL. Univariate and multivariate regression analyses were adopted to determine the independent differential factors between ICC and HCC. A nomogram was drawn according to these screened independent difference factors, and the total score of each patient was calculated using this established nomogram. The diagnostic ability of our nomogram was estimated by the ROC curve and AUC. Then, Z-test was applied to compare the difference between our nomogram and other model. The decision curve analysis (DCA) was used to assess the clinical utility value of the nomogram and other model by quantifying net benefits against a range of threshold probabilities (18). We further evaluated whether the use of indicator variables with missing data biased our results by performing multivariate multiple imputation analysis. We repeated all analyses with the complete data (19–21). The nomogram and DCA were established with R (http://www.R-project.org) and EmpowerStats software (www.empowerstats.com, Boston MA, USA) (22). Other analyses were performed by IBM SPSS software (version 25.0, USA) and MedCalc (version 20.0.8, Belgium). The $p<0.05$ was considered statistically significant.

RESULTS

Patient Demographics and Clinicopathologic Variables

During the study period, a total of 1,591 consecutive patients who underwent hepatectomy for primary hepatic carcinoma and met the inclusion criteria were enrolled. Among them, 1,197 and 394 patients formed the training and validation cohort, respectively. In the training group, 865 HCC patients and 332 ICC patients were included. The validation cohort consisted of 295 HCC patients and 99 ICC patients. The demographics and clinicopathological variables of the training and validation cohort patients are listed in **Table 1**. A comparison of baseline data showed that there were no significant differences in general conditions and other indicators between the former two cohorts. Meanwhile, the baseline clinicopathological data were compared between ICC and HCC of training cohort (**Table 2**).

Univariate and Multivariate Analysis of Independent Differences Between ICC and HCC Patients

As shown in **Table 3**, the univariate analysis of training cohort indicated that except for a few indicators (such as Log ALT, Log AST, TP, and ALB), all other indicators were potential difference factors between ICC and HCC patients ($p < 0.01$). All these potential difference factors were then brought into multivariate logistic regression. Only Log AFP (OR = 0.46; 95% CI, 0.31–0.68, $p = 0.0001$), Log PIVKA-II (OR = 0.19; 95% CI, 0.12–0.29, $p< 0.0001$), Log CA199 (OR = 2.88; 95% CI, 1.95–4.26, $p< 0.0001$), Log CA125 (OR = 2.75; 95% CI, 1.5–5.01, $p = 0.001$), and HBV (OR = 0.13; 95% CI, 0.08–0.22, $p< 0.0001$) were the independent difference for the presence of ICC and HCC.

Development and Validation of a Nomogram for the Differential Diagnosis Between ICC and HCC

The independent difference factors between ICC and HCC were further used to establish the nomogram for ICC risk assessment (**Figure 2**). In addition, we also established the model

TABLE 1 | Baseline characteristics of the development and validation groups.

Variables	Training (n = 1197)	Validation (n = 394)	*p*-value
Age (years)	57.82 (10.36)	57.77 (10.12)	0.942
Sex			0.642
Male	931 (77.78%)	302 (76.65%)	
Female	266 (22.22%)	92 (23.35%)	
PLT (10^9/L)	190.19 (91.19)	185.18 (86.14)	0.338
RBC (10^{12}/L)	4.42 (0.62)	4.38 (0.66)	0.252
WBC (10^9/L)	5.99 (2.75)	5.86 (2.63)	0.391
AFP (ng/mL)	9.20 (2.70–181.50)	8.94 (2.90–195.05)	0.575
AFP-L3%	4.60 (0.50–32.40)	3.50 (0.50–19.98)	0.143
CEA (ng/ml)	2.83 (1.80–4.57)	2.83 (1.88–4.30)	0.837
CA125 (U/ml)	14.80 (9.71–29.43)	13.56 (8.91–28.19)	0.099
CA199 (IU/ml)	21.20 (11.94–56.00)	21.45 (11.57–58.75)	0.851
PIVKA-II (mAU/ml)	114.00 (27.78–1266.06)	146.92 (28.25–1776.50)	0.374
AST (U/L)	33.00 (24.00–55.00)	37.00 (25.00–60.75)	0.036
ALT (U/L)	29.00 (19.00–51.00)	32.50 (20.00–53.00)	0.212
TP (g/L)	69.66 (7.25)	70.01 (7.28)	0.411
ALB (g/L)	39.89 (5.31)	39.47 (5.24)	0.181
GGT (U/L)	55.00 (29.00–131.00)	60.00 (32.00–148.50)	0.083
TBIL (μmol/L)	16.50 (12.34–23.56)	16.69 (12.00–22.38)	0.721
DBIL (μmol/L)	3.64 (2.60–5.71)	3.70 (2.52–5.65)	0.727
HBV			0.448
No	383 (32.00%)	118 (29.95%)	
Yes	814 (68.00%)	276 (70.05%)	
HCV			0.126
No	1,166 (97.41%)	389 (98.73%)	
Yes	31 (2.59%)	5 (1.27%)	
Clinicopathological staging			0.648
Well differentiation	176 (14.70%)	56 (14.21%)	
Moderate differentiation	720 (60.15%)	247 (62.69%)	
Poor differentiation	301 (25.15%)	91 (23.10%)	

Categorical variables are expressed as frequency. Continuous variables are expressed as mean (SD) or median with interquartile range (IQR).
PLT, platelet; RBC, red blood cell; WBC, white blood cell; AFP, α-fetoprotein level; AFP-L3, an isoform of AFP characterized by the presence of an a 1–6-linked residue on the AFP carbohydrate side chain; CA199, carbohydrate antigen 199; CEA, carcinoembryonic antigen; PIVKA-II, protein induced by vitamin K absence or antagonist-II; CA125, carbohydrate antigen 125; ALT, alanine transaminase; AST, aspartate transaminase; GGT, gamma glutamyl transpeptidase; TP, total protein; ALB, albumin; TBIL, total bilirubin; DBIL, direct bilirubin; HBV, hepatitis B virus; HCV, hepatitis C virus.

incorporating AFP and CA199, which was commonly used at present in clinical. Compared with this model (AUC = 0.887; 95% CI, 0.865–0.910), the nomogram could distinguish ICC and HCC better with the AUC of 0.951 (95% CI, 0.938–0.964) (**Figure 3A**, $p < 0.0001$). In the validation cohort, compared with the model (AUC = 0.903, 95% CI: 0.865~0.942), the nomogram displayed the higher AUC of 0.958 (95% CI, 0.938–0.978) for the differentiation of ICC and HCC (**Figure 3B**, $p = 0.0026$). Diagnostic efficacies of the nomogram and compared model for distinguishing between ICC and HCC are listed in **Table 4**. After integrating patient preferences into the analysis, DCA displayed that both the nomogram and model would offer net benefits over the "treat-all" or "treat-none." Upon further investigation, using this nomogram to distinguish ICC from HCC showed greater benefit when compared to the former model (**Figures 4A, B**).

DISCUSSION

ICC has higher malignancy and poorer prognosis than HCC, whose morbidity and mortality rates have the tendency of heightening in recent years. Several etiological danger factors and clinical features of ICC and HCC are consistent with each other. However, it is widely accepted that resection of ICC is the only chance for cure,while the treatments for HCC patients include liver transplant, resection, radiofrequency ablation (RFA) and vascular interventional. Thus, histological analyses of tumor biopsies are required to discriminate ICC from HCC, which is important to provide appropriate treatment strategies as shown in international guidelines (5, 23). However, tumor biopsy is not allowed in most cases due to the advanced stage of disease and concomitant risks. Therefore, there is an urgent need for the accurate noninvasive way to correctly distinguish ICC and HCC (24–26).

AFP is a glycoprotein whose elevation is usually related to HCC. However, it does not increase significantly in about 35%–40% of HCC patients, especially for patients with small hepatocellular carcinoma (27, 28). PIVKA-II, also called des-γ-carboxyprothrombin (DCP), has been regarded as the ideal biomarker for the diagnosis and evaluation of HCC in recent years (28, 29). CA199 is a glycoprotein macromolecule that has been used as the marker in digestive system tumors and hepatobiliary disease (30, 31). CA125 is a mucin-type glycoprotein, sometimes named cancer antigen 125, produced by the mucin 16 (MUC16) gene (32). AFP and CA199 are often

TABLE 2 | Demographic information and clinicopathological characteristics of the training cohort.

Variables	HCC (n=865)	ICC (n=332)	*p*-value
Age (years)	57.15 (10.19)	59.56 (10.59)	<0.001
Sex			<0.001
Male	718 (83.01%)	213 (64.16%)	
Female	147 (16.99%)	119 (35.84%)	
PLT (10^9/L)	170.98 (84.26)	240.22 (89.68)	<0.001
RBC (10^{12}/L)	4.46 (0.61)	4.33 (0.63)	0.001
WBC (10^9/L)	5.54 (2.54)	7.17 (2.92)	<0.001
AFP (ng/ml)	35.90 (4.20–558.10)	2.69 (1.87–4.43)	<0.001
AFP–L3%	10.00 (0.50–38.70)	0.50 (0.50–0.50)	<0.001
CEA (ng/ml)	2.50 (1.69–3.88)	3.90 (2.13–11.55)	<0.001
CA125 (U/ml)	13.04 (9.09–22.27)	23.90 (12.48–80.55)	<0.001
CA199 (IU/ml)	17.16 (10.90–29.48)	125.00 (23.91-1000.00)	<0.001
PIVKA-II (mAU/ml)	367.01 (49.08–2839.86)	27.66 (20.77–42.09)	<0.001
AST (U/L)	34.00 (25.00–53.00)	31.00 (22.00–61.00)	0.133
ALT (U/L)	30.00 (20.00–49.00)	27.00 (16.75–63.00)	0.138
TP (g/L)	69.87 (7.11)	69.12 (7.57)	0.106
ALB (g/L)	40.05 (5.32)	39.47 (5.25)	0.092
GGT (U/L)	49.00 (27.00–102.00)	87.50 (37.75–268.75)	<0.001
TBIL (μmol/L)	16.40 (12.47–22.60)	16.93 (12.00–36.61)	0.013
DBIL (μmol/L)	3.67 (2.67–5.44)	3.60 (2.50–12.12)	0.026
HBV			<0.001
No	123 (14.22%)	260 (78.31%)	
Yes	742 (85.78%)	72 (21.69%)	
HCV			0.144
No	839 (96.99%)	327 (98.49%)	
Yes	26 (3.01%)	5 (1.51%)	
Clinicopathological staging			0.009
Well differentiation	114 (13.18%)	62 (18.67%)	
Moderate differentiation	542 (62.66%)	178 (53.61%)	
Poor differentiation	209 (24.16%)	92 (27.71%)	

Categorical variables are expressed as frequency. Continuous variables are expressed as mean (SD) or median with interquartile range (IQR).

PLT, platelet; RBC, red blood cell; WBC, white blood cell; AFP, α-fetoprotein level; AFP-L3, an isoform of AFP characterized by the presence of an a 1–6-linked residue on the AFP carbohydrate side chain; CA199, carbohydrate antigen 199; CEA, carcinoembryonic antigen; PIVKA-II, protein induced by vitamin K absence or antagonist-II; CA125, carbohydrate antigen 125; ALT, alanine transaminase; AST, aspartate transaminase; GGT, gamma glutamyl transpeptidase; TP, total protein; ALB, albumin; TBIL, total bilirubin; DBIL, direct bilirubin; HBV, hepatitis B virus; HCV, hepatitis C virus.

used to distinguish ICC and HCC. The results, however, have been unsatisfactory. Nomograms can be used for accurate assessment and identification of diseases, which provides a more simple but highly effective method for disease diagnosis and prognostic evaluation (33–35). The aim of our study was to establish such an efficient diagnostic nomogram model for clinical differentiation between ICC and HCC based on demographic characteristics and the routine laboratory tests. In this study, we found that HBV, Log AFP, Log CA199, Log CA125, and Log PIVKA-II were the independent elements of differentiation between them through the univariable and multivariable logistic regression. Based on these independent difference factors, we established a nomogram which displayed high accuracy by the AUC of 0.951 and 0.958 in the training and validation groups, respectively. Among those factors, HBV, Log AFP, and Log PIVKA-II were negatively correlated to ICC, while Log CA199 and Log CA125 were the positive factors for ICC. It is well known that the main danger factors for HCC are chronic infection with HBV or HCV, aflatoxin-contaminated foods, and so on. Furthermore, HBV infection is likely the predominant determinant of HCC in China (1). High levels of AFP and PIVKA-II are more common in HCC than ICC, the opposite of the CA199 and CA125.

The traditional model including AFP and CA199 was used as control. Compared to the control model (AUC = 0.887), the AUC of our nomogram was better at 0.951. This role of our nomogram was confirmed by the validation group with the AUC of 0.958. Previously, nomogram was evaluated using ROC and AUC, which lacked of the evaluation of clinical value. DCA could compensate for this deficiency, which is an effective method to assess the clinical benefits (36–38). The results of DCA showed that more benefits were increased through making use of our nomogram to differentiate ICC from HCC compared to the control model. Several models have been put forward to distinguish ICC from HCC. A nomogram combining six serum N-glycans was established for discriminating between ICC and HCC by Huang and collaborators. However, they found that the diagnostic performance of the nomogram might be better for those with poor liver function (39). Comprehensive analysis of metabolomics of ICC and HCC have been reported in recent years. Banales et al. (5) developed a nomogram based on serum metabolites (such as amino acids and sphingomyelins) that provided high values to distinguish patients with ICC from those with HCC. However, the detection of metabolites required special instruments and equipment, and the process was complex, which limited their clinical applications. Wang et al. (3) proposed a nomogram

TABLE 3 | Univariate and multivariate logistic regression analysis of ICC presence based on preoperative data in training cohort.

Variables	Univariable		Multivariable	
	OR (95%CI)	*p*-value	OR (95%CI)	*p*-value
Age (years)	1.02 (1.01, 1.04)	0.003	NA	
Sex		<0.0001		
Male	reference		reference	
Female	2.73 (2.05, 3.63)		NA	
PLT (10^9/L)	1.01 (1.01, 1.01)	<0.0001	NA	
RBC (10^{12}/L)	0.72 (0.58, 0.88)	0.0012	NA	
WBC (10^9/L)	1.24 (1.18, 1.31)	<0.0001	NA	
Log AFP (ng/ml)	0.24 (0.19, 0.30)	<0.0001	0.47 (0.32, 0.69)	0.0001
Log AFP-L3%	0.35 (0.30, 0.42)	<0.0001	NA	
Log CEA (ng/ml)	5.46 (3.92, 7.62)	<0.0001	NA	
Log CA125 (U/ml)	4.35 (3.28, 5.77)	<0.0001	2.74 (1.50, 5.01)	0.001
Log CA199 (IU/ml)	7.68 (5.90, 9.98)	<0.0001	2.88 (1.95, 4.25)	<0.0001
Log PIVKA-II (mAU/ml)	0.20 (0.16, 0.26)	<0.0001	0.19 (0.13, 0.30)	<0.0001
Log AST (U/L)	1.02 (0.69, 1.53)	0.9105	NA	
Log ALT (U/L)	1.12 (0.80, 1.57)	0.5168	NA	
TP (g/L)	0.99 (0.97, 1.00)	0.106	NA	
ALB (g/L)	0.98 (0.96, 1.00)	0.0927	NA	
Log GGT (U/L)	3.32 (2.53, 4.36)	<0.0001	NA	
Log TBIL (μmol/L)	3.69 (2.60, 5.24)	<0.0001	NA	
Log DBIL (μmol/L)	2.82 (2.17, 3.66)	<0.0001	NA	
HBV		<0.0001		<0.0001
No	reference		reference	
Yes	0.05 (0.03, 0.06)		0.13 (0.08, 0.22)	
HCV		0.1516		
No	reference		reference	
Yes	0.49 (0.19, 1.30)		NA	

Categorical variables are expressed as frequency. Continuous variables are expressed as mean (SD) or median with interquartile range (IQR).
PLT, platelet; RBC, red blood cell; WBC, white blood cell; AFP, α-fetoprotein level; AFP-L3, an isoform of AFP characterized by the presence of an a 1–6-linked residue on the AFP carbohydrate side chain; CA199, carbohydrate antigen 199; CEA, carcinoembryonic antigen; PIVKA-II, protein induced by vitamin K absence or antagonist-II; CA125, carbohydrate antigen 125; ALT, alanine transaminase; AST, aspartate transaminase; GGT, gamma glutamyl transpeptidase; TP, total protein; ALB, albumin; TBIL, total bilirubin; DBIL, direct bilirubin; HBV, hepatitis B virus; HCV, hepatitis C virus; NA, Not applicable.

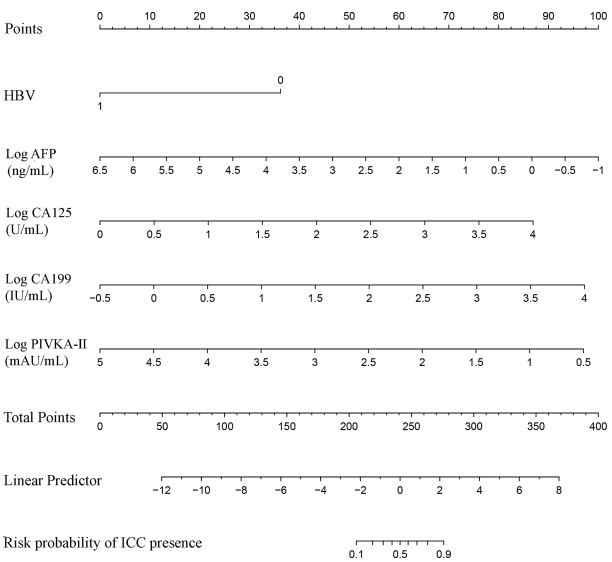

FIGURE 2 | The nomogram discriminates ICC from HCC. To use the nomogram, find the position of each variable on the corresponding axis, then draw a line to the points axis at the top of the nomogram to calculate the respective points for each parameter; finally, add the total points from all parameters and draw a line from the total points axis to the risk probability axis at the bottom of the nomogram to determine ICC presence probabilities.

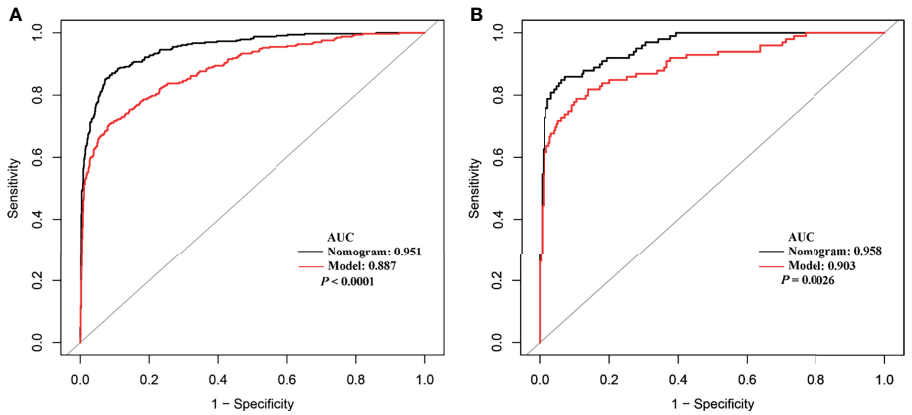

FIGURE 3 | The receiver operating characteristic curves of the nomogram and model from development cohort **(A)** and validation cohort **(B)**.

TABLE 4 | Diagnostic efficacies of the nomogram and compared model for distinguishing between ICC and HCC.

Group	Variables	Nomogram	Model
Training cohort	AUC (95% CI)	0.951 (0.938–0.964)	0.887 (0.865–0.910)
	Sensitivity	85.24%	70.78%
	Specificity	92.72%	91.56%
	NPV	94.24%	89.09%
	PPV	81.79%	76.30%
Validation cohort	AUC (95% CI)	0.958 (0.938–0.978)	0.903 (0.865–0.942)
	Sensitivity	84.85%	78.79%
	Specificity	93.90%	89.49%
	NPV	94.86%	92.63%
	PPV	82.35%	71.56%

Nomogram consists of HBV, Log AFP, Log CA199, Log CA125, and Log PIVKA-II; model includes Log AFP and Log CA199.
AUC, area under the receiver operating characteristic curve; NPV, negative predictive value; PPV, positive predictive value; AFP, α-fetoprotein level; CA199, carbohydrate antigen 199; PIVKA-II, protein induced by vitamin K absence or antagonist-II; CA125, carbohydrate antigen 125; HBV, hepatitis B virus.

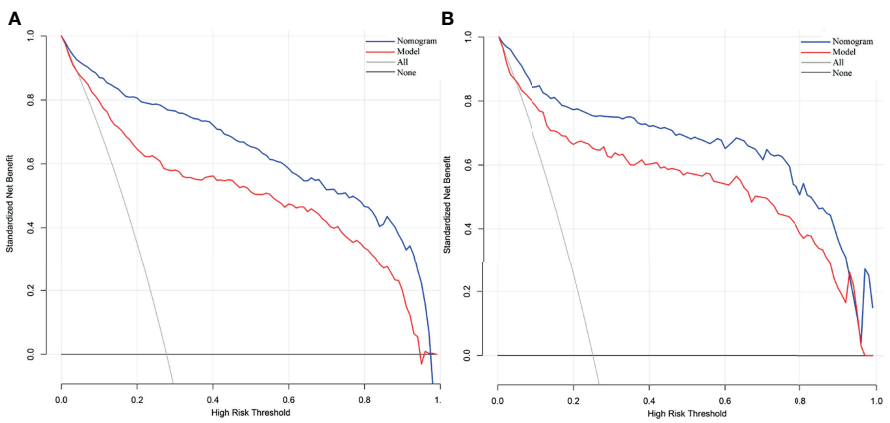

FIGURE 4 | Decision curve analysis of our nomogram and model from development cohort **(A)** and validation cohort **(B)**. The net benefit versus the risk threshold probability is plotted. The x- and y-axes show the risk threshold probability and net benefit, respectively. A model is only clinically useful if it has a higher net benefit than the default treat-all and treat-none. It is clear from the graph that both the nomogram and model are superior to either treat-all or none strategy. Besides that, using the nomogram to distinguish ICC from HCC may get more benefit compared with model.

integrating six preoperative variables (gender, HBsAg, AST, AFP, CEA, and CA199) to discriminate ICC from HCC. AFP and CA199 were the independent difference factors between HCC and ICC, which was consistent with our research conclusion. However, the six variables of the nomogram were all categorical variables, which were difficult to quantify. The continuous variables included in our nomogram have been analyzed after logarithmic transformation, which can facilitate quantitative statistics. Furthermore, our nomogram recruits PIVKA-II, regarded as a better marker for HCC diagnosis that greatly improves the differential diagnostic capability between ICC and HCC. Above all, variables of our nomogram were preoperative routine tests, providing possible evidence for clinical application extensively. Nevertheless, some limitations of our study should be recognized. The data of this study were obtained from a single institution; thus, external and large samples are needed for further validation. In addition, since variables of our nomogram were closely related with the differentiation of liver cancer, the diagnostic value of the nomogram might be better for those with poor differentiation.

CONCLUSION

In conclusion, we demonstrated that HBV, Log AFP, Log CA199, Log CA125, and Log PIVKA-II were the independent differential factors between ICC and HCC. The nomogram incorporating these five commonly assessed preoperative factors was established for optimal discrimination between them. Further application of this nomogram in multicenter investigations may confirm its clinical value.

DATA AVAILABILITY STATEMENT

The original contributions presented in the study are included in the article/supplementary material. Further inquiries can be directed to the corresponding authors.

ETHICS STATEMENT

The studies involving human participants were reviewed and approved by Ethics Committee of the Shandong Provincial Hospital Affiliated to Shandong First Medical University. The data were anonymous, and the requirement for informed consent was therefore waived.

AUTHOR CONTRIBUTIONS

ZL and YW conceived the project and designed the experiments. CP performed the data extraction and analyzation. YS and XW wrote and revised the manuscript. All authors contributed to the article and approved the submitted version.

FUNDING

This work was supported by the grants from the Medicine and Health Science and Technology Development Plan of Shandong Province (No. 2019WS474 http://sdkyxm.wsglw.net/).

REFERENCES

1. Sung H, Ferlay J, Siegel RL, Laversanne M, Soerjomataram I, Jemal A, et al. Global Cancer Statistics 2020: GLOBOCAN Estimates of Incidence and Mortality Worldwide for 36 Cancers in 185 Countries. *CA Cancer J Clin* (2021) 71(3):209–49. doi: 10.3322/caac.21660
2. Petrick JL, Braunlin M, Laversanne M, Valery PC, Bray F, McGlynn KA. International Trends in Liver Cancer Incidence, Overall and by Histologic Subtype, 1978-2007. *Int J Cancer* (2016) 139(7):1534–45. doi: 10.1002/ijc.30211
3. Wang M, Gao Y, Feng H, Warner E, An M, Jia J, et al. A Nomogram Incorporating Six Easily Obtained Parameters to Discriminate Intrahepatic Cholangiocarcinoma and Hepatocellular Carcinoma. *Cancer Med* (2018) 7 (3):646–54. doi: 10.1002/cam4.1341
4. Xue TC, Zhang BH, Ye SL, Ren ZG. Differentially Expressed Gene Profiles of Intrahepatic Cholangiocarcinoma, Hepatocellular Carcinoma, and Combined Hepatocellular-Cholangiocarcinoma by Integrated Microarray Analysis. *Tumour Biol* (2015) 36(8):5891–9. doi: 10.1007/s13277-015-3261-1
5. Banales JM, Iñarrairaegui M, Arbelaiz A, Milkiewicz P, Muntané J, Muñoz-Bellvis L, et al. Serum Metabolites as Diagnostic Biomarkers for Cholangiocarcinoma, Hepatocellular Carcinoma, and Primary Sclerosing Cholangitis. *Hepatology* (2019) 70(2):547–62. doi: 10.1002/hep.30319
6. Chaisaingmongkol J, Budhu A, Dang H, Rabibhadana S, Pupacdi B, Kwon SM, et al. Common Molecular Subtypes Among Asian Hepatocellular Carcinoma and Cholangiocarcinoma. *Cancer Cell* (2017) 32(1):57–70.e3. doi: 10.1016/j.ccell.2017.05.009
7. Massarweh NN, El-Serag HB. Epidemiology of Hepatocellular Carcinoma and Intrahepatic Cholangiocarcinoma. *Cancer Control* (2017) 24 (3):1073274817729245. doi: 10.1177/1073274817729245
8. Chen L, Zeng F, Yao L, Fang T, Liao M, Long J, et al. Nomogram Based on Inflammatory Indices for Differentiating Intrahepatic Cholangiocarcinoma From Hepatocellular Carcinoma. *Cancer Med* (2020) 9(4):1451–61. doi: 10.1002/cam4.2823
9. Ejaz A, Cloyd JM, Pawlik TM. Advances in the Diagnosis and Treatment of Patients With Intrahepatic Cholangiocarcinoma. *Ann Surg Oncol* (2020) 27 (2):552–60. doi: 10.1245/s10434-019-07873-z
10. Forner A, Reig M, Bruix J. Hepatocellular Carcinoma. *Lancet* (2018) 391 (10127):1301–14. doi: 10.1016/s0140-6736(18)30010-2
11. Rahnemai-Azar AA, Weisbrod A, Dillhoff M, Schmidt C, Pawlik TM. Intrahepatic Cholangiocarcinoma: Molecular Markers for Diagnosis and Prognosis. *Surg Oncol* (2017) 26(2):125–37. doi: 10.1016/j.suronc.2016.12.009
12. Li L, Che L, Tharp KM, Park HM, Pilo MG, Cao D, et al. Differential Requirement for *De Novo* Lipogenesis in Cholangiocarcinoma and Hepatocellular Carcinoma of Mice and Humans. *Hepatology* (2016) 63 (6):1900–13. doi: 10.1002/hep.28508
13. Kim R, Lee JM, Shin CI, Lee ES, Yoon JH, Joo I, et al. Differentiation of Intrahepatic Mass-Forming Cholangiocarcinoma From Hepatocellular Carcinoma on Gadoxetic Acid-Enhanced Liver MR Imaging. *Eur Radiol* (2016) 26(6):1808–17. doi: 10.1007/s00330-015-4005-8
14. Lei Z, Li J, Wu D, Xia Y, Wang Q, Si A, et al. Nomogram for Preoperative Estimation of Microvascular Invasion Risk in Hepatitis B Virus-Related Hepatocellular Carcinoma Within the Milan Criteria. *JAMA Surg* (2016) 151(4):356–63. doi: 10.1001/jamasurg.2015.4257
15. Zou Q, Li J, Wu D, Yan Z, Wan X, Wang K, et al. Nomograms for Pre-Operative and Post-Operative Prediction of Long-Term Survival of Patients Who Underwent Repeat Hepatectomy for Recurrent Hepatocellular Carcinoma. *Ann Surg Oncol* (2016) 23(8):2618–26. doi: 10.1245/s10434-016-5136-0

16. Ferrone CR, Kattan MW, Tomlinson JS, Thayer SP, Brennan MF, Warshaw AL. Validation of a Postresection Pancreatic Adenocarcinoma Nomogram for Disease-Specific Survival. *J Clin Oncol* (2005) 23(30):7529–35. doi: 10.1200/jco.2005.01.8101
17. Filion KB, Azoulay L, Platt RW, Dahl M, Dormuth CR, Clemens KK, et al. A Multicenter Observational Study of Incretin-Based Drugs and Heart Failure. *N Engl J Med* (2016) 374(12):1145–54. doi: 10.1056/NEJMoa1506115
18. Yang J, Zhu S, Yong J, Xia L, Qian X, Yang J, et al. A Nomogram for Preoperative Estimation of Microvascular Invasion Risk in Hepatocellular Carcinoma: Single-Center Analyses With Internal Validation. *Front Oncol* (2021) 11:616976. doi: 10.3389/fonc.2021.616976
19. Melamed A, Margul DJ, Chen L, Keating NL, Del Carmen MG, Yang J, et al. Survival After Minimally Invasive Radical Hysterectomy for Early-Stage Cervical Cancer. *N Engl J Med* (2018) 379(20):1905–14. doi: 10.1056/NEJMoa1804923
20. Farrar D, Fairley L, Santorelli G, Tuffnell D, Sheldon TA, Wright J, et al. Association Between Hyperglycaemia and Adverse Perinatal Outcomes in South Asian and White British Women: Analysis of Data From the Born in Bradford Cohort. *Lancet Diabetes Endocrinol* (2015) 3(10):795–804. doi: 10.1016/s2213-8587(15)00255-7
21. White IR, Royston P, Wood AM. Multiple Imputation Using Chained Equations: Issues and Guidance for Practice. *Stat Med* (2011) 30(4):377–99. doi: 10.1002/sim.4067
22. Wang K, Zuo P, Liu Y, Zhang M, Zhao X, Xie S, et al. Clinical and Laboratory Predictors of in-Hospital Mortality in Patients With Coronavirus Disease-2019: A Cohort Study in Wuhan, China. *Clin Infect Dis* (2020) 71(16):2079–88. doi: 10.1093/cid/ciaa538
23. Bridgewater J, Galle PR, Khan SA, Llovet JM, Park JW, Patel T, et al. Guidelines for the Diagnosis and Management of Intrahepatic Cholangiocarcinoma. *J Hepatol* (2014) 60(6):1268–89. doi: 10.1016/j.jhep.2014.01.021
24. El-Diwany R, Pawlik TM, Ejaz A. Intrahepatic Cholangiocarcinoma. *Surg Oncol Clin N Am* (2019) 28(4):587–99. doi: 10.1016/j.soc.2019.06.002
25. Kelley RK, Bridgewater J, Gores GJ, Zhu AX. Systemic Therapies for Intrahepatic Cholangiocarcinoma. *J Hepatol* (2020) 72(2):353–63. doi: 10.1016/j.jhep.2019.10.009
26. Lee AJ, Chun YS. Intrahepatic Cholangiocarcinoma: The AJCC/UICC 8th Edition Updates. *Chin Clin Oncol* (2018) 7(5):52. doi: 10.21037/cco.2018.07.03
27. Afshar M, Fletcher P, Bardoli AD, Ma Y, TPunia P. Non-Secretion of AFP and Neutrophil Lymphocyte Ratio as Predictors for Survival in Hepatocellular Carcinoma Patients Treated With Sorafenib: A Large UK Cohort. *Oncotarget* (2018) 9(24):16988–95. doi: 10.18632/oncotarget.24769
28. Qi F, Zhou A, Yan L, Yuan X, Wang D, Chang R, et al. The Diagnostic Value of PIVKA-II, AFP, AFP-L3, CEA, and Their Combinations in Primary and Metastatic Hepatocellular Carcinoma. *J Clin Lab Anal* (2020) 34(5):e23158. doi: 10.1002/jcla.23158
29. Park SJ, Jang JY, Jeong SW, Cho YK, Lee SH, Kim SG, et al. Usefulness of AFP, AFP-L3, and PIVKA-II, and Their Combinations in Diagnosing Hepatocellular Carcinoma. *Med (Baltimore)* (2017) 96(11):e5811. doi: 10.1097/md.0000000000005811
30. Huang D, Lin Q, Song J, Xu B. Prognostic Value of Pretreatment Serum CA199 in Patients With Locally Advanced Rectal Cancer Treated With CRT Followed by TME With Normal Pretreatment Carcinoembryonic Antigen Levels. *Dig Surg* (2021) 38(1):24–9. doi: 10.1159/000508442
31. Teng D, Wu K, Sun Y, Zhang M, Wang D, Wu J, et al. Significant Increased CA199 Levels in Acute Pancreatitis Patients Predicts the Presence of Pancreatic Cancer. *Oncotarget* (2018) 9(16):12745–53. doi: 10.18632/oncotarget.23993
32. Dochez V, Caillon H, Vaucel E, Dimet J, Winer N, Ducarme G. Biomarkers and Algorithms for Diagnosis of Ovarian Cancer: CA125, HE4, RMI and ROMA, a Review. *J Ovarian Res* (2019) 12(1):28. doi: 10.1186/s13048-019-0503-7
33. Nassiri F, Mamatjan Y, Suppiah S, Badhiwala JH, Mansouri S, Karimi S, et al. DNA Methylation Profiling to Predict Recurrence Risk in Meningioma: Development and Validation of a Nomogram to Optimize Clinical Management. *Neuro Oncol* (2019) 21(7):901–10. doi: 10.1093/neuonc/noz061
34. Serenari M, Han KH, Ravaioli F, Kim SU, Cucchetti A, Han DH, et al. A Nomogram Based on Liver Stiffness Predicts Postoperative Complications in Patients With Hepatocellular Carcinoma. *J Hepatol* (2020) 73(4):855–62. doi: 10.1016/j.jhep.2020.04.032
35. Berardi G, Morise Z, Sposito C, Igarashi K, Panetta V, Simonelli I, et al. Development of a Nomogram to Predict Outcome After Liver Resection for Hepatocellular Carcinoma in Child-Pugh B Cirrhosis. *J Hepatol* (2020) 72(1):75–84. doi: 10.1016/j.jhep.2019.08.032
36. Zhang Z, Rousson V, Lee WC, Ferdynus C, Chen M, Qian X, et al. Decision Curve Analysis: A Technical Note. *Ann Transl Med* (2018) 6(15):308. doi: 10.21037/atm.2018.07.02
37. Sande SZ, Li J, D'Agostino R, Yin Wong T, Cheng CY. Statistical Inference for Decision Curve Analysis, With Applications to Cataract Diagnosis. *Stat Med* (2020) 39(22):2980–3002. doi: 10.1002/sim.8588
38. Vickers AJ, van Calster BSteyerberg EW. A Simple, Step-by-Step Guide to Interpreting Decision Curve Analysis. *Diagn Progn Res* (2019) 3:18. doi: 10.1186/s41512-019-0064-7
39. Huang C, Xu X, Wang M, Xiao X, Cheng C, Ji J, et al. Serum N-Glycan Fingerprint Helps to Discriminate Intrahepatic Cholangiocarcinoma From Hepatocellular Carcinoma. *Electrophoresis* (2021) 42(11):1187–95. doi: 10.1002/elps.202000392

Conflict of Interest: The authors declare that the research was conducted in the absence of any commercial or financial relationships that could be construed as a potential conflict of interest.

Publisher's Note: All claims expressed in this article are solely those of the authors and do not necessarily represent those of their affiliated organizations, or those of the publisher, the editors and the reviewers. Any product that may be evaluated in this article, or claim that may be made by its manufacturer, is not guaranteed or endorsed by the publisher.

Copyright © 2022 Si, Wang, Pan, Wang and Lu. This is an open-access article distributed under the terms of the Creative Commons Attribution License (CC BY). The use, distribution or reproduction in other forums is permitted, provided the original author(s) and the copyright owner(s) are credited and that the original publication in this journal is cited, in accordance with accepted academic practice. No use, distribution or reproduction is permitted which does not comply with these terms.

frontiers | Frontiers in Surgery

ORIGINAL RESEARCH
published: 12 April 2022
doi: 10.3389/fsurg.2022.895982

The Effect of Anlotinib Combined with anti-PD-1 in the Treatment of Gastric Cancer

Wubin Zheng†, Guoqiang Sun†, Zhitao Li†, Fan Wu, Guangshun Sun, Hongyong Cao, Jin Zhou* and Yong Ma**

Department of General Surgery, Nanjing First Hospital, Nanjing Medical University, Nanjing, Jiangsu, China

OPEN ACCESS

Edited by:
Qi Liu,
Shanghai Cancer Center, Fudan University, China

Reviewed by:
Alessandro Rizzo,
Bari John Paul II Cancer Institute, National Cancer Institute Foundation (IRCCS), Italy
Andrea Botticelli,
Sapienza University of Rome, Italy

****Correspondence:***
Hongyong Cao
caohongy6167@163.com;
Jin Zhou
georgenjmu@163.com;
Yong Ma
yma0917@163.com

†These authors have contributed equally to this work.

Speciality section:
This article was submitted to Surgical Oncology, a section of the journal Frontiers in Surgery

Received: *14 March 2022*
Accepted: *29 March 2022*
Published: *12 April 2022*

Citation:
Zheng W, Sun G, Li Z, Wu F, Sun G, Cao H, Zhou J and Ma Y (2022) The Effect of Anlotinib Combined with anti-PD-1 in the Treatment of Gastric Cancer. Front. Surg. 9:895982. doi: 10.3389/fsurg.2022.895982

Background: Protein tyrosine kinase (PTK) signaling pathway has been confirmed to be involved in the proliferation, differentiation and migration of tumor cells. Anlotinib, as a multi-target tyrosine kinase inhibitor, which can inhibit the expression of vascular endothelial growth factor receptor (VEGFR), has been confirmed to have significant therapeutic effects on non-small cell lung cancer, medullary thyroid carcinoma, and soft tissue sarcoma, but the therapeutic effect on gastric cancer (GC) is still unclear.

Methods: Anlotinib was screened out of 880 drugs through Cell Counting Kit 8 (CCK-8) technology. TCGA was used to detect the expression of VEGFR in GC, and Kaplan-Meier Plotter was used to analyze the correlation between the expression of VEGFR and the survival rate of GC patients. The impacts exerted by anlotinib to GC cell proliferating, migrating and invading processes were assessed through wound healing assay, transwell assay, and proliferation assay in vitro. In vivo experiments of GC were performed in C57/B6 mouse model to evaluate the function of anlotinib and PD-1 antibody.

Results: It was found from more than compunds that anlotinib has a significant inhibitory effect on GC cells. In vitro experiments show that anlotinib can significantly inhibit the proliferation, invasion and proliferation of GC cells. The expression level of VEGFR is related to the prognosis and survival of GC. GC patients with low expression of VEGFR have better survival. Anlotinib can inhibit the expression of PD-L1, and achieve better therapeutic effects after combined with PD-1 antibody.

Conclusion: The present study reveals that anlotinib down regulates PD-L1. The combination of anlotinib and PD-1 monoclonal antibody is beneficial to GC therapy.

Keywords: anlotinib, gastric cancer, PD1, immunotherapy, VEGFR - vascular endothelial growth factor receptor

INTRODUCTION

Gastric cancer (GC) is one of the most common malignant tumors worldwide, with the 5th highest incidence rate and the 3rd highest mortality rate among all malignant tumors, after lung cancer and liver cancer (1). Due to the insidious symptoms of GC, patients are often diagnosed with progressive or even advanced GC, and the survival period is extremely low. With the rapid

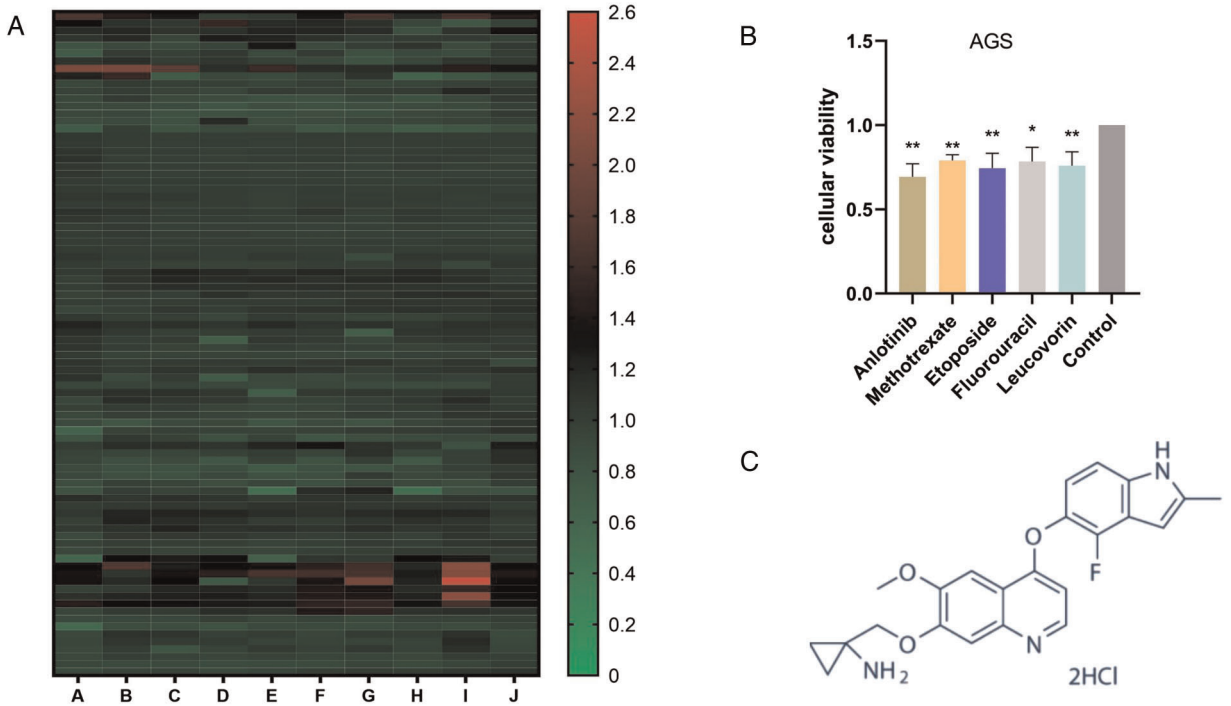

FIGURE 1 | Screening of the inhibitory effects of multiple drugs on GC cells: (**A**) The proliferation of more than 880 drugs after treatment of GC cells. (**B**) Compared with the four drugs commonly used in GC chemotherapy, Anlotinib has a more obvious inhibitory effect on the proliferation of GC cells. (**C**) Anlotinib compound structure. (Picture from www.selleck.cn). $^{*}P < 0.05$; $^{**}P < 0.01$.

development of treatment technology in recent years, the survival rate of patients with progressive gastric cancer is only about 20% (2). To date, surgery is still the main treatment modality for GC, while for those without surgical indications or who need to be supplemented with chemotherapy before and after surgery. The current first-line chemotherapy for gastric cancer is fluorouracil in combination with platinum ± epirubicin/docetaxel/irinotecan as recommended by the National Comprehensive Cancer Network (NCCN) in 2016. Nevertheless, the survival rate of GC patients is still extremely low, indicating that finding new and effective chemotherapeutic drugs to improve the treatment effect and prolong the survival rate of GC patients is still the top priority of gastric cancer treatment at present. In recent years, molecular targeted drugs have become a popular research topic because of their high efficiency and low toxicity in treating cancers such as breast, colorectal, thyroid, and non-small cell lung cancer. At the same time, TKIs plus immunotherapy have gradually been widely used in gastric cancer and other malignant tumors, and have received good feedback (3–5).

Tumor metastasis (especially peritoneum and liver) and hypoproteinemia are important factors affecting the survival of GC patients. The protein tyrosine kinase (PTK) signaling pathway is involved in the proliferation, differentiation and migration of tumor cells. Interfering or blocking the PTK pathway can stop the growth of tumor cells and thus achieve therapeutic effects (6). Anrotinib is a multi-target tyrosine kinase inhibitor, an orally administered small molecule drug that exerts an inhibitory effect on tumor angiogenesis and tumor cell proliferation by selectively inhibiting vascular endothelial growth factor receptor (VEGFR), fibroblast growth factor receptor (FGFR) and platelet-derived growth factor receptor (PDGFR) (7). Current researches have demonstrated that anlotinib has significant therapeutic effects on non-small cell lung cancer, medullary thyroid cancer, and soft tissue sarcoma, significantly prolonging overall survival (OS) and progression-free survival (PFS) with the adverse effects were small (8–10). However, there is still a lack of evidence for the efficacy of this treatment in GC.

GC evades the immune system by down-regulating tumor expression, up-regulating immune checkpoints, inactivating cytotoxic T cells and altering the tumor immune microenvironment. Anti-tumor therapies that inhibit negative immunoregulatory mechanisms, namely immune check-point blockade (ICB), have become a hot topic of current research. The application of PD-1(programmed death 1)/PD-L1 (programmed death ligand 1) inhibitors to block the immune checkpoint is the most promising ICB therapy (11, 12). It has been reported that PD-1 /PD-L1 expression is detected abnormally in GC patients and is closely related to tumor progression and patient prognosis. The effectiveness of

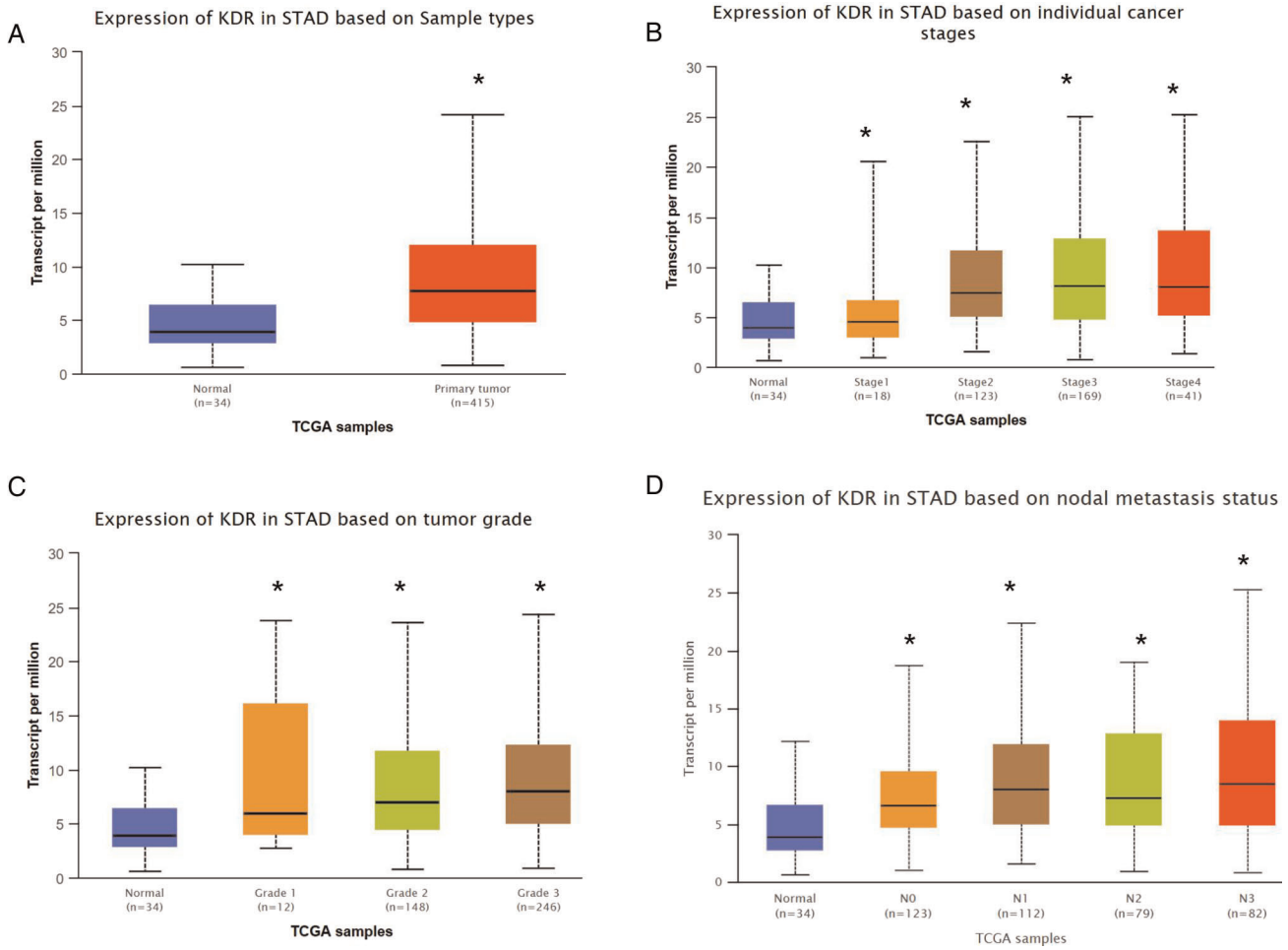

FIGURE 2 | VEGFR expression in GC. (**A**) VEGFR expression based on sample type. (**B**) VEGFR expression based on individual cancer stages. (**C**) VEGFR expression based on tumor grade. (**D**) VEGFR expression based on nodal metastasis status. *$p < 0.05$.

anlotinib and PD-1 antibody in the treatment of GC is currently unclear, and further studies are needed to provide guidance for the clinical treatment of GC.

MATERIALS AND METHODS

Cell Cultures

Human GC cell lines (AGS, MKN-45) were provided by Shanghai Institutes for Biological Sciences in China. All cells were grown in a humidified incubator at 37°C with 5% CO2 in RPMI-1640 medium (Biological Industries, Israel) containing 10% fetal bovine serum (Gibco, Austria) and 1% penicillin-streptomycin.

Quantitative Reverse Transcription Polymerase Reaction (qRT-PCR)

Total RNAs from cells were extracted using TRIzol reagent (Invitrogen, USA) according to the manufacturer's instructions. Overall RNAs were reverse transcribed to cDNA by a reverse transcription kit (Takara, Japan). We quantified PD-L1 mRNA and performed PCR assays based on the SYBR Green PCR kit (Takara, Japan) and based on a SYBR Green PCR Kit (RiboBio, China). Before calculating, the levels of mRNA expression status were normalized with GAPDH.

VEGFR Expression Level Analysis and Clinicopathological Analysis

The expression of VEGFR in GC tissues and corresponding normal tissues was investigated using TCGAportal. VEGFR expression was compared in GC patients of various types, stages, grades, and nodal metastasis status using UALCAN. Kaplan-Meier Plotter was used to compare correlations between VEGFR expression and overall survival (OS), post-progression survival (PPS), and first progression survival (FP). Tumor Immune Single-cell Hub (TISCH) was used to provide detailed cell-type annotation at the single-cell level, enabling the exploration of TME across different cancer types including GC.

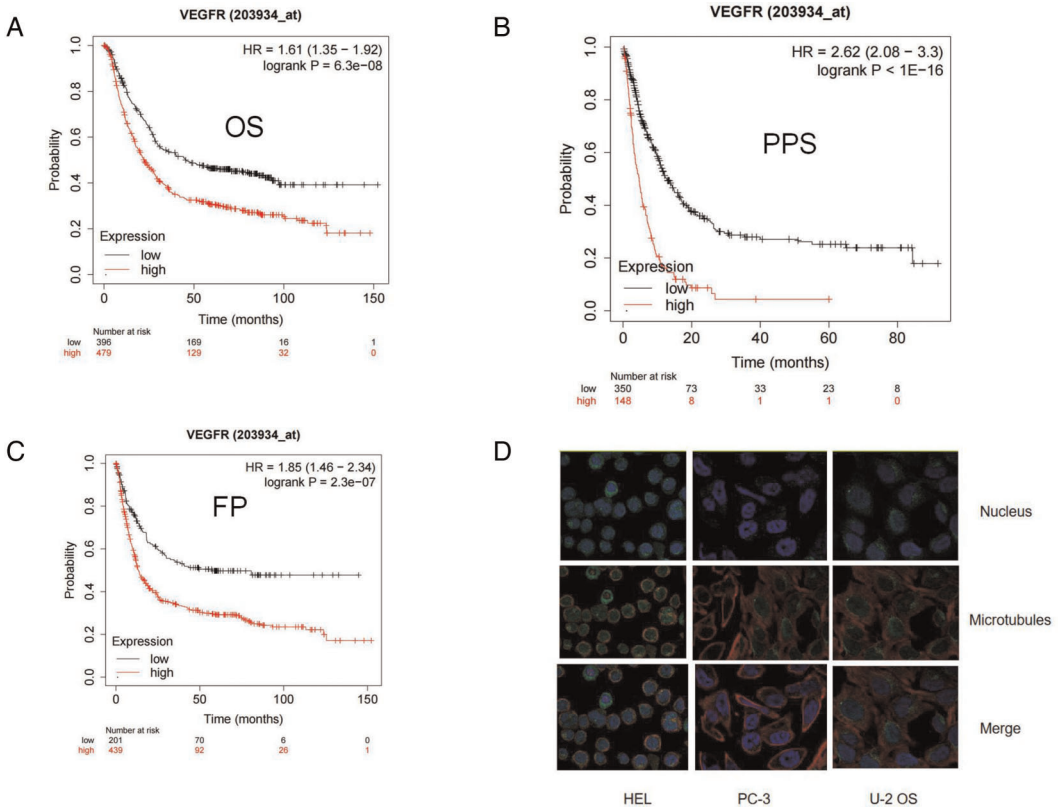

FIGURE 3 | High expression of VEGFR indicated a worse GC clinical prognosis from Kaplan Meier Plotter. (**A**-**C**) Kaplan Meier survival curve showed the relationship between PARP and overall survival (OS), post-progression survival (PPS), and first progression survival (FP) in GC patients. (**D**) The location of VEGFR in cell.

Tools for VEGFR Location in Cells

The Human Protein Atlas, compiling numerous reports and tissue, cell and pathology atlas forms, and gene data in cells and tissues, was utilized for obtaining VEGFR location in cells.

Tool for Immune-Related Analysis of VEGFR

TISIDB was adopted for delving into the spearman correlations between VEGFR and immune-modulator expression.

Cell Counting Kit-8 Proliferation Assay

To detect the inhibitory effect of drugs on cell proliferation, researchers used the CCK-8 kit (Ribobio, China). Drug Screening: GC cells (2,000/well) were spread in 96-well plates and cultured for 24 h. The drug to be screened was added to each well at a concentration of 5 μM. After a 24-hour incubation period in a humidified incubator at 37°C with 5% CO2, 10 μl of CCK-8 reagent was added to each well and the incubation was continued for 2 h before the absorbance at 450 nm was measured using an enzyme marker. Selleck (USA) provided the drug to be screened as well as the anlotinib used in the assay.

Wound Healing Assay

After the fusion of both AGS or MKN-45 cell lines reached 90%, artificial linear incisions were created with a standard 200 μl pipette tip, washed twice with PBS to remove any free-floating cells and debris, and replaced with new medium. 5 μM and 10 μM of anlotinib were added to the medium and equal concentrations of dimethyl sulfoxide (DMSO) were added to the control group. The plates were incubated at 37°C with 5% CO2 in a humidified incubator. At different time points (0 h, 24 h, 48 h), the wound healing within the scratch line was observed, and representative scratch lines were photographed.

Transwell Assay

Anlotinib was added to the GC cell lines after they had reached 90% fusion, and equal concentrations of dimethyl sulfoxide (DMSO) were added to the control group. The plates were then placed in a humidified incubator at 37°C with 5% CO2 for 24 h. Complete the inoculation of GC cell lines according to the manufacturer's instructions. The upper chamber was added with 200 μl RPMI-1640 medium and 4×10^6 GC cells (with or without treatment with anlotinib) and the lower chamber was added with 700 μl RPMI-1640 medium containing 10% fetal bovine serum as a chemotactic agent.

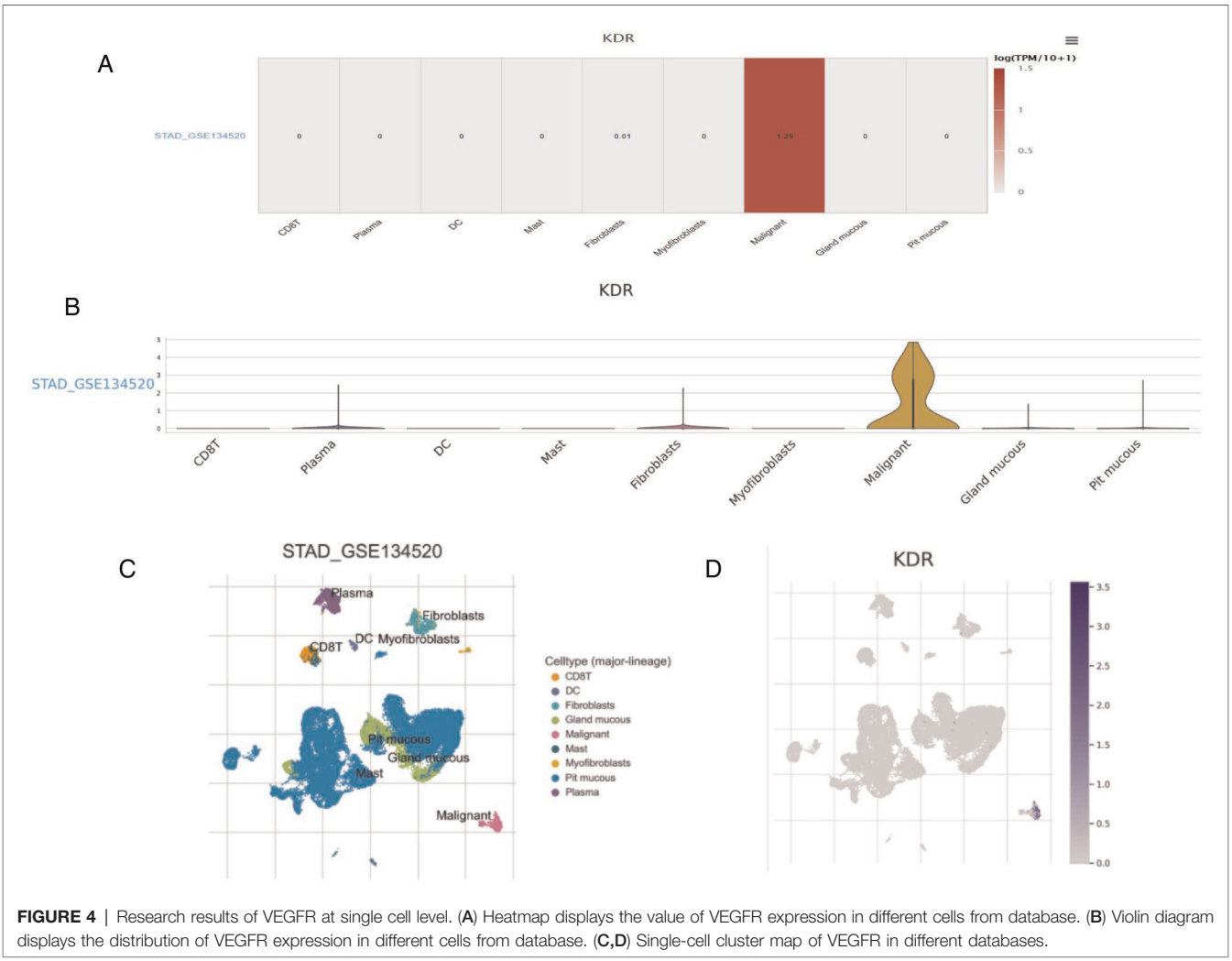

FIGURE 4 | Research results of VEGFR at single cell level. (**A**) Heatmap displays the value of VEGFR expression in different cells from database. (**B**) Violin diagram displays the distribution of VEGFR expression in different cells from database. (**C,D**) Single-cell cluster map of VEGFR in different databases.

The upper chamber was fixed with formaldehyde and stained with 0.1% crystal violet for 15 min after 24 h of culture. Finally, under an inverted microscope, the treated cell lines were photographed and counted.

Colony Formation Assay

AGS and MKN-45 cell lines were spread into six-well plates at a density of 1,000 cells/well, and they were treated with anlotinib, respectively, and equal concentrations of DMSO were added to the control group. The six-well plates were incubated for 14 days at 37°C with 5% CO2 in a humidified incubator. The cell colonies were fixed using formaldehyde and stained with 0.1% crystal violet for 15 min. The colonies were photographed and counted. All assays were carried out in triplicate.

Western Blotting

Abcam Corporation (UK) provided the anti-PD-L1 antibody. GADPH was obtained by lysing cells in RIPA lysis buffer (RIPA, Beyotime, China). The protrin blocked using 5% skim milk powder received the incubation using primary antibody, anti-GADPH and anti-PD-L1, at 4°C for 12 h. After that, the synthesized membranes were incubated for 2 h with a secondary antibody (1:5,000). Lastly, with enhanced chemiluminescence kit (Pierce, USA). Image J was using to analyze the images of western blot, and the quantitative expression level of proteins were examined as the band-intensity.

Mice Model

The animal experiment was approved by Nanjing Medical University's animal management committee, and all experiment procedures and animal caring conformed to the institutional ethics directions for animals-related experimental processes. For GC study, we conducted the random separation of 20 male C57/B6 mice aged 5 weeks in anlotinib, PD-1 monoclonal antibody (BP0273, bioxcell, USA), anlotinib+ PD-1 monoclonal antibody, PBS ($n = 5$ for the respective group) in a range of MFC cells. In the mice inguen, MFC cells were injected subcutaneously. The researchers killed all the mice in

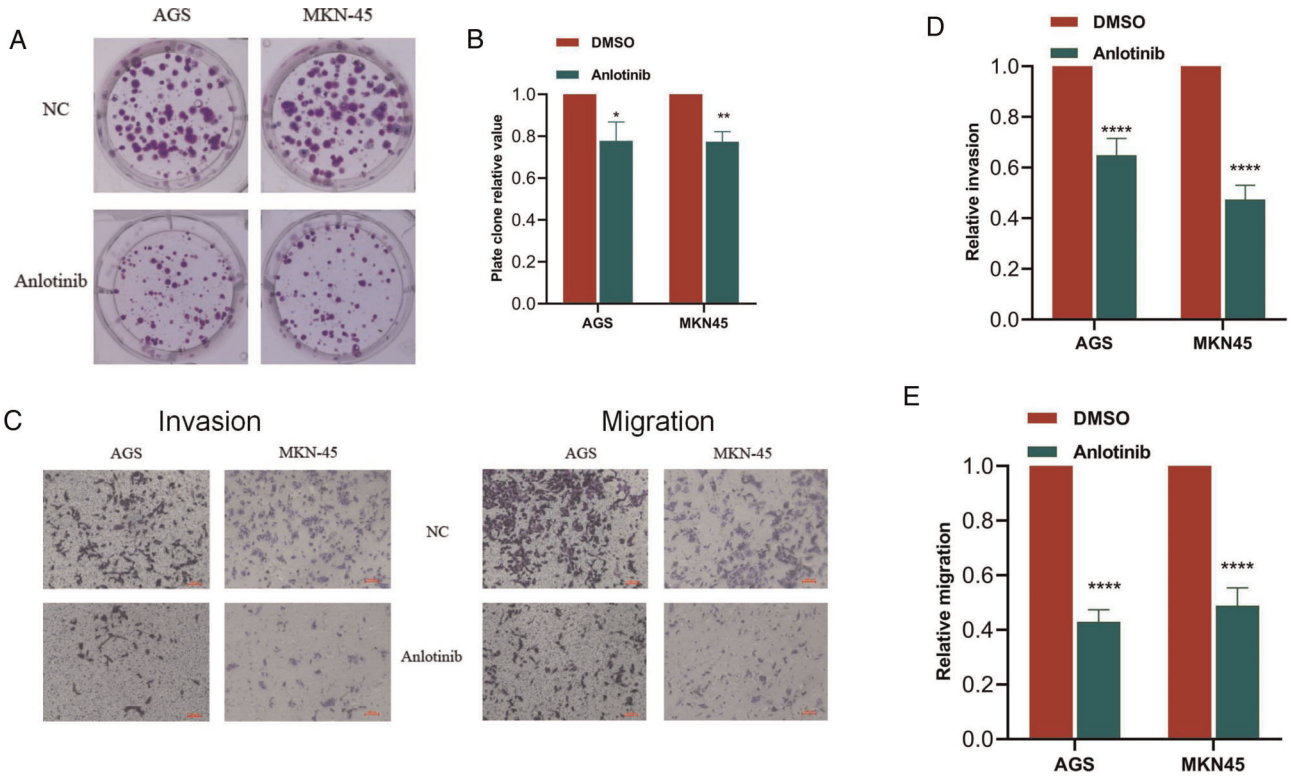

FIGURE 5 | Anlotinib can significantly inhibit the proliferation, migration and invasion of GC cells. (**A,B**) Plate cloning assays proved that Anlotinib can significantly inhibit the proliferation of GC cells. (**C**-**E**) The results of transwell migration and invasion assays proved that Anlotinib can inhibit the migration and invasion of GC cells. $^{*}P < 0.05$; $^{**}P < 0.01$; $^{****}P < 0.0001$.

the experiment, collected tumor sizes and weighed tumors for further experimental tests.

Statistical Analysis

We compared continuous information based on an individual *t*-experiment in the two groups.We carried out the analyses largely based on Graphpad Prism 8.0 (USA), and *p*-value <0.05 was reported with statistics-related significance.

RESULTS

Comprehensive High-Throughput Screening Shows that Anlotinib has a Significant Inhibitory Effect on GC Cells

We used CCK-8 experiment to detect the cell proliferation efficiency of 880 kinds of drugs after drug treatment, and the experimental results found that anlotinib has obviously inhibitory effect on GC cell proliferation (**Figure 1A**). After the initial screening was completed, we used the same experiment to compare anlotinib with traditional gastric cancer chemotherapy drugs such as Methotrexate, Etoposide, Fluorouracil and Leucovorin. The cell proliferation results indicated that anlotinib's inhibitory effect on GC cells is better than traditional drugs (**Figure 1B**). The structure of anlotinib is shown in the **Figure 1C**, and we decided to study the role of anlotinib in the treatment of GC.

VEGFR is Significantly Correlated with Clinical Prognosis

To further explore the prognostic potential of VEGFR (the target of anlotinib) in GC, TCGA portal and Kaplan-Meier Plotter were used.

The TCGA portal showed that the expression of VEGFR in tumor tissues was obvious higher than that in normal tissues (**Figure 2A**). The expression level of VEGFR in different stages, tumor grades,or lymph node metastasis of individual cancer indicated that the expression level of VEGFR in GC tissues was also higher than normal tissues (**Figures 2B–D**). The prognostic potential of VEGFR in GC was further examined using Kaplan-Meier Plotter. The results showed that GC patients with higher VEGFR expression had lower overall survival (OS), post-progression survival (PPS), and first progression survival (FP) (**Figures 3A–C**).

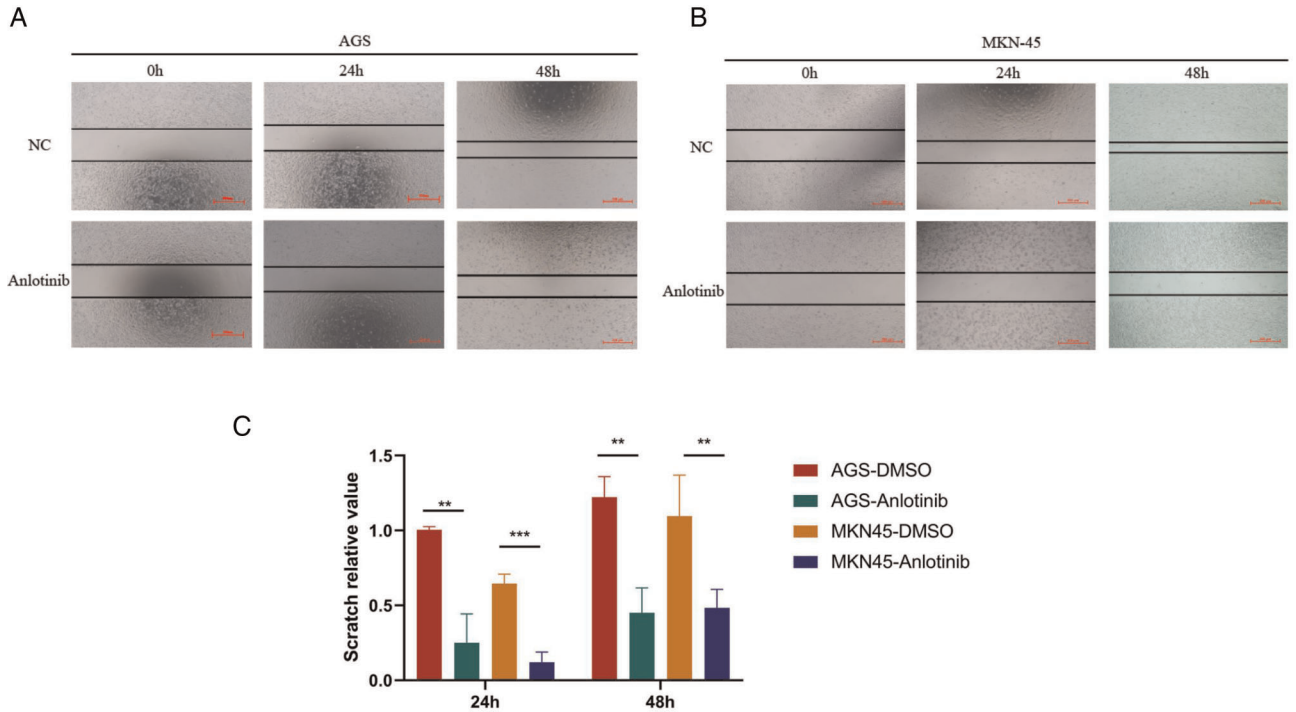

FIGURE 6 | Scratch test results of Anlotinib in GC cells. (**A–C**) Scratch assay proved that Anlotinib can inhibit the migration of GC cells. $^{*}P < 0.05$; $^{**}P < 0.01$; $^{***}P < 0.001$.

Research Results of VEGFR at Single Cell Level

We studied the expression of VEGFR at the single cell level. **Figures 4A,B** showed the distribution of VEGFR expression in GC database. In database GSE134520, the VEGFR was enriched at the malignant, fibroblasts, and plasma cell clusters (**Figures 4C,D**). These results suggest that VEGFR mainly function in malignant other than other cells. Moreover, according to the human protein atlas database, VEGFR is located in the cell membrane in cells (**Figure 3D**).

Anlotinib Inhibits the Proliferation, Invasion and Migration of GC Cells

For gaining insights into the effects exerted by anlotinib on the biological behaviors of GC cells, we used anlotinib to treat GC cell lines including AGS and MKN-45 respectively. The results of plate cloning experiments show that anlotinib can inhibit the proliferation of GC cells (**Figures 3A,B**). The transwell assay revealed that anlotinib can significantly inhibit the invasion and migration potential of GC cells, compared with the untreated group (**Figures 5C–E**). At the same time, wound healing assay once again confirmed that in GC cell lines, the wound healing rate of GC cells treated with anlotinib was significantly lower than the control group (**Figures 6A–C**).

VEGFR Expression was Correlated with Immune Factors

Existing studies have confirmed that the immune system is closely related to the occurrence and development of tumors. Therefore, we studied the relationship between the expression of VEGFR and immune factors. As shown in **Figures 7A,B**, there was a strong positive correlation between the expression of immunoinhibitors (CD274,TIGIT,CTLA4,HAVCR2) and the expression of VEGFR.

The Combined use of Anlotinib and anti-PD-1 has a Significant Inhibitory Effect on GC Cells

Next, we needed to explore whether the effect of anlotinib on the expression of PD-L1 in GC cells is consistent with the above results.

QRT-PCR results showed that the expression of PD-L1 in GC cells treated with anlotinib was significantly lower than that in the control group (**Figure 8A**). Western blotting analysis results from the protein expression level suggested that anlotinib can significantly reduce the expression of PD-L1 relative to the control group (**Figures 8B,C**). To examine the association between anlotinib and the growth of GC in vivo, we injected MFC cells into subcutaneous groin of C57/B6 mice, and then we administered intraperitoneally anlotinib or

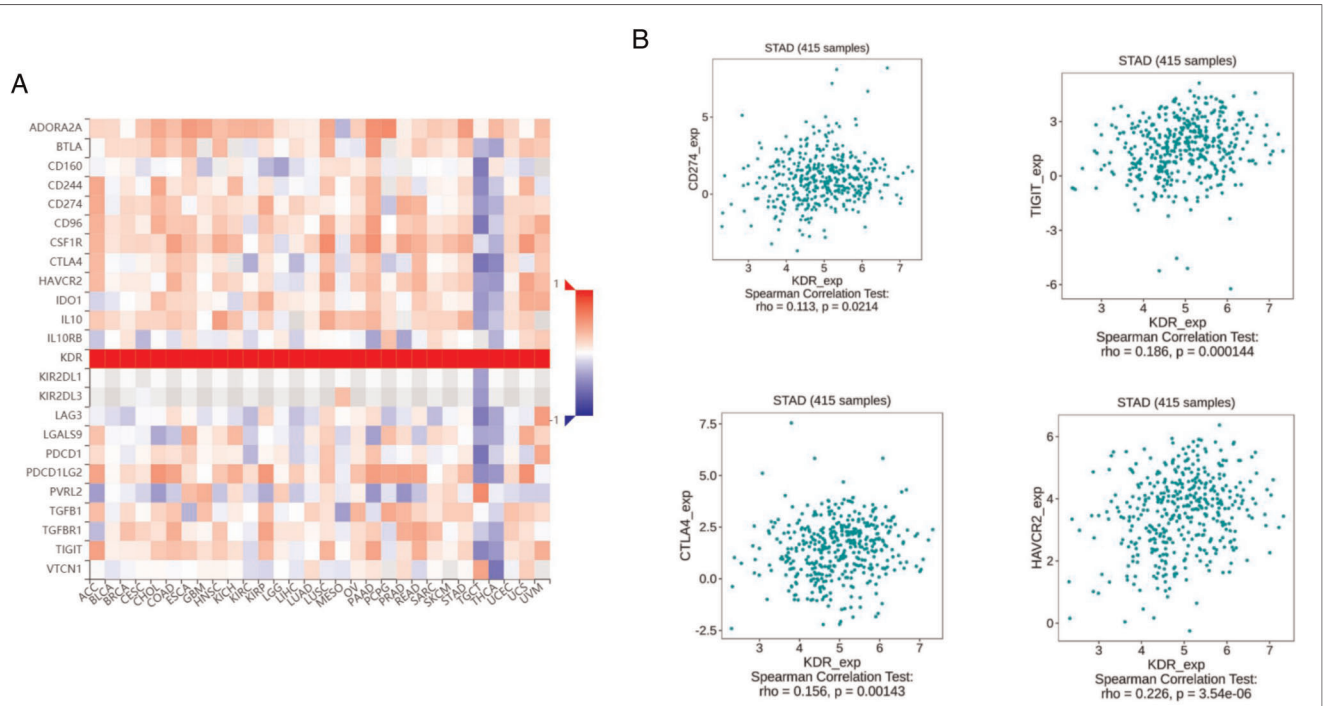

FIGURE 7 | Correlation between VEGFR expression and immunoinhibitors in GC. (**A**) The heat map shows the correlation between VEGFR and immunosuppressive factors in different cancers. (**B**) Line graph shows the correlation of VEGFR with specific immune indicators in GC.

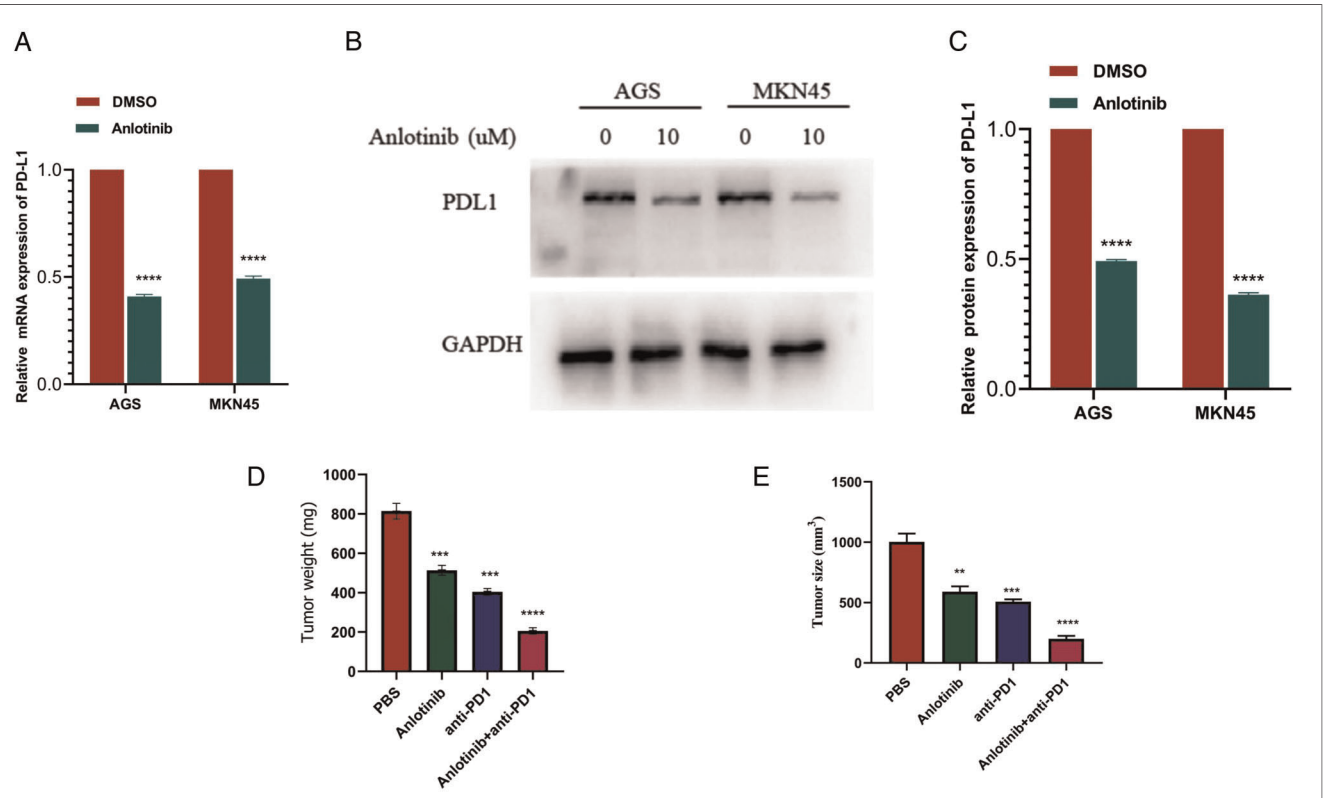

FIGURE 8 | Anlotinib combined with anti-PD-1 has a significant therapeutic effect on GC. (**A**) QRT- PCR results show that Anlotinib can significantly reduce the expression of PD-L1. (**B,C**) Western blotting experiment proved that Anlotinib can significantly reduce PD-L1 expression. (**D**) The relative weights of tumors were evaluated in C57BL/6 mice. (**E**) The relative tumor sizes were evaluated in C57BL/6 mice. ***$P < 0.001$; ****$P < 0.0001$.

PD-1 antibody alone or in combination to mice and analyzed tumor growth in 20 days, as well as weight of tumors after the mice were killed. As indicated from the results, the combination group of anlotinib combined with PD-1 monoclonal antibody has a better inhibitory effect on tumors, compared with the single-drug group and the control group (**Figures 8D,E**).

DISCUSSION

Although in the past few decades, the preoperative or postoperative chemotherapy regimen for GC has gradually been determined as fluorouracil combined with platinum ± epirubicin/docetaxel/irinotecan, but the current five-year survival rate of GC patients is still low, and the five-year survival rate for advanced GC patients with tumor metastasis is lower. Therefore, researchers are still looking for better new and effective chemotherapeutics that can prolong the survival rate of patients and improve the treatment effect.

In the past five years, ICB therapy has revolutionized the treatment of some solid tumors or hematological tumors, and there are still multiple new studies, hoping that ICB therapy can be more widely used in other tumor treatment areas in the future (4, 5). TKIs combined with immunotherapy is a brand-new weapon for tumor treatment in recent years. This method has not only been used in the treatment of GC, but also widely used in other tumors, and the therapeutic effect has been gradually verified in the laboratory and clinical practice.

Anlotinib is a multi-target tyrosine kinase inhibitor, an oral small molecule drug that selectively inhibits vascular endothelial growth factor receptor, fibroblast growth factor receptor, platelet-derived growth factor receptor. It plays an important role in inhibiting tumor angiogenesis and tumor cell proliferation. Studies have shown that the antiangiogenic effect of anlotinib is comparable to Sunitinib and stronger than that of Sorafenib (13). In the past, anlotinib was only used in the fields of non-small cell lung cancer (14), medullary thyroid carcinoma (15), soft tissue sarcoma (16), and it has a good therapeutic effect. However, the effect of anlotinib on GC is still lacking researching. Immunotherapy is the current research hotspot in the field of tumor treatment. ICB therapy, especially PD-1/PD-L1 inhibitors, is the most promising treatment method among them. Carrilizumab is a classic PD-1 inhibitor that has been frequently used in clinical practice recently. A large part of patients with gastric cancer can detect the abnormal expression of PD-1/PD-L1, so the therapeutic effect of carrilizumab in GC is worthwhile expect. Li et al. (17) found that antiangiogenic drugs also play a regulatory role in suppressing immune signals, including the expression of PD-1 in tumor infiltrating T cells. In addition, several studies have suggested that antiangiogenic agents may increase the efficacy of immune checkpoint inhibitors, and the combination of two pathway inhibitors is often feasible (18, 19).

Our research first found that the inhibitory effect of anlotinib on GC cells is not inferior to that of classic GC chemotherapy drugs through reasonable screening of a large number of drugs. Then, we used the TCGA public database to analyze and found that the low expression of VEGFR can significantly improve the prognosis of GC and prolong survival. In addition, according to Kaplan-Meier univariate survival analysis, we found that the OS, FP, and PPS of GC patients with low VEGFR expression were significantly longer than those with high VEGFR expression. The results of in vitro experiments can prove that anlotinib can significantly inhibit the proliferation and invasion of GC cells, and it is obviously concentration-dependent. The results of tumor formation experiments in mice prove that anlotinib has a significant therapeutic effect on tumor tissues, and it can significantly enhance the efficacy when used in combination with PD-1 monoclonal antibody.

However, our study of anlotinib still has certain limitations. First, we only found that anlotinib has a therapeutic effect on GC, but did not further explore the mechanism of the inhibitory effect. At the same time, the GC cell lines we selected in the cell experiment validation did not include HER2 negative, which cannot explain the therapeutic effect of anlotinib on HER2 negative GC. These will be reflected in the team's future research.

In conclusion, our study found that anlotinib, as a multi-target tyrosine kinase inhibitor, can significantly inhibit the proliferation and invasion of GC cells, and has a significant therapeutic effect on GC tumor tissues. Moreover, when used in combination with PD-1 inhibitors, anlotinib can significantly improve the efficacy. Our research may provide a new drug choice for the chemotherapy of GC.

DATA AVAILABILITY STATEMENT

The datasets presented in this study can be found in online repositories. The names of the repository/repositories and accession number(s) can be found in the article/supplementary material.

ETHICS STATEMENT

The animal study was reviewed and approved by Nanjing First Hospital.

AUTHOR CONTRIBUTIONS

WZ completed the paper writing and experiments, GS, ZL, FW, GS completed the data analysis, HC, JZ, YM completed the experimental design and project support. All authors contributed to the article and approved the submitted version.

FUNDING

This research was supported by Jiangsu Natural Science Foundation (SBK2019021253).

REFERENCES

1. Sung H, Ferlay J, Siegel RL, Laversanne M, Soerjomataram I, Jemal A, et al. Global cancer statistics 2020: GLOBOCAN estimates of incidence and mortality worldwide for 36 cancers in 185 Countries. *CA Cancer J Clin*. (2021) 71(3):209–49. doi: 10.3322/caac.21660
2. Jaberi MK, Gholami A, Cheraghian B,, Abolghasemi J, Solaymani-Dodaran M, Madani AH, et al. Survival rate of patients with gastric cancer in Hormozgan Province, Iran. *Med J Islam Repub Iran*. (2019) 33:74. doi: 10.34171/mjiri.33.74
3. Ricci AD, Rizzo A, Rojas Llimpe FL, Di Fabio F, De Biase D, Rihawi K. Novel HER2-directed treatments in advanced gastric carcinoma: anotHER paradigm shift? *Cancers (Basel)*. (2021) 13(7):1664. doi: 10.3390/cancers13071664
4. Rizzo A, Brandi G. Biochemical predictors of response to immune checkpoint inhibitors in unresectable hepatocellular carcinoma. *Cancer Treat Res Commun*. (2021) 27:100328. doi: 10.1016/j.ctarc.2021.100328
5. Rizzo A, Dadduzio V, Ricci AD, Massari F, Di Federico A, Gadaleta-Caldarola G, et al. Lenvatinib plus pembrolizumab: the next frontier for the treatment of hepatocellular carcinoma? *Expert Opin Investig Drugs*. (2021) 30:1–8. doi: 10.1080/13543784.2021.1948532
6. Power DG, Kelsen DP, Shah MA. Advanced gastric cancer–slow but steady progress. *Cancer Treat Rev*. (2010) 36(5):384–92. doi: 10.1016/j.ctrv.2010.01.005
7. Lin B, Song X, Yang D, Bai D, Yao Y, Lu N. Anlotinib inhibits angiogenesis via suppressing the activation of VEGFR2, PDGFRbeta and FGFR1. *Gene*. (2018) 654:77–86. doi: 10.1016/j.gene.2018.02.026
8. Sun Y, Niu W, Du F, Du C, Li S, Wang J, et al. Safety, pharmacokinetics, and antitumor properties of Anlotinib, an oral multi-target tyrosine kinase inhibitor, in patients with advanced refractory solid tumors. *J Hematol Oncol*. (2016) 9(1):105. doi: 10.1186/s13045-016-0332-8
9. Shen G, Zheng F, Ren D, Du F, Dong Q, Wang Z, et al. Anlotinib: a novel multi-targeting tyrosine kinase inhibitor in clinical development. *J Hematol Oncol*. (2018) 11(1):120. doi: 10.1186/s13045-018-0664-7
10. Han B, Li K, Wang Q, Zhang L, Shi J, Wang Z, et al. Effect of anlotinib as a third-line or further treatment on overall survival of patients with advanced non-small cell lung cancer: the ALTER 0303 phase 3 randomized clinical trial. *JAMA Oncol*. (2018) 4(11):1569–75. doi: 10.1001/jamaoncol.2018.3039
11. Lote H, Cafferkey C, Chau I. PD-1 and PD-L1 blockade in gastrointestinal malignancies. *Cancer Treat Rev*. (2015) 41(10):893–903. doi: 10.1016/j.ctrv.2015.09.004
12. Garon EB, Rizvi NA, Hui R, Leighl N, Balmanoukian AS, Eder JP, et al. Pembrolizumab for the treatment of non-small-cell lung cancer. *N Engl J Med*. (2015) 372(21):2018–28. doi: 10.1056/NEJMoa1501824
13. Wang J, Zhao Y, Wang Q, Zhang L, Shi J, Wang Z, et al. Prognostic factors of refractory NSCLC patients receiving Anlotinib hydrochloride as the third- or further-line treatment. *Cancer Biol Med*. (2018) 15(4):443–51. doi: 10.20892/j.issn.2095-3941.2018.0158
14. Han BH, Li K, Wang QM, Zhang L, Shi J, Wang Z, et al. Effect of anlotinib as a third-line or further treatment on overall survival of patients with advanced non-small cell lung cancer the ALTER 0303 phase 3 randomized clinical trial. *JAMA Oncol*. (2018) 4(11):1569–75. doi: 10.1001/jamaoncol.2018.3039
15. Sun Y, Du F, Gao M, Ji Q, Li Z, Zhang Y, et al. Anlotinib for the treatment of patients with locally advanced or metastatic medullary thyroid cancer. *Thyroid*. (2018) 28(11):1455–61. doi: 10.1089/thy.2018.0022
16. Chi Y, Fang Z, Hong X, Yao Y, Sun P, Wang G, et al. Safety and efficacy of anlotinib, a multikinase angiogenesis inhibitor, in patients with refractory metastatic soft-tissue sarcoma. *Clin Cancer Res*. (2018) 24(21):5233–8. doi: 10.1158/1078-0432.CCR-17-3766
17. Li B, Lalani AS, Harding TC, Luan B, Koprivnikar K, Huan Tu G, et al. Vascular endothelial growth factor blockade reduces intratumoral regulatory T cells and enhances the efficacy of a GM-CSF-secreting cancer immunotherapy. *Clin Cancer Res*. (2006) 12(22):6808–16. doi: 10.1158/1078-0432.CCR-06-1558
18. Assi HI, Kamphorst AO, Moukalled NM, Ramalingam SS. Immune checkpoint inhibitors in advanced non-small cell lung cancer. *Cancer*. (2018) 124(2):248–61. doi: 10.1002/cncr.31105
19. Furue M, Ito T, Wada N, Wada M, Kadono T, Uchi H. Melanoma and immune checkpoint inhibitors. *Curr Oncol Rep*. (2018) 20(3):29. doi: 10.1007/s11912-018-0676-z

Conflict of Interest: The authors declare that the research was conducted in the absence of any commercial or financial relationships that could be construed as a potential conflict of interest.

Publisher's Note: All claims expressed in this article are solely those of the authors and do not necessarily represent those of their affiliated organizations, or those of the publisher, the editors and the reviewers. Any product that may be evaluated in this article, or claim that may be made by its manufacturer, is not guaranteed or endorsed by the publisher.

Copyright © 2022 Zheng, Sun, Li, Wu, Sun, Cao, Jin and Ma. This is an open-access article distributed under the terms of the Creative Commons Attribution License (CC BY). The use, distribution or reproduction in other forums is permitted, provided the original author(s) and the copyright owner(s) are credited and that the original publication in this journal is cited, in accordance with accepted academic practice. No use, distribution or reproduction is permitted which does not comply with these terms.

frontiers | Frontiers in Oncology

ORIGINAL RESEARCH
published: 27 April 2022
doi: 10.3389/fonc.2022.899759

Prognostic Nomogram Based on the Metastatic Lymph Node Ratio for $T_{1-4}N_{0-1}M_0$ Pancreatic Neuroendocrine Tumors After Surgery

Jingxiang Shi[1,2,3,4], *Sifan Liu*[5], *Jisen Cao*[1,2,3,4], *Shigang Shan*[1,2,3,4], *Chaoyi Ren*[1,2,3,4], *Jinjuan Zhang*[1,2,3,4*] *and Yijun Wang*[1,2,3,4*]

[1] Department of Hepatobiliary Surgery, The Third Central Hospital of Tianjin, Tianjin, China, [2] Tianjin Key Laboratory of Extracorporeal Life Support for Critical Diseases, The Third Central Hospital of Tianjin, Tianjin, China, [3] Artificial Cell Engineering Technology Research Center, The Third Central Hospital of Tianjin, Tianjin, China, [4] Tianjin Institute of Hepatobiliary Disease, The Third Central Hospital of Tianjin, Tianjin, China, [5] School of Statistics, Tianjin University of Finance and Economics, Tianjin, China

OPEN ACCESS

Edited by:
Ravindra Deshpande,
Wake Forest School of Medicine,
United States

Reviewed by:
Kondapa Bobba,
University of California, San Francisco,
United States
Ganesh Raut,
Washington University in St. Louis,
United States

***Correspondence:**
Yijun Wang
wangyijun_carl@163.com
Jinjuan Zhang
15522242886@163.com

Specialty section:
This article was submitted to Gastrointestinal Cancers: Hepato Pancreatic Biliary Cancers, a section of the journal Frontiers in Oncology

Received: 19 March 2022
Accepted: 31 March 2022
Published: 27 April 2022

Citation:
Shi J, Liu S, Cao J, Shan S, Ren C, Zhang J and Wang Y (2022) Prognostic Nomogram Based on the Metastatic Lymph Node Ratio for $T_{1-4}N_{0-1}M_0$ Pancreatic Neuroendocrine Tumors After Surgery. Front. Oncol. 12:899759. doi: 10.3389/fonc.2022.899759

Purpose: This study aimed to investigate the prognostic significance of the metastatic lymph node ratio (LNR) in patients with pancreatic neuroendocrine tumors (pNETs) and to develop and validate nomograms to predict 5-, 7-, and 10-year overall survival (OS) and cancer-specific survival (CSS) rates for pNETs after surgical resection.

Methods: The demographics and clinicopathological information of $T_{1-4}N_{0-1}M_0$ pNET patients between 2004 and 2018 were extracted from the Surveillance, Epidemiology and End Results database. X-tile software was used to determine the best cutoff value for the LNR. Patients were randomly divided into the training and the validation groups. A Cox regression model was used in the training group to obtain independent prognostic factors to develop nomograms for predicting OS and CSS. The concordance index (C-index), calibration curves, area under the receiver operating characteristic curve (AUC) and decision curve analysis (DCA) were used to assess the nomograms. Patients were divided into four groups according to the model scores, and their survival curves were generated by the Kaplan–Meier method.

Results: A total of 806 patients were included in this study. The best cutoff value for the LNR was 0.16. The LNR was negatively correlated with both OS and CSS. Age, sex, marital status, primary site, grade, the LNR and radiotherapy were used to construct OS and CSS nomograms. In the training group, the C-index was 0.771 for OS and 0.778 for CSS. In the validation group, the C-index was 0.737 for OS and 0.727 for CSS. The calibration curves and AUC also indicated their good predictability. DCA demonstrated that the nomograms displayed better performance than the American Joint Committee on Cancer (AJCC) TNM staging system (8th edition). Risk stratification indicated that patients with higher risk had a worse prognosis.

Conclusions: The LNR is an independent negative prognostic factor for pNETs. The nomograms we built can accurately predict long-term survival for pNETs after surgery.

Keywords: lymph node ratio, pancreatic neuroendocrine tumors, nomogram, overall survival, cancer-specific survival

INTRODUCTION

Pancreatic neuroendocrine tumors (pNETs) are relatively rare tumors that originate from the pancreatic neuroendocrine system (1). According to the US epidemiology survey, its incidence is less than 1 in 100,000 people, representing nearly 10% of all pancreatic tumors (2, 3). Owing to the advancement of imaging and endoscopic techniques, the detection rate of pNETs has gradually increased in recent years (4). PNETs are classified as functional and nonfunctional types based on whether they secrete hormones associated with a clinical syndrome, while nonfunctional pNETs account for most of them (4, 5). One of the characteristics of pNETs is heterogeneity. Generally, they exhibit indolent clinical features; however, they may become invasive and transform rapidly in some circumstances (6).

Surgical resection is an effective treatment for pNETs without metastases (7). One SEER database study demonstrated that surgery might greatly improve survival compared with nonsurgery interventions (114 months vs. 35 months) (8). Other studies reported that the 5-year survival rate after surgical resection of pNETs was approximately 80% (6, 9). However, due to the rarity of this disease, studies on prediction models for pNETs after surgery are deficient.

Recently, the metastatic lymph node ratio (LNR), defined as the proportion of positive nodes to total examined nodes, has been an important prognostic factor for many tumors. You et al. (10) pointed out that the LNR might predict the prognosis of patients with pancreatic cancer. Zhang et al. (11) demonstrated that the LNR was a strong negative prognostic factor for patients with colorectal cancer. Two other studies also indicated that it was negatively related to the survival of patients with gastric and small intestinal neuroendocrine tumors (12, 13). However, there are no reports of nomograms of long-term survival after resection of pNETs that incorporate LNR data.

Therefore, based on the Surveillance, Epidemiology, and End Results (SEER) database, the present study attempted to explore the correlation between the LNR and the prognosis of pNET patients and to construct nomograms to predict 5-, 7-, and 10-year overall survival (OS) and cancer-specific survival (CSS) rates for pNETs after surgery.

MATERIALS AND METHODS

Data Collection

The SEER database is an authoritative cancer statistics database in the United States, covering approximately 30% of the US population (9). Data were extracted from the SEER database with SEER*Stat Software (version 8.3.9.2), and the Incidence SEER Research Plus Data, 9 Registries, Nov 2020 Sub (1975-2018) dataset was selected for analysis (username for login: 15881-Nov2020). Patients diagnosed with pNETs from 2004 to 2018 were identified retrospectively. The corresponding selection formula in the software was as follows: Site and Morphology, "Site recode ICD-O-3/WHO 2008" (Pancreas) and "ICD-O-3 Hist/behav" (8013/3, 8150/3-8156/3, 8240/2, 8240/3-8246/3, 8246/2, 8249/3). The following variables were extracted from the database: patient ID, age, sex, race, marital status, year of diagnosis, primary site, histologic type, grade, diagnostic confirmation, tumor size, T stage, N stage, M stage, American Joint Committee on Cancer (AJCC) TNM staging system, surgery at the primary site, the scope of regional lymph node surgery, radiation recode, chemotherapy recode, regional nodes examined, regional nodes positive, survival months, vital status recode, SEER cause-specific death classification, first malignant primary indicator and sequence number.

Data Processing

Patients conforming to any of the following criteria were excluded: 1) surgery was not performed; 2) no regional nodes examined or the number of regional lymph nodes removed was unknown; 3) the AJCC TNM staging system belonged to M1; 4) not the first malignant tumor or multiple primary tumors; and 5) missing or unknown clinical information.

Age was regarded as a continuous variable, and other factors were treated as categorical variables. Patients who were widowed, divorced, single or separated were considered unmarried. (C25.4, islets of Langerhans), (C25.7, other specified parts of the pancreas), (C25.8, overlapping lesion of the pancreas) and (C25.9, pancreas, NOS) in the primary site were considered other. The staging system was adjusted according to the 8th edition AJCC. OS was defined as survival time until death by any cause or last follow-up, and CSS was defined as survival time until death due to pNETs (9).

Construction and Validation of the Nomograms

The overall patients were randomly divided into a training cohort and a validation cohort at a ratio of 7:3. For the training group, univariate and multivariate Cox regression analyses were used to screen out significant variables. After that, all the independent prognostic factors in multivariate analysis were used to construct nomograms using the package "rms" in R software (14). The validation cohort was used to perform an external validation of the nomograms.

To assess the accuracy of the nomograms, we calculated Harrell's concordance index (C-index) and drew calibration curves of the training and validation groups for internal and external validation (15). The area under the receiver operating characteristic curve (AUC) was also used to evaluate the

predictive value (15). In addition, we used decision curve analysis (DCA) to determine the 5-, 7-, and 10-year survival rates of the two groups (16). Furthermore, DCA was applied to compare the AJCC staging system (8th edition), the LNR and the nomograms.

Statistical Analysis

All statistical tests were performed using R statistical software (version 4.1.2, https://www.r-project.org, Vienna, Austria). Categorical variables were expressed as frequencies and percentages. Continuous variables were presented as the mean with standard deviation. The optimal cutoff value for the LNR was determined by the X-tile program (17). Survival curves were generated by the Kaplan–Meier method and analyzed by the log-rank test. Variables with $P < 0.2$ in univariate analysis were subjected to multivariate analysis. $P < 0.1$ in multivariate analysis was considered clinically significant. Pearson's correlation was performed to detect collinearity among the variables. A correlation coefficient < 0.7 between two variables indicated no multicollinearity (18). Tolerance and variance inflation factor (VIF) were also used to evaluate multicollinearity between variables, with tolerance < 0.1 and VIF > 10 indicating multicollinearity (19). $P < 0.05$ was considered statistically significant.

RESULTS

Patient Characteristics

A total of 806 patients with $T_{1\text{-}4}N_{0\text{-}1}M_0$ pNETs were enrolled in this study, of which 564 cases were randomly assigned to the training group, while 242 cases were assigned to the validation group (**Figure 1**). The clinicopathological characteristics of patients in the 2 cohorts are summarized in **Table 1**. In the training group, 75 patients (13.3%) died from pNETs, and 23 (4.1%) patients died from other causes, while in the validation group, the numbers were 27 (11.2%) and 5 (2.1%), respectively. The optimal cutoff value for the LNR was 0.16. Therefore, patients were divided into three groups (LNR1: 0, LNR2: ≤ 0.16 and LNR3: > 0.16). Patients in the high LNR group had poorer OS and CSS than those in the relatively low LNR group (**Figures 2A, B**).

Variable Screening and Nomogram Construction

For the training cohort, the univariate analysis for OS revealed that age, sex, marital status, primary site, grade, tumor size, T stage, LNR, radiotherapy and chemotherapy were significantly associated with survival. Additionally, age, sex, marital status, primary site, grade, tumor size, T stage, LNR, radiotherapy, chemotherapy and lymph node dissection were significantly associated with CSS. The multivariate Cox regression analyses revealed that age, sex, marital status, primary site, grade, LNR and radiotherapy were significant for both OS and CSS (**Tables 2**, **3**). Therefore, these factors were included in the construction of the nomograms. Every variable was given a score in these two nomograms. Users could obtain the total score based on the individual scores of those factors and estimate the probability of survival for 5, 7 and 10 years (**Figures 3A, B**).

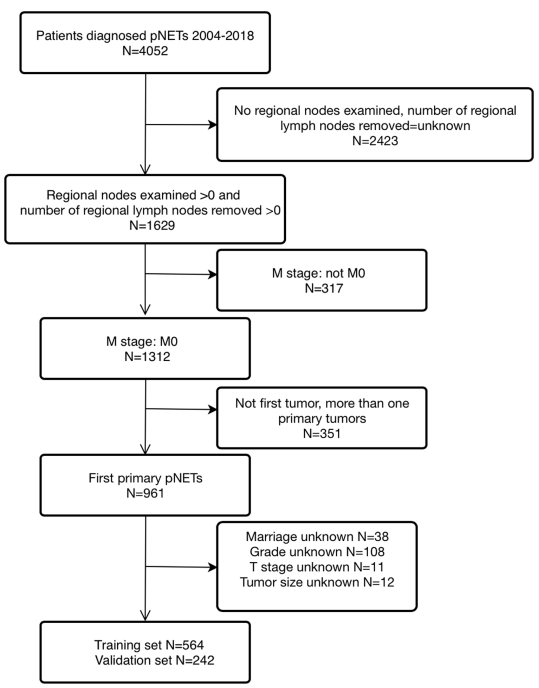

FIGURE 1 | This is the flow chart of enrolled patients.

TABLE 1 | Patient demographics and pathological characteristics.

Variables	Training group	Validation group
Age (year)	56.43±13.73	57.82±13.93
Sex		
Female	264 (46.8)	117 (48.3)
Male	300 (53.2)	125 (51.7)
Race		
White	413 (73.2)	183 (75.6)
Black	68 (12.1)	26 (10.7)
Others	83 (14.7)	33 (13.6)
Marriage		
Married	364 (64.5)	168 (69.4)
Unmarried	200 (35.5)	74 (30.6)
Primary site		
Head	170 (30.1)	77 (31.8)
Body	80 (14.2)	33 (13.6)
Tail	238 (42.2)	103 (42.6)
Other	76 (13.5)	29 (12)
Grade		
I	399 (70.7)	170 (70.2)
II	133 (23.6)	58 (24)
III	26 (4.6)	13 (5.4)
IV	6 (1.1)	1 (4)
Tumor size (cm)		
≤3	347 (61.5)	145 (59.9)
>3	217 (38.5)	97 (40.1)
T stage		
T1	196 (34.8)	73 (30.2)
T2	210 (37.2)	96 (39.7)
T3	142 (25.2)	69 (28.5)
T4	16 (2.8)	4 (1.7)
N stage		
N0	381 (67.6)	159 (65.7)
N1	183 (32.4)	83 (34.3)
Radiotherapy		
Yes	13 (2.3)	6 (2.5)
No	551 (97.7)	236 (97.5)
Chemotherapy		
Yes	34 (6)	15 (6.2)
No	530 (94)	227 (93.8)
Lymph nodes removed		
1 to 3	97 (17.2)	52 (21.5)
4 and more	467 (82.8)	190 (78.5)
AJCC TNM stage		
I	136 (24.1)	46 (19.0)
II	235 (41.7)	109 (45.0)
III	193 (34.2)	87 (36.0)

There was no significant correlation between the screened variables for the overall dataset, the training or the validation groups (**Figure 4**). Furthermore, the tolerance was >1, and the VIF was <10 for the three groups, proving no collinearity among the factors.

Nomogram Validation

The two nomograms were validated both internally and externally. In the internal validation, the C-index was 0.771 for OS and 0.778 for CSS. In the external validation, the C-index was 0.737 for OS and 0.727 for CSS. The calibration plots were close to the standard curves for OS (**Figure 5A**) and CSS (**Figure 6A**) in the training group and for OS (**Figure 5E**) and CSS (**Figure 6E**) in the validation group. The AUC values for predicting 5-, 7-, and 10-year OS rates were 0.804, 0.797 and 0.799 in the training group (**Figure 7A**) and 0.777, 0.770 and 0.822 in the validation group, respectively (**Figure 7B**). For the 5-, 7-, and 10-year CSS rates, the AUC values were 0.799, 0.790 and 0.786 in the training group (**Figure 7C**) and 0.740, 0.644 and 0.687 in the validation group (**Figure 7D**). For both the training and validation groups, the DCA curves for OS (**Figures 5B–D, F–H**) and CSS (**Figures 6B–D, F–H**) indicated that our nomograms displayed better performance than the AJCC staging system (8th edition), and the LNR was an important factor for predicting patient prognosis.

Risk Stratification

To determine the performance of the established nomograms in stratifying the risk of pNETs patients, we divided them into four

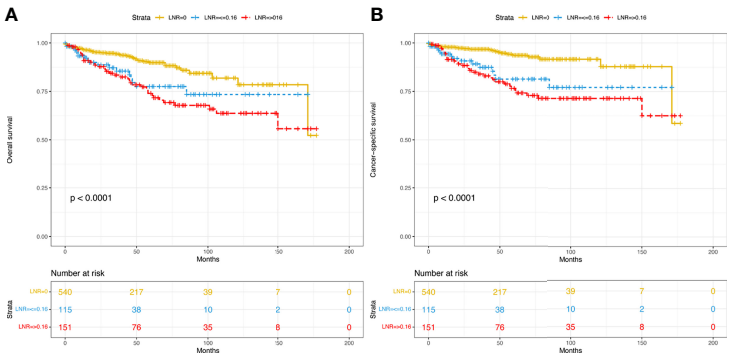

FIGURE 2 | Kaplan–Meier curves of OS **(A)** and CSS **(B)** for patients with different LNRs in the overall dataset. OS, overall survival; CSS, cancer-specific survival; LNR, lymph node ratio.

TABLE 2 | Variables associated with overall survival (OS) according to the Cox proportional hazards regression model in the training cohort.

	Univariate analysis		Multivariate analysis	
	HR (95% CI)	***P***	**HR (95% CI)**	***P***
Age (years)	1.04 (1.02-1.06)	<0.001	1.04 (1.02-1.06)	<0.001
Sex				
Female	0.63 (0.40-1.01)	0.057	0.50 (0.30-0.84)	0.008
Male	Reference		Reference	
Race				
White	Reference			
Black	1.04 (0.52-2.11)	0.897		
Others	0.56 (0.24-1.31)	0.181		
Marriage				
Married	Reference		Reference	
unmarried	1.72 (1.09-2.71)	0.019	1.96 (1.19-3.23)	0.008
Primary site				
Head	Reference		Reference	
Body	0.73 (0.37-1.44)	0.360	0.75 (0.34-1.65)	0.476
Tail	0.41 (0.24-0.72)	0.002	0.52 (0.28-0.97)	0.033
Other	0.60 (0.30-1.19)	0.145	0.89 (0.42-1.88)	0.766
Grade				
I, II	Reference		Reference	
III, IV	10.05 (6.05-16.7)	<0.001	4.66 (2.35-9.22)	<0.001
Tumor size				
≤3 cm	Reference		Reference	
>3 cm	1.81 (1.14-2.85)	0.011	0.96 (0.40-2.35)	0.935
T stage				
T1	Reference		Reference	
T2	0.94 (0.50-1.75)	0.843	0.67 (0.32-1.41)	0.293
T3	2.10 (1.19-3.70)	0.010	1.50 (0.51-4.39)	0.462
T4	1.29 (0.30-5.55)	0.731	0.78 (0.17-3.62)	0.750
LNR				
0	Reference		Reference	
≤0.16	2.42 (1.29-4.54)	0.006	1.71 (0.81-3.59)	0.159
>0.16	2.67 (1.61-4.44)	<0.001	2.32 (1.36-3.93)	0.002
Radiotherapy				
Yes	9.01 (4.73-17.21)	<0.001	2.27 (0.87,5.90)	0.092
No	Reference		Reference	
Chemotherapy				
Yes	3.36 (1.88-6.01)	<0.001	1.21 (0.51-2.91)	0.669
No	Reference		Reference	
Lymph nodes removed				
1 to 3	Reference			
4 and more	1.42 (0.75-2.70)	0.281		

LNR, lymph node ratio.

TABLE 3 | Variables associated with cancer-specific survival (CSS) according to the Cox proportional hazards regression model in the training cohort.

Variables	Univariate analysis		Multivariate analysis	
	HR (95% CI)	*P*	HR (95% CI)	*P*
Age (years)	1.02 (0.99-1.04)	0.106	1.02 (0.99-1.04)	0.077
Sex				
Female	0.66 (0.38-1.16)	0.152	0.58 (0.32-1.08)	0.085
Male	Reference		Reference	
Race				
White	Reference			
Black	1.20 (0.54-2.68)	0.661		
Others	0.71 (0.28-1.79)	0.463		
Marriage				
Married	Reference		Reference	
unmarried	1.95 (1.13-3.36)	0.016	2.05 (1.12-3.74)	0.020
Primary site				
Head	Reference		Reference	
Body	0.32 (0.11-0.92)	0.035	0.42 (0.13-1.34)	0.143
Tail	0.30 (0.15-0.60)	<0.001	0.45 (0.21-0.98)	0.044
Other	0.61 (0.29,1.31)	0.206	1.15 (0.49,2.68)	0.746
Grade				
I, II	Reference		Reference	
III, IV	11.71 (6.46-21.2)	<0.001	5.54 (2.41-12.72)	<0.001
Tumor size				
≤3 cm	Reference		Reference	
>3 cm	1.94 (1.12-3.37)	0.019	0.71 (0.21-2.36)	0.574
T stage				
T1	Reference		Reference	
T2	0.86 (0.38-1.91)	0.707	0.69 (0.28-1.73)	0.434
T3	2.63 (1.33-5.22)	0.006	2.12 (0.51-8.80)	0.301
T4	2.07 (0.46-9.26)	0.341	1.47 (0.30-7.23)	0.638
LNR				
0	Reference		Reference	
≤0.16	3.79 (1.76-8.16)	<0.001	1.72 (0.68-4.39)	0.252
>0.16	4.76 (2.53-8.95)	<0.001	3.24 (1.65-6.36)	<0.001
Radiotherapy				
Yes	12.2 (6.06-24.4)	<0.001	2.44 (0.90-6.64)	0.081
No	Reference		Reference	
Chemotherapy				
Yes	4.89 (2.60-9.18)	<0.001	1.46 (0.58-3.71)	0.420
No	Reference		Reference	
lymph nodes removed				
1 to 3	Reference		Reference	
4 and more	2.28 (0.91-5.74)	0.08	1.35 (0.50-3.65)	0.558

LNR, lymph node ratio.

groups according to the scores for OS (Min-67.9, 67.9-83.1, 83.1-100.2, 100.2-Max) and the scores for CSS (Min-91.7, 91.7-117.2, 117.2-150.6, 150.6-Max). Statistically significant differences in OS (**Figures 8A, B**) and CSS (**Figures 8C, D**) were found among the four groups in both the training and validation groups.

DISCUSSION

PNETs are heterogeneous tumors with different prognoses. Therefore, predicting the outcomes of these patients is complicated. In this study, we screened data from the SEER database and studied the factors affecting the long-term survival of $T_{1\text{-}4}N_{0\text{-}1}M_0$ pNET patients after surgery. After that, we constructed nomograms to predict the 5-, 7-, and 10-year OS rates and CSS rates for these patients. Considering the importance of the LNR, we included it in the nomograms. The relatively high C-indices and values of AUC in the training and validation cohorts proved the good clinical predictive ability of the nomograms. The calibration plots also demonstrated their reasonable prediction probability.

The LNR has been increasingly recognized as a strong predictor of survival for many neoplasms. Teng et al. (20) noted that the LNR was a significant negative predictive variable for the OS of breast cancer patients. Tol et al. (21) reported that the LNR was an important predictor of poor survival in ampullary cancer. Using SEER data regarding pNETs, Liu et al. (22) suggested that the LNR, but not the total number of examined lymph nodes or lymph node metastasis, was an adverse prognostic factor for OS.

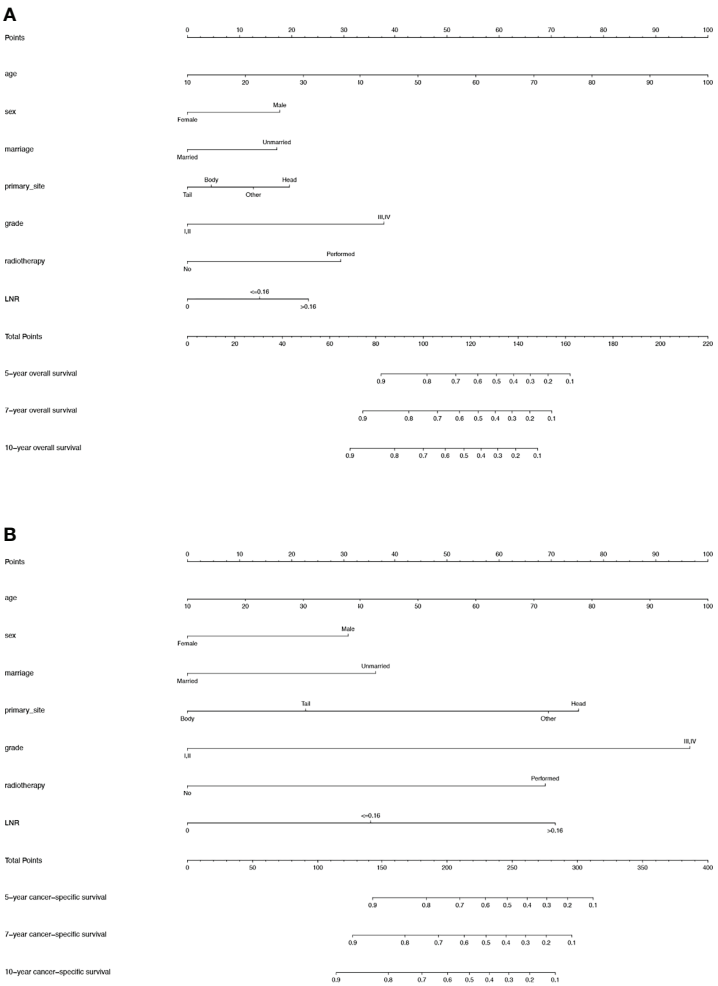

FIGURE 3 | **(A)** Nomogram used to predict the 5-, 7- and 10-year OS rates of patients with $T_{1\text{-}4}N_{0\text{-}1}M_0$ pNETs after surgery. **(B)** Nomogram used to predict the 5-, 7- and 10-year CSS rates of patients with $T_{1\text{-}4}N_{0\text{-}1}M_0$ pNETs after surgery. OS, overall survival; pNETs, pancreatic neuroendocrine tumors; CSS, cancer-specific survival.

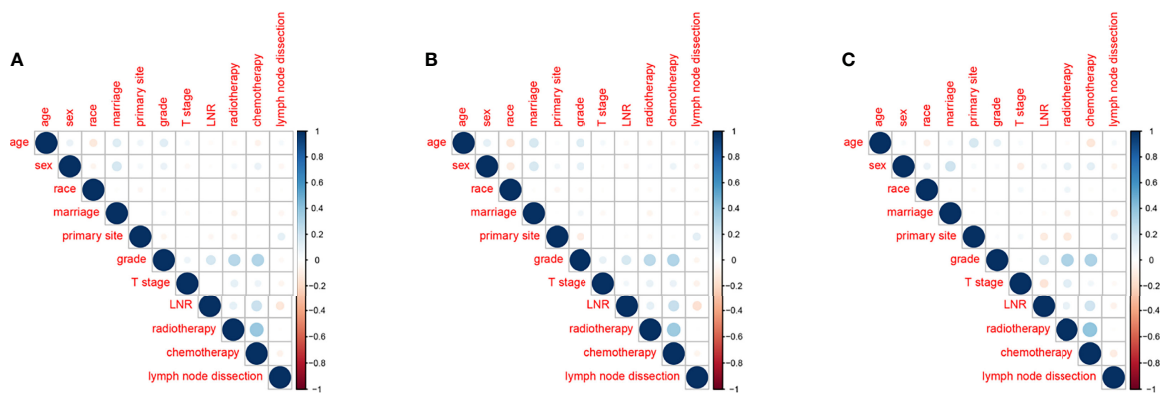

FIGURE 4 | Correlations between variables in the overall dataset **(A)**, the training group **(B)** and the validation group **(C)**.

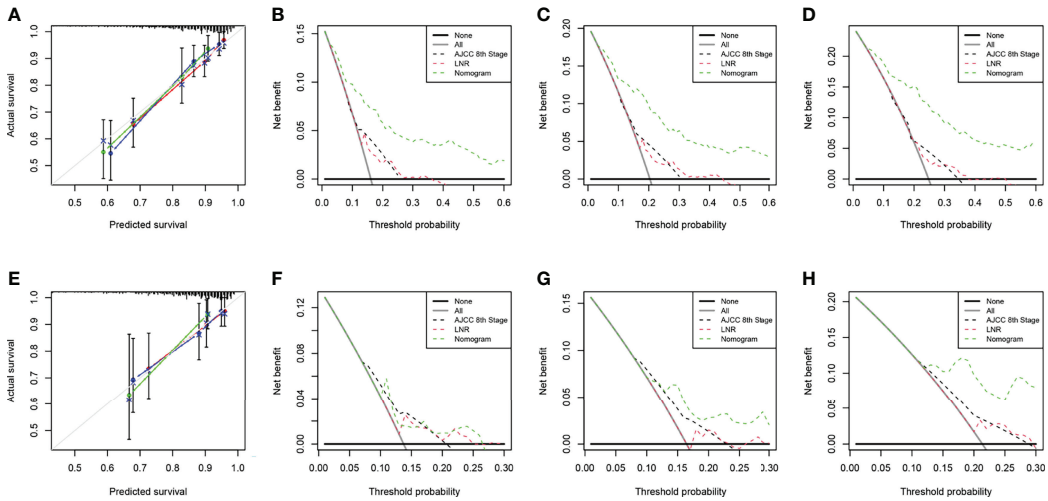

FIGURE 5 | Calibration curve of the nomogram for OS prediction from the training group **(A)** and the validation group **(E)**. Decision curve analysis of the AJCC 8th edition staging system, nomogram and the LNR for the 5- **(B)**, 7- **(C)** and 10-year **(D)** OS rates of patients with $T_{1\text{-}4}N_{0\text{-}1}M_0$ pNETs from the training group. Decision curve analysis of the AJCC 8th edition staging system, nomogram and the LNR for the 5- **(F)**, 7- **(G)** and 10-year **(H)** OS rates of patients with $T_{1\text{-}4}N_{0\text{-}1}M_0$ pNETs from the validation group. OS, overall survival; LNR, lymph node ratio; pNETs, pancreatic neuroendocrine tumors. For calibration curves, red, blue and green lines represent 5, 7, and 10 years, respectively.

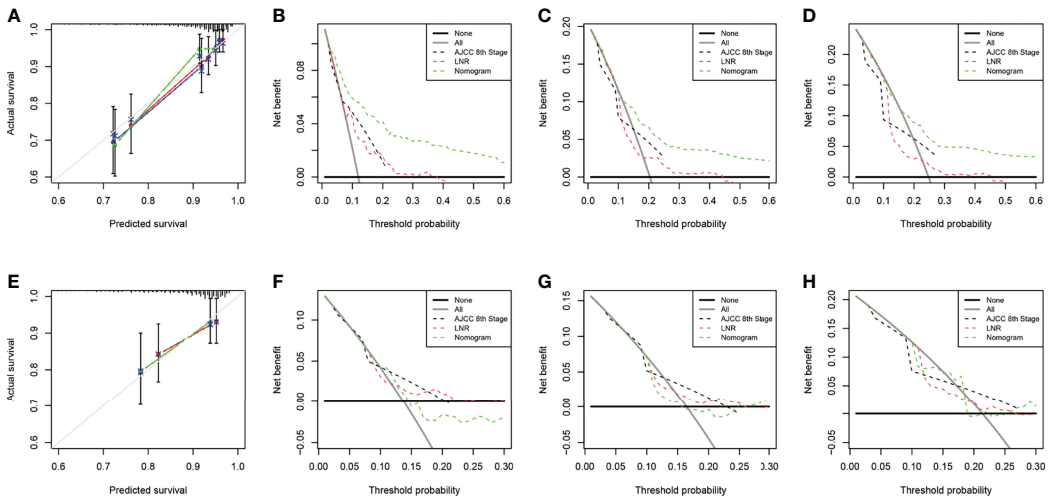

FIGURE 6 | Calibration curve of the nomogram for CSS prediction from the training group **(A)** and the validation group **(E)**. Decision curve analysis of the AJCC 8th edition staging system, nomogram and the LNR for the 5- **(B)**, 7- **(C)** and 10-year **(D)** CSS rates of patients with $T_{1\text{-}4}N_{0\text{-}1}M_0$ pNETs from the training group. Decision curve analysis of the AJCC 8th edition staging system, nomogram and the LNR for the 5- **(F)**, 7- **(G)** and 10-year **(H)** CSS rates of patients with $T_{1\text{-}4}N_{0\text{-}1}M_0$ pNETs from the validation group. CSS, cancer-specific survival; LNR, lymph node ratio; pNETs, pancreatic neuroendocrine tumors. For calibration curves, red, blue and green lines represent 5, 7, and 10 years, respectively.

Heidsma et al. (23) pointed out lymph node status (yes/no presence of positive node) was an independent factor to predict 5-year recurrence after resection of grade 1 and 2 nonfunctional pNETs. Ricci et al. (24) indicated that the LNR > 0.07 was associated with lower recurrence-free survival (RFS), whereas Boninsegna et al. (25) identified an LNR > 0.2 as an independent indicator of poor RFS. Another study showed that an LNR ≥ 0.5 was associated with worse CSS and that the LNR-based staging system was better than the 8th edition AJCC N staging (26). Similar to previous reports, this study showed that the LNR was a poor independent prognostic factor for both OS and CSS. Moreover, the LNR, being a ratio, eliminates the variability in lymph node sampling during surgery and is more suitable for evaluation of prognosis.

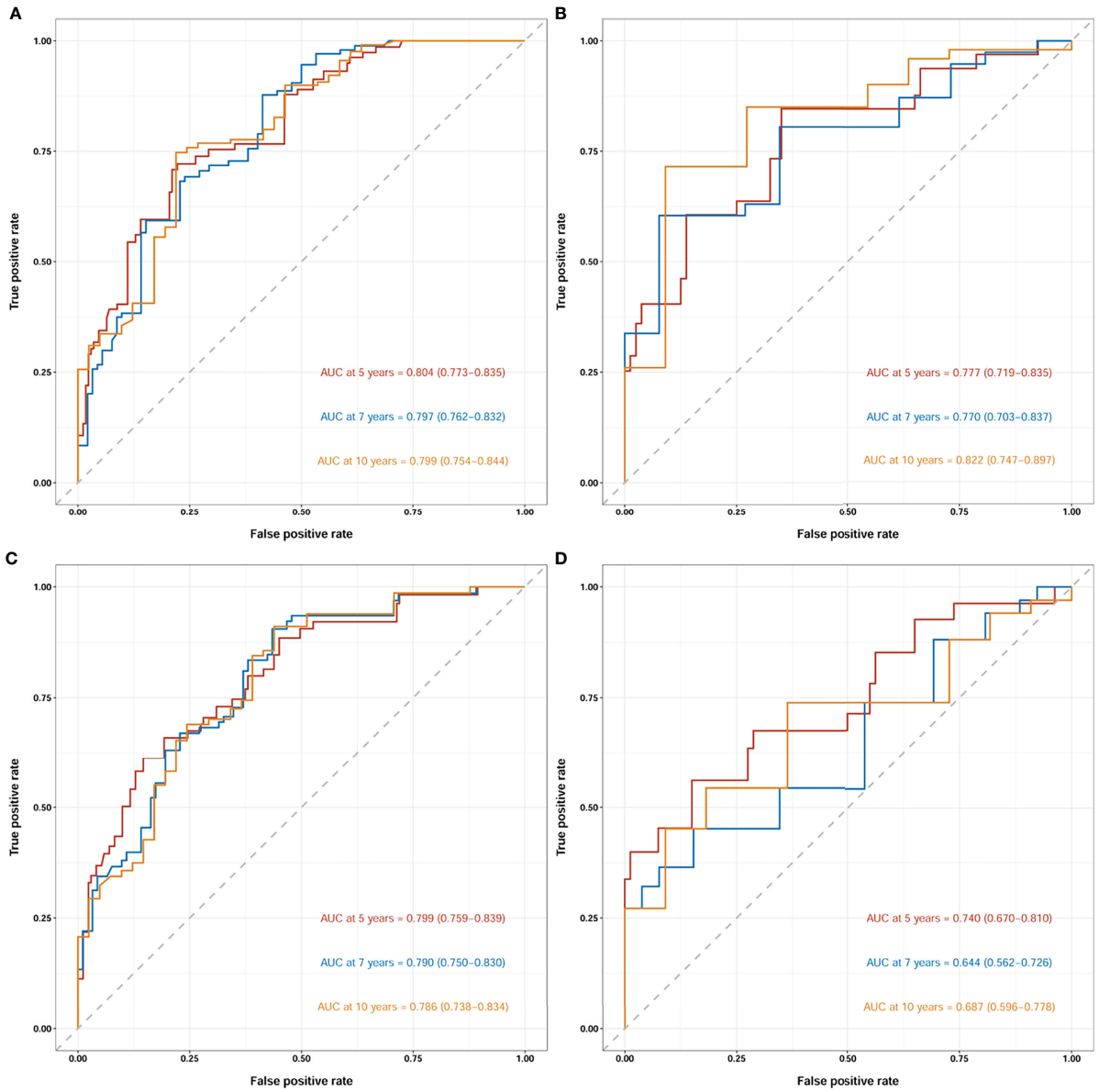

FIGURE 7 | Receiver operating characteristic curves (ROCs) of the nomogram for OS prediction **(A**, training group; **B**, validation group**)** and CSS prediction **(C**, training group; **D**, validation group**)**. OS, overall survival; CSS, cancer-specific survival; AUC, area under the receiver operating characteristic curve. For ROCs, red represents 5 years, blue represents 7 years and yellow represents 10 years.

In addition to LNR, several other variables were included in the established nomograms, such as age, sex, marital status, primary site, grade and radiotherapy. Several studies have indicated that age significantly impacts the survival of pNET patients (9, 27, 28). A similar negative effect was observed in this study. There are two possible reasons for this. First, tumor resistance in elderly patients is poorer than that in young patients due to physical aging; thus, the CSS of these patients is poor (14). Second, there are far more age-related comorbid conditions in elderly patients than in young patients; therefore, the OS of elderly patients is poor. Female patients had more favorable prognoses than male patients, which was in agreement with the conclusion of Miao et al. (29). Marital status was also shown to affect both OS and CSS, consistent with previous reports (29, 30). This is because married patients usually have better psychological mentation and socioeconomic status, which may indicate a better prognosis. Similar to a previous study, the primary site of the tumor was associated with survival (29). Furthermore, histologic grade, which is an inherent characteristic of tumors, was a critical factor in predicting the prognosis of pNET patients in this study. Similar results were found in previous reports (9, 31, 32). Interestingly, this study

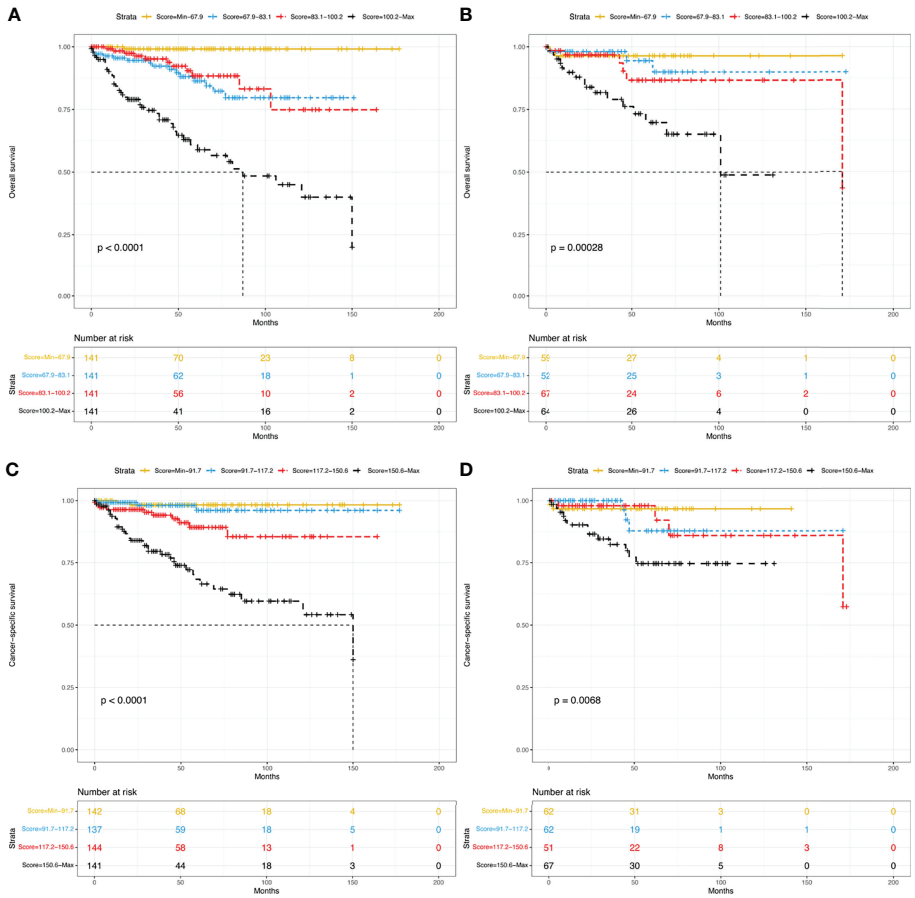

FIGURE 8 | Kaplan–Meier curves of risk stratification within the training group for OS **(A)** and CSS **(C)** and within the validation group for OS **(B)** and CSS **(D)**. OS, overall survival; CSS, cancer-specific survival.

showed that radiotherapy had some impact on survival. Iwata et al. (33) pointed out radiotherapy was an effective treatment for local disease control. However, the number of patients in that research was too small. The effect of radiotherapy on pNETs requires large sample studies.

For the first time, we developed and validated nomograms to predict 5-, 7-, and 10-year OS and CSS for $T_{1\text{-}4}N_{0\text{-}1}M_0$ pNET patients after surgery. The nomograms included not only clinicopathological factors but also demographic factors and were more precise than the conventional staging system. Furthermore, we compared the nomograms with the AJCC TNM staging system (8th edition). DCA curves proved that our nomograms prediction ability was better than the AJCC TNM staging system. In addition, the nomograms were composed of variables that are readily available in clinical practice. With this easily used system, doctors could evaluate the risk factors for patients more precisely. Risk stratification demonstrated good applicability for patients in different stages. Therefore, patients with high risks of poor prognosis may benefit from adjuvant therapy. These may promote more specialized individualized treatment for this heterogeneous neoplasm.

There were some limitations in this study. First, it was a retrospective study based on the SEER database, and this may lead to the risk of potential selection bias. Second, several important clinicopathological factors, such as carbohydrate antigen 19-9 (CA19-9), Ki-67 index, surgical margin status, chemotherapy regimens and radiation technology, were not included due to the limitation of the SEER database, which might affect the results.

In conclusion, the present study identified that the LNR is an independent prognostic factor for pNETs. We established nomograms based on the SEER database to predict long-term survival for pNETs after surgery. These nomograms could help clinicians make tailored treatment plans for patients.

DATA AVAILABILITY STATEMENT

The datasets presented in this study can be found in online repositories. The names of the repository/repositories and accession number(s) can be found in the article/**Supplementary Material**.

AUTHOR CONTRIBUTIONS

JS, JZ and YW: study design and revision of the manuscript. JS: performed the literature search and wrote the manuscript. JC and SS: data collection. SL and CR: statistical analysis. JZ and YW: study supervision. All authors read and approved the final manuscript.

FUNDING

This work was supported by the Tianjin Health Bureau under Grant (No. 2014KR04) and the Key Research Project of Tianjin Health and Family Planning Commission (No. 15KG114).

ACKNOWLEDGMENTS

The authors sincerely thank the Surveillance, Epidemiology, and End Results (SEER) program for providing high-quality open resources for researchers.

SUPPLEMENTARY MATERIAL

The Supplementary Material for this article can be found online at: https://www.frontiersin.org/articles/10.3389/fonc.2022.899759/full#supplementary-material.

REFERENCES

1. Halfdanarson TR, Rabe KG, Rubin J, Petersen GM. Pancreatic Neuroendocrine Tumors (PNETs): Incidence, Prognosis and Recent Trend Toward Improved Survival. *Ann Oncol* (2008) 19:1727–33. doi: 10.1093/annonc/mdn351
2. Vaghaiwalla T, Keutgen XM. Surgical Management of Pancreatic Neuroendocrine Tumors. *Surg Oncol Clin N Am* (2020) 29:243–52. doi: 10.1016/j.soc.2019.11.008
3. Dasari A, Shen C, Halperin D, Zhao B, Zhou S, Xu Y, et al. Trends in the Incidence, Prevalence, and Survival Outcomes in Patients With Neuroendocrine Tumors in the United States. *JAMA Oncol* (2017) 3:1335–42. doi: 10.1001/jamaoncol.2017.0589
4. Zhang Z, Liu M, Ji S, Luo G, Xu W, Liu W, et al. Prognostic Value and Clinical Predictors of Lymph Node Metastases in Pancreatic Neuroendocrine Tumors. *Pancreas* (2020) 49:381–6. doi: 10.1097/MPA.0000000000001493
5. Fathi AH, Romanyshyn J, Barati M, Choudhury U, Chen A, Sosa JA. Predicting Aggressive Behavior in Nonfunctional Pancreatic Neuroendocrine Tumors With Emphasis on Tumor Size Significance and Survival Trends: A Population-Based Analysis of 1787 Patients. *Am Surg* (2020) 86:458–66. doi: 10.1177/0003134820919730
6. Tanaka M, Heckler M, Mihaljevic AL, Probst P, Klaiber U, Heger U, et al. Systematic Review and Metaanalysis of Lymph Node Metastases of Resected Pancreatic Neuroendocrine Tumors. *Ann Surg Oncol* (2021) 28:1614–24. doi: 10.1245/s10434-020-08850-7
7. Rosenblum RE, Harris CK, Baeg KJ, Starr JA, Brais LK, Stashek KM, et al. Predictors of Recurrence and Survival in Patients With Surgically Resected Pancreatic Neuroendocrine Tumors. *Pancreas* (2020) 49:249–54. doi: 10.1097/MPA.0000000000001477
8. Hill JS, McPhee JT, McDade TP, Zhou Z, Sullivan ME, Whalen GF, et al. Pancreatic Neuroendocrine Tumors: The Impact of Surgical Resection on Survival. *Cancer* (2009) 115:741–51. doi: 10.1002/cncr.24065
9. Song Z, Wang S, Wu Y, Zhang J, Liu S. Prognostic Nomograms to Predict Overall Survival and Cancer-Specific Survival of Patients With Pancreatic Neuroendocrine Tumors: A Population-Based Study. *Pancreas* (2021) 50:414–22. doi: 10.1097/MPA.0000000000001779
10. You MS, Lee SH, Choi YH, Shin BS, Paik WH, Ryu JK, et al. Lymph Node Ratio as Valuable Predictor in Pancreatic Cancer Treated With R0 Resection and Adjuvant Treatment. *BMC Cancer* (2019) 19:952. doi: 10.1186/s12885-019-6193-0
11. Zhang CH, Li YY, Zhang QW, Biondi A, Fico V, Persiani R, et al. The Prognostic Impact of the Metastatic Lymph Nodes Ratio in Colorectal Cancer. *Front Oncol* (2018) 8:628. doi: 10.3389/fonc.2018.00628
12. Li J, Lin Y, Wang Y, Lin H, Lin F, Zhuang Q, et al. Prognostic Nomogram Based on the Metastatic Lymph Node Ratio for Gastric Neuroendocrine Tumour: SEER Database Analysis. *ESMO Open* (2020) 5:e000632. doi: 10.1136/esmoopen-2019-000632
13. Wu L, Chen F, Chen S, Wang L. The Lymph Node Ratio Optimizes Staging in Patients With Small Intestinal Neuroendocrine Tumors. *Neuroendocrinology* (2018) 107:209–17. doi: 10.1159/000491017
14. Liao Y, Yin G, Fan X. The Positive Lymph Node Ratio Predicts Survival in $T_{1\text{-}4}n_{1\text{-}3}m_0$ Non-Small Cell Lung Cancer: A Nomogram Using the SEER Database. *Front Oncol* (2020) 10:1356. doi: 10.3389/fonc.2020.01356
15. Heagerty PJ, Zheng Y. Survival Model Predictive Accuracy and ROC Curves. *Biometrics* (2005) 61:92–105. doi: 10.1111/j.0006-341X.2005.030814.x
16. Fitzgerald M, Saville BR, Lewis RJ. Decision Curve Analysis. *JAMA* (2015) 313:409–10. doi: 10.1001/jama.2015.37
17. Camp RL, Dolled-Filhart M, Rimm DL. X-Tile: A New Bio-Informatics Tool for Biomarker Assessment and Outcome-Based Cut-Point Optimization. *Clin Cancer Res* (2004) 10:7252–9. doi: 10.1158/1078-0432.CCR-04-0713
18. Waldmann P. On the Use of the Pearson Correlation Coefficient for Model Evaluation in Genome-Wide Prediction. *Front Genet* (2019) 10:899. doi: 10.3389/fgene.2019.00899
19. Marcoulides KM, Raykov T. Evaluation of Variance Inflation Factors in Regression Models Using Latent Variable Modeling Methods. *Educ Psychol Meas* (2019) 79:874–82. doi: 10.1177/0013164418817803
20. Teng J, Abdygametova A, Du J, Ma B, Zhou R, Shyr Y, et al. Bayesian Inference of Lymph Node Ratio Estimation and Survival Prognosis for Breast Cancer Patients. *IEEE J BioMed Health Inform* (2020) 24:354–64. doi: 10.1109/JBHI.2019.2943401
21. Tol JA, Brosens LA, Van Dieren S, Van Gulik TM, Busch OR, Besselink MG, et al. Impact of Lymph Node Ratio on Survival in Patients With Pancreatic and Periampullary Cancer. *Br J Surg* (2015) 102:237–45. doi: 10.1002/bjs.9709
22. Liu P, Zhang X, Shang Y, Lu L, Cao F, Sun M, et al. Lymph Node Ratio, But Not the Total Number of Examined Lymph Nodes or Lymph Node Metastasis, is a Predictor of Overall Survival for Pancreatic Neuroendocrine Neoplasms After Surgical Resection. *Oncotarget* (2017) 8:89245–55. doi: 10.18632/oncotarget.19184
23. Heidsma CM, Van Roessel S, Van Dieren S, Engelsman AF, Strobel O, Buechler MW, et al. International Validation of a Nomogram to Predict Recurrence After Resection of Grade 1 and 2 Nonfunctioning Pancreatic Neuroendocrine Tumors. *Neuroendocrinology* (2021). doi: 10.1159/000518757
24. Ricci C, Casadei R, Taffurelli G, Buscemi S, D'Ambra M, Monari F, et al. The Role of Lymph Node Ratio in Recurrence After Curative Surgery for Pancreatic Endocrine Tumours. *Pancreatology* (2013) 13:589–93. doi: 10.1016/j.pan.2013.09.001
25. Boninsegna L, Panzuto F, Partelli S, Capelli P, Delle Fave G, Bettini R, et al. Malignant Pancreatic Neuroendocrine Tumour: Lymph Node Ratio and Ki67 are Predictors of Recurrence After Curative Resections. *Eur J Cancer* (2012) 48:1608–15. doi: 10.1016/j.ejca.2011.10.030
26. Gaitanidis A, Patel D, Nilubol N, Tirosh A, Kebebew E. A Lymph Node Ratio-Based Staging Model Is Superior to the Current Staging System for Pancreatic Neuroendocrine Tumors. *J Clin Endocrinol Metab* (2018) 103:187–95. doi: 10.1210/jc.2017-01791
27. Liao T, Su T, Huang L, Li B, Feng LH. Development and Validation of a Novel Nomogram for Predicting Survival Rate in Pancreatic Neuroendocrine Neoplasms. *Scand J Gastroenterol* (2022) 57:85–90. doi: 10.1080/00365521.2021.1984571
28. Strosberg JR, Cheema A, Weber J, Han G, Coppola D, Kvols LK. Prognostic Validity of a Novel American Joint Committee on Cancer Staging Classification for Pancreatic Neuroendocrine Tumors. *J Clin Oncol* (2011) 29:3044–9. doi: 10.1200/JCO.2011.35.1817
29. Miao DL, Song W, Qian J, Zhu ZG, Wu Q, Lv CG, et al. Development and Validation of a Nomogram for Predicting Overall Survival in Pancreatic Neuroendocrine Tumors. *Transl Oncol* (2018) 11:1097–103. doi: 10.1016/j.tranon.2018.06.012

30. Zhou H, Zhang Y, Song Y, Tan W, Qiu Z, Li S, et al. Marital Status is an Independent Prognostic Factor for Pancreatic Neuroendocrine Tumors Patients: An Analysis of the Surveillance, Epidemiology, and End Results (SEER) Database. *Clin Res Hepatol Gastroenterol* (2017) 41:476–86. doi: 10.1016/j.clinre.2017.02.008
31. Zhang C, Wu Y, Zhuang H, Li D, Lin Y, Yin Z, et al. Establishment and Validation of an AJCC-Stage and Histologic Grade-Based Nomogram for Pancreatic Neuroendocrine Tumors After Surgical Resection. *Cancer Manag Res* (2019) 11:7345–52. doi: 10.2147/CMAR.S200340
32. Raj N, Valentino E, Capanu M, Tang LH, Basturk O, Untch BR, et al. Treatment Response and Outcomes of Grade 3 Pancreatic Neuroendocrine Neoplasms Based on Morphology: Well Differentiated Versus Poorly Differentiated. *Pancreas* (2017) 46:296–301. doi: 10.1097/MPA.0000000000000735
33. Iwata T, Ueno H, Itami J, Ito Y, Inaba K, Morizane C, et al. Efficacy of Radiotherapy for Primary Tumor in Patients With Unresectable Pancreatic Neuroendocrine Tumors. *Jpn J Clin Oncol* (2017) 47:826–31. doi: 10.1093/jjco/hyx081

Conflict of Interest: The authors declare that the research was conducted in the absence of any commercial or financial relationships that could be construed as a potential conflict of interest.

Publisher's Note: All claims expressed in this article are solely those of the authors and do not necessarily represent those of their affiliated organizations, or those of the publisher, the editors and the reviewers. Any product that may be evaluated in this article, or claim that may be made by its manufacturer, is not guaranteed or endorsed by the publisher.

Copyright © 2022 Shi, Liu, Cao, Shan, Ren, Zhang and Wang. This is an open-access article distributed under the terms of the Creative Commons Attribution License (CC BY). The use, distribution or reproduction in other forums is permitted, provided the original author(s) and the copyright owner(s) are credited and that the original publication in this journal is cited, in accordance with accepted academic practice. No use, distribution or reproduction is permitted which does not comply with these terms.

frontiers | Frontiers in Medicine

REVIEW
published: 28 April 2022
doi: 10.3389/fmed.2022.886996

Berberine as a Potential Agent for the Treatment of Colorectal Cancer

Xi Jiang[1], *Zhongxiu Jiang*[2], *Min Jiang*[3] *and Yan Sun*[4]*

[1] Department of Cardiology, Shengjing Hospital of China Medical University, Shenyang, China, [2] Department of Oncology, Shengjing Hospital of China Medical University, Shenyang, China, [3] Department of Gastroenterology, First Affiliated Hospital of China Medical University, Shenyang, China, [4] Department of Gastroenterology, Shengjing Hospital of China Medical University, Shenyang, China

Colorectal cancer (CRC) is one of the most commonly diagnosed and deadly malignancies worldwide. The incidence of CRC has been increasing, especially in young people. Although great advances have been made in managing CRC, the prognosis is unfavorable. Numerous studies have shown that berberine (BBR) is a safe and effective agent presenting significant antitumor effects. Nevertheless, the detailed underlying mechanism in treating CRC remains indistinct. In this review, we herein offer beneficial evidence for the utilization of BBR in the management and treatment of CRC, and describe the underlying mechanism(s). The review emphasizes several therapeutic effects of BBR and confirms that BBR could suppress CRC by modulating gene expression, the cell cycle, the inflammatory response, oxidative stress, and several signaling pathways. In addition, BBR also displays antitumor effects in CRC by regulating the gut microbiota and mucosal barrier function. This review emphasizes BBR as a potentially effective and safe drug for CRC therapy.

Keywords: berberine, colorectal cancer, antitumor, gut microbiota, mucosal barrier

OPEN ACCESS

Edited by:
Qi Liu,
Fudan University, China

Reviewed by:
Dhirendra Pratap Singh,
National Institute of Occupational Health (ICMR), India
Saeed Mohammadian Haftcheshmeh,
Neyshabur University of Medical Sciences, Iran
Doaa Ghareeb,
Alexandria University, Egypt
Ahmed Soffar,
Alexandria University, Egypt

***Correspondence:**
Yan Sun
yans1986@sina.com

Specialty section:
This article was submitted to Gastroenterology, a section of the journal Frontiers in Medicine

Received: *01 March 2022*
Accepted: *29 March 2022*
Published: *28 April 2022*

Citation:
Jiang X, Jiang Z, Jiang M and Sun Y (2022) Berberine as a Potential Agent for the Treatment of Colorectal Cancer. Front. Med. 9:886996. doi: 10.3389/fmed.2022.886996

INTRODUCTION

Colorectal cancer (CRC), one of the most common cancers worldwide, has been reported as the third most common cancer in men (10%) and second most common in women (9.2%) (1), accounting for the fourth most common cause of cancer-related death (2). It is a heterogeneous disease with multifarious, hereditary, and biological characteristics. Subtypes of CRC have been demonstrated to present different prognoses and therapeutic responses (3). The incidence rate of CRC has been decreasing in many developed countries; nevertheless, the prevalence has increased in adults younger than 50 years of age in numerous economically underdeveloped countries (4, 5). Although tremendous improvements have been made in the diagnosis and management of CRC, the prognosis remains poor (6). Currently, treatment for CRC mainly includes surgery, radiotherapy, and chemotherapy (7). For unresectable tumors, chemotherapy is a fundamental and indispensable therapeutic regimen. The common cytotoxic chemotherapy drugs include 5-fluorouracil (5-FU), irinotecan, oxaliplatin, raltitrexed, and lonsurf, as well as molecular-targeted agents, such as anti-vascular endothelial growth factor (VEGF) therapies (e.g., bevacizumab, Ziv-aflibercept, ramucirumab, and regorafenib) and anti-epidermal growth factor receptor (EGFR) drugs (e.g., cetuximab and panitumumab) (8). However, these cytotoxic chemotherapy drugs kill tumor cells by direct cytotoxicity and have poor selectivity for tumors; therefore, these drugs not only kill tumor cells but also kill normal cells (9). Moreover, the mucosal barrier tends to be disrupted by common chemotherapeutic drugs, initiating intestinal mucositis (IM). This disruption

is unfavorable for the later treatment of CRC (10). In addition, chemotherapy usually causes gastrointestinal (GI) epithelium injury, which is mediated at least in part by the activation of an inflammatory cascade (10). Furthermore, several limitations and adverse effects have also been reported during molecular-targeted therapy. Molecular-targeted therapy is relatively expensive, and patients might require multiple targeted agents. Level 3 or level 4 adverse events can be infrequently detected, and their incidence might increase when two or more targeted agents are combined (11). Furthermore, CRC involves multiple pathways, whereas conventional drugs only target one aspect. In addition, there is a substantially increased economic burden due to management. Therefore, more effective treatment approaches and medical interferences with safety and high efficacy are urgently needed. Traditional Chinese medicine (TCM) has been extensively acknowledged as a typical complementary and alternative treatment in China for patients with tumors (12). As a typical Chinese herbal medicine-derived phytochemical, berberine (BBR) and its derivatives have attracted increasing attention in cancer treatment. The current review highlights several beneficial properties of BBR and could provide novel insights into CRC treatment (13, 14).

COLORECTAL CANCER

Epidemiology of Colorectal Cancer

According to a report from 40 European countries, an estimated 3.91 million new cases of cancer occurred in Europe in 2018, including 500,000 CRC cases. There were ∼272,000 (13.2%) cases in men and 228,000 (12.3%) cases in women (15). In addition, 1.9 million incident cases and 0.9 million deaths worldwide were estimated to occur in 2020 (3). The overall incidence of CRC has been declining in many economically advanced countries; however, reports from the United States and other economically advanced countries, such as Australia, Canada, and Norway, have demonstrated that the prevalence is increasing in adults younger than 50 years of age (4, 5, 16–20). For example, the incidence of colon cancer increased by 1.8, 2.9, 2.9, and 3.1% per year in the United Kingdom (UK), New Zealand, Australia, and Denmark, respectively, in people younger than 50 years old, and the incidence of rectal cancer in the same age group also increased by 1.4, 2.6, and 3.4% per year in the UK, Australia, and Canada, respectively (20). Moreover, it has been reported that the incidence of colon cancer in individuals aged 20–29 years old increased by 9.3% every year from 2004 to 2014 in Australia, while the incidence of rectal cancer increased by 7.1% each year between 1993 and 2014 (17). The mortality of CRC has been reported to be decreased in many longstanding and economically advanced countries, such as the United States, Australia, New Zealand, most Western European countries (Austria and the UK.), some Asian countries (Japan), and Eastern European countries (the Czech Republic and Slovakia.) (21, 22). Effective prevention, early diagnosis through screening, interventions to reduce risk factors, and/or improvement of treatment strategies could contribute to reduced mortality (23). Nevertheless, mortality is still on the rise in both men and women in many low-income countries and regions, such as Mexico, Chile, and elsewhere in Latin America (21, 24, 25). CRC represents a huge burden globally on family and society and has a positive relationship with socioeconomic status (26–28). This burden is estimated to continue to increase due to the growth and aging of the population, as well as due to the adoption of high-risk behaviors and lifestyles, particularly in less economically developed countries (29, 30).

Prevalent Sites and Risk Factors of Colorectal Cancer

Colorectal cancer is usually observed in the proximal colon (41%), distal colon (22%), and rectum (28%) (31). Nevertheless, there can be differences in the location depending on age and gender (32). It has been reported that the most frequent sites of CRC in young patients are the rectum and the sigmoid colon (33). Genetic and environmental risk factors have been demonstrated to play critical roles in the progression and development of CRC. A number of molecular genetic markers have been identified for the diagnosis, prognosis, and treatment of CRC, such as *KRAS*, *ERBB2*, *MLH*, and *NAV2/TCF7L* (34, 35). An increasing amount of evidence has supported associations between a positive family history of CRC and an increased risk for CRC (36–38). The reported heritability of CRC ranges from 12 to 35% according to twin and family studies (39, 40). Although tremendous advances have been made in the genome-wide association studies of CRC (41, 42), there remain many elusive factors affecting heritability (43). Hereditary colorectal cancer syndromes affect people with a high lifetime risk of developing CRC caused by an inherited or *de novo* germline mutation, accounting for 5–10% of all CRCs (44, 45). This subgroup can be divided into nonpolyposis and polyposis syndromes. The former includes Lynch syndrome, and the latter contains familial adenomatous polyposis (FAP), Peutz-Jeghers syndrome, and MUTYH-associated polyposis (MAP). Polyposis syndromes are more effortlessly diagnosed by doctors due to the number of polyps; however, nonpolyposis syndromes are commonly overlooked because these patients present few adenomas, and these adenomas are morphologically similar to sporadic lesions. Hence, systematic molecular investigation in subjects of any age or subgroup of subjects <70 years of age might improve the diagnosis of this genetic syndrome. Moreover, some basic diseases, such as inflammatory bowel disease (IBD) and type 2 diabetes mellitus (T2DM), are also well known to be associated with CRC (46, 47). In addition, several acquired environmental lifestyles have been recognized as important risk factors for CRC, such as obesity and overweight (48), lack of physical exercise (49), excessive drinking (50), smoking (51, 52), high Diet Inflammatory Index (DII) scores (53, 54), and sedentary lifestyles (55). Additionally, some factors, such as healthy diet structure (e.g., fiber-containing foods, calcium supplements, milk intake, vitamins, fish intake, and phenol intake) and physical activity, have been described to reduce the risk factors of CRC (56–59). However, some of the data have been inconsistent, and the effect on rectal cancer vs. colorectal cancer may also be different. Furthermore, healthy lifestyle habits have been shown to improve the prognosis and mortality of CRC survivors (60, 61). In addition, male sex, increasing age, race, and

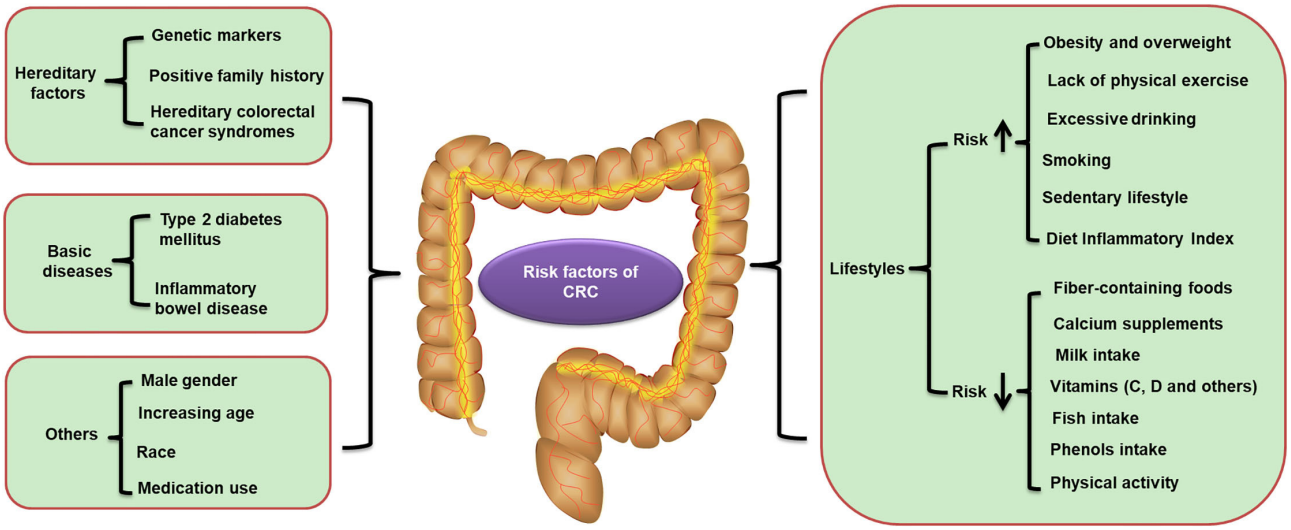

FIGURE 1 | Risk factors of CRC. CRC, colorectal cancer.

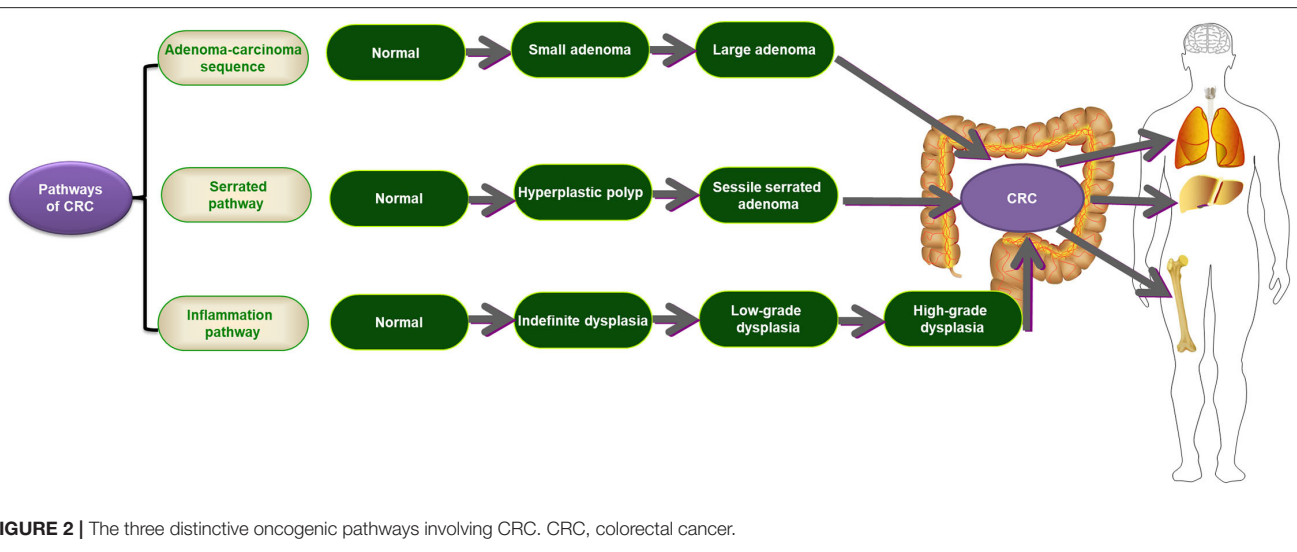

FIGURE 2 | The three distinctive oncogenic pathways involving CRC. CRC, colorectal cancer.

medical intake have also been demonstrated to play critical roles in the progression and development of CRC (62–64) (**Figure 1**).

Carcinogenic Pathways of Colorectal Cancer

There are three distinctive oncogenic pathways involved in CRC, including the adenoma-carcinoma sequence, serrated pathway, and inflammatory pathway (**Figure 2**). The adenoma-carcinoma sequence is a typical pathway that can explain ∼60–90% of sporadic CRC. In this classic pathway, normal cells are driven to transfer to small adenomas, then to large adenomas, and finally to malignancies by the gradual accumulation of genetic and epigenetic changes (65). Several factors have been confirmed to play imperative roles in this pathway, including male sex, increasing age, positioning in the distal colon, tobacco and alcohol use, and a high-fat diet (66, 67). This pathway is primarily characterized by chromosomal instability (CIN) and is related to the development of the CIN-positive subtype. Inactivating mutations in adenomatous polyposis coli (*APC*), a well-known tumor suppressor gene, have been demonstrated in more than 70% of adenomas and CRCs (68, 69). In addition, some mutations in other genes, such as *KRAS*, *TP53*, *SMAD4*, and *PIK3CA*, also contribute to this model (70, 71). Recently, the serrated pathway was described as one of the CRC subsets, accounting for ∼10–15% of sporadic CRCs (30). In this model, serrated polyps are considered precursor lesions to CRC, and they are characterized by the transformation of normal cells to hyperplastic polyps (HPs), then to sessile serrated adenoma (SSA), and ultimately to CRC (72, 73). The *BRAF* mutation and CpG island methylator phenotype (CIMP)

have significant involvement in this pathway (72, 74). The inflammatory pathway is another distinctive oncogenic pathway involved in CRC. It is highlighted by the progression of normal cells to indefinite dysplasia, then to low-grade dysplasia, next to high-grade dysplasia, and finally to CRC, stimulated by chronic inflammation (75). However, this pathway only accounts for <2% of all CRCs (30, 76). IBD, especially ulcerative colitis (UC), is representative of this pathway. Unlike the above two precursor lesions, chronic inflammation-induced dysplasia usually appears as a flat mucosa with multifocality. Different from the adenoma-carcinoma sequence, mutations of *TP53* are an early event in this model (75).

Management of Colorectal Cancer

Endoscopic resection can be performed as a minimally invasive method for early-stage colon cancer. It includes endoscopic mucosal resection (EMR), endoscopic submucosal dissection (ESD), and endoscopic full-thickness resection. The choice of endoscopic resection method depends on the size of T1 cancers. However, some individuals with T1 cancers who experience endoscopic resection require additional colectomy with lymph node dissection due to lymph node metastases (77). Surgery is the cornerstone and one of the most effective management options for CRC. However, the surgical approach for colon cancer is dependent on the tumor location and anatomic relationship with blood vessels. Currently, laparoscopy has become a standard method for CRC in many countries. Compared to conventional open surgery, laparoscopic resection is a minimally invasive technique that can expedite gastrointestinal function recovery and reduce the length of hospital stay, particularly for elderly patients (78). In addition, it has been shown that laparoscopic resection is associated with reduced postoperative mortality, and there are no adverse effects on long-term survival (79, 80). More recently, robotic colectomy has emerged as a popular method for the treatment of CRC (81). Although robotic colectomy can decrease the length of stay, it costs more and requires a longer operation time than laparoscopic colectomy, and no significant differences have been observed in perioperative and short- or long-term outcomes (82, 83). In addition to surgery for CRC, several drugs have been permitted for CRC management in clinical trials. The Food and Drug Administration (FDA)-approved anticancer drugs include 5 cytotoxics (5-FU, capecitabine, TAS-102, irinotecan, and oxaliplatin) and eight biologics/targets (cetuximab, panitumumab, bevacizumab, Ziv-aflibercept, regorafenib, ramucirumab, pembrolizumab, and nivolumab). As a standard first-line chemotherapy drug, 5-FU plays significant role in palliative and adjuvant systemic therapy for CRC. Nevertheless, some adverse effects of these drug treatments have been reported, such as diarrhea, gastrointestinal tract injury, stomachache, and fever (84–86). Compared to chemotherapy, immunotherapy could prompt the memory function of the adaptive immune system and trigger the immune system against tumors, achieving long-term durable responses. Furthermore, fewer adverse effects have been observed in immunotherapy because of immune tolerance.

Berberine

Source and Metabolites of Berberine

Berberine, also known as *Coptis rhizome*, is a pentacyclic isoquinoline alkaloid. It can be found in the Chinese herb *Coptis chinensis* and numerous Berberis plants, such as *Berberis aristata* (81), *Berberis vulgaris* (87), and *Berberis darwinii* (88). The molecular formula of BBR is $C_{20}H_{18}NO_4$, and the molecular weight is 336.337 g/mol. The isoquinoline alkaloids in Huanglian extracts include BBR, xanthophylline, epiberberine, and pharmacophorine. BBR is mainly metabolized in the intestine and liver (89, 90). With the involvement of cytochrome and UDP glucuronosyltransferase (UGT), BBR could be metabolized in liver cells (91). There are four major types of BBR metabolites: berberrubine, thalifendine, demethyleneberberine, and jatrorrhizine (92). However, the number of metabolites varies by species. For example, 16 and 11 metabolites were identified in rats (93) and mice (91), respectively.

Pharmacological Effects of Berberine

Berberine has been used as an important TCM for a long period of time owing to its extraordinary efficiency, such as in alleviating fever, dispelling fire, drying dampness, cooling blood, and detoxifying toxins. Recently, an increasing number of studies have reported regarding the novel pharmacological effects of BBR. For instance, BBR exerts remarkable anti-inflammatory (94–96), antiviral (97), antioxidant (98), antidiabetic (99), immunosuppressive (100), cardiovascular (101, 102), and neuroprotective (103) activities. Therefore, BBR could be utilized to treat various disorders (104–107), including metabolic, cardiovascular, digestive, and neurological diseases. It has been demonstrated that BBR displays protective effects against digestive diseases by inhibiting toxins and bacteria and fortifying the intestinal mucosa (108). Moreover, BBR has been confirmed to regulate glucolipid metabolism, ameliorate energy consumption, and decrease body weight (106). Furthermore, BBR also presents strong cardiovascular protection and neuroprotective effects by improving cardiovascular hemodynamics, reducing hypertension, and attenuating atherosclerosis progression (101, 109).

Antitumor Effects of Berberine

Emerging evidence has shown that BBR exerts anticancer effects in several malignancies (110–112). BBR has been reported to inhibit cancer cell proliferation by affecting the cell cycle and autophagy and stimulating cell apoptosis. For example, BBR could induce G1 cycle arrest in A549 lung cancer cells by decreasing the levels of cyclin D1 and cyclin E1 (113). BBR could inhibit the expression of cyclin D1 in HepG2 liver cancer cells (114). BBR also induced G1 cycle arrest by inhibiting cyclin B1 expression and CDC2 kinase in some cancer cells (115). Moreover, BBR has been suggested to induce autophagy in glioblastoma by targeting the AMP-activated protein kinase (AMPK)/mechanistic target of rapamycin (mTOR)/ULK1 pathway (116) and in liver cancer cells by stimulating the release of beclin-1 from the Bcl-2/beclin-1 complex (117). In addition, BBR has been revealed to stimulate

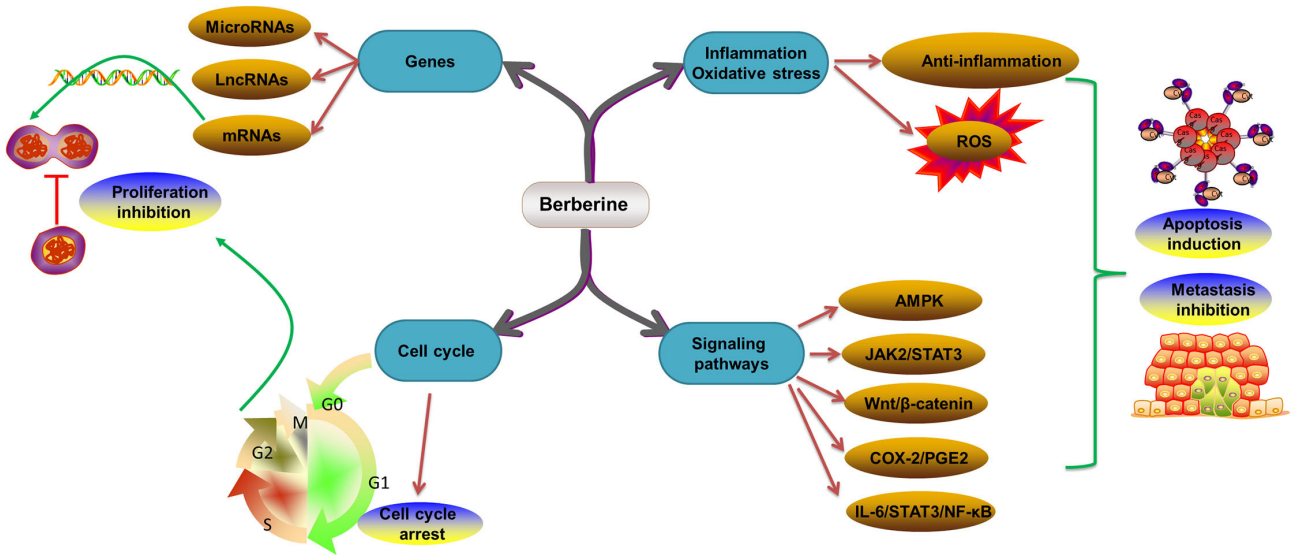

FIGURE 3 | Molecular mechanism of BBR in the treatment of CRC. CRC, colorectal cancer; BBR, berberine; ROS, reactive oxygen species; AMPK, AMP-activated protein kinase; STAT3, signal transducer and activator of transcription 3; COX-2, cyclooxygenase-2; PGE2, prostaglandin E2; IL-6, interleukin 6; NF-κB, nuclear factor kappa B.

apoptosis in leukemia by upregulation of caspase-8 and caspase-9 (118) and in skin squamous cell carcinoma A431 cells by increasing cytochrome C levels (119). In addition, BBR has been confirmed to inhibit cell migration and invasion by inhibiting the expression of epithelial–mesenchymal transition (EMT) and metastasis-related proteins, such as matrix metalloproteinases (MMPs) and E-cadherin, the tumor microenvironment, and/or the caspase-1/interleukin (IL)-1β and nuclear factor kappa B (NF-κB) signaling pathways (120–123). Interestingly, canadine, a derivative of flavopiridol, has been shown to improve cancer-induced muscle wasting (124). Furthermore, BBR has shown antitumor effects by interacting with microRNAs (125) and inhibiting telomerase activity (126).

Molecular Mechanism of Berberine in the Treatment of Colorectal Cancer

Numerous studies have revealed that BBR is a safe and effective treatment for CRC (127–129). The reported mechanisms include regulation of gene expression (microRNAs, long noncoding RNAs (lncRNAs), and mRNAs) (130–133), growth factors (EGFR) (134), cell cycles (135), signaling pathways (AMPK, JAK2/signal transducer and activator of transcription 3 (STAT3), Wnt/β-catenin, IL-6/STAT3/NF-κB, and cyclooxygenase-2 (COX-2)/prostaglandin E2 (PGE2) pathways) (13, 129, 136), inflammation, and oxidative stress (**Figure 3**). The effects and molecular mechanism of BBR in the treatment of CRC are summarized in **Table 1**.

Effects of Berberine on Gene Expression and Cell Cycle in Colorectal Cancer

Abnormal expression of miRNAs, lncRNAs, and mRNAs has been implicated in cancer development, including CRC. Based on the recently established evidence, BBR shows important regulatory effects on gene expression that are dysregulated in CRC, making it a potential agent for managing cancers. For example, BBR was reported to regulate the miR-21/integrin β4 (ITGβ4)/programmed cell death 4 (PDCD4) axis to exert anticancer effects on the CRC cell line HCT116 (137). In addition, BBR could decrease the expression levels of miR-429 while upregulating the expression of E-cadherin and partitioning defective 3 (Par-3) in CRC (132). Moreover, the combination of NVP-AUY922 and BBR induced cell growth arrest by suppressing cyclin-dependent kinase 4 (CDK4) expression and inducing miR-296-5p-mediated inhibition of the peptidylprolyl cis/trans isomerase NIMA-interacting 1 (Pin1)-β-catenin-cyclin D1 signaling pathway in CRC (129). In addition, BBR has been confirmed to prevent the proliferation and migration of CRC cells by decreasing glucose-regulated protein 78 (GRP78) (131). Furthermore, the lncRNA cancer susceptibility 2 (CASC2)/zeste 2 polycomb repressive complex 2 subunit (EZH2) /Bcl-2 axis was identified in BBR-induced CRC cell apoptosis (138). Huang et al. also suggested that DNA (cytosine-5)-methyltransferase PliMCI (DNMTs) and its targeted miRNAs were involved in the therapeutic effects of BBR on CRC (139). The cell cycle is an extremely conserved, ordered, and complex process that controls DNA replication and mitosis. It is regulated by many mechanisms to ensure that correct cell division occurs (146). Several reports have suggested that BBR can induce cell cycle arrest to inhibit cancer development. For instance, Huang et al. demonstrated that BBR induced G0/G1 cell cycle arrest in CRC and then further inhibited cell proliferation (130). Samad et al. found that BBR could also cause G0/G1 cell cycle arrest by regulating CCDN1 and CDK4 in the CRC cell line HCT116 and inhibiting telomerase activity (135). Soffar suggested that BBR

TABLE 1 | The effects and molecular mechanism of BBR in the treatment of CRC.

Authors and references	Publish year	Cell line/animals/tissues	Effect of BBR	Mechanism	Experimental model
Zhang (130)	2020	HCT116 and SW480 cell lines, male BALB/c nude mice	Anti-proliferation, induces apoptosis and cell cycle arrest	Downregulates IGF2BP3	*In vitro* and *in vivo*
Gong (131)	2020	SW480 and HT-29 cell lines	Anti-proliferation, anti-migration, and induces apoptosis	Downregulates GRP78	*In vitro*
Liu (132)	2016	*In vitro* culture of colorectal tissue	/	Reduces miR-429, E-cadherin, and Par3	*In vitro*
Dai (133)	2019	HT29 and HCT116 cell lines	Promotes apoptosis	Increases lncRNA CASC2	*In vitro*
Wang (134)	2013	IMCE and HT-29 cell lines, nude mice, and *APC* $^{min/+}$ mice	Anti-proliferation, induces apoptosis and cell cycle arrest	Downregulates EGFR and activates Cbl	*In vitro* and *in vivo*
Samad (135)	2021	HCT116 cell line	Anti-proliferation, inhibits telomerase activity and induces cell cycle arrest and telomere Erosion	Increases CCND1 and downregulates CDK4, TERT, and TERC	*In vitro*
Liu (136)	2015	SW620 and LoVo cell lines, male BALB/C nude mice	Anti-proliferation, inhibits invasion and metastasis	Reduces levels of COX-2/PGE2, phosphorylation of JAK2 and STAT3, and expression of MMP-2/-9.	*In vitro* and *in vivo*
Lü (137)	2018	HCT116 cell line	Anti-proliferation, and induces apoptosis	Regulates the microRNA-21-ITG?4-PDCD4 axis	*In vitro*
Su (129)	2015	HCT-15, HCT116WT, and HT-29 cell lines	Anti-proliferation	Enhances the antitumor activity of NVP-AUY922	*In vitro*
Dai (138)	2019	HT-29, HCT116, SW480, SW620 and LoVo cell lines	Anti-proliferation, promotes apoptosis, and inhibits migration and invasion	Increases lncRNA CASC2 and regulates EZH2/Bcl-2 axis	*In vitro*
Huang (139)	2017	Primary culture of colon tissues from neonatal rats	Anti-proliferation	Mediates the expression of DNMTs and target miRNAs	*In vitro*
Soffar (140)	2019	HCT116 spheroids	Anti-proliferation, induces cell cycle arrest	Induces G1-phase cell cycle delay and decreases the S-phase fraction of cells	*In vitro*
Liu (141)	2020	DLD-1 and Caco-2 cell lines	Anti-proliferation, induces cell cycle arrest	Inhibits the SCAP/SREBP-1 signaling pathway-mediated lipogenesis	*In vitro*
Li (142)	2015	HCT116, SW480 and LOVO cell lines, female FVB mice	Anti-inflammation, anti-proliferation, and induces apoptosis	Suppresses COX-2 expression via regulating AMPK pathway	*In vitro* and *in vivo*
Li (143)	2017	IMCE, RAW 264.7 macrophages, and HCT116 cell lines, C57BL/6J-*APC*$^{min/+}$ mice	Anti-inflammation, and anti-proliferation	Interferes with inflammatory response-driven EGFR signaling pathway	*In vitro* and *in vivo*
Wu (144)	2012	HCT116 cell line, female SD rats	Anti-proliferation, induces apoptosis and cell cycle arrest	Targets Wnt/β-catenin signaling pathway	*In vitro* and *in vivo*
Deng (145)	2022	C57BL/6 male mice	Anti-inflammation, improves intestinal barrier function, modulates gut microbiota dysbiosis	Inhibition of the JNK/STAT3 and β-Catenin pathways	*In vivo*

BBR, berberine; CRC, colorectal cancer; IGF2BP3, insulin like growth factor 2 mRNA binding protein 3; GRP78, glucose-regulated protein 78; miR, microRNA; lncRNA, long non-coding RNA; CASC2, cancer susceptibility candidate 2; EGFR, epidermal growth factor receptor; Cb1, cannabinoid receptor 1; CCND1, cyclin D1; CDK4, cyclin-dependent kinase; TERT, telomerase reverse transcriptase; TERC telomerase RNA component; COX-2, cyclooxygenase-2; PGE2, prostaglandin E2; STAT, signal transducer and activator of transcription; MMP, matrix metalloproteinase; ITG?4, integrin subunit beta 4; PDCD4, programmed cell death 4; EZH2, zeste 2 polycomb repressive complex 2 subunit; DNMTs, DNA methyltransferases; SCAP, SREBP cleavage-activating protein; SREBP1, sterol-regulatory element binding protein 1; AMPK, AMP activated protein kinase; SD, sprague dawely.

diminished CRC cancer cell growth by modulating G1-phase cell cycle delay (140). In addition, Liu and coauthors observed that BBR suppressed cell proliferation by inducing G0/G1 phase cell cycle arrest in CRC cells (141). Therefore, the anti-proliferation effect of BBR might largely contribute to G0/G1 cell cycle arrest in CRC.

Effects of Berberine on Inflammation, Oxidative Stress, and Signaling Pathways in Colorectal Cancer

An important relationship has been confirmed between chronic inflammation and CRC development. It has been estimated that ∼15–20% of cancer-related deaths involve an inflammatory response (147). CRC is colitis-associated cancer and patients with Crohn's disease (CD) or UC who develop CRC present an unfavorable prognosis (148, 149). This phenomenon might be explained by the chronic inflammatory response in the intestinal tract being able to trigger tumorigenesis and stimulate malignancy development (13). In addition, oxidative stress also plays a very important role in IBD carcinogenesis (66). During inflammation, activated inflammatory cells (neutrophils, macrophages, etc.) produce high levels of reactive oxygen species (ROS), including superoxide radicals, hydroxyl radicals, and hydrogen peroxide, which are important substances that contribute to tumorigenesis. Oxygen radicals can lead to abnormal DNA and RNA synthesis, and abnormal protein assembly and DNA repair (150). Moreover, oxygen radicals can also cause microsatellite instability (MSI) (151) and hypermethylation (152). In addition, oxygen radicals can activate genes that promote the production of free radicals, such as nitric oxide (NO) synthase and COX-2, allowing for a progressive inflammatory response and carcinogenesis (153). Therefore, inhibition of the inflammatory response and oxidative stress are beneficial for cancer treatment. BBR was reported to inhibit azoxymethane and dextran sulfate sodium (AOM/DSS)-induced CRC in a mouse model by suppressing COX-2 expression and regulating the AMPK pathway (142). Another discovery indicated that BBR inhibited the migration and invasion of CRC cells *via* the COX-2/PGE2-mediated JAK2/STAT3 signaling pathway (136). Additionally, Li and coauthors confirmed that BBR inhibited colitis-associated CRC by inhibiting inflammatory responses and subsequently suppressed EGFR signaling-involved tumor cell growth (143). Furthermore, BBR exerts its anti-inflammatory role in UC by modulating the IL-6/STAT3/NF-κB signaling pathway (154). BBR was described to inhibit the proliferation of CRC cells by inactivating the Wnt/β-catenin signaling pathway (144). Thus, BBR could be used as a critical anti-inflammatory and antioxidant agent in CRC.

Gut Microbiota, Mucosal Barrier, and Colorectal Cancer

Gut Microbiota and Colorectal Cancer

The colon is covered with a mass of microorganisms. It has been reported that more than 500–1,000 species and a total of 10^{13} bacteria settle in the colon and other parts of the large intestine of adult humans. The diversity and composition of the microbiota could be changed by a variety of factors, such as age, dietary habits, pharmacotherapy, and psychological stress. (155, 156). The intestinal microflora is often considered an important organ acquired by the human body, which can protect the host from pathogenic bacteria, promote the host's digestion and absorption, affect drug metabolism and carcinogenesis, influence the absorption and distribution of fat, and regulate energy metabolism and the innate and acquired immune systems (157). Dysbiosis is an imbalance in the function or structure of gut microbiota and has been responsible for many disorders, including CRC. Noteworthy changes have been reported in specific bacterial clusters in CRC subjects (158). For instance, commensal bacterial species (such as *Faecalibacterium*, *Blautia*, and *Roseburia*) are found to be decreased, while harmful bacterial inhabitants (such as *Akkermansia*, *Fusobacterium nucleatum*, and *Clostridium difficile*) are extensively enriched in CRC (159). Dysbiosis in the gut microbiota could contribute to the development of CRC by modulating several different mechanisms, such as the inflammatory response, immune regulation, DNA damage, and the production of metabolites responsible for cancer development or suppression (160–164). Beneficial bacteria might compete for attachment sites to reduce the abundance of pathogenic bacteria and avoid infection. However, the pathogenic bacteria could increase intestinal permeation and are very closely related to the colon inflammatory response, which might be an important issue for the promotion of CRC (165). Furthermore, microbial metabolites, such as short-chain fatty acids (SCFAs), might also participate in the development of CRC. SCFAs have been reported to regulate the differentiation of Th1/Th17 cells and production of IL-10 by increasing the expression of transcription factor B lymphocyte-induced maturation protein 1 (Blimp-1) to maintain intestinal homeostasis (166). In addition, *Fusobacterium nucleatum* changed microbial structures and activated JAK-STAT and mitogen-activated protein kinase (MAPK) pathways, promoting the release of inflammatory factors (128). Moreover, the gut microbiota causes immune repair by modulating the intestinal barrier.

Effects of Berberine on Gut Microbiota and Mucosal Barrier

Common chemotherapeutic drugs tend to disrupt the mucosal barrier, which is detrimental to the late treatment of CRC (10). In addition, chemotherapy generally induces gastrointestinal (GI) epithelium damage that is at least partially intermediated by the activation of the inflammatory cascade (10). For example, 5-FU, a standard first-line treatment for CRC individuals, promotes apoptosis of epithelial cells and inhibits mucosal proliferation, while apoptotic cells can further promote inflammation. In contrast, BBR can inhibit tumor growth through meditation of the intestinal flora and mucosal barrier, and generally and ultimately improve weight loss (167). Moreover, BBR has been reported to modulate the composition of intestinal flora and significantly reduce flora diversity. For instance, BBR was demonstrated to inhibit the relative abundance of some of the intestinal flora, such as *Desulfovibrio*, *Lactobacillus acidophilus*, *Eubacterium*, *Lactococcus lactis*, and *Bacteroides* (168, 169), while it enriched *Bacteroides* in the colon and terminal ileum of C57BL/6 mice (169). In addition, it has been also demonstrated

that BBR significantly reduced the relative abundances of both *Firmicutes* (such as *Lactobacillus* sp.) and *Bacteroidetes* in the gut of high-fat diet (HFD)-fed mice, indicating that the antimicrobial activity of BBR may be responsible for its anti-obesity effects (170). *Akkermansia muciniphila* (*A. muciniphila*) is a member of beneficial microbiota and a dedicated intestinal mucin degrader (171). Abnormal production and expression of mucin damage the mucinous layer, bringing bacteria into close contact with the intestinal epithelial cells and possibly triggering adverse host response and subsequent CRC development (172). BBR has been revealed to increase the growth of the populations of the symbiotic genus *Akkermansia* (173) and may further have effects on mucin expression. Moreover, BBR could modulate the gut microbiota in the colon by impacting the Treg/Th17 balance, reducing the levels of proinflammatory factors, including IL-17, IL-21, IL-22, IL-23, and IL-25, and increasing the levels of anti-inflammatory factors, such as IL-10 (174). In addition, BBR reduced bacterial endotoxins in the blood and alleviated the inflammatory response (175). Furthermore, it has been demonstrated that BBR decreases mucosal damage by modulating the levels of polyamines. Wu et al. (176) found that BBR could downregulate the levels of polyamine metabolism-associated proteins, including ornithine decarboxylase (ODC), c-myc, and hypoxia-inducible factor 1 subunit alpha (HIF-1α), and upregulate the levels of polyamine metabolic enzymes, including ornithine decarboxylase antizyme 1 (OAZ1) and spermidine/spermine N1-acetyltransferase (SSAT). At the same time, BBR could decrease the permeability of intestinal mucosa by modulating zonula occludens-1 (ZO1) and occludin (OCLN) (176). More recently, Deng and coauthors found that preadministration of BBR suppressed CRC development by inhibiting inflammation and proliferation and maintaining intestinal homeostasis (145).

Indoleamine-2, 3-Dioxygenase, Colorectal Cancer, and Berberine

Indoleamine 2,3-dioxygenase (IDO) is a key inflammatory cytokine-inducible rate-limiting enzyme of tryptophan catabolism, which includes three types, namely, IDO1, IDO2, and tryptophan 2,3-dioxygenase (TDO2). IDO has been demonstrated to play significant roles in the inhibition of intracellular pathogen replication and immunomodulation (177, 178). IDO is constitutively expressed in several human and mouse cells. It can catalyze the oxidative catabolism of tryptophan to kynurenine (179). In addition, IDO1 exerts its immunosuppressive effect by inhibiting the macrophage response and effector T cells by tryptophan starvation of sensitive T cells or accumulation of toxic metabolites (kynurenine) produced by tryptophan metabolism, subsequently inducing cell cycle arrest and effector T-cell death in the tumor microenvironment (180). In addition, the activity of IDO1 has been reported to directly stimulate cancer growth and proliferation by the production of kynurenine and the activation of β-catenin signaling (181). Previous studies discovered that IDO1 was highly expressed in CRC and was also correlated with impaired clinical outcomes (182–185). Therefore, targeting IDO1 for the treatment of cancer could be considered as an immunosuppressive-targeted strategy (177). Interestingly, BBR revealed uncompetitive and reversible inhibitory activity on IDO1, which might be due to direct binding to heme iron or occupation of the presumed tryptophan-binding site (186). Recently, a series of novel BBR derivatives targeting IDO1 has been designed to reduce the activity of IDO1. Wang et al. observed that compounds 2i and 2n of BBR displayed anticancer activity by increasing the specific lysis of natural killer (NK) cells to A549 cells through IDO1 (187). Both compounds repressed interferon (IFN)-γ-induced IDO1 expression *via* activation of AMPK and inhibition of STAT1 phosphorylation. Nevertheless, there have been no related studies about the effects of BBR on CRC *via* inhibition of IDO1 activity. Hence, compounds 2i and 2n could be selected as IDO1 modulators for small-molecule CRC immunotherapy for further investigation.

Limitations and Side Effects of Berberine

Although BBR presents valuable and promising biological effects in the management of cancers, the side effects of BBR cannot be overlooked (188). BBR should not be administered to infants with jaundice, pregnant women, or nursing women because of the potential risk of bilirubin-induced brain injury (189). In addition, intravenous administration of BBR can cause allergic reactions (190). Additionally, arrhythmia has been reported in hypervagotonic individuals after the administration of BBR (191). Other side effects, including nausea, cramping, diarrhea, flatulence, vomiting, rash, fever, constipation, and stomachache, have also been reported (192–194). Furthermore, a high dosage of BBR could cause low blood pressure, dyspnea, flu-like symptoms, and cardiac injury (190). Moreover, BBR can regulate the activity of P-glycoprotein (P-gp), and potential drug-drug interactions (DDIs) are observed when BBR is coadministered with P-gp substrates (195–197). For example, BBR in combination with P-gp inhibitor tetrandrine (Tet) can significantly improve the pharmacokinetics and hypoglycemic efficacy of BBR (196). Codelivery of the P-gp inhibitor tariquidar and BBR reversed the multiple drug resistance (MDR) in the K562/DOXO cell line (198). In addition, the efficiency of BBR is limited by its low bioavailability due to its poor absorption rate in the gut, low solubility in water, and fast metabolism. Studies have shown that the oral bioavailability of BBR is 0.68% in rats (199). Therefore, searching for novel methods to improve the absorption of BBR in the gut might be beneficial for the treatment of cancer. Previous studies have suggested complexation with C60 fullerene (200), solid lipid nanoparticles (SLNs) encompassing BBR by the spray-drying method (201), combining it with p-gp inhibitors (such as tariquidar and tetrandrine) (196, 198), and modification to berberine organic acid salts (BOAs) (168). However, the above-mentioned strategies were mostly tested in animals and must be demonstrated in human clinical trials.

In recent years, increasing evidence has suggested that nanoparticle (NP)-based delivery systems could be a great potential strategy to improve the therapeutic effects of BBR as an anticancer drug (202, 203). NPs, with a small diameter of 5–200 nm, are important artificial components of nanomedicine and play a key role as a therapeutic drug delivery system. NPs can effectively detect cancer and elucidate cancer-related

mechanisms, especially as therapeutic delivery vehicles (204). NPs have unique physical and chemical properties, as well as powerful biological functions. They can effectively protect cargo from the degradation of enzymes and mechanisms (205). Several categories of nanoscale drug delivery vehicles have been demonstrated, and some of them have been applied in nanomedicine for tumor management, such as liposomes, carbon nanotubes, hydrogels, polymeric nanoparticles, and magnetic nanoparticles (206). BBR-loaded polymeric NPs (polyamidoamine dendrimers, chitosan NPs, and dextran NPs), metal NPs (iron-oxide NPs and mesoporous silica NPs), lipid NPs (liposomes), and carbon NPs (carbon dots and graphene NPs) have been revealed to have potential antitumor effects in different trials and experiments (203). Nonetheless, further studies regarding the efficacy of BBR in combination with different conventional anticancer drugs will pave the way for the use of BBR as a component of cancer chemotherapy.

CONCLUSION AND FUTURE CHALLENGES

Berberine exerts widespread pharmacological activities in different disorders. In this review, the functions of BBR are systematically explored and the antitumor effects on CRC, as well as the underlying mechanisms, are delineated. This review confirms that BBR has antibacterial, anti-inflammatory, antioxidant, antitumor, and hypoglycemic effects and cardiovascular and cerebrovascular protective functions. Furthermore, BBR exerts antitumor effects in CRC by modulating miRNA, lncRNA, and mRNA expression, inducing cell cycle arrest, inhibiting cell proliferation, stimulating cell apoptosis, and suppressing inflammation and oxidative stress *via* several signaling pathways. In addition to the above-mentioned functions, BBR has also revealed powerful antitumor activity in CRC by modulating the gut microbiota and mucosal barrier, which is good news for the search for natural antitumor drugs; however, to date, studies of the antitumor effects of BBR have been mainly performed in *in vitro* and a few *in vivo* models. Hence, *in vivo* studies, especially human studies, are warranted to further elucidate and confirm the therapeutic effects of BBR. Moreover, innovative approaches to adjust the BBR structure into more promising derivatives with stronger antitumor effects or to synergize with other chemotherapeutic drugs to improve the anticancer effects of BBR are needed. In summary, BBR is a safe, inexpensive, and effective long-term application for the treatment of cancers.

AUTHOR CONTRIBUTIONS

YS conceived the project and drafted the manuscript. XJ and ZJ performed research studies. MJ collected background information. All authors reviewed and approved the manuscript.

REFERENCES

1. Wild CP, Stewart BW, Wild C. *World Cancer Report 2014*: World Health Organization Geneva, Switzerland (2014).
2. Maida M, Macaluso FS, Ianiro G, Mangiola F, Sinagra E, Hold G, et al. Screening of colorectal cancer: present and future. *Expert Rev Anticancer Ther.* (2017) 17:1131–46. doi: 10.1080/14737140.2017.1392243
3. Xi Y, Xu P. Global colorectal cancer burden in 2020 and projections to 2040. *Transl Oncol.* (2021) 14:101174. doi: 10.1016/j.tranon.2021.101174
4. Siegel RL, Fedewa SA, Anderson WF, Miller KD, Ma J, Rosenberg PS, et al. Colorectal cancer incidence patterns in the United States, 1974-2013. *J Ntl Cancer Inst.* (2017) 109:djw322. doi: 10.1093/jnci/djw322
5. Larsen IK, Bray F. Trends in colorectal cancer incidence in Norway 1962-2006: an interpretation of the temporal patterns by anatomic subsite. *Int J Cancer.* (2010) 126:721–32. doi: 10.1002/ijc.24839
6. Sałaga M, Zatorski H, Sobczak M, Chen C, Fichna J. Chinese herbal medicines in the treatment of IBD and colorectal cancer: a review. *Curr Treat Options Oncol.* (2014) 15:405–20. doi: 10.1007/s11864-014-0288-2
7. Zhang Y, Chen Z, Li J. The current status of treatment for colorectal cancer in China: a systematic review. *Medicine.* (2017) 96:e8242. doi: 10.1097/MD.0000000000008242
8. Yau TO. Precision treatment in colorectal cancer: Now and the future. *JGH Open.* (2019) 3:361–9. doi: 10.1002/jgh3.12153
9. Chari RV. Targeted cancer therapy: conferring specificity to cytotoxic drugs. *Acc Chem Res.* (2008) 41:98–107. doi: 10.1021/ar700108g
10. Lee CS, Ryan EJ, Doherty GA. Gastro-intestinal toxicity of chemotherapeutics in colorectal cancer: the role of inflammation. *World J Gastroenterol.* (2014) 20:3751–61. doi: 10.3748/wjg.v20.i14.3751
11. Xie YH, Chen YX, Fang JY. Comprehensive review of targeted therapy for colorectal cancer. *Signal Transduct Targeted Ther.* (2020) 5:22. doi: 10.1038/s41392-020-0116-z
12. Kong MY Li LY, Lou YM, Chi HY, Wu JJ. Chinese herbal medicines for prevention and treatment of colorectal cancer: From molecular mechanisms to potential clinical applications. *J Integr Med.* (2020) 18:369–84. doi: 10.1016/j.joim.2020.07.005
13. Hallajzadeh J, Maleki Dana P, Mobini M, Asemi Z, Mansournia MA, Sharifi M, et al. Targeting of oncogenic signaling pathways by berberine for treatment of colorectal cancer. *Med Oncol (Northwood, London, England).* (2020) 37:49. doi: 10.1007/s12032-020-01367-9
14. Chen YX, Gao QY, Zou TH, Wang BM, Liu SD, Sheng JQ, et al. Berberine versus placebo for the prevention of recurrence of colorectal adenoma: a multicentre, double-blinded, randomised controlled study. *Lancet Gastroenterol Hepatol.* (2020) 5:267–75. doi: 10.1016/S2468-1253(19)30409-1
15. Ferlay J, Colombet M, Soerjomataram I, Dyba T, Randi G, Bettio M, et al. Cancer incidence and mortality patterns in Europe: Estimates for 40 countries and 25 major cancers in 2018. *Eur J Cancer (Oxford, England: 1990).* (2018) 103:356–87. doi: 10.1016/j.ejca.2018.07.005
16. Bailey CE, Hu CY, You YN, Bednarski BK, Rodriguez-Bigas MA, Skibber JM, et al. Increasing disparities in the age-related incidences of colon and rectal cancers in the United States, 1975-2010. *JAMA Surg.* (2015) 150:17–22. doi: 10.1001/jamasurg.2014.1756
17. Feletto E, Yu XQ. Trends in Colon and Rectal Cancer Incidence in Australia from 1982 to 2014: Analysis of Data on Over 375,000 Cases. *Cancer Epidemiol Biomarkers Prev.* (2019) 28:83–90. doi: 10.1158/1055-9965.EPI-18-0523
18. Brenner DR, Ruan Y, Shaw E, De P, Heitman SJ, Hilsden RJ. Increasing colorectal cancer incidence trends among younger adults in Canada. *Prevent Med.* (2017) 105:345–9. doi: 10.1016/j.ypmed.2017.10.007
19. Dairi O, Anderson JC, Butterly LF. Why is colorectal cancer increasing in younger age groups in the United States? *Expert Rev Gastroenterol Hepatol.* (2021) 15:623–32. doi: 10.1080/17474124.2021.1876561
20. Araghi M, Soerjomataram I, Bardot A, Ferlay J, Cabasag CJ, Morrison DS, et al. Changes in colorectal cancer incidence in seven high-income countries: a population-based study. *Lancet Gastroenterol Hepatol.* (2019) 4:511–8. doi: 10.1016/S2468-1253(19)30147-5

21. Center MM, Jemal A, Smith RA, Ward E. Worldwide variations in colorectal cancer. *CA Cancer J Clin.* (2009) 59:366–78. doi: 10.3322/caac.20038
22. Bosetti C, Levi F, Rosato V, Bertuccio P, Lucchini F, Negri E, et al. Recent trends in colorectal cancer mortality in Europe. *Int J Cancer.* (2011) 129:180–91. doi: 10.1002/ijc.25653
23. Edwards BK, Ward E, Kohler BA, Eheman C, Zauber AG, Anderson RN, et al. Annual report to the nation on the status of cancer, 1975-2006, featuring colorectal cancer trends and impact of interventions (risk factors, screening, and treatment) to reduce future rates. *Cancer.* (2010) 116:544–73. doi: 10.1002/cncr.24760
24. Bosetti C, Bertuccio P, Malvezzi M, Levi F, Chatenoud L, Negri E, et al. Cancer mortality in Europe, 2005-2009, and an overview of trends since 1980. *Ann Oncol.* (2013) 24:2657–71. doi: 10.1093/annonc/mdt301
25. Chatenoud L, Bertuccio P, Bosetti C, Malvezzi M, Levi F, Negri E, et al. Trends in mortality from major cancers in the Americas: 1980–2010. *Ann Oncol.* (2014) 25:1843–53. doi: 10.1093/annonc/mdu206
26. Sharma R. An examination of colorectal cancer burden by socioeconomic status: evidence from GLOBOCAN 2018. *EPMA J.* (2020) 11:95–117. doi: 10.1007/s13167-019-00185-y
27. Douaiher J, Ravipati A, Grams B, Chowdhury S, Alatise O, Are C. Colorectal cancer-global burden, trends, and geographical variations. *J Surg Oncol.* (2017) 115:619–30. doi: 10.1002/jso.24578
28. Luengo-Fernandez R, Leal J, Gray A, Sullivan R. Economic burden of cancer across the European Union: a population-based cost analysis. *Lancet Oncol.* (2013) 14:1165–74. doi: 10.1016/S1470-2045(13)70442-X
29. Favoriti P, Carbone G, Greco M, Pirozzi F, Pirozzi RE, Corcione F. Worldwide burden of colorectal cancer: a review. *Updates Surg.* (2016) 68:7–11. doi: 10.1007/s13304-016-0359-y
30. Keum N, Giovannucci E. Global burden of colorectal cancer: emerging trends, risk factors and prevention strategies. *Nature reviews Gastroenterology & hepatology.* (2019) 16:713–32. doi: 10.1038/s41575-019-0189-8
31. Cheng L, Eng C, Nieman LZ, Kapadia AS, Du XL. Trends in colorectal cancer incidence by anatomic site and disease stage in the United States from 1976 to 2005. *Am J Clin Oncol.* (2011) 34:573–80. doi: 10.1097/COC.0b013e3181fe41ed
32. Thanikachalam K, Khan G. Colorectal Cancer and Nutrition. *Nutrients.* (2019) 11:164. doi: 10.3390/nu11010164
33. O'Connell JB, Maggard MA, Livingston EH, Yo CK. Colorectal cancer in the young. *Am J Surg.* (2004) 187:343–8. doi: 10.1016/j.amjsurg.2003.12.020
34. Comprehensive molecular characterization of human colon and rectal cancer. *Nature.* (2012) 487:330–7. doi: 10.1038/nature11252
35. Kudryavtseva AV, Lipatova AV, Zaretsky AR, Moskalev AA, Fedorova MS, Rasskazova AS, et al. Important molecular genetic markers of colorectal cancer. *Oncotarget.* (2016) 7:53959–83. doi: 10.18632/oncotarget.9796
36. Henrikson NB, Webber EM, Goddard KA, Scrol A. Piper M. Family history and the natural history of colorectal cancer: systematic review. *Genet Med.* (2015) 17:702–12. doi: 10.1038/gim.2014.188
37. Slattery ML, Levin TR, Ma K, Goldgar D, Holubkov R, Edwards S. Family history and colorectal cancer: predictors of risk. *Cancer Causes Control.* (2003) 14:879–87. doi: 10.1023/B:CACO.0000003840.94591.76
38. Pesola F, Eloranta S, Martling A, Saraste D, Smedby KE. Family history of colorectal cancer and survival: a Swedish population-based study. *J Intern Med.* (2020) 287:723–33. doi: 10.1111/joim.13036
39. Czene K, Lichtenstein P, Hemminki K. Environmental and heritable causes of cancer among 96 million individuals in the Swedish Family-Cancer Database. *Int J Cancer.* (2002) 99:260–6. doi: 10.1002/ijc.10332
40. Lichtenstein P, Holm NV, Verkasalo PK, Iliadou A, Kaprio J, Koskenvuo M, et al. Environmental and heritable factors in the causation of cancer—analyses of cohorts of twins from Sweden, Denmark, and Finland. *N Engl J Med.* (2000) 343:78–85. doi: 10.1056/NEJM200007133430201
41. Thomas M, Sakoda LC, Hoffmeister M, Rosenthal EA, Lee JK, van Duijnhoven FJB, et al. Genome-wide modeling of polygenic risk score in colorectal cancer risk. *Am J Hum Genet.* (2020) 107:432–44. doi: 10.1016/j.ajhg.2020.07.006
42. Simmer F, Brinkman AB, Assenov Y, Matarese F, Kaan A, Sabatino L, et al. Comparative genome-wide DNA methylation analysis of colorectal tumor and matched normal tissues. *Epigenetics.* (2012) 7:1355–67. doi: 10.4161/epi.22562
43. Jiao S, Peters U, Berndt S, Brenner H, Butterbach K, Caan BJ, et al. Estimating the heritability of colorectal cancer. *Hum Mol Genet.* (2014) 23:3898–905. doi: 10.1093/hmg/ddu087
44. Chew MH, Tan WS, Liu Y, Cheah PY, Loi CT, Tang CL. Genomics of Hereditary Colorectal Cancer: Lessons Learnt from 25 Years of the Singapore Polyposis Registry. *Ann Acad Med Singapore.* (2015) 44:290–6.
45. Syngal S, Brand RE, Church JM, Giardiello FM, Hampel HL, Burt RW. ACG clinical guideline: Genetic testing and management of hereditary gastrointestinal cancer syndromes. The American journal of gastroenterology. (2015) 110:223–62. doi: 10.1038/ajg.2014.435
46. Dyson JK, Rutter MD. Colorectal cancer in inflammatory bowel disease: what is the real magnitude of the risk? *World J Gastroenterol.* (2012) 18:3839–48. doi: 10.3748/wjg.v18.i29.3839
47. Krämer HU, Schöttker B, Raum E, Brenner H. Type 2 diabetes mellitus and colorectal cancer: meta-analysis on sex-specific differences. *Eur J Cancer (Oxford, England: 1990).* (2012) 48:1269–82. doi: 10.1016/j.ejca.2011.07.010
48. Kyrgiou M, Kalliala I, Markozannes G, Gunter MJ, Paraskevaidis E, Gabra H, et al. Adiposity and cancer at major anatomical sites: umbrella review of the literature. *BMJ (Clinical research ed).* (2017) 356:j477. doi: 10.1136/bmj.j477
49. Keighley MR, O'Morain C, Giacosa A, Ashorn M, Burroughs A, Crespi M, et al. Public awareness of risk factors and screening for colorectal cancer in Europe. *Eur J Cancer Prevent.* (2004) 13:257–62. doi: 10.1097/01.cej.0000136575.01493.9b
50. Cai S, Li Y, Ding Y, Chen K, Jin M. Alcohol drinking and the risk of colorectal cancer death: a meta-analysis. *Eur J Cancer Prevent.* (2014) 23:532–9. doi: 10.1097/CEJ.0000000000000076
51. Botteri E, Borroni E, Sloan EK, Bagnardi V, Bosetti C, Peveri G, et al. Smoking and Colorectal Cancer Risk, Overall and by Molecular Subtypes: a Meta-Analysis. *Am J Gastroenterol.* (2020) 115:1940–9. doi: 10.14309/ajg.0000000000000803
52. Botteri E, Iodice S, Bagnardi V, Raimondi S, Lowenfels AB, Maisonneuve P. Smoking and colorectal cancer: a meta-analysis. *JAMA.* (2008) 300:2765–78. doi: 10.1001/jama.2008.839
53. Luu HN, Wang R, Shivappa N, Hébert JR, Koh W-P, Yuan J-M, et al. prospective study of dietary inflammatory index scores and colorectal cancer risk: The Singapore Chinese Health Study. *AACR.* (2018). doi: 10.1158/1538-7445.AM2018-5264
54. Chan DS, Lau R, Aune D, Vieira R, Greenwood DC, Kampman E, et al. Red and processed meat and colorectal cancer incidence: meta-analysis of prospective studies. *PLoS ONE.* (2011) 6:e20456. doi: 10.1371/journal.pone.0020456
55. Nguyen LH, Liu PH, Zheng X, Keum N, Zong X, Li X, et al. Sedentary behaviors, TV viewing time, and risk of young-onset colorectal cancer. *JNCI Cancer Spectrum.* (2018) 2:pky073. doi: 10.1093/jncics/pky073
56. Alegria-Lertxundi I, Aguirre C, Bujanda L, Fernández FJ, Polo F, Ordovás JM, et al. Food groups, diet quality and colorectal cancer risk in the Basque Country. *World J Gastroenterol.* (2020) 26:4108–25. doi: 10.3748/wjg.v26.i28.4108
57. Baena R, Salinas P. Diet and colorectal cancer. *Maturitas.* (2015) 80:258–64. doi: 10.1016/j.maturitas.2014.12.017
58. Azeem S, Gillani SW, Siddiqui A, Jandrajupalli SB, Poh V, Syed Sulaiman SA. Diet and colorectal cancer risk in Asia—a systematic review. *Asian Pac J Cancer Prevent.* (2015) 16:5389–96. doi: 10.7314/APJCP.2015.16.13.5389
59. Borzì AM, Biondi A, Basile F, Luca S. Olive oil effects on colorectal cancer. *Nutrients.* (2018) 11:32. doi: 10.3390/nu11010032
60. Balhareth A, Aldossary MY. Impact of physical activity and diet on colorectal cancer survivors' quality of life: a systematic review *World J Surg Oncol.* (2019) 17:153. doi: 10.1186/s12957-019-1697-2
61. Schlesinger S, Walter J, Hampe J, von Schönfels W, Hinz S, Küchler T, et al. Lifestyle factors and health-related quality of life in colorectal cancer survivors. *Cancer Causes Control.* (2014) 25:99–110. doi: 10.1007/s10552-013-0313-y
62. Brenner H, Hoffmeister M, Arndt V, Haug U. Gender differences in colorectal cancer: implications for age at initiation of screening. *Br J Cancer.* (2007) 96:828–31. doi: 10.1038/sj.bjc.6603628

63. Low EE, Demb J, Liu L, Earles A, Bustamante R, Williams CD, et al. Risk factors for early-onset colorectal cancer. *Gastroenterology.* (2020) 159:492–501.e7. doi: 10.1053/j.gastro.2020.01.004
64. Sineshaw HM, Robbins AS, Jemal A. Disparities in survival improvement for metastatic colorectal cancer by race/ethnicity and age in the United States. *Cancer Causes Control.* (2014) 25:419–23. doi: 10.1007/s10552-014-0344-z
65. Bae JM, Kim JH, Kang GH. Molecular subtypes of colorectal cancer and their clinicopathologic features, with an emphasis on the serrated neoplasia pathway. *Arch Pathol Lab Med.* (2016) 140:406–12. doi: 10.5858/arpa.2015-0310-RA
66. Zauber AG, Winawer SJ, O'Brien MJ, Lansdorp-Vogelaar I, van Ballegooijen M, Hankey BF, et al. Colonoscopic polypectomy and long-term prevention of colorectal-cancer deaths. *N Engl J Med.* (2012) 366:687–96. doi: 10.1056/NEJMoa1100370
67. Vacante M, Ciuni R, Basile F. Gut microbiota and colorectal cancer development: a closer look to the adenoma-carcinoma sequence. *Biomedicines.* (2020) 8:489. doi: 10.3390/biomedicines8110489
68. Kinzler KW, Vogelstein B. Lessons from hereditary colorectal cancer. *Cell.* (1996) 87:159–70. doi: 10.1016/S0092-8674(00)81333-1
69. Fearon ER. Molecular genetics of colorectal cancer. *Annu Rev Pathol.* (2011) 6:479–507. doi: 10.1146/annurev-pathol-011110-130235
70. Vacante M, Borzì AM, Basile F, Biondi A. Biomarkers in colorectal cancer: current clinical utility and future perspectives. *World J Clinical Cases.* (2018) 6:869–81. doi: 10.12998/wjcc.v6.i15.869
71. Sievers CK, Grady WM, Halberg RB, Pickhardt PJ. New insights into the earliest stages of colorectal tumorigenesis. *Expert Rev Gastroenterol Hepatol.* (2017) 11:723–9. doi: 10.1080/17474124.2017.1330150
72. Leggett B, Whitehall V. Role of the serrated pathway in colorectal cancer pathogenesis. *Gastroenterology.* (2010) 138:2088–100. doi: 10.1053/j.gastro.2009.12.066
73. Kedrin D, Gala MK. Genetics of the serrated pathway to colorectal cancer. *Clin Transl Gastroenterol.* (2015) 6:e84. doi: 10.1038/ctg.2015.12
74. Yamane L, Scapulatempo-Neto C, Reis RM, Guimarães DP. Serrated pathway in colorectal carcinogenesis. *World J Gastroenterol.* (2014) 20:2634–40. doi: 10.3748/wjg.v20.i10.2634
75. Itzkowitz SH, Yio X. Inflammation and cancer IV. Colorectal cancer in inflammatory bowel disease: the role of inflammation. *Am J Physiol Gastrointest Liver Physiol.* (2004) 287:G7–17. doi: 10.1152/ajpgi.00079.2004
76. Triantafillidis JK, Nasioulas G, Kosmidis PA. Colorectal cancer and inflammatory bowel disease: epidemiology, risk factors, mechanisms of carcinogenesis and prevention strategies. *Anticancer Res.* (2009) 29:2727–37.
77. Watanabe T, Muro K, Ajioka Y, Hashiguchi Y, Ito Y, Saito Y, et al. Japanese Society for Cancer of the Colon and Rectum (JSCCR) guidelines 2016 for the treatment of colorectal cancer. *Int J Clin Oncol.* (2018) 23:1–34. doi: 10.1007/s10147-017-1101-6
78. Itatani Y. Kawada K. Treatment of Elderly Patients with Colorectal Cancer. *Biomed Res Int.* (2018) 2018:2176056. doi: 10.1155/2018/2176056
79. Panis Y, Maggiori L, Caranhac G, Bretagnol F, Vicaut E. Mortality after colorectal cancer surgery: a French survey of more than 84,000 patients. *Ann Surg.* (2011) 254:738–43. doi: 10.1097/SLA.0b013e31823604ac
80. Vallance AE, Keller DS, Hill J, Braun M, Kuryba A, van der Meulen J, et al. Role of emergency laparoscopic colectomy for colorectal cancer: a population-based study in England. *Ann Surg.* (2019) 270:172–9. doi: 10.1097/SLA.0000000000002752
81. Addison P, Agnew JL, Martz J. Robotic Colorectal Surgery. *Surg Clin North Am.* (2020) 100:337–60. doi: 10.1016/j.suc.2019.12.012
82. Ezekian B, Sun Z, Adam MA, Kim J, Turner MC, Gilmore BF, et al. Robotic-assisted versus laparoscopic colectomy results in increased operative time without improved perioperative outcomes. *J Gastrointest Surg.* (2016) 20:1503–10. doi: 10.1007/s11605-016-3124-0
83. Park JS, Kang H, Park SY, Kim HJ, Woo IT, Park IK. et al. Long-term oncologic after robotic versus laparoscopic right colectomy: a prospective randomized study. *Surg Endosc.* (2019) 33:2975–81. doi: 10.1007/s00464-018-6563-8
84. Chamseddine AN, Ducreux M, Armand JP, Paoletti X, Satar T, Paci A, et al. Intestinal bacterial β-glucuronidase as a possible predictive biomarker of irinotecan-induced diarrhea severity. *Pharmacol Ther.* (2019) 199:1–15. doi: 10.1016/j.pharmthera.2019.03.002
85. Cheng KW, Tseng CH, Tzeng CC, Leu YL, Cheng TC, Wang JY, et al. Pharmacological inhibition of bacterial β-glucuronidase prevents irinotecan-induced diarrhea without impairing its antitumor efficacy in vivo. *Pharmacol Res.* (2019) 139:41–9. doi: 10.1016/j.phrs.2018.10.029
86. Hattori T, Imaoka A. Irinotecan-induced gastrointestinal damage impairs the absorption of dabigatran etexilate. *Biopharm Drug Dispos.* (2019) 40:315–24. doi: 10.1002/bdd.2205
87. Suau R, Rico R, López-Romero JM, Nájera F, Cuevas A. Isoquinoline alkaloids from Berberis vulgaris subsp. australis. *Phytochemistry.* (1998) 49:2545–9. doi: 10.1016/S0031-9422(98)00121-6
88. Habtemariam S. The therapeutic potential of Berberis darwinii stem-bark: quantification of berberine and in vitro evidence for Alzheimer's disease therapy. *Nat Prod Commun.* (2011) 6:1089–90. doi: 10.1177/1934578X1100600809
89. Liu Y, Hao H, Xie H, Lv H, Liu C, Wang G. Oxidative demethylenation and subsequent glucuronidation are the major metabolic pathways of berberine in rats. *J Pharm Sci.* (2009) 98:4391–401. doi: 10.1002/jps.21721
90. Wang K, Feng X, Chai L, Cao S, Qiu F. The metabolism of berberine and its contribution to the pharmacological effects. *Drug Metab Rev.* (2017) 49:139–57. doi: 10.1080/03602532.2017.1306544
91. Guo Y, Li F, Ma X, Cheng X, Zhou H, Klaassen CD. CYP2D plays a major role in berberine metabolism in liver of mice and humans. *Xenobiotica.* (2011) 41:996–1005. doi: 10.3109/00498254.2011.597456
92. Qiu F, Zhu Z, Kang N, Piao S, Qin G, Yao X. Isolation and identification of urinary metabolites of berberine in rats and humans. *Drug Metab Dispos.* (2008) 36:2159–65. doi: 10.1124/dmd.108.021659
93. Kwon M, Lim DY, Lee CH, Jeon J-H, Choi M-K, Song I-S. Enhanced intestinal absorption and pharmacokinetic modulation of berberine and its metabolites through the inhibition of p-glycoprotein and intestinal metabolism in rats using a berberine mixed micelle formulation. *Pharmaceutics.* (2020) 12:882. doi: 10.3390/pharmaceutics12090882
94. Kuo CL, Chi CW, Liu TY. The anti-inflammatory potential of berberine in vitro and in vivo. *Cancer Lett.* (2004) 203:127–37. doi: 10.1016/j.canlet.2003.09.002
95. Haftcheshmeh SM, Abedi M, Mashayekhi K, Mousavi MJ, Navashenaq JG, Mohammadi A, et al. Berberine as a natural modulator of inflammatory signaling pathways in the immune system: Focus on NF-κB, JAK/STAT, and MAPK signaling pathways. *Phytother Res.* (2022) 36:1216–30. doi: 10.1002/ptr.7407
96. Mohammadian Haftcheshmeh S. Momtazi-Borojeni AA. Berberine as a promising natural compound for the treatment of periodontal disease: a focus on anti-inflammatory properties. *J Cell Mol Med.* (2021) 25:11333–7. doi: 10.1111/jcmm.17019
97. Warowicka A, Nawrot R, Gozdzicka-Józefiak A. Antiviral activity of berberine. *Arch Virol.* (2020) 165:1935–45. doi: 10.1007/s00705-020-04706-3
98. Rajasekhar K, Samanta S, Bagoband V, Murugan NA, Govindaraju T. Antioxidant berberine-derivative inhibits multifaceted amyloid toxicity. *iScience.* (2020) 23:101005. doi: 10.1016/j.isci.2020.101005
99. Ni WJ, Ding HH, Tang LQ. Berberine as a promising anti-diabetic nephropathy drug: an analysis of its effects and mechanisms. *Eur J Pharmacol.* (2015) 760:103–12. doi: 10.1016/j.ejphar.2015.04.017
100. Li YH, Xiao HT, Hu DD, Fatima S, Lin CY, Mu HX, et al. Berberine ameliorates chronic relapsing dextran sulfate sodium-induced colitis in C57BL/6 mice by suppressing Th17 responses. *Pharmacol Res.* (2016) 110:227–39. doi: 10.1016/j.phrs.2016.02.010
101. Feng X, Sureda A, Jafari S, Memariani Z, Tewari D, Annunziata G, et al. Berberine in cardiovascular and metabolic diseases: from mechanisms to therapeutics. *Theranostics.* (2019) 9:1923–51. doi: 10.7150/thno.30787
102. Fatahian A, Haftcheshmeh SM, Azhdari S, Farshchi HK, Nikfar B, Momtazi-Borojeni AA. Promising anti-atherosclerotic effect of berberine: evidence from in vitro, in vivo, and clinical studies. *Rev Physiol Biochem Pharmacol.* (2020) 178:83–110. doi: 10.1007/112_2020_42
103. Yuan NN, Cai CZ, Wu MY, Su HX Li M, Lu JH. Neuroprotective effects of berberine in animal models of Alzheimer's disease: a systematic review of pre-clinical studies. *BMC Complement Altern Med.* (2019) 19:109. doi: 10.1186/s12906-019-2510-z
104. Neag MA, Mocan A, Echeverría J, Pop RM, Bocsan CI, Crişan G, et al. Berberine: botanical occurrence, traditional uses, extraction methods, and

relevance in cardiovascular, metabolic, hepatic, and renal disorders. *Front Pharmacol.* (2018) 9:557. doi: 10.3389/fphar.2018.00557
105. Wang S, Xu Z, Cai B, Chen Q. Berberine as a Potential multi-target agent for metabolic diseases: a review of investigations for berberine. *Endocr Metab Immune Disord Drug Targets.* (2021) 21:971–9. doi: 10.2174/1871530320666200910105612
106. Och A, Och M, Nowak R, Podgórska D, Podgórski R, Berberine. A herbal metabolite in the metabolic syndrome: the risk factors, course, and consequences of the disease. *Molecules.* (2022) 27:1351. doi: 10.3390/molecules27041351
107. Song D, Hao J, Fan D. Biological properties and clinical applications of berberine. *Front Med.* (2020) 14:564–82. doi: 10.1007/s11684-019-0724-6
108. Yu M, Jin X, Liang C, Bu F, Pan D, He Q, et al. Berberine for diarrhea in children and adults: a systematic review and meta-analysis. *Therap Adv Gastroenterol.* (2020) 13:1756284820961299. doi: 10.1177/1756284820961299
109. Aski ML, Rezvani ME, Khaksari M, Hafizi Z, Pirmoradi Z, Niknazar S, et al. Neuroprotective effect of berberine chloride on cognitive impairment and hippocampal damage in experimental model of vascular dementia. *Iran J Basic Med Sci.* (2018) 21:53–8.
110. Liu D, Meng X, Wu D, Qiu Z, Luo H, A. Natural Isoquinoline Alkaloid With Antitumor Activity: Studies of the Biological Activities of Berberine. *Front Pharmacol.* (2019) 10:9. doi: 10.3389/fphar.2019.00009
111. Qi HW, Xin LY, Xu X, Ji XX, Fan LH. Epithelial-to-mesenchymal transition markers to predict response of Berberine in suppressing lung cancer invasion and metastasis. *J Transl Med.* (2014) 12:22. doi: 10.1186/1479-5876-12-22
112. Li H, Guo L, Jie S, Liu W, Zhu J, Du W, et al. Berberine inhibits SDF-1-induced AML cells and leukemic stem cells migration via regulation of SDF-1 level in bone marrow stromal cells. *Biomed Pharmacother.* (2008) 62:573–8. doi: 10.1016/j.biopha.2008.08.003
113. Xiao Y, Tian C, Huang T, Han B, Wang M, Ma H, et al. 8-Cetylberberine inhibits growth of lung cancer in vitro and in vivo. *Life Sci.* (2018) 192:259–69. doi: 10.1016/j.lfs.2017.11.012
114. Wang N, Wang X, Tan HY, Li S, Tsang CM, Tsao SW, et al. Berberine suppresses cyclin D1 expression through proteasomal degradation in human hepatoma cells. *Int J Mol Sci.* (2016) 17:1899. doi: 10.3390/ijms17111899
115. Li XK, Motwani M, Tong W, Bornmann W, Schwartz GK. Huanglian, A chinese herbal extract, inhibits cell growth by suppressing the expression of cyclin B1 and inhibiting CDC2 kinase activity in human cancer cells. *Mol Pharmacol.* (2000) 58:1287–93. doi: 10.1124/mol.58.6.1287
116. Wang J, Qi Q, Feng Z, Zhang X, Huang B, Chen A, et al. Berberine induces autophagy in glioblastoma by targeting the AMPK/mTOR/ULK1-pathway. *Oncotarget.* (2016) 7:66944–58. doi: 10.18632/oncotarget.11396
117. Wang N, Feng Y, Zhu M, Tsang CM, Man K, Tong Y, et al. Berberine induces autophagic cell death and mitochondrial apoptosis in liver cancer cells: the cellular mechanism. *J Cell Biochem.* (2010) 111:1426–36. doi: 10.1002/jcb.22869
118. Okubo S, Uto T, Goto A, Tanaka H, Nishioku T, Yamada K, et al. Berberine Induces apoptotic cell death via activation of caspase-3 and−8 in HL-60 human leukemia cells: nuclear localization and structure-activity relationships. *Am J Chin Med.* (2017) 45:1497–511. doi: 10.1142/S0192415X17500811
119. Li DX, Zhang J, Zhang Y, Zhao PW, Yang LM. Inhibitory effect of berberine on human skin squamous cell carcinoma A431 cells. *Genet Mol Res.* (2015) 14:10553–68. doi: 10.4238/2015.September.8.17
120. Jin H, Jin X, Cao B, Wang W. Berberine affects osteosarcoma via downregulating the caspase-1/IL-1β signaling axis. *Oncol Rep.* (2017) 37:729–36. doi: 10.3892/or.2016.5327
121. Ma W, Zhu M, Zhang D, Yang L, Yang T, Li X, et al. Berberine inhibits the proliferation and migration of breast cancer ZR-75-30 cells by targeting Ephrin-B2. *Phytomedicine.* (2017) 25:45–51. doi: 10.1016/j.phymed.2016.12.013
122. Chu SC Yu CC, Hsu LS, Chen KS, Su MY, Chen PN. Berberine reverses epithelial-to-mesenchymal transition and inhibits metastasis and tumor-induced angiogenesis in human cervical cancer cells. *Mol Pharmacol.* (2014) 86:609–23. doi: 10.1124/mol.114.094037
123. Liu JF, Lai KC. Berberine Inhibits Human Melanoma A375.S2 Cell Migration and Invasion via Affecting the FAK, uPA, and NF-κB Signaling Pathways and Inhibits PLX4032 Resistant A375.S2 Cell Migration In Vitro. *Molecules.* (2018) 23:2019. doi: 10.3390/molecules23082019
124. Lee H, Lee SJ, Bae GU, Baek NI, Ryu JH. Canadine from corydalis turtschaninovii stimulates myoblast differentiation and protects against myotube atrophy. *Int J Mol Sci.* (2017) 18:2748. doi: 10.3390/ijms18122748
125. Wang N, Zhu M, Wang X, Tan HY, Tsao SW, Feng Y. Berberine-induced tumor suppressor p53 up-regulation gets involved in the regulatory network of MIR-23a in hepatocellular carcinoma. *Biochim Biophys Acta.* (2014) 1839:849–57. doi: 10.1016/j.bbagrm.2014.05.027
126. Fu L, Chen W, Guo W, Wang J, Tian Y, Shi D, et al. Berberine Targets AP-2/hTERT, NF-κB/COX-2, HIF-1α/VEGF and Cytochrome-c/Caspase Signaling to Suppress Human Cancer Cell Growth. *PLoS ONE.* (2013) 8:e69240. doi: 10.1371/journal.pone.0069240
127. Tong M, Liu H, Hao J, Fan D. Comparative pharmacoproteomics reveals potential targets for berberine, a promising therapy for colorectal cancer. *Biochem Biophys Res Commun.* (2020) 525:244–50. doi: 10.1016/j.bbrc.2020.02.052
128. Yu YN, Yu TC, Zhao HJ, Sun TT, Chen HM, Chen HY, et al. Berberine may rescue Fusobacterium nucleatum-induced colorectal tumorigenesis by modulating the tumor microenvironment. *Oncotarget.* (2015) 6:32013–26. doi: 10.18632/oncotarget.5166
129. Su Y-H, Tang W-C, Cheng Y-W, Sia P, Huang C-C, Lee Y-C, et al. Targeting of multiple oncogenic signaling pathways by Hsp90 inhibitor alone or in combination with berberine for treatment of colorectal cancer. *Biochimica et Biophysica Acta (BBA)-Mol Cell Res.* (2015) 1853:2261–72. doi: 10.1016/j.bbamcr.2015.05.012
130. Zhang Y, Liu X, Yu M, Xu M, Xiao Y, Ma W, et al. Berberine inhibits proliferation and induces G0/G1 phase arrest in colorectal cancer cells by downregulating IGF2BP3. *Life Sci.* (2020) 260:118413. doi: 10.1016/j.lfs.2020.118413
131. Gong C, Hu X, Xu Y, Yang J, Zong L, Wang C, et al. Berberine inhibits proliferation and migration of colorectal cancer cells by downregulation of GRP78. *Anticancer Drugs.* (2020) 31:141–9. doi: 10.1097/CAD.0000000000000835
132. Liu H, Huang C, Wu L, Wen B. Effect of evodiamine and berberine on miR-429 as an oncogene in human colorectal cancer. *Onco Targets Ther.* (2016) 9:4121–7. doi: 10.2147/OTT.S104729
133. Dai W, Mu L, Cui Y, Li Y, Chen P, Xie H, et al. Berberine promotes apoptosis of colorectal cancer via regulation of the long non-coding RNA (lncRNA) cancer susceptibility candidate 2 (CASC2)/AU-Binding Factor 1 (AUF1)/B-Cell CLL/Lymphoma 2 (Bcl-2) Axis. *Med Sci Monit Int Med J Exp Clin Res.* (2019) 25:730–8. doi: 10.12659/MSM.912082
134. Wang L, Cao H, Lu N, Liu L, Wang B, Hu T, et al. Berberine inhibits proliferation and down-regulates epidermal growth factor receptor through activation of Cbl in colon tumor cells. *PLoS ONE.* (2013) 8:e56666. doi: 10.1371/journal.pone.0056666
135. Samad MA, Saiman MZ, Abdul Majid N. Berberine inhibits telomerase activity and induces cell cycle arrest and telomere erosion in colorectal cancer cell line, HCT 116. *Molecules.* (2021) 26:376. doi: 10.3390/molecules26020376
136. Liu X, Ji Q, Ye N, Sui H, Zhou L, Zhu H, et al. Berberine inhibits invasion and metastasis of colorectal cancer cells via COX-2/PGE2 mediated JAK2/STAT3 signaling pathway. *PLoS ONE.* (2015) 10:e0123478. doi: 10.1145/2818302
137. Lü Y, Han B, Yu H, Cui Z, Li Z, Wang J. Berberine regulates the microRNA-21-ITG?4-PDCD4 axis and inhibits colon cancer viability. *Oncol Lett.* (2018) 15:5971–6.
138. Dai W, Mu L, Cui Y, Li Y, Chen P, Xie H, et al. Long non-coding RNA CASC2 enhances berberine-induced cytotoxicity in colorectal cancer cells by silencing BCL2. *Mol Med Rep.* (2019) 20:995–1006. doi: 10.3892/mmr.2019.10326
139. Huang C, Liu H, Gong XL, Wu LY, Wen B. Effect of evodiamine and berberine on the interaction between DNMTs and target microRNAs during malignant transformation of the colon by TGF-β1. *Oncol Rep.* (2017) 37:1637–45. doi: 10.3892/or.2017.5379
140. Soffar AA. Berberine attenuates cancer cell growth via modulating the cell cycle dynamics but not apoptosis in human colorectal HCT-116 3D spheroid model. *J Biosci Appl Res.* (2019) 5:236–45. doi: 10.21608/jbaar.2019.146799

141. Liu Y, Hua W, Li Y, Xian X, Zhao Z, Liu C, et al. Berberine suppresses colon cancer cell proliferation by inhibiting the SCAP/SREBP-1 signaling pathway-mediated lipogenesis. *Biochem Pharmacol.* (2020) 174:113776. doi: 10.1016/j.bcp.2019.113776
142. Li W, Hua B, Saud SM, Lin H, Hou W, Matter MS, et al. Berberine regulates AMP-activated protein kinase signaling pathways and inhibits colon tumorigenesis in mice. *Mol Carcinog.* (2015) 54:1096–109. doi: 10.1002/mc.22179
143. Li D, Zhang Y, Liu K, Zhao Y, Xu B, Xu L, et al. Berberine inhibits colitis-associated tumorigenesis via suppressing inflammatory responses and the consequent EGFR signaling-involved tumor cell growth. *Lab Invest.* (2017) 97:1343–53. doi: 10.1038/labinvest.2017.71
144. Wu K, Yang Q, Mu Y, Zhou L, Liu Y, Zhou Q, et al. Berberine inhibits the proliferation of colon cancer cells by inactivating Wnt/β-catenin signaling. *Int J Oncol.* (2012) 41:292–8.
145. Deng J, Zhao L, Yuan X, Li Y, Shi J, Zhang H, et al. Pre-administration of berberine exerts chemopreventive effects in aom/dss-induced colitis-associated carcinogenesis mice via modulating inflammation and intestinal microbiota. *Nutrients*. (2022) 14:726. doi: 10.3390/nu14040726
146. Vermeulen K, Van Bockstaele DR, Berneman ZN. The cell cycle: a review of regulation, deregulation and therapeutic targets in cancer. *Cell Prolif.* (2003) 36:131–49. doi: 10.1046/j.1365-2184.2003.00266.x
147. Shacter E, Weitzman SA. Chronic inflammation and cancer. *Oncology (Williston Park, NY)*. (2002) 16:217–26.
148. Watanabe T, Konishi T, Kishimoto J, Kotake K, Muto T, Sugihara K. Ulcerative colitis-associated colorectal cancer shows a poorer survival than sporadic colorectal cancer: a nationwide Japanese study. *Inflamm Bowel Dis.* (2011) 17:802–8. doi: 10.1002/ibd.21365
149. Zhen Y, Luo C, Zhang H. Early detection of ulcerative colitis-associated colorectal cancer. *Gastroenterol Rep (Oxf).* (2018) 6:83–92. doi: 10.1093/gastro/goy010
150. Carini F, Mazzola M, Rappa F, Jurjus A, Geagea AG, Al Kattar S, et al. Colorectal carcinogenesis: role of oxidative stress and antioxidants. *Anticancer Res.* (2017) 37:4759–66. doi: 10.21873/anticanres.11882
151. Jackson AL, Chen R, Loeb LA. Induction of microsatellite instability by oxidative DNA damage. *Proc Natl Acad Sci USA*. (1998) 95:12468–73. doi: 10.1073/pnas.95.21.12468
152. Kraus S, Arber N. Inflammation and colorectal cancer. *Curr Opin Pharmacol.* (2009) 9:405–10. doi: 10.1016/j.coph.2009.06.006
153. Federico A, Morgillo F, Tuccillo C, Ciardiello F, Loguercio C. Chronic inflammation and oxidative stress in human carcinogenesis. *Int J Cancer.* (2007) 121:2381–6. doi: 10.1002/ijc.23192
154. Zhu L, Gu P, Shen H. Protective effects of berberine hydrochloride on DSS-induced ulcerative colitis in rats. *Int Immunopharmacol.* (2019) 68:242–51. doi: 10.1016/j.intimp.2018.12.036
155. Azimirad M, Rostami-Nejad M, Rostami K, Naji T, Zali MR. The susceptibility of celiac disease intestinal microbiota to clostridium difficile infection. *Am J Gastroenterol.* (2015) 110:1740–1. doi: 10.1038/ajg.2015.360
156. Rostami Nejad M, Ishaq S, Al Dulaimi D, Zali MR, Rostami K. The role of infectious mediators and gut microbiome in the pathogenesis of celiac disease. *Arch Iran Med.* (2015) 18:244–9.
157. Li D, Wang P, Wang P, Hu X, Chen F. The gut microbiota: a treasure for human health. *Biotechnol Adv.* (2016) 34:1210–24. doi: 10.1016/j.biotechadv.2016.08.003
158. Saffarian A, Mulet C, Regnault B, Amiot A, Tran-Van-Nhieu J, Ravel J. Crypt- and mucosa-associated core microbiotas in humans and their alteration in colon cancer patients. *mBio*. (2019) 10:e01315–19. doi: 10.1128/mBio.01315-19
159. Wang T, Cai G, Qiu Y, Fei N, Zhang M, Pang X, et al. Structural segregation of gut microbiota between colorectal cancer patients and healthy volunteers. *ISME J.* (2012) 6:320–9. doi: 10.1038/ismej.2011.109
160. Rubinstein MR, Wang X, Liu W, Hao Y, Cai G, Han YW. Fusobacterium nucleatum promotes colorectal carcinogenesis by modulating E-cadherin/β-catenin signaling via its FadA adhesin. *Cell Host Microbe.* (2013) 14:195–206. doi: 10.1016/j.chom.2013.07.012
161. Kostic AD, Chun E, Robertson L, Glickman JN, Gallini CA, Michaud M, et al. Fusobacterium nucleatum potentiates intestinal tumorigenesis and modulates the tumor-immune microenvironment. *Cell Host Microbe.* (2013) 14:207–15. doi: 10.1016/j.chom.2013.07.007
162. Wong SH. Yu J. Gut microbiota in colorectal cancer: mechanisms of action and clinical applications. *Nat Rev Gastroenterol Hepatol*. (2019) 16:690–704. doi: 10.1038/s41575-019-0209-8
163. Cipe G, Idiz UO, Firat D, Bektasoglu H. Relationship between intestinal microbiota and colorectal cancer. *World J Gastrointest Oncol.* (2015) 7:233–40. doi: 10.4251/wjgo.v7.i10.233
164. Loke YL, Chew MT, Ngeow YF, Lim WWD, Peh SC. Colon carcinogenesis: the interplay between diet and gut microbiota. *Front Cell Infect Microbiol.* (2020) 10:603086. doi: 10.3389/fcimb.2020.603086
165. Dzutsev A, Goldszmid RS, Viaud S, Zitvogel L, Trinchieri G. The role of the microbiota in inflammation, carcinogenesis, and cancer therapy. *Eur J Immunol.* (2015) 45:17–31. doi: 10.1002/eji.201444972
166. Sun M, Wu W, Chen L, Yang W, Huang X, Ma C, et al. Microbiota-derived short-chain fatty acids promote Th1 cell IL-10 production to maintain intestinal homeostasis. *Nat Commun.* (2018) 9:3555. doi: 10.1038/s41467-018-05901-2
167. Habtemariam S. Berberine pharmacology and the gut microbiota: a hidden therapeutic link. *Pharmacol Res.* (2020) 155:104722. doi: 10.1016/j.phrs.2020.104722
168. Cui HX, Hu YN, Li JW, Yuan K, Guo Y. Preparation and evaluation of antidiabetic agents of berberine organic acid salts for enhancing the bioavailability. *Molecules (Basel, Switzerland)*. (2018) 24:103. doi: 10.3390/molecules24010103
169. Guo Y, Zhang Y, Huang W, Selwyn FP, Klaassen CD. Dose-response effect of berberine on bile acid profile and gut microbiota in mice. *BMC Complement Altern Med.* (2016) 16:394. doi: 10.1186/s12906-016-1367-7
170. Xie W, Gu D, Li J, Cui K, Zhang Y. Effects and action mechanisms of berberine and Rhizoma coptidis on gut microbes and obesity in high-fat diet-fed C57BL/6J mice. *PLoS ONE.* (2011) 6:e24520. doi: 10.1371/journal.pone.0024520
171. van Passel MW, Kant R, Zoetendal EG, Plugge CM, Derrien M, Malfatti SA, et al. The genome of Akkermansia muciniphila, a dedicated intestinal mucin degrader, and its use in exploring intestinal metagenomes. *PLoS ONE.* (2011) 6:e16876. doi: 10.1371/journal.pone.0016876
172. Coleman OI, Haller D. Microbe-Mucus Interface in the Pathogenesis of Colorectal Cancer. *Cancers*. (2021) 13:616. doi: 10.3390/cancers13040616
173. Wang H, Guan L, Li J, Lai M, Wen X. The effects of berberine on the gut microbiota in Apc (min/+) mice fed with a high fat diet. *Molecules (Basel, Switzerland)*. (2018) 23:2298. doi: 10.3390/molecules23092298
174. Cui H, Cai Y, Wang L, Jia B, Li J, Zhao S, et al. Berberine regulates Treg/Th17 balance to treat ulcerative colitis through modulating the gut microbiota in the colon. *Front Pharmacol.* (2018) 9:571. doi: 10.3389/fphar.2018.00571
175. He Y, Yuan X, Zuo H, Sun Y, Feng A. Berberine exerts a protective effect on gut-vascular barrier via the modulation of the Wnt/beta-catenin signaling pathway during sepsis. *Cell Physiol Biochem*. (2018) 49:1342–51. doi: 10.1159/000493412
176. Wu YY Li TM, Zang LQ, Liu B, Wang GX. Effects of berberine on tumor growth and intestinal permeability in HCT116 tumor-bearing mice using polyamines as targets. *Biomed Pharmacother.* (2018) 107:1447–53. doi: 10.1016/j.biopha.2018.08.130
177. Selvan SR, Dowling JP, Kelly WK, Lin J. Indoleamine 2,3-dioxygenase (IDO): biology and target in cancer immunotherapies. *Curr Cancer Drug Targets.* (2016) 16:755–64. doi: 10.2174/1568009615666151030102250
178. King NJ, Thomas SR. Molecules in focus: indoleamine 2,3-dioxygenase. *Int J Biochem Cell Biol.* (2007) 39:2167–72. doi: 10.1016/j.biocel.2007.01.004
179. Ciorba MA. Indoleamine 2,3 dioxygenase in intestinal disease. *Curr Opin Gastroenterol.* (2013) 29:146–52. doi: 10.1097/MOG.0b013e32835c9cb3
180. Moffett JR, Namboodiri MA. Tryptophan and the immune response. *Immunol Cell Biol.* (2003) 81:247–65. doi: 10.1046/j.1440-1711.2003.t01-1-01177.x
181. Thaker AI, Rao MS, Bishnupuri KS, Kerr TA, Foster L, Marinshaw JM, et al. IDO1 metabolites activate β-catenin signaling to promote cancer cell proliferation and colon tumorigenesis in mice. *Gastroenterology*. (2013) 145:416–25.e1-4. doi: 10.1053/j.gastro.2013.05.002

182. Hacking S, Vitkovski T, Jain S, Jin C, Chavarria H, Wu D, et al. Clinical significance of program death ligand-1 and indoleamine-2,3-dioxygenase expression in colorectal carcinoma. *Appl Immunohistochem Mol Morphol.* (2021) 29:201–8. doi: 10.1097/PAI.0000000000000868
183. Ferdinande L, Decaestecker C, Verset L, Mathieu A, Moles Lopez X, Negulescu AM, et al. Clinicopathological significance of indoleamine 2,3-dioxygenase 1 expression in colorectal cancer. *Br J Cancer.* (2012) 106:141–7. doi: 10.1038/bjc.2011.513
184. Chen IC, Lee KH. Expression Pattern and Clinicopathological Relevance of the Indoleamine 2,3-Dioxygenase 1/Tryptophan 2,3-Dioxygenase Protein in Colorectal Cancer. *Dis Markers.* (2016) 2016:8169724. doi: 10.1155/2016/8169724
185. Ma WJ, Wang X, Yan WT, Zhou ZG, Pan ZZ, Chen G, et al. Indoleamine-2,3-dioxygenase 1/cyclooxygenase 2 expression prediction for adverse prognosis in colorectal cancer. *World J Gastroenterol.* (2018) 24:2181–90. doi: 10.3748/wjg.v24.i20.2181
186. Yu CJ, Zheng MF, Kuang CX, Huang WD, Yang Q. Oren-gedoku-to and its constituents with therapeutic potential in Alzheimer's disease inhibit indoleamine 2, 3-dioxygenase activity in vitro. *J Alzheimer's Dis.* (2010) 22:257–66. doi: 10.3233/JAD-2010-100684
187. Wang YX, Pang WQ, Zeng QX, Deng ZS, Fan TY, Jiang JD, et al. Synthesis and biological evaluation of new berberine derivatives as cancer immunotherapy agents through targeting IDO1. *Eur J Med Chem.* (2018) 143:1858–68. doi: 10.1016/j.ejmech.2017.10.078
188. Mohammadzadeh N, Mehri S, Hosseinzadeh H. Berberis vulgaris and its constituent berberine as antidotes and protective agents against natural or chemical toxicities. *Iran J Basic Med Sci.* (2017) 20:538–51.
189. Tan YZ, Chan WA, Tan BY, Heng WJ, Tang LF, Hao LJ, et al. Study on the interactions of berberine displace other drug from their plasma proteins binding sites. *Chin Pharmacol Bull.* (2002) 5:576–8.
190. Bagade A, Tumbigeremutt V, Pallavi G. Cardiovascular effects of berberine: a review of the literature. *J Restor Med.* (2017) 6:37–45. doi: 10.14200/jrm.2017.6.0100
191. Cannillo M, Frea S, Fornengo C, Toso E, Mercurio G, Battista S, et al. Berberine behind the thriller of marked symptomatic bradycardia. *World J Cardiol.* (2013) 5:261–4. doi: 10.4330/wjc.v5.i7.261
192. Yin J, Xing H, Ye J. Efficacy of berberine in patients with type 2 diabetes mellitus. *Metabolism.* (2008) 57:712–7. doi: 10.1016/j.metabol.2008.01.013
193. Dong H, Wang N, Zhao L, Lu F. Berberine in the treatment of type 2 diabetes mellitus: a systemic review and meta-analysis. *Evid Based Complement Alternat Med.* (2012) 2012:591654. doi: 10.1155/2012/591654
194. Fang L-H, Wang J-H, Du G-H. *Berberine. Natural Small Molecule Drugs from Plants*. Berlin: Springer (2018). p. 371–7. doi: 10.1007/978-981-10-8022-7_62
195. Qiu W, Jiang XH, Liu CX, Ju Y, Jin JX. Effect of berberine on the pharmacokinetics of substrates of CYP3A and P-gp. *Phytother Res.* (2009) 23:1553–8. doi: 10.1002/ptr.2808
196. Shan YQ, Zhu YP, Pang J, Wang YX, Song DQ, Kong WJ, et al. Tetrandrine potentiates the hypoglycemic efficacy of berberine by inhibiting P-glycoprotein function. *Biol Pharm Bull.* (2013) 36:1562–9. doi: 10.1248/bpb.b13-00272
197. Zhang Y, Guo L, Huang J. Inhibitory effect of berberine on broiler p-glycoprotein expression and function: in situ and in vitro studies. *Int J Mol Sci.* (2019) 20:1966. doi: 10.3390/ijms20081966
198. Vanti G, Coronnello M, Bani D. Co-delivery of berberine chloride and tariquidar in nanoliposomes enhanced intracellular berberine chloride in a doxorubicin-resistant K562 cell line due to P-gp overexpression. *Pharmaceutics*. (2021) 13:306. doi: 10.3390/pharmaceutics13030306
199. Chen W, Miao YQ, Fan DJ, Yang SS, Lin X, Meng LK, et al. Bioavailability study of berberine and the enhancing effects of TPGS on intestinal absorption in rats. *AAPS PharmSciTech.* (2011) 12:705–11. doi: 10.1208/s12249-011-9632-z
200. Grebinyk A, Prylutska S, Grebinyk S, Evstigneev M, Krysiuk I, Skaterna T, et al. Antitumor efficiency of the natural alkaloid Berberine complexed with C60 fullerene in Lewis lung carcinoma in vitro and in vivo. *Cancer Nanotechnol.* (2021) 12:1–18. doi: 10.1186/s12645-021-00096-6
201. Nguyen MC-N, Le KN-M, Huynh NT-T, Nguyen TT-T, Bui HT-X, Nguyen VH, editors. Solid lipid nanoparticles containing berberine by spray-drying method. Cham: Springer International Publishing (2022). doi: 10.1007/978-3-030-75506-5_25
202. Sahibzada MUK, Sadiq A, Faidah HS, Khurram M, Amin MU, Haseeb A, et al. Berberine nanoparticles with enhanced in vitro bioavailability: characterization and antimicrobial activity. *Drug Des Devel Ther.* (2018) 12:303–12. doi: 10.2147/DDDT.S156123
203. Majidzadeh H, Araj-Khodaei M, Ghaffari M, Torbati M, Ezzati Nazhad Dolatabadi J, Hamblin MR. Nano-based delivery systems for berberine: a modern anti-cancer herbal medicine. *Colloids Surf B, Biointer.* (2020) 194:111188. doi: 10.1016/j.colsurfb.2020.111188
204. Xin Y, Yin M, Zhao L, Meng F, Luo L. Recent progress on nanoparticle-based drug delivery systems for cancer therapy. *Cancer Biol Med.* (2017) 14:228–41. doi: 10.20892/j.issn.2095-3941.2017.0052
205. Bregoli L, Movia D, Gavigan-Imedio JD, Lysaght J, Reynolds J, Prina-Mello A. Nanomedicine applied to translational oncology: a future perspective on cancer treatment. *Nanomed Nanotechnol Biol Med.* (2016) 12:81–103. doi: 10.1016/j.nano.2015.08.006
206. Batra H, Pawar S, Bahl D. Curcumin in combination with anti-cancer drugs: a nanomedicine review. *Pharmacol Res.* (2019) 139:91–105. doi: 10.1016/j.phrs.2018.11.005

Conflict of Interest: The authors declare that the research was conducted in the absence of any commercial or financial relationships that could be construed as a potential conflict of interest.

Publisher's Note: All claims expressed in this article are solely those of the authors and do not necessarily represent those of their affiliated organizations, or those of the publisher, the editors and the reviewers. Any product that may be evaluated in this article, or claim that may be made by its manufacturer, is not guaranteed or endorsed by the publisher.

Copyright © 2022 Jiang, Jiang, Jiang and Sun. This is an open-access article distributed under the terms of the Creative Commons Attribution License (CC BY). The use, distribution or reproduction in other forums is permitted, provided the original author(s) and the copyright owner(s) are credited and that the original publication in this journal is cited, in accordance with accepted academic practice. No use, distribution or reproduction is permitted which does not comply with these terms.

frontiers | Frontiers in Surgery

ORIGINAL RESEARCH
published: 29 April 2022
doi: 10.3389/fsurg.2022.864593

Impact of Examined Lymph Node Count on Precise Staging and Long-term Survival After Neoadjuvant Therapy for Carcinoma of the Esophagus: A SEER Database Analysis

Tao Bao[1], *Lei Bao*[2] *and Wei Guo*[1]*

[1]Department of Thoracic Surgery, Daping Hospital, Army Medical University, Chongqing, China, [2]Computer Teaching and Research Office, Army Academy of Artillery and Air Defense, Hefei, China

OPEN ACCESS

Edited by:
Qi Liu,
Shanghai Cancer Center, Fudan University, China

Reviewed by:
Mohamed Kamel,
College of Medicine, Central Michigan University, United States
Matthew Fox,
University of Louisville, Louisville, United States

***Correspondence**:
Wei Guo
weiguodpyy@163.com

Speciality section:
This article was submitted to Surgical Oncology, a section of the journal Frontiers in Surgery

Received: 28 January 2022
Accepted: 11 April 2022
Published: 29 April 2022

Citation:
Bao T, Bao L and Guo W (2022) Impact of Examined Lymph Node Count on Precise Staging and Long-term Survival After Neoadjuvant Therapy for Carcinoma of the Esophagus: A SEER Database Analysis.
Front. Surg. 9:864593.
doi: 10.3389/fsurg.2022.864593

Purpose: To identify the optimal number of lymph nodes dissected during esophagectomy following neoadjuvant therapy for carcinoma of the esophagus by using the Surveillance, Epidemiology and End Results Registry (SEER) database.

Patients and Methods: Patients who underwent neoadjuvant Chemoradiotherapy (nCRT) plus esophagectomy with EC from 2001–2016 were analyzed retrospectively in the SEER database. We analyzed the correlation between the lymphadenectomy count and nodal stage migration and overall survival (OS) by using a binary logistic regression model and Cox proportional hazards regression. The curves of the odds ratios (ORs) of nodal stage migration and hazard ratios (HRs) of OS were smoothed using the LOWESS technique, and the cutoff points were determined by the Chow test. The OS curves were calculated with the Kaplan-Meier method.

Results: Among the 4,710 patients analyzed in the SEER database, a median of 12 lymph nodes (IQR, 7–19) were harvested. There was a significantly proportional increase in nodal stage migration (OR, 1.017; 95% CI, 1.011 to 1.023; $P < 0.001$) and serial improvements in OS among node-negative patients (HR, 0.983; 95% CI, 0.977 to 0.988; $P < 0.001$) with an increased ELN count after adjusting for the T stage. The corresponding cutoff point of the 16 ELNs was calculated for the OR of stage migration by the Chow test. For those with node-negative and node-positive diseases, no significant trend of survival benefit that favored a more extensive lymphadenectomy was demonstrated (HR, 1.001; 95% CI, 0.989 to 1.012; $P = 0.906$; and HR, 0.996; 95% CI, 0.985 to 1.006; $P = 0.405$, respectively).

Conclusion: On the basis of these results, we recommend that at least 16 ELNs be removed for accurate nodal staging as well as for obtaining a therapeutic benefit after nCRT for EC. Furthermore, once precise nodal staging has been achieved, patient survival does not improve with additional ELN dissection after nCRT, regardless of pathological nodal staging (negative or positive).

Keywords: esophageal carcinoma, esophagectomy, neoadjuvant treatment, lymphadenectomy, survival, SEER

INTRODUCTION

Esophageal cancer is ranked seventh in cancer incidence rates (572,000 cases) and sixth for cancer deaths (508,000 cases) worldwide, with a poor prognosis and high mortality rate (1). For patients with potentially curable localized tumors, surgical resection via esophagectomy with two- or three-field lymphadenectomy is still the primary form of treatment, with a 5-year survival rate of 23–41% (2). With regard to the count of the examined lymph nodes, the current National Comprehensive Cancer Network (NCCN) guidelines recommend that at least 15 examined lymph nodes (ELNs) should be achieved in patients undergoing esophagectomy without preoperative treatment for adequate nodal staging (3).

For patients with locally advanced disease, neoadjuvant chemotherapy or chemoradiotherapy prior to surgery has been revealed to be associated with a significant improvement in overall survival (4, 5). Concerning the extent of lymphadenectomy, several previous studies have demonstrated that high lymph node retrieval was associated with accurate staging and excellent outcomes (6–9). Kamel MK and colleagues (10) analyzed the National Cancer Database of 14,503 esophageal cancer patients and revealed that the cutoff number of resected LNs after induction chemoradiation that was associated with the highest survival benefit was 20 nodes. In contrast, another study conducted by Zhan et al. (11) demonstrated that 18, 19, and 28 ELNs could achieve accurate N0, N1, and N2 staging for patients with neoadjuvant therapy. However, the optimal count of ELN dissection post nCRT for carcinoma of the esophagus has not yet been well established. Moreover, the real value of extended lymphadenectomy following neoadjuvant treatment in EC is still elusive and debatable.

The purpose of the present study was to use the Surveillance, Epidemiology, and End Results (SEER) database to investigate the optimal count of ELN dissection and the real value of extended lymphadenectomy among patients who underwent neoadjuvant treatment followed by esophagectomy with lymphadenectomy at a population-based level.

MATERIALS AND METHODS

Patient Population

All cases were obtained from the National Cancer Institute's SEER database (http://www.seer.cancer.gov) with the use of SEER*Stat version 8.3.8 software: SEER 18 Regs Custom Data (with additional treatment field), Nov 2018 Sub (1975–2016 varying) database. Using the "Primary Site-labeled" variable, we chose tumor cases from the primary site of the esophagus diagnosed between 2001 and 2016. Only patients who received radiation (with or without chemotherapy) prior to surgery were included in this study. Patients with any of the following criteria were excluded: surgery alone, unknown regional nodes examined or positive, and unknown survival time. Information on the age at diagnosis, sex, race, size of the tumor, histologic type, grade, primary site, American Joint Committee on Cancer (AJCC) stage (6th ed or 7th ed), radiation sequence with surgery, chemotherapy recode (yes or no), regional nodes examined, regional nodes positive, distant metastasis, cause of death, and survival time was collected. Patients were staged according to the seventh edition of the TNM classification.

Approval for the study by the local institutional review board and written consent were not required because it was a public database of clinical research.

Statistical Analysis

Categorical data were compared using Pearson chi-square tests or Fisher's exact test, and continuous data were compared using ANOVA. A binary logistic regression model and Cox proportional hazards regression were carried out to determine the correlation between ELNs and stage migration (node negative versus node positive) and OS. The survival rate was calculated using the Kaplan-Meier method, and a log-rank test was used to assess the survival differences between groups. Statistical analyses were performed by using IBM SPSS 25.0 software (IBM, Inc.). P values of less than 0.05 were considered statistically significant.

In accordance with the procedures previously described by Liang et al. (12), the curves of the odds ratios (ORs; stage migration) of each ELN count compared with one ELN (as a reference) were smoothed using the locally weighted scatterplot smoother (LOWESS) technique with a bandwidth of 2/3 (default). The structural break points were determined by the Chow test, which were considered the threshold of clinical impact. Then, the curves of hazard ratios (HRs; OS) of more ELN counts compared with the threshold ELN count (as a reference) were smoothed to characterize the relationship between survival and the extended ELN yield. Both the LOWESS and Chow tests were performed by using Python version 3.7 software (Python Software Foundation, Delaware).

RESULTS

Patient Characteristics

A query of the SEER Database resulted in a total of 4,710 patients who received nCRT followed by esophagectomy that were performed for cancer between 2001 and 2016. The characteristics of the patients are described in **Table 1**. The study group consisted of 750 women and 3,960 men, with a median age of 61 years (range: 23–88) and a distinct preponderance of adenocarcinoma histology (adenocarcinoma: others, 3.5:1). The distribution of ELNs is shown in **Figure 1**, with a median number of harvested ELNs of 12 (range: 7–19). Furthermore, the median number of ELNs increased from 9 in 2001 to 2004 to 15 in 2013 to 2016.

Correlation between ELNs and Stage Migration

The median number of ELNs differed significantly within subgroups of the histologic type (AC: SCC: others: NOS, 14.3:13.2:13.9:10.7; $P = 0.01$), T stage (T0: T1: T2: T3: T4: TX,

TABLE 1 | Patient demographics.

Characteristic	Value
Number of patients	4,710
Age (years)	
Median (range)	61 (23–88)
Sex	
Male	3,960
Female	750
Race	
White	4,292
Black	233
Others	185
Tumor location	
Upper third	76
Middle third	534
Lower third	3,824
Esophagus, NOS	224
Histology	
AC	3,664
SCC	943
Others[a]	63
Carcinoma, NOS	40
Tumor cell differentiation	
Well differentiated	223
Moderately differentiated	1,980
Poorly differentiated	2,507
T stage	
T0	2
T1	471
T2	628
T3	2,343
T4	235
Unknown	1,031
N stage	
N0	2,918
N1	1,124
N2	480
N3	188
Median HLN count (IQR)	
Overall	12 (7–19)
No. regroup (2001–2004)	9 (5–14)
No. regroup (2005–2008)	10 (6–17)
No. regroup (2009–2012)	13 (7–20)
No. regroup (2013–2016)	15 (10–21)
Year of diagnosis	
2001–2004	718
2005–2008	1,027
2009–2012	1,288
2013–2016	1,677

AC, Adenocarcinoma; SCC, Squamous Cell Carcinoma; NOS, not otherwise specified.

[a]*Includes neuroendocrine carcinoma, small cell carcinoma, large cell neuroendocrine carcinoma.*

10.0:13.1:13.8:14.8:13.7:13.3; $P < 0.01$) and N stage (N0: N1: N2: N3, 13.4:13.9:16.0:21.7; $P < 0.01$). There was a significantly proportional increase in the N stage (from N0 to N1, N2, and N3), with an increasing ELN count after adjusting for the T stage (OR, 1.017; 95% CI, 1.011 to 1.023; $P < 0.001$; **Table 2**). However, after stratification by histologic type, only a consistent trend was observed in patients with AC with an increasing ELN count (OR, 1.021; 95% CI, 1.014 to 1.028; $P < 0.001$).

Correlation between ELNs and OS

After adjusting for the T stage, a greater number of ELNs was significantly associated with a better OS among patients with node-negative (N0) disease (HR, 0.983; 95% CI, 0.977 to 0.988; $P < 0.001$) and patients with node-positive (N1, N2, and N3) disease (HR, 0.985; 95% CI, 0.979 to 0.992; $P < 0.001$). However, after stratification by histologic type, only a consistent trend was observed in patients with AC, with the exception of node-negative patients with SCC (HR, 0.986; 95% CI, 0.975 to 0.997; $P < 0.001$; **Table 2**).

Cut-Point Analysis for Nodal Stage Migration and Validation

As shown in **Figure 2**, the fitting curves for the OR of nodal stage migration were smoothed using the LOWESS technique. The corresponding cutoff point of 16 ELNs was calculated for the OR of stage migration by the Chow test.

At the time of analysis, the median follow-up was 62.0 months. For node-negative patients, the five-year survival rates and median survival time were 59.2% and 72.0 months (95% confidence interval, 61.5 to 79.5 months), respectively, among patients with ELN count ≥16 and 52.9% and 48.6 months (95% confidence interval, 40.0 to 52.5 months), respectively, among those with ELN count <16 ($P < 0.001$; **Figure 3**). With regard to node-positive patients, the five-year survival rates and median survival time were 32.2% and 29.0 months (95% confidence interval, 25.7 to 32.2 months), respectively, among patients with ELN count ≥16 and 24.2% and 21.0 months (95% confidence interval, 18.8 to 23.1 months), respectively, among those with ELN count < 16 ($P < 0.001$; **Figure 4**).

Impact of Extended Lymphadenectomy

For those with node-negative and node-positive diseases, the curves of the hazard ratios (HRs; OS) of each ELN count (>16 nodes) compared with 16 ELNs (as a reference) were smoothed using the LOWESS technique and are shown in **Figure 5** and **Figure 6**, respectively; however, they failed to demonstrate a significant trend of survival benefit that favored a more extensive lymphadenectomy (HR, 1.001; 95% CI, 0.989 to 1.012; $P = 0.906$; and HR, 0.996; 95% CI, 0.985 to 1.006; $P = 0.405$, respectively).

DISCUSSION

The importance of the number of ELNs during esophagectomy alone for staging accuracy and long-term survival has been well documented and acknowledged (13–18). Accordingly, the NCCN guidelines recommend that at least 15 lymph nodes (LNs) should be removed in patients undergoing

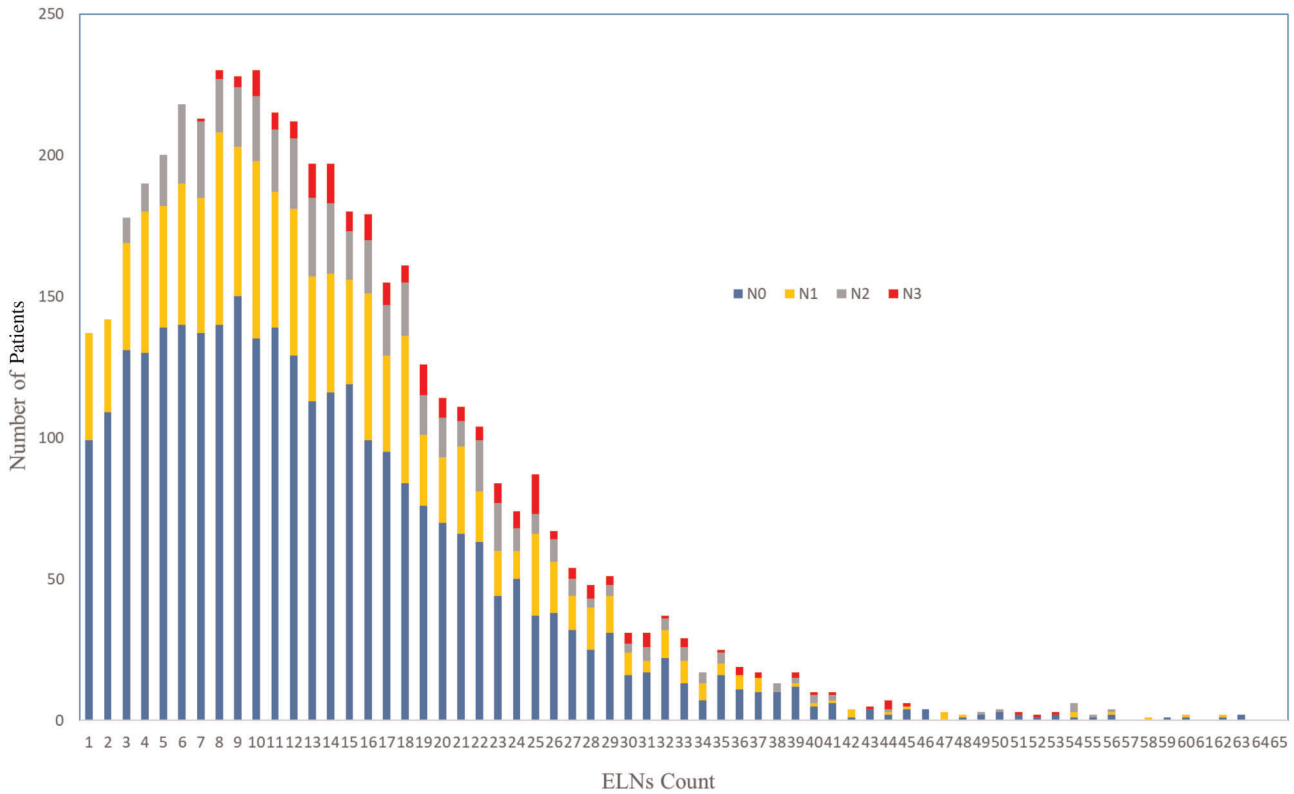

FIGURE 1 | Distribution of examined lymph nodes.

TABLE 2 | Number of ELNs (as a continuous variable) and Stage Migration and OS, Stratified by Histologic Subgroups, Adjusted for T stage.

Histology	Stage Migration		OS (Node-Negative)		OS (Node-Positive)	
	Sig.	OR (95% CI)	Sig.	HR (95% CI)	Sig.	HR (95% CI)
Overall	<0.001	1.017 (1.011–1.023)	<0.001	0.983 (0.977–0.988)	<0.001	0.986 (0.981–0.992)
AC	<0.001	1.021 (1.014–1.028)	<0.001	0.981 (0.974–0.988)	<0.001	0.985 (0.979–0.992)
SCC	0.649	1.003 (0.989–1.018)	0.011	0.986 (0.975–0.997)	0.925	0.999 (0.984–1.015)
Other[a]	0.926	0.997 (0.945–1.052)	0.773	0.993 (0.944–1.044)	0.056	0.941 (0.884–1.002)

AC, Adenocarcinoma; CI, Confidence Interval; HR, Hazard Ratio; OS, Overall Survival; OR, Odds Ratio; SCC, Squamous Cell Carcinoma.
[a]*Includes neuroendocrine carcinoma, small cell carcinoma, large cell neuroendocrine carcinoma and NOS.*

esophagectomy without preoperative treatment for adequate nodal staging (3). However, the impact of neoadjuvant treatment on the dissemination and the pattern of lymph node distribution has not been well established. Moreover, the potential effect of extensive lymphadenectomy on survival after surgery following neoadjuvant therapy remains controversial. The optimum lymphadenectomy during esophagectomy in patients after receiving neoadjuvant treatment has not yet been well identified. The study by Castoro and associates (19) on 402 patients with cancer of the esophagus or esophagogastric junction demonstrated that not only did the frequency of lymph node metastases decrease after neoadjuvant chemoradiotherapy (nCRT) but also the nodal localization and pattern were significantly modified. Moreover, in the Dutch CROSS trial, the median (interquartile range) number of resected nodes for patients who underwent surgery alone and received multimodality treatment was 18 (12–27) and 14 (9–21), with 2 (1–6) and 0 (0–1) resected positive nodes, respectively (20). Similarly, randomized clinical trials published in the New England Journal of Medicine have also revealed that there was a significant trend toward less advanced nodal disease in the perioperative chemotherapy group than in the surgery group (84.4% vs. 70.5%, $P = 0.01$) (4). Therefore, the question arises whether suboptimal lymphadenectomy affects the accuracy of nodal stage or long-term outcome after nCRT in patients with EC.

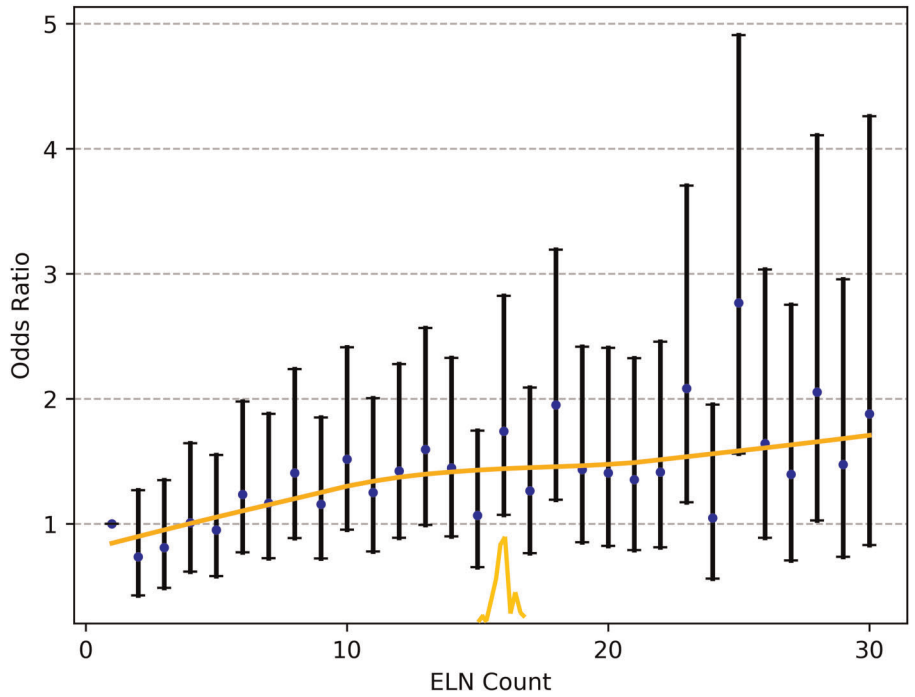

FIGURE 2 | The fitting curves for the OR of nodal stage migration were smoothed using the LOWESS technique, and the corresponding cutoff point of the ELNs was calculated by the Chow test. ELN, examined lymph node. OR, odds ratio.

A limited number of LNs harvested in EC patients after nCRT may lead to inaccurate nodal staging, particularly with regard to those with nodal upstaging. As Meguid et al. (21) reported, almost seventy percent of EC patients are partial responders and nonresponders to nCRT. In the current study, the US SEER Database was analyzed and the data clearly indicated that a larger number of LNs dissection was correlated with a higher proportion of more advanced nodal stage cases in SCC and AC post neoadjuvant treatment. Furthermore, our results suggested that at least 16 nodes should be removed to avoid nodal staging migration during esophagectomy for patients undergoing nCRT, which is mainly consistent with the NCCN guideline recommendations for those undergoing surgery alone (15 ELNs). Similarly, Stiles et al. (7) revealed that optimal lymphadenectomy, as defined by the WECC, may also be applicable to cases of esophagectomy following neoadjuvant therapy, particularly those who were not downstaged by pathological tumor depth classification and those with persistent nodal metastases.

A second question concerning long-term effects is whether overall survival may be improved by extended lymphadenectomy for patients treated with nCRT. Some investigators believe that resecting more LNs is helpful for accurate nodal staging and decreasing the chance of undiscovered positive LNs. For patients with node-positive disease (not declared as node-negative disease due to fewer ELNs), adjuvant treatment after surgery could improve the OS. In addition, extended nodal resection would benefit the clearance of micrometastases and residual lesions after neoadjuvant therapy and reduce the risk of local recurrence. For example, Solomon and colleagues (22) analyzed the SEER database of 4,224 patients and showed that there is a cooperative survival benefit for neoadjuvant radiation and adequate lymphadenectomy (ELNs $\geq$18) in patients with node-positive esophageal adenocarcinoma. Furthermore, a meta-analysis conducted by Visser et al. (8) demonstrated a survival benefit of high lymph node yield on overall survival (HR = 0.82; 95% CI = 0.73–0.92; $P < 0.01$). In contrast, however, in the present study, our results showed that once precise nodal staging (>16 nodes) had been achieved, patient survival did not improve with additional LNs dissection after nCRT, regardless of nodal stage (negative or positive). As stated by, the total number of ELNs was significantly associated with survival for patients in the surgery-alone arm ($P = 0.007$) but not in the nCRT arm ($P = 0.98$). Similarly, Shridhar et al. (23) noted that the number of LNs harvested during esophagectomy after nCRT does not impact OS or disease-free survival (DFS). Furthermore, Noordman BJ et al. (24) revealed that compared to surgery alone, the addition of nCRT may reduce the need for extended lymphadenectomy to improve long-term survival in patients with esophageal adenocarcinoma. This difference in effect of lymphadenectomy might be partially explained by the sterilization of micrometastases after nCRT and high local tumor control rate of radiotherapy on the regional lymph nodes. It has been

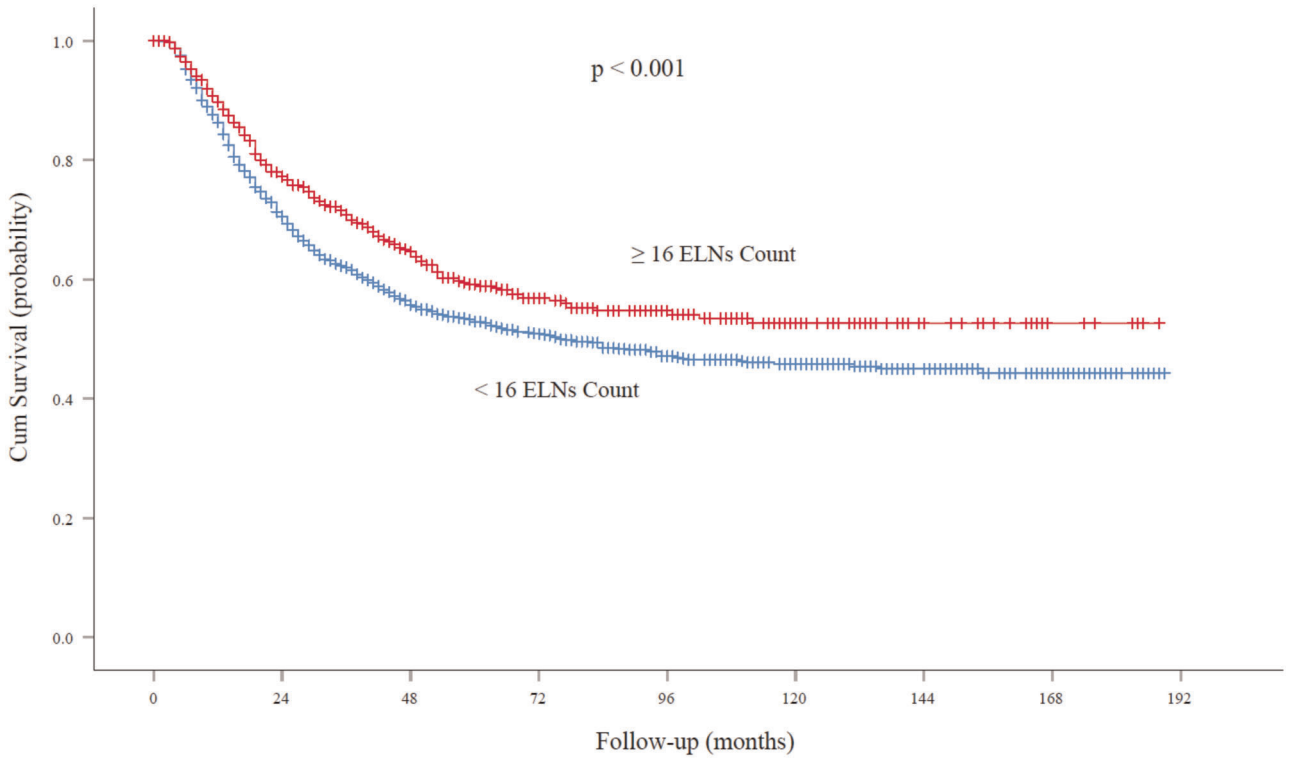

FIGURE 3 | Overall survival rates among patients with node-negative EC at the cutoff point of 16 ELNs. ELN, examined lymph node. EC, esophageal cancer.

reported that the pathological complete response rate was 19–40% in neoadjuvant CRT (25, 26). Moreover, several previous studies (24, 25) revealed that the number of resected LNs and the number of resected positive LNs were significantly decreased in patients treated with nCRT than in those treated with surgery alone, suggesting that the clinical importance of extended lymphadenectomy to improve the locoregional control rate may differ between surgery after nCRT and surgery alone. In addition, As Patti et al. (27) demonstrated, it is not the extent of lymphadenectomy that dictates outcomes but rather the tumor biology and the stage of the tumor during the surgery. In addition, a more extensive lymphadenectomy does have the disadvantage of greater surgical morbidity, which confers a large negative impact on survival after esophagectomy for cancer (8, 28). Further studies with larger study populations or other methods are required to better elucidate the role of extended lymphadenectomy following neoadjuvant treatment.

Finally, it should be noted that there are several other factors that may influence the long-term outcomes in patients undergoing lymphadenectomy post nCRT, including ELN location and ratio and extracapsular ELN involvement. In detail, a study by Phillips (6) concluded that omitting lymphatic dissection of hepatic, celiac, and splenic nodes may lead to a very limited number of extra cancer-related deaths, and thus, the extent of lymphadenectomy post neoadjuvant chemotherapy must be correlated with the node location. With regard to the ELN ratio, Mariette and colleagues (29) demonstrated that the ratio between metastatic and examined lymph nodes is an important predictor of a poor prognosis, especially for inadequately staged EC patients following nCRT. In addition, D'Journo et al. (30) found that extension of tumor cells through the nodal capsule into the fatty tissue seems to be an independent negative prognostic factor affecting survival in patients with locally advanced EC treated with nCRT and surgery.

This study has several limitations. First, it was retrospective, and some important patient clinicopathological features were rather limited, such as the variations in radiation doses and range over the study period, the usage of different combinations of chemotherapeutic agents, various therapeutic modalities given following surgery, various degrees of pathologic tumor response to neoadjuvant therapy, the incidence of postoperative complications, the lack of standardized staging due to missing data of clinical TNM stage, and resection margin status (R0, R1 or R2), all of which have the potential to modulate the treatment effect. Additionally, owing to the limitations of the database, we did not further associate the number of ELNs with their locations (cervical, mediastinal or abdominal), surgical approach (transthoracic or transhiatal), or surgeon/hospital esophagectomy volume, which might affect the ELN status

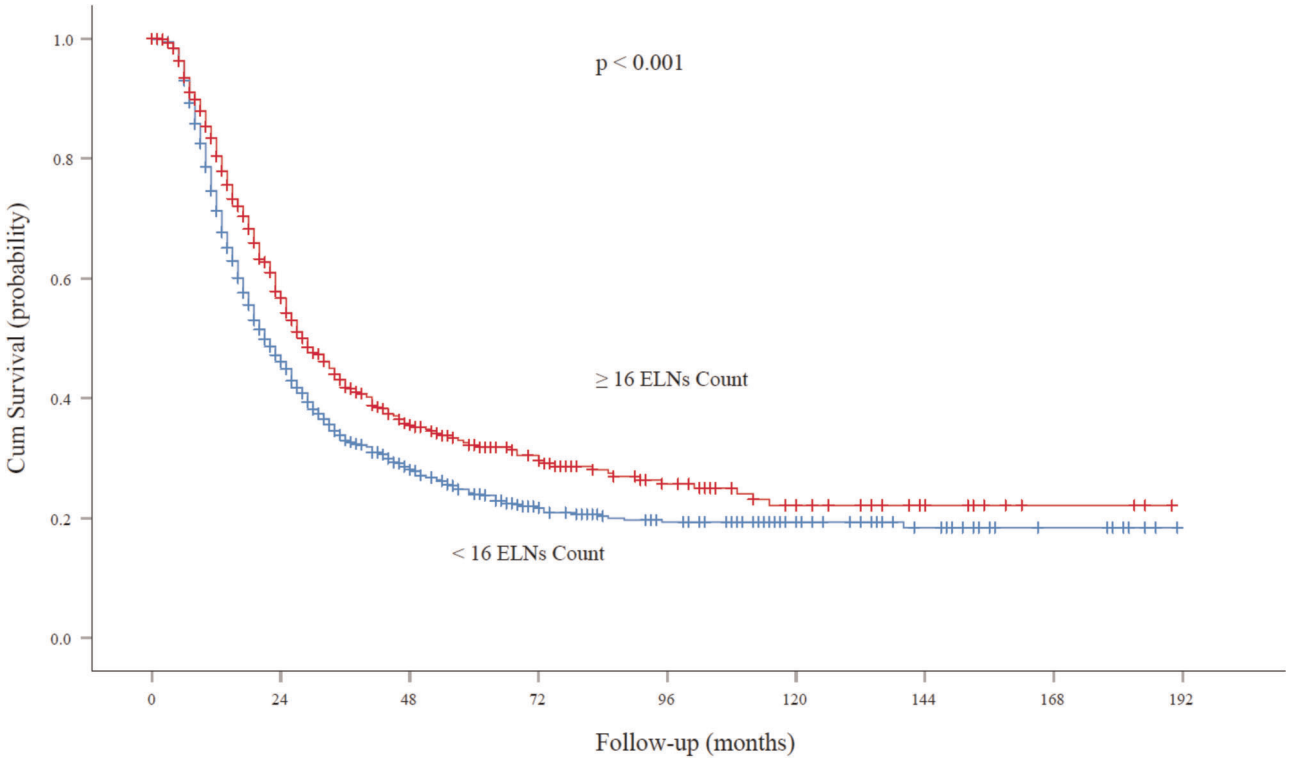

FIGURE 4 | Overall survival rates among patients with node-positive EC at the cutoff point of 16 ELNs. ELN, examined lymph node. EC, esophageal cancer.

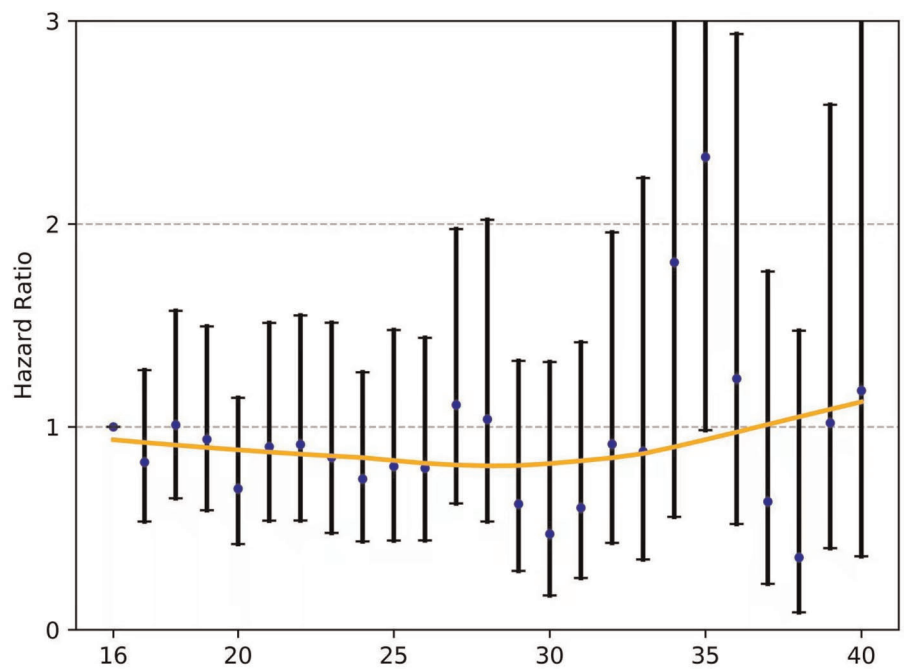

FIGURE 5 | The fitting curves for the HR of each ELN count (>16 nodes) compared with 16 ELNs (as a reference) among patients with node-negative EC were smoothed using the LOWESS technique. ELN, examined lymph node. EC, esophageal cancer. OR, odds ratio.

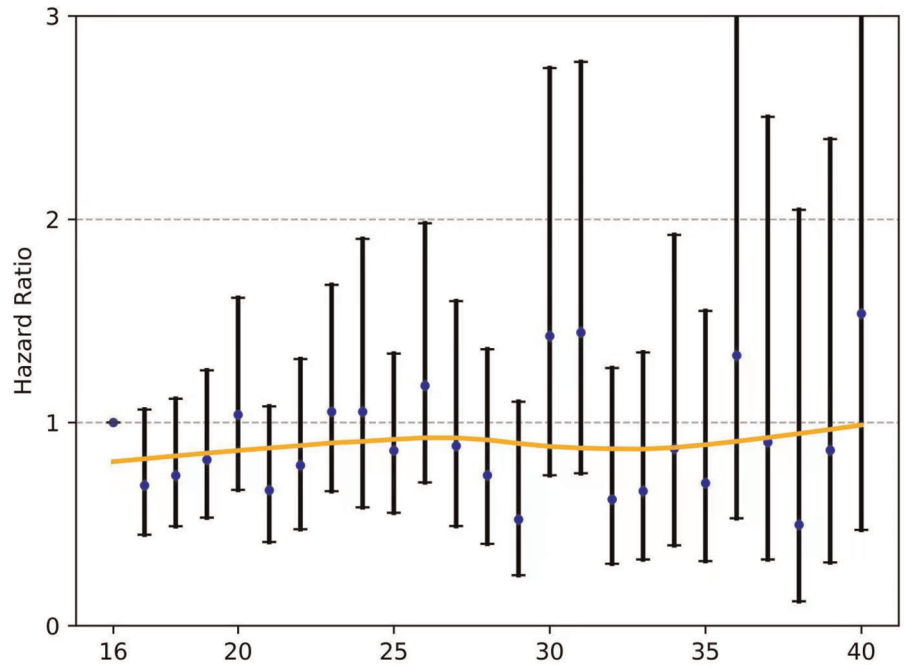

FIGURE 6 | The fitting curves for the HR of each ELN count (>16 nodes) compared with 16 ELNs (as a reference) among patients with node-positive EC were smoothed using the LOWESS technique. ELN, examined lymph node. EC, esophageal cancer. OR, odds ratio.

and long-term outcomes as previously reported. We suggest a future prospective randomized trial with a larger study population or other methods to validate our results.

In conclusion, our data suggest that at least 16 ELNs should be achieved for accurate nodal staging as well as for obtaining a therapeutic benefit for patients undergoing nCRT. Furthermore, once precise nodal staging has been achieved, patient survival does not improve with additional LNs dissection after nCRT, regardless of the pathological nodal staging (negative or positive). These findings have important clinical implications and should be considered when performing esophagectomy for patients post nCRT.

DATA AVAILABILITY STATEMENT

The raw data supporting the conclusions of this article will be made available by the authors, without undue reservation.

ETHICS STATEMENT

Approval for the study by the local institutional review board and written consent were not required because it was a public database of clinical research that only contains de-identified patient data.

AUTHOR CONTRIBUTIONS

TB and WG conceived and designed the experiments. TB and LB collected the data and draw the graphs. LB contributed analysis tools. LB and TB analyzed the data. TB wrote the manuscript. TB and LB contributed equally to this work and are co-first authors.

ACKNOWLEDGMENTS

We acknowledged the SEER database for the provided data for the research.

REFERENCES

1. Arnold M, Abnet CC, Neale RE, Vignat J, Giovannucci EL, McGlynn KA, et al. Global burden of 5 major types of gastrointestinal cancer. *Gastroenterology*. (2020) 159(1):335–49.e15. doi: 10.1053/j.gastro.2020.02.068
2. Short MW, Burgers KG, Fry VT. Esophageal cancer. *Am Fam Physician*. (2017) 95(1):22–8.
3. NCCN Clinical Practice Guidelines in Oncology- Esophageal and Esophagogastric Junction Cancers (2018 Version I). Available at: http://www.nccn.org (Accessed March 16, 2018).
4. Cunningham D, Allum WH, Stenning SP, Thompson JN, Van de Velde CJ, Nicolson M, et al. Perioperative chemotherapy versus surgery alone for resectable gastroesophageal cancer. *N Engl J Med*. (2006) 355(1):11–20. doi: 10.1056/NEJMoa055531

5. van Hagen P, Hulshof MC, van Lanschot JJ, Steyerberg EW, van Berge Henegouwen MI, Wijnhoven BP, et al. Preoperative chemoradiotherapy for esophageal or junctional cancer. *N Engl J Med*. (2012) 366(22):2074–84. doi: 10.1056/NEJMoa1112088
6. Phillips AW, Lagarde SM, Navidi M, Disep B, Griffin SM. Impact of extent of lymphadenectomy on survival, post neoadjuvant chemotherapy and transthoracic esophagectomy. *Ann Surg*. (2017) 265(4):750–6. doi: 10.1097/SLA.0000000000001737
7. Stiles BM, Nasar A, Mirza FA, Lee PC, Paul S, Port JL, et al. Worldwide Oesophageal Cancer Collaboration guidelines for lymphadenectomy predict survival following neoadjuvant therapy. *Eur J Cardiothorac Surg*. (2012) 42 (4):659–64. doi: 10.1093/ejcts/ezs105
8. Visser E, Markar SR, Ruurda JP, Hanna GB, van Hillegersberg R. Prognostic value of lymph node yield on overall survival in esophageal cancer patients: a systematic review and meta-analysis. *Ann Surg*. (2019) 269(2):261–8. doi: 10.1097/SLA.0000000000002824
9. Markar SR, Noordman BJ, Mackenzie H, Findlay JM, Boshier PR, Ni M, et al. Multimodality treatment for esophageal adenocarcinoma: multi-center propensity-score matched study. *Ann Oncol*. (2017) 28(3):519–27. doi: 10.1093/annonc/mdw560
10. Kamel MK, Harrison S, Lee B, Port JL, Stiles BM, Altorki NK. Extended lymphadenectomy improves survival after induction chemoradiation for esophageal cancer: a propensity matched analysis of the national cancer database. *Ann Surg*. (2021). doi: 10.1097/SLA.0000000000005197. Epub ahead of print.
11. Zhan C, Shi Y, Jiang W, Sun F, Li M, Lu T, et al. How many lymph nodes should be dissected in esophagectomy with or without neoadjuvant therapy to get accurate staging? *Dis Esophagus*. (2020) 33(1):doz009. doi: 10.1093/dote/doz009
12. Liang W, He J, Shen Y, Shen J, He Q, Zhang J, et al. Impact of examined lymph node count on precise staging and long-term survival of resected non-small-cell lung cancer: a population study of the US SEER database and a chinese multi-institutional registry. *J Clin Oncol*. (2017) 35 (11):1162–70. doi: 10.1200/JCO.2016.67.5140
13. Rizk NP, Ishwaran H, Rice TW, Chen LQ, Schipper PH, Kesler KA, et al. Optimum lymphadenectomy for esophageal cancer. *Ann Surg*. (2010) 251 (1):46–50. doi: 10.1097/SLA.0b013e3181b2f6ee
14. Rizk N, Venkatraman E, Park B, Flores R, Bains MS, et al. The prognostic importance of the number of involved lymph nodes in esophageal cancer: implications for revisions of the American jJoint Committee on Cancer staging system. *J Thorac Cardiovasc Surg*. (2006) 132(6):1374–81. doi: 10.1016/j.jtcvs.2006.07.039
15. Greenstein AJ, Litle VR, Swanson SJ, Divino CM, Packer S, Wisnivesky JP. Effect of the number of lymph nodes sampled on postoperative survival of lymph node-negative esophageal cancer. *Cancer*. (2008) 112(6):1239–46. doi: 10.1002/cncr.23309
16. Schwarz RE, Smith DD. Clinical impact of lymphadenectomy extent in resectable esophageal cancer. *J Gastrointest Surg*. (2007) 11(11):1384–93. doi: 10.1007/s11605-007-0264-2
17. Peyre CG, Hagen JA, DeMeester SR, Altorki NK, Ancona E, Griffin SM, et al. The number of lymph nodes removed predicts survival in esophageal cancer: an international study on the impact of extent of surgical resection. *Ann Surg*. (2008) 248(4):549–56. doi: 10.1097/SLA.0b013e318188c474
18. Hu Y, Hu C, Zhang H, Ping Y, Chen LQ. How does the number of resected lymph nodes influence TNM staging and prognosis for esophageal carcinoma? *Ann Surg Oncol*. (2010) 17(3):784–90. doi: 10.1245/s10434-009-0818-5
19. Castoro C, Scarpa M, Cagol M, Ruol A, Cavallin F, Alfieri R, et al. Nodal metastasis from locally advanced esophageal cancer: how neoadjuvant therapy modifies their frequency and distribution. *Ann Surg Oncol*. (2011) 18(13):3743–54. doi: 10.1245/s10434-011-1753-9
20. Koen Talsma A, Shapiro J, Looman CW, van Hagen P, Steyerberg EW, van der Gaast A, et al. Lymph node retrieval during esophagectomy with and without neoadjuvant chemoradiotherapy: prognostic and therapeutic impact on survival. *Ann Surg*. (2014) 260(5): 786–92; discussion 792-3. doi: 10.1097/SLA.0000000000000965
21. Meguid RA, Hooker CM, Taylor JT, Kleinberg LR, Cattaneo SM 2nd, Sussman MS, et al. Recurrence after neoadjuvant chemoradiation and surgery for esophageal cancer: does the pattern of recurrence differ for patients with complete response and those with partial or no response? *J Thorac Cardiovasc Surg*. (2009) 138(6):1309–17. doi: 10.1016/j.jtcvs.2009.07.069
22. Solomon N, Zhuge Y, Cheung M, Franceschi D, Koniaris LG. The roles of neoadjuvant radiotherapy and lymphadenectomy in the treatment of esophageal adenocarcinoma. *Ann Surg Oncol*. (2010) 17(3):791–803. doi: 10.1245/s10434-009-0819-4
23. Shridhar R, Hoffe SE, Almhanna K, Weber JM, Chuong MD, Karl RC, et al. Lymph node harvest in esophageal cancer after neoadjuvant chemoradiotherapy. *Ann Surg Oncol*. (2013) 20(9): 3038–43. doi: 10.1245/s10434-013-2988-4
24. Noordman BJ, van Klaveren D, van Berge Henegouwen MI, Wijnhoven BPL, Gisbertz SS, Lagarde SM, et al. Impact of surgical approach on long-term survival in esophageal adenocarcinoma patients with or without neoadjuvant chemoradiotherapy. *Ann Surg*. (2018) 267(5):892–7. doi: 10.1097/SLA.0000000000002240
25. Robb WB, Dahan L, Mornex F, Maillard E, Thomas PA, Meunier B, et al. Impact of neoadjuvant chemoradiation on lymph node status in esophageal cancer: post hoc analysis of a randomized controlled trial. *Ann Surg*. (2015) 261(5):902–8. doi: 10.1097/SLA.0000000000000991
26. Visser E, van Rossum PSN, Ruurda JP, van Hillegersberg R. Impact of lymph node yield on overall survival in patients treated with neoadjuvant chemoradiotherapy followed by esophagectomy for cancer: a population-based cohort study in the Netherlands. *Ann Surg*. (2017) 266:863–9. doi: 10.1097/SLA.0000000000002389
27. Patti MG. Survival after lymphadenectomy in patients with esophageal cancer: a controversial issue. *JAMA Surg*. (2016) 151(1):40. doi: 10.1001/jamasurg.2015.2599
28. Booka E, Takeuchi H, Nishi T, Matsuda S, Kaburagi T, Fukuda K, et al. The impact of postoperative complications on survivals after esophagectomy for esophageal cancer. *Medicine (Baltimore)*. (2015) 94(33):e1369. doi: 10.1097/MD.0000000000001369
29. Mariette C, Piessen G, Briez N, Triboulet JP. The number of metastatic lymph nodes and the ratio between metastatic and examined lymph nodes are independent prognostic factors in esophageal cancer regardless of neoadjuvant chemoradiation or lymphadenectomy extent. *Ann Surg*. (2008) 247(2): 365–71. doi: 10.1097/SLA.0b013e31815aaadf
30. D'Journo XB, Avaro JP, Michelet P, Trousse D, Tasei AM, Dahan L, et al. Extracapsular lymph node involvement is a negative prognostic factor after neoadjuvant chemoradiotherapy in locally advanced esophageal cancer. *J Thorac Oncol*. (2009) 4(4):534–9. doi: 10.1097/JTO.0b013e31819c862d

Conflict of Interest: The authors declare that the research was conducted in the absence of any commercial or financial relationships that could be construed as a potential conflict of interest.

Publisher's Note: All claims expressed in this article are solely those of the authors and do not necessarily represent those of their affiliated organizations, or those of the publisher, the editors and the reviewers. Any product that may be evaluated in this article, or claim that may be made by its manufacturer, is not guaranteed or endorsed by the publisher.

Copyright © 2022 Guo, Bao and Bao. This is an open-access article distributed under the terms of the Creative Commons Attribution License (CC BY). The use, distribution or reproduction in other forums is permitted, provided the original author(s) and the copyright owner(s) are credited and that the original publication in this journal is cited, in accordance with accepted academic practice. No use, distribution or reproduction is permitted which does not comply with these terms.

frontiers | Frontiers in Oncology

ORIGINAL RESEARCH
published: 24 May 2022
doi: 10.3389/fonc.2022.876668

Splenic Volume, an Easy-To-Use Predictor of HCC Late Recurrence for HCC Patients After Hepatectomy

Tongdi Fang[1,2], *Guo Long*[1,2], *Xingyu Mi*[1,2], *Wenxin Su*[1,2], *Lei Mo*[1,2] *and Ledu Zhou*[1,2*]

[1] Department of General Surgery, The Xiangya Hospital of Central South University, Changsha, China, [2] National Clinical Research Center for Geriatric Disorders, Xiangya Hospital, Central South University, Changsha, China

Purpose: The high recurrence rate of hepatocellular carcinoma (HCC) has a poor impact on the quality of life and survival time of patients. Especially for late recurrence, poor data are available in analysis. We aim to evaluate whether the splenic volume (SV) measured from preoperative CT images could predict late recurrence in HCC patients after hepatectomy.

Patients and Methods: A cohort of 300 HCC patients hospitalized at Xiangya Hospital of Central South University between January 2015 and June 2018 was retrospectively analyzed. The SV was calculated by using automated volumetry software from preoperative CT images. A total of 300 HCC patients were separated into the early recurrence cohort (n=167), the late recurrence cohort (n=39), and the no recurrence cohort (n=94) according to whether there is a recurrence and the recurrence time. Univariate and multivariate Cox analyses were performed to identify the independent risk factors of both early and late recurrence.

Results: AFP, Microvascular invasion (MVI), satellitosis, and BCLC staging were independent risk factors of HCC early recurrence. Splenic volume (HR=1.003, 95% CI:1.001-1.005, P<0.001) was the only predictor of HCC late recurrence. Based on X-tile software, 133 non-early recurrence patients were divided into two groups according to SV: low SV (<165ml, n=45) and high SV (≥165ml, n= 88). The low SV group had a significantly better RFS compared with the high SV group (P=0.015). Nomogram was built on the base of SV to get the probability of 3-year RFS, 4-year RFS, and 5-year RFS.

Conclusion: In our study, we drew a conclusion that splenic volume was the only predictor of HCC late recurrence because of its association with portal hypertension and liver cirrhosis. High splenic volume often indicated a worse recurrence.

Keywords: splenic volume (SV), hepatocellular carcinoma, recurrence, nomogram, liver cirrhosis

OPEN ACCESS

Edited by:
Qi Liu,
Fudan University, China

Reviewed by:
Alessandro Vitale,
University Hospital of Padua, Italy
Kristin Sheffield,
Eli Lilly, United States
Matteo Donadon,
Humanitas University, Italy

***Correspondence:**
Ledu Zhou
zhould@csu.edu.cn

Specialty section:
This article was submitted to Gastrointestinal Cancers: Hepato Pancreatic Biliary Cancers, a section of the journal Frontiers in Oncology

Received: *15 February 2022*
Accepted: *25 April 2022*
Published: *24 May 2022*

Citation:
Fang T, Long G, Mi X, Su W, Mo L and Zhou L (2022) Splenic Volume, an Easy-To-Use Predictor of HCC Late Recurrence for HCC Patients After Hepatectomy. Front. Oncol. 12:876668. doi: 10.3389/fonc.2022.876668

INTRODUCTION

In the past few decades, hepatocellular carcinoma (HCC) has risen to become the sixth most aggressive malignancy and the fourth-leading cause of cancer-related deaths worldwide (1). Among the various therapeutic approaches, hepatic resection (HR) is presently considered one of the most curative modalities for HCC patients (2). With the continuous improvement of perioperative

management and operation techniques over the past few years, although the overall survival time of the patient has been prolonged, the recurrence of HCC after hepatectomy remains high (3). As reported by the literature, the cumulative 5-year recurrence rate for HCC patients after hepatic resection was approximately 80% in most centers (4, 5).

The potential mechanism of postoperative recurrence could be an intrahepatic relapse of the primary tumor (considered as early recurrence) or the emergence of *de novo* multicentric tumor (stated as late recurrence). Therefore, according to the time to postoperative recurrence, we artificially divided the recurrence of liver cancer into early recurrence (recurrence within 24 months) and late recurrence (recurrence over 24 months) (6–9). Numerous recent studies have shown that early recurrence is related to biological characteristics of tumors such as tumor size, tumor numbers, tumor differentiation, microscopic vascular invasion (MVI), and satellitosis (10–12). There is a lack of data to predict late recurrence. Scholars tend to accept the view that late recurrence is commonly associated with the intrinsic liver condition, like liver cirrhosis (13, 14).

Liver cirrhosis is closely related to portal hypertension (PH) and PH could influence the natural history of the underlying liver condition in return (15). We couldn't accurately assess PH clinically without some invasive methods. The spleen is a sensitive organ to PH alteration and responds promptly in the form of splenomegaly. Moreover, splenomegaly can contribute to the progression of PH by increasing splenic blood flow (16). However, the relationship between splenomegaly and liver cirrhosis or PH is controversial. This is partly because the spleen is irregular in shape and the spleen size is measured by longitudinal spleen axis on ultrasound or CT images, which makes it not as accurate as three-dimensional measurement.

Recently, liver computed tomography (CT) volumetry has been used to help assess liver volume in clinical practice (17, 18). Especially, when considering the future liver remnant (FLR) volume, we can use three-dimensional CT reconstruction to accurately represent the remaining liver volume (19). Similarly, with the same use of three-dimensional CT volumetry software, the splenic volume could be feasible to obtain. Some studies have shown that spleen volume measured by CT is a dependable indicator for liver fibrosis, cirrhosis, and portal hypertension (20). As far as we know, the role of splenic volume as a predictor of HCC late recurrence has never been explored. Therefore, this study aimed to assess whether the SV measured by 3D reconstruction could predict HCC late recurrence after hepatectomy.

PATIENTS AND METHODS

Patients

A total of 320 patients meeting the inclusion criteria had undergone curative liver resection between January 2015 and June 2018 at XiangYa Hospital. Considering the exclusion criteria, we excluded 11 patients due to recurrent tumors and nine patients were excluded because of receiving anticancer treatments prior to hepatectomy. None of the patients had splenomegaly due to other causes such as hematological diseases. At last, our study included 300 HCC patients who underwent curative liver resection between January 2015 and June 2018 at XiangYa Hospital, Central South University.

Before hepatectomy, the splenic volume was measured using three-dimensional CT reconstruction for each patient. The study was under the permission of the Ethics Committee of the Xiangya Hospital and complied with the Declaration of Helsinki. Because of the retrospective nature of the study, the ethics committee did not require patient consent to review their medical data. The selection of HCC patients for hepatectomy in our study was based on Barcelona Clinic Liver Cancer (BCLC) criteria.

The inclusion criteria included: 1) diagnosis of HCC; 2) no simultaneous malignancies; 3) R0 resection confirmed by the postoperative pathological examination; 4) patients underwent a CT examination before surgery; 5) aged above 18 years old.

The exclusion criteria included: 1) patients were considered to have recurrent tumors; 2) patient received radiofrequency ablation (RA), transarterial chemoembolization (TACE), or other anticancer treatments before hepatectomy; 3) splenomegaly from other causes, like hematological diseases.

Follow-up and Endpoints

Routine examinations were required for all patients every 2 to 3 months after surgery in the first 2 years, including liver function tests, tumor markers, and liver ultrasound. A confirmatory computed tomography (CT) and/or magnetic resonance imaging (MRI) scan were performed if necessary. After 2 years of follow-up, we reduced the frequency of follow-up visits to every 3 to 6 months. The endpoint of the study was recurrence-free survival (RFS), which was measured as the time from the end of surgery to recurrence or metastasis (including death due to recurrence or metastasis), or the last follow-up date. The patients with a recurrence or metastasis within 24 months after hepatectomy were allocated into the early recurrence cohort, and those with a relapse or metastasis over 24 months were put into the late recurrence cohort. The patients without relapse or metastasis until the last follow-up date were allocated into the no recurrence cohort. Patients followed up for 2 years at least or having recurrence after surgery were collected. The follow-up endpoint was July 1, 2020.

Splenic Volume Calculation

All patients received an abdominal CT scan before surgery. By using a medical image analysis procedure (Myrian®; Intrasense S.A.S., Montpellier, France), a three-dimensional reconstruction of the spleen was performed for automated volumetry, and the results were modified by manual tracking of splenic margin following automated reconstruction by two experienced observers. The final SV was calculated after volumetry of the spleen (example shown in **Figure 1**).

Clinicopathologic Variables

The following factors were analyzed: age (time of surgery), gender, preoperative serum examination including routine

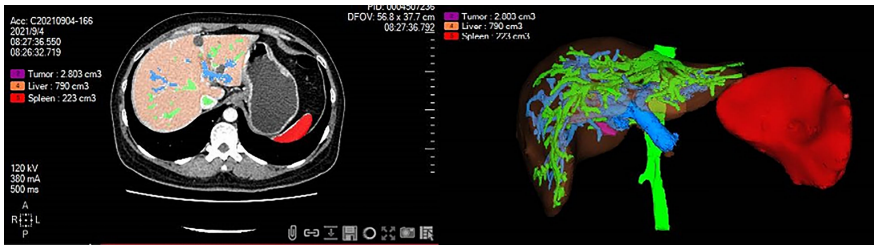

FIGURE 1 | Three-dimensional reconstruction of the spleen was performed for automated volumetry by using medical image analysis software. The splenic volume was calculated after volumetry of the spleen. Red color, spleen; Purple color, tumor; Orange color, liver; Green color, hepatic vein; Blue color, portal vein.

blood, liver function, coagulation function, serum alpha-fetoprotein (AFP), hepatitis B surface antigen (HBsAg), spenic volume, and postoperative clinicopathological data including tumor size, tumor number, tumor differentiation, satellitosis, liver cirrhosis, microvascular invasion (MVI), and tumor stage (BCLC staging).

Statistical Analysis

We collected patients who were followed up for 2 years to identify the independent factors associated with early recurrence. Then, those without relapse within 2 years were reanalyzed to recognize the independent variables related to late recurrence.

Continuous variables were expressed as mean ± standard deviation and analyzed using t-tests. Categorical variables were shown as frequency (percentage) and chi-square test was performed for comparison. Univariable and multivariate Cox analyses were performed for identifying the associated factors of RFS. In order to verify the significance of our findings and their potential application in clinical practice, we built a prediction model (nomogram) based on the independent late recurrence predictors by using the *R* (version 4.0.3). According to optimal cutoff values determined by X-tile software, the included patients were divided into two sub-groups. Recurrence-free survival (RFS) analyses were assessed by using the Kaplan-Meier (K-M) curve and a log-rank test. Statistical analysis was performed using SPSS 26.0 for windows (SPSS, Chicago, IL, USA) and R 4.1.1 software (Institute for Statistics and Mathematics). $P< 0.05$ was considered statistically significant.

RESULT

Clinicopathologic Characteristics

A total of 300 patients who met the inclusion and exclusion criteria were included. They were followed up for at least 2 years from the surgery date until the last follow-up date or until having HCC recurrence. Clinicopathologic characteristics of the three groups are comparatively shown in **Table 1**. Of 300 included patients, 167 out of 300 (55.7%) patients had an early recurrence, 39 out of 300 (13.0%) patients developed a late recurrence, and 94 (31.3%) patients didn't have recurrence (shown in **Figure 2**).

In the whole cohort, the average age at diagnosis was 50.4 ± 11.0 years old. The majority of patients (87%) were male and 85% of patients were infected with HBV, and cirrhosis was observed in 227 (75.7%) patients. The mean size of the tumor was (6.38 ± 3.97) cm and 102 (34.0%) patients had multiple tumors. The mean splenic volume was (260.22 ± 160.89) ml. Between three sub-group cohorts, the early recurrence cohort had a larger tumor size (7.42 ± 4.11) cm and a higher proportion of MVI (53.9%), satellitosis (32,9%), multiple tumors (46.7%), and poor tumor differentiation (24.6%). The late recurrence cohort had a larger splenic volume (304.50 ± 178.83) ml than others.

As for short-term complications, 75 Complications occurred in 50 patients among 300 HCC patients. Among them, liver failure was observed in 30 (10%) patients, with pleural effusion in 15 (5%) patients, biliary fistula in 11 (3.6%) patients, pulmonary infection in 10 (3.3%) patients, abdominal bleeding in six (2%) patients, and upper gastrointestinal bleeding in three (1%)patients.

Analyses of Risk Factors for HCC Recurrence

Early Recurrence (<2 Years)

Total clinicopathologic factors of 300 patients were taken into univariate and multivariate Cox analyses to identify independent risk factors. The univariate Cox analysis revealed that age, HBsAg, platelet, TBil, AST, AFP, tumor size, tumor number, MVI, satellitosis, BCLC staging, and tumor differentiation were potential risk factors of HCC early recurrence. Then, all the above factors were taken into multivariate Cox analysis. It suggested that AFP, MVI, satellitosis, and BCLC staging were independent risk factors of HCC early recurrence (shown in **Table 2**). The curve of RFS is shown in **Figure 3**.

Late Recurrence (>2 Years)

The same clinicopathologic factors of 133 patients were taken into univariate and multivariate Cox analyses to identify independent risk factors. The univariate analysis suggested that platelet (P=0.038) and splenic volume (P=0.001) were potential risk factors of HCC late recurrence. For further multivariate analysis, only splenic volume (HR=1.003, 95%CI:1.001-1.005, P=0.001) was an independent risk factor of HCC late recurrence (shown in **Table 3**). (HR=1.003 means: for every 1 mL increase

TABLE 1 | Demographics and clinical data of study population.

	Whole cohort (N=300)	Early recurrence (N=167)	Late recurrence (N=39)	No recurrence (N=94)
Age, yr (mean ± SD)	50.38 ± 11.02	48.96 ± 11.54	52.40 ± 8.84	52.14 ± 10.58
Male, n (%)	261 (87)	146 (87.4)	36 (92.3)	79 (84)
Female, n (%)	39 (13)	21 (12.6)	3 (7.7)	15 (16)
HBsAg (+), n (%)	255 (85)	149 (89.2)	32 (82.1)	74 (78.7)
Cirrhosis, n (%)	227 (75.7)	133 (79.6)	31 (79.5)	63 (67)
Neutrophil, 10^9L (mean ± SD)	3.47 ± 1.34	3.53 ± 1.40	3.12 ± 1.37	3.48 ± 1.21
Lymphocyte,10^9L (mean ± SD)	1.52 ± 0.67	1.52 ± 0.79	1.39 ± 0.41	1.58 ± 0.49
Platelet,10^3L (mean±SD)	167.00 ± 70.94	172.50 ± 78.52	140.53 ± 67.27	168.10 ± 54.16
TBil, μmol/L (mean ±SD)	13.13 ± 6.02	13.58 ± 7.05	12.27 ± 4.21	12.62 ± 4.46
Alb, g/L (mean ±SD)	41.26 ± 4.59	40.79 ± 4.86	41.93 ± 4.72	41.75 ± 3.99
ALT, U/L (mean ±SD)	39.91 ± 26.09	41.50 ± 26.58	41.27 ± 18.95	36.40 ± 27.56
AST, U/L (mean ±SD)	47.44 ± 34.47	52.78 ± 38.36	41.90 ± 20.35	40.09 ± 30.07
PT, s (mean ±SD)	13.55 ± 1.10	13.57 ± 1.13	13.68 ± 0.97	13.46 ± 1.10
Tumor size, cm (mean ±SD)	6.38 ± 3.97	7.42 ± 4.11	5.29 ± 3.14	4.97 ± 3.47
AFP, ng/ml, n (%)	191 (63.7)	91 (54.5)	30 (76.9)	70 (74.5)
≤400	109 (36.3)	76 (45.5)	9 (23.1)	24 (25.5)
>400				
Tumor number, n (%)	198 (66.0)	89 (53.3)	30 (76.9)	79 (84)
1	102 (34.0)	78 (46.7)	9 (23.1)	15 (16)
>2				
MVI, n (%)	169 (56.3)	77 (46.1)	27 (69.2)	65 (69.1)
No	131 (43.7)	90 (53.9)	12 (30.8)	29 (30.9)
Yes				
Satellitosis, n (%)	65 (21.7)	55 (32.9)	4 (10.3)	6 (6.4)
Splenic volume, mL (mean ±SD)	260.22 ± 160.89	272.47 ± 174.92	304.50 ± 178.83	219.19 ± 111.36
BCLC staging, n (%)	187 (62.3)	76 (45.5)	29 (74.4)	82. (87.2)
A	67 (22.3)	51 (30.5)	7 (17.9)	9 (9.6)
B	46 (15.3)	40 (24)	3 (7.7)	3 (3.2)
C				
Differentiation, n (%)	13 (4.3)	3 (1.8)	1 (2.6)	9 (9.6)
Well	226 (75.3)	123 (73.7)	34 (87.2)	69 (73.4)
Moderate	61 (20.3)	41 (24.6)	4 (10.3)	16 (17)
Poor				
Recurrence, n (%)	206 (68.7)	167 (55.7)	39 (13.0)	0

AFP, alpha-fetoprotein; ALB, albumin; ALT, alanine transaminase; TBIL, total bilirubin; AST, aspartate transaminase; MVI, microvascular invasion; PT, prothrombin time; BCLC, Barcelona Clinic Liver Cancer; HBsAg, hepatitis be antigen.

in splenic volume, a 0.3% increase in risk of late recurrence (0.3% as 1.003-1 = 0.003)). With the help of X-tile software, we figured splenic volume = 165 ml as an optimal cut-off value. Based on this cut-off value, the 133 patients were divided into two groups: low SV (<165ml, n=45), and high SV (≥165ml, n= 88) (shown in **Figure 4**). Subsequently, the survival analysis of RFS was performed by Kaplan–Meier method between two groups (shown in **Figure 5**). Among patients who survived without a recurrence within 24 months (time origin from 24 months), the median RFS was 816 days (95% CI: 544–1087 days) in the high SV group and it didn't reach the median RFS in the low SV group. The low SV group had a significantly better RFS compared with the high SV group (P=0.015). Especially, 3- and 5-year RFS rates were 70% and 36% in the high SV group, while they were up to 89% and 71% in the low group.

Comparison Between Two Groups

Clinicopathological factors are compared according to two groups (shown in **Table 4**). Patients with low SV had a higher platelet count than those with high SV (189.49 ± 55.92 vs 145.06 ± 56.05, P<0.001). Also, the proportion of cirrhosis is lower in the low SV group (55.6%vs78.4%, P=0.006). However, there was no significant difference between the two groups in tumor-related factors, such as tumor size (P=0.071), AFP (P=0.436), MVI (P=0.729), BCLC staging (P=0.073), and tumor differentiation (P=0.084). Of 133 included patients, 33 out of 88 (37.5%) patients developed a recurrence in the high SV group, and six out of 45 (13.3%) patients developed a recurrence in the low SV group (P=0.004). Therefore, we can get the conclusion that after excluding tumor-related factors (related to early recurrence), splenic volume is the only predictive factor for late HCC recurrence.

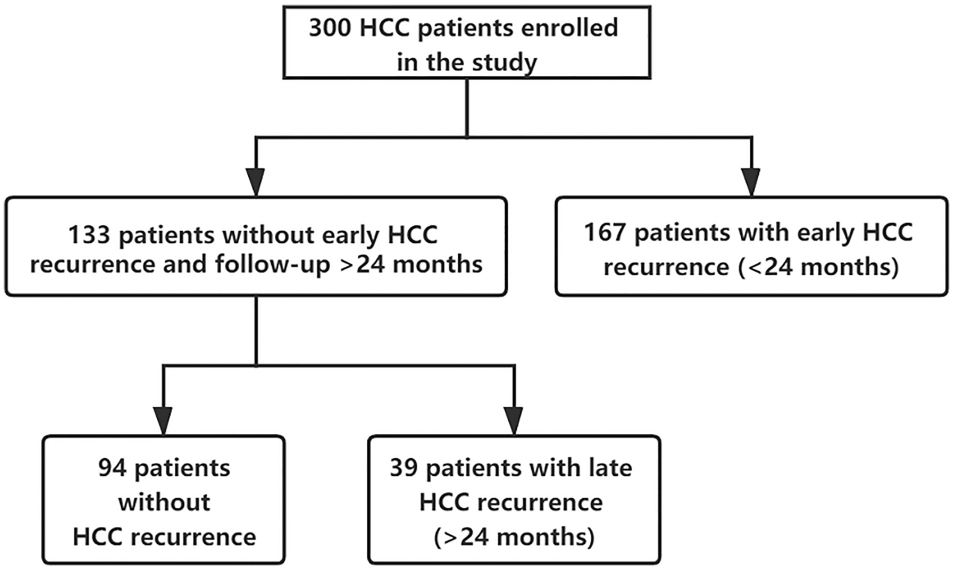

FIGURE 2 | Flowchart of this study.

TABLE 2 | Univariable and multivariable analyses for independent variables associated with HCC early recurrence.

Variables	Univariable cox regression		Multivariable cox regression	
N=300	**HR (95%CI)**	**P value**	**HR (95%CI)**	**P value**
Age, years	0.979 (0.965-0.993)	0.004	0.995 (0.979-1.011)	0.311
Gender, (Female vs Male)	0.987 (0.625-1.559)	0.955		
HBsAg, (Yes vs No)	1.656 (1.015-2.702)	0.043	1.425 (0.849-2.393)	0.144
Cirrhosis, (Yes vs No)	1.380 (0.947-2.012)	0.094		
Neutrophil, 10^9/L	1.068 (0.957-1.191)	0.241		
Lymphocyte, 10^9/L	0.976 (0.765-1.244)	0.842		
Platelet, 10^9/L	1.003 (1.001-1.005)	0.013	1.002 (1.000-1.005)	0.127
TBil, μmol/L	1.027 (1.003-1.052)	0.029	1.018 (0.995-1.041)	0.196
Alb, g/L	0.967 (0.934-1.001)	0.057		
ALT, U/L	1.003 (0.998-1.008)	0.292		
AST, U/L	1.006 (1.003-1.010)	<0.001	0.999 (0.993-1.004)	0.915
PT, s	1.031 (0.893-1.189)	0.679		
AFP, (>400 vs ≤ 400ng/ml)	2.143 (1.578-2.910)	<0.001	1.758 (1.286-2.404)	**<0.001**
Tumor size, cm	1.094 (1.061-1.128)	<0.001	0.998 (0.950-1.049)	0.811
Tumor number, (≥2 vs 1)	2.452 (1.805-3.332)	<0.001	1.332 (0.714-2.482)	0.566
MVI, (Yes vs No)	2.138 (1.576-2.902)	<0.001	1.423 (1.020-1.985)	**0.038**
Satellitosis	2.795 (2.017-3.875)	<0.001	1.551 (1.031-2.333)	**0.035**
Splenic volume (mL)	1.000 (1.000-1.001)	0.280		
BCLC staging		<0.001		**<0.001**
A	reference		reference	
B	2.795 (1.954-3.998)		1.920 (1.229-2.999)	
C	4.512 (3.058-6.659)		3.114 (2.007-4.833)	
Differentiation		0.006		0.244
well	reference		reference	
moderate	3.127 (0.994-9.832)		2.134 (0.673-6.771)	
poor	4.793 (1.483-15.489)		2.457 (0.741-8.149)	

AFP, alpha-fetoprotein; HBsAg, hepatitis be antigen; ALB, albumin; ALT, alanine transaminase; TBIL, total bilirubin; AST, aspartate transaminase; PT, prothrombin time; MVI, microvascular invasion; BCLC, Barcelona Clinic Liver Cancer; HR, Hazard Ratio. 'P < 0.05' was highlighted in bold.

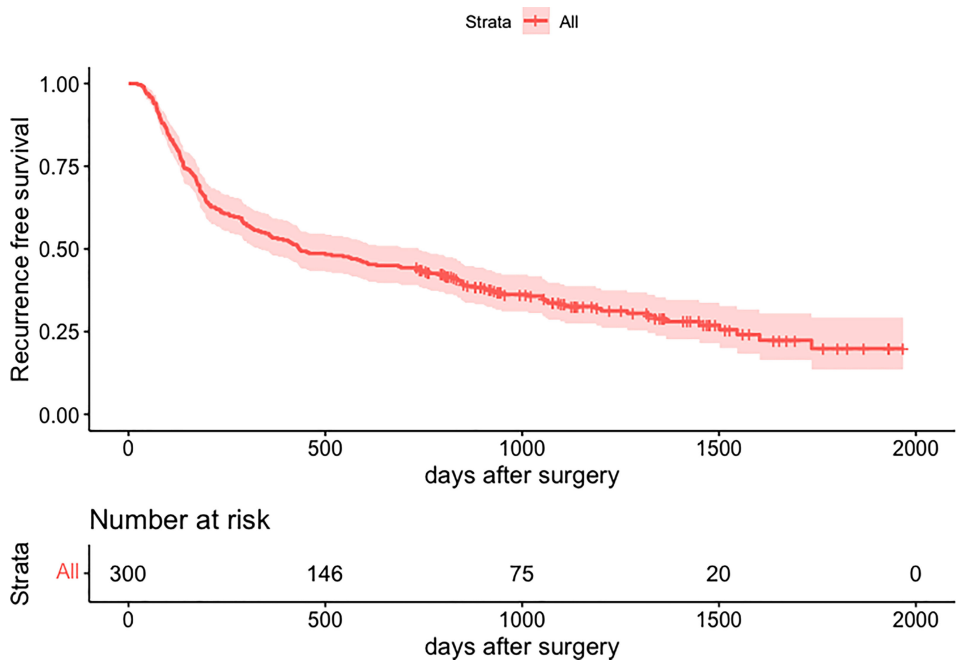

FIGURE 3 | Kaplan-Meier curve for recurrence-free survival of 300 patients. HCC, hepatocellular carcinoma.

TABLE 3 | Univariable and multivariable analyses for independent variables associated with HCC late recurrence.

Variables	Univariable cox regression		Multivariable cox regression	
N=133	**HR(95%CI)**	**P value**	**HR(95%CI)**	**P value**
Age, years	1.005 (0.972-1.040)	0.761		
Gender, (Female vs Male)	0.472 (0.145-1.536)	0.212		
HBsAg, (Yes vs No)	0.914 (0.401-2.081)	0.830		
Cirrhosis, (Yes vs No)	1.818 (0.834-3.961)	0.132		
Neutrophil, 10^9/L	0.857 (0.658-1.116)	0.251		
Lymphocyte, 10^9/L	0.574 (0.287-1.147)	0.116		
Platelet, 10^9/L	0.994 (0.988-1.000)	0.038	0.999 (0.992-1.006)	0.760
TBil, μmol/L	1.017 (0.946-1.093)	0.655		
Alb, g/L	1.004 (0.933-1.081)	0.914		
ALT, U/L	1.004 (0.994-1.013)	0.456		
AST, U/L	0.999 (0.990 1.009)	0.859		
PT, s	1.098 (0.858-1.404)	0.458		
AFP, (>400 vs ≤ 400ng/ml)	0.936 (0.444-1.976)	0.863		
Tumor size, cm	1.016 (0.930-1.110)	0.723		
Tumor number, (≥2 vs 1)	1.575 (0.744-3.335)	0.235		
MVI, (Yes vs No)	0.889 (0.450-1.757)	0.734		
Satellitosis	2.093 (0.733-5.976)	0.168		
Splenic volume (mL)	1.003 (1.001-1.005)	0.001	1.003 (1.001-1.005)	**0.001**
BCLC staging		0.168		
A	reference			
B	1.980 (0.862-4.551)			
C	2.116 (0.634-7.059)			
Differentiation		0.237		
well	reference			
moderate	4.200 (0.574-30.734)			
poor	2.454 (0.273-22.039)			

AFP, alpha fetoprotein; HBsAg, hepatitis be antigen; ALB, albumin; TBIL, total bilirubin; ALT, alanine transaminase; AST, aspartate transaminase; PT, prothrombin time; MVI, microvascular invasion; BCLC, Barcelona Clinic Liver Cancer. 'P < 0.05' was highlighted in bold.

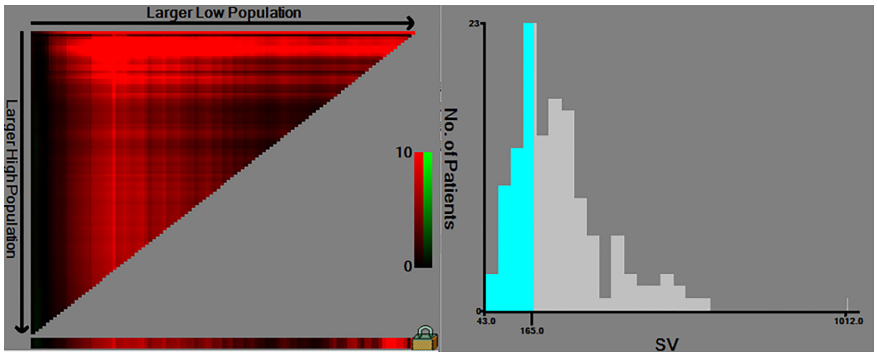

FIGURE 4 | The cut-off values were calculated by using X-tile based on the SV. The cut-off values were 167 for RFS. SV, splenic volume; RFS, recurrence-free survival.

Nomogram for Late Recurrence Based on SV

Nomograms are novel prediction models widely used for cancer prognoses such as recurrence or death (21). A late recurrence prediction model of HCC patients was conducted based on splenic volume. By calculating the preoperative SV of patients, we could simply get the probability of 3-year RFS, 4-year RFS, and 5-year RFS (shown in **Figure 6**).

DISCUSSION

Although surgical resection is beneficial to HCC patients, the high recurrence rate of HCC patients after hepatectomy remains the most serious challenge for both clinical surgeons and patients (9). Therefore, to better improve the management of these patients, identifying predictors of recurrence after hepatectomy is indispensable.

The determination of cut-off time between the early and the late recurrence has always been a focus of debate because of their distinct physiopathologic mechanism and strategies of surveillance, prevention, and management of HCC recurrence. Although a few studies (22, 23) suggested that less than 1 year from resection to recurrence has a worse prognosis, the cut-off of 2 years after hepatectomy has been widely accepted by researchers (6–9). Our study that there are completely different independent factors between early and late recurrence may indirectly support this point of view.

The risk factors for early HCC recurrence are mainly tumor-related, which is consistent with our study. In our study, we found that AFP (>400ng/ml), MVI, satellitosis, and BCLC staging were independent risk factors of HCC early recurrence through the multivariable Cox regression analysis. AFP serves as

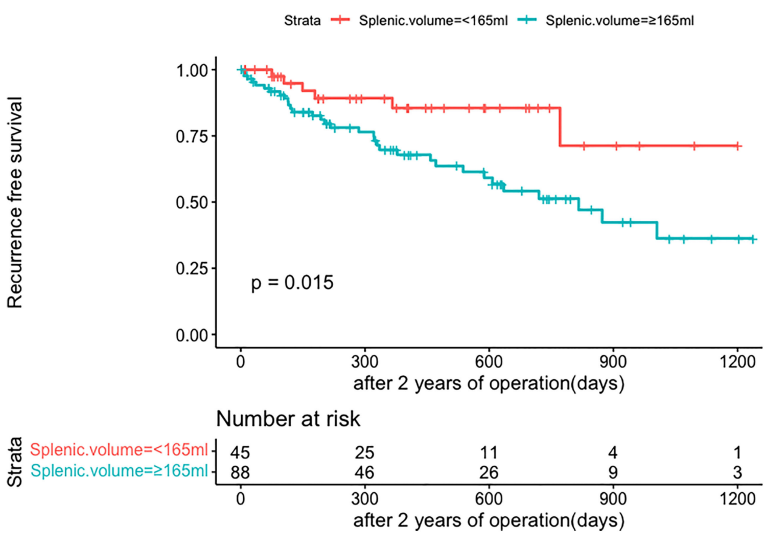

FIGURE 5 | Comparison of RFS in late recurrence patients between two groups (SV<165ml, SV≥165ml). RFS, recurrence-free survival; SV, splenic volume.

TABLE 4 | Comparison of clinicopathological factors between high splenic volume and low splenic volume group.

	High splenic volume (N=88)	Low splenic volume (N=45)	P value
HBsAg (+), n (%)	71 (80.7)	35 (77.8)	0.694
Cirrhosis, n (%)	69 (78.4)	25 (55.6)	0.006
Platelet,10^3L (mean ± SD)	145.06 ± 56.05	189.49 ± 55.92	<0.001
Tumor size, cm (mean ± SD)	5.40 ± 3.78	4.43 ± 2.30	0.071
AFP, ng/ml, n (%)	68 (77.3)	32 (71.1)	0.436
≤400	20 (22.7)	13 (28.9)	
>400			
Tumor number, n (%)	71 (80.7)	38 (84.4)	0.593
1	17 (19.3)	7 (15.6)	
>2			
MVI, n (%)	60 (68.2)	32 (71.1)	0.729
No	28 (31.8)	13 (28.9)	
Yes			
Satellitosis, n (%)	10 (11.4)	0	0.045
BCLC staging, n (%)	71 (80.7)	40 (88.9)	0.073
A	11 (12.5)	5 (11.1)	
B	6 (6.8)	0	
C			
Differentiation, n (%)	6 (6.8)	4 (8.9)	0.084
Well	73 (83.0)	30 (66.7)	
Moderate	9 (10.2)	11 (24.4)	
Poor			
Recurrence, n (%)	33 (37.5)	6 (13.3)	0.004

Data are expressed as mean ± SD or n (%).
AFP, α-fetoprotein level; HBsAg, hepatitis be antigen; MVI, microvascular invasion; BCLC, Barcelona Clinic Liver Cancer.

a surrogate marker for tumor differentiation as well as vascular invasion and high-level AFP was reported to be linked to HCC recurrence (24, 25). Microvascular invasion (MVI) is defined as the presence of tumor cell clusters in the branch of the portal or hepatic vein under microscopy (26). Obviously, the presence of MVI signifies the invasion of tumor cells into the vessel. Roayaie et al. suggested that MVI is an extremely important factor that can accurately predict the risk of recurrence (27). As for satellitosis, it refers to small metastases around the main tumor. In general, satellitosis originated from MVI, indicating that tumor metastasis has entered a late pathological stage (28). Several articles (29, 30) revealed that HCC patients with satellitosis had a worse overall survival than those without satellitosis. Our study further confirmed that satellitosis is a risk factor for early recurrence. Among many liver cancer staging systems, The Barcelona Clinic Liver Cancer (BCLC) system is currently the most widely applied system around the world. The unique advantage of BCLC staging is that the patient's performance status, tumor burden, and liver function are considered comprehensively (31, 32). Advanced-stage HCC (BCLC-C HCC) patients have tumors that have spread beyond the liver, as well as vascular invasion. Similarly, BCLC staging has been widely validated and associated with the prognosis of HCC patients by several multicenter studies (33, 34).

Subsequently, patients without early recurrence were accepted into our further analysis for late recurrence. After multivariate analysis, splenic volume was the only predictor of HCC late recurrence. The curves for late HCC recurrence-free survival showed a statistically significant difference: patients with SV ≥165 ml had a higher recurrence rate. And for patients with SV <165 ml, fewer than half of them relapsed during the study period. Through comparison between the low SV and the high SV groups, we found that most tumor-related variables (tumor size, AFP, MVI, BCLC staging, and tumor differentiation) didn't add a contribution to late recurrence. So according to the cut-off of 165 ml, we could preoperatively classify patients as high or low late recurrence of the crowd based on actual splenic volume (after excluding early recurrence-related factors). To obtain the late recurrence rate more accurately, we developed the nomogram based on SV. Depending on the specific value of SV, we could get the likelihood of the 3-year RFS, 4-year RFS, and 5-year RFS, which greatly facilitates individualized clinical surveillance and prevention of HCC recurrence.

There is no doubt that the risk factors for early HCC recurrence are biological characteristics of the tumor (10–12). Whereas, there are poor data for predicting late recurrence (35). It is widely acknowledged that the severity of chronic liver conditions (like liver cirrhosis) plays a significant role to some degree (13, 14). It is proven that the severity of portal

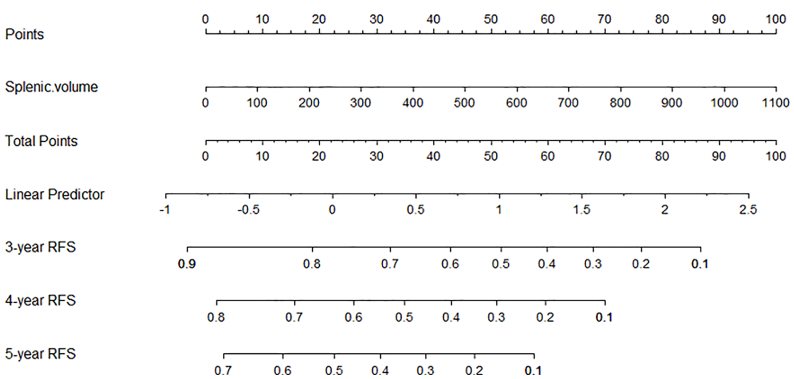

FIGURE 6 | The nomogram was developed based on SV. An individual SV value is drawn upward to determine points. Because there is only one variable, the points are the total points, and a line is drawn downward to the likelihood of 3-year RFS, 4-year RFS, and 5-year RFS.

hypertension accelerates the natural process of chronic liver disease, including HCC occurrence (36). Admittedly, the recurrence of HCC after 2 years of surgery was considered as a result of the development of *de novo* tumors or new malignant clones (9), which additionally confirms that late recurrence is correlated to the underlying liver condition. Therefore, we could assess the degree of liver cirrhosis by calculating the level of portal hypertension. In clinical, the Hepatic Venous Pressure Gradient (HVPG) is viewed as the gold standard for diagnosing PH. Due to its invasion, many scholars were devoted to searching for a non-invasive and simple method to evaluate HVPG. Both spleen size and platelet count were reported to serve as surrogate markers in assessing HVPG (37). In our univariate analysis for late recurrence, splenic volume (P=0.001) and platelet count (P=0.038) are risk factors, which supported previous theoretical research. It is well known that thrombocytopenia is caused by hypersplenism secondary to splenomegaly and is also one of the complications of portal hypertension. In our further multivariate analysis, however, the splenic volume (P=0.001) may play a more dominant role than platelet count (P=0.760).

HCC patients are often accompanied by congestive splenomegaly due to the background of cirrhosis. It is often seen in the increase of splenic vein pressure caused by the increase of portal vein pressure, which makes it difficult for the blood of the spleen to return, and then causes the blood stasis of the spleen, resulting in splenomegaly (38). In other words, Splenomegaly is regarded as an important symbol of cirrhosis and portal hypertension. Takeishi et al. showed that splenic volume could help predict HCC prognosis after hepatectomy, and combined splenectomy with hepatectomy can reduce tumor recurrence in patients with splenomegaly (39). Some studies (40, 41) have also found that HCC patients with splenomegaly tend to have a poor liver function. And for those patients, the incidence of tumor-related complications was significantly increased after surgeries, leading to a poor prognosis. It has also been discovered that the spleen plays an essential role in immunity. In Hashimoto's article (42), patients with splenomegaly have a higher number of CD4+ regulatory T cells, PD-L1, and PD-L2 expression cells than those without splenomegaly, implying that patients with splenomegaly have poor tumor immunity. The inhibitory influence of CD4+ Treg cells on immune function is mainly reflected in the inhibition of activation and proliferation of helper T cells and cytotoxic T cells, and it has been found that CD4+ Treg cells are involved in the formation of tumor immune tolerance and the inhibition of anti-tumor immune response (43). Similarly, cells expressing both PD-L1 and PD-L2 are crucial in the mechanism of tumor immune escape of the tumor microenvironment. In conclusion, decreased tumor immunity caused by splenomegaly may be one of the reasons for liver cancer recurrence.

For patients with large SV, liver transplantation has incomparable advantages compared with other treatment methods. It is the only method that can completely cure cirrhosis, HCC, and portal hypertension. However, because liver transplantation has high requirements for doctors, hospital equipment and conditions, as well as patient economy, not all patients have conditions to accept liver transplantation first. For those patients who cannot accept liver transplantation, the treatment of hepatocellular carcinoma should be given priority (re-resection). Therefore, for those patients with large SV, if they cannot accept primary liver transplantation (PLT), we'll consider hepatectomy first. Salvage liver transplantation (SLT) could be performed after several times of HCC recurrence or liver failure. It was shown that overall survival and disease-free survival were the same after PLT or SLT (44).

Our study makes use of splenic volume to predict HCC late recurrence. Patients only need a preoperative CT scan, and SV is automatically obtained by using three-dimensional CT volumetry software. Another advantage of using SV as a predictor is that in comparison to liver volume, splenic volume in adults is not affected by age, BMI, or other factors (45).

However, the current study has several limitations. Firstly, the possibility of selection bias certainly exists because of its retrospective nature. All data come from a single center and the late recurrence group had a small number of patients, which might make our results less convincing. Secondly, for developing the nomogram, the perfect design is to set up a training cohort and use other data to set up a validation cohort. This is really the shortcoming of our experiment. In fact, building a nomogram is not the main point of our article. Our team did not spend a lot of words describing the nomogram. Also, three-dimensional reconstruction of the spleen is not common in other hospitals. We have difficulty getting patient data from other hospitals as a validation cohort. Thirdly, we ignored the effect of anti-tumor therapy, such as antiviral drugs and neo/adjuvant systemic therapy, on the recurrence of liver cancer after surgery because we couldn't control the duration time and dose of therapy used by patients. A future multicenter prospective study is necessary.

CONCLUSION

In conclusion, our study verified that tumor-related factors are predictors of HCC early recurrence and splenic volume was related to HCC late recurrence because of its association with cirrhosis and PH. With the increase of SV, the probability of late recurrence also increases. This finding could assist us in guiding the clinical surveillance and prevention of HCC recurrence.

DATA AVAILABILITY STATEMENT

The original contributions presented in the study are included in the article/**Supplementary Material**. Further inquiries can be directed to the corresponding author.

ETHICS STATEMENT

The study was approved by the ethics committee of Xiangya Hospital of Central South University.

AUTHOR CONTRIBUTIONS

TF and LZ contributed to conception and design of the study. TF and LM organized the database. TF and GL performed the statistical analysis. TF wrote the first draft of the manuscript. TF wrote sections of the manuscript. All authors contributed to the article and approved the submitted version.

FUNDING

This work was supported by the grants National Nature Science Foundation of China (NO. 81771932).

ACKNOWLEDGMENTS

The authors thank Dong Wang, from the Affiliated Hospital of Qingdao University, for providing us with some useful suggestions for this manuscript.

SUPPLEMENTARY MATERIAL

The Supplementary Material for this article can be found online at: https://www.frontiersin.org/articles/10.3389/fonc.2022.876668/full#supplementary-material

REFERENCES

1. Bray F, Ferlay J, Soerjomataram I, Siegel RL, Torre LA, Jemal A. Global Cancer Statistics 2018: GLOBOCAN Estimates of Incidence and Mortality Worldwide for 36 Cancers in 185 Countries. *CA Cancer J Clin* (2018) 68 (6):394–424. doi: 10.3322/caac.21492
2. Kulik L, Heimbach JK, Zaiem F, Almasri J, Prokop LJ, Wang Z, et al. Therapies for Patients With Hepatocellular Carcinoma Awaiting Liver Transplantation: A Systematic Review and Meta-Analysis. *Hepatology* (2018) 67(1):381–400. doi: 10.1002/hep.29485
3. Yang JD, Hainaut P, Gores GJ, Amadou A, Plymoth A, Roberts LR. A Global View of Hepatocellular Carcinoma: Trends, Risk, Prevention and Management. *Nat Rev Gastroenterol Hepatol* (2019) 16(10):589–604. doi: 10.1038/s41575-019-0186-y
4. Taura K, Ikai I, Hatano E, Fujii H, Uyama N, Shimahara Y. Implication of Frequent Local Ablation Therapy for Intrahepatic Recurrence in Prolonged Survival of Patients With Hepatocellular Carcinoma Undergoing Hepatic Resection: An Analysis of 610 Patients Over 16 Years Old. *Ann Surg* (2006) 244(2):265–73. doi: 10.1097/01.sla.0000217921.28563.55
5. Hanazaki K, Kajikawa S, Shimozawa N, Mihara M, Shimada K, Hiraguri M, et al. Survival and Recurrence After Hepatic Resection of 386 Consecutive Patients With Hepatocellular Carcinoma. *J Am Coll Surg* (2000) 191(4):381–8. doi: 10.1016/S1072-7515(00)00700-6
6. Cha C, Fong Y, Jarnagin WR, Blumgart LH, DeMatteo RP. Predictors and Patterns of Recurrence After Resection of Hepatocellular Carcinoma. *J Am Coll Surg* (2003) 197(5):753–8. doi: 10.1016/j.jamcollsurg.2003.07.003
7. Marasco G, Colecchia A, Colli A, Ravaioli F, Casazza G, Bacchi Reggiani ML, et al. Role of Liver and Spleen Stiffness in Predicting the Recurrence of Hepatocellular Carcinoma After Resection. *J Hepatol* (2019) 70(3):440–8. doi: 10.1016/j.jhep.2018.10.022
8. Imamura H, Matsuyama Y, Tanaka E, Ohkubo T, Hasegawa K, Miyagawa S, et al. Risk Factors Contributing to Early and Late Phase Intrahepatic Recurrence of Hepatocellular Carcinoma After Hepatectomy. *J Hepatol* (2003) 38(2):200–7. doi: 10.1016/S0168-8278(02)00360-4
9. Portolani N, Coniglio A, Ghidoni S, Giovanelli M, Benetti A, Tiberio GA, et al. Early and Late Recurrence After Liver Resection for Hepatocellular Carcinoma: Prognostic and Therapeutic Implications. *Ann Surg* (2006) 243 (2):229–35. doi: 10.1097/01.sla.0000197706.21803.a1
10. Zhou YM, Yang JM, Li B, Yin ZF, Xu F, Wang B, et al. Risk Factors for Early Recurrence of Small Hepatocellular Carcinoma After Curative Resection. *Hepatobil Pancreat Dis Int* (2010) 9(1):33–7.
11. Shimoda M, Tago K, Shiraki T, Mori S, Kato M, Aoki T, et al. Risk Factors for Early Recurrence of Single Lesion Hepatocellular Carcinoma After Curative Resection. *World J Surg* (2016) 40(10):2466–71. doi: 10.1007/s00268-016-3529-7
12. Poon RT, Fan ST, Ng IO, Lo CM, Liu CL, Wong J. Different Risk Factors and Prognosis for Early and Late Intrahepatic Recurrence After Resection of Hepatocellular Carcinoma. *Cancer* (2000) 89(3):500–7. doi: 10.1002/1097-0142(20000801)89:3<500::AID-CNCR4>3.0.CO;2-O
13. Poon RT. Differentiating Early and Late Recurrences After Resection of HCC in Cirrhotic Patients: Implications on Surveillance, Prevention, and Treatment Strategies. *Ann Surg Oncol* (2009) 16(4):792–4. doi: 10.1245/s10434-009-0330-y
14. Xu XF, Xing H, Han J, Li ZL, Lau WY, Zhou YH, et al. Risk Factors, Patterns, and Outcomes of Late Recurrence After Liver Resection for Hepatocellular Carcinoma: A Multicenter Study From China. *JAMA Surg* (2019) 154(3):209–17. doi: 10.1001/jamasurg.2018.4334
15. Gatta A, Bolognesi M, Merkel C. Vasoactive Factors and Hemodynamic Mechanisms in the Pathophysiology of Portal Hypertension in Cirrhosis. *Mol Aspects Med* (2008) 29(1-2):119–29. doi: 10.1016/j.mam.2007.09.006
16. Berzigotti A, Zappoli P, Magalotti D, Tiani C, Rossi V, Zoli M. Spleen Enlargement on Follow-Up Evaluation: A Noninvasive Predictor of Complications of Portal Hypertension in Cirrhosis. *Clin Gastroenterol Hepatol* (2008) 6(10):1129–34. doi: 10.1016/j.cgh.2008.05.004
17. Lim MC, Tan CH, Cai J, Zheng J, Kow AW. CT Volumetry of the Liver: Where Does it Stand in Clinical Practice? *Clin Radiol* (2014) 69(9):887–95. doi: 10.1016/j.crad.2013.12.021
18. Zou H, Tao Y, Wang ZM. Integration of Child-Pugh Score With Future Liver Remnant Yields Improved Prediction of Liver Dysfunction Risk for HBV-related Hepatocellular Carcinoma Following Hepatic Resection. *Oncol Lett* (2017) 13(5):3631–7. doi: 10.3892/ol.2017.5919
19. Wigmore SJ, Redhead DN, Yan XJ, Casey J, Madhavan K, Dejong CH, et al. Virtual Hepatic Resection Using Three-Dimensional Reconstruction of Helical Computed Tomography Angioportograms. *Ann Surg* (2001) 233 (2):221–6. doi: 10.1097/00000658-200102000-00011
20. Li WX, Zhao XT, Chai WM, Zhu NY, Du LJ, Huang W, et al. Hepatitis B Virus-Induced Liver Fibrosis and Cirrhosis: The Value of Liver and Spleen Volumetry With Multi-Detector Spiral Computed Tomography. *J Dig Dis* (2010) 11(4):215–23. doi: 10.1111/j.1751-2980.2010.00441.x
21. Iasonos A, Schrag D, Raj GV, Panageas KS. How to Build and Interpret a Nomogram for Cancer Prognosis. *J Clin Oncol* (2008) 26(8):1364–70. doi: 10.1200/JCO.2007.12.9791
22. He W, Peng B, Tang Y, Yang J, Zheng Y, Qiu J, et al. Nomogram to Predict Survival of Patients With Recurrence of Hepatocellular Carcinoma After Surgery. *Clin Gastroenterol Hepatol* (2018) 16(5):756–64 e10. doi: 10.1016/j.cgh.2017.12.002
23. Tabrizian P, Jibara G, Shrager B, Schwartz M, Roayaie S. Recurrence of Hepatocellular Cancer After Resection: Patterns, Treatments, and Prognosis. *Ann Surg* (2015) 261(5):947–55. doi: 10.1097/SLA.0000000000000710
24. Hameed B, Mehta N, Sapisochin G, Roberts JP, Yao FY. Alpha-Fetoprotein Level > 1000 Ng/Ml as an Exclusion Criterion for Liver Transplantation in Patients With Hepatocellular Carcinoma Meeting the Milan Criteria. *Liver Transpl* (2014) 20(8):945–51. doi: 10.1002/lt.23904
25. Ding HF, Zhang XF, Bagante F, Ratti F, Marques HP, Soubrane O, et al. Prediction of Tumor Recurrence by Alpha-Fetoprotein Model After Curative Resection for Hepatocellular Carcinoma. *Eur J Surg Oncol* (2021) 47(3 Pt B):660–6. doi: 10.1016/j.ejso.2020.10.017
26. Jonas S, Bechstein WO, Steinmuller T, Herrmann M, Radke C, Berg T, et al. Vascular Invasion and Histopathologic Grading Determine Outcome After Liver Transplantation for Hepatocellular Carcinoma in Cirrhosis. *Hepatology* (2001) 33(5):1080–6. doi: 10.1053/jhep.2001.23561

27. Roayaie S, Blume IN, Thung SN, Guido M, Fiel MI, Hiotis S, et al. A System of Classifying Microvascular Invasion to Predict Outcome After Resection in Patients With Hepatocellular Carcinoma. *Gastroenterology* (2009) 137 (3):850–5. doi: 10.1053/j.gastro.2009.06.003
28. Okusaka T, Okada S, Ueno H, Ikeda M, Shimada K, Yamamoto J, et al. Satellite Lesions in Patients With Small Hepatocellular Carcinoma With Reference to Clinicopathologic Features. *Cancer* (2002) 95(9):1931–7. doi: 10.1002/cncr.10892
29. Lim C, Mise Y, Sakamoto Y, Yamamoto S, Shindoh J, Ishizawa T, et al. Above 5 Cm, Size Does Not Matter Anymore in Patients With Hepatocellular Carcinoma. *World J Surg* (2014) 38(11):2910–8. doi: 10.1007/s00268-014-2704-y
30. Meniconi RL, Komatsu S, Perdigao F, Boelle PY, Soubrane O, Scatton O. Recurrent Hepatocellular Carcinoma: A Western Strategy That Emphasizes the Impact of Pathologic Profile of the First Resection. *Surgery* (2015) 157 (3):454–62. doi: 10.1016/j.surg.2014.10.011
31. Llovet JM, Bru C, Bruix J. Prognosis of Hepatocellular Carcinoma: The BCLC Staging Classification. *Semin Liver Dis* (1999) 19(3):329–38. doi: 10.1055/s-2007-1007122
32. Llovet JM, Zucman-Rossi J, Pikarsky E, Sangro B, Schwartz M, Sherman M, et al. Hepatocellular Carcinoma. *Nat Rev Dis Primers* (2016) 2:16018. doi: 10.1038/nrdp.2016.18
33. Zhong JH, Ke Y, Gong WF, Xiang BD, Ma L, Ye XP, et al. Hepatic Resection Associated With Good Survival for Selected Patients With Intermediate and Advanced-Stage Hepatocellular Carcinoma. *Ann Surg* (2014) 260(2):329–40. doi: 10.1097/SLA.0000000000000236
34. Tsilimigras DI, Bagante F, Sahara K, Moris D, Hyer JM, Wu L, et al. Prognosis After Resection of Barcelona Clinic Liver Cancer (Bclc) Stage 0, A, and B Hepatocellular Carcinoma: A Comprehensive Assessment of the Current Bclc Classification. *Ann Surg Oncol* (2019) 26(11):3693–700. doi: 10.1245/s10434-019-07580-9
35. Jung KS, Kim SU, Choi GH, Park JY, Park YN, Kim DY, et al. Prediction of Recurrence After Curative Resection of Hepatocellular Carcinoma Using Liver Stiffness Measurement (Fibroscan(R)). *Ann Surg Oncol* (2012) 19 (13):4278–86. doi: 10.1245/s10434-012-2422-3
36. Ripoll C, Groszmann RJ, Garcia-Tsao G, Bosch J, Grace N, Burroughs A, et al. Hepatic Venous Pressure Gradient Predicts Development of Hepatocellular Carcinoma Independently of Severity of Cirrhosis. *J Hepatol* (2009) 50 (5):923–8. doi: 10.1016/j.jhep.2009.01.014
37. Berzigotti A, Seijo S, Arena U, Abraldes JG, Vizzutti F, Garcia-Pagan JC, et al. Elastography, Spleen Size, and Platelet Count Identify Portal Hypertension in Patients With Compensated Cirrhosis. *Gastroenterology* (2013) 144(1):102–11 e1. doi: 10.1053/j.gastro.2012.10.001
38. Pozo AL, Godfrey EM, Bowles KM. Splenomegaly: Investigation, Diagnosis and Management. *Blood Rev* (2009) 23(3):105–11. doi: 10.1016/j.blre.2008.10.001
39. Takeishi K, Kawanaka H, Itoh S, Harimoto N, Ikegami T, Yoshizumi T, et al. Impact of Splenic Volume and Splenectomy on Prognosis of Hepatocellular Carcinoma Within Milan Criteria After Curative Hepatectomy. *World J Surg* (2018) 42(4):1120–8. doi: 10.1007/s00268-017-4232-z
40. Bae JS, Lee DH, Yoo J, Yi NJ, Lee KW, Suh KS, et al. Association Between Spleen Volume and the Post-Hepatectomy Liver Failure and Overall Survival of Patients With Hepatocellular Carcinoma After Resection. *Eur Radiol* (2021) 31(4):2461–71. doi: 10.1007/s00330-020-07313-7
41. Peng W, Zhang XY, Li C, Wen TF, Yan LN, Yang JY. Spleen Stiffness and Volume Help to Predict Posthepatectomy Liver Failure in Patients With Hepatocellular Carcinoma. *Med (Baltimore)* (2019) 98(18):e15458. doi: 10.1097/MD.0000000000015458
42. Hashimoto N, Shimoda S, Kawanaka H, Tsuneyama K, Uehara H, Akahoshi T, et al. Modulation of CD4(+) T Cell Responses Following Splenectomy in Hepatitis C Virus-Related Liver Cirrhosis. *Clin Exp Immunol* (2011) 165 (2):243–50. doi: 10.1111/j.1365-2249.2011.04393.x
43. Ruter J, Barnett BG, Kryczek I, Brumlik MJ, Daniel BJ, Coukos G, et al. Altering Regulatory T Cell Function in Cancer Immunotherapy: A Novel Means to Boost the Efficacy of Cancer Vaccines. *Front Biosci (Landmark Ed)* (2009) 14:1761–70. doi: 10.2741/3338
44. Majno PE, Sarasin FP, Mentha G, Hadengue A. Primary Liver Resection and Salvage Transplantation or Primary Liver Transplantation in Patients With Single, Small Hepatocellular Carcinoma and Preserved Liver Function: An Outcome-Oriented Decision Analysis. *Hepatology* (2000) 31(4):899–906. doi: 10.1053/he.2000.5763
45. Prassopoulos P, Daskalogiannaki M, Raissaki M, Hatjidakis A, Gourtsoyiannis N. Determination of Normal Splenic Volume on Computed Tomography in Relation to Age, Gender and Body Habitus. *Eur Radiol* (1997) 7(2):246–8. doi: 10.1007/s003300050145

Conflict of Interest: The authors declare that the research was conducted in the absence of any commercial or financial relationships that could be construed as a potential conflict of interest.

Publisher's Note: All claims expressed in this article are solely those of the authors and do not necessarily represent those of their affiliated organizations, or those of the publisher, the editors and the reviewers. Any product that may be evaluated in this article, or claim that may be made by its manufacturer, is not guaranteed or endorsed by the publisher.

Copyright © 2022 Fang, Long, Mi, Su, Mo and Zhou. This is an open-access article distributed under the terms of the Creative Commons Attribution License (CC BY). The use, distribution or reproduction in other forums is permitted, provided the original author(s) and the copyright owner(s) are credited and that the original publication in this journal is cited, in accordance with accepted academic practice. No use, distribution or reproduction is permitted which does not comply with these terms.

frontiers | Frontiers in Oncology

ORIGINAL RESEARCH
published: 26 May 2022
doi: 10.3389/fonc.2022.897218

The Percentage of Signet Ring Cells Is Inversely Related to Aggressive Behavior and Poor Prognosis in Mixed-Type Gastric Cancer

Luigi Marano[1], Maria Raffaella Ambrosio[2,3], Luca Resca[1], Ludovico Carbone[1], Osvaldo Carpineto Samorani[1], Roberto Petrioli[4], Vinno Savelli[1], Maurizio Costantini[2], Lara Malaspina[2], Karol Polom[5], Ivano Biviano[6], Daniele Marrelli[1] and Franco Roviello[1]*

[1] Department of Medicine, Surgery and Neurosciences, Unit of General Surgery and Surgical Oncology, University of Siena, Siena, Italy, [2] Pathology Unit, University of Siena, Siena, Italy, [3] Pathology Unit, Azienda USL Toscana Nord-Ovest, Pisa, Italy, [4] Department of Medicine, Surgery and Neurosciences, Unit of Medical Oncology, University of Siena, Siena, Italy, [5] Department of Surgical Oncology, Medical University of Gdansk, Gdansk, Poland, [6] Gastroenterology and Operative Endoscopy Unit, AOU Senese, Siena, Italy

OPEN ACCESS

Edited by:
Chang-In Choi,
Pusan National University Hospital,
South Korea

Reviewed by:
Veronica De Simone,
Agostino Gemelli University Polyclinic (IRCCS), Italy
Jaques Waisberg,
Faculdade de Medicina do ABC, Brazil
Marta Goglia,
Sapienza University of Rome, Italy

***Correspondence:**
Luigi Marano
luigi.marano@unisi.it
orcid.org/0000-0002-9777-9588

Specialty section:
This article was submitted to Surgical Oncology, a section of the journal Frontiers in Oncology

Received: 15 March 2022
Accepted: 15 April 2022
Published: 26 May 2022

Citation:
Marano L, Ambrosio MR, Resca L, Carbone L, Carpineto Samorani O, Petrioli R, Savelli V, Costantini M, Malaspina L, Polom K, Biviano I, Marrelli D and Roviello F (2022) The Percentage of Signet Ring Cells Is Inversely Related to Aggressive Behavior and Poor Prognosis in Mixed-Type Gastric Cancer. Front. Oncol. 12:897218. doi: 10.3389/fonc.2022.897218

Background and Objectives: Only recently the percentage of signet ring cells (SRCs) in gastric cancer (GC) has been proposed as an independent predictor of survival. High amounts of SRCs have been related to lower recurrence and mortality rates, better prognosis, and favorable clinicopathological features in a poorly cohesive histotype. It is not known what the effect of SRC percentage in mixed-type GC is. We investigate the role of SRCs as a prognostic marker in mixed-histotype GC.

Methods: A retrospective analysis was performed through a prospectively maintained database of patients with diagnosed "mixed-type" gastric carcinoma, defined according to 2019 WHO classification. These patients underwent surgery between 1995 and 2016, and their tissue samples were stored in a tissue bank. All slides were analyzed, and patients were divided into three groups according to the percentage of SRCs: "Group 1" (displaying ≤10% of SRCs), "Group 2" (displaying <90% but >10% of SRCs), and "Group 3" (displaying ≥90% of SRCs). We compared clinical and pathological features as well as prognostic factors between the different groups.

Results: Among 164 enrolled patients, 68.9% were male and 31.1% were female ($p = 0.612$). The mean (±SD) age at diagnosis was 71.4 ± 9.6 years. Ninety-eight (59.7%) patients were classified as "Group 1", 66 (40.3%) as "Group 2", and none as "Group 3". Five-year overall survival was remarkably higher in Group 2 (73.8%) in comparison to Group 1 (35.4%), $p <$ 0.001. Mortality risk was three times higher in patients with ≤10% SRC pattern compared to

those with >10% [HR 2.70 (95% CI 1.72–4.24)]. After adjusting according to potential confounding factors, SRC percentage was still an independent predictor of survival.

Conclusions: The proportion of SRCs is inversely related to aggressive behavior and poor prognosis in mixed-type GCs, highlighting the role of SRC amount as an independent predictor of survival.

Keywords: mixed-type gastric cancer, signet ring cell, prognosis, histology, poorly cohesive

INTRODUCTION

Gastric cancer (GC) is the fifth most diagnosed malignancy worldwide with over 1 million estimated new cases annually (1). Due to its intratumoral and intertumoral huge heterogeneity, several classifications have been proposed to categorize different morphological subtypes of GC. The most commonly used classifications are those published by the Japanese Gastric Cancer Association (JGCA) (2), the World Health Organization (WHO) (3), and Lauren (4). However, a categorization into a few macro groups is burdened by excessive internal heterogeneity, resulting in conflicting evidence about the ability of the histopathological phenotype to predict patient prognosis or response to therapy. In 2019, the European Chapter of the International Gastric Cancer Association (IGCA) proposed the adoption of the recent fifth edition of the WHO classification for each newly diagnosed GC (5, 6). The latest classification recognized five main histological subtypes of GC: tubular, papillary, mucinous, poorly cohesive, and mixed adenocarcinomas. The latter account for 6%–27% of all GCs and are characterized by the coexistence of two or more distinct histological components: glandular (tubular/papillary) and signet ring cell (SRC)/poorly cohesive. Recently, the percentage of SRC was proposed as an independent prognostic factor of cancer-related survival in a poorly cohesive histotype, and high amounts of SRC were related to lower recurrence and mortality rates, better prognosis, and most advantageous clinicopathological features (6–8). Surprisingly, clinicopathological and prognostic aspects of mixed histotype have not been deeply investigated. Available data suggest that patients with mixed adenocarcinomas had a poorer prognosis (9, 10) and higher incidence of lymph node metastasis than those with only one component. Furthermore, to the best of our knowledge, no previous research has studied the connection between the amount of SRCs and biological as well as prognostic differences of mixed GC.

We conducted this study to compare the clinicopathological features and the prognostic differences of mixed GC according to the percentage of SRCs.

PATIENTS AND METHODS

A retrospective analysis was performed through a prospectively maintained database of adult patients from the Division of Surgical Oncology at the University of Siena, Italy. These patients all underwent upfront surgery for GC between 1995 and 2016, and their tissue samples were available for research at an institutionally approved tissue bank. Only patients with confirmed "mixed" gastric carcinoma, according to the last WHO classification (3), submitted to surgical treatment with curative purpose, were recruited for the analysis. All enrolled patients were then reclassified into the three groups according to the percentage of cells with signet ring features as proposed by the European Chapter of IGCA (6): Group 1 (presenting ≤10% of SRCs), Group 2 (presenting <90% but >10% of SRCs), and Group 3 (presenting ≥90% of SRCs).

Electronic medical records and pathological reports were thoroughly analyzed to acquire information related to age, sex, tumor size, location, depth of invasion, perineural/lymphovascular invasion, lymph node metastases, and TNM (8th edition) according to the American Joint Committee on Cancer Staging Manual (11).

Treatment Strategy and Clinical Information

Patients underwent similar management, according to the recommendations of the multidisciplinary team. Serosal invasion and minimal peritoneal disease were evaluated utilizing an optimized dedicated protocol through contrast-enhanced thoracoabdominal computed tomography (CT), with the help of an experienced radiologist. In selected cases, where CT scan results were doubtful and peritoneal carcinosis could not be ruled out, staging laparoscopy with a cytological examination of peritoneal lavage was also performed.

Experienced surgeons performed surgery according to treatment guidelines published by the Japanese Gastric Cancer Association (ver. 4) (12). The first-line treatment to remove the primary tumor consisted of total or subtotal gastrectomy. Combined visceral resections were conducted to remove all visible lesions, in a case-by-case evaluation. D1 lymphadenectomy was carried out in cases of early GC. When gastric wall layers deeper than muscularis propria were involved, D2 or D3 lymphadenectomy was performed.

Death within 90 days of surgery was considered as postoperative mortality. Systemic chemotherapy treatment consisting of a combination of fluoropyrimidine and platinum regimens was administered to patients after complete recovery and hospital discharge. Eventually, biological therapy was added, according to patients' general status and multidisciplinary evaluations.

Follow-Up

After surgery, patients were examined at set intervals for both surgical and oncological follow-up. Blood tests (including tumor

biomarkers), as well as CT, were performed every 3 months for the first 2 years, every 6 months from years 3 to 5, and yearly after that date, unless otherwise requested according to clinical status.

We differentiated recurrence as loco-regional relapse, distant organ metastasis, and peritoneal dissemination. Cancer recurrence at the anastomotic site or around the surgical area was included in the loco-regional relapse group. On the other hand, liver and other extra-abdominal site metastases, and nodal metastases beyond regional nodes were classified as distant recurrences.

Tumor recurrence was evaluated through clinical findings, radiological exams, endoscopic examination, and/or tissue biopsy.

Histopathological Assessment

Two pathologists (MA and LMal), experts in the gastro-intestinal pathology field, blindly reviewed hematoxylin and eosin (H&E) slides obtained from the patients enrolled in the study. All the cases were re-classified according to the last WHO classification (3) and IGCA classification (6). The mixed histotype was also confirmed using E-cadherin immunohistochemistry, which should be restricted to the SRC/poorly cohesive component. Moreover, in the poorly cohesive component, the percentage of SRC in respect to the whole morphology was assessed.

Study Endpoints and Definition

The main goal of this study was to compare the overall survival (OS), defined as the interval time from the date of intervention until the death of any cause or last available contact, in the three groups. The recurrence-free survival (RFS) was also investigated, from the day of intervention until loco-regional or distant recurrence evidence. The secondary aims were a comparative analysis of clinicopathological features, mortality, morbidity, and prognostic factors for survival.

Statistical Analysis

The data we gathered were analyzed and found to be normally distributed using the Shapiro–Wilk *W* test. These data are presented as means ± standard deviation (SD). An unpaired *t*-test, or Pearson's chi-squared (χ^2), was used appropriately to assess differences among groups. We used the reverse Kaplan–Meier method to estimate the median follow-up time (13). OS and RFS analyses were carried out between Group 1, Group 2, and Group 3 GC patients with curative resection with the use of the Kaplan–Meier estimation method and compared using the log-rank test. Hazard ratios (HRs) were calculated using the Cox proportional hazards regression with 95% confidence intervals to account for risk factors. The endpoint is defined as death from cancer. The model included the following covariates: age (<60 years and ≥60 years), lymph node metastasis (negative and positive), lymphovascular invasion (negative and positive), perineural invasion (negative and positive), EGC/AGC (early gastric cancer and advanced gastric cancer), TNM stage (1–2 and 3–4), and SRC proportion (Group 1 and Group 2). Variables were selected using the stepwise forward procedure, and *p*-values < 0.05 were considered significant for their inclusion. *p*-values > 0.1 were considered significant for their removal. At each step, the variable with the highest statistic score was added by the model. Global χ^2 changes from each previous step and residual χ^2 were calculated at each step. Beta coefficients, HRs, and their 95% confidence interval were estimated for each significant variable and compared with its reference category. Missing items were excluded or analyzed in a separate group if exceeding 5%. A *p*-value < 0.05 was considered statistically significant, and all statistical analyses were performed using the SPSS version 26.0 software package for Mac (IBM Corp., Chicago, IL, USA).

The present study complies with STROBE (Strengthening the Reporting of Observational Studies in Epidemiology) guidelines (**Supplementary Table 1**) (14).

RESULTS

Clinicopathological and Surgical Characteristics of Patients With Poorly Cohesive Carcinoma

Of 682 GC patients, 263 (38.6%) were confirmed as papillary, tubular, or mucinous histotype. Two hundred fifty-five patients (37.4%) were diagnosed as "poorly cohesive", while 164 (24%) were confirmed as mixed histotype according to the last WHO classification (3). These patients were included in our study, and the specimens of all mixed cancers were available in an institutionally approved tissue bank (**Figure 1**). The proportion of female was 31.1% (*n* = 51) and the mean (±SD) age at diagnosis was 71.4 ± 9.6 years. Twenty-five cases (15.2%) were diagnosed with EGC and 139 (84.8%) were diagnosed with AGC; in most cases, the lesions started from the distal part of the stomach (50%). **Table 1** summarizes the clinicopathological characteristics of 164 patients with mixed-type gastric carcinoma. In all cases, surgery was meant to be curative. Total gastrectomy was carried out in 33.5% (*n* = 55), while subtotal gastrectomy was performed in 66.5% (*n* = 109). D2 was the most common lymphadenectomy, while D1 was executed in 26.2% (*n* = 43) and D3 was executed in 8.5% (*n* = 14) of patients. At the histopathological evaluation, most cancers were pT3–4 (61%, *n* = 100) and pN+ (52.4%, *n* = 86), and with lymphovascular invasion (47.9%, *n* = 58) and neural invasion (17.6%, *n* = 21) (**Table 2**). No postoperative deaths were registered. After surgery, 95 patients (57.9%) completed systemic chemotherapy, while the remaining were not able to start the treatment due to postoperative complications that delayed discharge and recovery.

Clinicopathological and Surgical Characteristics of Patients Grouped by Proportion of SRC

Ninety-eight (59.7%) patients were classified as "Group 1" (**Figure 2**), 66 (40.3%) patients were classified as "Group 2" (**Figure 3**), and none of the 164 patients were considered as "Group 3". The maximum value of the SRC percentage was 40%. **Tables 1**, **2** also summarize the analysis of the clinicopathological and surgical characteristics of Group 1 and Group 2. A higher proportion of patients in Group 1 had a G3 grading (34.7% vs. 16.7%, $p < 0.001$) and almost none had a G1 grading (5.1% vs. 21.2%, $p < 0.001$). Group 2 had a lower mean tumor size (±SD) (42.5 ± 24.1 vs. 56.7 ± 26.4 mm, $p < 0.001$), and a lower

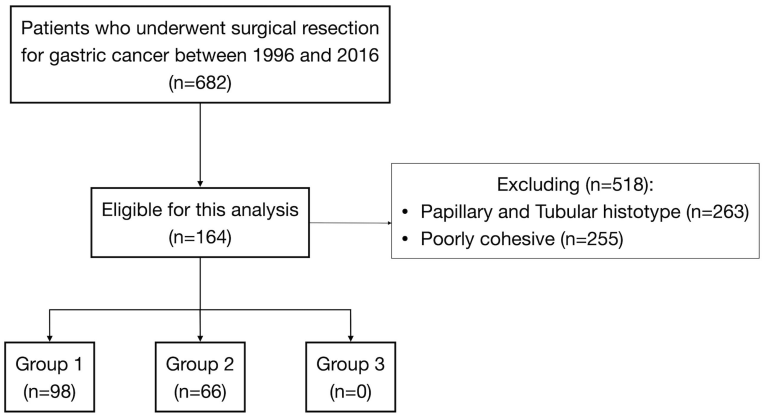

FIGURE 1 | Flow diagram of patient selection among 682 patients submitted to surgical resection for gastric cancer.

TABLE 1 | Clinicopathological characteristics of patients with mixed-type gastric cancer according to SRC percentage.

Variables	All patients (*n* = 164)	SRC ≤ 10 (*n* = 98)	SRC > 10 (*n* = 66)	*p*-value
Age (years) mean ± SD	71.4 ± 9.6	71.2 ± 9.4	71.7 ± 9.8	0.763
Gender				0.612
Female	51 (31.1)	29 (29.6)	22 (33.3)	
Male	113 (68.9)	69 (70.4)	44 (66.7)	
Location of tumor				0.499
Upper third	22 (23.4)	14 (14.3)	8 (12.1)	
Middle third	52 (31.7)	29 (29.6)	23 (34.8)	
Lower third	82 (50)	50 (51)	32 (48.5)	
Diffuse	8 (4.8)	5 (5.1)	3 (4.5)	
EGC/AGC				**0.000**
Early Gastric Cancer	25 (15.2)	5 (5.1)	20 (30.3)	
Advanced Gastric Cancer	139 (84.8)	93 (94.9)	46 (69.7)	
Adjacent organs infiltration				0.261
No	149 (90.9)	87 (88.8)	62 (93.9)	
Yes	15 (9.1)	11 (11.2)	4 (6.1)	
Grading				**0.001**
G1	19 (11.6)	5 (5.1)	14 (21.2)	
G2	22 (56.1)	53 (54.1)	39 (59.1)	
G3	45 (27.4)	34 (34.7)	11 (16.7)	
Tumor size (mm), mean ± SD	50.9 ± 26.4	56.7 ± 26.4	42.5 ± 24.1	**0.001**
Staging-T				**0.000**
T1–2	64 (39)	21 (21.4)	43 (65.2)	
T3–4	100 (61)	77 (78.6)	23 (34.8)	
Staging-N				**0.000**
N0	78 (47.6)	26 (26.5)	52 (78.8)	
N+	86 (52.4)	72 (73.5)	14 (21.2)	
Staging-M				0.786
M0	153 (93.3)	91 (92.9)	62 (93.9)	
M1	11 (6.7)	7 (7.1)	4 (6.1)	
AJCC TNM Stage 8th ed.				**0.000**
Ia	23 (14)	4 (4.1)	19 (28.8)	
Ib	27 (16.5)	9 (9.2)	18 (27.3)	
IIa	26 (15.9)	10 (10.2)	16 (24.2)	
IIb	15 (9.1)	11 (11.2)	4 (6.1)	
IIIa	14 (8.5)	12 (12.2)	2 (3)	
IIIb	14 (8.5)	13 (13.3)	1 (1.5)	
IIIc	27 (16.5)	25 (25.5)	2 (3)	
IV	18 (11)	14 (14.3)	4 (6.1)	

Data are expressed as n (%) unless otherwise specified and percentages are given according to number of patients per line after exclusion of patients with potential missing data. SD, standard deviation; SRC, signet ring cell; EGC, early gastric cancer; AGC, advanced gastric cancer; AJCC, American joint committee on cancer. P values in bold are statistically significant.

TABLE 2 | Surgical characteristics of patients with mixed-type gastric cancer according to SRC percentage.

Variables	All patients (*n* = 164)	SRC ≤ 10 (*n* = 98)	SRC > 10 (*n* = 66)	*p*-value
Lymphovascular invasion				**0.001**
Negative	63 (38.4)	26 (26.5)	37 (56.1)	
Positive	58 (35.4)	44 (44.9)	14 (21.2)	
Perineural invasion				0.155
Negative	98 (59.8)	52 (53.1)	46 (69.7)	
Positive	21 (12.8)	16 (16.3)	5 (7.6)	
Surgical procedure				**0.085**
Total gastrectomy	55 (33.5)	36 (36.7)	19 (28.8)	
Subtotal gastrectomy	109 (66.5)	62 (63.2)	47 (71.2)	
Lymphadenectomy				0.392
D1	43 (26.2)	27 (27.6)	16 (24.2)	
D2	107 (65.2)	65 (66.3)	42 (63.6)	
D3	14 (8.5)	6 (6.1)	8 (12.1)	
Resection of other organs				0.440
No	148 (90.2)	87 (88.8)	61 (92.4)	
Yes	16 (9.8)	11 (11.2)	5 (7.6)	
Radicality				**0.006**
R0	123 (75)	65 (66.3)	58 (87.9)	
R1	20 (12.2)	17 (17.3)	3 (4.5)	
R2	21 (12.8)	16 (16.3)	5 (7.6)	
Proximal margin infiltration				0.217
Negative	147 (98.7)	83 (97.4)	63 (100)	
Positive	2 (1.3)	2 (2.4)	0	
Distal margin infiltration				0.192
Negative	147 (96.1)	83 (94.3)	64 (98.5)	
Positive	6 (3.9)	5 (5.7)	1 (1.5)	

Data are expressed as n (%) unless otherwise specified and percentages are given according to number of patients per line after exclusion of patients with potential missing data. SD, standard deviation; SRC, signet ring cell. P values in bold are statistically significant.

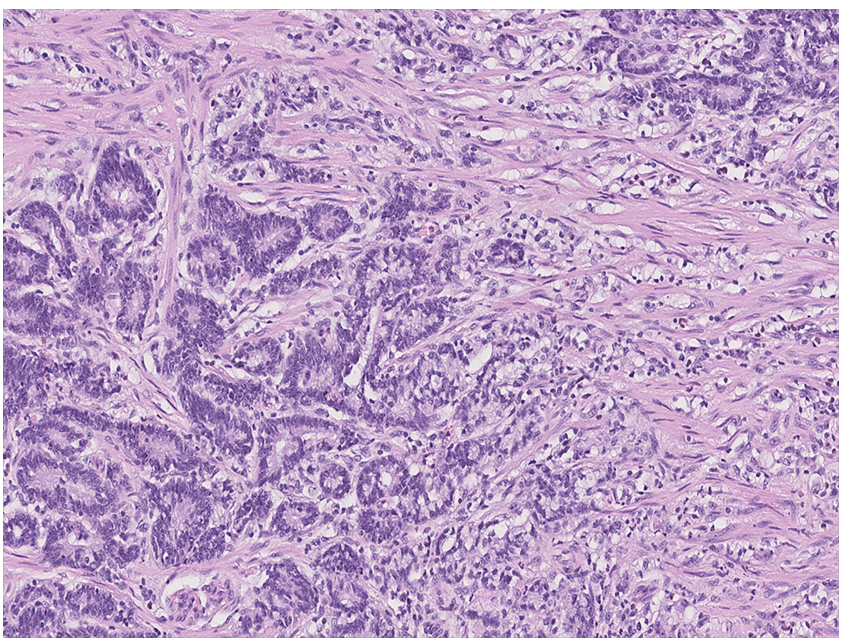

FIGURE 2 | Photomicrograph of mixed-type gastric cancer with moderately differentiated tubular adenocarcinoma on the left and ≤10% SRC carcinoma on the right (Group 1).

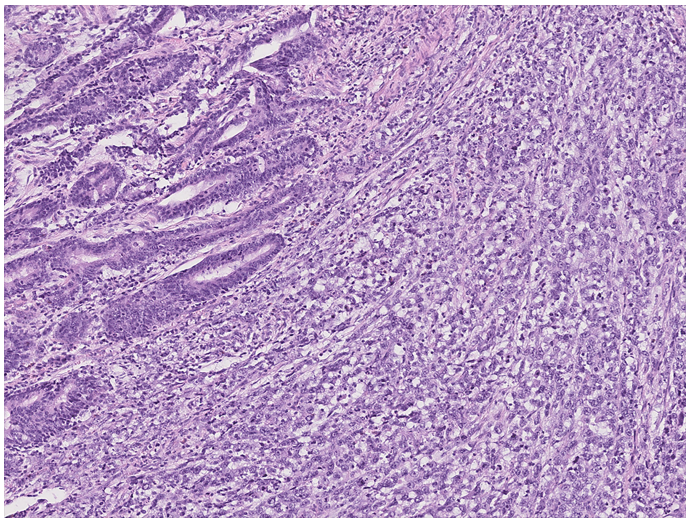

FIGURE 3 | Photomicrograph of mixed-type gastric cancer with moderately differentiated tubular adenocarcinoma on the left and 10%–90% SRC carcinoma on the right (Group 2).

proportion of Group 2 patients had AGC (69.7% vs. 94.9%, $p < 0.001$). The prevalence of SRC >10% was 80% (20/25) in ECG and 33.1% (46/139) in AGC patients. Additionally, Group 1 more frequently observed serosal invasion, positive peritoneal cytology, nodal involvement, neural and lymphovascular invasion, and R+ resection than Group 2. In Group 1, the median of positive nodes was 11 (range, 1–86) tumors compared to 1 (range, 1–54) in Group 2 ($p < 0.001$).

Survival Analysis

One hundred twenty-three patients who received curative resection (R0) were suitable for survival analysis. The median follow-up was 153 months [95% CI 144.3–161.7]. The median OS time for the entire group of patients with mixed-type GC was 69 months [95% CI 36.2–101.8]. The 5-, 10-, and 15-year OS rates were 53.3%, 37.8%, and 24.6%, respectively. The median RFS for the whole cohort was 10 months [95% CI 7.9-12.1], with a 3-year RFS rate of 11.4%.

Survival analyses were conducted with the mixed-type GCs grouped according to SRC proportion. The median OS in Group 1 was 25 months [95% CI 17.1–32.9] and that in Group 2 was 123 months [95% CI 52.8–193.2], with 5-year OS of 35.4% and 73.8% and 10-year OS of 25.7% and 51.5%, $p < 0.001$ (**Figure 4**). The median RFS in Group 1 was 9 months [95% CI 7.1–10.9] and 39 months [95% CI 0–78.6] in Group 2, with 3-year RFS of 0% and 66.7%, respectively, $p = 0.03$ (**Figure 5**).

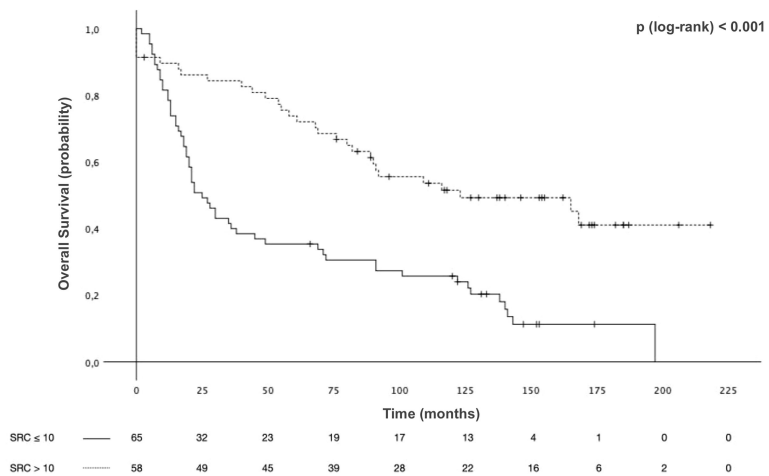

FIGURE 4 | Overall survival (OS) of patients with mixed-type gastric cancers stratified by signet ring cell (SRC) proportion.

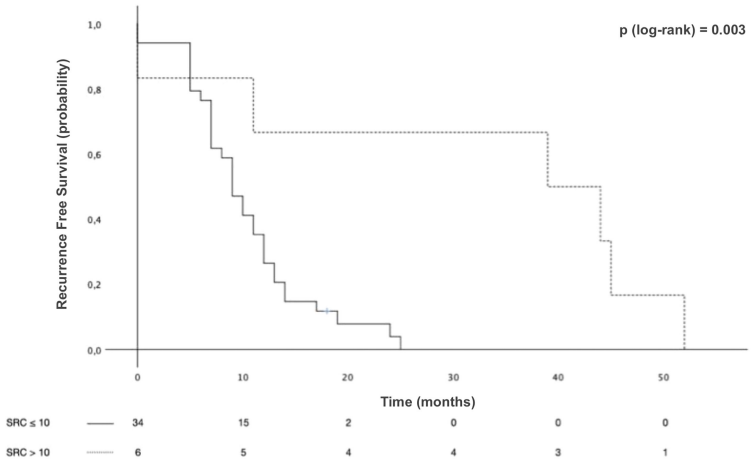

FIGURE 5 | Recurrence-free survival (RFS) of patients with mixed-type gastric cancers stratified by signet ring cell (SRC) proportion.

Interestingly, Group 2 showed better median OS [168 months (95% CI 65.3–270.6)] among patients with EGC, compared to Group 1 [69 months, (95% CI 0–152.7)], $p < 0.001$. Results for AGC patients were similar, with a median OS of 123 months [95% CI 43.4-202.6] for Group 2, compared with a median OS of 22 months [95% CI 13.4-30.6] for Group 1, $p < 0.001$. Given the poor prognosis found in univariate analysis for these variables, a multivariable model was constructed to adjust for potential confounding factors, which is illustrated in **Table 3**. The increase in mortality risk was about threefold in patients with ≤10% SRC pattern compared to those with >10% [HR 2.70 (95% CI 1.72–4.24), $p < 0.001$]. After adjusting for potential confounding factors, the SRC percentage was still an independent predictor of survival. Lymph node metastasis served as another independent prognostic factor.

DISCUSSION

Our results showed that a high percentage of SRCs in mixed-type GC was linked to the most favorable clinicopathological characteristics as well as better survival outcomes, providing new insight into the evidence of the prognostic value of SRC also in mixed-type GC.

TABLE 3 | Univariate analysis of factors affecting survival and hazard ratios for risk factors of mortality.

Variable	Category	*N*	Median overall survival (months) [95% CI]	Univariate analysis (*p* value)	Multivariate analysis		
					HR	95% CI	*p*-value
Gender	Male	83	58 [20.8–95.2]	0.552			
	Female	40	89 [63.8–114.2]				
Age	<60 years	12	140 [NR]	0.080			
	≥60 years	111	68 [41.6–94.4]				
Lymph node metastasis	Negative	72	116 [86.1–145.9]	**0.000**	1		
	Positive	51	21 [13.1–28.9]		2.1	[1.03–4.29]	**0.041**
Lymphovascular invasion	Negative	77	101 [68.1–133.9]	**0.000**	1		
	Positive	40	21 [17.3–24.7]		1.1	[0.52–2.20]	0.855
Perineural invasion	Negative	76	80 [50.4–109.6]	**0.006**	1		
	Positive	11	17 [8.7–25.3]		1.5	[0.62–3.46]	0.391
EGC/AGC	Early Gastric Cancer	25	116 [22.4–209.6]	**0.012**	1		
	Advanced Gastric Cancer	98	49 [16.2–81.8]		1.04	[0.43–2.47]	0.937
TNM stage	T1–2	60	109 [72.7–145.3]	**0.000**	1		
	T3–4	63	25 [10.4–39.6]		1.8	[0.88–3.54]	0.108
Adjuvant chemotherapy	Yes	95	118 [84.3–147.2]	**0.000**	1		
	No	69	23 [15.1–35.7]		2	[1.02–3.76]	**0.045**
Signet ring cells proportion	SRC ≤ 10	65	25 [17.1–32.9]	**0.000**	1.8	[1.04–3.19]	**0.035**
	SRC > 10	58	123 [52.8–193.2]		1		

Overall survival is illustrated as median with 95% CI. HR, hazard ratio; CI, confidence interval; NR, not reached; EGC, early gastric cancer; AGC, advanced gastric cancer; SRC, signet ring cell. P values in bold are statistically significant.

GCs exhibit a highly heterogeneous nature in terms of histological type and differentiation (1, 15). In the age of tailored surgery, it has been of greater interest not only to merely classify the tumor from a histological point of view but also to establish a pathological classification system with an independent prognostic peculiarity pursuing personalized clinical management. Although several classification systems for GC have been proposed over the years (3, 4, 16–21), the question of which of them may be relevant in the clinical setting has not yet been answered. Additionally, it would appear that the 50% SRC threshold proposed in the previous classifications has been vague. The World Health Organization (WHO) classification system is recognized as one of the most detailed among all classification systems and is employed by several researchers investigating the pathological and prognostic aspects of GC (1). Additionally, the 5th update of WHO classification has led to a marked improvement in GC knowledge. The mixed type has been described as a distinct histopathological entity that includes both glandular (tubular/papillary) and SRC/poorly cohesive components. Similarly, the Lauren classification, with a comparable significance to that provided by WHO, also identifies mixed type as a distinct category with a mixture of intestinal and diffuse components (4, 22). Evidence gathered over the last years has shown conflicting results, and the prognostic impact of this histotype is still debated among the scientific community, with some authors describing the mixed type as a predictor of poor prognosis and high risk of lymph node metastasis (23–25) and others reporting similar outcomes compared with other histotypes (26, 27).

Our group previously reported that the percentage of SRCs is inversely related to tumor aggressiveness in poorly cohesive GCs confirming the role of SRC pattern as an independent predictor of survival (8). By extending the concept of this new evidence to mixed histology, we can postulate that the inconsistent findings of previous studies (23–28) could be explained by the heterogeneity of SRC components. To the best of our knowledge, our study is the first to evaluate the clinicopathological aspects and prognostic outcomes of mixed-type GCs according to SRC percentages. Nonetheless, the retrospective design and the small sample size could affect our results in terms of bias.

As discussed, several studies showed that mixed histotype is associated with aggressive behavior, such as tumor size, lymphatic invasion, and lymph node metastasis (23, 29, 30). On the other hand, Zhong et al. (26), in a retrospective study on a total of 298 patients, stated that histological mixed type was not an independent risk factor for lymph node metastasis and was not associated with more aggressive characteristics in comparison with other histotypes. The same results were also obtained by Min et al. (27) on a cohort of 1577 patients.

In an attempt to explain the discrepancies arising from previous studies, this paper introduces new and intriguing evidence as regards the mixed-type GCs. By evaluating histopathological characteristics and prognoses, we observed that compared with those with more than 10% of SRCs, cancer patients with less than 10% of SRCs were younger and were more frequently associated with increased size, depth of invasion, nodal involvement, and advanced pathologic stage at diagnosis. Additionally, our data highlighted a distinctive tendency toward a survival difference according to SRC percentage between the two groups of mixed-type GC. Definitively, according to this research, the SRC pattern was an independent factor predicting prognosis in mixed-type GC patients.

Molecular mechanisms underlying the unfavorable behavior are still unclear. Anyway, it has been postulated that more aggressive clinicopathological as well as morphological findings of mixed-type cancers (10, 31) could be attributed to the angiogenetic process and cell proliferation, to cytosine-phosphate-guanine (CpG) island hypermethylation (32), or to the unregulated expression of proteins such as Ki-67, E-cadherin, and VEGF proteins, which were involved in proliferation (10), adhesion, and angiogenesis activities (10, 28). Interestingly, some researchers argued that mixed type would undergo transitional events leading to phenotype transformation along with cancer progression (33). Based on this finding, further research aiming at SRC amount comparison between endoscopic biopsies and resected specimens could be conducted.

We provide compelling evidence suggesting that distinct clinicopathological and prognostic findings are associated with the amount of SRCs in mixed-type gastric tumors. The significance of these different SRC percentages has not been investigated deeper, and our focus on the clinical outcome rather than genetic alterations could represent a limit for our study. Nevertheless, our data have confirmed, through undeniable evidence, that the SRC pattern is an independent predictor of survival also in mixed-type GC. Results demonstrate that a lower SRC proportion is associated with poorer OS. Thus, the proportion of SRCs can be considered a marker of differentiation.

In conclusion, the percentage of SRCs is inversely related to aggressive behavior and poor prognosis in mixed-type GCs, highlighting the role of SRC amount as an independent predictor of survival. Further studies are needed to investigate specific genetic and molecular profiles underlying the SRC effects to reach a clearer interpretation of these findings.

DATA AVAILABILITY STATEMENT

The raw data supporting the conclusions of this article will be made available by the authors, without undue reservation.

ETHICS STATEMENT

The studies involving human participants were reviewed and approved by the Institutional Review Committee of the University of Siena. The patients/participants provided their written informed consent to participate in this study.

AUTHOR CONTRIBUTIONS

Study concepts: LMar, FR, MA, and KP. Study design: LMar, FR, OS, and KP. Data acquisition: LMar, MA, LR, LMal, and KP. Quality control of data and algorithms: VS, MC, LMal, RP, IB, and OS. Data analysis and interpretation: LMar, DM, and MA. Statistical analysis: LMar, LR, RP, and IB. Manuscript preparation: LMar, DM, FR, VS, LR, RP, MA, and MC. Manuscript editing: LR, LC, RP, MA, and OS. Manuscript review: LMar, MA, MC, VS, LR, LC, IB, and KP. All authors contributed to the article and approved the submitted version.

ACKNOWLEDGMENTS

The authors express their special thanks to Antonia Carbone for her assistance with English editing.

SUPPLEMENTARY MATERIAL

The Supplementary Material for this article can be found online at: https://www.frontiersin.org/articles/10.3389/fonc.2022.897218/full#supplementary-material

REFERENCES

1. Sentani K, Imai T, Kobayashi G, Hayashi T, Sasaki N, Oue N, et al. Histological Diversity and Molecular Characteristics in Gastric Cancer: Relation of Cancer Stem Cell-Related Molecules and Receptor Tyrosine Kinase Molecules to Mixed Histological Type and More Histological Patterns. *Gastric Cancer* (2021) 24:368–81. doi: 10.1007/s10120-020-01133-w
2. Japanese Gastric Cancer Association. Japanese Classification of Gastric Carcinoma: 3rd English Edition. *Gastric Cancer* (2011) 14:101–12. doi: 10.1007/s10120-011-0041-5
3. WHO Classification of Tumours Editorial Board: WHO Classification of Tumours - 5th Edition. World Health Organization Press (2019). p. 539.
4. Lauren P. The Two Histological Main Types Of Gastric Carcinoma: Diffuse And So-Called Intestinal-Type Carcinoma. An Attempt At A Histo-Clinical Classification. *Acta Pathol Microbiol Scand* (1965) 64:31–49. doi: 10.1111/apm.1965.64.1.31
5. Nagtegaal ID, Odze RD, Klimstra D, Paradis V, Rugge M, Schirmacher P, et al. The 2019 WHO Classification of Tumours of the Digestive System. *Histopathology* (2020) 76:182–8. doi: 10.1111/his.13975
6. Mariette C, Carneiro F, Grabsch HI, van der Post RS, Allum W, de Manzoni G, et al. Consensus on the Pathological Definition and Classification of Poorly Cohesive Gastric Carcinoma. *Gastric Cancer* (2019) 22:0. doi: 10.1007/s10120-018-0868-0
7. Bencivenga M, Treppiedi E, Dal Cero M, Torroni L, Verlato G, Iglesias M, et al. The Amount of Signet Ring Cells Is Significantly Associated With Tumour Stage and Survival in Gastric Poorly Cohesive Tumours. *J Surg Oncol* (2020) 121(7):1084–9. doi: 10.1002/jso.25885
8. Roviello F, Marano L, Ambrosio MR, Resca L, D'Ignazio A, Petrelli F, et al. Signet Ring Cell Percentage in Poorly Cohesive Gastric Cancer Patients: A Potential Novel Predictor of Survival. *Eur J Surg Oncol* (2021) 48(3):561–9. doi: 10.1016/j.ejso.2021.09.003
9. Dong X, Sun G, Qu H, He Q, Hao Z. Prognostic Significance of Signet-Ring Cell Components in Patients With Gastric Carcinoma of Different Stages. *Front Surg* (2021) 8:642468. doi: 10.3389/fsurg.2021.642468
10. Chu Y, Mao T, Li X, Jing X, Ren M, Huang Z, et al. Predictors of Lymph Node Metastasis and Differences Between Pure and Mixed Histologic Types of Early Gastric Signet-Ring Cell Carcinomas. *Am J Surg Pathol* (2020) 44:934–42. doi: 10.1097/PAS.0000000000001460
11. Brierley J, Gospodarowicz MK: TNM Classification of Malignant Tumours, 8th Edition. Wiley-Blackwell Press (2016). p. 63.
12. Japanese Gastric Cancer Association. Japanese Gastric Cancer Treatment Guidelines 2014 (Ver. 4). *Gastric Cancer* (2017) 20:1–19. doi: 10.1007/s10120-016-0622-4
13. Xue X, Agalliu I, Kim MY, Wang T, Lin J, Ghavamian R, et al. New Methods for Estimating Follow-Up Rates in Cohort Studies. *BMC Med Res Methodol* (2017) 17:155. doi: 10.1186/s12874-017-0436-z
14. von Elm E, Altman DG, Egger M, Pocock SJ, Gøtzsche PC, Vandenbroucke JP. The Strengthening the Reporting of Observational Studies in Epidemiology (STROBE) Statement: Guidelines for Reporting Observational Studies. *Int J Surg* (2014) 12:1495–9. doi: 10.1016/j.ijsu.2014.07.013
15. Boccardi V, Marano L, Rossetti RRA, Rizzo MR, di Martino N, Paolisso G. Serum CD26 Levels in Patients With Gastric Cancer: A Novel Potential Diagnostic Marker. *BMC Cancer* (2015) 15:703. doi: 10.1186/s12885-015-1757-0
16. Goseki N, Takizawa T, Koike M. Differences in the Mode of the Extension of Gastric Cancer Classified by Histological Type: New Histological Classification of Gastric Carcinoma. *Gut* (1992) 33:606–12. doi: 10.1136/gut.33.5.606
17. Ming SC. Gastric Carcinoma. A Pathobiological Classification. *Cancer* (1977) 39:2475–85. doi: 10.1002/1097-0142(197706)39:6<2475::aid-cncr2820390626>3.0.co;2-l
18. Grundmann E, Schlake W. Histological Classification of Gastric Cancer From Initial to Advanced Stages. *Pathol Res Pract* (1982) 173:260–74. doi: 10.1016/S0344-0338(82)80088-5
19. Carneiro F, Seixas M, Sobrinho-Simões M. New Elements for an Updated Classification of the Carcinomas of the Stomach. *Pathol Res Pract* (1995) 191:571–84. doi: 10.1016/S0344-0338(11)80878-2
20. Ychou M, Boige V, Pignon J-P, Conroy T, Bouché O, Lebreton G, et al. Perioperative Chemotherapy Compared With Surgery Alone for Resectable Gastroesophageal Adenocarcinoma: An FNCLCC and FFCD Multicenter Phase III Trial. *J Clin Oncol* (2011) 29:1715–21. doi: 10.1200/JCO.2010.33.0597
21. Berlth F, Bollschweiler E, Drebber U, Hoelscher AH, Moenig S. Pathohistological Classification Systems in Gastric Cancer: Diagnostic Relevance and Prognostic Value. *World J Gastroenterol* (2014) 20:5679–84. doi: 10.3748/wjg.v20.i19.5679
22. Chen Y-C, Fang W-L, Wang R-F, Liu C-A, Yang M-H, Lo S-S, et al. Clinicopathological Variation of Lauren Classification in Gastric Cancer. *Pathol Oncol Res* (2016) 22:197–202. doi: 10.1007/s12253-015-9996-6
23. Komatsu S, Ichikawa D, Miyamae M, Shimizu H, Konishi H, Shiozaki A, et al. Histological Mixed-Type as an Independent Prognostic Factor in Stage I Gastric Carcinoma. *World J Gastroenterol* (2015) 21:549–55. doi: 10.3748/wjg.v21.i2.549
24. Pyo JH, Lee H, Min BH, Lee JH, Choi MG, Lee JH, et al. Early Gastric Cancer With a Mixed-Type Lauren Classification Is More Aggressive and Exhibits Greater Lymph Node Metastasis. *J Gastroenterol* (2017) 52:594–601. doi: 10.1007/s00535-016-1254-5
25. Shimizu H, Ichikawa D, Komatsu S, Okamoto K, Shiozaki A, Fujiwara H, et al. The Decision Criterion of Histological Mixed Type in "T1/T2" Gastric Carcinoma–Comparison Between TNM Classification and Japanese Classification of Gastric Cancer. *J Surg Oncol* (2012) 105:800–4. doi: 10.1002/jso.23010
26. Zhong Q, Sun Q, Xu G-F, Fan X-Q, Xu Y-Y, Liu F, et al. Differential Analysis of Lymph Node Metastasis in Histological Mixed-Type Early Gastric Carcinoma in the Mucosa and Submucosa. *World J Gastroenterol* (2018) 24:87–95. doi: 10.3748/wjg.v24.i1.87
27. Min BH, Kim KM, Park CK, Lee JH, Rhee PL, Rhee JC, et al. Outcomes of Endoscopic Submucosal Dissection for Differentiated-Type Early Gastric Cancer With Histological Heterogeneity. *Gastric Cancer* (2015) 18:618–26. doi: 10.1007/s10120-014-0378-7
28. Zhao B, Huang R, Lu H, Mei D, Bao S, Xu H, et al. Risk of Lymph Node Metastasis and Prognostic Outcome in Early Gastric Cancer Patients With Mixed Histologic Type. *Curr Probl Cancer* (2020) 44(6):100579. doi: 10.1016/j.currproblcancer.2020.100579
29. Watanabe G, Ajioka Y, Takeuchi M, Annenkov A, Kato T, Watanabe K, et al. Intestinal Metaplasia in Barrett's Oesophagus may be an Epiphenomenon Rather Than a Preneoplastic Condition, and CDX2-Positive Cardiac-Type Epithelium Is Associated With Minute Barrett's Tumour. *Histopathology* (2015) 66:201–14. doi: 10.1111/his.12486

30. Hanaoka N, Tanabe S, Mikami T, Okayasu I, Saigenji K. Mixed-Histologic-Type Submucosal Invasive Gastric Cancer as a Risk Factor for Lymph Node Metastasis: Feasibility of Endoscopic Submucosal Dissection. *Endoscopy* (2009) 41:427–32. doi: 10.1055/s-0029-1214495
31. Imamura T, Komatsu S, Ichikawa D, Kawaguchi T, Kosuga T, Okamoto K, et al. Early Signet Ring Cell Carcinoma of the Stomach Is Related to Favorable Prognosis and Low Incidence of Lymph Node Metastasis. *J Surg Oncol* (2016) 114:607–12. doi: 10.1002/jso.24377
32. Piessen G, Messager M, Leteurtre E, Jean-Pierre T, Mariette C. Signet Ring Cell Histology Is an Independent Predictor of Poor Prognosis in Gastric Adenocarcinoma Regardless of Tumoral Clinical Presentation. *Ann Surg* (2009) 250:878–87. doi: 10.1097/SLA.0b013e3181b21c7b
33. Luinetti O, Fiocca R, Villani L, Alberizzi P, Ranzani GN, Solcia E. Genetic Pattern, Histological Structure, and Cellular Phenotype in Early and Advanced Gastric Cancers: Evidence for Structure-Related Genetic Subsets and for Loss of Glandular Structure During Progression of Some Tumors. *Hum Pathol* (1998) 29:702–9. doi: 10.1016/s0046-8177(98)90279-9

Conflict of Interest: The authors declare that the research was conducted in the absence of any commercial or financial relationships that could be construed as a potential conflict of interest.

Publisher's Note: All claims expressed in this article are solely those of the authors and do not necessarily represent those of their affiliated organizations, or those of the publisher, the editors and the reviewers. Any product that may be evaluated in this article, or claim that may be made by its manufacturer, is not guaranteed or endorsed by the publisher.

Copyright © 2022 Marano, Ambrosio, Resca, Carbone, Carpineto Samorani, Petrioli, Savelli, Costantini, Malaspina, Polom, Biviano, Marrelli and Roviello. This is an open-access article distributed under the terms of the Creative Commons Attribution License (CC BY). The use, distribution or reproduction in other forums is permitted, provided the original author(s) and the copyright owner(s) are credited and that the original publication in this journal is cited, in accordance with accepted academic practice. No use, distribution or reproduction is permitted which does not comply with these terms.

frontiers | Frontiers in Surgery

ORIGINAL RESEARCH
published: 27 May 2022
doi: 10.3389/fsurg.2022.918198

Comparison of Four Lymph Node Staging Systems in Gastric Adenocarcinoma after Neoadjuvant Therapy – A Population-Based Study

Hongkun Lai[1,2†], *Jiabin Zheng*[2†] *and Yong Li*[2,1*]

[1]The Second School of Clinical Medicine, Southern Medical University, Guangzhou, China, [2]Department of Gastrointestinal Surgery, Guangdong Provincial People's Hospital; Guangdong Academy of Medical Sciences, Guangzhou, China

OPEN ACCESS

Edited by:
Qi Liu,
Shanghai Cancer Center,
Fudan University, China

Reviewed by:
Jingyu Deng,
Tianjin Medical University Cancer Institute and Hospital, China
Ahmed Farag El-Kased,
University of Menoufia, Egypt

***Correspondence:**
Yong Li
liyong@gdph.org.cn

[†]These authors have contributed equally to this work

Specialty section:
This article was submitted to Surgical Oncology, a section of the journal Frontiers in Surgery

Received: 12 April 2022
Accepted: 05 May 2022
Published: 27 May 2022

Citation:
Lai H, Zheng J and Li Y (2022) Comparison of Four Lymph Node Staging Systems in Gastric Adenocarcinoma after Neoadjuvant Therapy – A Population-Based Study. Front. Surg. 9:918198. doi: 10.3389/fsurg.2022.918198

Introduction: Neoadjuvant treatment leads in a reduction in positive lymph nodes and examined lymph nodes (ELN), which may affect assessment of lymph node staging and postoperative treatment.We aimed to compare the staging systems of lymph node ratio (LNR), the positive logarithm ratio of lymph nodes (LODDS), negative lymph nodes (NLN), and the 8th AJCC ypN stage for patients with gastric adenocarcinoma after neoadjuvant therapy.

Materials and Methods: Data was collected from the Surveillance, Epidemiology, and End Results database and 1,551 patients with gastric adenocarcinoma who underwent neoadjuvant therapy and radical surgery were enrolled. Harrell's concordance index, the Receiver Operative Curve, the likelihood ratio test, and the Akaike information criterion were used to compare the predictive abilities of the different staging systems.

Results: Among the 1,551 patients, 689 (44.4%) had ELN < 16 and node-negative patients accounted for 395 (25.5%). When regarded as the categorical variable, LNR had better discrimination power, higher homogeneity, and better model fitness for CSS and OS compared to other stage systems, regardless of the status of ELN. When regarded as the continuos variable, LODDS outperformed others for CSS. Furthermore, the NLN staging system performed superior to others in node-negative patients.

Conclusions: LNR had a better predictive performance than ypN, LODDS and NLN staging systems regardless of the status of ELN when regarded as the categorical variable, whereas LOODS became the better predictive factor for CSS when regarded

Abbreviations: OS, overall survival; CSS, cancer specific survival; N, number; IQR, interquartile range; HR, hazard ratio; CI, confidence interval; LN, lymph node; ELN, Examined lymph nodes; PLN, number of positive lymph nodes; LNR, lymph node ratio; LODDS, log odds of positive lymph node/ positive logarithm ratio of lymph nodes; NLN, negative lymph node; C-index, Harrell's concordance index; ROC, the Receiver Operative Curve; LR test,the likelihood ratio test; AIC, the Akaike information criterion; NAT, neoadjuvant therapy; SEER database, Surveillance, Epidemiology, and End Result (SEER) database.

as the continuos variable. In node-negative patients, NLN might be a feasible option for evaluating prognosis. A combination of LNR and NLN should be considered as user-friendly method in the clinical prognostic assessment.

Keywords: neoadjuvant therapy, prognosis, lymph node classification, gastric adenocarcinoma, lymph node ratio, positive logarithm ratio of lymph node, negative lymph node

INTRODUCTION

At present, neoadjuvant therapies have become the standard for the management of patients with locally advanced gastric adenocarcinoma in western countries, based on the results of randomized controlled trials [1–6]. Compared with patients with initial surgical resection, fewer examined lymph nodes (ELN) and positive lymph nodes (PLN) were harvested in patients receiving neoadjuvant therapy (NAT) [7], particularly in patients treated with neoadjuvant radiation [8]. As a result, neoadjuvant therapy increased the number of node-negative patients as well as those with insufficient ELN [7], and it may not accurately assess lymph node status following NAT. However, the lymph node (LN) status in the AJCC ypTNM stage system is still based on the number of PLN and it is recommended to harvest at least 16 LN to reduce the stage migration. It was proved that ELN in node-negative patients after NAT was an independent prognostic factor and the patients had better survival with ELN increased, suggesting that patients with insufficient ELN may be underestimated and when ELN increased, the patients may upstage to ypN1 or ypN2 [9]. Previous research suggested that LN status could aid in determining postoperative treatment in patients with pathological complete response [10–12]. Currently, the 8th edition AJCC ypTNM stage system is the most widely used to predict the prognosis of patients receiving NAT. Lymph node ratio (LNR) has been shown to be an alternative prognostic factor in a variety of cancers, and it has been proposed that it may reduce the N-stage migration effect [13–16]. However, in several studies, it was suggested that for patients with no metastatic lymph node, LNR does not outperform the ypN stage system [8, 17]. Moreover, LODDS is the logarithm of the ratio between PLN and negative lymph nodes (NLN) and has been proven to reduce the stage migration in many cancers, including pancreatic cancer and gastric adenocarcinoma [8, 18, 19]. Some studies have shown that NLN is also an alternative stage for a predictive prognosis for gastric adenocarcinoma and breast cancer [20, 21]. However, most previous studies have focused on patients who have not received preoperative treatment [22–26]. Whether the conclusions from these studies could be extended to patients after NAT remains unclear. In this study, we aimed to identify the best staging system among ypN, LNR, LODDS, and NLN for the prediction of prognosis in patients with gastric adenocarcinoma after NAT.

MATERIALS AND METHODS

All procedures involving human participants in this study comply with the Declaration of Helsinki (revised in 2013). Due to the retrospective nature of the study, the requirement for informed consent was abandoned. SEER*Stat software (Version 8.3.2) was used to collect data from the Surveillance, Epidemiology, and End Result (SEER) database (1973–2016). 1,551 patients with primary gastric adenocarcinoma who received NAT and surgical resection were enrolled (**Figure 1**).

Patients

Data collected included patient demographic information, clinicopathological characteristics, and survival. The inclusion criteria were as follows: (1) Age $\geq$18 years. (2) There is no history of the malignant tumor. (3) The histopathological diagnosis is gastric adenocarcinoma (5) Completed follow-up and the postoperative survival time $\geq$2 months. (6) Neoadjuvant therapy is performed before the operation. The primary outcomes were cancer-specific survival (CSS) and overall survival (OS). CSS is defined as the time from diagnosis to cancer-specific death, and OS is defined as the interval between the date of diagnosis and the date of all-cause death.

Tumor Stage and LN Classifications

We defined the tumor stage using the 8th edition AJCC ypTNM staging system and conducted an appropriate conversion in patients whose tumor stage was presented with old TNM editions. 8th AJCC ypN stage (ypN0: no PLN, ypN1: 1–2 PLN, ypN2: 3–6 PLN, ypN3: PLN $\geq$ 7) is the current standard for the lymph node stage of gastric adenocarcinoma. LNR is the ratio of the number of PLN to the number of ELN (LNR = PLN/ELN). [27] Use Xtile software (Yale University, New Haven, CT, USA) to obtain the best cut-off value of three alternative staging systems (LNR, LOODS, NLN) and divide the patients into 4 groups,respectively [28]. LNR:LNR1:0; LNR2: $0.01 \leq LNR \leq 0.14$; LNR3: $0.14 < LNR \leq 0.37$, LNR4: LNR >0.37. LODDS is the logarithm of (PLN + 0.5)/(NLN + 0.5). The patients were designated according to cut-off values of −2.75, −1.61 and −0.51: LODDS1: $LODDS \leq -2.75$; LODDS2: $-2.75 < LODDS \leq -1.61$; LODDS3: $-1.61 < LODDS \leq -0.51$; LODDS4:$LODDS > -0.51$. NLN is the value of (ELN-PLN).NLN was designed into NLN1: NLN1 (NLN > 21), NLN2 ($13 < NLN \leq 21$), NLN3 ($8 < NLN \leq 13$), NLN4 ($NLN \leq 7$). We analyzed the four staging systems as categorical and continuous variables, respectively.

Statistical Analysis

R software (version 3.61) and SPSS 25.0 (IBM SPSS Inc.) were used for statistical analysis. The baseline characteristics of patients were statistically analyzed by quantitative values and median interquartile differences (IQRs). Baseline factors related to CSS and OS were evaluated by univariate and

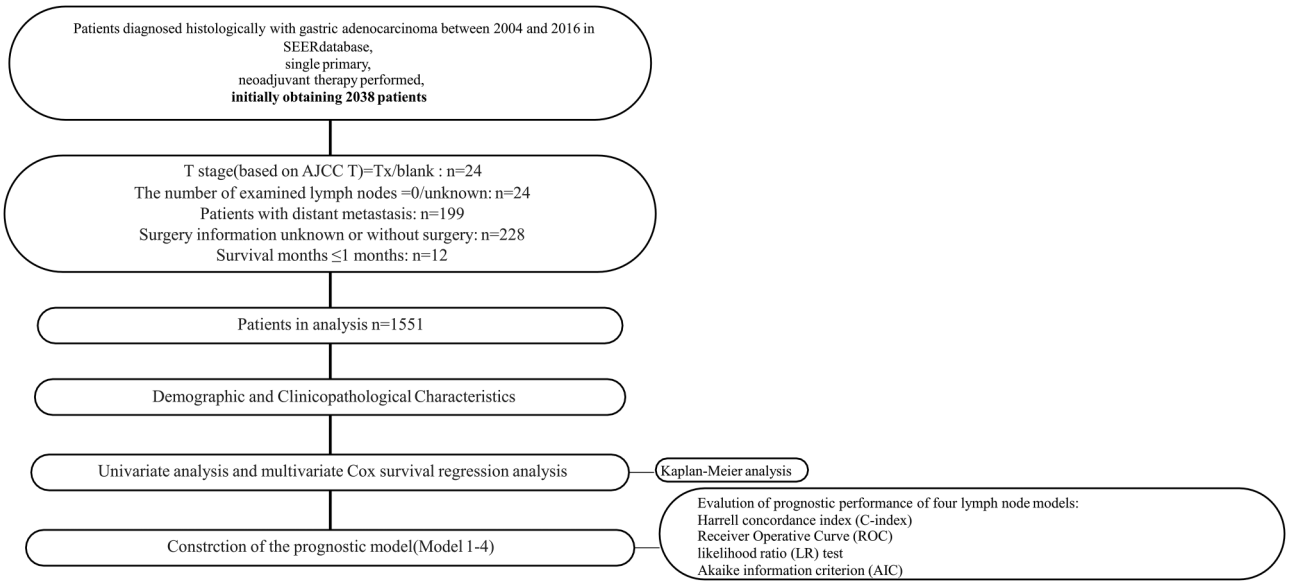

FIGURE 1 | Research flowchart.

multivariate Cox survival Regression Analysis. Multivariate analysis models included the covariates T stage, age, histological grade, tumor location, histological type, and each staging system, that is, ypN stage (Model1), LNR (Model2), LODDS (Model3), NLN (Model4). The Kaplan-Meier method was used to estimate CSS and OS, and the Log-rank test was used to verify the survival difference of each subgroup. The performance of the prognostic system has been proved to be evaluated by the discriminatory power (the survival of patients in different stages of each system is more different) and homogeneity (the survival of patients of the same category is less different in each system) [29–31]. Harrell's c index (C-index) and the Receiver Operative Curve (ROC) were performed to compare the discriminatory power among different systems. Model fit was evaluated using the Akaike information criterion (AIC) [31]. The likelihood ratio test (LR test) was calculated using Cox regression to measure homogeneity; a higher likelihood ratio test indicates better homogeneity. An internal validation procedure using 2,000 bootstraps was applied to the calculation of the C-index and Confidence Intervals. All tests are two-sided tests, and $p < 0.05$ is considered statistically significant.

RESULTS

Demographic and Clinicopathological Characteristics

A total of 1,551 patients were eligible for inclusion in this study. The patients' characteristics are summarized in **Table 1**. 395 (25.5%) were female and 1,156 (74.5%) male. 589(38.0%)were more than 65 years old. After NAT, most patients were found to have poorly or undifferentiated adenocarcinoma. Patients had a median of 17 lymph nodes examined. Among them, ELN ≥ 16 was 862 (55.6%) and ELN < 16 was 689 (44.4%), and node-negative patients were 395 (25.5%), and the median number of lymph node metastases was 2 (range from 0 to 47). The overall survival time have been described in section "Survival Analysis" below.

Univariate Analysis and Multivariate Analysis

As shown in **Table 1**, grade, histologic type, tumor size, ypT category, ELN, ypN stage, LODDS, LNR, NLN were significantly correlated with CSS, and age, grade, histologic type, tumor size, four lymph node staging schemes, ELN were significantly correlated with OS. Based on the univariate analysis and clinical practice, ypN (Model1), LNR (Model2), LODDS (Model3), and NLN (Model4) were respectively included in different multivariate Cox regression models for CSS and OS. As shown in **Tables 2**, **3**, in the multivariate Cox regression models, four lymph node staging schemes (ypN, LNR, LODDS and NLN) were independent prognostic factors for CSS and OS.

Survival Analysis

The median CSS and OS of patients were 29 and 27 months, and death caused by gastric adenocarcinoma was observed in 872 (56.2%) patients while 975 (62.9%) patients died from any causes. As shown in **Table 1** and **Figure 2**, four lymph node staging schemes were correlated to CSS and OS and pairwise survival in different schemes between subgroups was statistically significant.

The 3-year CSS and OS rates in the ypN0 group ($n = 395$), ypN1 group ($n = 413$), ypN2 group ($n = 404$) and ypN3 group ($n = 339$) were 55.8%, 36.7%, 21.5%, 13.3% and 46.6%, 31.7%,

TABLE 1 | Baseline characteristics and univariate analysis for CSS and OS in gastric adenocarcinoma patients after NAT.

Characteristic	*N* (%/IQR)	CSS		OS	
	1,551	Hazard ratio (95% CI)	*p*-value	Hazard ratio (95% CI)	*p*-value
Age					
≤65	962 (62.0)	1.00			1
>65	589 (38.0)	1.09 (0.95–1.25)	0.24	1.16 (1.02–1.32)	0.03
Race					
White	1,198 (77.2)	1.00		1	
Black	147 (9.5)	0.97 (0.77–1.22)	0.78	0.94 (0.76–1.18)	0.60
Other	206 (13.3)	0.79 (0.64–0.97)	0.03	0.83 (0.69–1.02)	0.07
Sex					
Female	395 (25.5)	1.00		1	
Male	1,156 (74.5)	0.97 (0.84–1.13)	0.71	1.02 (0.88–1.18)	0.76
Location					
Upper	928 (59.8)	1.00		1	
Middle	259 (16.7)	0.78 (0.64–0.95)	≤0.01	0.82 (0.69–0.99)	0.04
Lower	188 (12.1)	0.87 (0.7–1.08)	0.21	0.87 (0.71–1.07)	0.20
Overlapping	106 (6.8)	1.22 (0.95–1.58)	0.12	1.18 (0.92–1.52)	0.19
NOS	70 (4.5)	1.46 (1.08–1.96)	≤0.01	1.51 (1.14–2)	≤0.01
Histologic type					
Adenocarcinoma	1,225 (79.0)	1.00		1	
Signet ring cell carcinoma	326 (21.0)	1.38 (1.18–1.61)	≤0.01	1.32 (1.14–1.53)	≤0.01
Grade					
G1/G2	399 (25.7)	1.00		1	
G3/G4	1,053 (67.9)	1.42 (1.21–1.67)	≤0.01	1.33 (1.15–1.55)	≤0.01
Unknown	99 (6.4)	1.20 (0.88–1.62)	0.24	1.1 (0.82–1.47)	0.51
Tumor size					
≤2 cm	204 (13.2)	1.00		1	
>2 cm, ≤5 cm	590 (38.2)	1.25 (1–1.56)	0.05	1.25 (1.01–1.54)	0.04
>5 cm	476 (30.8)	1.46 (1.16–1.83)	≤0.01	1.43 (1.16–1.78)	≤0.01
Linitis plastica	27 (1.7)	1.73 (1.06–2.82)	0.03	1.71 (1.07–2.72)	0.02
Uknown	249 (16.1)	1.18 (0.92–1.53)	0.20	1.18 (0.92–1.5)	0.19
ypT category					
ypT1	124 (8.0)	1.00		1	
ypT2	159 (10.3)	1.62 (1.11–2.39)	≤0.01	1.45 (1.03–2.05)	0.03
ypT3	652 (42.0)	2.28 (1.65–3.15)	≤0.01	1.94 (1.46–2.59)	≤0.01
ypT4a	506 (32.6)	2.80 (2.02–3.88)	≤0.01	2.38 (1.79–3.18)	≤0.01
ypT4b	110 (7.1)	3.41 (2.33–5)	≤0.01	2.9 (2.06–4.1)	≤0.01
Positive lymph nodes	2.00 [0.00, 6.00]	0.99 (0.99–1)	≤0.01	1.06 (1.05–1.07)	≤0.01
Examined lymph nodes	17.00 [11.00, 25.00]	1.07 (1.06–1.08)	≤0.01	0.99 (0.99–1)	≤0.01
ypN category					
ypN0	395 (25.5)	1.00		1	
ypN1	413 (26.6)	1.60 (1.31–1.97)	≤0.01	1.52 (1.26–1.84)	≤0.01
ypN2	404 (26.0)	2.11 (1.73–2.58)	≤0.01	1.89 (1.57–2.28)	≤0.01
ypN3	339 (21.9)	3.40 (2.77–4.17)	≤0.01	3.08 (2.55–3.73)	≤0.01
ELN (categorical)					
ELN ≥ 16	862 (55.6)	1.00		1	
ELN < 16	689 (44.4)	1.17 (1.02–1.33)	0.02	1.15 (1.01–1.3)	0.03

(*continued*)

TABLE 1 | Continued

Characteristic	*N* (%/IQR)	CSS		OS	
	1,551	Hazard ratio (95% CI)	*p*-value	Hazard ratio (95% CI)	*p*-value
Lymph node ratio	0.14 [0.00, 0.37]	6.85 (5.44–8.64)	≤0.01	6.49 (5.2–8.1)	≤0.01
LNR category					
LNR1	395 (25.5)	1.00		1	
LNR2	394 (25.4)	1.36 (1.1–1.68)	≤0.01	1.28 (1.05–1.55)	0.02
LNR3	376 (24.2)	2.11 (1.72–2.59)	≤0.01	1.91 (1.58–2.31)	≤0.01
LNR4	386 (24.9)	3.81 (3.13–4.65)	≤0.01	3.48 (2.9–4.18)	≤0.01
LODDS	−1.61 [−2.75, −0.51]	1.40 (1.34–1.46)	≤0.01	1.38 (1.32–1.43)	≤0.01
LODDS category					
LODDS1	394 (25.4)	1.00		1	
LODDS2	389 (25.1)	1.45 (1.17–1.79)	≤0.01	1.32 (1.08–1.61)	≤0.01
LODDS3	384 (24.8)	2.20 (1.79–2.7)	≤0.01	1.97 (1.62–2.38)	≤0.01
LODDS4	384 (24.8)	3.94 (3.22–4.82)	≤0.01	3.55 (2.95–4.28)	≤0.01
NLN	13.00 [7.00, 21.00]	0.97 (0.96–0.98)	≤0.01	0.97 (0.97–0.98)	≤0.01
NLN category					
NLN1	359 (23.1)	1		1	
NLN2	383 (24.7)	1.32 (1.07–1.64)	≤0.01	1.31 (1.07–1.6)	≤0.01
NLN3	403 (26.0)	1.8 (1.47–2.21)	≤0.01	1.72 (1.42–2.09)	≤0.01
NLN4	406 (26.2)	2.29 (1.87–2.8)	≤0.01	2.19 (1.82–2.65)	≤0.01
Chemotherapy					
None	14 (0.9)	1.00		1	
Yes	1,537 (99.1)	1.51 (0.68–3.37)	0.31	1.49 (0.71–3.15)	0.29
Radiotherapy					
None	660 (42.6)	1.00		1.00	
Radiation prior to surgery	668 (43.1)	1.18 (1.01–1.36)	0.03	1.20 (1.05–1.39)	≤0.01
Radiation after surgery	201 (13.0)	1.22 (1.00–1.50)	0.05	1.20 (0.99–1.46)	0.07
Radiation before and after surgery	22 (1.4)	1.04 (1.57–1.90)	0.90	1.12 (0.64–1.94)	0.70

OS, overall survival; CSS, cancer specific survival; N, number; IQR, interquartile range; HR, hazard ratio; CI, confidence interval; ELNs, Examined lymph nodes; PLN, number of positive lymph nodes; LNR, lymph node ratio; LODDS, log odds of positive lymph node; NLN, negative lymph node.

18.9%, 10.3%, respectively. The 3-year CSS and OS rates in the LNR1 group ($n = 395$), LNR 2 group ($n = 394$), LNR 3 group ($n = 376$) and LNR 4 group ($n = 386$) were 52.3%, 40.3%, 23.3%, 10.2% and 46.0%, 35.6%, 20.4%, 7.4% respectively. The 3-year CSS and OS rates in the LOODS1 group ($n = 394$), LOODS2 group ($n = 389$), LOODS3 group ($n = 384$) and LOODS4 group ($n = 384$) were 54.8%, 38.0%, 24.0%, 10.3% and 48.5%, 33.5%, 20.9%, 7.4%, respectively. The 3-year CSS and OS rates in the NLN1 group ($n = 359$), NLN 2 group ($n = 383$), NLN 3 group ($n = 403$) and NLN 4 group ($n = 406$) were 47.6%, 36.6%, 26.2%, 21.9% and 42.8%, 31.0%, 22.7%, 18.3%, respectively.

Prognostic Performance of Four Lymph Node Models

As shown in **Tables 4**, **5**, when regarded as the categorical variables, LNR and LODDS had better performance than ypN and NLN schemes with higher C-index, lower AIC, higher LR test. Interestingly, when assessed as the continuous variables, the predictive performance of all staging systems were improved and LODDS outperformed other staging systems for CSS with higher C-index (CSS: 0.665), lower AIC (CSS: 11,422.83), higher LR test (CSS: 278.6) as well as LNR had better performance for OS with C-index (0.661), AIC (12,720.98), LR test (283.2). Additionally, as shown in **Figure 3**, based on the analysis of ROC curves, when regarded as the categorical variable, LNR and LODDS showed the superior discriminatory power for OS (LNR: 5-year CSS:0.751, 5-year OS:0.749;)(LODDS: 5-year CSS:0.751, 5-year OS:0.748;) to ypN (categorical:5-year CSS:0.740, 5-yearvOS:0.739;), NLN (categorical: 5-year CSS:0.708, 5-year OS: 0.702;) and the same result appeared when referring to CSS. The similar findings persisted when values of schemes were analyzed as the continuous variables (**Figure 4**).

TABLE 2 | Multivariate Cox regression analysis of prognostic predictors for OS in gastric adenocarcinoma patients after NAT.

Characteristic	Model 1 (ypN)		Model 2 (LNR)		Model 3 (LODDS)		Model 4 (NLN)	
OS	Hazard ratio (95% CI)	*p*-value	Hazard ratio (95% CI)	*p*-value	Hazard ratio (95% CI)	*p* value	Hazard ratio (95% CI)	*p*-value
Age								
≤65	1.00		1.00		1.00		1.00	
>65	1.21 (1.06–1.38)	≤0.01	1.22 (1.07–1.39)	≤0.01	1.22 (1.07–1.39)	≤0.01	1.21 (1.06–1.38)	≤0.01
Histologic type								
Adenocarcinoma	1.00		1.00		1.00		1.00	
Signet ring cell carcinoma	1.23 (1.04–1.44)	≤0.01	1.21 (1.03–1.43)	0.02	1.21 (1.03–1.42)	0.02	1.20 (1.02–1.41)	0.03
Grade								
G1/G2	1.00		1.00		1.00		1.00	
G3/G4	1.12 (0.95–1.32)	0.18	1.14 (0.97–1.34)	0.12	1.15 (0.97–1.35)	0.10	1.21 (1.03–1.42)	0.02
Unknown	0.91 (0.68–1.23)	0.55	0.91 (0.68–1.23)	0.55	0.92 (0.68–1.23)	0.57	1.00 (0.74–1.34)	0.98
Location								
Upper	1.00		1.00		1.00		1.00	
Middle	0.76 (0.63–0.92)	≤0.01	0.76 (0.63–0.92)	≤0.01	0.76 (0.63–0.92)	≤0.01	0.80 (0.66–0.97)	0.02
Lower	0.77 (0.63–0.96)	0.02	0.77 (0.62–0.95)	≤0.01	0.77 (0.62–0.95)	≤0.01	0.79 (0.64–0.97)	0.02
Overlapping	0.93 (0.72–1.22)	0.62	0.94 (0.72–1.22)	0.63	0.94 (0.72–1.23)	0.64	0.99 (0.76–1.3)	0.97
NOS	1.06 (0.78–1.43)	0.72	1.03 (0.77–1.4)	0.82	1.04 (0.77–1.4)	0.82	1.17 (0.86–1.58)	0.31
Tumor size								
≤2 cm	1.00		1.00		1.00		1.00	
>2 cm, ≤5 cm	1.06 (0.86–1.32)	0.57	1.10 (0.88–1.36)	0.40	1.11 (0.89–1.37)	0.36	1.19 (0.96–1.47)	0.12
>5 cm	1.04 (0.83–1.31)	0.74	1.06 (0.85–1.34)	0.60	1.08 (0.86–1.35)	0.53	1.24 (0.99–1.56)	0.06
Linitis plastica	1.17 (0.72–1.92)	0.52	1.16 (0.71–1.9)	0.55	1.17 (0.72–1.92)	0.52	1.08 (0.66–1.77)	0.75
Uknown	1.00 (0.78–1.28)	0.99	1.03 (0.81–1.32)	0.81	1.03 (0.8–1.32)	0.82	1.05 (0.82–1.35)	0.69
ypT category								
ypT1	1.00		1.00		1.00		1.00	
ypT2	1.29 (0.91–1.83)	0.15	1.25 (0.88–1.77)	0.21	1.26 (0.89–1.79)	0.19	1.31 (0.92–1.85)	0.13
ypT3	1.49 (1.11–2)	≤0.01	1.41 (1.05–1.9)	0.02	1.41 (1.05–1.9)	0.02	1.64 (1.23–2.2)	≤0.01
ypT4a	1.65 (1.22–2.23)	≤0.01	1.57 (1.16–2.12)	≤0.01	1.56 (1.15–2.11)	≤0.01	1.81 (1.34–2.44)	≤0.01
ypT4b	1.89 (1.31–2.72)	≤0.01	1.79 (1.25–2.59)	≤0.01	1.80 (1.25–2.59)	≤0.01	2.15 (1.5–3.08)	≤0.01
ypN category								
ypN0	1.00							
ypN1	1.38 (1.14–1.68)	≤0.01						
ypN2	1.81 (1.49–2.21)	≤0.01						
ypN3	2.95 (2.39–3.64)	≤0.01						
ELN (categorical)								
ELN ≥ 16	1.00		1.00		1.00		1.00	
ELN < 16	1.41 (1.23–1.62)	≤0.01	1.08 (0.95–1.24)	0.25	1.04 (0.91–1.19)	0.57	0.59 (0.48–0.71)	≤0.01
LNR category								
LNR1			1.00					
LNR2			1.19 (0.97–1.46)	0.09				
LNR3			1.71 (1.4–2.09)	≤0.01				
LNR4			3.01 (2.47–3.66)	≤0.01				
LODDS category								
LODDS1					1.00			
LODDS2					1.23 (1.01–1.51)	0.04		

(*continued*)

TABLE 2 | Continued

Characteristic	Model 1 (ypN)		Model 2 (LNR)		Model 3 (LODDS)		Model 4 (NLN)	
OS	Hazard ratio (95% CI)	*p*-value	Hazard ratio (95% CI)	*p*-value	Hazard ratio (95% CI)	*p* value	Hazard ratio (95% CI)	*p*-value
LODDS3					1.74 (1.43–2.13)	≤0.01		
LODDS4					3.06 (2.51–3.74)	≤0.01		
NLN category								
NLN1							1.00	
NLN2							1.39 (1.13–1.7)	≤0.01
NLN3							2.61 (2.07–3.29)	≤0.01
NLN4							3.35 (2.6–4.31)	≤0.01

OS, overall survival; N, number; IQR, interquartile range; HR, hazard ratio; CI, confidence interval; ELNs, Examined lymph nodes; PLN, number of positive lymph nodes; LNR, lymph node ratio; LODDS, log odds of positive lymph node; NLN, negative lymph node.

Prognostic Performance of Lymph Node Models in the Subgroups of <16 ELN and ≥16 ELN

We did a subgroup analysis based on the ELN for patients with insufficient ELN. When seen as the categorical variables, pairwise survival in ypN and NLN staging between subgroups was statistically significant. However, as shown in **Figure 5**, no significant differences were found between the LNR1 and LNR2 groups (OS: $p = 0.26$, CSS: $p = 0.28$), the LNR2 and LNR3 groups (OS: $p = 0.07$), or the LODDS1 and LODDS2 groups (OS: $p = 0.34$, CSS: $p = 0.21$). As shown in **Table 4**, LNR had better discrimination power (CSS: 0.654, OS: 0.649), higher homogeneity (CSS: 112.1, OS: 110.9), and better model fitness (CSS: 4,848.91, OS: 5,391.14) for CSS and OS compared to other staging systems. When lymph node staging systems were viewed as continuous variables shown in **Table 5**, a similar result was obtained.

For patients with adequate ELN, when assessed as the categorical variable, as shown in **Figure 6**, pairwise survival in LNR, LOODS, and NLN staging between subgroups was statistically significant. However, there was no significant difference between the ypN1 and ypN2 groups (OS: $p = 0.06$). Furthermore, As shown in **Table 4**, LNR had better prognostic performance than others, with a higher C-index (CSS: 0.677, OS: 0.669), lower AIC (CSS: 5,408.93, OS: 6,019.71) and higher LR test (CSS: 156.8, OS: 159.7). When viewed as a continuous variable shown in **Table 5**, LNR had greater discriminatory power (CSS: 0.678, OS: 0.671). In comparison, LODDS had a lower AIC (CSS: 5,392.99, OS: 6,003.26) and a higher LR test (CSS: 168.8, OS: 172.1).

Prognostic Performance of Lymph Node Models in the ypN0 Subgroup

Lymph node downstaging is common among patients treated with NAT, resulting in an increasement in the frequency of node-negative patients and patients with inadequate ELN. However, as shown in **Figure 7**, LNR and ypN staging systems demonstrated no predictive value in node-negative patients, whereas LODDS and NLN could still be utilized to stratify patients. As demonstrated in **Tables 4**, **5**, regardless of whether the variable is considered categorical or continuous in nature, NLN showed superior predictive performance for CSS and OS. Given the simplicity with which NLN may be calculated, it seems that NLN might be a feasible option for evaluating prognosis in ypN0 patients.

Distributive Correlation Between LODDS, LNR, and NLN

Figure 8 showed that LNR has a substantial correlation with LODDS, NLN. Furthermore, there was still heterogeneity in survival in patients with node-negatvie or no negative lymph node, which was well stratified by the NLN and LODDS when compared to the ypN and LNR staging schemes. As LNR increased, LODDS increased nonlinearly. The correlation is heterogeneous when the LNR approaches extreme levels, demonstrating that the NLN and LODDS systems might differentiate survival in patients with extreme LNR scores.

DISCUSSION

At present, NCCN guidelines recommend at least 16 lymph nodes should be harvested to decrease stage migration regardless of the initial treatment. However, following neoadjuvant therapy, there is a decrease in ELN and PLN as a result of stromal atrophy, fibrosis, and lymph node shrinking [7, 32–34]. It was demonstrated that lymph node status after NAT was still an important predictor of prognosis and that adequate N stage assessment may aid in post-operative treatment decision [10–12]. Thus, relying exclusively on the ypN stage to determine LN status may understage patients, thereby influencing postoperative treatment decision-making and prognosis. As a result, we sought to determine the optimal staging system among ypN, LNR, LODDS, and NLN in assisting in post-operative care of patients with gastric adenocarcinoma following NAT.

TABLE 3 | Multivariate Cox regression analysis of prognostic predictors for CSS in gastric adenocarcinoma patients after NAT.

Characteristic	Model1 (ypN)		Model2 (LNR)		Model3 (LODDS)		Model4 (NLN)	
CSS	Hazard ratio (95% CI)	*p*-value	Hazard ratio (95% CI)	*p*-value	Hazard ratio (95% CI)	*p*-value	Hazard ratio (95% CI)	*p*-value
Age								
≤65	1.00		1.00		1.00		1.00	
>65	1.14 (1.00–1.31)	0.06	1.15 (1.00–1.32)	0.04	1.15 (1.00–1.32)	0.05	1.14 (0.99–1.31)	0.06
Histologic type								
Adenocarcinoma	1.00		1.00		1.00		1.00	
Signet ring cell carcinoma	1.26 (1.06–1.49)	≤0.01	1.24 (1.05–1.47)	≤0.01	1.23 (1.04–1.46)	0.02	1.23 (1.04–1.46)	0.02
Grade								
G1/G2	1.00		1.00		1.00		1.00	
G3/G4	1.18 (0.99–1.41)	0.06	1.20 (1.01–1.43)	0.04	1.21 (1.02–1.45)	0.03	1.28 (1.08–1.53)	≤0.01
Unknown	0.98 (0.72–1.34)	0.91	0.99 (0.72–1.35)	0.94	0.99 (0.73–1.36)	0.97	1.08 (0.79–1.47)	0.63
Location								
Upper	1.00		1.00		1.00		1.00	
Middle	0.71 (0.58–0.87)	≤0.01	0.71 (0.58–0.87)	≤0.01	0.71 (0.58–0.87)	≤0.01	0.75 (0.61–0.92)	≤0.01
Lower	0.76 (0.61–0.94)	≤0.01	0.75 (0.60–0.94)	≤0.01	0.75 (0.60–0.94)	0.01	0.77 (0.61–0.96)	0.02
Overlapping	0.95 (0.72–1.25)	0.70	0.95 (0.72–1.25)	0.70	0.95 (0.72–1.25)	0.72	1.01 (0.76–1.33)	0.95
NOS	1.00 (0.72–1.37)	0.98	0.97 (0.71–1.34)	0.87	0.98 (0.71–1.34)	0.88	1.10 (0.80–1.51)	0.56
Tumor size								
≤2 cm	1.00		1.00		1.00		1.00	
>2 cm, ≤5 cm	1.04 (0.82–1.31)	0.75	1.08 (0.86–1.36)	0.51	1.09 (0.86–1.37)	0.48	1.17 (0.93–1.47)	0.19
>5 cm	1.01 (0.80–1.29)	0.91	1.05 (0.82–1.34)	0.70	1.06 (0.83–1.35)	0.63	1.23 (0.97–1.57)	0.08
Linitis plastica	1.13 (0.67–1.9)	0.64	1.13 (0.67–1.89)	0.65	1.14 (0.68–1.91)	0.62	1.05 (0.63–1.77)	0.85
Uknown	0.97 (0.74–1.26)	0.81	1.01 (0.78–1.31)	0.95	1.00 (0.77–1.31)	0.97	1.03 (0.79–1.34)	0.84
ypT category								
ypT1	1.00		1.00		1.00		1.00	
ypT2	1.41 (0.96–2.08)	0.08	1.36 (0.92–2.00)	0.13	1.38 (0.93–2.03)	0.11	1.45 (0.98–2.13)	0.06
ypT3	1.67 (1.19–2.34)	≤0.01	1.58 (1.13–2.21)	≤0.01	1.59 (1.13–2.22)	0.01	1.90 (1.36–2.64)	≤0.01
ypT4a	1.84 (1.31–2.59)	≤0.01	1.75 (1.24–2.46)	≤0.01	1.74 (1.24–2.45)	≤0.01	2.09 (1.49–2.92)	≤0.01
ypT4b	2.12 (1.42–3.17)	≤0.01	2.01 (1.34–3.01)	≤0.01	2.02 (1.35–3.02)	≤0.01	2.49 (1.67–3.70)	≤0.01
ypN category								
ypN0	1.00							
ypN1	1.44 (1.16–1.77)	≤0.01						
ypN2	1.99 (1.61–2.45)	≤0.01						
ypN3	3.20 (2.56–4.01)	≤0.01						
ELN (categorical)								
ELN ≥ 16	1.00		1.00		1.00		1.00	
ELN < 16	1.45 (1.26–1.67)	≤0.01	1.09 (0.95–1.26)	0.22	1.04 (0.90–1.20)	0.57	0.58 (0.48–0.71)	≤0.01
LNR category								
LNR1			1.00					
LNR2			1.26 (1.01–1.57)	0.04				
LNR3			1.85 (1.50–2.29)	≤0.01				
LNR4			3.19 (2.59–3.94)	≤0.01				
LODDS category								
LODDS1					1.00			
LODDS2					1.34 (1.08–1.66)	≤0.01		

(*continued*)

TABLE 3 | Continued

Characteristic	Model1 (ypN)		Model2 (LNR)		Model3 (LODDS)		Model4 (NLN)	
CSS	**Hazard ratio (95% CI)**	***p*-value**	**Hazard ratio (95% CI)**	***p*-value**	**Hazard ratio (95% CI)**	***p*-value**	**Hazard ratio (95% CI)**	***p*-value**
LODDS3					1.91 (1.53–2.36)	≤0.01		
LODDS4					3.30 (2.66–4.10)	≤0.01		
NLN category								
NLN1							1.00	
NLN2							1.39 (1.12–1.73)	≤0.01
NLN3							2.73 (2.13–3.48)	≤0.01
NLN4							3.44 (2.64–4.49)	≤0.01

CSS, cancer specific survival; N, number; IQR, interquartile range; HR, hazard ratio; CI, confidence interval; ELN, Examined lymph nodes; PLN, number of positive lymph nodes; LNR, lymph node ratio; LODDS, log odds of positive lymph node; NLN, negative lymph node.

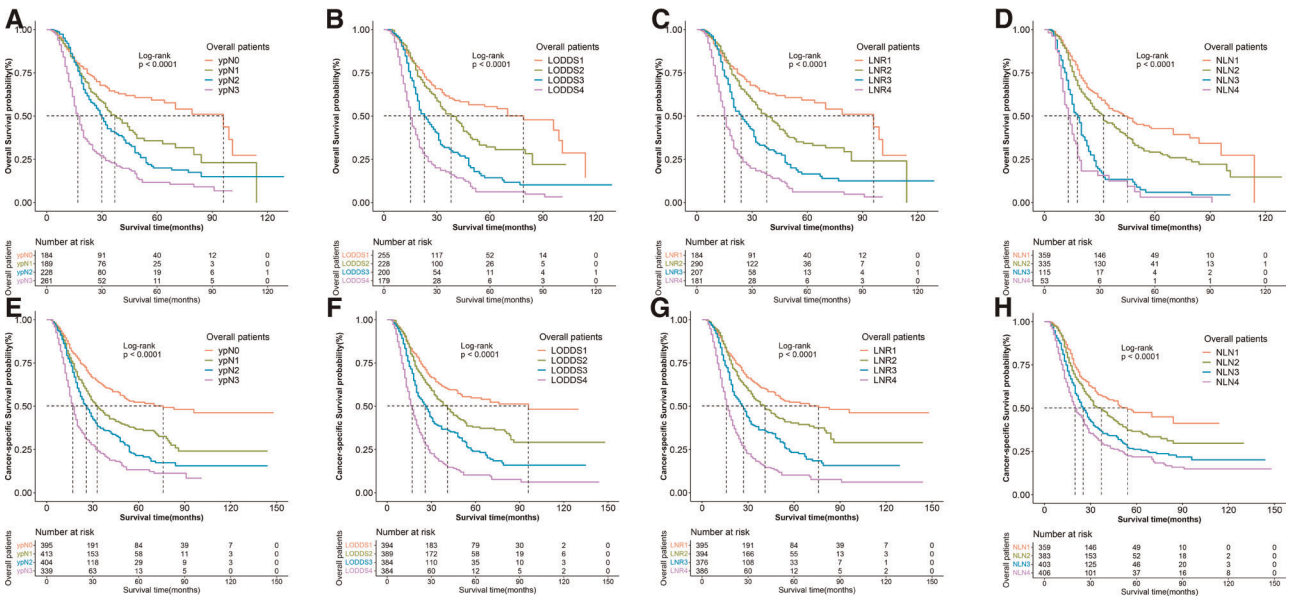

FIGURE 2 | Kaplan–Meier survival curves of OS according to (**A**) N stage, (**B**) LODDS, (**C**) LNR, and (**D**) NLN staging systems and CSS according to (**E**) N stage, (**F**) LODDS, (**G**) LNR and (**H**) NLN staging system for gastric adenocarcinoma patients after NAT.OS, overall survival; CSS, cancer specific survival; LNR, lymph node ratio; LODDS, log odds of positive lymph node; NLN, negative lymph node; NAT, neoadjuvant therapy.

Currently, the eighth edition of the AJCC N staging has been criticized for requiring sufficient lymph node resection to minimize staging migration. In the past, some researchers proposed the optimal number of examined lymph nodes and several alternative methods of calculating the lymph node status. However, the majority of these studies were conducted on patients who have not had preoperative therapy, and their applicability to patients who have received preoperative treatment has not been established. The current study is one of the biggest database analyses yet conducted to evaluate the four staging systems used in gastric adenocarcinoma following preoperative therapy, as well as the first report to evaluate the prognostic power of four staging systems among patients with less extended lymph node dissection (less than 16 lymph nodes harvested) following NAT. It was discovered that four lymph node staging schemes were capable of stratifying patients for CSS and OS, and that all four were significant independent prognostic variables in multivariate analysis. LNR and LODDS outperformed other alternative staging systems regardless of whether the variable was categorical or continuous in nature. It's worth noting that the NLN staging system outperformed others among node-negative patients.

It was demonstrated that LNR and LODDS integrated the ELN and PLN to minimize stage migration in a variety of cancers, and both outperformed the N stage for prognosis prediction [8, 13, 15, 16, 18]. Similarly, when the LNR and LOODS staging systems

TABLE 4 | Predictive performance of different staging systems in subgroups when LN status assessed as categorical varaible.

Study cohort (categorical)	Overall			ELNs < 16			ELNs ≥ 16			N0		
	AIC	C-index (95% CI)	LR test	AIC	C-index (95% CI)	LR test	AIC	C-index (95% CI)	LR test	AIC	C-index (95% CI)	LR test
CSS												
Model 1 (ypN)	11,472.87	0.653 (0.624–0.664)	232.6	4,858.80	0.651 (0.602–0.658)	102.1	5,435.35	0.662 (0.616–0.672)	130.4			
Model 2 (LNR)	11,445.35	0.661 (0.633–0.672)	260.1	4,848.91	0.654 (0.603–0.660)	112.1	5,408.93	0.677 (0.635–0.688)	156.8			
Model 3 (LODDS)	11,448.15	0.661 (0.632–0.671)	257.3	4,851.36	0.654 (0.602–0.659)	109.5	5,411.16	0.675 (0.634–0.686)	154.6	1,675.01	0.667 (0.582–0.669)	45.80
Model 4 (NLN)	11,508.48	0.643 (0.613–0.653)	197.3	4,891.65	0.627 (0.578–0.638)	67.23	5,432.53	0.659 (0.611–0.664)	133.2	1,671.14	0.675 (0.587–0.674)	51.68
OS												
Model 1 (ypN)	12,781.56	0.645 (0.616–0.655)	226.6	5,406.97	0.640 (0.593–0.647)	95.04	6,048.28	0.654 (0.610–0.662)	131.1			
Model 2 (LNR)	12,745.24	0.656 (0.629–0.666)	262.9	5,391.14	0.649 (0.603–0.657)	110.9	6,019.71	0.669 (0.629–0.680)	159.7			
Model 3 (LODDS)	12,748.61	0.656 (0.629–0.666)	259.5	5,393.35	0.649 (0.602–0.656)	108.7	6,020.50	0.669 (0.628–0.679)	158.9	2,012.14	0.664 (0.589–0.669)	56.34
Model 4 (NLN)	12,812.02	0.638 (0.609–0.646)	196.1	5,435.69	0.621 (0.571–0.626)	64.33	6,043.23	0.653 (0.610–0.661)	136.2	2,007.88	0.672 (0.596–0.675)	62.60

ELN, Examined lymph nodes;LNR, lymph node ratio; LODDS, log odds of positive lymph node; NLN, negative lymph node; C-index, Harrell's concordance index; ROC, the Receiver Operative Curve; LR test, the likelihood ratio test; AIC, the Akaike information criterion.

TABLE 5 | Predictive performance of different staging systems in subgroups when LN status assessed as continuous varaible.

Study cohort (continuous)	Overall			ELNs < 16			ELNs ≥ 16			N0		
	AIC	C-index (95% CI)	LR test	AIC	C-index (95% CI)	LR test	AIC	C-index (95% CI)	LR test	AIC	C-index (95% CI)	LR test
CSS												
Model 1 (ypN)	11,474.82	0.652 (0.625–0.663)	226.7	4,853.54	0.651 (0.605–0.661)	103.3	5,426.91	0.664 (0.623–0.6745)	134.8			
Model 2 (LNR)	11,428.77	0.665 (0.638–0.677)	272.7	4,835.69	0.659 (0.613–0.670)	121.2	5,399.79	0.678 (0.637–0.689)	161.9			
Model 3 (LODDS)	11,422.83	0.665 (0.639–0.678)	278.6	4,841.13	0.658 (0.612–0.669)	115.8	5,392.99	0.677 (0.635–0.690)	168.8	1,670.67	0.670 (0.592–0.679)	48.15
Model 4 (NLN)	11,511.07	0.643 (0.615–0.657)	190.4	4,876.43	0.636 (0.589–0.648)	80.4	5,449.78	0.652 (0.611–0.667)	112.00	1,666.38	0.673 (0.594–0.680)	52.43
OS												
Model 1 (ypN)	12,776.81	0.647 (0.622–0.658)	227.3	5,400.24	0.642 (0.598–0.652)	97.8	6,033.89	0.660 (0.620–0.671)	141.5			
Model 2 (LNR)	12,720.98	0.661 (0.636–0.673)	283.2	5,374.12	0.655 (0.610–0.665)	123.9	6,007.54	0.671 (0.631–0.683)	167.8			
Model 3 (LODDS)	12,723.34	0.660 (0.634–0.672)	280.8	5,384.00	0.653 (0.610–0.664)	114.0	6,003.26	0.668 (0.630–0.684)	172.1	2,009.66	0.667 (0.595–0.675)	56.82
Model 4 (NLN)	12,816.52	0.638 (0.611–0.651)	187.6	5,419.04	0.632 (0.587–0.643)	79.0	6,062.16	0.646 (0.607–0.659)	113.2	2,005.81	0.670 (0.599–0.678)	60.67

ELN, Examined lymph nodes;LNR, lymph node ratio; LODDS, log odds of positive lymph node; NLN, negative lymph node; C-index, Harrell's concordance index; ROC, the Receiver Operative Curve; LR test, the likelihood ratio test; AIC, the Akaike information criterion.

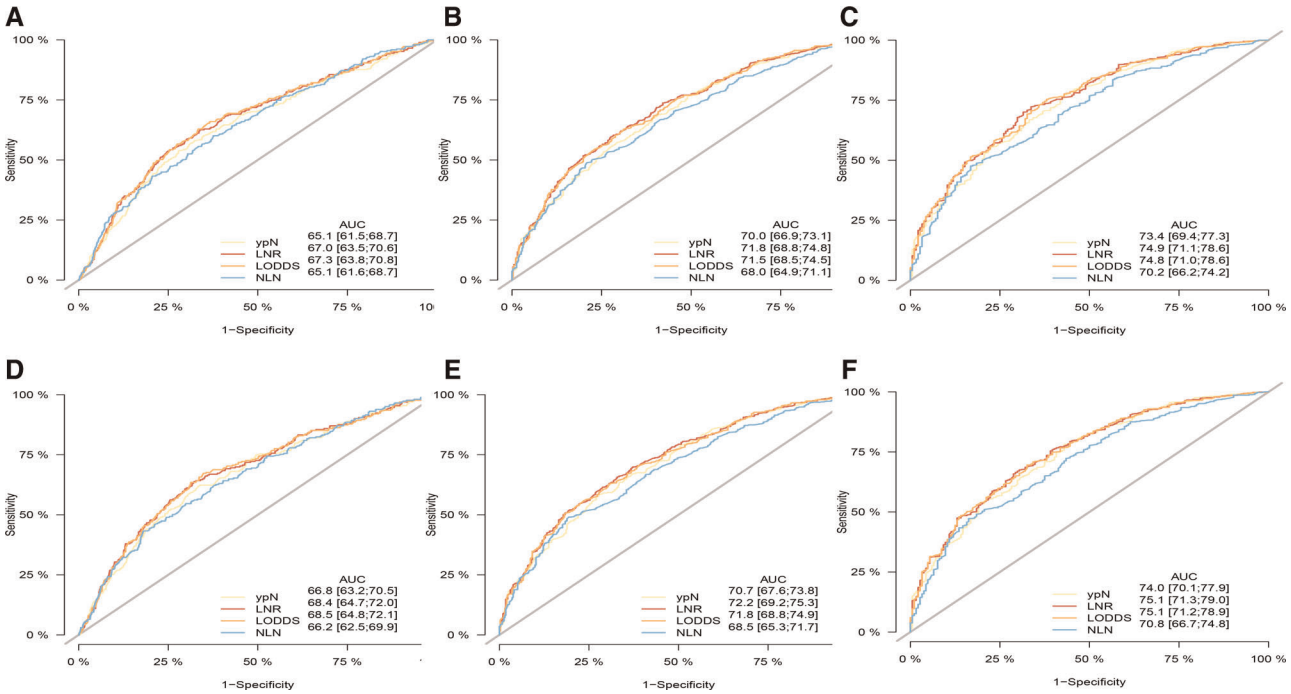

FIGURE 3 | ROC curve of the ypN stage, LNR, LODDS and NLN in the prediction of prognosis of gastric adenocarcinoma patients after NAT at 1 (**A**), 3 (**B**), 5 (**C**) year point for OS and 1 (**D**), 3 (**E**), 5 (**F**) year point for CSS when LN status assessed as categorical varaible. OS, overall survival; CSS, cancer specific survival; ROC, receiver operative curve; LNR, lymph node ratio; LODDS, log odds of positive lymph node; NLN, negative lymph node.

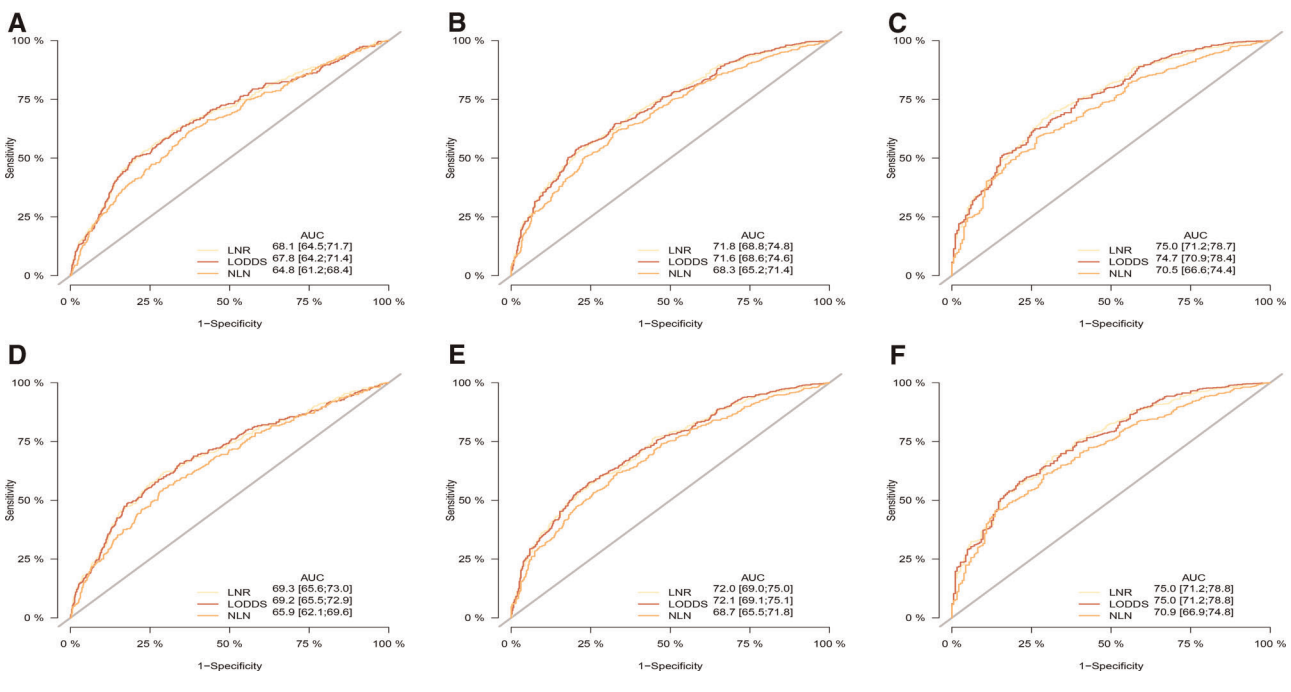

FIGURE 4 | ROC curve of the ypN stage, LNR, LODD and NLN in the prediction of prognosis of gastric adenocarcinoma patients after NAT at 1 (**A**), 3 (**B**), 5 (**C**) year point for OS and 1 (**D**), 3 (**E**), 5 (**F**) year point for CSS when LN status assessed as continuous varaible, OS, overall survival; CSS, cancer specific survival; ROC, receiver operative curve; LNR, lymph node ratio; LODDS, log odds of positive lymph node; NLN, negative lymph node.

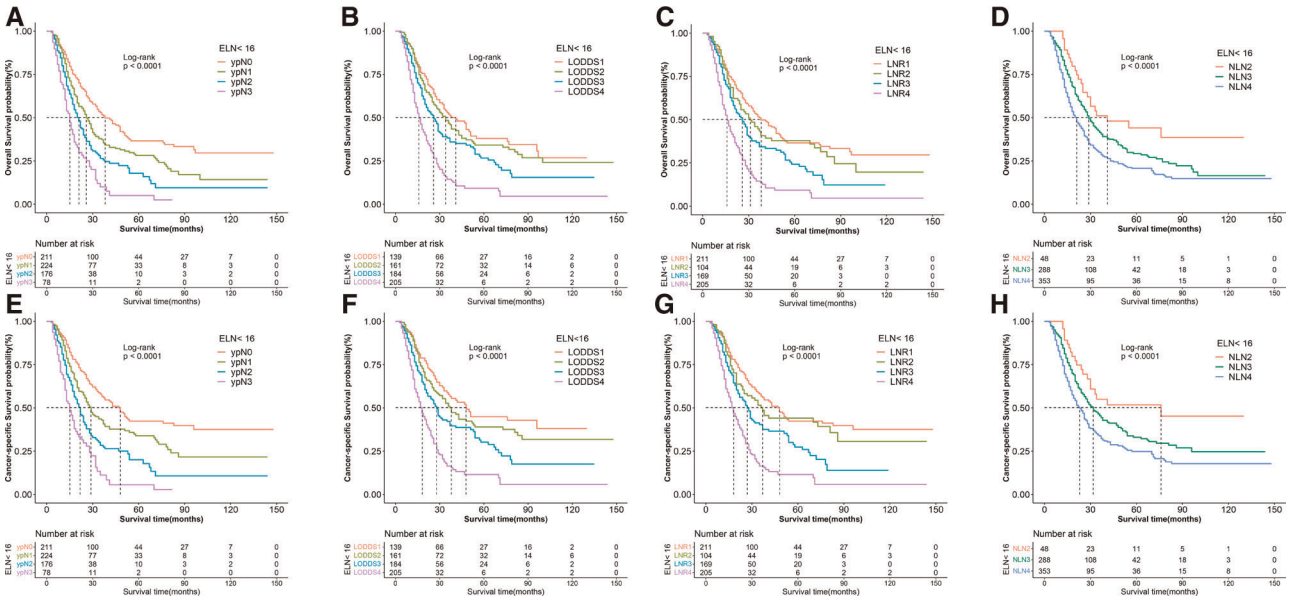

FIGURE 5 | Kaplan–Meier survival curves of OS according to (**A**) ypN (**B**) LODDS, (**C**) LNR, and (**D**) NLN staging system and CSS according to (**E**) ypN, (**F**) LODDS, (**G**) LNR and (**H**) NLN staging system for gastric adenocarcinoma patients after NAT with ELN < 16. OS, overall survival; CSS, cancer specific survival; LNR, lymph node ratio; LODDS, log odds of positive lymph node; NLN, negative lymph node; NAT, neoadjuvant therapy.

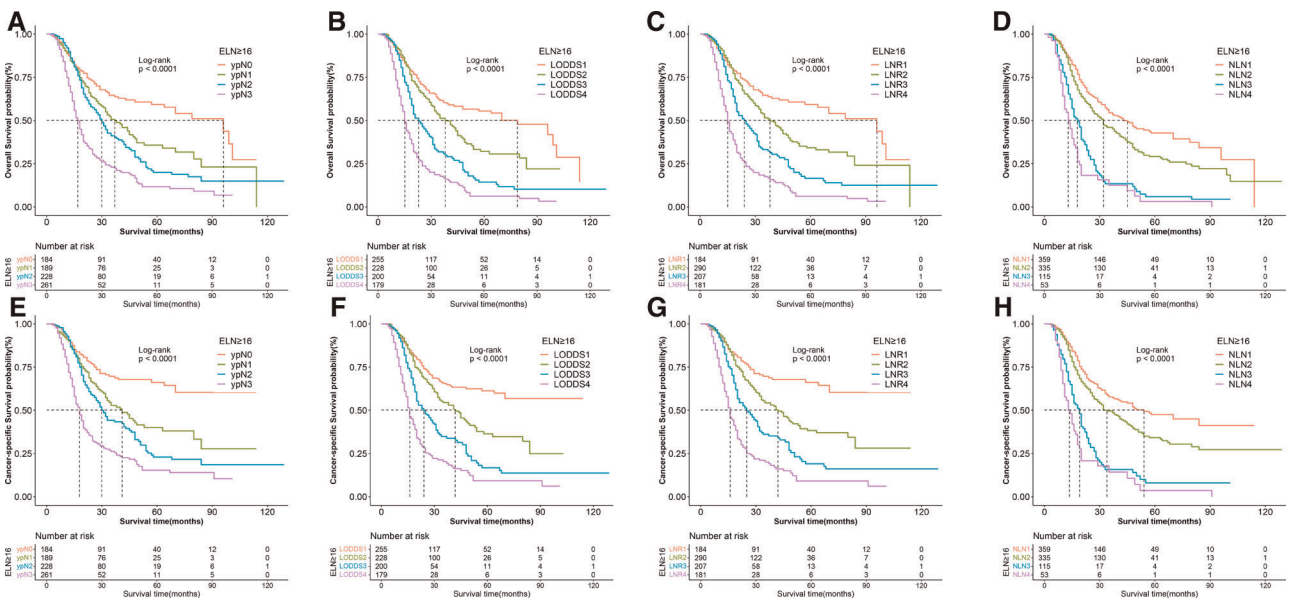

FIGURE 6 | Kaplan–Meier survival curves of OS according to (**A**) ypN, (**B**) LODDS, (**C**) LNR, and (**D**) NLN staging system and CSS according to (**E**) ypN, (**F**) LODDS, (**G**) LNR and (**H**) NLN staging system for gastric adenocarcinoma patients after NAT with ELN ≥ 16. OS, overall survival; CSS, cancer specific survival; LNR, lymph node ratio; LODDS, log odds of positive lymph node; NLN, negative lymph node; NAT, neoadjuvant therapy.

were applied in gastric adenocarcinoma following neoadjuvant treatment, similar conclusions were observed. However, in reviewing the literature, which of the two systems has the superior predictive ability remains controversial. Smith, Nelson, and Schwarz et al. validated the finding that LNR was the best staging scheme for predicting prognosis in patients with

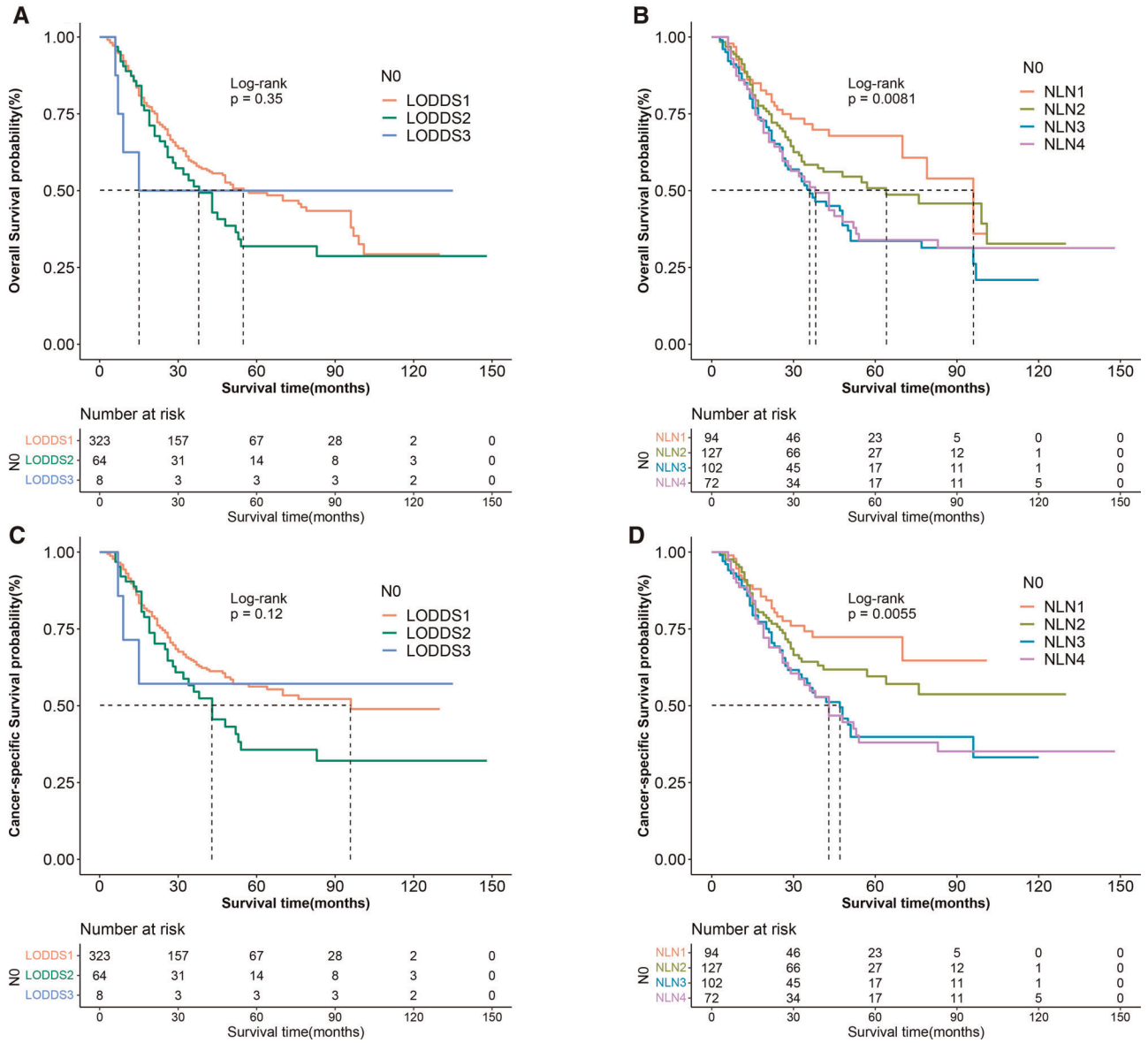

FIGURE 7 | Kaplan–Meier survival curves of OS according to (**A**) LOODS, (**B**) NLN staging system and CSS according to (**C**) LODDS, and (**D**) NLN staging system for gastric adenocarcinoma patients after NAT with ypN0. (OS, overall survival; CSS, cancer specific survival; LODDS, log odds of positive lymph node; NLN, negative lymph node; NAT, neoadjuvant therapy.

resectable gastric adenocarcinoma when used as a categorical variable [35], whereas Wang et al found that LODDS showed a prognostic superiority over both pN and LNR staging systems, when assessed as categorical variable [36]. Interestingly, in a multi-institutional database study, Spolverato et al found that LNR assess LN status with great predictive power when assessed as the categorical variable, while LOODS became the better predictive factor when regarded as the continuos variable for gastric adenocarcinoma patients without neoadjuvant therapy [17]. In the current study, similar findings were observed that LNR had better predictive ability than LODDS when regarded as the categorical variable, whereas LOODS became the better predictive factor for CSS when regarded as the continuos variable. A possible explanation for this might be that when stratifying patients based on LN status, numerous alternative "optimal" cutoffs have been suggested for each system. For instance, Marchet et al. proposed the four-category cutoff for LNR as 0–10%–25%, whereas Sun et al selected 0–20%–50%. In addition, Wang et al advocated the five-category cutoff based on LNR. However, the factors related to the cutoff selection may include the many aspects including the different statistical methods, the invloved patients selected form different countries, and patients following different preoperative treatments and so on [8, 17, 37].

When further exploited the relationship between the two staging systems, in patients reaching extremely low or high LNR scores, LNR staging system failed to stratify the prognosis. When seen in the scatter plot (**Figure 8**), as LNR was increased, LODDS nonlinearly increased. However, when the LNR approaches extreme LNR levels, the connection between the two variables becomes heterogeneous, showing that the LODDS system is capable of discriminating between patients with varying survival status due to their high LNR score. These results may seem self-evident. However, most doctors would agree that patients with one ELN and one PLN have a different prognosis when compared with those with twelve ELN and twelve PLN.

In our multivariate Cox regression analysis, ELN was an independent prognostic factor, suggesting that checking more than 16 lymph nodes can achieve better survival and help predict the prognosis of patients accurately. Patients with insufficient lymph node harvest accounted for 44.4 percent of total patients in our research, indicating the outcome of preoperative therapy. Hence, we performed subgroup analysis based on the ELN. When assessed as the categorical variable, LNR had the better prognostic performance than others regardless of the status of ELN. When the lymph node staging systems were regarded as continuous variable, LNR persisted to have better discrimination ability for OS. However, this result has not previously been described. Yang et al found that LODDS showed better predictive performance than pN, LNR, and NLN among adenocarcinoma of esophagogastric junction patients with ≤16 ELN [38]. Xu et al proposed that LODDS was a better prognostic factor for DFS than ypN staging or the LNR-based system in patients with rectal cancer after NAT, particularly in patients with insufficent ELN [8]. In a retrospective study, Spolverato et al found LOODS outperformed LNR when less than 10 lymph node harvested in gastric cancer with cancer-directed sugery [17]. Some researchers previously stated that one of the limitations of any LN ratio scheme is an inadequate number of LNs, and emphasized that utilizing an LN ratio scheme does not effectively compensate for low LN counts [37, 39, 40]. This discrepancy may be explained by the fact that preoperative therapy increased the frequency of node-negative patients who serve as respond a critical indicator of the efficacy of preoperative treatment. In a retrospective study including 316 patients with gastric cancer following NAT, Ikoma et al found similar survival in patients achieveing ypN0 regardless of the

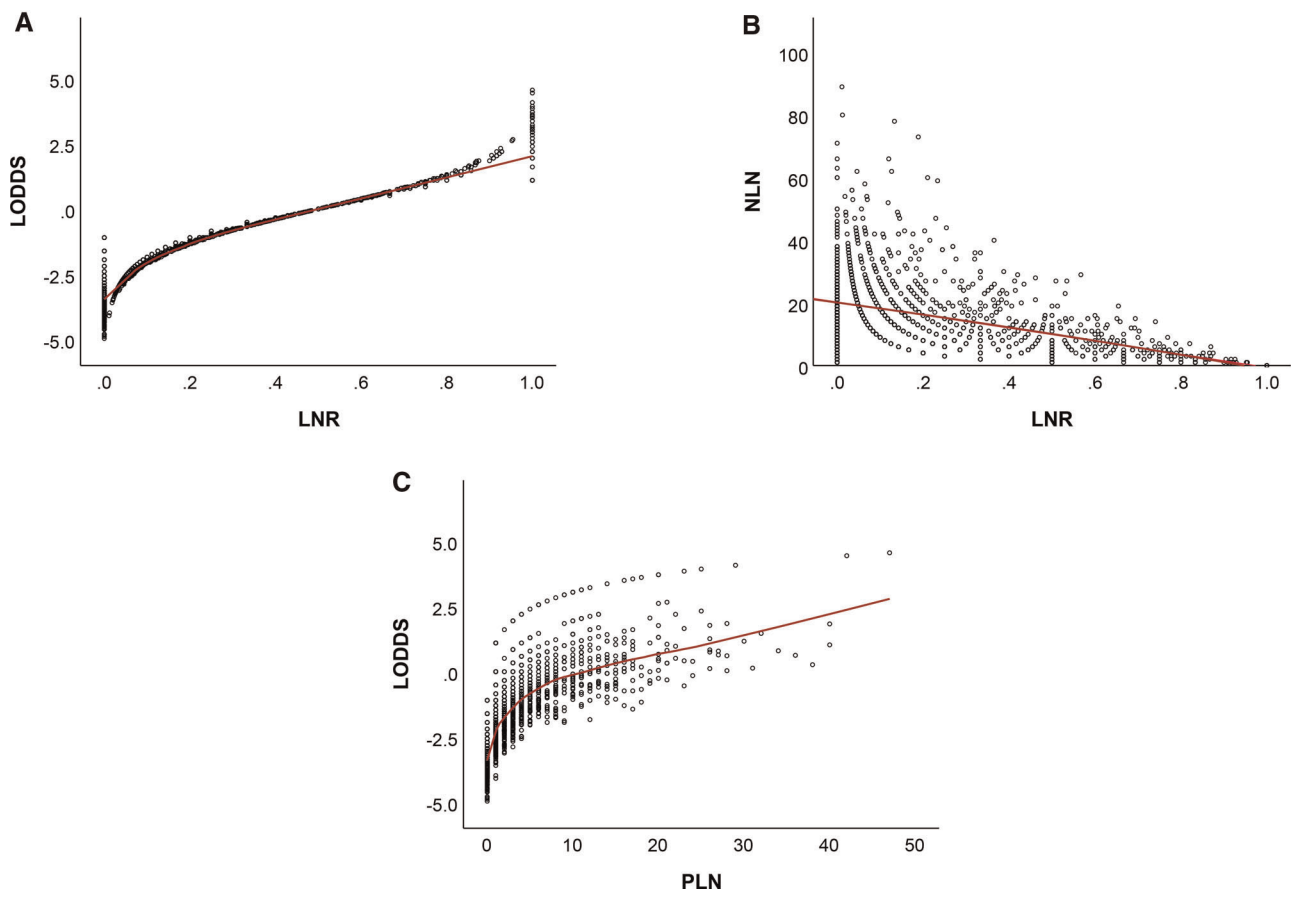

FIGURE 8 | Distribution of LNR vs LODDS (**A**), NLN (**B**), and PLN vs LODDS (**C**). LNR, lymph node ratio; LODDS, log odds of positive lymph node; NLN, negative lymph node; PLN, number of positive lymph nodes.

clinical N stage, suggesting that ypN0 status is an important hallmark demonstrating the effectiveness of preoperative therapy. Therefore, the homogeneity and model fit of LNR staging system has been improved within LNR1 group. There was the evidence that LNR had better discriminating capacity and homogeneity than LODDS in our investigation.

Indeed, in node-negative patients, ELN has been shown to be a indepent prognostic factor and is equal to NLN [9]. LODDS is different from ELN but still reply on ELN. In our study, ELN was an independent prognostic factor with CSS and OS in multivariate Cox regression analysis. Analyed by Kaplan-Meier method and Log-rank test, no statistically significant difference were observed between LODDS subgroups while there was significantly different in NLN (NLN1 vs NLN4, $P < 0.05$; NLN2 vs NLN4, $P< 0.05$). Furthermore, NLN outperformed LODDS with better discrimination power, higher homogeneity and better model fitness for CSS and OS. Considering the user-friendly calculation of NLN, it should be recommended in clinical prognostic assessment as a substitute for assessing lymph node status in ypN0 patients.

Even though the three alternative staging schemes (LNR, LODDS,and NLN) outperformed the ypN stage in different aspects, it is currently not widely applied in clinical practice. There could be several explanations for this, including the following: To begin, unlike the ypN stage, consensus on the cut-off value for alternative systems remains elusive. Secondly, when referring to LOODS, the calculation is not user-friendly and inconvenient. Finally, except for patients at high risk of N stage migration, it failed to provide a significant improvement in predicted prognosis.

For the reasons stated above, when LN status were seen as continuous factors rather than categorical variables, the predictive performance of three staging systems (LNR, LODDS, and NLN) was enhanced. Spolverato et al. concluded in a similar manner that staging methods should evaluate LN status as continuous variables rather than using indiscriminate categorical cutoffs for patients with gastric adenocarcinoma undergoing cancer-directed surgery [17]. Thus, our findings implies that in gastric adenocarcinoma following NAT, the staging system should consider LN status as a continuous variable rather than a heterogeneous categorical variable.

This study has some limitations. To begin, unavoidable deviations occur as a result of the retrospective experimental design. To ensure the reliability of the results, they must be validated in large, multi-center, prospective clinical trials. Second, the SEER database's lack of comprehensive data (such as surgical margin status, etc.) precludes future in-depth research. Finally, because our study excluded patients in stage IV, the impact on these patients remains unknown.

CONCLUSIONS

LNR had a better predictive performance than ypN, LODDS and NLN staging systems regardless of the status of ELN when regarded as the categorical variable, whereas LOODS became the better predictive factor for CSS when regarded as the continuos variable. In node-negative patients, NLN might be a feasible option for evaluating prognosis and a combination of LNR and NLN should be considered as user-friendly method in the clinical prognostic assessment.

DATA AVAILABILITY STATEMENT

The datasets presented in this study can be found in online repositories. The names of the repository/repositories and accession number(s) can be found in the article.

ETHICS STATEMENT

All procedures performed in studies involving human participants were in accordance with the ethical standards of the institutional and/or national research committee and with the 1964 Helsinki Declaration and its later amendments or comparable ethical standards. No ethics approval was declared because the SEER is a publicly available database. Written informed consent for participation was not required for this study in accordance with the national legislation and the institutional requirements.

AUTHOR CONTRIBUTIONS

All authors have helped in performing this research; Conception and design: HL, JZ, YL. Collection and assembly of data: HL, JZ. Data analysis and interpretation: HL, JZ, YL. All authors contributed to the article and approved the submitted version.

FUNDING

This study was funded by Guangdong Provincial People's Hospital, "Guangdong Outstanding Young Medical Talent", for individualized precision treatment of adenocarcinoma of esophagogastric junction (KJ012019439) and was supported by National key Clinical Specialty Construction Project (2021-2024, No. 2022YW030009).

REFERENCES

1. Joshi S, Badgwell B. Current treatment and recent progress in gastric cancer. *CA Cancer J Clin*. (2021) 71(3):264–79. doi: 10.3322/caac.21657
2. Zhang X, Liang H, Li Z, Xue Y, Wang Y, Zhou Z, et al. Perioperative or postoperative adjuvant oxaliplatin with S-1 versus adjuvant oxaliplatin with capecitabine in patients with locally advanced gastric or gastro-oesophageal junction adenocarcinoma undergoing D2 gastrectomy (RESOLVE): an open-label, superiority and non-inferiority, phase 3 randomised controlled trial. *Lancet Oncol*. (2021) 22(8):1081–92. doi: 10.1016/S1470-2045(21)00297-7
3. Ychou M, Boige V, Pignon J, Conroy T, Bouché O, Lebreton G, et al. Perioperative chemotherapy compared with surgery alone for resectable

gastroesophageal adenocarcinoma: an FNCLCC and FFCD multicenter phase III trial. *J Clin Oncol*. (2011) 29(13):1715–21. doi: 10.1200/JCO.2010.33.0597
4. Al-Batran S, Homann N, Pauligk C, Goetze T, Meiler J, Kasper S, et al. Perioperative chemotherapy with fluorouracil plus leucovorin, oxaliplatin, and docetaxel versus fluorouracil or capecitabine plus cisplatin and epirubicin for locally advanced, resectable gastric or gastro-oesophageal junction adenocarcinoma (FLOT4): a randomised, phase 2/3 trial. *Lancet (London, England)*. (2019) 393(10184):1948–57. doi: 10.1016/S0140-6736(18)32557-1
5. Cunningham D, Allum W, Stenning S, Thompson J, Van de Velde C, Nicolson M, et al. Perioperative chemotherapy versus surgery alone for resectable gastroesophageal cancer. *N Engl J Med*. (2006) 355(1):11–20. doi: 10.1056/NEJMoa055531
6. Schuhmacher C, Gretschel S, Lordick F, Reichardt P, Hohenberger W, Eisenberger C, et al. Neoadjuvant chemotherapy compared with surgery alone for locally advanced cancer of the stomach and cardia: European Organisation for Research and Treatment of Cancer randomized trial 40954. *J Clin Oncol*. (2010) 28(35):5210–8. doi: 10.1200/JCO.2009.26.6114
7. Lane WO, Nussbaum DP, Sun Z, Blazer DG. Preoperative radiation therapy in the surgical management of gastric and junctional adenocarcinoma: should lymph node retrieval guidelines be altered? *J Surg Oncol*. (2018) 117(8):1708–15. doi: 10.1002/jso.25068
8. Xu T, Zhang L, Yu L, Zhu Y, Fang H, Chen B, et al. Log odds of positive lymph nodes is an excellent prognostic factor for patients with rectal cancer after neoadjuvant chemoradiotherapy. *Ann Transl Med*. (2021) 9(8):637. doi: 10.21037/atm-20-7590
9. MingHua Z, KeCheng Z, ZhenYu C, Lin C, ChunXi W, ZeLong Y. Impact of lymph nodes examined on survival in ypN0 gastric cancer patients: a population-based study. *J Gastrointest Surg*. (2021) 25(4):919–25. doi: 10.1007/s11605-020-04579-6
10. Ikoma N, Estrella J, Hofstetter W, Das P, Minsky B, Ajani J, et al. Nodal downstaging in gastric cancer patients: promising survival if ypN0 is achieved. *Ann Surg Oncol*. (2018) 25(7):2012–7. doi: 10.1245/s10434-018-6471-0
11. Ma F, Zhang Y, Peng L, Zhang Z, Yang W, Chai J, et al. Which is the optimal management for locally advanced gastric cancer patients with TRG 0 and 1 after R0 resection? *Ann Transl Med*. (2020) 8(15):948. doi: 10.21037/atm-20-3986
12. Deng L, Groman A, Jiang C, Perimbeti S, Gabriel E, Kukar M, et al. Association of preoperative chemosensitivity with postoperative survival in patients with resected gastric adenocarcinoma. *JAMA Netw Open*. (2021) 4(11):e2135340. doi: 10.1001/jamanetworkopen.2021.35340
13. Che K, Wang Y, Wu N, Liu Q, Yang J, Liu B, et al. Prognostic nomograms based on three lymph node classification systems for resected gastric adenocarcinoma: a large population-based cohort study and external validation. *Ann Surg Oncol*. (2021) 28(13):8937–49. doi: 10.1245/s10434-021-10299-1
14. Kim S, Cho S, Lee J, Moon H, Noh W, Youn H, et al. Clinical relevance of lymph node ratio in breast cancer patients with one to three positive lymph nodes. *Br J Cancer*. (2013) 109(5):1165–71. doi: 10.1038/bjc.2013.465
15. Prassas D, Verde P, Pavljak C, Rehders A, Krieg S, Luedde T, et al. Prognostic discrimination of alternative lymph node classification systems for patients with radically resected non-metastatic colorectal cancer: a cohort study from a single tertiary referral center. *Cancers*. (2021) 13(15):3898. doi: 10.3390/cancers13153898
16. Detering R, Meyer V, Borstlap W, Beets-Tan R, Marijnen C, Hompes R, et al. Prognostic importance of lymph node count and ratio in rectal cancer after neoadjuvant chemoradiotherapy: results from a cross-sectional study. *J Surg Oncol*. (2021) 124(3):367–77. doi: 10.1002/jso.26522
17. Spolverato G, Ejaz A, Kim Y, Squires MH, Poultsides G, Fields RC, et al. Prognostic performance of different lymph node staging systems after curative intent resection for gastric adenocarcinoma. *Ann Surg*. (2015) 262(6):991–8. doi: 10.1097/SLA.0000000000001040
18. Chen Y, Wang M, Li Y, Li P, Ouyang S, Xu H, et al. Prognostic performance of different lymph node classification systems in young gastric cancer. *J Gastrointest Oncol*. (2021) 12(4):1285–300. doi: 10.21037/jgo-21-185
19. Arrington A, O'Grady C, Schaefer K, Khreiss M, Riall T. Significance of lymph node resection after neoadjuvant therapy in pancreatic, gastric, and rectal cancers. *Ann Surg*. (2020) 272(3):438–46. doi: 10.1097/SLA.0000000000004181
20. Huang C, Lin J, Zheng C, Li P, Xie J, Lin B. Effect of negative lymph node count on survival for gastric cancer after curative distal gastrectomy. *Eur J Surg Oncol*. (2011) 37(6):481–7. doi: 10.1016/j.ejso.2011.01.012
21. Wu S, Wang Y, Zhou J, Sun J, Li F, Lin H, et al. Number of negative lymph nodes should be considered for incorporation into staging for breast cancer. *Am J Cancer Res*. (2015) 5(2):844–53. https://www.ncbi.nlm.nih.gov/pmc/articles/PMC4396037/
22. Che K, Wang Y, Wu N, Liu Q, Yang J, Liu B, et al. Prognostic nomograms based on three lymph node classification systems for resected gastric adenocarcinoma: a large population-based cohort study and external validation. *Ann Surg Oncol*. (2021) 28(13):8937–49. doi: 10.1245/s10434-021-10299-1
23. Zhang Y, Liu D, Zeng D, Chen C. Lymph node ratio is an independent prognostic factor for patients with siewert Type II adenocarcinoma of esophagogastric junction: results from a 10-year follow-up study. *J Gastrointest Cancer*. (2021) 52(3):983–92. doi: 10.1007/s12029-020-00468-y
24. Zhou Z, Xie X, Hao N, Diao D, Song Y, Xia P, et al. Different lymph node staging systems for patients with adenocarcinoma of esophagogastric junction. *Curr Med Res Opin*. (2018) 34(6):963–70. doi: 10.1080/03007995.2018.1429390
25. Xu J, Cao J, Wang L, Wang Z, Wang Y, Wu Y, et al. Prognostic performance of three lymph node staging schemes for patients with Siewert type II adenocarcinoma of esophagogastric junction. *Sci Rep*. (2017) 7(1):10123. doi: 10.1038/s41598-017-09625-z
26. Spolverato G, Ejaz A, Kim Y, Squires M, Poultsides G, Fields R, et al. Prognostic performance of different lymph node staging systems after curative intent resection for gastric adenocarcinoma. *Ann Surg*. (2015) 262(6):991–8. doi: 10.1097/SLA.0000000000001040
27. Camp R, Dolled-Filhart M, Rimm D. X-tile: a new bio-informatics tool for biomarker assessment and outcome-based cut-point optimization. *Clin Cancer Res*. (2004) 10(21):7252–9. doi: 10.1158/1078-0432.CCR-04-0713
28. Camp RL, Dolled-Filhart M, Rimm DL. X-tile: a new bio-informatics tool for biomarker assessment and outcome-based cut-point optimization. *Clin Cancer Res*. (2004) 10(21):7252–9. doi: 10.1158/1078-0432.CCR-04-0713
29. Harrell F, Califf R, Pryor D, Lee K, Rosati R. Evaluating the yield of medical tests. *JAMA*. (1982) 247(18):2543–6. doi: 10.1001/jama.1982.03320430047030
30. Harrell F, Lee K, Mark D. Multivariable prognostic models: issues in developing models, evaluating assumptions and adequacy, and measuring and reducing errors. *Stat Med*. (1996) 15(4):361–87. doi: 10.1002/(SICI)1097-0258(19960229)15:4<361::AID-SIM168>3.0.CO;2-4
31. Vrieze S. Model selection and psychological theory: a discussion of the differences between the Akaike information criterion (AIC) and the Bayesian information criterion (BIC). *Psychol Methods*. (2012) 17(2):228–43. doi: 10.1037/a0027127
32. Park I, Yu C, Lim S, Yoon Y, Kim C, Kim T, et al. Prognostic implications of the number of retrieved lymph nodes of patients with rectal cancer treated with preoperative chemoradiotherapy. *J Gastrointest Surg*. (2014) 18(10):1845–51. doi: 10.1007/s11605-014-2509-1
33. Damin DC, Rosito MA, Contu PC, Tarta C, Ferreira PR, Kliemann LM, et al. Lymph node retrieval after preoperative chemoradiotherapy for rectal cancer. *J Gastrointest Surg*. (2012) 16(8):1573–80. doi: 10.1007/s11605-012-1916-4
34. Shridhar R, Dombi GW, Finkelstein SE, Meredith KL, Hoffe SE. Improved survival in patients with lymph node-positive gastric cancer who received preoperative radiation: an analysis of the Surveillance, Epidemiology, and End Results database. *Cancer*. (2011) 117(17):3908–16. doi: 10.1002/cncr.25995
35. Smith DD, Nelson RA, Schwarz RE. A comparison of five competing lymph node staging schemes in a cohort of resectable gastric cancer patients. *Ann Surg Oncol*. (2014) 21(3):875–82. doi: 10.1245/s10434-013-3356-0

36. Wang X, Appleby DH, Zhang X, Gan L, Wang JJ, Wan F. Comparison of three lymph node staging schemes for predicting outcome in patients with gastric cancer. *Br J Surg*. (2013) 100(4):505–14. doi: 10.1002/bjs.9014
37. Sun Z, Zhu GL, Lu C, Guo PT, Huang BJ, Li K, et al. The impact of N-ratio in minimizing stage migration phenomenon in gastric cancer patients with insufficient number or level of lymph node retrieved: results from a Chinese mono-institutional study in 2159 patients. *Ann Oncol*. (2009) 20 (5):897–905. doi: 10.1093/annonc/mdn707
38. Yang Y, Zheng J, Li Y. Comparison of 4 lymph node staging systems for the prognostic prediction of esophagogastric junction adenocarcinoma with ≤15 retrieved lymph nodes. *Eur J Surg Oncol*. (2022) 48(5):1017–24. doi: 10.1016/j.ejso.2021.11.133
39. Bando E, Yonemura Y, Taniguchi K, Fushida S, Fujimura T, Miwa K. Outcome of ratio of lymph node metastasis in gastric carcinoma. *Ann Surg Oncol*. (2002) 9(8):775–84. doi: 10.1007/BF02574500
40. Inoue K, Nakane Y, Iiyama H, Sato M, Kanbara T, Nakai K, et al. The superiority of ratio-based lymph node staging in gastric carcinoma. *Ann Surg Oncol*. (2002) 9(1):27–34. doi: 10.1245/aso.2002.9.1.27

Conflict of Interest: The authors declare that the research was conducted in the absence of any commercial or financial relationships that could be construed as a potential conflict of interest.

Publisher's Note: All claims expressed in this article are solely those of the authors and do not necessarily represent those of their affiliated organizations, or those of the publisher, the editors and the reviewers. Any product that may be evaluated in this article, or claim that may be made by its manufacturer, is not guaranteed or endorsed by the publisher.

Copyright © 2022 Lai, Zheng and Li. This is an open-access article distributed under the terms of the Creative Commons Attribution License (CC BY). The use, distribution or reproduction in other forums is permitted, provided the original author(s) and the copyright owner(s) are credited and that the original publication in this journal is cited, in accordance with accepted academic practice. No use, distribution or reproduction is permitted which does not comply with these terms.

frontiers | Frontiers in Oncology

GENERAL COMMENTARY
published: 02 June 2022
doi: 10.3389/fonc.2022.901010

Commentary: The Tumor Markers and Blood Inflammation Markers Are More Likely to Be the Indicators for Differentiating Benign and Malignant Pancreatic Mucinous Cystic Neoplasms

Jiang Liu[1], *Ying Xing*[2] *and Liqi Sun*[2]*

[1] Department of Gastroenterology, Huzhou Hospital of Zhejiang University, Affiliated Central Hospital Huzhou University, Huzhou, China, [2] Department of Gastroenterology, 72nd Group Army Hospital, Huzhou University, Huzhou, China

OPEN ACCESS

Edited by:
Qi Liu,
Fudan University, China

Reviewed by:
Uma Kundu,
University of Texas MD Anderson Cancer Center, United States
Nikolaos Machairas,
National and Kapodistrian University of Athens, Greece

***Correspondence:**
Liqi Sun
zjhzslqsmmu@qq.com

Specialty section:
This article was submitted to Gastrointestinal Cancers: Hepato Pancreatic Biliary Cancers, a section of the journal Frontiers in Oncology

Received: *21 March 2022*
Accepted: *16 May 2022*
Published: *02 June 2022*

Citation:
Liu J, Xing Y and Sun L (2022) Commentary: The Tumor Markers and Blood Inflammation Markers Are More Likely to Be the Indicators for Differentiating Benign and Malignant Pancreatic Mucinous Cystic Neoplasms. Front. Oncol. 12:901010. doi: 10.3389/fonc.2022.901010

Keywords: mucinous cystic neoplasm (MCN), serous cystic neoplasm, serum tumor markers, blood inflammation markers, EUS – endoscopic ultrasonography

A Commentary on

The Tumor Markers and Blood Inflammation Markers Are More Likely to Be the Indicators for Differentiating Benign and Malignant Pancreatic Mucinous Cystic Neoplasms
By Wang H, Chen S, Shu X, Liu Z, Liu P, Zhu Y, Zhu Y and Xiong H (2022). Front. Oncol. 12:831355. doi: 10.3389/fonc.2022.831355

To the editor:

We read with great interest the article by Wang et al. (1) which identified the value of carbohydrate antigen 19-9 (CA19-9) and [lymphocyte × albumin (ALB), LA] in differentiating serous cystic neoplasms (SCNs) and mucinous cystic neoplasms (MCNs). We appreciated the great efforts that the authors made to help the management of pancreatic cystic neoplasms (PCNs). However, some concerns arise which may limit the strength of the evidence level of this study.

First, it is widely acknowledged that a high level of CA19-9 is associated with advanced PCNs. The value of inflammatory markers based on circulating blood cells in predicting advanced PCNs is not well studied. The hypothesis that CA19-9 and inflammatory markers may be useful in differentiating MCN and SCN raised by the authors is mostly based on studies that focus on pancreatic cancer and other malignant tumors. However, MCNs are premalignant tumors, only 10%–17% of which will harbor malignancy (2). The hypothesis may not be applicable to PCN due to lack of reference support. Moreover, the cyst fluid CA19-9 has little value in distinguishing mucinous and non-mucinous PCNs and even the value of cyst fluid carcinoma embryonic antigen (CEA) was doubted at present (2). The conclusions are opposite to the statement in the introduction section raised by authors.

Second, eight MCNs were reported to have a malignant transformation in the study cohort. It means that the MCN patients had a more malignant rate than SCNs (18.8% vs 0%, P = 0.008). Hence, the results of the study merely indicate that CA19-9 and LA may be useful in differentiating benign and malignant tumors. The eight cases with malignancy should be excluded to further identify whether these indicators are still useful in differentiating MCNs and SCNs.

Third, the lymphocyte and ALB change greatly due to food intake and activity, even in the morning and evening of the day. At what time lymphocyte and ALB are tested should be clearly clarified. The analysis of LA is meaningless if they were evaluated at various stages of diseases (preoperative or postoperative, early tumor stage or later tumor stage, etc.). To avoid bias, each patient's nutritional state should be further assessed, too.

Fourth, the value of cytology obtained by endoscopic ultrasound-guided fine-needle aspiration (EUS-FNA) is limited in differentiating MCNs and SCNs with 42% sensitivity (3). Only about 35% of cytologic samples obtained by EUS-FNA were informative (4). The reported accuracy of EUS morphology alone for differentiating mucinous from non-mucinous PCNs is relatively low (48%–94%) (5). Although cytology obtained by EUS-FNA is highly specific (83%–100%), it is relatively insensitive (27–48%) (5). In general, the value of EUS-FNA in making a specific subtype of PCNs is limited. We noticed in Supplementary Table 2 that six SCN patients underwent EUS-FNA alone to make a final diagnosis. SCN was one of the non-mucinous PCN types. So, what are the diagnostic criteria of SCN without cytology? Imaging diagnoses are not definite diagnoses.

Fifth, only eight patients with malignant MCNs in this study were correctly resected. Even the patients who had a low level of cyst fluid CEA underwent surgery. The indications for surgery should be clarified.

Sixth, the authors stated that "The results of the ROC curve showed that the AUC values of serum CA199 and LA in differentiating SCNs and MCNs were 0.6734 and 0.6765, respectively, indicating that they have a certain value in the differential diagnosis of SCNs and MCN". However, with AUC <0.7, we may not be able to say the indicators had certain values.

Seventh, MCNs and mucinous ovarian tumors both originate from primordial germ cells, and ovarian-like stroma can be obtained from the tissue of MCNs (6); thus, MCNs may have an increased CA125 level as well as ovarian tumors. CA125 may be a better indicator than CA19-9 in differentiating SCNs and MCNs (7).

In general, the study provided a new thought to help us understand MCNs and SCNs better. However, great bias may exist in this study and the concerns prevent the study from making strong conclusions. The predictive efficacy of CA199 and LA still needs to be verified in future clinical work.

AUTHOR CONTRIBUTIONS

LS was responsible for the study design/planning, study conduct, and revision of the paper. JL wrote this paper. YX assisted in writing and revising the paper. All authors contributed to the article and approved the submitted version.

REFERENCES

1. Wang H, Chen S, Shu X, Liu Z, Liu P, Zhu Y, et al. The Value of Serum Tumor Markers and Blood Inflammation Markers in Differentiating Pancreatic Serous Cystic Neoplasms and Pancreatic Mucinous Cystic Neoplasms. *Front Oncol* (2022) 12:831355. doi: 10.3389/fonc.2022.831355
2. Stark A, Donahue TR, Reber HA, Hines OJ. Pancreatic Cyst Disease: A Review. *JAMA* (2016) 315(17):1882–93. doi: 10.1001/jama.2016.4690
3. Gillis A, Cipollone I, Cousins G, Conlon K. Does EUS-FNA Molecular Analysis Carry Additional Value When Compared to Cytology in the Diagnosis of Pancreatic Cystic Neoplasm? A Systematic Review. *HPB (Oxford)* (2015) 17 (5):377–86. doi: 10.1111/hpb.12364
4. Faias S, Cravo M, Pereira da Silva J, Chaves P, Dias Pereira A. Endoscopic Ultrasound With Fine Needle Aspiration is Useful in Pancreatic Cysts Smaller Than 3 Cm. *BMC Gastroenterol* (2020) 20(1):413. doi: 10.1186/s12876-020-01565-9
5. European Study Group on Cystic Tumours of the Pancreas. European Evidence-Based Guidelines on Pancreatic Cystic Neoplasms. *Gut* (2018) 67 (5):789–804. doi: 10.1136/gutjnl-2018-316027
6. Crinò SF, Bernardoni L, Gabbrielli A, Capelli P, Salvia R, Rusev BC, et al. Beyond Pancreatic Cyst Epithelium: Evidence of Ovarian-Like Stroma in EUS-Guided Through-The-Needle Micro-Forceps Biopsy Specimens. *Am J Gastroenterol* (2018) 113(7):1059–60. doi: 10.1038/s41395-018-0124-6
7. Sun LQ, Peng LS, Guo JF, Jiang F, Cui F, Huang HJ, et al. Validation of Serum Tumor Biomarkers in Predicting Advanced Cystic Mucinous Neoplasm of the Pancreas. *World J Gastroenterol* (2021) 27(6):501–12. doi: 10.3748/wjg.v27.i6.501

Conflict of Interest: The authors declare that the research was conducted in the absence of any commercial or financial relationships that could be construed as a potential conflict of interest.

Publisher's Note: All claims expressed in this article are solely those of the authors and do not necessarily represent those of their affiliated organizations, or those of the publisher, the editors and the reviewers. Any product that may be evaluated in this article, or claim that may be made by its manufacturer, is not guaranteed or endorsed by the publisher.

Copyright © 2022 Liu, Xing and Sun. This is an open-access article distributed under the terms of the Creative Commons Attribution License (CC BY). The use, distribution or reproduction in other forums is permitted, provided the original author(s) and the copyright owner(s) are credited and that the original publication in this journal is cited, in accordance with accepted academic practice. No use, distribution or reproduction is permitted which does not comply with these terms.

frontiers | Frontiers in Oncology

ORIGINAL RESEARCH
published: 07 June 2022
doi: 10.3389/fonc.2022.874749

Adjuvant Chemotherapy Benefit in Elderly Stage II/III Colon Cancer Patients

Xin Chen[1†], Junhao Tu[2†], Xiaolan Xu[3†], Wen Gu[1†], Lei Qin[1], Haixin Qian[1], Zhenyu Jia[4], Chuntao Ma[3] and Yinkai Xu[1*]*

[1] Department of General Surgery, The First Affiliated Hospital of Soochow University, Suzhou, China, [2] Department of General Surgery, Suzhou Wuzhong People's Hospital, Suzhou, China, [3] Department of Gastroenterology, Xiangcheng People's Hospital, Suzhou, China, [4] Department of Gastroenterology, The First Affiliated Hospital of Soochow University, Suzhou, China

OPEN ACCESS

Edited by:
Qi Liu,
Fudan University, China

Reviewed by:
Ziv Radisavljevic,
Brigham and Women's Hospital and Harvard Medical School, United States
Kondapa Bobba,
University of California, San Francisco, United States

***Correspondence:**
Yinkai Xu
xuyinkai@suda.edu.cn;
xuyinkaii@163.com
Chuntao Ma
xwqsu@163.com

[†]These authors have contributed equally to this work

Specialty section:
This article was submitted to Surgical Oncology, a section of the journal Frontiers in Oncology

Received: 12 February 2022
Accepted: 06 May 2022
Published: 07 June 2022

Citation:
Chen X, Tu J, Xu X, Gu W, Qin L, Qian H, Jia Z, Ma C and Xu Y (2022) Adjuvant Chemotherapy Benefit in Elderly Stage II/III Colon Cancer Patients. Front. Oncol. 12:874749. doi: 10.3389/fonc.2022.874749

Background: Studies providing more evidence to guide adjuvant chemotherapy decisions in elderly colon cancer patients are expected.

Methods: We obtained data from the Surveillance, Epidemiology and End Results (SEER) database between 2004 and 2012. Kaplan-Meier survival curves were constructed to calculate the cancer-specific survival (CSS) rate, and comparisons of survival difference between different subgroups were performed using the log-rank test. Multivariate Cox proportional hazards regression models were carried out to estimate hazard ratio (HR) and 95% confidence intervals (CIs) of different clinicopathological characteristics.

Results: In stage II colon cancer patients aged 70 years or older, the Kaplan-Meier survival analysis showed that the 5-year CSS rates of no chemotherapy and chemotherapy groups were 82.0% and 72.4%, respectively ($P < 0.001$). In stage III colon cancer patients aged 70 years or older, the Kaplan-Meier survival analysis showed that the 5-year CSS rates of no chemotherapy and chemotherapy groups were 50.7% and 61.3%, respectively ($P < 0.001$). Patients with chemotherapy receipt were independently associated with a 35.8% lower cancer-specific mortality rate (HR = 0.642, 95% CI: 0.620-0.665, $P < 0.001$) compared with those who did not receive chemotherapy.

Conclusions: Adjuvant chemotherapy should be considered during the treatment of stage III colon cancer patients aged 70 years or older, but the chemotherapy benefit in elderly stage II colon cancer is suboptimal.

Keywords: chemotherapy, survival, elderly, stage II/III, colon cancer

INTRODUCTION

As an important public health issue, colorectal cancer (CRC) is the third most commonly diagnosed cancer and the fourth most common cause of cancer death around the world (1).

With the aging of the population, the elderly occupies a sizable proportion of colon cancer patients and 60% percent of them are diagnosed over the age of 65 years (2). Older patients with colon cancer are reported to have worse survival compared with younger patients (3–6).

In 2001, a well-known randomized controlled trial reported that 5-FU-based adjuvant therapy could improve patient outcomes without a significant increase in toxic effects in selected elderly patients with colon cancer (7). Nonetheless, elderly CRC patients have been underrepresented in clinical trials, which has been a long-standing issue and needs further attention (8). In clinical trials, patients who are aged 65 years or older account for only 40% of patients, compared to 72% of the US population. Moreover, patients who are aged 70 years or older account for only 14% in clinical trials (9).

It has been previously proposed that 5-FU-based adjuvant therapy has shown comparable toxicity rates and similar survival benefits in elderly colon cancer patients compared with younger patients (7, 10). However, these studies were conducted before the incorporation of oxaliplatin into the 5-FU-based adjuvant therapy. In 2004, the addition of oxaliplatin to 5-FU/leucovorin (LV) chemotherapy was shown to improve disease-free survival (DFS) rate by 24% and reduce mortality rate by 14% compared with 5-FU/LV therapy alone in the MOSAIC trial (11).

In 2013, a study in Korea evaluated the efficacy of adjuvant chemotherapy in elderly colon cancer patients, which showed the survival benefit in stage III colon cancer patients offered by adjuvant chemotherapy, but the number of patients included in their study was too small (n= 382) (12). Therefore, the efficacy of adjuvant therapy has been reported in only a highly selected group of elderly colon cancer patients and studies providing more evidence to guide adjuvant chemotherapy decisions in elderly colon cancer patients are expected.

METHODS

Data Source

In this retrospective analysis, we obtained data from the Surveillance, Epidemiology and End Results (SEER) database between 2004 and 2012, which was maintained by the National Cancer Institute and covered basic information for ~28% of the US population. A flowchart of cohort ascertainment is shown in **Figure 1**. The patient information of the SEER database is publicly available and the SEER database is free of any sensitive patient information or identifiers. Therefore, the collection of it did not require informed consent and the ethical approval was not required for this study. From the database, the following patient and tumor information was collected: survival status, survival months, TNM stage, race, sex, year of diagnosis, tumor grade, primary tumor site, histology, treatment, and patient age.

Statistical Analysis

The cancer-specific survival (CSS) was the time from the initial colon cancer diagnosis to colon cancer-associated death. Only

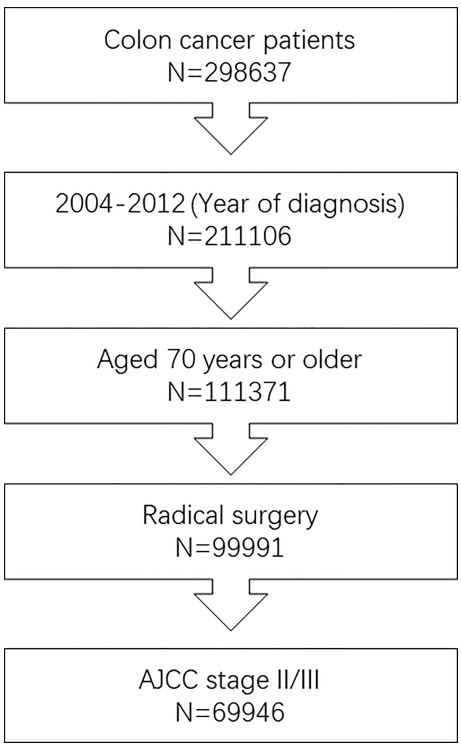

FIGURE 1 | Flowchart of cohort ascertainment in this study. We included 69,946 stage II/III patients aged 70 years or older diagnosed with colon cancer between 2004 and 2012.

deaths caused by colon cancer were regarded as events, and deaths from other causes were censored at the date of death. Chi-square test was performed to compare categorical data. Kaplan-Meier survival curves were plotted to calculate the CSS rate, and comparisons of survival difference between different subgroups were performed using the log-rank test. Multivariate Cox proportional hazards regression models were conducted to estimate hazard ratio (HR) and 95% confidence intervals (CIs) of different clinicopathological characteristics as follows: TNM stage, race, sex, year of diagnosis, tumor grade, primary tumor site, histology, and chemotherapy. The statistical analyses were conducted by using the statistical software package SPSS 23.0 (IBM Corp, Armonk, NY). All statistical tests were two-sided and a P value less than 0.05 was regarded as statistically significant.

RESULTS

Baseline Characteristics of Stage II/III Colon Cancer Patients

Finally, we included 69,946 stage II/III patients aged 70 years or older diagnosed with colon cancer between 2004 and 2012. In patients with known TNM stage, 35,099 (50.2%) patients were diagnosed with stage II colon cancer, which was comparable to stage III colon cancer patients; in colon cancer patients with known race, patients of white race (59,226, 84.7%) were far more prevalent than other races (10,720, 15.3%); in colon patients with known gender, male (31,024, 44.4%) patients were less prevalent than female (38,922, 55.6%) patients; in colon patients with known year of diagnosis, more patients were diagnosed with colon cancer between 2004 and 2008 (41,357, 59.1%) than between 2009 and 2012 (28,589, 40.9%); in colon patients with known tumor grade, grade I/II (50,234, 71.8%) patients were far more than grade III/IV (18,261, 26.1%) patients; in colon patients with known primary tumor site, patients with right colon cancer (48,640, 69.5%) were significantly more than patients with left colon cancer (21,306, 30.5%); in colon patients with known histology, patients with adenocarcinoma (61,708, 88.2%) were far more than patients with mucinous adenocarcinoma/signet ring cell carcinoma (8238, 11.8%).

Table 1 summarized the demographic and clinicopathological characteristics of stage II/III colon cancer patients by the receipt of chemotherapy. Significant differences were found in TNM stage, race, sex, year of diagnosis, tumor grade, and primary tumor site by the receipt of chemotherapy. Stage III (81.7% vs. 39.8%), other races (17.0% vs. 14.8%), male (48.0% vs. 43.2%), year of diagnosis between 2009 and 2012 (42.0% vs. 40.5%), grade III/IV (30.7% vs. 24.7%), and left colon cancer (32.9% vs. 29.7%) were more likely to be associated with the receipt of adjuvant chemotherapy ($P < 0.05$).

Table 2 summarizes the demographic and clinicopathological characteristics of colon cancer patients by different stages. Significant differences were found in the receipt of adjuvant chemotherapy, race, tumor grade, and histology. Compared with stage II patients, stage III colon cancer patients were more likely to be associated with the receipt of adjuvant chemotherapy (39.2% vs. 8.7%), other races (16.6% vs. 14.0%), grade III/IV (32.6% vs. 19.6%), and mucinous adenocarcinoma/signet ring cell carcinoma (12.1% vs. 11.5%) with two-sided P values less than 0.05.

TABLE 1 | Clinicopathological characteristics of colon cancer patients by the receipt of chemotherapy.

Variables	Chemotherapy (%)		P value
	No (N=53,233)	Yes (N=16,713)	
Stage			<.001
II	32,046 (60.2)	3053 (18.3)	
III	21,187 (39.8)	13,660 (81.7)	
Race			<.001
White	45,349 (85.2)	13,877 (83.0)	
Other	7884 (14.8)	2836 (17.0)	
Sex			<.001
Male	22,995 (43.2)	8029 (48.0)	
Female	30,238 (56.8)	8684 (52.0)	
Year of diagnosis			.001
2004-2008	31,656 (59.5)	9701 (58.0)	
2009-2012	21,577 (40.5)	7012 (42.0)	
Grade			<.001
I/II	39,007 (73.3)	11,227 (67.2)	
III/IV	13,128 (24.7)	5133 (30.7)	
Unknown	1098 (2.1)	353 (2.1)	
Primary tumor site			<.001
Right colon	37,422 (70.3)	11,218 (67.1)	
Left colon	15,811 (29.7)	5495 (32.9)	
Histology			.385
Adenocarcinoma	46,995 (88.3)	14,713 (88.0)	
Mucinous adenocarcinoma/signet ring cell carcinoma	6238 (11.7)	2000 (12.0)	

TABLE 2 | Clinicopathological characteristics of colon cancer patients by stage group.

Variables	(%)		P value
	II (N=35099)	III (N=34847)	
Chemotherapy			<.001
No	32,046 (91.3)	21,187 (60.8)	
Yes	3053 (8.7)	13,660 (39.2)	
Race			<.001
White	30,170 (86.0)	29,056 (83.4)	
Other	4929 (14.0)	5791 (16.6)	
Sex			.977
Male	15,566 (44.3)	15,458 (44.4)	
Female	19,533 (55.7)	19,389 (55.6)	
Year of diagnosis			.051
2004-2008	20,880 (59.5)	20,477 (58.8)	
2009-2012	14,219 (40.5)	14,370 (41.2)	
Grade			<.001
I/II	27,528 (78.4)	22,706 (65.2)	
III/IV	6886 (19.6)	11,375 (32.6)	
Unknown	685 (2.0)	766 (2.2)	
Primary tumor site			.874
Right colon	24,398 (69.5)	24,242 (69.6)	
Left colon	10,701 (30.5)	10,605 (30.4)	
Histology			.009
Adenocarcinoma	31,077 (88.5)	30,631 (87.9)	
Mucinous adenocarcinoma/signet ring cell carcinoma	4022 (11.5)	4216 (12.1)	

The Effect of Adjuvant Chemotherapy in Stage II Colon Cancer Patients Aged 70 Years or Older

In stage II colon cancer patients aged 70 years or older, the Kaplan-Meier survival analysis showed that the 5-year CSS rates of no chemotherapy and chemotherapy groups were 82.0% and 72.4%, respectively ($P < 0.001$), indicating a relatively poor survival of stage II colon cancer patients with the receipt of chemotherapy (**Figure 2A**).

Apart from this, we performed multivariate Cox proportional analysis of CSS for the prognostic characteristics in colon cancer patients. As shown in **Table 3**, for the whole cohort, race, tumor grade, primary tumor site, and the receipt of chemotherapy were independent prognostic determinants of CSS in stage II colon cancer patients aged 70 years or older. Using the white race as a reference, other races (HR = 1.137, 95% CI: 1.064-1.216, $P < 0.001$) had a poorer prognosis; using grade I/II as a reference, grade III/IV (HR = 1.178, 95% CI: 1.108-1.253, $P < 0.001$) had a poorer prognosis; using the right colon as a reference, the left colon (HR = 1.420, 95% CI: 1.349-1.495, $P < 0.001$) had a poorer prognosis. More importantly, patients with chemotherapy receipt were independently associated with a 44.6% higher cancer-specific mortality rate (HR = 1.446, 95% CI: 1.346-1.554, $P < 0.001$) compared with those who do not receive chemotherapy after adjusting for TNM stage, race, sex, year of diagnosis, tumor grade, primary tumor site, and histology.

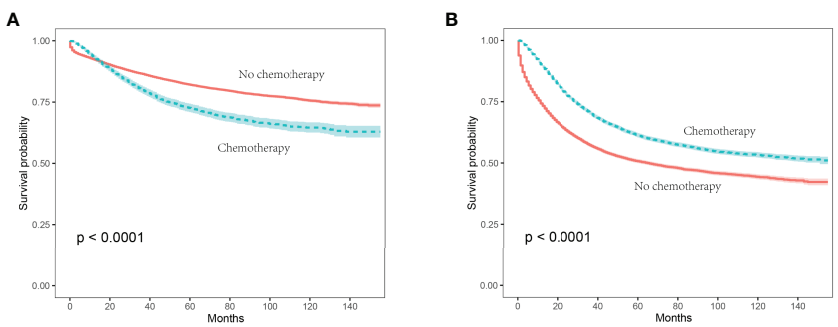

FIGURE 2 | Kaplan-Meier survival curves were plotted to calculate the CSS rate, and comparisons of survival difference between chemotherapy and no chemotherapy subgroups were performed using the log-rank test. **(A)** In stage II colon cancer patients, the 5-year CSS rates of no chemotherapy and chemotherapy groups were 82.0% and 72.4%, respectively ($P < 0.001$); **(B)** in stage III colon cancer patients aged 70 years or older, the 5-year CSS rates of no chemotherapy and chemotherapy groups were 50.7% and 61.3%, respectively ($P < 0.001$).

TABLE 3 | Multivariate Cox regression analyses for survival in stage II colon cancer.

Variables	N	Stepwise multivariate analysis	
		HR (95%CI)	P value
Race			<.001
White	30,170	1.0	
Other	4929	1.137 (1.064-1.216)	
Sex			0.520
Male	15,566	1.0	
Female	19,533	1.016 (0.967-1.068)	
Year of diagnosis			0.281
2004-2008	20,880	1.0	
2009-2012	14,219	0.972 (0.923-1.024)	
Grade			<.001
I/II	27,528	1.0	
III/IV	6886	1.178 (1.108-1.253)	
Unknown	685	1.385 (1.177-1.629)	
Primary tumor site			<.001
Right colon	24,398	1.0	
Left colon	10,701	1.420 (1.349-1.495)	
Histology			0.058
Adenocarcinoma	31,077	1.0	
Mucinous adenocarcinoma/signet ring cell carcinoma	4022	0.925 (0.853-1.003)	
Chemotherapy			<.001
No	32,046	1.0	
Yes	3053	1.446 (1.346-1.554)	

The Effect of Adjuvant Chemotherapy in Stage III Colon Cancer Patients Aged 70 Years or Older

In stage III colon cancer patients aged 70 years or older, the Kaplan-Meier survival analysis showed that the 5-year CSS rates of no chemotherapy and chemotherapy groups were 50.7% and 61.3%, respectively (P < 0.001), indicating a relatively poor survival of stage III colon cancer patients without the receipt of chemotherapy (**Figure 2B**).

The results of multivariate Cox proportional analysis of CSS for the prognostic characteristics in colon cancer patients are shown in **Table 4**. For the whole cohort, race, year of diagnosis, tumor grade, histology, and the receipt of chemotherapy were independent prognostic determinants of CSS in stage III colon cancer patients aged 70 years or older. Using the white race as a reference, other races (HR = 1.089, 95% CI: 1.042-1.139, P < 0.001) had a poorer prognosis; using year of diagnosis between 2004 and 2008 as a reference, year of diagnosis between 2009 and 2012 (HR = 0.938, 95% CI: 0.906-0.971, P < 0.001) had a more favorable prognosis; using grade I/II as a reference, grade III/IV (HR = 1.435, 95% CI: 1.385-1.487, P < 0.001) had a poorer prognosis; using adenocarcinoma as a reference, mucinous adenocarcinoma/signet ring cell carcinoma (HR = 1.077, 95% CI: 1.023-1.133, P = 0.004) had a poorer prognosis. Furthermore, patients who received chemotherapy were independently associated with a 35.8% lower cancer-specific mortality rate (HR = 0.642, 95% CI: 0.620-0.665, P < 0.001) compared with those who did not receive chemotherapy after adjusting for TNM stage, race, sex, year of diagnosis, tumor grade, primary tumor site, and histology.

DISCUSSION

The risk of oncogenesis is highly associated with advanced age and the elderly occupy a sizable proportion of colon cancer patients. In clinical practice, physicians are more prone to bias that advanced age could not tolerate chemotherapy or that the survival benefit of adjuvant therapy is not worth the risks in these elderly patients (12). In fact, clinicians should rely more on an assessment of biological age rather than chronological age in making treatment decisions for colon cancer patients (13). In addition, older patients were more likely to experience surgical complications than younger patients and patient's suboptimal postoperative recovery would also affect performance status, making these patients not willing to receive adjuvant chemotherapy (14). As a key factor affecting chemotherapy receipt, older age was associated with decreased receipt of chemotherapy (15, 16).

Surgical treatment is the most important treatment modality for colon cancer. However, it has recently been found that conventional colon surgery may not be sufficient when compared with standard surgery for rectal cancer (total mesorectal excision, TME) (17–19). Resection along the embryonic avascular mesorectal fascia plane could yield a complete specimen, including regional lymphatics, blood vessels, and surrounding adipose tissue bounded by the mesorectum (20). This could reduce the rate of local recurrence and improve disease-free and overall survival, and more research about this is needed in the future (21).

The first adjuvant chemotherapy regimen to demonstrate efficacy in colon cancer was the FULV regimen, which reduced

TABLE 4 | Multivariate Cox regression analyses for survival in stage III colon cancer.

Variables	N	Stepwise multivariate analysis	
		HR (95%CI)	P value
Race			<.001
White	29,056	1.0	
Other	5791	1.089 (1.042-1.139)	
Sex			.866
Male	15,458	1.0	
Female	19,389	0.997 (0.964-1.032)	
Year of diagnosis			<.001
2004-2008	20,477	1.0	
2009-2012	14,370	0.938 (0.906-0.971)	
Grade			<.001
I/II	22,706	1.0	
III/IV	11,375	1.435 (1.385-1.487)	<.001
Unknown		1.231 (1.099-1.379)	<.001
Primary tumor site			.657
Right colon	24,242	1.0	
Left colon	10,605	0.992 (0.955-1.029)	
Histology			.004
Adenocarcinoma	30,631	1.0	
Mucinous adenocarcinoma/signet ring cell carcinoma	4216	1.077 (1.023-1.133)	
Chemotherapy			<.001
No	21,187	1.0	
Yes	13,660	0.642 (0.620-0.665)	

the five-year risk of death by approximately 15% compared with surgery alone (22–24). Then in the MOSAIC study, the researchers found that the addition of oxaliplatin for 6 months (FOLFOX or CAPOX regimen) increased the efficacy of chemotherapy, which could increase the 6-year DFS and OS rates to 73.3% and 78.5%, respectively, as compared to 67.4% and 76% for fluoropyrimidine alone, and this result was confirmed in subsequent NSABPC-07 and XELOXA trials (11, 25–27).

However, the effectivity of adjuvant chemotherapy in elderly colon cancer patients was not clear, which was partially attributed to the problem that elderly colon cancer patients have been underrepresented or even excluded in clinical trial (28–31). It has been reported that only 35% of the patients > 65 years were asked by clinical investigators to participate in clinical trials, whereas 51% of patients < 65 years were asked for such trials (32). Hence, we conducted this retrospective analysis aiming to provide more evidence to guide adjuvant chemotherapy decisions in elderly colon cancer patients.

In this study, with 69,946 stage II/III patients aged 70 years or older identified, we conducted a retrospective analysis to assess the efficacy of adjuvant therapy in stage II/III colon cancer patients aged 70 years or older. First, Chi-square test of the baseline characteristics showed that stage III, other races, male, diagnosed between 2009 and 2012, grade III/IV, and left colon cancer were more likely to be associated with the receipt of adjuvant chemotherapy; compared with stage II patients, stage III colon cancer patients were more likely to be associated with the receipt of adjuvant chemotherapy than other races, grade III/IV, and mucinous adenocarcinoma/signet ring cell carcinoma. Then, the effect of adjuvant chemotherapy was assessed in stage II colon cancer patients aged 70 years or older. The Kaplan-Meier survival analysis indicated a relatively poor survival of stage II colon cancer patients with the receipt of chemotherapy and the 5-year CSS rates of no chemotherapy and chemotherapy groups were 82.0% and 72.4%, respectively ($P < 0.001$). Multivariate Cox proportional analysis indicated that race, tumor grade, primary tumor site, and the receipt of chemotherapy were independent prognostic determinants of CSS in stage II colon cancer patients aged 70 years or older. More importantly, patients with chemotherapy receipt were independently associated with a 44.6% lower cancer-specific mortality rate compared with those who do not receive chemotherapy after adjusting for TNM stage, race, sex, year of diagnosis, tumor grade, primary tumor site, and histology, which was in line with the result of the Kaplan-Meier survival analysis.

Finally, the effect of adjuvant chemotherapy was assessed in stage III colon cancer patients aged 70 years or older. The Kaplan-Meier survival analysis indicated a relatively poor survival of stage II colon cancer patients with the receipt of chemotherapy and the 5-year CSS rates of no chemotherapy and chemotherapy groups were 50.7% and 61.3%, respectively ($P < 0.001$). Multivariate Cox proportional analysis indicated race, year of diagnosis, tumor grade, histology, and the receipt of chemotherapy were independent prognostic determinants of CSS in stage III colon cancer patients aged 70 years or older. What is more, patients with chemotherapy receipt were independently associated with a 35.8% lower cancer-specific mortality rate compared with those who did not receive chemotherapy after adjusting for TNM stage, race, sex, year of diagnosis, tumor grade, primary tumor site, and histology.

In 2013, Kim et al. evaluated the efficacy of adjuvant chemotherapy in 382 elderly colon cancer patients and showed

the survival benefit in stage III colon cancer patients offered by adjuvant chemotherapy though adjuvant chemotherapy was not effective in elderly patients with stage II colon cancer, which was consistent with our findings. Therefore, the present study further confirmed Kim et al.'s viewpoint that adjuvant chemotherapy should be considered for stage III colon cancer patients aged 70 years or older, but the chemotherapy benefit in elderly stage II colon cancer was not truly clear.

According to the clinical practice guidelines promulgated by the American Society of Clinical Oncology (ASCO), stage II colon cancer patients with high-risk factors (including T4, sampling of fewer than 12 lymph nodes in the surgical specimen, perineural or lymphovascular invasion, poorly or undifferentiated tumor grade, intestinal obstruction, tumor perforation, or grade BD3 tumor budding) should be offered adjuvant chemotherapy (33). Those stage II colon cancer patients without high-risk factors did not receive adjuvant chemotherapy and usually had a good prognosis, which might also be a cause of suboptimal chemotherapy benefit in elderly stage II colon cancer. However, our analysis did not address this aspect owing to the lack of information about high-risk factors, and this aspect should be explored in future studies.

Taken together, here we have conducted a retrospective study with a large sample size and provide more evidence for that adjuvant chemotherapy should be considered in the treatment for stage III colon cancer patients aged 70 years or older, but the chemotherapy benefit in elderly stage II colon cancer is suboptimal. Future prospective studies to validate our results are therefore highly warranted. Moreover, clinical researchers should support more elderly patients to participate in relevant randomized controlled clinical studies in the future.

We also acknowledge that there are flaws in this study. First, as mentioned above, our research does not address the aspect of whether high-risk factors were the cause of suboptimal chemotherapy benefit in elderly stage II colon cancer owing to the lack of information about high-risk factors. Second, comorbidities and performance status of patients which could influence their willingness to accept chemotherapy are not available because of the inherent limitations of the database. Finally, there are inherent drawbacks of the retrospective study design, prospective studies to validate our results are therefore highly warranted.

In conclusion, this work provides further evidence that adjuvant chemotherapy should be considered in the treatment for stage III colon cancer patients aged 70 years or older, but the chemotherapy benefit in elderly stage II colon cancer is suboptimal. Moreover, clinical researchers should support more elderly patients to participate in relevant randomized controlled clinical studies in the future.

DATA AVAILABILITY STATEMENT

Publicly available datasets were analyzed in this study. This data can be found here: The datasets analyzed in this study are collected from SEER repository (https://seer.cancer.gov/).

AUTHOR CONTRIBUTIONS

YX and CM conceived and designed the study; XC, JT, XX, and WG extracted and analyzed the data; XC, JT, XX, LQ, HQ, and ZJ participated in the interpretation of data, and wrote the manuscript; all authors read and approved the final manuscript.

REFERENCES

1. Cavers D, Calanzani N, Orbell S, Vojt G, Steele RJC, Brownlee L, et al. Development of an Evidence-Based Brief 'Talking' Intervention for non-Responders to Bowel Screening for Use in Primary Care: Stakeholder Interviews. *BMC Family Pract* (2018) 19:105. doi: 10.1186/s12875-018-0794-6
2. Kurniali PC, Hrinczenko B, Al-Janadi A. Management of Locally Advanced and Metastatic Colon Cancer in Elderly Patients. *World J Gastroenterol* (2014) 20:1910–22. doi: 10.3748/wjg.v20.i8.1910
3. Jessup JM, McGinnis LS, Steele GD Jr, Menck HR, Winchester DP. The National Cancer Data Base. Report on Colon Cancer. *Cancer* (1996) 78:918–26. doi: 10.1002/(SICI)1097-0142(19960815)78:4<918::AID-CNCR32>3.0.CO;2-W
4. Kune GA, Kune S, Field B, White R, Brough W, Schellenberger R, et al. Survival in Patients With Large-Bowel Cancer. A Population-Based Investigation From the Melbourne Colorectal Cancer Study. *Dis Colon Rectum* (1990) 33:938–46. doi: 10.1007/BF02139103
5. Dekker JW, van den Broek CB, Bastiaannet E, van de Geest LG, Tollenaar RA, Liefers GJ. Importance of the First Postoperative Year in the Prognosis of Elderly Colorectal Cancer Patients. *Ann Surg Oncol* (2011) 18:1533–9. doi: 10.1245/s10434-011-1671-x
6. Waldron RP, Donovan IA, Drumm J, Mottram SN, Tedman S. Emergency Presentation and Mortality From Colorectal Cancer in the Elderly. *Br J Surg* (1986) 73:214–6. doi: 10.1002/bjs.1800730320
7. Sargent DJ, Goldberg RM, Jacobson SD, Macdonald JS, Labianca R, Haller DG, et al. A Pooled Analysis of Adjuvant Chemotherapy for Resected Colon Cancer in Elderly Patients. *N Engl J Med* (2001) 345:1091–7. doi: 10.1056/NEJMoa010957
8. Herrera AP, Snipes SA, King DW, Torres-Vigil I, Goldberg DS, Weinberg AD. Disparate Inclusion of Older Adults in Clinical Trials: Priorities and Opportunities for Policy and Practice Change. *Am J Public Health* (2010) 100 Suppl 1:S105–12. doi: 10.2105/AJPH.2009.162982
9. Hutchins LF, Unger JM, Crowley JJ, Coltman CA Jr, Albain KS. Underrepresentation of Patients 65 Years of Age or Older in Cancer-Treatment Trials. *N Engl J Med* (1999) 341:2061–7. doi: 10.1056/NEJM199912303412706
10. Gill S, Loprinzi CL, Sargent DJ, Thomé SD, Alberts SR, Haller DG, et al. Pooled Analysis of Fluorouracil-Based Adjuvant Therapy for Stage II and III Colon Cancer: Who Benefits and by How Much? *J Clin Oncol* (2004) 22:1797–806. doi: 10.1200/JCO.2004.09.059
11. André T, Boni C, Mounedji-Boudiaf L, Navarro M, Tabernero J, Hickish T, et al. Oxaliplatin, Fluorouracil, and Leucovorin as Adjuvant Treatment for Colon Cancer. *N Engl J Med* (2004) 350:2343–51. doi: 10.1056/NEJMoa032709
12. Kim KY, Cha IH, Ahn JB, Kim NK, Rha SY, Chung HC, et al. Estimating the Adjuvant Chemotherapy Effect in Elderly Stage II and III Colon Cancer Patients in an Observational Study. *J Surg Oncol* (2013) 107:613–8. doi: 10.1002/jso.23290
13. Hayes L, Forrest L, Adams J, Hidajat M, Ben-Shlomo Y, White M, et al. Age-Related Inequalities in Colon Cancer Treatment Persist Over Time: A

Population-Based Analysis. *J Epidemiol Community Health* (2019) 73:34–41. doi: 10.1136/jech-2018-210842
14. Al-Refaie WB, Parsons HM, Henderson WG, Jensen EH, Tuttle TM, Vickers SM, et al. Major Cancer Surgery in the Elderly: Results From the American College of Surgeons National Surgical Quality Improvement Program. *Ann Surg* (2010) 251:311–8. doi: 10.1097/SLA.0b013e3181b6b04c
15. Abraham A, Habermann EB, Rothenberger DA, Kwaan M, Weinberg AD, et al. Adjuvant Chemotherapy for Stage III Colon Cancer in the Oldest Old: Results Beyond Clinical Guidelines. *Cancer* (2013) 119:395–403. doi: 10.1002/cncr.27755
16. Abrams TA, Brightly R, Mao J, Kirkner G, Meyerhardt JA, Schrag D, et al. Patterns of Adjuvant Chemotherapy Use in a Population-Based Cohort of Patients With Resected Stage II or III Colon Cancer. *J Clin Oncol* (2011) 29:3255–62. doi: 10.1200/JCO.2011.35.0058
17. Khani MH, Smedh K. Centralization of Rectal Cancer Surgery Improves Long-Term Survival. *Colorectal Dis* (2010) 12:874–9. doi: 10.1111/j.1463-1318.2009.02098.x
18. Wibe A, Møller B, Norstein J, Carlsen E, Wiig JN, Heald RJ, et al. A National Strategic Change in Treatment Policy for Rectal Cancer–Implementation of Total Mesorectal Excision as Routine Treatment in Norway. A National Audit. *Dis Colon Rectum* (2002) 45:857–66. doi: 10.1007/s10350-004-6317-7
19. Søndenaa K, Quirke P, Hohenberger W, Sugihara K, Kobayashi H, Kessler H, et al. The Rationale Behind Complete Mesocolic Excision (CME) and a Central Vascular Ligation for Colon Cancer in Open and Laparoscopic Surgery : Proceedings of a Consensus Conference. *Int J Colorectal Dis* (2014) 29:419–28. doi: 10.1007/s00384-013-1818-2
20. Enker WE, Kafka NJ, Martz J. Planes of Sharp Pelvic Dissection for Primary, Locally Advanced, or Recurrent Rectal Cancer. *Semin Surg Oncol* (2000) 18:199–206. doi: 10.1002/(SICI)1098-2388(200004/05)18:3<199::AID-SSU3>3.0.CO;2-4
21. Heald RJ, Ryall RD. Recurrence and Survival After Total Mesorectal Excision for Rectal Cancer. *Lancet* (1986) 1:1479–82. doi: 10.1016/S0140-6736(86)91510-2
22. Quasar Collaborative Group, Gray R, Barnwell J, McConkey C, Hills RK, Williams NS, et al. Adjuvant Chemotherapy Versus Observation in Patients With Colorectal Cancer: A Randomised Study. *Lancet* (2007) 370:2020–9. doi: 10.1016/S0140-6736(07)61866-2
23. Efficacy of Adjuvant Fluorouracil and Folinic Acid in Colon Cancer. International Multicentre Pooled Analysis of Colon Cancer Trials (IMPACT) Investigators. *Lancet* (1995) 345:939–44. doi: 10.1016/S0140-6736(95)90696-7
24. O'Connell MJ, Mailliard JA, Kahn MJ, Macdonald JS, Haller DG, Mayer RJ, et al. Controlled Trial of Fluorouracil and Low-Dose Leucovorin Given for 6 Months as Postoperative Adjuvant Therapy for Colon Cancer. *J Clin Oncol* (1997) 15:246–50. doi: 10.1200/JCO.1997.15.1.246
25. Yothers G, O'Connell MJ, Allegra CJ, Kuebler JP, Colangelo LH, Petrelli NJ, et al. Oxaliplatin as Adjuvant Therapy for Colon Cancer: Updated Results of NSABP C-07 Trial, Including Survival and Subset Analyses. *J Clin Oncol* (2011) 29:3768–74. doi: 10.1200/JCO.2011.36.4539
26. Kuebler JP, Wieand HS, O'Connell MJ, Smith RE, Colangelo LH, Yothers G, et al. Oxaliplatin Combined With Weekly Bolus Fluorouracil and Leucovorin as Surgical Adjuvant Chemotherapy for Stage II and III Colon Cancer: Results From NSABP C-07. *J Clin Oncol* (2007) 25:2198–204. doi: 10.1200/JCO.2006.08.2974
27. Haller DG, Tabernero J, Maroun J, de Braud F, Price T, Van Cutsem E, et al. Capecitabine Plus Oxaliplatin Compared With Fluorouracil and Folinic Acid as Adjuvant Therapy for Stage III Colon Cancer. *J Clin Oncol* (2011) 29:1465–71. doi: 10.1200/JCO.2010.33.6297
28. Landherr L, Nagykálnai T. Chemotherapy of Elderly Patients With Colorectal Cancer. *Magy Onkol* (2009) 53:97–105. doi: 10.1556/MOnkol.53.2009.2.1
29. Turner NJ, Haward RA, Mulley GP, Selby PJ. Cancer in Old Age–is it Inadequately Investigated and Treated? *Bmj* (1999) 319:309–12. doi: 10.1136/bmj.319.7205.309
30. Hodgson DC, Fuchs CS, Ayanian JZ. Impact of Patient and Provider Characteristics on the Treatment and Outcomes of Colorectal Cancer. *J Natl Cancer Inst* (2001) 93:501–15. doi: 10.1093/jnci/93.7.501
31. Lewis JH, Kilgore ML, Goldman DP, Trimble EL, Kaplan R, Montello MJ, et al. Participation of Patients 65 Years of Age or Older in Cancer Clinical Trials. *J Clin Oncol* (2003) 21:1383–9. doi: 10.1200/JCO.2003.08.010
32. Kemeny MM, Peterson BL, Kornblith AB, Muss HB, Wheeler J, Levine E, et al. Barriers to Clinical Trial Participation by Older Women With Breast Cancer. *J Clin Oncol* (2003) 21:2268–75. doi: 10.1200/JCO.2003.09.124
33. Baxter NN, Kennedy EB, Bergsland E, Berlin J, George TJ, Gill S, et al. Adjuvant Therapy for Stage II Colon Cancer: ASCO Guideline Update. *J Clin Oncol* (2021).

Conflict of Interest: The authors declare that the research was conducted in the absence of any commercial or financial relationships that could be construed as a potential conflict of interest.

Publisher's Note: All claims expressed in this article are solely those of the authors and do not necessarily represent those of their affiliated organizations, or those of the publisher, the editors and the reviewers. Any product that may be evaluated in this article, or claim that may be made by its manufacturer, is not guaranteed or endorsed by the publisher.

Copyright © 2022 Chen, Tu, Xu, Gu, Qin, Qian, Jia, Ma and Xu. This is an open-access article distributed under the terms of the Creative Commons Attribution License (CC BY). The use, distribution or reproduction in other forums is permitted, provided the original author(s) and the copyright owner(s) are credited and that the original publication in this journal is cited, in accordance with accepted academic practice. No use, distribution or reproduction is permitted which does not comply with these terms.

frontiers | Frontiers in Oncology

ORIGINAL RESEARCH
published: 08 June 2022
doi: 10.3389/fonc.2022.893268

Integration of Inflammation-Immune Factors to Build Prognostic Model Predictive of Prognosis and Minimal Residual Disease for Hepatocellular Carcinoma

Xin Xu[1,2†], Ao Huang[1,3†], De-Zhen Guo[1,3†], Yu-Peng Wang[1,3], Shi-Yu Zhang[1,3], Jia-Yan Yan[1,3], Xin-Yu Wang[1,3], Ya Cao[4], Jia Fan[1,3,5,6], Jian Zhou[1,3,5,6], Xiu-Tao Fu[1,3] and Ying-Hong Shi[1,3*]*

[1] Liver Cancer Institute, Zhongshan Hospital, Fudan University and Key Laboratory of Carcinogenesis and Cancer Invasion (Fudan University), Ministry of Education, Shanghai, China, [2] Department of Liver Oncology, Zhongshan Hospital, Fudan University, Shanghai, China, [3] Department of Liver Surgery and Transplantation, Zhongshan Hospital, Fudan University, Shanghai, China, [4] Cancer Research Institute, Xiangya School of Medicine, Central South University; Key Laboratory of Carcinogenesis and Cancer Invasion, Ministry of Education, Xiangya Hospital, Central South University, Changsha, China, [5] Institute of Biomedical Sciences, Fudan University, Shanghai, China, [6] State Key Laboratory of Genetic Engineering, Fudan University, Shanghai, China

Background: Tumor recurrence after hepatectomy is high for hepatocellular carcinoma (HCC), and minimal residual disease (MRD) could be the underlying mechanism. A predictive model for recurrence and presence of MRD is needed.

Methods: Common inflammation-immune factors were reviewed and selected to construct novel models. The model consisting of preoperative aspartate aminotransferase, C-reactive protein, and lymphocyte count, named ACLR, was selected and evaluated for clinical significance.

Results: Among the nine novel inflammation-immune models, ACLR showed the highest accuracy for overall survival (OS) and time to recurrence (TTR). At the optimal cutoff value of 80, patients with high ACLR (> 80) had larger tumor size, higher Edmondson's grade, more vascular invasion, advanced tumor stage, and poorer survival than those with low ACLR (≤ 80) in the training cohort (5-year OS: 43.3% vs. 80.1%, $P < 0.0001$; 5-year TTR: 74.9% vs. 45.3%, $P < 0.0001$). Multivariate Cox analysis identified ACLR as an independent risk factor for OS [hazard ratio (HR) = 2.22, $P < 0.001$] and TTR (HR = 2.36, $P < 0.001$). Such clinical significance and prognostic value were verified in validation cohort. ACLR outperformed extant models, showing the highest area under receiver operating characteristics curve for 1-, 3-, and 5-year OS (0.737, 0.719, and 0.708) and 1-, 3-, and 5-year TTR (0.696, 0.650, and 0.629). High ACLR correlated with early recurrence ($P < 0.001$) and extremely early recurrence ($P < 0.001$). In patients with high ACLR, wide resection margin might confer survival benefit by decreasing recurrence (median TTR, 25.5 vs. 11.4 months; $P = 0.037$).

OPEN ACCESS

Edited by:
Qi Liu,
Fudan University, China

Reviewed by:
Giuseppe Zimmitti,
Fondazione Poliambulanza Istituto Ospedaliero, Italy
Antonio Giovanni Solimando,
University of Bari Aldo Moro, Italy
Augusto Lauro,
Sapienza University of Rome, Italy

***Correspondence:**
Ying-Hong Shi
shi.yinghong@zs-hospital.sh.cn
Xiu-Tao Fu
fu.xiutao@zs-hospital.sh.cn

[†]These authors have contributed equally to this work

Specialty section:
This article was submitted to Gastrointestinal Cancers: Hepato Pancreatic Biliary Cancers, a section of the journal Frontiers in Oncology

Received: 10 March 2022
Accepted: 17 May 2022
Published: 08 June 2022

Citation:
Xu X, Huang A, Guo D-Z, Wang Y-P, Zhang S-Y, Yan J-Y, Wang X-Y, Cao Y, Fan J, Zhou J, Fu X-T and Shi Y-H (2022) Integration of Inflammation-Immune Factors to Build Prognostic Model Predictive of Prognosis and Minimal Residual Disease for Hepatocellular Carcinoma. Front. Oncol. 12:893268. doi: 10.3389/fonc.2022.893268

Conclusions: The novel inflammation-immune model, ACLR, could effectively predict prognosis, and the presence of MRD before hepatectomy and might guide the decision on resection margin for patients with HCC.

Keywords: prognostic model, inflammation, immunity, hepatocellular carcinoma, prognosis

INTRODUCTION

Hepatocellular carcinoma (HCC) is the sixth most common cancer and the fourth leading cause of cancer-related death worldwide. In China, where the hepatitis B infection rate is high, HCC ranks fourth in cancer morbidity and second in cancer mortality (1, 2). Despite advances in diagnosis and treatment, the prognosis of HCC remains dismal, and tumor recurrence stands as the major cause of poor outcomes (3, 4). Therefore, it is of unmet need to develop robust biomarkers and prognostic models to distinguish patients with HCC with high recurrence risk and poor survival.

It is well established that systemic inflammation and immunity play vital roles in the carcinogenesis and metastasis of cancers (5). In fact, emerging evidence has demonstrated the prognostic value of systemic inflammation and immune markers, including neutrophil (6, 7), lymphocyte (8), platelet (9), and C-reactive protein (CRP) (10, 11), in various cancers including HCC. Moreover, chronic liver inflammation, which commonly results in hepatic function damage, also participates in tumorigenesis (12, 13), and factors such as aspartate aminotransferase (AST) (14) and albumin (15) are found to be predictive of prognosis. On the basis of these markers, several models have been developed to predict outcomes, including Glasgow prognostic score (GPS) (16), modified GPS (mGPS) (17), prognostic nutritional index (PNI) (18), neutrophil-to-lymphocyte ratio (NLR) (19), platelet-to-lymphocyte ratio (PLR) (20), and systemic immune-inflammation index (SII) (21). Moreover, models that combine systemic inflammation and chronic liver inflammation indexes, such as aspartate aminotransferase–to-platelet ratio index (APRI) (22) and aspartate aminotransferase–to-lymphocyte ratio index (ALRI) (23), have also been reported.

However, the prognostic value of the current existing models is not fully satisfactory because most models were constructed with only two inflammation or immune factors, and it is proposed that the combination of three markers might achieve better prediction efficiency. Moreover, few models have addressed the underlying issue of tumor recurrence, especially considering that minimal residual disease (MRD) has been increasingly regarded as the fundamental reason for tumor recurrence. In this study, we thoroughly reviewed currently available models and scrutinized the factors that they had used. We then constructed novel models using different combinations of those factors, evaluated their predicting values, and chose the one with the highest predictive accuracy. The prognostic value and clinical implication of the selected model were further assessed and validated.

Abbreviations: AFP, alpha-fetoprotein; AJCC, American Joint Committee on Cancer; ALRI, aspartate aminotransferase–to-lymphocyte ratio index; APRI, aspartate aminotransferase–to-platelet ratio index; AST, aspartate aminotransferase; AUC, area under the curve; BCLC, Barcelona Clinic Liver Cancer; CI, confidence interval; CNLC, China Liver Cancer Staging; CRP, C-reactive protein; CT, computed tomography; GPS, Glasgow prognostic score; HCC, hepatocellular carcinoma; HR, hazard ratio; mGPS, modified Glasgow prognostic score; MRD, minimal residual disease; MRI, magnetic resonance imaging; NLR, neutrophil-to-lymphocyte ratio; OS, overall survival; PET-CT, positron emission tomography–computed tomography; PLR, platelet-to-lymphocyte ratio; PNI, prognostic nutritional index; ROC, receiver operating characteristics; SII, systemic immune-inflammation index; TTR, time to recurrence.

METHODS

Patient Inclusion

Patients with HCC who underwent curative hepatectomy at the Zhongshan Hospital Fudan University from January 2013 to December 2015 were retrospectively analyzed. The inclusion criteria were as follows: (a) HCC confirmed by pathology, (b) no preoperative anti-tumor treatment, and (c) R0 resection. The exclusion criteria were as follows: (a) incomplete clinicopathological information or follow-up data, (b) presence or history of malignancies in extrahepatic organs, and (c) had preoperative anti-tumor treatment. Clinicopathological data and preoperative laboratory test results of all included patients were retrieved from medical documents. The tumor stage was assessed according to the Barcelona Clinic Liver Cancer (BCLC) stage (24), American Joint Committee on Cancer (AJCC) stage (25), and China Liver Cancer Staging (CNLC) (26). Edmondson's grading system was used to grade tumor differentiation (27). The Child-Pugh score system was applied to evaluate liver function. The present study was conducted in accordance with the Strengthening the Reporting of Observational Studies in Epidemiology (STROBE) recommendations (28). This study was approved by the Zhongshan Hospital Research Ethics Committee (No. B2020-427).

Inflammation-Immune Models

Factors that constituted previously reported inflammation-immune prognostic models were analyzed, and frequently used key factors were selected for further model construction. The factors were first formulated into different combinations, and the one with the highest accuracy to predict outcomes in the training cohort was chosen and tested in the validation cohort. The one that had consistent and the highest prognostic value in both cohorts was finally identified as our goal model.

Follow-Up

Postoperative follow-up was first performed 1 month after hepatectomy and then every 3 months until death or loss to follow-up. At each follow-up, laboratory tests including serum α-fetoprotein (AFP), chest X-ray, and abdominal ultrasonography were given to each patient. If recurrence was suspected, then an abdominal computed tomography (CT) or magnetic resonance imaging (MRI) scan was performed for differential diagnosis. Moreover, chest CT was applied to diagnose pulmonary metastasis, and positron emission tomography–CT (PET-CT) was used when extrahepatic metastases were suspected. Time to recurrence (TTR) was defined as the time from hepatectomy to recurrence. Overall survival (OS) was defined as the interval between hepatectomy and death or the end of the study. The last follow-up was made on October 1, 2020.

Statistical Analysis

Statistical analyses were performed using R 4.0.4 software (R Foundation for Statistical Computing, Vienna, Austria). Continuous variables were summarized as median (interquartile range) or mean (standard deviation), and Wilcoxon rank sum test or t-test was applied to compare the differences between the two groups, respectively. Categorical variables were shown as frequency (percentage) and compared *via* chi-square test or Fisher's exact test. The optimal cutoff values of inflammation-immune models were defined *via* the "surminer" package using R. Area under the curve (AUC) of receiver operating characteristics (ROC) and C-index were used to assess the predictive values for OS, TTR, and 90-day recurrence. The cumulative survival and recurrence rates were calculated using the Kaplan–Meier method and the differences between the two groups were evaluated by the log-rank test. Univariate and multivariate analyses were performed using the Cox regression model and the hazard ratio (HR) and 95% confidence interval (CI) were calculated. *P*-value less than 0.05 was considered statistically significant.

RESULTS

Characteristics of Patients

A total of 1,031 patients with HCC were retrieved, and, among them, 617 patients treated between 2013 and 2014 constituted the training cohort, whereas 414 patients treated in 2015 were enrolled in the validation cohort. The baseline characteristics of patients in the two cohorts were comparable, and no significant differences were identified, except for gender and AFP (**Supplementary Table 1**). The median follow-up time was 60.9 months (0.5–90.6 months) in the training cohort and 54.8 months (0.4–69.9 months) in the validation cohort. During the follow-up, 305 (29.6%) patients died and 581 (56.4%) patients experienced tumor recurrence. There were no significant differences between training cohort and validation cohort regarding 5-year survival rate (29.8% vs. 27.5%, $P = 0.430$) and 5-year recurrence rate (54.6% vs. 58.9%, $P = 0.170$).

Construction and Selection of Novel Inflammation-Immune Model-ACLR

Thorough scrutiny of the existing inflammation-immune models (GPS, mGPS, PNI, NLR, PLR, SII, APRI, and ALRI; **Supplementary Table 2**) identified the five most frequently used factors: lymphocyte and albumin positively correlated with prognosis, whereas neutrophil, CRP, and AST negatively correlated with prognosis. These markers were subsequently selected, and nine novel inflammation-immune models were constructed (**Supplementary Figure 1**). The combination of these factors for each model was shown in **Supplementary Table 3**. For example, ACLR was calculated as follows: AST (U/L) × CRP (mg/L)/lymphocyte count ($\times 10^9$/L).

For each model, the optimal cutoff value was obtained as described above. The C-index and AUC of these models for predicting 1-, 3-, and 5-year OS and TTR were shown in **Table 1**. Among the nine models, ACLR harbored the highest predictive value for both survival and recurrence (cutoff value: 80; C-index for OS: 0.660; TTR: 0.608) in the training cohort. Then, the predictive performance was further assessed in the validation cohort with the same cutoff. Consistently, ACLR bears the highest predictive significance with a C-index of 0.729 and 0.642 for OS and TTR, respectively. According to these findings, ACLR was chosen as the target model in this study, and its predictive value and prognostic potential were further assessed in patients with HCC.

TABLE 1 | C-indexes and AUCs of the nine models in the training and validation cohort.

Model	Cutoff	OS in training (n = 617)				TTR in training (n = 617)				OS in validation (n = 414)				TTR in validation (n = 414)			
		C-index	1-year AUC	3-year AUC	5-year AUC	C-index	1-year AUC	3-year AUC	5-year AUC	C-index	1-year AUC	3-year AUC	5-year AUC	C-index	1-year AUC	3-year AUC	5-year AUC
ACLR	80.0	0.66	70.0	68.8	68.5	0.608	67.3	63.6	62.3	0.729	78.2	76.7	74.5	0.642	73.2	67.5	64.1
NALR	151.5	0.60	68.2	62.5	60.7	0.55	58.4	56.0	55.7	0.619	64.3	65.1	61.9	0.565	60.9	57.6	54.5
NCLR	6.24	0.652	69.1	67.8	67.8	0.594	65.4	61.9	60.4	0.714	76.6	76.4	72.8	0.625	72.8	64.7	62.8
ACBR	3.72	0.655	71.0	69.8	67.5	0.599	65.2	62.4	61.2	0.722	77.2	76.5	72.6	0.635	70.8	66.8	63.3
NABR	5.93	0.588	64.8	61.2	59.3	0.551	58.4	56.0	55.4	0.608	60.3	63.6	61.8	0.570	58.9	59.7	57.3
NCBR	0.195	0.644	68.3	67.9	67.4	0.595	65.9	61.9	60.8	0.693	74.2	73.3	71.0	0.622	72.4	64.1	63.6
ABLR	1.95	0.548	59.3	57.0	55.6	0.525	52.5	53.4	53.6	0.538	53.8	54.3	52.8	0.528	50.9	54.9	52.9
NBLR	0.030	0.521	55.1	53.1	51.7	0.509	53.1	51.1	50.0	0.512	50.2	51.8	51.4	0.500	51.0	49.8	48.0
CBLR	0.129	0.630	67.0	66.3	65.4	0.578	61.4	61.0	59.3	0.657	64.7	69.2	63.5	0.583	65.1	59.0	55.6

TABLE 2 | Univariate and multivariate analyses in the training cohort.

Variables	OS				TTR			
	Univariate analysis		Multivariate analysis		Univariate analysis		Multivariate analysis	
	HR (95% CI)	*P*-value	HR (95% CI)	*P*-value	HR (95% CI)	*P*-value	HR (95% CI)	*P*-value
Age, y (50: >50)	0.82 (0.61–1.10)	0.180			0.82 (0.66–1.03)	0.084	0.79 (0.63–0.98)	0.034
Gender (male: female)	1.15 (0.81–1.63)	0.448			0.98 (0.74–1.29)	0.887		
HBsAg (negative: positive)	0.95 (0.66–1.38)	0.805			1.19 (0.88–1.60)	0.251		
Cirrhosis (no: yes)	1.15 (0.86–1.54)	0.340			1.15 (0.92–1.43)	0.215		
Child-Pugh stage (A: B)	0 (0-Inf)	0.994			0 (0-Inf)	0.993		
AFP, ng/ml (≤20: >20)	1.68 (1.23–2.28)	0.001	1.24 (0.89–1.73)	0.199	1.57 (1.25–1.97)	<0.001	1.30 (1.02–1.66)	0.032
Tumor size, cm (≤5: >5)	3.57 (2.67–4.77)	<0.001	1.67 (1.16–2.41)	0.006	2.09 (1.69–2.60)	<0.001	1.31 (1.00–1.70)	0.048
Tumor number (solitary: multiple)	2.29 (1.72–3.05)	<0.001	1.96 (1.46–2.62)	<0.001	1.93 (1.54–2.42)	<0.001	1.74 (1.38–2.21)	<0.001
Edmondson grade (I/II: III/IV)	1.90 (1.43–2.53)	<0.001	1.26 (0.92–1.73)	0.157	1.36 (1.10–1.69)	0.005	1.05 (0.82–1.33)	0.700
Vascular invasion (no: yes)	3.01 (2.26–4.01)	<0.001	1.85 (1.36–2.53)	<0.001	1.81 (1.46–2.26)	<0.001	1.37 (1.08–1.74)	0.01
GPS	2.13 (1.68–2.70)	<0.001	1.12 (0.83–1.52)	0.462	1.51 (1.23–1.86)	<0.001	0.93 (0.72–1.21)	0.593
NLR (≤2.7: >2.7)	2.32 (1.72–3.13)	<0.001	1.34 (0.90–2.00)	0.155	1.52 (1.19–1.94)	0.001	1.12 (0.80–1.55)	0.51
PLR (≤133.1: >133.1)	2.42 (1.77–3.31)	<0.001	0.95 (0.6–1.49)	0.814	1.84 (1.42–2.38)	<0.001	1.24 (0.84–1.81)	0.276
SII (≤523.8: >523.8)	2.70 (1.98–3.67)	<0.001	1.11 (0.65–1.89)	0.705	1.67 (1.28–2.17)	<0.001	0.88 (0.56–1.39)	0.589
ACLR (≤80: >80)	3.92 (2.95–5.22)	<0.001	2.22 (1.50–3.27)	<0.001	2.36 (1.89–2.94)	<0.001	1.94 (1.44–2.61)	<0.001

High ACLR Correlated With Advanced Clinicopathological Features

We then first investigated the correlation between ACLR and clinicopathological factors of patients with HCC. In the training cohort, patients with high ACLR (> 80) tended to have tumors with advanced clinical phenotypes including larger tumor size ($P < 0.001$), higher Edmondson's grade ($P < 0.001$), more vascular invasion ($P < 0.001$), and higher AFP level ($P = 0.004$) (**Supplementary Figures 2A–D**). Correspondingly, patients with high ACLR were also diagnosed at advanced AJCC stage ($P < 0.001$), BCLC stage ($P < 0.001$), and CNLC stage ($P < 0.001$; **Figures 1A–C**).

To validate the clinical significance of ACLR, we performed correlation analysis of ACLR with clinicopathological factors in patients with HCC from the validation cohort. Similarly, high ACLR was also associated with larger tumor size ($P < 0.001$), higher Edmondson's grade ($P < 0.001$), vascular invasion ($P < 0.001$), higher AFP level ($P = 0.038$) (**Supplementary Figures 3A–D**), advanced AJCC stage ($P < 0.001$), BCLC stage ($P < 0.001$), and CNLC stage ($P < 0.001$) (**Figures 1D–F**).

High ACLR Predicted an Unfavorable Prognosis of HCC

To assess the value of preoperative ACLR as a prognostic biomarker, Kaplan–Meier analysis was performed. Patients in the training cohort were divided into two groups based on the optimal cutoff value of 80 for ACLR. Consistent with the result that high ACLR correlated with advanced HCCs, patients with high ACLR demonstrated significantly poorer survival than patients with low ACLR (≤ 80) (n: 183 vs. 434; 1-, 3-, and 5-year OS: 80.9%, 52.8%, and 43.3% vs. 95.8%, 85.8%, and 80.1%; median OS: 40.3 months vs. unreached; $P < 0.001$; **Figure 2A**). Correspondingly, the 1-, 3-, and 5-year cumulative recurrence rates in patients with high ACLR were 45.1%, 67.4%, and 74.9%, respectively, with a median TTR of 15.0 months, which were significantly poorer than those of patients with low ACLR (1-, 3-, and 5-year recurrence rates: 15.2%, 35.8%, and 45.3%; median TTR: 67.5 months; $P < 0.001$; **Figure 2B**).

Univariate Cox regression analysis identified that AFP level, tumor size, tumor number, Edmondson's grade, vascular invasion, GPS, NLR, PLR, SII, and ACLR were associated with both OS and TTR (**Table 2**). Subsequently, these factors were taken into multivariate Cox analysis and only tumor size, tumor number, vascular invasion, and ACLR were found to be independent risk factors for both OS and TTR (ACLR for OS: HR = 2.22, 95% CI, 1.50–3.27, $P < 0.001$; ACLR for TTR: HR = 2.36, 95% CI, 1.89–2.94, $P < 0.001$; **Table 2**).

Consistent Prognostic Value of ACLR in the Validation Cohort

Kaplan–Meier survival analysis and Cox regression analysis were then performed in the validation cohort. Patients with high ACLR showed significantly shorter OS than patients with ACLR ≤ 80 (n: 128 vs. 286; 1-, 3-, and 5-year OS: 71.9%, 47.4%, and 39.0% vs. 96.9%, 91.2%, and 85.9%; median OS: 31.0 months vs. unreached; $P < 0.001$; **Figure 2C**). Moreover, the cumulative recurrence rates for patients with high ACLR dramatically increased when compared with those for patients with low ACLR (1-, 3-, and 5-year recurrence rates: 56.2%, 77.8%, and 83.2% vs. 13.7%, 37.0%, and 50.3%; median TTR: 10.5 vs. 59.7 months; $P < 0.001$; **Figure 2D**). In the Cox regression model, both univariate and multivariate analysis verified that ACLR was an independent risk factor for both OS (HR = 4.16; 95% CI, 2.59–6.69; $P < 0.001$) and TTR (HR = 2.19; 95% CI, 1.59–3.03, $P < 0.001$; **Supplementary Table 4**) in patients with HCC of the validation cohort.

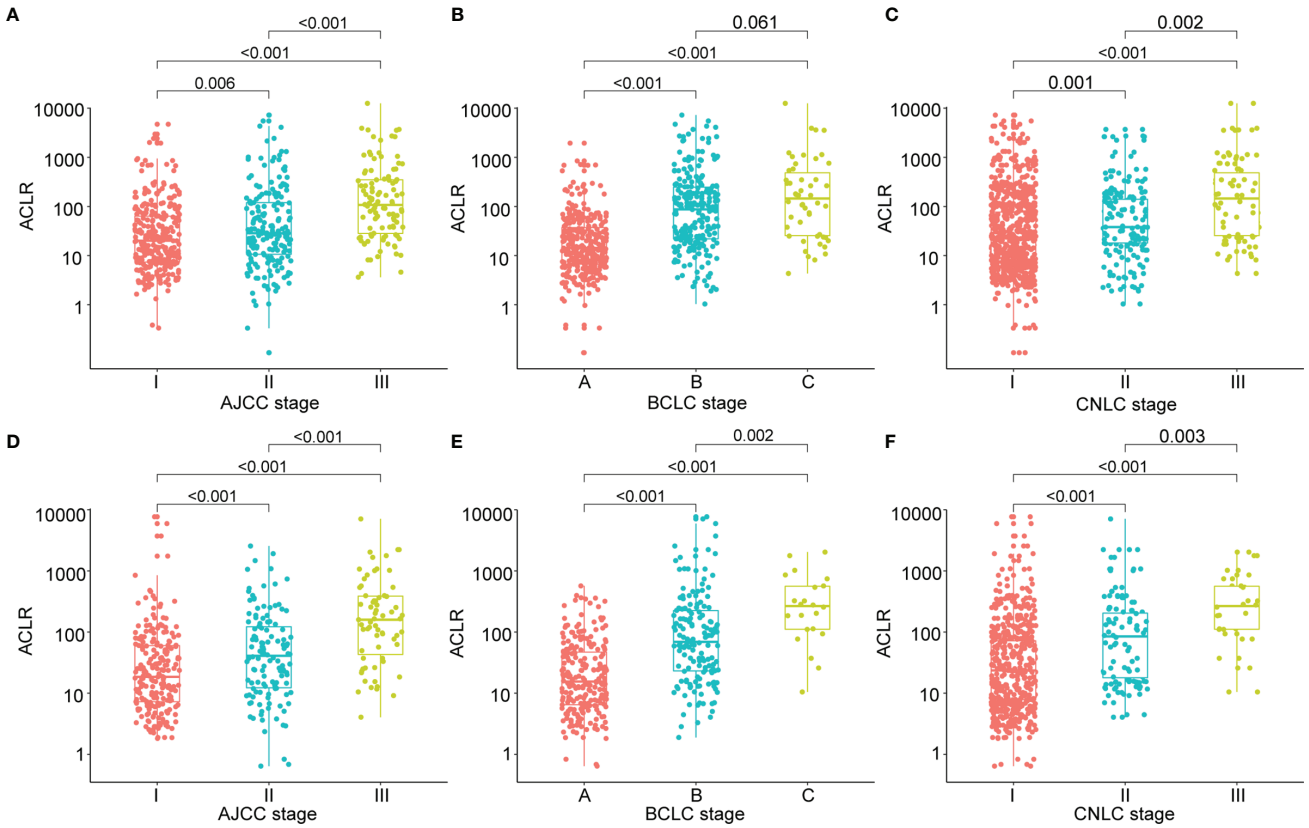

FIGURE 1 | Clinical significance of ACLR in patients with HCC from the training cohort and validation cohort. **(A–C)** Scattergrams of ACLR according to **(A)** AJCC stage, **(B)** BCLC stage, and **(C)** CNLC stage in patients with HCC from the training cohort. **(D–F)** Scattergrams of ACLR according to **(D)** AJCC stage, **(E)** BCLC stage, and **(F)** CNLC stage in patients with HCC from the validation cohort.

ACLR Outperformed Extant Inflammation-Immune Models on Prognostication

To further explore the prognostic value of ACLR, we compared ACLR with recently reported inflammation-immune models, including GPS, mGPS, PNI, NLR, PLR, SII, APRI, and ALRI, in the whole cohort. ROC analysis demonstrated that ACLR possessed the highest predictive accuracy for survival with the AUCs for 1-, 3-, and 5-year OS of 0.737, 0.719, and 0.708, respectively (**Figures 3A–C**). Meanwhile, the AUCs for 1-, 3-, and 5-year TTR were 0.696, 0.650, and 0.629, respectively, which were also the highest among all selected models (**Figures 3D–F**).

The Implication of ACLR for MRD and Resection Margin

Early recurrence, commonly resulting from MRD and occurring within 2 years after hepatectomy, indicated dismal outcomes for patients with HCC. Effective identification of these patients and timely application of adjuvant therapy might eliminate the potential minimal residual tumor cells and improve survival (29). Thus, we explored whether ACLR could accurately identify patients with a high risk of early recurrence. Indeed, patients with high ACLR were associated with higher early recurrence rate (62.4% vs. 29.2%, $P < 0.001$, **Figure 4A**). Moreover, high ACLR was also found to be related to extremely early recurrence (3-month after hepatectomy; 19.6% vs. 1.9%, $P < 0.001$, **Figure 4B**). Considering the extremely early recurrence might derive from the rapid development of disseminated tumor cells around the resection margin—in other words, MRD (30–32), we further explored the association of ACLR with recurrence around the resection margin. Factually, patients with high ACLR had a much higher recurrence rate around the resection margin than those with low ACLR (6.8% vs. 1.1%, P < 0.001, **Supplementary Figure 5A**).

Subsequently, we investigated the implication of ACLR for resection margin in patients with HCC. Patients were classified into wide resection margin group (margin > 1 cm; n = 168) or narrow resection margin group (margin ≤ 1 cm; n = 592) accordingly (26, 33, 34). In patients with high ACLR, both 2-year recurrence rate (48.8% vs. 69.7%; $P = 0.017$; **Figure 4C**) and TTR (median TTR, 25.5 vs. 11.4 months; $P = 0.037$, **Figure 4D**) were significantly better in the wide margin group than those in the narrow margin group. Meanwhile, wide margin also conferred a significant trend of longer OS compared with the narrow margin group (median OS, unreached vs. 29.9 months; $P = 0.088$; **Figure 4E**). By contrast, in patients with low ACLR, 2-year

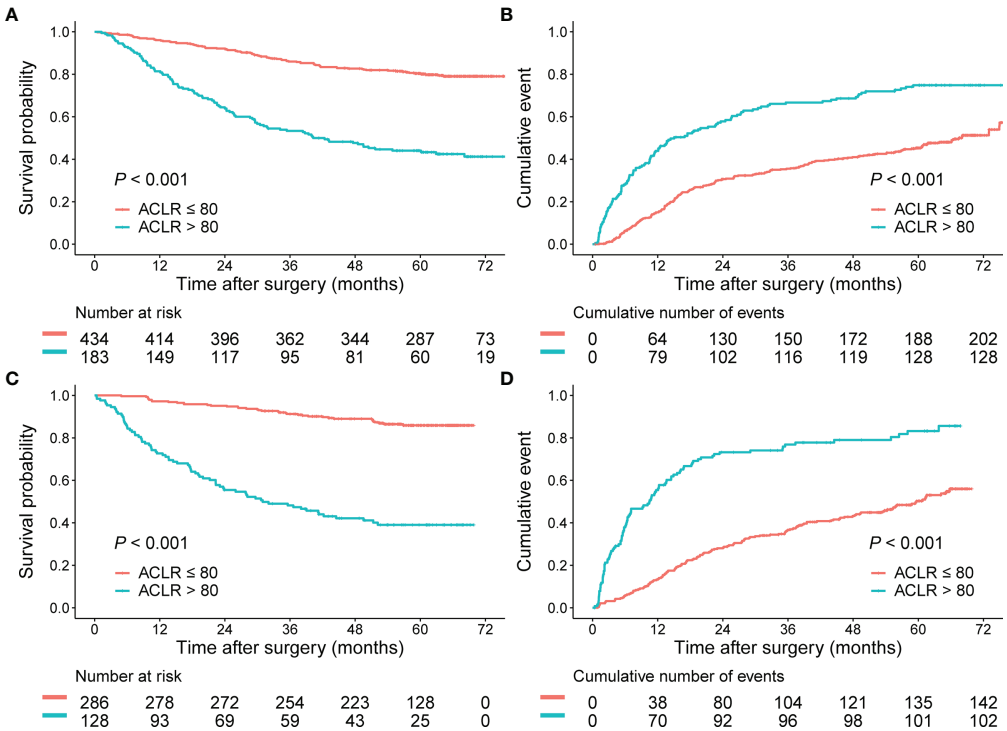

FIGURE 2 | Prognostic performance of ACLR in patients with HCC from the training cohort and validation cohort. **(A, B)** Kaplan–Meier analysis of OS **(A)** and recurrence rates **(B)** for patients with HCC stratified by ACLR (cutoff = 80) from the training cohort. **(C, D)** Kaplan–Meier analysis of OS **(C)** and recurrence rates **(D)** for patients with HCC stratified by ACLR (cutoff = 80) from the validation cohort.

recurrence rate (P = 0.660; **Supplementary Figure 4A**), TTR (P = 0.760; **Supplementary Figure 4B**), and OS (P = 0.480; **Supplementary Figure 4C**) were all comparable between patients with different margins. Consistently, we found that in patients with resection margin ≤ 1 cm, high ACLR indicated a higher risk of margin recurrence than those with low ACLR (7.2% vs. 1.0%; P < 0.001; **Supplementary Figure 5B**). However, in patients with surgical margin >1 cm, there was no difference in the margin recurrence risk between high and low ACLR patients (2.4% vs. 0.8%; P = 0.411; **Supplementary Figure 5C**).

DISCUSSION

Tumor recurrence remains the main obstacle to further improvement of survival in HCC. Accurate prediction of patients at high risk of recurrence before surgery, employment of proper resection margin during operation, and timely implementation of prophylactic treatment after hepatectomy would ensure a favorable outcome. Currently, few prognostic models have fulfilled such demand with acceptable accuracy, and novel models are still needed. Regarding this, we developed a new inflammation-immune model that could not only distinguish patients with high recurrence risk but also provide information possibly guiding the resection margin and choosing candidates for postoperative adjuvant therapy.

Different from previous studies that used fixed factors to construct models, we chose a novel strategy; we first analyzed the existing models and gathered the most common inflammation-immune factors. Then, we built nine models using the five common inflammation-immune factors with different combinations. This method was more comprehensive and objective because we had no presupposition which factors would be positively or negatively correlated with survival or recurrence. Only after comparing the prognostic value of all models that we had identified the combination of AST, CRP, and lymphocyte counts, namely, ACLR, as the target one with the best predictive performance in both the training and validation cohort. High ACLR was associated with advanced tumor characteristics and poorer prognosis than low ACLR. Multivariate Cox analyses also verified that high ACLR was an independent risk factor for both OS and TTR.

We also compared the newly built ACLR model with widely accepted prognostic ones, including GPS, NLR, PLR, and SII (16, 19–21). Although these models also showed satisfactory predictive efficiencies for both survival and recurrence in our cohort of patients, our model displayed some advantages, namely, the ability to predict early recurrence and indicate invasion margin. Notably, we found that high ACLR was strongly associated with early recurrence and extremely early recurrence. Early recurrence after radical resection is commonly considered the outcome of MRD, which could be hardly detected

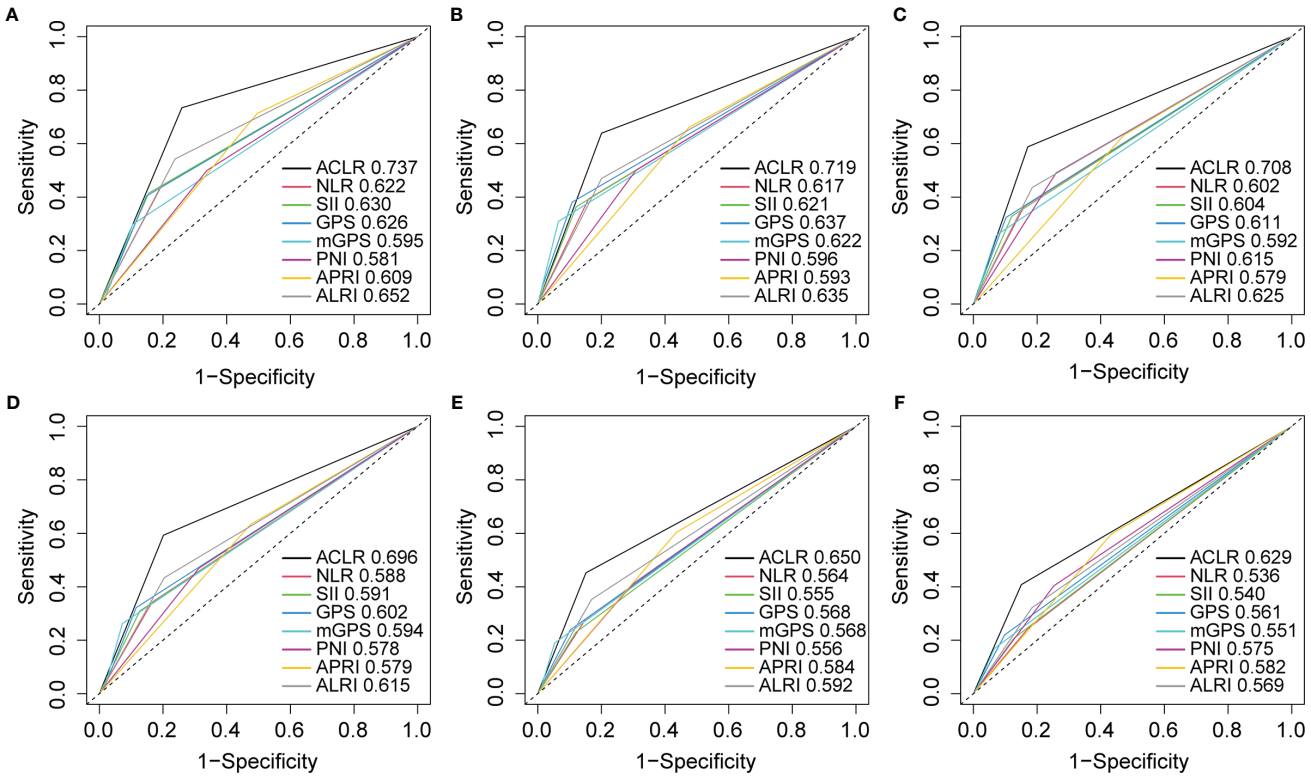

FIGURE 3 | Receiver operating characteristic (ROC) curves analysis to compare the predictive value of ACLR with other inflammation-immune models. **(A–C)** ROC curves of ACLR and other inflammation-immune models for **(A)** 1-, **(B)** 3-, and **(C)** 5-year OS in the whole cohort. **(D–F)** ROC curves of ACLR and other inflammation-immune models for **(D)** 1-, **(E)** 3-, and **(F)** 5-year TTR in the whole cohort.

using conventional imaging and serum tumor biomarkers (30, 35, 36). Currently, liquid biopsy had been proposed as a promising tool for MRD prediction in HCC. However, liquid biopsy is generally performed postoperatively and our model could be a viable option for MRD prediction before surgery.

Another interesting finding is that ACLR correlated with resection margin. It was reported that a wider resection margin could remove potential MRD around the tumor and decrease the early recurrence of patients with HCC after curative hepatectomy (34). However, for patients with HCC with large tumors or multiple lesions, especially on a cirrhotic background, a wide margin may leave insufficient liver remnant and lead to liver failure (37). Therefore, surgical outcome and liver function should be well balanced *via* choosing suitable resection margins for different patients with HCC. In the present study, a wide resection margin (>1 cm) could significantly decrease tumor recurrence after hepatectomy compared with a narrow margin for patients with HCC with high ACLR. Considering the fact that high ACLR correlated with vascular invasion and more advanced tumor phenotype, it is easy to understand such a connection: HCC with advanced phenotypes is at high risk of tumor dissemination into the microvascular around the resection margin and a wide resection margin would eradicate such MRD and decrease early recurrence. Thus, ACLR might serve as a biomarker for surgical oncologists to better prepare hepatectomy —making a wide resection margin in patients with high ACLR not only to minimize tumor recurrence risk but also to avoid the unnecessary sacrifice of hepatic reserve in patients with low ACLR and liver cirrhosis.

ACLR consists of three factors of which the associations with tumor progression and outcomes of HCC were well established. As a protein mainly synthesized in the acute phase of inflammation, CRP is stimulated by cytokines such as interleukin 6 and produced in the liver (38). CRP takes part in a wide range of inflammatory processes and connects the innate immune system with the adaptive immune system (39). Emerging evidence showed that CRP may also participate in tumor progression and metastasis in patients with HCC (40, 41). Meanwhile, several studies suggested elevated CRP predicted poor prognosis in both cirrhotic patients and patients with HCC (10, 42, 43). AST reflects damaged liver function, and increased AST might also indicate the activity of hepatitis B or C virus and progression of tumor (44). Immune response to malignancy depends on lymphocyte population, and decreased lymphocyte might lead to impaired defense against malignancy. Several pieces of evidence have showed that reduced lymphocytic infiltration in tumor was an independent risk factor in patients with HCC (45, 46). The combination of AST, CRP, and lymphocyte counts simultaneously reflects liver function damage, systemic inflammation, and immune response of

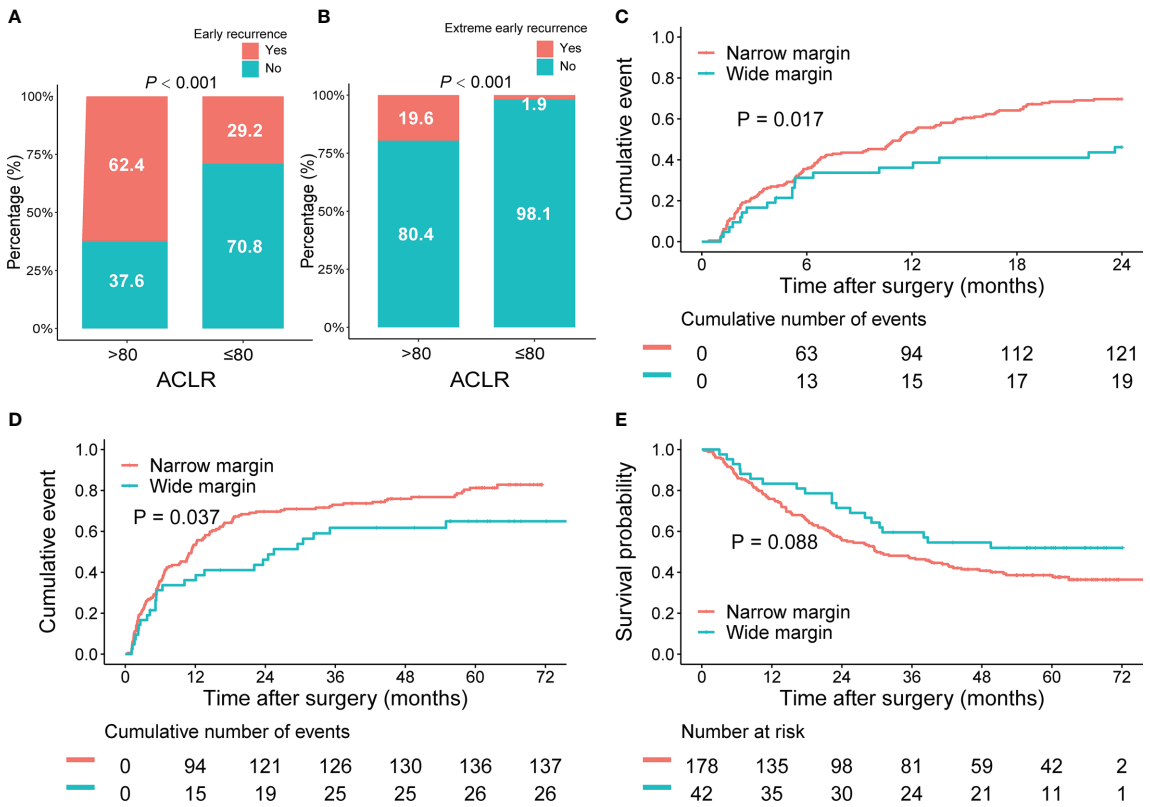

FIGURE 4 | Implications of ACLR for early recurrence and resection margin for patients with HCC of the whole cohort. **(A, B)** Comparison of **(A)** early recurrence and **(B)** extreme early recurrence rates between patients with HCC with high and low ACLR. **(C–E)** Kaplan–Meier analysis of 2-year cumulative recurrence rate **(C)**, TTR **(D)**, and OS **(E)** for patients with HCC with high ACLR, stratified by the resection margin.

patients with HCC. All three processes could affect the outcomes of patients with HCC after curative resection.

This study has some limitations. First, although ACLR could differentiate patients with HCC with poor prognosis and show good predictive value on early recurrence and extreme early recurrence, its accuracy for long-term prognosis is still unsatisfactory. This might be attributed to the recent advances in immunotherapy and targeted therapy that have prolonged the survival after recurrence. Second, the inflammation-immune model was only validated in another independent cohort from our center. Further external validation is still needed. In addition, all patients included in this study were from China and the predominant etiology was HBV infection. The clinical significance of ACLR in HCC with other etiology needs further investigation.

CONCLUSION

In conclusion, this study constructed a novel inflammation-immune model containing AST, CRP, and lymphocyte count, which not only could effectively predict prognosis and MRD for patients with HCC after curative resection but also might guide the clinical decision of optimal resection margin.

DATA AVAILABILITY STATEMENT

The raw data supporting the conclusions of this article will be made available by the authors, without undue reservation.

ETHICS STATEMENT

The studies involving human participants were reviewed and approved by the Zhongshan Hospital Research Ethics Committee. Written informed consent for participation was not required for this study in accordance with the national legislation and the institutional requirements.

AUTHOR CONTRIBUTIONS

Y-HS, XX, and X-TF designed the study and wrote the manuscript. D-ZG and AH performed the analysis of the data. Y-PW, S-YZ, J-YY, and X-YW collected patients' information and created the database. YC, JF, and JZ interpreted the data and revised the manuscript. All authors edited the manuscript. All authors contributed to the article and approved the submitted version.

FUNDING

This study was jointly supported by the National Key R&D Program of China (2019YFC1315800, 2019YFC1315802), National Natural Science Foundation of China (No.82150004, 82073217, 81830102), Fudan University (IDF152064/014), Zhongshan Hospital Fudan University (2021ZSYQ09), Shanghai Municipal Key Clinical Specialty, the Clinical Research Fundation of Shanghai Municipal Health Commission (No. 20204Y0226) and the Projects from the Shanghai Science and Technology Commission (No. 19XD1401100).

SUPPLEMENTARY MATERIAL

The Supplementary Material for this article can be found online at: https://www.frontiersin.org/articles/10.3389/fonc.2022.893268/full#supplementary-material

REFERENCES

1. Bray F, Ferlay J, Soerjomataram I, Siegel RL, Torre LA, Jemal A. Global Cancer Statistics 2018: GLOBOCAN Estimates of Incidence and Mortality Worldwide for 36 Cancers in 185 Countries. *CA Cancer J Clin* (2018) 68:394–424. doi: 10.3322/caac.21492
2. Galle PR, Forner A, Llovet JM, Mazzaferro V, Piscaglia F, Raoul JL, et al. EASL Clinical Practice Guidelines: Management of Hepatocellular Carcinoma. *J Hepatol* (2018) 69:182–236. doi: 10.1016/j.jhep.2018.03.019
3. Tabrizian P, Jibara G, Shrager B, Schwartz M, Roayaie S. Recurrence of Hepatocellular Cancer After Resection: Patterns, Treatments, and Prognosis. *Ann Surg* (2015) 261:947–55. doi: 10.1097/SLA.0000000000000710
4. Heimbach JK, Kulik LM, Finn RS, Sirlin CB, Abecassis MM, Roberts LR, et al. AASLD Guidelines for the Treatment of Hepatocellular Carcinoma. *Hepatology* (2018) 67:358–80. doi: 10.1002/hep.29086
5. Hanahan D, Weinberg RA. Hallmarks of Cancer: The Next Generation. *Cell* (2011) 144:646–74. doi: 10.1016/j.cell.2011.02.013
6. Margetts J, Ogle LF, Chan SL, Chan AWH, Chan KCA, Jamieson D, et al. Neutrophils: Driving Progression and Poor Prognosis in Hepatocellular Carcinoma? *Br J Cancer* (2018) 118:248–57. doi: 10.1038/bjc.2017.386
7. Ocana A, Nieto-Jiménez C, Pandiella A, Templeton AJ. Neutrophils in Cancer: Prognostic Role and Therapeutic Strategies. *Mol Cancer* (2017) 16:137. doi: 10.1186/s12943-017-0707-7
8. Afghahi A, Purington N, Han SS, Desai M, Pierson E, Mathur MB, et al. Higher Absolute Lymphocyte Counts Predict Lower Mortality From Early-Stage Triple-Negative Breast Cancer. *Clin Cancer Res* (2018) 24:2851–58. doi: 10.1158/1078-0432.CCR-17-1323
9. Lai Q, Vitale A, Manzia TM, Foschi FG, Levi Sandri GB, Gambato M, et al. Platelets and Hepatocellular Cancer: Bridging the Bench to the Clinics. *Cancers (Basel)* (2019) 11:1568–78. doi: 10.3390/cancers11101568
10. Sieghart W, Pinter M, Hucke F, Graziadei I, Schöniger-Hekele M, Müller C, et al. Single Determination of C-Reactive Protein at the Time of Diagnosis Predicts Long-Term Outcome of Patients With Hepatocellular Carcinoma. *Hepatology* (2013) 57:2224–34. doi: 10.1002/hep.26057
11. Hashimoto K, Ikeda Y, Korenaga D, Tanoue K, Hamatake M, Kawasaki K, et al. The Impact of Preoperative Serum C-Reactive Protein on the Prognosis of Patients With Hepatocellular Carcinoma. *Cancer* (2005) 103:1856–64. doi: 10.1002/cncr.20976
12. Ringelhan M, McKeating JA, Protzer U. Viral Hepatitis and Liver Cancer. *Philos Trans R Soc Lond B Biol Sci* (2017) 372:20160274–20162006. doi: 10.1098/rstb.2016.0274
13. Weber A, Boege Y, Reisinger F, Heikenwälder M. Chronic Liver Inflammation and Hepatocellular Carcinoma: Persistence Matters. *Swiss Med Wkly* (2011) 141:w13197. doi: 10.4414/smw.2011.13197
14. Zhou L, Wang SB, Chen SG, Qu Q, Rui JA. Prognostic Value of ALT, AST, and AAR in Hepatocellular Carcinoma With B-Type Hepatitis-Associated Cirrhosis After Radical Hepatectomy. *Clin Lab* (2018) 64:1739–47. doi: 10.7754/Clin.Lab.2018.180532
15. Antkowiak M, Gabr A, Das A, Ali R, Kulik L, Ganger D, et al. Prognostic Role of Albumin, Bilirubin, and ALBI Scores: Analysis of 1000 Patients With Hepatocellular Carcinoma Undergoing Radioembolization. *Cancers (Basel)* (2019) 11:879–85. doi: 10.3390/cancers11060879
16. Kinoshita A, Onoda H, Imai N, Iwaku A, Oishi M, Tanaka K, et al. The Glasgow Prognostic Score, an Inflammation Based Prognostic Score, Predicts Survival in Patients With Hepatocellular Carcinoma. *BMC Cancer* (2013) 13:52. doi: 10.1186/1471-2407-13-52
17. Chen H, Hu N, Chang P, Kang T, Han S, Lu Y, et al. Modified Glasgow Prognostic Score Might be a Prognostic Factor for Hepatocellular Carcinoma: A Meta-Analysis. *Panminerva Med* (2017) 59:302–07. doi: 10.23736/S0031-0808.16.03236-5
18. Man Z, Pang Q, Zhou L, Wang Y, Hu X, Yang S, et al. Prognostic Significance of Preoperative Prognostic Nutritional Index in Hepatocellular Carcinoma: A Meta-Analysis. *HPB (Oxford)* (2018) 20:888–95. doi: 10.1016/j.hpb.2018.03.019
19. Mano Y, Shirabe K, Yamashita Y, Harimoto N, Tsujita E, Takeishi K, et al. Preoperative Neutrophil-to-Lymphocyte Ratio is a Predictor of Survival After Hepatectomy for Hepatocellular Carcinoma: A Retrospective Analysis. *Ann Surg* (2013) 258:301–5. doi: 10.1097/SLA.0b013e318297ad6b
20. Ma W, Zhang P, Qi J, Gu L, Zang M, Yao H, et al. Prognostic Value of Platelet to Lymphocyte Ratio in Hepatocellular Carcinoma: A Meta-Analysis. *Sci Rep* (2016) 6:35378. doi: 10.1038/srep35378
21. Hu B, Yang XR, Xu Y, Sun YF, Sun C, Guo W, et al. Systemic Immune-Inflammation Index Predicts Prognosis of Patients After Curative Resection for Hepatocellular Carcinoma. *Clin Cancer Res* (2014) 20:6212–22. doi: 10.1158/1078-0432.CCR-14-0442
22. Shen SL, Fu SJ, Chen B, Kuang M, Li SQ, Hua YP, et al. Preoperative Aspartate Aminotransferase to Platelet Ratio is an Independent Prognostic Factor for Hepatitis B-Induced Hepatocellular Carcinoma After Hepatic Resection. *Ann Surg Oncol* (2014) 21:3802–9. doi: 10.1245/s10434-014-3771-x
23. Jin J, Zhu P, Liao Y, Li J, Liao W, He S. Elevated Preoperative Aspartate Aminotransferase to Lymphocyte Ratio Index as an Independent Prognostic Factor for Patients With Hepatocellular Carcinoma After Hepatic Resection. *Oncotarget* (2015) 6:19217–27. doi: 10.18632/oncotarget.4265
24. Bruix J, Llovet JM. Prognostic Prediction and Treatment Strategy in Hepatocellular Carcinoma. *Hepatology* (2002) 35:519–24. doi: 10.1053/jhep.2002.32089
25. Amin MB, Greene FL, Edge SB, Compton CC, Gershenwald JE, Brookland RK, et al. The Eighth Edition AJCC Cancer Staging Manual: Continuing to Build a Bridge From a Population-Based to a More "Personalized" Approach to Cancer Staging. *CA Cancer J Clin* (2017) 67:93–9. doi: 10.3322/caac.21388
26. Zhou J, Sun H, Wang Z, Cong W, Wang J, Zeng M, et al. Guidelines for the Diagnosis and Treatment of Hepatocellular Carcinoma (2019 Edition). *Liver Cancer* (2020) 9:682–720. doi: 10.1159/000509424
27. Wittekind C. Pitfalls in the Classification of Liver Tumors. *Pathologe* (2006) 27:289–93. doi: 10.1007/s00292-006-0834-1
28. von Elm E, Altman DG, Egger M, Pocock SJ, Gøtzsche PC, Vandenbroucke JP. The Strengthening the Reporting of Observational Studies in Epidemiology (STROBE) Statement: Guidelines for Reporting Observational Studies. *Epidemiology* (2007) 18:800–4. doi: 10.1097/EDE.0b013e3181577654
29. Wang Z, Ren Z, Chen Y, Hu J, Yang G, Yu L, et al. Adjuvant Transarterial Chemoembolization for HBV-Related Hepatocellular Carcinoma After Resection: A Randomized Controlled Study. *Clin Cancer Res* (2018) 24:2074–81. doi: 10.1158/1078-0432.CCR-17-2899
30. Okabe H, Yoshizumi T, Yamashita YI, Imai K, Hayashi H, Nakagawa S, et al. Histological Architectural Classification Determines Recurrence Pattern and Prognosis After Curative Hepatectomy in Patients With Hepatocellular Carcinoma. *PloS One* (2018) 13:e0203856. doi: 10.1371/journal.pone.0203856

31. Zhou KQ, Sun YF, Cheng JW, Du M, Ji Y, Wang PX, et al. Effect of Surgical Margin on Recurrence Based on Preoperative Circulating Tumor Cell Status in Hepatocellular Carcinoma. *EBioMedicine* (2020) 62:103107. doi: 10.1016/j.ebiom.2020.103107
32. Lim C, Compagnon P, Sebagh M, Salloum C, Calderaro J, Luciani A, et al. Hepatectomy for Hepatocellular Carcinoma Larger Than 10 Cm: Preoperative Risk Stratification to Prevent Futile Surgery. *HPB (Oxford)* (2015) 17:611–23. doi: 10.1111/hpb.12416
33. Shi M, Guo RP, Lin XJ, Zhang YQ, Chen MS, Zhang CQ, et al. Partial Hepatectomy With Wide Versus Narrow Resection Margin for Solitary Hepatocellular Carcinoma: A Prospective Randomized Trial. *Ann Surg* (2007) 245:36–43. doi: 10.1097/01.sla.0000231758.07868.71
34. Yang P, Si A, Yang J, Cheng Z, Wang K, Li J, et al. A Wide-Margin Liver Resection Improves Long-Term Outcomes for Patients With HBV-Related Hepatocellular Carcinoma With Microvascular Invasion. *Surgery* (2019) 165:721–30. doi: 10.1016/j.surg.2018.09.016
35. Uemura M, Sasaki Y, Yamada T, Gotoh K, Eguchi H, Yano M, et al. Serum Antibody Titers Against Hepatitis C Virus and Postoperative Intrahepatic Recurrence of Hepatocellular Carcinoma. *Ann Surg Oncol* (2014) 21:1719–25. doi: 10.1245/s10434-013-3417-4
36. Ben Lassoued A, Nivaggioni V, Gabert J. Minimal Residual Disease Testing in Hematologic Malignancies and Solid Cancer. *Expert Rev Mol Diagn* (2014) 14:699–712. doi: 10.1586/14737159.2014.927311
37. Rahbari NN, Garden OJ, Padbury R, Brooke-Smith M, Crawford M, Adam R, et al. Posthepatectomy Liver Failure: A Definition and Grading by the International Study Group of Liver Surgery (ISGLS). *Surgery* (2011) 149:713–24. doi: 10.1016/j.surg.2010.10.001
38. Peisajovich A, Marnell L, Mold C, Du Clos TW. C-Reactive Protein at the Interface Between Innate Immunity and Inflammation. *Expert Rev Clin Immunol* (2008) 4:379–90. doi: 10.1586/1744666X.4.3.379
39. Marnell L, Mold C, Du Clos TW. C-Reactive Protein: Ligands, Receptors and Role in Inflammation. *Clin Immunol* (2005) 117:104–11. doi: 10.1016/j.clim.2005.08.004
40. Park EJ, Lee JH, Yu GY, He G, Ali SR, Holzer RG, et al. Dietary and Genetic Obesity Promote Liver Inflammation and Tumorigenesis by Enhancing IL-6 and TNF Expression. *Cell* (2010) 140:197–208. doi: 10.1016/j.cell.2009.12.052
41. Maeda S, Hikiba Y, Sakamoto K, Nakagawa H, Hirata Y, Hayakawa Y, et al. Ikappa B Kinasebeta/Nuclear factor-kappaB Activation Controls the Development of Liver Metastasis by Way of Interleukin-6 Expression. *Hepatology* (2009) 50:1851–60. doi: 10.1002/hep.23199
42. Cervoni JP, Thévenot T, Weil D, Muel E, Barbot O, Sheppard F, et al. C-Reactive Protein Predicts Short-Term Mortality in Patients With Cirrhosis. *J Hepatol* (2012) 56:1299–304. doi: 10.1016/j.jhep.2011.12.030
43. Nagaoka S, Yoshida T, Akiyoshi J, Akiba J, Torimura T, Adachi H, et al. Serum C-Reactive Protein Levels Predict Survival in Hepatocellular Carcinoma. *Liver Int* (2007) 27:1091–7. doi: 10.1111/j.1478-3231.2007.01550.x
44. van Beek JH, de Moor MH, de Geus EJ, Lubke GH, Vink JM, Willemsen G, et al. The Genetic Architecture of Liver Enzyme Levels: GGT, ALT and AST. *Behav Genet* (2013) 43:329–39. doi: 10.1007/s10519-013-9593-y
45. Unitt E, Marshall A, Gelson W, Rushbrook SM, Davies S, Vowler SL, et al. Tumour Lymphocytic Infiltrate and Recurrence of Hepatocellular Carcinoma Following Liver Transplantation. *J Hepatol* (2006) 45:246–53. doi: 10.1016/j.jhep.2005.12.027
46. Unitt E, Rushbrook SM, Marshall A, Davies S, Gibbs P, Morris LS, et al. Compromised Lymphocytes Infiltrate Hepatocellular Carcinoma: The Role of T-Regulatory Cells. *Hepatology* (2005) 41:722–30. doi: 10.1002/hep.20644

Conflict of Interest: The authors declare that the research was conducted in the absence of any commercial or financial relationships that could be construed as a potential conflict of interest.

The handling editor QL declared a shared parent affiliation with the authors XX, AH, DG, YW, SZ, JY, XW, JF, JZ, XF, YS at the time of review.

Publisher's Note: All claims expressed in this article are solely those of the authors and do not necessarily represent those of their affiliated organizations, or those of the publisher, the editors and the reviewers. Any product that may be evaluated in this article, or claim that may be made by its manufacturer, is not guaranteed or endorsed by the publisher.

Copyright © 2022 Xu, Huang, Guo, Wang, Zhang, Yan, Wang, Cao, Fan, Zhou, Fu and Shi. This is an open-access article distributed under the terms of the Creative Commons Attribution License (CC BY). The use, distribution or reproduction in other forums is permitted, provided the original author(s) and the copyright owner(s) are credited and that the original publication in this journal is cited, in accordance with accepted academic practice. No use, distribution or reproduction is permitted which does not comply with these terms.

frontiers | Frontiers in Surgery

SYSTEMATIC REVIEW
published: 16 June 2022
doi: 10.3389/fsurg.2022.920595

Clinicopathological and Prognostic Value of USP22 Expression in Gastric Cancer: A Systematic Review and Meta-Analysis and Database Validation

Yuhang Wang[1,2†], Zirui Jia[1,2†], Jiacheng Gao[1,2†], Tingting Zhou[3], Xiangwen Zhang[1] and Guo Zu[1]**

[1]Department of General Surgery, The Dalian Municipal Central Hospital Affiliated of Dalian Medical University, Dalian, China, [2]Department of Graduate School, Dalian Medical University, Dalian, China, [3]Department of Neurology, The First Affiliated Hospital of Dalian Medical University, Dalian, China

OPEN ACCESS

Edited by:
Chang-In Choi,
Pusan National University Hospital,
South Korea

Reviewed by:
Guichuan Huang,
The Third Affiliated Hospital of Zunyi Medical University, China
Mingzhi Han,
University of Bergen, Norway

***Correspondence:**
Guo Zu
zushanghai@163.com
Xiangwen Zhang
dr-zhang@hotmail.com

†These authors share first authorship

Specialty section:
This article was submitted to Surgical Oncology, a section of the journal Frontiers in Surgery

Received: 14 April 2022
Accepted: 26 May 2022
Published: 16 June 2022

Citation:
Wang Y, Jia Z, Gao J, Zhou T, Zhang X and Zu G (2022) Clinicopathological and Prognostic Value of USP22 Expression in Gastric Cancer: A Systematic Review and Meta-Analysis and Database Validation. Front. Surg. 9:920595. doi: 10.3389/fsurg.2022.920595

Background: It has been reported that there is a correlation between the level of ubiquitin-specific protease 22 (USP22) and the clinicopathological parameters and prognosis of gastric cancer (GC) patients, but the conclusions are inconsistent. Hence, a meta-analysis must be conducted to clarify the relationship between USP22 expression and clinicopathological and prognostic value of GC patients to provide more accurate evidence.

Methods: According to the predetermined selection criteria, systematic file retrieval was performed. The hazard ratio (HR) or odds ratio (OR) and its 95% confidence interval (CI) were used to evaluate the relationship between USP22 expression and clinicopathological and prognostic value of GC patients.

Results: In a total of 802 patients, those with GC were finally included in 6 studies. The pooled results demonstrated that the expression of USP22 was significantly increased in GC tissues compared with control tissues (OR = 9.947, 95% CI, 6.074–16.291, $P = 0.000$), and USP22 expression was related to lymph node metastasis (OR = 2.415, 95% CI, 1.082, $P = 0.031$), distant metastasis (OR = 3.956, 95% CI, 1.365–11.464, $P = 0.011$) and TNM stage (OR = 2.973, 95% CI, 1.153–7.666, $P = 0.024$). Nevertheless, the expression of USP22 was not correlated with gender (OR = 1.202, 95% CI, 0.877–1.648, $P = 0.253$), age (OR = 1.090, 95% CI, 0.811–1.466, $P = 0.568$), tumor size (OR = 0.693,95% CI, 0.348–1.380, $P = 0.297$), tumor differentiation (OR = 1.830, 95%CI, 0.948–3.531, $P = 0.072$) and depth of invasion (OR = 2.320, 95% CI, 0.684–7.871, $P = 0.177$). Moreover, a high expression of USP22 predicted a poor overall survival (OS) in GC patients (HR = 2.012, 95% CI, 1.522–2.658, $P = 0.000$). The database of Kaplan–Meier plotter confirmed that a high expression of USP22 was correlated with poor prognostics in GC patients (HR = 1.41, 95% CI, 1.18–1.68, $P < 0.01$).

Conclusion: USP22 overexpression in GC tissues is positively related to lymph node metastasis, distant metastasis and TNM stage and indicates a poor clinical outcome of GC patients, but it is not associated with age, gender, depth of invasion, tumor differentiation and tumor size of GC patients.

Systematic Review Registration: https://www.crd.york.ac.uk/prospero/, identifier: 338361.

Keywords: USP22, gastric cancer, overall survival, clinicopathological parameters, meta-analysis

INTRODUCTION

Gastric cancer (GC), as a common malignant tumor, is the third leading cause of cancer death and ranks fifth in terms of cancer incidence (1). Although the treatment of GC has seen progress in the form of surgical technology, radiotherapy and chemotherapy, GC remains an important health issue worldwide. Most patients will already be in an advanced stage when they are diagnosed with GC, and the prognosis of advanced GC is extremely poor (2). Therefore, it is of great significance to find effective biomarkers to accurately determine the clinicopathological significance and prognosis of GC patients.

Ubiquitin-specific peptidase 22 (USP22), one of the highly conserved ubiquitin hydrolases, is involved in the formation of transcriptional protein acetylation composites. USP22 regulates gene transcription by catalyzing the removal of mono-ubiquitination of histones H2A and H2B (3). In recent years, USP22 has been reported as a member of 11 "Death-from-Cancer" genes (4, 5). It has been shown that USP22 is overexpressed in many solid tumors, for example, bladder cancer, breast cancer and colorectal cancer, which means that it is a potential cancer biomarker (6–8). Recently, an increasing number of evidence has also demonstrated that USP22 is overexpressed in GC (9–14). However, researchers have different conclusions about whether USP22 expression is related to clinicopathological parameters and clinical outcomes in patients with GC. Yang et al. indicated that a high expression of USP22 is correlated with prognosis and tumor differentiation of GC patients but not with tumor size (9). However, Liu et al. reported that in GC patients, USP22 expression is positively related to tumor size but not to tumor differentiation and prognosis (10). In order to resolve the current controversies, we conducted a systematic study and performed a meta-analysis on the correlation between USP22 and clinicopathological features and prognosis of GC patients.

METHODS

Search Studies

In order to collect all relevant data, we made a comprehensive survey on the Web of Science, PubMed, Embase, the Cochrane Library, CNKI and WanFang database, from inception to January 1, 2022. The following terms were used as keywords: ("gastric cancer" or "stomach cancer" or "gastric carcinoma") and ("USP22" or "Ubiquitin-specific peptidase 22"). Furthermore, the identified studies were manually inspected to improve the integrity of the eligible papers.

Inclusion and Exclusion Criteria

Articles must be in accordance with the following standards to be adopted: (1) the patients were definitively diagnosed with GC by pathology; (2) the relationship between USP22 expression and the clinicopathological parameters (age, gender, TNM stage, tumor differentiation, etc.) of GC patients was investigated; (3) the articles described the association between USP22 expression and medical outcomes in GC patients, including overall survival (OS); and (4) sufficient information was used to estimate the 95% CIs.

If the following criteria are met, the studies are excluded: (1) cell experiment; (2) case-only studies; (3) reviews, meta-analysis, letters and case reports; (4) non-original research; (5) other cancers; (6) repeat research based on the same database or patients; and (7) the patients received radiotherapy and chemotherapy before operation.

Data Extraction

The following information was identified and screened by two authors (Wang and Jia) from each eligible publication according to the prescribed standards: first author, publication year, country, study period, essay method, age, gender, tumor invasion, lymph node metastasis, distant metastasis, TNM stage, tumor differentiation, tumor size and OS. During this period, the different opinions were resolved by discussing all the contents with the third author (Gao) and reaching a consensus. The Newcastle–Ottawa Scale (NOS), with a score range of 0–9, was used to assess and score the quality of the study. When the score was 6 or higher, it was considered to be a high-quality literature.

Database Validation and Bioinformatics Analysis

The Kaplan–Meier Plotter database (http://www.kmplot.com) was used to analyze the effect of USP22 on OS in GC patients. The data of GC patients with USP22 expression was extracted from TCGA, GEO and the EGA database (https://www.cancer.gov/tcga).

Statistical Analysis

We extracted raw data from eligible studies to obtain combined odds ratio (OR), hazard ratio (HR) and 95% confidence interval (CI), which were used to evaluate the effect of USP22 on

clinicopathological parameters and OS in patients with GC. Statistical heterogeneity among studies was analyzed by using the Q-test and I^2 test. If the p-value was less than 0.05 or the I^2 value was greater than 50%, then significant heterogeneity existed in the data and the random effects model would be adopted. Otherwise, the fixed effects model would be used. In this meta-analysis, Stata 16.0 was used to analyze the extracted data.

RESULTS

Characteristics of Studies Included in Meta-Analysis

A total of 362 articles were selected in the relevant database. The recorded data of 35 articles were repeated from the same population. Among the 327 articles, 321 articles were excluded, and these contained other cancers ($N = 105$), review type ($N = 19$), non-original research ($N = 73$), repeat research ($N = 37$) and cell experiment ($N = 87$). Six articles were proved to be within the scope of the study and the average NOS score was 7 (**Figure 1**) (9–14). In total, 802 patients with GC were enrolled in our study. The basic information on these datasets is summarized in **Table 1**.

The Expression of USP22 in GC and Control Tissues

A total of 313 GC tissues and 158 control tissues were included to assess USP22 expression in GC patients. The results showed that the expression of USP22 was significantly increased in GC tissues compared with control tissues (OR = 9.947, 95% CI, 6.074–16.291, $P = 0.000$) (**Figure 2A**). There was no significant bias in the expression of USP22 of GC tissues and control tissues (Egger's test, $P = 0.413$) (**Figure 2B**).

USP22 Expression and Clinicopathological Factors

The association between USP22 expression and clinicopathological parameters is shown in **Figure 3** and **Table 2**. After systematic analysis, it was found that USP22 expression was not correlated with gender (OR = 1.202, 95% CI, 0.877–1.648, $P = 0.253$) (**Figure 3A**), age (OR = 1.090, 95% CI, 0.811–1.466, $P = 0.568$) (**Figure 3B**), tumor size (OR = 0.693,95% CI, 0.348–1.380, $P = 0.297$) (**Figure 3C**), tumor differentiation (OR = 1.830, 95%CI, 0.948–3.531, $P = 0.072$) (**Figure 3D**) and depth of invasion (OR = 2.320, 95% CI, 0.684–7.871, $P = 0.177$) (**Figure 3E**). However, the expression of USP22 was correlated with lymph node metastasis (OR = 2.415, 95% CI, 1.082, $P = 0.031$)

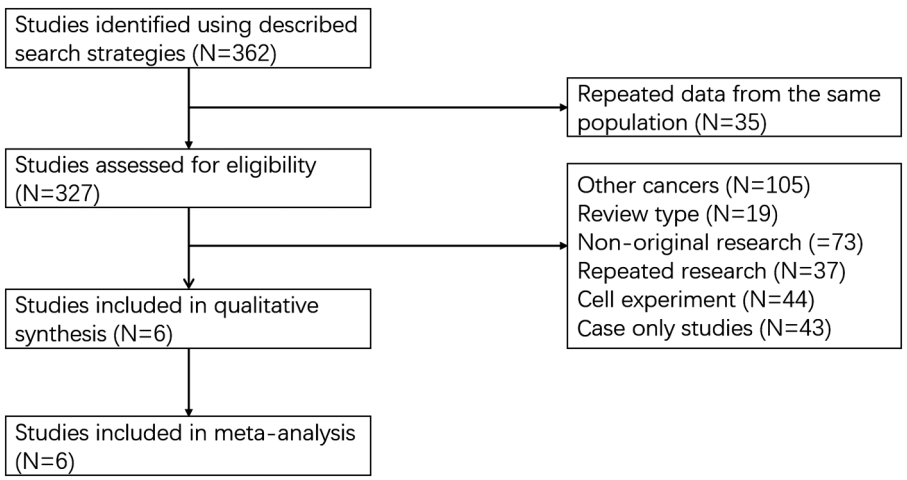

FIGURE 1 | Flow chart of research data screening.

TABLE 1 | Main characteristics and results of each study.

No.	Author	Year	Journal	Country	Study period	Sample size	M/F	Method	NOS
1	Liu	2019	Aging	China	2004.1–2008.12	186	119/67	IHC	8
2	Lim	2020	Cancer Cell International	China	2007.5–2008.2	88	65/23	IHC	7
3	Zheng	2019	Patholoay-Research and Practic	China	Not report	84	50/34	IHC	6
4	Deng	2011	Journal of Abdominal Surgery	China	2008.1–2009.7	100	66/34	IHC	7
5	Yang	2011	Cell Biochem Biophys	China	2004.1–2005.11	219	162/57	IHC	6
6	Yu	2016	Journal of Harbin Medical University	China	2004.1–2004.12	125	82/43	IHC	8

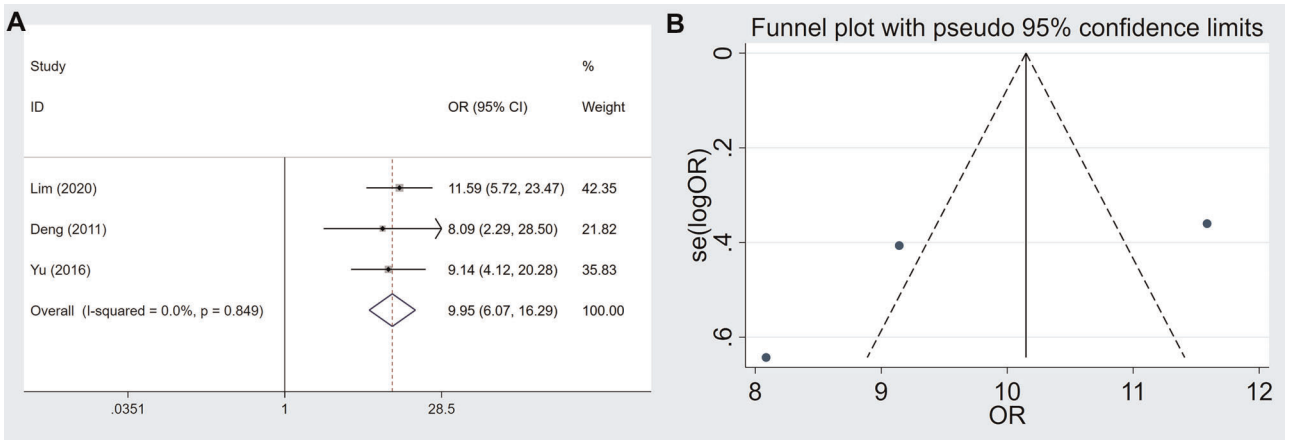

FIGURE 2 | Forest plots and funnel plots for the USP22 expression between GC and control tissues. (**A**) forest plots and (**B**) funnel plots.

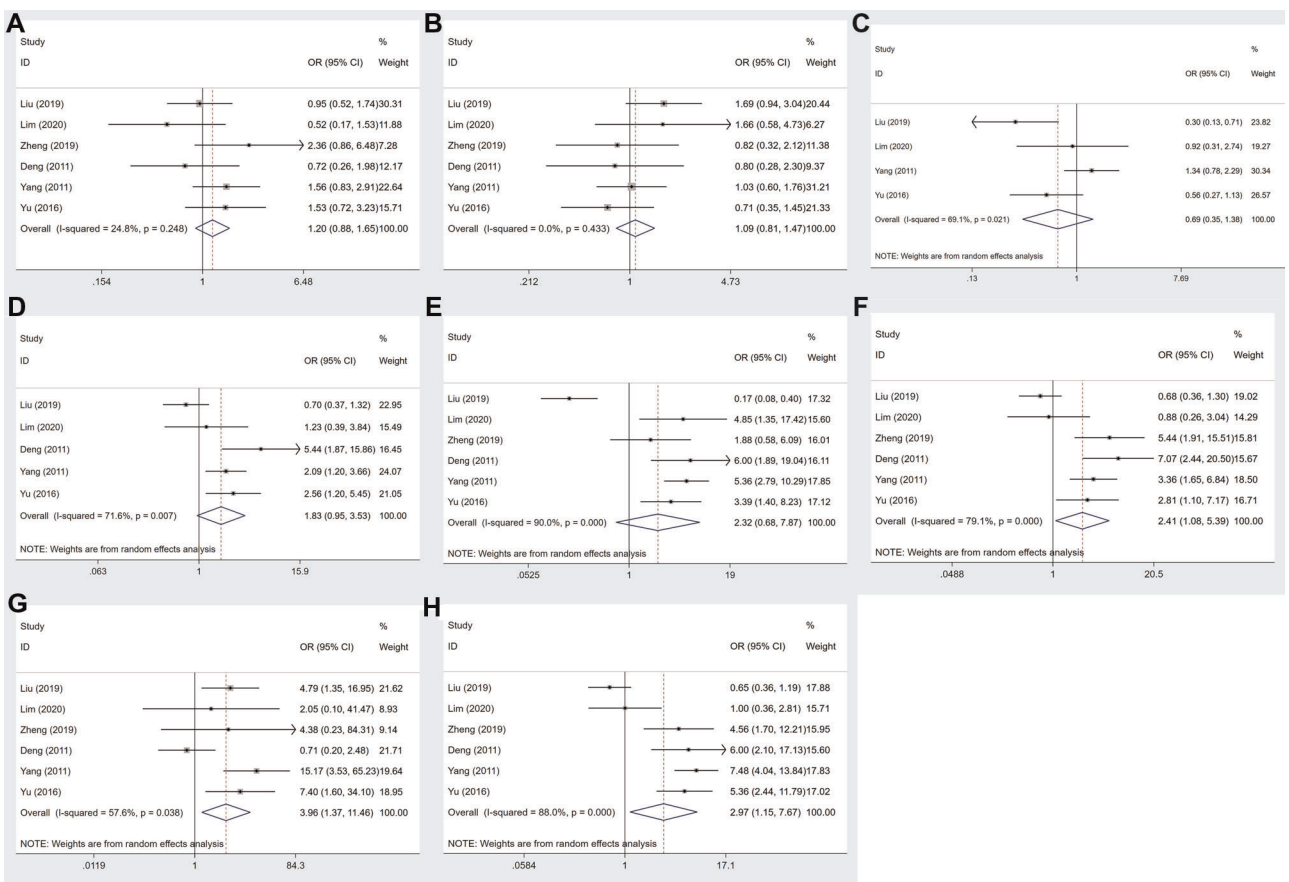

FIGURE 3 | Forest plots for the association of USP22 expression with clinicopathological parameters: (**A**) gender, (**B**) age, (**C**) tumor size, (**D**) tumor differentiation, (**E**) depth of invasion, (**F**) lymph node metastasis, (**G**) distant metastasis and (**H**) TNM stage.

TABLE 2 | The association between USP22 expression and clinicopathological factors in GC.

Factor	Number of studies	Number of patients	Pooled OR (95% CI)	*P* value	Heterogeneity		
					I^2 (%)	*P* value	Model
Gender (male vs. female)	1,2,3,4,5,6	802	1.202 (0.877–1.648)	0.253	24.8	0.248	Fixed
Age (≥60 vs. <60)	1,2,3,4,5,6	802	1.090 (0.811–1.466)	0.568	0.00	0.433	Fixed
Tumor size (≥5 vs. <5 cm)	1,2,5,6	618	0.693 (0.348–1.380)	0.297	69.1	0.021	Random
Tumor differentiation (well vs. poor)	1,2,4,5,6	718	1.830 (0.948–3.531)	0.072	71.6	0.007	Random
Depth of invasion (T_{3-4} vs. T_{1-2})	1,2,3,4,5,6	802	2.320 (0.684–7.871)	0.177	90.0	0.000	Random
Lymph node (yes vs. no)	1,2,3,4,5,6	802	2.415 (1.082–5.389)	0.031	79.1	0.000	Random
Distant metastasis (yes vs. no)	1,2,3,4,5,6	802	3.956 (1.365–11.464)	0.011	57.6	0.038	Random
TNM stage (III-IV vs. I-II)	1,2,3,4,5,6	802	2.973 (1.153–7.666)	0.024	88.0	0.000	Random

(**Figure 3F**), distant metastasis (OR = 3.956, 95% CI, 1.365–11.464, $P = 0.011$) (**Figure 3G**) and TNM stage (OR = 2.973, 95% CI, 1.153–7.666, $P = 0.024$) (**Figure 3H**).

Publication Bias of USP22 Expression and Clinicopathological Factors

Egger's test was selected for evaluating the publication bias. The conclusions drawn from the funnel plots suggested that there was no obvious bias in gender ($P = 0.635$) (**Figure 4A**), age ($P = 0.660$) (**Figure 4B**), tumor size ($P = 0.427$) (**Figure 4C**), differentiation ($P = 0.599$) (**Figure 4D**), invasion ($P = 0.937$) (**Figure 4E**), lymph node metastasis ($P = 0.358$) (**Figure 4F**), distant metastasis ($P = 0.851$) (**Figure 4G**) and TNM stage ($P = 0.740$) (**Figure 4H**).

USP22 Expression and OS of GC Patients

A total of 702 patients were included from four eligible articles, which provided us with data to evaluate the relationship between USP22 and OS. The data from the forest plot indicated that a high USP22 level predicted poor outcome in GC patients (HR = 2.012, 95% CI, 1.522–2.658, $P = 0.000$) (**Figure 5A**). No significant bias was found in the prognosis of patients with GC (Egger's test, $P = 0.227$) (**Figure 5B**).

Sensitivity analysis was performed to assess the stability of the meta-analysis results. After sequentially deleting each study, the results suggested no change in the overall results of OS, which meant that the result of our meta-analysis was highly stable (**Figure 5C**).

Database Validation and Bioinformatics Analysis

According to the database of the Kaplan–Meier plotter, the results suggested that USP22 overexpression expression was significantly related to poor OS (HR = 1.41, 95% CI, 1.18–1.68, $P < 0.01$) (**Figure 6**).

We conducted a subgroup analysis on the relationship between USP22 and prognosis in patients with GC. The results showed that there was no difference in the diagnostic value of USP22 in different T, N and TNM stages of GC patients (**Supplementary Figure S1**).

DISCUSSION

GC, as a gastrointestinal malignancy, is one of the most common causes associated with cancer deaths worldwide (15). In the past century, the morbidity and mortality rates of GC in most countries dropped steadily. But due to the changes in the age of population and diet structure, the increase in work pressure and Helicobacter pylori infection, the incidence rate of GC is still high (16). Recently, suitable biomarkers for early detection and diagnosis of GC have drawn the attention of researchers. For example, USP22 has been reported to be associated with clinicopathological features and clinical outcomes in numerous studies, but it has proved controversial. In this meta-analysis, we reported that USP22 expression was closely related to lymph node metastasis, distant metastasis and TNM stage in GC patients but not to age, gender, depth of invasion, tumor differentiation and tumor size. The high expression of USP22 suggested poor OS in GC patients, which might be an indicator of poor prognosis of GC patients.

USP22 is a catalytic subunit that regulates gene transcription by removing monoubiquitination of histones H2A and H2B. In addition, USP22 is involved in regulating the function of multiple non-histone targets, which are correlated with cancer progression and poor prognosis (17). Recently, some researchers have reported that USP22 plays a vital role in regulating the cell cycle and driving transcription (18–20). It has been proved that USP22 is one of the significant biomarkers of cancer stem cells (21, 22). USP22 overexpression has been reported in several human cancers such as bladder cancer, colorectal cancer and oral squamous cell carcinoma and is related to the clinicopathological parameters and prognosis of many types of cancers (23–29). Moreover, several studies have reported that a high level of USP22 is thought to play a significant role in patients with GC (9, 10, 21–24). Researchers have used the transwell migration and invasion assays to analyze the effect of USP22 on cell motility, and the results revealed that the migration of USP22 silenced cells is significantly reduced (10). Other researchers have also detected the expression of USP22 in GC samples, and the results showed that USP22 protein

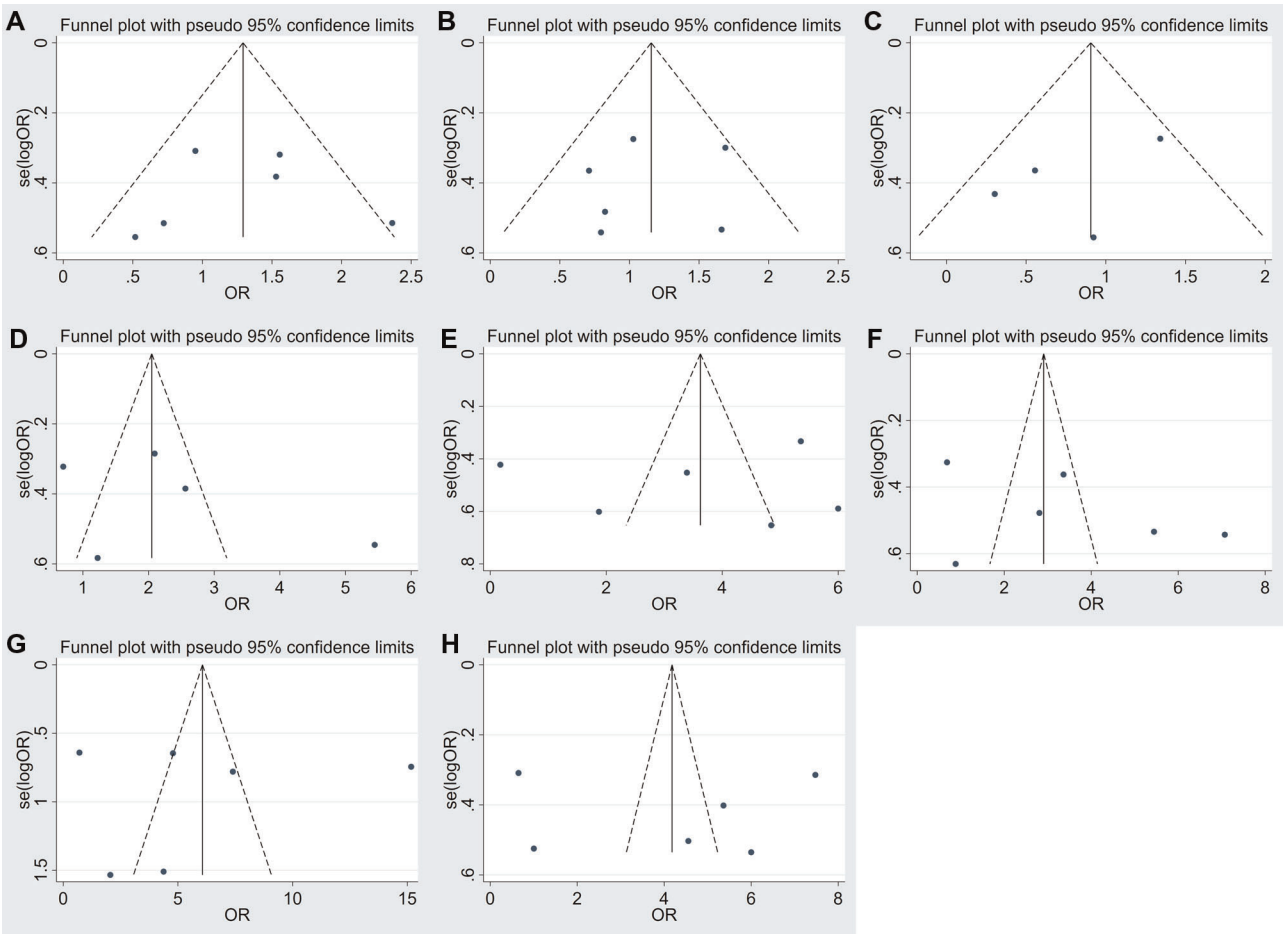

FIGURE 4 | Funnel plots for the association of USP22 expression with clinicopathological parameters: (**A**) gender, (**B**) age, (**C**) tumor size, (**D**) tumor differentiation, (**E**) depth of invasion, (**F**) lymph node metastasis, (**G**) distant metastasis and (**H**) TNM stage.

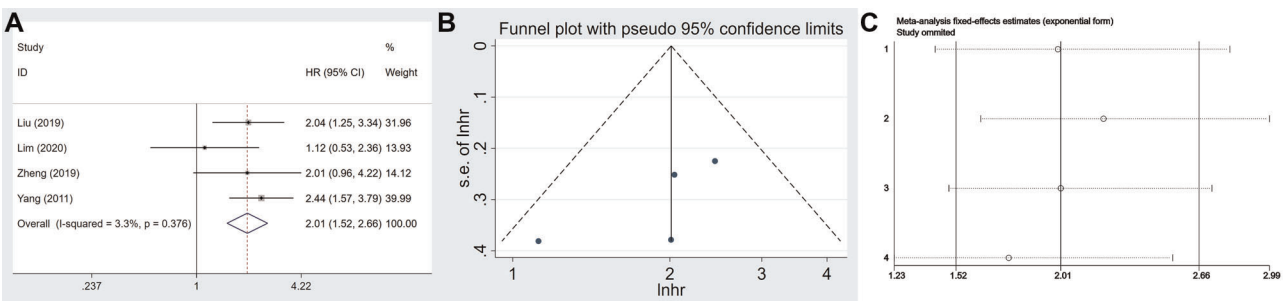

FIGURE 5 | The association of USP22 expression with the OS of GC patients: (**A**) forest plot, (**B**) funnel plots and (**C**) sensitivity analysis.

expression levels are obviously upregulated in GC patients with lymph node metastasis. However, the correlation between USP22 expression and lymph node metastasis of GC patients is still contradictory (9). Lim et al. examined USP22 protein expression in 88 GC tissue samples to investigate the role of USP22 in GC and found no clear relationship between USP22 overexpression and lymph node metastasis of GC (21). Meanwhile, USP22 is reported to promote GC distant

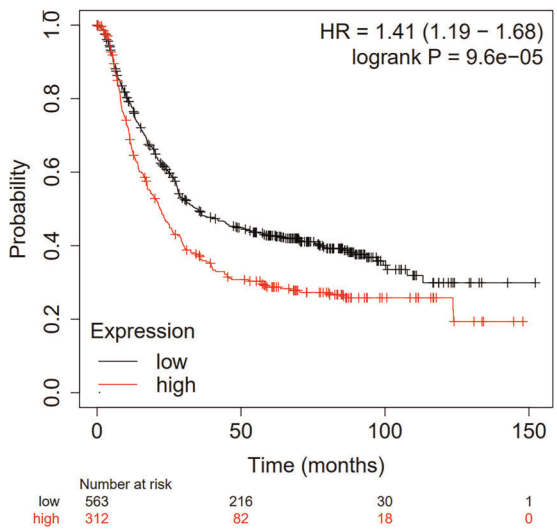

FIGURE 6 | Database validation to explore the relationship between USP22 expression and the OS of GC patients based on TCGA, GEO and EGA.

metastasis (9, 10, 23). However, Deng et al. showed that USP22 expression in GC tissues was not associated with distant metastasis. In addition, Lim et al. showed that the upregulation of the USP22 gene was not associated with the advanced TNM stage of GC, and these inconsistencies with other included studies might be due to the relatively small sample size of this study (9, 10, 22, 23, 24). In our meta-analysis, our results suggested that USP22 expression was correlated with lymph node metastasis, distant metastasis and the tumor TNM stage of GC patients.

Researchers have established tumor xenograft models in mice to evaluate the role of USP22 in tumor growth *in vivo*. They found that tumor growth was obviously reduced after the USP22 gene was knocked out (10). Furthermore, Liu et al. found that in GC patients, a high expression of USP22 was positively correlated with a tumor size of more than 5 cm (10). However, other authors indicated that no evidence of USP22 upregulation was found in GC patients (9, 11, 13). The authors reported that the expression level of USP22 was positively correlated with the T stage of GC (9–14). But Zheng et al. showed that the expression of USP22 was not related to the T stage of GC (12). The expression level of USP22 protein in GC tissue samples was negatively correlated with the degree of tumor differentiation (9, 10, 11, 13, 14). However, Lim et al. found no statistical difference after analyzing the relationship between USP22 expression and histological grade (11). Through a systematic study, our results suggested that USP22 expression was not associated with the depth of invasion, tumor differentiation and tumor size. However, the roles of depth of invasion, GC differentiation and tumor size for USP22 expression in GC patients need to be analyzed in a larger and randomized controlled trial sample. Therefore, further studies should be performed to detect the signal transduction pathway and the corresponding regulation mechanism of USP22 in GC cells and to further understand the role of USP22 in tumor genesis and the development of GC.

USP22 belongs to the ubiquitin specific protease family and is involved in the protein deubiquitination of histone or nonhistone proteins. USP22 was considered to be involved in many cancer types as an oncogene-like protein (23–29). In a variety of tumors, a high-expression of USP22 was thought to be associated with poor survival (30–32). Based on the findings of these studies, some researchers have attempted to evaluate the potential prognostic value of USP22 expression in GC patients. However, there is still no consensus on the OS of GC patients with USP22 expression. Lim et al. reported that no significant difference was found in the 5-year survival rate between USP22-negative and USP22-positive patients. However, some studies have shown that GC patients with an overexpression of USP22 have poorer survival rates than those with a low expression of USP22 (9, 10, 12, 13). In our study, the summarized results suggested that patients with an overexpression of USP22 tend to have a poor OS. The results were further validated in the TCGA database and then survival analysis was performed using the Kaplan–Meier plotter.

Valuable evidence in our meta-analysis has been provided for determining the relationship between USP22 expression and clinicopathologic parameters and prognosis of GC patients, which is helpful for clinical decision-making and promoting related research. Nevertheless, several potential limitations existing in the current meta-analysis should be removed. First, although we searched many websites such as PubMed and web of science, the account of the included literature is still small, which may cause bias in our conclusions. Second, the research groups are relatively small and are mostly from China, which may lead to a reduction of universality and heterogeneity. Furthermore, due to the unavailability of individual information, we could not consider some confounding factors such as smoking, surgery type and other environmental factors. In order to eliminate these limitations, high-quality studies are urgently needed in future work.

CONCLUSION

In conclusion, this meta-analysis demonstrates that USP22 expression is higher in GC tissues than in normal tissues. USP22 expression is associated with lymph node metastasis, distant metastasis, TNM stage and poor OS of GC patients but is not associated with age, gender, depth of invasion, tumor differentiation and tumor size. Database validation and bioinformatics analysis verify that USP22 may be an indicator of poor prognosis in GC patients. The findings of this study suggest that USP22 may be a potential poor prognostic marker of GC patients.

DATA AVAILABILITY STATEMENT

The original contributions presented in the study are included in the article/**Supplementary Material**, and further inquiries can be directed to the corresponding author/s.

AUTHOR CONTRIBUTIONS

XWZ and GZ conceived and designed the experiments; YHW, ZRJ and JCG performed the experiments; YHW, ZRJ and JC analyzed the data; YHW, ZRJ, JCG and TTZ contributed reagents/materials/analysis tools; YHW, ZRJ and JCG wrote the paper. All authors contributed to the article and approved the submitted version.

SUPPLEMENTARY MATERIAL

The Supplementary Material for this article can be found online at: https://www.frontiersin.org/articles/10.3389/fsurg.2022.920595/full#supplementary-material.

REFERENCES

1. Arnold M, Abnet CC, Neale RE, Vignat J, Giovannucci EL, McGlynn KA, et al. Global burden of 5 major types of gastrointestinal cancer. *Gastroenterology*. (2020) 159:335–49. doi: 10.1053/j.gastro.2020.02.068
2. Kim R, Ji JH, Kim JH, Hong JY, Lim HY, Kang WK, et al. Safety and anti-tumor effects of vismodegib in patients with refractory advanced gastric cancer: a single-arm, phase-II trial. *J Cancer*. (2022) 13:1097–102. doi: 10.7150/jca.67050
3. Roedig J, Kowald L, Juretschke T, Karlowitz R, Ahangarian Abhari B, Roedig H, et al. USP22 controls necroptosis by regulating receptor-interacting protein kinase 3 ubiquitination. *EMBO Rep*. (2021) 22:e50163. doi: 10.15252/embr.202050163
4. Glinsky GV, Berezovska O, Glinskii AB. Microarray analysis identifies a death-from-cancer signature predicting therapy failure in patients with multiple types of cancer. *J Clin Invest*. (2005) 115:1503–21. doi: 10.1172/JCI23412
5. Glinsky GV. Genomic models of metastatic cancer: functional analysis of death-from-cancer signature genes reveals aneuploid, anoikis-resistant, metastasis-enabling phenotype with altered cell cycle control and activated Polycomb Group (PcG) protein chromatin silencing pathway. *Cell Cycle*. (2006) 5:1208–16. doi: 10.4161/cc.5.11.2796
6. Lv L, Xiao XY, Gu ZH, Zeng FQ, Huang LQ, Jiang GS. Silencing USP22 by asymmetric structure of interfering RNA inhibits proliferation and induces cell cycle arrest in bladder cancer cells. *Mol Cell Biochem*. (2011) 346:11–21. doi: 10.1007/s11010-010-0585-4
7. Kim D, Hong A, Park HI, Shin WH, Yoo L, Jeon SJ, et al. Deubiquitinating enzyme USP22 positively regulates c-Myc stability and tumorigenic activity in mammalian and breast cancer cells. *J Cell Physiol*. (2017) 232:3664–76. doi: 10.1002/jcp.25841
8. Kosinsky RL, Saul D, Ammer-Herrmenau C, Faubion WA, Neesse A, Johnsen SA. USP22 suppresses SPARC expression in acute colitis and inflammation-associated colorectal cancer. *Cancers (Basel)*. (2021) 13:1817. doi: 10.3390/cancers13081817
9. Yang DD, Cui BB, Sun LY, Zheng HQ, Huang Q, Tong JX, et al. The co-expression of USP22 and BMI-1 may promote cancer progression and predict therapy failure in gastric carcinoma. *Cell Biochem Biophys*. (2011) 61:703–10. doi: 10.1007/s12013-011-9229-x
10. Liu H, Liu N, Zhao Y, Zhu X, Wang C, Liu Q, et al. Oncogenic USP22 supports gastric cancer growth and metastasis by activating c-Myc/NAMPT/SIRT1-dependent FOXO1 and YAP signaling. *Aging (Albany NY)*. (2019) 11:9643–60. doi: 10.18632/aging.102410
11. Lim C, Xu JC, Chen TY, Xu JX, Chen WF, Hu JW, et al. Ubiquitin-specific peptide 22 acts as an oncogene in gastric cancer in a son of sevenless 1-dependent manner. *Cancer Cell Int*. (2020) 10(20):45. doi: 10.1186/s12935-020-1137-y
12. Zheng H, Yu J, Li W, Yang D, Gao C, Zhang Q, et al. Is co-expression of USP22 and HSP90 more effective in predicting prognosis of gastric cancer? *Pathol Res Pract*. (2019) 215:653–9. doi: 10.1016/j.prp.2018.12.020
13. Yu JL, Yang DD, Zheng HQ. Expression of USP22 in gastric cancer and it significance. *J. Harbin Eng. Univ*. (2016) 50:533–5. doi: 1000-1905(2016) 06-0533-03
14. Deng MZ, Tao KX, Wang GB, Xinghua L. Expression of usp22 in gastric cancer and the clinical significance. *J Abdom Surg*. (2011) 24:302–3. doi: 10.3969/j.issn.1003-5591.2011.05.022
15. Sitarz R, Skierucha M, Mielko J, Offerhaus GJA, Maciejewski R, Polkowski WP. Gastric cancer: epidemiology, prevention, classification, and treatment. *Cancer Manag Res*. (2018) 7(10):239–48. doi: 10.2147/CMAR.S149619
16. Smyth EC, Nilsson M, Grabsch HI, van Grieken NC, Lordick F. Gastric cancer. *Lancet*. (2020) 396:635–48. doi: 10.1016/S0140-6736(20)31288-5
17. Prokakis E, Dyas A, Grün R, Fritzsche S, Bedi U, Kazerouni ZB, et al. USP22 promotes HER2-driven mammary carcinoma aggressiveness by suppressing the unfolded protein response. *Oncogene*. (2021) 40:4004–18. doi: 10.1038/s41388-021-01814-5
18. Yang X, Zang H, Luo Y, Wu J, Fang Z, Zhu W, et al. High expression of USP22 predicts poor prognosis and advanced clinicopathological features in solid tumors: a meta-analysis. *Onco Targets Ther*. (2018) 11:3035–46. doi: 10.2147/OTT.S148662
19. Hoeller D, Dikic I. Targeting the ubiquitin system in cancer therapy. *Nature*. (2009) 458:438–44. doi: 10.1038/nature07960
20. Ma Y, Fu HL, Wang Z, Huang H, Ni J, Song J, et al. USP22 maintains gastric cancer stem cell stemness and promotes gastric cancer progression by stabilizing BMI1 protein. *Oncotarget*. (2017) 8:33329–42. doi: 10.18632/oncotarget.16445
21. Zhang XY, Varthi M, Sykes SM, Phillips C, Warzecha C, Zhu W, et al. The putative cancer stem cell marker USP22 is a subunit of the human SAGA complex required for activated transcription and cell-cycle progression. *Mol Cell*. (2008) 29:102–11. doi: 10.1016/j.molcel.2007.12.015
22. Li ZH, Yu Y, Du C, Fu H, Wang J, Tian Y. RNA interference-mediated USP22 gene silencing promotes human brain glioma apoptosis and induces cell cycle arrest. *Oncol Lett*. (2013) 5:1290–4. doi: 10.3892/ol.2013.1188
23. Ning J, Zhang J, Liu W, Lang Y, Xue Y, Xu S. Overexpression of ubiquitin-specific protease 22 predicts poor survival in patients with early-stage non-small cell lung cancer. *Eur J Histochem*. (2012) 56:e46. doi: 10.4081/ejh.2012.e46
24. Piao S, Ma J, Wang W, Liu Y, Zhang M, Chen H, et al. Increased expression of USP22 is associated with disease progression and patient prognosis of salivary duct carcinoma. *Oral Oncol*. (2013) 49:796–801. doi: 10.1016/j.oraloncology.2013.03.454
25. Lv L, Xiao XY, Gu ZH, Zeng FQ, Huang LQ, Jiang GS. Silencing USP22 by asymmetric structure of interfering RNA inhibits proliferation and induces cell cycle arrest in bladder cancer cells. *Mol Cell Biochem*. (2011) 346:11–21. doi: 10.1007/s11010-010-0585-4
26. Liu YL, Yang YM, Xu H, Dong XS. Increased expression of ubiquitin-specific protease 22 can promote cancer progression and predict therapy failure in human colorectal cancer. *J Gastroenterol Hepatol*. (2010) 25:1800–5. doi: 10.1111/j.1440-1746.2010.06352.x
27. Piao S, Liu Y, Hu J, Guo F, Ma J, Sun Y, et al. USP22 is useful as a novel molecular marker for predicting disease progression and patient prognosis of oral squamous cell carcinoma. *PLoS One*. (2012) 7:e42540. doi: 10.1371/journal.pone.0042540
28. Li J, Wang Z, Li Y. USP22 nuclear expression is significantly associated with progression and unfavorable clinical outcome in human esophageal squamous cell carcinoma. *J Cancer Res Clin Oncol*. (2012) 138:1291–7. doi: 10.1007/s00432-012-1191-5
29. Schrecengost RS, Dean JL, Goodwin JF, Schiewer MJ, Urban MW, Stanek TJ, et al. USP22 regulates oncogenic signaling pathways to drive lethal cancer progression. *Cancer Res*. (2014) 74:272–86. doi: 10.1158/0008-5472.CAN-13-1954

30. Han B, Sun Y, Yang D, Zhang H, Mo S, Chen X, et al. USP22 promotes development of lung adenocarcinoma through ubiquitination and immunosuppression. *Aging (Albany NY)*. (2020) 12:6990–7005. doi: 10.18632/aging.103056
31. Zhibo Q, Lianxin L. Ubiquitin-specific protease 22 is associated with poor prognosis in neuroblastoma. *Adv Clin Exp Med*. (2020) 29:295–300. doi: 10.17219/acem/115089
32. Yuan X, Wang H, Xu A, Zhu X, Zhan Y, Wang W. Ubiquitin-specific peptidase 22 promotes proliferation and metastasis in human colon cancer. *Oncol Lett*. (2019) 18:5567–76. doi: 10.3892/ol.2019.10872

Conflict of Interest: The authors declare that the research was conducted in the absence of any commercial or financial relationships that could be construed as a potential conflict of interest.

Publisher's Note: All claims expressed in this article are solely those of the authors and do not necessarily represent those of their affiliated organizations, or those of the publisher, the editors and the reviewers. Any product that may be evaluated in this article, or claim that may be made by its manufacturer, is not guaranteed or endorsed by the publisher.

Copyright © 2022 Wang, Jia, Gao, Zhou, Zhang and Zu. This is an open-access article distributed under the terms of the Creative Commons Attribution License (CC BY). The use, distribution or reproduction in other forums is permitted, provided the original author(s) and the copyright owner(s) are credited and that the original publication in this journal is cited, in accordance with accepted academic practice. No use, distribution or reproduction is permitted which does not comply with these terms.

frontiers | Frontiers in Medicine

ORIGINAL RESEARCH
published: 16 June 2022
doi: 10.3389/fmed.2022.830595

Hepatic Arterial Infusion Chemotherapy With Folfirinox or Oxaliplatin Alone in Metastatic Colorectal Cancer

*Violaine Randrian[1], Simon Pernot[2], Baptiste Sionneau[3], Denis Smith[3], Annie Lim[4], Yann Touchefeu[5], Claire Gallois[6], Anthony Turpin[7], Sahir Javed[7], Rosine Guimbaud[8], Pascale Rivera[8], Mehdi Karoui[9], Edouard Auclin[10,11] and Julien Taieb[6]**

[1] Department of Hepato-Gastro-Enterology, CHU Poitiers, Poitiers, France, [2] Department of Medical Oncology, Institut Bergonié, Bordeaux, France, [3] Medical Oncology, Bordeaux University Hospital, Bordeaux, France, [4] Department of Gastroenterology, Clinique Santé Atlantique, Saint-Herblain, France, [5] Department of Hepatogastroenterology, Digestive Oncology, Nantes University Hospital, Nantes, France, [6] Department of Gastrointestinal Oncology, Université de Paris, Hôpital Européen Georges Pompidou, Paris, France, [7] Department of Oncology, CHU Lille, Lille, France, [8] Department of Digestive Oncology, IUCT-Rangueil, CHU Toulouse, Toulouse, France, [9] Department of Surgical Oncology, Université de Paris, Hôpital Européen Georges Pompidou, Paris, France, [10] Methodology and Quality of Life Unit in Oncology, University Hospital of Besançon, Bourgogne Franche-Comté University, INSERM, EFS BFC, UMR 1098, Interactions Hôte-Greffon-Tumeur/Ingénierie Cellulaire et Génique, Besançon, France, [11] Department of Medical Oncology, Université de Paris, Hôpital Européen Georges Pompidou, Paris, France

OPEN ACCESS

Edited by:
Qi Liu,
Fudan University, China

Reviewed by:
Louise Catherine Connell,
Cornell University, United States
Takeshi Aramaki,
Shizuoka Cancer Center, Japan

***Correspondence:**
Julien Taieb
Jtaieb75@gmail.com

Specialty section:
This article was submitted to Gastroenterology, a section of the journal Frontiers in Medicine

Received: *07 December 2021*
Accepted: *05 May 2022*
Published: *16 June 2022*

Citation:
Randrian V, Pernot S, Sionneau B, Smith D, Lim A, Touchefeu Y, Gallois C, Turpin A, Javed S, Guimbaud R, Rivera P, Karoui M, Auclin E and Taieb J (2022) Hepatic Arterial Infusion Chemotherapy With Folfirinox or Oxaliplatin Alone in Metastatic Colorectal Cancer. Front. Med. 9:830595. doi: 10.3389/fmed.2022.830595

Background: Hepatic arterial infusion (HAI) of chemotherapy is an option for the treatment of patients with liver metastases from colorectal cancer (LMCRC). Though HAI with oxaliplatin (HAI-Ox) is generally used, intravenous (IV) 5-fluoro-uracil (5FU)-oxaliplatin-irinotecan HAI (HAI-Folfirinox) is feasible and leads to curative-intent surgery in 30% of pretreated patients. We compared the efficacy and safety of HAI-Ox and HAI-Folfirinox.

Methods: Patients who underwent HAI chemotherapy for LMCRC were retrospectively included from 2008 to 2019 from six French expert centers.

Results: Data were collected from 273 previously treated patients with LMCRC. Patients received HAI-Folfirinox (n = 52) or HAI-Ox (n = 221) combined with IV chemotherapy. The objective response rate (ORR) was 43.2% in patients with HAI-Folfirinox and 45.9% (ns) in patients with HAI-Ox. Median overall survival (OS) was 17 months (95% CI: 15–32.3) with HAI-Folfirinox and 26.2 months (95% CI: 19.4–34.4; p = 0.1) with HAI-Ox. Median progression-free survival (PFS) was 7.9 months (95% CI: 4.9–10.3) with HAI-Folfirinox and 6.4 months (95% CI: 6.0–7.7; p = 0.6) with HAI-Ox. The secondary liver resection rate was 35.6% with HAI-Folfirinox and 16.7% with HAI-Ox (p = 0.007). Grade 2 and above toxicities were significantly more frequent with HAI-Folfirinox. In the global population, only 2 factors were prognostic for OS in multivariable analyses: liver-only disease [hazard ratio (HR): 0.4; 95% CI 0.20–0.83; p = 0.013] and local complications of the catheter (HR: 3.8; 95% CI 1.6–9.0; p = 0.002).

Conclusion: Hepatic arterial infusion results in high response rates, secondary resections, and long survival in pretreated patients with LMCRC.

Keywords: colorectal cancer, hepatic arterial infusion, liver metastases, cancer treatment, surgery

INTRODUCTION

Colorectal cancer (CRC) management raises new challenges as its incidence increases worldwide. As the first metastatic site, hepatic progression contributes to death in half of the patients with metastatic disease (1). This trend has prompted the medical community to elaborate more aggressive systemic and loco-regional approaches even after several lines of treatment (2, 3). Although hepatic arterial infusion (HAI) chemotherapy relies on a robust biological rationale, its development has been initially restricted by two limitations: first, the complexity of surgical removal of the catheter with a significant local complications rate and, second, extra-hepatic progressive lesions excluding patients from an HAI loco-regional treatment approach (4). With technical advances in catheter insertion through interventional radiology procedures (5), HAI chemotherapy has become an effective option for the treatment of patients with liver-dominant/exclusive disease. Moreover, the global strategy for the management of these patients has evolved, and HAI is now mostly used in combination with active systemic treatment, allowing better control of extrahepatic disease when limited (4).

Hepatic arterial infusion with oxaliplatin combined with intravenous (IV) 5-fluoro-uracil (5FU) has yielded positive results in patients harboring CRC liver metastases (6–8) (LMCRC), with a 16% secondary surgery rate (9). These preliminary results led to ongoing randomized phase III trials assessing HAI-Ox in the first- and second-line settings in non-resectable LMCRC (OSCAR NCT02885753, SULTAN NCT03164655) or in the adjuvant setting after liver surgery (PACHA-01, NCT02494973) (10).

The multicenter phase II trial, OPTILIV (11) has evaluated an intensified regimen with 5FU, oxaliplatin, and irinotecan administered intra-arterially combined with IV cetuximab in *RAS* wild-type patients with liver metastases from CRC after the failure of IV chemotherapy (12). About 30% of these heavily pretreated patients finally underwent hepatic resection. This regimen was associated with non-negligible grade 3–4 toxicities, in particular neutropenia (42.6%). To our knowledge, there is no study comparing HAI with oxaliplatin (HAI-Ox) and HAI with Folfirinox (HAI-Folfirinox) in patients with non-resectable LMCRC. In this multicenter retrospective study, we looked at HAI performance in pretreated patients with liver-dominant/exclusive mCRC and compared IV chemotherapy or targeted therapy combined with HAI-Ox or with HAI-Folfirinox. We assessed the efficacy and safety of these administration modalities in patients with disease refractory to standard therapies.

MATERIALS AND METHODS

Patients

Patients who underwent HAI chemotherapy for liver metastases from pathologically proven colorectal cancer refractory to at least one standard IV regimen were retrospectively included from 2008 to 2019.

Data were collected from routinely treated patients with HAI chemotherapy of six expert centers.

The study was performed according to the principles of the Declaration of Helsinki.

Treatments

Hepatic arterial infusion treatment was delivered through a catheter, which was implanted percutaneously by an interventional radiologist. This catheter was linked to an implantable port, intra-arterial catheter patency and hepatic artery skeletonization or occlusion were checked by contrast medium opacification before treatment initiation and every two courses of treatment. HAI-Ox was delivered at the dose of 85 mg/m^2 (86.5%) or 100 mg/m^2 (13.5%) in 2 h and IV chemotherapy with or without targeted therapy according to *RAS* status (bevacizumab or cetuximab). HAI-Folfirinox was based on the OPTILIV study protocol (11) as follows: 5-FU 2,800 mg/m^2, irinotecan 180 mg/m^2, and oxaliplatin 85 mg/m^2. HAI-Folfirinox was administered alone or in association with IV bevacizumab or cetuximab according to *RAS* status.

Data Collected

Data were collected retrospectively from electronic medical records. Included were demographic data (age and gender), disease characteristics (date of diagnosis of colorectal cancer and metastatic status, sites of metastases, number and distribution of liver metastases, and WHO PS), molecular data (*KRAS*, *RAS*, *BRAF*, and microsatellite instability status), laboratory parameters (bilirubin, ACE CA19-9 before treatment and during follow-up), previous treatments (surgical resection, radio-ablation, and previous systemic treatment lines), concomitant anti-cancer treatment (IV chemotherapy and targeted therapies), tolerability data (treatment-related toxicities, dose reductions, and treatment stop), and response to treatment and survival (objective hepatic and extra-hepatic response, date of hepatic and extra-hepatic progressions, last date of follow-up, and status at last follow-up).

Statistical Analysis

Progression-free survival (PFS) was defined as the time elapsed from the beginning of HAI treatment until progression (any site for global-PFS, hepatic for liver-PFS) or death (all causes). Overall survival (OS) was defined as the time elapsed from the beginning of HAI treatment until death (all causes).

Survival curves were estimated using the Kaplan-Meier method. Median follow-up and the 95% confidence intervals (CI) were calculated using the reverse Kaplan-Meier method.

The statistical association of patients with tumor-related characteristics and treatment with survival was first assessed by the univariate Cox proportional hazards model. Parameters with values of $p < 0.10$ in univariate analysis and/or clinically relevant variables were entered into the multivariable Cox-regression model. Values of $p < 0.05$ were considered statistically significant. All analyses were performed using R software version 2.15.2 (R Development Core Team, Vienna, Austria).

RESULTS

Patient Characteristics

We included 273 patients previously treated by one or more chemotherapy protocols (**Supplementary Table 1**). Among them, 52 (19.0%) received HAI-Folfirinox and 221 (81.0%) received HAI-Ox. The tumor molecular profile was only available for a subset of patients (109/273; 39.9%) according to the study period. *KRAS* status was available in 39.2% of patients. *KRAS* mutations were similar in the HAI-Folfirinox and HAI-Ox groups (31.6% vs. 43.0%; p = 0.124). *BRAF* mutations represented 7.4% of the 122 tumors analyzed and microsatellite instability represented 7.3% of the 69 tumors analyzed. The disease was liver-limited in 69.5% of patients and liver-dominant in the remaining 30.5%. Peritoneal, lung, and lymph node metastatic lesions were described in 5.6, 20.7, and 4.2% of patients, respectively, with no significant difference between the two groups (**Table 1**). All patients were previously treated with 5-FU. Most patients had previously received irinotecan (231/273; 84.9%) and oxaliplatin (231/273; 84.9%). HAI chemotherapy was proposed as a second-line or third-line treatment in 42.9 and 32.2% of cases, respectively.

Treatment

Patients in the HAI-Folfirinox group received a median of 4 cycles (range: 1–27) and patients in the HAI-Ox group received a median of 5 cycles (range: 1–17). HAI treatment was stopped for progression, unacceptable toxicity, failure of HAI, or upon patient decision. More patients in the HAI-Folfirinox group received only a short course of HAI chemotherapy (< 4 infusions in 37.2% as compared to 29.6% in the HAI-ox group; **Table 2**).

Concomitant IV cytotoxic chemotherapy was administered in 96.3% of patients in the HAI-Ox group and in no patients in the HAI-Folfirinox group. IV-targeted therapies were more frequently administered with HAI-Folfirinox (86.5%) than with HAI-Ox (37.3%), in particular for anti-epidermal growth factor receptor (EGFR; **Table 2**).

TABLE 1 | Characteristics of the extra-hepatic disease in the population.

Hepatic intra-arterial treatment	All patients *N* = 273	HAI-Folfirinox *N* = 52	HAI-Oxaliplatin *N* = 221	*p*
Peritoneal metastases				0.605
Yes	12 (5.6%)	0 (0.0%)	12 (6.2%)	
No	201 (94.4%)	18 (100.0%)	183 (93.9%)	
Unknown	60	34	26	
Lung metastases				1
Yes	9 (4.2%)	3 (16.7%)	41 (21.0%)	
No	204 (95.8%)	15 (83.3%)	154 (79.0%)	
Unknown	60	34	26	
Lymph node metastases				1
Yes	9 (4.2%)	0 (0.0%)	9 (4.6%)	
No	204 (95.8%)	18 (100.0%)	186 (95.4%)	
Unknown	52	34	26	

Efficacy

Considering the overall population treated with HAI in this cohort, 45.4% of patients presented an objective response, i.e., 11.5% with a complete response, 32.4% presented stable disease, and 22.2% presented primary progressive disease, leading to a disease control rate of 77.8% (**Table 3**). With a median follow-up of 30.6 months (95% CI: 21.7–39.9), median OS was 23.9 months (95% CI: 18.2–28.2). Median global PFS and hepatic PFS were 6.4 months (95% CI: 6.0–7.6) and 7.9 months (95% CI: 6.5–9.0), respectively (**Figures 1A,B**). HAI-Folfirinox, as compared to HAI-Ox, neither improve OS (median 17.0 months (95% CI: 15.0–32.3) vs. 26.2 months (95% CI: 19.4–34.4, p = 0.1) nor median PFS 5.9 months (95% CI: 4.9–10.3) vs. 6.4 months (95% CI: 6.0–7.7, p = 0.6), respectively.

No significant differences were observed in hepatic recurrences or in extra-hepatic recurrences depending on the type of HAI received (**Figures 1C,D**). Median extra-hepatic PFS was 8.1 months (95% CI: 5.0–18.2) and 7.9 months (95% CI: 6.1–9.2; p = 0.4) in patients treated with HAI-Folfirinox and HAI-Ox, respectively. Median hepatic-specific PFS was 7.7 months (95% CI: 6.0–13.5) and 8.7 months (95% CI: 6.8–9.2; p = 0.9) in patients treated with HAI-Folfirinox and HAI-Ox, respectively.

In the whole population, previous exposure to oxaliplatin led to similar median OS (23.6 months (95% CI: 17.7–31.2) vs. 23.9 months (95% CI: 16.0–46.3) without previous exposure to oxaliplatin; p = 0.7) and PFS 6.1 months (95% CI: 5.8–7.1) vs. 9.1 months (95% CI: 6.21–10.6) respectively; p = 0.9).

When looking at post-HAI treatments: 20.0% had a secondary hepatic resection and 12.8% had a secondary radiofrequency ablation. Secondary liver surgery was performed in 35.6% of patients treated with HAI-Folfirinox and 16.7% of patients treated with HAI-Ox (p = 0.007). The rate of secondary radiofrequency ablation was similar in the HAI-Folfirinox (16.7%) and HAI-Ox (12.4%, p = 0.7) groups.

TABLE 2 | Treatment delivery.

Hepatic arterial infusion treatment	All patients *N* = 273	HAI-folfirinox *N* = 52	HAI-oxaliplatin *N* = 221	*p*
Concomitant intravenous treatment				
None	7 (2.6%)	5 (13.5%)	2 (0.9%)	<0.001***
Cetuximab/ panitumumab	79 (28.9%)	29 (78.4%)	50 (23.0%)	<0.001***
Bevacizumab	34 (12.5%)	3 (8.1%)	31 (14.3%)	0.01*
5FU	209 (76.6%)	0 (0.0%)	209 (96.3%)	0.001**
Irinotecan	78 (28.6%)	0 (0.0%)	78 (35.9%)	0.318 ns
Oxaliplatin	5 (1.8%)	0 (0.0%)	5 (2.3%)	0.083 ns
Raltitrexed	3 (1.1%)	0 (0.0%)	3 (1.4%)	0.002*
Trifluridine-tipiracil	1 (0.4%)	0 (0.0%)	1 (0.5%)	<0.001***
Unknown	19	15	4	
Number of HAI infusions				
<4	82 (31.1%)	19 (37.2%)	63 (29.6%)	0.032*
4–8	130 (49.2%)	21 (41.2%)	109 (51.2%)	0.063 ns
≥9	52 (19.7%)	11 (21.6%)	41 (19.2%)	0.955 ns
Unknown	9	1	8	

Concomitant intravenous treatments and intra-arterial treatment duration.
**p < 0.05; **p < 0.01; and ***p < 0.001.*

TABLE 3 | Treatment efficacy: best response rates.

Type of HAI		All lines of treatment			Second line of treatment			Third and further lines of treatment		
		All *N* = 273	FOLFIRINOX *N* = 52	OX *N* = 221	All *N* = 116	FOLFIRINOX *N* = 24	OX *N* = 92	All *N* = 157	FOLFIRINOX *N* = 28	OX *N* = 129
Objective response rate	Yes	102 (45.4%)	19 (43.2%)	83 (45.9%)	51 (52.6%)	9 (40.9%)	42 (56.0%)	53 (39.3%)	10 (45.5%)	43 (38.1%)
	No	123 (54.7%)	25 (56.8%)	98 (54.1%)	46 (47.4%)	13 (59.1%)	33 (44.0%)	82 (60.7%)	12 (54.5%)	70 (61.9%)
	NA	48	8	40	20	2	17	22	6	15
Disease control rate	Yes	175 (77.8%)	33 (75.0%)	142 (78.5%)	80 (82.5%)	18 (81.8%)	62 (82.7%)	98 (39.0%)	15 (68.2%)	83 (73.5%)
	No	50 (22.2%)	11 (25.0%)	39 (21.5%)	17 (17.5%)	4 (18.2%)	13 (17.3%)	37 (60.3%)	7 (31.8%)	30 (26.5%)
	NA	48	8	40	19	2	17	22	6	16
Secondary hepatic resection	Yes	50 (20.1%)	16 (35.6%)*	34 (16.7%)*	31 (29.8%)	9 (40.9%)	22 (26.8%)	21 (14.2%)	7 (30.4%)	14 (11.2%)
	No	199 (79.9%)	29 (64.4%)	170 (83.3%)	73 (70.2%)	13 (59.1%)	60 (73.2%)	127 (85.8%)	16 (69.6%)	111 (88.8%)
	NA	24	7	17	13	2	11	11	5	6

HAI, hepatic arterial infusion.
**p < 0.05.*

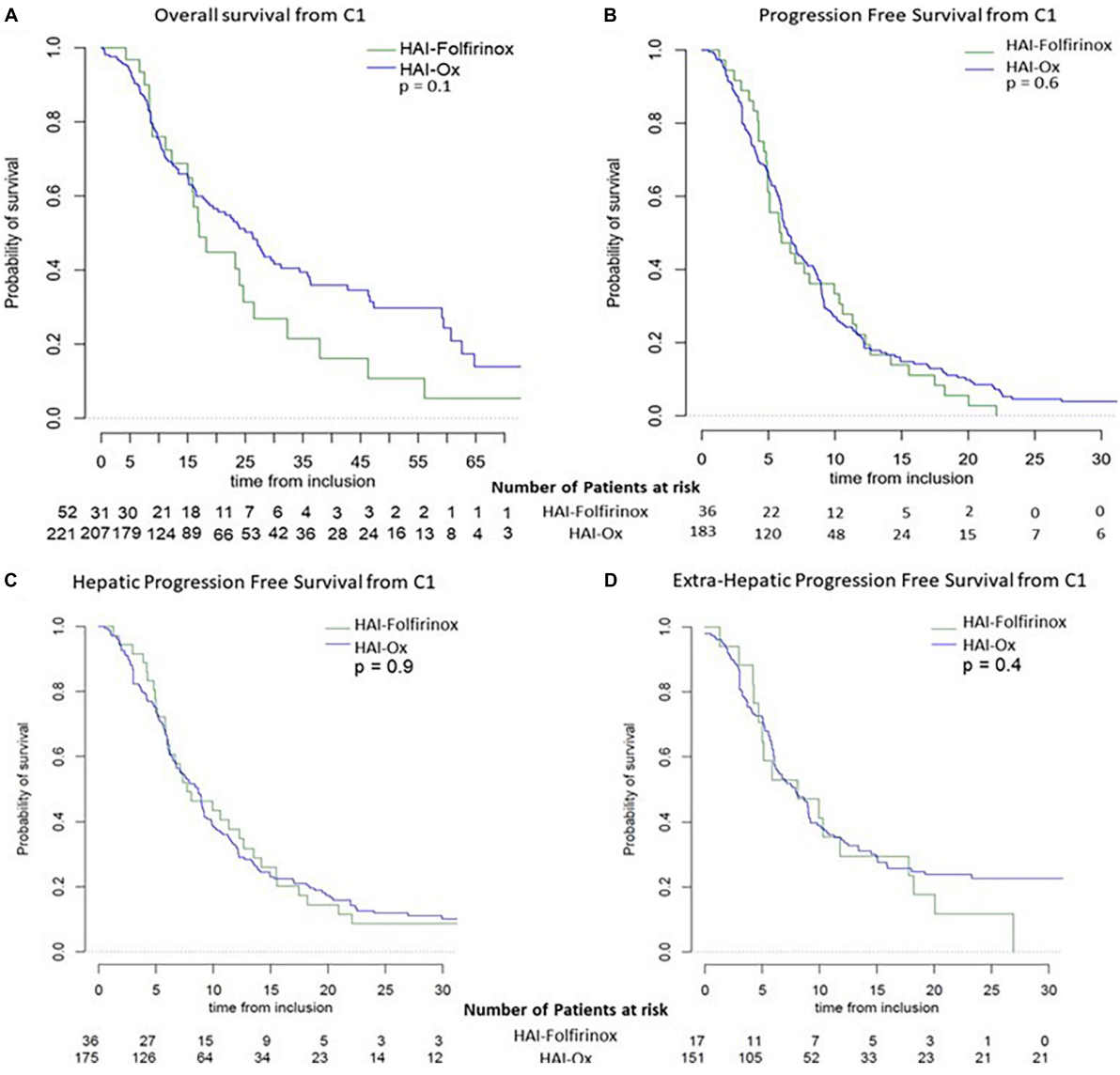

FIGURE 1 | Survival curves depend on HAI treatment. Overall survival **(A)** and progression-free survival **(B)** in patients with HAI-Folfirinox and HAI-Ox. Specific hepatic progression-free survival **(C)** and extra-hepatic progression-free survival **(D)** in patients with HAI-Folfirinox and HAI-Ox.

The use of HAI-Ox in second-line treatment as compared to later lines (**Table 3**) resulted in non-significant trends in secondary liver resections (26.8% vs. 11.2%; $p = 0.12$; **Figure 2A**), disease control rate (82.5% vs. 73.5%, $p = 0.50$; **Figure 2B**), and objective response rate (ORR; 56.0% vs. 38.1%, $p = 0.21$; **Figure 2C**). Similar trends were observed with HAI-Folfirinox. Patients on HAI chemotherapy had a median OS of 15.9 months (range 0.3–96.3) in second-line treatment and 11.2 months (range 0.6–70.9) beyond second line.

Tolerability

During treatment, a dose reduction was performed in 62.5% of patients in the HAI-Folfirinox group and in 34.1% in the HAI-Ox group ($p = 0.001$). Before HAI treatment, 91% of patients presented a grade of 0 or 1 neuropathy. During treatment, grade $\geq$ 2 neuropathy appeared in 20.4% of patients in the HAI-Folfirinox group and in 29.3% of patients in the HAI-Ox group (ns).

Vascular complications occurred in 21.0% of all HAI-treated patients and local complications (skin necrosis, hematoma, healing failure, and local infection) occurred in 23.8% of patients. Local complications were significantly more frequent in patients with HAI-Folfirinox (34.9% vs. 17.9%, $p = 0.01$). Grade $\geq$ 2 neutropenia (42.5% vs. 22.7%; $p < 0.001$), diarrhea (34.9% vs. 13.9%; $p = 0.005$), and vomiting (20.0% vs. 6.0%; $p = 0.006$) were also more frequent in patients with HAI-Folfirinox when compared with patients with HAI-Ox. Vascular complications included hepatic artery occlusion, catheter occlusion, arteritis, and shunts requiring radiologic embolization of extra-hepatic arteries, such as the gastroduodenal artery even without any ulcer diagnosed. Among vascular complications, hepatic artery occlusion was reported four times, each time in patients receiving HAI-Folfirinox. One toxic death occurred in each group (**Supplementary Table 2**).

Prognostic Factors in All Patients on Hepatic Arterial Infusion Treatments

In univariable analysis, parameters associated with poor OS were WHO-PS 2-3, peritoneal metastases, previous administration of irinotecan, bevacizumab treatment before HAI treatment, more than two previous treatment lines, and local complications related to the HAI catheter. Parameters associated with prolonged OS were liver metastases only and secondary hepatic resection (**Supplementary Table 3**).

In multivariable analysis, only 2 factors were associated with OS (**Supplementary Table 3**): the liver-only disease was associated with a prolonged OS (HR: 0.40; 95% CI 0.20–0.83; $p = 0.013$) and local complications related to HAI administration of the treatment were associated with a reduced OS (HR: 3.8; 95% CI 1.60–9.02; $p = 0.002$).

DISCUSSION

This study retrospectively compared HAI-Folfirinox to HAI-Ox in 273 patients with non-resectable liver metastases of colorectal cancer. Treatment was feasible and well tolerated in these patients with disease refractory to at least one line of treatment. Most of them had previously received IV oxaliplatin, irinotecan, and targeted therapies (bevacizumab or cetuximab). Treatment duration, PFS, and OS were similar between the two treatment modalities. HAI-Folfirinox was associated with significantly more secondary hepatic resections and more local complications linked to the catheter and treatment-related grade $\geq$ 2 toxicities, such as neutropenia, diarrhea, and vomiting. In multivariable analysis in the whole population receiving HAI, liver limited disease was associated with a prolonged OS whereas local complications were associated with shorter OS.

Hepatic Arterial Infusion Results in Longer Overall Survival

In our study, patients on HAI chemotherapy had a median OS of 15.9 months in second-line treatment and 11.2 months beyond the second line, as compared to reported OS of 13 months (13, 14) and 6 months, respectively, for IV treatment in the literature (15, 16). As for the ORR, we report a lower ORR (45.3%) than Ducreux et al. (6) (64%; 95% CI, 44–81%) and Boige et al. (9) (55%; 95% CI, 40–69%). In both studies, patients in second-line therapy were treated with HAI-Ox combined with IV 5-FU with a median of 8 or 9 cycles received. In Ducreux et al., they had not previously received oxaliplatin. It is worth noting that we analyzed a much larger population of non-selected patients with the extra-hepatic disease (30.5%), pretreated with targeted therapies, and cytotoxic chemotherapies, which may account for the lower ORR than expected. Altogether, our results promote HAI as an interesting option in LMCRC beyond first-line treatment. HAI treatment appeared well tolerated, especially when administered with oxaliplatin only. A randomized trial specifically designed to compare HAI treatment to IV chemotherapy in patients with non-resectable LMCRC after induction treatment is currently ongoing (17).

Hepatic Arterial Infusion to Increase Secondary Resection Rate

The use of HAI-Folfirinox relied on the resection rate of 16.7% and reported for patients treated with HAI-Folfirinox after two or three lines of treatment in the prospective OPTILIV trial (11). In terms of secondary resection, we noted a significantly higher secondary resection rate in patients with HAI-Folfirinox (35.6%). Our population included 42.9% of patients in a second-line setting, but the difference in secondary resection rate achieved was even greater between HAI-Folfirinox and HAI-Ox in third and further lines when compared with the second-line setting. Patients in the HAI-Ox group more often had extra-hepatic lesions (33.0% vs. 19.6%). The most frequent extra-hepatic lesions reported were lung metastases, which are less life threatening than peritoneal metastases. The peritoneal disease is rarely reported in this series: 0% in the HAI-Folfirinox group and 6.2% in the HAI-Ox group. The low number of patients concerned, resulting in a lack of statistical power, may account for the non-significance of the differences observed. In contrast with the OPTILIV trial, secondary surgical resection did not emerge as

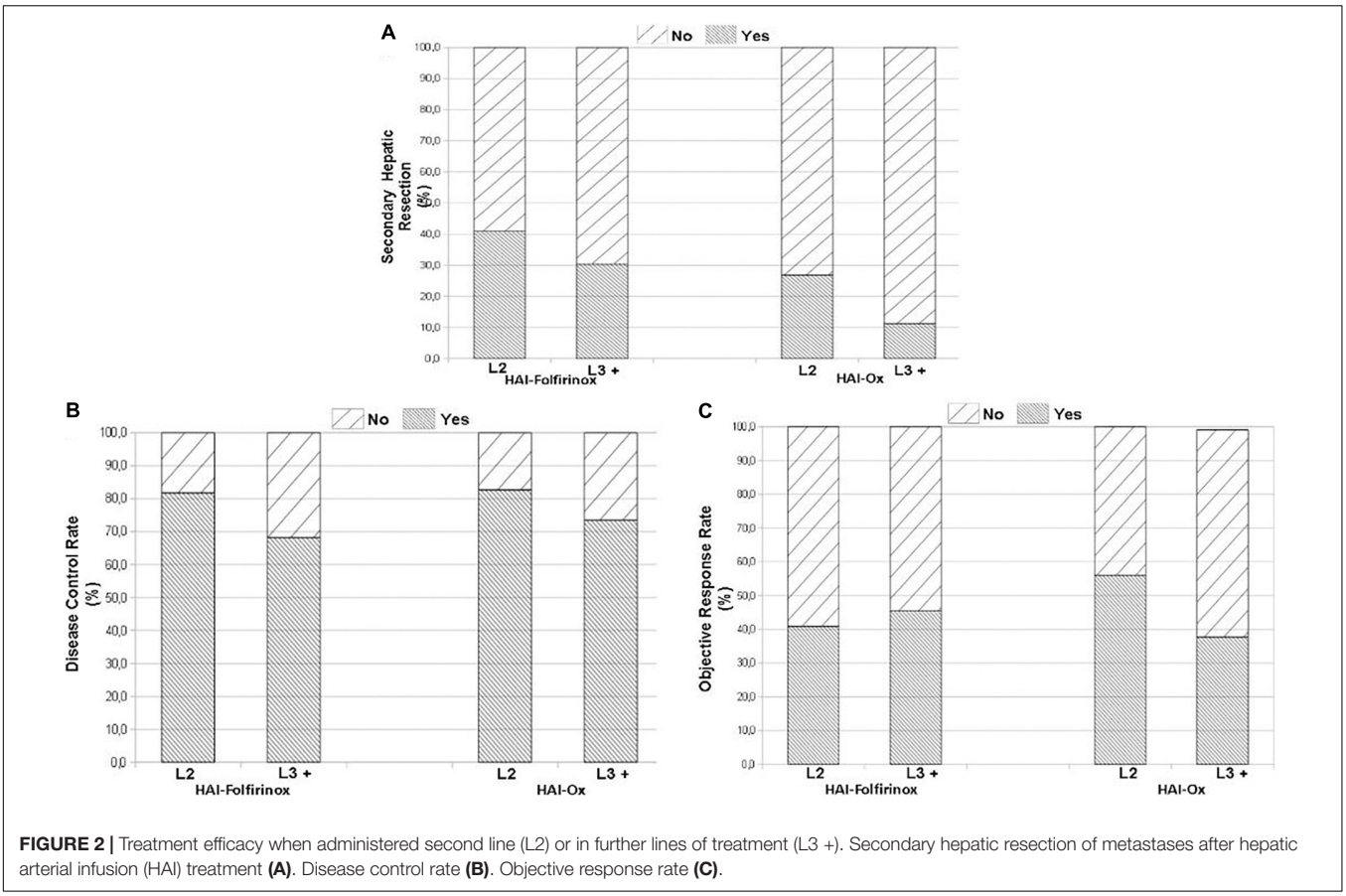

FIGURE 2 | Treatment efficacy when administered second line (L2) or in further lines of treatment (L3 +). Secondary hepatic resection of metastases after hepatic arterial infusion (HAI) treatment **(A)**. Disease control rate **(B)**. Objective response rate **(C)**.

a predictor of longer OS in this work. HAI-Folfirinox induced more toxicities than HAI-Ox and more than one-third of patients received less than 2 months of treatment. HAI-Folfirinox did not significantly improve median OS as compared to HAI-Ox. These results suggest that resection of hepatic metastases should not be the predominant parameter used to guide treatment decision after second-line treatment. The increasing life expectancy of patients with LMCRC justifies randomized trials with HAI to conclude with certainty that the resection rate correlates with OS (OSCAR NCT02885753, SULTAN NCT03164655).

Hepatic Arterial Infusion and Other Local Treatments

Other local treatments, such as chemoembolization with drug-eluting beads loaded with irinotecan (DEBIRI) (18) or selective internal radiation therapy (SIRT) (19), showed better OS than IV chemotherapy in patients pretreated for LMCRC. First attempts at comparing SIRT and HAI chemotherapy to set up the best treatment sequences have been published. They ruled in favor of HAI chemotherapy, which appeared as a predictor of longer OS (31.2 vs. 16.3 months; $p < 0.001$) when compared to SIRT (20). In addition, HAI is technically difficult after internal SIRT, which may affect the liver vasculature (21). Therefore, there is a need for HAI chemotherapy optimization. In this regard, previous reports suggest that several lines of HAI chemotherapy could be proposed before switching to another therapeutic strategy (22).

Limits and Strengths

The retrospective and non-randomized nature of our study limits the strength of the conclusions that can be drawn from this work. Especially, the period of inclusion from 2008 to 2019 accounts for a significant percentage of missing data in laboratory analyses. *BRAF* and *RAS* testing in France was recommended in 2014 and implemented in 2015. We were therefore not able to adjust data for *RAS* and *BRAF* status. In addition, the heterogeneity of previous lines of treatment and concomitant treatments to HAI may have introduced bias. Especially, the concomitant administration of cetuximab was unbalanced between the HAI-Folfirinox and HAI-oxaliplatin groups (78.4% vs. 23%, respectively). Although one of the largest series reported in HAI-treated patients, it remained too small for efficient application of a propensity score. These results show the importance of conducting randomized prospective studies in the field, which is the only method to build comparable treatment groups and determine the best HAI modalities.

Nevertheless, we report here, to our knowledge, the largest series of HAI-treated patients after failure of a first-line IV chemotherapy and the first series comparing two HAI regimens. As HAI chemotherapy is of particular interest in achieving resection of liver metastases (23), this study provides evidence

to help digestive oncologists and surgeons to adapt the modality of HAI treatment to their care objectives.

CONCLUSION

Hepatic arterial infusion treatment is an effective option in patients with LMCRC refractory to previous lines of treatments. Intensifying HAI treatment led to a higher rate of secondary hepatic resection with no significant impact on OS and PFS. Our study suggests that when resection is the main objective of the treatment, intensification of HAI can be proposed for selected patients.

DATA AVAILABILITY STATEMENT

The data that support the findings of this study are available from the corresponding author, upon reasonable request.

ETHICS STATEMENT

Ethical review and approval was not required for the study on human participants in accordance with the local legislation and institutional requirements. Written informed consent for participation was not required for this study in accordance with the national legislation and the institutional requirements.

AUTHOR CONTRIBUTIONS

VR completed the database, wrote, and revised the manuscript. SP initiated the project and the database. BS, DS, AL, YT, CG, AT, SJ, RG, PR, and MK reported cases to the study. EA performed the statistical analyses. JT initiated the study and supervised the project and the writing. All authors contributed to the article and approved the submitted version.

ACKNOWLEDGMENTS

We thank the Association des Gastro-Entérologues Oncologues (AGEO) for its support in English editing.

SUPPLEMENTARY MATERIAL

The Supplementary Material for this article can be found online at: https://www.frontiersin.org/articles/10.3389/fmed.2022.830595/full#supplementary-material

REFERENCES

1. Fong Y, Cohen AM, Fortner JG, Enker WE, Turnbull AD, Coit DG, et al. Liver resection for colorectal metastases. *J Clin Oncol.* (1997) 15:938–46. doi: 10.1200/JCO.1997.15.3.938
2. Van Cutsem E, Nordlinger B, Adam R, Köhne CH, Pozzo C, Poston G, et al. Towards a pan-European consensus on the treatment of patients with colorectal liver metastases. *Eur J Cancer.* (2006) 42:2212–21. doi: 10.1016/j.ejca.2006.04.012
3. Kennedy AS, McNeillie P, Dezarn WA, Nutting C, Sangro B, Wertman D, et al. Treatment parameters and outcome in 680 treatments of internal radiation with resin 90Y-microspheres for unresectable hepatic tumors. *Int J Radiat Oncol Biol Phys.* (2009) 74:1494–500. doi: 10.1016/j.ijrobp.2008.10.005
4. Jashodeep D, Narayan RR, Kemeny NE, D'Angelica MI. Role of hepatic artery infusion chemotherapy in treatment of initially unresectable colorectal liver metastases: a review. *JAMA Surg.* (2019) 154:768–76.
5. Tanaka T, Arai Y, Inaba Y, Matsueda K, Aramaki T, Takeuchi Y, et al. Radiologic placement of side-hole catheter with tip fixation for hepatic arterial infusion chemotherapy. *J Vasc Interv Radiol.* (2003) 14:63–8. doi: 10.1097/01.rvi.0000052292.26939.59
6. Ducreux M, Ychou M, Laplanche A, Gamelin E, Lasser P, Husseini F, et al. Hepatic arterial oxaliplatin infusion plus intravenous chemotherapy in colorectal cancer with inoperable hepatic metastases: a trial of the gastrointestinal group of the federation Nationale des centres de lutte contre le Cancer. *J Clin Oncol.* (2005) 23:4881–7. doi: 10.1200/JCO.2005.05.120
7. Goéré D, Deshaies I, de Baere T, Boige V, Malka D, Dumont F, et al. Prolonged survival of initially unresectable hepatic colorectal cancer patients treated with hepatic arterial infusion of oxaliplatin followed by radical surgery of metastases. *Ann Surg.* (2010) 251:686–91. doi: 10.1097/SLA.0b013e3181d35983
8. Goéré D, Benhaim L, Bonnet S, Malka D, Faron M, Elias D, et al. Adjuvant chemotherapy after resection of colorectal liver metastases in patients at high risk of hepatic recurrence: a comparative study between hepatic arterial infusion of oxaliplatin and modern systemic chemotherapy. *Ann Surg.* (2013) 257:114–20. doi: 10.1097/SLA.0b013e31827b9005
9. Boige V, Malka D, Elias D, Castaing M, De Baere D, Goere D, et al. Hepatic arterial infusion of oxaliplatin and intravenous LV5FU2 in unresectable liver metastases from colorectal cancer after systemic chemotherapy failure. *Ann Surg Oncol.* (2008) 15:219–26. doi: 10.1245/s10434-007-9581-7
10. Goéré D, Pignon JP, Gelli M, Elias D, Benhaim L, Deschamps F, et al. Postoperative hepatic arterial chemotherapy in high-risk patients as adjuvant treatment after resection of colorectal liver metastases – a randomized phase II/III trial – PACHA-01 (NCT02494973). *BMC Cancer.* (2018) 18:787. doi: 10.1186/s12885-018-4697-7
11. Lévi FA, Boige V, Hebbar M, Smith D, Lepère C, Focan C, et al. Conversion to resection of liver metastases from colorectal cancer with hepatic artery infusion of combined chemotherapy and systemic cetuximab in multicenter trial OPTILIV. *Ann Oncol.* (2016) 27:267–74. doi: 10.1093/annonc/mdv548
12. Falcone A, Ricci S, Brunetti I, Pfanner E, Allegrini G, Barbara C, et al. Phase III trial of infusional fluorouracil, leucovorin, oxaliplatin, and irinotecan (FOLFOXIRI) compared with infusional fluorouracil, leucovorin, and irinotecan (FOLFIRI) as first-line treatment for metastatic colorectal cancer: the gruppo oncologico nord ovest. *J Clin Oncol.* (2007) 25:1670–6. doi: 10.1200/JCO.2006.09.0928
13. Van Cutsem E, Tabernero J, Lakomy R, Prenen H, Prausová J, Macarulla T, et al. Addition of aflibercept to fluorouracil, leucovorin, and irinotecan improves survival in a phase III randomized trial in patients with metastatic colorectal cancer previously treated with an oxaliplatin-based regimen. *J Clin Oncol.* (2012) 30:3499–506. doi: 10.1200/JCO.2012.42.8201
14. Bennouna J, Sastre J, Arnold D, Österlund P, Greil R, Van Cutsem E, et al. Continuation of bevacizumab after first progression in metastatic colorectal cancer (ML18147): a randomised phase 3 trial. *Lancet Oncol.* (2013) 14:29–37. doi: 10.1016/S1470-2045(12)70477-1
15. Grothey A, Van Cutsem E, Sobrero A, Siena S, Falcone A, Ychou M, et al. Regorafenib monotherapy for previously treated metastatic colorectal cancer (CORRECT): an international, multicentre, randomised, placebo-controlled, phase 3 trial. *Lancet.* (2013) 381:303–12. doi: 10.1016/S0140-6736(12)61900-X
16. Mayer RJ, Van Cutsem E, Falcone A, Yoshino T, Garcia-Carbonero R, Mizunuma N, et al. Randomized trial of TAS-102 for refractory metastatic colorectal cancer. *N Engl J Med.* (2015) 372:1909–19. doi: 10.1056/NEJMoa1414325

17. Boilève A, Maillard A, Wagner M, Dromain C, Laurent C, Dupont Bierre E, et al. Treatment intensification with hepatic arterial infusion chemotherapy in patients with liver-only colorectal metastases still unresectable after systemic induction chemotherapy – a randomized phase II study – SULTAN UCGI 30/PRODIGE 53 (NCT03164655)– study protocol. *BMC Cancer*. (2020) 20:74. doi: 10.1186/s12885-020-6571-7
18. Fiorentini G, Aliberti C, Tilli M, Mulazzani L, Graziano F, Giordani P, et al. Intra-arterial infusion of irinotecan-loaded drug-eluting beads (DEBIRI) versus intravenous therapy (FOLFIRI) for hepatic metastases from colorectal cancer: final results of a phase III study. *Anticancer Res*. (2012) 32:1387–95.
19. Hendlisz A, Van den Eynde M, Peeters M, Maleux G, Lambert B, Vannoote J, et al. Phase III trial comparing protracted intravenous fluorouracil infusion alone or with yttrium-90 resin microspheres radioembolization for liver-limited metastatic colorectal cancer refractory to standard chemotherapy. *J Clin Oncol*. (2010) 28:3687–94. doi: 10.1200/JCO.2010.28.5643
20. Dhir M, Zenati MS, Jones HL, Bartlett DL, Choudry MHA, Pingpank JF, et al. Effectiveness of hepatic artery infusion (HAI) versus selective internal radiation therapy (Y90) for pretreated isolated unresectable colorectal liver metastases (IU-CRCLM). *Ann Surg Oncol*. (2018) 25:550–7. doi: 10.1245/s10434-017-6265-9
21. Pernot S, Velut G, Hampig Kourie R, Amouyal G, Sapoval M, Pointet AL, et al. 5-FU or mitomycin C hepatic arterial infusion after failure of arterial oxaliplatin in patients with colorectal cancer unresectable liver metastases. *Clin Res Hepatol Gastroenterol*. (2017) 42:255–60. doi: 10.1016/j.clinre.2017.11.004
22. Datta J, Narayan RR, Kemeny NE, D'Angelica MI. Role of hepatic artery infusion chemotherapy in treatment of initially unresectable colorectal liver metastases: a review. *JAMA Surg*. (2019) 154:768–76. doi: 10.1001/jamasurg.2019.1694
23. Kehm RD, Yang W, Tehranifar P, Terry MB. 40 years of change in age- and stage-specific cancer incidence rates in US women and men. *JNCI Cancer Spectr*. (2019) 3:kz038. doi: 10.1093/jncics/pkz038

Conflict of Interest: The authors declare that the research was conducted in the absence of any commercial or financial relationships that could be construed as a potential conflict of interest.

Publisher's Note: All claims expressed in this article are solely those of the authors and do not necessarily represent those of their affiliated organizations, or those of the publisher, the editors and the reviewers. Any product that may be evaluated in this article, or claim that may be made by its manufacturer, is not guaranteed or endorsed by the publisher.

Copyright © 2022 Randrian, Pernot, Sionneau, Smith, Lim, Touchefeu, Gallois, Turpin, Javed, Guimbaud, Rivera, Karoui, Auclin and Taieb. This is an open-access article distributed under the terms of the Creative Commons Attribution License (CC BY). The use, distribution or reproduction in other forums is permitted, provided the original author(s) and the copyright owner(s) are credited and that the original publication in this journal is cited, in accordance with accepted academic practice. No use, distribution or reproduction is permitted which does not comply with these terms.

frontiers | Frontiers in Medicine

CASE REPORT
published: 17 June 2022
doi: 10.3389/fmed.2022.856125

Type-1 Grade 2 Multi-Focal Gastric Neuroendocrine Tumors Secondary to Chronic Autoimmune Gastritis

*Ziqi Yu[1], Aiyao Wang[2], Chong Hu[2], Tao Yu[2] and Jianyong Chen[2]**

[1] Munich Medical Research School, Ludwig Maximilian University (LMU) of Munich, Munich, Germany, [2] Department of Gastroenterology and Hepatology, The First Affiliated Hospital of Nanchang Medical College, Jiangxi Provincial People's Hospital, Nanchang, China

Background: Chronic autoimmune gastritis (CAG) refers to chronic atrophic gastritis due to autoimmunity. Loss of gastric glands in CAG results in hypergastrinemia and achlorhydria leading to Vitamin B_{12} deficiency and hyperplasia of G cells and enterochromaffin-like (ECL) cells. Vitamin B_{12} deficiency could cause pernicious anemia and subacute combined degeneration, while G cells and ECL cells hyperplasia might develop gastric neuroendocrine tumor (G-NET).

Case Presentation: A 35-year-old Chinese female presented with multi-focal type-1 Grade 2 (G2) NETs with a 14-year history of pernicious anemia and subacute combined degeneration.

Conclusion: Here, we report a rare case of a Chinese patient presenting G-NET combined with pernicious anemia and subacute combined degeneration, which are secondary to chronic autoimmune gastritis. This case also illustrates the importance of routine gastroscopy in patients with Vitamin B_{12} deficiency.

Keywords: chronic autoimmune gastritis, atrophic gastritis, gastric neuroendocrine tumors, type-1 gastric carcinoid, G cell hyperplasia, ECL cell

OPEN ACCESS

Edited by:
Qi Liu,
Fudan University, China

Reviewed by:
Edith Lahner,
Sapienza University of Rome, Italy
Sohini Chakraborty,
New York University, United States

***Correspondence:**
Jianyong Chen
cjyacy69@163.com

Specialty section:
This article was submitted to Gastroenterology, a section of the journal Frontiers in Medicine

Received: *16 January 2022*
Accepted: *23 May 2022*
Published: *17 June 2022*

Citation:
Yu Z, Wang A, Hu C, Yu T and Chen J (2022) Type-1 Grade 2 Multi-Focal Gastric Neuroendocrine Tumors Secondary to Chronic Autoimmune Gastritis. Front. Med. 9:856125. doi: 10.3389/fmed.2022.856125

BACKGROUND

Atrophic gastritis is defined as chronic gastric inflammation referring to the disappearance of the gastric glands regardless of the metaplasia (1, 2). It mainly consists of a rare form of autoimmune gastritis (gastritis A) and a common form of *Helicobacter pylori* (H. pylori) associated with gastritis (gastritis B) (2, 3). Normally, for chronic autoimmune gastritis (CAG), women would have a higher prevalence with a 3:1 ratio to males (2, 4). The research found that the histologic change in CAG is a risk factor for gastric neuroendocrine tumor (G-NET) development (5, 6), and in patients with CAG, the annual incidence of G-NET was 0.68% per person-year (7, 8).

The G-NETs are rare neoplasms with origin in the peripheral neuroendocrine system in the stomach (9). G-NET could be subdivided into 4 types. Type-1 G-NETs predominantly occurred in females, representing 70–80% of G-NETs, and are gastrin-dependent (10). Normally, type-1 G-NETs are small multiple tumors around 1–2 cm located in the gastric body or fundus (6, 9, 11). Type-2 G-NETs take up 5% of the G-NETs. They are also gastrin dependent and normally associated with Zollinger-Ellison syndrome (ZES) or multiple endocrine neoplasias 1 (MEN1). They are also small and multiple tumors but have an equal prevalence in males and females

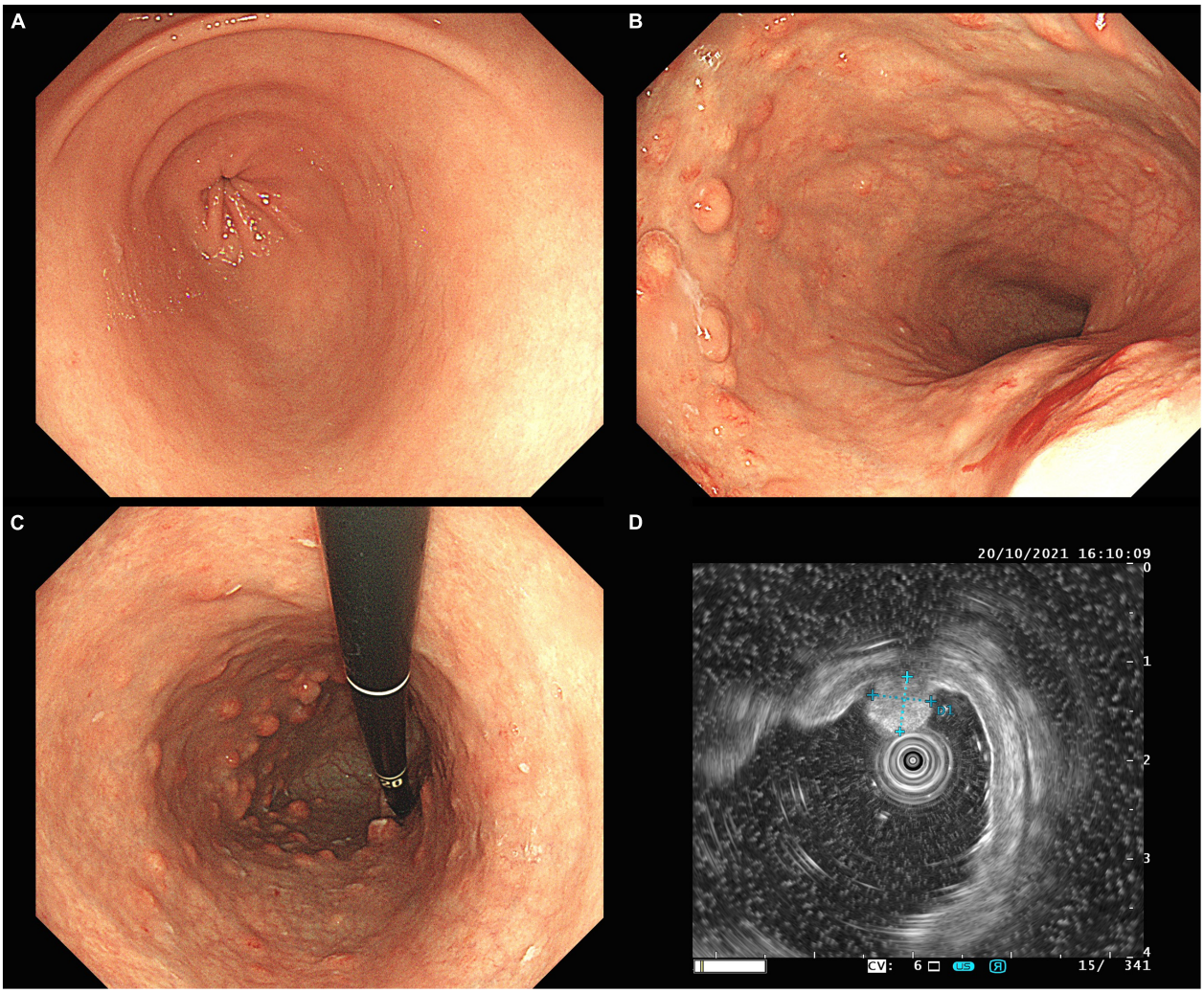

FIGURE 1 | Routine gastroscopy revealed smooth mucosa in the gastric antrum **(A)**, absence of gastric fold along the greater curvature of the gastric body **(B)**, pale appearance of mucosa, increased visibility of vasculature, and multiple gastric submucosal bulges within gastric body, and fundus **(B,C)**, EUS confirmed hyperechoic NETs originated from the muscularis mucosa, with an intact muscularis propria **(D)**.

(6, 9–11). Type-3 G-NETs comprise 10–15% of the G-NETs and are more frequently found in males. They are sporadic and gastrin-independent. They are normally single and larger than 1 cm, with high metastasis potential. In total, 25–40% of Type-3 G-NETs are malignant (6, 9, 10). The newly defined and rarest Type-4 G-NETs are also sporadic and gastrin-independent but with the highest metastasis potential (6, 10).

Besides, according to the mitotic rate and Ki-67 index, the World Health Organization (WHO) classified the NETs into Grade 1 to Grade 3. NETs with a low mitotic index (< 2) and Ki-67 proliferation index (< 3%) are classified as NET G1, NETs with the intermediate mitotic rate (2–20) and Ki-67 index (3–20%) are defined as NET G2, and NETs with the high mitotic rate (> 20) and Ki-67 index (> 20%) are named as NETs G3 (12).

In this report, we described a rare case of multiple Type-1 G2 G-NETs secondary to CAG. This patient also presented long-term pernicious anemia and subacute combined degeneration.

CASE PRESENTATION

A 35-year-old female with discomfort and fullness in the upper abdomen was admitted to our hospital. The patient was admitted due to fatigue in the lower limbs 14 years ago. She was diagnosed with pernicious anemia and subacute combined degeneration of the spinal cord in an outside hospital (laboratory results unavailable). Vitamin B_{12} and folic acid supplements were taken discontinuously but without symptomatic improvement. The patient has no family history of gastric disease. On admission, the patient was conscious and afebrile with normal vital signs. She has pale palpebral conjunctivas and fingernails with no other remarkable findings. Routine gastroscopy revealed autoimmune gastritis, multiple gastric submucosal bulges, and no endoscopic features related to H. pylori status according to the Kyoto classification (**Figures 1A–C**). Both the ^{13}C-Urea breath test (UBT) and rapid urease test showed negative results. Laboratory

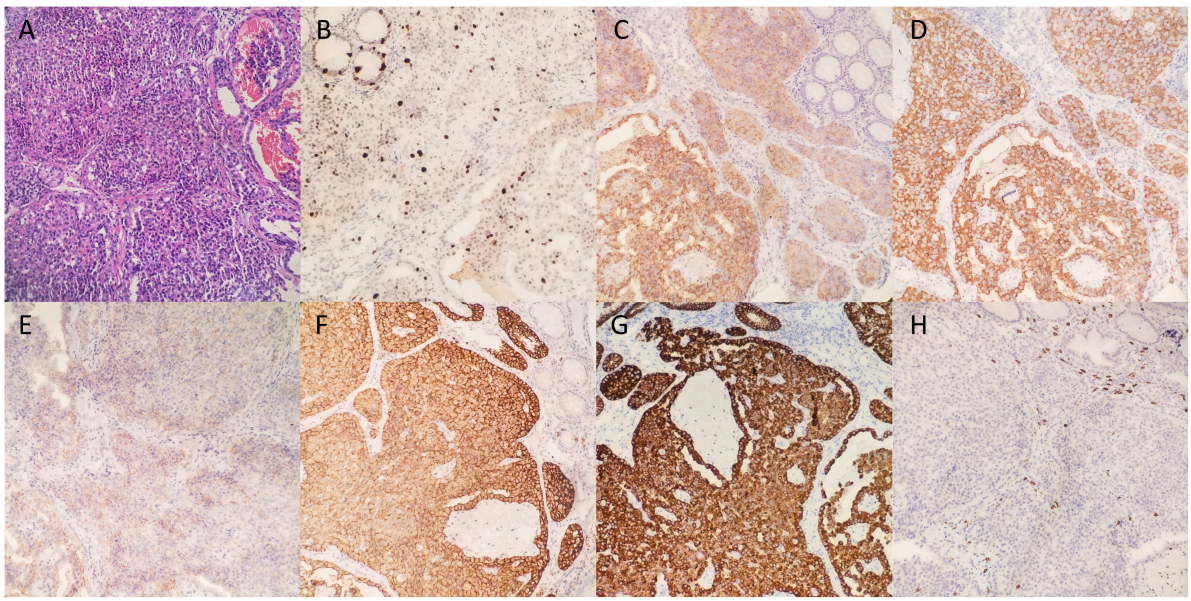

FIGURE 2 | Histological findings of pathological biopsies. **(A)** Hematoxylin and eosin staining (200x). **(B)** Ki-67 staining revealed the Ki-67 index was 15% and mitotic rate was 12. The carcinoid showed positive staining of CgA **(C)**, Syn **(D)**, CD56 **(E)**, SSTR2 **(F)**, CK **(G)**, and negative staining for CD117 **(H)**.

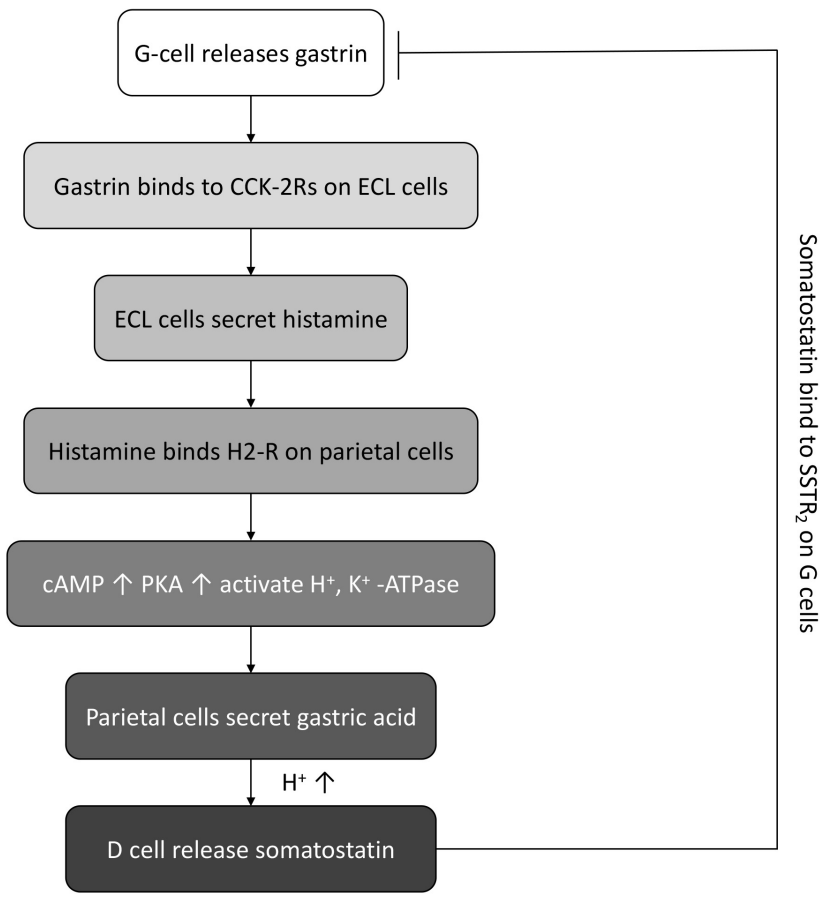

FIGURE 3 | The schematic diagram of normal feedback loop between gastrin, gastric acid, and somatostatin.

tests showed moderate anemia with decreased hemoglobin (80 g/L), serum iron (4 μmol/L) and serum ferritin of 6.17 ng/ml; normal vitamin B_{12} (1,271.70 pg/ml) and folic acid (> 30 ng/ml) level and elevated gastrin 17 (> 60 pmol/L), decreased pepsinogen I (PG I) (12.01 μg/L), normal pepsinogen II (PG II) (4.11 μg/L), lower PG I/II ratio (2.92), negative PCA (anti-parietal cell antibody), and negative IFA (anti-intrinsic factor antibody). Liver and kidney tests, urinalysis, stool routine tests, and tumor markers tests (CEA, AFP, CA19-9, and CA125) were unremarkable. The electrocardiogram showed sinus rhythm and frequent premature ventricular contractions. Thyroid ultrasound revealed no abnormalities. Cranial CT scan (plain scan) and chest and abdominal CT scan (plain and contrast-enhanced scan) revealed no abnormalities, except mild splenomegaly. Endoscopic ultrasonography (EUS) revealed multiple submucosal bulges (**Figure 1D**), which were confirmed as G2 NETs in the gastric fundus, gastric body junction, and gastric body by histopathological examination of endoscopic biopsies (**Figure 2**). We recommended endoscopic surveillance, endoscopic submucosal dissection, or somatostatin analogs for the treatment of the patient. The patient and the family chose endoscopic surveillance for further treatment. Therefore, we gave the symptomatic treatment of vitamin B_{12}, iron, and folic acid supplement and arranged a follow-up of gastroscopic surveillance every 6 months.

DISCUSSION AND CONCLUSION

The CAG is a chronic inflammatory disease that is due to an autoimmune parietal cell antibody targeting H^+, K^+ -ATPase on parietal cell or intrinsic factor. The infiltration of immune cells results in the destruction of parietal cells and other structures on oxyntic mucosa, which further leads to the destruction of the gastric gland (3, 13, 14).

In normal conditions, the antral G cells would secrete gastrin, which then binds to the cholecystokinin (CCK)-2 receptor on enterochromaffin-like (ECL) cells to stimulate the histamine release from ECL cells. Then, histamine binds to the G protein-coupled receptor H2 receptors on parietal cells. The activation of G protein-coupled receptor H2-R triggers the production of cAMP and the PKA signaling and further activates the H^+, K^+ -ATPase to pump out H^+, recycle K^+, and the concomitant secretion of Cl^-, leading to the secretion of gastric acid. Along with the enhancement of acidity, the D cells are activated and release the inhibitory somatostatin, which in turn binds the somatostatin receptor type 2 ($SSTR_2$) on G cells to inhibit the gastrin secretion (11, 15) (**Figure 3**).

However, regarding CAG, due to the destruction of parietal cells, the secretion of gastric acid and intrinsic factors are impaired. Gastric acid could exert multiple functions, such as Killing and preventing bacteria, digesting protein, and also inducing absorption of iron and vitamin B_{12} (15). The binding of intrinsic factors and vitamin B_{12} is also of vital importance to the absorption of vitamin B_{12} (16). Vitamin B_{12} is a co-factor in the reaction of the 5-methyl tetrahydrofolate (THF) converting to THF and also the conversion of homocysteine into methionine (17, 18). Deficiency in vitamin B_{12} could, on one hand, impair the *de novo* synthesis of purine and thymidylate, on the other hand, interfere with the DNA methyltransferase (19). Therefore, the deficiency of vitamin B_{12} could inhibit DNA synthesis and DNA repair after damage. Deficient DNA synthesis and repairment in pre-erythroblasts result in megaloblastic anemia; Vitamin B_{12} deficient megaloblastic anemia is also called pernicious anemia (20). Pernicious anemia could be asymptomatic for 4–5 years since the soluble vitamin B_{12} cobalamin could be reserved in the liver and could be used after vitamin B_{12} deficiency (18). Our patient has a 14-year-history of pernicious anemia, indicating a long-term history of CAG. Besides, vitamin B_{12} also plays a role in the synthesis of myelin sheaths that conducts nerve impulses (18). Therefore, vitamin B_{12} deficiency might also result in progressive fatigue, weakness, and numbness in the distal limbs. Unsteady gait, hearing loss, and urinary disorders might also be observed in these patients (18, 21). Our patient also reported a history of fatigue in lower limbs and subacute combined degeneration, this is also due to the neurological effect of vitamin B_{12} deficiency.

Moreover, deprived gastric acid secretion also results in the continuous secretion of gastrin and loss of negative feedback exerted by somatostatin by D cells. Since gastrin can stimulate cell proliferation, migration, and inhibit apoptosis (22, 23), continuous release of gastrin results in the hyperplasia of G cells and ECL cells. G cell and ECL cell hyperplasia could further induce the type-1 NETs (24). Type-1 NETs are mostly classified as Grade 1 (10).

The diagnosis criteria of CAG introduced in this study are mainly according to the Japanese criteria with at least two of the following three standards: (1) endoscopic reverse atrophy (severe atrophy in the corpus, while no or mild atrophy in the antral area); (2) hypergastrinemia, significantly decreased PG (pepsinogen) I or PG I/II, or positive PCA/IFA; (3) existence of ECL hyperplasia. Standard 1 is a must include standard (25). The laboratory result of our patient revealed elevated gastrin level, decreased PG I and decreased PG I/II level, and the gastroscopy exhibited reverse atrophy and multiple gastric submucosal bulges. Immunohistochemical expression showed a 15% Ki-67 index, a mitotic rate of 12, negative CD117 (−), positive epithelial marker CK (+), positive neuroendocrine markers synaptophysin (Syn) (+), positive CD56 (+), chromogranin A (CgA) (+), and positive prognosis marker SSTR2 (+) (**Figure 2**), indicating that our patient had multi-focal and well-differentiated epithelial Type-1 Grade2 G-NETs caused by CAG, which is a rare form in Type-1 G-NETs.

For treatment, simple endoscopic surveillance and endoscopic resection are recommended for type-1 G-NETs that are smaller than 20 mm by both National Comprehensive Cancer Network (NCCN) and European Neuroendocrine Tumor Society (ENETS) (26, 27). Antrectomy is also a potential treatment for recurrent or multi-focal G-NETs as it can eliminate the hypergastrinemia caused by G cells and also prevent the hyperplasia of ECL cells. However, the risks of complications should be made known to the patients (28). For well-localized G-NETs, endoscopic mucosal restriction (EMR) and endoscopic submucosal dissection (ESD) have been recommended. The

complete resection rate of EMR and ESD was 69 and 86%, respectively (29). Somatostatin analogs, which provide negative feedback by inhibiting gastrin secretion from G cells are also effective in treating type-1 G-NETs. However, they are not recommended due to the recurrence after cessation of medication and the high costs (30). In this case, our patient has type-1 G2 multi-focal G-NETs, with a size under 20 mm. EUS results indicated that the lesion is limited within the mucosa; meanwhile, cranial, chest, and abdominal CT scans exhibited no distant metastasis. The immunohistochemical result also showed positive SSTR2. Therefore, we suggested endoscopic surveillance, EMR, or somatostatin analogs for the treatment. However, the patient rejected EMR or somatostatin analogs treatment. Routine endoscopy was arranged for surveillance.

In conclusion, we report a rare case of type-1 G2 multi-focal G-NETs combined with pernicious anemia due to CAG. According to the medical history, the patient might have CAG underdiagnosed for more than 14 years. This also results in the development of type-1 G-NETs. Therefore, it is also suggested that patients with unknown reasons for vitamin B_{12} deficiency could undergo gastroscopy to exclude autoimmune gastritis.

DATA AVAILABILITY STATEMENT

The original contributions presented in this study are included in this article/supplementary material, further inquiries can be directed to the corresponding author/s.

ETHICS STATEMENT

The studies involving human participants were reviewed and approved by the Ethics committee of Jiangxi Provincial People's Hospital. The patients/participants provided their written informed consent to participate in this study.

AUTHOR CONTRIBUTIONS

ZY reviewed the literature and wrote the manuscript. AW performed the clinical endoscopic test. CH and TY collected the patient information. JC gave suggestions for revision. All authors have read and approved the final manuscript.

FUNDING

This study was supported by the National Natural Science Foundation of China (81960111) and the Natural Science Foundation of Jiangxi Province (20202BABL206013). ZY was supported by the China Scholarship Council (202008360174).

ACKNOWLEDGMENTS

We would like to thank Xiang Shen who polished the manuscript, and the excellent work of colleagues from the Department of Pathology. We also thank the patient, for the consent for participation and publication.

REFERENCES

1. Neumann WL, Coss E, Rugge M, Genta RM. Autoimmune atrophic gastritis–pathogenesis, pathology and management. *Nat Rev Gastroenterol Hepatol.* (2013) 10:529–41. doi: 10.1038/nrgastro.2013.101
2. Shah SC, Piazuelo MB, Kuipers EJ, Li D. AGA clinical practice update on the diagnosis and management of atrophic gastritis: expert review. *Gastroenterology.* (2021) 161:1325–32.e7. doi: 10.1053/j.gastro.2021.06.078
3. Nehme F, Rowe K, Palko W, Tofteland N, Salyers W. Autoimmune metaplastic atrophic gastritis and association with neuroendocrine tumors of the stomach. *Clin J Gastroenterol.* (2020) 13:299–307. doi: 10.1007/s12328-019-01074-7
4. Minalyan A, Benhammou JN, Artashesyan A, Lewis MS, Pisegna JR. Autoimmune atrophic gastritis: current perspectives. *Clin Exp Gastroenterol.* (2017) 10:19–27. doi: 10.2147/CEG.S109123
5. Vanoli A, La Rosa S, Luinetti O, Klersy C, Manca R, Alvisi C, et al. Histologic changes in type A chronic atrophic gastritis indicating increased risk of neuroendocrine tumor development: the predictive role of dysplastic and severely hyperplastic enterochromaffin-like cell lesions. *Hum Pathol.* (2013) 44:1827–37. doi: 10.1016/j.humpath.2013.02.005
6. Koseoglu H, Duzenli T, Sezikli M. Gastric neuroendocrine neoplasms: a review. *World J Clin Cases.* (2021) 9:7973–85.
7. Lahner E, Esposito G, Pilozzi E, Purchiaroni F, Corleto VD, Di Giulio E, et al. Occurrence of gastric cancer and carcinoids in atrophic gastritis during prospective long-term follow up. *Scand J Gastroenterol.* (2015) 50:856–65. doi: 10.3109/00365521.2015.1010570
8. Lenti MV, Rugge M, Lahner E, Miceli E, Toh B-H, Genta RM, et al. Autoimmune gastritis. *Nat Rev Dis Primers.* (2020) 6:56.
9. Sato Y, Hashimoto S, Mizuno K, Takeuchi M, Terai S. Management of gastric and duodenal neuroendocrine tumors. *World J Gastroenterol.* (2016) 22:6817–28.
10. McCarthy DM. Proton pump inhibitor use, hypergastrinemia, and gastric carcinoids-what is the relationship? *Int J Mol Sci.* (2020) 21:662. doi: 10.3390/ijms21020662
11. Burkitt MD, Pritchard DM. Review article: pathogenesis and management of gastric carcinoid tumours. *Aliment Pharmacol Ther.* (2006) 24:1305–20. doi: 10.1111/j.1365-2036.2006.03130.x
12. Nagtegaal, I. D., Odze, R. D., Klimstra, D., Paradis, V., Rugge, M., Schirmacher, P., et al. (2020). The 2019 WHO classification of tumours of the digestive system. *Histopathology* 2, 182–188. doi: 10.1111/his.13975
13. Park JY, Lam-Himlin D, Vemulapalli R. Review of autoimmune metaplastic atrophic gastritis. *Gastrointest Endosc.* (2013) 77:284–92. doi: 10.1016/j.gie.2012.09.033
14. Massironi S, Zilli A, Elvevi A, Invernizzi P. The changing face of chronic autoimmune atrophic gastritis: an updated comprehensive perspective. *Autoimmun Rev.* (2019) 18:215–22. doi: 10.1016/j.autrev.2018.08.011
15. Schubert ML. Gastric acid secretion. *Curr Opin Gastroenterol.* (2016) 32:452–60.
16. Watanabe F, Yabuta Y, Tanioka Y, Bito T. Biologically active vitamin B12 compounds in foods for preventing deficiency among vegetarians and elderly subjects. *J Agric Food Chem.* (2013) 61:6769–75. doi: 10.1021/jf401545z
17. Miller JW. Proton pump inhibitors, H2-receptor antagonists, metformin, and vitamin B-12 deficiency: clinical implications. *Adv Nutr.* (2018) 9:511S–8S. doi: 10.1093/advances/nmy023
18. Livzan MA, Gaus OV, Mozgovoi SI, Bordin DS. Chronic autoimmune gastritis: modern diagnostic principles. *Diagnostics (Basel).* (2021) 11:2113. doi: 10.3390/diagnostics11112113
19. Gan SH, Shaik MM. Chapter 11 - Epigenetics and migraine. In: Yasui DH, Peedicayil J, Grayson DR editors. *Neuropsychiatric Disorders and Epigenetics*. Boston, MA: Academic Press (2017). p. 215–31.

20. Yadav MK, Manoli NM, Madhunapantula SV. Comparative assessment of Vitamin-B12, folic acid and homocysteine levels in relation to p53 expression in megaloblastic anemia. *PLoS One.* (2016) 11:e0164559. doi: 10.1371/journal.pone.0164559
21. Zhang N, Li RH, Ma L, Li N, Shan PY, Wang XB, et al. Subacute combined degeneration, pernicious anemia and gastric neuroendocrine tumor occured simultaneously caused by autoimmune gastritis. *Front Neurosci.* (2019) 13:1. doi: 10.3389/fnins.2019.00001
22. Dimaline R, Varro A. Novel roles of gastrin. *J Physiol.* (2014) 592:2951–8. doi: 10.1113/jphysiol.2014.272435
23. Schubert ML. Functional anatomy and physiology of gastric secretion. *Curr Opin Gastroenterol.* (2015) 31:479–85. doi: 10.1097/MOG.0000000000000213
24. Vannella L, Sbrozzi-Vanni A, Lahner E, Bordi C, Pilozzi E, Corleto VD, et al. Development of type I gastric carcinoid in patients with chronic atrophic gastritis. *Aliment Pharmacol Ther.* (2011) 33:1361–9. doi: 10.1111/j.1365-2036.2011.04659.x
25. Kamada T, Maruyama Y, Monobe Y, Haruma K. Endoscopic features and clinical importance of autoimmune gastritis. *Dig Endosc.* (2022) 34:700–13. doi: 10.1111/den.14175
26. Kulke MH, Shah MH, Benson AB 3rd., Bergsland E, Berlin JD, Blaszkowsky LS, et al. Neuroendocrine tumors, version 1.2015. *J Natl Compr Canc Netw.* (2015) 13:78–108. doi: 10.6004/jnccn.2015.0011
27. Delle Fave G, Kwekkeboom DJ, Van Cutsem E, Rindi G, Kos-Kudla B, Knigge U, et al. ENETS Consensus Guidelines for the management of patients with gastroduodenal neoplasms. *Neuroendocrinology.* (2012) 95:74–87. doi: 10.1159/000335595
28. Gladdy RA, Strong VE, Coit D, Allen PJ, Gerdes H, Shia J, et al. Defining surgical indications for type I gastric carcinoid tumor. *Ann Surg Oncol.* (2009) 16:3154–60. doi: 10.1245/s10434-009-0687-y
29. Noh JH, Kim DH, Yoon H, Hsing LC, Na HK, Ahn JY, et al. Clinical outcomes of endoscopic treatment for Type 1 gastric neuroendocrine tumor. *J Gastrointest Surg.* (2021) 25:2495–502. doi: 10.1007/s11605-021-04997-0
30. Jianu CS, Fossmark R, Syversen U, Hauso O, Fykse V, Waldum HL. Five-year follow-up of patients treated for 1 year with octreotide long-acting release for enterochromaffin-like cell carcinoids. *Scand J Gastroenterol.* (2011) 46:456–63. doi: 10.3109/00365521.2010.539255

Conflict of Interest: The authors declare that the research was conducted in the absence of any commercial or financial relationships that could be construed as a potential conflict of interest.

Publisher's Note: All claims expressed in this article are solely those of the authors and do not necessarily represent those of their affiliated organizations, or those of the publisher, the editors and the reviewers. Any product that may be evaluated in this article, or claim that may be made by its manufacturer, is not guaranteed or endorsed by the publisher.

Copyright © 2022 Yu, Wang, Hu, Yu and Chen. This is an open-access article distributed under the terms of the Creative Commons Attribution License (CC BY). The use, distribution or reproduction in other forums is permitted, provided the original author(s) and the copyright owner(s) are credited and that the original publication in this journal is cited, in accordance with accepted academic practice. No use, distribution or reproduction is permitted which does not comply with these terms.

frontiers | Frontiers in Oncology

ORIGINAL RESEARCH
published: 20 June 2022
doi: 10.3389/fonc.2022.831614

Efficacy of Postoperative Adjuvant Transcatheter Arterial Chemoembolization in Hepatocellular Carcinoma Patients With Microscopic Portal Vein Invasion

*Yiwen Qiu, Yi Yang, Tao Wang, Shu Shen and Wentao Wang**

Department of Liver Surgery & Liver Transplantation Center, West China Hospital of Sichuan University, Chengdu, China

Background: Microscopic portal vein invasion (MPVI) strongly predicts poor prognosis in patients with hepatocellular carcinoma (HCC). This study aims to investigate the impact of MPVI on the efficacy of postoperative adjuvant transcatheter arterial chemoembolization (PA-TACE).

Methods: From April 2014 to July 2019, a total of 512 HCC patients who underwent curative liver resection (LR) with microscopic vascular invasion (MVI) confirmed by histopathological examination were enrolled and divided into LR alone and PA-TACE groups. They were subsequently stratified into subgroups according to the presence of MPVI. Recurrence-free survival (RFS) and overall survival (OS) were compared using Kaplan–Meier curves and the log-rank test. The efficacy of PA-TACE was tested using univariate and multivariate Cox regression analyses. Sensitivity analysis was conducted after propensity score matching (PSM).

Results: Among all patients, 165 (32.3%) patients underwent PA-TACE, and 196 (38.2%) patients presented MPVI. In the entire cohort, PA-TACE and the presence of MPVI were identified as independent predictors for RFS and OS (all $p<0.05$). In the subgroup analysis, patients without MPVI who received PA-TACE had significantly better outcomes than those who underwent LR alone before and after PSM (all $p<0.05$). For patients with MPVI, PA-TACE displayed no significant benefit in terms of improving either RFS or OS, which was consistent with the results from the PSM cohort.

Conclusion: Among the HCC patients without MPVI who underwent curative liver resection, those who received PA-TACE had better RFS and OS outcomes than those who underwent LR alone. For patients with MPVI, PA-TACE had no significant effect on either RFS or OS outcomes.

Keywords: Hepatocellular carcinoma, microvascular invasion, microscopic portal vein invasion, prognostic factor, adjuvant treatment

Abbreviations: HCC, Hepatocellular carcinoma; LR, liver resection; PA-TACE, postoperative adjuvant transcatheter arterial chemoembolization; MVI, microscopic vascular invasion; OS, overall survival; MPVI, microscopic portal vein invasion; MI, microvessel invasion; RFS, recurrence-free survival; PSM, propensity score matching.

OPEN ACCESS

Edited by:
Qi Liu,
Fudan University, China

Reviewed by:
Kwangyeol Paik,
Catholic University of Korea, South Korea
Tommaso Stecca,
ULSS2 Marca Trevigiana, Italy
Kazushi Numata,
Yokohama City University Medical Center, Japan

***Correspondence:**
Wentao Wang
wwtdoctor02@163.com

Specialty section:
This article was submitted to Surgical Oncology, a section of the journal Frontiers in Oncology

Received: *08 December 2021*
Accepted: *24 May 2022*
Published: *20 June 2022*

Citation:
Qiu Y, Yang Y, Wang T, Shen S and Wang W (2022) Efficacy of Postoperative Adjuvant Transcatheter Arterial Chemoembolization in Hepatocellular Carcinoma Patients With Microscopic Portal Vein Invasion. Front. Oncol. 12:831614. doi: 10.3389/fonc.2022.831614

INTRODUCTION

Primary liver cancer is the sixth most commonly diagnosed cancer and the third leading cause of cancer-related death worldwide, ranking fifth in terms of global incidence and second in terms of mortality for men (1). The most prevalent type of primary liver cancer is hepatocellular carcinoma (HCC), which comprises 75%-85% of all cases (2). In most regions with a high incidence of HCC, represented by eastern China, one of the key determinants is chronic HBV infection (3). The optimal therapeutics for early-stage HCC remains to be curative liver resection (LR) and liver transplantation in most instances (4). Unfortunately, it has a 5-year recurrence rate of over 50%, significantly increasing tumor-related mortality (5, 6). Thus, adjuvant therapies such as postoperative adjuvant transcatheter arterial chemoembolization (PA-TACE), kinase inhibitors and immune checkpoint inhibitors have been explored in many trials and are now utilized to improve the outcomes of liver resection (7, 8).

It is important to discover strong predictors of postoperative outcomes so that the proper population can be selected for adjuvant therapy to prevent recurrence (9). Microscopic vascular invasion (MVI), characterized as cancer cells invading the microscopic vessels in the peritumor liver parenchyma, has been perceived as a strong predictor for tumor recurrence and unsatisfactory overall survival (OS) among patients with HCC postoperatively (10). However, due to the various definitions and descriptions of MVI in different studies, the actual effect of MVI on the prognosis of HCC patients, particularly during the early stage, remains unclear and debated (11). A recent study suggested that MVI should be additionally segregated into microscopic vessel invasion (MI, defined as newly developed microscopic vascular structures in the peritumor liver parenchyma; microvessels have no obvious features of portal or hepatic vein or hepatic artery) and microscopic portal vein invasion (MPVI). The subclassification of MVI significantly affects the prognosis of HCC after liver resection (12) and can guide the selection of appropriate recipients for PA-TACE.

A variety of strategies employing PA-TACE have been proposed over the years, aiming to reduce recurrence after curative hepatectomy. Generally, PA-TACE is recommended for HCC patients at high recurrent risk (e.g., those have MVI, multiple lesions or gross vascular invasion) (13–15). An overall oncologic benefit of PA-TACE has been observed in selected patients (16). However, multiple studies have provided various and often conflicting results on the potency of PA-TACE in different patient populations (17). Regarding post-hepatectomy patients with MVI, the benefits of PA-TACE remain controversial (18). Therefore, it is necessary to explore which patients receive benefits from PA-TACE based on MVI subclassification.

In the present study, we explored the benefit of PA-TACE based on MVI subclassification. The outcomes of PA-TACE were evaluated in a large cohort of HCC patients who underwent curative LR and were stratified by the presence of MPVI using propensity score matching (PSM).

METHODS

Patients

This study was approved by the Ethics Committee of West China Hospital of Sichuan University (No. 2019-788) and was conducted in accordance with the Declaration of Helsinki. From April 2014 to July 2019, in West China Hospital, we studied the patient population with the following features in the present retrospective study. The inclusion criteria including 1) patients who underwent R0 liver resection confirmed at histopathological examination for early- or intermediate-stage HCC; 2) HCC confirmed by postoperative histopathological examination with MVI (i.e. microscopic tumor cells detected in the portal or hepatic vein of the surrounding liver parenchyma) (19); and 3) TACE as the only adjuvant treatment. The following were the exclusion criteria: 1) patients who received additional treatment (such as TACE, radiotherapy and sorafenib treatment) prior to curative LR; 2) with other synchronous malignancies or remote or lymph node metastasis; 3) with cardiopulmonary, renal, or cerebral dysfunction before LR; 4) with early recurrence within 1 month; and 5) loss to follow-up within 2 months after discharge. The patient selection flowchart is displayed in **Figure 1**.

Treatment

Following necessary preoperative examination, all patients initially underwent curative LR. postoperative histopathological examination confirmed a negative resection margin, and no detectable tumors were found by imaging examination in the remanent liver. Patient baseline data and other intraoperative parameters were collected. We recommended all patients to received PA-TACE at 1-3 months after the operation when their liver function reached the standard: Child-Pugh class A/B, with a serum bilirubin level 1.5 times the normal upper limit, alanine aminotransferase (ALT) and aspartate aminotransferase (AST) levels two times the normal upper limit. During PA-TACE, liver angiography and CT angiography was conducted to reveal any possible recurrence in the residual liver. Simultaneously, if no recurrence was found, an arterial catheter was inserted through the femoral artery using the Seldinger technique. We inserted the catheter into right or left hepatic artery. Through the catheter, we injected chemotherapeutic agents doxorubicin (20~30 mg/m^2) or pharmorubicin (20~40 mg/m^2) and lipiodol (3~5 mL). The dosage of lipiodol and doxorubicin was determined by body surface area and underlying liver function.

Subclassification of MVI

MVI was subclassified as follows (12): 1) microvessel invasion (MI), 2) microscopic portal vein invasion (MPVI), 3) microscopic hepatic vein invasion (MHVI), or 4) microscopic hepatic artery invasion (MHAI). Microvessels were prescribed as microscopic vascular structures resulting from angiogenesis in the tumor capsule or peritumor normal liver parenchyma; these microvessels have no obvious features of portal or hepatic vein or

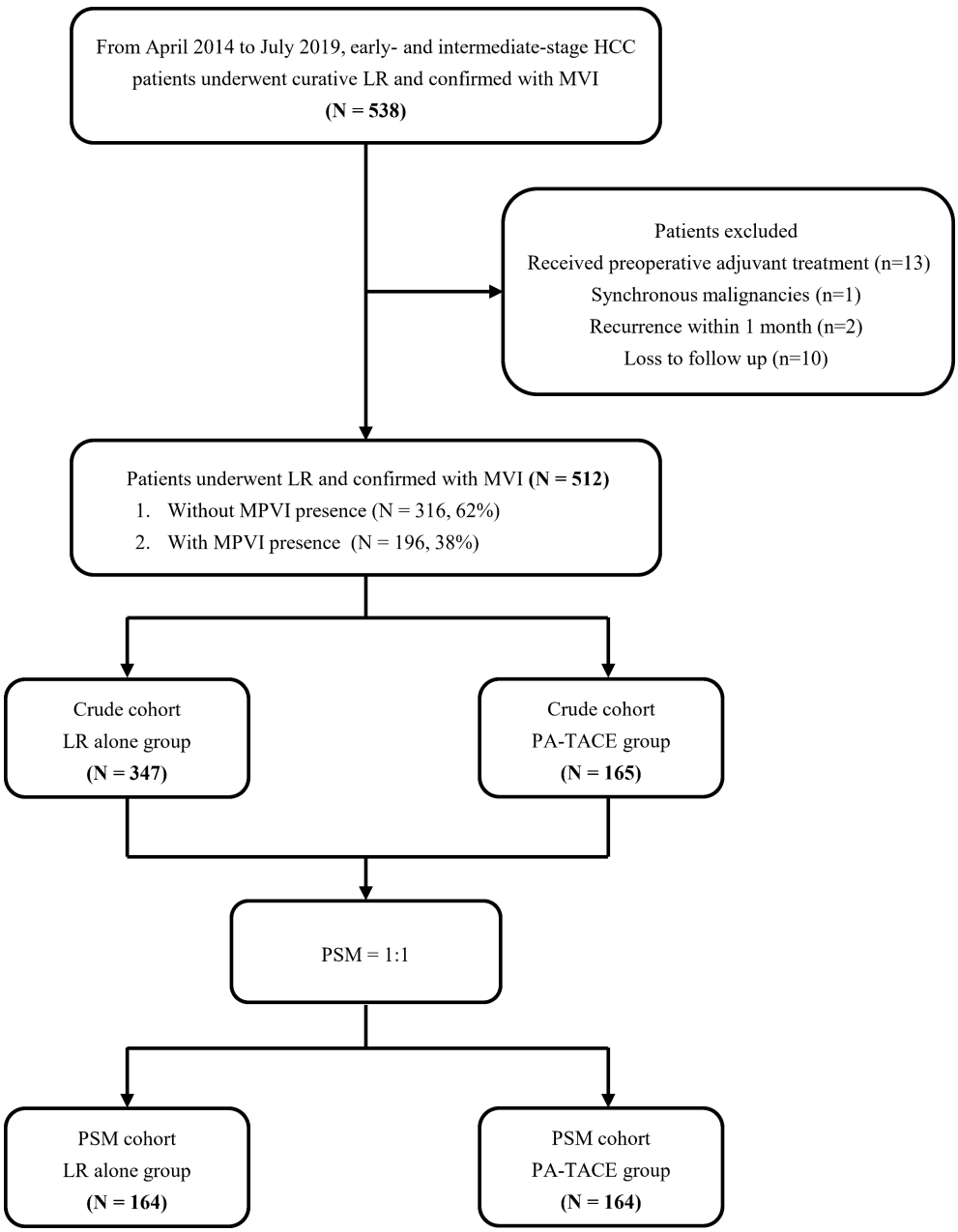

FIGURE 1 | Diagram of patient selection.

hepatic artery. In this study, MVI was subcategorized into a) without MPVI and b) with MPVI. Moreover, other pathological manifestations, including differentiation of tumor cells, microsatellites, and cirrhosis of liver parenchyma, were also recorded.

Follow-Up

In the first 2 years, the patients returned for follow-up visit every 2 months and received liver function assessments, tumor markers, and abdominal ultrasounds every time. All patients were followed up once every 3 months from the third year onward. We performed contrast-enhanced computed tomography (CT) or magnetic resonance imaging (MRI) at an 6-months interval or when recurrence/metastasis was suspected. Patients with CT or MRI images showing rapid tumor staining in the arterial phase that disappeared in the early venous phase combined with an increase in the serum AFP level were determined as recurrence. The main endpoint of the study was overall survival (OS, defined as the period between discharge and death), while recurrence-free survival (RFS, calculated from the

date of surgery to the date when recurrence and/or metastasis was confirmed) was the secondary endpoint.

Statistical Analysis

Parametric continuous data are expressed as the mean ± standard deviation (SD), and nonparametric data are expressed as the medians and interquartile ranges (Q1–Q3). Categorical data are expressed as numbers and percentages. Continuous variables were compared by Student's t test or the Mann–Whitney U test. Categorical variables were evaluated using the $\chi 2$ test or Fisher's exact test, as appropriate. Kaplan–Meier curves and the log-rank test were used to analyze DFS and OS. PA-TACE efficacy based on the MVI subclassification subgroups was assessed by Cox proportional hazards regression models. Propensity score matching (PSM) was used to reduce the differences in baseline characteristics. Variables that were not balanced in the LR alone group and PA-TACE group were entered into the propensity model with the use of a 1:1 matching protocol without replacement, with a caliper width equal to 0.02 of the SD of the logit of the propensity score. Kaplan–Meier curves and Cox regression analysis were conducted as sensitivity analyses for both the crude and PSM cohorts.

A 2-tailed P value<0.05 was considered to be statistically significant in all analyses. Empower (R) (www.empowerstats.com; X&Y solutions, Inc., Boston MA) was used for all statistical analyses.

RESULTS

Baseline and Clinicopathological Data of Patients

We enrolled 512 patients in this study, with 165 patients received PA-TACE. No serious adverse reactions occured. As displayed in **Table 1**, the BMI of patients who underwent LR alone was significantly lower than that of the PA-TACE group (22.5 ± 3.0 vs. 23.4 ± 2.9, p=0.010). Regarding perioperative data, the patients in the LR group had more blood loss (300 (10–7000) ml vs. 300 (15–5500) ml, p=0.003), more frequently required blood transfusion (10.4% vs. 3.6%, p=0.009) and more frequently had MPVI (42.4% vs. 29.7%, p=0.006) than patients in the PA-TACE group (**Table 2**). PSM process selected 164 pairs of patients who did and did not received PA-TACE with no significantly different variables between the two groups. The

TABLE 1 | Baseline data of all patients stratified by treatment.

Variables	Crude cohort			PSM cohort		
	LR (n = 347)	PA-TACE (n = 165)	P value	LR (n = 164)	PA-TACE (n = 164)	P value
Age, y	52 ± 11	50 ± 12	0.565	52 ± 12	51 ± 12	0.214
BMI, kg/m^2	22.6 ± 3.0	23.4 ± 2.9	0.010	22.8 ± 2.8	23.3 ± 2.8	0.137
Diameter, cm	4.9 ± 2.9	4.8 ± 2.9	0.531	5.0 ± 2.9	4.7 ± 2.9	0.278
PLT, ×10^9/L	161.8 ± 81.7	159.6 ± 83.3	0.649	145.0 (31.0-454.0)	138.0 (42.0-610.0)	0.807
ALT, U/L	49.7 ± 44.6	49.7 ± 57.2	0.598	37.0 (11.0-342.0)	35.0 (10.0-629.0)	0.991
TBIL, μmol/L	15.5 ± 16.1	15.9 ± 9.8	0.424	14.5 (2.4-44.6)	13.6 (3.5-100.0)	0.859
ALB, g/L	42.0 ± 4.4	41.9 ± 3.6	0.756	41.8 (27.1-52.4)	41.9 (28.9-55.3)	0.977
INR	1.1 ± 0.1	1.1 ± 0.1	0.991	1.0 (0.8-1.4)	1.0 (0.9-1.4)	0.913
Sex			0.255			0.261
male	305 (87.9%)	139 (84.2%)		145 (88.4%)	138 (84.1%)	
female	42 (12.1%)	26 (15.8%)		19 (11.6%)	26 (15.9%)	
Alcohol consumption			0.568			0.310
no	209 (60.2%)	95 (57.6%)		103 (62.8%)	94 (57.3%)	
yes	138 (39.8%)	70 (42.4%)		61 (37.2%)	70 (42.7%)	
Hypertension			0.422			0.592
no	305 (87.9%)	149 (90.3%)		145 (88.4%)	148 (90.2%)	
yes	42 (12.1%)	16 (9.7%)		19 (11.6%)	16 (9.8%)	
Diabetes			0.67			0.792
no	327 (94.2%)	157 (95.2%)		157 (95.7%)	156 (95.1%)	
yes	20 (5.8%)	8 (4.8%)		7 (4.3%)	8 (4.9%)	
HBsAg			0.683			0.884
negative	56 (16.1%)	29 (17.6%)		28 (17.1%)	29 (17.7%)	
positive	291 (83.9%)	136 (82.4%)		136 (82.9%)	135 (82.3%)	
AFP, ng/mL			0.054			0.054
≥400	208 (59.9%)	84 (50.9%)		102 (62.2%)	84 (51.2%)	
<400	139 (40.1%)	81 (49.1%)		62 (37.8%)	80 (48.8%)	
Number of tumors			0.092			0.273
single	231 (66.6%)	122 (73.9%)		112 (68.3%)	121 (73.8%)	
multiple	116 (33.4%)	43 (26.1%)		52 (31.7%)	43 (26.2%)	
Child–Pugh classification			0.835			1.000
A	342 (98.6%)	163 (98.8%)		162 (98.8%)	162 (98.8%)	
B	5 (1.4%)	2 (1.2%)		2 (1.2%)	2 (1.2%)	

PSM, propensity score matching; PA-TACE, postoperative adjuvant transhepatic arterial chemoembolization; TBIL, total bilirubin; TP, total protein; ALB, albumin; ALT, alanine aminotransferase; AFP, alpha-fetoprotein; PLT, platelets; INR, international normalized ratio; HBsAg, hepatitis B surface antigen.

TABLE 2 | Surgical and pathological data of all patients stratified by treatment.

Variables	Crude cohort			PSM cohort		
	LR (n=347)	PA-TACE (n = 165)	P value	LR (n = 165)	PA-TACE (n = 165)	P value
Blood loss, mL	300 (10-7000)	300 (15-5500)	0.003	300 (10-6000)	275 (15-5500)	0.110
Operation time, min	230 (50-555)	240 (60-430)	0.984	228 (100-505)	240 (60-430)	0.897
Approach of resection			0.150			0.897
Nonanatomical	189 (54.5%)	101 (61.2%)		98 (59.8%)	100 (61.0%)	
Anatomical	158 (45.5%)	64 (38.8%)		66 (40.2%)	64 (39.0%)	
Pringle maneuver			0.693			0.741
no	44 (12.7%)	23 (13.9%)		20 (12.2%)	22 (13.4%)	
yes	303 (87.3%)	142 (86.1%)		144 (87.8%)	142 (86.6%)	
Blood transfusion			0.009			0.777
no	311 (89.6%)	159 (96.4%)		157 (95.7%)	158 (96.3%)	
yes	36 (10.4%)	6 (3.6%)		7 (4.3%)	6 (3.7%)	
Differentiation			0.670			0.910
grades I-II	132 (38.0%)	66 (40.0%)		66 (40.2%)	65 (39.6%)	
grades III-IV	215 (62.0%)	99 (60.0%)		98 (59.8%)	99 (60.4%)	
Microsatellites			0.195			1.000
no	285 (82.1%)	143 (86.7%)		142 (86.6%)	142 (86.6%)	
yes	62 (17.9%)	22 (13.3%)		22 (13.4%)	22 (13.4%)	
MPVI			0.006			0.476
no	200 (57.6%)	116 (70.3%)		109 (66.5%)	115 (70.1%)	
yes	147 (42.4%)	49 (29.7%)		55 (33.5%)	49 (29.9%)	
Cirrhosis			0.548			0.377
no	176 (50.7%)	79 (47.9%)		86 (52.4%)	78 (47.6%)	
yes	171 (49.3%)	86 (52.1%)		78 (47.6%)	86 (52.4%)	

PSM, propensity score matching; PA-TACE, postoperative adjuvant transhepatic arterial chemoembolization; MPVI, microportal vein invasion.

median follow-up time was 26 (3-60) months for the crude cohort and 27 (3-60) months for the PSM cohort. The median interval between surgery and PA-TACE was 42 (28-97) days.

According to the postoperative histopathological examination, 42.4% (147/347) of the HCC patients who underwent LR alone presented MPVI versus 29.7% (49/165) of those who received PA-TACE. This difference in the incidence of MPVI was significant (p=0.006). The other pathological parameters showed no significant differences between the groups.

Overall Effect of PA-TACE on the RFS and OS Outcomes of HCC Patients With MVI

In the PSM cohort, the median RFS time for patients who underwent LR alone was shorter than that for patients who received PA-TACE (8.7 vs. 19.0 months, p=0.0032, **Figure 2A**).

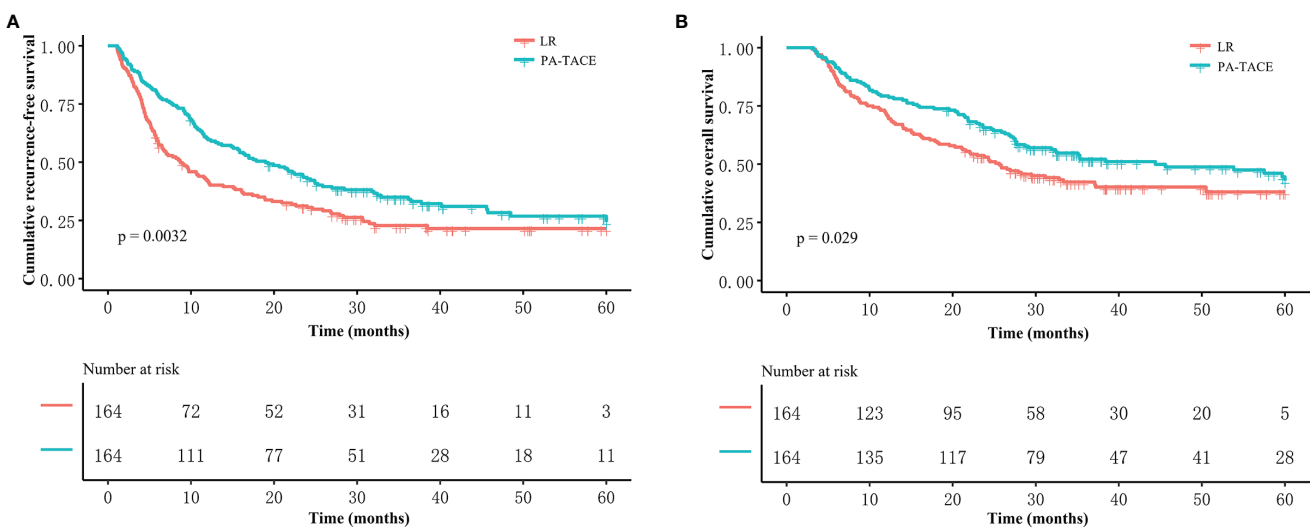

FIGURE 2 | Kaplan–Meier analysis of RFS and OS stratified by treatment in the PSM cohort. Patients who received PA-TACE had better RFS **(A)** and OS **(B)** than those who underwent liver resection alone.

The median OS time of the HCC patients with MVI was 24.6 months for the LR alone group and 44.4 months for the PA-TACE group. The OS of PA-TACE group was significantly superior to that for the LR alone group (1-, 3-, 5-year rates, 79.3%, 52.1%, 42.9% vs. 71.3%, 42.3%, 38.0%, p=0.029) in the PSM cohort (**Figure 2B**).

Univariate and multivariate regression analyses (**Table 3**) suggested that PA-TACE (HR 0.720, 95% CI 0.554-0.935, p= 0.014) and the presence of MPVI (HR 1.543, 95% CI 1.175-2.027, p=0.002) were independent predictors for RFS. Regarding OS, PA-TACE (HR 0.744, 95% CI 0.551-0.973, p= 0.041) and the presence of MPVI (HR 1.675, 95% CI 1.235-2.272, p=0.001) were also identified as independent predictors. The correlated results of the crude cohort were reported in **Supplementary File**, **Figure S1** and **Table S1**.

Effect of PA-TACE on RFS and OS Outcomes Based on the Subclassification of MVI

In the PSM cohort, among patients without MPVI, the RFS of the PA-TACE group was significantly better than that of the LR group (median RFS, 21.7 vs. 10.9 months; 1-, 3-, and 5-year rates, 67%, 38.1%, and 29.3% vs. 46.5%, 27.4%, and 25.5%, p=0.021, **Figure 3A**). Similarly, the OS of the PA-TACE group was significantly better than that of the LR group in patients without MPVI (median OS, 57.5 vs. 29.5 months; 1-, 3-, 5-year rates, 82.6%, 58.8%, 49.6% vs. 75.2%, 48.1%, 44.6%, p=0.039, **Figure 3C**). Moreover, univariate and multivariate regression analysis (**Table 4**) suggested that PA-TACE was a significant protective factor for both RFS (HR 0.726, 95% CI 0.475-0.986, p=0.043) and OS (HR 0.691, 95% CI 0.500-0.955, p=0.025). The correlated results of the crude cohort were reported in **Supplementary File**, **Figure S2A, C** and **Table S2**.

On the other hand, the RFS and OS of HCC patients with MPVI showed no significant differences between the PA-TACE and LR alone groups in both log-rank test (median RFS, 10.4 vs. 6.5 months, p=0.13; median OS, 27.3 vs. 17.9 months, p=0.26; **Figures 3B, D**) and regression analysis (RFS, 0.131; OS, p=0.266; **Table 5**). The correlated results of the crude cohort were reported in **Supplementary File**, **Figure S2B, D** and **Table S3**.

The Kaplan–Meier curves, RFS and OS stratified by treatment and the presence or absence of MPVI are displayed in **Figure 4** and **Table 6**. In a word, the RFS and OS remained better for the PA-TACE group than for the LR alone group in HCC patients without MPVI, which was not observed in HCC patients with the presence of MPVI.

DISCUSSION

To the best of our knowledge, this study is the first to analyze the effect of PA-TACE on RFS and OS outcomes among HCC

TABLE 3 | Univariate and multivariate analysis for RFS and OS in HCC patients with MVI in the PSM cohort.

Variables	RFS				OS			
	Univariate		Multivariate		Univariate		Multivariate	
	HR (95% CI)	p value	HR (95% CI)	p value	HR (95% CI)	p value	HR (95% CI)	p value
SEX, male	0.787 (0.536,1.156)	0.222			1.038 (0.685, 1.575)	0.859		
Age, y	**0.987 (0.976,0.999)**	**0.030**	**0.985 (0.974,0.997)**	**0.011**	0.991 (0.978, 1.004)	0.160		
BMI, kg/m^2	1.013 (0.968,1.060)	0.567			1.007 (0.956, 1.061)	0.785		
Alcohol consumption, yes	1.216 (0.937,1.577)	0.141			1.062 (0.785, 1.436)	0.695		
Hypertension, yes	0.676 (0.427,1.069)	0.094			0.635 (0.361, 1.117)	0.115		
Diabetes, yes	**0.415 (0.185,0.935)**	**0.034**	0.529 (0.233,1.202)	0.128	0.511 (0.210, 1.243)	0.139		
HBsAg, positive	1.408 (0.986,2.010)	0.060			**1.654 (1.067, 2.564)**	**0.025**	**1.714 (1.104, 2.662)**	**0.016**
AFP, <400 ng/mL	**0.715 (0.550,0.929)**	**0.012**	**0.741 (0.566,0.970)**	**0.029**	**0.734 (0.542, 0.995)**	**0.046**	0.762 (0.562, 1.034)	0.081
Diameter, cm	1.000 (0.955,1.046)	0.987			1.006 (0.957, 1.058)	0.807		
Number of tumors, multiple	**1.783 (1.360,2.338)**	**<0.001**	**1.473 (1.110,1.953)**	**0.007**	**1.588 (1.164, 2.164)**	**0.003**	1.281 (0.923, 1.777)	0.138
PLT, ×10^9/L	0.999 (0.998,1.001)	0.535			1.000 (0.998, 1.002)	0.769		
ALT, U/L	1.000 (0.998,1.003)	0.831			1.000 (0.997, 1.003)	0.558		
TBIL, μmol/L	1.013 (0.996,1.029)	0.129			1.011 (0.992, 1.030)	0.919		
ALB, g/L	1.000 (0.970,1.032)	0.985			0.990 (0.956, 1.025)	0.557		
INR	0.820 (0.195,3.445)	0.787			0.506 (0.095, 2.692)	0.424		
Child–Pugh classification, B	1.304 (0.484,3.510)	0.600			2.091 (0.775, 5.643)	0.145		
Approach of resection, anatomical	1.092 (0.841,1.418)	0.509			1.293 (0.961, 1.741)	0.090		
Pringle maneuver, yes	0.760 (0.530,1.090)	0.136			0.883 (0.582, 1.340)	0.559		
Blood loss, mL	1.000 (1.000,1.000)	0.375			1.000 (1.000, 1.000)	0.110		
Blood transfusion, yes	1.409 (0.768,2.582)	0.268			1.750 (0.924, 3.313)	0.086		
Operation time, min	1.001 (1.000,1.003)	0.086			1.001 (0.999, 1.003)	0.338		
PA-TACE, yes	**0.681 (0.527,0.881)**	**0.003**	**0.720 (0.554,0.935)**	**0.014**	**0.719 (0.534, 0.967)**	**0.029**	**0.744 (0.551, 0.973)**	**0.041**
Differentiation, grades 3-4	1.150 (0.883,1.497)	0.301			1.055 (0.780, 1.429)	0.727		
Microsatellites, yes	**1.782 (1.257,2.527)**	**0.001**	1.542 (1.070,2.222)	0.020	**1.814 (1.234, 2.667)**	**0.002**	**1.613 (1.077, 2.415)**	**0.020**
MPVI, yes	**1.621 (1.239,2.121)**	**<0.001**	**1.543 (1.175,2.027)**	**0.002**	**1.705 (1.261, 2.306)**	**0.001**	**1.675 (1.235, 2.272)**	**0.001**
Cirrhosis, yes	1.088 (0.842,1.406)	0.51772			0.970 (0.722, 1.302)	0.837		

RFS, recurrence free survival; OS, overall survival; HCC, hepatocellular carcinoma; PSM, propensity score matching; BMI, body mass index; HBsAg: hepatitis B surface antigen; AFP, alpha-fetoprotein; TBIL, total bilirubin; TP, total protein; ALB, albumin; ALT, alanine aminotransferase; PLT, platelets; INR, international normalized ratio; PA-TACE, postoperative adjuvant transhepatic arterial chemoembolization; MPVI, microportal vein invasion.

Bold values, statistical significant.

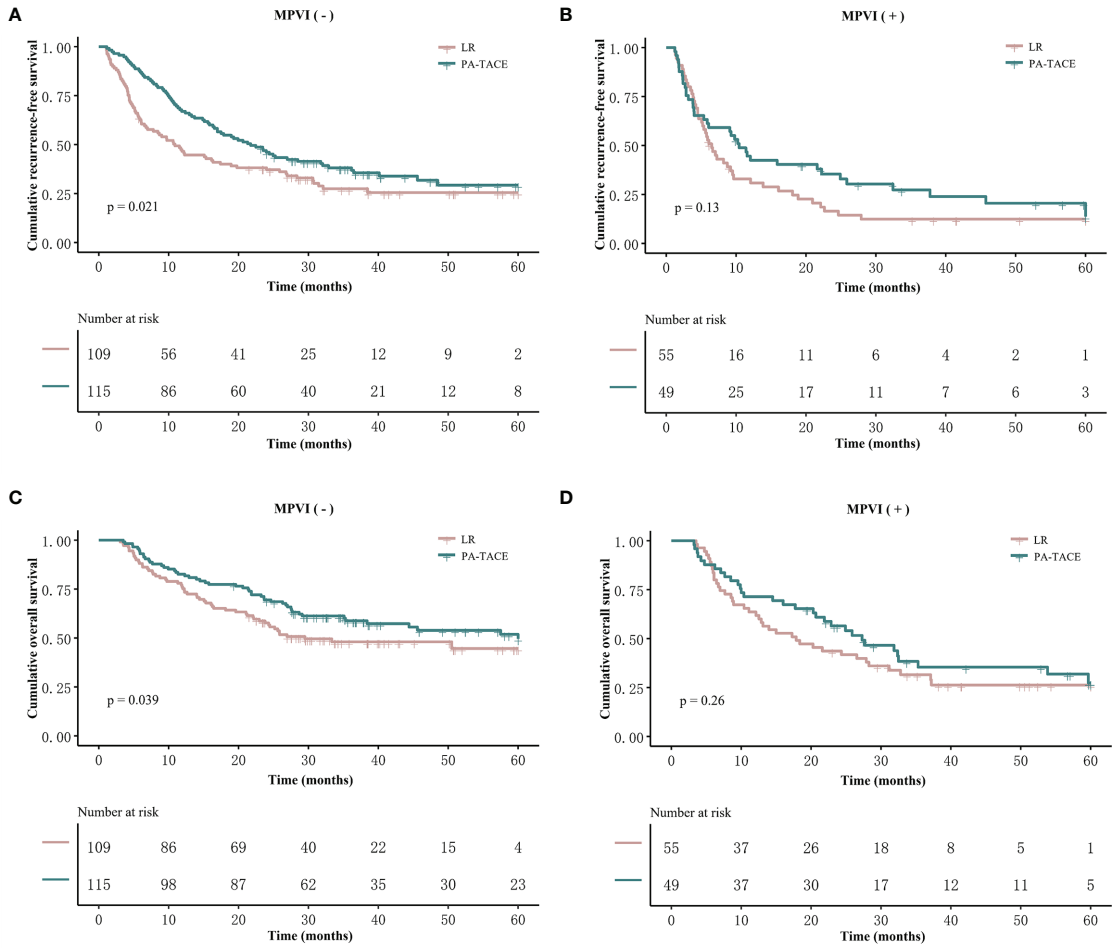

FIGURE 3 | Kaplan–Meier analysis of RFS and OS stratified by treatment and the presence or absence of MPVI in the PSM cohort. Patients without MPVI who received PA-TACE had better RFS **(A)** and OS **(C)** than those who underwent liver resection alone. The RFS **(B)** and OS **(D)** of patients with MPVI showed no significant differences between the PA-TACE and LR alone groups.

patients without or without MPVI. In the entire cohort, PA-TACE displayed consistent benefits in terms of improvements in RFS and OS outcomes both before and after PSM, which was subsequently confirmed in the subgroup analysis of HCC patients without MPVI. Intriguingly, this beneficial effect of PA-TACE in terms of improving RFS and OS was not observed in the subgroup of HCC patients with MPVI. The subclassification of patients based on MVI status (presence or absence) was also identified as an independent risk factor for HCC patients with MVI. These findings provide new information that can help identify suitable patient candidates for PA-TACE and guide clinical decisions.

MVI is a histopathological feature with an incidence of 15% to 74.4% (20, 21) and is routinely assessed in all patients who undergo liver resection. Despite the controversy regarding population selection, the predictive capability of MVI has been widely acknowledged and applied. Several studies have reported that MVI is significantly related to poor prognosis in patients with solitary HCC tumors ≤2 cm in size and stage II (based on TNM stage) disease (22–24). Recent studies have attempted to promote the application of MVI by further subclassification according to the number of tumor cells and infiltrated vessels, the distance of infiltrated vessels to the margin of the lesion, and the type of infiltrated vessels (25–29). For example, in the Practice Guidelines for the Pathological Diagnosis of Primary Liver Cancer developed by China (25), MVI is evaluated based on the number and distribution of invaded vessels as follows: 1) no MVI; 2) M1: <5 MVI and ≤1 cm away from tumor tissues; 3) M2: >5 MVI or >1 cm away from tumor tissues. However, the existing MVI classification uses parameters that are difficult to evaluate and generalize in routine clinical-pathological settings, which further complicates validation (30).

Discussion over the subtypes of MVI is not a new topic; in 2009, Shirabe et al. reported that the presence of MPVI is a poor prognostic factor in patients with HCC, and anatomical resection is recommended for these patients (30). Similar results were proposed by Fujita et al. in 2011 (29). Both studies subsequently classified patients with MPVI into high-risk (≥2 invaded vessels)

TABLE 4 | Univariate and multivariate analysis for RFS and OS in HCC patients without MPVI in the PSM cohort.

Variables	RFS				OS			
	Univariate		Multivariate		Univariate		Multivariate	
	HR (95% CI)	p value	HR (95% CI)	p value	HR (95% CI)	p value	HR (95% CI)	p value
SEX, male	1.218 (0.725, 2.045)	0.456			0.824 (0.509, 1.333)	0.431		
Age, y	**0.982 (0.966, 0.998)**	**0.031**	**0.980 (0.963, 0.997)**	**0.018**	**0.982 (0.968, 0.996)**	**0.012**	**0.980 (0.967, 0.994)**	**0.005**
BMI, kg/m2	1.007 (0.940, 1.079)	0.840			1.009 (0.952, 1.069)	0.766		
Alcohol consumption, yes	0.975 (0.659, 1.444)	0.900			1.322 (0.957, 1.827)	0.090		
Hypertension, yes	**0.449 (0.208, 0.966)**	**0.040**	0.889 (0.595, 1.329)	0.567	0.653 (0.383, 1.113)	0.117		
Diabetes, yes	0.434 (0.138, 1.369)	0.154			0.470 (0.192, 1.147)	0.097		
HBsAg, positive	**1.844 (1.011, 3.362)**	**0.046**	**2.192 (1.146, 4.190)**	**0.018**	1.410 (0.897, 2.217)	0.137		
AFP, <400 ng/mL	0.727 (0.491, 1.075)	0.110			1.000 (1.000, 1.000)	0.420		
Diameter, cm	0.956 (0.888, 1.029)	0.229			0.979 (0.921, 1.040)	0.494		
Number of tumors, multiple	**1.830 (1.224, 2.736)**	**0.003**	**1.563 (1.012, 2.414)**	**0.044**	**1.985 (1.406, 2.802)**	**<0.001**	**1.814 (1.268, 2.597)**	**0.001**
PLT, ×109/L	1.000 (0.997, 1.002)	0.709			0.999 (0.997, 1.001)	0.348		
ALT, U/L	1.001 (0.998, 1.004)	0.552			1.001 (0.999, 1.004)	0.326		
TBIL, μmol/L	0.988 (0.959, 1.017)	0.402			0.996 (0.973, 1.020)	0.760		
ALB, g/L	0.986 (0.944, 1.031)	0.547			1.005 (0.967, 1.044)	0.812		
INR	0.718 (0.085, 6.063)	0.761			0.603 (0.101, 3.590)	0.579		
Child–Pugh classification, B	**3.580 (1.133, 11.305)**	**0.030**	**4.522 (1.270, 16.107)**	**0.020**	2.024 (0.644, 6.363)	0.228		
Approach of resection, anatomical	1.283 (0.877, 1.878)	0.199			1.070 (0.775, 1.479)	0.681		
Pringle maneuver, yes	0.777 (0.450, 1.342)	0.366			0.869 (0.537, 1.405)	0.566		
Blood loss, mL	1.000 (1.000, 1.001)	0.717			1.000 (1.000, 1.000)	0.860		
Blood transfusion, yes	0.960 (0.237, 3.891)	0.955			0.976 (0.311, 3.062)	0.966		
Operation time, min	1.001 (0.999, 1.004)	0.296			1.001 (0.999, 1.003)	0.297		
PA-TACE, yes	**0.719 (0.491, 0.978)**	**0.032**	**0.726 (0.475, 0.986)**	**0.043**	**0.688 (0.500, 0.947)**	**0.022**	**0.691 (0.500, 0.955)**	**0.025**
Differentiation, grades 3-4	1.260 (0.850, 1.869)	0.249			1.336 (0.959, 1.860)	0.086		
Microsatellites, yes	**1.432 (0.828, 2.476)**	**0.199**	1.194 (0.671, 2.123)	0.546	**1.734 (1.101, 2.730)**	**0.017**	**1.388 (0.868, 2.222)**	**0.171**
Cirrhosis, yes	0.913 (0.625, 1.334)	0.638			1.088 (0.790, 1.498)	0.604		

RFS, recurrence free survival; OS, overall survival; HCC, hepatocellular carcinoma; PSM, propensity score matching; BMI, body mass index; HBsAg, hepatitis B surface antigen; AFP, alpha-fetoprotein; TBIL, total bilirubin; TP, total protein; ALB, albumin; ALT, alanine aminotransferase; PLT, platelets; INR, international normalized ratio; PA-TACE, postoperative adjuvant transhepatic arterial chemoembolization; MPVI, microportal vein invasion.
Bold values, statistical significant.

and low-risk (single invaded vessels), and the high-risk group displayed a worse prognosis than the low-risk group. Nevertheless, the subclassification of MVI in terms of the type of invaded vessels has not garnered much attention among the countless studies on the predictive capability of MVI. A recent multi-institutional study evaluated the value of anatomical resection in HCC patients with MPVI for the first time (31). Anatomical resection did not lead to any added benefit for RFS

TABLE 5 | Univariate analysis for RFS and OS of HCC patients with MPVI in the PSM cohort.

Variables	RFS		OS	
	HR (95% CI)	p value	HR (95% CI)	p value
SEX, male	0.690 (0.363, 1.310)	0.257	0.756 (0.375, 1.523)	0.434
Age, y	0.998 (0.978, 1.019)	0.877	1.004 (0.982, 1.026)	0.754
BMI, kg/m2	1.033 (0.962, 1.110)	0.368	1.015 (0.941, 1.095)	0.700
Alcohol consumption, yes	0.998 (0.642, 1.550)	0.993	1.189 (0.740, 1.912)	0.474
Hypertension, yes	1.054 (0.426, 2.610)	0.909	1.822 (0.784, 4.236)	0.163
Diabetes, yes	0.312 (0.043, 2.246)	0.248	0.957 (0.234, 3.917)	0.951
HBsAg, positive	1.587 (0.874, 2.881)	0.129	1.564 (0.818, 2.992)	0.176
AFP, <400 ng/mL	0.680 (0.438, 1.057)	0.087	0.725 (0.447, 1.174)	0.190
Diameter, cm	1.009 (0.942, 1.081)	0.799	1.050 (0.979, 1.127)	0.172
Number of tumors, multiple	1.295 (0.834, 2.012)	0.250	1.111 (0.683, 1.808)	0.671
PLT, ×109/L	1.000 (0.998, 1.003)	0.922	1.000 (0.997, 1.003)	0.933
ALT, U/L	0.996 (0.990, 1.003)	0.229	0.996 (0.989, 1.003)	0.254
TBIL, μmol/L	1.025 (1.005, 1.046)	0.013	**1.028 (1.004, 1.052)**	**0.020**
ALB, g/L	0.994 (0.944, 1.047)	0.822	0.992 (0.937, 1.050)	0.783
INR	1.315 (0.113, 15.273)	0.827	0.214 (0.013, 3.431)	0.276
Child–Pugh classification, B	0.547 (0.076, 3.961)	0.551	0.718 (0.099, 5.231)	0.744
Approach of resection, anatomical	1.255 (0.801, 1.965)	0.321	1.426 (0.886, 2.297)	0.144
Pringle maneuver, yes	0.767 (0.436, 1.352)	0.359	1.255 (0.653, 2.412)	0.496
Blood loss, mL	1.000 (1.000, 1.000)	0.920	1.000 (1.000, 1.000)	0.491
Blood transfusion, yes	1.315 (0.633, 2.733)	0.462	1.763 (0.843, 3.688)	0.132
Operation time, min	1.002 (0.999, 1.005)	0.172	1.000 (0.997, 1.003)	0.976
PA-TACE, yes	0.713 (0.460, 1.105)	0.131	0.763 (0.474, 1.229)	0.266
Differentiation, grades 3-4	0.813 (0.523, 1.266)	0.360	0.727 (0.451, 1.170)	0.189
Microsatellites, yes	1.691 (0.976, 2.930)	0.061	**2.279 (1.308, 3.971)**	**0.004**
Cirrhosis, yes	1.233 (0.800, 1.900)	0.342	1.217 (0.760, 1.949)	0.413

RFS, recurrence free survival; OS, overall survival; HCC, hepatocellular carcinoma; PSM, propensity score matching; BMI, body mass index; HBsAg, hepatitis B surface antigen; AFP, alpha-fetoprotein; TBIL, total bilirubin; TP, total protein; ALB, albumin; ALT, alanine aminotransferase; PLT, platelets; INR, international normalized ratio; PA-TACE, postoperative adjuvant transhepatic arterial chemoembolization; MPVI, microportal vein invasion.
Bold values, statistical significant.

and OS over nonanatomical resection in HCC patients who underwent curative LR and in all subgroup analyses, indicating that MPVI might be an unprecedented predictor for poor prognosis. Another study, by Kang et al., classified MVI into MI, MHVI and MPVI and reported that HCC patients with either MI or MPVI who underwent curative LR had poorer prognoses than those without MVI. The 5-year RFS rates were 75%, 45% and 25% in the no MVI, MI and MPVI groups, respectively, whereas the corresponding 5-year OS rates were 90%, 78%, and 55%, respectively (12). The potential for MPVI to be a strong predictor of HCC patient prognosis after curative hepatectomy warrants the further documentation of invaded vessels when MVI presents.

We conducted this study to clarify whether the high recurrence rate caused by MPVI can be reduced by PA-TACE. Unfortunately, PA-TACE did not lead to any significant improvement in the prognosis of HCC patients with MPVI. PA-TACE is used as a routine procedure to prevent recurrence in high-risk populations and has been reported to be significantly effective under various circumstances. Despite numerous retrospective studies presenting partially conflicting findings but overall benefit in terms of prognosis (18, 32), several randomized controlled studies have proven the efficacy of PA-TACE in selected patients (33–36), but concerns over the quality of the study design have been raised (17). Thus, the actual impact of PA-TACE on patient survival outcomes remains controversial, and an in-depth study is warranted to ensure that appropriate patient populations are selected for PA-TACE. To date, studies on HCC subpopulations that have huge tumors (≥10 cm) (37), exceed the Milan criteria (38), have multinodular tumors (39), have hepatic vein invasion (40) and have portal vein tumor thrombus (15) receive various degrees of benefit from PA-TACE. On the other hand, the negative finding reported in our study is a reminder to apply other therapies or combined modalities to mitigate the excessively high recurrence rate and improve OS outcomes in HCC patients with MPVI.

The MPVI-related poor prognosis might be explained as follows. The tumor tissue is fed mainly by the neovascular arterial vessels and drained through the peritumor portal vein (29). As a result, the spread of tumor cells *via* the portal vein has generally been recognized as the main mechanism for intrahepatic metastasis (41, 42). The tumor cells may disseminate to more distant and larger vessels through the portal venous system, which could hamper the curative effect of R0 hepatectomy with a general resection margin (1-2 cm). Wide and/or narrow surgical margins have been shown to be irrelevant to the prognosis of patients with MPVI (10). As a consequence, the increased burden of disseminated tumor cells may be the reason for the reduced benefit of PA-TACE.

Our study has some limitations. First, the retrospective design of this study inevitably introduced selection bias. Second, the study was conducted with a single-center cohort. The negative findings in HCC patients with MPVI should be interpreted with caution. The relatively low incidence of MPVI resulted in few HCC patients with MPVI receiving PA-TACE; that is, the

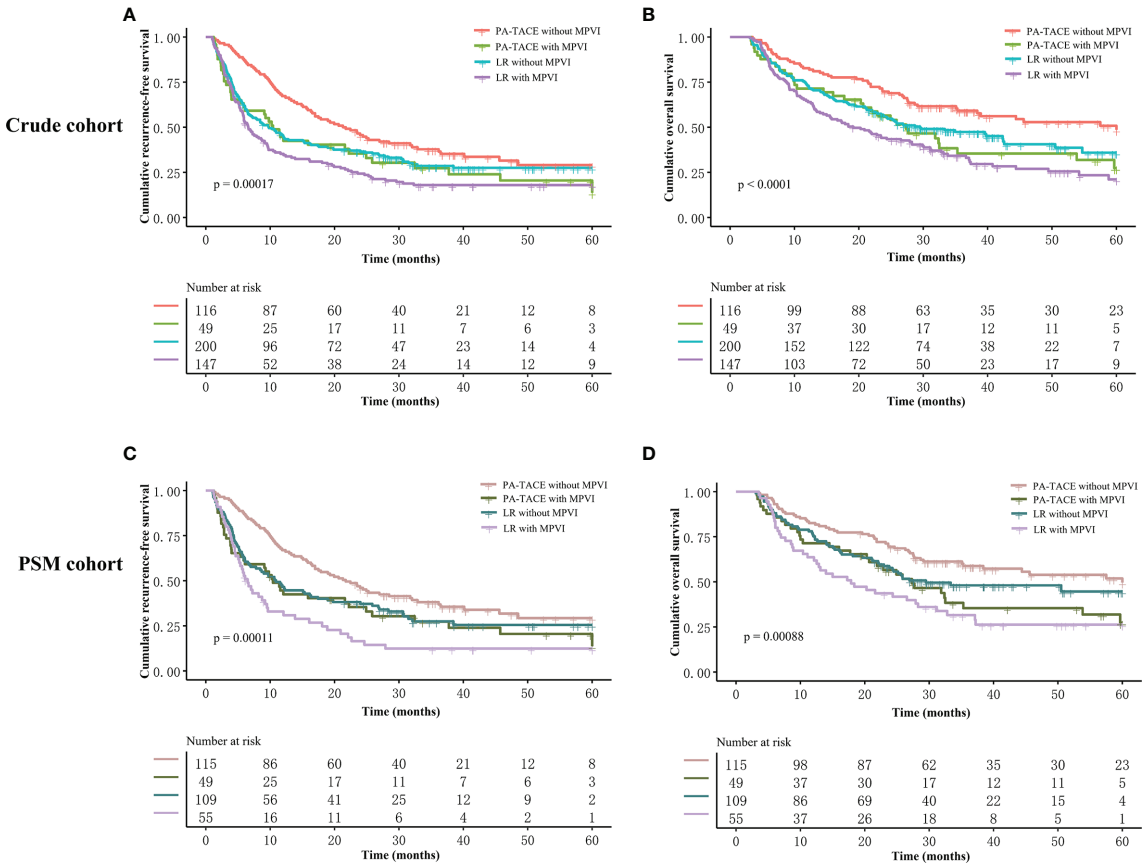

FIGURE 4 | Kaplan–Meier analysis of RFS and OS stratified by all subgroups before and after PSM. **(A)** RFS stratified by treatment and MPVI presence in crude cohort. **(B)** OS stratified by treatment and MPVI presence in crude cohort. **(C)** RFS stratified by treatment and MPVI presence in PSM cohort. **(D)** OS stratified by treatment and MPVI presence in PSM cohort.

TABLE 6 | recurrence-free survival and overall survival of HCC patients stratified by treatment before and after PSM.

RFS in crude cohort					
Stratification		**Median time**	**1-year rate**	**3-year rate**	**5-year rate**
Overall	LR alone	8.2	41.1%	24.1%	23.5%
	PA-TACE	18.9	60.5%	34.8%	26.7%
Without MPVI	LR alone	9.8	45.4%	28.6%	27.5%
	PA-TACE	21.5	67.2%	37.8%	29.1%
With MPVI	LR alone	6.6	35.3%	17.9%	17.9%
	PA-TACE	10.4	44.6%	27.3%	13.7%
OS in crude cohort					
Stratification		**Median time**	**1-year rate**	**3-year rate**	**5-year rate**
Overall	LR alone	24.5	69.5%	41.7%	28.8%
	PA-TACE	44.4	79.4%	52.4%	42.3%
Without MPVI	LR alone	29.5	73.0%	47.4%	35.9%
	PA-TACE	58.0	82.8%	59.2%	48.6%
With MPVI	LR alone	19.1	64.6%	34.2%	21.0%
	PA-TACE	27.3	71.4%	35.3%	27.3%
RFS in PSM cohort					
Stratification		**Median time**	**1-year rate**	**3-year rate**	**5-year rate**
Overall	LR alone	8.7	42.10%	22.80%	21.60%
	PA-TACE	19.0	60.30%	35.00%	24.40%
Without MPVI	LR alone	10.9	46.50%	27.40%	25.50%

(Continued)

TABLE 6 | Continued

RFS in crude cohort					
Stratification		**Median time**	**1-year rate**	**3-year rate**	**5-year rate**
	PA-TACE	21.7	67.00%	38.10%	29.30%
With MPVI	LR alone	6.5	32.90%	12.40%	12.40%
	PA-TACE	10.4	44.60%	27.30%	13.70%
OS in PSM cohort					
Stratification		**Median time**	**1-year rate**	**3-year rate**	**5-year rate**
Overall	LR alone	25.6	71.30%	42.30%	38.00%
	PA-TACE	44.4	79.30%	52.10%	42.90%
Without MPVI	LR alone	29.5	75.20%	48.10%	44.60%
	PA-TACE	57.5	82.60%	58.80%	49.60%
With MPVI	LR alone	17.9	63.60%	31.50%	26.30%
	PA-TACE	27.3	71.40%	35.40%	27.30%

HCC, hepatocellular carcinoma; PSM, propensity score matching; MPVI, microportal vein invasion.

efficacy of PA-TACE on HCC patients with MPVI was not sufficiently observed or evaluated. The findings in this study should not be used as justification for the complete refusal to perform PA-TACE for HCC patients with MPVI. Nevertheless, our study illustrates the need to document the subtypes of MVI. Further prospective studies are needed to explore the efficacy of PA-TACE in larger numbers of HCC patients with MPVI. A well-designed randomized controlled study is warranted to validate the impact of PA-TACE based on MVI subclassification.

CONCLUSION

In conclusion, among HCC patients who underwent curative liver resection without MPVI, those who received PA-TACE had better RFS and OS outcomes than those who underwent LR alone. For patients with MPVI, PA-TACE did not significantly improve either RFS or OS.

DATA AVAILABILITY STATEMENT

The raw data supporting the conclusions of this article will be made available by the authors, without undue reservation.

ETHICS STATEMENT

The studies involving human participants were reviewed and approved by the Ethics Committee of West China Hospital of Sichuan University. Written informed consent for participation was not required for this study in accordance with the national legislation and the institutional requirements.

AUTHOR CONTRIBUTIONS

YQ and WW participated in the research design. YQ participated in the writing of the paper. YQ, TW, and SS participated in the performance of the research. YQ and YY participated in the data analysis. All authors contributed to the article and approved the submitted version.

FUNDING

This research was supported by the Science and Technology Program of Sichuan Science and Technology Department (Nos. 2019YFS0029, 2019YFS0529), the National Natural Science Foundation of China (Nos. 81770566, 82000599) and the New Medical Technology Foundation of West China Hospital of Sichuan University (No. XJS2016004). The corresponding author WW is the guarantor.

SUPPLEMENTARY MATERIAL

The Supplementary Material for this article can be found online at: https://www.frontiersin.org/articles/10.3389/fonc.2022.831614/full#supplementary-material

REFERENCES

1. Sung H, Ferlay J, Siegel RL, Laversanne M, Soerjomataram I, Jemal A, et al. "Global Cancer Statistics 2020: GLOBOCAN Estimates of Incidence and Mortality Worldwide for 36 Cancers in 185 Countries.". *CA Cancer J Clin* (2021) 71:209–49. doi: 10.3322/caac.21660
2. Thun M, Linet MS, Cerhan JR, Haiman CA, Schottenfeld D. *Cancer Epidemiology and Prevention*. New York, NY, USA: Oxford University Press. (2017).
3. Chimed T, Sandagdorj T, Znaor A, Laversanne M, Tseveen B, Genden P, et al. "Cancer Incidence and Cancer Control in M Ongolia: Results From the N Ational C Ancer R Egistry 2008–12.". *Int J OF Cancer* (2017) 140:302–09. doi: 10.1002/ijc.30463
4. Yang JD, Heimbach JK. "New Advances in the Diagnosis and Management of Hepatocellular Carcinoma." *BMJ* (2020) 371:m3544. doi: 10.1136/bmj.m3544
5. Poon RT. "Prevention of Recurrence After Resection of Hepatocellular Carcinoma: A Daunting Challenge." *HEPATOLOGY* (2011) 54:757–59. doi: 10.1002/hep.24569

6. Dhir M, Melin AA, Douaiher J, Lin C, Zhen WK, Hussain SM, et al. "A Review and Update of Treatment Options and Controversies in the Management of Hepatocellular Carcinoma." *Ann OF Surg* (2016) 263:1112–25. doi: 10.1097/SLA.0000000000001556
7. Wang Z, Ren Z, Chen Y, Hu J, Yang G, Yu L, et al. "Adjuvant Transarterial Chemoembolization for HBV-Related Hepatocellular Carcinoma After Resection: A Randomized Controlled Study." *Clin Cancer Res* (2018) 24:2074–81. doi: 10.1158/1078-0432.CCR-17-2899
8. Cheng AL, Hsu C, Chan SL, Choo SP, Kudo M. "Challenges of Combination Therapy With Immune Checkpoint Inhibitors for Hepatocellular Carcinoma." *J OF Hepatol* (2020) 72:307–19. doi: 10.1016/j.jhep.2019.09.025
9. Imamura H, Matsuyama Y, Tanaka E, Ohkubo T, Hasegawa K, Miyagawa S, et al. "Risk Factors Contributing to Early and Late Phase Intrahepatic Recurrence of Hepatocellular Carcinoma After Hepatectomy." *J OF Hepatol* (2003) 38:200–07. doi: 10.1016/S0168-8278(02)00360-4
10. Zhang EL, Cheng Q, Huang ZY, Dong W. "Revisiting Surgical Strategies for Hepatocellular Carcinoma With Microvascular Invasion." *Front Oncol* (2021) 11:6913545. doi: 10.3389/fonc.2021.691354
11. Shindoh J, Andreou A, Aloia TA, Zimmitti G, Lauwers GY, Laurent A, et al. "Microvascular Invasion Does Not Predict Long-Term Survival in Hepatocellular Carcinoma Up to 2 Cm: Reappraisal of the Staging System for Solitary Tumors." *Ann OF Surg Oncol* (2013) 20:1223–29. doi: 10.1245/s10434-012-2739-y
12. Kang I, Jang M, Lee JG, Han DH, Joo DJ, Kim KS, et al. "Subclassification of Microscopic Vascular Invasion in Hepatocellular Carcinoma." *Ann Sug* (2021) 274(6):e1170–8. doi: 10.1016/j.ijsu.2020.01.048
13. Lee S, Kang TW, Song KD, Lee MW, Rhim H, Lim HK, et al. "Effect of Microvascular Invasion Risk on Early Recurrence of Hepatocellular Carcinoma After Surgery and Radiofrequency Ablation." *Ann Sug* (2021) 273:564–71. doi: 10.1097/SLA.0000000000003268
14. Wang H, Du PC, Wu MC, Cong WM. "Postoperative Adjuvant Transarterial Chemoembolization for Multinodular Hepatocellular Carcinoma Within the Barcelona Clinic Liver Cancer Early Stage and Microvascular Invasion." *Hepatobiliary Surg Nutr* (2018) 7:418–28. doi: 10.21037/hbsn.2018.09.05
15. Liu S, Guo L, Li H, Zhang B, Sun J, Zhou C, et al. "Postoperative Adjuvant Trans-Arterial Chemoembolization for Patients With Hepatocellular Carcinoma and Portal Vein Tumor Thrombus." *Ann Sug Oncol* (2018) 25:2098–104. doi: 10.1245/s10434-018-6438-1
16. Wei W, Jian PE, Li SH, Guo ZX, Zhang YF, Ling YH, et al. "Adjuvant Transcatheter Arterial Chemoembolization After Curative Resection for Hepatocellular Carcinoma Patients With Solitary Tumor and Microvascular Invasion: A Randomized Clinical Trial of Efficacy and Safety." *Cancer Commun (Lond)* (2018) 38:61. doi: 10.1186/s40880-018-0331-y
17. Esagian SM, Kakos CD, Giorgakis E, Burdine L, Barreto JC, Mavros MN. "Adjuvant Transarterial Chemoembolization Following Curative Hepatectomy Versus Hepatectomy Alone for Hepatocellular Carcinoma: A Systematic Review and Meta-Analysis of Randomized Controlled Trials. *" Cancers (Basel)* (2021) 13:2984. doi: 10.3390/cancers13122984
18. Chen ZH, Zhang XP, Zhou TF, Wang K, Wang H, Chai ZT, et al. "Adjuvant Transarterial Chemoembolization Improves Survival Outcomes in Hepatocellular Carcinoma With Microvascular Invasion: A Systematic Review and Meta-Analysis." *Eur J Surg Oncol* (2019) 45:2188–96. doi: 10.1016/j.ejso.2019.06.031
19. Zhang XP, Wang K, Wei XB, Li LQ, Sun HC, Wen TF, et al. "An Eastern Hepatobiliary Surgery Hospital Microvascular Invasion Scoring System in Predicting Prognosis of Patients With Hepatocellular Carcinoma and Microvascular Invasion After R0 Liver Resection: A Large-Scale, Multicenter Study.". *ONCOLOGIST* (2019) 24:e1476-88. doi: 10.1634/theoncologist.2018-0868
20. Rodríguez-Perálvarez M, Luong TV, Andreana L, Meyer T, Dhillon AP, Burroughs AK. "A Systematic Review of Microvascular Invasion in Hepatocellular Carcinoma: Diagnostic and Prognostic Variability." *Ann OF Surg Oncol* (2013) 20:325–39. doi: 10.1245/s10434-012-2513-1
21. Cucchetti A, Piscaglia F, Grigioni AD, Ravaioli M, Cescon M, Zanello M, et al. "Preoperative Prediction of Hepatocellular Carcinoma Tumour Grade and Micro-Vascular Invasion by Means of Artificial Neural Network: A Pilot Study." *J OF Hepatol* (2010) 52:880–88. doi: 10.1016/j.jhep.2009.12.037
22. Wang CC, Iyer SG, Low JK, Lin CY, Wang SH, Lu SN, et al. "Perioperative Factors Affecting Long-Term Outcomes of 473 Consecutive Patients Undergoing Hepatectomy for Hepatocellular Carcinoma." *Ann OF Surg Oncol* (2009) 16:1832–42. doi: 10.1245/s10434-009-0448-y
23. Shindoh J, Kobayashi Y, Kawamura Y, Akuta N, Kobayashi M, Suzuki Y, et al. "Microvascular Invasion and a Size Cutoff Value of 2 Cm Predict Long-Term Oncological Outcome in Multiple Hepatocellular Carcinoma: Reappraisal of the American Joint Committee on Cancer Staging System and Validation Using the Surveillance, Epidemiology, and End-Results Database." *Liver Cancer* (2020) 9:156–66. doi: 10.1159/000504193
24. Park S, Choi S, Cho YA, Sinn DH, Kim JM, Park CK, et al. "Evaluation of the American Joint Committee On Cancer (AJCC) 8th Edition Staging System for Hepatocellular Carcinoma in 1,008 Patients With Curative Resection.". *Cancer Res Treat* (2020) 52:1145–52. doi: 10.4143/crt.2020.208
25. Cong WM, Bu H, Chen J, Dong H, Zhu YY, Feng LH, et al. "Practice Guidelines for the Pathological Diagnosis of Primary Liver Cancer: 2015 Update." *World J Gastroenterol* (2016) 22:9279–87. doi: 10.3748/wjg.v22.i42.9279
26. Iguchi T, Shirabe K, Aishima S, Wang H, Fujita N, Ninomiya M, et al. "New Pathologic Stratification of Microvascular Invasion in Hepatocellular Carcinoma: Predicting Prognosis After Living-Donor Liver Transplantation." *TRANSPLANTATION* (2015) 99:1236–42. doi: 10.1097/TP.0000000000000489
27. Feng LH, Dong H, Lau WY, Yu H, Zhu YY, Zhao Y, et al. "Novel Microvascular Invasion-Based Prognostic Nomograms to Predict Survival Outcomes in Patients After R0 Resection for Hepatocellular Carcinoma.". *J Cancer Res Clin Oncol* (2017) 143:293–303. doi: 10.1007/s00432-016-2286-1
28. Sumie S, Nakashima O, Okuda K, Kuromatsu R, Kawaguchi A, Nakano M, et al. "The Significance of Classifying Microvascular Invasion in Patients With Hepatocellular Carcinoma." *Ann OF Surg Oncol* (2014) 21:1002–09. doi: 10.1245/s10434-013-3376-9
29. Fujita N, Aishima S, Iguchi T, Mano Y, Taketomi A, Shirabe K, et al. "Histologic Classification of Microscopic Portal Venous Invasion to Predict Prognosis in Hepatocellular Carcinoma." *Hum Pathol* (2011) 42:1531–38. doi: 10.1016/j.humpath.2010.12.016
30. Erstad Derek J, Tanabe Kenneth K. "Prognostic and Therapeutic Implications of Microvascular Invasion in Hepatocellular Carcinoma." *Ann OF Surg Oncol* (2019) 26:1474–93. doi: 10.1245/s10434-019-07227-9
31. Hidaka M, Eguchi S, Okuda K, Beppu T, Shirabe K, Kondo K, et al. "Impact of Anatomical Resection for Hepatocellular Carcinoma With Microportal Invasion (Vp1): A Multi-Institutional Study by the Kyushu Study Group of Liver Surgery." *Ann OF Surg* (2020) 271:339–46. doi: 10.1097/SLA.0000000000002981
32. Wang L, Ke Q, Lin N, Zeng Y, Liu J. "Does Postoperative Adjuvant Transarterial Chemoembolization Benefit for All Patients With Hepatocellular Carcinoma Combined With Microvascular Invasion: A Meta-Analysis." *Scand J Gastroenterol* (2019) 54:528–37. doi: 10.1080/00365521.2019.1610794
33. Peng BG, He Q, Li JP, Zhou F. "Adjuvant Transcatheter Arterial Chemoembolization Improves Efficacy of Hepatectomy for Patients With Hepatocellular Carcinoma and Portal Vein Tumor Thrombus." *Am J OF Surg* (2009) 198:313–18. doi: 10.1016/j.amjsurg.2008.09.026
34. Wei W, Jian PE, Li SH, Guo ZX, Zhang YF, Ling YH, et al. "Adjuvant Transcatheter Arterial Chemoembolization After Curative Resection for Hepatocellular Carcinoma Patients With Solitary Tumor and Microvascular Invasion: A Randomized Clinical Trial of Efficacy and Safety." *Cancer Commun (Lond)* (2018) 38:61. doi: 10.1186/s40880-018-0331-y
35. XU F. "Is Postoperative Adjuvant Transchatheter Arterial Chemoembolization Necessary for Small Hepatocellular Carcinoma Patients: A Randomized Controlled Trial." *Acad J Second Military Med Univ* (2012) (12):274–279. doi: 10.3724/SP.J.1008.2012.00274
36. Zhong C, Guo RP, Li JQ, Shi M, Wei W, Chen MS, et al. "A Randomized Controlled Trial of Hepatectomy With Adjuvant Transcatheter Arterial Chemoembolization Versus Hepatectomy Alone for Stage III a Hepatocellular Carcinoma.". *J Cancer Res Clin Oncol* (2009) 135:1437–45. doi: 10.1007/s00432-009-0588-2
37. Wang H, Yu H, Qian YW, Cao ZY, Wu MC, Cong WM. "Postoperative Adjuvant Transcatheter Arterial Chemoembolization Improves the Prognosis of Patients With Huge Hepatocellular Carcinoma.". *Hepatobiliary Pancreat Dis Int* (2021) 20:232–39. doi: 10.1016/j.hbpd.2020.12.018

38. Wang YY, Wang LJ, Xu D, Liu M, Wang HW, Wang K, et al. "Postoperative Adjuvant Transcatheter Arterial Chemoembolization Should be Considered Selectively in Patients Who Have Hepatocellular Carcinoma With Microvascular Invasion.". *HPB (Oxford)* (2019) 21:425–33. doi: 10.1016/j.hpb.2018.08.001
39. Qi YP, Zhong JH, Liang ZY, Zhang J, Chen B, Chen CZ, et al. "Adjuvant Transarterial Chemoembolization for Patients With Hepatocellular Carcinoma Involving Microvascular Invasion.". *Am J OF Surg* (2019) 217:739–44. doi: 10.1016/j.amjsurg.2018.07.054
40. Zhang XP, Liu YC, Chen ZH, Sun JX, Wang K, Chai ZT, et al. "Postoperative Adjuvant Transarterial Chemoembolization Improves Outcomes of Hepatocellular Carcinoma Associated With Hepatic Vein Invasion: A Propensity Score Matching Analysis.". *Ann OF Surg Oncol* (2019) 26:1465–73. doi: 10.1245/s10434-019-07223-z
41. Shi M, Zhang CQ, Zhang YQ, Liang XM, Li JQ. "Micrometastases of Solitary Hepatocellular Carcinoma and Appropriate Resection Margin.". *World J OF Surg* (2004) 28:376–81. doi: 10.1007/s00268-003-7308-x
42. Roayaie S, Blume IN, Thung SN, Guido M, Fiel MI, Hiotis S, et al. "A System of Classifying Microvascular Invasion to Predict Outcome After Resection in Patients With Hepatocellular Carcinoma.". *GASTROENTEROLOGY* (2009) 137:850–55. doi: 10.1053/j.gastro.2009.06.003

Conflict of Interest: The authors declare that the research was conducted in the absence of any commercial or financial relationships that could be construed as a potential conflict of interest.

Publisher's Note: All claims expressed in this article are solely those of the authors and do not necessarily represent those of their affiliated organizations, or those of the publisher, the editors and the reviewers. Any product that may be evaluated in this article, or claim that may be made by its manufacturer, is not guaranteed or endorsed by the publisher.

Copyright © 2022 Qiu, Yang, Wang, Shen and Wang. This is an open-access article distributed under the terms of the Creative Commons Attribution License (CC BY). The use, distribution or reproduction in other forums is permitted, provided the original author(s) and the copyright owner(s) are credited and that the original publication in this journal is cited, in accordance with accepted academic practice. No use, distribution or reproduction is permitted which does not comply with these terms.

frontiers | Frontiers in Oncology

ORIGINAL RESEARCH
published: 20 June 2022
doi: 10.3389/fonc.2022.926359

Development and Validation of Nomogram for Predicting Survival of Primary Liver Cancers Using Machine Learning

Rui Chen[1,2], Beining Hou[3], Shaotian Qiu[4], Shuai Shao[4,5], Zhenjun Yu[1,2], Feng Zhou[1,2], Beichen Guo[1,2], Yuhan Li[1,2], Yingwei Zhang[6] and Tao Han[1,2,4,5*]*

[1] Department of Hepatology and Gastroenterology, Tianjin Union Medical Center, Tianjin Medical University, Tianjin, China, [2] Department of Hepatology and Gastroenterology, The Third Central Clinical College of Tianjin Medical University, Tianjin, China, [3] School of Computer Science and Technology, Dalian University of Technology, Dalian, China, [4] Department of Hepatology and Gastroenterology, Tianjin Union Medical Center Affiliated to Nankai University, Tianjin, China, [5] Department of Hepatology and Gastroenterology, Tianjin Third Central Hospital Affiliated to Nankai University, Tianjin, China, [6] Beijing Key Laboratory of Mobile Computing and Pervasive Device, Institute of Computing Technology, Chinese Academy of Sciences, University of Chinese Academy of Sciences, Beijing, China

Background and Aims: Primary liver cancer (PLC) is a common malignancy with poor survival and requires long-term follow-up. Hence, nomograms need to be established to predict overall survival (OS) and cancer-specific survival (CSS) from different databases for patients with PLC.

Methods: Data of PLC patients were downloaded from Surveillance, Epidemiology, and End Results (SEER) and the Cancer Genome Atlas (TCGA) databases. The Kaplan Meier method and log-rank test were used to compare differences in OS and CSS. Independent prognostic factors for patients with PLC were determined by univariate and multivariate Cox regression analyses. Two nomograms were developed based on the result of the multivariable analysis and evaluated by calibration curves and receiver operating characteristic curves.

Results: OS and CSS nomograms were based on age, race, TNM stage, primary diagnosis, and pathologic stage. The area under the curve (AUC) was 0.777, 0.769, and 0.772 for 1-, 3- and 5-year OS. The AUC was 0.739, 0.729 and 0.780 for 1-, 3- and 5-year CSS. The performance of the two new models was then evaluated using calibration curves.

Conclusions: We systematically reviewed the prognosis of PLC and developed two nomograms. Both nomograms facilitate clinical application and may benefit clinical decision-making.

Keywords: primary liver cancer, SEER, TCGA, nomogram, cancer specific survival

OPEN ACCESS

Edited by:
Sanjit Mukherjee, National Institutes of Health (NIH), United States

Reviewed by:
Pijush Das, CSIR - Indian Institute of Chemical Biology, India
Arijita Sarkar, University of Southern California, United States
Weiqi Rong, Chinese Academy of Medical Sciences and Peking Union Medical College, China

***Correspondence:**
Yingwei Zhang
zhangyingwei@ict.ac.cn
Tao Han
hantaomd@126.com

Specialty section:
This article was submitted to Gastrointestinal Cancers: Hepato Pancreatic Biliary Cancers, a section of the journal Frontiers in Oncology

Received: *22 April 2022*
Accepted: *23 May 2022*
Published: *20 June 2022*

Citation:
Chen R, Hou B, Qiu S, Shao S, Yu Z, Zhou F, Guo B, Li Y, Zhang Y and Han T (2022) Development and Validation of Nomogram for Predicting Survival of Primary Liver Cancers Using Machine Learning. Front. Oncol. 12:926359. doi: 10.3389/fonc.2022.926359

INTRODUCTION

Primary liver cancer (PLC) is one of the most common malignancies of the digestive system, and its mortality rate in men and women has increased so that it now ranks fourth and seventh in terms of cancer-related deaths among global malignancies (1). Traditionally, tumors of the PLC at the pathological level can be subdivided into 3 groups: Hepatocellular carcinoma (HCC, comprising 75%-85% of cases), cholangiocarcinoma (CC, 10%-15%), and combined hepatocellular-cholangiocarcinoma (CHC) that is a rare primary liver cancer (2). Although the trend of PLC largely reflects the trend of HCC, there are notable exceptions (3). The main risk factors for liver cancer are chronic hepatitis B virus (HBV) or hepatitis C virus (HCV), eating aflatoxin-contaminated food, and heavy drinking. However, the main risk factors differ in different regions. As one of the malignant tumors, due to the low early diagnosis rate, high recurrence, and metastasis rate after resection, the 5-year survival rate of PLC has been maintained between 15% and 40% (2). With a poor prognosis and survival rates, HCC patients must have a long-term follow-up.

In the era of big data, various intelligent techniques can be used to optimize medical management plans, provide better patient care and treatment, improve population health and reduce costs (4). Surveillance, Epidemiology, and End Results (SEER) database, supported by the surveillance research program of the National Cancer Institute (NCI) Department of cancer control and Population Sciences, is one of the most representative large-scale tumor registration databases. It collects a large number of evidence-based medical data and provides systematic evidence and valuable first-hand information for clinicians' evidence-based practice and clinical medical research (5). The Cancer Genome Atlas (TCGA) project was jointly launched by the NCI and the National Human Genome Research Institute. At present, there is clinical and genetic information of more than 11,000 tumor patients with 33 cancers of more than 20 tissue types. In addition, the fields of big data and machine learning integrate genomics and other omics, as well as electronic health records (EHRs) and other clinical data, which in turn have the potential to transform medicine. Machine learning algorithms can predict the risk of individual patients and more accurately determine which patients will benefit the most from specific treatment (6, 7).

Nomogram is a common prediction model used to predict and quantify the probability of clinical events. It is of great value for clinical decision-making and risk stratification, especially for cancer patients (8). The nomogram of breast cancer, lung cancer, liver cancer (9–11), and other malignancies can help patients to predict the risks and benefits of treatment (12) (5). In recent years, there have been relatively few systematic review studies of liver cancer by combing two separate databases. Therefore, we decided to combine SEER and TCGA databases to construct nomograms to predict the prognosis of PLC and help provide new horizons for treatment.

MATERIALS AND METHODS

Data Collection

Clinical data were downloaded from the SEER data portal (www.seer.cancer.gov) and the TCGA data portal (https://portal.gdc.cancer.gov). Inclusion criteria included: a) complete clinical information; b) only one malignant primary tumor; c) the International Classification of Diseases for Oncology-3 (ICD-O-3) histology code: 8170/3: HCC, 8160/3: CC, 8180/3: CHC. Follow-up was suspended when patients with liver cancer died or lost contact. As SEER and TCGA data are open to the public, approval from a local ethics committee is not necessary.

The patient study variables we extracted and analyzed included baseline demographics and tumor characteristics. Baseline demographics include age(≤50y, 50–59y, 60 – 69y, 70–79y, ≥80y), race (White, Black, Other), gender (Female, Male) and time of diagnosis, survival time (months), follow-up and vital survival status. The main clinical variables were as follows: pathological type of liver cancer (HCC, CC, CHC), American Joint Committee on Cancer (AJCC) stage, and TNM staging were determined according to AJCC Cancer Staging Manual.

Overall survival (OS) or cancer-specific survival (CSS) was used as the endpoints of our study. OS represents the time duration from diagnosis to the date of death or last contact. CSS represents the time duration from diagnosis to the date of cancer death.

Statistical Analyses

To make full use of our data to build predictive models, we used python (version 3.8) to randomize data from SEER, taking the first 9161 as the training group, and the remaining 184 as the internal validation group while 172 patients from TCGA as the external validation group. We used the training group to build the prediction model and draw the nomogram. A validation group was used to validate the model.

For survival analyses, univariate Cox analysis was used to determine significant variables, defined as a p-value of less than 0.05, from clinical data. In all statistical analyses, P values were < 0.05 is considered significant. Univariate and multivariate Cox proportional hazards regression models were used to estimate hazard ratios (HR) and corresponding 95% confidential intervals (CI) for each potential prognostic variable. SPSS 25.0 (SPSS, Chicago, IL) was used for the above analysis. Based on the results of multivariate analysis, nomograms were developed to provide visual risk prediction. The nomogram was formulated based on the results of multivariate analysis using R software. The performance of the predictive prognostic model was evaluated by calculating the concordance index (c-index). Nomograms were calibrated for one -, three -, and five-year survival rates by comparing observed survival with predicted survival probabilities.

We performed statistical analysis with R version 4.1.2 (The R Foundation for Statistical Computing, Vienna, Austria). The software packages of R Project, such as "survival(3.2-13) survminer (0.4.9)", "survival (3.2-13 rms 6.2-0 Hmisc 4.6-0 grid

4.1.2 lattice 0.20-45 Formula 1.2-4 ggplot2 3.3.5)", "survival (3.2-13) rms (6.2-0)" and "survival (3.2-13) timeROC (0.4)" are used to draw Kaplan–Meier (KM), nomogram and calibration diagram and timeROC, while "timeroc" and "survival" are used to verify the model and conduct AUC analysis. All packages are installed by the Packages command installed from the R language functional network CRAN.

RESULTS

Patient Characteristics

According to the screening criteria, the data of 66039 patients were extracted from the SEER database. Subsequently, the data of 54588 patients were excluded because they did not have complete data. The final sample included 11451 patients in the entire cohort. Among them, 9161 (80%) patients were used as a training set to establish a predictive nomogram. The remaining 2290 (20%) patients were used to validate the nomogram. The external validation cohort included 172 patients from TCGA (**Supplementary Table 1**). The clinicopathological features of the training and validation cohort are shown in **Table 1**. All patients had complete information on survival time and cause of death. The median survival time of patients with liver cancer in this sample was 13.0 months. The 1-year, 3-year, and 5-year OS rate in the SEER population was 36.1%, 9.4%, and 2.2% respectively. While the 1 -, 3 -, and 5-year CSS were 51.5%, 29.7% and 21.5%, respectively.

Univariate and Multivariate Cox Proportional Hazard Analysis

We performed univariate and multivariate analyses to identify prognostic factors associated with the survival of PLC patients in the training cohort. In the univariate analysis, older age, higher TNM stage, higher pathologic stage, CHC, and American Indian/Alaska Native can predict worse OS and CSS. However, ethnicity and gender had no significant effect on OS or CSS (**Figures 1**, **2**).

Univariate Cox regression analysis of the training cohort revealed the role of the following parameters in predicting patient survival. Factors such as age, pathological type-CC, pathologic stage, stage T0, stage T1, and stage N were associated with patients' prognoses. All the above variables were statistically significant (all $P<0.05$) and were included in multivariate analysis. Among these factors, the pathologic stage (c-index=0.669) and T stage (c-index=0.643) had higher discriminatory power in predicting PLC survival compared with other factors. In the Cox analysis, the maximum number of iterations was 20.

Variables involved in the multivariate analysis of OS include pathological types, pathologic stage, TNM stage, and age. According to multivariate analysis, patients with younger age, disease type of CC, lower TNM stage and adequate treatment had improved outcomes. These factors were then incorporated into the prediction model (**Table 2**).

Development and Validation of a Prognostic Nomogram

Factors from the multivariate analysis were used to develop nomograms to calculate 1-,3 -, and 5-year OS or CSS probabilities (**Figure 3**). Each prognostic parameter was scored according to its prognostic value. The total score was used to predict 1 -, 3 -, and 5-year OS and CSS. Furthermore, the total score for all variables was converted into an estimate of the probability of death. The distinction between survival probabilities and actual observations was assessed using the c-index. The value of the c-index fluctuates between 0.5 and 1.0 representing random chance and 1.0 represents fully corrected discrimination (13). The c-index of the prognostic nomogram for OS prediction was 0.702 (95% CI, 0.696–0.708) in the training cohort and 0.702 (95% CI, 0.689–0.714) in the internal validation cohort. We tested the nomogram using an internal receiver operating characteristic (ROC) curve in the training cohort. The area under the curve (AUC) was 0.777, 0.769 and 0.772 for 1-,3- and 5-year OS respectively, with 0.739, 0.729 and 0.780 for 1-,3- and 5-year CSS (**Figure 4**). The calibration plot shows good agreement between the internal and external validation cohorts (**Figure 5**) (**Supplementary Figures 1**, **2**).

DISCUSSION

Worldwide, PLC is a common cause of cancer-related death. PLC death rates are increasing faster than any other cancer (14). In addition, PLC is the second most lethal tumor after pancreatic cancer. HCC accounts for the majority of PLC (15). The increasing number of deaths due to HCC is an increasing concern (16). Disease and tumor-related factors have a great impact on the treatment of PLC (17). CC is an epithelial cell malignancy, and most CCs are well, moderately, and poorly differentiated adenocarcinomas, with other histological subtypes, rarely occurring. Most CCs are new-onset, with no risk factors identified (18). Moreover, CHC is a rare and aggressive variant with features of both HCC and CC, and it is unclear whether treatments commonly used for PLC are effective. The prognosis of CHC is particularly poor due to its aggressive nature. The estimated incidence of CHC ranges from 1% to 14.2% (19) (20).

In this research, patients diagnosed with PLC were included in the analysis. With more than 60000 patients, we included 9161 patients with complete clinical information in the training set from the SEER database and 172 patients from TCGA. By univariate analysis, race, age, pathologic stage, primary diagnosis, and T and N stage were all related to liver cancer progression. In addition, we conducted the multivariate analysis using these significant variables in univariate analysis. In multivariable analyses, we demonstrated that older age, higher pathological stage, and more advanced T and N stages were independently associated with poor overall survival in PLC.

PLC incidence rates vary by race/ethnicity and state, largely because of differences in the prevalence of major risk factors and, to some extent, because of different access to high-quality care (21) (22). We can also know that social status is associated with better

TABLE 1 | Characteristics of 11,451 patients with Primary Liver Cancer in SEER, n (%).

Factors Total, n (%)	All cohort 11451	Train cohort 9161	Validation cohort 2290
Primary diagnosis			
HCC	10138 (88.5)	8111 (88.5)	2027 (88.5)
CC	1303 (11.4)	1043 (11.4)	260 (11.4)
CHC	10 (0.1)	7 (0.1)	3 (0.1)
Pathologic stage			
I	4634 (40.5)	3710 (40.5)	924 (40.3)
II	2227 (19.4)	1773 (19.4)	454 (19.8)
III	61 (0.5)	48 (0.5)	13 (0.6)
IIIA	919 (8.0)	728 (7.9)	191 (8.3)
IIIB	750 (6.5)	600 (6.5)	150 (6.6)
IIIC	190 (1.7)	150 (1.6)	40 (1.7)
IIINOS	10 (0.1)	7 (0.1)	3 (0.1)
IVA	632 (5.5)	522 (5.7)	110 (4.8)
IVB	2028 (17.7)	1623 (17.7)	405 (17.7)
T stage			
T0	6 (0.1)	5 (0.1)	1 (0.0)
T1	5094 (44.5)	4078 (44.5)	1016 (44.4)
T2	2212 (19.3)	1763 (19.2)	449 (19.6)
T2NOS	5 (0.0)	4 (0.0)	1 (0.0)
T2a	135 (1.2)	114 (1.2)	21 (0.9)
T2b	396 (3.5)	312 (3.4)	84 (3.7)
T3	169 (1.5)	143 (1.6)	26 (1.1)
T3NOS	14 (0.1)	11 (0.1)	3 (0.1)
T3a	1306 (11.4)	1053 (11.5)	253 (11.0)
T3b	1162 (10.1)	923 (10.1)	239 (10.4)
T4	451 (3.9)	365 (4.0)	86 (3.8)
TX	501 (4.4)	390 (4.3)	111 (4.8)
N stage			
N0	9905 (86.5)	7901 (86.2)	2004 (87.5)
N1	1167 (10.2)	957 (10.4)	210 (9.2)
NX	379 (3.3)	303 (3.3)	76 (3.3)
M stage			
M0	9423 (82.3)	7538 (82.3)	1885 (82.3)
M1	2028 (17.7)	1623 (17.7)	405 (17.7)
Race			
American Indian /Alaska Native	192 (1.7)	161 (1.8)	31 (1.4)
Asian or Pacific Islander	2083 (18.2)	1630 (17.8)	453 (19.8)
Black	1740 (15.2)	1415 (15.4)	325 (14.2)
White	7436 (64.9)	5955 (65.0)	1481 (64.7)
Ethnicity			
Non-Spanish-Hispanic-Latino	9999 (87.3)	8001 (87.3)	1998 (87.2)
Spanish-Hispanic-Latino	1452 (12.7)	1160 (12.7)	292 (12.8)
Gender			
Female	2910 (25.4)	2319 (25.3)	591 (25.8)
Male	8541 (74.6)	6842 (74.7)	1699 (74.2)
Age			
<50	692 (6.0)	541 (5.9)	151 (6.6)
50~59	3251 (28.4)	2631 (28.7)	620 (27.1)
60~69	4181 (36.5)	3349 (36.6)	832 (36.3)
70~79	2127 (18.6)	1686 (18.4)	441 (19.3)
≥80	1200 (10.5)	954 (10.4)	246 (10.7)

survival. In this research, we analyzed the association between ethnicity and race with tumor survival and found that survival was slightly lower in the American Indian/Alaska Native and black.

Many studies have shown that the TNM stage may be an important prognostic factor in HCC (23) (24). In the present study, we analyzed the relationship between the TNM stage and tumor survival and found that the higher the TNM stage, the worse the survival.

Hence, we plotted the nomogram according to independent prognostic factors in the multivariate. The data used were derived from the SEER database, which ensured the validity and reliability of our conclusions, as well as the internal and external validity of the nomograms. To validate this value and prevent overfitting of the current model, it is necessary to validate a new nomogram. Moreover, we validated the predictive value of the model by using both internal and external validation cohorts. In addition, we

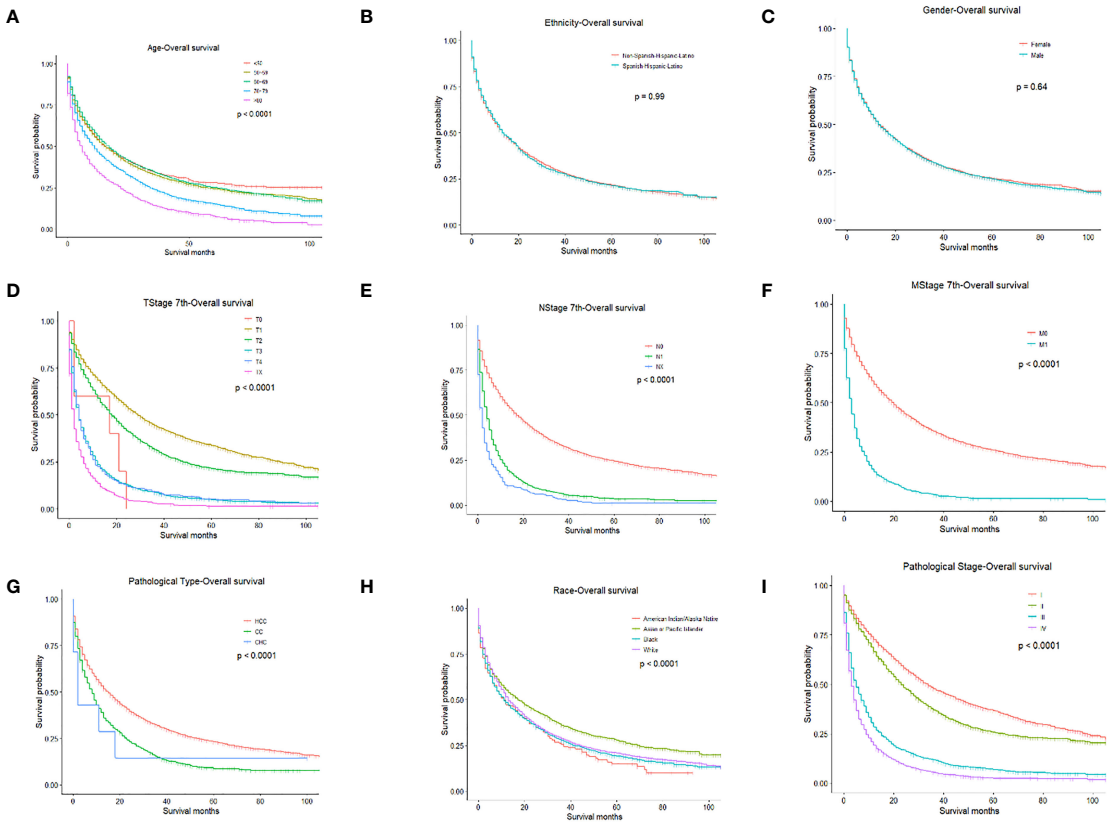

FIGURE 1 | OS for PLC patients stratified by **(A)** Age, p < 0.0001; **(B)** Ethnicity p = 0.990; **(C)** Gender, p = 0.640; **(D)** T-stage, p < 0.0001; **(E)** N-stage, p < 0.0001; **(F)** M-stage, p < 0.001; **(G)** Pathological Type, p < 0.0001; **(H)** Race, p < 0.0001; **(I)** Pathological Stage, p < 0.0001.

measured the accuracy of this model by ROC curve and a calibration plot, and the larger the AUC, the higher the accuracy of the model. The training cohort AUC was 0.777,0.769 and 0.772 for 1-,3- and 5-year OS and 0.739,0.729 and 0.780 for 1-,3- and 5-year CSS. All these results indicated that the model had good accuracy for the prediction of liver cancer survival. Meanwhile, the calibration curve also validated the model's prediction ability on the overall sample.

It has been reported that individualized prediction is considered a critical condition of predictive models (25). However, most current studies are based on a single database (26) (27). In this research, we mainly performed long-term follow-ups of patients with PLC. The main objective of this study was to use two databases to predict total and cancer-specific mortality in patients with liver cancer, which differs from currently published studies regarding predictive nomograms. The huge number of patients with PLC recorded in the SEER database helped us to build a more accurate model. In addition, the items included in the nomogram are common, easily accessible, and comprehensible items for physicians and patients in the clinic.

There are also relevant studies applied to predict cancer-specific diseases. Ni et al. (5) developed a hepatocellular carcinoma nomogram to predict cancer-specific mortality and overall mortality using the SEER database, which will help clinicians to obtain personal prediction information to determine whether patients are at high risk of death. Song et al. (28) created a pancreatic cancer survival nomogram to effectively predict patients' survival and use it in clinical practice. Similarly, Wang et al. (29) developed and validated a new nomogram for pulmonary invasive mucinous adenocarcinoma based on the SEER database, which is expected to provide new ideas for treatment. All of these studies are based on a bioinformatics database such as the SEER database to develop nomograms for multiple cancers that predict CSS characteristics to help clinicians make clinical decisions. In this research, we used two bioinformatics databases (SEER and TCGA databases) and developed two nomograms simultaneously. Making clinical decisions more convenient and effective.

Although we have developed powerful nomograms, there are still several limitations that must be acknowledged. Potential prognostic factors available in public databases are limited. Further analysis with a more complete data set may enhance the predictive power of this tool. Data from SEER and TCGA that did not report underlying chronic liver disease, laboratory studies to assess liver function, calculation of Child-Pugh score, or details of tumor characteristics were missing, which would be important for further treatment and thus impact survival.

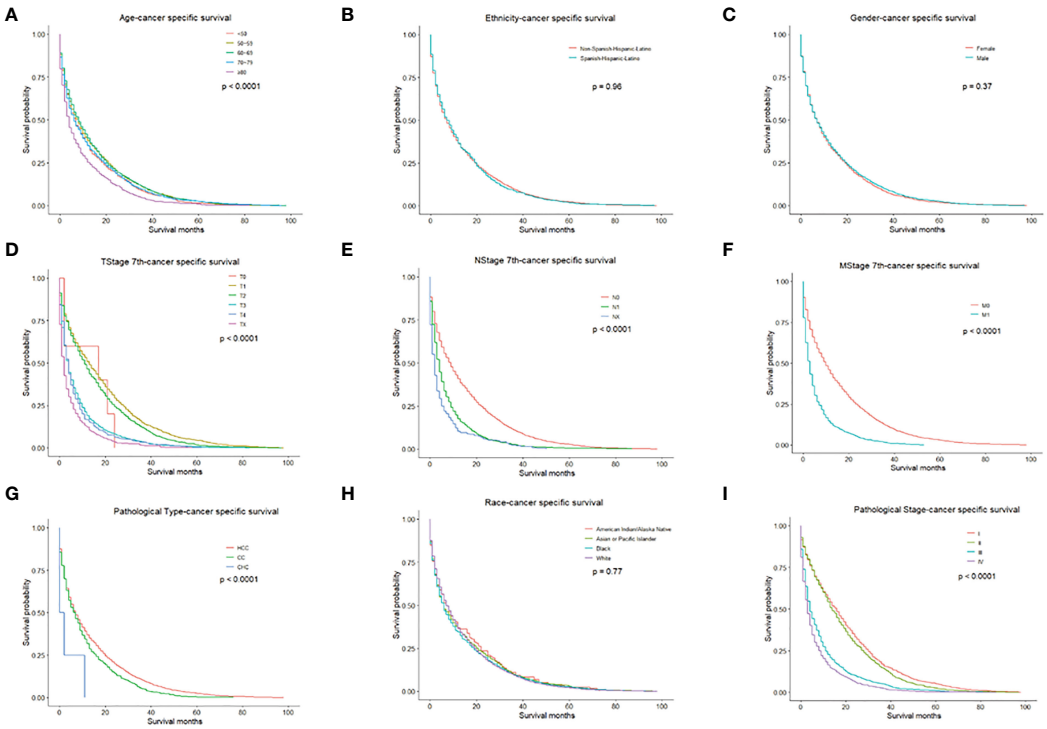

FIGURE 2 | CSS for PLC patients stratified by **(A)** Age, p < 0.0001; **(B)** Ethnicity p = 0.960; **(C)** Gender, p = 0.370; **(D)** T-stage, p < 0.0001; **(E)** N-stage, p < 0.0001; **(F)** M-stage, p < 0.001; **(G)** Pathological Type, p < 0.0001; **(H)** Race, p = 0.770; **(I)** Pathological Stage, p < 0.0001.

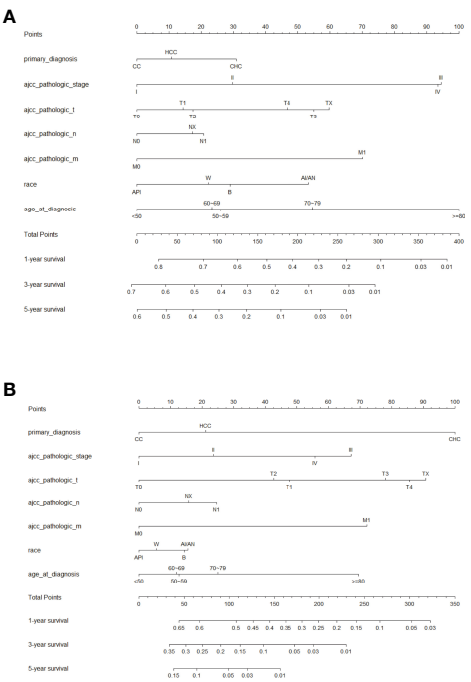

FIGURE 3 | Prognostic nomogram predicting the probability of 1-, 3- and 5-year **(A)** overall survival (OS) and **(B)** cancer-specific survival (CSS). Each subtype within these significant independent variables was assigned a score on the point scale. The total score is projected to the bottom scale. API, Asian or Pacific Islander; W, White; B, Black; AI/AN, American Indian/Alaska Native.

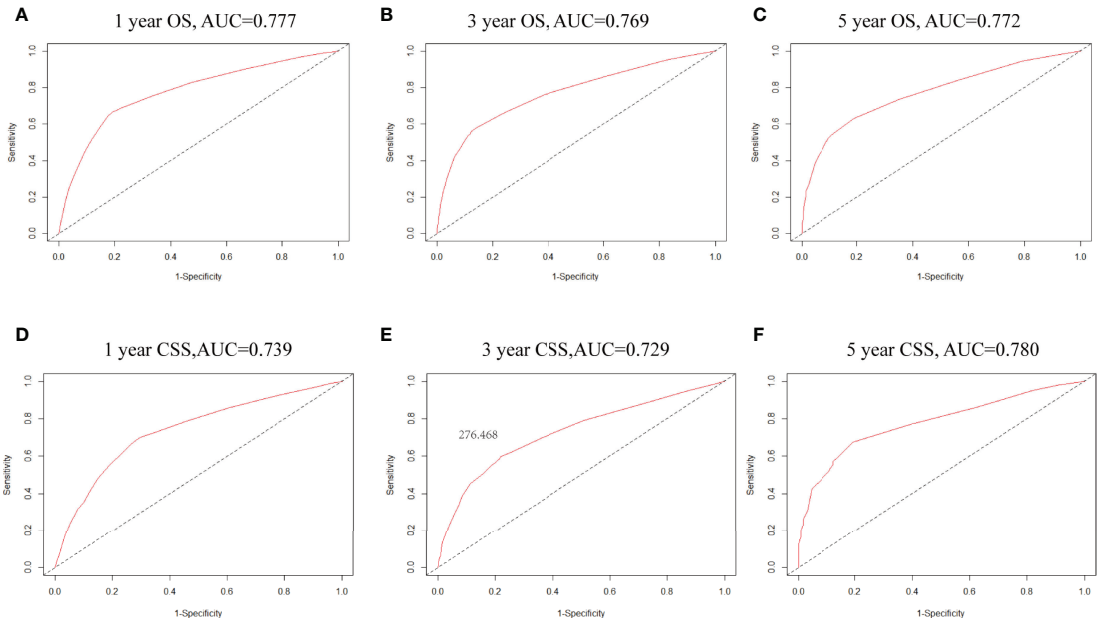

FIGURE 4 | **(A–C)** ROC curves for 1-, 3- and 5-year OS based on the nomogram. The AUC was 0.777,0.834 and 0.830, respectively; **(D–F)** ROC curves for 1-,3- and 5-year CSS. The AUC was 0.739,0.729 and 0.780, respectively.

However, data from the multicenter nature of the sources provide significant benefits. This model comprehensively evaluated the clinical features and treatment of liver cancer and provided ideas for improving the prognosis of liver cancer.

In conclusion, we conducted an analysis of the prognosis of PLC based on a large population in the SEER and TCGA databases. Reviewed the prognosis of PLC and developed and validated two new nomograms. We then elucidated the

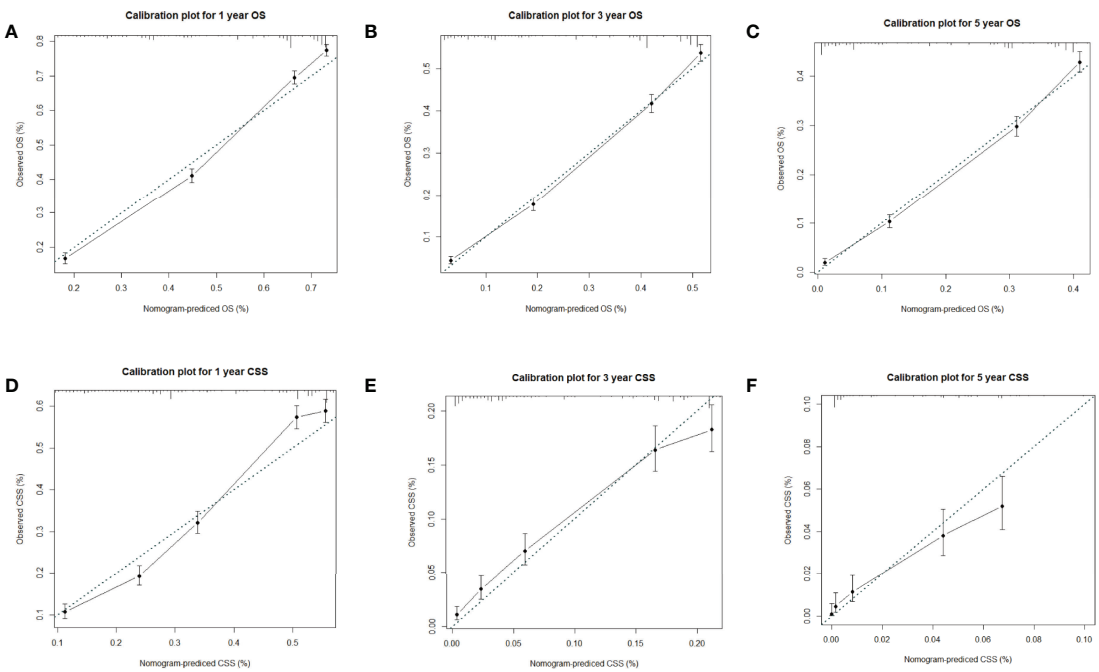

FIGURE 5 | **(A–C)** Calibration plots for 1-,3- and 5-year OS in the training cohort; **(D–F)** Calibration plots for 1-,3- and 5-year CSS in the training cohort.

TABLE 2 | Univariate and Multivariate Cox regression for OS.

Variables	Total (%)	Univariate analysis		Multivariate analysis	
		HR (95.0%CI)	p-value	HR (95.0%CI)	p-value
	9161				
primary_diagnosis					
HCC	8111 (88.5)	Reference	–	Reference	–
CC	1043 (11.4)	1.520 (1.419-1.629)	0.000	0.820 (0.731-0.921)	0.001
CHC	7 (0.1)	1.582 (0.710-3.523)	0.261	1.015 (0.451-2.285)	0.972
Pathologic stage					
I	3710 (40.5)	Reference	–	Reference	–
II	1773 (19.4)	1.276 (1.193-1.365)	0.000	1.664 (1.389-1.992)	0.000
III	48 (0.5)	2.533 (1.873-3.426)	0.000	2.512 (1.714-3.682)	0.000
IIIA	728 (7.9)	2.626 (2.409-2.863)	0.000	1.990 (1.665-2.379)	0.000
IIIB	600 (6.5)	3.819 (3.479-4.193)	0.000	2.397 (1.999-2.875)	0.000
IIIC	150 (1.6)	3.130 (2.640-3.712)	0.000	2.561 (2.007-3.269)	0.000
IIINOS	7 (0.1)	2.468 (1.108-5.501)	0.027	1.459 (0.409-5.205)	0.560
IVA	522 (5.7)	2.900 (2.627-3.202)	0.000	2.328 (1.965-2.758)	0.000
IVB	1623 (17.7)	4.821 (4.509-5.155)	0.000	3.962 (3.496-4.489)	0.000
T stage					
T0	5 (0.1)	Reference	–	Reference	–
T1	4078 (44.5)	0.393 (0.163-0.945)	0.037	1.085 (0.448-2.630)	0.856
T2	1763 (19.2)	0.466 (0.193-1.121)	0.088	0.826 (0.339-2.014)	–
T2NOS	4 (0.0)	0.850 (0.228-3.165)	0.808	1.302 (0.348-4.873)	–
T2a	114 (1.2)	0.782 (0.319-1.918)	0.591	1.182 (0.478-2.921)	–
T2b	312 (3.4)	1.092 (0.451-2.643)	0.846	1.519 (0.624-3.699)	–
T3	143 (1.6)	1.063 (0.435-2.594)	0.894	1.235 (0.500-3.052)	–
T3NOS	11 (0.1)	1.095 (0.374-3.205)	0.868	1.727 (0.462-6.451)	–
T3a	1053 (11.5)	1.073 (0.445-2.583)	0.876	1.396 (0.575-3.392)	–
T3b	923 (10.1)	1.506 (0.625-3.629)	0.361	1.787 (0.735-4.342)	–
T4	365 (4.0)	1.222 (0.505-2.954)	0.657	1.334 (0.548-3.248)	–
TX	390 (4.3)	1.855 (0.768-4.483)	0.170	1.553 (0.641-3.766)	–
N stage					
N0	7901 (86.2)	Reference	–	Reference	–
N1	957 (10.4)	2.395 (2.230-2.571)	0.000	1.157 (1.037-1.292)	0.009
NX	303 (3.3)	3.341 (2.969-3.759)	0.000	1.150 (1.000-1.323)	0.050
M stage					
M0	7538 (82.3)	Reference	–		.
M1	1623 (17.7)	3.279 (3.093-3.477)			
Race					
American Indian /Alaska Native	161 (1.8)	Reference	–	Reference	–
Asian or Pacific Islander	1630 (17.8)	0.744 (0.623-0.889)	0.001	0.639 (0.535-0.764)	0.000
Black	1415 (15.4)	0.930 (0.778-1.111)	0.423	0.814 (0.681-0.973)	–
White	5955 (65.0)	0.877 (0.739-1.040)	0.130	0.768 (0.647-0.912)	–
Ethnicity					
Non-Spanish-Hispanic-Latino	8001 (87.3)	Reference	–		–
Spanish-Hispanic-Latino	1160 (12.7)	1.000 (0.933-1.073)	0.995		–
Gender					
Female	2319 (25.3)	Reference	–		–
Male	6842 (74.7)	1.013 (0.960-1.068)	0.644		–
Age					
<50	541 (5.9)	Reference	–	Reference	–
50~59	2631 (28.7)	1.078 (0.966-1.203)	0.180	1.206 (1.079-1.347)	–
60~69	3349 (36.6)	1.043 (0.936-1.162)	0.446	1.195 (1.072-1.333)	–
70~79	1686 (18.4)	1.396 (1.246-1.563)	0.000	1.557 (1.389-1.745)	0.000
≥80	954 (10.4)	1.894 (1.679-2.137)	0.000	2.265 (2.005-2.558)	0.000

factors influencing the prognosis of PLC. These models give us a deeper understanding of PLC. They are expected to be used as stratification tools in clinical studies and as evidence for the development of interventions to improve survival.

DATA AVAILABILITY STATEMENT

The original contributions presented in the study are included in the article/**Supplementary Material**. Further inquiries can be directed to the corresponding authors.

ETHICS STATEMENT

This study was based on publicly available data from the SEER and TCGA database, and did not involve interaction with human subjects or the use of personally identifiable information. The study did not require informed consent for SEER and TCGA registration cases, and the author obtained a"limited use data agreement" from SEER. No trial registration was required.

AUTHOR CONTRIBUTIONS

Software, formal analysis, investigation, and writing of the original draft (YZ and TH), acquisition of the data (BH), analysis and interpretation of data (SS, ZY, and SQ), drafted the manuscript (RC), critical revision of the manuscript for important intellectual content (BG and FZ), and study supervision (YL). All authors reviewed and commented on the manuscript and approved the final version.

SUPPLEMENTARY MATERIAL

The Supplementary Material for this article can be found online at: https://www.frontiersin.org/articles/10.3389/fonc.2022.926359/full#supplementary-material

Supplementary Figure 1 | (A–C) Calibration plots for 1-,3- and 5-year OS in the internal validation cohort; **(D–F)** Calibration plots for 1-,3- and 5-year CSS in the internal validation cohort.

Supplementary Figure 2 | (A–C) Calibration plots for 1-,3- and 5-year OS in the external validation cohort.

Supplementary Table 1 | Characteristics of 172 patients with Primary Liver Cancer in TCGA.

REFERENCES

1. Siegel RL, Miller KD, Fuchs HE, Jemal A. Cancer Statistics, 2021. *CA Cancer J Clin* (2021) 71:7–33. doi: 10.3322/caac.21654
2. Kaplan DE, Mehta R, D'Addeo K, Gade TP, Taddei TH. Transarterial Chemoembolization Within First 3 Months of Sorafenib Initiation Improves Overall Survival in Hepatocellular Carcinoma: A Retrospective, Multi-Institutional Study With Propensity Matching. *J Vasc Interv Radiol* (2018) 29:540–9.e4. doi: 10.1016/j.jvir.2017.11.033
3. Sung H, Ferlay J, Siegel RL, Laversanne M, Soerjomataram I, Jemal A, et al. Global Cancer Statistics 2020: GLOBOCAN Estimates of Incidence and Mortality Worldwide for 36 Cancers in 185 Countries. *CA Cancer J Clin* (2021) 71:209–49. doi: 10.3322/caac.21660
4. Berwick DM, Nolan TW, Whittington J. The Triple Aim: Care, Health, and Cost. *Health Aff (Millwood)* (2008) 27:759–69. doi: 10.1377/hlthaff.27.3.759
5. Xiaofeng N. Development and Evaluation of Nomograms to Predict the Cancer-Specific Mortality and Overall Mortality of Patients With Hepatocellular Carcinoma. *BioMed Res Int* (2021) 2021:1658403. doi: 10.1155/2021/1658403
6. Weintraub WS, Fahed AC, Rumsfeld JS. Translational Medicine in the Era of Big Data and Machine Learning. *Circ Res* (2018) 123:1202–4. doi: 10.1161/CIRCRESAHA.118.313944
7. Telenti A, Lippert C, Chang PC, DePristo M. Deep Learning of Genomic Variation and Regulatory Network Data. *Hum Mol Genet* (2018) 27:R63–71. doi: 10.1093/hmg/ddy115
8. Balachandran VP, Gonen M, Smith JJ, DeMatteo RP. Nomograms in Oncology: More Than Meets the Eye. *Lancet Oncol* (2015) 16:e173–80. doi: 10.1016/S1470-2045(14)71116-7
9. Li Y, Liu W, Zhao L, Gungor C, Xu Y, Song X, et al. Nomograms Predicting Overall Survival and Cancer-Specific Survival for Synchronous Colorectal Liver-Limited Metastasis. *J Cancer* (2020) 11:6213–25. doi: 10.7150/jca.46155
10. Ma L, Deng K, Zhang C, Li H, Luo Y, Yang Y, et al. Nomograms for Predicting Hepatocellular Carcinoma Recurrence and Overall Postoperative Patient Survival. *Front Oncol* (2022) 12:843589. doi: 10.3389/fonc.2022.843589
11. Shen Q, Hu G, Wu J, Lv L. A New Clinical Prognostic Nomogram for Liver Cancer Based on Immune Score. *PLos One* (2020) 15:e0236622. doi: 10.1371/journal.pone.0236622
12. Xiao Z, Yan Y, Zhou Q, Liu H, Huang P, Zhou Q, et al. Development and External Validation of Prognostic Nomograms in Hepatocellular Carcinoma Patients: A Population Based Study. *Cancer Manag Res* (2019) 11:2691–708. doi: 10.2147/CMAR.S191287
13. Wolbers M, Koller MT, Witteman JC, Steyerberg EW. Prognostic Models With Competing Risks: Methods and Application to Coronary Risk Prediction. *Epidemiology* (2009) 20:555–61. doi: 10.1097/EDE.0b013e3181a39056
14. Ryerson AB, Eheman CR, Altekruse SF, Ward JW, Jemal A, Sherman RL, et al. Annual Report to the Nation on the Status of Cancer, 1975-2012, Featuring the Increasing Incidence of Liver Cancer. *Cancer* (2016) 122:1312–37. doi: 10.1002/cncr.29936
15. Villanueva A. Hepatocellular Carcinoma. *N Engl J Med* (2019) 380:1450–62. doi: 10.1056/NEJMra1713263
16. Jiaquan X. Trends in Liver Cancer Mortality Among Adults Aged 25 and Over in the United States, 2000-2016. *NCHS Data Brief* (2018) 314:1–8. doi: 10.1002/cncr.31869
17. Llovet J, Brú C, Bruix J. Prognosis of Hepatocellular Carcinoma: The BCLC Staging Classification. *Semin liver Dis* (1999) 19:329–38. doi: 10.1055/s-2007-1007122
18. Razumilava N, Gores GJ. Cholangiocarcinoma. *Lancet* (2014) 383:2168–79. doi: 10.1016/S0140-6736(13)61903-0
19. Koh KC, Lee H, Choi MS, Lee JH, Paik SW, Yoo BC, et al. Clinicopathologic Features and Prognosis of Combined Hepatocellular Cholangiocarcinoma. *Am J Surg* (2005) 189:120–5. doi: 10.1016/j.amjsurg.2004.03.018
20. Mitchell SW. Combined Hepatocellular Cholangiocarcinomas; Analysis of a Large Database. *Clin Med Pathol* (2008) 1:43–7. doi: 10.4137/cpath.s500
21. Jemal A, Ward EM, Johnson CJ, Cronin KA, Ma J, Ryerson B, et al. Annual Report to the Nation on the Status of Cancer, 1975-2014, Featuring Survival. *J Natl Cancer Inst* (2017) 109. doi: 10.1093/jnci/djx030
22. Krok-Schoen JL, Adams IK, Baltic RD, Fisher JL. Ethnic Disparities in Cancer Incidence and Survival Among the Oldest Old in the United States. *Ethn Health* (2020) 25:79–92. doi: 10.1080/13557858.2017.1395818
23. Minagawa M, Ikai I, Matsuyama Y, Yamaoka Y, Makuuchi M. Staging of Hepatocellular Carcinoma: Assessment of the Japanese TNM and AJCC/UICC TNM Systems in a Cohort of 13,772 Patients in Japan. *Ann Surg* (2007) 245:909–22. doi: 10.1097/01.sla.0000254368.65878.da
24. Chan AC, Fan ST, Poon RT, Cheung TT, Chok KS, Chan SC, et al. Evaluation of the Seventh Edition of the American Joint Committee on Cancer Tumour-Node-Metastasis (TNM) Staging System for Patients Undergoing Curative Resection of Hepatocellular Carcinoma: Implications for the Development of a Refined Staging System. *HPB (Oxford)* (2013) 15:439–48. doi: 10.1111/j.1477-2574.2012.00617.x
25. Zhou X, Wang W, Wang C, Zheng C, Xu X, Ni X, et al. DPP4 Inhibitor Attenuates Severe Acute Pancreatitis-Associated Intestinal Inflammation *via* Nrf2 Signaling. *Oxid Med Cell Longev* (2019) 2019:6181754. doi: 10.1155/2019/6181754
26. Hu C, Yang J, Huang Z, Liu C, Lin Y, Tong Y, et al. Diagnostic and Prognostic Nomograms for Bone Metastasis in Hepatocellular Carcinoma. *BMC Cancer* (2020) 20:494. doi: 10.1186/s12885-020-06995-y
27. Zhang Z, Zhao X, Li Z, Wu Y, Liu Y, Li Z, et al. Development of a Nomogram Model to Predict Survival Outcomes in Patients With Primary Hepatic

Neuroendocrine Tumors Based on SEER Database. *BMC Cancer* (2021) 21:567. doi: 10.1186/s12885-021-08337-y
28. Song W, Miao D-L, Chen L. Nomogram for Predicting Survival in Patients With Pancreatic Cancer. *OncoTargets Ther Volume* (2018) 11:539–45. doi: 10.2147/OTT.S154599
29. Wang Y, Liu J, Huang C, Zeng Y, Liu Y, Du J. Development and Validation of a Nomogram for Predicting Survival of Pulmonary Invasive Mucinous Adenocarcinoma Based on Surveillance, Epidemiology, and End Results (SEER) Database. *BMC Cancer* (2021) 21:148. doi: 10.1186/s12885-021-07811-x

Conflict of Interest: The authors declare that the research was conducted in the absence of any commercial or financial relationships that could be construed as a potential conflict of interest.

Publisher's Note: All claims expressed in this article are solely those of the authors and do not necessarily represent those of their affiliated organizations, or those of the publisher, the editors and the reviewers. Any product that may be evaluated in this article, or claim that may be made by its manufacturer, is not guaranteed or endorsed by the publisher.

Copyright © 2022 Chen, Hou, Qiu, Shao, Yu, Zhou, Guo, Li, Zhang and Han. This is an open-access article distributed under the terms of the Creative Commons Attribution License (CC BY). The use, distribution or reproduction in other forums is permitted, provided the original author(s) and the copyright owner(s) are credited and that the original publication in this journal is cited, in accordance with accepted academic practice. No use, distribution or reproduction is permitted which does not comply with these terms.

frontiers | Frontiers in Oncology

CASE REPORT
published: 23 June 2022
doi: 10.3389/fonc.2022.916457

Surgical Treatment of Intraductal Papillary Neoplasm of the Bile Duct: A Report of Two Cases and Review of the Literature

*Binjie Li, Zhiqiang Liu, Zhuo Meng, Mingyang Li, Weijun Tian and Quanyan Liu**

Department of Hepatobiliary Surgery, Tianjin Medical University General Hospital, Tianjin, China

OPEN ACCESS

Edited by:
Sanjit Mukherjee, National Institutes of Health (NIH), United States

Reviewed by:
Asit Kumar Manna, The University of Utah, United States
Abhisek Bhattacharya, National Institutes of Health (NIH), United States

***Correspondence:**
Quanyan Liu
spsslqy@vip.126.com

Specialty section:
This article was submitted to Gastrointestinal Cancers: Hepato Pancreatic Biliary Cancers, a section of the journal Frontiers in Oncology

Received: *09 April 2022*
Accepted: *16 May 2022*
Published: *23 June 2022*

Citation:
Li B, Liu Z, Meng Z, Li M, Tian W and Liu Q (2022) Surgical Treatment of Intraductal Papillary Neoplasm of the Bile Duct: A Report of Two Cases and Review of the Literature. Front. Oncol. 12:916457. doi: 10.3389/fonc.2022.916457

Intraductal papillary neoplasm of the bile duct (IPNB) is a rare bile duct tumor characterized by intraductal papillary or villous neoplasms covered by neoplastic epithelium with fine fibrovascular stalks in the dilated bile ducts (1). Its true etiology remains unknown. Herein, we report two cases of IPNB that underwent surgical resection. The first case was a 66-year-old male who complained of upper abdominal pain for three years. We found obstruction of the common bile duct and dilation of the intrahepatic and extrahepatic bile ducts after MRCP. Laparoscopic hepatic segmentectomy (S2, S3, S4), resection of the common bile duct, cholecystectomy, and hepaticojejunostomy were performed. The second case was a 67-year-old male with asymptomatic dilation of the intrahepatic duct. The patient underwent robot-assisted laparoscopic hepatic segmentectomy (S5, S6, S7, S8), resection of the common bile duct, hepaticojejunostomy and cholecystectomy.

Keywords: surgical treatment, intraductal papillary neoplasm of the bile duct, mutation, clinical features, prognosis

BACKGROUND

According to the 2019 World Health Organization (WHO) classification of digestive system tumors, intraductal papillary neoplasm of the bile duct (IPNB) is a rare tumor in the bile duct that is characterized by intraductal papillary or villous neoplasms covered by neoplastic epithelium with fine fibrovascular stalks in the dilated bile ducts (1, 2). IPNB is mainly reported in Far Eastern countries where hepatolithiasis and clonorchiasis are endemic (1). Based on a multicenter analysis, malignant features of tumors are observed in 43% of IPNB cases, and patient prognoses for malignant lesions are worse than for noninvasive lesions (3). Therefore, early identification and resection of lesions are significant, even in asymptomatic patients.

Here, we report two cases of surgical treatment of IPNB with a review of relevant literature; perhaps they could provide some information to understand this rare disease.

CASE PRESENTATION

Case 1

A 66-year-old man was referred to our hospital due to abdominal pain. Three years ago, he had presented with right upper quadrant abdominal pain, which worsened after meals, and the pain was more frequent in recent months. He had no noteworthy medical or family history. Physical examination was unremarkable.

Enhanced computed tomography (CT) at our hospital revealed interruption of the intrapancreatic common bile duct (**Figure 1B**) and dilatation of the extrahepatic and intrahepatic bile duct, which was especially obvious in the left lobe of the liver (**Figure 1A**). To evaluate dilatation of the bile duct, magnetic resonance cholangiopancreatography (MRCP) was performed. MRCP showed dilatation of the extrahepatic and intrahepatic bile ducts, irregular dilatation and thickening of the bile duct in the left lobe of the liver (**Figures 1C–H**). At the same time, there were localized nodular prominences in the bile duct lumen. Laboratory values on admission were as follows: tumor markers, alpha-fetoprotein (AFP) 2. 6 ng/mL (normal range 0.00-8.78 ng/mL), ferritin (Fer) 153.96 ng/mL (normal range 21.80–274. 66 ng/mL), carcinoembryonic antigen (CEA) 2. 57 ng/mL (normal range 0.00–5. 00 ng/mL), and cancer antigen 19-9 (CA199) 47. 85 U/mL (normal range 0.00–37.0 U/mL). A routine blood examination was not abnormal. The level of γ-glutamyltranspeptidase (γ-GTP) was elevated, 109 U/L (normal range 7–49 U/L) (**Table 1**).

After the relevant preoperative examination was completed, laparoscopic hepatic segmentectomy (S2, S3, S4), resection of the common bile duct, cholecystectomy, and hepaticojejunostomy were performed. On intraoperative cholangioscopy, we found the left hepatic duct filled with mucus and papillary protrusions adhering to the surface of the left hepatic duct (**Figure 1I**). No abnormalities were detected in the common bile duct. Laparoscopic hepatic segmentectomy (S2, S3, S4), resection of the common bile duct, cholecystectomy, and hepaticojejunostomy were performed. The bile duct was filled with greenish -yellow mucus -like sludge (**Figures 1J, K**). Microscopically, the intrahepatic bile duct, common bile duct and cystic duct were lined by papillary growth neoplasia with high-grade intraepithelial neoplasia (**Figures 1L, M**). Gene detection was performed using DNA extracted from paraffin-embedded bile ducts. Gene detection revealed KRAS codon 12 (p. G12F) mutation, and the mutation frequency was 62.9% (**Figure 1N**).

The postoperative course was uneventful, and the patient was discharged from the hospital on the 7th postoperative day. The patient had no recurrence and no complications for 8 months after surgery.

Case 2

A 67-year-old male with diabetes mellitus was admitted to our hospital due to finding dilatation of extrahepatic and intrahepatic bile ducts by accident during a routine medical examination 15

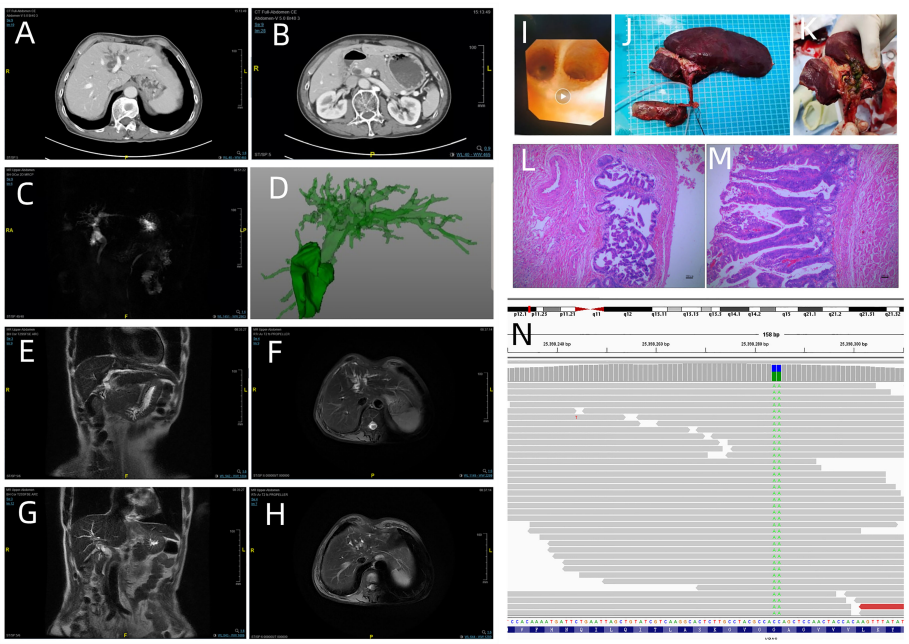

FIGURE 1 | Enhanced computed tomography showed dilatation of the intrahepatic bile duct in the left lobe of the liver **(A)** and common bile duct **(B)**; **(C)** (MRCP) and **(D)** (CT three dimensional reconstruction) revealed the dilatation of extrahepatic and intrahepatic bile duct; **(E)** (coronal view) and **(F)** (axial view). Irregular dilatation and thickening of the bile duct are visible in the left hepatic lobe; **(G)** (coronal view) and **(H)** (axial view) show dilatation of the bile duct in the right left hepatic lobe. **(I)** Intraoperative cholangioscopy findings: biliary papillomatosis in the left hepatic duct. **(J, K)** Macroscopic findings: the bile duct is filled with greenish- yellow mucus- like sludge. (**L**: magnification, x40 and **M**: magnification, x100; hematoxylin and eosin staining) Microscopic findings: the intrahepatic bile duct, common bile duct and cystic duct were lined by papillary growth neoplasia with high-grade intraepithelial neoplasia. **(N)** Next-generation sequencing results revealed the mutation of KRAS codon 12 (p.G12F).

TABLE 1 | Laboratory data before and after the surgery.

	Case 1			Case 2			Normal range
	Pre-operation	Post-operation (6 days)	Post-operation (8 months)	Pre-operation	Post-operation (10 days)	Post-operation (6 months)	
Tumor markers							
AFP	2. 6	–	–	1.97	–	1.54	0.00-8.78 ng/mL
Fer	153.96	–	–	288.81	–	195.62	21.80–274. 66 ng/mL
CEA	2. 57	–	–	4.91	–	2.65	0.00–5. 00 ng/mL
CA199	47. 85	–	28.65	95.00	–	35.55	0.00–37.00 U/mL
Routine blood tests							
WBC	4.21	7.15	5.74	9.81	9.02	–	3.50-9. 50×10^9/L
RBC	4.69	3.84	4.46	5.74	4.22	–	4.30 -5.80×10^12/L
Hb	139	118	131	163	122	–	130-175g/L
PLT	216	170	149	171	139	–	125-350×10^9/L
NEU%	65.3	69.7	62.4	77.0	70.4	–	40.0-75.0%
Liver function tests							
ALB	45	37	44	41	34	–	35-55 g/L
ALT	17	57	17	20	78	–	5-40 U/L
AST	19	24	21	17	27	–	5-40 U/L
ALP	90	58	42	104	68	–	40-150 U/L
γ-GTP	143	92	35	196	84	–	7-49 U/L

days ago. The patient was asymptomatic. He did not feel abdominal pain or abdominal distension. The patient did not have a history of viral hepatitis or alcoholic liver disease. There were no remarkable findings during the physical examination.

Dynamic upper abdominal computed tomography (CT) showed thickening of the distal common bile duct wall, luminal stenosis and dilatation of extrahepatic and intrahepatic bile duct, which was especially pronounced in the right lobe of the liver with a diameter of approximately 15 mm at its widest point (**Figures 2A, B**). Magnetic resonance cholangiopancreatography (MRCP) revealed that the common hepatic duct and intrahepatic bile duct were dilated (**Figures 2C, D, F**). The bile duct wall showed high intensity on diffusion-weighted imaging (**Figures 2E**). Laboratory test results included tumor markers, alpha-fetoprotein (AFP) 1. 97 ng/mL (normal range 0.00-8.78 ng/mL), ferritin (Fer) 288.81 ng/mL (normal range 21.80–274. 66 ng/mL), carcinoembryonic antigen (CEA) 4. 91 ng/mL (normal range 0.00–5. 00 ng/mL), and cancer antigen 19-9 (CA199) 95.00 U/mL (normal range 0.00–37.0 U/mL). Routine blood tests revealed a white blood cell count of 9.81×109/L (normal range 3.50-9. 50×109/L) and a neutrophilic granulocyte percentage of 77.0% (normal range 40.0-75.0%). The level of γ-glutamyltranspeptidase (γ-GTP) was elevated, 196 U/L (normal range 7–49 U/L) (**Table 1**). The diagnosis of intraductal papillary neoplasm of the bile duct (IPNB) was suspected based on the imaging and laboratory findings.

Intraoperative cholangioscopy was performed to evaluate the common bile duct. The common bile duct wall was rough and full of white flocculus (**Figures 2G, H**). Therefore, the patient underwent robot-assisted laparoscopic hepatic segmentectomy (S5, S6, S7, S8), resection of the common bile duct, hepaticojejunostomy and cholecystectomy. Grossly, the intrahepatic bile duct lumen was filled with yellow, gelatinous, sticky mucous masses. The diameter of the largest one was 18 mm. (**Figures 2I, J**) Pathologic findings were as follows: Intraductal papillary neoplasm of the bile duct (IPNB) with low-grade intraepithelial neoplasia, focal high-grade intraepithelial neoplasia; a large number of lymphocytes aggregated in the portal area with extensive bile duct proliferation (**Figures 2L, M**). The patient refused gene detection for financial reasons.

The patient's postoperative course was uneventful. The patient was discharged from our department 13 days after surgery. The patient was followed up for 6 months after the operation, and there were no signs of recurrence. (**Figure 2K**).

DISCUSSION

Intraductal papillary neoplasm of the bile duct (IPNB) is a rare bile duct tumor characterized by intraductal papillary or villous neoplasms covered by neoplastic epithelium with fine fibrovascular stalks in the dilated bile ducts (1).

IPNB is mainly found in patients in Eastern countries, such as Japan, and Korea, where hepatolithiasis and clonorchiasis, which are known to be major risk factors for IPNB, are endemic (4). IPNB shows a slight male predominance, and most patients are between 50 and 70 years of age is reported (4, 5).

However, the pathogenesis and nature of IPNB are still unclear. It is likely caused by cholestasis, biliary tract infection, and biliary tract cancer. Studies have found a mechanism for biliary tract cancer due to the progression of chronic inflammation to multistage carcinogenesis and eventually hyperplasia-dysplasia-carcinoma (6). Furthermore, chronic inflammation induces the production of reactive oxygen species and reactive nitrogen species, resulting in DNA damage, which plays an important role in carcinogenesis (7). IPNB symptoms include recurrent and intermittent abdominal pain, cholangitis, and jaundice. However, some patients are asymptomatic (3, 8). Histological types of IPNB have been classified into the following four types: gastric, intestinal, pancreaticobiliary, oncocytic, and IPMN, depending on morphologic appearance and mucin staining properties (9). GNAS and KRAS mutations detected in 50% and 46.2% of IPNBs are common in IPNBs. KRAS plays an important role in regulating cell growth and differentiation (10), A recent study has shown that KRAS mutation was detected in one

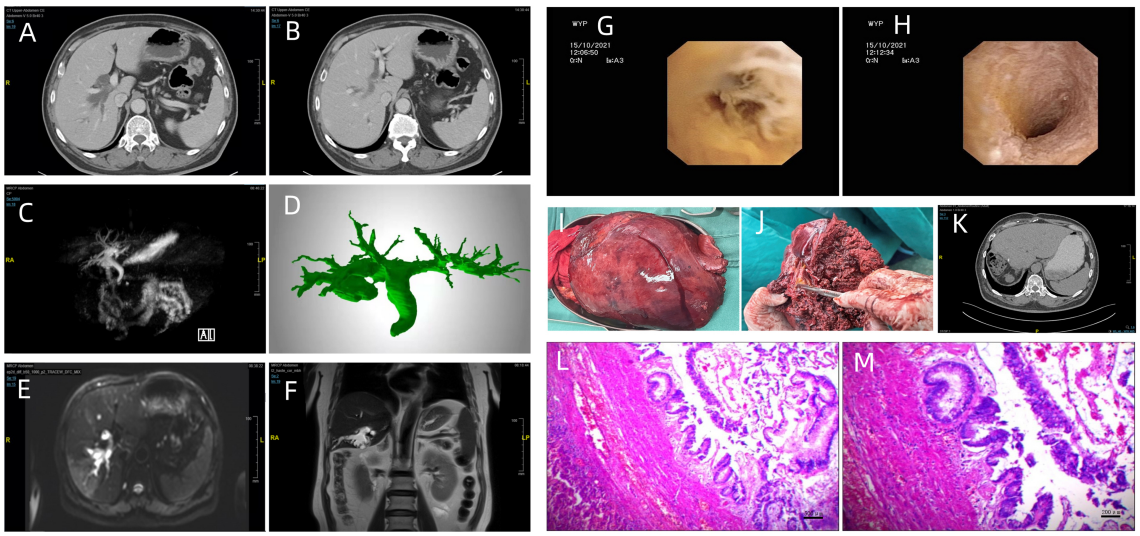

FIGURE 2 | **(A, B)** Enhanced computed tomography demonstrated thickening of the distal common bile duct wall, luminal stenosis, dilatation of extrahepatic and intrahepatic bile duct, especially more evident in the right lobe of liver; **(C)** (MRCP) and **(D)** (CT three dimensional reconstruction) revealed the dilatation of extrahepatic and intrahepatic bile duct; **(E)** (diffusion-weighted image) The bile duct showed high intensity; **(F)** (coronal view) showed the dilatation of intrahepatic bile duct in the right lobe of liver; Intraoperative cholangioscopy revealed the common bile duct wall was full of the white flocculus **(G)** and rough **(H)**; Grossly, the lumen of intrahepatic bile duct was full of yellow, gelatinous, sticky mucous masses **(I, J)**; abdominal computed tomography (CT) showed homogeneous liver parenchyma without bile duct dilation **(K)**; Microscopically, Intraductal papillary neoplasm of the bile duct(IPNB)with low-grade intraepithelial neoplasia, focal high-grade intraepithelial neoplasia; A large amount of lymphocytes aggregated portal area with extensive bile duct proliferation (**L**: magnification, x40 and **M**: magnification, x100; hematoxylin and eosin staining).

third of intrahepatic cholangiocarcinoma (ICC) and also one third of biliary intraepithelialneoplasia (BilINs) associated with hepatolithiasis (11). Moreover, the KRAS mutation rate in high-grade IPNBs, and invasive IPNBs is significantly higher than low- and intermediate-grade IPNBs. So KRAS mutation may contribute to the pathogenesis of IPNBs (12, 13). Research shows that the 5-year survival rate of patients undergoing R0 resection is 59.7%. However, it is still lower than that for patients with benign diseases and better than intrahepatic cholangiocarcinoma (14, 15).

Surgical resection is the first line treatment for patients with IPNB without distant metastasis because of recurrent cholangitis and obstructive jaundice (1, 16). Liver transplantation and pancreaticoduodenectomy can be theoretically regarded as the only curative treatment. However, liver transplantation is unsuitable for patients with advanced tumor invasion or positive lymph nodes (4). Recently, new approaches, such as RFA and APC, have been helpful for patients who are not candidates for surgery due to age or physical condition (17, 18).

To further investigate the clinical features and prognosis of IPNB, we gathered case reports of IPNB in PubMed (17–55). We searched PubMed for "Intraductal papillary neoplasm of the bile duct" and "case report" during 2002 to 2021. Case reports were included if they reported any aspect of the clinicopathological or surgical characteristics of patients with IPNB confirmed by pathology. Most patients were more than 45 years of age, with a median age of 69 years. Only two patients were younger than 45 years of age. Males slightly predominated the case reports. The geographic distribution of patients was not different from other reviews, with IPNB mainly in Asia. There was only one patient found in Africa. However, the patients was Japanese. The tumor size ranged from 10.6-130. 0 mm, with a median size of 52. 9 mm. IPNB can develop anywhere along the biliary tree, with 25.0% in the right lobe of the liver, 32.5% in the left lobe of the liver, 12.5% in the CBD, 17.5% in the extrahepatic duct and liver and 12.5% in other locations, including the whole liver or gallbladder. The common radiologic findings for IPNB are bile duct dilatation, intraductal mass and cystic lesion. Among all cases, 28 included information on tumor markers, the CA 19-9 of 10 cases was elevated, and 18 were not elevated. The type of surgery depended on various anatomical locations of the tumor and the physical qualifications of the patients. Hepatectomy, which accounted for 40%, was the main surgical approach. Twenty-five percent of patients underwent hepatectomy, extrahepatic bile duct resection, and hepaticojejunostomy. Five percent of patients underwent hepatectomy and segmental pancreatectomy. A total of 7.5% of patients underwent pancreatoduodenectomy. As a palliative treatment, endoscopic treatment is necessary for patients with poor physical conditions. It is worth mentioning that RFA and APC accounted for 7.5% of promising therapeutic strategies and are expected to bring new approaches for IPNB (**Table 2**). IPNB lesions frequently contain invasive components. Twenty-three cases (57.5%) contained evidence of high- grade cholangiocarcinoma, while 17 cases (42.5%) ranged from no invasion to medium-grade cholangiocarcinoma. Immunohistochemical data were available for 26 cases, from which we found that CK7 (42.3%), MUC5AC (53.8%) and MUC6 (53.8%) expression was common in the IPNB. Based on the recurrence-free survival (RFS) reported in 23 cases, we found that the range of RFS was 4.0-39.0 months, with a median of 14.0 months (**Table 3**).

TABLE 2 | The demographic characteristics, clinical features and surgical approaches of IPNB.

Feature	N(%)
Age (years)	
33-45	2 (5.0%)
45-57	4 (10.0%)
57-69	15 (37.5%)
69-81	12 (30.0%)
81-93	7 (17.5%)
Sex	
Male	22 (55.0%)
Female	18 (45.0%)
Region	28 (70.0%)
Asia	4 (10.0%)
America	7 (17.5%)
Europe	1 (2.5%)
Africa	
Tumor size (mm)	Range (10.6-130.0) Median (52.9)
Tumor location	
The right lobe of the liver	10 (25.0%)
The left lobe of the liver	13 (32.5%)
CBD	5 (12.5%)
Extrahepatic duct and liver	7 (17.5%)
Other	5 (12.5%)
Imaging findings	
Solid mass	9 (22.5%)
Cystic lesion	6 (15.0%)
Dilation of the bile duct	7 (17.5%)
Solid mass;cystic lesion	5 (12.5%)
Solid mass;dilation of the bile duct	5 (12.5%)
Cystic lesion;dilation of the bile duct	4 (10.0%)
Solid mass;cystic lesion;dilation of the bile duct	3 (7.5%)
Unknown	1 (2.5%)
Tumor marker (CA 19-9)	
Elevated	10 (25.0%)
Not elevated	18 (45.0%)
Unknown	12 (30.0%)
Surgical approaches	
Hepatectomy	16 (40.0%)
Hepatectomy;extrahepatic bile duct resection; hepaticojejunostomy	10 (25.0%)
Hepatectomy;segmental pancreatectomy	2 (5.0%)
Pancreatoduodenectomy	3 (7.5%)
Endoscopic treatment	3 (7.5%)
RFA and APC	3 (7.5%)
Other	2 (5.0%)
Unknown	1 (2.5%)

On further review of the literature, we could conclude that IPNB mainly behaves as in imaging solid mass, cystic lesion and dilation of the bile duct in imaging. Surgical resection is the major treatment for patients in fine condition, and interventional therapies such as RFA and APC are good choices for palliative treatments. Although most IPNB cases are high-grade intraepithelial neoplasia or invasive carcinoma in microscopically, surgical resection could make patients get satisfactory prognosis.

TABLE 3 | The pathological features and RFS of IPNB.

Tumor grade	N(%)
no invasion	5/40 (12.5%)
low grade	5/40 (12.5%)
low to intermediate grade	3/40 (7.5%)
intermediate grade	2/40 (5.0%)
intermediate to high grade	2/40 (5.0%)
high grade	8/40 (20%)
I PNB with cholangiocarcinoma	15/40 (37.5%)
Immunohistochemistry (+)	
CK7	11/26 (42.3%)
MUC5AC	14/26 (53.8%)
MUC6	14/26 (53.8%)
MUC1	5/26 (19.2%)
MUC2	3/26 (11.5%)
RFS (month)	Range (4.0-39.0) Median (14.0) N(23)

CONCLUSION

In summary, we report two cases of IPNB, a rare tumor of the hepatobiliary system, and analyze published case reports about IPNB. Since IPNB has a high potential for transforming into an invasive lesion, R0 surgical resection is preferred. At the same time, RFA and APC may be new palliative approaches for treating IPNB.

DATA AVAILABILITY STATEMENT

The datasets presented in this study can be found in online repositories. The names of the repository/repositories and accession number(s) can be found in the article/supplementary material.

AUTHOR CONTRIBUTIONS

BL designed the case report. ZL, QL, and WT participated in the operation and management of the patients. BL, ZM, and ML prepared radiological and histology figures. BL, ZL reviewed the literature and drafted the article. All authors contributed to the article and approved the submitted version.

REFERENCES

1. Ohtsuka M, Shimizu H, Kato A, Yoshitomi H, Furukawa K, Tsuyuguchi T, et al. Intraductal Papillary Neoplasms of the Bile Duct. *Int J Hepatol* (2014) 2014:459091. doi: 10.1155/2014/459091
2. Nakanuma Y, Basturk O, Esposito I, Klimstra DS, Komuta M, Zen Y. Intraductal Papillary Neoplasm of the Bile Ducts. In: *WHO Classification of Tumours. Digestive System Tumours, fifth ed.* Lyon: IARC (2019). p. 279–82.
3. Gordon-Weeks AN, Jones K, Harriss E, Smith A, Silva M. Systematic Review and Meta-Analysis of Current Experience in Treating IPNB: Clinical and Pathological Correlates. *Ann Surg* (2016) 263(4):656–63. doi: 10.1097/SLA.0000000000001426
4. Wan XS, Xu YY, Qian JY, Yang XB, Wang AQ, He L, et al. Intraductal Papillary Neoplasm of the Bile Duct. *World J Gastroenterol* (2013) 19 (46):8595–604. doi: 10.3748/wjg.v19.i46.8595
5. Wu X, Li B, Zheng C, Chang X, Zhang T, He X, et al. Intraductal Papillary Neoplasm of the Bile Duct: A Single-Center Retrospective Study. *J Int Med Res* (2018) 46(10):4258–68. doi: 10.1177/0300060518792800

6. Terada T, Nakanuma Y, Ohta T, Nagakawa T. Histological Features and Interphase Nucleolar Organizer Regions in Hyperplastic, Dysplastic and Neoplastic Epithelium of Intrahepatic Bile Ducts in Hepatolithiasis. *Histopathology* (1992) 21(3):233–40. doi: 10.1111/j.1365-2559.1992.tb00381.x
7. Aishima S, Kubo Y, Tanaka Y, Oda Y. Histological Features of Precancerous and Early Cancerous Lesions of Biliary Tract Carcinoma. *J Hepatobiliary Pancreat Sci* (2014) 21(7):448–52. doi: 10.1002/jhbp.71
8. Park HJ, Kim SY, Kim HJ, Lee SS, Hong GS, Byun JH, et al. Intraductal Papillary Neoplasm of the Bile Duct: Clinical, Imaging, and Pathologic Features. *AJR Am J Roentgenol* (2018) 211(1):67–75. doi: 10.2214/AJR.17.19261
9. Wang X, Cai YQ, Chen YH, Liu XB. Biliary Tract Intraductal Papillary Mucinous Neoplasm: Report of 19 Cases. *World J Gastroenterol* (2015) 21 (14):4261–7. doi: 10.3748/wjg.v21.i14.4261
10. Xiao HD, Yamaguchi H, Dias-Santagata D, Kuboki Y, Akhavanfard S, Hatori T, et al. Molecular Characteristics and Biological Behaviours of the Oncocytic and Pancreatobiliary Subtypes of Intraductal Papillary Mucinous Neoplasms. *J Pathol* (2011) 224(4):508–16. doi: 10.1002/path.2875
11. Hsu M, Sasaki M, Igarashi S, Sato Y, Nakanuma Y. KRAS and GNAS Mutations and P53 Overexpression in Biliary Intraepithelial Neoplasia and Intrahepatic Cholangiocarcinomas. *Cancer* (2013) 119(9):1669–74. doi: 10.1002/cncr.27955
12. Sasaki M, Matsubara T, Nitta T, Sato Y, Nakanuma Y. GNAS and KRAS Mutations are Common in Intraductal Papillary Neoplasms of the Bile Duct. *PloS One* (2013) 8(12):e81706. doi: 10.1371/journal.pone.0081706
13. Xian ZH, Qin C, Cong WM. KRAS Mutation and Immunohistochemical Profile in Intraductal Papillary Neoplasm of the Intrahepatic Bile Ducts. *Pathol Res Pract* (2018) 214(1):105–11. doi: 10.1016/j.prp.2017.10.017
14. Luvira V, Pugkhem A, Bhudhisawasdi V, Pairojkul C, Sathitkarnmanee E, Luvira V, et al. Long-Term Outcome of Surgical Resection for Intraductal Papillary Neoplasm of the Bile Duct. *J Gastroenterol Hepatol* (2017) 32 (2):527–33. doi: 10.1111/jgh.13481
15. Kawarada Y, Yamagiwa K, Das BC. Analysis of the Relationships Between Clinicopathologic Factors and Survival Time in Intrahepatic Cholangiocarcinoma. *Am J Surg* (2002) 183(6):679–85. doi: 10.1016/S0002-9610(02)00853-X
16. Krawczyk M, Ziarkiewicz-Wróblewska B, Podgórska J, Grzybowski J, Gierej B, Krawczyk P, et al. Intraductal Papillary Neoplasm of the Bile Duct - A Comprehensive Review. *Adv Med Sci* (2021) 66(1):138–47. doi: 10.1016/j.advms.2021.01.005
17. Arai J, Kato J, Toda N, Kurokawa K, Shibata C, Kurosaki S, et al. Long-Term Survival After Palliative Argon Plasma Coagulation for Intraductal Papillary Mucinous Neoplasm of the Bile Duct. *Clin J Gastroenterol* (2021) 14(1):314–8. doi: 10.1007/s12328-020-01199-0
18. Natov NS, Horton LC, Hegde SR. Successful Endoscopic Treatment of an Intraductal Papillary Neoplasm of the Bile Duct. *World J Gastrointest Endosc.* (2017) 9(5):238–42. doi: 10.4253/wjge.v9.i5.238
19. Nakagawa T, Arisaka Y, Ajiki T, Fujikura K, Masuda A, Takenaka M, et al. Intraductal Tubulopapillary Neoplasm of the Bile Duct: A Case Report and Review of the Published Work. *Hepatol Res* (2016) 46(7):713–8. doi: 10.1111/hepr.12604
20. Kunovsky L, Kala Z, Svaton R, Moravcik P, Mazanec J, Husty J, et al. Mucinous Cystic Neoplasm of the Liver or Intraductal Papillary Mucinous Neoplasm of the Bile Duct? A Case Report and a Review of Literature. *Ann Hepatol* (2018) 17(3):519–24. doi: 10.5604/01.3001.0011.7397
21. Apostolopoulos P, Ekmektzoglou KA, Paraskeva K, Dimopoulos K, Paparaskeva K, Alexandrakis G. Intraductal Papillary Neoplasm of the Bile Duct : Case Report and Review of the Literature. *Acta Gastroenterol Belg.* (2018) 81(1):97–9.
22. Nam NH, Taura K, Kanai M, Fukuyama K, Uza N, Maeda H, et al. Unexpected Metastasis of Intraductal Papillary Neoplasm of the Bile Duct Without an Invasive Component to the Brain and Lungs: A Case Report. *World J Gastroenterol* (2020) 26(3):366–74. doi: 10.3748/wjg.v26.i3.366
23. Tsujimae M, Sakai A, Masuda A, Inomata N, Masuda S, Gonda M, et al. A Case in Which an Intraductal Papillary Neoplasm of the Bile Duct Was Surgically Resected 12 Years After the Initial Diagnosis. *Intern Med* (2020) 59 (22):2879–83. doi: 10.2169/internalmedicine.4891-20
24. Peeters K, Delvaux P, Huysentruyt F. Intraductal Papillary Neoplasm of the Bile Duct: A Case Report. *Acta Chir Belg.* (2017) 117(4):260–3. doi: 10.1080/00015458.2016.1258785
25. Aliyev V, Yasuchika K, Hammad A, Tajima T, Fukumitsu K, Hata K, et al. A Huge Intraductal Papillary Neoplasm of the Bile Duct Treated by Right Trisectionectomy After Right Portal Vein Embolization. *Ann Hepatobiliary Pancreat Surg* (2018) 22(2):150–5. doi: 10.14701/ahbps.2018.22.2.150
26. Ma Z, Zhao F, Pan J, Lin G, Chen B, Fu W. Cystic Intraductal Papillary Neoplasms With Infiltrating Carcinoma of the Intrahepatic Bile Duct: A Case Report. *Med (Baltimore)* (2020) 99(3):e18758. doi: 10.1097/MD.0000000000018758
27. Tan Y, Milikowski C, Toribio Y, Singer A, Rojas CP, Garcia-Buitrago MT. Intraductal Papillary Neoplasm of the Bile Ducts: A Case Report and Literature Review. *World J Gastroenterol* (2015) 21(43):12498–504. doi: 10.3748/wjg.v21.i43.12498
28. Dutta S, Upadhyay P, Jain A, Nachiappa Ganesh R, Nelamangala Ramakrishnaiah VP. Intraductal Papillary Neoplasm of the Bile Duct: A Rare Case of Intrahepatic Space-Occupying Lesion. *Cureus* (2021) 13(2): e13063. doi: 10.7759/cureus.13063
29. Hokuto D, Nomi T, Yasuda S, Yoshikawa T, Ishioka K, Yamada T, et al. Long-Term Observation and Treatment of a Widespread Intraductal Papillary Neoplasm of the Bile Duct Extending From the Intrapancreatic Bile Duct to the Bilateral Intrahepatic Bile Duct: A Case Report. *Int J Surg Case Rep* (2017) 38:166–71. doi: 10.1016/j.ijscr.2017.07.031
30. Anjum MR, Dasari BVM, Menon S. Multiple Intraductal Papillary Neoplasms of the Bile Ducts: A Case Report. *VideoGIE* (2020) 6(1):22–3. doi: 10.1016/j.vgie.2020.08.008
31. Hachiya H, Kita J, Shiraki T, Iso Y, Shimoda M, Kubota K. Intraductal Papillary Neoplasm of the Bile Duct Developing in a Patient With Primary Sclerosing Cholangitis: A Case Report. *World J Gastroenterol* (2014) 20 (42):15925–30. doi: 10.3748/wjg.v20.i42.15925
32. Kitahama T, Yamane H, Mohri K, Fukuoka E, Yoshida T, Yamagishi T, et al. A Case of Intraductal Papillary Neoplasm of the Bile Duct Accompanied by Intraductal Papillary Mucinous Neoplasm of the Pancreas and Hepatocellular Carcinoma. *Clin J Gastroenterol* (2021) 14(5):1536–43. doi: 10.1007/s12328-021-01461-z
33. Kakisaka T, Kamiyama T, Yokoo H, Nakanishi K, Wakayama K, Tsuruga Y, et al. An Intraductal Papillary Neoplasm of the Bile Duct Mimicking a Hemorrhagic Hepatic Cyst: A Case Report. *World J Surg Oncol* (2013) 11:111. doi: 10.1186/1477-7819-11-111
34. Tsuchida K, Yamagata M, Saifuku Y, Ichikawa D, Kanke K, Murohisa T, et al. Successful Endoscopic Procedures for Intraductal Papillary Neoplasm of the Bile Duct: A Case Report. *World J Gastroenterol* (2010) 16(7):909–13. doi: 10.3748/wjg.v16.i7.909
35. Tominaga K, Kamimura K, Sakamaki A, Terai S. Intraductal Papillary Neoplasm of the Bile Duct: A Rare Liver Tumor Complicated by Malignancy. *Hepatol* (2017) 66(5):1695–7. doi: 10.1002/hep.29266
36. Shimoda T, Yoshida H, Hirakata A, Makino H, Yokoyama T, Maruyama H, et al. Surgical Resection of Cystic Intraductal Papillary Adenocarcinoma of the Bile Duct: Report of a Case. *J Nippon Med Sch* (2013) 80(3):234–9. doi: 10.1272/jnms.80.234
37. Tajima S, Ohata A, Koda K, Maruyama Y. Intraductal Papillary Neoplasm of the Bile Duct, Gastric Type, Arising in the Intrapancreatic Common Bile Duct Could Progress to Colloid Carcinoma: Report of a Case. *Int J Clin Exp Pathol* (2015) 8(5):5848–55.
38. Kang GH, Moon HS, Lee ES, Kim SH, Sung JK, Lee B, et al. A Case of Colloid Carcinoma Arising in Association With Intraductal Papillary Neoplasm of the Liver. *Korean J Gastroenterol* (2012) 60(6):386–90. doi: 10.4166/kjg.2012.60.6.386
39. Hasebe T, Sawada K, Hayashi H, Nakajima S, Takahashi H, Hagiwara M, et al. Long-Term Growth of Intrahepatic Papillary Neoplasms: A Case Report. *World J Gastroenterol* (2019) 25(36):5569–77. doi: 10.3748/wjg.v25.i36.5569
40. Okamoto T, Nakamura K, Fukuda K. Mucin-Producing Bile Duct Tumor Treated Successfully With Endoscopic Ultrasound-Guided Hepaticogastrostomy. *Clin J Gastroenterol* (2020) 13(5):812–7. doi: 10.1007/s12328-020-01123-6

41. Mo A, Brat G, Spolverato G, Pawlik TM. Intraductal Papillary Mucinous Neoplasm of the Liver: GI Image. *J Gastrointest Surg* (2015) 19(4):792–4. doi: 10.1007/s11605-015-2750-2
42. Lee JH, Kim HS, Park JH, Park JS. Intraductal Papillary Mucinous Neoplasm of the Biliary Tract With Cardiac Metastasis: A Case Report. *Med (Baltimore)* (2021) 100(3):e24310. doi: 10.1097/MD.0000000000024310
43. Nanashima A, Sumida Y, Tomoshige K, Takeshita H, Shibata K, Sawai T, et al. A Case of Intraductal Papillary Neoplasm of the Bile Duct With Stromal Invasion. *Case Rep Gastroenterol* (2008) 2(3):314–20. doi: 10.1159/000154818
44. Cocca S, Grande G, Reggiani Bonetti L, Magistri P, Di Sandro S, Di Benedetto F, et al. Common Bile Duct Lesions - How Cholangioscopy Helps Rule Out Intraductal Papillary Neoplasms of the Bile Duct: A Case Report. *World J Gastrointest Endosc.* (2020) 12(12):555–9. doi: 10.4253/wjge.v12.i12.555
45. Ishida M, Seki K, Honda K, Kimura T, Katayama K, Hirose K, et al. Intraductal Mucinous Tumors Occurring Simultaneously in the Liver and Pancreas. *J Gastroenterol* (2002) 37(12):1073–8. doi: 10.1007/s005350200181
46. Yokode M, Hanada K, Shimizu A, Minami T, Hirohata R, Abe T, et al. Intracholecystic Papillary Neoplasm of the Gallbladder Protruding Into the Common Bile Duct: A Case Report. *Mol Clin Oncol* (2019) 11(5):488–92. doi: 10.3892/mco.2019.1919
47. Hong MY, Yu DW, Hong SG. Intraductal Papillary Mucinous Neoplasm of the Bile Duct With Gastric and Duodenal Fistulas. *World J Gastrointest Endosc.* (2014) 6(7):328–33. doi: 10.4253/wjge.v6.i7.328
48. Kinoshita M, Asaoka T, Eguchi H, Hanaki T, Iwagami Y, Akita H, et al. A Case of Intraductal Papillary Neoplasm of the Bile Duct That Developed 38 Years After Choledochoduodenostomy With Invasive Adenocarcinoma and Lymph Node Metastasis. *Surg Case Rep* (2019) 5(1):93. doi: 10.1186/s40792-019-0651-4
49. Kung JWC, Parks RW, Ireland HM, Kendall TJ, Church NI. Intraductal Papillary Neoplasm of the Bile Duct: The Role of Single-Operator Cholangioscopy. *VideoGIE* (2017) 3(2):55–7. doi: 10.1016/j.vgie.2017.10.006
50. Parekh R, Krol G, Piraka C, Batra S. A Rare Case of Intraductal Papillary Mucinous Neoplasm of the Biliary Duct in a Patient With Prostate Adenocarcinoma. *Case Rep Gastroenterol* (2016) 10(3):743–8. doi: 10.1159/000450539
51. Carrafiello G, Bertolotti E, Sessa F, Cafaro T, Dionigi G, Genovese E, et al. Intraductal Papillary Mucinous Tumor of Bile Ducts Radiologic and Pathologic Features: A Case Report. *cases J* (2008) 1(1):319. doi: 10.1186/1757-1626-1-319
52. Fujita M, Wakui N, Yamauchi Y, Takeda Y, Sato T, Ueki N, et al. A Case of Branch Duct Type Intraductal Papillary Neoplasm of the Bile Duct Treated by Open Surgery After 11 Years of Follow-Up. *Mol Clin Oncol* (2013) 1(6):965–9. doi: 10.3892/mco.2013.160
53. Baltagiannis EG, Kalyvioti C, Glantzouni A, Batistatou A, Tzimas P, Glantzounis GK. Intrahepatic Intraductal Papillary Cystic Neoplasm of the Bile Duct: A Case Report. *Ann Med Surg (Lond)* (2021) 63:102167. doi: 10.1016/j.amsu.2021.02.013
54. Tang W, Qiu JG, Wei XF, Xiao H, Deng X, Wang SD, et al. Endoscopic Endoluminal Radiofrequency Ablation and Single-Operator Peroral Cholangioscopy System (SpyGlass) in the Diagnosis and Treatment of Intraductal Papillary Neoplasm of the Bile Duct: A Case Report and Literature Review. *Front Med (Lausanne)* (2021) 8:675720. doi: 10.3389/fmed.2021.675720
55. Baterdene N, Hwang S, Lee JW, Jung MJ, Shin H, Seo HK, et al. Surgical Treatment of Mucin-Producing Cholangiocarcinoma Arising From Intraductal Papillary Neoplasm of the Intrahepatic Bile Duct: A Report of 2 Cases. *Korean J Hepatobiliary Pancreat Surg* (2016) 20(3):137–43. doi: 10.14701/kjhbps.2016.20.3.137

Conflict of Interest: The authors declare that the research was conducted in the absence of any commercial or financial relationships that could be construed as a potential conflict of interest.

Publisher's Note: All claims expressed in this article are solely those of the authors and do not necessarily represent those of their affiliated organizations, or those of the publisher, the editors and the reviewers. Any product that may be evaluated in this article, or claim that may be made by its manufacturer, is not guaranteed or endorsed by the publisher.

Copyright © 2022 Li, Liu, Meng, Li, Tian and Liu. This is an open-access article distributed under the terms of the Creative Commons Attribution License (CC BY). The use, distribution or reproduction in other forums is permitted, provided the original author(s) and the copyright owner(s) are credited and that the original publication in this journal is cited, in accordance with accepted academic practice. No use, distribution or reproduction is permitted which does not comply with these terms.

frontiers | Frontiers in Oncology

ORIGINAL RESEARCH
published: 24 June 2022
doi: 10.3389/fonc.2022.879810

Regulation of Gamma-Aminobutyric Acid Transaminase Expression and Its Clinical Significance in Hepatocellular Carcinoma

Xiaoqiang Gao[1†], Xiaodong Jia[2†], Moyan Xu[3†], Jiao Xiang[4], Jin Lei[1], Yinyin Li[2], Yinying Lu[2,5,6*] and Shi Zuo[1*]*

[1] Department of Hepatobiliary Surgery, Affiliated Hospital of Guizhou Medical University, Guiyang, China, [2] Department of Liver Disease, Fifth Medical Center of Chinese People's Liberation Army General Hospital, Beijing, China, [3] Health Care Office, Chinese People's Liberation Army General Hospital, Beijing, China, [4] Education Department, Beijing Anzhen Hospital, Capital Medical University, Beijing, China, [5] Center for Synthetic and Systems Biology (CSSB), Tsinghua University, Beijing, China, [6] Guangdong Key Laboratory of Epigenetics, College of Life Sciences and Oceanography, Shenzhen University, Shenzhen, China

OPEN ACCESS

Edited by:
Sanjit Mukherjee, National Institutes of Health (NIH), United States

Reviewed by:
Hailong Wu, Shanghai University of Medicine and Health Sciences, China
Divya Rawat, Dr. Harisingh Gour Central University, India

***Correspondence:**
Shi Zuo
drzuoshi@gmc.edu.cn
Yinying Lu
luyinying1973@163.com
Yinyin Li
lhllyy@sohu.com

[†]These authors have contributed equally to this work and share first authorship

Specialty section:
This article was submitted to Gastrointestinal Cancers: Hepato Pancreatic Biliary Cancers, a section of the journal Frontiers in Oncology

Received: *20 February 2022*
Accepted: *23 May 2022*
Published: *24 June 2022*

Citation:
Gao X, Jia X, Xu M, Xiang J, Lei J, Li Y, Lu Y and Zuo S (2022) Regulation of Gamma-Aminobutyric Acid Transaminase Expression and Its Clinical Significance in Hepatocellular Carcinoma. Front. Oncol. 12:879810. doi: 10.3389/fonc.2022.879810

Background: Gamma-aminobutyric acid transaminase (ABAT) catalyzes the conversion of gamma-aminobutyric acid (GABA) into succinic semialdehyde. Although some evidence supports a key role of ABAT in the progression of hepatocellular carcinoma (HCC), no systematic analysis is available. Thus, this study aimed to investigate the possible mechanisms related to low ABAT expression and the prognostic value and potential functions of ABAT in HCC.

Methods: We obtained relevant datasets from the Encyclopedia of RNA Interactomes, MethSurv, cBioPortal, TISIDB and The Cancer Genome Atlas and used bioinformatic methods to analyze DNA methylation, copy number variation, gene mutation, and upstream microRNAs (miRNAs) of ABAT, exploring the potential relationship between ABAT expression and the prognosis, glycolysis, and immune infiltration in HCC.

Results: The results indicated that ABAT expression was lower in HCC tumor tissues than in normal tissues or adjacent tissues. Low ABAT expression was related to patient age, T stage classification, pathologic stage, histological grade, and alpha-fetoprotein level of HCC. Kaplan-Meier survival analyses indicated that low ABAT expression was correlated with poor HCC prognosis. ABAT was also verified as an independent risk factor in HCC *via* Cox multivariate analysis. Gene set enrichment analysis showed enrichment in various signaling pathways. Furthermore, DNA methylation, copy number variation, and gene mutation potentially induced low ABAT expression; miR-135a-5p was a potential upstream miRNA of ABAT. Additionally, ABAT expression was associated with glycolysis-related genes, infiltrated immune cells, immunoinhibitors, and immunostimulators in HCC.

Conclusions: Our study reveals that deficient ABAT expression is correlated with disease progression and poor prognosis in HCC because of its role in tumorigenesis and tumor immunity.

Keywords: gamma-aminobutyric acid transaminase, hepatocellular carcinoma (HCC), DNA methylation, copy number variation - CNV, gene mutation, miR-135a-5p, glycolysis (Warburg effect), immune infiltration

INTRODUCTION

Hepatocellular carcinoma (HCC) is a type of primary liver cancer accounting for more than 90% of primary liver cancer cases. The etiological factors of HCC include hepatitis virus infection, alcohol consumption, and nonalcoholic fatty liver disease (1). Despite multiple treatment modalities, the five-year survival rate for HCC remains below 20% worldwide. The failure of HCC screening resulting in late diagnosis, delayed treatment, and underuse of treatment methods in clinical practice may primarily cause the poor prognosis of HCC (2). Accordingly, accurate biomarkers are required for improved early-stage screening and diagnosis of HCC and for improving patient outcomes.

Gamma-aminobutyric acid (GABA) is an important neurotransmitter in the nervous system. The ionotropic GABA-A receptor (GABAA) and the metabotropic GABA-B receptor (GABAB) mediate the biological effects of GABA. GABA is involved in the growth and progression of tumors. Gamma-aminobutyric acid transaminase (ABAT) catalyzes the conversion of GABA into succinic semialdehyde and L-glutamate, and is expressed at low levels in basal-like breast cancer (BLBC), leading to an increase in GABA production. GABA then binds to the GABA-A receptor to increase the concentration of intracellular Ca^{2+}, promoting tumor progression by activating nuclear factor of activated T cells 1 (NFAT1) in BLBC cells (3). ABAT is still poorly expressed in HCC, which is correlated with a bad prognosis in patients with HCC, and the proliferation, migration, and invasion of HCC cells are inhibited by the overexpression of ABAT (4). Inconsistent with the study in BLBC (3), the low expression of ABAT may promote HCC progression through other signaling pathways than the GABA pathway. Firstly, GABA-A receptor activation induces the hyperpolarization of hepatic cells, which inhibits hepatic regeneration (5). Secondly, Baclofen, a GABAB receptor agonist, suppresses HCC cell growth by inducing G0/G1 phase arrest (6). Furthermore, GABA suppresses HCC cell migration and invasion through induction of the GABA-A receptor (7). The causes of the low expression of ABAT also remain obscure.

In the present study, we explored the correlation between ABAT and HCC using The Cancer Genome Atlas (TCGA) database. Gene set enrichment analysis (GSEA) was performed to elucidate the ABAT-related biological pathways in HCC. We analyzed DNA methylation, copy number variation, and gene mutations of *ABAT* using the MethSurv and cBioPortal databases. Upstream microRNAs (miRNAs) of ABAT were identified using the Encyclopedia of RNA Interactomes (ENCORI) and TCGA databases, and the relationship between ABAT and glycolysis was analyzed. The correlation of ABAT expression with immune cell infiltration and immunomodulatory molecules was investigated using the TISIDB and TCGA databases.

MATERIALS AND METHODS

ABAT Gene Expression Analysis With TCGA Database

HCC mRNA expression data were obtained from TCGA database (https://genome-cancer.ucsc.edu/). The R package "limma" was used to explore differential ABAT expression by analyzing the data after normalization. The R package "ggplot2" was utilized to draw plots.

Sample Collection

Tissue samples from 71 HCC patients who underwent surgical resection between 2013 and 2015 at the Department of Hepatic Surgery, in the Fifth Medical Center of the Chinese PLA General Hospital, Beijing, China, were collected. No anticancer treatments were administered to the patients before surgery. The follow-up endpoint for all patients was May 2020.

RNA Extraction and Quantitative Reverse Transcription Polymerase Chain Reaction

The total RNA content was extracted from the tumor tissues and adjacent non-tumor tissues (at least 2 cm away from the edge of the tumor) using the TRIzol method. Complementary DNA (cDNA) was synthesized based on the manufacturer's protocol (DBI Bioscience, Newark, DE, USA). qRT-PCR (Thermo Fisher Scientific, USA) was performed with cDNA and qPCR SuperMix (Takara Bio, Inc., Otsu, Japan). Each sample was tested in triplicate, and all samples were tested thrice. The specific primers of ABAT were as follows: 5`-AAGAGAGCCGAGGCAATTACC-3` and 5`-GCTCGCATTTTGAGGCTGTTG-3`. The GAPDH-specific primers were as follows: 5`-GGAGCGAGATCCCTCCAAAAT-3` and 5`-GGCTGTTGTCATACTTCTCATGG-3`. The forward primer of miR-135a-5p (poly (A)–tailing method) was as follows: 5`-TATGGCTTTTTATTCCTATGTGA-3`. Normalization of the results was done using the $2^{-\Delta\Delta Ct}$ value.

Western Blot

Eight pairs of HCC tissue samples were dissolved using radioimmunoprecipitation assay buffer (BIOSS, Beijing, China). A bicinchoninic acid protein assay kit (BIOSS, Beijing, China) was used to determine protein concentrations. Equivalent protein samples were separated using 12% sodium dodecyl sulfate-polyacrylamide gel electrophoresis and diverted onto a polyvinylidene fluoride membrane (Millipore, USA). The membrane was incubated with primary rabbit anti-human ABAT antibody (1:2000 dilution; Abcam, USA) overnight at 4° C after blocking, followed by Horseradish Peroxidase (HRP)-conjugated goat anti-rabbit secondary antibody (1:4000 dilution; Abcam, USA) for 2 h. Glyceraldehyde-3-phosphate dehydrogenase was used as the control. In the end, the membrane was rinsed with phosphate-buffered saline with 0.1% Tween 20 buffer thrice and scanned with a gel imaging system (Thermo, Waltham, USA).

Immunohistochemistry

Six pairs of paraffin-embedded samples were incubated with normal goat serum after rehydration and oxidation with hydrogen peroxide. Slides were incubated with primary rabbit anti-human ABAT antibody (1:100 dilution; Abcam, USA) overnight at 4°C followed by HRP-conjugated secondary antibody (Zhongshan Golden Bridge Biotechnology, China) for 30 min. Finally, the slides were sealed with resinene after incubation with 3,3-diaminobenzidine and counterstained with

hematoxylin. Five fields were randomly selected and imaged with a microscope (Olympus, Japan) at 200× magnification. Image Pro Plus software (version 7.0; USA) was utilized to analyze the results by calculating the average ratios of integrated optical density (IOD) to the positive area (IOD/pixel).

Relationships Between ABAT Expression, Clinical Phenotype, and Prognosis

Relevant data were extracted from each sample obtained from TCGA database. Ten clinical phenotypes were selected, namely, patient age, patient gender, T stage classification, N stage classification, M stage classification, pathologic stage, histologic grade, alpha-fetoprotein (AFP) level (ng/mL), Child-Pugh grade, and vascular invasion. The relationship between these clinical phenotypes and ABAT expression was explored. Correlation analysis was conducted using the R packages "limma" and "ggplot2." Overall survival (OS) was employed to explore the correlation between ABAT expression and patient prognosis. Survival analysis was carried out with the Kaplan-Meier method and log-rank test. The R packages "survival" and "survminer" were utilized to draw the curves.

Cox Regression Analysis

Logistic regression analysis was performed using the R packages "survival" and "forestplot" to further determine the effect of ABAT expression in HCC patients. A nomogram that predicted the 3- and 5-year survival probabilities based on the Cox regression analysis was drawn using the R package "rms." The C-index and calibration plot to assess the quality of the nomogram model were obtained using the R package "Hmisc." The C-index, calculated using a bootstrap method with 1000 resamples, was used to assess the discrimination of the nomogram.

GSEA

The R package "DESeq2" was utilized to identify the differentially expressed genes (DEGs) by comparing the low- and high-expression data of ABAT in HCC samples of TCGA database (HTseq-Count). The functional and pathway differences were determined by GSEA with the R package "ClusterProfiler." Adjusted $P < 0.05$ and false discovery rate (FDR) < 0.25 were deemed statistically significant.

Correlations of ABAT Expression With DNA Methylation, Copy Number Variation, and Gene Mutation

Gene expression is affected by many factors. To explore the aspects that affected the expression of ABAT, the MethSurv (https://biit.cs.ut.ee/methsurv/) and cBioPortal (www.cbioportal.org) databases were used to obtain data on ABAT methylation, copy number variation, and gene mutation in HCC. The data on copy number variation and gene mutation of ABAT were processed using GraphPad software (Version 8.4.3).

Candidate miRNA Prediction

ENCORI (https://starbase.sysu.edu.cn/), which contains seven programs, including TargetScan, miRanda, PicTar, PITA, miRmap, RNA22, and microT, was utilized to predict the upstream binding miRNAs of ABAT. Only the candidate miRNAs that appeared in at least five of the programs mentioned above were selected for further analysis. miRNA data for HCC were obtained from TCGA database. The "limma" and "ggplot2" R packages were used to explore the differential expression of the candidate miRNAs of ABAT in HCC, as well as to examine the correlation between the target miRNAs and ABAT.

Correlation Between ABAT and Glycolysis-Related Genes

Warburg has confirmed that increased glycolytic rate is an important feature of various cancers, including HCC. One cause of the "Warburg effect" is the overexpression of glycolysis-related enzymes (8). The expression of the glycolysis-related enzymes hexokinase 2 (HK2) (8), 6-phosphofructo-2-kinase/fructose 2,6-bisphosphatase 3 (PFKFB3) (9), pyruvate kinase M (PKM) (10), phosphoglycerate kinase 1 (PGK1) (11), and lactate dehydrogenase A (LDHA) (12) in HCC were evaluated using TCGA expression profile data. The correlation between ABAT and glycolysis-related enzymes was also determined. The results were displayed on a heat map.

Relationship Between ABAT Expression and Tumor Immunity

The ESTIMATE algorithm was used to determine the immune and stromal scores, after which the R software packages "estimate" and "limma" were used to investigate the relationships of the scores with ABAT expression, based on the levels of immune infiltration. The "ggplot2" package was used to evaluate the correlations between ABAT expression and both the levels of various immune cell infiltration and the representative immune regulatory molecules in HCC. In addition, the co-expression data of ABAT and immune-related genes, including genes encoding immune activation and immunosuppressive proteins, were collected with TISIDB (http://cis.hku.hk/TISIDB/).

Statistical Analysis

The comparisons between ABAT expression in HCC tissues and normal tissues or adjacent non-tumor tissues were drawn using t-test and Mann-Whitney test. The chi-square test was utilized to investigate the correlations between clinical characteristics and ABAT expression. The regulation of copy number variation and its relation to ABAT expression was analyzed using analysis of variance. Survival analyses in our study were performed using the Kaplan-Meier method, log-rank test, and Cox regression model. Statistical significance was set at $P < 0.05$. Majority of the statistical analyses were performed using R software (Version 4.0.2).

RESULTS

Differential Expression of ABAT Between HCC and Normal or Adjacent Tissue Samples

First, TCGA database was used to investigate the transcriptional level of ABAT. The expression of ABAT mRNA was lower in

HCC tissues than in normal tissues (P < 0.001) (**Figures 1A, B**). Furthermore, ABAT mRNA expression in different groups based on patient age, patient gender, T stage classification, histologic grade, pathologic stage, and vascular invasion was explored. ABAT mRNA expression in patients with HCC aged 60 years or younger was lower than that in patients older than 60 years (P = 0.004) (**Figure 1C**). The expression level of ABAT mRNA in patients with T3/T4 stage or G3/G4 grade of HCC was lower than that in patients with T1/T2 stage (P = 0.006) or G1/G2 grade (P < 0.001), respectively (**Figures 1E, F**). Patients in the late pathological stage had lower ABAT mRNA expression than that in patients in the early stage (P = 0.003) (**Figure 1G**).

We performed qRT-PCR to test ABAT expression in 71 pairs of HCC tissue samples, the result was displayed in **Figure 2A**. The results of western blotting and IHC were showed in **Figure 2B** and **Figure 2C**, respectively. Consistent with the results of bioinformatics analysis, the experimental results indicated that ABAT expression in HCC tissues was lower than that in the matched adjacent tissues.

Low ABAT Expression in HCC Is an Independent Risk Factor

Our results revealed that low ABAT mRNA expression was related to patient age (P = 0.011), T stage classification (P = 0.013), pathologic stage (P = 0.014), histologic grade (P < 0.001), and AFP level (P < 0.001) (**Table 1**). Survival analyses revealed that lower ABAT mRNA expression was correlated with poor OS in patients with HCC (P = 0.002) (**Figure 3A**), consistent with the qRT-PCR data (P = 0.0093) (**Figure 3B**). Subgroup analyses revealed that low expression of ABAT mRNA could affect OS in HCC patients aged below 60 years (P = 0.002), at T3/T4 stage (P = 0.007), and at pathological stage III/IV (P = 0.026) (**Figures 3C–I**). Univariate analysis showed that low ABAT expression, high T stage classification, advanced pathological stage, and distant metastasis were related to OS. Multivariate analysis indicated that low expression of ABAT was an independent risk factor for HCC patients (**Table 2**). We then created a nomogram to integrate ABAT as a biomarker of HCC by fitting the expression of ABAT, T stage

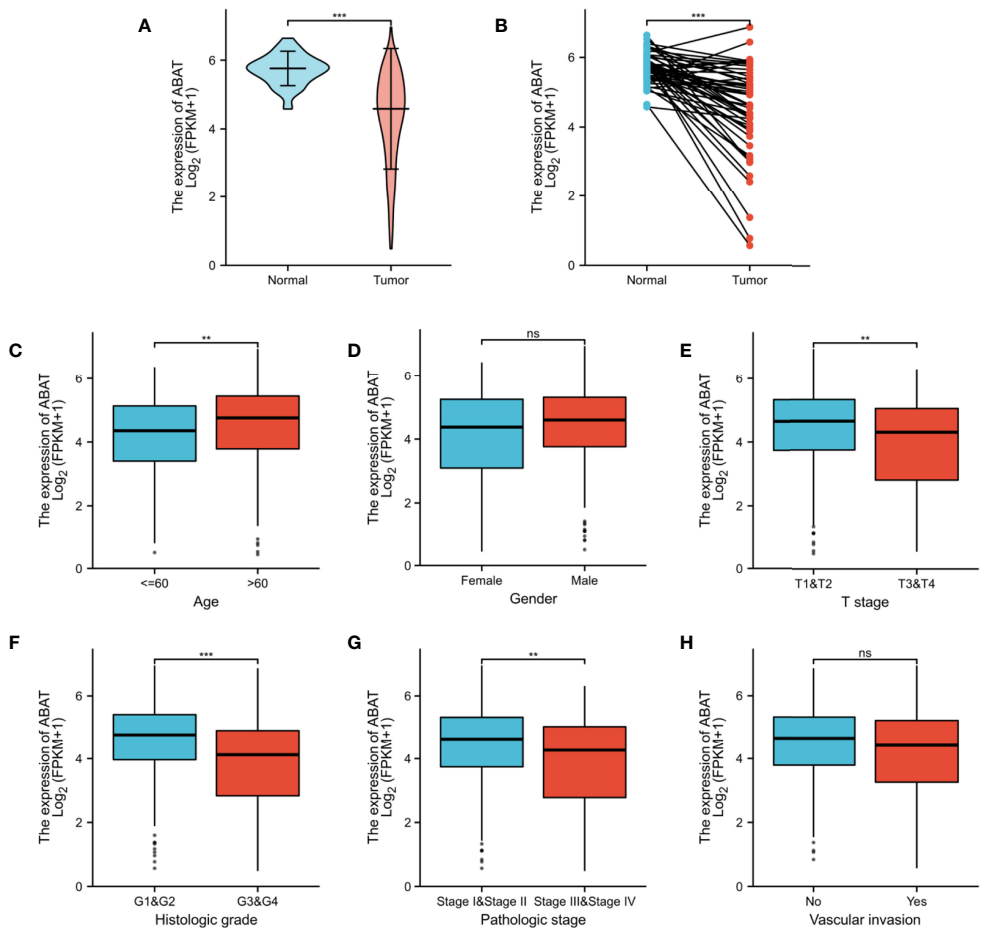

FIGURE 1 | ABAT mRNA expression and its association with clinical characteristics in HCC. **(A)** Expression level of ABAT mRNA in HCC tissues and normal tissues (P < 0.001). **(B)** Expression level of ABAT mRNA in HCC tissues and adjacent tissues (P < 0.001). Association of ABAT mRNA expression with **(C)** Age, **(D)** Gender, **(E)** T stage, **(F)** Histologic grade, **(G)** Pathologic stage, **(H)** Vascular invasion. NS: P = 0.05 or higher; **P < 0.01; ***P < 0.001.

classification, M stage, and pathological stage (**Figure 4A**). A worse prognosis factor was indicated by a higher nomogram score. The nomogram performance of ABAT was evaluated using a calibration curve. The C-index was 0.680 for ABAT. The prediction results were consistent with the observation results because the deviation line was close to the ideal curve in the calibration plot (**Figures 4B, C**).

ABAT-Related Signaling Pathways Identified *via* GSEA

Various signaling pathways were identified using GSEA, including "neutrophil degranulation," "cytokine to cytokine receptor interaction," "resolution of sister chromatid cohesion," "WNT signaling pathway," "FceRI-mediated NF-κB activation," "FceRI-mediated MAPK activation," "FCGR activation," and "CD22-mediated BCR regulation"; these were determined using the normalized enrichment score (NES), adjusted P-value, and FDR (**Table 3**, **Figure 5**).

DNA Methylation, Copy Number Variation, and Gene Mutation of ABAT

As shown in **Figure 6A**, ABAT expression had a negative correlation with its methylation level (R = -0.39, P < 0.0001). The effects of hypermethylation levels on ABAT expression and HCC prognosis were analyzed using MethSurv (**Figures 6B, C**). Hypermethylation level of ABAT correlated with a poor prognosis. The types of copy number variation include deep deletion, shallow deletion, diploid, gain, and amplification (13). From the cBioPortal data, we discovered that the proportions of ABAT gene shallow deletion, diploid, gain, and amplification were 28%, 60%, 11%, and 1%, respectively, in HCC (**Figure 7A**). **Figure 7B** shows the effect of copy number variation on ABAT gene expression. Compared to diploid, shallow deletion was associated with low expression of ABAT (P < 0.001). Gene mutation is an important factor affecting gene expression and our results revealed that the proportion of ABAT gene mutation in HCC was 1%, which was related to low ABAT expression (P < 0.001) (**Figures 7C, D**).

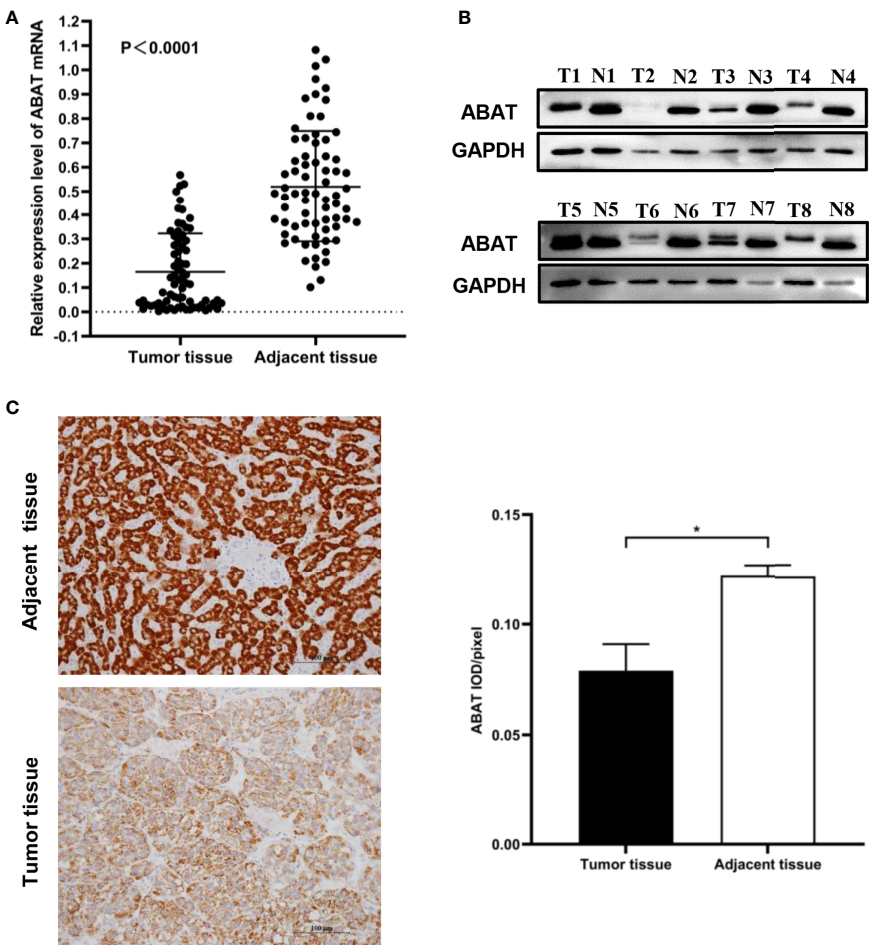

FIGURE 2 | Expression of ABAT in HCC. **(A)** qRT-PCR (P < 0.0001), **(B)** Western blot, and **(C)** IHC all showed that ABAT expression was lower in HCC tissues than in adjacent tissues. *P < 0.05.

TABLE 1 | Relationship between ABAT expression and clinical characteristics.

Clinical characteristics	Levels	Low expression N (%)	High expression N (%)	P
Age	<=60	101 (27.1%)	76 (20.4%)	0.011
	>60	85 (22.8%)	111 (29.8%)	
Gender	Female	63 (16.8%)	58 (15.5%)	0.658
	Male	124 (33.2%)	129 (34.5%)	
T stage	T1	79 (21.3%)	104 (28%)	0.013
	T2	49 (13.2%)	46 (12.4%)	
	T3	52 (14%)	28 (7.5%)	
	T4	6 (1.6%)	7 (1.9%)	
N stage	N0	135 (52.3%)	119 (46.1%)	0.626
	N1	3 (1.2%)	1 (0.4%)	
M stage	M0	143 (52.6%)	125 (46%)	0.626
	M1	3 (1.1%)	1 (0.4%)	
Pathologic stage	Stage I	76 (21.7%)	97 (27.7%)	0.014
	Stage II	44 (12.6%)	43 (12.3%)	
	Stage III	55 (15.7%)	30 (8.6%)	
	Stage IV	3 (0.9%)	2 (0.6%)	
Histologic grade	G1	19 (5.1%)	36 (9.8%)	< 0.001
	G2	78 (21.1%)	100 (27.1%)	
	G3	80 (21.7%)	44 (11.9%)	
	G4	8 (2.2%)	4 (1.1%)	
AFP (ng/ml)	<=400	86 (30.7%)	129 (46.1%)	< 0.001
	>400	51 (18.2%)	14 (5%)	
Child-Pugh grade	A	107 (44.4%)	112 (46.5%)	0.909
	B	11 (4.6%)	10 (4.1%)	
	C	0 (0%)	1 (0.4%)	
Vascular invasion	No	97 (30.5%)	111 (34.9%)	0.360
	Yes	58 (18.2%)	52 (16.4%)	

miR-135a-5p Might Be an Upstream miRNA of ABAT

Using the ENCORI database, we first identified nine upstream miRNAs that could potentially bind to ABAT. Cytoscape software was used to visualize the miRNA-ABAT regulatory network (**Figure 8A**). Based on the regulation mechanism of target genes by miRNAs, we expected that there would be a negative association between miRNAs and ABAT. Thus, the expression analysis of miRNAs in HCC was performed. Only miR-135a-5p had higher expression in HCC tissues than that in normal tissues (**Figures 8B–J**). According to TCGA data analysis, ABAT had a negative association with miR-135a-5p (**Figure 9A**).

We performed qRT-PCR to assess the expression of miR-135a-5p and ABAT mRNA in 7 pairs of HCC tissue samples. These results verified the above analysis (**Figures 9B–D**). Therefore, miR-135a-5p may be an upstream miRNA of ABAT.

Expression of Glycolysis-Related Genes Was Negatively Correlated With ABAT Levels

Subsequently, we explored the correlations between ABAT and glycolysis-related genes, which are vital for energy metabolism in HCC cells. The genes that we investigated included *HK2*, *PFKFB3*, *PKM*, *PGK1*, and *LDHA*. Our results revealed that the expression of glycolysis-related genes was negatively correlated with ABAT levels (**Figure 10A**).

Correlations Between ABAT Expression and Tumor Immunization

The tumor immune microenvironment acts as a vital factor in the occurrence and development of HCC (14). The stromal and immune cell scores in HCC were calculated using the ESTIMATE algorithm, and the correlations between ABAT and these two score types were analyzed. Immune cell score had negative correlation with ABAT expression levels ($R = -0.239$, $P < 0.001$) (**Figure 10B**), whereas stromal score was not significantly correlated ($R = -0.017$, $P = 0.748$) (**Figure 10C**). By exploring the relationships between ABAT and various immune-related cells in HCC, we determined the levels of infiltrating T cells and their different subgroups: T helper 1 (Th1) cells, T helper 2 (Th2) cells, CD8+ pan T (CD8+ T) cells, and effector memory T (Tem) cells, all of which, along with macrophages, had negative associations with ABAT expression levels. Conversely, the levels of infiltrating regulatory cells (Tregs), central memory T cells (Tcm), T helper 17 (Th17) cells, dendritic cells (DCs), and neutrophils had positive associations with ABAT expression (**Figure 11**). The correlations between ABAT expression levels and the genes encoding immune activation and immunosuppressive proteins were analyzed using TISIDB data. ABAT expression levels had positive correlations with some immune activators (**Figure 12A**) and negative correlations with almost all immunosuppressive factors (**Figure 12B**). Some representative molecules were displayed.

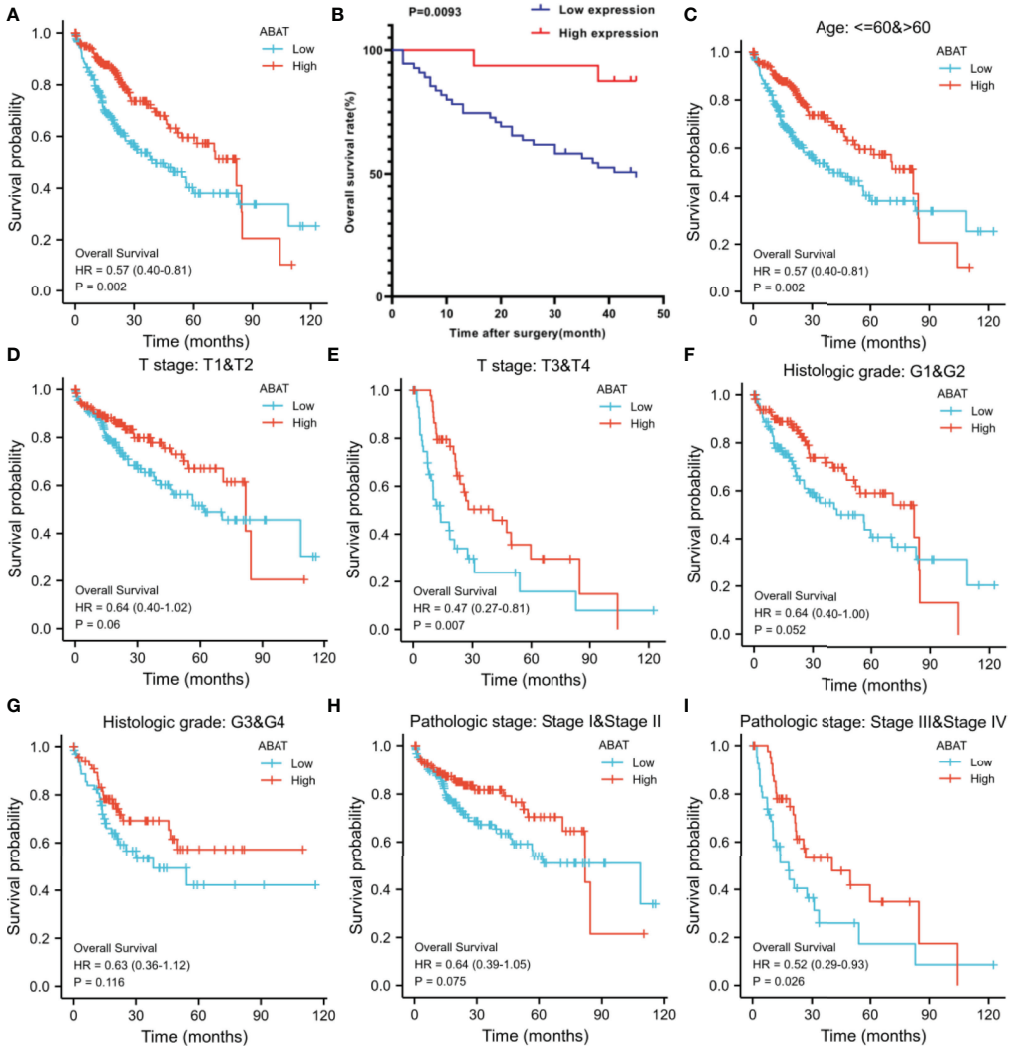

FIGURE 3 | Overall survival analyses with ABAT mRNA expression. **(A)** Survival curves in HCC for all cases from TCGA. **(B)** Survival curves in HCC with the results of qRT-PCR. **(C)** Age ≤ 60 or > 60, **(D)** T stage T1/T2, **(E)** T stage T3/T4, **(F)** Histologic grade G1/G2, **(G)** Histologic grade G3/G4, **(H)** Pathologic grade I/II, **(I)** Pathologic grade III/IV.

TABLE 2 | Univariate and multivariate Cox analysis of ABAT and other clinical pathological factors with OS in HCC patients.

Characteristics	Univariate analysis		Multivariate analysis	
	Hazard ratio (95% CI)	P value	Hazard ratio (95% CI)	P value
Age (years) (<= 60 vs > 60)	1.205 (0.850-1.708)	0.295		
Gender (Female vs Male)	0.793 (0.557-1.130)	0.200		
T stage (T1&T2 vs T3&T4)	2.598 (1.826-3.697)	<0.001	2.183 (0.296-16.098)	0.444
N stage (N0 vs N1)	2.029 (0.497-8.281)	0.324		
M stage (M0 vs M1)	4.077 (1.281-12.973)	0.017	1.827 (0.559-5.966)	0.318
Pathologic stage (I&II vs III&IV)	2.504 (1.727-3.631)	<0.001	1.299 (0.177-9.521)	0.797
Histologic grade (G1&G2 vs G3&G4)	1.091 (0.761-1.564)	0.636		
AFP (ng/ml) (<= 400 vs > 400)	1.075 (0.658-1.759)	0.772		
Child-Pugh grade (A vs B vs C)	1.595 (0.757-3.361)	0.219		
	2.138 (0.294-15.544)	0.453		
Vascular invasion (No vs Yes)	1.344 (0.887-2.035)	0.163		
ABAT (Low vs High)	0.571 (0.401-0.812)	0.002	0.451 (0.285-0.715)	<0.001

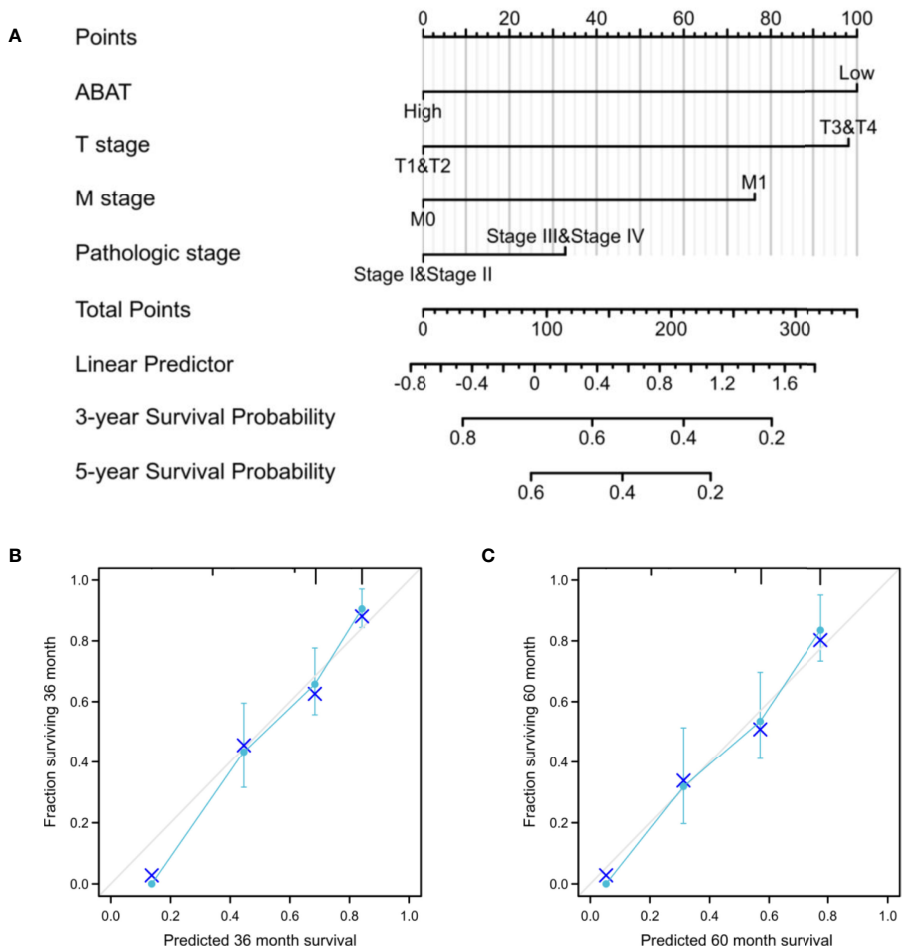

FIGURE 4 | Establishment and validation of a predictive nomogram. **(A)** Nomogram to predict the probability of 3- and 5-year OS for HCC. **(B)** The calibration plot of the nomogram for outcome prediction.

DISCUSSION

ABAT expression is downregulated in several types of cancer, including renal carcinoma (15), breast cancer (3, 16), and pancreatic cancer (17). Our study also showed that ABAT had lower expression in HCC tissues than that in normal tissues or adjacent non-tumor tissues, consistent with previous research (4). Downregulation of ABAT expression was correlated with patient age, tumor T stage classification, pathological stage, histologic grade, and AFP level of HCC and was an independent prognostic factor for HCC. Survival analysis validated that low ABAT expression was associated with poor prognosis in HCC. Similarly, loss of ABAT expression was previously documented to be strongly correlated with poor

TABLE 3 | Gene sets enriched in phenotype.

Gene set name	NES	MOMp-val	FDRq-val
REACTOME_NEUTROPHIL_DEGRANULATION	-1.364	0.001	0.039
KEGG_CYTOKINE_CYTOKINE_RECEPTOR_INTERACTION	-1.462	0.001	0.039
REACTOME_RESOLUTION_OF_SISTER_CHROMATID_COHESION	-1.575	0.001	0.039
PID_WNT_SIGNALING_PATHWAY	-1.715	0.001	0.039
REACTOME_FCERI_MEDIATED_NF_KB_ACTIVATION	-2.028	0.001	0.039
REACTOME_FCERI_MEDIATED_MAPK_ACTIVATION	-2.254	0.001	0.039
REACTOME_FCGR_ACTIVATION	-2.346	0.001	0.039
REACTOME_CD22_MEDIATED_BCR_REGULATION	-2.385	0.001	0.039

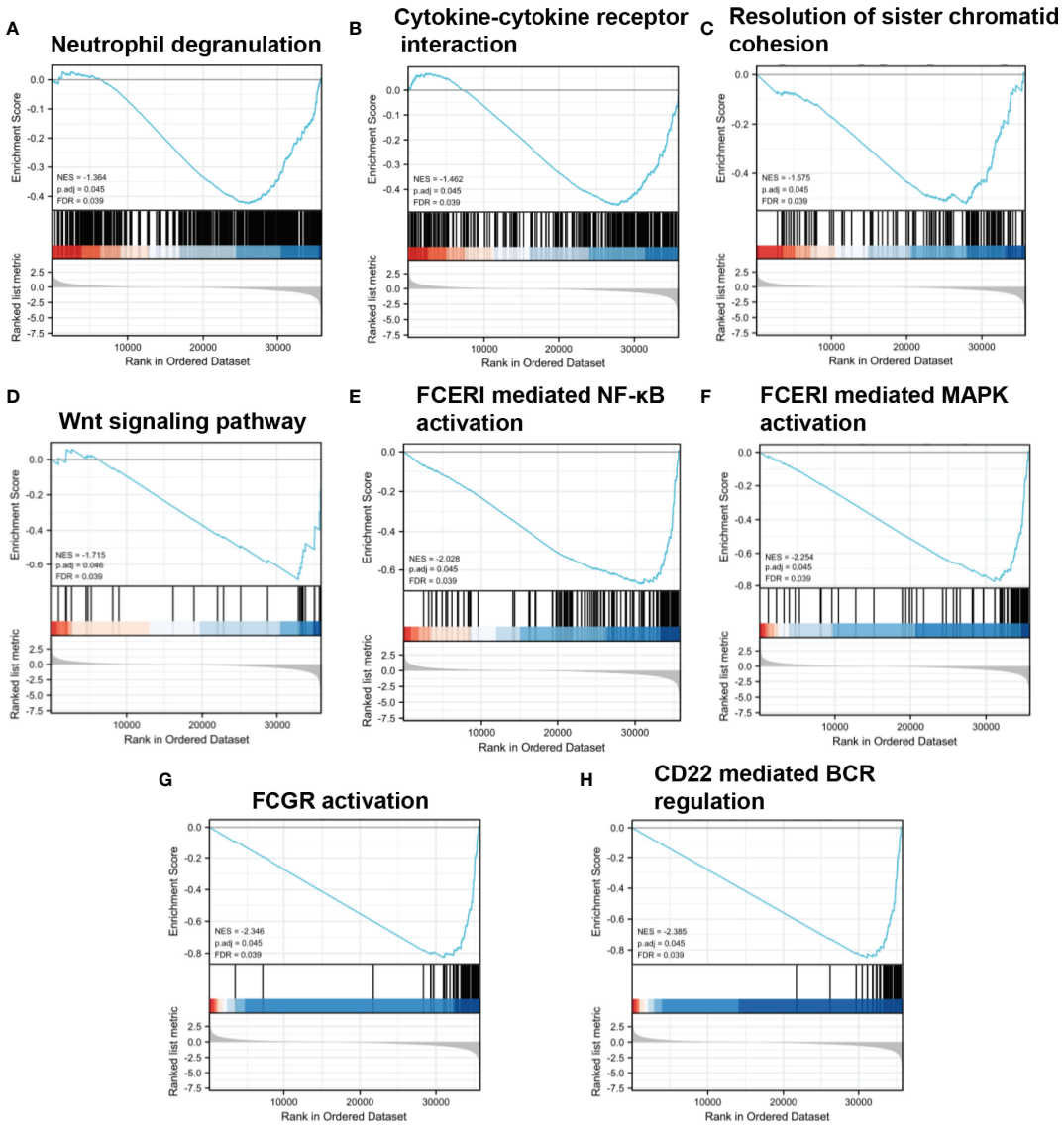

FIGURE 5 | Enrichment plots from GSEA. **(A–H)** NES, normalized ES; ADJ P-val, adjusted P-value; FDR, false discovery rate.

survival in basal-like breast cancer patients (3). Our results suggest that ABAT can be used as a biomarker for the determination of HCC prognosis.

Low expression of ABAT can increase the level of the substrate molecule, GABA, which can mediate the Ca^{2+}-NFAT1 axis to promote tumor growth and metastasis in BLBC (3). As mentioned previously, the ABAT-GABA-Ca^{2+} signaling pathway might not be the main mechanism affecting tumor prognosis in HCC. Therefore, we explored the possible associated molecular mechanisms using GSEA, which showed that in the low-expression ABAT phenotype, pathways such as "neutrophil degranulation," "cytokine to cytokine receptor interaction," "resolution of sister chromatid cohesion," "WNT signaling pathway," "FceRI-mediated NF-κB activation," "FceRI-mediated MAPK activation," "FCGR activation," and "CD22-mediated BCR regulation" were significantly differentially enriched. Among them, the tumor progression-related pathways were "resolution of sister chromatid cohesion" and "WNT signaling pathway." The WNT/β-catenin pathway can regulate embryonic development, cellular proliferation, and differentiation, and its aberrant expression is related to tumor stem cell maintenance, tumor progression, and drug resistance in HCC (18, 19). Additionally, the signaling pathways implicated in immune and inflammatory responses included "neutrophil degranulation," "cytokine to cytokine receptor interaction," "FceRI-mediated NF-κB activation," "FceRI-mediated MAPK activation," "FCGR activation," and "CD22-mediated BCR regulation." Inflammatory cytokines can drive the progression of HCC.

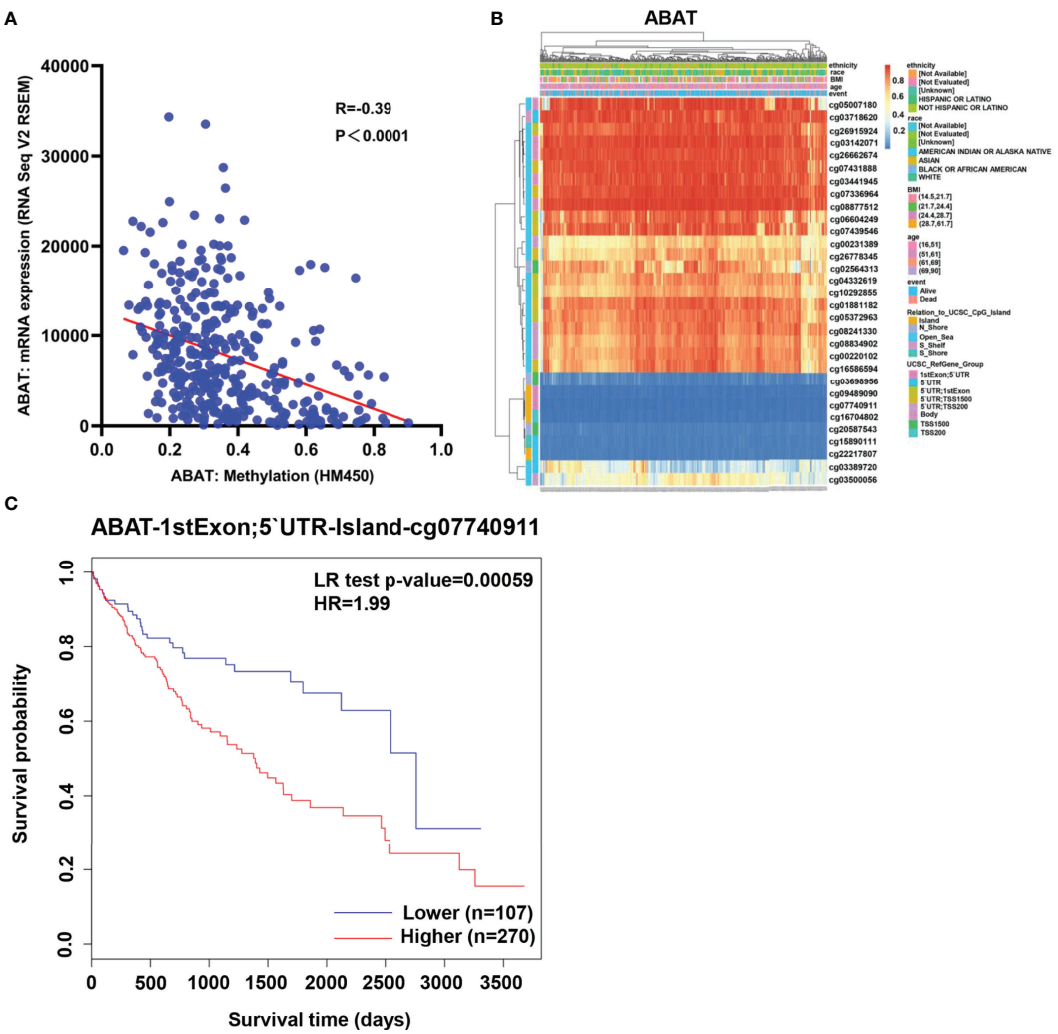

FIGURE 6 | Methylation of ABAT in HCC. **(A)** The correlation between ABAT methylation and its expression. **(B)** The visualization of the methylation level and the expression of ABAT. **(C)** The survival curves for promoter methylation of ABAT.

Furthermore, although adaptive immunity helps to eradicate early HCC, immune cells can also provoke HCC development. Therefore, the role of local immunity in HCC development is a complicated topic (20). Together, our results revealed that ABAT is involved in tumor progression and immune-related pathways.

We further investigated the mechanisms involved in low ABAT expression in HCC. ABAT hypermethylation, shallow deletion, and gene mutation were all associated with low ABAT expression in HCC, and patients with hypermethylations had a poor prognosis. DNA methylation, which regulates gene expression, is an epigenetic mechanism. Zhao et al. reported that ABAT expression was substantially downregulated in patients with myelodysplastic syndrome (MDS) compared with that in controls and that ABAT methylation level increased in MDS patients. ABAT methylation can affect MDS progression and is considered a sign of poor prognosis in hematological tumors (21). MiRNAs, a type of small endogenous RNAs, can regulate gene expression by targeting gene mRNAs (22). Bioinformatics analysis suggested that miR-135a-5p might be an upstream miRNA of ABAT, and our experimental results verified this. Indeed, miR-135a-5p can affect tumor progression by targeting correlated genes (23–25). Van Renne et al. found that miR-135a-5p upregulation in hepatitis C virus (HCV)-infected livers could drive HCV-associated hepatocarcinogenesis by targeting protein tyrosine phosphatase receptor delta (26). Yao et al. demonstrated that miR-135a-5p expression was upregulated in HCC and was negatively related to Krüppel-like Factor-4 expression, which promoted the proliferation and metastasis of HCC (27). Furthermore, miR-183-5p is the upstream miRNA of ABAT and can regulate cell functions in liver cancer (4), although this finding is inconsistent with our results. This may be because each miRNA can regulate the expression of multiple target genes, and each target gene can also be regulated by multiple miRNAs simultaneously (28).

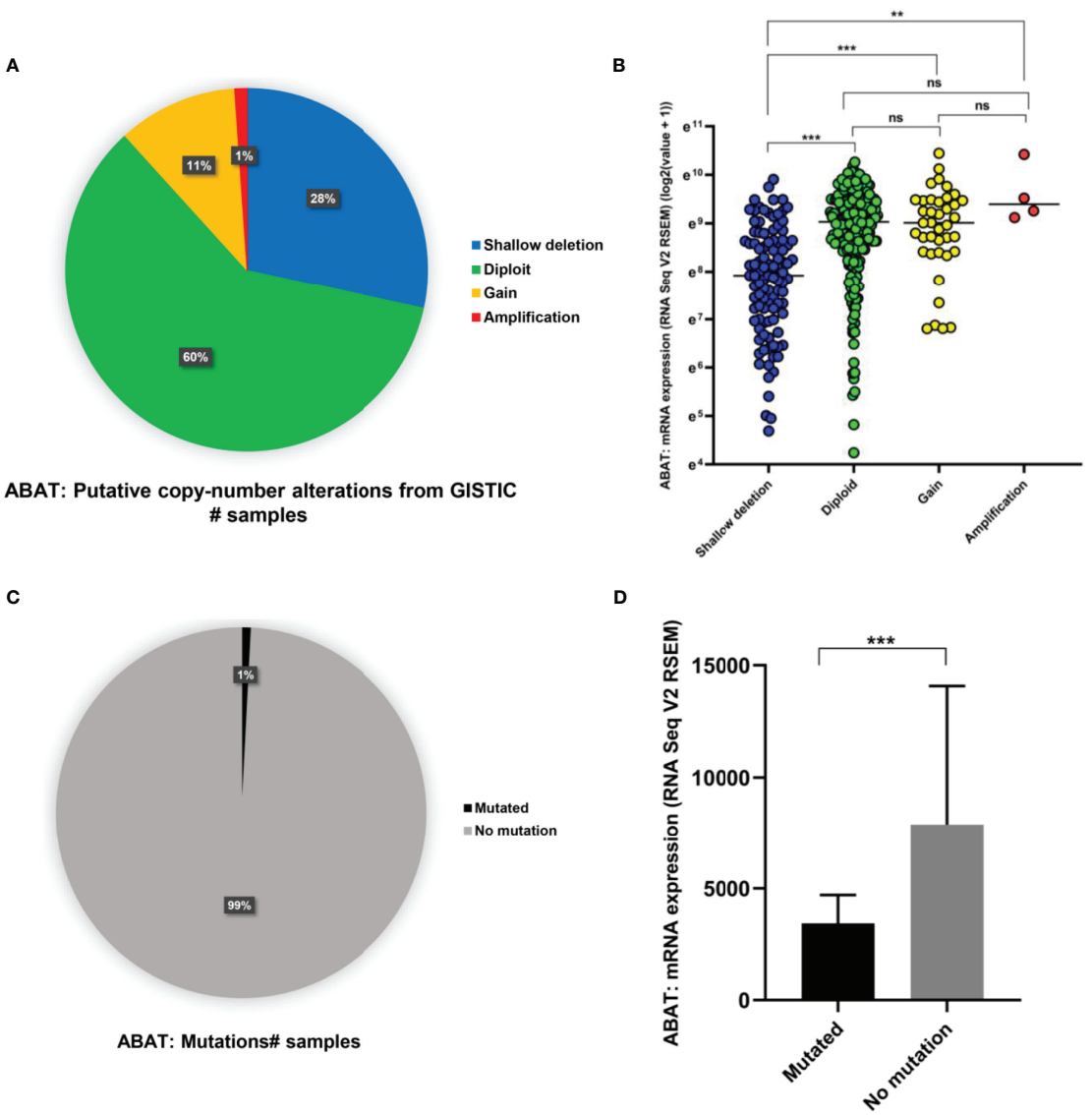

FIGURE 7 | Copy number variation and gene mutation of ABAT. **(A)** The proportion of various types of copy number variations of ABAT. **(B)** The effect of copy number variation on ABAT expression. **(C)** The proportion of gene mutation and no mutation of ABAT. **(D)** The effect of gene mutation on ABAT expression. NS, P = 0.05 or higher; **P < 0.01; ***P < 0.001.

Warburg first described the enhanced conversion of glucose into lactate in malignant tumors, even in an aerobic environment (29). This phenomenon is known as aerobic glycolysis or the Warburg effect. Aerobic glycolysis was first discovered in patients with HCC. It acts as a regulatory factor in the proliferation, angiogenesis, metastasis, and drug resistance of HCC (30). Our results determined that the expression of the glycolysis-related genes *HK2*, *PFKFB3*, *PKM*, *PGK1*, and *LDHA* were negatively correlated with ABAT expression levels. Sun et al. revealed that the androgen receptor could upregulate *HK2* expression, which induces glycolysis *via* the PKA/CREB signaling pathway, promoting the progression of HCC (8). Long et al. found that PFKFB3 expression was significantly upregulated in both HCC tissues and cell lines and was correlated with sorafenib resistance in HCC patients (9). The two isoforms of PKM, PKM1 and PKM2, are produced by the splicing of PKM. The long non-coding RNA LNCAROD could induce the upregulation of PKM2, eventually increasing cancer cell aerobic glycolysis, which is related to poor prognosis in HCC (10). PGK1 is an important glycolysis-related enzyme. Xie et al. observed that PGK1 was overexpressed in HCC tissues and that it could enhance the Warburg effect by inducing metabolic reprogramming; also, high PGK1 expression was correlated with bad prognosis in HCC patients (11). LDHA plays a vital

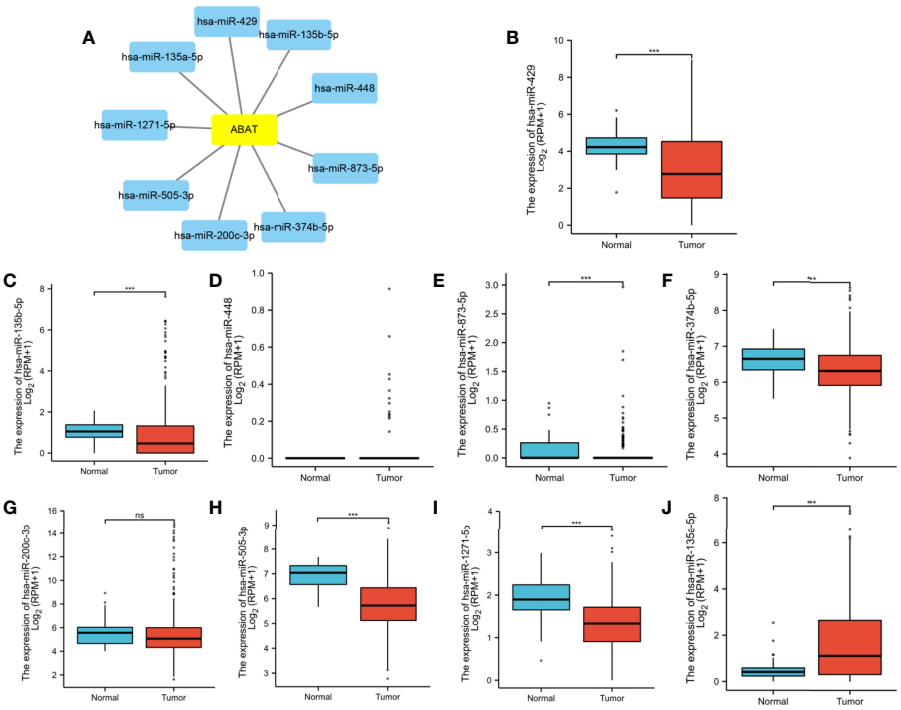

FIGURE 8 | **(A)** Establishment of miRNA-ABAT regulatory network with Cytoscape software and **(B–J)** the expression of candidate upstream miRNAs of ABAT in HCC tissues and normal tissues. NS, P = 0.05 or higher; ***P < 0.001.

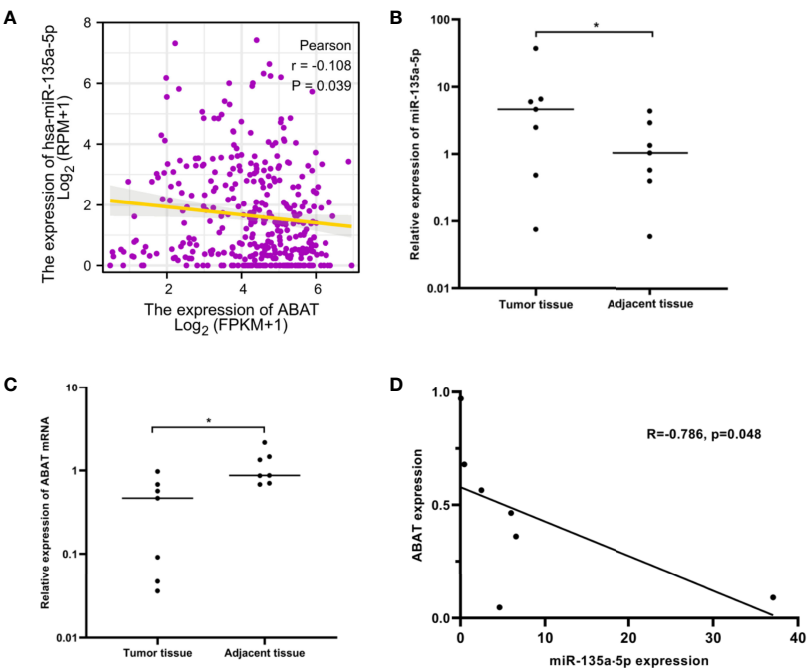

FIGURE 9 | miR-135a-5p expression and its correlation with ABAT in HCC. **(A)** The correlation between miR-135a-5p and ABAT was analyzed with TCGA data. **(B)** qRT-PCR for detection of miR-135a-5p in seven paired HCC and adjacent tissues. **(C)** qRT-PCR for detection of ABAT in seven paired HCC and adjacent tissues. **(D)** The correlation between miR-135a-5p and ABAT with qRT-PCR data. *P < 0.05.

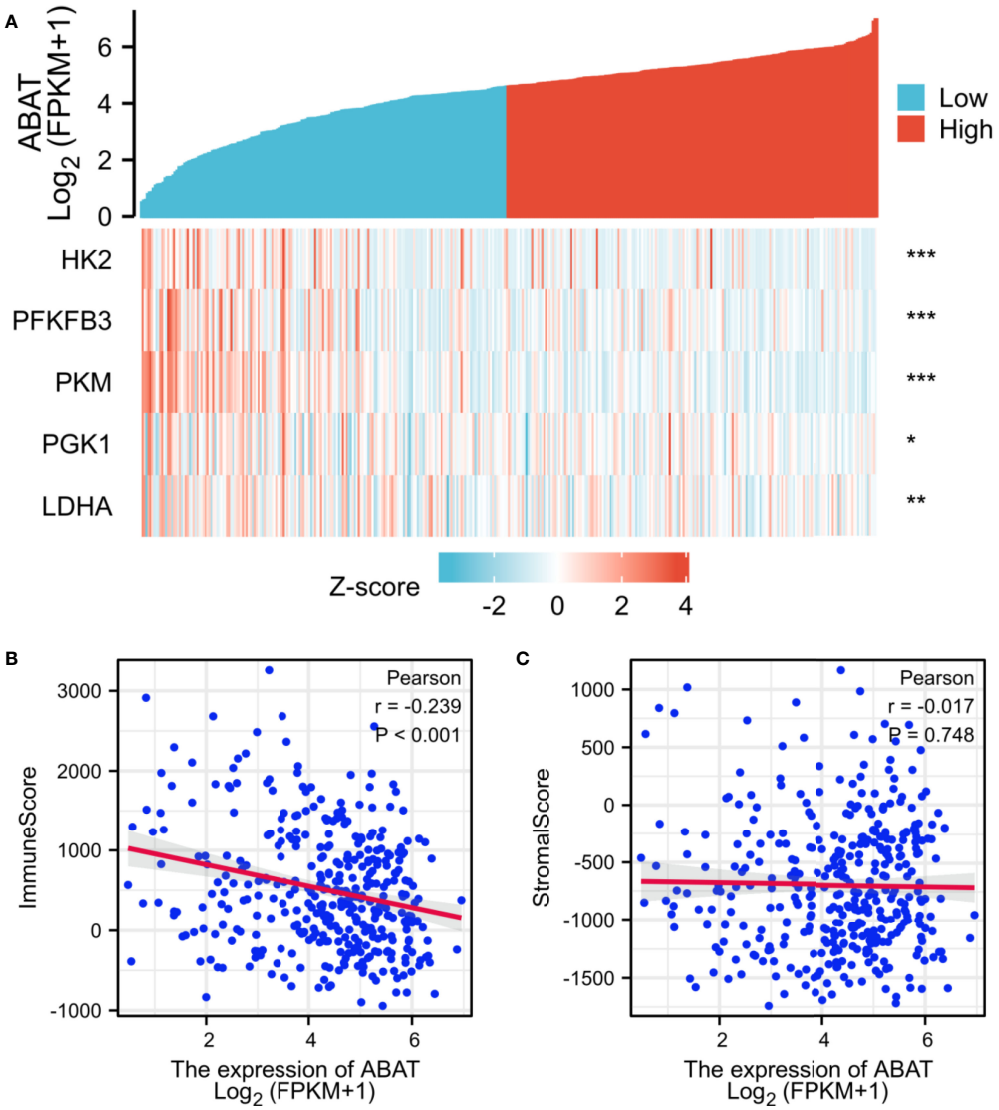

FIGURE 10 | Correlations between ABAT expression and glycolysis-related genes/tumor microenvironment. **(A)** The X-axis and Y-axis represent the samples and the glycolysis-related genes, respectively. Green and red tones indicate the downregulation and upregulation of genes, respectively. **(B)** Correlation between ABAT and immune score in HCC. **(C)** Correlation between ABAT and stromal score in HCC. *P < 0.05, **P < 0.01, ***P < 0.001.

role in non-neoplastic and neoplastic cells through the catalysis of pyruvate into lactate. Sheng et al. found that LDHA overexpression was correlated with a low apoptosis rate and high metastasis of HCC cells (12). Altogether, ABAT may be involved in the reprogramming of HCC energy metabolism.

Apart from cancer cells, the tumor microenvironment includes various components, including immune-related cells, stromal cells, fibroblasts, extracellular matrix, and signaling molecules, and is related to tumor growth, metastasis, and prognosis (31). Our results showed that most signaling pathways, as determined *via* GSEA, were implicated in the immune and inflammatory responses in HCC. Similarly, the ESTIMATE scores demonstrated that immune cell score was negatively correlated with ABAT expression levels. The ssGSEA revealed that the levels of infiltrating T cells and their different subgroups (Th1, Th2, CD8+ T, and Tem cells, as well as macrophages) were negatively associated with the ABAT expression levels. In contrast, ABAT expression levels were significantly associated with the infiltration levels of Treg, Tcm, Th17, and DC cells, as well as neutrophils. These results suggest that immune infiltration may be an aspect of ABAT-mediated carcinogenesis in HCC. Additionally, sufficient infiltration of immune cells and abundant expression of immune checkpoint molecules are all needed for the efficacy of immunotherapy (32). Our study validated the co-expression of ABAT with immune activation and immunosuppressive proteins. ABAT was

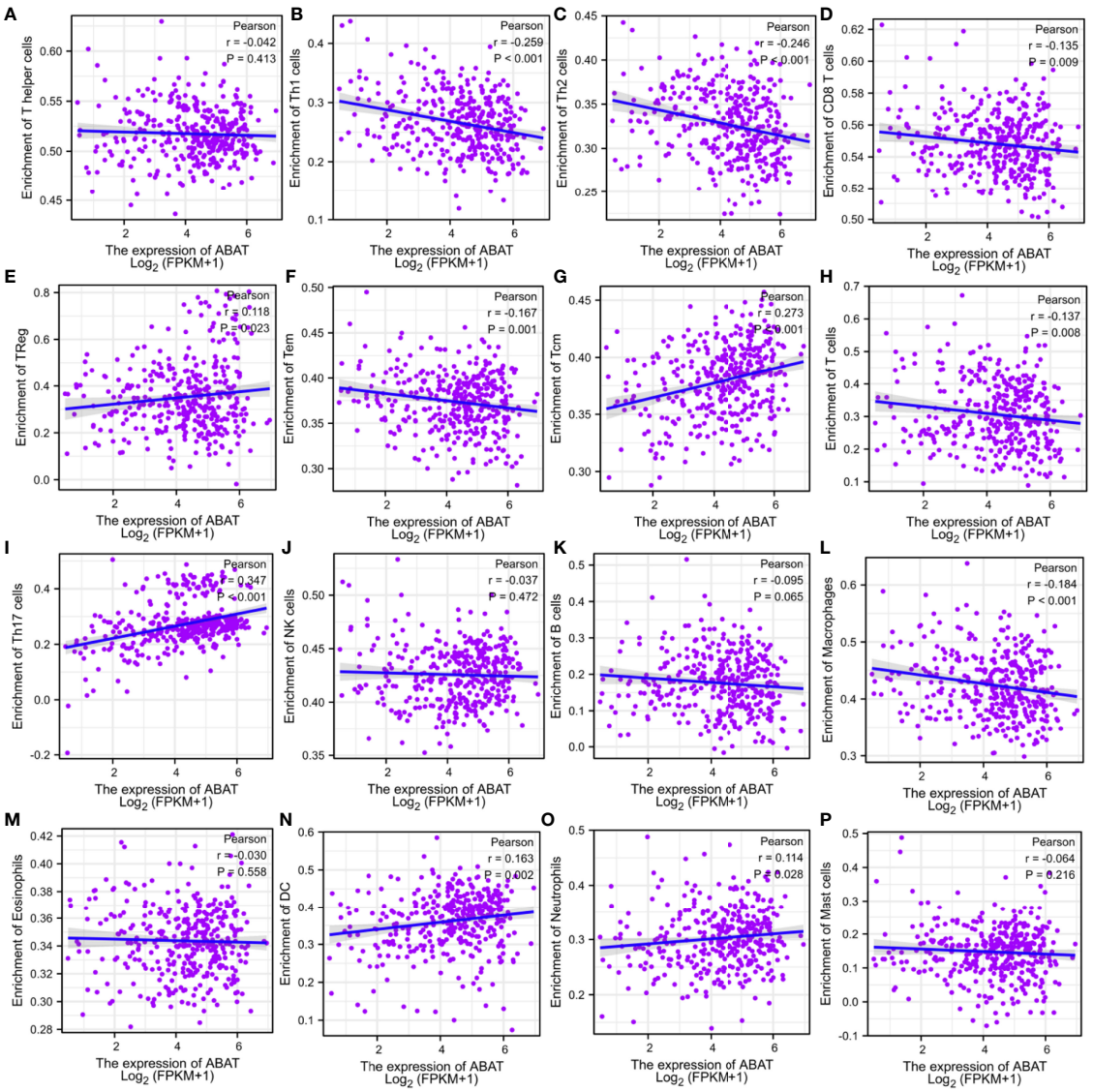

FIGURE 11 | **(A–P)** Relationship between ABAT expression and tumor infiltrating immune cells.

negatively correlated with almost all immunosuppressive factors, such as CTLA4, LGALS9, and TGFB1 in HCC, indicating that ABAT expression might be associated with the efficacy of immunotherapy in HCC.

This research also has certain limitations. First, the quality of the data from public databases could not be assessed. Second, the specific mechanism of ABAT in HCC could not be determined and needs further exploration.

In conclusion, our study confirmed that ABAT expression was downregulated in HCC. Low ABAT expression was associated with poor prognosis and was an independent risk factor in HCC patients. ABAT might promote tumor progression through a variety of signaling pathways, including the WNT signaling pathway, FceRI-mediated NF-κB activation, and FceRI-mediated MAPK activation. The mechanism of low ABAT expression might involve ABAT hypermethylation, shallow deletion, and gene mutation, and miR-135a-5p may be an upstream miRNA of ABAT. Furthermore, ABAT might be involved in energy metabolism reprogramming, immune cell infiltration, and the expression of immunosuppressive factors.

DATA AVAILABILITY STATEMENT

The datasets presented in this study can be found in online repositories. The names of the repository/repositories and accession number(s) can be found in the article/supplementary material.

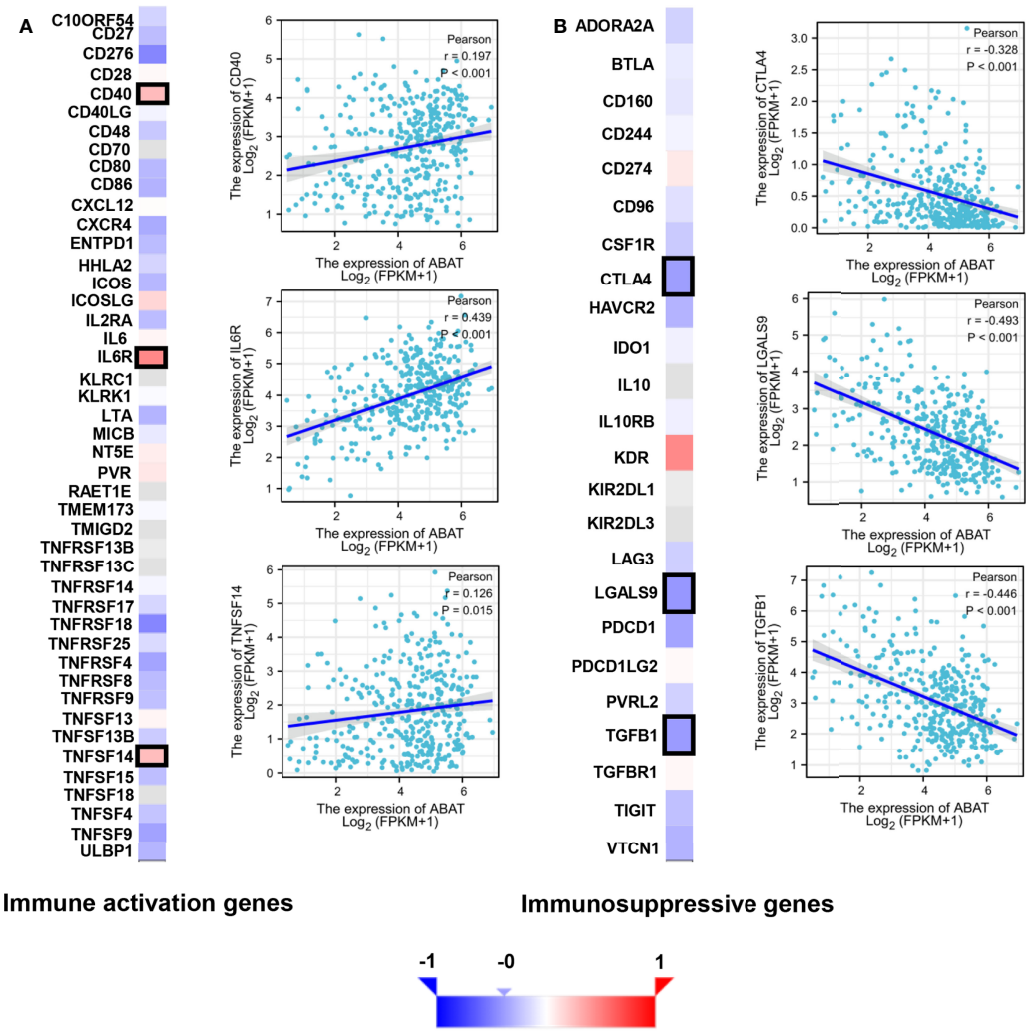

FIGURE 12 | Correlation of ABAT levels with the expression of immunomodulators in HCC. **(A)** The heatmap of the correlation with immune activation genes and display of three representative molecules. **(B)** The heatmap of the correlation with immunosuppressive genes and display of three representative molecules. The representative molecules are surrounded by black frames in the heatmaps.

ETHICS STATEMENT

The studies involving human participants were reviewed and approved by the Ethics Committee of the Fifth Medical Center of Chinese PLA General Hospital. Written informed consent was obtained from the individual(s) for the publication of any potentially identifiable images or data included in this article.

AUTHOR CONTRIBUTIONS

SZ and YLu designed this research. XG, XJ, JX, and JL collected the samples and data. XG and XJ conducted qRT-PCR, IHC, and western blotting and analyzed the data. XG wrote the first draft. SZ, YLu, MX, and YLi supervised the research and revised the manuscript. All authors contributed to the article and approved the submitted version.

FUNDING

This study was supported by grants from Natural Science Foundation of Beijing Municipality (7212099), National Natural Science Foundation of China (81902495), Medical Big Data and AI R & D Project of General Hospital (2019MBD-025), and Science Technology and Innovation Committee of Shenzhen Municipality (KCXFZ202002011006448).

ACKNOWLEDGMENTS

We would like to thank Editage (www.editage.cn) for English language editing.

REFERENCES

1. Gao Y, You M, Fu J, Tian M, Zhong X, Du C, et al. Intratumoral Stem-Like CCR4+ Regulatory T Cells Orchestrate the Immunosuppressive Microenvironment in HCC Associated With Hepatitis B. *J Hepatol* (2022) 76:148–59. doi: 10.1016/j.jhep.2021.08.029
2. Singal AG, Lok AS, Feng Z, Kanwal F, Parikh ND. Conceptual Model for the Hepatocellular Carcinoma Screening Continuum: Current Status and Research Agenda. *Clin Gastroenterol Hepatol* (2022) 20:9–18. doi: 10.1016/j.cgh.2020.09.036
3. Chen X, Cao Q, Liao R, Wu X, Xun S, Huang J, et al. Loss of ABAT-Mediated GABAergic System Promotes Basal-Like Breast Cancer Progression by Activating Ca2+-NFAT1 Axis. *Theranostics* (2019) 9:34–47. doi: 10.7150/thno.29407
4. Han H, Zhou S, Chen G, Lu Y, Lin H. ABAT Targeted by miR-183-5p Regulates Cell Functions in Liver Cancer. *Int J Biochem Cell Biol* (2021) 141:106116. doi: 10.1016/j.biocel.2021.106116
5. Minuk GY. GABA and Hepatocellular Carcinoma. *Mol Cell Biochem* (2000) 207:105–8. doi: 10.1023/a:1007062802164
6. Wang T, Huang W, Chen F. Baclofen, a GABAB Receptor Agonist, Inhibits Human Hepatocellular Carcinoma Cell Growth *In Vitro* and *In Vivo*. *Life Sci* (2008) 82:536–41. doi: 10.1016/j.lfs.2007.12.014
7. Chen ZA, Bao MY, Xu YF, Zha RP, Shi HB, Chen TY, et al. Suppression of Human Liver Cancer Cell Migration and Invasion *via* the GABAA Receptor. *Cancer Biol Med* (2012) 9:90–8. doi: 10.1007/s10620-020-06229-y
8. Sun RF, Zhao CY, Chen S, Yu W, Zhou MM, Gao CR, et al. Androgen Receptor Stimulates Hexokinase 2 and Induces Glycolysis by PKA/CREB Signaling in Hepatocellular Carcinoma. *Dig Dis Sci* (2021) 66:802–13. doi: 10.1007/s10620-020-06229-y
9. Long Q, Zou X, Song Y, Duan Z, Liu L. PFKFB3/HIF-1α Feedback Loop Modulates Sorafenib Resistance in Hepatocellular Carcinoma Cells. *BiochemBiophys Res Commun* (2019) 513:642–50. doi: 10.1016/j.bbrc.2019.03.109
10. Jia G, Wang Y, Lin C, Lai S, Dai H, Wang Z, et al. LNCAROD Enhances Hepatocellular Carcinoma Malignancy by Activating Glycolysis Through Induction of Pyruvate Kinase Isoform PKM2. *J Exp Clin Cancer Res* (2021) 40:299. doi: 10.1186/s13046-021-02090-7
11. Xie H, Tong G, Zhang Y, Liang S, Tang K, Yang Q. PGK1 Drives Hepatocellular Carcinoma Metastasis by Enhancing Metabolic Process. *Int J Mol Sci* (2017) 18:1630. doi: 10.3390/ijms18081630
12. Sheng SL, Liu JJ, Dai YH, Sun XG, Xiong XP, Huang G. Knockdown of Lactate Dehydrogenase A Suppresses Tumor Growth and Metastasis of Human Hepatocellular Carcinoma. *FEBS J* (2012) 279:3898–910. doi: 10.1111/j.1742-4658.2012.08748.x
13. Mermel CH, Schumacher SE, Hill B, Meyerson ML, Beroukhim R, Getz G. GISTIC2.0 Facilitates Sensitive and Confident Localization of the Targets of Focal Somatic Copy-Number Alteration in Human Cancers. *Genome Biol* (2011) 12:R41. doi: 10.1186/gb-2011-12-4-r41
14. Song M, He J, Pan QZ, Yang J, Zhao J, Zhang YJ, et al. Cancer-Associated Fibroblast-Mediated Cellular Crosstalk Supports Hepatocellular Carcinoma Progression. *Hepatology* (2021) 73:1717–35. doi: 10.1002/hep.31792
15. Lu J, Chen Z, Zhao H, Dong H, Zhu L, Zhang Y, et al. ABAT and ALDH6A1, Regulated by Transcription Factor HNF4A, Suppress Tumorigenic Capability in Clear Cell Renal Cell Carcinoma. *J Transl Med* (2020) 18:101. doi: 10.1186/s12967-020-02268-1
16. Jansen MP, Sas L, Sieuwerts AM, Van Cauwenberghe C, Ramirez-Ardila D, Look M, et al. Decreased Expression of ABAT and STC2 Hallmarks ER-Positive Inflammatory Breast Cancer and Endocrine Therapy Resistance in Advanced Disease. *Mol Oncol* (2015) 9:1218–33. doi: 10.1016/j.molonc.2015.02.006
17. Jiang Z, Zheng J, Liu J, Yang X, Chen K. Novel Branched-Chain Amino Acid-Catabolism Related Gene Signature for Overall Survival Prediction of Pancreatic Carcinoma. *J Proteome Res* (2022) 21:740–746. doi: 10.1021/acs.jproteome.1c00607
18. He S, Tang S. WNT/β-Catenin Signaling in the Development of Liver Cancers. *BioMed Pharmacother* (2020) 132:110851. doi: 10.1016/j.biopha.2020.110851
19. Vilchez V, Turcios L, Marti F, Gedaly R. Targeting Wnt/β-Catenin Pathway in Hepatocellular Carcinoma Treatment. *World J Gastroenterol* (2016) 22:823–32. doi: 10.3748/wjg.v22.i2.823
20. Yang YM, Kim SY, Seki E. Inflammation and Liver Cancer: Molecular Mechanisms and Therapeutic Targets. *Semin Liver Dis* (2019) 39:26–42. doi: 10.1055/s-0038-1676806
21. Zhao G, Li N, Li S, Wu W, Wang X, Gu J. High Methylation of the 4-Aminobutyrate Aminotransferase Gene Predicts a Poor Prognosis in Patients With Myelodysplastic Syndrome. *Int J Oncol* (2019) 54:491–504. doi: 10.3892/ijo.2018.4652
22. Diao H, Xu X, Zhao B, Yang G. Mir-135a-5p Inhibits Tumor Invasion by Targeting ANGPT2 in Gallbladder Cancer. *Mol Med Rep* (2021) 24:528. doi: 10.3892/mmr.2021.12167
23. Wang J, Yang J, Zhang H, Liao Y, Xu D, Ma S. Effects of miR-135a-5p and miR-141 on Proliferation, Invasion and Apoptosis of Colorectal Cancer SW620 Cells. *Oncol Lett* (2020) 20:914–20. doi: 10.3892/ol.2020.11598
24. Zhang Y, Jiang WL, Yang JY, Huang J, Kang G, Hu HB, et al. Downregulation of Lysyl Oxidase-Like 4 LOXL4 by miR-135a-5p Promotes Lung Cancer Progression *In Vitro* and *In Vivo*. *J Cell Physiol* (2019) 234:18679–87. doi: 10.1002/jcp.28508
25. Guo LM, Ding GF, Xu W, Ge H, Jiang Y, Chen XJ, et al. MiR-135a-5p Represses Proliferation of HNSCC by Targeting HOXA10. *Cancer Biol Ther* (2018) 19:973–83. doi: 10.1080/15384047.2018.1450112
26. Van Renne N, Roca Suarez AA, Duong FHT, Gondeau C, Calabrese D, Fontaine N, et al. miR-135a-5p-Mediated Downregulation of Protein Tyrosine Phosphatase Receptor Delta is a Candidate Driver of HCV-Associated Hepatocarcinogenesis. *Gut* (2018) 67:953–62. doi: 10.1136/gutjnl-2016-312270
27. Yao S, Tian C, Ding Y, Ye Q, Gao Y, Yang N, et al. Down-Regulation of Krüppel-Like Factor-4 by microRNA-135a-5p Promotes Proliferation and Metastasis in Hepatocellular Carcinoma by Transforming Growth Factor-β1. *Oncotarget* (2016) 7:42566–78. doi: 10.18632/oncotarget.9934
28. Lu TX, Rothenberg ME. MicroRNA. *J Allergy Clin Immunol* (2018) 141:1202–7. doi: 10.1016/j.jaci.2017.08.034
29. Vaupel P, Multhoff G. Revisiting the Warburg Effect: Historical Dogma Versus Current Understanding. *J Physiol* (2021) 599:1745–57. doi: 10.1113/JP278810
30. Feng J, Li J, Wu L, Yu Q, Ji J, Wu J, et al. Emerging Roles and the Regulation of Aerobic Glycolysis in Hepatocellular Carcinoma. *J Exp Clin Cancer Res* (2020) 39:126. doi: 10.1186/s13046-020-01629-4
31. Oura K, Morishita A, Tani J, Masaki T. Tumor Immune Microenvironment and Immunosuppressive Therapy in Hepatocellular Carcinoma: A Review. *Int J Mol Sci* (2021) 22:5801. doi: 10.3390/ijms22115801
32. Hu FF, Liu CJ, Liu LL, Zhang Q, Guo AY. Expression Profile of Immune Checkpoint Genes and Their Roles in Predicting Immunotherapy Response. *Brief Bioinform* (2021) 22:bbaa176. doi: 10.1093/bib/bbaa176

Conflict of Interest: The authors declare that the research was conducted in the absence of any commercial or financial relationships that could be construed as a potential conflict of interest.

Publisher's Note: All claims expressed in this article are solely those of the authors and do not necessarily represent those of their affiliated organizations, or those of the publisher, the editors and the reviewers. Any product that may be evaluated in this article, or claim that may be made by its manufacturer, is not guaranteed or endorsed by the publisher.

Copyright © 2022 Gao, Jia, Xu, Xiang, Lei, Li, Lu and Zuo. This is an open-access article distributed under the terms of the Creative Commons Attribution License (CC BY). The use, distribution or reproduction in other forums is permitted, provided the original author(s) and the copyright owner(s) are credited and that the original publication in this journal is cited, in accordance with accepted academic practice. No use, distribution or reproduction is permitted which does not comply with these terms.

frontiers | Frontiers in Surgery

CLINICAL TRIAL
published: 28 June 2022
doi: 10.3389/fsurg.2022.917352

Efficacy and Safety of Camrelizumab in Combination with Docetaxel + S-1 Sequenced by Camrelizumab + S-1 for Stage III (PD-1+/MSI-H/EBV +/dMMR) Gastric Cancer: Study Protocol for a Single-Center, Prospective, Open-Label, Single-Arm Trial

Zhongyi Dong†, Bo Ni†, Linxi Yang†, Yujing Guan, Chunchao Zhu, Enhao Zhao*, Gang Zhao, Xiang Xia and Zizhen Zhang**

Department of Gastrointestinal Surgery, Renji Hospital, School of Medicine, Shanghai Jiao Tong University, Shanghai, China

OPEN ACCESS

Edited by:
Qi Liu,
Fudan University, China

Reviewed by:
Manabu Ohashi,
Cancer Institute Hospital of Japanese Foundation for Cancer Research, Japan
Asit Kumar Manna,
The University of Utah, United States

***Correspondence:**
Zizhen Zhang
zhangzizhen@renji.com
Chunchao Zhu
zcczmy@hotmail.com
Enhao Zhao
zhaoenhao@renji.com

†*These authors have contributed equally to this work*

Specialty section:
This article was submitted to Surgical Oncology, a section of the journal Frontiers in Surgery

Received: *11 April 2022*
Accepted: *07 June 2022*
Published: *28 June 2022*

Citation:
Dong Z, Ni B, Yang L, Guan Y, Zhu C, Zhao E, Zhao G, Xia X and Zhang Z (2022) Efficacy and Safety of Camrelizumab in Combination with Docetaxel + S-1 Sequenced by Camrelizumab + S-1 for Stage III (PD-1+/MSI-H/EBV+/dMMR) Gastric Cancer: Study Protocol for a Single-Center, Prospective, Open-Label, Single-Arm Trial. Front. Surg. 9:917352. doi: 10.3389/fsurg.2022.917352

Background: Gastric cancer occupies the fourth highest morbidity rate of cancers worldwide. A higher incidence of gastric cancer had been found in East Asia compared to the other regions. Gastrectomy with radical lymph node dissection is the cornerstone of curative treatment for Stage III gastric cancer, and postoperative systemic chemotherapy with docetaxel, S-1 improved patients' disease-free survival rates. However, advances in immunotherapy bring innovations in the management of patients with gastric cancer. The objective of this study was to explore the efficacy and safety of camrelizumab in combination with docetaxel + S-1, sequenced by camrelizumab + S-1 in stage III gastric cancer patients who are EBV positive, with defective mismatch repair and CPS ≥5.

Methods and analysis: This prospective, open-label, single-arm trial was performed at Renji Hospital. In this study, a total of 70 adult patients aged 18–80 years with Stage III (PD-1+/MSI-H/EBV+/dMMR) gastric cancer confirmed by post-operative pathology will be enrolled after screening. Participants will receive the specific chemotherapy regimen until 1 year after the operation or until tumor recurrence or metastasis. The primary outcome is the 3-year disease-free survival rate measured by the Clopper-Pearson method and 95% confidence intervals. The secondary outcomes include overall survival, incidence and severity of adverse effects, and laboratory abnormalities. The

Abbreviations: EBV, Epstein-Barr virus; PD-1, Programed death 1 receptor; PD-L1, PD-1 ligand; MSI, Microsatellite instability; CPS, Combined positive score; CT, Computed tomography; MRI, Magnetic resonance imaging; CEA, Carcinoembryonic antigen; EUS, Endoscopic ultrasonography; CFDA, China Food and Drug Administration; CDHP, 5-chloro-2,4-dihydroxypyridine.

data will be analyzed by the Kaplan-Meier method and log-rank test. The patients will be followed up every 3 months with imaging investigation until clinical remission.

Ethics and dissemination: All participants will provide informed consent. The protocol has been approved by the Shanghai Jiaotong University School of Medicine, Renji Hospital Ethics Committee (KY2019-191). The results will be disseminated through peer-reviewed manuscripts, reports and presentations.

Clinical Trial Registration: ClinicalTrials.gov, identifier: ChiCTR1900027123. Registration date November 2019; first enrolment December 2019; expected end date December 2021; trial status: Ongoing.

Brief Abstract: A clinical trial for Stage III (PD-1+/MSI-H/EBV+/dMMR) gastric cancer patients who accepted anti-PD-1 therapy combined with docetaxel + S-1 as the first-line treatment and explored improvements in three-year disease-free survival rate.

Keywords: camrelizumab, docetaxel, gastric cancer, S-1, clinical protocols

BACKGROUND

Gastric cancer is one of the most common malignant tumors, accounting for 10%–15% of systemic malignancies (1). Its morbidity and mortality are ranked 4th and 2nd respectively in the world and second highest in China (2). Radical gastrectomy, D2 lymph node dissection and systemic chemotherapy were performed for advanced gastric cancer, whereas D1 + lymph node dissection with partial omentectomy, were performed for early gastric cancer (3). In addition to these standardized therapies, molecular-targeted drugs such as the human epidermal growth factor 2 (Herceptin) and the anti-angiogenic drug lapatinib have been gradually recognized in recent years. However, due to the high heterogeneity of gastric cancer and the lack of available targets, the clinical application of these drugs is still limited (4). With the development of research on Programmed Death Receptor-1(PD-1) and its ligand (PD-L1), immunotherapy has gained the attention of researchers in cancer treatment.

Multiple clinical studies have been carried out in the treatment of gastric cancer with immune checkpoint blockade therapy. Pembrolizumab, a PD-1 inhibitor binds PD-1, blocking the activation of PD-1 and PD-L1/2 signaling, and has been approved for melanoma treatment (5). A series of studies, such as KEYNOTE-012 and KEYNOTE-059, have confirmed its efficacy in advanced esophageal and gastric cancer with PD-L1-positive expression (6, 7). In KEYNOTE-062, all patients had a combined positive score (CPS) ≥1, and neither Pembro alone nor Pembro-Chemo significantly improved survival. However, for patients with CPS ≥ 10, the 12-month OS rate was 80% compared to 57% in this study (8). Based on these findings, PD-L1-positive patients are more likely to benefit from PD-1 immunotherapy, and the FDA has granted the accelerated approval of pembrolizumab for advanced gastric cancer treatment (7). In the treatment of metastatic colorectal cancer, the researchers found that patients with defective mismatch repair (dMMR) benefited more from PD-1 treatment than patients with proficient mismatch repair (pMMR), with some achieving lasting remission. A clinical trial conducted by Le et al. (9) not only demonstrated that gastric cancer patients with dMMR benefited more from PD-1 therapy but also confirmed that dMMR is an effective biomarker for response to PD-1 treatment. Panda et al. (10) reported PD-L1 antibody therapy that Epstein-Barr virus (EBV)-positive gastric cancer patients were treated with PD-L1 antibodies after the failure of standard multiline therapy. The analysis of tumor tissue specimens showed that it was negative for microsatellite instability and positive for EBV, suggesting that EBV might be a biomarker indicating sensitivity to PD-1 therapy.

In summary, this study will include patients with stage III gastric cancer who are EBV positive and have defective mismatch repair, CPS ≥5. These patients' response to traditional chemotherapy is not usually satisfactory and limited current means to effectively treat such patients (11, 12). We believe that our regimens may bring unexpected relief to them. And the study is designed to investigate the effects of immunotherapy combined with adjuvant chemotherapy on the 3-year disease-free survival (DFS) rate and overall survival (OS) in patients with stage III gastric cancer.

METHODS AND ANALYSIS

Study Design

The study was designed as a single-center, single group, prospective, open-label and single-arm research at Renji Hospital, Shanghai Jiao Tong University between Jan. 2020 and Dec. 2021. The data collection and analysis were completed to evaluate the efficacy and safety of camrelizumab in combination with docetaxel + S-1, sequenced by camrelizumab + S-1 as adjuvant therapy in stage III gastric cancer (PD-L1 + / MSI-H / EBV +/dMMR). The trial was in compliance with the applicable regulations and the Helsinki Declaration. Furthermore, the protocol has been approved by the Shanghai Jiaotong University School of Medicine, Renji Hospital Ethics Committee (KY2019-191) and registered in the Chinese Clinical Trial Registry (ChiCTR1900027123).

Study Participants

The written informed consent will be provided before starting the trial and then the participants will be screened by a gastrointestinal surgeon to establish whether they meet the eligibility criteria. The qualified patients will be admitted within 4 weeks after surgery and begin treatment. During the follow-up period, the patients will be scheduled for a return visit every 3 weeks and an imaging evaluation every 4 weeks until the end of the treatment. They will be assessed for the primary and secondary outcomes after the intervention and during the 3-year follow-up. The end of the trial is defined as the last follow-up date for the last patient. **Figure 1** summarizes the flow of participants.

Inclusion and Exclusion Criteria

Complete inclusion/exclusion criteria are detailed in **Table 1**.

Intervention

Camrelizumab

Camrelizumab (200 mg) was administered intravenously for 30 min (not less than 20 min, not more than 60 min, including flush time) every 3 weeks. Repeated every 21 days and 3 weeks for a course. The drug was discontinued 1 year after the operation or with tumor recurrence or metastasis, determined by imaging.

Camrelizumab dosing adjustment will not be allowed. However, if the patient develops severe complications, the researchers can suspend the medication.

Tegafur Gimeracil Oteracil Potassium

Tegafur 80–120 mg (adjusted dose by the researcher according to the patient's tolerance) d1-d14 taken orally followed by resting for 7 days. The cycle will be repeated every 21 days. And the course of treatment is 3 weeks and the drug will be discontinued 1 year after the operation or on tumor recurrence or metastasis, determined by imaging.

According to the patient's condition, the researcher will decide to adjust the drug dosage. Each dose was increased or decreased in the order of 40 mg, 50 mg, 60 mg and 75 mg. If the 40 mg dose is not tolerated, the drug administration will be discontinued.

Docetaxel

Docetaxel 40 mg/m2 (the dose is adjusted by the researcher according to the patient's tolerance level) is given intravenously for 1 h every 3 weeks from the second cycle to the seventh cycle. The drug was discontinued 1 year after the operation or on tumor recurrence or metastasis, determined by imaging.

The white blood cell count should be monitored regularly during the treatment. Docetaxel will only be given to patients with a neutrophil count greater than $1500/mm^3$. If severe neutropenia occurs ($<500/mm^3$ for 7 days or more), a reduction in dosage is recommended in the next course of treatment. If there is no improvement, further dose reduction or discontinuation will be recommended.

The treatment protocol described above will be given continuously for 1 year after the operation or until tumor recurrence or metastasis, determined by imaging. Safety visits and follow-ups will be performed after treatment. Cancer progression will also be followed up after the end of treatment for subjects who have non-disease progression and have completed the treatment.

Outcome Measures

Primary outcome

To observe and evaluate the 3-year disease-free survival (DFS) rate in patients with stage III gastric cancer (PD-L1 + / MSI-H / EBV +/dMMR).

Secondary outcome

1. To observe and evaluate the overall survival (OS) in patients with stage III gastric cancer (PD-L1 + / MSI-H / EBV +/dMMR).
2. To observe and evaluate the safety and adverse events in patients with stage III gastric cancer (PD-L1 + / MSI-H / EBV +/dMMR).

Sample Size Calculation

The sample size calculation will be based on the 3-year disease-free survival (DFS) rate of the included patients. The study was designed as a prospective single-arm trial, focusing on patients with stage III gastric cancer (PD-L1+/MSI-H/EBV+/dMMR). The sample size was estimated based on the following assumptions. According to previous literature, standard treatment has a 3-year disease-free survival rate of 67% (13). We estimate that PD-1 combined with adjuvant chemotherapy could result in a rate of 81%. It is expected that the studied regimen will achieve remission for a greater proportion of patients. Based on a two-tailed test of two independent means with a significance (α) level of 0.05% and at least 80% of the test efficacy, the number of participants determined was 62. If the loss rate does not exceed 10%, the minimum sample size for this study is 70 patients.

Statistical Analysis

The statistical analysis will be based on intention-to-treat (ITT) data or safety analysis set (SAT). The demographic characteristics of each group will be compared using the independent t-test and the chi-squared test for continuous variables and dichotomous variables. Measurement data will be expressed as mean, standard deviation, median, maximum, minimum. Enumeration data and ranked data will be expressed as a constituent ratio, rate, confidence interval. All statistical data will be analyzed by SPSS. The disease-free survival (DFS) rate will be estimated by Clopper-Pearson and the 95% confidence interval will be calculated. The overall survival (OS) rate will be analyzed by the Kaplan-Meier method and log-rank test. TTR is described by mean, standard deviation, median, maximum and minimum. Tumor markers associated with anti-PD-1 antibodies, such as levels of PD-L1 or other biomarkers in tumor tissue, will also be analyzed using descriptive statistics.

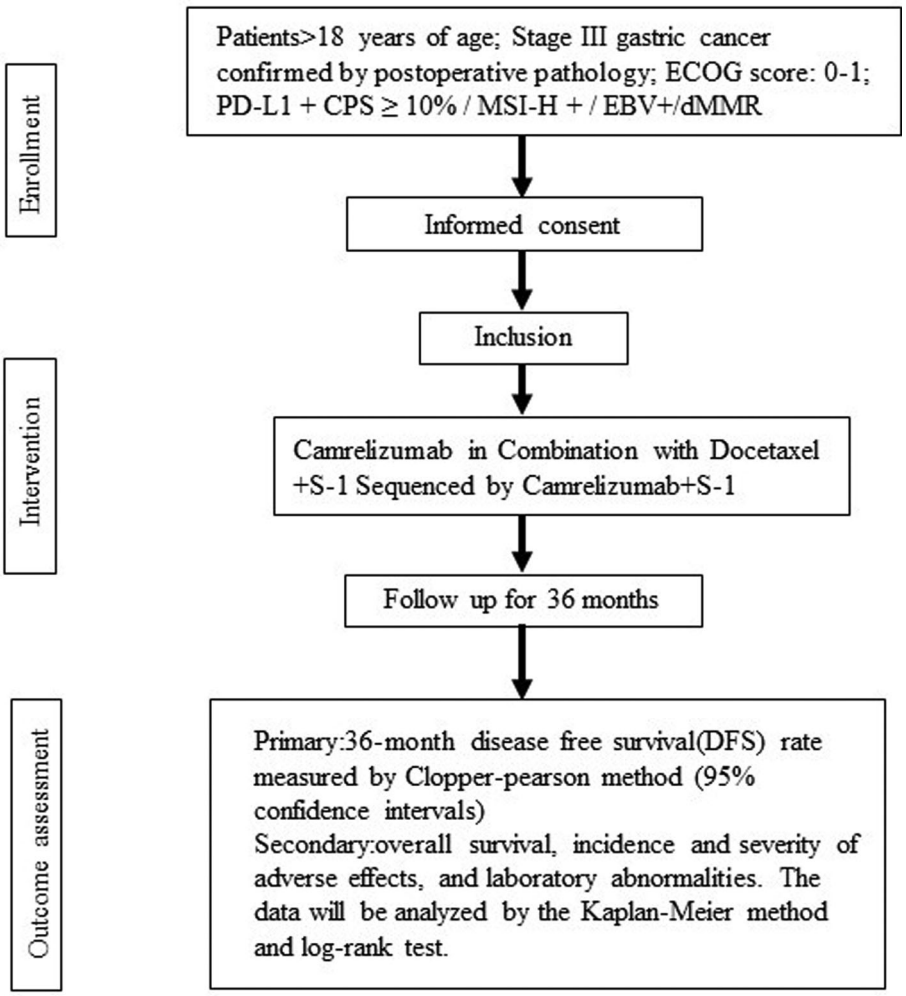

FIGURE 1 | Flowchart summarizing the trial procedure. Stage III gastric cancer participants in Camrelizumab in Combination with Docetaxel + S-1 Sequenced by Camrelizumab + S-1 for trial.

Data Collection and Monitoring

Data collection will include patient demographics and disease subclassification based on the Montreal Classification, such as clinical phenotype, disease location and surgical history. The collected patient demographic data will include the identity card number, sex, date of birth, age at diagnosis, duration, nationality, height and weight. Laboratory tests (including blood, urine, fecal occult blood test, liver/kidney function, blood glucose, serum electrolytes, serum proteins, clotting tests, thyroid function, tumor markers, etc.) should be completed within 14 days prior to the first treatment cycle Tumor imaging (including chest, abdomen, and pelvis CT scans; head CT or MRI and bone scans if clinically necessary) and echocardiography will be completed within 28 days. The participants and specific follow-up staff will screen for infectious diseases such as HIV, hepatitis B virus and hepatitis C virus.

Follow-up will be conducted by specific staff for all the participants enrolled in this study. The follow-up program will be established after the surgery and will be performed annually thereafter. In principle, all the examinations were suggested to be carried out in Renji Hospital. If the patients are reexamined in other hospitals, grade III, first-class hospitals are recommended and the follow-up staff will track and record the results. The tests included: (1) Adverse reactions; (2) Physical examination: superficial lymph nodes, abdomen, metastatic signs and so on; (3) Peripheral blood routine examination: HB, RBC, WBC, LYM, NEU, NEU%, PLT; (4) Blood biochemistry: albumin, prealbumin, total bilirubin, AST, ALT, creatinine, urea nitrogen, fasting blood-glucose; (5) Serum tumor markers: CEA, CA19-9, CA72-4; (6) Abdominal and pelvic CT.

All participants should be evaluated for safety and adverse events within 90 days of the last administration, and the patients' condition should be recorded. The following examinations should be performed on the 90th day of follow-up after treatment. (1) ECOG score standard; (2) Blood routine examination: hemoglobin, red blood cell, white blood

TABLE 1 | Inclusion and exclusion criteria.

Inclusion Criteria	(1) The patients voluntarily joined the study and signed the informed consent (2) ≥ 18 years old, ≤80 years old (3) Stage III gastric cancer confirmed by pathology (4) ECOG score: 0–1 (5) Detection of biomarkers in postoperative gastric cancer samples demonstrating PD-L1 + CPS ≥ 10% / MSI-H + / EBV+/dMMR (6) During the study treatment period and within 3 months after the end of the study treatment period, a medically recognized contraceptive measure (such as IUD, contraceptive pill or condom) should be used by the patients (7) The baseline blood routine and biochemical indexes of the selected patients should meet the specified standard
Exclusion Criteria	(1) Pregnant or lactating women; women of childbearing age with a positive pregnancy test (2) Have other malignant tumors in the past 5 years. Distant metastasis was diagnosed by CT /MR/ EUS (3) Received previous anti-tumor treatment (4) Uncontrollable pleural effusion, pericardial effusion, ascites or severe cardiovascular diseases (5) With gastroduodenal obstruction/bleeding, digestive dysfunction or malabsorption syndrome (6) Complicated with severe uncontrolled concurrent infection or other serious uncontrolled concomitant diseases, moderate or severe renal injury (7) Allergic reaction to the drugs used in this study (8) Steroid or other systemic immunosuppressive therapy was used within 14 days before admission (9) Patients who received study drug treatment within 4 weeks before enrollment (10) Active autoimmune diseases (11) History of primary immunodeficiency (12) Immunosuppressive drugs were used within 4 weeks prior to the first dose of study treatment (13) Received live attenuated vaccine within 4 weeks before the first dose of study treatment or during the study period (14) Active tuberculosis (15) History of allogeneic organ transplantation and allogeneic hematopoietic stem cell transplantation (16) HIV antibody positive, active hepatitis B or C (17) Other factors that may affect the safety or test compliance of the subjects according to the judgment of the researchers

cell, neutrophil count, and so on; (3) Routine urine test; (4) Blood biochemistry; (5) Evaluation for adverse events.

Combined with these results, the researchers assessed and recorded the postoperative survival status of all patients to determine tumor recurrence or metastasis. If patients refuse to be followed up according to our protocol, they will be recorded as missing cases and analyzed with those patients who met the study criteria at the end of the study.

After completion of the 90-day follow-up after discontinuation, the patients will enter the survival follow-up period. The participants, their family members, or local physicians are interviewed by telephone at least every three months. Follow-up staff will collect information on survival (date of death and cause of death) and post-treatment until either the end of death or the subject were lost to follow-up or the study was terminated by the researchers (**Table 2**).

Safety and Adverse Event Monitoring

An adverse event (AE) is any undesirable clinical event that occurs to a study participant during the study but does not necessarily have a causal relationship with the treatment. AEs may include any unexpected adverse symptom, sign, laboratory abnormality, or disease. For example:

(1) The original medical condition/disease is aggravated prior to entry into the clinical trial;
(2) Any new adverse medical condition (including symptoms, signs, recently diagnosed disease);
(3) Abnormal laboratory results with clinical significance.

The researchers will keep detailed records of any AE in the subjects.

Severe adverse event (SAE) refers to a medical event occurring during a clinical trial that requires hospitalization or prolonging the current hospitalization, causes persistent or significant disability, affects working capacity, endangers life, or results in congenital malformation/birth defect and other medical events. Hospitalization events exclude rehabilitation facilities, nursing homes, admission to a routine emergency room, day surgery (outpatient/ambulatory) and social reasons. Furthermore, if hospitalization or prolonged stay is unrelated to the exacerbation of AE, these events should not be included under SAE, such as annual physical examination, admission for pre-existing disease and so on. First, the subjects should sign an informed consent effective until 90 days after the last drug administration. The researchers should keep detailed records of symptoms, severity, association with the experimental drug, time of occurrence and treatment, measures that have been taken, time and manner of follow-up, and outcome. Any severe adverse event should immediately be reported by completing the SAE Report Form provided by the CFDA. Then the researcher should report the condition to the provincial, autonomous regional and municipal medical products administration, CFDA, and health administrative departments within 24 h and timely report to the ethics committee. SAEs occurring after 90 days following the last drug administration are generally not reported unless suspected to be related to the trial.

All AE/SAE should be followed up until disappearance, remission to baseline level, reaching a stable state, or a reasonable explanation (such as loss to follow-up, death).

Ethics and Dissemination

The study has been approved by Shanghai Jiaotong University School of Medicine, Renji Hospital Ethics Committee (KY2019-191) and registered in the Chinese Clinical Trial Registry (ChiCTR1900027123). The trial will be conducted according to the principles of the Declaration of Helsinki and in accordance with Good Clinical Practice (GCP) standards. Informed consent will be obtained by the coordinators or researchers associated with this protocol. It details the drug use, the course of the study, and the risks of the study are fully explained. Written informed consent must be obtained

TABLE 2 | Check and visit schedule.

Check/Visit	Screening[a]	1st cycle (21d) First Week C1/D1	2nd cycle (21d) Forth Week C2/D1 (±3d)	3rd cycle (21d) Seventh Week C3/D1 (±3d)	4th cycle (21d) Tenth Week C4/D1 (±3d)	5th cycle (21d) Thirteenth Week C5/D1(±3d)	6th–18th Cycle (21d) N week C6-C18/D1	Follow-up period		
								Finish/ Quit	Safety (every 30ds)	Survival (every3 mons)
ECOG Score	√	√	√	√	√	√	√	√	√	
Physical Examination	√					√	√	√	√	
Vital signs	√	√	√	√	√	√	√	√	√	
Blood routine[b]	√		√	√	√	√	√	√	√	
Urine Routine[c]	√		√	√	√	√	√	√	√	
Blood Biochemical[d]	√		√	√	√	√	√	√	√	
Occult blood test[e]	√									
Coagulation test[f]	√					√	√	√		
Thyroid function test[g]	√					√	√	√		
Pituitary-adrenal test[h]	√									
ECG[i]	√		√	√	√	√	√	√		
Imaging Evaluation[j]	√					√	√	√		
Pregnancy test[k]	√							√		
Adverse Events[l]	√	√	√	√	√	√	√	√	√	√
Tumor Markers[m]	√					√	√			
Quality of Life Score	√	√		√		√	√	√		
Compliance	√							√		

[a]*Screening: Tests and evaluations should be completed within 14 days prior to the first use of the drug. Tumor imaging and echocardiography can be completed in 28 days.*
[b]*Blood routine should include complete blood count and classification. If necessary, the researchers can perform additional tests.*
[c]*Routine urine tests include white blood cells, red blood cells, and urine proteins. Two consecutive urine protein test 2 + ~ 3 +, or proteinuria 4 +, requires 24-hour urinary protein quantification. Subjects with 24-hour urinary protein quantification more than 1 g during the screening period are not recommended.*
[d]*Blood biochemistry: Including ALT, AST, GGT, AKP, LDH, TP, ALB, TBIL, DBIL, GlU, IBIL, BUN or urea, Cr, K^+, Na^+, Cl^-, Ca^{2+}, Mg^{2+} . If necessary, the researchers can perform additional tests.*
[e]*Occult blood test: Eliminate dietary interference.*
[f]*Coagulation test: INR, APTT, PT, FIB.*
[g]*Thyroid function test: Serum FT3, FT4, TSH.*
[h]*Pituitary-adrenal test: Including Corticotropin, cortisol, sex hormones test.*
[i]*12-lead ECG: This should be completed before each administration of Camrelizumab. (Noting Qt, QTc, and P-R intervals)*
[j]*Imaging Evaluation: Baseline and postoperative radiographic evaluation were performed according to RECIST V1.1.*
[k]*Pregnancy test: Women of child-bearing age should perform blood or urine tests during the screening period (72 hours before first administration) and at the time of completion or withdrawal from the study.*
[l]*Adverse events: All adverse events were observed and recorded according to NCI CTCAE V5.0 standards.*
[m]*Tumor markers: CEA, CA199 and CA72-4 were detected before the first administration, every 4 cycles and the end of treatment.*

before proceeding with the study. Throughout the course of the clinical study, participants could withdraw their consent at any time. All the personal information about the subjects will be kept strictly confidential.

Results will be published in the open-access peer-reviewed medical literature as well as submitted for presentation at national and international meetings.

DISCUSSION

For decades, chemotherapy has remained the mainstay of effective treatment for advanced GC (14). For more than 50 years, the vast majority of chemotherapy regimens for gastric cancer have been based on the infusion of 5-FU (15). Although molecular targeted therapy is rapidly evolving in

individualized and precision medicine, only a few drugs have successfully been considered over conventional treatment (16). The CSCO guidelines suggest that patients with resectable gastric cancer receive postoperative adjuvant treatment. Furthermore, XELOX or S-1 alone are recommended for grade I tumors (17). In addition, S-1 is an oral 5-FU prodrug and has been widely accepted for the treatment of advanced GC in Japan (15). The JCOG9912 randomized trial showed that oral S-1 alone was as effective as a continuous infusion of fluorouracil for patients with metastatic gastric cancer (18). The main component of S-1 is tegafur with two enzyme inhibitors:5-chloro-2,4-dihydroxypyridine and potassium oxonate (19). It has been reported that CDHP enhances the anti-cancer activity of tegafur and Oxo blocks 5-FU phosphorylation, reducing local toxicity (20). Although S-1 monotherapy reduced the incidence of peritoneal metastasis, approximately 20%–30% of patients relapsed after one year (21).

Docetaxel, a cytotoxic anti-cancer agent, is a notable treatment option available for patients with advanced gastric cancer (22). Docetaxel can impair mitosis and induce apoptosis by suppressing the microtubule dynamics of the mitotic apparatus (23). It has not only revealed promising activity as a single agent but also showed efficacy in combination with S-1 (24). Several clinical trials of docetaxel in combination with S-1 have been conducted to explore the superiority over S-1 monotherapy. The randomized phase III study "JACCRO GC-07" (13), which compared S1/docetaxel vs. S-1 alone in 915 enrolled patients, showed significant superiority of S-1 plus docetaxel (65.9%) to S-1 (49.6%) for 3-year relapse-free survival (hazard ratio, 0.632; 99.99% CI, 0.400 to 0.998; stratified log-rank test, $P < .001$).

Although the DS regimen assessment results reported significant benefits for the patients, the advances in immunotherapy bring considerable changes. The "FORCE1" study (25) suggests that a large percentage of Chilean patients may be candidates for immunotherapy because of the prevalence of Epstein-Barr virus–related gastric cancer leading to microsatellite instability. Although only 5%–10% of adenocarcinomas are Epstein-Barr-virus (EBV)-associated gastric cancer worldwide, it is commonly believed that these patients have better disease courses and overall outcomes than Epstein-Barr negative patients. They potentially benefit from immunotherapy and have higher chances of survival (7).

Based on the results of these clinical studies, although guidelines recommend camrelizumab as a third-line treatment for gastric cancer, we would like to explore its efficacy and safety as a first-line treatment for patients with specific phenotypes of gastric cancer. To our knowledge, these strategies have not been compared in a clinical trial to date. Therefore, this study aims to investigate if camrelizumab, in combination with docetaxel + S-1, sequenced by camrelizumab + S-1treatment, can improve the outcome of patients who are EBV positive with defective mismatch repair and CPS $\geq$5.

However, this research has some shortcomings. Firstly, the number of eligible patients is relatively small. It may take long time and much money to enroll all patients. Secondly, the study we conducted is exploratory and subsequent large-scale clinical studies are still needed to provide higher level of evidence. Finally, the trial is open label so subjects and researchers can know what procedure was undertaken to treat.

The final review paper will be submitted to a peer-reviewed journal for publication and presented at relevant conferences (**Supplementary Table 1**).

DATA AVAILABILITY STATEMENT

The raw data supporting the conclusions of this article will be made available by the authors, without undue reservation.

ETHICS STATEMENT

Written informed consent was obtained from the individual(s) for the publication of any potentially identifiable images or data included in this article.

AUTHOR CONTRIBUTIONS

Conception and design: ZZ, GZ, XX, YJ. Principal investigators of the study: ZD, BN, LY. Revision of the study design and protocol: ZZ, GZ, XX, EZ, CZ. Study coordination: ZZ, XX, BN, LY. Acquisition of data and patient recruitment: LY, BN, ZD, XX, CZ. Statistical analysis: EHZ. Obtaining funding and supervision: ZZ. Drafting the manuscript: ZD, BN, LY. Revision and adaptation: All authors. All authors contributed to the article and approved the submitted version.

FUNDING

The study was sponsored by The National Natural Science Foundation of China (grant numbers: 81972206 and 82173215) and Jiangsu Hengrui Pharma. The funding department and Hengrui Pharma had no influence on the design of the trial and have no influence on the collection, analysis and interpretation of data, in writing the manuscript or in presenting the study results.

ACKNOWLEDGMENTS

We kindly thank the editor and reviewers for careful review and valuable comments, which have led to a significant improvement of the manuscript.

SUPPLEMENTARY MATERIAL

The Supplementary Material for this article can be found online at: https://www.frontiersin.org/articles/10.3389/fsurg.2022.917352/full#supplementary-material.

REFERENCES

1. Gao F, Li M, Xiang R, Zhou X, Zhu L, Zhai Y. Expression of CLDN6 in tissues of gastric cancer patients: Association with clinical pathology and prognosis. *Oncol Lett*. (2019) 17(5):4621–5. doi: 10.3892/ol.2019.10129
2. Zhuo S, Sun M, Bai R, Lu D, Di S, Ma T, et al. Long intergenic non-coding RNA 00473 promotes proliferation and migration of gastric cancer via the miR-16-5p/CCND2 axis and by regulating AQP3. *Cell Death Dis*. (2021) 12(5):496. doi: 10.1038/s41419-021-03775-9
3. Park KB, Yu B, Park JY, Kwon OK, Yu W. Impact of body mass index on quality of life after distal gastrectomy for gastric cancer. *Ann Surg Treat Res*. (2019) 96(5):250–8. doi: 10.4174/astr.2019.96.5.250
4. Bang YJ, Van Cutsem E, Feyereislova A, Chung HC, Shen L, Sawaki A, et al. Trastuzumab in combination with chemotherapy versus chemotherapy alone for treatment of HER2-positive advanced gastric or gastro-oesophageal junction cancer (ToGA): a phase 3, open-label, randomised controlled trial. *Lancet*. (2010) 376(9742):687–97. doi: 10.1016/S0140-6736(10)61121-X
5. Mahoney KM, Freeman GJ, McDermott DF. The next immune-checkpoint inhibitors: PD-1/PD-L1 blockade in melanoma. *Clin Ther*. (2015) 37 (4):764–82. doi: 10.1016/j.clinthera.2015.02.018
6. Muro K, Chung HC, Shankaran V, Geva R, Catenacci D, Gupta S, et al. Pembrolizumab for patients with PD-L1-positive advanced gastric cancer (KEYNOTE-012): a multicentre, open-label, phase 1b trial. *Lancet Oncol*. (2016) 17(6):717–26. doi: 10.1016/S1470-2045(16)00175-3
7. Fuchs CS, Doi T, Jang RW, Muro K, Satoh T, Machado M, et al. Safety and efficacy of pembrolizumab monotherapy in patients with previously treated advanced gastric and gastroesophageal junction cancer: phase 2 clinical KEYNOTE-059 trial. *JAMA Oncol*. (2018) 4(5):e180013. doi: 10.1001/jamaoncol.2018.0013
8. Shitara K, Ozguroglu M, Bang YJ, Di Bartolomeo M, Mandala M, Ryu MH, et al. Pembrolizumab versus paclitaxel for previously treated, advanced gastric or gastro-oesophageal junction cancer (KEYNOTE-061): a randomised, open-label, controlled, phase 3 trial. *Lancet*. (2018) 392 (10142):123–33. doi: 10.1016/S0140-6736(18)31257-1
9. Le DT, Durham JN, Smith KN, Wang H, Bartlett BR, Aulakh LK, et al. Mismatch repair deficiency predicts response of solid tumors to PD-1 blockade. *Science*. (2017) 357(6349):409–13. doi: 10.1126/science.aan6733
10. Panda A, Mehnert JM, Hirshfield KM, Riedlinger G, Damare S, Saunders T, et al. Immune activation and benefit from avelumab in EBV-positive gastric cancer. *J Natl Cancer Inst*. (2018) 110(3):316–20. doi: 10.1093/jnci/djx213
11. Haag GM, Czink E, Ahadova A, Schmidt T, Sisic L, Blank S, et al. Prognostic significance of microsatellite-instability in gastric and gastroesophageal junction cancer patients undergoing neoadjuvant chemotherapy. *Int J Cancer*. (2019) 144(7):1697–703. doi: 10.1002/ijc.32030
12. Kohlruss M, Grosser B, Krenauer M, Slotta-Huspenina J, Jesinghaus M, Blank S, et al. Prognostic implication of molecular subtypes and response to neoadjuvant chemotherapy in 760 gastric carcinomas: role of Epstein-Barr virus infection and high- and low-microsatellite instability. *J Pathol Clin Res*. (2019) 5(4):227–39. doi: 10.1002/cjp2.137
13. Yoshida K, Kodera Y, Kochi M, Ichikawa W, Kakeji Y, Sano T, et al. Addition of docetaxel to oral fluoropyrimidine improves efficacy in patients with stage III gastric cancer: interim analysis of JACCRO GC-07, a randomized controlled trial. *J Clin Oncol*. (2019) 37(15):1296–304. doi: 10.1200/JCO.18.01138
14. Cervantes A, Roda D, Tarazona N, Rosello S, Perez-Fidalgo JA. Current questions for the treatment of advanced gastric cancer. *Cancer Treat Rev*. (2013) 39(1):60–7. doi: 10.1016/j.ctrv.2012.09.007
15. Digklia A, Wagner AD. Advanced gastric cancer: Current treatment landscape and future perspectives. *World J Gastroenterol*. (2016) 22 (8):2403–14. doi: 10.3748/wjg.v22.i8.2403
16. Van Cutsem E, Sagaert X, Topal B, Haustermans K, Prenen H. Gastric cancer. *Lancet*. (2016) 388(10060):2654–64. doi: 10.1016/S0140-6736(16)30354-3
17. Wang FH, Shen L, Li J, Zhou ZW, Liang H, Zhang XT, et al. The Chinese Society of Clinical Oncology (CSCO): clinical guidelines for the diagnosis and treatment of gastric cancer. *Cancer Commun (Lond)*. (2019) 39(1):10. doi: 10.1186/s40880-019-0349-9
18. Boku N, Yamamoto S, Fukuda H, Shirao K, Doi T, Sawaki A, et al. Fluorouracil versus combination of irinotecan plus cisplatin versus S-1 in metastatic gastric cancer: a randomised phase 3 study. *Lancet Oncol*. (2009) 10(11):1063–9. doi: 10.1016/S1470-2045(09)70259-1
19. Kim HJ, Yun J, Kim HJ, Kim KH, Kim SH, Lee TH, et al. Phase II study of palliative S-1 in combination with cisplatin as second-line chemotherapy for gemcitabine-refractory pancreatic cancer patients. *Oncol Lett*. (2012) 3 (6):1314–8. doi: 10.3892/ol.2012.637
20. Zhang SC, Yu MY, Xi L, Zhang JX. Tegafur deteriorates established cardiovascular atherosclerosis in colon cancer: A case report and review of the literature. *World J Clin Cases*. (2019) 7(1):89–94. doi: 10.12998/wjcc.v7.i1.89
21. Sasako M, Sakuramoto S, Katai H, Kinoshita T, Furukawa H, Yamaguchi T, et al. Five-year outcomes of a randomized phase III trial comparing adjuvant chemotherapy with S-1 versus surgery alone in stage II or III gastric cancer. *J Clin Oncol*. (2011) 29(33):4387–93. doi: 10.1200/JCO.2011.36.5908
22. Wang M, You SK, Lee HK, Han MG, Lee HM, Pham TMA, et al. Development and evaluation of docetaxel-phospholipid complex loaded self-microemulsifying drug delivery system: optimization and in vitro/ex vivo studies. *Pharmaceutics*. (2020) 12(6):544. doi: 10.3390/pharmaceutics12060544
23. Kim E, Matsuse M, Saenko V, Suzuki K, Ohtsuru A, Mitsutake N, et al. Imatinib enhances docetaxel-induced apoptosis through inhibition of nuclear factor-kappaB activation in anaplastic thyroid carcinoma cells. *Thyroid*. (2012) 22(7):717–24. doi: 10.1089/thy.2011.0380
24. Japanese Gastric Cancer A. Japanese gastric cancer treatment guidelines 2010 (ver. 3). *Gastric Cancer*. (2011) 14(2):113–23. doi: 10.1007/s10120-011-0042-4
25. Cordova-Delgado M, Pinto MP, Retamal IN, Munoz-Medel M, Bravo ML, Fernandez MF, et al. High proportion of potential candidates for immunotherapy in a chilean cohort of gastric cancer patients: results of the FORCE1 study. *Cancers (Basel)*. (2019) 11(9):1275. doi: 10.3390/cancers11091275

Conflict of Interest: The authors declare that the research was conducted in the absence of any commercial or financial relationships that could be construed as a potential conflict of interest.

Publisher's Note: All claims expressed in this article are solely those of the authors and do not necessarily represent those of their affiliated organizations, or those of the publisher, the editors and the reviewers. Any product that may be evaluated in this article, or claim that may be made by its manufacturer, is not guaranteed or endorsed by the publisher.

Copyright © 2022 Dong, Ni, Yang, Zhu, Zhao, Zhao, Xia and Zhang. This is an open-access article distributed under the terms of the Creative Commons Attribution License (CC BY). The use, distribution or reproduction in other forums is permitted, provided the original author(s) and the copyright owner(s) are credited and that the original publication in this journal is cited, in accordance with accepted academic practice. No use, distribution or reproduction is permitted which does not comply with these terms.

frontiers | Frontiers in Surgery

ORIGINAL RESEARCH
published: 28 June 2022
doi: 10.3389/fsurg.2022.898952

SOX30 Overexpression Reflects Tumor Invasive Degree, Lymph Node Metastasis and Predicts Better Survival in Colorectal Cancer Patients: A Long-Term Follow-Up Cohort Study

Chao Li[1†], Pengfei Li[2†], Lulu Yu[1], Qingsen Sun[1], Bin Gu[1], Yanhua Sun[1] and Liansheng Sun[1]*

[1]Department of Gastrointestinal Surgery, Cangzhou People's Hospital, Cangzhou, China, [2]Department of Clinical Laboratory, Cangzhou People's Hospital, Cangzhou, China

OPEN ACCESS

Edited by:
Qi Liu,
Fudan University, China

Reviewed by:
Sohini Chakraborty,
New York University, United States
Konda Bobba,
University of California, United States
Ludovico Docimo,
University of Campania Luigi Vanvitelli, Italy
Jacek Kieżun,
University of Warmia and Mazury in Olsztyn, Poland

***Correspondence:**
Yanhua Sun
yan58581572@163.com

†These authors have contributed equally to this work

Specialty section:
This article was submitted to Surgical Oncology, a section of the journal Frontiers in Surgery

Received: 18 March 2022
Accepted: 03 June 2022
Published: 28 June 2022

Citation:
Li C, Li P, Yu L, Sun Q, Gu B, Sun Y and Sun L (2022) SOX30 Overexpression Reflects Tumor Invasive Degree, Lymph Node Metastasis and Predicts Better Survival in Colorectal Cancer Patients: A Long-Term Follow-Up Cohort Study. Front. Surg. 9:898952. doi: 10.3389/fsurg.2022.898952

Aims: Sex-determining region Y-box containing gene 30 (SOX30) takes part in the progression of several cancers, while its clinical engagement in colorectal cancer (CRC) is obscure. Therefore, this study aimed to explore the association of SOX30 with clinicopathological features and prognosis in CRC patients.

Methods: Tumor and adjacent noncancerous specimens of 195 CRC patients who received resection were acquired. Furthermore, an immunohistochemistry assay was performed to detect SOX30 protein expression in these specimens; meanwhile, SOX30 mRNA expression was determined by reverse transcription-quantitative polymerase chain reaction assay in 95 out of 195 specimens. Moreover, clinical characteristics and survival data (follow-up duration median (range): 71.0 (7.0-95.0) months) of CRC patients were gathered.

Results: SOX30 protein and mRNA expressions were both decreased in CRC tumor tissue compared to adjacent tissue (both $P < 0.001$). Furthermore, a negative correlation was found in tumor SOX30 protein expression with tumor size ($P = 0.049$), lymph node (LYN) metastasis ($P = 0.018$), T stage ($P = 0.001$), N stage ($P = 0.034$), and TNM stage ($P = 0.001$); tumor SOX30 mRNA expression was also negatively correlated with LYN metastasis ($P = 0.001$), T stage ($P = 0.019$), N stage ($P = 0.004$), and TNM stage ($P < 0.001$). Furthermore, tumor SOX30 protein expression was positively correlated with overall survival (OS) ($P = 0.017$), while tumor SOX30 mRNA expression was not correlated with OS ($P = 0.070$). Multivariate Cox's regression analysis illustrated that tumor SOX30 protein high expression was an independent factor for favorable OS (hazard ratio: 0.525, $P = 0.034$).

Conclusions: SOX30 has potential as a biomarker for the progression and prognostication of CRC, which might improve the management of CRC.

Keywords: sex-determining region Y-box containing gene 30, colorectal cancer, clinical characteristics, survival, disease progression

INTRODUCTION

Colorectal cancer (CRC) is one of the most common cancers and the major cause of cancerous mortality globally (1–3). According to the WHO cancer research center GLOBOCAN project, the morbidity and mortality of CRC worldwide in 2018 are approximately 1.8 million and 88 thousand, respectively (4). Generally, the treatments of CRC include resection, radiotherapy, chemotherapy combinations, and immunotherapy (5). Although great progress in the treatments of CRC, unfavorable long-term survival is still an obstinate problem in CRC patients (1, 2, 5). In consideration that CRC is still prevalent cancer with an unsatisfied cure rate and elevated recurrence, the exploration of prognostic factors to improve CRC management is crucial (1, 5).

Sex-determining region Y-box (SOX) transcription factors have been illustrated to be involved in tumor progression, such as tumorigenesis and metastasis (6). Among famously identified SOX transcription factors, SOX containing gene 30 (SOX30) is considered to be a suppressor of a variety of cancers, including hepatocellular carcinoma, lung cancer, ovarian cancer, etc. (7–12). For instance, SOX30 is able to repress tumor metastasis in lung cancer by regulating the Wnt signaling pathway (8); SOX30 also plays an anti-metastatic role in ovarian cancer through modulating the epithelial-mesenchymal transition (EMT) process (9); it has been illustrated that SOX30 has the capacity of inhibiting proliferation and invasion but promoting apoptosis of T24 and 5,673 cells to suppress the progression of bladder cancer (12). Besides, SOX30 is regarded as a prognostic biomarker in terminal ovarian cancer patients (9); elevated SOX30 expression is regarded as a predictor of better survival among non-small cell lung cancer patients (10). On the basis of the above-mentioned data, we speculated that SOX30 could show an association with the progression and prognosis of CRC, while the clinical value of SOX30 in CRC remains unclear.

Therefore, the purpose of this present study was to explore the correlation of SOX30 expression measured by both immunohistochemistry (IHC) and reverse transcription-quantitative polymerase chain reaction (RT-qPCR) with clinicopathological features and long-term prognosis in CRC patients.

METHODS

Patients

This retrospective study reviewed 195 CRC patients treated in the hospital between January 2013 and December 2017. The screening criteria for all subjects were: (i) diagnosed as primary CRC in accord with the European guidelines for colorectal cancer diagnosis (13); (ii) received tumor resections; (iii) had complete clinical characteristics and follow-up data; (iv) had available CRC specimens and paired adjacent noncancerous specimens to perform IHC assay. The exclusion criteria included: (i) diagnosed as relapsed CRC or secondary CRC at first admission; (ii) complicated with other carcinomas or malignancies at the time of diagnosis; (iii) had a history of chemotherapy, radiotherapy, or targeted therapy before resection. This study was approved by the Institutional Review Board of Cangzhou People's Hospital (ethics approval number: 20201127-2), and all patients or their statutory guardians signed the informed consent.

Collection of Data and Specimens

By reviewing the medical documents, the clinical characteristics were collected, including age, gender, pathological grade, tumor size, lymph node (LYN) status, and TNM stage. Besides, overall survival (OS) data of all patients were also gathered, and the last follow-up date was February 2021. For specimens, CRC and paired adjacent noncancerous specimens of 195 patients, which were fixed in formalin and embedded in paraffin (FFEP), were collected to assess the SOX30 protein expression. Among 195 patients, 95 pairs of cancerous and adjacent noncancerous specimens frozen in liquid nitrogen were also collected to evaluate the SOX30 mRNA expression.

SOX30 Protein Expression Detection

The SOX30 protein expression was assessed by IHC assay with 195 pairs of cancerous and adjacent tissue specimens. The rabbit anti-SOX30 polyclonal antibody (Thermo, Waltham, Massachusetts, USA) with 1:50 dilution was applied as the primary antibody, and the goat anti-rabbit IgG (H + L) (Thermo, Waltham, Massachusetts, USA) with 1:2,000 dilution was used as the secondary antibody. The process of the IHC assay was identical to the previous study (11). The assessment of the SOX30 protein expression was performed with a semi-quantitative scoring method as previously described (14). In brief, IHC staining results were observed by a light microscope. The intensity score of IHC staining was 0–3, while the density score of IHC staining was 0–4. The product of the intensity score and the density score generated a final IHC score, ranging from 0 to 12. The IHC score was evaluated by two pathologists in a blind manner. If the two pathologists gave different scores for the same sample, then the final IHC score of this sample was the mean value of the two IHC scores given by the two pathologists.

Western blot was conducted to verify the antibody against SOX30. After extracted by RIPA (Thermo, Waltham, Massachusetts, USA) and quantified by BCA kit (Beyotime, China), the protein was separated by sodium dodecyl sulfate polyacrylamide gel electrophoresis and transferred to polyvinylidene difluoride membranes (Beyotime, China). Then the membranes were incubated with primary antibodies (diluted at 1:2,000) at 4°C overnight, followed by secondary antibody incubation for 1 h at room temperature. After that, the brands were visualized by ECL kit (Yeason, China).

RT-qPCR Assay

After the collection of 95 paired frozen specimens, the RT-qPCR assay was used to evaluate the expression of SOX30 mRNA. Briefly, total RNA was extracted by TRIzol™ Reagent (Invitrogen, Carlsbad, California, USA) and reversely transcribed by iScript™ cDNA Synthesis Kit (Bio-Rad,

Hercules, California, USA). Afterwards, qPCR was performed by QuantiNova SYBR Green PCR Kit (Qiagen, Duesseldorf, Nordrhein-Westfalen, Germany). β-actin was used as an internal reference. Moreover, the relative expression of SOX30 mRNA was calculated by the $2^{-\Delta\Delta Ct}$ method. The PCR primer sequences were as follows: SOX30 forward: 5′-CCAAGCCC TGTCACACTTTT-3′ and reverse: 5′-AATCCTGTTGGCGCT CTCTA-3′; β-actin forward: 5′-CAATGACCCCTTCATTGA CC-3′ and reverse: 5′-GACAAGCTTCCCGTTCTCAG-3′.

Public Data for Prognostic Verification

We collected publicly available transcriptome data from two public databases to further verify the correlation of SOX30 expression with survival among CRC patients. A total of 597 CRC patients' SOX30 RNA Fragments Per Kilobase Million (FPKM) data were obtained from The Human Protein Atlas (derived from The Cancer Genome Atlas (TCGA)) (available at https://www.proteinatlas.org/ENSG00000039600-SOX30/pathology/colorectal+cancer). Besides, a total of 90 CRC patients' SOX30 Transcripts Per Million (TPM) data were obtained from GEPIA (available at http://gepia.cancer-pku.cn/detail.php?gene = SOX30###).

Statistical Analysis

SPSS V.19.0 software (IBM Corp., Armonk, New York, USA) was used for statistical analysis and GraphPad Prism 7.02 (GraphPad Software Inc., San Diego, California, USA) was used for graph making. Paired-samples *t* test and Wilcoxon signed-rank test were applied to compare the SOX30 expression between CRC and paired adjacent noncancerous specimens. For correlation analysis of SOX30 with other variables, the SOX30 protein expression was classified as low expression (IHC score ≤3) and high expression (IHC score >3), respectively; and the median mRNA expression (0.392) in tumor tissue was used to classify the SOX30 mRNA low expression (≤0.392) and SOX30 mRNA high expression (>0.392), respectively. The correlations of the two variables were evaluated by the Chi-square test and the Mantel-Haenszel Chi-square test. Correlations between the SOX30 expression and accumulating OS were evaluated by Kaplan-Meier curves and log-rank test. Prognostic factors were determined by Cox's proportional hazard regression model analysis. Statistical significance was concluded if a *P*-value <0.05 was presented in the corresponding analysis.

RESULTS

Clinical Characteristics of CRC Patients

Among 195 CRC patients, the mean age was 65.7 ± 10.3 years, meanwhile, there were 118 (60.5%) males and 77 (39.5%) females. Regarding patients with different pathological grades, there existed 27 (13.9%) patients with grade I, 135 (69.2%) patients with grade II, and 33 (16.9%) patients with grade III. In addition, the median tumor size was 4.5 (3.5–5.0) cm in patients. With respect to LYN metastasis, 126 (64.6%) patients had LYN metastasis and 69 (35.4%) patients had no LYN metastasis. In terms of T stages, there were 5 (2.6%) patients with T1, 23 (11.8%) patients with T2, 165 (84.6%) patients with T3, and 2 (1.0%) patients with T4. Regarding N stages, there existed 121 (62.1%), 50 (25.6%), and 24 (12.3%) patients with N0, N1, and N2 accordingly. Concerning TNM stages, there were 28 (14.4%), 93 (47.7%), and 74 (37.9%) patients with TNM stage I, stage II, and stage III, respectively (**Table 1**).

Comparison of SOX30 IHC Score and SOX30 mRNA Expression Between Tumor Tissue and Adjacent Tissue

SOX30 IHC score (mean ± standard deviation: 2.6 ± 1.6 vs. 5.5 ± 2.6) was decreased in tumor tissue compared to adjacent tissue ($P < 0.001$) (**Figures 1A,B**). Meanwhile, SOX30 mRNA expression (median (inter quartile range): 0.392 (0.221–0.744) vs. 1.000 (0.599–1.475)) was also reduced in tumor tissue compared to adjacent tissue ($P < 0.001$) (**Figure 1C**). In addition, antibody against SOX30 was verified by western blot, which showed that SOX30 detected by western blot was highly correlated with SOX30 detected by IHC (**Supplementary Figures 1A–C**).

TABLE 1 | Clinical characteristics of CRC patients.

Items	CRC patients (*N* = 195)
Age (years), mean ± SD	65.7 ± 10.3
Gender, No. (%)	
Male	118 (60.5)
Female	77 (39.5)
Pathological grade, No. (%)	
Grade I	27 (13.9)
Grade II	135 (69.2)
Grade III	33 (16.9)
Tumor size (cm), median (IQR)	4.5 (3.5–5.0)
LYN metastasis, No. (%)	
Negative	121 (62.1)
Positive	74 (37.9)
T stage, No. (%)	
T1	5 (2.6)
T2	23 (11.8)
T3	165 (84.6)
T4	2 (1.0)
N stage, No. (%)	
N0	121 (62.1)
N1	50 (25.6)
N2	24 (12.3)
TNM stage, No. (%)	
Stage I	28 (14.4)
Stage II	93 (47.7)
Stage III	74 (37.9)

CRC, colorectal cancer; SD, standard deviation; IQR, interquartile range; LYN, lymph node.

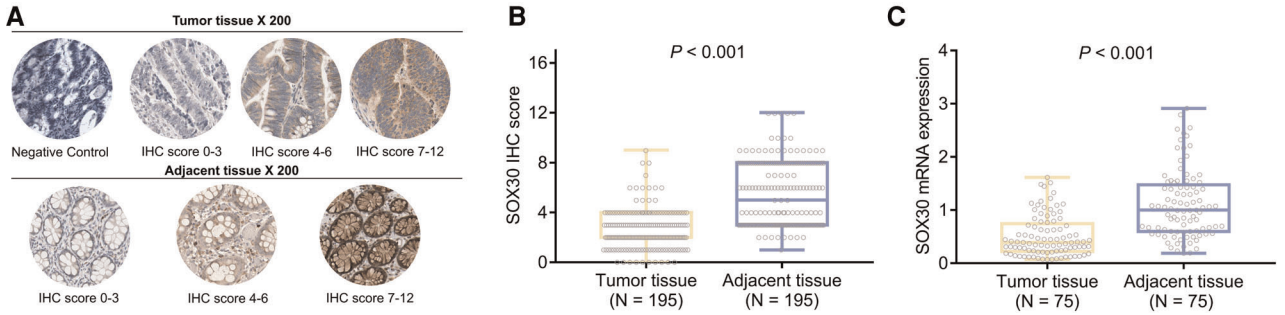

FIGURE 1 | SOX30 in CRC patients. IHC images of SOX30 expression in tumor tissue and adjacent tissue (**A**); comparison of SOX30 IHC score (**B**) and SOX30 mRNA expression (**C**) between tumor tissue and adjacent tissue. SOX30, sex-determining region Y-box containing gene 30; IHC, immunohistochemistry; CRC, colorectal cancer.

Correlation of Tumor SOX30 With Clinicopathological Features in CRC Patients

There were 145 CRC patients' tumor tissue IHC score ≤3 and 50 CRC patients' tumor tissue IHC score >3. Tumor SOX30 protein expression was negatively correlated with tumor size, LYN metastasis, T stage, N stage, and TNM stage (all $P < 0.05$); however, no correlation was found in tumor SOX30 protein expression with age, gender, or pathological grade (all $P > 0.05$). Furthermore, there were 46 CRC patients' tumor SOX30 mRNA expression ≤0.392 and 47 CRC patients' tumor SOX30 mRNA expression >0.392. Tumor SOX30 mRNA expression was negatively correlated with LYN metastasis, T stage, N stage, and TNM stage (all $P < 0.05$), while no correlation was found in tumor SOX30 mRNA expression with age, gender, pathological grade, or tumor size (all $P > 0.05$) (**Table 2**).

Correlation of Tumor SOX30 With Accumulating OS in CRC Patients

In order to explore the prognostic value of tumor SOX30 protein and mRNA expressions in CRC, we gathered the OS data of all CRC patients and we found that tumor SOX30 protein expression was positively correlated with accumulating OS ($P = 0.017$) (**Figure 2A**). However, tumor SOX30 mRNA expression was not correlated with accumulating OS ($P = 0.070$) (**Figure 2B**). Further subgroup analysis discovered that a positive correlation was only found in tumor SOX30 protein expression with OS in patients with TNM stage II ($P = 0.007$) (**Table 3**). In addition, data from The Human Protein Atlas (derived from The Cancer Genome Atlas (TCGA)) and GEPIA databases also revealed that SOX30 mRNA expression showed a tendency to be positively correlated with accumulating OS, but did not reach statistical significance (**Supplementary Figures 2A,B**).

Univariate and Multivariate Cox's Regression Model Analysis for OS

Univariate Cox's regression analysis showed that tumor SOX30 protein high expression was correlated with better OS (hazard ratio (HR): 0.494, $P = 0.020$); while higher pathological grade (HR: 1.322, $P < 0.001$), LYN metastasis (HR: 2.834, $P < 0.001$), higher N stage (HR: 2.232, $P < 0.001$) and higher TNM stage (HR: 2.164, $P < 0.001$) were all associated with poor OS. Moreover, multivariate Cox's regression analysis illustrated that tumor SOX30 protein high expression was independently associated with favorable OS (HR: 0.525, $P = 0.034$); while higher pathological grade (HR: 1.737, $P = 0.014$) and LYN metastasis (HR: 1.083, $P = 0.008$) were both independently correlated with poor OS (**Figure 3**).

DISCUSSION

In our study, we discovered several interesting results: (1) SOX30 protein and mRNA expressions were both reduced in CRC tumor tissue; (2) tumor SOX30 protein expression was negatively correlated with tumor size, LYN metastasis, T stage, N stage, and TNM stage; tumor SOX30 mRNA expression was negatively correlated with LYN metastasis, T stage, N stage, and TNM stage; (3) tumor SOX30 protein expression was positively correlated with accumulating OS, furthermore, tumor SOX30 protein high expression was independently associated with favorable OS.

SOX30 is reported to be a suppressor of several cancers, which exerts its function mainly through inhibition of the Wnt/β-catenin signaling pathway and activation of p53 transcription (15, 16). In terms of SOX30 expression in cancer, a previous study illustrated that SOX30 expression is reduced in breast cancer tissue compared to adjacent tissue (11). Another interesting study also reports that SOX30 expression is particularly reduced in non-small cell lung cancer tissues compared to adjacent noncancerous tissues (10). In our study, we found that tumor SOX30 protein and mRNA expressions were both reduced in CRC tumor tissue compared to adjacent tissue, which was partly consistent with previous studies (11, 15). Possible explanations might be that SOX30 downregulation might inhibit oncogenesis-related signaling pathways in CRC, such as Wnt and β-catenin signaling

TABLE 2 | Correlation of tumor SOX30 with clinicopathological features.

Items	SOX30 protein expression			SOX30 mRNA expression		
	Low	High	*P*-value	Low	High	*P*-value
Number of patients	145	50	0.080	46	47	0.507
Age, No. (%)						
<60 years	41 (28.3)	21 (42.0)		16 (34.8)	13 (27.7)	
≥60 years	104 (71.7)	29 (58.0)		30 (65.2)	34 (72.3)	
Gender, No. (%)			0.738			0.194
Female	56 (38.6)	21 (42.0)		13 (28.3)	20 (42.6)	
Male	89 (61.4)	29 (58.0)		33 (71.7)	27 (57.4)	
Pathological grade, No. (%)			0.892			0.852
Grade I	22 (15.2)	5 (10.0)		9 (19.6)	5 (10.6)	
Grade II	97 (66.9)	38 (76.0)		27 (58.7)	37 (78.7)	
Grade III	26 (17.9)	7 (14.0)		10 (21.7)	5 (10.6)	
Tumor size, No. (%)			0.049			0.132
<5 cm	91 (62.8)	39 (78.0)		26 (56.5)	34 (72.3)	
≥5 cm	54 (37.2)	11 (22.0)		20 (43.5)	13 (27.7)	
LYN metastasis, No. (%)			0.018			0.001
Negative	83 (57.2)	38 (76.0)		20 (43.5)	36 (76.6)	
Positive	62 (42.8)	12 (24.0)		26 (56.5)	11 (23.4)	
T stage, No. (%)			0.001			0.019
T1	2 (1.4)	3 (6.0)		0 (0.0)	1 (2.1)	
T2	12 (8.3)	11 (22.0)		1 (2.2)	6 (12.8)	
T3	129 (89.0)	36 (72.0)		44 (95.7)	40 (85.1)	
T4	2 (1.4)	0 (0.0)		1 (2.2)	0 (0.0)	
N stage, No. (%)			0.034			0.004
N0	83 (57.2)	38 (76.0)		20 (43.5)	36 (76.6)	
N1	42 (29.0)	8 (16.0)		20 (43.5)	8 (17.0)	
N2	20 (13.8)	4 (8.0)		6 (13.0)	3 (6.4)	
TNM stage, No. (%)			0.001			<0.001
Stage I	14 (9.7)	14 (28.0)		1 (2.2)	7 (14.9)	
Stage II	69 (47.6)	24 (48.0)		19 (41.3)	29 (61.7)	
Stage IIIs	62 (42.8)	12 (24.0)		26 (56.5)	11 (23.4)	

SOX30, sex determining region Y-box family factor 30; LYN, lymph node.

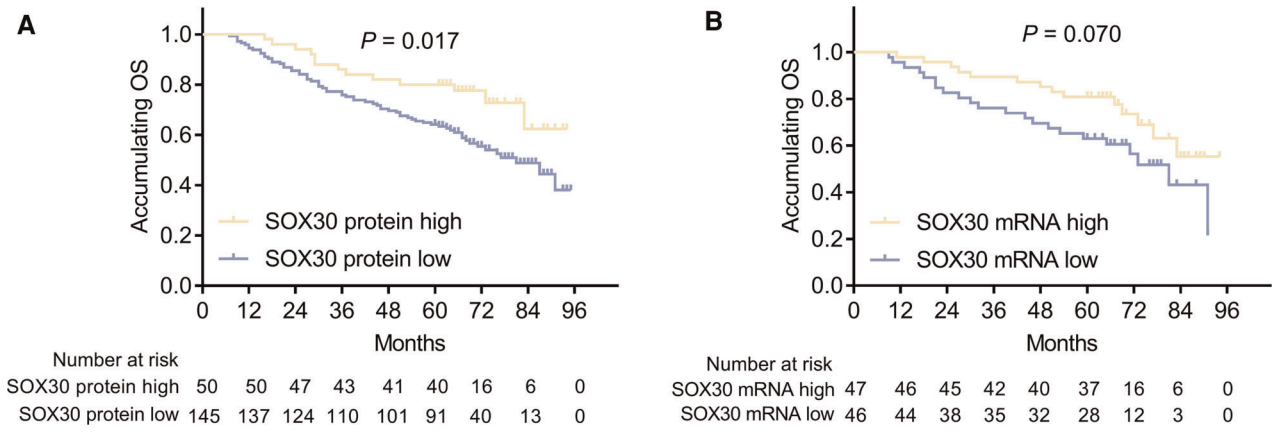

FIGURE 2 | Correlation between SOX30 expression and long-term prognosis among CRC patients. Correlation of SOX30 protein expression (**A**) and SOX30 mRNA expression (**B**) with accumulating OS. SOX30, sex-determining region Y-box containing gene 30; OS, overall survival; CRC, colorectal cancer.

TABLE 3 | Correlation of tumor SOX30 with OS in subgroups categorized by TNM stage.

Subgroup	Mean OS (months)				
	SOX30 protein high	**95% CI**	**SOX30 protein low**	**95% CI**	***P*-value**
TNM stage I	73.8	62.1–85.5	85.5	76.4–94.5	0.585
TNM stage II	89.2	82.9–95.6	72.0	64.9–79.1	0.007
TNM Stage III	55.4	39.8–71.1	57.9	49.9–65.9	0.740
	SOX30 mRNA high	**95% CI**	**SOX30 mRNA low**	**95% CI**	***P*-value**
TNM stage I	77.8	70.5–85.1	–	–	0.705
TNM stage II	79.7	70.3–89.1	62.2	50.5–73.9	0.178
TNM Stage III	68.6	54.5–82.7	64.1	52.1–76.2	0.812

SOX30, sex determining region Y-box family factor 30; OS, overall survival; CI, confidence interval.

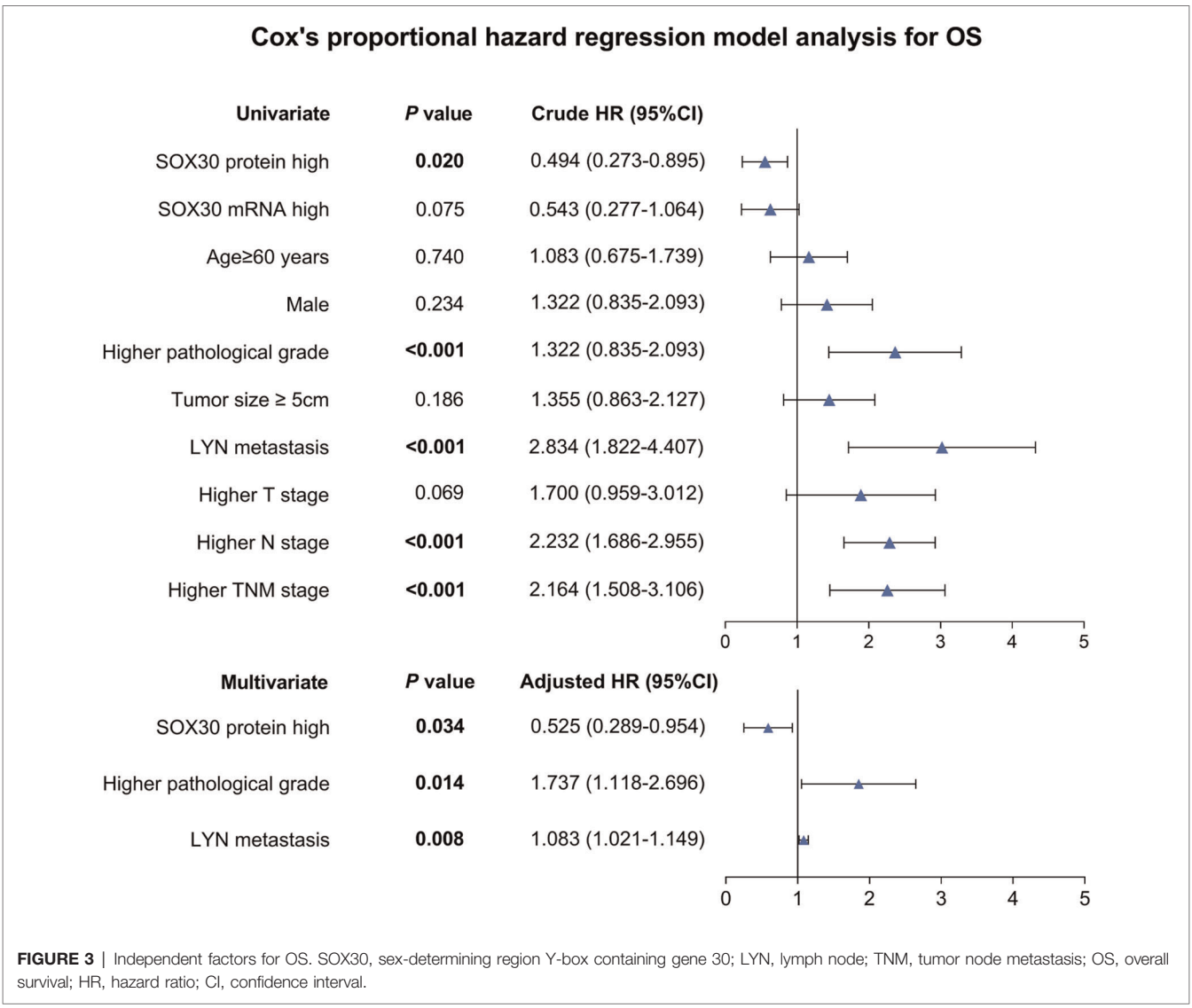

FIGURE 3 | Independent factors for OS. SOX30, sex-determining region Y-box containing gene 30; LYN, lymph node; TNM, tumor node metastasis; OS, overall survival; HR, hazard ratio; CI, confidence interval.

pathways (11, 15, 17). Therefore, SOX30 expression was decreased in CRC tumor tissue.

Regarding the correlation of SOX30 with clinicopathological features in cancers, it has been presented that elevated SOX30 expression is associated with deficient LYN metastasis and lower TNM stage in lung cancer patients (10); a negative association has been found between SOX30 and TNM stage in bladder cancer patients (12); moreover, SOX30 is also negatively associated with tumor size in hepatocellular carcinoma patients (7). In our study, negative associations were also found in tumor SOX30 with LYN metastasis, T stage, N stage, and TNM stage in CRC patients. The possible reasons would be that: (1) SOX30 might be able to suppress proliferation and promote apoptosis of CRC cells *via* activating p53 transcription, consequently inhibiting tumor growth of CRC (7, 18). Therefore, negative associations were found in tumor SOX30 with T stage in CRC patients; (2) SOX30 might suppress CRC cell metastasis and lymph node metastasis through attenuating Wnt-signaling by modulating the transcription of β-Catenin (8, 19). Thus, negative correlations were found in SOX30 with LYN metastasis, N stage, and TNM stage in CRC patients.

With respect to the association between SOX30 and prognosis in cancers, several studies have disclosed that SOX30 is correlated with a better prognosis (9, 11, 12). For instance, previous research has presented that a positive association is found between SOX30 expression and OS in bladder cancer patients (12). Another study also illustrates that increased SOX30 expression predicts more favorable OS in ovarian cancer patients (9). In the present study, a positive correlation was observed in tumor SOX30 expression with accumulating OS in total CRC patients, and in the TNM stage II subgroup; more notably, multivariate Cox's proportional hazards regression analysis presented that tumor SOX30 protein high expression was independently associated with favorable OS, which was partly consistent with previous studies (9, 11, 12). Potential explanations could be that: (1) SOX30 could decrease chemoresistance in CRC cells by promoting p53 transcriptional activation, thereby enhancing the effect of CRC therapy, which could directly improve the prognosis of CRC (7, 20); (2) tumor SOX30 was correlated with better tumor clinical features (above-mentioned), which could indirectly lead to better prognosis in CRC. Therefore, SOX30 was positively correlated with CRC prognosis.

There existed several limitations in our study: (1) we only recruited the patients who were diagnosed with primary CRC, the clinical value of SOX30 in patients with secondary CRC could be investigated in the future; (2) the present study was a retrospective study, which might exist a series of compound factors and bias; however, we tried to use multivariate Cox's regression model analysis to eliminate partial interfering factors; (3) the role of SOX30 in the regulatory mechanism of CRC could be investigated and further to explore the therapeutic value of SOX30 in CRC.

In conclusion, tumor SOX30 negatively associates with LYN metastasis, T stage, N stage, and TNM stage while positively relates to accumulating OS in CRC patients, suggesting SOX30 might be a possible biomarker of progression and prognosis of CRC.

DATA AVAILABILITY STATEMENT

The original contributions presented in the study are included in the article/**Supplementary Material**, further inquiries can be directed to the corresponding author/s.

ETHICS STATEMENT

The studies involving human participants were reviewed and approved by Institutional Review Board of Cangzhou People's Hospital. The patients/participants provided their written informed consent to participate in this study.

AUTHOR CONTRIBUTIONS

YS and LS conceived and designed the current study. CL, PL, and LY performed the experiments, interpreted the results, and contributed to manuscript writing. QS and BG contributed to data collection and analysis. All authors read and approved the final manuscript. All authors contributed to the article and approved the submitted version.

SUPPLEMENTARY MATERIAL

The Supplementary Material for this article can be found online at: https://www.frontiersin.org/articles/10.3389/fsurg.2022.898952/full#supplementary-material.

REFERENCES

1. Connell LC, Mota JM, Braghiroli MI, Hoff PM. The rising incidence of younger patients with colorectal cancer: questions about screening, biology, and treatment. *Curr Treat Options Oncol*. (2017) 18(4):23. doi: 10.1007/s11864-017-0463-3
2. Brenner H, Kloor M, Pox CP. Colorectal cancer. *Lancet*. (2014) 383 (9927):1490–502. doi: 10.1016/S0140-6736(13)61649-9
3. Haraldsdottir S, Einarsdottir HM, Smaradottir A, Gunnlaugsson A, Halfdanarson TR. Colorectal cancer - review. *Laeknabladid*. (2014) 100(2): 75–82. doi: 10.17992/lbl.2014.02.531
4. Bray F, Ferlay J, Soerjomataram I, Siegel RL, Torre LA, Jemal A. Global cancer statistics 2018: GLOBOCAN estimates of incidence and mortality worldwide for 36 cancers in 185 countries. *CA Cancer J Clin*. (2018) 68(6): 394–424. doi: 10.3322/caac.21492
5. Kuipers EJ, Grady WM, Lieberman D, Seufferlein T, Sung JJ, Boelens PG, et al. Colorectal cancer. *Nat Rev Dis Primers*. (2015) 1:15065. doi: 10.1038/nrdp.2015.65
6. Grimm D, Bauer J, Wise P, Kruger M, Simonsen U, Wehland M, et al. The role of SOX family members in solid tumours and metastasis. *Semin Cancer Biol*. (2020) 67(Pt 1):122–53. doi: 10.1016/j.semcancer.2019.03.004
7. Tao J, Liu Z, Wang Y, Wang L, Yin G, Yang W, et al. MicroRNA-645 represses hepatocellular carcinoma progression by inhibiting SOX30-mediated p53 transcriptional activation. *Int J Biol Macromol*. (2019) 121:214–22. doi: 10.1016/j.ijbiomac.2018.10.032

8. Han F, Liu WB, Shi XY, Yang JT, Zhang X, Li ZM, et al. SOX30 inhibits tumor metastasis through attenuating wnt-signaling via transcriptional and posttranslational regulation of beta-catenin in lung cancer. *EBioMedicine*. (2018) 31:253–66. doi: 10.1016/j.ebiom.2018.04.026
9. Han F, Liu WB, Li JJ, Zhang MQ, Yang JT, Zhang X, et al. SOX30 is a prognostic biomarker and chemotherapeutic indicator for advanced-stage ovarian cancer. *Endocr Relat Cancer*. (2019) 26(3):303–19. doi: 10.1530/ERC-18-0529
10. Liu C, Liu Y, Tian J, Zhang S, Li X, Zhai X, et al. High expression of SRY-box transcription factor 30 associates with well differentiation, absent lymph node metastasis and predicts longer survival in nonsmall-cell lung cancer patients. *Medicine (Baltimore)*. (2020) 99(20):e20122. doi: 10.1097/MD.0000000000020122
11. Peng H, Luo Y, Wu J, Yin W. Correlation of sex-determining region Y-box 30 with tumor characteristics and its prognostic value in breast cancer. *J Clin Lab Anal*. (2020) 34(6):e23232. doi: 10.1002/jcla.23232
12. Liu Y, Wang H, Zhong J, Wu C, Yang G, Zhong Y, et al. Decreased expression of SRY-box containing gene 30 is related to malignant phenotypes of human bladder cancer and correlates with poor prognosis. *BMC Cancer*. (2018) 18(1):642. doi: 10.1186/s12885-018-4560-x
13. Steele RJ, Rey JF, Lambert R. International agency for research on C. European guidelines for quality assurance in colorectal cancer screening and diagnosis. First edition–professional requirements and training. *Endoscopy*. (2012) 44(Suppl 3):SE106–15. doi: 10.1055/s-0032-1309796
14. Fu H, Jin C, Zhu Q, Liu T, Ke B, Li A, et al. Dysregulated expressions of PTEN, NF-kappaB, WWP2, p53 and c-Myc in different subtypes of B cell lymphoma and reactive follicular hyperplasia. *Am J Transl Res*. (2019) 11(2): 1092–101. PMID: 30899409; PMCID: PMC6413269
15. Fu Q, Sun Z, Yang F, Mao T, Gao Y, Wang H. SOX30, a target gene of miR-653-5p, represses the proliferation and invasion of prostate cancer cells through inhibition of Wnt/beta-catenin signaling. *Cell Mol Biol Lett*. (2019) 24:71. doi: 10.1186/s11658-019-0195-4
16. Han F, Liu W, Jiang X, Shi X, Yin L, Ao L, et al. SOX30, a novel epigenetic silenced tumor suppressor, promotes tumor cell apoptosis by transcriptional activating p53 in lung cancer. *Oncogene*. (2015) 34(33):4391–402. doi: 10.1038/onc.2014.370
17. Cheng X, Xu X, Chen D, Zhao F, Wang W. Therapeutic potential of targeting the Wnt/beta-catenin signaling pathway in colorectal cancer. *Biomed Pharmacother*. (2019) 110:473–81. doi: 10.1016/j.biopha.2018.11.082
18. Wang S, Zhang Y, Huang J, Wong CC, Zhai J, Li C, et al. TRIM67 activates p53 to suppress colorectal cancer initiation and progression. *Cancer Res*. (2019) 79(16):4086–98. doi: 10.1158/0008-5472.CAN-18-3614
19. Zhu L, Yang S, Zheng L, Zhang G, Cheng G. WNT/beta-catenin pathway activation via Wnt1 overexpression and Axin1 downregulation correlates with cadherin-catenin complex disruption and increased lymph node involvement in micropapillary-predominant lung adenocarcinoma. *J Thorac Dis*. (2020) 12(10):5906–15. doi: 10.21037/jtd-20-1495
20. Tracz-Gaszewska Z, Klimczak M, Biecek P, Herok M, Kosinski M, Olszewski MB, et al. Molecular chaperones in the acquisition of cancer cell chemoresistance with mutated TP53 and MDM2 up-regulation. *Oncotarget*. (2017) 8(47):82123–43. doi: 10.18632/oncotarget.18899

Conflict of Interest: The authors declare that the research was conducted in the absence of any commercial or financial relationships that could be construed as a potential conflict of interest.

Publisher's Note: All claims expressed in this article are solely those of the authors and do not necessarily represent those of their affiliated organizations, or those of the publisher, the editors and the reviewers. Any product that may be evaluated in this article, or claim that may be made by its manufacturer, is not guaranteed or endorsed by the publisher.

Copyright © 2022 Li, Li, Yu, Sun, Gu, Sun and Sun. This is an open-access article distributed under the terms of the Creative Commons Attribution License (CC BY). The use, distribution or reproduction in other forums is permitted, provided the original author(s) and the copyright owner(s) are credited and that the original publication in this journal is cited, in accordance with accepted academic practice. No use, distribution or reproduction is permitted which does not comply with these terms.

frontiers | Frontiers in Medicine

ORIGINAL RESEARCH
published: 30 June 2022
doi: 10.3389/fmed.2022.879986

Anti-colon Cancer Effects of *Dendrobium officinale* Kimura & Migo Revealed by Network Pharmacology Integrated With Molecular Docking and Metabolomics Studies

Shengchang Tao[1,2], *Jinyan Li*[1,3], *Huan Wang*[1,3], *Shaobo Ding*[2], *Weichao Han*[2], *Ruirong He*[2], *Zhiyao Ren*[3,4,5,6] *and Gang Wei*[1]*

[1] School of Pharmaceutical Sciences, Guangzhou University of Chinese Medicine, Guangzhou, China, [2] Department of Pharmacy, Affiliated Dongguan Hospital, Southern Medical University, Dongguan, China, [3] The Research Centre of Chinese Herbal Resource, Shaoguan Institute of Danxia Dendrobium Officinale, Shaoguan, China, [4] Department of Systems Biomedical Sciences, School of Medicine, Jinan University, Guangzhou, China, [5] NHC Key Laboratory of Male Reproduction and Genetics, Guangzhou, China, [6] Department of Central Laboratory, Family Planning Research Institute of Guangdong Province, Guangzhou, China

OPEN ACCESS

Edited by:
Qi Liu,
Fudan University, China

Reviewed by:
Gédéon Ngiala Bongo,
University of Kinshasa, Democratic Republic of Congo
Maria Eugenia Jaramillo-Flores,
Instituto Politécnico Nacional, Ciudad de México, Mexico

***Correspondence:**
Gang Wei
weigang021@outlook.com

Specialty section:
This article was submitted to Gastroenterology, a section of the journal Frontiers in Medicine

Received: 20 February 2022
Accepted: 23 May 2022
Published: 30 June 2022

Citation:
Tao S, Li J, Wang H, Ding S, Han W, He R, Ren Z and Wei G (2022) Anti-colon Cancer Effects of Dendrobium officinale Kimura & Migo Revealed by Network Pharmacology Integrated With Molecular Docking and Metabolomics Studies. Front. Med. 9:879986. doi: 10.3389/fmed.2022.879986

Objective: The present study aimed to investigate the potential mechanism of *Dendrobium officinale (D. officinale)* on colorectal cancer and the relevant targets in the pathway using a network pharmacological approach.

Methods: (1) We identified the major bioactive components of *D. officinale* by UPLC-ESI-MS/MS and established the in-house library by using the literature mining method. (2) Target prediction was performed by SwissADME and SwissTargetPrediction. (3) A protein–protein interaction (PPI) network and component–target–pathway network (C-T-P network) were constructed. (4) The GO pathways and the KEGG pathway enrichment analysis were carried out by the Metascape database. (5) Molecular docking was performed by AutoDock software. (6) A series of experimental assays including cell proliferation, cell invasion and migration, and TUNEL staining in CRC were performed in CRC cell lines (HT-29, Lovo, SW-620, and HCT-116) to confirm the inhibitory effects of *D. officinale*.

Results: (1) In total, 396 candidate active components of *D. officinale* were identified by UPLC-ESI-MS/MS and selected from the database. (2) From OMIM, GeneCards, DrugBank, and TTD databases, 1,666 gene symbols related to CRC were gathered, and (3) 34 overlapping gene symbols related to CRC and drugs were obtained. (4) These results suggested that the anti-CRC components of *D. officinale* were mainly apigenin, naringenin, caffeic acid, γ-linolenic acid, α-linolenic acid, cis-10-heptadecenoic acid, etc., and the core targets of action were mainly ESR1, EGFR, PTGS2, MMP9, MMP2, PPARG, etc. (5) The proliferation of muscle cells, the regulation of inflammatory response, the response of cells to organic cyclic compounds, and the apoptotic signaling pathway might serve as principal pathways for CRC treatment. (6) The reliability of some important active components and targets was further validated by molecular docking. The molecular docking analysis suggested an important role of apigenin, naringenin,

PTGS2, and MMP9 in delivering the pharmacological activity of *D. officinale* against CRC. (7) These results of the evaluation experiment *in vitro* suggested that *D. officinale* had a strong inhibitory effect on CRC cell lines, and it exerted anti-CRC activity by activating CRC cell apoptosis and inhibiting CRC cell migration and invasion.

Conclusion: This study may provide valuable insights into exploring the mechanism of action of *D. officinale* against CRC.

Keywords: *Dendrobium officinale*, UPLC-ESI-MS/MS, network pharmacology, colorectal cancer, molecular docking

INTRODUCTION

Colorectal cancer (CRC) is the third most common cancer after lung and breast cancers, and it is also the second leading cause of cancer-related mortality (1). *Dendrobium officinale* Kimura & Migo (*D. officinale*), a widely known traditional food–medicine herb, has been commonly employed in China and other Asian countries for thousands of years (2). According to Shennong's *Classic of Materia Medica*, the famous classic book of Chinese materia medica, it could benefit the intestines and stomach, supplementing body fluids (3). Also, the functions of benefiting the intestines and stomach, increasing saliva, nourishing Yin, and clearing heat were recorded by Chinese pharmacopeia (2020 edition). *D. officinale* has also been widely used as a traditional Chinese medicinal herb for thousands of years to treat gastrointestinal sickness in China (4). More importantly, their significant anti-CRC benefits have also been validated (1, 5–10).

However, previous studies have shown that *D. officinale* possesses a variety of active components, including polysaccharides (1, 6, 11, 12), flavonoids (13), alkaloids (14), amino acids (15), and bibenzyl (16). The underlying mechanisms of anti-colon cancer effects of *D. officinale* remain unclear because of the complex compositions. Moreover, the action mechanism of *D. officinale* inhibits the colon cancer cell growth, and metastasis is not clear, indicating the need for an investigation.

Traditional Chinese herb medicine or formulations contain multiple active components, targets, and pathways, which are not able to be elucidated by traditional methods (17). Fortunately, the approach of network pharmacology is an effective method to analyze traditional Chinese medicine for both prescription and single herb (18, 19) and provides a new perspective for studying Chinese herbal formulas (20). As a new paradigm in drug studies, derived from systems biology and bioinformatics, network pharmacology can reveal the underlying molecular mechanisms of Chinese herb medicine, *via* the construction and visualization of "medicine–target–disease" interaction network (21, 22). Network pharmacology can reflect the "multiple components–multiple targets–multiple pathways" of anticancer effects of Chinese herb medicine (23), which is potential to solve the same problems of the *D. officinale* methanolic extract.

This study investigated the potential mechanism of *D. officinale* on CRC and the relevant targets in the pathway. First, we identified the major bioactive components of *D. officinale* by UPLC-ESI-MS/MS and established the in-house library. Second, a series of network pharmacological analyses, including target prediction, GO and KEGG enrichment analysis, and network construction, were conducted to identify the CRC-related targets and potential mechanisms of *D. officinale*. Third, the reliability of some key active components and targets was further validated by molecular docking. Finally, a series of experimental assays including cell proliferation, cell invasion and migration, and TUNEL staining were performed in CRC cell lines to confirm the inhibitory effects of *D. officinale*. The workflow of our network pharmacological and experimental studies of *D. officinale* in CRC is shown in **Figure 1**. By characterizing the *D. officinale* composition and its therapeutic mechanisms on CRC, we laid the foundation for the clinical application of *D. officinale*.

MATERIALS AND METHODS

Chemicals and Reagents

D. officinale was collected from Shaoguan Hejiantang Ecological Agriculture Company Ltd. (latitude 24°80' N, longitude 113°59' E, Shaoguan, Guangdong, China) in June 2020 and was identified by Professor Yuechun Huang (Laboratory of the Department of Clinical Pharmacy, College of the First Clinical Medical, Guangzhou University of Chinese Medicine). The voucher specimen number was 57826, and a specimen was deposited in the School of Pharmaceutical Sciences, Guangzhou University of Chinese Medicine (Guangzhou, China).

The human colorectal cancer (CRC) cell lines HT-29, Lovo, SW-620, and HCT-116 were obtained from the Cell Line Bank of the Chinese Academy of Sciences (Shanghai, China). Reagents 5-fluorouracil (5-Fu), dimethyl sulfoxide (DMSO), and 3-[4,5-dimethylthiazol-2-yl]-2,5diphenyltetrazolium bromide (MTT) were purchased from Sigma Aldrich Co. (St. Louis, MO, USA). HPLC-grade acetonitrile, methanol, and acetic acid were purchased from Merck Millipore (Billerica, MA, USA). Ultrapure water was prepared using a Millipore Alpha-Q water system (Merck Millipore). All other reagents were of analytical grade; 24-well chambers with 8 μm pore size (#353097) and

Abbreviations: ADME, absorption, distribution, metabolism, and excretion; BC, betweenness centrality; CC, closeness centrality; CRC, colorectal cancer; *D. officinale*, *Dendrobium officinale*; DOME, *D. officinale* methanolic extract; DMSO, dimethyl sulfoxide; FBS, fetal bovine serum; GO, Gene Ontology; 5-Fu, 5-fluorouracil; C-T-P network, component–target–pathway network; KEGG, Kyoto Encyclopedia of Genes and Genomes; MF, molecular functions; MTT, 3-[4,5-dimethylthiazol-2-yl]-2,5-diphenyltetrazolium bromide; OMIM, Online Mendelian Inheritance in Man; PDB, Protein Data Bank; PPI, protein–protein interaction; STRING, Search Tool for the Retrieval of Interacting Genes/Proteins; TTD, Therapeutic Target Database.

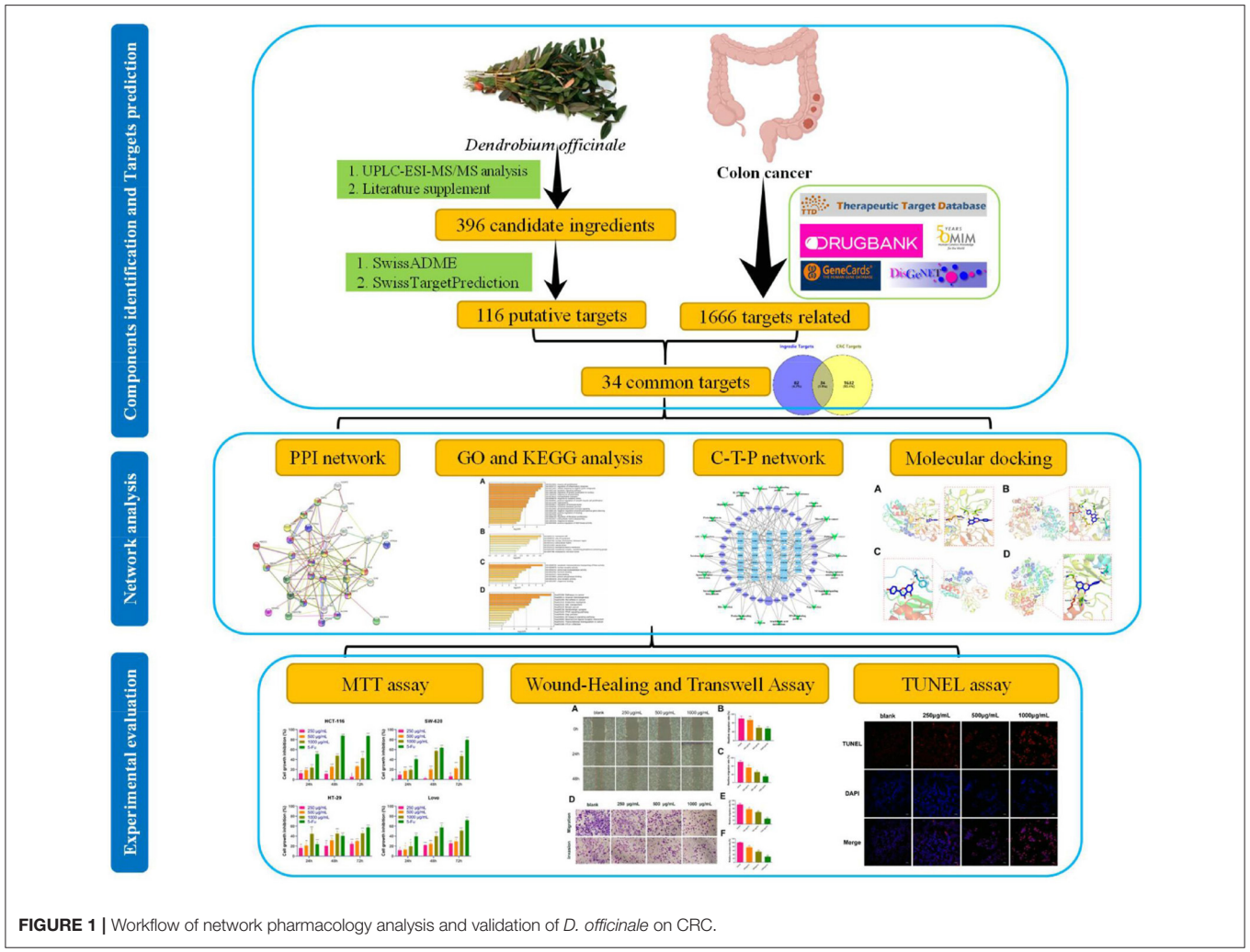

FIGURE 1 | Workflow of network pharmacology analysis and validation of *D. officinale* on CRC.

Matrigel matrix (#354263) were purchased from BD Biosciences (San Jose, CA, USA). Cell culture dishes and plates were purchased from Wuxi NEST biotechnology Co. (Wuxi, Jiangsu, China); 4% paraformaldehyde was purchased from Biosharp Life Sciences (Hefei, Anhui, China); 0.1% crystal violet was purchased from Beijing Leagene Biotech Co., Ltd (Beijing, China). The One Step TUNEL Apoptosis Assay kit (#C1089), Enhanced Immunostaining Permeabilization Solution (#P0097), and DAPI Staining Solution (#C1006) were purchased from Beyotime Biotechnology (Shanghai, China).

Sample Preparation

Leaves from fresh stems of *D. officinale* were removed and cleaned with tap water. Then, the vacuum freeze-dried stems were ground to a powder (MM 400, Retsch, Haan, Germany) at 30 Hz for 1.5 min in a grinder. The powder (100 mg) was extracted for 24 h at 4°C with 0.6 ml 70% aqueous methanol and vortexed six times to increase the extraction rate. After centrifuging at 10,000× *g* for 10 min, the supernatant was aspirated and filtered using a 0.22 μm microporous membrane for UPLC-ESI-MS/MS analysis.

Ultra-High-Performance Liquid Chromatography and Mass Spectrometry Conditions

The data acquisition instrument system included a UPLC-ESI-MS/MS system, which mainly includes UPLC (Shim-pack UFLC SHIMADZU CBM30A, SHIMADZU, Kyoto, Japan) coupled with an ESI-triple quadrupole linear ion trap MS/MS system (Applied Biosystems 4500 Q TRAP; AB SCIEX, Foster City, CA, USA).

The filtered supernatant was separated using an Acquity UHPLC HSS T3 C18 column (2.1 mm × 100 mm, 1.8 μm; Waters, Milford, MA, USA). The mobile phase consisted of 0.04% acetic acid in deionized water (mobile phase A) and 0.04% acetic acid in acetonitrile (mobile phase B). Separation was conducted using the following gradient elution: 0–10.00 min, 5–95% B; 10.00–11.00 min, 95% B; 11.0–11.10 min, 95–5% B; and 11.10–14.00 min, 5% B for equilibration of the column. The column temperature was maintained at 40°C. The flow rate was set at 0.35 ml/min, and the injection volume was 4 μL.

The mass spectrometry conditions were listed as follows: the electrospray ionization (ESI) temperature was 550°C, the ion spray voltage (IS) was 5,500 V (positive ion mode)/−4,500 V (negative ion mode), the curtain gas (CUR) was set to 30 psi, and the collision-induced dissociation (CAD) parameter was set high. In the triple quadrupole (QQQ), declustering potential (DP) and collision energy (CE) for individual multiple reaction monitoring (MRM) transitions were done with further DP and CE optimization (24, 25). Based on the self-built MetWare database (Wuhan Metware Biotechnology Co., Ltd., Wuhan, China), the material was characterized according to the secondary spectrum information.

Active Component Preparation From *D. officinale* and Target Prediction

The chemical composition of *D. officinale* was mainly obtained from UPLC-ESI-MS/MS analysis. Furthermore, we used the literature mining method (PubMed, CNKI.net, Cqvip.com, and Web of Science) to search for those that had been reported as the key active components of *D. officinale*, while had not been identified in UPLC-ESI-MS/MS analysis. The in-house library that covers all phytochemical constituents obtained from UPLC-ESI-MS/MS analysis and previously reported compounds from the literature is established in **Table 1** and **Supplementary Table 1**, including the compound name, molecular weight, molecular formula, ion mode, and related references. The in-house library totally acquired 396 active components after removing duplicates.

The molecular structures of the compounds were downloaded from the PubChem database (https://pubchem.ncbi.nlm.nih.gov/) or mapped with ChemDraw 18.0 software and were saved in the MDL sdf. format. All chemical structures were converted to the Mol2 format using ChemBio3D Ultra software and then were prepared and converted into SMILES files using Open Babel GUI software for subsequent analyses.

The SwissADME tool (http://www.swissadme.ch/) was used for analyzing active components with absorption, distribution, metabolism, and excretion (ADME) properties and druglikeness evaluation to screen for active components with potential therapeutic effects. The screening criterion we applied in this research were (1) pharmacokinetics "high" and (2) druglikeness (DL) with more than two "yes."

To obtain the targets of active components in *D. officinale*, SwissTargetPrediction (http://www.swisstargetprediction.ch/) (26) was employed to identify the targets. Finally, we totally acquired 116 genes after removing duplicates.

The target prediction results were sorted from high to low according to "probability," and a threshold (probability >0.5) was set to obtain more credible targets. The official names of drug targets were retrieved through the UniProtKB search function in the UniProt database (http://www.uniprot.org/).

Collection of Predicted Targets Related to Colon Cancer

"Colon cancer" was used as the keyword to obtain colon cancer-related targets. The known targets associated with colon cancer were derived from five databases, DisGeNet (https://www.disgenet.org/), Online Mendelian Inheritance in Man (OMIM, http://www.omim.org/), Therapeutic Target Database (TTD, http://database.idrb.cqu.edu.cn/TTD/), GeneCards (https://www.genecards.Org/), and DrugBank (http://www.drugbank.ca/). We searched these databases and totally acquired 1,666 genes after removing duplicates.

Protein–Protein Interaction (PPI) Network Construction and Analysis

To obtain overlapping targets, VENNY 2.1 (http://bioinfogp.cnb.csic.es/tools/venny/index.html) software was used to cross *D. officinale* active component targets with CRC-related targets. Then, network protein–protein interaction network was constructed by the Search Tool for the Retrieval of Interacting Genes/Proteins (STRING) online database (https://string-db.org/, version. 11.0), using the overlap targets between *D. officinale* active components targets and CRC-related targets (27), where the species was limited to "*Homo sapiens*," medium confidence of protein interaction data with a score > 0.400, and other basic settings were the default value.

To clarify the signaling pathways and function enrichment of potential target genes, Gene Ontology (GO) biological process enrichment analysis and Kyoto Encyclopedia of Genes and Genomes (KEGG) pathway enrichments analysis were conducted based on the Metascape database (http://metascape.org/gp/index.html) (28), using $P < 0.01$, min overlap genes = 3, and min enrichment factor > 1.5 as the cutoff criterion.

The PPI network was visualized utilizing Cytoscape v3.7.2 (www.cytoscape.org/) for further analyses (29, 30). The parameters "betweenness centrality (BC)," "closeness centrality (CC)," and "degree" were calculated using Network Analyzer to assess the topological importance of the nodes in the PPI network (31) and visualized the "component–target–pathway" network with the Merge feature of Cytoscape v3.7.2.

Molecular Docking

To evaluate the predicted targets, AutoDock software (4.2 version) was used to dock the structures of six active components, including apigenin, naringenin, caffeic acid, γ-linolenic acid, α-linolenic acid, and cis-10-heptadecenoic acid. These active components were docked with six candidate proteins, including ESR1 (PDB ID: 1hcq), EGFR (PDB ID: 5wb7), PTGS2 (PDB ID: 5f19), MMP9 (PDB ID: 1l6j), MMP2 (PDB ID: 1eak), and PPARG (PDB ID: 3e00), respectively. The 3D structures of ligands were obtained from the ZINC database (http://zinc.docking.org/) and saved as a mol2 file. The 3D crystal structures of the candidate protein were downloaded from the RCSB Protein Data Bank (PDB) database (https://www.rcsb.org/) and saved in the pdb format.

PyMOL software separated the original ligand from the target protein and removed the water molecule, phosphate, and other inactive ligands of the target protein (32). The protein and active components were saved in the pdb format. The AutoDockTools 1.5.6 was used to convert the pdb format of the active components and proteins to the pdbqt format. The active pocket parameters were set, and AutoDock was administered

TABLE 1 | Component identification results of 70% methanol extracts from *D. officinale*.

ID	Rt (min)	MW (g/mol)	Molecular Formula	Ionization Mode	Compounds	CAS
Flavonoids						
1	3.90	624.14	$C_{28}H_{32}O_{16}$	$[M–H]^-$	Isorhamnetin-3-O-rutinoside	604-80-8
2	4.09	304.05	$C_{15}H_{12}O_7$	$[M–H]^-$	Taxifolin	480-18-2
3	4.28	448.08	$C_{21}H_{20}O_{11}$	$[M+H]^+$	Quercitrin	522-12-3
4	3.73	610.13	$C_{27}H_{30}O_{16}$	$[M–H]^-$	Rutin	153-18-4
5	3.65	464.08	$C_{21}H_{20}O_{12}$	$[M–H]^-$	Hyperin	482-36-0
6	5.81	316.05	$C_{16}H_{12}O_7$	$[M–H]^-$	Isorhamnetin	480-19-3
7	3.75	432.09	$C_{21}H_{20}O_{10}$	$[M+H]^+$	Apigenin 5-O-glucoside	28757-27-9
8	3.98	464.08	$C_{21}H_{20}O_{12}$	$[M–H]^-$	Isoquercitrin	482-35-9
9	3.75	442.07	$C_{22}H_{18}O_{10}$	$[M–H]^-$	(-)-Catechin gallate	130405-40-2
10	3.80	464.08	$C_{21}H_{20}O_{12}$	$[M–H]^-$	Spiraeoside	20229-56-5
11	5.45	272.06	$C_{15}H_{12}O_5$	$[M–H]^-$	Pinobanksin	548-82-3
12	6.19	316.05	$C_{16}H_{12}O_7$	$[M–H]^-$	Rhamnetin (7-O-Methxyl Quercetin)	90-19-7
13	5.55	302.07	$C_{16}H_{14}O_6$	$[M+H]^+$	Homoeriodictyol	446-71-9
14	6.81	286.07	$C_{16}H_{14}O_5$	$[M+H]^+$	Isosakuranetin (4'-Methylnaringenin)	480-43-3
15	4.05	580.15	$C_{27}H_{32}O_{14}$	$[M–H]^-$	Narirutin	14259-46-2
16	3.18	594.13	$C_{27}H_{30}O_{15}$	$[M+H]^+$	Apigenin 6,8-C-diglucoside	23666-13-9
17	3.52	564.12	$C_{26}H_{28}O_{14}$	$[M+H]^+$	Isoschaftoside	52012-29-0
18	3.46	448.08	$C_{21}H_{20}O_{11}$	$[M+H]^+$	Orientin	28608-75-5
19	4.00	464.08	$C_{21}H_{20}O_{12}$	$[M–H]^-$	Gossypitrin	491-50-9
20	3.97	450.10	$C_{21}H_{22}O_{11}$	$[M–H]^-$	Astilbin	29838-67-3
21	3.70	432.09	$C_{21}H_{20}O_{10}$	$[M–H]^-$	Isovitexin	29702-25-8
22	3.46	448.08	$C_{21}H_{20}O_{11}$	$[M–H]^-$	HoMoorientin	4261-42-1
23	3.34	564.12	$C_{26}H_{28}O_{14}$	$[M+H]^+$	Schaftoside	51938-32-0
24	4.29	303.04	$C_{15}H_{11}O_7$	$[M]^+$	Delphinidin chloride	528-53-0
25	5.97	316.05	$C_{16}H_{12}O_7$	$[M+H]^+$	Tamarixetin	603-61-2
26	3.98	301.06	$C_{16}H_{13}O_6$	$[M]^+$	Peonidin	134-01-0
27	3.38	610.13	$C_{27}H_{30}O_{16}$	$[M+H]^+$	Luteolin 3',7-di-O-glucoside	52187-80-1
28	5.86	330.06	$C_{17}H_{14}O_7$	$[M–H]^-$	Di-O-methylquercetin	2068/2/2
29	3.96	578.14	$C_{27}H_{30}O_{14}$	$[M+H]^+$	Apigenin 7-rutinoside (Isorhoifolin)	552-57-8
30	3.79	594.13	$C_{27}H_{30}O_{15}$	$[M–H]^-$	Kaempferol 3-O-rutinoside (Nicotiflorin)	17650-84-9
31	5.54	272.06	$C_{15}H_{12}O_5$	$[M–H]^-$	Naringenin	480-41-1
32	3.72	434.10	$C_{21}H_{22}O_{10}$	$[M–H]^-$	Isohemiphloin	3682-02-8
33	3.77	448.08	$C_{21}H_{20}O_{11}$	$[M+H]^+$	Luteolin 7-O-glucoside (Cynaroside)	5373-11-5
34	5.47	272.06	$C_{15}H_{12}O_5$	$[M+H]^+$	Naringenin chalcone	73692-50-9
35	3.81	464.08	$C_{21}H_{20}O_{12}$	$[M–H]^-$	Quercetin 3-O-glucoside (Isotrifoliin)	21637-25-2
36	3.49	578.14	$C_{27}H_{30}O_{14}$	$[M+H]^+$	Vitexin 2"-O-β-L-rhamnoside	64820-99-1
37	5.01	284.06	$C_{16}H_{12}O_5$	$[M+H]^+$	Calycosin	20575-57-9
38	5.60	272.06	$C_{15}H_{12}O_5$	$[M+H]^+$	Butin	492-14-8
39	3.56	610.13	$C_{27}H_{30}O_{16}$	$[M–H]^-$	Bioquercetin	52525-35-6
40	5.74	300.05	$C_{16}H_{12}O_6$	$[M+H]^+$	Hispidulin	1447-88-7
41	5.90	330.06	$C_{17}H_{14}O_7$	$[M+H]^+$	Jaceosidin	18085-97-7
42	3.86	432.09	$C_{21}H_{20}O_{10}$	$[M+H]^+$	Apigenin-8-C-glucoside	3681-93-4
43	3.02	610.13	$C_{27}H_{30}O_{16}$	$[M+H]^+$	Luteolin-6,8-di-C-glucoside	29428-58-8
44	3.73	432.09	$C_{21}H_{20}O_{10}$	$[M+H]^+$	Genistein 8-C-glucoside	66026-80-0
45	3.77	446.10	$C_{22}H_{22}O_{10}$	$[M+H]^+$	Calycosin-7-glucoside	20633-67-4
46	5.63	270.04	$C_{15}H_{10}O_5$	$[M+H]^+$	Apigenin	520-36-5
47	3.31	610.13	$C_{27}H_{30}O_{16}$	$[M+H]^+$	Luteolin-7,3'-Di-O-β-D-Glucoside	257-724-7
48	3.75	594.13	$C_{27}H_{30}O_{15}$	$[M+H]^+$	Lonicerin	20633-84-5
49	3.55	578.14	$C_{27}H_{30}O_{14}$	$[M+H]^+$	Violanthin	40581-17-7

(Continued)

TABLE 1 | Continued

ID	Rt (min)	MW (g/mol)	Molecular Formula	Ionization Mode	Compounds	CAS
Lignans and Coumarins						
50	5.36	358.13	$C_{20}H_{22}O_6$	$[M–H]^-$	Pinoresinol	487-36-5
51	5.74	160.05	$C_{10}H_8O_2$	$[M+H]^+$	6-MethylCoumarin	92-48-8
52	2.71	340.07	$C_{15}H_{16}O_9$	$[M–H]^-$	Esculin(6,7-DihydroxyCoumarin-6-glucoside)	531-75-9
53	3.01	354.08	$C_{16}H_{18}O_9$	$[M+H]^+$	Scopolin	531-44-2
54	4.00	192.04	$C_{10}H_8O_4$	$[M+H]^+$	Scopoletin(7-Hydroxy-5-methoxycoumarin)	92-61-5
55	4.48	162.03	$C_9H_6O_3$	$[M–H]^-$	4-Hydroxycoumarin	1076-38-6
56	3.34	682.21	$C_{32}H_{42}O_{16}$	$[M–H]^-$	Pinoresinol diglucoside	63902-38-5
57	4.16	550.18	$C_{27}H_{34}O_{12}$	$[M–H]^-$	Eucommin A	99633-12-2
58	5.21	418.14	$C_{22}H_{26}O_8$	$[M–H]^-$	(+)-Syringaresinol	21453-69-0
59	5.30	388.13	$C_{21}H_{24}O_7$	$[M–H]^-$	Medioresinol	40957-99-1
60	7.82	368.11	$C_{21}H_{20}O_6$	$[M+H]^+$	Glycycoumarin	94805-82-0
Lipid						
61	7.48	314.22	$C_{18}H_{34}O_4$	$[M–H]^-$	9,10-Dihydroxy-12-octadecenoic acid	263399-34-4
62	9.03	296.21	$C_{18}H_{32}O_3$	$[M–H]^-$	13-Hydroxy-9,11-octadecadienoic acid	5204-88-6
63	9.03	296.21	$C_{18}H_{32}O_3$	$[M–H]^-$	9-Hydroxy-10,12-octadecadienoic acid	15514-85-9
64	10.85	228.19	$C_{14}H_{28}O_2$	$[M–H]^-$	Myristic Acid	544-63-8
65	0.76	257.10	$C_8H_{20}NO_6P$	$[M+H]^+$	Choline alfoscerate	28319-77-9
66	10.02	523.33	$C_{26}H_{54}NO_7P$	$[M+H]^+$	1-Stearoyl-sn-glycero-3-phosphocholine	19420-57-6
67	8.99	479.27	$C_{23}H_{46}NO_7P$	$[M–H]^-$	LysoPE 18:1	89576-29-4
68	11.38	242.21	$C_{15}H_{30}O_2$	$[M–H]^-$	Pentadecanoic Acid	1002-84-2
69	10.85	254.21	$C_{16}H_{30}O_2$	$[M–H]^-$	Palmitoleic Acid	373-49-9
70	10.78	278.21	$C_{18}H_{30}O_2$	$[M–H]^-$	γ-Linolenic Acid	506-26-3
71	10.56	278.21	$C_{18}H_{30}O_2$	$[M–H]^-$	α-Linolenic Acid	463-40-1
72	10.96	304.22	$C_{20}H_{32}O_2$	$[M–H]^-$	Arachidonic Acid	506-32-1
73	10.81	328.22	$C_{22}H_{32}O_2$	$[M–H]^-$	Cis-4,7,10,13,16,19-Docosahexaenoic Acid(C22:6n3)	6217-54-5
74	11.47	268.22	$C_{17}H_{32}O_2$	$[M–H]^-$	Cis-10-Heptadecenoic Acid	29743-97-3
75	12.11	282.23	$C_{18}H_{34}O_2$	$[M–H]^-$	Elaidic Acid	112-79-8
76	9.14	186.15	$C_{11}H_{22}O_2$	$[M–H]^-$	Undecylic Acid	112-37-8
77	7.19	272.21	$C_{16}H_{32}O_3$	$[M–H]^-$	16-Hydroxy hexadecanoic acid	506-13-8
78	11.05	284.25	$C_{18}H_{36}O_2$	$[M–H]^-$	Stearic Acid	57-11-4
79	11.90	282.23	$C_{18}H_{34}O_2$	$[M–H]^-$	11-Octadecanoic acid(Vaccenic acid)	506-17-2
80	6.53	216.16	$C_{12}H_{24}O_3$	$[M–H]^-$	12-Hydroxydodecanoic acid	505-95-3
81	8.74	495.30	$C_{24}H_{50}NO_7P$	$[M+H]^+$	LysoPC 16:0	17364-16-8
82	8.68	453.25	$C_{21}H_{44}NO_7P$	$[M+H]^+$	LysoPE 16:0	53862-35-4
83	8.91	278.21	$C_{18}H_{30}O_2$	$[M+H]^+$	Punicic acid	544-72-9
84	9.62	200.16	$C_{12}H_{24}O_2$	$[M–H]^-$	Lauric acid	143-07-7
85	8.92	296.21	$C_{18}H_{32}O_3$	$[M–H]^-$	9,10-EODE	65167-83-1
86	8.37	294.20	$C_{18}H_{30}O_3$	$[M–H]^-$	9-HOTrE	89886-42-0
87	9.12	294.20	$C_{18}H_{30}O_3$	$[M–H]^-$	9-KODE	54232-59-6
88	7.77	294.20	$C_{18}H_{30}O_3$	$[M–H]^-$	13-HOTrE(r)	74784-20-6
89	9.70	296.21	$C_{18}H_{32}O_3$	$[M–H]^-$	12,13-EODE	6799-85-5
90	11.01	310.26	$C_{20}H_{38}O_2$	$[M–H]^-$	Eicosenoic acid	26764-41-0
91	12.09	308.25	$C_{20}H_{36}O_2$	$[M–H]^-$	Eicosadienoic acid	5598-38-9
92	6.14	288.21	$C_{16}H_{32}O_4$	$[M–H]^-$	10,16-Dihydroxy-palmitic acid	3233-90-7
93	9.23	354.25	$C_{21}H_{38}O_4$	$[M+H]^+$	Glyceryl linoleate	26545-74-4
94	9.68	330.25	$C_{19}H_{38}O_4$	$[M+H]^+$	Glycerin Monopalmitate	542-44-9
95	7.30	301.27	$C_{18}H_{39}NO_2$	$[M+H]^+$	D-erythro-Dihydrosphingosine	764-22-7
Amino acids and their derivatives						
96	0.89	144.09	$C_7H_{14}NO_2^+$	$[M]^+$	Proline βine (ProBet)	1195-94-4

(Continued)

TABLE 1 | Continued

ID	Rt (min)	MW (g/mol)	Molecular Formula	Ionization Mode	Compounds	CAS
97	0.91	129.07	$C_6H_{11}NO_2$	$[M+H]^+$	Pipecolic acid	4043-87-2
98	0.89	143.09	$C_7H_{13}NO_2$	$[M+H]^+$	1,2-N-Methylpipecolic acid	7730-87-2
99	0.74	132.05	$C_4H_8N_2O_3$	$[M+H]^+$	L-Asparagine Anhydrous	70-47-3
100	0.76	131.05	$C_5H_9NO_3$	$[M+H]^+$	Trans-4-Hydroxy-L-proline	51-35-4
101	0.71	133.03	$C_4H_7NO_4$	$[M-H]^-$	L-Aspartic Acid	56-84-8
102	0.77	240.01	$C_6H_{12}N_2O_4S_2$	$[M+H]^+$	L-(-)-Cystine	56-89-3
103	1.20	131.09	$C_6H_{13}NO_2$	$[M+H]^+$	L-Leucine	61-90-5
104	1.13	181.07	$C_9H_{11}NO_3$	$[M+H]^+$	L-(-)-Tyrosine	60-18-4
105	0.68	155.06	$C_6H_9N_3O_2$	$[M+H]^+$	L-Histidine	71-00-1
106	0.84	117.07	$C_5H_{11}NO_2$	$[M+H]^+$	L-Valine	72-18-4
107	1.23	131.09	$C_6H_{13}NO_2$	$[M+H]^+$	L-Isoleucine	73-32-5
108	0.73	174.10	$C_6H_{14}N_4O_2$	$[M+H]^+$	L-(+)-Arginine	74-79-3
109	0.67	169.08	$C_7H_{11}N_3O_2$	$[M+H]^+$	3-N-Methyl-L-histidine	368-16-1
110	2.47	204.08	$C_{11}H_{12}N_2O_2$	$[M-H]^-$	L-Tryptophan	73-22-3
111	2.49	280.09	$C_{13}H_{16}N_2O_5$	$[M+H]^+$	Asp-phe	13433-09-5
112	3.52	312.13	$C_{18}H_{20}N_2O_3$	$[M+H]^+$	Phe-Phe	2577-40-4
113	1.92	188.10	$C_8H_{16}N_2O_3$	$[M+H]^+$	N-Glycyl-L-leucine	869-19-2
114	1.24	129.04	$C_5H_7NO_3$	$[M-H]^-$	5-Oxoproline	149-87-1
115	0.76	105.04	$C_3H_7NO_3$	$[M-H]^-$	D-Serine	312-84-5
116	0.75	303.13	$C_{12}H_{21}N_3O_6$	$[M+H]^+$	Nicotianamine	34441-14-0
117	0.79	131.05	$C_5H_9NO_3$	$[M+H]^+$	Cis-4-Hydroxy-D-proline	2584-71-6
118	1.35	131.09	$C_6H_{13}NO_2$	$[M+H]^+$	α-Aminocaproic acid	327-57-1
119	1.25	612.12	$C_{20}H_{32}N_6O_{12}S_2$	$[M-H]^-$	Oxidized Glutathione	121-24-4
120	2.29	236.10	$C_{12}H_{16}N_2O_3$	$[M+H]^+$	DL-Alanyl-DL-phenylalanine	1999-45-7
121	3.54	278.15	$C_{15}H_{22}N_2O_3$	$[M+H]^+$	Leucylphenylalanine	56217-82-4
122	1.86	188.10	$C_8H_{16}N_2O_3$	$[M+H]^+$	Glycylisoleucine	19461-38-2
123	2.26	222.09	$C_{11}H_{14}N_2O_3$	$[M+H]^+$	Glycylphenylalanine	721-66-4
124	3.83	246.09	$C_{13}H_{14}N_2O_3$	$[M-H]^-$	Acetyltryptophan	2280-01-5
125	0.79	115.06	$C_5H_9NO_2$	$[M+H]^+$	L-Proline	147-85-3
126	0.76	175.08	$C_6H_{13}N_3O_3$	$[M+H]^+$	L-Citrulline	372-75-8
127	0.83	147.05	$C_5H_9NO_4$	$[M+H]^+$	L-Glutamic acid	56-86-0
128	0.68	146.10	$C_6H_{14}N_2O_2$	$[M+H]^+$	L-(+)-Lysine	56-87-1
129	1.22	211.07	$C_{10}H_{13}NO_4$	$[M+H]^+$	(-)-3-(3,4-Dihydroxyphenyl)-2-methylalanine	555-30-6
130	1.02	188.10	$C_8H_{16}N_2O_3$	$[M+H]^+$	N6-Acetyl-L-lysine	692-04-6
131	0.75	160.08	$C_6H_{12}N_2O_3$	$[M-H]^-$	D-Alanyl-D-Alanine	923-16-0
132	1.17	188.07	$C_7H_{12}N_2O_4$	$[M-H]^-$	N-α-Acetyl-L-glutamine	2490-97-3
133	1.12	216.11	$C_8H_{16}N_4O_3$	$[M+H]^+$	N-α-Acetyl-L-arginine	155-84-0
134	0.72	169.08	$C_7H_{11}N_3O_2$	$[M+H]^+$	1-Methylhistidine	332-80-9
135	0.68	146.06	$C_5H_{10}N_2O_3$	$[M+H]^+$	L-Glutamine	56-85-9
136	0.73	190.08	$C_7H_{14}N_2O_4$	$[M+H]^+$	2,6-Diaminooimelic acid	583-93-7
137	1.20	137.08	$C_8H_{11}NO$	$[M+H]^+$	L-Tyramine	51-67-2
138	1.14	307.07	$C_{10}H_{17}N_3O_6S$	$[M-H]^-$	Glutathione reduced form	70-18-8
139	1.18	149.04	$C_5H_{11}NO_2S$	$[M+H]^+$	L-Methionine	63-68-3
140	1.58	220.08	$C_{11}H_{12}N_2O_3$	$[M+H]^+$	5-Hydroxy-L-tryptophan	56-69-9
141	0.84	117.07	$C_5H_{11}NO_2$	$[M+H]^+$	DL-Norvaline	760-78-1
142	1.40	162.04	$C_6H_{10}O_5$	$[M-H]^-$	3-Hydroxy-3-methylpentane-1,5-dioic acid	503-49-1
143	0.74	103.06	$C_4H_9NO_2$	$[M+H]^+$	2-Aminoisobutyric acid	62-57-7
144	0.75	103.06	$C_4H_9NO_2$	$[M+H]^+$	N,N-Dimethylglycine	1118-68-9
145	0.68	188.11	$C_7H_{16}N_4O_2$	$[M+H]^+$	H-HomoArg-OH	156-86-5
146	1.15	197.06	$C_9H_{11}NO_4$	$[M+H]^+$	3,4-Dihydroxy-DL-phenylalanine	63-84-3

(Continued)

TABLE 1 | Continued

ID	Rt (min)	MW (g/mol)	Molecular Formula	Ionization Mode	Compounds	CAS
147	3.90	290.11	$C_{15}H_{18}N_2O_4$	$[M–H]^-$	N-Acetyl-DL-tryptophan	87-32-1
148	1.91	165.07	$C_9H_{11}NO_2$	$[M+H]^+$	Phenylalanine	63-91-2
Alkaloids						
149	0.60	202.20	$C_{10}H_{26}N_4$	$[M+H]^+$	Spermine	71-44-3
150	0.78	117.07	$C_5H_{11}NO_2$	$[M+H]^+$	Betaine	107-43-7
151	3.79	550.12	$C_{24}H_{26}N_2O_{13}$	$[M+H]^+$	Batanin	7659-95-2
152	0.80	161.06	$C_6H_{11}NO_4$	$[M+H]^+$	DL-2-Aminoadipic acid	542-32-5
153	0.84	153.07	$C_8H_{11}NO_2$	$[M+H]^+$	Dopamine hydrochloride	62-31-7
154	5.77	270.08	$C_{16}H_{14}O_4$	$[M+H]^+$	Isomethacin	74560-05-7
155	1.89	135.05	$C_5H_5N_5$	$[M+H]^+$	Aminopurine	452-06-2
156	0.74	103.09	$C_5H_{13}NO$	$[M+H]^+$	Choline	62-49-7
157	2.27	234.12	$C_{13}H_{18}N_2O_2$	$[M+H]^+$	N-p-Coumaroyl putrescine	34136-53-3
158	0.64	130.11	$C_5H_{14}N_4$	$[M+H]^+$	Agmatine	306-60-5
159	2.47	117.05	C_8H_7N	$[M+H]^+$	Indole	120-72-9
160	2.42	473.14	$C_{20}H_{23}N_7O_7$	$[M+H]^+$	10-Formyl-THF	2800-34-2
161	6.53	342.26	$C_{19}H_{38}N_2O_3$	$[M+H]^+$	Cocamidopropyl βine	86438-79-1
162	0.79	137.04	$C_7H_7NO_2$	$[M+H]^+$	Trigonelline	535-83-1
163	0.72	130.10	$C_6H_{14}N_2O$	$[M+H]^+$	N-Acetylputrescine	18233-70-0
164	6.09	350.02	$C_{16}H_{11}N_2NaO_4S$	$[M–Na]^-$	Shikonin	523-44-4
165	9.01	516.31	$C_{33}H_{44}N_2O_3$	$[M+CH_3COOH-H]^-$	Dendrocrepine	51020-39-4
166	9.19	516.31	$C_{33}H_{44}N_2O_3$	$[M+CH_3COOH-H]^-$	Isodendrocrepine	50906-94-0
167	2.11	264.17	$C_{15}H_{24}N_2O_2$	$[M+H]^+$	Sophoranol	3411-37-8
168	1.20	131.09	$C_6H_{13}NO_2$	$[M+H]^+$	6-Deoxyfagomine	197449-09-5
169	2.94	310.15	$C_{16}H_{24}NO_5^+$	$[M]^+$	Sinapine	18696-26-9
170	2.88	280.14	$C_{15}H_{22}NO_4^+$	$[M]^+$	Feruloylcholine	85927-25-9
171	4.79	283.11	$C_{17}H_{17}NO_3$	$[M+H]^+$	N-p-Coumaroyltyramine	36417-86-4
172	6.03	624.22	$C_{36}H_{36}N_2O_8$	$[M+H]^+$	Cannabisin F	163136-19-4
173	4.76	313.13	$C_{18}H_{19}NO_4$	$[M+H]^+$	N-Trans-feruloyltyramine	66648-43-9
174	4.91	313.13	$C_{18}H_{19}NO_4$	$[M+H]^+$	N-Cis-feruloyltyramine	80510-09-4
Phenolic acids						
175	4.03	194.05	$C_{10}H_{10}O_4$	$[M–H]^-$	Ferulic acid	1135-24-6
176	3.38	198.04	$C_9H_{10}O_5$	$[M–H]^-$	Syringic acid	530-57-4
177	3.29	168.04	$C_8H_8O_4$	$[M–H]^-$	Vanillic acid	121-34-6
178	3.86	180.07	$C_{10}H_{12}O_3$	$[M–H]^-$	Coniferyl alcohol	458-35-5
179	4.09	152.04	$C_8H_8O_3$	$[M–H]^-$	2-Methoxybenzoic acid	529-75-9
180	2.74	354.08	$C_{16}H_{18}O_9$	$[M–H]^-$	Chlorogenic acid	327-97-9
181	3.97	152.04	$C_8H_8O_3$	$[M–H]^-$	Vanillin	121-33-5
182	3.69	122.03	$C_7H_6O_2$	$[M–H]^-$	4-Hydroxybenzaldehyde	123-08-0
183	3.05	138.03	$C_7H_6O_3$	$[M–H]^-$	4-Hydroxybenzoic acid	99-96-7
184	3.83	210.08	$C_{11}H_{14}O_4$	$[M–H]^-$	Sinapyl alcohol	537-33-7
185	2.85	154.02	$C_7H_6O_4$	$[M–H]^-$	2,4-Dihydroxy benzoic acid	89-86-1
186	2.72	342.11	$C_{16}H_{22}O_8$	$[M–H]^-$	Coniferin	531-29-3
187	3.31	786.22	$C_{35}H_{46}O_{20}$	$[M–H]^-$	Echinacoside	82854-37-3
188	4.28	666.18	$C_{31}H_{38}O_{16}$	$[M–H]^-$	2'-Acetylacteoside	94492-24-7
189	5.53	178.06	$C_{10}H_{10}O_3$	$[M–H]^-$	Trans-4-Hydroxycinnamic Acid Methyl Ester	19367-38-5
190	4.10	182.05	$C_9H_{10}O_4$	$[M–H]^-$	Syringic Aldehyde	134-96-3
191	4.09	194.05	$C_{10}H_{10}O_4$	$[M–H]^-$	Trans-ferulic acid	537-98-4
192	3.14	180.04	$C_9H_8O_4$	$[M–H]^-$	Caffeic acid	331-39-5
193	5.22	148.05	$C_9H_8O_2$	$[M–H]^-$	Cinnamic acid	140-10-3
194	3.05	138.06	$C_8H_{10}O_2$	$[M–H]^-$	Tyrosol	501-94-0
195	4.01	224.06	$C_{11}H_{12}O_5$	$[M–H]^-$	Sinapic acid	530-59-6

(Continued)

TABLE 1 | Continued

ID	Rt (min)	MW (g/mol)	Molecular Formula	Ionization Mode	Compounds	CAS
196	3.15	386.10	$C_{17}H_{22}O_{10}$	$[M-H]^-$	1-O-β-D-Glucopyranosyl sinapate	78185-48-5
197	3.79	164.04	$C_9H_8O_3$	$[M+H]^+$	p-Coumaric acid	501-98-4
198	4.43	208.06	$C_{11}H_{12}O_4$	$[M-H]^-$	Sinapinaldehyde	4206-58-0
199	2.30	316.10	$C_{14}H_{20}O_8$	$[M-H]^-$	Cimidahurinine	142542-89-0
200	2.45	154.02	$C7H_6O_4$	$[M-H]^-$	Gentisic acid	490-79-9
201	11.72	256.22	$C_{16}H_{32}O_2$	$[M-H]^-$	Hexadecanoic acid	1957/10/3
202	2.38	296.04	$C_{13}H_{12}O_8$	$[M-H]^-$	Cis-Coutaric acid	27174-07-8
203	2.87	354.08	$C_{16}H_{18}O_9$	$[M+H]^+$	4-Caffeoylquinic acid	905-99-7
204	9.71	148.01	$C_8H_4O_3$	$[M+H]^+$	Phthalic anhydride	85-44-9
205	1.75	170.02	$C_7H_6O_5$	$[M-H]^-$	Gallic acid	149-91-7
206	2.55	154.02	$C_7H_6O_4$	$[M-H]^-$	Protocatechuic acid	99-50-3
Nucleotides and their derivatives						
207	1.19	244.06	$C_9H_{12}N_2O_6$	$[M-H]^-$	Uridine	58-96-8
208	0.75	111.04	$C_4H_5N_3O$	$[M+H]^+$	Cytosine	71-30-7
209	1.13	125.05	$C_5H_7N_3O$	$[M+H]^+$	5-Methylcytosine	554-01-8
210	1.37	345.03	$C_{10}H_{12}N_5O_7P$	$[M-H]^-$	Guanosine 3',5'-cyclic monophosphate	7665-99-8
211	1.77	284.06	$C_{10}H_{12}N_4O_6$	$[M-H]^-$	Xanthosine	146-80-5
212	0.79	334.04	$C_{11}H_{15}N_2O_8P$	$[M+H]^+$	β-Nicotinamide mononucleotide	1094-61-7
213	1.84	329.04	$C_{10}H_{12}N_5O_6P$	$[M-H]^-$	Cyclic AMP	60-92-4
214	1.43	268.07	$C_{10}H_{12}N_4O_5$	$[M-H]^-$	9-(β-D-Arabinofuranosyl) hypoxanthine	7013-16-3
215	1.14	663.08	$C_{21}H_{27}N_7O_{14}P_2$	$[M+H]^+$	Nicotinic acid adenine dinucleotide	53-84-9
216	1.14	347.05	$C_{10}H_{14}N_5O_7P$	$[M+H]^+$	Adenosine 5'-monophosphate	61-19-8
217	1.12	566.03	$C_{15}H_{24}N_2O_{17}P_2$	$[M-H]^-$	Uridine 5'-diphospho-D-glucose	133-89-1
218	1.13	136.03	$C_5H_4N_4O$	$[M+H]^+$	Hypoxanthine	68-94-0
219	1.12	135.05	$C_5H_5N_5$	$[M+H]^+$	Adenine	73-24-5
220	0.85	151.04	$C_5H_5N_5O$	$[M+H]^+$	2-Hydroxy-6-aminopurine	3373-53-3
221	1.88	267.08	$C_{10}H_{13}N_5O_4$	$[M+H]^+$	Adenosine	58-61-7
222	2.08	242.08	$C_{10}H_{14}N_2O_5$	$[M+H]^+$	Thymidine	50-89-5
223	1.15	151.04	$C_5H_5N_5O$	$[M+H]^+$	Guanine	73-40-5
224	1.37	136.03	$C_5H_4N_4O$	$[M+H]^+$	Allopurinol	315-30-0
225	1.46	283.08	$C_{10}H_{13}N_5O_5$	$[M+H]^+$	Guanosine	118-00-3
226	1.68	267.08	$C_{10}H_{13}N_5O_4$	$[M+H]^+$	Deoxyguanosine	961-07-9
227	1.13	227.08	$C_9H_{13}N_3O_4$	$[M+H]^+$	Deoxycytidine	951-77-9
228	2.85	297.08	$C_{11}H_{15}N_5O_3S$	$[M+H]^+$	5'-Deoxy-5'-(methylthio)adenosine	2457-80-9
229	0.68	403.99	$C_9H_{14}N_2O_{12}P_2$	$[M-H]^-$	Uridine 5'-diphosphate	27821-45-0
230	1.14	331.05	$C_{10}H_{14}N_5O_6P$	$[M+H]^+$	2'-Deoxyadenosine-5'-monophosphate	653-63-4
231	1.23	324.02	$C_9H_{13}N_2O_9P$	$[M-H]^-$	Uridine 5'-monophosphate	58-97-9
232	2.17	383.09	$C_{14}H_{17}N_5O_8$	$[M+H]^+$	N6-Succinyl Adenosine	4542-23-8
233	0.82	243.07	$C_9H_{13}N_3O_5$	$[M+H]^+$	Cytidine	65-46-3
234	1.96	251.09	$C_{10}H_{13}N_5O_3$	$[M+H]^+$	Deoxyadenosine	958-09-8
235	2.23	311.11	$C_{12}H_{17}N_5O_5$	$[M+H]^+$	2-(Dimethylamino)guanosine	2140-67-2
Organic acid						
236	2.09	118.06	$C_5H_{10}O_3$	$[M-H]^-$	3-Hydroxy-3-methyl butyric acid	625-08-1
237	0.94	174.04	$C_7H_{10}O_5$	$[M-H]^-$	Shikimic acid	138-59-0
238	1.31	118.02	$C_4H_6O_4$	$[M-H]^-$	Succinic acid	110-15-6
239	4.43	188.09	$C_9H_{16}O_4$	$[M-H]^-$	Anchoic Acid	123-99-9
240	0.97	134.02	$C_4H_6O_5$	$[M-H]^-$	L-(-)-Malic acid	636-61-3
241	1.13	192.05	$C_7H_{12}O_6$	$[M-H]^-$	Kinic acid	77-95-2
242	0.84	192.02	$C_6H_8O_7$	$[M-H]^-$	Citric Acid	77-92-9
243	0.86	138.04	$C_6H_6N_2O_2$	$[M-H]^-$	UROCANIC ACID(RG)	104-98-3
244	0.95	166.04	$C_5H_{10}O_6$	$[M-H]^-$	D-Xylonic acid	526-91-0

(Continued)

TABLE 1 | Continued

ID	Rt (min)	MW (g/mol)	Molecular Formula	Ionization Mode	Compounds	CAS
245	1.11	116.01	$C_4H_4O_4$	$[M–H]^-$	Fumaric acid	110-17-8
246	1.32	118.02	$C_4H_6O_4$	$[M–H]^-$	Methylmalonic acid	516-05-2
247	2.08	132.04	$C_5H_8O_4$	$[M–H]^-$	2-Methylsuccinic acid	498-21-5
248	6.12	230.14	$C_{12}H_{22}O_4$	$[M–H]^-$	Dodecanedioic aicd	693-23-2
249	0.77	145.08	$C_5H_{11}N_3O_2$	$[M+H]^+$	4-Guanidinobutyric acid	463-00-3
250	2.64	154.02	$C_7H_6O_4$	$[M–H]^-$	2,3-Dihydroxybenzoic Acid	303-38-8
251	2.63	132.07	$C_6H_{12}O_3$	$[M–H]^-$	5-Hydroxyhexanoic acid	185956-02-9
252	5.02	202.11	$C_{10}H_{18}O_4$	$[M–H]^-$	Sebacate	111-20-6
253	1.00	131.09	$C_6H_{13}NO_2$	$[M+H]^+$	6-Aminocaproic acid	60-32-2
254	0.59	174.01	$C_6H_6O_6$	$[M+H]^+$	Trans-Citridic acid	4023-65-8
255	0.77	103.06	$C_4H_9NO_2$	$[M+H]^+$	γ-Aminobutyric acid	56-12-2
256	0.69	142.02	$C_6H_6O_4$	$[M–H]^-$	Trans,trans-Muconic acid	3588-17-8
Terpenes						
257	8.42	236.16	$C_{15}H_{24}O_2$	$[M+H]^+$	Prehelminthosporol	1619-13-2
258	11.20	286.21	$C_{20}H_{30}O$	$[M–H]^-$	Ferruginol	514-62-5
259	8.02	488.32	$C_{30}H_{48}O_5$	$[M–H]^-$	Rutundic acid	20137-37-5
260	2.42	376.12	$C_{16}H_{24}O_{10}$	$[M+NH_4]^+$	Adoxosidic acid	84375-46-2
Others						
261	1.49	122.04	$C_6H_6N_2O$	$[M+H]^+$	Nicotinamide	98-92-0
262	0.76	180.05	$C_6H_{12}O_6$	$[M–H]^-$	D-(+)-Glucose	50-99-7
263	0.77	152.06	$C_5H_{12}O_5$	$[M–H]^-$	Ribitol	488-81-3
264	0.74	182.07	$C_6H_{14}O_6$	$[M–H]^-$	D-Sorbitol	50-70-4
265	3.21	376.12	$C_{17}H_{20}N_4O_6$	$[M+H]^+$	Riboflavin	83-88-5
266	0.72	342.10	$C_{12}H_{22}O_{11}$	$[M–H]^-$	D-(+)-TrehaloseAnhydrous	99-20-7
267	0.73	152.06	$C_5H_{12}O_5$	$[M–H]^-$	D-Arabitol	488-82-4
268	0.76	152.06	$C_5H_{12}O_5$	$[M–H]^-$	L-Arabitol	7643-75-6
269	2.39	121.08	$C_8H_{11}N$	$[M+H]^+$	Phenethylamine	64-04-0
270	0.71	141.01	$C_2H_8NO_4P$	$[M–H]^-$	O-Phosphorylethanolamine	1071-23-4
271	0.69	260.02	$C_6H_{13}O_9P$	$[M–H]^-$	D-Glucose 6-phosphate	56-73-5
272	10.80	325.27	$C_{20}H_{39}NO_2$	$[M+H]^+$	N-Oleoylethanolamine	111-58-0
273	2.75	278.11	$C_{11}H_{22}N_2O_4S$	$[M–H]^-$	(R)-Pantetheine	496-65-1
274	0.75	342.10	$C_{12}H_{22}O_{11}$	$[M–H]^-$	Galactinol	3687-64-7
275	0.78	260.02	$C_6H_{13}O_9P$	$[M–H]^-$	Glucose-1-phosphate	59-56-3
276	0.78	182.07	$C_6H_{14}O_6$	$[M–H]^-$	Mannitol	87-78-5
277	0.73	342.10	$C_{12}H_{22}O_{11}$	$[M–H]^-$	Melibiose	585-99-9
278	2.28	219.10	$C_9H_{17}NO_5$	$[M+H]^+$	D-Pantothenic Acid	79-83-4
279	6.34	214.09	$C_{14}H_{14}O_2$	$[M–H]^-$	Dihydropinosylvin	14531-52-3
280	0.80	504.14	$C_{18}H_{32}O_{16}$	$[M–H]^-$	Panose	33401-87-5
281	0.69	422.06	$C_{12}H_{23}O_{14}P$	$[M–H]^-$	Trehalose 6-phosphate	4484-88-2
282	0.82	221.08	$C_8H_{15}NO_6$	$[M+H]^+$	N-Acetyl-D-galactosamine	1811-31-0
283	0.89	176.02	$C_6H_8O_6$	$[M–H]^-$	D-Glucurono-6,3-lactone	32449-92-6
284	0.82	342.10	$C_{12}H_{22}O_{11}$	$[M–H]^-$	Isomaltulose	13718-94-0
285	0.86	364.08	$C_{12}H_{21}O_{11}Na$	$[M+H]^+$	Turanose	547-25-1
286	1.11	123.03	$C_6H_5NO_2$	$[M+H]^+$	Nicotinic acid	59-67-6
287	0.77	152.06	$C_5H_{12}O_5$	$[M–H]^-$	Xylitol	87-99-0
288	0.74	180.05	$C_6H_{12}O_6$	$[M–H]^-$	Inositol	87-89-8
289	0.78	342.10	$C_{12}H_{22}O_{11}$	$[M–H]^-$	D-(+)-Sucrose	57-50-1
290	0.70	196.05	$C_6H_{12}O_7$	$[M–H]^-$	Gluconic acid	526-95-4
291	1.31	120.06	$C_7H_8N_2$	$[M+H]^+$	Benzamidine	618-39-3
292	2.29	205.12	$C_9H_{19}NO_4$	$[M+H]^+$	Pantothenol	16485-10-2
293	1.11	169.07	$C_8H_{11}NO_3$	$[M+H]^+$	Pyridoxine	65-23-6

(Continued)

TABLE 1 | Continued

ID	Rt (min)	MW (g/mol)	Molecular Formula	Ionization Mode	Compounds	CAS
294	0.75	182.07	$C_6H_{14}O_6$	$[M–H]^-$	Dulcitol	608-66-2
295	0.81	178.04	$C_6H_{10}O_6$	$[M–H]^-$	L-Gulonic-γ-lactone	1128-23-0
296	1.67	183.05	$C_8H_9NO_4$	$[M+H]^+$	4-Pyridoxic acid	82-82-6
297	4.53	188.09	$C_9H_{16}O_4$	$[M–H]^-$	Eucommiol	55930-44-4
298	4.68	228.07	$C_{14}H_{12}O_3$	$[M–H]^-$	9,10-Dihydrophenanthrene	776-35-2
299	3.55	410.17	$C_{21}H_{30}O_8$	$[M+H]^+$	Onitin-2'-O-D-glucoside	76947-60-9
300	6.10	242.08	$C_{15}H_{14}O_3$	$[M+H]^+$	Hircinol	41060-05-3
301	0.83	150.04	$C_5H_{10}O_5$	$[M–H]^-$	D-(-)-Arabinose	10323-20-3
302	6.76	270.04	$C_{15}H_{10}O_5$	$[M+H]^+$	Phosphoenolpyruvate	481-72-1
303	3.37	578.12	$C_{30}H_{26}O_{12}$	$[M+H]^+$	Procyanidin B3	23567-23-9
304	3.93	496.27	$C_{27}H_{44}O_8$	$[M+H]^+$	Podecdysone C	19458-46-9

for docking. When the binding energy was ≤ – 5.0 kJ/mol, the active component was considered to have good target binding activity (33).

Experimental Evaluation

Preparation of *D. officinale* Methanol Aqueous Extract

To prepare the DOME, the powdered samples (100 g) of dried stems of *D. officinale* were extracted with 2 L 70% methanol three times, each time for 2 h. The methanol extract was concentrated using a rotary evaporator, and the concentrate was freeze-dried under vacuum at −20°C by using a vacuum freeze dryer (SCIENTZ-10Z, Ningbo Scientz Biotechnology Co., Ltd., Ningbo, Zhejiang, China). Finally, the DOME was dissolved in DMSO to adjust the stock concentration (20%, w/v) and stored at −20°C for future study.

Wound Healing Migration Assay

Cell migration was evaluated with a wound healing assay. About 1×10^6 Lovo cells were seeded into 6-well plates prepared with five straight lines on the back and allowed to grow to 100% confluency in 10% fetal bovine serum (FBS) medium. Then, a clear cell-free line was manually created by scratching a single layer using a sterile 10 μL pipette tip in each well. After scratching, the wounded monolayers were washed three times with PBS and photographed using an inverted microscope (TS100, Nikon Corp., Tokyo, Japan) at 100 × magnification as the picture for 0 h. Then, the cells were exposed to DOME (0, 250, 500, and 1,000 μg/mL) in a 2.5% FBS medium for another 24 and 48 h, and photographed at 24 and 48 h under the microscope. The width of the scratch was measured by ImageJ software (National Institutes of Health, Bethesda, MD, USA) in 10 fields. The relative migration rate was calculated as follows:

$$\text{Relative migration rate of 24h } (\%) = \frac{1 - \text{treated group width at 24 h/treated group width at 0 h}}{1 - \text{ blank group width at 24 h /blank group width at 0 h}} \times 100\%$$

$$\text{Relative migration rate of 48h } (\%) = \frac{1 - \text{treated group width at 48 h/treated group width at 0 h}}{1 - \text{ blank group width at 48 h /blank group width at 0 h}} \times 100\%$$

Cell Viability

The CRC cell lines (HT-29, Lovo, SW-620, and HCT-116) were cultured in McCoy's 5A medium supplemented with 10% FBS, 100 U/ml penicillin, and 100 μg/ml streptomycin. All cultures were incubated at 37°C in an incubator with 5% CO_2.

The effect of the DOME on HT-29, Lovo, SW-620, and HCT-116 cell growth was assessed using an MTT assay. In brief, the cells in the logarithmic phase were seeded in 96-well plates at 1×10^4 cells/well. After incubation for 24 h, they were exposed to the DOME (0, 250, 500, and 1,000 μg/ml) for another 24, 48, and 72 h in triplicate. Then 5-Fu (50 μg/mL) was used as the positive control, 20 μL MTT solution (5 mg/ml) was added to each well, and the cells were incubated for 4 h at 37°C in an incubator with 5% CO_2. After discarding the supernatants, 100 μL DMSO was added, and the absorbance at 488 nm was measured using a microplate reader (Multiskan GO Microplate Spectrophotometer, Thermo Fisher Scientific, Waltham, MA, USA).

Transwell Migration and Invasion Assay

Migration and invasion were performed using 24-well chambers with 8 μm pore size. For the migration assay, Lovo cells were resuspended in 100 μL FBS-free medium (5×10^4 cells). Then, the cells were exposed to DOME (0, 250, 500, and 1,000 μg/ml) and added to the top chamber. After that, 800 μL medium supplemented with 20% FBS was added to the lower chamber. After incubation at 37°C with 5% CO_2 for 48 h, non-migrative Lovo cells on the upper chamber were carefully removed with a cotton swab. Then, the migrated Lovo cells were fixed in 4% paraformaldehyde for 20 min and stained with 0.1% crystal violet for 20 min. Migrated cell images were observed and photographed using an inverted fluorescence microscope (BX51, Olympus Optical Co. Ltd., Tokyo, Japan), at 200 × magnification. The images were quantitated using ImageJ software in six random fields.

For the invasion assay, the invasion capacity of Lovo cells was evaluated with the Matrigel matrix gel invasion assay. Then, the

invasion assay was similarly performed as the migration assay, except that the upper chamber was pre-coated with 100 μL Matrigel (300 μg/ml) overnight before seeding with Lovo cells. The relative migration or invasion rate was calculated as follows:

$$\text{Relative migration or invasion rate } (\%) = \frac{\text{Number of migration or invasion cells of treated group}}{\text{Number of migration or invasion cells of blank group}} \times 100\%$$

TUNEL Staining Assay

Apoptotic DNA fragmentation was examined using the One Step TUNEL Apoptosis Assay kit in accordance with the manufacturer's instructions. In brief, the Lovo cells were plated in the cell culture dish (35 mm) at a density of 1×10^5 cells/well. After culturing at 37°C in an incubator with 5% CO_2 for 24 h, the cells were treated with the DOME (0, 250, 500, and 1,000 μg/mL) in triplicate for another 48 h. After treatment, the Lovo cells were washed with PBS three times, fixed with 4% paraformaldehyde for 30 min, and permeabilized with Enhanced Immunostaining Permeabilization Solution for 5 min. The cells were then washed with PBS and incubated with TUNEL assay in the dark for 1 h at 37°C. The cells were also stained with DAPI for 10 min after a rinse with PBS to visualize cell nuclei. Cyanine 3 (Cy3)-labeled TUNEL-positive cells were imaged at ×200 magnification using a confocal laser scanning fluorescence microscope (Nikon A1 confocal, Nikon, Tokyo, Japan) with 550 nm excitation and 570 nm emission wavelengths. The cells with red fluorescence were defined as apoptotic cells.

RESULTS

Thirty Four Potential Active Components Were Focused on by Network Pharmacology Analysis

For comprehensive identification of *D. officinale* chemical constituents, 70% aqueous methanol of *D. officinale* was analyzed using UPLC-ESI-MS/MS both in positive and negative ion scanning modes. The corresponding total ion current diagrams are shown in **Supplementary Figures 1A,B**. In total, 304 *D. officinale* constituents were finally identified (**Table 1**). According to the literature, additional 92 active components were collected (**Supplementary Table 1**). The in-house library totally acquired 396 candidate active components. After screening by SwissADME online tools, we explored the drug targets for the aforementioned candidate active components in *D. officinale* using SwissTargetPrediction databases, which resulted in a total of 116 putative targets (**Supplementary Table 2**). At the same time, 1,666 colon cancer-related targets were gathered after removing overlapping targets among different databases with 12 targets from the DisGeNet database, 495 targets from the OMIM database, 1,263 targets from the GeneCards database, 37 targets from the DrugBank database, and eight targets from the TTD database (**Figure 2A**).

Then, we crossed 116 *D. officinale* active component targets with 1,666 CRC-related targets using VENNY 2.1 software (**Figure 2B**). As a result, 34 common targets were focused on, namely, CA9, CYP1B1, ABCC1, PLG, CYP19A1, HSD17B1, SHBG, ESR1, ESR2, EGFR, FLT3, CDK1, PTGS2, CDK6, GSK3B, TTR, CFTR, ABCG2, ALOX5, PARP1, ABCB1, PPARG, PPARD, PTGS1, TERT, ADORA3, HTR2A, LCK, CASP2, MMP9, MMP1, MMP2, PTPN1, and F2. 36 active components (**Supplementary Table 3**). These 34 targets were linked by a network pharmacology approach.

Construction and Analysis of Target PPI Network

The 34 common targets were submitted to STRING version 11.0 for PPI network construction (**Figure 2C**). As shown in **Figure 2C**, the results included a total of 34 nodes and 119 edges, the nodes that represent the target proteins and the edges that represent the interactions between the proteins. In this network interaction, the larger the degree is, the stronger the interaction relationship between the targets will be. It also indicates that this key target protein plays a pivotal role in regulating the network as the hub target (34). Then, Cytoscape 3.7.2 software was used for visualization and calculation of the topological parameters, such as degree, BC, and CC. Moreover, the top six targets were obtained using the value of degree as the condition for screening core targets, mainly involving ESR1, EGFR, PTGS2, MMP9, MMP2, and PPARG.

GO and KEGG Analysis

The Metascape database was used to carry out the GO enrichment analysis related to biological processes (BP), cellular components (CC), and molecular functions (MF) and KEGG pathway analysis of 34 common target genes. In the BP group, the most enriched genes concerned "muscle cell proliferation (GO:0033002)," "regulation of inflammatory response (GO:0050727)," "cellular response to organic cyclic compound (GO:0071407)," "apoptotic signaling pathway (GO:0097190)," and "regulation of protein localization to nucleus (GO:1900180)" (**Figure 3A**). The most enriched genes in the CC group were in "membrane raft (GO:0045121)," "side of membrane (GO:0098552)," and "nuclear chromosome, telomeric region (GO:0000784)" (**Figure 3B**). The genes in the MF group that were most enriched comprised "xenobiotic transmembrane transporting ATPase activity (GO:0008559)," "nuclear receptor activity (GO:0004879)," and "serine-type endopeptidase activity (GO:0004252)" (**Figure 3C**). KEGG pathway analysis indicated that "pathways in cancer (hsa05200)," "Ovarian steroidogenesis (hsa04913)," and "MicroRNAs in cancer (hsa05206)" were involved in the regulation of common target genes (**Figure 3D**). Details are listed in **Supplementary Table 4**. Based on these results, we were interested in and focused on the apoptotic signaling pathway, which was highly enriched in the GO and KEGG databases.

Analyses of the Component–Target–Pathway Network

According to the predicted results of the identified active components, key targets, and top 22 related pathways using the KEGG database (**Supplementary Table 4**), an integrated component–target–pathway network was constructed using Cytoscape.

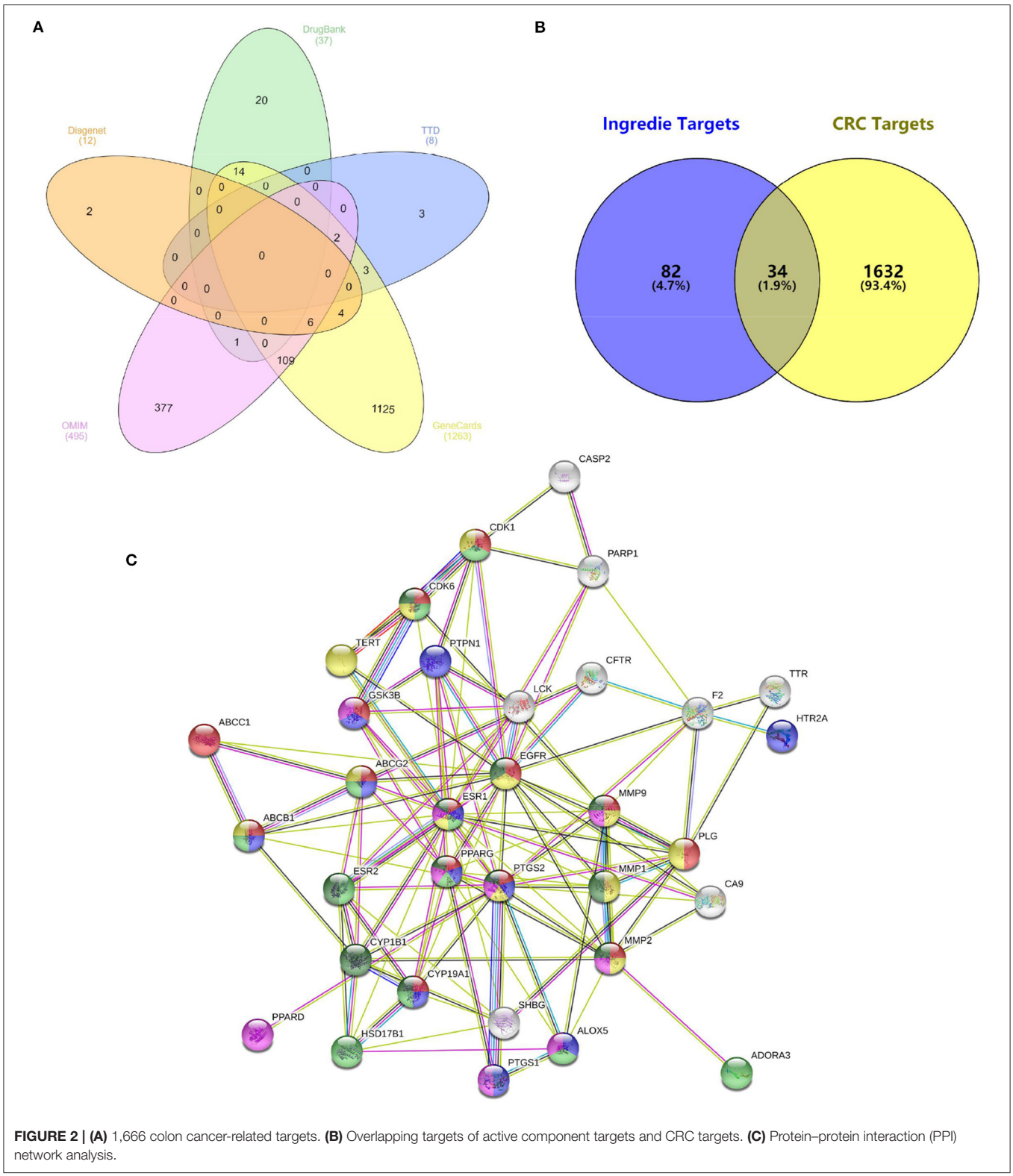

FIGURE 2 | (A) 1,666 colon cancer-related targets. **(B)** Overlapping targets of active component targets and CRC targets. **(C)** Protein–protein interaction (PPI) network analysis.

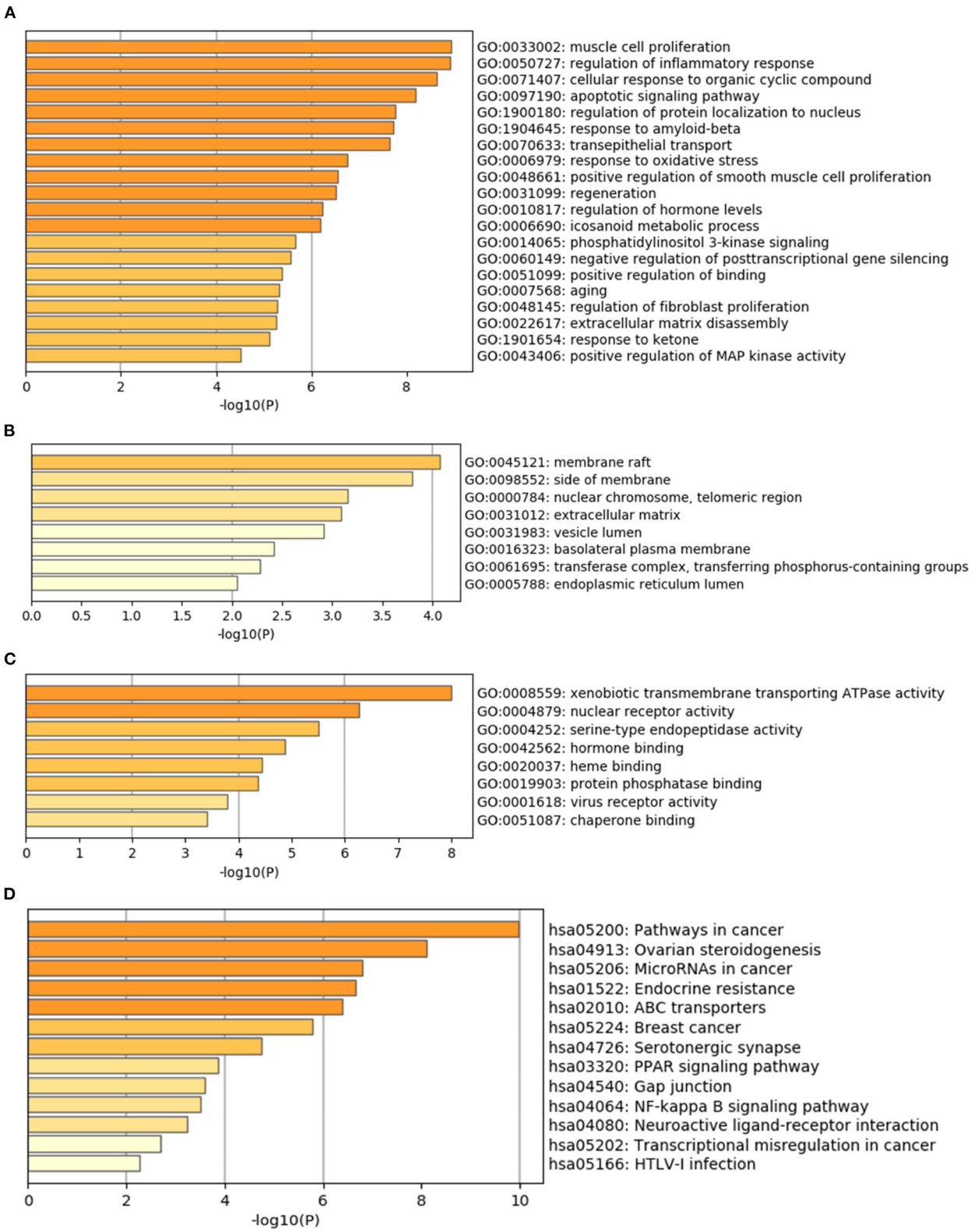

FIGURE 3 | GO and KEGG pathway enrichment analyses of 34 common target genes. **(A)** Biological process analysis. **(B)** Cellular component analysis. **(C)** Molecular function analysis. **(D)** KEGG pathway analysis.

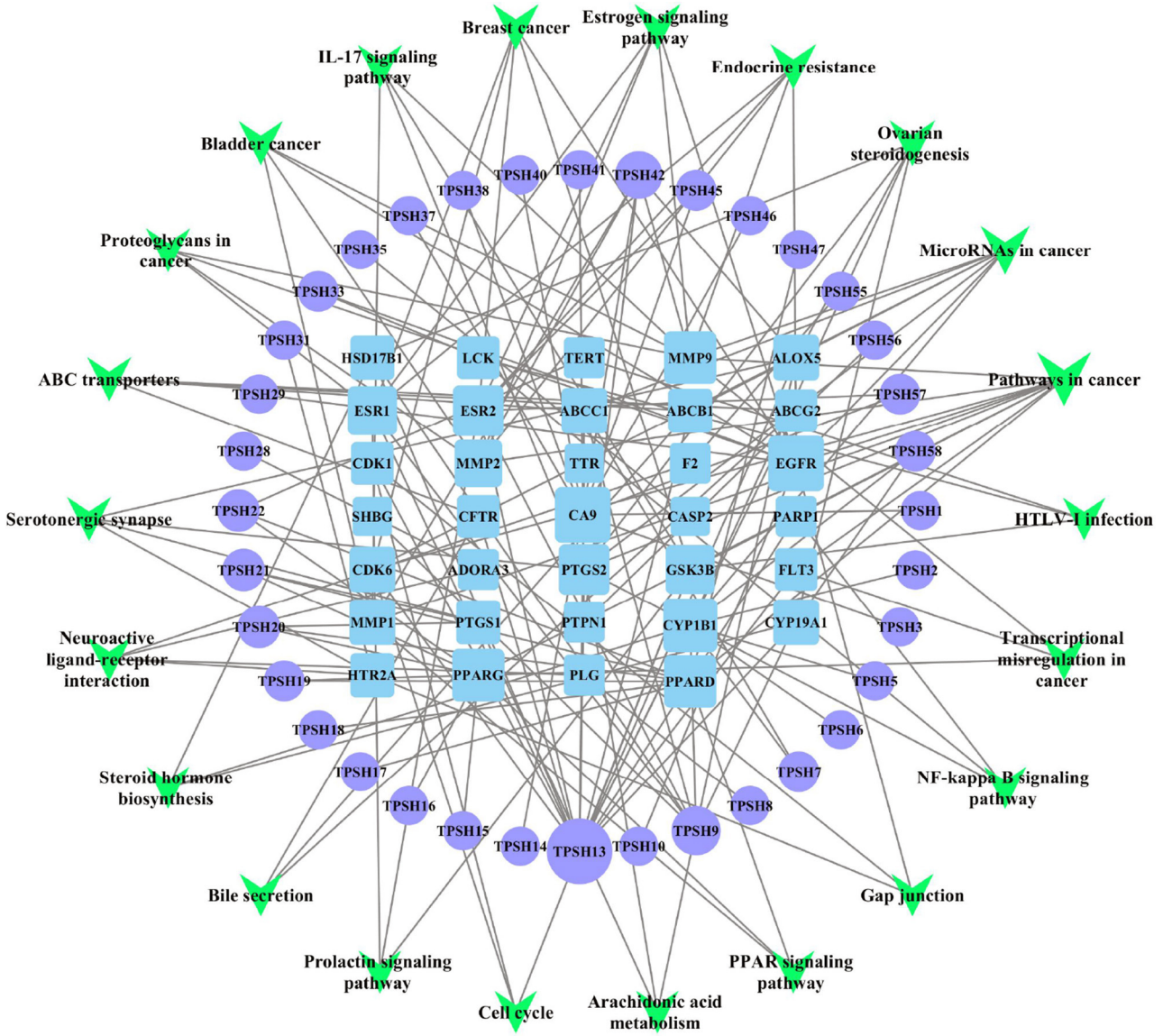

FIGURE 4 | Component–target–pathway (C-T-P) network of *D. officinale* for CRC. The purple circles represent the active components of *D. officinale*, the blue squares represent the common targets, and the green inverted triangles represent the main pathways. Node size is proportional to its degree. The larger the area is, the more important it is in the network.

As shown in **Figure 4**, 36 core active components were obtained, which were gallic acid, isorhamnetin, protocatechuic acid, homoeriodictyol, isosakuranetin (7'-methylnaringenin), tamarixetin, Di-O-methylquercetin, naringenin, naringenin chalcone, apigenin, scopoletin (7-hydroxy-5-methoxycoumarin), 13-hydroxy-9,11-octadecadienoic acid, 9-hydroxy-10,12-octadecadienoic acid, myristic acid, pentadecanoic acid, palmitoleic acid, γ-linolenic acid, α-linolenic acid, cis-10-heptadecenoic acid, L-glutamic acid, (-)-3-(3,4-dihydroxyphenyl)-2-methylalanine, 5-hydroxy-L-tryptophan, 3,4-dihydroxy-DL-phenylalanine, spermine, ferulic acid, syringic acid, trans-4-hydroxycinnamic acid methyl ester, trans-ferulic acid, caffeic acid, p-coumaric acid, gentisic acid, hexadecanoic acid, benzamidine, rutundic acid, p-hydroxy cinnamic acid, and 3',5, 5',7-tetrahydroxyflavanone (**Supplementary Table 3**). Apigenin, naringenin, caffeic acid, γ-linolenic acid, α-linolenic acid, cis-10-heptadecenoic acid, tamarixetin, palmitoleic acid, 3,4-dihydroxy-DL-phenylalanine, and p-coumaric acid were found to be the top 10 important active components in this network (**Supplementary Table 5**). Apigenin was the most important active component (degree = 17, BC = 0.6359, and CC = 0.4607), followed by naringenin (7, 0.3811, 0.3388). In addition, ESR1, EGFR, PTGS2, MMP9, MMP2, PPARG, PLG, CYP1B1, ESR2, and CYP19A1 were found to be the top 10 important targets in this network (**Supplementary Table 6**).

Molecular Docking

Molecular docking of the key active components of *D. officinale* (apigenin, naringenin, caffeic acid, γ-linolenic acid, α-linolenic acid, and cis-10-heptadecenoic acid) with the key target proteins (ESR1, EGFR, PTGS2, MMP9, MMP2, and PPARG) was performed by AutoDock 4.0.

The results showed that apigenin and naringenin are well-docked with PTGS2 and MMP9 and have a good affinity, suggesting that *D. officinale* has high accuracy in the treatment of CRC (**Supplementary Table 7**). Moreover, compared with other targets, the docking energy of apigenin with PTGS2 (−6.31 kJ/mol) was the lowest, indicating that the binding ability and stability of apigenin–PTGS2 complex were higher than those of the other targets. Apigenin was able to produce interaction with five amino acids within the binding pouch of PTGS2 such as ASN-34, GLN-327, ASP-157, GLN-461, and HIS-39 at bond lengths of 2.2, 2.1, 3.1, 2.0, 2.4, and 2.14 Å, respectively. The docking model is shown in **Figure 5B**. In addition, apigenin was docked with MMP9, and the binding energy was −5.20 kJ/mol. Also, apigenin was able to produce interaction with three amino acids within the binding pouch of MMP9 such as THR-246, ARG-332, and CYS-244 at bond lengths of 2.5, 1.7, and 2.4 Å, respectively. The docking model is shown in **Figure 5A**. The docking binding energies of naringenin with PTGS2 and MMP9 were −6.20 and −5.81 kJ/mol, respectively. Naringenin was able to produce interaction with four amino acids within the binding pouch of PTGS2 such as HIS-39, GLN-461, GLY-45, and GLN-327 at bond lengths of 1.8, 2.5, 2.1, 2.5, and 2.5 Å, respectively. Also, naringenin was able to produce interaction with one amino acid (PHE-107) within the binding pouch of MMP9 at a bond length of 2.1 Å. The docking model is shown in **Figures 5C,D**.

Experimental Evaluation

MTT Assay

To investigate the antitumor effect of the DOME on CRC, the treated HT-29, Lovo, SW-620, and HCT-116 cells were analyzed using an MTT assay. As shown in **Figure 6**, the results showed that the DOME decreased the proliferation of the four CRC cell lines in a dose- and time-dependent manner. In addition, the inhibitory rate was 1,000 μg/ml DOME ≤20% on the four CRC cells at 24 h, except the DOME on HT-29 cells (44.83%). However, the inhibitory rate was 1,000 μg/ml DOME ≥40% on these CRC cells at 48 h, which is close to the effect at 72 h. Therefore, this study chose 48 h as the time of the DOME on CRC cells in the subsequent experiments.

Wound Healing Migration Assay and Transwell Migration and Invasion Assay

Because MMP-2 and MMP-9 are important executors in cell migration and invasion, and based on the previous results in the component–target–pathway network analysis and molecular docking analysis, we further assessed the inhibitory effects of the DOME on the *in vitro* migration and invasion potential of Lovo cells using the wound healing migration assay and transwell assay, respectively. These results showed that the DOME significantly inhibited Lovo cell migration in a dose- and time-dependent manner (**Figures 7A–C**). To further assess the effects of the DOME on the migration of Lovo cells *in vitro*, the transwell migration assay was employed. The transwell migration assay also revealed that the DOME markedly weakened the migration ability of Lovo cells ($P < 0.01$, **Figures 7D–F**), further confirming the result of the wound healing assay.

Furthermore, cell invasion ability was determined by a transwell invasion assay. Compared to the blank group, the number of invaded cells in the DOME group was significantly reduced in a dose-dependent manner (**Figures 7E,F**). These results suggested that the DOME could suppress Lovo cell migration and invasion *in vitro*.

TUNEL Staining

According to the predicted results of the GO and KEGG pathway enrichment analyses and to further confirm the apoptosis-inducing activities of DOME in Lovo cells, TUNEL staining was also performed. The cell apoptosis in Lovo cells was determined with TUNEL assay after DOME treatments for 48 h. As shown in **Figure 8**, TUNEL-positive nuclei (representing apoptotic cells) were stained with red fluorescence, while total nuclei stained with DAPI and exhibited blue fluorescence. **Figure 8** shows that the DOME remarkably increased TUNEL-positive (red) cell number. The result demonstrated that the DOME induces apoptosis in Lovo cells, and this effect was significantly enhanced in a dose-dependent manner.

DISCUSSION

Currently, chemotherapy is the conventional treatment method for CRC, such as 5-Fu. However, chemotherapy has many adverse effects (35). A number of prior studies have shown that *D. officinale* exhibits excellent bioactivity against CRC (9, 10). Used as a medicine and food dual-use product for more than a thousand years, *D. officinale* has fewer side effects (1). However, the underlying mechanisms of anti-colon cancer effects of *D. officinale* remain unclear because of the complex compositions. The core active components and core target of *D. officinale*, which play the key role against the CRC, are unclear. We applied metabolomics combined with network pharmacology to screen the active components, drug targets, and singling pathway. Moreover, we performed further experimental validation using a series of cellular functional and molecular biological assays *in vitro*. Overall, our results did not only clarify the anti-CRC effective components and their potential targets of *D. officinale* but also offer in-depth knowledge of the molecular mechanisms of *D. officinale*.

In this study, 304 metabolites of active components in *D. officinale* 70% methanol extracts were determined by UPLC-ESI-MS/MS metabonomic analysis, while 178 compounds were identified by UPLC-MS/MS from the *D. officinale* anhydrous ethanol extracts as reported in the literature (36). It may be due to the different origins of *D. officinale* or the different extraction solvents used. Furthermore, in order to fully establish the component library of *D. officinale* and make the network pharmacological analysis more accurate (37), we used the literature mining method (PubMed, CNKI.net, Cqvip.com, and Web of Science) to search for those that had been reported

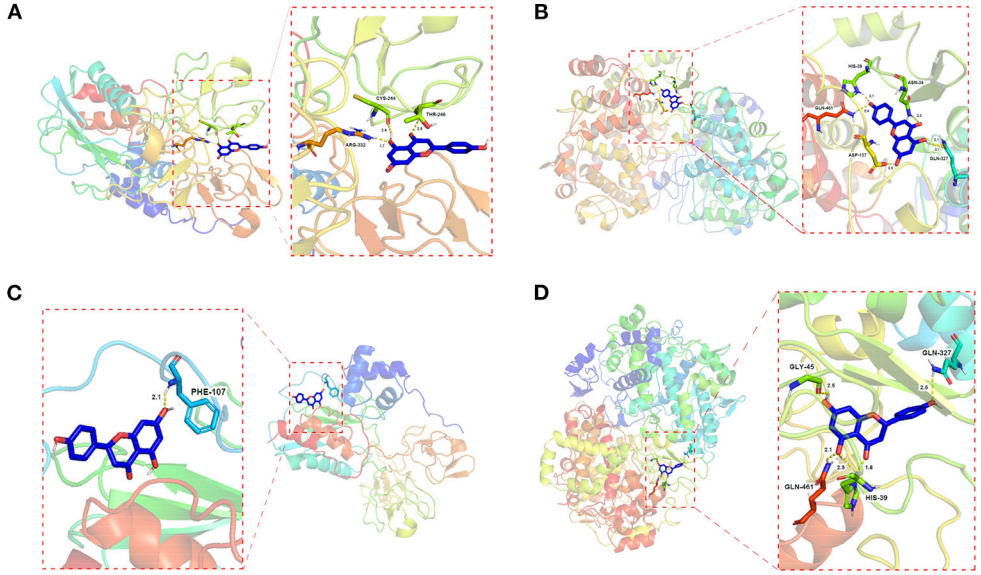

FIGURE 5 | Schematic (3D) representation of the molecular model of the active component combined with the target proteins. Components: apigenin. Target proteins: **(A)** MMP9; **(B)** PTGS2; components: naringenin. Target proteins: **(C)** MMP9; **(D)** PTGS2.

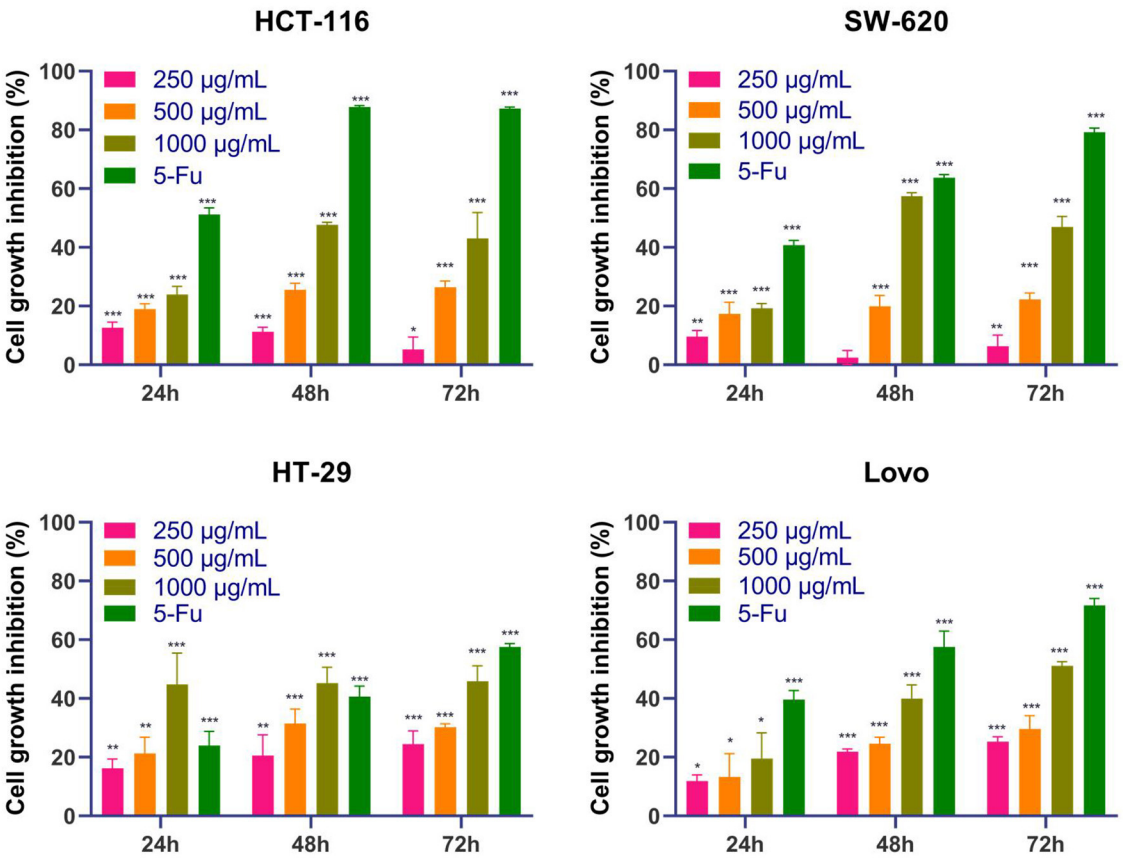

FIGURE 6 | Effects of DOME on the proliferation of CRC cell lines. The cell viability of HT-29, Lovo, SW-620, and HCT-116 cells treated with DOME for 24, 48, and 72 h were determined by MTT assay. The error bars represent SEM (*$P < 0.05$, **$P < 0.01$, ***$P < 0.001$, when compared with blank group).

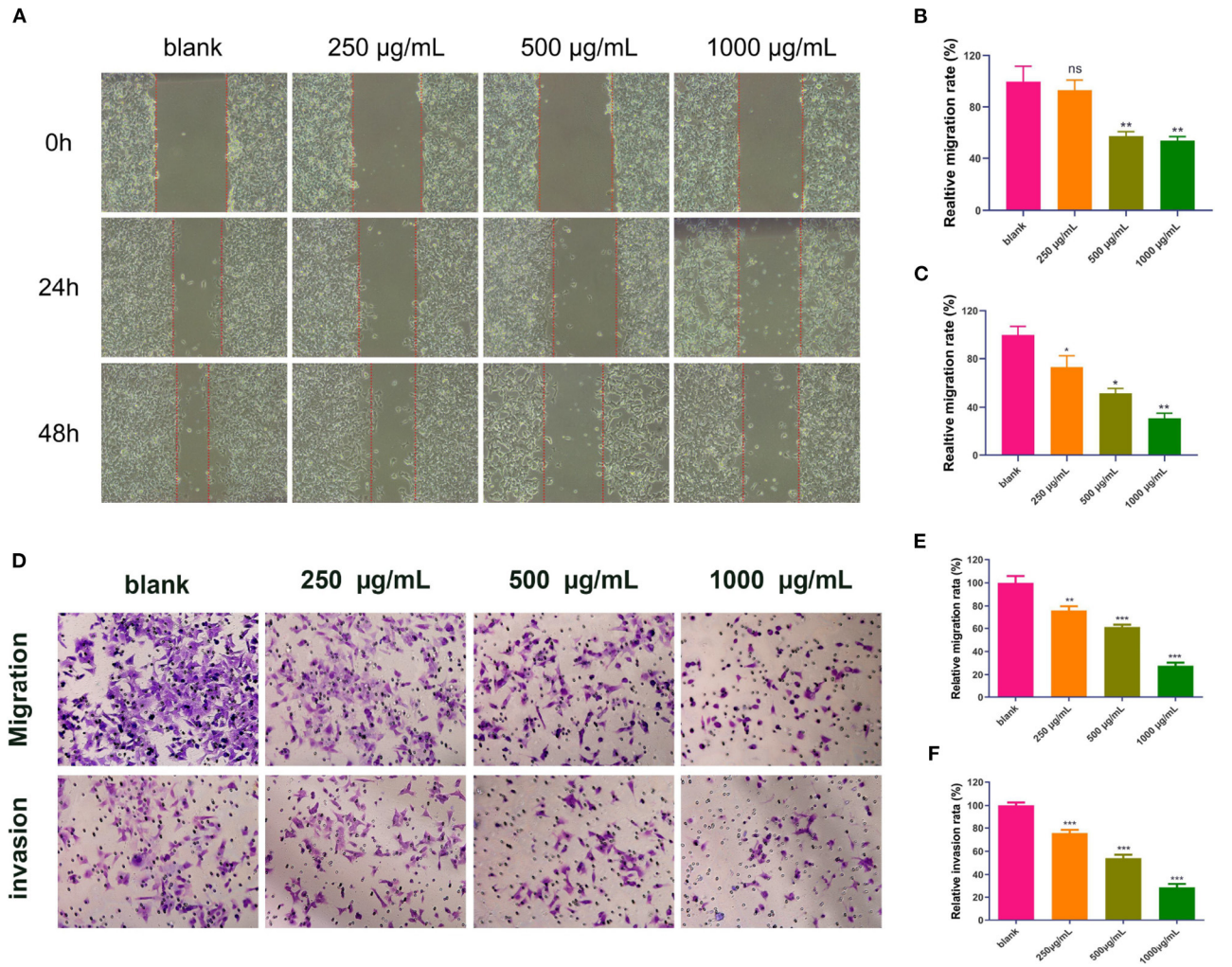

FIGURE 7 | DOME suppresses migration and invasion of Lovo cells. **(A)** Images of wound healing assay; quantification of wound healing assay in Lovo cells at 24 h **(B)** and 48 h **(C)**; **(D)** transwell assay in Lovo cells. **(E)** quantification of transwell migration assay in Lovo cells; **(F)** quantification of transwell invasion assay in Lovo cells. The error bars represent SEM (*$P < 0.05$, **$P < 0.01$, ***$P < 0.001$, when compared with the blank group).

as the key active components of *D. officinale*, while had not been identified in UPLC-ESI-MS/MS analysis. Overall, 92 active components of *D. officinale* were obtained. So, the in-house library totally acquired 396 active components. Subsequently, 116 putative targets were obtained by screening using the SwissADME online tools and SwissTargetPrediction databases. Then, 1,666 colon cancer-related targets were gathered from the DisGeNet database, OMIM database, GeneCards database, DrugBank database, and the TTD database (**Figure 2A**); 34 common targets were acquired after crossing 116 *D. officinale* active component targets with 1,666 CRC-related targets using VENNY 2.1 software.

Network pharmacology analysis results showed that the key active components mainly involved apigenin, naringenin, caffeic acid, γ-linolenic acid, α-linolenic acid, and cis-10-heptadecenoic acid, and the top six targets mainly involved ESR1, EGFR, PTGS2, MMP9, MMP2, and PPARG. These results involving key active components naringenin and caffeic acid were consistent with the literature report (36). The results of molecular docking suggested that the aforementioned key molecules are well-docked with important target proteins and have a good affinity, suggesting that *D. officinale* has high accuracy in the treatment of CRC (**Supplementary Table 7**). Moreover, the docking energy of apigenin with PTGS2 (−6.31 kJ/mol) was the lowest, followed by naringenin with PTGS2 (−6.20 kJ/mol), naringenin with MMP9 (−5.81 kJ/mol), and apigenin with MMP9 (−5.20 kJ/mol) (**Figure 5**), indicating that apigenin and naringenin in *D. officinale* were the most important active components, and PTGS2 and MMP9 were the most important targets that play the role of against CRC.

The finding that apigenin and naringenin were the most important active components is consistent with previous studies

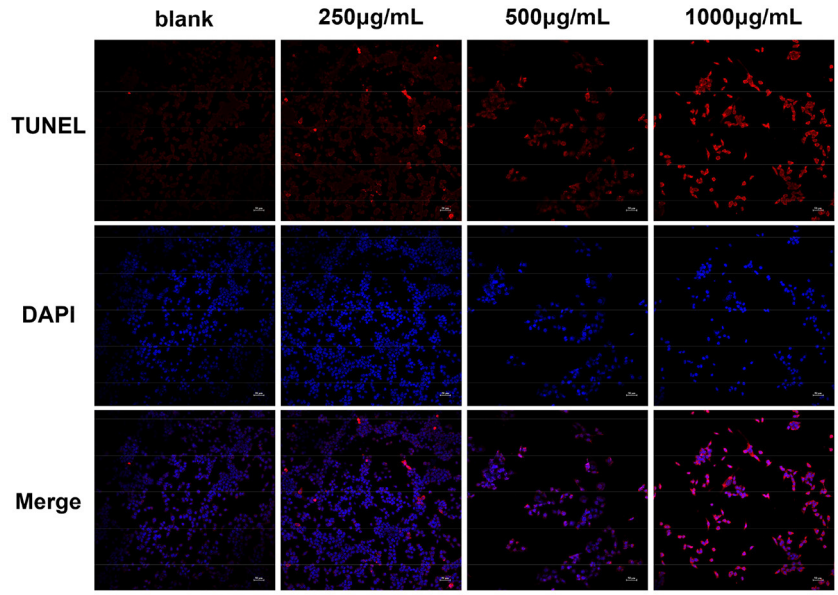

FIGURE 8 | Effect of DOME on cell apoptosis in Lovo cells. The cell apoptosis was determined using TUNEL assay, TUNEL-positive nuclei in red fluorescent color, and total nuclei staining with DAPI. Scale bar: 50 μm.

which have demonstrated that apigenin and naringenin have inhibitory effects against CRC (38–41). However, it is worth noting that the content of naringenin in *D. officinale* is much more than apigenin, consistent with a previous study (42). The study showed that the content of naringenin in *D. officinale* was generally higher, and the average mass fraction of the components reached 26.87 $\mu g \cdot g^{-1}$. Correspondingly, the component mass fraction of apigenin in *D. officinale* is $\leq 0.5\ \mu g \cdot g^{-1}$, it mainly exists in the form of flavonoid carbon glycosides, with apigenin as the core, rather than its free state (43–45). Therefore, naringenin might play a more important role than apigenin. However, there is also a possibility that the flavonoid carbon glycosides with apigenin as the nucleus degrade into free-state apigenin to exert anti-CRC effects.

MMP-2 and MMP-9 are important executors in cell migration and invasion (46, 47), and PTGS2 has been recognized to play an important role in regulating cell migration, invasion, and proliferation (48). In addition, in accordance with the results of molecular docking, a previous study has demonstrated that apigenin and naringenin can inhibit the invasion and migration of colon cancer cells by inhibiting the epithelial-to-mesenchymal transition (EMT) of CRC (49, 50). Hence, it could conceivably be hypothesized that the mechanism of *D. officinale* against CRC is closely related to the inhibition of tumor invasion and migration. The experiments of wound healing migration assay and transwell migration and invasion assay in this study further verified the conjecture. Despite these promising results, there were also some limitations to this research. We have not proven that apigenin and naringenin could exert anti-colon cancer effects *via* regulating PTGS2 and MMP9 with additional experiments in this study. The experimental evaluation was conducted only *in vitro*. Further *in vivo* animal experiments still need to be performed to confirm and validate these findings.

The GO and KEGG analysis results showed that the target proteins involved in the main pathways were "muscle cell proliferation (GO:0033002)," "regulation of inflammatory response (GO:0050727)," "cellular response to organic cyclic compound (GO:0071407)," "apoptotic signaling pathway (GO:0097190)," "regulation of protein localization to nucleus (GO:1900180)," "pathways in cancer" (hsa05200), "ovarian steroidogenesis" (has04913), and "microRNAs in cancer" (hsa05206) (**Figures 3A,D**). As shown in **Supplementary Figure 2**, the cancer-related KEGG pathways were determined as pathways related to the "pathways in cancer": PPAR signaling pathway, MAPK signaling pathway, calcium signaling pathway, cAMP signaling pathway, cytokine–cytokine receptor interaction, HIF-1 signaling pathway, cell cycle, p53 signaling pathway, mTOR signaling pathway, PI3K-Akt signaling pathway, apoptosis, Wnt signaling pathway, Notch signaling pathway, Hedgehog signaling pathway, TGF-beta signaling pathway, VEGF signaling pathway, focal adhesion, ECM–receptor interaction, adherens junction, JAK-STAT signaling pathway, and estrogen signaling pathway (51). Combined with the core protein targets analyzed in the previous network pharmacology (mainly ESR1, EGFR, PTGS2, MMP9, MMP2, PPARG, etc.), we speculate that the subcellular pathways that may play a role in inhibiting colon cancer proliferation, invasion, and migration are EGFR-associated signaling pathways (EGFR/Raf/MEK/ERK cascades) and PPAR signaling pathway. As shown in **Figure 4D**, "PPAR signaling pathway (hsa03320)" was also the eighth most enriched pathway in the KEGG pathway analysis. As shown in **Supplementary Figures 3**, **4**, combined with the protein targets screened in the previous network

pharmacology, we suppose miR-145 suppresses tumorigenesis and metastasis of the colorectal cancer cells by inhibiting the expression of EGFR. Dysregulation of specific miRNAs has been associated with certain types of cancer, where they may act as either oncogenes or tumor suppressors, depending on their target genes (52). For example, *in situ* hybridization detected accumulation of miR-145 in normal colon epithelia with no signal from adenocarcinomas cells. Loss of miR-145 in various tumors suggests its role as a tumor suppressor. miR-145 is downregulated in colorectal cancer (53, 54). In fact, miR-145 has been well-documented as a tumor suppressor gene in multiple tumor types because of its anti-proliferative and pro-apoptotic effects. Several reports suggest that miR-145 is a suppressor of metastasis. For example, miR-145 negatively regulates MUC1 and suppresses invasion and metastasis of breast cancer cells (55), and miR-145 suppresses proliferation, metastasis, and EMT of colorectal cancer *via* suppressing the EGFR-associated signaling pathway (56–58). In this study, other mechanisms in the aforementioned signal pathways might also play an important role. Further research is required to be performed to better understand the underlying mechanisms.

CONCLUSION

In conclusion, the present results demonstrated that the core active components are apigenin and naringenin, and the core targets are PTGS2 and MMP-9 when *D. officinale* exerts antitumor effects on CRC through a combination of network pharmacology, metabolomics, and molecular docking. Moreover, the apoptotic signaling pathway and inhibition of tumor invasion and migration signaling pathway had been validated to play a vital role in *D. officinale* against CRC. Our findings provided valuable insights into exploring the mechanism of action of *D. officinale* against CRC.

DATA AVAILABILITY STATEMENT

The datasets presented in this study can be found in online repositories. The names of the repository/repositories and accession number(s) can be found at: MetaboLights; MTBLS4678.

AUTHOR CONTRIBUTIONS

ST: conceptualization, data curation, writing—original draft preparation, writing—review and editing, and visualization. ST, JL, and HW: methodology and validation. ST, RH, and ZR: software. ST and HW: formal analysis. ST, SD, and WH: investigation. GW: resources, supervision, project administration, and funding acquisition. All authors contributed to the article and approved the submitted version.

FUNDING

This work was supported by the Innovation project of Dendrobium truth-seeking in Guangzhou University of Traditional Chinese Medicine (No. 2019shqz0209801), the 2018 Shaoguan City Science and Technology Plan Project: Special Project of Industry-University-Research Cooperation (No. 2018CS11919), and the 2019 Guangdong Province Special Fund for Science and Technology (Big project + task list) Project: Ecological Cultivation and Sustainable Utilization of Danxia *Dendrobium officinale*, a rare Southern Medicine in Guangdong Province (Nos. 2019gdskjzxzj-zt3-2 and 210316166270419).

SUPPLEMENTARY MATERIAL

The Supplementary Material for this article can be found online at: https://www.frontiersin.org/articles/10.3389/fmed.2022.879986/full#supplementary-material

REFERENCES

1. Tao S, Huang C, Tan Z, Duan S, Zhang X, Ren Z, et al. Effect of the polysaccharides derived from *Dendrobium officinale* stems on human HT-29 colorectal cancer cells and a zebrafish model. *Food Biosci.* (2021) 41:100995. doi: 10.1016/j.fbio.2021.100995
2. Ng TB, Liu J, Wong JH, Ye X, Wing Sze SC, Tong Y, et al. Review of research on Dendrobium, a prized folk medicine. *Appl Microbiol Biotechnol.* (2012) 93:1795–803. doi: 10.1007/s00253-011-3829-7
3. Liang J, Chen S, Chen J, Lin J, Xiong Q, Yang Y, et al. Therapeutic roles of polysaccharides from *Dendrobium officinale*on colitis and its underlying mechanisms. *Carbohydr Polymers.* (2018) 185:159–68. doi: 10.1016/j.carbpol.2018.01.013
4. Luo D, Qu C, Zhang Z, Xie J, Xu L, Yang H, et al. Granularity and laxative effect of ultrafine powder of *Dendrobium officinale*. *J Med Food.* (2017) 20:180–8. doi: 10.1089/jmf.2016.3827
5. Zhang K, Zhou X, Wang J, Zhou Y, Qi W, Chen H, et al. *Dendrobium officinale* polysaccharide triggers mitochondrial disorder to induce colon cancer cell death *via* ROS-AMPK-autophagy pathway. *Carbohydr Polymers.* (2021) 264:118018. doi: 10.1016/j.carbpol.2021.118018
6. Tao S, Ren Z, Yang Z, Duan S, Wan Z, Huang J, et al. Effects of different molecular weight polysaccharides from *Dendrobium officinale* Kimura & Migo on human colorectal cancer and transcriptome analysis of differentially expressed genes. *Front Pharmacol.* (2021) 12:704486. doi: 10.3389/fphar.2021.704486
7. Liang J, Li H, Chen J, He L, Du X, Zhou L, et al. *Dendrobium officinale* polysaccharides alleviate colon tumorigenesis *via* restoring intestinal barrier function and enhancing anti-tumor immune response. *Pharmacol Res.* (2019) 148:104417. doi: 10.1016/j.phrs.2019.104417
8. Li G, Sun P, Zhou Y, Zhao X, Chen F. Preventive effects of *Dendrobium candidum* Wall ex Lindl. on the formation of lung metastases in BALB/c mice injected with 26-M3.1 colon carcinoma cells. *Oncol Lett.* (2014) 8:1879–85. doi: 10.3892/ol.2014.2383
9. Wang Q, Sun P, Li G, Zhu K, Wang C, Zhao X. Inhibitory effects of *Dendrobium candidum* Wall ex Lindl. on azoxymethane- and dextran sulfate sodium-induced colon carcinogenesis in C57BL/6 mice. *Oncol Lett.* (2014) 7:493–8. doi: 10.3892/ol.2013.1728
10. Zhao X, Sun P, Qian Y, Suo H. *D. candidum* has *in vitro* anticancer effects in HCT-116 cancer cells and exerts *in vivo* anti-metastatic effects in mice. *Nutr Res Pract.* (2014) 8:487–93. doi: 10.4162/nrp.2014.8.5.487

11. Tao S, Lei Z, Huang K, Li Y, Ren Z, Zhang X, et al. Structural characterization and immunomodulatory activity of two novel polysaccharides derived from the stem of *Dendrobium officinale* Kimura et Migo. *J Funct Foods.* (2019) 57:121–34. doi: 10.1016/j.jff.2019.04.013
12. Yue H, Zeng H, Ding K. A review of isolation methods, structure features and bioactivities of polysaccharides from Dendrobium species. *Chin J Natural Med.* (2020) 18:1–27. doi: 10.1016/S1875-5364(20)30001-7
13. Zhiyao Ren, Xiaoyu Ji, Zhenbin Jiao, Yingyi Luo, Guo-Qiang Zhang, ShengchangTao, et al. Functional analysis of a novel C-glycosyltransferase in the orchid Dendrobium catenatum. *Horticult Res.* (2020) 7:1–18. doi: 10.1038/s41438-020-0330-4
14. Chen Y, Wang Y, Lyu P, Chen L, Shen C, Sun C. Comparative transcriptomic analysis reveal the regulation mechanism underlying MeJA-induced accumulation of alkaloids in *Dendrobium officinale*. *J Plant Res.* (2019) 132:419–29. doi: 10.1007/s10265-019-01099-6
15. Nie SP, Cui SW, Xie MY. *Glucomannans From Dendrobium officinale and Aloe. Bioactive Polysaccharides*. Elsevier Inc. (2018). p. 295–347.
16. Tang H, Zhao T, Sheng Y, Zheng T, Fu L, Zhang Y. *Dendrobium officinale* Kimura et Migo: a review on its ethnopharmacology, phytochemistry, pharmacology, and industrialization. *Evid Based Complement Altern Med.* (2017) 2017:7436259. doi: 10.1155/2017/7436259
17. Ma Y, Zhou K, Fan J, Sun S. Traditional Chinese medicine: potential approaches from modern dynamical complexity theories. *Front Med.* (2016) 10:28–32. doi: 10.1007/s11684-016-0434-2
18. Zhao J, Tian S, Lu D, Yang J, Zeng H, Zhang F, et al. Systems pharmacological study illustrates the immune regulation, anti-infection, anti-inflammation, and multi-organ protection mechanism of Qing-Fei-Pai-Du decoction in the treatment of COVID-19. *Phytomedicine.* (2021) 85:153315. doi: 10.1016/j.phymed.2020.153315
19. Ren L, Zheng X, Liu J, Li W, Fu W, Tang Q, et al. Network pharmacology study of traditional Chinese medicines for stroke treatment and effective constituents screening. *J Ethnopharmacol.* (2019) 242:112044. doi: 10.1016/j.jep.2019.112044
20. Zineh I. Quantitative systems pharmacology: a regulatory perspective on translation. *CPT Pharmacometr Syst Pharmacol.* (2019) 8:336–9. doi: 10.1002/psp4.12403
21. Ma YM, Zhang XZ, Su ZZ, Li N, Cao L, Ding G, et al. Insight into the molecular mechanism of a herbal injection by integrating network pharmacology and *in vitro*. *J Ethnopharmacol.* (2015) 173:91–9. doi: 10.1016/j.jep.2015.07.016
22. Li S, Zhang B. Traditional Chinese medicine network pharmacology: theory, methodology and application. *Chin J Natural Med.* (2013) 11:110–20. doi: 10.1016/S1875-5364(13)60037-0
23. Cao S, Han Y, Li Q, Chen Y, Zhu D, Su Z, et al. Mapping pharmacological network of multi-targeting Litchi ingredients in cancer therapeutics. *Front Pharmacol.* (2020) 11:451. doi: 10.3389/fphar.2020.00451
24. Chen W, Gong L, Guo Z, Wang W, Zhang H, Liu X, et al. A novel integrated method for large-scale detection, identification, and quantification of widely targeted metabolites: application in the study of rice metabolomics. *Mol Plant.* (2013) 6:1769–80. doi: 10.1093/mp/sst080
25. Chen L, Wu Q, He W, He T, Wu Q, Miao Y. Combined *de novo* transcriptome and metabolome analysis of common bean response to *Fusarium oxysporum* f. sp. phaseoli infection. *Int J Mol Sci.* (2019) 20:6278. doi: 10.3390/ijms20246278
26. Gfeller D, Grosdidier A, Wirth M, Daina A, Michielin O, Zoete V. SwissTargetPrediction: a web server for target prediction of bioactive small molecules. *Nucleic Acids Res.* (2014) 42:W32–8. doi: 10.1093/nar/gku293
27. Szklarczyk D, Gable AL, Lyon D, Junge A, Wyder S, Huerta-Cepas J, et al. STRING v11: protein-protein association networks with increased coverage, supporting functional discovery in genome-wide experimental datasets. *Nucleic Acids Res.* (2019) 47:D607–13. doi: 10.1093/nar/gky1131
28. Zhou Y, Zhou B, Pache L, Chang M, Khodabakhshi AH, Tanaseichuk O, et al. Metascape provides a biologist-oriented resource for the analysis of systems-level datasets. *Nat Commun.* (2019) 10:1523. doi: 10.1038/s41467-019-09234-6
29. Smoot ME, Ono K, Ruscheinski J, Wang PL, Ideker T. Cytoscape 2.8: new features for data integration and network visualization. *Bioinformatics.* (2011) 27:431–2. doi: 10.1093/bioinformatics/btq675
30. Shannon P, Markiel A, Ozier O, Baliga NS, Wang JT, Ramage D, et al. Cytoscape: a software environment for integrated models of biomolecular interaction networks. *Genome Res.* (2003) 13:2498–504. doi: 10.1101/gr.1239303
31. Assenov Y, Ramirez F, Schelhorn SE, Lengauer T, Albrecht M. Computing topological parameters of biological networks. *Bioinformatics.* (2008) 24:282–4. doi: 10.1093/bioinformatics/btm554
32. Warnecke A, Sandalova T, Achour A, Harris RA. PyTMs: a useful PyMOL plugin for modeling common post-translational modifications. *BMC Bioinformatics.* (2014) 15:370. doi: 10.1186/s12859-014-0370-6
33. Zhang ZJ, Wu WY, Hou JJ, Zhang LL, Li FF, Gao L, et al. Active constituents and mechanisms of Respiratory Detox Shot, a traditional Chinese medicine prescription, for COVID-19 control and prevention: network-molecular docking-LC-MS(E) analysis. *J Integr Med.* (2020) 18:229–41. doi: 10.1016/j.joim.2020.03.004
34. Ge Q, Chen L, Yuan Y, Liu L, Feng F, Lv P, et al. Network pharmacology-based dissection of the anti-diabetic mechanism of *Lobelia chinensis*. *Front Pharmacol.* (2020) 11:347. doi: 10.3389/fphar.2020.00347
35. Jin KT, Chen B, Liu YY, Lan HU, Yan JP. Monoclonal antibodies and chimeric antigen receptor (CAR) T cells in the treatment of colorectal cancer. *Cancer Cell Int.* (2021) 21:83. doi: 10.1186/s12935-021-01763-9
36. Wei L, Dong W, Han Z, Chen C, Jin Q, He J, et al. Network pharmacologic analysis of *Dendrobium officinale* extract inhibiting the proliferation of gastric cancer cells. *Front Pharmacol.* (2022) 13:832134. doi: 10.3389/fphar.2022.832134
37. Pan B, Wang Y, Wu C, Jia J, Huang C, Fang S, et al. A mechanism of action study on Danggui Sini decoction to discover its therapeutic effect on gastric cancer. *Front Pharmacol.* (2020) 11:592903. doi: 10.3389/fphar.2020.592903
38. Memariani Z, Abbas SQ, Ul Hassan SS, Ahmadi A, Chabra A. Naringin and naringenin as anticancer agents and adjuvants in cancer combination therapy: efficacy and molecular mechanisms of action, a comprehensive narrative review. *Pharmacol Res.* (2021) 171:105264. doi: 10.1016/j.phrs.2020.105264
39. Wang L, Zeng W, Wang L, Wang Z, Yin X, Qin Y, et al. Naringenin enhances the antitumor effect of therapeutic vaccines by promoting antigen cross-presentation. *J Immunol.* (2020) 204:622–31. doi: 10.4049/jimmunol.1900278
40. Li C, Lin D, Fu X, Zhang L, Fan Q, Liu Y, et al. Apigenin up-regulates transgelin and inhibits invasion and migration of colorectal cancer through decreased phosphorylation of AKT. *J Nutr Biochem.* (2013) 24:1766–75. doi: 10.1016/j.jnutbio.2013.03.006
41. Yang C, Song J, Hwang S, Choi J, Song G, Lim W. Apigenin enhances apoptosis induction by 5-fluorouracil through regulation of thymidylate synthase in colorectal cancer cells. *Redox Biol.* (2021) 47:102144. doi: 10.1016/j.redox.2021.102144
42. Lv C, Yang J, Kang C, Li Z, Guo L, Wang Y. Determination of 10 flavonoids by UPLC-MS /MS and analysis of polysaccharide contents and compositions in Dendrobii Officinalis Caulis from different habitats. *Chin J Exp Trad Med Formulae.* (2017) 23:47–52.
43. Zhou C, Xie Z, Lei Z, Huang Y, Wei G. Simultaneous identification and determination of flavonoids in *Dendrobium officinale*. *Chem Cent J.* (2018) 12:40. doi: 10.1186/s13065-018-0403-8
44. Ye Z, Dai JR, Zhang CG, Lu Y, Wu LL, Gong AGW, et al. Chemical differentiation of *Dendrobium officinale* and *Dendrobium devonianum* by using HPLC fingerprints, HPLC-ESI-MS, and HPTLC analyses. *Evid Based Complement Altern Med.* (2017) 2017:8647212. doi: 10.1155/2017/8647212
45. Zhang Y, Zhang L, Liu J, Liang J, Si J, Wu S. *Dendrobium officinale* leaves as a new antioxidant source. *J Funct Foods.* (2017) 37:400–15. doi: 10.1016/j.jff.2017.08.006
46. Muscella A, Vetrugno C, Cossa LG, Marsigliante S. TGF-beta1 activates RSC96 Schwann cells migration and invasion through MMP-2 and MMP-9 activities. *J Neurochem.* (2020) 153:525–38. doi: 10.1111/jnc.14913
47. Kalhori V, Tornquist K. MMP2 and MMP9 participate in S1P-induced invasion of follicular ML-1 thyroid cancer cells. *Mol Cell Endocrinol.* (2015) 404:113–22. doi: 10.1016/j.mce.2015.01.037
48. Cui HY, Wang SJ, Song F, Cheng X, Nan G, Zhao Y, et al. CD147 receptor is essential for TFF3-mediated signaling regulating colorectal

cancer progression. *Signal Transduct Target Ther.* (2021) 6:268. doi: 10.1038/s41392-021-00677-2
49. Tong J, Shen Y, Zhang Z, Hu Y, Zhang X, Han L. Apigenin inhibits epithelial-mesenchymal transition of human colon cancer cells through NF-kappaB/Snail signaling pathway. *Biosci Rep.* (2019) 39:BSR20190452. doi: 10.1042/BSR20190452
50. Shi X, Luo X, Chen T, Guo W, Liang C, Tang S, et al. Naringenin inhibits migration, invasion, induces apoptosis in human lung cancer cells and arrests tumour progression *in vitro*. *J Cell Mol Med.* (2021) 25:2563–71. doi: 10.1111/jcmm.16226
51. Ulgen E, Sezerman OU. driveR: a novel method for prioritizing cancer driver genes using somatic genomics data. *BMC Bioinformatics.* (2021) 22:263. doi: 10.1186/s12859-021-04203-7
52. Matthias Eder, Scherr M. MicroRNA and lung cancer. *N Engl J Med.* (2005) 352:2446–8. doi: 10.1056/NEJMcibr051201
53. Bandres E, Cubedo E, Agirre X, Malumbres R, Zarate R, Ramirez N, et al. Identification by Real-time PCR of 13 mature microRNAs differentially expressed in colorectal cancer and non-tumoral tissues. *Mol Cancer.* (2006) 5:29. doi: 10.1186/1476-4598-5-29
54. Kitade Y, Akao Y. MicroRNAs and their therapeutic potential for human diseases: microRNAs, miR-143 and−145, function as anti-oncomirs and the application of chemically modified miR-143 as an anti-cancer drug. *J Pharmacol Sci.* (2010) 114:276–80. doi: 10.1254/jphs.10R12FM
55. Sachdeva M, Mo YY. MicroRNA-145 suppresses cell invasion and metastasis by directly targeting mucin 1. *Cancer Res.* (2010) 70:378–87. doi: 10.1158/0008-5472.CAN-09-2021
56. Chen Q, Zhou L, Ye X, Tao M, Wu J. miR-145-5p suppresses proliferation, metastasis and EMT of colorectal cancer by targeting CDCA3. *Pathol Res Pract.* (2020) 216:152872. doi: 10.1016/j.prp.2020.152872
57. Guocheng Huang, Benlin Wei, Zebo Chen, Jingyao Wang, Liwen Zhao, Xiqi Peng, et al. Identification of a four-microRNA panel in serum as promising biomarker for colorectal carcinoma detection. *Biomark Med.* (2020) 14:749–60. doi: 10.2217/bmm-2019-0605
58. Niu Y, Zhang J, Tong Y, Li J, Liu B. miR-145-5p restrained cell growth, invasion, migration and tumorigenesis *via* modulating RHBDD1 in colorectal cancer *via* the EGFR-associated signaling pathway. *Int J Biochem Cell Biol.* (2019) 117:105641. doi: 10.1016/j.biocel.2019.105641

Conflict of Interest: The authors declare that the research was conducted in the absence of any commercial or financial relationships that could be construed as a potential conflict of interest.

Publisher's Note: All claims expressed in this article are solely those of the authors and do not necessarily represent those of their affiliated organizations, or those of the publisher, the editors and the reviewers. Any product that may be evaluated in this article, or claim that may be made by its manufacturer, is not guaranteed or endorsed by the publisher.

Copyright © 2022 Tao, Li, Wang, Ding, Han, He, Ren and Wei. This is an open-access article distributed under the terms of the Creative Commons Attribution License (CC BY). The use, distribution or reproduction in other forums is permitted, provided the original author(s) and the copyright owner(s) are credited and that the original publication in this journal is cited, in accordance with accepted academic practice. No use, distribution or reproduction is permitted which does not comply with these terms.

frontiers | Frontiers in Oncology

ORIGINAL RESEARCH
published: 01 July 2022
doi: 10.3389/fonc.2022.934045

Diagnostic Performance of LI-RADS Version 2018 for Primary Liver Cancer in Patients With Liver Cirrhosis on Enhanced MRI

Xinai Liu[1,2,3,4†], *Xiaoyan Ni*[2,3,4†], *Yubo Li*[1,2,3,4†], *Chun Yang*[2,3,4], *Yi Wang*[2,4], *Chunzheng Ma*[5*], *Changwu Zhou*[2,3,4*] *and Xin Lu*[2,3,4*]

[1] Department of Magnetic Resonance Imaging (MRI), Henan Provincial Hospital of Traditional Chinese Medicine (The Second Affiliated Hospital of Henan University of Traditional Chinese Medicine), Zhengzhou, China, [2] Department of Radiology, Zhongshan Hospital, Fudan University, Shanghai, China, [3] Shanghai Institute of Medical Imaging, Shanghai, China, [4] Department of Cancer Center, Zhongshan Hospital, Fudan University, Shanghai, China, [5] Department of Oncology, Henan Provincial Hospital of Traditional Chinese Medicine, Zhengzhou, China

OPEN ACCESS

Edited by:
Sanjit Mukherjee,
National Institutes of Health (NIH),
United States

Reviewed by:
Leonardo Centonze,
Niguarda Ca' Granda
Hospital, Italy
Roberto Cannella,
University of Palermo, Italy

***Correspondence:**
Xin Lu
luxcn@163.com
Changwu Zhou
changwu83@163.com
Chunzheng Ma
mchzh666@126.com

[†]These authors have contributed equally to this work

Specialty section:
This article was submitted to Gastrointestinal Cancers: Hepato Pancreatic Biliary Cancers, a section of the journal Frontiers in Oncology

Received: 02 May 2022
Accepted: 02 June 2022
Published: 01 July 2022

Citation:
Liu X, Ni X, Li Y, Yang C, Wang Y, Ma C, Zhou C and Lu X (2022) Diagnostic Performance of LI-RADS Version 2018 for Primary Liver Cancer in Patients With Liver Cirrhosis on Enhanced MRI. Front. Oncol. 12:934045. doi: 10.3389/fonc.2022.934045

Purpose: The study evaluated the diagnostic performance of the Liver Imaging Reporting and Data System (LI-RADS) version 2018 for differentiating hepatocellular carcinoma (HCC) from primary liver cancer in patients with liver cirrhosis based on the updated 2019 WHO classification.

Materials and Methods: From 2016 to 2021, 300 patients with surgically confirmed primary liver cancer (PLC) and liver cirrhosis based on the updated 2019 WHO classification were eligible for this retrospective study (100 cases in each of three groups including HCC, ICC, and cHCC-CCA). Two radiologists were blinded to the final diagnosis and independently assigned an LI-RADS category to each liver nodule. The diagnostic performances of the LR-5 category (definitely HCC), and the LR-M category (probably or definitely malignant, but not specific for HCC) were calculated in overall and small observations (<20 mm). Comparisons between groups of categorical variables were performed by one-way analysis of variance and the Chi-squared or Fisher's exact test.

Results: The mean age of 300 patients (226 men and 74 women) was 57.40 ± 11.05 years. The sensitivity and specificity of the LR-5 category for differentiating HCCs from other primary liver cancers were 81% (81 of 100) and 82% (164 of 200), respectively. The LR-M category had a sensitivity of 63% (126 of 200) for diagnosing non-HCCs (ICCs and cHCC-CCAs), with a specificity of 90% (90 of 100). The LR-5 category had a sensitivity of 82.5% (33 of 40) for diagnosing HCCs in small observations (<20 mm) with a specificity of 76.6% (59 of 77). On the contrary, LR-M demonstrated slightly higher specificity (93.8%) and sensitivity (73.8%) for diagnosing non-HCCs with tumor size <20 mm.

Conclusion: The LR-5 category as well as the LR-M category of Liver Imaging Reporting and Data System (LI-RADS) version 2018 can effectively distinguish hepatocellular

carcinoma from other primary hepatic malignancies in patients with liver cirrhosis, especially for small observations (<20 mm).

Keywords: hepatocellular carcinoma (HCC), primary liver cancer (PLC), cirrhosis, LI-RADS, combined hepatocellular-cholangiocarcinoma (cHCC-CC), intrahepatic cholangiocarcinoma (ICC)

INTRODUCTION

Primary liver cancer (PLC) is the fourth most common malignant tumor and the second leading cause of cancer-related death worldwide (1, 2), which seriously threatens the life and health of cirrhotic patients. Primary liver cancer mainly includes three pathological types: hepatocellular carcinoma (HCC), intrahepatic cholangiocarcinoma (ICC), and combined hepatocellular-cholangiocarcinoma (cHCC-CCA). Compared with other liver malignancies that require pathological confirmation, HCC can be diagnosed by non-invasive preoperative imaging features in at-risk patients (3).

The Liver Imaging Reporting and Data System (LI-RADS), as a comprehensive system for standardizing the terminology, technique, interpretation, reporting, and data collection of liver imaging in patients at risk of HCC, is being increasingly adapted by many academic and nonacademic clinical practices (4, 5). The latest v2018 LI-RADS has been released by adjusting the LR-5 criteria and threshold growth definition (size increase of a mass by 50% in 6 months) to be concordant with the American Association for the Study of Liver Diseases (AASLD) guidance for the definite diagnosis and management of HCC (6, 7). Despite the low incidence of ICC and cHCC-CCA, when ICC and cHCC-CCA exhibit similar risk factors to HCC, including cirrhosis and chronic viral hepatitis (8, 9), the distinction between non-HCC and HCC is important in terms of treatment and prognosis (6).

A recent investigation demonstrated the performance of LI-RADS 2017 for diagnosing HCC in patients with cirrhosis on MRI with gadoxetate disodium contrast agent (10). Although several studies (6, 7, 11, 12) have examined the performance of LI-RADS 2018 in patients at risk of HCC, these studies have yielded inconsistent results and were hampered by small patient populations and gadoxetate disodium contrast agent. Moreover, with the continuous feedback of user experience, the 2019 WHO classification (13) revised the definition and category of combined hepatocellular cholangiocarcinoma (cHCC-CCA) (14). The 2019 WHO classification (13) revised the diagnostic term for biphenotypic PLCs by including a list of all tumor components (15) and abandoned subtype classifications of typical HCCs or CCAs expressed by immunohistochemical stem cell markers and cholangiolocarcinomas (CLC) without an HCC component in subtypes with stem cell features (14).

Therefore, the main purpose is to evaluate the performance of LI-RADS 2018 for primary liver cancer in the background of liver cirrhosis on MRI combined with extracellular contrast agents based on the updated 2019 WHO classification and whether its efficacy also applies to small liver tumors (<20 mm).

MATERIALS AND METHODS

Study Population

This retrospective study was approved by the institutional review board of our institution with a waiver of the written informed consent requirement. From January 2016 to November 2021, patients with either cHCC-CCA or ICC who met the following

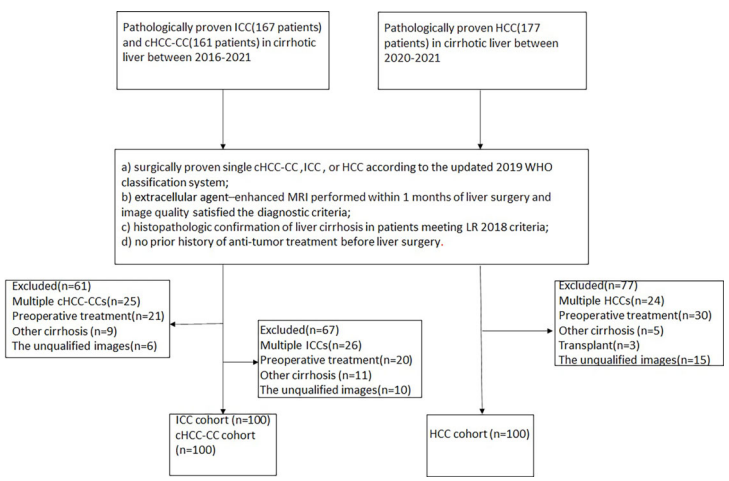

FIGURE 1 | Flowchart of the study cohort. HCC, hepatocellular carcinoma; ICC, intrahepatic cholangiocarcinoma; cHCC-CCA, combined hepatocellular carcinomacholangiocarcinoma.

criteria were enrolled: a) surgically proven single cHCC-CCA or ICC according to the updated 2019 WHO classification system; b) extracellular agent–enhanced MRI performed within 1 month of liver surgery and image quality satisfied the diagnostic criteria; c) histopathologic confirmation of liver cirrhosis in patients meeting the LR 2018 criteria; and d) no prior history of anti-tumor treatment before liver surgery. HCC patients meeting the above categories were selected at random during the latter 1 year of the study period (between 2020 and 2021). Ultimately, 300 patients were enrolled in this study, namely, 100 HCC, 100 ICC, and 100 cHCC-CCA patients. All patients had Child–Pugh class A cirrhosis. The flowchart of patient enrollment is provided in **Figure 1**.

Clinical Data Evaluation

The clinical data of the patients were retrospectively analyzed, namely, age, gender, HBV infection status, serum alpha-fetoprotein within 7 days before surgery (alpha fetoprotein, AFP), carcinoembryonic antigen (carcinoembryonic antigen, CEA) and carbohydrate antigen 19-9 (carbohydrate antigen 19-9, CA19-9), the critical value of AFP, CEA, and CA19-9. The cutoff values were 20 ng/ml, 5 ng/ml, and 37 U/ml, respectively.

MRI Acquisition

All patients were scanned with a 1.5-T MR scanner (uMR 560, United Imaging Healthcare) equipped with a 24-channel body array coil. Routine liver protocols consist of transverse T2-weighted imaging with fat-suppressed fast spin-echo sequence (T2WI), T1WI breath-hold in-phase and opposed-phase sequences, and diffusion-weighted imaging (DWI, b value = 0, 50, and 500 s/mm^2). Dynamic imaging was performed using a T1-weighted fat-suppressed breath-hold sequence. The arterial phase was acquired at 10–14 s when the contrast agent (gadolinium diethylenetriamine pentaacetic acid, Gd-DTPA; Magnevist, Bayer HealthCare) was administered in a vein at a dose of 0.1 mmol/kg at a rate of 2 ml/s. The portal venous phase and delayed phase sequences were acquired at 70–90 s and 160–180 s, respectively.

Image Feature Analysis

All MR images were retrospectively evaluated by two radiologists (CWZ and CY, who have 12 and 14 years of experience in abdominal imaging, respectively), who were blinded to the specific results of the pathological examination but were informed of the presence of tumor. They independently assigned an LI-RADS category to each nodule. All observers had access to all imaging studies through picture archiving and communication systems (PACS) from our institutions. A consensus was reached by discussion when there was disagreement between the two observers.

LI-RADS Major Features and Targetoid Mass Features

The following imaging characteristics of lesions were investigated on MR images according to LI-RADS version 2018 (8): nodule size, location, and presence or absence of major features (nonrim arterial phase hyperenhancement (APHE), non-peripheral washout, and enhancing capsule), and targetoid mass features (APHE), peripheral washout, delayed central enhancement, and targetoid restriction).

Ancillary Imaging Features

The ancillary imaging features in our study combined a part of LI-RADS 2018 ancillary and additional features (particularly prone to malignancy, not HCC) not included in the LI-RADS 2018 algorithm, which are beneficial for differential diagnosis according to the available literature (16, 17) and our clinical experience. The following ancillary imaging features favoring HCC were evaluated: a) nodule-in-nodule: smaller nodule with different imaging signs appeared in the mass; b) mosaic architecture: the interior of the mass was divided into multiple heterogeneous nodules or compartments, usually showed heterogeneous signal on T2WI; c) fat in mass: signal intensity reduced on T1WI opposed-phase images versus T1WI in-phase images; and d) blood products in mass: hyperintense on T1WI in- and opposed-phase images and hyperintense or heterogeneous on T2WI. Additionally, these other ancillary features favoring malignancy, not HCC in particular, based on the literature and experience were also evaluated: a) restricted diffusion: intensity on DWI, not attributable solely to T2 shine-through; b) mild-moderate T2 hyperintensity; c) peritumoral biliary dilatation; d) liver surface retraction: the liver surface was retracted by adjacent tumors; and e) corona enhancement: peri-observational enhancement in late arterial phase or early PVP attributable to venous drainage from tumor.

The radiologists assigned a LI-RADS category to each nodule. Nodules were classified as category LR-3 (intermediate probability of HCC), LR-4 (probably HCC), LR-5 (definitely HCC), LR-M (probably malignant, not specific for HCC), or LR-TIV (nodule with a definite tumor in the vein). Threshold growth was excluded because our study had only one preoperative MRI examination.

Statistical Analysis

Statistical analyses were performed using SPSS 26.0 (IBM). Continuous variables were expressed as mean ± standard deviation or median (interquartile range), while categorical variables were expressed as numbers and percentages. Inter-observer agreement of categorical variables was estimated by calculating Cohen's kappa statistics (0.0–0.2, poor; 0.2–0.4, fair; 0.4–0.6, moderate; 0.6–0.8, substantial; 0.8–1.0, perfect). Comparisons between groups of categorical variables were performed by one-way analysis of variance and the Chi-squared or Fisher's exact test.

RESULTS

Patient Clinical Data

The clinical characteristics of the 300 patients (226 men [mean age, 56.69 ± 11.21 years] and 74 women [mean age, 59.57 ± 10.34 years]; overall mean age, 57.40 ± 11.05 years) are summarized in **Table 1**. The cHCC-CCA cohort had a younger age and a smaller size than the ICC and HCC cohorts, and the differences were statistically

TABLE 1 | Clinical and pathological characteristics of study patients.

Variable	HCC (n = 100)	CHCC-CCA (n = 100)	ICC (n = 100)	P-value
Mean age (y) *	57.33 ± 10.85	54.8 ± 11.02	60.06 ± 10.76	0.001
All patients				0.24
Men	81	74	71	
Women	19	26	29	
Mean nodule size (mm) *	4.33 ± 3.21	3.82 ± 2.82	4.83 ± 2.81	0.22
Cause of cirrhosis				0.608
Hepatitis B	94	90	88	
Hepatitis C	4	6	6	
Alcoholism	2	4	6	
Tumor maker value				
AFP (≥20 ng/ml)	56	53	14	0.00
CEA (≥5 ng/ml)	7	13	14	0.24
CA 19-9 (≥37 U/ml)	11	24	42	0.00

Except where indicated, data are numbers of patients.
AFP, a-fetoprotein; CEA, carcinoembryonic antigen; CA 19-9, carbohydrate antigen 19-9; CHCC-CC, combined hepatocellular-cholangiocarcinoma; HCC, hepatocellular carcinoma; ICC, intrahepatic cholangiocarcinoma.
** Data are means ± standard deviations.*

significant (P = 0.001, 0.017, respectively). In all three groups, hepatitis B virus was the most common cause of liver cirrhosis. The CA19-9 >37 U/ml was more often in the ICC patients than in the cHCC-CCA or ICC patients, while the AFP >20 ng/ml was more often in the HCC and cHCC-CCA than ICC (all P<0.001).

MR Imaging Features

Table 2 summarizes the MRI features of HCCs, cHCC-CCAs, and ICCs. The three major features—nonrim APHE, non-peripheral washout, and enhancing capsule—were most frequently noted in HCCs (94, 86, and 82%, respectively), followed by cHCC-CCAs and ICCs (all P <0.001). The targetoid mass features—rim APHE, peripheral washout, delayed central enhancement, and targetoid restriction—were most common in ICC (78, 26, 74, and 27%, respectively), followed by cHCC-CCA and HCC (all P <0.001).

Fat in mass was more frequently noted in HCC (21% [21 of 100]) than in the other two cohorts (P <0.001), whereas liver surface retraction and corona enhancement were more common in ICC (40% [40 of 100], 43% [43 of 100]) than in the other two cohorts (P <0.001). Compared with HCC, peritumoral biliary dilatation was more common in cHCC-CCA and ICC (30 and 29%, respectively), and the differences were statistically significant (P <.001). Additionally, mosaic architecture-

TABLE 2 | Imaging characteristics of hepatic tumors in cirrhotic liver at gadopentetate acid-enhanced MRI.

Variable	HCC (n = 100)	CHCC-CC (n = 100)	ICC (n = 100)	P-value	Kappa value
Nodule size				0.036	
<10 mm	1	5	0		
10-19mm	15	18	10		
≥20 mm	84	77	90		
Major imaging features					
Nonrim arterial phase hyperenhancement	95	59	23	0.00	0.87
Nonperipheral washout	88	56	13	0.00	0.88
Enhancing capsule	83	53	24	0.00	0.94
Targetoid mass imaging features					
Rim arterial phase hyperenhancement	6	49	77	0.00	0.99
Peripheral washout	1	4	26	0.00	0.98
Delayed central enhancement	7	29	74	0.00	0.83
Targetoid restriction	6	24	27	0.00	0.72
Tumor in the vein	5	11	13	0.14	0.75
Ancillary imaging features					
Nodule-in-nodule	3	8	2	0.08	0.85
Mosaic	16	25	6	0.001	0.76
Fat in mass	21	7	1	0.00	0.58
Blood products in mass	17	15	7	0.08	0.89
Peritumoral biliary dilatation	7	30	29	0.00	0.90
Liver surface retraction	13	17	40	0.00	0.92
Corona enhancement	17	23	45	0.00	0.69
Restricted diffusion	99	94	98	0.09	1.0
Mild-moderate T2 hyperintensity	97	94	93	0.42	0.88

Data are numbers of lesions. CHCC-CC, combined hepatocellular-cholangiocarcinoma; HCC, hepatocellular carcinoma; ICC, intrahepatic cholangiocarcinoma.

ancillary imaging features favoring HCC were more common in HCC and cHCC-CCA than in ICC (P <0.001). However, the nodule-in-nodule, tumor in vein, and blood products in mass had no significant differences among HCCs, cHCC-CCAs, and ICCs (all P >0.05). Inter-observer agreements for each feature of the LI-RADS categorization are summarized in **Table 2**.

Diagnostic Performance of LR-5 and LR-M for HCC Versus Non-HCC Malignancies

The final LI-RADS categories of the 300 nodules included LR-3 in 8 nodules, LR-4 in 10 nodules, LR-5 in 117 nodules, LR-M in 136 nodules, and LR-TIV in 29 nodules (**Table 3**). In terms of the pathological diagnoses, the LI-RADS categories were inconsistent (P <0.001, **Table 3**): 81% of HCCs, 7% of ICCs, and 29% of cHCC-CCAs were classified as LR-5 (**Figure 2**), and 10% of HCCs, 73% of ICCs, and 53% of cHCC-CCAs were classified as LR-M (**Table 3**) (**Figures 3**, **4**). The sensitivity and specificity of the LR-5 category for differentiating HCCs from other primary liver cancers were 81% (81 of 100) and 82% (164 of 200), respectively. Furthermore, the specificity of the LR-5 category for differentiating between HCCs and ICCs was 93% (93 of 100) and 71% (71 of 100) between HCCs and cHCC-CCAs. Most false-positive diagnoses of HCC were due to 29 of 34 (85%) cHCC-CCAs with LR-5. The sensitivity and specificity of the LR-M category for differentiating non-HCCs (ICCs and cHCC-CCAs) from HCCs were 63% (126 of 200) and 90% (90 of 100), respectively. The sensitivity and specificity of the LR-5 category for diagnosing HCCs in small observations (<20 mm) were 82.5% (33 of 40) and 76.6% (59 of 77), respectively. The LR-5 category had a sensitivity of 82.1% (69 of 84) for diagnosing HCCs, with a specificity of 82.6% (138 of 167). The LR-M category had a sensitivity of 78.3% (18 of 23) for diagnosing non-HCCs (ICCs and cHCC-CCAs), with a specificity of 93.8% (15 of 16). Generally, LR-5 had lower sensitivity and specificity in small observations (<20 mm) than in overall observations. On the contrary, LR-M demonstrated slightly higher specificity and sensitivity for small observations (<20 mm) (**Table 4**).

Multivariate Analyses of Risk Factors for the MVI of the Primary Liver Cancer

According to the results of MVI-positive, 34 in HCC, 34 in cHCC-CCA, and 30 in ICC (P = 0.006, **Table 5**). In terms of MVI, the LI-RADS categories were inconsistent (P <0.001, **Table 5**): MVI positivity in HCC was mostly classified as LR-5 (61.8%, 21/34); MVI positivity was mostly classified as LR-M in cHCC-CCA (41.2%, 14/34) and ICC (67%, 20/30). Multivariate logistic regression analysis showed that tumor size (odds ratio [OR], 1.255, 95% confidence interval [CI], 1.091–1.444; p = 0.002), peripheral washout (OR, 4.891; 95% CI, 1.437–16.643; p = 0.011), and AFP ≥20 ng/ml (OR, 0.514; 95% CI, 0.291–0.910; p = 0.022) were independent variables associated with the MVI of PLC (**Table 5**).

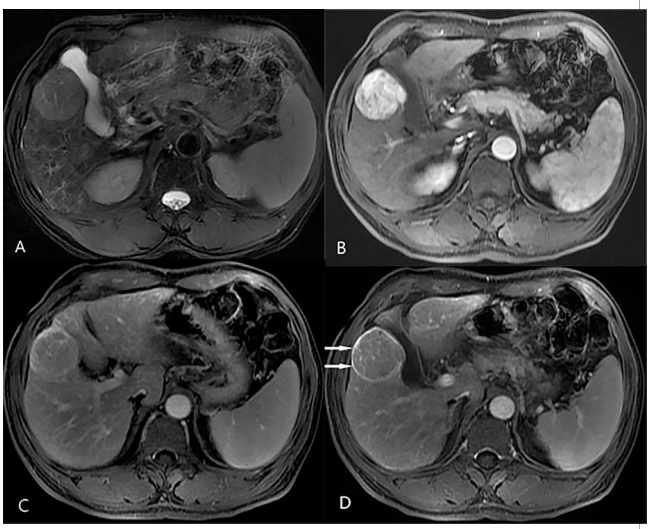

FIGURE 2 | Axial MR images in a 63-year-old man with hepatitis B-related liver cirrhosis and hepatocellular carcinoma that satisfies the LR-5 criteria. **(A)** T2-weighted image shows a 49-mm nodule with mildly homogeneous hyperintensity in hepatic segment V. The nodule shows non-rim hyperenhancement in **(B)** the arterial phase and nonperipheral washout in **(C)** the portal venous phase. An enhancing capsule is also observed in **(D)** the delay phase.

DISCUSSION

Our study evaluated the performance of LI-RADS 2018 for primary liver cancer in the background of liver cirrhosis on MRI combined with extracellular contrast agents based on the updated

TABLE 3 | Results of LI-RADS categorization of 300 hepatic tumors.

LR-category	All Tumors (n = 300)			Tumor size <20 mm (n = 300)			Tumor size ≥20 mm (n = 300)			P-value
	HCC (n = 100)	CHCC-CCA (n = 100)	ICC (n = 100)	HCC (n = 16)	CHCC-CCA (n = 23)	ICC (n = 10)	HCC (n = 84)	CHCC-CCA (n = 77)	ICC (n = 90)	0
LR-3	3	4	1	3 (18.8)	4 (17.4)	1 (10)	0	0	0	
LR-4	1	3	6	0	3 (13)	0	1 (1.2)	0	6 (6.7)	
LR-5	81	29	7	12 (75)	5 (21.7)	2 (20)	69 (82.1)	24 (31.2)	5 (5.6)	
LR-M	10	53	73	1 (6.3)	11 (47.8)	7 (70)	9 (10.7)	42 (54.5)	66 (73.3)	
LR-TIV	5	11	13	0	1 (2)	0	5 (6)	11 (14.3)	13 (14.4)	

Liver Imaging Reporting and Data System (LI-RADS) categories are defined as LR-3 (intermediate probability of HCC), LR-4 (probably hepatocellular carcinoma [HCC]), LR-5 (definitely HCC), LR-M (probably malignant, not specific for HCC), and LR-TIV (nodule with definite tumor in the vein). HCC, hepatocellular carcinoma; CHCC-CC, combined hepatocellular-cholangiocarcinoma; ICC, intrahepatic cholangiocarcinoma.

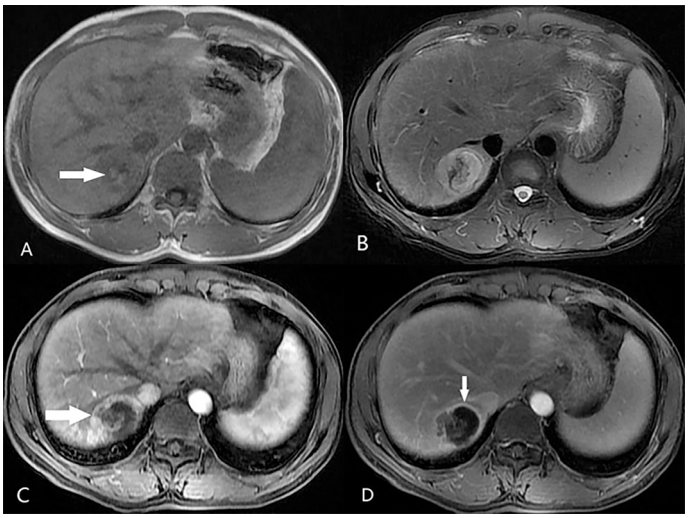

FIGURE 3 | A 48-year-old male patient with hepatitis B-related liver cirrhosis and HCC is categorized as LR-M category. **(A)** T1-weighted image shows a 36-mm nodule with blood product in mass (arrow) in hepatic segment VIII. The nodule shows heterogeneous hyperintensity on **(B)** T2-weighted image. **(C)** The arterial phase shows peripheral enhancement (arrow) on contrast-enhanced T1-weighted imaging with the contrast agent Gd-DTPA, and **(D)** the delay phase shows incompletely enhancing capsule (arrows).

2019 WHO classification. The results demonstrated that the sensitivity of the LR-5 category for differentiating HCCs from non-HCCs was consistent with that of the Lee et al. (6) study using LI-RADS 2018 and gadoxetate disodium contrast agent in all observations (81% vs 81%) and small observations (76% vs 75%). Our results had better sensitivity in the LR-5 category at the cost of reduced specificity than that of the previous studies (6, 12, 18, 19), which showed a range of sensitivity between 55.2 and 74%.

It should also be noted that the specificity of the LR-5 category was shown to be lower than that of the recent studies (4, 6, 12, 18, 19) by using LI-RADS v2017 or v2018 with gadoxetate disodium contrast agent. Intriguingly, in small observations (<20 mm), specificity was even lower than that in all observations (78.8% vs 82%). The reason, on one hand, may be the use of hepatobiliary phase imaging and, as shown in the study by Chen et al. (20), significantly higher specificity was

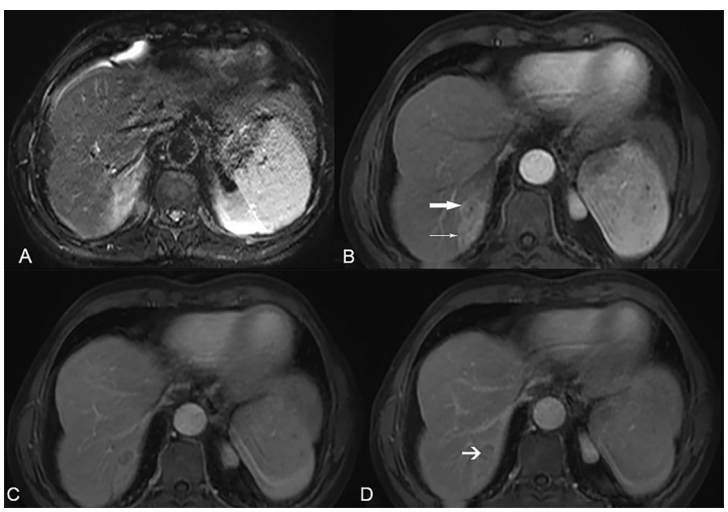

FIGURE 4 | A 61-year-old male patient with hepatitis B-related liver cirrhosis and cHCC-CCA is categorized as LR-M category. **(A)** T2-weighted image shows a 36-mm nodule with heterogeneous hyperintensity in hepatic segment VIII. **(B)** The arterial phase shows peripheral enhancement (arrow) and tumor thrombus in the bile duct (thin arrow) on contrast-enhanced T1-weighted imaging with the contrast agent Gd-DTPA. **(C)** The portal venous phase and **(D)** delay phase show targetoid appearance and the arrow shows progressively delayed central enhancement.

TABLE 4 | Diagnostic Performance of LR-5 and LR-M in primary liver cancer according to the size of the observation.

	LR-5		LR-M	
	sensitivity	**specificity**	**sensitivity**	**specificity**
overall	81 (81/100)	82 (164/200)	63 (126/200)	90 (90/100)
The size <20 mm	75 (12/16)	78.8 (26/33)	78.3 (18/23)	93.8 (15/16)
The size ≥20 mm	82.1 (69/84)	82.6 (138/167)	64.7 (108/167)	89.3 (75/84)

Data in parentheses were used to calculate percentages. LI-RADS, Liver Imaging Reporting and Data System.

observed than in studies of LI-RADS using extracellular contrast agents when the hepatobiliary phase images were added (21).

However, the most common cause of false-positive results was combined HCC-cholangiocarcinoma (cHCC-CCA). In other words, as demonstrated in a recent study (12, 22), cHCC-CCA, which mimics HCC, lowered the specificity of the LR-5 criteria. According to the previous study by Wang et al. (23) with the 2010 WHO classification, more cHCC-CCAs were misclassified

TABLE 5 | Clinical characteristics and multivariate analyses of risk factors for the MVI of primary liver cancer.

Variable	MVI-positive	MVI-negative	P-value	Multivariable Analysis	
	(n = 98)	(n = 202)		OR (95% CI)	P
Mean age (y)	57.21 ± 11.52	57.49 ± 10.85	0.279		
M:F ratio	73/25	153/49	0.813		
Mean nodule size (mm)	5.81 ± 3.63	3.61 ± 2.28	0.000	1.255 (1.091,1.444)	0.002
Cause of cirrhosis			0.542		
Hepatitis B	88 (89.8)	184 (91)			
Hepatitis C	7 (7.1)	9 (4.5)			
Alcoholism	3 (3.1)	9 (4.5)			
Pathology			0.006		
HCC	34 (34.7)	66 (32.7)			
ICC	30 (30.6)	70 (34.7)			
cHCC-CCA	34 (34.7)	66 (32.6)			
Tumor maker value					
AFP≥20 (ng/ml)	50 (51)	73 (36.1)	0.014	0.514 (0.291,0.910)	0.022
CEA≥5 (ng/ml)	14 (14.3)	20 (9.9)	0.261		
CA 19-9≥37(ng/ml)	26 (26.5)	51 (25.4)	0.83		
Major imaging features					
Arterial phase hyperenhancement	56 (57.1)	121 (59.9)	0.649		
Non-peripheral washout	53 (54.1)	104 (51.5)	0.673		
Enhancing capsule	51 (52)	109 (54)	0.755		
Targetoid mass imaging features					
Rim arterial phase hyperenhancement	47 (48)	85 (42.1)	0.336		
Peripheral washout	4 (4.1)	26 (12.9)	0.017	4.891 (1.437,16.643)	0.011
Delayed central enhancement	33 (33.7)	77 (38.1)	0.454		
Targetoid diffusion restriction	18 (18.4)	39 (19.3)	0.846		
Tumor in vein	20 (20.4)	9 (4.5)	0.000		
Ancillary imaging features					
Nodule-in-nodule	5 (5.1)	8 (4)	0.649		
Mosaic	24 (24.5)	23 (11.4)	0.003		
Fat in mass	10 (10.2)	19 (9.4)	0.826		
Blood products in mass	21 (21.4)	18 (8.9)	0.002		
Peritumoral biliary dilatation	31 (31.6)	35 (17.3)	0.005		
Liver surface retraction	34 (34.7)	36 (17.8)	0.001		
Corona enhancement	37 (37.8)	48 (23.8)	0.012		
Diffusion restriction	97 (99)	194 (96)	0.162		
Mild-hyper T2WI	97 (99)	187 (92.6)	0.021		
LR-category			0.000		
LR-3	0	8 (4)			
LR-4	1 (1.1)	7 (3.5)			
LR-5	36 (36.7)	81 (40.1)			
LR-M	41 (41.8)	97 (48)			
LR-TIV	20 (20.4)	9 (4.5)			

Data are the number of patients or lesions. Data are presented as count (percentage) and mean ± standard deviation. OR, odds ratio; CI, confidence interval.
Liver Imaging Reporting and Data System (LI-RADS) categories are defined as LR-3 (intermediate probability of HCC), LR-4 (probably hepatocellular carcinoma [HCC]), LR-5 (definitely HCC), LR-M (probably malignant, not specific for HCC), and LR-TIV (nodule with definite tumor in the vein).

as LR-5 with the updated 2019 WHO classification (29% vs 19.5%) in our study. Therefore, we speculated that the updated pathologic diagnosis of biphenotypic PLC in the 2019 WHO classification may impact the LI-RADS categorization of biphenotypic PLCs compared with previous classification systems. Although the result was inconsistent with that of Choi et al. (14), using the gadoxetate disodium contrast agent in patients at risk of HCC, they reported a much higher false-positive rate of LR-5 for cHCC-CCA.

Moreover, compared with the recent study by Yoon et al. (19) with cHCC-CCA in patients with cirrhosis, the rate classified as LR-M in cHCC-CCAs was decreased (58.8% vs 53%). The rate classified as LR-M in cHCC-CCAs was also even lower than that of recent studies (14, 19, 23) in patients at risk. That could explain why LI-RADS v2018 showed decreased specificity in the diagnosis of HCCs than recent reports with LI-RADS v2014 (21) and v2017 (4).

According to our results, LR-M has better specificity for differentiating non-HCCs (ICCs and cHCC-CCAs) from HCCs, which was similar to Lee et al. (6) using gadoxetate disodium contrast agents and LR2018 criteria, than that of the recent studies (10, 12, 18, 24). Particularly, in small observations (<20 mm), LR-M category had better sensitivity and specificity than that in all observations (78.3% vs 63%, 93.8% vs 90%, respectively). We speculate that there are two types of tumors that meet the LR-M criteria: "target sign" and "no target sign." For tumors<20 mm, the classification of LR-M mainly depends on the target sign. Therefore, the appearance of the target sign necessarily increases the sensitivity and specificity of tumors <20 mm. These results may contribute to risk-based personalized management. Generally, the LR-5 and LR-M category had maintained stable and good specificity and sensitivity in tumor with diameter of ≥20 mm, but the LR-5 category had relatively lower specificity and sensitivity for diagnosing HCC in small observations (<20 mm). Fortunately, the prognosis of most isolated small liver tumors is relatively good.

A previous study by Centonze et al. (25) with a retrospective cohort of 186 patients with HCC undergoing surgery resection reported that LR-5 patients presented with a higher prevalence of MVI, satellitosis, and capsule infiltration, whereas LI-RADS classification did not exert any statistically significant effect on overall survival and relapse-free survival. In our study, although MVI positivity was statistically significantly different in LI-RADS classification, LR classification was not an independent risk factor for predicting MVI in patients with the PLC. We speculated that the possible reason was the heterogeneity of the primary liver tumors. Our results also illustrated that tumor size, AFP ≥20 ng/ml and peripheral washout may indicate a higher risk of the MVI of the PLC. The results were consistent with the previous study by Zhou et al. (26), which showed that larger tumor size, higher AFP level, and CEUS LR-M were significantly correlated with the presence of MVI in HCC (all $p < 0.05$). According to the previous study by Wang et al. (23), the LR-category ($P = 0.857$) was not effective in predicting MVI of CHCC-CCA preoperatively, which was consistent with our study. The peripheral washout sign was one of the targetoid mass features in category LR-M. The results of MVI in our study may require further prospective studies to verify.

Our study also has several limitations. First, coincidentally, since the ICC cohort had the same number of cases as the cHCC-CCA cohort, we conducted our study retrospectively at random in the same number. It can lead to selection bias, where the proportion of ICC and cHCC-CCA is overestimated compared to the actual incidence of cirrhosis. Second, there were only 49 small observations (<20 mm), as many small HCCs were treated through local–regional treatment after having noninvasive diagnosis based on imaging features in our institution. Finally, we did not evaluate visibility at screening US and threshold growth, which might have caused an alteration of the sensitivity of LR-5 in the diagnosis of HCC.

In conclusion, our study demonstrates that the LR-5 category of Liver Imaging Reporting and Data System (LI-RADS) version 2018 based on the updated 2019 WHO classification with enhanced MRI with extracellular contrast agent had low specificity, particularly in small observations (<20 mm). Additionally, the LR-M category can effectively differentiate non-HCC malignancy from hepatocellular carcinoma (HCC) in cirrhosis.

DATA AVAILABILITY STATEMENT

The original contributions presented in the study are included in the article/supplementary material. Further inquiries can be directed to the corresponding authors.

ETHICS STATEMENT

The studies involving human participants were reviewed and approved by The Institutional Review Board of Zhongshan Hospital, Fudan University. The patients/participants provided their written informed consent to participate in this study. Written informed consent was obtained from the individual(s) for the publication of any potentially identifiable images or data included in this article.

AUTHOR CONTRIBUTIONS

XL had full access to all of the data in the study. XL, CM, CZ, and YW took responsibility for the integrity of the data and the accuracy of data analyses. YL and CZ designed the study. Due to computer spelling error, here is changed to YL, CY and YW conducted the analyses and interpreted the data. YL, XNL, and XN drafted the manuscript and have contributed equally to this work and share first authorship. All authors listed have made a substantial, direct, and intellectual contribution to the work and approved it for publication.

FUNDING

This study was supported by the Clinical Research Plan of SHDC (grant number SHDC2020CR1029B), the National Natural

Science Foundation of China (grant number 82171897), the Shanghai Municipal Key Clinical Specialty (grant number shslczdzk03202), the Clinical Research Project of Zhongshan Hospital, Fudan University (grant number 2020ZSLC61), and the Henan Provincial Universities Key Scientific Research Projects (grant number 21B320002).

REFERENCES

1. Elsayes KM, Hooker JC, Agrons MM, Kielar AZ, Tang A, Fowler KJ, et al. 2017 Version of LI-RADS for CT and MR Imaging: An Update. *Radiographics* (2017) 37(7):1994–2017. doi: 10.1148/rg.2017170098
2. Mittal S, El-Serag HB. Epidemiology of Hepatocellular Carcinoma: Consider the Population. *J Clin Gastroenterol* (2013) 47 Suppl(1539-2031 (Electronic): S2–6. doi: 10.1097/MCG.0b013e3182872f29
3. Kim JH, Joo I, Lee JM. Atypical Appearance of Hepatocellular Carcinoma and Its Mimickers: How to Solve Challenging Cases Using Gadoxetic Acid-Enhanced Liver Magnetic Resonance Imaging. *Korean J Radiol* (2019) 20 (7):1019–41. doi: 10.3348/kjr.2018.0636
4. Kierans AS, Makkar J, Guniganti P, Cornman-Homonoff J, Lee MJ, Pittman M, et al. Validation of Liver Imaging Reporting and Data System 2017 (LI-RADS) Criteria for Imaging Diagnosis of Hepatocellular Carcinoma. *J Magn Reson Imaging* (2019) 49(7):e205–e15. doi: 10.1002/jmri.26329
5. Sirlin CB. The LI-RADS Adventure-A Personal Statement. *Abdom Radiol (NY)* (2018) 43(1):1–2. doi: 10.1007/s00261-017-1386-y
6. Lee SM, Lee JM, Ahn SJ, Kang HJ, Yang HK, Yoon JH. LI-RADS Version 2017 Versus Version 2018: Diagnosis of Hepatocellular Carcinoma on Gadoxetate Disodium-Enhanced MRI. *Radiology* (2019) 292(3):655–63. doi: 10.1148/radiol.2019182867
7. Shao S, Liang Y, Kuang S, Chen J, Shan Q, Yang H, et al. Diagnostic Performance of LI-RADS Version 2018 in Differentiating Hepatocellular Carcinoma From Other Hepatic Malignancies in Patients With Hepatitis B Virus Infection. *Bosn J Basic Med Sci* (2020) 20(3):401–10. doi: 10.17305/bjbms.2019.4576
8. Chernyak V, Fowler KJ, Kamaya A, Kielar AZ, Elsayes KM, Bashir MR, et al. Liver Imaging Reporting and Data System (LI-RADS) Version 2018: Imaging of Hepatocellular Carcinoma in At-Risk Patients. *Radiology* (2018) 289 (3):816–30. doi: 10.1148/radiol.2018181494
9. Santillan C, Chernyak V, Sirlin C. LI-RADS Categories: Concepts, Definitions, and Criteria. *Abdom Radiol (NY)* (2018) 43(1):101–10. doi: 10.1007/s00261-017-1334-x
10. Choi SH, Lee SS, Park SH, Kim KM, Yu E, Park Y, et al. LI-RADS Classification and Prognosis of Primary Liver Cancers at Gadoxetic Acid-Enhanced MRI. *Radiology* (2019) 290(2):388–97. doi: 10.1148/radiol.2018181290
11. Fraum TJ, Cannella R, Ludwig DR, Tsai R, Naeem M, LeBlanc M, et al. Assessment of Primary Liver Carcinomas Other Than Hepatocellular Carcinoma (HCC) With LI-RADS V2018: Comparison of the LI-RADS Target Population to Patients Without LI-RADS-Defined HCC Risk Factors. *Eur Radiol* (2020) 30(2):996–1007. doi: 10.1007/s00330-019-06448-6
12. Kim Y-Y, Kim M-J, Kim EH, Roh YH, An C. Hepatocellular Carcinoma Versus Other Hepatic Malignancy in Cirrhosis: Performance of LI-RADS Version 2018. *Radiology* (2019) 291(1):72–80. doi: 10.1148/radiol.2019181995
13. Nagtegaal ID, Odze RD, Klimstra D, Paradis V, Rugge M, Schirmacher P, et al. The 2019 WHO Classification of Tumours of the Digestive System. *Histopathology* (2020) 76(2):182–8. doi: 10.1111/his.13975
14. Choi SH, Jeon SK, Lee SS, Lee JM, Hur BY, Kang H-J, et al. Radio-Pathologic Correlation of Biphenotypic Primary Liver Cancer (Combined Hepatocellular Cholangiocarcinoma): Changes in the 2019 WHO Classification and Impact on LI-RADS Classification at Liver MRI. *Eur Radiol* (2021) 31(12):9479–88. doi: 10.1007/s00330-021-07984-w
15. Brunt E, Aishima S, Clavien PA, Fowler K, Goodman Z, Gores G, et al. cHCC-CCA: Consensus Terminology for Primary Liver Carcinomas With Both Hepatocytic and Cholangiocytic Differentation. *Hepatology* (2018) 68(1):113–26. doi: 10.1002/hep.29789
16. Hwang J, Kim YK, Min JH, Choi SY, Jeong WK, Hong SS, et al. Capsule, Septum, and T2 Hyperintense Foci for Differentiation Between Large Hepatocellular Carcinoma (>/=5 Cm) and Intrahepatic Cholangiocarcinoma on Gadoxetic Acid MRI. *Eur Radiol* (2017) 27(11):4581–90. doi: 10.1007/s00330-017-4846-4
17. Choi SY, Kim YK, Min JH, Kang TW, Jeong WK, Ahn S, et al. Added Value of Ancillary Imaging Features for Differentiating Scirrhous Hepatocellular Carcinoma From Intrahepatic Cholangiocarcinoma on Gadoxetic Acid-Enhanced MR Imaging. *Eur Radiol* (2018) 28(6):2549–60. doi: 10.1007/s00330-017-5196-y
18. Ludwig DR, Fraum TJ, Cannella R, Ballard DH, Tsai R, Naeem M, et al. Hepatocellular Carcinoma (HCC) Versus Non-HCC: Accuracy and Reliability of Liver Imaging Reporting and Data System V2018. *Abdom Radiol (NY)* (2019) 44(6):2116–32. doi: 10.1007/s00261-019-01948-x
19. Yoon J, Hwang JA, Lee S, Lee JE, Ha SY, Park YN. Clinicopathologic and MRI Features of Combined Hepatocellular-Cholangiocarcinoma in Patients With or Without Cirrhosis. *Liver Int* (2021) 41(7):1641–51. doi: 10.1111/liv.14798
20. Chen N, Motosugi U, Morisaka H, Ichikawa S, Sano K, Ichikawa T, et al. Added Value of a Gadoxetic Acid-Enhanced Hepatocyte-Phase Image to the LI-RADS System for Diagnosing Hepatocellular Carcinoma. *Magn Reson Med Sci* (2016) 15(1):49–59. doi: 10.2463/mrms.2014-0149
21. Kim YY, An C, Kim S, Kim MJ. Diagnostic Accuracy of Prospective Application of the Liver Imaging Reporting and Data System (LI-RADS) in Gadoxetate-Enhanced MRI. *Eur Radiol* (2018) 28(5):2038–46. doi: 10.1007/s00330-017-5188-y
22. Fraum TJ, Tsai R, Rohe E, Ludwig DR, Salter A, Nalbantoglu I, et al. Differentiation of Hepatocellular Carcinoma From Other Hepatic Malignancies in Patients at Risk: Diagnostic Performance of the Liver Imaging Reporting and Data System Version 2014. *Radiology* (2018) 286 (1):158–72. doi: 10.1148/radiol.2017170114
23. Wang X, Wang W, Ma X, Lu X, Li S, Zeng M, et al. Combined Hepatocellular-Cholangiocarcinoma: Which Preoperative Clinical Data and Conventional MRI Characteristics Have Value for the Prediction of Microvascular Invasion and Clinical Significance? *Eur Radiol* (2020) 30(10):5337–47. doi: 10.1007/s00330-020-06861-2
24. Choi SY, Kim SH, Park CK, Min JH, Lee JE, Choi YH, et al. Imaging Features of Gadoxetic Acid-Enhanced and Diffusion-Weighted MR Imaging for Identifying Cytokeratin 19-Positive Hepatocellular Carcinoma: A Retrospective Observational Study. *Radiology* (2018) 286(3):897–908. doi: 10.1148/radiol.2017162846
25. Centonze L, De Carlis R, Vella I, Carbonaro L, Incarbone N, Palmieri L, et al. From LI-RADS Classification to HCC Pathology: A Retrospective Single-Institution Analysis of Clinico-Pathological Features Affecting Oncological Outcomes After Curative Surgery. *Diagnostics (Basel)* (2022) 12(1):160. doi: 10.3390/diagnostics12010160
26. Zhou H, Sun J, Jiang T, Wu J, Li Q, Zhang C, et al. A Nomogram Based on Combining Clinical Features and Contrast Enhanced Ultrasound LI-RADS Improves Prediction of Microvascular Invasion in Hepatocellular Carcinoma. *Front Oncol* (2021) 11:699290. doi: 10.3389/fonc.2021.699290

Conflict of Interest: The authors declare that the research was conducted in the absence of any commercial or financial relationships that could be construed as a potential conflict of interest.

Publisher's Note: All claims expressed in this article are solely those of the authors and do not necessarily represent those of their affiliated organizations, or those of the publisher, the editors and the reviewers. Any product that may be evaluated in this article, or claim that may be made by its manufacturer, is not guaranteed or endorsed by the publisher.

Copyright © 2022 Liu, Ni, Li, Yang, Wang, Ma, Zhou and Lu. This is an open-access article distributed under the terms of the Creative Commons Attribution License (CC BY). The use, distribution or reproduction in other forums is permitted, provided the original author(s) and the copyright owner(s) are credited and that the original publication in this journal is cited, in accordance with accepted academic practice. No use, distribution or reproduction is permitted which does not comply with these terms.

frontiers | Frontiers in Surgery

CASE REPORT
published: 06 July 2022
doi: 10.3389/fsurg.2022.926003

Undifferentiated Pleomorphic Sarcoma of the Duodenal Papilla: A Rare Case and Worth Discussing History

*Jianlong Wang[1], Bin Liu[2], Jiachao Hou[1] and Tao Li[1]**

[1]Department of General Surgery, The Second Hospital of Hebei Medical University, Shijiazhuang, China, [2]Central Laboratory, The Second Hospital of Hebei Medical University, Shijiazhuang, China

Background: Undifferentiated pleomorphic sarcoma (UPS) is a malignant tumor that originates in the mesenchymal tissue and is common in the extremities and retroperitoneum. Primary UPS of the duodenal papilla is rare and a distinct clinical entity.

Case presentation: In this report, a 48-year-old Chinese man was admitted to our hospital with symptoms of melena. The patient underwent choledochectomy and choledochaljejunostomy for obstructive jaundice 8 years before admission. Endoscopic examination after admission confirmed a mass located at the duodenal papilla. Then, the duodenal papilla and tumor resection were performed, and the histopathology report confirmed the diagnosis of UPS. The patient refused further treatment and died 2 months later due to local recurrence and intrahepatic metastasis.

Conclusions: It is rare that the mass in the duodenal papilla is diagnosed as UPS. The unpredicted behavior of these tumors warrants a careful plan considering their indolent nature and possible recurrence and metastasis. The prognosis was poor despite the early complete resection.

Keywords: undifferentiated pleomorphic sarcoma, duodenal papilla, duodenoscopy, duodenal papillectomy, case report

OPEN ACCESS

Edited by:
Qi Liu,
Fudan University, China

Reviewed by:
Masachika Ikegami,
Tokyo Metropolitan Komagome Hospital, Japan
Mariam Zaghloul,
Kafrelsheikh University, Egypt

****Correspondence:***
Tao Li
litao74102@126.com

Specialty section:
This article was submitted to Surgical Oncology, a section of the journal Frontiers in Surgery

Received: *22 April 2022*
Accepted: *03 June 2022*
Published: *06 July 2022*

Citation:
Wang J, Liu B, Hou J and Li T (2022) Undifferentiated Pleomorphic Sarcoma of the Duodenal Papilla: A Rare Case and Worth Discussing History. Front. Surg. 9:926003. doi: 10.3389/fsurg.2022.926003

INTRODUCTION

Undifferentiated pleomorphic sarcoma (UPS) is the most common soft tissue sarcomas in the elderly (1, 2). It is a neoplasm considered to originate from primitive mesenchymal cells, arising from soft tissue or bone, usually in the extremities or retroperitoneum (3). The Vater papilla region is uncommon and primary duodenal papilla UPS is exceedingly rare, with only one case confirmed in the literature to date (**Table 1**). At present, the epidemiology, diagnosis, and treatment of this disease remain unclear (4–6). The following case documents a primary lesion of the duodenum papilla, and its biological behavior characterizing a worth discussing history and an extremely poor prognosis.

TABLE 1 | Up-to-date review of cases of UPS around duodenal ampulla.

First author	Year	Age	Sex	Symptoms	Location	Treatment	Follow-up (months)
Margueles et al. (7)	1976	22	F	Postprandial pain, nausea	Head of pancreas	Pancreaticoduodenectomy	17 (alive)
Pascal et al. (8)	1989	39	M	Abdominal mass, reflux esophagitis	Head of pancreas	Pancreaticoduodenectomy	0 (died)
Suster et al. (9)	1989	71	M	Epigastralgia, nausea, jaundice	Head of pancreas	Pancreaticoduodenectomy	No-follow
Haba et al. (10)	1996	70	M	Vomiting, abdominal pain	Head of pancreas	Pancreaticoduodenectomy	22 (alive)
Mai et al. (11)	2002	71	F	Jaundice	Head of pancreas	Pancreaticoduodenectomy	24 (died)
Darvishian et al. (12)	2002	74	M	Accidentally discovered	Head of pancreas	Pancreaticoduodenectomy	4 (alive)
Yu et al. (13)	2008	67	M	Weight loss	Head of pancreas	Pancreaticoduodenectomy	11 (died)
Jarry et al. (14)	2010	45	M	Jaundice	Head of pancreas	Multidisciplinary treatment	11 (alive)
Sanei et al. (15)	2016	72	F	Abdominal pain	Head of pancreas	Pancreaticoduodenectomy	22 (alive)
Gilman et al. (16)	1986	29	F	Peritonitis	Duodenum	Pancreatoduodenectomy	0 (died)
Asai et al. (17)	1987	61	M	Epigastralgia	Duodenum	Resection	21 (alive)
Farinon et al. (18)	1999	61	F	Gastrointestinal bleeding	Duodenum	Pancreatoduodenectomy	2 (died)
Wang et al. (19)	2005	61	M	Gastrointestinal bleeding, weight loss	Duodenum	Pancreatoduodenectomy	24 (alive)
Tanaka et al. (17)	2005	53	M	Epigastralgia, fever	Duodenum	Chemotherapy	5 (died)
Makni et al. (20)	2011	63	M	Gastrointestinal bleeding, weight loss, vomiting	Duodenum	Gastroenteroanastomosis	4 (died)
Yuhei et al. (17)	2016	69	M	Epigastralgia, pancreatitis	Duodenum	Pancreatoduodenectomy	10 (alive)
Giuliani et al. (21)	2013	67	M	Jaundice	Duodenal papilla	Radiotherapy	No-follow
Present case	2018	48	M	Gastrointestinal bleeding	Duodenal papilla	Resection of tumor and duodenal papilla	2 (died)

UPS, undifferentiated pleomorphic sarcoma; M, male; F, female.

CASE PRESENTATION

A 48-year-old Chinese man was admitted with melena (hemoglobin = 64 g/L). Contrast-enhanced CT scans showed that the mass was located in the descending duodenum, a cross section of approximately 1.8 cm × 2.0 cm. The values of plain and three-phase contrast-enhanced CT scans were about 35/90/90/73HU (**Figure 1**). Duodenoscopy confirmed that the mass originated from the duodenal papilla and projected into the lumen of the duodenum without invading the intestinal wall (**Figure 2A**). Endoscopic biopsy of the tumor showed a proliferation of polygonal cells, which were a dense arrangement and accompanied by visible mitosis and pleomorphic giant cells. Tumor cells were positive for CD68, Ki67 (50%), and Vimentin (**Figures 2B–E**), while negative for CD117, CD20, CD3, CD34, chromogranin A, CK7, Desmin, DOG1, HMB-45, melon-A, and Synaptophysin (data not provided). Then, the diagnosis considered a high-grade sarcoma, and a complete resection of the tumor was recommended for further examination.

What is noteworthy is that the patient was admitted to our hospital 8 years ago with obstructive jaundice (bilirubin = 286 μmol/L, especially direct). Ultrasound and endoscopic retrograde cholangiopancreatography (ERCP) were performed at that time, both of which indicated mass in the distal common bile duct (**Figures 3A, B**). A biopsy specimen obtained from the mass revealed blood clots and multinucleated giant cell reaction (**Figure 3C**). Subsequently, the patient underwent cholecystectomy, choledochectomy, and Roux-en-Y hepaticojejunostomy. No mass was found in the bile duct during the operation, but stenosis was observed in the pancreatic segment of the common bile duct with a thickness of 0.3 cm. The distal bile duct was resected approximately 0.6 cm below the stenosis. Postoperative pathology showed chronic inflammation of the bile duct with mild hyperplasia of glandular epithelium and adenomyosis. The patient was asymptomatic for 8 years.

Based on medical history and the biopsy results during the second admission, the final surgical method was determined as

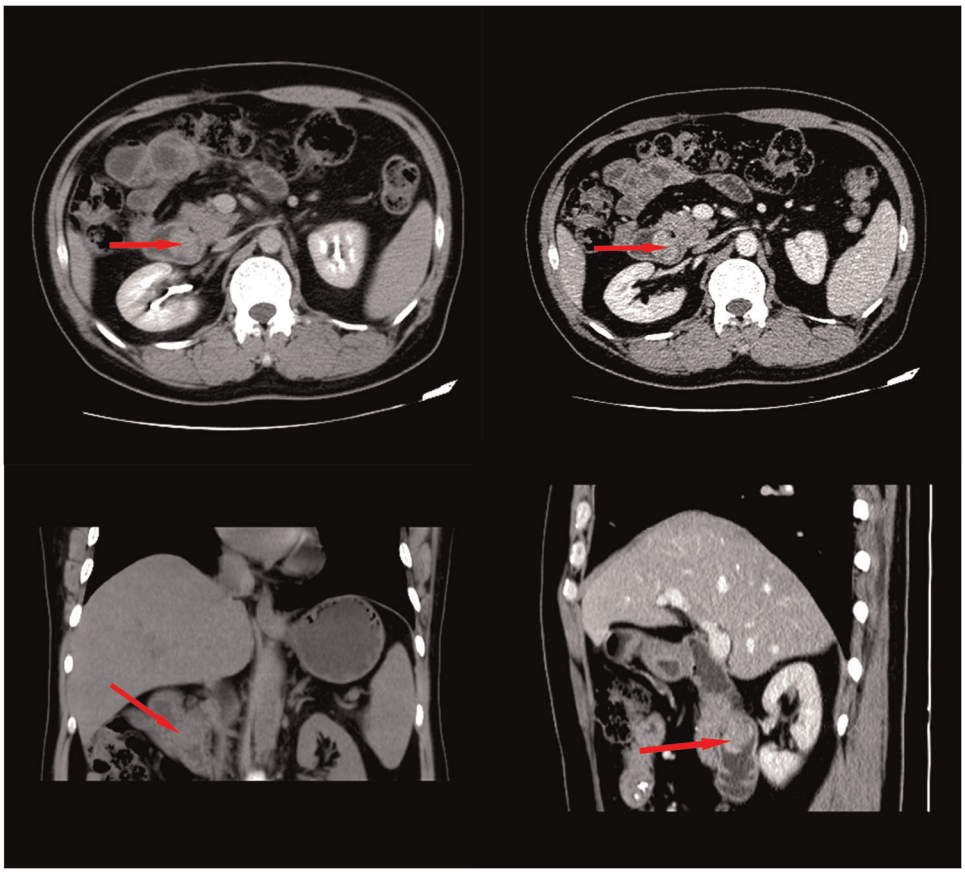

FIGURE 1 | Contrast-enhanced CT showed that the tumor was located in the duodenal cavity (approximately 1.8 cm × 2.2 cm) without penetrating the duodenal wall.

duodenal papilla and tumor resection, rather than pancreaticoduodenectomy. The histopathological findings revealed an UPS. Microscopically, multiple multinucleated osteoclast-like giant cells were evenly distributed on the mononucleated stromal cells. Giant cells contained numerous nuclei with eosinophilic cytoplasm. The pleomorphic stromal cells were spindle-shaped and atypical round, which were similar to the high-grade sarcoma. Nucleoli could be seen in several stromal cells. A small number of stromal cells showed a high degree of mitosis, which is a sign of malignancy. Immunohistochemical stains for CD68 and Vimentin were positive in the neoplastic cells, the proliferative marker Ki67 showing approximately 80% nuclear staining (**Figure 4**), and CD117, CD34, HMB45, CD45, CD56, S-100, smooth muscle actin (SMA), or desmin were negative (data not provided). The patient declined further chemotherapy and was discharged.

Two months later, the patient was admitted to our hospital again with complaints of melena. CT scan showed a recurrent duodenal mass and multiple metastatic foci in the liver (**Figure 5**), and the patient died of metastasis 2 weeks later. The episode of care is organized as a timeline in **Figure 6**.

DISCUSSION

UPS, or previously known malignant fibrous histiocytoma (MFH), is considered the most common type of soft tissue sarcoma. It often occurs in the limbs, trunk, and retroperitoneal tissues (3, 22), but it has been rarely observed in the digestive organ (15). The nomenclature and categorization of this neoplasm have changed several times over the years. In 2002, the World Health Organization (WHO) believed that MFH should be synonymous with UPS and divided into three subtypes, polymorphic MFH/UPS, giant cell MFH/with giant cell UPS, and inflammatory MFH/with prominent inflammation UPS (23). In 2013, the WHO removed MFH and replaced it with UPS, which was classified into the newly established undifferentiated soft tissue sarcoma (USTS), a group of polymorphic heterogenous stromal tumors with no clear differentiation direction (24, 25).

UPS located at the same site often have similar clinical features. UPS in the head of the pancreas is characterized by epigastric pain, nausea, and vomiting. Some patients may present with weight loss and abdominal mass. Jaundice is also possible, depending on whether the tumor is compressing or

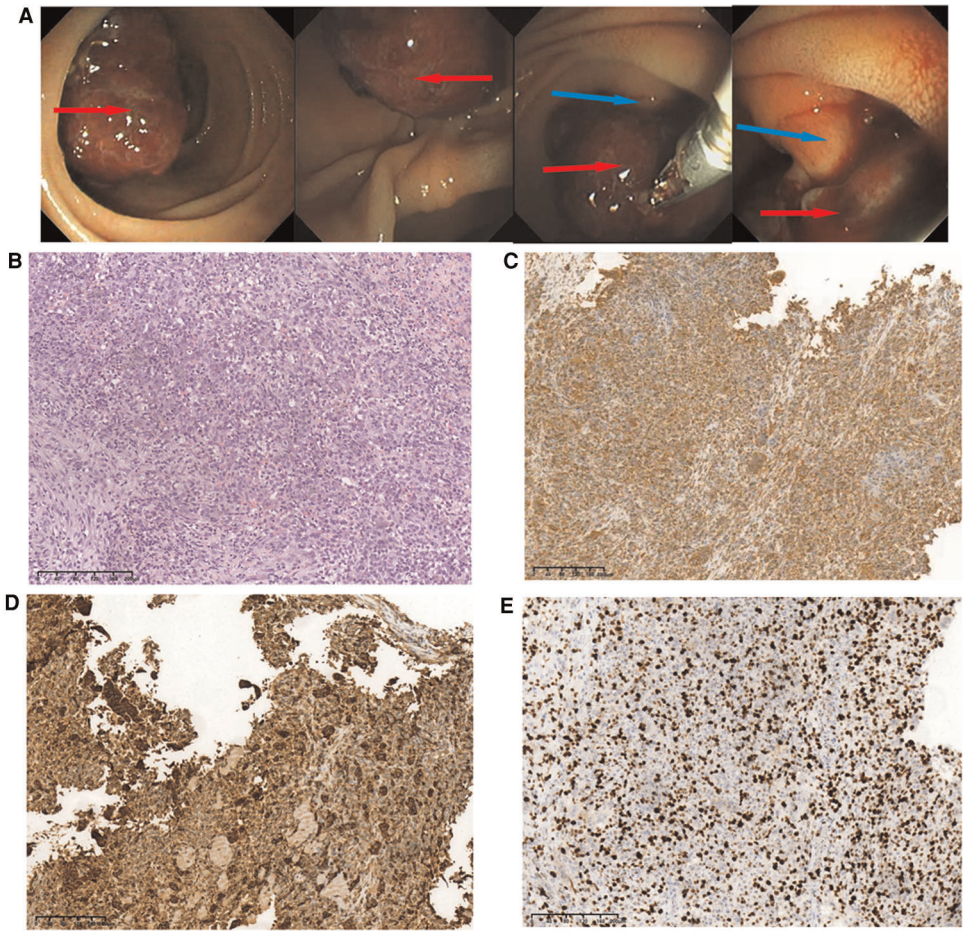

FIGURE 2 | Duodenoscopic images of the tumor and pathological results of endoscopic biopsy during hospitalization. (**A**) Duodenoscopic images of the tumor; the red arrow indicates tumor tissue, and the blue arrow indicates duodenal papilla. (**B**)Histopathological examination of the biopsy (H&E staining) of the tumor, original magnification, ×100. These cells were positive for Vimentin, ×100 (**C**), CD68, ×100 (**D**), and Ki-67 was about 50% upon immunostaining, ×100 (**E**).

invading the bile ducts. Primary UPS of the duodenum is often invasive and can penetrate the intestinal wall, leading to perforation or ulceration bleeding (20). Therefore, gastrointestinal bleeding and melena are the main symptoms of primary UPS in the duodenum. The symptoms caused by UPS arising in the Vater papilla region are similar to those caused by other tumors in this location and include melena, recurrent acute pancreatitis, jaundice, and abdominal pain. Similar to previous cases, melena was the main symptom accompanied by upper abdominal discomfort in this case. The difference is that this patient had undergone a Roux-en-Y hepaticojejunostomy, so jaundice was not present. The histopathology confirmed the diagnosis of UPS.

Patients with UPS in the duodenum often die months or years after diagnosis (18, 20). It is not clear whether the tumor has undergone a long growth process or grown rapidly from the beginning. The endoscopic biopsy result of 8 years ago showed blood clots and multinucleated giant cell reaction in this case, which could not be confirmed as UPS, giant cell tumor, or foreign body giant cell reflection now. A similar case has been reported in the central nervous system where a mass was found in the same area on a plain CT scan 5 years before the diagnosis of primary UPS in the brain (26). In addition, traumatic factors such as surgery are also one of the possible causes of UPS (27). The patient had undergone cholecystectomy and choledochectomy 8 years ago, and traumatic factors may have contributed to the occurrence of UPS in this rare site.

The diagnosis of UPS is important in its treatment process. UPS is defined as a group of sarcomas in which any attempt to disclose their line of differentiation has failed (28). Their immunophenotype is plastic and they may focally express CD34, SMA, and CD68. Immunohistochemistry can be used as a means to rule out melanoma, sarcomatoid carcinoma, and malignant lymphomas, which have respective tumor markers (29), but its role is still auxiliary. The diagnosis continues to presuppose thorough sampling and evaluation of hematoxylin–eosin-stained sections (29). Another differential

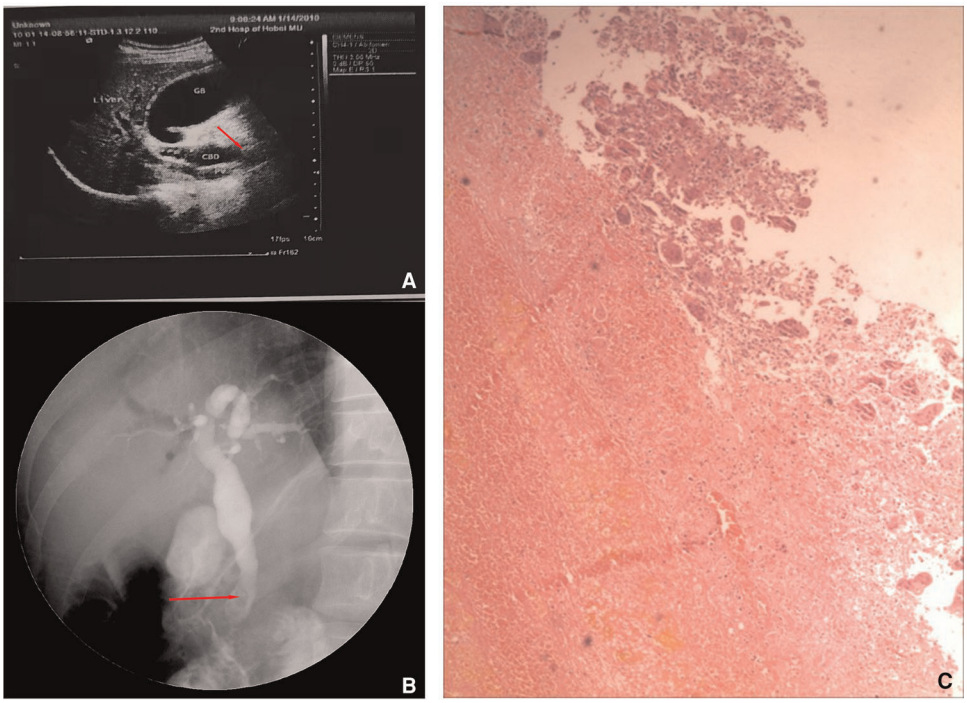

FIGURE 3 | Ultrasound, endoscopy, and biopsy results 8 years ago. Preoperative ultrasound (**A**) and endoscopic retrograde cholangiopancreatography (ERCP) images showed a mass (red arrow) in the distal bile duct (**B**), and the histological manifestation of biopsy specimen (**C**).

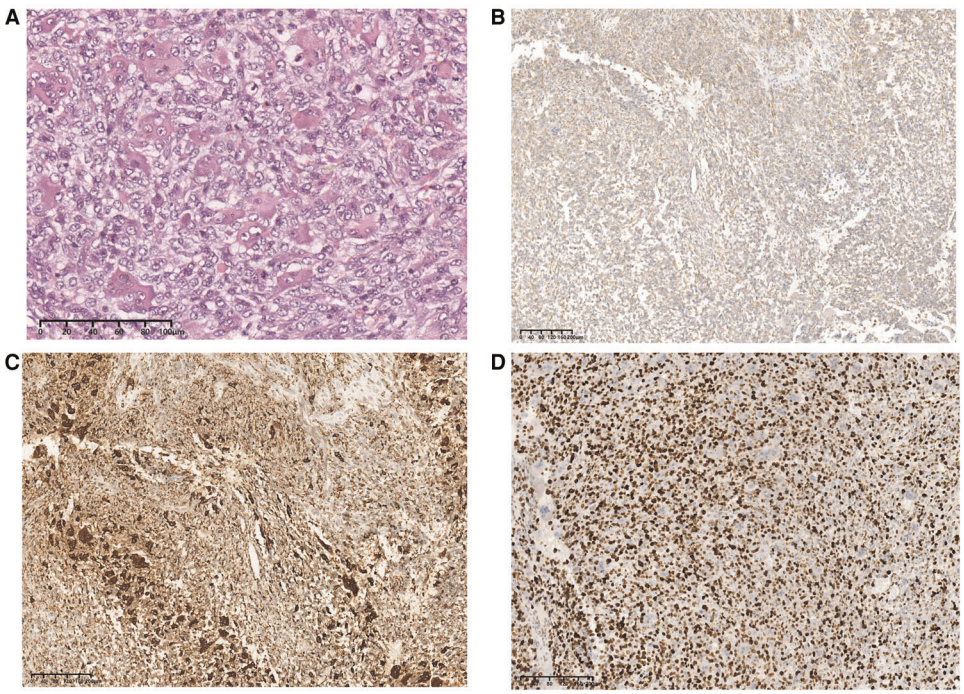

FIGURE 4 | Final pathological results after surgery. Histopathological examination of the tumor (H&E staining), original magnification, ×200 (**A**). These cells were positive for Vimentin, ×100 (**B**), CD68, ×100 (**C**), and Ki-67 was about 80% upon immunostaining, ×100 (**D**).

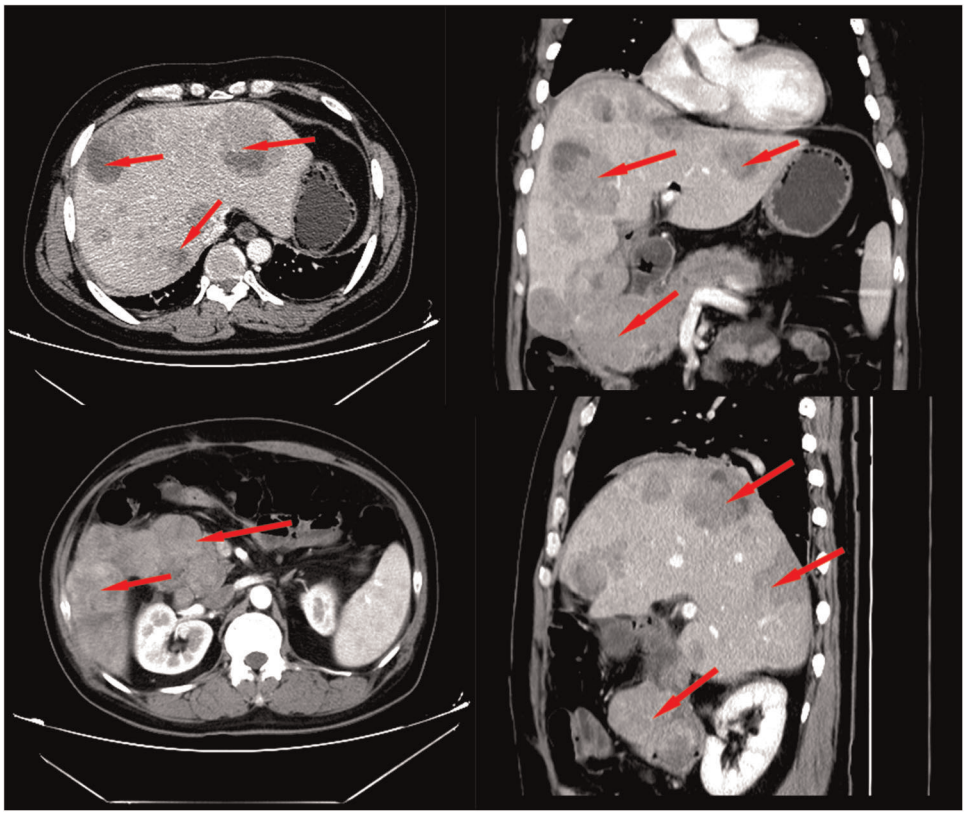

FIGURE 5 | Contrast-enhanced CT scan 2 months after surgery revealed local recurrence and intrahepatic metastasis.

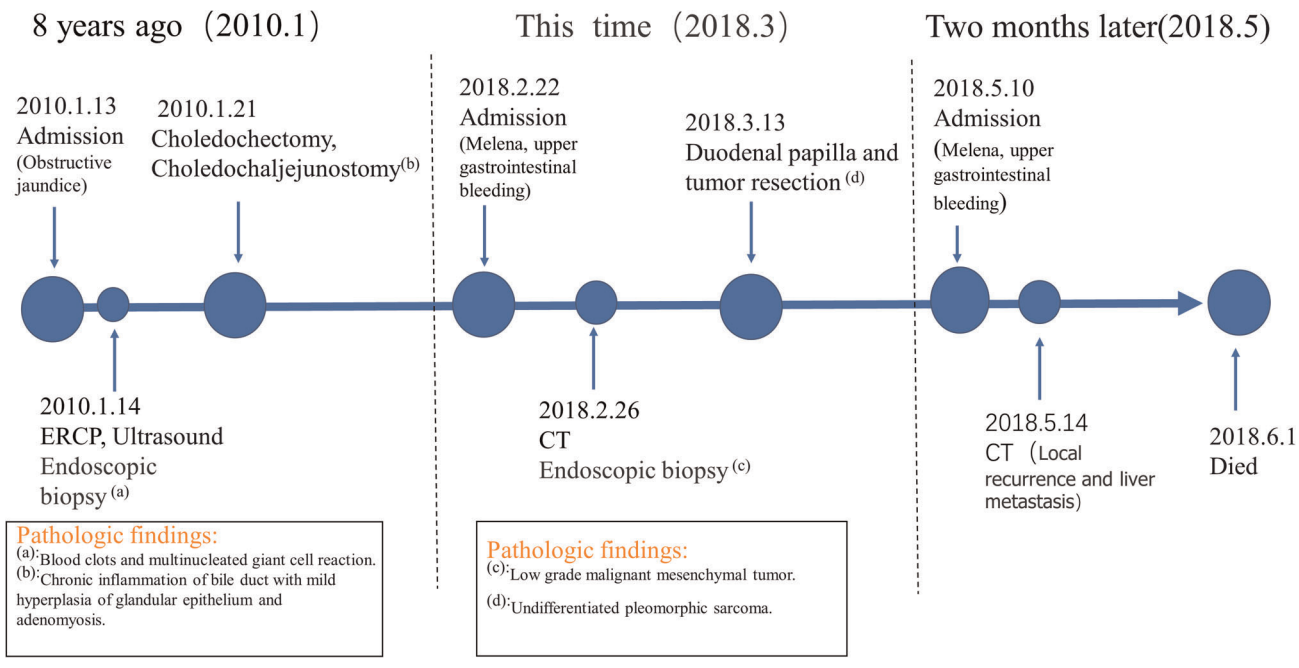

FIGURE 6 | A timeline with relevant data from the episode of care.

diagnosis of this case is giant cell tumor of soft tissue because of the existence of multinucleated giant cells (30, 31). However, considering the patient's high Ki67 index (80%) and rapidly progressing history, our final pathological diagnosis was UPS rather than a giant cell tumor of soft tissue (30, 32).

The surgical procedure, in this case, is different from the previous cases. Treatment with UPS emphasizes early complete resection of the tumor to obtain an adequate margin and reduce tumor recurrence. There is no consensus on what is an adequate margin distance for minimizing the risk of local recurrence. When UPS occurs in the extremities, the resection margin should be at least 1–3 cm away from the gross border (33, 34). However, if UPS is located in the retroperitoneum, complete compartmental resection will produce significantly better results (34, 35). Due to the low risk of lymphatic metastasis, routine lymph node dissection is not recommended during surgery (36). In this case, the tumor protruded into the intestinal lumen without invading the intestinal wall, and the intraoperative frozen section results showed a negative resection margin. Therefore, only the tumor and duodenal papilla were removed in this operation, instead of pancreaticoduodenectomy.

CONCLUSION

Primary UPS of the duodenal papilla is a highly malignant sarcoma with a poor prognosis. There are no specific clinical manifestations, which may only be jaundice with upper abdominal discomfort. When the tumor is enlarged and necrotic, upper gastrointestinal bleeding such as melena may occur. This tumor represents a challenge in management due to the lack of data in the literature. Early radical surgery is the key to better efficacy. The prognosis was poor despite the early complete resection. Early endoscopy in elderly patients with upper abdominal discomfort may yield early detection of this rare tumor, which needs to be verified in more cases.

DATA AVAILABILITY STATEMENT

The original contributions presented in the study are included in the article/Supplementary Material; further inquiries can be directed to the corresponding author.

ETHICS STATEMENT

Written informed consent was obtained from the individual(s) for the publication of any potentially identifiable images or data included in this article.

AUTHOR CONTRIBUTIONS

JW was responsible for the conception, design, and writing of the draft. BL, JH, and TL did the proof check. All authors contributed to the article and approved the submitted version.

FUNDING

This study was supported by the Medical Science Research Project of Hebei Province (No. 20211760) and the National Natural Science Foundation of China (No. 81402510).

REFERENCES

1. Weiss SW, Enzinger FM. Malignant fibrous histiocytoma: an analysis of 200 cases. *Cancer*. (1978) 41:2250–66. doi: 10.1002/1097-0142(197806)41:6<2250::aid-cncr2820410626>3.0.co;2-w
2. Liang Z, Han J, Tuo H, Xue D, Yu H, Peng Y. Undifferentiated pleomorphic sarcoma of the pancreas: a rare case report and literature review. *World J Surg Oncol*. (2022) 20:55. doi: 10.1186/s12957-022-02525-1
3. Winchester D, Lehman J, Tello T, Chimato N, Hocker T, Kim S, et al. Undifferentiated pleomorphic sarcoma: factors predictive of adverse outcomes. *J Am Acad Dermatol*. (2018) 79:853–9. doi: 10.1016/j.jaad.2018.05.022
4. Teng H, Xinghai Y, Wei H, Huang Q, Xiao J, Zhang C. Malignant fibrous histiocytoma of the spine: a series of 13 clinical case reports and review of 17 published cases. *Spine (Phila Pa 1976)*. (2011) 36:E1453–62. doi: 10.1097/BRS.0b013e318203e292
5. Takahashi H, Fujiwara T, Noro A, Orii S, Sato K, Sato S, et al. A case of malignant fibrous histiocytoma of mesentery of the ileum. *Nihon Shokakibyo Gakkai Zasshi*. (2000) 97:186–90. doi: 10.3919/ringe1963.54.2130
6. Pathak S, Soni TP, Gupta AK, Sharma LM. Retrovesical malignant fibrous histiocytoma: a rare tumor. *BMJ Case Rep*. (2017) 2017. doi: 10.1136/bcr-2017-222612
7. Margules RM, Allen RE, Dunphy JE. Pancreatic tumor of mesenchymal origin presenting as obstructive jaundice. *Am J Surg*. (1976) 131:357–9. doi: 10.1016/0002-9610(76)90131-8
8. Pascal RR, Sullivan L, Hauser L, Ferzli G. Primary malignant fibrous histiocytoma of the pancreas. *Hum Pathol*. (1989) 20:1215–7. doi: 10.1016/s0046-8177(89)80015-2
9. Suster S, Phillips M, Robinson MJ. Malignant fibrous histiocytoma (giant cell type) of the pancreas. A distinctive variant of osteoclast-type giant cell tumor of the pancreas. *Cancer*. (1989) 64:2303–8. doi: 10.1002/1097-0142(19891201)64:11<2303::aid-cncr2820641120>3.0.co;2-s
10. Haba R, Kobayashi S, Hirakawa E, Miki H, Okino T, Kurokawa T, et al. Malignant fibrous histiocytoma of the pancreas. *Pathol Int*. (1996) 46:515–9. doi: 10.1111/j.1440-1827.1996.tb03647.x
11. Mai G, Baer HU, Mittler M, Uhl W, Büchler MW, Rodriguez RU, et al. Malignant fibrous histiocytoma of the pancreas. *Pancreas*. (2002) 25:320–4. doi: 10.1097/00006676-200210000-00018
12. Darvishian F, Sullivan J, Teichberg S, Basham K. Carcinosarcoma of the pancreas: a case report and review of the literature. *Arch Pathol Lab Med*. (2002) 126:1114–7. doi: 10.5858/2002-126-1114-cotp
13. Yu RS, Wang JW, Chen Y, Ding WH, Xu XF, Chen LR. A case of primary malignant fibrous histiocytoma of the pancreas: CT and MRI findings. *World J Gastroenterol*. (2008) 14:2942–5. doi: 10.3748/wjg.14.2942
14. Jarry J, Belleannee G, Laurent C, Coindre JM, Evrard S. Primary malignant fibrous histiocytoma of the pancreas: benefit of the multidisciplinary approach. *Eur J Gastroenterol Hepatol*. (2010) 22:765–8. doi: 10.1097/MEG.0b013e32832e0a05
15. Sanei B, Kefayat A, Samadi M, Goli P, Sanei MH, Ghahremani F, et al. Undifferentiated pleomorphic sarcoma of pancreas: a case report and review of the literature for the last updates. *Case Rep Med*. (2018) 2018:1510759. doi: 10.1155/2018/1510759
16. Gilman JK, Sievers DB, Thornsvard CT. Malignant fibrous histiocytoma manifesting as a cavitary lung metastasis. *South Med J*. (1986) 79:376–8. doi: 10.1097/00007611-198603000-00031

17. Endo Y, Kobayashi T, Irie S, Mori K, Minamimura K, Hirata T, et al. Primary duodenal undifferentiated pleomorphic sarcoma that recurred after resection. *Jpn J Gastroenterol Surg*. (2016);49:989–96. doi: 10.5833/jjgs.2015.0190
18. Farinon AM, Bock E, Federico F, Rulli F, D'Antini P. Primary malignant fibrous histiocytoma of the duodenum. *Dig Surg*. (1999) 16:425–30. doi: 10.1159/000018760
19. Wang ZS, Xiong CL, Zhan N, Xiong GS, Li H, Hu H. Primary malignant fibrous histiocytoma of the small bowel: a report of an additional case in duodenum. *Int J Gastrointest Cancer*. (2005) 36:105–12. doi: 10.1385/ijgc:36:2:105
20. Makni A, Chebbi F, Azzouz H, Magherbi H, Jouini M, Kacem M, et al. A case of primary malignant fibrous histiocytoma of the duodenum. *Int J Surg Case Rep*. (2011) 2:103–5. doi: 10.1016/j.ijscr.2011.01.011
21. Giuliani J. Primary malignant fibrous histiocytoma of Vater's Papilla: first reported case. *J Gastrointest Cancer*. (2013) 44:366–7. doi: 10.1007/s12029-012-9439-5
22. Xu F, Zhao F, Feng X, Li C, Han D, Zheng S, et al. Nomogram for predicting cancer-specific survival in undifferentiated pleomorphic sarcoma: a surveillance, epidemiology, and end results-based study. *Cancer Control*. (2021) 28:10732748211036775. doi: 10.1177/10732748211036775
23. Matushansky I, Charytonowicz E, Mills J, Siddiqi S, Hricik T, Cordon-Cardo C. MFH Classification: differentiating undifferentiated pleomorphic sarcoma in the 21st Century. *Expert Rev Anticancer Ther*. (2009) 9:1135–44. doi: 10.1586/era.09.76
24. Kikuta K, Morioka H, Kawai A, Kondo T. Global protein-expression profiling for reclassification of malignant fibrous histiocytoma. *Biochim Biophys Acta*. (2015) 1854:696–701. doi: 10.1016/j.bbapap.2014.08.012
25. Jo VY, Fletcher CD. WHO Classification of soft tissue tumours: an update based on the 2013 (4th) edition. *Pathology*. (2014) 46:95–104. doi: 10.1097/pat.0000000000000050
26. Baehring JM, Alemohammed S, Croul SE. Malignant fibrous histiocytoma presenting as an intraventricular mass five years after incidental detection of a mass lesion. *J Neurooncol*. (2001) 52:157–60. doi: 10.1023/a:1010685020995
27. Froehner M, Gaertner HJ, Hakenberg OW, Wirth MP. Malignant fibrous histiocytoma of the ileum at a site of previous surgery: report of a case. *Surg Today*. (2001) 31:242–5. doi: 10.1007/s005950170177
28. Thway K, Fisher C. Undifferentiated and dedifferentiated soft tissue neoplasms: immunohistochemical surrogates for differential diagnosis. *Semin Diagn Pathol*. (2021) 38:170–86. doi: 10.1053/j.semdp.2021.09.005
29. Goldblum JR. An approach to pleomorphic sarcomas: can we subclassify, and does it matter? *Mod Pathol*. (2014) 27(Suppl 1):S39–S46. doi: 10.1038/modpathol.2013.174
30. Folpe AL, Morris RJ, Weiss SW. Soft tissue giant cell tumor of low malignant potential: a proposal for the reclassification of malignant giant cell tumor of soft parts. *Mod Pathol*. (1999) 12:894–902.
31. Carvalho SD, Pissaloux D, Crombé A, Coindre JM, Le Loarer F. Pleomorphic sarcomas: the state of the art. *Surg Pathol Clin*. (2019) 12:63–105. doi: 10.1016/j.path.2018.10.004
32. Xu Z, Qu W, Yu Y. Primary giant cell malignant fibrous histiocytoma of the lung: a rare case report and literature review. *Transl Cancer Res*. (2020) 9:7350–8. doi: 10.21037/tcr-20-2297
33. Jibbe A, Worley B, Miller CH, Alam M. Surgical excision margins for fibrohistiocytic tumors, including atypical fibroxanthoma and undifferentiated pleomorphic sarcoma: a probability model based on a systematic review. *J Am Acad Dermatol*. (2021). doi: 10.1016/j.jaad.2021.09.036. [Epub ahead of print]
34. Fujiwara T, Stevenson J, Parry M, Tsuda Y, Tsoi K, Jeys L. What is an adequate margin for infiltrative soft-tissue sarcomas? *Eur J Surg Oncol*. (2020) 46:277–81. doi: 10.1016/j.ejso.2019.10.005
35. Li B, Luo CH, Zheng W. Risk factors for recurrence and survival in patients with primary retroperitoneal tumors. *J Buon*. (2013) 18:782–7.
36. Gandhi J, Mehta S, Patel T, Gami A, Shah M, Jetly D. Metastasis of soft tissue sarcomas in lymph node: a cytomorphological study. *Diagn Cytopathol*. (2017) 45:784–8. doi: 10.1002/dc.23754

Conflict of Interest: The authors declare that the research was conducted in the absence of any commercial or financial relationships that could be construed as a potential conflict of interest.

Publisher's Note: All claims expressed in this article are solely those of the authors and do not necessarily represent those of their affiliated organizations, or those of the publisher, the editors and the reviewers. Any product that may be evaluated in this article, or claim that may be made by its manufacturer, is not guaranteed or endorsed by the publisher.

Copyright © 2022 Wang, Liu, Hou and Li. This is an open-access article distributed under the terms of the Creative Commons Attribution License (CC BY). The use, distribution or reproduction in other forums is permitted, provided the original author(s) and the copyright owner(s) are credited and that the original publication in this journal is cited, in accordance with accepted academic practice. No use, distribution or reproduction is permitted which does not comply with these terms.

frontiers | Frontiers in Oncology

ORIGINAL RESEARCH
published: 11 July 2022
doi: 10.3389/fonc.2022.944194

Overexpression of OAS1 Is Correlated With Poor Prognosis in Pancreatic Cancer

Lingling Lu[1†], Huaxiang Wang[1,2†], Jian Fang[3†], Jiaolong Zheng[4], Bang Liu[1], Lei Xia[3] and Dongliang Li[1,4]*

[1] Fuzong Clinical Medical College of Fujian Medical University, Fuzhou, China, [2] Department of Hepatobiliary and Pancreatic Surgery, Taihe Hospital, Affiliated Hospital of Hubei University of Medicine, Shiyan, China, [3] Department of Hepatobiliary Medicine, The Third Affiliated People's Hospital of Fujian University of Traditional Chinese Medicine, Fuzhou, China, [4] Department of Hepatobiliary Disease, The 900th Hospital of the People's Liberation Army Joint Logistics Support Force, Fuzhou, China

OPEN ACCESS

Edited by:
Sanjit Mukherjee,
National Institutes of Health (NIH),
United States

Reviewed by:
Ravi Kumar,
National Cancer Institute (NIH),
United States
Dipranjan Laha,
National Institutes of Health (NIH),
United States

***Correspondence:**
Dongliang Li
ldliang900@163.com

[†]These authors have contributed equally to this work and share first authorship

Specialty section:
This article was submitted to Gastrointestinal Cancers: Hepato Pancreatic Biliary Cancers, a section of the journal Frontiers in Oncology

Received: 14 May 2022
Accepted: 21 June 2022
Published: 11 July 2022

Citation:
Lu L, Wang H, Fang J, Zheng J, Liu B, Xia L and Li D (2022) Overexpression of OAS1 Is Correlated With Poor Prognosis in Pancreatic Cancer. Front. Oncol. 12:944194. doi: 10.3389/fonc.2022.944194

Background: OAS1 expression in pancreatic cancer has been confirmed by many studies. However, the prognostic value and mechanism of OAS1 in pancreatic cancer have not been analyzed.

Methods: The RNA-seq in pancreatic cancer were obtained by UCSC XENA and GEO database. In addition, immunohistochemical validation and analysis were performed using samples from the 900th hospital. The prognosis of OAS1 was evaluated by timeROC package, Cox regression analysis, and Kaplan-Meier survival curves. Then, the main functional and biological signaling pathways enrichment and its relationship with the abundance of immune cells were analyzed by bioinformatics.

Results: OAS1 was highly expressed in pancreatic cancer compared with normal pancreatic tissue. High OAS1 expression was associated with poor overall survival ($p<0.05$). The OAS1 was significantly correlated to TNM staging ($p=0.014$). The timeROC analysis showed that the AUC of OAS1 was 0.734 for 3-year OS. In addition, the expression of OAS1 was significantly correlated with the abundance of a variety of immune markers. GSEA showed that enhanced signaling pathways associated with OAS1 include Apoptosis, Notch signaling pathway, and P53 signaling pathway.

Conclusions: OAS1 is a valuable prognostic factor in pancreatic cancer. Moreover, it may be a potential immunotherapeutic target.

Keywords: pancreatic cancer, prognosis, OAS1, overall survival, immune infiltration

INTRODUCTION

Once pancreatic cancer has metastasized, the 5-year survival rate is as low as 2.9% (1). Early surgical intervention is still the radical cure. However, most patients with pancreatic cancer were found late and missed the best time for treatment. This may be related to the lack of early detection and identifiable symptoms and signs (2). With the development of multidisciplinary therapy, patients with pancreatic cancer can achieve better outcomes. However, the overall prognosis is still not satisfactory due to the high

tumor-specific mortality rate. and the annual mortality and morbidity rates are similar (3). The prognosis of pancreatic cancer is still worthy of special attention. However, there are many factors affecting the prognosis of patients, including not only the common tumor size, tumor stage (4) and the presence of disseminated tumor cells, but also the systemic inflammatory response (5), which reflects the response of the immune system to the proliferation and survival of tumor cells, which affects the ability of tumor cells to induce angiogenesis and metastasis and spread. In recent years, studies on tumor microenvironment (TME) have confirmed the key role of immune cells in the occurrence and development of cancer. Moreover, gene biomarkers have been widely explored in pancreatic cancer (6).

2',5'-oligoadenylate synthetase 1 (OAS1), a member of OAS family, has been shown to be a protein family of interferon-induced enzymes (7). The OAS family are involved in many intracellular functions, including induction of apoptosis, enhancement of IFN- α signal response, gene regulation, immune cell receptor regulation, and autophagy (8, 9). Moreover, OAS1 has been shown to be correlated with different subcellular components, such as mitochondria, nuclei, and rough/smooth microsomes (10, 11). It has been found that OAS1 is highly expressed in many tumors (12). And the high expression was related to worse prognosis in breast cancer (13). OAS1 may be associated with gastric cancer resistant to trastuzumab (14). It has been proved that down-regulating the expression of OAS1 can lead to the decrease of cell motility *in vitro* (15). In addition, OAS1 may be regulated by 17β-estradiol (E2) and play a key role in inducing apoptosis in cancer cells (16, 17). It is closely correlated with the occurrence and progress of gastric cancer (14), breast cancer (18), lung adenocarcinoma (19), and bladder cancer (20). However, the relationship between OAS1 and pancreatic cancer has not been clarified. Whether OAS1 can be used as a prognostic indicator of pancreatic cancer is worth exploring.

Here, it is particularly important to find reliable biomarkers related to prognosis in pancreatic cancer. We applied bioinformatics method to analyze the relationship between OAS1 and clinical information and overall survival (OS) of pancreatic adenocarcinoma (PAAD). Moreover, the immune-related database was used to analyze the relationship between OAS1 and tumor microenvironment. The aim was to explore the prognostic value of OAS1 in pancreatic cancer. In addition, Function analysis and GSEA were used to further enrich the signal pathways related to OAS1.

MATERIALS AND METHODS

Ethical Statement

All patients were included in the public database only after obtaining informed consent. Since all the research data are from open online databases, all informed consent can be guaranteed.

Differential Expression of OAS1

UCSC XENA (https://xenabrowser.net/datapages/) is a data analysis platform for cancer genomics, which includes data from TCGA, ICGC, and other projects. It can provide online analysis and data visualization. TCGA and GTEx RNAseq data in TPM format are processed through toil (21). This study extracted data of pancreatic adenocarcinoma (PAAD) from TCGA and corresponding normal tissue from GTEx. The R statistical language (version 3.6.3) and the ggplot2 package were used to analyze mRNA differential expression and for plotting. The GSE15471 dataset in the GEO (22) database was also used to evaluate the difference in OAS1 expression between pancreatic cancer and normal tissue. The Human Protein Atlas (https://www.proteinatlas.org/) (23) provides proteomic and transcriptome information for a variety of human samples, including monocytic, blood, tissue, and pathological maps. The database was applied to obtain the protein immunohistochemistry (IHC) of OAS1 in normal tissues and pancreatic cancer tissues.

Immunohistochemistry and Immunofluorescence

45 cases of pancreatic cancer tissue specimens were embedded in paraffin and cut into 4 μm sections. Next, the slides were then dewaxed with xylene at room temperature and then hydrated with degraded ethanol. Steam 20 minutes in sodium citrate buffer (PH 6.0) for antigen retrieval. H2O2 was used to inhibit endogenous peroxidase. The polyclonal rabbit anti-OAS1 antibody (1:100, LS-B6622, LifeSpan Biosciences) was added to the slices, incubated at room temperature for 1 hour, and washed in PBS for 3 times. Then, secondary antibody (PV-9001; goat anti-rabbit IgG polymer; Beijing Zhongshan Jinqiao Biotechnology Co., LTD) was added at room temperature and incubate for 30 minutes. Finally, diaminobenzidine (DAB) was used for 1 minute at room temperature, and the slides were stained with hematoxylin. We used a semi-quantitative scoring system to assess OAS1 protein expression. Score of 0 indicates no positive cells, while a score of 1 indicates less than 10% positive cells, 2 indicates 11%-25% positive cells, 3 indicates 26-50% positive cells, 4 indicates 51-75% positive cells, and 5 indicates greater than 75% positive cells. The scores of 0, 1 and 2 indicate the low expression of OAS1, while the higher the score, the higher the expression of OAS1. The score of IHC staining was performed by two experienced pathologists without knowing the patient's clinical information. All samples were taken from the 900th hospital of the People's Liberation Army Joint Logistics Support Force (Fujian, China). This study was approved by the Ethics Committee of the 900th hospital of the People's Liberation Army Joint Logistics Support Force and carried out in accordance with the Helsinki Declaration.

Similarly, paraffin blocks of pancreatic cancer were sectioned for dewaxing, rehydration, and antigen retrieval. They were then blocked with PBST containing 5% FBS for 30 min. Next, primary antibody (1:100, LS-B6622, LifeSpan Biosciences) was dropped and incubated at room temperature for 2 hours. Then the slides were washed with PBST and incubated with secondary antibody (1:1000, 8889s, CST) for 2 hours at room temperature. Finally, 4, 6-Diamidino-2-phenylindole (DAPI) (C1005, Beyotime Biotechanology, China) was stained for 4 minutes and observed by confocal laser scanning microscope.

Prognostic Value of OAS1

Extract the RNAseq data and clinical data from the TCGA-PAAD project, and eliminate the data with missing clinical information.

According to the median value of OAS1, they were divided into two groups: high expression group and low expression group. We used Kaplan-Meier survival curves to compare survival differences, and to study the relationship between OAS1 expression level and clinical outcome. Then using the survminer and survival package for statistical analysis of survival data. In addition, the independent prognostic factors were determined by Cox regression analysis. Using timeROC package to draw receiver operating characteristic (ROC) curve to evaluate the accuracy of OAS1 in survival prediction. OS is defined as the time between first diagnosis and death or the last observation point. Disease specific survival (DSS) was defined as the period from the date of diagnosis of pancreatic cancer to the recorded date of death due to pancreatic cancer. Progression free interval (PFI) is defined as the time between the start of follow-up and the first appearance of progression (24).

Immune Infiltration Analysis and Gene Alterations

TIMER (https://cistrome.shinyapps.io/timer/) was applied to analyze the relationship between gene expression and immune infiltrate or abundance online (25). In this work, TIMER data was used to identify the relationship between the expression of OAS1 and immune cells infiltration in pancreatic cancer. Furthermore, TISIDB (http://cis.hku.hk/TISIDB/) (26) was conducted to analyze the relationship between abundance of tumor-infiltrating lymphocytes (TILs) and expression of OAS1. Then for genetic changes of OAS1 gene, the data of cBioPortal (http://www.cbioportal.org/) (27) database were inquired, and the relationship between genetic alterations and clinical outcome, including OS and DFS, was obtained.

Functional Analysis and PPI Network Construction

The top 100 genes with the strongest correlation with OAS1 were found by using GEIPIA (http://gepia.cancer-pku.cn/index.html) (28) database and cBioportal database respectively, and the intersection was taken. Then, GO and KEGG (29) enrichment analysis of OAS1 related genes was carried out by using functional annotation tool in DAVID (https://david.ncifcrf.gov/) (30) database. In the process of GO and KEGG enrichment analysis, false discovery rate (FDR) < 0.5 or P<0.05 was used as the screening condition. In addition, the protein-protein interaction (PPI) network of OAS1-related genes was constructed in STRING (https://string-db.org/) (31) database and visualized in Cytoscape software (Version 3.7.1).

Gene Set Enrichment Analysis(GSEA)

GSEA is executed using GSEA software (version 4.0.3). Biological pathways associated with OAS1 were detected by gene enrichment analysis (GSEA). All the genetic data analyzed were obtained from TCGA database.

RESULTS

Elevated Expression of OAS1 in PAAD

We preliminarily evaluated the transcription levels of OAS1 in different human tumors by analyzing TCGA and GTEx RNA-seq data using the UCSC XENA database. OAS1 was highly expressed in 29 kinds of tumors including PAAD. It is interesting to note that OAS1 was only found to be significantly lower expressed in the tissues of kidney chromophobe (KICH) and Thymoma (THYM) than in the respective control tissues (**Figure 1A**). These results suggest that OAS1 is abnormally high expressed in most tumors. Then we compared OAS1 mRNA expression in 179 pancreatic cancer tissues and 171 normal tissues. The expression of OAS1 mRNA in PAAD tissue was significantly higher than that in normal pancreatic tissue (p<0.001, **Figure 1B**). In addition, we further analyzed the expression level of OAS1 in pancreatic cancer tissue using GEO data (GSE15471), and found that OAS1 mRNA in tumors was also significantly higher than that in normal tissue (p<0.001, **Figure 1C**). Overall, these results suggest that elevated expression of OAS1 in PAAD than in normal tissues.

We compared the protein expression of OAS1 between normal pancreatic tissue and pancreatic cancer tissue by HPA. As shown in **Figures 1D, E**, immunohistochemical staining also indicated OAS1 was upregulated in pancreatic cancer tissue.

OAS1 and the Clinicopathological Features in the Patients From the 900th Hospital

A total of 45 cases of pancreatic cancer samples from the 900th hospital of the People's Liberation Army Joint Logistics Support Force were collected. There were 14 females and 31 males. Mean age was 59.22 years (range 41-82). According to semi-quantitative scoring system, 45 cases of pancreatic cancer were divided into high expression group (n=23) and low expression group (n=22). The median overall survival was 21.0 months and 23.0 months for patients with high and low OAS1 expression, respectively. And the mean value of overall survival was 21.12 months and 25.18 months for patients with high and low OAS1 expression, respectively. As shown in **Figures 1F, G**, OAS1 expression was divided into high and low groups, and it was mainly expressed in the cytoplasm of pancreatic cancer cells. The immunofluorescence results showed that OAS1 was mainly observed in cytoplasm (**Figure 1H**). Furthermore, Kaplan-Meier survival curves showed that the high expression of OAS1 was related to the poor OS (p=0.020) in patients with pancreatic cancer (**Figure 2A**).

Survival Analysis

RNAseq data and clinical data from the TCGA-PAAD project were obtained for analysis. Samples are grouped according to the median value of OAS1 and then to study the correlation between the expression of OAS1 and the prognosis of patients with pancreatic cancer. Then we summarize the basic clinical features of the patient in **Table 1**. Of the 178 patients, 176 underwent surgery, including Whipple, total pancreatectomy, distal pancreatectomy, and other method. And postoperative residual tumors status can be obtained in 164 cases. Only one patient received neoadjuvant therapy. 118 out of the 178 patients received chemotherapy. The patients were treated with drugs, including "Gemcitabine", "Xeloda", "5-FU", "Tarceva", "Capecitabine", "Irinotecan". "Oxaliplatin", "Leucovorin", "Abraxane", "Cisplatin", "Docetaxel" "cyclophosphamide", and "gemzar". In addition, 45 of the 178

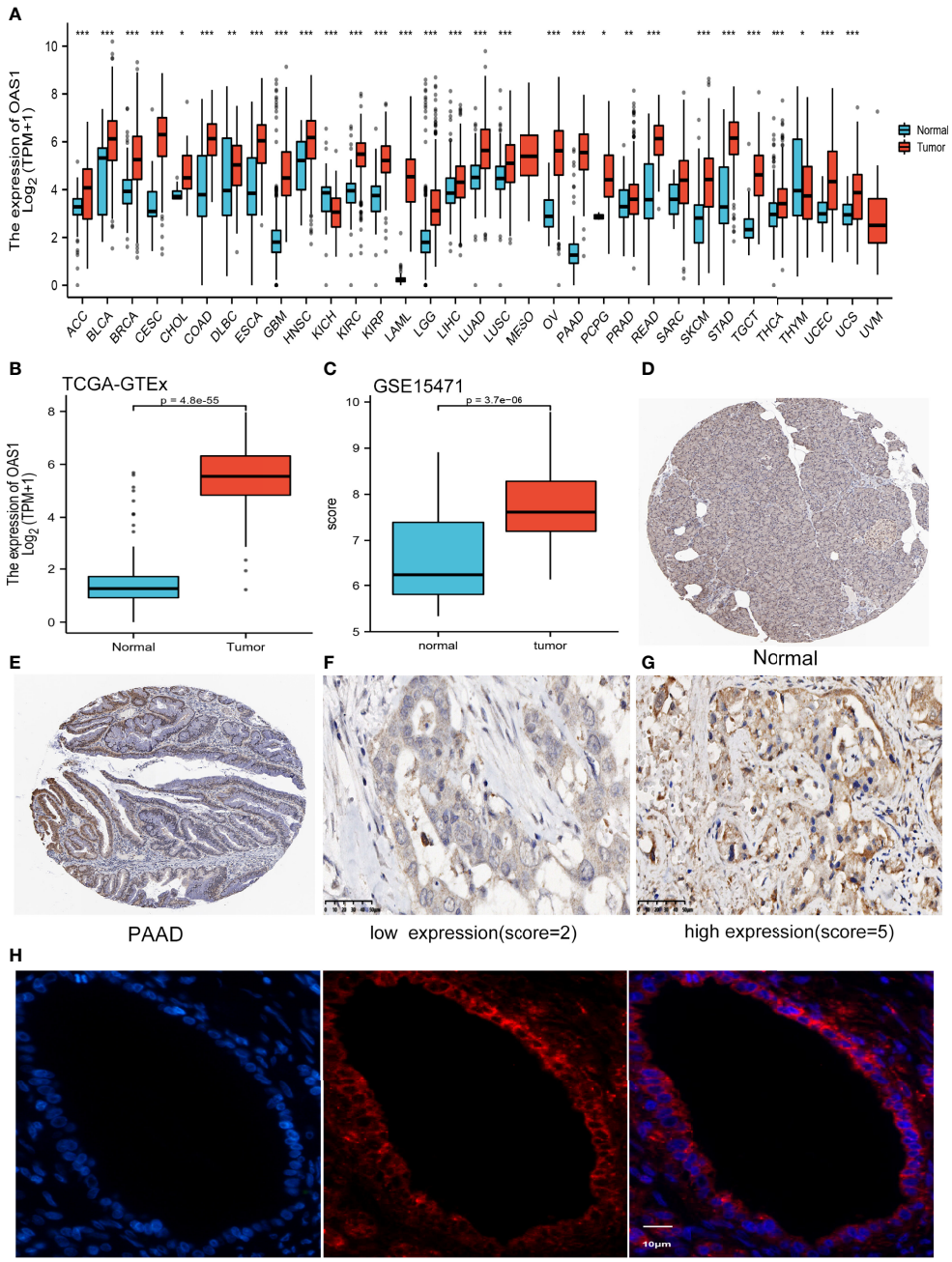

FIGURE 1 | The expression of OAS1 **(A)** OAS1 expression in different types of cancers (*P < 0.05, **P <0.01, ***P < 0.001). **(B)** OAS1 expression in pancreatic cancer and normal pancreatic tissue base on TCGA-PAAD. **(C)** OAS1 expression in pancreatic cancer and normal tissue base on GSE15471 of GEO. **(D, E)** The protein levels of OAS1 between normal pancreatic tissue and pancreatic cancer tissue based on HPA. **(F, G)** Representative Images of low **(F)** /High **(G)** protein expression of OAS1 in 45 patients with PAAD (original magnification:X400). **(H)** Localization of OAS1 (red) was observed by immunofluorescence confocal microscopy. The nuclei were stained (blue) with DAPI. Representative pictures are displayed.

patients received radiation therapy. The median survival time in individuals with low OAS1 expression was 23.4 years in comparison with the median survival time of 17.2 years in high OAS1 expression. Moreover, Kaplan-Meier survival curves showed that the prognostic value of OAS1 in pancreatic cancer (**Figure 2B**). The results indicated that the high expression of OAS1 was significantly correlated with the shorter OS of PAAD (HR 1.60, 95%CI,1.06-2.242; p=0.027). But we observed no significant relationship

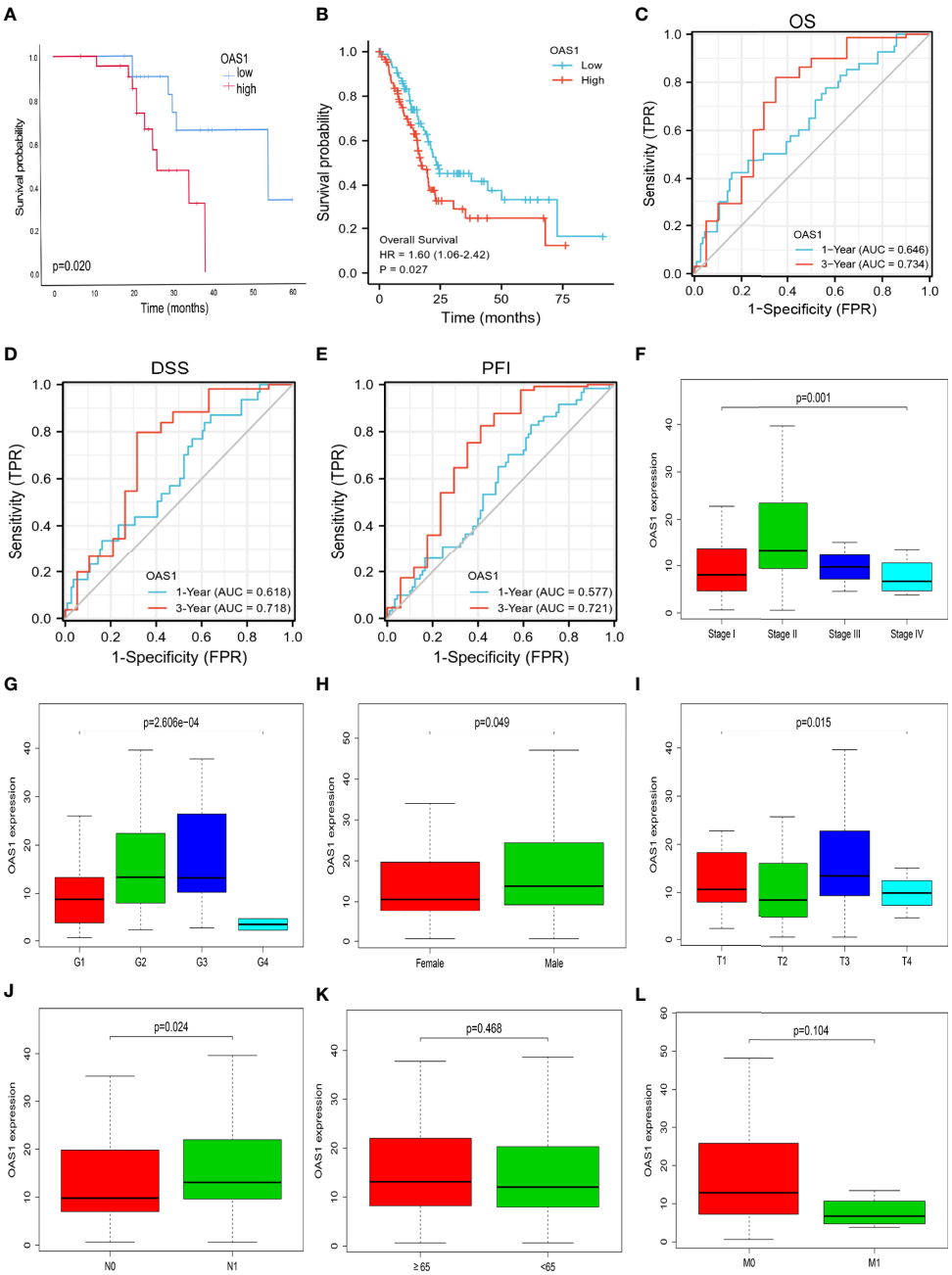

FIGURE 2 | **(A, B)** Kaplan-Meier survival curves for OAS1, and high expression of OAS1 has short overall survival in PAAD. The time-dependent ROC to assess the accuracy of OAS1 in predicting OS **(C)**, DSS **(D)**, and PFI **(E)** at 1 and 3 years. The relationships between OAS1 mRNA expression and clinical pathological characteristics. OAS1 mRNA expression was differentially expressed in different TNM stages **(F)**, grades **(G)**, gender **(H)**, T stages **(I)**, and N stages **(J)**. There was no difference in ages or M stages **(K, L)**.

between OAS1 expression and disease-free survival (p=0.17). The timeROC analysis showed that the AUC of OAS1 was 0.646 and 0.734 for 1- and 3-year OS, respectively (**Figure 2C**). The AUC for 1- and 3-year DSS were 0.618 and 0.717, respectively (**Figure 2D**), and the AUC for 1- and 3-year PFI were 0.577and 0.721, respectively (**Figure 2E**). These results showed the moderate predict performance of OAS1 and which is limited to 3-year OS, DSS, and PFI.

TABLE 1 | Baseline characteristics for patients with pancreatic cancer from TCGA.

Characteristic	Levels	Overall
n		178
T stage, n (%)	T1	7 (4%)
	T2	24 (13.6%)
	T3	142 (80.7%)
	T4	3 (1.7%)
N stage, n (%)	N0	50 (28.9%)
	N1	123 (71.1%)
	N2	0
M stage, n (%)	M0	79 (94%)
	M1	5 (6%)
Pathologic stage, n (%)	Stage I	21 (12%)
	Stage II	146 (83.4%)
	Stage III	3 (1.7%)
	Stage IV	5 (2.9%)
Gender, n (%)	Female	80 (44.9%)
	Male	98 (55.1%)
Race, n (%)	Asian	11 (6.3%)
	Black or African American	6 (3.4%)
	White	157 (90.2%)
Age, n (%)	<=65	93 (52.2%)
	>65	85 (47.8%)
Residual tumor, n (%)	R0	107 (65.2%)
	R1	52 (31.7%)
	R2	5 (3.1%)
Chemotherapy	No/unkown	60 (33.7%)
	Yes	118 (66.3%)
Radiation therapy, n (%)	No	118 (72.4%)
	Yes	45 (27.6%)
Histologic grade, n (%)	G1	31 (17.6%)
	G2	95 (54%)
	G3	48 (27.3%)
	G4	2 (1.1%)
Anatomic neoplasm subdivision, n (%)	Head of Pancreas	139 (78.1%)
	Other	39 (21.9%)
Smoker, n (%)	No	65 (45.1%)
	Yes	79 (54.9%)
Alcohol history, n (%)	No	65 (39.2%)
	Yes	101 (60.8%)
History of diabetes, n (%)	No	108 (74%)
	Yes	38 (26%)
History of chronic pancreatitis, n (%)	No	128 (90.8%)
	Yes	13 (9.2%)
OS event, n (%)	Alive	86 (48.3%)
	Dead	92 (51.7%)
DSS event, n (%)	Alive	100 (58.1%)
	Dead	72 (41.9%)
PFI event, n (%)	Alive	74 (41.6%)
	Dead	104 (58.4%)

Correlation Between OAS1 Expression and Clinicopathological Parameters

We obtained clinical data from the TCGA-PAAD project and studied the relationship between OAS1 and clinicopathological features, which is helpful to reveal the role of OAS1 in the progression of PAAD. As shown in **Figures 2F–L**, OAS1 mRNA expression was differentially expressed in different grades ($p<0.001$), gender ($p=0.049$), T stages ($p=0.015$), N stages ($p=0.024$), and TNM stages ($p=0.001$). There was no difference in age or M stage. Moreover, the Cox regression analysis was applied to analyze the prognostic factors. As shown in **Table 2**, the univariate analysis indicated that high OAS1 expression was correlated with the poorer OS (HR 1.545, 95%CI: 1.021-2.338, $p=0.040$). Other clinical parameters including T stage (HR 2.023, 95%CI: 1.072-3.816, $p=0.030$), and N stage (HR 2.154, 95%CI: 1.282-3.618, $p=0.004$) were also associated with the poorer overall survival. Multivariate analysis showed that only N staging (HR 1.870, 95%CI:1.079-3.240, $p=0.026$) was independently associated with OS.

Gene Alterations in OAS1 and Survival

We analyzed the gene alterations of OAS1 and their relationship with OS and DFS. As shown in **Figure 3A**, 10 of the 178 sequenced patients (5.62%) had gene alterations. In addition, the patient of

TABLE 2 | Univariate/multivariate Cox regression analysis.

		Univariate analysis		Multivariate analysis	
Characteristics	Total (N)	HR (95% CI)	P value	HR (95% CI)	P value
Gender (Male vs. Female)	178	0.809 (0.537-1.219)	0.311		
Age (>65 vs. <=65)	178	1.290 (0.854-1.948)	0.227		
Smoker (No vs. Yes)	144	0.921 (0.582-1.456)	0.724		
History of diabetes (No vs. Yes)	146	1.078 (0.619-1.878)	0.790		
T stage (T3&T4 vs. T1&T2)	176	2.023 (1.072-3.816)	**0.030**	1.261 (0.651-2.442)	0.492
N stage (N1 vs. N0)	173	2.154 (1.282-3.618)	**0.004**	1.870 (1.079-3.240)	0.026
M stage (M1 vs. M0)	84	0.756 (0.181-3.157)	0.701		
OAS1 (High vs. Low)	178	1.545 (1.021-2.338)	**0.040**	1.174 (0.768-1.795)	0.458

Bold values means that the P value < 0.05 were considered statistically significant.

altered group received a shorter OS (p<0.01; **Figure 3B**) and DFS (p<0.01; **Figure 3C**) than that of unaltered group. These results suggest that gene alteration of OAS1 may also significantly affect the prognosis of patients with pancreatic cancer.

OAS1 and Immune Cell Infiltration

TIMER database was used to investigate the correlation between the expression of OAS1 and immune cell infiltration in patients with PAAD. OAS1 expression had correlations with neutrophil (cor=0.302, p<0.001) and dendritic cell (cor=0.185, p<0.05) (**Figure 3D**). It highlights the key role of OAS1 in tumor immune infiltrating cells, neutrophils, and dendritic cells.

We also evaluated the relations between OAS1 expression and tumor-infiltrating lymphocytes (TILs) in the TISIDB database (**Figures 3E, F**). The expression of OAS1 was associated with activated CD4 T cell (rho=0.21, p<0.01), central memory CD8 T cell (rho=0.199, p<0.01), central memory CD4 T cell (rho=0.285, p<0.001), effector memory CD4 T cell (rho=-0.149, p<0.05), Type 17 T helper cell (rho=0.237, p<0.01), Type 2 T helper cell (rho=0.154, p<0.05), CD56bright natural killer cell (rho=0.365, p<0.001), CD56dim natural killer cell (rho=0.401, p<0.001), activated dendritic cell (rho=0.229, p<0.01), and eosinophil (rho=-0.202, p<0.01). Those results revealed that OAS1 may play a specific role in the immune infiltration of pancreatic cancer.

Functional Analysis and PPI Network Construction

Using cBioPortal and GEPIA database to find the top 100 genes with the strongest correlation with OAS1, and taking the intersection, 67 related genes can be obtained (**Figure 4A**). Then the 67 genes were analyzed by GO enrichment analysis including BP, CC, and MF (**Supplementary table 1**). GO-MF analysis showed that the related genes were most enriched by protein binding, ATP binding, and double-stranded RNA binding. Then visualize all the GO analysis results, as shown in **Figure 4B**. We also analyzed the related genes by KEGG enrichment analysis. In KEGG analysis, Cytosolic DNA-sensing pathway, RIG-I-like receptor signaling pathway, and Herpes simplex infection were enriched (**Figure 4C**). RIG-I-like receptor signaling pathway has been confirmed to be involved in the occurrence and development of tumors. The enrichment of the Herpes simplex infection suggests that the tumor may simulate immune mechanisms following viral infection. Finally, the interaction between these proteins is shown in **Figure 4D**.

GSEA Identifies OAS1-Related Signaling Pathways in Pancreatic Cancer

To explore the potential molecular function of OAS1 in pancreatic cancer, we conducted GSEA between low and high expression samples to predict OAS1-related signaling pathways. A total of 131 out of 178 gene sets are upregulated in the group of high OAS1 expression, and 47 out of 178 gene sets are upregulated in the group of low OAS1 expression. But only 20 signaling pathways were significantly enriched at NOM P < 0.05 (**Table 3**). Inhibitory signaling pathways associated with OAS1 include "Neuroactive ligand receptor interaction" and "Glycine serine and threonine metabolism". Enhanced signaling pathways associated with OAS1 include "Apoptosis", "Cytosolic and sensing pathway", "Glycerophospholipid metabolism", "Notch signaling pathway", and "P53 signaling pathway". The results of the GSEA are summarized in **Figure 4E**.

DISCUSSION

With the application of high-throughput sequencing, more and more studies have been conducted on the prognostic value of differential genes in pancreatic cancer in recent years. Song et al. found that the pyrolysis-related gene CASP4 can lead to the progression of pancreatic cancer by promoting fatty acid synthesis and accumulation (32). Other markers, such as AQP5, CDC25C, and TMEM170B, have been proved to be associated with the prognosis of pancreatic cancer (33–35). A specific single gene, or a group of genes, can predict the prognosis of the tumor in a corresponding way. The prediction model based on MCOLN1, PKD1, TRPC3, and TPRC7 can also predict the prognosis of pancreatic cancer (36). Zhang et al. found that most of the 21 immune-related prognostic genes of pancreatic cancer, including OAS1, were up-regulated in pancreatic cancer. OASL, as the most significant positive correlation with the expression of OAS1, was conformed that the high expression of OASL was also associated with poor OS in pancreatic cancer. This further speculates that OAS1 is related to the prognosis of pancreatic cancer (37).

In this study, OAS1 mRNA was significantly upregulated in patients with pancreatic cancer. Kaplan-Meier survival curve and

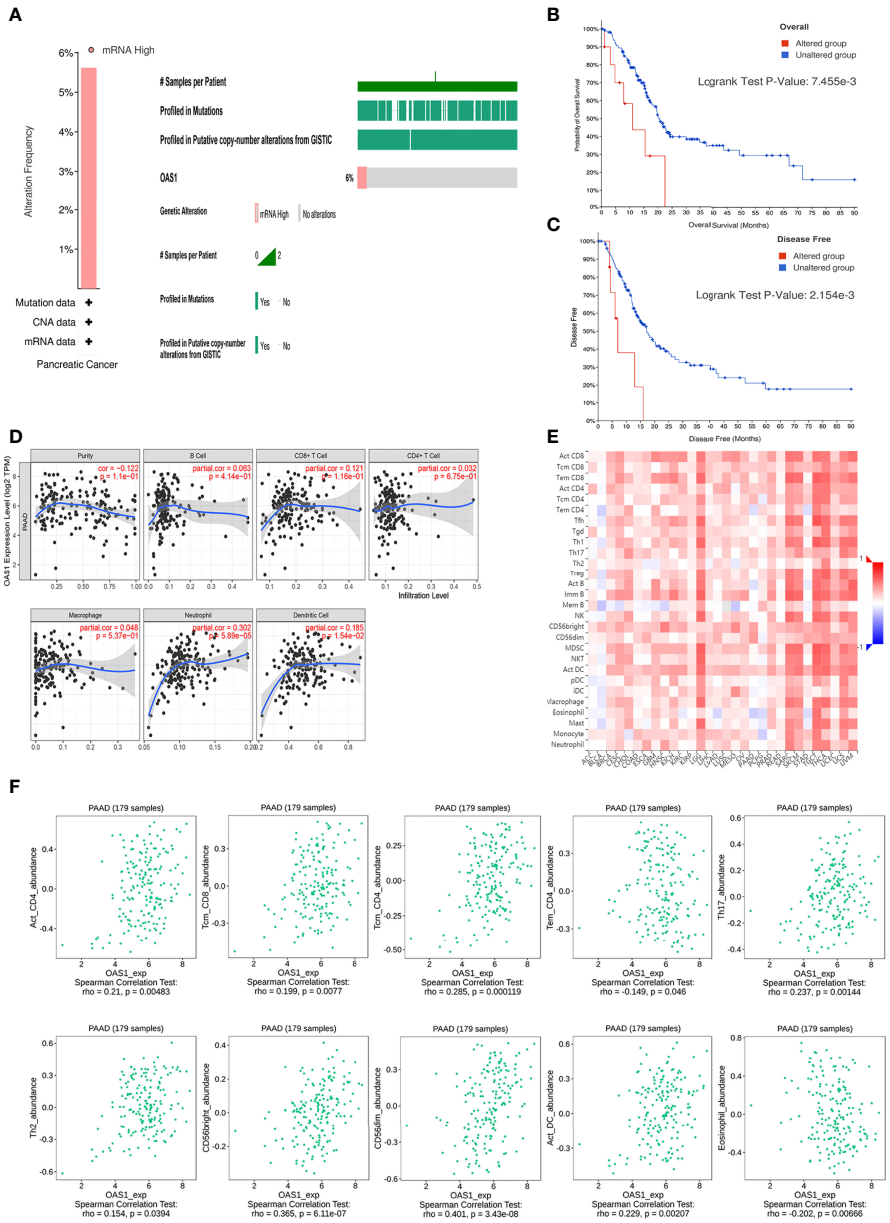

FIGURE 3 | Genetic alterations and immune infiltration. **(A)** Genetic alterations of OAS1 in patients with pancreatic cancer. The patient of altered group received a shorter OS **(B)** and DFS **(C)** than that of unaltered group. **(D)** OAS1 expression had correlations with neutrophil and dendritic cell. **(E)** correlations of OAS1 expression with TILs across human cancers. **(F)** The expression of OAS1 was associated with activated CD4 T cell, central memory CD8 T cell, central memory CD4 T cell, effector memory CD4 T cell, Type 17 T helper cell, Type 2 T helper cell, CD56bright natural killer cell, CD56dim natural killer cell, activated dendritic cell, and eosinophil.

univariate analysis showed that elevated OAS1 was associated with shorter OS. In addition, OAS1 has moderate predictive value in OS, DSS, and PFI at 3 years. The AUC of OAS1 was 0.734, 0.718, and 0.721 for 3-year OS, DSS, and PFI, respectively. Although the AUC was lower than that reported of PSMD6 (AUC=0.887) (38), it is higher than that of EIF4G1 (AUC=0.696) for 3-year OS (39). Furthermore, it has been reported that the gene prediction model performed well in predicting OS (AUC=0.680) and DSS (AUC=0.739) (36). Another model based on five prognostic molecules had AUC values of 0.72 and 0.67 at 1-and 2-years, respectively (40). Previous studies have reported the predictive value of a risk score constructed by combining OAS1 with 20 other prognostic genes in pancreatic cancer, and ROC evaluation showed good predictive value (AUC=0.833) (37).

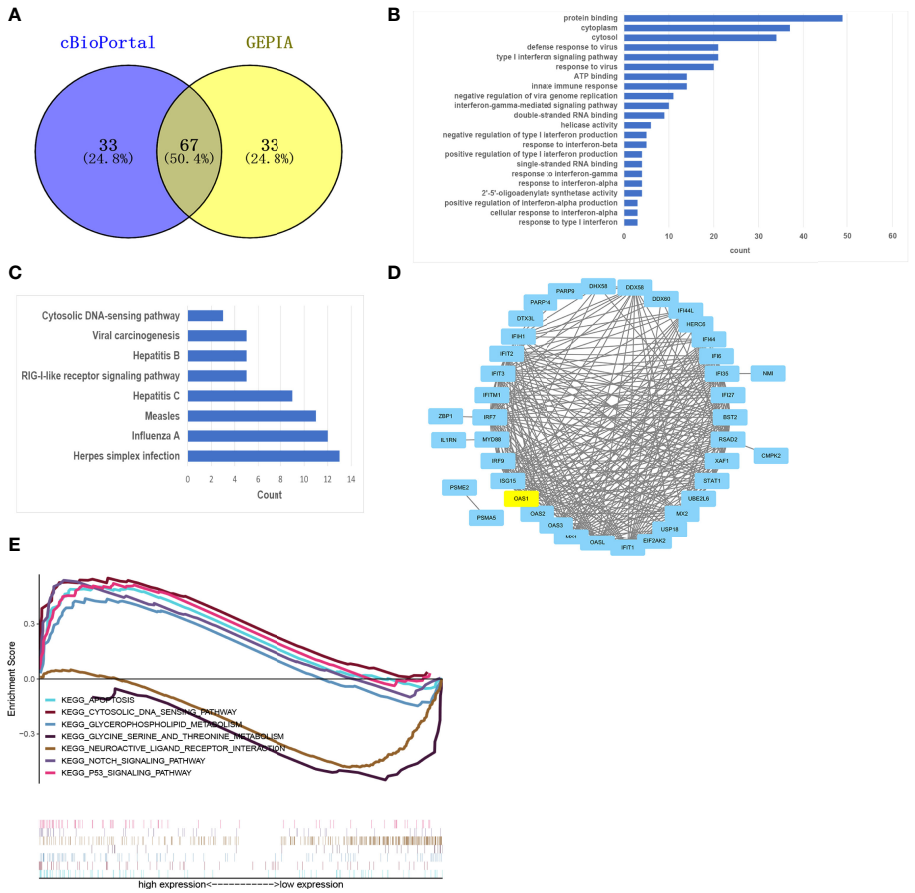

FIGURE 4 | Functional analysis and GSEA. **(A)** Venn plot showed overlapping genes in GEPIA and cBioPortal databases. **(B, C)** The 67 OAS1-related genes were analyzed by GO **(B)** and KEGG **(C)** enrichment analysis. **(D)** A PPI network of 67 OAS1-related genes was constructed and visualized. **(E)** GSEA identifies OAS1-related signaling pathways in pancreatic cancer.

Hence, OAS1 could be a biomarker for poor prognosis of patients with pancreatic cancer. In addition, it was found that OAS1 may play a key role in the immune infiltration of pancreatic cancer. Therefore, this study suggests that OAS1 may serve as a new prognostic biomarker for pancreatic cancer.

Recent studies have shown that elevated OAS1 is associated with short survival in many cancers, and it is an important biomarker of poor prognosis (13). Our study also found high expression of OAS1 in pancreatic cancer, consistent with those reports of abnormal expression of OAS1 in various cancers (13, 41). In breast cancer, elevated OAS1 is associated with poor prognosis. Qu et al. found that OAS1 is one of the high-risk genes for bladder cancer (42). Mandal et al. confirmed that the SNP of OAS1 rs2660 was associated with prostate cancer (43). Hence, OAS1 may play a carcinogenic or tumor suppressor role, affecting the development of cancers. However, the prognostic value of OAS1 in pancreatic cancer has not been studied. We speculate that OAS1 may be involved in the development of pancreatic cancer. Kaplan-Meier survival curves and univariate analysis were applied, the survival time of pancreatic cancer patients with high OAS1 expression was shorter than that of patients with low OAS1 expression. Therefore, we could speculate that OAS1 can be an important biomarker for poor prognosis of pancreatic cancer.

An important feature of PAAD microenvironment is its dense immunosuppressive stroma, which limits the infiltration of immune cells and therapeutic drug (44). Pancreatic ductal adenocarcinoma tumor cells usually account for only a small part of the tumor. Also, there are heterogeneous cell groups in TME, including immune cells, cancer-related fibroblasts (45), endothelial cells and neurons. As shown in **Figure 1**, OAS1 was also expressed in the stroma, especially in tumors with high expression of OAS1. But it is not clear what type of cell in the stroma is expressed. The dense stroma breaks down the tumor vascular system, limiting the delivery of nutrients and drugs (46, 47). This may also promote the insensitivity of pancreatic cancer to chemotherapy. Immune infiltration analysis revealed that OAS1 expression was associated with neutrophils and dendritic cells. This is consistent with previous findings that neutrophils are the predominant immune infiltrating cell type associated

TABLE 3 | Enrichment plots by GSEA.

Name	SIZE	ES	NES	NOM p-val	FDR q-val
KEGG_PROTEASOME	46	0.753654	1.784794	0.001930502	0.2470178
KEGG_BASE_EXCISION_REPAIR	35	0.74339	1.922512	0.001945525	0.06864582
KEGG_PATHOGENIC_ESCHERICHIA_COLI_INFECTION	56	0.61267	1.743762	0.002	0.2529717
KEGG_RIG_I_LIKE_RECEPTOR_SIGNALING_PATHWAY	70	0.538909	1.685073	0.008316008	0.22338139
KEGG_NOTCH_SIGNALING_PATHWAY	47	0.538491	1.704543	0.010288066	0.2797902
KEGG_CYTOSOLIC_DNA_SENSING_PATHWAY	54	0.550796	1.691296	0.012320329	0.25508887
KEGG_GLYCOSPHINGOLIPID_BIOSYNTHESIS_LACTO_AND_NEOLACTO_SERIES	26	0.518956	1.593648	0.014314928	0.3099594
KEGG_DRUG_METABOLISM_OTHER_ENZYMES	51	0.527769	1.581207	0.017045455	0.31012228
KEGG_P53_SIGNALING_PATHWAY	68	0.521419	1.658908	0.022044089	0.24438126
KEGG_PORPHYRIN_AND_CHLOROPHYLL_METABOLISM	40	0.526058	1.552143	0.023166023	0.32484913
KEGG_GLYCEROPHOSPHOLIPID_METABOLISM	77	0.438724	1.551786	0.023952097	0.3020833
KEGG_APOPTOSIS	87	0.502444	1.526006	0.026262626	0.2956351
KEGG_FC_GAMMA_R_MEDIATED_PHAGOCYTOSIS	96	0.505976	1.598625	0.034	0.37282383
KEGG_SPLICEOSOME	127	0.564458	1.598448	0.038240917	0.33185923
KEGG_ENDOCYTOSIS	181	0.426483	1.490546	0.03846154	0.30282775
KEGG_ARGININE_AND_PROLINE_METABOLISM	54	0.440407	1.475367	0.03960396	0.29238334
KEGG_PYRIMIDINE_METABOLISM	98	0.499027	1.565153	0.040462427	0.31966165
KEGG_RETINOL_METABOLISM	64	0.49851	1.493813	0.04423077	0.31135574
KEGG_NEUROACTIVE_LIGAND_RECEPTOR_INTERACTION	271	-0.48356	-1.71054	0.001992032	0.3879316
KEGG_GLYCINE_SERINE_AND_THREONINE_METABOLISM	31	-0.57781	-1.6636	0.016632017	0.30423322

with the OAS family (13). Neutrophils are involved in tumor metastasis through PI3K-Akt, cytokines (48), and circulating tumor cells-neutrophils cluster pattern (49). Furthermore, in our study, OAS1 was found to be associated with the expression of a variety of tumor-infiltrating immune cells, which is consistent with a recent study (50). These results indicated a possible correlation between OAS1 and immune infiltration in pancreatic cancer. Nevertheless, further studies are needed to verify.

Extensive DNA damage can lead to excessive synthesis of PAR, leading to energy depletion and/or activation of PAR-dependent programmed cell death pathways leading to cell death (12). And the high expression of OAS1 in cancer cells prevents cell death by inhibiting PAR synthesis and promotes their ability to survive DNA damage. Our study found that many OAS1-related pathways are involved in the development and progression of cancer. Those include the notch signaling pathway, and the P53 signaling pathway. However, OAS1 is not directly involved in these two pathways, and the specific mechanisms by which OAS1 affects these pathways remain unclear. The specific mechanism of OAS1 in the pathway needs to be verified in experiments. Although more and more studies have been conducted on OAS1, the OAS family has been neglected as drug targets, but their role in drug targets still has a lot of room for development. Recent studies have found that Asp75, Tyr230 and Gln229 residues in OAS1 interact with each other (51), which provided value for the development of OAS1 inhibitors.

In addition, the KEGG analysis found that RIG-I-like receptor signaling pathway was enriched. Interestingly, in another study, it was also found that LGALS9 as the prognostic marker of pancreatic cancer was also enriched in RIG-I-like receptor signaling pathway and Cytosolic DNA-sensing pathway (52). A previous study has found that up-regulation of RIG-I-like receptor signaling pathway can promotes migration and invasion of non-small cell lung cancer (53). However, the mechanism of this pathway in pancreatic cancer has not been elucidated. Following viral infection, researchers have discovered that tumor cells mimic innate immunity pathways (54). Activation of viral RNA recognition molecules (RIG-I and MDA5) in tumor cells induced immunogenic cell death (55, 56). Radiation and chemotherapy activate the RIG-I-like receptor pathway, which activates RIG-I, resulting in the physiologic responses to radio-/chemotherapy as an antiviral program (57).

Several limitations in our study should be noted. First, the sample size of pancreatic cancer in TCGA database are significantly smaller than those of other types of cancer, and some clinical data are missing, so it is necessary to expand the sample size for verification. Second, the mechanism of OAS1 in the development of pancreatic cancer was not explored in this study. the current findings identified significant characteristics associated with OAS1 prognosis only by exploring the hypothesized mechanisms. Although the possible mechanism of OAS1 can be preliminarily determined by the analysis of GO, KEGG and GSEA, it still needs further experiments to verify. This is of certain concern, as significant functional and physiological validations would be needed to propel that impressive dataset to the level of relevant biological insight. Finally, our study initially considers that OAS1 may be a potential therapeutic target, but this needs to be confirmed by further experiments.

In conclusion, the high expression of OAS1 is associated with poor prognosis of pancreatic cancer. OAS1 is a valuable prognostic factor in pancreatic cancer. Its close relationship with immune infiltration revealed that OAS1 may also be a potential therapeutic target, but further experimental confirmation is needed.

DATA AVAILABILITY STATEMENT

The datasets presented in this study can be found in online repositories. The names of the repository/repositories and accession number(s) can be found in the article/**Supplementary Material**.

ETHICS STATEMENT

The studies involving human participants were reviewed and approved by the Ethics Committee of the 900th hospital of the People's Liberation Army Joint Logistics Support Force. The patients/participants provided their written informed consent to participate in this study.

AUTHOR CONTRIBUTIONS

Study concept and design, all. Acquisition of data, LL, HW, JF, and DL. Analysis and interpretation of data, LL, HW, JF, BL, and JZ. Drafting of the manuscript, LL and HW. Contributed to study supervision and critical revision of the manuscript, all. All authors contributed to the article and approved the submitted version.

FUNDING

This study was supported by grants from Startup Fund for scientific research, Fujian Medical University (Grant number: 2019QH1285), the 900th hospital of the Joint Logistics Support Force Fund (Grant Number:2020Z12), the 900th hospital of the Joint Logistics Support Force Fund (Grant Number:2020Q02), and Guiding Project of Social Development of Fujian Province (Grant Number: 2021Y0062).

ACKNOWLEDGMENTS

The authors thank the contributors to GEO, TCGA, and other public databases for sharing open access PAAD expression profile data sets and gene-related information.

SUPPLEMENTARY MATERIAL

The Supplementary Material for this article can be found online at: https://www.frontiersin.org/articles/10.3389/fonc.2022.944194/full#supplementary-material

REFERENCES

1. Owens DK, Davidson KW, Krist AH, Barry MJ, Cabana M, Caughey AB, et al. Screening for Pancreatic Cancer: Us Preventive Services Task Force Reaffirmation Recommendation Statement. *JAMA* (2019) 322(5):438–44. doi: 10.1001/jama.2019.10232
2. Wolfgang CL, Herman JM, Laheru DA, Klein AP, Erdek MA, Fishman EK, et al. Recent Progress in Pancreatic Cancer. *CA Cancer J Clin* (2013) 63 (5):318–48. doi: 10.3322/caac.21190
3. Moore A, Donahue T. Pancreatic Cancer. *JAMA* (2019) 322(14):1426. doi: 10.1001/jama.2019.14699
4. Effenberger KE, Schroeder C, Hanssen A, Wolter S, Eulenburg C, Tachezy M, et al. Improved Risk Stratification by Circulating Tumor Cell Counts in Pancreatic Cancer. *Clin Cancer Res* (2018) 24(12):2844–50. doi: 10.1158/1078-0432.Ccr-18-0120
5. Vakkila J, Lotze MT. Inflammation and Necrosis Promote Tumour Growth. *Nat Rev Immunol* (2004) 4(8):641–8. doi: 10.1038/nri1415
6. Tang H, Jiang L, Stolzenberg-Solomon RZ, Arslan AA, Beane Freeman LE, Bracci PM, et al. Genome-Wide Gene-Diabetes and Gene-Obesity Interaction Scan in 8,255 Cases and 11,900 Controls From Panscan and Panc4 Consortia. *Cancer epidemiol Biomarkers Prev* (2020) 29(9):1784–91. doi: 10.1158/1055-9965.Epi-20-0275
7. Sarkar SN, Ghosh A, Wang HW, Sung SS, Sen GC. The Nature of the Catalytic Domain of 2'-5'-Oligoadenylate Synthetases. *J Biol Chem* (1999) 274 (36):25535–42. doi: 10.1074/jbc.274.36.25535
8. Justesen J, Hartmann R, Kjeldgaard NO. Gene Structure and Function of the 2'-5'-Oligoadenylate Synthetase Family. *Cell Mol Life Sci* (2000) 57(11):1593–612. doi: 10.1007/pl00000644
9. Rebouillat D, Hovanessian AG. The Human 2',5'-Oligoadenylate Synthetase Family: Interferon-Induced Proteins With Unique Enzymatic Properties. *J Interferon Cytokine Res* (1999) 19(4):295–308. doi: 10.1089/107999099313992
10. Hovanessian AG, Laurent AG, Chebath J, Galabru J, Robert N, Svab J. Identification of 69-Kd and 100-Kd Forms of 2-5a Synthetase in Interferon-Treated Human Cells by Specific Monoclonal Antibodies. *EMBO J* (1987) 6 (5):1273–80. doi: 10.1002/j.1460-2075.1987.tb02364.x
11. Chebath J, Benech P, Hovanessian A, Galabru J, Revel M. Four Different Forms of Interferon-Induced 2',5'-Oligo(a) Synthetase Identified by Immunoblotting in Human Cells. *J Biol Chem* (1987) 262(8):3852–7.
12. Kondratova AA, Cheon H, Dong B, Holvey-Bates EG, Hasipek M, Taran I, et al. Suppressing Parylation by 2',5'-Oligoadenylate Synthetase 1 Inhibits DNA Damage-Induced Cell Death. *EMBO J* (2020) 39(11):e101573. doi: 10.15252/embj.2019101573
13. Zhang Y, Yu C. Prognostic Characterization of Oas1/Oas2/Oas3/Oasl in Breast Cancer. *BMC Cancer* (2020) 20(1):575. doi: 10.1186/s12885-020-07034-6
14. Yu C, Xue P, Zhang L, Pan R, Cai Z, He Z, et al. Prediction of Key Genes and Pathways Involved in Trastuzumab-Resistant Gastric Cancer. *World J Surg Oncol* (2018) 16(1):174. doi: 10.1186/s12957-018-1475-6
15. Marino N, Collins JW, Shen C, Caplen NJ, Merchant AS, Gökmen-Polar Y, et al. Identification and Validation of Genes With Expression Patterns Inverse to Multiple Metastasis Suppressor Genes in Breast Cancer Cell Lines. *Clin Exp Metastasis* (2014) 31(7):771–86. doi: 10.1007/s10585-014-9667-0
16. Smekens M, Dumont JE, Degeyter A, Galand P. Effect of Estrogen Administration on Rat Liver 2-5a Synthetase Activity. *Biochim Biophys Acta* (1986) 887(3):341–4. doi: 10.1016/0167-4889(86)90164-3
17. Silvestro L, Viano I, Giubertoni M, Compagnoni G, Dianzani C, Di Carlo F, et al. Induction of 2'-5' Oligoadenylate Synthetase by 17 Beta-Oestradiol in a Human Breast Cancer Cell Line. *Pharmacol Res* (1989) 21(1):99–100. doi: 10.1016/1043-6618(89)90132-1
18. Lu D, Di S, Zhuo S, Zhou L, Bai R, Ma T, et al. The Long Noncoding Rna Tincr Promotes Breast Cancer Cell Proliferation and Migration by Regulating Oas1. *Cell Death Discovery* (2021) 7(1):41. doi: 10.1038/s41420-021-00419-x
19. Song C, Guo Z, Yu D, Wang Y, Wang Q, Dong Z, et al. A Prognostic Nomogram Combining Immune-Related Gene Signature and Clinical Factors Predicts Survival in Patients With Lung Adenocarcinoma. *Front Oncol* (2020) 10:1300. doi: 10.3389/fonc.2020.01300
20. Qiu H, Hu X, He C, Yu B, Li Y, Li J. Identification and Validation of an Individualized Prognostic Signature of Bladder Cancer Based on Seven Immune Related Genes. *Front Genet* (2020) 11:12. doi: 10.3389/fgene.2020.00012
21. Vivian J, Rao AA, Nothaft FA, Ketchum C, Armstrong J, Novak A, et al. Toil Enables Reproducible, Open Source, Big Biomedical Data Analyses. *Nat Biotechnol* (2017) 35(4):314–6. doi: 10.1038/nbt.3772
22. Edgar R, Domrachev M, Lash AE. Gene Expression Omnibus: Ncbi Gene Expression and Hybridization Array Data Repository. *Nucleic Acids Res* (2002) 30(1):207–10. doi: 10.1093/nar/30.1.207
23. Uhlén M, Fagerberg L, Hallström BM, Lindskog C, Oksvold P, Mardinoglu A, et al. Proteomics. Tissue-Based Map of the Human Proteome. *Sci (New York NY)* (2015) 347(6220):1260419. doi: 10.1126/science.1260419
24. Murakami R, Hirai T, Nakamura H, Furusawa M, Nakaguchi Y, Uetani H, et al. Recurrence Patterns of Glioblastoma Treated With Postoperative Radiation

Therapy: Relationship Between Extent of Resection and Progression-Free Interval. *Japanese J Radiol* (2012) 30(3):193–7. doi: 10.1007/s11604-011-0031-x
25. Li T, Fan J, Wang B, Traugh N, Chen Q, Liu JS, et al. Timer: A Web Server for Comprehensive Analysis of Tumor-Infiltrating Immune Cells. *Cancer Res* (2017) 77(21):e108–e10. doi: 10.1158/0008-5472.Can-17-0307
26. Ru B, Wong CN, Tong Y, Zhong JY, Zhong SSW, Wu WC, et al. Tisidb: An Integrated Repository Portal for Tumor-Immune System Interactions. *Bioinf (Oxford England)* (2019) 35(20):4200–2. doi: 10.1093/bioinformatics/btz210
27. Gao J, Aksoy BA, Dogrusoz U, Dresdner G, Gross B, Sumer SO, et al. Integrative Analysis of Complex Cancer Genomics and Clinical Profiles Using the Cbioportal. *Sci Signaling* (2013) 6(269):pl1. doi: 10.1126/scisignal.2004088
28. Tang Z, Li C, Kang B, Gao G, Li C, Zhang Z. Gepia: A Web Server for Cancer and Normal Gene Expression Profiling and Interactive Analyses. *Nucleic Acids Res* (2017) 45(W1):W98–w102. doi: 10.1093/nar/gkx247
29. Kanehisa M, Furumichi M, Sato Y, Ishiguro-Watanabe M, Tanabe M. Kegg: Integrating Viruses and Cellular Organisms. *Nucleic Acids Res* (2021) 49(D1): D545–d51. doi: 10.1093/nar/gkaa970
30. Huang da W, Sherman BT, Lempicki RA. Bioinformatics Enrichment Tools: Paths Toward the Comprehensive Functional Analysis of Large Gene Lists. *Nucleic Acids Res* (2009) 37(1):1–13. doi: 10.1093/nar/gkn923
31. Szklarczyk D, Gable AL, Nastou KC, Lyon D, Kirsch R, Pyysalo S, et al. The String Database in 2021: Customizable Protein-Protein Networks, and Functional Characterization of User-Uploaded Gene/Measurement Sets. *Nucleic Acids Res* (2021) 49(D1):D605–d12. doi: 10.1093/nar/gkaa1074
32. Song W, Liu Z, Wang K, Tan K, Zhao A, Li X, et al. Pyroptosis-Related Genes Regulate Proliferation and Invasion of Pancreatic Cancer and Serve as the Prognostic Signature for Modeling Patient Survival. *Discover Oncol* (2022) 13 (1):39. doi: 10.1007/s12672-022-00495-0
33. Chen G, Song H, Yang Z, Du T, Zheng Y, Lu Z, et al. Aqp5 Is a Novel Prognostic Biomarker in Pancreatic Adenocarcinoma. *Front Oncol* (2022) 12:890193. doi: 10.3389/fonc.2022.890193
34. Zhou C, Wang L, Hu W, Tang L, Zhang P, Gao Y, et al. Cdc25c Is a Prognostic Biomarker and Correlated With Mitochondrial Homeostasis in Pancreatic Adenocarcinoma. *Bioengineered* (2022) 13(5):13089–107. doi: 10.1080/21655979.2022.2078940
35. Zhang Z, Shang J, Dai Z, Yao Y, Shi Y, Zhong D, et al. Transmembrane Protein 170b Is a Prognostic Biomarker and Associated With Immune Infiltrates in Pancreatic Adenocarcinoma. *Front Genet* (2022) 13:848391. doi: 10.3389/fgene.2022.848391
36. Shi W, Li C, Wartmann T, Kahlert C, Du R, Perrakis A, et al. Sensory Ion Channel Candidates Inform on the Clinical Course of Pancreatic Cancer and Present Potential Targets for Repurposing of Fda-Approved Agents. *J personalized Med* (2022) 12(3):478–91. doi: 10.3390/jpm12030478
37. Zhang C, Zou Y, Zhu Y, Liu Y, Feng H, Niu F, et al. Three Immune-Related Prognostic Mrnas as Therapeutic Targets for Pancreatic Cancer. *Front Med (Lausanne)* (2021) 8:649326. doi: 10.3389/fmed.2021.649326
38. Zhou C, Li H, Han X, Pang H, Wu M, Tang Y, et al. Prognostic Value and Molecular Mechanisms of Proteasome 26s Subunit, Non-Atpase Family Genes for Pancreatic Ductal Adenocarcinoma Patients After Pancreaticoduodenectomy. *J Invest Surg Off J Acad Surg Res* (2022) 35 (2):330–46. doi: 10.1080/08941939.2020.1863527
39. Goh TS, Ha M, Lee JS, Jeong DC, Jung ES, Han ME, et al. Prognostic Significance of Eif4g1 in Patients With Pancreatic Ductal Adenocarcinoma. *OncoTar Ther* (2019) 12:2853–9. doi: 10.2147/ott.S202101
40. Guo JC, Zhang P, Zhou L, You L, Liu QF, Zhang ZG, et al. Prognostic and Predictive Value of a Five-Molecule Panel in Resected Pancreatic Ductal Adenocarcinoma: A Multicentre Study. *EBioMedicine* (2020) 55:102767. doi: 10.1016/j.ebiom.2020.102767
41. Luo Y, Chen L, Zhou Q, Xiong Y, Wang G, Liu X, et al. Identification of a Prognostic Gene Signature Based on an Immunogenomic Landscape Analysis of Bladder Cancer. *J Cell Mol Med* (2020) 24(22):13370–82. doi: 10.1111/jcmm.15960
42. Qu G, Liu Z, Yang G, Xu Y, Xiang M, Tang C. Development of a Prognostic Index and Screening of Prognosis Related Genes Based on an Immunogenomic Landscape Analysis of Bladder Cancer. *Aging (Albany NY)* (2021) 13(8):12099–112. doi: 10.18632/aging.202917
43. Mandal S, Abebe F, Chaudhary J. 2'-5' Oligoadenylate Synthetase 1 Polymorphism Is Associated With Prostate Cancer. *Cancer* (2011) 117 (24):5509–18. doi: 10.1002/cncr.26219
44. Encarnación-Rosado J, Kimmelman AC. Harnessing Metabolic Dependencies in Pancreatic Cancers. *Nat Rev Gastroenterol Hepatol* (2021) 18(7):482–92. doi: 10.1038/s41575-021-00431-7
45. Ho WJ, Jaffee EM, Zheng L. The Tumour Microenvironment in Pancreatic Cancer - Clinical Challenges and Opportunities. *Nat Rev Clin Oncol* (2020) 17 (9):527–40. doi: 10.1038/s41571-020-0363-5
46. Guillaumond F, Bidaut G, Ouaissi M, Servais S, Gouirand V, Olivares O, et al. Cholesterol Uptake Disruption, in Association With Chemotherapy, Is a Promising Combined Metabolic Therapy for Pancreatic Adenocarcinoma. *Proc Natl Acad Sci U.S.A.* (2015) 112(8):2473–8. doi: 10.1073/pnas.1421601112
47. Guillaumond F, Leca J, Olivares O, Lavaut MN, Vidal N, Berthezène P, et al. Strengthened Glycolysis Under Hypoxia Supports Tumor Symbiosis and Hexosamine Biosynthesis in Pancreatic Adenocarcinoma. *Proc Natl Acad Sci U.S.A.* (2013) 110(10):3919–24. doi: 10.1073/pnas.1219555110
48. Zhou SL, Dai Z, Zhou ZJ, Chen Q, Wang Z, Xiao YS, et al. Cxcl5 Contributes to Tumor Metastasis and Recurrence of Intrahepatic Cholangiocarcinoma by Recruiting Infiltrative Intratumoral Neutrophils. *Carcinogenesis* (2014) 35 (3):597–605. doi: 10.1093/carcin/bgt397
49. Szczerba BM, Castro-Giner F, Vetter M, Krol I, Gkountela S, Landin J, et al. Neutrophils Escort Circulating Tumour Cells to Enable Cell Cycle Progression. *Nature* (2019) 566(7745):553–7. doi: 10.1038/s41586-019-0915-y
50. Gonzalez KJ, Moncada-Giraldo DM, Gutierrez JB. In Silico Identification of Potential Inhibitors Against Human 2'-5'- Oligoadenylate Synthetase (Oas) Proteins. *Comput Biol Chem* (2020) 85:107211. doi: 10.1016/j.compbiolchem.2020.107211
51. Fan Y, Li T, Xu L, Kuang T. Comprehensive Analysis of Immunoinhibitors Identifies Lgals9 and Tgfbr1 as Potential Prognostic Biomarkers for Pancreatic Cancer. *Comput Math Methods Med* (2020) 2020:6138039. doi: 10.1155/2020/6138039
52. Tang XD, Zhang DD, Jia L, Ji W, Zhao YS. Lncrna Afap1-As1 Promotes Migration and Invasion of Non-Small Cell Lung Cancer *Via* Up-Regulating Irf7 and the Rig-I-Like Receptor Signaling Pathway. *Cell Physiol* (2018) 50 (1):179–95. doi: 10.1159/000493967
53. Matsumura T, Hida S, Kitazawa M, Fujii C, Kobayashi A, Takeoka M, et al. Fascin1 Suppresses Rig-I-Like Receptor Signaling and Interferon-B Production by Associating With Iκb Kinase ϵ (Ikkϵ) in Colon Cancer. *J Biol Chem* (2018) 293(17):6326–36. doi: 10.1074/jbc.M117.819201
54. Jiang LJ, Zhang NN, Ding F, Li XY, Chen L, Zhang HX, et al. Ra-Inducible Gene-I Induction Augments Stat1 Activation to Inhibit Leukemia Cell Proliferation. *Proc Natl Acad Sci U.S.A.* (2011) 108(5):1897–902. doi: 10.1073/pnas.1019059108
55. Besch R, Poeck H, Hohenauer T, Senft D, Häcker G, Berking C, et al. Proapoptotic Signaling Induced by Rig-I and Mda-5 Results in Type I Interferon-Independent Apoptosis in Human Melanoma Cells. *J Clin Invest* (2009) 119(8):2399–411. doi: 10.1172/jci37155
56. Ranoa DR, Parekh AD, Pitroda SP, Huang X, Darga T, Wong AC, et al. Cancer Therapies Activate Rig-I-Like Receptor Pathway Through Endogenous Non-Coding Rnas. *Oncotarget* (2016) 7(18):26496–515. doi: 10.18632/oncotarget.8420
57. Zhang C, Zou Y, Zhu Y, Liu Y, Feng H, Niu F, et al. Three Immune-Related Prognostic Mrnas as Therapeutic Targets for Pancreatic Cancer. *Front Med (Lausanne)* (2021) 8:649326. doi: 10.3389/fmed.2021.649326

Conflict of Interest: The authors declare that the research was conducted in the absence of any commercial or financial relationships that could be construed as a potential conflict of interest.

Publisher's Note: All claims expressed in this article are solely those of the authors and do not necessarily represent those of their affiliated organizations, or those of the publisher, the editors and the reviewers. Any product that may be evaluated in this article, or claim that may be made by its manufacturer, is not guaranteed or endorsed by the publisher.

Copyright © 2022 Lu, Wang, Fang, Zheng, Liu, Xia and Li. This is an open-access article distributed under the terms of the Creative Commons Attribution License (CC BY). The use, distribution or reproduction in other forums is permitted, provided the original author(s) and the copyright owner(s) are credited and that the original publication in this journal is cited, in accordance with accepted academic practice. No use, distribution or reproduction is permitted which does not comply with these terms.

frontiers | Frontiers in Oncology

ORIGINAL RESEARCH
published: 13 July 2022
doi: 10.3389/fonc.2022.916091

The Prognostic Value of Adjuvant Chemotherapy in Colon Cancer With Solitary Tumor Deposit

Qiangkang Lin, Huizhen Zhou, Si Shi, Jixu Lin and Wangxin Yan *

Department of Colorectal and Anal Surgery, The Third Affiliated Hospital of Shanghai University, Wenzhou People's Hospital, Wenzhou No. 3 Clinical Institute Affiliated to Wenzhou Medical University, Wenzhou, China

Purpose: The aim of this study is to investigate the survival benefit of adjuvant chemotherapy in patients with colon cancer with the solitary tumor deposit (TD).

Methods: The primary study outcomes used in this study were colon cancer–specific survival (CSS) and overall survival (OS). The differences of the distribution of categorical variables in patients with colon cancer with the solitary TD according to adjuvant chemotherapy administration were tested using the Pearson's chi-square test. The Kaplan–Meier method was utilized to evaluate CSS and OS. Hazard ratio (HR) and 95% confidence interval (CI) were calculated on the basis of Cox regression models to assess the prognostic value of different demographic and clinicopathological characteristics.

Results: A total of 877 patients with TanyN1cM0 colon cancer with solitary TD were identified in our analysis. It was found that OS (75.4% vs. 42.8% for 5-year OS rate, $p < 0.001$) and CSS (82.9% vs. 69.3% for 5-year CSS rate, $p < 0.001$) of patients with colon cancer with adjuvant chemotherapy administration were significantly better than those without adjuvant chemotherapy administration. Multivariate Cox survival analyses revealed that the overall and colon cancer–specific mortality risks of patients with adjuvant chemotherapy administration were decreased by 64.4% (HR = 0.356, 95% CI = 0.265–0.479, $p < 0.001$) and 57.4% (HR = 0.426, 95% CI = 0.286–0.634, $p < 0.001$) compared with those without adjuvant chemotherapy administration, respectively.

Conclusions: Adjuvant chemotherapy administration could significantly improve OS and CSS in patients with colon cancer with the solitary TD. This is the first study to investigate and demonstrate the survival benefit of adjuvant chemotherapy in patients with colon cancer with the solitary TD.

Keywords: adjuvant chemotherapy, colon cancer, solitary, tumor deposit, survival

OPEN ACCESS

Edited by:
Qi Liu,
Fudan University, China

Reviewed by:
Paul Willemsen,
Hospital Network Antwerp (ZNA), Belgium
Haruhiko Sugimura,
Hamamatsu University School of Medicine, Japan

***Correspondence:**
Wangxin Yan
wangxin__y@163.com

Specialty section:
This article was submitted to Surgical Oncology, a section of the journal Frontiers in Oncology

Received: *08 April 2022*
Accepted: *03 June 2022*
Published: *13 July 2022*

Citation:
Lin Q, Zhou H, Shi S, Lin J and Yan W (2022) The Prognostic Value of Adjuvant Chemotherapy in Colon Cancer With Solitary Tumor Deposit. Front. Oncol. 12:916091. doi: 10.3389/fonc.2022.916091

INTRODUCTION

Colorectal cancer is now the third most common cancer in the world and the second most common cause of cancer death (1). The tumor, node, metastasis (TNM) staging is the most generally used system for the diagnosis and treatment of colorectal cancer, and it has been continuously developed with the continuous progress of tumor treatment; the latest eight edition of the TNM staging system was published in 2017 (2, 3).

In the eighth edition of TNM staging, tumor deposit (TD) is defined as tumor foci located in the pericolonic or perirectal fat, away from the tumor invasion front, in the lymphatic drainage area of the tumor, with no identifiable residual lymph node tissue. In addition, the presence of TD is classified as N1c in the absence of lymph node metastasis (LNM) and TD has no impact on tumor stage in the presence of LNM. Previous studies have shown that TD is an independent and strong prognostic factor in patients with colorectal cancer after surgery, regardless of lymph node status (4–6). More importantly, many studies have shown that the number of TDs is independently associated with poor outcomes in patients with colorectal cancer and suggested adding TDs to the number of LNMs (7–9). A meta-analysis found that TD was a stronger prognostic factor than LNM or extramural vascular invasion for patients with colorectal cancer with liver, lung, and peritoneal metastases (10). In addition, TD is also significantly associated with higher local recurrence and worse prognosis in patients diagnosed with rectal adenocarcinoma (11, 12).

To date, however, no studies have evaluated the role of adjuvant chemotherapy in patients with colon cancer with solitary TD although adjuvant chemotherapy is routinely used in patients with N1c colorectal cancer. Recently, Korean researchers retrospectively analyzed the effect of adjuvant chemotherapy in 281 patients with colon cancer and found that adjuvant chemotherapy did not provide clear survival benefit for patients with colon cancer with solitary LNM (13). Therefore, it is reasonable to question the survival benefit of adjuvant chemotherapy in patients with colon cancer with solitary TD.

MATERIAL AND METHODS

Patients' Selection and Cohorts

Patients with solitary TD are a very small group of people in colon cancer; therefore, a large cancer database is utilized in this study. The National Cancer Institute's Surveillance, Epidemiology, and End Results (SEER) database is the largest cancer database in the United States, containing information on patient's age, sex, tumor stage, tumor site, tumor grade, treatment, and prognosis of malignant tumors in 18 population-based cancer registries, covering about one-third of the population in the country. We then extract the patient data from the SEER database (https://seer.cancer.gov). Because patient identification information has been removed in this database, ethics committee approval and patient informed consent are not required in this study.

As shown in **Figure 1**, we first selected patients diagnosed with colon cancer in the cancer database from 2010 to 2016, and patients who met the following criteria were further confirmed: treated with surgery, adenocarcinoma, without distant metastasis, and tumor grade is known. Finally, patients with TanyN1cM0 colon cancer with the solitary TD were selected for the analysis of this study.

Statistical Analysis

The primary study outcomes used in this study were colon cancer–specific survival (CSS) and overall survival (OS). CSS and OS were defined as the time between the cancer diagnosis and death due to colon cancer and death from any cause, respectively. Patients' demographic and clinicopathological characteristics were included as follows: T staging (T1, T2, T3, and T4), age at diagnosis (≤65 and >65 years old), gender (male and female), tumor location [right-sided colon (from caecum to transverse colon) and left-sided colon (from splenic flexure to rectosigmoid junction)], and tumor grade (grade I/II and grade III/IV).

The differences of the distribution of categorical variables in patients with colon cancer with the solitary TD according to adjuvant chemotherapy administration were tested using the Pearson's chi-square test. The Kaplan–Meier method was used to evaluate CSS and OS. The log-rank test was also carried out to assess whether the differences of CSS or OS rates between subgroups were statistically significant. Hazard ratio (HR) and 95% confidence interval (CI) were calculated on the basis of Cox regression models to assess the prognostic value of different demographic and clinicopathological characteristics. Statistically significant levels were two-tailed, and a p-value less than 0.05 was considered significant. Statistical analyses were conducted using the Statistical Package for the Social Sciences version 23.0 software (IBM Corporation, Chicago, IL, USA).

RESULTS

Patient Characteristics

As shown in **Figure 1**, a total of 877 patients with TanyN1cM0 colon cancer with solitary TD were identified in our analysis, among which 405 (46.2%) patients received adjuvant chemotherapy and 472 (53.8%) patients did not receive adjuvant chemotherapy; 29 (3.3%) patients were diagnosed with stage T1, 80 (9.1%) patients were diagnosed with stage T2, 567 (64.7%) patients were diagnosed with stage T3, and 201 (22.9%) patients were diagnosed with stage T4; 332 (37.9%) patients were less than 65 years old, and 545 (62.1%) patients were more than 65 years old; 453 (51.7%) patients were male, and 424 (48.3%) patients were female; 489 (55.8%) patients were diagnosed with right-sided colon cancer, and 388 (44.2%) patients were diagnosed with left-sided colon cancer; 727 (82.9%) patients were diagnosed with grade I/II colon cancer, and 150 (17.1%) patients were diagnosed with grade III/IV colon cancer.

Patients' demographic and clinicopathological characteristics according to adjuvant chemotherapy administration were shown in **Table 1**. There were no differences in T staging, gender, tumor grade, and number of lymph nodes examined between the two subgroups. Younger age (56.5% vs. 21.8% for ≤ 65 years old, $p < 0.001$) and left-sided colon cancer (48.6% vs. 40.5% for left-sided colon cancer, $p < 0.015$) were more likely to be associated with the adjuvant chemotherapy administration.

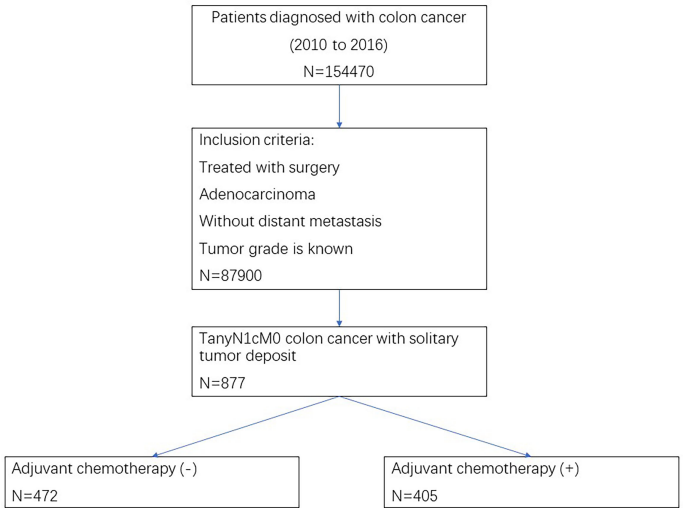

FIGURE 1 | Flow chart of case selection.

TABLE 1 | Clinicopathologic characteristics of colon cancer with solitary tumor deposit according to adjuvant chemotherapy administration.

Variables	Adjuvant Chemotherapy (–) (n = 472)	Adjuvant Chemotherapy (+) (n = 405)	*P*-value
T staging			0.111
T1	10 (2.1%)	19 (4.7%)	
T2	44 (9.3%)	36 (8.9%)	
T3	316 (66.9%)	251 (62.0%)	
T4	102 (21.6%)	99 (24.4%)	
Age at diagnosis (years)			<0.001
≤65	103 (21.8%)	229 (56.5%)	
>65	369 (78.2%)	176 (43.5%)	
Gender			0.807
Male	242 (51.3%)	211 (52.1%)	
Female	230 (48.7%)	194 (47.9%)	
Tumor location			0.015
Right-sided colon	281 (59.5%)	208 (51.4%)	
Left-sided colon	191 (40.5%)	197 (48.6%)	
Grade			0.259
I/II	385 (81.6%)	342 (84.4%)	
III/IV	87 (18.4%)	63 (15.6%)	
No. of lymph nodes examined			0.056
<12	76 (16.1%)	47 (11.6%)	
≥12	396 (83.9%)	358 (88.4%)	

Survival Benefit Conferred by Adjuvant Chemotherapy in All Patients With Colon Cancer With Solitary Tumor Deposit

As shown in **Figure 2**, the CSS and OS curves of patients with colon cancer with the solitary TD were generated using the Kaplan–Meier method. It was found that OS of patients with colon cancer with the solitary TD with adjuvant chemotherapy administration was significantly better than those without adjuvant chemotherapy administration (75.4% vs. 42.8% for 5-year OS rate, $p < 0.001$) and that CSS of patients with colon cancer with the solitary TD with adjuvant chemotherapy administration was significantly better than those without adjuvant chemotherapy administration (82.9% vs. 69.3% for 5-year CSS rate, $p < 0.001$).

Multivariate Cox survival analyses revealed that OS was significantly associated with T staging (HR = 2.018, 95% CI = 1.545–2.634, $p < 0.001$; **Table 2**), number of lymph nodes examined (HR = 0.587, 95% CI = 0.434–0.794, $p = 0.001$; **Table 2**), and age at diagnosis (HR = 1.987, 95% CI = 1.446–2.730, $p < 0.001$; **Table 2**) in all patients with colon cancer with solitary TD. Moreover, the overall mortality risk of all patients with adjuvant chemotherapy administration was decreased by 64.4% compared with those without adjuvant chemotherapy administration (HR = 0.356, 95% CI = 0.265–0.479, $p < 0.001$; **Table 2**). Multivariate Cox survival analyses revealed that CSS was significantly associated with T staging (HR = 3.497, 95% CI = 2.430–5.031, $p < 0.001$; **Table 2**), and number of lymph nodes examined (HR = 0.487, 95%

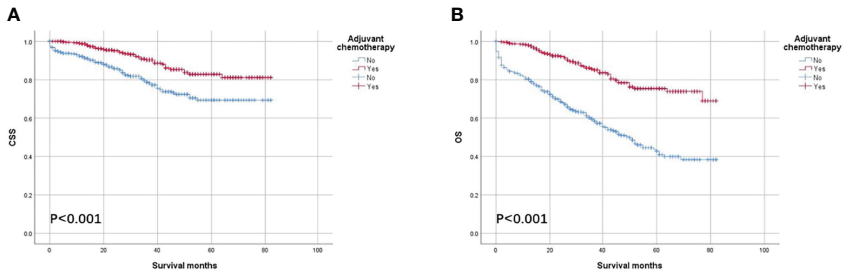

FIGURE 2 | Kaplan–Meier survival curves comparing **(A)** CSS and **(B)** OS according to the use of adjuvant chemotherapy in all patients with colon cancer with solitary tumor deposit.

TABLE 2 | Multivariate Cox regression analysis of prognostic factors for OS and CSS in colon cancer with solitary tumor deposit.

Variable	OS		CSS	
	HR (95% CI)	*P*-value	HR (95% CI)	*P*-value
T staging		<0.001		<0.001
T1–T3	1		1	
T4	2.018 (1.545–2.634)		3.497 (2.430–5.031)	
Adjuvant chemotherapy		<0.001		<0.001
No/unknown	1		1	
Yes	0.356 (0.265–0.479)		0.426 (0.286–0.634)	
Age at diagnosis (years)		<0.001		0.864
≤65	1		1	
>65	1.987 (1.446–2.730)		1.036 (0.691–1.554)	
Gender		0.135		0.967
Male	1		1	
Female	0.830 (0.650–1.060)		1.008 (0.707–1.435)	
Tumor location		0.264		0.544
Right-sided colon	1		1	
Left-sided colon	0.865 (0.670–1.116)		0.893 (0.619–1.287)	
Grade		0.296		0.895
I/II	1		1	
III/IV	1.176 (0.868–1.593)		0.970 (0.620–1.519)	
No. of lymph nodes examined		0.001		0.001
<12	1		1	
≥12	0.587 (0.434–0.794)		0.487 (0.323–0.734)	

CI = 0.323–0.734, p = 0.001; **Table 2**) in all patients with colon cancer with the solitary TD. Moreover, colon cancer–specific mortality risk of patients with adjuvant chemotherapy administration was decreased by 57.4% compared with those without adjuvant chemotherapy administration (HR = 0.426, 95% CI = 0.286–0.634, p < 0.001; **Table 2**).

Survival Benefit Conferred by Adjuvant Chemotherapy in Patients With T1–T3 Colon Cancer With Solitary Tumor Deposit

As shown in **Figure 3**, the CSS and OS curves of patients with T1–T3 colon cancer with the solitary TD were generated using the Kaplan–Meier method. It was found that OS of patients with T1–T3 colon cancer with the solitary TD with adjuvant chemotherapy administration was significantly better than those without adjuvant chemotherapy administration (80.5% vs. 48.1% for 5-year OS rate, p < 0.001; **Figure 3A**) and that CSS of patients with colon cancer with the solitary TD with adjuvant chemotherapy administration was significantly better than those without adjuvant chemotherapy administration (88.7% vs. 76.2% for 5-year CSS rate, p < 0.001; **Figure 3B**).

Multivariate Cox survival analyses revealed that OS was significantly associated with age at diagnosis (HR = 2.681, 95% CI = 1.804–3.983, p < 0.001; **Table 3**), and number of lymph nodes examined (HR = 0.602, 95% CI = 0.412–0.879, p = 0.009; **Table 3**) in patients with T1–T3 colon cancer with the solitary TD. Moreover, the overall mortality risk of patients with adjuvant chemotherapy administration was decreased by 65.4% compared with those without adjuvant chemotherapy administration (HR = 0.346, 95% CI = 0.239–0.500, p < 0.001; **Table 3**). Multivariate Cox survival analyses revealed that colon cancer–specific mortality risk of patients with adjuvant chemotherapy administration was decreased by 57.7% compared with those without adjuvant chemotherapy administration (HR = 0.423, 95% CI = 0.246–0.725, p = 0.002; **Table 3**).

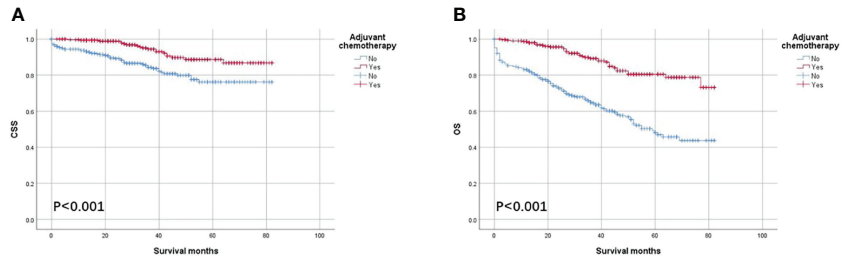

FIGURE 3 | Kaplan–Meier survival curves comparing **(A)** CSS and **(B)** OS according to the use of adjuvant chemotherapy in patients with T1–T3 colon cancer with solitary tumor deposit.

TABLE 3 | Multivariate Cox regression analysis of prognostic factors for OS and CSS in T1–T3 colon cancer with solitary tumor deposit.

Variable	OS		CSS	
	HR (95% CI)	*P*-value	HR (95% CI)	*P*-value
Adjuvant chemotherapy		<0.001		0.002
No/unknown	1		1	
Yes	0.346 (0.239–0.500)		0.423 (0.246–0.725)	
Age at diagnosis (years)		<0.001		0.123
≤65	1		1	
>65	2.681 (1.804–3.983)		1.519 (0.893–2.582)	
Gender		0.142		0.384
Male	1		1	
Female	0.800 (0.595–1.077)		0.812 (0.507–1.299)	
Tumor location		0.446		0.812
Right-sided colon	1		1	
Left-sided colon	0.887 (0.652–1.207)		0.946 (0.588–1.524)	
Grade		0.081		0.632
I/II	1		1	
III/IV	1.420 (0.958–2.105)		1.172 (0.612–2.244)	
No. of lymph nodes examined		0.009		0.018
<12	1		1	
≥12	0.602 (0.412–0.879)		0.509 (0.291–0.889)	

Survival Benefit Conferred by Adjuvant Chemotherapy in Patients With T4 Colon Cancer With Solitary Tumor Deposit

As shown in **Figure 4**, the CSS and OS curves of patients with T4 colon cancer with solitary TD were generated using the Kaplan–Meier method. It was found that OS of patients with T4 colon cancer with the solitary TD with adjuvant chemotherapy administration was significantly better than those without adjuvant chemotherapy administration (56.9% vs. 24.0% for 5-year OS rate, $p < 0.001$; **Figure 4A**) and that CSS of patients with colon cancer with the solitary TD with adjuvant chemotherapy administration was significantly better than those without adjuvant chemotherapy administration (61.5% vs. 42.3% for 5-year CSS rate, $p = 0.004$; **Figure 4B**).

Multivariate Cox survival analyses revealed that the overall mortality risk of patients with adjuvant chemotherapy administration was decreased by 68.4% compared with those without adjuvant chemotherapy administration in patients with T4 colon cancer with solitary TD (HR = 0.316, 95% CI = 0.188–0.531, $p < 0.001$; **Table 4**). In addition, colon cancer–specific mortality risk of patients with adjuvant chemotherapy administration was reduced by 63.3% compared with those without adjuvant chemotherapy administration (HR = 0.367, 95% CI = 0.196–0.686, $p = 0.002$; **Table 4**).

DISCUSSION

TD was first described in 1935 and was considered as the deposit of carcinoma cells at a distance from the primary growth (14). This definition has, in fact, changed in colorectal cancer over time. TDs were first introduced in the fifth edition of the The American Joint Committee on Cancer (AJCC)/TNM staging in 1997, where tumor nodules larger than 3 mm in diameter with no histological evidence of residual LN were classified as regional lymph node metastases, whereas tumor nodules smaller than 3 mm were classified in the T category (15).The presence of TD was classified as N1c in the absence of LNM, and the N1c classification was first introduced in the seventh edition of the AJCC/TNM staging to allow us to better understand the clinical significance of TD.

Notably, TD was redefined in the new TNM classification (eighth edition) released in early 2017, and its incidence was reported in previous literature to be between 18% and 25%

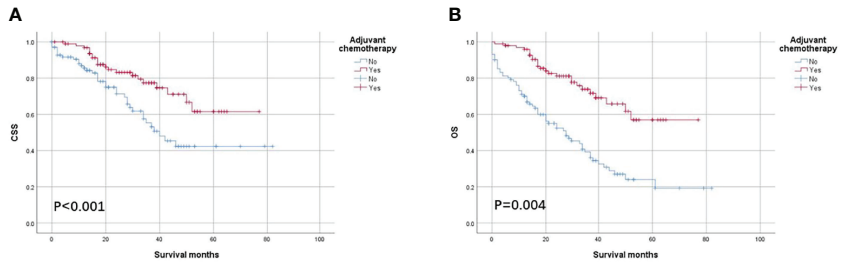

FIGURE 4 | Kaplan–Meier survival curves comparing **(A)** CSS and **(B)** OS according to the use of adjuvant chemotherapy in patients with T4 colon cancer with solitary tumor deposit.

TABLE 4 | Multivariate Cox regression analysis of prognostic factors for OS and CSS in T4 colon cancer with solitary tumor deposit.

Variable	OS		CSS	
	HR (95% CI)	*P*-value	HR (95% CI)	*P*-value
Adjuvant chemotherapy		<0.001		0.002
No/unknown	1		1	
Yes	0.316 (0.188–0.531)		0.367 (0.196–0.686)	
Age at diagnosis (years)		0.853		0.062
≤65	1		1	
>65	0.947 (0.532–1.686)		0.524 (0.267–1.032)	
Gender		0.655		0.225
Male	1		1	
Female	0.905 (0.585–1.401)		1.419 (0.807–2.497)	
Tumor location		0.195		0.298
Right-sided colon	1		1	
Left-sided colon	0.732 (0.456–1.174)		0.732 (0.406–1.317)	
Grade		0.934		0.676
I/II	1		1	
III/IV	1.020 (0.635–1.639)		0.875 (0.467–1.639)	
No. of lymph nodes examined		0.013		0.006
<12	1		1	
≥12	0.526 (0.316–0.874)		0.420 (0.227–0.780)	

(12, 16–18). Many previous studies have revealed that the presence of TD was a manifestation of more aggressive tumor biology and should be further investigated by researchers. Gopal et al. reported a trend toward decreased tumor response to neoadjuvant chemoradiotherapy in patients with N1c rectal cancer, which resulted in worse survival and recurrence in this group of patients (19% vs. 10%, p = 0.092 for 5-year local recurrence rate and 3.1 vs. 11.2 years for OS, p = 0.027) (12). Wei et al. found that the presence of TD was an important independent prognostic factor for rectal cancer following preoperative treatment (HR = 2.41, 95% CI =1.24–4.69, p = 0.01) (19). Another study showed that among patients with right-sided colon adenocarcinoma, N1c patients had significantly lower survival compared with N0 patients (20). A higher recurrence rate was also reported in patients with TD-positive colorectal cancer compared with patients with TD-negative colorectal cancer (65.1% vs. 39.1%) (21).

The survival benefit of chemotherapy in patients with colorectal cancer with TD has been inconsistent in previous studies because it was not clear whether the pN1c category was or was not equal to LNM (9). It was reported that the presence and number of TDs did not affect the benefit of chemotherapy in stage III colorectal cancer (22). It has also been shown that patients with TD did not show a benefit in disease-free survival following chemotherapy (23). However, a recent study found that chemotherapy was independently associated with better prognosis in patients with colorectal cancer with TD (HR = 0.542, 95% CI = 0.501–0.586) (24). Despite that, patients with colon cancer with the presence of TD should receive adjuvant chemotherapy after radical surgery according to clinical guidelines for colorectal cancer. Therefore, it is necessary to explore the clinical significance of TD in adjuvant chemotherapy for patients with colon cancer.

Recently, Yeom et al. conducted a retrospective study in 281 patients with colon cancer and found that adjuvant chemotherapy did not provide clear survival benefit for patients with colon cancer with solitary LNM (84.1% vs. 83.3%, p = 0.490 for 5-year disease-free survival). Therefore, it is reasonable to question the survival benefit of adjuvant chemotherapy in patients with colon cancer with solitary TD. In this study, it was found that adjuvant chemotherapy administration could significantly improve OS (75.4% vs.

42.8% for 5-year OS rate, $p < 0.001$) and CSS (82.9% vs. 69.3% for 5-year CSS rate, $p < 0.001$) in all patients with colon cancer with the solitary TD. Multivariate Cox survival analyses also showed that adjuvant chemotherapy administration was a good prognosis factor: The overall mortality risk of all patients with adjuvant chemotherapy administration was decreased by 64.4% compared with those without adjuvant chemotherapy administration, and colon cancer–specific mortality risk of patients with adjuvant chemotherapy administration was decreased by 57.4% compared with those without adjuvant chemotherapy administration. The survival benefit conferred by adjuvant chemotherapy in patients with colon cancer with solitary TD in our study was better than survival benefit conferred by chemotherapy in patients with colorectal cancer with TD as reported by Chen et al. (24).

Considering that adjuvant chemotherapy had definite survival benefit in T4 colon cancer, we then performed subgroup analyses according to T stage, and all patients were divided into T1–T3 and T4 subgroups (25–27). Again, subgroup analyses showed that adjuvant chemotherapy had obvious survival benefit in both patients with T1–T3 and T4 colon cancer with solitary TD, which further confirmed the above results. In patients with T1–T3 colon cancer with solitary TD, the overall and colon cancer–specific mortality risks of patients with adjuvant chemotherapy administration were decreased by 65.4% (HR = 0.346, 95% CI = 0.239–0.500, $p < 0.001$) and 57.7% (HR = 0.423, 95% CI = 0.246–0.725, $p = 0.002$) compared with those without adjuvant chemotherapy administration, respectively; in patients with T4 colon cancer with solitary TD, the overall and colon cancer–specific mortality risks of patients with adjuvant chemotherapy administration were decreased by 68.4% (HR = 0.316, 95% CI = 0.188–0.531, $p < 0.001$) and 63.3% (HR = 0.367, 95% CI = 0.196–0.686, $p = 0.002$) compared with those without adjuvant chemotherapy administration, respectively.

Taken together, our study suggests that adjuvant chemotherapy is warranted and has an obvious survival benefit in patients with colon cancer with the solitary TD. To our knowledge, this is the first time that the efficacy of adjuvant chemotherapy in patients with colon cancer with the solitary TD is proposed and explored. We screened the target population from more than 150,000 patients with colon cancer and performed this retrospective analysis, which provided a high quality of evidence for the use of adjuvant chemotherapy in patients with colon cancer with solitary TD and gave us a better understanding of the clinical significance of TD in colon cancer.

However, our study has some shortcomings. First, this study has the potential selection bias because of the nature of retrospective studies. Second, the patients included in the study have a long longitudinal span from 2010 to 2016, which may have a potential impact on the results of the analysis. Finally, because of database limitations, some important tumor or patient characteristics that may affect the prognosis of patients with colon cancer were not analyzed in this study. In particular, this cancer database did not capture information on specific chemotherapy regimens, so we did not analyze the effect of a particular chemotherapy regimen on the prognosis of patients with colon cancer, which should be deemed as one limitation of the present study. Therefore, the efficacy of adjuvant chemotherapy in patients with colon cancer with the solitary TD still deserves special attention from researchers in the future.

CONCLUSIONS

Adjuvant chemotherapy administration could significantly improve OS and CSS in patients with colon cancer with the solitary TD. This is the first study to investigate and demonstrate the survival benefit of adjuvant chemotherapy in patients with colon cancer with the solitary TD.

DATA AVAILABILITY STATEMENT

The raw data supporting the conclusions of this article are available from the corresponding author on reasonable request.

AUTHOR CONTRIBUTIONS

QL and WY conceived the project and wrote the manuscript. QL, SS, and JL collected the data. WY, HZ, and SS performed the data analyses. All authors contributed to the article and approved the submitted version.

REFERENCES

1. Bray F, Ferlay J, Soerjomataram I, Siegel RL, Torre LA, Jemal A. Global Cancer Statistics 2018: GLOBOCAN Estimates of Incidence and Mortality Worldwide for 36 Cancers in 185 Countries. *CA: Cancer J Clin* (2018) 68 (6):394–424. doi: 10.3322/caac.21492
2. Weiser MR. AJCC 8th Edition: Colorectal Cancer. *Ann Surg Oncol* (2018) 25 (6):1454–5. doi: 10.1245/s10434-018-6462-1
3. Liu Q, Luo D, Cai S, Li Q, Li X. Circulating Basophil Count as a Prognostic Marker of Tumor Aggressiveness and Survival Outcomes in Colorectal Cancer. *Clin Trans Med* (2020) 9(1):6. doi: 10.1186/s40169-019-0255-4
4. Lin Q, Wei Y, Ren L, Zhong Y, Qin C, Zheng P, et al. Tumor Deposit is a Poor Prognostic Indicator in Patients Who Underwent Simultaneous Resection for Synchronous Colorectal Liver Metastases. *OncoTar Ther* (2015) 8:233–40. doi: 10.2147/OTT.S71414
5. Zheng P, Chen Q, Li J, Jin C, Kang L, Chen D. Prognostic Significance of Tumor Deposits in Patients With Stage III Colon Cancer: A Nomogram Study. *J Surg Res* (2020) 245:475–82. doi: 10.1016/j.jss.2019.07.099
6. Yamano T, Semba S, Noda M, Yoshimura M, Kobayashi M, Hamanaka M, et al. Prognostic Significance of Classified Extramural Tumor Deposits and Extracapsular Lymph Node Invasion in T3-4 Colorectal Cancer: A Retrospective Single-Center Study. *BMC Cancer* (2015) 15:859. doi: 10.1186/s12885-015-1885-6
7. Wang S, Guan X, Ma M, Zhuang M, Ma T, Liu Z, et al. Reconsidering the Prognostic Significance of Tumour Deposit Count in the TNM Staging

System for Colorectal Cancer. *Sci Rep* (2020) 10(1):89. doi: 10.1038/s41598-019-57041-2
8. Pei JP, Zhang CD, Fu X, Ba Y, Yue S, Zhao ZM, et al. A Modified Tumor-Node-Metastasis Classification for Stage III Colorectal Cancers Based on Treating Tumor Deposits as Positive Lymph Nodes. *Front Med* (2020) 7:571154. doi: 10.3389/fmed.2020.571154
9. Delattre JF, Cohen R, Henriques J, Falcoz A, Emile JF, Fratte S, et al. Prognostic Value of Tumor Deposits for Disease-Free Survival in Patients With Stage III Colon Cancer: A *Post Hoc* Analysis of the IDEA France Phase III Trial (PRODIGE-GERCOR). *J Clin Oncol* (2020) 38(15):1702–10. doi: 10.1200/JCO.19.01960
10. Nagtegaal ID, Knijn N, Hugen N, Marshall HC, Sugihara K, Tot T, et al. Tumor Deposits in Colorectal Cancer: Improving the Value of Modern Staging-A Systematic Review and Meta-Analysis. *J Clin Oncol* (2017) 35 (10):1119–27. doi: 10.1200/JCO.2016.68.9091
11. Wang Y, Zhang J, Zhou M, Yang L, Wan J, Shen L, et al. Poor Prognostic and Staging Value of Tumor Deposit in Locally Advanced Rectal Cancer With Neoadjuvant Chemoradiotherapy. *Cancer Med* (2019) 8(4):1508–20. doi: 10.1002/cam4.2034
12. Gopal P, Lu P, Ayers GD, Herline AJ, Washington MK. Tumor Deposits in Rectal Adenocarcinoma After Neoadjuvant Chemoradiation are Associated With Poor Prognosis. *Modern Pathol* (2014) 27(9):1281–7. doi: 10.1038/modpathol.2013.239
13. Yeom SS, Lee SY, Kim CH, Kim HR, Kim YJ. The Prognostic Effect of Adjuvant Chemotherapy in the Colon Cancer Patients With Solitary Lymph Node Metastasis. *Int J colorectal Dis* (2019) 34(8):1483–90. doi: 10.1007/s00384-019-03346-7
14. Gabriel WB, Dukes C, Bussey HJR. Lymphatic Spread in Cancer of the Rectum. *BJS (British J Surgery)* (1935) 23(90):395–413. doi: 10.1002/BJS.1800239017
15. Delattre JF, Selcen Oguz Erdogan A, Cohen R, Shi Q, Emile JF, Taieb J, et al. A Comprehensive Overview of Tumour Deposits in Colorectal Cancer: Towards a Next TNM Classification. *Cancer Treat Rev* (2022) 103:102325. doi: 10.1016/j.ctrv.2021.102325
16. Nagtegaal ID, Tot T, Jayne DG, McShane P, Nihlberg A, Marshall HC, et al. Lymph Nodes, Tumor Deposits, and TNM: Are We Getting Better? *J Clin Oncol* (2011) 9(18):2487–92. doi: 10.1200/JCO.2011.34.6429
17. Ueno H, Mochizuki H, Shirouzu K, Kusumi T, Yamada K, Ikegami M, et al. Multicenter Study for Optimal Categorization of Extramural Tumor Deposits for Colorectal Cancer Staging. *Ann Surg* (2012) 255(4):739–46. doi: 10.1097/SLA.0b013e31824b4839
18. Zhang LN, Xiao WW, Xi SY, OuYang PY, You KY, Zeng ZF, et al. Tumor Deposits: Markers of Poor Prognosis in Patients With Locally Advanced Rectal Cancer Following Neoadjuvant Chemoradiotherapy. *Oncotarget* (2016) 7(5):6335–44. doi: 10.18632/oncotarget.6656
19. Wei XL, Qiu MZ, Zhou YX, He MM, Luo HY, Wang FH, et al. The Clinicopathologic Relevance and Prognostic Value of Tumor Deposits and the Applicability of N1c Category in Rectal Cancer With Preoperative Radiotherapy. *Oncotarget* (2016) 7(46):75094–103. doi: 10.18632/oncotarget.12058
20. Jin M, Roth R, Rock JB, Washington MK, Lehman A, Frankel WL. The Impact of Tumor Deposits on Colonic Adenocarcinoma AJCC TNM Staging and Outcome. *Am J Surg Pathol* (2015) 39(1):109–15. doi: 10.1097/PAS.0000000000000320
21. Belt EJ, van Stijn MF, Bril H, de Lange-de Klerk ES, Meijer GA, Meijer S, et al. Lymph Node Negative Colorectal Cancers With Isolated Tumor Deposits Should be Classified and Treated as Stage III. *Ann Surg Oncol* (2010) 17(12):3203–11. doi: 10.1245/s10434-010-1152-7
22. Shi M, Zhang H, Yao G, Wu J, Zhu C, Zhang X, et al. The Role of Tumor Deposits in Predicting the Efficacy of Chemotherapy in Stage III Colon Cancer. *Front Oncol* (2020) 10:586603. doi: 10.3389/fonc.2020.586603
23. Li X, An B, Zhao Q, Qi J, Wang W, Zhang D, et al. Impact of Tumor Deposits on the Prognosis and Chemotherapy Efficacy in Stage III Colorectal Cancer Patients With Different Lymph Node Status: A Retrospective Cohort Study in China. *Int J Surg (London England)* (2018) 56:188–94. doi: 10.1016/j.ijsu.2018.06.029
24. Chen J, Zhang Z, Ni J, Sun J, Ren W, Shen Y, et al. Predictive and Prognostic Assessment Models for Tumor Deposit in Colorectal Cancer Patients With No Distant Metastasis. *Front Oncol* (2022) 12:809277. doi: 10.3389/fonc.2022.809277
25. Verhoeff SR, van Erning FN, Lemmens VE, de Wilt JH, Pruijt JF. Adjuvant Chemotherapy is Not Associated With Improved Survival for All High-Risk Factors in Stage II Colon Cancer. *Int J Cancer* (2016) 139(1):187–93. doi: 10.1002/ijc.30053
26. Kumar A, Kennecke HF, Renouf DJ, Lim HJ, Gill S, Woods R, et al. Adjuvant Chemotherapy Use and Outcomes of Patients With High-Risk Versus Low-Risk Stage II Colon Cancer. *Cancer* (2015) 121(4):527–34. doi: 10.1002/cncr.29072
27. Babcock BD, Aljehani MA, Jabo B, Choi AH, Morgan JW, Selleck MJ, et al. High-Risk Stage II Colon Cancer: Not All Risks Are Created Equal. *Ann Surg Oncol* (2018) 25(7):1980–5. doi: 10.1245/s10434-018-6484-8

Conflict of Interest: The authors declare that the research was conducted in the absence of any commercial or financial relationships that could be construed as a potential conflict of interest.

Publisher's Note: All claims expressed in this article are solely those of the authors and do not necessarily represent those of their affiliated organizations, or those of the publisher, the editors and the reviewers. Any product that may be evaluated in this article, or claim that may be made by its manufacturer, is not guaranteed or endorsed by the publisher.

Copyright © 2022 Lin, Zhou, Shi, Lin and Yan. This is an open-access article distributed under the terms of the Creative Commons Attribution License (CC BY). The use, distribution or reproduction in other forums is permitted, provided the original author(s) and the copyright owner(s) are credited and that the original publication in this journal is cited, in accordance with accepted academic practice. No use, distribution or reproduction is permitted which does not comply with these terms.

frontiers | Frontiers in Surgery

TYPE Methods
PUBLISHED 14 July 2022
DOI 10.3389/fsurg.2022.956346

Check for updates

OPEN ACCESS

EDITED BY
Qi Liu,
Fudan University, China

REVIEWED BY
Miriam Dellino,
National Cancer Institute Foundation (IRCCS), Italy
Mohammad Esmaeil Akbari,
Shahid Beheshti University of Medical Sciences, Iran
Gerassimos Douridas,
Thriasio General Hospital, Greece

*CORRESPONDENCE
Jie Yin
yj232325@sina.com
Jun Zhang
zhangjun5986@ccmu.edu.cn

†These authors have contributed equally to this work.

SPECIALTY SECTION
This article was submitted to Surgical Oncology, a section of the journal Frontiers in Surgery

RECEIVED 30 May 2022
ACCEPTED 27 June 2022
PUBLISHED 14 July 2022

CITATION
Zhang H, Zheng Z, Liu X, Cai J, Yin J and Zhang J (2022) Exploring the scope of 4sb and 12a lymph node dissection for cT2-4 lower third gastric cancer: Study protocol for a prospective cohort trial.
Front. Surg. 9:956346.
doi: 10.3389/fsurg.2022.956346

COPYRIGHT
© 2022 Zhang, Zheng, Liu, Cai, Yin and Zhang. This is an open-access article distributed under the terms of the Creative Commons Attribution License (CC BY). The use, distribution or reproduction in other forums is permitted, provided the original author(s) and the copyright owner(s) are credited and that the original publication in this journal is cited, in accordance with accepted academic practice. No use, distribution or reproduction is permitted which does not comply with these terms.

Exploring the scope of 4sb and 12a lymph node dissection for cT2-4 lower third gastric cancer: Study protocol for a prospective cohort trial

Haiqiao Zhang†, Zhi Zheng†, Xiaoye Liu, Jun Cai, Jie Yin* and Jun Zhang*

Department of General Surgery, Beijing Friendship Hospital, Capital Medical University, Beijing, China

Background: Currently, the extent of 4sb and 12a lymph node dissection is not clear and is based on the personal understanding of the surgeon. It may result in damage to the splenic artery and portal vein, leading to surgical complications. Therefore, this study aims to explore the scope of 4sb and 12a lymph node dissection in cT2-4 lower third gastric cancer.

Methods: This is an ongoing prospective cohort trial. The total sample size required for the trial (March 2022 to February 2025) is approximately 524 patients. The participants are divided into the experimental (4sb first branch and 12a anterior lymphadenectomy) or control groups (traditional 4sb and 12a lymphadenectomy). Electronic data capture systems will be used to collect demographic, laboratory test, auxiliary examination, operation, postoperative condition, postoperative pathology, and follow-up data. The primary outcome is the 12a lymph node metastatic rate. Secondary outcomes include the pathology (consisting of the 4sb lymph node metastatic rate, the number of 4sb lymph nodes dissected, the number of 12a lymph nodes dissected and tumor pathological staging), a safety evaluation index (consisting of complications and mortality ≤30 days after surgery), an efficacy evaluation (consisting of operation data and postoperative recovery status), and follow-up data (consisting of 3-year or 5-year disease-free survival and overall survival).

Discussion: By exploring the scope of 4sb and 12a lymph node dissection on the premise of ensuring radical cure of the tumor, the operation is simplified, the operation time is shortened, the damage of important blood vessels is reduced, the intraoperative and postoperative complications are reduced, and the patient recovers as soon as possible. Our study is a prospective exploration of the pathology, safety, efficacy, and prognosis of the new and traditional methods of 4sb and 12a lymph node dissection.

Trial registration: Chinese Clinical Trial Registry, ChiCTR2200057698 (registration date: March 15, 2022).

KEYWORDS

12a, lymph node dissection, lymph node metastasis, gastric cancer, 4sb

Abbreviations: OS, overall survival; LNM, lymph node metastasis; LNs, lymph nodes; LGA, left gastroepiploic artery; PHA, proper hepatic artery; CT, computed tomography; EDC, electronic data capture; SAE, serious adverse event; ESEC, Efficacy and Safety Evaluation Committee; DSMC, Data and Safety Monitoring Committee.

Introduction

Over the last few years, gastric cancer has ranked fifth in morbidity and fourth in mortality among all cancers globally (1). In 2020, the number of new cases and deaths from gastric cancer in China were 478,000 and 375,000 respectively, accounting for 43.9% and 48.6% of the global new cases and deaths from gastric cancer (2). The prognosis of gastric cancer is poor and the 5-year overall survival (OS) rate is only 35.9% in China (3). Lymph node metastasis (LNM) is the main metastasis of gastric cancer. Therefore, strict implementation of intraoperative lymphadenectomy is essential. According to the European Society of Medical Oncology (ESMO), National Cancer Comprehensive Network (NCCN), and Japanese Gastric Cancer Association (JGCA), D2 lymphadenectomy is considered as the standard treatment for gastric cancer. However, the extent of 4sb and 12a lymph node dissection (LND) is undefinable according to these guidelines (4–6), it tends to be based more on the surgeon's personal understanding and experience.

Adequate lymphadenectomy contributes to the radical cure of tumors and improves the prognosis. Concurrently, it improves the accuracy of postoperative pathological results and guides patients' postoperative treatment. However, A study has shown that excessive lymphadenectomy is associated with higher postoperative mortality (7). Therefore, lymphadenectomy should be controlled within an appropriate range. According to the guidelines (4–6), the scope of 4sb LND is along the left gastroepiploic artery (LGA), including the root, and the scope of 12a LND is along the proper hepatic artery (PHA), and needs to expose the anterior wall of the portal vein.

The advantage of the traditional lymphadenectomy is that it thoroughly cleans the regional lymph nodes (LNs). However, there are important blood vessels around the 4sb and 12a LNs, such as the splenic artery and portal vein. The risk of vascular damage is higher, the operation is difficult, and the operation time is long. Patients with advanced lower third gastric cancer have a low rate of 4sb and 12a LNM, and the prognosis is poor. Therefore, we designed a new cleaning range. We divided the 4sb LNs into two parts, namely those at the root of the LGA and the peripheral LNs of the first branch. 12a LNs were divided into two parts, namely the anterior and posterior peripheral LNs of the PHA. According to the patient's condition, we will take the 4sb LND area as the first branch LNs of the LGA, saving those at the root, and take the 12a LNs in the anterior area of the PHA, saving those in the posterior area, in some patients. The purpose is to simplify the operation, shorten the operation time, reduce the surgical complications, and speed up the recovery of the patient while obtaining the same radical cure effect. However, the efficacy and safety of this new technique is still unclear.

Since the scope of 4sb and 12a LND is not uniform nationally and internationally and there are few studies on the effectiveness and safety of different anatomical scopes, clinical study on the scope of 4sb and 12a LND is necessary. Therefore, we designed this experiment to compare the pathology, safety, efficacy, and prognosis of the new and traditional methods of 4sb and 12a lymphadenectomy to provide a new, alternative lymphadenectomy for patients with gastric cancer.

Material and methods

Study design

This is a single-center prospective cohort study. The study period is from March 2022 to February 2025. 524 patients will participate in the study. The participants are divided into the experimental (4sb first branch and 12a anterior lymphadenectomy) or control groups (traditional 4sb and 12a lymphadenectomy). After providing informed consent, the participants will be assigned for surgical treatment by the surgeon to either the experimental or control group at a 1:1 ratio. If the patients in the experimental group are found to have positive 4sb and 12a LNs during preoperative imaging examination or during the operation, they will be included in the control group for traditional lymphadenectomy. **Figure 1** is a schematic diagram of the study process.

Inclusion and exclusion criteria

Participants need to meet the following inclusion criteria: (I) gastroscopy biopsy pathologically diagnosed as gastric cancer, with clinical stage $cT_{2-4}N_{-/+}M_0$ by abdominal enhanced computed tomography (CT) and ultrasound endoscopy in selected cases, and tumor location in the lower third of the stomach; (II) completion of laparoscopic distal gastric surgery with D2 lymphadenectomy, with or without conversion to laparotomy; (III) age 18–75 years, with no sex restrictions; (IV) cardiopulmonary function that can tolerate radical gastric cancer surgery; (V) ability to conform to the study protocol and sign the informed consent form; (VI) complete case information.

Patients that meet any of the following criteria are excluded from this study: (I) distant metastases found before or during the operation, and radical gastrectomy is not possible; (II) inability to tolerate anesthesia or surgery or refusal of surgery; (III) cerebrovascular injury or severe heart disease that have occurred within the past six months; (IV) a history of epilepsy, central nervous system disease or mental illness that inhibits cooperation with the study; (V) other diseases that seriously affect survival time; (VI) organ transplantation

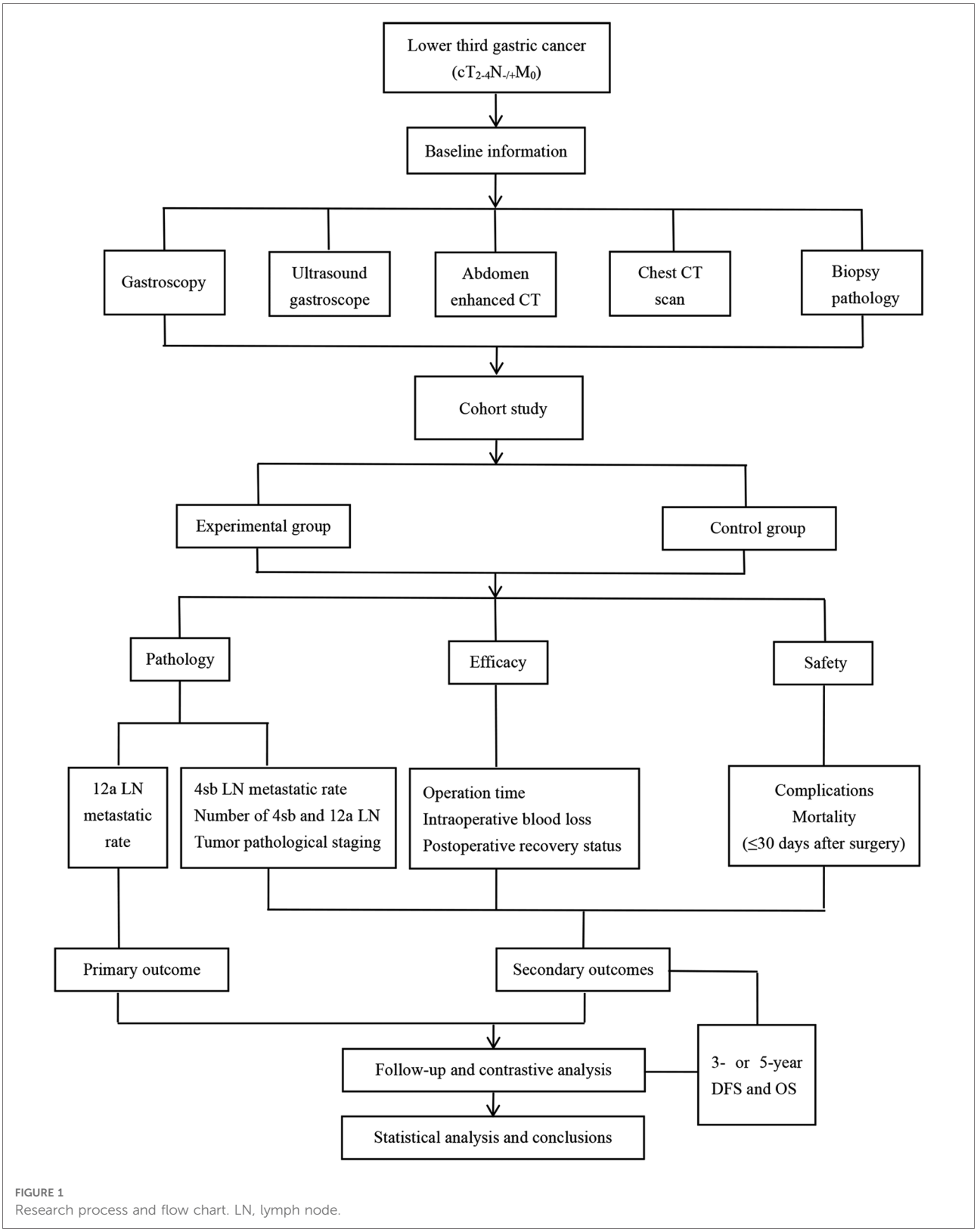

FIGURE 1
Research process and flow chart. LN, lymph node.

requiring immunosuppressive therapy; (VII) pregnancy or lactation; and (VIII) enrollment in other clinical study.

Participating surgeons

The surgeon's proficiency and experience in radical gastric cancer surgery with D2 lymphadenectomy have been found to affect the number of LNs dissected, postoperative recovery time, and postoperative complications (8). A meta-analysis has shown that if surgeons can perform 40 operations alone, they will be able to independently manage any issues encountered during the operation and ensure the operational standards and safety (8). The study medical team will be composed of two experienced surgeons and several experienced nurses, who will be responsible for performing operative and postoperative medical therapy. The two surgeons each completed at least 60 cases of laparoscopic radical gastric distal surgery with D2 lymphadenectomy.

Primary outcome

The primary outcome is the 12a lymph node metastatic rate. The 12a lymph node metastatic rate is equal to the number of patients with 12a LNM divided by the total number of patients enrolled.

Secondary outcomes

The secondary outcome has four parts: pathology data, efficacy index, safety index, and follow-up data. The pathology data comprises the 4sb lymph node metastatic rate, the number of 4sb LNs dissected, the number of 12a LNs dissected, and tumor pathological staging. The efficacy evaluation index comprises operation time, intraoperative blood loss, and postoperative recovery status (time to get out of bed, time to pass gas, time to liquid food intake, time to semi-liquid food intake, and postoperative hospital stay). The safety evaluation index comprises complications and mortality $\leq$30 days after surgery. Intraoperative complications include injuries of the hepatic artery, common bile duct, portal vein, spleen and pancreas. Postoperative complications include biliary fistula, delayed hepatic artery and portal vein hemorrhage, pancreatic fistula, and other pancreatic injury-related complications. Follow-up data comprises 3-year or 5-year disease-free survival and OS.

Interventions

First, all the patients will undergo laparoscopic surgery. Patients require gastroscopy biopsy pathology results to confirm the diagnosis, and endoscopic ultrasound and abdominal enhanced CT to evaluate the clinical stage and tumor location before surgery. To assess the general state of the patient and the risk of surgery, patients also need laboratory examinations including routine blood tests, blood biochemical tests, coagulation function tests, lung function tests, echocardiogram, and chest CT.

All patients will undergo supine and split leg surgery. We will use the following methods for puncture port placement: (a) Insert a 12 mm trocar through a 1 cm transverse incision under the navel to establish a pneumoperitoneum and maintain the pressure at 12–15 mmHg. This opening will also be used for observation. (b) Insert a 12 mm trocar 2 cm below the costal margin of the left anterior axillary line as the surgeon's main operation opening. (c) Insert a 5 mm trocar 1 cm above the navel of the left mid-clavicular line as an auxiliary operating opening for the surgeon. (d) Insert a 5 mm trocar 2 cm below the costal margin of the right anterior axillary line as a secondary operation opening for the assistant. (e) Insert a 12 mm trocar 1 cm below the midpoint of the connection between opening A and opening D as the assistant's main operation opening. The location of the puncture opening is shown in **Figure 2**.

Experimental group

We take the 4sb LNs at the first branch of the LGA and take the 12a LNs in the anterior area of the PHA. LNs in the two areas will be pathologically tested separately. The two groups

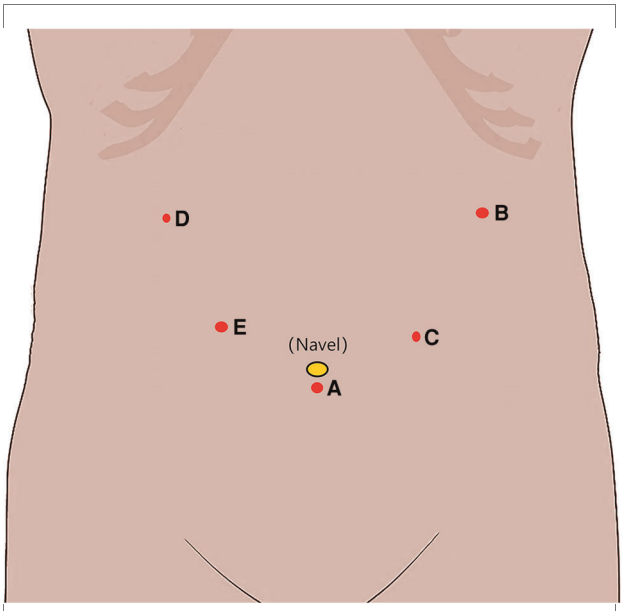

FIGURE 2
Puncture port placement.

of LNs will be separated and removed by the surgeon during the operation, rather than trimmed from the whole *ex vivo* pathological specimen.

The scope of 4sb LND is as follows: we choose to cut off the LGA at the beginning of the first branch of the LGA, and then sweep along the greater curvature to the LGA and the right gastroepiploic artery interchange (Figure 3).

The scope of 12a LND is as follows: (I) Upper border: the confluence of the right and left hepatic artery. (II) Lower border: the upper border of the pancreas at the origin of the PHA. (III) Right border: the left side of the bile duct. (IV) Left border: the left border of ligamentum hepatoduodenal. (V) Anterior border: the anterior hepatoduodenal ligament. (VI) Posterior border: the anterior side of the PHA (Figure 4).

Control group

We take the 4sb LNs at the first branch and the root of the LGA and take 12a LNs in the anterior and posterior areas of the PHA. LNs in the two areas will be pathologically tested separately. The two groups of LNs will be separated and removed by the surgeon during the operation, rather than trimmed from the whole *ex vivo* pathological specimen.

The scope of 4sb LND is as follows: we choose to cut off the LGA at the root of the LGA originating from the splenic artery, and then sweep along the greater curvature to the LGA and the right gastroepiploic artery interchange (Figure 3).

The scope of 12a LND is as follows: posterior border is the anterior side of the portal vein. The remaining borders are the same as the experimental group (Figure 4).

Perioperative treatment

Patients will receive symptom-based treatment after surgery, including electrocardiogram monitoring, intravenous fluid replacement, acid suppression, and pain relief. Routine blood tests, biochemical tests, measurement of drainage fluid amylase, and drainage fluid characteristics will be regularly monitored to observe whether bleeding, biliary fistula, and pancreatic injury-related postoperative complications occur. The discharge standards are as follows: gastrointestinal function is restored, the patient can have a semi-liquid diet, and the abdominal drainage tubes are removed.

Data collection

We will use numbers instead of the name and sex of the enrolled patient to protect the privacy of the patient. Electronic data capture (EDC) system will be used to

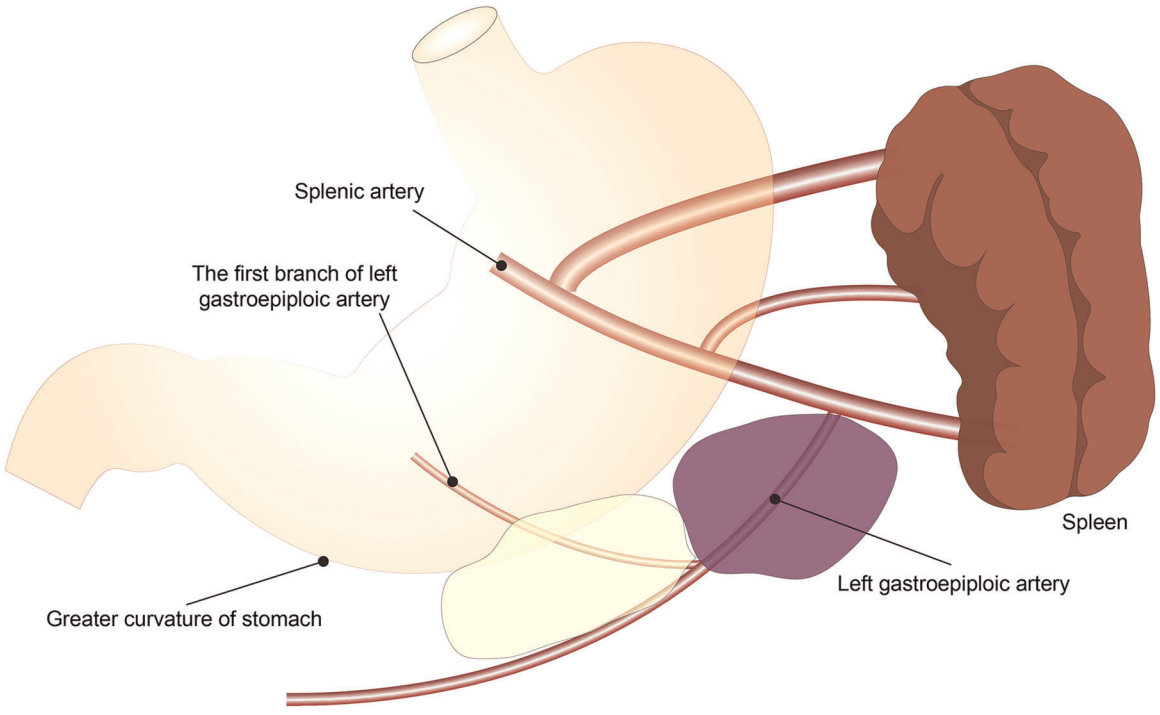

FIGURE 3
Schematic diagram of the scope of 4sb lymph node dissection. The yellow area is the experimental group, and the yellow plus purple area is the control group.

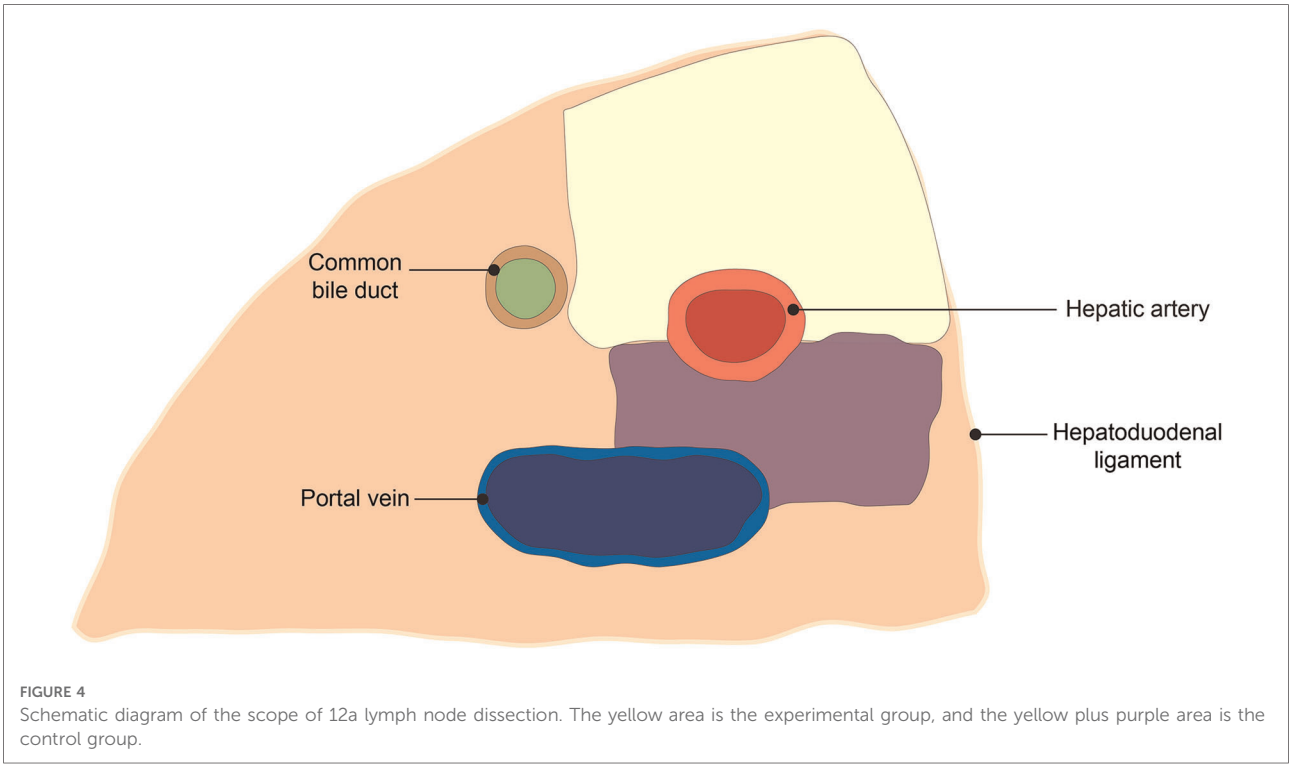

FIGURE 4
Schematic diagram of the scope of 12a lymph node dissection. The yellow area is the experimental group, and the yellow plus purple area is the control group.

collect clinical data. The following data will be collected: (I) demographic, including sex, age, body mass index and concomitant disease; (II) perioperative laboratory test results, including those of routine blood and biochemical tests; (III) auxiliary examination results, including those of gastroscopy biopsy, endoscopic ultrasound and abdominal enhanced CT; (IV) surgical data, including operation time, blood loss, surgical method, extent of lymphadenectomy and intraoperative complications; (V) postoperative recovery data including time to get out of bed, time to pass gas, time to liquid food intake, time to semi-liquid food intake, postoperative hospital stay; and (VI) postoperative pathology, including pathological stage, the number of 4sb and 12a LNs dissected and metastasis rate (Table 1).

Follow-up

We will arrange for a full-time nurse to be responsible for enrolled patients postoperative follow-up in the hospital, and the outpatient clinic after discharge. The follow-up time points are 3, 6, 12, 18, 24, 36, 48, and 60 months. During the follow-up period, the patients need to receive physical and laboratory examinations, chest CT, abdominal enhanced CT, and gastroscopy. Laboratory examinations will include routine blood and biochemical tests (Table 1).

Adverse events

A serious adverse event (SAE) refers to any adverse medical event, whether related to surgery or not. All SAEs will be recorded and reported to the ethics committee of Beijing Friendship Hospital within 24 h for enrolled patients. During the research period, the data monitoring committee will follow the standard procedures of clinical trials and supervise safety data in an unblinded manner.

Patients that have postoperative complications will receive the best therapy. Meanwhile, the enrollment will be suspended if the incidence of SAE exceeds 5% of enrolled patients. The Efficacy and Safety Evaluation Committee (ESEC) will evaluate whether to continue this study.

Monitoring and quality assurance

The 4sb and 12a LNs removed during the operation fixed with 10% neutral formalin and pathological examinations performed. Standardized procedures for LNs pathology are: (I) The LNs were initially retrieved by the surgeon and completely immersed in a 10% neutral formalin specimen bag containing 6–8 times the specimen volume within half an hour of being isolated. The sample will then be sent to the pathology department for further lymph node retrieval by a pathologist. Soaking time: 12–48 h. (II) Paraffin section production process: (A) Taking materials: first, remove the LNs soaked in 10%

TABLE 1 Checklist for clinical data collection and follow-up plan of enrolled patients.

	Baseline		Post-operation					Follow-up							
	Before operation	Operation	POD1	POD3	POD5	POD7	POD30	3 m	6 m	12 m	18 m	24 m	36 m	48 m	60 m
Inclusion/ Exclusion criteria	×														
Informed consent	×														
Demographic information	×														
Laboratory tests	×	×	×	×	×	×		×	×	×	×	×	×	×	×
Operation information		×													
Postoperative recovery status			×	×	×	×	×								
Physical examination	×							×	×	×	×	×	×	×	×
Chest CT	×									×		×	×	×	×
Abdomen enhanced CT	×							×	×	×	×	×	×	×	×
Gastroscopy	×									×		×	×	×	×
Ultrasound gastroscope	×														
Pathology	×					×									
Complications							×								
Mortality							×	×	×	×	×	×	×	×	×
Recurrence								×	×	×	×	×	×	×	×

"×", the need to collect the clinical data.
POD, postoperative day.

neutral formalin from the specimen bag and then remove the fat tissue around the nodes. The larger LNs can be cut into slices every 0.5 cm in parallel. The smaller LNs can be opened along the axis. (B) Fixation: 10% neutral formalin fixation is used for routine paraffin sections. (C) Dehydration: From low-concentration alcohol to high-concentration alcohol, step by step replacing the alcohol in time to ensure the concentration, so that the water in the tissue is completely removed. (D) Soaking wax: use 58%–60% melting point paraffin for 2 h, replace paraffin once every hour, to embed wax use 60%–62% paraffin. (E) Slice: The slice thickness is generally 3 μm. Bake slices in a 60°C incubator for 40 min. (III) Immunochemistry: place the sections in water, keep them at room temperature with 3% neutral formalin for a certain period, and wash the sections with distilled water and clean water. Then place the slices in a pressure cooker containing 1.1 L citric acid with pH 6.0, heat for 2 min and cool naturally, then take out and rinse twice with phosphate buffer saline, 2 min each time, add secondary antibody until the diaminobenzidine staining solution develops the color and compare the negative and positive of the antibody. (IV) Reading: finally, observe under a microscope to determine whether there are abnormal cells in the LNs to determine whether there is LNM. Lymph node micrometastasis will be defined as node-positive.

A Data and Safety Monitoring Committee (DSMC) was established, and is composed of senior professors, data administrators, ethics experts and statistician. We will clearly assign responsibilities to committee members and they will cooperate with each other. The DSMC can access the research data and other records unrestrictedly for quality assurance activities. Meanwhile, emergency review and assessment of safety-related issues can also be conducted. The DSMC is independent of research funders and has no competing interests.

Sample size

The sample size was calculated using PASS 11.0 software. The 12a lymph node metastatic rate was used as the main result in the sample size calculation. This study assumes that the 12a lymph node metastatic rate in the experimental group is not inferior to the control group. According to published literature (9), the 12a lymph node metastatic rate of the control group is estimated at 9.1%. Combined with clinical

practice, the non-inferiority threshold is set to −7.4%. The size of the two groups of patients was determined with a 1:1 design, setting a significance level of $\alpha = 0.025$ (unilateral), power at 80%, and loss to follow-up at 10%. We expect 524 patients to be registered, with 262 patients in each group.

Statistical analysis

The normally distributed data will be expressed as mean ± standard deviation, and independent sample t-test will be used for groups differences. The non-normally distributed data will be expressed by a median, and the Mann–Whitney U test will be used for groups differences. The count data will be described as frequency and percentage and Fisher's exact test will be used for groups differences. The survival curve will be analyzed with the use of Kaplan–Meier, and the log-rank test will be used to evaluate groups differences. The Cox proportional hazards model will be used to evaluate the hazard ratio. $P < 0.05$ is set as the significance level.

Interim analyses

When the number of enrolled patients reaches 262, we will perform statistical analysis on the primary and secondary outcomes. The independent statistical team will be responsible for the interim analysis and report the results to the DSMC. The DSMC will discuss the results and report to the ESEC. If the effectiveness and safety of the experimental group are significantly lower than that of the control group, the study will be suspended.

Dissemination plans

We plan to publish the results of short-term efficacy and safety studies in 2025, and the results of the long-term follow-up studies in 2030.

Trial status

The study was registered at the Chinese Clinical Trial Registry (http://www.chictr.org.cn), with number ChiCTR2200057698 on March 15, 2022. Currently, our research team has established the EDC systems to collect clinical data.

Discussion

LNM is an important factor affecting the 5-year OS rate of gastric cancer patients. Therefore, the prognostic value of D2 lymphadenectomy in gastric cancer needs to be further improved (10). Saito (11) found that in 239 cases of lower-third gastric cancer undergoing D2 lymphadenectomy, the lymph node metastatic rate in the 4sb group was 2.2%, which was related to LNs invasion and advanced gastric cancer. Shu (12) found that the metastasis rate of 12a LNs was 2.67% (11/413), which was related to tumor location, depth of tumor invasion and LNs stage. For patients with advanced gastric cancer (stages III/IV) located in the lower third of the stomach, the metastasis rate of 12a LNs increased to 10.7% (11/103). The recurrence-free survival rate and OS rate of patients with 12a LNM were significantly worse. Other studies have shown that the metastasis rate of 12a LNs is 1.7%–20% and it may be one of the most important factors affecting prognosis (7, 9, 10, 13–15). Therefore, accurate lymphadenectomy plays a positive role in the prognosis. However, the scope of 4sb and 12a LND in D2 lymphadenectomy is not clear. Lin (16) found that the unqualified rate of lymphadenectomy in 948 cases of laparoscopic total gastrectomy was 51.9%, and it gradually decreased with accumulated surgical experience. It is believed that the main reason for the unqualified LNs failure is the failure to dissect LNs at specific locations during the operation. Among them, the failure rate of the 12a LNs was higher (33.44%), and the No.4 LNs were lower (9.39%). This shows that a standardized and clear range of lymphadenectomy is significantly helpful for clinicians treating gastric cancer and undertaking complete D2 lymphadenectomy. However, there are few studies on the cleaning range of 4sb and 12a.

Huang (17) pointed out that the posterior boundary of 12a LND was defined as the anterior edge of the portal vein, so only the LNs in front of the portal vein were cleaned during the operation. Huang (14) published a new 12a LND sequence, suggesting that the portal vein should be exposed first and the LNs before the portal vein should be cleaned. However, we considered that the 12a lymph node metastatic rate is lower for advanced lower third gastric cancer, and LNM around the portal vein is even more rare. Therefore, we suggested that only the LNs area in the front of the PHA should be cleaned, retaining the LNs area around the portal vein. The same is true for the 4sb LNs. We suggested cleaning the LNs around the first branch of the LGA and retaining the LNs around the root of the LGA. Through such a cleaning method, under the premise of ensuring the radical cure of the tumor, the risk of damage to blood vessels and organs, and complications during surgery, are reduced.

Although ESMO, NCCN and JGCA regularly update the guidelines for treating gastric cancer, they are all updated in terms of indications of the extent of LND, and there is no further detailed update of the definition of LND (4–6). In addition, although there have been some studies on 4sb and 12a LNs, the majority are related to LNM and risk factors or

survival rates. Therefore, we are currently conducting a clinical trial to establish a safer 4sb and 12a LND range, to reduce the complication rate of D2 lymphadenectomy while obtaining the same radical cure effect.

Conclusion

The limitations of this study are that the quality of evidence is lower than that of a randomized controlled study and there may be selection bias. However, we will build iterations of future study protocols based on the findings. In addition, we will also recruit more patients to determine more effective 4sb and 12a LND protocols and to provide ideas and evidence for lymphadenectomy in collaboration with other research centers.

Data availability statement

The original contributions presented in the study are included in the article/Suplementary Material, further inquiries can be directed to the corresponding author/s.

Ethics statement

Written informed consent was obtained from the individual(s) for the publication of any potentially identifiable images or data included in this article.

Author contributions

Conceptualization: JZ and JY, Data curation: HZ and ZZ, Formal analysis: XL and JC, Funding acquisition: JZ and JY, Software: HZ, Supervision: JZ and JY, Writing—original draft: HZ and ZZ, Writing—review & editing: JZ and JY. All authors contributed to the article and approved the submitted version.

Funding

This work is supported by the Beijing Municipal Administration of Hospitals Incubating Program (No. PX2020001), the Research Foundation of Beijing Friendship Hospital, Capital Medical University (No. Y2018-3) and the Beijing Municipal Science & Technology Commission (No. D171100006517003).

The study conforms to the provisions of the Declaration of Helsinki (as revised in 2013). The study protocol has been approved by the Ethics Committee of Beijing Friendship Hospital, Capital Medical University (approval No.: 2019-P2-031-01). Informed consent has been obtained from the patient and approval has been obtained from the ethics committee.

Conflict of interest

The authors declare that the research was conducted in the absence of any commercial or financial relationships that could be construed as a potential conflict of interest.

Publisher's note

All claims expressed in this article are solely those of the authors and do not necessarily represent those of their affiliated organizations, or those of the publisher, the editors and the reviewers. Any product that may be evaluated in this article, or claim that may be made by its manufacturer, is not guaranteed or endorsed by the publisher.

References

1. Sung H, Ferlay J, Siegel RL, Laversanne M, Soerjomataram I, Jemal A, et al. Global cancer statistics 2020: GLOBOCAN estimates of incidence and mortality worldwide for 36 cancers in 185 countries. *CA Cancer J Clin.* (2021) 71 (3):209–49. doi: 10.3322/caac.21660

2. Zhang T, Chen H, Yin X, He Q, Man J, Yang X, et al. Changing trends of disease burden of gastric cancer in China from 1990 to 2019 and its predictions: findings from Global Burden of Disease Study. *Chin J Cancer Res.* (2021) 33(1):11–26. doi: 10.21147/j.issn.1000-9604.2021.01.02

3. Yang L, Zheng R, Wang N, Yuan Y, Liu S, Li H, et al. Incidence and mortality of stomach cancer in China, 2014. *Chin J Cancer Res.* (2018) 30(3):291–8. doi: 10.21147/j.issn.1000-9604.2018.03.01

4. Japanese gastric cancer treatment guidelines 2018 (5th edition). Gastric Cancer, 2020.

5. Ajani JA, D'Amico TA, Almhanna K, Bentrem DJ, Chao J, Das P, et al. Gastric cancer, version 3.2016, NCCN clinical practice guidelines in oncology. *J Natl Compr Canc Netw.* (2016) 14(10):1286–312. 3. doi: 10.6004/jnccn.2016.0137

6. Smyth EC, Verheij M, Allum W, Cunningham D, Cervantes A, Arnold D, ESMO Guidelines Committee. Gastric cancer: ESMO Clinical Practice Guidelines for diagnosis, treatment and follow-up. *Ann Oncol.* (2016) 27(Suppl 5):v38–49. doi: 10.1093/annonc/mdw350

7. Mocellin S, McCulloch P, Kazi H, Gama-Rodrigues JJ, Yuan Y, Nitti D. Extent of lymph node dissection for adenocarcinoma of the stomach. *Cochrane Database Syst Rev.* (2015) (8):CD001964. doi: 10.1002/14651858.CD001964.pub4

8. Zhou D, Quan Z, Wang J, Zhao M, Yang Y. Laparoscopic-assisted versus open distal gastrectomy with D2 lymph node resection for advanced gastric cancer: effect of learning curve on short-term outcomes. a meta-analysis. *J Laparoendosc Adv Surg Tech A.* (2014) 24(3):139–50. doi: 10.1089/lap.2013.0481

9. Yang K, Chen HN, Liu K, Zhang WH, Chen XZ, Chen XL, et al. The survival benefit and safety of No. 12a lymphadenectomy for gastric cancer patients with distal or total gastrectomy. *Oncotarget.* (2016) 7(14):18750–62. doi: 10.18632/oncotarget.7930

10. Huang X, Liu H, Hu Y, Yu J, Liao X, Li G. The poor prognosis of patients with stage III gastric cancer after D2 dissection is mainly due to lymphatic metastasis, especially the metastasis of No.12a LN: a nested case-control study. *Oncol Res Treat*. (2021) 44(6):313–21. doi: 10.1159/000512934

11. Saito R, Kawaguchi Y, Akaike H, Shiraishi K, Maruyama S, Shimizu H, et al. Prognostic significance of lymph node dissection along the upper-third-stomach in patients with lower-third gastric cancer. *Anticancer Res*. (2019) 39(3):1485–9. doi: 10.21873/anticanres.13266

12. Shu P, Sun X, Liu F, Fang Y, Shen K, Sun Y, et al. Pattern of No. 12a lymph node metastasis in gastric cancer. *Chin J Cancer Res*. (2021) 33(1):61–8. doi: 10.21147/j.issn.1000-9604.2021.01.07

13. Shirong C, Jianhui C, Chuangqi C, Kaiming W, Xinhua Z, Wu S, et al. Survival of proper hepatic artery lymph node metastasis in patients with gastric cancer: implications for D2 lymphadenectomy. *PLoS One*. (2015) 10(3):e118953. doi: 10.1371/journal.pone.0118953

14. Huang HP, Xiong WJ, Peng YH, Zheng YS, Luo LJ, Li J, et al. Safety and feasibility of No.12a lymph node dissection by portal vein approach in radical laparoscopic gastrectomy for gastric cancer. *Technol Cancer Res Treat*. (2020) 19:1079238925. doi: 10.1177/1533033820971277

15. Kumagai K, Hiki N, Nunobe S, Irino T, Ida S, Ohashi M, et al. Metastasis to the lymph nodes along the proper hepatic artery from adenocarcinoma of the stomach. *Langenbecks Arch Surg*. (2016) 401(5):677–85. doi: 10.1007/s00423-016-1429-9

16. Lin GT, Chen QY, Zheng CH, Li P, Xie JW, Wang JB, et al. Lymph node noncompliance affects the long-term prognosis of patients with gastric cancer after laparoscopic total gastrectomy. *J Gastrointest Surg*. (2020) 24(3):540–50. doi: 10.1007/s11605-019-04199-9

17. Huang Y, Zhu G, Zheng W, Hua J, Yang S, Zhuang J, et al. Scope definition and resection significance of No. 12a group lymph nodes in gastric cancer. *Mol Clin Oncol*. (2016) 5(2):257–62. doi: 10.3892/mco.2016.911

frontiers | Frontiers in Oncology

ORIGINAL RESEARCH
published: 14 July 2022
doi: 10.3389/fonc.2022.931414

Comparison of Long-Term Oncologic Outcomes Between Surgical T4 and T3 in Patients Diagnosed With Pathologic Stage IIA Right Colon Cancer

Youngbae Jeon[1†], *Kug Hyun Nam*[2†], *Seok Won Choi*[3], *Tae Sik Hwang*[4] *and Jeong-Heum Baek*[1*]

[1] Division of Colon and Rectal Surgery, Department of Surgery, Gil Medical Center, Gachon University College of Medicine, Incheon, South Korea, [2] Songdo General Surgery Clinic, Incheon, South Korea, [3] Pyeongtaek St. Mary's Hospital, Pyeongtaek, South Korea, [4] Yonsei Hang General Surgery Clinic, Incheon, South Korea

OPEN ACCESS

Edited by:
Qi Liu,
Fudan University, China

Reviewed by:
Sohini Chakraborty,
New York University, United States
Jagadeeswara Rao Bommi,
Case Western Reserve University, United States
Ayberk Dursun,
Ercis State Hospital, Turkey

***Correspondence:**
Jeong-Heum Baek
gsbaek@gilhospital.com

[†]These authors have contributed equally to this work and share first authorship

Specialty section:
This article was submitted to Surgical Oncology, a section of the journal Frontiers in Oncology

Received: 29 April 2022
Accepted: 23 June 2022
Published: 14 July 2022

Citation:
Jeon Y, Nam KH, Choi SW, Hwang TS and Baek J-H (2022) Comparison of Long-Term Oncologic Outcomes Between Surgical T4 and T3 in Patients Diagnosed With Pathologic Stage IIA Right Colon Cancer. Front. Oncol. 12:931414. doi: 10.3389/fonc.2022.931414

Purpose: T stage plays an important role in the classification of subgroups in stage II colon cancer. Patients with pathologic T4 are at high risk of recurrence and it is recommended to include adjuvant chemotherapy in the treatment plan, while this is not necessary in pathologic T3. There is a discrepancy between the surgical T stage (sT), as determined by the surgeon in the operative field, and pathologic T stage (pT). The pathologic stage is considered a standard prognostic factor, but it has not been established whether the surgical stage has an oncologic impact. The aim of this study was to compare oncologic outcomes between sT4 and sT3 in pathologic stage IIA right colon cancer.

Methods: Between January 2005 and December 2018, there were 354 patients who underwent right hemicolectomy performed by a single surgeon (JHB) at a tertiary hospital. The data from these patients were retrospectively collected and analyzed. Only those patients with pathologic stage IIA (pT3N0M0) right colon adenocarcinomas were included in this study. Patients with mucinous carcinoma, signet ring cell carcinoma, squamous cell carcinoma, or hereditary colon cancer, and who had emergent surgery were excluded. Finally, 86 patients were included in this study. The patients were categorized, according to their surgical records, into either the sT4 group (n=28) or the sT3 group (n=58).

Results: There were no statistical differences between the two groups in terms of age, sex, body mass index, comorbidities, cancer location, histologic grade, lymphovascular invasion, perineural invasion, number of harvested lymph nodes, and adjuvant chemotherapy. The 5-year overall survival rate was significantly different between the sT4 and sT3 groups (92.6% vs. 97.7%, p=0.024). In addition, the 5-year disease-free survival rate was significantly different between the sT4 and sT3 groups (88.6% vs. 97.7%, p=0.017). In the multivariate Cox regression analysis, a classification of sT4 was a significant independent predictive factor for recurrence (p = 0.023).

Conclusions: Long-term oncologic outcomes have shown significant differences between surgical T4 and T3 in pathologic stage IIA right colon cancer patients. Further large-scale, multicenter studies are required to verify the clinical impact of the surgical staging.

Keywords: surgical stage, colon cancer, oncologic outcomes, survival, recurrence

INTRODUCTION

Colorectal cancer is the third most commonly diagnosed malignant disease and the second leading cause of cancer-related death worldwide (1). The current standard practice for non-metastatic colon cancer is to perform either only surgery (including endoscopic resection) or surgery followed by adjuvant chemotherapy, depending on the pathologic staging results. The most widely used staging system for malignant tumors, including colon cancer, is the Tumor Nodes Metastasis (TNM) staging classification from the American Joint Committee on Cancer (AJCC) (2). It is widely accepted that TNM staging is a significant prognostic factor in oncologic outcomes (3, 4). The importance of tumor staging systems has increased over the past several decades as tailored therapies, which rely on an accurate understanding of the disease progression, become more prominent (5). The T stage plays an important role in the classification of cancer subgroups, especially in patients with stage II (T3 or T4, N0) colon cancer. Patients with pathologic T4 stage II colon cancer are recommended for adjuvant chemotherapy due to the high risk of recurrence, while patients with pathologic T3 stage II colon cancer are not (6, 7). Therefore, it is essential to distinguish patients in stage T4 from those in stage T3 to ensure they receive adjuvant therapy to improve their chances of survival.

In clinical practice, the surgical T stage (sT), which is determined by the surgeon in the operative field, is typically recorded. However, there is a discrepancy in staging between the sT and pathologic T stage (pT). The sT and pT staging were reported to be equivalent in 78.48% of colon cancer cases (8). Intraoperatively tumors suspected to be sT4 are often finally diagnosed as pT3 tumors. Thus, there are concerns regarding the underestimation of pT4. The pT stage has been considered a standard prognostic factor, but it is not established whether the sT stage has an oncologic impact. The aim of this study was to compare oncologic outcomes between sT4 and sT3 in pathologic stage IIA (pT3N0M0) of right colon cancer to explore the oncologic impact of the sT stage.

MATERIALS AND METHODS

Patient Selection and Surgical T Stage

Between January 2005 and December 2018, 354 patients underwent right hemicolectomy for right colon cancer, performed by a single surgeon (JHB) at a tertiary referral hospital, Gil Medical Center, Incheon, South Korea. All relevant data were retrospectively collected and analyzed. Only the medical records of patients with pathologic stage IIA (pT3N0M0) right colon adenocarcinomas were included in this study. Patients with mucinous carcinoma, signet ring cell carcinoma, squamous cell carcinoma, hereditary colon cancer, recurrent colon cancer, history of other malignancies, those who underwent emergent surgery, and those who had no information of surgical T stage in medical records were excluded. Finally, 86 patients were included in this study. The operative records of all patients were reviewed to obtain the sT, with 28 patients categorized into the sT4 group and 58 into the sT3 group. The pT was reported according to the AJCC TNM staging system, 7th and 8th editions (2, 9). The sT was assessed by a senior colorectal surgeon during surgery and checked against the gross specimen after resection. The sT3 was assessed by following surgical finding; The surgeon can detect the location of primary tumor under direct vision with the lesion appearing on the serosa of colorectal wall, but there were no invasion through the serosa, and no macroscopic adherence between tumor and either peritoneum or organ in surgical field. The sT4 was assessed by following surgical finding; The surgeon can detect the serosal invasion of the primary tumor, or the tumor macroscopically adheres or invades to adjacent organ or structure in surgical field (**Table 1**). Patient selection was performed by searching the Clinical Research Data Warehouse system at our institution and detailed data were retrospectively collected from the electronic medical records at the Gil Medical Center. Institutional review board approval was obtained from the Ethics Committee of the same hospital (approval no. GCIRB2021-349). Additionally, to identify the equivalency between sT3, 4 and pT3, 4, the distribution was investigated at all pTNM stages of right colon cancer.

Assessment Parameters

Selected clinical features, including age, sex, body mass index (BMI), American Society of Anesthesiology (ASA) score, comorbidities, tumor location, preoperative tumor marker levels, adjuvant chemotherapy, and histopathological outcomes were compared between the sT4 and sT3 groups. Overall survival was calculated from the date of surgery for colon cancer to the date of any cause of death, or loss of follow up. Disease-free survival was defined as the duration of time from the date of surgery for colon cancer to the date of local recurrence, distant metastasis, death, or loss of follow up.

Patient Follow-Up

The Gil Medical Center has preexisting follow up protocols in place for patients with cancer, therefore all patients diagnosed

Abbreviations: AJCC, American Joint Committee on Cancer; ASA, American Society of Anesthesiologist; BMI, body mass index; CEA, carcinoembryonic antigen; pT, pathological T stage; sT, surgical T stage; TNM, Tumor Nodes Metastasis.

TABLE 1 | Comparison between the pathologic T stage* and surgical T stage** in primary tumor (T) staging of patients with right colorectal cancer.

Primary tumor (T)	Pathologic T stage*	Surgical T stage**
Tx	Primary tumor cannot be assessed	Primary tumor cannot be assessed
T0	No evidence of primary tumor	No evidence of primary tumor
Tis	Carcinoma in situ, intramucosal carcinoma	Practically difficult to distinguish among Tis, T1, and T2
T1	tumor invades the submucosa	
T2	Tumor invades the muscularis propria	
T3	Tumor invades through the muscularis propria into pericolorectal tissues	The surgeon can detect the location of primary tumor under direct vision with the lesion appearing on the serosa of colorectal wall, but there were no invasion through the serosa, and no macroscopic adherence between tumor and either peritoneum or organ in surgical field.
T4	Tumor invades through the visceral peritoneum (T4a) or invades or adheres to adjacent organ or structure (T4b)	The surgeon can detect the serosal invasion of the primary tumor, or the tumor macroscopically adheres or invades to adjacent organ or structure in surgical field.

Pathological T stage is described based on the Tumor Nodes Metastasis staging classification from The American Joint Committee on Cancer, 7th and 8th editions.
**Surgical T stage is determined by the colorectal surgeon depending on the intraoperative findings.*

with stage IIA colon cancer were followed up every 3 months with serial carcinoembryonic antigen (CEA) levels and physical examination. Abdominopelvic computed tomography scans were performed annually for the first 5 years after surgery. Surveillance colonoscopies were performed every 2 - 3 years for the first 5 years. Patients with stage IIA colon cancer who have high risk factors for recurrence, including poorly differentiated histology, lymphovascular invasion, perineural invasion, perforation, obstruction, positive resection margin, or less than 12 harvested lymph nodes, are usually treated with adjuvant FOLFOX (folinic acid, fluorouracil, and oxaliplatin) chemotherapy for 12 cycles according to the current guidelines (10, 11).

Statistical Analysis

Continuous variables were analyzed using the Mann–Whitney U test, and categorical variables were compared using Pearson's chi-square test and Fischer's exact test. Survival analysis was performed using the Kaplan–Meier method and the log-rank test. Cox's proportional hazard model was used for multivariate analysis to identify factors predicting the prognosis. Significant differences between the two groups for each variable were defined as a two-tailed p-value < 0.05. All statistical analyses were performed using IBM SPSS Statistics for Windows, version 23 (IBM Corp., Armonk, N.Y., USA)

RESULTS

Patient Demographics

The baseline patient demographics are presented in **Table 2**. The median age was 69 years (range: 40 - 87 years) in the sT4 group and 66 years (range: 23 - 92 years) in the sT3 group. Fourteen (50.0%) patients in the sT4 group and 33 (56.9%) in the sT3 group, respectively, were men. The most common tumor location in both the groups was the ascending colon (60/86, 69.8%). Preoperative bowel obstruction and perforation were present in 11 (13.1%) and 8 (9.5%) patients, respectively. Twelve (42.9%) patients received adjuvant chemotherapy in the sT4 group and 24 (41.4%) patients were administered adjuvant chemotherapy in the sT3 group. There were no statistically significant differences between the two groups in terms of baseline clinical features.

Histopathological Characteristics

The histopathological characteristics are presented in **Table 3**. Moderately differentiated was the most common histological grade found in this study (71/86, 82.6%). Lymphovascular invasion and perineural invasion were found in 8 (28.6%) and 3 (10.7%) patients in the sT4 group, respectively, and 15 (25.9%) and 5 (8.6%) patients in the sT3 group, respectively. The median number of harvested lymph nodes was 26 (range: 8 - 60) in the sT4 group and 25 (range: 5 - 74) in the sT3 group. There were 3 (10.7%) patients in the sT4 group and 4 (6.9%) patients in the sT3 group who had high microsatellite instability. No statistically significant differences were identified between the two groups in terms of histopathological characteristics (**Table 3**).

Survival Outcomes and Predictive Factors

The 5-year overall survival rate was significantly different between the sT4 and sT3 groups (92.6% vs. 97.7%, p=0.024; **Figure 1**). The 5-year disease-free survival rate also showed a significant difference between the two groups (88.6% vs. 97.7%, p=0.017; **Figure 2**). The overall recurrence rate was 8.1% (7/86). The median follow-up period was 92.5 months in the sT4 group and 79.4 months in the sT3 group. Multivariate analysis of the overall survival by the Cox proportional hazard model showed no statistically significant predictive factors, but sT4 presented a trend toward significance [hazard ratio (HR), 8.007; 95% confidence interval (CI): 0.806 - 74.023, p = 0.067]. For disease-free survival, only sT4 showed a statistically significant difference (HR, 7.303; 95% CI: 1.314 - 40.596, p = 0.023) (**Table 4**).

TABLE 2 | Baseline patient demographics.

Variables	sT4 (n=28) n (%)	sT3 (n=58) n (%)	*p*
Age, years (range)	69 (40-87)	66 (23-92)	0.764
Sex			0.646
Male	14 (50.0)	33 (56.9)	
Female	14 (50.0)	25 (43.1)	
BMI, kg/m^2 (range)	21.8 (17.3-28.0)	22.9 (16.4-33.6)	0.253
ASA score			0.683
1	2 (7.1)	3 (5.2)	
2	23 (82.1)	45 (77.6)	
3	3 (10.7)	10 (17.2)	
Comorbidities			
Cardiovascular disease	13 (16.4)	33 (56.9)	0.489
Pulmonary disease	2 (7.1)	6 (10.3)	0.483
Diabetes mellitus	8 (28.6)	15 (25.9)	0.800
Location of tumor			0.945
Cecum	4 (14.3)	11 (19.0)	
Ascending colon	20 (71.4)	40 (69.0)	
Hepatic flexure	2 (7.1)	4 (6.9)	
Proximal transverse colon	2 (7.1)	3 (5.2)	
Preoperative CEA			1.000
≥5 ng/mL	4 (14.3)	9 (15.5)	
<5 ng/mL	23 (82.1)	45 (77.6)	
Unknown	1 (3.6)	4 (6.9)	
Presenting findings			
Bowel obstruction	5 (17.9)	6 (10.3)	0.327
Bowel perforation	3 (10.7)	5 (8.6)	0.712
Adjuvant chemotherapy	12 (42.9)	24 (41.4)	1.000

sT, surgical T stage; BMI, body mass index; ASA, American Society of Anesthesiologists; CEA, carcinoembryonic antigen.

Equivalency of the Pathologic T Stages and the Surgical T Stages

Distribution of the pathologic T3, 4 stages and the surgical T3, 4 stages in all pathologic TNM stages of right colon cancer was presented in **Table 5**. The patients who were recorded as sT3 were finally diagnosed with 87.8% of pT3, and 12.2% of pT4, respectively. The patients who were recorded as sT4 were finally diagnosed with 70.4% of pT3, and 29.6% of pT4.

DISCUSSION

The importance of tailored therapies in cancer management has increased in the last decades and as such, many studies have focused on identifying predictive clinicopathological factors. From this perspective, our study's aim of identifying the oncologic impact of the surgical T stage is in line with the current trends in cancer research. In our study, the sT4 group

TABLE 3 | Histopathological characteristics.

Variables	sT4 (n=28) n (%)	sT3 (n=58) n (%)	*p*
Histologic grade			1.000
Well differentiated	2 (7.1)	6 (10.3)	
Moderately differentiated	24 (85.7)	47 (81.0)	
Poorly differentiated	2 (7.1)	5 (8.6)	
Unknown	0 (0)	1 (1.7)	
Lymphovascular invasion			0.800
Present	8 (28.6)	15 (25.9)	
Absent	20 (71.4)	43 (74.1)	
Perineural invasion			0.679
Present	3 (10.7)	5 (8.6)	
Absent	19 (67.9)	35 (60.3)	
Unknown	6 (21.4)	18 (31.0)	
Harvested lymph node (range)	26 (8-60)	25 (5-74)	0.761
Microsatellite status			0.881
High	3 (10.7)	4 (6.9)	
Low or stable	12 (42.9)	26 (44.8)	
Unknown	13 (16.4)	28 (48.3)	

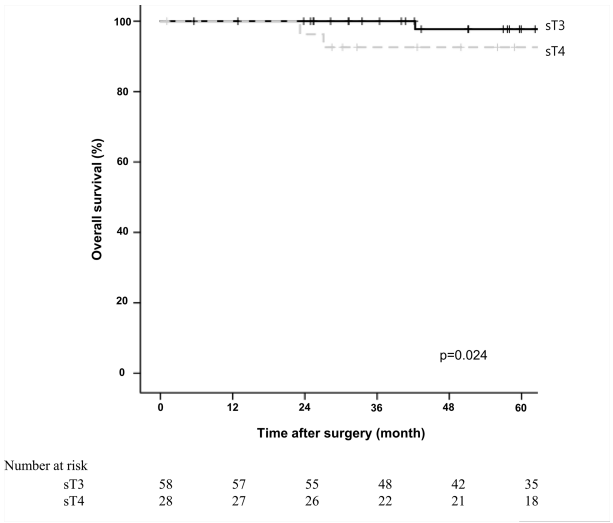

FIGURE 1 | Comparing overall survival for right colon adenocarcinoma between surgical stage T4 (sT4) and surgical stage T3 (sT3) in patients with pT3N0M0 by Kaplan-Meier curve. The 5-year overall survival rate of sT4 group was significantly lower than that of sT3 groups according to log-rank test (92.6% vs. 97.7%, *p*=0.024).

showed significantly lower overall survival rates and worse disease-free survival rates than those in the sT3 group. Furthermore, in the multivariate analysis, a staging of sT4 was the only significant predictive factor for recurrence. This implies that some of the patients who are diagnosed with pT3 may actually be pT4 and have been incorrectly classified. As mentioned above, surgical and pathologic T stages are matched in only 78.48% of colorectal cancer cases, and approximately 20% of patients are at risk of under or over treatment (8). Compton et al. insisted that peritoneal invasion is often underdiagnosed by pathologists when they only assessed by routine histologic examination, because documentation of peritoneal invasion required extensive sampling and serial sectioning (12). In the studies with cytologic examination of serosal scrapings, malignant cells presented 26% of tumor specimens which diagnosed as pT3 by histologic examination alone (13, 14). In

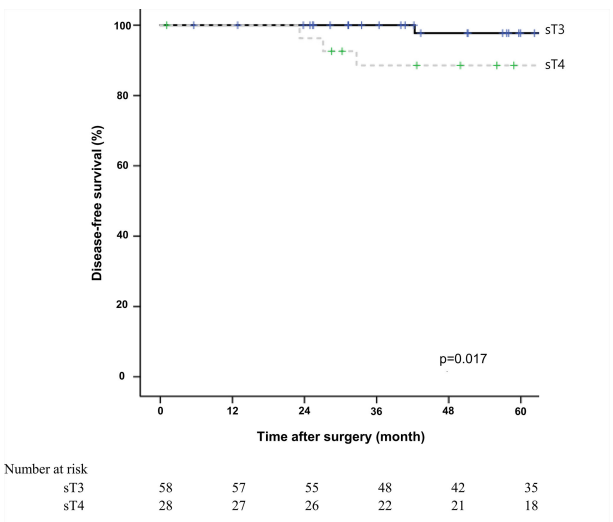

FIGURE 2 | Comparing disease-free survival for right colon adenocarcinoma between surgical stage T4 (sT4) and surgical stage T3 (sT3) in patients with pT3N0M0 by Kaplan-Meier curve. The 5-year disease-free survival rate of sT4 group was significantly lower than that of sT3 groups according to log-rank test (88.6% vs. 97.7%, *p*=0.017).

TABLE 4 | Univariate log-rank test and multivariate Cox proportional hazards model for survival.

Variables	Univariate log-rank test	Multivariate Cox regression analysis*		
	p	HR	95% CI	*p*
Overall survival				
Age ≥ 65 years	0.143	4.308	0.389-47.680	0.234
Male sex	0.972			
BMI ≥ 25	0.659			
Perforation	0.380			
Obstruction	0.400			
sT4	0.024**	8.007	0.866-74.023	0.067
Poorly differentiated	0.481			
Lymphovascular invasion	0.561			
Harvested LN < 12	0.010**	5.054	0.492-51-860	0.173
Adjuvant chemotherapy	0.553			
Disease-free survival				
Age ≥ 65 years	0.157	0.354	0.045-2.760	0.322
Male sex	0.484			
BMI ≥ 25	0.222			
Perforation	0.512			
Obstruction	0.548			
sT4	0.017**	7.303	1.314-40.596	0.023**
Poorly differentiated	0.781			
Lymphovascular invasion	0.424			
Harvested LN < 12	0.025**	2.938	0.304-28.376	0.352
Adjuvant chemotherapy	0.123	0.199	0.031-1.287	0.090

**After all variables that showed p ≥ 0.2 in univariate analysis were removed, multivariate Cox regression analysis was performed.*

***Statistical significance, p < 0.05.*

HR, hazard ratio; CI, confidence interval; BMI, body mass index; sT4, surgical stage T4; LN, lymph nodes.

our study, while the proportion of matching values of sT3 and pT3 was 87.8%, that of sT4 and pT4 was only 29.6%. It is assumed that the serosal lesions, which were only inflammatory changes, were also overestimated, because the surgeon recorded it as sT4 if there were any suspicions of serosal involvement or macroscopic tumor adherence.

It is also possible that sT4 itself, that is, the macroscopic tumor adherence, is an independent prognostic factor, even though the nature of tumor adherence represents a histologically malignant extension or only an inflammatory change. Several studies have emphasized the oncologic impact of macroscopic tumor adherence as a predictive factor for colorectal cancer (15–17). A study from Australia evaluated the associations between colorectal tumor adherence and other clinicopathological features in 268 patients with tumor adherence among 2504 patients who underwent colorectal surgeries (15). Adherent tumors were independently associated with pelvic recurrence (HR: 1.8, 95% CI: 1.2 - 2.7, p = 0.007), systemic recurrence (HR: 1.7, 95% CI: 1.1 - 2.4, p = 0.009), and poor overall survival (HR: 1.6, 95% CI: 1.3 - 2.0, $p < 0.001$) in rectal cancer, although there was no association between tumor adherence and survival in colon cancer. Another study proposed a revised pT category (r-pT) in colorectal cancer patients with a discrepancy between the surgical T stage and pathologic T stage (16). The patients with pT3 and sT4 were reclassified into r-pT4a and the patients with pT4a and sT4b were reclassified into r-pT4b. The r-pT stage showed superior predictive outcomes compared to the standard pT stage (Harrell's C: 0.668 vs. 0.636, p = 0.002) and presented an independent prognostic factor in multivariable regression analysis (HR: 1.846, 95% CI: 1.566 - 2.176, $p < 0.001$). This study was proposed as an alternative to overcome the weakness of the pathologically-oriented staging system. The last brief study also found that macroscopic serosal invasion, defined as tumor extent or colloid changes protruding from the surface of the serosa, was an independent risk factor for recurrence in multivariable survival analysis (HR: 4.750, 95% CI: 1.381 - 16.334, p = 0.013) among 375 patients with stage IIA colon cancer (17). They insisted that macroscopic serosal invasion in the operative findings may complement the shortcomings of the standard pathologic T category if there were inconsistencies between surgical and pathologic T stages. This is similar to our results and the assumptions of our study.

The surgical T stage is in accordance with the AJCC staging system but has a drawback in that it is difficult to distinguish between sTis, sT1, and sT2 in operative findings, while it is possible to distinguish between sT3 and sT4. Other studies have suggested the following criteria for the surgical T stage: sT1 lesions were

TABLE 5 | Distribution of the pathologic T3, 4 stages and the surgical T3, 4 stages in all pathologic TNM stages of right colon cancer.

	pT3, n (%)	pT4, n (%)	Total, n (%)
sT3, n (%)	65 (87.8)	9 (12.2)	74 (100)
sT4, n (%)	76 (70.4)	32 (29.6)	108 (100)

diagnosed when the lesion appeared normal, and this assessment was combined with the preoperative auxiliary examination; sT2 lesions were diagnosed when the lesion was mobile on the muscle layer of the colorectal wall; sT3 lesions were diagnosed when the tumor did not invade through the serosa, and the lesion appeared nodular on the serosal layer of the colorectal wall; sT4a lesions were diagnosed when serosal involvement was visible; and sT4b lesions were diagnosed when tumor directly invaded or was adherent to other organs or structures (16). In our study, we only focused on the surgical T stage in patients with pathological stage IIA. We did not find sTis, sT1, or sT2 lesions in pT3 patients; that is, all patients in pT3 were staged as sT3 or sT4. Furthermore, we believed that pathological assessment was sufficient for the stratification of T stages below T3, while operative findings were more important in distinguishing between T3 and T4 because T4 requires information regarding the relationship between the tumor and adjacent organs or structures.

The present study had several limitations. First, it was a retrospective, single-center analysis with a small population, which can lead to selection bias. The results of the multivariate Cox regression analysis were somewhat unrefined due to a small sample size (n=86), and a small number of events. Because there were quite a few patients who had no information of surgical T stage in their medical records, only small number of patients included in this study. It is the main drawback of our research. Second, we did not divide sT4a and sT4b, although the classification has been adapted from the 7th edition of the AJCC TNM staging classification. There were a couple of records filled with sT4a or sT4b, however, most of the records were filled with only just sT4. This is also considered a limitation of retrospective nature in this study. Third, we confined our study to patients with right colon adenocarcinoma to exclude the oncologic influence of tumor sidedness. Other tumor locations, including sigmoid colon cancer and rectal cancer, should also be evaluated. Fourth, the proportion of matching values between sT stage and pT stage was too low. Especially, only 30% of patients with sT4 were finally diagnosed with pT4, whereas 88% of patients with sT3 were finally diagnosed with pT3. Even considering the tendency of the surgeon to overestimate the surgical stages, it is necessary to assess the surgical T stage with clearer criteria. Finally, we did not check external validation. It is crucial to prove a prediction model's reproducibility and generalizability. Therefore, further researches should be prospective designed, and multicenter with big data studies. Nonetheless, this study has a strength in terms of identifying novel prognostic factors in the era of individual cancer therapy. In particular, the surgical T stage may estimate the patients' prognosis as a complementary factor to the pathologic findings. Furthermore, proper adjuvant chemotherapy or close follow up may be considered in patients with sT4 right colon cancer who are diagnosed with pathologic stage IIA through multidisciplinary discussion with pathologic review.

CONCLUSIONS

Comparative analysis of long-term oncologic outcomes showed significant differences between the sT4 and sT3 groups in pathologic stage IIA of patients with right colon adenocarcinoma. Surgical T stage may assist in distinguishing patients with a high risk of recurrence who are required adjuvant treatment to complement the surgical treatment. Our results suggest that multidisciplinary discussions, including those between surgeons and pathologists, are essential to manage colon cancer patients, especially when there is a discrepancy between the surgical and pathologic T stage. However, the limitations with small sample size and retrospective nature analysis should be overcome. Further large-scale prospective multicenter studies are needed to verify the oncologic impact of sT.

DATA AVAILABILITY STATEMENT

The raw data supporting the conclusions of this article will be made available by the authors, without undue reservation.

ETHICS STATEMENT

The studies involving human participants were reviewed and approved by Institutional review board approval was obtained from the Ethics Committee of Gil Medical Center, Gachon University College of Medicine (approval no. GCIRB2021-349). Written informed consent for participation was not required for this study in accordance with the national legislation and the institutional requirements.

AUTHOR CONTRIBUTIONS

YJ – data analysis and interpretation, drafting of manuscript and critical revision. KN – acquisition of data, data analysis and interpretation, and manuscript drafting. SC – acquisition of data. TH – acquisition of data. JH-B – conception and design of study, acquisition of data, critical revision of manuscript. All authors have approved the final version of the manuscript.

ACKNOWLEDGMENTS

We would like to thank Editage (www.editage.co.kr) for the English language editing.

REFERENCES

1. Sung H, Ferlay J, Siegel RL, Laversanne M, Soerjomataram I, Jemal A, et al. Global Cancer Statistics 2020: GLOBOCAN Estimates of Incidence and Mortality Worldwide for 36 Cancers in 185 Countries. *CA Cancer J Clin* (2021) 71:209–49. doi: 10.3322/caac.21660
2. Weiser MR. AJCC 8th Edition: Colorectal Cancer. *Ann Surg Oncol* (2018) 25:1454–55. doi: 10.1245/s10434-018-6462-1
3. O'Connell JB, Maggard MA, Ko CY. Colon Cancer Survival Rates With the New American Joint Committee on Cancer Sixth Edition Staging. *J Natl Cancer Inst* (2004) 96:1420–5. doi: 10.1093/jnci/djh275

4. Pestalozzi BC, Jäger D, Knuth A. Systemic Therapy for Colorectal Cancer. *Chirurg* (2005) 76:570–2. doi: 10.1007/s00104-005-1038-6
5. Elfaedy O, Owens P, Aakif M, Mansour E. Discrepancy in Colorectal Cancer Staging: A Single Center Experience. *World J Surg Surg Res* (2018) 1:1054.
6. Costas-Chavarri A, Nandakumar G, Temin S, Lopes G, Cervantes A, Correa M, et al. Treatment of Patients With Early-Stage Colorectal Cancer: ASCO Resource-Stratified Guideline. *J Glob Oncol* (2019) 5:1–19. doi: 10.1200/JGO.18.00214
7. Kannarkatt J, Joseph J, Kurniali PC, Al-Janadi A, Hrinczenko B. Adjuvant Chemotherapy for Stage II Colon Cancer: A Clinical Dilemma. *J Oncol Pract* (2017) 13:233–41. doi: 10.1200/JOP.2016.017210
8. Harisi R, Schaff Z, Flautner L, Winternitz T, Jaray B, Nemeth Z, et al. Evaluation and Comparison of the Clinical, Surgical and Pathological TNM Staging of Colorectal Cancer. *Hepatogastroenterology* (2008) 55:66–72.
9. Edge SB, Compton CC. The American Joint Committee on Cancer: The 7th Edition of the AJCC Cancer Staging Manual and the Future of TNM. *Ann Surg Oncol* (2010) 17:1471–4. doi: 10.1245/s10434-010-0985-4
10. National Comprehensive Cancer Network. *Colon Cancer Clinical Practice Guidelines in Oncology* (2022). Available at: http://www.nccn.org/professionals/physician_gls/pdf/colon.pdf (Accessed February 25, 2022).
11. Argiles G, Tabernero J, Labianca R, Hochhause D, Salazar R, Iveson T, et al. Localised Colon Cancer: ESMO Clinical Practice Guidelines for Diagnosis, Treatment and Follow-Up. *Ann Oncol* (2020) 31:1291–305. doi: 10.1016/j.annonc.2020.06.022
12. Compton C. Key Issues in Reporting Common Cancer Specimens: Problems in Pathologic Staging of Colon Cancer. *Arch Pathol Lab Med* (2006) 130:318–24. doi: 10.5858/2006-130-318-KIIRCC
13. Shepherd N, Baxter K, Love S. The Prognostic Importance of Peritoneal Involvement in Colonic Cancer: A Prospective Evaluation. *Gastroenterology* (1997) 112:1096–102. doi: 10.1016/s0016-5085(97)70119-7
14. Zeng Z, Cohen AM, Hajdu S, Sternberg SS, Sigurdson ER, Enker W. Serosal Cytologic Study to Determine Free Mesothelial Penetration of Intraperitoneal Colon Cancer. *Cancer* (1992) 70:737–40. doi: 10.1002/1097-0142(19920815)70:4<737::aid-cncr2820700404>3.0.co;2-s
15. Darakhshan A, Lin B, Chan C, Chapuis PH, Dent OF, Bokey L. Correlates and Outcomes of Tumor Adherence in Resected Colonic and Rectal Cancers. *Ann Surg* (2008) 247:650–8. doi: 10.1097/SLA.0b013e318163d264
16. Liang JW, Gao P, Wang ZN, Song YX, Xu YY, Wang MX, et al. The Integration of Macroscopic Tumor Invasion of Adjacent Organs Into TNM Staging System for Colorectal Cancer. *PloS One* (2012) 7:e52269. doi: 10.1371/journal.pone.0052269
17. Lee SY, Kim CH, Kim YJ, Kim HR. Macroscopic Serosal Invasion and Small Tumor Size as Independent Prognostic Factors in Stage IIA Colon Cancer. *Int J Colorectal Dis* (2018) 33:1139–42. doi: 10.1007/s00384-018-3048-0

Conflict of Interest: The authors declare that the research was conducted in the absence of any commercial or financial relationships that could be construed as a potential conflict of interest.

Publisher's Note: All claims expressed in this article are solely those of the authors and do not necessarily represent those of their affiliated organizations, or those of the publisher, the editors and the reviewers. Any product that may be evaluated in this article, or claim that may be made by its manufacturer, is not guaranteed or endorsed by the publisher.

Copyright © 2022 Jeon, Nam, Choi, Hwang and Baek. This is an open-access article distributed under the terms of the Creative Commons Attribution License (CC BY). The use, distribution or reproduction in other forums is permitted, provided the original author(s) and the copyright owner(s) are credited and that the original publication in this journal is cited, in accordance with accepted academic practice. No use, distribution or reproduction is permitted which does not comply with these terms.

frontiers | Frontiers in Medicine

ORIGINAL RESEARCH
published: 20 July 2022
doi: 10.3389/fmed.2022.888340

Intestinal Microbiota in Colorectal Adenoma-Carcinoma Sequence

Hanju Hua[1†], Yanhong Sun[2†], Xinjue He[3], Yi Chen[3], Lisong Teng[4*] and Chao Lu[3*]*

[1] Department of Colorectal Surgery, The First Affiliated Hospital, Zhejiang University, Hangzhou, China, [2] National Clinical Research Center for Child Health, National Children's Regional Medical Center, The Children's Hospital, Zhejiang University School of Medicine, Hangzhou, China, [3] Department of Gastroenterology, The First Affiliated Hospital, Zhejiang University School of Medicine, Hangzhou, China, [4] Department of Surgical Oncology, The First Affiliated Hospital, Zhejiang University School of Medicine, Hangzhou, China

OPEN ACCESS

Edited by:
Sanjit Mukherjee, National Institutes of Health (NIH), United States

Reviewed by:
Asit Kumar Manna, The University of Utah, United States
Abhisek Bhattacharya, National Institutes of Health (NIH), United States

***Correspondence:**
Yi Chen
zyyychen@zju.edu.cn
Lisong Teng
lsteng@zju.edu.cn
Chao Lu
zyyyluchao@zju.edu.cn

[†] These authors have contributed equally to this work

Specialty section:
This article was submitted to Gastroenterology, a section of the journal Frontiers in Medicine

Received: *02 March 2022*
Accepted: *12 May 2022*
Published: *20 July 2022*

Citation:
Hua H, Sun Y, He X, Chen Y, Teng L and Lu C (2022) Intestinal Microbiota in Colorectal Adenoma-Carcinoma Sequence. Front. Med. 9:888340. doi: 10.3389/fmed.2022.888340

Background: Most colorectal cancer (CRC) cases are sporadic and develop along the adenoma-carcinoma sequence. Intestinal microbial dysbiosis is involved in the development of colorectal cancer. However, there are still no absolute markers predicting the progression from adenoma to carcinoma. This study aimed to investigate the characteristics of intestinal microbiota in patients with colorectal adenoma and carcinoma and its correlations with clinical characteristics.

Methods: Fecal samples were collected from 154 patients with CRC, 20 patients with colorectal adenoma (AD) and 199 healthy controls. To analyze the differences in the intestinal microbiota, 16S rRNA gene sequencing was conducted.

Results: At the genus level, there were four significantly different genera among the three groups, namely Acidaminococcus, Alloprevotella, Mycoplasma, and Sphingobacterium, while Acidaminococcus significantly decreased with the order of Control-AD-CRC ($P < 0.05$). In addition, Parvimonas, Peptostreptococcus, Prevotella, Butyricimonas, Alistipes, and Odoribacter were the key genera in the network of colorectal adenoma/carcinoma-associated bacteria. The top 10 most important species, including *Butyricimonas synergistica*, *Agrobacterium larrymoorei*, *Bacteroides plebeius*, *Lachnospiraceae bacterium feline oral taxon 001*, *Clostridium scindens*, *Prevotella heparinolytica, bacterium LD2013*, *Streptococcus mutans*, *Lachnospiraceae bacterium 19gly4*, and *Eubacterium hallii*, showed the best performance in distinguishing AD from CRC (AUC = 85.54%, 95% CI: 78.83–92.25%). The clinicopathologic features, including age, gender, tumor location, differentiation degree, and TNM stage, were identified to be closely linked to the intestinal microbiome in CRC.

Conclusion: Several intestinal bacteria changed along the adenoma-carcinoma sequence and might be the potential markers for the diagnosis and treatment of colorectal adenoma/carcinoma. Intestinal microbiota characteristics in CRC should account for the host factors.

Keywords: intestinal microbiota, colorectal cancer, adenoma-carcinoma sequence, colorectal adenoma, 16S rRNA

INTRODUCTION

Colorectal cancer (CRC) is the fourth most deadly cancer worldwide (1). Due to the popularization of physical examination, the incidence and mortality of CRC in individuals over 50 years old have steadily decreased, while the incidence under the age of 50 has been on the rise (2). More than half of sporadic CRCs arise *via* adenoma-carcinoma sequence, starting as premalignant lesions represented by conventional, tubular, or tubulovillous adenomas (3). Therefore, understanding the characteristics of adenoma-carcinoma sequence is critical for CRC prevention. The pathogenesis of CRC is related to multiple factors, including diet, lifestyle, environmental factors, genetic mutation, and so on (4, 5). In recent years, an increasing number of studies have shown that intestinal microbiota play important roles in the development of CRC (6). Chen et al. reported that patients with CRC have shown reduced bacterial richness and diversity compared with those of healthy controls (7). According to metagenome-wide association study, Feng et al. found that fecal microbiome-based strategies may be propitious to the early diagnosis of CRC (8). It is reported that *Streptococcus bovis*, *Fusobacterium nucleatum*, and *Enterococcus faecalis* are closely related to the pathogenesis of CRC (9). In addition, *Escherichia coli*, as a class of symbiotic bacteria, has been reported higher levels of colonic colonization in CRC (10). On the other hand, some bacteria, such as *S. thermophilus* and *Clostridium butyicum* are depleted in CRC patients, which suggest that these bacteria may exert a protective effect against CRC (9). The results of the above studies show that there is currently no consistent result about intestinal microbiota and CRC. The relationship between the two is called "Alpha-Bug" (11) or "Driver-Passenger Model" (12) by researchers. Microbiota-associated mechanism in CRC carcinogenesis is highly complex, including biofilm, genotoxins, pathogenic bacteria, inflammation, metabolites, and oxidative stress (13).

Certain factors may affect the consistency of results in studies of the effect of gut microbiota on CRC, including the differences in samples (fecal or mucosal tissue), processing method (RT-PCR or high-throughput analyses), different stage of tumor or location differences between the left- and right-side (14). Therefore, there is controversy on markers predicting the progression of adenoma-carcinoma sequence.

In this study, the first purpose was to characterize the microbiota differences along the adenoma-carcinoma sequence based on 16s rRNA gene sequencing. The second aim was to explore the correlations between the intestinal microbiota and its clinical characteristics. Whether clinicopathologic features, including age, gender, tumor location, differentiation degree, and tumor node metastasis (TNM) stage, were closely linked to the intestinal microbiome in CRC.Based on the adenoma-carcinoma sequence, our findings provide more knowledge for elucidating the tumorigenesis and offer a basis for the development of more effective strategies for the clinical treatment of CRC in the future.

MATERIALS AND METHODS

Study Population and Sample

Participants were outpatients who received colonoscopies by experienced endoscopists in our hospital. The exclusion criteria included: (1) patients older than 90 years of age; (2) patients with a personal history of colorectal cancer, colorectal adenoma, inflammatory bowel disease (colitis-associated pathway is another different molecular pathways), or a family history of colorectal cancer (potential genetic confounding factors); (3) patients had used antibiotics within 2 months or received chemotherapy/radiation treatments within 6 months; (4) individuals who like red and processed meat. Informed consent was obtained from the participants and their privacy was respected. Fresh fecal samples ($\geq$ 1 g) were collected from all participants before colonoscopy and immediately frozen at -80°C until further processing for 16S rRNA gene sequencing analysis. The clinical characteristics of the patients were recorded, including age, sex, tumor size, location, TNM stage, differentiation degree, pathological pattern, and histology. In addition, there were no geographic differences among the patients included in the study, so there was no difference in dietary patterns. Types of adenomas followed the ICD10 and histological classification.

The study protocol was approved by the Medical Ethics Committee of the First Affiliated Hospital, Zhejiang University School of Medicine (2017-869).

DNA Extraction and 16s rRNA Gene Sequencing

Total genomic DNA extraction from fecal samples was performed using QIAamp DNA Stool Mini Kit (QIAGEN, Germany) following the manufacturer's instructions. The quality and concentration of DNA were verified with 2% agarose gel (Tanon, China) and NanoDrop spectrophotometer (Thermo Fisher Scientific, Waltham, MA, United States).

High-throughput Illumina sequencing of the V3–V4 variable regions of the 16S rRNA gene was performed using universal primers 343F (5′-TACGGRAGGCAGCAG-3′) and 798R (5′-AGGGTATCTAATCCT-3′). The PCR reaction was carried out with 15 μL of Phusion High-Fidelity PCR Master Mix (New England Biolabs), 0.2 μM of forward and reverse primers, and about 10 ng template DNA. Thermal cycling consisted of initial denaturation at 98°C for 1 min, followed by 30 cycles of denaturation at 98°C for 10 s, annealing at 50°C for 30 s, and elongation at 72°C for 30 s followed by a final extension of 5 min at 72°C.

The amplicon was purified with AMPure XP beads (Beckman Coulter, Brea, CA, United States) and subjected to a secondary PCR reaction. The final amplicon was quantified using a Qubit dsDNA assay Kit (Life Technologies, Carlsbad, CA, United States). Sequencing library was generated using TruSeq® DNA PCR-Free Sample Preparation Kit (Illumina, San Diego, CA, United States) following the manufacturer's recommendations and assessed on the Qubit® 2.0 Fluorometer (Thermo Fisher Scientific, Waltham, MA, United States) and

Agilent Bioanalyzer 2100 system. The library was sequenced on an Illumina NovaSeq platform and 250 bp paired-end reads were generated.

Bioinformatics and Statistical Analysis

The FASTQ files were processed using QIIME (V1.9.1[1]). Paired-end reads were merged using FLASH (V1.2.7[2]). Quality filtering on the raw tags was performed under specific filtering conditions to obtain high-quality clean tags. The effective tags were obtained by detecting chimera sequences and removing the chimera sequences using UCHIME algorithm (UCHIME Algorithm[3]) based on the reference database (Silva database[4]). Sequences with 97% sequence homology were assigned to the same operational taxonomic units (OTUs) by Uparse software (version 7.0.1001[5]). The representative sequence for each OTU was screened for further annotation. All representative reads were annotated and blasted against the SILVA database (version 123, see footnote 4) using RDP classifier (confidence threshold was 70%). OTUs abundance information was normalized using a standard of sequence number corresponding to the sample with the least sequences.

Alpha diversity and beta diversity analysis were performed by QIIME (version 1.9.1). Alpha diversity was applied for analyzing complexity of species diversity for samples. The community richness and diversity were described by the Chao index and Shannon index, respectively. Beta diversity analysis was used to evaluate comparisons between groups among samples and assessed by non-metric multidimensional scaling (NMDS) analysis and principal coordinates analysis (PCoA) by using weighted UniFrac distance matrix. Linear discriminant analysis (LDA) effect size (15) was used to identify differentially abundant bacterial taxa associated with groups of participants. The LDA value threshold was set at 4. *T*-test and Wilcox test were employed to assess the significance by QIIME (version 1.9.0).

RESULTS

Characteristics of Subjects

A total of 373 participants, including 154 patients with CRC (mean age 65.81 ± 10.98 years old, 63.64% male), 20 patients with AD (mean age 64.35 ± 12.89 years old, 75.00% male) and 199 healthy controls (mean age 59.48 ± 3.20 years old, 58.29% male) were enrolled in this study. The control group was younger, but we found the same conclusion after adjusting for age as a confounder. The clinical characteristics of the patients were shown in **Table 1**. The mean size of carcinoma was 4.55 ± 2.18 mm and most of the tumors were found in the left colon (75.97%). In the CRC group, the differentiation degree concentrated in the moderate degree (75.32%) and mainly tubular adenocarcinoma (85.06%).

[1]http://qiime.org/scripts/split_libraries_fastq.html

[2]http://ccb.jhu.edu/software/FLASH/

[3]http://www.drive5.com/usearch/manual/uchime_algo.html

[4]https://www.arb-silva.de/

[5]http://www.drive5.com/uparse/

Summarization of 16S rRNA Gene Sequencing Results

A total of 2,668 OTUs were generated from 164 patients' samples. A Venn diagram showed that 1,323 OTUs were shared between AD and CRC, while 113 unique OTUs existed in AD, and 1,232 unique OTUs existed in CRC (**Figure 1A**). Rarefaction curve and species accumulation boxplot were shown in **Figures 1B,C**. Moreover, the value of Good's coverage for each group was over 99.8% (**Figure 2A**). No significant difference in alpha diversity was observed between the AD and CRC group ($P = 0.95$ for Chao index, **Figure 2B**; $P = 0.74$ for Shannon index, **Figure 2C**).

A mild separation between AD and CRC was observed and no significant difference in microbiota composition was detected by PCoA analysis [Pr (> F) = 0.33 for weighted UniFrac distance, **Figure 3A**]. NMDS analysis also revealed that the microbiota composition between two groups was similar, and samples from AD and CRC mostly overlapped with one another (stress = 0.202 > 0.2, **Figure 3B**). The analysis of beta diversity revealed that fecal microbial communities between AD and CRC were not distinct from each other ($P = 0.88$ for weighted UniFrac

TABLE 1 | Demographic and clinical characteristics of patients and controls.

Characteristics	Control	AD	CRC
Number	199	20	154
Age, years	59.48 ± 3.20	64.35 ± 12.89	65.81 ± 10.98
Sex			
Male	116 (58.29%)	15 (75%)	98 (63.64%)
Female	83 (41.71%)	5 (25%)	56 (36.36%)
Location[a]			
Left	–	19 (95%)	117 (75.97%)
Right	–	1 (5%)	37 (24.03%)
Size, mm	–	–	4.55 ± 2.18
TNM stage[b]			
I	–	–	33
II	–	–	51
III	–	–	43
IV	–	–	10
NA	–	–	17
Differentiation degree			
Poor	–	–	9
Moderate	–	–	116
Well	–	–	9
NA	–	–	20
Pathological pattern			
Protrude	–	–	63
Ulcerative	–	–	69
NA	–	–	22
Histology			
Tubular	–	–	131
Mucinous	–	–	20
NA	–	–	3

CRC, colorectal cancer; AD, adenomas.

[a]The left colon was defined as the rectum, sigmoid, and descending colon; the right colon was defined as the transverse colon, ascending colon, and cecum.

[b]Tumor node metastasis (TNM) stage.

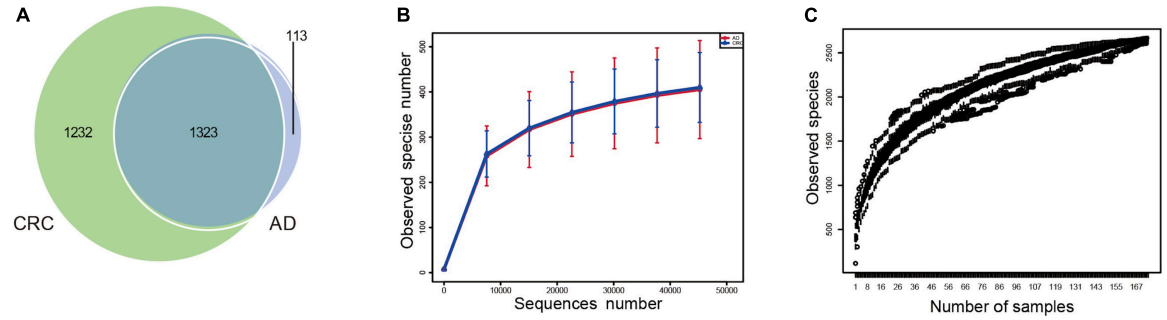

FIGURE 1 | (A) Venn diagram illustrating the total, unique, and shared number of OTUs predicted for AD and CRC group datasets; **(B)** Rarefaction curve of OTU; **(C)** Species accumulation boxplot.

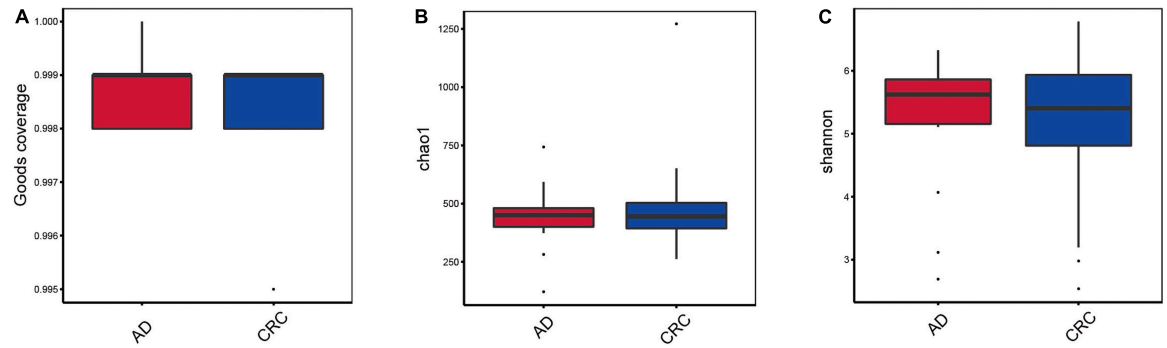

FIGURE 2 | (A) Box plot based on Good's coverage; **(B)** Alpha diversity analysis based on the Chao1 index in the AD and CRC group ($P = 0.95$); **(C)** Alpha diversity analysis based on the Shannon index in the AD and CRC group ($P = 0.74$).

distance, **Figure 3C**). However, there was more distribution in the control samples than that in AD or CRC samples both in the PCoA and NMDS plots (stress = 0.123 < 0.2, **Figures 3D,E**), suggesting that the fecal microbial communities between the Control and the AD or CRC group were different.

Specific Bacterial Taxa Associated With Adenoma-Carcinoma Sequence

The significant analysis based on Wilcox test showed that 115 genera of intestinal microbiota in patients with AD were distinct from that in controls. Correspondingly, there were 134 genera significantly different in patients with CRC compared with the control (**Figure 4A**). Within them, there were four significantly different genera among the three groups, namely Acidaminococcus, Alloprevotella, Mycoplasma, and Sphingobacterium (**Figure 4B**). Notably, the relative abundance of Acidaminococcus was decreased with the order of Control-AD-CRC. We further found that Parvimonas, Peptostreptococcus, Prevotella, Butyricimonas, Alistipes, and Odoribacter were key genera in the network of adenoma-carcinoma sequence (**Figure 4C**). Furthermore, Random Forest analysis suggested that a combination of the top 10 species showed the best performance in distinguishing AD patients from CRC (AUC = 85.54%, 95% CI: 78.83–92.25%, **Figure 4D**). Mean Decrease Gini (MDG) and Mean Decrease Accuracy (MDA) coefficients were used to rank the importance of the variables from Random Forest algorithm results (**Figures 4E,F**). The 10 most important species were *Butyricimonas synergistica*, *Agrobacterium larrymoorei*, *Bacteroides plebeius*, *Lachnospiraceae bacterium feline oral taxon 001*, *Clostridium scindens Clostridium scindens*, *Prevotella heparinolytica, bacterium LD2013*, *Streptococcus mutans*, *Lachnospiraceae bacterium 19gly4*, and *Eubacterium hallii.*

Association Between Fecal Microbiota and Colorectal Cancer Clinical Characteristics

To explore the correlations between intestinal microbiota and clinical characteristics of CRC, we created the correlation heatmap according to the different clinicopathologic features of CRC patients. As shown in **Figure 5A**, 154 patients were divided into two groups according to their ages: 13 CRC patients were younger than 50 years old and 141 patients were older than 50 years old, and 15 bacterial species were higher and another 15 bacterial species were significantly lower in the older patients than that in the younger patients. Stratified by gender, 5 bacterial species increased in female patients including *Prevotella sp. Marseille-P2931, Clostridium colinum*, *Bifidobacterium pseudocatenulatum*, *Gordonibacter sp. Marseille-P2775,* and *Saccharibacteria bacterium UB2523*, while other 11

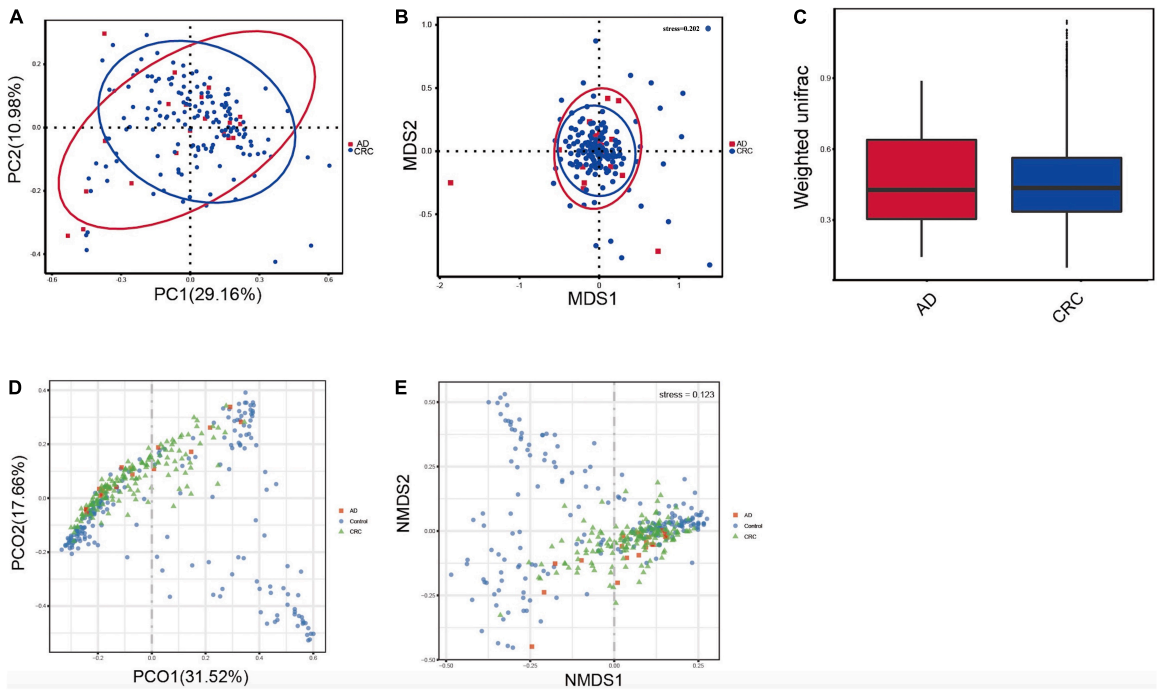

FIGURE 3 | (A) Principal coordinates analysis (PCoA) based on weighted unifrac distance matrix in the AD and CRC group [Pr (> F) = 0.33]; **(B)** Non-metric multidimensional scaling (NMDS) based on weighted unifrac distance matrix in the AD and CRC group (stress = 0.202); **(C)** Beta diversity analysis by weighted UniFrac distance in the AD and CRC group (P = 0.88); **(D)** Principal coordinates analysis (PCoA) based on weighted unifrac distance matrix among Control, AD, and CRC group; **(E)** Non-metric multidimensional scaling (NMDS) based on weighted unifrac distance matrix among Control, AD, and CRC group (stress = 0.123).

bacterial species were significantly enriched in male patients (**Figure 5B**). In addition, the microbiome was different between the patients with the tumor in the left and right colon, in which 17 bacterial species were found obviously changed (7 up and 10 down, left vs. right) (**Figure 5C**). Furthermore, we compared the relationship between microbiota and tumor stages in CRC (I–II vs. III–IV). The relative abundances of nine bacterial species, including *Porphyromonas uenonis*, *Clostridium colinum*, *Proteiniphilum sp.*, *Selenomonas ruminantium*, *Gordonibacter sp. Marseille-P2775*, *Akkermansia muciniphila*, *Rikenella microfusus*, *Dialister pneumosintes*, and *Weissella cibaria*, were significantly higher in the TNM stage III/IV group than in the TNM stages I/II group (**Figure 5D**).

DISCUSSION

In summary, our study identified colorectal adenoma/carcinoma-associated microbes in patients with AD/CRC compared with controls. CRC-associated bacteria altered with the colorectal adenoma-carcinoma sequence. Combining with the ten genera of adenoma-carcinoma sequence associated bacteria can effectively distinguish patients with AD and CRC. The host clinicopathologic features, such as age, sex, tumor location, differentiation degree, and TNM stage, were closely linked to the intestinal microbiome in CRC. Disease outcomes of CRC should account for microbiota characteristics and host factors in the future.

In this study, we found that the species richness and community diversity were not markedly altered between AD and CRC. There was only one family Prevotellaceae that was significantly enriched in CRC compared to AD by LEfSe analysis (data was not shown). The dominant gut microbiota at the genus level in CRC and AD was consistent with the studies reported (13, 16). These results suggest that the differences in microbiota between different studies are consistent, indicating that the differences in microbiota in AD and CRC are less likely to be affected by race, region, diet or others.

Moreover, *Acidaminococcus, Alloprevotella, Mycoplasma,* and *Sphingobacterium* were identified significantly altered among the three groups, in which *Acidaminococcus* was decreased with the order of control-AD-CRC. However, previous study reported that the enrichment of *Acidaminococcus intestini* was found to be higher in carcinomas than in controls and it was negatively correlated with the dietary indices (red meat and serum ferritin) (8). We believe that a single species does not reflect genus differences as a whole, thus leading to inconsistent results. In this study, *Alloprevotella* was enriched in CRC, which was consistent with previous reports on CRC gut microbiota in domestic populations (17). *Alloprevotella* was isolated from the human oral cavity (18), and we also observed the close relationship between colorectal adenoma/carcinoma and oral pathogens, such as *Parvimonas* and *Peptostreptococcus* in the network analysis (19). These bacteria were reported to be enriched in tumor tissues or feces of individuals with CRC or adenomas and involved in the carcinogenesis of CRC (20). Possible mechanisms of

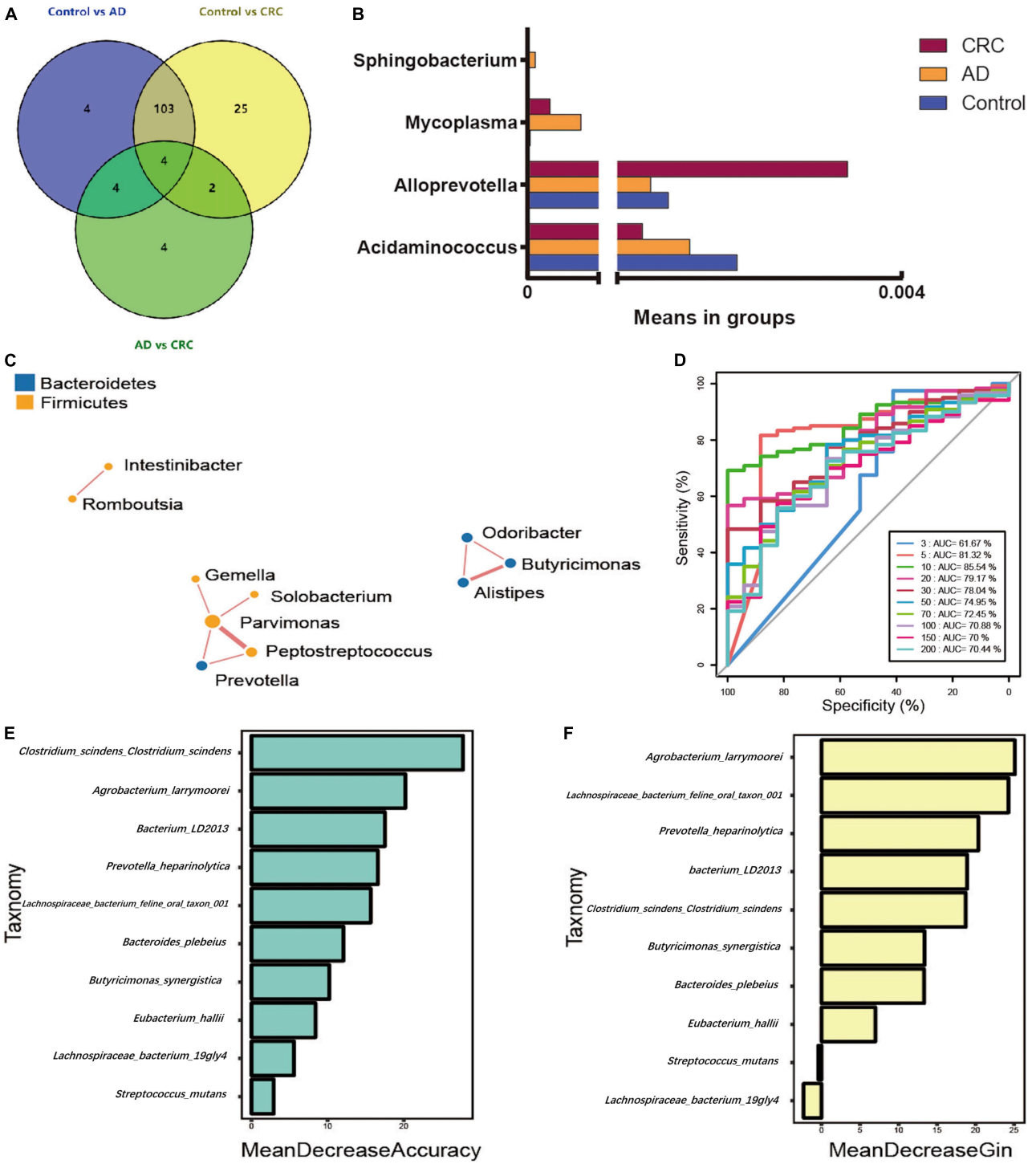

FIGURE 4 | (A) Venn diagram illustrating the total, unique, and shared number of significant pairwise difference at the genus level among the Control, AD, and CRC groups; **(B)** The relative abundance of the significant changed genera among the three groups; **(C)** Microbial association network for colorectal adenoma/carcinoma-associated genera; **(D)** Receiver operating curve (ROC) by Random Forest analysis for distinguishing AD patients from CRC; **(E)** Mean Decrease Accuracy (MDA) coefficients of the 10 most important species in distinguishing AD patients from CRC; **(F)** Mean Decrease Gini (MDG) coefficients of the 10 most important species in distinguishing patients with AD from patients with CRC.

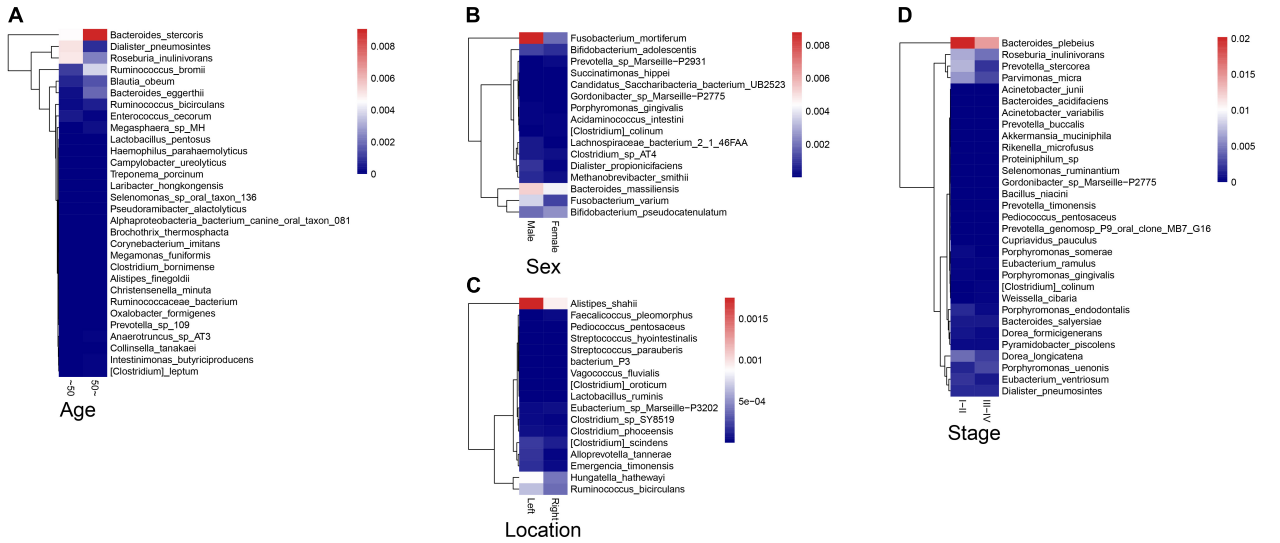

FIGURE 5 | Association between fecal microbiota and CRC clinical characteristics. **(A)** The correlation heatmap between intestinal microbiota and age of patients with CRC; **(B)** The correlation heatmap between intestinal microbiota and gender of patients with CRC; **(C)** The correlation heatmap between intestinal microbiota and the tumor location; **(D)** The correlation heatmap between intestinal microbiota and tumor stage.

pathogenicity include changes in permeability, and interference with signal pathways. Our results provided additional evidence that oral periodontopathic bacteria played an important role in the tumorigenesis of CRC.

Most importantly, our results showed that the combination of the 10 species can distinguish colorectal AD from CRC, which suggested that these 10 special species might be used as potential markers for diagnosing and predicting colorectal AD. Similarly, it was confirmed that CRC-associated bacteria were changed with the degree of malignancy and inflammatory factors (Plasma C-reactive protein and soluble tumor necrosis factor II) increased across the adenoma-carcinoma sequence (19). However, there are still no absolute markers predicting the progression from adenoma to carcinoma. The findings from the current study will contribute to develop the diagnostic biomarkers and therapeutic targets during the progression from adenoma to carcinoma.

Previous studies have shown that CRC-associated microbes varied with adenoma-carcinoma sequence and suggested that the fecal microbiota may contribute to the early diagnosis and treatment of CRC (21). It is known that short-chain fatty acids (SCFAs) producing bacteria is closely related to the occurrence of CRC (22). It may be due to the fact that SCFAs can reduce the expression of inflammatory factors by inhibiting the activation of NF-κB, which can produce anti-inflammatory effects and interfere with precancerous cells in the early stages of CRC development. The data from this study showed that SCFAs producing bacteria, *Eubacterium hallii,* changed in expression as adenoma-carcinoma sequence, which was consistent with results of a previous study. Moreover, a previous study had also reported *Gordonibacter* bacteremia in patients with CRC, indicating that *Gordonibacter sp.* may be related to the occurrence and development of CRC (23). These previous data exemplified can provide objective evidence to support the results of this study.

In addition, previous studies have reported that the composition and relative abundance of intestinal microbiome would be influenced by age, gender, race, or dietary habits (24, 25). Our study has reached similar conclusions. Relative abundance of several bacterial species was altered between different age or sex. Notably, firmicutes dramatically decreased in the old patients compared to the young patients. Consistent with the previous studies, our results also demonstrated that the microbiome was different between the patients with the tumor in the left and right colon (14). The relative abundance of *Bacteroides cellulosilyticus* was significantly increased with the order of differentiation degree in Poor-Moderate-Well and nine CRC-associated bacterial species were significantly higher in TNM stage III/IV group than in TNM stages I/II group. The differences in the microbiota of patients with different tumor location, differentiation degree, and stage provide strong evidence of the tumors–host heterogeneity.

Valuable results were obtained in this study, but there were still deficiencies and limitations. Although this paper revealed adenoma-carcinoma sequence associated intestinal bacteria, it does not provide a more in-depth analysis of the mechanism by which these bacteria participate in the occurrence of the mechanism. In addition, we conducted stratified analysis according to factors such as age, gender, location, and stage in order to further explore the influence of different factors on CRC and intestinal microbiome. However, based on the limitation of samples, the results were unstable. We were well aware of the limitations of results imposed by the lack of sample, and we are actively expanding the sample in order to make the results more reliable and to verify differentially expressed microbiota. Furthermore, this study did not conduct a more in-depth comparison of age subgroup analysis. The 50-year-old

distinction did not reflect the differences between different age groups very well, and we will make up for the deficiencies in follow-up research.

In conclusion, several intestinal bacteria changed along the adenoma-carcinoma sequence and might be the potential markers for the diagnosis and treatment of colorectal adenoma/carcinoma. Intestinal microbiota characteristics in CRC should account for the host factors.

DATA AVAILABILITY STATEMENT

The original contributions presented in the study are included in the article material, further inquiries can be directed to the corresponding authors.

ETHICS STATEMENT

The studies involving human participants were reviewed and approved by the Medical Ethics Committee of The First Affiliated Hospital, Zhejiang University School of Medicine. The patients/participants provided their written informed consent to participate in this study. Written informed consent was obtained from the individual(s) for the publication of any potentially identifiable images or data included in this article.

AUTHOR CONTRIBUTIONS

CL proposed the initial idea and designed the experiments. HH conducted the analysis and interpretation of data for the manuscript. XH and YS conducted the procedures. YS supervised and provided consultations during the whole study. YC revised the manuscript. LT solved problems of the knowledge points proposed by the reviewers and revised the final draft of the manuscript. All authors contributed to the article and approved the submitted version.

FUNDING

This study was supported by Zhejiang Medical and Health Science and Technology Plan Project (LY20H030005).

REFERENCES

1. Dekker E, Tanis PJ, Vleugels JLA, Kasi PM, Wallace MB. Colorectal cancer. *Lancet.* (2019). 394:1467–80. doi: 10.1016/s0140-6736(19)32319-0
2. Patel SG, Ahnen DJ. Colorectal cancer in the young. *Curr Gastroenterol Rep.* (2018) 20:15. doi: 10.1007/s11894-018-0618-9
3. Bae JM, Kim JH, Kang GH. Molecular subtypes of colorectal cancer and their clinicopathologic features, with an emphasis on the serrated neoplasia pathway. *Arch Pathol Lab Med.* (2016) 140:406–12. doi: 10.5858/arpa.2015-0310-RA
4. Hou N, Huo D, Dignam JJ. Prevention of colorectal cancer and dietary management. *Chin Clin Oncol.* (2013) 2:13. doi: 10.3978/j.issn.2304-3865.2013.04.03
5. Vacante M, Ciuni R, Basile F, Biondi A. Gut microbiota and colorectal cancer development: a closer look to the adenoma-carcinoma sequence. *Biomedicines.* (2020) 8:489. doi: 10.3390/biomedicines8110489
6. Tilg H, Adolph TE, Gerner RR, Moschen AR. The intestinal microbiota in colorectal cancer. *Cancer Cell.* (2018) 33:954–64. doi: 10.1016/j.ccell.2018.03.004
7. Chen W, Liu F, Ling Z, Tong X, Xiang C. Human intestinal lumen and mucosa-associated microbiota in patients with colorectal cancer. *PLoS One.* (2012) 7:e39743. doi: 10.1371/journal.pone.0039743
8. Feng Q, Liang S, Jia H, Stadlmayr A, Tang L, Lan Z, et al. Gut microbiome development along the colorectal adenoma-carcinoma sequence. *Nat Commun.* (2015) 6:6528. doi: 10.1038/ncomms7528
9. Cheng Y, Ling Z, Li L. The intestinal microbiota and colorectal cancer. *Front Immunol.* (2020) 11:615056. doi: 10.3389/fimmu.2020.615056
10. Veziant J, Gagnière J, Jouberton E, Bonnin V, Sauvanet P, Pezet D, et al. Association of colorectal cancer with pathogenic *Escherichia coli*: focus on mechanisms using optical imaging. *World J Clin Oncol.* (2016) 7:293–301. doi: 10.5306/wjco.v7.i3.293
11. Sears CL, Pardoll DM. Perspective: alpha-bugs, their microbial partners, and the link to colon cancer. *J Infect Dis.* (2011) 203:306–11. doi: 10.1093/jinfdis/jiq061
12. Tjalsma H, Boleij A, Marchesi JR, Dutilh BE. A bacterial driver-passenger model for colorectal cancer: beyond the usual suspects. *Nat Rev Microbiol.* (2012) 10:575–82. doi: 10.1038/nrmicro2819
13. Wong SH, Yu J. Gut microbiota in colorectal cancer: mechanisms of action and clinical applications. *Nat Rev Gastroenterol Hepatol.* (2019) 16:690–704. doi: 10.1038/s41575-019-0209-8
14. Flemer B, Lynch DB, Brown JM, Jeffery IB, Ryan FJ, Claesson MJ, et al. Tumour-associated and non-tumour-associated microbiota in colorectal cancer. *Gut.* (2017) 66:633–43. doi: 10.1136/gutjnl-2015-309595
15. Eckburg PB, Bik EM, Bernstein CN, Purdom E, Dethlefsen L, Sargent M, et al. Diversity of the human intestinal microbial flora. *Science.* (2005) 308:1635–8. doi: 10.1126/science.1110591
16. Saus E, Iraola-Guzmán S, Willis JR, Brunet-Vega A, Gabaldón T. Microbiome and colorectal cancer: roles in carcinogenesis and clinical potential. *Mol Aspects Med.* (2019) 69:93–106. doi: 10.1016/j.mam.2019.05.001
17. Chang H, Mishra R, Cen C, Tang Y, Ma C, Wasti S, et al. Metagenomic analyses expand bacterial and functional profiling biomarkers for colorectal cancer in a Hainan cohort, China. *Curr Microbiol.* (2021) 78:705–12. doi: 10.1007/s00284-020-02299-3
18. Zhang L, Liu Y, Zheng HJ, Zhang CP. The oral microbiota may have influence on oral cancer. *Front Cell Infect Microbiol.* (2019) 9:476. doi: 10.3389/fcimb.2019.00476
19. Zhang Y, Yu X, Yu E, Wang N, Cai Q, Shuai Q, et al. Changes in gut microbiota and plasma inflammatory factors across the stages of colorectal tumorigenesis: a case-control study. *BMC Microbiol.* (2018) 18:92. doi: 10.1186/s12866-018-1232-6
20. Flemer B, Warren RD, Barrett MP, Cisek K, Das A, Jeffery IB, et al. The oral microbiota in colorectal cancer is distinctive and predictive. *Gut.* (2018) 67:1454–63. doi: 10.1136/gutjnl-2017-314814
21. Nakatsu G, Li X, Zhou H, Sheng J, Wong SH, Wu WK, et al. Gut mucosal microbiome across stages of colorectal carcinogenesis. *Nat Commun.* (2015) 6:8727. doi: 10.1038/ncomms9727
22. Chen HM, Yu YN, Wang JL, Lin YW, Kong X, Yang CQ, et al. Decreased dietary fiber intake and structural alteration of gut microbiota in patients with advanced colorectal adenoma. *Am J Clin Nutr.* (2013) 97:1044–52. doi: 10.3945/ajcn.112.046607
23. Woo PC, Teng JL, Lam KK, Tse CW, Leung KW, Leung AW, et al. First report of *Gordonibacter pamelaeae* bacteremia. *J Clin Microbiol.* (2010) 48:319–22. doi: 10.1128/jcm.01459-09

24. Odamaki T, Bottacini F, Kato K, Mitsuyama E, Yoshida K, Horigome A, et al. Genomic diversity and distribution of *Bifidobacterium longum* subsp. longum across the human lifespan. *Sci Rep.* (2018) 8:85. doi: 10.1038/s41598-017-18391-x
25. Ishibashi KI, Nishioka M, Onaka N, Takahashi M, Yamanaka D, Adachi Y. Effects of *Euglena gracilis* EOD-1 ingestion on salivary IgA reactivity and health-related quality of life in humans. *Nutrients.* (2019) 11:1144. doi: 10.3390/nu11051144

Conflict of Interest: The authors declare that the research was conducted in the absence of any commercial or financial relationships that could be construed as a potential conflict of interest.

Publisher's Note: All claims expressed in this article are solely those of the authors and do not necessarily represent those of their affiliated organizations, or those of the publisher, the editors and the reviewers. Any product that may be evaluated in this article, or claim that may be made by its manufacturer, is not guaranteed or endorsed by the publisher.

Copyright © 2022 Hua, Sun, He, Chen, Teng and Lu. This is an open-access article distributed under the terms of the Creative Commons Attribution License (CC BY). The use, distribution or reproduction in other forums is permitted, provided the original author(s) and the copyright owner(s) are credited and that the original publication in this journal is cited, in accordance with accepted academic practice. No use, distribution or reproduction is permitted which does not comply with these terms.

frontiers | Frontiers in Oncology

TYPE Original Research
PUBLISHED 29 July 2022
DOI 10.3389/fonc.2022.964115

Check for updates

OPEN ACCESS

EDITED BY
Ravindra Deshpande,
Wake Forest School of Medicine,
United States

REVIEWED BY
Vipin Rawat,
University of Illinois at Chicago,
United States
Jagadeeswara Rao Bommi,
Case Western Reserve University,
United States
Gayatri Ramachandran,
University of Hyderabad, India

*CORRESPONDENCE
Fei Zhou
13816837501@sina.cn

SPECIALTY SECTION
This article was submitted to Gastrointestinal Cancers: Hepato Pancreatic Biliary Cancers, a section of the journal Frontiers in Oncology

RECEIVED 08 June 2022
ACCEPTED 05 July 2022
PUBLISHED 29 July 2022

CITATION
Shen F, Liu C, Zhang W, He S, Wang F, Wang J, Li Q and Zhou F (2022) Serum levels of IL-6 and CRP can predict the efficacy of mFOLFIRINOX in patients with advanced pancreatic cancer. *Front. Oncol.* 12:964115. doi: 10.3389/fonc.2022.964115

COPYRIGHT
© 2022 Shen, Liu, Zhang, He, Wang, Wang, Li and Zhou. This is an open-access article distributed under the terms of the Creative Commons Attribution License (CC BY). The use, distribution or reproduction in other forums is permitted, provided the original author(s) and the copyright owner(s) are credited and that the original publication in this journal is cited, in accordance with accepted academic practice. No use, distribution or reproduction is permitted which does not comply with these terms.

Serum levels of IL-6 and CRP can predict the efficacy of mFOLFIRINOX in patients with advanced pancreatic cancer

Feifei Shen[1], Chuan Liu[1], Weiguo Zhang[2], Sijia He[1], Fan Wang[1], Jingjue Wang[1], Qi Li[1] and Fei Zhou[1*]

[1]Department of Oncology, Shanghai General Hospital, Shanghai Jiaotong University School of Medicine, Shanghai, China, [2]Department of Radiology, Shanghai General Hospital, Shanghai Jiaotong University School of Medicine, Shanghai, China

Objectives: There is an urgent need for biomarkers that predict the survival outcome of patients diagnosed with metastatic pancreatic cancer, undergoing systemic chemotherapy. This study aimed to identify biomarkers associated with the survival of mPC patients treated with modified FOLFIRINOX (mFOLFIRINOX) as first-line chemotherapy.

Methods: This was a retrospective study of 30 patients with mPC who received mFOLFIRINOX between October 2018 and March 2021. Data on carcinoembryonic antigen (CEA), cancer antigen (CA)199, interleukin (IL)-6, C-reactive protein (CRP), neutrophils, platelets, lymphocytes, and albumin were collected and dichotomized using the upper or lower limit, as appropriate. These markers were examined for their association with progression-free survival (PFS). A receiver operating characteristic (ROC) curve analysis was used to explore a suitable model to predict mFOLFIRINOX effectiveness.

Results: IL-6 and CRP levels were associated with poor progression (P = 0.004 and P = <0.001, respectively) of mPC. The high IL-6 level was an independent poor prognostic factor for PFS (HR=4.66, 95%CI: 1.32-16.37, P=0.016) in the multivariable analysis. Patients with high IL-6 levels had a shorter PFS than those with low IL-6 levels (median PFS: 257 vs. 150 days, P=0.020). An increase in IL-6 and CRP levels during chemotherapy positively correlated with disease progression (P = <0.001 for both). The model combining IL-6 with CRP levels helped predict the outcomes of mPC patients treated with mFOLFIRINOX (AUC: 0.811, 95%CI: 0.639-0.983, P=0.003).

Conclusions: The serum levels of IL-6 and CRP might be considered as valuable biomarkers in predicting the outcomes of patients with mPC who received the mFOLFIRINOX regimen.

KEYWORDS

C-reactive protein, interleukin-6, inflammatory markers, metastatic pancreatic cancer, modified FOLFIRINOX

Introduction

Pancreatic cancer (PC) is a very lethal malignancy, with an incidence rate nearly equal to its mortality rate (1). The situation is even worse in China, where 83,600 new PC cases were reported in 2017, and an estimated 85,100 patients died (2). This was because most patients were not diagnosed timely, and 80%–90% of them were in an advanced stage at diagnosis and were unable to receive curative resection (3). The reported 5-year survival rate of PC is only 8% (1).

Systemic chemotherapy is the standard of care for patients with metastatic PC (mPC). The FOLFIRINOX regimen [oxaliplatin, irinotecan, leucovorin, and 5-fluorouracil (5-FU)] significantly improves overall survival (OS) compared with gemcitabine alone in patients with mPC, but it is associated with higher toxicity (4). The modified FOFIRINOX (mFOLFIRINOX) regimen was, therefore, suggested with the intention of reducing toxicity while preserving efficacy (5–7). It was also proven to be well tolerated and effective in Chinese patients (7). The overall response rate (ORR) of mFOLFIRINOX was reported to be 30%–53.5% (5–7). Although the TNM stage and serum carbohydrate antigen 199 (CA199) levels have been demonstrated to be associated with survival, their value in predicting the efficacy of mFOLFIRINOX is low (8, 9). Therefore, biomarkers that can effectively identify patients with mPC who will benefit from mFOLFIRINOX are urgently needed to improve patient management.

Inflammation predisposes individuals to the initiation, growth, progression, and metastatic spread of cancer (10). Inflammatory markers are associated with the prognosis of PC (11–19). One study showed that elevated serum C-reactive protein (CRP) levels were significantly associated with poor clinical outcomes in patients with PC (11), while another study found that the CRP-to-albumin ratio could be a significant and promising inflammatory prognostic score (12). In addition, many studies suggested that the changes in interleukin (IL) expression were associated with poor prognosis in advanced PC (APC) (13, 14). Furthermore, high CRP and IL-6 levels were associated with a poor response in patients with PC receiving first-line gemcitabine monotherapy (15, 16). Higher levels of tumor-infiltrating neutrophils were significantly associated with shorter survival, whereas higher levels of tumor-infiltrating lymphocytes, as well as low levels of platelets (PLT), were described as being positively correlated with extended OS and progression-free survival (PFS) in PC (17–19).

Therefore, it was hypothesized that inflammatory markers, such as CRP, ILs, tumor-infiltrating neutrophils and lymphocytes, and platelets, might be potential indicators for predicting the response of patients with mPC to mFOLFIRINOX. This study aimed to investigate the impact of these inflammatory markers on the outcomes of first-line mFOLFIRINOX chemotherapy in patients with mPC. The results of this study could help improve the management of mPC by identifying the patients who might benefit the most from mFOLFIRINOX.

Materials and methods

Study design and patients

This was a retrospective observational single-center study that included patients treated with mFOLFIRINOX at Shanghai General Hospital between October 2018 and March 2021. All patients included had been diagnosed with mPC by pathological and imaging examinations and had received mFOLFIRINOX as first-line chemotherapy. The patients who had clinical evidence of infection or another inflammatory disease during treatment were excluded (Figure 1). The study was approved by the ethics board of Shanghai General Hospital. The requirement for informed consent was waived by the committee due to the retrospective nature of the study.

Systemic chemotherapy

The mFOLFIRINOX regimen (oxaliplatin 68 mg/m^2 given as a 2-h intravenous infusion, immediately followed by irinotecan 135 mg/m^2 given as a 90-min intravenous infusion, then leucovorin 400 mg/m^2 delivered as a 2-h intravenous infusion, and finally 5-FU 2400 mg/m^2 given as a continuous intravenous infusion over a 46-h period) had been administered on day 1 and then repeated every 2 weeks until disease progression or patient refusal. Dose modification was allowed when unacceptable toxicity occurred.

Response assessment

Tumor response assessment was examined every three cycles of treatment by computed tomography (CT) or magnetic resonance imaging (MRI). The efficacy outcomes included complete response (CR), partial response (PR), progressive disease (PD), and stable disease (SD) according to the Response Evaluation Criteria in Solid Tumors version 1.1 (RECIST 1.1) (20). The best clinical response during chemotherapy for each patient was recorded as the tumor response. ORR was calculated as CR + PR/all evaluated patients. The disease control rate (DCR) was calculated as CR + PR + SD/all evaluated patients.

Data collection

The clinicopathological data including age, sex, surgical treatment before metastasis (yes or no), Eastern Cooperative Oncology Group (ECOG) score, body mass index (BMI), measurable metastatic site,

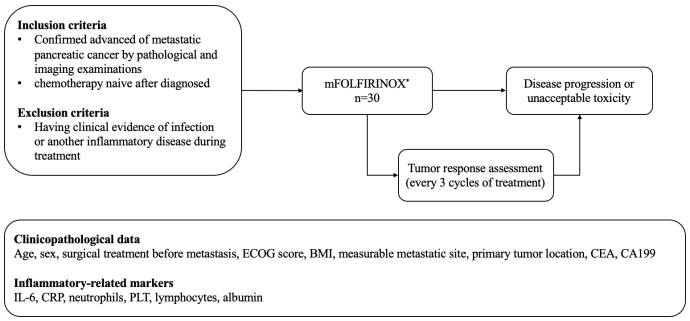

FIGURE 1
The mFOLFIRINOX regimen: oxaliplatin 68 mg/m^2 given as a 2-h intravenous infusion, then leycovorin 400 mg/m^2 delivered as a 2-h intravenous infusion, qnd finally 5-FU 2400 mg/m^2 given as a continous intravenous infusion over a 46-h period. The regimen had beeb administered on day 1 and the repeatedevery 2 weeks until disease progression or patient refusal. ECOG, Easteran Cooperative Oncology Group; BMI, body mass indez; CEA, carcinoembryonic antigen; CA199, cancerantigen199; IL-6 interleukin-6; CRP, C-reactive protein; PLT, platelets.

primary tumor location, carcinoembryonic antigen (CEA), and CA199 were collected from the patients' records. The other inflammatory-related markers, including IL-6, CRP, neutrophils, PLT, lymphocytes, and albumin, were also collected from the records. Blood samples had been obtained within 3 days before initiating treatment or during chemotherapy. CRP had been measured with an immunoturbidimetry assay. Serum IL-6, CA199, and CEA levels had been determined using electro-chemiluminescence immunoassay. As shown in Table 1, the normal reference value of IL-6 and CRP was 0–7 pg/mL and 0–10 mg/L, respectively. The other reference values were 0–40 U/mL for CA199, 0–5 ng/mL for CEA, 35–50 g/L for albumin, 85–303 × 10^9 for PLT, 2–7 × 10^9 for neutrophils, and 0.8–4 × 10^9 for lymphocytes. Using the upper limits of normal for IL-6 (>7 pg/mL), CRP (>10 mg/L), PLT (>303 × 10^9/L), neutrophils (>7 × 10^9/L), CA199 (>40 U/mL), and CEA (>5 ng/mL) as cutoff values, the patients were classified with low or high values for each of these markers. Using the lower limit of normal for lymphocytes (<0.8×10^9/L) and albumin (<35 g/L) as cutoff values, the patients were classified with low and high values. The definitions and cutoff values were based on previous reports (21–23). CEA, CA199, CRP, IL-6, neutrophils, PLT, lymphocytes, and albumin were tested at three-cycle intervals, at the same time as response evaluation. A dynamic increase was defined as two or more consecutive increases in the levels of tested markers compared with the last testing without a cutoff threshold. All markers described earlier were measured by the Department of Laboratory Medicine of Shanghai General Hospital (Shanghai Jiaotong University School of Medicine, Shanghai, China (using standard routine laboratory methods).

Survival data were obtained from the medical charts. PFS was defined as the time from the start of chemotherapy to documented disease progression or death, whichever occurred first.

Statistical analysis

Statistical analysis was performed using SPSS 20.0 (IBM Corp., NY, USA). The relationships between inflammatory markers and the clinical response were assessed using Fisher's

TABLE 1 The normal reference and cutoff values of serum markers.

	normal reference value	High	Low
IL-6 (pg/mL)	0 – 7	> 7	≤ 7
CRP (mg/L)	0 – 10	> 10	≤ 10
PLT (×10^9)	85 – 303	> 303	≤ 303
Neutrophil (×10^9)	2 – 7	> 7	≤ 7
CA199 (U/mL)	0 – 40	> 40	≤ 40
CEA (ng/mL)	0 – 5	> 5	≤ 5
Lymphocytes (×10^9)	0.8 – 4	≥ 0.8	< 0.8
albumin (g/L)	35 – 50	≥ 35	< 35

IL-6, interleukin-6; CRP, C-reactive protein; PLT: Platelets; CEA, carcinoembryonic antigen; CA199, Carbohydrate antigen 199.

exact test (for categorical variables) and Student's *t* test (for continuous variables). The correlations between dynamically changing inflammatory markers and the clinical response were evaluated using Spearman's rank correlation coefficient. Survival analysis was performed using the Kaplan-Meier method, and the curves were compared using the log-rank test. Multivariate analysis was performed using a stepwise forward Cox regression (likelihood ratio, enter $P < 0.05$, remove $P > 0.10$) with significant markers from the univariate analyses ($P < 0.05$); the results were presented as hazard ratio (HR) and 95% confidence interval (CI). Receiving operating characteristic (ROC) curve analysis was used to explore a combination of biomarkers based on the multivariate regression model to predict the efficacy (DCR) of the mFOLFIRINOX regimen in patients with mPC. Statistical significance was set at P <0.05 (two-sided).

Results

Characteristics of the patients

All the 36 patients included had stage IV PC. Six patients were excluded from data analysis: four received two or fewer cycles because of intolerable toxicity, one was lost to follow-up, and one received only one cycle for other reasons. Therefore, 30 patients were included in the evaluation of ORR and DCR.

As shown in Table 2, the median age was 63 years. Twenty-one (70.0%) patients were male, and nine (30.0%) were female. Most patients (70.0%) were ECOG 1, and one patient was ECOG 2. Eight (26.6%) patients had tumors located in the head of the pancreas, eleven (36.7%) in the body, and eleven (36.7%) in the tail. The most common metastatic sites were lymph nodes (56.7%) and the liver (56.7%). Patients received a median of 6 cycles, and 5 patients received at least 10 cycles. No patients had CR, 8 (26.7%) patients had PR, 18 (60.0%) had SD, and 4 (13.3%) had PD. The ORR was 26.7%, and the DCR was 86.7%. The median PFS was 189 (95% CI: 136–241) days (Supplementary Figure 1).

Correlation between inflammatory markers and effectiveness of mFOLFIRINOX

Among the inflammatory markers, IL-6 and CRP were significantly and positively associated with disease progression ($r = 0.515$, $P = 0.004$; and $r = 0.711$, $P = <0.001$, respectively) (Table 3). As shown in Figure 2, the serum IL-6 and CRP levels were higher in the PD group than in the DCR group ($P = 0.019$ and $P = 0.003$, respectively). Serum albumin levels were not different between the DCR and PD groups, and the serum levels of the other inflammatory markers were similar in the two groups (Table 3 and Supplementary Figure 2). Tumor markers, including CA199 and CEA, were not associated with the disease outcomes in this study (Table 3 and Supplementary Figure 2).

Correlation between dynamic changes in inflammation markers and clinical response to mFOLFIRINOX

To further describe the correlation between levels of IL-6 and CRP and clinical response, the dynamic changes in IL-6 and CRP were explored. Dynamic increases in IL-6 and CRP significantly correlated with the clinical response ($P = 0.005$ for IL-6; $P = 0.001$ for CRP) (Supplementary Table 1). As shown in Figure 3, the dynamic changes in IL-6 and CRP levels positively correlated with PD during chemotherapy (r= -0.599, P = <0.001 for IL-6; r = -0.711, P = <0.001 for CRP).

Correlation between IL-6 and CRP levels and the incidence of lung/liver metastasis at baseline

IL-6 was significantly and positively associated with CRP (r = 9.459, $P = 0.004$; and $r = 0.562$, $P = 0.001$, respectively) (Table 4). Since CRP is produced by the liver as part of the acute phase response, its levels correlate with cancer progression. The correlation between levels of IL-6 and CRP and the incidence of liver metastasis at baseline, as well as the correlation between the incidence of liver metastasis and the effectiveness of mFOLFIRINOX, were also explored. The correlation between levels of IL-6 and CRP and the incidence of lung metastasis was explored at the same time. The incidence of lung/liver metastasis at baseline was neither associated with baseline IL-6 or CRP levels nor with the best response to chemotherapy in this study (Table 3 and Supplementary Table 2).

Risk factors associated with the outcomes of patients with mPC

The univariate analyses showed that the liver metastasis (HR = 5.10, 95% CI: 1.38-18.79, $P = 0.014$), high IL-6 levels (HR = 3.77, 95% CI: 1.23-11.54, $P = 0.020$), and high CRP levels (HR = 4.26, 95% CI: 1.04-17.46, $P = 0.044$) were associated with a poorer PFS, while lung metastasis was associated with a better PFS (HR = 0.16, 95% CI: 0.35-0.78, $P = 0.024$) (Table 5 and Figures 4A–E). The multivariate analysis revealed lung metastasis as a good independent prognostic factor (HR = 0.13, 95% CI: 0.24-0.70, P = 0.018) and high IL-6 levels as a poor independent prognostic factor for PFS (HR = 4.66, 95% CI: 1.32-16.37, $P = 0.016$). (Table 3). As shown in Figure 4A, the median PFS in the IL-6-low group was 257

TABLE 2 Baseline characteristics of the patients.

Characteristics	Pancreatic cancer cases (n = 30)
Age, median (range), year	63 (59-68)
Sex, n (%)	
Male	21 (70.0)
Female	9 (30.0)
ECOG, n (%)[a]	
0	8 (26.7)
1	21 (70.0)
2	1 (3.3)
BMI, median (range), kg/m^2	20.6 (18.3-23.0)
Primary tumor location, n (%)	
Head	8 (26.6)
Body	11 (36.7)
Tail	11 (36.7)
Accept operation before metastasis, n (%)	
No	15 (50.0)
Yes	15 (50.0)
CA199, U/mL, n (%)	
>40	25 (83.3)
≤40	5 (16.7)
CEA, ng/mL, n (%)	
>5	16 (53.3)
≤5	14 (46.7)
Measurable metastatic site, n (%)	
Liver	17 (56.7)
Peripancreas	5 (16.7)
Lymph node	17 (56.7)
Lung	8 (26.6)
Peritoneal	7 (23.3)
Other	8 (26.7)
Clinical response, n (%)[b]	
CR	0
PR	8 (26.7)
SD	18 (60.0)
PD	4 (13.3)
CR + PR	8 (26.7)
CR + PR + SD	26 (86.7)

BMI, Body mass index; CA199, carbohydrate antigen 199; CEA, carcinoembryonic antigen; CR, complete response; ECOG, Eastern Cooperative Oncology Group; PD, progressive disease; PR, partial response; SD, stable disease.
The clinicopathological characteristics are expressed as the median (25th–75th percentile), and categorical data are expressed as n (%).
[a]ECOG performance status is assessed on five grades, with higher numbers indicating greater disability; a score of 0 indicates that the patient is fully active and able to carry on all pre-disease performance without restriction; a score of 1 indicates that the patient is restricted in physically strenuous activity but ambulatory and able to carry out work of a light or sedentary nature; a score of 2 indicates that the patient is ambulatory and capable of all self-care but unable to carry out any work activities; up and about more than 50% of waking hours.
[b]Clinical response was assessed according to the Response Evaluation Criteria in Solid Tumors version 1.1 (RECIST 1.1).

(95% CI: 237-276) days, which was significantly higher than that in the IL-6-high group (median PFS, 150 days; 95% CI:47-252, P = 0.020). Tumor markers, including CEA and CA199, were not associated with PFS in this study (P = 0.529 and P = 0.146, respectively) (Supplementary Figures 4A, B). So far, the median OS of these patients had not been reached.

ROC curve of the predictive model for the efficacy of mFOLFIRINOX in mPC

The inflammatory markers (IL-6 and CRP) were used for constructing a model to predict the effectiveness (DCR or not) of the mFOLFIRINOX regimen in patients with mPC. Concerning the possible predictive value of tumor biomarkers for the treatment response indicated in previous studies (8, 9, 24), CEA and CA199 were also added. As shown in Figure 5, the ROC analysis showed that the combination of IL-6 and CRP (AUC: 0.811, 95% CI: 0.639–0.983, P = 0.003) had a higher AUC compared with CRP alone (AUC: 0.767, 95% CI: 0.589–0.946, P = 0.011), IL-6 alone (AUC: 0.710, 95% CI: 0.524–0.896, P = 0.046), tumor markers (AUC: 0.640, 95% CI: 0.451–0.829, P = 0.184) alone, and their combination (IL-6 + CRP + tumor markers, AUC: 0.806, 95% CI: 0.633–0.979, P = 0.004).

Discussion

In this single-institution retrospective analysis, the median PFS was 189 days and the DCR was 86.7% among 30 patients with mPC treated with mFOLFIRINOX, which were comparable with previously reported findings (4–7). High levels of IL-6 and CRP were associated with poor treatment response. The dynamic increase in IL-6 and CRP levels during treatment was associated with a poor progression of mPC. High IL-6 was a predictor of poor PFS, while lung metastasis was a predictor of better PFS in the multivariate analysis. The model combining IL-6 with CRP showed a better value in predicting the outcomes of patients with mPC treated with mFOLFIRINOX. Furthermore, this study was novel in reporting the associations between the dynamic changes in serum IL-6 and CRP levels and clinical response.

CRP is synthesized by the hepatocytes and is one of the most commonly used markers to reflect systemic inflammation. In this study, the serum CRP levels were associated with the tumor response, which was consistent with previous findings. Indeed, Nurmi et al. (25) described the combination of CRP and CA19-9 as a useful prognostic marker in evaluating disease-specific survival of surgically treated patients with PC. Liu et al. (12) revealed an elevated CRP/albumin ratio as an independent factor for poor prognosis with the cutoff value of 0.180 in PC patients. The prognostic significance of the CRP/albumin ratio existed in Stages III and IV PC patients and had no connection with the primary tumor location. Mitsunaga et al. (16) investigated the serum levels of CRP and clinical outcomes in patients with APC treated with first-line gemcitabine monotherapy; low, intermediate, and high CRP levels were associated with a good, intermediate, and poor response to chemotherapy.

TABLE 3 Correlation between clinicopathological markers and clinical response in patients with mPC treated with mFOLFIRINOX.

	Clinical response			P^a	Spearman correlation	P^b
	PD	DCR				
		PR	SD			
IL-6 (pg/L)				**0.012**	**0.515**	**0.004**
High (>7)	4	2	5			
Low (≤7)	0	7	12			
CRP (mg/L)				**0.001**	**0.711**	**<0.001**
High (>10)	4	1	2			
Low (≤10)	0	8	15			
Albumin (g/L)				0.611	-0.109	0.568
High (≥35)	2	6	11			
Low (<35)	2	3	6			
Neutrophils ($\times10^9$/L)				0.360	0.135	0.478
High (>7)	1	1	2			
Low (≤7)	3	8	15			
Lymphocytes ($\times10^9$/L)				1.000	-0.154	0.417
High (≥0.8)	4	8	14			
Low (<0.8)	0	1	3			
Platelets ($\times10^9$/L)				1.000	-0.131	0.491
High (≤303)	0	0	3			
Low (>303)	4	9	14			
CA199 (U/mL)				0.557	0.196	0.299
High (>40)	4	6	14			
Low (≤40)	0	3	3			
CEA (ng/mL)				0.550	0.237	0.208
High (>5)	4	6	12			
Low (≤5)	0	3	5			
Liver metastasis				0.613	0.145	0.444
Yes	3	4	10			
no	1	5	7			
Lung metastasis				0.550	-0.237	0.208
Yes	0	3	5			
no	4	6	12			

CA199, Carbohydrate antigen 199; CEA, carcinoembryonic antigen; CR, complete response; CRP, C-reactive protein; DCR, CR + PR + SD; IL-6, interleukin-6; PD, progressive disease; PR, partial response; SD, stable disease.
[a]Fisher exact test. Statistical significance was set at P <0.05 (two-sided).
[b]Spearman's rank correlation coefficient. Statistical significance was set at P <0.05 (two-sided).
The bold values mean statistically significant.

Besides, the elevated CRP level was found to be statistically significant in patients with mPC receiving first-line chemotherapy, including FOLFIRINOX, monotherapy with gemcitabine, and doublet chemotherapy with gemcitabine in combination with cisplatin or oxaliplatin; it was also significantly associated with shorter PFS and OS (26, 27). These results implied that an underlying inflammatory state might play a role in resistance to systemic therapy or in increased tumor aggressiveness, thus supporting the conclusion of the present study that CRP was a possible biomarker predicting the efficacy of the mFOLFIRINOX regimen. This should be further explored in future studies.

IL-6 regulates the secretion of vascular endothelial growth factor (VEGF) in PC cells, thereby stimulating angiogenesis and tumor vascularization, resulting in lymphatic and distant metastasis and disease progression. High IL-6 levels predict poor PFS and poor response to gemcitabine monotherapy in patients with APC (15). A phase II trial reported that higher serum IL-6 levels before treatment were associated with a reduced response to therapy and worse OS in patients with APC treated with gemcitabine and curcumin (28). This study suggested that the serum levels of IL-6 were closely related to poor response and prognosis of mPC treated with mFOLFIRINOX, which was supported by the aforementioned

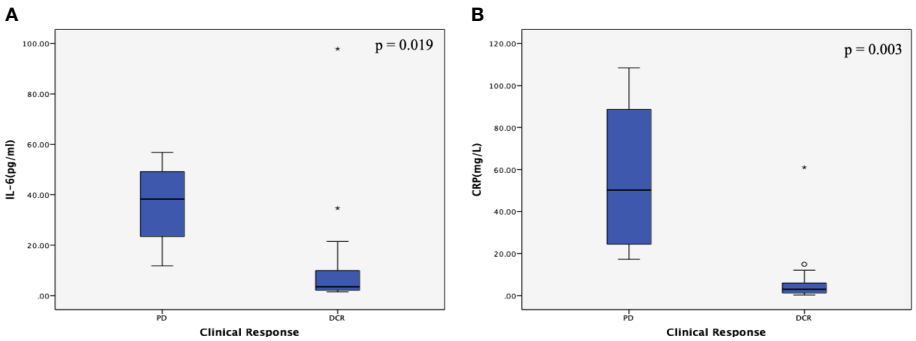

FIGURE 2
Correlations between inflammatory marker levels and the clinical response subgroup in patients with metastatic pancreatic cancer (mPC). **(A)** Correlation between interleukin (IL)-6 levels and the clinical response subgroup in patients with mPC. The serum IL-6 levels were higher in the PD group than in the DCR group (P = 0.019). **(B)** Correlation between C-reactive protein (CRP) levels and the clinical response subgroup in patients with mPC. The serum CRP levels were higher in the PD group than in the DCR group (P = 0.003). The *P* values were calculated using the Student's *t* test. The symbol * means abnormal values in the boxplot.

studies. In consideration of the complexity of the low half-life of IL-6, it may not be an ideal biomarker in clinical practice. A high serum level of CRP was reported to be related to a high serum IL-6 level in patients with treatment-naive APC (29). CRP may be a better substitute marker for IL-6 in predicting the efficacy of the mFOLFIRINOX regimen and PFS in patients with mPC. In the present study, IL-6 was significantly and positively associated with CRP in mPC patients who received the mFOLFIRINOX regimen as first-line chemotherapy. High levels of IL-6 and CRP were associated with poor treatment response, and they were also proved to be a predictor in the univariate analyses. The AUC of CRP alone was also higher than that of IL-6 alone. However, CRP was not associated with PFS in the multivariate analysis. The small sample size might have played a role in this result. The relationship between CRP and IL-6 in predicting PFS in patients with mPC should be further explored in future studies.

IL-6 induces metastasis through programming hematopoietic stem and progenitor cells toward tumor-supporting metastatic cells (30). Additionally, IL-6 affects monocyte-dendritic progenitors to differentiate into metastasis-promoting cells, thereby promoting tumor aggressiveness (30). An elevated CRP level may reflect a non-specific inflammatory response to tumor necrosis, which in turn indicates the levels of inflammatory cytokines such as IL-6. The production of inflammatory cytokines leads to the promotion of adhesion of circulating tumor cells to the vascular endothelium of distant organs by enhancing the E-selectin expression. This

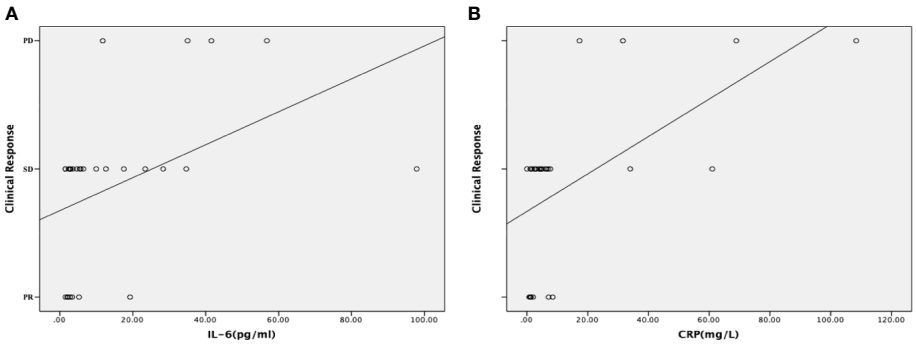

FIGURE 3
Correlations between the dynamic changes in inflammatory markers and the clinical response. **(A)** Correlation between the dynamic changes in the serum interleukin (IL)-6 level and the clinical response. The dynamic increases in the levels of IL-6 positively correlated with progressive disease (PD) during chemotherapy. **(B)** Correlation between the dynamic changes in the serum C-reactive protein (CRP) level and the clinical response. The dynamic increases in the levels of CRP positively correlated with progressive disease (PD) during chemotherapy. A scatter plot and a fitted curved were used to show the correlation more intuitively.

TABLE 4 Correlation between IL-6 and CRP levels in patients with mPC treated with mFOLFIRINOX.

	CRP (mg/L)		P^a	Correlation coefficient	P^b
	High (>10)	Low (≤10)			
IL-6 (pg/L)			0.004	0.562	0.001
High (>7)	6	5			
Low (≤7)	1	18			

CRP, C-reactive protein; IL-6, interleukin-6.
[a]The P values were calculated using Fisher's exact test.
[b] The P values were calculated using Spearman's rank correlation coefficient.
Statistical significance was set at P <0.05 (two-sided).

results in a microenvironment that favors tumor metastases (31, 32).The most common sites of metastasis in mPC are the liver, lung, regional lymph nodes, and peritoneum. Different metastatic patterns may involve different tumor biology and prognosis (33).

Kurokawa et al. (32) showed that liver metastasis occurred more frequently in high serum levels of CRP group in patients with pT2-T4 gastric cancer who underwent R0 resection. Kim et al. (34)revealed that IL-6 was significantly direct correlated with CRP, and it was an independent risk factor for progression to extensive hepatic metastasis in patients with PC. The correlation between lung metastasis and IL-6/CRP levels has not been found yet in published studies. In our study, IL-6 was significantly and positively associated with CRP in mPC patients, which was in line with Kim et al's study. However, the incidence of lung/liver metastasis at baseline was neither associated with baseline IL-6 or CRP levels nor with the best response to chemotherapy. The small sample size might have played a role in this result. The relationship between the lung/liver metastasis and CRP/IL-6 levels in predicting chemotherapy efficacy in mPC patients should be further explored in future studies.

Liver metastasis was a poor prognostic factor in this study, as supported by the MPACT study (35), while the presence of lung metastasis was considered as a good prognostic factor, which was also observed in other studies, but the mechanisms remain unclear.

Lung metastasis as the primary recurrence was reported as a favorable prognostic factor in patients with relapsed PC (36). Isolated lung metastases were demonstrated as a better prognosticator for OS in stage IV PC treated with palliative chemotherapy (37). Kruger et al. showed that limited disease (defined as metastatic disease of fewer than 10 metastases) confined to one lung might predict favorable outcomes in patients with PC without metastases to other organs (38). In addition, Lovecek et al. examined patients with PC who developed metachronous pulmonary metastases as the first site of recurrence after the curative-intent surgery. His result showed that patients with pulmonary metastases, including isolated pulmonary oligometastases, isolated pulmonary multiple metastases, and pulmonary metastases accompanied by other metastases, had prior DFS and OS compared with patients with nonpulmonary metastases (39). Patients with lung metastasis from PC had a better prognosis compared with those with other site metastases, which is still a controversial issue. Lung metastasis might confer less clinical-related complications compared with the complications that might be caused by local recurrence or liver metastasis, including biliary obstruction or gastric outlet obstruction. It might explain the better PFS or OS in patients with lung metastases. Patients with lung metastasis as the primary recurrence usually had lower pT category and less vascular invasion compared with patients with other metastases, and it might influence the prognosis (36). In the present study, all of the patients with lung metastasis also had other metastases. Patients with lung metastasis accompanied by other metastases had longer PFS compared with patients with non-lung metastasis. The difference between isolated lung metastasis and lung metastasis accompanied by other metastases in PFS of patients with mPC should be further studied in the future.

Circulating neutrophils (innate immune system) are thought to play a tumor-promoting role, while lymphocytes (adaptive immune system) play an anti-tumor role. High neutrophil counts were associated with a worse prognosis in patients with various cancers (40, 41). Angiogenesis is one of the most important causes of tumor proliferation and metastasis. Platelets contribute to tumor vascular growth through a number of platelet-derived angiogenic factors such as vascular endothelial growth factor (VEGF), platelet-derived growth factor, and hepatocyte growth factor. High platelet counts were associated with a worse prognosis in PC (42) and other cancer types (23, 43). Serum albumin is an important indicator of nutritional status. Hypoalbuminemia usually occurs in combination with poor performance status, weight loss, and nutritional deficiency, which negatively affect the prognosis of cancer patients. The relationship between hypoalbuminemia and poor survival may also depend on the systemic inflammatory response (44). A low serum albumin level was reported as a significant independent predictive factor for PFS in cancer patients (45–47). CEA and CA199 have been demonstrated to be predictive markers for the response to chemotherapy in PC (8, 48), with elevated serum values leading to poor OS (49, 50).

TABLE 5 Univariate and multivariate analyses of clinicopathological data and inflammatory markers in PFS.

Characteristics	Univariate analysis		Multivariate analysis	
	HR (95% CI)	P^c	HR (95% CI)	P^d
Age, year[a]		0.250		
>63	1 (ref)			
≤63	1.86 (0.64-5.43)			
Sex		0.624		
Female	1 (ref)			
Male	1.35 (0.40-4.48)			
ECOG[b]		**0.023**		
0	1 (ref)			
1–2	5.89 (1.27-21.73)			
BMI[a]		0.259		
>20.6	1 (ref)			
≤20.6	1.77 (0.65-4.81)			
Primary tumor location		0.735		
Head	1 (ref)			
Body	1.52 (0.41-5.56)			
Tail	1.54 (0.48-4.91)			
Operation before metastasis		0.405		
Yes	1 (ref)			
No	1.55 (0.55-4.37)			
CA199 (U/mL)		0.488		
≤40	1 (ref)			
>40	1.71 (0.37-7.81)			
CEA (ng/mL)		0.939		
≤5	1 (ref)			
>5	1.04 (0.38-2.84)			
Metastatic time		0.239		
Metachronous	1 (ref)			
Synchronous	1.92 (0.64-5.68)			
Measurable metastatic site				
Liver		**0.014**		0.132
No	1 (ref)		1 (ref)	
Yes	5.10 (1.38-18.79)		2.99 (0.72-12.44)	
Peripancreas		0.283		
No	1 (ref)			
Yes	2.27 (0.50-10.13)			
Lymph node		0.914		
No	1 (ref)			
Yes	0.94 (0.31-2.82)			
Lung		**0.024**		**0.018**
No	1 (ref)		1 (ref)	
Yes	0.16 (0.35-0.78)		0.13 (0.24-0.70)	
Peritoneal		0.982		
No	1 (ref)			
Yes	1.01 (0.27-3.71)			
Other		0.984		
No	1 (ref)			
Yes	1.01 (0.32-3.14)			

(Continued)

TABLE 5 Continued

Characteristics	Univariate analysis		Multivariate analysis	
	HR (95% CI)	P^c	HR (95% CI)	P^d
IL-6 (pg/mL)		**0.020**		**0.016**
≤7	1 (ref)		1 (ref)	
>7	3.77 (1.23-11.54)		4.66 (1.32-16.37)	
CRP (mg/L)		**0.044**		
≤10	1 (ref)			
>10	4.26 (1.04-17.46)			
Neutrophils ($\times10^9$/L)		0.114		
≤7	1 (ref)			
>7	4.01 (0.71-22.52)			
Lymphocytes ($\times10^9$/L)		0.829		
≥0.8	1 (ref)			
<0.8	1.25 (0.16-9.67)			
Platelets ($\times10^9$/L)		0.533		
≤303	1 (ref)			
>303	1.65 (0.35-7.46)			
Albumin (g/L)		0.061		
≥35	1 (ref)			
<35	3.16 (0.94-10.58)			

BMI, Body mass index; CA199, carbohydrate antigen 199; CEA, carcinoembryonic antigen; CI, confidence interval; CRP, C-reactive protein; ECOG, Eastern Cooperative Oncology Group; HR, hazard ratio; IL-6, interleukin-6.

[a]Using the median value as a cutoff value.

[b]ECOG performance status is assessed on five grades, with higher numbers indicating greater disability; a score of 0 indicates that the patient is fully active and able to carry on all pre-disease performance without restriction; a score of 1 indicates that the patient is restricted in physically strenuous activity but ambulatory and able to carry out work of a light or sedentary nature; a score of 2 indicates that the patient is ambulatory and capable of all self-care but unable to carry out any work activities; up and about more than 50% of waking hours.

[c]Univariable analyses were performed using the Kaplan–Meier method.

[d]Multivariable analysis was performed using a stepwise forward Cox regression (likelihood ratio, enter P <0.05, remove P >0.10) with significant markers from the univariate analysis (P < 0.05). The bold values mean statistically significant.

Several studies showed that CA199 reduction during chemotherapy was a potential predictor of efficacy (51, 52). However, in this study, neutrophils, lymphocytes, platelets, albumin, CEA, and CA199 did not correlate with the clinical response to mFOLFIRINOX or with PFS. In this study, the cutoff values were determined using the normal ranges, while previous studies used statistical methods to determine the cutoff. The sample size, as well as the type of therapy, might also play a role.

In the present study, the results suggested that IL-6 and CRP could effectively predict the clinical response to mFOLFIRINOX in mPC. CEA and CA199 were added to the predictive model because they are known to be markers of treatment response in PC (51, 52), but they did not improve the predictive value of IL-6 and CRP; the combination of IL-6 and CRP showed the best predictive value. This was supported by the fact that high IL-6 and CRP levels were associated with poorer PFS and that increases in IL-6 and CRP levels during treatment were associated with poorer prognosis. Nevertheless, models remain to be determined and improved for the prognosis of mPC. For now, the results suggested that patients with low IL-6 and low CRP levels before treatment might be those who would respond to mFOLFIRINOX. Additional studies are needed to refine these results.

This study had some limitations. The small sample size of this study might have prevented achieving sufficient power to detect survival differences between subgroups, which might be regarded as a major limitation. Additional data from other databases should be validated as well to provide a more powerful conclusion to avoid bias. However, no comparable published studies support a meta-analysis for external effectiveness in chemotherapy-naive mPC patients treated with the mFOLFIRINOX regimen as first-line chemotherapy. The results need to be validated using more samples in prospective studies. In addition, the retrospective nature of the study limited the analyzable data to those contained in the charts. A prospective cohort study may answer many questions regarding the markers of good response to mFOLFIRINOX.

In conclusion, higher IL-6 or CRP levels before or during chemotherapy positively correlated with PD. Higher serum levels of IL-6 and CRP might be predictors of a poor response to mFOLFIRINOX chemotherapy in patients with mPC. The combination of IL-6 and CRP might predict the response to mFOLFIRINOX. The relationship of inflammatory markers with the therapeutic effect of mFOLFIRINOX in patients with mPC deserves to be further investigated in the future.

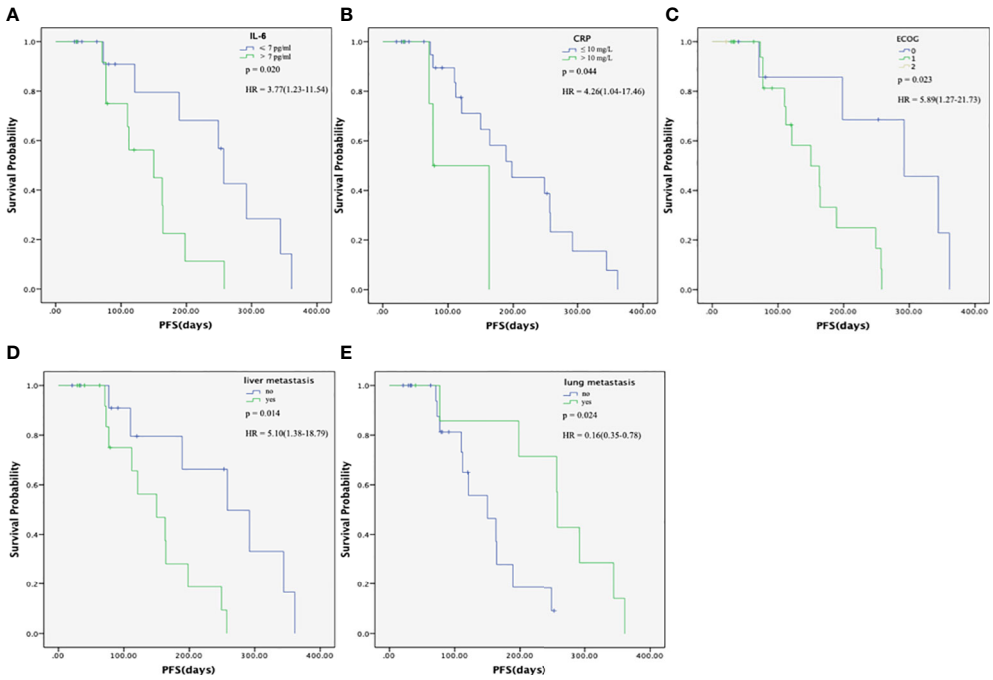

FIGURE 4
Progression-free survival (PFS) of patients with metastatic pancreatic cancer (mPC) treated with the modified FOLFIRINOX. **(A)** PFS in the interleukin (IL)-6-high and –low groups. The median PFS in the IL-6-low group was 257 (95% CI: 237-276) days, which was significantly higher than that in the IL-6-high group (median PFS, 150 days; 95% CI:47-252, P=0.020). **(B)** PFS in the C-reactive protein (CRP)-high and -low groups. The median PFS in the CRP-low group was 198 (95% CI: 42-353) days, which was significantly higher than that in the CRP-high group (median PFS, 163 days; 95% CI:28-297, P = 0.044). **(C)** PFS in the different ECOG groups. The median PFS was 292 (95% CI: 151-432) days and 150 (95% CI:81-218) days for ECOG score 0 and 1 group, respectively. **(D)** PFS according to the presence of liver metastasis. The median PFS in the non-liver metastasis group was 258 (95% CI:143-372) days, which was significantly higher than that in the liver metastasis group (median PFS, 150 days; 95% CI: 84-215, P = 0.014). **(E)** PFS, according to the presence of lung metastasis. The median PFS in the lung metastasis group was 258 (95% CI:255-260) days, which was significantly higher than that in the non-lung metastasis group (median PFS, 150 days; 95% CI: 86-213 P = 0.024). The PFS was calculated using the Kaplan-Meier method.

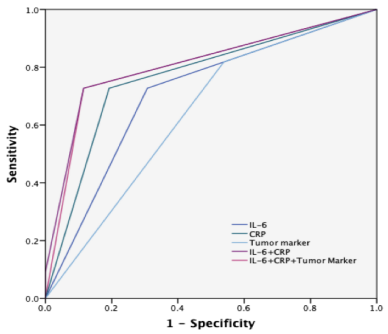

	AUC (95% CI)	P
IL-6+CRP	0.811 (0.639-0.983)	**0.003**
IL-6+CRP+tumor markers*	0.806 (0.633-0.979)	**0.004**
CRP	0.767 (0.589-0.946)	**0.011**
IL-6	0.710 (0.524-0.896)	**0.046**
Tumor markers*	0.640 (0.451-0.829)	0.184

* Tumor markers include CEA and CA199

FIGURE 5
Receiver operating characteristic (ROC) curves for predicting the efficacy of the mFOLFIRINOX regimen. ROC analyses of the prediction of the efficacy of mFOLFIRINOX using the inflammatory marker model, the tumor marker model, and the combined inflammatory and tumor marker model. The ROC analysis showed that the combination of IL-6 and CRP (AUC: 0.811, 95% CI: 0.639-0.983, P = 0.003) had a higher AUC compared with CRP alone (AUC: 0.767, 95% CI: 0.589-0.946, P = 0.011), IL-6 alone (AUC: 0.710, 95% CI: 0.524-0.896, P = 0.046), tumor markers (AUC: 0.640, 95% CI: 0.451-0.829. P = 0.184) alone, and their combination (IL-6 + CRP + tumor markers, AUC: 0. 806, 95% CI: 0.633-0.979, P = 0.004). AUC, Area under the curve. The symbol * is the annotation of tumor markers.

Data availability statement

The raw data supporting the conclusions of this article will be made available by the authors, without undue reservation.

Ethics statement

Ethical review and approval was not required for the study on human participants in accordance with the local legislation and institutional requirements. Written informed consent for participation was not required for this study in accordance with the national legislation and the institutional requirements.

Author contributions

(I) Conception and design, FZ; (II) Administrative support, none; (III) Provision of study materials or patients, FZ and QL; (IV) Collection and assembly of data, FS, WZ, CL, SH, FW, and JW; (V) Data analysis and interpretation, FS; (VI) Manuscript writing, all authors; (VII) Final approval of manuscript, all authors.

Conflict of interest

The authors declare that the research was conducted in the absence of any commercial or financial relationships that could be construed as a potential conflict of interest.

Publisher's note

All claims expressed in this article are solely those of the authors and do not necessarily represent those of their affiliated organizations, or those of the publisher, the editors and the reviewers. Any product that may be evaluated in this article, or claim that may be made by its manufacturer, is not guaranteed or endorsed by the publisher.

Supplementary material

The Supplementary Material for this article can be found online at: https://www.frontiersin.org/articles/10.3389/fonc.2022.964115/full#supplementary-material

References

1. Bray F, Ferlay J, Soerjomataram I, Siegel RL, Torre LA, Jemal A. Global cancer statistics 2018: GLOBOCAN estimates of incidence and mortality worldwide for 36 cancers in 185 countries. *CA Cancer J Clin* (2018) 68(6):394–424. doi: 10.3322/caac.21492

2. Xu XH, Zeng XY, Wang LJ, Liu YN, Liu JM, Qi JL, et al. The disease burden of pancreatic cancer in China in 1990 and 2017. *Zhonghua Liu Xing Bing Xue Za Zhi Zhonghua Liuxingbingxue Zazhi.* (2019) 40:1084–8. doi: 10.3760/cma.j.issn.0254-6450.2019.09.012

3. Levin B. *World cancer report 2014, World Health Organization 2015.* (2018).

4. Conroy T, Desseigne F, Ychou M, Bouché O, Guimbaud R, Bécouarn Y, et al. FOLFIRINOX versus gemcitabine for metastatic pancreatic cancer. *N Engl J Med* (2011) 364(19):1817–25. doi: 10.1056/NEJMoa1011923

5. Mahaseth H, Brutcher E, Kauh J, Hawk N, Kim S, Chen Z, et al. Modified FOLFIRINOX regimen with improved safety and maintained efficacy in pancreatic adenocarcinoma. *Pancreas* (2013) 42(8):1311—1315. doi: 10.1097/mpa.0b013e31829e2006

6. Stein SM, James ES, Deng Y, Cong X, Kortmansky JS, Li J, et al. Final analysis of a phase II study of modified FOLFIRINOX in locally advanced and metastatic pancreatic cancer. *Br J Cancer.* (2016) 114(7):737–43. doi: 10.1038/bjc.2016.45

7. Bai X, Su R, Ma T, Shen S, Li G, Lou J, et al. Modified FOLFIRINOX for advanced pancreatic cancer: a tertiary center experience from China. *Zhonghua Wai Ke Za Zhi.* (2016) 54(4):270–5. doi: 10.3760/cma.j.issn.0529-5815.2016.04.006

8. Morris-Stiff G, Taylor MA. Ca19-9 and pancreatic cancer: Is it really that good? *J Gastrointest Oncol* (2012) 3(2):88–9. doi: 10.3978/j.issn.2078-6891.2012.016

9. Mitsunaga S, Hasebe T, Iwasaki M, Kinoshita T, Ochiai A, Shimizu N. Important prognostic histological parameters for patients with invasive ductal carcinoma of the pancreas. *Cancer Sci* (2005) 96(12):858–65. doi: 10.1111/j.1349-7006.2005.00128.x

10. Greten FR, Grivennikov SI. Inflammation and cancer: Triggers, mechanisms, and consequences. *Immunity* (2019) 51(1):27–41. doi: 10.1016/j.immuni.2019.06.025

11. Szkandera J, Stotz M, Absenger G, Stojakovic T, Samonigg H, Kornprat P, et al. Validation of c-reactive protein levels as a prognostic indicator for survival in a large cohort of pancreatic cancer patients. *Br J Cancer.* (2014) 110(1):183–8. doi: 10.1038/bjc.2013.701

12. Liu Z, Jin K, Guo M, Long J, Liu L, Liu C, et al. Prognostic value of the CRP/Alb ratio, a novel inflammation-based score in pancreatic cancer. *Ann Surg Oncol* (2017) 24(2):561–8. doi: 10.1245/s10434-016-5579-3

13. Feng L, Qi Q, Wang P, Chen H, Chen Z, Meng Z, et al. Serum levels of IL-6, IL-8, and IL-10 are indicators of prognosis in pancreatic cancer. *J Int Med Res* (2018) 46(12):5228–36. doi: 10.1177/0300060518800588

14. Ramsey ML, Talbert E, Ahn D, Bekaii-Saab T, Badi N, Bloomston PM, et al. Circulating interleukin-6 is associated with disease progression, but not cachexia in pancreatic cancer. *Pancreatology* (2019) 19(1):80–7. doi: 10.1016/j.pan.2018.11.002

15. Mitsunaga S, Ikeda M, Shimizu S, Ohno I, Furuse J, Inagaki M, et al. Serum levels of IL-6 and IL-1β can predict the efficacy of gemcitabine in patients with advanced pancreatic cancer. *Br J Cancer.* (2013) 108(10):2063–9. doi: 10.1038/bjc.2013.174

16. Mitsunaga S, Ikeda M, Shimizu S, Ohno I, Takahashi H, Okuyama H, et al. C-reactive protein level is an indicator of the aggressiveness of advanced pancreatic cancer. *Pancreas* (2016) 45(1):110–6. doi: 10.1097/MPA.0000000000000465

17. Miksch R, Schoenberg M, Weniger M, Bösch F, Ormanns S, Mayer B, et al. Prognostic impact of tumor-infiltrating lymphocytes and neutrophils on survival of patients with upfront resection of pancreatic cancer. *Cancers* (2019) 11:39. doi: 10.3390/cancers11010039

18. Chen Y, Wang YR, Deng GC, Dai GH. CA19–9 decrease and survival according to platelet level in patients with advanced pancreatic cancer. *BMC Cancer.* (2019) 19(1):860. doi: 10.1186/s12885-019-6078-2

19. Ino Y, Yamazaki-Itoh R, Shimada K, Iwasaki M, Kosuge T, Kanai Y, et al. Immune cell infiltration as an indicator of the immune microenvironment of pancreatic cancer. *Br J Cancer.* (2013) 108(4):914–23. doi: 10.1038/bjc.2013.32

20. Eisenhauer EA, Therasse P, Bogaerts J, Schwartz LH, Sargent D, Ford R, et al. New response evaluation criteria in solid tumours: Revised RECIST guideline (version 1.1). *Eur J Cancer.* (2009) 45(2):228–47. doi: 10.1016/j.ejca.2008.10.026

21. Babic A, Schnure N, Neupane NP, Zaman MM, Rifai N, Welch MW, et al. Plasma inflammatory cytokines and survival of pancreatic cancer patients. *Clin Transl Gastroenterol* (2018) 9(4):145–5. doi: 10.1038/s41424-018-0008-5

22. Djaladat H, Bruins HM, Miranda G, Cai J, Skinner EC, Daneshmand S. The association of preoperative serum albumin level and American society of anesthesiologists (ASA) score on early complications and survival of patients

undergoing radical cystectomy for urothelial bladder cancer. *BJU Int* (2014) 113 (6):887–93. doi: 10.1111/bju.12240

23. Huszno J, Kolosza Z, Mrochem-Kwarciak J, Rutkowski T, Skladowski K. The role of neutrophil-lymphocyte ratio, platelet-lymphocyte ratio, and platelets in the prognosis of metastatic renal cell carcinoma. *Oncology* (2019) 97(1):7–17. doi: 10.1159/000498943

24. Gebhardt C, Meyer W, Reichel M, Wünsch PH. Prognostic factors in the operative treatment of ductal pancreatic carcinoma. *Langenbecks Arch Surg* (2000) 385(1):14–20. doi: 10.1007/s004230050004

25. Nurmi AM, Mustonen HK, Stenman UH, Seppänen HE, Haglund CH. Combining CRP and CA19-9 in a novel prognostic score in pancreatic ductal adenocarcinoma. *Sci Rep* (2021) 11(1):781–1. doi: 10.1038/s41598-020-80778-0

26. Schlick K, Magnes T, Huemer F, Ratzinger L, Weiss L, Pichler M, et al. C-reactive protein and Neutrophil/Lymphocytes ratio: Prognostic indicator for doubling overall survival prediction in pancreatic cancer patients. *J Clin Med* (2019) 8(11):1791. doi: 10.3390/jcm8111791

27. Markus M, Abendroth A, Noureddine R, Paul A, Breitenbuecher S, Virchow I, et al. Combined systemic inflammation score (SIS) correlates with prognosis in patients with advanced pancreatic cancer receiving palliative chemotherapy. *J Cancer Res Clin Oncol* (2021) 147(2):579–91. doi: 10.1007/s00432-020-03361-0

28. Pastorelli D, Fabricio ASC, Giovanis P, D'Ippolito S, Fiduccia P, Soldà C, et al. Phytosome complex of curcumin as complementary therapy of advanced pancreatic cancer improves safety and efficacy of gemcitabine: Results of a prospective phase II trial. *Pharmacol Res* (2018) 132:72–9. doi: 10.1016/j.phrs.2018.03.013

29. Miura T, Mitsunaga S, Ikeda M, Shimizu S, Ohno I, Takahashi H, et al. Characterization of patients with advanced pancreatic cancer and high serum interleukin-6 levels. *Pancreas* (2015) 44(5):756–63. doi: 10.1097/MPA.0000000000000335

30. Magidey-Klein K, Cooper TJ, Kveler K, Normand R, Zhang T, Timaner M, et al. IL-6 contributes to metastatic switch *via* the differentiation of monocytic-dendritic progenitors into prometastatic immune cells. *J Immunother Cancer.* (2021) 9(6):e002856. doi: 10.1136/jitc-2021-002856

31. Kim JM, Kwon CHD, Joh JW, Ko JS, Park JB, Lee JH, et al. C-reactive protein may be a prognostic factor in hepatocellular carcinoma with malignant portal vein invasion. *World J Surg Oncol* (2013) 11(1):92. doi: 10.1186/1477-7819-11-92

32. Kurokawa Y, Yamashita K, Kawabata R, Fujita J, Imamura H, Takeno A, et al. Prognostic value of postoperative c-reactive protein elevation versus complication occurrence: a multicenter validation study. *Gastric Cancer.* (2020) 23(5):937–43. doi: 10.1007/s10120-020-01073-5

33. Hani O, Petrausch U, Helbling D, Schmidt J, Mannhart M, Mehrabi A, et al. Prognostic value of site-specific metastases in pancreatic adenocarcinoma: A surveillance epidemiology and end results database analysis. *World J Gastroenterol* (2017) 23:1872. doi: 10.3748/wjg.v23.i10.1872

34. Kim HW, Lee JC, Paik KH, Kang J, Kim J, Hwang JH. Serum interleukin-6 is associated with pancreatic ductal adenocarcinoma progression pattern. *Med (Baltimore).* (2017) 96(5):e5926–6. doi: 10.1097/MD.0000000000005926

35. Tabernero J, Chiorean EG, Infante JR, Hingorani SR, Ganju V, Weekes C, et al. Prognostic factors of survival in a randomized phase III trial (MPACT) of weekly nab-paclitaxel plus gemcitabine versus gemcitabine alone in patients with metastatic pancreatic cancer. *Oncologist.* (2015) 20(2):143–50. doi: 10.1634/theoncologist.2014-0394

36. Zheng B, Ohuchida K, Yan Z, Okumura T, Ohtsuka T, Nakamura M. Primary recurrence in the lung is related to favorable prognosis in patients with pancreatic cancer and postoperative recurrence. *World J Surg* (2017) 41(11):2858–66. doi: 10.1007/s00268-017-4068-6

37. Liu KH, Hung CY, Hsueh SW, Chang PH, Chen YY, Lu CH, et al. Lung metastases in patients with stage IV pancreatic cancer: Prevalence, risk factors, and survival impact. *J Clin Med* (2019) 8(9):1402. doi: 10.3390/jcm8091402

38. Kruger S, Haas M, Burger PJ, Ormanns S, Modest DP, Westphalen CB, et al. Isolated pulmonary metastases define a favorable subgroup in metastatic pancreatic cancer. *Pancreatology* (2016) 16(4):593–8. doi: 10.1016/j.pan.2016.03.016

39. Lovecek M, Skalicky P, Chudacek J, Szkorupa M, Svebisova H, Lemstrova R, et al. Different clinical presentations of metachronous pulmonary metastases after resection of pancreatic ductal adenocarcinoma: Retrospective study and review of the literature. *World J Gastroenterol* (2017) 23(35):6420–8. doi: 10.3748/wjg.v23.i35.6420

40. Fankhauser CD, Sander S, Roth L, Gross O, Eberli D, Sulser T, et al. Systemic inflammatory markers have independent prognostic value in patients with metastatic testicular germ cell tumours undergoing first-line chemotherapy. *Br J Cancer.* (2018) 118(6):825–30. doi: 10.1038/bjc.2017.467

41. Feng F, Zheng G, Wang Q, Liu S, Liu Z, Xu G, et al. Low lymphocyte count and high monocyte count predicts poor prognosis of gastric cancer. *BMC Gastroenterol* (2018) 18(1):148. doi: 10.1186/s12876-018-0877-9

42. Wang H, Gao J, Bai M, Liu R, Li H, Deng T, et al. The pretreatment platelet and plasma fibrinogen level correlate with tumor progression and metastasis in patients with pancreatic cancer. *Platelets* (2013) 25. doi: 10.3109/09537104.2013.827782

43. Kizer NT, Hatem H, Nugent EK, Zhou G, Moore K, Heller P, et al. Chemotherapy response rates among patients with endometrial cancer who have elevated serum platelets. *Int J Gynecol Cancer Off J Int Gynecol Cancer Soc* (2015) 25 (6):1015–22. doi: 10.1097/IGC.0000000000000453

44. Crumley ABC, Stuart RC, McKernan M, McMillan DC. Is hypoalbuminemia an independent prognostic factor in patients with gastric cancer? *World J Surg* (2010) 34(10):2393–8. doi: 10.1007/s00268-010-0641-y

45. Fiala O, Pesek M FINEK J, Racek J, Minarik M, Benesova L, et al. Serum albumin is a strong predictor of survival in patients with advanced-stage non-small cell lung cancer treated with erlotinib. *Neoplasma* (2016) 63:471–6. doi: 10.4149/318_151001N512

46. Stenman M, Laurell A, Lindskog M. Prognostic significance of serum albumin in patients with metastatic renal cell carcinoma. *Med Oncol* (2014) 31 (3):841. doi: 10.1007/s12032-014-0841-7

47. Fan L, Chi C, Guo S, Wang Y, Cai W, Shao X, et al. Serum pre-albumin predicts the clinical outcome in metastatic castration-resistant prostate cancer patients treated with abiraterone. *J Cancer.* (2017) 8(17):3448–55. doi: 10.7150/jca.21134

48. Xu HX, Li S, Wu CT, Qi ZH, Wang WQ, Jin W, et al. Postoperative serum CA19-9, CEA and CA125 predicts the response to adjuvant chemoradiotherapy following radical resection in pancreatic adenocarcinoma. *Pancreatology* (2018) 18 (6):671–7. doi: 10.1016/j.pan.2018.05.479

49. Lee KJ, Yi SW, Chung MJ, Park SW, Song SY, Chung JB, et al. Serum CA 19-9 and CEA levels as a prognostic factor in pancreatic adenocarcinoma. *Yonsei Med J* (2013) 54(3):643–9. doi: 10.3349/ymj.2013.54.3.643

50. Imaoka H, Mizuno N, Hara K, Hijioka S, Tajika M, Tanaka T, et al. Prognostic impact of carcinoembryonic antigen (CEA) on patients with metastatic pancreatic cancer: A retrospective cohort study. *Pancreatology* (2016) 16(5):859–64. doi: 10.1016/j.pan.2016.05.007

51. Ishii H, Okada S, Sato T, Wakasugi H, Saisho H, Furuse J, et al. CA 19-9 in evaluating the response to chemotherapy in advanced pancreatic cancer. *Hepatogastroenterology* (1997) 44(13):279—283. doi: 10.1111/j.1523-5378.1997.tb00090.x

52. Halm U, Schumann T, Schiefke I, Witzigmann H, Mössner J, Keim V. Decrease of CA 19–9 during chemotherapy with gemcitabine predicts survival time in patients with advanced pancreatic cancer. *Br J Cancer.* (2000) 82(5):1013–6. doi: 10.1054/bjoc.1999.1035

frontiers | Frontiers in Oncology

TYPE Original Research
PUBLISHED 29 July 2022
DOI 10.3389/fonc.2022.964614

Check for updates

OPEN ACCESS

EDITED BY
Ravindra Deshpande,
Wake Forest School of Medicine,
United States

REVIEWED BY
Satheesh Sengodan,
National Cancer Institute at Frederick (NIH), United States;
Saratchandra Khumukcham
Duke University, United States

*CORRESPONDENCE
Dong-Sheng Huang
huangdshz99@hotmail.com
Lei Liang
liangl1992@hotmail.com

SPECIALTY SECTION
This article was submitted to Gastrointestinal Cancers: Hepato Pancreatic Biliary Cancers, a section of the journal Frontiers in Oncology

RECEIVED 08 June 2022
ACCEPTED 29 June 2022
PUBLISHED 29 July 2022

CITATION
Xu F-Q, Ye T-W, Wang D-D, Xie Y-M, Zhang K-J, Cheng J, Xiao Z-Q, Liu S-Y, Jiang K, Yao W-F, Shen G-L, Liu J-W, Zhang C-W, Huang D-S and Liang L (2022) Association of preoperative albumin–bilirubin with surgical textbook outcomes following laparoscopic hepatectomy for hepatocellular carcinoma. *Front. Oncol.* 12:964614. doi: 10.3389/fonc.2022.964614

COPYRIGHT
© 2022 Xu, Ye, Wang, Xie, Zhang, Cheng, Xiao, Liu, Jiang, Yao, Shen, Liu, Zhang, Huang and Liang. This is an open-access article distributed under the terms of the Creative Commons Attribution License (CC BY). The use, distribution or reproduction in other forums is permitted, provided the original author(s) and the copyright owner(s) are credited and that the original publication in this journal is cited, in accordance with accepted academic practice. No use, distribution or reproduction is permitted which does not comply with these terms.

Association of preoperative albumin–bilirubin with surgical textbook outcomes following laparoscopic hepatectomy for hepatocellular carcinoma

Fei-Qi Xu[1,2], Tai-Wei Ye[1,2], Dong-Dong Wang[1], Ya-Ming Xie[1], Kang-Jun Zhang[1], Jian Cheng[1], Zun-Qiang Xiao[1], Si-Yu Liu[3], Kai Jiang[1], Wei-Feng Yao[1], Guo-Liang Shen[1], Jun-Wei Liu[1], Cheng-Wu Zhang[1], Dong-Sheng Huang[1,4,5]* and Lei Liang[1,4]*

[1]General Surgery, Department of Hepatobiliary and Pancreatic Surgery and Minimal Invasive Surgery, Zhejiang Provincial People's Hospital, Affiliated People's Hospital, Hangzhou Medical College, Hangzhou, China, [2]The Second School of Clinical Medicine, Zhejiang Chinese Medical University, Hangzhou, China, [3]Department of Medical, Lishui Municipal Central Hospital, Lishui, China, [4]Department of Key Laboratory of Tumor Molecular Diagnosis and Individualized Medicine of Zhejiang Province, Zhejiang Provincial People's Hospital (People's Hospital of Hangzhou Medical College), Hangzhou, China, [5]School of Clinical Medicine, Hangzhou Medical College, Hangzhou, China

Background and aims: Recently, the effectiveness of "textbook outcomes (TO)" in the evaluation of surgical quality has been recognized by more and more scholars. This study tended to examine the association between preoperative albumin–bilirubin (ALBI) grades and the incidence of achieving or not achieving TO (non-TO) in patients with hepatocellular carcinoma (HCC) undergoing laparoscopic hepatectomy.

Methods: The patients were stratified into two groups: ALBI grade 1 (ALBI ≤ -2.60) and ALBI grade 2/3 (ALBI > -2.60). The characteristics of patients and the incidence of non-TO were compared. Multivariate analyses were performed to determine whether ALBI grade was independently associated with TO.

Results: In total, 378 patients were enrolled, including 194 patients (51.3%) in the ALBI grade 1 group and 184 patients (48.7%) in the ALBI grade 2/3 group. In the whole cohort, 198 patients (52.4%) did not achieve TO, and the incidence of non-TO in the ALBI grade 2/3 group was obviously higher than that in the ALBI grade 1 group (n = 112, 60.9% *vs.* n = 86, 44.3%, P = 0.001). The multivariate analyses showed that ALBI grade 2/3 was an independent risk factor for non-TO (OR: 1.95, 95%CI: 1.30–2.94, P = 0.023).

Conclusions: More than half (52.4%) of the patients with hepatocellular carcinoma did not achieve TO after laparoscopic hepatectomy, and preoperative ALBI grade 2/3 was significantly associated with non-TO. Improving the liver function reserve of patients before operation, thereby

reducing the ALBI grade, may increase the probability for patients to reach TO and enable patients to benefit more from surgery.

KEYWORDS

hepatocellular carcinoma, hepatectomy, albumin–bilirubin, textbook outcomes, laparoscopic

Introduction

Hepatocellular carcinoma (HCC) is the most common primary liver cancer, and it is expected that more than one million people will die from it in 2030 (1, 2). For resectable HCC patients, liver resection remains the preferred treatment with maximum benefit (3, 4). More and more minimally invasive procedures, especially laparoscopic, are being performed today, and their number has continued to grow exponentially (5–7).

The quality of surgery dramatically affects the short- and long-term prognosis of patients. Therefore, the evaluation of surgical quality is critical in clinical practice. In recent years, as a composite indicator, the effectiveness of "textbook outcomes (TO)" in evaluating surgical quality has been recognized by more and more scholars. TO can evaluate the overall quality of surgery more comprehensively than some other single-evaluation indexes, and it was a feasible and useful parameter for comparing the quality of institutions (8) as well as the assessment of patient-level outcomes, center designation, hospital performance, and quality metrics (9). At present, TO has been used to evaluate the quality of various types of surgery, and these studies have indicated that TO is associated with improved long-term outcomes after surgery (10–13).

Among many factors affecting the prognosis of HCC patients after hepatectomy, insufficient liver function reserve was considered as one of the most important risk factors (14). In 2015, Johnson et al. developed a new model for evaluating liver function, the albumin–bilirubin (ALBI) score (15). Once released, the model has been recognized by doctors for its good predictive value. Previous studies have shown that preoperative ALBI grade can affect the incidence of postoperative morbidity in patients with HCC, including liver failure, and a higher ALBI grade is an independent risk factor for prolonged hospital stay (16, 17). Therefore, in this study, we tended to study the association between preoperative ALBI grades and the incidence of TO or non-TO in patients with HCC undergoing laparoscopic hepatectomy.

Abbreviations: HCC, hepatocellular carcinoma; ALBI, albumin–bilirubin; TO, textbook outcomes; BMI, body mass index; PS, performance status; PLT, platelet count; HBV, hepatitis B virus; AFP, alpha-fetoprotein; MV, multivariable; NA, not available; OR, odds ratio; UV, univariable; CI, confidence interval.

Methods

Data source and patient selection

Patients with HCC who underwent laparoscopic hepatectomy in Zhejiang Provincial People's Hospital from January 2015 to December 2020 were selected. The exclusion criteria include (1) recurrent hepatocellular carcinoma (2), younger than 18 years old when diagnosed (3), conversion to open surgery, and (4) missing important data. According to the preoperative ALBI score [($\log_{10}$ bilirubin * 0.66) + (albumin * -0.085)], all patients were stratified as follows: ALBI grade 1 (ALBI ≤ -2.60) and ALBI grade 2/3 (ALBI > -2.60) (15). Patients with HCC were recognized by dynamic CT or MRI. If the imaging profile on CT or MR is specific for HCC (intense contrast uptake in the arterial phase followed by extracellular contrast wash-out in the venous and/or delayed phases), the diagnosis is established. Subsequently, the staging and treatment decisions for HCC are based on the Barcelona Clinic Liver Cancer staging standards. All patients with HCC were eventually diagnosed by the pathology of surgical specimens. This retrospective study complies with the Declaration of Helsinki and was approved by the institutional ethical committee, and the need for informed consent was waived.

Clinical characteristics and operative variables

The study variables were retrospectively collected from the medical record system of Zhejiang Provincial People's Hospital, including sex; age at diagnosis; body mass index (BMI); history of alcohol drinking, diabetes mellitus, and cigarette smoking; family history of HCC; performance status score; positivity of serum hepatitis B virus (HBV); presence of cirrhosis and portal hypertension; preoperative levels of alpha-fetoprotein (AFP); and platelet count. Tumor-related variables included tumor location, maximum diameter of tumor, tumor number, integrity of the tumor capsule, and macroscopic vascular

invasion. Surgical variables included intraoperative blood loss, operation time, type of resection, and extent of hepatectomy (major or minor). According to the Brisbane 2000 nomenclature of liver anatomy and resections, the type of resection was divided into anatomical and non-anatomical resection (18). All serological samples were taken in the morning when the patient had fasted for more than 8, and the data were obtained before any treatment and less than 1 week before surgery. All serological test variables were uniformly tested by the clinic lab of our hospital.

Definition of textbook outcome

TO is a composite indicator, which is composed of multiple indicators reflecting the short-term prognosis after surgery. We define it as follows (1): no morbidity within 30 days after surgery (2), no prolonged length of postoperative hospital stay (3), no perioperative blood transfusion (4), no readmission within 30 days after discharge (5), no mortality within 90 days after surgery, and (6) R0 resection. R0 resection was defined as microscopic resection margin that was negative (19). Postoperative morbidities included acute liver failure, hemorrhage, bile leakage, subdiaphragmatic effusion and abscess, infection in surgical incision, pulmonary infection, postoperative pleural effusion, postoperative subretinal effusion, and other complications. Prolonged length of postoperative hospital stay was defined as inpatient hospital stay that is longer than the 75th percentile of the postoperative length of stay (9 days). When a patient met the abovementioned six requirements, we determined that he reached TO. As such, non-TO was defined as follows: (1) morbidity occurred 30 days after operation, (2) prolonged length of postoperative stay, (3) perioperative blood transfusion, (4) readmission within 30 days after discharge, (5) postoperative 90-day mortality, and (6) R1 or R2 resection. R1 was defined as the presence of HCC upon microscopic observation. R2 was defined as the presence of HCC upon macroscopic observation. Meeting any of the points above is considered as non-TO.

Statistical analysis

Data analysis was performed using IBM SPSS, version 25.0 (SPSS Inc.). Categorical variables were compared using χ^2 test with the Yates correction or the Fisher's exact test as appropriate. Mann–Whitney *U*-test was used to compare the continuous variables. The baseline data of patients between ALBI grade 1 group and ALBI grade 2/3 group were compared. Significant variables ($P < 0.1$) in the univariable analysis were used to generate a multivariable logistic regression model. $P < 0.05$ was set as a statistically significant difference.

Results

Baseline characteristics

A total of 378 patients were enrolled in the whole cohort, including 194 cases (51.3%) in the ALBI grade 1 group and 184 cases (48.7%) in the ALBI grade 2/3 group (Figure 1). In the whole cohort, there was a total of 324 males (85.7%), more than half of whom had a history of chronic cirrhosis ($n = 245$, 64.8%), nearly a quarter of whom had portal hypertension ($n = 95$, 25.1%), only a minority of whom had family history of HCC ($n = 39$, 10.3%), and a minority of whom received major hepatectomy ($n = 46$, 12.2%). We can see that there is no significant difference in all clinical characteristics and surgically related variables between the ALBI grade 1 group and the ALBI grade 2/3 group (all $p > 0.05$) (Table 1).

Comparisons of TO and non-TO

In the whole cohort, a total of 198 cases (52.4%) did not achieve TO. There were 127 patients (33.6%) who experienced morbidity within 30 days after surgery, and 85 (22.5%) patients had a prolonged length of postoperative hospital stay. The median hospital stay was 8 (range, 6–9) days, and 96 (25.4%) patients received perioperative blood transfusion. Only a small number of patients experienced readmission within 30 days ($n = 6$, 1.6%), mortality within 90 days after surgery ($n = 3$, 0.8%), and R1 and R2 resection ($n = 3$, 0.8%).

Figure 2 describes the distribution of achieving a non-textbook outcome among two groups according to preoperative ALBI. As we can see in Table 2, the incidence of non-TO in the ALBI grade 2/3 group was significantly higher than that in the ALBI grade 1 group ($n = 112$, 60.9% *vs.* $n = 86$, 44.3%, $p = 0.001$). By comparing the distribution of achieving a non-TO, we can see that the number of patients who experienced morbidity within 30 days after surgery in the ALBI grade 2/3 group was significantly higher than that in the ALBI grade 1 group ($n = 78$, 42.4% *vs.* $n = 49$, 25.3%, $p < 0.001$). There were 50 (27.2%) patients with prolonged postoperative hospital stay in the ALBI grade 2/3 group, and the median postoperative hospital stay was 8 (7–10) days, while the ALBI grade 1 group had 35 (18%) patients, and the median hospital stay was 7 (7–9) days ($P < 0.001$). In the other four individual outcome parameters, there was no significant difference between the two groups ($P > 0.05$).

Independent risk factors associated with non-TO

Table 3 shows the results of the regression analyses for patients with HCC who did not achieve TO after laparoscopic hepatectomy. According to the results, ALBI grade 2/3 was an

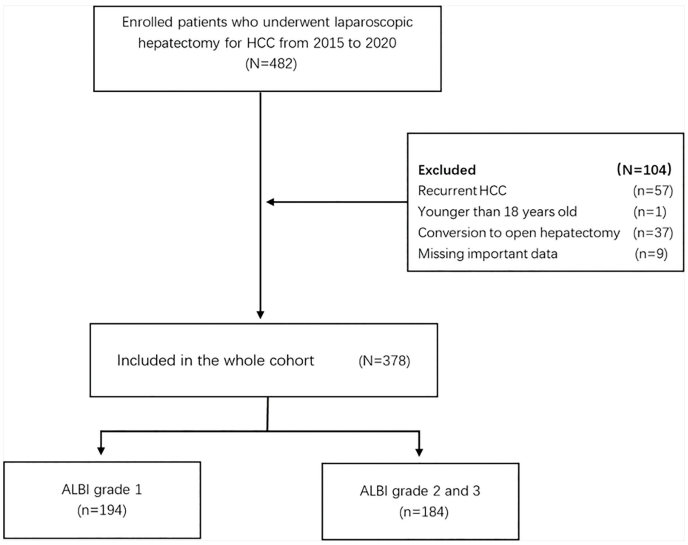

FIGURE 1
Flow chart of participant population. HCC, hepatocellular carcinoma; ALBI, albumin–bilirubin.

TABLE 1 Comparison of the clinical characteristics among the two groups according to preoperative albumin–bilirubin.

Variables	Overall (N = 378)	ALBI grade 1 (n = 194)	ALBI grade 2/3 (n = 184)	P
Male	324 (85.7%)	164 (84.5%)	160 (87.0%)	0.501
Age >60 years	155 (41.0%)	71 (36.6%)	84 (45.7%)	0.074
BMI[a]	22.9 (21.1–25.3)	23.1 (21.3–25.6)	22.7 (20.8–25.0)	0.164
Alcohol drinking	108 (28.6%)	50 (25.8%)	58 (31.5%)	0.216
Diabetes mellitus	48 (12.7%)	19 (9.8%)	29 (15.8%)	0.082
Cigarette smoking	153 (40.5%)	76 (39.2%)	77 (41.8%)	0.597
Family history of HCC	39 (10.3%)	21 (10.8%)	18 (9.8%)	0.739
Performance status ≥1	76 (20.1%)	32 (16.5%)	44 (23.9%)	0.072
HBV (+)	308 (81.5%)	159 (82.0%)	149 (81.0%)	0.806
Cirrhosis	245 (64.8%)	118 (60.8%)	127 (69.0%)	0.095
Portal hypertension	95 (25.1%)	41 (21.1%)	54 (29.3%)	0.066
AFP >400 ug/L	85 (22.5%)	42 (21.6%)	43 (23.4%)	0.689
PLT <100 μg/L	86 (22.8%)	37 (19.1%)	49 (26.6%)	0.080
Tumor in segment 7/8	115 (30.4%)	60 (30.9%)	55 (29.9%)	0.827
Maximum tumor size >2 cm	282 (74.6%)	137 (70.6%)	145 (78.8%)	0.068
Multiple tumors	56 (14.8%)	27 (13.9%)	29 (15.8%)	0.614
Incomplete capsule	248 (65.6%)	119 (61.3%)	129 (70.1%)	0.073
Microscopic vascular invasion	161 (42.6%)	82 (42.3%)	79 (42.9%)	0.896
Intraoperative blood loss >400 ml	81 (21.4%)	35 (18.0%)	46 (25.0%)	0.099
Operation time[a]	187.5 (140–250)	182.5 (130.0–240.0)	190.0 (150–258.8)	0.158
Non-anatomical resection	185 (48.9%)	97 (50.0%)	88 (47.8%)	0.673
Major hepatectomy	46 (12.2%)	20 (10.3%)	26 (14.1%)	0.256
TO/non-TO	180 (47.6%)/198 (52.4%)	108 (55.7%)/86 (44.3%)	72 (39.1%)/112 (60.9%)	0.001

[a]Values are median (range).
BMI, body mass index; HCC, hepatocellular carcinoma; HBV, hepatitis B virus; AFP, alpha-fetoprotein; PLT, platelet count; TO, textbook outcomes.

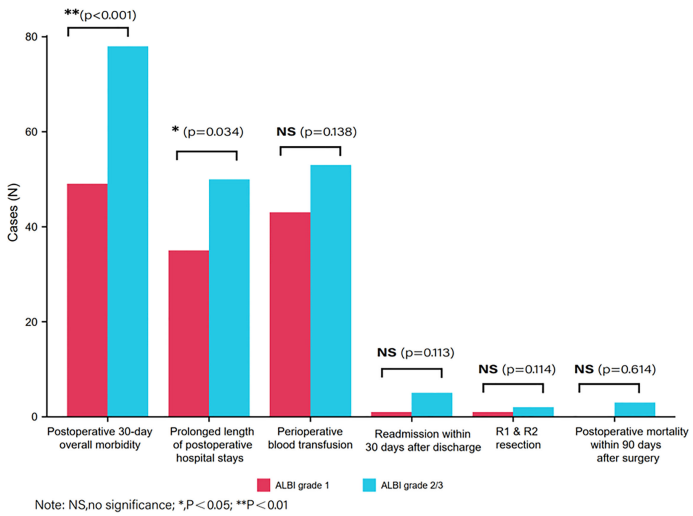

FIGURE 2
Distribution of achieving a non-textbook outcome between two groups according to preoperative albumin–bilirubin.

independent risk factor for non-TO (OR: 1.95, 95%CI: 1.30–2.94, $P = 0.023$). In addition, the multivariate regression analysis also shows that BMI ≥25 (OR: 1.87, 95%CI: 1.10–3.18, $P = 0.022$), diabetes mellitus (OR: 2.80, 95%CI: 1.32–5.94, $P = 0.007$), portal hypertension (OR: 2.01, 95%CI: 1.15–3.51, $P = 0.014$), multiple tumor (OR: 2.07, 95%CI: 1.02–4.19, $P = 0.043$), intraoperative blood loss >400 ml (OR: 4.73, 95%CI: 2.38–9.40, $P < 0.001$), operation time ≥180 min (OR: 2.25, 95%CI: 1.38–3.66, $P = 0.001$), and major hepatectomy (OR: 3.22, 95%CI: 1.40–7.42, $P = 0.006$) were also associated with a higher incidence of non-TO.

Discussion

The quality of surgery is closely related to the short- and long-term prognosis, so it is very important to evaluate the quality of surgery effectively. Surgical medical quality assessment is multidimensional and multi-level. For the evaluation of surgical quality, some single-evaluation indexes were used in the past, such as R0 resection, intraoperative blood loss, perioperative mortality, postoperative morbidity, and hospitalization time (20, 21); however, this often cannot accurately and comprehensively evaluate the surgical quality from multiple levels. Therefore, as a composite index, TO combines multiple parameters into a single defined quality index, which can more accurately evaluate the overall quality of surgery. Since Kolfschoten first proposed the concept of TO in 2013 and applied it to evaluate the quality of colon cancer surgery (12), TO is also gradually being used to evaluate the quality of other surgeries, including hepatectomy, liver transplantation, and other liver-related surgeries (22, 23).

In the present study, we employed the novel use of the indicator of TO to comprehensively evaluate perioperative outcomes for patients with HCC after hepatectomy. The results showed that 180 (47.6%) of the patients reached TO in

TABLE 2 Distribution of achieving non-textbook outcomes.

Distribution of non-textbook outcomes	Overall ($N = 378$)	ALBI grade 1 ($n = 194$)	ALBI grade 2/3 ($n = 184$)	P
Overall	198 (52.4%)	86 (44.3%)	112 (60.9%)	0.001
Morbidity within 30 days after surgery	127 (33.6%)	49 (25.3%)	78 (42.4%)	<0.001
Prolonged length of postoperative hospital stays[a]	85 (22.5%)	35 (18.0%)	50 (27.2%)	0.034
Postoperative hospital stays, days[b]	8 (6–9)	7 (7–9%)	8 (7–10%)	<0.001
Perioperative blood transfusion	96 (25.4%)	43 (22.2%)	53 (28.8%)	0.138
Readmission within 30 days after discharge	6 (1.6%)	1 (0.5%)	5 (2.7%)	0.113
Mortality within 90 days after surgery	3 (0.8%)	0	3 (1.6%)	0.114
R1 and R2 resection	3 (0.8%)	1 (0.5%)	2 (1.1%)	0.614

[a]Prolonged length of postoperative hospital stay was defined as an inpatient hospital stay longer than the 75th percentile of postoperative length of stay (9 days).
[b]Values are median (range).

TABLE 3 Univariable and multivariable logistic regression analyses of risk factors associated with non-TO following laparoscopic hepatectomy for HCC.

Variables	OR Comparison	UV OR (95%CI)	UV *P*	MV OR (95%CI)	MV *P*[a]
Sex	Male *vs.* female	0.94 (0.53–1.68)	0.834		
Age	>60 *vs.* ≤60 years	1.04 (0.69–1.56)	0.865		
BMI	≥25 *vs.* <25 kg/m^2	1.93 (1.21–3.08)	0.006	**1.87 (1.10–3.18)**	**0.022**
Alcohol drinking	Yes *vs.* no	1.26 (0.80–1.97)	0.313		
Diabetes mellitus	Yes *vs.* no	3.11 (1.56–6.19)	0.001	**2.80 (1.32–5.94)**	**0.007**
Cigarette smoking	Yes *vs.* no	1.13 (0.75–1.71)	0.549		
Family history of HCC	Yes *vs.* no	0.85 (0.44–1.65)	0.629		
Performance status	≥1 *vs.* <1	1.41 (0.85–2.35)	0.183		
HBV (+)	Yes *vs.* no	1.20 (0.72–2.03)	0.480		
Cirrhosis	Yes *vs.* no	1.65 (1.08–2.52)	0.022	NA	0.195
Portal hypertension	Yes *vs.* no	1.91 (1.18–3.09)	0.008	**2.01 (1.15–3.51)**	**0.014**
ALBI	Grade 2/3 *vs.* grade 1	1.95 (1.30–2.94)	0.001	**1.73 (1.08–2.77)**	**0.023**
AFP	>400 *vs.* ≤400 ug/L	1.32(0.81–2.14)	0.270		
PLT	<100 *vs.* >100 ug/L	1.35 (0.83–2.20)	0.225		
Tumor in segment 7/8	Yes *vs.* no	1.56 (1.00–2.43)	0.051	NA	0.379
Maximum tumor size	>2 *vs.* ≤2 cm	1.89 (1.18–3.02)	0.008	NA	0.420
Tumor number	Multiple *vs.* solitary	2.60 (1.40–4.82)	0.003	**2.07 (1.02–4.19)**	**0.043**
Capsule	Incomplete *vs.* complete	1.21 (0.79–1.85)	0.375		
Microscopic vascular invasion	Yes *vs.* no	1.67 (1.10–2.52)	0.015	NA	0.659
Intraoperative blood loss	>400 *vs.* ≤400 ml	6.72 (3.56–12.70)	<0.001	**4.73 (2.38–9.40)**	**<0.001**
Operation time	≥180 *vs.* <180 min	3.38 (2.20–5.16)	<0.001	**2.25 (1.38–3.66)**	**0.001**
Type of resection	Non-anatomical *vs.* anatomical	0.88 (0.59–1.32)	0.550		
Extent of hepatectomy	Major *vs.* minor	4.37 (2.04–9.33)	<0.001	**3.22 (1.40–7.42)**	**0.006**

[a]Those variables found to be significant at P <0.1 in the univariable analysis were entered into a multivariable logistic analysis.
BMI, body mass index; HCC, hepatocellular carcinoma; HBV, hepatitis B virus; AFP, alpha-fetoprotein; PLT, platelet count. MV, multivariable; NA, not available; OR, odds ratio; UV, univariable.
The bold values means that those variables found to be significant at P <0.05 in the multivariate analysis.

the cohort, which was higher than that in previous studies (33.3%) (24). Because the cohorts were all laparoscopic hepatectomy patients, excluding open surgery patients, and a previous meta-analysis showed that laparoscopic hepatectomy had a lower incidence of postoperative morbidity, shorter postoperative hospital stays, and less intraoperative blood loss than open hepatectomy (25–28), these factors may lead to higher TO rates in this cohort than that in other studies. It can be seen from the results of this study that the main influencing factors for non-TO were postoperative morbidity (33.6%), prolonged postoperative hospital stays (22.5%), and perioperative blood transfusion (25.4%), while there are very few patients with non-TO due to the other three factors.

Previous studies have shown that insufficient liver function reserve is considered one of the most important risk factors in various clinical and operative variables associated with postoperative morbidity (29–31). At present, Child–Pugh grading is widely used to evaluate liver function reserve; however, this indicator contains two subjective parameters (ascites and hepatic encephalopathy), which can lead to an inconsistent Child–Pugh classification due to the differences in subjective judgments among different observers. Johnson (15) established that the ALBI classification model only involves two simple objective indicators, which are convenient to calculate, and has been proved to be superior to the traditional Child–Pugh classification in evaluating liver function, postoperative liver failure, and prognosis of HCC (32, 33). A previous study demonstrated the relationship between BMI and TO in patients with HCC (34), but the association between liver function reserve and TO has not been reported. We can detect from the results of this study that ALBI grade 2/3 was an independent risk factor for non-TO [OR: 1.95 (1.30–2.94), $P = 0.023$]. Therefore, we may lower the preoperative AIBL grade of patients through preoperative albumin infusion and other interventions, thereby increasing the probability of TO and increasing the benefits of surgery.

According to the results of multivariate regression analyses, we found that, except ALBI grade 2/3, BMI ≥25, portal hypertension, blood loss >400 ml, and major liver resection were also independently associated with a higher incidence of non-TO, which was consistent with previous studies (34). In addition, this study showed that diabetes mellitus and operation time ≥180 min also play a negative effect on non-TO, which has not been reported before. The possible reason is that the immune

function of diabetic patients was worse than that of normal people, and the probability of postoperative morbidity such as infection was relatively high, resulting in an increase in the probability of non-TO. In addition, the prolongation of operation time often indicated the increase of intraoperative bleeding, which may lead to the increase of perioperative blood transfusion rate. On the other hand, the increase of operation time also increases the possibility of postoperative morbidity, such as infection, which will increase the probability of non-TO. It is worth noting that this study suggested that cirrhosis is not an independent risk factor of non-TO, which contradicted previous studies (34). The reason may be the following: first, the cohort of patients were resectable HCC patients, and the majority of patients in the cohort had cirrhosis in the compensatory phase; second, the vast majority of patients with cirrhosis in this cohort were cases of hepatitis B-related cirrhosis, most patients were regularly treated with antiviral therapy before surgery, the process of cirrhosis was effectively controlled, and only a small number (12.2%) of patients in this cohort received major hepatectomy, so the risk of postoperative liver failure was small. The abovementioned reasons may lead to cirrhosis not becoming an independent risk factor for non-TO.

There are several undeniable limitations in this study. First, this is a single-center, retrospective study; the retrospective design introduces the risk of selection bias. Second, the majority of the included patients were HBV-related HCC, and whether the same results exist in western countries (mainly HCV-related HCC) remains to be studied. Third, this study only enrolled patients undergoing laparoscopic hepatectomy. Compared with open hepatectomy, laparoscopic hepatectomy had a lower incidence of postoperative morbidities, less intraoperative blood loss, and shorter postoperative hospital stays (25–28). These factors can directly affect the probability of patients reaching TO. Fourth, the definition of TO, however, is arbitrary, subject to cultural differences, and might even change over time (35). Therefore, the definition of TO in this study was not necessarily applicable to other regions, which may also lead to differences in results.

In conclusion, more than half (52.4%) of patients with hepatocellular carcinoma did not achieve TO after laparoscopic hepatectomy, and preoperative ALBI grade 2/3 was independently associated with non-TO for HCC flowing laparoscopic hepatectomy. Improving the liver function reserve of patients before operation, thereby reducing the ALBI grade, may increase the probability for patients to reach TO and enable the patients to benefit more from surgery.

Data availability statement

The raw data supporting the conclusions of this article will be made available by the authors without undue reservation.

Ethics statement

This retrospective study complies with the Declaration of Helsinki and was approved by the institutional ethical committee and the need for informed consent was waived.

Author contributions

F-QX, T-WY, D-DW, and Y-MX contributed equally to this work. LL and Dong-Sheng Huang had full access to all the data in the study and takes responsibility for the integrity of the data and the accuracy of the data analysis. Study concept and design: F-QX, LL, and D-SH. Acquisition, analysis, or interpretation of data: T-WY, D-DW, Y-MX, K-JZ, JC, Z-QX, S-YL, W-FY, and KJ. Drafting of the manuscript: F-QX and T-WY. Critical revision of the manuscript for important intellectual content: G-LS, J-WL, and C-WZ. Statistical analysis: T-WY, D-DW, and Y-MX. Obtained funding: LL, W-FY, and KJ. Administrative, technical, or material support: C-WZ, D-SH, and LL. Study supervision: D-SH and LL. All authors listed have made a substantial, direct, and intellectual contribution to the work and approved it for publication.

Funding

Funding for this study was provided by Zhejiang Provincial People's Hospital (no. ZRY2020A004), Health Commission of Zhejiang Province (no. 2022KY532, no. 2018KY261, and no.2018277275), and General Scientific Research Project of the Education Department of Zhejiang Province (no. Y201840617). The funding sources had no role in the design and conduct of the study; collection, management, analysis, and interpretation of the data; preparation, review, or approval of the manuscript; and decision to submit the manuscript for publication.

Conflict of interest

The authors declare that the research was conducted in the absence of any commercial or financial relationships that could be construed as a potential conflict of interest.

Publisher's note

All claims expressed in this article are solely those of the authors and do not necessarily represent those of their affiliated organizations, or those of the publisher, the editors and the reviewers. Any product that may be evaluated in this article, or claim that may be made by its manufacturer, is not guaranteed or endorsed by the publisher.

References

1. Villanueva A. Hepatocellular carcinoma. *New Engl J Med* (2019) 380 (15):1450–62. doi: 10.1056/NEJMra1713263

2. Anstee QM, Reeves HL, Kotsiliti E, Govaere O, Heikenwalder M. From NASH to HCC: current concepts and future challenges. *Nat Rev Gastroenterol hepatol* (2019) 16(7):411–28. doi: 10.1038/s41575-019-0145-7

3. Yang JD, Heimbach JK. New advances in the diagnosis and management of hepatocellular carcinoma. *BMJ* (2020) 371:m3544. doi: 10.1136/bmj.m3544

4. Sirica AE, Gores GJ, Groopman JD, Selaru FM, Strazzabosco M, Wei Wang X, et al. Intrahepatic cholangiocarcinoma: Continuing challenges and translational advances. *Hepatol (Baltimore Md).* (2019) 69(4):1803–15. doi: 10.1002/hep.30289

5. Koffron AJ, Auffenberg G, Kung R, Abecassis M. Evaluation of 300 minimally invasive liver resections at a single institution: less is more. *Ann surgery.* (2007) 246 (3):385–92. doi: 10.1097/SLA.0b013e318146996c

6. Edwin B, Nordin A, Kazaryan AM. Laparoscopic liver surgery: new frontiers. *Scandinavian J Surg* (2011) 100(1):54–65. doi: 10.1177/145749691110000110

7. Hashizume M, Takenaka K, Yanaga K, Ohta M, Kajiyama K, Shirabe K, et al. Laparoscopic hepatic resection for hepatocellular carcinoma. *Surg endoscopy.* (1995) 9(12):1289–91. doi: 10.1007/BF00190161

8. van Roessel S, Mackay TM, van Dieren S, van der Schelling GP, Nieuwenhuijs VB, Bosscha K, et al. Textbook outcome: Nationwide analysis of a novel quality measure in pancreatic surgery. *Ann surgery.* (2020) 271(1):155–62. doi: 10.1097/SLA.0000000000003451

9. Tsilimigras DI, Pawlik TM, Moris D. Textbook outcomes in hepatobiliary and pancreatic surgery. *World J gastroenterol* (2021) 27(15):1524–30. doi: 10.3748/wjg.v27.i15.1524

10. Karthaus EG, Lijftogt N, Busweiler LAD, Elsman BHP, Wouters M, Vahl AC, et al. Textbook outcome: A composite measure for quality of elective aneurysm surgery. *Ann surgery.* (2017) 266(5):898–904. doi: 10.1097/SLA.0000000000002388

11. Busweiler LA, Schouwenburg MG, van Berge Henegouwen MI, Kolfschoten NE, de Jong PC, Rozema T, et al. Textbook outcome as a composite measure in oesophagogastric cancer surgery. *Br J surgery.* (2017) 104(6):742–50. doi: 10.1002/bjs.10486

12. Kolfschoten NE, Kievit J, Gooiker GA, van Leersum NJ, Snijders HS, Eddes EH, et al. Focusing on desired outcomes of care after colon cancer resections; hospital variations in 'textbook outcome'. *Eur J Surg Oncol* (2013) 39(2):156–63. doi: 10.1016/j.ejso.2012.10.007

13. Görgec B, Benedetti Cacciaguerra A, Lanari J, Russolillo N, Cipriani F, Aghayan D, et al. Assessment of textbook outcome in laparoscopic and open liver surgery. *JAMA surgery.* (2021) 156(8):e212064. doi: 10.1001/jamasurg.2021.2064

14. Fattovich G, Stroffolini T, Zagni I, Donato F. Hepatocellular carcinoma in cirrhosis: incidence and risk factors. *Gastroenterology* (2004) 127(5 Suppl 1):S35–50. doi: 10.1053/j.gastro.2004.09.014

15. Johnson PJ, Berhane S, Kagebayashi C, Satomura S, Teng M, Reeves HL, et al. Assessment of liver function in patients with hepatocellular carcinoma: a new evidence-based approach-the ALBI grade. *J Clin Oncol* (2015) 33(6):550–8. doi: 10.1200/JCO.2014.57.9151

16. Fagenson AM, Gleeson EM, Pitt HA, Lau KN. Albumin-bilirubin score vs model for end-stage liver disease in predicting post-hepatectomy outcomes. *J Am Coll Surgeons.* (2020) 230(4):637–45. doi: 10.1016/j.jamcollsurg.2019.12.007

17. Zou H, Wen Y, Yuan K, Miao XY, Xiong L, Liu KJ. Combining albumin-bilirubin score with future liver remnant predicts post-hepatectomy liver failure in HBV-associated HCC patients. *Live Int* (2018) 38(3):494–502. doi: 10.1111/liv.13514

18. Zhong JH, Ma L, Xiang BD, Li LQ, Yang T. We're still in an update process of the BCLC system. *Ann surgery.* (2018) 267(2):e23–e4. doi: 10.1097/SLA.0000000000001922

19. Hermanek P, Wittekind C. The pathologist and the residual tumor (R) classification. *Pathol Res practice.* (1994) 190(2):115–23. doi: 10.1016/S0344-0338(11)80700-4

20. Pascal L, Polazzi S, Piriou V, Cotte E, Wegrzyn J, Carty MJ, et al. Hospital length of stay reduction over time and patient readmission for severe adverse events following surgery. *Ann surgery.* (2020) 272(1):105–12. doi: 10.1097/SLA.0000000000003206

21. Haskins IN, DeAngelis EJ, Lambdin J, Amdur RL, Jackson HT, Vaziri K. Patient risk factors associated with increased morbidity and mortality following revisional laparoscopic bariatric surgery for inadequate weight loss or weight recidivism: an analysis of the ACS-MBSAQIP database. *Obes surgery.* (2020) 30 (12):4774–84. doi: 10.1007/s11695-020-04861-1

22. Merath K, Chen Q, Bagante F, Alexandrescu S, Marques HP, Aldrighetti L, et al. A multi-institutional international analysis of textbook outcomes among patients undergoing curative-intent resection of intrahepatic cholangiocarcinoma. *JAMA surgery.* (2019) 154(6):e190571. doi: 10.1001/jamasurg.2019.0571

23. Moris D, Shaw BI, Gloria J, Kesseli SJ, Samoylova ML, Schmitz R, et al. Textbook outcomes in liver transplantation. *World J surgery.* (2020) 44(10):3470–7. doi: 10.1007/s00268-020-05625-9

24. Merath K, Chen Q, Bagante F, Beal E, Akgul O, Dillhoff M, et al. Textbook outcomes among Medicare patients undergoing hepatopancreatic surgery. *Ann surgery.* (2020) 271(6):1116–23. doi: 10.1097/SLA.0000000000003105

25. Vibert E, Perniceni T, Levard H, Denet C, Shahri NK, Gayet B. Laparoscopic liver resection. *Br J surgery.* (2006) 93(1):67–72. doi: 10.1002/bjs.5150

26. Dagher I, Proske JM, Carloni A, Richa H, Tranchart H, Franco D. Laparoscopic liver resection: results for 70 patients. *Surg endoscopy.* (2007) 21 (4):619–24. doi: 10.1007/s00464-006-9137-0

27. Jin B, Chen MT, Fei YT, Du SD, Mao YL. Safety and efficacy for laparoscopic versus open hepatectomy: A meta-analysis. *Surg Oncol* (2018) 27(2):A26–a34. doi: 10.1016/j.suronc.2017.06.007

28. Kasai M, Cipriani F, Gayet B, Aldrighetti L, Ratti F, Sarmiento JM, et al. Laparoscopic versus open major hepatectomy: a systematic review and meta-analysis of individual patient data. *Surgery* (2018) 163(5):985–95. doi: 10.1016/j.surg.2018.01.020

29. Kauffmann R, Fong Y. Post-hepatectomy liver failure. *Hepatobiliary Surg Nutr* (2014) 3(5):238–46. doi: 10.3978/j.issn.2304-3881.2014.09.01

30. van Mierlo KM, Schaap FG, Dejong CH, Olde Damink SW. Liver resection for cancer: New developments in prediction, prevention and management of postresectional liver failure. *J hepatol* (2016) 65(6):1217–31. doi: 10.1016/j.jhep.2016.06.006

31. van den Broek MA, Olde Damink SW, Dejong CH, Lang H, Malagó M, Jalan R, et al. Liver failure after partial hepatic resection: definition, pathophysiology, risk factors and treatment. *Live Int* (2008) 28(6):767–80. doi: 10.1111/j.1478-3231.2008.01777.x

32. Zou H, Yang X, Li QL, Zhou QX, Xiong L, Wen Y. A comparative study of albumin-bilirubin score with child-pugh score, model for end-stage liver disease score and indocyanine green R15 in predicting posthepatectomy liver failure for hepatocellular carcinoma patients. *Digestive Dis (Basel Switzerland).* (2018) 36 (3):236–43. doi: 10.1159/000486590

33. Oh IS, Sinn DH, Kang TW, Lee MW, Kang W, Gwak GY, et al. Liver function assessment using albumin-bilirubin grade for patients with very early-stage hepatocellular carcinoma treated with radiofrequency ablation. *Digestive Dis Sci* (2017) 62(11):3235–42. doi: 10.1007/s10620-017-4775-8

34. Liu ZP, Yao LQ, Diao YK, Chen ZX, Feng ZH, Gu WM, et al. Association of preoperative body mass index with surgical textbook outcomes following hepatectomy for hepatocellular carcinoma: A multicenter study of 1206 patients. *Ann Surg Oncol* (2022). doi: 10.1245/s10434-022-11721-y

35. Mull HJ, Chen Q, Shwartz M, Itani KM, Rosen AK. Measuring surgical quality: which measure should we trust? *JAMA Surg* (2014) 149(11):1210–2. doi: 10.1001/jamasurg.2014.373

frontiers | Frontiers in Oncology

TYPE Original Research
PUBLISHED 29 July 2022
DOI 10.3389/fonc.2022.899761

Check for updates

OPEN ACCESS

EDITED BY
Ravindra Deshpande,
Wake Forest School of Medicine,
United States

REVIEWED BY
Hassan Alkharaan,
Prince Sattam Bin Abdulaziz University,
Saudi Arabia
Giovanni Butturini,
Casa di cura Pederzoli, Italy

*CORRESPONDENCE
Guangjun Shi
sgjzp@hotmail.com

SPECIALTY SECTION
This article was submitted to Gastrointestinal Cancers: Hepato Pancreatic Biliary Cancers, a section of the journal Frontiers in Oncology

RECEIVED 19 March 2022
ACCEPTED 27 June 2022
PUBLISHED 29 July 2022

CITATION
Yang Z and Shi G (2022) Comparison of clinicopathologic characteristics and survival outcomes between invasive IPMN and invasive MCN: A population-based analysis.
Front. Oncol. 12:899761.
doi: 10.3389/fonc.2022.899761

COPYRIGHT
© 2022 Yang and Shi. This is an open-access article distributed under the terms of the Creative Commons Attribution License (CC BY). The use, distribution or reproduction in other forums is permitted, provided the original author(s) and the copyright owner(s) are credited and that the original publication in this journal is cited, in accordance with accepted academic practice. No use, distribution or reproduction is permitted which does not comply with these terms.

Comparison of clinicopathologic characteristics and survival outcomes between invasive IPMN and invasive MCN: A population-based analysis

Zhen Yang and Guangjun Shi*

Department of Hepatopancreatobiliary Surgery, Qingdao Municipal Hospital, Qingdao University, Qingdao, China

Background: Intraductal papillary mucinous neoplasm (IPMN) and mucinous cystic neoplasm (MCN) are two main histological subtypes of pancreatic cystic neoplasms with rapidly increasing incidence recently. The natural histories, treatment patterns, and survival outcomes of invasive IPMN and invasive MCN have not been well explored.

Methods: Patients with a diagnosis of invasive IPMN and invasive MCN in the SEER database from 2000 through 2018 were retrospectively identified. Multivariable Cox regression analysis was conducted to determine the independent risk factors associated with overall survival (OS). Subgroup analyses of survival outcomes for invasive IPMN and invasive MCN were conducted. The OS for invasive IPMN was compared between patients who underwent surgery alone and those who received surgery plus chemotherapy by propensity score matching (PSM).

Results: A total of 2,505 patients were included, of whom 2,300 were diagnosed with invasive IPMN and 205 were diagnosed with invasive MCN. Half of the invasive IPMN (48.4%) and three-quarters of the invasive MCN (76.1%) patients were female. Of all patients, both the OS and cancer-specific survival were significantly better in the invasive MCN cohort compared to the invasive IPMN cohort. In subgroup analyses, while invasive MCN experienced better OS compared to invasive IPMN in the subgroups of patients with local–regional disease, the survival advantages disappeared in patients at a distant stage. In addition, surgery plus chemotherapy in invasive IPMN patients was associated with significantly better survival compared to surgery alone after PSM.

Conclusion: We examined the demographic and clinical characteristics between invasive IPMN and invasive MCN patients using a large-population-

based analysis. Although the OS is significantly better for invasive MCN *versus* invasive IPMN, the difference disappeared in patients with distant disease. A combination of surgery and chemotherapy in selected invasive IPMN patients could confer survival benefits compared to surgery alone.

KEYWORDS

IPMN, MCN, clinical characteristic, survival, treatment

Introduction

Pancreatic cystic neoplasms (PCNs) are regarded as challenging entities as they can exhibit a disease spectrum from benign to malignant lesions (1). The incidence of incidentally discovered PCNs has been gradually rising worldwide over the last few decades due to the increased use of cross-sectional imaging (2, 3). Intraductal papillary mucinous neoplasm (IPMN) and mucinous cystic neoplasm (MCN) are two main histological subtypes which have been recognized as precursors of pancreatic cancer (4). IPMN is a mucin-producing clinical entity arising from the pancreatic duct system, while MCN is a distinctive subtype with the presence of ovarian-type stroma and almost exclusively occurs in middle-aged females (5, 6). The risk of progression to malignancy varies between IPMN and MCN (7). However, the natural history and malignant potentials were not fully understood yet. Given the divergent malignant potentials and increasing frequency of these two predominant lesions, it is crucial to differentiate between these various types and formulate clinical guidelines for decision-making. Regarding the variable clinical course and limited high-quality research on invasive IPMN and invasive MCN, there also remain ambiguities in distinction between these two diseases. Moreover, the management of pancreatic cysts remains controversial (8, 9). The European guidelines suggest conservative treatment for IPMN and MCN with less than 4 cm in size and in the absence of worrisome features (10), while the international and American guidelines recommend aggressive surgical resection for all MCNs and IPMN >3 cm (11, 12). Additionally, larger population-based analyses investigating the clinicopathologic features and survival outcomes are scarce.

Thus, the purpose of this current study was to determine and compare the demographic and clinical characteristics of invasive IPMN *versus* invasive MCN as well as evaluate the treatment strategies using a large population in the United States.

Methods

Data regarding patients with invasive IPMN or invasive MCN between 2000 and 2018 were retrieved from the SEER database which represents about 30% of the population in the United States (13). The inclusion criteria were as follows: (1) patients with a histological confirmation of invasive IPMN or invasive MCN, (2) patients with invasive IPMN or invasive MCN labeled as the first and only primary tumor, and (3) patients with a follow-up duration of more than 1 month. Patients with missing information on survival status or treatment details were excluded. The parameters collected in our study included age at diagnosis (<70/≥70 years), gender (female/male), race (white/black/other), marital status (married/other), tumor size, tumor location (head/body and tail), tumor differentiation (well differentiated/poorly differentiated/unknown), lymph node status (positive/negative/unknown), tumor stage (localized/regional/distant), treatment details (surgery/chemotherapy/radiation), and survival data (time and status). The primary outcomes were overall survival (OS) and cancer-specific survival (CSS).

Statistical analysis

Continuous variables were presented as mean ± standard deviation and compared using independent-samples *t*-test, while categorical variables were described as number (percentage) and compared using chi-square analysis. OS and CSS were calculated by the Kaplan–Meier method, and comparisons were conducted with log-rank test. Univariate and multivariate COX analyses were performed to identify independent risk factors associated with OS or CSS. Additionally, in order to compare the efficacy between surgery and surgery plus chemotherapy in patients with invasive IPMN, propensity score matching (PSM) analysis was utilized to balance the baseline characteristics and increase between group comparability (14, 15). A p-value <0.05 was considered statistically significant. All analyses were performed by SPSS, version 26.0 and R version 4.0.3.

Results

During the study period, a total of 2,505 patients diagnosed with invasive IPMN (N = 2,300) or invasive MCN (N = 205)

between 2000 and 2018 in the United States with complete data were identified and analyzed in our study according to the inclusion and exclusion criteria. In the invasive IPMN cohort, most of the cases were localized at the pancreatic head (62.7%), with single tumor (94.0%), and only 42.6% received surgery. While in the invasive MCN cohort, the vast majority of patients were female (76.1%), younger than 70 years old (67.3%), white (76.1%), with single tumor (90.7%), and more than 85% had a surgical resection performed. In addition, invasive MCNs were more commonly found in the pancreatic body and tail (68.3%). As for the tumor characteristics, the tumor diameters were 4.26 ± 3.52 and 6.87 ± 8.08 cm in the invasive IPMN and invasive MCN groups, respectively. The most common tumor stage at presentation was distant in patients with invasive IPMN while localized in patients with invasive MCN. Unknown regional node status in these two cohorts accounted for 54.8 and 23.4%, respectively. The more detailed demographic and treatment data are summarized in Table 1. As presented in Table 1, the variables including gender, age at diagnosis, tumor size, tumor location and number, tumor stage, regional node status, distant metastasis, and treatment modalities were significantly different between invasive IPMN and MCN cohorts.

Survival outcomes

Of all patients in our study, both the OS and CSS were significantly better in the invasive MCN cohort compared to the invasive IPMN cohort (Figure 1). Among the patients with invasive IPMN, the 1-, 3-, and 5-year OS was 46.3, 22.2, and 16.6%, respectively. With respect to patients with invasive MCN, the 1-, 3-, and 5-year OS was 69.9, 49.7, and 45.3%, respectively. The median OS was 11 months for invasive IPMN and 36 months for invasive MCN. As for CSS, the survival probability at 1, 3, and 5 years was 48.3, 24.2, and 19.3% in the IPMN cohort, respectively, and 73.6, 55.2, and 52.4% in the MCN cohort, respectively. The median CSS was more favorable in the MCN group than in the IPMN group (Table 2).

As shown in Figure 2, the survival outcomes in all prespecified subgroups were estimated and compared according to age at diagnosis, sex, race, tumor location, tumor grade, and tumor stage, respectively. Significant differences were observed for OS in the subgroup analysis except for male, of tumor located at the pancreatic head, and distant disease (Figure 2). The 1-, 3-, and 5-year OS and CSS probabilities at different stages are summarized in Table 3.

Treatment patterns and the relative survival outcomes in invasive IPMN and MCN patients

The treatment patterns of the different stages are summarized in Table 4. Surgery remained the main treatment option for patients with localized disease in the invasive IPMN cohort, whereas chemotherapy was more commonly performed in the distant disease. IPMN patients at a localized stage who only underwent surgery were found to associate with a similar overall survival compared to surgery plus other treatment, whereas surgery plus chemotherapy provided survival benefits in patients with regional disease (Figures 3A, B). However, patients with distant disease were associated with poor prognosis, and there were no effective treatments as yet (Figure 3C). In terms of the patients with invasive MCN, we found that surgery yielded comparable survival results compared to surgery plus other treatments (Figure 3D).

Analysis of risk factors for OS in patients with invasive IPMN or MCN

On multivariate analysis of patients with invasive IPMN (n = 2,300), age at diagnosis, race, marital status, tumor location, tumor grade, tumor stage, regional nodes status, liver involvement, surgery, and radiation were significant prognostic factors for OS. With respect to OS in patients with invasive MCN, age at diagnosis, tumor grade, tumor stage, and surgery were independent risk factors (Table 5).

Comparison of therapeutic efficacy in patients with invasive IPMN after PSM

In order to examine the survival benefits of surgery plus chemotherapy in patients with invasive IPMN, we compared the therapeutic efficacy between surgery and surgery plus chemotherapy using the PSM method. Before PSM, age at diagnosis, tumor grade, and tumor stage were significantly different between the two cohorts. Surgery plus chemotherapy was more frequently performed in patients with older age (≥70), poorly differentiated tumor, and advanced stages. The overall survival was similar in the unmatched cohorts (Figure 4A). After PSM, 234 patients were matched in each group, and the baseline characteristics were well balanced between these two groups. As can be seen in Table 6, the vast majority of patients was at the regional and distant stages. Using matched data, surgery plus chemotherapy was associated with survival advantages than surgery alone for selected invasive IPMN patients (P = 0.0072) (Figure 4B).

Discussion

IPMN and MCN are the most common pancreatic cystic neoplasms. Differences in clinical characteristics and prognosis have not been well investigated in a large-cohort study. The current study demonstrated that the demographic and clinical

TABLE 1 Baseline characteristics of IPMN and MCN patients.

Variables	All patients (n = 2,505)	IPMN (n = 2,300)	MCN (n = 205)	P-value
Gender				**<0.001**
Male	1,236 (49.3%)	1,187 (51.6%)	49 (23.9%)	
Female	1,269 (50.7%)	1,113 (48.4%)	156 (76.1%)	
Age (years)				**0.019**
<70	1,494 (59.6%)	1,356 (59.0%)	138 (67.3%)	
≥70	1,011 (40.4%)	944 (41.0%)	67 (32.7%)	
Race				0.197
Black	279 (11.1%)	254 (11.0%)	25 (12.2%)	
White	2,011 (80.3%)	1,855 (80.7%)	156 (76.1%)	
Other	215 (8.6%)	191 (8.3%)	24 (11.7%)	
Tumor size (cm), ± SD	4.47 ± 4.14	4.26 ± 3.52	6.87 ± 8.08	**<0.001**
Marital status				0.893
Married	1,514 (60.4%)	1,391 (60.5%)	123 (60.0%)	
Other	991 (39.6%)	909 (39.5%)	82 (40.0%)	
Location				**<0.001**
Head	1,507 (60.2%)	1,442 (62.7%)	65 (31.7%)	
Body/tail	998 (39.8%)	858 (37.3%)	140 (68.3%)	
Grade				0.138
Well differentiated	966 (38.6%)	874 (38.0%)	92 (44.9%)	
Poorly differentiated	354 (14.1%)	326 (14.2%)	28 (13.6%)	
Unknown	1,185 (47.3%)	1,100 (47.8%)	85 (41.5%)	
Tumor number				**0.042**
Single	2,354 (94.0%)	2,168 (94.3%)	186 (90.7%)	
Multiple	151 (6.0%)	132 (5.7%)	19 (9.3%)	
Tumor stage				**<0.001**
Localized	437 (17.4%)	339 (14.7%)	98 (47.8%)	
Regional	898 (35.8%)	827 (36.0%)	71 (34.6%)	
Distant	1,170 (46.8%)	1,134 (49.3%)	36 (17.6%)	
Regional nodes positive				**<0.001**
Yes	517 (20.6%)	478 (20.8%)	39 (19.0%)	
No	680 (27.2%)	562 (24.4%)	118 (57.6%)	
Unknown	1,308 (52.2%)	1,260 (54.8%)	48 (23.4%)	
Liver involvement	293 (11.7%)	292 (12.7%)	1 (0.5%)	**<0.001**
Lung involvement	173 (6.9%)	172 (7.5%)	1 (0.5%)	**<0.001**
Surgery				**<0.001**
Done	1,155 (46.1%)	979 (42.6%)	176 (85.9%)	
None	1,350 (53.9%)	1,321 (57.4%)	29 (14.1%)	
Radiation				0.566
Done	523 (20.9%)	477 (20.7%)	46 (22.4%)	
None	1,982 (79.1%)	1,823 (79.3%)	159 (77.6%)	
Chemotherapy				**<0.001**
Done	1,426 (56.9%)	1,350 (58.7%)	76 (37.1%)	
None	1,079 (43.1%)	950 (41.3%)	129 (62.9%)	

IPMN, intraductal papillary mucinous neoplasm; MCN, mucinous cystic neoplasm; SD, standard deviation. Bold indicates significance.

characteristics were significantly different between invasive IPMN and invasive MCN using the SEER database. Compared with invasive IPMN patients, invasive MCN patients were more likely to be younger, female, with a larger tumor size, and with tumors of the pancreatic body or tail, and patients with invasive IPMN presented at more advanced tumor stages and were associated with worse long-term survival outcomes compared to those with invasive MCN. With respect to the management of

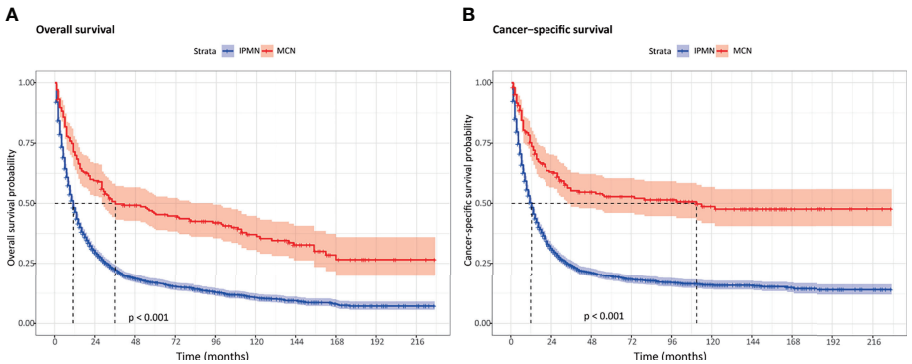

FIGURE 1
The overall survival and cancer-specific survival between invasive intraductal papillary mucinous neoplasm and invasive mucinous cystic neoplasm. **(A)** Overall survival. **(B)** Cancer-specific survival.

invasive IPMN, surgery remained the cornerstone of treatment for localized stage patients, while surgery plus chemotherapy may provide additional survival benefits in selected patients after adjusting for baseline characteristics, especially in patients with advanced stages.

Among the clinical variables, female sex predominance was observed in the invasive MCN cohort, which was in line with previous studies (16, 17), while the incidence rates of invasive IPMN were similar in both sexes. However, the exact cause of gender distribution was not well learned. Further studies are required to fully understand the gender differences of these two diseases.

It is noteworthy that the tumor size in patients with invasive MCN was significantly larger compared to that in patients with invasive IPMN. However, the survival outcomes were even worse in invasive IPMN patients, and the tumor size was not significantly associated with overall survival in invasive MCN patients. The underlying reason for the association between tumor size and prognosis remained unclear. Previous studies suggested that larger MCNs tend to be symptomatic and more indolent. Compared to invasive IPMN, invasive MCN was more commonly associated with a lower aggressive behavior (18).

In survival analysis, we found that the OS and CSS were significantly better in patients with invasive MCN compared to those with invasive IPMN. Interestingly, among patients who were with older age (≥70), male, other race, of tumors in the pancreatic head, and with distant disease, no significant survival differences were observed between invasive IPMN and MCN cohorts. This might be attributed to the limited samples of invasive MCN in these subgroups. Further investigations to account for this discrepancy based on a large sample size are needed to conduct a more specific and detailed subgroup analysis.

On the basis of available guidelines and consensus, surgical resection for resectable and borderline-resectable invasive IPMN patients has been strongly recommended due to the encouraging survival results following surgery (19, 20). In our study, a subgroup analysis of overall survival was performed according to the tumor stage. As shown in the stage-matched survival analysis, patients who only underwent surgery have a more favorable prognosis than those who received other treatments in localized stage. As for the regional stage, surgery plus chemotherapy tended to result in significantly better overall survival. In terms of the patients with invasive MCN, surgery alone was associated with a similar overall survival compared to

TABLE 2 Survival outcomes of patients with IPMN and MCN.

Outcomes		IPMN (n = 2,300)	MCN (n = 205)	P-value
Overall survival	1 year	46.3%	69.9%	$P < 0.001$
	3 year	22.2%	49.7%	$P < 0.001$
	5 year	16.6%	45.3%	$P < 0.001$
	Median	11 months	36 months	$P < 0.001$
Cancer-specific survival	1 year	48.3%	73.6%	$P < 0.001$
	3 year	24.2%	55.2%	$P < 0.001$
	5 year	19.3%	52.4%	$P < 0.001$
	Median	12 months	111 months	$P < 0.001$

IPMN, intraductal papillary mucinous neoplasm; MCN, mucinous cystic neoplasm.

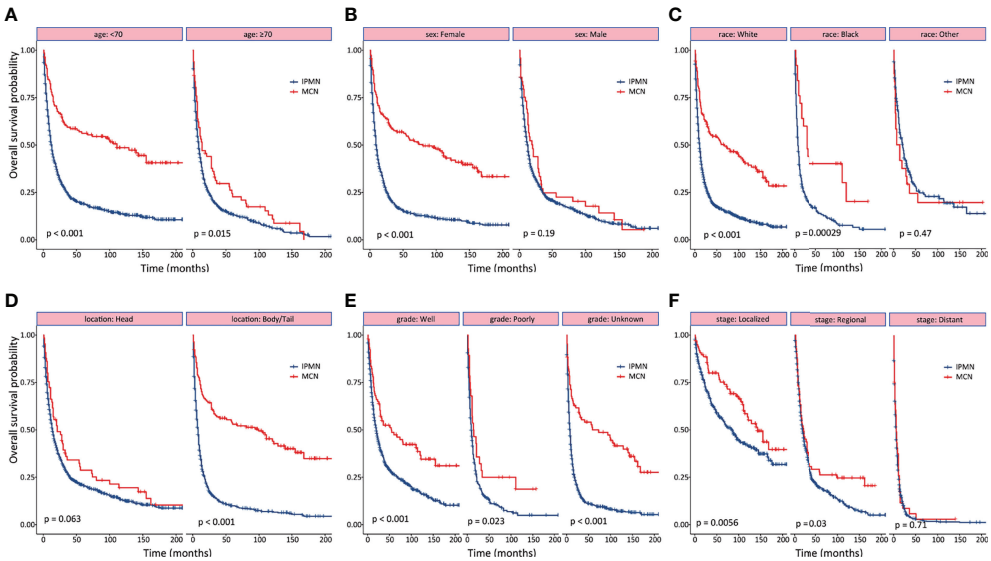

FIGURE 2
Subgroup analyses of overall survival between patients with invasive intraductal papillary mucinous neoplasm and invasive mucinous cystic neoplasm. **(A)** age. **(B)** gender. **(C)** race. **(D)** tumor location. **(E)** tumor differentiation. **(F)** tumor stage.

surgery plus chemotherapy in our study. According to the 2015 AGA and 2017 IAP guidelines (11, 12), surgery was strongly recommended for all MCNs regardless of the tumor diameter, whereas the 2018 European guideline suggested that surgical operations should only be performed in patients with a tumor size larger than 4 cm or with the presence of a nodule. Some studies argued that a conservative management for asymptomatic MCNs was feasible (21). A systematic review including 52 papers was conducted to investigate the natural history and prognosis of pancreatic MCNs, showing that the surveillance of MCNs less than 4 cm in size appeared to be acceptable and safe (22). Our study displayed that more than 85% of MCNs received surgery between 2000 and 2018, and the long-term survival outcomes were satisfactory. Given the small but measurable risk of malignant transformation, the observation strategy should be undertaken with caution. Further high-quality studies are needed to develop the optimal treatment strategies of invasive MCN.

In our large population-based analysis of 2,300 patients with invasive IPMN, multivariate COX regression analysis revealed that surgery was associated with improved overall survival, while chemotherapy was not the independent risk factor for overall survival in the entire study cohort. Several studies have substantiated the prognostic significance of surgical treatment. Unlike pancreatic ductal carcinoma, the impact of chemotherapy in patients with invasive IPMN is still a matter of debate. Within a study including 102 invasive IPMN patients treated between 1990 and 2016, Marchegiani *et al.* demonstrated that adjuvant chemotherapy could improve survival only in patients with positive nodal status and tubular differentiation

TABLE 3 Survival outcomes of patients with IPMN and MCN in different stages.

Outcomes		Localized		Regional		Distant	
		IPMN (n = 339)	MCN(n = 98)	IPMN (n = 827)	MCN(n = 71)	IPMN (n = 1,134)	MCN(n = 36)
Overall survival	1 year	82.4%	90.7%	62.6%	63.4%	23.8%	26.0%
	3 year	65.0%	79.7%	29.0%	30.7%	4.2%	5.8%
	5 year	56.2%	74.6%	19.4%	26.3%	2.5%	2.9%
	Median	NA	NA	18 months	20 months	6 months	6 months
Cancer-specific survival	1 year	83.5%	95.6%	64.8%	67.0%	25.5%	26.7%
	3 year	68.9%	88.2%	31.3%	34.5%	4.6%	6.0%
	5 year	63.0%	85.8%	22.2%	31.7%	2.9%	3.0%
	Median	NA	NA	20 months	23 months	6 months	7 months

IPMN, intraductal papillary mucinous neoplasm; MCN, mucinous cystic neoplasm.

TABLE 4 Treatment patterns of IPMN and MCN patients in different stages.

Patterns	IPMN			MCN		
	Localized (*n* = 339)	Regional (*n* = 827)	Distant (*n* = 1,134)	Localized (*n* = 98)	Regional (*n* = 71)	Distant (*n* = 36)
Surgery only	192	188	37	69	33	5
Chemotherapy only	12	72	565	0	1	5
Radiation only	2	8	23	0	0	1
Surgery–chemotherapy	57	177	46	13	6	8
Trimodality	27	213	19	14	22	4
None of the three	30	79	368	2	5	12

IPMN, intraductal papillary mucinous neoplasm; MCN, mucinous cystic neoplasm.

(23). In another retrospective study on 103 patients collected from 1993 to 2018, Rodrigues *et al.* examined the impact of adjuvant chemotherapy and found that it could not provide survival benefits in node-negative patients but even compromise the prognosis (24). However, a systematic review of 11 studies and 3,393 invasive IPMNs found that node-positive patients could benefit from adjuvant chemotherapy (25). In order to determine the potential role of chemotherapy in the invasive IPMN cohort, we assessed the outcomes between patients who underwent surgery alone and those who received surgery plus chemotherapy after adjusting for confounding by the PSM method. Using matching data, we found that surgery plus chemotherapy could confer survival benefits in invasive IPMN patients with older age and advanced stages. Our findings confirmed that the combination of surgery and chemotherapy would translate into survival benefits for these selected patients.

There were some limitations in our study. Firstly, the current study was limited by the retrospective design. Secondly, some important factors related to long-term survival were lacking, such as patients' performance status, surgical type and approach, underlying diseases, and comorbidities. Thirdly, disease recurrence and information on treatment schemes were not recorded in the SEER database. Finally, our analysis was based on populations in the United States, which might limit the generalization to other regions.

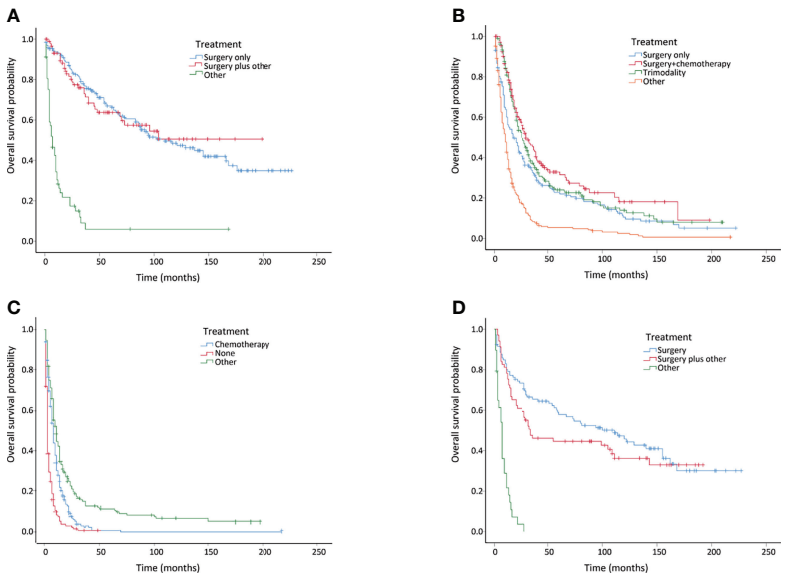

FIGURE 3
Kaplan–Meier curves of overall survival in invasive intraductal papillary mucinous neoplasm (IPMN) and invasive mucinous cystic neoplasm (MCN) patients with different treatments. **(A)** Invasive IPMNs with localized disease. **(B)** Invasive IPMNs with regional disease. **(C)** Invasive IPMNs with distant disease. **(D)** Entire invasive MCNs.

TABLE 5 Univariate and multivariate analysis for overall survival in IPMN and MCN patients.

Variables	IPMN				MCN			
	Univariate analysis		Multivariate analysis		Univariate analysis		Multivariate analysis	
	HR (95% CI)	*P*-value	HR (95% CI)	*P*-value	HR (95% CI)	*P*-value	HR (95% CI)	*P*-value
Gender								
Male	Ref		Ref		Ref		Ref	
Female	0.89 (0.81–0.97)	**0.008**	1.01 (0.92–1.11)	0.830	2.07 (1.43–3.00)	**<0.001**	1.32 (0.87–1.99)	0.189
Age (years)								
<70	Ref		Ref		Ref		Ref	
≥70	1.30 (1.19–1.43)	**<0.001**	1.37 (1.25–1.50)	**<0.001**	2.70 (1.90–3.83)	**<0.001**	2.30 (1.58–3.36)	**<0.001**
Race								
White	Ref		Ref		Ref		Ref	
Black	1.22 (1.06–1.40)	**0.006**	1.16 (1.01–1.34)	**0.047**	1.24 (0.74–2.07)	0.424	1.46 (0.85–2.49)	0.168
Other	0.70 (0.58–0.83)	**<0.001**	0.73 (0.61–0.87)	**<0.001**	2.03 (1.24–3.33)	**0.005**	1.18 (0.69–2.02)	0.548
Tumor size (cm)	1.01 (1.00–1.01)	**<0.001**	1.00 (0.99–1.01)	0.315	1.01 (0.99–1.01)	0.568		
Marital status								
Married	Ref		Ref		Ref			
Other	1.24 (1.13–1.36)	**<0.001**	1.24 (1.13–1.36)	**<0.001**	0.95 (0.67–1.34)	0.759		
Location								
Head	Ref		Ref		Ref		Ref	
Body/tail	1.55 (1.41–1.70)	**<0.001**	1.19 (1.08–1.32)	**0.001**	0.55 (0.39–0.79)	**0.001**	0.81 (0.53–1.22)	0.314
Grade								
Well differentiated	Ref		Ref		Ref		Ref	
Poorly differentiated	1.69 (1.47–1.95)	**<0.001**	1.39 (1.21–1.60)	**<0.001**	1.78 (1.08–2.92)	**0.023**	1.71 (1.01–2.91)	**0.047**
Unknown	1.86 (1.69–2.06)	**<0.001**	1.09 (0.97–1.22)	0.143	1.04 (0.71–1.51)	0.854	0.87 (0.57–1.33)	0.526
Tumor number								
Single	Ref				Ref			
Multiple	1.48 (0.68–3.22)	0.318			0.68 (0.38–1.24)	0.212		
Tumor stage								
Localized	Ref		Ref		Ref		Ref	
Regional	2.52 (2.12–2.99)	**<0.001**	1.93 (1.59–2.34)	**<0.001**	2.78 (1.85–4.15)	**<0.001**	2.21 (1.40–3.50)	**0.001**
Distant	6.66 (5.62–7.89)	**<0.001**	2.48 (2.02–3.05)	**<0.001**	8.85 (5.46–14.33)	**<0.001**	5.40 (2.92–9.97)	**<0.001**
Regional nodes positive								
Yes	Ref		Ref		Ref		Ref	
No	2.36 (2.04–2.75)	**<0.001**	1.73 (1.47–2.05)	**<0.001**	2.58 (1.66–4.01)	**<0.001**	1.01 (0.61–1.69)	0.966
Unknown	5.38 (4.72–6.14)	**<0.001**	1.79 (1.47–2.18)	**<0.001**	3.15 (2.10–4.72)	**<0.001**	1.55 (0.90–2.65)	0.112
Liver involvement	2.98 (2.56–3.46)	**<0.001**	1.24 (1.06–1.46)	**0.009**	1.08 (0.86–1.37)	0.514		
Lung involvement	2.07 (1.73–2.47)	**<0.001**	0.943 (0.78–1.14)	0.536	1.08 (0.85–1.36)	0.532		
Surgery								
None	Ref		Ref		Ref		Ref	
Done	0.23 (0.21–0.26)	**<0.001**	0.43 (0.36–0.52)	**<0.001**	0.15 (0.10–0.24)	**<0.001**	0.43 (0.21–0.88)	**0.021**
Radiation								
None	Ref		Ref		Ref			
Done	0.76 (0.68–0.84)	**<0.001**	0.82 (0.73–0.92)	**0.001**	0.93 (0.62–1.39)	0.716		
Chemotherapy								
None	Ref				Ref			
Done	0.91 (0.83–1.01)	0.053			1.07 (0.75–1.53)	0.693		

IPMN, intraductal papillary mucinous neoplasm; MCN, mucinous cystic neoplasm; Ref, reference. Bold indicates significance.

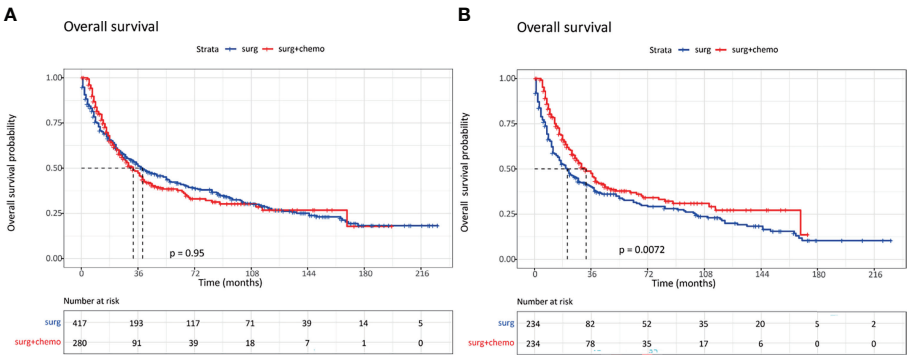

FIGURE 4
Kaplan–Meier curves of overall survival in invasive intraductal papillary mucinous neoplasm patients with surgery alone and surgery plus chemotherapy. **(A)** Survival curves in unmatched patients. **(B)** Survival curves in matched patients.

TABLE 6 Demographic and clinical characteristics of IPMN patients undergoing surgery or surgery plus chemotherapy before and after PSM.

Variables	Before PSM			After PSM		
	Surgery (n = 417)	Surgery + chemotherapy (n = 280)	P-value	Surgery (n = 234)	Surgery + chemotherapy (n = 234)	P-value
Gender			0.747			0.926
Male	236 (56.6%)	155 (55.4%)		125 (53.4%)	124 (53.0%)	
Female	181 (43.4%)	125 (44.6%)		109 (46.6%)	110 (47.0%)	
Age (years)			**<0.001**			0.778
<70	211 (50.6%)	181 (64.6%)		136 (58.1%)	139 (59.4%)	
≥70	206 (49.4%)	99 (35.4%)		98 (41.9%)	95 (40.6%)	
Race			0.172			0.077
Black	43 (10.3%)	18 (6.4%)		32 (13.7%)	17 (7.3%)	
White	338 (81.1%)	233 (83.2%)		178 (76.1%)	191 (81.6%)	
Other	36 (8.6%)	29 (10.4%)		24 (10.2%)	26 (11.1%)	
Tumor size (cm), ± SD	3.70 ± 2.67	4.25 ± 5.94	0.102			
Marital status			0.439			0.056
Married	256 (61.4%)	180 (64.3%)		135 (57.7%)	156 (66.7%)	
Other	161 (38.6%)	100 (35.7%)		99 (42.3%)	78 (33.3%)	
Location			0.988			0.525
Head	307 (73.6%)	206 (73.6%)		171 (73.1%)	177 (75.6%)	
Body/tail	110 (26.4%)	74 (26.4%)		63 (26.9%)	57 (24.4%)	
Grade			**<0.001**			0.929
Well differentiated	237 (56.8%)	178 (63.6%)		150 (64.1%)	147 (62.8%)	
Poorly differentiated	53 (12.7%)	62 (22.1%)		47 (20.1%)	47 (20.1%)	
Unknown	127 (30.5%)	40 (14.3%)		37 (15.8%)	40 (17.1%)	
Tumor number			0.121			1.000
Single	371 (89.0%)	259 (92.5%)		215 (91.9%)	215 (91.9%)	
Multiple	46 (11.0%)	21 (7.5%)		19 (8.1%)	19 (8.1%)	
Tumor stage			**<0.001**			1.000
Localized	192 (46.0%)	57 (20.4%)		57 (24.3%)	57 (24.3%)	
Regional	188 (45.1%)	177 (63.2%)		142 (60.7%)	142 (60.7%)	
Distant	37 (8.9%)	46 (16.4%)		35 (15.0%)	35 (15.0%)	

PSM, propensity score matching; SD, standard deviation. Bold indicates significance.

Conclusion

In conclusion, our study comprehensively investigated the clinicopathologic features, treatment patterns, and survival outcomes of patients with the two common subtypes of pancreatic cystic neoplasms, invasive IPMN and invasive MCN. While invasive MCN experienced better overall survival compared to invasive IPMN in the subgroups of patients with local–regional disease, the survival advantages disappeared in patients with distant disease. Furthermore, we found that the combination of surgery and chemotherapy was associated with survival benefits in selected invasive IPMN patients, especially those with older age and advanced tumor stages.

Data availability statement

Publicly available datasets were analyzed in this study.These data can be found here: https://seer.cancer.gov/.

Ethics statement

The studies involving human participants were reviewed and approved by the Qingdao Municipal Hospital. The current study is based on the SEER database, and the requirements for informed consent were waived off due to the retrospective design.

Author contributions

Conception and data collection: GS. Drafting and statistical analysis: ZY. All authors contributed to the article and approved the submitted version.

Funding

This study was supported by the Hepatobiliary and Pancreatic Cancer from Hubei Chen Xiaoping Foundationfor Scientific and Technological Development.(no. CXPJJH11900001-2019206)

Conflict of interest

The authors declare that the research was conducted in the absence of any commercial or financial relationships that could be construed as a potential conflict of interest.

Publisher's note

All claims expressed in this article are solely those of the authors and do not necessarily represent those of their affiliated organizations, or those of the publisher, the editors and the reviewers. Any product that may be evaluated in this article, or claim that may be made by its manufacturer, is not guaranteed or endorsed by the publisher.

References

1. van Huijgevoort NCM, Del Chiaro M, Wolfgang CL, van Hooft JE, Besselink MG. Diagnosis and management of pancreatic cystic neoplasms: current evidence and guidelines. *Nat Rev Gastroenterol Hepatol* (2019) 16(11):676–89. doi: 10.1038/s41575-019-0195-x

2. Chandwani R, Allen PJ. Cystic neoplasms of the pancreas. *Annu Rev Med* (2016) 67:45–57. doi: 10.1146/annurev-med-051914-022011

3. Burk KS, Knipp D, Sahani DV. Cystic pancreatic tumors. *Magn Reson Imaging Clin N Am* (2018) 26(3):405–20. doi: 10.1016/j.mric.2018.03.006

4. McGuigan A, Kelly P, Turkington RC, Jones C, Coleman HG, McCain RS. Pancreatic cancer: A review of clinical diagnosis, epidemiology, treatment and outcomes. *World J Gastroenterol* (2018) 24(43):4846–61. doi: 10.3748/wjg.v24.i43.4846

5. Keane MG, Afghani E. A review of the diagnosis and management of premalignant pancreatic cystic lesions. *J Clin Med* (2021) 10(6). doi: 10.3390/jcm10061284

6. Ketwaroo GA, Mortele KJ, Sawhney MS. Pancreatic cystic neoplasms: An update. *Gastroenterol Clin North Am* (2016) 45(1):67–81. doi: 10.1016/j.gtc.2015.10.006

7. Del Chiaro M, Verbeke C, Salvia R, Klöppel G, Werner J, McKay C, et al. European Experts consensus statement on cystic tumours of the pancreas. *Dig Liver Dis* (2013) 45(9):703–11. doi: 10.1016/j.dld.2013.01.010

8. Hasan A, Visrodia K, Farrell JJ, Gonda TA. Overview and comparison of guidelines for management of pancreatic cystic neoplasms. *World J Gastroenterol* (2019) 25(31):4405–13. doi: 10.3748/wjg.v25.i31.4405

9. Lanke G, Lee JH. Similarities and differences in guidelines for the management of pancreatic cysts. *World J Gastroenterol* (2020) 26(11):1128–41. doi: 10.3748/wjg.v26.i11.1128

10. European Study Group on Cystic Tumours of the Pancreas. European Evidence-based guidelines on pancreatic cystic neoplasms. *Gut* (2018) 67(5):789–804. doi: 10.1136/gutjnl-2018-316027

11. Tanaka M, Fernández-Del Castillo C, Kamisawa T, Jang JY, Levy P, Ohtsuka T, et al. Revisions of international consensus Fukuoka guidelines for the management of IPMN of the pancreas. *Pancreatology* (2017) 17(5):738–53. doi: 10.1016/j.pan.2017.07.007

12. Vege SS, Ziring B, Jain R, Moayyedi P. American Gastroenterological association institute guideline on the diagnosis and management of asymptomatic neoplastic pancreatic cysts. *Gastroenterology* (2015) 148(4):819–822; quize812-813. doi: 10.1053/j.gastro.2015.01.015

13. Doll KM, Rademaker A, Sosa JA. Practical guide to surgical data sets: Surveillance, epidemiology, and end results (SEER) database. *JAMA Surg* (2018) 153(6):588–9. doi: 10.1001/jamasurg.2018.0501

14. Benedetto U, Head SJ, Angelini GD, Blackstone EH. Statistical primer: propensity score matching and its alternatives. *Eur J Cardiothorac Surg* (2018) 53 (6):1112–7. doi: 10.1093/ejcts/ezy167

15. Kuss O, Blettner M, Börgermann J. Propensity score: an alternative method of analyzing treatment effects. *Dtsch Arztebl Int* (2016) 113(35-36):597–603. doi: 10.3238/arztebl.2016.0597

16. Luo G, Fan Z, Gong Y, Jin K, Yang C, Cheng H, et al. Characteristics and outcomes of pancreatic cancer by histological subtypes. *Pancreas* (2019) 48(6):817–22. doi: 10.1097/mpa.0000000000001338

17. Reid MD, Choi H, Balci S, Akkas G, Adsay V.. Serous cystic neoplasms of the pancreas: clinicopathologic and molecular characteristics. *Semin Diagn Pathol* (2014) 31(6):475–83. doi: 10.1053/j.semdp.2014.08.009

18. Griffin JF, Page AJ, Samaha GJ, Christopher A, Bhaijee F, Pezhouh MK, et al. Patients with a resected pancreatic mucinous cystic neoplasm have a better prognosis than patients with an intraductal papillary mucinous neoplasm: A

large single institution series. *Pancreatology* (2017) 17(3):490–6. doi: 10.1016/j.pan.2017.04.003

19. Hirono S, Yamaue H. Surgical strategy for intraductal papillary mucinous neoplasms of the pancreas. *Surg Today* (2020) 50(1):50–5. doi: 10.1007/s00595-019-01931-5

20. Bhardwaj N, Dennison AR, Maddern GJ, Garcea G. Management implications of resection margin histology in patients undergoing resection for IPMN: A meta-analysis. *Pancreatology* (2016) 16(3):309–17. doi: 10.1016/j.pan.2016.02.008

21. Talukdar R, Nageshwar Reddy D. Treatment of pancreatic cystic neoplasm: surgery or conservative? *Clin Gastroenterol Hepatol* (2014) 12(1):145–51. doi: 10.1016/j.cgh.2013.08.031

22. Nilsson LN, Keane MG, Shamali A, Millastre Bocos J, Marijinissen van Zanten M, Antila A, et al. Nature and management of pancreatic mucinous cystic neoplasm (MCN): A systematic review of the literature. *Pancreatology* (2016) 16(6):1028–36. doi: 10.1016/j.pan.2016.09.011

23. Marchegiani G, Andrianello S, Dal Borgo C, Secchettin E, Melisi D, Malleo G, et al. Adjuvant chemotherapy is associated with improved postoperative survival in specific subtypes of invasive intraductal papillary mucinous neoplasms (IPMN) of the pancreas: it is time for randomized controlled data. *HPB (Oxford)* (2019) 21(5):596–603. doi: 10.1016/j.hpb.2018.09.013

24. Rodrigues C, Hank T, Qadan M, Ciprani D, Mino-Kenudson M, Weekes CD, et al. Impact of adjuvant therapy in patients with invasive intraductal papillary mucinous neoplasms of the pancreas. *Pancreatology* (2020) 20(4):722–8. doi: 10.1016/j.pan.2020.03.009

25. Chong E, Ratnayake B, Dasari BVM, Loveday BPT, Siriwardena AK, Pandanaboyana S. Adjuvant chemotherapy in the treatment of intraductal papillary mucinous neoplasms of the pancreas: Systematic review and meta-analysis. *World J Surg* (2022) 46(1):223–34. doi: 10.1007/s00268-021-06309-8

frontiers | Frontiers in Oncology

TYPE Original Research
PUBLISHED 09 August 2022
DOI 10.3389/fonc.2022.913731

Check for updates

OPEN ACCESS

EDITED BY
Chang-In Choi,
Pusan National University Hospital,
South Korea

REVIEWED BY
Xiaojun Liu,
Gansu Provincial Hospital, China
Dario Lorenzin,
University Hospital Of Udine, Italy

*CORRESPONDENCE
Xiaolun Huang
huangxiaolun@med.uestc.edu.cn
Ying Shi
shiying_uestc@uestc.edu.cn

†These authors have contributed equally to this work

SPECIALTY SECTION
This article was submitted to Gastrointestinal Cancers: Hepato Pancreatic Biliary Cancers, a section of the journal Frontiers in Oncology

RECEIVED 06 April 2022
ACCEPTED 21 July 2022
PUBLISHED 09 August 2022

CITATION
Liang Y, Zhang Z, Zhong D, Lai C, Dai Z, Zou H, Feng T, Shang J, Shi Y and Huang X (2022) The prognostic significance of inflammation-immunity-nutrition score on postoperative survival and recurrence in hepatocellular carcinoma patients. *Front. Oncol.* 12:913731. doi: 10.3389/fonc.2022.913731

COPYRIGHT
© 2022 Liang, Zhang, Zhong, Lai, Dai, Zou, Feng, Shang, Shi and Huang. This is an open-access article distributed under the terms of the Creative Commons Attribution License (CC BY). The use, distribution or reproduction in other forums is permitted, provided the original author(s) and the copyright owner(s) are credited and that the original publication in this journal is cited, in accordance with accepted academic practice. No use, distribution or reproduction is permitted which does not comply with these terms.

The prognostic significance of inflammation-immunity-nutrition score on postoperative survival and recurrence in hepatocellular carcinoma patients

Yuxin Liang[1,2,3†], Zilong Zhang[1,2,3†], Deyuan Zhong[1,2,3], Chunyou Lai[1,2,3], Zonglin Dai[1,2,3], Haibo Zou[1,2], Tianhang Feng[1,2,3], Jin Shang[1,2,3], Ying Shi[1,2,3*] and Xiaolun Huang[1,2,3*]

[1]Department of Hepatobiliary-Pancreatic Surgery, Cell Transplantation Center, Sichuan Provincial People's Hospital, University of Electronic Science and Technology of China, Chengdu, China, [2]Clinical Immunology Translational Medicine Key Laboratory of Sichuan Province and Organ Transplant Research Institute, Sichuan Provincial People's Hospital, University of Electronic Science and Technology of China, Chengdu, China, [3]Chinese Academy of Sciences Sichuan Translational Medicine Research Hospital, Chengdu, China

Background: Inflammation, immunity, and nutrition status play important roles in tumorigenesis, progression, and metastasis. This study aimed to evaluate the prognostic value of Inflammation-Immunity-Nutrition Score (IINS) for overall survival (OS) and progression-free survival (PFS) in patients with hepatocellular carcinoma (HCC) undergoing radical surgery.

Methods: A total of 204 HCC patients who met the criteria were included in this retrospective study: 144 in the prediction model and 60 in the validation model. IINS was constructed based on the sum of classification scores of preoperative high-sensitivity C-reactive protein (hsCRP), lymphocyte (LYM), and albumin (ALB). The associations between the IINS group and the clinicopathologic characteristics were analyzed using Pearson's $\chi 2$ test or Fisher's exact test. Multivariate Cox regression analysis was used to evaluate variables significant on univariate analysis. Kaplan-Meier survival curves were conducted to investigate the prognostic values of IINS, Alpha-fetoprotein (AFP) and IINS-AFP classification. The prognostic performances of all the potential prognostic factors were further compared by receiver operating characteristic (ROC) curve, and time-dependent ROC curve. The internal validation and external validation were used to ensure the credibility of this prediction model.

Results: The patients were divided into low and high IINS groups according to the median of IINS. According to multivariate Cox regression analyses, the Barcelona Clinic Liver Cancer (BCLC) Stage (P=0.003), AFP (P=0.013), and IINS (P=0.028) were independent prognostic factors for OS, and BCLC Stage

(P=0.009), microvascular invasion (P=0.030), and IINS (P=0.031) were independent prognostic factors for PFS. High IINS group were associated with significantly worse OS and PFS compared with low IINS group (P<0.001; P=0.004). In terms of clinical prognosis, IINS-AFP classification was good in group I, moderate in group II, and poor in group III. Group I had a longer OS (P<0.001) and PFS (P=0.008) compared with group II and III. ROC analysis revealed that IINS-AFP classification had a better prognostic performance for OS (AUC: 0.767) and PFS (AUC: 0.641) than other predictors, excluding its slightly lower predictive power for PFS than IINS. The time-dependent ROC curves also showed that both IINS (12-month AUC: 0.650; 24-month AUC: 0.670; 36-month AUC: 0.880) and IINS-AFP classification (12-month AUC: 0.720; 24-month AUC: 0.760; 36-month AUC: 0.970) performed well in predicting OS for HCC patients. Furthermore, the internal validation and external validation proved that IINS had good predictive performance, strong internal validity and external applicability, and could be used to establish the prediction model.

Conclusion: Inflammation-immunity-nutrition score could be a powerful clinical prognostic indicator in HCC patients undergoing radical surgery. Furthermore, IINS-AFP classification presents better prognostic performance than IINS or AFP alone, and might serve as a practical guidance to help patients adjust treatment and follow-up strategies to improve future outcomes.

KEYWORDS

inflammation-immunity-nutrition score, alpha-fetoprotein, hepatocellular carcinoma, prognosis, recurrence

Introduction

Hepatocellular carcinoma (HCC), one of the most common malignant tumors, is also the leading cause of cancer-related death worldwide. Its global incidence continues to rise and might surpass an annual incidence of 1 million cases (1–3). For the treatment of patients with early-stage HCC, surgical resection, liver transplantation, and radiofrequency ablation are all first-line radical treatments (4, 5). Moreover, transarterial chemoembolization (TACE), targeted therapy, and immunotherapy are currently considered the three most promising approaches for patients with advanced HCC (3, 6–8). However, the high recurrence rate of HCC after curative surgery limits its therapeutic efficacy and leads to an overall 5-year survival of 50-70% (9). In recent years, an increasing number of potential prognostic indicators in clinical practice have been discovered to predict the postoperative prognosis of patients with liver cancer (10–12). However, these indicators are often limited to traditional clinicopathological parameters or the composite scores of peripheral inflammatory cells, such as neutrophils, lymphocytes, and platelets (10, 13, 14). Therefore, more comprehensive, easily accessible, and practical clinical prognostic indicators are required for predicting prognosis of postoperative HCC patients and help them improve the future outcome.

Inflammation, immunity, and nutrition status play important roles in tumorigenesis, progression, and metastasis (15, 16), and are widely considered as viable prognostic tools for clinical outcomes in HCC patients (10, 11, 13). Previous studies have clearly demonstrated that systemic inflammatory response biomarkers, such as neutrophil lymphocyte ratio (NLR), platelet lymphocyte ratio (PLR), systemic immune-inflammation index (SII), and systemic inflammation response index (SIRI) are reliable predictors for prognosis of HCC patients undergoing surgical treatment (10, 13, 14). High-sensitivity C-reactive protein (hsCRP) is the most sensitive protein synthesized by the liver to detect systemic inflammation, and it is closely related to the prognosis of HCC patients (15, 17, 18). In addition, serum albumin (ALB) is considered to be the simplest and effective factor reflecting human nutritional status and liver function, and is also the decisive factor of cancer cell immune response (5, 19).

In a recent study, the inflammation-immunity-nutrition score (IINS), which was constructed by the combination of hsCRP, lymphocyte (LYM), and ALB, has been proved to be a powerful prognostic predictor for overall survival (OS) in patients with colorectal cancer (20). However, whether IINS presents good prognostic performance in HCC patients who received radical resection has not been verified. Therefore, this study aimed to evaluate the prognostic value of IINS in HCC patients after radical surgery.

Materials and methods

Patients and study design

We retrospectively collected preoperative and postoperative clinicopathological data of HCC patients who received radical hepatectomy at the Sichuan Provincial People's Hospital between July 2017 and July 2021. All serum indicators were collected within 1 week before the operation. The inclusion criteria are as follows (1): histopathological evaluation confirmed HCC (2); received radical resection (3); no preoperative therapy for primary HCC (4); initial diagnosis rather than recurrent tumors (5); hepatectomy with tumor-negative resection margins (6); Eastern Cooperative Oncology Group (ECOG) performance status 0–1. The exclusion criteria are as follows (1): having history of malignancies or concurrent with other malignancies (2); incomplete clinical and follow-up data (3); having diseases of the hematologic system (4); preexisting autoimmune or systemic inflammatory disease (5); perioperative death (death within 30 days after surgery) or death from other diseases during follow-up. Pathological stage was confirmed according to the 7th American Joint Committee on Cancer staging. Finally, a total of 144 patients who were included from July 2017 to July 2021 were defined as the prediction model. The clinicopathological data of the other 60 patients were collected as the validation model for external validation. The flow chart of the study design is showed in Figure 1.

The experimental protocol was established, according to the ethical guidelines of the Helsinki Declaration and was approved by the Human Ethics Committee of Sichuan Academy of Medical Sciences and Sichuan Provincial People's Hospital (NO2021-447). Written informed consent was obtained from individual or guardian participants.

Definitions

According to the correlation between the three indicators and the patients' OS, the optimal cut-off values of hsCRP, ALB, and LYM were determined using the X-tile software version 3.6.1 (https://medicine.yale.edu/lab/rimm/research/software/, Yale University School of Medicine, New Haven, CT) (21). According to 2 cut-offs, hsCRP was divided into the following three groups: score 0: ≤ 2.47 mg/L, score 1: > 2.47 mg/L and ≤ 11.33 mg/L, score 2: > 11.33mg/L. And LYM and ALB were grouped as follows: LYM (score 0: > 1.60×10^9/L, score 1: > 0.84×10^9/L and ≤ 1.60×10^9/L, score 2: ≤ 0.84×10^9/L); ALB (score 0: > 39.8 g/L, score 1: > 35.2 g/L and ≤ 39.8 g/L, score 2: ≤ 35.2g/L). Then, the scores for hsCRP, LYM, and ALB were summed to obtain the inflammation-immunity-nutrition score (IINS). Since the median IINS was 2 in this study, IINS > 2 was defined as high IINS group.

To compare the prognostic valve of IINS with other predictors, we also investigated the prognostic performance of Child-Pugh grade, Barcelona Clinic Liver Cancer (BCLC) stage, alpha-fetoprotein (AFP), carcinoembryonic antigen (CEA), LYM, ALB, NLR, PLR, SII and SIRI for each patient. The

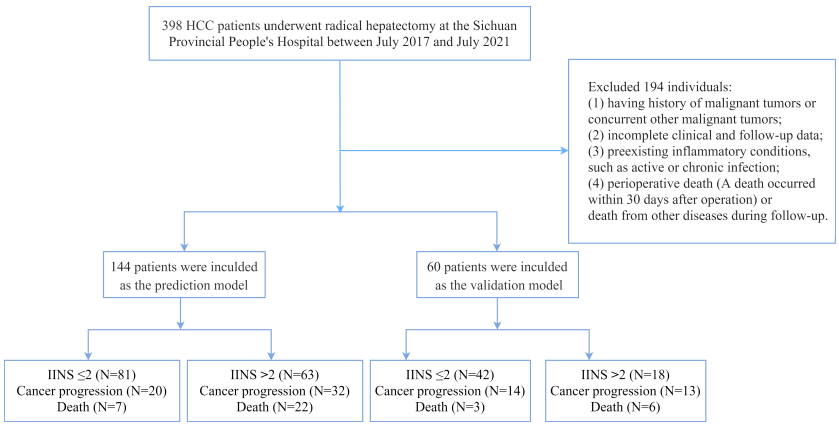

FIGURE 1
The flowchart of patients enrolled in this study. HCC, hepatocellular carcinoma; IINS, inflammation-immunity-nutrition score.

optimum cut-off values for NLR, PLR, AFP, CEA, LYM, SII and SIRI derived from receiver operating characteristic (ROC) curves are presented in Table 4 and Table 5. The NLR and PLR were defined as follows: NLR = neutrophil/lymphocyte counts and PLR = platelet/lymphocyte counts (13), whereas the SII was defined as platelet × neutrophil/lymphocyte counts (10). The SIRI was calculated by using the Qi's original formula: SIRI= monocytes × neutrophil/lymphocyte (22).

Follow up

After the surgery, survival data were obtained by outpatient visits and telephone follow-up every 3 months in the first year, and then every 6 months thereafter if there was no recurrence or metastasis. The primary outcome was overall survival (OS), which was counted as the interval from the date of curative surgery to the date of death, lost to follow-up, or the end of the follow-up (August 2021), whichever came first. And the secondary outcome was progression-free survival (PFS), which was defined as the interval from the date of curative surgery to the date of death, recurrence or metastasis, loss to follow-up, or the end of the follow-up (August 2021), whichever came first. Cancer progression was defined as tumor recurrence, metastasis, or death.

Statistical analysis

The associations between the IINS and the clinicopathologic characteristics were analyzed using Pearson's $\chi 2$ test or Fisher's exact test. Continuous data were expressed as mean ± SD. The area under the ROC curve (AUC) and optimal cutoff value that were calculated by predicting the OS and PFS for the NLR, PLR, AFP, CEA, LYM, SII, SIRI, and PNI are shown in Table 4 and Table 5. Survival curves were presented using the Kaplan–Meier method and the differences were compared by log rank test. Univariate and multivariate analyses were performed using the Cox proportional hazards model. Moreover, time-dependent ROC curves were used to detect the prognostic performance of IINS, AFP and IINS-AFP classification for OS, respectively. Compared with ordinary ROC curve, time-dependent ROC curve could observe the prognostic performance of indicators at specific time points after surgery (20). The validation of the prediction model includes internal validation and external validation. In the internal validation, the bootstrap method was used to test the internal validity of the prediction model. The clinicopathological data of 60 HCC patients were used as the external validation data. The C-Statistics representing the discrimination ability and the Hosmer-Lemeshow test (H-L test) representing the calibration ability were calculated separately. Two-tailed $P < 0.05$ was considered statistically significant. All statistical analyses were performed using SPSS statistical software (version 26; SPSS-IBM, Chicago, IL, USA) and GraphPad Prism version 9.2.0 (GraphPad, CA, USA).

Results

Patient characteristics

The baseline characteristics of all the 144 participants in the prediction model are shown in Table 1. A total of 123 (85.4%) patients were male, and the average age was 58 ± 12 years. 104 (72.2%) of them had hepatitis B virus infection, and their mean body mass index (BMI) was 22.66 ± 2.81. The mean SII and SIRI were 447.38 ± 410.79 and 1.67 ± 2.16, respectively. Child-Pugh grade A, B, C accounted for 96 (66.7%), 47 (32.6%), 1 (0.7%), respectively. The proportion of patients with BCLC stages of 0/A, B, and C were 52.8%, 15.3%, and 31.9%, respectively. A total of 118 (81.9%) patients had medium-high differentiation cancer. Microvascular invasion was noted in 51 (35.4%) patients and cirrhosis in 103 (71.5%) patients. After surgery, 75 (52.1%) patients underwent adjuvant transarterial chemoembolization (TACE). The median follow-up time of the study was 17 ± 10 months. At the end of follow-up, 52 (36.1%) presented cancer progression, and 29 (20.1%) patients died. Patients with high IINS were more likely to present cancer progression (61.5%) and death (75.9%).

Relationships between the inflammation-immunity-nutrition score and clinicopathologic characteristics

A total of 81 patients had low IINS, whereas 63 patients had high IINS. The relationship between clinicopathological factors and IINS are presented in Table 1. The patients with high IINS were more likely to have higher BCLC stage ($P = 0.001$), Child-Pugh grade ($P < 0.001$), NLR ($P < 0.001$), PLR ($P = 0.002$), SIRI ($P = 0.030$) and hsCRP levels ($P < 0.001$), more tumor numbers ($P = 0.031$), but lower ALB ($P < 0.001$) and LYM ($P < 0.001$) levels. All differences were statistically significant ($P < 0.05$). However, IINS was not associated with age, BMI, microvascular invasion, histopathological type, or cirrhosis.

Univariate and multivariate analyses of OS and PFS among the HCC patients

Univariate and multivariate analyses were performed for Child-Pugh grade, BCLC Stage, tumor number, microvascular invasion, AFP, ALB, IINS, and other clinicopathologic variables. Univariate Cox regression analysis revealed that BCLC Stage ($P < 0.001$), microvascular invasion ($P = 0.008$), AFP ($P = 0.002$), and IINS ($P = 0.001$) were all significantly associated with OS in HCC patients (Table 2). Moreover,

10.3389/fonc.2022.913731

TABLE 1 Associations of the IINS with the clinicopathologic characteristics of HCC patients in the prediction model.

	IINS value (0–6)			
Characteristics	**Overall (n = 144)**	**IINS≤2 (n=81)**	**IINS>2 (n=63)**	**P value**
Gender				**0.013**
Male	123 (85.4%)	71 (57.7%)	52 (42.3%)	
Female	21 (14.6%)	10 (47.6%)	11 (52.4%)	
Age, years	58 ± 12	59 ± 11	55 ± 13	0.089
BMI, kg/m^2	22.66 ± 2.81	22.63 ± 2.73	22.70 ± 2.93	0.844
Etiology of HCC				0.851
HBV	104 (72.2%)	59 (56.7%)	45 (43.3%)	
Others	40 (27.7%)	22 (55.0%)	18 (45.0%)	
ALB, g/L	36.96 ± 4.75	39.32 ± 3.80	33.92 ± 4.10	**<0.001**
LYM, $10^9/L$	1.62 ± 1.18	1.71 ± 0.73	1.51 ± 1.59	**<0.001**
hsCRP, mg/L	11.35 ± 21.96	2.76 ± 5.03	22.40 ± 29.32	**<0.001**
AFP, ng/mL	2019.93 ± 5180.67	923.23 ±3257.38	3429.96 ± 6679.91	0.175
CEA, ng/mL	13.85 ± 127.65	3.75 ± 9.75	26.84 ± 192.75	0.220
Child-Pugh grade				**<0.001**
A	96 (66.7%)	71 (74.0%)	25 (26.0%)	
B	47 (32.6%)	10 (21.3%)	37 (78.7%)	
C	1 (0.7%)	0 (0%)	1 (100.0%)	
BCLC stage				**0.001**
0/A	76 (52.8%)	52 (68.4%)	24 (31.6%)	
B	22 (15.3%)	12 (54.5%)	10 (45.6%)	
C	46 (31.9%)	17 (37.0%)	29 (63.0%)	
Microvascular invasion				0.553
No	93 (64.6%)	54 (58.1%)	39 (41.9%)	
Yes	51 (35.4%)	27 (52.9%)	24 (47.1%)	
NLR	2.88 ± 2.06	2.42 ± 1.91	3.48 ± 2.11	**<0.001**
PLR	114.37 ± 66.20	95.47 ± 43.19	138.67 ± 81.46	**0.002**
SII	447.38 ± 410.79	357.85 ± 265.98	562.49 ± 523.44	0.100
SIRI	1.67 ± 2.16	1.44 ± 4.60	1.97 ± 2.16	**0.030**
Histopathological type				0.870
Poorly differentiation	26 (18.1%)	15 (57.7%)	11 (42.3%)	
Medium-high differentiation	118 (81.9%)	66 (55.9%)	52 (36.1%)	
Tumor number				**0.031**
Single	94 (65.3%)	59 (62.8%)	35 (37.2%)	
Multiple	50 (34.7%)	22 (44.0%)	28 (56.0%)	
Cirrhosis				0.471
No	41 (28.5%)	25 (61.0%)	16 (39.0%)	
Yes	103 (71.5%)	56 (54.4%)	47 (32.6%)	
Postoperative adjuvant TACE	69 (47.9%)	40 (58.0%)	29 (42.0%)	0.691
No	75 (52.1%)	41 (54.7%)	34 (45.3%)	
Yes				
Cancer progression				**0.001**
No	92 (63.9%)	61 (66.3%)	31 (33.7%)	
Yes	52 (36.1%)	20 (38.5%)	32 (61.5%)	
Death				**<0.001**
No	115 (79.9%)	74 (64.3%)	41 (35.7%)	
Yes	29 (20.1%)	7 (24.1%)	22 (75.9%)	

BMI, Body Mass Index; HCC, hepatocellular carcinoma; HBV, hepatitis B virus; BCLC, Barcelona Clinic Liver Cancer; ALB, albumin; LYM, lymphocyte; hsCRP, high sensitivity C-reactive protein; AFP, alpha-fetoprotein; CEA, carcinoembryonic antigen; NLR, neutrophil–lymphocyte ratio; PLR, platelet–lymphocyte ratio; SII, systemic immune-inflammation index; SIRI, systemic inflammation response index; IINS, inflammation-immunity-nutrition score. Bold values means the P value is significant.

TABLE 2 Univariate and multivariate Cox regression analyses of the associations between the prognostic factors and the overall survival of the HCC patients.

Characteristics	Univariate Analysis		Multivariate Analysis	
	HR (95% CI)	P value	HR (95% CI)	P value
Child-Pugh grade (A vs. B-C)	1.557 (0.743-3.263)	0.241		
BCLC Stage (0-A vs. B-C)	6.629 (2.515-17.472)	**<0.001**	5.077 (1.758-14.660)	**0.003**
Tumor number (Single vs. Multiple)	1.978 (0.951-4.113)	0.068		
Microvascular invasion (No vs. Yes)	2.707 (1.292-5.670)	**0.008**	1.159 (0.519-2.590)	0.718
AFP, ng/mL (≤80.38 vs. >80.38)	3.288 (1.552-6.968)	**0.002**	2.692 (1.235-5.867)	**0.013**
BMI, kg/m2 (≤21.57 vs. >21.57)	0.554 (0.267-1.149)	0.113		
Cirrhosis (No vs. Yes)	1.063 (0.471-2.400)	0.883		
HBV infection (No vs. Yes)	1.647 (0.670-4.046)	0.277		
IINS (Low group vs. High group)	4.018 (1.716-9.408)	**0.001**	2.680 (1.113-6.449)	**0.028**

HCC, hepatocellular carcinoma; BCLC, Barcelona Clinic Liver Cancer; AFP, alpha-fetoprotein; BMI, Body Mass Index; IINS, inflammation-immunity-nutrition score. Bold values means the P value is significant.

BCLC Stage (P < 0.001), tumor number (P = 0.024), microvascular invasion (P < 0.001), and IINS (P = 0.005) had significant associations with PFS in HCC patients (Table 3). From the multivariate Cox regression analysis, we found that BCLC Stage (hazard ratio (HR): 5.077; 95% confidence interval (95% CI): 1.758-14.660; P = 0.003), AFP (HR: 2.692; 95% CI: 1.235-5.867; P = 0.013), and IINS (HR: 2.680; 95% CI: 1.113-6.449; P = 0.028) were significant prognostic markers for OS (Table 2). BCLC Stage (HR: 2.988; 95% CI: 1.311-6.807; P = 0.009), microvascular invasion (HR: 1.965; 95% CI: 1.069-

TABLE 3 Univariate and multivariate Cox regression analyses of the associations between the prognostic factors and the progression-free survival of the HCC patients.

Characteristics	Univariate Analysis		Multivariate Analysis	
	HR (95% CI)	P value	HR (95% CI)	P value
Child-Pugh grade (A vs. B-C)	1.046 (0.591-1.854)	0.876		
BCLC Stage (0-A vs. B-C)	3.286 (1.819-5.935)	**<0.001**	2.988 (1.311-6.807)	**0.009**
Tumor number (Single vs. Multiple)	1.895 (1.088-3.303)	**0.024**	0.762 (0.373-1.577)	0.456
Microvascular invasion (No vs. Yes)	2.799 (1.597-4.905)	**<0.001**	1.965 (1.069-3.610)	**0.030**
AFP, ng/mL (≤80.38 vs. >80.38)	1.475 (0.850-2.560)	0.167		
BMI, kg/m2 (≤21.57 vs. >21.57)	0.734 (0.424-1.270)	0.269		
Cirrhosis (No vs. Yes)	0.775 (0.430-1.399)	0.398		
HBV infection (No vs. Yes)	1.295 (0.690-2.429)	0.421		
IINS (Low group vs. High group)	2.225 (1.272-3.891)	**0.005**	1.874 (1.061-3.311)	**0.031**

HCC, hepatocellular carcinoma; BCLC, Barcelona Clinic Liver Cancer; AFP, alpha-fetoprotein; BMI, Body Mass Index; IINS, inflammation-immunity-nutrition score. Bold values means the P value is significant.

3.610; P = 0.030), and IINS (HR: 1.874; 95% CI: 1.061-3.311; P = 0.031) emerged as the powerful prognostic factors of PFS (Table 3).

Prognostic analysis of the inflammation-immunity-nutrition score in HCC patients

Patients with high IINS were associated with significantly worse OS and PFS compared with low IINS (HR: 4.013; 95% CI: 1.927-8.356; P < 0.001; Figure 2A; HR: 2.222; 95% CI: 1.281-3.855; P = 0.004; Figure 2B). Similar to IINS group, we found the OS and PFS of patients in the high AFP group (cutoff value = 80.38) were significantly worse than those in the low AFP group (HR: 3.281; 95% CI: 1.515-7.102; P < 0.001; Figure 3A; HR: 1.717; 95% CI: 0.980-3.009; P = 0.042; Figure 3B). Thus, IINS-AFP classification was formed by classifying patients using cut-off values of AFP and different IINS groups, and then dividing them into the following three groups: patients in low IINS group and with low AFP were group I, patients in high IINS group and with low AFP or in low IINS group and with high AFP were group II, patients in high IINS group and with high AFP were group III. We found that group I had a longer OS (Chi square: 24.03, P < 0.001, Figure 4A) and PFS (Chi square: 9.741, P = 0.008, Figure 4B) compared with group II and III.

ROC analysis of the characteristics in HCC patients

In our research, ROC analysis was used to evaluate the effect of different independent factors on prognosis. The results showed that the IINS-AFP classification (AUC: 0.767; 95% CI: 0.675-0.858; Table 4) was more predictive of OS in HCC patients than IINS (AUC: 0.760; 95% CI: 0.668-0.851; Table 4), although the difference was not statistically significant (P = 0.875). Moreover, the AUC of IINS-AFP classification for predicting OS was significantly higher than that of preoperative serum AFP levels (AUC: 0.668; 95% CI: 0.556-0.780; P = 0.043; Table 5) and other indicators. In terms of PFS, the AUC of IINS-AFP classification (AUC: 0.641; 95% CI: 0.546-0.735; P = 0.297; Table 5) was higher than that of other predictors, excluding its slightly lower predictive power than IINS (AUC: 0.679; 95% CI: 0.589-0.769; Table 5). In addition, the time-dependent ROC curves showed that both IINS (12-month AUC: 0.650, 24-month AUC: 0.670, 36-month AUC: 0.880) and IINS-AFP classification (12-month AUC: 0.720, 24-month AUC: 0.760, 36-month AUC: 0.970) performed well in predicting OS for HCC patients (Figure 5).

Validation and performance of the prediction model

To ensure the credibility of the prediction model, the performance of the model was quantified by assessing its discrimination and calibration abilities. The baseline characteristics of all the 60 participants in the validation model are shown in Supplemental Table 1. As shown in Table 6, the internal validation found the model to have strong internal consistency and moderate predictive validity for clinical prognosis. The predictive performances of the prediction model for OS and PFS as measured by the C-Statistics were good (C-Statistics = 0.759; C-Statistics = 0.668). The external validation showed that the C-Statistics of IINS in OS and PFS were 0.716 and 0.665, respectively, which also represented that IINS had strong discrimination ability and external applicability. In the Hosmer-Lemeshow test (H-L test), the P values for OS and PFS were 0.769 and 0.971, respectively, indicating a strong calibration ability of the model. Therefore, IINS had good predictive performance, strong internal validity and external applicability, and could be used to establish the prediction model for predicting postoperative survival and recurrence in patients with HCC.

Discussion

In this study, we found that IINS might serve as a robust prognostic score in HCC patients after hepatectomy. Our results showed that patients with low IINS had significantly better OS and PFS than those with high IINS, and IINS was an independent risk factor for the clinical outcomes of HCC patients. Further comparison revealed the better prognostic performance of IINS than other indicators, such as Child-Pugh grade, BCLC stage, AFP, CEA, neutrophil lymphocyte ratio (NLR), platelet lymphocyte ratio (PLR), systemic immune-inflammation index (SII), and systemic inflammation response index (SIRI). To the best of our knowledge, this retrospective study was the first to identify the predictive value of inflammation-immunity-nutrition score in HCC patients who received radical hepatectomy.

In recent years, a lot of studies have shown the prognostic values of prognostic biomarkers for cancer prognosis, and elevated NLR, PLR, SII, SIRI, and PLR are associated with poor OS or RFS of patients with liver cancer (5, 10, 13, 14). However, most of the current prognostic biomarkers are different combinations of the two indicators in serum detection, which cannot reflect the immune and nutritional functions of the body, and thus lead to inevitable bias and prediction inaccuracy (23). Therefore, the Inflammation-immunity-nutrition score, which is based on a combined score of preoperative hsCRP, LYM and ALB, has been proved to have

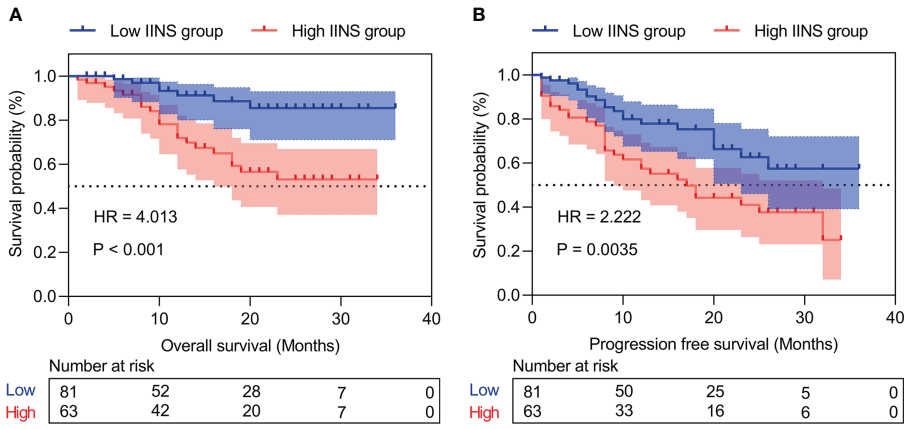

FIGURE 2
Kaplan-Meier curves of inflammation-immunity-nutrition score (IINS) for overall survival **(A)** and progression-free survival **(B)**. IINS, inflammation-immunity-nutrition score.

good prognostic performance in resectable CRC for OS (20), and the predictive value of IINS for HCC may also be explained by the role of these indicators. High IINS usually results from lymphopenia, hypoproteinemia, and increased hsCRP, suggesting high inflammatory response and low immune and nutritional status. Systemic inflammation is closely related to the proliferation, invasion and metastasis of malignant tumors (16, 24, 25), in which immune and nutritional status are important components of the inflammatory response (5). Furthermore, most liver cancers occur in chronically inflamed cirrhotic livers, this creates a pro-inflammatory environment that also promotes tumor formation and progression (25–28). Accumulating evidence has also suggested that hsCRP/LYM, hsCRP/ALB, and prognostic nutritional index (PNI) present powerful prognostic values in many types of cancer (5, 18, 19, 29). ALB is often used to assess liver function in patients with liver cancer, and hypoalbuminemia could reduce the systemic immune system, leading to tumor cell proliferation (5). Lymphocytes serve as the basis of cell-mediated anti-tumor immune responses, which could inhibit tumor cell proliferation and metastasis. Low lymphocyte counts could reduce the immune surveillance of cancer and lead to poor prognosis in various malignancies (30–32). As a result, IINS could be a practical, effective, and easily accessible clinical prognostic indicator for patients with HCC.

As an oncofetal antigen and a diagnostic marker for HCC, AFP has long been recognized as a useful predictor of the prognosis of liver cancer (33, 34). High AFP levels are usually associated with larger tumors, poorly differentiated histopathological type, and worse survival (35). This may be

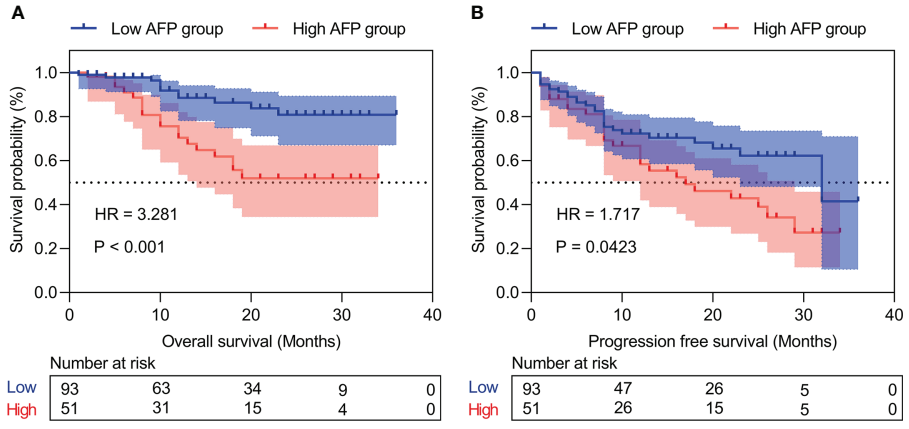

FIGURE 3
Kaplan-Meier curves of the different AFP levels for overall survival **(A)** and progression-free survival **(B)**. AFP, alpha-fetoprotein.

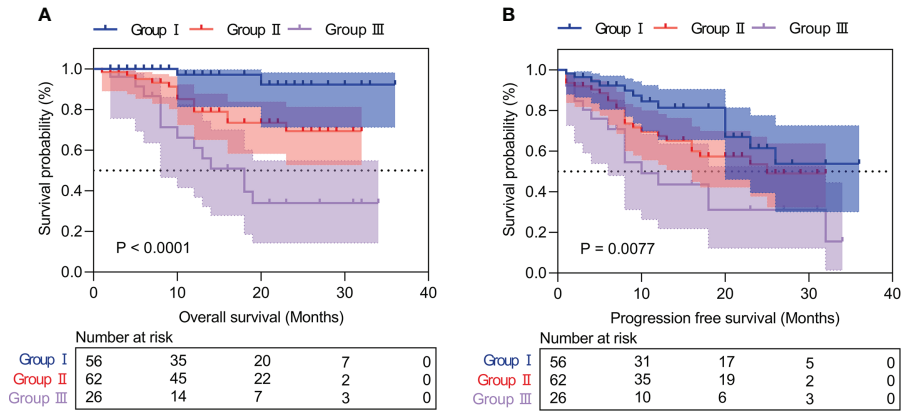

FIGURE 4
Kaplan-Meier curves of IINS-AFP classification for overall survival **(A)** and progression-free survival **(B)**. IINS, inflammation-immunity-nutrition score; AFP, alpha-fetoprotein.

explained by the relationship between high AFP levels and the role of VEGF and VEGFR-2 in angiogenesis and promoting the growth of various malignances, including HCC (36, 37). Therefore, AFP has been applied to various HCC prognostic scoring systems in clinical practice (12, 38).

Serum AFP level mainly reflects the pathological conditions and tumor activity, while IINS reflects the overall status of the patient, including inflammation, immune, and nutritional status. In the current study, we also innovatively combined the application of IINS and AFP, and then performed an individualized prediction of the postoperative prognosis of HCC patients. Our study revealed that IINS-AFP classification had a better prognostic performance for survival and recurrence than other predictors, excluding its slightly lower predictive power for PFS than IINS. According to prognosis, group I was good, group II was moderate, and group III was poor. For patients in group I or II, curative surgery rather than palliative resection should be the primary consideration in resectable cases. While for patients in group III, considering the high mortality and recurrence rates, surgeons should carefully evaluate whether they can implement aggressive surgical treatment. Early treatment such as TACE, targeted therapy, and immunotherapy may prolong the survival time and enhance the quality of life for them. Furthermore, IINS-AFP classification could also serve as a practical guidance to help patients adjust follow-up strategies and improve future outcomes.

This study also has several limitations. First, although the cutoff value of IINS derived from clinical reference value, it may vary in different studies due to different sample sizes and patient selection criteria. Second, this study included patients only from one center, and the sample size in the study was limited. Further multicenter, large-scale prospective studies are needed to validate our findings.

TABLE 4 Receiver operating characteristics analysis between IINS and other indicators in overall survival of the HCC patients.

Variables	Cut off value	AUC (95% CI)	Specificity	Sensitivity	P value
BCLC stage		0.751 (0.653-0.849)	0.617	0.828	**<0.001**
Child-Pugh grade		0.556 (0.435-0.677)	0.687	0.414	0.354
NLR	3.01	0.621 (0.500-0.743)	0.739	0.552	**0.044**
PLR	145.73	0.630 (0.502-0.758)	0.817	0.483	**0.031**
AFP	80.38	0.668 (0.556-0.780)	0.713	0.621	**0.005**
CEA	2.44	0.536 (0.451-0.620)	0.496	0.690	0.518
LYM	0.84	0.577 (0.492-0.659)	0.896	0.345	0.233
SII	517.02	0.621 (0.498-0.743)	0.791	0.483	**0.045**
SIRI	1.10	0.640 (0.520-0.759)	0.530	0.759	**0.020**
IINS		0.760 (0.668-0.851)	0.644	0.759	**<0.001**
IINS-AFP		0.767 (0.675-0.858)	0.470	0.931	**<0.001**

HCC, hepatocellular carcinoma; BCLC, Barcelona Clinic Liver Cancer; AFP, alpha-fetoprotein; CEA, carcinoembryonic antigen; LYM, lymphocyte; NLR, neutrophil–lymphocyte ratio; PLR, platelet–lymphocyte ratio; SII, systemic immune-inflammation index; SIRI, systemic inflammation response index; IINS, inflammation-immunity-nutrition score. Bold values means the P value is significant.

TABLE 5 Receiver operating characteristics analysis between IINS and other indicators in progression-free survival of the HCC patients.

Variables	Cut off value	AUC (95% CI)	Specificity	Sensitivity	P value
BCLC stage		0.674 (0.581-0.767)	0.644	0.667	**0.001**
Child-Pugh grade		0.513 (0.414-0.612)	0.687	0.414	0.793
NLR	2.59	0.664 (0.570-0.759)	0.733	0.556	**0.001**
PLR	109.9	0.614 (0.519-0.709)	0.633	0.537	**0.023**
AFP	305.21	0.549 (0.449-0.650)	0.778	0.352	0.328
CEA	2.44	0.566 (0.481-0.648)	0.522	0.654	0.188
LYM	0.92	0.572 (0.487-0.654)	0.848	0.346	0.165
SII	501.24	0.640 (0.545-0.736)	0.822	0.426	**0.005**
SIRI	1.03	0.649 (0.553-0.744)	0.533	0.722	**0.003**
IINS		0.679 (0.589-0.769)	0.656	0.593	**<0.001**
IINS-AFP		0.641 (0.546-0.735)	0.456	0.722	**0.005**

HCC, hepatocellular carcinoma; BCLC, Barcelona Clinic Liver Cancer; AFP, alpha-fetoprotein; CEA, carcinoembryonic antigen; LYM, lymphocyte; NLR, neutrophil–lymphocyte ratio; PLR, platelet–lymphocyte ratio; SII, systemic immune-inflammation index; SIRI, systemic inflammation response index; IINS, inflammation-immunity-nutrition score. Bold values means the P value is significant.

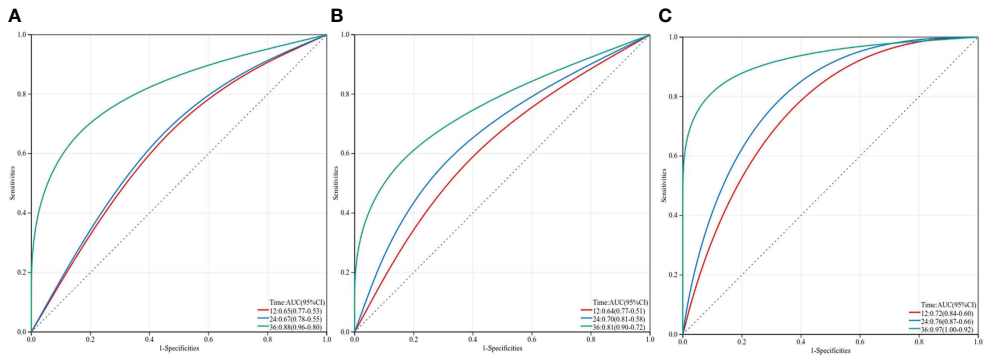

FIGURE 5
Three-year time-dependent ROC curves for overall survival of inflammation-immunity-nutrition score, AFP and IINS-AFP classification. IINS, inflammation-immunity-nutrition score; AFP, alpha-fetoprotein.

TABLE 6 Validation and performance of the prediction model for overall survival and progression-free survival.

Overall Survival	Inflammation-Immunity-Nutrition Score		
	Internal validation[b]		External validation[c]
C-Statistics (95% CI)	0.759 (0.652-0.866)		0.716 (0.523-0.908)
P value[a]		0.769	
Progression-free Survival	**Internal validation[b]**		**External validation[c]**
C-Statistics (95% CI)	0.668 (0.559-0.776)		0.665 (0.523-0.807)
P value[a]		0.971	

[a]Hosmer-Lemeshow test (H-L test); [b]the resampling sample size is 100; [c]the number of patients was 60.

Conclusion

Our study demonstrated that preoperative IINS could serve as a powerful prognostic predictor for HCC patients after radical surgery. Specifically, IINS-AFP classification presents better prognostic performance than IINS or AFP alone, which may provide a simple way to identify patients with poor prognosis and an opportunity to guide treatment and follow-up strategies to improve their prognosis.

Data availability statement

The raw data supporting the conclusions of this article will be made available by the authors, without undue reservation.

Ethics statement

The experimental protocol was established, according to the ethical guidelines of the Helsinki Declaration and was approved by the Human Ethics Committee of Sichuan Academy of Medical Sciences and Sichuan Provincial People's Hospital (NO2021-447). Written informed consent to participate in this study was provided by the participants' legal guardian/next of kin.

Author contributions

YL, ZZ was responsible for study conception and design, data acquisition, data analysis and drafting and revision of the manuscript. XH, YS was responsible for study conception and design, data analysis and drafting and revision of the manuscript. DZ, CL, ZD, HZ, TF were responsible for data acquisition. JS was responsible for drafting and revision of the manuscript. All authors contributed to the article and approved the submitted version.

Funding

This study was supported by Sichuan Province Science and Technology Support Program (No. 2018HH0062), and Sichuan Province Science and Technology Support Program (No. 2021YFH0187).

Conflict of interest

The authors declare that the research was conducted in the absence of any commercial or financial relationships that could be construed as a potential conflict of interest.

Publisher's note

All claims expressed in this article are solely those of the authors and do not necessarily represent those of their affiliated organizations, or those of the publisher, the editors and the reviewers. Any product that may be evaluated in this article, or claim that may be made by its manufacturer, is not guaranteed or endorsed by the publisher.

Supplementary material

The Supplementary Material for this article can be found online at: https://www.frontiersin.org/articles/10.3389/fonc.2022.913731/full#supplementary-material

References

1. Akinyemiju T, Abera S, Ahmed M, Alam N, Alemayohu MA, Allen C, et al. The burden of primary liver cancer and underlying etiologies from 1990 to 2015 at the global, regional, and national level: Results from the global burden of disease study 2015. *JAMA Oncol* (2017) 3(12):1683–91. doi: 10.1001/jamaoncol.2017.3055

2. Bray F, Ferlay J, Soerjomataram I, Siegel RL, Torre LA, Jemal A. Global cancer statistics 2018: GLOBOCAN estimates of incidence and mortality worldwide for 36 cancers in 185 countries. *CA: Cancer J Clin* (2018) 68(6):394–424. doi: 10.3322/caac.21492

3. Llovet JM, Montal R, Sia D, Finn RS. Molecular therapies and precision medicine for hepatocellular carcinoma. *Nat Rev Clin Oncol* (2018) 15(10):599–616. doi: 10.1038/s41571-018-0073-4

4. Cadier B, Bulsei J, Nahon P, Seror O, Laurent A, Rosa I, et al. Early detection and curative treatment of hepatocellular carcinoma: A cost-effectiveness analysis in France and in the united states. *Hepatol (Baltimore Md)* (2017) 65(4):1237–48. doi: 10.1002/hep.28961

5. Wang D, Hu X, Xiao L, Long G, Yao L, Wang Z, et al. Prognostic nutritional index and systemic immune-inflammation index predict the prognosis of patients with HCC. *J Gastrointestinal Surg Off J Soc Surg Alimentary Tract* (2021) 25 (2):421–7. doi: 10.1007/s11605-019-04492-7

6. Song JE, Kim DY. Conventional vs drug-eluting beads transarterial chemoembolization for hepatocellular carcinoma. *World J Hepatology* (2017) 9 (18):808–14. doi: 10.4254/wjh.v9.i18.808

7. Baur J, Ritter CO, Germer CT, Klein I, Kickuth R, Steger U. Transarterial chemoembolization with drug-eluting beads versus conventional transarterial chemoembolization in locally advanced hepatocellular carcinoma. *Hepatic Med Evidence Res* (2016) 8:69–74. doi: 10.2147/hmer.S105395

8. El-Khoueiry AB, Sangro B, Yau T, Crocenzi TS, Kudo M, Hsu C, et al. Nivolumab in patients with advanced hepatocellular carcinoma (CheckMate 040): an open-label, non-comparative, phase 1/2 dose escalation and expansion trial. *Lancet (London England)* (2017) 389(10088):2492–502. doi: 10.1016/s0140-6736(17)31046-2

9. Villanueva A, Hoshida Y, Battiston C, Tovar V, Sia D, Alsinet C, et al. Combining clinical, pathology, and gene expression data to predict recurrence of hepatocellular carcinoma. *Gastroenterology* (2011) 140(5):1501–12.e2. doi: 10.1053/j.gastro.2011.02.006

10. Hu B, Yang XR, Xu Y, Sun YF, Sun C, Guo W, et al. Systemic immune-inflammation index predicts prognosis of patients after curative resection for hepatocellular carcinoma. *Clin Cancer Res An Off J Am Assoc Cancer Res* (2014) 20 (23):6212–22. doi: 10.1158/1078-0432.Ccr-14-0442

11. Ji F, Liang Y, Fu S, Chen D, Cai X, Li S, et al. Prognostic value of combined preoperative prognostic nutritional index and body mass index in HCC after hepatectomy. *HPB Off J Int Hepato Pancreato Biliary Assoc* (2017) 19(8):695–705. doi: 10.1016/j.hpb.2017.04.008

12. Leung TW, Tang AM, Zee B, Lau WY, Lai PB, Leung KL, et al. Construction of the Chinese university prognostic index for hepatocellular carcinoma and comparison with the TNM staging system, the okuda staging system, and the cancer of the liver Italian program staging system: a study based on 926 patients. *Cancer* (2002) 94(6):1760–9. doi: 10.1002/cncr.10384

13. Lin WF, Zhong MF, Zhang YR, Wang H, Zhao HT, Cheng BB, et al. Prognostic role of platelet-to-Lymphocyte ratio in hepatocellular carcinoma with different BCLC stages: A systematic review and meta-analysis. *Gastroenterol Res practice* (2018) 2018:5670949. doi: 10.1155/2018/5670949

14. Xu L, Yu S, Zhuang L, Wang P, Shen Y, Lin J, et al. Systemic inflammation response index (SIRI) predicts prognosis in hepatocellular carcinoma patients. *Oncotarget* (2017) 8(21):34954–60. doi: 10.18632/oncotarget.16865

15. Crusz SM, Balkwill FR. Inflammation and cancer: advances and new agents. *Nat Rev Clin Oncol* (2015) 12(10):584–96. doi: 10.1038/nrclinonc.2015.105

16. Elinav E, Nowarski R, Thaiss CA, Hu B, Jin C, Flavell RA. Inflammation-induced cancer: crosstalk between tumours, immune cells and microorganisms. *Nat Rev Cancer* (2013) 13(11):759–71. doi: 10.1038/nrc3611

17. Ko YJ, Kwon YM, Kim KH, Choi HC, Chun SH, Yoon HJ, et al. High-sensitivity c-reactive protein levels and cancer mortality. *Cancer Epidemiology Biomarkers Prev Publ Am Assoc Cancer Research Cosponsored By Am Soc Prev Oncol* (2012) 21(11):2076–86. doi: 10.1158/1055-9965.Epi-12-0611

18. Liao M, Chen P, Liao Y, Li J, Yao W, Sun T, et al. Preoperative high-sensitivity c-reactive protein to lymphocyte ratio index plays a vital role in the prognosis of hepatocellular carcinoma after surgical resection. *OncoTargets Ther* (2018) 11:5591–600. doi: 10.2147/ott.S167857

19. Lu J, Xu BB, Zheng ZF, Xie JW, Wang JB, Lin JX, et al. CRP/prealbumin, a novel inflammatory index for predicting recurrence after radical resection in gastric cancer patients: *post hoc* analysis of a randomized phase III trial. *Gastric Cancer Off J Int Gastric Cancer Assoc Japanese Gastric Cancer Assoc* (2019) 22(3):536–45. doi: 10.1007/s10120-018-0892-0

20. Li XY, Yao S, He YT, Ke SQ, Ma YF, Lu P, et al. Inflammation-Immunity-Nutrition score: A novel prognostic score for patients with resectable colorectal cancer. *J Inflammation Res* (2021) 14:4577–88. doi: 10.2147/jir.S322260

21. Camp RL, Dolled-Filhart M, Rimm DL. X-Tile: a new bio-informatics tool for biomarker assessment and outcome-based cut-point optimization. *Clin Cancer Res An Off J Am Assoc Cancer Res* (2004) 10(21):7252–9. doi: 10.1158/1078-0432.Ccr-04-0713

22. Qi Q, Zhuang L, Shen Y, Geng Y, Yu S, Chen H, et al. A novel systemic inflammation response index (SIRI) for predicting the survival of patients with pancreatic cancer after chemotherapy. *Cancer* (2016) 122(14):2158–67. doi: 10.1002/cncr.30057

23. LC KA, Meugnier E, McLachlan GJ. Integrative mixture of experts to combine clinical factors and gene markers. *Bioinf (Oxford England)* (2010) 26 (9):1192–8. doi: 10.1093/bioinformatics/btq107

24. Candido J, Hagemann T. Cancer-related inflammation. *J Clin Immunol* (2013) 33 Suppl 1:S79–84. doi: 10.1007/s10875-012-9847-0

25. Coussens LM, Werb Z. Inflammation and cancer. *Nature* (2002) 420 (6917):860–7. doi: 10.1038/nature01322

26. Roth GS, Decaens T. Liver immunotolerance and hepatocellular carcinoma: Patho-physiological mechanisms and therapeutic perspectives. *Eur J Cancer (Oxford Engl 1990).* (2017) 87:101–12. doi: 10.1016/j.ejca.2017.10.010

27. Buonaguro L, Tagliamonte M, Petrizzo A, Damiano E, Tornesello ML, Buonaguro FM. Cellular prognostic markers in hepatocellular carcinoma. *Future Oncol (London England)* (2015) 11(11):1591–8. doi: 10.2217/fon.15.39

28. O'Rourke JM, Sagar VM, Shah T, Shetty S. Carcinogenesis on the background of liver fibrosis: Implications for the management of hepatocellular cancer. *World J Gastroenterology.* (2018) 24(39):4436–47. doi: 10.3748/wjg.v24.i39.4436

29. Oh TK, Choi YR, Cho JY, Yoon YS, Han HS, Park IS, et al. The high-sensitivity c-reactive Protein/Albumin ratio predicts long-term oncologic outcomes after curative resection for hepatocellular carcinoma. *J Clin Med* (2018) 7(6):139. doi: 10.3390/jcm7060139

30. Dunn GP, Old LJ, Schreiber RD. The immunobiology of cancer immunosurveillance and immunoediting. *Immunity* (2004) 21(2):137–48. doi: 10.1016/j.immuni.2004.07.017

31. Wu ES, Oduyebo T, Cobb LP, Cholakian D, Kong X, Fader AN, et al. Lymphopenia and its association with survival in patients with locally advanced cervical cancer. *Gynecologic Oncol* (2016) 140(1):76–82. doi: 10.1016/j.ygyno.2015.11.013

32. Cho Y, Park S, Byun HK, Lee CG, Cho J, Hong MH, et al. Impact of treatment-related lymphopenia on immunotherapy for advanced non-small cell lung cancer. *Int J Radiat Oncology Biology Physics* (2019) 105(5):1065–73. doi: 10.1016/j.ijrobp.2019.08.047

33. Tangkijvanich P, Anukulkarnkusol N, Suwangool P, Lertmaharit S, Hanvivatvong O, Kullavanijaya P, et al. Clinical characteristics and prognosis of hepatocellular carcinoma: analysis based on serum alpha-fetoprotein levels. *J Clin Gastroenterology.* (2000) 31(4):302–8. doi: 10.1097/00004836-200012000-00007

34. Wang X, Wang Q. Alpha-fetoprotein and hepatocellular carcinoma immunity. *Can J Gastroenterol Hepatology* (2018) 2018:9049252. doi: 10.1155/2018/9049252

35. Gomaa AI, Khan SA, Leen EL, Waked I, Taylor-Robinson SD. Diagnosis of hepatocellular carcinoma. *World J Gastroenterology.* (2009) 15(11):1301–14. doi: 10.3748/wjg.15.1301

36. Amini A, Masoumi Moghaddam S, Morris DL, Pourgholami MH. The critical role of vascular endothelial growth factor in tumor angiogenesis. *Curr Cancer Drug Targets* (2012) 12(1):23–43. doi: 10.2174/156800912798888956

37. Tugues S, Koch S, Gualandi L, Li X, Claesson-Welsh L. Vascular endothelial growth factors and receptors: anti-angiogenic therapy in the treatment of cancer. *Mol Aspects Med* (2011) 32(2):88–111. doi: 10.1016/j.mam.2011.04.004

38. Borzio M, Dionigi E, Rossini A, Marignani M, Sacco R, De Sio I, et al. External validation of the ITA.LI.CA prognostic system for patients with hepatocellular carcinoma: A multicenter cohort study. *Hepatol (Baltimore Md)* (2018) 67(6):2215–25. doi: 10.1002/hep.29662

frontiers | Frontiers in Oncology

TYPE Original Research
PUBLISHED 19 August 2022
DOI 10.3389/fonc.2022.968202

Check for updates

OPEN ACCESS

EDITED BY
Ravindra Deshpande,
Wake Forest School of Medicine,
United States

REVIEWED BY
Rajesh Kumar Kar,
Yale University, United States
Rui Liao,
First Affiliated Hospital of Chongqing Medical University, China
Alessandro Rizzo,
National Cancer Institute Foundation (IRCCS), Italy

*CORRESPONDENCE
Ying-Hong Shi
shi.yinghong@zs-hospital.sh.cn
Ying-Yong Hou
hou.yingyong@zs-hospital.sh.cn
Hao Zou
hzou@tsimage.cn

†These authors have contributed equally to this work

SPECIALTY SECTION
This article was submitted to Gastrointestinal Cancers: Hepato Pancreatic Biliary Cancers, a section of the journal Frontiers in Oncology

RECEIVED 13 June 2022
ACCEPTED 04 August 2022
PUBLISHED 19 August 2022

CITATION
Qu W-F, Tian M-X, Qiu J-T, Guo Y-C, Tao C-Y, Liu W-R, Tang Z, Qian K, Wang Z-X, Li X-Y, Hu W-A, Zhou J, Fan J, Zou H, Hou Y-Y and Shi Y-H (2022) Exploring pathological signatures for predicting the recurrence of early-stage hepatocellular carcinoma based on deep learning.
Front. Oncol. 12:968202.
doi: 10.3389/fonc.2022.968202

Exploring pathological signatures for predicting the recurrence of early-stage hepatocellular carcinoma based on deep learning

Wei-Feng Qu[1†], Meng-Xin Tian[2†], Jing-Tao Qiu[3†], Yu-Cheng Guo[3], Chen-Yang Tao[1], Wei-Ren Liu[1], Zheng Tang[1], Kun Qian[4], Zhi-Xun Wang[4], Xiao-Yu Li[3], Wei-An Hu[3], Jian Zhou[1], Jia Fan[1], Hao Zou[3,5*], Ying-Yong Hou[6*] and Ying-Hong Shi[1*]

[1]Department of Liver Surgery, Liver Cancer Institute, Zhongshan Hospital, Fudan University, Key Laboratory of Carcinogenesis and Cancer Invasion of Ministry of Education, Shanghai, China, [2]Department of General Surgery, Zhongshan Hospital, Fudan University, Shanghai, China, [3]Tsimage Medical Technology, Yihai Center, Shenzhen, China, [4]Department of Information and Intelligence Development, Zhongshan Hospital, Fudan University, Shanghai, China, [5]Center for Intelligent Medical Imaging & Health, Research Institute of Tsinghua University in Shenzhen, Shenzhen, China, [6]Department of Pathology, Zhongshan Hospital, Fudan University, Shanghai, China

Background: Postoperative recurrence impedes the curability of early-stage hepatocellular carcinoma (E-HCC). We aimed to establish a novel recurrence-related pathological prognosticator with artificial intelligence, and investigate the relationship between pathological features and the local immunological microenvironment.

Methods: A total of 576 whole-slide images (WSIs) were collected from 547 patients with E-HCC in the Zhongshan cohort, which was randomly divided into a training cohort and a validation cohort. The external validation cohort comprised 147 Tumor Node Metastasis (TNM) stage I patients from The Cancer Genome Atlas (TCGA) database. Six types of HCC tissues were identified by a weakly supervised convolutional neural network. A recurrence-related histological score (HS) was constructed and validated. The correlation between immune microenvironment and HS was evaluated through extensive immunohistochemical data.

Results: The overall classification accuracy of HCC tissues was 94.17%. The C-indexes of HS in the training, validation and TCGA cohorts were 0.804, 0.739 and 0.708, respectively. Multivariate analysis showed that the HS (HR= 4.05, 95% CI: 3.40-4.84) was an independent predictor for recurrence-free survival. Patients in HS high-risk group had elevated preoperative alpha-fetoprotein levels, poorer tumor differentiation and a higher proportion of microvascular invasion. The immunohistochemistry data linked the HS to local immune cell infiltration. HS was positively correlated with the expression level of peritumoral

$CD14^+$ cells (p= 0.013), and negatively with the intratumoral $CD8^+$ cells (p< 0.001).

Conclusions: The study established a novel histological score that predicted short-term and long-term recurrence for E-HCCs using deep learning, which could facilitate clinical decision making in recurrence prediction and management.

KEYWORDS

hepatocellular carcinoma, curative resection, recurrence, deep learning, pathological slides

Introduction

Hepatocellular carcinoma (HCC) is the sixth most common malignancy and the fourth leading cause of cancer related deaths worldwide (1). Several treatments including surgery, locoregional therapies, and immunotherapy have been adopted as standards of care according to different tumor stages (2–4). Curative resection offers a chance of improved survival for HCC patients, especially those with early-stage tumors that are defined as Barcelona Clinic Liver Cancer (BCLC) stages 0 and A (5). Although the 5-year survival rate can reach 70% in early-stage HCC patients (6), half of patients suffer recurrence after liver resection (7) due to the lack of approved adjuvant therapies. Therefore, the precise prediction of postoperative recurrence is urgently needed.

Common prognostic factors for predicting early-stage HCC recurrence include pathological features, clinical biomarkers and genetic signatures (8). Recently, Yuan et al. developed a CpG methylation signature to elucidate the recurrence patterns in early-stage HCC with concordance indexes (C-indexes) of approximately 0.7 in three datasets (9). Compared to traditional staging systems, radiomics models also showed favorable efficacy in the recurrence prediction of HCC patients within the Milan criteria (10). In terms of histological features, specific structures such as microvascular invasion (MVI) and tumor-infiltrating lymphocytes were associated with recurrence risk (11, 12). However, due to the high heterogeneity in HCC, valuable information based on whole-slide images (WSIs) has not been thoroughly detected. Furthermore, the correlation between pathological texture and recurrence remains unknown.

In the past decade, breakthroughs in artificial intelligence (AI) have made remarkable progress in cancer research (13, 14). With the increasingly high capacity of deep learning, a large amount of work involved in the histopathological fields has been carried out, including tumor diagnosis, subtyping, grading, staging, and prognostic prediction (15–17), as well as the identification of pathological features, biomarkers, and genetic changes (18, 19). The advent of digital WSIs of tissue has not only economized the great amount of time or manual labor needed but also potentiated mining of subvisual morphometric phenotypes and ultimately improved patient management or therapeutic decision-making. Previous studies have originally proposed survival indicators based on digital WSIs *via* deep learning (20, 21). Nevertheless, the existing computational methods can identify only basic HCC structures. Complex and rich information contained in architectural features such as the portal area and lymphocytes is still hampered to be expounded. Herein, we explored more distinctive histological features to further describe the recurrence patterns and clinicopathological information of early-stage HCC.

The present study successfully developed a convolutional neural network (CNN) based on six classes of HCC tissues (namely, tumor region, normal liver tissue, portal area, fibrosis, hemorrhage/necrotic area, and lymphocyte area) and constructed a histological score (HS) *via* least absolute shrinkage and selection operator (LASSO) Cox regression to assess patients' recurrence risk after hepatectomy. The novel model was validated in the three independent cohorts. By stratifying patients into different risk subgroups, their prognosis could be precisely appraised and multiomics characteristics were investigated.

Materials and methods

Patient cohort and study design

A total of 416 WSIs and 387 corresponding early-stage HCC patients who underwent radical resection at Zhongshan Hospital from January 2006 to December 2011 were retrospectively enrolled as the first dataset (Figure 1). The inclusion criteria were as follows: 1) pathologically proven HCC; 2) no neoadjuvant antitumor therapy; 3) Child–Pugh class A or B before surgery; and 4) BCLC stage 0-A. The exclusion criteria were as follows: 1) presence of other pathological types, such as intrahepatic cholangiocarcinoma (ICC) or combined hepatocellular cholangiocarcinoma (CHC); 2) previous

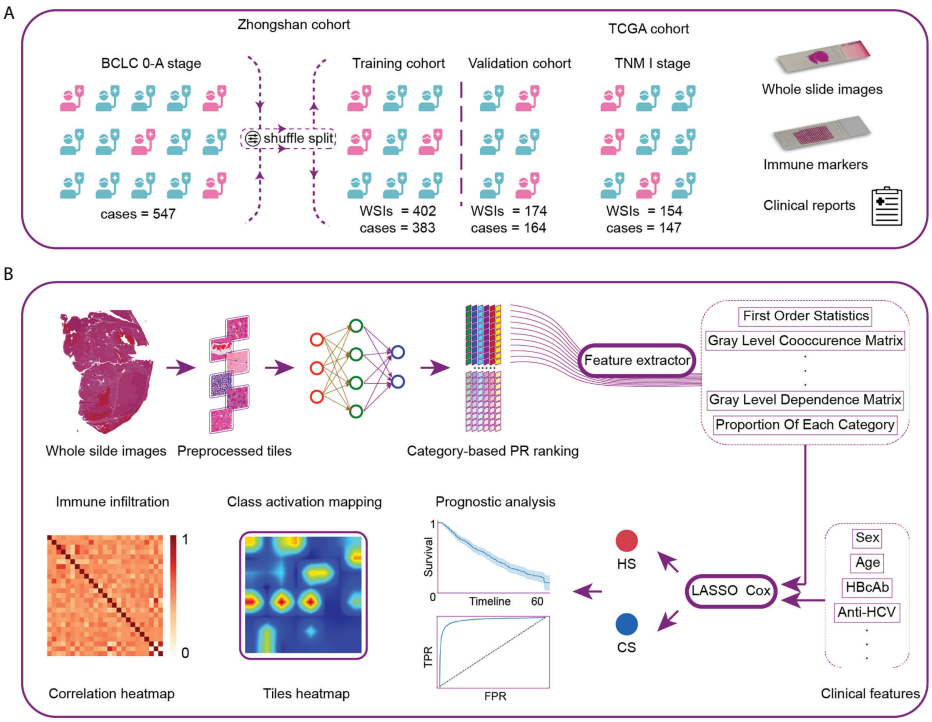

FIGURE 1
Workflow and general methodology of the study. **(A)** The recurrence-related scores were first developed and internally validated in a series of patients with BCLC stage 0-A treated by curative resection at Zhongshan Hospital. The scores were then externally validated by TNM-I stage patients in the TCGA cohort. **(B)** We first developed the neural network using 116 whole-slide images (WSIs) as the category-based training data. The network was then used to analyze the remaining WSIs and generate the classification maps. Pathological image features were extracted from typical tiles. Next, we constructed two recurrence prediction scores *via* LASSO-Cox. CS was composed of clinical and histological characteristics. HS was developed based on pure histological features. Finally, we analyzed the model discrimination ability, patient prognosis and local immune cell infiltration. TCGA, The Cancer Genome Atlas; PR, precision-recall; CS, combined score; HS, histological score; TPR, true positive rate; FPR, false positive rate.

antitumor treatment; 3) missing clinical information; and 4) death or disease recurrence within 1 month after resection. Data on tumor stages were collected according to the BCLC staging system (22) and China Liver Cancer (CNLC) (23) staging guidelines.

Following the same inclusion and exclusion criteria, another 160 patients who underwent curative partial hepatectomy at Zhongshan Hospital from October 2014 to December 2014 and 160 WSIs were enrolled as the second dataset. We combined the two datasets and randomized cases into the training and validation cohorts at a ratio of 7:3.

We enrolled 154 WSIs and 147 patients from The Cancer Genome Atlas (TCGA) database as the external validation cohort (https://portal.gdc.cancer.gov/). Due to the lack of information on BCLC staging, all the enrolled cases had tumor node metastasis (TNM) stage I disease, which fulfilled the criterion of BCLC stage 0-A.

The follow-up was censored in December 2019. Recurrence was the primary endpoint in the present study. HCC recurrence was defined as the appearance of a newly detected HCC tumor confirmed on two radiologic images, with or without an elevation in serum tumor markers. Time to recurrence (TTR) was defined as the time between surgery and recurrence or metastasis. Recurrence-free survival (RFS) and overall survival (OS) were the secondary endpoints. RFS was defined as the time from the date of hepatectomy to the date of recurrence, metastasis, death, or the last follow-up. OS was defined as the time between resection and death. The study obtained ethical approval from the Institutional Review Board of Zhongshan Hospital and complied with the standards of the Declaration of Helsinki. Informed consent was received from each patient before surgery.

Preparation of H&E staining and immunohistochemistry for immune markers

Hematoxylin and eosin (H&E) staining was performed on paraffin-embedded tissues that were at 4 μm thickness. Tissue

microarray (TMA) construction and immunohistochemistry for 28 immune markers were conducted as previously described (11, 24). Some of the previous data were used directly as a complement to the results (11).

Image annotation and processing

We randomly selected 116 WSIs for annotation in the Zhongshan cohort. Using ASAP 1.8, two pathologists manually annotated and fully examined the slides in six categories: tumor region, normal liver tissue, portal area, fibrosis, hemorrhage/necrotic area, and lymphocyte area. The annotated WSIs were divided into training, validation, and testing datasets at a ratio of 8:1:1. The annotated tissue areas were extracted based on the binary mask obtained by OTSU (25) and then divided into small squares, 299 pixels×299 pixels in size, called "tiles". After image incision, data enhancement methods were used to balance the number of tiles for the six categories (details are provided in the Supplementary Methods).

Standardization of TCGA diagnostic slides

Due to the disparity in the staining and scanning process between the Zhongshan and TCGA cohorts, the trained neural model could not be directly applied to the TCGA WSIs. We modified the traditional Reinhard algorithm (26) to standardize stainingin both the Zhongshan and TCGA cohorts.

Classification network

We mainly proposed training a classification network to discriminate six types of HCC tissues. Inception V3 (27) was used as the basic model. Classification maps were derived after image recognition. Morphological processing was utilized to optimize the original classification maps. We used the t-distributed stochastic neighbor embedding (t-SNE) algorithm to visualize the segmental results. The pathological signatures were then extracted from the ten tiles with the highest prediction probability for each type (details are provided in the Supplementary Methods).

Establishment of the histological score and combined score

LASSO Cox regression (9) was applied to obtain high-dimensional prognostic features in histology. With recurrence status and TTR as labels, a combined score (CS) was constructed by integrally analyzing the histological signatures and clinical markers. The clinical markers included sex, age, serum levels of alpha-fetoprotein (AFP) and alanine transaminase (ALT), and morphological information such as tumor number and size. In the same way, we constructed a histological score (HS) through pure histological features (details are provided in the online Supplementary Materials). The optimal cutoff value for survival time was obtained through the "survminer" package. The patients were then divided into high-risk and low-risk subgroups for further survival comparisons.

Correlation between HS and immune infiltration

To evaluate the correlation between the HS and immune infiltration conditions, we applied hierarchical clustering analysis for specific immune markers in the TMA. In the TCGA datasets, the CIBERSORT algorithm (28) was used to explore the quantity of tumor-infiltrating immune cells based on the transcriptome signature.

Statistical analysis

Continuous variables are expressed as the median (IQR) and were compared with using Mann–Whitney U test. Categorical variables are expressed as numbers and percentages, and were compared with the χ^2 test or Fisher's exact test. Kaplan–Meier curves with the log-rank test were used to compare survival. The LASSO Cox method was used to select independent factors associated with recurrence. Hazard ratios (HRs) and 95% confidence intervals (CIs) were also estimated by means of univariable and multivariable Cox analyses. A two-tailed p value> 0.05 was considered statistically significant. Model discrimination was assessed by the overall C-index, receiver operating characteristic (ROC) curve and net reclassification improvement (NRI) (29). Statistical analysis was performed using R-software 3.6.3 (R Foundation, Vienna, Austria) and SPSS ® 22.0 (IBM, Armonk, New York, USA).

Results

Patient demographics and clinical information

Supplementary Table S1 describes the demographic, clinical, and tumor characteristics of patients in the training and validation cohorts. The median ages in the training and validation cohorts were 53 years and 55 years, respectively. Most patients in both cohorts were male. More than 80% of patients were infected with hepatitis B virus (HBV) and diagnosed with liver cirrhosis. Over half of the patients

presented with elevated serum AFP levels in both cohorts (55.6% and 59.8%). Microvascular invasion was detected in 23.2% and 26.8% of patients in the training and validation cohorts, respectively. A majority of patients had a single lesion and were diagnosed as CNLC stage Ia. More patients were diagnosed with BCLC stage A than stage 0 in both cohorts. No significant differences were observed for the demographic information between the two cohorts.

After a median follow-up of 54.2 months (range, 3.0 to 64.6) for the Zhongshan population, 44.4% of patients (243/547) suffered tumor recurrence and 25.8% (141/547) died. The 1-, 3-, and 5-year recurrence rates were 17.1%, 33.1%, and 48.1%, respectively, and the 1-, 3-, and 5-year RFS rates were 82.2%, 66.4%, and 51.5%, respectively.

In terms of the TCGA cohort, the median follow-up time was 27.0 months (range, 1.1 to 115.9). A total of 38.8% of patients (57/147) suffered tumor recurrence and 21.1% (31/147) died. The 1-, 3-, and 5-year recurrence rates were 19.2%, 45.4%, and 62.0%, respectively, and the 1-, 3-, and 5-year RFS rates were 76.7%, 49.5%, and 34.5%, respectively.

Visualization of category-based HCC tissue

We first built the category-based model by training a classification network according to HCC tissue. The distribution of HCC tissues in a slide is displayed in Figure 2A. Corresponding histological images of the six categories before and after staining standardization are shown in Supplementary Figures S1A, B. Representative examples of the raw outputs of the classification network and their postprocessing results by morphology are revealed in Figure 2B, with different colors representing distinct tissue components. A visualization of a typical classification map in the TCGA cohort is shown in Supplementary Figure S1C.

After comprehensive training, we used the testing dataset to verify the performance of the computation network, which revealed an overall accuracy of 94.17%. Specifically, the accuracy values for normal liver tissue and tumor regions, shown in the confusion matrix (Figure 2C), were 0.984 and 0.950, respectively. A precision-recall (PR) curve rather than an ROC curve was applied to evaluate the model to minimize the imbalance. The area under the curve (AUC) values of each tissue type, except for the portal area, in our classification model exceeded 0.920 with the highest in tumor region classification (AUC= 0.997) (Figure 2D). Figure 2E shows the t-SNE visualization of the classification results. One thousand tiles were randomly selected for each tissue category.

We then used class activation mapping (CAM) (30) of the last convolution layer to visualize the outputs of each tissue category, where redder and bluer heatmaps indicated regions with higher or lower interest, respectively (Figure 2F).

Signature extraction and construction of prognostic scores

Next, we analyzed all 416 WSIs in the training cohort using the classification network and extracted pathological signatures from tiles of each type of HCC tissue. A total of 133 signatures and their coefficients were derived from LASSO Cox analysis (Supplementary Figure S2). Univariable Cox analysis of signatures that had a significant impact on RFS is shown in Supplementary Table S2.

HS and CS were then obtained by the sum of products by indexes and coefficients (details are provided in the Supplementary Methods). A calibration curve was constructed to evaluate the prediction accuracy. HS showed great concordance between the predicted and observed recurrence probabilities in the training, validation and TCGA cohorts (Figures 3A–C). Similarly, CS performed well in the training and validation cohorts (Supplementary Figure S3). To further compare the prediction reliability between the new scores and traditional biomarkers and stages, we carried out ROC curve analysis based on the cases in the training and validation cohorts. In terms of 1-year RFS, the AUC values of HS and CS were 0.837 and 0.857, respectively, much higher than those of clinical indicators such as AFP or liver cirrhosis, and the CNLC or BCLC staging systems (Figure 3D). The AUC values of HS and CS reached 0.857 and 0.852 for 3-year RFS prediction and 0.826 and 0.845 for 5-year RFS prediction, respectively (Figures 3E, F).

Comparison of HS and CS in predictive accuracy

The C-indexes of HS, CS and clinical signatures were calculated to estimate the possibility of using histological textures as a substitute for clinical indicators. Compared to the clinical signatures, HS and CS presented higher C-indexes in the Zhongshan datasets (Table 1). Specifically, the C-indexes of HS were 0.804, 0.739 and 0.708 in the training, validation and TCGA cohorts, respectively. Both HS and CS performed better than clinical signatures in RFS prediction (Supplementary Figure S4). Ultimately, ROC curves in the two Zhongshan datasets showed no significant differences between HS and CS for 1-year, 3-year, or 5-year RFS prediction (Supplementary Figure S5, Supplementary Table S3). The NRI elucidated the quantitative difference between HS and CS in TTR prediction (Supplementary Figure S6). Subsequently, the CS model was superior to HS in all three periods with a subtle advantage, but statistical significance was not reached ($p > 0.1$).

Survival prediction of novel pathological predictors

Optimal cutoff values for HS and CS were determined using the "survminer" package (31). All the patients were then divided into a

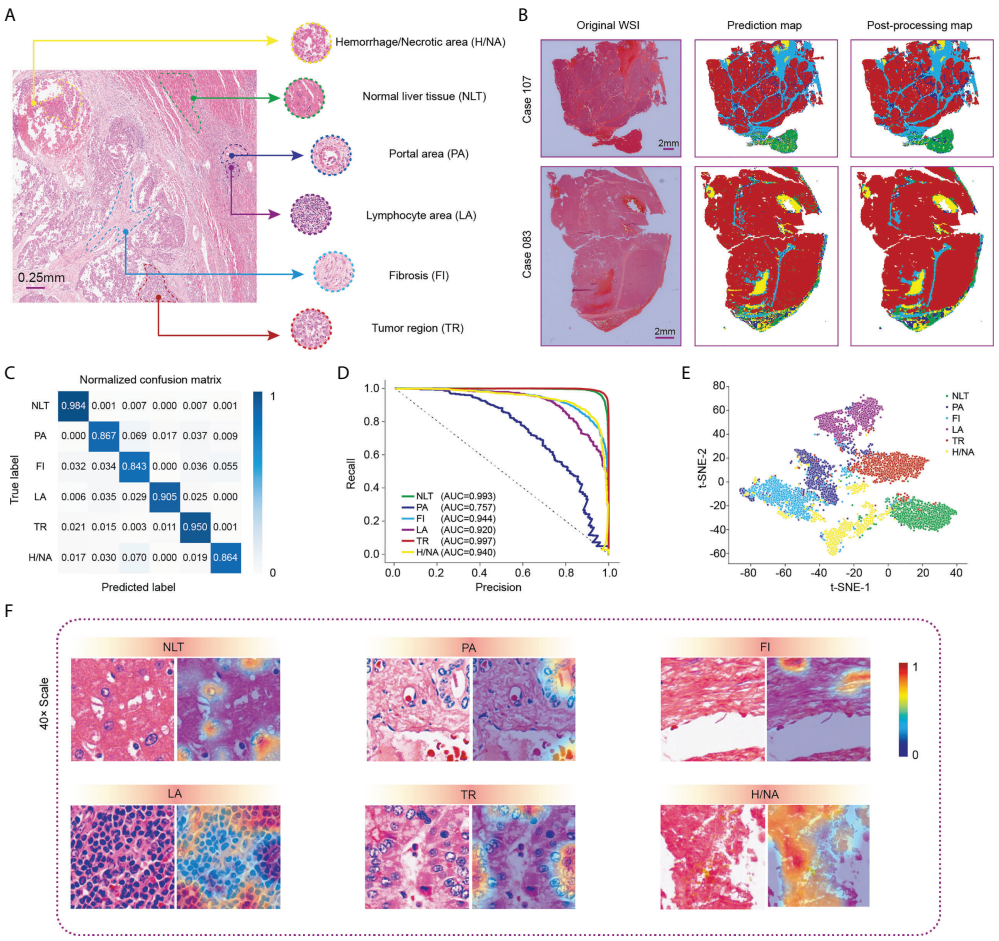

FIGURE 2
Visualization of WSI classification for HCC tissue in the Zhongshan cohort. **(A)** Six classic categories of HCC tissue, including normal liver tissue (NLT), portal area (PA), fibrosis (FI), lymphocyte area (LA), tumor region (TR) and hemorrhage/necrotic area (H/NA). **(B)** Two representative outputs of the classification network. Red represents TR, green represents NLT, light blue represents FI, dark blue represents PA, purple represents LCA, and yellow represents H/NA. **(C)** Precision-recall curve of category-based sampling. **(D)** Normalized confusion matrix for the classification network. **(E)** t-SNE analysis for visualization of six tissue categories. **(F)** CAM results for visualization of HCC tissues. HCC, hepatocellular carcinoma; CAM, class activation mapping; t-SNE, t-distributed stochastic neighbor embedding.

high-risk group (HS> -0.1605954, CS> 3.417892) and a low-risk group (HS≤ -0.1605954, CS≤ 3.417892). Figure 4 and Supplementary Figure S7 depict the survival curves of HS and CS, respectively. Generally, patients in the high-risk group from the three cohorts faced notable susceptibility to postoperative recurrence and poorer survival.

Prognostic predictors of RFS in early-stage HCC

We performed Cox proportional hazards regression analysis to explore the independent predictors for RFS in the training and validation cohorts (Table 2). Eleven candidates were proven to be significant in the univariable analysis and were then evaluated with multivariable Cox regression. The multivariable analysis revealed that MVI (HR= 1.459, 95% CI: 1.094-1.948) and HS (HR= 4.054, 95% CI: 3.397-4.838) were significant indicators.

The correlation between HS and clinicopathological characteristics

As shown in Figure 5, the clinical characteristics and prognostic value of HS were compared in the different risk subgroups, namely, the low-risk group (n= 332) and the high-risk group (n= 215). Compared to patients in the low-risk group, more patients in the high-risk group had elevated AFP levels (65.6% vs 51.2%). Moreover, HCCs in the high-risk group were characterized by poorer tumor differentiation, and a higher proportion of MVI.

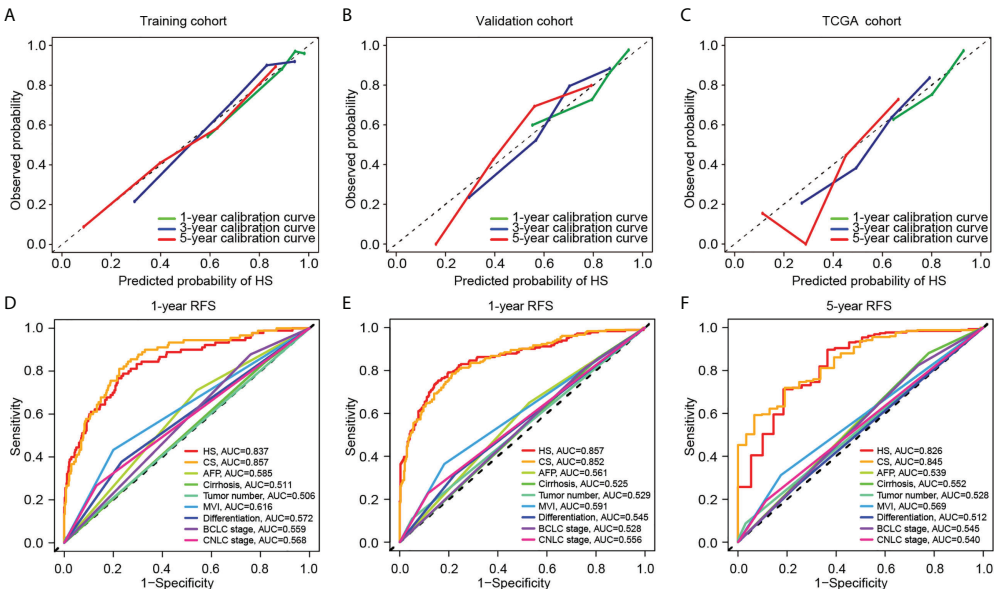

FIGURE 3
Comparison of predictive performance between two novel models. Upper: The calibration curves for TTR of HS in the training **(A)**, validation **(B)**, and TCGA cohort **(C)**. Down: The ROC curves for 1-year **(D)**, 3-year **(E)** and 5-year **(F)** RFS based on different clinicopathological features and stages. TCGA, The Cancer Genome Atlas; RFS, recurrence-free survival; HS, histological score; CS, combined score; AFP, alpha-fetoprotein; MVI, microvascular invasion; BCLC, Barcelona Clinic Liver Cancer; CNLC, China Liver Cancer; AUC, area under the curve.

Seventy-eight (23.5%) patients in the low-risk group experienced recurrence. Conversely, 76.7% of patients in the high-risk group suffered recurrence during the follow-up. In particular, HS was proven to be a prognostic factor in all the subgroups in terms of patients' clinicopathological characteristics.

The histological markers including proliferation indexes, therapeutic targets, and specific diagnostic markers have been reported to be an efficient indicator for HCC diagnosis and prognosis after resection (32–34). The immunohistochemistry (IHC) and quantitative analysis for six markers was performed in 160 patients (from October 2014 to December 2014). Compared to HS low-risk group, patients in the high-risk group had a higher expression of heat shock protein 70 (HSP70, p= 0.01). A slightly higher proportion of Ki-67$^+$ cells was observed in the high-risk group although significance was not reached (Supplementary Figure S8).

The correlation between pathological subtype and histologic features was also assessed. The results revealed that more patients (12%) in the HS high-risk subgroup were diagnosed with macrotrabecular-massive HCC (MTM-HCC) compared to 5% in the low-risk subgroup (Supplementary Figure S9).

The correlation between HS and the immune microenvironment

Using TMA data, we examined the expression patterns and distributions of 14 immune markers in 175 HCC patients with early-stage HCC (35). To investigate the relationship between HS and local immune status, we carried out clustering and correlation analysis (Figure 6A). We found that HS was positively correlated with the expression of peritumoral CD14 (p= 0.013, R= 0.187), but negatively correlated with the infiltration of intratumoral CD8 (p< 0.001, R= 0.275). Typical immunohistochemical images of the two markers are shown in Figure 6B. To investigate the interrelation between immune markers, we performed

TABLE 1 C-indexes of the novel scores.

Cohort	HS	CS	Clinical signatures
Training	0.804 (0.771-0.837)	0.809 (0.777-0.840)	0.653 (0.611-0.695)
Validation	0.739 (0.686-0.792)	0.754 (0.705-0.802)	0.686 (0.630-0.742)
TCGA	0.708 (0.635-0.780)		

∗ Values are presented as C-index (95% confidential interval). HS, histological score; CS, combined score; TCGA, The Cancer Genome Atlas.

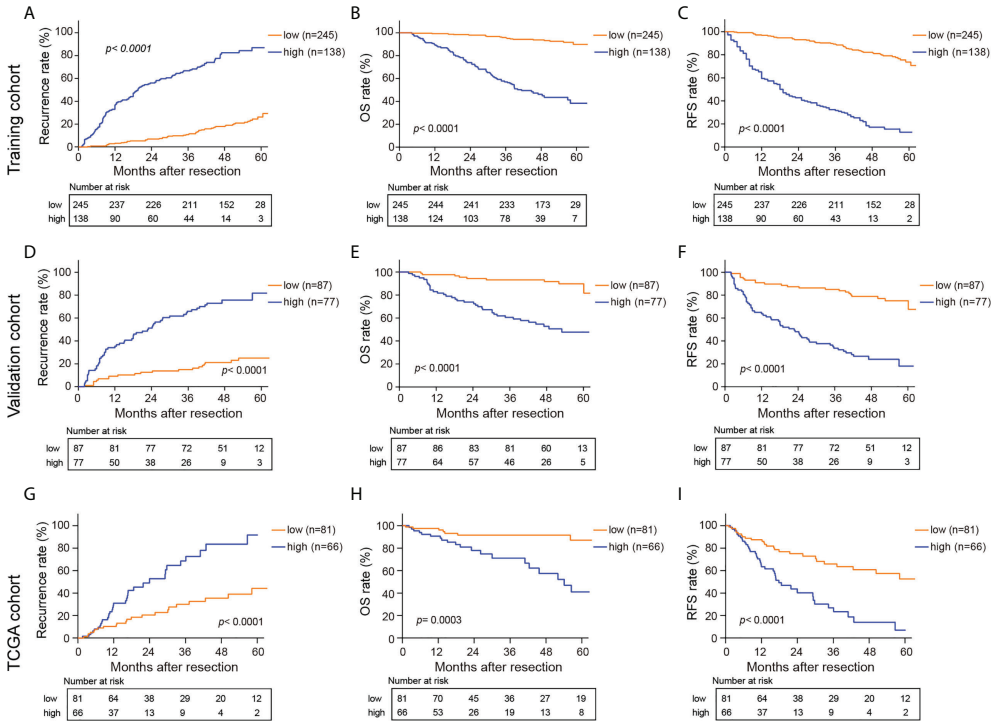

FIGURE 4
Kaplan-Meier curves for recurrence rate, OS, and RFS in the training **(A–C)**, validation **(D–F)** and TCGA cohorts **(G–I)** based on HS. HS, histological score; OS, overall survival; RFS, recurrence free survival.

correlation analysis in different risk subgroups of HS (Figures 6C, D). Compared to the low-risk group, the predominant immune cells in the high-risk group were characterized by CD66-, CD68-, CD103- and CXCR5-positive cells infiltrating both tumoral and peritumoral tissues, which implied that macrophages or neutrophils may play a potential role in the progression of recurrence.

The immune microenvironment of cases in the TCGA datasets was investigated by CIBERSORT algorithm (28). The boxplot revealed significantly higher expression of monocytes and lower expression of M2 macrophages in the HS low-risk subgroup (Figure 6E). HS was positively correlated with the infiltration of M2 macrophages (p= 0.011, R=0.275, Figure 6F). Similar findings suggested an increased interaction among

TABLE 2 Cox proportional hazards regression model showing the association of variables with RFS.

Variables	Univariate analysis			Multivariate analysis		
	HR	95%CI	*p* value	HR	95%CI	*p* value
HBsAg (yes/no)	1.487	(1.030-2.146)	0.034	1.066	(0.728-1.560)	0.743
Albumin, g/L	0.945	(0.938-0.993)	0.013	0.978	(0.948-1.009)	0.159
AFP (>20/≤20, ng/mL)	1.459	(1.125-1.890)	0.004	1.095	(0.835-1.435)	0.512
GGT, U/L	1.001	(1.000-1.003)	0.045	1.000	(0.999-1.002)	0.516
PT, s	1.131	(1.008-1.269)	0.037	1.047	(0.935-1.174)	0.425
Liver cirrhosis (yes/no)	1.666	(1.136-2.442)	0.008	1.389	(0.922-2.092)	0.116
Tumor number (multiple/single)	1.430	(1.009-2.027)	0.045	1.361	(0.870-2.129)	0.177
Tumor diameter, cm	1.108	(1.059-1.159)	<0.001	1.029	(0.981-1.079)	0.245
MVI (yes/no)	1.931	(1.475-2.527)	<0.001	1.459	(1.094-1.948)	0.010
Tumor differentiation (Edmondson-Steiner grade III-IV/I-II)	1.341	(1.018-1.765)	0.037	1.039	(0.782-1.380)	0.794
Histological score	4.263	(3.616-5.025)	<0.001	4.054	(3.397-4.838)	<0.001

∗Values are presented as HR and 95%CI. HR, hazard ratio; CI, confidence interval; HBsAg, Hepatitis B virus surface antigen; AFP, α-fetoprotein; GGT, γ-glutamyl transpeptidase; PT, prothrombin time; MVI, micro vascular invasion.

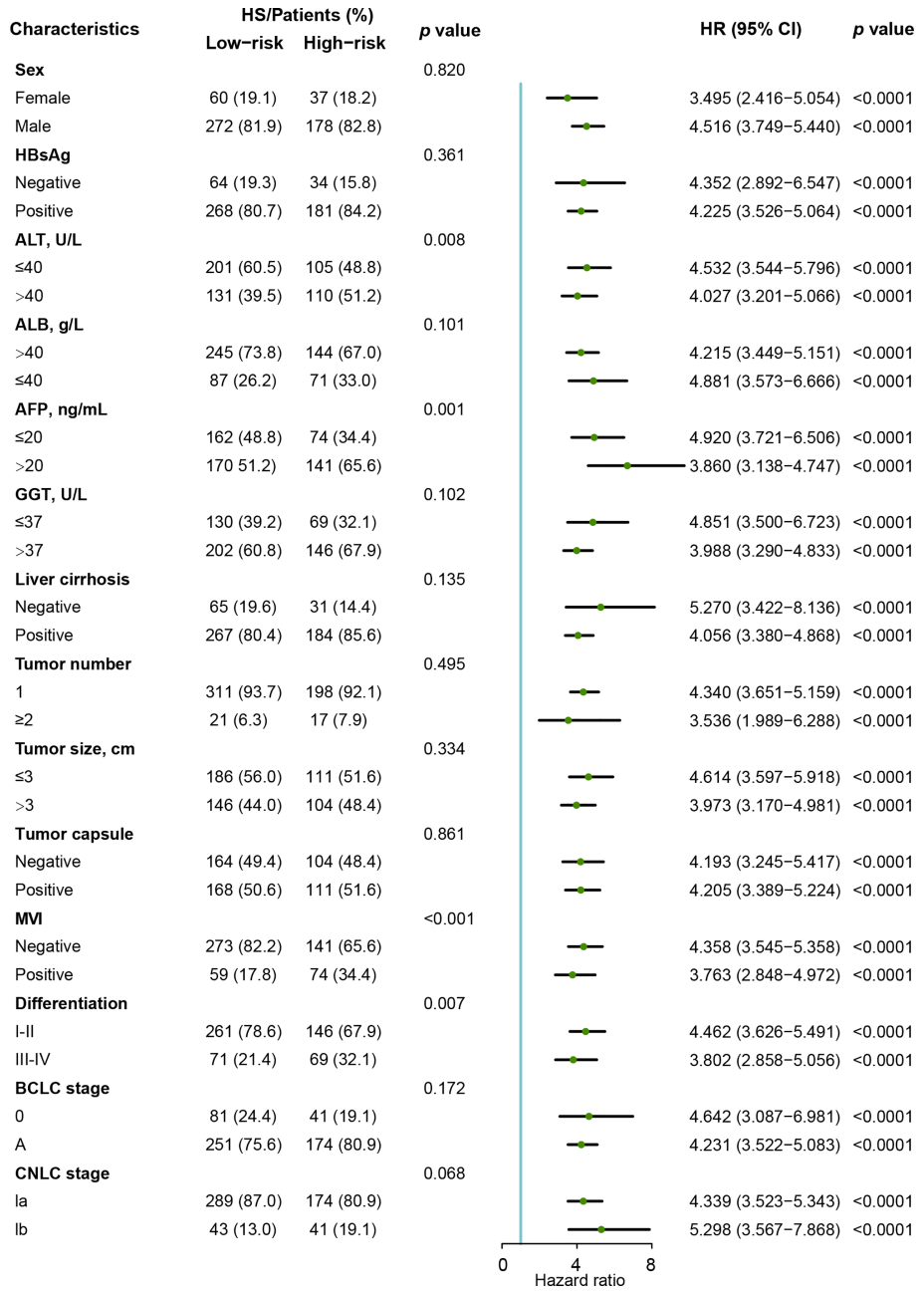

FIGURE 5
Forest plot of recurrence-free survival based on HS in the Zhongshan cohort. HS, histological score; HR, hazard ratio. ; CI, confidence interval; AFP, α-fetoprotein; ALT, alanine aminotransferase; ALB, albumin; GGT, γ-glutamyl transpeptidase; MVI, micro vascular invasion; CNLC, China Liver Cancer Staging; BCLC, Barcelona Clinic Liver Cancer.

macrophages, dendritic cells and other immune cells based on the corrplots in the TCGA database (Supplementary Figure S10).

Discussion

The emergence of AI has reformed multiple aspects of cancer management. The combination of deep learning and digital WSIs has alleviated the labor in detection and revealed the decent accuracy and efficacy for prognostic models in different solid tumors. The recurrence of early-stage HCC after resection remains a major obstacle in curative treatment. Although multiomics analysis highlighted potential recurrence-related determinants and therapeutic targets (8), its high cost and complexity have hindered its prevalent utilization. Herein, we

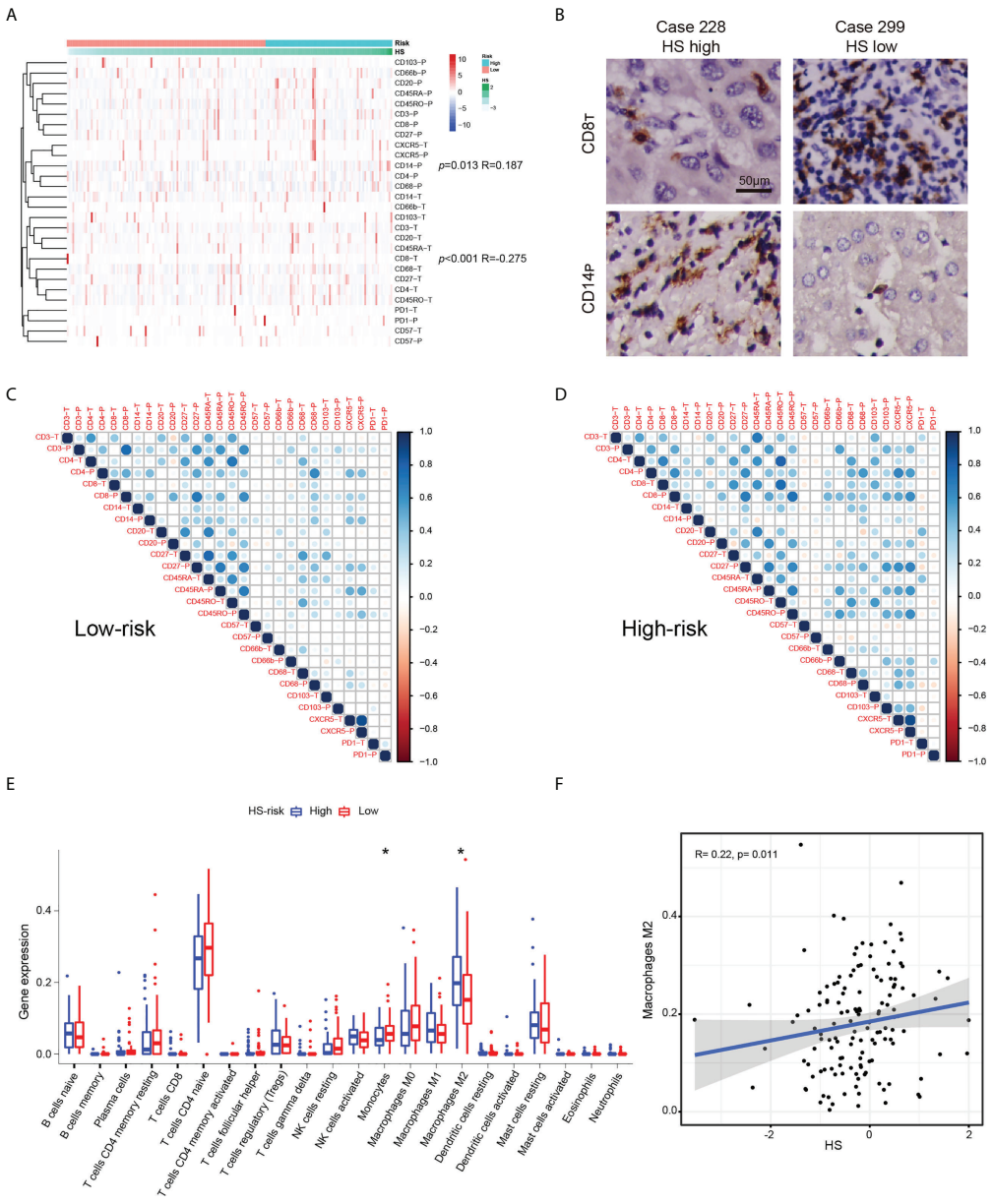

FIGURE 6
The relationship between HS and immune infiltration condition. **(A)** Heatmap and cluster analysis of the Zhongshan TMA. **(B)** Typical immunohistochemical pictures of $CD8_T$ AND $CD14_P$. **(C)** The corrplots of immune markers in the HS low-risk group. **(D)** The interaction analysis of immune markers in the HS high-risk group. **(E)** Boxplot of immune cells in the TCGA cohort. Data are compared using Wilcoxon test. *p < 0.05;. **(F)** Correlation analysis between HS and M2macrophages in the TCGA cohort. HS, histological score; TCGA, The Cancer Genome Atlas.

integrated a neural network with the massive WSIs of HCC patients in BCLC stage 0-A and successfully developed an efficient recurrence prediction index that was prognostic of OS, TTR, and RFS. The novel index was validated in three independent cohorts, demonstrating the generalizability of our approach. By analyzing substantial TMA data, we found that immune infiltration status could potentially provide prognostically valuable information on histological texture.

Recent studies on AI reported novel prognostic models for HCC patients based on pathological images. Saillard et al. established two independent scores using an unsupervised neural network algorithm and attention mechanism according to tumoral or nontumoral annotated tiles (20). Both models showed high accuracy in survival prediction and strong correlations between clinical characteristics. Gao et al. innovatively divided HCC slides into four categories,tumor

tissue, normal liver tissue, stroma, and necrosis, and then discriminated the features with high AUC values (21). The study developed and validated an efficient survival prediction model based on a large number of WSIs.

In these two previous studies, pathological signatures were directly generated and extracted by traditional CNNs. CNNs are usually regarded as a "black box", in which the data are processed through complex computing layers; thus, it is difficult to concretize and interpret the relevant features of samples. In the present research, we manually input abundant signatures of the most relevant tiles, automatically screened the signatures with the recurrence time as the labels *via* LASSO Cox regression, and visually presented the weight of each signature. This procedure bypassed the need for the manual recognition of numerous postprocess tiles. In addition, the image signatures that came from empirical utilization ensured the feasibility (36, 37).

Compared to reported studies, our study has advantages in terms of multicategory training, heatmap visualization, a more accurate prediction of recurrence and multifaceted analysis. HCC is highly heterogeneous with regard to not only genetics or epigenetics but also histology. Despite the classic histological categories mentioned above, the portal area and lymphocyte area are also important structures. Recently, tertiary lymphoid structures were proven to be a favorable factor for prognosis and recurrence status (38), and immune infiltration conditions are becoming more determinant in precision therapy (39). The portal area is a connective tissue among hepatic lobules consisting of branches of the hepatic artery, portal vein and hepatic ducts, in which lymphatic vessels and nerve fibers exist. It was reported that the number of portal areas and inflammation or iron deposition around the portal area were associated with the pathogenesis of HCC (40, 41). Herein, these two structures were originally annotated and trained in the study. The AUC value for the portal area was 0.757, lower than that of the other five tissues, which could be caused by poor structural purity and inadequate amounts. Technically, modified image standardization balanced the color differences among tiles, which raised the overall recognition accuracy for HCC structures up to 94.17%. We also applied the CAM method to visualize the importance of the local structure. As shown in Figure 2, cells attracted more attention for recurrence than cell-free areas such as fibrosis and necrosis areas, which made it easier for us to intuitively understand the microscopic information.

Subsequently, we established two recurrence prediction scores *via* LASSO Cox analysis and derived each score through the overall WSIs to maximally preserve the pathological signatures of all sections. Both scores showed great congruence with the recurrence probability and survival. No significant difference was found between HS and CS under NRI analysis, which consequently suggested the feasibility of the potential replacement of important clinical characteristics with pure histological features. In Gao et al's research, the newly constructed score aimed at OS and its median C-indexes reached 0.731 and 0.713 in two cohorts. Therefore, we specifically targeted recurrence conditions after resection and complemented the recurrence-related information in the TCGA database, which was not included in Gao's study. In our study, the C-indexes of HS for TTR prediction reached 0.804, 0.739 and 0.708 in the training, validation and TCGA cohorts, respectively.

We compared clinicopathological characteristics between the two risk subgroups. Notably, a larger proportion of MTM-HCC was found in the HS high-risk group, indicating that invisible information processed by deep learning could be explained by the specific texture of tumor cells. In contrast to Saillard et al's dissected tiles of MTM structures, we analyzed the pathological subtype by a whole slide, which was closer to the definition of MTM-HCC (42). As a rare and highly malignant tumor subtype of HCC, MTM-HCC was proven to be correlated with an increased recurrence risk and poor survival (42, 43). Our study supported this finding. Staining markers for pathological evaluation have gained increasing attention in postoperative management. HSP70 is identified as an upregulated marker in HCC components and performs its role at several points of apoptotic signaling (33). A significant difference was observed in the expression of HSP70 between two risk subgroups, which was consistent with the previous study (44).

The immune microenvironment plays a crucial role in tumor progression and recurrence. Using TMA data, we fully explored the relationship between HS and immune infiltration. CD14-P and CD8-T were shown to be of significance. Our results were supported by a previous study showing that high densities of both CD3(+) and CD8(+) T cells in both the interior and margin were significantly associated with a low rate of recurrence (p= 0.007) and prolonged RFS (p= 0.002) (45). A recent study reported that a high density of marginal $CCR1^+$ $CD14^+$ monocytes positively correlated with CCL15 expression and was an independent index for dismal survival (46). Moreover, peritumoral monocytes were found to promote HCC progression by inducing cancer cell autophagy (47), which probably led to the dense expression of CD14-P in patients with high recurrence risk.

From TCGA immune data, we observed that more M2 macrophages were aggregated in the tumor tissues of patients with high HS. This finding was consistent with the prognostic value and tumor biochemical modulation of M2 macrophages (48).

The correlation analysis in both the Zhongshan and TCGA cohorts implied different interaction patterns of immune markers. The stronger interactive effect of macrophages and dendritic cells in the HS high-risk subgroup highlighted the important status of antigen presentation during tumor progression. The result may offer new prospects for further fundamental research.

There are several limitations in our study. First, our training data came from a single institution. There may be image inconsistency in model validation; thus, standardization is an

essential step for processing. Second, the patients in both cohorts were predominantly infected with HBV, which reduced the representativity of an extensive HCC population. A more rigorous external validation dataset needs to be validated before routine clinical use. Third, our research carried out deep learning at the histologic level of WSIs. Further study could focus on single-cell discrimination, such as lymphocytes and cancer-associated fibroblasts. Fourth, AI-based study of multiomics sequencing information, more staining markers or images of multicomplex immunofluorescence could be further combined into the prediction model.

Conclusion

In conclusion, the study proposed an efficient recurrence prediction score for patients with early-stage HCC based on deep learning. The prognostic pathological features identified in digital WSIs composed a computable index to discriminate patients in terms of their relapse risk. The new model derived by weakly supervised training facilitated the classification process of typical HCC tissues, depicted the immune infiltration condition in intratumoral and peritumoral structures, and highlighted the clinical characteristics that were significant to prognosis. Further AI research may pay attention to interpretation at the cellular level and the integration of therapeutic decisions or multiomics sequencing.

Data availability statement

The raw data supporting the conclusions of this article will be made available by the authors, without undue reservation.

Ethics statement

The study obtained ethical approval from the Institutional Review Board of Zhongshan Hospital (B2021-611) and complied with the standards of the Declaration of Helsinki. Informed consent was received from each patient before the research.

Author contributions

(I) Conception and design: W-FQ, M-XT, Y-HS; (II) Administrative support: Y-HS, Y-YH, HZ; (III) Provision of study materials or patients: Y-HS, Y-YH, HZ, JZ, JF; (IV) Collection and assembly of data: W-FQ, M-XT, J-TQ, Y-CG, W-RL, ZT, C-YT, W-AH, X-YL, Z-XW, KQ; (V) Data analysis and interpretation: W-FQ, M-XT, J-TQ; (VI) Manuscript writing: W-FQ, M-XT, J-TQ; (VII) Final approval of manuscript: All authors.

Funding

This work was supported by grants from the National Natural Science Foundation of China (No.81773067, 81902963, 882073217, 82073218, and 82003084), Shanghai Sailing Program (19YF1407800), Intelligent Chronic Disease Management System Based on Edge and Cloud Computing Cooperation (2020-002), Shanghai Municipal Science and Technology Major Project (Grant No. 2018SHZDZX05). Shanghai Municipal Key Clinical Specialty. CAMS Innovation Fund for Medical Sciences (CIFMS) (2019-I2M-5-058). National Key R&D Program of China (2020YFE0202200, 2018YFF0301102 and 2018YFF0301105).

Conflict of interest

The authors declare that the research was conducted in the absence of any commercial or financial relationships that could be construed as a potential conflict of interest.

Publisher's note

All claims expressed in this article are solely those of the authors and do not necessarily represent those of their affiliated organizations, or those of the publisher, the editors and the reviewers. Any product that may be evaluated in this article, or claim that may be made by its manufacturer, is not guaranteed or endorsed by the publisher.

Supplementary material

The Supplementary Material for this article can be found online at: https://www.frontiersin.org/articles/10.3389/fonc.2022.968202/full#supplementary-material

References

1. Bray F, Ferlay J, Soerjomataram I, Siegel RL, Torre LA, Jemal A. Global cancer statistics 2018: GLOBOCAN estimates of incidence and mortality worldwide for 36 cancers in 185 countries. *CA Cancer J Clin* (2018) 68(6):394–424. doi: 10.3322/caac.21492

2. Llovet JM, De Baere T, Kulik L, Haber PK, Greten TF, Meyer T, et al. Locoregional therapies in the era of molecular and immune treatments for hepatocellular carcinoma. *Nat Rev Gastroenterol Hepatol* (2021) 18(5):293–313. doi: 10.1038/s41575-020-00395-0

3. Rizzo A, Ricci AD, Gadaleta-Caldarola G, Brandi G. First-line immune checkpoint inhibitor-based combinations in unresectable hepatocellular carcinoma: current management and future challenges. *Expert Rev Gastroenterol Hepatol* (2021) 15(11):1245–51. doi: 10.1080/17474124.2021.1973431

4. De Lorenzo S, Tovoli F, Barbera MA, Garuti F, Palloni A, Frega G, et al. Metronomic capecitabine vs. best supportive care in child-pugh b hepatocellular carcinoma: a proof of concept. *Sci Rep* (2018) 8(1):9997. doi: 10.1038/s41598-018-28337-6

5. Marrero JA, Kulik LM, Sirlin CB, Zhu AX, Finn RS, Abecassis MM, et al. Diagnosis, staging, and management of hepatocellular carcinoma: 2018 practice guidance by the american association for the study of liver diseases. *Hepatology* (2018) 68(2):723–50. doi: 10.1002/hep.29913

6. Tsilimigras DI, Bagante F, Sahara K, Moris D, Hyer JM, Wu L, et al. Prognosis after resection of barcelona clinic liver cancer (BCLC) stage 0, a, and b hepatocellular carcinoma: A comprehensive assessment of the current BCLC classification. *Ann Surg Oncol* (2019) 26(11):3693–700. doi: 10.1245/s10434-019-07580-9

7. Tabrizian P, Jibara G, Shrager B, Schwartz M, Roayaie S. Recurrence of hepatocellular cancer after resection: patterns, treatments, and prognosis. *Ann Surg* (2015) 261(5):947–55. doi: 10.1097/SLA.0000000000000710

8. Jiang Y, Sun A, Zhao Y, Ying W, Sun H, Yang X, et al. Proteomics identifies new therapeutic targets of early-stage hepatocellular carcinoma. *Nature* (2019) 567 (7747):257–61. doi: 10.1038/s41586-019-0987-8

9. Qiu J, Peng B, Tang Y, Qian Y, Guo P, Li M, et al. CpG methylation signature predicts recurrence in early-stage hepatocellular carcinoma: Results from a multicenter study. *J Clin Oncol* (2017) 35(7):734–42. doi: 10.1200/JCO.2016.68.2153

10. Ji GW, Zhu FP, Xu Q, Wang K, Wu MY, Tang WW, et al. Radiomic features at contrast-enhanced CT predict recurrence in early stage hepatocellular carcinoma: A multi-institutional study. *Radiology* (2020) 294(3):568–79. doi: 10.1148/radiol.2020191470

11. Liu WR, Tian MX, Tang Z, Fang Y, Zhou YF, Song SS, et al. Nine-factor-based immunohistochemistry classifier predicts recurrence for early-stage hepatocellular carcinoma after curative resection. *Br J Cancer* (2020) 123(1):92–100. doi: 10.1038/s41416-020-0864-0

12. Lim KC, Chow PK, Allen JC, Chia GS, Lim M, Cheow PC, et al. Microvascular invasion is a better predictor of tumor recurrence and overall survival following surgical resection for hepatocellular carcinoma compared to the milan criteria. *Ann Surg* (2011) 254(1):108–13. doi: 10.1097/SLA.0b013e31821ad884

13. Hosny A, Parmar C, Quackenbush J, Schwartz LH, Aerts H. Artificial intelligence in radiology. *Nat Rev Cancer* (2018) 18(8):500–10. doi: 10.1038/s41568-018-0016-5

14. Bhinder B, Gilvary C, Madhukar NS, Elemento O. Artificial intelligence in cancer research and precision medicine. *Cancer Discov* (2021) 11(4):900–15. doi: 10.1158/2159-8290.CD-21-0090

15. Bera K, Schalper KA, Rimm DL, Velcheti V, Madabhushi A. Artificial intelligence in digital pathology - new tools for diagnosis and precision oncology. *Nat Rev Clin Oncol* (2019) 16(11):703–15. doi: 10.1038/s41571-019-0252-y

16. Ahn JC, Connell A, Simonetto DA, Hughes C, Shah VH. Application of artificial intelligence for the diagnosis and treatment of liver diseases. *Hepatology* (2021) 73(6):2546–63. doi: 10.1002/hep.31603

17. Campanella G, Hanna MG, Geneslaw L, Miraflor A, Werneck Krauss Silva V, Busam KJ, et al. Clinical-grade computational pathology using weakly supervised deep learning on whole slide images. *Nat Med* (2019) 25(8):1301–9. doi: 10.1038/s41591-019-0508-1

18. Coudray N, Ocampo PS, Sakellaropoulos T, Narula N, Snuderl M, Fenyo D, et al. Classification and mutation prediction from non-small cell lung cancer histopathology images using deep learning. *Nat Med* (2018) 24(10):1559–67. doi: 10.1038/s41591-018-0177-5

19. Liao H, Long Y, Han R, Wang W, Xu L, Liao M, et al. Deep learning-based classification and mutation prediction from histopathological images of hepatocellular carcinoma. *Clin Transl Med* (2020) 10(2):e102. doi: 10.1002/ctm2.102

20. Saillard C, Schmauch B, Laifa O, Moarii M, Toldo S, Zaslavskiy M, et al. Predicting survival after hepatocellular carcinoma resection using deep learning on histological slides. *Hepatology* (2020) 72(6):2000–13. doi: 10.1002/hep.31207

21. Shi JY, Wang X, Ding GY, Dong Z, Han J, Guan Z, et al. Exploring prognostic indicators in the pathological images of hepatocellular carcinoma based on deep learning. *Gut* (2021) 70(5):951–61. doi: 10.1136/gutjnl-2020-320930

22. Llovet JM, Bru C, Bruix J. Prognosis of hepatocellular carcinoma: the BCLC staging classification. *Semin Liver Dis* (1999) 19(3):329–38. doi: 10.1055/s-2007-1007122

23. Xie DY, Ren ZG, Zhou J, Fan J, Gao Q. 2019 Chinese clinical guidelines for the management of hepatocellular carcinoma: Updates and insights. *Hepatobiliary Surg Nutr* (2020) 9(4):452–63. doi: 10.21037/hbsn-20-480

24. Gao Q, Qiu SJ, Fan J, Zhou J, Wang XY, Xiao YS, et al. Intratumoral balance of regulatory and cytotoxic t cells is associated with prognosis of hepatocellular carcinoma after resection. *J Clin Oncol* (2007) 25(18):2586–93. doi: 10.1200/JCO.2006.09.4565

25. Otsu N. A threshold selection method from gray-level histograms. *IEEE Trans syst. man cybern.* (1979) 9(1):62–6. doi: 10.1109/TSMC.1979.4310076

26. Reinhard E, Adhikhmin M, Gooch B, Shirley P. Color transfer between images. *IEEE Comput Graphics Appl* (2001) 21(5):34–41. doi: 10.1109/38.946629

27. Szegedy C, Vanhoucke V, Ioffe S, Shlens J, Wojna Z eds. Rethinking the inception architecture for computer vision. In: *2016 IEEE Conference on Computer Vision and Pattern Recognition (CVPR)*. 2016; Las Vegas, NV, USA: IEEE

28. Newman AM, Liu CL, Green MR, Gentles AJ, Feng W, Xu Y, et al. Robust enumeration of cell subsets from tissue expression profiles. *Nat Methods* (2015) 12 (5):453–7. doi: 10.1038/nmeth.3337

29. Leening MJ, Vedder MM, Witteman JC, Pencina MJ, Steyerberg EW. Net reclassification improvement: computation, interpretation, and controversies: a literature review and clinician's guide. *Ann Intern Med* (2014) 160(2):122–31. doi: 10.7326/M13-1522

30. Zhou B, Khosla A, Lapedriza A, Oliva A, Torralba A editors. Learning Deep Features for Discriminative Localization. *016 IEEE Conference on Computer Vision and Pattern Recognition (CVPR)*. CVPR (2016) Las Vegas, NV, USA: IEEE.

31. Xi J, Yin J, Liang J, Zhan C, Jiang W, Lin Z, et al. Prognostic impact of radiological consolidation tumor ratio in clinical stage IA pulmonary ground glass opacities. *Front Oncol* (2021) 11:616149. doi: 10.3389/fonc.2021.616149

32. Cao Y, Ke R, Wang S, Zhu X, Chen J, Huang C, et al. DNA topoisomerase IIalpha and Ki67 are prognostic factors in patients with hepatocellular carcinoma. *Oncol Lett* (2017) 13(6):4109–16. doi: 10.3892/ol.2017.5999

33. Wang C, Zhang Y, Guo K, Wang N, Jin H, Liu Y, et al. Heat shock proteins in hepatocellular carcinoma: Molecular mechanism and therapeutic potential. *Int J Cancer* (2016) 138(8):1824–34. doi: 10.1002/ijc.29723

34. Zhou F, Shang W, Yu X, Tian J. Glypican-3: A promising biomarker for hepatocellular carcinoma diagnosis and treatment. *Med Res Rev* (2018) 38(2):741–67. doi: 10.1002/med.21455

35. Tian MX, Liu WR, Wang H, Zhou YF, Jin L, Jiang XF, et al. Tissue-infiltrating lymphocytes signature predicts survival in patients with early/intermediate stage hepatocellular carcinoma. *BMC Med* (2019) 17(1):106. doi: 10.1186/s12916-019-1341-6

36. Klimov S, Miligy IM, Gertych A, Jiang Y, Toss MS, Rida P, et al. A whole slide image-based machine learning approach to predict ductal carcinoma *in situ* (DCIS) recurrence risk. *Breast Cancer Res* (2019) 21(1):83. doi: 10.1186/s13058-019-1165-5

37. Yu KH, Zhang C, Berry GJ, Altman RB, Re C, Rubin DL, et al. Predicting non-small cell lung cancer prognosis by fully automated microscopic pathology image features. *Nat Commun* (2016) 7:12474. doi: 10.1038/ncomms12474

38. Calderaro J, Petitprez F, Becht E, Laurent A, Hirsch TZ, Rousseau B, et al. Intra-tumoral tertiary lymphoid structures are associated with a low risk of early recurrence of hepatocellular carcinoma. *J Hepatol* (2019) 70(1):58–65. doi: 10.1016/j.jhep.2018.09.003

39. Sia D, Jiao Y, Martinez-Quetglas I, Kuchuk O, Villacorta-Martin C, Castro de Moura M, et al. Identification of an immune-specific class of hepatocellular carcinoma, based on molecular features. *Gastroenterology* (2017) 153(3):812–26. doi: 10.1053/j.gastro.2017.06.007

40. Lukacs-Kornek V. The role of lymphatic endothelial cells in liver injury and tumor development. *Front Immunol* (2016) 7:548. doi: 10.3389/fimmu.2016.00548

41. Chung JW, Shin E, Kim H, Han HS, Cho JY, Choi YR, et al. Hepatic iron overload in the portal tract predicts poor survival in hepatocellular carcinoma after curative resection. *Liver Int* (2018) 38(5):903–14. doi: 10.1111/liv.13619

42. Ziol M, Pote N, Amaddeo G, Laurent A, Nault JC, Oberti F, et al. Macrotrabecular-massive hepatocellular carcinoma: A distinctive histological subtype with clinical relevance. *Hepatology* (2018) 68(1):103–12. doi: 10.1002/hep.29762

43. Mule S, Galletto Pregliasco A, Tenenhaus A, Kharrat R, Amaddeo G, Baranes L, et al. Multiphase liver MRI for identifying the macrotrabecular-massive subtype of hepatocellular carcinoma. *Radiology* (2020) 295(3):562–71. doi: 10.1148/radiol.2020192230

44. Bauer K, Nitsche U, Slotta-Huspenina J, Drecoll E, von Weyhern CH, Rosenberg R, et al. High HSP27 and HSP70 expression levels are independent adverse prognostic factors in primary resected colon cancer. *Cell Oncol (Dordr)* (2012) 35(3):197–205. doi: 10.1007/s13402-012-0079-3

45. Gabrielson A, Wu Y, Wang H, Jiang J, Kallakury B, Gatalica Z, et al. Intratumoral CD3 and CD8 t-cell densities associated with relapse-free survival in HCC. *Cancer Immunol Res* (2016) 4(5):419–30. doi: 10.1158/2326-6066.CIR-15-0110

46. Liu LZ, Zhang Z, Zheng BH, Shi Y, Duan M, Ma LJ, et al. CCL15 recruits suppressive monocytes to facilitate immune escape and disease progression in hepatocellular carcinoma. *Hepatology* (2019) 69(1):143–59. doi: 10.1002/hep.30134

47. Chen DP, Ning WR, Li XF, Wei Y, Lao XM, Wang JC, et al. Peritumoral monocytes induce cancer cell autophagy to facilitate the progression of human hepatocellular carcinoma. *Autophagy* (2018) 14(8):1335–46. doi: 10.1080/15548627.2018.1474994

48. Yeung OW, Lo CM, Ling CC, Qi X, Geng W, Li CX, et al. Alternatively activated (M2) macrophages promote tumour growth and invasiveness in hepatocellular carcinoma. *J Hepatol* (2015) 62(3):607–16. doi: 10.1016/j.jhep.2014.10.029

COPYRIGHT

© 2022 Qu, Tian, Qiu, Guo, Tao, Liu, Tang, Qian, Wang, Li, Hu, Zhou, Fan, Zou, Hou and Shi. This is an open-access article distributed under the terms of the Creative Commons Attribution License (CC BY). The use, distribution or reproduction in other forums is permitted, provided the original author(s) and the copyright owner(s) are credited and that the original publication in this journal is cited, in accordance with accepted academic practice. No use, distribution or reproduction is permitted which does not comply with these terms.

frontiers | Frontiers in Medicine

TYPE Original Research
PUBLISHED 22 August 2022
DOI 10.3389/fmed.2022.977652

Check for updates

OPEN ACCESS

EDITED BY
Sanjit Mukherjee,
National Institutes of Health (NIH), United States

REVIEWED BY
Kondapa Bobba,
University of California, San Francisco, United States
Asit Kumar Manna,
The University of Utah, United States

*CORRESPONDENCE
Rui Sun
sunr@sysucc.org.cn
Weiwei Xiao
xiaoww@sysucc.org.cn

†These authors have contributed equally to this work and share first authorship

SPECIALTY SECTION
This article was submitted to Gastroenterology, a section of the journal Frontiers in Medicine

RECEIVED 24 June 2022
ACCEPTED 02 August 2022
PUBLISHED 22 August 2022

CITATION
Liu S, Yang S, Yu H, Luo H, Chen G, Gao Y, Sun R and Xiao W (2022) A nomogram for predicting 10-year cancer specific survival in patients with pathological T3N0M0 rectal cancer. *Front. Med.* 9:977652. doi: 10.3389/fmed.2022.977652

COPYRIGHT
© 2022 Liu, Yang, Yu, Luo, Chen, Gao, Sun and Xiao. This is an open-access article distributed under the terms of the Creative Commons Attribution License (CC BY). The use, distribution or reproduction in other forums is permitted, provided the original author(s) and the copyright owner(s) are credited and that the original publication in this journal is cited, in accordance with accepted academic practice. No use, distribution or reproduction is permitted which does not comply with these terms.

A nomogram for predicting 10-year cancer specific survival in patients with pathological T3N0M0 rectal cancer

Shuang Liu[1,2,3†], Shanfei Yang[1,2,3†], Haina Yu[1,2,3†], Huilong Luo[1,2,3], Gong Chen[2,3,4], Yuanhong Gao[1,2,3], Rui Sun[1,2,3*] and Weiwei Xiao[1,2,3*]

[1]Department of Radiation Oncology, Sun Yat-sen University Cancer Center, Guangzhou, China, [2]State Key Laboratory of Oncology in South China, Sun Yat-sen University Cancer Center, Guangzhou, China, [3]Collaborative Innovation Center for Cancer Medicine, Sun Yat-sen University Cancer Center, Guangzhou, China, [4]Department of Colorectal Surgery, Sun Yat-sen University Cancer Center, Guangzhou, China

Background: The pathological T3N0M0 (pT3N0M0) rectal cancer is the earliest stage and has the best prognosis in the locally advanced rectal cancer, but the optimal treatment remains controversial. A reliable prognostic model is needed to discriminate the high-risk patients from the low-risk patients, and optimize adjuvant chemotherapy (ACT) treatment decisions by predicting the likelihood of ACT benefit for the target population.

Patients and methods: We gathered and analyzed 276 patients in Sun Yat-sen University Cancer Center from March 2005 to December 2011. All patients underwent total mesorectal excision (TME), without preoperative therapy, and were pathologically proven pT3N0M0 rectal cancer with negative circumferential resection margin (CRM). LASSO regression model was used for variable selection and risk factor prediction. Multivariable cox regression was used to develop the predicting model. Optimum cut-off values were determined using X-Tile plot analysis. The 10-fold cross-validation was adopted to validate the model. The performance of the nomogram was evaluated with its calibration, discrimination and clinical usefulness.

Results: A total of 188 patients (68.1%) had ACT and no patients had adjuvant radiotherapy. Age, monocyte percentage, carbohydrate antigen 19–9, lymph node dissection numbers and perineural invasion (PNI) were identified as significantly associated variables that could be combined for an accurate prediction risk of Cancer Specific Survival (CSS) for pT3N0M0 patients. The model adjusted for CSS showed good discrimination with a C-index of 0.723 (95% CI: 0.652–0.794). The calibration curves showed that the nomogram adjusted for CSS was able to predict 3-, 5-, and 10-year CSS accurately. The corresponding predicted probability was used to stratify high and low-risk patients (10-year CSS: 69.1% vs. 90.8%, HR = 3.815, 95%CI: 2.102–6.924, $P < 0.0001$). ACT improved overall survival (OS) in the low-risk patients (10-year OS: 91.9% vs. 83.3%, HR = 0.338, 95% CI: 0.135–0.848, $P < 0.0001$), while it did not exhibit a significant benefit in the high-risk patients.

Conclusion: The present study showed that age, monocyte percentage, carbohydrate antigen 19–9, lymph node dissection numbers and PNI were independent prognostic factors for pT3N0M0 rectal cancer patients. A nomogram based on these prognostic factors effectively predicts CSS in patients, which can be conveniently used in clinical practice. ACT may improve overall survival in the low-risk patients. But the benefit of ACT was not seen in the high-risk patients.

KEYWORDS

pT3N0M0, rectal cancer, nomogram, CSS, adjuvant chemotherapy

Background

The pathological T3N0M0 (pT3N0M0) rectal cancer is the earliest stage and the best prognosis in the locally advanced rectal cancer. Although neoadjuvant chemoradiotherapy plus interval chemotherapy is the treatment for clinical T3N0M0 patients recommended by the guidelines (1), many patients do not receive neoadjuvant therapy due to the adverse symptoms and high costs. In addition, due to the inaccuracy of the image, some patients who were diagnosed clinical T1-2 might be confirmed T3 after total mesorectal excision (TME) surgery. For pT3N0M0 patients, positive circumferential resection margin (CRM) after surgery was considered to be an independent prognostic factor of clinical outcome (2, 3), and these patients require adjuvant chemoradiotherapy. As for pT3N0M0 patients with negative CRM, there has been little data to guide recommendations in adjuvant chemoradiotherapy. It was crucial to optimize and guide personalized treatment through further effective risk stratification for these patients.

Although it is difficult to stratify patients based on the traditional TNM staging system for pT3N0M0 rectal cancer with negative resection margin, clinical features and several potential prognostic factors warrant further studies. For the TNM staging system, the N factor depends on whether there is regional lymph node metastasis and the extent of metastasis The inadequate lymph nodes dissection examined results in an inaccurate number of positive lymph nodes and inaccurate staging (4, 5). Current guidelines especially recommended that at least 12 lymph nodes be resected and histologically evaluated (6–8). Furthermore, the adjuvant chemotherapy (ACT) regimen is determined by the number of lymph node dissection metastases (9).

The prognosis of rectal cancers is correlated with host- and tumor-related factors (10–12). Peripheral blood monocyte was one of the well-known indicators of the immune status of cancer patients (13, 14). Existing studies suggest that a decreased lymphocyte-to-monocyte ratio before treatment was independently associated with worse overall survival in rectal cancers who underwent surgery (15). Pretreatment lymphocyte count was also independently associated with ACT efficacy for the high-risk patients in Stage II rectal cancers (16). Further, we attempted to investigate other potential blood biomarkers and pathologic conditions included surgical margin status, tumor thrombus, perineural invasion (PNI) of patients' related disease outcomes in this study.

A previous study based on the Surveillance, Epidemiology, and End Results (SEER) database developed a risk-stratification model for pT3N0 rectal patients, which was composed of age, tumor differentiation, and the number of nodes resected (17). The long-term survival was better for low-risk patients than for high-risk patients (5-year CSS: 92.13% vs. 72.55%, $P < 0.001$). The sequential radiotherapy after surgery doubled 5-year CSS in high-risk patients (42.06% vs. 91.26%, $P = 0.001$), while showed no obvious survival benefit in the low-risk patients (93.36% vs. 96.38%, $P = 0.182$). The model may not be able to inaccurately predict clinical outcomes in the Chinese population because of ethnical diversity and environmental exposures. The 5-year CSS of overall cohort from SEER database was 86.31%, while the 5-year CSS in our study was 89.5%.

In this study, we combined the common clinical variables with potential prognostic indicators to develop a nomogram to predict CSS in patients with pT3N0M0 rectal cancer with negative CRM. We aimed to provide clinicians with more guidance to stratify those high-risk score patients who need more comprehensive treatment and closer follow-up to improve survival.

Patients and methods

Patients

We collected retrospective data about 276 patients with rectal cancer who underwent standard TME at Sun Yat-sen University Cancer Center from March 2005 to December 2011. The inclusion criteria were as follows: (1) pathological

diagnosis of rectal cancer; (2) postoperative pathological stage of pT3N0M0; (3) complete surgical resection; and (4) no preoperative therapy. Patients were excluded if they died of postoperative complications within 30 days or with positive surgical margins. This research was approved by the Ethical Committee of Sun Yat-sen University Cancer Center (B2022-005-01), and written informed consent was obtained from participants for the use of their clinical records in this study.

Preoperative examination and assessment

All eligible patients received complete preoperative evaluation. The clinical TNM (8th edition) stage was assessed according to endorectal ultrasound (EUS) and magnetic resonance imaging (MRI) and computed tomography (CT) scan in all patients.

The laboratory tests including routine blood tests, blood biochemistry, and assessment for tumor markers [carcinoembryonic antigen (CEA) and carbohydrate antigen 19-9 (CA199) level]. To exclude the influence of various comorbidities or other disease states, all included patients had no self-reported acute infections or colorectal disorders, indicating that the hematologic markers could represent the baseline value.

Surgical specimen and pathological assessment

Surgical resection was defined as radical when there was no evidence of distant metastases and tumor clearance was both macroscopically and histologically complete. All operations are performed by experienced colorectal surgeons in accordance with TME principles, and the surgical approaches included Hartmann, Dixon, and Miles surgery.

Two pathologists who were blinded to the clinical outcomes of the patients assessed all the resection specimens according to the eighth edition of the American Joint Committee on Cancer (AJCC) TNM staging category. Pathologic assessment included surgical margin status, tumor thrombus, PNI, positive lymph node numbers, and lymph node dissection numbers (LNDs).

Follow-up

The first follow-up evaluation was underwent 3–5 weeks after TME surgery. Follow-up after surgery was conducted every 3–6 months for the first 2 years after treatment, every 6 months for next 3 years, and annually after 5 years. Follow-up data were obtained from medical records, telephone calls, and the population death information registration system. CSS was defined as the time from initial diagnosis until the date of cancer-specific death. OS was calculated from initial diagnosis to death due to any cause or the last follow-up.

Statistical analysis

The least absolute shrinkage and selection operator (LASSO) method for features selection in Cox regression analysis was used to determine the most meaningful predictive clinicopathological factors. Statistical significance was defined as $P < 0.05$. X-tile software (Version 3.6.1) was used to determine the optimal cut-off values for continuous variables, including age, CA199, monocyte percentage (MONO%), and LNDs (18). The optimal cut-off values were 67 years for age, 27 U/ml for CA199, 7.6% for MONO%, and 12 for LNDs according to the X-tile software recommendation.

Nomogram model was utilized to generate the probability of 3, 5, and 10-year CSS. The "rms" package[1] within R project was utilized for nomogram model building and visualization. Candidate models were constructed for all possible feature combinations, and the final model with the highest C-index was chosen. Internal validation of the model was evaluated by bootstrapping using 1,000 samples. Calibration curves for 3-, 5-, and 10-year CSS were drawn to investigate the closeness between predicted survival and the actual survival. According to the nomogram model, we calculated the total points of each patient were by plus point from each characteristic. We further classified the patients into high-risk subgroup and low-risk subgroup based on the total points. All statistical tests in this study were performed in IBM SPSS statistics (Version 23.0), R project (Version 3.6.0), and X-tile (Version 3.6.1).

Results

Clinicopathologic characteristics of patients

A total of 276 patients were included in this study, 68.1% (n = 188) received ACT and 31.9% (n = 88) had no adjuvant chemotherapy (non-ACT). 138 patients received single-agent ACT (5-FU/LV: 5-fluorouracil/leucovorin or capecitabine) and 50 patients received multi-agent ACT (FOLFOX: 5-fluorouracil with oxaliplatin or Capeox: capecitabine with oxaliplatin). Fifty-one patients received ACT for 3 months or less, and 137 patients received ACT for more than 3 months. The mean duration of follow-up was 141.02 ± 6.12 years. The 10-year OS was 78.6% (217/276) and the 10-year CSS was 81.2% (224/276) for the whole population. **Table 1** presents the clinicopathologic

1 https://cran.r-project.org/web/packages/rms/index.html

TABLE 1 Baseline clinicopathologic characteristics of the patients with pT3N0M0 rectal cancer.

Characteristics	Total, n (%)	non-ACT, n (%)	ACT, n (%)	*P-value*
Total	276 (100%)	88 (31.9%)	188 (68.1%)	
Gender				1
Female	170 (61.6%)	54 (61.4%)	116 (61.7%)	
Male	106 (38.4%)	34 (38.6%)	72 (38.3%)	
Age				0.005
≤67 years	187 (67.8%)	49 (55.7%)	138 (73.4%)	
>67 years	89 (32.2%)	39 (44.3%)	50 (26.6%)	
Distance to anal verge				0.457
≤5 cm	66 (23.9%)	24 (27.3%)	42 (22.3%)	
>5 cm	210 (76.1%)	64 (72.7%)	146 (77.7%)	
Monocyte percentage (MONO%)				0.61
≤7.6%	152 (55.1%)	46 (52.3%)	106 (56.4%)	
>7.6%	124 (44.9%)	42 (47.7%)	82 (43.6%)	
Carcinoembryonic antigen (CEA)				0.034
Normal (≤ 5 ng/ml)	171 (62.0%)	63 (71.6%)	108 (57.4%)	
Elevated (> 5 ng/ml)	105 (38.0%)	25 (28.4%)	80 (42.6%)	
Carbohydrate antigen 19-9 (CA199)				0.01
≤27 U/ml	225 (81.5%)	80 (90.9%)	145 (77.1%)	
>27 U/ml	51 (18.5%)	8 (9.09%)	43 (22.9%)	
Surgery approach				0.958
Dixon	219 (79.3%)	71 (80.7%)	148 (78.7%)	
Miles	50 (18.1%)	15 (17.0%)	35 (18.6%)	
Hartmann	7 (2.54%)	2 (2.27%)	5 (2.66%)	
Lymph node dissection numbers (LNDs)				0.917
≤12	122 (44.2%)	38 (43.2%)	84 (44.7%)	
>12	154 (55.8%)	50 (56.8%)	104 (55.3%)	
Perineural invasion (PNI)				0.257
Negative	183 (66.3%)	63 (71.6%)	120 (63.8%)	
Positive	93 (33.7%)	25 (28.4%)	68 (36.2%)	

characteristics of all patients. Of all patients, 61.6% (n = 170) of patients were female and 67.8% (n = 187) patients were aged ≤ 67 years. The patients with low rectal cancer (distance to anal verge less than 5 cm) were 23.9% (n = 66). 79.3% (n = 219) patients received Dixon surgery, and 18.1% (n = 50) patients received Miles surgery.

ACT was more common among patients aged ≤ 67 years than among patients aged > 67 years (P = 0.005), among patients with CEA > 5 ng/ml than among those with ≤ 5 ng/ml (P = 0.034), and among patients with CA199 > 27 U/ml than among those with ≤ 27 U/ml (P = 0.01).

Independent prognostic factors of cancer specific survival

Univariate analysis was performed on all collected variables. The results revealed that age (P = 0.005), monocyte percentage (MONO%) (P < 0.001), carbohydrate antigen 19-9 (CA199) (P = 0.003), lymph node dissection numbers (LNDs) (P = 0.004), and PNI (P = 0.004) were considered significant predictors for CSS (Table 2). Multivariate Cox regression analysis showed age (HR = 1.877, 95%CI: 1.085–3.249, P = 0.024), MONO% (HR = 2.496, 95%CI: 1.415–4.403, P = 0.002), CA199 (HR = 2.306, 95%CI: 1.284–4.142, P = 0.005), LNDs (HR = 0.442, 95%CI: 0.251–0.778, P = 0.005), and PNI (HR = 2.126, 95%CI: 1.244–3.632, P = 0.006) were significantly associated with CSS (Table 2).

Subgroup analysis

Kaplan-Meier analysis showed that patients aged ≤ 67 years had a better prognosis than those aged > 67 years (10-year CSS: 85.6% vs. 71.9%, P = 0.004; Figure 1A). The patients with MONO% ≤ 7.6% had better outcomes than patients with MONO% > 7.6% (10-year CSS: 88.2% vs. 72.6%, P = 0.001; Figure 1B). The patients with CA199 ≤ 27 U/ml had an obvious advantage in survival than patients with CA199 > 27 U/ml (10-year CSS: 84.4% vs. 66.7%, P = 0.002; Figure 1C). The patients for whom ≤ 12 nodes had been resected had a poorer prognosis than patients for whom > 12 nodes had been resected (10-year CSS: 74.6% vs. 86.4%, P = 0.003; Figure 1D). The positive PNI was detrimental for patient survival (10-year CSS: negative vs. positive, 86.3% vs. 71.0%, P = 0.003; Figure 1E). However, no survival difference was observed between the patients who received ACT and those who did not (10-year CSS: 81.9% vs. 79.5%, P = 0.523; Figure 1F). These variables were also assessed when using OS as an endpoint. Similar findings were obtained (Supplementary Figures 1A–F).

TABLE 2 Prognostic factors of 10-year CSS in univariate analysis and multivariate analysis.

Characteristics	10-year CSS	Univariate analysis		Multivariate analysis	
		HR (95% CI)	*P-value*	HR (95% CI)	*P-value*
Gender (Male vs. Female)		0.608 (0.339–1.090)	0.095		
Age (≤67 years vs. > 67 years)	85.6% vs. 71.9%	2.140 (1.254–3.651)	0.005	1.877 (1.085–3.249)	0.024
Distance to anal (≤5 cm vs. > 5 cm)	84.4% vs. 80.0%	1.118 (0.589–2.124)	0.733		
Monocyte percentage (MONO%) (≤7.6% vs. > 7.6%)	88.2% vs. 72.6%	2.510 (1.435–4.390)	0.001	2.496 (1.415–4.403)	0.002
Carcinoembryonic antigen (CEA) (≤5 ng/ml vs. > 5 ng/ml)	82.5% vs. 79.9%	1.340 (0.784–2.293)	0.285		
Carbohydrate antigen 19-9 (CA199) (≤ 27 U/ml vs. > 27 U/ml)	84.4% vs. 66.7%	2.417 (1.359–4.296)	0.003	2.306 (1.284–4.142)	0.005
Surgery approach					
Dixon	81.3%	—			
Miles	82.0%	1.150 (0.591–2.239)	0.680		
Hartmann	71.4%	1.998 (0.482–8.275)	0.340		
Lymph node dissection numbers (LNDs) (≤12 vs. > 12)	74.6% vs. 86.4%	0.444 (0.257–0.767)	0.004	0.442 (0.251–0.778)	0.005
Perineural invasion (PNI) (Negative vs. Positive)	86.3% vs. 71%	2.182 (1.279–3.722)	0.004	2.126 (1.244–3.632)	0.006
Adjuvant chemotherapy (ACT)	79.5% vs. 81.9%	0.809 (0.463–1.416)	0.459		

Construction and internal validation of the nomogram for cancer specific survival

Based on the results of the LASSO regression and multivariate COX regression, the nomogram incorporating five predictors was established to predict CSS in pT3N0M0 rectal cancer patients following TME surgery (Figure 2A). According to our nomogram plot, total points of each pT3N0M0 rectal cancer patients was calculated as follows: Age > 67 years (69 points), CA199 > 27 U/ml (91 points), MONO% > 7.6% (100 points), LNDs ≤ 12 (89 points), and positive PNI (82 points). Each of these variables was assigned a score based on the point scale. By adding up the total point from all the variables, we could estimate 3-, 5-, and 10-year CSS probability. The C-index for the nomogram model was 0.723 (95% CI: 0.652–0.794). The calibration plots for 3-, 5-, and 10-year CSS probability also exhibited good internal consistency between the predicted CSS and the actual CSS (Figures 2B–D).

We used total point = 170, corresponding to a 5-year CSS probability of 80%, as a cut-off value to stratify patients. In our study, 123 patients with total point > 170 were classified as high-risk group (44.6%), and 153 patients with total point ≤ 170 were classified as low-risk group (55.4%). CCS was significantly higher in the low-risk group than in the high-risk group (10-year CSS: 69.1% vs. 90.8%, HR = 3.815, 95%CI: 2.102–6.924, $P < 0.0001$; Figure 3A). OS was also significantly higher in the low-risk group than in the high-risk group (10-year OS: 65.9% vs. 88.9%, HR = 3.485, 95%CI: 2.038–5.961, $P < 0.0001$; Figure 3D). And our model was superior to the previous model (17) (10-year CSS: 87.8% vs. 74.8%, HR = 2.445, 95%CI: 1.353–4.418, $P = 0.003$; 10-year OS: 87.8% vs. 69.6%, HR = 2.971, 95% CI: 1.696–5.204, $P < 0.0001$; Supplementary Figures 2A,B).

In the low-risk patients, the application of ACT could benefit the patient's survival (10-year CSS: 92.9% vs. 87%, HR = 0.411, 95% CI: 0.148–1.146, $P = 0.089$; 10-year OS: 91.9% vs. 83.3%, HR = 0.338, 95% CI: 0.135–0.848, $P < 0.0001$; Figures 3B,E). However, no survival difference was observed between high−risk patients who treated with surgery plus ACT vs. those who treated with surgery alone (10-year CSS: 67.6% vs. 69.7%, HR = 0.94, 95% CI: 0.468–1.887, $P = 0.861$; 10-year OS: 58.8% vs. 68.5%, HR = 0.814, 95% CI: 0.433–1.531, $P = 0.523$; Figures 3C,F).

Further analysis showed that there was no significant difference in survival between single-agent chemotherapy and multi-agent chemotherapy regimen (10-year CSS: 71.6% vs. 63.6%, HR = 1.609, 95%CI: 0.641–4.039, $P = 0.311$; 10-year OS: 70.1% vs. 63.6%, HR = 1.438, 95% CI: 0.586–3.529, $P = 0.380$); Supplementary Figures 3A,C). There was no apparent survival benefit between 3 months or less of ACT vs. more than 3 months of ACT (10-year CSS: 72.2% vs. 69.0%, HR = 1.095, 95%CI: 0.426–2.819, $P = 0.850$; 10-year OS: 72.2% vs. 67.6%, HR = 1.145, 95% CI: 0.453–2.894, $P = 0.783$; Supplementary Figures 3B,D).

Discussion

Firstly, to our knowledge, this was the first and only study of a nomogram for predicting CSS in patients with pT3N0M0 rectal cancer. Secondly, this model is established by screening the complete common preoperative laboratory test indicators and pathological outcomes, which makes it more accurate and more targeted. Age, MONO%, CA199, LNDs, and PNI were

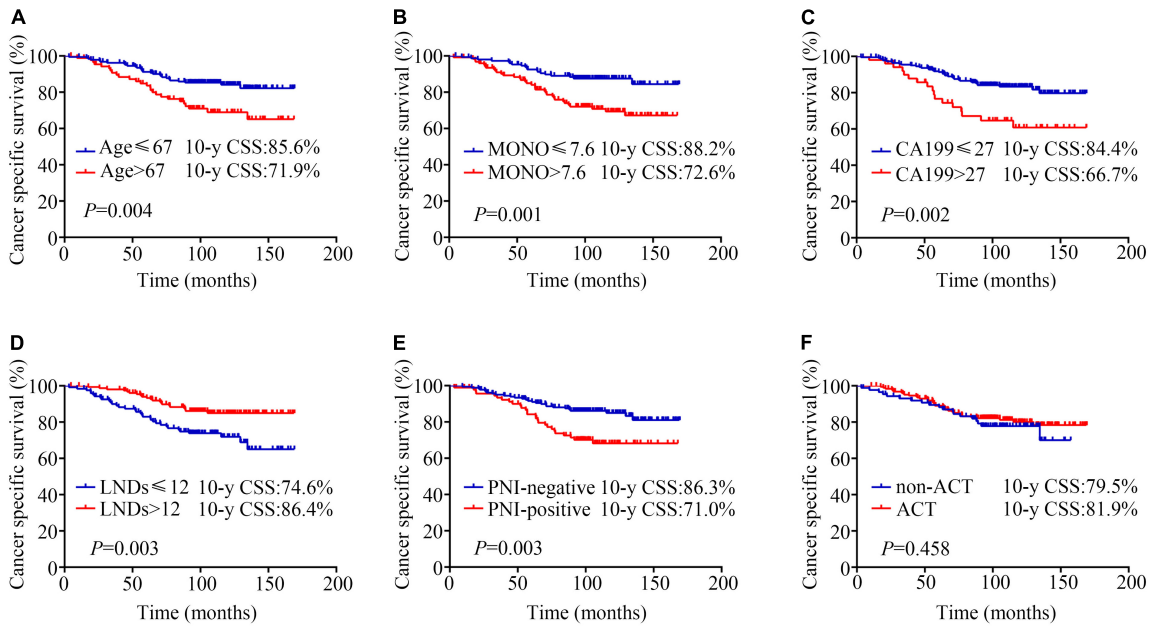

FIGURE 1
Kaplan-Meier analysis of cancer specific survival according to **(A)** age (≤67 years vs. > 67 years, 10-y CSS: 85.6% vs. 71.9%, *P* = 0.004); **(B)** monocyte percentage (MONO%) (≤ 7.6% vs. > 7.6%, 10-year CSS: 88.2% vs. 72.6%, *P* = 0.001); **(C)** carbohydrate antigen 19-9 (CA199) (≤27 U/ml vs. > 27 U/ml, 10-year CSS: 84.4% vs. 66.7%, *P* = 0.002); **(D)** lymph node dissection numbers (LNDs) (≤ 12 vs. > 12, 10-year CSS: 74.6% vs. 86.4%, *P* = 0.003); **(E)** perineural invasion (PNI) (negative vs. positive, 10-year CSS: 86.3% vs. 71%, *P* = 0.003); **(F)** adjuvant chemotherapy (ACT) (non-ACT vs. ACT, 10-year CSS: 79.5% vs. 81.9%, *P* = 0.458).

performed as independent factors to construct our prognostic nomogram model. Our nomogram had good discrimination (C-index = 0.723, 95% CI: 0.652–0.794; Figure 2A), which provided a convenient and feasible tool for predicting the risk of pT3N0M0 patients. Thirdly, our model effectively distinguishes high-risk and low-risk groups, which could guide the choice of postoperative treatment for T3N0M0 colorectal cancer patients. For Chinese patients, our nomogram (10-year CSS: 69.1% vs. 90.8%, HR = 3.815, 95%CI: 2.102–6.924, $P < 0.0001$; 10-year OS: 65.9% vs. 88.9%, HR = 3.485, 95%CI: 2.038–5.961, $P < 0.0001$; Figures 3A,D) had a better prediction effect than the previous risk-stratification model (17) (10-year CSS: 87.8% vs. 74.8%, HR = 2.445, 95%CI: 1.353–4.418, $P = 0.003$; 10-year OS: 87.8% vs. 69.6%, HR = 2.971, 95% CI: 1.696–5.204, $P < 0.0001$; Supplementary Figures 2A,B).

Over the years, several studies have focused on the role of adjuvant treatment including chemotherapy and radiotherapy in T3N0 patients (17, 19–21). Luke C. Peng et al. collected 4,724 patients with T3N0M0 rectal cancer diagnosed between 1998 and 2008 in the SEER database. The results demonstrated that adjuvant radiotherapy was significantly associated with improved CSS compared with surgery alone (HR = 0.688, 95% CI: 0.578–0.819, $P < 0.001$), while neoadjuvant radiotherapy had no significant benefits (HR = 0.863, 95% CI: 0.715–1.043, $P = 0.127$) (19). Another study reported that postoperative concurrent chemoradiotherapy could significantly decrease locoregional recurrence rate in patients with CRM- but having one risk factor (distance from anal verge ≤ 5 cm or distal resection margin ≤ 2 cm) (5-year locoregional recurrence free survival: 98.9% vs. 87.4%, $P = 0.006$) (21). Unlike these prior studies, our study focused on the effect of ACT alone. In the patients who were classified as low-risk patients according to this model (total points ≤ 170), the application of ACT after surgery could benefit the patient's survival (10-year OS: 91.9% vs. 83.3%, HR = 0.338, 95% CI: 0.135–0.848, $P < 0.0001$; Figure 3E), whereas high-risk patients had no significant survival benefit (10-year OS: 58.8% vs. 68.5%, HR = 0.814, 95% CI: 0.433–1.531, $P = 0.523$; Figure 3F). ACT alone might be insufficient for high-risk patients, and the combination of radiotherapy and chemotherapy should be considered.

In high-risk stage II colon cancer, the addition of oxaliplatin to fluoropyrimidine did not improve overall survival (22). For duration of ACT, the IDEA study showed that 6 months of ACT was not superior to 3 months of ACT in high-risk stage II colon cancer patients [5-year DFS: 3 months group vs. 6 months group = 80.7% vs. 83.9%, HR = 1.17, 80%CI: 1.05–1.31, P (for non-inferiority) = 0.39] (23, 24) Similar to these results, we did not find a population of high-risk patients who benefited from adjuvant therapy and regimens after grouping according to the existing model. Therefore, risk stratification by identifying precise predictors of adjuvant therapy benefit in the context of patient individualization is necessary for high-risk

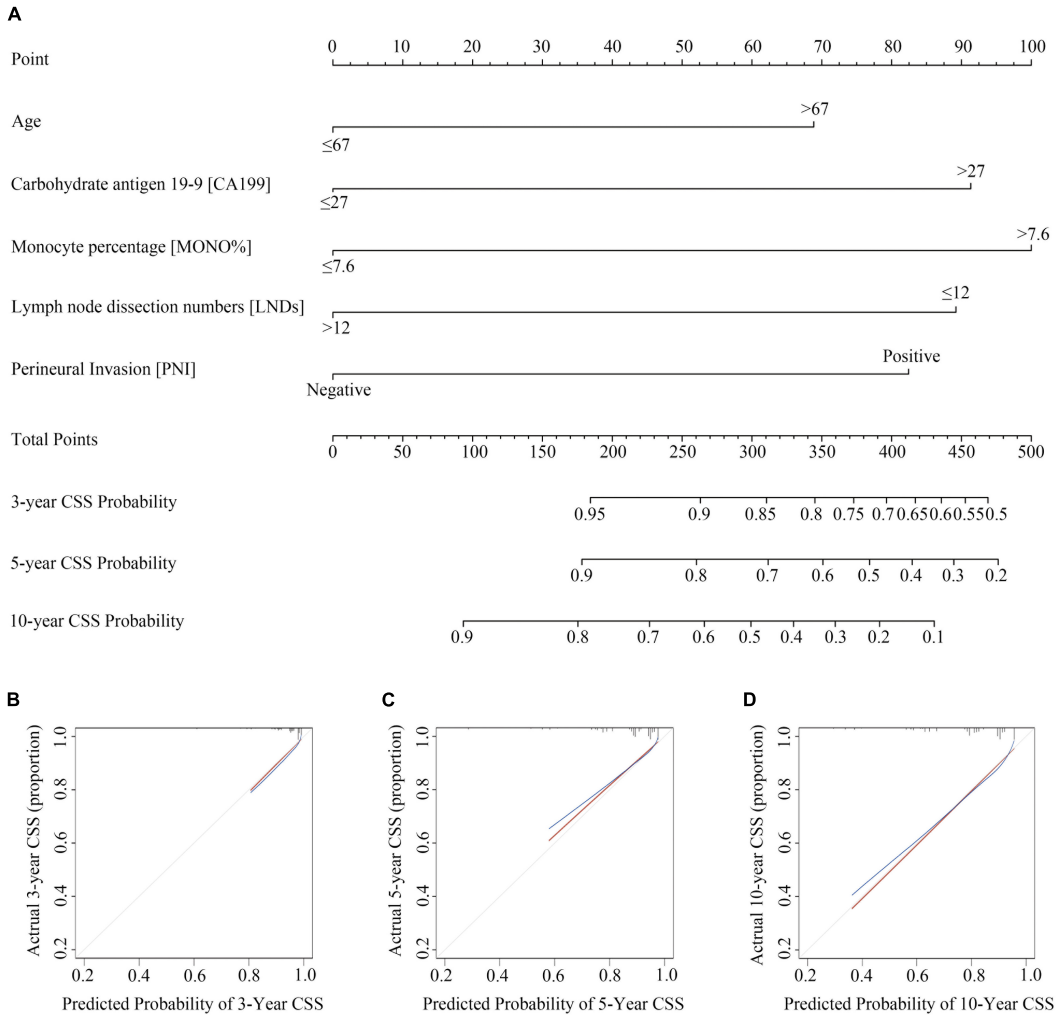

FIGURE 2
Construction and validation of Nomogram for cancer specific survival probability in pT3N0M0 rectal cancer patients. **(A)** The nomogram was developed with age, monocyte percentage (MONO%), carbohydrate antigen 19-9 (CA199), lymph node dissection numbers (LNDs), and perineural invasion (PNI); **(B–D)** calibration curves of the CSS nomogram, indicating the consistency between predicted and observed 3-, 5-, and 10-year outcomes.

patients. Mismatch repair (MMR) status may be considered one of the most powerful prognostic indicators (25). Detection of circulating tumor DNA (ctDNA) is also currently considered a useful tool to guide the application of ACT (26).

The TNM system is based on the depth of invasion, distant metastases and the number of positive lymph nodes. Indeed, accumulating studies have noted the predictive value of the lymph node status and lymph node ratio (LNR) in CRC. Notably, the 5-year survival of patients with negative lymph nodes (80%) was significantly higher than that (45%) of those with positive nodes ($P < 0.05$) (27). While the number of retrieved LNs is influenced by various factors including age and gender, the experience or skill of the surgeon and even the ethnicity of patients. Kidner et al. found that the 5-year survival rate of stage I/II patients with 1–4 lymph nodes removed was 48%, while that of patients with more than 20 lymph nodes removed was 65% (28). Another survival analysis determined that in patients with CRC without metastatic lymph nodes, the CSS of patients with 1–11 lymph nodes removed was significantly worse than that of patients with more than 12 lymph nodes removed (CSS: 62.3% vs. 75.1%, HR = 0.59, 95%CI: 0.41–0.84, $P = 0.004$) (29). In addition, Sarli et al. found that patients with no more than 9 lymph nodes examined have a similar 5-year survival rate to patients with 1–3 positive lymph nodes (51.3% vs. 52.6%), and postoperative chemotherapy recommend for N0 patients with only a few nodes examined (30). The NCCN and AJCC/UICC guidelines recommend at least 12 lymph nodes should be examined as the current standard for pathological examination in CRC surgery (31). Reviewing the presented data, 12 assessable lymph nodes

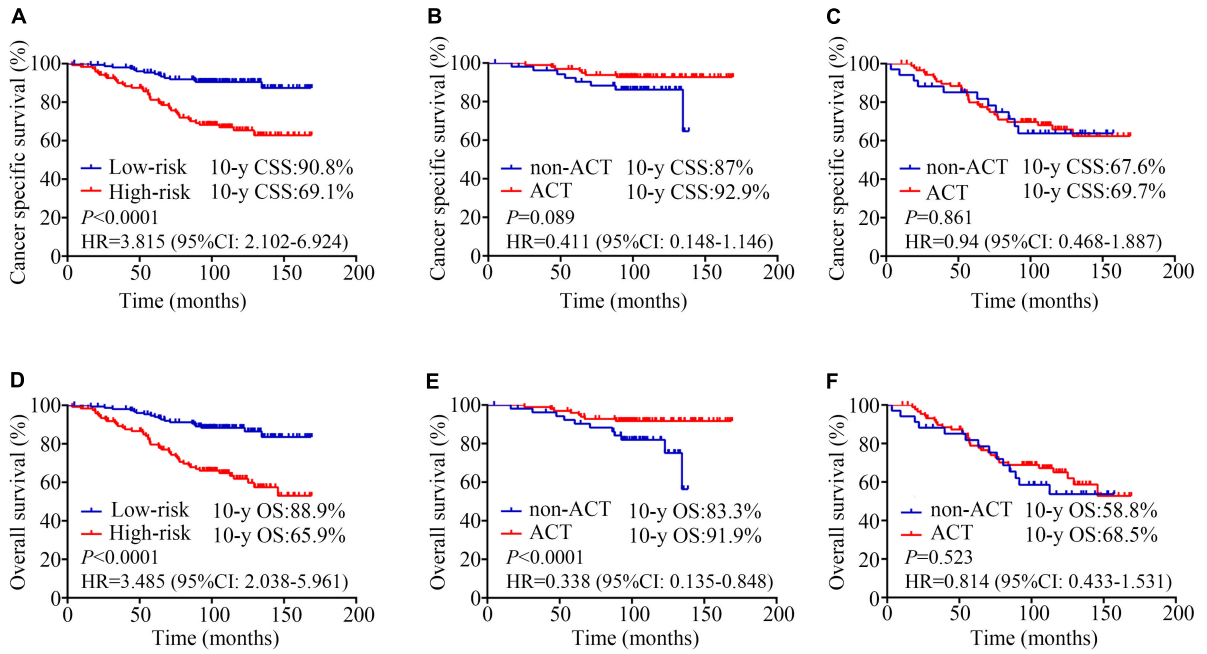

FIGURE 3
Kaplan-Meier analysis estimates. Cancer specific survival according to **(A)** risk stratifications (low-risk vs. high-risk, 10-year CSS: 69.1% vs. 90.8%, HR = 3.815, 95%CI: 2.102–6.924, $P < 0.0001$); **(B)** adjuvant chemotherapy (ACT) for low-risk patients (non-ACT vs. ACT, 10-year CSS: 92.9% vs. 87%, HR = 0.411, 95% CI: 0.148–1.146, $P = 0.089$); **(C)** adjuvant chemotherapy (ACT) for high-risk patients (non-ACT vs. ACT, 10-year CSS: 67.6% vs. 69.7%, HR = 0.94, 95% CI: 0.468–1.887, $P = 0.861$); Overall survival according to **(D)** risk stratifications (low-risk vs. high-risk, 10-year OS: 65.9% vs. 88.9%, HR = 3.485, 95%CI: 2.038–5.961, $P < 0.0001$); **(E)** adjuvant chemotherapy (ACT) for low-risk patients (non-ACT vs. ACT, 10-year OS: 91.9% vs. 83.3%, HR = 0.338, 95% CI: 0.135–0.848, $P < 0.0001$); **(F)** adjuvant chemotherapy (ACT) for high-risk patients (non-ACT vs. ACT, 10-year OS: 58.8% vs. 68.5%, HR = 0.814, 95% CI: 0.433–1.531, $P = 0.523$).

retrieved as adequate lymph node count could be a biomarker to evaluate the prognosis of pT3N0M0 rectal cancer. In our study, the 12 lymph nodes minimum for adequacy was achieved in over 50% of the total study cohort, and in the previous study, the rate ranged from 36 to 67% (32).

The expression of CA 199 occurs as a result of the presence of sialylated Lewis a blood group antigen, is a tumor-associated antigen elevated in many types of cancer (33). CA199 levels have also been demonstrated to be predictive of malignancy in numerous previous studies (34, 35). Several studies have expressed concern that it was one of the best available prognostic indicators in colorectal cancers (36, 37). Especially, Zheng et al. showed that a higher level of serum levels of CA19-9 may serve as a useful marker effective in identifying node-negative CRCs had a poor prognosis after surgery and chemotherapy (38).

PNI can occur when neoplastic cells are missed since they can travel along nerves far from the primary lesion. This hinders surgery's ability to establish local control over malignancy (39, 40). PNI is a strong prognostic factor for colorectal cancer, which is generally associated with worse oncological outcomes. In the eighth edition of TNM, PNI was introduced as a supporting factor (41). This study showed that PNI was an independent prognostic factor for cancer-specific survival in multivariate analysis (HR = 2.126, 95% CI: 1.244-3.632, $P = 0.006$) (42). A comprehensive meta-analysis has also shown that PNI was an independent prognostic factor for 5-year overall, 5-year disease-free, and 5-year cancer-specific survival in multivariate analysis (HR = 1.85, 95% CI: 1.63–2.12; HR = 2.35, 95% CI: 1.97–3.08; and HR = 1.91, 95% CI: 1.50–2.42, respectively) (42). And in our study, the overall incidence of PNI was found to be 33.7%, similar to the 33% found in a previous review (43).

Recent research revealed that cancer-associated inflammation may play an important play in rectal cancer progression and prognosis (44–46). Guo et al. proposed that inflammatory cells included monocyte and related cytokines infiltrate in the tumor microenvironment, which promotes tumor angiogenesis and proliferation, survival, and migration (47). In Hu et al. study, higher peripheral monocyte counts as a useful predictor of postoperative prognosis in CRC patients and were associated with a worse 5-year disease-free survival rate (48). An elevated preoperative peripheral blood monocyte count might reflect a high degree of immune suppression and high levels of inflammatory cytokines. Similar to our results, Liu et al. constructed and validated a nomogram included monocyte count (cut off value 0.43 in the validation set) to predict individual survival probability for stage II–III colorectal cancer (49).

This study is subject to two major limitations. First, it was a retrospective study involving a single institution. Second, it would be not feasible to perform an external validation cohort study limited by sample size now. Further study should focus on validating the model by building multicenter normalized database, which includes complete laboratory examination and pathological outcomes. It should be noted that the reference standards of the variables may be slightly different in multicenter data, due to the application of different equipment and technologies in different centers. The model may have to be carefully optimized by slightly adjusting the cut-off values of some variables.

Conclusion

Regardless of the above limitations, our study showed that age, preoperative monocyte percentage, preoperative CA199, lymph node dissection numbers, and PNI were considered significant predictors for CSS. ACT was associated with improved survival compared with TME alone in the low-risk patients. Appropriate intensive treatment and follow-up may improve the efficacy of treatment and survival for high-risk patients.

Data availability statement

The raw data supporting the conclusions of this article will be made available by the authors, without undue reservation.

Ethics statement

This research was approved by the Ethical Committee of Sun Yat-sen University Cancer Center (B2022-005-01). The patients/participants provided their written informed consent to participate in this study.

Author contributions

WX, RS, and SL helped to design and refine study strategy. SL and SY screened selected studies for inclusion and extracted relevant data. SL and HY carried out data collection and analysis. SL, SY, and HY contributed to the first draft of the manuscript. WX, RS, GC, and YG supervised the project and provided critical review of the manuscript. All authors were involved in the interpretation of data and results, contributed to the revision and refinement of the final manuscript, had full access to all study data, given final approval of this version of the manuscript to be published, and agreed to be accountable to all aspects of the work, and read and approved the final manuscript.

Funding

This work was supported by the 5010 Clinical Research Foundation of Sun Yat-sen University (Grant No. 5010-2018-04) and the Chinese Society of Clinical Oncology Grand (Grant No. Y-XD202001-0144).

Conflict of interest

The authors declare that the research was conducted in the absence of any commercial or financial relationships that could be construed as a potential conflict of interest.

Publisher's note

All claims expressed in this article are solely those of the authors and do not necessarily represent those of their affiliated organizations, or those of the publisher, the editors and the reviewers. Any product that may be evaluated in this article, or claim that may be made by its manufacturer, is not guaranteed or endorsed by the publisher.

Supplementary material

The Supplementary Material for this article can be found online at: https://www.frontiersin.org/articles/10.3389/fmed.2022.977652/full#supplementary-material

SUPPLEMENTARY FIGURE 1
Kaplan-Meier analysis of overall survival according to **(A)** age (≤ 67 vs. > 67 years, 10-y OS: 85.6% vs. 64%, $P < 0.0001$); **(B)** monocyte percentage (MONO%) (≤ 7.6% vs. > 7.6%, 10-year OS: 96.8% vs. 68.5%, $P < 0.0001$); **(C)** carbohydrate antigen 19-9 (CA199) (≤27 U/ml vs. > 27 U/ml, 10-year OS: 81.8% vs. 64.7%, $P = 0.003$); **(D)** lymph node dissection numbers (LNDs) (≤12 vs. > 12, 10-year OS: 72.1% vs. 83.8%, $P = 0.005$); **(E)** perineural invasion (PNI) (negative vs. positive, 10-year OS: 83.1% vs. 69.9%, $P = 0.013$); **(F)** adjuvant chemotherapy (ACT) (non-ACT vs. ACT, 10-year OS: 73.9% vs. 80.9%, $P = 0.113$).

SUPPLEMENTARY FIGURE 2
Kaplan-Meier analysis estimates of the previous risk-stratification model (17) in our patients. **(A)** Cancer specific survival according to risk stratifications (low-risk vs. high-risk, 10-year CSS: 87.8% vs. 74.8%, HR = 2.445, 95%CI: 1.353–4.418, $P = 0.003$); **(B)** overall survival according to risk stratifications (low-risk vs. high-risk, 10-y OS: 87.8% vs. 69.6%, HR = 2.971, 95% CI: 1.696–5.204, $P < 0.0001$).

SUPPLEMENTARY FIGURE 3
Kaplan-Meier analysis estimates for high-risk patients. Cancer specific survival according to **(A)** adjuvant chemotherapy (ACT) for single-agent chemotherapy vs. multi-agent chemotherapy regimen, (10-year CSS: 71.6% vs. 63.6%, HR = 1.609, 95%CI: 0.641–4.039, $P = 0.311$); **(B)** ACT for 3 months or less (≤3 months) vs. more than 3 months (>3 months), (10-year CSS: 72.2% vs. 69.0%, HR = 1.095, 95%CI: 0.426–2.819, $P = 0.850$); Overall survival according to **(C)** ACT for single-agent chemotherapy vs. multi-agent chemotherapy regimen, 10-year OS: 70.1% vs. 63.6%, HR = 1.438, 95% CI: 0.586–3.529, $P = 0.380$); **(D)** ACT for ≤ 3 months vs. >3 months, (10-year OS: 72.2% vs. 67.6%, HR = 1.145, 95% CI: 0.453–2.894, $P = 0.783$).

References

1. Dong C, Ding Y, Weng S, Li G, Huang Y, Hu H, et al. Update in version 2021 of Csco guidelines for colorectal cancer from version 2020. *Chin J Cancer Res.* (2021) 33:302–7. doi: 10.21147/j.issn.1000-9604.2021.03.02

2. Agger EA, Jörgren FH, Lydrup MA, Buchwald PL. Risk of local recurrence of rectal cancer and circumferential resection margin: population-based cohort study. *Br J Surg.* (2020) 107:580–5. doi: 10.1002/bjs.11478

3. Patel SH, Hu CY, Massarweh NN, You YN, McCabe R, Dietz D, et al. Circumferential resection margin as a hospital quality assessment tool for rectal cancer surgery. *J Am Coll Surg.* (2020) 230:1008–18.e5. doi: 10.1016/j.jamcollsurg.2020.02.033

4. Dai W, Li Y, Wu Z, Feng Y, Cai S, Xu Y, et al. Pathological nodal staging score for rectal cancer patients treated with radical surgery with or without neoadjuvant therapy: a postoperative decision tool. *Cancer Manag Res.* (2019) 11:537–46. doi: 10.2147/cmar.S169309

5. Fujino S, Miyoshi N, Ohue M, Ito A, Yasui M, Ogino T, et al. A new fat-dissociation method to detect lymph nodes in colorectal cancer: a prospective randomized study. *Sci Rep*. (2020) 10:20205. doi: 10.1038/s41598-020-77195-8

6. Glimelius B, Tiret E, Cervantes A, Arnold D. Rectal cancer: esmo clinical practice guidelines for diagnosis, treatment and follow-up. *Ann Oncol.* (2013) 24(Suppl. 6):vi81–8. doi: 10.1093/annonc/mdt240

7. Watanabe T, Muro K, Ajioka Y, Hashiguchi Y, Ito Y, Saito Y, et al. Japanese society for cancer of the colon and rectum (Jsccr) guidelines 2016 for the treatment of colorectal cancer. *Int J Clin Oncol.* (2018) 23:1–34. doi: 10.1007/s10147-017-1101-6

8. National Comprehensive Cancer Network. *Guidelines: Rectal Cancer (Version 2.2021)*. (2021). Available online at: https://www.nccn.org/professionals/physician_gls/pdf/rectal.pdf (accessed Octorber 25, 2021).

9. Schofield JB, Mounter NA, Mallett R, Haboubi NY. The importance of accurate pathological assessment of lymph node involvement in colorectal cancer. *Colorect Dis.* (2006) 8:460–70. doi: 10.1111/j.1463-1318.2006.01044.x

10. Iseki Y, Shibutani M, Maeda K, Nagahara H, Ohtani H, Sugano K, et al. Impact of the preoperative controlling nutritional status (conut) score on the survival after curative surgery for colorectal cancer. *PLoS One.* (2015) 10:e0132488. doi: 10.1371/journal.pone.0132488

11. Ikeya T, Shibutani M, Maeda K, Sugano K, Nagahara H, Ohtani H, et al. Maintenance of the nutritional prognostic index predicts survival in patients with unresectable metastatic colorectal cancer. *J Cancer Res Clin Oncol.* (2015) 141:307–13. doi: 10.1007/s00432-014-1799-8

12. Balkwill F, Mantovani A. Inflammation and cancer: back to virchow? *Lancet.* (2001) 357:539–45. doi: 10.1016/s0140-6736(00)04046-0

13. Lichtenstern CR, Ngu RK, Shalapour S, Karin M. Immunotherapy, inflammation and colorectal cancer. *Cells.* (2020) 9:618. doi: 10.3390/cells9030618

14. Craig SG, Humphries MP, Alderdice M, Bingham V, Richman SD, Loughrey MB, et al. Immune status is prognostic for poor survival in colorectal cancer patients and is associated with tumour hypoxia. *Br J Cancer.* (2020) 123:1280–8. doi: 10.1038/s41416-020-0985-5

15. Kozak MM, von Eyben R, Pai JS, Anderson EM, Welton ML, Shelton AA, et al. The prognostic significance of pretreatment hematologic parameters in patients undergoing resection for colorectal cancer. *Am J Clin Oncol.* (2017) 40:405–12. doi: 10.1097/coc.0000000000000183

16. Liang L, Zhu J, Jia H, Huang L, Li D, Li Q, et al. Predictive value of pretreatment lymphocyte count in stage ii colorectal cancer and in high-risk patients treated with adjuvant chemotherapy. *Oncotarget.* (2016) 7:1014–28. doi: 10.18632/oncotarget.5835

17. Huang YX, Lin YZ, Li JL, Zhang XQ, Tang LR, Zhuang QY, et al. Role of postoperative radiotherapy in Pt3n0 rectal cancer: a risk-stratification system based on population analyses. *Cancer Med.* (2019) 8:1024–33. doi: 10.1002/cam4.1991

18. Camp RL, Dolled-Filhart M, Rimm DL. X-tile: a new bio-informatics tool for biomarker assessment and outcome-based cut-point optimization. *Clin Cancer Res.* (2004) 10:7252–9. doi: 10.1158/1078-0432.Ccr-04-0713

19. Peng LC, Milsom J, Garrett K, Nandakumar G, Coplowitz S, Parashar B, et al. Surveillance, epidemiology, and end results-based analysis of the impact of preoperative or postoperative radiotherapy on survival outcomes for T3n0 rectal cancer. *Cancer Epidemiol.* (2014) 38:73–8. doi: 10.1016/j.canep.2013.12.008

20. de Paula TR, Gorroochurn P, Kiran RP, Keller DS. Does adjuvant chemotherapy improve survival in T3n0 rectal cancer? An evaluation of use and outcomes from the national cancer database (n.d.). *J Gastrointest Surg.* (2020) 24:1188–91. doi: 10.1007/s11605-020-04541-6

21. Baek JY, Yu JI, Park HC, Choi DH, Yoo GS, Lee WY, et al. Determining whether postoperative chemoradiotherapy is required in patients with pathologic T3n0 rectal cancer with negative resection margin. *Int J Colorectal Dis.* (2020) 35:2239–48. doi: 10.1007/s00384-020-03701-z

22. Tournigand C, André T, Bonnetain F, Chibaudel B, Lledo G, Hickish T, et al. Adjuvant therapy with fluorouracil and oxaliplatin in stage II and elderly patients (between ages 70 and 75 years) with colon cancer: subgroup analyses of the multicenter international study of oxaliplatin, fluorouracil, and leucovorin in the adjuvant treatment of colon cancer trial. *J Clin Oncol.* (2012) 30:3353–60. doi: 10.1200/jco.2012.42.5645

23. Iveson TJ, Sobrero AF, Yoshino T, Souglakos I, Ou FS, Meyers JP, et al. Duration of adjuvant doublet chemotherapy (3 or 6 months) in patients with high-risk stage II colorectal cancer. *J Clin Oncol.* (2021) 39:631–41. doi: 10.1200/jco.20.01330

24. Souglakos J, Boukovinas I, Kakolyris S, Xynogalos S, Ziras N, Athanasiadis A, et al. Three- versus six-month adjuvant folfox or capox for high-risk stage ii and stage iii colon cancer patients: the efficacy results of hellenic oncology research group (horg) participation to the international duration evaluation of adjuvant chemotherapy (idea) project. *Ann Oncol.* (2019) 30:1304–10. doi: 10.1093/annonc/mdz193

25. Sargent DJ, Marsoni S, Monges G, Thibodeau SN, Labianca R, Hamilton SR, et al. Defective mismatch repair as a predictive marker for lack of efficacy of fluorouracil-based adjuvant therapy in colon cancer. *J Clin Oncol.* (2010) 28:3219–26. doi: 10.1200/jco.2009.27.1825

26. Tie J, Cohen JD, Lahouel K, Lo SN, Wang Y, Kosmider S, et al. Circulating tumor DNA analysis guiding adjuvant therapy in stage II colon cancer. *N Engl J Med.* (2022) 386:2261–72. doi: 10.1056/NEJMoa2200075

27. Compton CC. Pathology report in colon cancer: what is prognostically important? *Digest Dis.* (1999) 17:67–79. doi: 10.1159/000016908

28. Kidner TB, Ozao-Choy JJ, Yoon J, Bilchik AJ. Should quality measures for lymph node dissection in colon cancer be extrapolated to rectal cancer? *Am J Surg.* (2012) 204:843–7; discussion 7–8. doi: 10.1016/j.amjsurg.2012.05.003

29. Duraker N, Civelek Çaynak Z, Hot S. The prognostic value of the number of lymph nodes removed in patients with node-negative colorectal cancer. *Int J Surg.* (2014) 12:1324–7. doi: 10.1016/j.ijsu.2014.10.038

30. Sarli L, Bader G, Iusco D, Salvemini C, Mauro DD, Mazzeo A, et al. Number of lymph nodes examined and prognosis of Tnm stage II colorectal cancer. *Eur J Cancer.* (2005) 41:272–9. doi: 10.1016/j.ejca.2004.10.010

31. Edge SB, Compton CC. The American joint committee on cancer: the 7th edition of the AJCC cancer staging manual and the future of TNM. *Ann Surg Oncol.* (2010) 17:1471–4. doi: 10.1245/s10434-010-0985-4

32. Arnold A, Kloor M, Jansen L, Chang-Claude J, Brenner H, von Winterfeld M, et al. The association between microsatellite instability and lymph node count in colorectal cancer. *Virch Arch.* (2017) 471:57–64. doi: 10.1007/s00428-017-2150-y

33. Berger AC, Garcia M Jr, Hoffman JP, Regine WF, Abrams RA, Safran H, et al. Postresection Ca 19-9 predicts overall survival in patients with pancreatic cancer treated with adjuvant chemoradiation: a prospective validation by Rtog 9704. *J Clin Oncol.* (2008) 26:5918–22. doi: 10.1200/jco.2008.18.6288

34. Fritz S, Hackert T, Hinz U, Hartwig W, Büchler MW, Werner J. Role of serum carbohydrate antigen 19-9 and carcinoembryonic antigen in distinguishing between benign and invasive intraductal papillary mucinous neoplasm of the pancreas. *Br J Surg.* (2011) 98:104–10. doi: 10.1002/bjs.7280

35. Kim JR, Jang JY, Kang MJ, Park T, Lee SY, Jung W, et al. Clinical implication of serum carcinoembryonic antigen and carbohydrate antigen 19-9 for the prediction of malignancy in intraductal papillary mucinous neoplasm of pancreas. *J Hepato Biliary Pancreat Sci.* (2015) 22:699–707. doi: 10.1002/jhbp.275

36. Takakura Y, Ikeda S, Imaoka Y, Urushihara T, Itamoto T. An elevated preoperative serum carbohydrate antigen 19-9 level is a significant predictor for peritoneal dissemination and poor survival in colorectal cancer. *Colorectal Dis.* (2015) 17:417–25. doi: 10.1111/codi.12865

37. Zhou W, Yang F, Peng J, Wang F, Lin Y, Jiang W, et al. High pretreatment serum Ca19-9 level predicts a poor prognosis for patients with stage III colon cancer after curative resection and adjuvant chemotherapy. *J Cancer.* (2019) 10:3810–8. doi: 10.7150/jca.31375

38. Zheng Z, Wang X, Huang Y, Lu X, Chi P. Predictive value of changes in the level of carbohydrate antigen 19-9 in patients with locally advanced rectal cancer treated with neoadjuvant chemoradiotherapy. *Colorectal Dis.* (2020) 22:2068–77. doi: 10.1111/codi.15355

39. Dunn M, Morgan MB, Beer TW. Perineural invasion: identification, significance, and a standardized definition. *Dermatol Surg.* (2009) 35:214–21. doi: 10.1111/j.1524-4725.2008.34412.x

40. Buchwald P, Olofsson F, Lörinc E, Syk I. Standard protocol for assessment of colon cancer improves the quality of pathology. *Colorectal Dis.* (2011) 13:e33–6. doi: 10.1111/j.1463-1318.2010.02454.x

41. Weiser MR. Ajcc 8th edition: colorectal cancer. *Ann Surg Oncol.* (2018) 25:1454–5. doi: 10.1245/s10434-018-6462-1

42. Knijn N, Mogk SC, Teerenstra S, Simmer F, Nagtegaal ID. Perineural invasion is a strong prognostic factor in colorectal cancer: a systematic review. *Am J Surg Pathol.* (2016) 40:103–12. doi: 10.1097/pas.0000000000000518

43. Liebig C, Ayala G, Wilks JA, Berger DH, Albo D. Perineural invasion in cancer: a review of the literature. *Cancer.* (2009) 115:3379–91. doi: 10.1002/cncr.24396

44. Rizzo A, Pallone F, Monteleone G, Fantini MC. Intestinal inflammation and colorectal cancer: a double-edged sword? *World J Gastroenterol.* (2011) 17:3092–100. doi: 10.3748/wjg.v17.i26.3092

45. Ye X, Wang R, Bhattacharya R, Boulbes DR, Fan F, Xia L, et al. *Fusobacterium nucleatum* subspecies animalis influences proinflammatory cytokine expression and monocyte activation in human colorectal tumors. *Cancer Prev Res.* (2017) 10:398–409. doi: 10.1158/1940-6207.Capr-16-0178

46. Balkwill F, Charles KA, Mantovani A. Smoldering and polarized inflammation in the initiation and promotion of malignant disease. *Cancer Cell.* (2005) 7:211–7. doi: 10.1016/j.ccr.2005.02.013

47. Guo G, Wang Y, Zhou Y, Quan Q, Zhang Y, Wang H, et al. Immune cell concentrations among the primary tumor microenvironment in colorectal cancer patients predicted by clinicopathologic characteristics and blood indexes. *J Immunother Cancer.* (2019) 7:179. doi: 10.1186/s40425-019-0656-3

48. Hu S, Zou Z, Li H, Zou G, Li Z, Xu J, et al. The preoperative peripheral blood monocyte count is associated with liver metastasis and overall survival in colorectal cancer patients. *PLoS One.* (2016) 11:e0157486. doi: 10.1371/journal.pone.0157486

49. Liu J, Huang X, Yang W, Li C, Li Z, Zhang C, et al. Nomogram for predicting overall survival in stage II-III colorectal cancer. *Cancer Med.* (2020) 9:2363–71. doi: 10.1002/cam4.2896

frontiers | Frontiers in Surgery

TYPE Original Research
PUBLISHED 01 September 2022
DOI 10.3389/fsurg.2022.981591

Check for updates

OPEN ACCESS

EDITED BY
Chang-In Choi,
Pusan National University Hospital, South Korea

REVIEWED BY
Ludovico Carbone,
University of Siena, Italy
Francesca Marcon,
IRCCS Ca 'Granda Foundation Maggiore Policlinico Hospital, Italy

*CORRESPONDENCE
Yiping Mou
yipingmou@126.com;
Tao Xia
xiatao13@163.com

†These authors have contributed equally to this work

SPECIALTY SECTION
This article was submitted to Surgical Oncology, a section of the journal Frontiers in Surgery

RECEIVED 29 June 2022
ACCEPTED 10 August 2022
PUBLISHED 01 September 2022

CITATION
Niu N, He Y, Mou Y, Meng S, Xu P, Zhou Y, Jin W, Lu C, Xu Y, Zhu Q and Xia T (2022) Clinical outcome comparison of laparoscopic radical antegrade modular pancreatosplenectomy vs. laparoscopic distal pancreatosplenectomy for left-sided pancreatic ductal adenocarcinoma surgical resection. Front. Surg. 9:981591. doi: 10.3389/fsurg.2022.981591

COPYRIGHT
© 2022 Niu, He, Mou, Meng, Xu, Zhou, Jin, Lu, Xu, Zhu and Xia. This is an open-access article distributed under the terms of the Creative Commons Attribution License (CC BY). The use, distribution or reproduction in other forums is permitted, provided the original author(s) and the copyright owner(s) are credited and that the original publication in this journal is cited, in accordance with accepted academic practice. No use, distribution or reproduction is permitted which does not comply with these terms.

Clinical outcome comparison of laparoscopic radical antegrade modular pancreatosplenectomy vs. laparoscopic distal pancreatosplenectomy for left-sided pancreatic ductal adenocarcinoma surgical resection

Nan Niu[1,2†], Yuhui He[1,2†], Yiping Mou[2*], Sijia Meng[2,3], Peng Xu[2,4], Yucheng Zhou[2], Weiwei Jin[2], Chao Lu[2], Yunyun Xu[2], Qicong Zhu[2] and Tao Xia[2*]

[1]Department of Surgery, The Second Clinical Medical College of Zhejiang Chinese Medical University, Hangzhou, China, [2]Department of General Surgery, Cancer Center, Division of Gastrointestinal and Pancreatic Surgery, Zhejiang Provincial People's Hospital, Affiliated People's Hospital, Hangzhou Medical College, Hangzhou, China, [3]Department of Surgery, Bengbu Medical College, Bengbu, China, [4]Department of Surgery, Qingdao University, Qingdao, China

Background: Laparoscopic radical antegrade modular pancreatosplenectomy (LRAMPS) is a validated surgical treatment for patients with left-sided pancreatic ductal adenocarcinoma (PDAC). In addition, laparoscopic distal pancreatectomy (LDPS) has purported benefits. However, there is a limited analysis comparing the results between LRAMPS and LDPS. Thus, this study aims to compare the short-term and long-term outcomes of patients who underwent LRAMPS and LDPS for PDAC treatment.

Methods: Patients with left-sided PDAC that underwent LRAMPS or LDPS from 2015 to 2021 were retrospectively identified. Demographic and clinic pathologic data were collected. Disease-free survival (DFS) and overall survival (OS) probabilities were obtained.

Results: The number of lymph nodes retrieved was significantly greater in the LRAMPS group than in the LDPS group. Several clinicopathological factors, including CA19-9 levels greater than 37 U/ml, positive lymph nodes, moderate to poor tumor differentiation, and peripancreas fat invasion, were associated with DFS. Moderate with poor tumor differentiation was associated with poor DFS (HR 0.568; 95% CI 0.373–0.921; $P = 0.021$). Levels of CA19-9 greater than 37 U/ml, CEA levels greater than 5 μg/ml, larger tumor size, positive lymph nodes, moderate with poor tumor differentiation, peripancreas fat invasion, and adjuvant chemotherapy were all associated with OS. LRAMPS nearly improved OS but did not reach statistical significance. Serum carcinoembryonic antigen (CEA) levels greater than 5 ug/ml (HR 1.693; 95% CI 1.200–1.132; $P = 0.001$), and positive lymph nodes (HR 2.410; 95% CI 1.453–3.995; $P = 0.001$) were independently associated with poor OS. Treatment with adjuvant chemotherapy

was associated with improved OS (HR 0.491; 95% CI 0.248–0.708; $P = 0.001$).
Conclusions: The LRAMPS procedure achieved comparable results to standard LDPS in terms of postoperative outcomes. Treatment with chemotherapy is important for the prognosis of patients with left-sided pancreatic cancer.

KEYWORDS

pancreatic cancer, laparoscopic distal pancreatosplenectomy, laparoscopic RAMPS, chemotherapy, survivability

Introduction

Surgical resection offers the only curative treatment for pancreatic ductal adenocarcinoma (PDAC). Specifically, distal pancreatectomy (DPS) is the standard procedure for left-sided PDAC resection, but it has a high rate of retroperitoneal margin positivity (62%), which indicates that cancerous tissue persists post-surgery. In 2003, Dr. Steven Strasberg introduced the radical antegrade modular pancreatosplenectomy (RAMPS) procedure (1). Compared to DPS, RAMPS attempts to achieve negative retroperitoneal margins and higher lymph node retrieval in order to improve survival outcomes (2, 3). Several studies have demonstrated that RAMPS increases the negative tangential margin rate and lymph node harvest (4). Furthermore, laparoscopic distal pancreatectomy (LDPS) has purported benefits for short-term and long-term outcomes compared to open DPS (5, 6). Similarly, laparoscopic RAMPS (LRAMPS) has been demonstrated to be more feasible (7–9). In a recent meta-analysis to date comparing minimally invasive RAMPS (MI-RAMPS) against open RAMPS, intra-operative blood loss was observed to be significantly reduced in MI-RAMPS, while lymph node yield was higher in O-RAMPS and there was no difference in overall survival (OS) (10). Modern chemotherapy has proven to be effective and improves the survival of PDAC. A previous study revealed chemotherapy to be an independent factor for OS after RAMPS and DPS (11). However, there is limited clinical outcome analysis comparing the LRAMPS and LDPS procedures with chemotherapy. Thus, we conducted this study to compare the short-term and long-term outcomes of patients who underwent LRAMPS and LDPS for left-sided PDAC treatment.

Methods

Patients

From May 2015 to May 2021, patients with left-sided PDAC that underwent LRAMPS or LDPS procedures performed by one surgeon were retrospectively identified from the database at Zhejiang Provincial People's Hospital. Patients with left-sided PDAC without any evidence of distant metastasis or vascular invasion beyond the celiac axis were included. Patients who underwent neoadjuvant therapy and vascular reconstruction were excluded. All acquisition methods were approved by the Institutional Review Board.

Demographic and clinic pathologic data were collected. Postoperative pancreatic fistula (POPF) was defined according to the International Study Group on Pancreatic Fistula Definition (ISGPF) (12). All patients with grades B and C were defined as having clinically significant POPF. The severity of complications was defined according to Clavien–Dindo classification system (13). Pathological data were classified using the eighth AJCC/UICC TNM. R1 margin status was defined as <1 mm from the edge of the specimen. Overall survival (OS) was defined as the duration of time between the date of surgery and the date of death. Disease-free survival (DFS) was similarly calculated as the interval between the date of surgery and the date of tumor recurrence. Adjuvant chemotherapy was recommended as routine therapy for patients who could tolerate the adverse effects. Chemotherapy regimens and duration were left to the discretion of the oncologist.

Operative procedures

The LRAMPS procedure was performed in our institution since 2017 as described by Strasberg et al. (1). Briefly, patients were placed in the supine position with their heads slightly elevated. Five trocars, including a camera port (10 mm) below the umbilicus and four additional working ports (one 12 mm and three 5 mm), were placed in the right flank, right upper flank, left upper flank, and left flank. The peritoneal cavity and liver surface were inspected to rule out metastasis. The gastrocolic ligament was divided to expose the anterior surface of the pancreas. The inferior border of the pancreas was mobilized to visualize the superior mesenteric vein and the portal vein. Furthermore, the pancreas was mobilized along the superior border to explore the common hepatic artery and to dissect the lymph nodes along the common hepatic and gastroduodenal arteries. The pancreas neck was then transected with an endoscopic linear stapler (Ethicon Endo-Surgery, PSE45A, Cincinnati, OH, USA). The splenic artery and vein were ligated and divided, respectively. Lymph nodes were dissected from the celiac axis down to the left side of the superior mesenteric artery. The distal pancreas was

dissected along with the soft tissue of the retroperitoneum in a medial-to-lateral manner. The short gastric vessels were ligated to mobilize the spleen and the lymph nodes along the splenic artery and hilum were removed. After complete resection of the distal pancreas and spleen, the tissue was removed through an enlarged umbilical incision with a specimen bag. The LDPS procedure was performed as previously described (14). The laparoscopic procedure was performed as the LRAMPS procedure. The lymph nodes along the celiac axis and superior mesenteric artery were dissected but the soft tissue of the retroperitoneum was reserved.

Statistical analysis

All statistical analyses were performed using SPSS v.22.0 and GraphPad Prism 8 software. All continuous variables were presented as median summative values with interquartile ranges (IQRs). Continuous variables were compared using the student's *t*-test or Wilcoxon rank test for parametric or nonparametric distributions, respectively. The chi-square or Fisher's exact tests were used to analyze categorical variables, as appropriate. OS and DFS were assessed using the Kaplan–Meier estimate method, and comparisons were conducted using the log-rank test. Only variables with *P*-value less than 0.05 in univariate analysis were included in a Cox proportional hazards model. *P*-values less than 0.05 were considered statistically significant.

Results

In total, 109 patients with left-sided PDAC underwent surgical resection. Clinic pathological characteristics of patients are summarized in Table 1.

Fifty (45.9%) patients underwent LRAMPS, and 59 (54.1%) patients underwent LDPS. Factors including sex, age, BMI, serum carbohydrate antigen (CA) 19-9 values, and serum carcinoembryonic antigen (CEA) values were confirmed to have no significant difference between the LRAMPS and LDPS groups. A total of 19 patients developed clinically significant POPF. Thirteen cases of grade B POPF occurred in the LDPS group. Moreover, one case of grade C and five cases of grade B POPF were confirmed in the LRAMPS group. No meaningful differences were found in operative time, estimated blood loss (EBL), clinically significant POPF, complications, or length of stay (Table 1).

There were no significant differences in the tumor size, level of differentiation, R0 resection margin, perineural invasion, vascular invasion, or peripancreas fat invasion. The number of lymph nodes retrieved was significantly greater in the LRAMPS group than in the LDPS group ($P = 0.035$). Furthermore, 49 (42.2%) patients received adjuvant chemotherapy and others rejected chemotherapy. Gemcitabine-based chemotherapy was administered as first-line chemotherapy for most patients; the remaining patients received FOLFIRINOX. The median follow-up period was 46.7 months.

TABLE 1 Clinicopathological characteristics of patients with left-side pancreatic ductal adenocarcinoma.

Variables	All cases ($N = 109$)	LRAMPS ($N = 50$)	LDPS ($N = 59$)	*P* value
Sex, female	41 (37.6%)	19 (38%)	22 (37.3%)	0.939
Age (years)	67 [38,88]	67 [44,87]	66 [38,88]	0.588
BMI (kg/m^2)	22.37 [14.76,30.47]	22.30 [17.58,30.09]	22.39 [14.76,30.47]	0.081
CA19-9 (>37 U/L)	83 (76.1%)	37 (74%)	46 (78%)	0.628
CEA (>5 U/L)	39 (35.8%)	18 (36%)	21 (35.6%)	0.965
Estimated blood loss (ml)	100 [40,300]	100 [50,300]	100 [40,200]	0.627
Operative time (min)	130 [90,310]	140 [100,310]	130 [90,230]	0.351
Pancreatic fistula, B and C	19 (17.4%)	6 (12%)	13 (22%)	0.169
Clavien–Dindo, I/II, III	98/11	46/4	52/7	0.505
Length of stay (days)	12 [7,56]	13 [7,56]	12[7,44]	0.940
Tumor size (cm)	3.5 [1.5,10]	3.5 [1.8,10]	3.5 [1.5–7.0]	0.799
Retrieved lymph nodes	9 [5,28]	11 [5,28]	7 [5–28]	0.035
Resection margin status	5 (9.4%)	3 (6%)	2 (3.4%)	0.659
Differentiation, well-moderate/moderate with poor	59/50	25/25	34/25	0.426
Perineural invasion, yes/no	86/23	44/6	42/17	0.056
Vascular invasion, yes/no	37/72	19/31	18/41	0.401
Peripancreas fat invasion, yes/no	77/32	34/16	43/16	0.577
Adjuvant chemotherapy, yes/no	48/61	23/27	25/34	0.704

LRAMPS, laparoscopic radical antegrade modular pancreatosplenectomy; LDPS, laparoscopic distal pancreatectomy; CA, carbohydrate antigen; CEA, carcinoembryonic antigen.

By the end of the follow-up period, disease recurrence occurred in 77 (70.64%) patients and 69 (63.3%) patients had died. The median DFS was 12.6 months and the median OS was 22.9 months. Finally, the 1-year, 3-year, and 5-year OS rates were 84.4%, 25.7%, and 12.8%, respectively.

Several clinicopathological factors were associated with DFS upon univariate analysis, including CA19-9 levels greater than 37 U/ml, positive lymph nodes, moderate with poor tumor differentiation, and peripancreas fat invasion. Neither surgical procedure nor adjuvant chemotherapy was found to affect DFS. Additionally, moderate with poor tumor differentiation was associated with poor DFS upon multivariate analysis (HR 0.568; 95% CI 0.373–0.921; $P = 0.021$) (Table 2).

Univariate analysis revealed CA19-9 levels greater than 37 U/ml, CEA levels greater than 5 ug/ml, larger tumor size, positive lymph nodes, moderate with poor tumor differentiation, peripancreas fat invasion, and adjuvant chemotherapy were associated with OS. LRAMPS trended to improve OS but did not reach statistical significance (28.83 months vs. 18.93 months, $P = 0.336$). Serum CEA levels greater than 5 μg/ml (HR 1.693; 95% CI 1.200–1.132; $P = 0.001$) and positive lymph nodes (HR 2.410; 95% CI 1.453–3.995; $P = 0.001$) were independently associated with poor OS. Treatment with adjuvant chemotherapy was associated with improved OS (HR 0.491; 95% CI 0.248–0.708; $P = 0.001$) (Table 3).

Cancer-positive lymph nodes were found to affect both DFS and OS. The LRAMPS procedure retrieved more lymph nodes than LDPS. However, the median OS of patients with positive lymph nodes that underwent LRAMPS and LDPS was 22.1 and 13.6 months, respectively, and did not reach statistical significance ($P = 0.156$). OS in patients with positive lymph nodes and treated with adjuvant chemotherapy was significantly different from untreated patients (33.5 months vs. 13.4 months, $P = 0.001$) (Figure 1). In the cancer-negative lymph node cohort, neither surgical procedure ($P = 0.502$) nor treatment with adjuvant chemotherapy ($P = 0.065$) was found to affect OS (Figure 2).

TABLE 2 Kaplan–Meier and Cox proportional hazard regression analysis of disease-free survival.

Variables	Univariate		Multivariate		
	Median survival (months)	*P* value	HR	95% CI	*P* value
Sex (male/female)	11.00/17.40	0.401			
Age (≤74/≥75 years)	12.60/12.10	0.601			
BMI (≤18.4/≥18.5 kg/m^2)	9.60/12.70	0.464			
CA19-9 (<37/≥37 U/L)	41.30/11.80	0.017	1.757	0.970–1.259	0.063
CEA (<5/≥5 U/L)	13.20/11.00	0.098			
LRAMPS/LDPS	11.80/14.70	0.544			
T (T1/T2, T3)	54.90/12.40	0.193			
Positive lymph nodes (yes/no)	9.70/15.60	0.003	1.352	0.793–2.303	0.268
Resection margin status (R0/R1)	12.60/12.10	0.922			
Differentiation (moderate with poor/well-moderate)	9.20/17.30	0.010	0.568	0.373–0.921	0.021
Perineural invasion (yes/no)	12.40/12.60	0.641			
Lymphatic invasion (yes/no)	16.20/12.10	0.757			
Peripancreas fat invasion (yes/no)	12.00/13.00	0.020	0.598	0.341–1.050	0.074
Adjuvant chemotherapy (yes/no)	17.40/11.8	0.095			

LRAMPS, laparoscopic radical antegrade modular pancreatosplenectomy; LDPS, laparoscopic distal pancreatectomy; CA, carbohydrate antigen; CEA, carcinoembryonic antigen.

Discussion

Curative surgery plays an essential role in the treatment of PDAC. R0 resection margin and radical N1 lymph node resection are major prognostic factors for patients with left-sided PDAC (15, 16). Many reports (11, 17) showed that RAMPS achieved improved R0 resection and regional lymph node retrieval compared to DPS as evident by reported outcomes. Due to these results, RAMPS became a mainstream surgical procedure for patients with left-sided PDAC. Over the past decade, the safety and feasibility of LDPS improved and demonstrated fewer complications with shortened hospital stays worldwide (5). Therefore, the LRAMPS procedure was mainly performed in high-volume pancreatic centers, where several reports indicated the improved safety and feasibility of LRAMPS (10).

TABLE 3 Kaplan–Meier and Cox proportional hazard regression analysis of overall survival.

Variables	Univariate		Multivariate		
	Median survival (months)	*P* value	HR	95% CI	*P* value
Sex (male/female)	20.00/28.83	0.425			
Age (≤74/≥75 years)	25.80/16.50	0.108			
BMI (≤18.4/≥18.5 kg/m^2)	21.80/24.27	0.697			
CA19-9 (<37/≥37 U/L)	46.33/20.00	0.019	1.680	0.893–3.161	0.107
CEA (<5/≥5 U/L)	26.43/16.60	0.010	1.963	1.200–3.212	0.007
LRAMPS/LDPS	18.93/28.83	0.336			
T (T1/T2, T3)	No/22.93	0.126			
Positive lymph nodes (yes/no)	16.80/29.53	0.002	2.410	1.453–3.995	0.001
Resection margin status (R0/R1)	22.93/33.27	0.822			
Differentiation (moderate with poor/well-moderate)	17.60/33.53	0.017	0.661	0.386–1.132	0.132
Perineural invasion (yes/no)	23.33/22.93	0.959			
Lymphatic invasion (yes/no)	22.93/23.33	0.642			
Peripancreas fat invasion (yes/no)	21.53/29.77	0.034	0.762	0.404–1.437	0.401
Adjuvant chemotherapy (yes/no)	33.53/16.50	0.001	0.419	0.248–0.708	0.001

LRAMPS, laparoscopic radical antegrade modular pancreatosplenectomy; LDPS, laparoscopic distal pancreatectomy; CA, carbohydrate antigen; CEA, carcinoembryonic antigen.

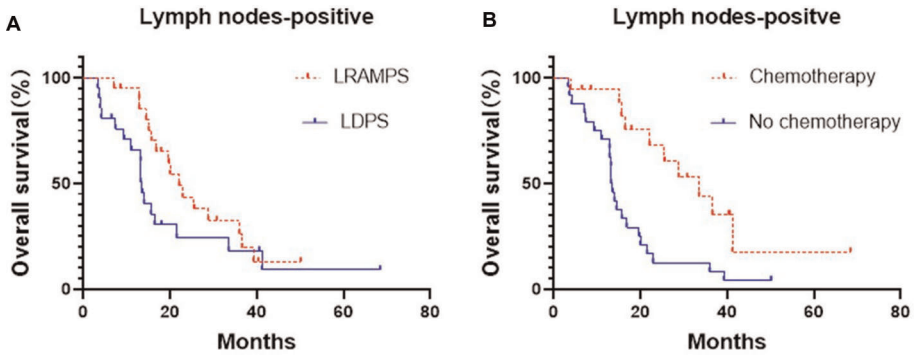

FIGURE 1
Median OS of positive lymph nodes patients, (A) LRAMPS: 22.1 months; LDPS: 13.57 months. (B) Chemotherapy: 33.5 months; no chemotherapy: 13.4 months.

The LRAMPS procedure is more complex than LDPS. Therefore, surgeons worried about longer operative times and perioperative complications when deciding between the two procedures. However, in the present study, there were no significant differences found in operative time, EBL, clinically significant POPF, complications, and length of stay between LRAMPS and LDPS groups. A large, multi-institutional study also revealed that there were no differences in rates of postoperative pancreatic fistula (16.5% vs. 17.8%, $P = 1.000$) and postoperative hemorrhage (5.9% vs. 3.6%, $P = 0.385$) between RAMPS and DPS groups (18). Furthermore, a meta-analysis indicated no significant differences were observed between RAMPS and DPS in terms of postoperative complications ($P = 0.87$), POPF ($P = 0.15$), mortality ($P = 0.80$), and length of stay ($P = 0.53$) (4).

This study demonstrated no significant difference in DFS or OS between LRAMPS and LDPS procedures and supported the findings of previous studies and meta-analyses of RAMPS and DPS (11, 18). Moreover, the results showed that adjuvant chemotherapy was associated with improved OS. It supported the consensus that adjuvant chemotherapy is indispensable for patients with PDAC. Survival is slowly increasing with a reported median OS of 54.4 months with adjuvant chemotherapy with FOLFIRINOX after surgery (19, 20).

Many RAMPS proponents argued that R0 resection and more lymph node retrieval can improve prognosis. In this study, the number of lymph nodes retrieved was significantly greater in the LRAMPS group than in the LDPS group. However, there was no significant difference in the survival of patients with positive lymph nodes that underwent LRAMPS or LDPS (22.1 months vs. 13.6 months, $P = 0.156$). In addition, we found no significant difference in the R0 resection margin. Moreover, OS in patients with positive lymph nodes and treated with adjuvant chemotherapy was significantly longer than in patients that did not receive adjuvant chemotherapy (33.5 vs. 13.4, $P = 0.001$). It was consistent with several reports between open RAMPS and DPS (11, 18). We hypothesize the survival of patients with positive lymph nodes was more likely determined by adjuvant chemotherapy because of biological properties rather than

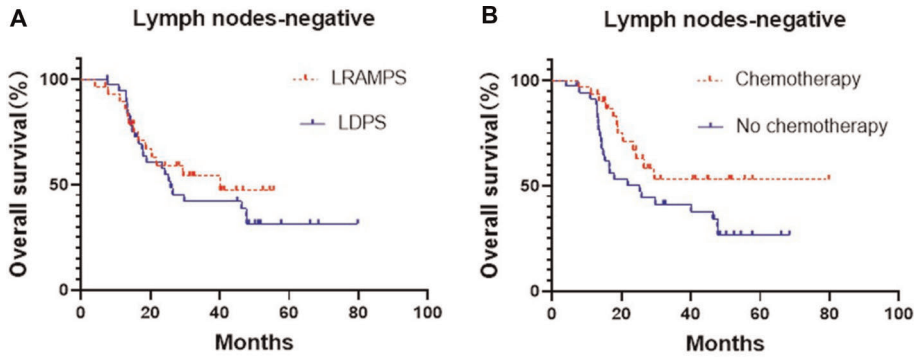

FIGURE 2
Median OS of negative lymph nodes patients, (A) LRAMPS: 40.1 months; LDPS: 25.8 months. (B) Chemotherapy: not reach; no chemotherapy: 25.3 months.

surgical procedures (21). Modern chemotherapy has proven to be effective and improve survival, even in the setting of an R1 resection (22, 23).

We acknowledge that this study has limitations. First, this was a retrospective, cohort study, which has inherent weaknesses. Second, some data, such as pancreatic parenchyma texture and the thickness of the pancreatic stump, were not elaborately collected and may affect the quality of the reported short-term outcomes. Finally, due to the limited number of patients who received adjuvant chemotherapy, the efficacy of different chemotherapy regimens could not be thoroughly evaluated.

Conclusions

The LRAMPS procedure achieves comparable results to standard LDPS regarding postoperative outcomes. Comparatively, LRAMPS retrieves more lymph nodes. In addition, positive lymph nodes correlated with both DFS and OS. However, LRAMPS is not associated with an improvement in either DFS or OS over LDPS. OS in patients with positive lymph nodes and treated with adjuvant chemotherapy was significantly better than in untreated patients. Treatment with chemotherapy is an important predictive factor procedure for the prognosis of patients with left-sided pancreatic cancer.

Data availability statement

The original contributions presented in the study are included in the article/Supplementary Material, further inquiries can be directed to the corresponding author/s.

Ethics statement

The studies involving human participants were reviewed and approved by Zhejiang Provincial People's Hospital Institutional Review Board. The patients/participants provided their written informed consent to participate in this study.

Author contributions

NN, YM, and TX contributed to the conception and design of the study. YHH, YCZ, WWJ, CL, QCZ, and YX organized the database. SM, PX, TX performed the statistical analysis. TX wrote the first draft of the manuscript. NN and YH wrote sections of the manuscript. All authors contributed to the article and approved the submitted version.

Funding

This work was supported by the Key Medical Science and Technology Project of Zhejiang Province (no. WKJ-ZJ-2201 to YPM), and Key Projects of Zhejiang Provincial Science and Technology (no. 2022C03099 to YPM).

Conflict of interest

The authors declare that the research was conducted in the absence of any commercial or financial relationships that could be construed as a potential conflict of interest.

Publisher's note

All claims expressed in this article are solely those of the authors and do not necessarily represent those of their affiliated organizations, or those of the publisher, the editors and the reviewers. Any product that may be evaluated in this article, or claim that may be made by its manufacturer, is not guaranteed or endorsed by the publisher.

References

1. Strasberg SM, Drebin JA, Linehan D. Radical antegrade modular pancreatosplenectomy. *Surgery*. (2003) 133(5):521–7. doi: 10.1067/msy.2003.146

2. Dai M, Zhang H, Li Y, Xing C, Ding C, Liao Q, et al. Radical antegrade modular pancreatosplenectomy (RAMPS) versus conventional distal pancreatosplenectomy (CDPS) for left-sided pancreatic ductal adenocarcinoma. *Surg Today*. (2021) 51(7):1126–34. doi: 10.1007/s00595-020-02203-3

3. Chun YS. Role of radical antegrade modular pancreatosplenectomy (RAMPS) and pancreatic cancer. *Ann Surg Oncol*. (2018) 25(1):46–50. doi: 10.1245/s10434-016-5675-4

4. Zhou Q, Fengwei G, Gong J, Xie Q, Liu Y, Wang Q, et al. Assessment of postoperative long-term survival quality and complications associated with radical antegrade modular pancreatosplenectomy and distal pancreatectomy: a meta-analysis and systematic review. *BMC Surg*. (2019) 19(1):12. doi: 10.1186/s12893-019-0476-x

5. Lee JM, Kim H, Kang JS, Byun Y, Choi YJ, Sohn HJ, et al. Comparison of perioperative short-term outcomes and oncologic long-term outcomes between open and laparoscopic distal pancreatectomy in patients with pancreatic ductal adenocarcinoma. *Ann Surg Treat Res*. (2021) 100(6):320–8. doi: 10.4174/astr.2021.100.6.320

6. de Rooij T, van Hilst J, van Santvoort H, Boerma D, van den Boezem P, Daams F, et al. Minimally invasive versus open distal pancreatectomy (LEOPARD): a multicenter patient-blinded randomized controlled trial. *Ann Surg*. (2019) 269(1):2–9. doi: 10.1097/SLA.0000000000002979

7. Larkins K, Rowcroft A, Pandanaboyana S, Loveday BPT. A systematic scoping review of the initial experience with laparoscopic radical antegrade modular pancreatosplenectomy for pancreatic malignancy. *Surg Endosc*. (2021) 35 (9):4930–44. doi: 10.1007/s00464-021-08528-5

8. Hirashita T, Iwashita Y, Fujinaga A, Nakanuma H, Tada K, Masuda T, et al. Surgical and oncological outcomes of laparoscopic versus open radical antegrade modular pancreatosplenectomy for pancreatic ductal adenocarcinoma. *Surg Today*. (2021) 52(2):224–30. doi: 10.1007/s00595-021-02326-1

9. Zhang H, Li Y, Liao Q, Xing C, Ding C, Zhang T, et al. Comparison of minimal invasive versus open radical antegrade modular pancreatosplenectomy (RAMPS) for pancreatic ductal adenocarcinoma: a single center retrospective study. *Surg Endosc*. (2021) 35(7):3763–73. doi: 10.1007/s00464-020-07938-1

10. Wu EJ, Kabir T, Zhao JJ, Sarr M, Abu Hilal M, Adham M, et al. Minimally invasive versus open radical antegrade modular pancreatosplenectomy: a meta-analysis. *World J Surg*. (2022) 46(1):235–45. doi: 10.1007/s00268-021-06328-5

11. Kim HS, Hong TH, You YK, Park JS, Yoon DS. Radical antegrade modular pancreatosplenectomy (RAMPS) versus conventional distal pancreatectomy for left-sided pancreatic cancer: findings of a multicenter, retrospective, propensity score matching study. *Surg Today*. (2021) 51(11):1775–86. doi: 10.1007/s00595-021-02280-y

12. Bassi C, Marchegiani G, Dervenis C, Sarr M, Abu Hilal M, Adham M, et al. The 2016 update of the International Study Group (ISGPS) definition and grading of postoperative pancreatic fistula: 11 years after. *Surgery*. (2017) 161(3):584–91. doi: 10.1016/j.surg.2016.11.014

13. Clavien PA, Barkun J, DE Oliveira ML, Vauthey JN, Dindo D, Schulick RD, et al. The Clavien–Dindo classification of surgical complications: five-year experience. *Ann Surg*. (2009) 250(2):187–96. doi: 10.1097/SLA.0b013e3181b13ca2

14. Xia T, Zhou JY, Mou YP, Xu XW, Zhang RC, Zhou YC, et al. Risk factors for postoperative pancreatic fistula after laparoscopic distal pancreatectomy using stapler closure technique from one single surgeon. *PLoS One*. (2017) 12(2): e0172857. doi: 10.1371/journal.pone.0172857

15. Rho SY, Hwang HK, Chong JU, Yoon DS, Lee WJ, Kang CM. Association of preoperative total lymphocyte count with prognosis in resected left-sided pancreatic cancer. *ANZ J Surg*. (2019) 89(5):503–8. doi: 10.1111/ans.15030

16. Sugawara T, Ban D, Nishino J, Watanabe S, Maekawa A, Ishikawa Y, et al. Prediction of early recurrence of pancreatic ductal adenocarcinoma after resection. *PLoS One*. (2021) 16(4):e0249885. doi: 10.1371/journal.pone.0249885

17. Trottman P, Swett K, Shen P, Sirintrapun J. Comparison of standard distal pancreatectomy and splenectomy with radical antegrade modular pancreato-splenectomy. *Am Surg*. (2014) 80(3):295–300. doi: 10.1177/000313481408000326

18. Sham JG, Guo S, Ding D, Shao Z, Wright M, Jing W, et al. Radical antegrade modular pancreatosplenectomy versus standard distal pancreatosplenectomy for pancreatic cancer, a dual-institutional analysis. *Chin Clin Oncol*. (2020) 9(4):54. doi: 10.21037/cco-20-6

19. Oneda E, Zaniboni A. Are we sure that adjuvant chemotherapy is the best approach for resectable pancreatic cancer? Are we in the era of neoadjuvant treatment? A review of current literature. *J Clin Med*. (2019) 8(11):1922. doi: 10.3390/jcm8111922

20. Motoi F, Unno M. Adjuvant and neoadjuvant treatment for pancreatic adenocarcinoma. *Jpn J Clin Oncol*. (2020) 50(5):483–9. doi: 10.1093/jjco/hyaa018

21. Wijetunga AR, Chua TC, Nahm CB, et al. Survival in borderline resectable and locally advanced pancreatic cancer is determined by the duration and response of neoadjuvant therapy. *Eur J Surg Oncol*. (2021) 47(10):2543–50. doi: 10.1016/j.ejso.2021.04.005

22. Zhang E, Wang L, Shaikh T, Pavlakis N, Clarke S, Chan DL, et al. Neoadjuvant chemoradiation impacts the prognostic effect of surgical margin status in pancreatic adenocarcinoma. *Ann Surg Oncol*. (2022) 29(1):354–63. doi: 10.1245/s10434-021-10219-3

23. Arrington AK, Hsu CH, Schaefer KL, O'grady CL, Khreiss M, Riall TS. Survival after margin-positive resection in the era of modern chemotherapy for pancreatic cancer: do patients still benefit? *J Am Coll Surg*. (2021) 233(1):100–9. doi: 10.1016/j.jamcollsurg.2021.02.020

frontiers | Frontiers in Oncology

TYPE Original Research
PUBLISHED 02 September 2022
DOI 10.3389/fonc.2022.975846

Check for updates

OPEN ACCESS

EDITED BY
Ravindra Deshpande,
Wake Forest School of Medicine,
United States

REVIEWED BY
Gayatri Ramachandran,
University of Hyderabad, India
Shuji Isaji,
Mie University Hospital, Japan
Shiva Basnet,
Tongji University, China

*CORRESPONDENCE
Jinghai Song
jhaisong2003@126.com

SPECIALTY SECTION
This article was submitted to Gastrointestinal Cancers: Hepato Pancreatic Biliary Cancers, a section of the journal Frontiers in Oncology

RECEIVED 22 June 2022
ACCEPTED 11 August 2022
PUBLISHED 02 September 2022

CITATION
Zheng Y, Lu Z, Shi X, Tan T, Xing C, Xu J, Cui H and Song J (2022) Lymph node ratio is a superior predictor in surgically treated early-onset pancreatic cancer.
Front. Oncol. 12:975846.
doi: 10.3389/fonc.2022.975846

COPYRIGHT
© 2022 Zheng, Lu, Shi, Tan, Xing, Xu, Cui and Song. This is an open-access article distributed under the terms of the Creative Commons Attribution License (CC BY). The use, distribution or reproduction in other forums is permitted, provided the original author(s) and the copyright owner(s) are credited and that the original publication in this journal is cited, in accordance with accepted academic practice. No use, distribution or reproduction is permitted which does not comply with these terms.

Lymph node ratio is a superior predictor in surgically treated early-onset pancreatic cancer

Yangyang Zheng[1,2], Zhenhua Lu[1], Xiaolei Shi[1], Tianhua Tan[1,2], Cheng Xing[1], Jingyong Xu[1], Hongyuan Cui[1] and Jinghai Song[1,2]*

[1]Department of General Surgery, Department of Hepato-bilio-pancreatic Surgery, Beijing Hospital, National Center of Gerontology, Institute of Geriatric Medicine, Chinese Academy of Medical Sciences, Beijing, China, [2]Graduate School of Peking Union Medical College, Chinese Academy of Medical Sciences, Beijing, China

Background: The prognostic performance of four lymph node classifications, the 8th American Joint Committee on Cancer (AJCC) Tumor Node Metastasis (TNM) N stage, lymph node ratio (LNR), log odds of positive lymph nodes (LODDS), and examined lymph nodes (ELN) in early-onset pancreatic cancer (EOPC) remains unclear.

Methods: The Surveillance, Epidemiology, and End Results (SEER) database was searched for patients with EOPC from 2004 to 2016. 1048 patients were randomly divided into training (n = 733) and validation sets (n = 315). The predictive abilities of the four lymph node staging systems were compared using the Akaike information criteria (AIC), receiver operating characteristic area under the curve (AUC), and C-index. Multivariate Cox analysis was performed to identify independent risk factors. A nomogram based on lymph node classification with the strongest predictive ability was established. The nomogram's precision was verified by the C-index, calibration curves, and AUC. Kaplan–Meier analysis and log-rank tests were used to compare differences in survival at each stage of the nomogram.

Results: Compared with the 8th N stage, LODDS, and ELN, LNR had the highest C-index and AUC and the lowest AIC. Multivariate analysis showed that N stage, LODDS, LNR were independent risk factors associated with cancer specific survival (CSS), but not ELN. In the training set, the AUC values for the 1-, 3-, and 5-year CSS of the nomogram were 0.663, 0.728, and 0.760, respectively and similar results were observed in the validation set. In addition, Kaplan–Meier survival analysis showed that the nomogram was also an important factor in the risk stratification of EOPC.

Conclusion: We analyzed the predictive power of the four lymph node staging systems and found that LNR had the strongest predictive ability. Furthermore,

the novel nomogram prognostic staging mode based on LNR was also an important factor in the risk stratification of EOPC.

KEYWORDS

early-onset pancreatic cancer, lymph node ratio, log odds of positive lymph nodes, examined lymph nodes, nomogram

Introduction

Pancreatic cancer is a highly lethal solid organ malignancy with a poor 5-year overall survival (OS) rate approaching 10% and is the third leading cause of cancer-related death in America (1). With increased incidence and mortality rates, and difficulty in developing effective therapies for pancreatic cancer, this type of malignancy is expected to be the second-leading cause of cancer-related death in developed countries by 2040 (2). Although pancreatic cancer is often thought of as a disease of older adults, with a higher incidence in people aged 60 to 70 years, some retrospective studies have observed an increase in the incidence in younger age groups. Sung et al. observed a significant increase in the incidence of pancreatic cancer in people under 50 years of age (3). Tavakkoli et al. found that the incidence of pancreatic cancer increased by 44% in black and 57% in white patients aged 30-39 years, highlighting the emerging challenge of early-onset pancreatic cancer (EOPC) (4). Currently, there is no international standard definition of early onset pancreatic cancer. In recent years, early onset pancreatic cancer has been defined in literatures as pancreatic cancer diagnosed before the age of 40, 45, 50 years (5–8). Considering that researchers often use the criterion of age < 50 years for EOPC in literatures and the American Gastrointestinal Association Institute recommended that screening for pancreatic cancer in high-risk groups should begin at age 50, we have defined EOPC as pancreatic cancer diagnosed at an age of less than 50 years in this study (8–13). One study reported that EOPC can result in up to one-third of the total years lost to disease, suggesting its impact on overall life expectancy (14). Patients with EOPC often contribute to the extra global cancer burden by bringing about years of life lost because of premature death; thus, improving its prognosis may dramatically help reduce the global burden of disease.

Abbreviations: AIC, Akaike information criterion; AJCC, American Joint Committee on Cancer; AOPC, Average age-onset pancreatic cancer; AUC, Area under the curve; CI, Confidence interval; CSS, Cancer specific survival; ELN, Examined lymph nodes; HR, Hazard ratio; LODDS, Log odds of positive lymph nodes; LNR, Lymph node ratio; PLN, Positive lymph node; ROC, Receiver operating characteristic; SEER, Surveillance Epidemiology and End Results; TNM, Tumor Node Metastasis (TNM).

Although the risk factors for EOPC are similar to those for average age-onset pancreatic cancer (AOPC), including obesity, smoking, and alcohol consumption, studies have further suggested that patients with EOPC may present unique clinical, pathological, and genomic features that may affect prognosis (8, 14–18). Some studies have also shown that patients with EOPC tend to be diagnosed at a later clinical stage. Consequently, these patients receive more aggressive treatment in the absence of significant comorbidities and have a better prognosis because of better functional reserve (8, 11, 19).

Among the predictors of postoperative survival, lymph node metastasis is a decisive factor for pancreatic cancer (20, 21). Therefore, accurate and efficient indicators for the evaluation of lymph node metastasis are necessary to provide individualized treatment and improve the prognosis of patients with EOPC. Little is known about the relationship between the prognosis of postoperative patients with EOPC and the new lymph node classifications. Nomogram is a predictive tool of visually assessing risk by providing a numerical estimate of the probability of a specific clinical event, while incorporating key factors of clinical outcome. Nomogram prognostic model has been used extensively in recent years for the prediction of most tumors. Some studies have shown that the predictive performance of nomogram is superior to that of TNM stage (22–24).

The purpose of the current study was to compare the predictive ability of four lymph node staging systems, namely, the 8th American Joint Committee on Cancer (AJCC) Tumor Node Metastasis (TNM) N stage, lymph node ratio (LNR), log odds of positive lymph nodes (LODDS), and examined lymph nodes (ELN), to screen the most effective factor in predicting cancer specific survival (CSS) in patients with EOPC who have undergone surgery and establish a novel nomogram prognostic staging model.

Materials and methods

Data collection in the SEER database

This retrospective study focused on patients diagnosed with EOPC who underwent radical surgery between 2004 and 2016.

All the data involved in this study were retrieved from the Surveillance, Epidemiology, and End Results (SEER) 18 registry research database (SEER*Stat 8.3.9). SEER database is a federally funded, private information-free, publicly available cancer reporting system. We have been granted access to the database data (SEER Stat username: 14866-Nov2020).

Patients diagnosed with EOPC were identified according to the site codes (C25.0-25.9) and histologic codes (8010, 8020, 8021,8022, 8050, 8140, 8141, 8230, 8260, 8450, 8453, 8471,8480, 8481and 8500) of the International Classification of Diseases for Oncology, 3rd edition (ICD-O-3). This study defined early-onset disease as a diagnosis before the age of 50. The inclusion criteria were as follows (1) patients diagnosed with EOPC were identified according to the site codes (C25.0-25.9) and histologic codes (8010, 8020, 8021,8022, 8050, 8140, 8141, 8230, 8260, 8450, 8453, 8471,8480, 8481and 8500) of the International Classification of Disease for Oncology, 3rd edition (ICD-O-3); (2) patients diagnosed before the age of 50 years; (3) patients with complete lymph node biopsy records; (4) patients undergoing radical surgery; and (5) patients with a survival time of more than one month after surgery. The exclusion criteria were as follows: (1) an unconfirmed diagnosis by histopathology; (2) incomplete clinicopathological data; (3) patients who died of causes other than pancreatic cancer or an unknown cause; (4) pancreatic operation without lymph node harvest; and (5) incomplete or absent information about survival time, overall life status, or other characteristics.

Ultimately, 1,048 patients with EOPC were enrolled in this study. The patients were randomly divided into a training set (n = 733) and validation set (n = 315) at a ratio of 7:3 (Table 1). Data on the were obtained: sex, age, race, year of diagnosis, histological grade, SEER historic stage, histology, tumor size, AJCC TNM stage, T/N/M stage, ELN, positive lymph node (PLN), LNR, and LODDS. The calculation formulas for LNR and LODDS are as follows: LNR = PLN/ELN; LODDS = log [(PLN + 0.05)/(ELN-PLN + 0.05)]. TNM stages of patients with EOPC in the SEER database were updated to align with the 8th edition of the AJCC criteria. In this study, cancer specific survival (CSS), defined as the date of diagnosis to the date of death from pancreatic cancer, was set as the end event.

Optimal cut-off points of the variables

The best cut-off values for age, tumor size, ELN, LNR, and LODDS were calculated using X-tile 3.6.1, based on the principles of maximum chi-squared value and minimum p-value (Table S1). The best cutoff point for age was 23 years, and the tumor size was 18 mm. As the best cut-off point for ELN was 6, ELN was divided into two groups: ELN1 (ELN ≤ 6) and ELN2 (ELN > 6). The best cut-off points for LNR were 0.04 and 0.17 mm, hence, LNR was divided into three groups, LNR1 (LNR ≤ 0.04), LNR2 (0.04 < LNR ≤ 0.17), and LNR3 (> 0.17). The best cut-off points for LODDS were -1.01 and -0.65 mm; thus, LODDS was divided into three groups: LODDS1 (LODDS ≤ -1.01), LODDS2 (−1.01 < LODDS ≤-0.65), and LODDS3 (LODDS > -0.65).

Statistical analysis

Continuous variables were expressed as medians (quartiles), while ranked or categorical variables were presented as numbers (percentages). Kaplan–Meier curves and log-rank tests were used to assess the effectiveness of N stage, ELN, LNR, and LODDS for prognostic stratification of EOPC. The C-index, Akaike information criterion (AIC), and receiver operating characteristic (ROC) area under the ROC curve (AUC) were used to compare the predictive performance of N stage, ELN, LNR, and LODDS. Independent risk factors for EOPC were identified using univariate and multifactorial Cox analyses. Corresponding hazard ratio (HR) and 95% confidence intervals (CI) were also calculated. Based on the results of the multifactorial analysis, a nomogram of EOPC was constructed to predict 1-, 3-, and 5-year CSS. In addition, the predictive performance of the nomogram was validated using AUC, calibration curve, AIC, and C-index, and compared with the AJCC TNM staging system. Risk scores were calculated on the nomogram, and risk stratification was performed using X-tile version 3.6.1, with three stages (I, II, and III). Kaplan–Meier analysis and log-rank tests were used to compare differences in survival at each stage. The study was statistically analyzed using R software (version.4.0.3; The R Project for Statistical Computing, TX, USA; http://www.r-project.org). Statistically significant difference was set at two-tailed $p < 0.05$.

Results

Clinicopathological characteristics

From 2004 to 2016, 1,048 patients with radically resected EOPC were included in this study. They were randomly divided into a training set (n =733) and validation set (n = 315) at a ratio of 7:3. Table 1 summarizes the clinical and pathological characteristics of the patients with EOPC. The median survival time was 20 months (IQR, 11–39 months), and the 1-, 3, and 5-year CSS rates were 74.6, 38.1, and 29.9%, respectively. Of the entire cohort (n =1048), 548 (52.3%) were men and 799 (76.2%) were white. A total of 1024 (97.7%) patients were aged > 23 years at the time of diagnosis, and the median age at diagnosis was 46 years (IQR, 42–48). A total of 712 (67.9%) patients had AJCC TNM stage I-II, and 67 (6.4%) patients had metastasis. There were 700 (66.8%) patients who underwent pancreatoduodenectomy (PD) and 117 (11.2%) who underwent total pancreatectomy (TP). At the same time, patients (677, 64.6%) had regional lymph node metastasis, and only 172 (16.4%) patients had an ELN ≤ 6.

10.3389/fonc.2022.975846

TABLE 1 Demographics and clinicopathologic characteristics of EOPC patients.

Variables	Total number, n (%) (n = 1048)	Training cohort, n (%) (n = 733)	Validation cohort, n (%) (n = 315)	P-value
Sex				1
female	500 (47.7)	350 (47.7)	150 (47.6)	
male	548 (52.3)	383 (52.3)	165 (52.4)	
age				0.44
≤23	24 (2.3)	19 (2.6)	5 (1.6)	
24-49	1024 (97.7)	714 (97.4)	310 (98.4)	
race				0.21
White	799 (76.2)	564 (76.9)	235 (74.6)	
Black	138 (13.2)	88 (12.0)	50 (15.9)	
Other	111 (10.6)	81 (11.1)	30 (9.5)	
Tumor location				0.70
head	715 (68.2)	496 (67.7)	219 (69.5)	
body/tail	210 (20.0)	147 (20.1)	63 (20.0)	
other	123 (11.7)	90 (12.3)	33 (10.5)	
Grade				0.71
Well	169 (16.1)	119 (16.2)	50 (15.9)	
Moderate	516 (49.2)	368 (50.2)	148 (47.0)	
Poor	337 (32.2)	229 (31.2)	108 (34.3)	
Undifferentiated	26 (2.5)	17 (2.3)	9 (2.9)	
Chemotherapy				0.97
None/Unknown	277 (26.4)	193 (26.3)	84 (26.7)	
Yes	771 (73.6)	540 (73.7)	231 (73.3)	
Beam Radiation				0.65
None/Unknown	616 (58.8)	427 (58.3)	189 (60.0)	
Yes	432 (41.2)	306 (41.7)	126 (40.0)	
Type of pancreatectomy				0.66
PD	700 (66.8)	496 (67.7)	204 (64.8)	
DP	168 (16.0)	116 (15.8)	52 (16.5)	
TP	117 (11.2)	81 (11.1)	36 (11.4)	
others	63 (6.0)	40 (5.5)	23 (7.3)	
Tumor size (mm)				0.36
≤ 18	112 (10.7)	77 (10.5)	35 (11.1)	
>18	936 (89.3)	656 (89.5)	280 (88.9)	
8th AJCC T stage				0.29
T1	172 (16.4)	128 (17.5)	44 (14.0)	
T2	494 (47.1)	340 (46.4)	154 (48.9)	
T3	322 (30.7)	219 (29.9)	103 (32.7)	
T4	60 (5.7)	46 (6.3)	14 (4.4)	
8th AJCC N stage				0.22
N0	371 (35.4)	267 (36.4)	104 (33.0)	
N1	430 (41.0)	288 (39.3)	142 (45.1)	
N2	247 (23.6)	178 (24.3)	69 (21.9)	
8th AJCC M stage				1
M0	981 (93.6)	686 (93.6)	295 (93.7)	
M1	67 (6.4)	47 (6.4)	20 (6.3)	
8th AJCC TNM stage				0.72
I	210 (20.0)	149 (20.3)	61 (19.4)	
II	502 (47.9)	343 (46.8)	159 (50.5)	

(Continued)

TABLE 1 Continued

Variables	Total number, n (%) (n = 1048)	Training cohort, n (%) (n = 733)	Validation cohort, n (%) (n = 315)	P-value
III	269 (25.7)	194 (26.5)	75 (23.8)	
IV	67 (6.4)	47 (6.4)	20 (6.3)	
ELN				0.61
ELN1	172 (16.4)	117 (16.0)	55 (17.5)	
ELN2	876 (83.6)	616 (84.0)	260 (82.5)	
LNR				0.59
LNR1	397 (37.9)	284 (38.7)	113 (35.9)	
LNR2	300 (28.6)	210 (28.6)	90 (28.6)	
LNR3	351 (33.5)	239 (32.6)	112 (35.6)	
LODDS				0.40
LODDS1	403 (38.5)	286 (39.0)	117 (37.1)	
LODDS2	254 (24.2)	183 (25.0)	71 (22.5)	

EOPC, early-onset pancreatic cancer; PD, pancreaticoduodenectomy; DP, distal pancreatectomy; TP, total pancreatectomy; ELN, examined lymph nodes; LNR, positive lymph node ratio; LODDS, log odds of positive lymph nodes.

Comparison of four lymph node staging systems

Univariate analysis based on the training set showed that 12 variables were strongly associated with cancer specific survival in patients with EOPC: sex, tumor location, grade, chemotherapy, tumor size, 8th AJCC T stage, 8th AJCC N stage, 8th AJCC M stage, 8th AJCC TNM stage, ELN, LNR, and LODDS (Table 2).

TABLE 2 Univariate analysis of prognostic factors associated with cancer-specific survival for EOPC patients in the training cohort.

Variables	Univariate analysis	
	HR (95% CI)	P-value
Sex		
male	Reference	
female	0.679 (0.564-0.818)	**<0.001**
age		
≤23	Reference	
24-49	1.964 (0.931-4.145)	0.076
race		
White	Reference	
Black	0.948 (0.712-1.263)	0.717
Other	0.890 (0.653-1.213)	0.460
Tumor location		
head	Reference	
body/tail	0.599 (0.462-0.776)	**<0.001**
other	0.953 (0.716-1.268)	0.743
Grade		
Well	Reference	
Moderate	2.196 (1.605-3.007)	**<0.001**
Poor	3.050 (2.203-4.224)	**<0.001**
Undifferentiated	2.075 (1.048-4.107)	**0.036**
Chemotherapy		
None/Unknown	Reference	
Yes	1.759 (1.388-2.229)	**<0.001**
Beam Radiation		
None/Unknown	Reference	
Yes	1.157 (0.962-1.391)	0.121
Tumor size (mm)		
≤ 18	Reference	
>18	2.008 (1.428-2.823)	**<0.001**
8th AJCC T stage		
T1	Reference	
T2	1.630 (1.240-2.142)	**<0.001**
T3	1.403 (1.045-1.883)	**0.024**
T4	2.349 (1.539-3.587)	**<0.001**
8th AJCC N stage		
N0	Reference	
N1	2.488 (1.974-3.135)	**<0.001**
N2	3.350 (2.601-4.314)	**<0.001**
8th AJCC M stage		
M0	Reference	
M1	1.962 (1.389-2.773)	**<0.001**
AJCC TNM stage		
I	Reference	
II	1.909 (1.439-2.534)	**<0.001**
III	3.165 (2.346-4.270)	**<0.001**
IV	3.809 (2.512-5.777)	**<0.001**

(Continued)

TABLE 2 Continued

Variables	Univariate analysis	
	HR (95% CI)	P-value
ELN		
ELN1	Reference	
ELN2	1.378 (1.062-1.787)	**0.016**
LNR		
LNR1	Reference	
LNR2	2.204 (1.732-2.804)	**<0.001**
LNR3	3.328 (2.641-4.194)	**<0.001**
LODDS		
LODDS1	Reference	
LODDS2	1.661 (1.296-2.128)	**<0.001**
LODDS3	2.841 (2.279-3.542)	**<0.001**

HR, hazard ratio; CI, confidence interval.
Significant p-values in bold (P<0.05).

In addition, Kaplan–Meier survival analysis and log-rank test revealed that the prognosis of patients with EOPC could be stratified by the 8th AJCC N stage, ELN, LNR, and LODDS (Figure 1).

In the training set, the C-indices for the N stage, ELN, LODDS, and LNR were 0.618, 0.518, 0.614, and 0.623, respectively. The AIC values for N stage, ELN, LODDS, and LNR were 8138.614, 8248.666, 8145.589, and 8119.163, respectively. The AUC values of the N stage, ELN, LODDS, and LNR for 1-year CSS were 0.643, 0.532, 0.623, and 0.635, respectively. The AUC values for the 3- year CSS of N stage, ELN, LODDS, and LNR were 0.688, 0.535, 0.680, and 0.702, respectively. The AUC values of N stage, ELN, LODDS, and LNR for 5- year CSS were 0.712, 0.547, 0.688, and 0.731, respectively. In conclusion, LNR had the highest C-index and AUC, with the lowest AIC, indicating that LNR had better predictive performance than N stage, ELN, and LODDS for CSS in patients with EOPC (Table 3). Based on the results of the

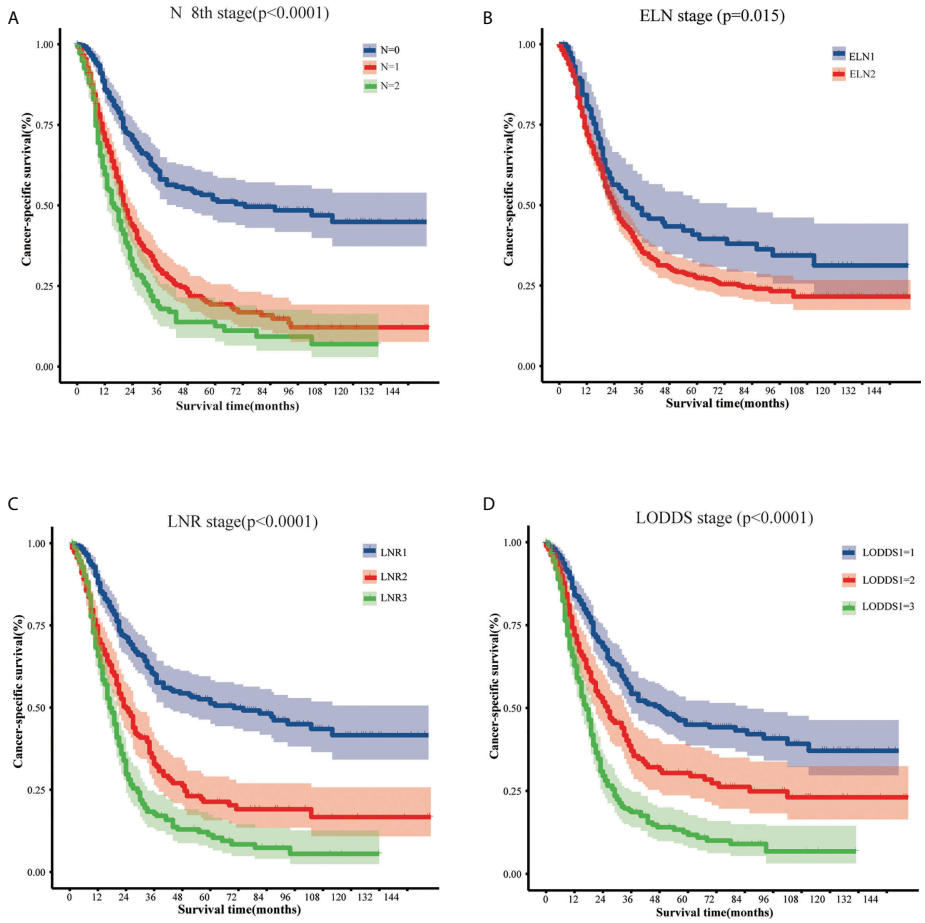

FIGURE 1
The cancer-specific survival of early-onset pancreatic cancer patients who underwent surgery stratified by different lymph node classifications: **(A)** 8th AJCC N stage, **(B)** the ELN stage, **(C)** the LNR stage, and **(D)** the LODDS stage. AJCC, American Joint Committee on Cancer; ELN, examined lymph nodes; LNR, lymph node ratio; LODDS, log odds of positive lymph nodes.

TABLE 3 Prognostic efficiency of different lymph node staging systems.

Systems	C-index	AIC	AUC		
			1-year CSS	3-year CSS	5-year CSS
N stage	0.618	8138.614	0.643	0.688	0.712
ELN	0.518	8248.666	0.532	0.535	0.547
LODDS	0.614	8145.589	0.623	0.680	0.688
LNR	**0.623**	8119.163	0.635	0.702	0.731

C-index, concordance index; AIC, Akaike information criterion; AUC, area under the receiver operating characteristic curve.
Significant values in bold.

univariate analysis combined with the same confounders, the N stage, ELN, LODDS, and LNR were incorporated into four different Cox regression models separately. Multivariate Cox regression analysis suggested that grade, tumor size, AJCC 8th M stage, AJCC 8th N stage, LODDS, LNR were independent prognostic indicators for CSS (Table S2; $p < 0.05$). However, ELN were not significantly associated with the prognosis of EOPC (Table S2; $p = 0.30$).

Construction and validation of the prognostic nomogram for CSS

A nomogram model for predicting cancer specific survival in patients with EOPC was developed (Figure 2) based on the above four independent risk factors: grade, tumor size, 8th AJCC M stage, and LNR. As shown in Figure 2, each factor of these variables was given a score on the point of the scale. Grades of differentiation well, moderate, poor, and undifferentiated were scored as 0, 60, 87 and 62, respectively. A tumor size ≤ 18 mm was scored as 0 and a tumor size > 18 mm was scored as 50. 8th AJCC M0 was scored as 0, and 8th AJCC M1 was scored as 55. LNR1 (LNR ≤ 0.04), LNR2 (0.04 < LNR ≤ 0.17), and LNR3 (> 0.17) were scored as 0, 61,100, respectively. By summing the scores for each variable, we can predict the CSS rates of 1-, 3-, and 5-year of patients with EOPC. For example, the probabilities of CSS rates of 1-, 3-, and 5-year for EOPC patients with Well-differentiated, tumor size ≤ 18 mm, LNR1 (LNR ≤ 0.04) and M0 ranged from 0.9 to 1, 0.8 to 1 and 0.8 to 1, respectively. However, the probabilities of CSS rates of 1-, 3-, and 5-year for EOPC patients with undifferentiated, tumor size > 18 mm, LNR3 (LNR > 0.17) and M1 ranged from 0.4 to 0.5, 0 to 0.1, and 0 to 0.1, respectively.

In the training set, the AUC values of the nomogram were 0.663, 0.728, and 0.760, respectively (Figures 3A–C), for predicting 1-, 3-, and 5- year CSS in patients with EOPC. Similar outcomes were observed in the validation set, where the AUC values of the nomogram were 0.674, 0.683, and 0.711

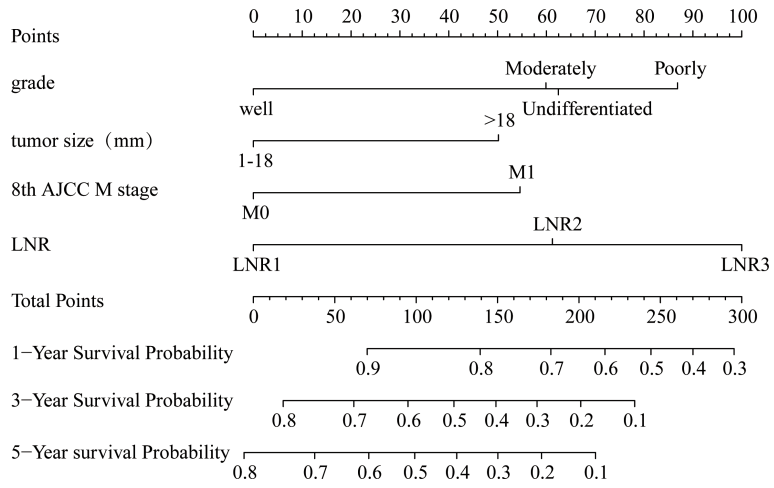

FIGURE 2
Nomogram for predicting the 1-, 3- and 5-year probabilities of cancer-specific survival in surgically treated early-onset pancreatic cancer patients in the training cohort. The nomogram was constructed by grade, tumor size, 8th AJCC M stage, and LNR. LNR, lymph node ratio; AJCC, American Joint Committee on Cancer.

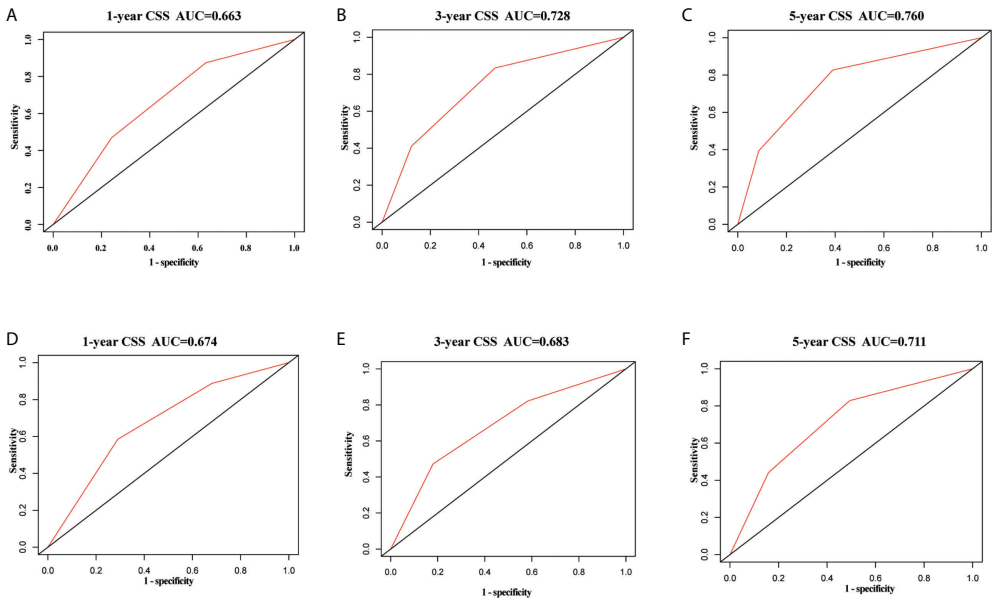

FIGURE 3
ROC curves of the nomogram for predicting cancer-specific survival in surgically treated early-onset pancreatic cancer patients. ROC curves of the nomogram predicting CSS for 1-year **(A)**, 3-year **(B)**, and 5-year **(C)** in the training set; ROC curves of the nomogram predicting CSS for 1-year **(D)**, 3-year **(E)**, and 5-year **(F)** in the validation set. ROC, receiver operating characteristic; CSS, cancer-specific survival.

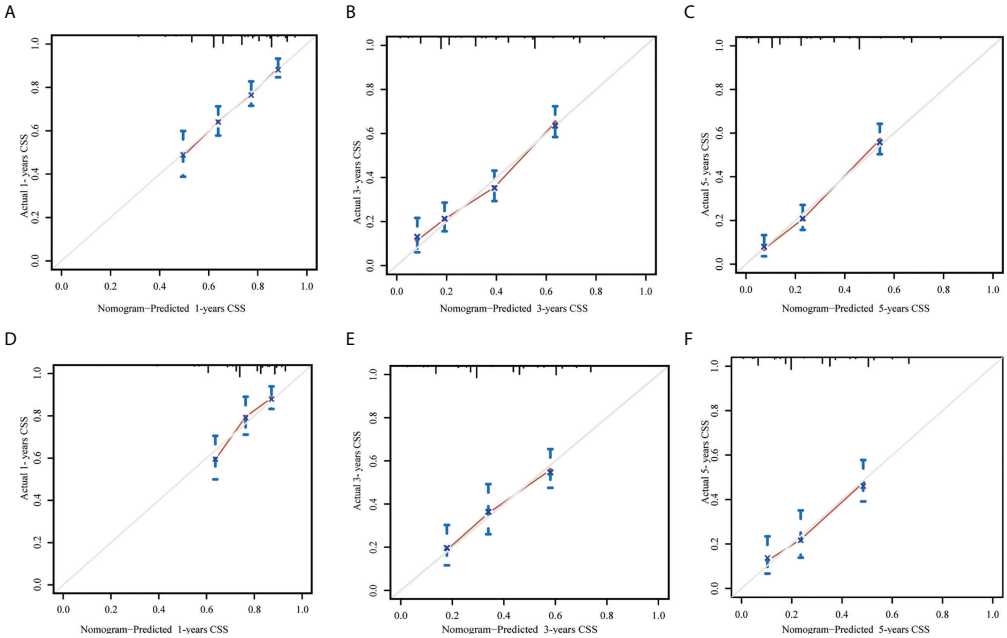

FIGURE 4
Calibration curves for predicting 1-, 3- and 5-year cancer-specific survival in patients with early-onset pancreatic cancer after surgery in the training set **(A–C**, respectively**)** and in the internal validation set **(D–F**, respectively**)**. The X-axis represented the nomogram-predicted probability of CSS and the Y-axis represented actual observed survival. The diagonal grey line represents an ideal evaluation where the predicted probabilities were identical to that of actual observed. CSS, cancer-specific survival.

for 1-, 3-, and 5-year CSS, respectively (Figures 3D–F). An optimal agreement was demonstrated by the calibration curves between the nomogram-predicted and measured 1-, 3-, and 5-year CSS in both the training (Figures 4A–C) and validation sets (Figures 4D–F).

To compare the performances of the nomogram and AJCC TNM stage, the C-index and AIC were calculated for both the training and validation cohorts (Table 4). In the training set, the C-indices of the nomogram and AJCC TNM stage for CSS prediction were 0.674 and 0.615, respectively. The AIC of the nomogram and AJCC TNM stage for CSS prediction were 5284 and 5370 respectively. The C-index of the nomogram was higher, and its AIC was lower than that of the AJCC TNM staging system. The results in the validation cohort were similar. The C-index of the nomogram was 0.668, which was higher than the AJCC TNM 0.594, and the AIC of the nomogram was 1955, which was lower than that of AJCC TNM 1997. In summary, these indicators demonstrated that the nomogram prognostic model showed superior performance to the AJCC TNM staging system.

Risk stratification based on the nomogram

In addition, the X-Tile software was used to determine the optimal cut-off values and establish a risk grading system. All patients were classified as low-risk (stage I, score: 0–136), medium-risk (stage II, score: 137–203), and high-risk (stage III, score: 204–292). Theoretically, the total scores range from 0 to 292. Kaplan–Meier curves (Figure 5) showed that the risk classification system had good stratification and differentiation in the training and validation sets, respectively.

Discussion

Recent studies have shown that lymph node metastasis affects the surgical-pathological staging, treatment planning, and prognosis of pancreatic cancer, making it important to properly assess the status of lymph node metastasis (25, 26).

TABLE 4 Prognostic efficiency of nomogram prognostic model and the 8th TNM.

Systems	C-index		AIC	
	Training cohort (n = 733)	Validation cohort (n = 315)	Training cohort (n = 733)	Validation cohort (n = 315)
Nomogram	**0.674**	**0.668**	**5284**	**1955**
8th TNM	0.615	0.594	5370	1997

C-index, concordance index; AIC, Akaike information criterion.
Significant values in bold.

To improve the accuracy of predicting pancreatic cancer prognosis, the American Joint Committee on Cancer (AJCC) published the 8th edition of the TNM classification. The 8th edition for the first time divided pancreatic cancer patients with lymph node metastases into three groups: N0 with no regional lymph nodes with metastases, N1 with one to three regional lymph nodes with metastases, and N2 with more than or equal to four regional lymph nodes with metastases. This reclassification emphasizes the importance of the number of positive lymph nodes in pancreatic cancer staging. Currently, the 8th AJCC TNM N stage remains the gold standard for assessing the status of lymph node metastasis for postoperative staging of pancreatic cancer. However, N staging is highly dependent on the number of positive lymph nodes, which is directly influenced by the total number of examined lymph nodes (ELN). Valsangkar et al. showed that the prognostic accuracy of any lymph node variable depends on the total number of examined lymph nodes (27). To ensure the accuracy of the N stage, the 8th AJCC guidelines state that the minimum number of lymph nodes to be detected should not be less than 12. However, in clinical practice, the number of retrieved lymph nodes depends on several factors, such as the extent of lymph node clearance, the operator's skill and experience, the condition of the specimen, and individual patient variation. Moreover, among patients following neoadjuvant chemotherapy, destruction and fibrosis of lymphatic vessels and lymph nodes are observed, which increases the rate of negative pathological lymph nodes and makes lymph node detection more difficult. For example, in this study, 37.4% of patients did not meet the criteria for a minimum of 12 lymph nodes to be detected, which could interfere with the performance of the 8th N stage.

Published retrospective studies have observed that a higher ELN is often associated with better prognosis in patients with pancreatic cancer, particularly in N0 patients. Zhu et al. analyzed 10,910 patients from the National Cancer Database and found that a higher ELN correlated with better survival, and the survival benefits of adjuvant radiation therapy may not compensate for inadequate lymph node dissection (28). A study conducted by Malleo et al. suggested that, among lymph node-negative patients, the 5-year survival rate was significantly lower in patients with ELN < 20 than in those with ELN ≥ 20 (33.5% vs. 67.6%) (29). ELN was recognized as an important prognostic factor for two reasons. First, a higher number of ELN increases the chance of eradicating isolated tumor cells and micrometastases in the lymph nodes (30–32). Second, correct regional lymph node staging can only be obtained based on adequate ELN (28, 29, 33, 34). To date, there is no consensus on the recommendations for minimum ELN numbers in pancreatic cancer patients. Several retrospective analyses have attempted to establish a standard, with recommendations for minimum ELN varying widely from 11 to 17 (33, 35–37).

As young people are often not considered to be at high risk for pancreatic cancer, early-onset pancreatic cancer can easily be

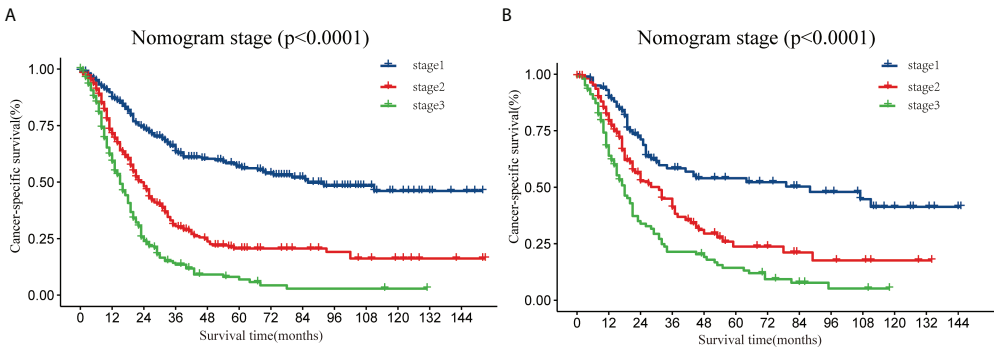

FIGURE 5
Analysis of the prognostic significance of the nomogram in surgically treated early-onset pancreatic cancer patients. Kaplan–Meier curves of CSS for all patients stratified by risk scores predicted by the nomograms in training set **(A)** and in the validation set **(B)**. CSS, cancer-specific survival.

overlooked, and the diagnosis is delayed. Ordonez et al. reported that early-onset pancreatic cancer tended to present with a later stage (stage 3 or 4 cancer) of disease than AOPC (62.1% vs. 55.2%; $p < 0.001$) (8). Previous studies have shown that patients with EOPC tend to receive more aggressive treatment in the absence of significant comorbidities and have better functional reserve. Saadat et al. found that EOPC patients received more chemotherapy (38% vs. 29%), chemoradiation (12% vs. 9.2%), and multimodal treatment (21% vs. 15%) compared with AOPC (11). Receiving more chemotherapy preoperatively tends to increase the difficulty of lymph node detection. This may explain the cut-off value of 6 for the ELN in this study, which is much smaller than the ELN in other studies. In this study, ELN was compared with other staging systems, and the predictive value of the model was assessed.

In recent years, LNR and LODDS staging systems have been gradually proposed in academia. As LNR and LODDS take into account both the number of positive lymph nodes and the number of examined lymph nodes, they are considered to have better staging ability for metastatic lymph nodes. Wu et al. retrospectively analyzed 177 patients who underwent pancreaticoduodenectomy and found that the LNR was an independent prognostic factor for pancreatic cancer (38). Slidell et al. divided 4,005 patients into LNR = 0, $0 < \text{LNR} \leq 0.2$, $0.2 < \text{LNR} \leq 0.4$, and LNR > 0.4, for survival analysis, and found that there was a significant difference in the overall survival among the four groups (39).The LNR combines the prognostic impact of both the number of positive lymph nodes and ELN, and reduces stage migration to some extent; however, it loses its inherent ability when N is 0 or when all intraoperative lymph nodes are detected positively, with an LNR value of 0 or 1. Some scientists have attempted to assess lymph node status using a new metric, which is the log odds of positive lymph nodes (LODDS).La et al. showed that LODDS and LNR were independent prognostic factors in patients with pancreatic cancer and that LODDS had a better prognostic power than LNR in N0 patients (40). However, after summarizing comparative studies of LNR and LODDS, we found no consensus on the advantages of LNR and LODDS. Ramacciato et al. found that ELN, LNR, and LODDS were useful for further prognostic stratification of N1 patients undergoing pancreatic resection combined with portal/superior mesenteric vein resection, while no one method was found to be superior to the other (41). Lee et al. evaluated several current lymph node-related prediction models in 2,584 patients and concluded that LNR and AJCC 8th edition N staging had better predictive value than LODDS regardless of the number of lymph nodes detected, whether R1 resection was performed, and the extent of surgical resection (42). Zou et al. found no significant difference in the concordance index (C-index) of the two prediction models by comparing LNR with N-staging, but N-staging was found to be clinically more accessible than LNR (43).

Recent research has shown that cancer is trending towards the younger population (44). As young people are not already a high-risk group for cancer, it is easy to delay diagnosis and treatment among young cancer patients. Constructing a postoperative predictive model in the hope of helping clinicians identify high-risk patients early and intervene as soon as possible is critical for improving the prognosis of patients with EOPC. However, no study has examined the prognostic significance and staging accuracy of the four current lymph node staging systems, 8th AJCC T stage,8th AJCC N stage, lymph node ratio (LNR), log odds of positive lymph nodes (LODDS), and examined lymph nodes (ELN) in early-onset pancreatic cancer.

In this study, univariate analysis showed that sex, tumor location, grade, chemotherapy, tumor size, 8th AJCC N stage, 8th AJCC M stage, AJCC TNM stage, ELN, LNR, and LODDS were strongly associated with CSS in patients with EOPC. The prognostic predictive performance of the LNR stage was also found to be superior to that of the 8th AJCC TNM N stage, ELN, and LODDS, according to an evaluation criterion consisting of

the C-index, AIC, and AUC values. Through multivariate Cox regression analyses, grade, tumor size, AJCC 8th M stage, AJCC 8th N stage, LODDS, LNR were verified as independent prognostic predictors for CSS with early-onset pancreatic cancer ($p < 0.05$). However, ELN were not significantly associated with the prognosis of EOPC ($p = 0.30$).

Based on four independent risk factors, including grade, tumor size, 8th AJCC M stage, and LNR, we constructed and validated a novel nomogram. A new LNR stage was obtained by stratifying the LNR risk score according to the principles of maximum chi-squared and minimum p-values using the X-tile software. Furthermore, Kaplan–Meier survival analysis showed that the LNR stage was not only strongly associated with the prognosis of EOPC but was also an important factor in the risk stratification of early-onset pancreatic cancer. The higher the LNR stage, the lower the CSS. Dai et al. confirmed similarly that a higher LNR was an independent prognostic factor of CSS based on their retrospective study of 1,386 pancreatic cancer (<45 years) (6). LNR has been also regarded as an independent prognostic factor that is strongly associated with the prognosis of various malignancies such as oral cancer, esophageal cancer, breast cancer and medullary thyroid cancer, etc (45–48). In studies of esophageal cancer and medullary thyroid cancer, LNR showed superior prognostic performance than N stage (46, 48).

To our knowledge, this study demonstrated for the first time that LNR is a more reliable prognostic staging indicator than AJCC 8th edition N-stage, ELN, and LODDS in early-onset pancreatic cancer. In addition, the performance of the nomogram was demonstrated to be more accurate and intuitive than that of the 8th AJCC TNM staging system. However, this study has several limitations. First, despite the large sample size, this was a retrospective study, and the findings need to be validated by prospective studies. Second, because this study used the SEER database, selection bias was likely to exist in our study. Third, the type of surgical resection (R0, R1, or R2) and other clinical information affecting patient survival (e.g., jaundice, CA199, neoadjuvant/adjuvant regimens) were not available from the SEER database; hence, they could not be included in the Cox regression model. Fourth, recurrence information was not available for SEER, and disease-free survival could not be assessed in this study.

Conclusions

In conclusion, this study retrospectively analyzed 1,048 patients with early-onset pancreatic cancer from the SEER database. Our results demonstrated that the LNR stage yielded superior prognostic efficiency compared with the 8th AJCC TNM N stage, LODDS, and ELN. In addition, N stage, LODDS, LNR were independent risk factors associated with cancer specific survival (CSS), but not ELN. The nomogram prognostic model based on LNR for predicting cancer specific survival in EOPC can be used to stratify patients with EOPC at high and low risk. This may complement the current 8th AJCC TNM staging system and help clinicians provide patients with EOPC with more individualized follow-up and treatment. Well-designed prospective clinical trials with appropriate sample sizes are required to verify these conclusions.

Data availability statement

The raw data supporting the conclusions of this article will be made available by the authors, without undue reservation.

Author contributions

YZ were involved in the final data collection, analysis, and manuscript writing. ZL, XS, and TT were involved in the data collection, ZL, CX, JX, and HC were involved in the data analysis. JS was involved in study design and responsible for the entire research project. All authors have agreed on the journal to which the article has been submitted, agree to be accountable for all aspects of the work criteria, made a significant contribution to the work reported, contributed to the article, and approved the submitted version.

Acknowledgments

The authors give special thanks to the National Cancer Institute for sharing the SEER data.

Conflict of interest

The authors declare that the research was conducted in the absence of any commercial or financial relationships that could be construed as a potential conflict of interest.

Publisher's note

All claims expressed in this article are solely those of the authors and do not necessarily represent those of their affiliated organizations, or those of the publisher, the editors and the reviewers. Any product that may be evaluated in this article, or claim that may be made by its manufacturer, is not guaranteed or endorsed by the publisher.

Supplementary material

The Supplementary Material for this article can be found online at: https://www.frontiersin.org/articles/10.3389/fonc.2022.975846/full#supplementary-material

References

1. Siegel RL, Miller KD, Fuchs HE, Jemal A. Cancer statistics, 2022. *CA Cancer J Clin* (2022) 72(1):7–33. doi: 10.3322/caac.21708

2. Rahib L, Wehner MR, Matrisian LM, Nead KT. Estimated projection of us cancer incidence and death to 2040. *JAMA Netw Open* (2021) 4(4):e214708. doi: 10.1001/jamanetworkopen.2021.4708

3. Sung H, Siegel RL, Rosenberg PS, Jemal A. Emerging cancer trends among young adults in the USA: Analysis of a population-based cancer registry. *Lancet Public Health* (2019) 4(3):e137–e47. doi: 10.1016/s2468-2667(18)30267-6

4. Tavakkoli A, Singal AG, Waljee AK, Elmunzer BJ, Pruitt SL, McKey T, et al. Racial disparities and trends in pancreatic cancer incidence and mortality in the united states. *Clin Gastroenterol Hepatol* (2020) 18(1):171–8.e10. doi: 10.1016/j.cgh.2019.05.059

5. Eguchi H, Kobayashi S, Gotoh K, Noda T, Doki Y. Characteristics of early-onset pancreatic cancer and its association with familial pancreatic cancer and hereditary pancreatic cancer syndromes. *Ann Gastroenterol Surg* (2020) 4(3):229–33. doi: 10.1002/ags3.12326

6. Dai D, Wang Y, Hu X, Jin H, Wang X. Prognostic analysis of very early onset pancreatic cancer: A population-based analysis. *PeerJ* (2020) 8:e8412. doi: 10.7717/peerj.8412

7. Takeda T, Sasaki T, Inoue Y, Okamoto T, Mori C, Mie T, et al. Early-onset pancreatic cancer: Clinical characteristics and survival outcomes. *Pancreatology* (2022) 22(4):507–15. doi: 10.1016/j.pan.2022.04.003

8. Ordonez JE, Hester CA, Zhu H, Augustine M, Porembka MR, Wang SC, et al. Clinicopathologic features and outcomes of early-onset pancreatic adenocarcinoma in the United States. *Ann Surg Oncol* (2020) 27(6):1997–2006. doi: 10.1245/s10434-019-08096-y

9. Aslanian HR, Lee JH, Canto MI. Aga clinical practice update on pancreas cancer screening in high-risk individuals: Expert review. *Gastroenterology* (2020) 159(1):358–62. doi: 10.1053/j.gastro.2020.03.088

10. LaPelusa M, Shen C, Arhin ND, Cardin D, Tan M, Idrees K, et al. Trends in the incidence and treatment of early-onset pancreatic cancer. *Cancers (Basel)* (2022) 14(2):283. doi: 10.3390/cancers14020283

11. Saadat LV, Chou JF, Gonen M, Soares KC, Kingham TP, Varghese AM, et al. Treatment patterns and survival in patients with early-onset pancreatic cancer. *Cancer* (2021) 127(19):3566–78. doi: 10.1002/cncr.33664

12. Campa D, Gentiluomo M, Obazee O, Ballerini A, Vodickova L, Hegyi P, et al. Genome-wide association study identifies an early onset pancreatic cancer risk locus. *Int J Cancer* (2020) 147(8):2065–74. doi: 10.1002/ijc.33004

13. Kadakia KC, Trufan SJ, Jagosky MH, Worrilow WM, Harrison BW, Broyhill KL, et al. Early-onset pancreatic cancer: An institutional series evaluating end-of-Life care. *Support Care Cancer* (2021) 29(7):3613–22. doi: 10.1007/s00520-020-05876-1

14. Raimondi S, Maisonneuve P, Löhr JM, Lowenfels AB. Early onset pancreatic cancer: Evidence of a major role for smoking and genetic factors. *Cancer Epidemiol Biomarkers Prev* (2007) 16(9):1894–7. doi: 10.1158/1055-9965.Epi-07-0341

15. Ben-Aharon I, Elkabets M, Pelossof R, Yu KH, Iacubuzio-Donahue CA, Leach SD, et al. Genomic landscape of pancreatic adenocarcinoma in younger versus older patients: Does age matter? *Clin Cancer Res* (2019) 25(7):2185–93. doi: 10.1158/1078-0432.Ccr-18-3042

16. McWilliams RR, Maisonneuve P, Bamlet WR, Petersen GM, Li D, Risch HA, et al. Risk factors for early-onset and very-Early-Onset pancreatic adenocarcinoma: A pancreatic cancer case-control consortium (Panc4) analysis. *Pancreas* (2016) 45(2):311–6. doi: 10.1097/mpa.0000000000000392

17. Ntala C, Debernardi S, Feakins RM, Crnogorac-Jurcevic T. Demographic, clinical, and pathological features of early onset pancreatic cancer patients. *BMC Gastroenterol* (2018) 18(1):139. doi: 10.1186/s12876-018-0866-z

18. Piciucchi M, Capurso G, Valente R, Larghi A, Archibugi L, Signoretti M, et al. Early onset pancreatic cancer: Risk factors, presentation and outcome. *Pancreatology* (2015) 15(2):151–5. doi: 10.1016/j.pan.2015.01.013

19. Miksad RA, Calip GS. Early-onset pancreatic cancer research: Making sense of confounding and bias. *Cancer* (2021) 127(19):3505–7. doi: 10.1002/cncr.33663

20. O'Connell JB, Maggard MA, Manunga JJr., Tomlinson JS, Reber HA, Ko CY, et al. Survival after resection of ampullary carcinoma: A national population-based study. *Ann Surg Oncol* (2008) 15(7):1820–7. doi: 10.1245/s10434-008-9886-1

21. Warschkow R, Tsai C, Köhn N, Erdem S, Schmied B, Nussbaum DP, et al. Role of lymphadenectomy, adjuvant chemotherapy, and treatment at high-volume centers in patients with resected pancreatic cancer-a distinct view on lymph node yield. *Langenbecks Arch Surg* (2020) 405(1):43–54. doi: 10.1007/s00423-020-01859-2

22. Song KJ, Arndt AT. Is a novel nomogram better than tnm staging at predicting survival in siewert type 2 adenocarcinoma? *Ann Surg Oncol* (2019) 26(5):1182–3. doi: 10.1245/s10434-019-07242-w

23. Bobdey S, Mair M, Nair S, Nair D, Balasubramaniam G, Chaturvedi P. A nomogram based prognostic score that is superior to conventional tnm staging in predicting outcome of surgically treated T4 buccal mucosa cancer: Time to think beyond tnm. *Oral Oncol* (2018) 81:10–5. doi: 10.1016/j.oraloncology.2018.04.002

24. Xie T, Wang X, Li M, Tong T, Yu X, Zhou Z. Pancreatic ductal adenocarcinoma: A radiomics nomogram outperforms clinical model and tnm staging for survival estimation after curative resection. *Eur Radiol* (2020) 30(5):2513–24. doi: 10.1007/s00330-019-06600-2

25. Belfiori G, Crippa S, Francesca A, Pagnanelli M, Tamburrino D, Gasparini G, et al. Long-term survivors after upfront resection for pancreatic ductal adenocarcinoma: An actual 5-year analysis of disease-specific and post-recurrence survival. *Ann Surg Oncol* (2021) 28(13):8249–60. doi: 10.1245/s10434-021-10401-7

26. Fukuda Y, Asaoka T, Maeda S, Hama N, Miyamoto A, Mori M, et al. Prognostic impact of nodal statuses in patients with pancreatic ductal adenocarcinoma. *Pancreatology* (2017) 17(2):279–84. doi: 10.1016/j.pan.2017.01.003

27. Valsangkar NP, Bush DM, Michaelson JS, Ferrone CR, Wargo JA, Lillemoe KD, et al. N0/N1, pnl, or lnr? the effect of lymph node number on accurate survival prediction in pancreatic ductal adenocarcinoma. *J Gastrointest Surg* (2013) 17(2):257–66. doi: 10.1007/s11605-012-1974-7

28. Zhu F, Wang H, Guirguis A, Ashamalla H. The value of total lymph nodes examined and number of positive lymph nodes in determining the role of adjuvant radiation in pancreatic cancer patients. *Pancreas* (2020) 49(3):435–41. doi: 10.1097/mpa.0000000000001512

29. Malleo G, Maggino L, Ferrone CR, Marchegiani G, Mino-Kenudson M, Capelli P, et al. Number of examined lymph nodes and nodal status assessment in distal pancreatectomy for Body/Tail ductal adenocarcinoma. *Ann Surg* (2019) 270(6):1138–46. doi: 10.1097/sla.0000000000002781

30. Komo T, Murakami Y, Kondo N, Uemura K, Hashimoto Y, Nakagawa N, et al. Prognostic impact of para-aortic lymph node micrometastasis in pancreatic ductal adenocarcinoma. *Ann Surg Oncol* (2016) 23(6):2019–27. doi: 10.1245/s10434-016-5120-8

31. Yekebas EF, Bogoevski D, Bubenheim M, Link BC, Kaifi JT, Wachowiak R, et al. Strong prognostic value of nodal and bone marrow micro-involvement in patients with pancreatic ductal carcinoma receiving no adjuvant chemotherapy. *World J Gastroenterol* (2006) 12(40):6515–21. doi: 10.3748/wjg.v12.i40.6515

32. Kayahara M, Funaki K, Tajima H, Takamura H, Ninomiya I, Kitagawa H, et al. Surgical implication of micrometastasis for pancreatic cancer. *Pancreas* (2010) 39(6):884–8. doi: 10.1097/MPA.0b013e3181ce6daa

33. Huang L, Jansen L, Balavarca Y, van der Geest L, Lemmens V, Koerkamp BG, et al. Significance of examined lymph node number in accurate staging and long-term survival in resected stage I-ii pancreatic cancer-more is better? A Large international population-based cohort study. *Ann Surg* (2021) 274(6):e554–e63. doi: 10.1097/sla.0000000000003558

34. Hua J, Zhang B, Xu J, Liu J, Ni Q, He J, et al. Determining the optimal number of examined lymph nodes for accurate staging of pancreatic cancer: An analysis using the nodal staging score model. *Eur J Surg Oncol* (2019) 45(6):1069–76. doi: 10.1016/j.ejso.2019.01.018

35. Pu N, Gao S, Beckman R, Ding D, Wright M, Chen Z, et al. Defining a minimum number of examined lymph nodes improves the prognostic value of lymphadenectomy in pancreas ductal adenocarcinoma. *HPB (Oxford)* (2021) 23(4):575–86. doi: 10.1016/j.hpb.2020.08.016

36. Huebner M, Kendrick M, Reid-Lombardo KM, Que F, Therneau T, Qin R, et al. Number of lymph nodes evaluated: Prognostic value in pancreatic adenocarcinoma. *J Gastrointest Surg* (2012) 16(5):920–6. doi: 10.1007/s11605-012-1853-2

37. Ashfaq A, Pockaj BA, Gray RJ, Halfdanarson TR, Wasif N. Nodal counts and lymph node ratio impact survival after distal pancreatectomy for pancreatic adenocarcinoma. *J Gastrointest Surg* (2014) 18(11):1929–35. doi: 10.1007/s11605-014-2566-5

38. Wu C, Hou SZ, Wu Z, Huang X, Wang Z, Tian B. Prognostic nomogram for patients undergoing radical pancreaticoduodenectomy for adenocarcinoma of the pancreatic head. *BMC Cancer* (2021) 21(1):624. doi: 10.1186/s12885-021-08295-5

39. Slidell MB, Chang DC, Cameron JL, Wolfgang C, Herman JM, Schulick RD, et al. Impact of total lymph node count and lymph node ratio on staging and survival after pancreatectomy for pancreatic adenocarcinoma: A Large, population-based analysis. *Ann Surg Oncol* (2008) 15(1):165–74. doi: 10.1245/s10434-007-9587-1

40. La Torre M, Nigri G, Petrucciani N, Cavallini M, Aurello P, Cosenza G, et al. Prognostic assessment of different lymph node staging methods for pancreatic cancer with R0 resection: Pn staging, lymph node ratio, log odds of positive lymph nodes. *Pancreatology* (2014) 14(4):289–94. doi: 10.1016/j.pan.2014.05.794

41. Ramacciato G, Nigri G, Petrucciani N, Pinna AD, Ravaioli M, Jovine E, et al. Prognostic role of nodal ratio, lodds, pn in patients with pancreatic cancer with venous involvement. *BMC Surg* (2017) 17(1):109. doi: 10.1186/s12893-017-0311-1

42. Lee W, Lee JB, Hong S, Park Y, Kwak BJ, Jun E, et al. Predictive performance of current nodal staging systems in various categories of pancreatic cancer. *Ann Surg Oncol* (2022) 29(1):390–8. doi: 10.1245/s10434-021-10641-7

43. Zou W, Wang Z, Wang F, Zhang G, Liu R. A nomogram predicting overall survival in patients with non-metastatic pancreatic head adenocarcinoma after surgery: A population-based study. *BMC Cancer* (2021) 21(1):524. doi: 10.1186/s12885-021-08250-4

44. Miller KD, Fidler-Benaoudia M, Keegan TH, Hipp HS, Jemal A, Siegel RL. Cancer statistics for adolescents and young adults, 2020. *CA Cancer J Clin* (2020) 70(6):443–59. doi: 10.3322/caac.21637

45. Voss JO, Freund L, Neumann F, Mrosk F, Rubarth K, Kreutzer K, et al. Prognostic value of lymph node involvement in oral squamous cell carcinoma. *Clin Oral Investig* (2022). doi: 10.1007/s00784-022-04630-7

46. Zhang Y, Cao Y, Zhang J, Huang M, Roy P, Huang B, et al. Lymph node ratio improves prediction of overall survival in esophageal cancer patients receiving neoadjuvant chemoradiotherapy: A national cancer database analysis. *Ann Surg* (2022). doi: 10.1097/sla.0000000000005450

47. Huang X, Luo Z, Liang W, Xie G, Lang X, Gou J, et al. Survival nomogram for young breast cancer patients based on the seer database and an external validation cohort. *Ann Surg Oncol* (2022) 29(9):5772–81. doi: 10.1245/s10434-022-11911-8

48. Prassas D, Kounnamas A, Cupisti K, Schott M, Knoefel WT, Krieg A. Prognostic performance of alternative lymph node classification systems for patients with medullary thyroid cancer: A single center cohort study. *Ann Surg Oncol* (2022) 29(4):2561–9. doi: 10.1245/s10434-021-11134-3

frontiers | Frontiers in Oncology

TYPE Case Report
PUBLISHED 20 September 2022
DOI 10.3389/fonc.2022.945689

Check for updates

OPEN ACCESS

EDITED BY
Qi Liu,
Fudan University, China

REVIEWED BY
Ajit Venniyoor,
The Royal Hospital, Oman
Hariharan Ramesh,
VPS Lakeshore Hospital, India
Giuseppe Zimmitti,
Fondazione Poliambulanza Istituto Ospedaliero, Italy

*CORRESPONDENCE
Jiangnan Hu
johu@stanford.edu
Zhen Wang
zhenwang1223@gmail.com

†PRESENT ADDRESS
Jiangnan Hu,
Department of Surgery, Stanford Cancer Institute, Stanford University School of Medicine, Stanford, CA, United States

SPECIALTY SECTION
This article was submitted to Surgical Oncology, a section of the journal Frontiers in Oncology

RECEIVED 16 May 2022
ACCEPTED 22 August 2022
PUBLISHED 20 September 2022

CITATION
Jin C, Hu J, Balapattabi K, Wang B, Hu S, Wang K, Fu L, Zhao X, Qian F and Wang Z (2022) Case report: A rare occurrence of triple malignancy of the stomach, rectum and liver in a single patient. *Front. Oncol.* 12:945689. doi: 10.3389/fonc.2022.945689

COPYRIGHT
© 2022 Jin, Hu, Balapattabi, Wang, Hu, Wang, Fu, Zhao, Qian and Wang. This is an open-access article distributed under the terms of the Creative Commons Attribution License (CC BY). The use, distribution or reproduction in other forums is permitted, provided the original author(s) and the copyright owner(s) are credited and that the original publication in this journal is cited, in accordance with accepted academic practice. No use, distribution or reproduction is permitted which does not comply with these terms.

Case report: A rare occurrence of triple malignancy of the stomach, rectum and liver in a single patient

Cancan Jin[1], Jiangnan Hu[2*†], Kirthikaa Balapattabi[3], Brian Wang[4], Sizhe Hu[1], Kangyi Wang[1], Liangbin Fu[1], Xiaokang Zhao[1], Feng Qian[1] and Zhen Wang[5*]

[1]Department of Oncology, Dongyang Hospital of Wenzhou Medical University, Dongyang, China, [2]Department of Dermatology and Cancer Center, Medical College of Wisconsin, Milwaukee, WI, United States, [3]Department of Physiology, Medical College of Wisconsin, Milwaukee, WI, United States, [4]Pathnova Laboratories Pte. Ltd., Singapore, Singapore, [5]Department of Colorectal Surgery, The Second Affiliated Hospital of Harbin Medical University, Harbin, China

Malignant tumors of the digestive system are common worldwide; however, it is extremely rare for more than two malignancies to occur simultaneously. Here, we report a case with a triple malignancy of the digestive system, including gastric, rectal, and hepatic tumors. The patient underwent surgical resection of three tumors followed by chemotherapy. Negative image-based screenings and the absence of serum tumor biomarkers elevation were found at 2.5 years after the surgery, indicating the absence of recurrence and metastasis of cancers.

KEYWORDS

gastric carcinoma, hepatocellular carcinoma, rectal carcinoma, surgery, immune checkpoint inhibitors

Background

Cancer is a leading cause of death worldwide and remains the major obstructive factor for a rise in global life expectancy. In 2020, the World Health Organization reported approximately 10 million cancer deaths worldwide. Colorectal and stomach cancer are the third and fourth leading causes of death, followed by liver cancer. According to a study done by the National Cancer Institute in 2011, the number of patients with multiple primary cancers is increasing dramatically (1).

Abbreviations: AFP, Alpha-fetoprotein; CapeOX, Capecitabine and Oxaliplatin; CEA, Carcinoembryonic Antigen; CSCO, Chinese Society of Clinical Oncology; HER-2, Human Epidermal Growth Factor Receptor 2; TNM, Tumor Node Metastasis.

In this report, we present a unique and important case of a patient with triple malignancy of the stomach, liver, and colorectum. The gold standard criteria outlined by Warren and Gates (2) was adapted for patient diagnosis: (i) Each tumor must have a clear image and histological confirmation of malignancy; (ii) Each tumor must be topographically distinct and separated by a healthy mucosa (at least 2 cm); (iii) The lesions must be primary, not metastases of each other. Fortunately, diagnostic equipment such as PET/CT has advanced to such a level that enables identification of multiple synchronous malignancies occurring in various organs like the thyroid, breast, head, neck, and others (3, 4).

Based on the diagnosis, the patient underwent surgical removal of the triple tumors and was given chemotherapy thereafter. Most encouragingly, no signs of recurrence or metastases have occurred so far. As triple primary malignancies are rare, no large case studies describing the characteristics and outcomes in such patients have been reported (see Table 1). The treatment plan for patients with multiple tumors presents many challenges, and a multidisciplinary approach with tailored decision-making for the individual patient helps to achieve optimum outcomes. It is our hope that detailing this rare clinical case including our strategies for patient care and management can serve as a reference for any similar future clinical cases.

Case presentation

A 64-year-old male patient presented with epigastric pain for half a month and the sensation of rectal tenesmus for more than three months. The timeline of events is presented Figure 1. According to the Chinese Society of Clinical Oncology (CSCO) guidelines, a gastroscopy was first performed where a tumor was found at the angular notch of the stomach (Figure 2A). Elevated alpha-fetoprotein (AFP) and carcinoembryonic antigen (CEA) serum levels were at 34.25 ng/ml and 30.11 ng/ml, respectively. There was also no indication of infection due to Hepatitis A, B, and C viruses.

To further determine the cause of increased AFP and CEA levels, contrast-enhanced computed tomography (CT) was performed that showed a primary tumor in the left lobe of the liver (Figures 3A, B), with possible existing carcinomas in the stomach (Figure 2B) and the rectum (Figure 4B). To assess the mass in the rectum, a colonoscopy revealed an erythematous mass located at roughly 10 cm away from the pectinate line. The mass had an uneven and brittle surface that was eroded, and also occupied about two-thirds of the intestinal lumen, resulting in colon stenosis. A biopsy indicated that the mass was a rectal adenocarcinoma which was prone to bleeding (Figure 4A).

A multidisciplinary team comprising a gastrointestinal surgeon, an oncology surgeon, a radiologist, a histopathologist, and an oncologist was then convened. Based on the findings, the team agreed that no tumors were found in other organs and that the patient could tolerate surgical treatment. Although most tumors are resectable, the simultaneous resection of multiple tumors poses a high risk. A decision was then reached to perform tumor resection in two stages.

The first stage involved radical gastrectomy of the stomach carcinoma, a left hemihepatectomy and cholecystectomy. During the operation, the samples from the lesion sites of stomach and liver were biopsied, both pathological examinations show malignant tumors (Figures 2C, 3C). The pathological analysis of the gastric tumor revealed an erythematous mass with an irregular border located at the anterior wall of the gastric antrum (size: 5 × 5 × 1 cm) and suggested an ulcer uplifted type of moderately differentiated adenocarcinoma that was immersed under the serous membrane. Lymphovascular emboli were present and perineural invasion was absent. Twenty-one surrounding

TABLE 1 Summary of cases with multiple primary tumors (three and above) reported in literature.

Author, Year	Age/Sex	Tumors Reported
Kim et al. (5), 2013	73/F	Thyroid carcinoma/Breast carcinoma/Pancreatic carcinoma/Gastrointestinal stromal tumor
Grace et al. (6), 2015	70/M	Glioblastoma/Schwannoma/Neuroendocrine tumor/Adenoma
Meeks et al. (7), 2016	95/F	Adenocarcinoma/Adenoma/Neuroendocrine tumor/Schwann cell hamartoma
Elec et al. (8), 2017	78/M	Prostate adenocarcinoma/Clear cell renal carcinoma/Papillary renal carcinoma/Bladder cancer
Nanashima et al. (9), 2017	67/M	Stomach/Sigmoid colon/Rectum/Pancreas carcinomas
Kataoka et al. (10), 2017	72/M	Pharyngeal squamous cell carcinoma/Esophageal squamous cell carcinoma/Esophageal adenocarcinoma
Wang et al. (11), 2019	56/F	Cervix/Endometrium/Ovary/Stomach carcinomas
Tanaka et al. (12), 2020	73/M	Stomach/Intrahepatic Bile Duct/Prostate carcinomas
Albaqmi et al. (13), 2020	63/M	Stomach/Colon/Kidney carcinomas
Takada et al. (14), 2020	89/M	Stomach/Lung/Breast carcinomas
Takada et al. (15), 2017	71/F	Breast/Duodenal/Lung carcinomas
Katz et al. (16), 2017	48/F	Colon/Ovary/Adrenal gland carcinomas
Sauri et al. (17), 2021	61/M	Stomach adenocarcinoma/Esophageal squamous cell carcinoma/Colon adenocarcinoma

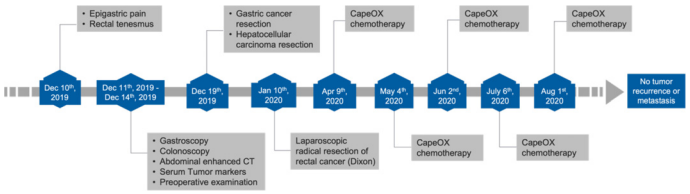

FIGURE 1
Timeline outlining clinical events.

lymph nodes around the stomach were removed, six of which were metastatic. The TNM (Tumor Node Metastasis) stage of the gastric cancer was $T_3N_{3a}M_0$ (stage IIIB). Histological analysis of the hemihepatectomy showed chronic cholecystitis and poorly differentiated adenocarcinoma (size: 10 × 10 cm) with a negative margin of resection. Immunohistochemistry interrogation revealed that it was CerbB-2 (-), P53 (-), Ki-67 (approximately 70% +), AFP (-), Hepatocyte (-), CD34 (-), CK20 (-), CDX2 (+), CK8 (-), CK19 (-), and Gly-3 (-). The liver mass was also confirmed to be malignant. In addition, based on the CT images, we found that the liver tumor was isolated and located in the left lobe with no signs of vascular invasion. Therefore, surgical resection was the primary treatment since the tumor was isolated and complete resection was feasible (18). However, we acknowledge that an in-depth pathological study could have been done to further identify the nature of the cancer.

The second stage was a laparoscopic radical resection of the rectal adenocarcinoma (Dixon). Pathological analysis showed a rectal ulcerative type of moderately differentiated adenocarcinoma (size: 7 × 4.5 × 1.5 cm) infiltrating the outer membrane with the presence of lymphovascular emboli and absence of perineural invasion (Figure 4C). All nineteen lymph nodes were surgically removed and there were no signs of lymph node metastasis. The TNM stage of the rectal cancer was $T_3N_0M_0$ (stage IIA).

Following the two-stage surgery, a combination chemotherapy with CapeOX (Capecitabine and Oxaliplatin) was given once a month for four consecutive months (Figure 1). Follow-up abdominal enhanced CT scan was done every 6 months and showed no tumor recurrence. In the most recent abdominal enhanced CT scan performed on May 26th, 2022, no tumor recurrence was indicated. AFP and CEA levels also declined to normal values postoperatively.

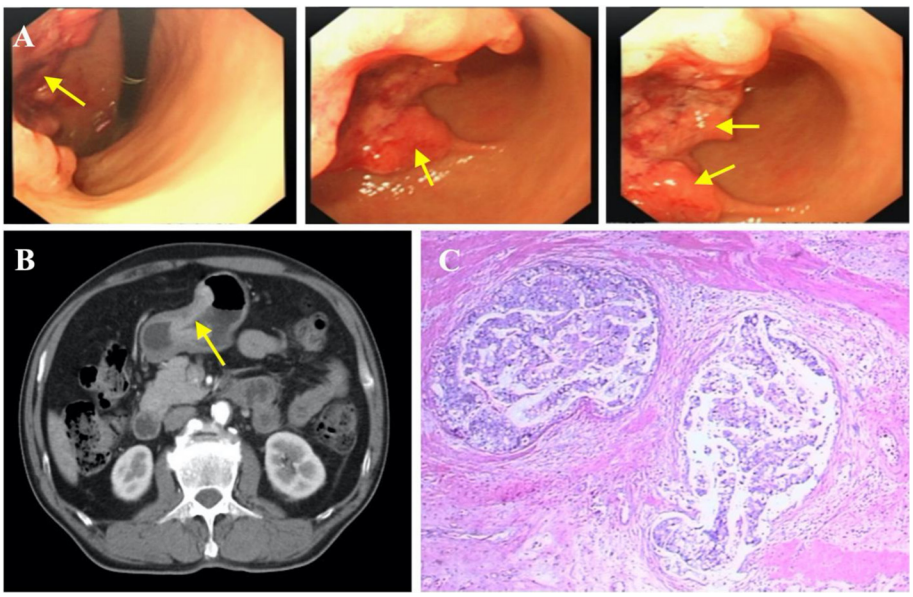

FIGURE 2
Diagnosis of gastric carcinoma. **(A)** Endoscopic images showing gastric cancer. **(B)** Gastric cancer (indicated by yellow arrow), specific enhancement pattern on multiphasic contrast-enhanced computed tomography (CT). **(C)** Representative histopathological image of gastric cancer.

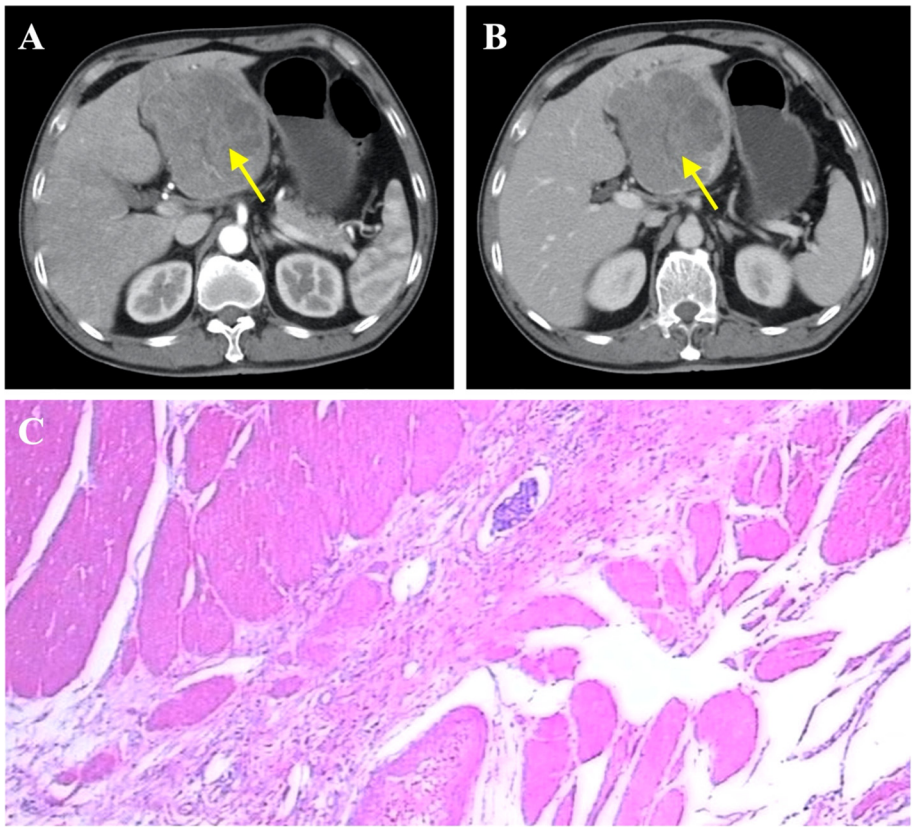

FIGURE 3
Diagnosis of primary liver cancer. **(A)** Liver cancer seen on contrast-enhanced CT (arterial phase), indicated by yellow arrow. **(B)** Liver cancer seen on contrast-enhanced CT (venous phase), indicated by arrow. **(C)** Representative histopathological image of liver cancer.

Discussion and conclusion

Here, we describe a triple primary malignancy in a patient who subsequently had successful treatment. The patient had no prior medical history of any serious illness. The patient, whose father died of pancreatic cancer in his 70s, was advised to undergo a genetic evaluation before surgery, but the patient refused. Considering available evidence for the etiology of multiple cancers, it is likely to be multifactorial with possible influences from the environment with likely minimal genetic influence. The patient had a remote smoking history (quit smoking 18 years ago), smoking about sixty cigarettes daily for twenty years. The patient also had a history of alcohol intake; ~250 ml distilled spirits daily for forty years. The occurrence of multiple tumors could be highly related to his living environment and lifestyle habits. When the patient came to the hospital, three tumors were diagnosed at the same time, so the sequence of tumor incidence was not clear.

Although simultaneous occurrence of multiple gastrointestinal tumors has been reported (Table 1), it is still an extremely rare phenomenon seen in less than 0.5% of patients with cancer (19–22). One problem presented by multiple primary tumors is the risk that they could have been metastatic in nature, and thus change oncosurgical management to include preoperative chemotherapy instead. To investigate this, we evaluated the nature of the liver tumors as the liver is known to be one of the most common sites for cancer metastasis and also due to its proximity to the GI tract. Abdominal CT scans show that the liver tumors present with an exophytic growth pattern and a necrotic core at the lesion site. Based on our team's collective experience, this was diagnosed as primary liver cancer. In addition, postoperative immunohistochemical analysis of the liver tumors revealed that they were all negative for AFP, Hep and Gly-3 markers, so the diagnosis of hepatocellular carcinoma was excluded. Moreover, the liver cancer cells showed no similarities when compared with the ones from the GI tumors. Taken together, we concluded that the liver tumors were primary in nature and had not metastasized from the gastric carcinoma.

The treatment of multiple primary cancers is still a challenge because of the lack of harmonized guidelines. However, surgical treatment is the standard of care for solid tumors in their early and advanced stages. For our patient, all tumors were resectable,

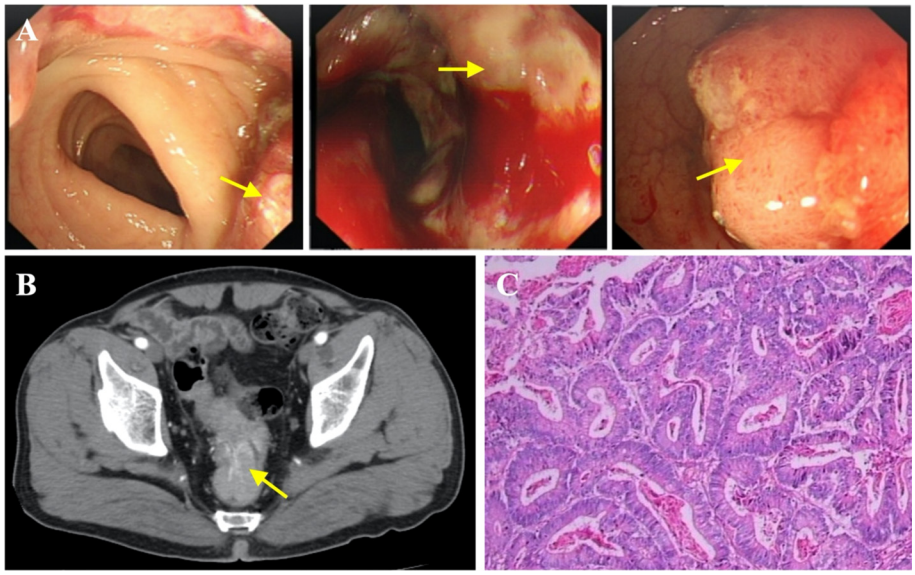

FIGURE 4
Diagnosis of rectal carcinoma. **(A)** Endoscopic images indicating rectal carcinoma (yellow arrow). **(B)** Contrast-enhanced CT showing rectal cancer. **(C)** Representative histopathological image of rectal carcinoma.

and a long-term survival was expected with radical resection. Given that the surgical resections of the gastric and rectal tumors were significantly invasive, other additional treatments such as chemotherapy and radiotherapy were needed to improve the surveillance. According to the 2021 CSCO guidelines for the diagnosis and treatment of gastric cancer, the CapeOX and SOX (Tegafur Gimeracil and Oteracil Porassium Capsule and Oxaliplatin) were recommended for postoperative adjuvant chemotherapy for stage IIIB gastric cancer. The rectal tumor was located at the rectosigmoid junction and invaded the serosa, but the surgically removed lymph nodes showed no infiltration of tumor cells. Histology of the dissected colonic tumor suggested adventitia infiltration, which suggests a high-risk factor for metastasis. Importantly, CapeOX chemotherapy can also be used for managing colorectal cancer (23). In addition, our clinical team proposed radiotherapy to the patient based on the stage of gastric cancer (IIIB), but he declined due to financial difficulties and the risk of adverse effects. Eventually, as reported (Figure 1), the patient was given CapeOX chemotherapy five times following CSCO's guidelines. In the course of chemotherapy, the patient developed myelosuppression and was unable to tolerate the side effects which led to the cessation of chemotherapy. The reference value of this case could be greatly increased if the entire chemotherapy was completed on time and in a standardized manner (for six consecutive months at a frequency of every three weeks). However, it has been 2.5 years since the patient was diagnosed with triple primary cancers and the latest follow-up examination results showed no signs of tumor recurrence or metastasis.

Recently, immune checkpoint inhibitors have been actively introduced into the management of gastrointestinal tumors, and their contribution, either as monotherapy or in combination is meaningful. Along with the development of precision medicine, immune checkpoint inhibitors will play a major life saving role in the treatment of gastrointestinal tumors. For our patient, we also proposed genetic testing for immunotherapy suitability, but he declined citing financial difficulty and personal reasons. In addition, HER-2 (Human Epidermal Growth Factor Receptor 2) expression was negative in the tumor biopsy, so targeted therapy with Herceptin was not applicable in this case (18).

We acknowledge that there were some shortcomings in our patient management since this is our first time experiencing a case of multiple synchronous tumors. The first being the irregularity of chemotherapy which could have affected full therapeutic benefits to be gained by the patient, but this factor was shown to be non-crucial since the patient is still in complete remission after 2.5 years. The second being the lack of relevant genetic tests conducted due to the patient's refusal, which immediately excluded him from potential immunotherapy and exposed him to higher risks due to invasive surgical procedures. Lastly, our lack of clinical experience could have made the treatment flawed. The fact that we did not first distinguish whether the liver tumor originated from the gastrointestinal tumor created an uncertainty in patient management.

In conclusion, a few lessons can be gleaned from our experience. In the case of multiple primary synchronous tumors, clinicians should evaluate the nature of these tumors i.e., primary or metastasized, as this determines the appropriate

oncosurgical plan for the patient. If the cancer has metastasized, neoadjuvant chemotherapy may be considered. Relevant genetic testing can also be subsidized by the healthcare institution or government and made available for those who present as candidates for suitable immunotherapy, which has shown great promise for GI tumors. Finally, a multidisciplinary approach to patient management has proven to be beneficial in that most aspects were covered to devise the best possible treatment plan.

Data availability statement

The original contributions presented in the study are included in the article. Further inquiries can be directed to the corresponding authors.

Ethics statement

The studies involving human participants were reviewed and approved by Dongyang Hospital of Wenzhou Medical University. The patients/participants provided their written informed consent to participate in this study.

Author contributions

CJ, JH, and ZW conceived and drafted the manuscript. KB, BW, SH, KW, LF, XZ, and FQ reviewed and edited the manuscript. All authors read and approved the final version of the manuscript.

Funding

This work was supported by Dongyang Hospital of Wenzhou Medical University and the Second Affiliated Hospital of Harbin Medical University.

Conflict of interest

Author BW was employed by Pathnova Laboratories Pte. Ltd.

The remaining authors declare that the research was conducted in the absence of any commercial or financial relationships that could be construed as a potential conflict of interest.

Publisher's note

All claims expressed in this article are solely those of the authors and do not necessarily represent those of their affiliated organizations, or those of the publisher, the editors and the reviewers. Any product that may be evaluated in this article, or claim that may be made by its manufacturer, is not guaranteed or endorsed by the publisher.

References

1. Bray F, Ferlay J, Soerjomataram I, Siegel RL, Torre LA, Jemal A. Global cancer statistics 2018: GLOBOCAN estimates of incidence and mortality worldwide for 36 cancers in 185 countries. *CA Cancer J Clin* (2018) 68(6):394–424. doi: 10.3322/caac.21492

2. Warren S. Multiple primary malignant tumors. a survey of the literature and a statistical study. *Am J Cancer* (1932) 16:1358–414.

3. Ishimori T, Patel PV, Wahl RL. Detection of unexpected additional primary malignancies with PET/CT. *J Nucl Med* (2005) 46(5):752–7.

4. Miyazaki T, Sohda M, Higuchi T, Tanaka N, Suzuki S, Sakai M, et al. Effectiveness of FDG-PET in screening of synchronous cancer of other organs in patients with esophageal cancer. *Anticancer Res* (2014) 34(1):283–7.

5. Kim JS, Chung C-Y, Park H-C, Myung D-S, Cho S-B, Lee W-S, et al. Synchronous quadruple primary tumors of thyroid, breast, pancreas, and stomach: A case report. *Anticancer Res* (2013) 33(5):2135–8.

6. Grace S, Muzaffar R, Veerapong J, Alkaade S, Poddar N, Phillips N, et al. Synchronous quadruple primary neoplasms: glioblastoma, neuroendocrine tumor, schwannoma and sessile serrated adenoma in a patient with history of prostate cancer. *Anticancer Res* (2015) 35(4):2121–7.

7. Meeks MW, Grace S, Chen Y, Petterchak J, Bolesta E, Zhou Y, et al. Synchronous quadruple primary neoplasms: Colon adenocarcinoma, collision tumor of neuroendocrine tumor and schwann cell hamartoma and sessile serrated adenoma of the appendix. *Anticancer Res* (2016) 36(8):4307–11.

8. Elec FI, Zaharie A, Ene B-M, Ghervan L. Quadruple primary urogenital cancers - a case report. *Int J Surg Case Rep* (2017) 39:239–44. doi: 10.1016/j.ijscr.2017.08.035

9. Nanashima A, Tominaga T, Nonaka T, Wakata K, Kunizaki M, Tobinaga S, et al. A case of multiple synchronous quadruple cancers of the stomach, sigmoid colon, rectum, and pancreas. *Int J Surg Case Rep* (2017) 35:4–7. doi: 10.1016/j.ijscr.2017.03.041

10. Kataoka S, Omae M, Horiuchi Y, Ishiyama A, Yoshio T, Hirasawa T, et al. Synchronous triple primary cancers of the pharynx and esophagus. *Clin J Gastroenterol* (2017) 10(3):208–13. doi: 10.1007/s12328-017-0734-3

11. Wang DD, Yang Q. Synchronous quadruple primary malignancies of the cervix, endometrium, ovary, and stomach in a single patient: A case report and review of literature. *World J Clin cases* (2019) 7(20):3364–71. doi: 10.12998/wjcc.v7.i20.3364

12. Tanaka S, Okazaki T, Owada Y, Iwabuchi S, Hosono M, Kawasaki K. A case of synchronous triple cancer of the stomach, intrahepatic bile duct, and prostate. *Gan To Kagaku Ryoho* (2020) 47(13):2346–8.

13. AlBaqmi KH, AlMudaiheem FA, Boghdadly S, AlHussaini KA, Shokor N, AlOudah N. Multiple primary malignancies of the colon, stomach, and kidney in a patient with bowel obstruction requiring emergency surgery: A case report. *Am J Case Rep* (2020) 21:e926472. doi: 10.12659/AJCR.926472

14. Takada K, Miyashita M, Kawajiri H. [A case of an elderly Male with breast cancer with synchronous triple cancer of the lung and stomach]. *Gan To Kagaku Ryoho* (2019) 46(13):2213–5.

15. Takada K, Kashiwagi S, Amano R, Goto W, Asano Y, Ohira G, et al. A case of synchronous triple cancer of the breast, duodenal and lung. *Gan To Kagaku Ryoho* (2017) 44(12):1074–6.

16. Katz H, Jafri H, Brown L, Pacioles T. Triple synchronous primary malignancies: A rare occurrence. *BMJ Case Rep* (2017) 2017. doi: 10.1136/bcr-2017-219237

17. Sauri FM, Zakarneh EA, Alessa MY, Sakr AH, Chung YS, Kim HS, et al. Triple synchronous primary neoplasms in the gastrointestinal tract. *Chin Med J (Engl)* (2021) 134(10):1233–5. doi: 10.1097/CM9.0000000000001389

18. Wang FH, Zhang X-T, Li Y-F, Tang L, Qu X-J, Ying J-E, et al. The Chinese society of clinical oncology (CSCO): Clinical guidelines for the diagnosis and treatment of gastric cancer, 2021. *Cancer Commun (Lond)* (2021) 41(8):747–95. doi: 10.1002/cac2.12193

19. Iioka Y, Tsuchida A, Okubo K, Ogiso M, Ichimiya H, Saito K, et al. Metachronous triple cancers of the sigmoid colon, stomach, and esophagus: Report of a case. *Surg Today* (2000) 30(4):368–71. doi: 10.1007/s005950050602

20. Tamura M, Shinagawa M, Funaki Y. Synchronous triple early cancers occurring in the stomach, colon and gallbladder. *Asian J Surg* (2003) 26(1):46–8; discussion 49. doi: 10.1016/S1015-9584(09)60216-5

21. Sato K, Maekawa T, Yabuki K, Tamasaki Y, Maekawa H, Kudo K, et al. A case of triple synchronous cancers occurring in the gallbladder, common bile duct, and pancreas. *J Gastroenterol* (2003) 38(1):97–100. doi: 10.1007/s005350300014

22. Leong BD, Ramu P, Kumar VM, Chuah JA. Synchronous adenocarcinoma of caecum, transverse colon and jejunum. *Med J Malaysia* (2008) 63(2):148–9.

23. Yoshino T, Argilés G, Oki E, Martinelli E, Taniguchi H, Arnold D. Pan-Asian adapted ESMO clinical practice guidelines for the diagnosis treatment and follow-up of patients with localised colon cancer. *Ann Oncol* (2021) 32(12):1496–510. doi: 10.1016/j.annonc.2021.08.1752

frontiers | Frontiers in Medicine

TYPE Original Research
PUBLISHED 30 September 2022
DOI 10.3389/fmed.2022.893252

Check for updates

OPEN ACCESS

EDITED BY
Qi Liu,
Fudan University, China

REVIEWED BY
Shuji Isaji,
Mie University Hospital, Japan
Apurva Patel,
Gujarat Cancer and Research Institute, India

*CORRESPONDENCE
Supinda Koonmee
suppun@kku.ac.th

SPECIALTY SECTION
This article was submitted to Gastroenterology, a section of the journal Frontiers in Medicine

RECEIVED 10 March 2022
ACCEPTED 25 July 2022
PUBLISHED 30 September 2022

CITATION
Aphivatanasiri C, Sa-Ngiamwibool P, Sangkhamanon S, Intarawichian P, Kunprom W, Thanee M, Prajumwongs P, Khuntikeo N, Titapun A, Jareanrat A, Thanasukarn V, Srisuk T, Luvira V, Eurboonyanun K, Promsorn J, Loilome W, Wee A and Koonmee S (2022) Modification of the eighth AJCC/UICC staging system for perihilar cholangiocarcinoma: An alternative pathological staging system from cholangiocarcinoma-prevalent Northeast Thailand. *Front. Med.* 9:893252. doi: 10.3389/fmed.2022.893252

COPYRIGHT
© 2022 Aphivatanasiri, Sa-Ngiamwibool, Sangkhamanon, Intarawichian, Kunprom, Thanee, Prajumwongs, Khuntikeo, Titapun, Jareanrat, Thanasukarn, Srisuk, Luvira, Eurboonyanun, Promsorn, Loilome, Wee and Koonmee. This is an open-access article distributed under the terms of the Creative Commons Attribution License (CC BY). The use, distribution or reproduction in other forums is permitted, provided the original author(s) and the copyright owner(s) are credited and that the original publication in this journal is cited, in accordance with accepted academic practice. No use, distribution or reproduction is permitted which does not comply with these terms.

Modification of the eighth AJCC/UICC staging system for perihilar cholangiocarcinoma: An alternative pathological staging system from cholangiocarcinoma-prevalent Northeast Thailand

Chaiwat Aphivatanasiri[1,2,3], Prakasit Sa-Ngiamwibool[1,2,3], Sakkarn Sangkhamanon[1,2,3], Piyapharom Intarawichian[1,2,3], Waritta Kunprom[1,2,3], Malinee Thanee[1,2,3], Piya Prajumwongs[1,2,3], Narong Khuntikeo[1,2,4], Attapol Titapun[1,2,4], Apiwat Jareanrat[1,2,4], Vasin Thanasukarn[1,2,4], Tharatip Srisuk[1,2,4], Vor Luvira[1,2,4], Kulyada Eurboonyanun[1,2,5], Julaluck Promsorn[1,2,5], Watcharin Loilome[1,2,6], Aileen Wee[7] and Supinda Koonmee[1,2,3]*

[1]Cholangiocarcinoma Screening and Care Program (CASCAP), Khon Kaen University, Khon Kaen, Thailand, [2]Cholangiocarcinoma Research Institute, Khon Kaen University, Khon Kaen, Thailand, [3]Department of Pathology, Faculty of Medicine, Khon Kaen University, Khon Kaen, Thailand, [4]Department of Surgery, Faculty of Medicine, Khon Kaen University, Khon Kaen, Thailand, [5]Department of Radiology, Faculty of Medicine, Khon Kaen University, Khon Kaen, Thailand, [6]Department of Biochemistry, Faculty of Medicine, Khon Kaen University, Khon Kaen, Thailand, [7]Department of Pathology, National University Hospital, Singapore, Singapore

Aim: This study aims to improve the classification performance of the eighth American Joint Committee on Cancer (AJCC) staging system for perihilar cholangiocarcinoma (pCCA) by proposing the Khon Kaen University (KKU) staging system developed in cholangiocarcinoma-prevalent Northeast Thailand.

Method: Four hundred eighty-eight patients with pCCA who underwent partial hepatectomy between 2002 and 2017 at the Srinagarind Hospital, Faculty of Medicine, Khon Kaen University, Thailand, were included. Overall survival (OS) related to clinicopathological features was analyzed using the Kaplan–Meier method. Logrank test was performed in univariate analysis to compare OS data of clinicopathological features to determine risk factors for poor survival. Significant features were further analyzed by multivariate analysis (Cox regression) to identify prognostic factors which were then employed to modify the eighth AJCC staging system.

Results: Multivariate analysis showed that growth pattern (HR = 4.67–19.72, $p < 0.001$), moderately and poorly differentiated histological grades (HR = 2.31–4.99, $p < 0.05$ and 0.001, respectively), lymph node metastasis

N1 and N2 (HR = 1.37 and 2.18, $p < 0.05$ and 0.01, respectively), and distant metastasis (HR = 2.11, $p < 0.001$) were independent factors when compared to their respective reference groups. There was a clear separation of patients with pCCA into KKU stage: I [OS = 116 months (mo.)], II (OS = 46 mo.), IIIA (OS = 24 mo.), IIIB (11 mo.), IVA (OS = 7 mo.), and IVB (OS = 6 mo.).

Conclusion: The new staging system was based on the incorporation of growth patterns to modify the eighth AJCC staging system. The classification performance demonstrated that the KKU staging system was able to classify and distinctly separate patients with pCCA into those with good and poor outcomes. It was also able to improve the stratification performance and discriminative ability of different stages of pCCA classification better than the eighth AJCC staging system. Hence, the KKU staging system is proposed as an alternative model to augment the accuracy of survival prognostication and treatment performance for patients with pCCA.

KEYWORDS

perihilar cholangiocarcinoma, eighth AJCC/UICC staging, KKU staging system, classification, growth pattern

Introduction

Cholangiocarcinoma (CCA) is a cancer of epithelial origin arising from different locations within the intra- and extrahepatic biliary tree. The incidence is remarkably high in Asian countries, especially in Thailand, which has the highest reported incidence in the world (1, 2). The major risk factor for Thai patients with CCA is evidently associated with the liver fluke, *Opisthorchis viverrini* (3–5). *O. viverrini* has been reported to enhance cholangiocarcinogenesis via several carcinogenic mechanisms (6, 7). In general, late presentations with locally advanced or metastatic disease contribute to high mortality and dismal response after surgery (8–10). CCA is classified into three types based on anatomical localization, namely, intrahepatic (iCCA), perihilar (pCCA), and distal (dCCA) CCA. This study focused on pCCA because it is the commonest type with distinct epidemiology and dismal outcomes after treatment (9, 11).

Perihilar CCA has a reported incidence rate of approximately 50–70% of all CCA (12, 13). By definition, pCCA is a tumor that is located in the extrahepatic biliary tree proximal to the origin of the cystic duct. Proximally, the tumor extends up to the secondary branches of the right and left hepatic ducts and invades the liver parenchyma (14). This results in the formation of three major types of growth patterns, comprising intraductal (ID), periductal infiltrating (PI), and mass-forming (MF) growth types, similar to iCCA (15–18). In pCCA, PI and MF growth patterns have been reported as risk factors for poor survival, while the ID pattern favors a good prognosis of patients with CCA in general (18). The survival time of patients with pCCA is poor, with overall survival of about 12 months. The survival time can be prolonged to 40 months by post-operative palliative treatment (11). Almost all prognostic studies focused on patients who have undergone resection. The dismal post-operative outcomes are attributed to tumor recurrence and advanced stage at presentation (10, 11). Present studies propose adjuvant therapy as an additional treatment option. Rizzo and Brandi (19) updated adjuvant therapy for CCA, especially in pCCA cases, based on the results of phase III studies in three clinical trials analyzing adjuvant systemic therapy in resected bile duct tumors, namely, the BILCAP (United Kingdom), the BCAT (Japan), and the PRODIGE-12/ACCORD-18 (France). Although these studies showed good outcomes, only the BILCAP trial demonstrated statistically significant outcomes and safety. Moreover, adjuvant therapy is still debatable and controversial in terms of safety and treatment efficiency issues in the CCA medical community. Another alternative treatment is immunotherapy for advanced CCA treatment suggested by Rizzo et al. (20). They reported that immune checkpoint inhibitors (ICI) can provide effective treatment in phases I–III of advanced CCA. ICI is deemed a new strategy to combat advanced CCA and there remains room for investigations to confirm performance and safety. Therefore, effective stratification of patients with pCCA is crucial for precise prognostic discrimination to improve treatment performance.

The American Joint Committee on Cancer (AJCC) and The Union for International Cancer Control (UICC) staging system are one of the most common strategies for the stratification of cancer staging. The eighth edition of the AJCC/UICC Staging Manual was recently updated (21). Several studies comparing stratification performances of the seventh and eighth editions have suggested that the latter has improved classification

(22–25). However, there have been observations that the overall performance of eighth AJCC staging to classify pCCA is not notably better. In fact, there are increasing reviews that the eighth AJCC has shown only slight improvement leading to calls for further refinements to improve the prognostic discriminative ability by applying prognostic factors (26–32). There are several reports of modifications of the eighth AJCC staging system using prognostic factors from multivariate analysis, such as invasive tumor thickness (ITT) (26, 27), tumor size (28), bilirubin level (29), and serum CA19-9 (30, 31), and creation of a new staging

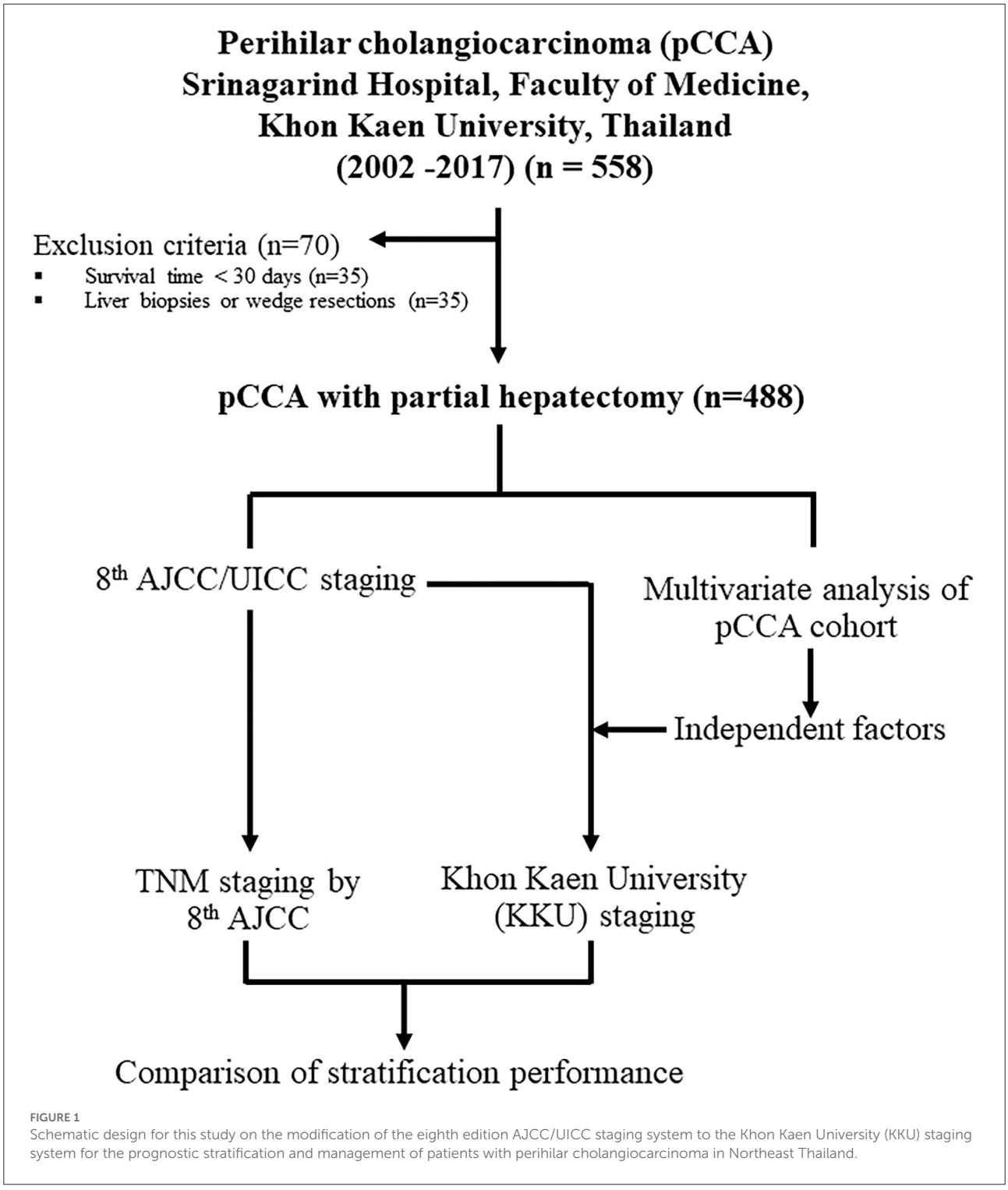

FIGURE 1
Schematic design for this study on the modification of the eighth edition AJCC/UICC staging system to the Khon Kaen University (KKU) staging system for the prognostic stratification and management of patients with perihilar cholangiocarcinoma in Northeast Thailand.

system (Mayo Clinic Staging System) (32). These modifications provide improvement in prognostication when compared to conventional classification by the eighth AJCC staging system.

This study, henceforth, aims to modify the eighth AJCC staging system for pCCA with the creation of an alternative staging system called the Khon Kaen University (KKU) staging system and to compare the prognostic and classifying ability of the two systems. All patients with pCCA with partial hepatectomy were stratified using the eighth AJCC staging system, and possible features significantly related to overall survival (OS) were analyzed by multivariate analysis to identify prognostic factors for poor survival. These prognostic factors were then employed to modify the eighth AJCC staging system to develop the KKU model.

Materials and methods

Patients

Between 2002 and 2017, 558 patients were diagnosed with pCCA at the Srinagarind Hospital, Faculty of Medicine, Khon Kaen University, Thailand. There were three groups of patients, namely, (i) those with liver biopsies or wedge resections (n = 35), (ii) those who survived less than 30 days after surgery with likely perioperative causes of death (n = 35), and (iii) those who underwent partial hepatectomies (n = 488). The first two groups were excluded. A final total of 488 patients was included. The experimental workflow is shown in Figure 1. This research was approved by the Ethics Committee for Human Research, Khon Kaen University (HE641499).

Recorded data

Patients underwent hepatectomy with the *en-bloc* resection of the tumor and extrahepatic bile duct according to the Bismuth-Corlette classification. The extent of the tumor was evaluated with pre-operative imaging by computerized tomography (CT) and magnetic resonance cholangiopancreatography (MRCP) (33, 34). Lymph node (LN) sites, namely, the common hepatic artery (LN8), hepatoduodenal ligament (LN12), and posterior pancreaticoduodenal node (LN13), were regularly resected. Combined vascular resection and reconstruction to the remnant side of the liver were performed if the tumor involved the portal vein or hepatic artery. Intraoperative data collection comprised sex, age, hepatic resection region, sample diameter, tumor diameter, growth patterns (ID, PI, and MF), surgical margin, and characteristics of surrounding organs.

The liver specimens were examined with relevant tissue blocks taken by a pathologist for routine tissue processing. The tumor sampling consisted of at least one block per centimeter of the largest dimension of tumor. Formalin-fixed paraffin-embedded (FFPE) tissue blocks were sectioned at 5 microns and stained with hematoxylin and eosin (H&E). Pathological diagnosis was reviewed under the 2019 World Health Organization (WHO) classification criteria (35). Four pathologists conducted a double-blind microscopic review of the tissue slides, and a consensus diagnosis was taken. The following histomorphological data were recorded: growth patterns, histological type, histological grade, surgical margin, lymphovascular invasion, and lymph node metastasis. Distant metastasis status was retrieved from the medical records. Finally, the gross examination and pathological data were used to determine pathological staging following the eighth AJCC staging manual (21) (Table 1).

TABLE 1 Definition of TNM categories of the eighth AJCC/UICC staging manual.

Tumor category (T)	Lymph node metastasis (N)	Distal metastasis (M)
T*is* = Carcinoma in *situ*//high-grade dysplasia	N0 = Negative lymph node	M0 = No distant metastasis
T1 = Tumor confined to the bile duct, with extension up to the muscle layer or fibrous tissue	N1 = One to three positive lymph nodes	M1 = Distant metastasis
T2 = Tumor invades beyond the wall of the bile duct:	N2 = Four or more positive lymph nodes	
T2a = Tumor invades beyond the wall of the bile duct to surrounding adipose tissue		
T2b = Tumor invades adjacent hepatic parenchyma		
T3 = Tumor invades unilateral branches of the portal vein or hepatic artery		
T4 = Tumor invades the main portal vein or its branches bilaterally, or the common hepatic artery; or unilateral second-order biliary radicals with contralateral portal vein or hepatic artery involvement		

Growth pattern proportion

The liver resection specimens were serially sectioned, photographed, and tumor growth pattern/s were recorded at the time of gross examination and subsequently confirmed histologically. The growth patterns were estimated as increments

of 10% to establish the proportion of each pattern, namely, ID, PI, MF, or combination of patterns (ID+PI, ID+MF, PI+MF, and ID+PI+MF).

Pathological diagnosis

There were four major histological types found in this study, namely, papillary adenocarcinoma, tubular adenocarcinoma, papillotubular adenocarcinoma, and adenocarcinoma, not otherwise specified (NOS). Papillary, tubular, and papillotubular adenocarcinomas were graded as well-or moderately differentiated carcinomas and diagnosed according to 2019 WHO classification criteria (35). Adenocarcinoma, NOS, was defined as poorly differentiated bile duct cancer lacking well-formed papillary or tubular formations.

Statistical analysis

Only patients with complete datasets were included in the statistical analyses. Categorical data were reported as counts and percentages. Clinicopathological features were compared using chi-square tests (χ2-Test), and continuous variables were compared using Student's *t*-tests. Survival analysis using the Kaplan–Meier model was applied for OS calculation, and the Logrank test was used for the comparison of OS for each clinicopathological feature. Patients with perioperative causes of death were excluded from this analysis (survival time <30 days). For growth pattern estimation, 20% was used as a cut-off value as this figure showed significantly different OS between each pattern. Statistically significant features from the Logrank test were further examined by multivariate analysis. Cox regression model was performed to identify independent factors in multivariate analysis.

Results

Basic clinicopathological characteristics of patients with perihilar cholangiocarcinoma

A total of 488 patients underwent partial hepatectomy for pCCA. There were two types of pCCA comprising non-invasive (tumor *in situ*, $n = 25$) and invasive tumors ($n = 463$); the non-invasive category was used as the baseline for good survival of patients with pCCA. The clinicopathological features are shown in Table 2. The median age of 58 (range, 33–78) years was used to separate the patients into two groups of ≤58 years ($n = 251$, 51.4%) and >58 years ($n = 237$, 48.6%). There were 344 men (70.5%) and 144 women (29.5%).

Gross examination revealed the median tumor size to be 4 cm (range, 0.2–24 cm). Based on tumor size, there were four

TABLE 2 Clinicopathological features of patients with perihilar cholangiocarcinoma.

Features	$n = 488$	%
Age (year)		
≤58	251	51.4
>58	237	48.6
Sex		
Male	344	70.5
Female	144	29.5
Tumor size (range, 0.2–24 cm)		
Tumor *in situ*	25	5.1
≤4	177	36.2
>4	155	31.8
Unknown	131	26.9
Growth pattern		
Tumor *in situ* (Intraductal growth, ID)	25	5.1
Intraductal growth (ID)	39	8
Periductal infiltrating (PI)	94	19.3
Mass forming (MF)	119	24.4
ID+PI	54	11.1
ID+MF	36	7.4
PI+MF	82	16.8
ID+PI+MF	39	8
Surgical margin (R)		
R0 (tumor *in situ*)	25	5.1
R0	180	36.9
R1	283	58
Histological types		
Tumor *in situ* (P or T)	25	5.1
Papillary (P)	196	40.2
Tubular (T)	180	36.9
Papillotubular (P+T)	19	3.9
Adenocarcinoma, NOS	68	13.9
Histological grade		
Well-differentiated (tumor *in situ*)	25	5.1
Well-differentiated	383	78.5
Moderately differentiated	56	11.5
Poorly differentiated	24	4.9
T categories		
T*is*	25	5.1
T1	40	8.2
T2a	125	25.6
T2b	197	40.4
T3	71	14.5
T4	30	6.2
Lymph node metastasis (N)		
N0 (tumor *in situ*)	25	5.1
N0	248	50.8
N1	182	37.3
N2	33	6.8

(Continued)

10.3389/fmed.2022.893252

TABLE 2 (Continued)

Features	$n = 488$	%
Distant metastasis (M)		
M0 (tumor *in situ*)	25	5.1
M0	415	85.1
M1	48	9.8

groups, namely, ≤4 cm (n = 177, 36.2%), >4 cm (n = 155, 31.8%), tumor *in situ* (n = 25, 5.1%), and unknown size (n = 131, 26.9%). The tumors exhibited a spectrum of gross growth patterns ranging from tumor *in situ* with ID (n = 25, 5.1%) to ID (n = 39, 8%), PI (n = 94, 19.3%), MF (n = 119, 24.4%), and combinations of ID+PI (n = 54, 11.1%), ID+MF (n = 36, 7.4%), PI+MF (n = 82, 16.8%), and ID+PI+MF (n = 39, 8%). The surgical margin was assessed microscopically to be free from tumor, R0 (tumor *in situ*, n = 25, 5.1%), R0 (n = 180, 36.9%), and involved by tumor, R1 (n = 283, 58%).

Pathological examination revealed the following histological types: tumor *in situ* with either papillary or tubular adenocarcinoma (n = 25, 5.1%); papillary adenocarcinoma (P) (n = 196, 40.2%); tubular adenocarcinoma (T) (n = 180, 36.9%); papillotubular adenocarcinoma (P+T) (n = 19, 3.9%); and adenocarcinoma, NOS (n = 68, 13.9%). Histological grades comprised well- (tumor *in situ*, n = 25, 5.1%), well- (n = 383, 78.5%), moderately (n = 56, 11.5%), and poorly differentiated carcinomas (n = 24, 4.9%).

According to the eighth AJCC staging system (Table 1), T categories comprised T*is* (n = 25, 5.1%), T1 (n = 40, 8.2%), T2a (n = 125, 25.6%), T2b (n = 197, 40.4%), T3 (n = 71, 14.5%), and T4 (n = 30, 6.2%). Lymph node metastasis (N) following the eighth AJCC staging system was divided into four groups: N0 (tumor *in situ*, n = 25, 5.1%), N0 (n = 248, 50.8%), N1 (n = 182, 37.3%), and N2 (n = 33, 6.8%). Distant metastasis (M) comprised M0 (tumor *in situ*, n = 25, 5.1%), M0 (n = 415, 85.1%), and M1 (n = 48, 9.8%). The metastatic sites, which were confirmed non-local invasion, included gallbladder (n = 20), falciform ligament (n = 2), hepatoduodenal tissue (n = 5), omentum (n = 10), peritoneum (n = 5), diaphragm (n = 5), and skull (n = 1). All data were further analyzed for survival times (univariate analysis by Logrank test) and prognostic risk factors (multivariate analysis by Cox regression).

Survival and univariate analysis of possible risk factors of patients with perihilar cholangiocarcinoma

The OS and 5-year survival rate (5y) of the 488 patients with pCCA were analyzed with the Kaplan–Meier model and the comparison of OS for the various clinicopathological features

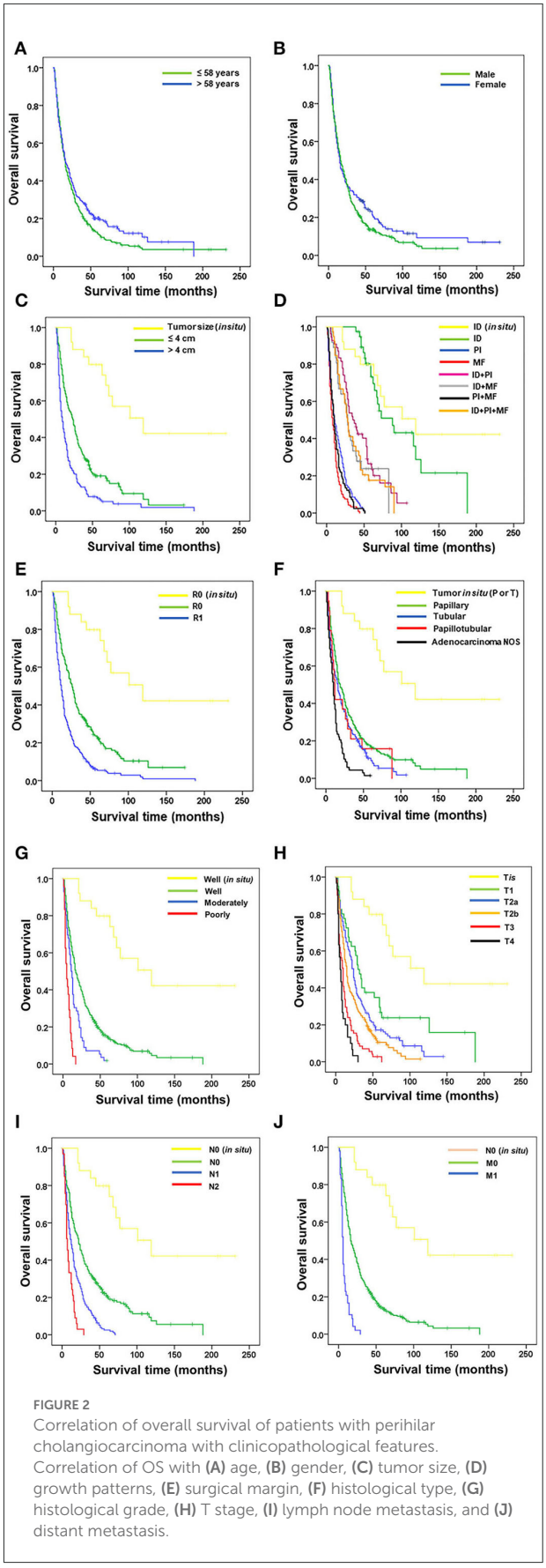

FIGURE 2
Correlation of overall survival of patients with perihilar cholangiocarcinoma with clinicopathological features. Correlation of OS with **(A)** age, **(B)** gender, **(C)** tumor size, **(D)** growth patterns, **(E)** surgical margin, **(F)** histological type, **(G)** histological grade, **(H)** T stage, **(I)** lymph node metastasis, and **(J)** distant metastasis.

TABLE 3 Univariate and multivariate analyses of survival in patients with perihilar cholangiocarcinoma.

Feature	Univariate analysis					Multivariate analysis		
	n = 488	OS (month)	5-year survival rates	HR (95% CI)	*p*-value	*n* = 331	HR (95% CI)	*p*-value
Age (yr)								
≤58	251	16	12%	1		-	-	-
>58	237	16	21%	0.84 (0.70–1.02)	0.068	-	-	-
Gender								
Male	344	16	14.2%	1		-	-	
Female	144	15	14.6%	0.86 (0.69–1.06)	0.153	-	-	-
Tumor size (range, 0.5–24 cm.)								
Tumor *in situ*	25	119	80%	0.23 (0.13–0.44)	<0.001	-	-	-
≤4 cm	177	23	20.1%	1		177	1	
>4 cm	155	9	7.7%	1.87 (1.49–2.36)	<0.001	154	1.22 (0.94–1.61)	0.141
Unknown	131	-	-	-	-	-	-	-
Surgical margin (R)								
R0 (Tumor *in situ*)	25	119	80%	0.25 (0.14–0.47)	<0.001	-	-	-
R0	180	23	23.3%	1		119	1	
R1	283	9	6.3%	1.96 (1.60–2.40)	<0.001	212	1.22 (0.93–1.60)	0.156
Growth pattern								
ID (*in situ*)	25	119	80%	0.70 (0.34–1.47)	0.349	-	-	-
ID	39	88	76.9%	1		27	1	
PI	94	10	0%	14.67 (8.61–24.99)	<0.001	53	19.72 (9.20–42.24)	<0.001
MF	119	8	0%	22.66 (13.31–38.57)	<0.001	97	19.37 (9.02–41.60)	<0.001
ID+PI	54	35	27.8%	3.52 (2.03–6.08)	<0.001	30	4.67 (2.14–10.20)	<0.001
ID+MF	36	28	25%	4.72 (2.59–8.59)	<0.001	29	6.15 (2.77–13.68)	<0.001
PI+MF	82	10	0%	16.95 (9.87–29.11)	<0.001	63	16.01 (7.51–34.12)	<0.001
ID+PI+MF	39	28	17.9%	4.43 (2.50–7.83)	<0.001	32	4.94 (2.32–10.51)	<0.001
Histological type								
Tumor *in situ*	25	119	80%	0.21 (0.11-−0.39)	<0.001	-	-	-
Papillary carcinoma	196	19	17.3%	1		137	1	
Tubular carcinoma	180	16	12.8%	1.30 (1.05–1.61)	<0.05	139	0.86 (0.65–1.13)	0.276
Papillotubular carcinoma	19	12	15.8%	1.19 (0.73–1.97)	0.488	15	-	-
Adenocarcinoma, NOS	68	10	1.8%	2.38 (1.78–3.18)	<0.001	40	0.56 (0.25–1.27)	0.164
Histological grade								
Well-differentiated (*in situ*)	25	119	80%	0.19 (0.11–0.35)	<0.001	-	-	-
Well-differentiated	383	17	15.4%	1		280	1	
Moderately differentiated	56	11	1.7%	1.83 (1.37–2.44)	<0.001	32	2.31 (1.19–4.49)	<0.05
Poorly differentiated	24	5	0%	4.32 (2.81–6.65)	<0.001	19	4.99 (2.02–12.29)	<0.001
T categories								
T*is*	25	119	80%	0.31 (0.16–0.62)	<0.01	-	-	-
T1	40	30	27.5%	1		26	1	
T2a	125	24	17.6%	1.49 (1.00–2.22)	<0.05	82	0.83 (0.48–1.44)	0.515
T2b	197	15	13.2%	2.00 (1.36–2.94)	<0.001	153	0.97 (0.57–1.66)	0.920
T3	71	10	2.8%	3.54 (2.30–5.44)	<0.001	47	1.23 (0.68–2.20)	0.496
T4	30	6	0%	5.37 (3.21–8.99)	<0.001	23	1.38 (0.70–2.71)	0.348
Lymph metastasis (N)								
N0 (*in situ*)	25	119	80%	0.23 (0.12–0.42)	<0.001	-	-	-
N0	248	22	22.2%	1		168	1	

(Continued)

TABLE 3 (Continued)

Feature	Univariate analysis					Multivariate analysis		
	n = 488	OS (month)	5-year survival rates	HR (95% CI)	*p*-value	*n* = 331	HR (95% CI)	*p*-value
N1	182	12	3.3%	2.01 (1.63–2.47)	<0.001	135	1.37 (1.04–1.80)	<0.05
N2	33	7	0%	3.66 (2.50–5.37)	<0.001	28	2.18 (1.39–3.44)	<0.01
Distal metastasis (M)								
M0 (*in situ*)	25	119	80%	0.19 (0.10–0.35)	<0.001	-	-	-
M0	415	16	14.7%	1		294	1	
M1	48	6	0%	3.49 (2.55–4.79)	<0.001	37	2.11 (1.44–3.10)	<0.001

with the Logrank test. There was no significant difference in the survival times of age and gender of patients. Therefore, neither did age nor gender affect the survival time in pCCA (Figures 2A,B, Table 3).

Non-invasive CCA served as a baseline for good survival time against which all other clinicopathological features were analyzed. Tumor size was available in 350 patients (Figure 2C, Table 3). Survival analysis showed that patients with tumor size >4 cm had significantly shorter survival time and 5-year survival rate than those with tumor size ≤4 cm (OS = 9 vs. 23 mo., 5y = 7.7% vs. 20.1%, $p < 0.001$), while those with tumor size ≤4 cm had significantly shorter survival time than those with tumor *in situ* (OS = 23 vs. 119 mo., 5y = 20.1 vs. 80%, $p < 0.001$).

Growth patterns identified by the surgeon-pathologist team included ID in non-invasive/*in situ* CCA, ID, PI, and MF, and combinations of ID+PI, ID+MF, PI+MF, and ID+PI+MF (Figure 2D, Table 3). Results showed that ID (OS = 88 mo.) had a significantly better survival time than PI (OS=88 vs 10 mo., 5y = 76.9 vs. 0%, $p < 0.001$), MF (OS = 88 vs. 8 mo., 5y = 76.9 vs. 0%, $p < 0.001$), ID+PI (OS = 88 vs. 35 mo., 5y = 76.9 vs. 27.8%, $p < 0.001$), ID+MF (OS = 88 vs. 28 mo., 5y = 76.9 vs. 25%, $p < 0.001$), PI+MF (OS = 88 vs. 10 mo., 5y = 76.9 vs. 0%, $p < 0.001$), and ID+PI+MF (OS = 88 vs. 28 mo., 5y = 76.9 vs. 17.9%, $p < 0.001$). However, there was no significant difference between ID and ID in non-invasive CCA (OS = 88 vs. 119 mo., 5y = 76.9 vs. 80%, $p = 0.349$).

Surgical margin (R) status was assessed microscopically (Figure 2E, Table 3). Patients having invasive CCA with positive surgical margins (R1) had survival time and rate significantly shorter than those with free surgical margins (R0) (OS = 9 vs. 23 mo., 5y = 6.3 vs. 23.3%, $p < 0.001$). In addition, the survival time of R0 in invasive CCA was significantly lower than R0 in non-invasive (tumor *in situ*) CCA (OS = 23 vs. 119 mo., 5y = 23.3 vs. 80%, $p < 0.001$).

Histological type was specified by the pathologist (Figure 2F, Table 3). Tubular and adenocarcinoma, NOS, types, had significantly shorter survival time and rate than papillary type, which was used as the reference group (OS = 16 vs. 19 mo., 5y = 12.8 vs. 17.3% $p < 0.05$) and (OS = 10 vs. 19 mo., 5y = 1.8 vs. 17.3%, $p < 0.001$), respectively. Additionally, the survival time of papillary type was shorter than histological types with *in situ* papillary or tubular types (OS = 19 vs. 119 mo., 5y = 17.3 vs. 80%, $p < 0.001$). No significance was recorded between papillary and papillotubular types (OS = 19 vs. 12 mo., 5y = 17.3 vs. 15.8%, $p = 0.488$).

Histological grades comprised well-, moderately, and poorly differentiated pCCA (Figure 2G, Table 3). The OS of patients with well-differentiated tumors was significantly higher than those with moderately (OS = 17 vs. 11 mo., 5y = 15.4 vs. 1.7%, $p < 0.001$) and poorly differentiated tumors (OS = 17 vs. 5 mo., 5y = 15.4 vs. 0%, $p < 0.001$). The OS of well-differentiated invasive CCA was markedly shorter than those with well-differentiated *in situ* tumors (OS = 17 vs. 119 mo., 5y = 15.4 vs. 80%, $p < 0.001$).

T categories according to the eighth AJCC staging system comprise T*is*, T1, T2a, T2b, T3, and T4 (Figure 2H, Table 3). Results of the survival analysis, using T1 as reference group, showed that T1 (OS = 30 mo.) was markedly better than T2a (OS = 30 vs. 24 mo., 5y = 27.5 vs. 17.6%, $p < 0.05$), T2b (OS = 30 vs. 15 mo., 5y = 27.5 vs. 13.2%, $p < 0.001$), T3 (OS = 30 vs. 10 mo., 27.5 vs. 2.8%, $p < 0.001$), and T4 (OS = 30 vs. 6 mo., 5y = 27.5 vs. 0%, $p < 0.001$), while OS of T1 was lower than T*is* (OS = 30 vs. 119 mo., 5y = 27.5 vs. 80%, $p < 0.01$).

As for lymph node metastasis (N) and distant metastasis (M) (Figures 2I,J, Table 3), results showed that patients who were either N1/N2 or M1 positive had remarkably shorter survival times than those with negative results (OS = 12 vs 22 mo., 5y = 3.3 vs. 22.2%, $p < 0.001$), (OS = 7 vs. 22 mo., 5y = 0 vs. 22.2%, $p < 0.001$), and (OS = 6 vs 16 mo., 5y = 0 vs. 14.7%, $p < 0.001$), respectively. As expected, invasive CCA with negative N and M status correlated with significantly shorter survival times than *in situ* tumors (OS = 22 vs. 119 mo., 5y = 22.2 vs. 80%, $p < 0.001$) and (OS = 16 vs. 119 mo., 5y = 14.7 vs. 80%, $p < 0.001$), respectively.

Significant factors such as age, tumor size, surgical margin, growth patterns, histological type, histological grade, and TNM categories were identified in the univariate analysis. These factors were selected for further investigation by multivariate analysis to identify independent factors for prognostication

in pCCA. For multivariate analysis, only invasive pCCA was analyzed after removing non-invasive/*in situ* cases.

Multivariate analysis of significant pathological features from univariate analysis

Univariate analysis of 331 patients identified tumor size, surgical margin, growth patterns, histological type, histological grade, T category, lymph node metastasis, and distant metastasis as having significantly affected survival times of patients with pCCA. Further analysis by multivariate analysis revealed that growth patterns, histological grade, lymph node metastasis, and distant metastasis were independent risk factors for the prediction of poor outcomes in patients with pCCA (Table 3).

For growth patterns, ID was used as a reference group for comparison with other growth patterns. Multivariate analysis showed that PI and MF had HR significantly higher than ID (HR = 19.72 and 19.37, $p < 0.001$), respectively. This finding was also found in the combination types; ID+PI, ID+MF, PI+MF, and ID+PI+MF showed HR significantly higher than ID (HR = 4.67, 6.15, 16.01, and 4.94, $p < 0.001$), respectively. We observed that OS of patients was increased when the growth patterns contained an ID component (ID+PI, ID+MF, and ID+PI+MF); henceforth, labeled as ID mixed types. Therefore, it was postulated that patients with pCCA with growth patterns lacking an ID component tended to do poorly. This finding suggested that the presence of ID components in growth patterns was a favorable prognostic factor for patients with pCCA. The corollary was that the lack of ID component was a poor prognostic factor.

For histological grades, the moderately and poorly differentiated tumors had HR markedly higher than the well-differentiated reference group (HR = 2.31, $p < 0.05$; and HR = 4.99, $p < 0.001$), respectively.

Lymph node metastasis and distant metastasis were consistent risk factors for poor prognosis. Multivariate results showed that positive lymph nodes (N1, N2) and distant metastasis had HR significantly greater than when they were negative (HR = 1.37 and 2.18, $p < 0.05$ and 0.01; and HR = 2.11, $p < 0.001$), respectively.

This study showed that growth patterns (PI, MF, and PI+MF), histological grade (moderate and poor differentiation), lymph node metastasis, and distant metastasis were prognostic risk factors for poor survival in patients with pCCA. Interestingly, growth patterns impacted the survival of patients with pCCA with high HR, and survival time changed between tumors with or without ID components. Therefore, this study aims to propose the incorporation of growth patterns for clustering patients with pCCA as an alternative tool for classifying such patients in our cohort. The limited number of cases in the higher histological grade groups precluded the incorporation of histological grade into the modification of the eighth AJCC staging system.

Stratification performance of the eighth AJCC/UICC staging system

To investigate the stratification performance of the eighth AJCC staging system, TNM staging was performed to classify pCCA according to the AJCC staging manual (Table 1). The results showed stage 0 ($n = 25$, OS = 119 mo., 5y = 80%), I ($n = 31$, OS = 39 mo., 5y = 35.5%), II ($n = 160$, OS = 26 mo., 5y = 26.3%), IIIA ($n = 35$, OS = 10 mo., 5y = 5.7%), IIIB ($n = 8$, OS = 4 mo., 5y = 0%), IIIC ($n = 153$, OS = 15 mo., 5y = 3.9%), IVA ($n = 28$, OS = 7 mo., 5y = 0%), and IVB ($n = 48$, OS = 6 mo., 5y = 0%). The stratification performance of the eighth AJCC staging system was inefficient in classifying and separating certain stages of patients with pCCA. The survival times and rates were equivocal and there was no significant difference between stages IIIA and IIIB; in fact, the survival times were shorter than for IIIC. Furthermore, stage IIIB had the shortest survival time when compared to IVA and IVB (Figure 3). This poor performance of the eighth AJCC staging system may impact prognosis and treatment decisions.

This study proposed an alternative staging system by employing prognostic factors from multivariate analysis to improve classification performance for pCCA. Our findings revealed that growth pattern has the highest impact on the survival of patients with pCCA. We hypothesize that the inclusion of a growth pattern subgroup may provide the necessary improvement required for pCCA classification.

Subgroup analysis of growth pattern and lymph node status

There were seven growth patterns based on various morphological proportions, comprising ID, PI, MF, ID+PI, ID+MF, PI+MF, and ID+PI+MF (Figure 4), and they were associated with different survival outcomes. Based on survival outcomes, the patients were classified into three groups comprising well (ID, OS = 88 mo.), moderate (ID+PI, ID+MF, and ID+PI+MF, OS = 35, 28, and 28 mo., respectively), and poor (PI, MF, and PI+MF, OS = 10, 8, and 10 mo., respectively) outcomes (Figure 2D, Table 3). Notably, the survival outcomes of patients were favorably associated with the presence of the ID component. Therefore, on the basis of the ID component, we stratified growth patterns into three subgroups: ID, ID mixed types (ID+PI, ID+MF, and ID+PI+F), and without ID mixed types (PI, MF, and PI+MF). In addition, this investigation excluded N2M0 ($n = 28$) and M1 ($n = 48$) status because they

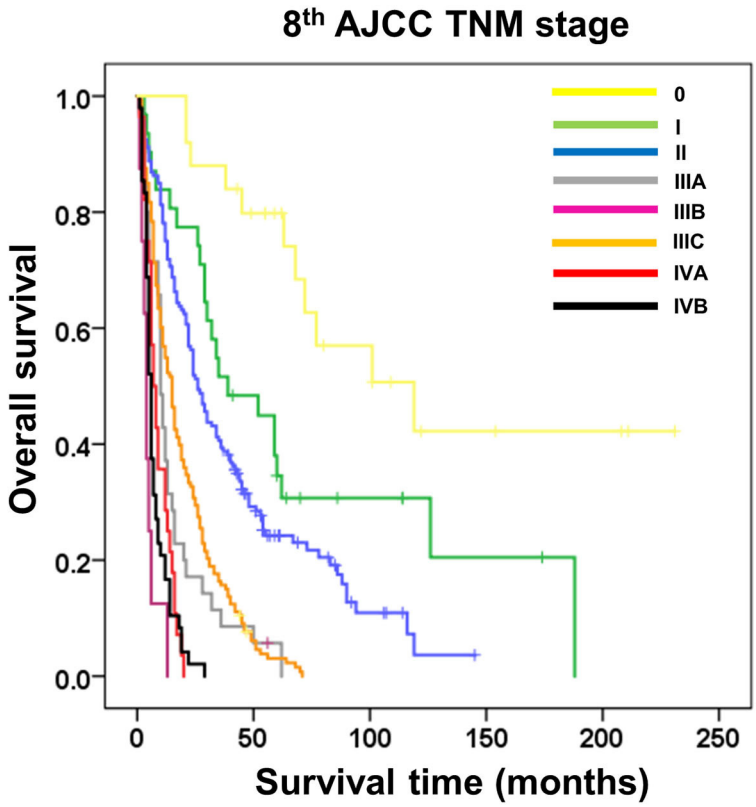

TNM stage	N (488)	OS (mo.)	5-year Survival rate	HR (95%CI)	*P value*
0	25	119	80%	0.38 (0.18-0.78)	<0.01
I	31	39	35.5%	1	
II	160	26	26.3%	1.62 (1.03-2.54)	<0.05
IIIA	35	10	5.7%	4.47 (2.59-7.70)	<0.001
IIIB	8	4	0%	17.57 (7.65-40.36)	<0.001
IIIC	153	15	3.9%	3.57 (2.26-5.63)	<0.001
IVA	28	7	0%	8.23 (4.61-14.72)	<0.001
IVB	48	6	0%	10.06 (5.93-17.06)	<0.001

FIGURE 3
Kaplan–Meier curve represented the overall survival of patients with perihilar cholangiocarcinoma with TNM stages by the eighth AJCC staging system. The table represented the outcomes of patients with TNM stage by the eighth AJCC staging system, namely, TNM stage, number of cases, overall survival, 5-year survival rate, hazard ratio, and *p*-value.

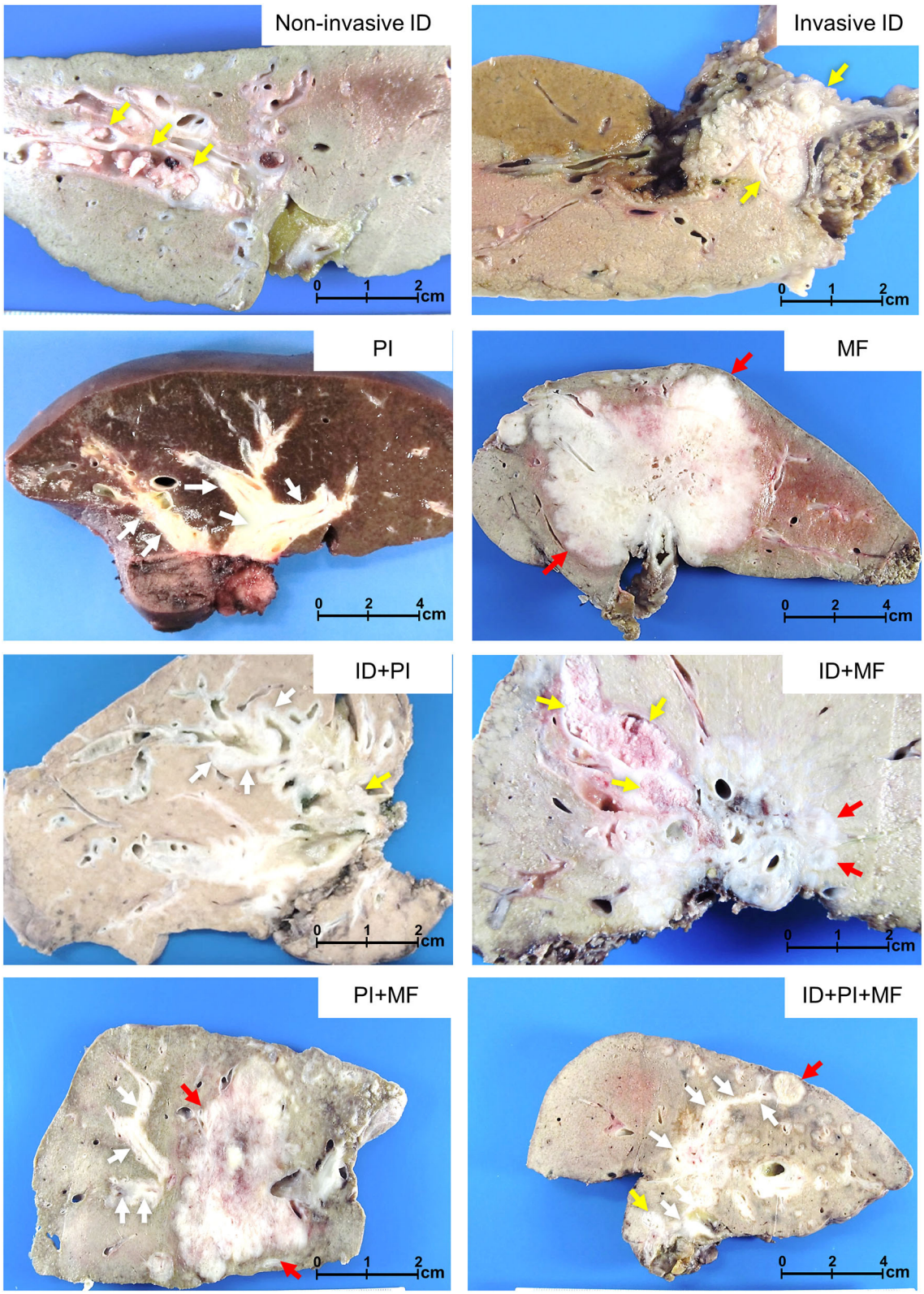

FIGURE 4
Growth patterns of perihilar cholangiocarcinoma. Non-invasive intraductal (ID), invasive ID, periductal infiltrating (PI), mass-forming (MF), and mixed types comprising ID+PI, ID+MF, PI+MF, and ID+PI+MF. Yellow, white, and red arrows indicate ID, PI, and MF, respectively.

represent late-stage disease and are well-known poor prognostic factors for pCCA.

This investigation aims to subclassify growth patterns with N0 and N1 status and to determine whether N status has any effect on influencing the survival time of various growth patterns when N status changes. To demonstrate this hypothesis, the growth pattern was divided into seven groups, comprising ID (*in situ*) as a baseline for good prognosis, ID/N0, ID/N1, ID mixed type/N0, ID mixed type/N1, without ID mixed type/N0, and without ID mixed type/N1.

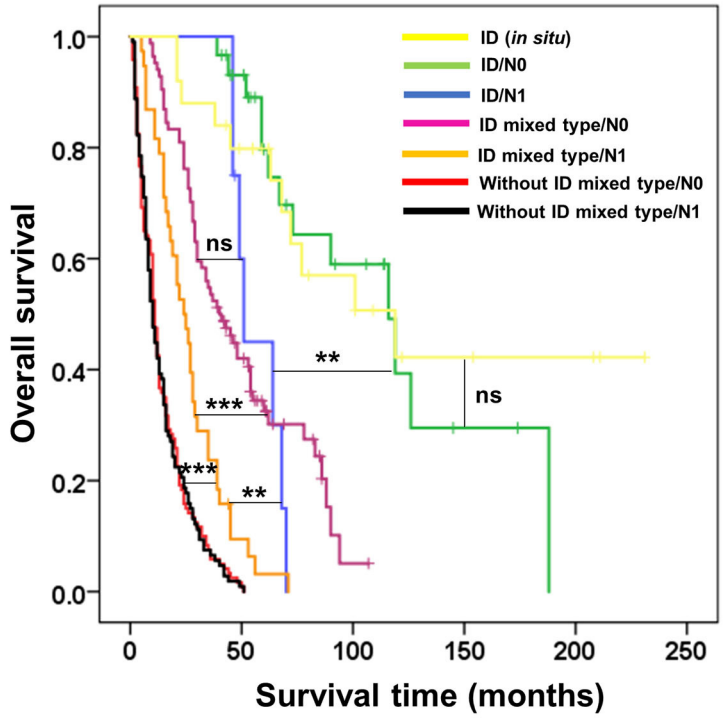

Subgroups of growth patterns	N (412)	OS (mo.)	5-year Survival rate	HR (95%CI)	*P* value
ID (*in situ*)	25	119	80%	0.94 (0.42-2.12)	0.888
ID/N0	30	116	83.3%	1	
ID/N1	8	51	50%	4.03 (1.55-10.48)	<0.01
ID mixed type/N0	84	40	35.7%	4.40 (2.32-8.37)	<0.001
ID mixed type/N1	38	24	5.3%	12.22 (6.08-24.57)	<0.001
without ID mixed type/N0	120	11	0%	26.50 (13.72-51.17)	<0.001
without ID mixed type/N1	107	10	0%	27.07 (13.97-52.46)	<0.001

FIGURE 5
Kaplan–Meier curve represented the overall survival of subgroup coordinating growth pattern and lymph node status (N0 and N1) in patients with perihilar cholangiocarcinoma. The table represented the outcomes of subgroup analysis, namely, subgroups of growth patterns, number of cases, overall survival, 5-year survival rate, hazard ratio, and *p*-value. $^{**}p < 0.01$, $^{***}p < 0.001$, and ns = no statistical significance.

The survival analysis showed that ID/N0 had OS and 5-year survival rate better than ID/N1 (OS = 116 vs. 51 mo., 5y = 83.3% vs. 50%, $p < 0.01$), ID mixed type/N0 (OS = 116 vs. 40 mo., 5y = 83.3 vs. 35.7%, $p < 0.001$), ID mixed type/N1 (OS = 116 vs 24 mo., 5y = 83.3 vs. 5.3%, $p < 0.001$), without ID mixed type/N0 (OS = 116 vs. 11 mo., 5y = 83.3 vs. 0%, $p < 0.001$), and without ID mixed type/N1 (OS = 116 vs. 40 mo., 5y = 83.3 vs. 0%, $p < 0.001$), while no significant difference was observed when compared with ID (*in situ*) (OS = 116 vs. 119 mo., 5y = 83.3 vs. 80%, $p = 0.888$).

Additionally, the comparison between subgroups found that ID/N1 and ID mixed type/N0 were not significantly different, while both ID/N1 and ID mixed type/N0 were markedly different when compared with ID mixed type/N1 ($p < 0.01$ and 0.001, respectively). Furthermore, ID mixed type/N1 had obviously better survival time than both without ID mixed type/N0 ($p < 0.001$) and without ID mixed type/N1 ($p < 0.001$), while the comparison of ID mixed type/N0 and without ID mixed type/N1 showed no significant difference (Figure 5). This information supported the hypothesis that the survival

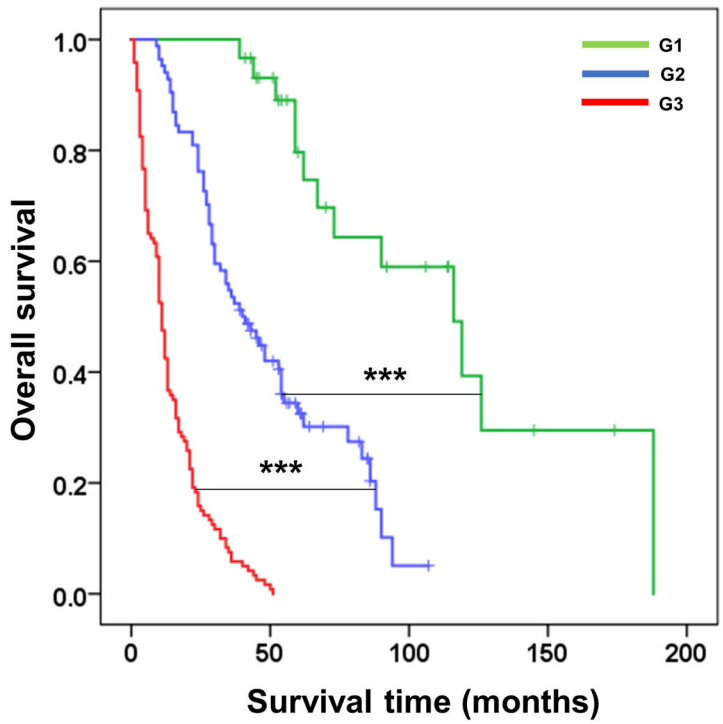

G category	N (234)	OS (mo.)	5-year Survival rate	HR (95%CI)	*P* value
G1	30	116	83.3%	1	
G2	84	40	35.7%	5.10 (2.47-10.53)	<0.001
G3	120	11	0%	28.60 (13.50-60.60)	<0.001

FIGURE 6
Kaplan–Meier curve represented the overall survival of the G category in the KKU staging system for classifying patients with perihilar cholangiocarcinoma. The table represented the outcomes of patients with G category classification, namely, groups, number of cases, overall survival, 5-year survival rate, hazard ratio, and *p*-value. ***$p < 0.001$.

time of growth pattern-classified patients was decreased when N1 appeared.

Creating growth pattern (G) category of the KKU staging system

From Figure 5, we found that N1 could upgrade the aggressive behavior of growth pattern-classified pCCA, such as in ID (N0/N1) and ID mixed type (N0/N1), while no difference was found in without ID mixed type (N0/N1). Therefore, we generated a new G category to replace the T category of the eighth AJCC staging system. The G category was created according to the survival analysis of subgroups of growth patterns without lymph node positivity.

There were three classes of the G category in this study, comprising G1 (ID/N0, $n = 30$), G2 (ID mixed type/N0, $n = 84$), and G3 (without ID mixed type/N0, $n = 120$). The survival analysis showed that G1 had OS and survival rate markedly better than G2 (OS = 116 vs. 40 mo., 5y = 83.3 vs. 35.7%, $p < 0.001$) and G3 (OS = 116 vs. 11 mo., 5y = 83.3 vs. 0%, $p<0.001$). Moreover, the comparison of survival time for each G category revealed a clear separation between each stage; G2 vs G3 ($p < 0.001$) (Figure 6).

Classification of patients with perihilar cholangiocarcinoma using the KKU staging system

According to Figures 5, 6, we proposed the KKU staging manual for classifying patients with pCCA (Table 4). G category was incorporated together with N and M categories (according to the eighth AJCC staging system) into the KKU stage: I (G1/N0/M0), II (G1/N1/M0 or G2/N0/M0), IIIA (G2/N1/M0), IIIB (G3/M0/M0 or G3/N1/M0), IVA (anyG/N2/M0), and IVB (anyG/anyN/M1). The results showed that patients with pCCA can be classified into seven stages, comprising KKU stage 0 ($n = 25$), I ($n = 30$), II ($n = 92$), IIIA ($n = 38$), IIIB ($n = 227$), IVA ($n = 28$), and IVB ($n = 48$). KKU stage 0 represents non-invasive tumor (carcinoma *in situ*//high-grade dysplasia) with good survival, while KKU stage I is a baseline for a good prognosis of invasive tumor which had similar outcomes as stage 0 (OS = 116 vs. 119 mo., 5y = 83.3 vs. 80%, $p = 0.888$).

The stratification performance demonstrated good separation between stages with overall survival and survival rate of KKU stage I being significantly better than for II (OS = 116 vs. 46 mo., 5y = 83.3 vs. 37%, $p < 0.001$), IIIA (OS = 116 vs. 24 mo., 5y = 83.3 vs. 5.3%, $p < 0.001$), IIIB (OS = 116 vs. 11 mo., 5y = 83.3 vs. 0%, $p < 0.001$), IVA (OS = 116 vs. 7 mo., 5y = 83.3 vs. 0%, $p < 0.001$), and IVB (OS = 116 vs. 6 mo., 5y = 83.3 vs 0%, $p < 0.001$).

TABLE 4 Definition of GNM categories of the KKU staging manual.

G category (G)	Lymph node metastasis (N)*	Distant metastasis (M)*
T*is* = Carcinoma in *situ*//high-grade dysplasia*	N0 = Negative lymph node	M0 = No distant metastasis
G1 = Pure intraductal growth pattern (ID)	N1 = One to three positive lymph nodes	M1 = Distant metastasis
G2 = With ID mixed types (ID+PI, ID+MF, ID+PI+MF)	N2 = Four or more positive lymph nodes	
G3 = Without ID mixed types (PI, MF, PI+MF)		
KKU staging system (GNM stage)		
Stage I	G1/N0/M0	
Stage II	G1/N1/M0, G2/N0/M0	
Stage IIIA	G2/N1/M0	
Stage IIIB	G3/N0/M0, G3/N1/M0	
Stage IVA	AnyG/N2/M0	
Stage IVB	AnyG/anyN/M1	

*According to the eighth AJCC staging system.
G1 was the growth pattern; ID.
G2 was the growth pattern; ID+PI, ID+MF, and ID+PI+MF.
G3 was the growth pattern; PI, MF, and PI+MF.

Moreover, the comparison of each stage showed good separation: II vs IIIA ($p < 0.001$), IIIA vs IIIB ($p < 0.001$), and IIIB vs. IVA ($p < 0.01$), and IVB ($p < 0.001$) (Figure 7). These findings support the contention that the KKU staging system has high performance to classify patients with pCCA in Thailand; thus, providing an alternative tool to overcome the weak classification ability of the eighth AJCC staging system.

Discussion

Nowadays, curative therapy for pCCA is limited to the surgical strategy with poor 5-year survival rates (11–13). Our study showed the survival rates of patients with pCCA at 1, 3, and 5 years after partial hepatectomy to be 58, 27, and 11.5%, respectively (Supplementary Figure 1). Previous reports have suggested that the major issue was late diagnosis with advanced disease (10, 11). About 56% of our cohort of patients with pCCA between 2002 and 2017 presented with advanced disease–40% stage III and 16% stage IV, based on the eighth AJCC staging system. This translated into a higher rate of surgical margin involvement with R1 as high as 58% when compared to the reported range of 11–39% in other cohorts (26, 27, 29, 31, 32, 36, 37). This clearly shows that early diagnosis is crucial for accurate clustering and treatment.

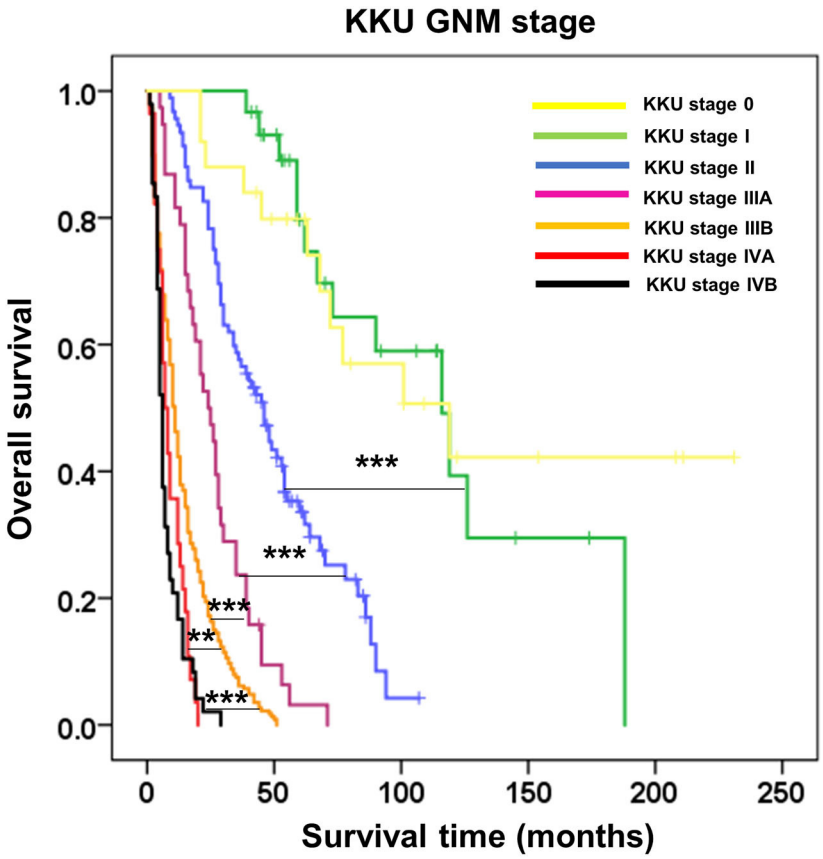

KKU stage	N (488)	OS (mo.)	5-year Survival rate	HR (95%CI)	*P* value
0	25	119	80%	0.94 (0.42-2.12)	0.888
I	30	116	83.3%	1	
II	92	46	37%	4.36 (2.31-8.26)	<0.001
IIIA	38	24	5.3%	12.25 (6.09-24.62)	<0.001
IIIB	227	11	0%	26.94 (14.11-51.44)	<0.001
IVA	28	7	0%	49.12 (23.29-103.62)	<0.001
IVB	48	6	0%	59.45 (29.34-120.49)	<0.001

FIGURE 7
Kaplan–Meier curve represented the overall survival of perihilar cholangiocarcinoma patients with GNM stages by the KKU staging system. The table represented the outcomes of patients with GNM stage by the KKU staging system, namely, KKU stage, number of cases, overall survival, 5-year survival rate, hazard ratio, and p-value. $^{**}p < 0.01$ and $^{***}p < 0.001$.

The current stratification tool for clustering pCCA is the eighth edition of the AJCC staging system (21). Several reports have suggested that the updated edition provided a better classification and stratification performance than the seventh edition (22–25, 38). Ruzzenente et al. (22) compared both editions of the AJCC staging system in 214 patients who

underwent surgery for pCCA at two Italian tertiary referral hepatobiliary centers. Based on the seventh edition, the 5-year OS rates were stage I (71%), II (34%), and IV (34%), while there were no patients who survived 5 years in stage IIIA, IIIB, and IV. The eighth edition, however, appeared to have improved discriminatory ability with consistent classification for 5-year OS in stage I (71%), II (35%), and better discrimination for stage IIIA (23%), IIIB (19%), and IIIC (22%). Interestingly, there was no 5-year OS for stages IVA and IVB. The C-index representing discriminatory performance was higher for the eighth than the seventh edition (0.624 vs. 0.619). Similarly, Lee et al. (24) showed in 348 patients who underwent hepatectomy that the stratification by the eighth edition of each group of T classification improved the clustering of patients with T3 and T4 when compared to the seventh edition. The eighth AJCC classification showed increase in OS of T3 (T1, 42.6%; T2, 31.2%; T3, 13.9%; T4, 15.1%; T1 vs. T2, $p = 0.260$; T2 vs. T3, $p = 0.001$; T3 vs. T4, $p = 0.996$), and decrease of OS of T4 and when each T stage was separated, especially T3 and T4. These results were greater than by classification by the seventh AJCC staging system (T1, 41.0%; T2, 30.5%; T3, 9.1%; T4, 25.7%; T2 vs. T3, $p< 0.001$; T3 vs. T4, $p = 0.013$). Gaspersz et al. (23) analyzed the eighth AJCC staging system in 248 patients with pCCA by separating them into (i) patients with curative-intent resection (18.1%) and (ii) patients with non-resection due to metastasis (81.9%). The prognostic accuracy (C-index) was performed for the comparison of stratification performance. The results showed that the eighth edition had C-index higher than seventh edition for both curative-intent resection (0.67 vs. 0.65) and non-resection (0.58 vs. 0.57).

Although the prognostic predictability of the eighth edition is improved, the overall performance remains unsatisfactory (22–25). Accordingly, when this study applied the eighth AJCC staging system to classify 488 patients who had undergone partial hepatectomy for pCCA, the OS and 5-year survival rate results were not consistent and were ambiguous for each stage. Furthermore, the survival analysis displayed ambiguous stratification in stages III and IV (OS = IIIC>IIIA>IVA>IVB>IIIB)—IIIB had poor survival time less than IIIA, IIIC, IVA and IVB; and IIIA was less than IIIC (Figure 3). These results may lead to errors in diagnosis, prognosis, and treatment plans.

Numerous studies have suggested additional factors to modify the eighth AJCC staging system for suitable and precise prognostic predictability of pCCA (26–32). Prognostic factors which are independent factors from the multivariate analysis are favored, one of which is invasive tumor thickness (ITT). The new T classification based on ITT better separates each T stage than the eighth AJCC staging system (26). Oba et al. (27) confirmed that although they used different ITT cut-off values, T classification by ITT was able to distinguish the T stage better than the eighth AJCC staging system. Zhang et al. (28) proposed tumor size as a prognostic factor. They suggested that larger tumor size (range, 22–33 mm or ≥33 mm) is associated with poor outcomes, such as advanced T stage, more positive regional lymph nodes, and more frequent vascular invasion. For this study, we applied the growth pattern to improve the predictive accuracy of the prognosis of the eighth AJCC staging system (18, 39). Moreover, Cheng et al. (40) proposed the incorporation of serum tumor markers; carcinoembryonic antigen (CEA) and carbohydrate antigen 19-9 (CA 19-9), into the TNM staging system to form the mTNM staging system. The classification performance of mTNM showed a better ability to separate each stage than the TNM staging system.

In this study, growth patterns, histological grades (moderate and poor differentiation), lymph node, and distant metastasis were found to be independent factors for predicting poor survival of patients with pCCA. Interestingly, the growth patterns that included PI, MF, ID+PI, ID+MF, PI+MF, and ID+PI+MF had an HR markedly higher than the ID growth pattern, which is viewed as a favorable prognostic marker in patients with iCCA (15, 18, 41). In this cohort, almost all the pCCA cases were found in the intrahepatic location. We demonstrated a spectrum of growth patterns—ID, PI, and MF, and combined types comprising ID+PI, ID+MF, PI+MF, and ID+PI+MF. The proportion of combined types was considered by a surgeon-pathologist team with a 20% cut-off. Based on multivariate analysis, growth pattern was considered a major prognostic factor for poor survival of patients with pCCA (Table 3). Moreover, although histological grade (moderate and poor differentiation) was an independent factor in the multivariate analysis, the data were not robust enough to support inclusion in the new staging system.

In applying prognostic factors to generate a new KKU staging system, we created a new G category to replace the T category of the eighth AJCC tagging system. The patients with pCCA were clustered into three groups comprising G1 (ID), G2 (ID mixed types: ID+PI, IP+MF, ID+PI+F), and G2 (PI, MF, without ID mixed type—PI+MF). The G category showed good separation—G1 vs. G2 and G2 vs. G3; and OS and survival rate were decreased when G was increased (OS and 5-year survival rate = G1>G2>G3). The KKU staging system retained the N and M categories of the eighth AJCC staging system because both categories were independent factors in this study. Moreover, we found that all growth patterns showed shorter survival when N1, N2, and M1 status appeared compared to those with negative status (Figure 5); except for N1 without ID mixed type (PI, MF, and PI+MF) which showed no difference when N0 vs. N1 was compared. G3 showed poor outcomes irrespective of N0 or N1. Supplementary Table 1 showed that G3 was significantly correlated with tumor size, high histological grade, and high T category in the eighth AJCC staging system; hence, the poor survival. Previous reports support our findings that PI and MF were correlated with poor survival of patients with CCA, while ID favored a good prognosis (15, 18, 42, 43).

Therefore, the GNM stage by the KKU staging manual was applied to classify patients with pCCA (Table 4), with the resultant seven stages: KKU stage 0, I, II, IIIA, IIIB, IVA, and IVB. The performance of the KKU staging system (Figure 7) was superior to the eighth AJCC staging system (Figure 3) for patients with pCCA in Thailand. We hope this improvement will provide for a more precise prognosis, diagnosis, and choice of treatment plan. Therefore, we proposed the KKU

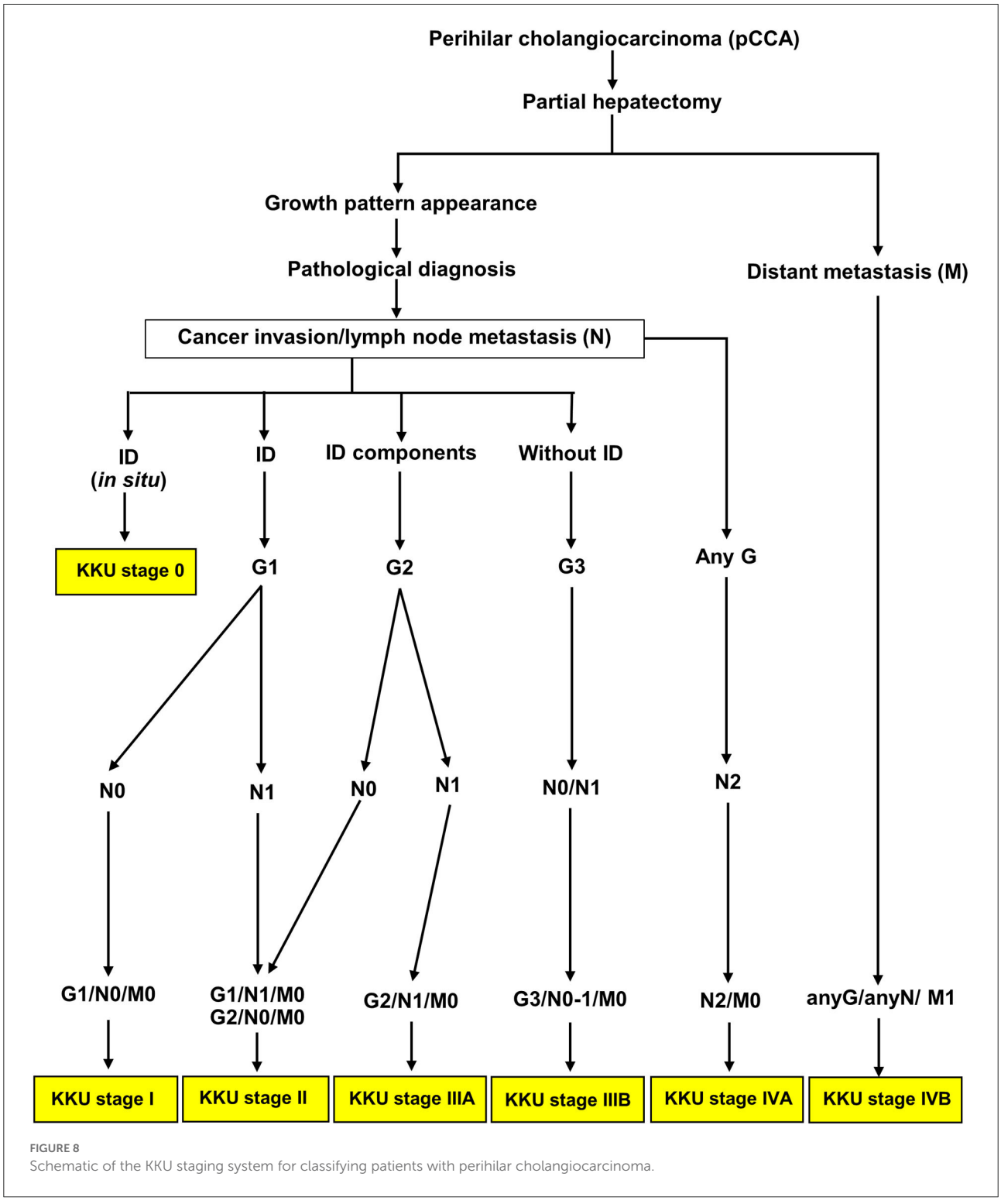

FIGURE 8
Schematic of the KKU staging system for classifying patients with perihilar cholangiocarcinoma.

staging system as an alternative tool for classifying patients with pCCA (Figure 8).

Our study has three major strengths. Northeast Thailand has the highest incidence of CCA worldwide. Furthermore, pCCA constituted the majority of the patients with CCA; thus, giving us a sizeable cohort for statistically significant analysis. Routine recording of growth pattern data has also enabled us to analyze and conclude that PI and MF patterns forebode poor prognostic outcomes (1, 15, 18).

However, there are several limitations to this study. The proposed KKU staging system was applied in a single institution in Northeast Thailand. Overall survival and not disease-specific survival were studied. The small number of patients in certain stages, such as stage IIIB, does not adequately represent the rest of the patient population. Histological grade and serum tumor markers (CEA and CA 19-9) are commonly reported characteristics in cancer prognostication and are important independent risk factors for stratifying patients; further analysis with a larger number of cases would be performed for subsequent incorporation into the KKU model. Post-operative complications are important and highly impact prognosis; however, this information was not available in our database. There was also no available follow-up data on adjuvant therapy, thereby significantly curtailing the evaluation of surgical margin status. Finally, the internal and external validation of the KKU staging system is needed to confirm and verify the discriminatory performance for the prognostic stratification of patients with pCCA.

For future perspective of this study, we believe that with validation from internal and external cohorts, the KKU staging system can be put into practice at our institute. Since growth pattern is routinely recorded in the pathological gross examination of CCA resection specimens, it may prove to be beneficial for stratification, prognostication, and planning for treatment or palliative care. Moreover, there is a prospect of applying the KKU staging system in a pre-operative setting. There are several studies in our institute, suggesting that pre-operative detection of ID lesions by radiology can be performed for early stages and for pre-invasive neoplasms of the bile ducts (44, 45). In 2017, Luvira V. and Eurboonyanun K. (co-authors in our study) investigated intraductal papillary neoplasms of the bile duct (IPNB) with survival correlation of patients with CCA via radiological–pathological staging. They created a new morphological classification of IPNB based on radiological–pathological appearance correlated with clinical findings, including outcomes. Their study showed that IPNB correlated with early stage and predicted survival very well (46, 47). In future, this study will be modified for incorporation into the KKU staging system in guiding the planning of surgical procedures.

In summary, in this study spanning 2002–2017, we updated significant information on the staging of pCCA. Approximately 56% of pCCA from Northeast Thailand presented with late-stage disease (TNM stage III, 40%) and distant metastasis (stage IV, 16%). All of these patients had poor survival outcomes. This study demonstrated that growth patterns, histological grade, lymph node, and distant metastasis are prognostic factors for poor outcomes. We propose a new KKU staging system by incorporating the growth pattern to modify and refine the eighth AJCC staging system for the evaluation of patients with pCCA. Our staging system showed prognostic ability better than the eighth AJCC staging system for the stratification of pCCA in Thailand. However, to put things in proper perspective, the KKU staging system is essentially employed for post-operative prognostic prediction and management planning; clinical pre-operative staging with radiological T of the eighth AJCC staging system still plays an important role in the pre-operative management plan. There is currently a prospective study where the KKU staging system is applied to patients with pCCA to validate its utility as a prognostic predictive tool and guidance to treatment options.

Data availability statement

The datasets presented in this study can be found in online repositories. The names of the repository/repositories and accession number(s) can be found in the article/Supplementary material.

Ethics statement

The studies involving human participants were reviewed and approved by the guidelines of the Declaration of Helsinki. This study was approved by the Ethics Committee for Human Research, Khon Kaen University (HE641499). The patients/participants provided their written informed consent to participate in this study.

Author contributions

Conceptualization: PS-N, SK, CA, SS, and PI. Funding acquisition and supervision: SK. Sample collection and diagnosis: PS-N, SK, CA, SS, PI, WK, NK, AT, AJ, VT, TS, VL, KE, WL, and JP. Analysis and interpretation of data: PS-N, SK, CA, and PP. Writing—original draft: PS-N, SK, CA, SS, PI, and PP. Writing—review and editing: PS-N, SK, CA, SS, PI, WK, MT, AW, and PP. All authors approved the final version of the manuscript.

Funding

We would like to acknowledge the Cholangiocarcinoma Screening and Care Program (CASCAP) under

Cholangiocarcinoma Research Institute (CARI), Khon Kaen University, Khon Kaen, Thailand, and the National Research Council of Thailand through Fluke Free Thailand project, Khon Kaen University through Cholangiocarcinoma Research Institute to support funding.

Acknowledgments

The authors would like to acknowledge Chawalit Pairojkul and Banchob Sripa of the Department of Pathology and Faculty of Medicine, Khon Kaen University, Thailand for helpful discussions. Additionally, all authors are truly grateful to Bandit Thinkhamrop, the director of Data Management and Statistical Analysis Center (DAMASAC), Faculty of Public Health, Khon Kaen University, Thailand for work on statistical analysis. This research is also indebted to all members of KKU, particularly the cohort members, and researchers at the Department of Pathology, Faculty of Medicine, Khon Kaen University for collecting and supporting the data.

Conflict of interest

The authors declare that the research was conducted in the absence of any commercial or financial relationships that could be construed as a potential conflict of interest.

Publisher's note

All claims expressed in this article are solely those of the authors and do not necessarily represent those of their affiliated organizations, or those of the publisher, the editors and the reviewers. Any product that may be evaluated in this article, or claim that may be made by its manufacturer, is not guaranteed or endorsed by the publisher.

Supplementary material

The Supplementary Material for this article can be found online at: https://www.frontiersin.org/articles/10.3389/fmed.2022.893252/full#supplementary-material

References

1. Banales JM, Cardinale V, Carpino G, Marzioni M, Andersen JB, Invernizzi P, et al. Expert consensus document: cholangiocarcinoma: current knowledge and future perspectives consensus statement from the European network for the study of cholangiocarcinoma (ENS-CCA). *Nat Rev Gastroenterol Hepatol.* (2016) 13:261–80. doi: 10.1038/nrgastro.2016.51

2. Global Burden of Disease Cancer C, Fitzmaurice C, Dicker D, Pain A, Hamavid H, Moradi-Lakeh M, et al. The global burden of cancer 2013. *JAMA Oncol.* (2015) 1:505–27. doi: 10.1001/jamaoncol.2015.0735

3. Elkins DB, Haswell-Elkins MR, Mairiang E, Mairiang P, Sithithaworn P, Kaewkes S, et al. A high frequency of hepatobiliary disease and suspected cholangiocarcinoma associated with heavy Opisthorchis viverrini infection in a small community in north-east Thailand. *Trans R Soc Trop Med Hyg.* (1990) 84:715–9. doi: 10.1016/0035-9203(90)90159-c

4. Haswell-Elkins MR, Satarug S, Tsuda M, Mairiang E, Esumi H, Sithithaworn P, et al. Liver fluke infection and cholangiocarcinoma: model of endogenous nitric oxide and extragastric nitrosation in human carcinogenesis. *Mutat Res.* (1994) 305:241–52. doi: 10.1016/0027-5107(94)90244-5

5. Sriamporn S, Pisani P, Pipitgool V, Suwanrungruang K. Kamsa-ard S, Parkin DM. Prevalence of Opisthorchis viverrini infection and incidence of cholangiocarcinoma in Khon Kaen, Northeast Thailand. *Trop Med Int Health.* (2004) 9:588–94. doi: 10.1111/j.1365-3156.2004.01234.x

6. Sripa B, Pairojkul C. Cholangiocarcinoma: lessons from Thailand. *Curr Opin Gastroenterol.* (2008) 24:349–56. doi: 10.1097/MOG.0b013e3282fbf9b3

7. Sripa B, Kaewkes S, Sithithaworn P, Mairiang E, Laha T, Smout M, et al. Liver fluke induces cholangiocarcinoma. *PLoS Med.* (2007) 4:e201. doi: 10.1371/journal.pmed.0040201

8. Rogers JE, Law L, Nguyen VD, Qiao W, Javle MM, Kaseb A, et al. Second-line systemic treatment for advanced cholangiocarcinoma. *J Gastrointest Oncol.* (2014) 5:408–13. doi: 10.3978/j.issn.2078-6891.2014.072

9. Chaiteerakij R, Harmsen WS, Marrero CR, Aboelsoud MM, Ndzengue A, Kaiya J, et al. A new clinically based staging system for perihilar cholangiocarcinoma. *Am J Gastroenterol.* (2014) 109:1881–90. doi: 10.1038/ajg.2014.327

10. Jarnagin WR, Fong Y, DeMatteo RP, Gonen M, Burke EC, Bodniewicz BJ, et al. Staging, resectability, and outcome in 225 patients with hilar cholangiocarcinoma. *Ann Surg.* (2001) 234:507–17. doi: 10.1097/00000658-200110000-00010

11. Groot Koerkamp B, Wiggers JK, Gonen M, Doussot A, Allen PJ, Besselink MGH, et al. Survival after resection of perihilar cholangiocarcinoma-development and external validation of a prognostic nomogram. *Ann Oncol.* (2015) 26:1930–5. doi: 10.1093/annonc/mdv279

12. Esnaola NF, Meyer JE, Karachristos A, Maranki JL, Camp ER, Denlinger CS. Evaluation and management of intrahepatic and extrahepatic cholangiocarcinoma. *Cancer.* (2016) 122:1349–69. doi: 10.1002/cncr.29692

13. DeOliveira ML, Cunningham SC, Cameron JL, Kamangar F, Winter JM, Lillemoe KD, et al. Cholangiocarcinoma: thirty-one-year experience with 564 patients at a single institution. *Ann Surg.* (2007) 245:755–62. doi: 10.1097/01.sla.0000251366.62632.d3

14. Razumilava N, Gores GJ. Cholangiocarcinoma. *Lancet.* (2014) 383:2168–79. doi: 10.1016/S0140-6736(13)61903-0

15. Yamasaki S. Intrahepatic cholangiocarcinoma: macroscopic type and stage classification. *J Hepatobiliary Pancreat Surg.* (2003) 10:288–91. doi: 10.1007/s00534-002-0732-8

16. Rizvi S, Gores GJ. Current diagnostic and management options in perihilar cholangiocarcinoma. *Digestion.* (2014) 89:216–24. doi: 10.1159/000360791

17. Joo I, Lee JM, Yoon JH. Imaging diagnosis of intrahepatic and perihilar cholangiocarcinoma: recent advances and challenges. *Radiology.* (2018) 288:7–13. doi: 10.1148/radiol.2018171187

18. Tawarungruang C, Khuntikeo N, Chamadol N, Laopaiboon V, Thuanman J, Thinkhamrop K, et al. Survival after surgery among patients with cholangiocarcinoma in Northeast Thailand according to anatomical and morphological classification. *BMC Cancer.* (2021) 21:497. doi: 10.1186/s12885-021-08247-z

19. Rizzo A, Brandi G. Pitfalls, challenges, and updates in adjuvant systemic treatment for resected biliary tract cancer. *Expert Rev Gastroenterol Hepatol.* (2021) 15:547–54. doi: 10.1080/17474124.2021.1890031

20. Rizzo A, Ricci AD, Brandi G. Recent advances of immunotherapy for biliary tract cancer. *Expert Rev Gastroenterol Hepatol.* (2021) 15:527–36. doi: 10.1080/17474124.2021.1853527

21. Amin MB, Edge SB, Greene FL, Byrd DR, Brookland RK, Washington MK, et al. *AJCC Cancer Staging Manual*. Cham: Springer International Publishing (2017).

22. Ruzzenente A, Bagante F, Ardito F, Campagnaro T, Scoleri I, Conci S, et al. Comparison of the 7th and 8th editions of the American joint committee on cancer staging systems for perihilar cholangiocarcinoma. *Surgery.* (2018) 164:244–50. doi: 10.1016/j.surg.2018.03.012

23. Gaspersz MP, Buettner S, van Vugt JLA, de Jonge J, Polak WG, Doukas M, et al. Evaluation of the new American joint committee on cancer staging manual 8th edition for perihilar cholangiocarcinoma. *J Gastrointest Surg.* (2020) 24:1612–8. doi: 10.1007/s11605-019-04127-x

24. Lee JW, Lee JH, Park Y, Lee W, Kwon J, Song KB, et al. Prognostic predictability of american joint committee on cancer 8th staging system for perihilar cholangiocarcinoma: limited improvement compared with the 7th staging system. *Cancer Res Treat.* (2020) 52:886–95. doi: 10.4143/crt.2020.023

25. Zhao J, Zhang W, Zhang J, Zhang Y, Ma WJ, Liu SY, et al. Survival analysis of patients with stage T2a and T2b perihilar cholangiocarcinoma treated with radical resection. *BMC Cancer.* (2020) 20:849. doi: 10.1186/s12885-020-07357-4

26. Shinohara K, Ebata T, Shimoyama Y, Nakaguro M, Mizuno T, Matsuo K, et al. Proposal for a new classification for perihilar cholangiocarcinoma based on tumour depth. *Br J Surg.* (2019) 106:427–35. doi: 10.1002/bjs.11063

27. Oba M, Nakanishi Y, Amano T, Okamura K, Tsuchikawa T, Nakamura T, et al. Stratification of post-operative prognosis by invasive tumor thickness in perihilar cholangiocarcinoma. *Ann Surg Oncol.* (2021) 28:2001–9. doi: 10.1245/s10434-020-09135-9

28. Zhang Y, Wu Z, Wang X, Li C, Chang J, Jiang W, et al. Development and external validation of a nomogram for predicting the effect of tumor size on survival of patients with perihilar cholangiocarcinoma. *BMC Cancer.* (2020) 20:1044. doi: 10.1186/s12885-020-07501-0

29. Li CX, Zhang H, Wang K, Wang X, Li XC. Preoperative bilirubin level predicts overall survival and tumor recurrence after resection for perihilar cholangiocarcinoma patients. *Cancer Manag Res.* (2019) 11:10157–65. doi: 10.2147/CMAR.S230620

30. Laoveeravat P, Jaruvongvanich V, Wongjarupong N, Linlawan S, Tanpowpong N, Phathong C, et al. Outcome and validation of a new clinically based staging system for predicting survival of perihilar cholangiocarcinoma patients. *JGH Open.* (2017) 1:56–61. doi: 10.1002/jgh3.12009

31. Lee JW, Lee JH, Park Y, Kwon J, Lee W, Song KB, et al. Prognostic impact of perioperative CA19-9 levels in patients with resected perihilar cholangiocarcinoma. *J Clin Med.* (2021) 10:345. doi: 10.3390/jcm10071345

32. Coelen RJS, Gaspersz MP, Labeur TA, van Vugt JLA, van Dieren S, Willemssen F, et al. Validation of the mayo clinic staging system in determining prognoses of patients with perihilar cholangiocarcinoma. *Clin Gastroenterol Hepatol.* (2017) 15:1930–9. doi: 10.1016/j.cgh.2017.04.044

33. Ebata T, Kamiya J, Nishio H, Nagasaka T, Nimura Y, Nagino M. The concept of perihilar cholangiocarcinoma is valid. *Br J Surg.* (2009) 96:926–34. doi: 10.1002/bjs.6655

34. Radtke A, Konigsrainer A. Surgical Therapy of Cholangiocarcinoma. *Visc Med.* (2016) 32:422–6. doi: 10.1159/000452921

35. Nagtegaal ID, Odze RD, Klimstra D, Paradis V, Rugge M, Schirmacher P, et al. The 2019 WHO classification of tumours of the digestive system. *Histopathology.* (2020) 76:182–8. doi: 10.1111/his.13975

36. Juntermanns B, Kaiser GM, Reis H, Gries S, Kasper S, Paul A, et al. Long-term Survival after resection for perihilar cholangiocarcinoma: Impact of UICC staging and surgical procedure. *Turk J Gastroenterol.* (2019) 30:454–60. doi: 10.5152/tjg.2019.18275

37. Ruzzenente A, Bagante F, Olthof PB, Aldrighetti L, Alikhanov R, Cescon M, et al. Surgery for Bismuth-Corlette Type 4 perihilar cholangiocarcinoma: results from a western multicenter collaborative group. *Ann Surg Oncol.* (2021) 28:7719–29. doi: 10.1245/s10434-021-09905-z

38. Hau HM, Meyer F, Jahn N, Rademacher S, Sucher R, Seehofer D. Prognostic relevance of the eighth edition of TNM classification for resected perihilar cholangiocarcinoma. *J Clin Med.* (2020) 9:3152. doi: 10.3390/jcm9103152

39. Deoliveira ML, Schulick RD, Nimura Y, Rosen C, Gores G, Neuhaus P, et al. New staging system and a registry for perihilar cholangiocarcinoma. *Hepatology.* (2011) 53:1363–71. doi: 10.1002/hep.24227

40. Cheng Z, Lei Z, Si A, Yang P, Luo T, Guo G, et al. Modifications of the AJCC 8th edition staging system for intrahepatic cholangiocarcinoma and proposal for a new staging system by incorporating serum tumor markers. *HPB.* (2019) 21:1656–66. doi: 10.1016/j.hpb.2019.05.010

41. Sriputtha S, Khuntikeo N, Promthet S, Kamsa-Ard S. Survival rate of intrahepatic cholangiocarcinoma patients after surgical treatment in Thailand. *Asian Pac J Cancer Prev.* (2013) 14:1107–10. doi: 10.7314/apjcp.2013.14.2.1107

42. Shimada K, Sano T, Sakamoto Y, Esaki M, Kosuge T, Ojima H. Surgical outcomes of the mass-forming plus periductal infiltrating types of intrahepatic cholangiocarcinoma: a comparative study with the typical mass-forming type of intrahepatic cholangiocarcinoma. *World J Surg.* (2007) 31:2016–22. doi: 10.1007/s00268-007-9194-0

43. Hwang S, Lee YJ, Song GW, Park KM, Kim KH, Ahn CS, et al. Prognostic impact of tumor growth type on 7th AJCC staging system for intrahepatic cholangiocarcinoma: a single-center experience of 659 cases. *J Gastrointest Surg.* (2015) 19:1291–304. doi: 10.1007/s11605-015-2803-6

44. Khuntikeo N, Titapun A, Chamadol N, Boonphongsathien W, Sa-Ngiamwibool P, Taylor-Robinson SD, et al. *In vitro* intraductal MRI and T2 mapping of cholangiocarcinoma using catheter coils. *Hepat Med.* (2020) 12:107–14. doi: 10.2147/HMER.S266841

45. Nakanuma Y, Uesaka K, Kakuda Y, Sugino T, Kubota K, Furukawa T, et al. Intraductal papillary neoplasm of bile duct: updated clinicopathological characteristics and molecular and genetic alterations. *J Clin Med.* (2020) 9:3991. doi: 10.3390/jcm9123991

46. Luvira V, Somsap K, Pugkhem A, Eurboonyanun C, Luvira V, Bhudhisawasdi V, et al. Morphological classification of intraductal papillary neoplasm of the bile duct with survival correlation. *Asian Pac J Cancer Prev.* (2017) 18:207–13. doi: 10.22034/APJCP.2017.18.1.207

47. Sungkasubun P, Siripongsakun S, Akkarachinorate K, Vidhyarkorn S, Worakitsitisatorn A, Sricharunrat T, et al. Ultrasound screening for cholangiocarcinoma could detect premalignant lesions and early-stage diseases with survival benefits: a population-based prospective study of 4,225 subjects in an endemic area. *BMC Cancer.* (2016) 16:346. doi: 10.1186/s12885-016-2390-2

frontiers | Frontiers in Oncology

TYPE Original Research
PUBLISHED 13 October 2022
DOI 10.3389/fonc.2022.961530

Check for updates

OPEN ACCESS

EDITED BY
Qi Liu,
Fudan University, China

REVIEWED BY
Hitomi Takada,
University of Yamanashi, Japan
Anne Rix,
RWTH Aachen University, Germany

*CORRESPONDENCE
Xiaoli Mai
maixl@njglyy.com
Decai Yu
yudecai@nju.edu.cn

†These authors have contributed equally to this work

SPECIALTY SECTION
This article was submitted to Gastrointestinal Cancers: Hepato Pancreatic Biliary Cancers, a section of the journal Frontiers in Oncology

RECEIVED 04 June 2022
ACCEPTED 03 October 2022
PUBLISHED 13 October 2022

CITATION
Zhang L, Cheng C, Li B, Chen J, Peng J, Cao Y, Yue Y, Mai X and Yu D (2022) Combined clinical features and MRI parameters for the prediction of VEGFR2 in hepatocellular carcinoma patients. *Front. Oncol.* 12:961530. doi: 10.3389/fonc.2022.961530

COPYRIGHT
© 2022 Zhang, Cheng, Li, Chen, Peng, Cao, Yue, Mai and Yu. This is an open-access article distributed under the terms of the Creative Commons Attribution License (CC BY). The use, distribution or reproduction in other forums is permitted, provided the original author(s) and the copyright owner(s) are credited and that the original publication in this journal is cited, in accordance with accepted academic practice. No use, distribution or reproduction is permitted which does not comply with these terms.

Combined clinical features and MRI parameters for the prediction of VEGFR2 in hepatocellular carcinoma patients

Laizhu Zhang[1†], Chunxiao Cheng[2†], Binghua Li[1], Jun Chen[3], Jin Peng[1], Yajuan Cao[1], Yang Yue[1], Xiaoli Mai[4*] and Decai Yu[1,2*]

[1]Hepatobiliary and Pancreatic Center & Liver Transplantation Center, the Affiliated Drum Tower Hospital, Medical School of Nanjing University, Nanjing, China, [2]Nanjing Drum Tower Hospital Clinical College of Nanjing University of Chinese Medicine, Nanjing, China, [3]Department of Pathology, the Affiliated Drum Tower Hospital, Medical School of Nanjing University, Nanjing, China, [4]Department of Radiology, the Affiliated Drum Tower Hospital, Medical School of Nanjing University, Nanjing, China

Purpose: To develop a prediction model for estimating the expression of vascular endothelial growth factor receptor 2 (VEGFR2) in hepatocellular carcinoma (HCC) patients using clinical features and the contrast-enhanced MRI Liver Imaging Reporting and Data System (LI-RADS).

Methods: A total of 206 HCC patients were subjected to preoperative contrast-enhanced MRI, radical resection, and VEGFR2 immunohistochemistry labeling. The intensity of VEGFR2 expression was used to split patients into either the positive group or the negative group. For continuous data, the Mann-Whitney U test was employed, and for categorical variables, the $\chi 2$ test was utilized.

Results: VEGFR2-positivity was identified in 41.7% (86/206) of the patients. VEGFR2-positive HCCs were confirmed by higher serum alpha-fetoprotein (AFP) levels, larger tumor dimensions (either on MRI or upon final pathology), and a higher LI-RADS score (all $p < 0.001$). LI-RADS scores and AFP levels were independent predictors for high VEGFR2 expression. These two parameters were used to establish a VEGFR2-positive risk nomogram, which was validated to possess both good discrimination and calibration. The area under the curve was 0.830 (sensitivity 83.6%, specificity 72.5%) and the mean absolute error was 0.021. The threshold probabilities ranged between 0.07 and 0.95, and usage of the model contributed net benefits.

Conclusion: A nomogram including clinical features and contrast-enhanced MRI parameters was developed and was demonstrably effective at predicting VEGFR2 expression in HCC patients.

KEYWORDS

hepatocellular carcinoma, LI-RADS, VEGFR2, nomogram, targeted therapy

Introduction

Liver cancer was the sixth most common cancer and the fourth leading cause of cancer death worldwide in 2018 (1). Hepatocellular carcinoma (HCC) was the most common kind of liver cancer, accounting for the vast majority of diagnoses and fatalities (2). Because the symptoms of HCC are relatively insidious, many patients have lost the opportunity for surgery when they are diagnosed. For advanced HCC, the treatment options are limited. Targeted therapy is one of the main choices for advanced HCC, with many associated molecular targeted drugs entering the clinic (3).

Vascular endothelial growth factor receptor 2 (VEGFR2) mRNA levels and expression are upregulated in HCC (4). The proliferation, migration, survival, and permeability of vascular endothelial cells are influenced by VEGF/VEGFR2 signaling cascades (5, 6), and these factors can modulate the efficacy of sorafenib therapy. Prior to sorafenib therapy, a lack of VEGFR2 expression in resected tumor tissues is linked to worse overall survival (7). Therefore, anti-angiogenic drugs that block the VEGFR/VEGFR2 pathway provide a new target for the clinical therapy of HCC, and many studies have demonstrated their validity and safety in advanced HCC (8, 9). VEGFR2 is the only target of apatinib and one of the main targets of other targeted drugs, including sorafenib and lenvetinib (10–12). As a result, VEGFR2 expression has important clinical significance due to its susceptibility to targeted therapy in HCC patients (7).

Preoperative examinations like contrast-enhanced MRI can dynamically display the blood supply of lesions and provide perfusion parameters. Furthermore, when combined with the LI-RADS score 2018 (13), these data can provide an assessment of the possibility of malignancy in liver nodules in the background of cirrhosis (14, 15). It has been demonstrated that the signal intensity in the arterial phase as well as the intensity heterogeneity are both positively correlated with VEGF expression in HCC (16). The perfusion markers of blood flow, blood volume in the artery phase, and the hepatic perfusion index were found to be higher with the increasing expression of VEGFR2, as determined by immunostaining (17, 18).

If we can effectively predict the expression of VEGFR2 in patients before undergoing pathological examination, more precise and individualized treatment plans can be made. Therefore, our objective was to find significant predictors for high VEGFR2 expression and to further develop a risk model for its prediction.

Materials and methods

Patients

Data was chosen from individuals who had either liver resections or transplants at our center from January 2018 to December 2020. The inclusion criteria were as follows: (1) MRI examination within the 2 weeks prior to surgery; (2) MRI images could clearly recognize the tumor; (3) the presence of primary HCC with no preoperative treatment, such as ablation, chemotherapy, immunotherapy or transarterial chemoembolization; (4) postoperative pathology confirmed the presence of HCC; (5) the clinical data was complete. A total of 206 participants were enrolled in our study (Figure 1). Twenty-six patients could not be contacted after radical resection in the follow-up. Thirty-five underwent liver transplants. The hospital review board gave its permission and all of the participants signed their written informed consent.

MRI examination

All MRI examinations were completed within two weeks prior to radical surgery. Patients were scanned in the supine position using a 3.0-T whole-body MRI scanner (uMR770, United Imaging, China) with a sixteen-channel phased-array coil centered over the belly. Before the MRI, all patients were required to fast for a minimum of 8 hours. A T1-weighted volume interpolated breath-hold gradient recall echo sequence was used to provide an unenhanced scan, dynamic contrast-enhanced phase, and hepatobiliary phase (HBP). The dynamic contrast-enhanced scan early arterial (EAP) and late arterial phases (LAP) were used to ensure that we could observe the enhancement of the tumor. A dosage of 0.025 mmol/kg Gd-EOB-DTPA (Primovist; Bayer HealthCare, Berlin, Germany) was administered at a rate of 2.0 mL/s, and then followed by a

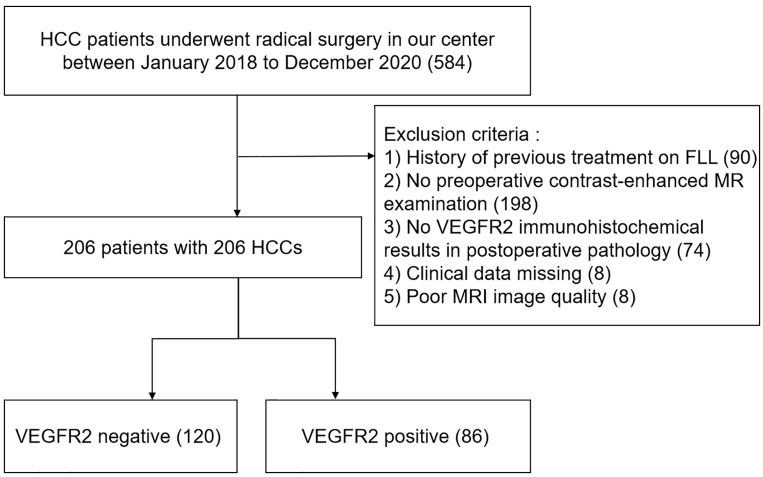

FIGURE 1
Flowchart of patient selection. HCC, hepatocellular carcinoma; MRI, contrast-enhanced magnetic resonance imaging; FLL, focal liver lesion; VEGFR2, vascular endothelial growth factor receptor 2.

30-mL saline flush at the same rate. Using bolus triggering, a dual arterial phase sequence was started 15-25 seconds after the contrast media arrived at the distal thoracic aorta, while the portal venous phase (PVP), delay phase (DP), and HBP were acquired at 1, 3, and 15 minutes after Gd-EOB-DTPA administration, respectively. The HBP images were used to assist in the diagnosis and demarcation of the tumor location.

Image analysis and LI-RADS interpretation

Three hepatologists and one radiologist independently assessed the results to obtain the LI-RADS score (DCY with 20 years of clinical experience, YJC with 13 years of clinical experience, and JP with 7 years of clinical experience). The final assessment was made by professor XLM (with 21 years of clinical experience).

A tumor is defined as having an LI-RADS score of 5 (LR-5) when presenting with a focal liver lesion (FLL) (>10mm) showing arterial phase hyperenhancement (APHE) and nonperipheral "washout" (WO) regardless of the presence of an enhancing capsule (EC). A tumor is defined as LR-4 if any of the following apply: (a) it is >20mm in size and shows APHE without WO or EC, or else shows no APHE with EC; (b) it is 10-19mm in size and shows APHE with EC and no WO; (c) it is <10mm in size and shows APHE with WO or EC. A tumor is defined as LI-3 if any of the following apply: (a) it is <20mm in size and shows APHE (no rim) with no WO or EC; (b) it shows no APHE and no EC; (c) it is <20mm in size and shows no APHE and has EC. Given that all patients studied were diagnosed with HCC, we did not use the category LI-RADS-M, which indicates cases as either 'probably' or 'definitely' malignant, non-specific to HCC.

Histopathological evaluation

After being fixed in 4% paraformaldehyde (pH 7.4, for 24 hours), resected samples were dehydrated, and embedded in paraffin. The nesting tissues were sectioned continuously at a thickness of 3.0 μm. The tissue slides were xylenated, hydrated in a series of alcohols, and then submerged in phosphate-buffered saline (PBS). Antigen retrieval was achieved in ethylene diamine tetraacetie acid (EDTA) buffer (pH 8.0, 100°C, 2.5 minutes). After washing with PBS, 100 μL of endogenous peroxidase blocking agent (3% H2O2) was added and incubated for 10 minutes at room temperature. Slides were incubated with primary antibodies against human VEGFR2 (1:500, ZSGB-BIO, Beijing, China, ZA-0287) for 60 minutes at 37°C. Next, they were treated with enzyme-labelled goat anti-mouse immunoglobulin G (IgG) polymer (ZSGB-BIO, Beijing, China, IB000087) for 30 minutes at 37°C. Then, 100 μl diaminobenzidine reagent (ZSGB-BIO, Beijing, China, MA-2000) was added and incubated at room temperature for 6 minutes. After washing with tap water, stained with hematoxylin staining solution for 30-60 seconds at room temperature, differentiate with hydrochloric acid and alcohol, and return to blue. All experiments were performed by the same team. The operators were independent of the diagnostic results.

We utilized the Remmele/Stegner immunoreactive score for the semi-quantitative assessment of VEGFR2 staining (IRS score) (19). All results were evaluated independently by YY (with 15 years of clinical experience) and JC (with 20 years of clinical experience). The extent scores representing the intensity of staining were "0" (unstained, negative), "1" (brown stained, weakly positive), "2" (dark brown stained, moderate positive), or "3" (darker brown, strongly positive). IRS scores were calculated by multiplying the extent scores with a factor based on the percentage of tumor cells that were positive (0–10%/1; 10–50%/2; 50–80%/3; 80–100%/4). We defined the IRS scores 0, 1, 2, 3 as negative and 4, 6, 8, 9, 12 as positive. For the cases where the pathological diagnosis results and histological staining results were not uniform, we adopted the feature that occupied a large area as the judgment result of the tumor.

Statistical analysis

For continuous variables, the Mann-Whitney U test was used. For categorical variables, the Chi-square test or Fisher's test was used where necessary. Univariate analysis was used to screen for potentially significant variables. Variables with $p<0.05$ that were screened out from the univariate analysis were entered into the multivariate analysis to determine the independent predictors. The "rms" package in R 3.5.2 (https://www.r-project.org/) was used to generate a nomogram utilizing the significant predictors. The internal discrimination validation was performed using the "pROC" package and 1,000 iterations of bootstrapping. We derived the corresponding AUC value, sensitivity, and differentiation specificity with 95% confidence intervals. Using the calibration plot of the 'rms' package, we visually evaluated the degree of either over- or underestimating the expected probability compared to the actual VEGFR2-positivity, which was internally verified with 1,000 cycles of bootstrapping. As previously stated, the "rmda" package was used to conduct decision curve analysis (DCA). SPSS 25.0 (IBM, USA) was used to conduct the statistical analysis. The statistical significance was set at $p<0.05$ for all two-sided tests.

Results

Table 1 provides a summary of the 206 patients' features. Of the 206 patients, 160 had a single tumor and 46 had multifocal tumors. For patients with multifocal tumors, we took the tumor with the largest diameter for each patient for subsequent study. Following a thorough pathological examination, these individuals were classified as either VEGFR2-positive (86/206, 41.7%) or VEGFR2-negative (120/206, 58.3%) according to the immunohistochemical results. Patients positive for VEGFR2 were confirmed to have higher serum AFP levels, larger tumor dimensions on ceMRI, higher LI-RADS scores, and larger tumor dimensions on final pathology (all $p<0.001$). In univariate logistic regression model analysis, tumor dimensions on both the ceMRI and LI-RADS scores were shown to be closely linked with the high expression of VEGFR2 (Table 2). In multivariate logistic analysis, only two predictors remained significant: AFP

TABLE 1 Characteristics of the 206 patients stratified by the VEGFR2 status of HCC.

Features	N=206	VEGFR2		p
		Negative (120)	Positive (86)	
Age (y)	59 (58-61)	60 (58-62)	58 (55-60)	0.126
Gender (male)	175 (85.0)	105 (87.5)	70 (81.4)	0.227
WBC (10^9/L)	5.4 (5.1-5.6)	5.3 (5.0-5.7)	5.4 (5.0-5.8)	0.956
Platelets (10^9/L)	153.4(143.3-163.2)	149.2 (136.7-161.7)	159.0 (142.4-175.5)	0.434
ALT (U/L)	54.2 (31.1-77.4)	68.7 (29.2-108.3)	34.0 (28.6-39.4)	0.353
AST (U/L)	64.8 (28.8-100.8)	85.9 (24.1-147.7)	35.4 (30.1-40.7)	0.698
TB (umol/L)	17.2 (13.3-21.0)	18.4 (11.9-25.0)	15.4 (13.6-17.2)	0.404
AFP (ng/ml)				<0.001
<400	164 (79.6)	107 (89.1)	57 (66.3)	
>400	42 (20.4)	13 (10.8)	29 (33.7)	
HBV infection				0.406
+	184 (89.3)	109 (90.8)	75 (87.2)	
-	22 (10.7)	11 (9.2)	11 (12.8)	
Liver cirrhosis (+)				<0.001
+	91 (44.2)	39 (32.5)	52 (60.5)	
-	115 (55.8)	81 (67.5)	34 (39.5)	

(Continued)

TABLE 1 Continued

Features	N=206	VEGFR2		p
		Negative (120)	Positive (86)	
Tumor dimension on ceMRI (cm)	4.8 (4.3-5.2)	4.1 (3.6-4.7)	5.7 (4.9-6.4)	<0.001
LI-RADS score				<0.001
3	63 (30.6)	57 (47.5)	6 (7.0)	
4	53 (25.7)	36 (30)	17 (19.8)	
5	90 (43.7)	27 (22.5)	63 (73.2)	
Tumor dimension on pathology (cm)	4.8 (4.3-5.2)	4.1 (3.6-4.7)	5.7 (4.9-6.4)	<0.001
pT stage				0.467
T1	105 (51.0)	65 (54.2)	40 (46.5)	
T2	74 (36.0)	39 (32.5)	35 (40.7)	
T3-4	27 (13.0)	16 (13.3)	11 (12.8)	
Edmondson-Steiner grade				0.908
I-II	92 (44.7)	54 (45)	38 (44.2)	
III-IV	114 (55.3)	66 (55)	48 (55.8)	
Focality				0.343
single	160 (77.7)	96 (80)	64 (77.4)	
multiple	46 (22.3)	24 (20)	22 (25.6)	
MVI				0.669
Positive	59 (28.6)	33 (27.5)	26 (30.2)	
Negative	147 (71.4)	87 (72.5)	60 (69.8)	

Continuous variables are presented as media (interquartile range, IQR), while categorical variables are presented as patients (%).
WBC, white blood cells; ALT, alanine aminotransferase; AST, aspartate; aminotransferase; AFP, alpha-fetoprotein; HBV, hepatitis B virus; ceMRI, contrast-enhanced magnetic resonance imaging; LI-RADS, Liver Imaging Reporting and Data System; MVI, microvascular invasion.

(odds ratio 7.648, 95% confidence intervals (CI) 2.849-20.531 p<0.001) and the LI-RADS score (odds ratio 30.430, 95% CI 10.278-90.096, p<0.001) (Table 3). Representative cases illustrating positive and negative VEGFR2 expression in resected samples were shown in Figure 2 and 3, respectively.

Furthermore, we tested the diagnostic performance of AFP and the LI-RADS score for VEGFR2-positivity in HCC using final pathology as a reference. The AUC area, sensitivity, and specificity of the LI-RADS scores were 0.790, 0.733, and 0.775, respectively. The AUC area, sensitivity, and specificity of AFP were 0.614, 0.337, and 0.892, respectively (Supplementary Figure 1).

Further, a VEGFR2-positive risk nomogram integrating these two predictors was created (Figure 4A). Bootstrapping was used to verify the nomogram internally. Nomogram discrimination was performed by ROC analysis with an AUC of 0.830 (95% CI 0.750, 0.866) (Figure 4B). The sensitivity and specificity of the results were 0.837 and 0.725, respectively. Furthermore, with a mean absolute error of 0.021, a bootstrapped calibration curve of the model revealed no adverse departure of the expected risk from the actual risk of VEGFR2-positivity (Figure 4C). The DCA curve was used to investigate its clinical benefits (Figure 5). With threshold probabilities ranging between 0.07 and 0.95, the model provides larger net advantages than intervening in either all or none of the patients.

Discussion

As far as we know, this is the first research of its kind in developing a model to predict VEGFR2 expression in HCC using a combination of clinical features and MRI data. The related sensitivity and specificity of the nomogram were 0.725 and 0.837, respectively.

VEGFR2, which is abundantly expressed in HCC and vessels, is linked to tumor biological behavior and 5-year survival rate in HCC patients (20). In our study, the disease-free survival (DFS, p=0.003) and overall survival (OS, p=0.010) time of the groups stratified by AFP (400 ng/ml) were significantly different (Supplementary Figure 2B, D). However, the DFS and OS of the subgroups divided by LI-RADS score and VEGFR2-positivity were not significantly different, possibly due

TABLE 2 Univariate logistic regression analyses for the prediction of VEGFR2-positive HCC.

Variable and intercept	Univariate logistic regression	
	OR (95%CI)	p
Age	0.979 (0.955-1.005)	0.111
Gender (male vs. female)	0.625 (0.290-1.345)	0.229
WBC (10^9/L)	1.021 (0.891-1.170)	0.768
platelets (10^9/L)	1.002 (0.998-1.006)	0.344
ALT (U/L)	0.994 (0.986-1.002)	0.160
AST (U/L)	0.997 (0.989-1.004)	0.393
TB (μmol/L)	0.995 (0.982-1.008)	0.478
AFP (>400ng/ml)	4.188 (2.020-8.680)	<0.001
HBV (+)	0.688 (0.284-1.669)	0.408
Liver cirrhosis (+)	3.176 (1.784-5.656)	<0.001
Tumor dimension on ceMRI (cm)	1.163 (1.060-1.277)	0.001
LI-RADS (5 vs. 3/4)	22.167(8.535-57.570)	<0.001

CI, confidence interval; OR, odds ratio; WBC, white blood cells; ALT, alanine aminotransferase; AST, aspartate aminotransferase; AFP, alpha-fetoprotein; HBV, hepatitis B virus; ceMRI, contrast-enhanced magnetic resonance imaging; LI-RADS, Liver Imaging Reporting and Data System.

TABLE 3 Multivariate logistic regression analyses for the prediction of VEGFR2-positive HCC.

Variable and intercept	Multivariate logistic regression	
	OR (95%CI)	p
AFP (>400ng/ml)	7.648 (2.849-20.531)	<0.001
Tumor dimension on ceMRI (cm)	1.036 (0.921-1.164)	0.558
LI-RADS (5 vs. 3/4)	30.430(10.278-90.096)	<0.001

AFP, alpha-fetoprotein; ceMRI, contrast-enhanced magnetic resonance imaging; LI-RADS, Liver Imaging Reporting and Data System.

to the sample size. Postoperative adjuvant therapy was also one of the critical factors influencing OS and DFS. VEGFR2 is a crucial target in anti-cancer therapy because it is an essential regulator of angiogenesis (21). Chu et al. revealed high VEGFR2 expression to be correlated with hepatic cirrhosis, and this finding was consistent with the results of the current study (17). However, HBV infection was not found to be a predictor of high VEGFR2 expression, and this result may have been partly due to differences in the conditions and nationality of the

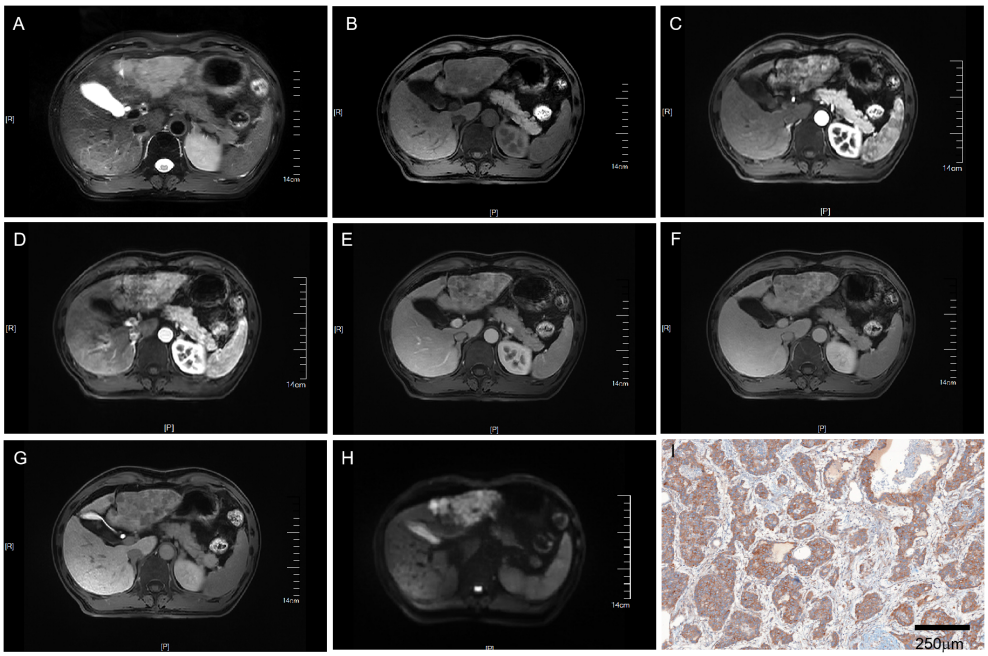

FIGURE 2
MRI of a VEGFR2-positive HCC patient with LI-RADS 5. Patient summary: a 50-year-old man with HCC in the left lobe of the liver, AFP level of 266ng/ml, lesion dimension on MRI of 8.1cm, and LI-RADS score of 5. **(A)** Axial T2-weighted MRI, **(B)** Axial T1-weighted MRI. **(C, D)** Early (15s) and late arterial phase (25s). **(E)** Portal venous phase (1min). **(F)** Delay phase (3min). **(G)** Hepatobiliary phase (15min). **(H)** Axial diffusion-weighted MRI. **(I)** VEGFR2-positivity in pathology. MRI, magnetic resonance imaging; LI-RADS, liver imaging reporting and data system; AFP, alpha-fetoprotein; VEGFR2, vascular endothelial growth factor receptor 2.

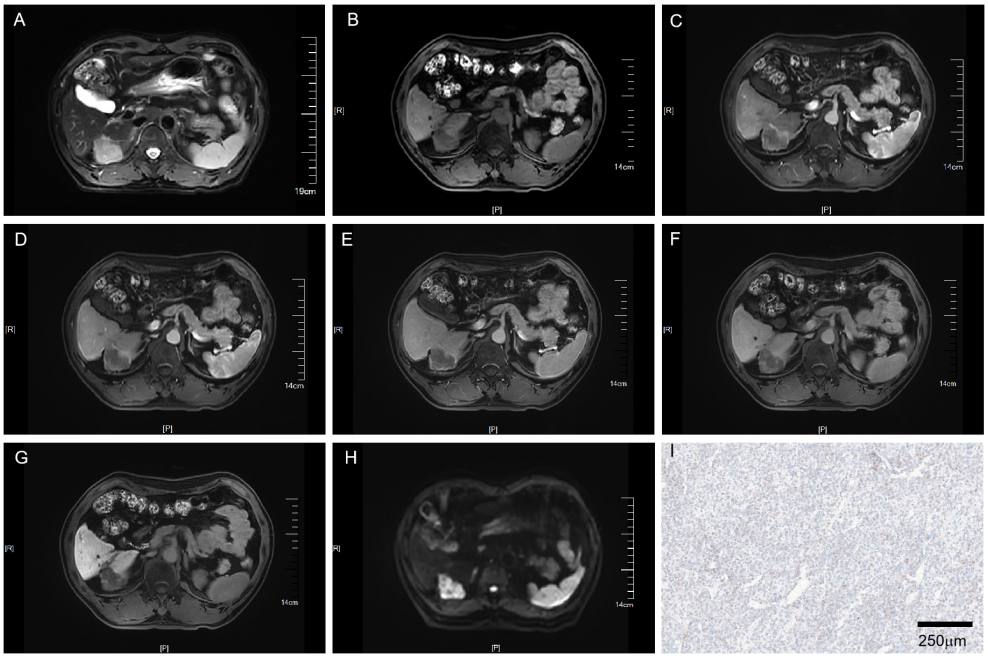

FIGURE 3
MRI of a VEGFR2-negative HCC patient with LI-RADS 3. Patient summary: a 59-year-old man with HCC in the right lobe of the liver, AFP level 2.7ng/ml, lesion dimension on MRI 3.8cm, and LI-RADS score of 3. **(A)** Axial T2-weighted MRI. **(B)** Axial T1-weighted MRI. **(C, D)** Early (15s) and late arterial phase (25s). **(E)** Portal venous phase (1min). **(F)** Delay phase (3min). **(G)** Hepatobiliary phase (15min). **(H)** Axial diffusion-weighted MRI. **(I)** VEGFR2-negative in pathology. MRI, magnetic resonance imaging; LI-RADS, liver imaging reporting and data system; AFP, alpha-fetoprotein; VEGFR2, vascular endothelial growth factor receptor 2.

patients in our center. In our study, the AFP level (>400 ng/ml), presence of liver cirrhosis (confirmed by pathology), and LI-RADS score were revealed to be independent predictors of VEGFR2 expression in HCC patients. Given that the LI-RADS scoring system is suitable for patients with either HBV infection, liver cirrhosis, or a history of HCC, we did not include liver cirrhosis in the model in order to minimize selection bias (13).

Previous research has shown that the LI-RADS score is associated with MVI, postoperative disease-free survival, and overall survival in HCC patients (22–25). Tumor proliferation and invasion require ample blood supply, and VEGFR2 is regarded to be one of the most essential regulators of angiogenesis (21). We speculated that the LI-RADS score could reflect the blood supply of hepatocellular carcinoma to a certain extent, and therefore illustrate the expression of VEGFR2 in HCC. Indeed, we found that the LI-RADS score was strongly correlated to the expression of VEGFR2 (odds ratio 40.825, $p<0.001$). Future studies using additional research centers and larger samples can further validate this finding. AFP has traditionally served as a biomarker for HCC, and its relationship with the behavior and prognosis of HCC has been validated (26, 27). We further validated the strong correlation between AFP and VEGFR2 expression, and these findings were consistent with the findings of Huang J et al. (20). It is possible that AFP is secreted more as the tumor proliferates, as VEGFR2 expression is positively correlated with tumor size (28). To explain its correlation from another perspective, high levels of serum AFP and the high expression of VEGFR2 both have been shown to predict poorer prognosis (20, 29), but the causal relationship remains unclear, and more studies are needed to further explore this.

Due to the poor performance of various factors in predicting VEGFR2 expression, the construction of additional models will be necessary. Based on recent studies that have observed significant differences in clinical and MRI parameters between high and low VEGFR2 expression, we aimed to establish a risk model that could predict high VEGFR2 expression. Variables incorporating both AFP levels and LI-RADS scores were found for nomogram generation using multivariate logistic regression analysis. With

10.3389/fonc.2022.961530

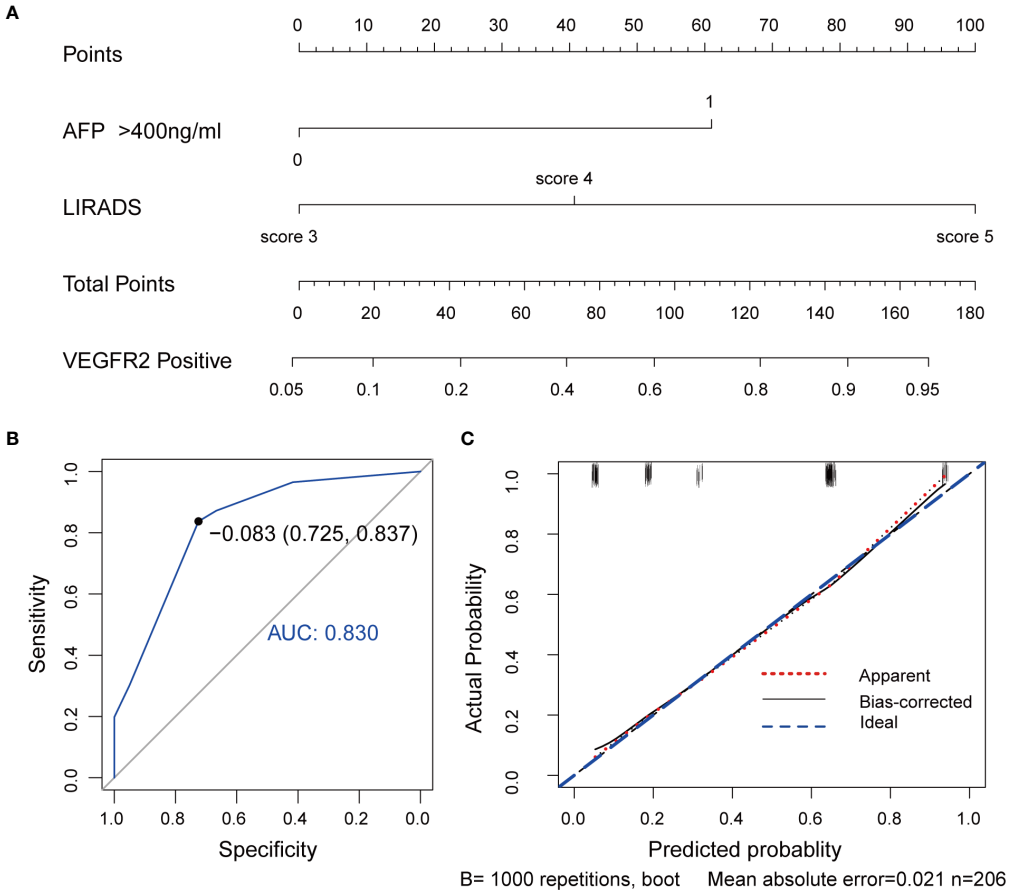

FIGURE 4
VEGFR2-positive-risk nomogram establishment and validation. **(A)** Risk nomogram incorporating AFP and the LI-RADS score for predicting high VEGFR2 expression in HCC patients. **(B)** ROC curve for the nomogram's VEGFR2-positive prediction AUC, sensitivity, and specificity. **(C)** Calibration curves illustrating the nomogram's calibration in terms of the agreement between the predicted risk of high VEGFR2 expression and the actual pathological VEGFR2 expression status. The 45° blue line represents a perfect prediction, the red dashed line shows the nomogram's predictive performance, and the black solid line is bias-corrected. The nomogram's forecast accuracy improves as the dashed line approaches the ideal line. AUC, area under the curve; AFP, alpha-fetoprotein, LI-RADS, Liver Imaging Reporting and Data System, VEGFR2, vascular endothelial growth factor receptor 2, ROC, receiver operating characteristic.

internal validation, the VEGFR2-positive-risk nomogram revealed a high degree of discrimination and calibration as well as significant net advantages under particular threshold probabilities. For individuals diagnosed with HCC, the associated VEGFR2-positivity risk may be computed using this nomogram. The risk of VEGFR2-positivity based on the nomogram suggests that this population might be more suitable for targeted therapies involving appropriately targeted drugs. This would be beneficial for the individualized treatment of HCC patients, as well as advantageous in reducing both medical costs and the social burden.

Our research has some limitations. Firstly, because the study had a retrospective design, there will certainly have been some degree of selection bias Secondly, based on the postoperative pathological results of all our patients being consistent with HCC, we did not use the classification category LI-RADS-M, and so the conclusions may be biased. Furthermore, this study only found a correlation between the LI-RADS score and VEGFR2 expression without offering a convincible mechanistic cause. We therefore advise that further studies be performed for verification and elucidation. Thirdly, in cases involving multiple lesions, we only selected the largest lesions for study, which introduced unreliability due to tumor heterogeneity.

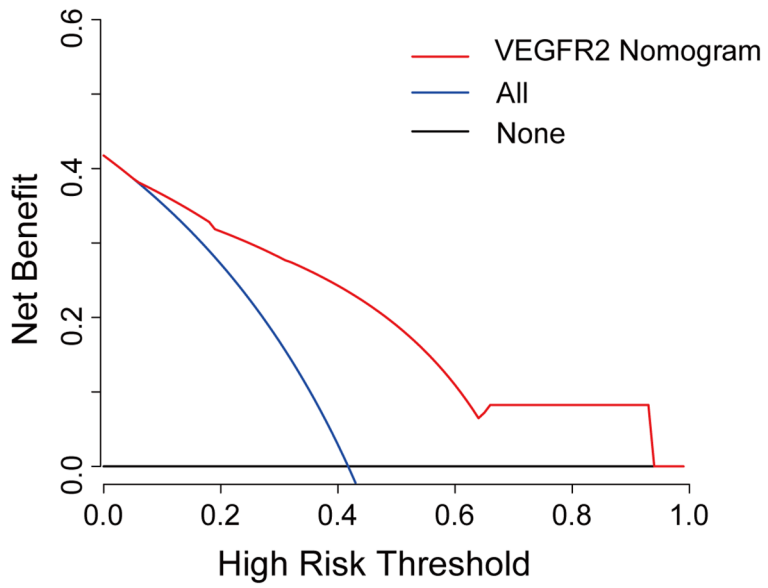

FIGURE 5
Decision curve analysis for the VEGFR2-positive-risk nomogram. The red line represents the nomogram, the blue line represents the condition that all patients are VEGFR2-positive, and the black line represents the condition that no patient harbors detectable VEGFR2 expression. The decision curve reveals that utilizing the VEGFR2-positive-risk model to forecast VEGFR2 expression offers a greater benefit than intervening in either all or none of the patients when the threshold probability ranges from 0.07 to 0.95.

Fourthly, we only studied the ability of MR to discriminate VEGFR2. Other necessary imaging tests, such as contrast-enhanced CT and ultrasonography, are warranted to provide further data. Lastly, this was a unicentric respective study. We only conducted internal validation because of the sample size, and hence, external validation sourced from other centers will be required in the future.

Conclusion

In conclusion, both the AFP level and LI-RADS score are significant predictors for VEGFR2 expression in HCC. By integrating them, we built a model to predict VEGFR2 expression among HCC patients. With internal validation, the model demonstrated good diagnostic performance. Considerable net advantages could be acquired under particular threshold probabilities.

Data availability statement

The raw data supporting the conclusions of this article will be made available by the authors, without undue reservation.

Ethics statement

The studies involving human participants were reviewed and approved by Nanjing Drum Tower Hospital Medical Ethics Committee. The patients/participants provided their written informed consent to participate in this study. Written informed consent was obtained from the individual(s) for the publication of any potentially identifiable images or data included in this article.

Author contributions

LZ and CC contributed equally. DY and XM are the corresponding authors. All authors contributed to the article and approved the submitted version.

Funding

This work was supported by the National Natural Science Foundation of China (No. 81871967).

Conflict of interest

The authors declare that the research was conducted in the absence of any commercial or financial relationships that could be construed as a potential conflict of interest.

Publisher's note

All claims expressed in this article are solely those of the authors and do not necessarily represent those of their affiliated organizations, or those of the publisher, the editors and the reviewers. Any product that may be evaluated in this article, or claim that may be made by its manufacturer, is not guaranteed or endorsed by the publisher.

Supplementary material

The Supplementary Material for this article can be found online at: https://www.frontiersin.org/articles/10.3389/fonc.2022.961530/full#supplementary-material

References

1. Bray F, Ferlay J, Soerjomataram I, Siegel RL, Torre LA, Jemal A. Global cancer statistics 2018: GLOBOCAN estimates of incidence and mortality worldwide for 36 cancers in 185 countries. *CA Cancer J Clin* (2018) 68:394–424. doi: 10.3322/caac.21492

2. McGlynn KA, Petrick JL, El-Serag HB. Epidemiology of hepatocellular carcinoma. *Hepatology* (2021) 73 Suppl 1:4–13. doi: 10.1002/hep.31288

3. Llovet JM, Kelley RK, Villanueva A, Singal AG, Pikarsky E, Roayaie S, et al. Hepatocellular carcinoma. *Nat Rev Dis Primers* (2021) 7:6. doi: 10.1038/s41572-020-00240-3

4. Peng S, Wang Y, Peng H, Chen D, Shen S, Peng B, et al. Autocrine vascular endothelial growth factor signaling promotes cell proliferation and modulates sorafenib treatment efficacy in hepatocellular carcinoma. *Hepatology* (2014) 60:1264–77. doi: 10.1002/hep.27236

5. Kwon JH, Lee N, Park JY, Yu YS, Kim JP, Shin JH, et al. Actionable gene expression-based patient stratification for molecular targeted therapy in hepatocellular carcinoma. *PloS One* (2013) 8:e64260. doi: 10.1371/journal.pone.0064260

6. Saharinen P, Eklund L, Pulkki K, Bono P, Alitalo K. VEGF and angiopoietin signaling in tumor angiogenesis and metastasis. *Trends Mol Med* (2011) 17:347–62. doi: 10.1016/j.molmed.2011.01.015

7. Hu Y, Qin T, Li S, Zhang T, Xue J. Efficacy and safety of SBRT combined with camrelizumab and apatinib in HCC patients with PVTT: Study protocol of a randomized controlled trial. *Front Oncol* (2020) 10:1589. doi: 10.3389/fonc.2020.01589

8. Matsuki M, Hoshi T, Yamamoto Y, Ikemori-Kawada M, Minoshima Y, Funahashi Y, et al. Lenvatinib inhibits angiogenesis and tumor fibroblast growth factor signaling pathways in human hepatocellular carcinoma models. *Cancer Med* (2018) 7:2641–53. doi: 10.1002/cam4.1517

9. Tian S, Quan H, Xie C, Guo H, Lü F, Xu Y, et al. YN968D1 is a novel and selective inhibitor of vascular endothelial growth factor receptor-2 tyrosine kinase with potent activity *in vitro* and in vivo. *Cancer Sci* (2011) 102:1374–80. doi: 10.1111/j.1349-7006.2011.01939.x

10. Yang C, Qin S. Apatinib targets both tumor and endothelial cells in hepatocellular carcinoma. *Cancer Med* (2018) 7:4570–83. doi: 10.1002/cam4.1664

11. Tang W, Chen Z, Zhang W, Cheng Y, Zhang B, Wu F, et al. The mechanisms of sorafenib resistance in hepatocellular carcinoma: theoretical basis and therapeutic aspects. *Signal Transduct Target Ther* (2020) 5:87. doi: 10.1038/s41392-020-0187-x

12. Zhao Y, Zhang YN, Wang KT, Chen L. Lenvatinib for hepatocellular carcinoma: From preclinical mechanisms to anti-cancer therapy. *Biochim Biophys Acta Rev Cancer* (2020) 1874:188391. doi: 10.1016/j.bbcan.2020.188391

13. Chernyak V, Fowler KJ, Kamaya A, Kielar AZ, Elsayes KM, Bashir MR, et al. Liver imaging reporting and data system (LI-RADS) version 2018: Imaging of hepatocellular carcinoma in At-risk patients. *Radiology* (2018) 289:816–30. doi: 10.1148/radiol.2018181494

14. Huang Z, Meng X, Xiu J, Xu X, Bi L, Zhang J, et al. MR imaging in hepatocellular carcinoma: correlations between MRI features and molecular marker VEGF. *Med Oncol* (2014) 31:313. doi: 10.1007/s12032-014-0313-0

15. Ippolito D, Sironi S, Pozzi M, Antolini L, Ratti L, Alberzoni C, et al. Hepatocellular carcinoma in cirrhotic liver disease: Functional computed tomography with perfusion imaging in the assessment of tumor vascularization. *Acad Radiol* (2008) 15:919–27. doi: 10.1016/j.acra.2008.02.005

16. Thaiss WM, Kaufmann S, Kloth C, Nikolaou K, Bösmüller H, Horger M. VEGFR-2 expression in HCC, dysplastic and regenerative liver nodules, and correlation with pre-biopsy dynamic contrast enhanced CT. *Eur J Radiol* (2016) 85:2036–41. doi: 10.1016/j.ejrad.2016.09.012

17. Chu JS, Ge FJ, Zhang B, Wang Y, Silvestris N, Liu LJ, et al. Expression and prognostic value of VEGFR-2, PDGFR-β, and c-met in advanced hepatocellular carcinoma. *J Exp Clin Cancer Res* (2013) 32:16. doi: 10.1186/1756-9966-32-16

18. Kanematsu M, Osada S, Amaoka N, Goshima S, Kondo H, Moriyama N. Expression of vascular endothelial growth factor in hepatocellular carcinoma and the surrounding liver: correlation with MR imaging and angiographically assisted CT. *Abdom Imaging* (2006) 31:78–89. doi: 10.1007/s00261-005-0091-4

19. Remmele W, Stegner HE. [Recommendation for uniform definition of an immunoreactive score (IRS) for immunohistochemical estrogen receptor detection (ER-ICA) in breast cancer tissue]. *Pathologe* (1987) 8:138–40.

20. Huang J, Zhang X, Tang Q, Zhang F, Li Y, Feng Z, et al. Prognostic significance and potential therapeutic target of VEGFR2 in hepatocellular carcinoma. *J Clin Pathol* (2011) 64:343–8. doi: 10.1136/jcp.2010.085142

21. Nakamura K, Zen Y, Sato Y, Kozaka K, Matsui O, Harada K, et al. Vascular endothelial growth factor, its receptor flk-1, and hypoxia inducible factor-1alpha are involved in malignant transformation in dysplastic nodules of the liver. *Hum Pathol* (2007) 38:1532–46. doi: 10.1016/j.humpath.2007.03.002

22. Chen J, Zhou J, Kuang S, Zhang Y, Xie S, He B, et al. Liver imaging reporting and data system category 5: MRI predictors of microvascular invasion and recurrence after hepatectomy for hepatocellular carcinoma. *AJR Am J Roentgenol* (2019) 213:821–30. doi: 10.2214/AJR.19.21168

23. Zhou H, Sun J, Jiang T, Wu J, Li Q, Zhang C, et al. A nomogram based on combining clinical features and contrast enhanced ultrasound LI-RADS improves prediction of microvascular invasion in hepatocellular carcinoma. *Front Oncol* (2021) 11:699290. doi: 10.3389/fonc.2021.699290

24. Granata V, Fusco R, Setola S, Picone C, Vallone P, Belli A, et al. Microvascular invasion and grading in hepatocellular carcinoma: correlation with major and ancillary features according to LIRADS. *Abdominal Radiol (New York)* (2019) 44:2788–800. doi: 10.1007/s00261-019-02056-6

25. Choi SH, Lee SS, Park SH, Kim KM, Yu E, Park Y, et al. LI-RADS classification and prognosis of primary liver cancers at gadoxetic acid-enhanced MRI. *Radiology* (2019) 290:388–97. doi: 10.1148/radiol.2018181290

26. Carr BI, Akkiz H, Üsküdar O, Yalçın K, Guerra V, Kuran S, et al. HCC with low- and normal-serum alpha-fetoprotein levels. *Clin Pract (Lond)* (2018) 15:453–64. doi: 10.4172/clinical-practice.1000393

27. Tsilimigras DI, Moris D, Hyer JM, Bagante F, Ratti F, Marques HP, et al. Serum α-fetoprotein levels at time of recurrence predict post-recurrence outcomes following resection of hepatocellular carcinoma. *Ann Surg Oncol* (2021) 28:7673–83. doi: 10.1245/s10434-021-09977-x

28. Carr BI, Guerra V, Giannini EG, Farinati F, Ciccarese F, Rapaccini GL, et al. Significance of platelet and AFP levels and liver function parameters for HCC size and survival. *Int J Biol Markers* (2014) 29:e215–223. doi: 10.5301/jbm.5000064

29. Yao M, Zhao J, Lu F. Alpha-fetoprotein still is a valuable diagnostic and prognosis predicting biomarker in hepatitis b virus infection-related hepatocellular carcinoma. *Oncotarget* (2016) 7:3702–8. doi: 10.18632/oncotarget.6913

frontiers | Frontiers in Surgery

TYPE Original Research
PUBLISHED 10 November 2022
DOI 10.3389/fsurg.2022.986696

Check for updates

OPEN ACCESS

EDITED BY
Qi Liu,
Fudan University, China

REVIEWED BY
Natale Calomino,
University of Siena, Italy
Vincenzo Lizzi,
Azienda Ospedaliero-Universitaria Ospedali Riuniti di Foggia, Italy
Alfredo Colombo,
Casa Di Cura Macchiarella, Italy
Fabrizio Urraro,
University of Campania Luigi Vanvitelli, Italy

*CORRESPONDENCE
Lisong Teng
lsteng@zju.edu.cn

SPECIALTY SECTION
This article was submitted to Surgical Oncology, a section of the journal Frontiers in Surgery

RECEIVED 05 July 2022
ACCEPTED 24 October 2022
PUBLISHED 10 November 2022

CITATION
Chen Y, Chen Y, Wen L, Tou L, Wang H and Teng L (2022) PN3b as an independent risk factor for poor prognosis and peritoneal recurrence in Borrmann type IV gastric cancer: A retrospective cohort study.
Front. Surg. 9:986696.
doi: 10.3389/fsurg.2022.986696

COPYRIGHT
© 2022 Chen, Chen, Wen, Tou, Wang and Teng. This is an open-access article distributed under the terms of the Creative Commons Attribution License (CC BY). The use, distribution or reproduction in other forums is permitted, provided the original author(s) and the copyright owner(s) are credited and that the original publication in this journal is cited, in accordance with accepted academic practice. No use, distribution or reproduction is permitted which does not comply with these terms.

PN3b as an independent risk factor for poor prognosis and peritoneal recurrence in Borrmann type IV gastric cancer: A retrospective cohort study

Yiran Chen[1], Yanyan Chen[1], Liping Wen[1], Laizhen Tou[2], Haiyong Wang[1] and Lisong Teng[1]*

[1]Department of Surgical Oncology, The First Affiliated Hospital, College of Medicine, Zhejiang University, Hangzhou, China, [2]Department of Gastrointestinal Surgery, Lishui Hospital, College of Medicine, Zhejiang University, Lishui, China

Background: The clinicopathological features and surgical treatment strategies of Borrmann type IV gastric cancer (GC) remain controversial. Peritoneal metastasis is the most common recurrence pattern in patients with Borrmann type IV GC.

Methods: Among 2026 gastric cancer between January 2009 and August 2019, 159 cases of Borrmann type IV GC were included in this study (7.8%). We retrospectively analyzed the clinicopathological characteristics and prognosis of these patients. Univariate and multivariate Cox proportional hazards were applied to identify independent prognostic factors. Predictors related to peritoneal metastasis of type IV GC were analyzed by multivariate Cox regression analysis.

Results: Borrmann type IV gastric cancer was associated with more advanced clinicopathological features at diagnosis than the other Borrmann type GC. Of the 159 patients with Borrmann type IV GC, the median OS was 23 months. The number of patients with peritoneal metastasis was 43, accounted for 27.0% of all the patients and 87.8% of the patients with distant metastasis. Multivariate analyses revealed lymph node metastasis to be independent prognostic factor for survival in Borrmann type IV GC patients. pN3b and tumor size > 50 mm showed to be risk factors for peritoneal metastasis.

Conclusions: Borrmann type IV GC is an important independent prognostic factor. pN3b is an independent prognostic factor and a predictor of peritoneal metastasis in patients with Borrmann type IV GC.

KEYWORDS

gastric cancer, peritoneal metastasis, lymph node metastasis, Borrmann type, signet ring cell carcinoma

Introduction

Gastric cancer (GC) is one of the most common malignancies in the world, with more than 1.8 million new cases worldwide in 2020 and an estimated 770,000 deaths, making it the fifth most frequently diagnosed cancer and the fourth in mortality (1). The Borrmann type proposed in 1926 provides a relatively accurate description of the

gross morphology of advanced gastric cancer (2), among which Borrmann type IV GC accounts for about 8%–13% (3–6). Borrmann type IV GC, including linitis plastica, are characterized by poorly differentiated tumor cells with diffusely infiltrative involvement of the stomach (5, 7, 8). The patients were frequently associated with poor tumor differentiation, lymph node metastases, peritoneal metastases, serosal invasion, lymphatic invasion, and poor prognosis (4, 9–11). Peritoneal metastasis (PM) represents the most common type of recurrence in advanced GC and is considered as an independent factor for poor prognosis (12). Although the treatments of peritoneal metastasis in gastric cancer have made some progress, its prognosis is still poor (13, 14). Early detection and intervention are still the main way to prolong the life of patients. Lee et al. reported that Borrmann type IV gastric cancer is an independent risk factor for peritoneal recurrence (15). However, in Borrmann type IV GC, the risk factors of peritoneal recurrence have not been well studied. Prognostic factors have the potential to play an important role in improving health, including clinical practice, healthcare research, and the development, evaluation, and targeting of interventions (16). Therefore, in our study, we described the clinicopathological features of Borrmann type IV gastric cancer and focus on the risk factors for PM in this special type of gastric cancer.

Material and methods

Probands

Between January 2009 and August 2019, 2026 gastric cancer patients underwent gastric resection at the department of surgical oncology, the First Affiliated Hospital, Zhejiang University. Among these patients, 159 cases of Borrmann type IV GC were included in further analysis (7.8%). In addition, 761 cases of Borrmann type I–III GC were selected for comparison with Borrmann type IV GC. The inclusion criteria for patients were as follows: (i) patients diagnosed with gastric cancer with pT2 or more from January 2009 to August 2019; (ii) patients received radical gastrectomy or palliative gastrectomy in the department of surgical oncology; and (iii) patients had complete clinical data and pathologic specimens available for reevaluation. The exclusion criteria for patients included: (i) patients diagnosed with combined primary malignant cancer; (ii) patients had history of severe underlying diseases; and (iii) missing information for key variants. The specific patient selection pathway is shown in **Figure 1**. Each patient was consented to collecting research data once the hospital file is created. Outcomes of our interest, that is, overall survival (OS) and time to first recurrence (RFS), were collected during the follow-up period (median follow-up time 38 months, ranging from 1 month to 122 month). 18 Borrmann type IV GC patients were lost in post-operative follow-up. Age, gender, CEA and CA19-9 level before surgery, surgical intervention, pathological features including histological type, tumor location, tumor size, depth of tumor invasion and lymph node metastasis, were retrospectively collected from the medical record system of our institution. The tumors were staged according to the eighth edition of AJCC/UICC TNM staging system.

Statistical analysis

The clinicopathological features between Borrmann type IV GC and Borrmann type I–III GC were compared using Chi-square or Fisher's exact test. Log-rank tests were used to analyze survival curves which were created using Kaplan-Meier analysis. Information obtained from the univariate analysis was applied to a survival analysis with covariates using the Cox model of proportional hazards (forward likelihood ratio model). Subsequently, Cox proportional hazard regression (enter model) was used to examine the effect of different clinicopathological features and treatment on PM in patients with Borrmann type IV gastric cancer and predict the independent risk factors of PM in such patients. Statistical analysis was performed using SPSS 26.0 software. In all statistical analyses, $P < 0.05$ was considered significant.

Results

Characteristics of Borrmann type IV GC patients

Borrmann type IV GC patients showed significant differences in the distribution of gender, operation type, surgical curability, tumor size, differentiation, depth of invasion, lymph node metastasis, distant metastasis and stage comparing with other Borrmann types of gastric cancer (**Supplementary Table S1**). Multivariate analysis showed that Borrmann type IV GC was an independent prognostic factor (**Supplementary Figures S1, S2** and **Supplementary Table S2**) after adjusting for age, gender, residual tumor, differentiation, TNM stage, serum CEA and CA19-9 level. The clinicopathological features of Borrmann type IV GC patients are shown in **Table 1**. Of 159 patients with Borrmann type IV GC who underwent gastrectomy, 89 (56.0%) were male and 70 (44.0%) were female. The mean age was 59-year-old (range 16 to 87). Total gastrectomy was performed in 97 patients (61.0%) and subtotal gastrectomy was performed in 62 patients (39.0%). D2/D2 + lymphadenectomy was applied to all stage I–III patients. 7 patients received D2 lymph node dissection including splenectomy because of tumor invasion. The average number of lymph nodes examined was 26.8. Among the 26 patients diagnosed as stage IV, 8 patients received palliative resection due to gastrointestinal bleeding or

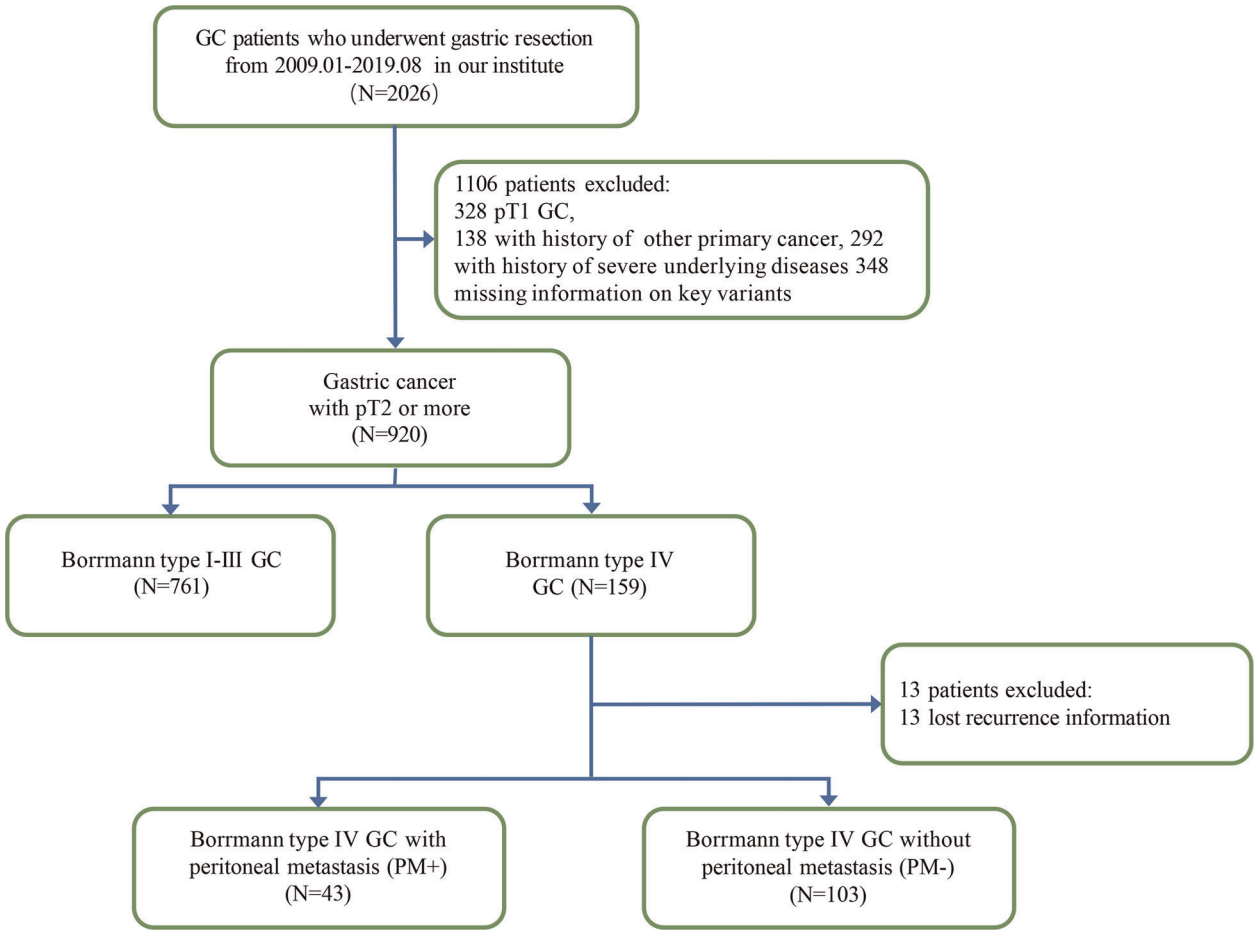

FIGURE 1
Study workflow diagram (GC, gastric cancer; PM, peritoneal metastasis).

obstruction and others were found to have distant metastasis during the operation or post-operative pathology confirmed distant metastasis. 12 cases (7.6%) underwent extended surgical resection due to tumor invasion or concurrent indications for resection. Among these patients, 115 patients received at least 1 cycle of first-line chemotherapy (platinum- or taxane-based), in which 25 patients received neoadjuvant chemotherapy and 109 patients received adjuvant chemotherapy. The purpose of these patients receiving chemotherapy included not only preoperative drawdown and postoperative adjuvant, but also conversion chemotherapy.

Prognostic significance of Borrmann type IV GC

The median OS of patients with Borrmann type IV GC was 23 months, and the 5-year survival rate was 25.1% (**Supplementary Figure S3**). Univariate Cox analysis revealed that residual tumor, tumor size, lymph node metastasis, distant metastasis, serum CEA and CA19-9 level were significantly associated with OS (**Table 1** and **Supplementary Figures S4A–F**). Multivariate analysis showed that N category and distant metastasis were the independent prognostic factors (**Figure 2A**) after adjusting for age, CEA, CA199 and tumor size. As for patients who received R0 resection, only distant metastasis was the independent prognostic factors after adjusting for age, lymph node metastasis, CEA, CA199 and tumor size (**Figure 2B**). Notably, pN3b was associated with the worst prognosis, which was significantly worse than pN3a (**Table 1** and **Figure 3A**).

Risk factors for peritoneal metastasis of Borrmann type IV GC

43 patients developed PM, accounting for 27% of all patients and 87.8% of the patients with distant metastasis. Among them, 23 patients had synchronous PM and 20 developed metachronous PM (peritoneal recurrence). The median OS of patients with

TABLE 1 Clinicopathological features and survival analysis of patients with Borrmann type IV gastric cancer.

Factors	Borrmann IV GC ($n = 159$)	Median OS (month)	Hazard Ratio (95% CI)	*P* Value
Age	16–87 (59)			
Gender				
Female	70 (44.0%)	24	Reference	
Male	89 (56.0%)	21	1.166 (0.746–1.822)	0.494
Operation				
Distal gastrectomy	55 (34.6%)	49	Reference	0.029
Total gastrectomy	97 (61.0%)	18	2.341 (1.388–3.947)	
Proximal gastrectomy	2 (1.3%)	1	9.124 (2.079–40.041)	
Residual gastrectomy	5 (3.1%)	–	0.676 (0.090–5.067)	
Residual Tumor				
R0	123 (77.4%)	32	Reference	<0.001
R1[#]	20 (12.6%)	16	2.273 (1.280–4.034)	
R2	11 (6.9%)	7	3.368 (1.518–7.472)	
NA	5 (3.1%)	–	–	
Tumor Size				
≤50 mm	57 (35.8%)	47	Reference	<0.001
>50 mm	102 (64.2%)	18	2.458 (1.468–4.113)	
Tumor Location				
Upper 1/3	10 (6.3%)	13	Reference	0.003
Upper-middle	7 (4.4%)	26	0.315 (0.067–1.487)	
Middle 1/3	35 (22.0%)	23	0.516 (0.219–1.219)	
Middle-lower	18 (11.3%)	19	0.741 (0.297–1.845)	
Lower 1/3	55 (34.6%)	35	0.496 (0.222–1.107)	
Entire	29 (18.2%)	10	1.580 (0.692–3.606)	
Residual stomach	5 (3.1%)	–	0.254 (0.032–2.039)	
Depth of Invasion				
T2	8 (5.0%)	–	Reference	0.071
T3	50 (31.4%)	26	6.026 (0.810–44.840)	
T4a	75 (47.2%)	20	8.056 (1.108–58.566)	
T4b	26 (16.4%)	17	7.999 (1.036–61.761)	
Lymph Node Metastasis				
N0	19 (11.9%)	47	Reference	<0.001
N1	17 (10.7%)	49	1.004 (0.251–4.015)	
N2	29 (18.2%)	26	2.888 (0.971–8.593)	
N3a	43 (27.0%)	27	2.777 (0.959–8.037)	
N3b	51 (32.1%)	14	5.732 (2.010–16.348)	
Distant Metastasis				
M0	133 (83.6%)	29	Reference	<0.001
M1	26 (16.4%)	6	3.684 (2.178–6.232)	
TNM Stage				
I	5 (3.1%)	–	–	<0.001
II	22 (13.8%)	47	Reference	
III	106 (66.6%)	23	3.030 (1.212–7.574)	
IV	26 (16.4%)	6	9.292 (3.436–25.127)	
CEA				
≤5.0 ng/ml	109 (68.6%)	24	Reference	0.038
>5 ng/ml	32 (20.1%)	13	1.720 (1.019–2.906)	

(*continued*)

TABLE 1 Continued

Factors	Borrmann IV GC ($n = 159$)	Median OS (month)	Hazard Ratio (95% CI)	P Value
NA	18 (11.3%)	–	–	
CA19-9				
≤37 U/ml	106 (67.3%)	26	Reference	0.002
>37 U/ml	34 (21.4%)	12	2.167 (1.300–3.612)	
NA	18 (11.3%)	–	–	
Chemotherapy				
No	38 (23.9%)	16	Reference	0.035
Yes*	115 (72.3%)	29	0.591 (0.362–0.964)	
NA	6 (3.8%)	–	–	

Abbreviations: NA, not available.
#R1, postoperative pathology showed positive surgical margin.
*Including the patients received neoadjuvant chemotherapy ($n = 25$) and adjuvant chemotherapy ($n = 109$).

PM was significantly shorter than that of patients without PM (16 months vs. 29 months, $P = 0.001$, Supplementary Figure S5). The 3-year survival rate was 12.7%. 1-year survival rate of patients with synchronous PM was 22.5% and that of patients who develop metachronous PM (peritoneal recurrence) was 77.4%. The median OS after metachronous PM was 11 months. Among 159 patients with Borrmann type IV GC, 103 patients were followed up to date or died without peritoneal recurrence or metastasis. To investigate the risk factors for PM in patients with Borrmann type IV GC, we selected these 103 patients and 43 patients with PM for comparative analysis. The clinicopathological features are presented in Table 2. Through univariate Cox analysis, we found that there were significant differences in the prognosis and recurrence risk between pN3b and other N categories (Figures 3A,B). Therefore, when discussing the risk factors for peritoneal recurrence, we divided the N category into N0-3a and N3b with lymph node metastasis >15 as cut-off value.

Univariate Cox analysis showed that factors related to PM were regional lymph node metastasis, tumor size, residual tumor and preoperative CA19-9 level (Table 2). Multivariate cox regression analysis revealed that pN3b ($P = 0.04$) and tumor size >50 mm ($P = 0.03$) were the independent risk factors of PM after adjusting for age and CA199 (Figure 4A). Meanwhile, univariate and multivariate analysis was also performed separately for the patients who received R0 resection (Supplementary Table S3 and Figure 4B). The results indicated that pN3b and signet ring cell carcinoma were significant risk factors for peritoneal recurrence of Borrmann type IV GC.

Discussion

The incidence of Borrmann type IV gastric cancer has a large deviation in previous reports, ranging from 8 to 20% (3, 4, 9). In recent years, many relevant studies have shown that Borrmann type IV gastric cancer was characterized as higher female/male ratio, poorer differentiation, higher risk of serosal infiltration, lymph node metastasis and peritoneal metastasis, and poor prognosis (4, 9). Lee et al. reported that Borrmann type IV gastric cancer is an independent risk factor for peritoneal recurrence (15). In this study, we mainly included patients who underwent gastrectomy, and the incidence of Borrmann type IV GC was about 7.8%. Due to the aggressiveness of Borrmann type IV GC, many patients had already lost the opportunity for surgical treatment when they were diagnosed, so our incidence rate was slightly lower than that shown in relevant reports. Many studies have reported the prognostic factors of Borrmann type IV GC. For instance, Yamashita et al. suggested that elder age, T category, N category, peritoneal dissemination, CY1/CYX and margin status are prognostic factors of Borrmann type IV GC, in which elder age, T category and peritoneal dissemination are independent prognostic factors (17). Univariate analysis by Yook et al. found that tumor location, occupied region, invasion depth, lymph node metastasis and pTNM stage were correlated with the prognosis of Borrmann type IV gastric cancer after radical surgery (18). The multivariate analysis indicated that only tumor location and pTNM stage were independent factors affecting the prognosis of Borrmann type IV gastric cancer after radical surgery. In this study, a multivariate analysis of 159 patients showed that pN3b ($P = 0.03$), along with residual tumor, was a significant independent prognostic factor of Borrmann type IV GC, which was basically consistent with previous reports. The treatment options for Borrmann type IV GC are difficult and controversial because of its high incidence of peritoneal metastasis and poor prognosis. Early detection of Borrmann IV gastric cancer by endoscope remain difficult due to the diffuse invasion of cancer cells to the mucosa lamina propria and no obvious ulcer or mucosal surface uplift (3, 8). At diagnosis, cancer cells often penetrate the serous membrane

A

		Univariable analysis		Multivariable analysis	
Variable		**Median OS (m)**	***P* value**	**Hazard ratio(95%CI)**	***P* value**
Age	< 60	27		Reference	
	≥ 60	23	0.194	1.09 (0.64, 1.86)	0.75
LNM	N0–N3a	35		Reference	
	N3b	14	< 0.001	1.99 (1.10, 3.60)	0.02
M	M0	29		Reference	
	M1	6	< 0.001	1.92 (0.99, 3.70)	0.05
CEA	≤ 5.00ng/ml	24		Reference	
	> 5.00ng/ml	13	0.038	1.48 (0.86, 2.52)	0.15
CA199	≤ 37.00U/ml	26		Reference	
	> 37.00U/ml	12	0.002	1.47 (0.82, 2.65)	0.20
Size	≤ 50mm	47		Reference	
	> 50mm	18	< 0.001	1.51 (0.82, 2.80)	0.19

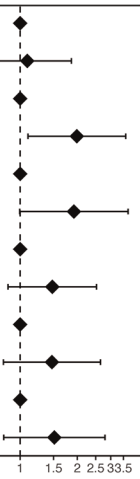

B

		Univariable analysis		Multivariable analysis	
Variable		**Median OS (m)**	***P* value**	**Hazard ratio(95%CI)**	***P* value**
Age	< 60	27		Reference	
	≥ 60	23	0.194	1.55 (0.77, 3.12)	0.22
LNM	N0–N3a	35		Reference	
	N3b	14	< 0.001	1.42 (0.68, 2.97)	0.35
M	M0	29		Reference	
	M1	6	< 0.001	3.04 (1.16, 7.95)	0.02
CEA	≤ 5.00ng/ml	24		Reference	
	> 5.00ng/ml	13	0.038	1.84 (0.91, 3.70)	0.09
CA199	≤ 37.00U/ml	26		Reference	
	> 37.00U/ml	12	0.002	1.04 (0.45, 2.40)	0.93
Size	≤ 50mm	47		Reference	
	> 50mm	18	< 0.001	1.66 (0.78, 3.50)	0.19

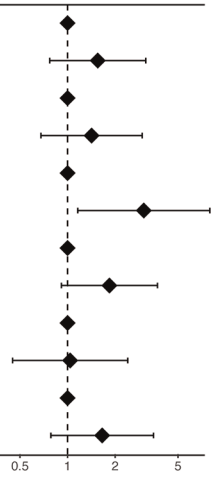

FIGURE 2
Cox proportional hazard regression models and forest plot for overall survival. (A) Forest plot displaying the results of hazard ratio for overall survival of patients with Borrmann type IV gastric cancer; (B) Forest plot displaying the results of hazard ratio for overall survival of patients with B-4 GC after receiving R0 resection. (LNM, lymph node metastasis; M, distant metastasis; CI, confidence interval).

and have lymph node metastasis. Curative resection (R0 resection) is critical for treatment of this GC subtype (4, 5).

Previous reports have shown that nearly 20% of patients with GC were diagnosed with PM before or during surgery, and about 50% of patients developed PM after radical surgery (19, 20). Patients with PM had a poor prognosis with a median OS of less than 2 years (19, 21). PM eventually lead to refractory ascites, intestinal obstruction and cachexia, which are the main causes of death of gastric cancer (20). Many clinical studies have investigated the risk factors of PM in GC. Huang BJ et al. suggested that patients with Borrmann III/IV and N3 should be closely followed to detect peritoneal metastasis (22). Several other studies have shown a significantly close relationship between lymph node metastasis and PM (23, 24). Among the characteristics of Borrmann type IV GC, it is worth noting that the incidence of PM is much higher than other types (9). This is also one of the main reasons for the poor prognosis of this GC subtype. It is noteworthy that the tendency of Borrmann type IV to develop PM was concurrent with a lower risk of liver

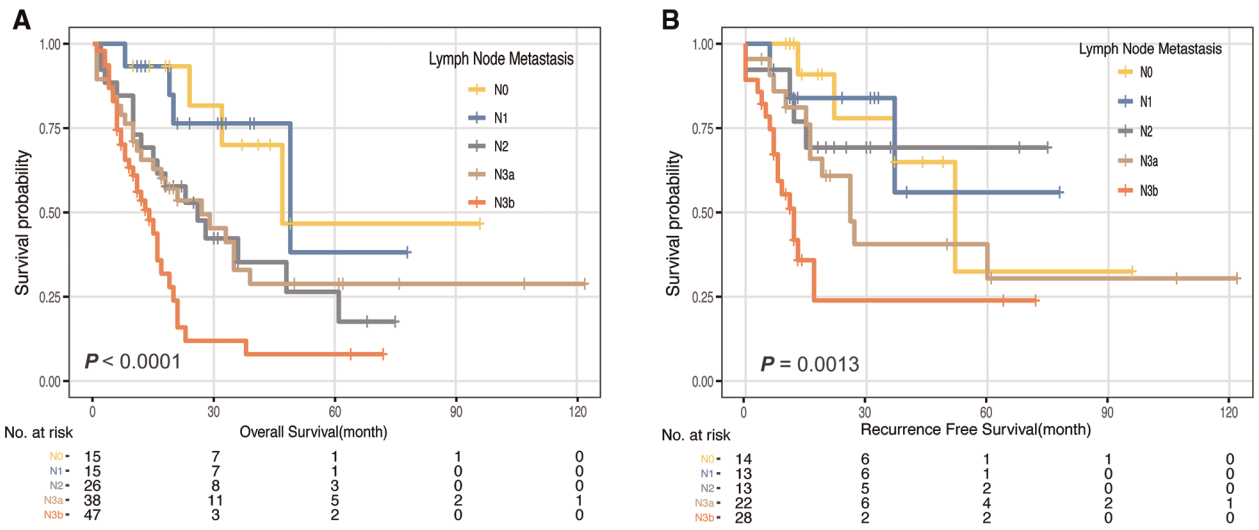

FIGURE 3
Kaplan-Meier curve of pN stage. (A) Kaplan-Meier curves of overall survival (OS) according to N category in Borrmann type IV gastric cancer. (B) Kaplan-Meier curves of recurrence-free survival (RFS) according to N category in Borrmann type IV gastric cancer.

metastasis, suggesting a specific pattern of metastasis (9). Consistently, among 49 who developed distant metastasis in our cohort, 43 (87.8%) developed PM but only 3 (6.1%) developed liver metastasis. Otsuji E et al. considered lymph node metastasis as an independent risk factor for PM of Borrmann type IV GC in 1999 in a cohort of 150 patients (25). In addition, Dong RZ et al. concluded that extracapsular lymph node spread (ECS) is an independent prognostic factor and an adverse factor for PM in patients with Borrmann type IV gastric cancer with radical resection (3). Otherwise, there are few studies focus on the risk factors associated with peritoneal metastasis of Borrmann type IV GC. In this study, we found that regional lymph node metastasis and tumor size were the variables that independently correlated with PM. Furthermore, pN3b and signet ring cell carcinoma were the independent predictor of PM in patients who had received R0 resection (peritoneal recurrence).

Among several clinicopathologic factors, the tumor size clinically served as a simple predictor of tumor progression (26). Previous study reported that tumor size was strongly correlated with the depth of invasion, degree of lymph node metastasis, and stage of the disease. Saito et al. (27) reported that tumor size might be a good indicator in the prediction of recurrence site as well as serve as a simple predictor of survival of patients with gastric cancer. These results indicate that tumor size provides important information about the malignant potential of tumors. Patients with larger tumors may need more aggressive treatment and more frequent postoperative re-examination.

Gastric signet ring cell carcinoma (GSRC) is a typical diffuse infiltrating gastric cancer with low differentiation, strong invasiveness and poor prognosis (28–31). Most of GSRCs were Borrmann type III and IV gastric cancer (30). Previous studies [6,8] found that GSRC showed a higher incidence of peritoneal metastasis (30, 32) and was an independent factor affecting lymph node metastasis (32), while the latter was an independent prognostic factor of advanced GC (32). These results suggest that one of the reasons for the poor prognosis of gastric SRCC is the tendency of lymph node metastasis. In our study, GSRC was an independent risk factor of peritoneal recurrence which suggested that carefully follow-up examinations and more aggressive treatment may be necessary for Borrmann type IV GC with SRC after surgery.

Regional lymph node metastasis played an important role in predicting prognosis and peritoneal recurrence in our study, especially pN3b. The American Joint Committee on Cancer (AJCC) TNM staging system is currently recognized as the best malignant tumor staging system in the world, and its latest 8th edition was published in October 2016, replacing the 7th edition since 2009 (33–35). Although the 7th edition divided N3 into N3a and N3b, it did not impact the TNM staging of GC. However, a study of over 25,000 GC patients from 15 countries found that N3a and N3b two subgroups of patients with significant differences of its survival. Subsequently, in the updated 8th edition of TNM staging system, N3a and N3b largely impact the tumor staging (33, 35). The new grading system has been validated in national databases to verify its predictive power and accuracy (36–39). Some studies have identified that patients with pN3a and pN3b presented distinct survival outcomes (34, 40), which is consistent with our results (**Table 1** and **Supplementary Table S4**). Yonemura Y. et al. reported trans-lymphatic

TABLE 2 Clinicopathological features between PM (+) and PM (–) patients with Borrmann type IV gastric cancer.

Factors	PM (−) ($n = 103$)	PM (+) ($n = 43$)	Odds Ratio (95%CI)	*P* value
Gender				
Female	45 (72.6%)	17 (27.4%)	Reference	
Male	58 (69.0%)	26 (31.0%)	0.963 (0.474–1.958)	0.917
Age				
<60	45 (64.3%)	25 (35.7%)	Reference	
≥60	58 (76.3%)	18 (23.7%)	0.613 (0.293–1.283)	0.194
Signet ring cell				
No	78 (70.9%)	32 (29.1%)	Reference	
Yes	25 (69.4%)	11 (30.6%)	1.417 (0.651–3.084)	0.380
CEA				
≤5.0 ng/ml	71 (71.0%)	29 (29.0%)	Reference	
>5.0 ng/ml	21 (72.4%)	8 (27.6%)	1.341 (0.506–3.557)	0.555
NA	11	6		
Depth of Invasion				
T2–3	42 (76.4%)	13 (23.6%)	Reference	
T4	61 (67.0%)	30 (33.0%)	1.486 (0.712–3.102)	0.292
Residual Tumor				
R0	85 (75.9%)	27 (24.1%)	Reference	
R1[#]	11 (57.9%)	8 (42.1%)	3.145 (1.297–7.654)	
R2	3 (30.0%)	7 (70.0%)	8.534 (3.052–23.865)	<0.001[a]
Lymph Node Metastasis				
N0-3a	75 (75.8%)	24 (24.2%)	Reference	
N3b	28 (59.6%)	19 (40.4%)	3.349 (1.610–6.966)	0.001
Tumor Size				
≤50 mm	43 (81.1%)	10 (18.9%)	Reference	
>50 mm	60 (64.5%)	33 (35.5%)	3.350 (1.439–7.797)	0.005
CA19-9				
≤37 U/ml	73 (73.0%)	27 (27.0%)	Reference	
>37 U/ml	19 (65.5%)	10 (34.5%)	2.613 (1.124–6.072)	0.026
NA	11	6		
Chemotherapy				
No	28 (82.4%)	6 (17.6%)	Reference	
Yes*	71 (66.4%)	36 (33.64%)	3.096 (0.736–13.027)	0.088
NA	4	1	–	

Abbreviations: PM, peritoneal metastasis; NA, not available.
[a]Fisher's exact test, others using Pearson's Chi square test.
[#]R1, postoperative pathology showed positive surgical margin.
*Including the patients received neoadjuvant chemotherapy ($n = 23$) and adjuvant chemotherapy ($n = 102$).

metastasis as one of the PM formation concepts (41). In our study, univariate Cox analysis showed that pN3b was significantly different from other N stages in predicting prognosis and peritoneal recurrence in Borrmann type IV GC (**Figures 3A,B**). This might be because more tumor cells exist in patients with lymph node metastasis, spreading through the lymphatic system, also patients with pN3b indicates a more locally advanced disease, which might thus be accompanied by a higher incidence of transperitoneal spread. Therefore, we conclude that for patients with Borrmann type IV GC, lymph node metastasis greater than 15 is a better cut-off value to predict poor prognosis and high incidence of peritoneal recurrence. Thus, we could make more effort for these patients in order to improve their prognosis. Firstly, routine gastroscopy physical examination and early detection of cancer without lymph node metastasis may be effective means of prevention. Secondly, for patients with N3b indicated by preoperative imaging examination, it is more necessary to

A

Variable		Univariable analysis Odds Ratio (95%)	*P* value	Multivariable analysis Hazard ratio (95%CI)	*P* value
Age	< 60	Reference		Reference	
	≥ 60	0.61 (0.29, 1.28)	0.19	0.57 (0.22, 1.44)	0.23
Residual Tumor	R0	Reference		Reference	
	R1	3.15 (1.30, 7.65)		2.80 (1.00, 7.86)	0.05
	R2	8.53 (3.05, 23.87)	<0.001	18.28 (5.27, 63.40)	<0.001
LNM	N0–N3a	Reference		Reference	
	N3b	3.35 (1.61, 6.97)	0.001	2.56 (1.04, 6.30)	0.04
CA199	≤ 37.00U/ml	Reference		Reference	
	> 37.00U/ml	2.61 (1.12, 6.07)	0.03	0.83 (0.27, 2.49)	0.73
Size	≤ 50mm	Reference		Reference	
	> 50mm	3.35 (1.44, 7.80)	0.005	3.30 (1.13, 9.66)	0.03

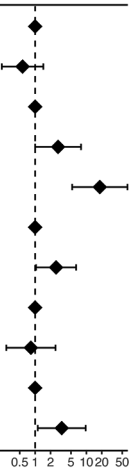

B

Variable		Univariable analysis Odds Ratio (95%)	*P* value	Multivariable analysis Hazard ratio (95%CI)	*P* value
Age	< 60	Reference		Reference	
	≥ 60	0.81 (0.31, 2.06)	0.65	0.42 (0.15-1.24)	0.117
LNM	N0–N3a	Reference		Reference	
	N3b	4.58 (1.75, 12.00)	0.002	5.64(1.66-19.20)	0.006
SRC	No	Reference		Reference	
	Yes	3.14 (1.03, 9.58)	0.045	3.50 (1.13-10.90)	0.030
Size	≤ 50mm	Reference		Reference	
	> 50mm	2.83 (1.00, 7.97)	0.05	1.93 (0.59-6.33)	0.280

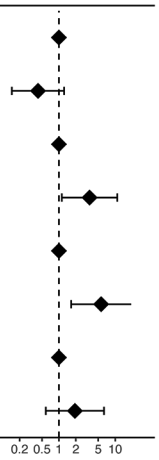

FIGURE 4
Cox proportional hazard regression models and forest plot for recurrence free survival. (A) Forest plot of data from multivariate cox regression revealing factors independently associated with peritoneal metastasis of patients with Borrmann type IV gastric cancer. (B) Forest plot of data from multivariate cox regression revealing factors independently associated with peritoneal metastasis of patients with Borrmann type IV gastric cancer after receiving R0 resection. (LNM, lymph node metastasis; SRC, signet ring cell; CI, confidence interval).

perform neoadjuvant therapy and more active treatment measures including prophylactic intraperitoneal chemotherapy to achieve the purpose of a better prognosis. Last but not least, more intensive follow-up for N3b patients may be meaningful for early detection and intervention of metachronous peritoneal metastasis to improve the outcomes of patients with Borrmann type IV GC.

Whereas, there are some limitations of our study. This study is a retrospective and single-institution study and only those patients who referred to our hospital for surgery were enrolled. A very few patients had less than 16 lymph nodes dissected due to the lack of standardization of surgical methods in the early years. For Borrmann I–III GC, we lacked some information on recurrence, making it difficult for us to make a more accurate comparison. These limitations can lead to biases that may affect the accurate evaluation. A multicenter, prospective study is needed to validate these results in a larger population in future. Also, neoadjuvant therapy plays an important role in the treatment of Borrmann type IV GC due to its malignant biological behavior.

However, pN stage is inferred from pathological findings which might not be disadvantageous in choosing treatment options.

Conclusion

In summary, retrospective analysis of clinicopathological factors in Borrmann type IV GC revealed that lymph node metastasis, specifically pN3b, as an independent prognostic factor. Lymph node status and tumor size were identified as independent predictors of PM. Importantly, pN3b is an important predictive factor for worse prognosis and peritoneal recurrence after radical surgery in patients with Borrmann type IV GC.

Data availability statement

The raw data supporting the conclusions of this article will be made available by the authors, without undue reservation.

Ethics statement

The studies involving human participants were reviewed and approved by Ethics Committee of The First Affiliated Hospital, College of Medicine, Zhejiang University (No. IIT20210588A). The patients/participants provided their written informed consent to participate in this study. Written informed consent was obtained from the individual(s) for the publication of any potentially identifiable images or data included in this article.

Author contributions

YC and YC are responsible for the study concept and design. YC and LW are responsible for the acquisition of data and the development of methodology. YC, XC and YC are responsible for the analysis and interpretation of data. YC, LT and YC are responsible for the writing of the manuscript, HW and LT are responsible for the review and/or revision of the manuscript. All authors contributed to the article and approved the submitted version.

Funding

This work was supported by grants from: Project of the regional diagnosis and treatment centre of the Health Planning Committee (No. JBZX-201903), Science and Technology Project of Zhejiang Province (2021C03119), Chinese Medicine Technology Project of Zhejiang Province (2020ZZ013) and Youth Project of Zhejiang Provincial Natural Science Foundation (LQ18H160012).

Conflict of interest

The authors declare that the research was conducted in the absence of any commercial or financial relationships that could be construed as a potential conflict of interest.

Publisher's note

All claims expressed in this article are solely those of the authors and do not necessarily represent those of their affiliated organizations, or those of the publisher, the editors and the reviewers. Any product that may be evaluated in this article, or claim that may be made by its manufacturer, is not guaranteed or endorsed by the publisher.

Supplementary material

The Supplementary Material for this article can be found online at: https://www.frontiersin.org/articles/10.3389/fsurg.2022.986696/full#supplementary-material.

References

1. Sung H, Ferlay J, Siegel RL, Laversanne M, Soerjomataram I, Jemal A, et al. Global cancer statistics 2020: gLOBOCAN estimates of incidence and mortality worldwide for 36 cancers in 185 countries. *CA Cancer J Clin*. (2021) 71 (3):209–49. doi: 10.3322/caac.21660

2. Borrmann R Geschwulste des magens und des duodenums. In: F Henke, O Lubarsch, editors. *Handbuch spez pathol anat und histo*. Berlin: Springer Verlag (1926). p. 812–1054.

3. Dong RZ, Guo JM, Zhang ZW, Zhou YM, Su Y. Prognostic impact and implications of extracapsular lymph node spread in borrmann type IV gastric cancer. *Oncotarget*. (2017) 8(57):97593–601. doi: 10.18632/oncotarget.18400

4. An JY, Kang TH, Choi MG, Noh JH, Sohn TS, Kim S. Borrmann type IV: an independent prognostic factor for survival in gastric cancer. *J Gastrointest Surg*. (2008) 12(8):1364–9. doi: 10.1007/s11605-008-0516-9

5. Kim DY, Kim HR, Kim YJ, Kim S. Clinicopathological features of patients with borrmann type IV gastric carcinoma. *ANZ J Surg*. (2002) 72(10):739–42. doi: 10.1046/j.1445-2197.2002.02523.x

6. Huang JY, Wang ZN, Lu CY, Miao ZF, Zhu Z, Song YX, et al. Borrmann type IV gastric cancer should be classified as pT4b disease. *J Surg Res*. (2016) 203 (2):258–67. doi: 10.1016/j.jss.2016.04.026

7. Furukawa H, Hiratsuka M, Iwanaga T. A rational technique for surgical operation on borrmann type 4 gastric carcinoma: left upper abdominal evisceration plus Appleby's Method. *Br J Surg*. (1988) 75(2):116–9. doi: 10.1002/bjs.1800750209

8. Zhao X, Huang K, Zhu Z, Chen S, Hu R. Correlation between expression of leptin and clinicopathological features and prognosis in patients with gastric

cancer. *J Gastroenterol Hepatol*. (2007) 22(8):1317–21. doi: 10.1111/j.1440-1746.2007.04941.x

9. Luo Y, Gao P, Song Y, Sun J, Huang X, Zhao J, et al. Clinicopathologic characteristics and prognosis of Borrmann type IV gastric cancer: a meta-analysis. *World J Surg Oncol*. (2016) 14(1):49. doi: 10.1186/s12957-016-0805-9

10. Chen CY, Wu CW, Lo SS, Hsieh MC, Lui WY, Shen KH. Peritoneal carcinomatosis and lymph node metastasis are prognostic indicators in patients with borrmann type IV gastric carcinoma. *Hepatogastroenterology*. (2002) 49 (45):874–7.

11. Zhu YL, Yang L, Sui ZQ, Liu L, Du JF. Clinicopathological features and prognosis of Borrmann type IV gastric cancer. *J BUON*. (2016) 21(6):1471–5.

12. Chu DZ, Lang NP, Thompson C, Osteen PK, Westbrook KC. Peritoneal carcinomatosis in nongynecologic malignancy. A prospective study of prognostic factors. *Cancer*. (1989) 63(2):364–7. doi: 10.1002/1097-0142(19890115)63:2<364::AID-CNCR2820630228>3.0.CO;2-V

13. Bonnot PE, Piessen G, Kepenekian V, Decullier E, Pocard M, Meunier B, et al. Cytoreductive surgery with or without hyperthermic intraperitoneal chemotherapy for gastric cancer with peritoneal metastases (CYTO-CHIP study): a propensity score analysis. *J Clin Oncol*. (2019) 37(23):2028–40. doi: 10.1200/JCO.18.01688

14. Fujitani K, Yang HK, Mizusawa J, Kim YW, Terashima M, Han SU, et al. Gastrectomy plus chemotherapy versus chemotherapy alone for advanced gastric cancer with a single non-curable factor (REGATTA): a phase 3, randomised controlled trial. *Lancet Oncol*. (2016) 17(3):309–18. doi: 10.1016/S1470-2045(15)00553-7

15. Lee JH, Son SY, Lee CM, Ahn SH, Park DJ, Kim HH. Factors predicting peritoneal recurrence in advanced gastric cancer: implication for adjuvant intraperitoneal chemotherapy. *Gastric Cancer*. (2014) 17(3):529–36. doi: 10.1007/s10120-013-0306-2

16. Riley RD, Hayden JA, Steyerberg EW, Moons KG, Abrams K, Kyzas PA, et al. Prognosis research strategy (PROGRESS) 2: prognostic factor research. *PLoS Med*. (2013) 10(2):e1001380. doi: 10.1371/journal.pmed.1001380

17. Yamashita K, Hosoda K, Katada N, Moriya H, Mieno H, Higuchi K, et al. Survival outcome of Borrmann type IV gastric cancer potentially improved by multimodality treatment. *Anticancer Res*. (2015) 35(2):897–906.

18. Yook JH, Oh ST, Kim BS. Clinicopathological analysis of Borrmann type IV gastric cancer. *Cancer Res Treat*. (2005) 37(2):87–91. doi: 10.4143/crt.2005.37.2.87

19. Katai H, Ishikawa T, Akazawa K, Isobe Y, Miyashiro I, Oda I, et al. Five-year survival analysis of surgically resected gastric cancer cases in Japan: a retrospective analysis of more than 100,000 patients from the nationwide registry of the Japanese gastric cancer association (2001–2007). *Gastric Cancer*. (2018) 21 (1):144–54. doi: 10.1007/s10120-017-0716-7

20. Yonemura Y, Bandou E, Kawamura T, Endou Y, Sasaki T. Quantitative prognostic indicators of peritoneal dissemination of gastric cancer. *Eur J Surg Oncol*. (2006) 32(6):602–6. doi: 10.1016/j.ejso.2006.03.003

21. Nashimoto A, Akazawa K, Isobe Y, Miyashiro I, Katai H, Kodera Y, et al. Gastric cancer treated in 2002 in Japan: 2009 annual report of the JGCA nationwide registry. *Gastric Cancer*. (2013) 16(1):1–27. doi: 10.1007/s10120-012-0163-4

22. Huang B, Sun Z, Wang Z, Lu C, Xing C, Zhao B, et al. Factors associated with peritoneal metastasis in non-serosa-invasive gastric cancer: a retrospective study of a prospectively-collected database. *BMC Cancer*. (2013) 13:57. doi: 10.1186/1471-2407-13-57

23. Yoshida M, Sugino T, Kusafuka K, Nakajima T, Makuuchi R, Tokunaga M, et al. Peritoneal dissemination in early gastric cancer: importance of the lymphatic route. *Virchows Arch*. (2016) 469(2):155–61. doi: 10.1007/s00428-016-1960-7

24. Tanaka T, Kumagai K, Shimizu K, Masuo K, Yamagata K. Peritoneal metastasis in gastric cancer with particular reference to lymphatic advancement; extranodal invasion is a significant risk factor for peritoneal metastasis. *J Surg Oncol*. (2000) 75(3):165–71. doi: 10.1002/1096-9098(200011)75:3<165::AID-JSO3>3.0.CO;2-5

25. Otsuji E, Yamaguchi T, Sawai K, Sakakura C, Okamoto K, Takahashi T. Regional lymph node metastasis as a predictor of peritoneal carcinomatosis in patients with Borrmann type IV gastric carcinoma. *Am J Gastroenterol*. (1999) 94(2):434–7. doi: 10.1111/j.1572-0241.1999.873_b.x

26. Adachi Y, Oshiro T, Mori M, Maehara Y, Sugimachi K. Tumor size as a simple prognostic indicator for gastric carcinoma. *Ann Surg Oncol*. (1997) 4 (2):137–40. doi: 10.1007/BF02303796

27. Saito H, Osaki T, Murakami D, Sakamoto T, Kanaji S, Oro S, et al. Macroscopic tumor size as a simple prognostic indicator in patients with gastric cancer. *Am J Surg*. (2006) 192(3):296–300. doi: 10.1016/j.amjsurg.2006.03.004

28. Taghavi S, Jayarajan SN, Davey A, Willis AI. Prognostic significance of signet ring gastric cancer. *J Clin Oncol*. (2012) 30(28):3493–8. doi: 10.1200/JCO.2012.42.6635

29. Chon HJ, Hyung WJ, Kim C, Park S, Kim JH, Park CH, et al. Differential prognostic implications of gastric signet ring cell carcinoma: stage adjusted analysis from a single high-volume center in Asia. *Ann Surg*. (2017) 265 (5):946–53. doi: 10.1097/SLA.0000000000001793

30. Kao YC, Fang WL, Wang RF, Li AF, Yang MH, Wu CW, et al. Clinicopathological differences in signet ring cell adenocarcinoma between early and advanced gastric cancer. *Gastric Cancer*. (2019) 22(2):255–63. doi: 10.1007/s10120-018-0860-8

31. Jiang CG, Wang ZN, Sun Z, Liu FN, Yu M, Xu HM. Clinicopathologic characteristics and prognosis of signet ring cell carcinoma of the stomach: results from a Chinese mono-institutional study. *J Surg Oncol*. (2011) 103 (7):700–3. doi: 10.1002/jso.21878

32. Li C, Kim S, Lai JF, Hyung WJ, Choi WH, Choi SH, et al. Advanced gastric carcinoma with signet ring cell histology. *Oncology*. (2007) 72(1-2):64–8. doi: 10.1159/000111096

33. Amin MB, Greene FL, Edge SB, Compton CC, Gershenwald JE, Brookland RK, et al. The eighth edition AJCC cancer staging manual: continuing to build a bridge from a population-based to a more "personalized" approach to cancer staging. *CA Cancer J Clin*. (2017) 67(2):93–9. doi: 10.3322/caac.21388

34. Sano T, Coit DG, Kim HH, Roviello F, Kassab P, Wittekind C, et al. Proposal of a new stage grouping of gastric cancer for TNM classification: international gastric cancer association staging project. *Gastric Cancer*. (2017) 20(2):217–25. doi: 10.1007/s10120-016-0601-9

35. Amin MB ES, Greene FL. *AJCC Staging manual*. 8th ed. New York: Springer (2017).

36. Lu J, Zheng CH, Cao LL, Li P, Xie JW, Wang JB, et al. The effectiveness of the 8th American joint committee on cancer TNM classification in the prognosis evaluation of gastric cancer patients: a comparative study between the 7th and 8th editions. *Eur J Surg Oncol*. (2017) 43(12):2349–56. doi: 10.1016/j.ejso.2017.09.001

37. Xi H, Zhang K, Wei B, Chen L. Significance and contemplation of clinical diagnosis and therapy on the renewal of the eighth edition of gastric cancer TNM staging system. *Zhonghua Wei Chang Wai Ke Za Zhi*. (2017) 20(2):166–70.

38. In H, Solsky I, Palis B, Langdon-Embry M, Ajani J, Sano T. Validation of the 8th edition of the AJCC TNM staging system for gastric cancer using the national cancer database. *Ann Surg Oncol*. (2017) 24(12):3683–91. doi: 10.1245/s10434-017-6078-x

39. Kim SG, Seo HS, Lee HH, Song KY, Park CH. Comparison of the differences in survival rates between the 7th and 8th editions of the AJCC TNM staging system for gastric adenocarcinoma: a single-institution study of 5,507 patients in Korea. *J Gastric Cancer*. (2017) 17(3):212–9. doi: 10.5230/jgc.2017.17.e23

40. He X, Wu W, Lin Z, Ding Y, Si J, Sun LM. Validation of the American joint committee on cancer (AJCC) 8th edition stage system for gastric cancer patients: a population-based analysis. *Gastric Cancer*. (2018) 21(3):391–400. doi: 10.1007/s10120-017-0770-1

41. Yonemura Y, Ishibashi H, Mizumoto A, Nishihara K, Liu Y, Wakama S, et al. Mechanisms of peritoneal metastasis formation. In: O Glehen, A Bhatt, editors. *Pathology of peritoneal metastases: The unchartered fields*. Singapore: Springer Singapore (2020). p. 1–26.

frontiers | Frontiers in Oncology

TYPE Original Research
PUBLISHED 23 January 2023
DOI 10.3389/fonc.2022.977111

Check for updates

OPEN ACCESS

EDITED BY
Sanjit Mukherjee,
National Institutes of Health (NIH),
United States

REVIEWED BY
Hui Li,
Chongqing University, China
Zhaohui Tang,
Shanghai Jiao Tong University, China
Seogsong Jeong,
CHA University, Republic of Korea

*CORRESPONDENCE
Di Tang
tangdi@mail.sysu.edu.cn
Tong Zhang
zhjeff72@sina.com

†These authors have contributed equally to this work

SPECIALTY SECTION
This article was submitted to Surgical Oncology, a section of the journal Frontiers in Oncology

RECEIVED 24 June 2022
ACCEPTED 28 December 2022
PUBLISHED 23 January 2023

CITATION
Deng G, Ren J-k, Wang H-t, Deng L, Chen Z-b, Fan Y-w, Tang Y-j, Zhang T and Tang D (2023) Tumor burden score dictates prognosis of patients with combined hepatocellular cholangiocarcinoma undergoing hepatectomy. *Front. Oncol.* 12:977111. doi: 10.3389/fonc.2022.977111

COPYRIGHT
© 2023 Deng, Ren, Wang, Deng, Chen, Fan, Tang, Zhang and Tang. This is an open-access article distributed under the terms of the Creative Commons Attribution License (CC BY). The use, distribution or reproduction in other forums is permitted, provided the original author(s) and the copyright owner(s) are credited and that the original publication in this journal is cited, in accordance with accepted academic practice. No use, distribution or reproduction is permitted which does not comply with these terms.

Tumor burden score dictates prognosis of patients with combined hepatocellular cholangiocarcinoma undergoing hepatectomy

Gang Deng[1†], Jun-kai Ren[2†], Hai-tao Wang[1], Liang Deng[1], Zu-bing Chen[1], You-wen Fan[1], Ya-jun Tang[1], Tong Zhang[2*] and Di Tang[1*]

[1]Department of General Surgery, the Seventh Affiliated Hospital of Sun Yat-sen University, Shenzhen, China, [2]Department of Hepatic Surgery and Liver Transplantation Center, the Third Affiliated Hospital of Sun Yat-sen University, Guangzhou, China

Background: The prognostic value of the tumor burden score (TBS) in patients with combined hepatocellular-cholangiocarcinoma (cHCC-CCA) remains unknown. This study aimed to investigate the impact of TBS on long-term outcomes after surgery.

Methods: Patients who underwent radical-intent resection between June 2013 and December 2019 were retrospectively reviewed. Kaplan–Meier curves were used to analyze patient survival, and disease-free survival (DFS) and overall survival (OS) were examined in relation to TBS.

Results: A total of 178 patients were included in this study, with 119 in the training cohort and 59 in the validation cohort. Kaplan–Meier curves showed that TBS was a strong prognostic indicator in patients with cHCC-CCA. Elevated TBS was associated with poorer DFS and OS (both P-value < 0.001) and was identified as an independent prognostic indicator. In addition, the prognostic value of TBS outperformed tumor size and number alone, microvascular invasion, and lymph node invasion. The prognostic significance of TBS was confirmed by the internal validation cohort.

Conclusions: The present study suggested the significance of tumor morphology in assessing the prognosis of patients with cHCC-CCA who undergoing curative resection. The TBS is a promising prognostic index in patients with cHCC-CCA. Elevated TBS was related to a lower long-term survival rate and was identified as an independent risk factor for poor DFS and OS. Further research is needed to verify our results.

KEYWORDS

combined hepatocellular-cholangiocarcinoma, tumor burden score, curative resection, overall survival, tumor relapse

Introduction

Combined hepatocellular-cholangiocarcinoma (cHCC-CCA) is a rare subtype that accounts for less than 5% of all primary liver cancers (1). Histologically, cHCC-CCA exhibits both hepatocytic and biliary differentiation. The prognosis of cHCC-CCA is generally worse than that of hepatocellular carcinoma (HCC) and similar to that of intrahepatic cholangiocarcinoma (ICC) (2). Among various therapeutic strategies, surgical resection remains the only curative option for patients with cHCC-CCA (3). However, the 5-year tumor relapse rate exceeds 80% after hepatectomy, and the 5-year overall survival (OS) rate was less than 30% (4).

Conventionally, the tumor-node-metastasis staging system is applied for the prognostic classification of patients with solid malignancies (5, 6). To date, the American Joint Committee on Cancer (AJCC) staging system is the most widely used for the clinical classification of cHCC-CCA (7). In the eighth edition, the T1 category was reclassified using a maximum tumor size of 5 cm, emphasizing the effect of tumor size on outcomes. Moreover, tumor multifocality exerts an equivalent prognostic effect to macrovascular invasion (8).

Recently, a new metric called "tumor burden score (TBS)", calculated on the basis of tumor size and tumor number, was proposed for risk stratification in multifocal tumors (9). Emerging evidence has shown the promising potential of TBS in stratifying the prognosis of patients with colorectal liver metastasis, HCC, and ICC who underwent surgical resection (10–13). Nevertheless, the prognostic value of TBS in patients with cHCC-CCA has not been evaluated. The present study aimed to investigate the prognostic significance of TBS in surgically treated patients with cHCC-CCA and to compare its predictive accuracy with the other prognostic factors.

Methods

Patients

This study was approved by the Ethics Committees of the relevant institutions and was performed in accordance with the Declaration of Helsinki (14). Surgically treated patients with cHCC-CCA from the Seventh Affiliated Hospital of Sun Yat-Sen University and the Third Affiliated Hospital of Sun Yat-Sen University between June 2013 and December 2019 were retrospectively reviewed. The diagnosis was confirmed by pathological examination. The exclusion criteria were as follows: patients with recurrent cHCC-CCA, tumors with positive surgical margin, tumors with local organ invasion, patients who did not undergo resection with curative intent, and those with incomplete clinical data. The included patients were reviewed for basic information, laboratory parameters, and histological and gross tumor features. In addition, all patients were required to sign a consent form for clinical research prior to hepatectomy. The patients were randomly divided into the training cohort and the validation cohort using 2:1 patient matching.

Follow-up

Tumor markers and contrast-enhanced ultrasonography were performed every month for the first 3 months following surgery, then every 3 months for 1 year, and every half year thereafter. For patients who opted not to go back to the hospital for re-examination, a telephone follow-up survey was carried out. The patients were followed until December 2021 or death. OS was calculated from the date of hepatic resection to the date of the last follow-up or death. In contrast, disease-free survival (DFS) was defined as the interval between the date of hepatic resection and the earliest evidence of recurrence or last follow-up.

TBS evaluation

TBS was defined as previously reported (9), using the formula: TBS^2 = (maximum tumor diameter)^2 + (lesion number)^2. The maximum tumor diameter and lesion number were obtained from preoperative contrast-enhanced CT scan examination and confirmed by the final pathological report. The optimal cutoff value of TBS was determined by X-tile (version 3.6.1, Yale University) (15). Patients were categorized into the high-TBS group and the low-TBS group according to the cutoff value. The ability of TBS to predict prognosis was validated using the internal validation cohort.

Statistical analysis

Variables were presented as frequency (%), and continuous variables were compared using the student's t-test or Wilcoxon rank sum test. Categorical variables were analyzed by the chi-square or Fisher's exact test, as appropriate. Bivariate survival analyses were performed using Kaplan–Meier curves, and their differences were tested by log-rank test. Cox proportional hazard models (enter method) were employed to assess the potential independent prognostic risk factors and to present adjusted hazard ratio. Variables that were statistically significant in univariate analyses (P-value < 0.05) were entered into multivariate analyses. Adjusted hazard ratios identified by multivariate analyses exhibited risk ratios for tumor relapse or death. However, tumor size and tumor number were excluded from multivariate analyses to avoid collinearity bias (16). The areas under the receiver operator characteristic curve were used to evaluate the predictive accuracy of the significant indicators identified in multivariate analyses. All analyses were performed by MedCalc (version 20.0.3.0, Ostend, Belgien) and SPSS (version 24.0, Chicago, IL, United States). A P-value < 0.05 was considered statistically significant.

Results

Patient characteristics

A total of 203 patients who underwent hepatic resection with curative intent between January 2012 and December 2019 were pathologically diagnosed as cHCC-CCA. Among them, 11 patients were associated with recurrent tumors, five patients with positive surgical margins, seven patients with local organ invasion, and two patients had incomplete clinical data. Finally, 178 patients (150 male patients and 128 female patients) were included in the present

analysis (119 in the training cohort and 59 in the validation cohort), as shown in Figure 1. Among the enrolled patients, 142 (79.8%) were aged less than 60 years, 77 (43.3%) exhibited a maximum tumor diameter of less than 5 cm, and 104 (58.4%) had solitary tumors. No significant difference in baseline characteristics was observed between the training and validation cohorts (Table 1).

Association between TBS and clinicopathologic features

The optimal cutoff value of TBS was identified as 5.2 after calculating by using the X-tile (the detailed information was shown in Supplementary Figures 1, 2). In the training cohort, 54 (45.4%) patients were classified into the low-TBS group, and 65 (54.6%) were classified into the high-TBS group. The mean TBS value was 3.77 in the low-TBS group. Patients in the high-TBS group were associated with greater frequency of capsular invasion (P-value = 0.012) and lymph node invasion (P-value = 0.036) (Table 2).

The association between TBS and clinicopathological features was verified in the validation cohort (Supplementary Table 1). In brief, 20 (33.9%) patients were classified into the low-TBS group, whereas 39 (66.1%) patients were classified into the high-TBS group. The frequency of capsular invasion, lymph node invasion, and microvascular invasion MVI was comparable between the two groups.

Among the enrolled patients, three (1.7%) patients received neoadjuvant therapy, and 52 (29.2%) patients were treated with adjuvant chemotherapy. As displayed in Table 1, no significant difference was found between the derivation and validation cohorts. Stratified by TBS, postoperative chemotherapy was comparable between the two groups (P-value = 0.521, Table 2). In addition, univariate analyses identified that adjuvant chemotherapy might not be a prognostic factor for OS and DFS (Table 3). Our results were consistent with previous studies, showing that adjuvant treatment did not influence survival outcomes (17). Collectively, these results implied that cHCC-ICC should be considered as a distinct entity requiring specific therapeutic strategies, especially adjuvant treatments after curative resection.

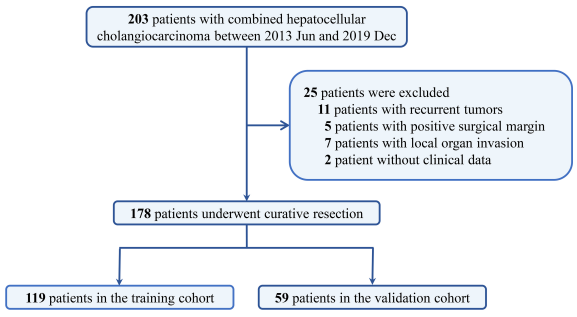

FIGURE 1
The selection diagram of combined hepatocellular-cholangiocarcinoma patients.

Association between TBS and patient prognosis

As shown in Figure 2, patients with a maximum tumor diameter of less than 5 cm were associated with longer DFS but similar OS compared with those with tumor size larger than 5 cm (Figures 2A, D). In addition, patients with solitary tumors were associated with longer DFS but similar OS compared with those with multiple tumors (Figures 2B, E). The patients were stratified into two groups on the basis of TBS. The patients in the low-TBS group were associated with better OS and a lower rate of tumor relapse compared with those with high TBS (Figures 2C, F). The Cox regression models indicated that high TBS was an independent risk factor for poor OS [hazard ratio (HR) = 2.361; 95% confidence interval (CI), 1.417–3.934; P-value < 0.001] and DFS (HR = 2.643; 95% CI, 1.629–4.288; P-value < 0.001) (Table 3). Furthermore, MVI and lymph node invasion were also independent prognostic indicators for poor OS and DFS.

In the internal validation cohort, patients with solitary tumors were associated with better OS and similar DFS compared with those with multiple tumors. Patients in the low-TBS group were associated with better prognoses. Consistently, Cox regression models identified high TBS as an independent prognostic indicator for poor OS and DFS (Figure 3; Supplementary Table 2).

The predictive accuracy of TBS was compared with tumor size, tumor number, MVI, and lymph node invasion. As shown in Supplementary Table 3, TBS showed the highest area under curve (AUC) in predicting OS (0.689; 95% CI, 0.584–0.782) and DFS (0.772; 95% CI, 0.672–0.853), indicating that TBS was the most effective in predicting patient prognosis. Subsequently, the specificity and sensitivity of these indicators were compared. In addition, the AUCs of TBS based on those previously reported cutoff values were compared, revealing that the present TBS cutoff value was the most accurate in predicting long-term outcomes for patients with cHCC-ICC (Supplementary Table 4).

Discussion

Epidemiologically, cHCC-CCA is a rare subtype of primary liver cancer, accounting for less than 5% of the cases (1). cHCC-ICC may exhibit both hepatocytic and biliary differentiation (2). The likelihood of viral hepatitis in patients with cHCC-ICC is intermediate between HCC and ICC (18, 19). In addition, cHCC-ICC cells may produce AFP and CA19-9. Clinically, a simultaneous increase in serum levels of both markers strongly suggests the diagnosis of cHCC-ICC. Nevertheless, only a minority of patients were associated with an increase in both serum markers. The clinical symptoms of cHCC-ICC are most often associated with advanced tumoral disease and are not apparent in the early stage. Therefore, more than half of the patients were diagnosed at advanced stages. Currently, there is no therapeutic guideline for cHCC-CCA, and curative resection is considered the most effective treatment (20). However, the long-term outcome of patients with cHCC-CCA is still poor due to rapid progression and frequent tumor relapse. Improving the prognosis of patients with cHCC-CCA remains a medical challenge. The present study demonstrated that TBS, calculated on the basis of the maximum

10.3389/fonc.2022.977111

TABLE 1 Baseline patient characteristics between training and validation cohort.

Variables	All patients (*n* = 178)	Training cohort (*n* = 119)	Validation cohort (*n* = 59)	P-value
Age				0.553
<60	142 (79.8)	93 (78.2)	49 (83.1)	
≥60	36 (20.2)	26 (21.8)	10 (16.9)	
Sex				0.386
Male	150 (84.3)	98 (82.4)	52 (88.1)	
Female	28 (15.7)	21 (17.6)	7 (11.9)	
AFP, ng/ml				0.867
<8	61 (34.3)	40 (33.6)	21 (35.6)	
≥8	117 (65.7)	79 (66.4)	38 (64.4)	
CA19-9 value, U/ml				0.872
<37	78 (43.8)	53 (44.5)	25 (42.4)	
≥37	93 (54.4)	66 (55.5)	34 (57.6)	
HBsAg, +/−				0.621
Positive	116 (65.2)	76 (63.9)	40 (67.8)	
Negative	62 (34.8)	43 (36.1)	19 (32.2)	
Cirrhosis				0.875
Positive	83 (46.6)	56 (47.1)	27 (45.8)	
Negative	95 (53.4)	63 (52.9)	32 (54.2)	
Tumor size, cm				0.842
<5	77 (43.3)	52 (43.7)	25 (42.4)	
≥5	101 (56.7)	67 (56.3)	34 (57.6)	
Tumor number				0.757
Solitary	104 (58.4)	71 (59.7)	33 (55.9)	
Multiple	74 (41.6)	48 (40.3)	26 (44.1)	
Differentiation				0.642
Well	28 (15.7)	19 (16.0)	9 (15.3)	
Moderate-poor	150 (84.3)	100 (84.0)	50 (84.7)	
Capsular invasion				0.741
Positive	113 (63.5)	77 (64.7)	36 (61.0)	
Negative	65 (36.5)	42 (35.3)	23 (39.0)	
MVI				0.730
Positive	51 (28.7)	32 (26.9)	19 (32.2)	
Negative	127 (70.8)	87 (72.3)	40 (67.8)	
Lymph node invasion				0.878
Positive	19 (10.7)	13 (10.9)	6 (10.2)	
Negative	159 (89.3)	106 (89.1)	53 (89.8)	
Adjuvant chemotherapy				0.423
Yes	52 (29.2)	40 (33.6)	12 (20.3)	
No	109 (61.2)	67 (56.3)	42 (71.1)	

(Continued)

TABLE 1 Continued

Variables	All patients (*n* = 178)	Training cohort (*n* = 119)	Validation cohort (*n* = 59)	P-value
Unknown	17 (9.6)	12 (10.1)	5 (8.6)	
TBS grade				0.151
Low	74 (41.6)	54 (45.4)	20 (33.9)	
High	104 (58.4)	65 (54.6)	39 (66.1)	

AFP, alpha-fetoprotein; CA19-9, carbohydrate antigen 19-9; MVI, microvascular invasion; TBS, tumor burden score.

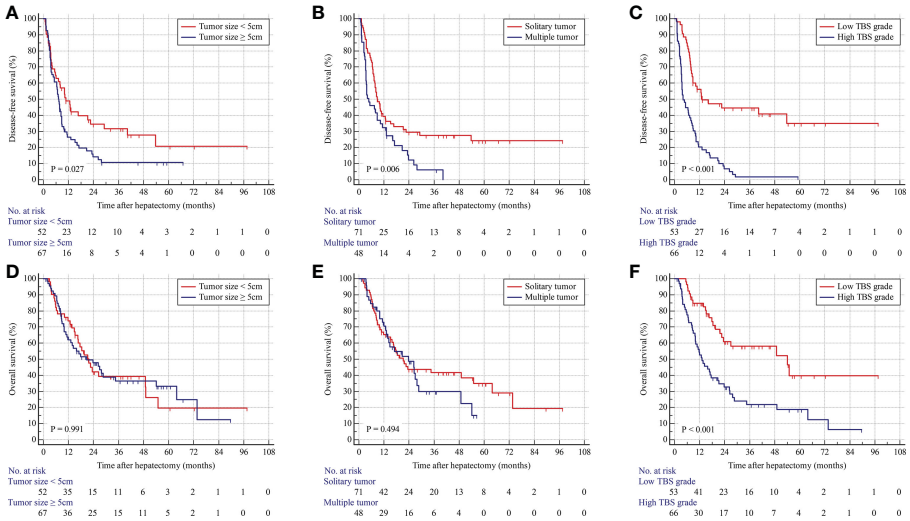

FIGURE 2
Kaplan–Meier curves for DFS and OS stratified by tumor size **(A, D)**, tumor number **(B, E)**, and TBS grade **(C, F)** in the derivation cohort.

TABLE 2 Correlation between TBS grade and clinicopathological characteristics in training cohort.

Variables	Low-TBS grade (*n* = 54)	High-TBS grade (*n* = 65)	P-value
Age			0.377
<60	40 (74.1)	53 (81.5)	
≥60	14 (25.9)	12 (18.5)	
Sex			0.815
Male	45 (83.3)	53 (81.5)	
Female	9 (16.7)	12 (18.5)	
AFP, ng/ml			0.079
<8	23 (42.6)	17 (26.2)	
≥8	31 (57.4)	48 (73.8)	
CA19-9 value, U/ml			0.272
<37	29 (53.7)	26 (40.0)	
≥37	25 (46.3)	39 (60.0)	
HBsAg, +/−			0.187
Positive	38 (70.4)	38 (58.5)	

(Continued)

10.3389/fonc.2022.977111

TABLE 2 Continued

Variables	Low-TBS grade (n = 54)	High-TBS grade (n = 65)	P-value
Negative	16 (29.6)	27 (41.5)	
Cirrhosis			0.202
Positive	29 (53.7)	27 (41.5)	
Negative	25 (46.3)	38 (58.5)	
Tumor size, cm			<0.001*
<5	51 (94.4)	1 (1.5)	
≥5	3 (5.6)	64 (98.5)	
Tumor number			0.005*
Solitary	40 (74.1)	31 (47.7)	
Multiple	14 (25.9)	34 (52.3)	
Differentiation			0.924
Well	9 (16.7)	10 (15.4)	
Moderate-poor	45 (83.3)	55 (84.6)	
Capsular invasion			0.012*
Positive	28 (51.9)	49 (75.4)	
Negative	26 (48.1)	16 (24.6)	
MVI			0.154
Positive	11 (20.4)	21 (32.3)	
Negative	43 (79.6)	44 (67.7)	
Lymph node invasion			0.036*
Positive	2 (3.7)	11 (16.9)	
Negative	52 (96.3)	54 (83.1)	
Adjuvant chemotherapy			0.521
Yes	17 (31.5)	23 (35.4)	
No	32 (59.3)	35 (53.8)	
Unknown	5 (9.2)	7 (10.8)	
TBS value	3.77 (0.94)	9.15 (2.38)	<0.001*

AFP, alpha-fetoprotein; CA19-9, carbohydrate antigen 19-9; MVI, microvascular invasion; TBS, tumor burden score; TBS value was showed as mean (standard deviation); *statistically significant.

TABLE 3 Identification of prognostic factors for overall survival and disease-free survival in the training cohort.

Variables	Overall survival				Disease-free survival			
	Univariate		Multivariate		Univariate		Multivariate	
	HR (95% CI)	P-value	HR (95% CI)	P-value	HR (95% CI)	P-value	HR (95% CI)	P-value
Sex (F/M)	0.647 (0.331–1.266)	0.204			0.935 (0.558–1.569)	0.800		
Age (≥60/<60)	1.325 (0.711–2.471)	0.376			1.429 (0.853–2.395)	0.175		
AFP (≥8/<8)	1.525 (0.914–2.544)	0.106			1.714 (1.093–2.689)	0.019*	1.436 (0.892–2.310)	0.136

(Continued)

10.3389/fonc.2022.977111

TABLE 3 Continued

Variables	Overall survival				Disease-free survival			
	Univariate		Multivariate		Univariate		Multivariate	
	HR (95% CI)	P-value	HR (95% CI)	P-value	HR (95% CI)	P-value	HR (95% CI)	P-value
CA19–9 (≥37/<37)	1.325 (0.817–2.151)	0.254			1.479 (0.967–2.262)	0.071		
HBsAg	1.244 (0.750–2.064)	0.397			1.208 (0.782–1.865)	0.394		
Cirrhosis	1.118 (0.700–1.784)	0.641			1.132 (0.751–1.705)	0.555		
Tumor size (≥5/<5)	1.003 (0.624–1.613)	0.991			1.597 (1.056–2.416)	0.027*		
Tumor number (multiple/solitary)	1.189 (0.724–1.950)	0.494			1.751 (1.154–2.656)	0.006*		
Differentiation (moderate-poor/well)	1.111 (0.399–1.648)	0.563			1.131 (0.512–2.495)	0.761		
Liver capsule invasion	1.166 (0.719–1.892)	0.534			1.358 (0.879–2.098)	0.168		
MVI	1.977 (1.206–3.242)	0.007*	2.289 (1.374–3.813)	0.001*	1.660 (1.063–2.592)	0.026*	1.654 (1.054–2.597)	0.029*
Lymph node invasion	2.727 (1.386–5.366)	0.004*	2.546 (1.255–5.164)	0.010*	1.695 (1.124–2.557)	0.012*	1.576 (1.006–2.469)	0.047*
Adjuvant chemotherapy	0.821 (0.534–1.342)	0.556			0.751 (0.512–1.273)	0.329		
TBS grade (high/low)	2.510 (1.524–4.133)	<0.001*	2.361 (1.417–3.934)	<0.001*	3.177 (2.040–4.949)	<0.001*	2.643 (1.629–4.288)	<0.001*

M, male; F, female; MVI, microvascular invasion; CA19-9, carbohydrate antigen 19-9; HR, hazard ratio; CI, confidence interval; *statistically significant.

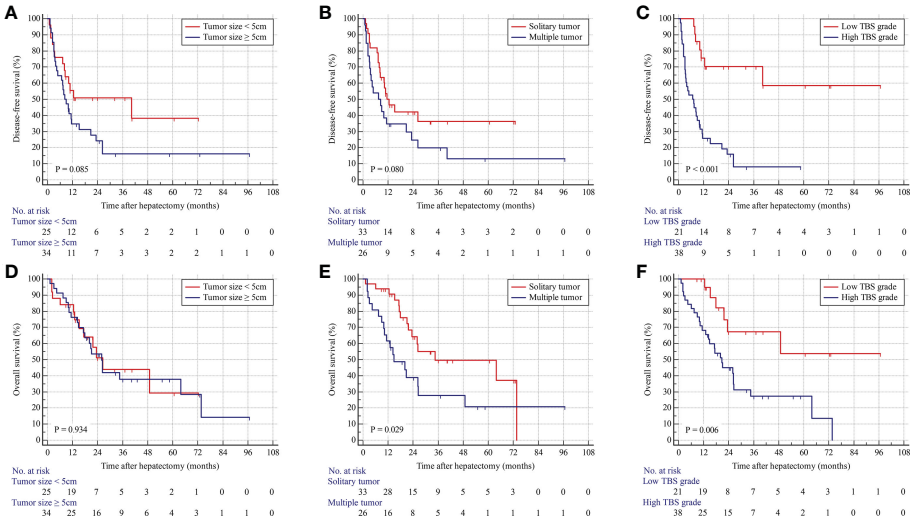

FIGURE 3
Kaplan–Meier curves for DFS and OS stratified by tumor size **(A, D)**, tumor number **(B, E)**, and TBS grade **(C, F)** in the validation cohort.

tumor diameter and the number of lesions, was a stable and independent prognostic indicator for both DFS and OS in patients with cHCC-CCA who undergoing radical hepatic resection.

The staging strategy for cHCC-CCA was first incorporated into the ICC-tumor-node-metastasis (TNM) staging system in the seventh edition of the AJCC staging manual (21), in which tumor size was not included as a factor. However, in the eighth edition, the T1 stage was stratified into T1a and T1b on the basis of tumor size with a cutoff value of 5 cm. T2a and T2b were merged into T2, which represented the equivalent effect of tumor multifocality and vascular invasion (8). A growing number of studies have identified tumor size as an independent prognostic predictor for poor survival outcomes in patients with cHCC-CCA (22, 23). Our results in this study reflected the previous findings that patients with tumor size > 5 cm were associated with faster tumor relapse. However, the prognostic value of the number of lesions in patients with cHCC-CCA has been controversial. Kim et al. suggested that patients with solitary tumors were associated with a superior prognosis than those with multiple lesions (24), whereas Jiang et al. demonstrated that the tumor number was not a prognostic indicator for cHCC-CCA after curative resection (25). Our results revealed that multiple tumor lesions were associated with worse DFS but similar OS compared with those with solitary lesions. Nevertheless, the prognostic value of tumor size and tumor number in patients with cHCC-CCA should be confirmed by future studies with larger sample sizes.

TBS was defined as the distance from the origin of a Cartesian plane using maximum tumor size as the X-axis and tumor number as the Y-axis (9). As previously reported, TBS is a valuable tool in evaluating prognosis for colorectal liver metastases, HCC, and ICC (13, 26, 27). The present study assessed the significance of TBS in dictating the prognosis of patients with cHCC-CCA after curative liver resection. Elevated TBS grade was associated with poor DFS and OS and was identified as a stable, independent prognostic indicator for long-term outcomes. Notably, the predictive effect of TBS outperformed tumor size and number alone and MVI and lymph node invasion in evaluating DFS and OS.

The following limitations should be considered when interpreting our results. First, this was a retrospective study with a limited number of cases, which might involve selection bias or unmeasured confounding factors. Second, although the cutoff value for TBS was validated by our internal validation cohort, its applicability to overseas patient populations remains unknown. In addition, as only surgically treated patients with cHCC-CCA (a limited part of the overall population of patients with cHCC-CCA) were included in the analyses, the results are only applicable to patients who undergoing curative resection.

In conclusion, this study suggests the significance of tumor morphology in assessing the prognosis of patients with cHCC-CCA who undergoing curative resection. The TBS, based on the maximum tumor diameter and lesion number, is a promising index in the prognostic evaluation of patients with cHCC-CCA. Elevated TBS was associated with worse long-term survival and was identified as an independent risk factor for poor DFS and OS. Nevertheless, these results should be verified by further studies.

Data availability statement

The original contributions presented in the study are included in the article/Supplementary Material. Further inquiries can be directed to the corresponding authors.

Ethics statement

The studies involving human participants were reviewed and approved by Seven Affiliated Hospital of Sun Yat-sen University. The patients/participants provided their written informed consent to participate in this study.

Author contributions

Conceptualization: GD, TZ, and DT. Data curation: GD, Z-BC, and Y-WF. Formal analysis: GD, J-KR, and Y-JT. Supervision: TZ and DT. Writing—original draft: GD, J-KR, and H-TW. All the authors approved the final version of manuscript.

Funding

This work was supported by Natural Science Foundation of Guangdong Province (2019A1515011850 and 2022A1515012224).

Conflict of interest

The authors declare that the research was conducted in the absence of any commercial or financial relationships that could be construed as a potential conflict of interest.

Publisher's note

All claims expressed in this article are solely those of the authors and do not necessarily represent those of their affiliated organizations, or those of the publisher, the editors and the reviewers. Any product that may be evaluated in this article, or claim that may be made by its manufacturer, is not guaranteed or endorsed by the publisher.

Supplementary material

The Supplementary Material for this article can be found online at: https://www.frontiersin.org/articles/10.3389/fonc.2022.977111/full#supplementary-material

References

1. Sung H, Ferlay J, Siegel RL, Laversanne M, Soerjomataram I, Jemal A, et al. Global cancer statistics 2020: GLOBOCAN estimates of incidence and mortality worldwide for 36 cancers in 185 countries. *CA Cancer J Clin* (2021) 71:209–49. doi: 10.3322/caac.21660

2. Brunt E, Aishima S, Clavien PA, Fowler K, Goodman Z, Gores G, et al. cHCC-CCA: Consensus terminology for primary liver carcinomas with both hepatocytic and cholangiocytic differentation. *Hepatology* (2018) 68:113–26. doi: 10.1002/hep.29789

3. Kim KH, Lee SG, Park EH, Hwang S, Ahn CS, Moon DB, et al. Surgical treatments and prognoses of patients with combined hepatocellular carcinoma and cholangiocarcinoma. *Ann Surg Oncol* (2009) 16:623–9. doi: 10.1245/s10434-008-0278-3

4. Yamashita YI, Aishima S, Nakao Y, Yoshizumi T, Nagano H, Kuroki T, et al. Clinicopathological characteristics of combined hepatocellular cholangiocarcinoma from the viewpoint of patient prognosis after hepatic resection: High rate of early recurrence and its predictors. *Hepatol Res* (2020) 50:863–70. doi: 10.1111/hepr.13507

5. Zhang F, Hu K, Tang B, Tian M, Lu S, Yuan J, et al. A new scoring method for personalized prognostic prediction in patients with combined hepatocellular and cholangiocarcinoma after surgery. *J Gastrointest Surg* (2021) 25:971–82. doi: 10.1007/s11605-020-04618-2

6. Li H, Lan T, Liu H, Liu C, Dai J, Xu L, et al. IL-6-induced cGGNBP2 encodes a protein to promote cell growth and metastasis in intrahepatic cholangiocarcinoma. *Hepatology* (2022) 75:1402–19. doi: 10.1002/hep.32232

7. Hou GM, Liu HL, Wu H, Zeng Y. Prediction of prognosis for cHCC-CC patients after surgery: Comparison of tumor marker score based on AFP, CEA, CA19-9, and other clinical stages. *Ann Surg Oncol* (2021) 28:7647–60. doi: 10.1245/s10434-021-09949-1

8. Cheng Z, Lei Z, Si A, Yang P, Luo T, Guo G, et al. Modifications of the AJCC 8th edition staging system for intrahepatic cholangiocarcinoma and proposal for a new staging system by incorporating serum tumor markers. *HPB (Oxford)* (2019) 21:1656–66. doi: 10.1016/j.hpb.2019.05.010

9. Sasaki K, Morioka D, Conci S, Margonis GA, Sawada Y, Ruzzenente A, et al. The tumor burden score: A new "Metro-ticket" prognostic tool for colorectal liver metastases based on tumor size and number of tumors. *Ann Surg* (2018) 267:132–41. doi: 10.1097/SLA.0000000000002064

10. Ho SY, Liu PH, Hsu CY, Ko CC, Huang YH, Su CW, et al. Tumor burden score as a new prognostic marker for patients with hepatocellular carcinoma undergoing transarterial chemoembolization. *J Gastroenterol Hepatol* (2021) 36(11):3196–203. doi: 10.1136/gutjnl-2021-IDDF.78

11. Elfadaly AN, Tsilimigras DI, Hyer JM, Paro A, Bagante F, Ratti F, et al. Impact of tumor burden score on conditional survival after curative-intent resection for hepatocellular carcinoma: A multi-institutional analysis. *World J Surg* (2021) 45 (11):3438–48. doi: 10.1007/s00268-021-06265-3

12. Moris D, Shaw BI, McElroy L, Barbas AS. Using hepatocellular carcinoma tumor burden score to stratify prognosis after liver transplantation. *Cancers (Basel)* (2020) 12 (11):3372. doi: 10.3390/cancers12113372

13. Li H, Liu R, Qiu H, Huang Y, Liu W, Li J, et al. Tumor burden score stratifies prognosis of patients with intrahepatic cholangiocarcinoma after hepatic resection: A retrospective, multi-institutional study. *Front Oncol* (2022) 12:829407. doi: 10.3389/fonc.2022.829407

14. Carlson RV, Boyd KM, Webb DJ. The revision of the declaration of Helsinki: past, present and future. *Br J Clin Pharmacol* (2004) 57:695–713. doi: 10.1111/j.1365-2125.2004.02103.x

15. Camp RL, Dolled-Filhart M, Rimm DL. X-Tile: a new bio-informatics tool for biomarker assessment and outcome-based cut-point optimization. *Clin Cancer Res* (2004) 10:7252–9. doi: 10.1158/1078-0432.CCR-04-0713

16. Chan AWH, Zhong J, Berhane S, Toyoda H, Cucchetti A, Shi K, et al. Development of pre and post-operative models to predict early recurrence of hepatocellular carcinoma after surgical resection. *J Hepatol* (2018) 69:1284–93. doi: 10.1016/j.jhep.2018.08.027

17. Liu WR, Tian MX, Tao CY, Tang Z, Zhou YF, Song SS, et al. Adjuvant transarterial chemoembolization does not influence recurrence-free or overall survival in patients with combined hepatocellular carcinoma and cholangiocarcinoma after curative resection: a propensity score matching analysis. *BMC Cancer* (2020) 20:642. doi: 10.1186/s12885-020-07138-z

18. Taguchi J, Nakashima O, Tanaka M, Hisaka T, Takazawa T, Kojiro M. A clinicopathological study on combined hepatocellular and cholangiocarcinoma. *J Gastroenterol Hepatol* (1996) 11:758–64. doi: 10.1111/j.1440-1746.1996.tb00327.x

19. Tickoo SK, Zee SY, Obiekwe S, Xiao H, Koea J, Robiou C, et al. Combined hepatocellular-cholangiocarcinoma: a histopathologic, immunohistochemical, and *in situ* hybridization study. *Am J Surg Pathol* (2002) 26:989–97. doi: 10.1097/00000478-200208000-00003

20. Beaufrère A, Calderaro J, Paradis V. Combined hepatocellular-cholangiocarcinoma: An update. *J Hepatol* (2021) 74:1212–24. doi: 10.1016/j.jhep.2021.01.035

21. Edge SB, Compton CC. The American joint committee on cancer: the 7th edition of the AJCC cancer staging manual and the future of TNM. *Ann Surg Oncol* (2010) 17:1471–4. doi: 10.1245/s10434-010-0985-4

22. Xu J, Li S, Feng Y, Zhang J, Peng Y, Wang X, et al. The Fibrinogen/Albumin ratio index as an independent prognostic biomarker for patients with combined hepatocellular cholangiocarcinoma after surgery. *Cancer Manag Res* (2022) 14:1795–806. doi: 10.2147/CMAR.S361462

23. Kim JH, Yoon HK, Ko GY, Gwon DI, Jang CS, Song HY, et al. Nonresectable combined hepatocellular carcinoma and cholangiocarcinoma: analysis of the response and prognostic factors after transcatheter arterial chemoembolization. *Radiology* (2010) 255:270–7. doi: 10.1148/radiol.09091076

24. Kim M, Hwang S, Ahn CS, Kim KH, Moon DB, Ha TY, et al. Postresection prognosis of combined hepatocellular carcinoma-cholangiocarcinoma according to the 2010 world health organization classification: single-center experience of 168 patients. *Ann Surg Treat Res* (2021) 100:260–9. doi: 10.4174/astr.2021.100.5.260

25. Jiang XX, Huang XT, Huang CS, Chen LH, Liang LJ, Yin XY. Long-term outcome and prognostic factors of combined hepatocellular carcinoma and cholangiocarcinoma after curative resection. *Gastroenterol Rep (Oxf)* (2020) 8:134–42. doi: 10.1093/gastro/goaa003

26. Cao Y, Ke S, Deng S, Yan L, Gu J, Mao F, et al. Development and validation of a predictive scoring system for colorectal cancer patients with liver metastasis: A population-based study. *Front Oncol* (2021) 11:719638. doi: 10.3389/fonc.2021.719638

27. Müller L, Hahn F, Auer TA, Fehrenbach U, Gebauer B, Haubold J, et al. Tumor burden in patients with hepatocellular carcinoma undergoing transarterial chemoembolization: Head-to-Head comparison of current scoring systems. *Front Oncol* (2022) 12:850454. doi: 10.3389/fonc.2022.850454

Frontiers in Oncology

Advances knowledge of carcinogenesis and tumor progression for better treatment and management

The third most-cited oncology journal, which highlights research in carcinogenesis and tumor progression, bridging the gap between basic research and applications to imrpove diagnosis, therapeutics and management strategies.

Discover the latest Research Topics

See more →



Frontiers

Avenue du Tribunal-Fédéral 34
1005 Lausanne, Switzerland
frontiersin.org

Contact us

+41 (0)21 510 17 00
frontiersin.org/about/contact